ACTA CHEMICA SCANDINAVICA 15 (1961) 1–10

On the Complex Chemistry of the Tervalent Rare-Earth Ions

VI. A Study of the Complex Formation between Gadolinium and Glycolate Ions in an Anion Exchanger

ARTUR SONESSON

Department of Inorganic and Physical Chemistry, University of Lund, Lund, Sweden

The complex formation between gadolinium and glycolate ions in an anion exchanger phase has been studied at 20°C, a resin with quarternary ammonium groups (Dowex 1 × 4) being used. The glycolate concentration of the resin was varied widely by exchange for perchlorate ions. The amount of water of the resin phase was determined and the ionic strength of the resin phase was calculated formally. The ionic strength of the water phase was approximately constant, 0.21 M.

The glycolate concentration of the two phases was determined by oxidation with potassium permanganate in a solution made alkaline by sodium carbonate.

It was found that the ligand number of the resin phase could not be calculated in the whole concentration range as the ionic strength probably varied too widely, owing to the dependence of the swelling upon the glycolate load on the exchanger.

Approximate values of $K \cdot \beta_{n\mathrm{R}}$, where K is a constant, were determined, but it was not possible to compute K. The values of $K \cdot \beta_{n\mathrm{R}}$ (n = 1, 2, 3, 4) are of the same order of magnitude as the potentiometrically obtained complexity constants for a water solution. It seems probable that only the first anionic complex is formed in the resin phase.

Complexity constants of the gadolinium-glycolate system are also reported for solutions with the ionic strengths 0.21 M and 3.0 M.

The method of calculation given by Fronæus *et al.*[1] has been used. As to the notations and the equations used for the calculations, the reader is referred to the previous papers [1,2].

In this investigation the ionic strength of the water phase was kept approximately constant (I = 0.21 M). Therefore the complexity constants for the water phase may be considered as approximately constant.

For the distribution of a tervalent ion species, M^{3+}, between a water phase and a resin phase, both containing the ligand A^-, we have the Donnan equilibrium

$$f_{\mathrm{MR}} \cdot [\mathrm{M}^{3+}]_{\mathrm{R}} \cdot f_{\mathrm{AR}}^{3} \cdot [\mathrm{A}^-]_{\mathrm{R}}^{3} = K_{\mathrm{a}} \cdot f_{\mathrm{ML}} \cdot [\mathrm{M}^{3+}]_{\mathrm{L}} \cdot f_{\mathrm{AL}}^{3} \cdot [\mathrm{A}^-]_{\mathrm{L}}^{3} \qquad (1)$$

Here we mean by f the activity coefficient, by K_a the thermodynamic equilibrium constant, and by the indices R and L the resin phase and the water phase, respectively.

For the distribution of the uncharged third complex MA_3 between the two phases, we have

$$[MA_3]_R = l_3 \cdot [MA_3]_L \tag{2}$$

where l_3 is the distribution coefficient for the third complex.

It is now easily seen from eqns. (1) and (2) that

$$K_a = l_3 \cdot \frac{f_{3R}}{f_{3L}} \cdot \frac{\beta_{3L}^{(a)}}{\beta_{3R}^{(a)}} \tag{3 a}$$

Here, f_3 is the activity coefficient for the third, uncharged complex, and we may assume that $f_{3R} \approx f_{3L} \approx 1$. $\beta_3^{(a)}$ is the thermodynamic complexity constant, and β_3, the concentration complexity constant for the third complex.

In the following we use a concentration constant K, defined

$$K = l_3 \cdot \frac{\beta_{3L}}{\beta_{3R}} \tag{3 b}$$

Thus
$$K = K_a \cdot (f_{ML} \cdot f_{AL}^3) \cdot (f_{MR} \cdot f_{AR}^3)^{-1} \tag{3 c}$$

According to Fronæus [1], (*cf.* IV eqn 21) we have for a tervalent ion

$$K \cdot X([A]_R) = \varphi \cdot X([A]_L) \cdot \frac{[A]_R^3}{[A]_L^3} \tag{4}$$

where
$$X([A]_R) = 1 + \sum_{n=1}^{N} \beta_{nR} \cdot [A]_R \tag{4 a}$$

The function $X([A]_L)$ is formed in the corresponding way.

If corresponding values of $K \cdot X_R$ and $[A]_R$ are known *, it ought to be possible to calculate $K \cdot \beta_{nR}$ and perhaps also K.

If the activity coefficients for the two phases are constant under the experimental conditions, the ligand number, $\bar{n}_R$, of the resin phase can be obtained according to Fronæus [1]:

$$\bar{n}_R = 3 + \frac{d \ln \varphi}{d \ln [A]_R} + (\bar{n} - 3) \cdot \frac{d \ln [A]_L}{d \ln [A]_R} \tag{5}$$

Thus, to be able to compute $\bar{n}_R$ and β_{nR}, we must know $\varphi = C_{MR} \cdot C_{ML}^{-1}$ (*i.e.*, the distribution of gadolinium ions between the resin phase and the water phase), $[A]_L$ and $[A]_R$ (*i.e.*, the concentration of free glycolate ions in both the phases), $\bar{n}_L$ and $X([A]_L)$ (*i.e.*, the complexity constants for the outer solution). Also, we must know the volume of the inner solution to be able to express β_{nR} in the usual way (M^{-n}).

* X_R and X_L are used as abbreviations for $X([A]_R)$ and $X([A]_L)$, respectively.

MEASUREMENTS

The complex solutions had the starting composition

$$C'_M \text{ mM } Gd(ClO_4)_3 + C'_{HA} \text{ mM HAcOH} + C'_A \text{ mM NaAcOH} + (200 - C'_A) \text{ mM } NaClO_4 \quad (7)$$

$AcOH^-$ is the glycolate ion. The ratio C'_{HA}/C'_A was 0.49. C'_M was kept constant at 0.0975 mM. The gadolinium perchlorate contained the radioactive isotope ^{153}Gd. The pH of the starting solution of $Gd(ClO_4)_3$ was about 4.5. The initial ionic strength of the solutions was always 0.20 M.

The anion-exchanger Dowex 1 × 4 was used for this investigation. It was converted in the glycolate form and air-dried. The glycolate amount was found to be 3.05 mequiv. per gram air-dried resin.

15 ml of the complex solution was shaken with 1 g of the air-dried, glycolate-saturated exchanger for 20 h in a thermostat at 20°C.

The distribution $\varphi = C_{MR} \cdot C_{ML}^{-1}$ was determined by means of the radioactive isotope in the way described before (Sonesson [2]). The exchanger was carefully separated from the outer solution (solution A) by means of a small glass-filter funnel. The exchanger was then eluted with regard to both gadolinium ions and glycolate ions by means of 20 ml 2 M $NaClO_4$ in small portions, and the "resin solution" (solution B, diluted to 25 ml) was obtained.

However, a certain amount of solution A adhered to the funnel and to the particles of the resin and could not be removed before the elution. An approximate value of the volume of the adhering solution was obtained in the following way. In special measurements with $C'_M = 0$, the resin was separated from the solution in exactly the same way as before. The resin and the funnel was washed rapidly with cold water. Then both the outer solution A and the wash water was analysed. After having determined the total concentration of HAcOH + NaAcOH and the amount of HAcOH, we could calculate the amount of NaAcOH in both the solutions. The sodium glycolate in the wash solution ought to have come from solution A adsorbed to the funnel and the resin. Calculations showed that 0.20—0.25 ml of solution A was adsorbed *. Therefore in the calculations of C_{MR} and $[AcOH^-]_R$ corrections have been made for 0.20 ml outer solution adsorbed. This correction term is perhaps too high. A part of the glycolate now assumed to be adsorbed may have been present in the resin phase as non-exchange electrolyte according to the Donnan equilibrium.

It was found that the resin was radioactive after it had been eluted with 20 ml 2 M $NaClO_4$. Thus, it still contained gadolinium ions, possibly as hydrolytic products precipitated in the resin during the elution. It is also possible that $Gd(AcOH)_3$ has been precipitated in the resin phase, as the glycolate is rather slightly soluble. Therefore, the resin was eluted a second time, now with 2 ml warm 2 M $HClO_4$ in small portions. After this elution the resin showed very low activity. The solution was diluted to 25 ml and analysed on both gadolinium and glycolate ions. When the total value of C_{MR} was to be cal-

* In separate measurements it was found that about 30 % of the solution assumed adsorbed should adhere to the resin and the rest to the funnel.

culated the gadolinium content of this last solution had to be taken into consideration. The content of glycolate ions was, however, always so low that it could be neglected.

The total concentration of glycolic acid + sodium glycolate, *i.e.*, $C_{HA} + C_{NaA}$, was determined through oxidation by potassium permanganate in solutions made alkaline by sodium carbonate. To a known volume of the glycolate solution was added sodium carbonate solution and a known amount of potassium permanganate so large that the glycolate was quantitatively oxidized to carbon dioxide when the permanganate was reduced to manganese dioxide *. The solution was warmed in a glass flask fitted with a condenser (all in glass) for 30 min. on a boiling water bath. Then the solution was acidified with sulphuric acid and a known amount of sodium oxalate was added to a slight excess. Finally the excess of oxalate was back-titrated with permanganate.

This method of determining the glycolate proved, however, somewhat uncertain, because permanganate ions have a tendency to decompose spontaneously in alkaline solutions. Therefore, we had to use two different values for the permanganate titer, one "alkaline titer" for the permanganate heated in alkaline solution, and another "acid titer" for the permanganate added for the back-titration in acid solution.

The degree of decomposition seemed to depend on the purity of the permanganate solution, on the way in which the analysis was performed, and on the nature of the glass wall of the flask in which the solution was heated. Therefore, the stock solution of permanganate was boiled and filtered several times before it was used. All analyses were performed in exactly the same way using only two sets of flasks and condensers, for which it was checked that the same degree of decomposition occurred.

The "acid titer" of the permanganate solution was determined in the usual manner by means of sodium oxalate. The "alkaline titer" was determined by oxidizing a known amount of glycolic acid in the way described above. Several determinations were performed with varying amounts of glycolic acid. With few exceptions the values obtained for the "alkaline titer" deviated less than 0.3 % from the mean value. The "alkaline titer" was about 2.5 % lower than the "acid titer".

For every solution the determination of the total concentration $C_{HA} + C_{NaA}$ was performed at least twice. The uncertainty of $C_{HA} + C_{NaA}$ was estimated at $\pm$ 3 %.

After having determined C_{HA} by titration with sodium hydroxide, we could compute C_{NaA}, *i.e.*, the concentration of free glycolate ions, [$AcOH^-$]. Correction terms depending on the protolyze of glycolic acid and of the complex formation between gadolinium and glycolate ions could be neglected. The random errors of [$AcOH^-$] were estimated at $\pm$ 4 %.

To be able to express $[AcOH^-]_R$ in mole per liter, we must determine the volume of the water in the resin phase. This was done by determining the water content of the air-dried resin and by measuring the swelling of the air-

* As it was found in the literature that calcium ions catalyse the reaction, calcium nitrate was added in small amounts. Any significant effect of this was, however, not observed.

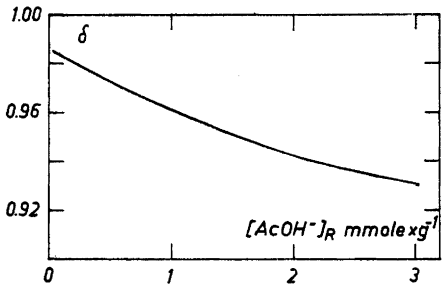

Fig. 1. The variation of the swelling factor δ with the concentration of glycolate ions in the resin phase. The total amount of water was $[15(1-\delta) + 0.13]$ g per g air-dried resin in the glycolate form.

dried resin in buffer solutions with $C'_M = 0$. In the latter case the concentration of sodium ions was determined firstly with no resin present ($[Na^+]'$), and secondly when equilibrium was reached between 1 g air-dried resin and 15 ml buffer solution ($[Na^+]''$) *. The ratio $[Na^+]'/[Na^+]'' = \delta$ is called the swelling factor. The value of δ was determined for different values of C'_A (ionic strength always 0.20 M). The variation of δ with $[AcOH^-]_R$ is shown in Fig. 1. The volume of water absorbed by the resin was 15 (1—δ) ml per gram air-dried resin.

The glycolate-saturated resin contained in the air-dried state 0.13 g water per g resin. It was determined as the loss of weight when the resin was slowly heated to 100°C.

Thus per g air-dried and glycolate-saturated resin there was taken up totally $[15(1-\delta) + 0.13]$ g water. All this water cannot be considered as free solvent in the resin phase, as a part of it is surely bound in hydrated ions. Since the amount of absorbed water increases strongly with increasing $[AcOH^-]_R$, it is probable that the absorbed water is to a rather large extent bound by the glycolate ions. It is, however, impossible to estimate through the measurements done, to what extent the absorbed water shall be counted as free solvent. Nor have any investigations of this problem been found in the literature.

Table 1. The complexity constants β_n and the stability constants $b_n = \beta_n \cdot \beta_{n-1}^{-1}$ ($b_1 = \beta_1$) for the gadolinium glycolate system at different values of the ionic strength. The constants at the ionic strength 1.0 M have been determined by measurements with a cation exchanger. In the other cases potentiometric measurements have been performed. The temperature has always been 20°C.

Ionic strength	β_1 M^{-1}	β_2 M^{-2}	β_3 M^{-3}	β_4 M^{-4}	β_5 M^{-5}	β_6 M^{-6}	b_1	b_2	b_3	b_4	b_5	b_6
0.21 M	540	$61 \cdot 10^3$	$20 \cdot 10^5$	$130 \cdot 10^5$	$10 \cdot 10^6$	—	540	115	33	6.5	0.8	—
1.0 M	350	$30 \cdot 10^3$	$7 \cdot 10^5$	—	—	—	350	85	23	—	—	—
2.0 M	300	$27 \cdot 10^3$	$6 \cdot 10^5$	$26 \cdot 10^5$	$1 \cdot 10^6$	—	300	90	23	4	0.4	—
3.0 M	390	$40 \cdot 10^3$	$13 \cdot 10^5$	$65 \cdot 10^5$	$6 \cdot 10^6$	$4 \cdot 10^6$	390	105	33	5	0.9	0.7

* The concentration of sodium ions was determined by means of a cation exchanger column in the hydrogen state. In this way the total concentration of sodium salts and glycolic acid was obtained. Then the concentration of glycolic acid was determined separately and the concentration of sodium ions could be computed.

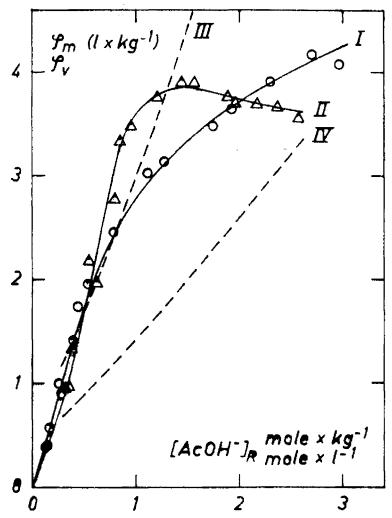

Fig. 2. The variation of the distribution $\varphi = C_{MR} \cdot C_{ML}^{-1}$ with the glycolate concentration of the resin phase, $[AcOH^-]_R$. Curve I (symbol O) shows φ_m and is obtained when $[AcOH^-]_R$ is expressed in moles per kg resin. Curve II (symbol △) shows φ_v when $[AcOH^-]_R$ is expressed in moles per liter water in the resin phase. The figures show the values obtained experimentally. Curves III and IV have been calculated, both with $[AcOH^-]_R$ expressed in moles per liter. Curve III has been obtained with the values of $K \cdot \beta_{nR}$ given in Table 4 and therefore it should be valid for the ionic strength 6 to 8 M. For the calculation of curve IV, the values of β_n obtained potentiometrically at the ionic strength 3 M have been used. It has also been assumed that $K = 1$.

To be able to compute $K \cdot X_R$ by means of eqn. (4), we must know the X_L-function for the water phase. This function and the complexity constants were determined by a potentiometric investigation in the way described in part III (Sonesson [3]). Sodium perchlorate was added to give the ionic strength 0.21 M as this was a mean value of the ionic strength of the water phase in the experiments with the anion exchanger ($\delta = 0.95$). The complexity constants at the ionic strength 3.0 M were also determined potentiometrically, as it was probable that in our measurements with the anion exchanger the ionic strength of the resin phase was about 3 M at high values of $[AcOH^-]_R$. In Table 1 the values of the complexity constants obtained at different values of the ionic strength have been collected (Sonesson [2,3]).

DISCUSSION OF THE RESULTS

The experimentally obtained values of φ, $[AcOH^-]_R$ and $[AcOH^-]_L$ are shown in Table 2. The glycolate concentration of the resin phase is given both in moles per kg resin and in moles per liter inner solution. The function $\varphi([AcOH^-]_R)$ is shown in Fig. 2.

To be able to calculate $\bar{n}_R$ according to eqn. (5), $\log \varphi$ is plotted as a function of $\log [AcOH^-]_R$. Curve I in Fig. 3 is obtained if $[AcOH^-]_R$ is expressed in moles per kg (*i.e.* $\varphi = \varphi_m$), and curve II if $[AcOH^-]_R$ is given in moles per liter (*i.e.*

Table 2. The experimentally obtained values of φ and the concentrations of free glycolate ions in the water phase and in the resin phase ($[AcOH^-]_L$ and $[AcOH^-]_R$, respectively). The starting concentration of gadolinium (C'_M) was 0.0975 mM. φ_m and φ_v are the φ-values when $[AcOH^-]_R$ is expressed in moles per kilogram resin and in moles per liter solvent, respectively. I_R is the calculated ionic strength of the resin phase.

$[AcOH^-]_L$ M	$[AcOH^-]_R$ mole·kg^{-1}	φ_m l·kg^{-1}	g H_2O per g resin	$[AcOH^-]_R$ M	φ_v	I_R M
0.183	0.13	0.38	0.40	0.325	0.95	7.6
0.182	0.15	0.40	0.415	0.360	0.96	7.3
0.194	0.17	0.57	0.43	0.395	1.32	7.1
0.201	0.25	1.00	0.46	0.545	2.17	6.6
0.200	0.29	0.90	0.46	0.630	1.96	6.6
0.204	0.40	1.40	0.505	0.795	2.77	6.0
0.201	0.44	1.73	0.52	0.845	3.33	5.9
0.203	0.54	1.96	0.565	0.955	3.47	5.4
0.206	0.79	2.45	0.655	1.205	3.74	4.7
0.208	1.12	3.02	0.775	1.445	3.90	3.9
0.208	1.26	3.13	0.805	1.565	3.89	3.8
0.210	1.75	3.47	0.925	1.89	3.75	3.3
0.211	1.93	3.64	0.985	1.96	3.70	3.1
0.212	2.30	3.91	1.06	2.17	3.69	2.9
0.215	2.70	4.17	1.14	2.37	3.66	2.7
0.216	2.97	4.08	1.15	2.58	3.55	2.65

$\varphi = \varphi_v$). The last term of eqn. (5), *i.e.* $(\bar{n}-3) \cdot d \ln [A]_L / d \ln [A]_R$, is only a small correction term, as $[AcOH^-]_L$ varies only slightly with $[AcOH^-]_R$ except at the lowest values of $[AcOH^-]_R$ (Table 2). The ligand number of the water phase is about 3.6 at $[AcOH^-]_L = 0.2$ M. Thus $(\bar{n}-3) \cdot d \ln [AcOH^-]_L / d \ln [AcOH^-]_R$ does not exceed 0.1 (for $[AcOH^-]_R > 0.5$ M it is lower than 0.05), irrespective of the way in which $[AcOH^-]_R$ is expressed.

The ligand number $\bar{n}_R$ obtained from curve II in Fig. 3 will, to begin with, increase with increasing $[AcOH^-]_R$, as seen in Table 3. From a maximum

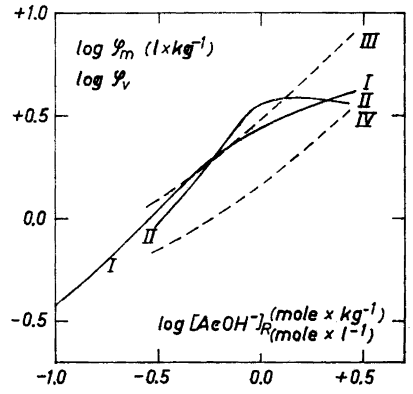

Fig. 3. Curves showing log φ as a function of log$[AcOH^-]_R$. The curves correspond to the curves with the same number in Fig. 2.

value of about 4.3 at $[AcOH^-]_R \approx 0.5$ M, it decreases to about 3.0 for $[AcOH^-]_R \geq 1.5$ M. Also, curve I gives a decrease of $\bar{n}_R$, though the decrease is not so pronounced (from 4.1 at 0.3 M to 3.4 at 3 M).

It can, however, not be correct that $\bar{n}_R$ decreases when $[AcOH^-]_R$ increases. One of the possible reasons why incorrect values of $\bar{n}_R$ are obtained, may be the variation of the volume and thereby also the ionic strength of the resin solution. If all the water absorbed is considered as solvent, the ionic strength varies as shown in Table 2. As seen in Table 1 the complexity constants increase, especially the last ones, when the ionic strength increases from 2 M to 3 M, and it is likely that the β_n-values are still higher at higher values of the ionic strength. As the highest values of the ionic strength in the resin phase are reached at the lowest values of $[AcOH^-]_R$, it is evident that $\varphi = l_3 \cdot \alpha_3/\alpha_{3R}$ (Fronæus[1]) must increase more slowly with $[AcOH^-]_R$ than if the ionic strength had been constant. Therefore, applying eqn. (5), we must obtain too low values of $\bar{n}_R$. Another reason for the incorrect values of $\bar{n}_R$ may be a variation of K with the ionic strength.

In calculating $K \cdot X_R$ according to eqn. (4) we have taken the values φ_v and $[A]_R$ from the curves in Fig. 2. The values of $K \cdot X_R$ are given in Table 3. The values in brackets are obtained by extrapolations of the corresponding curves and are therefore very uncertain.

It was not possible to obtain a value of K by extrapolation of $K \cdot X_R$ to $[A]_R = 0$. The values of $K \cdot \beta_{nR}$ have been calculated by extrapolations of

Table 3. Computation of the $K \cdot X([A]_R)$-function from the experimentally obtained values of the glycolate concentrations $[AcOH^-]_R$ and $[AcOH^-]_L$, and of the distribution φ_v (with $[AcOH^-]_R$ expressed in moles per liter). The $X([A]_L)$-function, i.e. the $X([A])$-function for the glycolate concentrations in the water phase given in the $[AcOH^-]_L$-column at the ionic strength 0.21 M, has been obtained potentiometrically.

The ligand number $\bar{n}_R$ has been calculated according to eqn. (5) from curve I in Figure 3. I_R is the ionic strength of the resin phase.

$[AcOH^-]_R$ M	I_R M	φ_v	$[AcOH^-]_L$ M	$\bar{n}_R$	$\varphi_v \frac{[A]_R^3}{[A]_L^3}$	$X([A]_L) \cdot 10^{-3}$ $I = 0.21$ M	$K \cdot X([A]_R) \cdot 10^{-5}$
0							
0.10	8.5	(0.30)		4.1			(0.03)
0.20	8.1	(0.60)		4.1			(0.32)
0.30	7.7	0.90	(0.17)	4.1	5.0	23.8	1.19
0.40	7.3	1.25	0.19	4.2	11.7	35.5	4.15
0.50	7.0	1.65	0.197	4.3	27.0	40.0	10.8
0.60	6.6	2.05	0.200	4.3	55.4	42.1	23.3
0.80	6.0	2.95	0.203	4.1	180	44.4	80.0
1.00	5.3	3.60	0.204	3.6	424	45.0	191
1.20	4.7	3.75	0.206	3.2	742	46.8	347
1.50	3.8	3.85	0.208	3.0	1 445	48.5	701
1.70	3.5	3.80	0.209	3.0	2 045	49.3	1 008
2.00	3.0	3.75	0.211	3.0	3 200	51.0	1 630
2.20	2.8	3.70	0.213	3.0	4 080	52.7	2 150
2.50	2.6	3.65	0.215	3.0	5 740	54.5	3 130
2.70	2.5	3.60	0.216	3.0	7 030	55.2	3 880

$K \cdot X_{nR}$ to $[A]_R = 0$ (Table 4) *. They must, however, be considered rather approximate (especially $K \cdot \beta_{1R}$) as the extrapolations were very difficult. The values obtained may be considered valid at the ionic strength 6 to 8 M, *i.e.* the ionic strength at low glycolate concentrations.

From the values of $K \cdot \beta_{3R} = 1 \times 10^6$ M^{-3} and $\beta_{3L} = 2 \times 10^6$ M^{-3} we can calculate a value of l_3. Eqn. (3 b) gives us $l_3 = 0.5 \pm 0.2$.

The stability constants $b_n = \beta_n \cdot \beta_{n-1}^{-1}$ ($b_1 = \beta_1$) calculated from the values of $K \cdot \beta_{nR}$ in Table 4, have the following values

$$b_{2R} \geq 100; \qquad b_{3R} \sim 10; \qquad b_{4R} \sim 15$$

These stability constants are of the same order of magnitude as those in Table 1, but the increase of b_{3R} to b_{2R} seems to be somewhat greater than the increase of b_3 to b_2 shown in the table. Therefore, we may expect that $b_{1R} = \beta_{1R}$ is somewhat greater than $b_1 = \beta_1$. Thus, as we have obtained $K \cdot \beta_{1R} \leq 1 \times 10^3$, it seems probable that $K \approx 1$. This value of K should be valid for the ionic strength 6 to 8 M. It is not possible to calculate a value of K at lower ionic strength, but it seems more probable that K increases than decreases for

Table 4. Calculation of the values of $K \cdot \beta_{nR}$ by extrapolations of the $K \cdot X_{nR}$-functions to $[AcOH^-]_R = 0$. The X([A])-function in the last but one column has been obtained potentiometrically at the ionic strength 3 M for the glycolate concentrations given in the first column. The X([A])-function in the last column has been calculated with the potentiometrically obtained complexity constants under the assumption that only the four first complexes are formed.

The following values of $K \cdot \beta_{nR}$ were obtained: $K \cdot \beta_{1R} \leq 1 \times 10^3$ M^{-1}; $K \cdot \beta_{2R} \approx 1 \times 10^5$ M^{-2}; $K \cdot \beta_{3R} = 1 \times 10^6$ M^{-3}; $K \cdot \beta_{4R} \approx 10$ à 20×10^6 M^{-4}; $K \cdot \beta_{5R} < 10 \times 10^6$ M^{-5}.

$[AcOH^-]_R$ M	$K \cdot X([A]_R) \cdot 10^{-4}$	$K \cdot X_{1R} \times 10^{-4}$ M^{-1}	$K \cdot X_{2R} \times 10^{-5}$ M^{-2}	$K \cdot X_{3R} \times 10^{-6}$ M^{-3}	$K \cdot X_{4R} \times 10^{-6}$ M^{-4}	I_R M	$X([A]) \times 10^{-4}$ $I = 3$ M	$X([A]) \times 10^{-4}$ $I = 3$ M $\beta_1 \ldots \beta_4$
0		*≤ 0.1*	*1*	*1*	*10—20*			
0.10	(0.3)	3	3	2	10	8.5	0.25	0.24
0.20	(3.2)	16	8	3.5	13	8.1	2.54	
0.30	11.9	40	13.5	4.2	11	7.7	11.4	9.1
0.40	41.5	104	26	6.5	14	7.3	35.0	
0.50	108	216	43	8.5	15	7.0	87	58
0.60	233	390	65	10.5	16	6.6	188	
0.80	800	1 000	125	15.5	18	6.0	663	
1.00	1 910	1 910	190	19	18	5.3	1 830	780
1.20	3 470	2 890	240	20	16	4.7	4 380	
1.50	7 010	4 670	310	21	13	3.8	12 900	3 800
1.70	10 080	5 930	350	21	12	3.5	24 200	6 100
2.00	16 300	8 150	410	20	10	3.0	61 700	11 500
2.20	21 500	9 760	445	20	8.5	2.8	92 900	16 600
2.50	31 300	12 500	500	20	7.5	2.6	184 000	27 500
2.70	38 800	14 400	535	19.5	7	2.5	319 000	37 700

* The values of $K \cdot \beta_{1R}$ and $K \cdot \beta_{2R}$ have been obtained by extrapolations of log $K \cdot X_{1R}$ and log $K \cdot X_{2R}$ to $[A]_R = 0$.

decreasing ionic strength (*cf.* the variation of β_3 in Table 1; l_3 may be assumed constant).

A comparison of $K \cdot X_R$ with the potentiometrically obtained values of X([A]) for $I = 3$ M (Table 4) shows that the two sets of values agree rather well for $[AcOH^-]_R < 1\,000$ mM. However, at higher values of $[AcOH^-]_R$, when the ionic strength of the resin phase probably is rather near 3 M, $K \cdot X_R$ is lower than X([A]), and the difference between the two functions increases for increasing values of $[AcOH^-]_R$. At high glycolate concentrations the values of $K \cdot X_R$ correspond better to an X([A])-function calculated by means of the potentiometrically obtained complexity constants, if it is assumed that only the first four complexes can be formed in the resin phase (the last column in Table 4). It cannot be decided from the $K \cdot X_{4R}$-function in Table 4 if a fifth complex is formed, but if the estimated value of K is correct, the coincidence at high glycolate concentrations between the $K \cdot X_R$-function and the X-function in the last column of Table 4, must indicate that the complex formation in the resin phase is chiefly completed when the fourth complex has been formed. It is true that for lower glycolate concentrations the $K \cdot X_R$-function is considerably higher than the calculated X-function but this may depend on the fact that in this concentration range the ionic strength of the resin phase is considerably higher than 3 M.

The values of φ shown by curve III in Fig. 2 have been calculated assuming that only four complexes are formed in the resin phase with the values of $K \cdot \beta_{nR}$ given in Table 4 ($K \cdot \beta_{4R} = 15 \times 10^6$ M^{-4}). Thus, curve III should show the function $\varphi([AcOH^-]_R)$ if the ionic strength of the resin phase had been constantly 6 to 8 M. Curve IV shows the same function for the case that the ionic strength of the resin phase had been 3 M constantly, assuming that the complexity constants are the same in a resin phase as in a water phase of the same ionic strength, and that the constant K has a value of about 1. Curve II shows the function obtained experimentally when $[AcOH^-]_R$ is given in moles per liter.

At low values of $[AcOH^-]_R$ the coincidence between curve III and curve II is rather good. At higher concentrations, when the ionic strength becomes lower than 4 M, curve II approaches towards curve IV. Thus it seems probable that at least at this ionic strength the values of $K \cdot \beta_{nR}$ are about the same as the β_n-values for a water phase of the ionic strength 3 M.

I wish to express my sincere thanks to Professor Sture Fronæus for the valuable aid he has given me in different respects.

Further I wish to thank Fil. mag. Lennart Månsson for his valuable assistance in the measurements.

REFERENCES

1. Fronæus, S. *et al. Acta Chem. Scand. To be published.*
2. Sonesson, A. *Acta Chem. Scand.* **13** (1959) 1437.
3. Sonesson, A. *Acta Chem. Scand.* **13** (1959) 998.

Received September 19, 1960.

ACTA CHEMICA SCANDINAVICA 15 (1961) 11–15

Effects of Ionizing Radiation on Arylesterase and Cholinesterase

KLAS-BERTIL AUGUSTINSSON, GUNNEL JONSSON and BERNDT SPARRMAN

Institute of Organic Chemistry and Biochemistry, University of Stockholm, Sweden

The effects of ^{60}Co γ-irradiation on arylesterase and cholinesterase of human blood plasma were compared using solid preparations of purified enzymes containing various amounts of water. In the case of cholinesterase a water content of 12 % exerted maximum protection against irradiation. Such a protection by water was not observed with arylesterase. In aqueous solutions cholinesterase was more resistant to irradiation by γ-rays than was arylesterase when irradiation was performed in an atmosphere of nitrogen.

It is generally believed that ionizing radiation inactivates enzymes by direct action in dried preparations, and by means of free radicals formed from the ionization of water in dilute aqueous solutions [1]. In the present study the effects of ^{60}Co γ-irradiation on two esterases, acetylarylesterase and butyrylcholinesterase, were compared using solid preparations of partly purified esterases equilibrated to different water contents. Arylesterase was recently shown to be a sulphydryl enzyme in contrast to cholinesterase, the activity of which is not dependent on the presence of free —SH groups in the same high degree as arylesterase [2].

MATERIALS AND METHODS

Materials. Arylesterase was prepared from human serum according to a partly modified method No. 6 of Cohn *et al.*[3]; a homogeneous, finely powdered sample of this preparation was used throughout the experiments. The cholinesterase preparation was obtained from the same source by the same fractionation procedure and was similarly homogeneous. Both preparations contained one single esterase, and neither preparation showed any activity of the other. These preparations were dried over silica-gel at room-temperature and equilibrated to different water contents (see below). After irradiation they were dissolved in a bicarbonate-CO_2 buffer, the composition of which was dependent on the esterase studied, to give a concentration of 0.15 mg arylesterase and 0.50 mg cholinesterase per ml, respectively (unless otherwise stated), corrections being made for the water content. In order to get clear solutions of the arylesterase preparation these were gently shaken under running water (40 – 41°C) for one min. The cholinesterase prepara-

tion was readily soluble in water, except for preparations subjected to irradiation in the presence of NO. For esterase determinations, 0.4 ml portions of these enzyme solutions were used.

In the experiments with irradiation of esterase in aqueous solutions, these were prepared similarly before irradiation.

Phenyl acetate was used as substrate for arylesterase, solutions being prepared with a bicarbonate-CO_2 buffer containing 0.0336 M $NaHCO_3$ and 0.001 M $CaCl_2$. In the experiments with cholinesterase, acetylcholine chloride was used as substrate, solutions being prepared in a bicarbonate-CO_2 buffer containing 0.115 M NaCl, 0.0336 M $NaHCO_3$ and 0.0012 M $MgCl_2$. The final concentration of each substrate (1.6 ml used for esterase determination) in the reaction mixture during activity measurement was 0.01 M (total reaction mixture, 2.00 ml).

Equilibration of esterase preparations to different water contents. Before irradiation the esterase samples, in small polyethylene tubes, were kept for 48 h in desiccators containing solutions giving different humidities. To each desiccator two wash-bottles, containing the same solution, were connected and a slow stream of air was pumped through the system. The driest samples were equilibrated by means of concentrated sulphuric acid, and the other water contents were obtained by means of solutions of potassium hydroxide in distilled water.

Radiation source. Irradiation of the esterase samples was performed in a ^{60}Co γ-source ("Hot Pot" from Picker, Cleveland, Ohio, USA) containing 2 750 Curies of ^{60}Co and with a maximum dose rate of 670 000 r/h. The dose rate in the experiments described was 570 000 r/h. The temperature measured with a N. T. C. resistor did not exceed 37°C during the irradiation, and the controls were also kept under similar temperature conditions.

Irradiation performance. The polyethylene tubes, containing 12—15 mg of the esterase preparation to be irradiated, were transformed to vacuum glass tubes (Thunberg tubes) allowing the samples to be kept in any desired gas atmosphere during irradiation. The standard procedure involved three washings with nitrogen and 10 min evacuation with an oil pump between the nitrogen fillings after which the desired gas could be filled in. After irradiation for various lengths of time, depending on the required dose, the gas atmosphere was not altered for 6—8 h before enzyme activity measurements, thus allowing the after-effects to occur in the irradiation atmosphere.

In the experiments with aqueous solutions, 2—4 ml was irradiated in glass tubes. When irradiation was performed in N_2-atmosphere, the gas was bubbled through the solutions in small wash-bottles for 5 min before the bottles were carefully sealed and placed in the irradiation chamber.

Control experiments have shown that the composition of the tubes (glass, polyethylene, *etc.*) has no measurable influence, *i.e.*, electronequilibrium is present.

Enzyme activity measurements. Manometric determinations were made at 25°C by the Warburg technique [2]. Esterase activity was expressed in μl CO_2 evolved in 30 min, corrections being made for spontaneous hydrolysis of the substrates. The percentage of remaining esterase activity after irradiation was plotted as a function of irradiation dose (in r) on semilogarithmic paper.

RESULTS

Activity-dose relationship for solid preparations and aqueous solutions. Solid preparations with known water content (4—12 %) of partly purified esterases were irradiated with doses varying from 1.0 to 11.0×10^6 r. In all experiments performed the activities decreased exponentially in relation to the dose. A similar relationship was found with aqueous solutions of the same preparation (*cf. Fig. 2*). This indicated that both esterase preparations used were homogeneous as far as the active component was concerned. The dose corresponding to 37 % remaining activity was extrapolated from these dose curves and used when the irradiation effects on preparations with various water contents were compared.

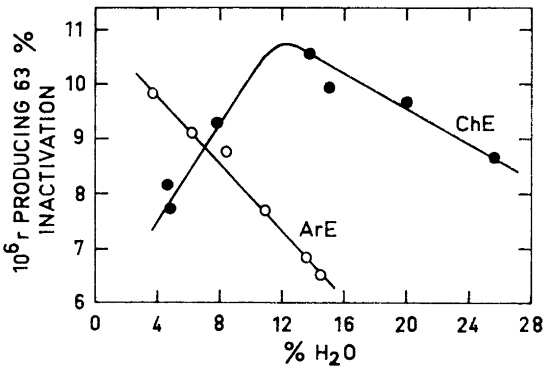

Fig. 1. Influence of the water content on inactivation of the esterases by ^{60}Co γ-irradiation. The 63 % inactivation values were extrapolated from dose-activity curves obtained in irradiation experiments with a series of solid preparations (ArE, arylesterase; ChE, cholinesterase) containing the same amount of water.

Influence of the water content on the irradiation effect. With increasing water content the sensitivity to γ-irradiation of the arylesterase preparations was increased. Fig. 1 illustrates the linear relationship between the water content and the irradiation dose which produces 63 % esterase inactivation. The influence of the water content in the case of cholinesterase was strikingly different. With increasing water content, up to about 12 %, the esterase was increasingly protected from inactivation. In the presence of higher (> 12 %) water contents this enzyme behaved similarly to arylesterase, *i.e.*, the inactivation by γ-irradiation increased proportionally to the amount of water present. These were the experimental results when irradiation was performed in an atmosphere of air.

Due to practical difficulties in obtaining reproducible water contents of the preparations when in equilibrium with other atmcspheres than air, similar irradiation experiments performed in atmospheres of N_2 or NO have not yet given conclusive results. However, enzyme inactivation by γ-irradiation of arylesterase did not seem to differ greatly when irradiation was performed in air, N_2 and NO with water contents varying between 4 and 8 %. In the case of cholinesterase, the irradiation had less effect when carried out in the absence of air (preparations in equilibrium with N_2) with water contents varying between 5 and 12 %. The solid cholinesterase preparation used seemed to be partially denaturated when irradiated in an atmosphere of NO.

Loss of esterase activity on irradiation of aqueous solutions. Fig. 2 illustrates the loss of esterase activity in aqueous solutions of arylesterase and cholinesterase subjected to ^{60}Co γ-irradiation, as a function of dose. With increasing dose the activity decreased more rapidly the lower the initail enzyme concentration. When the solutions were irradiated in the absence of air (solutions equilibrated with N_2; curve C) cholinesterase was relatively more resistant to the inactivating effect of γ-rays than was arylesterase.

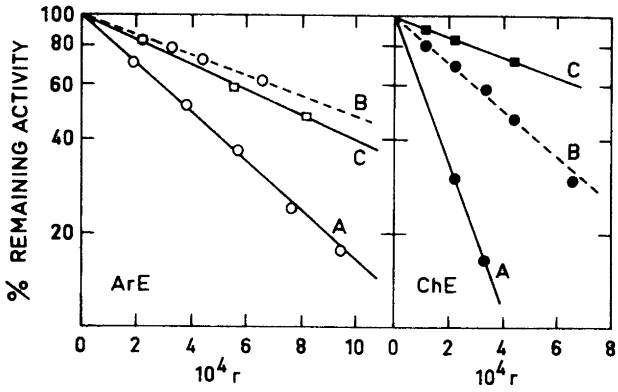

Fig. 2. Decrease of esterase activity of aqueous solutions of purified preparations of arylesterase (ArE) and cholinesterase (ChE) after irradiation with ^{60}Co γ-rays. A and B refer to irradiation performed in an atmosphere of air, C in that of N_2. Protein concentration in A and C was 0.15 mg/ml, in B 0.50 mg/ml.

DISCUSSION

The results reported above with irradiation of solid enzymes may be of some importance in view of the fact that a maximum protection by water against radiation has been found also in seeds [4] and starch [5] at about the same water content as in the case of cholinesterase. This seems to indicate that the same or similar effects are involved. With arylesterase, such a protection by water was not observed, which may be due to the dependence on —SH groups for the activity of this enzyme. It is well-known that these groups are sensitive to irradiation. An increasing degree of hydration, therefore, may render the energy transfer from the "hit points" in the molecule to the —SH groups easier, thus increasing the inactivation of the enzyme.

Cholinesterase activity is not as dependent on —SH groups as arylesterase activity, but the same theory may also be used to explain the increasing protective effect of water up to 12 % H_2O for cholinesterase. The increasing water content makes the energy transfer to the —SH groups easier, thus protecting the more essential part(s) of the active enzyme surface. This difference between the two enzymes supports the hypothetical explanations of the water effect given by Ehrenberg [4,5]. The increase in sensitivity with increasing water content higher than 12 % is not yet possible to explain clearly. Other types of reactions are possibly becoming predominant in this case, *i.e.*, the energy transfer takes other pathways which leads to a destruction of the sensitive sites in the active surface before energy can be trapped by —SH groups.

Arylesterase and cholinesterase behaved differently also when irradiated in aqueous solutions. The difference in resistance to irradiation, performed in an atmosphere of nitrogen, needs further studies in order to be explained. It indicates, however, that there is some fundamental difference in the mechanism of action of ionizing radiation for the two esterases studied. The difference in behaviour may also be of some value in understanding the role of

—SH groups in enzyme action, which has been found to differ for the two types of esterase by other experiments.

This investigation has been supported by grants from the *Swedish Natural Science Research Council* and the *Swedish Agriculture Research Council.* Our thanks are due to Dr. Lars Ehrenberg for fruitful discussions.

REFERENCES

1. Bacq, Z. M. and Alexander, P. *Fundamentals of radiobiology*, Butterworth, London 1955.
2. Augustinsson, K.-B. *Acta Chem. Scand.* **13** (1959) 571, 1081, 1097.
3. Cohn, E. J., Gurd, F. R. N., Surgenor, D. M., Barnes, B. A., Brown, R. K., Derouaux, G., Gillespie, J. M., Kahnt, F. W., Lever, W. F., Liu, C. H., Mittelman, D., Mouton, R. F., Schmid, K. and Uroma, E. *J. Am. Chem. Soc.* **72** (1950) 465.
4. Ehrenberg, L. *Bot. Notiser* **108** (1955) 184.
5. Ehrenberg, L. *Radiobiology Conference*, Cambridge 1955, p. 114.

Received September 7, 1960.

ACTA CHEMICA SCANDINAVICA 15 (1961) 16–30

Refinement of the Crystal Structure of β-Arabinose

ASBJØRN HORDVIK*

Chemical Institute, University of Bergen, Bergen, Norway

The crystal and molecular structure of β-arabinose has been determined more accurately by means of ($F_o - F_c$) synthesis in *a*-axis and *c*-axis projections. The hydrogen atoms have been located and included in the calculations, and corrections have been made for individual and anisotropic thermal vibrations of carbon and oxygen atoms.

The mean length of C—C bonds is 1.535 Å, and the mean length of C—O bonds, excluding C_1-O_1, is 1.434 Å. The bond C_1-O_1 is 1.382 ± 0.012 Å, and deviates significantly from the mean value.

The mean value of the angles in the pyranose ring (excluding $C_1-O_5-C_5$) is 109.5°, equal to the tetrahedral angle. The angle $C_1-O_5-C_5 = 112.7 \pm 0.6°$ deviates significantly from the mean value, and so does the angle $O_5-C_1-O_1 = 113.0 \pm 0.7°$.

All the oxygen atoms and hydroxyl hydrogen atoms are engaged in hydrogen bonds, one of which is found to be as long as 3.035 ± 0.008 Å. O_3 takes part in three hydrogen bonds and has roughly tetrahedral surroundings.

The approximate crystal structure of β-arabinose has been determined earlier by means of the *a*-axis and *c*-axis projections [1]. It was, however, found desirable to try to obtain more information on details in the structure, particularly because the general interest in sugar structures in recent years seems to be focused on structural details. In order to know accurately the hydrogen bonding system in the crystal, it would be necessary to locate the hydrogen atoms. Regarding the angle $C_1—O_5—C_5$ in the pyranose ring, there seems to be some disagreement in the literature [2,3], and it was hoped that a new detailed structure determination of a pyranose sugar might give more reliable information about this angle. In the same way it would be valuable to have an accurate determination of the length of the bond $C_1—O_1$, which in sugars is usually reported to be shorter than the normal C—O single bond [2,3]. The apparent reactivity of O_1 might be related to such a shortened bond, and this might therefore be a point of interest for the study of the chemical reactions of pyranoses.

Two short axes and the space group $P2_12_12_1$ make β-arabinose suitable for two-dimensional refinement.

* Present address: University College of Addis Abæba, Ethiopia.

CRYSTAL DATA

The X-ray data on which the preliminary structure determination was based [1], did not seem good enough for a more accurate structure analysis. A new series of X-ray photographs were therefore taken, using Cu$K\alpha$ radiation. The crystals had cross-sections of about 0.1 × 0.1 mm. The unit cell dimensions were redetermined from high order reflections on Weissenberg photographs, using a crystal coated with KCl powder. As lattice parameter of KCl the value 6.293 Å was used [4].

The following axial lengths were derived:

$a = 6.535 \pm 0.007$ Å, $b = 19.467 \pm 0.020$ Å, $c = 4.841 \pm 0.005$ Å

The relative intensities of the reflections were corrected for "spot shape" effect [5].

The carbon and oxygen contributions to the calculated structure factors were based on the atomic scattering curves of Berghuis *et al.*[6], and the hydrogen contributions were based on the curve of Viervoll and Øgrim [7].

REFINEMENT OF THE STRUCTURE

The c-axis projection. About twenty successive (F_o—F_c) refinements were carried out in order to bring the discrepancy factor $R_{hk0} = (\Sigma|F_o—F_c|)/\Sigma|F_o|$ from 0.30 to the final value 0.055. After the twelfth step, nine of the hydrogen atoms were projected from a molecular model on to the difference map, Fig. 1a,

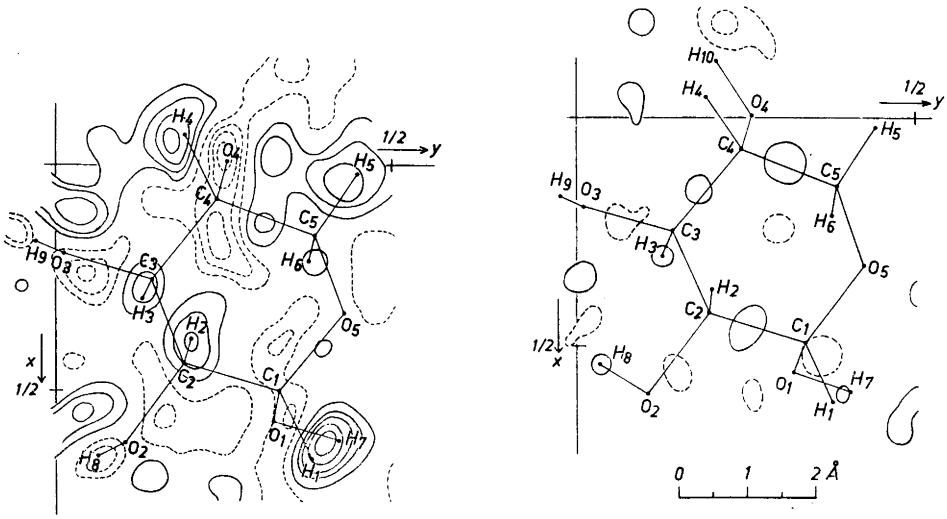

Fig. 1. (a) The twelfth difference projection of β-arabinose along the *c* axis, with hydrogen atoms *not* subtracted, and (b) the final difference projection along the same axis, with hydrogen atoms subtracted. Contour lines at intervals of 0.2 e·Å^{-3}, with negative lines dashed. The zero line is omitted. The maxima in the middle of $C_1—C_2$, $C_3—C_4$ and $C_4—C_5$ indicate asymmetry in the electron clouds due to the bonding electrons.

using a model with C—H = 1.09 Å and O—H = 0.96 Å. Fig. 1a shows that the six hydrogen atoms bound to carbon could be placed in positive areas on the map. Assuming H_7, H_8 and H_9 to be engaged in hydrogen bonding and lying near the straight line between adjacent oxygens, H_7 could be placed in a positive area, but H_8 and H_9 had to be placed in a negative. The negative area might however be due to anisotropic thermal vibrations of O_3. It was possible to place H_{10} in a positive area on the connecting line O_4....O_2, in agreement with the assumption that it should be engaged in a hydrogen bond. The distance O_4....O_2 (Fig. 4) did however seem rather long, about 3.0 Å, and might not correspond to a hydrogen bond. Even if it was assumed that the other positive areas in the neighbourhood of O_4 (Fig. 1a) were due to anisotropic vibrations of this atom, it was thought better to wait for the correct position of H_{10} to reveal itself during the further refinement. H_{10} was therefore not included in the first calculations, during which corrections were made for the thermal parameters of the heavy atoms only. For atoms with anisotropic thermal vibration the following formula was used, where ψ is the angle between the direction of maximum vibration and the b-axis, and φ is the angle between the normal of the reflecting plane and the direction of maximum vibration: $F = f_o \cdot A \exp[-(B + \Delta B \cos^2\varphi) \sin^2\Theta/\lambda^2] + f_o \cdot D \exp[-(B + \Delta B \cos^2(180° - 2\psi \pm \varphi))\sin^2\Theta/\lambda^2]$.

Positive sign before φ for $0° < \psi < 90°$ and negative sign for $90° < \psi < 180°$

A and D means:

$h + k$ equal, $A = 2\cos 2\pi hx \cos 2\pi ky - 2\sin 2\pi hx \sin 2\pi ky$

$D = 2\cos 2\pi hx \cos 2\pi ky + 2\sin 2\pi hx \sin 2\pi ky$

$h + k$ odd, $A = +2\cos 2\pi hx \cos 2\pi ky - 2\sin 2\pi hx \sin 2\pi ky$

$D = -2\cos 2\pi hx \cos 2\pi ky - 2\sin 2\pi hx \sin 2\pi ky$

When it became evident from the difference map that sufficient corrections had been made for the vibrations of the atoms, H_{10} had appeared as a maximum of height 0.4 e·Å^{-2}, on the line O_4....O_2'. H_8 was now situated in a minimum, —0.3 e·Å^{-2}, and was moved to a maximum, 0.6 e·Å^{-2}, at a distance of about 0.5 Å from the line O_2.....O_3'. The insertion of H_{10} and the shift of H_8 seemed to cause a better agreement between F_c and F_o, and the discrepancy factor became slightly smaller. During the whole refinement process, the hydrogen coordinates were changed only three times. All coordinates were finally adjusted [8] on the basis of gradients still present at some atomic positions in the last difference map.

Table 1. Reflections affected by secondary extinction.

Reflection	$\lvert F_c \rvert$	$\lvert F_o \rvert$	$\lvert F_o \rvert$ corrected
040	37.2	30.4	34.6
060	29.5	25.3	27.0
110	26.0	23.1	25.2
120	36.1	32.4	36.8
170	43.3	38.4	42.0
180	36.2	34.6	37.0
210	42.8	40.8	45.6
240	69.6	59.4	71.2

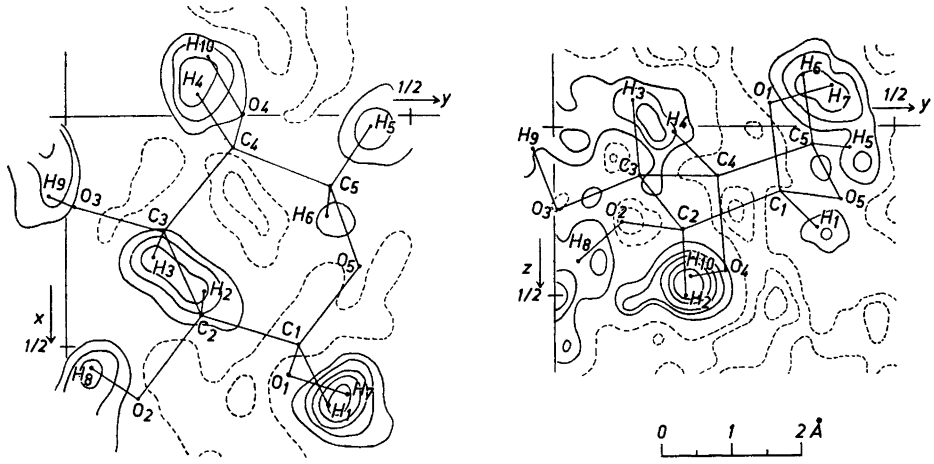

Fig. 2. The final difference projections of β-arabinose (a) along the *c* axis and (b) along the *a* axis, with hydrogen atoms *not* subtracted. Contour lines at intervals of 0.2 e·Å^{-3}, with negative lines dashed. The zero line is omitted.

In the course of the refinement process it was found that F_o values for the largest structure factors were systematically too low as compared with F_c. This might be due to secondary extinction, and the relevant reflections were for a few refinement cycles omitted from the calculations. Corrections for secondary extinction were then made according to the formula of Lipson [9], and the corrected reflections were again included in the synthesis.

The a-axis projection. Eight succesive refinements were carried out before R_{0kl} had dropped to 0.144. At this point the difference map showed positive areas for all hydrogen atoms in positions which agreed with the *y* coordinates found in the *c*-axis projection, and the hydrogen atoms were accordingly included in the calculations. Corrections were made for individual and anisotropic

Table 2. Individual and anisotropic temperature factors and the angle φ between the direction of maximum vibration and the *b*-axis.

	c-axis projection			*a*-axis projection		
Atom	φ(°)	B(Å^2)	ΔB(Å^2)	φ(°)	B(Å^2)	ΔB(Å^2)
C_1		3.2			3.0	
C_2		3.0			3.0	
C_3		3.0			3.0	
C_4		3.5			4.0	
C_5		3.5			4.5	
O_1	0	3.5	0.5		3.2	
O_2		4.0		135	2.3	1.2
O_3	63	3.0	4.0		3.2	
O_4	0	3.7	3.5	35	4.0	2.6
O_5		3.2		74	2.0	2.0
H_{1-10}		3.5			3.5	

Table 3. Atomic coordinates, in fractions of corresponding cell edges. The y coordinates are mean values of y coordinates from the a- and c-axis projections.

Atom	x	y	z
C_1	0.493	0.4172	0.188
C_2	0.431	0.3469	0.2985
C_3	0.251	0.3198	0.131
C_4	0.0695	0.3712	0.149
C_5	0.150	0.4414	0.053
O_1	0.5625	0.4099	−0.080
O_2	0.6075	0.3019	0.271
O_3	0.191	0.2545	0.237
O_4	−0.004	0.3781	0.426
O_5	0.325	0.4632	0.211
H_1	0.628	0.442	0.290
H_2	0.376	0.347	0.500
H_3	0.303	0.311	−0.078
H_4	−0.043	0.343	0.007
H_5	0.024	0.472	0.064
H_6	0.220	0.439	−0.149
H_7	0.600	0.454	−0.120
H_8	0.539	0.267	0.392
H_9	0.173	0.237	0.067
H_{10}	−0.125	0.352	0.444

thermal vibrations of carbon and oxygen atoms. After four cycles the discrepancy factor was reduced to the final value of $R_{0kl} = 0.067$. As in the c-axis projection the atomic coordinates were finally adjusted on the basis of the final difference map.

DISCUSSION OF RESULTS

Accuracy. The standard deviation in electron density, evaluated as the root-mean-square of the figures in the difference maps, is 0.13 e·Å^{-2} in the c-axis projection and 0.16 e·Å^{-2} in the a-axis projection. The standard deviation in atomic coordinates was estimated from the gradients and the curvatures of the electron density peaks [10]. The curvatures 67.2 e·Å^{-4} and 83.6 e·Å^{-4} which were used for C and O, respectively, are the mean values of well resolved carbon and oxygen peaks in the c-axis projection. For the hydrogen atoms a curvature of 10 e·Å^{-4} was used as a rough estimate.

Table 4. Standard deviation in atomic coordinates.

		c-axis projection	a-axis projection
O	$\sigma(x)$	0.005 Å	
	$\sigma(y)$	0.006 Å	
	$\sigma(z)$		0.007 Å
C	$\sigma(x)$	0.006 Å	
	$\sigma(y)$	0.007 Å	
	$\sigma(z)$		0.009 Å
H	$\sigma(x)$	0.04 Å	
	$\sigma(y)$	0.05 Å	
	$\sigma(z)$		0.06 Å

Table 5. Bond lengths in β-arabinose.

	Length(Å)	Standard deviation(Å)		Length(Å)	Standard deviation(Å)
C_1-C_2	1.524	0.009	C_1-H_1	1.13	0.05
C_2-C_3	1.523	0.009	C_2-H_2	1.04	0.06
C_3-C_4	1.554	0.009	C_3-H_3	1.08	0.06
C_4-C_5	1.537	0.010	C_4-H_4	1.15	0.05
C_1-O_1	1.382	0.012	C_5-H_5	1.02	0.05
C_2-O_2	1.454	0.008	C_5-H_6	1.08	0.06
C_3-O_3	1.426	0.009	O_1-H_7	0.91	0.05
C_4-O_4	1.431	0.012	O_2-H_8	1.00	0.05
C_5-O_5	1.440	0.008	O_3-H_9	0.90	0.06
C_1-O_5	1.421	0.008	O_4-H_{10}	0.94	0.05

On account of overlapping, the errors in calculated bond lengths (Table 5) and bond angles (Table 6) may be larger than should be expected from the calculated standard deviations. However, the correspondence between the two independently determined sets of y coordinates, one from each zone, indicates that the estimates are of reasonable order of magnitude. The average difference between independently determined y coordinates are 0.006 Å for C and 0.008 Å for O atoms, and with respect to the overlapped atoms the y-differences are 0.002 Å, 0.006 Å and 0.002 Å for C_1, O_1, and O_4, and none for C_4. The standard deviations in bond lengths, calculated on the basis of the values in Table 5, are 0.012 Å for C—C (1.535 Å), and C—O (1.434 Å) bonds, and 0.04 Å for C—H (1.08 Å) and O—H (0.94 Å) bonds.

Bond lengths. The approximate molecular structure of β-arabinose has been described elsewhere [1]. Bond lengths and bond angles as derived from the present refinement and listed in Tables 5 and 6, may now be compared with those from other sugar investigations, of which the structure analysis

Table 6. Bond angles in β-arabinose.

	Angle(°)	Standard deviation(°)		Angle(°)
$C_1-C_2-C_3$	109.2	0.6	$O_5-C_1-H_1$	107
$C_2-C_3-C_4$	109.7	0.6	$O_1-C_1-H_1$	101
$C_3-C_4-C_5$	107.1	0.6	$C_2-C_1-H_1$	116
$C_4-C_5-O_5$	111.9	0.6	$C_1-C_2-H_2$	115
$C_5-O_5-C_1$	112.7	0.6	$C_3-C_2-H_2$	104
$O_5-C_1-C_2$	109.5	0.6	$O_2-C_2-H_2$	111
$O_5-C_1-O_1$	113.0	0.7	$C_2-C_3-H_3$	108
$C_2-C_1-O_1$	108.9	0.7	$C_4-C_3-H_3$	113
$C_1-C_2-O_2$	107.3	0.6	$O_3-C_3-H_3$	106
$C_3-C_2-O_2$	110.8	0.6	$C_3-C_4-H_4$	98
$C_2-C_3-O_3$	109.3	0.6	$C_5-C_4-H_4$	118
$C_4-C_3-O_3$	110.1	0.6	$O_4-C_4-H_4$	113
$C_3-C_4-O_4$	111.7	0.7	$C_4-C_5-H_5$	103
$C_5-C_4-O_4$	108.3	0.7	$O_5-C_5-H_5$	116
$C_1-O_1-H_7$	101		$C_4-C_5-H_6$	112
$C_2-O_2-H_8$	90		$O_5-C_5-H_6$	99
$C_3-O_3-H_9$	93		$H_5-C_5-H_6$	115
$C_4-O_4-H_{10}$	109			

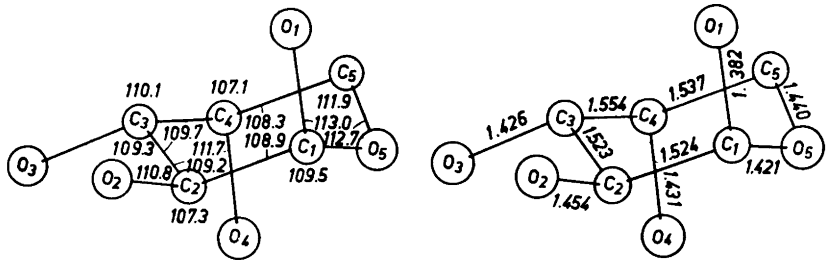

Fig. 3. Bond angles (°, left) and bond lengths (Å, right) in the β-arabinose molecule.

of α-rhamnose monohydrate [3] is presumably the most accurate. In β-arabinose the mean of C—C bonds is 1.535 Å. No individual C—C bond differs significantly from this mean value which agrees with the corresponding value for α-rhamnose, 1.532 Å. The mean value of C—O bonds, excluding C_1—O_1, is 1.434 Å in β-arabinose, exactly the same as in α-rhamnose. The bond C_1—O_1 is found to be 1.382 Å in β-arabinose and 1.376 Å in α-rhamnose, and both values differ significantly from the mean value 1.434 Å. According to Pauling [11] a C—O bond of 1.38 Å should correspond to 9% double bond character.

A detailed discussion of C—H and O—H bond lengths is hardly warranted in view of the uncertainty in the coordinates of the hydrogen atoms. The mean values of the six C—H and four O—H bonds should, however, be fairly accurate, and permit a comparison with C—H and O—H bonds reported in other X-ray investigations. In some recent X-ray analyses C—H bond lengths have been found shorter than would be expected from the currently accepted values [12,13], which are 1.09—1.11 Å for sp^3-hybridized and 1.07—1.09 Å for sp^2-hybridized carbon. Thus Tomiie *et al.*[14] reported a C(sp^2)-H bond of 0.94 Å in diformylhydrazine, and Marsh [15] found a C(sp^3)-H distance of 0.91 Å in glycine. In salicylic acid a C(sp^2)-H distance of 0.89 Å has been reported by Cochran. [16] Bommel and Bijvoet [17] found C(sp^3)-H bonds of 1.00—1.02 Å in ammonium hydrogen D-tartrate. The mentioned bond lengths appear to be significantly shorter than the normal C—H bond lengths, and the authors assume the shortening to be caused by a displacement of the electron cloud in the hydrogen atom towards the adjacent atom. The maximum of electron density might therefore be located nearer to this atom and give a shortened "bond" as result. The theoretical treatment by Cochran [18] of the electron distribution in the benzene molecule, indicates that the displacement of the maximum in the hydrogen electron cloud ought not be as drastic as found in salicylic acid. The calculated displacement in benzene was about 0.03 Å. In α-pyridone Penfold [19] found the mean value of C(sp^2)-H bond lengths to be 1.04 Å, in agreement with Cochran's theoretical results. For β-arabinose the mean length of C(sp^3)—H bonds is found to be 1.08 Å, and thus there seems to be only slight displacement of the maximum in the hydrogen electron cloud in agreement with Cochran's calculted shortening in benzene, and with α-pyridone.

McDonald [20] has derived a theoretical expression for the relation between electron distribution and temperature factor in a hydrogen peak. A rough estimate of the electron density at the hydrogen positions in β-arabinose gave as a mean 0.7 e·Å^{-2} at a temperature factor $B = 3.5$ Å^2 which agrees with McDonald's results. The mean length of O—H bonds in β-arabinose is 0.94 Å and agrees with those found by Cochran for salicylic acid, but it seems that a higher value might have been expected since the hydrogen atoms are engaged in hydrogen bonding [17].

Bond angles. Taking a difference of more than three times the standard deviation as real, it appears from Table 6 that some of the angles in β-arabinose deviate significantly from the tetrahedral angle. Among these are $C_5—O_5—C_1 = 112.7°$, $C_3—C_4—C_5 = 107.1°$ and $C_4—C_5—O_5 = 111.9°$ which belong to the pyranose ring. The mean value of the ring angles, excluding $C_5—O_5—C_1$, is 109.5°. The hetero atom O_5 seems to have caused a change in the angles $C_3—C_4—C_5$ and $C_4—C_5—O_5$. This seems likely because they are situated in the apparently most flexible part of the ring on account of absence of a hydroxyl group on C_5. However, O_5 might also have been expected to cause a change in the angles $C_1—C_2—C_3$ and $O_5—C_1—C_2$. Since the deviation of the angles $C_1—C_2—C_3$ and $C_3—C_4—C_5$ from their mean 108.2° and the deviations of the angles $C_4—C_5—O_5$ and $O_5—C_1—C_2$ from their mean 110.7° are not significant, a structure in which O_5 has caused deviations from the "ideal" chair form on both sides of the pyranose ring may be possible. The angle $C_1—O_5—C_5$ is in the literature reported to be 120° in α-rhamnose [3] and 111° for α-glucose [2]. In α-rhamnose the angle differs significantly from the tetrahedral angle, but the value appears surprisingly large.

The angles which include a hydroxyl oxygen atom $O_5—C_1—O_1 = 113.0°$, $C_1—C_2—O_2 = 107.3°$ and $C_3—C_4—O_4 = 111.7°$ appear to differ significantly from the tetrahedral value. The deviations may be due to repulsion between adjacent oxygen atoms, and this seems to agree with the fact that the greatest deviation is found in the angle $O_5—C_1—O_1$ where the repulsion on account of the O—O distance is presumably greatest. Exluding $O_5—C_1—O_1$, the mean value of the other angles including hydroxyl oxygen atom is 109.5°. The standard deviation in O—C—H and C—C—H angles, calculated on the basis of their deviations from 109.5°, was found to be 6°, which agrees with the values derived from the standard deviation of the atomic coordinates. This seems to confirm that the standard deviations in hydrogen coordinates have been correctly estimated. The mean value of the four C—O—H angles is 98°. A smaller than tetrahedral angle may here be expected on account of lone pair repulsion [21].

Hydrogen bonds. The intermolecular O—O distances, given in Table 7, correspond to hydrogen bonds. The distance $O_4.....O_2' = 3.035$ Å is rather long, but as H_8 is located near the connecting line it is probably engaged in a hydrogen bond between these atoms. Next to the O—O distances listed in Table 7, the closest approach of any two oxygen in the structure is 3.55 Å.

The environment of O_2 makes an interesting feature in the crystal structure, as O_2 is engaged in three hydrogen bonds. These bonds and $O_2—C_2$ are arranged in a roughly tetrahedral manner (Fig. 5). The fact that H_8 is displaced from the straight line connecting O_2 and O_3 makes for a better tetrahedral

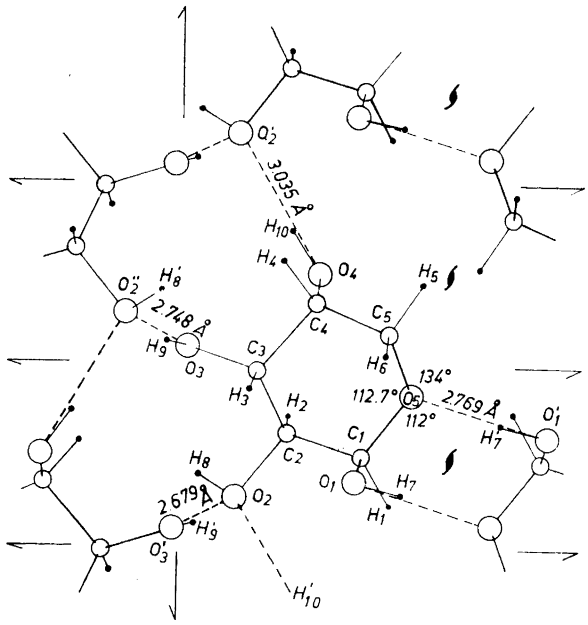

Fig. 4. The *c*-projection of the crystal structure of β-arabinose. Dashed lines indicate hydrogen bonds.

coordination, and supports the contention that O_2 is engaged in three hydrogen bonds.

O_3 takes part in two hydrogen bonds, O_1, O_4, and O_5 in one. O_3—C_3, O_3—H_9, and O_3....H_8' lie nearly in a plane as the sum of the angles at O_3 is

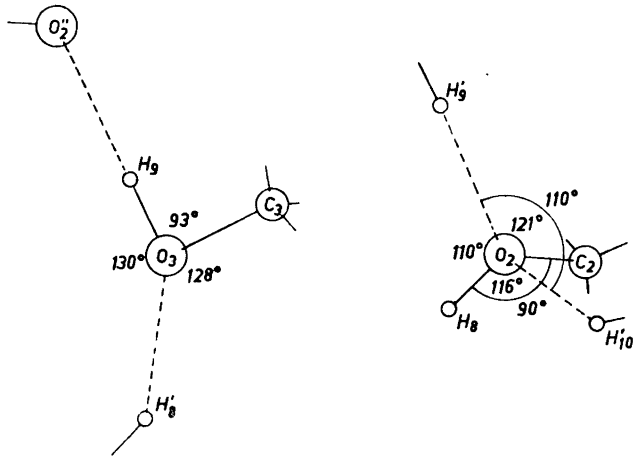

Fig. 5. Details in the crystal structure of β-arabinose at O_2 and O_3.

Table 7. Intermolecular O—O distances corresponding to hydrogen bonds, and angles at O atoms.

	Length(Å)	Standard deviation(Å)
$O_3...O_3'$	2.679	0.010
$O_3...O_2''$	2.748	0.010
$O_4...O_2'$	3.035	0.008
$O_5...O_1'$	2.769	0.009

Angles at O_2	Angle(°)
$H_8-O_2..H_{10}'$	116
$H_8-O_2..H_9'$	110
$H_8-O_2-C_2$	90
$H_{10}'..O_2-C_2$	110
$H_9'..O_2..H_{10}'$	110
$H_9'..O_2-C_2$	121

Angles at O_3	Angle(°)
$H_8'..O_3-C_3$	128
$H_8'..O_3-H_9$	130
$H_9-O_3-C_3$	93

Angles at O_5	Angle(°)
$C_5-O_5..H_7'$	134
$C_1-O_5..H_7'$	112
$C_5-O_5-C_1$	112,7

351° (Fig. 5), and the same holds for O_5—C_5, O_5—C_1 and O_5....H_7', as the sum of the angles at O_5 is 359° (Fig. 4). The direction of maximum thermal vibration of O_3 and O_5 is perpendicular to these planes. As regards O_1, O_2 and O_4 the direction of maximum vibration is about perpendicular to the C—O bonds. Thus the molecules are linked together in a three-dimensional array by hydrogen bonds in which all the available hydrogen and oxygen atoms take part.

The optical analogy between galactose and arabinose once made it difficult to designate the arabinose anomeres according to Hudson's rules [22]. The difficulty seems to have been due to the incompleteness of experimental evidence regarding the chair-formed pyranose ring and the conversion forms.

In 1909 Hudson set forth his well-known rules [23]. These were based on the suggestion that the principle of optical superposition holds for the sugars. Consequently the interest was focused on the configurations of the sugars. A relation between molecular configuration and the optical properties expressed in the α- and β-designations was sought for [22,24–26]. In 1933 the term "anomeres" was introduced by Riiber and Sørensen [25] as the class name for α- and β-forms of reducing sugars and their glycosides. Criticism was made to Hudson's rules, especially with respect to arabinose [25]. In 1947 Hassel and Ottar advanced the assumption that the six-membered pyranose ring is chair formed [27]. Each pyranose sugar should then theoretically have two chair forms, one being formed from the other by conversion of the ring, and a new problem arose concerning the relative stability of the two conversion forms. This problem was first attacked by Hassel and Ottar, who introduced what has been called the "Hassel-Ottar effect" [27], and the problem has later been approached from several different viewpoints [28].

If one adopts Reeves' symbols [29] C1 and 1C for the two possible chair forms of D-sugars, it appears that the configuration of substituents 1—5 (other than hydrogen atoms) is 1*a*5*e* and 1*e*5*a* for C1 and 1C α-D-aldohexoses,

and likewise the β-forms have the configurations 1*e*5*e* and 1*a*5*a* for C1 and 1C, respectively. For aldopentoses exactly the same holds for 1—4 hydroxyl groups. α- and β-forms are consequently related to the configuration, as in fact anticipated by Hudson.

The present work has shown that the usual crystalline form of arabinose, which according to Hudson's rules is designated β-arabinose, has the configuration 1*a*2*e*3*e*4*a*. β-L-Arabinose must thus have the conversion form C1 which is the same as for α-D-galactose. Since the 1,2,3,4 hydroxyl groups in β-L-arabinose and α-D-galactose have the same configuration, the analogy in optical properties between the two sugars is explained.

Structure of β-arabinose and other pyranoses in relation to molecular criterions. For the eight aldohexoses and four aldopentoses some desirable information concerning the configuration is still missing. Half a century of research in sugar chemistry has not yet led to unambigous configurations for α- and β-forms for all [28].

Apart from the altroses, taloses and lyxoses, the expected configuration of an aldohexose or aldopentose in crystalline form follows from Reeves' investigations [29], and the molecular configurations of α-glucose [2], α-rhamnose [2], α-xylose [30] and β-arabinose, the only ones which so far have been determined by X-ray crystallographic methods, agree with Reeves' results. Reeves supposes that altroses and lyxoses exist in both conversion forms in aqueous solution, and this has later received support from work by Whiffen [31]. Mill's arguments against Reeves' "Δ 2 effect" are interesting, but do not seem to have any influence on Reeves' stability scheme. On the basis of the relative stability of α- and β-pyranosides to acid, Edward [33] discussed the problem that it is the *less* stable glucose anomer, α-glucose, which crystallizes from aqueous solution. This is explained by Edward as due to dipole-dipole interaction between the polar group on C_1 and the lone pair electrons on the ring oxygen. An axial alkoxyl group on C_1 is, according to Edward, more stable than an equatorial alkoxyl group on C_1. As to the pure pyranoses Edward believed that better opportunities for hydrogen bonding from equatorial C_1-hydroxyl group to the solvent may overcome the mentioned effect, and thus favour the anomer which has an equatorial hydroxyl group on C_1.

The distance from the oxygen atom on C_1 to the ring oxygen atom is probably independent of *e* or *a* position of the former. The difference in repulsive force between the oxygen atoms in the two configurations should therefore be mainly due to the change in relative orientation of dipoles. The direction of the dipole resulting from C_1—O_5 and C_5—O_5 is fixed in relation to the molecule, but the dipole resulting from C_1—O_1 and O_1—H will change its direction as O_1—H is rotated about the C_1—O_1 bond. It seems therefore that this dipole-dipole interaction may be quite as considerable for an axial as for an equatorial hydroxyl group on C_1. Hydrogen bonding in a solution or a crystal may fix the direction of the dipole C_1—O_1—H and thus also the magnitude of the repulsive force. It therefore seems likely that the explanation of the fact that α-glucose and not β-glucose crystallizes from an aqueous solution might be found in the crystal energy of α-glucose *versus* that of β-glucose rather than in the dipole effect. A survey of the usual crystalline form of the aldohexoses and aldopentoses [34,35] and their suggested configurations [29] seem-

Table 8. Observed and calculated *hk*0 and 0*kl* structure factors for β-arabinose.

k	F_o	F_c	*k*	F_o	F_c	*k*	F_o	F_c
	*hk*0 zone		13	3.8	− 3.6	19	4.3	− 3.0
			14	18.8	+18.0	20	6.5	− 5.4
	0*k*0		15	6.7	− 7.4	21	8.2	+ 8.0
2	9.7	− 9.6	16	8.3	− 7.3			
4	34.6	−37.2	17	11.5	+12.1		5*k*0	
6	27.0	−29.5	18	2.9	− 3.1	1	< 3.0	+ 0.6
8	9.1	− 9.6	19	< 3.1	− 0.8	2	< 3.0	− 0.4
10	13.0	−14.7	20	< 2.9	− 1.1	3	14.4	+15.5
12	< 2.6	+ 0.1	21	3.9	+ 3.1	4	20.1	+21.4
14	12.2	−12.0	22	< 2.4	+ 0.4	5	3.3	− 3.4
16	4.1	+ 5.0	23	3.0	+ 2.1	6	9.0	+ 8.9
18	15.0	−15.0				7	< 3.2	− 1.1
20	4.1	+ 3.1		3*k*0		8	6.8	− 5.7
22	< 2.6	+ 2.3	1	9.8	− 9.0	9	4.2	− 5.3
24	6.2	+ 4.9	2	12.2	+13.4	10	3.0	+ 2.6
			3	6.6	+ 5.8	11	< 3.2	− 1.0
	1*k*0		4	5.6	− 5.5	12	< 3.2	− 1.1
1	25.2	+26.0	5	15.0	−14.8	13	< 3.1	+ 1.0
2	36.8	−36.1	6	25.8	+25.0	14	3.0	+ 1.8
3	< 1.4	− 0.7	7	21.0	−21.0	15	< 2.8	+ 0.4
4	14.2	−14.3	8	19.2	+18.1	16	2.9	− 2.6
5	17.7	+18.2	9	5.8	− 6.2	17	< 2.5	− 0.7
6	18.7	−20.4	10	13.7	−13.7	18	3.3	− 2.7
7	42.0	−43.3	11	11.7	+11.8	19	4.1	− 3.0
8	37.0	−36.2	12	18.0	+19.0			
9	14.8	−14.7	13	23.8	+23.2		6*k*0	
10	5.0	− 6.1	14	< 3.2	+ 0.8	0	< 3.2	+ 1.8
11	29.2	+30.4	15	< 3.2	0.0	1	< 3.2	− 1.5
12	7.8	+ 7.5	16	< 3.2	0.0	2	10.8	+11.5
13	10.7	+10.9	17	< 3.2	+ 1.8	3	< 3.2	− 0.8
14	< 2.9	0.0	18	< 3.0	− 0.6	4	5.8	+ 5.9
15	8.9	− 9.7	19	< 2.9	− 0.4	5	< 3.2	+ 0.6
16	12.5	+12.1	20	6.2	− 5.2	6	9.4	−10.2
17	21.9	−22.6	21	< 2.4	+ 2.0	7	8.9	− 9.0
18	4.0	− 4.6	22	< 2.0	− 0.3	8	< 3.1	+ 1.8
19	< 3.2	+ 1.5				9	3.1	+ 1.7
20	3.6	+ 3.4		4*k*0		10	5.2	− 5.0
21	5.5	+ 4.2	0	< 2.5	+ 4.3	11	< 2.9	− 0.9
22	< 2.6	+ 0.6	1	< 2.6	+ 1.1	12	2.8	− 3.3
23	< 2.3	+ 0.2	2	< 2.6	− 0.8	13	4.0	+ 3.8
24	< 1.9	− 0.2	3	19.8	+20.5	14	< 2.4	− 1.2
			4	15.8	−15.6	15	< 2.2	− 0.6
	2*k*0		5	3.9	+ 2.3	16	< 2.0	− 0.3
0	33.7	+31.9	6	3.9	− 4.8			
1	45.6	+42.8	7	5.5	+ 5.9		7*k*0	
2	19.4	+19.4	8	9.4	+ 9.5	1	3.4	− 3.3
3	6.6	− 7.0	9	8.4	− 7.9	2	< 2.9	− 1.0
4	71.2	−69.6	01	4.8	+ 4.5	3	2.8	+ 2.7
5	25.3	+25.2	11	18.8	+18.8	4	2.5	− 2.7
6	13.0	−12.9	12	8.2	+ 9.8	5	< 2.8	+ 0.5
7	24.0	−24.1	13	< 3.2	− 0.9	6	5.4	− 5.5
8	17.2	+15.6	14	3.8	− 3.5	7	< 2.6	− 0.3
9	22.7	−23.3	15	< 3.2	+ 1.0	8	< 2.5	− 0.2
10	20.6	+20.6	16	< 3.0	+ 1.1	9	< 2.4	+ 1.7
11	< 2.6	+ 0.6	17	< 3.0	− 0.4	10	3.1	− 3.7
12	2.6	− 2.4	18	< 2.7	< 2.0	11	< 2.1	+ 1.0

Table. 8 (cont)

k	F_o	F_c	k	F_o	F_c	k	F_o	F_c
12	< 1.9	+ 1.6	21	5.9	− 5.4	18	11.1	+10.0
			22	2.0	− 1.3	19	< 2.0	− 0.2
	8*k*0		23	2.6	− 2.2	20	7.4	− 7.0
0	< 2.0	− 0.6	24	5.4	+ 6.7	21	8.4	+ 8.6
1	< 2.0	− 1.5						
2	< 2.0	− 1.2		0*k*2			0*k*4	
3	< 1.9	+ 0.4	0	40.7	−41.2	0	5.6	+ 5.4
4	< 1.8	− 0.2	1	< 1.6	+ 2.1	1	13.1	−11.7
5	< 1.8	− 0.3	2	25.8	−25.1	2	7.4	+ 6.6
6	< 1.6	− 0.1	3	13.2	−13.1	3	< 2.5	+ 2.4
			4	32.3	+31.9	4	14.4	+14.9
			5	16.1	+15.5	5	11.6	+12.9
	0*kl* zone		6	2.2	+ 3.1	6	2.6	+ 3.5
			7	1.8	+ 1.0	7	2.2	− 2.6
	0*k*0		8	3.1	+ 3.4	8	< 2.5	− 0.5
2	11.4	+10.2	9	13.9	−15.1	9	8.1	− 8.3
4	32.5	−34.8	10	9.2	− 9.5	10	6.9	+ 6.3
6	28.7	+28.3	11	4.7	+ 4.8	11	2.6	+ 2.2
8	10.0	− 8.7	12	< 2.4	+ 0.3	12	< 2.4	− 1.7
10	15.4	+13.5	13	4.9	+ 4.8	13	1.6	+ 1.6
12	< 2.1	− 0.7	14	7.9	− 8.6	14	< 2.3	+ 0.5
14	15.4	+15.2	15	< 2.5	− 1.0	15	4.4	− 4.4
16	4.3	+ 5.0	16	2.2	+ 1.4	16	< 1.9	− 0.1
18	18.2	+18.6	17	6.4	+ 5.5	17	3.3	+ 3.0
20	3.8	+ 3.6	18	12.2	−12.3	18	3.3	+ 3.4
22	2.2	− 1.7	19	7.6	+ 6.7			
24	5.4	+ 6.5	20	6.0	− 5.8		0*k*5	
			21	1.7	− 1.9	1	4.2	− 3.4
	0*k*1		22	3.4	− 3.7	2	< 2.4	− 1.6
1	22.0	+25.0	23	3.0	− 3.4	3	1.9	− 2.2
2	91.2	+89.0				4	< 2.4	+ 0.7
3	35.2	−33.7		0*k*3		5	7.5	+ 7.9
4	21.1	+19.8	1	9.3	− 7.8	6	5.1	+ 5.7
5	38.0	+38.4	2	8.5	− 8.7	7	3.6	+ 3.6
6	28.5	+27.1	3	9.1	+ 9.2	8	< 2.2	− 0.6
7	10.2	−11.0	4	1.9	+ 2.0	9	4.4	+ 5.0
8	19.6	−18.6	5	4.7	− 5.5	10	3.2	+ 3.4
9	22.5	−21.4	6	17.9	−17.3	11	1.6	− 1.4
10	12.2	+12.1	7	2.8	− 3.2	12	3.2	+ 2.2
11	10.1	+ 9.9	8	8.2	− 8.2	13	< 1.6	− 0.1
12	< 2.2	− 2.4	9	4.9	− 5.2	14	2.4	− 3.8
13	11.2	+10.0	10	4.6	+ 4.2			
14	8.7	− 9.6	11	3.3	+ 2.7		0*k*6	
15	< 2.4	− 1.7	12	3.1	+ 3.8	0	2.9	− 4.1
16	< 2.5	− 2.4	13	4.0	− 4.5	1	< 1.4	+ 0.3
17	< 2.5	+ 0.6	14	9.5	− 9.9	2	1.4	− 2.1
18	< 2.5	0.0	15	3.1	− 2.7	3	6.5	+ 7.6
19	3.1	+ 3.9	16	5.4	+ 5.4	4	1.6	− 2.2
20	7.6	+ 8.2	17	4.0	− 4.0	5	2.6	− 2.9

ingly gives support to this idea. Thus allose crystallizes from dilute methano with equatorial hydroxyl 1*e*, and mannose crystallizes from ethanol with equatorial hydroxyl 1*e*. With respect to mannose it is interesting to note that the "Δ 2" form seems to crystallize rather than the 1*a*2*a* form. Further gulose

(sirup) seems to appear in β-form with 1*e*. Galactose crystallizes from water or a boiling saturated alcoholic solution in the α-form with 1*a*, but when a large excess of ice-NaCl cooled absolute alcohol is added to a solution of galactose of 0°C, the β-form with 1*e* crystallizes. Lyxose and altrose are known in α- and β-form respectively, but the configuration in which they crystallize can hardly be decided because both conversion forms, as mentioned above, seem to exist in aqueous solution. Proton magnetic resonance spectra of acetylated pyranoses [36] in chloroform show that both acetylated α-D-lyxose and α-D-altrose appear in the C1 configuration, but this does not tell which conversion form would be found in crystals of the pure sugars. Crystalline talose is known in α-form (from ethanol) and β-form (from methanol), but infrared measurements [37] seem to indicate that both conversion forms exist in solution. It has been found that the usual crystalline form of glucose [2], xylose [28] and arabinose [1] have 1*a* configuration, and the same is assumed to be the case with ribose.

REFERENCES

1. Furberg, S. and Hordvik, A. *Acta Chem. Scand.* **11** (1957) 1594.
2. McDonald, T. R. R. and Beevers, C. A. *Acta Cryst.* **5** (1952) 654.
3. McGeachin, H. McD. and Beevers, C. A. *Acta Cryst.* **10** (1957) 227.
4. Westman, S. and Magnéli, A. *Acta Chem. Scand.* **11** (1957) 1587.
5. Broomhead, J. M. *Acta Cryst.* **1** (1948) 324.
6. Berghuis, J., Haanappel, I. M., Potters M., Loopstra, B. O., MacGillavry, C. H. and Veenendaal, A. L. *Acta Cryst.* **8** (1955) 478.
7. Viervoll, H. and Øgrim, O. *Acta Cryst.* **2** (1949) 277.
8. Lipson, H. and Cochran, W. *The Determination of Crystal Structures. The Crystalline State*, Vol. III. W. Bragg (Ed.) G. Bell and Sons Ltd., London 1953, p. 301.
9. Pimock, P. R., Taylor, C. A. and Lipson, H. *Acta Cryst.* **9** (1956) 173.
10. Jeffrey, G. A. and Cruickshank, D. W. J. *Quart. Revs. (London)* **7** (1953) 335.
11. Pauling, L. *The Nature of the Chemical Bond*, 2nd Ed., Cornell University Press, Ithaca 1948.
12. Brown, M. G. *Trans. Faraday Soc.* **55** (1959) 694.
13. Costain, C. C. and Stoicheff, B. P. *J. Chem. Phys.* **30** (1959) 777.
14. Tomiie, Y., Koo, C. H. and Nitta, I. *Acta Cryst.* **11** (1958) 774.
15. Marsh, R. E. *Acta Cryst.* **11** (1958) 654.
16. Cochran, W. *Acta Cryst.* **6** (1953) 260.
17. Bommel, A. J. and Bijvoet, J. M. *Acta Cryst.* **11** (1958) 61.
18. Cochran, W. *Acta Cryst.* **9** (1956) 924.
19. Penfold, B. R. *Acta Cryst.* **6** (1953) 591.
20. McDonald, T. R. R. *Acta Cryst.* **9** (1956) 162.
21. Gillespie, R. J. and Nyholm, R. S. *Quart. Revs. (London)* **11** (1957) 339.
22. Riiber, C. N. and Sørensen, N. A. *Kgl. Norske Videnskab. Selskabs Skrifter* **1938** No.1.
23. Hudson, C. S. *J. Am. Chem. Soc.* **31** (1909) 66.
24. Boeseken, J. *Advances in Carbohydrate Chem.* **4** (1949) 189.
25. Riiber, C. N. and Sørensen, N. A. *Kgl. Norske Videnskab. Selskabs Skrifter* **1933** No. 7.
26. Jackson, E. L. and Hudson, C. S. *J. Am. Chem. Soc.* **59** (1937) 994.
27. Hassel, O. and Ottar, B. *Acta Chem. Scand.* **1** (1947) 929.
28. Ferrier, R. J. and Overend, W. G. *Quart. Revs. (London)* **8** (1959) 265.
29. Reeves, R. E. *J. Am. Chem. Soc.* **72** (1950) 1499.
30. Woolfson, M. M. *Acta Cryst.* **11** (1958) 393.
31. Reeves, R. E. *Ann. Rev. Biochem.* **27** (1958) 15.
32. Mills, J. A. *Advances in Carbohydrate Chem.* **10** (1955) 1.

33. Edward, J. T. *Chem. & Ind. (London)* **1955** 1102.
34. Beilstein's *Handbuch der Organischen Chemie.* Vol **31** Part. 1 (*Kohlenhydrate*). Julius Springer, Berlin 1938.
35. Rodd, E. H. *Chemistry of Carbon Compounds.* Vol. 1 Part B, Elsevier Publishing Company, New York 1952.
36. Lemieux, R. U., Kullning, R. K. Bernstein, H. J. and Schneider, W. G. *J. Am Chem. Soc.* **80** (1958) 6098.
37. Neely, W. B. *Advances in Carbohydrate Chem.* **12** (1957) 13.

Received June 28, 1960.

ACTA CHEMICA SCANDINAVICA 15 (1961) 31–35

The Ag-Rich Side of the Binary Phase Diagrams Ag/Au and Ag/Cu as Studied by Zone Refining

J. MARKALI

Central Institute for Industrial Research, Blindern, Norway

P. THORESEN*

Department of Physics, University of Oslo, Blindern, Norway

The Ag-rich side of the system Ag/Au and Ag/Cu has been investigated by the zone refining method. The opening angle of the liquidus-solidus gap of the system Ag/Au is in disagreement with older data, but is indistinguishable from the recent reinvestigation of the system. The system Ag/Cu also deviates from the commonly accepted phase diagram in that the opening angle is greater than that commonly accepted. Determinations of the segregation coefficients as a function of concentration of solute in the concentration range investigated show that the ratio of the activities departs markedly from the ratio of concentrations for Cu in Ag for concentrations above 0.5 atomic %. No such departure was found in the system Ag/Au in the concentration range investigated. The obvious usefulness of the zone refining method in the determination of the opening angle of the liquidus/solidus gap in binary systems is shown.

Since the invention of the zone refining method by Pfann [1], several practical consequences of the invention have been evaluated and have been used in many laboratories. Much work has also been done on the evaluation of concentration profiles, based on either the simple or the more complicated equations describing this process.

It is usual to define the distribution coefficient as the ratio between the solubilities in the solid and the liquid states:

$$k_0 = \frac{c_s}{c_l}$$

* Present address: Royal Norwegian Defence Research Establishment, Kjeller, Norway.

If k_0 can be found by experiment, the opening angle between the liquidus- and the solidus-curve can be determined to the same degree of accuracy as the liquidus-curve. It is well known that the accuracy in determining the liquidus-curve is much higher than that of the solidus-curve. The accuracy of the opening angle in the binary phase-diagrams so far published is probably low.

Since most binary phase-diagrams have few or no experimental data for very low concentrations of the components, the beginning of the curves are more artistic than real. The steadily growing interest in pure and ultrapure materials requires more exact data. Determination of k_0 by zone refining experiments is one way of obtaining more exact information.

Following Burton and Schlichter [3] one can define an effective distribution coefficient

$$k = \frac{k_0}{k_0 + (1 - k_0)\exp - v\delta/D}$$

where δ is the extension of the diffusion layer, v the velocity of the zone and D the diffusivity in the liquid. It is customary to rearrange this equation in the forms

$$\ln\left(\frac{1}{k} - 1\right) = \ln\left(\frac{1}{k_0} - 1\right) - v\delta/D \text{ for } k_0 < 1$$

and

$$\ln\left(1 - \frac{1}{k}\right) = \ln\left(1 - \frac{1}{k_0}\right) - v\delta/D \text{ for } k_0 > 1$$

D is usually known and δ is usually unknown. δ/D can be calculated or estimated. As δ/D is nearly independent of the zone velocity it can also be found or eliminated by zone refining experiments at different zone velocities. If D for the solute in question is unknown, but known for another solute, it can be determined by zone refining of the two systems in question.

EXPERIMENTAL

The specimens were contained in a graphite crucible and heated by induction. The silver did not stick to the graphite and the zone was thoroughly stirred. Purified nitrogen was used as inert atmosphere and the zone velocity was quite low, 1.51×10^{-2} mm/sec. The geometry of the melted zone was determined by quenching experiments. We tried to achieve nearly optimum conditions for zone refining.

The concentration profiles were determined from different methods:

1) neutron activation analysis,
2) radioactive tracer technique,
3) chemical analysis,
4) direct spectrographic analysis.

All of these methods were used to evaluate the usefulness of the different methods for this and other similar problems [4].

The amount of solute used for analysis by neutron activation, was determined from calculations of the neutron flux available, the time of irradiation and the type of solute to be determined. In the cases where neutron activation and radioactive tracers were used, the registration of the concentration profiles after the zone refining experiments was done by picking out the characteristic radiation in a β spectrometer. In the cases where radioactive tracers were used, the concentration profiles were also determined by a direct photographic method.

An estimate of the error for the different methods was made.

Direct spectrographic methods gave the poorest results and in our case the radioactive tracer technique seemed to be the most useful method for determining small amounts of solute.

THE SYSTEM Ag–Au

By comparing the experimental concentration profiles and the deduced k-values with the concentration profiles and the effective k-values given by Pfann [5], the k-value was found to differ only slightly from the k_0-value. The comparison of the experimental and theoretical concentration profiles for 10 passes of the zone showed $1.08 < k < 1.10$. Assuming a maximum (the least favourable) value of $\delta/D = 100$ sec/cm the result is $1.08 < k_0 < 1.12$.

Fig. 1 gives the opening angle for the phase diagram ($k_0 = 1.11$) as found by the experiments and that taken from Metals Reference Book [2]. The disagreement is evident.

In 1954, Wagner [6] calculated the width of the gap between the liquidus and the solidus to be 1.3°K at 50 atomic % Au. The system was more recently reinvestigated by White *et al.*[7] based on the measured thermodynamic properties of the solid and liquid alloys. They determined the gap between the liquidus and solidus to be 1.5°K at 50 atomic % Au. In a recent paper White [8] has confirmed the results also by thermal analysis. The opening angle taken from the work of White *et al.*[7] cannot be distinguished from that of the present investigation. This does not only confirm the usefulness of the zone refining method in determining the opening angle of binary phase diagrams, but it also shows that for the concentrations used (starting concentration = 1 %), there is apparently no deviation from ideality. Therefore $a_1/a_2 = c_1/c_2$, where a_1 and a_2 are the activities of the two components and c_1 and c_2 the corresponding concentrations.

THE SYSTEM Ag–Cu

The concentration profils after zone refining for specimens with Cu as solute did not correspond with concentration profiles calculated for a number of k-values and zone passes. The reason for this may be found in the invalidity

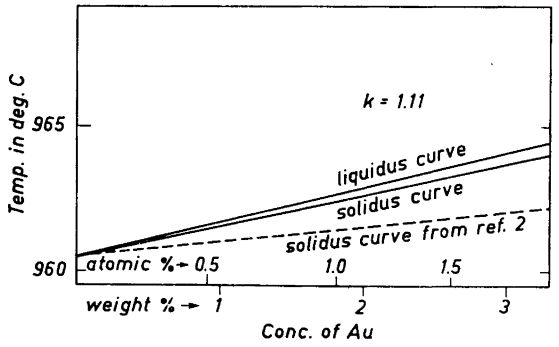

Fig. 1. The Ag-rich side of the phase diagram Ag/Au.

of the assumptions made in the evaluation of the zone refining formulae, *i.e.* at the solute concentrations used, the solution deviated from ideality. At too high solute concentrations this will cause a variation of k with concentration in part of the specimen. From the experimental concentration profiles it was possible to calculate the k-value continuously from 0.05 % — 2.5 % Cu. The calculation was based on the concentration profiles from the purest part of the rod. The values of these for 1, 3, 5 and 10 zone passes were compared with those from theory. The amount of copper in the distance from the starting end of the rod was calculated ($c_l(x)$), and the calculations were compared with the amount of copper in the solidified rod ($c_s(x)$).

The equation:

$$k(x) = k(c_l(x)) = \frac{c_s(x)}{c_l(x)}$$

gives the k-value as a function of the concentration in the liquid zone. The solidus' curve in the phase diagram could then be calculated, based on the liquidus curve. The results are given in Fig. 2, where the opening angle is greater than that found in Ref.[2]. At about 0.5 % Cu, the numerical value of the gradient begins to decrease, owing to departure from ideality ($a_1/a_2 \neq c_1/c_2$). The first part of the curve represents the correct gradient based on a k_0-value of 0.41 and a k-value of 0.45. This allows not only a determination of k- and k_0-values which determines the opening angle of the phase diagram (equilibrium diagram), but also gives measure for the departure from ideality, (a_1/a_2 compared with c_1/c_2).

CONCLUSION

It may be expected that the deviation from ideality starts at lower concentrations of copper in silver than of gold in silver.

It is shown that opening angles in binary diagrams can be determined with a high degree of accuracy by use of the zone refining method, provided that the concentration profiles can be exactly determined.

It is also shown that the method can give informations regarding deviations from ideality as a function of concentration of solute.

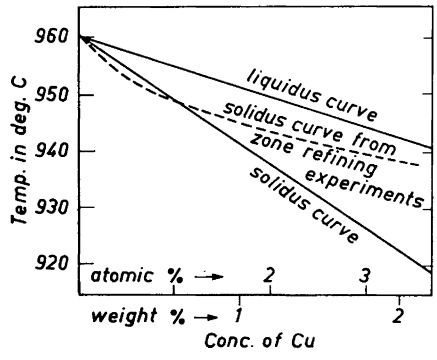

Fig. 2. The Ag-rich side of the phase diagram Ag/Cu.

REFERENCES

1. Pfann, W. G. *J. Metals* **4** (1952) 747.
2. Smithells, C. J. *Metals Reference Book*, Butterworths, London 1955.
3. Burton, J. A. and Schlichter, W. P. *Transistor Technology*, Van Nostrand, Princeton, N. J. 1958, Vol. I, Chapt. 5.
4. Thoresen, P. *Thesis*, University of Oslo, 1959.
5. Pfann, W. G. *Zone Melting*, Wiley & Sons, Inc., New York 1958.
6. Wagner, C. *Acta Met.* **2** (1954) 242.
7. White, J. L., Orr, R. L. and Hultgren, R. *Acta Met.* **5** (1957) 747.
8. White, J. L. *Trans. Met. Soc. AIME* **215**, (1959) 178.

Received September 14, 1960.

ACTA CHEMICA SCANDINAVICA 15 (1961) 36–46

Studies on Peroxy Compounds VII *

The Copper Salt Catalyzed Decomposition of *t*-Butyl Perbenzoate in the Presence of Benzyl Sulphides

SVEN-OLOV LAWESSON and CURT BERGLUND

Department of Organic Chemistry, Chemical Institute, University of Uppsala, Uppsala, Sweden

It has been shown that when *t*-butyl peroxide is decomposed in a benzyl sulphide, the benzyl radical formed dimerizes but no fragmentation is observed. When *t*-butyl perbenzoate is decomposed in the same types of substrates and with catalytic amounts of cuprous chloride present, no dimer but only the corresponding benzoyloxy compound is isolated. Also, when the perester is decomposed in the presence of benzyl alcohol, cuprous chloride has a stabilizing effect giving the dibenzyl acetal of benzaldehyde; without cuprous chloride, benzaldehyde is the sole product. Cuprous chloride has no effect in the case of benzyl mercaptan; dibenzyl disulphide is formed in both reactions. When the benzoyloxy compound of dibenzyl sulphide is heated stilbene is formed.

Recently Huang and coworker [1] showed by decomposing *t*-butyl peroxide in the presence of different benzyl ethers that the generated radical II either dimerizes, undergoes fragmentation or both as follows:

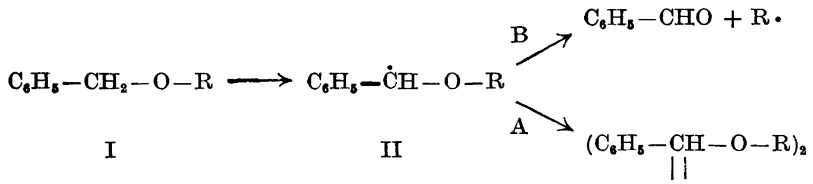

(1)

The reaction takes different courses depending upon the group R. As the reaction is not favoured if a very energetic radical R· is formed it is clear that for R = methyl or phenyl dimerization occurs exclusively (route A), thus revealing the high reactivity of the methyl and phenyl radicals. With R = ben-

* Part VI. Lawesson, S.-O. and Grōwall, S. *Acta Chem. Scand.* 14 (1960) 1445.

zyl, only fragmentation according to route B is observed, and with R = *i*-propyl *etc.* both fragmentation and dimerization occur which indicates that these radicals R· (R = C_2H_5, *i*-C_3H_7) are somewhere inbetween the methyl and phenyl ones on one side and benzyl on the other in regard to reactivity and stability.

Lawesson and Berglund [2,3] have studied the copper salt catalyzed decomposition of *t*-butyl perbenzoate in the presence of benzyl ethers and found that the benzoyloxy group is introduced according to the following formulas:

$$\underset{\text{I}}{C_6H_5-CH_2-O-R} \longrightarrow \underset{\text{II}}{C_6H_5-\dot{C}H-O-R} \longrightarrow C_6H_5-\underset{\displaystyle OCOC_6H_5}{\underset{|}{CH}}-O-R \qquad (2)$$

R = C_6H_5, CH_3, *i*-C_3H_7, *t*-C_4H_9

This would indicate that the intermediate radical II (eqn. 2) is in some way stabilized by the presence of the copper salt. No fragmentation or dimerization is observed. When dibenzyl ether is used as a substrate, the dibenzyl acetal of benzaldehyde is isolated, which is a rather unexpected result. We cannot give an exact explanation of this at present, but for reasons which appear in the sequel, a hypothesis is presented (see below).

In connection with this it may be mentioned that Lawesson and Busch [4] have investigated the reaction of acetals with radicals, and it has been shown that dibenzylacetal of benzaldehyde with *t*-butoxy radicals gives benzyl benzoate, benzaldehyde, dibenzyl and *meso*-dihydrobenzoin dibenzoate.

From the work of Lawesson and Berglund [2,3], the effect of cuprous salt has been shown to be of certain importance in modifying the course of the reaction when benzylic ethers (I) are transformed into the corresponding radicals (II) and then allowed to react with a benzoyloxy radical. Our recently outlined research plan [2] was therefore continued, and this paper deals with the work on sulphur homologues of the benzyl ethers.

As a free radical of a benzyl ether dimerizes, fragments or both according to eqn. 1, it was of a special interest to ascertain how radicals of benzyl sulphides would react under similar conditions. From the work of Huang *et al.*[1], we know that for benzyl ether [R = benzyl (eqn. 1)] fragmentation is the main process. Therefore, it was logical to start with dibenzyl sulphide as an assumed extreme case. If the sulphide would react in the same way as the corresponding ether, thiobenzaldehyde (as a trimer) and dibenzyl would be the supposed products. We found that the only product, besides starting material, which could be isolated was the dimer according to the following formulas:

$$C_6H_5CH_2-S-CH_2-C_6H_5 \longrightarrow C_6H_5\dot{C}H-S-CH_2-C_6H_5 \longrightarrow (C_6H_5-\underset{|}{CH}-S-CH_2-C_6H_5)_2 \qquad (3)$$

The illustrated difference between benzyl ethers and thio ethers may be explained as follows: sulphur but not oxygen can stabilize an unpaired electron on an adjacent carbon atom, and the following mesomeric interaction would explain the stabilization [5,6]

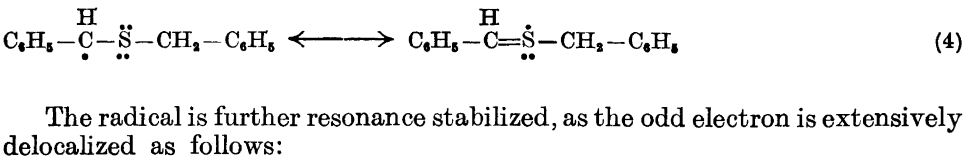

(4)

The radical is further resonance stabilized, as the odd electron is extensively delocalized as follows:

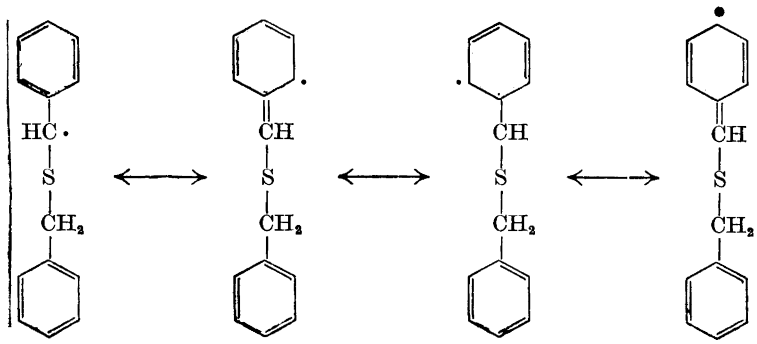

As radicals of benzyl sulphides do not undergo fragmentation but only dimerization, decomposition of peroxides in the presence of benzyl sulphides in contrast to benzyl ethers seems to be a simpler case. A survey of the literature shows that as late as 1957 Horner and coworkers[7] investigated the reaction between diacyl peroxides and certain sulphides in chloroform whereby benzoic acid, benzoic anhydride, the sulphoxides and, in a few cases, the corresponding benzoyloxy compounds were isolated.

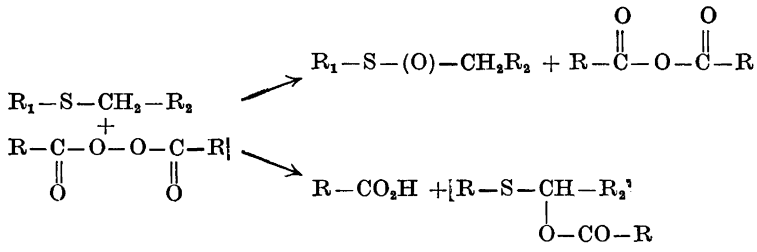

(5)

The only sulphide of benzylic type investigated was dibenzyl sulphide.

In our studies of copper salt catalyzed decomposition of *t*-butyl perbenzoate in the presence of different types of benzyl sulphides, we have found that the benzoyloxy group is introduced on the methylene group according to the following formulas:

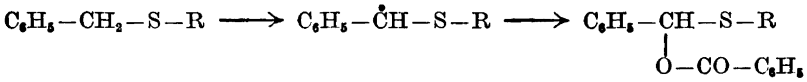

(6)

R = CH_3, C_2H_5, *i*-C_3H_7, *i*-C_4H_9, *t*-C_4H_9, C_6H_5

The principle of the method is to add *t*-butyl perbenzoate to a preheated benzene solution of the substrate in the presence of catalytic amounts of cuprous chloride. The temperature is maintained close to 80°C, and the reaction is followed by titration or by observation of the infra-red curves. The *t*-butyl perbenzoate carbonyl group absorbs at 1 775 cm^{-1}, and the disappearence of this peak indicates the disappearence of the perester. After the formed benzoic acid is isolated by extraction, the benzoyloxy compound is isolated by extremely careful distillation. Too strong heat *etc.* can cause an immediate decomposition of the benzoyloxy compound, and like their corresponding ether homologues, these compounds are sensitive to air (oxygen); also when stored for six months in a closed vial over nitrogen, benzoic acid precipitates and a strong smell of thiobenzaldehyde is noticed.

In the case of dibenzyl sulphide, the reaction with *t*-butyl perbenzoate is quite normal. After the excess of substrate (dibenzyl sulphide) is distilled off from the reaction mixture, it is demonstrated by IR that the crude, neutral residue contains a benzoate. However, every attempt to purify it by distillation was futile as benzoic acid was always formed. By oxidizing the sulphide with potassium permanganate in glacial acetic acid, the corresponding sulphone was obtained and shown to be the authentic Horner compound [7]. In one experiment when an attempt was made to fractionate the benzoate using a 20 cm high column, *trans*-stilbene and benzoic acid were isolated. The formation of stilbene calls our attention to a paper by Bordwell and Cooper [8] who isolated *trans*-stilbene from benzyl α-chlorobenzyl sulphone (actually an example of the Ramberg-Bäcklund reaction [9-11]). We hope to continue our research on pyrolysis of α-benzoyloxy sulphides to find out more thoroughly the scope of our findings.

As there are some apparent differences between radicals of benzyl ethers and thioethers, we considered it pertinent to make a similar comparison between benzyl alcohol and benzyl mercaptan. With hydroxy compounds, similar investigations have been made earlier and Bartlett and Nozaki's results [12] are wellknown: induced decomposition of benzoyl peroxide in primary and secondary alcohols can be described by the following reaction scheme in agreement with other known radical reactions.

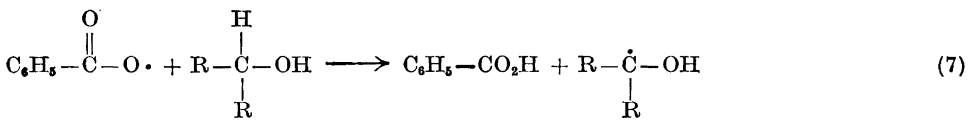

(7)

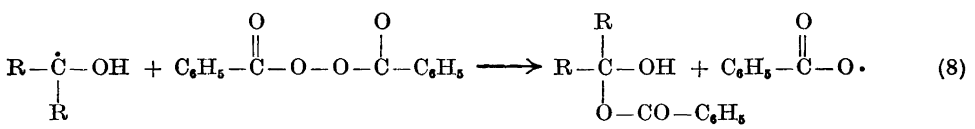

(8)

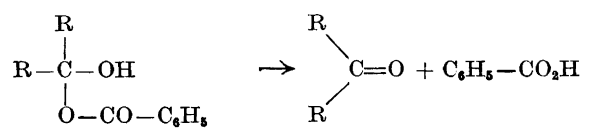

(9)

In our case, when *t*-butyl perbenzoate was decomposed in the presence of benzyl alcohol and catalytic amounts of cuprous chloride, the sole product which could be isolated was di-benzylacetal of benzaldehyde. The same product [3] was obtained when *t*-butyl perbenzoate was decomposed in the presence of dibenzyl ether. From the work of Urry and coworkers [13], it is also known that a *t*-butoxy radical abstracts a hydrogen attached to the carbon bearing the —OH; thus the following reaction scheme is postulated:

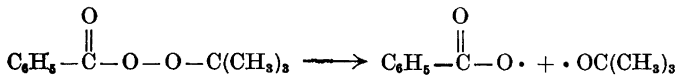

(10)

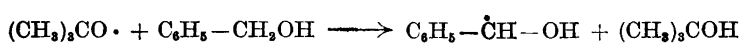

(11)

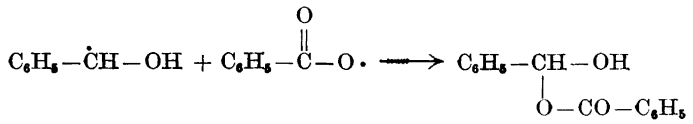

(12)

It is not probable that the intermediate radical in eqn. 11 should undergo fragmentation,

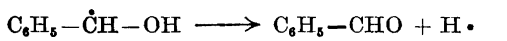

(13)

as this (eqn. 13) would lead to a high energy hydrogen radical. As no dimer is isolated, the copper salt stabilizes the radical and thus prevents a possible dimerization;

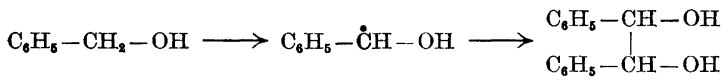

(14)

Instead, the stabilized benzyl radical with the benzoyloxy radical gives an acylal (eqn. 12), but the fate of this intermediate is unknown except that the final product has been characterized. As we have not been able to prepare dibenzyl acetal of benzaldehyde from benzaldehyde, benzyl alcohol and benzoic acid, the hypothesis that the acylal decomposes into benzaldehyde and benzoic acid is very uncertain.

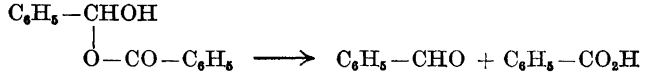

(15)

However, as we have now shown that reflux of ethanol with the benzoate of benzyl ethyl ether gives the acetal (eqn. 16),

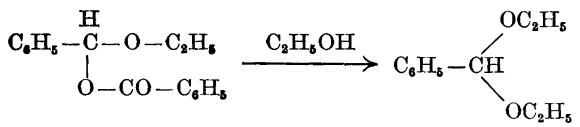

(16)

it would not be out of order to envisage an exchange as follows:

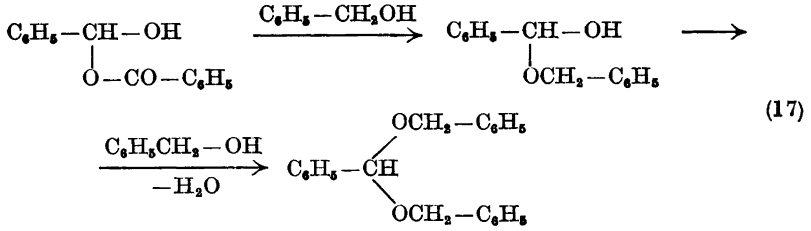

(17)

When *t*-butyl perbenzoate is decomposed in benzyl alcohol but with no cuprous chloride present, no high-boiling product was isolated but only benzaldehyde. As *t*-butyl perbenzoate gives different kinds of radicals when heated,

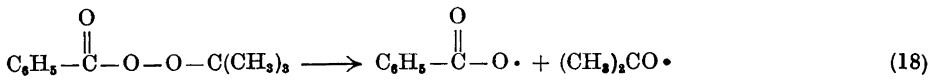

(18)



(19)

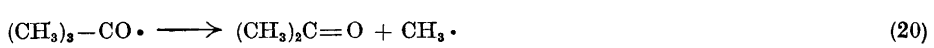

(20)

different alternatives are possible and no clear-cut reaction seems to be valid.

From the work of Bartlett *et al.*[12] the proposal of an acylal as an intermediate (*cf.* eqns. 7—9) has been made which then decomposes into the corresponding carbonyl compound and benzoic acid. Since the decomposition of the acylal according to eqn. 15 is prevented when cuprous chloride is present, this would indicate that also at that stage of the reaction transition metal salts are of a certain importance.

The results of Sosnovsky and Yang [14] are different from ours in this case and their findings that benzaldehyde and benzoic acid are formed, when cuprous bromide is present, have not been observed by us.

In the case of benzyl mercaptan, the only product found was dibenzyl disulphide. The presence of copper salt seems to be of no importance in this case. The *t*-butoxy radical attacks on the S—H bond and not the C—H bond, and the proposal for the formation of disulphide under radical conditions is

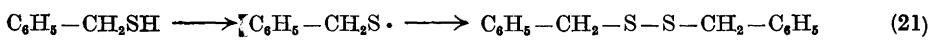

(21)

From the results presented in this investigation, the presence of copper salt leads to a different type of reactions. No conventional free radical intermediate seems to exist which would give the dimer, but a mechanism of a concerted type, where the copper salt is of a profound importance. Kharasch and Sosnovsky [15] have shown that in olefins, transition metal salts such as copper or cobalt salts are effective but that zinc or magnesium salts are ineffective. In the case of copper salt, the valence is of no importance as the same

results are obtainable with cuprous or cupric salts. Based on cuprous salt, these authors offer an explanation of the copper salt catalysed decomposition of peresters in the presence of olefins according to the following formulas:

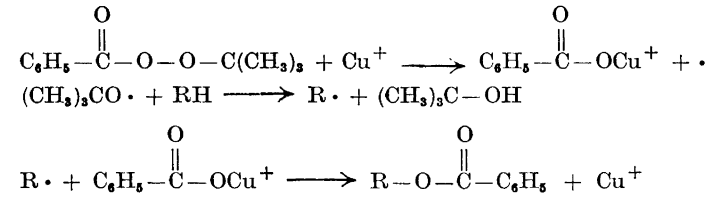

(22)

(23)

(24)

Denney *et al.*[17], on the other hand, working solely with cupric salts suggest a complex between the cupric ion, a benzoyloxy, and a *t*-butoxy radical which then coordinates to the olefin. Probably in a concerted manner, the displacement of the allylic hydrogen by the benzoyloxy group follows the abstraction of the hydrogen atom by the *t*-butoxy radical.

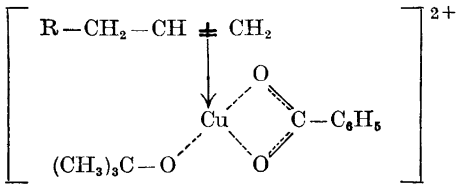

At this point, neither of these mechanisms can be ruled out as two types of complexes might exist. However, in all our reactions, we have used cuprous chloride as a catalyst and have never observed divalent copper in the reaction mixture after the reaction has ended (determined by electron magnetic resonance). Further we have used divalent copper salt in one experiment and even in that case no divalent copper was observed. This would indicate that the Denney-complex in its present form might exist, but that the fate of it and the finer details of the mechanism are still unknown.

EXPERIMENTAL

The reactions between *t*-butyl perbenzoate and the benzyl sulphides were carried out in an atmosphere of dry, oxygenfree nitrogen. All sulphides were distilled prior to use. Commercial (Light) *t*-butyl perbenzoate (n_D^{20} = 1.5000) was used in all experiments withour further purification. No reaction was considered complete unless the reaction mixture gave a negative peroxide test. The rate of the decomposition of the perester was followed by titration according to the method of Silbert and Swern [18]. The infra-red spectra measurements were made on a Perkin-Elmer Model 21, double beam spectrophotometer and an Infracord. The analyses were made by Alfred Bernhardt, Mülheim (Ruhr) and The Analytical Department, Uppsala University. Boiling and melting points are uncorrected.

Starting material

Preparations of sulphides. Benzyl—S—R (R = methyl, ethyl, *i*-propyl, *i*-butyl, *n*-butyl, benzyl) were prepared by adding the corresponding halogen compound to benzyl mercaptide [19]. Benzyl *t*-butyl sulphide was prepared in analogy with Ipatieff's *et al.*[20] preparation of phenyl *t*-butyl sulphide. Benzyl phenyl sulphide was prepared from thiophenol and benzylchloride [21].

Benzyl t-butyl sulphide. 250 g of 75 % sulphuric acid was placed in a three-necked 500 ml flask, fitted with a mechanical stirrer, an inlet-tube to the bottom of the flask and a dropping funnel. The flask was surrounded by an ice-water bath. *Iso*butylene was bubbled through the rapidly stirred acid until 44 g (0.8 mole) was absorbed. Then, 43 g (0.35 mole) of benzyl mercaptan was added drop-wise. When the addition was complete, crushed ice was poured down into the flask while the flask still was surrounded by the ice-water bath. The solution was then twice extracted with ether. The ether extract was washed with water, alkali and water till neutral, then dried over anhydrous sodium sulphate and distilled. B.p. 114–115°C/10 mm Hg, n_D^{20} = 1.5283, Weight 54.5 g, Yield 87 %. Lit.[22] report b.p. 115–116°C/15 mm Hg.

Experiments

The reaction of t-butyl perbenzoate and benzyl phenyl sulphide. A 500 ml three-necked flask was fitted with a stirrer, a dropping funnel and a reflux condenser, the top of which was connected to a gas collector. 200 ml of anhydrous benzene, 0.1 g of cuprous chloride and 37 g (0.185 mole) of benzyl phenyl sulphide (m.p. 40–42°C) were placed in the flask. The system was swept with nitrogen gas, and the flask was maintained at an oil bath temperature of 80°C. 20 ml (0.1 mole) of *t*-butyl perbenzoate in 50 ml of benzene was added dropwise during half an hour. A blue colour appeared rapidly, and the reaction progress was followed by titration of the peroxy compound in the following way: To a 2 ml sample of the solution were added 2 ml of a saturated sodium iodide solution and 10 ml of glacial acetic acid containing a trace of ferric chloride. The final solution was allowed to stand in the dark for 10 min, 50 ml of water was added, and then the iodine liberated was titrated with 0.1 M sodium thiosulphate. No gas evolution was observed. After 3.5 h, the reaction was complete. The solution was washed with a 2 M NaOH solution. The benzene phase was then washed with water until neutral and dried over sodium sulphate. The alkaline solution was acidified with 2 M HCl. The precipitated benzoic acid was filtered off, dried and weighed (1.3 g). From the organic phase, the benzene was removed under reduced pressure. In this and all following distillations, pure nitrogen was drawn through the capillary. The excess benzyl phenyl sulphide was first collected, b.p. 90–105°C/0.1 mm Hg. The benzoyloxy compound was then collected at 165–170°C/0.05 mm Hg. The compound solidified, and part of it was recrystallized from ethanol and petroleum ether. The melting point was 64.5–65.5°C. 13.5 g. Yield 42 %. (Found: C 75.16; H 5.24; S 9.90. Calc. for $C_{20}H_{16}O_2S$ (320.19): C 74.99; H 5.03; S 9.99).

The reaction of t-butyl perbenzoate and benzyl methyl sulphide. 0.2 mole of *t*-butyl perbenzoate were added dropwise during 35 min to a refluxing benzene solution (300 ml), containing 53 g (0.375 mole) of redistilled benzyl methyl sulphide (n_D^{20} = 1.5582) and 0.1 g of cuprous chloride. The reaction was complete after 3 h at an oil bath tempereture of 80°C. No gas was collected. The blue solution was extracted with a 2 M NaOH solution, washed with water until neutral and dried over sodium sulphate. From the alkaline washings 5.2 g of benzoic acid were obtained. After the solvent had been removed from the organic phase the residue was distilled and gave 30 g of the starting compound, b.p. 70–75°/0.3 mm Hg. The benzoyloxy compound was obtained at b.p. 140–145°C/0.1 mm Hg. Weight 39 g. Yield 76 %. The benzoyloxy compound crystallized immediately and part of it was recrystallized from petroleum ether. M.p. 44–46°C. (Found: C 69.49; H 5.46; S 12.27. Calc. for $C_{15}H_{14}O_2S$ (258.22): C 69.79; H 5.42; S 12.39).

The reaction of t-butyl perbenzoate and benzyl ethyl sulphide. *t*-Butyl perbenzoate (0.2 mole) in 50 ml of anhydrous benzene was added dropwise to 65 g (0.43 mole) of benzyl ethyl sulphide (n_D^{20} = 1.5508) and 0.1 g of CuCl in 300 ml benzene, kept at an oil bath temperature of 80°C. After 2 h, the reaction was complete and no gas evolution was observed. The work-up was performed as above. The alkaline solution gave 4.5 g benzoic acid. Distillation of the organic phase first gave benzyl ethyl sulphide (n_D^{20} = 1.5512) 39 g and then the benzoate, b.p. 140–150°C/0.3 mm Hg. Weight 29 g. Yield 53 %. The benzoyloxycompound crystallized, and part of it was recrystallized from petroleum ether. M.p. 29–32°C. (Found: C 70.73; H 6.03; S 11.71. Calc. for $C_{16}H_{16}O_2S$ (272.23): C 70.57; H 5.92; S 11.75).

The reaction of t-butyl perbenzoate and benzyl i-propyl sulphide. A flask containing 200 ml of anhydrous benzene, 0.1 g of CuCl and 40 g (0.28 mole) of redistilled benzyl *i*-propyl sulphide (n_D^{20} = 1.5393) was maintained at an oil bath temperature of 70°C. 0.1 mole of *t*-butyl perbenzoate in 25 ml of benzene was added during 15 min. Titration showed that the reaction was almost immediately complete, and the reaction mixture was cooled. The alkaline washings gave 3.5 g of benzoic acid. The neutral benzene solution was dried and the benzene and excess of sulphide was removed under reduced pressure. The rest solidified in contact with cold petroleum ether. After recrystallization the melting point was 28—29°C. Weight: 8 g. Yield 28 %. (Found: C 71.16; H 6.27; S 11.12. Calc. for $C_{17}H_{18}O_2S$ (286.24): C 71.31; H 6.34; S 11.17).

The reaction of t-butyl perbenzoate and benzyl i-butyl sulphide. *t*-Butyl perbenzoate (0.15 mole) was added dropwise to a refluxing benzene solution (200 ml) containing 59 g (0.33 mole) of benzyl *i*-butyl sulphide (n_D^{20} = 1.5234) and 0.1 g of cuprous chloride. After refluxing for 2 h at 80°C, the reaction was complete. No gas evolution was observed. The reaction mixture was washed with 2 M NaOH, then with water and finally dried over sodium sulphate. The alkaline solution was acidified and the precipitated benzoic acid dried and weighed (7.8 g). From the organic solution, benzene and excess of benzyl *i*-butylsulphide were removed under reduced pressure. The benzoyloxy compound was obtained at 135—140°C/0.1 mm Hg. Weight 21 g. Yield 47 %. The product solidified and part of it was recrystallized from petroleum ether. M.p. 53—54°C. (Found: C 71.33; H 6.71; S 10.63. Calc. for $C_{18}H_{20}O_2S$ (300.25): C 71.98; H 6.71; S 10.66).

The reaction of t-butyl perbenzoate and benzyl t-butyl sulphide. In a flask containing 300 ml of anhydrous benzene were placed 50 g (0.28 mole) of redistilled benzyl *t*-butyl sulphide (n_D^{20} = 1.5283) and 0.1 g of cuprous chloride. 0.2 mole of *t*-butyl perbenzoate dissolved in 50 ml of benzene were added dropwise during 15 min to the benzene sulphide solution which was kept in an oil bath at a temperature of 75°C. After 45 min, the reaction was almost complete. No gas evolution was observed. After the solution had been washed with a 2 M NaOH solution and with water in the usual way, it was dried over sodium sulphate. Benzoic acid (3 g) was obtained from the alkaline washings. Benzene was removed from the organic phase, the remainder was distilled and benzyl *t*-butyl sulphide (18 g) was collected first, b.p. 114— 120°C/10 mm Hg (n_D^{20} = 1.5272). The distillation residue, 39 g (65 %), crystallized in contact with cold petroleum ether M.p. 73—77°C. Recrystallization gave a m.p. of 77—78°C. (Found: C 71.75; H 6.75; S 10.55. Calc. for $C_{18}H_{20}O_2S$ (300.25): C 71.98; H 6.71; S 10.66).

The reaction of t-butyl perbenzoate and dibenzyl sulphide. In an oil bath with a temperature of 85°C were placed a flask containing 300 ml of benzene, 80 g (0.37 mole) of dibenzyl sulphide (m.p. 149°) and 0.1 g of CuCl. 0.2 mole of *t*-butyl perbenzoate in 50 ml of benzene was added dropwise. The reaction was complete after 2 h, 15 min. The alkaline washings gave 2.5 g of benzoic acid. The benzene and excess of the dibenzyl sulphide were removed. The residue was weighed and found to be 56 g. It was shown by infrared measurements to contain an ester group.

A. 15 g of the crude benzoyloxy compound of dibenzyl sulphide was distilled without any special precautions. At 175—195°C/0.2 mm Hg a red coloured crystalline fraction was obtained. The compound was dissolved in ether, washed with 2 M NaOH and water and dried. Benzoic acid (3.2 g) was precipitated from the alkaline washings. When ether was removed 2.7 g of a compound precipitated which was shown to be *trans*-stilbene by IR, elemental analysis and mixed melting point. Yield 32 %. (Found: C 93.15; H 6.67. Calc. for $C_{14}H_{21}$ (180.24): C 93.29; H 6.71). M.p. and mixed m.p. 123—124°C.

B. In another attempt to distil the compound under so mild conditions as possible no stilbene was obtained but only the expected benzoyloxy compound in a form not sufficiently pure for analyses. Every attempt to crystallize it was unsucessful. Instead, the crude benzoyloxy compound was dissolved in acetic acid, and an excess of 4 % $KMnO_4$ solution was added. After extraction with chloroform, washing with water until neutral, removal of the solvent, the corresponding sulphone crystallized. After several recrystalizations the melting point was 121—123°C. Mixed melting point with the Horner compound was not depressed *.

* We wish to express our cordial thanks to Professor Dr. L. Horner for providing us with a sample of this material.

The reaction of dibenzyl sulphide and t-butylperoxide. In a 100 ml flask equipped with a mechanical stirrer and a reflux condenser were placed 23 g (0.108 mole) of dibenzyl sulphide and 10 g of *t*-butyl peroxide. The mixture was maintained at an oil bath temperature of 125°C for 53 h. By distillation, 11.5 g dibenzyl sulphide were recovered and from the residue 8.3 g of a product crystallized in contact with cold *i*-propyl ether. After several recrystallizations from *i*-propyl ether and also from ethanol, the melting point was found to be 133–134°C. The infra-red spectrum was mainly identical with that of the dibenzyl sulphide, and the compound was the dimer. (Found: C 78.41; H 6.20; S 14.87; mol. wt. in benzene 401. Calc. for $C_{28}H_{26}S_2$ (426.62): C 78.82; H 6.14; S 15.00).

The reaction of t-butyl perbenzoate and benzyl mercaptan. A flask containing 125 ml of anhydrous benzene, 0.1 g of CuCl and 27 g (0.22 mole) of redistilled benzyl mercaptan ($n_D^{20} = 1.5738$) was maintained at an oil bath temperature of 80°C. 20 ml (0.1 mole) of *t*-butyl perbenzoate in 15 ml of benzene was added dropwise during 10 min. The solution was at once discoloured and when the titration indicated that no perester was left, the solution was cooled immediately, and washed with 2 M NaOH and water. 12.5 g of benzoic acid was precipitated. After removing benzene, the distillation residue (22 g) solidified and was recrystallized from petroleum ether. M.p. 67–69°. The compound was dibenzyl disulphide which was demonstrated by mixed melting point (not depressed) and by identical infra-red spectra.

The reaction of t-butyl perbenzoate and benzyl alcohol. 54 g (0.5 mole) of benzyl alcohol and 0.1 g of cuprous chloride in 200 ml of benzene were heated to 105°C under a nitrogen atmosphere, and 0.2 mole of *t*-butyl perbenzoate was thereafter added dropwise during 30 min. After 5 h, all peroxide was consumed, and the work-up was performed in the usual way. Isolated benzoic acid was equal to 22.2 g. Of the starting material 31.8 g was recovered. No benzaldehyde could be isolated, and the main fraction of the acetal distilled at 150–155°C/0.05 mm Hg, $n_D^{20} = 1.5781$ (Lit.[3]: $n_D^{20} = 1.5776$). Yield 24 g. IR-spectra of dibenzyl acetal of benzaldehyde and the main fraction were superimposable.

The reaction of t-butylperbenzoate and benzyl alcohol without cuprous chloride. Benzyl alcohol, 108 g (1 mole) and 14 ml (0.07 mole) of *t*-butyl perbenzoate in 150 ml of benzene were reacted in the usual way for 9 h. The reaction mixture was extracted with 2 M NaOH and then with water until neutral and finally dried over $MgSO_4$. The alkaline washings gave 9 g of benzoic acid. The distillation gave 9 g of benzaldehyde.

The reaction of t-butyl peroxide with benzyl alcohol. 44 g of redistilled benzyl alcohol and 8 g of *t*-butyl peroxide were refluxed for 20 h at 130°C. Distillation gave starting material (smell of benzaldehyde) and a solid, which after recrystallization from ethanol gave 9 g (42 %) of mesohydrobenzoin, m.p. and mixed m.p. 135–136°C.

The reaction of an acylal with ethanol. The benzoyloxy compound of benzyl ethyl ether (95 g) was refluxed under a nitrogen atmosphere for 5 h with 30 ml of ethanol. The alcohol was then stripped off, ether was added and the benzoic acid was extracted with sodium bicarbonate (isolated benzoic acid = 4.2 g). The ether phase was washed until neutral with water, dried over sodium sulphate and distilled. The main fraction was obtained at b.p. 93–95°C/11 mm Hg Weight 3.2 g. IR and vapor phase diagrams of the last fraction showed that one pure compound had been isolated and was identical in all respects with the diethyl acetal of benzaldehyde.

Acknowledgements. The authors are indebted to Professor A. Fredga for his kind interest and for all facilities put at their disposal. A grant from *Magnus Bergwall's Stiftelse* is gratefully acknowledged.

REFERENCES

1. Huang, R. L. and Si-Hoe, S. S. in Waters, W. A. *Vistas in Free Radical Chemistry*, Pergamon Press, London 1959, p. 242.
2. Lawesson, S.-O. and Berglund, C. *Tetrahedron Letters* **2** (1960) 4.
3. Lawesson, S.-O. and Berglund, C. *Arkiv Kemi* **16** (1960) 287.
4. Lawesson, S.-O. and Busch, T. *In preparation.*
5. Price, C. C. and Zomlefer, J. *J. Am. Chem. Soc.* **72** (1950) 14.
6. Price, C. C. and Morita, H. *J. Am. Chem. Soc.* **75** (1953) 4747.
7. Horner, L. and Jürgens, E. *Ann.* **602** (1957) 135.

8. Bordwell, F. G. and Cooper, G. D. *J. Am. Chem. Soc.* **73** (1950) 5187.
9. Ramberg, L. and Bäcklund, B. *Arkiv Kemi Mineral. Geol.* **13 A** (1940) No. 27.
10. Bäcklund, B. *Diss.* Uppsala University 1945.
11. Scholnick, F. *Extensions of the Ramberg and Bäcklund reaction, University Microfilms,* (1955).
12. Bartlett, P. D. and Nozaki, K. *J. Am. Chem. Soc.* **69** (1947) 2299.
13. Urry, W. H., Stacey, F. W., Huyser, E. S. and Juveland, O. O. *J. Am. Chem. Soc.* **76** (1954) 450.
14. Sosnovsky, G. and Yang, N. C. *J. Org. Chem.* **25** (1960) 899.
15. Kharasch, M. S. and Sosnovsky, G. *J. Am. Chem. Soc.* **80** (1958) 756.
16. Kharasch, M. S., Sosnovsky, G. and Yang, N. C. *J. Am. Chem. Soc.* **81** (1959) 5819.
17. Denney, D. B., Denney, D. Z. and Feig, G. *Tetrahedron Letters* **15** (1959) 19.
18. Silbert, L. S. and Swern, D. *Anal. Chem.* **30** (1958) 385.
19. Büchi, J., Prost, M., Eichenberger, H. und Lieberherr, R. *Helv. Chim. Acta* **35** (1952) 1527.
20. Ipatieff, V. N., Pines, H. and Friedman, B. S. *J. Am. Chem. Soc.* **60** (1938) 2731.
21. Pummerer, R. *Ber.* **43** (1910) 1401.
22. Rheinboldt, H., Mott, F. and Motzkus, E. *J. prakt. Chem.* **134** (1932) 257.

Received August 25, 1960.

ACTA CHEMICA SCANDINAVICA 15 (1961) 47–61

The Solution Chemistry of Copper and Nickel Complexes with Dimethylglyoxime

DAVID DYRSSEN and MARGARETA HENNICHS

Department of Inorganic Chemistry, Royal Institute of Technology, Stockholm 70, Sweden

The distribution of $^{64}Cu(II)$ at 25°C between chloroform and 0.1 M perchlorate solutions has been studied as a function of H^+ and HA (dimethylglyoxime) in the aqueous phase and of B (quinoline or dodecylamine) in the organic phase. From the data the following constants have been calculated:
$CuA_2 \rightleftharpoons CuA_2$(in $CHCl_3$);log $\lambda_2 = -0.93 \pm 0.05$
$Cu^{2+} + 2A^- \rightleftharpoons CuA_2$; log $K_1K_2 = 19.24 \pm 0.06$
CuA_2 (in $CHCl_3$) + B (in $CHCl_3$) $\rightleftharpoons CuA_2B$ (in $CHCl_3$); log $\varkappa_B = 2.04$ (quinoline) and 3.36 (dodecylamine). The data give no evidence of CuA^+; we conclude that log $K_1 \leq$ log $K_2 - 1.2$.

The solubility of CuA_2 in 0.1 M $NaClO_4$ and chloroform has been determined. The solutions were saturated by slow filtration through columns packed with solid radioactive CuA_2. Results: $7.9_1 \times 10^{-3}$ M (0.1 M $NaClO_4$), $1.05_3 \times 10^{-3}$ M (wet chloroform) and $1.02_3 \times 10^{-3}$ M (dry chloroform). From a study of the solubility of CuA_2 in 0.1 M $Na(OH,ClO_4)$ the hydrolysis constant of CuA_2 was determined: log $\varkappa_H = -10.60$. The solubility of NiA_2 in chloroform solutions of quinoline or dodecylamine was studied and no reaction between NiA_2 and B was found.

These results are compared with previous data[5] on NiA_2 and it is concluded that the large differences between NiA_2 and CuA_2 are due to the fact that Cu^{2+} in CuA_2 has a tendency to be five-coordinated while Ni^{2+} in NiA_2 has only the coordination number of four.

An important contribution to the understanding of the differences of properties between Ni and Cu-complexes with dimethylglyoxime (HA) has recently been made by Frasson, Bardi and Bezzi [1] by their X-ray determination of the crystal structure of the copper salt, CuA_2. This, together with the determination of the structure of NiA_2 by Godycki and Rundle [2], means that we are now well-informed about the structures of the two compounds in the solid state and can make some guesses about the linkages that determine the lattice energy. In the case of copper, Cu_2A_4 dimers are formed in the crystal, while in the case of nickel NiA_2 monomers are formed. These units are probably linked with each other in the crystal by van der Waals' forces, but in the case

of NiA_2 there may also exist long Ni—Ni bonds (3.245 Å against 2.492 Å in the metal [3] and 3.084 Å in NiF_2, which has a rutile lattice [4]).

In the solid medium with its rather high density of bond-forming atoms (N and O) nickel has a coordination number of four in NiA_2, except for the two rather long and probably weak metal bonds, while copper forms an additional coordinate link with an oxygen atom in the neighboring CuA_2 molecule and therefore has a coordination number of five in the crystal state. Consequently, Cu does not lie in the same plane as the four metalbonding N atoms of dimethylglyoxime, while Ni does.

It is thus quite possible that the forces between the NiA_2 or Cu_2A_4 molecules in the solid state (lattice energy) may be of the same order of magnitude and that the solubilities in inert non-solvating solvents may therefore also be about the same for the two salts. A more complete understanding of the differences between NiA_2 and CuA_2 may therefore be obtained from a study of the solution chemistry of the two complexes.

The work reported here includes the determination of the complexity constants for the reaction $M^{2+} + 2A^- \rightleftharpoons MA_2$ by the distribution technique (*cf.* Dyrssen, Krašovec, and Sillén [5] for nickel), of the distribution constants of MA_2 between chloroform and water, and of the solubilities of MA_2 in chloroform. Furthermore, the reaction $MA_2 + B \rightleftharpoons MA_2B$ (B = quinoline or *n*-dodecylamine) was studied in chloroform.

EXPERIMENTAL

Chemicals. Chloroform ("Merck's p.a. für Chromatographie") was washed with distilled water to remove the 1 % abs. alcohol and to saturate the solvent with water. Dimethylglyoxime (Kebo's p.a. reagent for nickel) was not further purified or recrystallized. *n*-Dodecylamine (two white crystallized products from Fluka and Light & Co) had a melting point of 26—28°C and was not further purified. Care was taken to avoid contact with CO_2 when handling the amine or its solution in chloroform. Quinoline (synthetic product, Kebo puriss., b.p. 235—237°C) and triethanolamine (Fluka, Switzerland, colorless puriss. quality) were also used without further purification. The $NaClO_4$ was made according to a technique used in this laboratory [6]. Other chemicals ($HClO_4$, NH_3, alcohol, *etc.*) were of analytical grade.

The radioactive copper, 12.8 h ^{64}Cu, was obtained by irradiation of weighed pieces (about 200 mg) of pure sheet-copper in the Swedish reactor R 1; the neutron flux used was between 5 and 20 $\times$ 10^{11} n cm^{-2} sec^{-1}. After irradiation the copper was dissolved in conc. HNO_3. This solution was evaporated to dryness and the copper nitrate was dissolved in 25 ml of 0.1 M $HClO_4$. This stock solution was then further diluted with 0.1 M $NaClO_4$. The purity of the ^{64}Cu nuclide was checked by following the decay over a week.

The radioactive CuA_2 was synthetized according to Tschugaeff [7]. However, his method was slightly modified as follows: 10 mmoles of dimethylglyoxime (HA) were dissolved in a hot solution of 2 ml of conc. NH_3 $\times$ 20 ml of abs. alcohol. 5 ml of a hot solution of 1 M $CuSO_4$ with radioactive ^{64}Cu was added. On chilling, CuA_2 crystallized out of the dark solution. The crystals were washed with alcohol and dried on filter paper at room temperature.

NiA_2 was simply precipitated from a saturated solution of dimethylglyoxime in water with a solution of $NiCl_2$.

Analytical procedures. For the analysis of dimethylglyoxime in 0.1 M $NaClO_4$ and in chloroform solutions, the dimethylglyoxime was reacted with an excess of nickel chloride in an alcohol-chloroform mixture using triethanolamine as a proton-acceptor. The UV light absorption of the NiA_2 formed was measured at 365 mμ. At this wave-length the absorption did not seem to vary with the conc. of quinoline in the chloroform solution. The extinction coefficient of NiA_2 at 365 mμ is 3 356 M^{-1} cm^{-1}. The same wave-length

was used for the determination of the solubility of NiA_2 in chloroform solutions of quinoline or dodecylamine.

The analysis of the conc. of copper was made radiometrically utilizing the annihilation radiation of the positrons formed in the decay of ^{64}Cu. The gamma quanta were counted in a Tracerlab SC-57 low background well scintillation counter connected with a Tracerlab SC-18A Superscaler or SC-73 Versa/matic II scaler.

Solubility experiments. Solutions of quinoline or *n*-dodecylamine in chloroform were saturated with dimethylglyoxime or its nickel and copper salts, NiA_2 and CuA_2, by filtering the solutions through columns with a bed 7—10 cm thick at a flow rate of about 1 cm min^{-1}. It is an experience at our laboratory that solutions that flow from such columns are saturated. This was checked in our case by filtering some solutions twice through a column (or back-washing), and by variation of the flow rate and column height. The results agreed also with experiments where equilibrium was obtained by shaking the solutions over night. These experiments confirm that the diffusion layer outside the surface of the solid phase is much more effectively broken down in a filtering column than in a shaking process. Solutions of 0.1 M $NaClO_4$ + 0.0001 M $HClO_4$ were saturated with dimethylglyoxime in a similar manner and the solubility of CuA_2 in 0.1 M Na(OH, ClO_4) was studied by the same technique.

Distribution experiments. The two phases (15 ml of each) were made up as follows. The organic phase was either pure chloroform or a solution of quinoline or *n*-dodecylamine in chloroform. Dimethylglyoxime was added as a saturated solution (0.005 M) in 0.1 M $NaClO_4$ (+ 0.0001 M $HClO_4$). The hydrogen ion concentration of the aqueous layer ($[H^+]$) was adjusted with three solutions: 0.09 M $NaClO_4$ + 0.01 M $HClO_4$, 0.09 M $NaClO_4$ + 0.01 M Na-acetate, and 0.09 M $NaClO_4$ + 0.01 M NaOH. The final volume of the aqueous phase (15 ml) was made up with 0.1 M $NaClO_4$ after addition of radioactive copper (see above).

The two phases were shaken for 1—18 h and centrifuged. No heating of the solutions was observed after 10 min centrifugation [8]. The value of $-\log [H^+]$ was measured with a glass electrode standardized against a solution of 0.01 M $HClO_4$ + 0.09 M $NaClO_4$ ($-\log [H^+] = 2.00$). The copper concentration of each phase was measured radiometrically as described above. Care was taken not to contaminate the sample of the chloroform layer with the more active aqueous layer. No difficulties were met in obtaining material balance; the sum of intensities of the two phases was constant for each sample of irradiated copper when corrected for the decay of ^{64}Cu.

All experiments were carried out at 25°C in constant temperature rooms and the ionic strength of the aqueous solutions was kept constant at 0.1 M using mainly $NaClO_4$.

SYMBOLS AND EQUILIBRIUM CONSTANTS

HA = dimethylglyoxime, $CH_3C(:NOH)C(:NOH)CH_3$
B = quinoline, C_9H_7N, or *n*-dodecylamine, $C_{12}H_{25}NH_2$
HAc = acetic acid, CH_3COOH

$$K_a = [H^+][A^-][HA]^{-1}$$
$$K_d = [HA]_{org}[HA]^{-1}$$
$$K_B = [HAB]_{org}[HA]_{org}^{-1}B]_{org}^{-1}$$
$$K_{B2} = [HAB_2]_{org}[HA]_{org}^{-1}[B]_{org}^{-2}$$

$$\beta_1 = [MA^+][M^{2+}]^{-1}[A^-]^{-1};\ M = Ni \text{ or } Cu$$
$$\beta_2 = [MA_2][M^{2+}]^{-1}[A^-]^{-2};\ \beta_1 = K_1;\ \beta_2 = K_1K_2$$
$$\lambda_2 = [MA_2]_{org}[MA_2]^{-1}$$
$$\varkappa_B = [MA_2B]_{org}[MA_2]_{org}^{-1}[B]_{org}^{-1}$$
$$\varkappa_H = [H^+][MA_2OH^-][MA_2]^{-1}$$

q = net distribution ratio (org/aq)
$[HA]_{tot}$ = initial total conc. of HA in the aqueous phase
$[Cu]_{tot}$ = initial total conc. of copper in the aqueous phase.

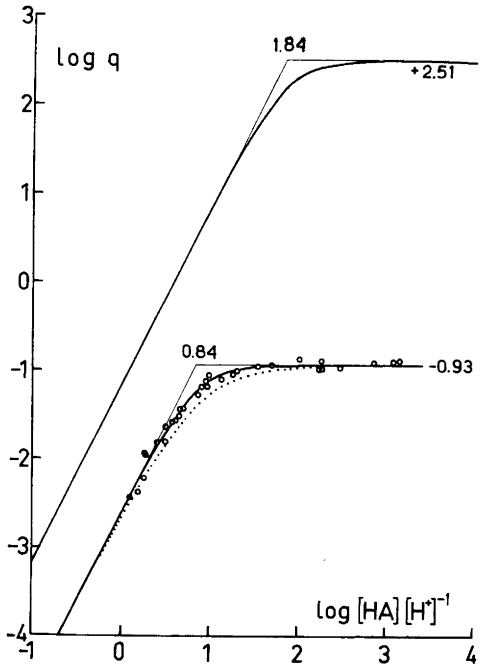

Fig. 1. Distribution of nickel (upper curve) and copper between chloroform and 0.1 M $NaClO_4$ as a function of log [HA] $-$log [H+]. Normalised curves $Y = -\log(1 + pv + v^2)$, $X = -\log v$ in position of best fit, for $p = 0$ (full-drawn) and $p = 1$ (dotted). The thin lines are the asymptotes.

COMPLEX FORMATION OF CuA_2

Recently it has been shown by Dyrssen, Krašovec, and Sillén [5] that the complex formation of nickel with dimethylglyoxime could be studied by the distribution method with reasonably good accuracy. This method is also used here for the determination of β_2 and λ_2 for the copper-dimethylglyoxime-chloroform system. The general equations in our previous paper [5] will not be repeated here. The distribution data are given in Table 1 and plotted as log q against log $[HA][H^+]^{-1}$ in Fig. 1.

[HA], the free conc. of dimethylglyoxime in the aqueous phase, was calculated from the initial conc. of HA, $[HA]_{tot}$, with the following two equations, which allow for the amount of free HA in the organic phase, $[HA]_{org}$, and the small amount bound to Cu as CuA_2 both in the organic and aqueous phase (equal volumes of each phase):

$$[CuA_2] = \frac{[Cu]_{tot}}{1 + \lambda_2 + 10^{1.82}[H^+]^2[HA]_{tot}^{-2}}$$

$$[HA] = \frac{[HA]_{tot} - 2(1 + \lambda_2)[CuA_2]}{1 + K_d}$$

Table 1. Distribution of Cu^{2+} between chloroform and 0.1 M perchlorate solutions at 25°C. The concentrations refer to the initial total concentrations in the aqueous phase. The data are plotted in Fig. 1 as log q against log [HA] − log [H+].

$[Cu]_{tot}$ 10^{-4} M	$[Ac]_{tot}$ 10^{-3} M	$[HA]_{tot}$ 10^{-3} M	log q	−log[H+]
0.0396	3.33	1.57	−2.44	2.94
1.186	1.20	1.57	−2.38	3.03
0.593	0	1.57	−2.22	3.10
0.459	3.33	0.78	−1.94	3.51
0.777	3.33	1.67	−1.95	3.19
3.11	1.33	1.67	−1.81	3.28
0.777	3.33	1.67	−1.81	3.29
0.777	3.33	1.67	−1.64	3.30
0.406	1.33	1.58	−1.59	3.44
3.11	3.33	1.67	−1.59	3.43
0.459	3.33	1.56	−1.43	3.50
0.459	3.33	1.56	−1.52	3.49
3.11	3.33	1.67	−1.43	3.58
0.593	1.33	1.57	−1.18	3.77
0.395	1.33	1.57	−1.26	3.72
0.406	1.33	1.58	−1.12	3.80
3.11	3.33	1.67	−1.27	3.78
0.344	2.67	2.34	−1.05	3.66
1.186	2.93	1.58	−1.18	3.85
0.395	1.33	1.57	−1.10	3.97
0.813	0	3.15	−1.05	3.81
0.0396	3.33	1.57	−1.01	4.13
0.0396	3.33	1.57	−0.95	4.37
0.0396	2.00	3.15	−0.94	4.23
0.406	2.00	3.15	−0.87 *	4.56
0.115	3.33	2.34	−0.88 *	4.91
1.24	3.33	1.56	−0.98 *	5.14
1.24	3.33	1.56	−0.97 *	5.17
1.24	3.33	1.56	−0.98 *	5.17
0.932	5.00	1.25	−0.96 *	5.47
0.0115	3.33	0.78	−0.90 *	6.00
0.0115	3.33	1.56	−0.89 *	5.92
0.0115	3.33	2.34	−0.88 *	5.81

* λ_2 was calculated from these experiments by dividing the sum of counts per minute of the organic layers (23 778) with the corresponding value of the aqueous layers (201 800).

The constants $\lambda_2 = 10.^{-0.93}$ and $10^{1.82}$ were obtained from a plot log q against log $[HA]_{tot}[H^+]^{-1}$. $K_d = 0.0786$ was obtained by dividing the solubility of dimethylglyoxime in $CHCl_3$ (saturated with water), 3.94×10^{-4} M, by that in 0.1 M $NaClO_4$ + 0.0001 M $HClO_4$, 5.01×10^{-3} M. In most experiments (see Table 1) $[Cu]_{tot}$ is considerably smaller than $[HA]_{tot}$. It can therefore not be a serious error to neglect the amount of A bound as CuA^+.

The influence of the acetate ions on the distribution is greater in the case of copper than in the case of nickel as $\lambda_2\beta_2$ and λ_2 for MA_2 are smaller and the constants for the formation of MAc^+ and MAc_2 are larger than for nickel. However, at low values of $[A^-]$ (low pH) the formation of acetic acid will predominate over the formation of copper acetate complexes, and at high values of $[A^-]$ the dominating complex will be CuA_2. If one uses the stability constants for the copper-acetate system given by Pedersen [9] and corrected with Kielland's [10] activity factors, it can be calculated for the acetate concentrations used, that the lowering of log q is less than 0.05 in the most sensitive region. This

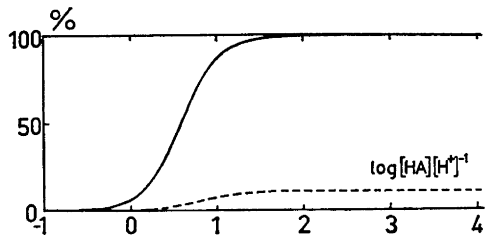

Fig. 2. Percentage of nickel (full-drawn curve) and copper (dashed curve) distributed between chloroform and 0.1 M $NaClO_4$ as a function of log [HA] $-$log [H+]. The curves are valid for equal volumes of both phases. The maximum extraction is determined by $100\ \lambda_2(1 + \lambda_2)^{-1}$.

was confirmed experimentally by varying the amount of acetate buffer in the aqueous phase; no systematic deviations can be observed. As the acetate ion concentration must be kept below 0.005 M, the buffering capacity of the aqueous phase is not very large. We therefore believe that the scattering of the data in Fig. 1 is due in part to errors in the measurement of $-\log [H^+]$ of the sampled aqueous layers. This error is of course not serious for the horizontal part of the curve.

The variation of log q with log $[HA][H^+]^{-1}$ plotted in Fig. 1 is ascribed to reactions between Cu^{2+} and HA and we may compare the data with those in the study of the complex formation with nickel [5] (*cf.* p. 57, Fig. 2 in that work; the signs of the two axes have there been reversed to simplify the comparison with solubility data). It may then be seen that the data can be fitted to the normalized curve [5,11] $Y = -\log(1 + pv + v^2)$, $X = -\log v$ with $p = 0$ (full-drawn curve in Fig. 1), but not with $p = 1$ (dotted). Thus no evidence is found of CuA^+ in appreciable amounts just as in the case with nickel [5], and the same conclusion may be drawn about the parameter $p = \sqrt{K_1/K_2} \leq 0.25$. Using the value of the horizontal asymptote of the distribution curve, log $\lambda_2 = -0.93$, calculated from the data in Table 1, we find from the position of the best fit with the other data for the reaction

$$Cu^{2+} + 2\,HA \rightleftharpoons CuA_2 + 2\,H^+$$

the equilibrium constant

$$\log \beta_2 + 2 \log K_a = -2(0.84 \pm 0.03)$$

from the point of intersection between the asymptotes in Fig. 1. Using log $K_a = -10.46$ calculated from solubility data [5,12] we obtain log $\beta_2 = 19.24 \pm 0.06$.

We have thus determined the following set of equilibrium constants for the $CHCl_3$ -0.1 M $NaClO_4$ system at 25°C:

log λ_2: $+ 2.51 \pm 0.10$ (Ni) and -0.93 ± 0.05 (Cu)
log β_2: 17.24 ± 0.07 (Ni) and 19.24 ± 0.06 (Cu)

The distribution curves determined by these constants and log $K_a = -10.46$ are shown as full-drawn curves in Fig. 1. It may be seen that, at all values of

log $[HA][H^+]^{-1}$, the extraction of Ni is much larger than the extraction of Cu, the larger value of β_2 for Cu being unable to counterbalance the large difference in log λ_2. Fig. 2 shows the percentage extraction for the two metals as a function of log $[HA][H^+]^{-1}$. The fact that nickel is readily extracted with dimethylglyoxime and chloroform while copper is not, is well-known to analytical chemists even if the explanations given hitherto have been based on insufficient experimental data.

The values of λ_2 and β_2 will be further discussed below.

FORMATION OF MIXED COMPLEXES WITH QUINOLINE AND DODECYLAMINE

The reason why λ_2 is so low for CuA_2 in comparison with NiA_2 is probably that Cu^{2+} in CuA_2 has a tendency to coordinate with H_2O and to be linked thereby with the water lattice. NiA_2 on the other hand does not form any strong bonds with water, so it will have a fairly large value of λ_2. Dimethylglyoxime itself (HA) can form hydrogen bonds both as an acceptor and donor and consequently K_d is rather small.

If Cu^{2+} in CuA_2 can be five-coordinated also in solution it should be possible to form a mixed complex (adduct) CuA_2B in the organic phase with a hydrophobic uncharged ligand B (base) and thus increase the distribution ratio q for copper:

$$q = \frac{[CuA_2]_{org} + [CuA_2B]_{org}}{[Cu^{2+}_{aq}] + [CuA_2]}$$

If we carry out the experiment in the range where $[Cu^{2+}] \ll [CuA_2]$ the expression for q is simplified:

$$q = \lambda_2 + \lambda_2 \varkappa_B [B]_{org}$$

Table 2. Distribution of Cu^{2+} between solutions of quinoline in chloroform and 0.1 M perchlorate solutions buffered with acetate. The concentrations refer to the initial conc. in the aqueous (copper, dimethylglyoxime and acetate) or organic phase (quinoline). The data are plotted in Fig. 2 as log q against log $[B]_{org}$.

$[Cu]_{tot}$ 10^{-4} M	$[Ac]_{tot}$ 10^{-3} M	$[HA]_{tot}$ 10^{-3} M	$[B]_{tot}$ 10^{-3} M	$-\log [H^+]$	log q
1.22	2.00	1.58	1.67	4.46	−0.90
0.988	3.33	1.58	3.33	4.30	−0.83
1.22	2.00	1.58	5.00	4.51	−0.76
0.395	3.33	1.57	6.66	4.43	−0.74
1.22	2.00	1.58	10.0	4.54	−0.63
0.395	3.33	1.57	16.7	4.47	−0.50
1.22	2.00	1.58	23.3	4.63	−0.38
1.15	1.67	2.09	33.3	4.20	−0.33
0.156	3.33	1.56	66.6	5.88	−0.03
0.156	3.33	1.56	133.5	6.03	+ 0.28
0.156	3.33	1.56	267	6.34	+ 0.55
1.15	1.67	2.09	534	4.86	+ 0.79
1.15	2.09	2.09	1 000	5.37	+ 1.02

Table 3. Distribution of Cu^{2+} between solutions of *n*-dodecylamine in chloroform and 0.1 M perchlorate solutions buffered with 0.1 mmole NH_3 per 15 ml. The initial total conc. of dimethylglyoxime in the aqueous phase was 1.66×10^{-3} M and the value of $-\log [H^+]$ varies between 8.6—8.9.

$[Cu]_{tot}$ 10^{-4} M	$[B]_{tot}$ M	log q	log q $-\log[B]_{org}$
0.479	0.005	0.19	2.49
0.958	0.0133	0.59	2.47
0.0271	0.0133	0.56	2.44
0.479	0.02	0.75	2.45
0.271	0.02	0.74	2.44
0.958	0.04	1.04	2.44
0.958	0.05	1.17	2.47
0.271	0.06	1.14	2.36
0.479	0.1	1.40	2.40
0.0271	0.1	1.43	2.43
0.0271	0.133	1.55	2.43
0.271	0.22	1.67	2.33
0.958	0.5	1.92	2.22
0.271	0.5	1.75	2.05
0.271	1	1.47	1.47

The mean value of log q $[B]_{org}^{-1}$ for $[B]_{tot} \leq 0.22$ M is 2.43 ± 0.05, which is equal to log $\lambda_2 \varkappa_B$ (see text).

Quinoline and *n*-dodecylamine were chosen as B-ligands of different basicity. The hydrocarbon parts of these molecules are so large that the amount of B in the aqueous phase is negligible *, and the formation of CuA_2B in the aqueous phase may therefore be neglected. The pH of the aqueous phase was so high that the amount of BH^+ could be neglected too.

The value of λ_2 for Ni is so large (log $\lambda_2 = 2.51$) that the distribution method is not very suitable for a study of a complex formation between NiA_2 and quinoline and dodecylamine. We therefore chose to study the solubility of NiA_2 in chloroform solutions of quinoline and dodecylamine. The same method was also used to study reactions between HA and B (see below the results with CuA_2 and NiA_2).

Results. The data are given in Tables 2 (CuA_2-quinoline), 3 (CuA_2-dodecylamine), 4 (HA-quinoline), and 5 (HA-dodecylamine). The copper data are plotted in Fig. 3 and the HA-data in Fig. 5 as log q and log S against log $[B]_{org}$.

The data with quinoline in Fig. 3 can be fitted with the normalized [11] curve $Y = \log (1 + v)$; $X = \log v$, which indicates that in addition to $CuA_2(H_2O)_x$ (x is not determined in these experiments where the activity of H_2O is constant) a 1:1 complex is formed with quinoline and that Cu^{2+} can attain a coordination number of at least five in CuA_2. No experiments with dodecylamine were made with $[B]_{org}$ between 0 and 0.005 M since it was feared that the correction for the amount of dodecylamine bound to HA would be too large (see below). For this reason we did not obtain the part of

* The distribution constant of quinoline between chloroform and 0.1 M $NaClO_4$ was determined as 471 ± 3 by S. Ekberg.

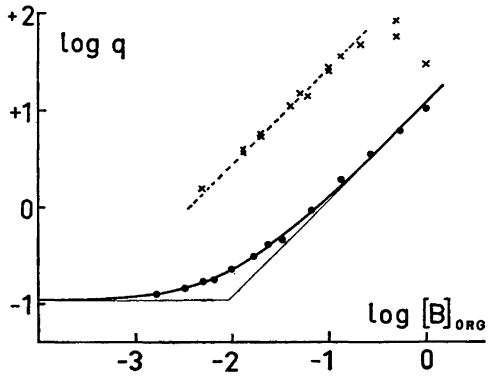

Fig. 3. Distribution of copper between chloroform and 0.1 M $NaClO_4$ as a function of the quinoline (full-drawn curve) or dodecylamine (dashed line with slope 1) concentration in the chloroform phase. The normalised curve $Y = \log (1 + v)$, $X = \log v$ is fitted to the data.

the curve, where appreciable amounts of both CuA_2 and CuA_2B are present in the organic phase. Deviations at $[B]_{org} > 0.22$ M are probably due to the self-association of dodecylamine in chloroform (*cf.* Fig. 5).

The equilibrium constant $\varkappa_B$ of the reaction CuA_2 (in $CHCl_3$) + B (in $CHCl_3$) $\rightleftharpoons$ CuA_2B (in $CHCl_3$) is obtained from the intercept of the two asymptotes, $\log q = \log \lambda_2$ ($Y=0$) and $\log q = \log \lambda_2 \varkappa_B [B]_{org}$ ($Y=X$), to the curve (Fig. 3):

$$\log \varkappa_B = 2.04 \quad (B = \text{quinoline})$$
$$\log \varkappa_B = 3.36 \quad (B = \text{dodecylamine})$$

Fig. 4 shows that the solubility of NiA_2 is very little increased by the addition of quinoline or dodecylamine to the chloroform phase; the decrease at high $[B]_{org}$ is probably due to self-association of B. From the experiments we conclude that Ni^{2+} is four-coordinated in NiA_2. The value of the solubility of NiA_2 in chloroform, saturated with water, obtained by us is 4.75×10^{-4} M, which agrees very well with the value of 4.8×10^{-4} M determined by Christopherson and Sandell [12], who saturated their solutions by shaking for 6 hours.

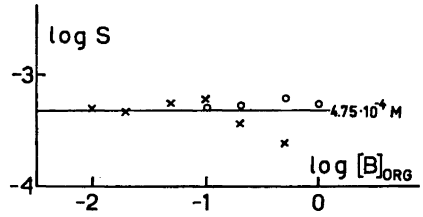

Fig. 4. Solubility of NiA_2 in solutions of quinoline (O) or dodecylamine (×) in chloroform.

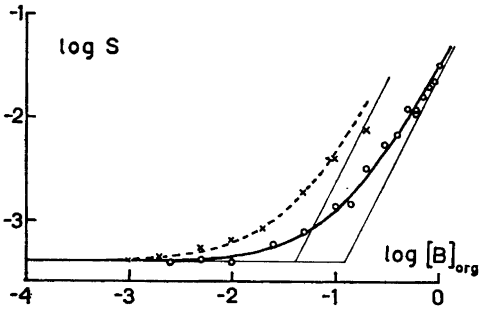

Fig. 5. The solubility of dimethylglyoxime in chloroform as a function of the conc. of quinoline (full-drawn curve) or dodecylamine (dashed curve). The normalised curve $Y = \log (1 + pv + v^2)$, $X = \log v$ is fitted to the data. The best fit was obtained with $p = 2$.

Table 4. Solubility of dimethylglyoxime in wet chloroform solutions of quinoline at 25°C. Values of S in mmoles per liter and molar conc. of quinoline: 0.392 (0), 0.391 (0.0025), 0.405 (0.005), 0.389 (0.01), 0.583 (0.025), 0.769 (0.05), 1.383 (0.1), 1.430 (0.14), 3.20 (0.2), 5.36 (0.3), 6.79 (0.4), 11.98 (0.5), 11.47 (0.6), 10.64 (0.6), 15.53 (0.7), 19.58 (0.8), 22.4 (0.9), 32.0 (1).

Table 5. Solubility of dimethylglyoxime in wet chloroform solutions of dodecylamine at 25°C. Values of S in mmoles per liter and molar conc. of dodecylamine: 0.403 (0.00098), 0.439 (0.00196), 0.534 (0.0049), 0.638 (0.0098), 0.823 (0.0196), 1.86 (0.049), 3.97 (0.098), 7.42 (0.196).

Table 6. Distribution of Cu^{2+} between chloroform and aqueous solutions containing dimethylglyoxime and NH_3. Values of log q and molar conc. of NH_3 in the aqueous phase: −0.91 (0.0067), −0.81 (0.0333), −0.91 (0.167), −1.31 (0.6).

That also B can react with dimethylglyoxime itself is obvious from Tables 4 and 5 and Fig. 5, which shows the increase of the solubility of HA with $[B]_{org}$. The data seem to approach a line with slope 2, which corresponds to the formation of HAB_2; each hydrogen in the oxime groups seems to form a hydrogen bond with the acceptor molecule B. Using the technique of curve-fitting [11,13] it was found that a curve $Y = \log (1 + 2v + v^2)$, $X = \log v$ fitted the data reasonably well except for dodecylamine concentrations above 0.1 M where probably self-association occurs (*cf.* Fig. 3). The equation of the curves can be derived as follows.

$$S = [HA] + [HAB] + [HAB_2] = [HA](1 + K_B[B]_{org} + K_{B_2}[B]^2_{org})$$

The equations of the two asymptotes to the curve log S (log $[B]_{org}$) are

$$\log S = \log [HA] = \log S_0$$
$$\log S = \log S_0 K_{B_2}[B]^2_{org}$$

The parameters S_0 and K_{B_2} are obtained from the point of intercept of the asymptotes: $S_0 = 3.94 \times 10^{-4}$ M and log $K_{B_2} = 1.80$ (quinoline) and 2.74 (dodecylamine). From the difference between S and S_0 at this point we obtain K_B: log $K_B = 1.20$ (quinoline) and 1.67 (dodecylamine) (*cf.* Ref.[13]). The value of S_0 agrees fairly well with Christopherson and Sandell's value [12] 4.5×10^{-4} M and very well with the value of Babko and Mikkel'son [14] 3.96×10^{-4} M.

The reactions between HA and B lower the value of [HA] in the aqueous phase, and will disturb an investigation of the complex formation of MA_2 and B if the value of log $[HA][H^+]^{-1}$ is not sufficiently high. With quinoline the correction in the calculation of the conc. of free B, $[B]_{org}$, is small as the total conc. of HA is always below 0.0021 M. This is not quite true with dodecylamine, which reacts more readily with HA.

REACTIONS BETWEEN CuA_2 AND NH_3

The investigations with quinoline and dodecylamine showed clearly that CuA_2 could react with a base in chloroform and it was therefore thought worthwhile to see if the distribution ratio of copper could be lowered by the addition of NH_3 to the aqueous phase. Such an experiment might indicate the existence of a five-coordinated copper complex, CuA_2NH_3. The data in Table 6 show, however, that q is very little affected by the addition of NH_3 at pH where the hydrolysis of CuA_2 may be neglected (see below). We therefore conclude that for NH_3-concentrations less than 0.2 M, $CuA_2(H_2O)$ is the dominating complex in the aqueous phase. This is in agreement with the fact that the equilibrium constant for the reaction $Cu(NH_3)_4^{2+} + NH_3 \rightleftharpoons Cu(NH_3)_5^{2+}$ is small [15]. It can then be concluded that the method [16] of removing CuA_2 from the chloroform layer by shaking the chloroform with dilute ammonia, is an effect due to a low value of λ_2, and not due to the formation of a CuA_2NH_3 complex. In this procedure the nickel content in the organic phase is not appreciably lowered [16] if the pH is sufficiently high.

THE SOLUBILITIES OF NiA_2 AND CuA_2

It is a well-known fact that the Ni^{2+} but not Cu^{2+} may be precipitated from aqueous solutions with dimethylglyoxime. Following Godycki and Rundle [2], Sharpe and Wakefield [17] suggested that the forces in the solid state and especially the Ni—Ni bond offered an explanation of the great difference in solubility between the copper and nickel complex. The new X-ray data [1] on CuA_2 and the fact that CuA_2 is known to be less extractable [18] than NiA_2 in spite of the fact that Cu^{2+} forms stronger complexes [19], suggested, however, that solvation effects should be much more important.

If this was true the solubility of the two salts in an organic non-solvating solvent should not be very different. We obtained the following results for chloroform, which presumably does not coordinate with the central atom:

For NiA_2: 4.75×10^{-4} M (wet)
For CuA_2: $10.5_3 \times 10^{-4}$ M (wet) and $10.2_3 \times 10^{-4}$ M (dry)

The values of the solubilities of the salts in 0.1 M $NaClO_4$ saturated with chloroform can be estimated by dividing the solubilities in chloroform with λ_2:

For NiA_2: $\lambda_2^{-1} \times 4.75 \times 10^{-4} = (1.5 \pm 0.3)\ 10^{-6}$ M
For CuA_2: $\lambda_2^{-1} \times 10.5_3 \times 10^{-4} = (9 \pm 1)\ 10^{-3}$ M

The estimated value for NiA_2 agrees fairly well with a value given by Christopherson and Sandell [12] for 0.05 M NaCl saturated with $CHCl_3$: 1.23×10^{-6} M and for CuA_2 in 0.1 M $NaClO_4$ the value measured by us is $7.9_1 \times 10^{-3}$ M, which also agrees reasonably well with the estimated value.

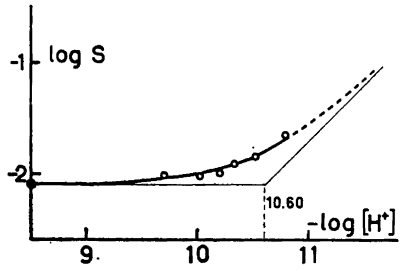

Fig. 6. The solubility of CuA_2 in 0.1 M $Na(OH, ClO_4)$ as a function of $-\log [H^+]$. The normalised curve $Y = \log (1 + v)$; $X = \log v$ is fitted to the data utilizing the solubility in 0.1 M $NaClO_4$, 7.91×10^{-3} M, $\log S = -2.10$, as the value of the horizontal asymptote (thin line).

From these experiments we conclude that lattice the energies of the two salts are about the same, and that the large difference in water-solubility must be due to solvation of CuA_2, which thereby is linked to the water lattice. Furthermore, we conclude from the solubilities of CuA_2 in dry and wet chloroform, that the complex may be unhydrated in wet chloroform. This conclusion could not be drawn from the distribution experiments.

The crystal structure of CuA_2 and experiments reported above suggest that copper may be five-coordinated in CuA_2 and form a monohydrate, $CuA_2(H_2O)$, in water. The low solubility of NiA_2 in water is then partly due to the forces in the solid state and partly to the fact that it contains hydrophobic groups and no tendency to be five- or six-coordinated (and solvated). The importance of the forces in the solid state (but not necessarily the Ni—Ni bond) is shown by the fact that the ethylmethylglyoxime nickel salt is more soluble in water [20] despite the increased size of the hydrophobic groups. How much the long Ni—Ni bond contributes to the lattice energy is still open to speculation.

THE HYDROLYSIS OF CuA_2H_2O

If it is correct that CuA_2 can coordinate with a water molecule it should be possible to find a complex CuA_2OH^- in alkaline solutions provided the hydrolysis of CuA_2H_2O is not too weak.

As chloroform reacts with alkali we preferred to study the hydrolysis of CuA_2H_2O by measuring the solubility of CuA_2 in 0.1 M $Na(OH,ClO_4)$ as a function of $-\log [H^+]$. As seen from Fig. 6 the solubility increases with pH ($-\log [H^+]$) and the data could be fitted to the normalized curve $Y = \log (1 + v)$, $X = \log v$. In addition to CuA_2 there must then be a complex with one proton less than in CuA_2. Our guess is CuA_2OH^-, but the proton can equally well come from one of the hydrogen bridges in CuA_2. To explain the experimental curve we shall write the solubility of CuA_2 as

$$S = [CuA_2H_2O] + [CuA_2OH^-] = [CuA_2H_2O](1 + \varkappa_H[H^+]^{-1})$$

In the neutral range (0.1 M $NaClO_4$)

$$S = [CuA_2H_2O] = 7.91 \times 10^{-3} \text{ M}$$

We then obtain

$$\log S = -2.10 + \log (1 + \varkappa_H[H^+]^{-1})$$

The constant $\varkappa_H$ may be found from the position of the asymptotes to the curve at the best fit: log $\varkappa_H = -10.60$.

This value may be compared [15] with log $*K_1 \sim -7$ for the hydrolysis of $Cu(H_2O)_n^{2+}$. Obviously, the hydrolysis of CuA_2H_2O is much weaker than the hydrolysis of the charged aqueous complex. Alternatively it can be said that the complex formation with the strong base OH^- is much weaker. Using log $[H^+][OH^-] = -13.81$ in 0.1 M $NaClO_4$ we may calculate log K_1 as 3.21 for $CuA_2 + OH^- \rightleftharpoons CuA_2OH^-$.

CONCLUSIONS

From distribution experiments no evidence is found of the presence of significant amounts of CuA^+, and it is concluded that log $K_1 \leq$ log $K_2 - 1.2$ as in the case of nickel [5]. As this is not true for either ethylenediamine [15], acetylacetone [15], or *β-iso*propyltropolone [21,22] we conclude that the formation of the second complex is favored by the formation of two hydrogen bonds.

The distribution of copper can be increased by the addition of a base (quinoline or dodecylamine) to the chloroform phase. The reaction, which is an example of the so-called "synergic" effect [24], can be written as follows:

$$CuA_2(org) + B(org) \rightleftharpoons CuA_2B(org) \qquad (\text{eq. const. } \varkappa_B)$$

Dodecylamine is a stronger base than quinoline and consequently gives a higher value of $\varkappa_B$. The solubility of NiA_2 in chloroform is very little affected by the addition of quinoline or dodecylamine. From these experiments it is concluded that Cu^{2+} has a tendency to be five-coordinated in CuA_2 while Ni^{2+} in NiA_2 has not.

From the values of the distribution constants of NiA_2 and CuA_2 it is concluded that the large difference can only be explained by the fact that the CuA_2 complex is solvated in the aqueous phase. As CuA_2 is five-coordinated in the crystal state as well as in chloroform solutions of quinoline or dodecylamine it seems probable that the primary complex in the aqueous phase is CuA_2H_2O. This complex is then linked with the water lattice. — For *β-iso*propyltropolone [22] we obtained $\lambda_2(Cu) > 10\,000 > \lambda_2(Ni) > 100$, and the copper salt of tropolone is planar (four-coordination) in the crystal state[23]. The difference between dimethylglyoxime and *β-iso*propyltropolone as chelate-forming ligands may be explained by the smaller tendency of the two dimethylglyoximate ions to fill the electron gaps in the Cu^{2+} ion. In the Cu(II) di*iso*propyltropolonate complex the gaps are probably more effectively filled and no coordination power is left.

The solubilities of NiA_2 and CuA_2 have been determined in wet chloroform, and were found to be not very different. From these experiments it is concluded that the lattice energy is about the same for both complexes and that the long Ni—Ni bonds in NiA_2 are weak. The large difference in water solubility can be explained by the solvation of CuA_2 and is a consequence of the tendency of Cu^{2+} to be five-coordinated in CuA_2. The low solubility of NiA_2 in water is an effect of the weak tendency of NiA_2 to co-ordinate water molecules.

As pH increases, the solubility of CuA_2 in 0.1 M $Na(OH,ClO_4)$ will increase The data show that one proton comes off, and our guess is that this is not a proton from one of the two strong hydrogen bridges but one from the associated water molecule in CuA_2H_2O.

Note. When our work was completed we obtained a microfilm of a thesis by D. Fleischer [25] with the title "A thermodynamic study of some factors affecting the stability and solubility of metal chelates". This work contains a determination of the solubilities of the nickel and copper salts of dimethylglyoxime in water, chloroform, benzene and *n*-heptane at various temperatures. The following values were obtained at 25°C (Ni, Cu): 1.05×10^{-6}, 5.68×10^{-3} M (H_2O); 4.62×10^{-4}; 1.24×10^{-3} M ($CHCl_3$); 7.53×10^{-5}, 4.5×10^{-5} M (C_6H_6); 2.5×10^{-7}, 1.84×10^{-7} M (C_7H_{16}). The values for water and chloroform are not very different from our values. The heats of solution ($\Delta H°$) in water were 9.0 kcal (Ni) and 0.0 kcal (Cu). According to Fleischer [25] this difference must be due to larger solvation energy of CuA_2 in water and to the fact that copper can exhibit a coordination number higher than four. Fleischer [25] also states that the addition of *n*-butylamine permitted quantitive extraction of CuA_2 into chloroform. From the solubilities in benzene and heptane Fleischer [25] concludes that the crystalline CuA_2 is more stable than NiA_2 by about two or three kilocalories. On the whole Fleischer's data and conclusions agree with our results, and as the two investigations have been carried out independently still more reliance can be placed on the present explanation of the chemical differences between NiA_2 and CuA_2.

Note added in proof. The spectra of 5×10^{-4} M CuA_2 in 0.1 M $NaClO_4$ with 1.503×10^{-3} M HA has recently been studied in our laboratory as a function of $-\log [H^+]$ by Mrs. Solveig Ekberg and Mr. Sven Hansson. The light absorption between 350 and 450 mμ increases from 10 to 90 % between $-\log [H^+] = 3$ and 4, but the shape of the curve remains unchanged. As neither Cu^{2+} nor HA absorbs light in this region, the experiments indicate that below pH = 7 CuA_2 is the only complex formed: $Cu^{2+} + 2HA \rightleftharpoons CuA_2 + 2H^+$. From the data the equilibrium constant of this reaction could be calculated as $\log \beta_2 K_a^2 = -2(0.85 \pm 0.04)$. This value is in complete agreement with the result from the extraction work reported above.

Acknowledgements. The present investigation has been supported by the *Swedish Council for Atomic Research* (AFR) and *Swedish Natural Science Research Council* (NFR). Valuable criticism on the manuscript has been made by the head of the department, professor Lars Gunnar Sillén. The English has been revised by Dr. Valentine Tyrrell.

REFERENCES

1. Frasson, E., Bardi, R. and Bezzi, S. *Acta Cryst.* **12** (1959) 201.
2. Godycki, L. E. and Rundle, R. E. *Acta Cryst.* **6** (1953) 487.
3. Pearson, W. B. *Lattice Spacings and Structures of Metals and Alloys*, Pergamon Press, London 1957.
4. Haendler, H. M., Patterson, W. L., Jr. and Bernard, W. J. *J. Am. Chem. Soc.* **74** (1952) 3167.
5. Dyrssen, D., Krašovec, F. and Sillén, L. G. *Acta Chem. Scand.* **13** (1959) 50.
6. "*Some laboratory methods* . . . , Department of Inorganic Chemistry, Royal Institute of Technology, Stockholm", manuscript, 1959.
7. Tschugaeff, L. *Z. anorg. Chem.* **46** (1905) 144.
8. Higgins, C. E. and Baldwin, W. H. *Anal. Chem.* **32** (1960) 236.
9. Pedersen, K. J. *Kgl. Danske Vidensk. Selskab. Math.-fys. Medd.* **22** (1945) No. 12.
10. Kielland, J. *J. Am. Chem. Soc.* **59** (1937) 1675.
11. Sillén, L. G. *Acta Chem. Scand.* **10** (1956) 186.
12. Christopherson, H. and Sandell, E. B. *Anal. Chem. Acta* **10** (1954) 1.
13. Dyrssen, D. and Sillén, L. G. *Acta Chem. Scand.* **7** (1953) 663.
14. Babko, A. K. and Mikkel'son, P. B. *Ukrain. Khim. Zhur.* **21** (1955) 388.

15. Bjerrum, J., Schwarzenbach, G. and Sillén, L. G. *Stability Constants* I and II, The Chemical Society, Spec. Publ. No. 6 and 7, London 1958.
16. Alexander, O. R., Godar, E. M. and Linde, N. J. *Ind. Eng. Chem., Anal. Ed.* **18** (1946) 206.
17. Sharpe, A. G. and Wakefield, D. B. *J. Chem. Soc.* **1957** 281.
18. Sandell, E. B. Colorimetric Determinations of Traces of Metals, Interscience Publishers, New York 1950.
19. Charles, R. G. and Freiser, H. *Anal. Chim. Acta* **11** (1954) 101.
20. Cox, E. G., Sharratt, E., Wardlaw, W. and Webster, K. C. *J. Chem. Soc.* **1936** 129.
21. Dyrssen, D. Intern. Conf. on Coordination Chemistry, London 1959.
22. Dyrssen, D. *To be published.*
23. Robertson, J. M. *J. Chem. Soc.* **1951** 1222.
24. Irving, H. and Edgington, D. N. *Proc. Chem. Soc.* **1959** 360.
25. Fleischer, D. *Thesis*, Univ. Pittsburgh 1959, *Univ. Microfilms* 59—2396, Ann Arbor, Michigan.

Received August 31, 1960.

ACTA CHEMICA SCANDINAVICA 15 (1961) 62–68

Preliminary Investigations of the Reactions of the Hexaquo Chromium(III) Ion with α,α′-Dipyridyl and with *o*-Phenanthroline

RICHARD G. INSKEEP* and JANNIK BJERRUM

Chemistry Department A, Technical University of Denmark Copenhagen, Denmark

The investigation of the reactions of the α,α′-dipyridyl-hexaquo chromium(III) system and the *o*-phenanthroline-hexaquo chromium(III) system in acid solution has been initiated. In the case of the phenanthroline system, spectral studies indicate the initial reaction to be first order in chromium and first order in phenanthroline. The dipyridyl system is analogous. In each of the two systems, a diaquobis(diamine)chromium(III) nitrate is isolated and indirect evidence indicates that this salt is the *trans*-diaquo compound. A second product, probably the *cis*-diaquo compound, remained in the solution. There was no indication of tris(diamine)chromium(III) formation.

Complexes of α,α′-dipyridyl and of *o*-phenanthroline and metal(III) ions are not usually prepared by the direct addition of the bases to the aqueous metal(III) salt solution because of the possibility of hydroxide precipitation (*e.g.* chromium [1]) or of the formation of some basic salt (*e.g.* iron [2]). The usual path of preparation is the reaction of the base with a lower oxidation state metal ion and oxidation of this complex to the desired (III)-oxidation state (*e.g.* chromium [3,4]).

We find in the case of the hexaquo chromium(III) ion that if rather than using the free base, the acid salt of the base is used, no hydroxide precipitation occurs and complex formation takes place. Solutions of various concentrations of dipyridylium nitrate and hexaquo chromium(III) nitrate when mixed in the pH range 1.5—3.0 slowly change colour from the characteristic hexaquo chromium(III) ion colour to wine red. The change in light absorption was followed with a Cary recording spectrophotometer. Fig. 1 gives the spectrum at various times of a sample containing dipyridylium nitrate and hexaquo chromium(III) nitrate maintained at 60°C.

* United States National Science Foundation Science Faculty Fellow on leave of absence from the Department of Chemistry, University of Vermont, Burlington, Vermont, U.S.A.

THE REACTION OF *o*-PHENANTHROLINE WITH HEXAQUO CHROMIUM(III) ION IN ACID SOLUTION

The *o*-phenanthroline-hexaquo chromium(III) system exhibits similar behaviour as shown in Fig. 1 for the dipyridyl system. The phenanthroline system was extensively investigated by following the change in visible absorption of samples of various reactant concentrations in constant salt medium of 1.0 M sodium nitrate maintained at 60°C. The short wavelength band of hexaquo chromium(III) ion is obscured by the nitrate and the phenanthroline absorptions, but the long wavelength band at 574 mμ with an $\varepsilon_{max.}$ of 15.5 was free of these interferences. The band envelope of the reactant band, intermediate band and the products bands changed with time and the maximum asymptotically approached 505 mμ with an apparent $\varepsilon_{max.}$ of 54.

An orange-red salt separated from this reaction mixture. It had an absorption band with a maximum at 495 mμ and an $\varepsilon_{max.}$ of 40.7 in a solution 1.0 M in sodium nitrate indicating the presence of a second, more strongly absorbing product, which was not isolated. The absorbance of the liquid remaining from the crystallization indicated that this product had an approximate maximum at 510 mμ and an approximate $\varepsilon_{max.}$ of 60. Examination of the family of curves obtained from the time study of a single sample indicates that these envelopes could be explained by four bands: the reactant chromium band, an intermediate band at 525—530 mμ and two product bands, one at 495 mμ and another at 510 mμ.

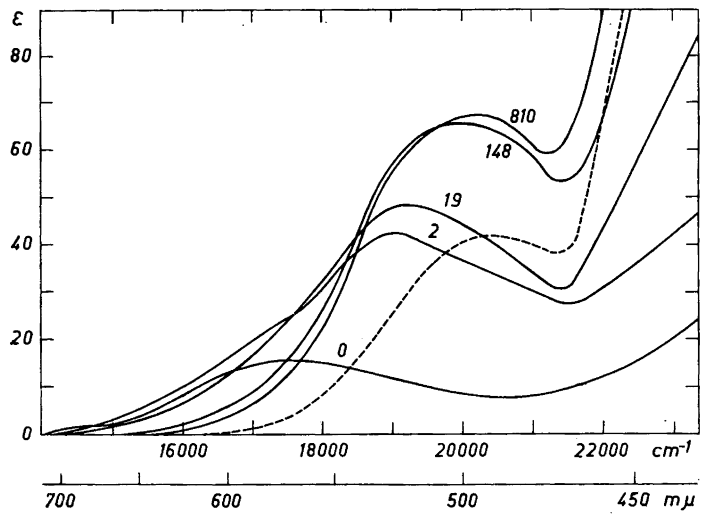

Fig. 1. Spectra of a mixture 0.0214 M in $Cr(H_2O)_6(NO_3)_3$, 0.171 M in dipy · HNO_3, 1.0 M in $NaNO_3$ and 0.01 M in HNO_3 followed in time at 60°C. The numbers on the solid line spectra indicate the time in hours that the mixture had been maintained at 60°C before samples were taken and measured at 25°C. The dashed line spectrum is that of $[Cr(dipy)_2(H_2O)_2](NO_3)_3$ isolated from the mixture.
Abscissae: Wave number in cm^{-1}, and wavelength in mμ.
Ordinate: The molar decadic extinction coefficient ε.

Table 1. Initial rate dependence of chromium ion concentration, phenanthrolinium ion concentration, and hydrogen ion concentration.

$[Cr(H_2O)_6^{3+}]$	$[phenH^+]$	$[H_3O^+]$	$[Cr^{3+}]$ reacted in 100 h at 60°C.*
0.0214	0.0288	0.12	0.00026
0.0214	0.0576	0.12	0.00056
0.0214	0.0864	0.12	0.00075
0.0214	0.0288	0.040	0.00086
0.0214	0.0576	0.040	0.00162
0.0214	0.0864	0.040	0.00259
0.0214	0.0288	0.020	0.00186
0.0214	0.0576	0.020	0.00308
0.0214	0.0864	0.020	0.00458
0.0117	0.0390	0.013	0.00457
0.0234	0.0390	0.013	0.00633
0.0351	0.0390	0.013	0.00842

The initial rate of change of the band envelope varied directly with chromium ion concentration and with phenanthrolinium ion concentration. In the pH range (1.0—3.0) this initial rate is inhibited by the hydrogen ion concentration approximately inversely first order (see Table 1). These experiments lead to an initial rate law:

$$\frac{+ d[H^+]}{dt} = k \frac{[phenH^+]\,[Cr(H_2O)_6^{3+}]}{[H^+]} \qquad (1)$$

A series of experiments was tried where the release of hydrogen ions was followed at 60°C by a Radiometer Titrator maintaining pH = 2.2 by the controlled addition of standard sodium hydroxide. These experiments met with but limited success; one moderately successful run with the concentrations: $[Cr(H_2O)_6^{3+}] = 0.0214$ M, $[phenH^+] = 0.0856$ M, and pH = 2.20 gave an initial proton release of 0.149 mM per hour. Inserting in (1) this run gives a rate constant of $k = 0.513 \times 10^{-3}$ h^{-1}.

Since the acid salt of the base is also in equilibrium with the free base and the hydrogen ions ($pK_a = 4.96$ at 25°C [5] and ~4.3 at 60°C)

$$[phen] = 10^{-4.3} \frac{[phenH^+]}{[H^+]} \qquad (2)$$

Substitution of (2) into (1) gives:

$$\frac{+[H^+]}{dt} = 10.3 \cdot [phen]\,[Cr(H_2O)_6^{3+}] \qquad (3)$$

This rate expression with $k_1 = 10.3$ M^{-1}.h^{-1} (or 2.85×10^{-3}M^{-1}. sec^{-1}) confirms that a mono(diamine) complex corresponding to the intermediate band at 525—530 mμ is the first reaction product.

* Estimated from the optical density at 505 mμ of the samples at the end of 100 h compared to the optical density of the samples at this wavelength after a very long time (as much as 1 500 h).

PREPARATION OF SALT ISOLATED FROM REACTION MIXTURE

The first samples of the salt obtained were a by-product of the spectral-kinetic studies. A more direct preparation is by refluxing 100 ml of a mixture of 0.1 M $Cr(H_2O)_6(NO_3)_3$ and 0.4 M phenHNO_3 in water for a period of 8 h. Four aliquots of sodium hydroxide were added to the reflux mixture to neutralize the hydrogen ions released at the end of 1, 3, 5, and 7 h. At the end of this period sufficient nitric acid was added to lower the pH to 1; approximately one half of the water was evaporated and upon cooling the salt crystallized out. The salt was recrystallized from 0.1 M nitric acid, washed with 0.1 M nitric acid and dried in a desiccator over sulfuric acid. The approximate yield under these conditions based on the total chromium was 60 %.

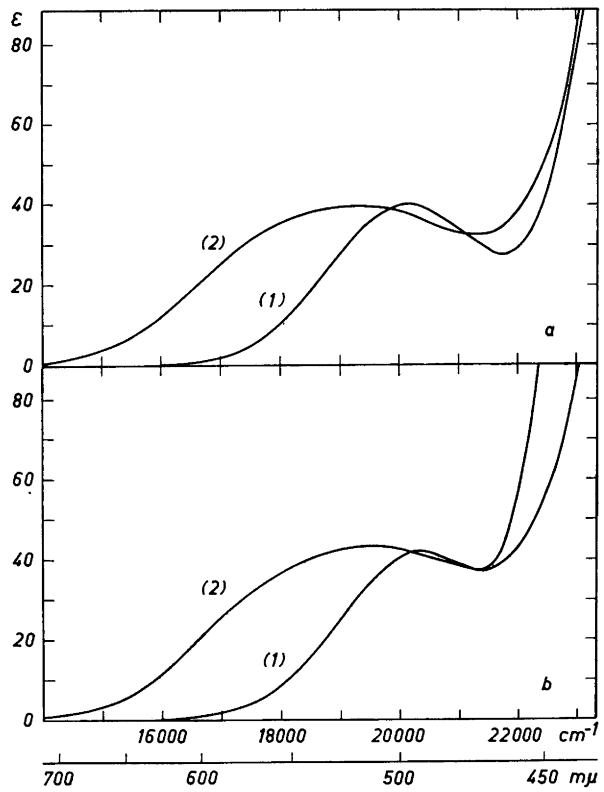

Fig. 2. Spectra of the bis(diamine)chromium(III) complexes in 1 M $NaNO_3$. a: Spectra of the $[Cr(phen)_2(H_2O)_2]^{3+}$ (1) and $[Cr(phen)_2(OH)_2]^{+}$ (2). b: Spectra of the $[Cr(dipy)_2(H_2O)_2]^{3+}$ (1) $[Cr(dipy)_2(OH)_2]^{+}$ (2). Abscissae and ordinate: Same as Fig. 1.

A carbon hydrogen nitrogen analysis * of the isolated salt indicated a C:H:N ratio of 24:23:7 and a possible formula of:

$$[Cr(phen)_2(H_2O)_2](NO_3)_3 \cdot \tfrac{3}{2} H_2O$$

and a formula weight of 661. (Found: C 43.30; H 3.40; N 14.71; Cr 7.60. Calc. for $CrC_{24}H_{23}N_7O_{12\frac{1}{2}}$: C 43.65; H 3.48; N 14.81; Cr 7.85).

S. E. Rasmussen of this laboratory determined the dimensions of the unit cell and found the crystal to be orthorhombic and probably of the space group $Pba2, C^8_{2v}$ No. 32.

The axes are:

$$a = 9.49 \text{ Å} \qquad b = 32.2 \text{ Å} \qquad c = 9.03 \text{ Å}$$

This combined with the density of 1.57 g/cm^3 gives a formula weight of 4 × 652. A general position of the space group is fourfold.

The absorption spectrum of this salt varied with the pH. Fig 2a gives the spectrum of the diaquo salt in 0.1 M nitric acid and also the spectrum of the corresponding dihydroxo complex in 0.1 M sodium hydroxide. The potentiometric titration, using glass and calomel electrodes, of the salt in 1 M sodium nitrate solution gives a curve typical of a dibasic acid with approximate $pK_1 = 3.4$ and $pK_2 = 6.0$ and a formula weight of 666. The approximate solubility of the salt in water is 0.05 moles per liter.

A solution of the purified salt dissolved in an aqueous solution of 1 M sodium nitrate and 0.16 M phenanthrolinium nitrate and placed in a thermostated oven at 60°C for a period of six weeks showed no shift in the wavelength of absorption but underwent a decrease in absorbance, a behaviour that cannot be explained by the formation of a tris(phenanthroline)chromium(III) ion with its lower wavelength of absorption nor by interconversion of the salt to the more strongly coloured form that we have as yet been unable to obtain from the reaction mixture. Such a behaviour could be explained by postulating that the equilibrium is at a position intermediate between the mono(phenanthroline)chromium(III) ion and the bis(diamine) ion for these concentrations.

THE α,α′-DIPYRIDYL-CHROMIUM(III) REACTION

The case of the reaction of α,α′-dipyridylium nitrate with hexaquo chromium(III) nitrate in a 1.0 M aqueous sodium nitrate solution of initial pH = 2.0 is very similar to the more extensively studied phenanthroline case. The main differences are: (1) the initial rate of reaction is nearly tenfold greater for the same initial concentrations; (2) the mono(dipyridyl) chromium band is distinctly resolved from the reactant band and product bands; and, (3) the bis(diamine) salt isolated was formed to a lesser extent, more soluble and more difficult to crystallize.

Fig. 1 illustrates the dipyridyl case. The solution was 0.0214 M in hexaquo chromium(III) nitrate, 0.171 M in dipyridylium nitrate, 1.0 M in sodium

* We are indebted to Mr. Preben Hansen who carried out the C, H, and N determinations n Prof. K. A. Jensen's laboratory.

nitrate and initial pH = 2.0. The band envelopes of the reactant band, intermediate band and the products bands changed with time and asymptotically approached 495 mμ and an apparent $\varepsilon_{max.} = 68$. An orange salt isolated from this mixture had an absorption band with a maximum at 490 mμ and an $\varepsilon_{max.} = 42.8$. Again, a more strongly absorbing second product with a somewhat different wavelength of absorption is indicated but not isolated.

PREPARATION OF DIAQUOBIS(DIPYRIDYL)CHROMIUM(III) NITRATE

A direct preparation of this salt is effected by the refluxing of 100 ml of an aqueous mixture 0.1 M in $Cr(H_2O)_6(NO_3)_3$ and 0.4 M in dipyHNO_3 for a period of 4 h periodically neutralizing the hydrogen ions released with sodium hydroxide. At the end of this period the unreacted dipyridyl was precipitated from the solution with sodium hydroxide and the solution filtered. The pH of the filtrate is lowere to 1 with nitric acid and it is evaporated to approximately 20 ml. The solution is allowed to stand for several hours and crystals form. These are recrystallized from 0.1 HNO_3, washed with 0.1 M HNO_3 and dried over sulfuric acid. Approximate yield based on the chromium is 35 %.

A carbon-hydrogen nitrogen analysis of this orange salt indicated a C:H:N ratio of 20:21:7 and a possible formula of:

$$[Cr(dipy)_2(H_2O)_2](NO_3)_3 \cdot \tfrac{1}{2} H_2O$$

and a formula weight of 595. (Found: C 40.70; H 3.57; N 16.55. Calc. for $CrC_{20}H_{21}N_7O_{11\frac{1}{2}}$: C 40.35; H 3.53; N 16.45).

The absorption spectrum varied with pH. Fig. 2b gives the spectrum of the diaquo salt in 0.1 M nitric acid and also the spectrum of the dihydroxo complex in 0.1 M sodium hydroxide. The potentiometric titration of the salt in 0.1 M sodium nitrate solution also gives a curve typical of a dibasic acid with approximate $pK_1 = 3.5$ and $pK_2 = 6.1$ and a formula weight of 586. The approximate solubility of the salt in water is 0.6 moles per liter.

DISCUSSION

Diamines such as α,α′-dipyridyl and *o*-phenanthroline will react directly with hexaquo chromium(III) in aqueous solution in the pH range 1.5—3.0. A mono complex is first formed and the reaction continues to form a bis(diamine) ion. There is no direct evidence as to whether the diaquobis(diamine) ions formed are the *cis*- or the *trans*-diaquo ions. In complex ions of this type the *trans* forms are the lesser soluble entities. In the case of the *cis*- and the *trans*-diaquobis(ethylenediamine)chromium(III) ions, Woldbye [6] reports that the long wavelength chromium band has an $\varepsilon_{max.}$ of approximately 30 in the case of the *trans* compound but an $\varepsilon_{max.}$ of over 60 for the *cis* compound. Therefore, we believe the salt isolated to be the *trans*-diaquo compound and that the more soluble, more strongly light absorbing *cis*-diaquo compound remains in solution. The rates of formation are slow but the rates of *cis-trans* interconversion and decomposition are very slow, even at 100°C; thus indicating a large stability constant.

No evidence of a tris(diamine) complex ion formation was detected. The principal *trans*-diaquo product is extremely stable and cannot add a third diamine molecule without rearrangement and the less abundant *cis*-diaquo compound must react with the excess amine exceedingly slowly.

We wish to thank our colleagues in Chemistry Department A, particularly Professor S. E. Rasmussen, presently of Aarhus University, for many stimulating and helpful discussions.

REFERENCES

1. Pfeiffer, P. and Werdelmann, B. *Z. anorg. Chem.* **263** (1950) 31.
2. Blau, F. *Monatsh.* **19** (1898) 647.
3. Hammett, L. P., Walden, G. H. and Edmonds, S. M. *J. Am. Chem. Soc.* **56** (1934) 1092.
4. Barbieri, G. A. and Tettamanzi, A. *Atti reale accad.nazl. Lincei* **15** (1932) 877.
5. Lee, T. S., Kolthoff, I. M. and Leussing, D. L. *J. Am. Chem. Soc.* **70** (1948) 2348.
6. Woldbye, F. *Acta Chem. Scand.* **12** (1958) 1079.

Received August 26, 1960.

ACTA CHEMICA SCANDINAVICA 15 (1961) 69–77

Benzaurinstudien

VI. Gleichgewichte und Reaktionskinetik des 4″-Chlor-3,3′-dimethylbenzaurins in wässrigen Lösungen

HANS GUSTAF HANSSON

Abteilung für anorganische und physikalische Chemie des Chemischen Instituts der Universität Lund, Schweden

In three previous papers [1-3] the equilibrium conditions of benzaurin and four of its derivatives were described according to the same equilibrium system including three coloured "anhydrous" forms and three colourless "carbinolic" forms. The equilibrium constants of the protolytic reactions between the "anhydrous" forms and between the "carbinolic" forms, and of the hydration reactions between corresponding "carbinolic" and "anhydrous" forms were determined by light absorption measurements at different pH-values. The velocity constants of the slow hydration reactions, which, when starting from the "anhydrous" forms, appear as a gradual fading of the solutions until equilibrium is reached, were determined, by following the light absorption as a function of time.

In the present paper the results from a corresponding investigation of 4″-chloro-3,3′-dimethyl-benzaurin are presented. Unfortunately they are incomplete, mainly because of the impossibility of obtaining reproducable equilibrium values of the light absorption in alkaline solutions. This impossibility seems to be due to the fact that the hydration reactions of this derivative are slower than for the derivatives investigated previously, and because of the longer waiting-times for equilibrium the disturbance effect of irreversible reactions are more pronounced here.

The measurements were performed at 20°C, at the ionic strength 0.50 M and in a solvent with the composition 98 % water + 2 % acetone.

A summary and a discussion of the results in the series "Benzaurinstudien" is published elsewhere [4].

In einigen früheren Arbeiten [1-3] wurde über Untersuchungen über das Protolysenschema bei fünf Farbstoffen des Benzaurintypus berichtet. Die Untersuchungen wurden mit Hilfe von Lichtextinktionsmessungen ausgeführt. Die Farbstoffe konnten prinzipiell durch dasselbe Gleichgewichtsschema, welches drei gefärbte "Anhydridformen" und drei farblose "Karbinolformen" enthält, beschrieben werden. In diesem Aufsatz werden die Resultate

bei Messungen von 4″-Chlor-3,3′-dimethyl-benzaurin dargelegt. Da auch dieser Farbstoff demselben Schema wie die früher untersuchten folgt, werden sowohl die abgekürzten Formeln R, G_1 und G_2 (gefärbt) und F_1, F_2 und F_3 (farblos), wie die Gleichgewichtskonstanten K_1, K_2, K_3, K_4, K_5, K_6 und K_7 und die Geschwindigkeitskonstanten k_1, k_2, k_3 und k_4 wie früher [1-3] definiert.

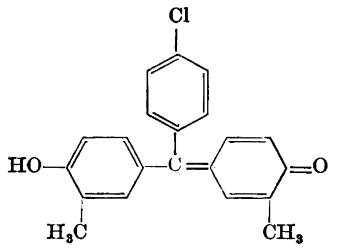

4″-Chlor-3,3′-dimethyl-benzaurin. Anhydrid (G_1).

Wie es beim Benzaurin [2] und 4″-Chlor-benzaurin [2] auch der Fall war, zeigte der vorliegende Farbstoff schlecht reproduzierbare Gleichgewichtsextinktionen (E_∞) in alkalischen Lösungen mit pH $> \sim 9$. Bei 4″-Chlor-3,3′-dimethyl-benzaurin sind die Hydratationsreaktionen ausserdem langsamer, die Wartezeiten vor der Messung von E_∞ folglich länger und die Einwirkung von störenden irreversiblen Prozessen grösser. Die Resultate unten sind deshalb unvollständig. Von den Gleichgewichtskonstanten konnten nur K_1, K_2, K_7 und das Produkt K_3K_6 ermittelt werden, und von den Geschwindigkeitskonstanten k_1 und k_2. Die für die Berechnungen verwendeten Formeln sind alle in den früheren Arbeiten [1-2], auf die Hinweise gemacht werden, abgeleitet worden. Formel (1; II.) bedeutet z.B. Formel (1) in der Arbeit "Benzaurinstudien II." [1].

MESSUNGEN UND ERGEBNISSE

Präparat. Das in einer früheren Arbeit [4] beschriebene Perchlorat des Farbstoffes wurde verwendet. Die Stammlösungen, die in Bezug auf den Farbstoff von der Stärke (1,5—3,8) $\times 10^{-4}$ M waren, wurden durch Auflösen einer eingewogenen Menge Perchlorat in wasserfreiem Aceton bereitet. Um die Haltbarkeit [2] zu erhöhen, wurden die Stammlösungen mit Triäthylamin bis zu einer Stärke von 1×10^{-2} M versetzt [2,3].

Puffersubstanzen waren Dinatriumhydrogenphosphat — Natriumhydroxyd, Borsäure — Natriumhydroxyd, Natriumdihydrogenphosphat — Dinatriumhydrogenphosphat in folgenden ungefähren pH-Intervallen: $9{,}8 < \text{pH} < 11{,}6$; $7{,}8 < \text{pH} < 9{,}7$; $5{,}7 < \text{pH} < 7{,}8$. In den sauren Lösungen mit pH $< 1{,}36$, die bei der Bestimmung von K_7 zur Verwendung kamen, wurde $[H^+]$ durch Zusatz einer bestimmten Menge HCl definiert. In alkalischen Lösungen mit pH $> 11{,}6$ wurde $[OH^-]$ durch Zusatz einerbestimmten Menge NaOH definiert. Für $K_w = [H^+] \cdot [OH^-]$ ist der früher [1] bestimmte Wert $1{,}22 \times 10^{-14}$ werwendet worden.

Die experimentellen Vorrichtungen waren die gleichen wie bei den früheren Untersuchungen [1]. Folglich wurden die Lichtextinktionen in einem Beckman-Quarz-Spektrophotometer, Modell DU, bei der Temperatur 20°C, gemessen. Die Zusammensetzung des Lösungsmittels in den Messlösungen war durchgehend 98 % Wasser und 2 % Aceton und die Ionenstärke 0,50 M. Als Zusatzsalz wurde NaCl verwendet.

Bei der Bereitung der Messlösungen wurden zu 49,0 ml Puffer 1,046 ml Acetonstammlösung des Farbstoffes mittels einer Injektionsspritze hinzugefügt. Das Volumen der Spritze war durch Auswägen mit Wasser ermittelt worden. Die $[H^+]$-Konzentration wurde, sofern sie nicht durch HCl- oder NaOH-Zusatz definiert war, mit Chinhydron- oder Platinwasserstoffgaselektroden gemessen.

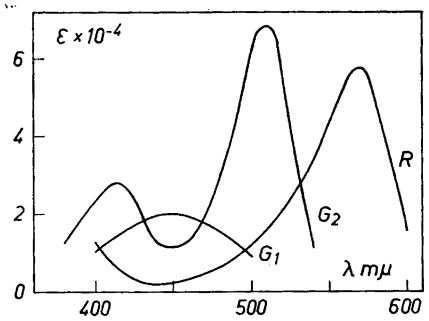

Fig. 1. Lichtabsorptionskurven. R ist das blaurote Ion $[(OC_6H_3CH_3)_2C(C_6H_4Cl)]^+$, G_1 das gelbe Molekül $(HOC_6H_3CH_3)C(C_6H_4Cl)$-$(CH_3C_6H_3O)$ und G_2 das gelbrote Ion $[(HOC_6H_3CH_3)_2C(C_6H_4Cl)]^+$.

Die verwendeten Chemikalien waren pro-analysi-Produkte, meistens von Baker oder Merck.

Die Unsicherheit in den bestimmten Konstanten beträgt normalerweise 2 — 5 Einheiten in der letzten Ziffer.

Die Geschwindigkeitskonstanten sind mit Brigg'schen Logarithmen berechnet worden und enthalten also die Grösse $^{10}\log e$.

Bezeichnungen C = die Gesamtkonzentration des Farbstoffes
d = die Schicht-(Kyvetten-)dicke
ε = der molekulare Lichtextinktionskoeffizient

E = die Lichtextinktion (E_0 bei der Zeit Null; E_∞ beim Gleichgewicht).
E_R (E_{G_1}, E_{G_2}) = die Lichtextinktion für eine Lösung, in der
C = [R] ([G_1], [G_2]) bei unverändertem d ist.

λ = die Wellenlänge; t = die Zeit

Die Lichtabsorptionskurven für die gefärbten Formen R, G_1 und G_2 finden sich in Figur 1 wieder, in der ε als Funktion von λ in mμ aufgetragen ist. Die R-Kurve wurde bei pH = 9,19 mit $d = 2$ cm und $C = 7{,}5 \times 10^{-6}$ M aufgenommen. Aus den gemessenen E-Werten wurde ε_R berechnet, wobei sämtliche in der Lösung vorliegenden Formen berücksichtigt wurden.

Die Kurve für G_1 wurde beim pH = 5,98(5) mit $d = 5$ cm und $C = 3{,}21 \times 10^{-6}$ M aufgenommen. Durch Extrapolation wurde E_0 erhalten und daraus ε_{G_1} in derselben Weise wie früher [1–3].

Die G_2-Kurve wurde in einer Lösung mit $[H^+] = 1{,}00$ M aufgenommen. d war 5 cm und $C = 3{,}21 \times 10^{-6}$ M. Aus den gemessenen E-Werten wurde E_{G_2} mit Hilfe der Formel (6; III.)[2] berechnet, und aus E_{G_2} wurde ε_{G_2} erhalten.

Es wurden folgende Daten für die Maxima erhalten:

$(\varepsilon_R)_{max} = 5{,}8 \times 10^4$ bei $\lambda \approx 570$ mμ
$(\varepsilon_{G_1})_{max} = 1{,}9(7) \times 10^4$ bei $\lambda \approx 450$ mμ
$(\varepsilon_{G_2})_{max} = 6{,}8 \times 10^4$ bei $\lambda \approx 510$ mμ
$(\varepsilon_{G_2})_{max} = 2{,}8(3) \times 10^4$ bei $\lambda \approx 415$ mμ

Bestimmung von K_1 erfolgte im Gebiet $7{,}4 < pH < 8{,}4$ mit $d = 5$ cm und $C = 3{,}21 \times 10^{-6}$ M. Für eine Reihe von Lösungen wurde E bei $\lambda = 570$

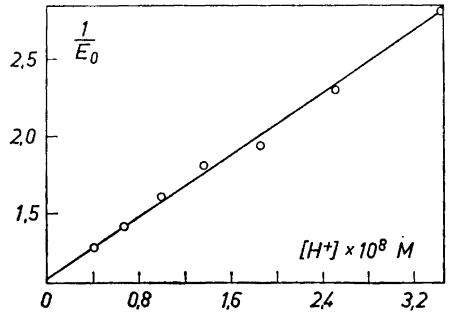

Fig. 2. $1/E_0$ als Funktion von $[H^+]$ für die Bestimmung von K_1 (und E_R). $\lambda = 570$ mμ, $d = 5$ cm und $C = 3{,}21 \times 10^{-6}$ M.

mμ (Absorptionsmaximum von R) als Funktion der Zeit gemessen und durch Extrapolation wurde E_0 erhalten. In Figur 2 ist $1/E_0$ als Funktion von $[H^+]$ aufgetragen. Die Kurve ist eine Gerade nach Formel (1; II.)[1]

$$\frac{1}{E_0} = \frac{1}{E_R} + \frac{K_1 \times [H^+]}{E_R}$$

Durch graphische Bestimmung wurde

$$K_1 = 0{,}46(3) \times 10^8,\ 1/K_1 = 2{,}1(6) \times 10^{-8},\ E_R = 0{,}92(7)$$

erhalten.

Bestimmung von K_3K_6 wurde im Gebiet $8{,}2 < \mathrm{pH} \leq 9{,}2$ ausgeführt; d war 2 cm und $C = 7{,}8(5) \times 10^{-6}$ M. Nachdem Gleichgewicht eingetreten war, wurde E_∞ bei $\lambda = 570$ mμ gemessen. Durch Korrektion für $[G_1]$ wurde E'_∞ berechnet [1]. In Figur 3 ist $1/E'_\infty$ als Funktion von $[H^+]$ aufgetragen. Mit Ausnahme von den niedrigeren Werten von $[H^+]$ (wo $[F_3]$ nicht vernachlässigt werden kann) liegen die Punkte auf einer Geraden nach Formel (3; II.)[1]

$$\frac{1}{E_\infty} = \frac{1 + 1/K_6}{E_R} + \frac{1}{E_R \times K_3K_6} \times [H^+]$$

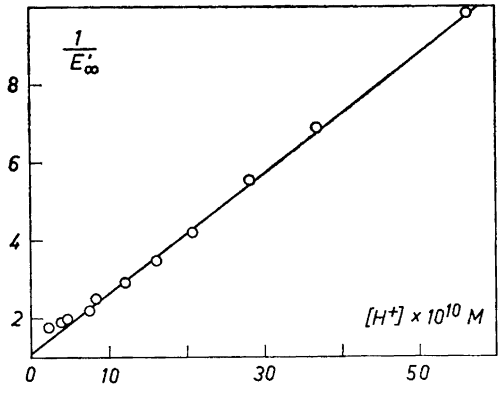

Fig. 3. $1/E'_\infty$ als Funktion von $[H^+]$ für die Bestimmung von K_3K_6. $\lambda = 570$ mμ $d = 2$ cm und $C = 7{,}8(5) \times 10^{-6}$ M.

Durch graphische Bestimmung wurde

$$K_3K_6 = 0{,}7(2) \times 10^{-9}$$

erhalten. Für E_R wurde dabei 0,908 eingesetzt, erhalten (nach Korrektion für $[G_1]$) als der Mittelwert aus fünf durch Extrapolation bestimmten E_0-Werten im Gebiet $8{,}5 < pH < 9{,}7$. Dadurch dass K_6 gross ist (wahrscheinlich > 7) gestattete die graphische Bestimmung keine Berechnung von K_6.

Eine Bestimmung von $K_5 = K_6/K_4$ *und* K_6 aus Formel (4; II.)[1] konnte nicht erfolgen, da reproduzierbare Gleichgewichtsextinktionen (E_∞) im aktuellen pH-Gebiet nicht erhalten werden konnten.

Bestimmung von K_2 wurde im Gebiet $7{,}8 < pH < 8{,}4$ ausgeführt. Für vier Lösungen, identisch mit vier von denen, die bei der Bestimmung von K_1 zur Verwendung kamen, wurde E_∞ mit $d = 5$ cm und bei $\lambda = 570$ mμ gemessen. Danach wurde K_2 aus Formel (6; II.)[1] berechnet.

$$K_2 = \frac{E_R - E_\infty\,(1 + K_1 \cdot [H^+] + 1/K_6)}{E_\infty \cdot K_1 \cdot [H^+]}$$

Für das Glied $1/K_6$, welches ein Korrektionsglied ist, wurde 0,1 eingesetzt. Für E_R wurde 0,927 eingesetzt, welches teils bei der Bestimmung von K_1 oben erhalten wurde, teils als der Mittelwert $0{,}927 \pm 0{,}005$ aus fünf E_0-Werten. Die E_0-Werten waren durch Extrapolation auf die Zeit Null bei der Bestimmung der Reaktionsgeschwindigkeit in fünf verschiedenen alkalischen Lösungen erhalten worden. Die Resultate sind in Tabelle 1 zusammengefasst. Als Mittelwert wurde $K_2 = 29(,2)$ erhalten.

Aus den oben bestimmten Konstanten erhält man das Produkt $K_1 \cdot K_2 \cdot K_3K_6 = 0{,}97$

Bestimmung von K_7 wurde im Gebiet $pH < 1{,}36$ ausgefürt, in dem das Gleichgewicht zwischen F_1, G_1 und G_2 sich fast momentan einstellt. Die Messungen der Lichtextinktionen, E, wurden bei $\lambda = 510$ mμ (Absorptionsmaximum von G_2) gemacht; d war 5 cm und $C = 3{,}21 \times 10^{-6}$ M.

Zuerst wurde eine Mess-serie bei der Ionenstärke 1,00 M zur Bestimmung von E_{G_1} gemacht. $[H^+]$ variierte zwischen 0,087 und 1,00 M. In Fig. 4 ist $[H^+] / \left(E - \frac{E_{G_1}}{1 + K_2}\right)$ als Funktion von $[H^+]$ * aufgetragen. Man erhält nach Formel (7; III.)[2] eine Gerade.

$$\frac{[H^+]}{E - \frac{E_{G_1}}{1 + K_2}} = \frac{K_7(1 + K_2)}{E_{G_2} - \frac{E_{G_1}}{1 + K_2}} + \frac{[H^+]}{E_{G_2} - \frac{E_{G_1}}{1 + K_2}}$$

Durch graphische Bestimmung wurde

$$E_{G_2} = 1{,}10(0); \quad (K_7(1 + K_2) = 0{,}50(3))$$

erhalten.

* Für $E_{G_1}/(1 + K_2)$ wurde 0,006 eingesetzt, welches durch Messen von E bei pH = 4,07 (Acetatpuffer) erhalten wurde.

Tabelle 1. Messungen bei 570 mμ zur Bestimmung von K_2; $d = 5$ cm und $C = 3{,}21 \times 10^{-6}$ M.

[H+] × 10^9 M	13,6(3)	9,9(4)	6,70	4,06
$E\infty$	0,045	0,062	0,092	0,134
K_2	29,9	29,1	27,9	29,9

Danach wurde eine Mess-serie bei der Ionenstärke 0,50 M mit demselben λ, d und C durchgeführt. $[H^+]$ variierte zwischen 0,0436 und 0,500 M. In Fig. 5 ist $\left(E - \frac{E_{G_1}}{1+K_2}\right)/(E_{G_1}-E)$ mit $E_{G_1} = 1{,}10$ als Funktion von $[H^+]$ aufgetragen, was eine Gerade durch Origo nach Formel (8; III.)[2] gibt.

$$\frac{E - \frac{E_{G_1}}{1+K_2}}{E_{G_1}-E} = \frac{[H^+]}{K_7(1+K_2)}$$

Graphische Bestimmung der Neigung ergab das Resultat $K_7(1 + K_2) = 0{,}69(0)$. Einsetzen von $K_2 = 29(,2)$ ergab $K_7 = 2{,}2(8) \times 10^{-2}$.*

Die Geschwindigkeitskonstante k des Aufhellungs- (Hydratations-) prozesses wurde durch Messung von E als Funktion von t und Berechnung von k aus Formel (7; II.)[1] bestimmt.

$$k = \frac{1}{t} \cdot \ln \frac{E_0 - E_\infty}{E - E_\infty}$$

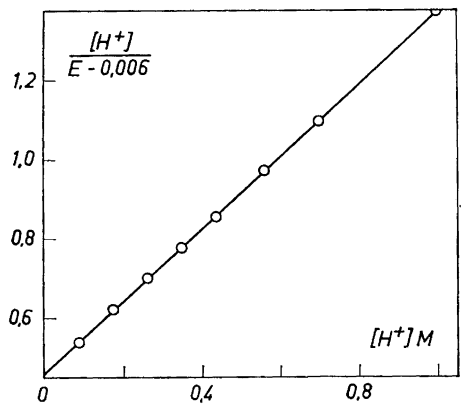

Fig. 4. $[H^+]/\left(E - \frac{E_{G_1}}{1+K_2}\right)$ als Funktion von $[H^+]$ für die Bestimmung von E_{G_1}. $\lambda = 510$mμ, $d = 5$ cm und $C = 3{,}21 \times 10^{-6}$ M. Die Ionenstärke = 1,00 M.

* Die Verwendung von Formel (7; III.)[2] in dieser Serie ergab das Resultat (siehe Fig. 5 a):

$$E_{G_1} = 1{,}11(4);\ K_7(1+K_2) = 0{,}70(4);\ K_7 = 2{,}3(3) \times 10^{-2}$$

Das Ergebnis oben zeigt, dass der bei der Ionenstärke 1,00 M oben bestimmte Wert von E_{G_1} innerhalb der Fehlergrenze mit diesem bei der Ionenstärke 0,50 M erhaltenen Wert übereinstimmt. Eine entsprechende Übereinstimmung ist früher bei Benzaurin[2] festgestellt worden.

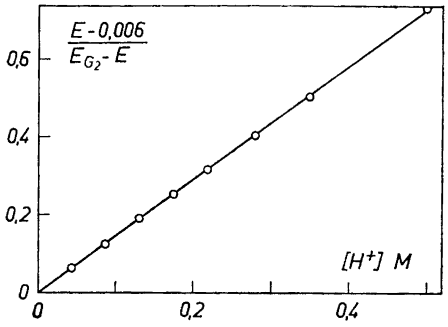

Fig. 5. $\left(E-\frac{E_{G_1}}{1+K_2}\right)/(E_{G_1}-E)$ als Funktion von [H+] für die Bestimmung von K_7. [λ = 510 mμ, d = 5 cm und C = 3,21 × 10^{-6} M. Die Ionenstärke = 0,50 M.

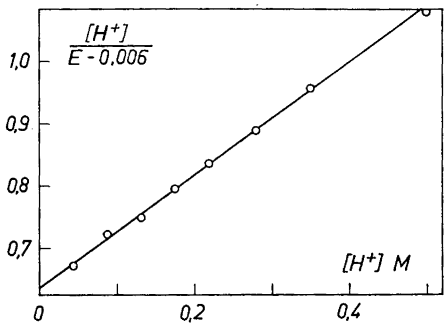

Fig. 5a. [H+]/$\left(E-\frac{E_{G_1}}{1+K_2}\right)$ als Funktion von [H+]. (Siehe Fussnote Seite 74). λ = 510 mμ, d = 5 cm und C = 3,21 × 10^{-6} M. Die Ionenstärke = 0,50 M.

Die Messungen von E fanden bei λ = 450 mμ (Absorptionsmaximum von G_1) für pH < 7 und bei λ = 570 mμ (Absorptionsmaximum von R) für pH > 7 statt. Für 8,5 < pH < 9,7 war d = 2 cm und C = 7,8(5) × 10^{-6} M; für die übrigen pH-Werte war d = 5 cm und C = 3,21 × 10^{-6} M.

Die Resultate gehen aus Figur 6, die k als Funktion von pH wiedergibt, hervor. Im Gebiet 9,6 < pH < 11,5 war es nicht möglich E_∞ zufriedenstellend zu bestimmen. E_∞ war jedoch zu gross, um vernachlässigt werden zu können; daher konnten in diesem Gebiet keine quantitativen Resultate erhalten werden.

k ist eine zusammengesetzte Geschwindigkeitskonstante, die aus den einzelnen Konstanten nach Formel (8; II.)[1] gebildet wird

$$k = \frac{k_2 \cdot [H^+]^2 + k_4 \cdot K_3 \cdot [H^+]}{[H^+]^2 + K_3 \cdot [H^+] + K_3 \cdot K_4} + \frac{k_1 \cdot K_1 \cdot [H^+] + k_3}{1 + K_1 \cdot [H^+]}$$

Bestimmung von k_1 und k_2 erfolgte im Gebiet 5,7 < pH < 6,6. In diesem Gebiet, wo die Reaktion $G_1 + H_2O \rightleftharpoons F_1$ dominiert und die Reaktion $R + H_2O \rightleftharpoons F_3$ unberücksichtigt gelassen wird, gilt Formel (9; II.)[1]

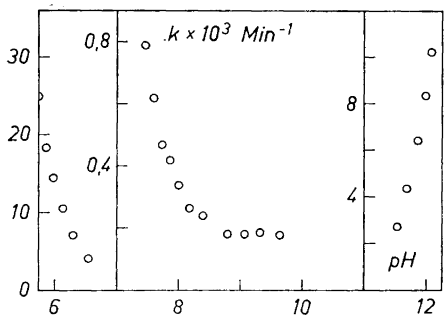

Fig. 6. Die Geschwindigkeitskonstante k als Funktion von pH. Die experimentell gefundenen Werte sind mit O bezeichnet.

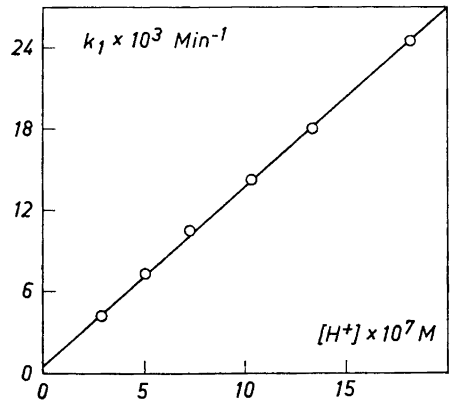

Fig. 7. Die Geschwindigkeitskonstante k_1 als Funktion von [H+].

$$k = k_1 \cdot \frac{K_1 \cdot [H^+]}{1 + K_1 \cdot [H^+]} + k_2$$

Durch Einsetzen in Formel (9; II.)[1] von der Relation $k_2 = k_1/K_2$, den oben erhaltenen Werten von K_1 und K_2 (0,46 $\times$ 10^8 bzw. 29) und zusammengehörigen, experimentell bestimmten Werten von k und [H$^+$] wurde k_1 bei verschiedenen [H$^+$]-Werten berechnet. Es zeigte sich, dass k_1, wie früher, linear mit [H$^+$] nach Formel (10; II.)[1] wächst.

$$k_1 = k_1^\circ + k_1' \cdot [H^+]$$

In Figur 7 ist k_1 als Funktion von [H$^+$] aufgetragen. Durch graphische Bestimmung wurde $k_1^\circ = 5 \times 10^{-4}$ und $k_1' = 1{,}3(2) \times 10^4$ erhalten. Folglich ist, mit [H$^+$] in Mol/l,

$k_1 = 5 \times 10^{-4} + 1{,}3(2) \times 10^4\,[H^+]$; $k_2 = 0{,}17 \times 10^{-4} + 4{,}5 \times 10^2\,[H^+]$ Min^{-1}.

Bestimmung von k_3 und k_4 konnte nicht erfolgen, da diese voraussetzt, dass die Konstanten K_4 und K_6 bekannt sind (siehe Formel (12; II.)[1]). Aus Figur 6 geht jedoch hervor, dass die starke Zunahme von k mit dem pH-Wert auf eine solche starke Zunahme von k_3 (und k_4) mit [OH$^-$] zurückzuführen sein muss — wie es schon bei den früher untersuchten Farbstoffen beobachtet werden konnte.

Tabelle 2. Zusammenfassung der Ergebnisse. [H+] in Mol/l.

K_7	$1/K_1$	$K_3 \cdot K_6$	K_2	k_1 Min^{-1}	k_2 Min^{-1}
$2{,}2(8) \times 10^{-2}$	$2{,}1(6) \times 10^{-8}$	$0{,}7(2) \times 10^{-9}$	29,(2)	$5 \times 10^{-4} + 1{,}3(2) \times 10^4 [H^+]$	$0{,}17 \times 10^{-4} + 4{,}5 \times 10^2 [H^+]$

DISKUSSION

Die erhaltenen, in Tabelle 2 zusammengefassten Resultate, können in erster Linie mit den für 4''-Chlor-benzaurin bestimmten Konstanten [2] am besten verglichen werden. Das Einführen der Methylgruppen hat die Hydratation kräftig verringert; K_2 hat mit dem Faktor 4,7 abgenommen. Ferner haben sich die Protolysenkonstanten verringert, K_7 und $1/K_1$ beide mit dem Faktor 2,1. (Auch K_3 dürfte kleiner geworden sein). Die Reaktionsgeschwindigkeit der Aufhellung (Hydratation) hat kräftig abgenommen und ist durchgehend 5 bis 10 mal geringer.

Die Lage der Lichtabsorptionsmaxima hat sich verändert. Durch die Einführung der Methylgruppen haben sich das ε_R-Maximum und das grosse ε_{G_1}-Maximum um etwa 15 mμ, und das kleine ε_{G_1}-Maximum um etwa 5 mμ gegen Rot verschoben.

Eine Zusammenfassung der Ergebnisse in der Serie "Benzaurinstudien" erscheint anderswo [6].

Der Verfasser dankt herzlich Herrn Professor Sven Bodforss, Herrn Professor Sture Fronæus und Herrn Dozent Rune Cigén für wertvolle Ratschläge und Diskussionen.

Fräulein Lena Hansson war als Assistentin tätig. Die Arbeit wurde mit finanzieller Hilfe von dem *Schwedischen naturwissenschaftlichen Forschungsrat*, Stockholm, und der *Mathematisch-naturwissenschaftlichen Fakultät der Universität Lund* durchgeführt.

Die Übersetzung ins Deutsche wurde von Fil.mag. Ingrid Wartenberg besorgt.

LITERATUR

1. Hansson, H. G. *Acta Chem. Scand.* **13** (1959) 1309 (= Benzaurinstudien II.).
2. Hansson, H. G. *Acta Chem. Scand.* **14** (1960) 407 (= Benzaurinstudien III.).
3. Hansson, H. G. *Acta Chem. Scand.* **14** (1960) 2021 (= Benzaurinstudien V.).
4. Hansson, H. G. und Nilsson, O. *Kgl. Fysiograf. Sällskap. Lund, Förh.* **29** (1959) No. 9 (= Benzaurinstudien I.).
5. Hansson, H. G. und Nilsson, O. *Kgl. Fysiograf. Sällskap. Lund, Förh.* **30** (1960) No. 3 (= Benzaurinstudien IV.).
6. Hansson, H. G. *Svensk Kem. Tidskr.* **78** (1961) *Im Drucke.*

Eingegangen am 3. Oktober 1960.

ACTA CHEMICA SCANDINAVICA 15 (1961) 78–86

Studies on Arabogalactans

V. Barry Degradation of the Arabogalactans from Western Larch. A Kinetic Study of the Mild Acid Hydrolysis of Arabogalactan A

HANS O. BOUVENG

Träkemiska avdelningen, Svenska Träforskningsinstitutet, Stockholm Ö, Sweden

Arabogalactan A and B from Western Larch heartwood were subjected to periodate oxidation and then Barry degradation. Hydrolysis of degraded and methylated arabogalactan B gave 2,4-di-*O*-methyl-D-galactose, 2,4,6-tri-*O*-methyl-D-galactose and 2,3,4,6-tetra-*O*-methyl-D-galactose as main products together with smaller amounts of 2-*O*-methyl-D-galactose, 4-*O*-methyl-D-galactose, 2,6-di-*O*-methyl-D-galactose, 2,3,4-tri-*O*-methyl-D-galactose, 2,5-di-*O*-methyl-L-arabinose and 2,3,5-tri-*O*-methyl-L-arabinose.

The kinetics of the hydrolysis of arabogalactan A in 0.005 N hydrochloric acid were studied. The velocity constants for the hydrolysis of the L-arabinofuranose and 3-*O*-β-L-arabinopyranosyl-L-arabinofuranose residues were estimated as 7.4×10^{-4} and 2.9×10^{-4}, respectively, (min, Brigg's logarithms); that for the easily-hydrolysed galactose residues was not less than 1.0×10^{-4}.

Previous papers of this series have described the fractionation of the arabogalactans from Western larch (*Larix occidentalis* Nutt.) into two components, A and B, and an investigation of these by the methylation technique [1–3]. The complexity of polysaccharide A has been demonstrated [2]. In the present investigation the procedure developed by Barry [4] for the degradation of periodate-oxidised polysaccharides has been applied to the polysaccharides for the elucidation of further structural details.

Arabogalactan B consumed 0.96 mole of oxidant on periodate oxidation with the liberation of 0.44 mole of formic acid per mole of anhydrosugar. This is equivalent to an oxidation of 44 molar % of the residues in the polysaccharide as terminal and 6-substituted galactose and terminal, pyranosidic arabinose and of 8 % as terminal furanosidic arabinose, which agrees fairly well with methylation data (41.0 and 7.6 molar %, respectively) [3].

The oxidised polysaccharide was degraded by treatment with phenyl hydrazine and acetic acid as devised by Barry [4] to give a polysaccharide fraction together with glyoxal *bis*-phenylhydrazone, glyceroosazone and L-ara-

binoosazone. The lowmolecular weight fragments were identified by chromatography on dimethyl sulphoxide-impregnated paper [5]. Neither galactoosazone nor any oligosaccharide osazone could be detected. The degraded polysaccharide contained 10.9 molar % of arabinose. A calculation from methylation data of the arabinose content of the non-oxidisable residues in the original polysaccharide gave a value of 16.3 %. Thus about one third of the arabinose was split off as osazone during the degradation. This could be explained by direct hydrolysis of arabinofuranose residues during the degradation but the virtual absence of arabinoosazone among the products formed on degradation of oxidised arabogalactan A indicates however that the hydrolysis, if any, of furanosidic linkages is very minute under the conditions used. The results show rather that about one third of the 3-substituted arabinofuranose residues in polysaccharide B are linked through the 6-position to galactose residues carrying no other substituents (I) while the remainder and also the 3-substituted arabinofuranose residues in polysaccharide A are linked to non-oxidisable galactose residues, for instance II.

β-L-Ara*p* 1——3 L-Ara*f* 1——6 β-D-Gal*p* 1—— I

β-L-Ara*p* 1——3 L-Ara*f* 1——6 β-D-Gal*p* 1—— II
3
|

The degraded polysaccharide was subjected to a further periodate oxidation and subsequent Barry degradation. A polymeric material could be isolated from the reaction mixture and on partial hydrolysis this gave as main product a homologuous series of oligosaccharides made up from β-1→3-linked galactose. Only faint traces of arabinose and of the 1→6-linked galactobiose were found. This makes it probable that the backbone of the polysaccharide consists of β-1→3-linked galactose residues.

Methylation of the first degradation product and hydrolysis of the methylated material gave the different methyl ethers shown in Table 1. The methylation steps were accompanied by severe losses, probably due to the low solubility of the methylated product and thus the results may not be fully representative for the original polysaccharide.

The high proportion of 2,4,6-tri-*O*-methyl-D-galactose gives further evidence of a backbone in the polysaccharide made up of 1→3-linked galactopyranose residues. The finding that practically no 1→6-linkages remain on further oxidation and Barry degradation of the polysaccharide suggests that the 2,4-di-*O*-methyl-D-galactose corresponds to residues in the main backbone carrying short branches, mainly single D-galactopyranose residues, at the 6-position. The 4-*O*-methyl-D-galactose is probably an artifact.

Table 1. Methyl ethers from methylated and hydrolysed degraded arabogalactan B.

Methyl ether	Molar %	Methyl ether	Molar %
2-Methylgalactose	3.2	2,4,6-Trimethylgalactose	38.9
4-Methylgalactose	1.6	2,3,4,6-Tetramethylgalactose	21.6
2,4-Dimethylgalactose	18.5	2,5-Dimethylarabinose	1.7
2,6-Dimethylgalactose	4.8	2,3,5-Trimethylarabinose	6.5
2,3,4-Trimethylgalactose	3.3		

Table 2. Methyl ethers corresponding to non-oxidisable residues from methylated and hydrolysed arabogalactan B.

Methyl ether	Molar %	Methyl ether	Molar %
2-Methylgalactose	4.9	2,4,6-Trimethylgalactose	8.5
2,4-Dimethylgalactose	66.7	2,5-Dimethylarabinose	11.5
2,6-Dimethylgalactose	8.3		

The 2,3,5-tri-*O*-methyl-L-arabinose arises from 3-substituted arabinofuranose residues in undegraded arabogalactan B. The presence of 2,5-di-*O*-methyl-L-arabinose is in agreement with the previously assumed [3] occurrence of residues of type III in the original polysaccharide.

L-Ara(*p* or *f*) 1———3 L-Ara*f* 1———3 L-Ara*f* 1——— III

The methylation data given in Table 1 can profitably be compared with those obtained from the original polysaccharide. Table 2 shows the proportions of the methyl ethers [3] related to *non-oxidised* residues in arabogalactan B (the release of part of the arabinose as osazone is accounted for).

Comparison of Tables 1 and 2 shows that the main part of the terminal galactopyranose residues in the degraded polysaccharide originates from doubly substituted galactopyranose residues in the undegraded polysaccharide represented by the 2,4-di-*O*-methyl-D-galactose in Table 2. Heavily ramified elements like IV are thus not infrequent in arabogalactan B.

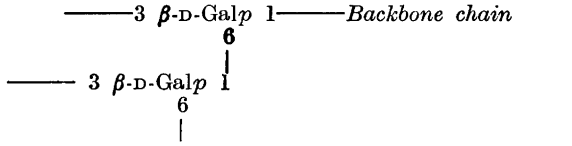

IV

As can be seen from Tables 1 and 2 there is an actual decrease of about 40 % in the residues corresponding to 2-*O*-methyl-D-galactose and 2,6-di-*O*-methyl-D-galactose. The remainder must be substituted by nonoxidisable (3-substituted) residues in the original polysaccharide.

As yet no unambiguous proof has been advanced that the 2-*O*- and 2,6-di-*O*-methyl-D-galactoses found in hydrolysates from methylated larch arabogalactans [1,3,6,7] have any structural significance. Partial hydrolysis would afford the corresponding 1,4-linked disaccharide but only in about the same amounts as would be expected to be formed by acid reversion of galactose [8]. A trial experiment was made, in which the hydrolysis was carried out in steps with intermediate withdrawal of low-molecular weight material in order to increase the yield of disaccharides. After fractionation of the hydrolysate by carbon column chromatography, one fraction was found by paper chromatography and electrophoresis in borate buffer to contain traces of a disaccharide with the same mobility as 4-*O*-β-D-galactopyranosyl-D-galactose [9]. However the large amounts of 3-*O*-β-D-galactopyranosyl-D-galactose accompanying it made any proper characterisation impossible.

Arabogalactan A consumed 1.01 mole of periodate with the liberation of 0.45 mole of formic acid per mole of anhydrohexose. This is equivalent to an oxidation of 45 molar % of the sugar residues in the polysaccharide as terminal and 6-substituted galactose and terminal, pyranosidic arabinose and of 11 % as terminal furanosidic arabinose. An estimate of these oxidisable residues from the methylation data [1] for comparison gave low values as the recovery of the corresponding methyl ethers was incomplete because of their slight volatility. Correction for these losses (*cf.* Ref.[3]) gave residues of 42 and 12 %, respectively, in fair agreement with the above values. No arabinoosazone or galactoosazone was observed among the degradation products formed on treatment with phenylhydrazine-acetic acid. The virtual absence of galactoosazone from the degradation products from the two polysaccharides excludes the presence of structural elements that contain 3-substituted galactose residues separated from the main chain by residues substituted only in the 6-position (V). Both degraded arabogalactans gave single, slightly oval spots with M_G values of 0.4—0.5 on electrophoresis on glass fibre sheets. Degraded polysaccharide A after mild hydrolysis unlike the original polysaccharide [2] gave one spot only on electrophoresis.

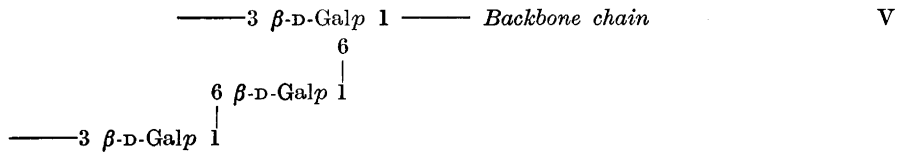

V

The results obtained in this series of investigations have shown few marked dissimilarities between the two arabogalactans from Western larch heartwood. Their molecular weights calculated from sedimentation constants differ considerably (4.3 and 1.4 for polysaccharide A and B, respectively). Polysaccharide A unlike B gives two distinct polymeric fragments when subjected to mild hydrolysis. The reason for this behaviour is not clearly understood.

The results of methylation and periodate oxidation studies show only slight differences in the proportions of different types of substituted galactose residues. The arrangement of the arabinose residues is, however, obviously different [1,3] but results of investigations of other larch arabogalactans [2,6,7] indicate that the arrangement as well as the amount of these residues can vary considerably in these polysaccharides. Polysaccharide A appears to be somewhat more branched than B. It also has a slightly higher proportion of residues that can form borate complexes. These residues include terminal and 6-substituted galactose and terminal pyranosidic arabinose, the total amount of which is equivalent to the amount of formic acid liberated on periodate oxidation of the polysaccharides. This slight difference does not, however, seem sufficiently large to account for the difference in rate of migration of the polysaccharides on electrophoresis in borate buffer (M_G values 0.76 and 0.63, respectively). Any comparison of the two polysaccharides in these respects is however open to criticism as long as the structural background of the splitting of polysaccharide A into the two polymeric fragments A I and A II [2] is not accounted for.

The results of this series of investigation and of investigations of similar arabogalactans (presumably of type A [2]) from European larch (*Larix decidua* Miller) [6,12] and tamarack (*L. laricina* (Du Roi) Koch) [1] make it possible to outline a general structure for these complicated polysaccharides. They contain a backbone made up mainly, or possibly exclusively, of β-1→3-linked D-galactopyranose residues. This backbone is ramified by substitution at the 6-positions and the low proportion of 2,4,6-tri-*O*-methyl-D-galactose found in the hydrolysates from the methylated polysaccharides indicates that few if any of the 6-positions in these backbone residues are unsubstituted. No regular pattern for the side-branching is discernible. Calculations from the data obtained from methylated Western larch arabogalactan B and from the products of periodate oxidation and Barry degradation, indicate that two thirds of the residues in this polysaccharide occur in the side-chains, that is, each side-chain contains an average of two residues. The non-terminal galactose seems largely to be 6-substituted and there are indications of residues in the side-chains of the B polysaccharide that are substituted in both the 3- and 6-positions. The arrangement of the arabinose is presumably variable. It occurs as single terminal furanosidic residues, as biosidic residues and to some extent as chains of three residues (III).

The structural significance of the 2-*O*- and 2,6-di-*O*-methyl-D-galactose found in the hydrolysates from methylated larch arabogalactans has not been unequivocally proved. Undermethylation or demethylation during hydrolysis might explain their appearance but this is contradicted by their virtual absence from the hydrolysate of an otherwise similar arabogalactan isolated from maple sap.[13]

Several investigations [6,10,11] have shown that significant amounts of D-galactose and 6-*O*-β-D-galactopyranosyl-D-galactose are liberated in addition to furanosidically linked L-arabinose and 3-*O*-β-L-arabinopyranosyl-L-arabinose when larch arabogalactans are subjected to acid hydrolysis under very mild conditions, for instance 0.01 N acid at 100°. This suggests that D-galactofuranosidic residues are present in the polysaccharide but careful investigations [3,6] have failed to give any positive evidence for the presence of such residues.

A semi-quantitative estimate was made of the hydrolysis constants for L-arabinose and 3-*O*-β-L-arabinopyranosyl-L-arabinose and for D-galactose together with 6-*O*-β-D-galactopyranosyl-D-galactose in the hydrolysis of arabogalactan A with 0.005 N hydrochloric acid at about 95°. Samples were withdrawn at suitable intervals and the amounts of the different saccharides were estimated by hypoiodite oxidation [14] after separation on thick filter paper. The results are shown in Table 3. The velocity constants are calculated assuming a monomolecular reaction, that is $kt = -\log (c_o - c)/c_o$, and extrapolated to time 0. When the hydrolysis had proceeded for 9 h, about half of the arabinose originally present had been split off and the k values had decreased up to 15 %. Methylation data gave the amount (c_o) of each saccharide in the starting material. However, the amount of galactose and 6-β-galactobiose originally accessible to hydrolysis under these conditions is not known and suitable values must be chosen arbitrarily. The first value (25 molar % of the original polysaccharide) assumes that the main part of the terminal galactose residues is hydrolysed at a uniform rate while the second value (10 %)

Table 3. Velocity constants (min. and Brigg's logarithms) for the hydrolysis of some saccharides from arabogalactan A in 0.005 N hydrochloric acid at 95°.

Saccharide	$k \times 10^4$
L-Arabinofuranose	7.4
3-*O*-β-L-Arabinopyranosyl-L-arabinofuranose	2.9
D-Galactopyranose + 6-*O*-β-D-galactopyranosyl-D-galactopyranose, 25 %	1.0
» , 10 %	2.5

corresponds to the minimum value given by the results from various experiments that have been made in this series of investigations on the mild hydrolysis of the polysaccharide.

As can be seen from Table 3 these galactopyranosidic residues are hydrolysed at almost the same rate as the arabinofuranosidic. The hydrolysis rates for pyranosides and furanosides normally differ [15] by a factor of about 10^3.

EXPERIMENTAL

All melting points are corrected. All evaporations were done under reduced pressure.

Chromatography. Papers: Whatman No. 1 and Schleicher and Schüll 602 hP. Solvents: Butanol, ethanol, water, 10:3:5, and benzene, dimethyl sulphoxide (DMSO), 20:1 (for chromatography on DMSO-impregnated paper [5]). Spray reagent: anisidine hydrochloride. The osazones required no spray reagent.

Electrophoresis. Papers: Whatman No. 1 and Schleicher and Schüll glass fibre sheets. Buffer: 0.1 M borate buffer of pH 10. Spray reagents: Anisidine hydrochloride and α-naphthol-sulphuric acid in butanol.

Periodate oxidation of arabogalactan B. Periodate oxidations were done in 0.125 M sodium periodate at room temperature. The oxidation of arabogalactan B was complete in 4 h, 0.96 mole of periodate being consumed and 0.44 mole of formic acid liberated. The overoxidation was 0.03 mole in 24 h.

Barry degradation of oxidised arabogalactan B. Arabogalactan B (10 g) was oxidised for 6 h and then ethylene glycol was added to destroy excess periodate. The solution was freed from iodate by precipitation with lead acetate and filtration. Excess lead ion was precipitated with sulphuric acid. The solution was filtered and neutralised and then phenylhydrazine (25 ml) and acetic acid (12 ml) were added. The yellow flocculent precipitate formed was recovered on a glass filter and thoroughly washed with water. It contained 11.57 % nitrogen. An oxidised polysaccharide-phenylhydrazine complex of the type described by Barry *et al.*[16] and with a composition in accord with the methylation data for arabogalactan B [3] would contain 11.68 % nitrogen.

The precipitate was dispersed in aqueous ethanol (400 ml), acetic acid (60 ml) and phenylhydrazine (30 ml) and refluxed for 4 h. The dark-coloured solution was concentrated and the glyoxal *bis*-phenylhydrazone which crystallised (m.p. and mixed m.p. 168—170°) was removed by filtration. Water was then added to the solution and it was exhaustively extracted, first with benzene and then with ether. The extracts were examined by chromatography on paper impregnated with DMSO [5]. As well as glyoxal *bis*-phenylhydrazone this also indicated the presence of glycerosazone and L-arabinoosazone. No galactoosazone was observed. The ether extract contained mainly phenylhydrazine acetate.

The extracted aqueous solution was concentrated and run into ethanol to give the degraded arabogalactan as a yellow precipitate. After purification by reprecipitation the polysaccharide was obtained as a pale yellow powder (3.94 g) containing 3.1 % nitrogen. It was later found that the nitrogen content could be greatly reduced by treatment of the polysaccharide with hot 20 % acetic acid for 20—60 min. Arabinose constituted 10.9 % of the reducing sugars in the polysaccharide.

Table 4. Fractionation of methylated and hydrolysed, degraded arabogalactan B.

Fract.	mmole (tot)	Sugars	%	mmole
24—32	0.096	2-Methylgalactose	66	0.063
		4-Methylgalactose	34	0.033
33—48	0.342	2,4-Dimethylgalactose		
49—60	0.120	2,4-Dimethylgalactose	21	0.025
		2,6-Dimethylgalactose	79	0.095
61—80	0.100	2,3,4-Trimethylgalactose	66	0.066
		2,5-Dimethylgalactose	34	0.034
81—143	0.775	2,4,6-Trimethylgalactose		
Residue	0.558	2,3,4,6-Tetramethylgalactose	77	0.430
		2,3,5-Trimethylarabinose	23	0.129

Parts of the extracts and the filtrate from the precipitated polysaccharide were taken to dryness and then dissolved in ethanol and treated with Amberlite IR 120 in the acid form. An oligosaccharide osazone would, according to Finan and O'Colla [17], be hydrolysed by this treatment to give a reducing saccharide with one residue less. No reducing saccharides were detected on chromatography of the supernatant liquid and thus no larger fragments could have been split off as osazones during the degradation.

Methylation of degraded arabogalactan B. The degraded polysaccharide (3.0 g) was methylated first with dimethyl sulphate in aqueous 30 % sodium hydroxide, then twice with methyl iodide and barium oxide in dimethylformamide (DMFA) [2,18] and finally twice with methyl iodide and silver oxide in DMFA. The final product (0.85 g) was difficult to free from impurities and it was not possible to obtain a reliable methoxyl analysis. No unmethylated monomer was detected on chromatography of a hydrolysed sample.

Hydrolysis of methylated, degraded arabogalactan B and fractionation of the hydrolysate. The methylated polysaccharide (0.6 g) was first treated with hot formic acid (50 ml) for 1 h. After evaporation of the formic acid it was hydrolysed completely by using 0.5 N sulphuric at 100° for 16 h. This procedure has been found to cause very little degradation and demethylation. The hydrolysate was fractionated on a carbon-Celite column (3.5 × 46 cm) using 5 l 6→35 % aqueous ethanol as eluant. Mixed fractions were subfractionated on thick filter paper and the amount of reducing sugar in the various fractions was estimated by hypoiodite oxidation [14]. The results of the fractionations are summarised in Tables 1 and 4.

*Characterisation of the methyl ethers. 2-O-Methyl-*D*-galactose, 4-O-methyl-*D*-galactose* and *2,6-di-O-methyl-*D*-galactose* were indistinguishable from authentic specimens on paper chromatography and on paper electrophoresis.

*2,5-Di-O-methyl-*L*-arabinose* and *2,3,4-tri-O-methyl-*D*-galactose* were indistinguishable from authentic specimens on normal paper chromatography and on chromatography on paper impregnated with DMSO.

*2,4-Di-O-methyl-*D*-galactose.* The ether was recrystallised from ethyl acetate-methyl ethyl ketone, m.p. 100°; the aniline derivative had m.p. 216—218°, undepressed on admixture with authentic 2,4-di-*O*-methyl-D-galactosyl-*N*-phenylamine.

*2,4,6-Tri-O-methyl-*D*-galactose.* The ether was recrystallised from ethanol-*iso*propyl ether, m.p. 101—104°; the aniline derivative had m.p. 176—178°, undepressed on admixture with authentic 2,4,6-tri-*O*-methyl-D-galactosyl-*N*-phenylamine.

*2,3,4,6-Tetra-O-methyl-*D*-galactose.* The aniline derivative had m.p. 199—200°, undepressed on admixture with authentic 2,3,4,6-tetra-*O*-methyl-D-galactosyl-*N*-phenylamine.

*2,3,5-Tri-O-methyl-*L*-arabinose.* The ether was converted to the amide of the corresponding acid. It had m.p. 138—140° after recrystallisation from ethyl acetate, in good agreement with values previously reported [19].

Periodate oxidation and Barry degradation of arabogalactan A. Arabogalactan A on oxidation with periodate consumed 1.01 mole of oxidant with the liberation of 0.45 mole of formic acid per mole anhydrohexose. The oxidised polysaccharide was degraded in the same manner as arabogalactan B to yield a polysaccharide material containing 8.1 %

arabinose (arabinose content calculated from methylation data 6.2 %). Neither L-arabinoosazone nor D-galactoosazone was observed among the degradation products.

Miscellaneous experiments on degraded arabogalactans A and B. Both polysaccharides yielded arabinose only on hydrolysis in 0.01 N hydrochloric at 100° for 2 h. They travelled as single spots on electrophoresis in borate buffer both before and after mild hydrolysis.

When subjected to graded hydrolysis (0.1 N hydrochloric acid), both afforded 3-*O*- and 6-*O*-β-D-galactopyranosyl-D-galactose but the proportion of the latter was less than in case of the original polysaccharides.

Degraded arabogalactan B was subjected to a second periodate oxidation followed by Barry degradation. As the polysaccharide gave a rather dark solution, no estimate of the consumption of oxidant could be made. A polysaccharide fraction could be isolated as a brownish powder and this on hydrolysis for 2 h in 0.1 N hydrochloric acid at 100° gave the following saccharides as main products (the fractions R_M/n^{20} are given in brackets): D-galactose (0.36), 3-*O*-β-D-galactopyranosyl-D-galactose (0.35), a trisaccharide (0.35), a tetrasaccharide (0.33) and higher oligosaccharides. The similarity of the R_M/n fractions indicates that the polymeric material consisted mainly of straight chains of β-1→3-linked D-galactopyranose residues. Only faint traces of arabinose and 6-*O*-β-D-galactopyranosyl-D-galactose appeared on the chromatogram.

Partial hydrolysis of arabogalactan A. Arabogalactan A (4.0 g = 25.6 mmole of anhydrosugar) was hydrolysed in 0.005 N hydrochloric acid (200 ml) at about 95°. Samples of suitable size (2—4 ml) were withdrawn at intervals and run into ethanol to precipitate polymeric material which was removed by filtering. After reprecipitation of the solids and filtering, the oligosaccharides in the combined filtrates were separated on prewashed Schleicher and Schüll 602 hP papers. The amounts of L-arabinose, D-galactose and 6-*O*-β-D-galactopyranosyl-D-galactose were estimated by hypoiodite oxidation directly after elution from the papers. As the 3-*O*-β-L-arabinopyranosyl-L-arabinose might not be stable at the pH used for the hypoiodite oxidation [21], the eluate containing it was taken to dryness and dissolved in hot ethanol. Any hemicellulosic material from the paper was removed by filtering the hot solution. The solvent was evaporated and the disaccharide was hydrolysed in 0.5 N sulphuric acid. The solution was neutralised with sodium bicarbonate and the amount of arabinose present was estimated by hypoiodite oxidation. The results of the hydrolysis are given in Table 5.

Calculation of the hydrolysis constants. The velocity constants for the hydrolysis of L-arabinose, 3-β-arabinobiose and of D-galactose together with 6-β-galactobiose were calculated from the curves constructed from the values given in Table 5. Only the values from the first nine hours should be taken into consideration as the secondary hydrolysis of the disaccharides taking place during this short period can probably be disregarded. Methylation data [1] gave the following proportions in molar % of hydrolysable residues (c_0) in the starting material: arabinofuranose 12 % = 3.07 mmole; 3-β-arabinobiose 3 % = 0.77 mmole; D-galactose + 6-β-galactobiose 25 % = 6.40 mmole (assuming that the main part of the terminal galactose and galactobiose residues was hydrolysed at an uniform rate) and 10 % = 2.56 mmole (assuming that only part of the residues was sensitive to hydrolysis under the conditions used). The results of the calculation are summarised in Table 3.

Table 5. Saccharides formed on hydrolysis of 4.0 g of arabogalactan A in 0.005 N hydrochloric acid at 95° (mmole).

Time, h	L-arabinose	D-galactose	3-*O*-β-L-arabinopyranosyl-L-arabinose	6-*O*-β-D-galactopyranosyl-D-galactose
0.5	0.165			
1	0.267	0.073	0.027	
2	0.636	0.150	0.056	0.036
4	1.04	0.242	0.097	0.048
6	1.37	0.368	0.165	0.092
8.5	1.66	0.452	0.216	0.102
23.5	2.70	1.13	0.284	0.194
30	2.88	1.43	0.270	0.238

The author is greatly indebted to Professor Bengt Lindberg for his keen interest in this work and to Miss Anita Myhrman for her skilful assistance.

REFERENCES

1. Bouveng, H. O. and Lindberg, B. *Acta Chem. Scand.* **12** (1958) 1977.
2. Bouveng, H. O. *Acta Chem. Scand.* **13** (1959) 1869.
3. Bouveng, H. O. *Acta Chem. Scand.* **13** (1959) 1877.
4. Barry, V. C. *Nature* **152** (1943) 538.
5. Wickberg, B. *Acta Chem. Scand.* **12** (1958) 615.
6. Aspinall, G. O., Hirst, E. L. and Ramstad, E. *J. Chem. Soc.* **1958** 593.
7. Adams, G. A. *Can. J. Chem.* **38** (1960) 280.
8. Thompson, A., Anno, K., Wolfrom, M. L. and Inatome, M. *J. Am. Chem. Soc.* **76** (1954) 1309.
9. Bouveng, H. O. and Meier, H. *Acta Chem. Scand.* **13** (1959) 1884.
10. Jones, J. K. N. *J. Chem. Soc.* **1953** 1672.
11. Bouveng, H. O. and Lindberg, B. *Acta Chem. Scand.* **10** (1958) 1515.
12. Aspinall, G. O., Cairncross, J. M. and Nicholson, A. *Proc. Chem. Soc.* **1959** 270.
13. Bishop, C. T. *Private communication.*
14. Hirst, E. L., Hough, L. and Jones, J. K. N. *J. Chem. Soc.* **1949** 57.
15. Pigman, W. W. and Goepp, R. M. *Chemistry of the Carbohydrates*, New York 1948, p. 206.
16. Barry, V. C. and Mitchell, P. W. D. *J. Chem. Soc.* **1953** 3631.
17. Finan, P. A. and O'Colla, P. S. *Chem. & Ind. London* **1955** 1387.
18. Kuhn, R., Baer, H. H. and Seeliger, A. M. *Ann.* **611** (1958) 236.
19. Maher, G. G. *Advances in Carbohydrate Chem.* **10** (1955) 263.
20. French, D. and Wild, G. M. *J. Am. Chem. Soc.* **75** (1953) 2612.
21. Whistler, R. L. and BeMiller, J. N. *Advances in Carbohydrate Chem.* **13** (1958) 289.

Recived September 9, 1960.

ACTA CHEMICA SCANDINAVICA 15 (1961) 87–95

Phenyl*iso*cyanate Derivatives of Carbohydrates

HANS O. BOUVENG

Träkemiska avdelningen, Svenska Träforskningsinstitutet, Stockholm Ö, Sweden

An investigation was made of a method of locating the acetyl groups in partially acetylated carbohydrates using phenyl*iso*cyanate for introducing protective substituents. It was found that the derived phenylcarbamoyl groups sometimes undergo acyl migration but that generally the reagent is suitable for use in the determination of the substituent distribution in partially acetylated 1→4-linked xylans and glucans.

Locating the *O*-acetyl groups in partially acetylated carbohydrates is complicated by their lability. It seemed that locating these groups might be facilitated by using phenyl*iso*cyanate for the introduction of protective groups. In the procedure used here the acetyl groups are replaced by methyl groups according to the reaction sequence I—V (R = phenylcarbamoyl group, Ph · NH · CO—). The *O*-methyl groups are then easily localised by standard methods.

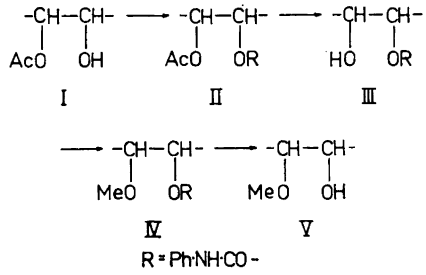

Such a procedure must satisfy the following requirements: (a) Phenyl*iso*cyanate should react quantitatively with the free hydroxyl groups under conditions that do not affect the acetyl groups; (b) The derived phenylcarbamoyl groups should not be affected by the deacetylation; (c) The phenylcarbamoyl groups should not migrate on methylation of the deacetylated products; (d) The phenylcarbamoyl groups should be easily removed to give the partially methylated compound.

To investigate these points the reaction sequence I—V or part of it was applied to the following D-glucose derivatives:

Methyl 2,3,4-tri-*O*-acetyl-α-D-glucopyranoside;
Methyl 6-*O*-acetyl-β-D-glucopyranoside;
Methyl β-D-glucopyranoside 2,3-di(phenylcarbamate);
1,2-*O*-*iso*propylidene-3-*O*-acetyl-α-D-glucofuranose;
1,2-*O*-*iso*propylidene-6-*O*-acetyl-α-D-glucofuranose.

Phenyl*iso*cyanate is known to react quantitatively with hydroxyl groups and it is possible to prepare fully substituted glycosides quite readily.[1] The reaction is usually carried out in pyridine but neutral solvents such as benzene can also be used[2]. It has been claimed[3,4] that when partially acetylated carbohydrates are treated with phenyl*iso*cyanate, no migration of the acetyl groups takes place. The absence of migration was confirmed by conversion of methyl 2,3,4-tri-*O*-acetyl-α-D-glucopyranoside to 2,3,4-tri-*O*-methyl-D-glucose by application of the reaction sequence I—V followed by hydrolysis.

After substitution of the free hydroxyl groups in the partially acetylated derivative, deacetylation was carried out at room temperature in methanol or ethanol-acetone containing about 2 % of sulphuric or hydrochloric acid. The reaction was complete after 20—50 h. The stability of the phenylcarbamoyl group to acid hydrolysis was shown by treating methyl α-D-glucopyranoside 6-phenylcarbamate for 20 h with 3 % sulphuric acid at 100°. Only a faint trace of glucose was detected on chromatography of the hydrolysate.

Boiling sodium methoxide solution has been used to remove phenylcarbamoyl groups in carbohydrates[2]. Thus methyl α-D-glucopyranoside 6-phenylcarbamate, prepared by treatment of methyl 2,3,4-tri-*O*-acetyl-α-D-glucopyranoside with phenyl*iso*cyanate followed by deacetylation[3], gave methyl α-D-glucopyranoside in good yield when treated for 1 h with 1.5 equivalents of sodium methoxide in boiling methanol. Phenylcarbamates are, however, rapidly N-methylated when treated with iodomethane and silver oxide in *N*,*N*-dimethylformamide (DMFA) and this increases the resistance to alkaline hydrolysis. Lithium aluminium hydride (LAH) has previously been used for reductive removal of phenylcarbamoyl groups[5]. It was now found that *N*-methyl-phenylcarbamoyl groups also reacted smoothly with LAH using dioxan or tetrahydrofuran as solvent. The reductive removal was complete in 3—4 h.

The phenylcarbamates are carboxylic esters. These groups would therefore be expected to undergo acyl migration when the steric conditions are favourable, in an analogous way to the ready migration of the otherwise extremely stable mesitoyl group to the C_2 hydroxyl when 1-*O*-mesitoyl-2,3,4,6-tetra-*O*-acetyl-α-D-glucose is deacetylated in methanolic ammonia at 0°[6]. Acyl migration in carbohydrates has been reviewed by Pacsu[7] and Sugihara[8]. Lately Bonner[9] has devoted a series of investigations to the subject. The migration is assumed to proceed over an orthoester intermediate[10] and it is noticeable that it is possible to construct molecular models of orthoester intermediates in all cases where the course of an acyl migration has been established.

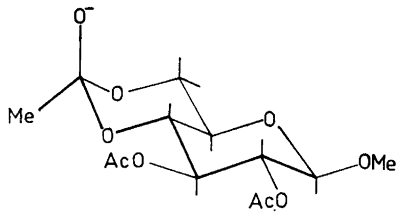

VI

Migration of an acetyl group from the C_4 to the C_6 hydroxyl group in D-glucose is known to take place very easily, for instance on methylation of its 2,3,4-tri-*O*-acetyl derivatives [11,12]. The assumed intermediate (VI) consists of two strainless 6-membered rings with the glucose in the C*1* conformation. To test whether phenylcarbamoyl groups are liable to migrate or not, an examination was made of the products formed on methylation of methyl β-D-glucopyranoside 2,3,4-tri(phenylcarbamate), prepared by treatment of methyl 6-*O*-acetyl-β-D-glucopyranoside with phenyl*iso*cyanate and subsequent deacetylation. The main methylation product was a crystalline compound (yield 67 %, calculated as methyl mono-*O*-methyl-β-D-glucopyranoside tri-(*N*-methyl-phenylcarbamate) which on reduction with LAH gave crystalline methyl 4-*O*-methyl-β-D-glucopyranoside. In addition to the crystalline compound, which must be assigned a methyl 4-*O*-methyl-β-D-glucopyranoside 2,3,6-tri-(*N*-methyl-phenylcarbamate) structure, there was also obtained some non-crystalline material. On reduction with LAH and subsequent hydrolysis this gave 4-*O*-methyl-D-glucose as main product together with a quantity of 6-*O*-methyl-D-glucose corresponding to 5—10 % of the original methyl β-D-glucopyranoside 2,3,4-tri(phenylcarbamate). It is thus obvious that the phenylcarbamate group can migrate. The small amount of 6-*O*-methyl-D-glucose found indicates, however, that some methylation of the 6-positions occurred before the migration took place. The methyl 4-*O*-methyl-β-D-glucopyranoside obtained on methylation of methyl 2,3,4-tri-*O*-acetyl-β-D-glucopyranoside [12] was also accompanied by a small amount of the 2-*O*-methyl isomer showing that in this case some migration from the C_2 to the C_4 hydroxyl took place before the methylation of the C_4 hydroxyl was completed.

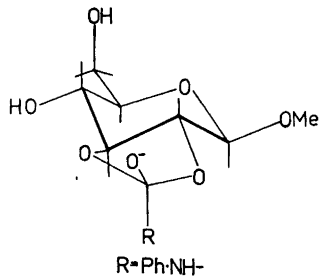

VII

The main purpose of the present investigation was to find a suitable procedure for determining the distribution of substituents in the partially acetylated xylan from birch wood [13] and in partially acetylated cellulose. A migration of acyl groups from the C_2 to the C_3 hydroxyl groups does not seem to be possible by the accepted mechanism as the formation of an intermediate orthoester (VII) would require a considerable distortion of bonds. The same applies for migration from the C_2 to the C_6 hydroxyl in cellulose. Inspection of molecular models shows that migration might be possible over a somewhat hindered intermediate (VIII) from the C_3 to the C_6 hydroxyl groups in

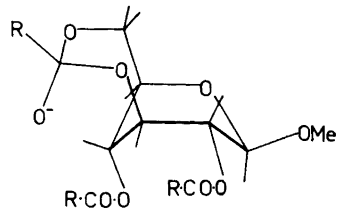

R= Ph·NH-

VIII

glucopyranose structures with 1 C and 1 B conformations. To investigate this, methyl β-D-glucopyranoside 2,3-di(phenylcarbamate) was methylated with iodomethane and silver oxide in DMFA and the product was reduced with LAH and hydrolysed. Crystalline 4,6-di-*O*-methyl-D-glucose was the sole product. This shows that neither $C_3 \rightarrow C_6$ nor $C_3 \rightarrow C_4$ migration took place. As no $C_3 \rightarrow C_4$ migration occurred the inference might be drawn that neither would $C_2 \rightarrow C_3$ migration occur in glucose or xylose as the $C_2 - C_3$ and $C_3 - C_4$ groupings are conformationally similar. It appears from this that the reaction sequence I—V should therefore be applicable to the determination of the substituent distribution in partially acetylated 1 → 4-linked xylans and glucans.

Josephson [14] has investigated the kinetics of the rearrangement of 1,2-*O*-*iso*propylidene-3-*O*-acetyl-α-D-glucofuranose (IX) to the 6-*O*-acetyl isomer (X). For an intended comparison of the rates of migration of acetate and phenylcarbamoyl groups, analoguous 3- and 6-phenylcarbamoyl D-glucofuranose derivatives were prepared. IX and X were treated with phenyl*iso*cyanate to give the 5,6- (XI) and 3,5-di(phenylcarbamates) (XII), respectively. These were then deacetylated with simultaneous glycosidation according to Haworth and Porter [15] yielding the amorphous 5,6- and 3,5-di(phenylcarbamates) of methyl D-glucofuranoside (XIII and XIV, respectively), mainly as the β-anomers [15]. It was anticipated that the 3-*O*-phenylcarbamoyl group in XIV would migrate to the 6-position by analogy with the behaviour of the 3-*O*-acetyl group in IX. No change in the optical rotation was, however, observed when XIV was treated with saturated ammoniacal methanol. On treatment with silver oxide in DMFA the specific rotation in methanol changed from —35° to —26°. The same treatment of XIII had no effect on its rotation (—14°).

The infrared spectra of XIV and of its derived product XV were very similar except that XIV showed a weak band at 1 800 cm^{-1} and XV a weak band

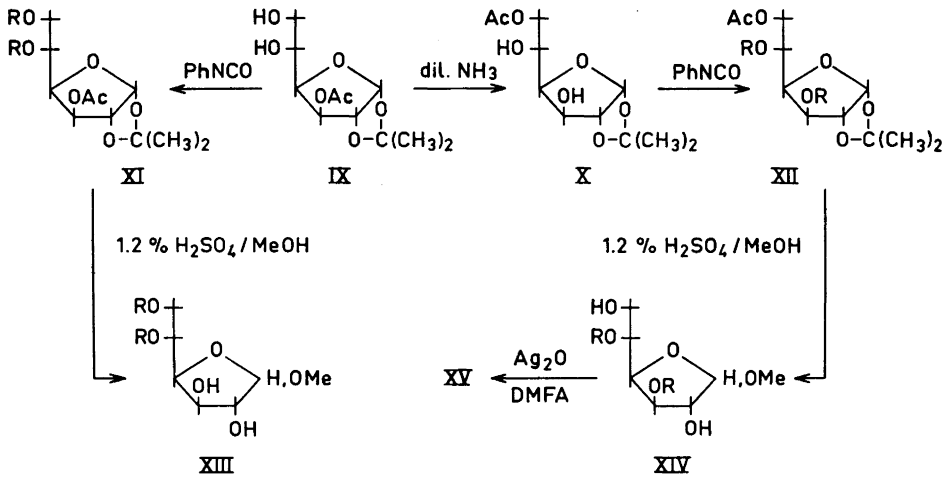

at 1 650 cm^{-1}. These spectra were, however, easily distinguished from that of XIII, especially in the regions for the amide I (1 700 — 1 725 cm^{-1}) and amide II (1 540 — 1 550 cm^{-1}) bands, the bands for the C-O stretching vibration of the ester groups (1 200 — 1 260 cm^{-1}) and the bands associated with the stretching mode of C-O bonds in hydroxyl groups (1 040 — 1 125 cm^{-1})[16].

XV, on acetylation with acetic anhydride in pyridine solution, gave a heterogeneous product which probably consisted of a mixture of the acetates obtained on acetylation of XIII and XIV.

XIV was methylated twice with iodomethane and silver oxide in DMFA solution. The syrupy methylation product was reduced with LAH and then hydrolysed. The hydrolysate contained a mixture of 2-*O*-methyl-D-glucose (21 %), 2,3-di-*O*-methyl-D-glucose (55 %) and 2,6-di-*O*-methyl-D-glucose (24 %). Only traces of mono-*O*-methyl-D-glucoses other than 2-*O*-methyl-D-glucose were observed.

The 2,3-di-*O*-methyl-D-glucose results from methylation of the C_3 hydroxyl subsequent to the migration of the 3-*O*-phenylcarbamate group. The not unsignificant amount of 2,6-di-*O*-methyl-D-glucose found shows that methylation of the C_6 hydroxyl takes place at a rate comparable to that of the migration. The presence of 2-*O*-methyl-D-glucose among the products is difficult to explain. The interpretation of this and of the ambiguous results from the IR studies and from the acetylation experiments must await further investigation.

EXPERIMENTAL

All melting points were corrected. All evaporations were done under reduced pressure.

Methyl α-D-glucopyranoside 6-phenylcarbamate. Methyl 2,3,4-tri-*O*-acetyl-α-D-glucopyranoside 6-phenylcarbamate[3], m.p. 146—148° (2.0 g), was dissolved in 2 % methanolic hydrochloric acid (40 ml). The solution was stored at room temperature until the optical rotation was constant (30 h). It was then neutralised and concentrated to a small volume. The product that crystallised (1.25 g, 87 %) was recrystallised several times from etha-

nol, m.p. 182—184°, $[\alpha]_D^{20}$ +93° (*c*, 0.5 in ethanol). Hearon *et al.*[3] report m.p. 131—133° for methyl α-D-glucopyranoside 6-phenylcarbamate. (Found: C 52.1; H 6.2; N 4.3. Calc. for $C_{14}H_{19}O_7N$: C 53.7; H 6.1; N 4.5.)

Methylation of methyl α-D-glucopyranoside 6-phenylcarbamate. Methyl α-D-glucopyranoside 6-phenylcarbamate (0.98 g) was methylated with iodomethane and silver oxide in DMFA [17]. The reaction mixture was filtered and the filtrate taken to dryness. Extraction of the residue with hot chloroform and concentration of the extract gave the methylation product as a light-coloured glass (1.07 g).

2,3,4-Tri-O-methyl-D-glucose. Part of the methylated methyl α-D-glucopyranoside 6-phenylcarbamate was used in less successful attempts to remove the *N*-methyl-phenylcarbamoyl group by alkaline hydrolysis. A portion (0.20 g) was instead treated for 3 h with excess lithium aluminium hydride (LAH) in hot dioxan. Excess water and then dilute sulphuric acid were added to the cooled reaction mixture. It was filtered, the filtrate was taken to dryness and the product obtained was dissolved in 0.5 N sulphuric acid and kept at 100° overnight. After neutralisation and concentration of the solution the product was purified by distillation to give a colourless syrup (87 mg), $[\alpha]_D^{20}$ +96° (*c*, 0.5 in chloroform). The product was indistinguishable from 2,3,4-tri-*O*-methyl-D-glucose on chromatography and its aniline derivative had m.p. 144—146°, undepressed on admixture with authentic 2,3,4-tri-*O*-methyl-D-glucosyl-*N*-phenylamine.

Methyl 6-O-acetyl-β-D-glucopyranoside 2,3,4-tri(phenylcarbamate). Methyl 6-*O*-acetyl-β-D-glucopyranoside was prepared by treatment of methyl β-D-glucopyranoside (15 g) with 0.9 equiv. of acetic anhydride in pyridine at room temperature overnight. Water was then added and the mixture was concentrated with further addition of water to remove the acetic acid. The resulting aqueous solution of the reaction product was then extracted continuously with hot chloroform, first for 3 h and then exhaustively. The 3-hour extract contained mainly di-, tri- and tetraacetylated products. The second extract was concentrated to dryness and then dissolved in ethanol-ether. On scratching, crude methyl 6-*O*-acetyl-β-glucopyranoside (3.33 g, 18 %) crystallised. It was recrystallised from ethanol-ether, $[\alpha]_D^{20}$ —34° (*c*, 2.0 in water), m.p. 128—129°, undepressed on admixture with an authentic specimen [18].

The methyl 6-*O*-acetyl-β-D-glucopyranoside (2.00 g) was treated for 3 h with phenyl*iso*cyanate (1.2 equiv.) in anhydrous pyridine (25 ml) at 100°. Anhydrous methanol was then added to destroy excess phenyl*iso*cyanate and the solution was boiled for another 10 min. and then poured into cold water. The crystalline precipitate formed was collected on a glass filter and dried. It was recrystallised from ethanol-acetone giving needles, m.p. 221—221.5°, $[\alpha]_D^{20}$ —19° (*c*, 1.0 in pyridine). Yield 4.55 g (91 %). (Found: C 60.6; H 5.1; N 7.4. Calc. for $C_{30}H_{31}O_{10}N_3$. C 60.1; H 5.1; N 7.2.)

Methyl β-D-glucopyranoside 2,3,4-tri(phenylcarbamate). Methyl 6-*O*-acetyl-β-D-glucopyranoside 2,3,4-tri(phenylcarbamate) (3.8 g) was dissolved in acetone (100 ml) and ethanol containing 10 % concentrated hydrochloric acid (100 ml). When the optical rotation was constant (24 h) the solution was neutralised with aqueous sodium hydrogen carbonate. After concentration to about one third the solution was poured into water. The precipitated product was recrystallised from aqueous acetone giving large needles, m.p. 218—219°, $[\alpha]_D^{20}$ —3° (*c*, 1.0 in pyridine). Hearon *et al.*[4] report somewhat different constants for methyl β-D-glucopyranoside 2,3,4-tri(phenylcarbamate) and for the methyl β-D-glucopyranoside 2,3-di(phenylcarbamate) described below. To make sure that no migration had occurred during the isolation of methyl β-D-glucopyranoside 2,3,4-tri(phenylcarbamate) it was reacetylated to give a crystalline material, m.p. 220.5—221°, undepressed on admixture with methyl6-*O*-acetyl-β-D-glucopyranoside 2,3,4-tri(phenylcarbamate). (Found: C 61,1; H 5.3; N 7.4. Calc. for $C_{28}H_{29}O_9N_3$: C 61.1; H 5.3; N 7.6.)

Methylation of methyl β-D-glucopyranoside 2,3,4-tri(phenylcarbamate). Methyl β-D-glucopyranoside 2,3,4-tri(phenylcarbamate) (2.36 g) was methylated twice with iodomethane and silver oxide in DMFA. The reaction product was isolated as previously described. It crystallised on concentration of a methanolic solution. Recrystallisation from aqueous methanol gave large prisms, m.p. 133—134°, $[\alpha]_D^{20}$ +25° (*c*, 1.0 in pyridine). Yield 1.75 g (67 %). (Found: C 63.1; H 5.8; N 7.0; OCH_3 10.4; (N)-CH_3 7.1. Calc. for methyl mono-

O-methyl-β-D-glucopyranoside tri-(*N*-methyl-phenylcarbamate) ($C_{32}H_{37}O_9N_3$): C 63.1; H 6.1; N 6.9; OCH_3 10.2; (N)-CH_3 7.1.)

Reduction of methylated methyl β-D-glucopyranoside 2,3,4-tri(phenylcarbamate). The above compound (1.64 g) in dioxan was refluxed for 4 h with excess LAH. After removal of inorganic material the solution was taken to dryness to give a rapidly crystallising glass (0.58 g = 96 %). Recrystallisation from ethyl acetate gave large, non-dichroic plates, m.p. 90—91°, $[\alpha]_D^{20}$ —17° (*c*, 1.0 in water). The molten compound solidified to fan-like dichroic crystals, m.p. 102—104°. The latter melting point and the optical rotation are in agreement with the values reported for methyl 4-*O*-methyl-β-D-glucopyranoside [12].

A hydrolysed sample of the product was indistinguishable from authentic 4-*O*-methyl-D-glucose on paper chromatography and paper electrophoresis in borate buffer.

The non-crystalline material in the mother liquors from the methylated methyl β-D-glucopyranoside 2,3,4-tri(phenylcarbamate), on reduction with LAH and subsequent hydrolysis gave a syrupy product (0.16 g). Paper electrophoresis of this product in borate buffer showed the presence of 4-*O*-methyl-D-glucose and 6-*O*-methyl-D-glucose in proportions of about 3 : 1, together with a faint trace of D-glucose.

Methyl 4,6-O-ethylidene-β-D-glucopyranoside 2,3-di(phenylcarbamate). Methyl 4,6-*O*-ethylidene-β-D-glucopyranoside 2,3-di(phenylcarbamate) was prepared from methyl 4,6-*O*-ethylidene-β-D-glucopyranoside following the procedure previously described. It had m.p. 224—225°, $[\alpha]_D^{20}$ —165° (*c*, 1.0 in pyridine). (Found: C 60.1; H 5.5; N 6.4. Calc. for $C_{23}H_{26}O_8N_2$: C 60.3; H 5.7; N 6.1.)

Methyl β-D-glucopyranoside 2,3-di(phenylcarbamate). Methyl 4,6-*O*-ethylidene β-D-glucopyranoside di(phenylcarbamate) (4.37 g) was dissolved in hot ethanol (60 ml) and 0.5 N sulphuric acid (30 ml). After boiling for 3 h the solution was neutralised with barium carbonate and filtered. The filtrate was taken to dryness. The residue was triturated with ether giving small needles, m.p. 195°. This product was recrystallised from aqueous acetone, m.p. 205—207°, $[\alpha]_D^{20}$ —118° (*c*, 1.0 in pyridine). Yield 3.24 g (79 %). Found: C 56.3; H 5.6; N 6.7. Calc. for $C_{21}H_{24}O_8N_2$. C 58.3; H 5.6; N 6.5.) A sample of the substance was acetylated with acetic anhydride in pyridine solution to give a product that melted at 215—216° in good agreement with the value [3] previously reported for methyl 4,6-di-*O*-acetyl β-D-glucopyranoside 2,3-di(phenylcarbamate).

Methylation of methyl β-D-glucopyranoside 2,3-di(phenylcarbamate(. The methyl β-D-glucopyranoside 2,3-di(phenylcarbamate) was methylated with iodomethane and silver oxide in DMFA. After isolation in the usual manner the product was obtained as a glass, $[\alpha]_D^{20}$ +24° (*c*, 1.0 in pyridine), which did not crystallise.

Methyl 4,6-di-O-methyl-β-D-glucopyranoside and 4,6-di-O-methyl-D-glucose. The above methylation product was treated with excess LAH and the reduced product was worked up as usual. After removal of inorganic material it crystallised on concentration of its ethereal solution. Recrystallisation from ethyl ether-*iso*propyl ether gave long needles, m.p. 73.5—75°, $[\alpha]_D^{20}$ —28° (*c*, 1.0 in chloroform).

A portion of this compound was hydrolysed in 0.5 N sulphuric acid. The isolated product crystallised from ethyl acetate-ethyl ether as small needles, $[\alpha]_D^{20}$ +109° → +64° (*c*, 0.5 in water), m.p. 155—157°. The m.p. agrees with that reported for the expected 4,6-di-*O*-methyl-α-D-glucose [19], and it was not depressed on admixture with an authentic specimen of this ether. M.p. 52—54°and $[\alpha]_D^{20}$ —28° are reported for its methyl β-glucopyranoside. The m.p. reported above for this substance indicates that it was obtained as a different crystal modification.

*1,2-O-*Iso*propylidene-3-O-acetyl-α-D-glucofuranose 5,6-di(phenylcarbamate) (XI).* 1,2-*O*-*Iso*propylidene-3-*O*-acetyl-α-D-glucofuranose, m.p. 124—125°, $[\alpha]_D^{20}$ —27° (*c*, 1.0 in ethanol) prepared as described by Josephson [14] was treated for 2.5 h with 2.4 equiv. of phenyl*iso*cyanate in hot DMFA solution. The product was isolated as previously described and appeared as microscopic needles, melting at 186—188° with partial recrystallisation. The molten sample crystallised on cooling and was used for inoculating a hot methanolic solution of the product which then crystallised as long, silky needles, m.p. 196—196.5°,

$[\alpha]_D^{20}$ +42° (*c*, 1.0 in pyridine). (Found: C 60.1; H 5.7; N 5.7. Calc. for $C_{25}H_{28}O_9N_2$. C 60.0; H 5.6; N 5.6.)

1,2-O-Isopropylidene-6-O-acetyl-α-D-glucofuranose 3,5-di(phenylcarbamate) (XII). 1,2-*O-Iso*propylidene-3-*O*-acetyl-α-D-glucofuranose was dissolved in a minimum of aqueous ethanol and a few drops of ammonia were added. Crystals started immediately to separate from the solution. It was concentrated and the product was filtered off. The yield of 1,2-*O-iso*propylidene-6-*O*-acetyl-α-D-glucofuranose was 85 %, m.p. 144—145°, $[\alpha]_D^{20}$ −4° (*c*, 1.0 in ethanol). It was treated with phenyl*iso*cyanate giving the 3,5-di(phenylcarbamate) as flat needles, crystallised from methanol, m.p. 218—219°, $[\alpha]_D^{20}$ +9° (*c*, 1.0 in pyridine). (Found: C 60.0; H 5.7; N 5.7. Calc. for $C_{25}H_{28}O_9N_2$: C 60.0; H 5.6; N 5.6.)

Methyl (α,β)-D-glucofuranoside 3,5- and 5,6-di(phenylcarbamates). XI and XII were deacetylated with simultaneous glycosidation in dry methanol containing 1.2 % sulphuric acid.[15] The reactions were followed polarimetrically and were complete in 50 h. The solutions were neutralised by slowly adding dilute methanolic ammonia until a precipitate of ammonium sulphate formed. After filtration the solutions were taken to dryness and the residues extracted with warm ethyl ether. On concentration of the extracts the products were obtained as amorphous powders soluble in ethanol and warm ether and insoluble in chloroform. The methyl (α,β)-D-glucofuranoside 5,6-di(phenylcarbamate) (XIII) had $[\alpha]_D^{20}$ −14° (*c*, 1.0 in methanol) and the methyl (α,β)-D-glucofuranoside 3,5-di(phenylcarbamate) (XIV) $[\alpha]_D^{20}$ −35° (*c*, 1.0 in methanol).

Treatment of XIII with saturated methanolic ammonia or with silver oxide in DMFA, as expected, had no effect on its optical rotation. Saturated methanolic ammonia had no effect on XIV but silver oxide in DMFA changed its specific rotation in methanol to −26°. This compound (XV) was obtained as an amorphous powder after isolation and purification in the same way as the products from methylations with iodomethane and silver oxide in DMFA.

Acetylation of XIII, XIV and XV. These were acetylated with acetic anhydride in pyridine. The products were recrystallised from ethanol-ether. Acetylated XIII formed non-dichroic needles recrystallising at 150° to larger, dichroic crystals, m.p. 189—191°. Acetylated XIV formed small non-dichroic needles, m.p. 179—180°. Acetylated XV consisted of small non-dichroic needles, melting at 180° leaving larger dichroic crystals which melted at 189°. Too little material was available for further investigations but it seemed probable that the latter acetate consisted of a mixture of the first two.

Methylation of methyl (α,β)-D-glucofuranoside 3,5-di(phenylcarbamate). The amorphous 3,5-di(phenylcarbamate) XIV (1.87 g) was methylated twice with iodomethane and silver oxide in DMFA. The product (1.80 g) was treated with excess LAH. The reduced material was then hydrolysed in 0.1 N sulphuric acid at 100° overnight. After neutralisation and concentration a lightcoloured syrup (0.75 g) was obtained. This was shown by paper chromatography to contain a mixture of three components indistinguishable from authentic 2-*O*-, 2,3-di-*O*- and 2,6-di-*O*-methyl-D-glucose. The proportions of the three ethers (21, 55 and 24 %, respectively) were estimated quantitatively by hypoiodite oxidation [20] after fractionation on thick filter paper. The 2,3-di-*O*-methyl-D-glucose appeared considerably enriched in the extract on continuous extraction of an aqueous solution of the ethers with hot chloroform. The 2-*O*-methyl-D-glucose and 2,6-di-*O*-methyl-D-glucose were separated by chromatography on thick filter paper.

The 2-*O*-methyl-D-glucose had m.p. 153—154° underpressed on admixture with an authentic specimen. It was indistinguishable from the authentic ether on electrophoresis in borate buffer of pH 10. The 2,3-di-*O*-methyl-D-glucose was characterised as the 1,4,6-triazobenzoate, m.p. 183—185°, $[\alpha]_D^{20}$ −29° (*c*, 1.0 in chloroform) and the 2,6-di-*O*-methyl-D-glucose as the 1,3,4-triazobenzoate, m.p. 203—205°, $[\alpha]_D^{20}$ −250° (*c*, 1.0 in chloroform).

Acknowledgements: The author is indebted to Professor Bengt Lindberg for many valuable discussions throughout this work, to Miss Anita Myhrman for skilful assistance and to Dr. D. J. Bell, Edinburgh, for a gift of 4,6-di-*O*-methyl-D-glucose.

REFERENCES

1. Wolfrom, M. L. and Pletcher, D. E. *J. Am. Chem. Soc.* **62** (1940) 1151.
2. Salmon, M. R. and Powell, G. *J. Am. Soc.* **61** (1939) 3507.
3. Hearon, W. M., Hiatt, G. D. and Fordyce, C. R. *J. Am. Chem. Soc.* **66** (1944) 995.
4. Bredereck, H., Wagner, A., Faber, G., Huber, N., Immel, G. and Kreiselmeier, H. *Ber.* **91** (1958) 2819.
5. Gaylord, N. G. *Reduction with complex metal hydrides.* Interscience, New York 1956 p. 636.
6. Wood, H. B. and Fletcher, H. G. *J. Am. Chem. Soc.* **78** (1956) 2849.
7. Pacsu, E. *Advances in Carbohydrate Chem.* **1** (1945) 77.
8. Sugihara, J. M. *Advances in Carbohydrate Chem.* **8** (1953) 1.
9. Bonner, W. A. *J. Am. Chem. Soc.* **80** (1958) 3372, 3697.
10. Fischer, E. *Ber.* **53** (1920) 1621.
11. Haworth, W. N., Hirst, E. L. and Teece, E. G. *J. Chem. Soc.* **1931** 2858.
12. Bouveng, H. O., Lindberg, B. and Theander, O. *Acta Chem. Scand.* **11** (1957) 1788.
13. Bouveng, H. O., Garegg, P. J. and Lindberg, B. *Acta Chem. Scand.* **14** (1960) 742.
14. Josephson, K. *Ann.* **472** (1929) 217.
15. Haworth, W. N. and Porter, C. R. *J. Chem. Soc.* **1929** 2796.
16. Bellamy, L. J. *The Infra-red Spectra of Complex Molecules*, Methuen, London 1958.
17. Kuhn, R., Trischmann, H. and Löw, I. *Angew. Chem.* **67** (1955) 32.
18. Croon, I. and Gierer, J. *Unpublished results.*
19. Bourne, E. J. and Peat, S. *Advances in Carbohydrate Chem.* **5** (1950) 145.
20. Hirst, E. L., Hough, L. and Jones, J. K. N. *J. Chem. Soc.* **1949** 57.

Received September 22, 1960.

ACTA CHEMICA SCANDINAVICA 15 (1961) 96–100

Phenyl*iso*cyanate Derivatives of Carbohydrates

II. Location of the *O*-Acetyl Groups in Birch Xylan

HANS O. BOUVENG

Träkemiska avdelningen, Svenska Träforskningsinstitutet, Stockholm, Sweden

The distribution of the *O*-acetyl groups in glucuronoxylan from birch wood was re-investigated using phenylcarbamoyl groups as protective substituents. The isolated polysaccharide contained 13.2 % of *O*-acetyl. 58.1 % of the D-xylose residues carried no *O*-acetyl groups, 11.8 % were substituted in the 2-position, 24.0 % in the 3-position and 6.1 % in both the 2- and 3-positions.

While investigating the properties of dimethyl sulphoxide (DMSO) as extractive agent in the isolation of wood hemicelluloses, Hägglund *et al.*[1] isolated a partly acetylated glucuronoxylan from birch wood holocellulose. Subsequently, a good yield of the polysaccharide was obtained by extraction of birch wood holocellulose[2] (prepared by chlorination of the wood followed by extraction with ethanolic ethanolamine) with DMSO. Methylation studies conducted on the partly acetylated glucuronoxylan indicated that the acyl groups (identified as *O*-acetyl groups) were mainly attached at the 3-positions in the original polysaccharide. The procedure employed, however, was inadequate for an unambiguous location of the *O*-acetyl groups in as much as approximately 30 % of these groups were hydrolysed during the methylation of the polysaccharide.

The previous paper in this series[3] investigated the possibility to umambiguously locate *O*-acetyl groups in partly acetylated carbohydrates. This procedure has now been applied to the *O*-acetylated birch wood glucuronoxylan.

Glucuronoxylan, containing 13.2 % of *O*-acetyl, was obtained by extracting birch wood holocellulose (prepared by the chlorite method) with DMSO. Treatment of a solution of the polysaccharide in hot, anhydrous dimethylformamide (DMFA) with an excess of phenyl*iso*cyanate transformed the free hydroxyl groups to phenylcarbamoyl groups.

The polysaccharide derivative thus obtained was insoluble in all the common solvents except anhydrous DMSO and anhydrous (or slightly moist) DMFA. Deacetylation of the material was attempted by dissolving it in DMFA and adding a small amount of aqueous sulphuric acid. The hydrolysing effi-

ciency of that medium gradually decreased however, due to the hydrolysis of the solvent into formic acid and dimethyl amine. The procedure was repeated once. Subsequent methylation showed that about 40 % of the *O*-acetyl groups were removed by this treatment.

Further deacetylation was effected by dissolving the partially deacetylated and methylated glucuronoxylan phenylcarbamoyl derivative in moist tetrahydrofuran containing sulphuric acid. *O*-methyl groups were substituted for all *O*-acetyl groups by alternate deacetylations and methylations.

The methylations were conducted in DMFA[4] with iodomethane and silver oxide. The solubility properties of the product required a modified isolation procedure, by which it was separated from the silver salts by precipitation of the polysaccharide in ethanolic potassium cyanide. Although this procedure gave very good yields of product, its use is limited to materials that are insoluble in ethanol.

The *O*-methylglucuronoxylan phenylcarbamoyl derivative was treated with lithium aluminium hydride in tetrahydrofuran solution to give a good yield of the corresponding partly *O*-methylated glucoxylan. This was hydrolysed and the hydrolysate fractionated on a carbon-Celite column. The mixed fractions were fractionated further by paper chromatography and paper electrophoresis in borate buffer of pH 9.4. Fractionation by chromatography on filter paper impregnated with borate buffer of pH 10[5] was tried but some alkaline degradation of the 3-*O*-methyl-D-xylose occurred during some part of the process. The amount of sugar in each fraction was estimated by hypoiodite oxidation [6]. The results of the fractionation are summarised in Table 1.

The results given in Table 1 show that the 2- and 3-positions in the original polysaccharide are substituted by *O*-acetyl groups in the ratio 1: 1.7. This result agrees fairly well with that previously obtained[2] which indicated that the birch xylan was substituted by *O*-acetyl groups mainly at the 3-positions.

The amount of 4-*O*-methyl-D-glucose found is much less than is required by the molar ratio of the D-xylopyranose and 4-*O*-methyl-D-glucuronic acid residues (91.5 : 8.5) in the original polysaccharide. This is explained by the reaction of phenyl*iso*cyanate with the carboxylic groups of the uronic residues giving *N*-phenylamide groups.[7] The main part of the amide bonds is apparently not hydrolysed during the deacetylations and the corresponding residues are converted into 4-*O*-methyl-6-deoxy-6-*N*-phenylamino-D-glucose residues.[8] The latter substance was not encountered in the hydrolysate. The 4-*O*-methyl-D-glucose found might correspond to uronic acid *N*-phenyl amide residues that were hydrolysed during the deacetylations. The carboxyl groups

Table 1. Methyl ethers from the hydrolysed, partly methylated glucoxylan.

Sugars	Mole %
Xylose	57.5
2-Methylxylose	11.7
3-Methylxylose	23.8
2,3-Dimethylxylose	6.0
4-Methylglucose	1.0

liberated would be esterified during the methylations and subsequently converted to hydroxyl groups by treatment with lithium aluminium hydride. Hence, it was not possible to obtain meaningful values for the nitrogen and methoxyl contents in the corresponding polysaccharide derivatives. The values given in the experimental part are calculated assuming either that the *N*-phenyl amide groups were unaffected during the deacetylations or that they were removed completely.

The values given in Table 1 correspond to an *O*-methyl glucoxylan containing 10.0 % methoxyl (methoxyl content of the unhydrolysed polysaccharide as analysed, 10.2 %). These values are lower than those (11.7 — 12.3 %) calculated on basis of the methylated glucuronoxylan phenylcarbamate. The low methoxyl content might be explained by the fact that fractionation of the polysaccharide occurred during the isolation.

EXPERIMENTAL

All melting points were corrected. All evaporations were conducted under reduced pressure.

Chromatography. Papers: Whatman No. 1 and 3 MM and Schleicher & Schüll 602 hP. These papers were also used impregnated with 0.1 M sodium borate buffer of pH 10[8]. Spray reagent: Anisidine hydrochloride.

Isolation of O-acetylated birch xylan. Acetone-extracted wood meal (1—2 mm) from a freshly cut log of *Betula verrucosa* Erh. was delignified by the chlorite method[9] at 60° and pH 4.7 to give a holocellulose containing less than 1 % of lignin.

The holocellulose (230 g) was extracted three times at room temperature with 2 l portions of dimethyl sulphoxide (DMSO). Three volumes of ethanol and a small amount of glacial acetic acid were added to the extracts and the precipitated hemicellulose was recovered on a glass filter. The third extract gave only a small amount of precipitate.

The hemicellulose was dissolved in water and insolubles were removed by filtration. The filtrate was acidified with glacial acetic acid and added to ethanol. The precipitated hemicellulose was recovered by filtration, thoroughly washed with ethanol and ether and subsequently dried. The product thus obtained for use in the present investigation was a white powder. Yield 14 g, $[\alpha]_D^{20}$ −54° (*c*, 1.0 in water). Anal. Uronic acid (as glucuronic acid) 10.5 %; *O*-acetyl (as CH_3CO) 13.2 %.

The residual holocellulose was impregnated with 5 % ethanolic monoethanolamine, dried, and extracted three times with DMSO.

Product yield following the isolation and purification procedure described above was 13 g of hemicellulose, $[\alpha]_D^{20}$ −56° (*c*, 1.0 in water). Anal. Uronic acid 13.9 %; *O*-acetyl 9.1 %.

Chromatographic analysis of the two samples after hydrolysis indicated that D-xylose was the only aldose present.

Treatment of birch O-acetyl xylan with phenylisocyanate. After drying in vacuum over phosphorus pentoxide, the polysaccharide (8.0 g) was dissolved in anhydrous *N,N*-dimethyl formamide (DMFA, 200 ml). Phenyl*iso*cyanate (20 ml) was added and the solution kept at 100° for 3 h. It was then poured into ethanol to produce a voluminous precipitate which was collected on a glass filter, washed with ethanol and ether and dried. The treatment with phenyl*iso*cyanate was repeated once and after a final purification by reprecipitation, the product was obtained as a coarse, yellowish powder (15.2 g), $[\alpha]_D^{20}$ −92° (*c*, 1.0 in DMFA), soluble in DMFA and in anhydrous DMSO. However, the addition of only small amounts of water to the DMSO solution of polysaccharide caused an immediate precipitation. (Found: N 6.41 %; CH_3CO 5.83 %. Calc.: N 6.53 %; CH_3CO 6.01 %.)

Deacetylation and methylation of the birch O-acetyl xylan phenylcarbamate. Deacetylation of the above product (14.4 g) was first accomplished by treating it at room tempera-

ture with a mixture of DMFA (250 ml) and 33 % aqueous sulphuric acid (15 ml) for 20 h. After isolation by precipitation in ethanol the treatment was repeated once.

The product was methylated with iodomethane (20 ml) and silver oxide (20 g) in DMFA (100 ml), the reaction time in all methylations being 35—45 h. After trial experiments which involved some loss of material (yield after the first methylation 9.0 g, OCH_3, 2.30 %), the following procedure was adopted for the isolation of the methylated product: The solids in the methylation mixture were centrifuged and washed with DMFA. The combined centrifugates were poured into ethanol (about 1.5 l) containing about 10 g of potassium cyanide in a small amount of water. The solution was allowed to stand for about 15 min with occasional stirring, after which the white, flocculent precipitate was collected on a glass filter, washed with ethanol and ether, and then dried. The yields produced by this procedure were 95—98 %.

The product was dissolved in DMFA (100 ml) and subjected to three additional methylations using half of the amounts of the reagents noted above. These treatments failed to raise the methoxyl content above 2.60 %, indicating that only about 40 % of the *O*-acetyl groups were removed at the deacetylation stage.

Complete deacetylation was effected by dissolving the material in tetrahydrofuran (280 ml) containing aqueous 33 % sulphuric acid (20 ml), the reaction being conducted at room temperature. This process was repeated twice, all treatments being followed by two methylation steps. The total time for these acid deacetylation treatments was about 5 days. Following the last methylation the product was dissolved in tetrahydrofuran, filtered, precipitated in ethyl ether, finally being obtained as a white powder (5.2 g), $[\alpha]_D^{20}$ −7° (*c*, 1.0 in DMFA). (Found: OCH_3 5.22 %; N 6.50 %. Calc.: OCH_3 5.0 — 5.8 %; N 6.1 — 6.4 %.)

Added in proof. It has later been shown that a material with better solubility properties is obtained by conversion of the phenylcarbamoyl into *N*-methyl-phenylcarbamoyl groups. Therefore, the best procedure for deacetylation of the *O*-acetyl glucuronoxylan phenylcarbamate involves an initial *N*-methylation of the phenylcarbamoyl groups with iodomethane and silver oxide. The product obtained is then deacetylated with sulphuric acid in moist tetrahydrofuran.

Reduction of the methylated xylan phenylcarbamoyl derivative. The above product (4.80 g) was placed in a 500 ml flask fitted with a condenser and dissolved in anhydrous tetrahydrofuran (200 ml). The addition of lithium aluminium hydride (300 mg) caused the solution to gelatinise. The gel dispersed by gentle warming on a steam bath. More lithium aluminium hydride (1.2 g) was added and the reaction mixture agitated with a magnetic stirrer; the gel dissolved gradually. The mixture was gently agitated overnight at room temperature and thereafter refluxed for 1 h to ensure complete reaction. After adding water the reaction mixture was neutralised with dilute phosphoric acid, this acid being used in order to convert the hydroxides into salts with low solubility in water. The reaction mixture was filtered, the solids washed with cold water and the combined filtrates were concentrated and added to ethanol. The precipitate thus formed was collected on a glass filter, washed with ethanol and ether and dried. Inorganic salts were removed by dissolving the product in cold water, filtering and precipitating it in ethanol: the process was repeated. It was finally obtained as a white powder, $[\alpha]_D^{20}$ −86° (*c*, 1.0 in water). Yield 1.64 g = 84 %. (Found: OCH_3 10.2 %; Calc.: OCH_3 11.7 — 12.3 %.)

Table 2. Fractionation of hydrolysed *O*-methyl glucoxylan.

Fract. No.	mmoles (total)	Sugars	% of fraction	mmoles
23—38	4.42	Xylose		
39—96	3.05	Xylose	4.8	0.15
		2-Methylxylose	30.5	0.93
		3-Methylxylose	62.0	1.89
		4-Methylglucose	2.7	0.08
Residue	0.48	2,3-Dimethylxylose		

Chromatographic analysis on paper impregnated with borate buffer showed that the hydrolysed sample contained D-xylose, 2-*O*-methyl-D-xylose, 3-*O*-methyl-D-xylose, 2,3-di-*O*-methyl-D-xylose and 4-*O*-methyl-D-glucose.

Hydrolysis and fractionation of the O-methyl glucoxylan. The polysaccharide (1.3 g) was hydrolysed in 0.5 N sulphuric acid at 100° overnight and then neutralised with barium carbonate. The salts were filtered and the hydrolysate concentrated to a small volume and added to the top of a carbon-Celite column (3.5 by 43 cm) and the components were eluted with 5 1 2 → 20 % aqueous ethanol, 30 ml fractions being collected. The column was finally washed with 50 % aqueous ethanol. Mixed fractions were resolved on thick filter paper impregnated with borate buffer. The fractionations are summarised in Table 2.

By resolving a sample of fracs. 39—96 on ordinary filter paper an estimate of the relative amounts of D-xylose, 4-*O*-methyl-D-glucose and 2-*O*-methyl-D-xylose + 3-*O*-methyl-D-xylose was possible. In a separate experiment the monomethylxyloses were isolated; after resolving the fraction by paper electrophoresis in borate buffer of pH 9.4 the relative amounts of 2-*O*-methyl-D-xylose and 3-*O*-methyl-D-xylose were estimated. The data in Table 2 were then calculated from the values obtained.

Characterisation of the components. 4-O-Methyl-D-glucose. This substance was chromatographically indistinguishable from an authentic specimen both on ordinary paper and on paper impregnated with borate buffer.

α-D-Xylose. The sugar had $[\alpha]_D^{20}$ +18° (*c*, 1.0 in water, final value) and m.p. and mixed m.p. 144—146°.

2-O-Methyl-β-D-xylose. The ether had $[\alpha]_D^{20}$ −21 → +34° (*c*, 1.0 in water) and m.p. and mixed m.p. 130—132°.

3-O-Methyl-α-D-xylose. The ether had m.p. and mixed m.p. 95—97°.

2,3-Di-O-methyl-D-xylose. The ether had $[\alpha]_D^{20}$ +23° (*c*, 0.6 in water). It was converted to its aniline derivative, m.p. and mixed m.p. 126—128°.

The author is indebted to Professor Bengt Lindberg for the many valuable discussions throughout this work and to Miss Anita Myhrman for skilful assistance.

REFERENCES

1. Hägglund, E., Lindberg, B. and McPherson, J. *Acta Chem. Scand.* **10** (1956) 1160.
2. Bouveng, H. O., Garegg, P. J. and Lindberg, B. *Acta Chem. Scand.* **14** (1960) 742.
3. Bouveng, H. O. *Acta Chem. Scand.* **15** (1961). 87.
4. Kuhn, R., Trischmann, H. and Löw, I. *Angew. Chem.* **67** (1955) 32.
5. Wachtmeister, C. A. *Acta Chem. Scand.* **5** (1951) 976.
6. Hirst, E. L., Hough, L. and Jones, J. K. N. *J. Chem. Soc.* **1949** 57.
7. Naegeli, C. and Tyabji, A. *Helv. Chim. Acta* **17** (1934) 931; **18** (1935) 142.
8. Gaylord, N. G. *Reduction with Complex Metal Hydrides*, Interscience, New York 1956, p. 544.
9. Timell, T. E. and Jahn, E. C. *Svensk Papperstidn.* **54** (1951) 831.

Received October 14, 1960.

ACTA CHEMICA SCANDINAVICA 15 (1961) 101–120

Studies on the Hydrolysis of Metal Ions

32. The Uranyl Ion, UO_2^{2+}, in Na_2SO_4 Medium

ALF PETERSON*

Department of Inorganic Chemistry, Royal Institute of Technology, Stockholm 70, Sweden

The hydrolysis of UO_2^{2+} has been studied in a 1.5 M (sodium)-sulfate medium at 25°C by electrometric titration using glass electrodes. The total uranium concentration ranged between 0.0003 and 0.04 M. Special studies were made on similar cells without uranyl or with uranyl at acidities giving neglible hydrolysis. The results make it reasonable to assume K ($HSO_4^- \rightleftharpoons H^+ + SO_4^{2-}$) $\approx$ 0.4 M and to neglect $Na^+ - SO_4^{2-}$ complexing. K ($Na^+ + SO_4^{2-} \rightleftharpoons NaSO_4^-$) is estimated to be $\leq$ 0.13 M^{-1}. The average number of sulfate groups bound per uranyl group was found to lie between 2 and 3 with a probable value of about 2.9. The sulfate groups of the uranyl sulfate complexes seem to have somewhat lower affinity for protons than the free sulfate ions.

The present data indicate the formation of "core + links" complexes of the general formula $UO_2((OH)_2UO_2)_n^{2+}$. "Direct analysis" indicates that at least the first four complexes, $(UO_2)_2(OH)_2^{2+}$, $(UO_2)_3(OH)_4^{2+}$, $(UO_2)_4(OH)_6^{2+}$, $(UO_2)_5(OH)_8^{2+}$, exist.

If only these are assumed to exist, the best values for the equilibrium constants k_n of the reaction, $(n+1)UO_2^{2+} + 2nH_2O \rightleftharpoons UO_2((OH)_2UO_2)_n^{2+} + 2n\,H^+$, are $\log k_1 = -8.17$, $\log k_2 = -16.20$, $\log k_3 = -24.51$ and $\log k_4 = -32.14$. The data were also well explained by theory "IIIc"[1], assuming an infinite series of complexes with $\log k_n = -(7.66n + \log n! + 0.52)$, thus $\log k_1 = -8.18$, $\log k_2 = -16.15$, $\log k_3 = -24.29$ and $\log k_4 = -32.56$.

Some years ago, the hydrolysis of the ion UO_2^{2+} in a perchlorate medium was studied by Ahrland *et al.*[2-3]. The hydrolysis products were found to be polynuclear and of a "core + links" type, $UO_2((OH)_2UO_2)_n^{2+}$. The data were best explained with an unlimited mechanism, assuming the formation of complexes with all integral values for n, "hypothesis III"[1]. With this approximation of the real mechanism, the equilibrium constant for the first reaction,

* Present address: Section for Chemical Engineering, AB Atomenergi, Stockholm 9, Sweden.

$UO_2^{2+} + 2H_2O + UO_2^{2+} \rightleftharpoons UO_2(OH)_2UO_2^{2+} + 2H^+$, was found to be $k_1 = 10^{-6.05 \pm 0.10}$ and for all following reactions, $UO_2((OH)_2UO_2)_n^{2+} + 2H_2O + UO_2^{2+} \rightleftharpoons UO_2((OH)_2UO_2)_{n+1}^{2+} + 2H^+$, the constants were $k = 10^{-6.35 \pm 0.1}$.

It was considered valuable to study the hydrolysis of UO_2^{2+} in other ionic media and for this investigation 1.5 M Na_2SO_4 was chosen.

SYMBOLS

In general, the symbols are those used in the previous papers of this series. $b = [UO_2^{2+}]$, concentration of free UO_2^{2+}; B = total concentration of U(VI); $c = [SO_4^{2-}]$; C = total concentration of sulfate (4); E = measured emf in mV (2); $E_0 = E + 59.16 \log h - E_j$ (2); E_j = liquid junction potential (2); $E' = E + 59.16 \log H$ (5); E_0', defined by (6); F, defined by (12); $g(u) = \Sigma\, k_n u^n$ (10), (9); $h = [H^+]$; H = total analytical excess concentration of hydrogen ions, assuming no hydrolysis (3); k_n = equilibrium constant for $(n+1)\ UO_2^{2+} + 2nH_2O \rightleftharpoons UO_2((OH)_2UO_2)_n^{2+} + 2nH^+$ (10); k, k_0 = constants in "hypothesis IIIc": $k_n = k_0 k^n\,(n!)^{-1}$ (17); K = dissociation constant of HSO_4^- (3); K_1 = complex formation constant of $MgSO_4$ (44); n = number of links per "core + links" complex; $\bar{n}$ = average number of links per complex (11); $\bar{n}_S$ = average number of sulfate groups bound per uranyl group (4); $u = h^{-2}b$ (9), (8b); $v_{1/2}$ = value of v for $y = 1/2$ (19); $w = k_1^{-1}k_2 u$ (15); $x = \log B - 2 \log h$ (7); $x_{1/2}$ = value of x for $y = 1/2$ (18); $y = Z/2$ (7); Z = average number of OH bound per UO_2^{2+} (1); $\alpha = k_1 k_2^{-2} k_3$ (13).

Concentrations and equilibrium constants are expressed in M (mole l^{-1}) as a rule, but in the text and headings the convenient unit mM is sometimes used.

As usual, all species may, in addition to the formula as written, contain a certain number of medium ions and solvent molecules.

METHOD OF MEASUREMENT

This study of the hydrolysis of uranium(VI) in sulfate solution was made as a series of potentiometric titrations at 25°C. All solutions were made 1.5 M in sulfate by the addition of sodium sulfate. This was done in order to make possible the use of concentrations instead of activities in the formulas for emf and equilibrium constants.

In each titration, the total uranyl concentration, B, was kept constant while H, the analytical concentration of H^+, was varied. The free concentration of H^+, h, was measured with a glass electrode. The average number of hydroxyl groups bound per uranyl group, Z, was calculated from

$$Z = (h + [HSO_4^-] - H)/B \qquad (1)$$

The data could then be plotted in the form $Z(\log h)_B$.

The cell used was

— glass electrode | solution S | SE +

SE, the reference electrode, was

SE = Ag, AgCl | 10 mM Ag_2SO_4, 1 490 mM Na_2SO_4 | 1 500 mM Na_2SO_4

Solution S had the composition

S = B mM UO_2SO_4, $H/2$ mM H_2SO_4, (1 500 — B — $H/2$) mM Na_2SO_4

For the cell used, the measured emf may be written

$$E = E_0 - 59.16 \log h + E_j \quad (2)$$

From the definitions it follows:

$$h[SO_4^{2-}] = K[HSO_4^-]; \; H = h + [HSO_4^-] - BZ \quad (3)$$

and

$$C = [SO_4^{2-}] + [HSO_4^-] + \bar{n}_S B \quad (4)$$

We will introduce the quantity E' defined by

$$E' = E + 59.16 \log H \quad (5)$$

In the Appendix, equations are treated which are identical with (1) — (5) except that BZ is neglected, so, in the final result (30), H should strictly speaking be replaced by $(H + BZ)$. Moreover, the limiting value for $[SO_4^{2-}]$ at low acidities, c_0, is $(C - \bar{n}_S B)$ and not C. According to (30), for $H \ll C$, E' (H) approximates to a straight line which (for H, or rather $H + BZ$, $\rightarrow 0$) extrapolates to

$$E_0' = E_0 + 59.16 \log [1 + (C - \bar{n}_S B) K^{-1}] \quad (6)$$

The experimental record, E' *versus* H for constant B, gave straight lines for intermediate concentrations where the hydrolysis was neglible (Fig. 9). These lines gave E_0' by extrapolation and, from this quantity, E_0 was calculated using eqn. (6). The values $K = 0.4$ M and $\bar{n}_S = 2.9$ were used (see Appendix). Since the hydrolysis of the uranyl ion took place at pH > 3, no correction in E for the liquid junction potential was needed.

Reagents and Analysis

Uranyl sulfate was prepared from an especially pure UO_3 sample obtained from AB Atomenergi, Stockholm. After ignition to U_3O_8 at 850°C, a weighed amount was dissolved in an equivalent amount of sulfuric acid by the aid of H_2O_2 (Merck p.a.). After boiling, the solution was diluted with water to an exactly known volume. The concentration of uranium was checked by ignition to U_3O_8 and the sulfate concentration was checked by passing a sample through a hydrogen-saturated cation exchanger and titrating with NaOH.

Sodium sulfate. The p.a. quality of Merck was recrystallized from water several times and dried in an oven to constant weight.

Sulfuric acid solutions were prepared from the p.a. quality of Merck and standardized against standard NaOH.

Sodium hydroxide. A 50 % solution was prepared from the E.K.A. product. Dilute solutions were prepared from water or sodium sulfate solutions and 50 % NaOH, filtered through a Jena G 4 filter. The alkaline solutions were standardized against recrystallized hydrazine sulfate (Merck p.a.).

Silver sulfate solution was prepared from the p.a. quality of Baker without purification.

Water. Deaerated distilled water was always used.

Apparatus

The apparatus was of the type generally used for studying hydrolysis mechanisms in this institute [4].

Two glass electrodes were used, one Radiometer G 102 BK and one Jena 9006 gaf. The silver-silver chloride electrode was prepared according to Brown [5].

A valve potentiometer, Radiometer PHM 3 ik, was used for the emf measurements and the emf values were read to 0.1 mV.

Agitation in the titration vessel was arranged by bubbling nitrogen gas through the solution, and, in addition, swirling after each addition from the burets. The nitrogen was purified by washing with 10 % NaOH and 10 % H_2SO_4. Before entering the titration vessel, the gas was saturated with water by passing it through two wash bottles containing 1.5 M sodium sulfate.

Procedure

The measurements were made in a room thermostated to 25 ± 1°C with the cell in an oil thermostat set at 25.0 ± 0.1°C.

The procedure may be best described by giving, as an example, one of the titrations with B = 40 mM.

The following solutions were used

A = 40 mM UO_2SO_4, 1 460 mM Na_2SO_4
B = 40 mM UO_2SO_4, 75 mM H_2SO_4, 1 385 mM Na_2SO_4
C = 80 mM UO_2SO_4, 1 420 mM Na_2SO_4
D = 188.3 mM NaOH, 1 500 mM Na_2SO_4

At the start of the titration, 50 ml of A and 5 ml of B were put into the titration vessel. Equal amounts of C and D were added from burets at intervals and the emfs were record-

Table 1. A titration with B = 40 mM

$$E_0 = 108.1 - 59.16 \log\left(1 + \frac{1.5 - 0.04 \times 2.9)}{0.4}\right) = 69.7 \text{ mV}$$

v_A ml	v_B ml	v_C ml	v_D ml	H M × 10^3	E mV	E' mV	$-\log h$	h M × 10^3	Z
50.00	5.00			13.64	218.4	108.0			
		2.00	2.00	6.34	238.2	108.1	2.848	1.42	0.000
		3.00	3.00	3.05	255.9		3.147	0.713	0.003
		4.01	4.00	−0.081	287.7		3.684	0.207	0.025
		6.01	6.00	−5.683	320.1		4.232	0.059	0.149
		8.00	8.00	−10.65	329.7		4.394	0.040	0.271
		11.00	11.00	−17.16	337.8		4.531	0.029	0.432
		13.00	13.00	−20.96	341.8		4.599	0.025	0.527
		15.00	15.00	−24.41	345.3		4.658	0.022	0.613
		18.00	18.00	−29.00	349.8		4.734	0.018	0.727
		21.00	21.00	−33.03	353.8		4.802	0.016	0.828
		24.00	24.00	−36.59	357.5		4.864	0.014	0.916
		29.02	29.00	−41.72	363.5		4.966	0.011	1.044
		34.00	34.00	−45.95	369.3		5.064	0.009	1.150
	15.00			−31.22	351.9		4.770	0.017	0.783
	30.00			−12.85	332.7		4.445	0.036	0.325
	42.60			−0.076	288.2		3.693	0.203	0.025
	55.00			10.68	224.7	108.1	2.620	2.40	0.000
	90.00			34.13	194.7	107.9			

Table 2. Data Z (log h) at various total concentrations of uranyl ion, B.

B = 0.040 M. Z, −log h: (R) 0.000, 2.620 (b); 0.000, 2.848; 0.003, 3.147; 0.025, 3.684; 0.025, 3.693 (b); 0.149, 4.232; 0.271, 4.394; 0.325, 4.445 (b); 0.432, 4.531; 0.527, 4.599; 0.613, 4.658; 0.727, 4.734; 0.783, 4.770 (b); 0.828, 4.802; 0.916, 4.864; 1.044, 4.966; 1.150, 5.064 — (J) 0.024, 3.657; 0.180, 4.279; 0.328, 4.445; 0.518, 4.594; 0.674, 4.700; 0.807, 4.788; 0.920, 4.869; 1.047, 4.971; 1.177, 5.092; 1.284, 5.211; 1.373, 5.333; 1.448, 5.459.

B = 0.020 M. Z, −log h: (R) 0.000, 2.920; 0.003, 3.233; 0.030, 3.950; 0.083, 4.247; 0.143, 4.391; 0.262, 4.545; 0.376, 4.646; 0.688, 4.856; 0.875, 4.981; 1.040, 5.114; 1.194, 5.258; 1.268, 5.339; 1.339, 5.432 — (J) 0.027, 3.913; 0.353, 4.623; 0.652, 4.829; 0.913, 5.008; 1.142, 5.198; 1.345, 5.434.

B = 0.010 M. Z, −log h: (R) −0.002, 2.909; 0.028, 4.180; 0.039, 4.265; 0.086, 4.447; 0.205, 4.649; 0.376, 4.802; 0.542, 4.916; 0.704, 5.022; 0.859, 5.127; 1.007, 5.237; 1.151, 5.364; 1.290, 5.516; 1.358, 5.605; 1.425, 5.708 — (J) 0.031, 4.150; 0.124, 4.517; 0.229, 4.667; 0.368, 4.791; 0.504, 4.887; 0.636, 4.973; 0.764, 5.058; 0.889, 5.142; 1.010, 5.235; 1.157, 5.367; 1.298, 5.524; 1.438, 5.729.

B = 0.005 M. Z, −log h: (R) −0.006, 3.511; −0.006, 3.869; 0.061, 4.537; 0.372, 4.948; 0.683, 5.156; 0.986, 5.362; 1.278, 5.643 — (J) 0.037, 4.363; 0.139, 4.696; 0.256, 4.846; 0.363, 4.938; 0.471, 5.014; 0.676, 5.147; 0.867, 5.274; 1.049, 5.409; 1.214, 5.560 — (J) 0.039, 4.375; 0.166, 4.740; 0.308, 4.890; 0.449, 4.997; 0.590, 5.090; 0.729, 5.178; 0.866, 5.271; 1.001, 5.370; 1.134, 5.489; 1.265, 5.627; 1.394, 5.803.

B = 0.0025 M. Z, −log h: (R) −0.009, 3.800; 0.342, 5.081; 0.488, 5.184; 0.630, 5.276; 0.771, 5.367; 0.908, 5.460; 1.042, 5.565; 1.173, 5.685; 1.302, 5.828; 1.430, 6.008 — (J) 0.045, 4.625; 0.126, 4.848; 0.264, 5.015; 0.380, 5.110; 0.495, 5.186; 0.719, 5.328; 0.935, 5.477; 1.144, 5.651; 1.346, 5.877 — (J) 0.047, 4.588; 0.137, 4.857; 0.242, 4.985; 0.458, 5.157; 0.673, 5.294; 0.887, 5.433; 1.098, 5.595; 1.308, 5.813.

B = 0.00125 M. Z, −log h: (J) −0.001, 4.081 (b); 0.020, 4.513 (b); 0.059, 4.786; 0.085, 4.875 (b); 0.109, 4.938; 0.120, 4.960 (b); 0.159, 5.026 (b); 0.166, 5.039; 0.284, 5.169; 0.398, 5.261; 0.505, 5.333; 0.588, 5.384 (b); 0.607, 5.396; 0.704, 5.458; 0.881, 5.572; 1.041, 5.683 — (J) 0.059, 4.784; 0.202, 5.083; 0.365, 5.233; 0.529, 5.343; 0.693, 5.448; 0.846, 5.553; 1.015, 5.670; 1.174, 5.800; 1.330, 5.976; 1.485, 6.200.

B = 0.00063 M. Z, −log h: (J) 0.074, 4.968; 0.187, 5.203; 0.317, 5.337; 0.447, 5.433; 0.573, 5.518; 0.698, 5.596; 0.818, 5.672; 0.935, 5.744; 1.048, 5.829; 1.156, 5.922; 1.263, 6.032.

B = 0.00031 M. Z, −log h: (J) 0.093, 5.151; 0.180, 5.325; 0.338, 5.491; 0.504, 5.607; 0.722, 5.743; 0.937, 5.883; 1.148, 6.045; 1.353, 6.258.

(b) indicates backtitration data
(R) ((J)) the titration has been performed with the Radiometer (Jena) electrode.

ed. At the end of the titration, the hydrolysis was reversed by adding portions of B from a buret in order to make sure that the equilibria were completely reversible. The titration data will be found in Table 1.

In some instances, especially for the lower concentrations, only A, C, and D type solutions were used and E_0 was determined separately in a solution of known H value.

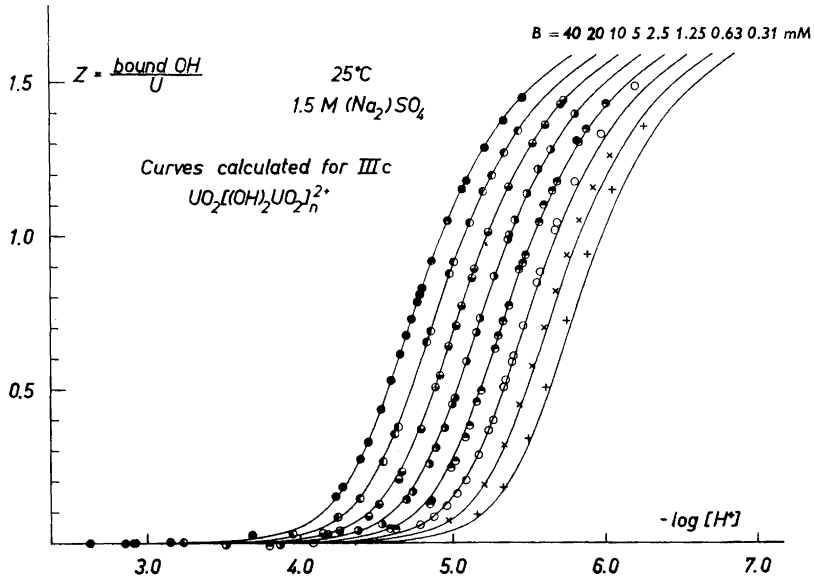

Fig. 1. Experimental data plotted as Z $(-\log h)_B$. Curves calculated assuming "mechanism IIIc" ($k_0 = 0.30$, $\log k = -7.66$).

DATA AND RESULTS

Formula of the complexes

The data were first calculated* (Tab. 2) and plotted in the form $Z(\log h)_B$, see Fig. 1. The curves for different values of B do not coincide but are nearly parallel with a nearly constant spacing of 0.15 log h units. Since the concentrations have a constant ratio of 2, $\Delta \log B = 0.30$ and thus $(\Delta \log B / \Delta \log h)_Z = 2$, which implies that polynuclear species of the formula $UO_2((OH)_2UO_2)_n^{2+}$ are formed in the hydrolysis process [6]. The data were therefore plotted in a diagram with

$$y = Z/2;\ x = \log B - 2 \log h \qquad (7)$$

From Fig. 2, it is seen that the points fall on practically the same curve (however there are systematic but small divergences for B values of 1.25 mM and lower). One can thus conclude that the main hydrolysis products are polynuclear with the formula given above.

The next step is to deduce which complexes occur and the equilibrium constants for the formation of these complexes.

* As seen, *e.g.* from the data in Table 1 and eqn. (6), the value for E_0 depends on the value assumed for K. A reasonable shift of K will, however, only shift the log h scale by a constant, and not affect the Z values. The conclusions on the species found will thus not be affected, though the equilibrium constants will be shifted, as given by eqns. (21) and (22).

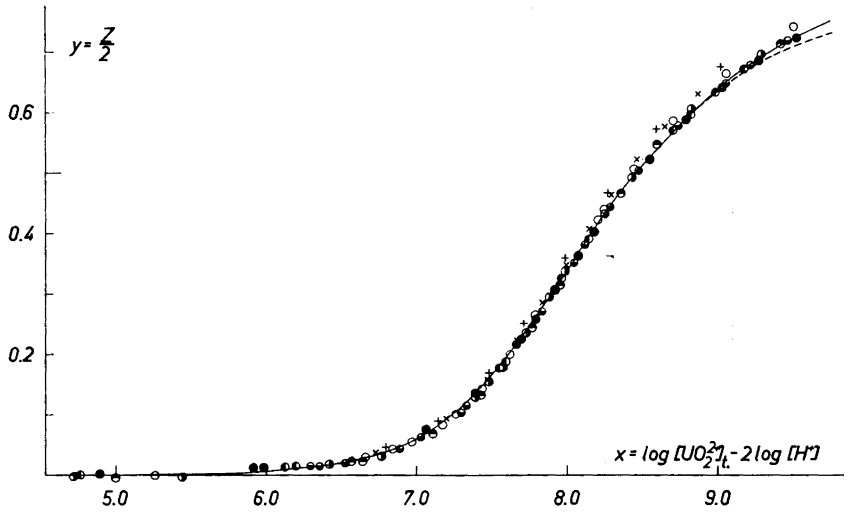

Fig. 2. Experimental data plotted as $y(x)$. Full drawn curve calculated assuming "mechanism IIIc" ($k_0 = 0.30$, $\log k = -7.66$). Broken curve calculated assuming the existence of only the first four complexes ($\log k_1 = -8.17$; $\log k_2 = -16.20$; $\log k_3 = -24.51$; $\log k_4 = -32.14$).

Direct analysis of the $y(x)$ curve

A smooth curve was drawn through the data $y(x)$ with no weight given to the points for $B = 1.25$ mM and lower.

The analysis of this curve was performed according to AB II [1]. The function $g(u)$ is calculated from the data by means of the following equations

$$\log (1 + g) = \int_{-\infty}^{x} y \, dx + \log (1 - y) + y \log e \tag{8a}$$

$$\log u = x - y \log e - \int_{-\infty}^{x} y \, dx \tag{8b}$$

The variables u and g are

$$u = bh^{-2} = [UO_2^{2+}]h^{-2} \tag{9}$$

$$g = \Sigma k_n u^n = k_1 u + k_2 u^2 + \ldots \tag{10}$$

Thus, $g(u)$ is a power series, the coefficients of which are equilibrium constants k_n for the formation of the complexes.

From the $g(u)$ data, we can calculate the average number of links per complex

$$\bar{n} = \frac{d \log g}{d \log u} = \frac{y}{1 - y - F^{-1}} \tag{11}$$

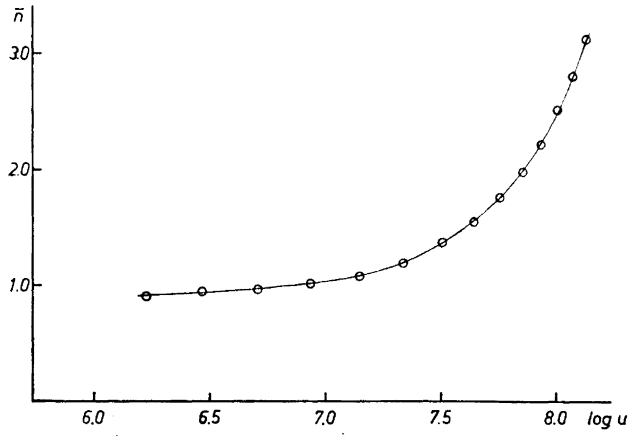

Fig. 3. $\bar{n}$ (eqn. 11) as a function of log u.

where

$$\log F = y \log e + \int_{-\infty}^{x} y \, dx \tag{12}$$

From Fig. 3 where $\bar{n}$ (log u) is plotted, $\bar{n}$ is seen to start at about 1.0 and rise uniformly to a value of 3.1 for the highest log u value. This would imply that complexes with more than three "links" are formed.

Neglecting, for the moment, this result and assuming that only the first three complexes exist, we may write

$$gu^{-1}k_1^{-1} = 1 + k_2k_1^{-1}u + k_3k_1^{-1}u^2 = 1 + w + a\,w^2 \tag{13}$$

$$\log (1 + w + aw^2) = \log gu^{-1} - \log k_1 \tag{14}$$

$$\log w = \log u + \log k_2 - \log k_1 \tag{15}$$

A family of normalized curves, log $(1 + w + aw^2)$ *versus* log w, was compared with the experimental curve, log gu^{-1} *versus* log u, and an attempt was made to fit them together. An acceptable fit was obtained for low values of g; at the highest g values, there were deviations so that the existence of at least a fourth complex had to be considered.

From the position of best fitting, it was estimated that log $k_1 = -8.17 \pm 0.01$ and log $k_2 = -16.20 \pm 0.05$.

Rewriting eqn. (10) and assuming the existence of four complexes, we obtain

$$(gu^{-1} - k_1 - k_2u)\, u^{-2} = k_3 + k_4u \tag{16}$$

A family of curves, $(gu^{-1} - k_1 - k_2u)u^{-2}$ *versus* u, was calculated for various sets of values for k_1 and k_2. The best straight lines were obtained with the two sets given in Fig. 4. From the intercepts and slopes of the lines, it is possible to obtain k_3 and k_4.

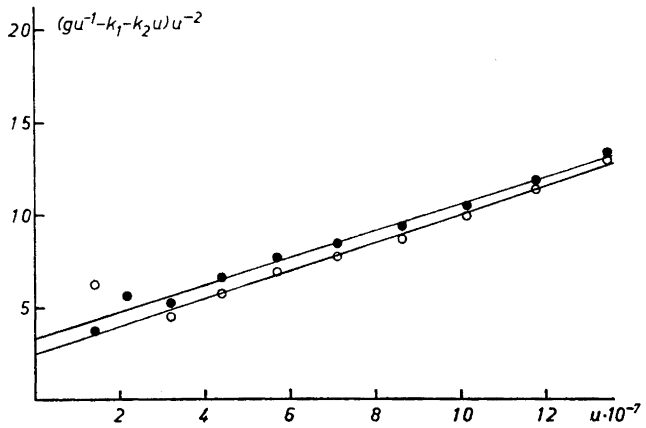

Fig. 4. $(gu^{-1} - k_1 - k_2u)u^{-2}$ (eqn. 16) as a function of u. Dots calculated from experimental values assuming log $k_1 = -8.17$, log $k_2 = -16.22$. Open circles calculated from the same experimental values assuming log $k_1 = -8.18$; log $k_2 = -16.17$).

By means of this direct analysis of the curve $y(x)$, an acceptable fit can be obtained with log $k_1 = -8.17 \pm 0.01$, log $k_2 = -16.20 \pm 0.03$, log $k_3 = -24.51 \pm 0.09$ and log $k_4 = -32.14 \pm 0.02$.

Testing of simple mechanisms

The $y(x)$ curve was independently compared with curves calculated for various simple mechanisms discussed in AB II (hypotheses II, III a, b, and c). A good fit was obtained with only one of them, namely hypothesis III c. In this hypothesis, it is assumed that complexes with all values of n are formed and that the equilibrium constant, k_n, is given by

$$k_n = k_0 k^n (n!)^{-1} \tag{17}$$

which means that the formation of higher complexes becomes increasingly difficult.

k_0 may be obtained from the comparison discussed above and k from the following equation

$$\log k = \log 2 + k_0 v_{1/2}^2 e^{v_{1/2}} - x_{1/2} \tag{18}$$

where $v_{1/2}$ is taken from the equation

$$e^{v_{1/2}} (v_{1/2} - 1) = k_0^{-1} \tag{19}$$

and $x_{1/2}$ is the value of x for $y = 1/2$.

As k_0 was seen to be about 0.3, k_0 values of 0.29, 0.30 and 0.31 were tried and gu^{-1} was calculated from

$$gu^{-1} = k_0 u^{-1} (e^{ku} - 1) \tag{20}$$

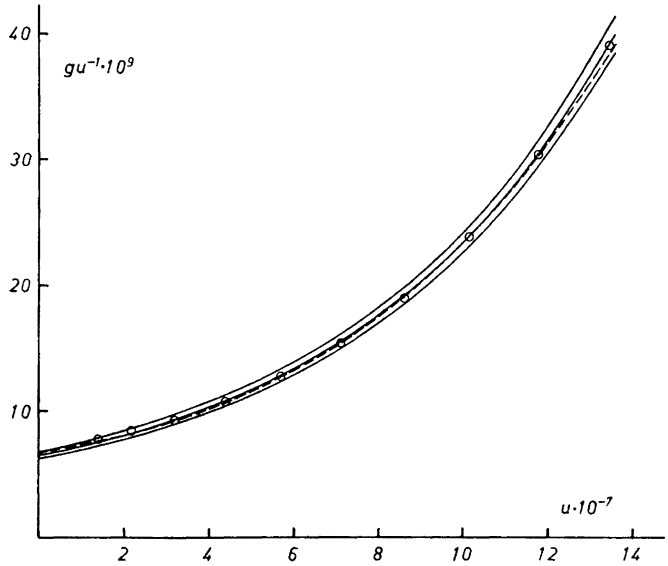

Fig. 5. gu^{-1} (eqn. 20) as a function of u. Solid lines calculated with "IIIc", log k = -7.66 and k_0 = 0.31 (upper), 0.30 (middle) and 0.29 (lower line). Broken curve calculated with only four complexes, constants like in Fig. 2.

and plotted against u. From the comparison in Fig. 5 with experimental points, it is seen that $k_0 = 0.30$ gives the best fit.

With log $k = -7.66 \pm 0.01$, log $k_0 = -0.52 \pm 0.01$ and log $k_n = -(7.66\,n + \log n! + 0.52)$, the following constants were calculated for the "IIIc" approximation. Log $k_1 = -8.18$, log $k_2 = -16.15$, log $k_3 = -24.29$, log $k_4 = -32.56$. If "IIIc" was the real mechanism, the mean deviations would be $\pm\ 0.01(n + 1)$.

The $y(x)$ curves calculated from III c and from direct analysis are given in Fig. 2 and are seen to practically coincide except for the highest x values. Here, the experimental determinations favor hypothesis III c or a limited series with more than four complexes.

If in the future, a more reliable value K' for K is found, it will be quite easy to calculate better values k_n' for the constants k_n. From (3), (4) and the equation

$$k_n = \frac{[UO_2((OH)_2UO_2)_n^{2+}]\,[H^+]^{2n}}{[UO_2^{2+}]^{n+1}} \tag{21}$$

we get

$$\log k_n' = \log k_n + 2n \log \left(\frac{K'(C + K - \bar{n}_S B)}{K\,(C + K' - \bar{n}_S B)}\right) \tag{22}$$

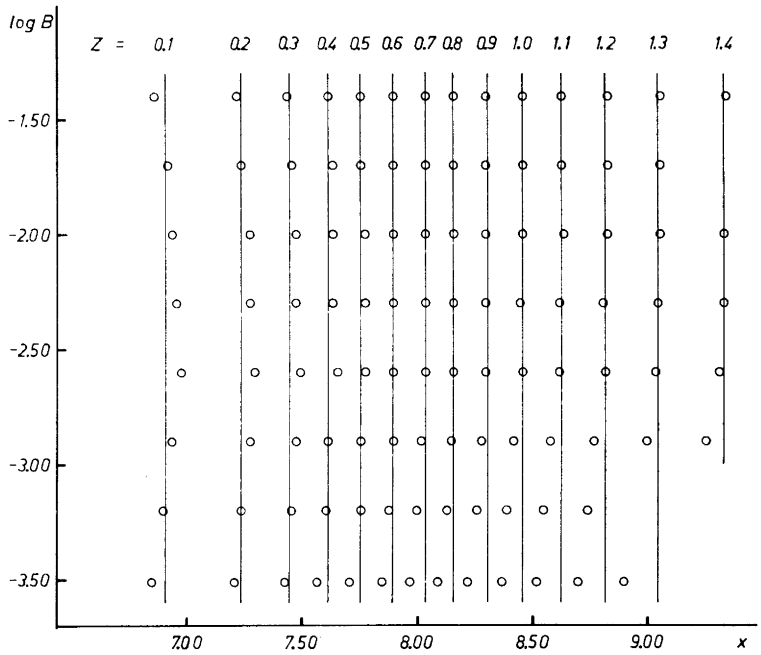

Fig. 6. log B as a function of x for Z values 0.1 to 1.4. Circles: experimental points. The lines are calculated assuming "mechanism IIIc" ($k_0 = 0.30$, log $k = -7.66$).

where the correction term $\bar{n}_S B$ is of minor importance. When B varies from 0 to 0.04 M, the change in log k_4 is only 0.01.

Deviations from the "core + links" mechanism

In Fig. 6, the experimental results are plotted as log $B(x)_Z$. It is seen that there are systematic deviations from the "core + links" curve. These deviations may be explained in several ways:

a) It was assumed that besides the main complexes, $UO_2((OH)_2UO_2)_n^{2+}$, there is also present the mononuclear species UO_2OH^+ or the dinuclear complex $(UO_2)_2OH^{3+}$. These assumptions were tested with methods outlined in AB IV[7] but none of them could explain the deviations nor could a combination of the assumptions be satisfactorily applied. As indicated by the recent work of Hietanen and Dunsmore, there may also be larger complexes containing more OH than the "core + links" formulas.

b) One may suspect the uncertainty in K (the dissociation constant of HSO_4^-) to be responsible for the deviations. However, a change in the value of K within the possible limits merely moves the $Z(\log h)_B$ curves along the (—log h) axis without changing the form of the curves or the spacing between them.

c) A third possible explanation is the presence of impurities in the sodium sulfate. In the preliminary titrations, the p.a. product of Merck was used without purification. It was not possible, however, to get stable potentials in titrations with the lower uranium concentrations, thus indicating slow hydrolysis and precipitation reactions. After several recrystallisations, stable and reversible potentials were obtained for even the lowest uranium concentrations. However, the titration curves (Fig. 1) for the lower concentrations ($\leq$ 2.5 mM) moved to the right the more purified the sodium sulfate became, *i.e.* the deviations became smaller. Thus, the deviations from the "core + links" mechanism may partly be attributable to the presence of impurities still left in the sodium sulfate. The question must, however, be left open for the time being.

Supersaturation of the solutions

The titrations were in general continued until the potentials became unstable, indicating that precipitation had started. This happened when Z had reached values around 1.4. However, precipitation did occur at much lower Z values if the solutions were left overnight. This means that a great number of the measurements have probably been made in supersaturated solutions. However, as pointed out by Biedermann and Schindler [8], a true picture of the hydrolysis equilibria in the clear solution will still be obtained provided the rate of precipitation is negligible compared with that of the hydrolysis.

COMMENTS

The data obtained in this investigation indicate that the hydrolysis of the uranyl ion in a sulfate medium gives the same type of products, $UO_2((OH)_2UO_2)_n^{2+}$, as in a perchlorate medium. The range of hydrolysis, however, lies about one pH unit higher for the sulfate medium. This is explained by the rather strong complex formation between uranyl and sulfate ions ($\bar{n}_S = 2.9$) in 1.5 M sodium sulfate.

It is interesting to note that probably all basic uranyl sulfates described in literature can be written as containing groups $UO_2((OH)_2UO_2)_n^{2+}$, *e.g.*

Zippeite [9]	$UO_2((OH)_2UO_2)_1SO_4 \cdot 4H_2O$
Synthetic compound [10]	$UO_2((OH)_2UO_2)_2SO_4$
"	$UO_2((OH)_2UO_2)_3SO_4 \cdot 4H_2O$
Johannite [9]	$CuUO_2((OH)_2UO_2)_1(SO_4)_2 \cdot 6H_2O$
Uranopilite [9]	$UO_2((OH)_2UO_2)_5SO_4 \cdot 12H_2O$

In addition, there seems to be evidence for the existence of the compound $(NH_4)_6UO_2((OH)_2UO_2)_7(SO_4)_4$ [11].

APPENDIX

Liquid junction potential and sulfate complexing

General equations. For the cell
— glass electrode | H M H^+, B M UO_2^{2+}, $(2C—H—2B)$ M Na^+, C M SO_4^{2-} |
or Pt, H_2
| C M Na_2SO_4 | 0.02 M Ag^+, $(2C - 0.02)$M Na^+, C M SO_4^{2-} | AgCl, Ag^+ we may write

$$E = E_0 - RTF^{-1} \ln h + E_j \tag{23}$$

Introducing

$$E' = E + RTF^{-1} \ln H \tag{24}$$

we get

$$E' = E_0 + RTF^{-1} \ln (Hh^{-1}) + E_j \tag{25}$$

We shall first consider cells where $B = 0$, thus no uranyl is present.
Combining

$$h [SO_4^{2-}] = K [HSO_4^-] \tag{26}$$

and

$$H = h + [HSO_4^-] \tag{27}$$

we get

$$E' = E_0 + RTF^{-1} \ln (1 + K^{-1} c) + E_j \tag{28}$$

where

$$c = [SO_4^{2-}] \tag{29}$$

For values of H which are not too large, we may write (c_0 is the value for c when $H = 0$)

$$E' = E_0 + RTF^{-1} \ln(1 + c_0K^{-1}) + H(dE'/dH)_{H=0} \tag{30}$$

By differentiating (28) we find

$$(dE'/dH)_{H=0} = RTF^{-1} (K + c_0)^{-1} (dc/dH)_{H=0} + (dE_j/dH)_{H=0} \tag{31}$$

Na_2SO_4 medium; $Na^+ — SO_4^{2-}$ complexing neglected

Assuming $B = 0$ and no complex formation between Na^+ and SO_4^{2-} we have

$$c = C — [HSO_4^-] \tag{32}$$

Combining (26), (27) and (32) gives

$$c^2 + c(K + H — C) — KC = 0 \tag{33}$$

We differentiate with respect to the variables c and H which gives an expression for dc/dH. This is simplified for small H values where we may set $H \approx 0$ and $c \approx c_0 = C$

$$(dc/dH)_{H=0} = —C(C + K)^{-1} \tag{34}$$

E_j may be written according to Hendersons's formula

$$E_j = RTF^{-1}(D'' - D')(S'' - S')^{-1}\ln(S''/S') \tag{35}$$

where

$$D = (\Sigma c_i l_i)_{\text{cations}} - (\Sigma c_i l_i)_{\text{anions}} \tag{36}$$

$$S = (\Sigma c_i z_i l_i)_{\text{cations}} + (\Sigma c_i |z_i| l_i)_{\text{anions}} \tag{37}$$

c_i is the concentration of an ion, l_i its equivalent conductance and z_i its charge. Further, ′ indicates the solution which faces the positive pole of the cell and ″ the solution which faces the negative pole.

From (26), (27) and (32), we get

$$h = HK(C + K)^{-1} \tag{38}$$

By insertion of (36), (37), and (38) into (35) we get (39)

$$E_j = \frac{RT[K(l_H - l_{Na}) + C(l_{SO_4} - l_{HSO_4} - l_{Na})]}{F[K(l_H - l_{Na}) + C(l_{HSO_4} - 2l_{SO_4} - l_{Na})]}$$

$$\ln\left(1 + \frac{HK(l_H - l_{Na}) + HC(l_{HSO_4} - 2l_{SO_4} - l_{Na}}{2C(C + K)\Lambda_{Na_2SO_4}}\right)$$

Transforming the "ln" expression into a series and using only the first term and differentiating E_j with respect to H, we find

$$(dE_j/dH)_{H=0} = \frac{RT}{F}\frac{K(l_H - l_{Na}) + C(l_{SO_4} - l_{HSO_4} - l_{Na})}{2C(C + K)\Lambda_{Na_2SO_4}} \tag{40}$$

Insertion into (30) gives

$$E' = E_0 + RTF^{-1}\ln(1 + CK^{-1}) + H(dE'/dH)_{H=0} \tag{41}$$

where

$$(dE'/dH)_{H=0} =$$

$$= \frac{RT}{F(C + K)}\left(\frac{K(l_H - l_{Na}) + C(l_{SO_4} - l_{HSO_4} - l_{Na})}{2C\Lambda_{Na_2SO_4}} - \frac{C}{C + K}\right) \tag{42}$$

In Fig. 7, the experimental results $E'(H)$ of a number of titrations are given. As is expected from (42), a straight line is obtained (the lowest line in Fig. 7). From the slope, we find $dE'/dH = -7.7$ mV M^{-1} (see Fig. 11).

To determine K from the experimental data $E(H)$, values would have been required for l_H, l_{SO_4}, l_{HSO_4} and l_{Na} in 1.5 M Na_2SO_4 at 25°C. Such values are, however, not available with the required accuracy. If the rather vague estimates which can be made about them are put into (42), the result is that K is of the order of 0.1 — 0.5 M.

In Fig. 8, the values of Baes [12] and Young *et al.*[13] are given for K in H_2SO_4, NH_4HSO_4, $NaHSO_4$ and Na_2SO_4 at various concentrations and 25°C. These

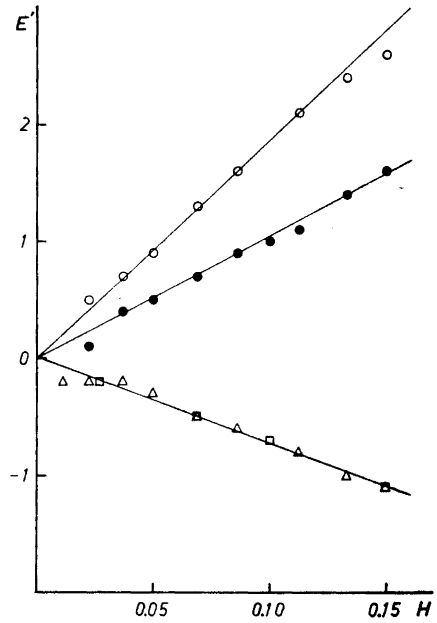

Fig. 7. E' (eqn. 24) as a function of H. Open circles: 1 M $MgSO_4$ (glass electrode). Dots: 1.5 M $MgSO_4$ (glass electrode). Triangles: 1.5 M Na_2SO_4 (glass electrode). Squares: 1.5 M Na_2SO_4 (hydrogen electrode).

values are based on Raman data. The diagram indicates that K is about 0.4 M in 1.5 M Na_2SO_4.

As will be shown below, applying (55) gives a maximum value, $K \leq 0.5$ M.

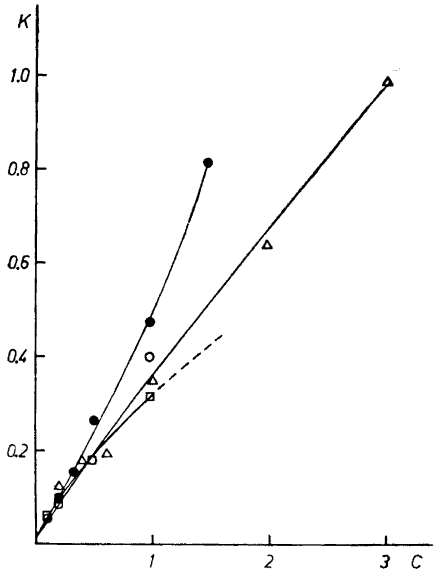

Fig. 8. Plot of K against C, sulfate concentration [12,13]. Dots: H_2SO_4. Open circles: $NaHSO_4$. Triangles: NH_4HSO_4. Squares: Na_2SO_4.

In conclusion, we can therefore state that $K \approx 0.4$ M in 1.5 M Na_2SO_4 at 25°C.

Inserting $K = 0.4$ M and $dE'/dH = -7.7$ mV^{-1} into (31) we obtain $dE_j/dH = 3.0$ mV M^{-1} and by the aid of (38) we find $dE_j/dh = 14$ mV M^{-1}, which is nearly the same values as for 3 M $NaClO_4$.

$MgSO_4$ medium; $Mg^{2+} - SO_4^{2-}$ complexing neglected

In Fig. 7, the data $E'(H)$ are given not only for 1.5 M Na_2SO_4 but also for 1 and 1.5 M $MgSO_4$. For all these solutions, we obtained approximately straight lines with the difference that dE'/dH is positive for $MgSO_4$ and negative for Na_2SO_4.

In the same way as for Na_2SO_4 an expression can be deduced for dE'/dH at low H-values.

$$(dE'/dH)_{H=0} =$$

$$= \frac{RT}{F(C+K)}\left(\frac{K(l_H - 0.5\, l_{Mg}) + C(l_{SO_4} - l_{HSO_4} - 0.5\, l_{Mg})}{2C\Lambda_{MgSO_4}} - \frac{C}{C+K}\right) \quad (43)$$

Some tentative calculations show that, in order to make dE'/dH positive with $MgSO_4$, either K must have a value several times greater than that for 1.5 M Na_2SO_4, which seems improbable, or some species must be assumed which we have neglected.

Complexes $MgSO_4$ ($NaSO_4^-$) in the media

Let us assume that magnesium and sulfate ions form a complex with each other. We can then no longer set $c_0 = C$ as was done in the derivation of (42) and (43).

In (31), which is still valid, the last term, $(dE_j/dH)_{H=0}$ is likely to be positive. We shall derive expressions for $(dc/dH)_{H=0}$, starting with $MgSO_4$, and then show how $(dE'/dH)_{H=0}$ can have opposite signs for $MgSO_4$ and Na_2SO_4.

We define the equilibrium constant K_1 as follows:

$$[MgSO_4] = [Mg^{2+}]\,[SO_4^{2-}]K_1 = [Mg^{2+}]cK_1 \quad (44)$$

We then have

$$[H^+]_{tot} + hK^{-1}(K + c) = H \quad (45)$$

$$[Mg^{2+}]_{tot} = [Mg^{2+}](1 + cK_1) = C - 0.5\,H \quad (46)$$

$$[SO_4^{2-}]_{tot} = c(1 + hK^{-1} + [Mg^{2+}]K_1) = C \quad (47)$$

Eliminating $[Mg^{2+}]$ and h, we get

$$c + Hc(K + c)^{-1} + cK_1(1 + cK_1)^{-1}(C - 0.5\,H) = C \quad (48)$$

We now differentiate with respect to the variables c and H which gives an expression for dc/dH. This is simplified for small H values where we may set $[Mg^{2+}] \approx c \approx c_0$ and (*cf.* 47) $C \approx c_0 + c_0^2K_1$ (49)

$$\left(\frac{dc}{dH}\right)_{H=0} = -c_0\frac{2 - K_1(K - c_0)}{2(K + c_0)(1 + 2c_0K_1)} \quad (50)$$

It is possible to eliminate c_0 from (50) using (49). The resulting equation, however, seems more complicated than (49) and (50) taken together.
In the case of Na_2SO_4, we get in the same way

$$(dc/dH)_{H=0} = -c_0 \frac{1 - KK_1}{(K + c_0)(1 + 2c_0K_1 + CK_1)} \quad (51)$$

where in this case K_1 is the formation constant of $NaSO_4^-$.

For 1.5 M Na_2SO_4, $dE'/dH = -7.7$ mV M^{-1}. By combining literature data for equivalent conductances and transference numbers, the following probable values of equivalent conductance have been estimated: $l_H = 230$, $l_{Na} = 14$, $l_{SO_4} = 24$ and $l_{HSO_4} = 14$. It is found from (40), by insertion of these values, that $(dE_j/dH)_{H=0}$ will be positive as long as $K > 0.03$. By changing the values above by 20 % and combining these values in the most unfavourable manner, it is further found that $(dE_j/dH)_{H=0}$ will be positive as long as $K > 0.14$. It thus seems quite plausible to assume $(dE_j/dH)_{H=0} \geq 0$. It then follows from (31) (with $K = 0.4$ M) that $K_1 < 0.13$ M^{-1} and $c_0 > 1.1$ M.

In the case of $MgSO_4$, it is seen from (50) that dc/dH will be positive if K_1 is sufficiently large. To make dE'/dH positive, it is not necessary that the first term in dE'/dH should be positive. It is sufficient that its absolute value is $< dE_j/dH$ since dE_j/dH is probably positive.

For dilute solutions ($C \to 0$) experimental values for K_1 are given in the literature [14]: for $MgSO_4$ $K_1 \approx 200$ M^{-1} and for $NaSO_4^-$ $K_1 \approx 5$ M^{-1}. For strong solutions no experimental values could be found, but an estimate can be made, using the similarity between simple 2—2-sulfates pointed out by Leden[16]. For $CdSO_4$ also, $K_1 \approx 200$ M^{-1} at extreme dilution but [16] in 3 M $NaClO_4$ it is ≈ 7 M^{-1}. It is then fair to assume that in 1.5 M sulfate media K_1 ($MgSO_4$) is of the order of ten whereas K_1 ($NaSO_4^-$) is much lower. The formation constant for $MgSO_4$, using the same E_j as for Na_2SO_4 and with eqns. (31) and (50), gives K_1 of the order of 100. This indicates that the complex formation is considerable; exactly for this reason the contribution from the liquid junction potential will probably be greater which will decrease the value for K_1. The order of ten seems quite reasonable.

The complex formation between uranyl and sulfate ions in 1.5 M Na_2SO_4

When uranyl ions are present in the solutions under non-hydrolyzing conditions and $\bar{n}_S$ is the average number of sulfate groups bound per uranyl group, we have

$$c = C - \bar{n}_S B - [HSO_4^-] - [NaSO_4^-] \quad (52)$$

Let us first neglect $[NaSO_4^-]$. Combining eqns. (25), (26), (27), and (52) we get

$$E' = E_0 + RTF^{-1} \ln(1 + (C - [HSO_4^-] - \bar{n}_S B)K^{-1}) + E_j. \quad (52\,a)$$

When $H \to 0$, $[HSO_4^-] \to 0$ and we obtain

$$E_0' = E_0 + RTF^{-1} \ln (1 + (C - \bar{n}_S B)K^{-1}) \quad (6)$$

We define

$$\Delta E = E'_{B=0,H=0} - E'_{B=B,H=0} \quad (53)$$

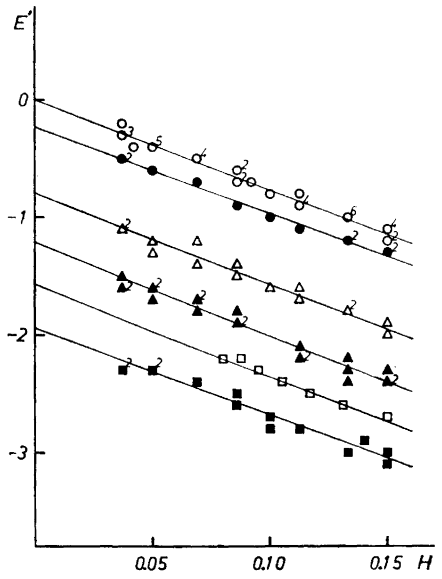

Fig. 9. E' as a function of H. Open circles: $B = 0$. Dots: $B = 5$ mM. Open triangles: $B = 20$ mM. Black triangles: $B = 30$ mM. Open squares: $B = 40$ mM. Black squares: $B = 50$ mM. The figures in the plot indicate the number of points with the same values.

The lines are calculated according to the method of least squares.

From (53) and (6), it follows that

$$\bar{n}_S = B^{-1}(K+C)(1-e^{-\Delta EF/RT}) \tag{54}$$

The experimental plot, $E'(H)$, gives straight lines for constant B, Fig. 9. By extrapolation to $H = 0$, we get E_0'.

From Fig. 10, it is seen that, for $B = 0$, we have

$$\bar{n}_S(C + K)^{-1} = 1.6 \pm 0.1 \tag{55}$$

which indicates that the value for $\bar{n}_S$ in 1.5 M Na_2SO_4 is ≈ 3.0 (with $K = 0.4$). Since no evidence has been found for complexes with more than three SO_4^{2-} per UO_2^{2+}, we may assume that $\bar{n}_S$ must have a value not greater than 3.0 and (55) then gives that $K \leq 0.5$ M in 1.5 M Na_2SO_4.

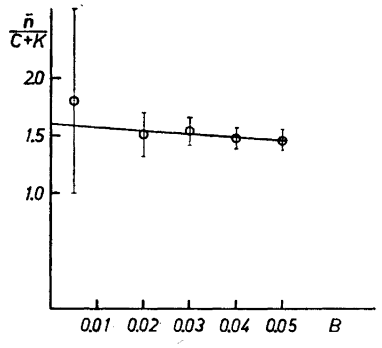

Fig. 10. $\bar{n}_S(C + K)^{-1}$ (eqn. 54) as a function of B.

If we assume the existence of $NaSO_4^-$, we get

$$\bar{n}_S = B^{-1}(K + c_0)(1 - e^{-\Delta EF/RT}) \quad (56)$$

$\bar{n}_S$ will thus become lower. For the probable maximum value of $K_1 = 0.13$ M^{-1} (see above), we have $c_0 \approx 1.1$ M which gives by inserting into (56) that $\bar{n}_S$ is between 2.3 and 2.6. Assuming a maximum value of 3.0 for $\bar{n}_S$ gives $K \leq 0.9$.

In conclusion, it may be stated that there are on an average between 2 and 3 sulfate groups bound per uranyl group in 1.5 M Na_2SO_4, with a probable value of nearly 3. It may be noted that a calculation of $\bar{n}_S$ by means of Ahrland's [15] values for 1 M $NaClO_4$ gives a value of 2.9.

The proton affinity of uranyl sulfate complexes

When protons are brought into solutions containing uranyl and sulfate ions, the protons can combine both with the free sulfate ions and with the sulfate groups in the uranyl sulfate complexes. In the following an attempt is made to determine the extent of the second mechanism.

The equilibrium constant for the dissociation of protons from the bisulfate groups formed with the uranyl sulfate complexes is supposed to be constant and is designed by L. We then have

$$C = c\,(1 + hK^{-1}) + \bar{n}_S B \quad (57)$$

$$H = h + hcK^{-1} + \bar{n}_S B \frac{h}{h + L} \quad (58)$$

Inserting eqn. (58) into

$$E' = E_0 + RTF^{-1}\ln(Hh^{-1}) + E_j \quad (25)$$

and differentiating we get

$$(dE'/dH)_{H=0} = RTF^{-1}(K + C - \bar{n}_S B + \bar{n}_S BKL^{-1})^{-1}(dc/dH)_{H=0} + (dE_j/dH)_{H=0} \quad (59)$$

By combining (57) and (58) we get after differentiating

$$(dc/dH)_{H=0} = -\frac{C - \bar{n}_S B}{C - \bar{n}_S B + K + \bar{n}_S BKL^{-1}} \quad (60)$$

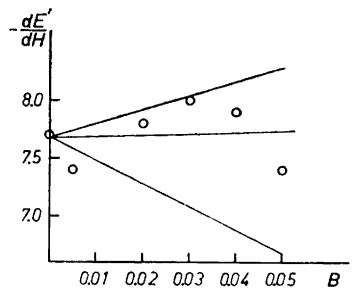

Fig. 11. $-dE'/dH$ (eqn. 61) as a function of B. Upper line: $L^{-1} = 0$. Lowest line: $L = K$.

Inserting this into (4) gives

$$(\mathrm{d}E'/\mathrm{d}H)_{H=0} = -RTF^{-1}\frac{C-\bar{n}B}{(C+K-\bar{n}_S B+\bar{n}_S BKL^{-1})^2} + (\mathrm{d}E_j/\mathrm{d}H)_{H=0} \qquad (61)$$

First we will assume that no protons combine with the sulfate groups linked to the uranyl ions, *i.e.*, $L^{-1} = 0$.

$$(\mathrm{d}E'/\mathrm{d}H)_{H=0} = -RTF^{-1}\frac{C-\bar{n}_S B}{(C+K-\bar{n}_S B)^2} + (\mathrm{d}E_j/\mathrm{d}H)_{H=0} \qquad (61\,a)$$

Inserting $C = 1.5$, $K = 0.4$ and $\bar{n}_S = 2.9$ we find that $(\mathrm{d}E'/\mathrm{d}H)_{H=0}$ will diminish with 0.6 mV M^{-1} when B rises from 0 to 0.05 M.

Second it will be assumed that $L = K$, *i.e.*, $KL^{-1} = 1$.

$$(\mathrm{d}E'/\mathrm{d}H)_{H=0} = -RTF^{-1}\left(\frac{C-\bar{n}_S B}{(C+K)^2}\right) + (\mathrm{d}E_j/\mathrm{d}H)_{H=0} \qquad (61\,b)$$

In this case the slope will rise with 1.0 mVM^{-1} when B rises from 0 to 0.05 M.

From the results given in Fig. 11 we can conclude that $0 < L^{-1} < K^{-1}$, *i.e.*, the protons probably do combine with the sulfate groups attached to the uranyl ions, but not as easily as with the free sulfate ions.

Acknowledgements. Thanks are due to professor Lars Gunnar Sillén for his support and inspiring criticism. The author is also very indebted to his Chief, Dr. Erik Svenke, who made it possible for him to do this work. Thanks are also due to Drs. George Biedermann, Sirkka Hietanen, Nils Ingri, and Åke Olin for many valuable discussions. This work is part of a program financially supported by *Statens råd för atomforskning (Swedish Atomic Research Council)* and *Statens Naturvetenskapliga Forskningsråd (Swedish Natural Science Research Council)*. The English in this manuscript has been revised by D. G. Gillam.

REFERENCES

1. Sillén, L. G. *Acta Chem. Scand.* **8** (1954) 318 (AB II).
2. Ahrland, S. *Acta Chem. Scand.* **3** (1949) 374.
3. Ahrland, S., Hietanen, S. and Sillén, L. G. *Acta Chem. Scand.* **8** (1954) 1907 (Part 10).
4. Forsling, W., Hietanen, S. and Sillén, L. G. *Acta Chem. Scand.* **6** (1952) 901 (Part 3).
5. Brown, A. S. *J. Am. Chem. Soc.* **56** (1934) 646.
6. Sillén, L. G. *Acta Chem. Scand.* **8** (1954) 299 (AB I).
7. Biedermann, G. and Sillén, L. G. *Acta Chem. Scand.* **10** (1956) 1011 (AB IV).
8. Biedermann, G. and Schindler, P. *Acta Chem. Scand.* **11** (1957) 731.
9. Strunz, H. *Mineralogische Tabellen*, 3. Aufl., Akademische Verlagsgesellschaft Geest und Portig K.-G., Leipzig 1957, p. 213.
10. *Gmelins Handbuch der Anorganischen Chemie*, System—Nr 55, 8. Aufl., Verlag Chemie, Berlin 1936, p. 156.
11. Peterson, A. *To be published.*
12. Baes, C. F., Jr. *J. Am. Chem. Soc.* **79** (1957) 5611.
13. Hamer, W. J. *The Structure of Electrolytic Solutions*, Wiley and Sons, New York 1959, p. 35.
14. Bjerrum, J., Schwarzenbach, G. and Sillén, L. G. *Stability Constants*, Part II, The Chemical Society, London 1958, p. 80.
15. Ahrland, S. *Acta Chem. Scand.* **5** (1951) 1151.
16. Leden, I. *Acta Chem. Scand.* **6** (1952) 971.

Received August 8, 1960.

ACTA CHEMICA SCANDINAVICA 15 (1961) 121–140

On the Accuracy of Heat of Combustion Data Obtained with a Precision Moving-Bomb Calorimetric Method for Organic Bromine Compounds

LARS BJELLERUP

Department of Organic Chemistry, University of Lund, Lund, Sweden

The purpose of the investigation has been to establish the accuracy of results obtainable with a recent high-precision moving-bomb method for measuring heats of combustion at 25°C of solid and liquid organic bromine compounds. The approach has been to compare, for five selected bromine compounds, heats of formation calculated from heat of combustion data obtained by the given method, with those derived from calorimetric data on heats of reactions other than combustion. The purification of samples of the following compounds is described: 1,2-dibromobutane, 1,2-dibromo*cyclo*hexane, 1-bromopropane, 2-bromopropane and 2-bromobutane. Data on density and refractive index for the spectral lines D, Hα and Hβ, at 20 and 25°C of the purified samples are given and compared with corresponding data from previous investigations. The following values, in kcal/mole, are reported for the heat of combustion, $-\Delta Hc°$, at 25°C, of the liquid sample in gaseous oxygen to form gaseous carbon dioxide, liquid water and liquid bromine, with reactants and products in their thermodynamic standard states: 1,2-dibromobutane 614.26 ± 0.52, 1,2-dibromo*cyclo*hexane 867.54 ± 0.60, 1-bromopropane 491.54 ± 0.34, 2-bromopropane 490.42 ± 0.42, 2-bromobutane 646.52 ± 0.30. Standard heats of formation at 25°C calculated from the heat of combustion data are compared with values calculated from reaction-calorimetric data on heats of addition of bromine (in three cases) and hydrogen bromide (in six cases) to unsaturated hydrocarbons, and from data on the heat of hydrogenation of 1-bromopropane to propane. In the first three cases the heat of formation values from combustion data were found to disagree with those from reaction-calorimetric data by as much as two to three kcal/mole, but in all other cases the values obtained from the two types of calorimetric data were virtually the same. The results of the comparison are discussed and it is concluded that the combustion calorimetric method for organic bromine compounds can give heats of combustion accurate within error limits of approximately 0.01 %.

Two previous papers [1,2] described a moving-bomb method for combustion calorimetry of organic bromine compounds and the method of reducing the observed heats of combustion to standard conditions. It was found that

results were of an immediate precision [3 (p. 430)] slightly better than 0.01 %. Although this precision was satisfactorily high, undetected systematic errors might render the accuracy [3] of obtained heat of combustion data much lower than this. It has been necessary, therefore, to determine the absolute accuracy of the method, and the results of the investigation are reported here.

METHOD

There are several possible ways of investigating the accuracy of the results obtainable by the application of a given method for the determination of the heats of combustion of organic compounds [4 (p. 216)]. One is to compare results of combustion experiments with other appropriate calorimetrically determined heats of reaction. Since the principal use for heat of combustion data is to derive corresponding heats of formation, the approach made here is to compare, for certain selected bromine compounds, heats of formation calculated both from heat of combustion data and from calorimetric data on heats of reactions other than combustion.

The selection of compounds for this comparison was governed by various considerations. One was that comparison should be based on heats of formation calculated from data obtained in as many different high-precision calorimetric investigations on heats of reaction as are available. Suitable investigations have already been reported on the heats of: (i) gas-phase addition of bromine to certain alkenes [6], (ii) liquid-phase addition of bromine to certain *cyclo*alkenes and alkenes [7], (iii) gas-phase addition of hydrogen bromide to *cyclo*propane and certain alkenes [8–10], and (iv) gas-phase reduction of 1-bromopropane to propane [11]. Secondly, since it was originally intended to apply the present bomb-calorimetric technique to some lower mono- and dibromoalkanes, it was clearly advantageous to choose the substances for comparison from this class of compounds. Accordingly, the following compounds were chosen: 1,2-dibromobutane, 1,2-dibromo*cyclo*hexane, 1-bromopropane, 2-bromopropane and 2-bromobutane. The purification of samples of these compounds and the determination of their heats of combustion is described in the following section.

HEAT OF COMBUSTION MEASUREMENTS

Apparatus and Procedure

Two different calorimetric systems, A and B, were used in the heat of combustion measurements. Calorimeter A has been described in detail in Ref.[1] and calorimeter B, which was an earlier model of calorimeter A, has been described briefly in Refs. [4,12] Calorimeter A was used for the measurements on the samples of 1,2-dibromobutane and 1,2-dibromo*cyclo*hexane and calorimeter B for 1-bromopropane and 2-bromobutane. Measurements on the 2-bromopropane sample were made with both calorimeters.

The experimental procedures used in experiments with calorimeters A and B have been described in Ref.[1] and Refs.[4,12], respectively. In both cases, volatile liquid combustion samples were sealed in soft-glass ampoules [13(p. 45)] and a baffle (top) [13(p. 48), 14(p. 145)] was used when required.

Possible systematic errors in results obtained with calorimeters A and B have been discussed in Ref.[1] and Refs.[15,16], respectively.

Materials

Benzoic acid. The benzoic acid samples used in the calibration experiments with calorimeters A and B were National Bureau of Standards standard sample 39g[17] and 39f[18], respectively.

Paraffin oil. The two paraffin oil samples used as auxiliary material in the combustion experiments with the bromine compounds were both redistilled mineral oils. The sample used in experiments with calorimeter A, Paraffin oil USBM-P3a, has been described previously [1(p. 1531)]. The sample used in experiments with calorimeter B, Paraffin oil L, was found to have a percentage composition corresponding to the empirical formula $CH_{1.97}$ and a density of 0.8838 g/ml at 20.00°C.

Bromine compounds. The bromine compound samples were all obtained by careful purification of commercial products except for the 1,2-dibromo*cyclo*hexane, the original sample of which was synthesized as described below. The various original samples were first treated chemically and then purified by successive fractional distillations at two or more different pressures. The all-glass, packed distilling column was equipped with controlled heating element jacket and a total condensation—variable takeoff head [19]. The material in the still pot was heated with a near infrared heat lamp, which gave a very smooth boiling even at rather low distillation pressures. The efficiency of the column, as determined with a carbon tetrachloride—benzene mixture [20], was found to be equivalent to 24 theoretical plates for total reflux at a distillation rate of about 6 ml/min. The progress of each distillation was followed by measuring the density of the successive fractions of the distillate. The density measurements were made with a standard Ostwald-Sprengel pycnometer to an accuracy estimated at ± 0.0001 g/ml. The fractionation was continued until more than 75 % of the distillate in a distillation was collected at a constant density, and until two distillations at different pressures gave distillates having the same density within the uncertainty of the density measurements. This last precaution precluded the presence of azeotropic mixtures. Details on the purification of the various samples follow.

1,2-Dibromobutane. A 500 g sample (Eastman Organic Chemicals) with the density $d_4^{20} = 1.7926$, $d_4^{25} = 1.7844$ was treated in order with conc. sulfuric acid, water, 10 % sodium carbonate solution and water, and was finally dried with calcium chloride. The product was purified by six successive fractional distillations at the following pressures: 100, 45, 20, 50, 20 and 25 mm. In the final distillation 80 % (77 g) of the distillate was collected over a density range of 0.0002 g/ml.

1,2-Dibromocyclohexane. This substance was prepared from *cyclo*hexene by the addition of bromine in carbon tetrachloride containing a little ethyl alcohol [21]. The product, 640 g, was treated with ethyl alcoholic potassium hydroxide *etc.*, as described in Note 7 of Ref.[21], and dried first with calcium chloride and then with phosphorus pentoxide. The dry sample was purified by successive fractionations at pressures 50, 20, 8, 7, and 20 mm. In the final distillation 80 % (82 g) of the distillate was collected over a density range of 0.0002 g/ml.

1-Bromopropane. A commercial sample (Columbia Organic Chemicals) was treated with phosphorus pentoxide. The resulting 168 g were purified by three successive fractional distillations at pressures 755, 360, and 755 mm, respectively. All the distillate (25 g) in the final distillation was, except for the first few grams, collected over a boiling temperature range of 0.02°C and a corresponding density range of 0.0003 g/ml.

2-Bromopropane. A commercial sample (Columbia Organic Chemicals) was treated in order with conc. hydrochloric acid, 10 % sodium bicarbonate solution and water. The product was dried with calcium chloride and with phosphorus pentoxide and the resulting 155 g were fractionated by successive distillations at pressures 740, 750, and 760 mm. In the final distillation 80 % (19 g) of the distillate was collected over a boiling range of 0.01°C corresponding to a density range of 0.0004 g/ml.

2-Bromobutane. A 100 g sample (Columbia Organic Chemicals) was purified by successive fractional distillations at 750 and 170 mm pressure, respectively. In the final distillation 75 % (39 g) of the distillate was collected over a density range of 0.0001 g/ml. This product was dried with calcium sulfate and subjected to simple distillation at 290 mm. The middle fraction from this distillation was used in the heat of combustion experiments.

Table 1. Comparison with earlier data of density and refractive index data for the samples prepared in the present investigation.

Compound and reference	Density g/ml		Refractive index					
			D		$H\alpha$		$H\beta$	
	20°	25°	20°	25°	20°	25°	20°	25°
1,2-Dibromobutane								
Present investigation	1.7954	1.7870	1.5149	1.5125	1.5113	1.5089	1.5238	1.5213
Dillon, Young and Lucas [23]	1.7951	1.7870	1.5150	1.5125				
1,2-Dibromo*cyclo*hexane								
Present investigation	1.7903	1.7833	1.5529	1.5506	1.5492	1.5469	1.5620	1.5598
Goering and Sims [24]		1.784		1.5507				
Winstein [25]		1.7826		1.5507				
1-Bromopropane								
Present investigation	1.3550	1.3465	1.4346	1.4320	1.4318	1.4292	1.4412	1.4385
Tschamler, Richter and Wettig [26]		1.3467	1.43419					
Skau and McCullough [27]		1.3455						
Timmermans and Martin [28]	1.35135	1.34305	1.43435	1.43175	1.43180	1.42920	1.44119	1.43854
2-Bromopropane								
Present investigation	1.3142	1.3055	1.4255	1.4226	1.4228	1.4200	1.4321	1.4293
Skau and McCullough [27]		1.3063						
Timmermans and Martin [29]	1.31389	1.30554	1.43562	1.42277	1.42286	1.42006	1.43230	1.42940
2-Bromobutane								
Present investigation	1.2607	1.2533	1.4370	1.4345	1.4342	1.4318	1.4435	1.4410
Skau and McCullough [27]		1.2530						
Timmermans and Delcourt[30]	1.26086	1.25365			1.43434	1.43204	1.44369	1.44124
Lucas, Dillon and Young [31]	1.2607	1.2534	1.4374					

Table 1 gives the results of density measurements, at 20 and 25°C, and refractive indices for the spectral lines D, $H\alpha$ and $H\beta$, at 20 and 25°C, of the samples used in the heat of combustion experiments. The densities were determined as described above and the refractive indices were measured with a calibrated Pulfrich refractometer, giving refractive index values within error limits of $\pm$ 0.0001. For comparison with earlier data on density and refractive index of highly purified samples of the various compounds, the results from certain selected (*cf.* Ref.[22]) previous investigations [23–31] are also listed in Table 1.

RESULTS

The results of the calibration experiments with benzoic acid are presented in Tables 2 and 3, those of the combustion experiments with the paraffin oils in Tables 4 and 5, and those with the various bromine compounds in Tables 6 and 7. The symbols have the same significance as in corresponding Tables of Ref.[1] The additional symbols denote:

Table 2. Results of calibration experiments on calorimeter A.

t_h = 25.0°C V(Bomb) = 0.2670 liter; m^i(Cont.) = 20.745 g; ε^i(Cont.) = 3.198 cal/deg

t_i = 24.1°C $V^i(H_2O$ tot.) = 0.810 ml; $-\Delta Ec/M$(Benzoic acid NBS 39g) = 6 317.83 ± 0.62 cal/g[a]

P^i(gas.) = 30.0 atm; m(Pt) = 8.528 g

$-\Delta Ec/M$(Fuse) = 3 971 ± 4 cal/g

m' g	m''' g	Δt deg	$-\Delta E(HNO_3)$ cal	$-\Delta E_{I.B.P.}/\Delta t$ cal/deg
0.80083	0.00551	0.87575	1.50	5 804.04
0.80130	0.00554	0.87649	0.60	5 801.64
0.80069	0.00548	0.87560	2.10	5 804.57
0.80132	0.00551	0.87608	0.65	5 804.41
0.80065	0.00564	0.87577	1.35	5 803.03
0.80141	0.00550	0.87610	0.45	5 804.66
0.80173	0.00568	0.87667	0.60	5 804.18
0.80149	0.00539	0.87659	0.35	5 801.38
			Mean	5 803.49
			Standard deviation of mean	± 0.47

ε°(Calor.) = 5 821.01 ± 0.47 cal/deg

[a] At 25°C under the actual bomb conditions.

ε^f(Cont.) the energy equivalent of the final contents of the bomb

$-\Delta E_{oxid.}(As_2O_3)$ the heat evolved per mole of the reaction $As_2O_3(aq) + O_2(g) \rightarrow As_2O_5(aq)$, *cf.* Refs.[1(p. 1525–26), 2(p. 621)].

m(glass) the mass of the glass ampoule containing the combustion sample.

It should be noted that, (i) the results listed in Tables 2, 4, and 6 were all obtained in experiments with calorimeter A and those in Tables 3, 5, and 7 in experiments with calorimeter B; (ii) the reference temperature, t_h, was 25.0°C in experiments with calorimeter A and 20.0°C in experiments with calorimeter B; and (iii) 0.810 ml of water was introduced into the bomb in the calibration as well as the combustion experiments on paraffin oil with calorimeter A, while in the corresponding experiments with calorimeter B 30 ml of arsenious oxide solution were placed in the bomb.

Calculation of results. The results of the calibration experiments given in Table 2 were calculated as described in Ref.[1] For the calibration experiments given in Table 3, however, this method of calculation had to be modified as follows. Firstly, since all experiments with calorimeter B were so arranged that $t_h = t_i$, eqn. 14 of Ref.[1] changed to:

$$\varepsilon^\circ(\text{Calor.}) = -\Delta E_{I.B.P.} / \Delta t + C_p(H_2O)m^i(\text{Cont.}) - \varepsilon^f(\text{Cont.}) \quad (1)$$

Secondly, the computation of the heat of combustion of the standard benzoic acid under the actual bomb conditions of the calibration experiments,

Table 3. Results of calibration experiments on calorimeter B.

t_h=20.0°C t_i=20.0°C P^i(gas.)= 30 atm	V(Bomb)=0.2750 liter V^i(soln.)=0.03001 liter C^i(soln.)=0.0625$_5$ mole As_2O_3/liter	m(Pt)=4.722 g; m^i(Cont.)=45.69 g $-\Delta Ec°/M$(Benzoic acid NBS 39f) =6 314.12 ± 0.62 cal/g at 20°C $-\Delta Ec°/M$(Fuse) = 3 971 ± 4 cal/g	ε^f(Cont.) = 32.17 cal/deg

m′ g	m‴ g	Δt deg	$-\Delta E(CO_2)$ cal	$-\Delta E(HNO_3)$ cal	$-\Delta E_\Sigma$ cal	$-\Delta E_{I.B.P.}/\Delta t$ cal/deg
0.73458	0.00491	0.99413	15.31	1.45	−1.91	4 704.01
0.73404	0.00469	0.99289	15.30	0.80	−1.91	4 704.90
0.73319	0.00494	0.99202	15.28	0.75	−1.91	4 704.55
0.73340	0.00420	0.99144	15.28	1.30	−1.91	4 706.24
0.73508	0.00503	0.99438	15.32	0.85	−1.91	4 705.88
0.73450	0.00497	0.99384	15.31	1.50	−1.91	4 705.16
					Mean	4 705.12
					Standard deviation of mean	± 0.34
					$\varepsilon°$(Calor.) = 4 718.62 ± 0.34 cal/deg	

$-\Delta Ec/M$(Benzoic acid), from the certified value under certificate conditions [18] could not be made using the factor given in the certificate [18] since the actual bomb conditions differred too radically from the certificate conditions. Therefore, eqn. 15 of Ref.[1] could not be used in its original form for computation of $-\Delta E_{I.B.P.}$. Instead the standard heat of combustion per gram of the benzoic acid sample, $-\Delta Ec°/M$(Benzoic acid), was calculated from the certificate value using the Washburn reduction as given in Ref.[2] For the individual cali-

Table 4. Results of combustion experiments on paraffin oil USBM-P3a.

Calorimeter A				
t_h = 25.0°C	V(Bomb) = 0.2670 liter	$\varepsilon°$(Calor.) = 5 821.01 ± 0.47 cal/deg	ε(Calor.) = 5 800.63 cal/deg	
t_i = 24.1°C	V^i(H_2O tot.) = 0.810 ml		ε^i(Cont.) = 3.21 cal/deg	
P^i(gas.) = 30.0 atm; m(Pt) = 8.528 g		$-\Delta Ec°/M$(Fuse) = 3 971 ± 4 cal/g		

m'' g	m''' g	Δt deg	$-\Delta E(CO_2)$ cal	$-\Delta E(HNO_3)$ cal	$-\Delta E_\Sigma$ cal	$-\Delta Ec°/M$ cal/g
0.44937	0.00529	0.85422	0.49	1.60	−1.07	10 978.9
0.45589	0.00534	0.86696	0.49	1.70	−1.07	10 983.5
0.45438	0.00596	0.86388	0.49	0.30	−1.07	10 978.2
0.45502	0.00592	0.86522	0.49	1.75	−1.07	10 977.1
0.45967	0.00598	0.87429	0.49	2.04	−1.07	10 979.4
0.45470	0.00526	0.86428	0.49	0.90	−1.07	10 980.4
					Mean	10 979.6
					Standard deviation of mean	± 0.9

Table 5. Results of combustion experiments on paraffin oil L.

Calorimeter B

t_h = 20.0°C V(Bomb) = 0.2750 liter $\varepsilon°$(Calor.) = 4 718.62 ± 0.34 cal/deg
t_i = 20.0°C V^i(soln.) = 0.03001 liter
P^i(gas.) = 30.0 atm C^i(soln.) = 0.0625$_5$ mole As_2O_3/liter $-\Delta Ec°/M$(Fuse) = 3 971 ± 4 cal/g

m'' g	m''' g	m(Pt) g	ε(Calor.) cal/deg	ε^f(Cont.) cal/deg	Δt deg	$-\Delta E(CO_2)$ cal	$-\Delta E(HNO_3)$ cal	$-\Delta E_\Sigma$ cal	$-\Delta Ec°/M$ cal/g
1.42465	0.00444	4.722	4 673.25	32.30	0.99644	11.26	1.20	0.08	10 970.9
1.42516	0.00497	4.722	4 673.25	32.30	0.99824	11.28	0.90	0.08	10.973.4
1.42491	0.00410	4.722	4 673.25	32.30	0.99709	11.26	1.45	0.08	10 974.1
1.42428	0.00468	7.002	4 670.97	32.37	0.99452	11.25	2.15	0.08	10 971.6
1.42474	0.00475	4.90	4 673.07	32.30	0.99711	11.26	2.10	0.08	10 970.5
								Mean	10 972.1
								Standard deviation of mean	± 0.7

bration experiments the quantities $-\Delta E(CO_2)$ and $-\Delta E_\Sigma$ were then computed, as given in Ref.[2], and finally the $-\Delta E_{I.B.P.}$ values were calculated from the following modification of eqn. 15 of Ref.[1]:

$$-\Delta E_{I.B.P.} = -m'\Delta Ec°/M(\text{Benzoic acid}) - m'''\Delta Ec°/M(\text{Fuse}) - \Delta E(CO_2) - -\Delta E(HNO_3) + \Delta E_\Sigma \quad (2)$$

The results of the combustion experiments listed in Tables 4—7 were calculated as given in Ref.[1] by use of the following main equations:

$$\varepsilon(\text{Calor.}) = \varepsilon°(\text{Calor.}) - C_P(H_2O)m^i(\text{Cont.}) \quad (3)$$

$$-\Delta E_{I.B.P.} = [\varepsilon(\text{Calor.}) + \varepsilon^i(\text{Cont.}) \text{ or } \varepsilon^f(\text{Cont.})]\Delta t \quad (4)$$

$$-\Delta Ec°/M = \frac{1}{m'}\{-\Delta E_{I.B.P.} - [-\Delta E(As) - \Delta E(Oil) - \Delta E(Fuse) - -\Delta E(CO_2) - \Delta E(HNO_3) - \Delta E(Au) - \Delta E(Pt)] - \Delta E(HBr) - \Delta E_\Sigma\} \quad (5)$$

The two last $-\Delta Ec°/M$ values given for 2-bromopropane in Table 7 were obtained by conversion from 25°C to 20°C of the two $-\Delta Ec°/M$ values given for 2-bromopropane in Table 6. In the calculations the following values were used for the heat capacity, $C_P°$, at 25°C of liquid 2-bromopropane, gaseous oxygen, gaseous carbon dioxide, liquid water and liquid bromine, respectively: 33 (estimated), 7.017 (Ref.[32]), 8.874 (Ref.[32]), 17.996 (Ref.[32]) and 17.00 (Ref.[33]) cal/deg mole.

Unit of energy. Auxiliary quantities. The results are given in terms of the defined thermochemical calorie equal to 4.1840 abs. joules. The $-\Delta Ec°/M$ values refer to the reaction represented by eqn. 6, in which all reactants and products are in their thermodynamic standard states [32] at the temperature t_h:

$$C_aH_bO_cBr_d(liq) + (a + b/4 - c/2)\,O_2(g) \rightarrow \rightarrow a\,CO_2(g) + b/2\,H_2O(liq) + d/2\,Br_2(liq) \quad (6)$$

Table 6. Results of combustion experiments on bromine compounds.

Calorimeter A

t_h = 25.0°C; t_i = 24.1°C; P^i(gas.) = 30.0 atm; V(Bomb) = 0.2670 liter; V^i(soln.) = 0.03005 liter; C^i(soln.) = 0.0628$_5$ mole As_2O_3/liter; $\varepsilon°$(Calor.) = 5 821.01 ± 0.47 cal/deg; $-\Delta Ec°/M$(Oil) = 10 979.6 ± 0.9 cal/g; $-\Delta Ec°/M$(Fuse) = 3 971 ± 4 cal/g; $-\Delta E_{oxid.}(As_2O_3) = (77.4 \pm 0.1) \times 10^3$ cal/mole

m' g	m'' g	m''' g	m(glass) g	ε(Calor.) cal/deg	ε^i(Cont.) cal/deg	Δt deg	$n^f(As_2O_5)$ mole	$-\Delta E(CO_2)$ cal	$-\Delta E(HNO_3)$ cal	$-\Delta E$(Au) cal	$-\Delta E$(Pt) cal	$-\Delta E$(HBr) cal	$-\Delta E\Sigma$ cal	$-\Delta Ec°/M$ cal/g
1,2-Dibromobutane														
m(Pt) = 17.996 g														
0.642508	0.256444	0.005881	0.0519	5 762.40	32.51	0.82059	0.001431	10.02	1.60	0.08	0.04	31.36	0.16	2 840.8
0.622896	0.293647	0.005703	0.0654	5 762.37	32.45	0.88110	0.001383	10.76	1.20	0.04	0.07	30.40	0.02	2 842.1
0.626494	0.299904	0.005083	0.0676	5 762.36	32.45	0.89452	0.001405	10.93	1.65	0.10	0.05	30.58	0.02	2 840.7
0.627561	0.299733	0.005228	0.0607	5 762.36	32.45	0.89433	0.001394	10.93	1.55	0.09	0.07	30.63	0.02	2 837.8
0.624233	0.296261	0.005153	0.0649	5 762.37	32.45	0.88572	0.001400	10.83	0.75	0.08	0.04	30.47	0.02	2 835.0
0.606059	0.308427	0.005378	0.0621	5 762.37	32.45	0.90001	0.001357	11.01	1.10	0.09	0.06	29.58	0.03	2 837.9
0.609773	0.304134	0.005177	0.0610	5 762.38	32.45	0.89377	0.001373	10.93	0.65	0.09	0.05	29.76	0.03	2 839.1
													Mean	2 839.1
													Standard deviation of mean	± 0.9$_0$
1,2-Dibromo*cyclo*hexane														
m(Pt) = 17.673 g														
0.633191	0.242096	0.005299	0.0393	5 762.76	32.38	0.86786	0.001280	10.90	0.35	0.07	0.04	27.53	0.00	3 580.8
0.613328	0.249100	0.005608	0.0439	5 762.77	32.38	0.86858	0.001243	10.95	0.50	0.06	0.03	26.67	0.00	3 579.1
0.619436	0.264593	0.005484	0.0489	5 762.74	32.40	0.90134	0.001242	11.32	1.00	0.08	0.02	26.94	0.01	3 575.6
0.626006	0.263931	0.005447	0.0574	5 762.73	32.40	0.90458	0.001249	11.36	1.00	0.04	0.06	27.22	0.01	3 579.4
0.622097	0.257557	0.005821	0.0411	5 762.75	32.40	0.89044	0.001254	11.18	0.60	0.04	0.05	27.05	0.01	3 580.4
													Mean	3 579.1
													Standard deviation of mean	± 0.9$_2$
2-Bromopropane														
m(Pt) = 17.673 g														
0.48086	0.309334	0.005420	0.0524	5 762.83	32.44	0.93053	0.000916	11.25	1.75	0.03	0.03	20.52	0.25	3 975.3
0.47680	0.284761	0.005933	0.0601	5 762.85	32.43	0.88164	0.000913	10.61	1.25	0.03	0.02	20.35	0.29	3 979.2
													Mean: See Table 7 and text	

Table 7. Results of combustion experiments on bromine compounds (Continued).

Calorimeter B

t_h = 20.0°C; t_i = 20.0°C; P^i(gas.) = 30.0 atm; V(Bomb) = 0.2750 liter; V^i(soln.) = 0.03001 liter; C^i(soln.) = 0.0625$_5$ mole As_2O_3/liter; $\varepsilon°$(Calor.) = 4 718.62 ± 0.34 cal/deg; $-\Delta Ec°/M$(Oil) = 10 972.1 ± 0.7 cal/g; $-\Delta Ec°/M$(Fuse) = 3 971 ± 4 cal/g; $-\Delta E_{oxid.}(As_2O_3) = (77.4 \pm 0.1) \times 10^3$ cal/mole

m' g	m'' g	m''' g	m(glass) g	ε(Calor.) cal/deg	ε^f(Cont.) cal/deg	Δt deg	$n^f(As_2O_3)$ mole	$-\Delta E(CO_2)$ cal	$-\Delta E(HNO_3)$ cal	$-\Delta E$(Au) cal	$-\Delta E$(Pt) cal	$-\Delta E$(HBr) cal	$-\Delta E\Sigma$ cal	$-\Delta Ec°/M$ cal/g
1-Bromopropane														
m(Pt) = 6.580 g in the first two experiments and 15.740 g in the following														
0.56036	0.21550	0.00466	0.074	4 670.98	32.28	0.99741	0.001095	10.83	2.75	0.04	0.10	24.83	0.41	3 988.2
0.55444	0.21451	0.00444	0.083	4 670.97	32.28	0.99012	0.001094	10.75	1.10	0.04	0.10	24.56	0.41	3 993.0
0.53588	0.22392	0.00507	0.085	4 661.82	32.55	0.99743	0.001049	10.84	0.80	0.04	0.10	23.74	0.40	3 986.8
0.53311	0.22257	0.00495	0.084	4 661.83	32.55	0.99182	0.001041	10.78	0.35	0.04	0.10	23.62	0.40	3 988.7
0.55786	0.21257	0.00476	0.087	4 661.81	32.57	0.98990	0.001086	10.74	0.60	0.04	0.10	24.72	0.41	3 989.0
													Mean	3 989.1
													Standard deviation of mean	± 1.0$_4$
2-Bromopropane														
m(Pt) = 15.740 g														
0.53496	0.22100	0.00451	0.090	4 661.83	32.54	0.98825	0.001042	10.74	0.90	0.05	0.10	23.70	0.42	3 978.1
0.51190	0.23375	0.00465	0.090	4 661.84	32.54	0.99814	0.000994	10.88	0.45	0.05	0.10	22.68	0.39	3 979.6
0.54035	0.22111	0.00496	0.092	4 661.82	32.54	0.99427	0.001051	10.80	0.55	0.05	0.10	23.94	0.41	3 984.9
														3 976.7[a]
														3 980.6[a]
													Mean	3 980.0
													Standard deviation of mean	± 1.4$_0$
2-Bromobutane														
m(Pt) = 5.764 g														
0.63617	0.14915	0.00457	0.119	4 671.74	32.20	1.00450	0.001106	10.90	2.40	0.03	0.08	25.32	0.42	4 711.2
0.62907	0.15489	0.00452	0.122	4 671.74	32.19	1.01008	0.001109	10.98	1.10	0.03	0.08	25.04	0.42	4 707.5
0.62596	0.14437	0.00443	0.120	4 671.76	32.18	0.98261	0.001095	10.65	1.60	0.03	0.08	24.92	0.43	4 710.8
0.63471	0.14290	0.00478	0.098	4 671.77	32.20	0.98840	0.001114	10.71	1.15	0.03	0.08	25.27	0.43	4 710.9
													Mean	4 710.1
													Standard deviation of mean	± 0.8$_7$

[a] These values were obtained by reduction from 25°C to 20°C of the two $-\Delta Ec°/M$ values given in Table 6 (see text).

For both samples of benzoic acid the certified value [17,18] for the heat of combustion under certificate conditions is 26.4338 ± 0.0026 abs. kj/g mass which is equal to 6317.83 ± 0.62 cal/g mass. This value was recalculated, by the method given in Ref.[2], to give the value 6312.92 ± 0.62 cal/g mass for the standard heat of combustion per gram mass of the sample, $-\Delta Ec^\circ/M$, at 25°C. This was converted to apply to 20°C by use of the following values at 25°C for the heat capacity, C_P°, of crystalline benzoic acid, gaseous oxygen, gaseous carbon dioxide and liquid water, respectively: 35.088 (Ref.[34]), 7.017 (Ref.[32]), 8.874 (Ref.[32]) and 17.996 (Ref.[32]) cal/deg mole. The value thus obtained for the standard heat of combustion at 20°C of the benzoic acid samples was 6314.12 ± 0.62 cal/g mass. In addition to the numerical quantities given above and in Ref.[2] the values listed in Table 8 were used in the calculation of the results. The symbols in Table 8 denote: ϱ the density, c_P the specific heat, and $(\partial E/\partial P)_T$ the energy of compression of the substance. The $(\partial E/\partial P)_T$ values were calculated, unless otherwise stated, from the corresponding density data using the approximate relation $(\partial E/\partial P)_T = -T(\partial V/\partial T)_P$ as discussed in Ref.[36(p. 542–43)].

Final over-all precision. The standard deviations of the means given in Tables 2—7 are measures of the immediate precision [3(p. 430)] of the various results. The over-all precision [3(p. 430)] of the $-\Delta Ec^\circ/M$ mean value obtained for each bromine compound was estimated by calculation of the corresponding final over-all standard deviation [3(p. 432)] as recommended in Ref.[3] The method of calculation given in Ref.[3], however, needs modification in order to be applicable to results from combustion experiments in which a considerable part of the total amount of heat evolved is associated with the combustion of an auxiliary material, the heat of combustion of which has been determined separately. The final over-all standard deviations given in Table 9 were obtained as follows.

Table 8. Auxiliary quantities for calculation of results.

Substance	ϱ g/ml		c_P cal/g deg 25°C	$(\partial E/\partial P)_T$ cal/g atm 20–25°C
	20°C	25°C		
Benzoic acid	1.323 [a]	1.320 [b]	0.287 [c]	−0.0029 [d]
Paraffin oil USBM-P3a	0.8755 [e]	0.8724 [e]	0.53 [f]	−0.0060
Paraffin oil L	0.8838 [g]		0.53 [h]	−0.0060 [h]
Fuse		1.5 [i]	0.4 [j]	−0.007 [k]
1,2-Dibromobutane	1.7954 [g]	1.7870 [g]	0.20 [l]	−0.0038
1,2-Dibromo*cyclo*hexane	1.7903 [g]	1.7833 [g]	0.16 [l]	−0.0032
1-Bromopropane	1.3550 [g]	1.3465 [g]	0.269 [m]	−0.0066
2-Bromopropane	1.3142 [g]	1.3055 [g]	0.27 [l]	−0.0072
2-Bromobutane	1.2607 [g]	1.2533 [g]	0.27 [l]	−0.0066

[a] Calculated from the value for the density at 25°C and the average of the two values for the coefficient of cubical expansion, γ, given in Ref.[35]; [b] Ref.[35]; [c] Ref.[34]; [d] Calculated from the aforementioned average value of the coefficient of cubical expansion, $\gamma = 0.00054$ deg^{-1}; [e] Ref.[1(p. 1531)]; [f] Ref.[37(p. 93)]; [g] This work; [h] Taken as the same as that for Paraffin oil USBM-P3a; [i] Ref.[37(p. 81)]; [j] Ref.[37(p. 93)]; [k] Ref.[37(p. 90)]; [l] Estimated; [m] Ref.[38].

If the "second-order" quantities in eqns. 14 and 15 of Ref.[1] are neglected, the mean values of the energy equivalent of the calorimeter, ε°(Calor.), and the heat of combustion of the auxiliary oil, $-\Delta Ec^\circ/M$(Oil), can be obtained from the following approximation equations:

$$\varepsilon^\circ(\text{Calor.}) = -\Delta Ec/M(\text{Benzoic acid})(m/\Delta t)_{\text{b.a.}} \tag{7}$$

$$-\Delta Ec^\circ/M(\text{Oil}) = \varepsilon^\circ(\text{Calor.})(\Delta t/m)_{\text{oil}} = -\Delta Ec/M(\text{Benzoic acid})(m/\Delta t)_{\text{b.a.}}(\Delta t/m)_{\text{oil}} \tag{8}$$

in which $-\Delta Ec/M$(Benzoic acid) is the "accepted" value for the heat of combustion of the benzoic acid used in the calibration experiments, $(m/\Delta t)_{\text{b.a.}}$ is the mean of the individual values obtained for the ratio of benzoic acid mass to temperature rise in the calibration experiments, and $(\Delta t/m)_{\text{oil}}$ is the mean of the individual values obtained for the ratio of temperature rise to paraffin oil mass in the experiments by which the heat of combustion of the paraffin oil sample was determined. All three values, $-\Delta Ec/M$(Benzoic acid), $(m/\Delta t)_{\text{b.a.}}$, and $(\Delta t/m)_{\text{oil}}$, carry with them standard deviations, s_1, s_2, and s_3, respectively, which are estimated according to the procedure described in Ref.[3] Further, if the uncertainties in the "second-order" quantities $-\Delta E$(Fuse), $-\Delta E(HNO_3)$, $-\Delta E$(Au), $-\Delta E$(Pt), $-\Delta E$(HBr) and $-\Delta E_\Sigma$ in eqn. 29 of Ref.[1] are neglected and the same quantities removed from the equation, the following approximate equation is obtained for calculation of the results of the combustion experiments with bromine compounds:

$$-\Delta Ec^\circ/M(\text{Compound}) = \frac{1}{m'}\left\{-\Delta E_{\text{I.B.P.}} - [-\Delta E(\text{As}) - \Delta E(\text{Oil}) - -\Delta E(CO_2)]\right\} = \frac{1}{m'}\left\{\varepsilon^\circ(\text{Calor.})\,\Delta t - n^{\text{f}}(As_2O_5)\,[-\Delta E_{\text{oxid.}}(As_2O_3)] - m''[-\Delta Ec^\circ/M(\text{Oil})] - n^{\text{f}}(CO_2\text{ diss.})[-\Delta E_{\text{soln.}}(CO_2)]\right\} \tag{9}$$

where $-\Delta E_{\text{oxid.}}(As_2O_3)$ and $-\Delta E_{\text{soln.}}(CO_2)$ denote the same quantities as do the symbols $-\Delta E$(reaction 21) and $-\Delta E$(reaction 24) in Ref.[1], and $n^{\text{f}}(As_2O_5)$ and $n^{\text{f}}(CO_2$ diss.) denote the number of moles of As_2O_5 and of CO_2 in the final bomb solution. Combination of eqn. 9 with eqns. 7 and 8 leads to the following equation:

$$-\Delta Ec^\circ/M(\text{Compound}) = \frac{1}{m'}\left\{-\Delta Ec/M(\text{Benzoic acid})(m/\Delta t)_{\text{b.a.}}\Delta t - -n^{\text{f}}(As_2O_5)[-\Delta E_{\text{oxid.}}(As_2O_3)] - m''\Delta Ec/M(\text{Benzoic acid})(m/\Delta t)_{\text{b.a.}}(\Delta t/m)_{\text{oil}} - -n^{\text{f}}(CO_2\text{ diss.})\,[-\Delta E_{\text{soln.}}(CO_2)]\right\} \tag{10}$$

from which it can be deduced [3] to what extent the standard deviations in the values $-\Delta Ec/M$(Benzoic acid), $(m/\Delta t)_{\text{b.a.}}$, $(\Delta t/m)_{\text{oil}}$, $-\Delta E_{\text{oxid.}}(As_2O_3)$ and $-\Delta E_{\text{soln.}}(CO_2)$ are carried over into the value obtained for $-\Delta Ec^\circ/M$(Compound). The final over-all standard deviation, $s_{\text{over-all}}$, to be assigned to the mean value obtained for $-\Delta Ec^\circ/M$(Compound) can thus be obtained from the equation (*cf.* Ref.[13(p. 74)]):

$$\frac{s_{\text{over-all}}}{-\Delta Ec^\circ/M(\text{Compound})} = \sqrt{\sum_1^6 \left(f_i \times \frac{s_i}{q_i}\right)^2} \qquad (11)$$

where the quantities s_i are the standard deviations of the mean values q_i obtained from the sets of observations leading to the following quantities:

$q_1 = -\Delta Ec/M$(Benzoic acid)	the "accepted" heat of combustion of the benzoic acid standard sample
$q_2 = \varepsilon^\circ$(Calor.)	the energy equivalent of the calorimetric system
$q_3 = -\Delta Ec^\circ/M$(Oil)	the heat of combustion of the auxiliary oil
$q_4 = -\Delta E_{\text{soln.}}(CO_2)$	the heat of solution of carbon dioxide in final bomb solution
$q_5 = -\Delta E_{\text{oxid.}}(As_2O_3)$	the heat of oxidation of arsenious oxide in bomb solution
$q_6 = -\Delta Ec^\circ/M$(Compound)	the heat of combustion of the compound under investigation,

and where the factors f_i are defined by the relations:

$$f_1 = f_2 = \left\{-\Delta E_{\text{I.B.P.}} - [-\Delta E(\text{Oil})]\right\} / -\Delta E(\text{Compound})$$
$$f_3 = -\Delta E(\text{Oil}) / -\Delta E(\text{Compound})$$
$$f_4 = -\Delta E(CO_2) / -\Delta E(\text{Compound})$$
$$f_5 = -\Delta E(\text{As}) / -\Delta E(\text{Compound})$$
$$f_6 = 1$$

in which $-\Delta E_{\text{I.B.P.}}$, $-\Delta E$(Compound), $-\Delta E$(Oil), $-\Delta E(CO_2)$ and $-\Delta E$(As), respectively, are rough means of the individual values, obtained in the various combustion experiments, for the heat effects associated with the actual amounts of the following reactions occurring in the bomb process: (i) the entire isothermal bomb process, (ii) the combustion of the bromine compound, (iii) the combustion of the auxiliary oil, (iv) the solution of carbon dioxide in the final bomb solution, and (v) the oxidation of arsenious oxide.

In the calculation of the final over-all standard deviations given in Table 9 the following values were used for the ratios s_i/q_i:

$s_1/q_1 = 0.5 \times 10^{-4}$, $s_2/q_2 = 0.8 \times 10^{-4}$ (Table 6) and 0.7×10^{-4} (Table 7), $s_3/q_3 = 0.8 \times 10^{-4}$ (Table 6) and 0.6×10^{-4} (Table 7), $s_4/q_4 = 350 \times 10^{-4}$, $s_5/q_5 = 13 \times 10^{-4}$. As is seen, the factors f_1 and f_2 were approximately equal to 1 for all the combustion experiments of the present investigation.

Derived data. Recalculation by conventional methods [37(p. 103–4)] of the $-\Delta Ec^\circ/M$ mean values given in Tables 6 and 7 yielded the values listed in Table 9 for the standard energies of combustion, ΔEc°, at 25°C and 20°C, and the standard enthalpies of combustion, ΔHc°, at 25°C for the various compounds. The data given in Table 9 refer to the combustion reaction represented by eqn. 6, in which all reactants and products are in their standard states [32].

HEATS OF FORMATION

For comparison of the results from the heat of combustion experiments with appropriate data from reaction-calorimetric studies, heat of formation values for the selected compounds were calculated from both sets of data.

Table 9. Derived standard heats of combustion.

Compound and state	Molecular weight [a]	$-\Delta Ec°$ at 25°C kcal/mole	$-\Delta Ec°$ at 20°C kcal/mole	$-\Delta Hc°$ at 25°C kcal/mole
1,2-Dibromobutane(liq)	215.940	613.08 ± 0.52 [b]		614.26 ± 0.52 [b]
1,2-Dibromo*cyclo*hexane(liq)	241.978	866.06 ± 0.60		867.54 ± 0.60
1-Bromopropane(liq)	123.005		490.68 ± 0.34 [b]	491.54 ± 0.34
2-Bromopropane(liq)	123.005		489.56 ± 0.42	490.42 ± 0.42
2-Bromobutane(liq)	137.032		645.43 ± 0.30	646.52 ± 0.30

[a] Computed from the 1957 table of atomic weights [39].
[b] The uncertainties in this column are equal to twice the final over-all standard deviation; see text for comments.

Heats of formation from heat of combustion data.

For the compounds listed in Table 9 standard heats of formation, $\Delta Hf°$, at 25°C, referring to reaction 12, were calculated from the $-\Delta Hc°$ values

$$a\ C(c, \text{graphite}) + b/2\ H_2(g) + d/2\ Br_2(liq) \rightarrow C_aH_bBr_d(liq) \qquad (12)$$

given in Table 9 and the selected values [32] for the standard heats of formation of gaseous carbon dioxide [40] −94.0539 ± 0.0108 kcal/mole and liquid water [41] 68.3174 ± 0.0096 kcal/mole. The value for carbon dioxide is corrected to the present atomic weight of 12.011 for carbon. The derived standard heats of formation for the liquid compounds are given in column 2 of Table 10. In column 3 of the same table are listed heats of vaporization, ΔHv, at 25°C, for the various compounds, calculated from data given in Refs.[7,42–44]. In column 4 of Table 10 are given the resulting standard heats of formation, at 25°C, of the compounds in the gaseous state. Actually, the values given in this column apply to the bromine compounds at their saturation pressures at 25°C. It can, however, be estimated that reduction of the values to apply to the bromine compounds in a state of unit fugacity (1 atm) will change the values with

Table 10. Standard heats of formation from heat of combustion data.

Compound	$\Delta Hf°$(liq) at 25°C kcal/mole	ΔHv [a] at 25°C kcal/mole	$\Delta Hf°$(g) at 25°C [b] kcal/mole
1,2-Dibromobutane	−35.23 ± 0.52 [c]	10.80 ± 0.20 [d]	−24.43 ± 0.58 [e]
1,2-Dibromo*cyclo*hexane	−38.37 ± 0.60	12.10 ± 0.35	−26.27 ± 0.70
1-Bromopropane	−29.73 ± 0.34	7.75 ± 0.20	−21.98 ± 0.40
2-Bromopropane	−30.85 ± 0.42	7.30 ± 0.20	−23.55 ± 0.46
2-Bromobutane	−37.12 ± 0.31	8.45 ± 0.25	−28.66 ± 0.40

[a] For the process $C_aH_bBr_d(liq) \rightarrow C_aH_bBr_d(g)$, at saturation pressure at 25°C.
[b] See text for comments.
[c] The uncertainties in this column are equal to twice the final over-all standard deviation [3].
[d] The uncertainties in this column are estimates.
[e] The uncertainties in this column are equal to twice the final over-all standard deviation (including the estimated uncertainties assigned to the ΔHv values in column 3) [3].

only a few hundredths of a kcal/mole. Only for 2-bromopropane will the reduction amount to the order of 0.10 kcal/mole. Therefore the given values have been listed as standard heats of formation.

Heats of formation from reaction-calorimetric data

1,2-Dibromobutane. The heat of formation of 1,2-dibromobutane can be calculated from two different sets of reaction-calorimetric data: (i) Conn, Kistiakowsky and Smith [6] found for the reaction butene-1(g) + bromine(g) → 1,2-dibromobutane(g), at 355°K and 1 atm total pressure, $\Delta H = -29.58 \pm 0.40$* kcal/mole. This value corresponds to $\Delta H = -29.66 \pm 0.40$ kcal/mole for the reaction at 298°K, assuming the following heat capacity values, C_P°, in cal/mole deg, for the various compounds in the gaseous state: butene-1 [45] 20.57 at 300°K and 26.04 at 400°K; bromine [46] 8.62 at 300°K and 8.78 at 400°K; 1,2-dibromobutane [47] 30.35 at 300°K and 33.48 at 350°K. By combining this ΔH_{298} value with the standard heats of formation at 25°C of gaseous butene-1 [45,48,49], —0.03 ± 0.20 kcal/mole, and gaseous bromine [33], + 7.45 kcal/mole, a value of —22.24 ± 0.45 kcal/mole is derived for the standard heat of formation, ΔHf°, at 25°C of gaseous 1,2-dibromobutane. (ii) Lister [7] studied the reaction butene-1(in CCl_4 solution) + bromine(liq) → → 1,2-dibromobutane(in CCl_4 solution) at 27°C and obtained $\Delta H = -26.921 \pm 0.276$ ** kcal/mole. From this value and auxiliary data he calculated $\Delta H = -28.900 \pm 0.600$ kcal/mole for the reaction butene-1(g) + bromine(g) → 1,2-dibromobutane(g) at 27°C. Assuming this same value to apply at 25°C, and combining it with the standard heat of formation at 25°C of gaseous butene-1, given above, and with the enthalpy of vaporization of bromine, 7.466 kcal/mole, used by Lister in his calculations, the standard heat of formation, ΔHf°, at 25°C of gaseous 1,2-dibromobutane is calculated to be —21.46 ± 0.63 kcal/mole.

1,2-Dibromocyclohexane. Lister [7] investigated the reaction *cyclo*hexene(in CCl_4 solution) + bromine(liq) → 1,2-dibromo*cyclo*hexane(in CCl_4 solution) at 27°C, and reported $\Delta H = -30448 \pm 124$ cal/mole (the error limits are the average deviation from the mean of six experiments), but considered the true uncertainty in the result to be ± 300 cal/mole. The heats of solution at 27°C of liquid *cyclo*hexene and liquid 1,2-dibromo*cyclo*hexane in carbon tetrachloride were also measured in order to derive from the observed ΔH, the appropriate value for the reaction *cyclo*hexene(liq) + bromine(liq) → 1,2-dibromo*cyclo*hexane(liq). The observed heats of solution were small and Lister therefore chose to take them as zero, allowing an extra uncertainty of ± 1 % from this cause. This leads to $\Delta H = -30.45 \pm 0.42$ kcal/mole for the reaction *cyclo*hexene(liq) + Br_2(liq) → 1,2-dibromo*cyclo*hexane(liq) at 27°C. The same value can be applied to 25°C without appreciable error. Combining this value with the standard heat of formation, ΔHf°, at 25°C of liquid *cyclo*hexene [50], —9.70 ± 0.19 kcal/mole, yields for the standard heat of formation, ΔHf°, at 25°C of liquid 1,2-dibromo*cyclo*hexane a value of —40.15 ± 0.46 kcal/mole.

* The uncertainty is twice the "estimated total probable error" given in Ref.[6]
** The uncertainty is the average deviation from the mean of three experiments.

1-Bromopropane. Two independent heat of formation values can be calculated for 1-bromopropane from the following heat of reaction data: (i) Lacher, Kianpour and Park [10] measured for the reaction *cyclo*propane(g) + hydrogen bromide(g) → 1-bromopropane(g) at 401°K $\Delta H = -25\,790 \pm 320$ cal/mole. This needed correction for the small amount of 2-bromopropane formed in the reaction *, yielding finally $\Delta H = -25\,784 \pm 320$ cal/mole at 401°K. This value can be converted to apply to 298°K assuming the following values, in cal/mole deg, for the heat capacity, C_P°, of the various compounds in the gaseous state: for *cyclo*propane [51] 13.44 at 300°K and 18.33 at 400°K; for hydrogen bromide [46] 6.96 at 300°K and 6.98 at 400°K; for 1-bromopropane [47] 21.13 at 300°K and 25.93 at 400°K. The value obtained for the reaction at 298°K is $\Delta H = -25.854 \pm 0.320$ kcal/mole. Combination of this value with the standard heats of formation at 25°C of gaseous *cyclo*propane[52], $+12.74 \pm 0.14$ kcal/mole, and gaseous hydrogen bromide [32], -8.66 ± 0.20 ** kcal/mole, yields for the standard heat of formation, ΔHf°, at 25°C of gaseous 1-bromopropane a value of -21.77 ± 0.40 kcal/mole. (ii) Lacher *et al.*[11] measured for the reaction 1-bromopropane(g) + hydrogen(g) → propane(g) + hydrogen bromide(g) at 521°K $\Delta H = -13\,100 \pm 376$ cal/mole. This value can be converted to give $\Delta H = -12\,330 \pm 376$ cal/mole for the same reaction at 298°K, if the following values, in cal/mole deg, are used for the heat capacities, C_P°, of the various compounds in the gaseous state: for 1-bromopropane [47] 21.13 at 300°K and 25.93 at 400°K; for hydrogen [46] 6.97 at 400°K and 7.43 at 500°K; for propane [45] 22.54 at 400°K and 27.02 at 500°K; for hydrogen bromide [46] 6.98 at 400°K and 7.04 at 500°K. Combination of this ΔH_{298} value with the standard heats of formation at 25°C of gaseous propane [45,54], -24.820 ± 0.142 kcal/mole, and gaseous hydrogen bromide [32], yields for the standard heat of formation, ΔHf°, at 25° C of gaseous 1-bromopropane a value of -21.15 ± 0.45 kcal/mole.

2-Bromopropane. The enthalpy change for the reaction propene(g) + HBr(g) → 2-bromopropane(g) has been measured twice: Lacher, Walden, Lea and Park [8] obtained in 1950 at 367°K $\Delta H = -20\,140 \pm 240$ cal/mole and Lacher, Kianpour and Park [10] obtained in 1957 at 401°K $\Delta H = -20\,430 \pm 150$ cal/mole. After correction for the small amount of 1-bromopropane formed in the reactions (*cf.* footnote *), the two values become $\Delta H_{367} = -20\,170 \pm 240$ cal/mole and $\Delta H_{401} = -20\,460 \pm 150$ cal/mole. These values can be converted to apply to 298°K by use of the heat capacity values given above for hydrogen bromide and the following values, in cal/mole deg, for the heat capacity, C_P°, of propene [45] 15.34 at 300°K and 19.10 at 400°K; and of 2-bromopropane [47] 21.59 at 300°K and 26.41 at 400°K. The two values thus obtained for the reaction at 298°K are $\Delta H = -20.14 \pm 0.24$ kcal/mole and $\Delta H = -20.44 \pm 0.15$ kcal/mole. Combination of these values with the standard heats of formation at 25°C of gaseous propene [45,49], $+4.879 \pm 0.122$ kcal/mole, and gaseous hydrogen bromide [32], yields for the standard heat of formation, ΔHf°, at 25°C of gaseous 2-bromopropane -23.92 ± 0.33 and -24.22 ± 0.28 kcal/mole, respectively.

* For the isomerization 2-bromopropane(g) → 1-bromopropane(g) at 401°K ΔH was taken as 2 000 cal/mole.

** This uncertainty is estimated, *cf.*, however, Ref.[53]

2-Bromobutane. Heat of formation values can be calculated for 2-bromobutane from heat of reaction data obtained by Lacher, Billings, Campion, Lea and Park [9] for the following three reactions: (i) butene-1(g) + hydrogen bromide(g) → 2-bromobutane(g), $\Delta H_{367} = -20\,150$ * ± 180 cal/mole; (ii) *cis*-butene-2(g) + hydrogen bromide(g) → 2-bromobutane(g), $\Delta H_{373} = 18\,344 \pm 157$ cal/mole; and (iii) *trans*-butene-2(g) + hydrogen bromide(g) → 2-bromobutane(g), $\Delta H_{383} = -17\,340 \pm 135$ cal/mole. These ΔH values can be converted to 298°K using the heat capacity values given above for hydrogen bromide and the following values, in cal/mole deg, for the heat capacity, C_P°, of butene-1 [45] 20.57 at 300°K and 26.04 at 400°K; of *cis*-butene-2 [45] 18.96 at 300°K and 24.33 at 400°K; of *trans*-butene-2 [45] 21.08 at 300°K and 26.02 at 400°K; and of 2-bromobutane [47] 26.75 at 300°K and 33.22 at 400°K. For the three reactions at 298°K the following ΔH values are obtained: —20.09 ± 0.18, —18.43 ± 0.16, —17.28 ± 0.14 kcal/mole, respectively. Combination of these values with the standard heats of formation at 25°C of gaseous butene-1 [45,48,49], —0.03 ± 0.19 kcal/mole, gaseous *cis*-butene-2 [45,48,49], —1.67 ± 0.30 kcal/mole, gaseous *trans*-butene-2 [45,48,49], —2.67 ± 0.24 kcal/mole, and gaseous hydrogen bromide [32], yields for the standard heat of formation, ΔHf°, at 25°C of gaseous 2-bromobutane the values (i) —28.75 ± 0.34, (ii) —28.76 ± 0.39 and (iii) —28.61 ± 0.34 kcal/mole, respectively.

Table 11. Comparison of standard heats of formation from various methods.

Compound and state	ΔHf° at 25°C kcal/mole		Difference between the heat of formation values from the two sets of data kcal/mole
	From heat of combustion data [a]	From reaction calorimetry data [b]	
1,2-Dibromobutane(g)	−24.43 ± 0.58 [c]	−22.24 ± 0.45 [c]	−2.19 ± 0.73 [c]
	−24.43 ± 0.58	−21.46 ± 0.63	−2.97 ± 0.78 [d]
1,2-Dibromo*cyclo*hexane(liq)	−38.37 ± 0.60	−40.15 ± 0.46	+1.78 ± 0.76
1-Bromopropane(g)	−21.98 ± 0.40	−21.77 ± 0.40	−0.21 ± 0.57
	−21.98 ± 0.40	−21.15 ± 0.45	−0.83 ± 0.60
2-Bromopropane(g)	−23.55 ± 0.46	−23.92 ± 0.33	+0.37 ± 0.57
	−23.55 ± 0.46	−24.22 ± 0.28	+0.67 ± 0.54
2-Bromobutane(g)	−28.66 ± 0.40	−28.75 ± 0.34	+0.09 ± 0.53
	−28.66 ± 0.40	−28.76 ± 0.39	+0.10 ± 0.56
	−28.66 ± 0.40	−28.61 ± 0.34	−0.05 ± 0.53

[a] This work.
[b] See text and Fig. 1 for references.
[c] The uncertainties in this column are equal to twice the final over-all standard deviation [s].
[d] This uncertainty is lower than the combined uncertainties of the two heat of formation values given in the preceding columns since the uncertainty in the heat of vaporization of 1,2-dibromobutane cancels in the difference.

* This value has been corrected for the small amount of 1-bromobutane, formed in the reaction, by taking ΔH_{367} as 2 000 cal/mole for the isomerization 2-bromobutane(g) → 1-bromobutane(g).

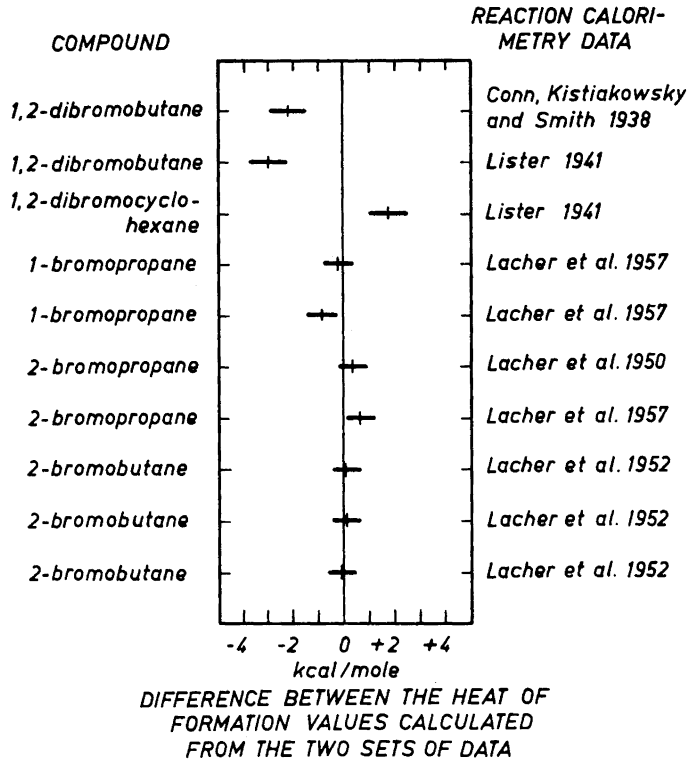

Fig. 1. Plot of the differences between the standard heats of formation calculated from heats of combustion from this work and those calculated from reaction calorimetry data from previous work. The lengths of the horizontal lines represent the uncertainties assigned to the observed differences.

The various heat of formation values obtained from the reaction-calorimetric data are listed in column 3 of Table 11.

COMPARISON OF HEATS OF FORMATION FROM THE VARIOUS METHODS AND DISCUSSION OF RESULTS

The standard heats of formation calculated from the heat of combustion data of the present investigation and from calorimetric data on heats of reactions other than combustion are compared in Table 11. The results of the comparison are shown graphically in Fig. 1. The references to the reaction calorimetry investigations are also listed in Fig. 1.

It is seen from Table 11 and Fig. 1 that the first three differences in column 4 of Table 11 are numerically greater than zero by amounts significantly greater than the uncertainties assigned to the various differences. The remain-

ing seven differences are, however, virtually equal to zero. This means that for the dibromides the heats of formation calculated from heats of combustion disagree with those obtained from the heats of *addition of bromine* to the corresponding unsaturated hydrocarbons, whereas for the monobromides the heats of formation obtained from heats of combustion are in good accord with those calculated from the heats of *addition of hydrogen bromide* to the corresponding unsaturated hydrocarbons, and from the heat of *reduction* of 1-bromopropane *with hydrogen*. It seems possible that although the precision in measurement of the heats of addition of bromine was good, the over-all accuracy was less than that obtained in the heats of addition of hydrogen bromide, because of the following facts: (i) The addition of hydrogen bromide to unsaturated compounds of the type considered here and under the given conditions is known to proceed chemically more cleanly than the addition of bromine; (ii) The main reaction product in the heat of addition of bromine experiments was identified only by measurement of its refractive index at a single temperature, whereas in the heat of addition of hydrogen bromide experiments the products, collected at the exit of the calorimeter, were quantitatively analyzed by infrared absorption spectrophotometry; (iii) As is seen from Fig. 1, the heat of formation obtained for 1,2-dibromobutane from the heat of combustion is numerically *greater*, by approximately 3 kcal/mole, than that obtained from the heat of addition of bromine to butene-1 as measured by Lister, whereas for 1,2-dibromo*cyclo*hexane the heat of formation obtained from the heat of combustion is numerically *less*, by approximately 2 kcal/mole, than that obtained from the heat of addition of bromine to *cyclo*hexene, which latter value was measured by Lister with the same apparatus and technique as for the addition of bromine to butene-1. This fact suggests that the discordance between the heats of formation from the two sets of data, for these two points of comparison is not due to a constant systematic error in one or both of the two experimental methods; (iv) As discussed by Lister [7(p. 148)] an inconsistency is found in the heats of hydrogenation [55,56] and addition of bromine [6,7] to *cis*-butene-2 and *cyclo*hexene. The heats of hydrogenation of the two compounds are, within the experimental errors, the same, whereas the heat of addition of bromine to *cyclo*hexene is numerically 3.3 kcal/mole *greater* than that to *cis*-butene-2. These results are definitely incompatible with one another.

For these reasons it seems justifiable to place more weight on the good accord of the heat of combustion data with the data on heats of addition of hydrogen bromide [8-11] than on the discord with the data on heats of addition of bromine [6,7]. It can therefore be concluded that, although the cause of certain discrepancies still has to be found, enough evidence has been obtained to prove that the moving-bomb method for combustion calorimetry of organic bromine compounds is capable of giving heats of combustion having an accuracy corresponding to the precision of the observed results. It has previously been found [1] that with the given method results of an immediate precision slightly better than 0.01 % can be obtained.

Acknowledgement. The author's thanks are due to the *Swedish Natural Science Research Council*, the *Swedish Technical Research Council*, *Kungl. Fysiografiska Sällskapet i Lund* and *Doktor P. Håkanssons Stiftelse* for financial support of this investigation.

REFERENCES

1. Bjellerup, L. *Acta Chem. Scand.* **13** (1959) 1511.
2. Bjellerup, L. *Acta Chem. Scand.* **14** (1960) 617.
3. Rossini, F. D. and Deming, W. E. *J. Wash. Acad. Sci.* **29** (1939) 416.
4. Smith, L. and Bjellerup, L. *Combustion in a Bomb of Organic Bromine Compounds*, Chapter 9 of Ref.[5]
5. Rossini, F. D. (Ed.) *Experimental Thermochemistry*, Interscience, New York 1956.
6. Conn, J. B., Kistiakowsky, G. B. and Smith, E. A. *J. Am. Chem. Soc.* **60** (1938) 2764.
7. Lister, M. W. *J. Am. Chem. Soc.* **63** (1941) 143.
8. Lacher, J. R., Walden, C. H., Lea, K. R. and Park, J. D. *J. Am. Chem. Soc.* **72** (1950) 331.
9. Lacher, J. R., Billings, T. J., Campion, D. E., Lea, K. R. and Park, J. D. *J. Am. Chem. Soc.* **74** (1952) 5291.
10. Lacher, J. R., Kianpour, A. and Park, J. D. *J. Phys. Chem.* **61** (1957) 1124.
11. Lacher, J. R. *Personal communication* (1957).
12. Bjellerup, L. and Smith, L. *Kgl. Fysiograf. Sällskap. Lund, Förh.* **24** (1954) 21.
13. Sunner, S. *Studies in Combustion Calorimetry Applied to Organo-Sulphur Compounds* (Diss.) University, Lund 1949.
14. Hubbard, W. N., Katz, C. and Waddington, G. *J. Phys. Chem.* **58** (1954) 142.
15. Sunner, S. and Bjellerup, L. *Acta Chem. Scand.* **5** (1951) 261.
16. Bjellerup, L. and Sunner, S. *Rec. trav. chim.* **73** (1954) 862.
17. *Provisional Certificate of Analysis of Standard Sample 39 g, Benzoic Acid*, National Bureau of Standards, Washington, D.C., 1949.
18. *Certificate for Standard Sample 39f, Benzoic Acid*, National Bureau of Standards, Washington, D.C., 1944 (with Supplementary Note 1946).
19. Willingham, C. B. and Rossini, F. D. *J. Research Natl. Bur. Standards* **37** (1946) 15.
20. Stage, H. and Schultze, G. R. *Oel u. Kohle* (1944) 90.
21. Snyder, H. R. and Brooks, L. A. *Org. Syntheses Coll. Vol.* **2** (1943) 171.
22. Timmermans, J. *Physico-Chemical Constants of Pure Organic Compounds*, Elsevier Amsterdam 1950.
23. Dillon, R. T., Young, W. G. and Lucas, H. J. *J. Am. Chem. Soc.* **52** (1930) 1953.
24. Goering, H. L. and Sims, L. L. *J. Am. Chem. Soc.* **77** (1955) 3465.
25. Winstein, S. *J. Am. Chem. Soc.* **64** (1942) 2792.
26. Tschamler, H., Richter, E. and Wettig, F. *Sitz. ber. Akad. Wiss. Wien, Math. naturw. Kl. Abt. II b* **158** (1949) 856.
27. Skau, E. L. and McCullough, R. *J. Am. Chem. Soc.* **57** (1935) 2439.
28. Timmermans, J. and Martin, F. *J. chim. phys.* **23** (1926) 747, p. 776.
29. Timmermans, J. and Martin, F. *J. chim. phys.* **25** (1928) 411, p. 423.
30. Timmermans, J. and Delcourt, Y. *J. chim. phys.* **31** (1934) 85, p. 96.
31. Lucas, H. J., Dillon, R. T. and Young, W. G. *J. Am. Chem. Soc.* **52** (1930) 1949.
32. Rossini, F. D., Wagman, D. D., Evans, W. H., Levine, S. and Jaffe, I. *Selected Values of Chemical Thermodynamic Properties*, Circular of the National Bureau of Standards 500, U.S. Government Printing Office, Washington, D. C., 1952.
33. Stull, D. R. and Sinke, G. C. *Thermodynamic Properties of the Elements*, American Chemical Society, Washington, D.C., 1956.
34. Furukawa, G. T., McCoskey, R. E. and King, G. J. *J. Research Natl. Bur. Standards* **47** (1951) 256.
35. Jessup, R. S. *J. Research Natl. Bur. Standards* **36** (1946) 421.
36. Washburn, E. W. *Bur Standards J. Research* **10** (1933) 525.
37. Hubbard, W. N., Scott, D. W. and Waddington, G. *Standard States and Corrections for Combustions in a Bomb at Constant Volume*, Chapter 5 of Ref.[5]
38. Kurbatov, V. Ya. *Zhur. Obshchei Khim.* **18** (1948) 372–87; *Chem. Abstr.* **43** (1949) 30*a*.
39. Wichers, E. *J. Am. Chem. Soc.* **80** (1958) 4121.
40. Prosen, E. J., Jessup, R. S. and Rossini, F. D. *J. Research Natl. Bur. Standards* **33** (1944) 447.
41. Wagman, D. D., Kilpatrick, J. E., Taylor, W. J., Pitzer, K. S. and Rossini, F. D. *J. Research Natl. Bur. Standards* **34** (1945) 143.

42. Stull, D. R. *Ind. Eng. Chem.* **39** (1947) 517.
43. Dreisbach, R. R. *Pressure-Volume-Temperature Relationships of Organic Compounds*, 3rd Ed., Handbook Publishers, Sandusky 1952.
44. Jordan, T. E. *Vapor Pressure of Organic Compounds*, Interscience, New York 1954.
45. *Selected Values of Properties of Hydrocarbons and Related Compounds*, American Petroleum Institute Research Project 44, Carnegie Institute of Technology, Pittsburgh, Pennsylvania.
46. *Selected Values of Chemical Thermodynamic Properties, Series III*, Circular of the National Bureau of Standards 500, Washington, D.C.
47. McCullough, J. P. *Personal communication* (1957).
48. Prosen, E. J., Maron, F. W. and Rossini, F. D. *J. Research Natl. Bur. Standards* **46** (1951) 106.
49. Prosen, E. J. and Rossini, F. D. *J. Research Natl. Bur. Standards* **36** (1946) 269.
50. Epstein, M. B., Pitzer, K. S. and Rossini, F. D. *J. Research Natl. Bur. Standards* **42** (1949) 379.
51. Kistiakowsky, G. B. and Rice, W. W. *J. Chem. Phys.* **8** (1940) 610.
52. Knowlton, J. W. and Rossini, F. D. *J. Research Natl. Bur. Standards* **43** (1949) 113.
53. Lacher, J. R., Casali, L. and Park, J. D. *J. Phys. Chem.* **60** (1956) 608.
54. Prosen, E. J. and Rossini, F. D. *J. Research Natl. Bur. Standards* **34** (1945) 263.
55. Kistiakowsky, G. B., Ruhoff, J. R., Smith, H. A. and Vaughan, W. E. *J. Am. Chem. Soc.* **57** (1935) 876.
56. Kistiakowsky, G. B., Ruhoff, J. R., Smith, H. A. and Vaughan, W. E. *J. Am. Chem. Soc.* **58** (1936) 137.

Received July 14, 1960.

ACTA CHEMICA SCANDINAVICA 15 (1961) 141–153

Structural Changes Induced in Solid Dextran by Irradiation with Gamma Rays *

KIRSTI A. GRANATH and PER-OLOF KINELL**

Research Laboratories, Pharmacia Ltd., and Institute of Physical Chemistry, University of Uppsala, Uppsala, Sweden

Dextran samples with various molecular properties have been irradiated in air and in vacuum by cobalt-60 gamma rays. Degradation occurs as is evidenced from changes in molecular weight. The rate of degradation is faster in oxygen but less reproducible. The energy per broken bond is in vacuum the same for all samples (19 eV) and it does not change with increasing dosage up to 18 Mrad. Gel filtration experiments have shown that irradiation in oxygen gives a molecular weight distribution which contains a larger weight fraction of low molecular material. Electron spin resonance data show that very stable free radicals are formed. A hypothesis has been put forward that primarily a radical ion is formed which then dissociates into a positive ion and an alkoxy radical. The change in branching during the degradation indicates that simultaneous bond scission and rearrangements of the molecules occur. An increase in branching is typical for molecules having an initially low degree of branching, while a high number of branches originally will lead to the formation of less branched molecules. This is explained as due to the spatial conditions along the chain. In all cases the polymolecularity of the samples increases during the degradation.

Dextran intended for clinical use is generally obtained by acid hydrolysis and fractionation of raw dextran [1]. It is, however, also possible to achieve the necessary reduction in molecular weight of the original material by the action of enzymes [2], ultrasonics [3], and by means of high energy radiation [4,5]. The present investigation was carried out in order to study the changes occurring in the molecular properties of the material when subjected in the solid state to the ionizing action of the γ-rays from the isotope cobalt-60. This study has been concerned mainly with changes in the degree of branching and in the molecular heterogeneity at different doses of absorbed energy. It was, however, also considered useful if some information about the mechanism of the degradation could be obtained from electron spin resonance studies of

* Part of this investigation was presented at the First Nordic Meeting on Food Preservation by Ionizing Radiations, held at Risö, Denmark, 25—26th April, 1960 (Risö Report No. 16, p. 23).

** Present address: AB Atomenergi, Studsvik, Tystberga, Sweden.

the free radicals formed during the irradiation. Therefore, some measurements made with regard to this [6] have been discussed in the present study.

Previous investigations on dextran exposed to ionizing radiation (γ-rays) [7] in both aqueous solution and in the solid state have shown that the rate of depolymerization in the former case is significantly faster than in the latter. Further, it was shown that the branching of the molecules did not change during the irradiation and therefore the degradation must predominantly take place through the breaking of the 1→ 6-glucosidic linkages. Lang *et al.*[8] have shown (γ-rays) that in aqueous solution the degradation rate decreases with increasing molecular weight. The depolymerization induced by irradiation of dilute aqueous solutions proceeds faster in the absence than in the presence of air [9].

As regards the formation of additional degradation products, *e.g.* low molecular weight material from the glucose units, no such products have been identified after irradiation of dextran. On the other hand the existence of acidic groups in irradiated materials has been proven, *e.g.* for glucose [10], dextran [10], and starch [11].

The molecular weight distribution of the dextran seems to be dependent upon the method of degradation: a broader distribution is obtained after irradiation than after acid hydrolysis [8,12]. The distribution can also change with the degree of degradation. This has been shown to be the case with polymethyl methacrylate treated in solution with ultrasonic waves [13]. In this case the heterogeneity passes a maximum during the intermediate phase of the degradation.

Samples that have been irradiated have given a lower value for the exponent α in the viscosity molecular weight relation ($[\eta] = K \cdot M^{\alpha}$)[4]. This has been explained as due to a more dense molecular structure caused by increased branching during the irradiation. However, increased heterogeneity will also affect the α value in the same direction [12] and, therefore, such an explanation cannot be regarded as adequately confirmed.

EXPERIMENTAL

Some preliminary irradiation experiments were performed in order to get information about the importance of the physical state of the samples and the influence of oxygen and moisture content. It was then found that both the size and density of the dextran grains and the oxygen content were significant factors. Moisture contents less than 5 % did not seem to have any pronounced effect on the degradation. The latter result is, however, contrary to the findings on other polysaccharides for instance starch [11] and cellulose [14].

Samples. For the present work three dextran fractions were selected representing different degrees of branching and molecular heterogeneities. These samples included two partially hydrolyzed Swedish dextrans

478—I—A with high molecular weight, very marked heterogeneity but moderately branched,

823—327—VI with intermediate molecular weight, low heterogeneity and low degree of branching,

and one dextran of German origin

Onkotin 179 with low molecular weight, moderate heterogeneity but a high degree of branching.

The characterizing data on these samples, *i.e.* number and weight average molecular weights, heterogeneities and degrees of branching are given in Table 1.

Pretreatment. In order to eliminate as far as possible any dependence of the degradation rate on the size and porosity of the dextran particles all samples were pretreated in the same way. The polysaccharide was dissolved in distilled water to a 5 % solution. This was then dropwise added to pure ethanol with continuous and vigorous stirring. The final ethanol concentration was adjusted to at least seven volumes ethanol per one volume original solution. By means of this procedure dextran was precipitated as fluffy flakes. These were filtered off and dried.

Irradiation. About 300 mg of the dextran sample was placed in carefully cleaned glass ampoules. These were evacuated to about 0.01 mm Hg pressure and heated to 60—70°C for several hours. The ampoules were then either hermetically closed directly or after the admittance of air. The irradiation was done in the gamma field from a 100 curie ^{60}Co freely radiating source described by Kinell and Larsson [15]. The dose rate was measured by the ferric ion dosimetry technique and was found to be about 60 000 rad/h at the points where the ampoules were placed. The total dose was controlled by recording the irradiation time making due corrections for the decay of ^{60}Co. The temperature was kept at 20°C.

Number average molecular weight. The number average molecular weight, M_n, was determined by Somogyi's phosphate method [16] using isomaltose as a standard. In this method the terminal aldehyde group of the dextran molecule reduces an alkaline copper phosphate reagent. As it was not immediately evident that reducing end-groups were formed during the degradation after irradiation as in acid hydrolysis, some check measurements were made. Applying Somogyi's method to glucose irradiated to a dose of 5.4 Mrad the true molecular weight of 180 was obtained (it has been found that at doses of 10—100 Mrad some decomposition of the glucose molecule occurs [17]). This shows that the reducing groups are within experimental errors intact.

Further osmotic measurements were made on a dextran sample irradiated to a dose of 27 Mrad and then dialysed before the measurements. A molecular weight of 9 500 was obtained compared to the value 8 500 from Somogyi's method.

Weight average molecular weight. The weight average molecular weight, M_w, were determined by the light scattering technique using a Brice-Phoenix photometer and applying the same experimental procedure that has been described previously [19].

Degree of branching. For this purpose the periodate oxidation method by Jeanes and Wilham [20] in a modification earlier described [19] was used. Due corrections were introduced for the amount of formic acid formed by the terminal end-groups.

Gel filtration experiments. In order to study the molecular weight distribution after irradiation the gel filtration method [21,22] was used. The two samples investigated had been given a dose of about 18 Mrad, one of them in air and the other in vacuum. 5 ml of a 10 % solution was filtered through a column packed with a dextran gel (Sephadex ,Pharmacia) having a water regain of 7.7 g/g. A number of fractions were collected and analyzed for their amount of dextran by the anthrone method [23]. The number average molecular weights were determined by the end-group method for some of the fractions.

RESULTS

Number of broken bonds. The number of broken bonds per monomer unit, *i.e.* the fracture density, p, induced by the radiation at a certain dose, r, has been calculated from the M_n values.

Then

$$p = m\left(\frac{1}{M_n} - \frac{1}{M_{n_0}}\right).$$

where m is the molecular weight of the monomer unit and M_{n_0} is the original molecular weight of the sample. The data obtained are collected in Table 1. In Fig. 1 the p values are given as a function of the dose in Mrad. The sensitivity towards radiation induced fracture as expressed through the proportionality factor p_o,

$$p = p_o r,$$

Table 1. Degradation data for dextran samples irradiated by cobalt-60 γ-rays. r = dose in Mrad; p = fracture density; M_n and M_w = number and weight averages of molecular weight; q = number of 1→6-linkages per monomer unit.

r	M_n	$\frac{10^6}{M_n}$	$p \cdot 10^3$	M_w	$\frac{M_w}{M_n}$	q
478—I—A irradiated in air.						
0	275 000	3.6	0	2 180 000	7.9	0.915
6.2	11 200	89.3	13.9	300 000	26.8	0.918
11.25	7 700	130.5	20.5	159 000	20.8	0.904
15.1	6 800	147.0	23.2	105 000	15.5	0.955
18.0	5 200	192.0	30.5	75 800	14.6	0.955
478—I—A irradiated in vacuum.						
0	275 000	3.6	0	2 180 000	7.9	0.915
7.3	22 100	45.3	6.8	205 000	9.3	0.895
10.6	14 800	68.0	10.4	134 000	9.1	0.894
14.0	12 700	79.6	12.3	89 300	7.1	—
17.35	10 300	96.7	15.1	69 400	6.7	0.893
Onkotin 179 irradiated in air.						
0	33 500	29.8	0	125 000	3.7	0.700
6.2	11 800	84.7	8.9	68 500	5.8	0.852
13.5	7 700	130.0	16.2	57 800	7.5	0.852
18.0	5 700	174.2	23.4	45 700	7.9	0.850
Onkotin 179 irradiated in vacuum.						
0	33 500	29.8	0	125 000	3.7	0.700
4.5	19 100	52.4	3.7	77 500	4.1	0.785
11.9	11 000	90.6	9.9	66 700	6.0	0.794
18.4	8 700	115.7	14.0	52 600	6.1	0.803
823—327—VI irradiated in air.						
0	106 000	9.4	0	143 000	1.3	0.940
2.1	21 900	45.7	5.9	90 900	4.2	—
4.1	13 500	74.0	10.5	74 600	5.5	0.889
7.0	9 500	105.2	15.5	63 300	6.7	0.910
12.1	6 150	162.6	24.8	55 200	9.0	0.931
17.1	5 300	190.4	29.3	42 600	8.1	—
823—327—VI irradiated in vacuum.						
0	106 000	9.4	0	143 000	1.3	0.940
3.1	30 300	33 6	3.9	94 300	3.1	0.896
6.0	21 300	46.9	6.1	79 400	3.7	0.913
11.3	14 200	70.8	10.0	66 200	4.7	0.915
14.0	12 100	82 7	11.9	52 600	4.4	0.902
18.1	11 100	89.7	13.0	50 500	4.5	0.908

is higher in the presence of oxygen than in vacuum. The non-linear dependence of p on r for samples 478—I—A and 823—327—VI is not definitely ascertained. The difference between these two samples and Onkotin 179 may depend upon different accessibilities of various parts of the polymer in a degradation mechanism, where the presence of oxygen is important. In vacuum all three samples show the same behaviour within experimental errors. The p_o values per Mrad radiation dose are given in Table 2.

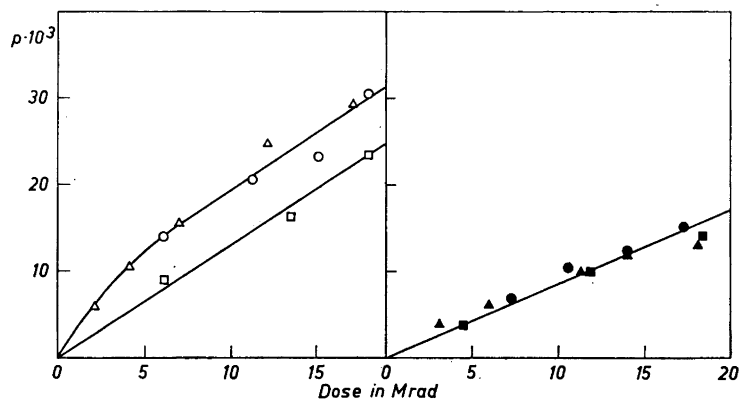

Fig. 1. The fracture density as a function of radiation dose. The following notations have been used

Sample	Air	Vacuum
478—I—A	○	●
823—327—VI	△	▲
Onkotin 179	□	■

Radiation yield. From the p_o values the yield of fractures per 100 eV, G, can easily be calculated [24],

$$G = 0.96 \times 10^6 \frac{p_o}{m}$$

The data are given in Table 2. These values compare with the value $G = 7.1$ obtained from data on irradiation of dextran with 800 keV electrons [4] and $G = 10$ for cellulose [25]. For amylopectin the value $G = 14.5$ has been reported [11]. Converting the G values into energies per bond fracture we get the values in the last column of Table 2.

Degree of branching. The degree of branching of the dextran molecules measured as the number, q, of 1→6 linkages is also given in Table 1. The most

Table 2. Radiation yield data for dextran.

Sample	Fracture density per unit dose (in Mrad)	G value Fractures/100 eV	Energy per broken bond eV
Air:			
478—I—A, 823—327—VI	$\sim 1.8 \times 10^{-3}$	11	~ 9
Onkotin 179	1.3×10^{-3}	7.7	13
Vacuum:			
478—I—A, 823—327—VI, Onkotin 179	0.87×10^{-3}	5.2	19
Dextran [4]	—	—	14
Cellulose [25]	—	—	10
Amylopectin [11]	—	—	7

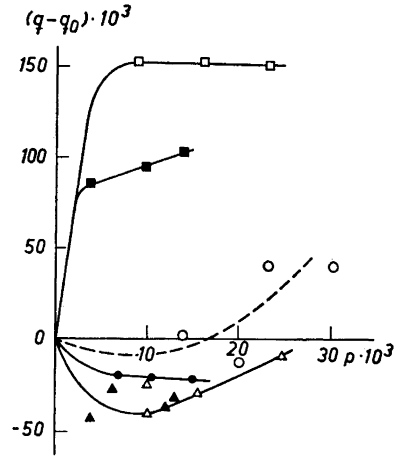

Fig. 2. Change in number of branches as a function of the fracture density. For symbols *cf.* Fig. 1

highly branched species is Onkotin 179. Samples 478—I—A and Onkotin 179 show a decrease in degree of branching when irradiated in air. In vacuum 478—I—A becomes more branched as the radiation dose increases but for Onkotin 179 the number of branches still decreases. Both in air and in vacuum the degree of branching of sample 823—327—VI increases at low doses, whereas at higher doses it has a tendency to decrease. The change of the degree of branching, given as the quantity $q-q_o$, with the fracture density, p, is given in Fig. 2.

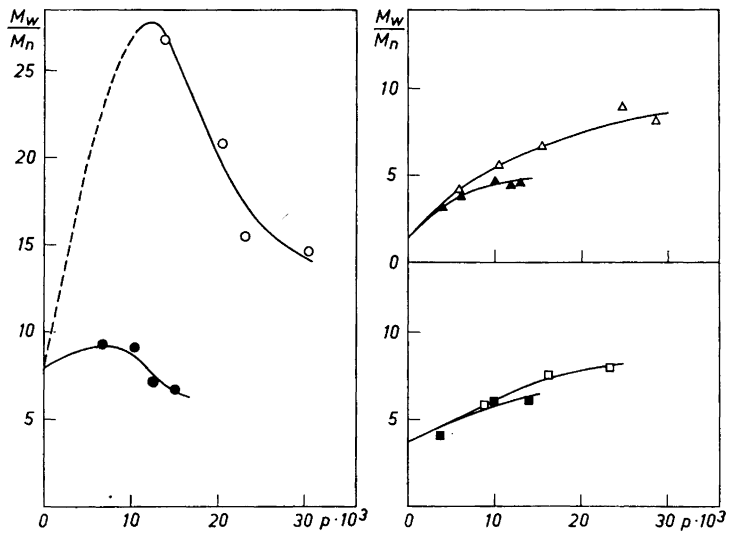

Fig. 3. Polymolecularity measured as M_w/M_n as a function of fracture density. For symbols *cf.* Fig. 1.

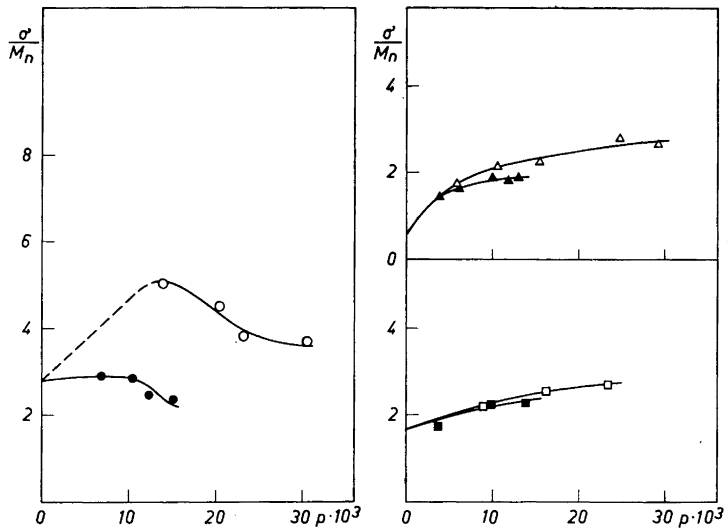

Fig. 4. Polymolecularity, measured as σ/M_n, as a function of fracture density. For symbols *cf.* Fig. 1.

Polymolecularity. The change in molecular weight distribution during the degradation has been measured as the ratio M_w/M_n. The values obtained are given in Table 1. In Fig. 3 the variation with the fracture density is given. As a further measure of the heterogeneity the quantity σ/M_n, where $\sigma = \sqrt{M_n(M_w - M_n)}$ is the mean deviation from the number average molecular weight, has been used and plotted against the fracture density in Fig. 4. The molecular weight distributions for the two samples of 478—I—A irradiated

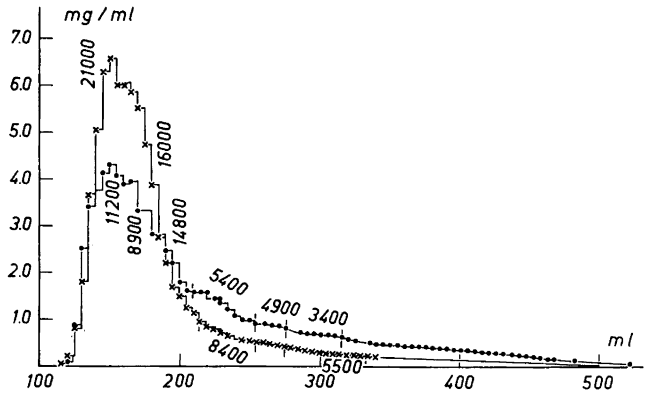

Fig. 5. Distribution curves from gel filtration experiments. ●——● refers to irradiation in air.

Table 3. Number average molecular weights of some fractions obtained by using the gel filtration technique on samples from 478—I—A.

Irradiation in vacuum Dose: 17.35 Mrad. $M_w/M_n = 6.7$		Irradiation in air Dose: 18.0 Mrad. $M_w/M_n = 14.6$	
Amount of fraction %	M_n	Amount of fraction %	M_n
8.0	>21 000	9.3	>11 200
36.6	21 000	24.6	11 200
17.2	16 000	12.9	8 900
10.0	14 800	11.6	5 400
7.0	8 400	4.2	4 900
3.8	5 500	7.9	3 400
5.0	< 5 500	12.3	< 3 400

to 18 Mrad are given in Fig. 5. Some pertinent data for these samples are also given in Table 3.

Electron spin resonance measurements. Some studies have been undertaken in order to get information about the free radicals formed during the irradiation of dextran [6]. Irradiated samples were investigated both for the number of free radicals formed and for their structure. The number was found to be proportional to the dose given. The resonance spectrum obtained is shown in Fig. 6. It corresponded to a g value of 2.005 and the line width was 26 gauss. The line has a hyperfine splitting which is quite evident but not very well resolved. The splitting was estimated to 3—6 gauss. The life time of the radicals was measured at 20°C and 50°C. The decay was found to be very slow at the lower temperature and a change was hardly detectable: a half life of about 12.5 weeks was estimated. At the higher temperature a more rapid decay was observed during the first day, half life 8.5 h. Later the decay was considerably reduced: half life 12.5 days. The decay curve at 50°C is given in Fig. 7.

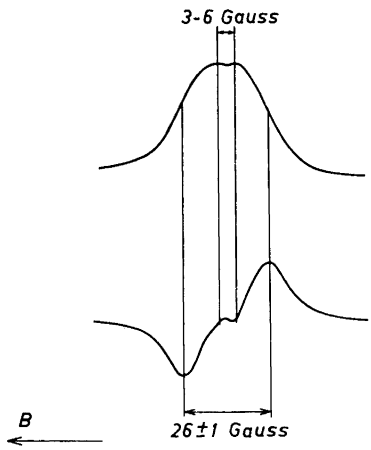

Fig. 6. Spin resonance spectrum of irradiated dextran. The arrow indicates increasing magnetic field.

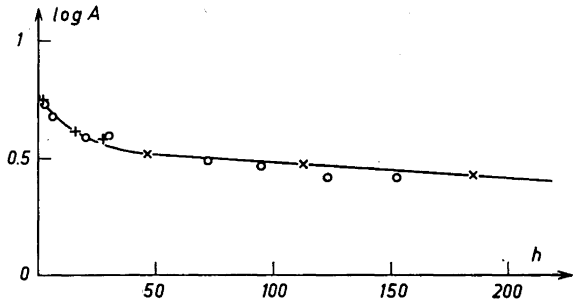

Fig. 7. Decay curve for free radicals at 50°C. A is the number of free radicals. The doses are: 4 Mrad (O), 6.5 Mrad (+).

DISCUSSION

An essential point in the present work is the correct determination of the number of broken bonds. Each broken linkage between two glucose units will increase the number of molecules by one. The number of molecules counted after a certain dose of radiation depends upon the type of end-group formed because of the chemical end-group method employed. Somogyi's method only detects reducing end-groups, *i.e.* groups having the configuration

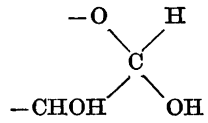

at carbon atom number 1. If other types of end-groups are formed an error will be introduced. The necessary condition for obtaining reducing end-groups is that one hydrogen atom and one hydroxyl group are present and that these can be attached to the O and C atoms of the broken glucosidic linkage. A reducing group could be formed by intramolecular transfer of a hydrogen atom over a C—C bond distance but that process would introduce steric strain in the hydrogen donor glucose unit and is therefore unlikely to occur. If the degradation reaction proceeded predominantly in the solid phase one would expect the water content in the material to exert a pronounced effect. This is not the case. With respect to the long half life of the free radicals formed in the solid state only very slow reactions in which these radicals take part are likely to occur. Therefore, most of the energy deposited in the solid samples through the radiation is probably stored and possible reactions only start when the samples are dissolved in water. Then reducing end-groups can be formed because there is no lack of water. The irradiation of glucose shows that the reducing groups themselves are not influenced by the radiation. The rather good agreement between the molecular weight values obtained by Somogyi's method and the osmotic measurement gives no evidence that any appreciable errors should be introduced when using Somogyi's method for obtaining the number of broken bonds.

The influence of oxygen on the degradation is not very easy to interpret. The reproducibility seems to be low and also the size of the dextran grains appears of importance. The results from the gel filtration fractionation shows that the molecular weight distribution is not exactly the same after degradation in air and in vacuum. The weight fraction of low molecular weight material is higher after irradiation in air.

The radiation yields given in Table 2 correspond to an energy per broken bond of the order of 10—20 eV. This value is much higher than the real bond energy. Some significant values are, 3.64 eV for C—C bonds, 3.45 eV for C—O bonds and 4.54 eV for O—H bonds. From these figures it seems most reasonably to presume a higher probability of cleavage for C—C or C—O bonds. On the other hand these figures refer to the formation of bonds in molecules in their ground state. The conditions must be quite different when the molecule is excited or ionized. The first ionization potential for organic molecules is around 10 eV. This is the lowest amount of energy that must be transferred to the molecule from the gamma quantum in order to produce an ionization. In practice about three times this value is necessary for the formation of an ion pair.

Chain scission will only occur for broken C—O bonds outside the glucose unit, *i.e.* in the glucosidic links. If the immediate result of the gamma quantum is to remove one of the p_z electrons from the ether oxygen then the following two radical ions can be formed

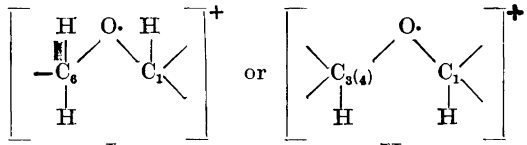

I II

depending upon which type of glucosidic linkage is attacked. In this connection it may be mentioned that the binding energy of 1 → 4-linkages is about 0.13 eV (3 kcal/mole) lower than the binding energy of a 1 → 6-linkage [26]. Further it has been observed that 1 → 4-linkages break down about four times faster than 1 → 6-linkages [27]. As the 1 → 4- and 1 → 3-linkages are very similar, the 1 → 3-linkage is also probably weaker than the 1 → 6-linkage. The radical ion may dissociate into one free radical and one positive ion

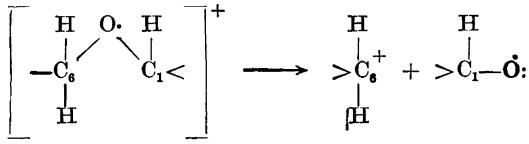

(1)

When examining the electron spin resonance spectra, one finds that the observed hyperfine structure may indicate a weak interaction with one proton spin. It means that the electron spin density for the carbon atom C_1 might attain a low value but in the radical ions it would have to be zero for the C_3 and C_6 carbon atoms. Alkoxy radicals of the type RO· exhibit a hyperfine

pattern which suggests weak interaction with the α hydrogens but negligible interaction with the β hydrogens [28]. Due to the proximity of the C_1 carbon atom to another oxygen atom the coupling of the electron spin to the proton spins of the hydrogens at the C_3 and C_6 carbon atoms may be still more reduced. Then either of the radicals I and II or the radical formed during the dissociation would have a structure in accordance with the electron spin resonance spectrum. Further the absence of any additional hyperfine structure with lines separated by 20—30 gauss typical for hydrocarbon radicals would support the hypothesis put forward in the reaction (1) that a positive hydrocarbon-like ion is formed. There is nothing in the existing data which contradicts the possibility that this reaction proceeds in solid material. When dissolving the irradiated dextran in water the following reactions may occur,

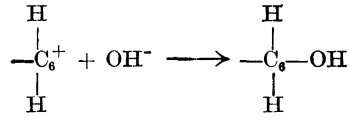

(2)

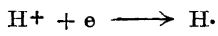

(3)

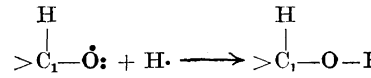

(4)

The last group constitutes a reducing end-group. The hypothesis presented here for the cleavage process of the glucosidic bonds is only a tentative approach to a certainly very complicated mechanism.

That the changes are rather complicated is evident from the changes in degree of branching occurring during the degradation process. The variation of the number of branches per monomer unit (the $q - q_0$ values in Fig. 2) during the irradiation differs very much between the three samples. Onkotin 179 has a high original degree of branching and it undergoes a considerable degradation as far as the branches are concerned during the first part of the breakdown process. In the presence of oxygen the unbranching will finally cease. In vacuum degradation proceeds continually but at a much lower rate. The behaviour of sample 478—I—A in air is not very clear. Initially the degree of branching seems to remain constant but subsequently unbranching probably begins. In vacuum the number of branches per monomer increases at the same time as the fracture density increases. For the sample 823—327—VI the enhanced degree of branching is quite evident both in the presence of air and in vacuum. The degree of branching has an optimum value after which it starts to decrease. It is evident that rather complicated processes must occur and the behaviour of the samples can only be explained if it is assumed that the units which once have been cut off have the ability to reunite with the macromolecules at different points. What is happening is then a combined degradation and rearrangement. In Onkotin 179 which is heavily branched the cut off units are most likely rather small [29]. These units will preferably be attached to the chain ends because of the limited space available along the chains. Finally a structure of the polymer molecule is

obtained which undergoes a "normal" degradation. In the case of 478—I—A in vacuum and 823—327—VI both in vacuum and in air the cut off units will preferably attach themselves to glucose units somewhere along the chain to form new branches. The initially low degree of branching of these samples gives the spatial requirements for favouring such an attachment. After a certain degree of branching has been reached the probability for branch formation along the chain is reduced and then attachement to the chain end will start to dominate, which results in a lowering of the degree of branching in the same way as for Onkotin 179. It should be mentioned that the same general connection between initial degree of branching and the branching behaviour during degradation has also been found in acid hydrolysis of dextran [12]. The possibility of branching through rearrangement has previously been discussed for dextran molecules [30] but mainly with regard to its influence on the molecular properties. This problem of degradation and increase in degree of branching is evidently closely related to the question of simultaneous bond scission and crosslinking.

Figs. 3 and 4 give the general behaviour of the samples as far as changes in polymolecularity are concerned. All three samples show the same tendency to become more polymolecular when degradation increases. In air the heterogeneity of sample 478—I—A reaches a maximum after which the sample becomes progressively more homogeneous. The other two samples show little difference between irradiation in air and in vacuum but a tendency to form a maximum heterogeneity is exhibited. The higher polymolecularities in air compared to vacuum indicates that in the presence of oxygen smaller fragments are cut off. This will effect the M_n value more than the M_w value. Also with respect to polymolecularity the acid hydrolysis gives the same general picture [12].

Acknowledgements. The authors are much indebted to Professors The Svedberg, Stig Claesson, and Kai Siegbahn for their interest in this work and for the facilities put at their disposal.

REFERENCES

1. Ingelman, B. and Halling, M. *Arkiv Kemi* **1** (1949) 61.
2. Ingelman, B. *Acta Chem. Scand.* **2** (1948) 803.
3. Stacey, M. *Research* **4** (1951) 48. Lockwood, A. *Chem. & Ind. London* **1951** 46.
4. Price, F., Bellamy, W. and Lawton, E. *J. Phys. Chem.* **58** (1954) 21.
5. U.S. Patent 2,867,571 (1959).
6. Kinell, P.-O., Granath, K. and Vänngård, T. *Arkiv Fysik* **13** (1958) 272.
7. Ricketts, C. and Rowe, C. *Chem. & Ind. London* **1954** 189.
8. Lang, R., Schmitt, E., Henley, E. and Gaden, E. *Termination Report* (1956) April 15, United States Atomic Energy Comm.
9. Phillips, G. and Moody, G. *J. Chem. Soc.* **1958** 3534.
10. Moody, G. and Phillips, G. *Chem. & Ind. London* **1959** 1247.
11. Ehrenberg, L., Jaarma, M. and Zimmer, E. *Acta Chem. Scand.* **11** (1957) 950.
12. Granath, K. *Unpublished.*
13. Schmid, G., Schneider, Ch. and Henglein, A. *Kolloid. Z.* **148** (1956) 73.
14. Scocca, P. and Brenner, F. Abstr. of Papers, ACS Meeting 122, Sept. 1952.
15. Kinell, P.-O. and Larsson, B. *Risö Report* No. 16 (1960) p. 9.
16. Isbell, H., Snyder, C., Holt, N. and Dryden, M. *J. Research Natl. Bur. Standards* **50** (1953) 81.

17. Saeman, J., Millett, M. and Lawton, E. *Ind. Eng. Chem.* **44** (1952) 2848.
18. Peat, S., Whelan, W. and Roberts, J. *J. Chem. Soc.* **1956** 2258.
19. Granath, K. *J. Colloid. Sci.* **13** (1958) 308.
20. Jeanes, A. and Wilham, C. *J. Am. Chem. Soc.* **72** (1950) 2655.
21. Porath, J. and Flodin, P. *Nature* **183** (1959) 1657.
22. Flodin, P. and Granath, K. *Symposium über Makromoleküle*, Wiesbaden 1959.
23. Scott, T. and Melvin, E. *Anal. Chem.* **25** (1953) 1656.
24. Charlesby, A. *Atomic Radiation and Polymers*, Pergamon Press, Oxford 1960, p. 137.
25. Ref.[24], p. 361.
26. Jeanes, A., Schieltz, N. and Wilham, C. *J. Biol. Chem.* **176** (1948) 617.
27. Swanson, M. and Cori, C. *J. Biol. Chem.* **172** (1948) 797; Carlqvist, B. *Acta Chem. Scand.* **2** (1948) 759.
28. *Technical Information Bulletin from the Radio-Frequency Spectroscopy Laboratories of the Instrument Division, Varian Associates*, Palo Alto, Calif. **2** (1959) No. 4.
29. Van Cleve, J., Schaefer, W. and Rist, C. *J. Am. Chem. Soc.* **78** (1956) 4435.
30. Bovey, F. *J. Polymer Sci* **35** (1959) 183.

Received September 8, 1960.

ACTA CHEMICA SCANDINAVICA 15 (1961) 154–158

Dihydrochalcones from the Fronds of *Pityrogramma chrysophylla* var. *marginata*, Domin

MARTIN NILSSON

Organisk-kemiska Institutionen, Kungl. Tekniska Högskolan, Stockholm, Sweden

2′,6′-Dihydroxy-4′-methoxydihydrochalcone (I) and 2′,6′-dihydroxy-4,4′-dimethoxydihydrochalcone (II) were isolated from the fronds of the title fern and were also prepared by hydrogenolysis of the appropriate, known, flavanones.

Recently ceroptene, the yellow pigment of the "goldenbacked fern", *Pityrogramma triangularis*, was re-investigated in this laboratory and was found to be a C-methylated chalcone derivative [1,2]. In the same genus there are also ferns, which are characterised by a white coating on the back of the fronds and in an early investigation of such a "silver fern", *P. calomelanos* (the genus then was given as *Gymnogramme*), Zopf isolated a colourless compound, m.p. 141—142° ($C_{20}H_{22}O_6$?), which he named calomelanene [3].

A sample of another silver fern, *P. chrysophylla* var. *marginata* Domin, has now been available for investigation. The white coating was removed by extraction with ether. From the extract a colourless phenol, m.p. 173—175°, was obtained merely by recrystallisation. The mother liquors also contained a small amount of another phenolic component, m.p. 143—145°, which was isolated by partition chromatography.

The compound, m.p. 175°, analysed for $C_{16}H_{16}O_4$ and contained one methoxyl group. It gave rapidly a bright red colour with diazotised benzidine and a strong, brownish red colour with iron(III)chloride. The infrared spectrum indicated the presence of an *o*-hydroxyacylophenone structure, a non-chelated hydroxyl group and a mono-substituted benzene ring.

Among known compounds with these structural features a phenol, m.p. 165°, identified as 2′,6′-dihydroxy-4′-methoxydihydrochalcone (I), has been isolated from the essential oil of *Populus balsamifera* L. by Goris and Canal [4], who also prepared it by mono-methylation of 2′,4′,6′-trihydroxydihydrochalcone [5].

The structure of the present phenol at first was determined indirectly. A Houben-Hoesch condensation of phloroglucinol monomethylether and β-phenylpropionitrile afforded a compound, m.p. 194—197°, which by analogy with acylations with acetonitrile [6] and benzonitrile [7] should be 2′,4′-dihydroxy-

6′-methoxydihydrochalcone. On methylation with diazomethane 2′-hydroxy-4′,6′-dimethoxydihydrochalcone was obtained. The same dimethyl ether was formed on methylation of the natural product also. The position of the methoxyl group was not, however, yet rigidly proved. Hydrogenolysis of flavanones to dihydrochalcones has been successfully applied, *e.g.* for the conversion of naringenin to phloretin [8]. In the present case catalytic hydrogenation of 5-hydroxy-7-methoxyflavanone gave a compound identical with the natural product, m.p. 175°, thereby conclusively proving it to be 2′,6′-dihydroxy-4′-methoxydihydrochalcone (I).

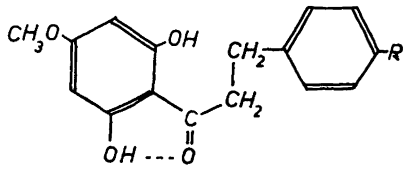

I R = H

II R = OCH_3

The other compound, m.p. 145°, had the composition $C_{17}H_{18}O_5$ and contained two methoxyl groups. The colour reactions and the spectra were largely similar to those of the first dihydrochalcone. However in the infrared spectrum the absorptions due to the mono-substituted benzene ring were absent and a new band at 815 cm^{-1} indicated the presence of two adjacent hydrogen atoms on an aromatic ring. It seemed reasonable to assume the new compound to be a dimethyl ether of phloretin (2′,4,4′,6′-tetrahydroxydihydrochalcone). This was proved by methylation with diazomethane to give phloretin trimethyl ether. The positions of the methoxyl groups were established by hydrogenolysis of 5-hydroxy-4′,7-dimethoxyflavanone to give a compound identical with the natural product, which is therefore 2′,6′-dihydroxy-4,4′-dimethoxydihydrochalcone (II).

The problem of defining the position of the methoxyl groups in phloroacylophenone monomethyl ethers is a classical one, which in this case was easily solved by relating the products to known flavanones. In other cases it has been solved by more laborious procedures involving alternating methylation and ethylation [6] or ethylation followed by oxidation to quinones [7]. The infrared spectra of the present dihydrochalcones and some related compounds indicate that the choice between 2-O-methyl- and 4-O-methylphloroacylophenones can be made by a study of the 1500—1700 cm^{-1} region of the infrared spectra. The results indicated in Fig. 1 are selfexplanatory. Essentially analogous spectra were recorded for 2-O-methyl- and 4-O-methylphloroacetophenone and for the corresponding phloretin dimethyl ethers. Thus the 4-O-methylphloroacylophenones investigated show a fairly sharp chelate carbonyl absorption band at *ca.* 1 640 cm^{-1} whereas the 2-O-methylphloroacylophenones are characterised by a broad band near 1 620 cm^{-1}. Also in the 1 500—1 600 cm^{-1} region the absorption patterns are different and characteristic.

Dihydrochalcones are apparently not very widely spread in nature. In the bibliography of Karrer [9] only phloretin, asebogenin and 2′,6′-dihydroxy-4′-methoxydihydrochalcone are mentioned. Of these phloretin and asebogenin seem to occur in nature only as glucosides.

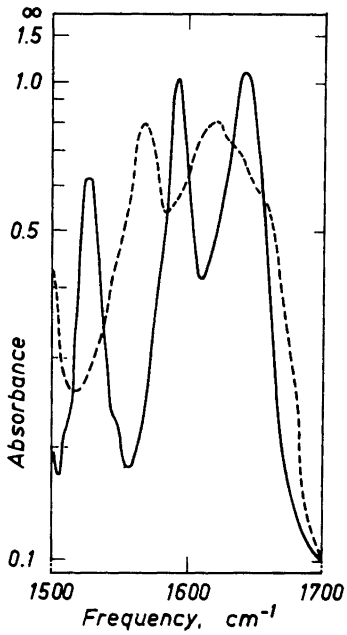

Fig. 1. Part of the infrared spectra for 2′,6′-dihydroxy-4′-methoxydihydrochalcone (I, ——) and 2′,4′-dihydroxy-6′-methoxydihydrochalcone (II, — —). Potassium bromide discs, 13 mm diam., 1 mg of sample.

As for the "calomelanene" mentioned in the introduction it seems that the composition $C_{17}H_{18}O_5$ would fit as well as that proposed by Zopf, who did not perform any determination of the molecular weight or methoxyl content. It is therefore very probable that calomelanene is identical with the 2′,6′-dihydroxy-4,4′-dimethoxydihydrochalcone.

EXPERIMENTAL

The melting points were determined on a Kofler block. The infrared spectra were recorded on a Perkin Elmer No. 21 instrument (sodium chloride prism and potassium bromide discs) and the ultraviolet spectra on a Beckman DK-2 spectrophotometer (solvent ethanol).

Isolation procedures. Air-dried fronds and stems of *Pityrogramma chrysophylla* var. *marginata* collected and identified in the Royal Botanic Gardens, Kew, Richmond, Surrey, England, during the autumn 1958 (7.1 g) were rapidly extracted with ether. The extract was filtered and on evaporation afforded a somewhat waxy material (1.04 g), which melted with some decomposition at 147—165°. Recrystallisation from benzene gave a crystalline material, m.p. 166—170° (0.35 g).

The material in the mother liquors was partitioned between light petroleum (b.p. 40—60°) and dimethyl sulphoxide. The petroleum phase on evaporation gave a colourless wax, m.p. 50—66° (0.1 g), the infrared spectrum of which indicated the presence of hydrocarbons and small amounts of ketones and alcohols. The benzidine test indicated that no phenolic material was present in this fraction. The dimethyl sulphoxide solution was poured into a large excess of water and the mixture was exhaustively extracted with ether. The ether extract after washing and drying was evaporated to give a solid (0.5 g).

Chromatography on paper impregnated with an ethylenediaminetetraacetic acid buffer using dimethyl sulphoxide as the stationary and *iso*propyl ether as the mobile phase according to Wachtmeister and Wickberg [10] showed the presence of the compound isolated

above (R_F 0.20) and another phenolic component (R_F 0.13). There was also a minor component (R_F 0.08).

The mixture was separated by chromatography on a silica gel column impregnated with dimethyl sulphoxide using *iso*propyl ether as the eluant [11]. It was also found advantageous to treat the silica gel with EDTA-buffer. The silica gel was pretreated with nitric acid (*d* 1.42), washed with water and then with a buffer containing 0.015 M disodium-EDTA and 0.005 M EDTA and dried at 120° without any additional washing with water. This chromatography gave a further amount of the compound, m.p. *ca.* 170°, and the compound, R_F 0.13 (60 mg, m.p. *ca.* 140°).

Investigation of the compound m.p. ca. *170°.* Recrystallisation from benzene and sublimation (0.005 mm) gave the pure compound as plates, m.p. 173—175°. (Found: C 70.5; H 5.9; O 23.3; CH_3O 11.1. Calc. for $C_{16}H_{16}O_4$: C 70.6; H 5.9; O 23.5; CH_3O (one) 11.4.)

Infrared spectrum: 3 240 m, 3 050 w, 3 000 w, 2 960 w, 2 930 w, 2 850 w, 2 800—2 400 w, 1 640 s, 1 590 s, 1 525 m, 1 500 w, 1 470 w, 1 435 m, 1 430 m, 1 385 m, 1 360 m, 1 330 w, 1 300 m, 1 230 m, 1 215 s, 1 160 m, 1 080 m, 1 065 w, 1 040 w, 1 030 w, 980 w, 960 m, 905 w, 845 w, 810 s, 765 w, 750 m, 725 w, and 700 cm^{-1} m.

Ultraviolet absorptions: $\lambda_{shoulder}$ 330 mμ (log ε 3.5), λ_{max} 285 (4.37), 226 (4.29) and 210 (4.38).

Compound m.p. ca. *140°.* Recrystallisation from benzene and sublimation gave plates, m.p. 142—145°. (Found: C 66.8; H 6.0; CH_3O 19.8. Calc. for $C_{17}H_{18}O_5$: C 67.5; H 6.0; CH_3O (two) 20.5.)

Infrared spectrum: 3 220 m, 3 020 w, 2 980 w, 2 920 w, 2 810 w, 2 800—2 400 w, 1 640 s, 1 610 m, 1 590 s, 1 525 m, 1 510 s, 1 465 m, 1 440 s, 1 425 m, 1 390 m, 1 360 m, 1 295 m, 1 245 s, 1 220 m, 1 210 s, 1 175 m, 1 160 m, 1 100 w, 1 075 m, 1 060 w, 1 030 m, 975 w, 960 m, 905 w, 855 w, 815 m, 805 s, 790 w and 720 cm^{-1} w.

Ultraviolet absorptions: $\lambda_{shoulder}$ 330 mμ (log ε 3.5), λ_{max} 286 (4.34), 225 (4.40) and 210 (4.33).

Houben-Hoesch acylations. A mixture of phloroglucinol monomethyl ether [12] (0.01 mole), β-phenylpropionitrile [13] or β-(*p*-methoxyphenyl)-propionitrile [15] (0.01 mole) and freshly fused zinc chloride (*ca.* 1 g) in dry ether (50 ml) was saturated with dry hydrogen chloride at 0° and left in the refrigerator for 2—4 days. The supernatant was discarded, the remaining oil or crystalline mixture was washed with small portions of ether and then boiled with water (100 ml) for 1 h and left to cool. The phloroacylophenones crystallised in a fairly pure state in ca 60 % yield. Water of crystallisation was present but was readily removed by drying at 100°.

2′,4′-Dihydroxy-6′-methoxydihydrochalcone was obtained as needles from benzene, m.p. 194—197° (strong sublimation). (Found: C 70.9; H 6.1; CH_3O 11.3. Calc. for $C_{16}H_{16}O_4$: C 70.6; H 5.9; CH_3O 11.4). (Lit. m.p. 189° [15]).

2′,4′-Dihydroxy-4,6′-dimethoxydihydrochalcone crystallised as needles from benzene, m.p. 175—177°. (Found: C 67.8; H 6.0; CH_3O 20.3. Calc. for $C_{17}H_{18}O_5$: C 67.5; H 6.0; CH_3O 20.5).

Methylations. Treatment of 2′,4′-dihydroxy-6′-methoxydihydrochalcone with excess diazomethane in methanol-ether overnight afforded a quantitative yield of 2′-hydroxy-4′,6′-dimethoxydihydrochalcone, which was recrystallised from methanol and from *cyclo*hexane to give prisms, m.p. 106—108°. (Found: C 71.4; H 6.4; CH_3O 21.3. Calc. for $C_{17}H_{18}O_4$: C 71.3; H 6.3; CH_3O 21.7.) It gave a strong brownish red colour with iron(III)-chloride.

Methylation of the phenol, m.p. 173—175°, afforded the same compound, m.p. and mixed m.p. 105—107°. The infrared spectra were identical.

Similarly methylations of 2′,4′-dihydroxy-4,6′-dimethoxydihydrochalcone and the phenol, m.p. 143—145°, afforded phloretin trimethyl ether, m.p. and mixed m.p. 108—110°

Hydrogenations. 5,7-Dihydroxyflavanone was prepared according to Rosenmund's method and was methylated with diazomethane to give 5-hydroxy-7- methoxyflavanone, m.p. 100—102°.

The flavanone (20 mg), palladised charcoal (20 mg, 10 %) and ethanol (10 ml) were shaken in a hydrogen atmosphere for 48 h. Paper chromatography then indicated that most of the starting material had been consumed and that a compound with the same R_F-value as the phenol, m.p. 173—175°, had been formed. The hydrogen consumption was not measured. After filtering the solvent was evaporated and the residue recrys-

tallised from benzene and sublimed to afford a product, m.p. 172—174°, alone or in admixture with the natural product. The infrared spectra were identical.

Naringenin was prepared by acid hydrolysis of commercial naringin (Eastman) and was methylated with diazomethane to 5-hydroxy-4′,7-dimethoxyflavanone, m.p. 119—120°. Hydrogenation as above furnished a product with the same R_F value as the phenol, m.p. 143—145°, and after recrystallisation from benzene and sublimation the identity of the two products was proved by mixed melting point determination and comparison of the infrared spectra.

Acknowledgements. I wish to thank Dr. G. Taylor, Royal Botanic Gardens, Kew, for the fern material, Professor H. Erdtman for his encouraging interest, Miss Gurli Hammarberg for the spectral measurements, Mr. E. Pettersson for technical assistance and Dr. B. R. Thomas for linguistic criticism.

REFERENCES

1. Nilsson, M. *Acta Chem. Scand.* **13** (1959) 750.
2. Forsén, S. and Nilsson, M. *Acta Chem. Scand.* **13** (1959) 1383.
3. Zopf, W. *Ber. deut. botan. Ges.* **24** (1906) 264.
4. Goris, A. and Canal, H. *Compt. rend.* **201** (1935) 1435.
5. Goris, A. and Canal, H. *Compt. rend.* **201** (1935) 1520.
6. Sonn, A. *Ber.* **61** (1928) 2300.
7. Späth, E. and Wessely, F. *Monatsh.* **49** (1928) 229.
8. Rosenmund, K. W. and Rosenmund, M. *Ber.* **61** (1928) 2608.
9. Karrer, W. *Konstitution und Vorkommen der organischen Pflanzenstoffe*, Birkhäuser Verlag, Basel 1958, p. 189.
10. Wachtmeister, C. A. and Wickberg, B. *Acta Chem. Scand.* **12** (1958) 1335.
11. Lindberg, B. and Wickberg, B. *Arkiv Kemi* **13** (1958—59) 447.
12. Zemplén, G., Bognár, R. and Thiele, K. *Ber.* **77** (1944) 446.
13. Klarmann, E. *J. Am. Chem. Soc.* **48** (1926) 2358.
14. Evans, W. L. and Walker, N. *J. Chem. Soc.* **1947** 1571.
15. Zemplén, G., Bognár, R. and Mechner, J. *Ber.* **77** (1944) 99.

Received September 17, 1960.

ACTA CHEMICA SCANDINAVICA 15 (1961) 159–166

On the Reaction between Platinum and Sulfur, Selenium, or Tellurium. I. Preparation of PtS, $PtSe_{0.80}$, and PtTe

ARNE KJEKSHUS

Kjemisk Institutt A, Universitetet i Oslo, Blindern, Norway

The direct syntheses of PtS, $PtSe_{0.80}$ and PtTe from different materials of platinum have been studied by means of X-ray and metallographic methods in the temperature region 700—1 150°C. While these compounds are easily prepared from powdered platinum in this temperature range, the results are dependent upon temperature for platinum plate or wire. At temperatures below the melting point of the compounds layers of di- and "mono"-chalkogenides are formed on the platinum plates and platinum wires during the reaction. The reaction apparently ceases when one half of the platinum has reacted. A possible explanation is proposed in terms of the existing theories for oxidation.

The reaction of sulfur, selenium and tellurium with platinum to form platinum "mono"-chalkogenides has been studied by many investigators [1–11]. A literature survey of the earlier studies on the platinum chalkogenides has been given by Grønvold *et al.*[1] According to Grønvold *et al.*[1], compounds with formal oxidation number +2 (+8/5) and +4 were found to exist by means of X-ray and density measurements, *cf.* Table 1. While "mono"-chalkogenides can be easily obtained from fine powdered platinum [1], attempts to make "mono"-chalkogenides from platinum plate or wire resulted in heterogeneous products with platinum and platinum di-chalkogenides as main constituents.

The published data indicate that the nature of the platinum metal is of fundamental importance in the reaction and new experiments were carried out to examine the difference between powdered platinum, platinum plate and platinum wire.

EXPERIMENTAL

Most of the platinum metal used in this study was platinum wire from Johnsen Matthey & Co., Ltd. A spectrographic analysis of the platinum showed about 0.05 % Au, 0.05 % Cu, 0.02 % Ir, 0.01 % Pd and 0.01 % Rh. No analysis was made on gaseous impurities (O_2, N_2, H_2) and carbon.

Sulfur from Schering-Kahlbaum A. G. (Sulfur cryst. puriss.) was purified by double distillation in a silica apparatus. Only the middle fractions were used. The highly purified

Table 1. Crystallographic data for the platinum chalkogenides.

Phase	Structure type	a(Å)	b(Å)	c(Å)	β(°)
PtS	B 17	3.4700		6.1096	
PtS_2	C 6	3.5432		5.0388	
$Pt_{10}Se_8$	MONOCL.	6.5806	4.6248	11.145	78.40
$PtSe_2$	C 6	3.7278		5.0813	
PtTe	ORTHOR.	6.6144	5.6360	11.865	
$PtTe_2$	C 6	4.0259		5.2209	

selenium was a gift from Bolidens Gruvaktiebolag, Sweden. It carried the analysis: 0.0002 % Cu, 0.0007 % Fe, 0.003 % Te, 0.01 % S and 0.003 % non volatile matter. Tellurium from The British Drug Houses Ltd. was purified by vacuum distillation in a silica apparatus. According to the spectrographic analysis the distilled product contained less than 0.01 % Fe and only traces of Al, Mg and Pb.

The samples were prepared by heating accurately weighed quantities of platinum and sulfur, selenium or tellurium, respectively, in evacuated and sealed, transparent silica tubes. Before each experiment the platinum specimens were degreased in chloroform and acetone, and finally rinsed in distilled water. The platinum wire, with diameter 0.45 mm, was cut into specimens about 30 mm long. The platinum sheets were cut into specimens about 10 × 3 × 0.2 mm.

The reaction of platinum with sulfur, selenium or tellurium was studied at temperatures between 700 and 1 150°C. By means of a variac the temperature of the heating furnace was kept constant within ± 5°C. The Pt/Pt-Rh thermocouple of the furnace was calibrated with a standard couple. Before the start of the run, the furnace was at room temperature. The furnace reached the desired temperature in a period of about one hour.

The X-ray diffraction investigation of the reaction products was carried out in powder cameras with 114.6 mm effective diameter, using filtered CuK-radiation. X-Ray photographs were taken on samples both from the total amount of the platinum chalkogenide scales and from different layers of the heterogeneous reaction product.

The thickness of the unreacted nucleus of platinum was measured with a micrometer.

The preparation of metallographic specimens proved difficult as the brittle chalkogenide layer became crushed and displaced during the grinding and polishing. The procedure which was adopted was to use araldite as the mounting material. After grinding, polishing with a fine grained diamond paste and final polishing with levigated alumina, transverse sections of the specimens were examined.

The microindentation hardness testing was performed with a Reichert microhardness tester (No. 1109) used in connection with a Reichert universal camera microscope (model MeF). The indenter was a Vickers pyramid. Variations in microhardness at a single load over transverse sections of the specimens were recorded. A comparatively low load — 8.4 g — was chosen. The cross sections to be tested, were always etched in 10 % NaCN + 10 % $(NH_4)_2S_2O_8$ (1 : 1 by volume) prior to the hardness measurements.

RESULTS

A. Fine powdered platinum

In agreement with the results of Grønvold *et al.*[1] both the "mono"-chalkogenides and the di-chalkogenides of platinum could be easily prepared from fine powdered platinum. According to the present results the reactions were

completed and homogeneous samples were obtained after heat treatment at 825°C for 2—4 days, depending on the chalkogen used.

The "mono"-chalkogenides PtS, $PtSe_{0.80}$ and PtTe were also obtained by adding platinum in the right proportion to the di-compounds and heating the samples at 825°C for 5 days.

B. Platinum sheet or wire

Melted samples. X-Ray powder photographs of melted alloys with composition $PtSe_{0.80}$, prepared from platinum sheet or wire and selenium showed the presence of Pt, $PtSe_{0.80}$ and $PtSe_2$. In agreement with the results of Grønvold *et al.*[1] this sample became homogenized on heating the finely ground alloys at 825°C, which is below the peritectic temperature.

According to the present results PtTe was obtained from platinum plate or wire and tellurium heated to the melting point or just below.

Attempts to synthesize the PtS phase by a similar method from the same platinum material failed, because PtS decomposes instead of melting. Neither could the samples be heated to a sufficiently high temperature since the sulfur pressure [4,12,13] made the quartz tubes burst.

Below the melting points. Experiments were made in the temperature region below 1 100°C for PtS and $PtSe_{0.80}$ and below 900°C for PtTe. The characteristic feature of these experiments is the growth after a short time of coatings of platinum chalkogenides on the plates and wires. The platinum chalkogenides form well adherent coatings. Unlike many other metal chalkogenide coatings these coatings did not spall during or after cooling of the specimens down to room temperature.

The results of the thickness measurements for the unreacted nucleus of the platinum wires are listed in Table 2. The thickness of the nucleus is found

Table 2. Thicknesses of unreacted platinum in platinum wires.

Sample	Melting point (°C)	Temperature (°C)	Thickness (mm) of platinum nucleus after			X-Ray photographs of layers show
			10 days	30 days	50 days	
PtS	Decomposes	700	0.43	0.43	0.43	PtS
		825	0.32	0.32	0.32	90—95 % PtS_2 10— 5 % PtS
		1 000		0.32		
$PtSe_{0.80}$	1 055 ± 15	825	0.35	0.34	0.34	85—90 % $PtSe_2$ 15—10 % $PtSe_{0.80}$
		1 000		0.34	0.34	
PtTe	925 ± 15	700		0.32	0.31	90—95 % $PtTe_2$ 10— 5 % PtTe
		825	0.31	0.31	0.31	
		900	Homogeneous product			PtTe

to be ≈ 0.32 mm, *i.e.*, nearly equal to the value $\frac{1}{\sqrt{2}} d \left(\frac{1}{\sqrt{2}} 0.45 \approx 0.32 \right)$ one would expect to find when one half of the platinum has reacted. The thickness of the unreacted nucleus does not change within the limits of the experimental error after ten days, *cf.* Table 2. Since no visible amounts of the metalloids are seen in the tubes a reaction of the type:

$$Pt + X_2 = PtX_2 \quad (X = S, Se \text{ or } Te)$$

is expected to have taken place.

X-Ray photographs of the platinum chalkogenide layers show that two phases are present. According to the X-ray photographs 90—95 % is found to be di-chalkogenides (PtS_2, $PtSe_2$ or $PtTe_2$) and 10—5 % "mono"-chalkogenides (PtS, $PtSe_{0.80}$ or PtTe). The X-ray results are accordingly in close agreement with the results of the thickness measurements.

Further X-ray studies indicate that the chalkogenide coatings are composed of two different layers. Fig. 1a is a drawing of the idealized distribution of the layers found on a sulfurized platinum wire. Next to the platinum core is found the PtS layer and further away the PtS_2 layer. A similar distribution of layers is found in the experiments to prepare $PtSe_{0.80}$ and PtTe. When platinum and tellurium react at 900 °C the X-ray photographs taken of the reaction product show that only PtTe is present. Fig. 1b shows the results which indicate that the wire form is preserved, while a hole appears in the centre of the wire. Similar holes seem also to be present in samples of PtS_2, $PtSe_2$ and $PtTe_2$, prepared from platinum sheet. The same was evidently also observed by Thomassen [9] by the preparation of platinum di-chalkogenides from platinum plates.

The surface appearance of the reacted specimens is dependent upon the reagent (sulfur, selenium or tellurium), temperature, pressure and the duration of the reaction. Initially the platinum chalkogenides formed do not lead to continuous chalkogenide scales, but nucleation of the platinum chalkogenides takes place in spots on the surface.

After a short time layers of a rather uniform thickness have grown up on the plates and wires. Fig. 2a shows a platinum sheet heated with sulfur for 1 day at 825°C. X-Ray photographs of the platinum sulfide layer gave the picture of the PtS_2-phase and the strongest reflections from the PtS-phase. At 700°C (*cf.* Table 2) this sulfide layer does not increase much in thickness

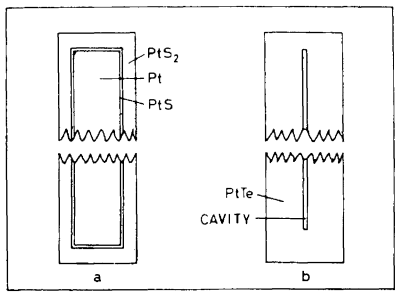

Fig. 1. The idealized distribution of the platinum chalkogenide layers on a platinum wire viewed in centralincision. *a*, Weighed quantities correspond to PtS. Temperature 825°C; *b*, PtTe prepared at 900°C.

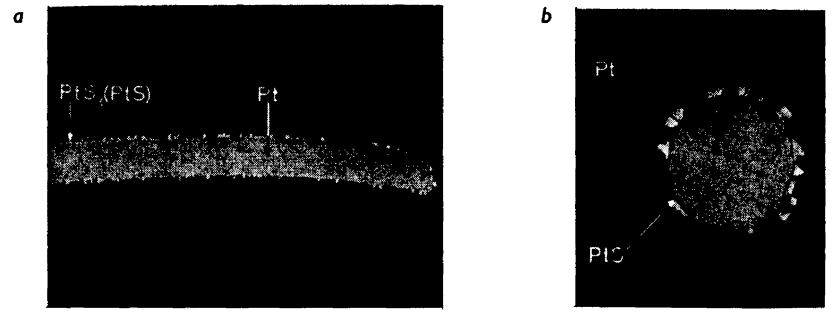

Fig. 2. Metallographic cross-section of platinum specimen heated with sulfur for *a*, 1 day at 825°C; *b*, 50 days at 700°C. Polarized light. 40 ×.

with time. Fig. 2b shows the cross-section of a platinum wire heated with sulfur for 50 days at 700°C.

Prolonged heating at higher temperatures leads to thick, well adherent platinum chalkogenide scales. The appearance of platinum sheet specimens after heat treatment at 825°C with selenium and tellurium is shown in Figs. 3a and b, respectively. In the case of platinum wire a distinct splitting of the di-chalkogenide layer along the wire is seen. Figs. 4a and b show cross section of wires heated with selenium and tellurium, respectively. As might be seen from the pictures, a preferred orientation normal to the metal surface is generally found in the "mono"-chalkogenide layers while recrystallization has taken place in the di-chalkogenide layers.

All the micrographs discussed so far, *cf.* Figs. 2—4, are from samples with weighed quantities corresponding to the "mono"-chalkogenides. Figs. 5a and b show the cross section of a platinum wire heated with a selenium amount corresponding to the formula $PtSe_{1.75}$ for 10 days at 825°C. The occurrence of the characteristic splitting is still more pronounced throughout the $PtSe_2$ layer in this sample.

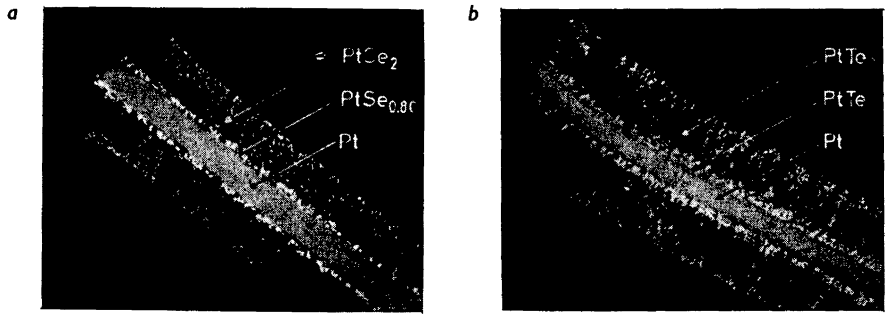

Fig. 3. Metallographic cross-section of platinum specimen heated with *a*, selenium (weighed quantities corresponds to $PtSe_{0.80}$); *b*, tellurium (weighed quantities corresponds to PtTe) for 10 days at 825°C. Polarized light. Platinum sheet turned 45° to incident beam. 40 ×.

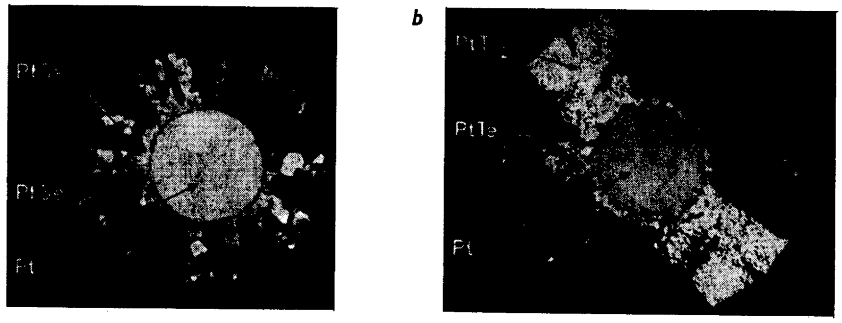

Fig. 4. Cross-section of platinum wire heated with *a*, selenium (weighed quantities corresponds to $PtSe_{0.80}$); *b*, tellurium (weighed quantities corresponds to PtTe) for 10 days at 825°C. Polarized light. 40 ×.

The results of the micro indentation hardness measurements in the metal core show an increase in the hardness near the platinum/platinum chalkogenide interface. Except for the platinum telluride samples the depth of contamination is found to be about 5—10 μ. The hardness curve for a representative platinum/platinum telluride sample is found in Fig. 6.

DISCUSSION

From thermodynamic reasoning one might expect to find in the case of the reaction between platinum and sulfur, selenium, or tellurium, a sequence of the platinum chalkogenides in the layers with the "mono"-chalkogenides near the platinum/platinum chalkogenide phase boundary and the di-chalkogenides in the outer part of the layers. Both the X-ray diffraction and metallographic studies show that this occurs.

A mixture of platinum metal and one of the platinum di-chalkogenides is thermodynamically unstable at the temperatures in question. The reason

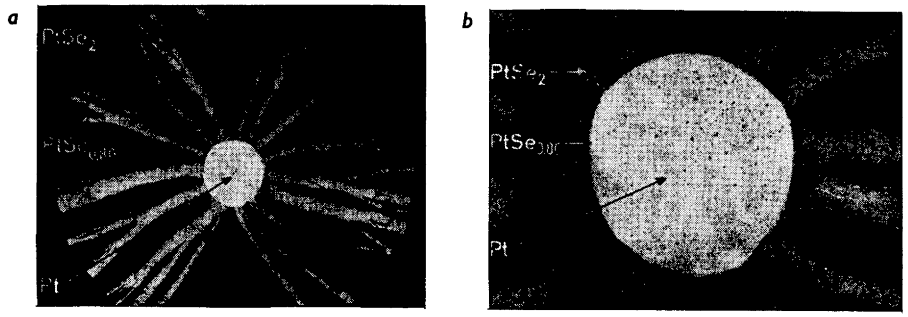

Fig. 5. Cross-section of platinum wire heated with selenium for 10 days at 825°C. Vertical illumination. *a*, 40 ×; *b*, 125 ×.

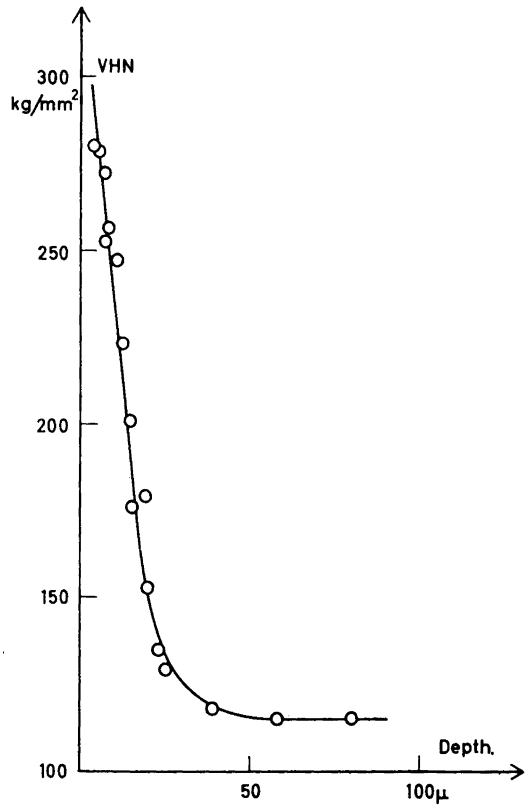

Fig. 6. Micro indentation hardness *versus* depth for a platinum sheet heated with tellurium for 10 days at 825°C.

why a reaction to form the "mono"-chalkogenides does not take place rapidly is that the reactants are separated by the intermediate layer of the "mono"-chalkogenides. Actually the reaction has to occur by diffusion of ions and electrons through the "mono"-chalkogenide layers and by reactions in the phase boundaries, *cf.* Fig. 7. Because of the observed holes in the samples of PtS_2, $PtSe_2$, $PtTe_2$ and PtTe (900°C) there are reasons for assuming

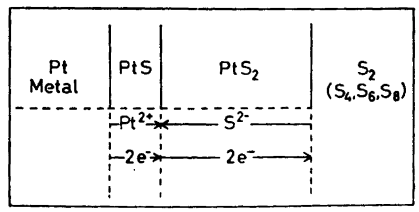

Fig. 7. A possible model for diffusion of ions and electrons in the platinum sulfide layers.

that platinum atoms or ions and electrons migrate through the "mono"-chalkogenide layers. Sulfur, selenium or tellurium atoms or ions and electrons diffuse in the di-chalkogenide layers. When unreacted sulfur, selenium or tellurium is present there is a considerable vapour pressure in the tubes. This pressure drops to the equilibrium pressure platinum di-chalkogenide/platinum "mono"-chalkogenide when the reaction to di-chalkogenide (and small amount of "mono"-chalkogenide) is completed. On the basis of the existing theories of oxidation the reaction velocity should be dependent upon this pressure. A considerably smaller rate might thus be expected from the moment no more unreacted sulfur, selenium or tellurium is left.

From the present study further information about the diffusion of atoms in the chalkogenide layers and reactions in the phase boundaries can not be obtained. It is, however, planned to carry out a detailed study of the kinetics of these reactions and to determine the ratelimiting step.

Acknowledgements. The author wishes to thank Professor Haakon Haraldsen for his interest in this study and for placing laboratory facilities at his disposal. Thanks are also due to Dosent Fredrik Grønvold at Kjemisk Institutt, and Dr. Earl A. Gulbrandsen (guest at S. I.), Dr. Per Kofstad, and siviling. Hallstein Kjøllesdal at Sentralinstitutt for Industriell Forskning for inspiring discussions.

REFERENCES

1. Grønvold, F., Haraldsen, H. and Kjekshus, A. *Acta Chem. Scand.* **14** 1960) 1879.
2. Davey, E. *Phil. Mag.* **40** (1812) 28; *Journal f. Chem. u. Phys.* **10** (1814) 382.
3. Bannister, R. and Hey, H. M. *Mineralog. Mag.* **23** (1932) 188.
4. Biltz, W. and Juza, R. *Z. anorg. u. allgem. Chem.* **190** (1930) 161.
5. Vauquelin, L. N. *Ann. chim. et phys.* **5** (1817) 260; *Journal f. Chem. u. Phys.* **20** (1818) 394.
6. Schneider, R. *Ann. Physik* **138** (1869) 604; **148** (1873) 625.
7. Wöhler, L., Ewald, K. and Krall, H. G. *Ber.* **66B** (1933) 1638.
8. Roessler, F. *Z. anorg. Chem.* **9** (1895) 31.
9. Thomassen, L. *Z. physik. Chem.* **B2** (1929) 349.
10. Roessler, C. *Z. anorg. Chem.* **15** (1897) 405.
11. Groeneveld Meijer, W. O. J. *Am. Mineralogist* **40** (1955) 647, 693.
12. Braune, H., Peter, S. and Neveling, V. *Z. Naturforsch.* **6a** (1951) 32.
13. Richardson, F. D. and Jeffes, J. H. *J. Iron Steel Inst. (London)* **171** (1952) 165.

Received September 7, 1960.

ACTA CHEMICA SCANDINAVICA 15 (1961) 167–174

The Crystal Structure of $SbCl_5 \cdot PO(CH_3)_3$

CARL-IVAR BRÄNDÉN and INGVAR LINDQVIST

Institute of Chemistry, University of Uppsala, Uppsala, Sweden

The crystal structure of $SbCl_5 \cdot PO(CH_3)_3$ has been determined and refined from three-dimensional X-ray data. The compound is isomorphous with $SbCl_5 \cdot POCl_3$. The Sb—O and P—O bond lengths are 1.99 ± 0.02 Å and 1.61 ± 0.02 Å, respectively. The Sb—O—P bond angle is 139.0° ± 2.4°.

Comparisons are made with the structures of $PO(CH_3)_3$ and $SbCl_5 \cdot POCl_3$. The predictions of the bond length variations in these compounds based on the theory for inductive effects on polar bonds has been confirmed. The nature of the P—O bond is briefly discussed.

The compounds $PO(CH_3)_3$ and $POCl_3$ both form adducts with a great number of Lewis acids. Sheldon and Tyree [1] have concluded from the shifts in the phosphoryl-bond stretching frequency that the oxygen atom functions as the donor atom in both these molecules; this was also found in the structure determination of $SbCl_5 \cdot POCl_3$[2]. We have found it interesting to compare the structures of the two similar addition compounds $SbCl_5 \cdot POCl_3$ and $SbCl_5 \cdot PO(CH_3)_3$.

CRYSTAL DATA

Single crystals of the compound $SbCl_5 \cdot PO(CH_3)_3$ were prepared by Olovsson in a way described earlier [3]. The crystals were stable in air during the time of exposure.

The unit cell dimensions of these orthorhombic crystals are very similar to those of $SbCl_5 \cdot POCl_3$, and the two compounds belong to the same space-group *Pnma* (extinctions $0kl$ for $k + l$ odd and $hk0$ for h odd).

The cell-dimensions of $SbCl_5 \cdot PO(CH_3)_3$ were determined from powder photographs taken in a camera of the Guinier type using $CrK\alpha_1$-radiation and with silicon ($a = 5.4306$ Å) as internal standard. They are listed below together with those of $SbCl_5 \cdot POCl_3$.

$SbCl_5 \cdot PO(CH_3)_3$	$SbCl_5 \cdot POCl_3$
$a = 16.66 \pm 0.02$ Å	$a = 16.42 \pm 0.01$ Å
$b = 8.205 \pm 0.01$ Å	$b = 8.06 \pm 0.01$ Å
$c = 8.865 \pm 0.01$ Å	$c = 8.93 \pm 0.02$ Å

The crystals are needle-shaped with the a-axis as needle-axis. A needle was cut in an approximately cubic form (0.005 × 0.005 × 0.006 mm) and mounted with the c-axis as rotation axis. Weissenberg photographs were taken. 8 zones (0—7) were recorded with CuK-radiation using the multiple-film technique. In order to get a connection between the zones a needle was mounted along the a-axis (dimensions 0.01 × 0.02 × 0.25 mm) and 2 zones (0—1) were recorded in a similar way. (We are indebted to Mr. A. Czartoryski for help with the X-ray work.)

The 420 independent intensities were estimated visually. The relative $|F|^2$-values were obtained after correction using a modified Lu-procedure [4].

The number of molecules in the unit cell is 4. No correction was made for absorption errors, the linear absorption coefficient is 303.1 cm^{-1} for Cu$K\alpha$.

DETERMINATION OF THE ATOMIC POSITIONS

As this compound has very similar cell-dimensions and belongs to the same space-group as $SbCl_5 \cdot POCl_3$, it was assumed that the two structures were isomorphous. The intensities of the two compounds showed rather close agreement.

From the final parameters of the Sb, 5Cl and P positions of $SbCl_5 \cdot POCl_3$, the signs were determined for 300 of 420 observed $F(h,k,l)$. This, and the following calculations were made on the electronic computer BESK in Stockholm, using the programs made by Åsbrink *et al.*[5] and Westman *et al.*[6] For the structure-factor program the constants given by Vand *et al.*[7] were used. The signs thus obtained were used for a three-dimensional electron density calculation. New parameters for the assumed positions were then obtained and the O-atom was located.

New signs were determined and from a difference synthesis with (F_{obs} — F_{Sb}) as Fourier coefficients approximate coordinates could be assigned to the C-atoms.

REFINEMENT AND ASSESSMENT OF ACCURACY

In order to avoid termination errors in the localization of the maxima, the refinement of the coordinates was carried out in the following way. (Unfortunately a least-squares program is not yet available for the computer BESK, so that this method could not be used.)

One F_{obs} and one F_{calc} synthesis were calculated and backshift corrections were applied to the Sb-parameters.

One difference synthesis with ($F_{obs} - F_{Sb}$) and one synthesis with ($F_{Cl} + F_P + F_O + F_C$) as Fourier coefficients were then computed. Back-shift cor-

rections were applied to the Cl-, P-, O- and C_2-parameters. C_2 is the carbon atom in the eight-fold position 8(d) of *Pnma*. A back-shift correction applied to the parameters of atom C_1 would, however, bring that atom too close to the P atom, the bond length would only be of the order of 1.4 Å. The reason for this is probably that the $F_{obs} - F_{Sb}$ synthesis is affected by errors of different kind, such as termination effects, errors due to anisotropic thermal vibration of the Sb atom and errors in the observed F-values. From the shape of the $(CH_3)_3PO$-part of the molecule, it may be safely assumed, however, that the position of C_1 is not entirely wrong. In all similar structures it has been found that there are only small changes in the structure of the donor molecule by adduct formation $|SbCl_5 \cdot POCl_3$[2], $(TiCl_4 \cdot POCl_3)_2$[8] and $SnCl_4 \cdot 2POCl_3$[9]$|$.

In order to try to locate this atom more accurately, without making corrections for these errors, a difference-synthesis was calculated where the contributions from all atoms except the C_1-atom were subtracted from the observed F-values. The C_1-position derived from this function gave a more reasonable P—C distance, but the peak was rather broad, and the maximum position could not be located with good accuracy.

At this stage ln F_{obs}/F_{calc} was plotted against the calculated intensity giving a straight line. The linear variation of ln F_{obs}/F_{calc} was assumed to depend mainly on secondary extinction [10] and the correction was applied to the observed F-values.

Two successive back-shift corrections were then carried out, in the same way as before, for the Cl, P, O and C_2 atoms. No correction was applied to C_1 and no attempt made to locate the hydrogen atoms.

Cruickshank's method [11] was used to obtain an estimate of the standard deviations in the atomic coordinates. The last backshift corrections gave smaller shifts than the standard deviations.

In order to get better accuracy in the coordinates of atom C_1 a new difference synthesis was calculated in the same way as before. The maximum was, however, still rather broad. No attempt was made to estimate the standard deviations of the parameters of this atom.

The standard deviations obtained are given in Table 1 together with the final parameters. Using a temperature-factor of 4.07 Å^2 the reliability index $R = \Sigma||F_{obs}| - |F_{calc}||/\Sigma|F_{obs}|$ for all observed reflections is 0.13.

Table 1. Final atomic parameters and their standard deviations.

Atom	x	y	z	$\sigma(x)$ Å	$\sigma(y)$ Å	$\sigma(z)$Å
Sb	0.1454	0.2500	0.0710	0.002	—	0.002
Cl_1	0.2615	0.2500	0.9269	0.010	—	0.011
Cl_2	0.0258	0.2500	0.2150	0.011	—	0.013
Cl_3	0.2240	0.2500	0.2871	0.016	—	0.016
Cl_6	0.1424	0.9641	0.0541	0.011	0.012	0.011
P	0.0794	0.2500	0.7074	0.009	—	0.010
O	0.0749	0.2500	0.8890	0.019	—	0.021
C_1	0.4800	0.2500	0.8800			
C_2	0.1397	0.0707	0.6375	0.04	—	0.06

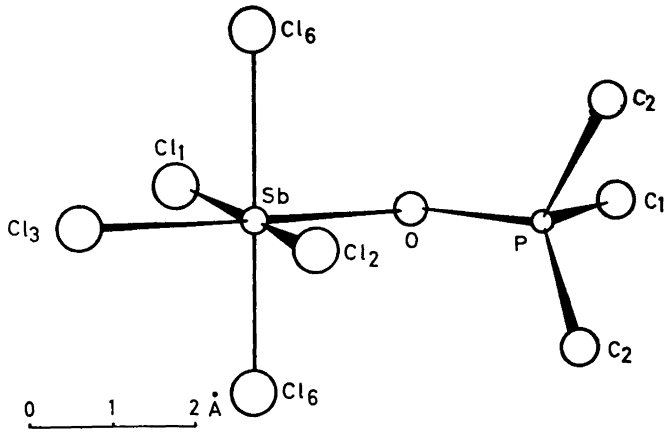

Fig. 1. The molecule of the addition compound $SbCl_5 \cdot PO(CH_3)_3$.

A copy of the observed and calculated F-values can be obtained from this Institute by request.

DESCRIPTION AND DISCUSSION OF THE STRUCTURE

The main features of the structures of $SbCl_5 \cdot PO(CH_3)_3$ and $SbCl_5 \cdot POCl_3$ are the same. The structure of one adduct molecule is given in Fig. 1. The bond lengths and bond angles are given in Table 2 together with their standard deviations. The shortest packing distances are given in Table 3.

The bond lengths in this compound offer interesting comparisons with those in the corresponding adduct $SbCl_5 \cdot POCl_3$ and in the free donor molecule $PO(CH_3)_3$[12]. A number of points are discussed in the following.

Table 2. Bond distances and bond angles in $SbCl_5 \cdot PO(CH_3)_3$ and their standard deviations

	Distance (Å)	S.D. (Å)		Angle (°)	S.D.(°)
$Sb-Cl_1$	2.32	0.012	$O-Sb-Cl_1$	92.7	0.7
$Sb-Cl_2$	2.37	0.012	$Cl_1-Sb-Cl_3$	89.1	0.5
$Sb-Cl_3$	2.32	0.016	$Cl_3-Sb-Cl_2$	91.7	0.5
$Sb-Cl_6$	2.35	0.012	Cl_2-Sb-O	86.6	0.7
$Sb-O$	1.99	0.02	$Cl_6-Sb-Cl_6$	172.3	0.4
$P-O$	1.61	0.02	Cl_6-Sb-O	86.4	0.6
$P-C_1$	1.85		$Cl_6-Sb-Cl_1$	89.0	0.4
$P-C_2$	1.89	0.05	$Cl_6-Sb-Cl_3$	93.7	0.5
			$Cl_6-Sb-Cl_2$	90.9	0.4
			$Sb-O-P$	139.0	1.3
			$O-P-C_2$	110.7	1.9
			$O-P-C_1$	111.9	
			C_1-P-C_2	109.8	
			C_2-P-C_2	102.4	2.4

Table 3. Packing distances in $SbCl_5 \cdot PO(CH_3)_3$ (*cf.* Fig. 2 in the structure of $SbCl_5 \cdot POCl_3$ (Ref.[2]) where Cl_4 should be replaced by C_1 and Cl_5 by C_2.)

	Distance (Å)
$Cl_1 - C_1$	3.66
$Cl_{6A} - Cl_{1B}$	4.07
$Cl_{6A} - C_{1E}$	3.95
$Cl_{6A} - C_{2B}$	3.72
$Cl_{6A} - Cl_{3C}$	3.69
$C_{2A} - Cl_{3C}$	3.72
$C_{2A} - Cl_{1C}$	3.62
$C_{2A} - C_{1D}$	4.01
$C_{2A} - Cl_{2E}$	4.03

1. Firstly the predictions based on the theory for inductive effects on polar bonds proposed by Lindqvist [13] can be checked. If we compare $SbCl_5 \cdot PO(CH_3)_3$ with $SbCl_5 \cdot POCl_3$ we have to consider the inductive effect of the substitution of chlorine for the methyl group. This corresponds to an increased electron withdrawal from the phosphorus atom and complete predictions have been made for this case [13]. The P-O bond should be stronger, because the net charge on the oxygen atom is negative, and the Sb-O bond should be weaker because the net charge on the antimony atom is positive (see the reference paper for details.) The P-O bond length has actually decreased from 1.61 to 1.46 Å, and the Sb-O bond length increased from 1.99 to 2.18 Å. (The last values are those found in the $POCl_3$ adduct.) The predictions are thus fully confirmed and this example can be added to the examples presented in Table 4 of the earlier reference [13].

2. A comparison with the free donor molecule shows the effect of addition reactions, which also was discussed by Lindqvist [13]. The adduct formation would, according to that picture, cause an electron withdrawal from the donor atom. This would give rise to a loss of bond energy for the P-O bond, because the net charge on the phosphorus atom is positive. (The further assumption is then made that no important change of the valence state of the donor atom has taken place.) The P-O bond length has actually increased from 1.48 to 1.61 Å by the adduct formation, a very obvious effect.

The effect on the adjacent P-C bond is more difficult to predict. The net charge on the carbon atom in the phosphine $P(CH_3)_3$ is certainly negative, but in the oxide $PO(CH_3)_3$, the electron attraction of the oxygen atom probably has reduced this negative net charge appreciably as a secondary effect. It is then difficult to make safe predictions about the inductive effect, (the limitations are discussed in the above-mentioned paper [13]). The experimental values for the P-C bonds in the present compound are rather uncertain. The bond length has increased from 1.81 to 1.87 Å (averaged values) but the standard deviation might be as large as 0.1 Å. The P-C asymmetric stretching frequency shows, on the other hand, a positive shift, which might indicate a bond strengthening [14]. The problem is thus still open for discussion at this point.

3. It is a striking fact that, in the two $SbCl_5$ adducts compared, bond lengths between the same atoms show appreciable differences. The variations can be discussed in a very approximately resonance language. In the $POCl_3$ adduct the non-bonding structure $Cl_3P{=}O\ldots SbCl_5$ would dominate, while in the $PO(CH_3)_3$ adduct the semipolar form $(CH_3)_3P^+{-}O{-}\overline{SbCl_5}$ would be most important. In the free donor molecules the forms $Cl_3P{=}O$ and $(CH_3)_3P{=}O$ would dominate. Such an explanation can, however, only be used if multiple bonds are involved, although similar effects are obtained in all types of compounds [13]. It thus seems preferable to consider the inductive effect as the primary effect in all cases. The large magnitude of the effect of the substitution of Cl for CH_3 may, however, indicate that the polarizability is large for the P-O bond. This might be due to the existence of a double bond P=O, and to the possibility of a delocalization of electrons according to the resonance formulation.

This idea is supported by the results of an interesting theoretical discussion of the S—O bonds in sulfoxides and sulfones. Moffitt [15] has attributed all heteropolarity to the π electrons because these are more readily polarized than the σ electrons. It thus seems very probable that the P—O bonds in phosphine oxides and $POCl_3$ are double bonds in the same sense as the S—O bonds in sulfoxides and sulfones.

On the other hand there is a distinction between our approach and the suggestion: «If the bond were purely $P^+{-}O^-$ we should expect that an increase in electronegativity of the groups attached to phosphorus could only decrease the strength of the P—O bond» [16]. As has been shown in the discussion of inductive effects [13] an *increase* of the strength of a single bond can also be predicted, and is actually found in many cases. In a double bond, however, the inductive effect will mainly work on the π electrons and simple resonance formulations are possible in many cases.

4. Another approach has recently been suggested by Lindqvist [17], starting from a molecular model with an idealized electron density distribution. Predictions were then made about the deviations from this idealized structure obtaining in the real compound. These predictions were mainly based on a consideration of inductive effects, as changes in hybridization were supposed to be negligible. In this way it was predicted that in $SbCl_5 \cdot POCl_3$ the term $\{|Sb{-}Cl|-|Sb{-}O|-0.32\}$ Å should be equal in magnitude to the term $\{|P{-}Cl|-|P{-}O|-0.32\}$ Å, but different in sign. The actual values are -0.17 and $+0.18$ Å (all details are given in reference 17). It was also predicted that the corresponding terms in $SbCl_5 \cdot PO(CH_3)_3$ should be smaller in magnitude. The term $\{|Sb{-}Cl|-|Sb{-}O|-0.32\}$ Å is actually 0.03 Å in the present compound, thus vanishing within the limits of experimental error.

The other term $\{|P{-}C|-|P{-}O|-0.12\}$ Å has also decreased to 0.14 Å, but we have already pointed out that the limits of error for the P—C bond lengths are rather large, maybe of the order of 0.1 Å. Even if this uncertainty is considered, however, the difference does not seem to have changed as much as on the acceptor side. Lindqvist in his prediction [17] assumed that the negative net charge on the carbon atom would be large enough to permit predictions valid for clearly polar bonds. In point 2 of this discussion it was pointed out that the case is more doubtful. The result therefore does not inva-

lidate the reasoning based on an idealized electron distribution but caution should be exercised in the application to bonds of low polarity.

5. If is a very interesting fact that the difference |Sb—Cl| — |Sb—O| does not differ significantly from the predicted value 0.32 Å for the idealized electron distribution. This means that the attraction of the electrons on the bridging oxygen atom is almost equal on both sides. The Sb—O bond should therefore be of the same length as in compounds with symmetrical oxygen bridges. No accurate structure determinations have, however, been reported of such compounds.

If the anomaly on the donor side is mainly due to the P—C bond, we would expect, in the same way that the P—O bond would be similar in length to that in symmetric P—O—P bridges. A few examples of relatively accurate structure determinations have been reported for compounds of this type. The recommended average value given in *Tables of Interatomic Distances* [18] is 1.63 ± 0.01 Å, while our experimental value is 1.61 ± 0.02 Å. A detailed account has then not been taken of possible inductive effects, but the agreement seems promising.

6. The much larger effect on the $PO(CH_3)_3$ molecule by adduct formation is also reflected in the fact that it is a much better donor molecule than $POCl_3$. This has been shown by spectroscopic [19] and thermochemical studies [20]. In the discussion of the thermochemical balance for donor-acceptor reactions [13] it was pointed out that both the strength of the new donor-acceptor bond and the inductive effects on adjacent bonds must be considered. The comparison of the two adducts discussed here shows that the weakening of the P—O bond is an important part of the thermochemical balance, even if it is more than compensated by the larger gain of energy in the donor-acceptor bond Sb—O.

7. The Sb—Cl bond lengths are not significantly different from those in the $POCl_3$ adduct, the average value being 2.34 Å compared with 2.33 Å. These values are significantly shorter than the bond length 2.47 Å found in $SbCl_6^-$. This difference has been discussed by Lindqvist [13]. The Sb—O—P bond angle in this compound is slightly smaller than in $SbCl_5 \cdot POCl_3$; no reasonable explanation of this fact is suggested.

We wish to thank Professor Hägg for all facilities put at our disposal. This work has been sponsored by a grant from *Air Force Office of Scientific Research of the Air Research and Development Command, United States Air Force,* through its European Office under Contract No. AF 61(052)—43. This grant is gratefully acknowledged. Facilities for use of the electronic digital computer BESK were given by the *Swedish Board for Computing Machinery.*

REFERENCES

1. Sheldon, J. C. and Tyree, S. Y. *J. Am. Chem. Soc.* **80** (1958) 4775.
2. Lindqvist, I and Brändén, C.-I. *Acta Cryst.* **12** (1959) 642.
3. Lindqvist, I. and Olovsson, G. *Acta Chem. Scand.* **13** (1959) 1753.
4. Löfgren, T. *Acta Cryst.* **13** (1960) 156.
5. Åsbrink, S., Blomqvist, G. and Westman, S. *Arkiv Kemi* **14** (1959) 545.
6. Westman, S., Blomqvist, G. and Åsbrink, S. *Arkiv Kemi* **14** (1959) 535.
7. Vand, V., Eiland, P. F. and Pepinsky, R. *Acta Cryst.* **10** (1957) 303.
8. Brändén, C.-I. and Lindqvist, I. *Acta Chem. Scand.* **14** (1960) 726.

9. Brändén, C.-I. *To be published.*
10. Vand, V. *J. Applied Phys.* **26** (1955) 1191.
11. Cruickshank, D. W. J. *Acta Cryst.* **2** (1949) 65.
12. Wang, H. K. Forsvarets forskningsinstitutt (Norway) Intern rapport IR-K-225 (1960).
13. Lindqvist, I. *Nova Acta Regiae Soc. Sci. Upsaliensis* (IV) **17** (1960) No. 11.
14. Zackrisson, M. and Aldén, K.-I. *Acta Chem. Scand.* **14** (1960) 994.
15. Moffitt, W. *Proc. Roy. Soc. London A* **200** (1950) 409.
16. Cotton, F. A., Barnes, R. D. and Bannister, E. *J. Chem. Soc.* **1960** 2199.
17. Lindqvist, I. *Acta Chem. Scand.* **14** (1960). 1112
18. *Tables of Interatomic Distances.* Chemical Society, London, Special Publ. (1958) No. 12.
19. Kinell, P.-O., Lindqvist, I. and Zackrisson, M. *Acta Chem. Scand.* **13** (1959) 190.
20. Lindqvist, I. and Zackrisson, M. *Acta Chem. Scand.* **14** (1960) 453.

Received September 27, 1960.

ACTA CHEMICA SCANDINAVICA 15 (1961) 175–189

Equilibrium Studies of Polyanions

7. The First Step in the Acidification of WO_4^{2-}; Equilibria in 3 M $NaClO_4$ at 25° C

YUKIYOSHI SASAKI

Department of Inorganic Chemistry, The Royal Institute of Technology, Stockholm 70, Sweden

The reaction between H^+ and the wolframate ion, WO_4^{2-}, has been studied at 25°C in 3 M $NaClO_4$ medium using a glass electrode. The main reaction was found to be: $7\ H^+ + 6\ WO_4^{2-} \rightleftharpoons 3\ H_2O + HW_6O_{21}^{5-}$ with the equilibrium constant $\log K = 60.68 \pm 0.03$. On further acidification, a range with slow reactions was encountered. The product $HW_6O_{21}^{5-}$, which is probably identical with the "para-wolframate A" of Souchay and others, undergoes a slow reaction which does not seem however to affect the present data.

It is well known that isopolyanions are formed when acid is added to a wolframate solution, and that polywolframate salts may be crystallized from the solution.

The crystal structures. The crystal structure for the sodium "parawolframate", $Na_{10}W_{12}O_{41}(H_2O)_{28}$, has been subjected to an X-ray investigation by Lindqvist [1] who found that it contains separate groups $W_{12}O_{46}^{20-}$. Keggin [2] pointed out the apparent isomorphism (powder photographs) of the "metawolframate", $K_4H_4W_{12}O_{40}(H_2O)_{18}$, and the wolframosilicate, $K_4SiW_{12}O_{40}(H_2O)_{18}$. Since, according to him, the latter salt contains discrete groups $SiW_{12}O_{40}^{4-}$, he concluded that the metawolframate contains groups $H_2W_{12}O_{40}^{6-}$. This view has been supported by preparative work of Schott and Harzdorf [3].

Work on solutions. Wolframate solutions of pH > 10 contain the mononuclear species WO_4^{2-}, as has been proved repeatedly, for instance by spectrophotometric [7] and cryoscopic [12] work. The wolframate ion, WO_4^{2-}, has also been found in several crystal structures [4–6].

Jander and his coworkers [7–9] concluded, mainly from their measurements of diffusion coefficients, that the dominant complex between pH = 8 and pH = 6 is $HW_6O_{21}^{5-}$. Further addition of acid leads to the formation of $H_3W_6O_{21}^{3-}$ and, in concentrated solutions, a more condensed anion, $H_6W_{12}O_{40}^{6-}$, is also formed [10,11].

Later on, Souchay [12] studied the wolframate ions by potentiometric, cryoscopic, and polarographic methods. His conclusion was that there are two "parawolframates" of the same formula, $HW_6O_{21}^{5-}$. "Parawolframate A" is slowly transformed into an ion, "parawolframate B", which differs from "A" in some reactions. For example, A but not B forms wolframosilicate with silicate anions. If more acid is added, parawolframate A yields "ψ-metawolframate", $H_3W_6O_{21}^{3-}$, whereas B does not seem to react with H^+.

If a solution of ψ-metawolframate is boiled, it is transformed into "metawolframate", $H_6W_{12}O_{42}^{6-}$. According to Souchay, this reaction does not occur at room temperature.

After some additional experiments, Jander and Krüerke [13] accepted Souchay's picture of the situation with the modification that, according to Jander, there are also two different anions with the formula $H_3W_6O_{21}^{3-}$, namely "metawolframate A" and "ψ-metawolframate".

Another mononuclear species, HWO_4^-, was claimed by Jander and Krüerke[13] and recently by Schwarzenbach and Meier [14]. Ripan and co-workers [15], from conductiometric and emf work, also found support for the formulae $HW_6O_{21}^{5-}$ and $H_3W_6O_{21}^{3-}$. Pan and Hseu[17,18] reported the existence of the complexes $W_2O_7^{2-}$, $W_3O_{11}^{4-}$, $HW_6O_{21}^{5-}$, $H_2W_6O_{21}^{4-}$, and $H_3W_6O_{21}^{3-}$. Another set of complexes, $H_3W_2O_9^{3-}$, $H_4W_3O_{13}^{4-}$, $W_3O_{13}^{8-}$, $H_{10}W_{12}O_{46}^{10-}$, and $H_2W_{12}O_{46}^{6-}$, were claimed by Freedman [16] who like Pan and Hseu mainly drew his conclusions from the bends on titration curves.

Bettinger and Tyree [19] concluded from light-scattering data, that a triwolframate ion predominates in the range between mono- and hexawolframates.

Spitsyn and Pirogova [20,21] used dialysis techniques to measure the molecular weight of the wolframate complexes present in solutions. They concluded that the general formula of the products obtained on acidification of a Na_2WO_4 solution can be written $(HW_6O_{21}^{5-}(H_2O)_x)_n$ where $n = 1$ at pH = 6 to 6.5, and $n = 8$ at pH = 5.0 to 5.8. In solutions prepared by dissolving parawolframate crystals, the molecular weight corresponded to $W_{12}O_{41}^{10-}(H_2O)_{28}$ before boiling the solution, and $HW_6O_{21}^{5-}$ $(H_2O)_{13.5}$ after boiling. According to Spitsyn and Pirogova, solutions of metawolframate crystals contain complexes with molecular weights fifty times greater than that of $WO_4^{2-}(H_2O)_2$.

The present work was started in order to study the wolframate ions by methods previously used in this Department for other systems. Considerable difficulties were met with due to slow attainment of equilibrium in certain pH and concentration ranges. However, enough data were obtained to study the equilibrium of the first reaction step at 25°C.

SYMBOLS

The symbols used in this paper conform with few exceptions, to those in the papers "AB I" and "AB II" (Sillén[23,24]):

B = total W concentration; b = concentration of WO_4^{2-}; c_n = concentration of a complex with n links (10); E = measured emf in mV; $E_o = E - E_j - 59.15 \log h$ (1); $E_j(h)$ = liquid junction potential as a function [29] of h; $E_{oqh} = E_o$ for the quinhydrone electrode; $E_{og} = E_o$ for a glass electrode;

$F = B/b$ (11); $g = \Sigma k_n u^n$ (12,15): H = total (analytical) excess concentration of H^+ calculated assuming no reaction with WO_4^{2-}; $h = [H^+]$; $\boldsymbol{h}$ = normalized variable, corresponding to h, defined by (22); k = constant defined by (20); $K = k_5 = \beta_{76}$ equilibrium constant of (17); $k_n = \beta_{t_n,n+1}$; n = number of "links" (H_tWO_4) per complex; $\bar{n}$ average number of "links" per complex (10); p = number of H^+ in complex; $\bar{p}$ = average number of H^+ per complex (excepting WO_4^{2-}), (5); P = unique value of p (21); q = number of W per complex; $\bar{q}$ = average number of W per complex (excepting WO_4^-), (6); Q = unique value of q (21); R = reciprocal of the average degree of condensation (3); t = number of H^+ per "link" (7); $u = bh^t$ (13, 14); $x = t \log h + \log B$ (9); $y = Z/t$ (8); Z = average number of H^+ bound per WO_4^{2-} (7); $z = Z-2$ = average charge per W; β_{pq} = equilibrium constant of the reaction $pH^+ + qWO_4^{2-} \rightleftharpoons H_pW_qO_{4q}^{p-2q}$*.

EXPERIMENTAL

Methods

As in studies on other systems, the aim was to obtain data $Z(\log h)_B$ (see list of symbols) in a wide range and to use them to calculate the formulas and formation constants of the species present.

In order to keep the activity factors of the wolframates and other anionic species as constant as possible during the acidification, $[Na^+]$ was kept at 3 M in all solutions by adding $NaClO_4$.

Glass electrodes were used in all measurements of $[H^+] = h$ because preliminary experiments had shown that, in part of the range we had to cover, the solutions were too alkaline for the use of a quinhydrone electrode and also because the hydrogen electrode is reported to reduce wolframate solutions [22].

Most of the experiments were carried out as "titrations", *i.e.* by adding perchloric acid to the Na_2WO_4 solution at 25 ± 0.1°C and keeping B, the total concentration of W, constant by adding an appropriate amount of Na_2WO_4 solution from another buret. Reverse titrations were also performed. Wolframate concentrations from 0.0012 M to 0.16 M were used in eight independent titrations. Some spectrophotometric measurements were made at 25°C and with the same ionic medium in order to construct the extinction curves for the species present.

Chemicals and apparatus

Sodium perchlorate was prepared from Na_2CO_3 (Merck p.a.) and $HClO_4$ (Kebo p.a.) as described previously [26]. After a recrystallization from water, it was kept as a ~ 5 M solution in a Pyrex glass bottle. Possible impurities are Fe and Al. Any traces of these present were concentrated by extraction with oxine and chloroform and the absorption peaks of the oxine complexes of these elements were searched for using a Hilger Uvispec Spectrophotometer.

In a 5 M $NaClO_4$ solution which had been kept in a Pyrex bottle for about two months, the amount of Al found corresponded to 0.003 mM Al in 3 M $NaClO_4$ solution. No definite evidence for Fe was found and, from the sensitivity of the method, it was calculated that there was at most 0.0003 mM Fe in 3 M $NaClO_4$. No Cl^- or SO_4^{2-} could be detected with $AgNO_3$ and $BaCl_2$.

---

* In this paper, WO_4^{2-} is treated as the central group and H^+ as the ligand. If, instead, WO_4^{2-} is considered as the ligand (*i.e.* in the IUPAC Tables of Stability constants [25]), the order of the subscripts should be reversed: K for (17) is β_{67} instead of β_{76} *etc.*

Sodium wolframate (Merck p.a.) was recrystallized twice from water under a stream of nitrogen. In this way, a certain impurity (probably Al and Fe) was removed which precipitates from solutions of the commercial reagent on the addition of NaOH. The purified product was heated to *ca.* 150°C, after which it was dissolved in twice-distilled water and freed from carbon dioxide at room temperature using nitrogen. The solution was filtered through a glass filter G 4 and diluted to give a stock solution with *ca.* 1.5 mole W/kg solution. The stock solution was kept in a polythene bottle.

In the solution thus prepared, no Tyndall effect could be detected even when a strong light beam was used. On the other hand, solutions of commercial sodium wolframate gave a strong Tyndall effect even after long boiling.

Analysis: A known amount of solution was evaporated and dried in an oven at 150°C overnight. Weighing the residue as Na_2WO_4 gave quite reproducible results. To determine the concentration of Na^+, a known amount of stock solution was diluted and passed through a column of OH^--saturated anion exchanger Dowex-2 and the OH^- set free was titrated potentiometrically with acid [27]. The reliability of the method was tested using Na_2SO_4.

The values for $[Na^+]$ obtained by ion exchange and by weighing agreed within less than 0.1 %.

A few hours before each experiment the wolframate solutions for the equilibrium "titrations" were prepared from measured quantities of the stock solutions of Na_2WO_4 and $NaClO_4$. Both solutions were first diluted separately with boiled distilled water and then mixed in a measuring flask. Otherwise, when concentrated solutions of Na_2WO_4 and $NaClO_4$ are mixed, a white precipitate occurs which does not dissolve on dilution or shaking.

Perchloric acid, sodium hydroxide and *silver perchlorate* were prepared and standardized as described previously [34]. The Ag,AgCl electrodes were made by Brown's method [28].

Radiometer Red glass electrodes (Copenhagen, type 202 B) were used throughout all the work. The electrodes were tested against a quinhydrone electrode in a phosphate solution containing 3 M Na^+ to which acid was gradually added. The potential difference between the glass and quinhydrone electrodes remained constant to within 0.1 mV throughout the pH range used, from 2 to 7.1. (See also "Determination of h" below.)

The emf was read to 0.1 mV by means of a Radiometer PHM3i valve potentiometer.

The "titration vessel" containing the equilibrium mixture was kept in an oil thermostat at 25± 0.1°C placed in a room thermostated at 25°C.

PROCEDURE

The cell may be written as follows:

glass electrode/solution//SE

where the reference half-cell is

SE = 3 M $NaClO_4$ // 2.990 M $NaClO_4$, 0.010 M $AgClO_4$ / AgCl, Ag

At the beginning of each titration, the solution in the vessel had the composition 3 M Na^+, B M WO_4^{2-} and (3 — 2B) M ClO_4^-. To this solution, equal volumes were added from two burets, one containing $HClO_4$ and 3 M $NaClO_4$ and the other 2B M WO_4^{2-}, 3 M Na^+ and (3—4B) M ClO_4^-. In this way, the total wolframate content, B, was kept constant throughout the titration.

Nitrogen gas was bubbled continuously through the solution to keep out CO_2 and, after each addition of acid, the solution was shaken to prevent any local excess of acid.

Determination of h

From the measured E, $h = [H^+]$ is calculated [39] from

$$E = E_o + E_j(h) + 59.15 \log h \qquad (1)$$

In the present study, the liquid-junction potential E_j was negligible because always $h < 10^{-3}$ M.

In our preliminary experiments, the constant E_o was determined in an independent "titration" in the same medium, 3 M $Na(ClO_4)$, in which acid was added in the absence of wolframate. However, we soon found that, for most of our glass electrodes, the values for E_o measured before and after a wolframate titration disagreed. Sometimes a discrepancy of 2 mV was met with. This may be connected with the large jump in pH between the Na_2WO_4 solution with pH about 8 and the acidic solution with $h \sim 0.1$ M in which the value for E_o was determined. Some preliminary attempts were made to calibrate the glass electrode by using it, instead, in alkaline solutions of known $[OH^-]$, with or without wolframate present, but these were abandoned when a better calibration method was found.

In the following, the E_o for the glass electrode was determined by measuring its potential in a phosphate solution 3 M in $Na(ClO_4)$ and with h close to that of the wolframate solutions studied. This reference solution was prepared by mixing solutions of Na_3PO_4, $HClO_4$ and $NaClO_4$. The hydrogen ion concentration in this solution, h, was determined accurately by means of a quinhydrone electrode (using a Leeds and Northrup compensator, type K). The standard potential, E_{oqh}, of the quinhydrone electrode had been determined earlier by means of an acidic solution of known h.

Thus, we knew for the phosphate buffer, $E_{qh} - E_{oqh} = 59.15 \log h$, with an accuracy of 0.03 mV, and the E_o for the glass electrode was calculated from $E_{og} = E_g - E_{qh} + E_{oqh}$. In the "titrations" given here, E_{og} determined in this way before and after the main titration differed by at most $\pm$ 0.2 mV.

Knowing E_{og}, h could be calculated for each solution using (1). Since, from the analytical composition of the solutions, we knew B (the total W concentration) and H (the analytical H^+ excess), we could easily calculate Z, (the average number of H^+ bound per WO_4^{2-}), by means of the equation

$$H - h = BZ \qquad (2)$$

Equilibration

Whereas solutions with $Z < 1.15$ seem in general to give reversible equilibria, irreversible phenomena and slow reactions were met with at higher values for Z. It thus seems convenient to discuss first of all the range $Z < 1.15$ and thereafter higher Z values.

For $Z < 1.15$, and especially at the lowest values for Z, it appears that the equilibrium was established quickly since stable potentials were obtained almost instantaneously. In the solutions with the highest B values, a white precipitate was observed immediately after the addition of acid but it dissolved quickly on vigorous shaking. At the three highest concentrations used, $B =$ 0.040, 0.080, and 0.160 M, the dissolution of the precipitate was slower already at $Z \sim 0.7$ to 1.0, and the solution began to show a strong Tyndall effect. Even if the emf seemed to have settled within some 10 minutes (in the other solutions for $Z < 1.15$, the emf became constant practically immediately) these solutions may not correspond to true equilibrium. In Fig. 1, which

contains the data obtained, the theoretical curves are dotted within this "colloidal" region.

To test the reversibility, two reverse titrations were performed, both at $B = 0.020$ M, in which an alkaline solution was added to a solution with $Z \sim 1.10$. As seen from Fig. 1, the points fall on the same curve for increasing and decreasing Z. On the other hand, starting from a value for $Z > 1.15$, the titration curves with decreasing and increasing Z did not coincide.

The region $Z > 1.15$, may be described as an "instability range", analogous to those found in the silicate [30] and vanadate [31,32] systems.

In a titration with increasing Z the emf was found, at a point with $Z > 1.15$, to drift slowly for several days without reaching a stationary value. The drift is in the direction of decreasing h (Z increasing, but very little).

In two parallel experiments, the titrations with acid described above were continued to $Z = 1.35$. In one case, we had $B = 0.04$ M. In the other, the original value of B was 0.08 M; the solution was then diluted with an equal amount of 3 M $NaClO_4$ to give a solution which should have had, like the previous one, $B = 0.04$ M and $Z = 1.35$. However, the emfs observed with the two solutions and hence their h values differed considerably. Even after two weeks, the difference was about 10 mV. These experiments indicated that the equilibration is very slow, and it did not therefore seem advisable to keep solutions of known Z in glass bottles for a long time in order to obtain equilibrium ("point titration"). It was thus decided that if equilibria were to be obtained in this range, it would be necessary to work at higher temperatures.

RESULTS

The experimental data are given in Fig. 1 and in Table 1 in the form Z $(\log h)_B$. Obviously, the points for different B values fall on different curves,

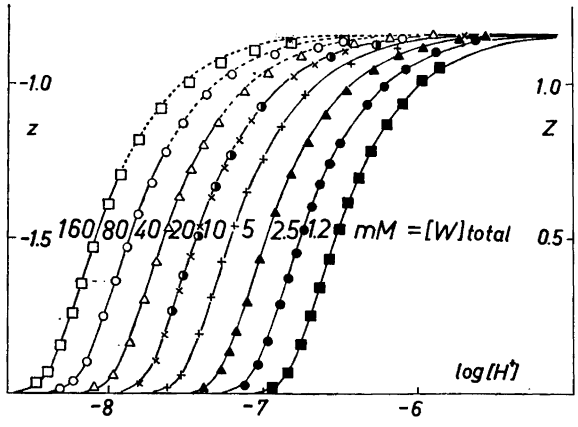

Fig. 1. z (average charge per W) and Z (number of protons bound per WO_4^{2-}) as functions of log $[H^+]$. The half-filled symbols for $B = 20$ mM represent data obtained by a reverse titration. The lines are calculated curves for the reaction (17) and log $K = 60.67$.

Table 1. Wolframate acidification at 25°C in 3 M $Na(ClO_4)$. Data Z (log h)$_B$ obtained with glass electrode.

B = 0.00125 M. Z — log. h:				0.019,	6.951;	0.029,	6.931;	0.049,	6.882;		
0.069,	6.852;	0.108,	6.809;	0.157,	6.769;	0.204,	6.735;	0.252,	6.706;		
0.298,	6.676;	0.345,	6.647;	0.390,	6.615;	0.435,	6.586;	0.480,	6.557;		
0.524,	6.524;	0.567,	6.495;	0.610,	6.464;	0.653,	6.427;	0.695,	6.393;		
0.736,	6.360;	0.778,	6.316;	0.818,	6.275;	0.870,	6.209;	0.900,	6.170;		
0.938,	6.111;	0.979,	6.038;	1.010,	5.979;	1.040,	5.910;	1.055,	5.866;		
1.086,	5.780;	1.100,	5.726;	1.116,	5.666;	1.130,	5.606;	1.145,	5.540;		
1.159,	5.469;	1.174,	5.382.								
B = 0.0025 M. Z, —log h:				0.029,	7.129;	0.049,	7.102;	0.069,	7.071;		
0.094,	7.044;	0.108,	7.029;	0.126,	7.012;	0.172,	6.980;	0.218,	6.950;		
0.254,	6.924;	0.288,	6.901;	0.331,	6.875;	0.373,	6.848;	0.454,	6.796;		
0.531,	6.747;	0.605,	6.693;	0.676,	6.633;	0.744,	6.571;	0.809,	6.502;		
0.873,	6.427;	0.935,	6.336;	0.993,	6.226;	1.048,	6.082;	1.104,	5.885;		
1.123,	5.775;	1.144,	5.634;	1.154,	5.548;	1.164,	5.450;	1.174,	5.357;		
B = 0.0050 M. Z, — log h:				0.017,	7.396;	0.024,	7.371;	0.042,	7.335;		
0.055,	7.313;	0.074,	7.286;	0.105,	7.256;	0.134,	7.232;	0.163,	7.207;		
0.201,	7.188;	0.245,	7.151;	0.294,	7.115;	0.342,	7.088;	0.431,	7.036;		
0.510,	6.985;	0.582,	6.931;	0.647,	6.879;	0.706,	6.828;	0.761,	6.775;		
0.809,	6.720;	0.856,	6.664;	0.899,	6.601;	0.939,	6.540;	0.976,	6.473;		
1.010,	6.388;	1.041,	6.297;	1.058,	6.246;	1.073,	6.182;	1.088,	6.136;		
1.115,	5.972;	1.128,	5.866;	1.141,	5.741;	1.153,	5.572;				
B = 0.0100 M. Z, — log h:				0.019,	7.624;	0.034,	7.582;	0.047,	7.558;		
0.059,	7.538;	0.083,	7.509;	0.108,	7.486;	0.132,	7.465;	0.192,	7.418;		
0.252,	7.377;	0.311,	7.342;	0.369,	7.308;	0.426,	7.273;	0.483,	7.232;		
0.539,	7.191;	0.594,	7.147;	0.649,	7.117;	0.703,	7.065;	0.756,	7.009;		
0.808,	6.960;	0.861,	6.887;	0.913,	6.818;	0.964,	6.730;	1.016,	6.612;		
1.066,	6.436;	1.116,	6.130;	1.135,	5.956;	1.160,	5.602.				
B = 0.0200 M. Z, — log h:				0.013,	7.891;	0.022,	7.846;	0.028,	7.824;		
0.034,	7.802;	0.046,	7.776;	0.059,	7.758;	0.083,	7.729;	0.107,	7.702;		
0.160,	7.660;	0.189,	7.639;	0.218,	7.619;	0.274,	7.584;	0.329,	7.548;		
0.383,	7.514;	0.441,	7.474;	0.488,	7.448;	0.538,	7.411;	0.587,	7.376;		
0.635,	7.338;	0.683,	7.303;	0.729,	7.256;	0.774,	7.210;	0.818,	7.166;		
0.861,	7.110;	0.883,	7.083;	0.904,	7.049;	0.945,	6.983;	0.986,	6.899;		
1.025,	6.801;	1.064,	6.670;	1.084,	6.586;	1.099,	6.500;	1.106,	6.473;		
1.114,	6.415;	1.121,	6.331;	1.129,	6.226;	1.151,	5.903;	1.159,	5.695;		
1.160,	5.404;	— — —	1.129,	6.273*;	1.089,	6.569*;	1.045,	6.759*;			
0.931,	7.019*;	0.771,	7.218*;	0.668,	7.318*;	0.511,	7.433*;	0.382,	7.528*;		
0.271,	7.607*;										
B = 0.0399 M. Z, — log h:				0.018,	8.101;	0.026,	8.049;	0.042,	8.008;		
0.058,	7.979;	0.074,	7.956;	0.090,	7.940;	0.105,	7.923;	0.135,	7.898;		
0.165,	7.874;	0.194,	7.852;	0.232,	7.824;	0.269,	7.802;	0.302,	7.781;		
0.365,	7.741;	0.424,	7.702;	0.480,	7.666;	0.533,	7.628;	0.584,	7.592;		
0.632,	7.555;	0.678,	7.516;	0.722,	7.475;	0.761,	7.437;	0.800,	7.394;		
0.838,	7.349;	0.871,	7.301;	0.909,	7.249;	0.974,	7.131;	1.007,	7.060;		
1.034,	6.980;	1.063,	6.887;	1.090,	6.760;	1.129,	6.426;	1.147,	6.189;		
1.157,	5.908.										

* An asterisk indicates data from a reverse titration.

B = 0.0797 M. Z, – log h:				0.016,	8.321;	0.022,	8.295;	0.028,	8.270;
0.034,	8.253;	0.041,	8.234;	0.071,	8.189;	0.087,	8.169;	0.102,	8.153;
0.132,	8.126;	0.162,	8.101;	0.192,	8.077;	0.250,	8.042;	0.307,	8.001;
0.364,	7.966;	0.419,	7.930;	0.473,	7.891;	0.526,	7.856;	0.578,	7.817;
0.635,	7.776;	0.680,	7.732;	0.732,	7.688;	0.778,	7.643;	0.873,	7.526;
0.965,	7.374;	1.009,	7.267;	1.031,	7.210;	1.053,	7.137;	1.074,	7.043;
1.096,	6.933;	1.117,	6.647;	1.138,	6.490;	1.150,	6.103.		
B = 0.1604 M. Z, – log h:				0.014,	8.571;	0.025,	8.500;	0.033,	8.471;
0.040,	8.453;	0.055,	8.426;	0.071,	8.402;	0.100,	8.371;	0.129,	8.343;
0.158,	8.319;	0.193,	8.294;	0.227,	8.268;	0.260,	8.246;	0.292,	8.226;
0.355,	8.185;	0.386,	8.167;	0.415,	8.147;	0.473,	8.108;	0.529,	8.069;
0.556,	8.049;	0.582,	8.030;	0.608,	8.011;	0.633,	7.991;	0.675,	7.949;
0.705,	7.927;	0.775,	7.861;	0.818,	7.812;	0.921,	7.670;	1.007,	7.487;
1.042,	7.381;	1.069,	7.281;	1.082,	7.217;	1.109,	7.061;	1.122,	6.928;
1.132,	6.825;	1.141,	6.578;	1.148,	6.475;	1.160,	5.511.		

thus showing that polynuclear complexes are formed. Moreover, the curves seem to be practically parallel.

Two different approaches were made in order to find out the main reaction and the equilibrium constant involved. In the "integration method" no further assumption was made about the system apart from those that the activity factors can be considered constant and that the law of mass action is obeyed. In the "core and links" approach, it was assumed that the curves are exactly parallel as they seem to be.

"Integration method"

An integration method has been developed by Sillén [33] which makes it possible to compute the average composition of the complexes from $Z(\log h)_B$ data without any special assumption being necessary provided that equilibrium data of sufficient accuracy are available over a sufficient concentration range. In the present case the reagents are

$$A = H^+, \quad B = WO_4^{2-}, \quad a = h, \quad b = [WO_4^{2-}]$$

and we have data from $\log h \sim -8.5$ upwards. Using the equations given in Ref.[33] (see also Refs.[32,34]) we have for R (the average number of free molecules per W = the reciprocal value of the average number of W per W complex) and $b = [WO_4^{2-}]$:

$$R = 1 + \int_0^Z \left(\frac{\partial \log h}{\partial \log B}\right)_Z dZ \tag{3}$$

$$\log b = \log B + R - 1 - \int_{-8.5}^{\log h} Z \, d \log h \tag{4}$$

Because of the steepness of the curves, there is no need to consider the residual integral beyond —8.5.

Now, we may subtract b from B (the total concentration of W) and from BR (the total molecular concentration of W complexes), and thus calculate $\bar{p}$ and $\bar{q}$ which give the average number of H^+ and WO_4^{2-} per complex in all W-complexes except WO_4^{2-}:

$$\bar{p} = \frac{BZ}{BR - b} \qquad (5) \qquad\qquad \bar{q} = \frac{B - b}{BR - b} \qquad (6)$$

Table 2 gives the result of an numerical integration of $Z(\log h)_B$ for $B = 0.02$ M. It is seen that $\bar{p} \sim 7$ to 8 and $\bar{q} \sim 6$ to 7. Both values are rather constant which indicates that one polynuclear complex predominates among the reaction products. With $p = 7$ and $q = 6$, the main reaction would be

$$7H^+ + 6WO_4^{2-} \rightleftharpoons HW_6O_{21}^{5-} + 3H_2O \qquad (17)$$

if the complex is written with as little water as possible. However, this first survey would also leave the reaction products, $W_6O_{20}^{4-}$, $W_7O_{24}^{6-}$, and $HW_7O_{25}^{7-}$, as possibilities to be further investigated.

"Core and links" approach

If the curves $Z(\log h)_B$ are exactly parallel, with a constant spacing, this would indicate that all complexes present in appreciable amounts have the general formula $B(A_tB)_n$ where

$$t = -\left(\frac{\partial \log B}{\partial \log h}\right)_Z \qquad (7)$$

is a constant and n may have one or several values (Sillén [23,24]).

By measuring the spacing between the experimental curves (Fig. 1), we found $t = 1.40 \pm 0.03$.

In the following analysis of the data, we shall follow the methods and notations of ABII [24]. Fig. 2 gives

$$y = Z/t = Z/1.4 \qquad (8)$$

Table 2. Analysis of the $Z(\log h)$ for $B = 0.02$ M

Z	R	$\frac{b}{B}$	$\bar{p}$	$\bar{q}$
0.075	0.946	0.937	8.52	7.13
0.125	0.910	0.894	7.91	6.68
0.175	0.874	0.853	8.33	6.98
0.225	0.838	0.809	7.73	6.54
0.275	0.802	0.767	7.79	6.59
0.325	0.766	0.722	7.35	6.28
0.375	0.731	0.681	7.50	6.45
0.425	0.695	0.638	7.40	6.30
0.475	0.659	0.596	7.55	6.40
0.525	0.623	0.555	7.63	6.46
0.575	0.588	0.509	7.27	6.21
0.625	0.552	0.468	8.41	7.16

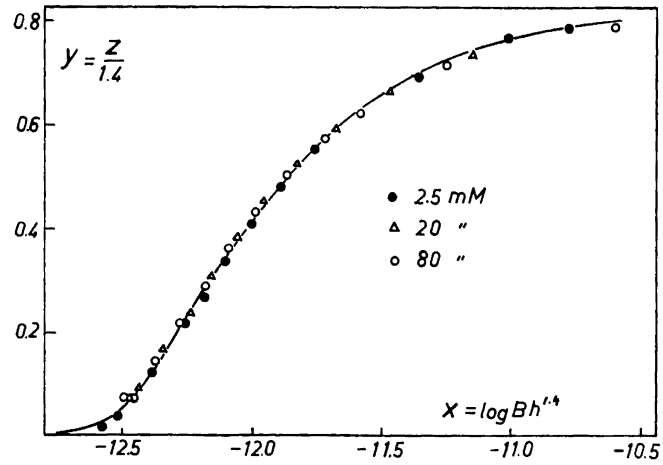

Fig. 2. $y = z/1.4$ as a function of $x = \log Bh^{1.4}$. The curve is calculated from eqns. (22) and (23) in ABII for $N = 5$ and $\log K = 60.70$.

as a function of

$$x = \log B + t \log h = \log B + 1.4 \log h \tag{9}$$

All of the experimental points in this diagram fall on a single curve within the experimental accuracy, as required if t in (7) is constant.

To find the value, or values, of n, one may either carry out a "direct analysis" of the function $y(x)$ or compare it with a group of theoretical curves.

Direct analysis. From the relationship between B, b, t and Z, it can be shown that

$$\bar{n} = \frac{y}{1 - y - bB^{-1}} \tag{10}$$

(*viz.* $BZ = t \Sigma n c_n$; $B = b + \Sigma (n+1)c_n$; $\bar{n} \Sigma c_n = \Sigma n c_n$; $Z = ty$)

Table 3. Direct analysis of $y(x)$

y	F^{-1}	$\bar{n}$	$\log u$	$\log g$	$\log K_5$
0.025	0.972	8.62	−12.57	−2.525	60.33
0.050	0.942	6.49	−12.51	−2.087	60.46
0.075	0.913	6.75	−12.49	−1.915	60.54
0.10	0.884	6.28	−12.46	−1.745	60.56
0.15	0.824	5.79	−12.43	−1.502	60.65
0.20	0.762	5.30	−12.38	−1.305	60.60
0.25	0.701	5.10	−12.36	−1.155	60.65
0.30	0.639	4.98	−12.35	−1.026	60.73
0.35	0.579	4.98	−12.32	−0.917	60.69
0.40	0.520	5.02	−12.30	−0.814	60.69
0.45	0.458	4.93	−12.28	−0.702	60.70
0.50	0.397	4.88	−12.26	−0.589	60.71
0.55	0.339	5.42	−12.24	−0.487	60.72
0.60	0.280	5.03	−12.21	−0.372	60.68

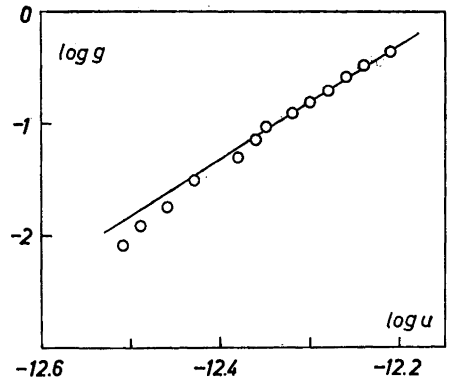

Fig. 3. Direct analysis of the curve $y(x)$ in Fig. 2, log g as a function of log u. A straight line with slope 5 is shown at the position of best fit.

Here, $\bar{n}$ is the average number of links $H_{1.4}WO_4$ per complex, and bB^{-1}, which cannot be measured directly, can be calculated from the curve $y(x)$ by means of the formula (derived from ABII [24]; eqns. 14, 8a and 5a).

$$\log F = \log Bb^{-1} = y \log e + \int_{-\infty}^{x} y\mathrm{d}x \tag{11}$$

From smoothed curves through the points (x, y), the values of $\bar{n}$ given in Table 3 were obtained. If the first less accurate values are excluded, the table indicates a constant value $\bar{n} = N = 5$ so there is no need to assume higher complexes in any appreciable amount.

The same conclusion and also the same equilibrium constant are obtained from another type of diagram (Fig. 3). Log g has been plotted as a function of log u where g and u were calculated from:

$$g = F(1 - y) - 1 \tag{12}$$

$$u = 10^x F^{-1} \tag{13}$$

using the experimental values for x and y and also the F calculated by means of (11). As shown in AB II [24] (eqns. 5a, 14 and 15), provided the "core and links" complexes predominate, u and g calculated in this way are the quantities:

$$u = bh^t \quad (14); \qquad g = \Sigma\, k_n u^n \tag{15}$$

Here, k_n is the equilibrium constant for the reaction

$$n\mathrm{tA} + (n+1)\mathrm{B} \rightleftharpoons B(A_tB)_n \tag{16}$$

In our case, we remember that $A = H^+$, $B = WO_4^{2-}$, and $t \sim 1.40 \pm 0.03$. As seen from Fig. 3, the slope agrees well with the theoretical one for $n = 5$. The points in the lower left corner of the diagram are those most sensitive

to experimental error. At any rate, the slope corresponding to $n = 6$ would not fit the data at all. Besides with $n = 6$ the formula of the complex would not contain an integral number of atoms. With $n = 5$ and $t = 1.4$, the formula of the complex is $H_7W_6O_{24}^{5-}$ or $HW_6O_{21}^{5-}$. We shall use the second formula; if nothing is known about the structure of a complex it is often preferred to write it with as little water as possible.

The main reaction is thus

$$7H^+ + 6WO_4^{2-} \rightleftharpoons HW_6O_{21}^{5-} + 3\ H_2O \qquad K = K_5 = \beta_{76} \tag{17}$$

The other possible reaction products suggested by the "integration method", $W_6O_{20}^{4-}$, $W_7O_{24}^{6-}$, and $HW_7O_{25}^{7-}$, were definitely ruled out, since they give t values of 1.6, 1.33 and 1.17, respectively. Such values would give a spacing between the curves different from that observed.

Since from (15), $g = K_5u^5$ we may find the equilibrium constant for reaction (17) either from the intercepts of log g(log u) or numerically, using for instance the equation

$$\log K = \log g - 5\,x + 5 \log F \tag{19}$$

The results of numerical calculations with (19) are given in Table 3. There is no trend in the values except for the very first ones and the average is

$$\log K = 60.68 \pm 0.03$$

(The first three points were excluded when calculating the average.)

From the graph, the value for log K was found to be:

$$\log K = 60.69 \pm 0.02$$

Fig. 1 shows theoretical curves $Z(-\log h)_B$ calculated for the reaction and the constant thus obtained. The agreement with the experimental points is satisfactory.

Curve fitting

The experimental curve $y(x)$ was also compared with various families of theoretical curves calculated for various mechanisms (AB II)[24]. It was found to fit very well with the curve calculated by assuming only one complex with $n = N = 5$ which supports the previous results. From the position of best fit, we may calculate $K = k^5$ using (AB II [24], eqn. 24):

$$x_{\frac{1}{2}} = \log 2 - \log k + \log N - (1 + N^{-1}) \log (N - 1) \tag{20}$$

The result was log $K = 60.70 \pm 0.05$

Another type of curve-fitting was tried, once the formula of the complex was established, by constructing $Z(\log h)_B$ curves. We start from eliminating b

$$B = b + QKb^Qh^P \quad (21a); \quad BZ = PKb^Qh^P \tag{21b}$$

$P = tN$ and $Q = 1 + N$ are the values for p and q in the complex in the present case, $P = 7$, $Q = 6$. We may introduce a normalized function $\boldsymbol{h}$ making

$$7(\log \boldsymbol{h} - \log h) = \log K + 5 \log B - \log 7 \tag{22}$$

Elimination of b and $\boldsymbol{h}$ from (21) and (22) then gives

$$7 \log \boldsymbol{h} = \log Z - 6 \log (1 - 6 Z 7^{-1}) \quad (23)$$

One may construct a diagram $Z(\log h)$ using eqn. (23) and compare this curve with each separate curve $Z(\log h)_B$. From the value of best fit, one finds $(\log \boldsymbol{h} - \log h)$ and thus, using (22), $\log K$. The average value found was $\log K = 60.67 \pm 0.05$.

There was no trend among the different B values which also supports our conclusion that the main reaction is (17).

SPECTROPHOTOMETRIC EXPERIMENTS

Knowing what the main reaction was, we intended to construct the extinction curve for the anion, $HW_6O_{21}^{5-}$, by measuring absorption spectra of wolframate solutions with different values for Z and B. However, we soon found that the extinction coefficient drifted with time and that Beer's law is valid only in freshly mixed solutions or solutions which contain excess NaOH. In the course of a few hours or a day, a new species was apparently formed with a much stronger absorption in the range 2 500 — 3 250 Å. This species may be identical with the "parawolframate B" of Souchay whereas the ions formed immediately on equilibrium would be identical with his "parawolframate A"[12].

Whatever the nature of this slow reaction, it is so slow that it does not seem to influence the results of the emf studies described here, but, because of the strong absorption of the new species, it made the spectrophotometric work very difficult.

COMPARISON WITH PREVIOUS WORK

Our conclusion that the main complex is $HW_6O_{21}^{5-}$ agrees with the results of Jander, Souchay and others quoted in the introduction. On the other hand, our results do not support the existence of the species with 2 or 3 W suggested by Freedman, Pan and Hseu and others. Nor do our data seem to support the existence of complexes with 12 W or more in freshly prepared solutions [21]. We have not been able to locate any earlier equilibrium constants for the wolframate-hexawolframate equilibrium.

A few words must be said about HWO_4^- and H_2WO_4. Schwarzenbach and Meier [13] mixed two streams of solutions containing, respectively, wolframate and acid, and placed a glass electrode immediately after the mixing point. Their data gave evidence for HWO_4^- and H_2WO_4, with the average equilibrium constant $\frac{1}{2}\beta_{21} = 4.05$ (see footnote, page 177). It seems that, under these conditions, the polynuclear complex did not have time to form. By comparison with the present data, one finds that the mononuclear complexes would form an appreciable fraction of the total W only at much lower values for B (0.01 to 0.001 mM) than those practicable in the present work.

On the other hand, in the molybdate system, where the same emf methods were applied [35], definite evidence was found indicating the existence of the mononuclear species $HMoO_4^-$.

Future work. It is planned to investigate the wolframate equilibria at higher temperatures with a new technique for emf-titration [37]. In this way, it is hoped to reach equilibrium within a reasonable time, which may thus throw more light on the mechanism of the slow reactions.

From wolframate solutions of pH $\sim$ 5.2, a sodium "parawolframate" $Na_{10}W_{12}O_{41}(H_2O)_{28}$ crystallizes slowly [36]. Souchay for various reasons has concluded that this phase contains "parawolframate B" ions. According to a recent X-ray investigation by Lindqvist[1], it contains discrete anions, with 12 W-atoms, whereas Souchay considers that the "parawolframate B" contains 6 W. This problem would be worth further investigation.

Acknowledgement. The author is deeply indebted to Professor Lars Gunnar Sillén for his kind help and advice.

He also wishes to thank Drs. Georg Biedermann, Nils Ingri and Åke Olin for many discussions during the present work and Mr. Frans Ericson for making the apparatus needed.

Mr. Val Tyrrell kindly corrected the English of this paper.

The present work has been supported by the *Air Force Office of Scientific Research of the Air Research and Development Command, United States Air Force,* by its European Office under contract no. AF 61(052)—162.

REFERENCES

1. Lindqvist, I. *Acta Cryst.* **5** (1952) 667.
2. Keggin, J. F. *Nature* **131** (1933) 908; **132** (1933) 351; *Proc. Roy. Soc.* London, *Ser. A.* **144** (1934) 75.
3. Schott, G. and Harzdorf, C. *Z. anorg. allgem. Chem.* **288** (1956) 15.
4. *Strukturberichte* **I** (1931), 347, 386; **II** (1937) 83.
5. Lindqvist, I. *Acta Chem. Scand.* **4** (1950) 1066.
6. Sillén, L. G. and Nylander, A. L. *Arkiv-Kemi, Mineral. Geol.* **17A** (1943) No. 4.
7. Jander, G., Mojert, D. and Aden, T. *Z. anorg. allgem. Chem.* **180** (1929) 129.
8. Jander, G. and Heukeshoven, W. *Z. anorg. allgem. Chem.* **187** (1930) 60.
9. Jahr, K. F. and Witzman, H. *Z. anorg. allgem. Chem.* **208** (1932) 145.
10. Jander, G. *Z. physik. Chem.* **A 187** (1940) 149.
11. Jander, G. and Exner, F. *Z. physik. Chem.* **A 190** (1942) 195.
12. Souchay, P. *Ann. Chim. Paris* **18** (1943) 61, 169.
13. Jander, G. and Krüerke, U. *Z. anorg. allgem. Chem.* **265** (1951) 244.
14. Schwarzenbach, G. and Meier, J. *J. Inorg. & Nuclear Chem.* **8** (1958) 302.
15. Ripan, R. and Puşcaşin, M. *Acad. populare Romîne Studii cercetări chim.* **IX** (1958) 7.
16. Freedman, M. L. *J. Am .Chem. Soc.* **80** (1958) 2072.
17. Pan, K. and Hseu, T. M. *Bull. Chem. Soc. Japan* **26** (1953) 126.
18. Pan, K., Lin, S. F. and Sheng, S. T. *Bull, Chem. Soc. Japan* **26** (1953) 131.
19. Bettinger, D. J. and Tyree, S. Y., Jr. *J. Am. Chem. Soc.* **79** (1957) 3355.
20. Spitsyn, V. I. and Pirogova, G. N. *Doklady Akad. Nauk S.S.S.R.* **115** (1957) 322.
21. Spitsyn, V. I. and Pirogova, G. N. *Zhur. Neorg. Khim.* **2** (1957) 2102.
22. Britton, H. T. S. *J. Chem. Soc.* **1927** 147.
23. Sillén, L. G. *Acta Chem. Scand.* **8** (1954) 299 (ABI).
24. Sillén, L. G. *Acta Chem. Scand.* **8** (1954) 318 (ABII).
25. Bjerrum, J., Schwarzenbach, G. and Sillén, L. G. *Stability constants, Part II, Inorganic ligands,* The Chemical Society Special Publication No. 7 (1958).
26. Biedermann, G. *Arkiv Kemi* **9** (1956) 277.
27. Samuelson, O. and Schramm, K. *Svensk Kem. Tidskr.* **63** (1951) 307.
28. Brown, A. S. *J. Am. Chem. Soc.* **56** (1934) 646.
29. Biedermann, G. and Sillén, L. G. *Arkiv Kemi* **5** (1953) 425.

30. Lagerström, G. *Acta Chem. Scand.* **13** (1959) 722.
31. Sillén, L. G. *Quart. Revs. London* **13** (1959) 146.
32. Ingri, N. and Brito, F. *Acta Chem. Scand.* **13** (1959) 1971.
33. Sillén, L. G. Mimeographed lecture sheets: *Studies on Chemical Equilibria* (MIT, 1957).
34. Ingri, N., Lagerström, G., Frydman, M. and Sillén, L. G. *Acta Chem. Scand.* **11** (1957) 1034.
35. Sasaki, Y., Lindquist, I. and Sillén, L. G. *J. Inorg. & Nuclear Chem.* **9** (1959) 93.
36. Saddington, K. and Cahn, R. W. *J. Chem. Soc.* **1950** 3526.
37. Biedermann, G. *To be published.*

Received August 4, 1960.

ACTA CHEMICA SCANDINAVICA 15 (1961) 190–210

The Complex Formation between Copper(II) Ion and Methoxyacetate, Ethoxyacetate, (Ethylthio)acetate, and Thiodiacetate Ions

ARVID SANDELL

Department of Inorganic and Physical Chemistry, Chemical Institute, University of Lund, Lund, Sweden

The complexity constants of the mononuclear complexes formed by copper(II) ion in water solution with methoxyacetate, ethoxyacetate, (ethylthio)acetate, and thiodiacetate ions have been determined by potentiometric methods at 20.0°C. The investigations have been carried out in a perchlorate medium at ionic strength $I = 1.0$ M. The constants obtained are collected in Tables 11 and 12.

The complex formation between copper(II) ions and both acetate and glycolate ions in water solution is well known [1,2], showing a considerably greater stability of the glycolate complexes than of the acetate complexes. For the copper(II) alkoxyacetate systems, however, no determination of stability constants seems to have been published so far.

In recent years a number of investigations have been published permitting a comparison of the complex formation tendency between metal central ions and ligands containing oxygen or bivalent sulphur, as donor atoms. Copper(II) systems have been investigated in respect to comparatively complicated polydentate ligands (*e.g.*, $Me{\cdot}X{\cdot}CH_2{\cdot}CH_2{\cdot}N(CH_2{\cdot}COOH)_2$ and $X[CH_2{\cdot}CH_2{\cdot}N(CH_2{\cdot}COOH)_2]_2$ where X = oxygen or sulphur) [1]. The investigation reported here, including the copper(II) (ethylthio)acetate and the copper(II) thiodiacetate systems, makes such a comparison possible on simpler types of ligands.

The measurements have been performed potentiometrically, thus acquiring high accuracy, which permits a determination of the stability constants of even the third and fourth complexes. The copper(II) (ethylthio)acetate system has been investigated by measuring the free ligand concentration and the other three systems by measuring the free central ion concentration.

SUMMARY OF THE PRINCIPLES FOR CALCULATION OF THE COMPLEXITY CONSTANTS

The methods of calculation are elaborated by Bjerrum [3], Leden [4] and Fronæus [2]. Only a short summary is given here.

1. Calculation from the measurements of the free ligand concentration

Assuming formation in solution of only mononuclear complexes MA_1 MA_2. . .MA_N between the central ion M (total concentration C_M) and the ligand A (total concentration C_A), the complexity constant β_n is defined by

$$\beta_n = \frac{[MA_n]}{[M][A]^n}$$

corresponding to the equilibrium

$$M + nA \rightleftharpoons MA_n$$

which is valid for the formation of the complex MA_n.

Using β_n, we obtain

$$C_M = [M] \cdot X \tag{1}$$

$$C_A = [A] + [M] \cdot [A] \cdot X' \tag{2}$$

where $X = X([A])$ and $X' = X'([A])$, are defined by

$$X = 1 + \sum_{n=1}^{N} \beta_n \cdot [A]^n$$

and

$$X' = \frac{d\,X([A])}{d[A]}$$

The ligand number $\bar{n}$ is defined by Bjerrum [3] as

$$\bar{n} = \frac{C_A - [A]}{C_M} \tag{3}$$

The curve obtained by plotting $\bar{n}$ as a function of [A] is known as the complex formation curve.

From eqns. (1), (2), and (3), we get

$$\frac{X'}{X} = \frac{\bar{n}}{[A]} \tag{4}$$

which on integration leads to

$$\ln X([A]_j) = \int_0^{[A]_j} \frac{\bar{n}}{[A]} \cdot d[A] \tag{5}$$

Evaluating this integral, which has to be done graphically, leads to a set of corresponding values of X and [A] for the system under investigation, thus enabling the determination of the different complexity constants. In the present paper this determination is carried out by successive extrapolation to [A] = 0 of the following functions

$$X_1 = \frac{X-1}{[A]} = \beta_1 + \beta_2[A] + \beta_3[A]^2 + \ldots$$
$$X_2 = \frac{X_1-\beta_1}{[A]} = \beta_2 + \beta_3[A] + \ldots . \qquad (6)$$

and so forth.

If the formation of polynuclear complexes is not negligible, $\frac{\bar{n}}{[A]}$ will not be a function only of [A].

Assuming formation of mono- and dinuclear complexes and introducing (*cf.* Fronæus [2])

$$\beta'_n = \frac{[M_2A_n]}{[M]^2[A]^n}$$

and

$$Y([A]) = \sum_{n=1}^{L} \beta'_n[A]^n$$

the total concentrations of central ion and ligand will be

$$C_M = [M]\cdot X + 2[M]^2\cdot Y$$
$$C_A = [A] + [M]\cdot X'\cdot[A] + [M]^2\cdot Y'\cdot[A]$$

From these equations we arrive at

$$\frac{\bar{n}}{[A]} = \frac{X' + [M]\cdot Y'}{X + 2[M]\cdot Y} \qquad (7)$$

Thus $\frac{\bar{n}}{[A]}$ is found to be a function of both [A] and [M]. However, it is still possible to compute the constants, β_n, of the mononuclear complexes by arranging the investigation to include measurements at different values of C_M and using the fact that

$$\lim_{C_M \to 0} \frac{\bar{n}}{[A]} = \frac{X'}{X} \qquad (8)$$

The calculation can then be performed as described above.

If $C_A \to 0$, then $[M] \to C_M$. Applying this to eqn. (8) we arrive at

$$\lim_{C_A \to 0} \frac{\bar{n}}{[A]} = \beta_1 + C_M\cdot\beta_1' \qquad (8')$$

Hence it follows that an increase of C_M at low [A] must cause an increase of $\frac{\bar{n}}{[A]}$, if both mono- and dinuclear complexes are formed.

2. Calculation from the measurements of the free central ion concentration

Assuming only mononuclear complexes to be formed and using the same symbols as above, we can write eqn. (1)

$$\frac{C_M}{[M]} = X[A] \tag{1'}$$

In emf measurements of the free central ion concentration, E_M is determined

$$E_M = \frac{RT}{\nu F} \ln \frac{C_M}{[M]} \tag{9}$$

Keeping C_M constant (or a known function of C_A) and varying C_A within a measurement gives us C_A as a function of E_M. Repeating this operation with other C_M-values results in a set of curves on plotting C_A against E_M.

From these curves we obtain a set of corresponding values $(C_M, C_A)_j$ for every arbitrarily chosen value of $E_M = E_{M_j}$. As E_{M_j} is constant within a set, it follows from eqns. (9), (1'), and (4) that X_j, $[A]_j$, and $\bar{n}_j$, are also constant. For every E_{M_j}, eqn. (3) is the equation of a straight line

$$C_A = \bar{n}_j C_M + [A]_j \tag{3'}$$

from which $[A]_j$ can be determined by extrapolation to $C_M = 0$. Thus, corresponding values of [A] and X[A] have been obtained and the complexity constants can be determined from eqns. (6). The ligand number, $\bar{n}$, can be calculated by the aid of these constants and compared with the slope, $\bar{n}_j$, of eqn. (3').

If both mono- and dinuclear complexes are present in the solution, we obtain

$$\frac{C_M}{[M]} = X + 2[M]\cdot Y \tag{1''}$$

and

$$E_M = \frac{RT}{\nu F} \ln(X + 2[M]Y) \tag{9'}$$

If we put $E_M = E_{M_j}$, we obtain a set of corresponding values $(C_M, C_A)_j$ as before. Keeping E_M constant will not cause [A], X([A]), and Y([A]) to be constant, and plotting $(C_M, C_A)_j$ will not result in a straight line. However, extrapolation to $C_M = [M] = 0$ will lead to

$$E_{M_j} = \frac{RT}{\nu F} \ln X([A]_j) \qquad (9'')$$

and $$C_A = [A]_j$$

resulting in corresponding values of [A] and X([A]).

If the complex formation is very strong, the values of $[A]_j$ will be too small to be determined with sufficient accuracy for small C_A. However, if only mononuclear complexes are formed, $\bar{n}_j$ can be determined from eqn. (3') for every X_j, and corresponding values of [A] and X([A]) can be calculated by the aid of

$$\log \frac{[A]_j}{[A]_o} = \int_{X([A]_o)}^{X([A]_j)} \frac{1}{\bar{n}} \cdot d \log X \qquad (10)$$

obtained by integration of eqn. (4).

$[A]_o$ has to be determined from eqn. (3') by extrapolation at a comparatively high value of C_A.

THE GRAPHICAL REPRESENTATION OF THE COMPLEX SYSTEMS

At any value of [A] the composition of a complex system can be computed by means of the determined complexity constants. If only mononuclear complexes are formed the following equations are valid

$$\alpha_o = \frac{[M]}{C_M} = \frac{1}{X} \qquad (11)$$

$$\alpha_n = \frac{[MA_n]}{C_M} = \frac{\beta_n [A]^n}{X}; \; n \geq 1 \qquad (12)$$

The ligand number, $\bar{n}_1$, for the mononuclear complexes can be calculated at any [A] according to

$$\bar{n}_1 = \sum_{n=1}^{N} \frac{n\beta_n [A]^n}{1 + \beta_n [A]^n} \qquad (13)$$

In the systems investigated by measurements of the free central ion concentration, values of the ligand number for the mononuclear complexes can be calculated according to the approximate equation

$$\bar{n}_1 = \frac{\Delta E_M}{\frac{RT}{\nu F} \Delta \ln [A]} \qquad (14)$$

obtained from eqns. (1), (4), and (9). This equation is applied to every two consecutive points of the titration curve and the calculated $\bar{n}_1$ is ascribed to the geometrical mean of the [A] values in question.

CALCULATIONS FROM EXPERIMENTAL DATA

1. *Ligand measurements.* With C'_A and C'_{HA} denoting the stoichiometric concentrations of the ligand ion and its corresponding acid, and $[H^+]'$ the hydrogen ion concentration in the buffer solution, we have

$$K_c = \frac{[H^+]'(C'_A + [H^+]')}{C'_{HA} - [H^+]'} \tag{15}$$

if the central ion concentration is zero.

In a solution with the same C'_A and C'_{HA} but with the total central ion concentration C_M, we denote the concentrations of hydrogen ion by $[H^+]$, of free ligand ions by [A], and of unprotolysed acid by [HA]. If the concentration $C_H = \alpha \cdot C_M$ of free perchloric acid in the stock solution of central ion is taken into consideration, we get the equation

$$K_c = \frac{[H^+][A]}{C'_{HA} + C_H - [H^+]} \tag{16}$$

Putting $C'_{HA} = \delta \cdot C'_A$, we obtain from eqns. (15) and (16)

$$[A] = \frac{[H^+]'}{[H]} \cdot \frac{(C'_A + [H^+]')(\delta C'_A + C_H - [H^+])}{\delta C'_A - [H^+]'} \tag{17}$$

The ligand number, $\bar{n}$, is obtained from

$$\bar{n} = \frac{C'_A + [H^+] - C_H - [A]}{C_M} \tag{18}$$

The determination of $[H^+]$ and $[H^+]'$ was carried out with the aid of the element (25), the emf of which is denoted by E and E', respectively. The slope of the glass electrode was found to be 57.3 mV. Hence,

$$E' - E = E_A = 57.3 \log \frac{[H^+]}{[H^+]'} \tag{19}$$

2. *Central ion measurements.* Using the same symbols as above, we obtain the total ligand concentration in the solution

$$C_A = C'_A + [H^+] - C_H$$

E denotes the emf of an element of the type (21), and E_o the emf of the same element, if $C_M = 0$. The difference between E and E_o is denoted by E_M.

$$E_M = 29.08 \log \frac{C_M}{[M]} \tag{20}$$

EXPERIMENTAL

Chemicals

Copper (II) perchlorate was prepared in the following manner. Copper(II) oxide was precipitated from a hot solution of copper(II) sulphate (Merck's p.a.) by sodium carbonate (Merck's p.a.), washed, and dissolved in perchloric acid (Baker's analysed). The precipitation was repeated four times and the copper(II) perchlorate was recrystallized several times. An approximately 1/3 M stock solution was prepared and the copper(II) concentration determined by electrolysis after addition of sulphuric acid. No foreign ions could be detected in the stock solution.

Copper amalgam, 2.01 % by weight, was prepared by electrolysing a solution of copper(II) sulphate, with pure mecury as cathode. The amalgam was stored under dilute perchloric acid in a closed bottle.

Sodium perchlorate was prepared from perchloric acid (Baker's analysed), sodium carbonate (Merck's p.a.), and carbonate-free sodium hydroxide.

Ethoxyacetic acid was prepared from freshly distilled monochloracetic acid and sodium ethoxide [5]. Purification was by repeated vacuum distillation, dry nitrogen being led through the distillation apparatus. The fraction boiling at 8 torr at 96.5 ± 0.2°C was collected. The equivalent weight was determined by titration with NaOH to 104.1 (calc. 104.1).

A buffer was prepared by adding a calculated amount of carbonate-free sodium hydroxide solution to a weighed portion of the free acid. The buffer was analysed with the aid of a cation exchange resin in the hydrogen form.

In an analogous manner *methoxyacetic acid* was prepared. The portion collected boiled at 98.0 ± 0.2°C at 9 torr, and was a colourless, hygroscopic liquid, which crystallised on cooling (m.p. + 9°C).

A buffer was prepared from 68.69 g of freshly distilled acid, care being taken to prevent humidity from the air being absorbed during weighing. The buffer was then analysed with the aid of a cation exchange resin. Result: $[HA] + [A^-] = 1.526$ M (calc. 1.525 M with equiv. wt. 90.1).

(Ethylthio)acetic acid was prepared from freshly distilled mercaptoacetic acid and ethyl bromide by a method described for similar substances by Larsson [6]. Synthesis and purification were carried out in absence of oxygen. The collected portion, a colourless liquid, boiled at 117.3°C at 10 torr. The equivalent weight was determined to 120.1. (calc. 120.2). A buffer was made and analysed in the same way as with ethoxyacetic acid.

Thiodiacetic acid was prepared and purified according to the method of Lovén [7] and had a melting point of 129°C, and an equivalent weight of 75.0 (calc. 75.1). A stock solution of the disodium salt was prepared by neutralizing the acid with carbonate-free sodium hydroxide.

Quinhydrone was Merck's p.a.

Method

The methoxy- and ethoxyacetate systems were investigated by central ion measurements. The emf, E (mV), of elements of the following composition was measured.

−Cu(Hg)	C_M mM $Cu(ClO_4)_2$ C'_A mM NaA $\delta \cdot C'_A$ mM HA $NaClO_4$ to $I = 1.00$ M	1.00 M $NaClO_4$	10.00 mM $HClO_4$ 990 mM $NaClO_4$ Quinhydrone	* Au +(21)

* The right hand half-cell is in this paper denoted by RE.

The solutions in the left hand half-cell were prepared by adding increasing volumes of solution S_2 to a known volume of a solution S_1.

	S_1	S_2	
$Cu(ClO_4)_2$	C_M	C_M	mM
NaA	0	$C°_A$	mM
HA	0	$C°_{HA}$	mM
$NaClO_4$	$1\,000 - 3\ C_M$	$1\,000 - 3\ C_M - C°_A$	mM

(22)

The thiodiacetate system was investigated by the same method with the exception that no buffer solution was used. The elements had here the composition:

$-Cu(Hg)$	C_M mM $Cu(ClO_4)_2$ C'_A mM Na_2A $NaClO_4$ to $I = 1.00$ M	$NaClO_4$ 1.00 M	RE +

(23)

and the solutions S_1 and S_2 had the composition:

	S_1	S_2	
$Cu(ClO_4)_2$	C_M	C_M	mM
Na_2A	0	$C°_A$	mM
$NaClO_4$	$1\,000 - 3\ C_M$	$1\,000 - 3\ C_M - 3\ C°_A$	mM

(24)

A stream of oxygen-free nitrogen was led through the solution in the left half-cell before the amalgam was put into the electrode vessel. Good mixing of the solutions during the titration was brought about by the nitrogen stream and by stirring the amalgam with a glass rod. Before entering the electrode vessel, the nitrogen had bubbled through a 1.00 M $NaClO_4$ solution to attain the correct vapour pressure. Within one minute the potentials reached stable values and could with very few exceptions, be reproduced within 0.1 mV (in the thiodiacetate system 0.3 mV). Every titration series was repeated at least once.

For the measurements, a Wulff's potentiometer was used, in connection with a Cambridge Light Spot Galvanometer used as a zero instrument.

The investigation of the (ethylthio)acetate system was performed by the ligand measurement method, a glass electrode being used to determine the hydronium ion concentration in the complex solution.

The emf of the following cell

$-$Glass-electrode	C_M mM $Cu(ClO_4)_2$ C'_A mM NaA $C'_{HA} = \delta\ C'_A$ mM HA $NaClO_4$ to $I = 1.00$ M	$NaClO_4$ 1.00 M	RE +

(25)

was determined by means of a Radiometer PHM3 valve potentiometer.

During a titration series C_M was kept constant and C'_A was varied by mixing solutions analogous to S_1 and S_2 in (22). As before, a stream of nitrogen was used for mixing the solutions and keeping them free from oxygen. The titration series were repeated at least once and the potentials were stable and reproducible in general within 0.2 mV.

MEASUREMENTS

The copper(II) perchlorate. In order to determine the concentration of free perchloric acid in the stock solution, $[H^+]$ was measured by a glass electrode ($I = 1.00$ M), at different copper(II) perchlorate concentrations, C_M. The results are collected in Table 1. The values in the fourth column are those found by Pedersen [8] in solutions of pure copper(II) nitrate. Thus the figures

Table 1. The hydronium ion concentration in the copper(II) perchlorate solution at different C_M.

$C_M \times 10^3$ M	$[H^+] \times 10^5$ M	$([H^+]/C_M) \times 10^4$	$([H^+]/C_M)_P \times 10^4$
10.00	0.48	48	16
20.00	13.7	68	12
50.00	41.9	84	8.8

in the third column indicate an excess of free perchloric acid in the stock solution.

From these measurements, the excess of perchloric acid cannot be calculated, owing to the influence of hydrolysis. To eliminate this the following method was employed.

The emf was measured for the cell

−Au	c M $HClO_4$ $NaClO_4$ to I = 1.00 M Quinhydrone	$NaClO_4$ 1.00 M	200 mM $Cu(ClO_4)_2$ c M $HClO_4$ $NaClO_4$ to I = 1.00 M Quinhydrone	Au +

This emf (E mV) can be written

$$E = E_1 + \frac{RT}{F} \ln \frac{c+h}{c} = E_1 + \frac{RT}{F} \ln \left(1 + \frac{h}{c}\right)$$

For small values of $\frac{h}{c}$ we arrive at

$$E = E_1 + \frac{RT}{F} \cdot \frac{h}{c} = E_1 + k \cdot h \cdot \frac{1}{c}$$

If c is sufficiently increased the hydrolysis will be totally depressed and h will attain a limit value h_o, corresponding to the concentration of free perchloric acid in the copper(II) perchlorate solution.

Plotting E against c^{-1} will give a curve which, for small values of c^{-1}, will be approximately a straight line, from the slope S of which we will obtain

$$h_o = \lim_{c^{-1} \to 0} h = \frac{S}{k}$$

where $k = 25.26$ mV.

h_o was found to be 2.0×10^{-3} M and $E_1 = 1.6$ mV. Thus $\frac{h_o}{C_M} = \alpha = 1.0 \times 10^{-2}$.

The copper (II) methoxyacetate system. This system was investigated by central ion measurements as described above. In order to suppress the hydrolysis of the copper(II) ions the measurements were carried out in a buffer (element 21).

It was concluded that the complex solutions were not reduced by the amalgam, since the potentials were well reproducible and remained constant for several hours.

To find out if complex formation occurred between the free acid and the central ion, the emf of the following elements was measured:

—Cu(Hg)	20 mM $Cu(ClO_4)_2$ 100 mM $HClO_4$ C_{HA} mM HA $NaClO_4$ to $I = 1.00$ M	$NaClO_4$ 1.00 M	RE+

When C_{HA} was increased from 0 to 300 mM the potential decreased 0.7 mV. Obviously no complex formation occurred since this should have caused an increase of the potential.

The dissociation constant, K_c, of the methoxyacetic acid at $I = 1.00$ M was determined from the emf of the following element:

—Au	C'_A mM NaA $\delta C'_A$ mM HA $NaClO_4$ to $I = 1.00$ M Quinhydrone	$NaClO_4$ 1.00 M	RE+

where $\delta = 0.515$.

In the range $0.005 \text{ M} \leq C'_A \leq 0.670$ M, the constant was found to be

$$K_c = (4.3 \pm 0.1) \times 10^{-4} \text{ M}$$

Table 2. Determination of corresponding values of C_A and E_M for the copper(II) methoxyacetate system.

$C_M = 10.0$ mM $E_o = 300.2$ mV		$C_M = 20.0$ mM $E_o = 291.4$ mV		$C_M = 33.3$ mM $E_o = 285.0$ mV	
C_A mM	E_M mV	C_A mM	E_M mV	C_A mM	E_M mV
20.5	9.5	27.1	9.6	34.8	9.5
30.3	13.3	36.4	12.6	51.2	14.1
39.2	16.4	53.6	17.8	67.0	18.2
51.4	20.1	70.2	22.2	82.3	21.8
67.2	24.5	86.1	26.1	97.0	25.2
82.5	28.2	101.5	29.5	118.1	29.5
97.2	31.5	123.5	33.8	151	35.5
118.3	35.5	158	39.7	181	40.3
151	41.0	189	44.3	263	51.0
220	50.2	275	54.6	310	55.8
263	55.1	383	64.5	367	61.1
373	65.0	474	71.3	429	66.3
453	71.0	518	74.2	495	71.1
566	78.3	592	78.9	566	75.9
647	82.9	676	83.7	647	80.8
725	87.0	758	87.8	725	85.1

Table 3. Determination of [A] and X_1 for the copper(II) methoxyacetate system.

E_M mV	C_A mM for C_M = 33.3 mM	C_M = 20.0 mM	C_M = 10.0 mM	C_M = 0 mM	X	X_1 M^{-1}	$\bar{n}$ *cf.*eqn.(3′)
10.0	35.9	28.2	21.6	15.7	2.21	76.9	0.62
11.0	39.5	31.2	24.2	17.8	2.39	78.1	0.67
13.0	46.7	37.5	29.4	22.2	2.80	81.0	0.76
15.0	54.6	44.0	35.1	27.0	3.28	84.4	0.84
18.0	66.4	54.4	44.3	35.2	4.16	89.7	0.95
20.0	74.6	61.7	51.1	41.3	4.87	93.8	1.01
30.0	120.8	104.0	90.4	77.5	10.77	126	1.31
35.0	148.1	130.2	115.5	102	16.00	147	1.40
40.0	179	160	145	130	23.77	175	1.47
45.0	215	194	179	163	35.2	210	1.57
55.0	302	279	263	245	77.8	314	
65.0	413	390	373	356	171.8	480	
70.0	479	456	440	423	255.3	601	1.7
75.0	552	530	512	495	379	764	
80.0	634	612	596	580	564	970	1.6
85.0	724	702	687	671	838	1 247	

The experimental results from the complex measurements are collected in Tables 2 and 3.

By graphical extrapolation of the functions X_1, X_2, and X_3, to [A] = 0, the complexity constants were determined:

$$\beta_1 = (66 \pm 3) \quad M^{-1}$$
$$\beta_2 = (640 \pm 50) \quad M^{-2}$$
$$\beta_3 = (1\,300 \pm 300) \quad M^{-3}$$
$$\beta_4 = (600 \pm 300) \quad M^{-4}$$

β_4 was obtained from the slope of the function $X_3([A])$.

The copper (II) ethoxyacetate system. The measurements were performed in the same way as in the methoxyacetate system.

No complex formation could be found between the free acid and the copper(II) ion and the potentials were stable and well reproducible.

For the buffer solution used, δ had the value 0.500, and the dissociation constant K_c at I = 1.00 M was found to be

$$K_c = (3.5 \pm 0.1) \times 10^{-4} \text{ M}$$

The experimental results are collected in Tables 4 and 5.

Graphical extrapolation gave the constants:

$$\beta_1 = (62 \pm 3) \quad M^{-1}$$
$$\beta_2 = (740 \pm 50) \quad M^{-2}$$
$$\beta_3 = (1\,600 \pm 300) \quad M^{-3}$$
$$\beta_4 = (600 \pm 300) \quad M^{-4}$$

β_4 was obtained from the slope of $X_3([A])$.

Table 4. Determination of corresponding values of C_A and E_M for the copper(II) ethoxyacetate system.

C_M = 5.00 mM E_o = 308.9 mV		C_M = 10.0 mM E_o = 300.2 mV		C_M = 20.0 mM E_o = 291.4 mV		C_M = 33.3 mM E_o = 285.0 mV	
C_A mM	E_M mV	C_A mM	E_M mV	C_A mM	E_M mV	C_A mM	E_M mV
9.6	5.6	16.5	7.7	17.1	6.2	16.9	4.6
18.3	9.7	23.6	10.5	27.4	9.6	36.7	10.1
30.6	14.7	30.1	12.9	36.2	12.5	59.9	16.2
46.3	20.1	41.6	16.9	46.7	15.5	80.9	21.4
65.0	25.4	60.1	22.4	65.1	20.8	98.6	25.4
81.9	30.0	74.2	26.1	83.6	25.6	121.3	30.1
100.1	33.6	96.5	31.4	94.0	28.0	150.0	35.4
110.6	35.8	117.5	35.8	108.1	31.0	450	69.4
137.4	40.7	150.1	41.5	136.6	36.5	492	72.5
168.4	45.5	180.1	45.8	199.8	46.3	563	77.5
243.2	55.0	261.8	55.9	273.3	55.3	643	82.7
287.8	59.8	371	66.3	381	65.5		
341	64.8	450	72.5	470	72.6		
400	69.8	563	80.3	588	80.7		
450	73.7	643	85.2	671	85.8		

The copper(II) (ethylthio)acetate system. For this system, two formation constants in 50 % dioxane at 30°C are reported by Irving and Fernelius [9].

The system could not be investigated by means of copper amalgam or quinhydrone since the potentials did not attain stable values and obviously

Table 5. Determination of [A] and X_1 for the copper(II) ethoxyacetate system.

E_M mV	C_A mM for C_M = 33.3 mM	C_M = 20.0 mM	C_M = 10.0 mM	C_M = 5.0 mM	C_M = 0 mM	X	X_1 M^{-1}	$\bar{n}$ *cf.*eqn.(3')
10.0	36.2	28.6	22.3	19.2	16.2	2.208	74.6	0.61
12.0	43.9	34.9	27.7	23.9	20.4	2.586	77.7	0.72
16.0	59.2	48.3	38.9	34.1	29.8	3.55	85.5	0.90
20.0	75.2	62.2	51.7	45.9	41.1	4.87	94.2	1.05
24.0	92.4	77.2	66.1	59.8	54.2	6.69	104.9	1.16
35.0	148	128.5	114	107	99	16.00	151.2	1.46
40.0		157	141	133	125	23.77	182	1.6
45.0		190.5	174	165	156	35.2	220	1.7
50.0		228	211.5	202	193	52.4	266	1.8
55.0		271	254	243	234	77.8	328	1.9
60.0		321	301	290	280	115.6	409	2.1
65.0		378	355	344	333	171.8	513	2.2
70.0	458	436	417	403	396	255.3	642	
75.0	526	504	485		468	379	808	
80.0	600	578	560		543	564	1 036	

some reaction occurred between the complex solution and the electrode material. Thus a yellow precipitate is formed if the complex solution is shaken with metallic copper or copper amalgam.

Using a glass electrode instead of quinhydrone to determine the hydronium ion concentration of the complex solutions gave stable potentials reproducible in general within 0.2 mV.

The present investigation was carried out by measuring the emf of the element (25) as described above.

By measurements in buffer solutions of known pH the slope of the glass electrode was found to be 57.3 mV.

Immediately before and after each titration series the asymmetry potential of the glass electrode was controlled in a reference methoxyacetate buffer of approximately the same pH as the complex solutions. A determination of $[H^+]$ in this buffer by quinhydrone gave the value 2.228×10^{-4} M and the mean value of the emf of the cell

— Glass-electrode	Reference buffer	$NaClO_4$ 1.00 M	RE +

was, in a series of determinations, 390.8 mV. All potential readings were corrected to this reference potential, thus avoiding the influence of slow variations in the asymmetry potential of the glass electrode.

For the buffer used δ had the value 0.510.

In the range 4 mM $\leqq C'_A \leqq$ 50 mM, the mean value of the dissociation constant, K_c, of the acid is

$$K_c = (2.43 \pm 0.03) \times 10^{-4} \text{ M}$$

A spectrophotometrical examination of the solutions A—F below showed that, within experimental error, the concentration of unprotolysed (ethylthio)-acetic acid had no influence on the shape of the light absorption curve. Thus it was assumed that any complex formation between copper(II) ion and the unprotolysed acid could be neglected.

	A	B	C	D	E	F	
$Cu(ClO_4)_2$	10	—	10	10	10	10	mM
$Et{\cdot}S{\cdot}CH_2{\cdot}COOH$	—	15	15	15	150	15	mM
$Et{\cdot}S{\cdot}CH_2{\cdot}COO^-$	—	—	—	—	—	30	mM
$HClO_4$	880	880	880	10	100	—	mM
$NaClO_4$ to I = 1.00 M							

The complex formation caused a considerable alteration of the absorption spectrum curve, especially in the ultraviolet range. Even in solution C, the C_A- of which was calculated to be 4×10^{-6} M, this effect was noticeable as a slight increase of the absorption with its maximum value at the wave length 330 mμ. The absorption curves of the two solutions D and E, with C_A- calculated to 3.4×10^{-4} M and 3.6×10^{-4} M, were almost identical and showed a strong absorption in the ultraviolet range.

Table 6. Determination of corresponding values of [A⁻] and $\frac{\bar{n}}{[A]}$ for $C'_A < 50$ mM in the copper (II) (ethylthio)acetate system.

	C_M = 10.0 mM			C_M = 20.0 mM			C_M = 50.0 mM			C_M = 80.0 mM		
C'_A mM	E_A mV	[A] mM	$\frac{\bar{n}}{[A]}$ M^{-1}	E_A mV	[A] mM	$\frac{\bar{n}}{[A]}$ M^{-1}	E_A mV	[A] mM	$\frac{\bar{n}}{[A]}$ M^{-1}	E_A mV	[A] mM	$\frac{n}{[A]}$ M^{-1}
	—	0	374	—	0	382	—	0	399	—	0	418
3.83	32.6	0.95	338	44.5	0.53	356						
5.64	32.8	1.42	320	45.7	0.78	346	62.5	0.33	379			
9.05	32.1	2.41	290	46.4	1.28	326	65.0	0.52	370			
12.23	30.5	3.51	257	46.2	1.79	308	66.1	0.71	359			
15.19	28.6	4.75	226	45.5	2.32	290	66.7	0.89	351	76.3	0.555	371
19.92	25.6	7.08	185	44.1	3.27	263	67.2	1.19	338	77.3	0.737	358
25.8	21.7	10.79	141	41.3	4.81	223	67.2	1.58	323	77.9	0.97	346
30.9	18.8	14.5	114	38.4	6.52	190	66.7	1.97	307	78.0	1.19	335
37.4	15.8	19.85	88.8	34.6	9.25	154	65.8	2.51	288	78.0	1.47	323
49.8	12.0	30.9	61.8	27.3	16.6	100	63.5	3.75	252	77.3	2.08	299

For $C'_A \leq 50$ mM, measurements with the cell (25) were carried out with four different C_M. The results are collected in Table 6.

For every C_M-value, $\frac{\bar{n}}{[A]}$ was plotted against [A] and the curve extrapolated to [A] = 0.

Table 7. Determination of corresponding values of [A] and $\frac{\bar{n}}{[A]}$ for $C'_A > 50$ mM in the copper(II) (ethylthio)acetate system.

	C_M = 26.7 mM			C_M = 53.3 mM			C_M = 80.0 mM			C_M = 100.0 mM		
C_A' mM	E_A mV	[A] mM	$\frac{\bar{n}}{[A]}$ M^{-1}	E_A mV	[A] mM	$\frac{\bar{n}}{[A]}$ M^{-1}	E_A mV	[A] mM	$\frac{\bar{n}}{[A]}$ M^{-1}	E_A mV	[A] mM	$\frac{\bar{n}}{[A]}$ M^{-1}
63.4	30.9	18.33	92.5	62.1	5.10	217.5	75.9	2.86	273	83.3	2.07	308
85.6	21.9	35.7	52.6	54.5	9.50	151.2	72.6	4.50	229	81.2	3.13	270
106.4	16.9	54.2	36.1	45.3	17.23	97.3	68.0	6.81	184.7	78.4	4.42	235
139.4	12.4	85.0	24.0	32.1	38.5	49.1	57.7	13.67	115.3	72.1	7.59	175.1
180.8	9.5	123.8	17.2	22.5	73.6	27.3	42.3	33.2	55.6	60.8	15.68	105.5
216	7.7	159.3	13.4	17.8	106.3	19.4	32.3	59.4	33.0	48.9	30.4	61.1
287	5.7	229	9.5	12.6	173.6	12.2	21.8	120.2	17.3	32.4	78.5	26.5
349	4.8	288	7.9	10.0	234.0	9.2	16.9	177.5	12.0	24.6	130.3	16.7
498				7.2	374	6.2	11.5	315	7.2	14.4	280	7.7
596				6.3	464	5.3	9.5	408	5.7	12.0	369	6.1
697				5.3	564	4.4	8.1	505	4.8	10.2	464	5.0

Table 8. X-functions obtained by graphical integration of the $\frac{\bar{n}}{[A]}$-function for the copper(II) (ethylthio)acetate system.

[A] mM	X([A])	X_1 M^{-1}	X_2 M^{-2}	X_3 M^{-3}
0	*1*	*365*	*56 000*	*76 000*
1.00	1.420	420		
2.00	1.948	474		
4.00	3.343	586		
6.00	5.19	698		
8.00	7.49	811		
12.00	13.45	1 038		
16.00	21.26	1 266		
20.00	31.0	1 500		
100.0	676	6 750	63 800	
150.0	1 593	10 610	68 300	
200.0	2 950	14 730	71 800	
300	7 220	24 100	79 000	77 000
400	13 900	34 700	86 000	75 000
500	23 600	47 200	94 000	76 000

These curves did not quite coincide for small [A], which could indicate a very slight formation of polynuclear complexes.

If the values of $\lim_{C_A \to 0} \frac{\bar{n}}{[A]}$ were plotted against C_M a straight line was obtained. This is in accordance with the theory if mono- and dinuclear complexes are formed.

From eqn. (8′) β_1 was found to be (370 ± 5) M^{-1}.

If the change in activity coefficients can be neglected in this concentration range ([A] < 3 mM), β'_1 can be estimated to (600 ± 200) M^{-2}.

A similar titration series was performed where C'_A was increased to 700 mM. These results are collected in Tables 7 and 8.

The $\frac{\bar{n}}{[A]}$ functions for the different C_M-values all coincide well, especially for 4 mM < [A] < 300 mM. Thus, for [A] > 4 mM, the mean values of $\frac{\bar{n}}{[A]}$ have been plotted against corresponding [A]. On this curve the graphical integration has been carried out.

Graphical extrapolation gave the constants:

$$\beta_1 = (365 \pm 10) \quad M^{-1}$$
$$\beta_2 = (58\,000 \pm 2\,000) \quad M^{-2}$$
$$\beta_3 = (70\,000 \pm 5\,000) \quad M^{-3}$$

The copper(II) thiodiacetate system. Tichane and Bennet [10], who have investigated this system in 0.1 M KCl at 30.0°, report two stability constants, $\log K_1 = 4.5$ and $\log K_2 = 2.8$, but they do not mention any higher complexes.

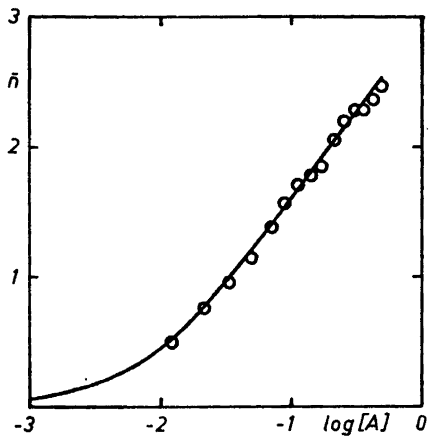

Fig. 1. The complex formation curve of the copper(II) ethoxyacetate system. The fulldrawn curve represents $\bar{n}_1$ computed by means of eqn. (13). $\bar{n}_1$ from eqn. (14) is denoted by (O).

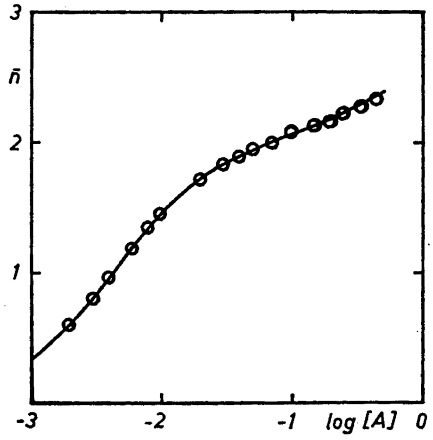

Fig. 2. The complex formation curve of the copper(II) (ethylthio)acetate system. The fulldrawn curve represents $\bar{n}_1$ computed by means of eqn. (13). The sign (O) refers to $\bar{n}_1$ obtained from Tables 6 and 7.

To find out if there is any formation of higher complexes, an investigation has been carried out by emf measurements of the concentration of free central ion in the same way as for the copper(II) methoxyacetate system (element 23).

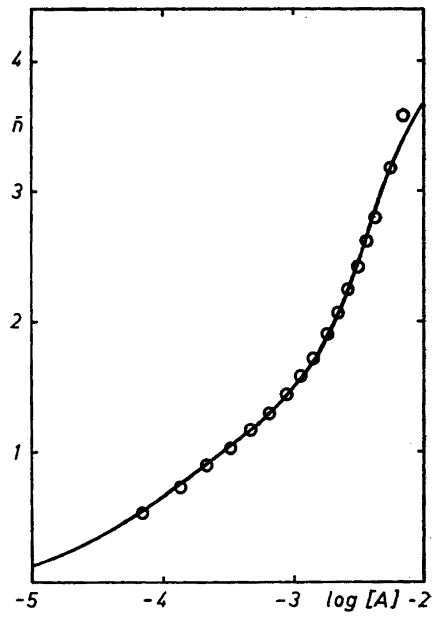

Fig. 3. The complex formation curve of the copper(II) thiodiacetate system. The fulldrawn curve represents $\bar{n}_1$ computed by means of eqn. (13), and the sign (O) refers to $\bar{n}_1$ obtained from eqn. (14).

However, a buffer solution of the ligand could not be used owing to the formation of the ion HA^-. Therefore the complex solutions were prepared from a stock solution of 1/3 M disodium thiodiacetate. The systematic error caused by the hydrolysis of the copper ions was supposed to be negligible owing to the relatively strong complexity of the system under investigation.

Some reaction occurs between the complex solutions and the copper amalgam as in the (ethylthio)acetate system. However, the reaction rate is slow and the potentials measured in some sample solutions showed good constancy during as long a time as required for a titration series.

The titrations were repeated several times and the reproducibility of the potentials was in general 0.3 mV.

At higher C_M a bluish white precipitate was easily formed which was supposed to be the neutral complex. (Found: Cu 30.0 %. Calc. for $CuS(CH_2 \cdot COO)_2$: Cu 30.0 %).

This tendency of the neutral complex to precipitate from the complex solution made it necessary to use $C_M \leq 5$ mM. If Cu^+ is formed in noticeable amounts in the complex solutions in contact with copper amalgam during the titration, this could give rise to considerable errors in the calculated complexity constants, especially at these small C_M (*cf.* Fronæus [2]). However, checking by measuring in freshly mixed complex solutions, the compositions of which were chosen to cover the titration series, gave the same potential readings as in the titrations (within the same limits of error).

A separate control was made in a solution with $C_M = 5$ mM and $C_A = 20$ mM through which nitrogen was bubbled for several hours. Amalgam was put in the oxygen-free solution and samples taken from this solution after 10 and 45 min. The samples were analysed by means of EDTA according to Schwarzenbach [11], and showed an increase in the consumption of titrator of about 2 %.

A similar experiment with $CuSO_4$-solution showed no increase in the metal ion concentration in the solution.

Table 9. Determination of corresponding values of C_A and E_M for the copper(II) thiodiacetate system.

C_M = 5.00 mM		C_M = 2.00 mM		C_M = 1.00 mM		C_M = 0.50 mM	
C_A mM	E_M mV	C_A mM	E_M mV	C_A mM	E_M mV	C_A mM	E_M mV
2.97	10.6	1.06	8.3	0.59	9.1	0.388	9.3
5.88	26.8	2.09	20.7	1.15	20.2	0.51	12.9
8.74	42.6	3.11	32.5	1.70	29.3	0.87	22.8
11.54	55.6	4.10	42.2	2.48	40.2	1.32	32.4
14.29	66.1	5.08	50.2	3.21	48.6	1.94	42.9
19.63	84.5	6.04	57.6	4.14	58.1	2.83	55.1
27.3	105.3	7.44	66.8	5.41	68.4	3.67	64.7
34.5	120.2	8.81	75.4	6.74	78.2	4.44	72.3
		12.3	92.2	8.42	88.9	5.49	81.1
		15.2	104.3	10.00	97.6	6.67	89.4
				12.4	107.6		

Table 10. Determination of [A] and X-functions for the copper(II) thiodiacetate system.

E_M mV	$\bar{n}$	$\int_{X([A]_0)}^{X([A])} \frac{1}{\bar{n}} d \log X$	[A] mM	X([A])	$X_1 \times 10^{-3}$ M^{-1}	$X_2 \times 10^{-7}$ M^{-2}	$X_3 \times 10^{-9}$ M^{-3}	$X_4 \times 10^{-11}$ M^{-4}
			0	*1*	*15.0*	*1.2*	*0.4*	*8*
15	0.73	1.7058	0.138	3.279	16.5			
20	0.90	1.4974	0.22	4.873	17.6	1.18		
25	1.03	1.3216	0.33	7.239	18.9	1.18		
30	1.17	1.1664	0.48	10.77	20.4	1.13		
35	1.30	1.0284	0.66	16.00	22.7	1.17		
40	1.44	0.8974	0.89	23.77	25.6	1.19		
45	1.58	0.7854	1.15	35.24	29.8	1.29		
70	2.43	0.3476	3.14	255.3	81.0	2.10	2.87	7.9
75	2.62	0.2805	3.67	379	103	2.40	3.27	7.8
80	2.80	0.2176	4.24	564	133	2.78	3.77	7.9
90	3.19	0.1003	5.56	1245	224	3.76	4.68	7.7
100	3.59	0	7.00	2748	392	5.39	6.0	8.0

This minute effect on the composition of the complex solutions caused by reaction with the amalgam was not considered to influence seriously the possibility of a fairly accurate determination of the complexity constants for the system under investigation, particularly as the amalgam was not allowed to be in contact with a complex solution for more then 10 to 15 min in the measurements.

If only mononuclear complexes are formed, C_A will be a linear function of C_M if E_M is constant (eqn. 3'). This was the case with this system.

Owing to the strong complexity, the values of [A] had to be determined by numerical integration according to eqn. (10).

The value of $[A]_0$ had to be determined by extrapolation. In this case the value at the highest E_M obtained (100 mV, corresponding to $X([A]_0)=2\ 750$) was chosen. Extrapolation gave $[A]_0 = 7.00$ mM.

The results are collected in Tables 9 and 10.

The following constants were obtained by graphical extrapolation:

$$\beta_1 = (1.5 \pm 0.1) \times 10^4 \quad M^{-1}$$
$$\beta_2 = (1.2 \pm 0.2) \times 10^7 \quad M^{-2}$$
$$\beta_3 = (4 \pm 2) \times 10^8 \quad M^{-3}$$
$$\beta_4 = (8 \pm 3) \times 10^{11} \quad M^{-4}$$

β_4 was obtained from the slope of the function $X_3([A])$.

DISCUSSION

The complex formation curves for the methoxyacetate and the ethoxyacetate systems are almost identical and one of them is reproduced in Fig. 1. The ligand number $\bar{n}$ attains here a highest value of 2.5. The steep form of the curve indicates the presence of a fourth complex. These curves coincide

Table 11. The logarithms of the complexity constants determined at 20.0°C and ionic strength 1.00 M.

Systems	log β_1	log β_2	log β_3	log β_4
Cu^{2+} – Me·O·CH_2·COO^-	1.82	2.81	3.11	2.8
Cu^{2+} – Et·O·CH_2·COO^-	1.79	2.87	3.20	2.8
Cu^{2+} – Et·S·CH_2·COO^-	2.56	4.76	4.85	—
Cu^{2+} – $S(CH_2 \cdot COO^-)_2$	4.18	7.08	8.6	11.9

well in their general shape with the corresponding curve for the copper(II) acetate system according to Fronæus [2]. This might indicate that the complex formation should occur mainly in the same way as in the acetate system.

For the (ethylthio)acetate system the complex formation curve is of a somewhat different form (Fig. 2). With increasing [A], the value of the ligand number rapidly increases to $\bar{n} \simeq 1.6$. Then the curve becomes flatter, indicating a wide range of existence of the second complex. The ligand number reaches approximately the same value as in the ethoxyacetate system but on account of the flat course of the curve, there seems to be no reason to take more than three complexes into consideration.

The complex formation curve for the thiodiacetate system as presented in Fig. 3, indicates a relatively wide range of existence of the first complex, since the slope of the curve is comparatively small within the range $0.5 < \bar{n} < 1.5$. The ligand number reaches a value of 3.7, indicating the for-

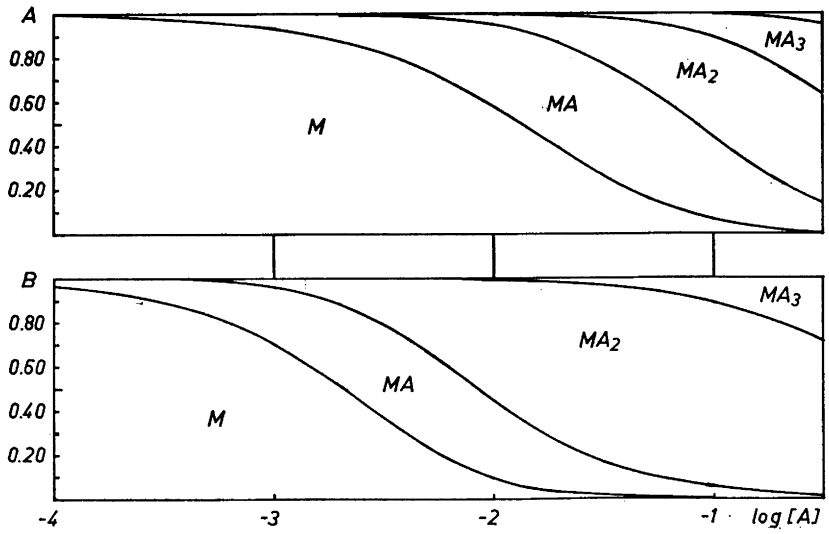

Fig. 4. The distribution of the central ion between the mononuclear complexes with varying [A] according to eqns. (11) and (12) in: A, the copper(II) ethoxyacetate system; B, the copper(II) (ethylthio)acetate system.

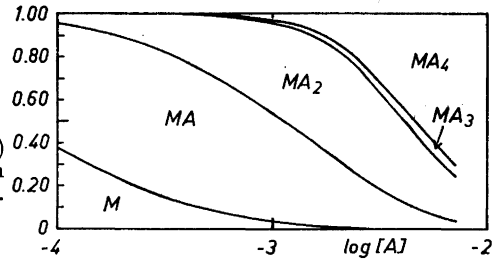

Fig. 5. The distribution of the copper(II) ion between the mononuclear complexes in the thiodiacetate system according to eqns. (11) and (12).

mation of at least four complexes. The steep form of the curve at $\bar{n} > 2$ points to a narrow range of existence of the third complex.

From the complexity constants, β_n, the stability constants, b_n,

$$b_n = \frac{[MA_n]}{[MA_{n-1}][A]}$$

have been calculated and brought together in Table 12. For the sake of survey the constants of the copper(II) acetate system according to Fronæus [2] have been included.

A comparison between the constants for the acetate system on one hand and for the methoxyacetate and ethoxyacetate on the other hand, strengthens the assumption made above that the formation of the complexes within these systems follows mainly the same scheme. Except for the slightly higher values of b_1 in the alkoxyacetate systems, there is no evidence for chelate formation.

For the (ethylthio)acetate system the situation is quite different. The high values of b_1 and b_2 indicate that the first two complexes are mainly chelates with the sulphur atom strongly bound to the central atom. With regard to the small value of b_3, the third ligand can be considered to co-ordinate monodentately. The high value of the quotient $\frac{b_2}{b_3}$ expresses the predominance of the second complex.

An interpretation of the data obtained in the investigation of the thiodiacetate system is far more difficult. On account of the experiences from the

Table 12. The stability constants calculated from the determined complexity constants.

Systems	b_1 M^{-1}	b_2 M^{-1}	b_3 M^{-1}	b_4 M^{-1}	$\frac{b_1}{b_2}$	$\frac{b_2}{b_3}$	$\frac{b_3}{b_4}$
Cu^{2+} — Me·O·CH_2·COO^-	66	9.7	2.0	0.46	6.8	4.9	4.3
Cu^{2+} — Et·O·CH_2·COO^-	62	11.9	2.2	0.38	5.2	5.4	5.8
Cu^{2+} — Et·S·CH_2·COO^-	365	160	1.2		2.3	130	
Cu^{2+} — S(CH_2·COO^-)$_2$	15 000	800	33	2 000	19	24	0.02
Cu^{2+} — CH_3·COO^- (according to Fronæus[2])	47	9.6	2.6	0.65	4.9	3.7	4.0

(ethylthio)acetate system, however, it may be reasonable to regard the ligand ion as tridentate, capable of filling two or three of the planarly disposed co-ordination positions of the four-co-ordinated copper(II) ion. The great stability of the first two complexes may therefore be attributed to chelating. The value of the constant b_4, obtained in this investigation, is largely influenced by any imperfections in the applied methods. The unexpectedly high value of b_4 can be due to this. However, it may be mentioned that Fronæus [2] observed a similar effect in the copper(II) tartrate system.

Finally, I wish to express my gratitude to my teachers, Professor S. Bodforss and Professor S. Fronæus, who interested me in complex chemistry, put the best working facilities at my disposal, and stimulated this work by many valuable discussions.

REFERENCES

1. Bjerrum, J., Schwarzenbach, G. and Sillén, L. G. *Stability Constants*, Part I, Organic Ligands, The Chemical Society, London 1957.
2. Fronæus, S. *Komplexsystem hos koppar.* (Diss.) University, Lund 1948.
3. Bjerrum, J. *Metal Ammine Formation in Aqueous Solution* (Diss.) University, Copenhagen 1941.
4. Leden, I. *Potentiometrisk undersökning av några kadmiumsalters komplexitet* (Diss.) University, Lund 1943.
5. Blatt, A. H. (Ed.) *Organic Syntheses, Coll. Vol.* **2** (1946) 260.
6. Larsson, E. *Ber.* **63 I** (1930) 1347.
7. Lovén, J. M. *Ber.* **27** (1894) 3059.
8. Pedersen, K. J. *Kgl Danske Videnskab. Selskab, Mat.-fys. Medd.* **20** (1943) No. 7, p. 21.
9. Irwing, R. J. and Fernelius, W. C. *J. Phys. Chem.* **60** (1956) 1427.
10. Tichane, R. M. and Bennet, W. E. *J. Am. Chem. Soc.* **79** (1957) 1293.
11. Schwarzenbach, G. *Die Komplexometrische Titration*, Stuttgart 1955, p. 68.

Received July 22, 1960.

ACTA CHEMICA SCANDINAVICA 15 (1961) 211–230

Short Communications

Chalcones from the Fronds of *Pityrogramma chrysophylla*, var. *heyderi*

MARTIN NILSSON

Organisk-kemiska Institutionen, Kungl. Tekniska Högskolan, Stockholm, Sweden

In continuation of the studies on frond pigments of the "ceraceus" ferns [1-3] the pigments of *Pityrogramma chrysophylla* (Sw.) Link, var. *heyderi* (Lauche) Domin, have now been investigated. This fern has an orange-coloured coating on the back of the fronds.

P. chrysophylla Kaulf. and *P. sulphurea Desv.* have been investigated by Zopf [4] (the genus then was given as *Gymnogramme*). He isolated a red material, m.p. 159°, which analysed for $C_{18}H_{18}O_5$. This "gymnogrammen" on boiling with ethanol was converted into colourless "gymnogrammidin", m.p. 114–115° (no analysis).

A similar material was obtained from *P. chrysophylla* var. *heyderi* in the present investigation. It proved to be a mixture which was separated by chromatography to give two main coloured components. Both pigments had indefinite melting points around 160°, which were not improved by recrystallisation. On vacuum distillation both were converted into colourless compounds, m.p. 100–102° and 119–120°. These rearrangement products were found to be flavanones and comparison with authentic material showed them to be (±)-5-hydroxy-7-methoxyflavanone and (±)-5-hydroxy-4′,7-dimethoxyflavanone, respectively.

The infrared and ultraviolet spectra of the pigments clearly indicate that these are the corresponding chalcones: 2′,6′-dihydroxy-4′-methoxychalcone (I) and 2′,6′-dihydroxy-4,4′-dimethoxychalcone (II). Of these only I has been observed before — it was obtained by Lindstedt [5] in a small amount on acidification of an alkaline solution of the corresponding flavanone and was found to cyclise very readily. Appreciable amounts of the flavanones were also isolated from the extracts.

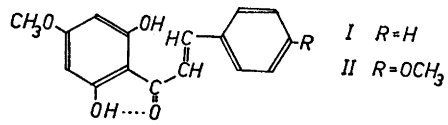

I R=H
II R=OCH_3

In the *Pityrogramma* species hitherto investigated all pigments on the back of the fronds are of the $C_6C_3C_6$-type. Whereas in *P. chrysophylla* var. *heyderi* the orange colour is due to the chalcones I and II the white coating of var. *marginata* contains the corresponding dihydrochalcones [3]. In *P. triangularis* on the other hand the yellow pigment, although closely related to the chalcone I, is 3′,3′-dimethylated preventing aromaticity of the phloroglucinoid nucleus [1,2].

The gymnogrammen described by Zopf could be identical with the chalcone II.

Experimental. Melting points were determined on a Kofler block. The infrared spectra were recorded on Perkin Elmer No. 21 instrument (sodium chloride prism, potassium bromide discs) and the ultraviolet spectra on a Beckman DK-2 spectrophotometer (ethanol solutions).

Isolation. The samples of *P. chrysophylla* var. *heyderi* were collected and identified in the Royal Botanic Gardens at Kew in the autumn 1958. Fresh fronds and stems (147 g) were extracted with ether and the material obtained partitioned between dimethyl sulphoxide and *cyclo*hexane as described earlier [3]. A wax fraction (1.7 g, m.p. 40–75°) and a pigment fraction (4.9 g, m.p. 130–140°) were

obtained. Recrystallisation from benzene gave a bright red, crystalline material, m.p. 140—156°. Paper chromatography (*iso*propylether, dimethyl sulphoxide, EDTA treated paper [3]) showed the presence of two phenolic components, R_F 0.26 and 0.18. The mother liquors contained small amounts of a further slow-moving component (R_F 0.15) and two rapid components (R_F 0.57 and 0.38). The latter gave a brown colour with the benzidine reagent only after addition of sodium carbonate.

Separation of the mixtures as described for the dihydrochalcones [3] gave the following components: R_F *0.57*, 0.3 g; *0.38*, 0.2 g; *0.26*, 0.3 g and *0.18*, 1 g.

The R_F 0.57 product was recrystallised from methanol and sublimed, colourless plates, m.p. 100—102° identical with (±)-5-hydroxy-7-methoxyflavanone [3] (mixed m.p. and IR).

The R_F 0.38 product was recrystallised from methanol and sublimed to give colourless needles, m.p. 119—120°, identical with (±)-5-hydroxy-4′,7-dimethoxyflavanone [3] (mixed m.p. IR).

The R_F 0.26 product was recrystallised from benzene giving red prisms, m.p. 156—167°. The melting point range was not improved by repeated crystallisations. The infrared spectrum showed a broad band between 3 200 and 2 400 cm^{-1} and absorptions at 1 635, 1 610 and 825 cm^{-1}. The ultraviolet spectrum showed a broad maximum at 355 mμ (log ε 4.70). On attempted sublimation (130°, 0.005 mm) a colourless oil distilled. It solidified on cooling and proved to be identical with (±)-5-hydroxy-4′,7-dimethoxyflavanone (mixed m.p., IR). On standing, particularly in solution, the pigment was slowly converted into the flavanone.

The R_F 0.18 product on recrystallisation from benzene gave red prisms with an indefinite melting point, 156—162°. Relevant infrared absorptions were observed at 3 200—2 400, 1 635, 745 and 685 cm^{-1}. The ultraviolet spectrum showed a broad absorption at 340 mμ (log ε 4.74). Thermal rearrangement as described above gave (±)-5-hydroxy-7-methoxyflavanone in almost quantitative yield (identified by mixed m.p. and IR).

Acknowledgements. I thank Dr. G. Taylor, Royal Botanic Gardens, Kew, for a generous supply of fern material, Professor H. Erdtman for his interest in the work, Miss Gurli Hammarberg for the spectra and Mr. E. Pettersson for technical assistance. Dr. I. Wellings has checked the English.

1. Nilsson, M. *Acta Chem. Scand.* **13** (1959) 750.
2. Forsén, S. and Nilsson, M. *Acta Chem. Scand.* **13** (1959) 1383.
3. Nilsson, M. *Acta Chem. Scand.* **15** (1961) 154.
4. Zopf, W. *Ber. deut. botan. Ges.* **24** (1906) 264.
5. Lindstedt, G. *Acta Chem. Scand.* **4** (1950) 1042.

Received December 16, 1960.

Gel Filtration Chromatography in the Separation of Human Serum

GUNNAR LUNDBLAD

Statens Bakteriologiska Laboratorium, Stockholm, Sweden

It has been reported by Alridge [1], Mounter and Whittaker [2], Augustinsson [3], and Marton and Kalow [4] that human plasma contains arylesterase activity.

In connection with investigations of cytolytic serum factors [5,6], it was noticed that the arylesterase activity of various fractions obtained in continuous (courtain) flow electrophoresis of human serum had such values that the presence of two arylesterases is indicated.

It can now be reported that two different arylesterases have been partly separated in fractions from human serum. As found in the investigations cited [5,6], there is one heat labile (56°C for 30 min.) arylesterase in human serum which is not influenced by EDTA and one heat stabile arylesterase which is completely inactivated by EDTA.

Experimental. Normal human serum from healthy blood donors (10 ml) was fractionated at +4°C with ammonium sulphate at pH 5.2. The sediments from 0—50, 50—60, and 60—70 % saturation were dissolved in 5 ml portions and for desalting filtered through Sephadex [7] G-25 columns 2 × 28 cm, equilibrated with 0.9 % NaCl. The supernatant from 70 % saturation was filtered too. The different solutions were at the desalting by Sephadex filtration collected in 3 ml fractions and the optical density at 280 mμ was measured as well as protein nitrogen and arylesterase activity. All fractions filtered were free from ammonium

obtained. Recrystallisation from benzene gave a bright red, crystalline material, m.p. 140—156°. Paper chromatography (*iso*propylether, dimethyl sulphoxide, EDTA treated paper [3]) showed the presence of two phenolic components, R_F 0.26 and 0.18. The mother liquors contained small amounts of a further slow-moving component (R_F 0.15) and two rapid components (R_F 0.57 and 0.38). The latter gave a brown colour with the benzidine reagent only after addition of sodium carbonate.

Separation of the mixtures as described for the dihydrochalcones [3] gave the following components: R_F *0.57*, 0.3 g; *0.38*, 0.2 g; *0.26*, 0.3 g and *0.18*, 1 g.

The R_F 0.57 product was recrystallised from methanol and sublimed, colourless plates, m.p. 100—102° identical with (±)-5-hydroxy-7-methoxyflavanone [3] (mixed m.p. and IR).

The R_F 0.38 product was recrystallised from methanol and sublimed to give colourless needles, m.p. 119—120°, identical with (±)-5-hydroxy-4′,7-dimethoxyflavanone [3] (mixed m.p. IR).

The R_F 0.26 product was recrystallised from benzene giving red prisms, m.p. 156—167°. The melting point range was not improved by repeated crystallisations. The infrared spectrum showed a broad band between 3 200 and 2 400 cm^{-1} and absorptions at 1 635, 1 610 and 825 cm^{-1}. The ultraviolet spectrum showed a broad maximum at 355 mμ (log ε 4.70). On attempted sublimation (130°, 0.005 mm) a colourless oil distilled. It solidified on cooling and proved to be identical with (±)-5-hydroxy-4′,7-dimethoxyflavanone (mixed m.p., IR). On standing, particularly in solution, the pigment was slowly converted into the flavanone.

The R_F 0.18 product on recrystallisation from benzene gave red prisms with an indefinite melting point, 156—162°. Relevant infrared absorptions were observed at 3 200—2 400, 1 635, 745 and 685 cm^{-1}. The ultraviolet spectrum showed a broad absorption at 340 mμ (log ε 4.74). Thermal rearrangement as described above gave (±)-5-hydroxy-7-methoxyflavanone in almost quantitative yield (identified by mixed m.p. and IR).

Acknowledgements. I thank Dr. G. Taylor, Royal Botanic Gardens, Kew, for a generous supply of fern material, Professor H. Erdtman for his interest in the work, Miss Gurli Hammarberg for the spectra and Mr. E. Pettersson for technical assistance. Dr. I. Wellings has checked the English.

1. Nilsson, M. *Acta Chem. Scand.* **13** (1959) 750.
2. Forsén, S. and Nilsson, M. *Acta Chem. Scand.* **13** (1959) 1383.
3. Nilsson, M. *Acta Chem. Scand.* **15** (1961) 154.
4. Zopf, W. *Ber. deut. botan. Ges.* **24** (1906) 264.
5. Lindstedt, G. *Acta Chem. Scand.* **4** (1950) 1042.

Received December 16, 1960.

Gel Filtration Chromatography in the Separation of Human Serum

GUNNAR LUNDBLAD

Statens Bakteriologiska Laboratorium, Stockholm, Sweden

It has been reported by Alridge [1], Mounter and Whittaker [2], Augustinsson [3], and Marton and Kalow [4] that human plasma contains arylesterase activity.

In connection with investigations of cytolytic serum factors [5,6], it was noticed that the arylesterase activity of various fractions obtained in continuous (courtain) flow electrophoresis of human serum had such values that the presence of two arylesterases is indicated.

It can now be reported that two different arylesterases have been partly separated in fractions from human serum. As found in the investigations cited [5,6], there is one heat labile (56°C for 30 min.) arylesterase in human serum which is not influenced by EDTA and one heat stabile arylesterase which is completely inactivated by EDTA.

Experimental. Normal human serum from healthy blood donors (10 ml) was fractionated at +4°C with ammonium sulphate at pH 5.2. The sediments from 0—50, 50—60, and 60—70 % saturation were dissolved in 5 ml portions and for desalting filtered through Sephadex [7] G-25 columns 2 × 28 cm, equilibrated with 0.9 % NaCl. The supernatant from 70 % saturation was filtered too. The different solutions were at the desalting by Sephadex filtration collected in 3 ml fractions and the optical density at 280 mμ was measured as well as protein nitrogen and arylesterase activity. All fractions filtered were free from ammonium

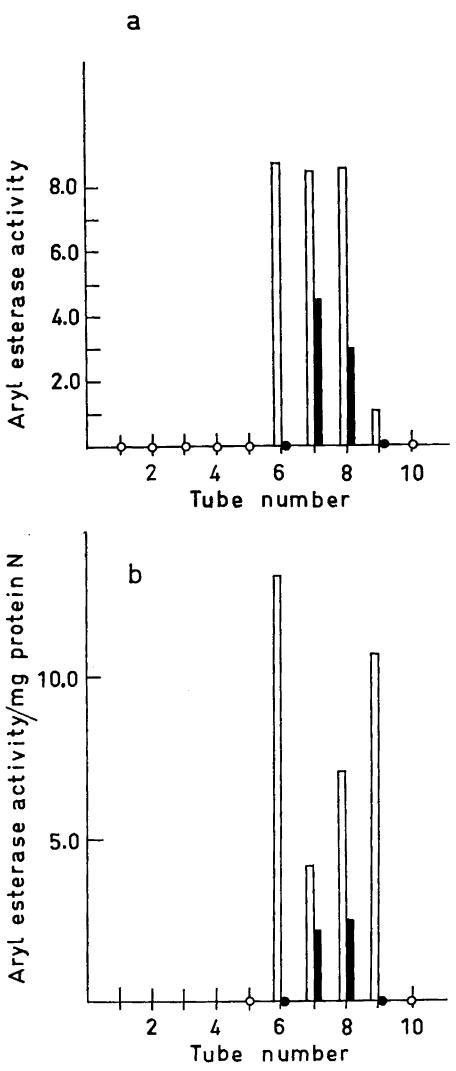

Fig. 1. Arylesterase activity in normal human serum fraction, precipitated at 60—70 % ammonium sulphate saturation. The precipitate was dissolved in 5 ml 0.9 % NaCl and filtered through a Sephadex G-25 column and collected in 3 ml fractions. Open areas: total arylesterase activity. Dark areas: heat stabile arylesterase activity. Substrate: phenylacetate in Tris buffer at pH 8.0. a: activity per volume; b: activity per mg protein nitrogen.

sulphate. Phenylacetate was used as substrate and the hydrolysis was measured by titration of liberated carboxyl groups. The assay mixture consisted of 0.50 ml sample and 3.00 ml 0.04 M phenylacetate in 0.1 M tris buffer at pH 8.0. The mixtures were incubated at 25°C for 60 min. The determinations were duplicates and controls for nonenzymatic hydrolysis were always run. The esterase activity was assayed in unheated samples as well as in samples heated at 56°C for 30 min.

Results. As can be seen in the figure, which shows the arylesterase activity of the precipitate from 60—70 % ammonium sulphate saturation, separation occurs after the gel filtration. In tube number 6 there is only the heat labile arylesterase. In tube number 7, however, more than 50 % of the activity remained after heating and in tube number 8 there is about 40 % of the heat stabile arylesterase present. In tube number 9 there is only a weak activity of the heat labile enzyme. The distribution of the two arylesterases was confirmed when the activity was tested in presence of EDTA in a final concentration of 0.001 M. Thus, it appeared that the esterase activity in tubes number 7 and 8 was completely removed with the agent but remained the same without EDTA in tubes number 6 and 9. Eserine sulphate ($M \times 10^{-4}$) had no effect, thus indicating the absence of cholinesterase. The precipitate from 50—60 % ammonium sulphate saturation and the supernatant after 70 % saturation had rather strong arylesterase activity, but only from the heat labile enzyme.

1. Alridge, W. N. *Biochem. J.* **53** (1953) 110.
2. Mounter, L. A. and Whittaker, V. P. *Biochem. J.* **54** (1953) 551.
3. Augustinsson, K.-B. *Nature* **181** (1958) 1786; *Acta Chem. Scand.* **13** (1959) 571, 1097.
4. Marton, A. and Kalow, W. *Can. J. Biochem. Physiol.* **37** (1959) 1367.
5. Paulsson, J.-E., Björklund, B. and Björklund, V. *Med. Riksstämman Stockholm* 1960; *Acta Pathol. Microbiol. Scand. In press.*
6. Lundblad, G., Paulsson, J.-E., von Zeipel, E. and Björklund, B. *Med. Riksstämman Stockholm* 1960; *Acta Pathol. Microbiol. Scand. In press.*
7. Porath, J. and Flodin, P. *Nature* **183** (1959) 1657.

Received December 21, 1960.

X-Ray Study on Solid Solutions of Oxygen in Hafnium

TORE DAGERHAMN

Institute of Inorganic and Physical Chemistry, University of Stockholm, Stockholm, Sweden

In connection with studies on the titanium-oxygen and zirconium-oxygen systems which are being conducted at this Institute, an investigation has been made of the solubility of oxygen in the hexagonal close-packed modification of hafnium.

Hafnium metal (Imperial Chemical Industries Ltd., crystal bar, Hf min. 98.5 % with Zr 1.0 – 1.5 % and O 400 ppm as major impurities) and hafnium dioxide obtained by heating the metal in a stream of oxygen were used to prepare several samples within the composition range $HfO_{0-0.5}$. Mixtures of the starting materials were arc-melted in an argon atmosphere and then heat-treated in evacuated silica capsules for one month at 600°C followed by quenching in water. X-Ray powder photographs were taken in a Guinier focusing camera using $CuK\alpha_1$ radiation. Details of the methods used in the preparative and X-ray work have been given in previous articles [1,2].

The results of the investigation are summarized in Table 1 and Fig. 1. The introduction of oxygen in solid solution increases the hafnium lattice parameters a and c over the entire range of solubility. The axial ratio c/a, however, is practically constant after a slight rise at low oxygen contents. The limit of solubility was found to be at 20.6 at. % ($HfO_{0.26}$). Samples with higher oxygen contents contain dioxide as the additional phase.

Table 1. Unit-cell parameters for samples HfO_x heat-treated at 600°C for 1 month.

x	a (Å)	c (Å)	c/a	
0.00	3.1969	5.0604	1.5829	
0.10	3.2044	5.0830	1.5863	
0.15	3.2072	5.0889	1.5867	
0.20	3.2112	5.0942	1.5864	
0.25	3.2142	5.0983	1.5862	
0.30	3.2148	5.1006	1.5866	(two-phase region)
0.35	3.2145	5.0990	1.5863	» » »
0.40	3.2150	5.0990	1.5860	» » »
0.50	3.2147	5.1003	1.5866	» » »

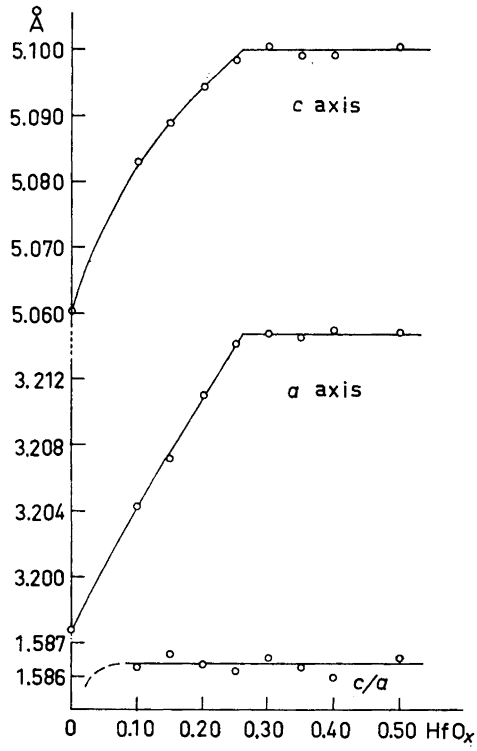

Fig. 1. Unit-cell parameters for samples HfO_x heat-treated at 600°C for 1 month.

As is the case for the titanium-oxygen and zirconium-oxygen solid solutions, the oxygen atoms dissolved in hafnium must occupy interstitial positions in the metal structure. The powder photographs of the specimens HfO_x did not show any extra lines which indicates that the distribution of the interstitial atoms is a random one at all concentrations of oxygen.

A comparison with the titanium-oxygen [1] and zirconium-oxygen [3] systems indicates a decrease in the solubility limit in the order $TiO_{0.50}$, $ZrO_{0.40}$ and $HfO_{0.26}$. The appearance of ordered arrangements of the interstitial oxygen atoms and the peculiar shape of the lattice parameter curves observed for the former two systems entirely lack a counterpart in the solid solutions of oxygen in hafnium.

The author wishes to express his gratitude to Dr. Arne Magnéli and Fil.kand. Bo Holmberg for their kind interest in this investigation which was undertaken in connection with research programmes financially supported by the *Swedish Natural Science Research Council* and by the *AB Atomenergi Ltd.*

1. Andersson, S., Collén, B., Kuylenstierna, U. and Magnéli, A. *Acta Chem. Scand.* **11** (1957) 1641.
2. Westman, S. and Magnéli, A. *Acta Chem. Scand.* **11** (1957) 1587.
3. Holmberg, B. and Dagerhamn, T. *To be published in Acta Chem. Scand.*

Received December 17, 1960.

On Light-Induced Phosphorylation and Oxidation of Reduced Diphosphopyridine Nucleotide in *Rhodospirillum rubrum*

MARGARETA BALTSCHEFFSKY

Wenner-Gren Institute, University of Stockholm, Sweden

The highest values yet reported for the specific activity of bacterial light-induced phosphorylation, have been obtained with isolated chromatophores from the photosynthetic bacterium *Rhodospirillum rubrum*, which has been ground with alumina (Alcoa A-301) in order to rupture the intact cells [1]. During the last year we have also used sand (Baker, purified) as an abrasive instead of alumina, and these preparations have usually shown a higher photophosphorylating activity when compared to alumina-ground preparations from the same batch of bacteria. However, the yield has been considerably lower. The reduced diphosphopyridine nucleotide oxidase (DPNH-oxidase) activity in "sand-preparations" and "alumina-preparations" has also been investigated. Its distribution between various fractions depends on the method of preparation. The DPNH-oxidase has been partly purified.

Table 1. Comparison of light-induced phosphorylation in preparations made with sand and with alumina. The values are given as μmoles orthophosphate esterified per hour per mg chlorophyll. Phosphorylation was determined as in Ref.[2] The 25 000 *g* fraction was used.

Batch	Alumina	Sand
1	320	480
2	280	530
3	420	540
4	620	490
5	230	530

The cells were grown, harvested and ground with alumina according to previously described methods [2]. When sand grinding was employed the procedure was as follows: the paste of wet bacteria was weighed and transferred to an ice-cold mortar. Cold sand in an amount equivalent to twice the weight of the bacteria was added, the mixture was ground for 3 min and subsequently extracted with ice-cold 0.2 M glycylglycine buffer, pH 7.4, 2 ml for each gram of bacteria. The extracted material was centrifuged 10 min at 10 000 *g*, the sediment discarded and the supernatant centrifuged 1 h at 25 000 *g* or 40 000 *g*. The latter force brings down all or almost all the colored material in contrast to its effect on "alumina preparations" where more than one third of the colored material normally remains in the supernatant. This indicates that "sand preparations" contain larger particles, presumably more "intact" chromatophores.

Table 2. Typical distributions of DPNH-oxidase activity in preparations from two batches of *Rhodospirillum rubrum*. The activity was measured at 340 mμ in a Beckman DK2 spectrophotometer. The values are given as μM (μmoles per liter) DPNH oxidized per min per mg protein. The initial concentration of DPNH was 10^{-4} M.

Batch	Abrasive	Fraction		
		25 000 *g*	100 000 *g*	Supernatant
5	Alumina	2.6	5.5	7.3
5	Sand	5.8	13.3	1.8
8	Alumina	10.0	4.3	11.1
8	Sand	21.0	3.3	2.2

The author wishes to express his gratitude to Dr. Arne Magnéli and Fil.kand. Bo Holmberg for their kind interest in this investigation which was undertaken in connection with research programmes financially supported by the *Swedish Natural Science Research Council* and by the *AB Atomenergi Ltd.*

1. Andersson, S., Collén, B., Kuylenstierna, U. and Magnéli, A. *Acta Chem. Scand.* **11** (1957) 1641.
2. Westman, S. and Magnéli, A. *Acta Chem. Scand.* **11** (1957) 1587.
3. Holmberg, B. and Dagerhamn, T. *To be published in Acta Chem. Scand.*

Received December 17, 1960.

On Light-Induced Phosphorylation and Oxidation of Reduced Diphosphopyridine Nucleotide in *Rhodospirillum rubrum*

MARGARETA BALTSCHEFFSKY

Wenner-Gren Institute, University of Stockholm, Sweden

The highest values yet reported for the specific activity of bacterial light-induced phosphorylation, have been obtained with isolated chromatophores from the photosynthetic bacterium *Rhodospirillum rubrum*, which has been ground with alumina (Alcoa A-301) in order to rupture the intact cells [1]. During the last year we have also used sand (Baker, purified) as an abrasive instead of alumina, and these preparations have usually shown a higher photophosphorylating activity when compared to alumina-ground preparations from the same batch of bacteria. However, the yield has been considerably lower. The reduced diphosphopyridine nucleotide oxidase (DPNH-oxidase) activity in "sand-preparations" and "alumina-preparations" has also been investigated. Its distribution between various fractions depends on the method of preparation. The DPNH-oxidase has been partly purified.

Table 1. Comparison of light-induced phosphorylation in preparations made with sand and with alumina. The values are given as μmoles orthophosphate esterified per hour per mg chlorophyll. Phosphorylation was determined as in Ref.[2] The 25 000 *g* fraction was used.

Batch	Alumina	Sand
1	320	480
2	280	530
3	420	540
4	620	490
5	230	530

The cells were grown, harvested and ground with alumina according to previously described methods [2]. When sand grinding was employed the procedure was as follows: the paste of wet bacteria was weighed and transferred to an ice-cold mortar. Cold sand in an amount equivalent to twice the weight of the bacteria was added, the mixture was ground for 3 min and subsequently extracted with ice-cold 0.2 M glycylglycine buffer, pH 7.4, 2 ml for each gram of bacteria. The extracted material was centrifuged 10 min at 10 000 *g*, the sediment discarded and the supernatant centrifuged 1 h at 25 000 *g* or 40 000 *g*. The latter force brings down all or almost all the colored material in contrast to its effect on "alumina preparations" where more than one third of the colored material normally remains in the supernatant. This indicates that "sand preparations" contain larger particles, presumably more "intact" chromatophores.

Table 2. Typical distributions of DPNH-oxidase activity in preparations from two batches of *Rhodospirillum rubrum*. The activity was measured at 340 mμ in a Beckman DK2 spectrophotometer. The values are given as μM (μmoles per liter) DPNH oxidized per min per mg protein. The initial concentration of DPNH was 10^{-4} M.

Batch	Abrasive	Fraction		
		25 000 *g*	100 000 *g*	Supernatant
5	Alumina	2.6	5.5	7.3
5	Sand	5.8	13.3	1.8
8	Alumina	10.0	4.3	11.1
8	Sand	21.0	3.3	2.2

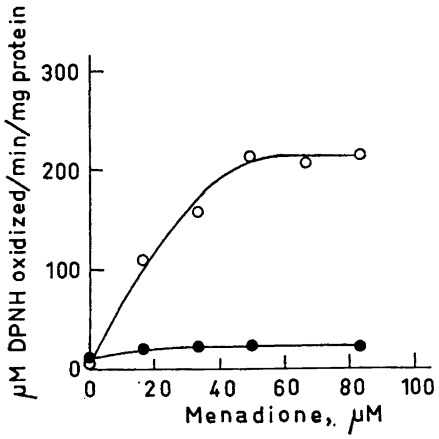

Fig. 1. The stimulation by menadione on DPNH-oxidase activity in the supernatant after centrifugation at 100 000 *g* (O) and the "100 000 *g*-fraction" (●). The DPNH-oxidation was measured at 340 mμ in a Beckman DK2 spectrophotometer. The reaction volume was 3 ml. The initial concentration of DPNH was 10^{-4} M. Sand preparation.

Table 1 gives a comparison of light-induced phosphorylation in five preparations made with sand and alumina, respectively, from five consecutive batches of bacteria. As a complement to this table it may be mentioned that in the former kind of preparation an activity as high as 800 μmoles of orthophosphate esterified per hour per mg chlorophyll (3 ml, 30°C) has been obtained, in the latter the highest value has been 650.

A marked difference between the two types of preparations is found in the relative distribution of the DPNH-oxidase activity in different fractions (Table 2). In "alumina preparations" it is high in the supernatant after centrifugation at 100 000 *g*, but in "sand preparations" the activity in the supernatant is quite low, most of it being found in the chromatophores (washed or unwashed). This is taken as a second indication that the sand-method causes less disruption of chromatophore structure than the alumina-method.

The DPNH-oxidase is stimulated by menadione, as is shown in Fig. 1. It is seen that the stimulation is much higher in the supernatant than in the chromatophore fraction. Possibly the particle-bound DPNH-oxidase is not as accessible to menadione as the solubilized activity in the supernatant.

The DPNH-oxidase in the supernatant after centrifugation at 100 000 *g* has been partially purified by ammonium sulfate fractionation. The fraction between 35 and 45 % saturation contained the highest activity per unit protein and gave, when dialyzed against distilled water, through which a continuous, oxidizing air-stream was led, a precipitate. This could be separated by centrifugation and dissolved in either 0.2 M glycylglycine buffer of pH 7.4 or by adding a small volume of DPNH in substrate amounts. The product so obtained gave a 4-fold increase in specific DPNH-oxidase activity as compared to the supernatant. Horio and Kamen [3] have recently reported DPNH-oxidizing activities with a citrate extract from whole lyophilized bacteria. Their most active fraction came from 45-65 % saturation with ammonium sulfate. They got a 10-fold purification of the DPNH-2,6-dichlorophenol-indophenol reductase activity, however, with complete loss of DPNH-oxidase activity.

Further studies are in progress and a more detailed account will be published.

Many thanks are due to professor Olov Lindberg and Dr. Herrick Baltscheffsky for continuous support.

1. Smith, L. and Baltscheffsky, M. *J. Biol Chem.* **234** (1959) 1575.
2. Baltscheffsky, H. *Biochim. et Biophys. Acta* **40** (1960) 1.
3. Horio, T. and Kamen, M. *Biochim. et Biophys. Acta* **43** (1960) 382.

Received December 22, 1960.

Note on a Phase Transition in VO_2

SVEN WESTMAN

Institute of Inorganic and Physical Chemistry, University of Stockholm, Stockholm, Sweden

It has been shown by Andersson [1,2] that the crystal structure of the room-temperature form of vanadium dioxide constitutes a deformation, akin to the MoO_2 structure [3], of the rutile-type structure, with the following relations [2] existing between the rutile-type subcell and the monoclinic unit cell of VO_2:

$$a = 2c_r, \quad b = a_r, \quad c = a_r - c_r$$

A sample of VO_2 was obtained by mixing appropriate amounts of V_2O_5 (L.K.B. Forskningslaboratorium, reagent grade) and V_2O_3 (obtained by hydrogen reduction of V_2O_5) and heating at 900°C for 20 days in an evacuated silica tube. The sample was quenched in water from the annealing temperature.

By heating the sample in a furnace [4] attached to a recording diffractometer, the powder diffractogram was registered at various temperatures. It was found to change, rapidly and reversibly, at ~70°C, the most obvious feature being the disappearance (on raising the temperature) of all reflexions *hkl* with *h* odd. The effect was still more strikingly demonstrated by single-crystal photographs taken at about 180°C (Cu$K\alpha$ radiation). Using these X-ray data, the crystal structure of the high-temperature form was derived and found to be essentially of the rutile type. A small splitting, less than the $\alpha_1 - \alpha_2$ separation, of the 101 and 210 powder reflexions (rutile indexing) indicates a slight residual deformation of the rutile-type cell.

The following structural data were obtained (180°C):

Space-group: $P4_2/mnm$ (No. 136)
Unit cell dimensions: $a = 4.530 \pm 0.009$ Å
$c = 2.869 \pm 0.006$ Å
Cell content: 2 VO_2
2 V in 2(*a*): 0,0,0; $\frac{1}{2},\frac{1}{2},\frac{1}{2}$
4 O in 4(*f*): *x*,*x*,0 etc.
$x = 0.305 \pm 0.003$

The reliability factor *R*, for all observed reflexions, was found to be = 0.12.

The transition [5-12] is accompanied by changes in the expansion coefficient, the electrical resistivity and the magnetic susceptibility.

The lengthening, at the transformation temperature, of the short metal-metal distances [2] (2.65 Å) present in the low-temperature form, to 2.87 Å is in accordance with the unpariring of electron spins [12] (breaking of metal-metal bonds [3,13]) indicated by the magnetic data.

The oxygen-oxygen contact distances parallel to and at righ angles to the *c* axis are 2.87 Å and 2.50 Å, respectively. The latter one is notably shorter than the corresponding distance in low-VO_2 [2] (2.62 Å) along a shared edge of the oxygen octahedra surrounding two metal atoms that form a doublet.

Inclined to the [001] direction the O—O distances are 2.73 Å, *i.e.* their changes at the phase transition are quite small (*cf.* Ref.[2]).

Thanks are due to the principal investigator of this programme, Dr. Arne Magnéli, for his never-failing interest in this study.

The investigation has been sponsored in part by the *Office, Chief of Research and Development, U.S. Department of Army*, through its European Research Office, and in part by the *Swedish Natural Science Research Council.*

1. Andersson, G. *Acta Chem. Scand.* **8** (1954) 1599.
2. Andersson, G. *Acta Chem. Scand.* **10** (1956) 623.
3. Magnéli, A. and Andersson, G. *Acta Chem. Scand.* **9** (1955) 1378.
4. Magnéli, A., Andersson, S., Westman, S., Åsbrink, S. and Holmberg, B. *Final Technical Report* **1** DA—91—508—EUC—245.
5. Jaffray, J. and Dumas, D. *J. recherches centre natl. recherche sci. Labs Bellevue (Paris)* **27** (1954) 360.
6. Hoschek, E. and Klemm, W. *Z. anorg. Chem.* **226** (1936) 359.
7. Hoschek, E. and Klemm, W. *Z. anorg. Chem.* **242** (1939) 63.
8. Perakis, N. and Wucher, I. *Compt. rend.* **235** (1952) 354.
9. Perakis, N. *J. phys. radium.* **8** (1927) 473.
10. Klemm, W. and Grimm, L. *Naturwiss.* **27** (1939) 787.
11. Cook, O. A. *J. Am. Chem. Soc.* **69** (1947) 331.
12. Rüdorff, W., Walter, G. and Stadler, J. *Z. anorg. u. allgem. Chem.* **297** (1958) 1.
13. Marinder, B.-O. and Magnéli, A. *Acta Chem. Scand.* **11** (1957) 1635.

Received December 19, 1960.

Zur Oxydation mit Chinonen

HANS-DIETER BECKER und ERICH ADLER

Institutionen för organisk kemi, Chalmers Tekniska Högskola, Göteborg, Schweden

Braude, Brook und Linstead [1] untersuchten Chinone mit hohem Redoxpotential auf ihre Verwendbarkeit als Dehydrierungsmittel. Dabei fanden sie, dass 2,3-Dichlor-5,6-dicyan-1,4-benzochinon (DDB) Hydroaromaten schon bei Zimmertemperatur dehydriert. In siedendem Dioxan oder Benzol gehen Δ^4- oder $\Delta^{4,6}$-Steroid-3-ketone in Gegenwart von DDB in die entsprechenden $\Delta^{1,4}$- bzw. $\Delta^{1,4,6}$-3-Ketone über [2]. Durch Einwirkung von DDB bei Zimmertemperatur auf α,β-ungesättigte Steroid-alkohole gelang kürzlich Burn, Kirk und Weston [3] die selektive Oxydation der Allylalkoholgruppe.

In Hinblick auf ligninchemische Fragestellungen untersuchten wir jetzt die Oxydation einiger Benzylakohole mit DDB. Es zeigte sich, dass Benzylalkohole bei Zimmertemperatur in die entsprechenden Car-

Tabelle 1. Oxydation einiger Benzylalkohole mit 2,3-Dichlor-5,6-dicyan-1,4-benzochinon.

Alkohol	Oxydationsprodukt	Mol DDB / Mol Alkohol	Ausbeute Mol DDH / Mol Alkohol	Reaktionszeit (Stunden)
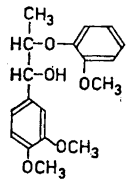	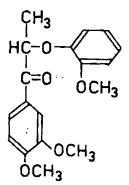	1.4	0.87	24
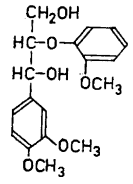	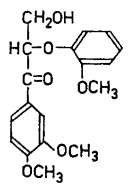	2.9	0.96	19
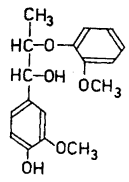	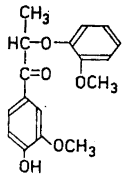	1.2	0.96	23
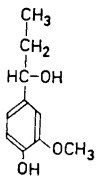	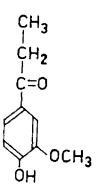	2.2	0.89	18

bonylverbindungen übergeführt werden. Gesättigte Alkoholgruppen wurden dabei nicht angegriffen.

Überraschenderweise gelang die selektive Oxydation der Benzylalkoholgruppe auch, wenn die *p*-Stellung durch Hydroxyl substituiert war. Hierin erweist sich das DDB dem für die selektive Oxydation von Benzylalkoholen ebenfalls verwendbaren aktiven Mangandioxyd überlegen, da letzteres auch die phenolische Hydroxylgruppe angreift [4].

Tabelle 1 gibt eine Übersicht über die von uns vorläufig untersuchten Reaktionen. Diese wurden, wie für Allylalkohole beschrieben [3], in trockenem Dioxan ausgeführt. Vom auskristallisierten 2,3-Dichlor-5,6-dicyan-hydrochinon (DDH) wurde abgesaugt und die Lösung über eine Säule von Al_2O_3 filtriert, worauf mit Äther nachgewaschen wurde. Aus den vereinigten Filtraten kristallisierten beim Eindunsten die entsprechenden Carbonylverbindungen; sie wurden durch Vergleich der IR-Spektren mit authentischem Material identifiziert.

Früher war bereits die Oxydation von Benzylalkoholen mit Tetrachlor-*o*-benzochinon von Braude und Mitarb.[5] untersucht worden, jedoch waren die Ausbeuten hierbei unbefriedigend.

Über die Verwendung von 2,3-Dichlor-5,6-dicyan-1,4-benzochinon zu analytischen Untersuchungen am Lignin soll später berichtet werden.

Wir danken *Statens Naturvetenskapliga Forskningsråd* für die Gewährung eines Forschungsbeitrages.

1. Braude, E. A., Brook, A. G. und Linstead, R. P. *J. Chem. Soc.* **1954** 3569.
2. Burn, D., Kirk, D. N. und Petrow, V. *Proc. Chem. Soc. (London)* **1960** 14.
3. Burn, D., Petrow, V. und Weston, G. O. *Tetrahedron Letters No.* **9** (1960) 14.
4. Freudenberg, K. und Grion, G. *Chem. Ber.* **92** (1959) 1355.
5. Braude, E. A., Linstead, R. P. und Wooldridge, K. R. *J. Chem. Soc.* **1956** 3070.

Eingegangen am 19. Dezember 1960.

The Sulfonation of Iodobenzene

N. HESSELBJERG CHRISTENSEN

Danish Atomic Energy Commission, Risø, Denmark

The anhydride of the *p*-iodobenzenesulfonic acid, pipsan, labelled with ^{131}I or ^{35}S, has become an invaluable tool in the determination of steroid hormones in submicrogramme quantities [1-3].

The preparation of the pipsan by conventional methods [1] has proved impractical from the point of view of radiation protection. It was therefore found of interest to study the formation of arylsulfonic acid anhydride from aryl halide and oleum at room temperature. This type of reaction has been known for many years [4,5], and recently Lukashevich [6] has worked out approximate conditions for separation of such compounds.

The original method of recovering the anhydride is to pour the sulfonation mixture on to ice, whereby the insoluble anhydride precipitates. The present paper describes a method of isolating pipsan from the sulfonation mixture without the use of ice or water. The modification proves of benefit, especially in a remote handling procedure [7]. Further, the conditions for optimal separation of the pipsan have been studied in detail.

Sulfonations of iodobenzene conducted on a semi-micro scale with varying amounts of oleum containing varying amounts of SO_3 revealed that within a rather narrow range of conditions the sulfonic acid anhydride separated rapidly in a yield of 50–60 %, which is at least as good as the yield reported by Lukashevich [6].

Experimental. The samples of oleum were prepared by mixing "60 % free SO_3" (p.a.) oleum and conc. sulfuric acid (p.a.), and the contents of total SO_3 in the mixtures were determined by titration according to Rosin [8]. The iodobenzene was a British Drug Houses preparation, "not less than 98 %". Weighed amounts of the components (0.5 g of iodobenzene and 0.5—4 g of oleum) were mixed in 10 ml centrifuge tubes and kept at 0° for 3 h, whereupon the precipitate, if any, was centrifuged down and the supernatant removed. The precipitate was washed consecutively with 5 ml of acetic acid anhydride, 2 × 4 ml of

bonylverbindungen übergeführt werden. Gesättigte Alkoholgruppen wurden dabei nicht angegriffen.

Überraschenderweise gelang die selektive Oxydation der Benzylalkoholgruppe auch, wenn die *p*-Stellung durch Hydroxyl substituiert war. Hierin erweist sich das DDB dem für die selektive Oxydation von Benzylalkoholen ebenfalls verwendbaren aktiven Mangandioxyd überlegen, da letzteres auch die phenolische Hydroxylgruppe angreift [4].

Tabelle 1 gibt eine Übersicht über die von uns vorläufig untersuchten Reaktionen. Diese wurden, wie für Allylalkohole beschrieben [3], in trockenem Dioxan ausgeführt. Vom auskristallisierten 2,3-Dichlor-5,6-dicyan-hydrochinon (DDH) wurde abgesaugt und die Lösung über eine Säule von Al_2O_3 filtriert, worauf mit Äther nachgewaschen wurde. Aus den vereinigten Filtraten kristallisierten beim Eindunsten die entsprechenden Carbonylverbindungen; sie wurden durch Vergleich der IR-Spektren mit authentischem Material identifiziert.

Früher war bereits die Oxydation von Benzylalkoholen mit Tetrachlor-*o*-benzochinon von Braude und Mitarb.[5] untersucht worden, jedoch waren die Ausbeuten hierbei unbefriedigend.

Über die Verwendung von 2,3-Dichlor-5,6-dicyan-1,4-benzochinon zu analytischen Untersuchungen am Lignin soll später berichtet werden.

Wir danken *Statens Naturvetenskapliga Forskningsråd* für die Gewährung eines Forschungsbeitrages.

1. Braude, E. A., Brook, A. G. und Linstead, R. P. *J. Chem. Soc.* **1954** 3569.
2. Burn, D., Kirk, D. N. und Petrow, V. *Proc. Chem. Soc. (London)* **1960** 14.
3. Burn, D., Petrow, V. und Weston, G. O. *Tetrahedron Letters No.* **9** (1960) 14.
4. Freudenberg, K. und Grion, G. *Chem. Ber.* **92** (1959) 1355.
5. Braude, E. A., Linstead, R. P. und Wooldridge, K. R. *J. Chem. Soc.* **1956** 3070.

Eingegangen am 19. Dezember 1960.

The Sulfonation of Iodobenzene

N. HESSELBJERG CHRISTENSEN

Danish Atomic Energy Commission, Risø, Denmark

The anhydride of the *p*-iodobenzenesulfonic acid, pipsan, labelled with ^{131}I or ^{35}S, has become an invaluable tool in the determination of steroid hormones in submicrogramme quantities [1-3].

The preparation of the pipsan by conventional methods [1] has proved impractical from the point of view of radiation protection. It was therefore found of interest to study the formation of arylsulfonic acid anhydride from aryl halide and oleum at room temperature. This type of reaction has been known for many years [4,5], and recently Lukashevich [6] has worked out approximate conditions for separation of such compounds.

The original method of recovering the anhydride is to pour the sulfonation mixture on to ice, whereby the insoluble anhydride precipitates. The present paper describes a method of isolating pipsan from the sulfonation mixture without the use of ice or water. The modification proves of benefit, especially in a remote handling procedure [7]. Further, the conditions for optimal separation of the pipsan have been studied in detail.

Sulfonations of iodobenzene conducted on a semi-micro scale with varying amounts of oleum containing varying amounts of SO_3 revealed that within a rather narrow range of conditions the sulfonic acid anhydride separated rapidly in a yield of 50–60 %, which is at least as good as the yield reported by Lukashevich [6].

Experimental. The samples of oleum were prepared by mixing "60 % free SO_3" (p.a.) oleum and conc. sulfuric acid (p.a.), and the contents of total SO_3 in the mixtures were determined by titration according to Rosin [8]. The iodobenzene was a British Drug Houses preparation, "not less than 98 %". Weighed amounts of the components (0.5 g of iodobenzene and 0.5—4 g of oleum) were mixed in 10 ml centrifuge tubes and kept at 0° for 3 h, whereupon the precipitate, if any, was centrifuged down and the supernatant removed. The precipitate was washed consecutively with 5 ml of acetic acid anhydride, 2 × 4 ml of

ether and 4 ml of pentane, dried in a stream of nitrogen and weighed. The yield is calculated as per cent of the theoretical from iodobenzene.

The dried crude product melts rather unsharp at 190—205° and is insoluble in cold water and only slowly soluble in boiling water. A quick way to effect hydrolysis is to expose the anhydride to steam.

In all instances the products were completely soluble in water after hydrolysis, indicating absence of any sulfone. By titration with 0.1 N NaOH, the crude, hydrolyzed product was found to have a neutralization equivalent weight of 280 ± 5 (calc. 275).

The crude product may be recrystallized from pure acetic acid anhydride, acetonitrile, nitromethane and chloroform. By dissolving in hot, purified and anhydrous chloroform and reprecipitating with four volumes of pentane, the acid anhydride separates in 70—80 % yield, m.p. 207—213°, previously reported: 220—221° [1], eqiv.wt. 280.

On comparison of the infra-red spectra of the recrystallized material with a specimen prepared according to Bojesen [1] it was concluded that the product prepared in oleum contained about 95 % of the *para* isomeride. Neither sulfone nor sulfonic acid could be detected, but an isomeric anhydride may be present as a contaminant.

Anhydrous *p*-iodobenzenesulfonic acid was prepared by hydrolysis of the anhydride and drying *in vacuo* at 100°. It is very hygroscopic, readily soluble in cold water and has a m.p. of about 70°.

Results and discussion. On the arbitrary assumption that oleum consists of 100 % H_2SO_4 and free SO_3, the mole ratios H_2SO_4/C_6H_5I and free SO_3/C_6H_5I have been calculated for each experiment. From Fig. 1 it is seen that regardless of the H_2SO_4/C_6H_5I ratio, the maximum yields are obtained with a free SO_3/C_6H_5I ratio of 1.0—1.6.

Free SO_3/C_6H_5I: 0 — 1.0. In this range the iodobenzene dissolves in the oleum and the mixture takes on a faintly yellow colour, but hardly any precipitation of anhydride occurs. After some minutes, however, colourless needles start to appear, and with low contents of H_2SO_4 the mixture soon solidifies to a mass of crystals soluble in acetic anhydride and water. These crystals are probably iodobenzenesulfonic acid.

Free SO_3/C_6H_5I: 1.0 — 1.6. This is the range for optimal yields of acid anhydride. The mixture is instantaneously coloured deeply yellow-brown, and after a while the colourless anhydride starts precipitating. With stirring, the precipitation seems to be complete after half an hour.

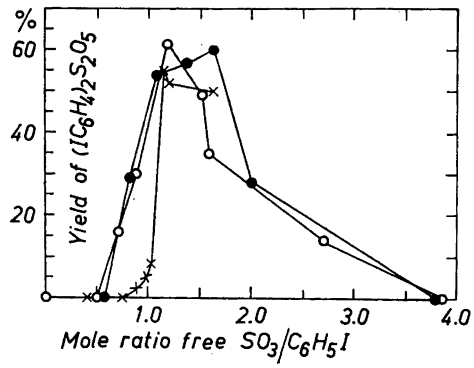

Fig. 1. Yields of iodobenzenesulfonic acid anhydride formed by sulfonation of iodobenzene with oleum (100 % H_2SO_4 + free SO_3), 3 h at 0°. × = 0.6—1.2, ● = 1.8—3.6 and ○ = 5.2—8.2 moles of H_2SO_4 pr mole of C_6H_5I.

Free SO_3/C_6H_5I: 1.6 — 4.5. With increasing contents of SO_3 the reaction mixture becomes a dark violet or black tar and the yield of anhydride decreases. The reason for the colour-formation is apparently not destruction of iodobenzene, since on dissolving the tar in acetic acid anhydride an orange gel is formed. If the tar is poured on to ice the colour disappears completely, *cf.* also observations by Willgerodt *et al.*[11] It should be noticed that the stoicheiometric equation $3SO_3 + 2C_6H_5I \rightarrow (IC_6H_4)_2S_2O_5 + H_2SO_4$ demands a ratio of 1.5. The reason why the yields do not exceed 60 %, even at the ratio 1.5, is probably competitive reactions. With increasing SO_3/C_6H_5I-ratios these reactions may become predominant. Under analogous conditions the formation of pyrosulfonic acids, disulfonic acids and SO_3-adducts has been described by various authors [9,10].

The restricted yield cannot be wholly explained by solubility of the sulfonic acid anhydride in the cold oleum. When the supernatants from the sulfonation mixtures were poured on to ice-water, only a slight turbidity was formed. It is also noteworthy in this respect that maximum yields of 60 % are obtained regardless the size of the reaction volumes (as defined by the H_2SO_4/C_6H_5I ratio).

Iodine-131-labelled pipsan, prepared after this method, has now for one year been successfully applied by The Institute of Experimental Medicine, University of Copenhagen, for making indicators used in routine analyses of steroid hormones.

1. Bojesen, E. *Scand. J. Clin. Lab. Invest.* **8** (1956) 55.
2. Bojesen, E. and Degn, H. *Advance Abstr. short Comm. 1st Intern. Congr. Endocrinol.* Copenhagen 1960, p. 1057.
3. Svendsen, R. *Acta Endocrinol.* **35** (1960) 161.
4. Rosenberg, J. *Ber.* **19** (1886) 652.
5. Neumann, G. S. *Ann.* **241** (1887) 33.
6. Lukashevich, V. O. *Doklady Akad. Nauk S.S.S.R.* **99** (1954) 995; *Chem. Abstr.* **50** (1956) 217.
7. Christensen, N. H. *Proc. Conf. Use Radioisotopes Phys. Sci. and Ind. Copenhagen.* IAEA Vienna 1961, no. 244. *In press.*
8. Rosin, J. *Reagent Chemicals and Standards,* 3rd Ed., van Nostrand Co., New York 1955, p. 458.
9. Lukashevich, V. O. *Proc. Acad. Sci. U.S.S.R., Sect. Chem.* **112** (1957) 133, (English translation).
10. Courtot, C. and Bonnet, J. *Compt. rend.* **182** (1926) 855.
11. Willgerodt, E. and Waldeyer, O. *J. prakt. Chem.* **59** (1899) 194.

Received December 21, 1960.

On the Reaction of 2,4-Dihydroxy-1,4-benzoxazin-3-one to 2(3)-Benzoxazolinone

ERKKI HONKANEN
and ARTTURI I. VIRTANEN

Laboratory of the Foundation for Chemical Research, Biochemical Institute, Helsinki, Finland

In earlier papers [1,2] from this laboratory it was confirmed that the aglucone, 2,4-dihydroxy-1,4-benzoxazin-3-one, isolated from crushed rye seedlings and its 7-methoxy derivative [3] from wheat and maize plants undergoes a reaction by heating in aqueous solution, upon which 2(3)-benzoxazolinone (or its 6-methoxy derivative) is formed by simultaneous liberation of formic acid. Later a similar reaction was found to occur also by heating of 4-hydroxy-1,4-benzoxazine-2,3-dione (III)[4], carbon dioxide being split off.

Theoretically there are two possibilities for the formation of the formic acid: from carbon atom 2 or 3. To solve this problem an aglucone (II) labelled with ^{14}C at the position 2 was synthesized by an analogous procedure as in the case of the syntheses of the normal aglucone [5] from *o*-methoxymethoxyphenylhydroxylamine (I) and dibromoacetyl-2-^{14}C chloride. The needed dibromoacetyl-2-^{14}C chloride was prepared by the following reactions from diethyl-(malonate-2-^{14}C).

After heating the aqueous solution of II, the radioactivity was found in the formic acid, and we conclude that the formic acid originates from carbon atom 2 in II. Nothing certain can be said about the reaction mechanism. A prerequisite for this reaction seems to be the easy rupture of the bond between the oxygen and carbon atom 2 and the presence of the N-hydroxyl group. The compound IV [4] which has a simple ether linkage and the compound V[5] which has no N-hydroxyl group are quite stable in boiling aqueous solution.

Dibromoacetyl-2-^{14}C chloride. A mixture of 1.85 mg (0.025 mC) of diethyl-(malonate-2-^{14}C)* and 500 mg of diethylmalonate in 10 ml of 2 N hydrochloric acid was heated for 24 h at 50°C. The solution was then evaporated to dryness under reduced pressure. The residue was dissolved in 1 ml of 2 N hydrochloric acid, the solution cooled below +5°C, and 350 μl of bromine were added. After standing for 2 h the solvent was evaporated in vacuum. The residue (dibromomalonic acid) was then decarboxylated to dibromoacetic acid by heating for 1 h at 130°C. Two ml of thionyl chloride were added after cooling, and the mixture was boiled for 1 h on a water bath. The excess of thionyl chloride was then removed under reduced pressure, and the residue was used without further purification for the following reaction.

2,4-Dihydroxy-1,4-benzoxazin-3-one-2-^{14}C. A solution of the above dibromoacetyl-2-^{14}C chloride in 10 ml of dry ether was added under cooling to a solution of *o*-methoxymethoxyphenylhydroxylamine prepared from 0.5 g of *o*-

* A product of The Radiochemical Centre.

Iodine-131-labelled pipsan, prepared after this method, has now for one year been successfully applied by The Institute of Experimental Medicine, University of Copenhagen, for making indicators used in routine analyses of steroid hormones.

1. Bojesen, E. *Scand. J. Clin. Lab. Invest.* **8** (1956) 55.
2. Bojesen, E. and Degn, H. *Advance Abstr. short Comm. 1st Intern. Congr. Endocrinol.* Copenhagen 1960, p. 1057.
3. Svendsen, R. *Acta Endocrinol.* **35** (1960) 161.
4. Rosenberg, J. *Ber.* **19** (1886) 652.
5. Neumann, G. S. *Ann.* **241** (1887) 33.
6. Lukashevich, V. O. *Doklady Akad. Nauk S.S.S.R.* **99** (1954) 995; *Chem. Abstr.* **50** (1956) 217.
7. Christensen, N. H. *Proc. Conf. Use Radioisotopes Phys. Sci. and Ind. Copenhagen.* IAEA Vienna 1961, no. 244. *In press.*
8. Rosin, J. *Reagent Chemicals and Standards,* 3rd Ed., van Nostrand Co., New York 1955, p. 458.
9. Lukashevich, V. O. *Proc. Acad. Sci. U.S.S.R., Sect. Chem.* **112** (1957) 133, (English translation).
10. Courtot, C. and Bonnet, J. *Compt. rend.* **182** (1926) 855.
11. Willgerodt, E. and Waldeyer, O. *J. prakt. Chem.* **59** (1899) 194.

Received December 21, 1960.

On the Reaction of 2,4-Dihydroxy-1,4-benzoxazin-3-one to 2(3)-Benzoxazolinone

ERKKI HONKANEN
and ARTTURI I. VIRTANEN

Laboratory of the Foundation for Chemical Research, Biochemical Institute, Helsinki, Finland

In earlier papers [1,2] from this laboratory it was confirmed that the aglucone, 2,4-dihydroxy-1,4-benzoxazin-3-one, isolated from crushed rye seedlings and its 7-methoxy derivative [3] from wheat and maize plants undergoes a reaction by heating in aqueous solution, upon which 2(3)-benzoxazolinone (or its 6-methoxy derivative) is formed by simultaneous liberation of formic acid. Later a similar reaction was found to occur also by heating of 4-hydroxy-1,4-benzoxazine-2,3-dione (III)[4], carbon dioxide being split off.

Theoretically there are two possibilities for the formation of the formic acid: from carbon atom 2 or 3. To solve this problem an aglucone (II) labelled with ^{14}C at the position 2 was synthesized by an analogous procedure as in the case of the syntheses of the normal aglucone [5] from *o*-methoxymethoxyphenylhydroxylamine (I) and dibromoacetyl-2-^{14}C chloride. The needed dibromoacetyl-2-^{14}C chloride was prepared by the following reactions from diethyl-(malonate-2-^{14}C).

After heating the aqueous solution of II, the radioactivity was found in the formic acid, and we conclude that the formic acid originates from carbon atom 2 in II. Nothing certain can be said about the reaction mechanism. A prerequisite for this reaction seems to be the easy rupture of the bond between the oxygen and carbon atom 2 and the presence of the N-hydroxyl group. The compound IV [4] which has a simple ether linkage and the compound V[5] which has no N-hydroxyl group are quite stable in boiling aqueous solution.

Dibromoacetyl-2-^{14}C chloride. A mixture of 1.85 mg (0.025 mC) of diethyl-(malonate-2-^{14}C)* and 500 mg of diethylmalonate in 10 ml of 2 N hydrochloric acid was heated for 24 h at 50°C. The solution was then evaporated to dryness under reduced pressure. The residue was dissolved in 1 ml of 2 N hydrochloric acid, the solution cooled below +5°C, and 350 μl of bromine were added. After standing for 2 h the solvent was evaporated in vacuum. The residue (dibromomalonic acid) was then decarboxylated to dibromoacetic acid by heating for 1 h at 130°C. Two ml of thionyl chloride were added after cooling, and the mixture was boiled for 1 h on a water bath. The excess of thionyl chloride was then removed under reduced pressure, and the residue was used without further purification for the following reaction.

2,4-Dihydroxy-1,4-benzoxazin-3-one-2-^{14}C. A solution of the above dibromoacetyl-2-^{14}C chloride in 10 ml of dry ether was added under cooling to a solution of *o*-methoxymethoxyphenylhydroxylamine prepared from 0.5 g of *o*-

* A product of The Radiochemical Centre.

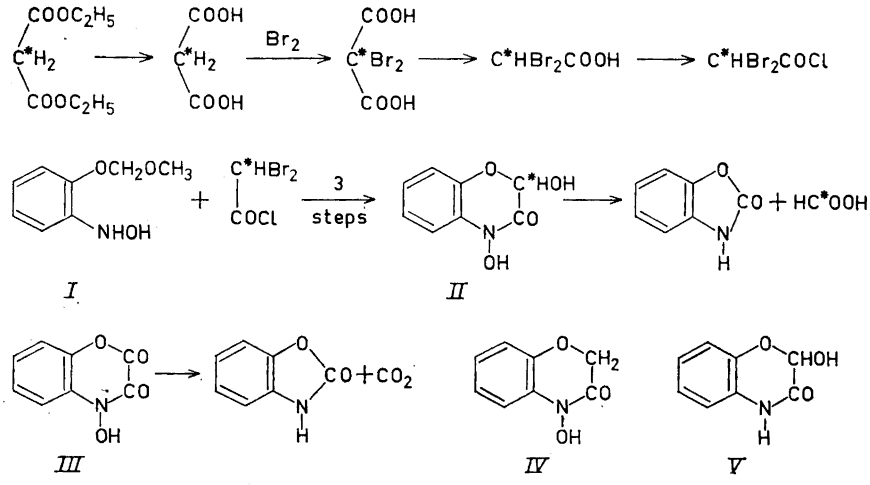

methoxymethoxynitrobenzene [5] in 10 ml of dry ether. The preparation was then carried out by a similar procedure as in the case of the synthesis of 2,4-dihydroxy-1,4-benzoxazin-3-one [5], with the difference that the reaction time with methanol-hydrochloric acid was reduced from 30 min to 10 min and that with the sodium hydroxide solution from 2 h to 20 min. The yield was by this means increased about three times. The product was crystallized from a mixture of ethyl acetate-petroleum ether. Total yield (from diethylmalonate) 21 mg (3.7 %).

Conversion of 2,4-*dihydroxy*-1,4-*benzoxazin*-3-*one*-2-^{14}*C to benzoxazolinone.* 21 mg of the 2-^{14}C-labelled aglucone was dissolved in 1 000 ml of water and heated for 30 min at 100°C. 10 mg of sodium hydrogen carbonate was added and the cooled solution extracted 4—5 times with ether. The water solution as well as the ether extract were evaporated to dryness under reduced pressure. The radioactivity was then measured in both residues. The activity of the sodium formate fraction was about 20 times higher than that of the benzoxazolinone fraction. The low activity which was obtained in benzoxazolinone may be due to the coloured impurities formed as by-products in the reaction.

This investigation belongs to a research project under U.S. Public Law No. 480, 83rd Congress.

1. Virtanen, A. I. and Hietala, P. K. *Acta Chem. Scand.* **14** (1960) 499.
2. Hietala, P. K. and Virtanen, A. I. *Ibid.* **14** (1960) 502.
3. Wahlroos, Ö. and Virtanen, A. I. *Ibid.* **13** (1959) 1906.
4. Honkanen, E. and Virtanen, A. I. *Ibid.* **14** (1960) 1214.
5. Honkanen, E. and Virtanen, A. I. *Ibid.* **14** (1960) 504.

Received December 20, 1960.

Estimation of "Uncondensed" Phenolic Units in Spruce Lignin

ERICH ADLER and KNUT LUNDQUIST

Institutionen för organisk kemi, Chalmers Tekniska Högskola, Göteborg, Sweden

Previous work by Freudenberg and several other authors (for literature, see Ref.[1]) has established the presence of two general types of arylpropane units in conifer lignin. One of them is characterised by an unsubstituted 6-position ("uncondensed" units, I and Ia, with free and etherified phenolic hydroxyl group, respectively). In the other type ("condensed" units, II and IIa) the 6-position is substituted by a carbon atom, either of an aromatic ring (diphenyl structure) or of the side-chain of an adjacent arylpropane unit. The coumaran system, in which R and R′ are two carbon atoms of the hydrofuran ring, is an important representative of type IIa.

Various attempts have been made to estimate the relative amounts of these two types of units in lignin. From the yields of vanillin obtained on nitrobenzene oxidation, Leopold [2] concluded that lignin contains about equal amounts of both types. Mikawa and co-workers [3], studying the Mannich reaction of a thiolignin, reached the conclusion that 25—40 % of the phenolic nuclei (I and II) of this material were "uncondensed" (I).

We wish to report that the number of "uncondensed" units with a free phenolic hydroxyl group (I) can be estimated by means of an oxidation with potassium nitrosodisulphonate, $ON(SO_3K)_2$ (Fremy's salt). Teuber and Staiger [4] have shown that this reagent yields *o*-benzoquinones when acting on 4-substituted guaiacol compounds. In extension of this work, a variety of lignin model compounds of type I has now been found to be readily converted into the exceptionally stable 3-methoxy-1,2-benzoquinones (III). For instance, quinone IV (m.p. 69—70°) was obtained from ethylguaiacylcarbinol methyl ether. Similarly, dihydro-dehydrodi*iso*eugenol gave an *o*-quinone of m.p. 98—99°, and (+)-pinoresinol yielded the expected bis-*o*-quinone (decomp. >170°, phenazine derivative, decomp. >200°). Guaiacol compounds which were substituted in both the 4- and 6-positions, *i.e.*, models for the "condensed" type II, were not appreciably attacked by Fremy's salt.

The above-mentioned model *o*-quinones of type III, dissolved in glycol monomethyl ether-water (3 : 2), had very similar absorption curves with a main maximum at 365—367 mμ and a broad maximum or shoulder at about 465 mμ (*cf.* Ref.[5]); the ε_{max} values, based on one phenolic guaiacyl equivalent of the starting material, were 2 500 and 700—800, respectively. Spectrophotometric examination of the reaction between the phenols and Fremy's salt indicated a 90 % yield of the *o*-quinones.

For the application of Teuber's reaction to lignin, the following two exceptions were important. Firstly, guaiacol compounds of type I, which carried a keto

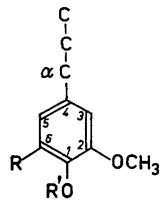

I. R = R′ = H
Ia. R = H; R′ = C
II. R = C; R′ = H
IIa. R = C; R′ = C

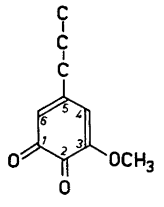

III

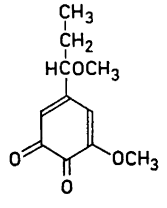

IV

group in the α-position (*e.g.*, 4-propioguaiacone), did not react with Fremy's salt, the 6-position being deactivated by the 4-carbonyl substituent. Secondly, when treated with Fremy's salt, guaiacylcarbinols (type I, the α-C carrying H and OH) suffered *p*-oxidative cleavage rather than the normal *o*-oxidation. For instance, guaiacylethylcarbinol gave methoxy-*p*-quinone and propionic aldehyde. (As mentioned above, the corresponding carbinol methyl ether reacted in the normal way, yielding the *o*-quinone IV.) Similarly, dehydrodivanillyl acohol (V[6]) was oxidised to the di-*p*-quinone VII, m.p. 200°. The methyl ether VI, formed from V in methanolic hydrochloric acid (20°), was not attacked by Fremy's salt.

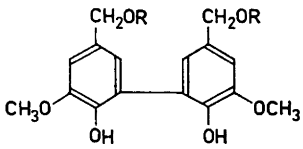

V. R=H
VI. R=CH_3

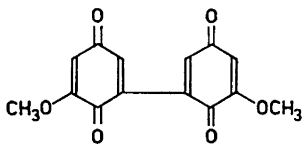

VII

The findings just mentioned made it necessary to remove the minor amounts of α-keto and α-carbinol groups present in the phenolic units of lignin. Björkman lignin was therefore reduced with sodium borohydride and subsequently treated with a solution of 0.15 N HCl in methanol-dioxan 1 : 1 (20°, 48 h); these operations converted the α-groupings mentioned into >CH(OCH_3) groupings [7].

Oxidation of this pretreated lignin in glycol monomethyl ether-water with Fremy's salt produced a red solution, the absorption spectrum of which was very similar to that of the model *o*-quinones in the same solvent. Comparison of the ε-values of the oxidised lignin solution in the range above 360 mμ with those of the solutions of the similarly produced model *o*-quinones indicated the presence of 0.15 — 0.18 "uncondensed" phenolic units (I) per methoxyl group of the lignin. Since Björkman lignin contains about 0.30 phenolic hydroxyl groups per OCH_3, the result obtained means that, of the total of phenolic guaiacylpropane units (I + II), 50—60 % are of the "uncondensed" type (I) and 40—50 %, *i.e.* 0.12 — 0.15 units per OCH_3, of the "condensed" type (II).

The results reported here give no information regarding the ratio between "uncondensed" and "condensed" units of the non-phenolic type (Ia and IIa). As shown before [8], lignin contains about 0.08 coumaran units per OCH_3; thus, "condensed" units of this type would make up about 12 % of the non-phenolic portion of the lignin molecule. The distribution of the remaining types of "condensed" units, especially the diphenyl elements, will be discussed in a forthcoming detailed publication.

Financial support of this work by *Statens Tekniska Forskningsråd* is gratefully acknowledged.

1. Adler, E. and Gierer, J. in Treiber, E. *Die Chemie der Pflanzenzellwand*, Springer-Verlag 1957, p. 446.
2. Leopold, B. *Svensk Kem. Tidskr.* **64** (1952) 18.
3. Mikawa, H., Sato, K., Takasaki, C. and Ebisawa, K. *Bull. Chem. Soc. Japan* **29** (1956) 259.
4. Teuber, H.-J. and Staiger, G. *Chem. Ber.* **88** (1955) 802.
5. Adler, E., Magnusson, R., Berggren, B. and Thomelius, H. *Acta Chem. Scand.* **14** (1960) 515.
6. Adler, E. and Hernestam, S. *Acta Chem. Scand.* **9** (1955) 319.
7. Adler, E. *Proc. Fourth Intern. Congr. Biochem.*, Vienna 1958, vol. II, p. 137.
8. Adler, E., Delin, S. and Lundquist, K. *Acta Chem. Scand.* **13** (1959) 2149.

Received January 5, 1961.

Communic Acid, a New Diterpene Acid from *Juniperus communis* L.

V. P. ARYA, C ENZELL, H. ERDTMAN and T. KUBOTA

Organisk-kemiska institutionen, Kungl. Tekniska Högskolan, Stockholm, Sweden

A new diterpene acid, communic acid (Ia) has been isolated as its sodium salt, $C_{20}H_{29}O_2Na \cdot H_2O$, m.p. 228–230°, $[\alpha]_D$ +25° (methanol) from the bark of the common juniper, *Juniperus communis* L. The free acid, which easily polymerises, furnishes with diazomethane a stable methyl ester $C_{21}H_{32}O_2$, m.p. 105–106°, $[\alpha]_D$ +47°, λ_{max} 232 mμ (ε 25 000). The ester gave a maleic anhydride adduct, $C_{25}H_{34}O_5$, m.p. 169–171°, $[\alpha]_D$ +85° and on ozonisation furnished formaldehyde in an amount indicative of the presence of two terminal methylene groups.

Methyl communate rapidly consumed one mole of hydrogen on catalytic hydrogenation (Pd/C, ethanol) giving methyl dihydrocommunate (II), $C_{21}H_{34}O_2$, b.p. 148–149°/0.5 mm, n_D^{23} 1.5062, $[\alpha]_D$ +55° which gave formaldehyde on ozonolysis in an amount indicative of one terminal methylene group.

Other products of ozonolysis of methyl dihydrocommunate and methyl communate include a keto-acid, $C_{16}H_{24}O_5$ (III), m.p. 171–172°, $[\alpha]_D$ +12°, semicarbazone, $C_{17}H_{27}O_5N_3$, m.p. 200–201°.

Methyl communate was reduced with lithium aluminium hydride to communol (IV), $C_{20}H_{32}O$, b.p. 65°/0.01 mm. $[\alpha]_D$ +18°, λ_{max} 233 mμ (ε 22 000), 3,5-dinitrobenzoate, $C_{27}H_{34}O_6N_2$, m.p. 115–117°, maleic anhydride adduct, $C_{24}H_{34}O_4$, m.p. 185–187°, $[\alpha]_D$ +49°. Reduction of communol in propanol with sodium gave *iso*dihydrocommunol (V), $C_{20}H_{34}O$, b.p. 95°/0.1 mm, 3,5-dinitrobenzoate, $C_{27}H_{36}O_6N_2$, m.p. 107–108°.

Torulosol [1] (VI), a new diterpene alcohol, which has been correlated with manool and with agathene dicarboxylic acid, gave on treatment with acetic anhydride and acetic acid mixture (1:1), the triene-ol (VII), λ_{max} 227 mμ (ε 27 000), 3,5-dinitrobenzoate, $C_{27}H_{34}O_6N_2$, m.p. 73–74°. Reduction of this triene-ol in propanol with sodium gave the dihydroderivative (V), the 3,5-dinitrobenzoate of which was identical with *iso*-dihydrocommunol 3,5-dinitrobenzoate.

The identity of the two dihydro-derivatives (V) of (IV) and (VII), the difference (5 mμ) between the U.V. absorption maxima of (IV) and (VII) and the formation of the C_{16}-keto-acid (III) on ozonolysis of methyl communate show that communic acid possesses the structure and configuration (Ia).

Full details of this work including spectral data and direct correlations to agathene dicarboxylic acid will be described shortly elsewhere.

The U.V. spectra were taken in ethanol and optical rotations in chloroform solutions, unless otherwise stated. We thank Miss G. Hammarberg for these measurements. Satisfactory analyses were obtained for the compounds described, and we are grateful to Dr. A. Wettstein, Ciba Ltd., Basel, for several of them.

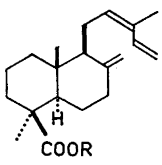

Ia R=H
Ib R=CH_3

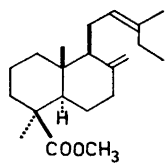

II

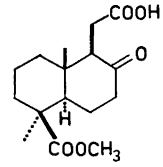

III

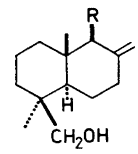

IV R=$-CH_2-CH=C(CH_3)-CH=CH_2$
V R=$-CH_2-CH_2-C(CH_3)=CH-CH_3$
VI R=$-CH_2-CH_2-C(CH_3)(OH)-CH=CH_2$
VII R=$-CH_2-CH_2-C(=CH_2)-CH=CH_2$

This research was supported in part by the *Swedish Technical Research Council* and by the *Office of Research and Development, U.S. Army Department*, through its European Office. Part of this work was carried out during the tenure of a Post-doctoral Fellowship by one of us (V.P.A.) awarded by *Ciba Fellowship Trust*, Cambridge.

1. Enzell, C. *Svensk Kem. Tidskr.* **72** (1960) 602.

Received January 14, 1961.

Cytochrome c from *Salmonella typhimurium*

MARK RICHMOND and NIELS OLE KJELDGAARD

Universitetets Mikrobiologiske Institut, Øster Farimagsgade 2 A, København K, Denmark

In the course of growth experiments with *Salmonella typhimurium*, it was found that organisms grown in a simple synthetic medium with L-glutamate as sole carbon source were pink when looked at in bulk by transmitted light. Glucose grown organisms of the same strain were white or pale cream under similar conditions and a difference spectrum (glutamate cells/glucose cells) taken at high suspension densities showed strong absorption bands in the regions 400—420, 515—530 and 540—560 mμ for glutamate grown cells. These absorption bands suggested that the pink colour was due to cytochromes. Treatment of a dense suspension of glutamate grown bacteria (*ca.* 8 g wet weight of bacteria in all) as described by Tissières [1] produced material with the absorption spectrum shown in Fig. 1. Sharp peaks were found at 416, 525 and 551 mμ in the reduced form and at 409 mμ in the oxidised form. These peaks are located in exactly the same positions as the absorption peaks of the cytochrome C_4 isolated by Tissières [1] from *Azotobacter vinelandii*.

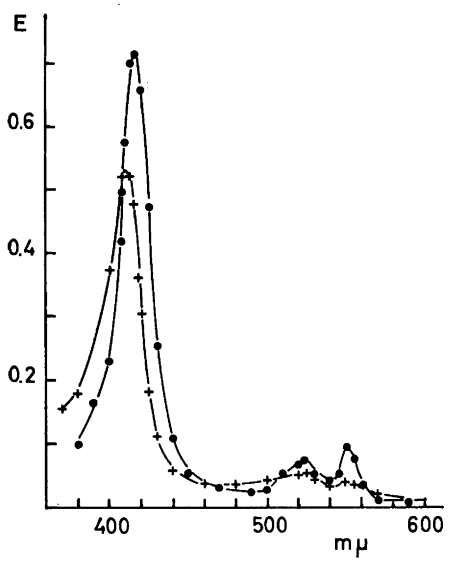

Fig. 1. Absorption spectra (1.0 cm light path) of the oxidised (+) and reduced (●) forms of the cytochrome preparation extracted from *Salmonella typhimurium*. The cytochrome was reduced with $Na_2S_2O_4$.

Table 1. Relative extinction coefficients of bacterial cytochrome c preparations.

Organism	Reduced			Oxidised
A.vinelandii	E_{416}	E_{525}	E_{551}	E_{409}
(C_4)	9.0	1.0	1.32	6.8
S.typhimurium	9.6	1.0	1.3	7.1

Comparison of the quantitative relationship between the extinction coefficients at the absorption peaks for these cytochromes (see Table 1) shows that the *Salmonella typhimurium* cytochrome is very similar to that from *Azotobacter vinelandii*, at least as far as absorption properties are concerned.

One of us (MR) would like to acknowledge the receipt of a CIBA Fellowship in support of this work.

1. Tissières, A. *Biochem. J.* **64** (1956) 582.

Received January 15, 1961.

This research was supported in part by the *Swedish Technical Research Council* and by the *Office of Research and Development, U.S. Army Department*, through its European Office. Part of this work was carried out during the tenure of a Post-doctoral Fellowship by one of us (V.P.A.) awarded by *Ciba Fellowship Trust*, Cambridge.

1. Enzell, C. *Svensk Kem. Tidskr.* **72** (1960) 602.

Received January 14, 1961.

Cytochrome c from *Salmonella typhimurium*

MARK RICHMOND and NIELS OLE KJELDGAARD

Universitetets Mikrobiologiske Institut, Øster Farimagsgade 2 A, København K, Denmark

In the course of growth experiments with *Salmonella typhimurium*, it was found that organisms grown in a simple synthetic medium with L-glutamate as sole carbon source were pink when looked at in bulk by transmitted light. Glucose grown organisms of the same strain were white or pale cream under similar conditions and a difference spectrum (glutamate cells/glucose cells) taken at high suspension densities showed strong absorption bands in the regions 400—420, 515—530 and 540—560 mμ for glutamate grown cells. These absorption bands suggested that the pink colour was due to cytochromes. Treatment of a dense suspension of glutamate grown bacteria (*ca.* 8 g wet weight of bacteria in all) as described by Tissières [1] produced material with the absorption spectrum shown in Fig. 1. Sharp peaks were found at 416, 525 and 551 mμ in the reduced form and at 409 mμ in the oxidised form. These peaks are located in exactly the same positions as the absorption peaks of the cytochrome C_4 isolated by Tissières [1] from *Azotobacter vinelandii*.

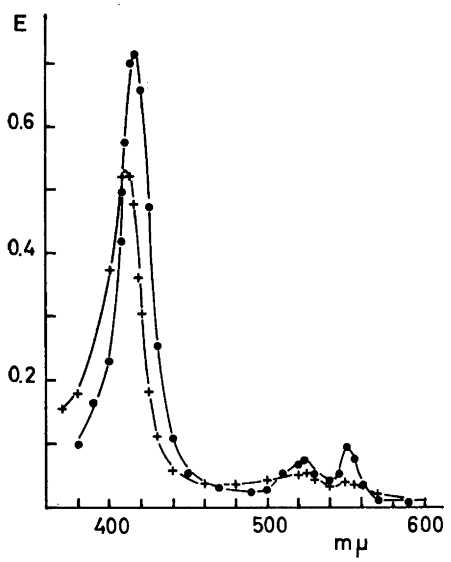

Fig. 1. Absorption spectra (1.0 cm light path) of the oxidised (+) and reduced (●) forms of the cytochrome preparation extracted from *Salmonella typhimurium*. The cytochrome was reduced with $Na_2S_2O_4$.

Table 1. Relative extinction coefficients of bacterial cytochrome c preparations.

Organism	Reduced			Oxidised
A.vinelandii	E_{416}	E_{525}	E_{551}	E_{409}
(C_4)	9.0	1.0	1.32	6.8
S.typhimurium	9.6	1.0	1.3	7.1

Comparison of the quantitative relationship between the extinction coefficients at the absorption peaks for these cytochromes (see Table 1) shows that the *Salmonella typhimurium* cytochrome is very similar to that from *Azotobacter vinelandii*, at least as far as absorption properties are concerned.

One of us (MR) would like to acknowledge the receipt of a CIBA Fellowship in support of this work.

1. Tissières, A. *Biochem. J.* **64** (1956) 582.

Received January 15, 1961.

On the Dithiocyanation of Pyrrole

ERIK SÖDERBÄCK, SALO GRONOWITZ and ANNA-BRITTA HÖRNFELDT

Chemical Institute, University of Uppsala, Sweden

Some years ago one of us (E.S.) investigated the thiocyanation of aromatic compounds with thiocyanogen, using aluminium chloride as catalyst [1]. It was found that pyrrole reacted smoothly with thiocyanogen in benzene or ether solution even in the absence of aluminium chloride, yielding a dithiocyanopyrrole. At that time it was generally accepted [2] (*cf.* also recent reviews in Refs.[3-5]) that substitution in the pyrrole nucleus occurred in the α-position; hence it was assumed that the compound obtained in these reactions was α,α'-dithiocyanopyrrole.

Later Matteson and Snyder [6,7] succeeded to monothiocyanate pyrrole with thiocyanogen in methanol at $-70°$, or with cupric thiocyanate in methanol at 0°. They gave convincing evidence that the monothiocyanopyrrole of m.p. 41.5–43° was 3-thiocyanopyrrole. This result throws doubt on the structure assigned to the dithiocyanopyrrole and we have therefore reinvestigated this problem.

Treatment of 3-thiocyanopyrrole with thiocyanogen in methanol at $-70°$ or in ether at 0° gave a dithiocyanopyrrole which in all respects (m.p., mixed m.p. and IR-spectra) was identical with that obtained according to Söderbäck [1]. If we assume that no rearrangement of the 3-thiocyano group had occurred under these mild conditions, we can conclude that the product is not the 2,5-isomer.

As the position in which monothiocyanation occurs is rather unexpected, it is difficult to predict the directing effect of the first introduced thiocyano group on further thiocyanation. It should be noted that the effect of the 3-thiocyano group must be different on its two *ortho* positions. Although one can assume that the inductive effect is similar in the 2- and 4-positions, the conjugative effect of this group (+M or −M) can be relayed to the 2-positions (Resonance forms II and III) only, if we assume that resonance structures with long bonds like IV have low weights.

We proved the structure of the dithiocyanopyrrole by investigating its NMR-spectrum. In solvents like acetone and dioxane, the spectrum consists of a broad NH resonance and of a doublet with splitting of 2.6 c/s (Fig. 1). In more basic

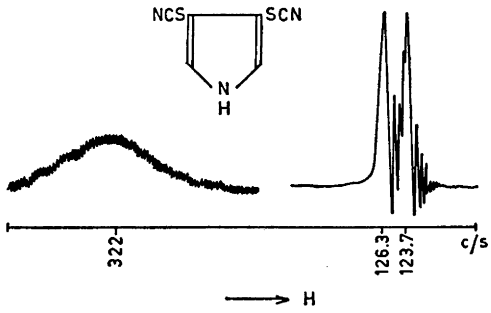

Fig. 1. NMR-spectrum of 3,4-dithiocyanopyrrole in (14 wt %) dioxane solution at 40 Mc/s. The solvent is used as internal reference.

solvents like N,N-dimethyl formamide, one sharp peak is obtained for the ring hydrogens. As it is highly improbable that the chemical shifts for the hydrogens in the 2,3- or 2,4-isomer could coincide in all the solvents investigated, this result shows that the compound obtained is the symmetric 3-4-dithiocyanopyrrole. The splitting in the NMR-spectrum is due to the J_{NH-2} coupling and is of the magnitude found by Abraham and Bernstein [8] in other pyrroles. Additional evidence is obtained

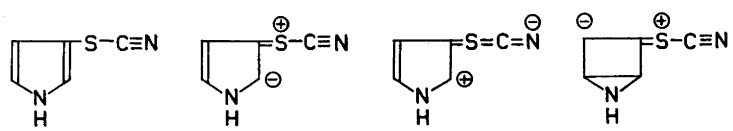

from the NMR-spectrum of the N-methylated dithiocyanopyrrole [1], which also shows a sharp peak for the ring hydrogens.

The reactivity of the β-hydrogens in the thiocyanation reaction is also evident from the ease with which 2,5-dimethylpyrrole is dithiocyanated at −70° to 2,5-dimethyl-3,4-dithiocyanopyrrole.

Experimental. 3,4-Dithiocyanopyrrole. A solution of thiocyanogen in ether was prepared from 6.5 g (0.020 mole) of lead thiocyanate and 2.8 g (0.018 mole) of bromine in 30 ml of dry ether at 0°. The light yellow ethereal solution was decanted and the precipitated lead bromide washed with 20 ml of dry ether. 2.0 g (0.016 moles) of 3-thiocyanopyrrole [7] in 15 ml of dry ether was added to the cooled ethereal thiocyanogen and the resulting solution allowed to stand at 0° for 30 min. The ether phase was washed with sodium bicarbonate and water and dried over magnesium sulphate. Evaporation of the ether yielded 2.0 g (69 %) of crude dithiocyanopyrrole. One recrystallization from water yielded 1.4 g (50 %) of pure 3,4-dithiocyanopyrrole, m.p. 113—114°. This compound was identical (IR-spectra and mixed m.p.) with the dithiocyanopyrrole prepared according to Söderbäck [1]. The NMR-spectrum in dioxane solution (14 % by weight) showed the broad NH resonance at 8.1 ppm from the solvent peak, and a doublet due to the α-hydrogens centered at 3.1 ppm from the solvent peak with a splitting of 2.6 c/s. In acetone solution (27 % by weight) the shifts were 9.9 ppm and 4.6 ppm, respectively, and the splitting 2.5 c/s. In N,N-dimethyl formamide solution (33 % by weight) the ring hydrogens give a sharp peak at —1.2 ppm from the hydrogen attached to the carbonyl group of the reference solvent.

2,5-Dimethyl-3,4-dithiocyanopyrrole. Method I. To a solution of thiocyanogen in methanol, prepared at —70° from 20 g (0.21 mole) of potassium thiocyanate in 25 ml of methanol, was added rapidly a precooled (—70°) solution of 4.7 g (0.050 mole) of 2,5-dimethylpyrrole [9] in 12.5 ml of methanol. After 10 min. the cooling-bath was removed and when the temperature had risen to —25°, the reaction mixture was poured into 200 g of ice followed by the addition of 30 g of sodium chloride. After the ice had melted, the precipitated product was filtered off, dissolved in ether and reprecipitated by the addition of petrolether, to give 8.2 g (78 %) of product, m.p. 136—140°. Recrystallization from a benzene-ligroin (2:1) mixture gave 6.0 g (57 %) of pure 2,5-dimethyl-3,4-dithiocyanopyrrole, m.p. 138.5—139.5°. Additional recrystallization did not raise the m.p. (Found: C 46.16; H 3.27; N 19.92; S 30.51. Calc. for $C_8H_7N_3S_2$ (209.3): C 45.91; H 3.37; N 20.08; S 30.64).

Method II. 2,5-Dimethyl-3,4-dithiocyanopyrrole was prepared also according to the description given by Söderbäck [1] for the dithiocyanation of pyrrole. From 70 g (0.22 mole) of lead thiocyanate, 32 g (0.20 mole) of bromine, 300 ml of benzene and 9.5 g (0.10 mole) of 2,5-dimethylpyrrole [9] was obtained 15.5 g (74 %) of 2,5-dimethyl-3,4-dithiocyanopyrrole, m.p. 138—140°. Its IR-spectrum was identical to that of the product obtained by method I.

The melting-points were determined with a hot stage microscope. The NMR-spectra were obtained with a Varian Associates model V-4300-B high-resolution spectrometer operating at 40.00 Mc/s and a flux-stabilized 12 in. magnet equipped with shimcoils from the same company. The magnet sweep was calibrated with the modulation side-band technique using a 50.00 ± 0.05 c/s modulation frequency obtained from the power line.

Note added in proof (February, 21). Recent results obtained in these laboratories seem to indicate that the monothiocyanopyrrole obtained by Snyder *et al.* is, nevertheless, the *2-isomer*. In such a case the present investigation proves the dithiocyanopyrrole to be the 2,5-isomer as originally suggested by Söderbäck.

Acknowledgements. Thanks are due to Mr. Bo Gestblom for recording the NMR-spectra.

1. Söderbäck, E. *Acta Chem. Scand.* **8** (1954) 1851.
2. Elderfield, R. C. *Heterocyclic Compounds I*, Chapter 6, New York 1950.
3. Albert, A. *Heterocyclic Chemistry*, Chapter 5, Bristol 1959.
4. Treibs, A. and Fritz, G. *Ann.* **611** (1958) 162.
5. Katritzky, A. R. and Lagowski, J. M. *Heterocyclic Chemistry*. Chapter 4, London 1960.
6. Matteson, D. S. and Snyder, H. R. J. *J. Am. Chem. Soc.* **79** (1957) 3610.
7. Matteson, D. S. and Snyder, H. R. J. *J. Org. Chem.* **22** (1957) 1500.
8. Abraham, R. J. and Bernstein, H. J. *Can. J. Chem.* **37** (1959) 1056.
9. Young, D. M. and Allen, C. F. H. *Org. Syntheses*, Coll. Vol. **2** (1946) 219.

Received January 16, 1961.

Die Messung der Rotationsdispersion als Hilfsmittel für die Untersuchung chemischer Zeit- und Gleichgewichtsreaktionen

O. KLING*

Chemisches Laboratorium A, Technische Hochschule, Kopenhagen, Dänemark

Die weitgehenden Analogien zwischen spektraler Absorption und optischer Drehung deuten darauf hin, dass die Messung der optischen Aktivität dieselbe Bedeutung erlangen kann wie sie die Spektralphotometrie heute besitzt. Die allgemeine Form des Lambert—Beer'schen Gesetzes für ein Mehrkomponentensystem lautet

$$E_{ges} = \sum_i E_i = \sum_i \varepsilon_i \cdot c_i \cdot d \qquad (1)$$

wobei E_{ges} die Gesamtextinktion des Systems und E_i die Extinktion, ε_i der molare dekadische Extinktionskoeffizient und c_i die Konzentration der i-ten Komponente in Mol/l ist. d ist die Schichtdicke in cm[1].

Für die optische Drehung gilt im allgemeinen eine analoge Beziehung

$$a_{ges} = \sum_i a_i = \sum_i \frac{[M]_i}{100} \cdot c_i \cdot d \qquad (2)$$

Dabei ist a_{ges} der Gesamtdrehwinkel des Mehrkomponentensystems mit dem Einzeldrehwert a_i, dem molaren Drehwert $[M]_i$ und der Konzentration c_i (Mol/l) der i-ten Komponente. d ist ebenfalls die Schichtdicke in cm. Die Abhängigkeit des Extinktionskoeffizienten von der Wellenlänge λ liefert die "typische Farbkurve" oder das "charakteristische Absorptionsspektrum" der betreffenden Substanz [1]. Der Zahlenwert des molaren Drehvermögens $[M]$ als Funktion der Wellenlänge ist die "Rotationsdispersion" (vgl. z.B. Ref. 2).

Bei der spektralphotometrischen Untersuchung chemischer Zeit- und Gleichgewichtsreaktionen findet man bisweilen, dass die erhaltenen Absorptionskurven an einer oder mehreren Stellen durch gemeinsame Schnittpunkte laufen. Die Bedingungen für das Auftreten dieser sogenannten "isosbestischen Punkte" (Punkte gleichbleibender Extinktion)[3,4] auch bei komplizierten Systemen und die Schlussfolgerungen, die daraus gezogen werden können, sind bereits an anderer Stelle ausführlich dargestellt [5,6].

Die Untersuchung chemischer Reaktionen mit Hilfe von Messungen der Rotationsdispersion lässt auf Grund der völligen Analogie der Gll. (1) und (2) erwarten, dass die dabei sukzessive erhaltenen Drehwertkurven unter bestimmten Bedingungen ebenfalls gemeinsame Schnittpunkte konstanten Drehwinkels liefern. Solche ausgezeichneten Punkte sind auch bereits beobachtet worden [7]. In Anlehnung an A. Thiel [3], der die Bezeichnung "isosbestische Punkte" in der Spektralphotometrie einführte, wird vorgeschlagen, die entsprechenden Punkte im Falle der Rotationsdispersion "isodinetische Punkte" * zu nennen. Diese Bezeichnung erscheint wegen des philologischen Zusammenhangs [3] und auch aus phonetischen Gründen günstiger als "isorotatorisch" und ähnliche Wortbildungen.

Die Bedingungen, unter denen bei der Messung der Rotationsdispersion isodinetische Punkte zu erwarten sind, entsprechen völlig denen, die das Auftreten isosbestischer Punkte in der Spektralphotometrie bestimmen. Die hierfür abgeleiteten Beziehungen [5,6] können völlig analog übernommen werden, indem anstelle des Extinktionskoeffizienten ε der molare Drehwert $[M]$ eingesetzt wird. Es ist jedoch zu berücksichtigen, dass ε immer ≥ 0 ist, während $[M]$ positive und negative Werte annehmen kann.

Daraus ergeben sich für die isodinetischen Punkte besondere quantitative Unterschiede gegenüber den isosbestischen Punkten. So ist z.B. bei der Interpretation von Racemisierungsreaktionen von Bedeutung, ob die isodinetischen Punkte auf der Nullinie des $[M]/\lambda$-Diagramms oder abseits davon liegen. Da sich die entsprechenden Beziehungen in konkreten Fällen leicht ableiten lassen [6], sei an dieser Stelle auf eine ausführliche Diskussion verzichtet.

Die fortschreitende Entwicklung automatischer Spektralpolarimeter der verschiedensten Systeme macht es möglich, Rotationsdispersionskurven optisch aktiver

* Derzeitige Anschrift: Institut für physikalische Chemie, Universität Frankfurt a.M., Deutschland.

* griech. δινητός, im Kreise gedreht, drehbar.

Lösungen relativ einfach zu ermitteln. Kinetische und Gleichgewichtsuntersuchungen mit Hilfe der optischen Drehung bei monochromatischer Strahlung sollten darum auf kolorimetrie-analoge Messungen (wie z.B. die Saccharimetrie) beschränkt bleiben, bei denen es nicht auf die Kenntnis des Chemismus selbst sondern nur auf seine exakte Reproduzierbarkeit ankommt. In allen anderen Fällen sollten quantitative Messungen bei einzelnen Wellenlängen erst dann erfolgen, wenn vorher die Änderung der Rotationsdispersion in einem grösseren Spektralbereich untersucht wurde. Das Auftreten oder Nichtvorhandensein isodinetischer Punkte liefert dann bereits wichtige Hinweise auf den Reaktionsverlauf.

Die Anwendbarkeit der Messung der optischen Drehung ist naturgemäss zunächst auf Systeme beschränkt, die optisch aktive Zentren enthalten. Sie wird jedoch oft noch weiter eingeschränkt dadurch, dass die Rotationsdispersion oft nicht konzentrationsunabhängig ist, wie in Gl. (2) vorausgesetzt, und auch durch andere Lösungspartner stark beeinflusst werden kann. Dies bietet jedoch andrerseits die Möglichkeit des Einsatzes optisch aktiver "Indikatoren" zur Untersuchung optisch inaktiver Systeme. Bei diesen indirekten Methoden wirken Konzentrations- und sonstige Änderungen der Ausgangslösungen auf den Indikator ein und können dadurch messend verfolgt werden. Die Anwendung empfindlicher, automatischer Spektralpolarimeter als Hilfsmittel für die Aufklärung chemischer Probleme eröffnet somit ein weites Arbeitsgebiet, dessen Möglichkeiten heute erst zum Teil übersehen werden können.

Der Verfasser dankt Herrn Prof. J. Bjerrum und F. Woldbye für ihr förderndes Interesse an dieser Arbeit, die im Rahmen eines Auslandsstipendiums der *Deutschen Forschungsgemeinschaft* durchgeführt wurde.

1. Kortüm, G. *Kolorimetrie, Photometrie und Spektrometrie.* Springer 1955, 3. Aufl., S. 28.
2. Kortüm, G. *Die Dispersion der optischen Drehung amorpher Systeme.* Ferd. Enke, Stuttgart 1922.
3. Thiel, A. *Fortschr. Chem., Physik u. physik. Chem.* **19** (1924) 36.
4. Weigert, F. *Ber.* **49** (1916) 1527.
5. Schläfer, H. L. und Kling, O. *Angew. Chem.* **68** (1956) 667.
6. Kling, O. und Schläfer, H. L. *Z. Elektrochem.* (1961) *Im Druck.*
7. Woldbye, F. *Optical Rotatory Dispersion of Transition Metal Complexes,* European Research Office, U.S. Army, Frankfurt a.M. 1959.

Eingegangen am 14. Januar 1961.

ACTA CHEMICA SCANDINAVICA 15 (1961) 231–241

Heats of Combustion and Formation of the 1-Bromoalkanes from C_4 through C_8

LARS BJELLERUP

Department of Organic Chemistry, University of Lund, Lund, Sweden

The heats of combustion of highly purified samples of five 1-bromoalkanes have been determined with a moving-bomb calorimetric method.

The purification of samples of the following compounds is described: 1-bromobutane, 1-bromopentane, 1-bromohexane, 1-bromoheptane and 1-bromooctane. Data on density and refractive index for the spectral lines D, Hα and Hβ, at 20 and 25°C, of the purified samples are given and compared with corresponding data from previous investigations.

The following values, in kcal/mole, are reported for the heat of combustion, $-\Delta Hc°$, at 25°C, of the liquid sample in gaseous oxygen to form gaseous carbon dioxide, liquid water and liquid bromine, with reactants and products in their thermodynamic standard states: 1-bromobutane 649.17 ± 0.30, 1-bromopentane 805.30 ± 0.34, 1-bromohexane Sample I 962.82 ± 0.36, 1-bromohexane Sample II 961.91 ± 0.38, 1-bromoheptane 1118.52 ± 0.38, 1-bromooctane 1274.52 ± 0.54.

Combination of these values with the known standard heats of formation of carbon dioxide and water and with values for the heats of vaporization of the various bromine compounds yields the following values, in kcal/mole, for the heat of formation, $-\Delta Hf°$, at 25°C, of the gaseous compound from carbon(graphite), gaseous hydrogen and liquid bromine, with reactants and products in their thermodynamic standard states: 1-bromobutane 25.67 ± 0.40, 1-bromopentane 31.02 ± 0.46, 1-bromohexane 34.97 ± 0.48 (Sample I) and 35.88 ± 0.49 (Sample II), 1-bromoheptane 40.69 ± 0.52, 1-bromooctane 46.26 ± 0.65.

The derived heat of formation data are discussed and found to be internally consistent with the possible exception of the heat of formation value derived from the heat of combustion of Sample I of 1-bromohexane.

Modern experimental data from which heats of formation for monobromoalkanes can be calculated, are available only for ethyl bromide [1], the two propyl bromides [2–5] and *sec.*-butyl bromide [5,6]. Experimental data on other members of this class of compounds are therefore needed and, as a first step

in this direction, heats of combustion have been determined, with the moving-bomb method, for carefully purified samples of the C_4—C_8 1-bromoalkanes. The observed bomb-calorimetric data have been reduced to standard heats of combustion and the latter then combined with heats of formation for carbon dioxide and water to yield standard heats of formation for the given compounds.

This paper describes the purification of the samples and the heat of combustion experiments and presents the observed and derived heat of combustion and formation data.

MATERIALS

Benzoic acid. The benzoic acid samples used in the calibration experiments with the calorimeters A and B were National Bureau of Standards standard sample 39g[7] and 39f[8], respectively.

Paraffin oils. The paraffin oil samples used as auxiliary material in the combustion experiments with the bromine compounds were the same as those described in Ref.[5]

Bromine compounds. The bromine compound samples were all obtained by careful purification of commercial products. The latter were first treated chemically and then purified by successive fractional distillations at two or more different pressures, using the same apparatus and technique as described in Ref.[5] Details of the purification of the various samples follow.

1-Bromobutane. The commercial sample (Columbia Organic Chemicals) was treated with phosphorus pentoxide. The resulting 180 g were purified by two successive fractional distillations at pressures 750 and 340 mm, respectively. In the final distillation 80 % (53 g) of the distillate was collected over a density range of 0.0003 g/ml. The second half (27 g) of this distillate, all of which was collected at constant density, was treated with calcium sulfate and subjected to simple distillation at atmospheric pressure. The middle fraction from this distillation was used in the heat of combustion experiments.

1-Bromopentane. The commercial sample (Columbia Organic Chemicals) was treated with phosphorus pentoxide. The resulting 83 g were purified by two fractional distillations at pressures 760 and 41 mm, respectively. In the final distillation 80 % (23 g) of the distillate was collected at constant density. This product was treated with calcium sulfate and distilled at 64 mm. A middle fraction from this distillation was used in the heat of combustion experiments.

1-Bromohexane Sample I. After treatment of the commercial sample (Columbia Organic Chemicals) with phosphorus pentoxide the product (100 g) was fractionally distilled at 160 mm, and 90 % (85 g) of the distillate was collected over a density range of 0.0004 g/ml. Several fractions were discolored. Therefore, all fractions of the 85 g of distillate collected were combined and treated first with 10 % sodium bicarbonate solution and then with water, and then dried with calcium chloride and finally with phosphorus pentoxide. The dry sample was purified by successive fractionations at pressures 20 and 60 mm, respectively. All the distillate (16 g) in the final distillation was collected over a density range of 0.0002 g/ml. This product was treated with calcium sulfate and subjected to simple distillation at 8 mm. A middle fraction from this distillation was used in the heat of combustion experiments.

1-Bromohexane Sample II. The commercial sample (Kebo) was treated successively with 48 % hydrobromic acid, water, 10 % sodium carbonate solution and water. The product was dried with calcium chloride and with calcium sulfate and the resulting 1 000 g were fractionated by successive distillations at pressures 200, 100, and 50 mm. In the final distillation 77 % (240 g) of the distillate was collected over a density range of 0.0002 g/ml (the whole distillate was collected over a density range of 0.0005 g/ml). The fractions making in all 240 g were combined into one sample. A vapor phase chromatographic test on the sample did not indicate the presence of any impurities. Part of this sample, after treatment with calcium sulfate and simple distillation, was used in the heat of combustion experiments.

1-Bromoheptane. The commercial sample (Columbia Organic Chemicals) was treated in order with conc. hydrochloric acid, water, 10 % sodium bicarbonate solution and water,

Table 1. Comparison with earlier data of density and refractive index data for the samples prepared in the present investigation.

Compound and reference	Density g/ml		Refractive index					
			D		$H\alpha$		$H\beta$	
	20°	25°	20°	25°	20°	25°	20°	25°
1-BROMOBUTANE								
Present investigation	1.2758	1.2686	1.4398	1.4374	1.4371	1.4347	1.4463	1.4438
Tschamler, Richter and Wettig [9]		1.2694	1.43981					
Skau and McCullough [10]		1.2686						
Lucas, Dillon and Young [11]	1.2756	1.2686	1.4403					
Timmermans and Martin [12]	1.27568	1.26844	1.43975	1.43725	1.43690	1.43440	1.44615	1.44355
1-BROMOPENTANE								
Present investigation	1.2186	1.2123	1.4444	1.4420	1.4418	1.4394	1.4509	1.4485
Skau and McCullough [10]		1.2121						
1-BROMOHEXANE								
Present investigation Sample I	1.1745	1.1688	1.4475	1.4452	1.4449	1.4426	1.4539	1.4516
Present investigation Sample II	1.1745	1.1686	1.4475	1.4454	1.4446	1.4425	1.4537	1.4513
Tschamler, Richter and Wettig [9]		1.1690						
1-BROMOHEPTANE								
Present investigation	1.1402	1.1348	1.4503	1.4481	1.4477	1.4456	1.4566	1.4544
Deffet [13]	1.1399	1.1345			1.4477	1.4456	1.4568	1.4546
1-BROMOOCTANE								
Present investigation	1.1129	1.1077	1.4526	1.4505	1.4499	1.4478	1.4588	1.4567
Deffet [13]	1.1129	1.1078			1.4501	1.4481	1.4592	1.4572

and then dried first with calcium chloride and finally with phosphorus pentoxide. The resulting 83 g were purified by successive fractional distillations at pressures 105 and 45 mm, respectively. In the final distillation all the distillate was collected over a density range of 0.0001 g/ml. Part of this distillate was used in the heat of combustion experiments without further treatment.

1-Bromooctane. The commercial sample (Kebo) was treated in order with conc. sulfuric acid, water, 10 % sodium carbonate solution and water. The product was dried with calcium chloride and the resulting 515 g were fractionated by successive distillations at pressures 100 and 40 mm. In the final distillation 89 % (318 g) of the distillate were collected over a density range of 0.0002 g/ml. Part of this distillate was dried with calcium sulfate and distilled at 2 mm. A middle fraction was taken for the combustion experiments.

Table 1 gives the densities, at 20 and 25°C, and refractive indices for the spectral lines D, $H\alpha$ and $H\beta$, at 20 and 25°C, of the samples used in the heat of combustion experiments. The density measurements were made with a standard Ostwald-Sprengel pycnometer to an accuracy estimated at $\pm$ 0.0001 g/ml and the refractive indices were measured with a calibrated Pulfrich refractometer, giving refractive index values within estimated error limits of $\pm$ 0.0001.

For comparison with earlier data on density and refractive index of highly purified samples of the various compounds, the results from certain selected previous investigations [9-13] are also listed in Table 1.

Table 2. Results of combustion experiments on 1-bromobutane, 1-bromopentane, 1-bromohexane Sample I, and 1-bromoheptane.

Calorimeter B

t_h = 20.0°C; t_i = 20.0°C; P^i(gas.) = 30.0 atm; V(Bomb) = 0.2750 liter; V^i(soln.) = 0.03001 liter; C^i(soln.) = 0.0625$_5$ mole As_2O_3/liter; ε°(Calor.) = 4 718.62 ± 0.34 cal/deg; $-\Delta Ec°$/M(Oil) = 10 972.1 ± 0.7 cal/g; $-\Delta Ec°$/M(Fuse) = 3 971 ± 4 cal/g; m(Pt) = 5.764 g; $-\Delta E_{oxid.}(As_2O_3)$ = (77.4 ± 0.1) × 10^3 cal/mole

m′ g	m″ g	m‴ g	m(glass) g	ε(Calor.) cal/deg	ε^f(Cont.) cal/deg	Δt deg	$n^f(As_2O_3)$ mole	$-\Delta E(CO_2)$ cal	$-\Delta E(HNO_3)$ cal	$-\Delta E$(Au) cal	$-\Delta E$(Pt) cal	$-\Delta E$(HBr) cal	$-\Delta E\Sigma$ cal	$-\Delta Ec°/M$ cal/g
1-BROMOBUTANE														
0.60492	0.15996	0.00455	0.111	4 671.77	32.19	0.99982	0.001057	10.86	1.75	0.03	0.08	24.08	0.40	4 727.7
0.61800	0.16166	0.00479	0.112	4 671.76	32.19	1.01765	0.001087	11.04	1.05	0.03	0.08	24.60	0.40	4 729.6
0.62208	0.14750	0.00438	0.110	4 671.77	32.19	0.98858	0.001085	10.71	1.75	0.03	0.08	24.76	0.40	4 731.0
													Mean	4 729.4
													Standard deviation of mean	± 0.7$_6$[a]
1-BROMOPENTANE														
0.60170	0.12956	0.00451	0.139	4 671.78	32.23	1.00033	0.000945	10.87	1.80	0.03	0.06	21.69	0.38	5 322.0
0.59458	0.13210	0.00477	0.094	4 671.83	32.23	0.99816	0.000944	10.85	0.90	0.03	0.06	21.44	0.38	5 321.4
0.57889	0.14080	0.00460	0.136	4 671.80	32.23	1.00054	0.000919	10.88	1.10	0.03	0.06	20.87	0.38	5 323.1
													Mean	5 322.2
													Standard deviation of mean	± 0.7$_9$[a]
1-BROMOHEXANE Sample I														
0.66101	0.06811	0.00480	0.123	4 671.79	32.24	0.99492	0.000954	10.76	1.50	0.02	0.04	21.81	0.38	5 824.1
0.64126	0.08200	0.00459	0.110	4 671.81	32.25	1.00187	0.000926	10.86	1.15	0.02	0.04	21.16	0.36	5 820.8
0.62659	0.09517	0.00477	0.096	4 671.83	32.26	1.01468	0.000898	11.01	1.50	0.02	0.04	20.67	0.34	5 823.5
													Mean	5 822.8
													Standard deviation of mean	± 0.7$_3$[a]
1-BROMOHEPTANE														
0.63811	0.05940	0.00492	0.105	4 671.84	32.27	1.00078	0.000858	10.87	1.20	0.02	0.06	19.38	0.36	6 233.5
0.59224	0.08533	0.00476	0.104	4 671.86	32.27	0.99951	0.000792	10.89	1.20	0.02	0.06	17.99	0.34	6 233.2
0.60950	0.06559	0.00487	0.094	4 671.87	32.27	0.97711	0.000821	10.62	1.30	0.02	0.06	18.51	0.35	6 235.9
0.63266	0.06649	0.00472	0.109	4 671.84	32.27	1.01014	0.000849	10.97	0.95	0.02	0.06	19.22	0.36	6 236.1
													Mean	6 234.7
													Standard deviation of mean	± 0.6$_5$[a]

[a] This value has been estimated as given in text.

Table 3. Results of combustion experiments on 1-bromohexane Sample II.

Calorimeter A

$t_h = 25.0°C$ V(Bomb) = 0.2670 liter $\varepsilon°$(Calor.) = 5 822.45 ± 0.33 cal/deg m(Pt) = 8.854 g in expt. no.1-6; 18.424 g in expt. no.7-10

$t_i = 24.1°C$ V^i(soln.) = 0.03015 liter in expt. no. 1—3; 0.03005 liter in expt. no. 4—10 $-\Delta Ec°$/M(Oil) = 10 971.6 ± 0.6 cal/g in expt. no. 1—6; 10 984.4 ± 1.2 cal/g in expt.no. 7—10

P^i(gas.) = 30.0 atm C^i(soln.) = 0.0629$_1$ mole As_2O_3/liter $-\Delta Ec°$/M(Fuse) = 3 971 ± 4 cal/g $-\Delta E_{oxid.}(As_2O_3)$ = (77.4 ± 0.1) × 10^3 cal/mole

Expt. No.	m′ g	m″ g	m‴ g	m(glass) g	ε(Calor.) cal/deg	ε^i(Cont.) cal/deg	Δt deg	$n^f(As_2O_3)$ mole	$-\Delta E(CO_2)$ cal	$-\Delta E(HNO_3)$ cal	$-\Delta E$(Au) cal	$-\Delta E$(Pt) cal	$-\Delta E$(HBr) cal	$-\Delta E_\Sigma$ cal	$-\Delta Ec°/M$ cal/g
1	0.653639	0.116178	0.005679	0.0832	5772.98	32.22	0.88903	0.000917	10.62	2.40	0.01	0.03	20.77	0.31	5 814.9
2	0.595775	0.149650	0.005203	0.1040	5772.98	32.22	0.89298	0.000858	10.72	1.00	0.03	0.02	18.92	0.29	5 811.6
3	0.631233	0.131386	0.005126	0.0875	5772.98	32.22	0.89433	0.000913	10.71	0.90	0.02	0.03	20.06	0.32	5 810.8
4	0.606192	0.143907	0.005543	0.0901	5773.09	32.12	0.89349	0.000853	10.67	2.10	0.01	0.05	19.25	0.33	5 817.8
5	0.662344	0.112724	0.005433	0.0932	5773.06	32.12	0.89143	0.000949	10.61	1.15	0.02	0.03	21.06	0.32	5 816.8
6	0.649002	0.122353	0.005368	0.1039	5773.05	32.13	0.89604	0.000925	10.67	1.20	0.01	0.03	20.63	0.31	5 817.2
7	0.703072	0.090822	0.005107	0.0799	5763.50	32.43	0.89231	0.001018	10.60	1.30	0.02	0.03	22.36	0.32	5 811.4
8	0.661589	0.112691	0.004821	0.0818	5763.52	32.42	0.89196	0.000948	10.62	0.95	0.02	0.04	21.03	0.32	5 818.0
9	0.688238	0.105649	0.005043	0.0824	5763.50	32.42	0.90595	0.000993	10.80	1.40	0.03	0.04	21.88	0.27	5 816.8
10	0.685332	0.098890	0.005264	0.0786	5763.51	32.42	0.89000	0.000981	10.58	1.25	0.04	0.04	21.79	0.32	5 815.4
														Mean	5 815.1
														Standard deviation of mean	± 0.8$_3$

Table 4. Results of combustion experiments on 1-bromooctane.

Calorimeter A

t_h = 25.0°C — V(Bomb) = 0.2670 liter — $\varepsilon°$(Calor.) = 5 821.01 ± 0.47 cal/deg — m(Pt) = 17.994 g

t_i = 24.1°C — V^i(soln.) = 0.03005 liter — $-\Delta Ec°/M$(Oil) = 10 979.6 ± 0.9 cal/g — ε^i(Cont.) = 32.41 cal/deg

P^i(gas.) = 30.0 atm — C^i(soln.) = 0.0628$_5$ mole As_2O_3/liter — $-\Delta Ec°/M$(Fuse) = 3 971 ± 4 cal/g — $-\Delta E_{oxid.}(As_2O_3)$ = (77.4 ± 0.1) × 10^3 cal/mole

m′ g	m″ g	m‴ g	m(glass) g	Δt deg	$n^f(As_2O_5)$ mole	$-\Delta E(CO_2)$ cal	$-\Delta E(HNO_3)$ cal	$-\Delta E$(Au) cal	$-\Delta E$(Pt) cal	$-\Delta E$(HBr) cal	$-\Delta E\Sigma$ cal	$-\Delta Ec°/M$ cal/g
0.651095	0.066860	0.005858	0.0548	0.88031	0.000788	10.49	0.30	0.05	0.02	17.67	0.30	6 589.1
0.648572	0.086604	0.005344	0.0491	0.91399	0.000796	10.91	0.65	0.04	0.02	17.60	0.31	6 582.4
0.674744	0.068958	0.005302	0.0409	0.91130	0.000834	10.85	0.65	0.03	0.01	18.31	0.31	6 588.1
0.654363	0.079064	0.005559	0.0422	0.90671	0.000810	10.81	0.30	0.03	0.02	17.76	0.31	6 584.2
0.647449	0.070521	0.005679	0.0623	0.88248	0.000791	10.52	0.65	0.02	0.03	17.57	0.31	6 583.6
0.651145	0.072602	0.005523	0.0610	0.89100	0.000772	10.62	1.15	0.03	0.03	17.67	0.31	6 589.4
0.653175	0.069570	0.005142	0.0649	0.88707	0.000811	10.57	0.15	0.02	0.01	17.73	0.31	6 584.4
											Mean	6 585.9
											Standard deviation of mean	± 1.0$_9$

HEAT OF COMBUSTION MEASUREMENTS

Apparatus and procedure

The same calorimetric systems, A and B, and the same experimental procedures used in the work reported in Ref.[5] were used in the present heat of combustion measurements. Calorimeter A was used for the measurements on the samples of 1-bromohexane Sample II and 1-bromooctane and calorimeter B for 1-bromobutane, 1-bromopentane, 1-bromohexane Sample I and 1-bromoheptane.

Results

The results of the combustion experiments are presented in Tables 2—4. The symbols have the same significance as in corresponding tables of Refs.[5,14]. It should be noted that, (i) the results listed in Table 2 were obtained in experiments with calorimeter B and those in Tables 3 and 4 in experiments with calorimeter A; and (ii) the reference temperature, t_h, was 20.0°C in experiments with calorimeter B and 25.0°C in experiments with calorimeter A.

Calculation of results. The results were calculated as given in Ref.[14] by use of eqns. 3—5 of Ref.[5]

Unit of energy. Auxiliary quantities. The results are given in terms of the defined thermochemical calorie equal to 4.1840 abs. joules. The $-\Delta E_c^\circ/M$ values refer to the reaction represented by eqn. 1, in which all reactants and products are in their thermodynamic standard states [15] at the temperature t_h:

$$C_nH_{2n+1}Br(liq) + (6n+1)/4\ O_2(g) \rightarrow n\ CO_2(g) + (2n+1)/2\ H_2O(liq) + \tfrac{1}{2}Br_2\ (liq) \qquad (1)$$

For both samples of benzoic acid used in calibration experiments with the two calorimeters the certified value [7,8] for the heat of combustion under certificate conditions is 26.4338 ± 0.0026 abs. kj/g mass which is equal to 6 317.83 ± 0.62 cal/g mass. This value is recalculated, as given in Refs.[5,16], to give the values 6 312.92 ± 0.62 and 6 314.12 ± 0.62 cal/g mass for the standard heat of combustion per gram mass of the sample, $-\Delta E_c^\circ/M$, at 25°C and 20°C, respectively.

In addition to the numerical quantities given in Ref.[5] (Table 8) the values listed in Table 5 were used in the calculation of the results. The symbols in Table 5 denote: ϱ the density, c_p the specific heat, and $(\partial E/\partial P)_T$ the energy of compression of the substance. The density values are from the present paper. The specific heat values for 1-bromobutane, 1-bromopentane and 1-bromohexane were obtained from data given in Ref.[17] by plotting and extrapolation, and the specific heat values for 1-bromoheptane and 1-bromooctane were estimated by analogy with the three lower homologues. The $(\partial E/\partial P)_T$ values were calculated from the corresponding density data using the approximate relation $(\partial E/\partial P)_T = -T(\partial V/\partial T)_P$ as discussed in Ref.[18] (p. 542–43)

Uncertainties. The standard deviations of mean given in Tables 3 and 4 were calculated in the conventional way [19] (p. 433). Because of the small number of experiments on each of the compounds listed in Table 2 the standard deviations of mean in this table were calculated by the method given in Ref.[20] (p. 73–74) utilizing all 13 individual experiments of the table.

Table 5. Auxiliary quantities for calculation of results [a].

Compound (liq)	ϱ g/ml		c_P cal/g deg 25°C	$(\partial E/\partial P)_T$ cal/g atm 20–25°C
	20°C	25°C		
1-Bromobutane	1.2758	1.2686	0.27	−0.0064
1-Bromopentane	1.2186	1.2123	0.28	−0.0061
1-Bromohexane	1.1745	1.1687	0.30	−0.0060
1-Bromoheptane	1.1402	1.1348	0.31	−0.0060
1-Bromooctane	1.1129	1.1077	0.32	−0.0060

[a] See text for comments.

The final over-all standard deviations [19 (p. 432)] given in Table 6 were calculated by the method described in Ref.[5 (p. 130)] using the following values for the ratios s_i/q_i:

$s_1/q_1 = 0.5 \times 10^{-4}$; $s_2/q_2 = 0.7 \times 10^{-4}$ (Table 2), 0.6×10^{-4} (Table 3) and 0.8×10^{-4} (Table 4); $s_3/q_3 = 0.6 \times 10^{-4}$ (Table 2), 1.0×10^{-4} (Table 3) and 0.8×10^{-4} (Table 4); $s_4/q_4 = 350 \times 10^{-4}$; $s_5/q_5 = 13 \times 10^{-4}$.

Derived standard heats of combustion

The $-\Delta Ec^\circ/M$ mean values given in Tables 2—4, on recalculation by conventional methods [21 (p. 103–4)], gave the values listed in Table 6 for the standard energies of combustion, ΔEc°, at 20°C and 25°C, and the standard enthalpies of combustion, ΔHc°, at 25°C for the various compounds. The data refer to the combustion reaction represented by eqn. 1, in which all reactants and products are in their standard states. The uncertainties were calculated as described in the preceding section.

Table 6. Derived standard heats of combustion.

Compound and state	Molecular weight [a]	$-\Delta Ec^\circ$ at 20°C kcal/mole	$-\Delta Ec^\circ$ at 25°C kcal/mole	$-\Delta Hc^\circ$ at 25°C kcal/mole
1-Bromobutane(liq)	137.032	648.08±0.30[b]		649.17±0.30[b]
1-Bromopentane(liq)	151.059	803.97±0.34		805.30±0.34
1-Bromohexane(liq)				
Sample I	165.086	961.26±0.36		962.82±0.36
Sample II			959.99±0.38[b]	961.91±0.38
1-Bromoheptane(liq)	179.113	1 116.72±0.38		1 118.52±0.38
1-Bromooctane(liq)	193.140		1 272.00±0.54	1 274.52±0.54

[a] Computed from the 1957 table of atomic weights[23].

[b] The uncertainties in this column are equal to twice the final over-all standard deviation; see text for comments.

Table 7. Derived standard heats of formation.

Compound	$\Delta Hf°$(liq) at 25°C kcal/mole	ΔHv[a] at 25°C kcal/mole	$\Delta Hf°$(g)[b] at 25°C kcal/mole
1-Bromobutane	−34.47 ± 0.31[c]	8.80 ± 0.25[d]	−25.67 ± 0.40[e]
1-Bromopentane	−40.72 ± 0.35	9.70 ± 0.30	−31.02 ± 0.46
1-Bromohexane Sample I	−45.57 ± 0.37	10.60 ± 0.30	−34.97 ± 0.48
Sample II	−46.48 ± 0.39	10.60 ± 0.30	−35.88 ± 0.49
1-Bromoheptane	−52.24 ± 0.39	11.55 ± 0.35	−40.69 ± 0.52
1-Bromooctane	−58.61 ± 0.55	12.35 ± 0.35	−46.26 ± 0.65

[a] For the process $C_aH_bBr_d(liq) \rightarrow C_aH_bBr_d(g)$, at saturation pressure at 25°C.
[b] See text for comments.
[c] The uncertainties in this column are equal to twice the final over-all standard deviation[19].
[d] The uncertainties in this column are estimates.
[e] The uncertainties in this column are equal to twice the final over-all standard deviation (including the estimated uncertainties assigned to the ΔHv values in column 3)[19].

HEATS OF FORMATION

Standard heats of formation, $\Delta Hf°$, at 25°C, referring to reaction 2,

$$n\ C(c, \text{graphite}) + (2n+1)/2\ H_2(g) + \tfrac{1}{2}\ Br_2(liq) \rightarrow C_nH_{2n+1}Br(liq) \quad (2)$$

were calculated from the $-\Delta Hc°$ values given in Table 6 and the selected values [15] for the standard heats of formation of gaseous carbon dioxide [24], −94.0539 ± 0.0108 kcal/mole, and liquid water [25], 68.3174 ± 0.0096 kcal/mole. The value for carbon dioxide is corrected to the present atomic weight of 12.011 for carbon. The derived standard heats of formation for the liquid compounds are given in column 2 of Table 7. In column 3 are listed heats of vaporization, ΔHv, at 25°C for the various compounds, calculated from data in Refs.[26,27]. Resulting standard heats of formation, at 25°C, of the compounds in the gaseous state are listed in column 4. Actually, the values given in this column apply to the compounds at their saturation pressures at 25°C. It can, however, be estimated [27] that reduction of the values to apply to the compounds in a state of unit fugacity (1 atm) will change the values by less than a few hundredths of a kcal/mole. Therefore the given values have been listed as standard heats of formation.

DISCUSSION OF RESULTS

The internal consistency of the derived heat of formation data in Table 7 can be checked in the following way.

It has been shown [28] that for several homologous series of hydrocarbons the standard heats of formation of the gaseous compounds can be expressed by the following relation:

$$\Delta Hf°_{298.15}\ [Y—(CH_2)_m—H,\ gas] = A + Bm + \delta \quad (3)$$

Table 8. Values of δ in the relation $\Delta Hf°_{298.15}$ [$CH_2Br-(CH_2)_m-H$, gas] = A + B × m + δ for the standard heats of formation, in the gaseous state at 25°C, of the 1-bromoalkanes

m	A + B × m kcal/mole	$\Delta Hf°_{298.15}$ kcal/mole	$\delta = \Delta Hf°_{298.15} - (A + B \times m)$ kcal/mole
A = −11.164 kcal/mole, B = −4.926 kcal/mole			
4	−30.87	−31.02 ± 0.46	−0.15 ± 0.46
5 (Sample I)	−35.79	−34.97 ± 0.48	+ 0.82 ± 0.48
5 (Sample II)	−35.79	−35.88 ± 0.49	−0.09 ± 0.49
6	−40.72	−40.69 ± 0.52	+ 0.03 ± 0.52
7	−45.65	−46.26 ± 0.65	−0.61 ± 0.65
A = −11.364 kcal/mole, B = −4.926 kcal/mole			
2	−21.22	−21.98 ± 0.40[a]	−0.76 ± 0.40
3	−26.14	−25.67 ± 0.40	+ 0.47 ± 0.40
4	−31.07	−31.02 ± 0.46	+ 0.05 ± 0.46
5	−35.99	−35.88 ± 0.49	+ 0.11 ± 0.49
6	−40.92	−40.69 ± 0.52	+ 0.23 ± 0.52
7	−45.85	−46.26 ± 0.65	−0.41 ± 0.65

[a] Ref.[5]

where $(CH_2)_m$—H is a *n*-alkyl group bonded to any end group Y (methyl, vinyl, phenyl, *cyclo*pentyl, *cyclo*hexyl), A is a constant characteristic of the end group, B is a constant for all *n*-alkyl series, independent of Y, and δ is a term which has a small finite value for the lower members of a series and becomes zero for the higher members, beginning near m = 4. Choosing the bromomethyl group as end group for the 1-bromoalkanes, CH_2Br—$(CH_2)_m$—H, and using the same relation 3 and the same numerical value of B, —4.926 kcal/mole, as for the various hydrocarbon series, a value for A can be calculated from the derived heat of formation values for 1-bromopentane, 1-bromohexane Samples I and II, 1-bromoheptane and 1-bromooctane, for which compounds $m \geq 4$ and for which δ in eqn. 3 therefore can be assumed to be zero. The value obtained for A is —11.164 kcal/mole. Using this figure the δ values given in the upper part of Table 8 are obtained. It is seen that only in the case of Sample I of 1-bromohexane does the value of δ differ significantly from zero. Preference may therefore be given to the heat of formation value obtained for Sample II of 1-bromohexane. Accordingly a different value for A can be calculated from the same heat of formation data as above with exclusion of that for Sample I of 1-bromohexane. The value —11.364 kcal/mole is thus obtained for A. Corresponding δ values are given in the lower part of Table 8.

The given discussion has thus shown that the heat of formation data derived from the heat of combustion values obtained in the present investigation are internally consistent when the heat of formation derived from the heat of combustion of Sample I of 1-bromohexane is excluded. It has also been

shown that the standard heats of formation at 25°C of the C_5—C_8 1-bromoalkanes can be expressed by the relation:

$$\Delta Hf°_{298.15}\ [CH_2Br—(CH_2)_m—H,\ gas] = —11.364 — 4.926 \times m\ kcal/mole \quad (m = 4, 5, 6, 7).$$

Acknowledgement. The author's thanks are due to the *Swedish Natural Science Research Council*, the *Swedish Technical Research Council, Kungl. Fysiografiska Sällskapet i Lund* and *Doktor P. Håkanssons Stiftelse* for financial support of this investigation.

REFERENCES

1. Lane, M. R., Linnett, J. W. and Oswin, H. G. *Proc. Roy. Soc. London* **216** (1953) 361.
2. Lacher, J. R., Walden, C. H., Lea, K. R. and Park, J. D. *J. Am. Chem. Soc.* **72** (1950) 331.
3. Lacher, J. R., Kianpour, A. and Park, J. D. *J. Phys. Chem.* **61** (1957) 1124.
4. Lacher, J. R. *Personal communication* (1957).
5. Bjellerup, L. *Acta Chem. Scand.* **15** (1961) 121.
6. Lacher, J. R., Billings, T. J., Campion, D. E., Lea, K. R. and Park, J. D. *J. Am. Chem. Soc.* **74** (1952) 5291.
7. *Provisional Certificate of Analysis of Standard Sample 39g, Benzoic Acid*, National Bureau of Standards, Washington, D.C., 1949.
8. *Certificate for Standard Sample 39f, Benzoic Acid*, National Bureau of Standards, Washington, D.C., 1944 (with Supplementary Note 1946).
9. Tschamler, H., Richter, E. and Wettig, F. *Sitz. ber. Akad. Wiss. Wien, Math. naturw. Kl. Abt. II b* **158** (1949) 856.
10. Skau, E. L. and McCullough, R. *J. Am. Chem. Soc.* **57** (1935) 2439.
11. Lucas, H. J., Dillon, R. T. and Young, W. G. *J. Am. Chem. Soc.* **52** (1930) 1949.
12. Timmermans, J. and Martin, F. *J. chim. phys.* **23** (1926) 747, p. 779.
13. Deffet, L. *Bull. soc. chim. Belges* **40** (1931) 385.
14. Bjellerup, L. *Acta Chem. Scand.* **13** (1959) 1511.
15. Rossini, F. D., Wagman, D. D., Evans, W. H., Levine, S. and Jaffe, I. *Selected Values of Chemical Thermodynamic Properties*, Circular of the National Bureau of Standards 500, U.S. Government Printing Office, Washington, D.C., 1952.
16. Bjellerup, L. *Acta Chem. Scand.* **14** (1960) 617.
17. Deese Jr., R.F. *J. Am. Chem. Soc.* **53** (1931) 3673.
18. Washburn, E. W. *Bur. Standards J. Research* **10** (1933) 525.
19. Rossini, F. D. and Deming, W. E. *J. Wash. Acad. Sci.* **29** (1939) 416.
20. Sunner, S. *Studies in Combustion Calorimetry Applied to Organo-Sulphur Compounds* (Diss.) University, Lund 1949.
21. Hubbard, W. N., Scott, D. W. and Waddington, G. *Standard States and Corrections for Combustions in a Bomb at Constant Volume* Chapter 5 of Ref.[22]
22. Rossini, F. D. (Ed.) *Experimental Thermochemistry*, Interscience, New York 1956.
23. Wichers, E. *J. Am. Chem. Soc.* **80** (1958) 4121.
24. Prosen, E. J., Jessup, R. S. and Rossini, F. D. *J. Research Natl. Bur. Standards* **33** (1944) 447.
25. Wagman, D. D., Kilpatrick, J. E., Taylor, W. J., Pitzer, K. S. and Rossini, F. D. *J. Research Natl. Bur. Standards* **34** (1945) 143.
26. Stull, D. R., *Ind. Eng. Chem.* **39** (1947) 517.
27. Dreisbach, R. R. *Pressure-Volume-Temperature Relationships of Organic Compounds*, 3rd Ed., Handbook Publishers, Sandusky 1952.
28. Prosen, E. J., Johnson, W. H. and Rossini, F. D. *J. Research Natl. Bur. Standards* **37** (1946) 51.

Received October 13, 1960.

ACTA CHEMICA SCANDINAVICA 15 (1961) 242–248

Synthesis and Metabolism of Δ^4-Cholestene-7α-ol-3-one

Bile Acids and Steroids 108

HENRY DANIELSSON

Department of Chemistry, Karolinska Institutet, Stockholm, Sweden

A method of preparing Δ^4-cholestene-7α-ol-3-one is described. This compound can be obtained in low yield (4–5 %) from 3β-benzoxy-7α-tetrahydro-2′-pyranyloxycholesterol by hydrolysis of the 3β-benzoxy group, Oppenauer oxidation at this position followed by reduction with sodium borohydride yielding a 3-hydroxy-7-pyranyl ether with the double bond in the 4-position. Hydrolysis of this product followed by selective oxidation at the 3-position with manganese dioxide yielded Δ^4-cholestene-7α-ol-3-one.

Randomly tritium-labelled Δ^4-cholestene-7α-ol-3-one, prepared biosynthetically by incubation of labelled 7α-hydroxycholesterol with mouse liver homogenates, has been administered to bile-fistula rats, and the labelled products in the bile have been separated with chromatography and partly identified. Δ^4-Cholestene-7α-ol-3-one is metabolized in part to chenodeoxycholic acid and to cholic acid. In addition several unidentified bile acids of polarity similar to that of cholic as well as of chenodeoxycholic acid are formed.

7α-Hydroxycholesterol has been shown to be converted to both cholic and chenodeoxycholic acid in the rat *in vivo* [1] and this compound has been suggested as a possible intermediate in the formation of bile acids from cholesterol. The metabolism of 7α-hydroxycholesterol in mouse liver homogenates has recently been studied in this laboratory [2]. One of the products formed was found to be somewhat less polar than 7α-hydroxycholesterol, suggesting the presence of a keto group instead of a hydroxyl in this compound. This metabolite was not identical with 7-ketocholesterol and the possibility that oxidation had occurred at the 3-position with the formation of Δ^4- or Δ^5-cholestene-7α-ol-3-one appeared likely. While this work was in progress Yamasaki *et al.*[3] reported that 7α-hydroxycholesterol was metabolized in rat liver homogenates to a compound, which on grounds of its spectrographic properties was suggested to be Δ^4-cholestene-7α-ol-3-one. Any further characterization of the metabolite was not reported.

Greenhalgh *et al.*[7] have reported the synthesis of Δ^4-cholestene-7β-ol-3-one and also some early steps in the synthesis of the 7α-epimer, but these

authors were not able to obtain any Δ^4-cholestene-7α-ol-3-one because of its ready dehydration in the final steps of the synthesis. In this communication will be described the synthesis of Δ^4-cholestene-7α-ol-3-one and the metabolism of this compound in the bile-fistula rat.

EXPERIMENTAL

All rotations were taken in chloroform solutions. Melting points are uncorrected.

7α-Hydroxycholesteryl benzoate. This compound was prepared from cholesteryl benzoate using the method of Bide *et al.*[4] for synthesis of 7α-bromo-cholesteryl benzoate and that of Schaltegger and Müllner [5] for conversion of the 7α-bromo- into the 7α-hydroxycompound.

The *7α-bromo-cholesteryl benzoate* synthesized had m.p. 139—140°, $[\alpha]_D^{23}$° −175° (*c*, 1.0); reported [4] m.p. 140°, $[\alpha]_D$ −172° and the *7α-hydroxycholesteryl benzoate* had m.p. 167—168°, $[\alpha]_D^{23}$° −50° (*c*, 1.0); reported [6] m.p. 167—168°, $[\alpha]_D$ −50.5°.

3β-Benzoxy-7α-tetrahydro-2′-pyranyloxycholesterol. 4 g of 7α-hydroxycholesteryl benzoate were dissolved in 40 ml of dihydropyran and 8 drops of phosphorus oxychloride added as described by Greenhalgh *et al.*[7] The solution was kept at room temperature for 2 h. Afterwards it was made alkaline with methanolic potassium hydroxide, diluted with water and extracted twice with ether The ether extracts were washed with water until neutral and taken to dryness Crystallization twice from acetone/water gave 3.6 g of *3β-benzoxy-7α-tetrahydro-2′-pyranyloxycholesterol*, m.p. 140—141°, $[\alpha]_D^{23}$° −106° (*c*, 1.0). (Found: C 79.0; H 9.7. Calc. for $C_{39}H_{58}O_4$: C 79.25; H 9.9.)

7α-Tetrahydro-2′-pyranyloxycholesterol. The foregoing benzoxypyranyl ether (3.6 g) was dissolved in 50 ml of methanol and treated with 50 ml of 10 % potassium hydroxide in methanol under reflux for 30 min. Isolation by ether extraction and crystallization from methanol/water gave 2.8 g 7α-tetrahydro-2′-pyranyloxycholesterol, m.p. 138°, $[\alpha]_D^{23}$° −138° (*c*, 1.1); reported [7] m.p. 137—140°. (Found: C 77.1; H 11.2. (The material had been dried *in vacuo* (0.1 mm Hg) over phosphorus pentoxide 24 h at room temperature.) Calc. for $C_{32}H_{54}O_3$: C 78.95; H 11.2; Calc. for $C_{32}H_{54}O_3 + CH_3OH$: C 76.5; H 11.1.)

Δ^4-Cholestene-7α-ol-3-one. 2.5 g of foregoing hydroxy-pyranyl ether in 50 ml of dry benzene were heated under reflux for 2 h with 20 ml of a 25 % solution of aluminum *tert.*-butoxide in toluene and 36 ml of acetone as described by Greenhalgh *et al.*[7] The mixture was then acidified with 0.2 N hydrochloric acid, diluted with water and extracted twice with ether. The ether extracts were washed neutral and evaporated to dryness. To the residue were added a few ml of xylene and the solution was again evaporated to dryness. The resultant product showed two absorption maxima, at 243 mμ and at 285 mμ. The ratio of the absorption at 243 to that at 285 mμ was 3.2. Assuming that all material obtained were the desired product, 7α-tetrahydro-2′-pyranyloxy-cholest-4-en-3-one, the molar extinction coefficient at 243 mμ was 8 900. An ε of 15 000—16 000 was expected of this compound [7,12] and the content of it in the oxidation mixture would then be about 60 %. Attempts to crystallize the mixture failed. In an effort to remove unchanged starting material and the material giving rise to the absorption at 285 mμ, presumably $\Delta^{4,6}$-cholestadiene-3-one, the mixture was chromatographed on a 90 g column of Hostalene (Farbwerke Hoechst G.m.b.H., W-Germany) using phase system I [8]. The purification obtained was not very satisfactory. Although much of the starting material could be removed, the compounds giving rise to the absorption at 243 and 285 mμ, respectively, showed similar chromatographic properties in this system. The molar extinction coefficient at 243 mμ of the ultraviolet-absorbing material had increased to 11 000 after chromatography, but the ratio of absorption at 243 to 285 mμ had decreased to 2.6. No crystalline material could be obtained. Efforts to separate the α,β-unsaturated ketone from the cholestadienone with other phase systems [8] were not successful. Chromatography on aluminum oxide, either Merck (Merck A.G., W-Germany) or Woelm (M. Woelm, Eschwege, W-Germany), grade I, caused dehydration of the α,β-unsaturated ketone and mainly material absorbing at 285 mμ was recovered. Chromatography on weaker aluminum oxide was not tried at this stage.

As found by Greenhalgh *et al.*[7] hydrolysis with dilute hydrochloric acid of the α,β-unsaturated ketone to remove the protecting pyranyl ether group causes dehydration at the 7α-position with formation of $\Delta^{4,6}$-cholestadiene-3-one. It appeared possible to overcome this difficulty by removing the protecting pyranyl ether group after reduction of the ketone to the alcohol and then obtain the desired Δ^4-cholestene-7α-ol-3-one by selective oxidation of the allylic alcohol group at the 3-position.

The chromatographed material (1.7 g) was reduced with 1.7 g of sodium borohydride in 200 ml of methanol for 1 h at room temperature. The solution was then cooled, acidified with 0.2 N hydrochloric acid and extracted with ether. No crystalline material could be obtained. Attempts to separate the dienol, formed from the cholestadienone, from the hydroxy-pyranyl ether by reversed phase partition chromatography [8] were unsuccessful.

1 g of the reduction mixture was hydrolyzed with 100 ml of 0.08 % hydrochloric acid in absolute ethanol for 1 h at room temperature *. The hydrolysis mixture was then made alkaline with methanolic potassium hydroxide, diluted with water and extracted with ether. The washed ether extracts were taken to dryness, the residue dissolved in 200 ml of chloroform and then stirred at room temperature for 24 h with 10 g of manganese dioxide, prepared as described by Mancera *et al.*[9] The solution was then filtered, evaporated to dryness and the residue chromatographed on a 45 g column of hydrophobic Hyflo Supercel (Johns Manville and Co., USA) using phase system III [8]. After elution with 3 000 ml of mobile phase only one main peak of ultraviolet-absorbing material, appearing at 2 000 ml of effluent, had been eluted. This material, which had its absorption maximum at 243 mμ and no absorption at 285 mμ, was rechromatographed on a 13.5 g column using phase system I. The main fraction weighed 77 mg and had a molar extinction coefficent of 15 200. Crystallization from methanol/water afforded 42 mg as needles of Δ^4-cholestene-7α-ol-3-one, m.p. 183—184°; $[\alpha]_D^{23°}$ + 67° (*c*, 0.82); λ_{max}, 242.5 mμ ε = 16 100. (Found: C 81.1; H 10.9. Calc. for $C_{27}H_{44}O_2$: C 80.95; H 11.1.) Further recrystallization from acetone/water and hexane did not change the melting point or the optical rotation.

Δ^4-Cholestene-7α-ol-3-one acetate. 28 mg of foregoing hydroxy-ketone were dissolved in 1 ml of dry pyridine and 0.5 ml of acetic anhydride and left at room temperature for 24 h. The mixture was worked up in the usual manner and crystallized from methanol/water yielding 20 mg, m.p. 136—137°. Recrystallization from hexane afforded 10 mg as needles of *Δ^4-cholestene-7α-ol-3-one acetate*, m.p. 144—145°, $[\alpha]_D^{23°}$ + 20° (*c*, 0.82); λ_{max}, 238 mμ ε = 16 300. (Found: C 78.4; H 10.2. Calc. for $C_{29}H_{46}O_3$: C 78.65; H 10.5.)

Δ^4-Cholestene-7β-ol-3-one. This compound was prepared exactly as described by Greenhalgh *et al.*[7] and had m.p. 182—183°, $[\alpha]_D^{23°}$ + 62° (*c*, 0.52); reported [7] m.p. 183.5—184°, $[\alpha]_D$ + 63°.

Animal experiments. Randomly tritium-labelled Δ^4-cholestene-7α-ol-3-one was prepared by incubating tritium-labelled 7α-hydroxycholesterol with mouse liver homogenates [2] and was purified by chromatography with phase system III [8]. The identity of the labelled compound was established by chromatography together with unlabelled material, synthesized as described above, and crystallization to constant specific activity both as free sterol and as acetate.

White male rats (Sprague-Dawley, weighing about 250 g) were provided with bile fistula in the usual manner. The bile was saponified with 1 N potassium hydroxide over night at 110°. The free bile acids were extracted with ether and then chromatographed with phase system F 1 [10] to separate the cholic and the chenodeoxycholic acid fraction. The cholic acid fraction was rechromatographed with phase system C 1 [10] and the chenodeoxycholic acid fraction with phase system F 1.

* Exposure for longer times, 3 h to 6 days, gave with time lower and lower yields as measured by the amount of Δ^4-cholestene-7α-ol-3-one formed after oxidation of the hydrolysis mixture with manganese dioxide.

RESULTS AND DISCUSSION

Chemical synthesis of Δ^4-cholestene-7α-ol-3-one. The physical properties of Δ^4-cholestene-7α-ol-3-one and Δ^4-cholestene-7β-ol-3-one were found to be strangely similar with respect to melting point and optical rotation. The 7α-epimer synthesized as described above had m.p. 183—184° and $[\alpha]_D$ + 67° while the 7β-epimer has m.p. 183.5—184° and $[\alpha]_D$ + 63° [7]. The same physical constants were obtained in repeated syntheses of Δ^4-cholestene-7α-ol-3-one, and synthesis of the 7β-epimer according to Greenhalgh *et al.*[7] gave a product with the same properties as the one described by these authors. That the two compounds were not identical could be shown by mixed melting point determination, chromatography and preparation of the acetates. There was a substantial depression of the melting point on admixture of the epimer (155—165°), the two compounds separated completely on thin layer chromatography (see Fig. 1) and the physical constants of the acetate of the 7α-epimer were

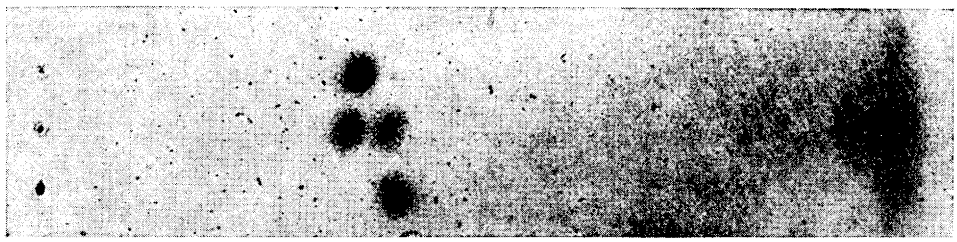

Fig. 1. Thin layer chromatography of Δ^4-cholestene-7β-ol-3-one (uppermost), Δ^4-cholestene-7α-ol-3-one (lower) and a mixture of these (middle) according to the method of Van Dam *et al.*[11] Mobile phase: benzene/ethyl acetate 2:1 (v/v).

quite different from those of the 7β-epimer. In addition, oxidation of 7β-tetrahydro-2′-pyranyloxycholesterol under the same conditions used for the 7α-epimer proceeded much slower and yielded preponderantly a cholestadienone [12].

Readings of the optical rotation of samples of the 7α-compound crystallized from different solvents and obtained from different syntheses all gave values for $[\alpha]_D$ between + 67° and + 70°. This value is worth noting as it could be expected to be *less* positive than that of the 7β-epimer. In spite of the large "positive" contribution to the M_D by the shift of the double bond from the 5- to the 4-position [13], the large difference in rotation of 7α-hydroxycholesterol ($[\alpha]_D$ —92°) and 7β-hydroxycholesterol ($[\alpha]_D$ + 7°) was thought to be noticeable also in the epimeric 7-hydroxy-Δ^4-cholestene-3-ones. In fact, the $[\alpha]_D$ of the 7α-acetate was substantially less positive (+ 20°) than that of the 7β-acetate (+ 77°).

Metabolism of Δ^4-cholestene-7α-ol-3-one. The labelled Δ^4-cholestene-7α-ol-3-one was prepared biosynthetically by incubation of tritium-labeled 7α-hydroxycholesterol with mouse liver homogenates [2]. The identity of the isolated

product with the compound synthesized chemically was established by co-chromatography and isotope dilution.

Tritium-labelled Δ^4-cholestene-7α-ol-3-one in an emulsion stabilized with serum albumin was injected intraperitoneally into a bile fistula rat. After 24 h 35 % of the injected dose had been excreted in bile. In this connection it should be pointed out that a considerable part of the tritium label can be expected to be located in the terminal *iso*propyl group of the injected compound [14], as it was prepared from 7α-hydroxycholesterol which in turn had been synthesized from cholesterol labelled with tritium according to Bloch and Rittenberg [15]. This tritium will be lost in the degradation of the side-chain to the C_{24}-length, hence the per cent radioactivity excreted in bile can be regarded as a minimum figure.

After preliminary chromatographic purification of the saponified bile, the cholic acid fraction was rechromatographed with phase system C 1. As is seen in Fig. 2 the radioactivity is distributed in three main peaks, one appear-

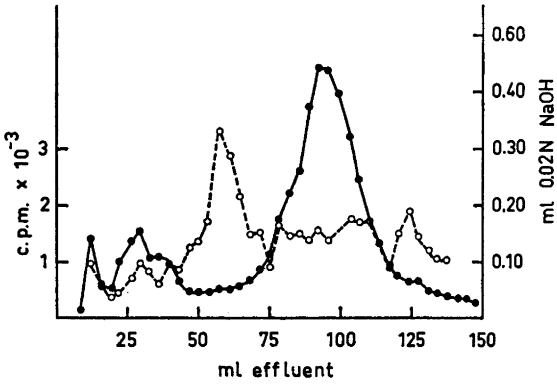

Fig. 2. Chromatography of the cholic acid fraction of the first 24 h portion of bile from bile fistula rat injected with Δ^4-cholestene-7α-ol-3-one. Column: 4.5 g hydrophobic Hyflo Supercel. Phase system C 1. Broken line: radioactivity. Solid line:titration values.

ing before the titration peak of cholic acid, one within the cholic acid peak and one shortly after. The main part of the cholic acid peak was rerun on a column with phase system C 1 and the radioactivity coincided with the titration peak (Fig. 3). The identity of this labelled material with cholic acid was established by isotope dilution. The radioactive material eluted shortly after cholic acid (Fig. 2) has the same elution volume as one of the metabolites of chenodeoxycholic acid, 3α-,6β-,7β-trihydroxycholanic acid, while no clue is at present available to the structure of the radioactive acid eluted before the cholic acid.

The chenodeoxycholic acid fraction was rechromatographed with phase system F 1 (Fig. 4). Part of the radioactivity coincided with the titration peak of chenodeoxycholic acid and the identity was established by isotope dilution. The structures of the radioactive acids eluted before and after chenodeoxycholic acid are not known and have not yet been further investigated.

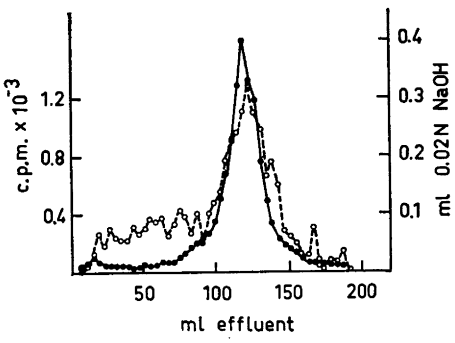

Fig. 3. Rechromatography of the cholic acid peak, Fig. 2. Column: 4.5 g hydrophobic Hyflo Supercel. Phase system C 1.

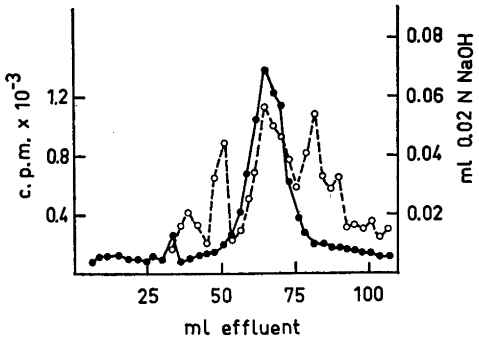

Fig. 4. Chromatography of the chenodeoxycholic acid fraction of the first 24 h portion of bile. Column: 4.5 g hydrophobic Hyflo Supercel. Phase system F 1.

In repeated experiments the same results were obtained and the radioactive acid which is more polar than cholic acid accounted for somewhat more of the activity excreted in bile than did cholic acid. Also, the radioactive acid eluted after chenodeoxycholic acid contained more radioactivity than did the chenodeoxycholic acid.

The findings of Lindstedt [1] and Bergström and Lindstedt [16] that 7*α*-hydroxycholesterol and 3*α*-,7*α*-dihydroxycoprostane are converted to both chenodeoxycholic and cholic acid in the rat have led Yamasaki *et al.*[3] to suggest these sterols as intermediates in the degradation of cholesterol to bile acids and that 7*α*-hydroxycholesterol is converted into 3*α*-,7*α*-dihydroxycoprostane *via* the intermediate formation of Δ^4-cholestene-7*α*-ol-3-one. At present, there is no definite proof available that 7*α*-hydroxycholesterol or 3*α*-,7*α*-dihydroxycoprostane are intermediates [1] nor has the postulated conversion of 7*α*-hydroxycholesterol to 3*α*-,7*α*-dihydroxycoprostane been shown. The results obtained on the metabolism of Δ^4-cholestene-7*α*-ol-3-one in the bile fistula rat should be interpreted with caution in relation to the possibility that this compound might be an intermediate in the conversion of cholesterol to bile acids. It does not appear unlikely that the enzymes involved in the catabolism of cholesterol to bile acids are arranged in an orderly manner passing their substrates along to next enzyme. When a sterol is administered extrahepatically and when no sizeable pool of this compound is present in the liver, the quantitative relations between its different metabolites might be quite different from those found when the compound is formed and metabolized *in situ*.

Cholic acid and chenodeoxycholic acid are present in rat bile in the proportion of about 8:2 and when labelled cholesterol is administered to a bile fistula rat these acids will be labelled to this proportion. When labelled 7*α*-hydroxycholesterol and 3*α*-,7*α*-dihydroxycoprostane are administered approximately 50 % of the radioactivity excreted in bile is present as chenodeoxycholic acid. In this investigation it was found that Δ^4-cholestene-7*α*-ol-3-one was metabolized to both cholic and chenodeoxycholic acid but also to other unidentified

acids. However, as discussed above, it cannot be excluded on these grounds that Δ^4-cholestene-7α-ol-3-one, 7α-hydroxycholesterol and 3α-,7α-dihydroxycoprostane might be intermediates in the degradation of cholesterol to bile acids. To clarify these points, the conversion of cholesterol to these compounds should be established.

Acknowledgements. The valuable technical assistance of Miss Birgitta Holmberg and Miss Marie-Louise Reinius is gratefully acknowledged. Thanks are also due to Dr. Peter Eneroth for help with thin layer chromatography.

This work is part of investigations supported by *The National Heart Institute*, Bethesda, Md., USA, (Grant H-2842) and has also been supported by a grant from *Karolinska Institutets Reservationsanslag.*

REFERENCES

1. Lindstedt, S. *Acta Chem. Scand.* **11** (1957) 417.
2. Danielsson, H. *Arkiv Kemi* **17** (1961). *In press.*
3. Yamasaki, K., Noda, F. and Shimizu, K. *J. Biochem. Tokyo* **46** (1959) 739, 747.
4. Bide, H. E., Henbest, H. B., Jones, E. R. H., Peevers, R. W. and Wilkinson, P. A. *J. Chem. Soc.* **1948** 1783.
5. Schaltegger, H. and Müllner, F. X. *Helv. Chim. Acta* **34** (1951) 1096.
6. Henbest, H. B. and Jones, E. R. H. *J. Chem. Soc.* **1948** 1792.
7. Greenhalgh, C. W., Henbest, H. B. and Jones, E. R. H. *J. Chem. Soc.* **1952** 2375.
8. Danielsson, H. *Biochim. et Biophys. Acta* **27** (1958) 401.
9. Mancera, O., Rosenkranz, G. and Sondheimer, F. *J. Chem. Soc.* **1953** 2189.
10. Norman, A. and Sjövall, J. *J. Biol. Chem.* **233** (1958) 872.
11. Van Dam, M. J. D., De Kleuver, G. J. and De Heus, J. G. *J. Chromatography* **4** (1960) 26.
12. Danielsson, H. and Issidorides, C. H. *To be published.*
13. Fieser, L. F. and Fieser, M. *Steroids*, Reinhold Publ. Co., N.Y., 1959, p. 178.
14. Fukushima, D. K. and Gallagher, T. F. *J. Biol. Chem.* **198** (1952) 861.
15. Bloch, K. and Rittenberg, D. *J. Biol. Chem.* **149** (1943) 505.
16. Bergström, S. and Lindstedt, S. *Biochem. et Biophys. Acta* **19** (1956) 556.

Received January 4, 1961.

ACTA CHEMICA SCANDINAVICA 15 (1961) 249–259

Studies on Peroxy Compounds VIII *

The Preparation of Acylals and Related Compounds by Copper Salt Catalyzed Reaction of *t*-Butyl Perbenzoate with Simple Ethers and Sulphides

SVEN-OLOV LAWESSON, CURT BERGLUND and SUSANNE GRÖNWALL

Department of Organic Chemistry, Chemical Institute, University of Uppsala, Uppsala, Sweden

The thermal decomposition of *t*-butyl perbenzoate in the presence of simple ethers and sulphides has been studied. Cuprous chloride has been shown to have a stabilizing effect on the intermediate radical. Instead of dimerization of the substrate, the benzoyloxy group is introduced in the *α*-position. The benzoates of anisole, phenetole, *t*-butyl *iso*-butyl ether, *n*-butyl-allyl ether, *sec*-butyl allyl ether, *t*-butyl allyl ether and di-*n*-butyl ether have thus been prepared. In the last mentioned case, the corresponding *α*-butoxy compound has also been formed; the mechanism of this is discussed. Likewise, the benzoyloxy compounds of phenyl methyl sulphide, phenyl ethyl sulphide, *t*-butyl ethyl sulphide, *n*-butyl allyl sulphide and di-*n*-butyl sulphide have been smoothly prepared. When the last mentioned compound was heated, benzoic acid was split off, resulting in an *α,β*-unsaturated sulphide. Similarly, when attempts were made to purify the benzoyloxycompound of phenyl *n*-amyl sulphide, benzoic acid was split off with the formation of the unsaturated sulphide.

In two earlier papers [1,2] in this series, Lawesson and Berglund have shown that benzyl ethers or sulphides do not undergo fragmentation or dimerization when treated with *t*-butyl perbenzoate in the presence of catalytic amounts of cuprous chloride but instead, the benzoyloxy group is introduced according to the following equations:

$$\underset{\text{I}}{C_6H_5-CH_2-X-R} \rightarrow \underset{\text{II}}{C_6H_5-\dot{C}H-X-R} \rightarrow \underset{\text{III}}{C_6H_5-\underset{\displaystyle O-COC_6H_5}{\underset{|}{C}}H-X-R} \qquad (1)$$

X = O, S; R = alkyl, aryl

* Part VII: Ref.[2]

This gives a method of preparing acylals [3] of different types. That the copper salt in some way stabilizes the radical II is in keeping with the fact that in its absence a free radical II (X = O), obtained by heating benzyl ethers with *t*-butyl peroxide, either undergoes fragmentation, dimerization or both, according to the following [4]:

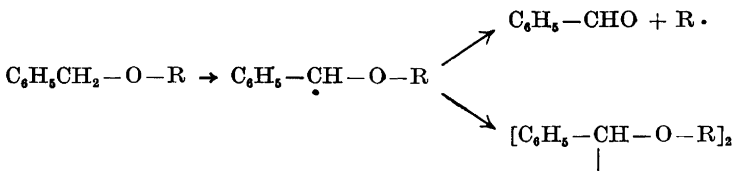

(2)

A benzyl sulphide when treated in the same way, gives a free radical II (X = S) which, probably due to the sulphur atom, does not undergo fragmentation but only dimerizes [2,5]:

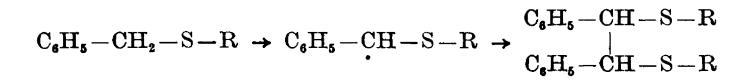

(3)

The question arises, which hydrogen is removed from the benzyl compound? As the most stable radical is preferentially formed, it is clear that the hydrogen abstraction is mainly from the CH_2-group between the phenyl group and the hetero atom, the extensively delocalized odd electron in II resulting in a resonance-stabilized radical.

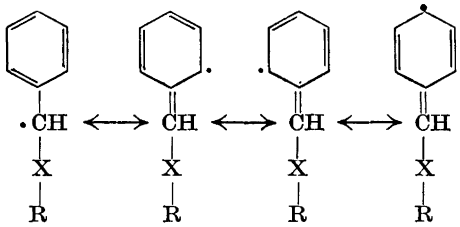

In the case of benzyl sulphides, the stabilization of the radical II (X = S) might also be explained by the following mesomeric interaction [6,7].

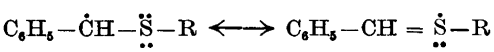

The reaction of certain acyl peroxides with simple ethers was first investigated by Cass [8-10] who, by studying the decomposition of benzoyl peroxide in diethyl ether, isolated 1-ethoxy-1-benzoyloxy ethane and benzoic acid as main products. The kinetics of this reaction has also been elucidated by Nozaki and Bartlett [11] and the mechanism recently worked out by Denney and Feig [12]. It may be concluded from these investigations that a hydrogen is preferentially removed from the α-carbon and that the intermediate radical formed does not undergo any fragmentation whatsoever.

Recently, Johnston and Williams [13] have studied the reaction of *t*-butyl peroxide with aromatic compounds with side chains and found that toluene, for instance, gives dibenzyl smoothly with a stabilized benzyl-type radical as an intermediate. However, anisole gives only polymeric material, probably due to the fact that the intermediate free radical is extremely short-lived and not stabilized by resonance. Sosnovsky [14] and the present authors [15] have studied the reaction between *t*-butyl perbenzoate and di-*n*-butyl ether in the presence of cuprous salts.

Apart from the studies made recently by us [2,5] only one other investigation of the reaction between peroxides and sulphides has been reported up till now. Horner and Jürgens [16] found as late as 1956 that diacyl peroxides with sulphides give the corresponding sulphoxide and the α-acyloxy compound of the sulphide. The peroxide is thereby converted into the anhydride and acid, respectively, according to the following formulas:

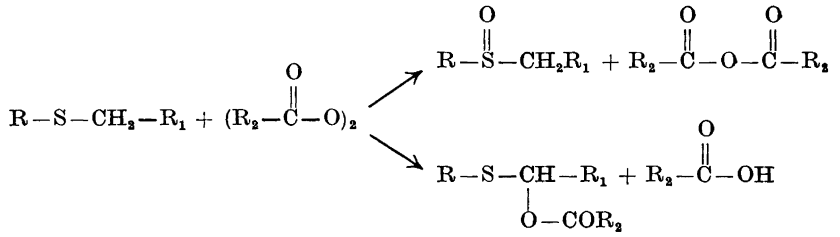

The Pummerer reaction [17–19] between a sulphoxide and an anhydride gives also an acyloxy compound:

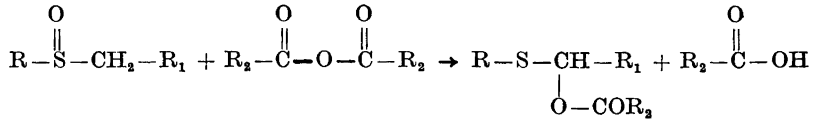

To complete the project previously outlined [20] we describe in this paper the results of the reaction of *t*-butyl perbenzoate with simple ethers and thioethers. The general idea of our earlier investigations has been to show that the presence of cuprous chloride is of primary importance in the decomposition rate of the perester as well as for stabilizing the formed radical of the substrate. We have confirmed earlier results that *t*-butyl perbenzoate decomposes slowly on heating alone, whereas the presence of cuprous chloride greatly accelerates rupture of the oxygen-oxygen bond. The stabilizing effect is easily understood by referring to eqns. 1—3. As has been pointed out by Cass for the case of simple ethers and by Horner for the case of sulphides the corresponding ether or sulphide radicals are relatively stable and the effect of the cuprous salt is supposed to prevent dimerization.

In our investigations, a dilute perbenzoate solution was added to the preheated substrate admixed with catalytic amounts of cuprous chloride and the consumption of the peroxy compound was then followed by titration or by infra-red measurements. Generally, the substrate was kept at a rather low

temperature in order to prevent decomposition of the benzoyloxy compound. After the benzoic acid, invariably formed, was extracted, the remainder was fractionated giving the acylals.

Johnston's and William's result [13] that anisole when heated with *t*-butyl peroxide, does not give any well-defined products is the only published example which we know where complications arise. We have therefore also investigated a series of compounds of similar type.

Phenyl alkyl ethers. Anisole IVa and phenetole IVb give the corresponding benzoyloxy compound Va and Vb smoothly.

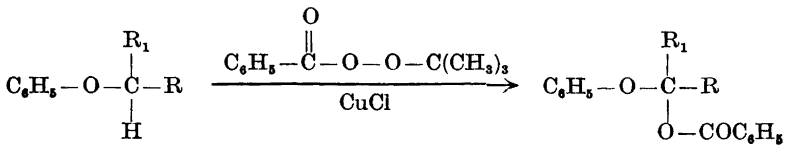

IVa	$R = R_1 = H$	Va	$R = R_1 = H$
IVb	$R = H$; $R_1 = CH_3$	Vb	$R = H$; $R_1 = CH_3$
IVc	$R = H$; $R_1 = n\text{-}C_4H_9$	Vc	$R = H$; $R_1 = n\text{-}C_4H_9$

In the case of anisole, only one structure is possible as the benzoyloxy group does not enter a common non-activated aromatic substrate. The position of the benzoyloxy group in Vb was established by hydrolysis which gave acetaldehyde. Furthermore we were unable to isolate any benzoate when phenyl *iso*propyl ether was used as substrate. As cumene [21] and 2-phenylbutane [22] do give the benzoyloxy compound, steric hindrance is apparently not the cause of this failure. We are rather inclined to believe that the instability of the benzoate formed causes it to decompose during the reaction. When phenyl *n*-amyl ether IVc was used as the substrate the benzoate Vc was obtained in rather low yield, and attempts to purify the compound for anlyses were futile.

Phenyl alkyl sulphides were also investigated and from phenyl methyl sulphide VIa and phenyl ethyl sulphide VIb the corresponding benzoates VIIa and VIIb were obtained.

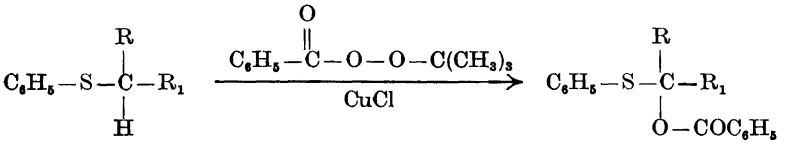

VIa	$R = R_1 = H$	VIIa	$R = R_1 = H$
VIb	$R = H$; $R_1 = CH_3$	VIIb	$R = H$; $R_1 = CH_3$

Phenyl *iso*propyl sulphide did not give any isolable benzoyloxy compound either. In the case of phenyl *n*-amyl sulphide (VI $R = H$; $R_1 = n\text{—}C_4H_9$) all attempts to purify the formed benzoate were futile. Decomposition occurred

and benzoic acid was split off, giving an unsaturated sulphide according to the following scheme:

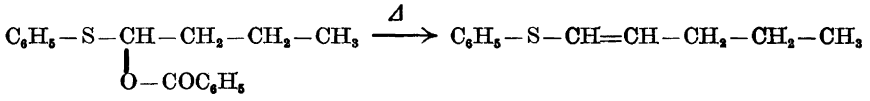

Phenyl allyl sulphide did react normally with *t*-butyl perbenzoate, infra-red measurements showing a benzoate to be present in the crude product, but all attempts to get a pure neutral product by distillation proved futile.

Di-alkyl ethers. All ethers except those having only one hydrogen on the α-carbons gave the corresponding benzoyloxy compound smoothly. Thus *t*-butyl *sec*-butyl ether and di-*iso*propyl ether gave no benzoate even when the reaction temperature was low. Quantitative yields of benzoic acid were isolated, indicating that the acylal formed is unstable and decomposes even at a moderate temperature. The allylic ethers investigated gave the benzoyloxy compound rapidly and although a few of them are quite unstable in air it was possible to get them in a pure state. *n*-Butyl allyl ether VIIIa thus gave the benzoate IXa,

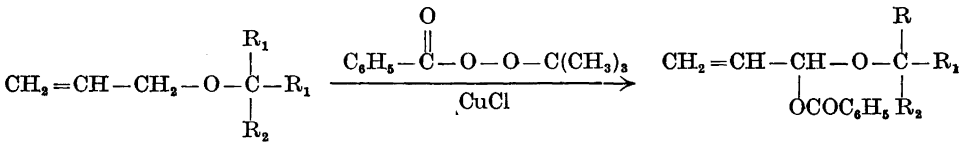

VIIIa	$R = R_1 = H$; $R_2 = C_3H_7$	IXa	$R = R_1 = H$; $R_2 = C_3H_7$
VIIIb	$R = H$; $R_1 = CH_3$; $R_2 = C_2H_5$	IXb	$R = H$; $R_1 = CH_3$; $R_2 = C_2H_5$
VIIIc	$R = R_1 = R_2 = CH_3$	IXc	$R = R_1 = R_2 = CH_3$

sec-butyl allyl ether VIIIb the corresponding acylal IXb and finally *t*-butyl allyl ether VIIIc the corresponding benzoyloxy compound IXc. As the allylic position is more activated than the other α-position, the hydrogen is preferrentially abstracted from here giving the corresponding acylal. Thus there is little doubt about the position of the benzoyloxy group in the case of IXa and IXc. However, some uncertainty was to be expected with respect to the *sec*-butyl allyl ether. As it is well-known that reactivity increases with decreasing C—H bond strength and increasing resonance stabilization of the radical produced, since hydrogen atoms are always substituted at rates which are in the order primary < secondary < tertiary, the tertiary hydrogen of the *sec*-butyl group could have been substituted besides one of the allylic hydrogens. However, the product isolated is certainly IXc as we have never been able to prepare a tertiary benzoate, though possibly the primary product could have been a mixture.

With di-*n*-butyl ether we were able to isolate the α-benzoyloxy compound X in 50 % yield [15] after a nine hours long reaction time.

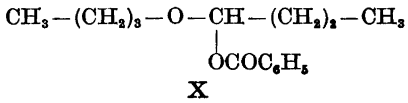

X

A careful investigation of the fore-runs revealed that a 15 % yield of an *a*-butoxy compound XI* also had been formed.

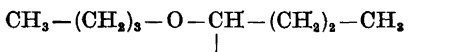

XIa R = *n*-C_4H_9 ; XIb R = *t*-C_4H_9

The benzoyloxy groups is supposed to substitute an *a*-hydrogen first which compound then reacts with *t*-butanol to give the acetal XIb. We have partly confirmed this as X when heated with *t*-butanol gives the *t*-butoxy compound XIb. By heating X for 24—30 h benzoic acid is eliminated but an unsaturated ether is not found and only ill defined products were formed. This indicates that the Sosnovsky mechanism (route A) might be an over simplification and before his interpretation is accepted a reinvestigation is needed.

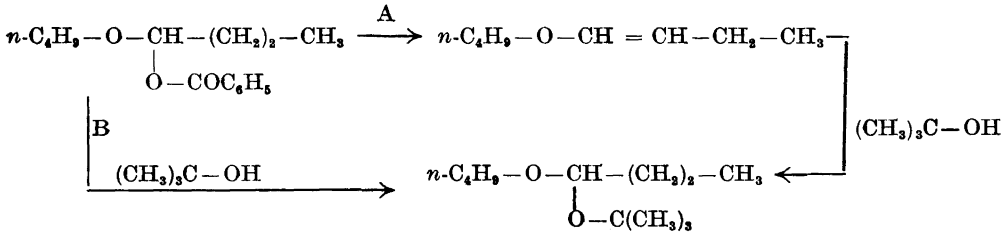

Since it has been shown in an earlier investigation [2] that a benzoyloxy group is displaced by an alkoxy group, route B might be considered as an alternative to route A.

Di-alkyl sulphides. *t*-Butyl ethyl sulphide XII and di- *n*-butyl sulphide XIV smoothly give the corresponding benzoyloxy compound XIII and XV.

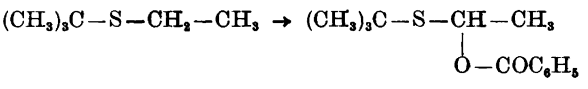

XII XIII

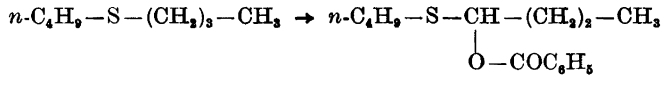

XIV XV

When *t*-butyl *iso*propyl sulphide was reacted with *t*-butyl perbenzoate in the presence of cuprous chloride, quantitative yields of benzoic acid was isolated. In contradistinction to the findings with the corresponding oxygen analog, the benzoyloxy group in XV is not displaced by the alkoxy group when

* *Added in proof:* Lawesson and Berglund, (*Arkiv Kemi* (1961), *in press*) have shown that this acetal is XIa,

heated with *t*-butanol or any other alcohol. Furthermore, when heated in benzene, benzoic acid is split off and an unsaturated sulphide XVI is formed.

$$CH_3(CH_2)_3-S-\underset{\displaystyle O-CO-C_6H_5}{\underset{|}{CH}}-(CH_2)_2CH_3 \xrightarrow{\Delta} CH_3(CH_2)_3-S-CH=CH-CH_2CH_3$$

XVI

EXPERIMENTAL

The reactions described were carried out in an atmosphere of nitrogen. All ethers and sulphides were distilled prior to use. Commercial (Light) *t*-butyl perbenzoate ($n_D^{20} = 1.5000$) was used. The progress of the reactions was followed either by titration according to the method of Silbert and Swern [23] or by IR-measurements. The infra-red spectra were recorded either on a Perkin-Elmer Model 21, double beam spectrophotometer or on a Perkin-Elmer Infracord. The analyses were made by Alfred Bernhardt, Mülheim (Ruhr), and The Analytical Department, Uppsala University. Boiling and melting points are uncorrected.

Starting materials

Preparation of ethers and sulphides. The anisole, phenetole, *n*-butyl ether and *iso*-propyl ether used were of commercial grade. Phenyl−S−R (R = CH_3, C_2H_5, *i*-C_3H_7, $CH_2-CH=CH_2$, *n*-C_5H_{11}) were prepared by adding the appropriate chloride to sodium thiophenolate [24]. Phenyl−O−R′(R′ = *i*-C_5H_7, *n*-C_5H_{11}) were made by reacting the appropriate chlorides with sodium phenolate. *t*-Butyl−S−R″ (R″ = C_2H_5, *i*-C_3H_7) was prepared in a manner analogous to the synthesis of phenyl *t*-butyl sulphide by Ipatieff *et al.*[25] *t*-Butyl−O−R‴ (R‴ = *sec*−C_4H_9, *i*-C_4H_9) was prepared according to Lawesson and Yang [26] whilst allyl−O−R⁗ (R⁗ = *n*-C_4H_9, *sec*-C_4H_9) according to Talley *et al.*[27] Di-*n*-butyl sulphide was prepared by adding *n*-butyl bromide to *n*-butyl mercaptid and *t*-butyl allyl ether according to the general method by Norris and Rigby [28].

Preparation of t-butyl-sec-butyl ether. *t*-Butylperbenzoate (0.3 mole) in 200 ml of ether was slowly added to a vigorously stirred solution of *sec*-butylmagnesium bromide (0.5 mole in 200 ml of ether) at 0°−5°. Stirring was continued overnight, after which the mixture was poured into ice-water containing hydrochloric acid. After extraction with ether, washing with 2 M NaOH and water, the ether phase was dried. Distillation gave 21 g (54 %) of *t*-butyl *sec*-butyl ether $n_D^{20} = 1.3972$, b.p. 114−115°. (C 73.40; H 14.08. Calc. C 73.78; H 13.92.)

Preparation of t-butyl isobutyl ether. *t*-Butyl perbenzoate (0.4 mole) in 100 ml of ether was dropped to a Grignard reagent (0.6 mole) in 500 ml of ether at 0−5°. The work-up was performed as in the case of *t*-butyl *sec*-butyl ether. 30 g, yield 58 %, b.p. 110−111°C, $n_D^{20} = 1.3912$. (C 73.72; H 14.00. Calc. C 73.78; H 13.92.)

Preparation of t-butyl allyl ether. 174 g of allyl alcohol was added to a cooled mixture of 29.4 ml conc. sulphuric acid and 296 ml of water. The flask was warmed to 70° and *t*-butyl alcohol (30 ml) was added dropwise. The product was distilled slowly, the distillation temperature being maintained at 80° by the occasional addition of *t*-butanol, a total of 105 ml being added. The product was washed 15 times with water. When all the alcohol was removed the two layers separated immediately. The product was dried over Na_2SO_4, warmed with sodium to reflux temperature for one hour and distilled. 28 g of *t*-butyl allyl ether, b.p. 100°, $n_D^{20} = 1.4078$, was obtained. [Lit.[27] $n_D^{20} = 1.4011$].

Preparation of t-butyl ethyl sulphide. Into an ice-cold mixture of 220 g of sulphuric acid and 75 ml of water in a 500 ml flask equipped with a stirrer, gas-inlet tube and a reflux condenser was bubbled 15 g (0.26 mole) of *iso*butylene, followed by the dropwise addition of 15 g (0.21 mole) of ethyl mercaptan. The mixture was allowed to stand in the ice bath for half an hour whereupon crushed ice was added. The mixture was extracted three times with ether. The combined ether extracts were washed with 2 M NaOH and water

until neutral, dried over sodium sulphate and the ether driven off. 14 g (57 %) of the sulphide, b.p. 120°, $n_D^{20} = 1.4429$, was obtained. [Lit. values [29], b.p. 120.4°, $n_D^{25} = 1.4390$].

Preparation of t-butyl isopropyl sulphide. 35 g (0.61 mole) of *iso*butylene was added to a mixture of 220 g of conc. H_2SO_4 and 75 g of water in the apparatus described above, followed by 30 g (0.4 mole) of *iso*propyl mercaptan. The neutral and dry product was distilled giving 37 g (70 %) of the sulphide, b.p. 129—131°, $n_D^{20} = 1.4412$.

Socony-Vacuum Laboratories report b.p. 40—42°/31—32 mm Hg.

Reactions with *t*-butyl perbenzoate

The reaction with anisole. To a flask containing 50 ml (0.5 mole) of redistilled anisole ($n_D^{20} = 1.5178$), 300 ml of dry benzene and 0.1 g of CuCl, was added 40 ml (0.2 mole) of *t*-butyl perbenzoate during ½ h. The mixture was maintained at gentle reflux for 23 h, when it was extracted with 2 M NaOH and washed with water till neutral. The alkaline washings gave 11.5 g of benzoic acid. Distillation of the dried organic solution gave 34 g of anisole, b.p. 60—65° / 20 mm Hg ($n_D^{20} = 1.5180$), 2.3 g of benzoic acid, b.p. 80—100° / 0.1 mm Hg and the benzoyloxy compound, b.p. 135—140°/0.1 mm Hg. The last fraction solidified and part of it was recrystallized from petroleum ether. M.p. 35—36°. Yield 23 %. Distillation residue, 13 g. (C 73.74; H 5.35. Calc. C 73.67; H 5.30.)

The reaction with phenetole. 40 ml (0.2 mole) of *t*-butyl perbenzoate in 50 ml of benzene was added dropwise to 65 g (0.53 mole) of redistilled phenetole ($n_D^{20} = 1.5065$) in 300 ml of benzene and 0.1 g of CuCl. The solution was maintained at gentle reflux for 20 h. After washing and drying in the usual manner 9.8 g of benzoic acid precipitated out. After the benzene and excess of phenetole had distilled off, 18 g (37 %) of *o*-benzoyloxy phenetole, b.p. 108—110°/0.05 mm Hg, $n_D^{20} = 1.5512$, was obtained. (C 74.31; H 5.80. Calc. C 74.36; H 5.83.)

Hydrolysis. To a 4 g sample of Vb was added 50 ml of methanol and hydrochloric acid in slight excess. The mixture was allowed to stand for half an hour at 20° whereupon a solution of 2,4-dintrophenylhydrazine in hydrochloric acid was added. The mixture was shaken for 60 min, cooled and filtered. Acetaldehyde 2,4-dinitrophenyl hydrazone was obtained in 71 % yield, m.p. 165—167° after recrystallization from ethanol. Mixed melting point with an authentic sample of the acetaldehyde derivative showed no depression. A strong smell of phenol was apparent in the aqueous phase.

The reaction with phenyl methyl sulphide. 40 ml (0.2 mole) of *t*-butyl perbenzoate was added dropwise during 50 min. to a mixture of 150 ml of benzene, 35 g (0.28 mole) of redistilled thioanisole ($n_D^{20} = 1.5868$) and 0.1 g of CuCl maintained at 70—75°. The reaction was complete after 5.5 h. The alkaline washings gave 3.4 g of benzoic acid. After drying and distilling off the benzene and excess of thioanisole, 23 g (47 %) of the benzoyloxy compound, b.p. 150—155°/0.15 mm Hg, $n_D^{20} = 1.5978$, was obtained. Horner and Jürgens [16] had a b.p. of 145—146°/0.5 mm Hg.

The reaction with phenyl ethyl sulphide. 200 ml of benzene, 39 g (0.28 mole) of redistilled phenyl ethyl sulphide ($n_D^{20} = 1.5669$) and 0.1 g of CuCl were placed in the reaction flask and maintained at an oil bath temperature of 110°. 30 ml (0.15 mole) of *t*-butylperbenzoate was added dropwise during 55 min. After 2.25 h, the reaction was complete. The mixture was worked up as usual, giving 4.2 g of benzoic acid from the alkaline washings. Distillation gave 24 g (62 %) of the benzoyloxy compound, b.p. 121—122°/0.1 mm Hg, $n_D^{20} = 1.5823$. (C 69.90; H 5.58; S 12.36. Calc. C 69.75; H 5.46; S 12.39.)

The reaction with phenyl n-amyl sulphide. *t*-Butyl perbenzoate (0.2 mole) was added during 30 min. to a refluxing mixture of 150 ml of benzene, 68 g (0.38 mole) of phenyl *n*-amyl sulphide ($n_D^{20} = 1.5397$) and 0.1 g of cuprous chloride. The reaction was complete after heating for 13 h at an oil bath temperature of 100°. The alkaline washings gave 6.3 g of benzoic acid. After distilling off the benzene and excess of sulphide at reduced pressure, the benzoyloxy compound decomposed at a distilling temperature of 100—120°/0.1 mm Hg, and 27 g of distillate were collected in the receiver. The distillate was taken up in

ether, washed with 2 M NaOH, then with water until neutral and dried. 9.1 g of benzoic acid was recovered from the alkaline washing. Distillation of the ether phase gave 12.5 g (35 %) of the unsaturated sulphide, b.p. 72—73°/0.3 mm Hg, n_D^{20} = 1.5650. (C 74.20; H 7.76; S 17.83. Calc. C 74.13; H 7.92; S 17.96.)

The reaction with t-butyl isobutyl ether. 0.1 mole of *t*-butyl perbenzoate was added during 20 min. to a mixture of 200 ml of benzene, 23 g (0.177 mole) of redistilled *t*-butyl *iso*butyl ether (n_D^{20} = 1.3912) and 0.1 g of cuprous chloride, maintained at an oil bath temperature of 120°. The reaction was complete, after 16 h, whereupon the mixture was worked up, giving 7 g of benzoic acid. The neutral and dry benzene solution was distilled giving 12 g of *t*-butyl *iso*butyl ether and 8.3 g (33 %) of the benzoyloxy compound, b.p. 53°/1.5 mm Hg, n_D^{20} = 1.5042. (C 71.17; H 8.60. Calc. C 71.97; H 8.86.)

The reaction with n-butyl allyl ether. *t*-Butyl perbenzoate (0.2 mole) was added dropwise to 51 g (0.45 mole) of *n*-butyl allyl ether and 0.1 g of cuprous chloride in 300 ml of benzene, maintained at 95°. Th reaction mixture was heated for 2 h, after which time no perester was present. Benzoic acid (12.5 g) was recovered from the alkaline washings. The neutral and dry benzene solution was distilled giving 16.6 g (35 %) of the benzoyloxy compound, b.p. 96—99°/0.05 mm Hg, n_D^{20} = 1.4792. (C 71.56; H 7.77. Calc. C 71.77; H 7.74.)

The reaction with sec-butyl allyl ether. *t*-Butyl perbenzoate (0.2 mole) was added during 30 min. to a refluxing mixture of 300 ml of benzene, 48 g (0.42 mole) of *sec*-butyl allyl ether and 0.1 g of cuprous chloride. After refluxing for 5.5 h at an oil bath temperature of 100°, the mixture was worked up as usual giving 7.5 g of benzoic acid. After distilling off the benzene and excess *sec*-butyl allyl ether, 20 g (43 %) of the benzoyloxy compound, b.p. 84—86°/0.05 mm Hg, n_D^{20} = 1.4968, was obtained. (C 71.27; H 7.68. Calc. C 71.77; H 7.74.)

The reaction with t-butyl allyl ether. To 28 g (0.24 mole) of *t*-butyl allyl ether (n_D^{20} = 1.4078) and 0.1 g of cuprous chloride in 150 ml dry benzene, maintained at an oil bath temperature of 105°, *t*-butyl perbenzoate (0.1 mole) in 25 ml benzene was added during 35 min. After heating for 2 h, titration showed that no perester was present. The mixture was worked up as usual, yielding 0.5 g benzoic acid. Fractionation gave 17 g (74 %) of the benzoyloxy compound, b.p. 94—96°/0.3 mm Hg, n_D^{20} = 1.4863. (C 71.24; H 7.45; Calc. C 71.77; H 7.74.)

The reaction with di-n-butyl ether. Into a flask containing 300 ml of dry benzene was introduced 52 g (0.4 mole) of di-*n*-butyl ether (n_D^{20} = 1.4205) and 0.1 g of cuprous chloride. *t*-Butyl perbenzoate (0.2 mole) dissolved in 50 ml of benzene was added during 10 min. and the mixture maintained at 90° for 9 h. After washing with 2 M sodium hydroxide and water in the usual way, the organic phase was dried over magnesium sulphate. The alkaline washings yielded 11 g of benzoic acid. The organic phase was fractionated under vacuum to give 6 g (15 %) of *a*-butoxy *n*-butyl ether, b.p. 59—60°/0.3 mm Hg, n_D^{20} = 1.4182. (C 71.23; H 12.75. Calc. C 71.23; H 12.95). Sosnovsky gives for 1-*n*-butoxy-1-*t*-butoxy butane b.p. 100°/17 mm Hg, n_D^{25} = 1.4148.

25 g (50 %) of a higher boiling fraction consisting of *a*-benzoyloxy di-*n*-butyl ether, b.p. 97—98°/0.3 mm Hg, n_D^{20} = 1.4837, was then obtained. (C 72.25; H 8.91. Calc. C 71.97; H 8.86.)

Decomposition of a-benzoyloxy di-n-butyl ether in t-butanol. 21 g (0.084 mole) of the benzoyloxy compound was heated during 15 h at 140° in 18 g (0.24 mole) of *t*-butanol. The solution was then dissolved in ether and extracted with 2 M NaOH, from which 7.5 g benzoic acid was recovered. The neutral and dry ether solution was fractionated giving 8.5 g (50 %) of the *a*-*t*-butoxy di-*n*-butyl ether, b.p. 92°/10 mm Hg, n_D^{20} = 1.4183. (C 71.34; H 13.00. Calc. C 71.23; H 12.95.)

The reaction with t-butyl ethyl sulphide. 0.1 mole of *t*-butyl perbenzoate was added dropwise to a mixture of 200 ml of benzene, 14 g (0.12 mole) of *t*-butyl ethyl sulphide (n_D^{20} = 1.4429) and 0.1 g of cuprous chloride at 125°. After 6.5 h, the reaction was complete and the mixture worked up as usual yielding 5.6 g of benzoic acid. The neutral

and dry benzene solution was distilled giving 12 g (50 %) of benzoate, b.p. 93—95°/0.4 mm Hg, n_D^{20} = 1.5216. (C 65.90; H 7.46; S 13.31. Calc. C 65.51; H 7.60; S 13.43.)

The reaction with di-n-butyl sulphide. 40 ml (0.2 mole) of *t*-butyl perbenzoate in 50 ml of benzene was added during 40 min. to a mixture of 200 ml of dry benzene, 0.1 g of cuprous chloride and 60 g (0.41 mole) of redistilled di-*n*-butyl sulphide (n_D^{20} = 1.4540) at 80°. After 3 h the mixture was worked up as usual, giving 3.6 g of benzoic acid After distilling off the benzene and the excess of sulphide 35 g (66 %) of the benzoyloxy compound, b.p. 108—109°/0.2 mm Hg, was obtained. (C 67.57; H 8.09; S 11.98. Calc. C 67.63; H 8.31; S 12.02.)

Decomposition of α-benzoyloxy di-n-butyl sulphide. a) 8.5 g (0.032 mole) of α-benzoyloxy di-*n*-butyl sulphide was refluxed during 6 h with 30 ml abs. ethanol. The ethanol was then removed under vacuum, the residue taken up in ether and the benzoic acid (3.8 g) extracted with 2 M NaOH. Distillation gave 3 g of a compound, b.p. 76—79°/10 mm Hg, n_D^{20} = 1.4730. Horner and Kaiser [17] report b.p. 19.1°/0.3 mm Hg and n_D^{20} = 1.4750 for $C_4H_9-S-CH=CH-C_2H_5$.

b) 17 g (0.064 mole) of the benzoyloxy compound was refluxed with 75 ml of *t*-butanol during 9 h and the mixture worked up as above. 7.3 g of the unsaturated sulphide, b.p. 83°/15 mm Hg, n_D^{20} = 1.4741, was obtained.

The reaction of t-butyl perbenzoate with n-butyl allyl sulphide. 0.2 mole of *t*-butyl perbenzoate was added during 1 h to a mixture of 200 ml of benzene, 53 g (0.4 mole) of redistilled *n*-butyl allyl sulphide and 0.1 g of cuprous chloride, maintained at gentle reflux temperature (80°). The reaction was complete after 2 h. The mixture was worked up as usual, giving 4.3 g of benzoic acid. Fractionation gave 31 g (61 %) of the benzoyloxy compound, b.p. 122—124°/0.3 mm Hg, n_D^{20} = 1.5380. (C 66.53; H 6.71; S 12.61. Calc. C 67.17; H 7.25; S 12.79.)

Thanks are due to Professor A. Fredga for his keen interest in this work. A grant from *Magnus Bergwalls Stiftelse* is gratefully acknowledged.

REFERENCES

1. Lawesson, S.-O. and Berglund, C. *Arkiv Kemi* (1960). **16** (1960) 287.
2. Lawesson, S.-O. and Berglund, C. *Acta Chem. Scand.* **15** (1961) 36.
3. Hurd, C. D. and Green, F. O. *J. Am. Chem. Soc.* **63** (1941) 2201.
4. Huang, R.-L. and Si-Hoe, S. S. in Waters, W. A. *Vistas in Free Radical Chemistry*, Pergamon Press, London 1959, p. 242.
5. Lawesson, S.-O. and Busch, T. *To be published.*
6. Price, C. C. and Zomlefer, J. *J. Am. Chem. Soc.* **72** (1950) 14.
7. Price, C. C. and Morita, H. *J. Am. Chem. Soc.* **75** (1953) 4747.
8. Cass, W. E. *J. Am. Chem. Soc.* **68** (1946) 1976.
9. Cass, W. E. *J. Am. Chem. Soc.* **69** (1947) 500.
10. Cass, W. E. *J. Am. Chem. Soc.* **72** (1950) 4915.
11. Nozaki, K. and Bartlett, P. D. *J. Am. Chem. Soc.* **68** (1946) 1686.
12. Denney, D. B. and Feig, G. *J. Am. Chem. Soc.* **81** (1959) 5322.
13. Johnston, K. M. and Williams, G. H. *J. Chem. Soc.* **1960** 1168.
14. Sosnovsky, G. *J. Org. Chem.* **25** (1960) 874.
15. Lawesson, S.-O., Berglund, C. and Grönwall, S. *Acta Chem. Scand.* **14** (1960) 944.
16. Horner, L. and Jürgens, E. *Ann.* **602** (1957) 135.
17. Horner, L. and Kaiser, P. *Ann.* **626** (1959) 19.
18. Horner, L. *Ann.* **631** (1960) 198.
19. Pummerer, R. *Ber.* **43** (1910) 1401.
20. Lawesson, S.-O. and Berglund, C. *Tetrahedron Letters* **2** (1960) 4.
21. Kharasch, M. S. and Fono, A. *J. Org. Chem.* **23** (1958) 324.
22. Hallgarten, P. A. *Personal communication.*

23. Silbert, L. S. and Swern, D. *Anal. Chem.* **30** (1958) 385.
24. Reid, E. E. *Organic Chemistry of bivalent sulfur*, Vol. II. Chemical Publication Co. New York 1960.
25. Ipatieff, V. N., Pines, H. and Friedman, B. S. *J. Am. Chem. Soc.* **60** (1938) 2731.
26. Lawesson, S.-O. and Yang, N.C. *J. Am. Chem. Soc.* **81** (1959) 4230.
27. Talley, E. A., Hunter, A. S. and Yanovsky, E. *J. Am. Chem. Soc.* **73** (1951) 3528.
28. Norris, J. F. and Rigby, G. W. *J. Am. Chem. Soc.* **54** (1932) 2088.
29. McAllan, D. T., Cullum, T. V., Dean, R. A. and Fidler, F. A. *J. Am. Chem. Soc.* **73** (1951) 3627.

Received September 13,1960.

ACTA CHEMICA SCANDINAVICA 15 (1961) 260–270

Studies on Peroxy Compounds XI *

The Introduction of the *t*-Butoxy- and Benzoyloxy Groups into Malonic Esters — a Novel Method for the Preparation of Tartronates

SVEN-OLOV LAWESSON, TAMARA BUSCH and (in part) CURT BERGLUND

Department of Organic Chemistry, Chemical Institute, University of Uppsala, Uppsala, Sweden

In contrast to reactions in alcoholic solutions, the sodium derivative of diethyl malonate in benzene gives with *t*-butyl peracetate, diethyl O-*t*-butyl tartronate and with benzoyl peroxide, diethyl O-benzoyl tartronate together with small amounts of diethyl dibenzoyloxy malonate. Substituted sodium malonates give no O-*t*-butyl tartronates with peresters but with benzoyl peroxide, the corresponding benzoyl tartronates are formed smoothly. A representative series of alkyl, aryl, aralkyl and chloro-substituted diethyl malonates have been shown to give high yields of benzoyl tartronates which, in a few cases, have been characterized as diethyl tartronates and tartronic acids.

In a recent investigation [1] of the reactions between Grignard reagents and peroxy compounds, it was found that in the case of *t*-butyl perbenzoate the oxygen-oxygen bond is ruptured, thus affording a novel and convenient method for the preparation of *t*-butyl ethers, according to the following scheme:

$$RMgX + C_6H_5\overset{\overset{O}{\|}}{C}-O-O-C(CH_3)_3 \longrightarrow RO-C(CH_3)_3 \qquad (1)$$

Similarly, when benzoyl peroxide was allowed to react with Grignard reagents, the oxygen-oxygen bond seems to be initially ruptured. As a logical continuation of this investigation, we felt that instead of using organo-metallics, enolates or more precisely the sodium derivative of so called active methylene compounds, ought to be investigated. The *t*-butoxy group would thus be introduced into malonates to give O-*t*-butyl tartronates, in an analogous

* Part X. Lawesson, S.-O. and Berglund, C. *Angew. Chem.* **73** (1961) 65.

way to the ether synthesis (eqn. 1). Such types of compounds cannot be prepared by reacting a sodium alkoxide with diethyl bromomalonate, since this gives tetraethyl ethanecarboxylate instead. However, simple diethyl *n*-alkyl tartronates have been prepared in recent years by the following method [2–4]:

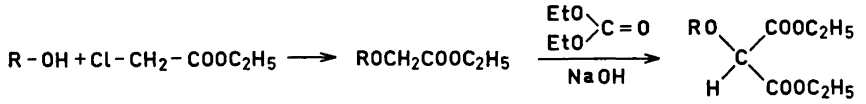

(2)

$R = CH_3, C_2H_5, \underline{n}\text{-}C_3H_7, \underline{n}\text{-}C_4H_9, C_6H_5CH_2.$

We have found that by reacting *t*-butyl peracetate with the sodium compound of diethyl malonate, diethyl O-*t*-butyl tartronate was obtained in 27 % yield [5], in addition to tar and polymeric products. Under similar conditions, *t*-butyl perbenzoate gave only ill-defined products. We also tried this reaction with substituted malonic esters but no reaction product could be isolated. Thus, attempts at introducing the *t*-butoxy group into diethyl malonate under the described conditions do not seem to hold much promise nor are they applicable to preparative purposes. When we used ethanol as solvent, the malonate was always recovered unchanged, and ethyl benzoate was isolated, indicating that the peroxy compound reacted faster with the sodium alcoholate than with the sodium malonate. Milas *et al.*[6] similarly obtained methyl benzoate and *t*-butyl hydroperoxide when *t*-butyl perbenzoate was treated with sodium methoxide.

Since the reactions between *t*-butyl peracetate (perbenzoate) and sodium compounds of malonates were sluggish, we turned our attention to benzoyl peroxide. It has long been known that when benzoyl peroxide is treated with sodium alkoxide in ethanol, perbenzoic acid is formed; because of this, and also due to certain preliminary experiments, ethanol was considered unsuitable as the reaction medium. Tetrahydrofuran was not used as solvent because benzoyl peroxide underwent induced decomposition in it. Since benzene was found to be a convenient solvent, it was used in all subsequent experiments. We found that the oxygen-oxygen bond in benzoyl peroxide is split by the sodium compound according to the following [7]:

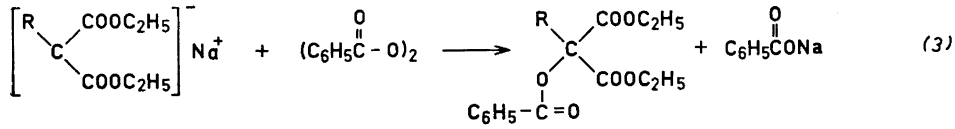

(3)

In an earlier work [8] with ethyl benzoylacetate the same observation had also been made.

The benzoyl tartronic esters were prepared from benzoyl peroxide and the sodium derivative of malonic ester as follows. Sodium hydride and malonic ester were warmed together in benzene, the solution cooled to 0—4° and treated dropwise with benzoyl peroxide in benzene; after stirring overnight, the ben-

zoic acid was extracted with alkali, the benzene distilled off and the residue fractionated. The malonate is always used in excess, hence generally no peroxide is left at the end of the reaction. When necessary, unreacted peroxides are destroeyd by treatment with sodium iodide in glacial acetic acid containing catalytic amounts of ferrous salt.

The O-benzoyl tartronates are stable compounds which, when stored for 1—2 years in closed vials, do not seem to decompose. They occur as very viscous liquids and might be suitable as plastizisers. When heated with glacial acetic acid, no exchange of acyloxy groups was observed, nor was any other reaction detected.

A single attempt to react benzoyl peroxide with ethoxymagnesium malonate in ether, according to Lund, was unsuccessful. Whereas no tartronate was detected, some decomposition of the benzoyl peroxide was observed.

Acyloxy compounds of malonates have been prepared earlier. Conrad and Brückner [9] reacted diethyl bromomalonate with potassium acetate in absolute ethanol and obtained diethyl acetyl tartronate. Dimroth and Schweizer [10] found that when diethyl malonate is treated with lead tetraacetate, the acetoxy group is easily introduced. Diethyl benzoyl tartronate was first prepared by Jackson and Phinney [11] by heating diethyl tartronate with benzoyl chloride under pressure. These authors gave no analytical data as they had difficulties with the final purification. Cope and Field [12], during an investigation on the reactions of Grignard reagents with diethyl mesoxalate acording to eqn. 4, have also prepared diethyl O-benzoyl-1-naphthyl tartronate from diethyl 1-naphthyl tartronate according to Jackson and Phinney's method.

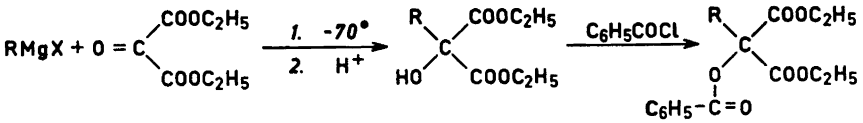

(4)

We have prepared diethyl O-benzoyl 1-naphthyl tartronate in almost quantitative yields according to eqn. 3 (R = 1-naphthyl). Although elementary analyses and molecular weight determinations were theoretical, we found a slightly higher melting point than did Cope and Field, and the mixed melting point with their compound showed a small depression. The infrared spectrum showed minor differences, too. We believe that Cope's and our compounds are identical but that crystal effects for instance might account for the differences observed.

We have prepared a series of benzoyl tartronates with various substituents and it was observed that good yields of the corresponding tartronates were obtained almost irrespective of the size of the substituent. Unlike the case with substituted diethyl malonate, the reaction between the unsubstituted compound and benzoyl peroxide seemed at first to be anomalous. Carbon dioxide was evolved and quantitative yields of benzoic acid were not isolated, indicating that in this case a free-radical reaction might be taking place. It is well-known that the scission of benzoyl peroxide is a two-step process and if a free-radical mechanism is involved a sequence of reactions could be

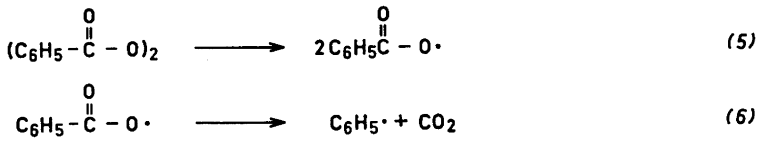

(5)

(6)

easily postulated. However, eventually we found that if redistilled diethyl malonate and twice recrystallized benzoyl peroxide were used, no gas evolution occurs and quantitative yields of benzoic acid are isolated. Both the monosubstituted malonate (main product) and the disubstituted one are produced. Since no gas was evolved when the sodium derivative of substituted malonates reacts with benzoyl peroxide, a conventional free-radical mechanism involving the benzoyloxy radical might be questioned. The reaction may instead be formulated in the following way:

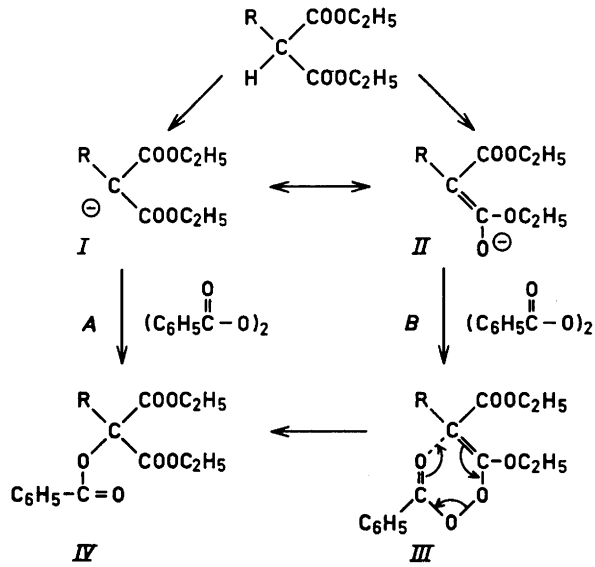

Scheme 1.

It is known from the work by Walling and especially by Denney that reactions of nucleophiles (phosphines [13], phenoles [14], amines [15]) proceed by initial displacement on one of the peroxide oxygens, the oxygen-oxygen bond being the weakest in the molecule. We believe that either form of the malonate, I or II (Scheme 1) will react according to route A or B. In route A the carbanion I will attack the oxygen-oxygen bond directly, giving the tartronate IV. The transition state III in route B might be formed by a nucleophilic attack of the enolate II on the oxygen-oxygen bond and is an unstable perester which then forms the tartronate IV by an intramolecular rearrangement.

Finally it must be stressed that from a mechanistic point of view a benzoyloxy radical is not eliminated but as this question may not be answered without a study with isotopic benzoyl peroxide (carbonyl ^{18}O), this matter will be reserved for a further publication.

Besides the alkyl and aryl substituted malonic esters we have also investigated some other compounds in this series. Tricarbethoxymethane reacted violently with sodium hydride in benzene and gave a sodium derivative which, with benzoyl peroxide, gave the corresponding benzoate. Diethyl benzoyl malonate did not react with sodium hydride in benzene. The sodium hydride became deactivated, possibly due to the hydride being covered with a layer of the initially formed sodium compound. Diethyl O-benzoyl tartronate reacted rapidly with sodium hydride but when treated with benzoyl peroxide, only an ill-defined thick oil was initially isolated in low yield. After some time diethyl dibenzoyloxy malonate cyrstallized out. When the above mentioned sodium tartronate was allowed to react with benzoyl chloride, however, the benzoyl group was introduced in high yield.

Because of the difficulties at first encountered with the unsubstituted malonates, which, if not absolutely pure, caused induced decomposition of the peroxide, resulting in undesirable side-reactions and reduced yields, we tried working with diethyl chloro malonate, intending to prepare the tartronates according to the following scheme:

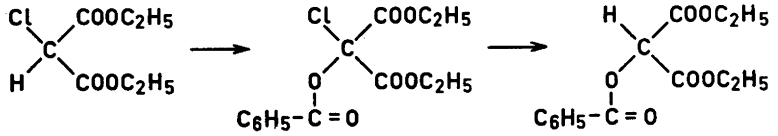

(7)

Diethyl chloromalonate reacted rapidly with sodium hydride without any dechlorination and the reaction with benzoyl peroxide ran smoothly to give the corresponding O-benzoyl tartronate in high yield. Elimination of chlorine from mono-chloro and dichloro malonates with Grignard reagents has been tried earlier [16,17] but with little success. We found, however, that a Grignard reagent is very convenient in our case as it neither attacked the ester group nor did it cause other side-reactions, possibly because addition to the carbonyl group occurs very slowly or because of steric hindrance. When phenylmagnesium bromide was used, chlorobenzene was isolated according to eqn. 8.

It is known that in the case of 1-halosubstituted ketones, the elimination proceeds through an intermediate enolate and it is possible that the halogen

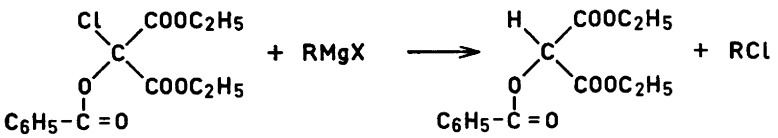

(8)

$R = C_6H_5$; X = Br.

elimination in this case also proceeds *via* a somewhat similar mechanism involving a six-membered ring as an intermediate according to scheme 2.

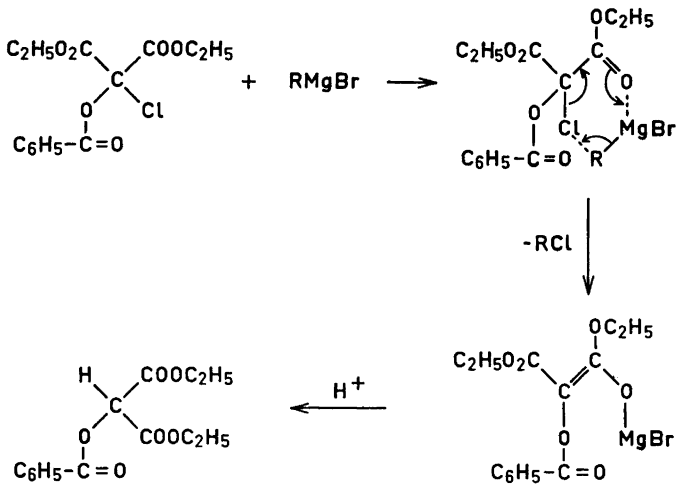

Scheme 2.

In order to characterize these new benzoyl tartronates further and to explore the possibilities of using this method for the preparation of tartronates and tartronic acids, we investigated the hydrolysis of some of these compounds.

Acids and bases are unsuitable for the hydrolysis of O-benzoyl tartronates since mixtures of acids are formed which are difficult to separate. However, by alcoholysis reesterification will take place and ethyl benzoate is easily distilled off from the tartronate. In some cases the tartronate was isolated and shown to be an authentic hydroxy malonate. The tartronic acids were easily prepared from the tartronate (which usually were not isolated) by acid hydrolysis. Decarboxylation occurred when diethyl O-benzoyl phenyl tartronate was alcoholyzed and then hydrolyzed, giving mandelic acid as the sole product. From the work of Cope and McElvain [18] it is known that alcoholic sodium ethoxide smoothly cleaves dialkylated malonic esters into the substituted acetic ester according to two possible routes. In our case, however, we cannot as yet say by which mechanism is the cleavage of the benzoyl tartronates effected by the ethoxide ion.

EXPERIMENTAL

The reactions between benzoyl peroxide and the sodium derivative of malonates were carried out in an atmosphere from which moisture was rigidly excluded. Benzoyl peroxide was recrystallized at low temperature from methanol and chloroform. *t*-Butylperacetate (Lupersol ≠ 7) was supplied by Lucidol Division, Wallace and Tiernan, Inc., Buffalo, N.Y. and used without further purification. The experiments with Grignard reagents were carried out in nitrogen, and pure magnesium (Dow) was used. The sodium hydride (Kebo) was the ordinary laboratory reagent. The gas generated during the reaction was collected over saturated aqueous sodium chloride, saturated with carbon dioxide.

The infra-red spectra were recorded on a Perkin-Elmer Model 21, double beam spectrophotometer. The analyses were made by Dr. Alfred Bernhardt, Mülheim (Ruhr) and at The Analytical Department of Uppsala University. Boiling and melting points are uncorrected.

Starting material. Commercial diethyl malonate was used after distillation (n_D^{20} = 1.4143).

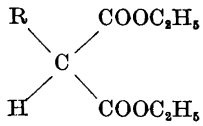

R	B.p.°C	mm Hg	n_D^{20}
CH_3 [19]	96	15	1.4178
C_2H_5 [20]	97	15	1.4178
n-C_3H_7 [21]	100	10	1.4219
allyl [22]	117	10	1.4349
n-C_4H_9 [23]	113	12	1.4243
i-C_4H_9 [24]	112–114	12	1.4223
$C_6H_5CH_2$ [25]	169	12	1.4869
C_6H_5 [26]	160	10	1.4918
1-$C_{10}H_8$ [27]	59–60*	—	—
Cl [28]	118	16	1.4247
$-COOC_2H_5$ [29]	130	10	1.4297

* M.p.

The substituted malonates (R = ethyl, allyl, *n*-propyl, *n*-butyl, *iso*butyl, benzyl) were prepared by alkylation of diethyl malonate in the usual way. The methyl, phenyl and 1-naphthyl derivatives were prepared *via* the corresponding ethoxalyl derivative; diethyl chloromalonate [28] was prepared by chlorinating diethyl malonate with sulphuryl chloride. Tricarbethoxymethane [29] was prepared from sodium malonate and ethyl chloroformate and diethyl oxomalonate [30], b.p. 103–108°C/15 mm Hg, n_D^{20} = 1.4195, from diethyl malonate and oxides of nitrogen.

Preparation of diethyl O-t-butyl tartronate. 5 g of sodium hydride was placed into a three-necked flask fitted with stirrer, reflux condenser and a dropping funnel and covered with 800 ml of benzene. 0.15 mole of *t*-butyl peracetate in benzene was added and heat was applied for a few minutes until the exothermic reaction started. After 90 min, when the reaction seemed to cease, the clear, yellow solution was heated for 8 h at 60°C. Peroxide test: neg. The solution was poured into water, the organic phase separated, the aqueous phase extracted twice with ether and the combined extracts washed neutral with water and finally dried over sodium sulphate. Distillation gave a fore-run of diethyl malonate and a fraction with b.p. 68–70°/0.2 mm Hg. Redistillation gave the pure compound b.p. 67–68°/0.2 mm Hg, n_D^{20} = 1.4298. Yield 9.4 g (27 %). (Found: C 56.93; H 8.78. Calc. C 56.88; H 8.68).

Preparation of 5-t-butoxy barbituric acid. 2 g of diethyl t-butyl tartronate (n_D^{20} = 1.4290) and 0.73 g of urea in 25 ml of ethanol was refluxed gently for 3 h with sodium alcoholate in alcohol. The solution was then poured into 25 ml of water, extracted with benzene and the aqueous phase acidified. White, fine crystals began to precipitate out. After standing the mixture in a refrigerator for some time, the product was separated, washed with water and benzene and dried in air. M.p. 187–189°C. (Found: C 47.96; H 6.04. Calc. C 47.99; H 6.04).

Diethyl O-benzoyl tartronate. 3.6 g (0.15 mole) of sodium hydride was covered with 300 ml of benzene and treated with 24 g (0.15 mole) of diethyl malonate, to give a yellow

porridge-like mixture of the sodium derivative. 24.2 g (0.1 mole) of benzoyl peroxide in 200 ml of dry benzene was added during 60 min to the sodium diethyl malonate, cooled to 0—4°. After standing overnight, the mixture was poured into cold water and acidified with hydrochloric acid. The benzene layer was separated and the aqueous phase extracted several times with ether. The combined organic layers were extracted with sodium hydroxide solution to remove benzoic acid, washed neutral with water and dried over sodium sulphate. 12 g of benzoic acid were recovered from the acidified alkali extract. The solvents were distilled off and the residue was fractionated. A fore-run of diethyl malonate (6 g) was followed by the main fraction, b.p. 145°/0.5 mm Hg, $n_D^{20} = 1.4890$. Weight 15.5 g. Yield 55 %. The tartronate solidified when treater with light petroleum. Recrystallisation from pet. ether and ether gave crystalline plates, m.p. 57—58°C. (Found: C 60.36; H 5.80. Calc. for $C_{14}H_{16}O_6$: C 59.99; H 5.75).

In one experiment, diethyl dibenzoyloxy malonate was isolated in 7 % yield. B.p. 170—180°C/0.1 mm Hg. M.p. 118—121°C (from pet. ether + ether). Found: C 63.25; H 5.10. Calc. for $C_{20}H_{20}O_8$: C 62.99; H 5.04).

Diethyl dibenzoyloxy malonate was also obtained when 0.1 mole of diethyl O-benzoyl tartronate in 150 ml of benzene was treated with 2.4 g of sodium hydride followed by the addition of 18 g of benzoyl peroxide (in 200 ml of benzene) in the usual way. Only 5 g of benzoic acid was isolated. When the organic phase was worked-up in the usual manner, a thick, viscous oil was initially obtained which, after storing in the cold, afforded 2.2 g of white crystals identical in every respect to authentic diethyl dibenzoyloxy malonate.

Dimethyl O-benzoyl tartronate. 0.1 mole of sodium dimethyl malonate in 150—200 ml of benzene was treated at 0°C with 0.075 mole of benzoyl peroxide in benzene. B.p. (of the tatronate) 133°/0.2 mm Hg. M.p. 45—47°C (from pet.ether). Weight 17.2 g. Yield 68 % (Found: C 57.40; H 4.80. Calc for $C_{12}H_{12}O_6$: C 57.14; H 4.80).

Diethyl O-benzoyl methyl tartronate. This was prepared from 0.15 mole of methyl sodium diethyl malonate in 200 ml of benzene, and 0.1 mole of benzoyl peroxide in 150—200 ml of benzene, as described above. No gas was evolved. The product distilled at 143—146°/0.6 mm Hg. $n_D^{20} = 1.4893$. Weight 26.6 g. Yield 90 %. (Found: C 64.70; H 6.48. Calc. for $C_{15}H_{18}O_6$: C 64.73; H 6.52).

Diethyl O-benzoyl ethyl tartronate. Prepared from 0.15 mole of ethyl sodium diethyl malonate and 0.1 mole of benzoyl peroxide. No gas was evolved. A thick colourless oil of b.p. 137°/0.15 mm Hg, $n_D^{20} = 1.4890$ was obtained. Weight 23.2 g. Yield 75 %. Found: C 62.23; H 6.50. Calc. for $C_{16}H_{20}O_6$: C 62.32; H 6.54).

Diethyl O-benzoyl n-*propyl tartronate.* Prepared from 0.15 mole of the appropriate sodium compound and 0.1 mole of benzoyl proxide. No gas was evolved. A viscous oil of b.p. 136—138°/0.15 mm Hg $n_D^{20} = 1.4880$ was obtained. Weight 26.8 g. Yield 83 %. (Found: C 63.25; H 6.62. Calc. for $C_{17}H_{22}O_6$: C 63.34; H 6.88).

Diethyl O-benzoyl allyl tartronate. Prepared from 0.21 mole of diethyl allyl malonate and 0.175 mole of benzoyl peroxide. No gas was evolved. Quantitative yields of benzoic acid were isolated. A colourless thick oil of b.p. 145°/0.5 mm Hg, $n_D^{20} = 1.4959$, was obtained. Wight 31.4 g. Yield 56 %. (Found: C 63.65; H 6.28. Calc. for $C_{17}H_{21}O_6$: C 63.74; H 6.29).

Diethyl O-benzoyl n-*butyl tartronate.* Prepared from 0.15 mole of diethyl *n*-butyl malonate and 0.1 mole of benzoyl peroxide. (The sodium derivative was soluble in benzene.) A viscous oil of b.p. 140°/0.15 mm Hg, $n_D^{20} = 1.4870$, was obtained. Weight: 28.9 g. Yield 86 %. (Found: C 64.22; H 7.28. Calc. for $C_{18}H_{24}O_6$: C 64.27; H 7.19).

Diethyl O-benzoyl iso*butyl tartronate.* From 0.1 mole of diethyl *iso*butyl malonate (its sodium derivative is soluble in benzene) and 0.1 mole of benzoyl peroxide. No gas was evolved. The product has b.p. 128—130°/0.1 mm Hg, $n_D^{20} = 1.4873$. Weight 19 g. Yield 56 %. (Found: C 67.22; H 7.28. Calc. for $C_{18}H_{24}O_6$: C 67.27; H 7.19).

Diethyl O-benzoyl phenyl tartronate. Prepared from 0.15 mole of diethyl phenyl malonate and 0.1 mole of benzoyl peroxide. Quantitative yields of benzoic acid were isolated. No gas was evolved. B.p. 184°/0.12 mm Hg, m.p. 80—81°C (from pet. ether). Weight 29.3 g. Yield 82 %. (Found: C 67.57; H 5.59. Calc. for $C_{20}H_{20}O_6$: C 67.40; H 5.66).

Diethyl O-benzoyl 1-naphthyl tartronate. Prepared from 0.1 mole of the appropriate malonate and 0.075 mole of benzoyl peroxide. No gas was evolved. Quantitative yields of benzoic acid were isolated. Needles of m.p. 116–117.5° (from pet. ether) were obtained. Mixed m.p. 111–113°C *. Weight 29.6 g. Yield 97 %. (Found: C 70.92; H 5.51; mol.wt. 398. Calc. for $C_{24}H_{22}O_6$: C 70.92; H 5.46; mol. wt. 406.4).

Diethyl O-benzoyl benzyl tartronate. Prepared from 0.25 mole of diethyl benzyl malonate and 0.2 mole of benzoyl peroxide. No gas was evolved and quantitative yields of benzoic acid were isolated. B.p. 172°/0.1 mm Hg, $n_D^{20} = 1.5255$. Weight 59.2 g. Yield 80 %. (Found: C 68.17; H 5.93. Calc. for $C_{21}H_{22}O_6$: C 68.09; H 5.99).

Diethyl O-benzoyl chloro tartronate. 0.15 mole of diethyl chloromalonate was added slowly at room temp. to 0.15 mole of sodium hydride covered with 200 ml of dry benzene, and the mixture stirred for 5 h. Benzoyl peroxide (0.1 mole) in benzene was added in the usual way. No gas was evolved. Quantitative yields of benzoic acid were isolated. An almost colourless oil of b.p. 140°/0.3 mm Hg, $n_D^{20} = 1.4982$, was obtained. Weight 23.5 g. Yield 75 % (Found: C 53.74; H 4.74. Calc for $C_{14}H_{15}O_6Cl$: C 53.43; H 4.80.)

Diethyl O-benzoyl carbethoxy tartronate. 0.2 mole of sodium hydride was covered with with 400 ml of benzene to which 0.2 mole of tricarbethoxymethane was added dropwise. After 3 h, the hydride was consumed and 0.1 mole of benzoyl peroxide in 200 ml of benzene was added to the cooled sodium compound. No gas evolution was observed. Quantitative yields of benzoic acid were isolated. White plates (from ethanol) of m.p. 59–60°C were obtained. Weight 32.4 g. Yield 92 %. (Found: C 57.95; H 5.75. Calc for $C_{17}H_{20}O_8$: C 57.95; H 5.72). Upon recrystallization, two fractions were obtained, one with m.p. 49–51° and the other with m.p. 59–61°C (from ether and pet. ether). Elementary analyses were identical. After 6 months' storage in closed vials both samples had m.p. 59–60°C.

Preparation of diethyl O-benzoyl tartronate from diethyl O-benzoyl chlorotartronate. a). 24.3 g of diethyl O-benzoyl chloro tartronate was dissolved in 200 ml of dry ether and cooled to 0°C. Ethylmagnesium bromide (from 3 g of magnesium and 8.4 g of ethyl bromide) in 125 ml of ether was added dropwise during one hour. The mixture was stirred overnight then poured into water and extracted with ether. The ether phase was extracted with alkali and dried over sodium sulphate. After the solvent had been distilled off a solid residue was obtained. M.p. 57–59° (from ether and pet. ether). Mixed m.p. with an authentic sample showed no depression. Weight 20.3 g. Yield 95 %.

b). Phenylmagnesium bromide (from 15.7 g of bromobenzene and 3 g of magnesium) in 100 ml of dry ether was added dropwise to an ice-cold solution of 32 g of diethyl O-benzoyl chlorotartronate in 200 ml of ether. A yellow precipitate was immediately formed and the mixture stirred for 15 h. Water + hydrochloric acid was added to decompose the magnesium complex. After extracting with ether the combined ether layers were washed with water till neutral and dried over sodium sulphate. The ether was distilled off and a low-boiling fraction of b.p. 130–136°C was obtained. Redsitillation gave a product, $n_D^{20} = 1.5254$, which was in all respects identical with chlorobenzene, b.p. 132°C, $n_D^{20} = 1.5247$. When the residue in the distillation flask was cooled a solid precipitated. Recrystallization from ether and pet. ether gave white plates with m.p. 59–60°C. Mixed melting point with autentic diethyl O-benzoyl tartronate gave no depression.

Diethyl benzoyl O-benzoyl tartronate. 2.4 g of sodium hydride was covered with 75 ml of tetrahydrofuran and 23 g of diethyl O-benzoyl tartronate in 150 ml of tetrahydrofuran was added dropwise. A violent evolution of hydrogen was observed and after one hour all hydride was consumed and a clear solution had been formed. 17 g of benzoyl chloride was added all at once (room-temp.) and after stirring for 1–2 min the mixture was neutral and was poured out onto water. The organic layer was separated, the water phase shaken with ether three times and the combined extracts washed once with water and dried over sodium sulphate. After concentration distillation gave a small fraction of benzoyl chloride but attempted distillation of the rest caused decomposition. By adding ligroin a white powder precipitated (16.5 g) and repeated recrystallization from pet.ether + ether

* We wish to express our cordial thanks to Prof Arthur C. Cope of Massachusetts Institute of Technology for providing us with a sample of this compound.

gave white needles, m.p. 80—82°C. Yield 52 %. (Found: C 65.64; H 5.28. Calc for $C_{21}H_{20}O_7$: C 65.61; H 5.24).

Preparation of tartronic acid. Sodium alcoholate, prepared from 2.3 g (0.10 mole) of sodium in 100 ml of absolute ethanol, was added to 12 g of diethyl O-benzoyl tartronate in 50 ml of ethanol. The mixture was stirred for 34 h at room temperature. It was then poured into water, and extracted with ether 3—4 times. The combined extracts were washed neutral with water, dried over sodium sulphate and distilled. Ethyl benzoate, b.p. 86°C/10 mm Hg, $n_D^{20} = 1.5047$, was obtained. Yield 3.9 g (60 %). The aqueous phase was acidified and extracted with ether during 48 h. Concentration of the dried ether phase gave 4.1 g of a solid, which after recrystallization from pet. ether (b.p. 60—71°C) and ether gave white crystals, m.p. 176—178°C. (Lit. 178°C).

n-*Propyl tartronic acid.* 26.2 g (0.08 mole) of diethyl *n*-propyl O-benzoyl tartronate was added to a sodium alcoholate solution (from 3.7 g of sodium in 50 ml of ethanol) at room temperature and stirred for 18 h. The mixture was worked up as above, giving 9.2 g (76 %) of ethyl benzoate and 6.9 g (54 %) of *n*-propyltartronic acid, m.p. 124—124.5° (from ether and pet. ether) (Lit. 122°).

iso*Butyl tartronic acid.* Sodium alcoholate (from 3.2 g of sodium in 75 ml of ethanol) was added dropwise to 23 g (0.07 mole) of diethyl *iso*butyl O-benzoyl tartronate at room temperature and stirred for 18 h. The usual work up yielded 7.5 g (55 %) of ethyl benzoate and 11.6 g (94 %) of *iso*butyl tartronic acid, m.p. 126—126.5°C (from pet.ether and ether) (Lit. 107°C). (Found: C 47.55, H 6.92. Calc for $C_7H_{12}O_5$: C 47.72, H 6.87.)

Benzyl tartronic acid. Sodium alcoholate, from 2.6 g (0.12 mole) of sodium in 50 ml of absolute alcohol, was added to 15.7 g (0.06 mole) of diethyl benzoyl tartronate at room temperature. The mixture was stirred for 18 h and worked up as above, yielding 5 g (56 %) of ethylbenzoate and 7.6 g (60 %) benzyltartronic acid, m.p. 156—160°C (from ether and pet.ether).

Ethanolysis and hydrolysis of diethyl phenyl O-benzoyl tartronate. Sodium alcoholate, prepared from 2.3 g (0.1 mole) of sodium in 100 ml of ethyl alcohol, was added dropwise to a solution of 18.4 (0.05 mole) of diethyl phenyl O-benzoyl tartronate in 100 ml of ethyl alcohol; after stirring overnight, the mixture was poured into water, extracted with ether 3 times, washed neutral, dried and distilled: 6 g (80 %) of ethyl benzoate was obtained. The aqueous phase was acidified and extracted continuously during 26 h with ether. 6.3 g (83 %) of mandelic acid was isolated from the ether phase. Recrystallization from formic acid gave pure crystals, m.p. 118—121°; on admixture with authentic mandelic acid, no depression of the melting point was observed.

Ethanolys of diethyl n-*butyl O-benzoyl tartronate.* Sodium alcoholate, prepared from 3.2 g (0.14 mole) of sodium and 75 ml of water-free ethanol, was added dropwise to 23 g (0.07 mole) of diethyl *n*-butyl O-benzoyl tartronate and stirred for 24 h at room temperature. The mixture was poured into water and extracted 2 times with ether. 8.7 g (83 %) of ethyl benzoate was isolated from the ether phase. The water phase was neutralized to pH 7 and extracted with ether 10—15 times at low temperature. The combined ether extracts were dried over sodium sulphate, concentrated and distilled; giving 4.5 g (29 %) of diethyl *n*-butyl tartronate, b.p. 120—123°/10 mm Hg, $n_D^{20} = 1.4292$, identical to a sample prepared as follows:

To 31.3 g (0.18 mole) of diethyl oxomalonate in 100 ml of toluene, cooled to —70°C was added *n*-butylmagnesium bromide (from 4.3 g of magnesium and 24.6 g of *n*-butyl bromide) in 150 ml of ether during 90 min. When the temperature of the reaction mixture had risen to about 0°C, the mixture was poured into water and dilute hydrochloric acid. The water phase was extracted 10—15 times with cold ether, the combined organic layers dried over sodium sulphate and finally distilled; giving 22.5 g (54 %) of diethyl *n*-butyl tartronate, b.p. 117—120°/12 mm Hg, $n_D^{20} = 1.4288$. (Found: C 56.94, H 8.72. Calc. for $C_{11}H_{20}O_5$: C 56.88, H 8.68.)

Ethanolysis of diethyl benzyl O-benzoyl tartronate. 0.1 mole of sodium ethoxide was prepared in the usual way from 2.3 g of sodium in 125 ml of absolute ethanol. The alcoholate was added dropwise with stirring to a cooled (0—5°C) solution of 18.6 g (0.05 mole) of diethyl benzyl O-benzoyl tartronate in 100 ml of ethanol. Stirring was continued for 22 h. The mixture was poured into water and extracted repeatedly with ether. Ethyl benzoate, b.p. 81/10 mm Hg, $n_D^{20} = 1.5068$, was isolated from the ether phase. Yield

6.1 g (81 %). The water phase was neutralized to pH 7 and extracted 10 times with cold ether. The ether was dried, concentrated and distilled, giving 7.4 g (58 %) of diethyl benzyl tartronate, b.p. 102—104°/0.1 mm Hg, $n_D^{20} = 1.4952$. (Found: C 63.37; H 6.98.) Calc for $C_{14}H_{18}O_6$: C 63.14, H 6.81).

Preparation of diethyl benzyl tartronate according to Cope. Benzylmagnesium chloride was prepared from 3 g (0.13 mole) of magnesium and 13 g (0.12 mole) of benzyl chloride in 150 ml of ether. 18.4 g (0.11 mole) of diethyl oxomalonate, in 175 ml of ether was cooled to —70°C and the Grignard reagent added dropwise during 25 min. Stirring was continued for another 45 min, whereupon the mixture was poured into ice-water and hydrochloric acid. After extraction of the water phase with ether six times, the combined extracts were dried, concentrated and distilled giving 10.3 g (35 %) of product, b.p. 101—103°/0.1 mm Hg, $n_D^{20} = 1.4955$.

Acknowledgements. The authors are indebted to the head of this Institute, Professor A. Fredga, for the facilities put at their disposal and for his interest in this work. A grant from the *Swedish Natural Science Research Council* is gratefully acknowledged.

REFERENCES

1. Lawesson, S.-O. and Yang, N. C. *J. Am. Chem. Soc.* **81** (1959) 4230.
2. Ames, D. E. and Bowman, R. E. *J. Chem. Soc.* **1951** 1079.
3. Hammond, K. M., Fisher, N., Morgan, E. N., Tanner, E. M. and Franklin, C. S. *J. Chem. Soc.* **1957** 1062.
4. Wallingford, V. H., Homeyer, A. H. and Jones, D. M. *J. Am. Chem. Soc.* **63** (1941) 2056.
5. Lawesson, S.-O. and Berglund, C. *Acta Chem. Scand.* **13** (1959) 1716.
6. Milas, N. A. and Surgenor, D. M. *J. Am. Chem. Soc.* **68** (1946) 642.
7. Lawesson, S.-O. and Busch, T. *Acta Chem. Scand.* **13** (1959) 1716.
8. Bradley, W. and Robinson, R. *J. Chem. Soc.* **1928** 1541.
9. Conrad, M. and Brückner, C. *Ber.* **24** (1891) 2993.
10. Dimroth, O. and Schweizer, R. *Ber.* **56** (1923) 1375.
11. Jackson, C. L. and Phinney, J. I. *Am. Chem. J.* **21** (1899) 418.
12. Cope, A. C. and Field, L. *J. Org. Chem.* **14** (1959) 856.
13. Greenbaum, M. A., Denney, D.B. and Hoffman, A. K. *J. Am. Chem. Soc.* **78** (1956) 2563.
14. Walling, C. and Hodgdon, R. *J. Am. Chem. Soc.* **80** (1958) 228.
15. Denney, D. B. and Denney, D. Z. *J. Am. Chem. Soc.* **82** (1960) 1389.
16. Lemaire, J. *Bull acad. roy. Belg.* **1909**, 83.
17. Lemaire, J. *Rec. trav. chim.* **29** (1910) 22.
18. Cope, A. C. and McElvain, S. M. *J. Am. Chem. Soc.* **54** (1932) 4319.
19. *Org. Syntheses*, Coll. Vol. II (1943) 279.
20. Connor, R. *J. Am. Chem. Soc.* **55** (1933) 4597.
21. Bischoff, C. A. *Ber.* **28** (1895) 2616.
22. Conrad, M. and Bischoff, C. A. *Ann.* **204** (1880) 166.
23. *Org. Syntheses* Coll. Vol. I (1932) 245.
24. Fischer, E. and Schmitz, W. *Ber.* **39** (1906) 351.
25. Conrad, M. *Ann.* **204** (1880) 174.
26. *Org. Syntheses*, Coll. Vol. II (1943) 288.
27. Blicke, F. F. and Feldkamp, R. F. *J. Am. Chem. Soc.* **66** (1944) 1087.
28. MacBeth, A. K. *J. Chem. Soc.* **121** (1922) 1116.
29. Lawesson, S.-O., Busch, T. and Jönsson, P. G. *Unpublished results.*
30. *Org. Syntheses*, Coll. Vol. I (1932) 266.

Received December 28, 1960.

ACTA CHEMICA SCANDINAVICA 15 (1961) 271–276

Conjugate Additions of Grignard Reagents to alpha, beta-Unsaturated Esters

VIII. Further Studies on the Effect of Cuprous Chloride

JON MUNCH-PETERSEN and VIGGO KØGS ANDERSEN

Organisk-kemisk Laboratorium, Polyteknisk Læreanstalt, Copenhagen, Denmark

The yields of 1,4-addition products from *sec*-butyl crotonate and Grignard reagents are improved by cuprous chloride catalysis provided that the catalyst is added to the Grignard reagent in small portions concurrently with the addition of the ester solution, whereas the catalyst has little effect when added in one portion before the ester addition starts (except in the case of methylmagnesium bromide). This and other evidence for a limited life time of cuprous chloride in the Grignard reagent solution is presented.

Certain problems relating to the reactivities of crotonic, tiglic and cinnamic esters are considered.

In previous communications the effect of cuprous chloride in promoting 1,4-addition of Grignard reagents to α,β-unsaturated esters has been discussed, *e.g.* the reaction of *n*-butylmagnesium bromide with *sec*-butyl crotonate:

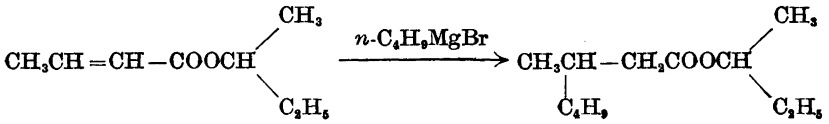

It was first thought [1] that this catalyst was essential to secure any reasonable yield of conjugate addition product, even with *sec*-butyl esters, the use of which effectively prevents addition to the carbonyl group. Later it was found that the results of the first paper could not be reproduced in all cases, and a reinvestigation [2] led to a somewhat different procedure according to which the use of cuprous chloride was abandoned. The use of *sec*-butyl esters and a somewhat larger excess of Grignard reagent were proved to be sufficient conditions for a generally applicable procedure, although the yield of *sec*-butyl 3-methylheptanoate from *sec*-butyl crotonate and *n*-butylmagnesium bromide by the new procedure (70—75 %) was not quite so high as that originally obtained by the cuprous chloride method. The reason for the non-reproducibility of the original procedure was not found.

In later work again, cuprous chloride has been found to exert a strong influence in certain other cases. Thus, the reaction of methylmagnesium bromide resulted in 1,4-addition only when cuprous chloride had been added to the Grignard reagent prior to the ester [3], and it was found that even ethyl [4] and methyl [1] crotonate with *n*-butylmagnesium bromide in the presence of cuprous chloride gave 1,4-addition products in good yields, although in the latter case a secondary acetoacetic ester condensation took place. In the case of acetylenic esters cuprous chloride is able to bring about a complete change in orientation from 1,2- to 1,4-addition [5].

Recently cuprous chloride was found to catalyze reduction of the double bonds of citraconic and mesaconic esters in competition with conjugate addition of *n*-butylmagnesium bromide [6]. A suggestion concerning the possible mode of action of cuprous chloride was advanced, the essentials of which were a) the formation of a cuprous alkyl from cuprous chloride and the Grignard reagent according to Gilman [7]:

$$RMgBr + CuCl \rightarrow RCu + MgBrCl \quad (1)$$

and b) the coordination of the cuprous ion from the cuprous alkyl with the ethylenic α-carbon atom of the α,β-unsaturated ester, combined with the concept of a cyclic electron shift operating within a six-membered ring. These ideas, which appear to be quite useful in explaining the effects of cuprous chloride in the work of this series, will be further set out in a forthcoming publication [8] (p. 282—283).

The purpose of this communication is to report some experiments which have been carried out as a consequence of the above-mentioned considerations.

It has long since been realized that when cuprous chloride is added to the Grignard reagent (*e.g.*, *n*-butylmagnesium bromide) in ether solution at 0°, a black precipitate appears, generally after 10—15 min. Presumably copper is formed according to the following equation [7]:

$$2\,RCu \rightarrow R{-}R + 2\,Cu \quad (2)$$

In order to test this assumption an experiment was carried out, in which an excessively large amount of cuprous chloride was used.

In a run with 0.4 mole (56.8 g) of *sec*-butyl crotonate the Grignard reagent was prepared from 1.25 g-atom of magnesium and 1.56 mole of *n*-butyl bromide (as compared with 1.0 g-atom and 1.3 mole, resp. in the usual runs[2].) The Grignard solution was cooled in an ice-salt bath for 15 min. Cuprous chloride was added gradually in small portions from a small flask, connected with one of the side-necks of the reaction vessel. A total of 36.4 g (0.36 mole, 25 mole per cent with respect to the Grignard reagent) was added during about 30 min. After approximately one fourth of the amount of cuprous chloride had been added a vigorous reaction set in with evolution of enough heat to cause the ether to boil violently, mercury thereby being blown out of the mercury seal. Immediately the reaction mixture acquired a shiny red colour and a black precipitate formed. The rest of the cuprous chloride could now be added without any further vigorous reaction. The ester was then added during 3 h as previously described, but the yield of 1,4-addition product was only 28 %

The black precipitate, which was filtered from the reaction mixture before this was worked up, was almost certainly copper, since it became warm on exposure to the air and gained in weight It dissolved in nitric but not in hydrochloric acid When boiled with the latter acid the precipitate turned red.

Table 1. Yields of conjugate addition products from Grignard reagents and *sec*-butyl esters of *α,β*-unsaturated esters. Unless otherwise indicated, product data are published previously [1-3].

α,β-Unsaturated *sec*-butyl ester	Grignard reagent RMgBr R	Product: *sec*-butyl ester	Temp. °C	Yield %		
				no catalyst	CuCl one portion	CuCl small portions
Crotonic	*n*-C_4H_9	3-methylheptanoic	0	70–75	70–75	80–85
»	C_2H_5	3-methylvaleric	0 −10	78	 56[a]	 79
»	*n*-C_3H_7	3-methylhexanoic[b]	0 −10	60–66	56–59 65	69–74 88
»	*iso*-C_3H_7	3,4-dimethylvaleric	0 −10	51–57	58 71	64–71 80
»	*tert*-C_4H_9[c]	3,4,4-trimethylvaleric	0 −10	14	14 15	27 48[d]
»	CH_3	*iso*valeric	−10	0	51–59	61–65
Tiglic	*n*-C_4H_9	2,3-dimethylheptanoic	0	70	50[e]	55
»	CH_3	3,4-dimethylpentan-2-one[f]	−10	0	63	65[g]
Cinnamic	*n*-C_4H_9	3-phenylheptanoic	0	36	42	50
»	CH_3	4-phenylpentan-2-one[f]	−10	0	51	49
Sorbic[g]	*n*-C_4H_9	*n*-butylhexenoic[h]	0	30–40	30–58	72

[a]Ref.[1]: the excess of Grignard reagent was 25 % only. [b]The data for this ester are given in Ref.[11] (p. 298). [c]*tert*-Butylmagnesium chloride was used. [d]This yield has been further improved by using a larger excess of Grignard reagent [11]. [e]The previously reported [1] complete failure of this conjugate addition has been found erroneous. [f]1,2 + 1,4-addition product = saturated ketone. [g]Yield corrected for 19 % recovered unreacted *sec*-butyl tiglate. The reaction mixture was stirred for 2.5 h at room temperature, while in the one-portion reaction it was left over-night [3]. [h]Mixture of isomers [8].

This experiment lends support to the idea that cuprous chloride as such has a limited life time in the Grignard reagent solution. Previously it has been found [1] that this "coupling" reaction takes place much more readily with the

lower Grignard reagents such as methyl- and ethylmagnesium bromide than with *n*-butylmagnesium bromide, and in order to secure a catalytic effect of cuprous chloride towards these two Grignard reagents it is, therefore, necessary to cool the reaction mixture in ice-salt (—8 to —15°). It has now been found (*cf.* Table 1) that strong cooling also is favourable in the cases of *n*-propyl- and *iso*propylmagnesium bromides as well as *tert*-butylmagnesium chloride. With *n*-butylmagnesium bromide (and higher alkylmagnesium bromides), on the other hand, the coupling reaction takes place instantaneously at room temperature, but at 0° it is sufficiently delayed to render a catalytic effect possible. These observations are in accordance with the findings of Gilman [7] that cuprous-organic compounds are formed according to (1) and will decompose according to (2), and that the lower cuprous alkyls are very unstable; no comparison between the stabilities of lower and higher cuprous alkyls was, however, reported.

An investigation has now been carried out to see whether the catalytic effect of cuprous chloride (with respect to 1,4-addition) was improved by adding it in small portions at regular intervals during the addition of the ester to the Grignard reagent rather than adding it in one portion before the ester.

In the case of *sec*-butyl crotonate this was indeed the case (Table 1).

As in the standard procedure[2] the Grignard reagent was prepared from 25 g (1.04 g-atom) of magnesium and 178 g (1.30 mole) of *n*-butyl bromide in 300 ml of ether. Likewise the ester (0.4 mole) dissolved in 400 ml of ether was then added over 3 h to the cooled (*cf.* Table 1) Grignard reagent. Cuprous chloride was used in the following way: 1.4 g of cuprous chloride (1.4 mole per cent with respect to the Grignard reagent) was added, concurrently with the ester, in 0.2 g portions at half-hourly intervals, the first portion being added just before ester addition and the last one just after. Commercial cuprous chloride (E. Merck, Darmstadt, Germany, *p.a.*) was used without previous reduction or drying.

The yield, which is around 70—75 % in the uncatalyzed reaction and is unaffected by cuprous chloride added all at once [2], is, by portion-wise addition of cuprous chloride, increased by at least 10 % to 80—85 %.

Under these conditions the yield with ethyl crotonate was only 70 %, being the same as when cuprous chloride was added in one portion [4].

It should be mentioned that the so-called "inverse" addition of the Grignard reagent *to* the ester solution containing the cuprous chloride (*cf.* Ref.[6]) results in the formation of a non-distillable oil and only 2—3 % of 1,4-addition product. A similar result was previously obtained with citraconic ester [6], and it appears as if the "inverse" addition procedure is of value only in the case of alkylidene-cyanoacetic and -malonic esters [5,6].

In the case of *sec*-butyl tiglate, however, no increase in the yield of 1,4-addition product with *n*-butylmagnesium bromide has been obtained. On the contrary, some drop in yield as compared with the uncatalyzed reaction was encountered. The reason for the inhibitory effect of cuprous chloride in this case is not clear, and since the by-products actually produced have not, so far, been investigated, any comment on this point would be of little value.

In the uncatalyzed reaction of *sec*-butyl cinnamate with *n*-butylmagnesium bromide we have been unable to reproduce the previously reported [2] yield (52 %). The reason

for this has not yet been found. The favourable effect of cuprous chloride on the yield in this case appears, however, to be established. Considerable amounts of the condensation-addition product, analogous to that described from the reaction with crotonic ester [1] were obtained in all reactions with cinnamic ester, but when cuprous chloride was added in small portions the yield of simple 1,4-addition product was 50 % as compared to 36 % in the uncatalyzed reaction.

The results with *sec*-butyl sorbate, which support the views here presented, are described in the following paper of this series [8] (p. 277).

Reactions involving methylmagnesium bromide lead to conjugate addition, only when cuprous chloride is present and the reaction mixture is cooled in ice-salt during the addition of the ester [3]; otherwise 1,2-addition takes place and no conjugate addition products are formed. With tiglic and cinnamic esters, however, the cuprous chloride catalyzed conjugate addition does not, as with crotonic ester, result in *simple* 1,4-addition; 1,2-addition occurs as well, and the products are saturated ketones [3]. In these reactions of methylmagnesium bromide the step-wise addition of cuprous chloride hardly offers any advantage over the one-portion addition method.

In the addition of ethylmagnesium bromide to *sec*-butyl crotonate the uncatalyzed reaction (at 0°) gives as high a yield (78 %) as does the cuprous chloride catalyzed reaction (cooled in ice-salt). Apparently, here the 1,2-addition is no serious side-reaction, and the low stability of the cuprous alkyl in this case prevents its catalytic effect to improve the yield of simple 1,4-addition product over that obtained in the uncatalyzed reaction.

The reactions with methylmagnesium bromide are of interest in other respects. The results with tiglic and cinnamic esters raise the question as to which one of the two addition types (1,2 or 1,4) takes place first. Most likely the saturated ketone is the result of a primary 1,2-addition followed by a subsequent 1,4-addition to the α,β-usaturated ketone [10]:

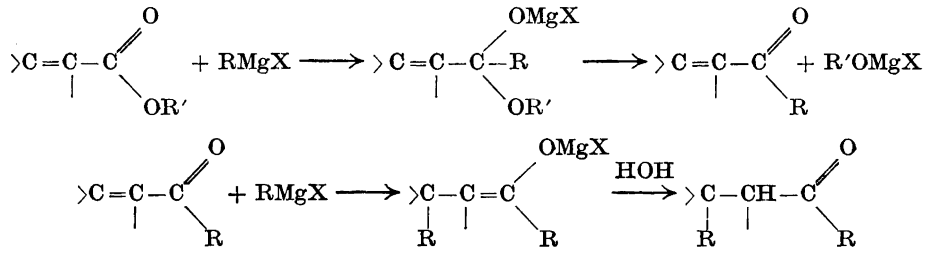

The two addition reactions may thus both occur in the etheral reaction mixture, whereas the reverse order of addition: a primary 1,4-addition followed by a 1,2-addition to the carbonyl group of the saturated ester could hardly be visualized as taking place:

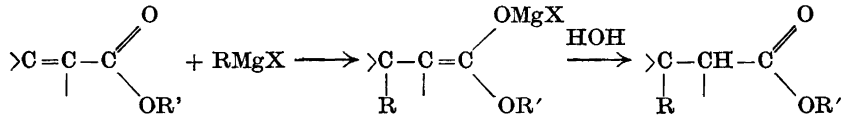

since the primary addition product must be hydrolyzed before being able to undergo 1,2-addition.

This implies that tiglic and cinnamic esters are less reactive than crotonic ester towards 1,4-addition, since this addition occurs in good yield in the latter case, but does not take place in the former case unless the α,β-unsaturated ester is first transformed into the more reactive α,β-unsaturated ketone. Since none of this ketone has ever been obtained, the 1,4-addition to the ketone must be rapid compared to the primary 1,2-addition to the ester.

Further evidence for these ideas is found in the fact that *sec*-butyl tiglate, in contrast to both *sec*-butyl crotonate and ethyl tiglate, did not give complete reaction by stirring for two hours at room temperature after the addition of the ester, but had to stand overnight; otherwise unreacted ester was recovered.

The authors are indebted to *Otto Mønsteds Fond* for financial support.

REFERENCES

1. Munch-Petersen, J. *J. Org. Chem.* **22** (1957) 170.
2. Munch-Petersen, J. *Acta Chem. Scand.* **12** (1958) 967.
3. Munch-Petersen, J. *Acta Chem. Scand.* **12** (1958) 2007.
4. Munch-Petersen, J. *Acta Chem. Scand.* **12** (1958) 2046.
5. Bretting, C., Munch-Petersen, J., Møller Jørgensen, P. and Refn, S. *Acta Chem. Scand.* **14** (1960) 151.
6. Bjerl Nielsen, E., Munch-Petersen, J., Møller Jørgensen, P. and Refn, S. *Acta Chem. Scand.* **13** (1959) 1943.
7. Gilman, H. and Straley, J. M. *Rec. trav. chim.* **55** (1936) 821.
8. Munch-Petersen, J., Bretting C., Møller Jørgensen, P., Refn, S., Andersen, V. K. and Jart, A. *Acta Chem. Scand.* **15** (1961) 277.
9. Brändström, A. and Forsblad, I. *Arkiv Kemi* **6** (1954) 561.
10. *Cf.* Kohler, E. P. *Am. Chem. J.* **36** (1906) 529 [*Chem Zentr.* **1907 I** 559].
11. Munch-Petersen, J. and Andersen, V. K. *Acta Chem. Scand.* **15** (1961) 293.

Received September 27, 1960.

ACTA CHEMICA SCANDINAVICA 15 (1961) 277—292

Conjugate Additions of Grignard Reagents to alpha, beta-Unsaturated Esters

IX. 1,4- and 1,6-Additions of *n*-Butylmagnesium Bromide to the *sec*-Butyl Ester of Sorbic Acid

JON MUNCH-PETERSEN, CLAUS BRETTING, PEER MØLLER JØRGENSEN, SUSANNE REFN and VIGGO KØGS ANDERSEN

Organisk-kemisk Laboratorium, Polyteknisk Læreanstalt, Copenhagen, Denmark

AAGE JART

Dansk Fedtforskningsinstitut, Copenhagen, Denmark

The uncatalyzed addition of *n*-butylmagnesium bromide to *sec*-butyl sorbate results in both conjugate addition and 1,2-addition. The conjugate addition is predominantly a 1,4-addition, although 1,6-addition takes place to a considerable degree. When the addition is carried out in the presence of cuprous chloride no 1,2-addition product can be isolated, and the conjugate addition takes place in good yield and almost exclusively as 1,6-addition. A mechanism which accounts for these results is suggested.

The identification and estimation of compounds has been accomplished by means of gas-liquid chromatography, infra-red spectroscopy and conventional chemical investigations.

The addition of a Grignard reagent, *e.g.* *n*-butylmagnesium bromide, to a sorbic ester may in principle lead to the formation of the following compounds, either by 1,2-additions (to the carbonyl group), by 1,4-addition (to the α,β-double bond) or by 1,6-additions (to the 2,4-diene system or to the γ,δ-double bond):

$$CH_3CH=CH-CH=CH-COOR' \xrightarrow{C_4H_9MgBr}$$

1,2-additions

$CH_3CH=CH-CH=CH-CO-C_4H_9$ I

$CH_3CH=CH-CH=CH-C(OH)(C_4H_9)_2$ II

1,4-addition

$CH_3CH=CH-\underset{\displaystyle C_4H_9}{\underset{|}{CH}}-CH_2COOR'$ III

1,6-additions

$$CH_3CH(C_4H_9)-CH=CH-CH_2COOR' \quad IV$$

$$CH_3CH(C_4H_9)-CH_2CH=CH-COOR' \quad V$$

Furthermore, products resulting from the occurrence of combinations of these addition types could be formed, such as:

$$CH_3CH=CH-CH(C_4H_9)-CH_2CO-C_4H_9 \quad VI$$

In the literature additions of Grignard reagents to the double bonds of 2,4-alkadienoic esters are apparently only reported by Kohler and his school. Kohler and Butler [1] added phenylmagnesium bromide to methyl β-vinylacrylate and obtained exclusively (75 %) 1,3-diphenylpent-4-en-1-one as the result of one 1,2- and one 1,4-addition (*cf.* VI, above). With methyl cinnamylidenemalonate and phenylmagnesium bromide Reimer [2] found only 1,4-addition, and the same was the case in the reaction of ethyl cinnamylidenecyanoacetate with phenyl- and ethylmagnesium bromides [3]. The methyl ester of α-phenyl-cinnamylideneacetic acid did only with difficulty react at all and gave phenyl 1,2,4-triphenylbut-3- enyl ketone as the result of one 1,2- and one 1,4-addition [4]. Kohler [5] also reports the exclusive 1,4-addition of phenylmagnesium bromide (and benzylmagnesium chloride) to cinnamylideneacetophenone, and Fuson and Libby [6] find that the additions of phenylmagnesium bromide to sorbomesitylene and to sorbodurene take place as 1,4-additions only.

If the β-carbon atom is substituted so as to form a hindrance to 1,4-addition, only 1,2-addition takes place: methyl β-phenyl-cinnamylideneacetate thus gives the tertiary alcohol (1,1,3,5-tetraphenylpenta-2,4-dien-1-ol) with phenylmagnesium bromide [1].

1,6-Additions of Grignard reagents have been described in more special cases [7]. Thus Fuson *et al.*[8] describe the *para*-substitution by Grignard alkyls in the phenyl ring of phenyl duryl ketone and similar sterically hindered ketones. Here the 1,6-addition is followed by the loss of a molecule of hydrogen. Julian *et al.*[9] report the 1,6-addition to certain methylenequinones, *e.g.* methyleneanthrone and fuchsone, resulting in the creation of aromaticity in the rings. In no case, however, has 1,6-addition been observed in a simple linear diene-carbonyl system.

With other nucleophilic reagents, on the other hand, such as the anions of malonic, cyanoacetic and acetoacetic esters, additions take place predominantly as 1,6-additions [10]. Thus the δ-substituted compounds are formed from sorbic and β-vinylacrylic esters [1,11], *e.g.*

$$CH_3CH=CH-CH=CH-COOCH_3 + CH_2(COOCH_3)_2 \xrightarrow{NaOCH_3} CH_3CH(CH(COOCH_3)_2)-CH=CH-CH_2COOCH_3$$

Table 1. Additions of *n*-butylmagnesium bromide to *sec*-butyl sorbate.

Catalyst	Type of products	Yield %		Type of conjugate addition % of total [a]		
		0.1 mole scale	0.2 mole scale	1,4	1,6-(α,δ)	1,6-(γ,δ)
None	conj. add.	40	30	73—75	7—7	20—18
	1,2-add. + conj. add.	20	30	>95	trace	trace
	condensation + conj. add.		0			
CuCl-catalyzed, one portion	conj. add.	52—58	30—35[b]	3—8	24—21	73—71
	1,2-add. + conj. add.	0	0			
	condensation + conj. add.	+	20			
CuCl-catalyzed, step-wise addition	conj. add.	72	72	2	24	74
	1,2-add. + conj. add.	0	0			
	condensation + conj. add.	+	+			

[a] The figures are roughly estimated accurate to the nearest 0.5, 2 and 5 % for the values: below 10 %, around 20 % and 70 %, respectively. Two figures in a column represent results from two determinations.

[b] The ratios between the isomers given are those for 0.1 mole runs only.

although some 1,4-addition occurs as well (in the above reaction to an extent of 7—10 %[12]) depending on the possible presence of substituent alkyl groups at the carbon atoms α,β, and γ[13,14]; thus γ-methylsorbic ester gives 75 % 1,4-addition of ethyl cyanoacetate. The addition of ethyl acetoacetate to sorbic ester has been reported to give high yield of 1,6-addition product, although the possibility that small amounts of 1,4-addition product have been formed can not be excluded [15]. It should be noted that in these cases of 1,6-additions the 1,6-adducts have been reported to be of the type V, that is the β,γ-unsaturated ester.

The analogous reaction of 1-cyanobuta-1,3-diene, which is the "vinylog" of acrylonitrile, has likewise been described to give 1,6-addition of active hydrogen compound [16]. In this reaction, which is analogous to the cyanoethylation, the yields are low, and the possibility of 1,4-addition is not considered by the authors.

Summarizing, it appears as if conjugate additions to an unhindered 2,4-dienic carbonyl compound take place essentially as 1,6-additions when the addends are sodium derivatives of active hydrogen compounds, whereas essentially 1,4-addition occurs when the addends are Grignard reagents.

The present paper describes additions of *n*-butylmagnesium bromide to *sec*-butyl sorbate under conditions which have previously been found favour-

able for conjugate addition [17–19]. The addition products have been subjected to identification work in order to solve the question of 1,4-*versus* 1,6-addition. The effect of cuprous chloride on the course of the addition has been investigated. Also the possible formation of two types of 1,6-addition products (IV and V, above) has been touched upon. The results are summarized in Table 1.

By the uncatalyzed addition of *n*-butylmagnesium bromide to *sec*-butyl sorbate a fair yield of a product was obtained, which distilled within a rather narrow boiling point range, but showed a greatly fluctuating refractive index. This fraction was found to be a mixture of addition products, and by saponification it could be separated in an acidic and a somewhat smaller non-acidic fraction; both of these fractions gave products with sharp boiling points and refractive indices (but the occurrence of a smaller, somewhat higher boiling fraction was noted in each case). Microanalyses of samples of the constant boiling fractions were consistent with the calculated values for a *n*-butylhexenoic acid and a *n*-butyl *n*-butylpentenyl ketone, respectively. The acid is the result of a simple conjugate addition of the Grignard reagent to one double bond of the unsaturated ester, while the ketone is the product of one 1,2-addition (to the ester carbonyl group) and one conjugate addition.

The ketonic product was found (as described below) to be essentially one single isomer, namely the 1,2 + 1,4-addition product (VI).

The acidic product was identified (as described below) as a mixture of about 75 % 1,4-addition product (type III): 3-propenylheptanoic acid and 25 % 1,6-addition products (types IV and V): 5-methylnon-3- and -2-enoic acids.

$$\underset{\text{1,4-adduct: acid}_{III}}{CH_3CH=CH-\underset{C_4H_9}{\underset{|}{CH}}-CH_2COOH}$$

$$\underset{\text{1,6-}(\alpha,\delta)\text{-adduct: acid}_{IV}}{CH_3\underset{C_4H_9}{\underset{|}{CH}}-CH=CH-CH_2COOH} \qquad \underset{\text{1,6-}(\gamma,\delta)\text{-adduct: acid}_{V}}{CH_3\underset{C_4H_9}{\underset{|}{CH}}-CH_2CH=CH-COOH} \qquad (1)$$

The ratios between the two 1,6-adducts were approximately 3 to 1, the α,β-unsaturated acid$_V$ being the one present in the larger amount.

In the cuprous chloride catalyzed reactions the yields of conjugate addition products were considerably better and no ketonic product was obtained. Here the favourable effect of stepwise addition of the cuprous chloride recently found [19] (p. 271) is very pronounced. Furthermore, in the one-portion cuprous chloride catalyzed reaction the yield was much lower when the reaction was run on a larger scale. The dependency on the scale of the run was not found when the cuprous chloride was added in smaller portions concurrently with the addition of the ester. This result is consistent with the view [19] that cuprous chloride is active only for a short period in the Grignard reagent solution. The primarily formed cuprous alkyl (RCu, *cf.* below) will gradually decompose into copper metal and hydrocarbon (R—R), and since the addition time for the ester has to be proportional with the scale of the run [20], the catalyst added in the start is probably only active during the addition of the first minor part of the ester.

As may be seen from Table 1 some effect of the scale of the run has also been encountered in the uncatalyzed reaction.

In the catalyzed reactions a higher-boiling product was formed. It was only estimated and isolated in one case. It showed the correct analysis for an ester of a dibasic acid, analogous to the high-boiling glutaric esters formed as by-products from crotonic and other esters [20] by a primary intermolecular Michael condensation, leading to a dimer, followed by a conjugate addition. The infra-red spectrum showed the characteristic absorption for *sec*-butyl esters [21], but the product was not further investigated.

The composition of the acid mixture from the cuprous chloride catalyzed reactions was found (see below) to be remarkably different from that encountered in the uncatalyzed reaction. In this case the product to an extent of more than 90 % was the 1,6-addition products, the ratio of which still was: γ,δ-adduct to α,δ-adduct approximately 3 to 1. Less than 10 % of 1,4-addition product was apparently formed.

DISCUSSION

Apart from substituent influences, such as steric, polarization and hyperconjugation effects, which are considered absent in the diene system of sorbic ester *, two factors seem to be important for the competition between 1,4- and 1,6-additions. In a freely conducting, linear conjugated system polarity is most strongly developed at the ends of the system [14]. Since the reaction consists in an attack by a nucleophilic reagent on a positively charged carbon atom, this terminal polarization will obviously favour 1,6-addition to sorbic ester. On the other hand, if the nucleophilic reagent is one like the Grignard reagent, the magnesium atom of which is known to have a fairly strong tendency for coordination with the oxygen of the carbonyl group, a mechanism involving a cyclic, synchronous electron shift should be energetically favourable. Such a mechanism has been proposed by Lutz and Reveley [22] for the conjugate addition of Grignard reagents to α,β-unsaturated systems, and it has been discussed in previous communications of this series [21,23]:

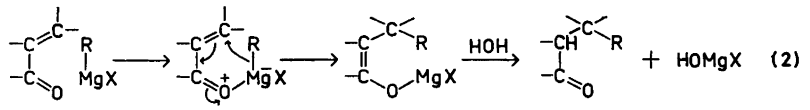

This mechanism involves an electron shift within a *six*-membered ring, and the preference for it will thus favour 1,4-addition over 1,6-addition, which could only arise from a similar mechanism within a sterically much less favourable *eight*-membered ring.

The addition of the sodium derivatives of active hydrogen compounds are examples of the Michael addition reaction. As discussed by Ingold [14], this is a reversible process, which in the cases reported has most likely been run to

* That this is not strictly true is shown by the above cited 7 – 10 % 1,4-Michael addition actually observed in the case of sorbic ester, in contrast to the case of β-vinylacrylic ester which gives exclusively 1,6-addition [1,11,12].

equilibrium, and the resulting addition is therefore probably thermodynamically controlled. This may in most cases, including that of sorbic ester, account for the above-mentioned reported additions.

On the other hand the addition of a Grignard reagent is probably kinetically controlled, and here, although the terminal polarization will favour 1,6-addition, the operation of the cyclic mechanism readily accounts for the predominance of 1,4-addition of Grignard reagents. The results with sorbic ester in the uncatalyzed reaction thus lends further support to the cyclic mechanism.

Cuprous chloride catalysis. As to the effect of cuprous chloride to cause the drastic change in orientation, two viewpoints could be put forward. The generally experienced effect (also found in the work here described) of this catalyst to promote conjugate addition over 1,2-addition in α,β-unsaturated systems [18,24] could be ascribed to a tendency of the cuprous ion to coordinate with the double bond, thus making this more vulnerable for attack of nucleophilic reagents by increasing its polarization (*cf.* below). One would expect that the carbon atom with which the cuprous ion should preferably coordinate would be the α-carbon, and in the case of the diene system the result might then be an increase of the polarization through the full conjugated system; thus the fractional positive charge at the terminal δ-carbon atom should increase. Furthermore, it must be assumed [25] that the cuprous chloride, when added to the Grignard solution, will react to form the cuprous alkyl:

$$\mathrm{RMgBr} + \mathrm{CuCl} \longrightarrow \mathrm{MgBrCl} + \mathrm{RCu}$$

which will then coordinate with the alkenic carbon; thus the following cyclic mechanism, leading to 1,6-addition (and involving a *six*-membered ring) is rendered possible [26]:

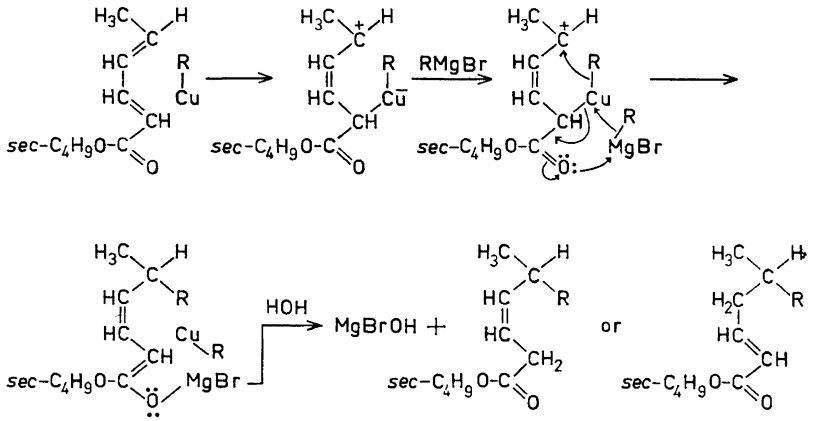

This mechanism accounts for the change in orientation of conjugate addition by the presence of cuprous chloride, and it is consistent with the previously suggested mode of action for cuprous chloride in promoting reduction

of the carbon-carbon double bond in citraconic and mesaconic esters by means of *n*-butylmagnesium bromide [21].

It should be mentioned that a similar cyclic mechanism, involving *two* molecules of cuprous alkyl, one of which coordinates with the α-carbon atom, could explain the above-mentioned *general* effect of cuprous chloride to catalyze the conjugate addition in competition with the 1,2-addition [18,21,24] and the condensation-addition process [20,19]:

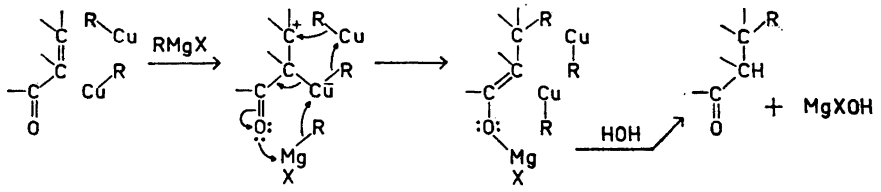

This mechanism is analogous to that suggested by Swain and Boyles [27] for the addition of Grignard reagents to carbonyl groups. In this way all known effects of cuprous chloride on Grignard reactions with α,β-unsaturated esters could be accounted for on the same basis, *viz.* the concept of cuprous ion-alkene carbon coordination.

However, this mechanism implies that the tendency to addition of the cuprous alkyl to the carbon-carbon unsaturated system is greater than for the alkylmagnesium bromide to add to the carbonyl group. Although Gilman has stated [28] that alkylmagnesium halides are more reactive towards addition to carbonyl groups than are cuprous alkyls, it must be remembered that in the case of α,β-unsaturated carbonyl compounds the reactivity of the carbonyl group is strongly reduced by the conjugation with the double bond, and, conversely, the electrophilic reactivity of the β-carbon atom of the double bond correspondingly enhanced. Thus Gilman's reactivity sequence is not likely to be valid in this case. On the contrary, it could be considered as a reasonable assumption that cuprous alkyls are more reactive than Grignard reagents towards addition to an α,β-unsaturated carbonyl compound.

The question of the relative amounts of the two 1,6-adducts [28a] has not really been considered, since the ratio between them should be dependent on the course of the secondarily occurring tautomerization only. Furthermore, the possibility of migration of the double bond during the saponification could not be entirely excluded, although, apparently such a transformation is not encountered in the case of the 1,4-adduct. The infrared spectrum of the adduct-ester from the cuprous chloride catalyzed addition did not show the absorption characteristic for conjugated carbon-carbon double bonds (1 600—1 650 cm^{-1}) as did the spectrum of the acid obtained from it (*cf.* Table 2), and the ester carbonyl band (1 740 cm^{-1}) was found above the region usually assigned to α,β-unsaturated ester carbonyl (1 730—1 717 cm^{-1}). These facts, however, do not necessarily exclude the possibility that the ester also is α,β-unsaturated [29].

The questions of the composition of the ketonic adduct obtained in the uncatalyzed reaction and of the non-formation of such a ketonic adduct in the cuprous chloride catalyzed reaction are considered in the experimental part.

IDENTIFICATION AND ESTIMATION OF ISOMERIC ACIDS

This was accomplished by means of gas-liquid chromatography and infra-red spectroscopy (besides conventional chemical analytical methods). The problem was attacked in two ways: investigation of the mixture of unsaturated acids obtained by saponification of the primary products (*cf.* Table 2), and investigation of saturated acids produced by the oxidative degradation of the unsaturated acids.

Identification of unsaturated acids. By fractional distillation the mixtures of acids could be separated in only two fractions, one boiling at 98—99°/0.6 mm and one at 110—110.5°/0.7 mm, both fractions giving correct analyses for $C_{10}H_{18}O_2$. The product from the uncatalyzed addition process consisted almost exclusively of the low-boiling acid.

Infra-red spectroscopy indicated a double bond in the α,β-position to the carboxyl group [29a] in the secound of these fractions, whereas this conjugation was absent in the first fraction.

Table 2. C_{10}-Acids from adducts and authentic samples. Physical data and analyses. (Calc. for $C_{10}H_{18}O_2$ (170.24): C 70.54; H 10.66; neutr. equiv. 170.24).

Acid	b.p. °C/mm Hg	Ref. index at °C	Analyses	Infra-red spectrum
No. 1. from non-cat. addition	98—101/0.7 118—121/3	1.4462 at 25° 1.4494 at 20°	neutr. equiv. 172	similar to those of nos. 2, 4 and 5
No. 2. low-boil. from CuCl-cat. addition	98—99/0.6	1.4485 at 20°	C 70.65 H 10.60	similar to those of nos. 1, 4 and 5
No. 3. high-boil. from CuCl-cat. addition	110—110.5/0.7	1.4623 at 20°	C 70.45 H 10.66	similar to that of no. 6, bands at 1 707 cm^{-1}(C=O) and 1 655 cm^{-1} (C=C)[a]
No. 4. authentic $acid_{III}$ (mixture[b])	92/0.5	1.4471 at 20°	C 70.55 H 10.49	similar to those of nos. 1, 2 and 5
No. 5. authentic $acid_{IV}$	102/1	1.4481 at 20°	C 70.35 H 10.63	similar to those of nos. 1, 2 and 4
No. 6. authentic $acid_{V}$	110—111/0.9	1.4610 at 25°	C 70.45 H 10.46	similar to that of no. 3.

[a] Characteristic absorptions for α,β-unsaturated acids [29a].
[b] See experimental part, p. 288.

The three possible isomeric acids: $acid_{III}$, $acid_{IV}$ and $acid_{V}$ (*cf.* (1), p. 280) were synthesized independently by other routes, as described below. Of these (*cf.* Table 2), acid III (the 1,4-adduct) and $acid_{IV}$ (the 1,6-(α,δ)-adduct) had very similar physical properties (boiling points, refractive indices and infra-red spectra), and these properties were largely in agreement with those of the lower-boiling acid-fraction obtained by the addition reactions. The properties of the higher-boiling acid-fraction, on the other hand, were very nearly the same as those of the authentic 1,6-(γ,δ)-adduct ($acid_{V}$).

By gas chromatography, however, the acids from the addition reactions were further separated, and *the components were identified* as $acid_{III}$, $acid_{IV}$ and $acid_{V}$ (1). All three isomeric acids were found in both the above-mentioned fractions. The lower-boiling fractions (from the uncatalyzed as well as from the catalyzed addition) were, essentially, mixtures of acid III and acid IV, whereas the higher-boiling fraction (from the catalyzed reaction only) was practically pure $acid_{V}$.

In order to *estimate the ratios of isomeric adducts* in the products, the two addition reactions were repeated twice and, after saponification, the crude acidic reaction products were analyzed gas-chromatographically, giving, in average, the results of Table 1.

Further evidence of the *identities* of the acid-isomers was obtained by oxidative degradation with alkaline potassium permanganate. By this treatment the three isomers should give, as main products, *n*-butylsuccinic acid, 2-methylhexanoic acid and 3-methylheptanoic acid, respectively:

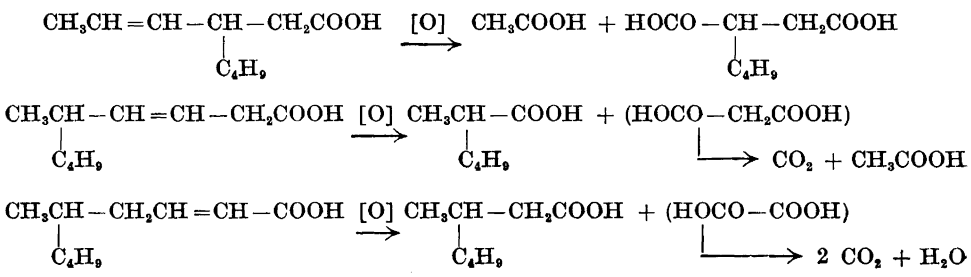

These three acids were synthesized independently as authentic samples (see experimental part), and by gas-chromatographic investigation the oxidation products were found to be, essentially, mixtures of them. *n*-Butylsuccinic acid, which is a solid (m.p. 81°), was isolated analytically pure, and it was further identified by comparison with the authentic sample, also with respect to infra-red spectrum and mixed melting point.

The ketonic product from the uncatalyzed reaction appears, according to the gas-chromatographic analysis, to contain only one compound. The infra-red spectrum showed a ketonic carbonyl group but no indication of conjugated carbon-carbon double bond. This ketone was identified as the 1,2 + 1,4-addition product (VI) by comparison of its data with those of ketonic samples synthesized from the acidic addition products. However, this does not necessarily mean that only this kind of 1,2 + conjugate addition occurs (see experimental part).

GAS-LIQUID CHROMATOGRAPHIC IDENTIFICATIONS AND DETERMINATIONS

The instrument used was a Griffin and George apparatus, mark II.

The acids were separated as the methyl esters into which they were converted by treatment for 5 min. with a 2 % solution of diazomethane in ether, followed by evaporation of the excess of diazomethane and ether on the steam-bath [30]. The column consisted of 1.8 m of Celite 545 with 25 % of "Apiezon" grease M. Helium was used as the carrier gas with a flow rate of 1 l per h. The operating temperature was 160° and the sample size was 10—20 mg.

In the case of the ketonic products the column consisted of 0.9 m of Celite 545 with 30 % of silicone elastomer E 301. The operating temperature was 180° while the other conditions were the same as those for the methyl esters.

The retention times are given in Table 3.

The quantitative determinations are based upon the assumption that the areas under the recorded peaks are proportional to the molar percentages of the corresponding components in the mixtures. Previously, quantitative analyses of methyl esters of *straight chain* fatty acids [31] have indicated that, by using this principle of calculation, the values obtained for the components being present in large quantities may be somewhat too high. Such an uncertainty may be eliminated by calibrating the instrument on pure compounds. Although the error thus introduced is unknown in the present case, it is probably small and certainly not of major importance for the problems under discussion in this work. No attempt has, therefore, been made to calibrate the instrument with respect to the components analyzed.

EXPERIMENTAL

Microanalyses are by Mr. Preben Hansen, Microanalytical Division, The Chemical Laboratory, The University of Copenhagen. Fractional distillations were through a simple 45 cm × 8 mm Podbielniak-type coloumn with a tantalum wire spiral, a heated jacket and a partial reflux head.

All products were checked by infra-red spectroscopy on solutions in carbon tetrachloride, using a Beckman IR2 single-beam spectrophotometer with sodium chloride optics. The spectra were recorded by one of us (S.R.) except for the spectra of acid$_{IV}$, ketone$_{none}$ and ketone$_{CuCl}$, which were measured by Mrs. Inger Grete Krogh Andersen, M.Sc.

Table 3. Gas-liquid chromatographic retention times (min) for addition products.

Type of product	Type of adduct		
	1,4	1,6-(α,δ)	1,6-(γ,δ)
Methyl ester of acid	31	37	61
Ketone	26	29	47

sec-*Butyl sorbate was prepared* from commercial acid (Fluka, *purum*) using the general esterification procedure previously described [20], b.p. 105°/17 mm, n_{20}^{D} 1.4846, yield 85 %. (Neutr.equiv. found: 167.6. Calc. for $C_{10}H_{16}O_2$: 168.23).

Non-catalyzed additions of n-*butylmagnesium bromide to* sec-*butyl sorbate* were carried out in 0.1 or 0.2 mole scales as previously described [17]: The solution of *n*-butylmagnesium bromide was prepared during about 1 h from 12.6 g (0.52 g-atom) of magnesium and 85 g (0.62 mole) of *n*-butyl bromide dissolved in 240 ml of ether. The solution was effectively stirred and cooled in ice-water during 15 min; then 33.6 g (0.2 mole) of *sec*-butyl sorbate, dissolved in 200 ml of ether, was added dropwise over a period of about 3 h. When the addition was completed, stirring was continued in the ice-bath for another 15 min and for 1 h at room temperature. The reaction mixture was then poured onto a mixture of ice, concentrated hydrochloric acid (55 ml) and ether (100 ml) under vigorous shaking and worked up the conventional way [20]. When only 0.1 mole of ester was used the addition time was about 1.5 h.

The fractional distillations gave, in 65 % yield, a product with boiling point range 77—101°/0.7 mm and refractive index range n_D^{25} 1.4426—1.4767. Most of this product (75 %) distilled at 77—82°/0.7 mm and had n_D^{25} 1.4430, but showed by elementary analysis the carbon content too high for the simple conjugate addition product. This product, on saponification (see below), gave a 50 % yield of an acid (compound 1, Table 2). In addition a 35 % yield of a non-acidic ketonic product, b.p. 85—86°/1 mm, n_D^{20} 1.4500, was obtained. (Found: C 79.90; H 12.40. Calc. for $C_{14}H_{26}O$ (210.35): C 79.93; H 12.46).

Cuprous chloride catalyzed addition of n-*butylmagnesium bromide to* sec-*butyl sorbate* differed from the non-catalyzed addition in that 1.5 mole per cent of cuprous chloride * was added to the Grignard reagent after cooling in ice-water for 15 min, either in one portion just before addition of the ester is started [18] or in small portions at intervals of 20—30 min throughout the addition of the ester solution [19].

By the distillation was obtained a mixture of simple conjugate addition products: *sec*-butyl *n*-butylhexenoates (III, IV and V), b.p. 82°/0.9 mm, n_D^{25} 1.4383. (Found: C 74.40; H 11.47. Calc. for $C_{14}H_{26}O_2$ (226.25): C 74.28; H 11.58). A higher-boiling fraction, b.p. 151—154°/0.9 mm, n_D^{25} 1.4622, is probably a condensation-addition product (*cf.* above, p. 281). (Found: C 72.80; H 10.38. Calc. for $C_{24}H_{42}O_4$ (394.58): C 73.05; H 10.73).

The lower-boiling ester-mixture was saponified (see below). No non-acidic fraction was found (*cf.* below). The acidic fraction distilled over a long boiling point range. By careful fractionation two samples were obtained: a low-boiling fraction (compound 2, Table 2) and a high-boiling fraction (compound 3, Table 2).

Saponifications of esters were carried out essentially as previously described [20]: The ester, dissolved in ethanol was refluxed with a three-fold excess of potassium hydroxide for at least 8 h. The ethanol, 2-butanol and other non-acidic products were removed by distillation and extraction, and the acidic products were then obtained by acidification and extraction.

Preparation of authentic adduct-acids. For the use in the gas-chromatographic and spectroscopic identification work (above) the acids corresponding to the three types of adducts (III, IV and V) were prepared ** as authentic samples (see Table 2). Of these, $acid_{III}$, 3-propenylheptanoic acid (compound 4, Table 2) was prepared by the malonic ester synthesis from 4-bromoöct-2-ene. This "allylic" bromide was obtained by the action of phosphorus tribromide on the

* With respect to the Grignard reagent, *e.g.* 0.75 g of cuprous chloride to 0.2 mole of ester.

** The valuable participation in this synthetic work by Mr. Henrik Brink Clausen, Miss Jette Holmblad, Mr. Steffen Jacobsen, Mr. Axel Sonne and Mr. Peter Tommerup, students at the Polyteknisk Læreanstalt for the M.Sc. degree in chemical engineering, is gratefully acknowledged.

corresponding alcohol, prepared from crotonaldehyde and *n*-butylmagnesium bromide *:

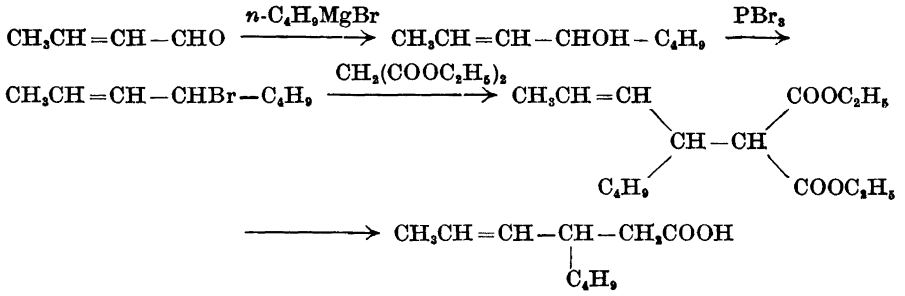

It was expected that this acid$_{III}$-sample should be a mixture of this acid and the isomeric 3-methylnon-4-enoic acid, resulting from an allylic inversion at one of the steps above:

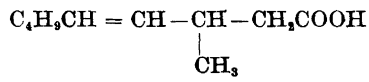

This mixture should, however, be just as useful for the identification by gas chromatography as the pure acid $_{III}$. This proved also to be the case. The product was found to contain about 50 % of acid$_{III}$, which was easily recognized, but the remainder consisted of not one, but two isomeric acids amounting to about 20 and 30 %, resp., of the mixture.

The following data was found for the intermediate compounds. The alcohol, oct-2-en-4-ol, was prepared in 65 % yield according to Hurd and Puterbaugh [32a], b.p. 77–80°/13 mm, n_D^{20} 1.4417 (rep.[32a] 74°/8 mm, n_D^{20} 1.4395). The gas-chromatographic analysis indicated a mixture of two compounds, but the amount of one of them was only about 15 %. The bromide, 4-bromoöct-2-ene, was obtained in about 45 % yield using a procedure given by Jones *et al.*[33] for methallyl bromide; b.p. 67–69°/10 mm, n_D^{25} 1.4631 (rep.[34] b.p. 76°/18 mm, n_D^{25} 1.4632). The gas-chromatographic analysis indicated the presence of two bromides, representing about 15 and 85 %, resp., of total. The alkylated malonic ester, diethyl 2-propenylhexan-1,1-dicarboxylate, was prepared in 52 % yield as described for *n*-butylmalonic ester in *Organic Syntheses* [35], b.p. 98–100°/0.6 mm, n_D^{25} 1.4422. (Found: C 66.70; H 9.56. Calc. for $C_{15}H_{26}O_4$ (270.36): C 66.63; H 9.69). The gas-chromatographic analysis showed the presence of three compounds, the percentages being approximately 40, 45 and 15 %, resp. The last step in the above sequence, the hydrolysis and decarboxylation of the malonic ester, was carried out essentially as described in *Organic Syntheses* for 3-methylpentanoic acid [36]. However, decarboxylation did not take place as readily as there indicated, and, consequently the acid distilled off only very slowly. The crude reaction mixture (probably mainly un-decarboxylated malonic acid) was

* This sequence of reactions were suggested to us by the analogous preparation of 3-methylhex-4-enoic acid [32] by Jack W. Ralls and William J. Weston of United States Department of Agriculture, Agricultural Research Service, Western Utilization and Development Division, Albany 10, California. This information was kindly placed at our disposal by Dr. Jack W. Ralls, who reports the preparation in high purity of methyl 3-methylhex-4-enoate in an overall yield of 56 % from the corresponding alkylated malonic ester, which in turn was obtained in 84 % yield. The methyl 3-methylhex-4-enoate was found by gas chromatography to consist of one single compound.

subjected to distillation *in vacuo*. Now decarboxylation did take place, and a crude acid, b.p. 140°/20 mm, was obtained. After redistillation (*cf.* Table 2) the yield of $acid_{III}$ was 69 %.

The problem of the identities of the isomers in the malonic ester and the $acid_{III}$ preparation has not yet been solved but is the subject of further studies.

$Acid_{IV}$ and $acid_V$ were both obtained by the condensation of 3-methylheptaldehyde with malonic acid:

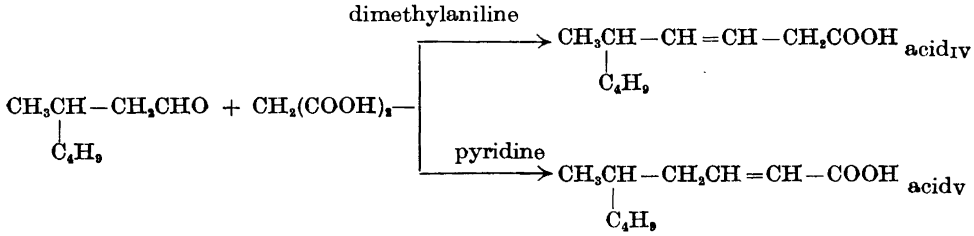

The use of pyridine, according to the general procedure given in *Organic Syntheses* [37], leads to the predominant formation of the α,β-unsaturated $acid_V$, whereas the use of other amine bases, such as dimethylaniline, according to Boxer and Linstead [38], gives the β,γ-unsaturated $acid_{IV}$.

The 3-methylheptaldehyde, b.p. 50—52°/10 mm, was secured in 40 % yield by the Rosenmund reduction [39] of the acid chloride. Toluene was used as the solvent instead of xylene in order to facilitate separation of the aldehyde by fractional distillation. 3-Methylheptanoyl chloride, b.p. 70—72°/10 mm, was obtained in about 90 % yield from the acid by means of thionyl chloride. The preparation of 3-methylheptanoic acid (*cf.* below) is previously described [20].

Preparation of authentic adduct-ketones. The corresponding authentic ketones proved considerably more difficult to obtain. After several unsuccessful attempts to synthesize them along independent routes, two ketonic samples were prepared using the acid-mixtures from the adducts as starting materials: the lower-boiling acid from the uncatalyzed addition reaction (compound 1, Table 2; mainly the 1,4-adduct) and the acid-mixture from the cuprous chloride catalyzed reaction (compounds 2 + 3, Table 2; essentially 1,6-adducts). These acid-mixtures were converted into the crude acid chlorides (b.p. 95—105°/15 mm and 73—80°/1.2 mm, resp.) in 80—90 % yields by treatment with thionyl chloride at room temperature for several hours. From the acid chlorides the crude *n*-butyl ketones were prepared (in yields of 68 and 35 %, resp.) using the cadmium reaction as described by Cason [40]: The acid chloride, dissolved in benzene, was added to di-*n*-butylcadmium in benzene, prepared from *n*-butylmagnesium bromide and dry cadmium chloride.

Purified samples of the two ketones showed the following physical data (calc. for $C_{14}H_{26}O$ (210.35): C 79.93; H 12.46):

$Ketone_{none}$ (from the "non-catalyzed adduct-acid mixture"), b.p. 81—83°/0.7 mm, n_D^{25} 1.4444. (Found: C 79.95; H 12.60.)

$Ketone_{CuCl}$ (from the "cuprous chloride catalyzed adduct-acid mixture"), b.p. 89—92°/0.5 mm, n_D^{25} 1.4492. (Found: C 78.20; H 12.23.)

Comparison of their infra-red spectra with the spectrum of the ketonic product, obtained directly by the addition reaction, indicated this ketone to be identical with $ketone_{none}$, that is the 1,2 + 1,4-addition product VI. Whereas this compound did not show infra-red absorption characteristic for an α,β-unsaturated ketone (the C=O band being at 1 715 cm^{-1}), this was indeed the case with $ketone_{CuCl}$, which showed a split C=O absorption with peaks at 1 685 and 1 665 cm^{-1} and a strong C=C band at 1 610 cm^{-1} [41].

The gas-chromatographic analyses of the two ketonic samples indicated $ketone_{none}$ to be essentially one single compound, identical with the ketonic adduct. $Ketone_{CuCl}$, on the other hand, contained two compounds, of which the one present in the smaller quantity (about 15 %) was identical with $ketone_{none}$ (and the ketonic adduct), whereas the one present in the larger amount (about 85 %) had a longer retention time (*cf.* Table 3).

$Ketone_{CuCl}$ was obtained only in a poor yield, a large amount of non-distillable polymeric products being formed. As the elementary analysis (above) showed, the product is not pure. However the infra-red spectrum and the gas-chromatographic analysis indicated that it is essentially the α,β-unsaturated 1,6-(γ,δ)-ketone, as expected since it is obtained from an acid-product consisting mainly of the corresponding unsaturated acid. Several attempts were made to purify $ketone_{CuCl}$ in order to obtain a sample showing the correct elementary analysis. Each time the major part of the product was lost because of extensive polymerization. The instability of the α,β-unsaturated ketone towards polymerization not only explains the low yield and purity of $ketone_{CuCl}$, but also the fact that $ketone_{CuCl}$ contains as much as 15 % of the 1,4-ketone (VI) while the acid from which it is made only contains a few percent of 1,4-acid ($acid_{III}$). Likewise, the $ketone_{none}$ is almost 100 % 1,4-ketone (VI) while the acid mixture from which this ketone is derived contains 20 % of α,β-unsaturated acid ($acid_V$). In fact, the easy polymerization of the α,β-unsaturated ketone under alkaline conditions is probably also the reason for the two encountered results: a) the ketone obtained in the uncatalyzed reaction is almost 100 % 1,4-ketone (VI) in contrast to the corresponding acid-adduct which contains as much as 20 % of α,β-unsaturated acid ($acid_V$), and b) no ketonic adduct whatsoever is obtained in the cuprous chloride catalyzed reaction, although it would indeed have been reasonable to expect at least some 1,6-ketone. The latter may very well form, however, but one would expect it to be mainly the α,β-unsaturated ketone, which will polymerize. Thus the percentages given in Table 1 for the ketonic adducts do probably not give the true picture of the 1,2 + conjugate additions which have actually taken place.

Oxidative cleavage. Unsaturated acids were oxidized essentially according to the procedure of *Organic Syntheses* [42] for the preparation of azelaic acid from castor oil. In a 2 l three-necked flask, fitted with mechanical stirring, 98 g (0.62 mole) of potassium permanganate was dissolved in 1 200 ml of water. The solution was heated to 35°, and 20 g (0.118 mole) of unsaturated acid, dissolved in a solution of 10 g (0.18 mole) of potassium hydroxide in 250 ml of water, was added in one portion. In 5 min the temperature rose to 60—65° and stayed there for about 1 h. The reaction mixture was now subject to filtration which was very slow (several hours), and the manganese dioxide was washed twice with hot water. The alkaline solution was evaporated to about 750 ml, and, after acidification, continuously extracted with ether for 24 h. The ether solution was dried over sodium sulfate, and the ether and most of the acetic acid (*cf.* p. 285) was distilled. The residue was subjected to gas-liquid chromatography, and the components: *n*-butyl-

succinic, 2-methylhexanoic, and 3-methylheptanoic acids were identified by comparison of the retention times with those of the authentic samples described below.

In the case of the acid-fraction from the uncatalyzed reaction, the residue solidified and a 65 % yield of *n*- butylsuccinic acid was obtained. However, by the gas-chromatographic analysis 2-methylhexanoic and 3-methylheptanoic acids were found as well. In the case of the acid-product from the cuprous chloride catalyzed reaction *n*-butylsuccinic acid crystallized in the otherwise liquid residue. Also here all three possible degradation products were found.

Authentic *n-butylsuccinic acid*, m.p. 81°, was obtained by saponification (se above) of its *sec*-butyl ester, which was available from the addition of *n*-butylmagnesium bromide to *sec*-butyl maleate [21]. Authentic *2-methylhexanoic acid*, b.p. 104—105°/15 mm, n_D^{25} 1.4220, neutr. equiv. 132 (calc. for $C_7H_{14}O_2$: 130.18), was prepared by the malonic ester synthesis from diethyl methylmalonate and *n*-butyl bromide according to the procedure of *Organic Syntheses* [35,36]. Authentic *3-methylheptanoic acid*, b.p. 116°/10 mm, was obtained by saponification (se above) of its *sec*-butyl ester, which was available by the addition of *n*-butylmagnesium bromide to *sec*-butyl crotonate [17,19].

Also the *ketone* obtained by the addition process was subjected to oxidative cleavage, ozonization being applied in this case [43]. The crude ozonides were oxidized with peracetic acid, the resulting acid mixture transformed into methyl esters as above [30], and analyzed by gas chromatography. Although no proper identification was attained because of the lack of an authentic sample of the main cleavage product, further evidence for the identity of the ketone with VI was found in the fact that the cleavage product was a large-molecule acid, with a retention time far above those of 2-methylhexanoic and 3-methylheptanoic acids (*cf.* above) which would have been the main cleavage products from 1,2 + 1,6-addition product ketones.

The authors want to express their gratitude towards *Otto Mønsteds Fond* and *Det Teknisk-Videnskabelige Forskningsråd* for financial support.

REFERENCES

1. Kohler, E. P. and Butler, F. R. *J. Am. Chem. Soc.* **48** (1926) 1036.
2. Reimer, M. *Am. Chem. J.* **38** (1907) 227 [*Chem. Zentr.* **1907 II**, 1240].
3. Mcleod, A. L. *Am. Chem. J.* **44** (1910) 331 [*Chem. Zentr.* **1910 II**, 1706].
4. Reimer, M. and Reynolds, G. P. *Am. Chem. J.* **40** (1908) 428 [*Chem. Zentr.* **1909 I**, 71].
5. Kohler, E. P. *Am. Chem. J.* **31** (1904) 642 [*Chem. Zentr.* **1904 II**, 444].
6. Fuson, R. C. and Libby, W. H. *J. Org. Chem.* **16** (1951) 626.
7. Gaertner, R. *Chem. Revs.* **45** (1949) 49; Kharasch, M. S. and Reinmuth, O. *Grignard Reactions of Nonmetallic Substances*, Prentice-Hall, New York 1954, p. 234 ff.
8. Fuson, R. C. and McKusick, B. C. *J. Am. Chem. Soc.* **65** (1943) 60; Fuson, R. C. and Tull, R. *J. Am. Chem. Soc.* **71** (1949) 2543; Fuson, R. C., Emmons, W. D. and Smith, S. G. *J. Am. Chem. Soc.* **77** (1955) 2503.
9. Julian, P. L. and Cole, W. *J. Am. Chem. Soc.* **57** (1935) 1607; Julian, P. L. and Gist, W. J. *J. Am. Chem. Soc.* **57** (1935) 2030.
10. Ralls, J. W. *Chem. Revs.* **59** (1959) 329.
11. Farmer, E. H. and Healy, A. T. *J. Chem. Soc.* **1927** 1060.
12. Farmer, E. H. and Metha, T. N. *J. Chem. Soc.* **1930** 1610.
13. Farmer, E. H. and Metha, T. N. *J. Chem. Soc.* **1931** 1904; Bloom, J. and Ingold, C.K. *J. Chem. Soc.* **1931** 2765.
14. Ingold, C. K. *Structure and Mechanism in Organic Chemistry*, Cornell University Press, Ithaca, N.Y. 1953, p. 697—699.
15. Ames, D. E. and Bowman, R. E. *J. Chem. Soc.* **1950** 329.
16. Charlish, J. L., Davies, W. H. and Rose, J. D. *J. Chem. Soc.* **1948** 232.
17. Munch-Petersen, J. *Acta Chem. Scand.* **12** (1958) 967.
18. Munch-Petersen, J. *Acta Chem. Scand.* **12** (1958) 2007; 2046.
19. Munch-Petersen, J. and Andersen, V. K. *Acta Chem. Scand.* **15** (1961) 271.
20. Munch-Petersen, J. *J. Org. Chem.* **22** (1957) 170.

21. Bjerl Nielsen, E., Munch-Petersen, J., Møller Jørgensen, P. and Refn, S. *Acta Chem. Scand.* **13** (1959) 1943.
22. Lutz, R. E. and Reveley, W. G. *J. Am. Chem. Soc.* **63** (1941) 3180.
23. Munch-Petersen, J., Møller Jørgensen, P. and Refn, S. *Acta Chem. Scand.* **13** (1959) 1955.
24. Bretting, C., Munch-Petersen, J., Møller Jørgensen, P. and Refn, S. *Acta Chem. Scand.* **14** (1960) 151.
25. Gilman, H. and Straley, J. M. *Rec. trav. chim.* **55** (1936) 821.
26. *Cf.* Ref.[21], p. 1950.
27. Swain, C. G. and Boyles, H. B. *J. Am. Chem. Soc.* **73** (1951) 870.
28. Gilman, H. in Gilman, H. *Organic Chemistry*, 2nd, Ed., Vol. **I**, John Wiley and Sons, New York 1943, p. 520.
28a. Ingold[14], pp. 696 and 562 ff.
29. Bellamy, L. J. *The Infra-Red Spectra of Complex Molecules*, Methuen, 2nd. Ed. 1958. *a.* pp. 168 and 41. *b.* pp. 179 and 181.
30. Jart, Aa. *Oléagineux* **14** (1959) 651.
31. Jart, Aa. *Acta Chem. Scand.* **13** (1959) 1723.
32. See also Bergmann, E. *Helv. Chim. Acta* **20** (1937) 590.
32a. Hurd, C. D. and Puterbaugh, M. P. *J. Org. Chem.* **2** (1937) 381.
33. Jones, W. J., Davies, W. C., Bowden, S. T., Edwards, C., Davis, V. E. and Thomas, L. H. *J. Chem. Soc.* **1947** 1448.
34. Karasev, K. I. and Khabarova, *J. Gen. Chem.* **10** (1940) 1645 [Beilstein, *Drittes Ergänzungswerk* **I** [1] 840; *cf. Chem. Abstracts* **35** (1941) 3225].
35. Adams, R. and Kamm, R. M. *Organic Syntheses* Coll. Vol. **I** (1941) 250.
36. Vliet, E. B., Marvel, C. S. and Hsueh, C. N. *Organic Syntheses* Coll. Vol. **II** (1943) 416.
37. Allen, C. F. H. and Van Allan, J. *Organic Syntheses* **24** (1944) 92.
38. Boxer, S. E. and Linstead, R. P. *J. Chem. Soc.* **1931** 740.
39. Hershberg, E. B. and Cason, J. *Organic Syntheses* **21** (1941) 84.
40. Cason, J. and Prout, F. S. *Organic Syntheses* **28** (1948) 75; Cason, J. and Rapoport, H. *Laboratory Text in Organic Chemistry*, Prentice-Hall, New York 1950, p. 325.
41. Bellamy[29], pp. 136 and 41.
42. Hill, J. W. and McEwen, W. L. *Organic Syntheses* Coll. Vol. **II** (1943) 53.
43. Jart, Aa. *To be published.*

Received September 27, 1960.

ACTA CHEMICA SCANDINAVICA 15 (1961) 293–299

Conjugate Additions of Grignard Reagents to alpha, beta-Unsaturated Esters

X. Possible Influence of the Halogen in the Grignard Reagent

JON MUNCH-PETERSEN and VIGGO KØGS ANDERSEN

Organisk-kemisk Laboratorium, Polyteknisk Læreanstalt, Copenhagen, Denmark

The yields of simple conjugate addition products from *sec*-butyl crotonate and alkylmagnesium halides decrease in the sequence Cl ≧ Br ≫ I. In the cuprous chloride catalyzed reaction the yields from the three halides are equal and the same as those from the chlorides in the uncatalyzed reaction (about 80–85 %). Improvements of the preparative procedure for 3-methylalkanoic acids have been attained in certain cases. Thus, from *tert*-butylmagnesium chloride a 78 % yield of β,γ,γ-trimethylvaleric ester has been obtained.

In most discussions of reactions involving Grignard reagents the significance of the halogen is largely neglected. The relative reactivities of the different halides (I > Br > Cl) in the *preparation* of the Grignard reagents are well-known, and this knowledge suitably coupled with considerations of availability and ease of handling of the halides and of the alkylmagnesium halides is usually decisive for the choice of the Grignard reagent. Thus, in series of Grignard reagents investigated, most halides employed are bromides, but as the methylmagnesium halide the iodide is often used and as the *tert*-butyl- and benzylmagnesium halides the chlorides.

However, it appears to be a widely accepted implicit assumption that the opposite sequence: Cl > Br > I holds true for the reactivities of the Grignard reagents [1].

The present paper describes the results of conjugate additions of some alkylmagnesium halides to *sec*-butyl crotonate under conditions which have previously [2,3] been found favourable for 1,4-addition of alkylmagnesium bromides;

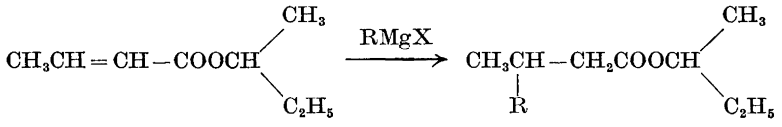

The reactions were carried out by the slow addition of the ester to an excess of cooled Grignard reagent, uncatalyzed [2] as well as cuprous chloride catalyzed [3], the catalyst being applied in small portions throughout the addition of the ester.

It is seen (Tables 1 and 2) that the bromides are quite satisfactory as compared to the other two halides, and, all circumstances considered, probably would be the preferred halides in many cases. Although alkylmagnesium chlorides may give better yields (and cuprous chloride catalysis is rendered unnecessary), the alkyl chlorides are less reactive towards magnesium and the preparation of the Grignard reagents from them is, therefore, somewhat more troublesome. In case of the lower alkyls the alkyl chlorides also have the disadvantage of being very low boiling. The alkylmagnesium chlorides are, furthermore, considerably less soluble in ether, a fact which with *tert*-butyl- and methylmagnesium chlorides causes the reaction mixture to become heterogenous. The iodides, as represented by *n*-butyl-, *n*-propyl- and methylmagnesium iodides, are definitely inferior to the other two halides.

Naturally, an evaluation of the effect of variations in the halogen moiety on a Grignard reagent is difficult. In the first place the extent to which various competing reactions occur should be estimated, and, in the second place, a large number of factors must be considered in the attempted interpretation, such as electronegativities of organic radicals, steric effects, and solubilities of reactants and products.

One of the few accounts in the literature, known to the present authors, which deal with the relative reactivities of alkylmagnesium chlorides, bromides and iodides *, is a paper by Wotiz, Hollingsworth and Dessy [6], who have determined the rate of extraction of a proton from an alkyne by means of a series of Grignard reagents. These may be arranged according to increasing reactivity as follows:

$$CH_3MgI,\ CH_3MgBr < CH_3MgCl < n\text{-}C_3H_7MgBr < C_2H_5MgI$$

$$< C_2H_5MgBr < C_2H_5MgCl < iso\text{-}C_3H_7MgBr < \text{allylMgBr}$$

This sequence indicates that alkylmagnesium chlorides are more reactive than bromides which are again more reactive than iodides, and the results are thus in accordance with the above-mentioned generally assumed reactivity order [1]. It should be noted, however, that the differences due to changes in the halogen moiety are smaller than the differences caused by varying the alkyls of the Grignard reagents. In this reaction with alkynes, coordination of the magnesium atom should be insignificant and the steric requirements on the Grignard reagent should be small. Thus the above results may be considered to give the order of nucleophilic reactivities of the Grignard reagents.

However, the general statement that the sequence of the reactivities of the Grignard reagents is the reverse of the sequence of the reactivities of the corresponding halides towards magnesium [1] is apparently not in accordance

* Gilman[5] also reports decreasing reactivities for the *n*-butylmagnesium halides: Cl > Br > I in the reduction of azobenzene.

with Wotiz' above-mentioned results, this divergence being especially evident in the case of allylmagnesium bromide (*cf.* also below).

In contrast to the above-mentioned reaction of Grignard reagents with alkynes [7], the addition of Grignard reagents to α,β-unsaturated carbonyl compounds is generally believed to take place according to a mechanism [8] which involves the primary coordination of magnesium with carbonyl oxygen, followed by a cyclic synchronous electron shift within a six-membered ring, resulting in the transfer of the alkyl group to the β-carbon atom. Therefore, although here again the nucleophilic reactivity of the alkyl group should be of importance, also the electrophilic reactivity of the magnesium atom as well as the spatial properties of the Grignard reagents as a whole may play a significant role. Furthermore, the situation is in this case still more complex. A variety of competing reactions may take place besides the 1,4-addition, *e.g.* 1,2-additions [9], condensation reactions [4] and reductions [10], and it is hard to say how the probability of the occurrence of these processes is influenced by the different factors. Again the case of allylmagnesium bromide is illustrative. As mentioned above, its nucleophilic reactivity is found to be exceptionally high. In the reaction with α,β-unsaturated esters, this Grignard reagent gives, exclusively and in high yields, 1,2-addition products under conditions which in the case of other Grignard reagents lead to 1,4-addition only [11]. Furthermore, addition to the carbonyl group of the so-called "butenyl" Grignard reagent is taking place with sterically hindered ketones which are reduced by other Grignard reagents [12]. The peculiar reactivity of the allylic Grignard reagents is presumably caused by a special mechanism operating [12,11].

Also, as mentioned above, the solubilities of the alkylmagnesium halides differ considerably, and this fact may strongly affect the results. Thus methyl-, ethyl- and *tert*-butylmagnesium chlorides are slurries of greyish-white precipitates in ether. Wotiz, Hollingsworth and Dessy [6] state that such precipitates consist of magnesium chloride. This being true would — according to the Schlenk equilibrium — mean that the metalloörganic compounds in these cases to a much larger extent are dialkylmagnesiums than alkylmagnesium halides (or a complex between dialkylmagnesium and magnesium halide, as recently suggested by Dessy [13]). The former are believed to be less reactive than the latter as regards coordination of magnesium with the carbonyl oxygen [14]. Since the above-mentioned mechanism [3] involves such a complex formation and since, furthermore, a large excess of Grignard reagent is essential for obtaining high yields of simple 1,4-addition products from α,β-unsaturated esters and Grignard reagents [2], the relatively lower yields from *tert*-butyl- and methylmagnesium chloride may in part be accounted for on the basis of the low solubility of these Grignard reagents. Especially the strongly improved yield from the soluble *tert*-butylmagnesium bromide indicates that the solubility may be important. Also the significant rise in the yield obtained from the chloride when a greater amount of Grignard reagent is used (see experimental part) could be taken as an evidence that the low solubility causes the excess of Grignard reagent to be too small in the usual procedure to provide favourable conditions for the 1,4-addition. It is consistent with these interpretations that at 0° (*cf.* below), the yield from the soluble *tert*-butylmagnesium bromide is unaffected by such an increase in the quantity of the

Table 1. Additons of Grignard reagents (RMgX) to *sec*-butyl crotonate; % 1,4-addition.

R	Temp. °C	X					
		Cl		Br		I	
		uncat.	CuCl	uncat.	CuCl	uncat.	CuCl
n-C_4H_9	0	85	85	70–75	82–85	45	86
n-C_3H_7	0	86	89	60–66	69–74	43	84
	−10				88		
iso-C_3H_7[a]	0	78–82	82–85	51–57	64–71		
	−10				80		
tert-C_4H_9[a,b]	0	14 (22)	27 (60–78)	50	52 (49)		
	−10		48 (65)	39	62 (78)		
CH_3	−10	0	55–65	0	61–65	0	27–29

[a] *Iso*propyl- and *tert*-butylmagnesium iodides were not included since the yields of Grignard reagents in these cases were so low due to side-reactions that the results of the addition reactions would be of no significance (*cf.* Ref.[1], p. 32; Tschelinzew, W. *Zhur. Russ. Fiz. Khim. Obshchestva* **36** (1903) 549 [*Chem. Zentr.* **1904 II**, 183]). [b] The percentages given in parentheses are the yields obtained by using a greater excess of Grignard reagent (see experimental part).

Grignard reagent used. In the case of *n*-butylmagnesium chloride the reaction mixture remained homogeneous, and because of the greater nucleophilic reactivity of the chloride the yield is somewhat higher (in the uncatalyzed reaction) than when the bromide is used.

In the case of the methylmagnesium halides the insoluble chloride gives the *same* yield of simple 1,4-addition product as does the bromide. The relative solubilities may, as with the *tert*-butylmagnesium halides, be the reason why the chloride does not give *higher* yield than the bromide.

An indication of a steric effect could perhaps be found in the relative amounts of 1,2-addition products in the cases of methylmagnesium chloride and bromide (Table 2). Whereas considerable amounts of 1,2-addition products are formed from the chloride, 1,2-addition takes place only to a negligible degree when the bromide is used. Instead the amounts of polymerization products is correspondingly increased. In the case of the iodide (*cf.* below) the smaller nucleophilic reactivity seems to influence the 1,4-addition principally, resulting in enhanced polymerization as well as some increase in 1,2-addition.

Table 2. Additions of methylmagnesium halides to *sec*-butyl crotonate at −10°; yields (%) of 1,2 + 1,4-addition product (methyl *iso*butyl ketone), 1,4-addition product (*sec*-butyl isovalerate) and higher-boiling residue.

Product	CH_3MgCl	CH_3MgBr	CH_3MgI
1,2 + 1,4	11–16	0–5	17–18
1,4	55–65	61–65	29–27
residue	18–20	25–27	48

As to the iodides (*cf.* note[a], Table 1), they are probably less reactive as nucleophilic reagents, and furthermore, the iodine atom may constitute a steric hindrance to 1,4-addition as well as to 1,2-addition. Whereas the catalytic effect of cuprous chloride is strong enough to overcome the decreased reactivity in the cases of *n*-butyl- and *n*-propylmagnesium iodides (*cf.* Table 1), the corresponding methyl reagent is too unreactive, even in the presence of cuprous chloride, to enable the 1,4-addition to compete successfully with the polymerization. A similar result appears to have been found by Hauser *et al.*[15] from the reaction between *tert*-butyl cinnamate and methylmagnesium iodide in refluxing ether. Thus, although these authors were unable to realize appreciable 1,4-addition (in contrast to what was the case in the reaction with phenylmagnesium bromide), they apparently also obtained very low yield of 1,2-addition products; these were not isolated and the yields are not given. Probably mostly polymerization took place *. When, in the present investigation, the reaction between *sec*-butyl crotonate and methylmagnesium iodide ** was carried out uncatalyzed (at 0° as well as at −10°) no 1,4-addition product was found, less polymerization took place (16 %), much unreacted ester was recovered (about 20 %), and a mixture of low-boiling compounds was obtained, probably the 1,2-addition products: methyl *iso*butyl ketone and propenyldimethylcarbinol, as evidenced by boiling points and refractive indices. The presence of the latter compound was further indicated by the production of water during the distillation.

The effect of cuprous chloride. *n*-Alkylmagnesium chlorides (as well as *iso*propylmagnesium chloride) give, even in the absence of this catalyst, the maximum yields, whereas these yields are obtained from the corresponding bromides and iodides only when cuprous chloride is present.

With the *n*-propylmagnesium halides, however, it was found that, whereas the cuprous chloride exerts its full effect at 0° towards *n*-propylmagnesium

* In contrast, Kohler[16] reports the formation of considerable amounts of 1,2-addition product (tertiary alcohol) from methyl cinnamate and methylmagnesium iodide, although the yield is not given in this case either.

** Very similar results were encountered with methylmagnesium chloride and bromide.

iodide, this is not the case towards *n*-propylmagnesium bromide unless the reaction mixture is more strongly cooled (to about —10°)[3], *cf.* Table 1. This observation is subject to further studies.

The reaction at 0° with *tert*-butylmagnesium chloride is catalyzed by cuprous chloride, whereas the reaction with *tert*-butylmagnesium bromide is not. Also here there is a significant effect of stronger cooling. At the very low temperature also *tert*-butylmagnesium bromide is somewhat insoluble in ether, and positive effects of cuprous chloride as well as of a larger excess of Grignard reagent are indeed observed (*cf.* Table 1).

The methylmagnesium halides give simple conjugate addition products only when the reactions are cuprous chloride catalyzed and carried out at —10° [9].

EXPERIMENTAL

Analyses are by Mr. Preben Hansen, Microanalytical Division, The Chemical Laboratory, The University of Copenhagen. Fractional distillations were through a simple 45 cm × 8 mm Podbielniak type column with a tantalum wire spiral, a heated jacket and a partial reflux head.

Alkyl halides were either commercial products or they were prepared and/or purified according to conventional methods. *tert*-Butyl bromide, b.p. 71—74°, was obtained in 57 % yield according to Norris [17] by distillation of a mixture of *tert*-butyl alcohol and hydrobromic acid.

Grignard reagents. Alkyl bromides and iodides reacted spontaneously with magnesium when the reaction flask, containing the magnesium, had been flushed with dry nitrogen at about 100° for 10 min and during the subsequent cooling to 35—40°. By the preparation of the alkylmagnesium chlorides a small amount of the corresponding alkyl bromide or iodide was sometimes used as an initiator for the reaction.

The conjugate addition reactions were carried out as previously described [2,3], generally with 0.2 mole of ester.

The addition of *n*-propylmagnesium halides to *sec*-butyl crotonate has not been described previously. The product is *sec*-butyl 3-methylhexanoate, b.p. 87°/12 mm, n_D^{25} 1.4164. (Found: C 71.00; H 11.94. Calc. for $C_{11}H_{22}O_2$ (186.29): C 70.91; H 11.91.)

The addition reactions with *tert*-butylmagnesium halides were carried out also (*cf.* Table 1) with a much larger excess of Grignard reagent, but otherwise according to the general procedure, except that the magnesium turnings were those from May and Baker (Dagenham, England). These turnings are much more finely cut than those ordinarily used for Grignard reactions, and they have been found especially suited for the preparation of Grignard reagents from very reactive halides (*cf.* Ref.[11]), in the case of which there is a considerable risk for reaction between the Grignard reagent and unreacted halide. The Grignard reagent for 0.2 mole of ester was prepared by the slow addition of 0.8 mole of the *tert*-butyl halide (dissolved in 400 ml of ether) to 2 g-atoms of magnesium (suspended in 100 ml of ether) under vigorous stirring (*cf.* Ref.[18]). The product, *sec*-butyl 3,4,4-trimethylvalerate, b.p. 97—99°/14 mm, n_D^{25} 1.4248 (rep.[4] b.p. 95°/12 mm, n_D^{25} 1.4231) was obtained in 60—78 % yield, from *tert*-butyl chloride or bromide.

The authors want to express their gratitude towards *Otto Mønsteds Fond* for financial support.

REFERENCES

1. *Cf.* Kharasch, M. S. and Reinmuth, O. *Grignard Reactions of Nonmetallic Substances*, Prentice-Hall, New York 1954, p. 20.
2. Munch-Petersen, J. *Acta Chem. Scand.* **12** (1958) 967.
3. Munch-Petersen, J. and Andersen, V. K. *Acta Chem. Scand.* **15** (1961) 271.

4. Munch-Petersen, J. *J. Org. Chem.* **22** (1957) 170.
5. Gilman, H., Heck, L. L. and St. John, N. B. *Rec. trav. chim.* **49** (1930) 212.
6. Wotiz, J. H., Hollingsworth, C. A. and Dessy, R. E. *J. Am. Chem. Soc.* **77** (1955) 103.
7. *Cf.* Dessy, R. E., Wotiz, J. H. and Hollingsworth, C. A. *J. Am. Chem. Soc.* **79** (1957) 358.
8. See, *e.g.*, Lutz, R. E. and Reveley, W. G. *J. Am. Chem. Soc.* **63** (1941) 3180; Johnson, J. R. in Gilman, H. *Organic Chemistry*, 2nd. Ed., Vol. **II**, John Wiley and Sons, New York 1943, p. 1881–1882; Alexander, E. R. *Principles of Ionic Organic Reactions*, John Wiley and Sons, New York 1950, p. 193–194; Royals, E. E. *Advanced Organic Chemistry* Prentice-Hall, Englewood Cliffs, N.J. 1954, p. 699.
9. *Cf.* Munch-Petersen, J. *Acta Chem. Scand.* **12** (1958) 2007.
10. Bjerl Nielsen, E., Munch-Petersen, J., Møller Jørgensen, P. and Refn, S. *Acta Chem. Scand.* **13** (1959) 1943.
11. Munch-Petersen, J., Møller Jørgensen, P. and Refn, S. *Acta Chem. Scand.* **13** (1959) 1955.
12. Young, W. G. and Roberts, J. D. *J. Am. Chem. Soc.* **67** (1945) 319; **68** (1946) 1472 and further references given there; Wilson, K. W., Roberts, J. D. and Young, W. G. *J. Am. Chem. Soc.* **72** (1950) 218; *cf.* Alexander, E.R.[8], p. 287; Royals, E.E.[8], p. 696.
13. Dessy, R., E. Handler, G. S., Wotiz, J. H. and Hollingsworth, C. A. *J. Am. Chem. Soc.* **79** (1957) 3476; Dessy, R. E and Handler, G. S. *J. Am. Chem. Soc.* **80** (1958) 5824; *cf.* Dessy, R. E. and Jones, R. M. *J. Org. Chem.* **24** (1959) 1685.
14. See Rochow, E. G., Hurd, D. T. and Lewis, R. N. *The Chemistry of Organometallic Compounds*, John Wiley and Sons, New York 1957, p. 83.
15. Hauser, C. R., Yost, R. S. and Ringler, B. I. *J. Org. Chem.* **14** (1949) 261.
16. Kohler, E. P. and Heritage, G. *Am. Chem. J.* **33** (1905) 21 [*Chem. Zentr.* **1905 I**, 521].
17. Norris, J. F. *Am. Chem. J.* **38** (1907) 627.
18. Gilman, H. and McGlumphy, J. H. *Bull. soc. chim. France* [4] **43** (1928) 1322 [Shirley, D. A. *Preparation of Organic Intermediates*, John Wiley and Sons, New York 1951, p. 5].

Received September 27, 1960.

ACTA CHEMICA SCANDINAVICA 15 (1961) 300–320

Anodic Dissolution of Iron

I. General Mechanism

K. A. CHRISTIANSEN, H. HØEG, KIRSTEN MICHELSEN, G. BECH NIELSEN and H. NORD

Chemistry Department A, Technical University of Denmark, Copenhagen, Denmark

It is suggested that the kinetics of the anodic dissolution of iron is essentially governed by a mechanism in which the pH dependent and potential dependent dissociation of chemisorbed water plays a dominating role. The steps in this mechanism are

$LOH_2 \rightleftharpoons LOH^- + H^+$	Bond weakening
$LOH^- \rightleftharpoons FeOH^+ + 2e^-$	Bond breaking
$FeOH^+ \rightarrow Fe^{++} + OH^-$	Solvation
$LOH^- \rightarrow FeO + H^+ + 2e^-$	Passivation
$FeO + H^+ \rightleftharpoons FeOH^+$	Activation

LOH_2 is a surface iron atom, still belonging to the metal lattice, with a chemisorbed watermolecule. LOH^- is a surface iron atom with a chemisorbed hydroxyl ion. $FeOH^+$ and FeO are adsorbed oxidized forms and Fe^{++} the solvated ferrous ion.

The system of differential equations for this mechanism is derived and solved for steady state conditions. The resulting kinetic expression is

$$s = \frac{N}{A + B \cdot h + C/h}$$

where s is the rate of dissolution and N the number of sites on the surface, able to accomodate water molecules and hence to go through the series of steps described above. A, B and C are functions of potential dependent rate constants and h is the concentration of proton donor in the solution. Experiments illustrating the qualitative validity of this expression are described.

A more thorough analysis of the mechanism, both for steady state and for non steady state experimental conditions, is given, and compared with experimental results, quantitative as well as qualitative. It is shown that the general mechanism given above is in good agreement, both with new experimental findings of the present paper and with results from other laboratories.

An interesting consequence of the above is that the mechanism of passivity is the electrostatic repulsion of hydrogen ions, necessary for the dissolution of surface oxide layers. The striking influence of oxygen, dissolved in the aqueous phase, and of hydrogen, dissolved in the metal phase, is discussed on the basis of new experiments.

The apparent complexity of the anodic dissolution of iron, a process which has long been a problem of major interest, is well illustrated by the observed effects of increasing positive (anodic) potential and of the addition of hydrogen ions. When iron dissolves as an anode under conditions where the Tafel equation [1]

$$E = a + b \log i \qquad \text{I}$$

is obeyed, it has been reported that b (the voltage change which changes the anodic current by a factor of ten) may have values from well above 100 mV [2] to below 20 mV [3]. As current theories of electrode kinetics would suggest a value around 58 mV [4,5] for the simple reaction

$$Fe \rightarrow Fe^{++} + 2e^{-}$$

it has hitherto not been possible to give any theoretical explanation for either of these extreme values. Some workers [6-9] maintain that 29 mV is the typical value of b in acid solution and ascribe this value to a mechanism with a "transition complex" containing two iron atoms about to dissolve, or to a mechanism in which each sequence of steps containing one rate determining step, involves the dissolution of two iron atoms.

One interesting feature of the behaviour of iron is its dissolution (no applied potential) in strong non-oxidizing acid. Stern [10a] has found that the velocity of the process

$$Fe + 2H^{+} \rightarrow Fe^{++} + H_2$$

is very nearly independent of acid concentration in the range $4 \geq pH \geq 1$ in agreement with the work of Bonhoeffer and Heusler [8] and others. At the same time the potential of this corroding iron electrode decreases nearly 58 mV per pH unit.

In spite of the above agreement between different experimentalists some doubt nevertheless remains as yet other workers [7,11] have found some increase in corrosion rate with increasing acidity, and a change of potential somewhat less than 58 mV/pH unit. It may be relevant that Stern [10b] has also found that his results quoted above are valid for pure iron only and that small amounts of phosphorus or sulphur in the iron change the picture drastically. In this connection it is also important that Hoar and Hurlen [6] found that while the Tafel line for the anodic dissolution of iron is nearly independent of impurities in the iron the Tafel lines for cathodic production of hydrogen show the highest "hydrogen overvoltage" for the purest iron. Thus it may be that the results obtained by Stern and by Bonhoeffer and Heusler are very nearly correct and that the other workers used less pure conditions. If this is not so it is still certain that a change in acidity gives an opposing change of potential so the actual rate of spontaneous dissolution of iron in strong acid is rather insensitive to change in acid concentration.

This striking feature has provoked the senior author of the present paper [12] to suggest that a rate determining step in this process is independent of potential. A change in acidity causes a corresponding change in potential so the actual "equilibrium" concentration of a "transition complex" containing the catalyzing hydroxyl ion [13,14] is nearly independent of acidity within the limits of pH

quoted above. The transformation of this species into the final corrosion product, the ferrous ion, would then occur according to a potential independent rate law. The hydrogen evolution must then occur according to a similar pattern. These points of view will be amplified in the following and some experimental evidence for their validity presented.

The complexity of the corroding iron electrode is also reflected in the existence of the passivity phenomena. It is well known that the practical corrosionist to a certain extent protects iron from corrosion in an aqueous medium by rendering this medium alkaline. According to some of the authors mentioned above hydroxyl ions catalyze anodic dissolution of iron, as does positive potentials. Yet alkaline environments and high potentials are features generally associated with the passive state, in which the corrosion of iron is strongly inhibited. There is general agreement in the literature that the passive state of iron is due to some kind of oxide layer on iron, but at the same time there is strong controversy about the nature of this layer as far as thickness and composition is concerned. Though interesting in itself this controversy seems to be somewhat irrelevant at the present time; it seems to us that one is still faced with the problem of how an oxide layer is able to protect iron from corrosion; why it will not dissolve away under strongly oxidizing conditions but does so under more reducing conditions. It is generally assumed that the transition between the active and the passive state of iron is discontinuous, a definite potential, the so called Flade potential [15] governed at 25°C by the equation [16]

$$E_F = 0.590—0.058 \text{ pH}$$

separating a negative potential region where iron is active and a positive region in which iron is passive. It is shown in the present paper that this relationship is an artefact, that the transition between a fully passive state and a fully active state is smooth and continuous, both in neutral and in strongly acid environment. It is proposed, that the mechanism of passivity is electrostatic repulsion from the oxide layer of hydrogen ions necessary for the dissolution of the oxide layer.

THE MECHANISM

The model of the iron electrode on which the following is based is a very simple one. Water is chemisorbed to the surface in a such way that there is a constant potential difference between the interior of the iron phase and the surface of chemisorbed water. Any change of potential between the iron electrode and the liquid is essentially restricted to the region outside this layer of water. A change of iron potential in a positive direction will increase the tendency of the adsorbed water to transfer hydrogen ions to the solution, *i.e.* the adsorbed water is behaving as an acid the strength of which is potential dependent. The degree of ionization of this adsorbed "acid" water is thus determined both by the pH of the bulk solution and also by the electrode potential.

It is now suggested that the bond between a surface iron atom still belonging to the metal lattice is stable when the iron atom is accommodating an

adsorbed water molecule, but has a certain probability of breaking when a hydroxyl ion is adsorbed. This would give the following sequence of reactions:

$$LOH_2 \rightleftharpoons LOH^- + H^+ \quad (\pm 1)$$
$$LOH^- \rightleftharpoons FeOH^+ + 2e^- \quad (\pm 2)$$

where LOH_2 represents a surface iron atom with a chemisorbed water molecule, the iron atom still belonging to the metal lattice. LOH^- is an iron atom, also belonging to the lattice, with a hydroyl ion, and $FeOH^+$ is a hydroxy ferrous ions which still belongs to the surface but no longer to the metal lattice.

The anodic dissolution of an iron atom is finally completed by a solvation step:

$$FeOH^+ \rightarrow Fe^{++} + OH^- \quad (+ 3)$$

When anodic dissolution is proceeding at a potential far from the equilibrium potential of the Fe/Fe^{++} electrode, *i.e.* when the anodic dissolution is independent of the ferrous concentration in the solution, it should not be necessary to take a step (— 3) into consideration.

The potential dependence of the rate constants corresponding to these steps might possibly be derived in the following way:

Step 1. The quotient k_{+1}/k_{-1}, where k_{+1} and k_{-1} are

rate constants for the first step forwards and backwards, respectively, should be the equilibrium constant for the protolytic reaction ($\pm$ 1). According to the picture given above a change of potential (η) between metal phase and solution (iron electrode and reference electrode) would involve an identical change between the region in which the hydrogen ion is situated when belonging to the LOH_2 acid and the phase where there is free hydrogen ion. This may of course be a somewhat crude picture of the actual (unknown) situation but seems nevertheless to give a very satisfactory working hypothesis. According to this hypothesis the equilibrium constant for this reaction shall have the form

$$K_{1,\eta} = K_{1,0} \exp\ (F \cdot \eta / RT) \qquad \text{II}$$

where $K_{1,0}$ is the value of K_1 at an arbitrary reference potential ($\eta = 0$). This is a simple consequence of Boltzmann's distribution law. We then have

$$\frac{k_{1,\eta}}{k_{-1,\eta}} = \frac{k_{1,0}}{k_{-1,0}} \cdot \frac{\exp\ (\alpha \cdot F \cdot \eta / RT)}{\exp\ (-(1-\alpha) F \cdot \eta / RT)} \qquad \text{III}$$

This equation is valid for any value of α as far as the formal relationship between rate constants and equilibrium constants is concerned. There are however good reasons for giving the value 0.50 to α. The exponential factors in nominator and denominator governs the influence of electrical forces on the transport of the hydrogen ion in either direction through the diffuse part of the electrical double layer at the iron surface. According to the picture given above potential changes between metal interior and liquid interior are restricted to this part of the double layer. It is true that the thickness of this layer, like the radius of the ionic atmosphere in the Debye-Hückel theory of

ionic solutions, is strongly influenced by, *e.g.*, concentration and charge type of electrolytes in the solution, but the part of the total potential drop found in the diffuse part of the double layer is hardly changed very much. Probably electrode kinetics will in the future turn out to be the best source of information about the actual double layer structure.

Step 2. The second step in the mechanism suggested above does not involve transference of charged species between two phases. Therefore the rate constants of this step should not directly be functions of potential. They might be functions of, *e.g.*, availability of electrons and hence may be linear functions of potential and double layer capacity, but for the present it seems adequate simply to regard k_2 and k_{-2} as potential independent.

Step 3. k_3 is a little more obscure as the fate of the hydroxyl ion is unpredictable. If the solvation process were transference of $FeOH^+$ through the double layer the potential dependence of k_3 should be the same as for k_1. There is experimental evidence which could mean that the constant k_3 depends on potential according to the law expected for transfer of a double charged particle and this will be maintained throughout in the following discussion.

The water molecules, of course, are to be considered as a two basic acid. As we shall see later the process (+ 2) is probably fairly slow, so that at high potentials or at high pH values, (+ 2) must compete with

$$LOH^- \rightarrow FeO + H^+ + 2e^- \quad (+ 4)$$

We suppose that this splitting off of the second proton leads to immediate bond breaking between surface iron atom and lattice, and that the FeO formed remains on the surface as a constituent of the passivity oxide layer. It will not solvate unless a hydrogen ion is taken up:

$$FeO + H^+ \rightleftharpoons FeOH^+ \quad (\pm 5)$$

It seems reasonable to believe that if the bonding between surface iron and lattice is indefinitely stable when water is adsorbed and is less stable when one hydrogen is split off, then the bond will break immediately when both hydrogen ions are split off. The constants k_4, k_5, and k_{-5} will all have potential dependence corresponding to transference of one hydrogen ion. There is no reason to believe that the back reaction (—4) will play any significant part in the mechanism of the iron electrode.

To summarise, the proposed mechanism is:

LOH_2	$\rightleftharpoons LOH^- + H^+$	(± 1)	Bond weakening
LOH^-	$\rightleftharpoons FeOH^+ + 2e^-$	(± 2)	Bond breaking
$FeOH^+$	$\rightarrow Fe^{++} + OH^-$	$(+ 3)$	Solvation
LOH^-	$\rightarrow FeO + H^+ + 2e^-$	$(+ 4)$	Passivation
$FeO + H^+$	$\rightleftharpoons FeOH^+$	(± 5)	Activation

with the corresponding rate constants (η in mV)

$$\begin{aligned}
\log k_{1,\eta} &= \log k_{1,0} + \eta/116 \\
\log k_{-1,\eta} &= \log k_{-1,0} - \eta/116 \\
\log k_{2,\eta} &= \log k_{2,0} \\
\log k_{-2,\eta} &= \log k_{-2,0} \\
\log k_{3,\eta} &= \log k_{3,0} + \eta/58 \\
\log k_{4,\eta} &= \log k_{4,0} + \eta/116 \\
\log k_{5,\eta} &= \log k_{5,0} - \eta/116 \\
\log k_{-5,\eta} &= \log k_{-5,0} + \eta/116
\end{aligned} \qquad \text{IV}$$

OVERALL STEADY STATE KINETICS

The mechanism outlined above gives the following overall steady state kinetic expression:

$$s = \frac{N}{A + B\,h + C/h} \qquad \text{V}$$

In this expression s is the velocity of iron dissolution per unit of anode area. N is the number of iron atoms per unit anode area which are able to accommodate a water molecule and hence to go through the sequence of events described above. A, B and C are functions of the rate constants given above. h is the hydrogen ion concentration.

The definition of the parameters of V is deliberately crude. In the calculation of the actual number of sites on the iron surface it is of course necessary also to take into account the fact that other species than water can, and will, adsorb on to the iron surface. Some foreign adsorbed species may promote corrosion, others may protect the host iron atom from oxidation or at least from solvation. The protolytic reactions must be highly dependent on the availability of acid-base systems in the solution apart from water molecules. Therefore the above mechanism can, even if it turns out to be essentially correct, only represent a fairly crude picture of the complete mechanism of the iron electrode. With these reservations V is derived as follows:

The surface concentrations of the forms LOH_2, LOH^-, $FeOH^+$, and FeO are, respectively, a_2, a_1, b_1, and b_0. Hence

$$a_2 + a_1 + b_1 + b_0 = N \qquad \text{VI}$$

According to the mechanism these surface concentrations obey the differential equations

$$\left.\begin{aligned}
\frac{da_2}{dt} &= -k_1 a_2 + k_{-1} h a_1 + k_3 b_1 \\
\frac{da_1}{dt} &= k_1 a_2 - k_{-1} h a_1 - k_2 a_1 + k_{-2} b_1 - k_4 a_1 \\
\frac{db_1}{dt} &= k_2 a_1 - k_{-2} b_1 - k_3 b_1 + k_5 h b_0 - k_{-5} b_1 \\
\frac{db_0}{dt} &= k_4 a_1 - k_5 h b_0 + k_{-5} b_1
\end{aligned}\right\} \qquad \text{VII}$$

The term $k_3 b_1$ in the expression for a_2 indicates that LOH_2 is reformed by immediate adsorption of a new water molecule at the surface iron atom exposed after solvation of the ferrous ion. As the four equations of VII through VI are interrelated we have four independent equations with four unknowns, *viz.* the four surface concentrations. The dependent parameter of greatest interest is the corrosion rate introduced by the equation

$$s = k_3 b_1 \qquad \text{VIII}$$

It is of course a hopeless task to attempt to give general solutions for this system of differential equations when the potential dependence of the rate constants is considered, although it would not be difficult to investigate the properties of the system on an analogue computer and to compare its behaviour with that of the actual iron electrode. Here, however we can only give the steady state solution, obtained by equating the differential quotients of VII to zero, eliminating the surface concentrations and thus determining s.

The result is

$$\frac{N}{s} = \frac{1}{k_1} + \frac{1}{k_3} + \frac{1}{k_2 + k_4} + \frac{k_{-2}}{k_3(k_2 + k_4)} + \frac{\frac{k_{-1}}{k_1} + \frac{k_{-1}k_{-2}}{k_1 k_3}}{k_2 + k_4} \cdot h + \frac{\frac{k_{-2}k_4}{k_3 k_5} + \frac{k_4 k_{-5}}{k_3 k_5} + \frac{k_4}{k_5} + \frac{k_2 k_{-5}}{k_3 k_5}}{k_2 + k_4} \cdot \frac{1}{h} \qquad \text{IX}$$

which is seen to be of the same form as V.

The following experiments are meant to illustrate the most general applicability of this expression.

Fig. 1 shows examples of the dependence of the velocity of anodic dissolution on pH as measured by the anodic current at constant potential. The curves have maxima in accordance with V and IX, proving that the hydrogen ions both catalyze and inhibit the anodic dissolution. A complete quantitative analysis of these experiments would seem to be of little value at present; the system is too complicated. Thus comparison of the three curves for three acetate concentrations shows immediately that not only pH, but also sodium acetate or acetic acid concentration has influence on the integral behavior of the iron electrode.

Fig. 2 shows the influence of potential on the corrosion rate at three fixed pH values. It is seen that the influence of increasing potential is very similar to that of increasing pH as shown in Fig. 1. The accordance between IX and the experiments of Fig. 2 follows from the potential dependence of the terms of the denominator of V (IX):

$$A = 1/k_1 + 1/k_3 + 1/(k_2 + k_4) + k_{-2}/k_3(k_2 + k_4)$$

If $k_4 \ll k_2$ the numbers —1, —2, 0, —2 give the factor of 10 by which these terms are changed when the potential of the iron electrode is changed 116 mV

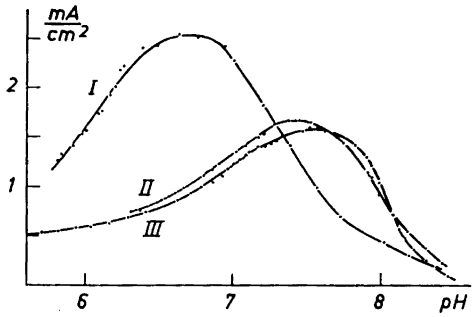

Fig. 1. Rate of anodic dissolution *vs.* pH;
Temp. 25.0°C;
Potential: $E_h = -210$ mV:
Electrode area: 2.40 cm²
Medium: I 0.100 M sodium acetate
II 0.500 M sodium acetate
III 1.000 M sodium acetate

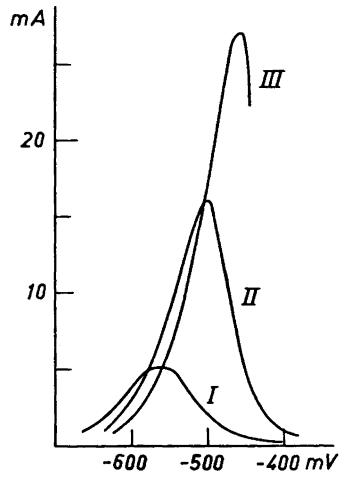

Fig. 2. Rate of anodic dissolution *vs.* potential;
Temp. 25.0°C:
Reference electrode: Ag/AgCl; 0.1 M HCl;
Medium: 1 M sodium acetate, 2×10^{-3} M *o*-phenanthroline;
Scanning rate: 5 mV/sec;
Electrode area: 2.40 cm²;
pH: I 7.65
II 7.07
III 6.76

in anodic direction. It is seen that A decreases with increasing positive potential. Hence the A term is most significant at negative potentials.

$$B = [k_{-1}/k_1 + k_{-1}k_{-2}/k_1k_3]/(k_2 + k_4)$$

Again, provided $k_4 \ll k_2$ the numbers —2 and —4 give the factor of ten by which the two terms in the square brackets are changed when the potential is changed 116 mV. Also the term $B \cdot h$ decreases with increasing potential.

$$C = (k_{-2}k_4/k_3k_5 + k_4k_{-5}/k_3k_5 + k_4/k_5 + k_2k_{-5}/k_3k_5]/(k_2 + k_4)$$

Still retaining the assumption $k_4 \ll k_2$ which may be reasonable at not too positive potentials the exponents are 0, + 1, + 2, and 0, respectively. Hence the term C/h must increase with increasing anodic potential.

This means, that at fixed pH the denominator of V must go through a minimum, and therefore the steady state corrosion rate through a maximum when measured as a function of potential. The two functions of potential $B \cdot h$ and C/h must be shifted with increasing h in such a way, that the maximum at lower pH values occurs at potentials where the potential function A is greater. Hence the value of the maximum corrosion rate must decrease with increasing pH, as in fact seen on Fig. 2. This result is of course of

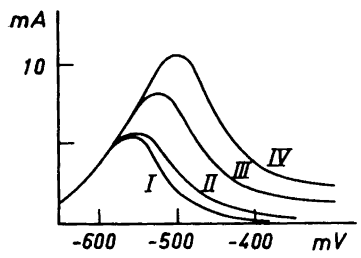

Fig. 3. Rate of anodic dissolution *vs.* potential;

Temperature: 25.0°C;
Reference electrode: Ag/AgCl; 0.1 M HCl;
Medium: as Fig. 2. I;
Rate of scanning: I 5 mV/sec
II 20 mV/sec
III 100 mV/sec
IV 200 mV/sec

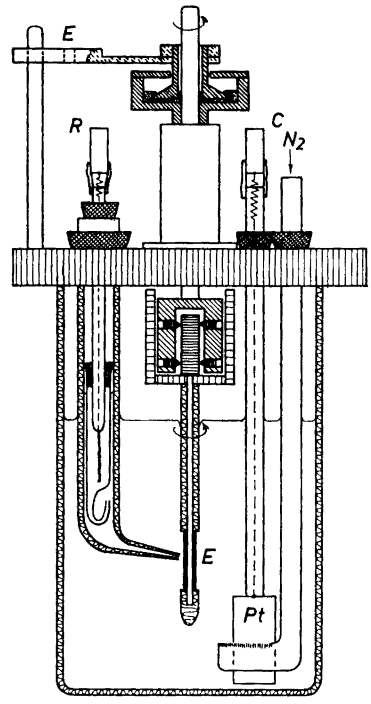

Fig. 4. Reaction vessel with electrode system. Volume: 400 ml, R, reference electrode; E, Experimental electrode (iron); C, counter electrode (platinum).

practical interest as it shows that the highest possible value of iron corrosion rate decreases strongly with increasing pH. It is on the other hand clear from Fig. 2 that when rather negative potentials only are considered the rate of corrosion at constant potential now increases with increasing pH. Fig. 3 shows the influence of increase of scanning rate. It is clear, that when the steady state condition is not fulfilled IX will not be the solution of VI, VII and VIII. It is seen that the corrosion rate shoots up to higher maximum values when the potential is changed at a rather fast rate. It should be emphasized that the measured anodic current under non steady state conditions comprises both anodic dissolution and change of charge of double layer, *e.g.* by change in the degree of acid dissolution of the adsorbed water molecules. It is of course hopeless to attempt a quantitative analytical theory for the

Fig. 5. Simple potentiostat:

E, experimental electrode;
R, reference electrode;
C, counter electrode;
P_1, potential selector;
MA, current measuring device;
K_1, DC amplifier. Usually Kintel BFO 111. (gain: ca -10^6. bandwidth: DC–40KC, zero point stability: ca 2 μV).

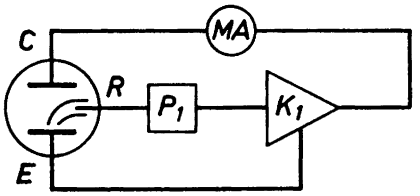

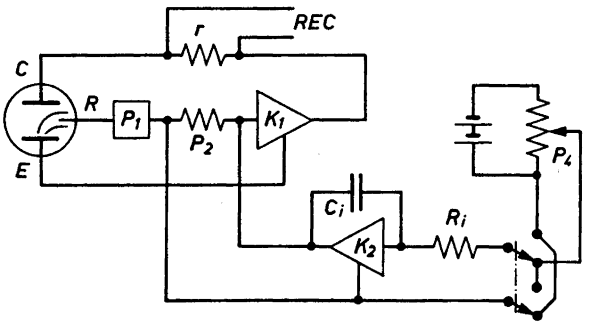

Fig. 6. Fully electronic polarograph. Details of potentiostat part as Fig. 5. Sliding potential provided by the integrator consisting of the amplifier K_2, the condenser C_i and the resistance R_i. Direction and rate of scanning determined by choice of C_i, R_i and of sign and magnitude of the potential P_4. Example: $C_i = 1$ μF, $R_i = 1$ MΩ gives scanning rate = P_4 mV/sec. Current measuring device generally an X-Y recorder (Moseley Autograph 2 S. 10″ × 15″), the X position of which is controlled by the sliding potential.

Fig. 7. Potentiostat with coulombmeter. Details of the potentiostat as for Fig. 5. The amplifier K_3 forms together with R_i and C_i an integrator, the output of which is proportional to the amount of electricity passed through the resistance r during the time elapsed since C_i was last short-circuited. Recorder: Moseley Autograph X-Y recorder 10″ × 15″.

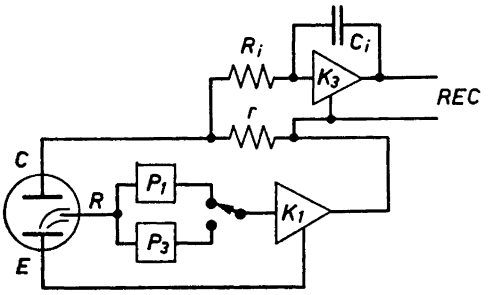

experiments of Fig. 3. A numerical solution of the system of differential equations governing the iron electrode for such conditions would on the other hand be of great value for assigning definite values to the numerous rate constants of the iron electrode.

EXPERIMENTAL PROCEDURES

The experiments described in this paper were all carried out at 25°C. The electrolysis system had three electrodes (Fig. 4): the iron electrode, the reference electrode with Luggin capillary and a platinum counter electrode. The iron was supplied by Wacuum Schmeltze, Hanau, Germany, as 4 mm rods, described as "Rein Eisen, gasfrei". The

limits of impurities are fairly generous (*e.g.*, C 0.02 %; Ni 0.1 %) but the quality was considered satisfactory for the experiments described in this paper (see remarks on the paper by Hoar and Hurlen [6], p. 301). The rods were cut in 20 mm length and a 2 mm hole drilled through the whole length. The cylinders were suspended in a lathe, ground with suitable grades of emery paper and finished with diamond powder polishing. They were mounted in an electrode holder of glass as seen on Fig. 4 so that only the outer cylindrical area was exposed (apparent area: *ca* 2.4 cm²). The electrode holder was designed so that the electrode could be rotated and easily well centered. The cylindrical electrode form was chosen becuase all points on the electrode can be regarded identical, both electrically and hydrodynamically. The stirring rate was generally about 1 000 revolutions/min and none of the phenomena discussed in this paper were changed appreciably by change of rate of stirring, *i.e.* there was no transport control.

The reference electrodes were in most cases silver/silver chloride electrodes, 0.1 M HCl, which are about 290 mV more positive than the normal hydrogen electrode.

The platinum counter electrodes were generally screened from the bulk of solution in such a way that they were placed in a glass tube, connected with the rest of the system through a sintered glass plate. Nitrogen, freed from oxygen by means of a Meyer-Ronge apparatus [17] was bubbled through the solutions, unless otherwise stated. Most of the electrolysis experiments were carried out at controlled potential. The active elements of the potentiostats were analogue computer amplifiers, either those from a small Donner computer or KINTEL B F O 111 amplifiers. These latter amplifiers are especially attractive for electrode kinetic purposes as they are floating, thus making it possible to choose freely the point of the electrolysis system to be earthed. Fig. 5 shows the basic wiring for a potentiostat. In Fig. 6 is shown the system used for experiments of the type shown in Figs. 2 and 3, a second amplifier connected as integrator providing the scanning potential. Fig. 7 shows a setup in which a second amplifier is used as an integrator to record the number of coulumbs passed through the electrode rather than the current.

Solutions were made up with doubly distilled water and materials of analytical reagent grade. Most solutions contained 2—4 mmole of *o*-phenanthroline to keep the ferrous ion produced on the "polarographically inert" *o*-phenanthroline complex form. This measure was found to increase the reproducibility of experiments enormously, without changing the nature of the results obtained. Experiments have shown, that the adsorption of *o*-phenanthroline is too slow to compete with adsorption of water or other solution constituents, provided the electrode is continuously corroding.

INFLUENCE OF HYDROGEN

Fig. 8 demonstrates the reproducibility attained by the experimental procedure outlined above, and also one of the pitfalls which had to be overcome before high reproducibility was obtained. The experiments were carried out with the circuit of Fig. 5. The bellshaped curve I represents two identical experimental runs with the same electrode, which had never been polarized

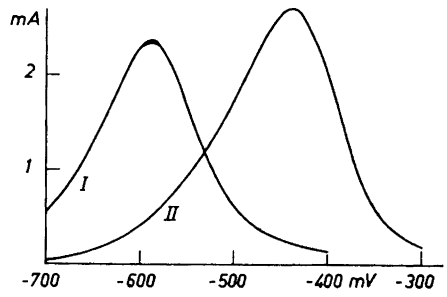

Fig. 8. Rate of anodic dissolution *vs.* potential;
Medium: 0.5 M sodium acetate, 0.002 M *o*-phenanthroline. pH: 7,95;
Temp. 25.0°C; Reference electrode: Ag/AgCl, 0.1 M HCl;
Rate of scanning: 4 mV/sec.
Electrode area: 2.36 cm².
I Two identical runs with nonhydrogenated electrode.
II Same experiment after cathodic polarization.

cathodically. Curve II represents a similar run with the same electrode after the electrode had been held at a more negative potential with hydrogen evolution for some time (a few minutes). The shift towards more positive potentials cannot possibly be attributed to an adsorption phenomenon, as something like 100 atomic layers of iron are stripped off in each run. The almost identical shape of the two curves indicates, that the rate-determining phenomena in the two cases are also the same, *i.e.* that the "zero charge potential", the potential at which the electrode acts on the hydrogen ions of the chemisorbed water with zero coulombic force, is shifted by diffusion of hydrogen into the electrode. The shift persists for about half an hour after the cathodic treatment.

Hoar and Hurlen [6] have found that their potential dependent rate laws for anodic dissolution and cathodic deposition of iron combine to give the accepted standard potential of the iron/ferrous ion electrode. The drastic influence of hydrogen on the iron electrode, which we have found in acid solution also, suggests that this relationship cannot be expected to hold under all conditions. We have found that there is no shift when the solution contains nitrate ion. The explanation given here seems to be the only one reasonable, and supports the point of view that the influence of change of potential is essentially electrostatic as suggested in the discussion above.

THE ACTIVE IRON ELECTRODE

The expression IX is too complicated to warrant a detailed analysis at present. It is however a promising feature that most of the terms of IX are strongly potential dependent. This means that when the potential of the iron electrode is changed it can be expected that the various terms change in relative significance to an extent which makes it possible to isolate the influence on the overall kinetics of at least some of the terms. In this way it may be possible to identify such terms and hence to prove more directly the correctness or not of some of the aspects of the mechanism given above. It may be reasonable to assume that the surface species FeO, which according to the mechanism suggested in this paper is at least a precursor of the passive layer of the iron electrode, is absent from the electrode mechanism when the potential is sufficiently negative. Under such conditions IX is reduced to

$$\frac{N}{s} = \frac{1}{k_1} + \frac{1}{k_2} + \frac{1}{k_3} + \frac{k_{-2}}{k_2 k_3} + \left[\frac{k_{-1}}{k_1 k_2} + \frac{k_{-1}k_{-2}}{k_1 k_2 k_3}\right] \cdot h \qquad \text{X}$$

When this relationship holds, a plot of the inverse corrosion rate against acidity at constant potential should be a straight line with intercept on ordinate

$$A = \frac{1}{k_1} + \frac{1}{k_2} + \frac{1}{k_3} + \frac{k_{-2}}{k_2 k_3} \qquad \text{XI}$$

and slope

$$B = \frac{k_{-1}}{k_1 k_2} + \frac{k_{-1}k_{-2}}{k_1 k_2 k_3} \qquad \text{XII}$$

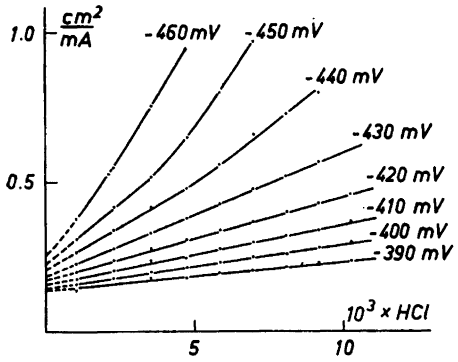

Fig. 9. Reciprocal rate of anodic dissolution against concentration of hydrochloric acid. Medium: 1 M sodium chloride, 0.004 M *o*-phenanthroline.

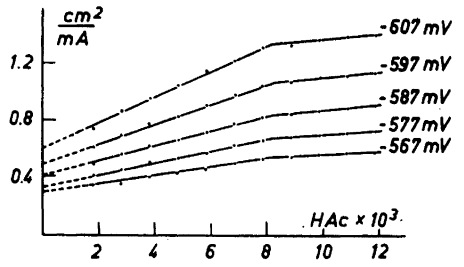

Fig. 10. Reciprocal rate of anodic dissolution against acetic acid concentration. Medium: 1 M sodium acetate, 0.004 M *o*-phenanthroline.

We have, in disagreement with some earlier workers, found, that it is generally not possible to obtain a Tafel line for the overall corrosion rate of the iron electrode. This should be possible if only one term of IX is significant for the overall kinetics. We have, however, found that X often reproduces data of experiments at lower potentials (where the electrode is active) reasonably well. Examples are shown in Figs. 9 and 10, which are for a hydrochloric

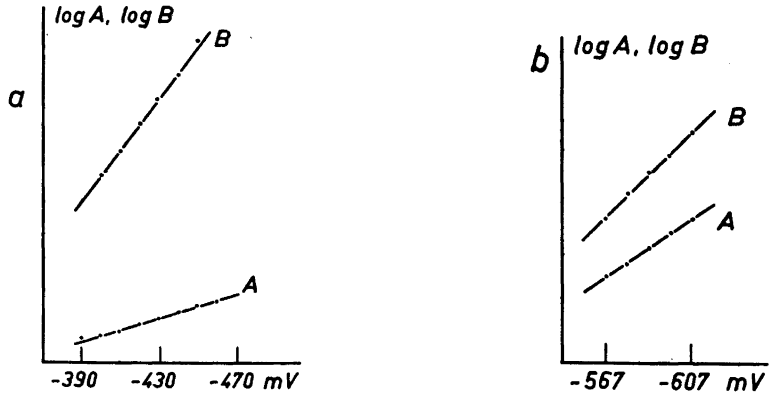

Fig. 11. Tafel lines for intercepts (A) and slopes (B) from the experiments on Figs. 9. and 10, respectively.

a) the hydrochloric acid experiment

$$\frac{d\,\eta}{d\log A} = 170 \text{ mV}; \frac{d\,\eta}{d\log B} = 61 \text{ mV}$$

b) the acetic acid experiment

$$\frac{d\,\eta}{d\log A} = 116 \text{ mV}; \frac{d\,\eta}{d\log B} = 86 \text{ mV}$$

acid and an acetate/acetic acid system, respectively. Fig. 9 shows very good agreement with X at a number of potentials. The curvature of the upper curves undoubtedly reflects the fact that when acidity is high and potential low the hydrogen evolution on the electrode is not fully suppressed; hence the electrode is changed as decribed above. Both the slopes and the intercepts of Fig. 9 give good Tafel lines as shown on Fig. 11. The slope of the line for B corresponds to a factor of ten change for 61 mV, not much different from the 58 mV slope expected if only the first term of XII were significant (*cf.* p. 307). The slope of the line for A is near 170 mV suggesting that both the term $1/k_1$ (corresponding to $b = 116$ mV) and the term $1/k_2$ (with no potential dependence) are significant. The experimental data for A from Fig. 9 fit a Tafel line with slope 116 mV after subtraction of a suitable contribution from the term $1/k_2$.

Fig. 10 shows also good agreement with X at lower acidities. At high acidities the inverse rate is too low, *i.e.* the rate too high, for the simple expression. Other experiments with the acetic acid system have shown that a plateau is reached on which the electrode seems to be fully covered with adsorbed acetic acid and where the rate follows a 116 mV slope Tafel law. In this state the rate of corrosion seems to be governed by splitting off of one proton from adsorbed acetic acid. The B values from the steep parts of Fig. 10 obey, as again seen on Fig. 11, a Tafel equation with $b = 80$ mV whereas the A values from Fig. 10 give a b value close to 116 mV. It is seen that these findings are in substantial agreement with the general picture given in the present paper.

In the introduction we have mentioned the papers by Hoar and Hurlen [6,7] and by Bonhoeffer and Heusler [8,9], in which it was found, that the overall kinetics of the anodic dissolution obeys a Tafel type equation with $b =$ ca. 29 mV. It is seen, again from the discussion on p. 307, that this is the b value corresponding to the second term of XII. This would be the leading term of XII if

$$k_{-2} \ll k_3 \qquad \text{XIII}$$

It is reasonable to postulate, that a major difference between the experimental conditions of the workers mentioned above and ours is the validity of XIII. In their case, iron electrodes were heated in hydrogen flames before experiments and hydrogen gas was thoroughly bubbled through solutions during experiments. In our case, no such pretreatment of electrodes was performed, and nitrogen was used to keep oxygen away from the electrode system during experiments. It is not unlikely that the probability of the reaction (—2), which is a reduction, is strongly influenced by hydrogen dissolved in the iron phase. The validity for the hydrogen treated electrode of our mechanism in connection with the assumption XIII is in Heuslers [9] case strongly supported by his own experiments. Heusler changed the potential of an iron electrode suddenly from a steady state condition at a constant potential to another constant potential and found that the rate of anodic dissolution changed, immediately according to a $b = 58$ mV law, and after a slower transition, to a new steady state corrosion rate, related to the original steady state rate according to a $b = 29$ mV law. Considering that the measured rate is governed by VIII this result is understandable; the immediate response to a change of

potential would be a change of k_3 according to a 58 mV law, followed by a slow change of the concentration of the surface species b_1, also increased by a factor of 10 when the potential is changed 58 mV, provided the dominating species on the surface is adsorbed, undissociated water. That would give

1) a fast change of dissociation of water when potential is changed so

$$a_1 = a_2 \frac{k_1}{k_{-1}} = NK_1 \qquad \text{XIV}$$

2) slow equilibrium adjustment of b_1 according to

$$b_1 = a_1 \frac{k_2}{k_{-2}} \qquad \text{XV}$$

and therefore an overall change of two factors of ten for 58 mV change of potential. This explanation of the 29 mV Tafel lines for anodic dissolution of iron is amplified, still with reference to Heuslers interesting experiments, when the differential equation for b_1 is considered:

$$\frac{\mathrm{d}b_1}{\mathrm{d}t} = k_2 a_1 - k_{-2} b_1 - k_3 b_1 \qquad \text{XVI}$$

The solution of XVI, when from an arbitrary steady state condition a_1 is suddenly changed to a new value a_1', is:

$$b_1 = a_1' \frac{k_2}{k_{-2} + k_3} - (a_1' - a_1) \frac{k_2}{k_{-2} + k_3} \exp\left[-(k_{-2} + k_3)t\right] \qquad \text{XVII}$$

If the steady state velocities according to VIII, based on a_1' and a_1, but both with the new value of k_3, are called s_{st} and s_{min}, respectively, we have:

$$s = s_{st} - (s_{st} - s_{min}) \exp\left(-t/\tau\right) \qquad \text{XVIII}$$

where $1/\tau = k_{-2} + k_3$.

XVIII is identical with eqn. (1) of Heusler's paper. τ is in his experiments independent of potential and is about 0.3 sec. It is strongly suggested that this is the potential independent value of $1/k_{-2}$. We have found similar time constants in our experiments, but of much higher values (several seconds). It is therefore suggested, that one of the differences between the hydrogen treated iron electrode and our non treated electrodes is, that for the hydrogen treated electrode the assumption XIII is valid, and hence the term with $b = 29$ mV of XII the leading one, whereas in our case the first term of XII was the dominating one.

It is of course possible to investigate a differential equation of the form XVI for experimental conditions other than those mentioned above. An analogue to XVI is valid for the acid dissociation of the adsorbed water:

$$\frac{\mathrm{d}a_1}{\mathrm{d}t} = k_1 a_2 - k_{-1} h a_1 - k_2 a_1 \qquad \text{XIX}$$

This may be solved analytically for small changes of potential as linear functions of time. If we neglect both oxidized forms in VI, we have

$$\frac{\mathrm{d}a_1}{\mathrm{d}t} = k_1 N - (k_1 + h k_{-1} + k_2) \cdot a_1 \qquad \text{XX}$$

We want to solve this equation for the condition

$$\eta = \eta_0 + \alpha t \qquad \text{XXI}$$

where $\alpha t \ll 116$ mV. The initial condition is

$$0 = k_{1,0}N - (k_{1,0} + k_{-1,0}h + k_2) \cdot a_{1,0} \qquad \text{XXII}$$

where the indices 0 refer to a steady state at the potential η_0. We define, introducing XXI

$$\left.\begin{aligned} k_1 &= k_{1,0} \exp\left(\tfrac{1}{2} \cdot \frac{zF}{RT} \cdot \alpha \cdot t\right) \sim k_{1,0}(1 + \beta \cdot t) \\ k_{-1} &= k_{-1,0}(1 - \beta \cdot t) \\ a_1 &= a_{1,0} + \Delta a_1 \end{aligned}\right\} \qquad \text{XXIII}$$

k_2 is potential independent.
Introduction of these expressions in XX and combination with XXII gives:

$$\begin{aligned} \frac{\mathrm{d}a_1}{\mathrm{d}t} = \frac{\mathrm{d}\,\Delta a_1}{\mathrm{d}t} = {} & [k_{1,0}N - (k_{1,0} - k_{-1,0}h)a_{1,0}]\beta t \\ & -[k_{1,0} + k_{-1,0}h + k_2]\Delta a_1 \\ & + \text{terms of higher order} \end{aligned} \qquad \text{XXIV}$$

which we write

$$\frac{\mathrm{d}\,\Delta a_1}{\mathrm{d}t} = Kt - L \cdot \Delta a_1 \qquad \text{XXV}$$

As $\Delta a_1 = 0$ for $t = 0$ we have

$$\Delta a_1 = \frac{K}{L} \cdot t - \frac{K}{L^2}\,(1 - \exp\,(-Lt)) \qquad \text{XXVI}$$

An increase of a_1 is seen experimentally as an anodic current:

$$\Delta a_1 = \frac{1}{F} \cdot \Delta q = \frac{1}{F} \cdot C \cdot \Delta\eta = \frac{1}{F} \cdot C \cdot \alpha \cdot t$$

where C is a formal capacity.
For large t the exponential term of XXVI vanishes, so

$$\frac{\mathrm{d}\,\Delta a_1}{\mathrm{d}t} = \frac{K}{L} \text{ and } C = F \cdot \frac{K}{L}$$

or

$$C = \frac{N(2hk_{-1}k_1 + k_1k_2) \cdot z \cdot F^2}{(k_1 + k_{-1}h + k_2)^2 RT} \qquad \text{XXVII}$$

The potential dependencies of the kinetic constants imply that C is small at extreme potential values and has a maximum somewhere in the potential region where corrosion is significant. We have determined the total double layer capacities of iron electrodes by an impulse method, details of which will be reported in a later paper: a result is seen in Fig. 12. It is seen that the

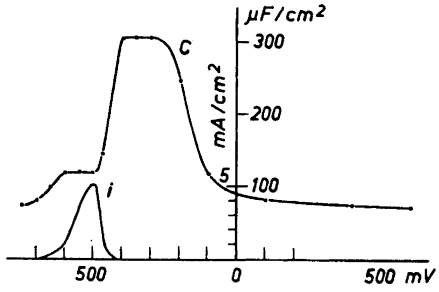

Fig. 12. *C*, capacity of iron electrode *vs.* potential;
i, anodic dissolution rate *vs.* potential;
Medium: 1.00 M sodium acetate, 0.002 M *o*-phenanthroline. pH 7.05; Temp. 25.0°C.

double layer capacity has high values at intermediate potentials as expected from the theory. The integral

$$\int \frac{C}{F} \, d\eta = 10^{-9} \text{ mole/cm}^2$$

taken over the potential region where C is high, should be an expression for the amount of hydrogen ion given off by the electrode going from fully active to fully passive electrode state. The estimated experimental value given is reasonable for a monomolecular layer of water.

It is seen from XXVI that a transition phenomenon should be shown by such capacity measurements. The values of $L = k_1 + k_{-1}h + k_2$ actually observed were about 10^3—10^4 sec^{-1}, nearly independent of h and with the higher values at the more positive potentials. It appears that the observed values essentially represent k_1. It has not however hitherto been possible to obtain very accurate data for capacities and time constants because of inherent noise. We intend to return to these phenomena in future work.

Fig. 13 shows the result of some experiments, which typify the behaviour of the iron electrode. A potentiostat was programmed to change the potential of an iron electrode in a triangular way. The total change of potential was 59 mV the scanning time was 10 sec. for a full period. It is seen that the measured corrosion current was throughout lower for increasing potentials than for decreasing potentials.

Very similar hysteresis phenomena were, as seen on Fig. 14, observed when an analogue computer solved a differential equation of the type XIX for the condition that k_1 and $k_{-1}h$ were exponential functions of time. There is a striking resemblance between the behaviour of the electrode system and of the analogue computer. A quantitative agreement was not obtained, as the three first steps of the general mechanism must have had an influence on the overall kinetics, but only two steps were actually incorporated in the "mechanism" of the computer. The computer at our disposal was too small to accomodate a more correct representation of the corroding iron electrode. The comparison of Figs. 13 and 14 does, however, illustrate that the various hysteresis phenomena, so typical for the kinetic behaviour of solid electrodes, often do reflect quite simple aspects of the electrode reaction studied. Hence the investigation of such phenomena should be worth while if appropriate means of calculation are at disposal.

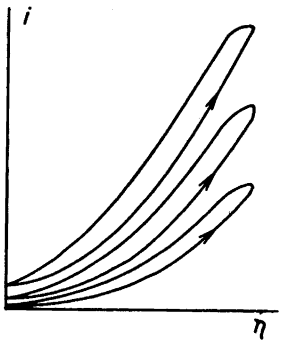

Fig. 13. See text. Medium: 0.5 M sulphuric acid.

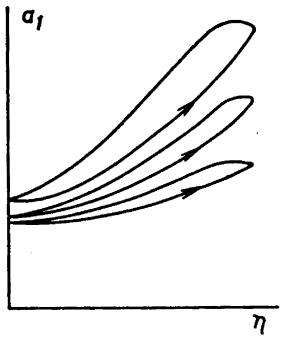

Fig. 14. See text.

THE PASSIVE STATE

The mechanism for the iron electrode suggested in this paper would seem to involve that the passive layer is of monomolecular thickness. It is well known from many investigations, that this is not so. The surface species FeO occurring in our mechanism must therefore essentially be regarded a precursor for the passive layer as this is described in the literature [4]. We have on the other hand found that both the passivation of iron and the reactivation necessitate much less exchange of electricity than generally assumed. In neutral or weakly alkaline solutions we have been able to passivate rotating iron electrodes, suddenly rised to a potential in the passive region, with a few millicoulombs/cm^2. Fig. 15 shows a direct recording of the amount of electricity passed through an iron electrode the first few seconds after a sudden potentiostatic reactivation. It is seen that there is an immediate demand for cathodic current amounting to about one millicoulomb/cm^2, followed by a slower anodic corrosion current. Whether the cathodic current represents a reduction of the passive layer or not it is still certain, that some mechanism for the transport of electricity between electrode surface and solution must exist. As the solution does not contain reducible matter we can think of no better explanation than that the cathodic current is a manifestation of a transport of hydrogen ion from the solution to the passive layer. That would also explain why both the electrode potential and the pH of the solution are so important for the state of the iron electrode.

The mechanism of passivity given here is *not* in accordance with the existence of a sharp transition between a passive and an active state of the iron electrode. Fig. 16 shows that when the potential of a passive iron electrode is carefully changed to more negative values, it is possible to obtain a smooth increase in anodic current with decreasing potential. It is seen that two of the Tafel lines have slopes of 58 mV, and one of them somewhat less. These values are in reasonable accordance with the discussion on p. 302; whether or not they are actually determined exactly by the terms of the factor C they do

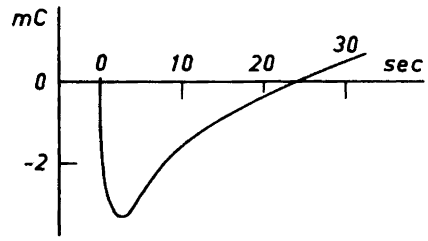

Fig. 15. Direct recording of amount of electricity passed through an iron electrode after change of potential at time zero. Medium: 1 M sodium hydrogen carbonate. 10 % CO_2 in gasphase. Temp. 25.0°C. Electrode area, 2.41 cm^2.

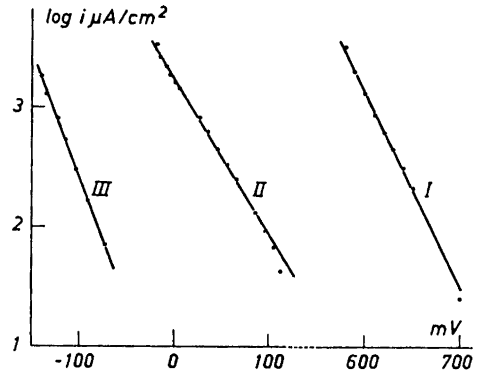

Fig. 16. Tafel lines for reactivation of passive electrodes.
I 0.5 M sulphuric acid
II 1.0 M sodium acetate + acetic acid, pH 5.75
III 0.5 M sodium chloride + 0.5 M sodium acetate
+ acetic acid, pH 6.75.

support the point of view of a catalytic influence of hydrogen ion, taken up by the passive layer, as the mechanism of the effect demonstrated in Fig. 16. Inversely; the mechanism of passivity must be the electrostatic repulsion of hydrogen ions, in the absence of which the solvation step, which completes the anodic dissolution of iron, is impossible.

INFLUENCE OF DISSOLVED OXYGEN

A passive iron electrode will, according to our experience, not reduce dissolved oxygen at potentials, where oxygen is reduced readily on, *e.g.*, a silver electrode. At somewhat more negative potentials, where iron becomes active it will reduce oxygen. It is of great interest that an electrode which according to a potential-anodic dissolution diagram for oxygenfree solution should be slightly active, will not corrode at that potential in the presence of oxygen. It seems, that the difference between the active iron electrode and the silver electrode on one hand, and the passive iron electrode on the other hand, might very well be the availability of hydrogen for a reaction such as

$$O_2 + 4e^- + 4H^+ \rightarrow 2H_2O$$

The slightly active electrode would then become passive because this reaction removes the hydrogen ion from the surface of the iron electrode. In accordance with this point of view oxygen is found to catalyse the anodic dissolution at more negative potentials, *i.e.* at the ascending branch of the potential-corrosion rate diagram. It seems that presence of oxygen causes a change of

behaviour of the iron electrode corresponding to a change of potential towards more positive values, *i.e.* towards conditions with lower steady state surface concentration of hydrogen.

CONCLUDING REMARKS

The mechanism of the anodic dissolution of iron given in this paper is obviously very crude. It seems however, that all known features of the behaviour of the iron electrode are reasonably well explained by this mechanism and there should be every reason to study its implications more closely, as we intend to do in coming papers.

A question which must arise in this connection is the power of resolution of kinetic methods altogether. The mathematical image of the mechanism is the differential equations of VIII; once their validity is established the mechanism is also proved valid. In this sense, the word mechanism only means the sequence of events an iron atom must go through from the time it belongs to the metal lattice till it is solvated or till it is embedded into a passive layer in a more or less oxidized form. In a wider sense the mechanism is not understood until not only the sequence of events, but also the nature of each event is more precisely understood. To obtain such understanding it is essential that the numerous rate constants of the electrode are ascribed absolute values in their dependence on thermodynamic parameters such as temperature, potential and properties of solvent. It is interesting, that the velocity and the parameter N are inseparable according to the steady state solution of the kinetic equations, and also that, however accurate are the data for the experimentally accessible parameters of IX or X, it will not be possible to separate the various rate constants without auxiliary assumptions, *e.g.* those of IV. Even so can IX and X only provide the rate constants multiplied by N. That this is a special feature of the steady state solutions of the kinetic equations is seen from the solutions for non steady state conditions. In these solutions the exponential terms involved contain naked rate constants. This opens up a way of determining the important parameter N. Future work may thus disclose whether the active corrosion process is confined to special active sites, *e.g.* lattice defects, to all iron atoms in a monomolecular surface layer or may be to a spongy layer of a thickness corresponding to several atomic layers.

REFERENCES

1. Tafel, J. *Z. physik. Chem.* **50** (1905) 641.
2. Okamota, G., Nagayama, M. and Sato, N. *CITCE* **8** (1958) 72.
3. Hoar, T. P. *Private communication.*
4. Hoar, T. P. *Modern Aspects of Electrochemistry* No. 2 (Ed. J. O'M. Bockris) (1959) 262 (This excellent review contains 351 references).
5. Bockris, J. O'M. *Modern Aspects of Electrochemistry* (Ed. J. O'M. Bockris) (1954) 180.
6. Hoar, T. P. and Hurlen, T. *CITCE* **8** (1958) 445.
7. Hurlen, T. *Teknisk Ukeblad* **1958** 95, 119.
8. Bonhoeffer, K. F. and Heusler, K. E. *Z. physik. Chem. N. F.* **8** (1956) 390.

9. Heusler, K. E. *Z. Elechtrochem.* **62** (1958) 582.
10. Stern, M. *J. Electrochem. Soc.* **102** (1955) a. 609; b. 663.
11. Makrides, A. C., Komodromos, N. M. and Hackerman, N. *Ibid.* 363.
12. Nord, H. *Ingeniøren* **1958** 261.
13. Kabanov, B., Burstein, R. and Frumkin, A. *Discussions Faraday Soc.* **1** (1947) 259.
14. Bonhoeffer, K. F. and Heusler, K. E. *Z. Elektrochem.* **61** (1957) 122.
15. Flade, F. *Z. physik. Chem.* **76** (1911) 513.
16. Frank, U. F. *Z. Naturforsch.* **4a** (1949) 378.
17. Meyer, F. R. and Ronge, G. *Angew. Chem.* **52** (1939) 637.

Received September 7, 1960.

ACTA CHEMICA SCANDINAVICA 15 (1961) 321–324

The Phosphorus Turn-over Rate of Human Red Cell Mononucleotides

E. PITKÄNEN

From the First Department of Medicine, University of Helsinki, Finland

A two dimensional paper chromatographical method was used for the study of human red cell mononucleotides *. ATP, ADP, GTP, GDP and an uridine containing mononucleotide were found constantly. The labelling of the mononucleotides was investigated after incubation with radioactive phosphate. ADP and GTP were shown to have a phosphorus turn-over rate almost as high as the ATP turn-over rate.

The presence of ATP and ADP in human red cell has been amply demonstrated (review in Whittam [1]). More recently, the concentration of the two nucleotides has been adequately determined by enzymic [2] and paper chromatographical [3–5] means and with the use of ion-exchange chromatography [6–8]. The presence of small amounts of GTP and AMP has also been verified.

The adenine nucleotide phosphorus has a high turn-over rate [9,10]. By means of differential hydrolysis Gourley[9] showed a high labelling of the labile phosphorus of ATP while the stable phosphorus labelling was lower. The great number of various organic phosphates present in the red cells makes, however, an adequate study of the nucleotide labelling difficult. The procedure used in the present work allowed a means for the estimation of the amount and the degree of labelling of the nucleotides after incubation of the red cells with radioactive phosphorus.

MATERIAL AND METHODS

The nucleotides were purchased from the Sigma Chemical Co, St Louis, Mo., and from Boehringer and Soehne, Mannheim, Germany, radioactive orthophosphate from the Radiochemical Centre, Amersham, England, Norite A was a produce of N.V. Norit — Vereeniging Verkoop Centrale, Amsterdam. Myokinase was purchased from Boehringer and Soehne. ATP was determined enzymatically in the presence of glyceraldehyde phosphate dehydrogenase, phosphoglycerate kinase, 3-phosphoglycerate and reduced diphosphopyridine nucleotide. The reagents were purchased from Boehringer and Soehne.

* The following abbreviations are used in the text: EDTA, ethylene diamine tetra acetic acid, pH 7.4; ATP, adenosine triphosphate; ADP, adenosine diphosphate; AMP, adenosine monophosphate; GTP, guanosine triphosphate; GDP, guanosine diphosphate.

Venous blood samples, approximately 10 ml each, were taken in tubes containing 0.5 ml of 0.2 M EDTA solution with simultaneous samples for the hematocrite and serum phosphorus determinations. Aliquots of 2 ml were immediately transferred into 50 ml Erlenmeyer bottles and about two million c.p.m. of radioactive phosphate was added. The bottles were filled with a gas mixture containing nitrogen, oxygen and carbon dioxide (75:20:5), corked and incubated for 15 min at 37°. The samples were subsequently chilled to + 2°, washed twice with physiological saline and 9 ml of 10 % trichloroacetic acid was added. The extract, after centrifugation, was neutralized to pH 8—8,5, 0.5 ml of 25 % solution of Ba-acetate and 60 ml of ethanol were added. The precipitate was allowed to settle down for 30 min, centrifuged down and washed once with ethanol. The precipitate was then suspended in 5 ml of water and enough Amberlite (IR-120, in acid form) was added to solubilize totally the precipitate.

The solution was neutralized to pH 6—7 and pressed through a Norit A column (1.5 cm length, 0.5 cm diam.). The column was washed with 10 ml of water and eluted with 5 ml of a mixture containing ethanol, ammonia and water (5:3:2). The eluate was evaporated to a small volume under a current of nitrogen and submitted to paper chromatography.

Whatman No. 3 MM chromatographical paper sheets were washed with 0.01 M EDTA solution, water and *n*-propanol by allowing the solvents to run through the paper, one day each. The sample was transferred to the paper by means of a capillary to make a spot, 0.5 cm wide and 1 cm long.

The solvents were slightly modified from those used by Hanes and Isherwood [11] and Miettinen [12]. In the first run *tert.* butanol: formic acid: water: ammonia (8:3:4:0.03, 8 h), and in the second run *n*-propanol:ammonia:water (6:3:1, 20 h) were used.

The spots were localized under ultraviolet light, outlined with pencil, cut off and eluted with 0.1 M tris buffer, pH 7.1, by means of a capillary. The volume was adjusted to 0.5 ml. The absorption spectra of the spots were determined in Beckman DU spectrophotometer in 0.5 ml cuvettes having a light path of 1 cm. The radioactivity of the samples was subsequently determined in an Ekco Model M-6 Geiger-Müller tube. Generally, the counts were taken over a period of 5 min.

Suitable blank areas on the chromatograms were treated similarly.

The total amount of ATP in blood samples was determined by the glyceraldehyde phosphate dehydrogenase reaction. The total amount of the other nucleotides was computed using the ratio of total ATP to ATP in the chromatogram as a correction factor.

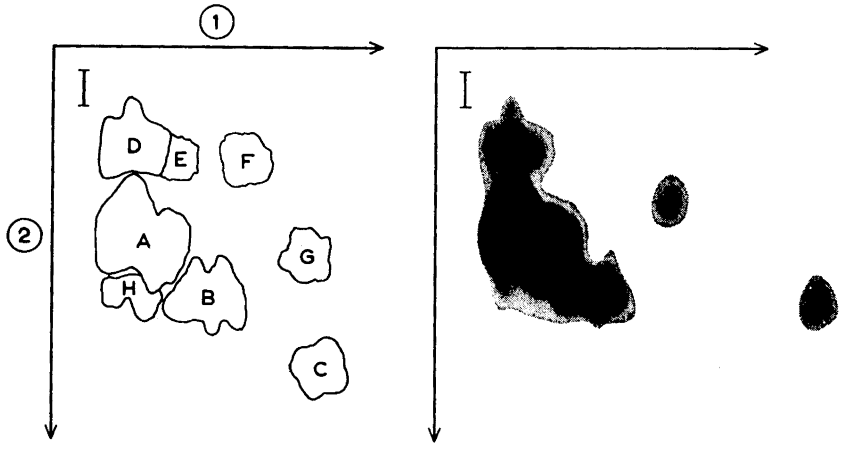

Fig. 1. Diagramatic representation and radioautogram of red cell mononucleotides after two-dimensional separation by paper chromatography.

RESULTS AND DISCUSSION

Eight ultraviolet light absorbing spots were visible in the chromatograms.

A) was the largest spot with a spectrum identical to that of adenosine. It was identified as ATP by means of the glyceraldehyde phosphate dehydrogenase reaction.

B) also showed the absorption spectrum of adenosine. It's R_F value was indentical with that of ADP. It also showed the glyceraldehyde phosphate dehydrogenase reaction after addition of myokinase.

C) A weak spot with a spectrum of adenosine was occasionally found at this area. The R_F values of AMP coincided with that of this spot. No radioactivity was found in the spot.

D) and E) were not well separated from each other. The two spots had spectra identical with that of guanosine. D) has been further identified as GTP by means of it's R_F value. E) has been tentatively identified as GDP.

F) The weak spot has not been identified.

G) has a spectrum identical with that of uridine. The compound has not been further identified, however. The spot showed no radioactivity.

H) was a weak spot and it was found inconsistently. It had a spectrum of adenosine, and is presumed to be ADP, a breakdown product of ATP, formed during the run with the acid solvent.

A weak and indistinct spot was seldom found in the area between A, D and E. The eluate of the area showed consistently a spectrum of adenosine. The area also had radioactivity, which, however, mostly was due to the phosphate liberated from ATP during the run.

The amount of the four nucleotides that were found constantly in the blood samples are shown in Table 1. The ratio of ATP/ADP, roughly 8:2, is similar to the value found by Greenwalt [5], Bishop [6], Mills [7] and Hannon [2] but is somewhat lower than that found by Vogel [4]. The amount of GTP is consistent with the results of Mills [7].

Table 1. The amount of labelling of mononucleotides after incubation with radioactive phosphorus in eight samples of human red cells.
The amounts expressed as μg of mononucleotide/ml of red cells. Amount of radioactive phosphorus was two million counts per min. for 1 ml of red cells. The labelling corrected for 3 mg phosphorus in 100 ml plasma.

ATP			ADP			GTP			GDP	
μg	c.p.m.	Counts per μg	μg	c.p.m.	Counts per μg	μg	c.p.m.	Counts per μg	μg	c.p.m.
229	35 350	154	32	4 370	136	6.8	860	108	1.9	80
425	34 450	81	85	6 170	72	14	304	20	3.7	—
347	44 030	126	35	4 580	130	21	810	39	5.1	—
587	65 214	111	77	6 362	82	22	1 150	50	6.5	103
533	42 100	78	61	3 105	50	32	1 406	43	5.7	43
634	60 500	95	62	2 580	41	38	1 010	23	8.5	—
560	88 950	158	94	12 460	132	26	1 834	70	7.4	71
400	74 226	185	69	9 769	141	9.3	1 227	130	3	70

The highest uptake of phosphorus was found in ATP. It suggests, in accordance with Gourley [9] that ATP is one of the key substances in the uptake of phosphorus from plasma into the cell. ADP, however, showed a labelling almost as high as that of ATP. It suggests that, in addition to the adenylate kinase system, another pathway exists in the red cell for the labelling of the ADP-phosphorus. The lack of any detectable AMP in most of the samples also suggests that the adenylate kinase pathway is inhibited in the red cell.

A remarkably high phosphorus uptake was found also in GTP.

REFERENCES

1. Whittam, R. *J. Physiol.* **140** (1958) 479.
2. Hannon, J. P. *J. Appl. Physiol.* **12** (1958) 211.
3. Vogel, G. *Arch. exptl. Pathol. Pharmakol. Naunyn-Schmiedeberg's* **233** (1958) 499.
4. Prankerd, T. A. J. and Altman, K. I. *Biochem. J.* **58** (1954) 622.
5. Greenwalt, T. J. and Ayers, V. E. *Blood* **60** (1960) 698.
6. Bishop, C., Rankine, D. M. and Talbot, J. H. *J. Biol. Chem.* **234** (1959) 1233.
7. Mills, G. C. and Summers, L. B. *Arch. Biochem. Biophys.* **84** (1959) 7.
8. Bartlett, G. R. *J. Biol. Chem.* **234** (1959) 449.
9. Gourley, D. R. H. *Arch. Biochem. Biophys.* **40** (1952) 1.
10. Yoshikawa, H., Nakao, M., Miyamoto, K. and Yanagisawa, I. *J. Biochem. Tokyo* **46** (1959) 83.
11. Hanes, C. S. and Isherwood, F. A. *Nature* **164** (1949) 1107.
12. Miettinen, J. K. and Savioja, T. *Acta Chem. Scand.* **13** (1959) 1693.

Received October 7, 1960.

ACTA CHEMICA SCANDINAVICA 15 (1961) 325–341

Isoelectric Fractionation, Analysis, and Characterization of Ampholytes in Natural pH Gradients. I. The Differential Equation of Solute Concentrations at a Steady State and its Solution for Simple Cases

HARRY SVENSSON

The Gates and Crellin Laboratories of Chemistry, California Institute of Technology, Pasadena, Calif., USA, and Department of Bacteriology, Karolinska Institutet, Stockholm, Sweden

The properties of natural pH gradients formed by stationary electrolysis are analyzed and compared with those of artificial pH gradients. The pH of a pure ampholyte solution is calculated, and the difference between this and its isoelectric pH is used to prove that a stationary state is characterized by mutually balancing diffusional and electric mass flows. The differential equation of the concentration of a component contributing to a natural pH gradient is formulated. It is shown that such components have to be defined as acids, bases, or ampholytes, and that the mobilities or transference numbers entering the differential equations must be ascribed to these ion constituents of the protolytes which are not H^+ or OH^-. Solutions to the differential equation are presented for a one-component system and for a trace component present in a large excess of other components. The practical significance of the results for fractionation and characterization of ampholytes is discussed. Thus it is proved that the pH at the concentration maximum of an ampholyte is identical with its isoelectric point, which should be of value for direct measurement of isoelectric points. The concentrations of acids and bases or, more generally, of the most acidic and the most basic components present in the system, are shown to increase steadily towards the anode and cathode, respectively, without developing maxima in the mathematical sense. It is shown that the electrokinetic properties of proteins make them especially suitable to isoelectric fractionation, whereas simple ampholytes are extremely useful as "carrier electrolytes" in work with proteins. By a proper choice of simple ampholytes and their concentrations, it is possible in principle to obtain pH gradients of any desired extension and shallowness, but for the present a sufficient number of suitable simple ampholytes is not available.

Isoelectric precipitation is a standard procedure for fractionation and purification of proteins. Isoelectric fractionation by electrical transport has also been used for a very long time, especially for group separations of amino acids and peptides (see the author's [1] review of 1948). However, the resolving power of these methods has stayed far behind that obtainable by moving boundary or zone electrophoresis using differences in electric mobility at a constant pH. A renewed interest in isoelectric methods has now been evoked through a series of articles by Kolin [2-6] and through the experiments described by Hoch and Barr [7] and by MacDonald and Williamson [8].

Isoelectric analysis and fractionation by electric transport is based on sending a direct current through a system of electrolytes such that pH increases gradually from anode to cathode. If the pH gradient can be kept reasonably stable during the time for an experiment, proteins and other ampholytes will be repelled from both electrodes and collect in a region where the local pH is identical with the isoelectric point of the ampholyte. This principle can be applied in a number of different ways depending on the nature of the pH gradient and also on the principle selected for stabilizing the system against remixing by uncontrolled convection.

ARTIFICIAL pH GRADIENTS

The authors just mentioned used artificial pH gradients, that is, they applied their samples in a mixing zone between two buffers of different pH's. Such a method puts great demands on the selection of the two buffers in order to secure a sufficient stability of the pH gradient. Since all buffers are composed of electrolytes, any artificial pH gradient is subject to changes caused by electric migration of the buffer ions. Needless to say, the migration of the pH gradient has to be slower than that of the components to be separated. Since the latter retard to zero mobility in the isoelectric state, it is evident that artificial pH gradients can never be expected to give more than quasi-equilibrium positions of isoelectric compounds. The length of a run may thus often be critical and difficult to predict.

The most favourable buffer systems are pairs of buffers containing the same ion species, *e.g.* two acetate buffers with pH's including the isoelectric points of the proteins. The differences between them is a certain concentration of excess acetic acid, which is very slightly ionized. This constituent is thus almost stationary. According to Kohlrausch's [9] electro-migration laws, the salt concentration also remains constant as long as the buffer reservoir suffices. A pH gradient of this kind is consequently very stable.

Kolin used a mixture of sodium acetate and sodium barbital as the basic, and the same solution mixed with hydrochloric acid as the acidic buffer. Hoch and Barr used a phosphate buffer of pH 7.4 as the basic, and mono-sodium phosphate as the acidic buffer. MacDonald and Williamson applied their samples in a region containing only distilled water between highly conducting anolytes containing hydrochloric or citric acid and catholytes with sodium hydroxyde or sodium citrate.

Artificial pH gradients, if properly selected, have the advantage that the conductance and field strength can be freely chosen and kept constant during the experiment.

NATURAL pH GRADIENTS

The numerous workers who have applied stationary electrolysis have allowed the electric current to create the pH gradient, usually in an apparatus with several compartments separated by membranes. The mechanism of this procedure is the following. Let us suppose that the electrolytic solution does not contain any ions, except the water ions, that can undergo oxidation or reduction at the electrodes. This is essentially the case with sodium sulphate in low concentrations. One then gets evolution of hydrogen at the cathode and of oxygen at the anode (which should be of platinum or carbon), while sodium hydroxyde collects in the catholyte and sulphuric acid in the anolyte. If remixing is prevented in some way or other, the final result is a partial or complete separation of acid and base, with or without a layer of pure water between them, depending on the current density.

If now ampholytes are added to the system, they will acquire a positive charge in the anolyte and a negative charge in the catholyte. Repulsion from both electrodes causes them to migrate towards the center of the apparatus. Between the acid and the alkali, they lose their charges and stop migrating. The final positions of the various ampholytes will be according to the sequence of their isoelectric points, the more basic ones being concentrated near the alkali, the more acidic ones closer to the acid. The ultimate course of pH from anode to cathode will be dictated by the isoelectric points of the ampholytes and by the concentrations and buffering properties of all protolytes in the system.

Subsequently a pH gradient thus formed will be called a natural pH gradient because it is the type of gradient which the current itself has created. For this reason, it is characterized by a complete stability. It is understood, then, that every artificial pH gradient must be reshaped into the natural pH gradient, provided that a sufficient time for electrolysis is allowed and that the system is stabilized against remixing. It is also obvious that an artificial pH gradient made up so as to imitate a natural one can be expected to get a very high stabiltiy.

If the extreme pH's given by sulphuric acid and sodium hydroxyde are not required, there is reason to choose a salt of a weaker acid and a weaker base, *e.g.* ammonium acetate, instead of sodium sulphate, provided that the acid withstands anodic oxidation and the base cathodic reduction. The pH's below 2 and above 12 are then not obtainable, and the whole apparatus can be better utilized for the pH range really needed. If still more restricted pH ranges are sufficient, it may be suitable to exclude all salts and to use only ampholytes and/or acids and bases too weak for mutual salt formation (boric acid, phenols, aromatic amines). For instance, for separations in the range between pH 3 and 4, a mixture of picolinic acid (isoelectric point 3.16), glutamic acid (IP 3.22), nicotinic acid (IP 3.44), anthranilic acid (IP 3.53), and *m*-aminobenzoic acid (IP 3.93) is adequate. In this way restricted pH gradients of any desired

shallowness can be created if suitable ampholytes are available. This is of great importance for high-resolution separations and for handling greater quantities of material.

The unlimited stability of natural pH gradients makes them very attractive, but unfortunately the method is so far hampered by some serious drawbacks. Its most severe limitation lies in the fact that one cannot choose the conductance throughout the system. The conductance generally becomes extremely low round the neutral point, which results in an excessive heating there. This limits the current that can be sent through to such a low value that one gets only a poor separation in other pH regions. Another experimental difficulty of great importance is the scarcity of suitable ampholytes for certain pH regions. Consequently, in spite of the elegance of the method and the simplicity of the equipment required, not much can be expected from natural pH gradients unless one acquires a clear understanding of the reasons for these difficulties and tries to find remedies. In this and following articles it will be shown that it should be possible to increase the versatility and capability of natural pH gradients quite considerably. This relates to refined isoelectric analysis in density gradients as well as to large-scale fractionation in multi-membrane apparatuses.

METHODS FOR STABILIZATION OF ELECTROLYTIC SOLUTION

All workers who have used natural pH gradients hitherto have applied multi-membrane equipment. In such a set-up, the separation occurs in the pores of the membranes, and the compartments between them, which are continuously homogenized by natural convection or mechanical stirring, merely serve as reservoirs for scaling up the capacity. The stabilizing principle is thus a capillary system. The same is the case in the experiments described by Hoch and Barr [7] and MacDonald and Williamson [8], who used ordinary paper electrophoresis equipment.

Kolin applied artificial pH gradients in vertical density gradient columns. The use of such columns in combination with natural pH gradients has recently been successfully explored by the present author and will be the subject of a forthcoming article in this series. It may be mentioned already now that such a procedure, although subject to the difficulties mentioned above, offers great advantages through the extreme simplicity of the equipment. Since the electrode reactions constitute an essential part of the separation process, special electrode vessels with comparatively large volumes of buffer are not to be used. In principle, only a test-tube and two platinum electrodes are required. However, since one electrode has to be at the bottom, it is also necessary to have a gas-escape tube around it. Devices for cooling and for taking fractions also have to be added if the apparatus is to be used for other than demonstration purposes.

THE pH OF A SOLUTION OF A PURE AMPHOLYTE

The pH of a solution of a pure ampholyte is known by experience to be approximately its isoelectric pH. A simple consideration of the electro-neutral-

ity condition reveals, however, that there must be a difference between the actual pH and the isoelectric point, pI. An ampholyte isoelectric at pH 3 gives in solution a hydrogen ion concentration of about 10^{-3} moles per liter. Since the ampholyte is the only possible source of anions, a concentration of the same magnitude must exist in the anionic form, and consequently it is not isoelectric. In the technique under discussion here, it is of interest to know something about the discrepancy between actual and isoelectric pH's, and further how it varies with the properties of the ampholyte.

The difference pH — pI can easily be derived theoretically if only two pK values of the ampholyte exert a measurable influence on its isoelectric point. This is the case for all well-known and easily available low-molecular ampholytes. Actually their isoelectric points can be calculated as the arithmetic mean between two adjacent pK values.

The following notation is convenient, all K quantities having the same dimension of concentration. Known quantities are:

K_1 = first dissociation constant of ampholyte when titrated with acid from isoelectric state;
K_2 = first dissociation constant of ampholyte when titrated with base from isoelectric state;
K^2 = ion product of water = 10^{-14} at 25°C;
K_i = $\sqrt{K_1 K_2}$ = isoelectric constant of ampholyte;
pK_1 = $-\log K_1$;
pK_2 = $-\log K_2$;
pI = $-\log K_i = (pK_1 + pK_2)/2$ = isoelectric point of ampholyte;
C = total concentration of ampholyte in moles per liter.

Unknown quantities are:

h = hydrogen ion concentration;
C_+ = concentration of cationic ampholyte;
C_- = concentration of anionic ampholyte;
C_0 = concentration of undissociated and zwitterionic ampholyte.

Leaving activity coefficients without consideration, one has the following four equations:

$$h\,C_0 = K_1 C_+ \tag{1}$$

$$h\,C_- = K_2 C_0 \tag{2}$$

$$h + C_+ = K^2/h + C_- \tag{3}$$

$$C = C_+ + C_- + C_0 \tag{4}$$

of which (3) expresses the electro-neutrality condition. Elimination of C_+ and C_- between (1), (2), and (4) gives the following relation between C_0 and C:

$$C_0(h^2 + K_1 h + K_1 K_2) = K_1\,h\,C \tag{5}$$

The ion concentrations can then be expressed in h and known quantities:

$$C_+(h^2 + K_1 h + K_1 K_2) = C\,h^2 \tag{6}$$

$$C_-(h^2 + K_1 h + K_1 K_2) = C\,K_1 K_2 \tag{7}$$

They can then be introduced into the electro-neutrality condition, which gives the equation:

$$Ch(K_i^2 - h^2) = (h^2 - K^2)(K_i^2 + K_1 h + h^2) \quad (8)$$

This equation contains h as the only unknown quantity, but it is of the fourth degree.

On consideration of practical examples one finds, however, that the degree falls to three and that the resulting equation is easily solved numerically by successive approximation. Thus ampholytes isoelectric below pH 6 give h^2 values at least 100 times greater than K^2; thus this quantity can be omitted. For all acidic ampholytes, one consequently gets the following third-degree equation:

$$C(K_i^2 - h^2) = K_i^2 h + K_1 h^2 + h^3 \quad (9)$$

On the other hand, for ampholytes isoelectric above *pH* 8, h^2 can be neglected beside K^2. Thus all basic ampholytes obey the equation:

$$Ch(h^2 - K_i^2) = K^2(K_i^2 + K_1 h + h^2) \quad (10)$$

For neutral ampholytes, isoelectric between pH 6 and 8, such simplifications are not possible, but for those no calculation at all is necessary. The pH of such solutions coincides with the isoelectric point to a very high precision at concentrations of practical interest.

Since the pH of the solution is known to be approximately equal to pI, $h = K_i$ is used as a first approximation on the right-hand side of (9) or (10) in order to gain a first approximation of $(K_i^2 - h^2)$. This gives a second approximation of h which, on insertion on the right-hand side, gives a second approximation of $(K_i^2 - h^2)$ and a third approximation of h. In most cases the second approximation of h is accurate enough, and in all cases tested by the author the third one has been correct to less than 0.01 pH unit. Thus, for glutamic acid, with the numerical figures:

$$pK_1 = 2.19 \quad pI = 3.22 \quad C = 0.1$$

one gets a pH of 3.24 in the second, and the same figure in the third approximation. Aspartic acid, with the numerical figures:

$$pK_1 = 1.88 \quad pI = 2.765 \quad C = 0.0563$$

gives pH 2.84 in the second and 2.82 in the third approximation.

On the right-hand side of eqns. (9) and (10), the second term is always the biggest one. However, when K_1 and K_2 both approach K_i, the other two terms also become important. One thus finds the difference pH — pI to be the bigger, the closer together the two pK values of the ampholyte.

The dependence on concentration is easily understood from eqn. (8). The quantity $(K_i^2 - h^2)$ is inversely proportional to concentration, and h approaches K (pH approaches 7) as C approaches zero, which must be expected.

CONSEQUENCES FOR THE THEORY OF THE NATURAL pH GRADIENT

The existence of the difference pH — pI enables one to draw some logical conclusions which are helpful for a proper understanding of a natural pH gradient. As will be shown below, these consequences involve valuable information regarding the concentration distribution of ampholytes and concerning the possibility of direct measurement of isoelectric points.

Hitherto available experimental evidence supports the view that it is possible to reach a steady state by prolonged electrolysis under the conditions defined earlier. A steady state includes the demand of a stationary solvent, that is, absence of electro-osmosis by the use of a density gradient as stabilizing agent, or an electrically inert capillary system, or possibly a hydrodynamic back-flow of solvent balancing the electro-osmotic flow. All these alternatives are experimentally possible. If somebody is worried about the continuous consumption of water in the form of hydrogen and oxygen at the electrodes, he can imagine a hydrogen electrode as the anode and a device conducting the hydrogen formed at the cathode to this anode. In such an idealized stationary state, which is most suited for a theoretical attack, the only thing that happens is a continuous circulatory flow of hydrogen. All other chemical components are stationary, they do not change their concentrations anywhere in the system.

Let us first consider a point in the system where an ampholyte is the only solute. The existence of such a point is evident from the fact that there may be only one component plus the solvent in the whole system; the possibility of complete purification by stationary electrolysis is thus not anticipated. It has been proved in last section that the pH at such a point is a little closer to 7 (in water) than the pI of the ampholyte. Thus the latter must possess a small net charge and take part in the transport of current. The ampholyte is consequently bound to migrate electrically, which seems to be in conflict with the supposition of a steady state. This incongruity can only be solved by assuming a mass flow in the other direction, caused by something else than electric attraction and repulsion. Since convection and other transport of solvent have been ruled out, the only possible cause of such a flow is diffusion. One must consequently conclude that *at any point in a natural pH gradient where there is an ampholyte in a pure state, this ampholyte must necessarily have a concentration gradient directed towards the anode for acidic and towards the cathode for basic ampholytes*, the magnitude of this gradient being such that the mass flow due to diffusion balances the electric migration.

The same reasoning applied to acids and bases leads to a similar conclusion. However, the demand for purity can be omitted since no impurity can reverse the electric charge of a non-amphoteric ion constituent. Thus, *the uninterrupted electric migration of acids towards the anode and of bases towards the cathode is balanced by a diffusion flow away from the electrodes.* The steady state is consequently characterized by acid and alkali concentration gradients directed towards the respective electrodes.

Hydrogen is the only substance that exhibits a net mass flow through the apparatus at a steady state. It should be pointed out that it is erroneous to conclude from this fact that the transference number of the hydrogen ion con-

stituent H^+ is unity throughout the system. The definition of a transference number (Hartley and Moilliet [10]) is based on the mass flow *due to electric migration alone.* The protolytic ion constituents, although with a net mass flow of zero, exhibit electric migration and thus have finite transference numbers.

The impossibility for an ampholyte to have a constant concentration in a pure state leads either to the conclusion that it is nowhere pure (which is in conflict with experimental evidence and with the possibility of a one-component system), or to the consequence that it must have a maximum concentration somewhere, since the amount of the ampholyte is finite. If the ampholyte is an end component collecting at one of the electrodes, its highest concentration is found in contact with that electrode. This is no maximum in the mathematical sense, since the concentration gradient for end components is finite all the way to the electrode. If the ampholyte is an intermediate component collecting in an isoelectric zone, its maximum concentration has a vanishing gradient. It follows that there can be no diffusional mass flow at this point, and hence no electric migration either. It is hereby proved that *the pH at the concentration maximum of an ampholyte in a natural pH gradient is its isoelectric point.* Another corollary is, however, that *the ampholyte is necessarily contaminated by the adjacent component at its point of maximum concentration.*

On the other side of the maximum (the side towards the electrode) the pH is lower than pI for acidic, and higher than pI for basic ampholytes, the reason for this being an increased contamination by the adjacent ampholytes. On each side of the maximum, the electric migration is towards the top, and the diffusion flow away from it.

The steady state concentration distribution of ampholytes is thus characterized by a series of bell-shaped curves, one for each ampholyte that does not collect at an electrode. The pH's at the concentration maxima represent the exact isoelectric points of the ampholytes, but the overlapping of the various curves is so extensive that, going from the electrodes towards the neutral point, the concentration of one ampholyte has never reached zero at the concentration maximum of next ampholyte. The experimental implications of these conclusions will be further considered in the discussion.

DIFFERENTIAL EQUATION OF THE CONCENTRATION DISTRIBUTION OF A PROTOLYTE IN A NATURAL pH GRADIENT

After the qualitative considerations in last section, it is easy to formulate the differential equation of the concentration course of an electrolytic component, regardless whether it is an ampholyte or a non-ampholyte or whether it is an end or intermediate component. This equation is:

$$\frac{Cui}{q\varkappa} = D\,\frac{\mathrm{d}C}{\mathrm{d}x} \tag{11}$$

where:

C = concentration of component and ion constituent in arbitrary mass units per arbitrary volume unit;

u = electric mobility in $cm^2\ volt^{-1}\ sec^{-1}$ of ion constituent except H^+ and OH^-, with positive sign for cationic and negative sign for anionic migration;
i = electric current in amperes;
q = cross-sectional area in cm^2 of electrolytic medium, measured perpendicularly to the direction of current;
$\varkappa$ = conductance of medium in $ohm^{-1}\ cm^{-1}$;
D = diffusion coefficient in $cm^2\ sec^{-1}$ of component corresponding to the ion constituent with mobility u.
x = coordinate along the direction of current, thus x increasing from 0 at the anode towards the cathode.

Each term in eqn. (11) expresses the mass flow per second and cm^2 of the cross-section, that to the left being the electric, that to the right the diffusional mass flow.

It is necessary to stay a little at the concepts of component and ion constituent. The latter term is the concept defined by MacInnes [11]. The left-hand side of (11) necessarily refers to an ion constituent in contrast to a chemical component since the latter, if ionized, has at least two mobilities, one cationic and one anionic. On the right-hand side, there is a diffusion coefficient which must refer to a component since D is not defined as the selfdiffusion coefficient of an ion. The fact that one side of the equation describes the mass flow of an ion constituent, the other the mass flow of a chemical component, necessitates such a definition of the latter that an experimental determination of both mass flows amounts to measurements of mass transports of one and the same ion constituent. In other words, un unambiguous correspondence between component and ion constituent is required.

This condition is only satisfied by regarding every base, every acid, and every ampholyte present in the system as components thereof, and by ascribing the mobility u to that ion constituent which is not H^+ or OH^-. In this way eqn. (11) loses application to the two solvent ions. This is natural concerning H^+ since it exhibits a finite net mass flow. With a hydrogen electrode as anode, OH^- *is* stationary, and eqn. (11) should be valid using the concentration and diffusion coefficient of water. However, this is superfluous since the concentration course of water is unambiguously defined by those of the solute species.

In the case of capillary systems as stabilizing agents, the cross-sectional area q and the conductance $\varkappa$ refer to the whole medium including the solid phase. Now there are no good methods for conductance measurements of such media. Some experimental workers then prefer to measure the conductance of the free liquid and to determine experimentally the cross-sectional area of free liquid in the capillary system. Already this leads to doubtful results, and in addition there is the phenomenon of surface conductance, which is different from conductance in bulk solution, at least for electrically active capillary systems. Capillary systems are thus very difficult to master in quantitative measurements.

Like most differential equations in physics and chemistry, eqn. (11) is rather useless without solutions pertaining to specific experimental conditions.

The impossibility of formulating a simple general solution is evident from the fact that one is concerned with a system of mutually dependent differential equations. The conductance and the mobilities are complicated functions of all solute concentrations. However, because of the ease with which rigorous and approximate solutions can be derived for a couple of simple cases, these will be considered in the next two sections.

SOLUTION OF THE DIFFERENTIAL EQUATION FOR A ONE-COMPONENT SYSTEM. CONCENTRATION DISTRIBUTION OF A PURE END COMPONENT

If the differential equation is written in the form:

$$i \frac{\mathrm{d}x}{q} = \frac{\varkappa D \, \mathrm{d}C}{C u} \tag{12}$$

all concentration-dependent quantities are collected to the right, while q, which may be a function of x due to the construction of the apparatus or due to electro-osmosis, is to the left. Only the current is always independent of both x and C. The general solution is:

$$i \int \frac{\mathrm{d}x}{q} = \int \frac{\varkappa D \, \mathrm{d}C}{C u} \tag{13}$$

The cross-sectional area is either constant or can be measured as a function of x. By suitable experiments, it is also possible to represent, $\varkappa$ D, and u as functions of C graphically or mathematically by curve-fitting procedures. In each case, it is therefore possible to obtain a rigorous numerical integration of the differential equation.

Since the transference number T of an ion constituent is given by the equation:

$$T = \frac{FCzu}{\varkappa} \tag{14}$$

where $F = 96\,500$ coulombs per equivalent is the Faraday constant and z is the valence, with plus or minus sign, of the ion constituent, the solution (13) can also be given in the form:

$$i \int \frac{\mathrm{d}x}{q} = Fz \int \frac{D}{T} \, \mathrm{d}C \tag{15}$$

This is more convenient since it only contains two C-dependent quantities that have to be measured.

Eqn. (15) is still an exact solution, applicable to all experimental conditions. The equation:

$$\frac{ix}{FqzD} = \int \frac{\mathrm{d}C}{T} \tag{16}$$

is restricted to experimental conditions giving a constant cross-section and has an exactness corresponding to the constancy of D. The concentration has to be given in moles per cm^3, a restriction that imposes eqn. (14).

For a detailed discussion of the meaning of a transference number of an ampholyte, reference must be made to a previous article on that subject (Svensson [12]). It may suffice to tell here that, according to the modern perception of ampholytes as protolytes over the entire pH range, it is logical and rational to regard H^+ as the positive ion constituent of every ampholyte. It follows that the ampholytic ion constituent is always negative, even that of arginine. The number z for ampholytes is thus a negative integer equal to the number of acidic groups in the molecule.

The transference number is also a signed quantity, as is evident from eqn. (14). A positive product zu gives a positive transference number, and *vice versa*. Ampholytes have negative transference numbers below their isoelectric points.

To go one step further in approximation and simplification, one can make use of the fact that even transference numbers are in many cases essentially independent of concentration. Then the solution of the differential equation becomes especially simple and is best given in the form:

$$C = \frac{Ti\,(x-b)}{FDzq} \tag{17}$$

where $Tib/FDzq$ is the integration constant. The validity of this equation is of course restricted to the space between the electrodes (the interval between $x = 0$ and $x = a$) and to positive concentrations. The coordinate b may assume any positive and negative values. Negative b values may be obtained for Tz positive and means that the concentration is finite and steadily increasing from anode to cathode. Positive b values greater than a may be obtained for negative Tz values and means that the concentration is finite and steadily increasing from cathode to anode. Positive b values smaller than a, finally, means that the concentration drops to zero somewhere in the apparatus, and eqn. (17) is then restricted to the interval between b and that electrode where the component exists. For the interval between b and the other electrode, one has instead:

$$C = 0 \tag{18}$$

which also satisfies the differential equation (11).

The numerical value of b for given experimental conditions can be calculated in terms of the total mass m of the component present in the apparatus. To that end, C is multiplied by q and integrated over the interval for which eqn. (17) is applicable. For b outside the electrodes, this interval is the whole apparatus, and the integration gives the relation:

$$m = \frac{Tia}{2FDz}\,(a - 2b) \tag{19}$$

Insertion of b from (19) into (17) then gives:

$$C = \bar{C} + \frac{T\,i}{2FDzq}\,(2x - a) \tag{20}$$

where C is the mean concentration. This equation is valid for currents lower than the limiting value:

$$i = \pm \frac{2FDzm}{T\,a^2} \tag{21}$$

for which the concentration drops to zero at one of the electrodes. The sign making i positive is valid.

For currents stronger than (21), the concentration reaches zero between the electrodes, and the integration must consequently be carried out from the anode to b if Tz is negative, and from b to the cathode if Tz is positive. One finds for Tz positive:

$$m = \frac{Ti\ (a-b)^2}{2FDz} \tag{22}$$

$$C = \frac{2m\ (x-b)}{q(a-b)^2} \tag{23}$$

and for Tz negative:

$$m = -\frac{Tib^2}{2FDz} \tag{24}$$

$$C = \frac{2m\ (b-x)}{qb^2} \tag{25}$$

Comparison between the eqns. (21), (22), and (24) now reveals that the current necessary for confining the component to a distance c from the electrode at which it collects, is given by the equation:

$$i = \pm \frac{2FDzm}{T\,c^2} \tag{26}$$

If the current density i/q is squared and then divided by the conductance, one obtains the Joule heat per cm^3 of the medium:

$$w = \frac{i^2}{q^2\varkappa} = \frac{4F^2D^2z^2m^2}{T^2q^2b^4\varkappa} \tag{27}$$

Knowing that the minimum conductance is that of the pure solvent and that evacuation of electrolytes really occurs in this process, this equation may be of value in the design of apparatus, especially its cooling system. The conductance of electrolyzed water may be as low as $5 \cdot 10^{-8}$ ohm^{-1} cm^{-1}.

THE CONCENTRATION DISTRIBUTION OF AN INTERMEDIATE COMPONENT

One single component in a system becomes necessarily an end component, that is, it concentrates at one electrode if it concentrates at all. This is true for ampholytes as well as for acids and bases. Glutamic acid, if present alone, can never reach its isoelectric state and is thus attracted by the anode all the time and everywhere, just like sulphuric acid.

The condensation of an ampholyte into an isoelectric zone thus requires at least two components. The system of two or more differential equations (11) is, however, not solvable by simple mathematical means. The resulting pH and conductivity courses of multi-component systems at a steady state thus cannot be calculated, but they can be roughly predicted from the amounts, isoelectric points, and conductances of the components of the system. For example, if comparatively much glutamic acid is present, one can expect to get an extended region with a very shallow pH gradient around the isoelectric point (3.22) of glutamic acid, and with a conductance not lower than that of pure glutamic acid solutions of concentrations corresponding to that in the apparatus. On the other hand, if no suitable ampholytes isoelectric between pH 5 and 7 are available, then the pH gradient in this region must be expected to be rather steep.

Since it is possible to make experimental records of pH and conductance for each system, it will now be assumed that this has been done and that consequently pH and $\varkappa$ are known functions of x. The differential equation (11) can then be applied to an additional component added in so small amounts that it cannot materially alter the concentration distribution of the other, the "carrier" components. This case has a considerable interest for work with proteins in systems of low-molecular ampholytes.

If eqn. (11) is written in the form:

$$\frac{i}{q}\,\frac{u\mathrm{d}x}{\varkappa} = D\,\frac{\mathrm{d}C}{C} \tag{28}$$

it is seen that it is possible to integrate it if u is known as a function of pH and D as a function of C. Specifically, if the conductance, the diffusion coefficient, and the derivative:

$$p = -\,\frac{\mathrm{d}u}{\mathrm{d}x} = -\,\frac{\mathrm{d}u}{\mathrm{d(pH)}}\,\frac{\mathrm{d(pH)}}{\mathrm{d}x} \tag{29}$$

can be regarded as constant within the protein zone, then $u = -\,px$, and one obtains the following analytical solution:

$$C = C_0 \exp\left(-\,\frac{pix^2}{2q\varkappa D}\right) \tag{30}$$

where x is now defined as being $= 0$ at the concentration maximum C_0. This is a Gaussian concentration distribution with the inflexion points at

$$x_i = \pm\sqrt{\frac{q\,\varkappa\,D}{p\,i}} \tag{31}$$

The relation between the maximum concentration and the total amount of ampholyte is:

$$m = C_0\sqrt{\frac{2\,q^3\,\varkappa\,D}{p\,i}} \tag{32}$$

Eqn. (31) shows that proteins are especially suitable for isoelectric condensation, partly because of their low diffusion coefficients, partly due to to their steep mobility curves in the isoelectric range (large value of the slope $du/d(pH)$). The low conductance generally obtained in stationary electrolysis also contributes to give very narrow protein zones. This in turn increases the exactness of the assumption of constant p and $\varkappa$.

If the conductance is not constant, but a linear or quadratic function of x, it is still possible to integrate the differential equation analytically. For

$$\varkappa = \varkappa_0 + rx \tag{33}$$

the author has found the solution:

$$C = C_0 \exp\left[\frac{pi\varkappa_0}{Dqr^2} \ln\left(1 + \frac{rx}{\varkappa_0}\right) - \frac{pix}{Dqr}\right] \tag{34}$$

which is a skew concentration distribution. For

$$\varkappa = \varkappa_0 + sx^2 \tag{35}$$

the solution is found to be:

$$C = C_0 \left(1 + \frac{sx^2}{\varkappa_0}\right)^{-pi/2sqD} \tag{36}$$

DISCUSSION

In 1941, Tiselius [13] described the steady state in stationary electrolysis as a dynamic equilibrium between diffusion and electric migration. He also gave the differential equation (11) in a slightly different form. This interpretation has now been substantiated, and the differential equation has been thoroughly interpreted and solved for two simple cases. End components, which may be acids, bases, or ampholytes, have concentrations steadily increasing towards the electrodes, while intermediate components, which must be ampholytes, have bell-shaped concentration courses. Thus the stationary state of an end component resembles that in sedimentation equilibrium, while the condensation of ampholytes in zones is much akin to the condensation of macromolecules into isodensity bands in the ultracentrifugal technique developed by Meselson *et al.*[14]

At first glance, it appears as self-evident that the pH's of the ampholyte zones are their isoelectric pH's. However, a closer analysis of the differential equation and of equations for the pH of pure ampholyte solutions reveals that pH varies throughout an ampholyte zone, and that a pure ampholyte in solution is non-isoelectric. It has now been shown that the pH at the concentration maximum of an ampholyte in a natural pH gradient is its exact isoelectric point, which is possible due to a contamination at this point by the adjacent component. This should be of great importance for experimental work. There is no other direct way of measuring isoelectric points than by way of the solubility minimum. The moving boundary method of electrophoresis

offers an indirect way which is rather laborious. At least four experiments at different pH's are required for each ionic strength. Extrapolation to zero ionic strength amounts to about 16 experiments. Mobility measurements in paper or other solid support is hampered by great uncertainty and inaccuracy. Stationary electrolysis seems to offer great advantages in this respect, since a pH measurement at the point of maximum concentration is all that is needed. Moreover, the medium is salt-free, so the isoelectric point obtained refers to essentially zero ionic strength.

The solution of the differential equation given for a one-component system shows that an end component exhibits a linear concentration course if the diffusion coefficient and the transference number as defined in the text are constant, or, more generally, have a constant ratio. For higher electric loads, the concentration drops to zero at a distance from the repelling electrode, leaving a region of pure solvent there. This result of the theory checks completely with measurements on sulphuric acid and sodium hydroxyde performed by Tiselius [13].

The complete understanding of the behaviour of a one-component system facilitates considerably the interpretation of more complicated systems. It should be remembered that the process separates the components to a large extent, and that in the steady state only two or three components coexist. Thus, since a region of pure solvent has been shown to develop at one electrode when only an acid or a base is present, then one must conclude that the same may happen in the center of the apparatus when the electrolysis is started with a salt. This was probably the case in Tiselius' experiment with egg albumin and hemoglobin.

One consequence of the diffusion-electromigration theory is that one ampholyte necessarily extends to and beyond the concentration maximum of the adjacent one. Every ampholyte is therefore more or less contaminated already at the centre of its zone. The ampholyte becomes the more contaminated the closer together two adjacent isoelectric points. A complete separation of ampholytes, with regions of pure solvent between component zones, is a theoretical impossibility unless they are isoelectric on either side of the neutral point.

This fact puts a definite limit to the purity obtainable of low-molecular ampholytes by stationary electrolysis. No important advances in this application over those already described in the literature are to be expected. However, this behaviour of low-molecular ampholytes is very favourable for work with proteins. If a system of simple ampholytes is used as "carrier" electrolytes in the separation of proteins, the overlapping concentration curves of the former result in very smooth changes from one isoelectric pH to the next, and in a helpful buffering capacity even at pH's between the available isoelectric points. In combination with the favourable pH-mobility curves of proteins, this opens possibilities for highresolution isoelectric fractionation of proteins.

Schumacher [15] has recently presented a general theory of "focusing ion exchange", which term includes the condensation of ampholytes in isoelectric zones as a special case. His solution of the differential equation for the case of a constant pH gradient (his eqn. (15)) is rather complex, but the corresponding concentration distribution (his Fig. 3) resembles very much the distribu-

tions according to the simple solutions (30), (34), and (36). The discrepancy between his and the present results seems to depend upon fundamentally different physico-chemical approaches. Thus, while in the present treatment mobilities and diffusion coefficients refer to ion constituents and chemical components, respectively, and are experimentally measurable as functions of pH, Schumacher has introduced separate u and D values for the cationic and anionic subspecies. It is also remarkable that the uncharged subspecies have been left without consideration although they are present in most cases (for protolytes: always), take part in the exchange reactions, and contribute to the diffusional flow.

Another difference in approach lies therein that a constant pH gradient was assumed by Schumacher, whereas a constant mobility gradient $\mathrm{d}u/\mathrm{d}x = p$ underlies the solutions (30), (34), and (36) in the present treatment.

Experimental workers in this field have paid great attention to the electrochemical behaviour of the membranes in equipment where such have been used. Electropositive membranes at the anode and negative ones at the cathode is a recommendation one frequently finds in this literature. In terms of quantities used in this theory, the desirable properties of the membranes can be specified as follows.

If the transference number (14) is introduced directly into the differential equation (11), one obtains:

$$\frac{\mathrm{d}C}{\mathrm{d}x} = \frac{Ti}{FDzq} \tag{37}$$

The higher the concentration gradient, the better is the confinement of an end component to the electrode, and the more effective is the separation as a whole. It is seen that the concentration gradient is directly proportional to the transference number of that ion constituent which is not H^+ or OH^-. Electropositive membranes give increased transference numbers to anions, electronegative ones to cations, which explains the recommendations mentioned above.

It should be of special interest to study the applicability of amphoteric membranes, since they would automatically acquire the selectivity desired. The transference numbers would then be expected to change from membrane to membrane, the concentration course of an end component would no longer be linear, but curved so as to improve the confinement to one electrode.

Acknowledgement. This work was started in 1959 at California Institute of Technology. and the author wishes to express his sincere thanks to Professor Linus Pauling for his kind invitation and for laboratory facilities during a period of six months. It was completed at the Department of Bacteriology, Karolinska Institutet, Stockholm, and the author is indebted to Professor Berndt Malmgren for laboratory space during 1960. Grants covering the traveling costs to California were received from the *Natural Science* and the *Technical Research Councils of Sweden*, and the work in Pasadena was made possible by financial support from California Institute of Technology and from LKB-Produkter, Stockholm. From 1960, this research is supported by the *Natural Science*, the *Technical*, and the *Medical Research Councils of Sweden*, which is gratefully acknowledged.

REFERENCES

1. Svensson, H. *Advances in Protein Chem.* **4** (1948) 251.
2. Kolin, A. *J. Chem. Phys.* **22** (1954) 1628.
3. Kolin, A. *J. Chem. Phys.* **23** (1955) 407.
4. Kolin, A. *Proc. Natl. Acad. Sci. U.S.* **41** (1955) 101.
5. Kolin, A. in Glick, D., *Methods in Biochemical Analysis* **6** (1958) 254.
6. Kolin, A. *Proc. Natl. Biophys. Conf. 1957*, Yale University Press, New Haven, Conn. (1959) p. 125.
7. Hoch, H. and Barr, G. H. *Science* **122** (1955) 243.
8. MacDonald, H. J. and Williamson, M. B. *Naturwiss.* **42** (1955) 461.
9. Kohlrausch, F. *Ann. Physik* **62** (1897) 209.
10. Hartley, G. S. and Moilliet, J. L. *Proc. Roy. Soc. London* **A 140** (1933) 141.
11. MacInnes, D. A. *The Principles of Electrochemistry*, New York 1939.
12. Svensson, H. *Science Tools* **3** (1956) 30.
13. Tiselius, A. *Svensk Kem. Tidskr.* **58** (1941) 305.
14. Meselson, M., Stahl, F. W. and Vinograd, J. *Proc. Natl. Acad. Sci. U. S.* **43** (1957) 581.
15. Schumacher, E. *Helv. Chim. Acta* **40** (1957) 2322.

Received September 10, 1960.

ACTA CHEMICA SCANDINAVICA 15 (1961) 342–348

The Crystal Structure of Re_2P

STIG RUNDQVIST

Institute of Chemistry, University of Uppsala, Uppsala, Sweden

The crystal structure of Re_2P has been determined by X-ray powder methods. The structure belongs to the $C23$ type. The dimensions of the orthorhombic unit cell are: $a = 5.540$ Å; $b = 2.939$ Å; $c = 10.040$ Å. The space group is $Pnma$, with $4Re_I$ in $4(c)$: $x = 0.829_5$; $z = 0.065_5$; $4Re_{II}$ in $4(c)$: $x = 0.852_0$; $z = 0.785_0$; and 4P in $4(c)$: $x = 0.395$; $z = 0.110$. The Re_2P structure is compared with that of Ru_2P, and notable differences are indicated.

In previous communications [1–5] on the crystal chemistry of phosphides of the Group VIII metals, the structures of several phosphides with the composition Me_2P have been described. Among the phosphides of the Group VII transition metals, Mn_2P is known to be isostructural with Fe_2P (the revised $C22$ type [1]), but the structure of Re_2P has not been determined previously. The present investigation was undertaken in view of the possible structural relationships between Re_2P and the phosphides of the platinum metals.

EXPERIMENTAL

Rhenium phosphides were prepared by heating rhenium powder (Heraeus, Hanau, Germany, claimed purity 99.8 %) and red phosphorus (purity higher than 99 %) in evacuated and sealed silica tubes at temperatures up to 1 100°C. No attack on the tube walls was detected and chemical analysis was not carried out. Powder photographs were taken in Guinier-type focussing cameras using Cu$K\alpha$ radiation. For the lattice parameter measurements, silicon ($a = 5.4306$ Å) was used as an internal calibration standard and the accuracy obtained was estimated to be greater than 0.05 %. Intensities of the powder lines were measured on photometer records of the films using methods similar to those described by Hägg and Regnström [6]. Relative $|F|$-values were calculated from the equation derived by Hägg [7]. No absorption correction was applied. Fourier summations were made on an analogue computer of the Hägg-Laurent type, constructed by T. Lundström [8]. Structure factor calculations were made on the electronic digital computer BESK using a program devised by Åsbrink *et al.*[9] For the calculations of the atomic scattering factors, expressions of the type

$$f_i = A_i \cdot \exp\left(-\frac{a_i}{\lambda^2}\sin^2\Theta\right) + B_i \cdot \exp\left(-\frac{b_i}{\lambda^2}\sin^2\Theta\right) + C_i \cdot \exp\left(-\frac{c_i}{\lambda^2}\sin^2\Theta\right) + D_i$$

were used. The constants A_i, B_i, C_i and a_i, b_i, c_i have been calculated by Appel [10] on the basis of scattering factor tables given for rhenium by Thomas and Umeda [11] and for phosphorus by Tomiie and Stam [12]. The following constants were used:

	A_i	B_i	C_i	a_i	b_i	c_i
Re	25.854	28.303	19.925	0.170	1.885	15.175
P	1.447	7.971	5.588	0.001	1.528	37.194

For rhenium, the real part of the dispersion correction, calculated by Dauben and Templeton [13] to be -6 units, was inserted as the constant D_i in the above expression.

THE RHENIUM-PHOSPHORUS SYSTEM

The rhenium-phosphorus system was investigated earlier by Haraldsen [14]. He found four intermediate phases with the compositions Re_2P, ReP, ReP_2 and ReP_3. No crystallographic data were reported.

In the present investigation, alloys with phosphorus contents varying from 0 to 50 atom % were prepared. The products were obtained as blue-black powders which oxidized slowly in air.

The powder photographs showed the existence of Re_2P and ReP, and furthermore the existence of the two-phase regions Re + Re_2P and Re_2P + ReP was established. This shows that Re_2P and ReP are the only intermediate phases in the region 0—50 atom % phosphorus (at least at temperatures between 800° and 1 100°C). Within the limits of experimental errors (less than 0.05 %) the lattice parameters of Re_2P were unchanged in two-phase Re + ReP and Re_2P + ReP alloys. It is therefore concluded that Re_2P has a narrow homogeneity range.

Re_2P alloys were heated for several weeks at 1 000°C in silica tubes, but single-crystals suitable for X-ray work were not formed. Re_2P alloys were also heated at temperatures up to the melting point in an argon-filled arc furnace, but they decomposed rapidly, evolving phosphorus fumes. The powder method was therefore the only possible means for the structure determination.

THE STRUCTURE DETERMINATION OF Re_2P

The reflexions in the powder pattern of Re_2P were indexed on the basis of an orthorhombic unit cell with the dimensions: $a = 5.540$ Å; $b = 2.939$ Å; $c = 10.040$ Å. The cell volume of 163.5 Å indicates that the unit cell contains eight rhenium and four phosphorus atoms. Accordingly a value of 16.4 g·cm^{-3} is obtained for the calculated density. The experimental value quoted by Haraldsen [14] is 15.5 g·cm^{-3}.

($hk0$) reflexions were observed only for $h = 2n$ and ($0kl$) reflexions for $k + l = 2n$. It was noted further that the intensity distribution of the ($h0l$) reflexions was closely similar to that of the ($h2l$). These observations, combined with the small value of 2.939 Å for b strongly suggest that the Re_2P structure is based on the space group *Pnma* with all the atoms in the 4(c) positions.

Table 1 X-Ray powder data for Re_2P (Cu$K\alpha$ radiation, $\lambda_{CuK\alpha} = 1.5418$ Å)

hkl	$\sin^2\Theta_{obs} \times 10^4$	$\sin^2\Theta_{calc} \times 10^4$	$\lvert F\rvert_{obs}$	F_{calc}	I_{obs}	I_{calc}
002	236	236	41.1	− 47.6	11.2	15.0
101	252	252	109.4	113.3	153.5	164.3
102	430	429	39.6	45.0	12.7	16.5
103	725	724	29.7	− 31.2	3.8	4.2
011	746	746	98.0	102.9	38.8	42.8
200	774	774	177.6	−173.8	61.0	58.5
201	832	832	112.9	−106.9	45.7	41.1
111	939	939		191.7	288.0	235.5
004		942		84.6		11.5
202	1 008	1 009	29.9	− 21.5	2.7	1.4
112	—	1 116		8.5	259.5	0.4
104	1 136	1 136	310.9	298.1		238.5
013	1 216	1 217	383.6	−381.0	371.0	376.0
203	1 303	1 304	343.1	336.9	282.5	273.0
113	1 411	1 410	26.6	− 29.0	3.2	3.8
210	1 460	1 461	381.5	377.8	320.0	313.5
211	1 520	1 519	13.9	− 17.0	0.8	1.2
105	1 666	1 666	76.9	81.2	11.3	12.7
212	1 697	1 696	46.0	− 48.3	8.0	8.8
204	1 715	1 716	26.6	− 33.1	1.3	2.1
301	1 800	1 800		−191.3	156.3	65.8
114	1 820	1 823		−158.6		90.5
302	1 976	1 976		− 62.4	56.5	6.4
213	1 992	1 991		121.0		48.0
006	2 121	2 120	177.9	−190.9	24.7	28.4
015	2 161	2 160	67.0	− 63.1	6.8	6.1
205	2 243	2 246	42.4	42.3	2.7	2.7
303	2 270	2 271	32.0	35.1	1.5	1.8
106	2 313	2 314	18.7	− 22.6	0.5	0.8
115	2 354	2 353	62.2	66.4	10.9	13.0
214	2 404	2 403	60.5	62.5	10.9	11.6
311	2 489	2 487	24.2	− 18.7	1.7	1.0
312	2 662	2 663		40.5	4.4	4.4
304	—	2 683		20.5		0.6
020	2 748	2 748	343.1	−333.4	78.8	74.3
206	2 895	2 894	58.4	70.3	4.5	6.5
215	2 934	2 933		53.9	9.3	7.7
313	2 956	2 958		− 23.0		1.4
022	—	2 984		28.2	13.1	1.0
121	3 000	3 000		− 67.5		11.8
116		3 001		23.5		1.4
107	3 079	3 079		−156.3	57.4	31.8
400	3 092	3 094		−204.7		27.2
401	3 154	3 153		32.4	2.9	1.4
122	3 178	3 177		− 27.6		2.0
305	3 212	3 213	53.8	− 62.5	3.8	5.1
402	3 332	3 330		62.5	174.5	5.1
314	3 371	3 370		235.7		146.3
123	3 470	3 471	20.0	19.1	1.1	1.0
220	3 522	3 522	103.9	106.5	14.5	15.3
017	—	3 573		− 14.5	59.4	0.3
221	3 580	3 580		65.7		11.8
216		3 581		−134.2		49.0
403	3 625	3 625	156.0	−163.2	33.6	36.7

Table 1. Cont.

hkl	$\sin^2\Theta_{obs} \times 10^4$	$\sin^2\Theta_{calc} \times 10^4$	$\|F\|_{obs}$	F_{calc}	I_{obs}	I_{calc}
207	—	3 660		9.4	4.1	0.1
024	3 690	3 690		− 52.2		3.8
222	—	3 757		13.4		0.5
117	3 767	3 766		−219.5	206.0	137.0
008		3 770		−136.4		13.4
410	3 780	3 781		−180.1		46.1
411	3 839	3 840		− 71.7	139.2	15.0
306	3 860	3 861		− 30.7		1.4
124	3 883	3 884		−188.5		104.0
315	3 898	3 900		65.0		12.4
108	3 963	3 963	97.3	94.2	14.2	13.3
412	—	4 017		− 13.8	153.5	0.6
404	4 035	4 037		− 44.8		3.1
223	4 053	4 052		−216.9		145.3
413	4 312	4 311		146.8	64.3	71.3
217	—	4 347		23.7		1.9
125	4 416	4 414		− 54.3	13.9	10.1
224	4 465	4 464		22.1		1.7
208	4 548	4 543		74.2	71.8	9.8
316		4 548		− 26.9		2.6
321		4 548		126.6		57.0
405	4 571	4 567		− 69.4		8.5
307	4 627	4 627		225.6	100.0	93.3
118	4 648	4 650		− 72.5		19.6
322	4 725	4 724		42.8	13.8	7.0
414		4 724		− 42.3		6.8
026	4 866	4 868		129.6	41.1	34.0
501	4 891	4 894		77.5		12.1

In order to determine the atomic parameters, the Patterson sections $P(x0z)$ and $P(x\frac{1}{2}z)$ were calculated. On account of overlaps only 32 reflexions were clearly resolved on the photometer curves. For most of the remaining lines, individual $|F|^2$ values were calculated using the sum of the intensities obtained from the photometer curves and the ratio of the intensities estimated visually on the powder films.

Table 2. Interatomic distances in Re_2P (Å). (Distances shorter than 3.5 Å listed)

	Re_I	Re_{II}	P
Re_I	2.73 (2) 2.939 (2)	2.74 (2) 2.82, 2.83(2)	2.4_5, 2.6_1 (2) 3.1_7, 3.2_8
Re_{II}	2.74 (2) 2.82, 2.83 (2)	2.86 (2) 2.939 (2)	2.2_7 (2) 2.6_9 (2)
P	2.4_5, 2.6_1 (2) 3.1_7, 3.2_8	2.2_7 (2) 2.6_9 (2)	2.9_0 (2) 2.939 (2)

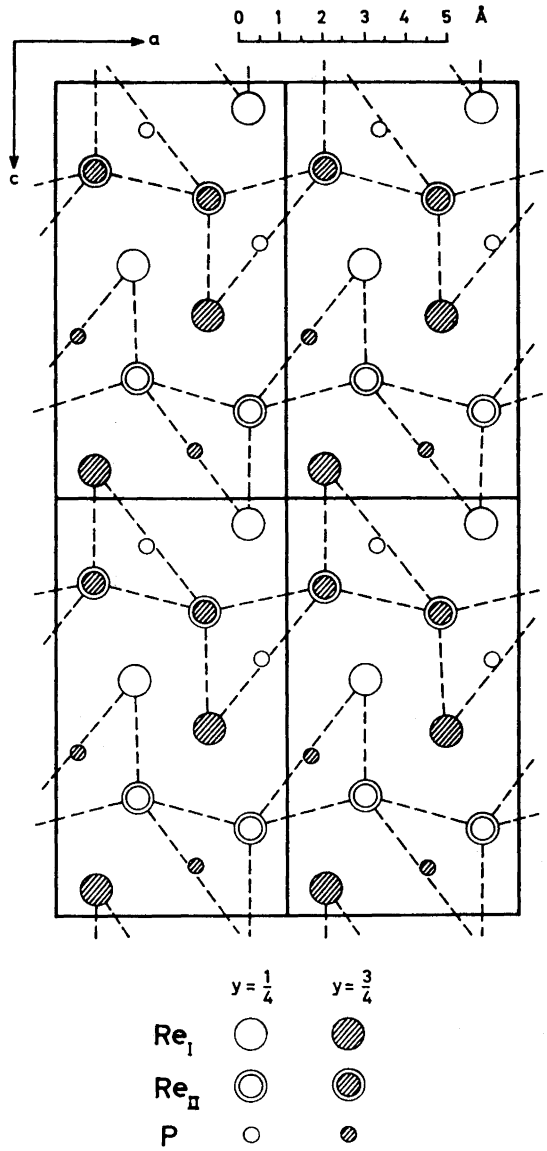

Fig. 1. The structure of Re_2P projected on (010).

All strong maxima in the two Patterson sections can be interpreted as arising from eight rhenium atoms situated in two sets of 4(*c*) positions of space-group *Pnma*. On the basis of parameter values obtained from the Patterson maps, the signs of most of the structure factors were determined, and the

electron density function was calculated in the section $\varrho(x\frac{1}{4}z)$. In addition to the expected rhenium maxima, positive regions corresponding to a 4(*c*) set of phosphorus atoms were discernible.

The structure was then refined by successive difference syntheses. After two cycles, the signs of the structure factors became constant. In the further refinements, only the $|F|$ values of the 32 well resolved reflexions were used, and the final R-value for these reflexions was found to be 0.047. An isotropic temperature factor with $B = 1.52$ Å^2 was applied. X-ray powder data for Re_2P are given in Table 1.

The final structure data of Re_2P are as follows:

Space group *Pnma* — (D_{2h}^{16}) No. 62

$a = 5.540$ Å; $b = 2.939$ Å; $c = 10.040$ Å; $U = 163.5$ Å^3

All atoms are in 4(*c*) positions with the parameter values:

	x	z
Re_I	0.829_5	0.065_5
Re_{II}	0.852_0	0.785_0
P	0.395	0.110

An estimation of the errors in the atomic positions using Cruickshanks [15] equation indicated the following standard deviations: rhenium positions 0.02 Å; phosphorus positions 0.07 Å.

Interatomic distances are listed in Table 2.

DESCRIPTION AND DISCUSSION OF THE STRUCTURE

Fig. 1 shows a projection on the *ac*-plane of the Re_2P structure. As seen from the general arrangement of the atoms, the structure can be classified as belonging to the *C*23 type. In a previous paper [5] the structures of Co_2P and Ru_2P, both of which have the *C*23 structure, were treated. The atomic radius of ruthenium is not very different from that of rhenium. Nevertheless, the structures of Re_2P and Ru_2P show significant differences, which are clearly seen when the interatomic distances are compared.

As a basis for the comparison, the following atomic radii may be taken, for phosphorus the tetrahedral covalent radius $r_P = 1.10$ Å, for rhenium and ruthenium the Goldschmidt radii for 12-coordination $r_{Re} = 1.37_5$ Å and $r_{Ru} = 1.33_5$ Å (as given by Hume-Rothery and Raynor [16]). Details of the atomic coordination in Re_2P and Ru_2P are summarized below. Only distances less than 3.5 Å are considered.

Compound	Atom	Number of close metal neighbours	Average distances
Re_2P	Re_I	9	$2.81 = 2r_{Re} + 0.06$
	Re_{II}	9	$2.84 = 2r_{Re} + 0.09$
	P	9	$2.67 = r_{Re} + r_P + 0.19$
Ru_2P	Ru_I	8	$2.82 = 2r_{Ru} + 0.15$
	Ru_{II}	10	$2.93 = 2r_{Ru} + 0.26$
	P	9	$2.49 = r_{Ru} + r_P + 0.05$

(It should be noted that whilst the accuracy of individual Re—P distances is not great, the average value is more reliable.)

It is evident that by comparison with the values quoted for the atomic radii of Ru, Re and P, the average Me—Me distances are shorter and the Me—P distances longer in Re_2P than in Ru_2P.

Acknowledgements. This work has been financially supported by the *Swedish State Council of Technical Research* and by the *Air Force Office of Scientific Research of the Air Research and Development Command, United States Air Force,* through its European Office under Contract No. AF 61(052)—40. Facilities for the use of the electronic digital computer BESK were granted by the *Swedish Board for Computing Machinery.*

The author is much indebted to professor G. Hägg for valuable comments on the manuscript The author also wishes to thank Mr. S. Wahlgren for taking the photometer records, and Dr. B. Aronsson for interesting discussions.

REFERENCES

1. Rundqvist, S. and Jellinek, F. *Acta Chem. Scand.* **13** (1959) 425.
2. Rundqvist, S. and Larsson, E. *Ibid.* **13** (1959) 551.
3. Rundqvist, S. *Nature* **185** (1960) 31.
4. Rundqvist, S. and Hede, A. *Acta Chem. Scand.* **14** (1960) 893.
5. Rundqvist S. *Ibid.* **14** (1960) 1961.
6. Hägg, G. and Regnström, G. *Arkiv Kemi, Mineral. Geol.* **18 A** (1944) Nr. 5.
7. Hägg, G. quoted in Berger, S. *Acta Chem. Scand.* **7** (1953) 612.
8. Lundström, T. and Klimecki, V. *J. Sci. Instr. In print.*
9. Åsbrink, S., Blomqvist, G. and Westman, S. *Arkiv Kemi* **14** (1959) 545.
10. Appel, K. *Technical Note from the Quantum Chemistry Group, University of Uppsala.*
11. Thomas, L. H. and Umeda, K. *J. Chem. Phys.* **26** (1957) 293.
12. Tomiie, Y. and Stam, C. H. *Acta Cryst.* **11** (1958) 126.
13. Dauben, C. H. and Templeton, D. H. *Ibid.* **8** (1955) 841.
14. Haraldsen, H. *Z. anorg. Chem.* **221** (1935) 397.
15. Cruickshank, D. W. J. *Acta Cryst.* **2** (1949) 65.
16. Hume-Rothery, W. and Raynor, G. *The structure of metals and alloys.* The Institute of Metals, London 1954.

Received October 5, 1960.

ACTA CHEMICA SCANDINAVICA 15 (1961) 349–356

Organophosphorus Analogues of Tropic Acid Esters

2. Tautomerism of Phenyl-diethoxyphosphoryl Acetaldehyde

L. LARSSON and L.-E. TAMMELIN

Research Institute of National Defence, Dept. 1, Sundbyberg 4, Sweden

In part 1 of this investigation it has been proposed that phenyl-diethoxyphosphoryl acetaldehyde exists in both keto and enolic forms. Ethyl formyl-phenyl-acetate has in earlier literature been considered to exist in two enolic forms, *cis* and *trans*.

In this paper the structures of these compounds have been further elucidated by IR-spectra, protolytic titration with pK_a determination, and spectrophotometric determination of the coloured iron(III) complex concentration as a function of time. It has been confirmed that phenyl-diethoxyphosphoryl acetaldehyde in carbon tetrachloride and *iso*propanol solutions exists in keto and *cis* enolic forms. From IR-spectra it is evident that ethyl formyl-phenyl-acetate in carbon tetrachloride, besides existing in the enolic form, also exists in the keto form. In none of these two compounds has support been found for the existence of a *trans* enolic form or for enolization of the phosphoryl group.

In an earlier paper [1] the synthesis and properties of 2-phenyl-2-diethoxyphosphoryl ethanol has been described. An intermediate compound in this synthesis was phenyl-diethoxyphosphoryl acetaldehyde (for formulae see "Discussion"). This compound, which is closely related to ethyl formyl-phenyl-acetate, was shown to have the property of changing in refractive index and infrared spectrum, after distillation, during a period of eight days at room temperature. It was also pointed out in part 1 of this series [1] that an enolization evidently occurred which was a likely explanation of the observed phenomena. However, no consideration was given to the possibility of *cis-trans* isomerism of the enolic form. Such properties have been indicated by several authors [2,3,4] in the case of ethyl formyl-phenyl-acetate. Another possibility for consideration is the enolization of the phosphoryl group. Investigations in order to obtain a more detailed description of phenyl-diethoxyphosphoryl acetaldehyde seemed thus an interesting study. Comparison of infrared spectra of phosphoryl and carbonyl analogues, determination of the keto-enol equilibrium and determination of the acid equilibrium constant of the enolic forms are the experiments chosen for this purpose.

EXPERIMENTAL

2,4-Dinitrophenylhydrazine was used as aldehyde carbonyl reagent.

Phenyl-diethoxyphosphoryl methane, phenyl-diethoxyphosphoryl acetaldehyde and 2-phenyl-2-diethoxyphosphoryl ethanol were prepared as described in part 1.

Ethyl phenyl-acetate was commercial (B.p. 90–91°/5 mm).

Ethyl formyl-phenyl-acetate was prepared analogously to the phenyl-diethoxyphosphoryl acetaldehyde. 1.5 moles of sodium were allowed to react with 2 moles of ethyl formate in 200 ml of ether, in a round bottomed flask fitted with a reflux condenser. One mole of ethyl phenyl-acetate in 250 ml of ether was added when all sodium had been consumed. The mixture was boiled for 4 h and then stirred at room temperature for 24 h, after which the ether solution was extracted with 2 × 200 ml of water. The pH of this extract was adjusted to 10 and the solution extracted with 3 × 100 ml of ether, the ether extracts being discarded. The aqueous solution was acidified with sulfuric acid to pH ~ 3 and percolated with ether for 12 h. The ether extract thus obtained was evaporated, giving a viscous residue. The residue was dissolved in benzene and the benzene evaporated; this operation was repeated twice. Finally, the product was distilled, the first 5 ml of distillate being discarded (B.p. 110°/6 mm Hg). Yield 55 %. $n_D^{25} = 1.5295$. (Found: C 68.9; H 6.3. Calc. for $C_{11}H_{12}O_3$ (192.2): C 68.8; H 6.3.)

Tropic acid ethyl ester was prepared by hydrogenation of ethyl formyl-phenyl-acetate, using sodium borohydride (SWS, Metal Hydrides Incorporated, Beverly, Mass.). 100 g of the sodium borohydride preparation (12.5 %) in 100 ml of water was neutralized with carbon dioxide to pH ~11. One mole of ethyl formyl-phenyl-acetate in 300 ml of methanol was added. Five min after the addition the mixture was hydrolysed with a dilute solution of hydrochloric acid. The methanol was evaporated under reduced pressure and the residual solution extracted with ether. The final product was obtained by fractional distillation of the ether extract (B.p. 145°/5 mm Hg). Yield 70 %. $n_D^{25} = 1.5192$. (Found: C 67.4; H 6.9. Calc. for $C_{11}H_{14}O_3$ (194.2): C 68.0; H 7.3.)

Infrared spectrophotometric measurements. The infrared spectra were recorded on a Perkin-Elmer spectrophotometer, Model 21, equipped with a rock salt prism. 0.2 M solutions in carbon tetrachloride were used, and the thickness of the cell was about 0.1 mm. In addition a 0.02 M solution of phenyl-diethoxyphosphoryl acetaldehyde in a 1.0 mm cell and a 0.2 M solution in *iso*propanol and cell thickness 0.1 mm were recorded. The following settings were used: resolution 927; response 2:1170; gain 5.7, suppression 3; speed about 1 μ/min; scale 5 cm/μ.

Determination of dissociation constants. The dissociation constants of phenyl-diethoxyphosphoryl acetaldehyde and corresponding carbonyl analogue were determined at 25°C with a recording titrator [5]. The compounds were dissolved in 0.100 M potassium chloride and the concentration of the compounds was approximately 5.0 mM. Titration was performed in an atmosphere of nitrogen with 0.0990 M sodium hydroxide, which was added in 0.1 ml portions every third minute to permit the restoration of the keto-enol equilibrium. The pH-meter was standardized against two buffer solutions, 0.05 M potassium hydrogen *o*-phthalate (pH = 4.01) and 0.01 M borax (pH = 9.18).

The mixed dissociation constant is defined by

$$K_a' = \frac{a_{H^+} \times [E^-]}{[E] + [K]}$$

where $[E^-]$ is the concentration of the enolate ion and [E] and [K] the concentrations of the enolic and keto forms, respectively. In the actual pH-range a_{H^+} and a_{OH^-} can be neglected as terms and thus $[E^-] = [Na^+]$ and $[E] + [K] = C - [Na^+]$ are obtained, where C is the total concentration which was calculated from the titration curve. The equivalence point was obtained by plotting $\Delta V/\Delta$pH against V (see Tables 1 and 2). The activity factor of the enolate ion, f_{E^-}, was estimated at 0.82[6], and the thermodynamic dissociation constant was calculated from

$$pK_a = pK_a' - \log f_{E^-} = pK_a' + 0.09$$

Formation of iron (III) complex. At zero time one part of a 0.25 mM or 0.50 mM solution of phenyl-diethoxyphosphoryl acetaldehyde in *iso*propanol was added to one

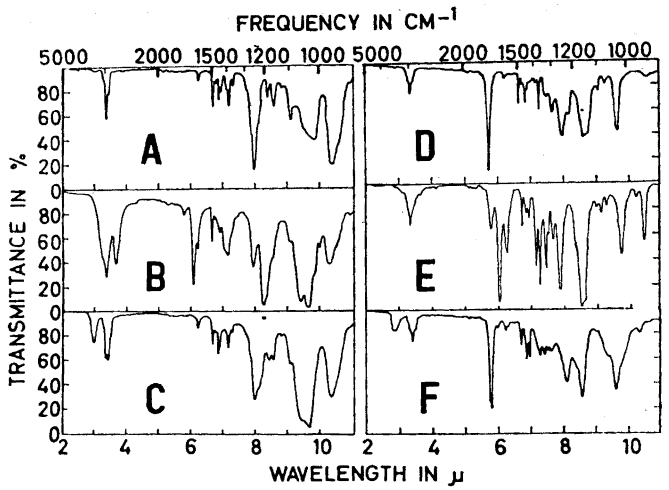

Fig. 1. Infrared absorption spectra of A. $\varphi CH_2PO(OC_2H_5)_2$; B. $\varphi CH(CHO)PO(OC_2H_5)_2$; C. $\varphi CH(CH_2OH)PO(OC_2H_5)_2$; D. $\varphi CH_2COOC_2H_5$; E. $\varphi CH(CHO)COOC_2H_5$; F. $\varphi CH(CH_2OH)COOC_2H_5$.

part of a 25 mM solution of iron(III) perchlorate in *iso*propanol. The optical density of the coloured complex was read at 4 500 Å at intervals until the development of colour terminated. A Beckmann spectrophotometer, Model B, with a 1 cm cell was used.

The molecular weight of phenyl-diethoxyphosphoryl acetaldehyde was determined with an isothermal distillation method using carbon tetrachloride as a solvent and azobenzene as a reference [11].

RESULTS

The following group frequency assignements can be made from the infrared spectra of the compounds [7,8] (Fig. 1).

The 3 000 cm^{-1} region. The absorption bands at 3 015—2 875 cm^{-1} can be assigned to various CH stretching frequencies. The bands of the two carbinol derivatives (C and F) at 3 500—3 355 cm^{-1} can be ascribed to weakly hydrogen bonded OH frequencies, whereas the two bands of the aldehydes (B and E) at about 3 060 cm^{-1} and 2 730 cm^{-1} can probably be attributed to = C—H frequencies, and resonance stabilized intramolecular hydrogen bonded OH frequencies of the enolic forms, respectively.

Ten times dilution of solution B did not change the frequencies of its absorption bands in this region, nor did the relation between their densities change. Thus, only one O—H bond, which is intramolecular hydrogen bonded, has been found in B.

The 1 740—1 630 cm^{-1} region. The absorption band at about 1 730 cm^{-1} occurring in the spectra of phenyl-diethoxyphosphoryl acetaldehyde (B) and the three carbonyl derivatives (D, E, F) is ascribed to the C=O stretching frequencies and the very strong band of ethyl formylphenyl-acetate (E) at 1 660 cm^{-1} arises from a strongly hydrogen bonded C=O group. In the hydrogenated form (F) the C=O band occurs at 1 725 cm^{-1} indicating a much weaker hyd-

rogen bond than in (E). The band of (B) at 1 635 cm^{-1} can probably be attributed to the C=C bond of the enolic from of (B). The corresponding band of the enolic form of (E) is presumably overlapped by the band at 1 660 cm^{-1}.

The 1 600—1 300 cm^{-1} region. The two bands occurring in all the spectra at 1 600 cm^{-1} and at 1 495—1 490 cm^{-1} are caused by vibrations of the benzene nucleus. The 1 600 cm^{-1} band is accentuated by the aliphatic C=C absorption in B and by C=O in E. Most of the other absorption bands in this region can be ascribed to C—H bending vibrations.

The 1 270—1 200 cm^{-1} region. At about 1 250 cm^{-1} the three phosphorus compounds have an absorption band which originates from the P=O bond. Compound (B), however, shows an additional very strong band at 1 200 cm^{-1} which probably originates from a hydrogen bonded P=O group. In this range absorption caused by the ester linkage C—O is also expected to occur (See D, E, F).

At lower frequencies absorption bands characteristic of C—OC, C—OP and CO—P bonds are found.

A change in infrared spectrum of phenyl-diethoxyphosphoryl acetaldehyde occurs when the compound is stored for a week at room temperature, as appears from Fig. 2. The absorption of the bands in the 3 000 cm^{-1} region increases, especially that attributed to the hydrogen bonded band at 2 730 cm^{-1}, and the one attributed to H—C= at 3 060 cm^{-1}. The C=O band at 1 725 cm^{-1} decreases and a new band ascribed to the C=C group appears at 1 635 cm^{-1}. The simultaneous increase of this band and the ones at 3 060 and 2 730 cm^{-1} supports the assumption that the band at 1 635 cm^{-1} is caused by vibrations of the C=C bond. The obvious increase of the absorption at 1 410

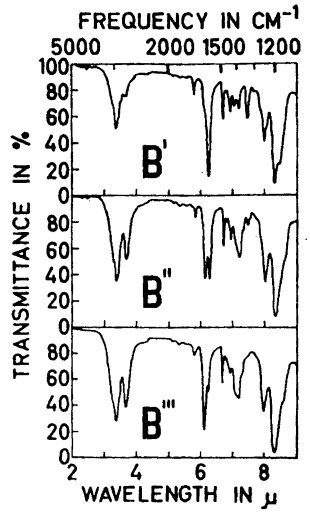

Fig. 2. Change in infrared absorption spectra from B′ to B‴ of phenyl-diethoxyphosphoryl acetaldehyde during a period of eight days after distillation. B‴ represents the final stage.

Table 1. Dissociation constant of phenyl-diethoxy-phosphoryl acetaldehyde at 25°C Total amount = 0.1899 mmoles.

V ml NaOH	pH	[E⁻] mM	[E] + [K] mM	pK'_a
0.600	6.66	1.46	3.22	7.00
0.700	6.76	1.70	2.97	7.00
0.800	6.87	1.94	2.71	7.02
0.900	6.95	2.18	2.46	7.00
1.000	7.04	2.42	2.22	7.00
1.100	7.13	2.65	1.97	7.00
1.200	7.22	2.88	1.73	7.00
1.300	7.32	3.11	1.48	7.00
			Mean value	7.00
			pK_a =	7.09

cm^{-1} may possibly arise from O—H bending vibrations, and moreover the band at 1 200 cm^{-1} originating from the hydrogen bonded P=O group shows an increase in absorption.

At the *protolytic titration* of phenyl-diethoxyphosphoryl acetaldehyde and corresponding carbonyl analogue, it was observed that after every addition of alkali the pH, after an instantaneous increase, slowly decreased some tenths of units, and that equilibrium was reached after one to two min. This fact indicates a transformation of the compounds from a keto to an enolic form. The dissociation constants of the two compounds are given in Tables 1 and 2.

The *optical density of iron (III) complex*, after reaching a constant value, D_∞, has been found to be proportional to the concentration of phenyl-diethoxyphosphoryl acetaldehyde. The formation of the complex follows first-order kinetics as appears in Fig. 3. The quotient $a = D_0/(D_\infty - D_0)$, where D_0 is the optical density at the instant of mixing, and the rate constant of the complex formation, β, obtained from the slope of the line in Fig. 3, are

Table 2. Dissociation constant of ethyl formyl-phenyl-acetate at 25°C. Total amount = 0.1917 mmoles.

V ml NaOH	pH	[E⁻] mM	[E] + [K] mM	pK'_a
0.601	6.78	1.47	3.26	7.13
0.700	6.88	1.71	3.01	7.13
0.801	6.97	1.94	2.76	7.12
0.900	7.06	2.18	2.51	7.12
1.000	7.15	2.42	2 26	7 12
1 100	7 24	2 65	2.01	7.12
1.200	7.33	2.88	1.77	7.12
1.300	7.43	3.12	1.53	7.12
			Mean value	7.12
			pK_a =	7.21

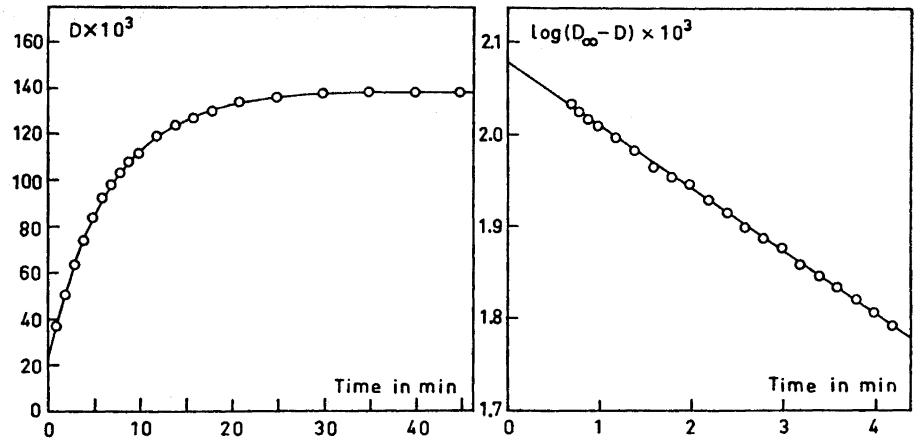

Fig. 3. Increase in optical density at 4 500 Å after addition of excess of iron(III) ions to an *iso*propanol solution of phenyldiethoxyphosphoryl acetaldehyde.

given in Table 3. For the significance of these constants see "Discussion".

The addition of 2,4-dinitrophenylhydrazine to phenyl-diethoxyphosphoryl acetaldehyde in alkaline solution produces a wine-red colour [9].

The molecular weight of phenyl-diethoxyphosphoryl acetaldehyde was found to be 260 (Calc. 256.2).

DISCUSSION

An obstacle in determining the possible tautomeric forms of phenyl-diethoxyphosphoryl acetaldehyde was the fact that the enolic form did not consume bromine in aqueous solution. Such investigations have been made earlier [2] with the analogous ethyl formyl-phenyl-acetate, and the amount of enolic double bonds was found to exceed the amount of compound able to form iron(III) complex. The difference was interpreted as due to the presence of a *trans* enolic form.

Table 3. The constants of the keto-enol equilibrium, α, and enolization rate, β, of phenyl-diethoxy-phosphoryl acetaldehyde in *iso*propanol.

C	$\alpha = \frac{D_0}{D\infty - D_0}$	$\beta \times 10^3$ sec^{-1}
0.50	0.18	2.4
0.50	0.14	2.4
0.50	0.18	2.5
0.25	0.12	2.8
0.25	0.16	2.6
0.25	0.16	(3.7)
Mean value	0.16	2.5

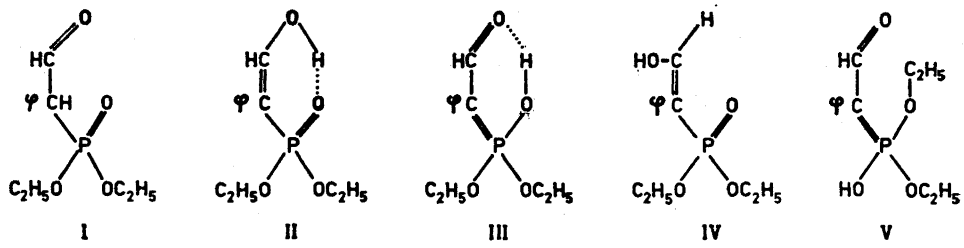

Fig. 4. A priori possible structures of phenyl-diethoxyphosphoryl acetaldehyde. Present experiments exclude III and V and give no support for IV.

The following is a discussion on how the results in this work support or exclude the *a priori* possible forms I—V (Fig. 4). Infrared spectra, especially B in Fig. 1 and Fig. 2, indicate that at least two of the forms given in Fig. 4 exist simultaneously in carbon tetrachloride solution. The discussion on the forms I—V is thus limited to the problem of which of these forms exist in considerable amounts. Influence of the solvent is realized but considered to cause only moderate changes in the concentration relations.

Formula I is the only form capable of showing simultaneously a carbonyl group and a slow neutralization, and thus represents one of the forms existing in considerable amounts.

Much more complicated than to demonstrate the presence of a keto form is the problem concerning which enol forms could be present. Here two oxygen atoms could act as proton acceptors and for each case one *cis* and one *trans* form have to be considered. Formulae II to V all have hydroxyl groups.

The content of C=C was shown to increase during enolization which indicates presence of II and IV. Formulae III and V show C=P and P—OH structures, but no absorption bands which could be attributed to these bonds have been observed. Moreover, phenyl-diethoxyphosphoryl acetaldehyde and ethyl formyl-phenyl-acetate show very similar pK_a values, indicating a carbonyl enolization. The pK_a-value itself (7.09) of the organic phosphorus compound is far above that which could be expected from a P—OH structure. It is thus reasonable to exclude formulae III and V.

Formulae II and IV now remain as possible forms, and the choice between these forms or their coexistence is mainly founded on the comparison of the infrared spectra in the 3 000 cm^{-1} region at different concentrations. The *trans* form IV would most probably have been represented by two hydroxyl absorption bands, one for free hydroxyl and one for intermolecular hydrogen bonded hydroxyl. Such bands would also show changes in density and frequency, respectively, on dilution. None of these effects could be demonstrated. Only one band corresponding to an intramolecular hydrogen bonded hydroxyl group was found. It might be inferred that absorption bands from other types of hydroxyl groups are covered in the 3 000 cm^{-1} region. Such covered bands are, however, unlikely because of the results from the dilution experiments, and also because of the propotional increase of the hydroxyl band to

the band ascribed to the =C—H group (Fig. 2). Furthermore the molecular weight obtained shows that no association occurs in carbon tetrachloride solution. The instantaneous formation of a coloured iron(III) complex also indicates a *cis* enolic group. Formula II must thus be considered to represent an existing form.

The kinetic results from the experiments with iron(III) complex (Fig. 3 and Table 3) can be given the following interpretations. Since the *trans* form can be excluded and the *cis* form is the only one capable of yielding a coloured complex instantaneously in the presence of excess of iron(III) ions, D_0 is proportional to the concentration of *cis* enol and enolate, [E], and D_∞ proportional to the total concentration, [E] + [K]. This gives

$$a = \frac{D_0}{D_\infty - D_0} = \frac{[E]}{[K]}$$

i.e. a is the equilibrium constant for $K \rightleftharpoons E$. Furthermore, under such conditions, the transformation of K → E is the rate determining step in the colour reaction, and β is thus the enolization rate constant.

Altogether, the present results give strong support to the view that phenyl-diethoxyphosphoryl acetaldehyde and ethyl formylphenyl-acetate exist in keto and *cis* enolic forms, and no support to the existence of a *trans* enolic form in either of the compounds. This conclusion is also supported by the opinion that the thermochemical stabilities of the keto and *cis* enolic forms are much higher than that of the *trans* enolic form [10].

Our sincere thanks are due to the Head of this Institute, Prof. G. Ljunggren, for his kind interest in this work.

REFERENCES

1. Tammelin, L.-E. and Fagerlind, L. *Acta Chem. Scand.* **14** (1960) 1353.
2. Dieckmann, W. *Chem. Ber.* **50** (1917) 1375.
3. Morton, R. A. and Rogers, E. *J. Chem. Soc.* **1926** 716.
4. Henecka, H. *Chem. Ber.* **81** (1948) 189.
5. Larsson, L. and Hansen, B. *Svensk Kem. Tidskr.* **68** (1956) 521.
6. Kielland, J. *J. Am. Chem. Soc.* **59** (1937) 1675.
7. Bellamy, L. J. *The infrared spectra of complex molecules.* Methuen, London 1954.
8. Ketelaar, J. A. A. and Gersmann, H. R. *Rec. trav. chim.* **78** (1959) 190.
9. Lappin, G. R. and Clark, L. C. *Anal. Chem.* **23** (1951) 541.
10. Wheland, G. W. *Advanced organic chemistry.* Chapman and Hall, London 1949, p. 613.
11. Childs, C. E. *Anal. Chem.* **26** (1954) 1963.

Received September 30, 1960.

ACTA CHEMICA SCANDINAVICA 15 (1961) 357–369

Carbonyl Groups in Lignin

II *. Catalytic Hydrogenation of Model Compounds Containing Aryl Carbinol, Aryl Carbinol Ether, Ethylene and Carbonyl Groups **

ERICH ADLER and JOSEF MARTON

Institutionen för organisk kemi, Chalmers Tekniska Högskola, Göteborg, Sweden

The catalytic hydrogenation of a variety of lignin model compounds containing aryl carbinol, aryl carbinol ether, ethylene and carbonyl groups has been examined. In a reaction mixture containing 93 % acetic acid as a solvent, Pd-$BaSO_4$ as a catalyst and HCl as a promoter, hydrogenolysis of the aryl carbinols I and their methyl ethers proceeded readily, but the rate of reaction was decreased if the β- and γ-positions of the propane side-chain were substituted by hydroxyl groups. Further inhibition was produced by a β-guaiacoxy substituent and especially by the simultaneous presence of a β-guaiacoxy and a γ-hydroxy substituent (guaiacylglycerol-β-guaiacyl ether type). Cyclic benzyl ethers, as in pinoresinol or in phenylcoumarans, were readily opened by hydrogenolysis.

Ethylenic bonds, either conjugated with the aromatic ring (as in coniferyl alcohol) or isolated (as in eugenol) were rapidly saturated.

Keto groups conjugated with the aromatic ring (α-keto groups) were reduced at satisfactory rates. In coniferyl aldehyde both the carbonyl and the ethylenic group were rapidly hydrogenated. Isolated keto groups (β-keto groups), however, reacted extremely slowly.

In a few experiments a nickel boride catalyst and an alkaline solvent were used. In this system the rate of hydrogenation decreased in the following series: C = C > β-CO groups > α-CO groups. No appreciable hydrogenolysis of aryl carbinols and aryl carbinol ethers took place.

The original purpose of the investigations reported in the present and the following paper was the conversion, by catalytic hydrogenolysis, of the aryl carbinol and aryl carbinol ether groups (I) of Björkman lignin into groupings of type II. The presence of the groupings of type I in lignin was suggested

* Part I, see Ref.[16a]

** Preliminary communication, Marton, J., Tionde Nordiska Kemistmötet, Stockholm, 1959, Abstracts of Papers, *Svensk Kem. Tidskr.* **71** (1959) 439.

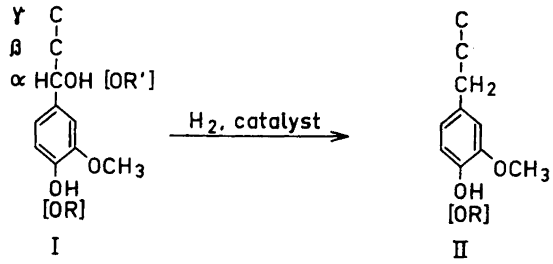

I II

by B. Holmberg and is supported by numerous arguments based on model studies as well as by analytical results and enzymatic syntheses (for literature, see Refs.[1,2]). It seemed that a detailed study of the hydrogenolysis of these groups might give new information on their occurrence and frequency in lignin and on the relative proportion of the various types indicated in formula I (free or etherified hydroxyl groups). Furthermore, the reductive removal of the highly reactive benzyl alcoholic hydroxyl groups would greatly reduce the tendency of lignin to undergo condensation reactions under the influence of acid or alkali, and a lignin product containing groups of type II instead of type I should therefore be a suitable starting material for degradation experiments.

Mild catalytic hydrogenation of lignin would also involve the reduction of ethylenic and carbonyl groups present, and therefore, in an investigation of the hydrogenation reaction, the changes brought about by the latter reactions would have to be taken into consideration. As will be shown in the following paper, hydrogenolysis of benzyl alcohol and ether groupings in lignin was only partially successful. On the other hand a study of the simultaneous reduction of ethylenic and carbonyl groups provided valuable structural information, and therefore the hydrogenation work is reported in this series of papers on "Carbonyl Groups in Lignin".

The present publication describes hydrogenation experiments with various lignin model compounds, mainly of the guaiacyl- and veratrylpropane type, containing aryl carbinol, aryl carbinol ether, ethylene, and carbonyl groups.

In order to avoid unwanted hydrogenation of the aromatic nuclei, the experiments were carried out under mild conditions, *i.e.*, at room temperature and ordinary pressure. In view of the solubility properties of Björkman lignin, acetic acid containing 7 % of water was chosen as a solvent for the model compounds. Palladium chloride on barium sulphate (5 % $PdCl_2$), prehydrogenated in the solvent immediately before the addition of the substrate, was found to be a highly active and suitable catalyst.

The activity of the freshly reduced catalyst (preparation, see Exptl.) in 93 % acetic acid was greater than that of the commonly used palladium or platinum catalysts (*cf.*, *e.g.*, Ref.[3]). This is evidently due to the presence of the hydrochloric acid formed in the prehydrogenation. The hydrochloric acid also catalysed a more or less complete acetylation of the non-reducible alcoholic hydroxyl groups present in a number of the model substances studied (as well as in lignin) (*cf.* also Ref.[4]). This side-reaction could be suppressed by the addition of sodium acetate but the activity of the catalyst was decreased at the same time. If the $PdCl_2$-$BaSO_4$ catalyst after hydrogenation was washed until free from HCl, as generally recommended [3], before being added to the reaction mixture, its

activity was considerably diminished, and the original activity was not restored on subsequent addition of hydrochloric acid. For instance, hydrogenolysis of benzyl alcohol with the acid-free prehydrogenated catalyst was eight times slower than with the catalyst prehydrogenated *in situ*, *i.e.*, with the promoting hydrochloric acid present, as used here. Addition of HCl or $HClO_4$ to the system containing the prehydrogenated and washed catalyst only restored the activity to about 50 % of that obtained without washing after prehydrogenation. This indicates that washing changes the surface structure of the catalyst.

Methylcellosolve and dioxan, which are good solvents for Björkman lignin, were used in some model experiments instead of 93 % acetic acid. In methylcellosolve, the rate of hydrogenolysis of aryl carbinols was usually lower than in the acetic acid. Dioxan could not be used, as it dissolved the palladium chloride; subsequent prehydrogenation produced a palladium precipitate with very slight activity.

Platinum on asbestos showed little activity in the hydrogenolysis of most of the guaiacyl carbinols studied.

A few hydrogenation experiments were carried out in an alkaline medium in the presence of the nickel boride catalyst described by Paul *et al.*[5] This system was of special interest in view of the solubility of lignin in dilute alkali.

HYDROGENOLYSIS OF THE BENZYL-OXYGEN LINKAGE

Although numerous benzyl alcohols and benzyl ethers have been subjected to hydrogenolysis [6], very little is known about the reactivity of compounds of the guaiacyl ethyl carbinol type (structure I) characteristic of lignin. In a short communication, Japanese workers [7] have recently reported some experiments with C_6—C_2 compounds, showing that, as expected, only hydroxyl groups in the benzyl position are reduced.

In the present work, an examination was first made of the guaiacyl and veratryl ethyl carbinols III—X which formed suitable models for two of the possible variants of structure I, *i.e.*, the free carbinols with a free phenolic hydroxyl and with an etherified phenolic hydroxyl. For comparison, some experiments were carried out with benzyl alcohol and with vanillyl and veratryl

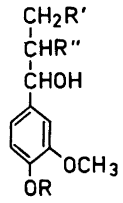

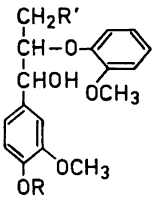

III : R = R' = R" = H
IV : R = CH_3; R' = R" = H
V : R = CH_3; R' = H; R" = OH
VI : R = H; R' = R" = OH
VII: R = CH_3; R' = R" = OH

VIII: R = R' = H
IX : R = CH_3; R' = H
X : R = CH_3; R' = OH

Table 1. Hydrogenolysis of aryl carbinols. Catalyst: $PdCl_2$-$BaSO_4$. Solvent: 93 % acetic acid.

Substance	Amount of substance, mmole	Amount of catalyst, g	Time required for consumption of 0.5 mole of H_2 per mole of substance, $t_{½}$ (min)
Benzyl alcohol	1	0.05	1.5
	1	0.1	1
Vanillyl alcohol	1	0.05	4.5
	1	0.1	2
Veratryl alcohol	1	0.05	9
	1	0.1	2
Ethyl guaiacyl carbinol (III)	1	0.1	16
	1	0.2	3.5 [a]
	1	0.5	1.5 [b]
Ethyl veratryl carbinol (IV)	1	0.1	3 [a]
Methyl*iso*eugenolglycol (V), α-form [8,c]	0.5	0.2	94
	0.5	0.5	47
Methyl*iso*eugenolglycol (V), β-form [8,c]	0.5	0.2	64
	0.5	0.5	25 [b]
Guaiacylglycerol (VI), m.p. 83—84° [25,d]	0.5	0.5	32 [b]
Veratrylglycerol (VII), m.p. 109—110° [9,e]	0.5	0.5	33
*Iso*eugenolglycol-β-guaiacyl ether (VIII) [10]	0.5	0.2	77
	0.5	0.5	50
Methyl*iso*eugenolglycol-β-guaiacyl ether (IX)	0.5	0.2	130
	0.5	0.5	76 [b]
Veratrylglycerol-β-guaiacyl ether (X) [11].	0.5	0.5	140 [b,f]

[a] For further details of this experiment, see Experimental.

[b] See also Fig. 1.

[c] It has been shown [24] that the α-form [8] is the D,L-*erythro* isomer, the β-form the D,L-*threo* isomer of V.

[d] It has been shown [24] that the crystalline form of guaiacylglycerol, m.p. 83—84°, is the D,L-*erythro* isomer.

[e] It has been shown [24] that the veratrylglycerol isomer of m.p. 109—110° is the D,L-*threo* isomer.

[f] Reduction incomplete after 24 h.

alcohols. The results are summarised in Table 1, in which the rates of hydrogenolysis are expressed as the time $t_{½}$ (min) required for the uptake of 0.5 mole of hydrogen per mole of substance. The total hydrogen uptake in most cases was close to the expected 1 mole of hydrogen per mole. Hydrogenation curves for several of these compounds are shown in Fig. 1.

The results obtained show that substituents at the β and γ positions in the propane side-chain had a marked effect on the rate of hydrogenolysis. This can be illustrated by the following examples. Using 0.1 g of the $PdCl_2$-$BaSO_4$ catalyst and 1 mmole of ethyl veratryl carbinol (IV) in 15 ml of the solvent, 1 mole of hydrogen was consumed in about 40 min, $t_{½}$ being 3 min. (4-Propyl-

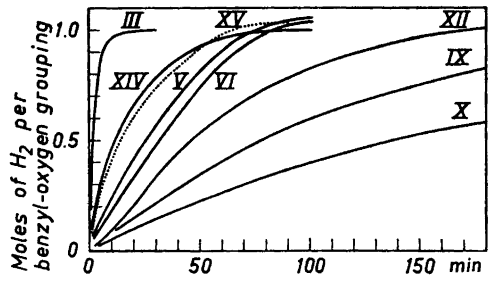

Fig. 1. Hydrogenolysis of some aryl carbinols and aryl carbinol ethers. Experimental conditions, see Tables 1 and 2. Substances see p. 359 and below.

veratrol was recovered from the reaction mixture.) The presence of a hydroxyl group in the β-position (methyl*iso*eugenol glycol, V, β-form [8]) caused the hydrogenolysis of the α-hydroxyl group to proceed at a considerably lower rate, $t_{1/2}$ being 25 min, even though a greater amount of catalyst was used than in the hydrogenolysis of IV described above. An additional hydroxyl substituent in the γ-position (veratrylglycerol, VII [9]) caused a further slight decrease in the rate of hydrogenolysis. Considerable inhibition of hydrogenolysis was caused by a guaiacoxy substituent in the β-position (IX [10], $t_{1/2}$ = 76 min), and hydrogenolysis was extremely slow, when the β-carbon atom carried a guaiacoxy group and the γ-carbon atom a hydroxyl group (veratrylglycerol-β-guaiacyl ether, X [11], $t_{1/2}$ = 140 min).

There was no marked difference in the rates of hydrogenolysis of the veratryl compounds and their phenolic (guaiacyl) analogues (see Table 1 and Fig. 1).

Experimental evidence has been given [12] for the view that one fourth to one third of the arylpropane units of lignin are of the guaiacylglycerol-β-aryl ether type (*cf.* model compound X). On the basis of the model experiments

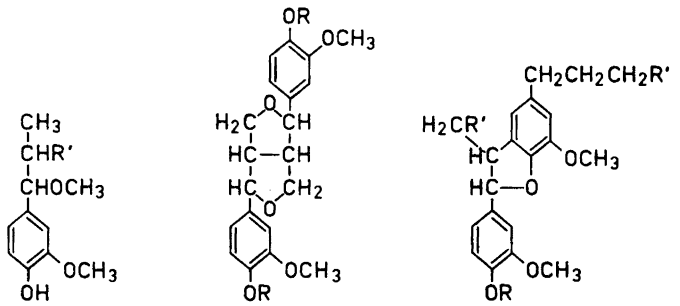

XI : R' = H
XII: R' = O- 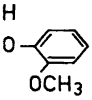

XIII : R = H
XIV : R = CH_3

XV : R = R' = H
XVI : R = CH_3; R' = H
XVII : R = H ; R' = OH

Table 2. Hydrogenolysis of aryl carbinol ethers. Catalyst: $PdCl_2$-$BaSO_4$. Solvent: 93 % acetic acid.

Substance	Amount of substance, mmole	Amount of catalyst, g	Time required for consumption of 0.5 mole of H_2 per mole of substance, $t_{½}$ (min)
Diveratryl ether [13]	0.5	0.05	8.5
	0.5	0.1	2
Ethyl guaiacyl carbinol -α-methyl ether (XI) [24]	1	0.05	27
	1	0.1	10
	1	0.2	2.5 [a]
*Iso*eugenolglycol-α-methyl-β-guaiacyl ether (XII) [10]	0.5	0.5	45 [b]
Pinoresinol (XIII)	0.5	0.2	22 [c]
			91 [d]
Pinoresinol dimethyl ether (XIV)	0.5	0.1	30 [c]
			101 [d]
	0.5	0.2	15 [c]
			50 [d]
	0.5	0.5	4 [c]
			14 [d,b]
Dihydro-dehydrodi*iso*-eugenol (XV)	1	0.2	61
	0.5	0.2	36
	0.5	0.5	14 [b]
Dihydro-dehydrodi*iso*-eugenol methyl ether (XVI)	0.5	0.2	47
Dihydro-dehydrodiconiferyl alcohol (XVII)	0.5	0.2	23

[a] For further details of this experiment, see Experimental.
[b] See also Fig. 1.
[c] $t_{½}$ for the consumption of the first mole of hydrogen per mole of substance.
[d] $t_{½}$ for the consumption of the second mole of hydrogen per mole of substance.

reported above, it can therefore be predicted that the hydrogenolysis of a considerable proportion of the aryl carbinol groups present in lignin will be extremely slow.

Substances XI—XVII and diveratryl ether [13] were investigated as model compounds for the aryl carbinol ether groupings postulated in lignin (*cf.* formula I, with OR′ or with OR and OR′, R and R′ being C-atoms of the propane side-chains in adjacent monomers) (Table 2 and Fig. 1). The calculated amount of hydrogen (1 mole of H_2 per benzyl ether group) was consumed in all cases, and the rate of the reaction was similar to that found for the corresponding model compound with a free carbinol group (*e.g.* the pairs III, XI and VIII, XII). The presence of a guaiacoxy substituent in the β-position (XII) again caused a very marked inhibition. Hydrogenolysis of the cyclic benzyl alkyl ether linkages present in pinoresinol (XIII) and its dimethyl ether (XIV) and of the cyclic benzyl aryl ether bonds of the phenylcoumaran derivatives XV, XVI, and XVII proceeded with remarkable ease, if sufficient catalyst was used (*cf.* the low rate of hydrogenolysis of XV and XVI with Pd-black in glacial acetic acid previously reported [14]).

HYDROGENATION OF ETHYLENE GROUPS

In view of the fact that ethylenic linkages are present in lignin, albeit only in small amount (see the following communication), a few unsaturated model compounds were subjected to hydrogenation under the conditions described above (Table 3).

Table 3. Hydrogenation of ethylene groups. Catalyst: $PdCl_2$-$BaSO_4$. Solvent: 93 % acetic acid.

Substance	Amount of substance, mmole	Amount of catalyst, g	Time required for consumption of 0.5 mole of H_2 per mole of substance, $t_{½}$ (min)
Eugenol	1	0.1	2
Dehydrodi*iso*eugenol (XVIII)	2	0.2	1 [a]
Coniferyl alcohol (XIX)	1	0.2	1
α-(2-Methoxy-4-methylphenoxy)-coniferyl alcohol (XX) [26]	0.25	0.1	1.5
Dehydrodiconiferyl alcohol (XXI)	0.5	0.2	0.5 [a]

[a] Refers to the consumption of the first mole of hydrogen (reduction of the ethylenic bond); a second mole of hydrogen (hydrogenolysis of the furan ring) was consumed at a much lower rate (*cf.* XV and XVII in Table 2).

Eugenol, a model for possible structures containing isolated ethylenic bonds, was rapidly hydrogenated as were double bonds conjugated with the aromatic ring in compounds XVIII—XXI. Because of this rapid C=C hydrogenation, the cinnamyl alcohols XIX—XXI, although they are vinylogous benzyl alcohols, did not undergo hydrogenolysis at the carbinol group. The phenylcoumaran derivatives (XVIII, XXI), after the rapid hydrogenation of the unsaturated side-chain, consumed further hydrogen at a low rate due to hydrogenolysis of the dihydrofuran ring (*cf.* above).

The solvent-catalyst system used in this work has been found to be very suitable for the preparation [15] of dihydrodehydrodiconiferyl alcohol (XVII) from XXI; sodium acetate was added as a buffering agent, thus preventing acetylation of the alcoholic hydroxyl groups which would otherwise be catalysed by the hydrochloric acid formed in the prehydrogenation of the catalyst. Although the rate of hydrogenation was somewhat lower in the presence of sodium acetate, the conversion XXI → XVII was complete in 5 min.

HYDROGENATION OF CARBONYL GROUPS

The carbonyl groups in lignin include (1) aldehyde groups in structures of the coniferyl aldehyde type, (2) keto groups conjugated with the aromatic ring and (3) isolated keto groups (in the *β*-position of the propane side-chain). The results obtained with models for these types of carbonyl-containing lignin

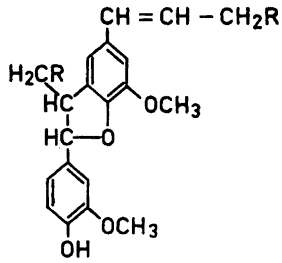

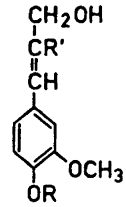

XVIII: R = H XIX: R = R' = H

XXI : R = OH XX : R = H; R' = 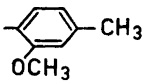

structures are given in Table 4. Hydrogenation curves for some of these compounds are shown in Fig. 2.

Coniferyl aldehyde (XXII) and its methyl ether (XXIII) were readily hydrogenated, 2 moles of hydrogen being consumed at a nearly constant rate. This indicates that hydrogenation of the ethylenic bond and the carbonyl group proceeded simultaneously at approximately equal rates, with the formation of dihydroconiferyl alcohol (*cf.* below).

Hydrogenation of the conjugated aryl ketones (XXIV—XXXIV) involves reduction to the corresponding aryl carbinol, followed by hydrogenolysis. Both steps proceeded with great ease in the case of 4-propioguaiacone (XXIV) and its methyl ether (XXV). A hydroxyl group on the terminal carbon atom of the side-chain had some inhibiting effect (β-hydroxypropioveratrone, XXVI). The presence of a hydroxyl substituent on the carbon atom adjacent to the keto group (XXVII, XXVIII) did not inhibit the first step, but caused the second step to proceed at a markedly lower rate, as expected from the behaviour of the glycols V and VI (see Table 1). Ethoxy, acetoxy, and guaiacoxy substituents adjacent to the keto group (XXIX—XXXIII) caused some inhibition of the first step, and the combination of guaiacoxy and hydroxyl substituents, as in XXXIV, produced further inhibition. In general, however, the reduction of the conjugated keto groups proceeded more easily than the subsequent hydrogenolysis of the carbinol groups formed.

The reduction of isolated keto groups (in XXXV—XXXVII) proved to be extremely difficult. Thus, the α-keto groups of the diketones XXXVIII and XXXIX were readily reduced to $-CH_2-$, but the β-keto groups remained practically unaffected. (The guaiacylacetone and veratrylacetone formed were identified with authentic material by comparison of the infrared spectra.)

It may be of interest to note that, in contrast to their resistance to catalytic hydrogenation, β-keto groups are rapidly reduced by sodium borohydride. Furthermore, while the catalytic hydrogenation of α-keto groups was comparatively easy in both guaiacyl and veratryl compounds, borohydride reduction of the phenolic α-ketones has been found [16] to proceed much more slowly than the reduction of the non-phenolic α-ketones.

Table 4. Hydrogenation of carbonyl compounds.

Substance	Amount of substance, mmole	Amount of catalyst, g	$t_{1/2}$ (min) for consumption, per mole of substance, of 1st mole of H_2[a]	2nd mole of H_2[b]
Vanillin	1	0.1	1.5	1.5
Veratraldehyde	1	0.1	1.5	2
Coniferyl aldehyde (XXII)	0.5	0.1	1.5	1.5 [c]
Methylconiferyl aldehyde (XXIII)	0.5	0.1	1.5	1.5
4-Propioguaiacone (XXIV)	0.5	0.2	1	2 [d]
4-Propioveratrone (XXV)	0.5	0.2	1.5	2.6 [d]
β-Hydroxypropioveratrone (XXVI)[27]	0.5	0.2	4	7.5 [c]
α-Hydroxypropioguaiacone (XXVII) [27]	0.5	0.5	1	21
α-Hydroxypropioveratrone (XXVIII) [27]	0.5	0.5	1	88
α-Ethoxypropioguaiacone (XXIX)[27]	0.25	0.2	7	73
α-Ethoxypropioveratrone (XXX) [27]	0.5	0.5	14	65
α-Acetoxypropioveratrone (XXXI)[27]	0.5	0.5	8.5	60
α-Guaiacoxypropioguaiacone (XXXII) [10]	0.5	0.5	5.5	28 [c]
α-Guaiacoxypropioveratrone (XXXIII) [10]	0.5	0.5	7.5	56 [c]
α-Guaiacoxy-β-hydroxypropioveratrone (XXXIV) [11]	0.5	0.5	51	110 [c]
Guaiacylacetone (XXXV) [27]	0.5	0.5	250 [e]	—
Veratrylacetone (XXXVI) [27]	0.5	0.5	250 [e]	—
ω-Hydroxy-guaiacylacetone (XXXVII) [27]	0.5	0.5	e, c	—
Vanilloyl methyl ketone (XXXVIII) [27]	0.5	0.2	0.5	3
Veratroyl methyl ketone (XXXIX)[27]	0.5	0.2	1	4

[a] Reduction of carbonyl group to carbinol group.
[b] Hydrogenolysis of aryl carbinol group formed in the first step; for XXII and XXIII, however, see text, p. 364.
[c] See also Fig. 2.
[d] See also Experimental.
[e] Reaction incomplete after 24 h.

SOME EXPERIMENTS WITH A NICKEL BORIDE CATALYST

The results of reductions using the nickel boride catalyst of Paul *et al.*[5] are shown in Table 5. As expected, ethylenic bonds (XIX, XL) were readily reduced. Hydrogenation of keto groups however, proceeded slowly, and hydrogenolysis of aryl carbinols was extremely slow. It was therefore possible to obtain ethyl veratryl carbinol (IV) by hydrogenation of vinyl or ethynyl veratryl carbinol (XL, XLI). Thus, unlike the palladium-HCl system, the nickel boride-alkali system showed a marked selectivity with the three types of groupings investigated. There were also differences in the activity of the two hydrogenation systems in the reduction of different carbonyl compounds; with nickel boride an isolated keto group (XXXVI) was more easily reduced than a conjugated keto group while the palladium catalyst showed a reversed sequence of activity.

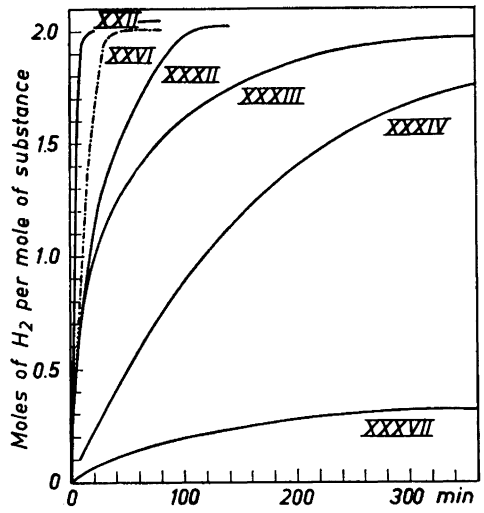

Fig. 2. Catalytic hydrogenation of some carbonyl-containing lignin model compounds. Experimental conditions, see Table 4. Substances see p. 367.

Dihydroconiferyl alcohol (XLII), m.p. 63° (65° according to Semetskina and Shorigina [17]), was obtained by hydrogenation of coniferyl alcohol over nickel boride. Hydrogenation of veratrylacetone (XXXVI) gave veratrylpropanol-2 (XLIII), m.p. 40°.

Table 5. Hydrogenation of some model compounds in the presence of a nickel boride catalyst. Reaction mixture: 1 mmole of substance, about 0.2 g of catalyst (see Experimental), 15 ml of ethanol (or aqueous ethanol, 1:1, in the case of phenolic compounds), 0.5 ml of 1 N aqueous NaOH. Atmospheric pressure, room temperature.

Substance	Time required for consumption of 0.5 mole of H_2 per mole of substance, $t_{½}$ (min)
Vinyl veratryl carbinol (XL)	4
Coniferyl alcohol (XIX)	5 [a]
Ethynyl veratryl carbinol (XLI)	18 [a,b]
Veratrylacetone (XXXVI)	23 [a]
β-Hydroxypropioveratrone (XXVI)	45
4-Propioguaiacone (XXIV)	80
α-Guaiacoxypropioguaiacone (XXXII)	360
Benzyl alcohol	150
Ethyl veratryl carbinol (IV)	c

[a] See also Experimental.

[b] Refers to the consumption of the first mole of hydrogen; a second mole was consumed at a similar rate.

[c] Only 0.1 mole of H_2 per mole of IV had been consumed after 360 min.

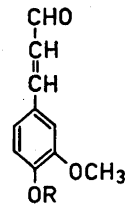

XXII : R = H
XXIII : R = CH_3

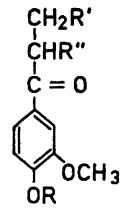

XXIV : R = R' = R" = H
XXV : R = CH_3; R' = R" = H
XXVI : R = CH_3; R' = OH; R" = H
XXVII : R = R' = H; R" = OH
XXVIII : R = CH_3; R' = H; R" = OH
XXIX : R = R' = H; R" = OC_2H_5
XXX : R = CH_3; R' = H; R" = OC_2H_5
XXXI : R = CH_3; R' = H; R" = $OCOCH_3$

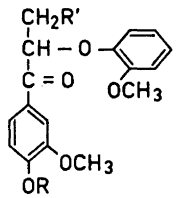

XXXII : R = R' = H
XXXIII : R = CH_3; R' = H
XXXIV : R = CH_3; R' = OH

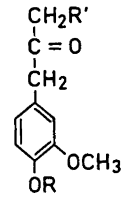

XXXV : R = R' = H
XXXVI : R = CH_3; R' = H
XXXVII : R = H; R' = OH

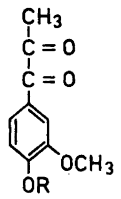

XXXVIII : R = H
XXXIX : R = CH_3

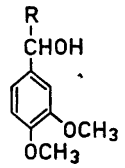

XL : R = CH=CH_2
XLI : R = C≡CH

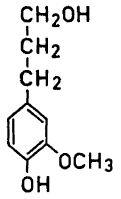

XLII

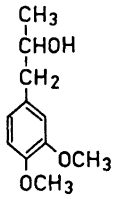

XLIII

EXPERIMENTAL

$PdCl_2$-$BaSO_4$ Catalyst. Barium sulphate was prepared as described by Mozingo [3]. Palladium chloride (2 g) was dissolved in 12 % aqueous hydrochloric acid (15 ml) by

heating for about 1 h on a steam bath. The solution was added to a paste of barium sulphate (22 g) and distilled water (17 ml), and after thorough stirring the mixture was slowly taken to dryness on a steam bath. The product, which should have a uniform brown colour, was dried at 105°. When stored in a dark bottle, its activity remained unchanged for several months. The product was powdered before use.

Hydrogenation procedure. Hydrogenation of the lignin model compounds was carried out at room temperature and atmospheric pressure in a semi-micro apparatus, which was a modification of that described by Frampton *et al.*[18]

The catalyst (0.05—0.5 g) was suspended in 10 ml of acetic acid containing 7 % of water, and hydrogenated (about 30 min), before adding the substrate (0.5—2 mmole) dissolved in 5 ml of the same solvent. A magnetic stirrer was used.

Nickel boride catalyst containing chromium boride as a promoter was prepared according to Paul *et al.*[5] The catalyst, stored under ethanol, lost its activity in a few days.

For the hydrogenation experiments (see Table 5), the ethanol was decanted and 0.2 g of the wet catalyst was added to a mixture of 10 ml of ethanol (ethanol-water 1:3, in the hydrogenation of phenolic substances) and 0.5 ml of 1 N aqueous sodium hydroxide, and prehydrogenated. Freshly prepared catalyst consumed about 5 ml of hydrogen. (If no hydrogen is consumed in the prehydrogenation, the catalyst is no longer active.) A solution of the compound to be investigated (1 mmole) in ethanol (5 ml) was then added and hydrogenation carried out at room temperature and normal pressure (see above).

In the following the results of some of the hydrogenations listed in Tables 1—5 are briefly reported.

Hydrogenation of ethyl guaiacyl carbinol (III), ethyl guaiacyl carbinol methyl ether (XI) and 4-propioguaiacone (XXIV). One mmole of the compound and 0.2 g of $PdCl_2$-$BaSO_4$ catalyst were used in each experiment and the hydrogenation was carried out as described above. III and XI consumed 1 mmole, XXIV consumed 2 mmoles of hydrogen. When hydrogen consumption had ceased, the catalyst was removed by centrifuging, the solvent was evaporated and the residue dissolved in ether. The product obtained from the ethereal solution in each case was a light oil, which distilled at 0.3 mm Hg and 100° (bath temperature). The distilled oil (yield, about 80 %) was identified by refractive index (n_D^{20}, 1.5220) and comparison of infrared absorption spectra as *4-n-propylguaiacol* (*coerulignol*).

Hydrogenation of ethyl veratryl carbinol (IV) and 4-propioveratrone (XXV) with $PdCl_2$-$BaSO_4$ in the same way yielded *4-n-propylveratrol*[19]; n_D^{20}, 1.5175. (Found: OCH_3 34.3. Calc. for $C_{11}H_{16}O_2$: OCH_3 34.4.)

Hydrogenation of methylisoeugenolglycol-β-guaiacyl ether (IX) (0.5 mmole) with $PdCl_2$-$BaSO_4$ (0.5 g) for 24 h (see Fig. 1) gave a viscous oil, which distilled at 0.04 mm Hg and 210° (bath temperature). As expected for the *guaiacyl ether of veratrylpropanol-2*, the infrared spectrum of the product showed no hydroxyl absorption unlike the spectrum of IX which has a strong band at 3 500 cm^{-1}.

Hydrogenation of dihydro-dehydrodiisoeugenol methyl ether (XVI) (0.5 mmole) with $PdCl_2$-$BaSO_4$ (0.2 g) for 3 h (hydrogen consumption, 0.5 mmole) gave a viscous oil, which distilled at 0.04 mm Hg and 180° (bath temperature). (For *1-(3,4-dimethoxyphenyl)-2-(6-hydroxy-5-methoxy-3-propylphenyl)-propane* a distillation temperature of about 218° at 1.5 mm Hg has been reported [14].) The phenolic hydroxyl group liberated by the hydrogenolysis of XVI gives a band at 3 540 cm^{-1} in the infrared spectrum of the reaction product.

Hydrogenation of dehydrodiconiferyl alcohol (XXI) (1 mmole) with $PdCl_2$-$BaSO_4$ (0.2 g) in the presence of anhydrous sodium acetate (0.03 g), for 5 min (1 mmole of H_2 consumed), gave *dihydro-dehydrodiconiferyl alcohol (XVII)*, m.p. 120°, as reported by Freudenberg and Hübner [15].

Hydrogenation of ethynyl veratryl carbinol (XLI) [20]. A solution of XLI (2 mmole) in ethanol was added to a suspension of prehydrogenated nickel boride catalyst (about 0.2 g) in alkaline ethanol (see general procedure given above) and the mixture was stirred under hydrogen. The calculated amount of hydrogen (4 mmole, *i.e.*, 2 mole of H_2/mole) was consumed in about 1 h. The catalyst was removed by centrifugation and the solution was neutralised and then taken to dryness under reduced pressure. The residue on recrystallisation from ether-light petroleum gave colourless needles, m.p. 35°, identified by infrared absorption spectrum and mixed m.p. as *ethyl veratryl carbinol (IV)*. (This

substance, described by Roberti *et al.*[21] as an oil, b.p. 102—103° at 0.2 mm, was previously obtained in this institute [10] as a crystalline solid, m.p. 35—36°.)

On similar hydrogenation of *vinyl veratryl carbinol* (XL) [22], 1 mole of hydrogen per mole was consumed with the production of IV.

Hydrogenation of coniferyl alcohol (XIX) with the nickel boride catalyst was complete after 20 min, 1 mole of hydrogen per mole being consumed. The oily reaction product crystallised from ether-light petroleum, after seeding with crystals of dihydroconiferyl alcohol (XLII) [23]; m.p. and mixed m.p. 63°. This substance has been obtained previously as an oil, b.p. 196°/16 mm (Pearl [17]), and as a solid, m.p. 65° (Semetskina and Shorigina [17]).

Hydrogenation of veratrylacetone (XXXVI) with the nickel boride catalyst was complete after 80 min, 1 mole of hydrogen per mole being consumed. The oily reaction product crystallised from ether-light petroleum, yielding the previously unknown *1-(3,4-dimethoxyphenyl)-n-propan-2-ol (XLIII)* as needles, m.p. 40° (Found: C 67.07; H 8.11. Calc. for $C_{11}H_{16}O_3$: C 67.32; H 8.22.)

Financial support from *Statens Tekniska Forskningsråd* is gratefully acknowledged. The authors also wish to thank Mrs. Terezia Marton for valuable assistance.

REFERENCES

1. Adler, E. and Gierer, J. in Treiber, E. *Chemie der Pflanzenzellwand*, Springer-Verlag 1957, p. 446.
2. Freudenberg, K. a) *Proc. IVth Intern. Congr. Biochem.* Vienna 1958, Pergamon Press, Vol. II, p. 121. b) *Chem. Ber.* **92** (1959) LXXXIX.
3. Mozingo, R. *Org. Syntheses* **26** (1946) 77.
4. Kindler, K. and Helling, H. G. *Chem. Ber.* **90** (1957) 750.
5. Paul, B., Buisson, P. and Joseph, N. *Compt. rend* **232** (1951) 627; *Ind. Eng. Chem.* **44** (1952) 1006.
6. Hartung, W. H. and Simonoff, R. in Adams, R. *Organic Reactions* **7** (1953) 263.
7. Nakano, J., Ishizu, A. and Migita, N. *J. Chem. Soc. Japan* **61** (1958) 1080.
8. Kolokolow, M. *J. Russ. Phys. Chem. Soc.* **29** (1897) 23; *Chem. Zentr.* **1897, I**, 915.
9. Adler, E. and Björkqvist, K. J. *Acta Chem. Scand.* **5** (1951) 241.
10. Adler, E. and Delin, S. *Unpublished.*
11. Adler, E., Lindgren, B. O. and Saedén, U. *Svensk Papperstidn.* **55** (1952) 245.
12. Adler, E., Pepper, J. M. and Eriksoo, E. *Ind. Eng. Chem.* **49** (1957) 1391.
13. Lindgren, B. O. *Acta Chem. Scand.* **4** (1950) 1370.
14. Aulin-Erdtman, G. *Svensk Papperstidn.* **56** (1953) 91.
15. Freudenberg, K. and Hübner, H. H. *Chem. Ber.* **85** (1952) 11.
16. a) Adler, E. and Marton, J. *Acta Chem. Scand.* **13** (1959) 75; b) Marton, J. *Proc. IVth Intern. Congr. Biochem.* Vienna 1958, Pergamon Press, Vol. II, p. 154.
17. Semetskina, A. F. and Shorigina, N. N. *Zhur. Obshcheĭ Khim.* **28** (1958) 3265. *Cf.* also Pearl, I. A. *J. Org. Chem.* **24** (1959) 736.
18. Frampton, V. L., Edwards, J. D. and Henze, H. R. *J. Am. Chem. Soc.* **73** (1951) 4432.
19. Ciamician, G. and Silber, P. *Ber.* **23** (1890) 1166.
20. Clapperton, E. T. and MacGregor, W. S. *J. Am. Chem. Soc.* **71** (1949) 3234.
21. Roberti, P. C., York, R. F. and MacGregor, W. S. *J. Am. Chem. Soc.* **73** (1950) 5760. *Cf.* Béhal, A. and Tiffeneau, M. *Bull. soc. chim. France* [4], **3** (1908) 309 and also Müller, A., Raitschewa, M. and Papp, M. *Ber.* **75** (1942) 692.
22. Marton, J. and Eriksson, E. *Unpublished.*
23. Adler, E. and Lindberg, U. H. *Unpublished.*
24. Adler, E. and Gustafsson, B. *Unpublished.*
25. Adler, E. and Eriksoo, E. *Acta Chem. Scand.* **9** (1955) 34.
26. Freudenberg, K. and Müller, H. G. *Ann.* **584** (1953) 40.
27. For references see Brauns, F. E. *The Chemistry of Lignin*, Academic Press, New York 1952, p. 476.

Received October 3, 1960.

ACTA CHEMICA SCANDINAVICA 15 (1961) 370–383

Carbonyl Groups in Lignin

III. Mild Catalytic Hydrogenation of Björkman Lignin

JOSEF MARTON and ERICH ADLER

Institutionen för organisk kemi, Chalmers Tekniska Högskola, Göteborg, Sweden

Björkman lignin was subjected to catalytic hydrogenation at room temperature in 93 % acetic acid in the presence of a Pd-$BaSO_4$ catalyst promoted by HCl (system A) or in alkaline solution with a nickel boride catalyst promoted by chromium boride (system B). The hydrogen consumption amounted to 0.5–0.6 moles of H_2/OCH_3 in system A, and to nearly 0.3 moles of H_2/OCH_3 in system B. Hydrogenation of the aromatic nuclei was negligible in both systems.

In system A only a minor fraction of the benzyl alcohol and benzyl ether groups suffered hydrogenolysis. The resistant main part of these groupings may belong to elements of the arylglycerol-β-aryl ether structure (V), which in model experiments was found to be hydrogenolysed very slowly. In system B the benzyl alcohol and benzyl ether groupings remained entirely intact.

In accordance with previous results, Björkman lignin was found to contain 0.03–0.04 cinnamaldehyde units per OCH_3. In addition, 0.03 ethylene groups were found, presumably present in cinnamyl alcohol units. These conclusions were reached by spectrochemical examination of the hydrogenated lignin products. Hydrogenation in system B indicated a total carbonyl content of about 0.2 CO/OCH_3, which is in harmony with the value previously found by oximation.

In Part II [1], experiments regarding the catalytic hydrogenation, at room temperature, of a great variety of lignin model compounds was reported. In the majority of the experiments 93 % acetic acid was used as a solvent, and the catalyst was prepared by hydrogenating $PdCl_2$-$BaSO_4$ immediately before the addition of the substance to be examined. The reaction mixture then contained a small amount of hydrochloric acid produced in the prehydrogenation of the catalyst. Some experiments were carried out in alkaline solution, with a nickel boride catalyst activated with chromium boride.

The results obtained with the palladium catalyst may be summarised as follows.

a) The benzyl-oxygen linkage of guaiacyl and veratryl ethyl carbinols (I) and their methyl ethers (II) was rapidly cleaved by hydrogenolysis, oxygen-containing substituents in the β and γ positions decreasing the rate of the reaction. The benzyl ether ring

was easily opened by hydrogenolysis in the two dimeric structures III (pinoresinol) and IV (phenylcoumaran type) and their ethers.

b) Hydrogenolysis of the benzyl-oxygen linkage was very slow in models representing the important lignin dimer structure V. Evidently, the β-aroxyl substituent and the γ-carbinol group decrease the reactivity of the benzyl grouping.

c) Ethylenic bonds either conjugated with the aromatic ring (as in coniferyl alcohol, VI) or isolated (as in eugenol) were rapidly hydrogenated under the conditions used.

d) Keto groups conjugated with the aromatic ring (α-carbonyl groups) were reduced at satisfactory rates in guaiacyl as well as in veratryl compounds (VIII). In coniferyl aldehyde (VII) both the carbonyl and the ethylenic groups were rapidly hydrogenated.

e) Isolated keto groups (β-carbonyl groups, IX) reacted extremely slowly.

It could not be expected, of course, that the potentially reducible elements present in lignin would react with hydrogen at the same rates as the corresponding structures examined in the model compounds. In the polymeric lignin

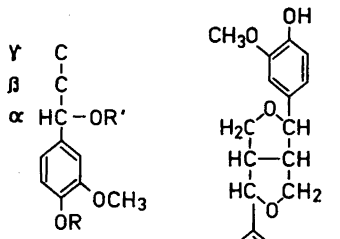

I: R = H or CH_3; R' = H

II: R = H or CH_3; R' = CH_3

III

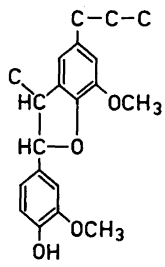

IV

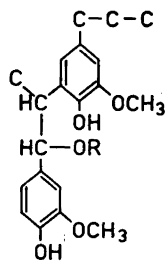

IVa

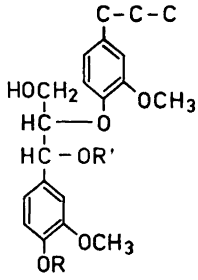

V: R = R' = H or C

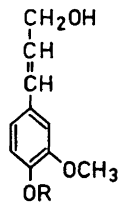

VI: R = H or C

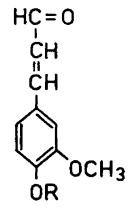

VII: R = H or C

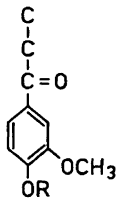

VIII: R = H or C

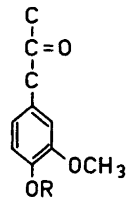

IX: R = H or C

Table 1. Catalytic hydrogenation of lignin preparations (room temperature).

Expt.	Lignin preparation	Reaction mixture	H_2-pressure; time	Hydrogen consumption, moles of H_2 per OCH_3
1	Björkman lignin (Bj.L.)	0.1 g lignin, 0.5 g $PdCl_2$-$BaSO_4$, 15 ml 93 % HOAc	atm. press.; 24 h	0.5—0.6
2	Bj.L., reduced with $NaBH_4$	as in expt. 1	atm. press.; 24 h	0.3—0.4
3	Bj.L.	as in 1, plus 0.05 g NaOAc	atm. press.; 24 h	0.2—0.3
4	Bj.L., methylated with CH_3OH-HCl	as in 3	atm. press.; 24 h	0.4—0.5
5	Bj.L.	1.2 g lignin, 8 g $PdCl_2$-$BaSO_4$, 100 ml 93 % HOAc	4 atm.; 70 h	not determined
6	Bj.L., methylated with CH_3OH-HCl	as in expt. 5	4 atm.; 70 h	» »
7	Bj.L.	1.0 g lignin, 0.7 g Ni-Cr-boride, 0.5 g NaOH in 50 ml EtOH-H_2O (1:1)	atm. press.; 6 h	0.3

these elements are probably less accessible to the action of the catalyst and therefore will react more slowly. It was hoped, however, that the relative order of reactivity of the various structures in lignin would be similar to that observed in the low-molecular model compounds and that a study of the hydrogenation of lignin would provide information regarding the occurrence and the relative number of these structural elements.

A. HYDROGENATION OF BJÖRKMAN LIGNIN OVER PALLADIUM

When a solution of Björkman lignin in 93 % acetic acid was stirred in a hydrogen atmosphere over the prehydrogenated $PdCl_2$-$BaSO_4$ catalyst at atmospheric pressure, 0.4—0.5 moles of H_2/OCH_3 were consumed during a period of 4—5 h, values of 0.5—0.6 moles of H_2/OCH_3 being attained after about 24 h (Fig. 1, curve *a*, and Table 1, expt. 1). The hydrogen consumption was only 0.2—0.3 moles per OCH_3, if sodium acetate was added to the reaction mixture to eliminate the promoting action of the small amount of hydrogen chloride formed in the prehydrogenation of the $PdCl_2$ catalyst (Table 1, expt. 3). The hydrogenation of a Björkman lignin preparation, which had been pretreated with sodium borohydride [2] (see also Exptl.), resulted in the uptake of 0.3—0.4 moles of H_2/OCH_3 (Table 1, expt. 2). Experiments were also carried out at a hydrogen pressure of 4 atm. over a period of 70 h (Table 1, expt. 5).

The hydrogenated lignins recovered from the reaction mixtures in about 90 % yield were practically white. The IR absorption in the region of 1 700

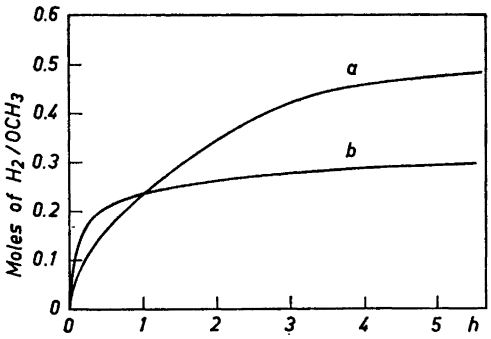

Fig. 1. Hydrogenation of Björkman lignin with a Pd-catalyst (curve *a*, exptl. conditions see Table 1, expt. 1) and a nickel boride catalyst (curve *b*, exptl. conditions see Table 1, expt. 7).

—1 665 cm^{-1} (aryl ketone and coniferyl aldehyde groupings) was considerably lower than in untreated Björkman lignin [3].

Due to the presence of HOAc and HCl in the reaction mixture, partial acetylation of hydroxyl groups of the lignin took place, as indicated by analysis (the product obtained in expt. 1, Table 1, contained 0.68 CH_3CO/OCH_3) as well as by an absorption band at 1 740 cm^{-1}. It is well-known, however, that acetylation of benzyl alcohol groups would not prevent the hydrogenolysis of such groups. This was also confirmed in the model experiments [1].

Fig. 2 gives the UV absorption curves of untreated Björkman lignin and of two of the hydrogenated products. The absorption values of the latter products at 280 mμ are only slightly lower than the corresponding value for Björkman lignin and are similar to that found for sodium borohydride-reduced lignin. This proves that no appreciable hydrogenation of the aromatic nuclei has taken place.

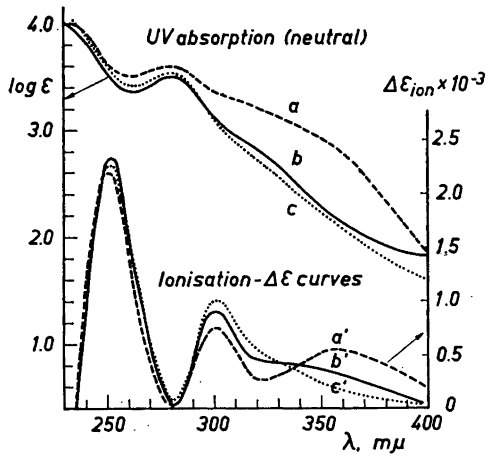

Fig. 2. UV-absorption in neutral solution and ionisation-$\Delta\varepsilon$ curves. Solvents: Ethanol-ethylcellosolve (9:1) and 0.1 N NaOH in ethanol-ethylcellosolve-water (4:1:5), respectively. Curves *a* and *a'*: Untreated Björkman lignin. Curves *b* and *b'*: Hydrogenated Björkman lignin ($PdCl_2$-$BaSO_4$, 4 atm. H_2; see Table 1, expt. 5). Curves *c* and *c'*: $NaBH_4$-reduced and subsequently hydrogenated Björkman lignin ($PdCl_2$-$BaSO_4$; see Table 1, expt. 2).

1. The benzyl alcohol and benzyl ether groupings in lignin.

According to the model experiments reported in Part II [1], it could be expected that the benzyl alcohol and benzyl ether groupings (structural types I, R and R′ = H or C, III, IV, V) assumed to be present in untreated lignin or sodium borohydride reduced lignin, would undergo hydrogenolysis.

Hydrogenolysis of benzyl-oxygen linkages such as are present in structures of type I, R′ = C, would involve a degradation of the lignin molecules. However, the solubility of the hydrogenated products did not differ significantly from that of original Björkman lignin, which tends to indicate that such hydrogenolysis did not occur to any great extent.

A closer examination of the behaviour of the benzyl alcohol and benzyl ether groups in the hydrogenation of Björkman lignin was made by studying the reaction of the hydrogenated products with cold methanolic hydrochloric acid. As demonstrated previously, Brauns lignin [4] as well as Björkman lignin [5,6] are methylated by this reagent, the latter lignin acquiring an average of 0.56 moles of OCH_3 per OCH_3 originally present. Since the borohydride-reduced lignins were methylated similarly, this introduction of OCH_3 could not be due to acetal formation, but was ascribed to the etherification and trans-etherification of benzyl alcohol and benzyl ether groups, respectively. Model experiments [4-8] showed that both guaiacyl and veratryl carbinols and their noncyclic ethers (types I, II and V) are etherified and trans-etherified, respectively, by CH_3OH-HCl at 20°. Under similar conditions, pinoresinol (III) yielded a resinous product with unchanged methoxyl content, and its dimethyl ether as well as the phenylcoumarans of type IV remained unaffected [6,7].

Reductive cleavage of the benzyl-oxygen linkages in lignin elements of types I, II, III, and V would cause such elements to become unreactive towards methanolic hydrochloric acid. It was found, however, that untreated as well as borohydride-reduced Björkman lignin, when subjected to catalytic hydrogenation (Table 1, expts. 1, 2, 5) and subsequently treated with cold methanolic hydrochloric acid, acquired 0.40—0.45 moles of OCH_3 per OCH_3 originally present. As there is no reason to doubt the correctness of the view that the presence of benzyl alcohol and benzyl ether groups in lignin is essentially responsible for this type of methylation, the result obtained indicates that the majority of these groups has resisted the hydrogenolytic attack. Only about 0.1 benzyl alcohol (benzyl ether) groups seem to have been removed.

Since hydrogen was consumed and, as will be shown below, ethylenic bonds and carbonyl groups were reduced, the fact that the majority of the benzyl-oxygen linkages survived, cannot be attributed to a general inefficiency of the hydrogenation system. It rather suggests that the benzyl-oxygen groups in lignin mainly belong to structural type V (arylglycerol-β-aryl ether type). In our model experiments (see Ref.[1], Table 1 and Fig. 1) these were found to be hydrogenolysed more slowly than the model types not carrying the β-aroxyl and γ-hydroxyl substituents. This would be in harmony with the view [9,10] that type V constitutes a quantitatively important structural element in lignin.

A Björkman lignin preparation which had been treated with CH_3OH-HCl (OCH_3 content, 22.33 %, corresponding to an uptake of 0.56 OCH_3 per OCH_3 originally present) was hydrogenated in the presence of sodium acetate (Table 1, expt. 4). Only 0.14–0.17 OCH_3 per OCH_3 originally present in the untreated lignin were removed. (In the absence of a buffering agent (expt. 6), 0.34 OCH_3 were eliminated, but in this case the HCl present may have caused some hydrolytic cleavage of the benzyl methyl ether groups.) Model experiments (see Ref.[1], Table 2 and Fig. 1) had shown that benzyl ether models of type V (R′ = CH_3) carrying a β-aroxyl substituent undergo hydrogenolysis at a considerably lower rate than corresponding ethers lacking the β-aroxyl substituent. The slow and highly incomplete removal of OCH_3 on hydrogenation of methylated lignin seems to be in harmony with the suggestion that methylation had mainly taken place at aryl carbinol (ether) structures of type V.

As mentioned above, pinoresinol (III) and the phenylcoumarans (type IV) as well as the methyl ethers of III and IV are not methylated by methanolic hydrochloric acid at room temperature [6,7]. Methylation of the hydrogenated lignin products would therefore give no information whether or not hydrogenolysis of these cyclic benzyl ether groupings has taken place. In the model experiments [1], compounds of type III and IV were more susceptible to hydrogenolysis than those of type V. Since the hydrogenolytic opening of the hydrofuran rings of pinoresinol [11] and of phenylcoumarans involves the liberation of one aliphatic OH/OCH_3 and of 0.5 phenolic OH/OCH_3, respectively, similar reactions, if occurring in the catalytic hydrogenation of lignin, would be reflected in an increase of the number of hydroxyl groups.

The interpretation of such hydroxyl increase, however, is difficult. The hydrogenation of lignin will involve not only the hydrogenolytic liberation of aliphatic and phenolic OH, but also the formation of OH groups by the reduction of CO groups, and, furthermore, the disappearance of OH groups by reduction of aryl carbinol groupings. Estimation of the total number of acetylatable OH in hydrogenated lignins (from expts. 1 and 5, Table 1) indicated an increase of about 0.2 OH/OCH_3 as a result of the hydrogenation. Without going into details, this figure might be tentatively interpreted as involving, *inter alia*, the hydrogenolysis of pinoresinol elements amounting to about 10 % of the lignin molecule.

The liberation of phenolic hydroxyl which must take place on hydrogenolysis of the hydrofuran ring of phenylcoumarans seemed to provide a measure of the latter reaction. By the periodate method [2] as well as the ionisation-$\Delta\varepsilon$ method [12], the number of phenolic OH in hydrogenated lignin (from expt. 5, Table 1) was found to be only 0.05 phenolic OH/OCH_3 higher than in untreated lignin. Assuming that the hydrogenolysis of the coumaran elements was complete, and that phenolic OH was liberated solely from such elements *, the figure obtained would indicate that 10 % of the lignin molecule

* Recently, K. Freudenberg and B. Lehmann [*Chem. Ber.* **93** (1960) 1354] briefly reported that the reaction mixture obtained on enzymatic dehydrogenation of coniferyl alcohol yielded two derivatives of guaiacylglycerol-β-coniferyl ether, each carrying a second aryl ether group in the α-position. If such α-aryl ether structures were present in lignin, their hydrogenolysis would also give rise to the liberation of phenolic hydroxyl, although they might be expected to react very slowly, in analogy to the carbinols and carbinol methyl ethers of similar type (V). On the basis of the finding that the methylation of Björkman lignin with cold CH_3OH-HCl did not bring about any significant liberation of phenolic OH, whereas a benzyl aryl ether model (veratryl 2-methoxyphenyl ether) readily suffered methanolysis (Adler, E. and Gierer, J., in Treiber, E., *Die Chemie der Pflanzenzellwand*, Springer-Verlag, Berlin, Göttingen, Heidelberg, 1957, p. 471; and Ref.[6]), it was concluded that benzyl aryl ether linkages are very scarce in lignin.

was made up of dimeric elements of the phenylcoumaran type (IV). By converting the phenylcoumaran elements into phenylcoumarone structures, Adler, Delin and Lundqvist [13] recently estimated the amount of these elements to be nearly 20 % of the lignin molecule. The latter figure, however, may include "open" dimeric elements of type IVa, which also would yield the phenylcoumarone structure under the experimental conditions used.

On the basis of the results reported above, of the 0.5—0.6 moles of H_2/OCH_3 consumed by the lignin, 0.1—0.2 moles may be attributed to the hydrogenolysis of benzyl alcohol and benzyl ether groupings (including pinoresinol structures) and 0.05 moles to the hydrogenolytic opening of phenylcoumaran structures. As will be shown in the following section, the remainder of the hydrogen consumed may be ascribed in part to the hydrogenation of carbonyl and ethylene groups.

2. Hydrogenation of carbonyl and ethylene groups

As shown in Part II [1], keto groups adjacent to the guaiacyl or veratryl nucleus (α-keto groups) are reduced in the Pd-HCl system, the rate of consumption of the first mole of H_2 (aryl-CO— → aryl-CHOH—) being markedly higher than that of the second mole of H_2 (aryl-CHOH— → aryl-CH_2—). Coniferyl aldehyde and coniferyl alcohol were readily reduced to dihydroconiferyl alcohol. The occurrence and extent of the corresponding reactions in Björkman lignin have now been examined by $\Delta\varepsilon$ methods as introduced by Aulin-Erdtman [12].

In the range above 300 mμ, the ultraviolet absorption of hydrogenated Björkman lignin (Fig. 2, curve *b*, left hand ordinate) was markedly lower than that of untreated Björkman lignin (curve *a*), indicating the loss of chromophores with ethylenic and carbonyl groups conjugated with the aromatic

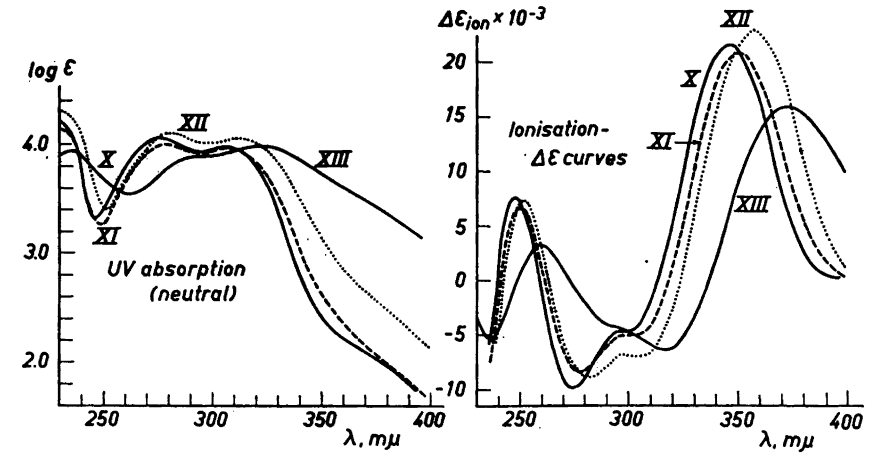

Fig. 3. UV-absorption (in neutral solution) and ionisation-$\Delta\varepsilon$ curves of some guaiacylpropanone models. 4-Propioguaiacone (X); α-hydroxypropioguaiacone (XI); α-guaiacoxypropioguaiacone (XII); vanilloyl methyl ketone (XIII). Neutral solvent, ethanol-water (1:1). Alkaline solvent, 0.1 N NaOH in ethanol-water (1:1).

nuclei. By subtracting the ε values of curves *a* and *b* from those obtained for the solutions of the corresponding products in 0.1 N NaOH (which are not included in Fig. 2), the ionisation-$\Delta\varepsilon$ curves [12] (Fig. 2, curves *a'* and *b'*) were constructed. In curve *b'*, the long-wave $\Delta\varepsilon$-maximum at 357 mμ present in *a'* is missing, which indicates that the hydrogenation had resulted in the reduction of α-keto groups of phenolic guaiacyl propane units.

A comparison of the ionisation-$\Delta\varepsilon$ curves of a few phenolic α-ketones (Fig. 3) shows that α-guaiacoxy-propioguaiacone (XII) [7] gives a $\Delta\varepsilon$-maximum at 357 mμ, *i.e.* at the position characteristic of the corresponding maximum for Björkman lignin, whereas the $\Delta\varepsilon$-maxima for propioguaiacone (X) and α-hydroxypropioguaiacone (XI) are found at somewhat shorter wave-length values, and that of vanilloyl methyl ketone (XIII) at a higher wave-length.

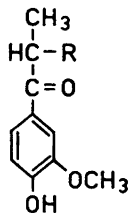

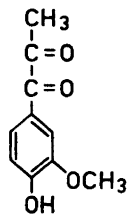

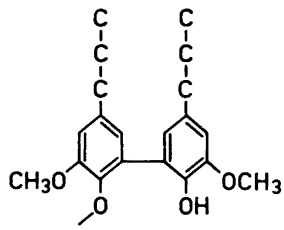

X : R = H XIII XIV

XI : R = OH

XII : R = O– 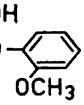

The similarity of the absorption curve of catalytically hydrogenated lignin (Fig. 2, curve *b*) with that of a lignin which had been treated with borohydride prior to the hydrogenation (Fig. 2, curve *c*) also supports the view that the conjugated carbonyl groups were reduced by the hydrogenation.

It may also be noted that the ionisation-$\Delta\varepsilon$ curve of borohydride-reduced and subsequently hydrogenated lignin (Fig. 2, curve *c'*) still shows a smoothly descending branch above 320 mμ. According to Aulin Erdtman [12], this region of the difference curve is to be attributed to 6,6'-dehydrodiguaiacyl elements (XIV), in which at least one of the two nuclei is phenolic. Comparison of the $\Delta\varepsilon$ values of curve *c'* with those of appropriate models [12] indicates that the Björkman lignin examined contained 0.06 6,6'-dehydrodiguaiacyl elements per OCH_3. A similar value has been reported [12] for Brauns lignin.

The difference between the $\Delta\varepsilon$ values, at 357 mμ, of curves *a'* and *c'* (Fig. 2) should be a measure of the number of phenolic guaiacyl-α-ketone elements (type VIII, R = H). Based on model substance XII, the difference value (350) would indicate the presence of 0.015 phenolic units VIII per OCH_3 in Björkman lignin. This value is in satisfactory agreement with that obtained previously by means of the borohydride-reduction-$\Delta\varepsilon$ method (about 0.01) [3].

As shown recently [3], the presence of phenolic as well as non-phenolic aryl-α-ketones and coniferyl aldehyde units can be demonstrated by studying the spectral changes occurring when lignin is reduced with sodium borohydride in alkaline solution ("$\Delta\varepsilon_r$ curves"). Similar examination of catalytically

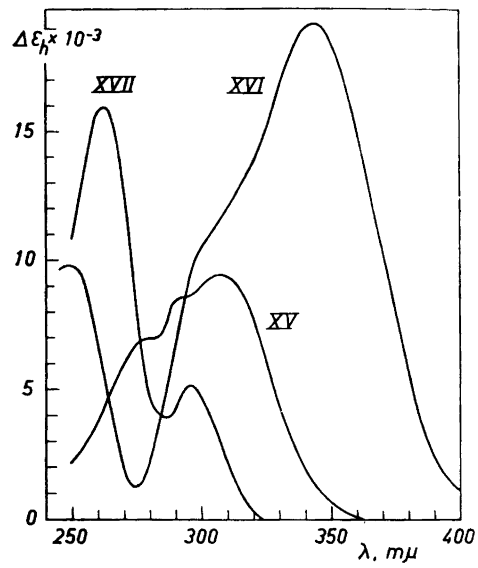

Fig. 4. Hydrogenation-$\Delta\varepsilon$ curves of some model compounds. α-Guaiacoxypropioveratrone (XV); *iso*propylconiferyl aldehyde (XVI); *iso*propylconiferyl alcohol (XVII). Solvent: 93 % acetic acid. Catalyst: $PdCl_2$-$BaSO_4$.

hydrogenated Björkman lignin gave no appreciable decrease of absorption in the wave-length region of 300—400 mμ. This shows clearly that not only the phenolic but also the non-phenolic α-ketone and coniferyl aldehyde units, originally present in the lignin, have been hydrogenated. The absence of coniferyl aldehyde groupings in the hydrogenated products is also obvious from the failure of the latter products to give specific colour reactions, *e.g.*, with *p*-aminobenzoic acid [3].

Finally, a closer examination of the spectral changes effected by the hydrogenation gave qualitative and quantitative information regarding not only the carbonyl groups but also the ethylenic groupings in Björkman lignin.

In Fig. 4, the spectral changes taking place on catalytic hydrogenation of the conjugated ethylene and carbonyl groups of model substances XV—XVII in 93 % acetic acid are represented as "hydrogenation-$\Delta\varepsilon$ curves" [12] ("$\Delta\varepsilon_h$ curves").

The $\Delta\varepsilon_h$ curve for the unknown *iso*propylconiferyl alcohol (XVII) was obtained by considering the $\Delta\varepsilon_h$ and $\Delta\varepsilon_r$ curves for *iso*propylconiferyl aldehyde (XVI) [14] (see Fig. 4). The $\Delta\varepsilon_h$ curve represents the spectral changes involved when both the carbonyl and ethylenic groups are reduced (*i.e.* XVI → XVIII). The $\Delta\varepsilon_r$ curve (see Ref.[3], Fig. 3) represents the spectral change involved when only the carbonyl group is reduced (XVI → XVII). The difference between these two curves should approximate the $\Delta\varepsilon_h$ curve for XVII. This curve, shown in Fig. 4, is very similar to the $\Delta\varepsilon_h$ curve of coniferyl alcohol (*cf.* Aulin-Erdtman and Hegbom [12b]. Whereas the latter authors presented the hydrogenation difference curves by negative values, the corresponding positive values are used in the present paper.)

In Table 2, the position and height of the maxima of the $\Delta\varepsilon_h$ curves of these and two further model compounds are summarised. There was no appreciable difference between the $\Delta\varepsilon_h$ maxima for the non-phenolic com-

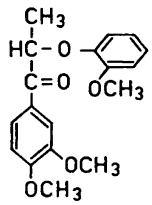

XV

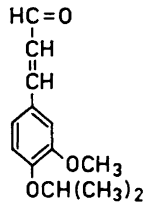

XVI

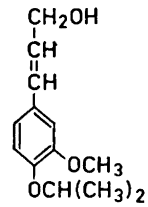

XVII

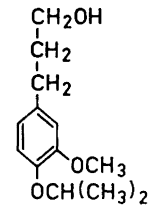

XVIII

pounds given in Fig. 4 and Table 2, and the corresponding analogues with a free phenolic hydroxyl group.

Fig. 5 gives the $\Delta\varepsilon_h$ curves for two hydrogenations with Björkman lignin, one at atmospheric pressure (Table 1, expt. 1) the other at 4 atmospheres (expt. 5). In spite of the pressure difference, the two experiments yielded similar curves, both curves exhibiting a plateau at 260 mμ, a maximum at 308 mμ and a shoulder at about 340 mμ. Comparison with the model experiments (Fig. 4) shows that these features are to be attributed to the hydrogenation of C=C bonds conjugated with aromatic rings (model XVII), α-keto groups (model XV), and cinnamaldehyde side-chains (model XVI), respectively. On the basis of the $\Delta\varepsilon_h$ values obtained for the models (Fig. 4 and Table 2), the $\Delta\varepsilon_h$ values of the lignin curves (Fig. 5) indicate that the following amounts (per OCH_3) of the various chromophores have been hydrogenated:

0.03 cinnamyl alcohol groups (type VI)
0.03—0.04 cinnamaldehyde groups (type VII)
0.05 aryl-α-ketone groups (type VIII)

The number of cinnamyl alcohol groupings (type VI) is in accordance with that estimated by Lindgren and Mikawa [15] by means of a colour reaction. The values for cinnamaldehyde and α-ketone groups are satisfactorily close to those obtained by means of the $\Delta\varepsilon_r$ method (0.03—0.04 cinnamaldehyde and 0.06—0.07 α-CO groups)[3]. It may also be noted that the three figures are

Table 2. Maxima of the "hydrogenation-$\Delta\varepsilon$ curves" of some model substances.

Substance	maximum		maximum	
	λ (mμ)	$\Delta\varepsilon_h \times 10^{-3}$	λ (mμ)	$\Delta\varepsilon_h \times 10^{-3}$
α-Guaiacoxy-propioveratrone (XV)[7] (see Fig. 4)	280	7.0	308	9.5
ω-Hydroxy-propioveratrone	273	8.9	305	9.0
*Iso*propylconiferyl aldehyde (XVI)[14] (see Fig. 4)	250	9.8	343	19.3
*Iso*propylconiferyl alcohol (XVII) (see Fig. 4)	262	16.0	295	5.1
Dehydrodi*iso*eugenol [12]	269	16.5	298	5.0

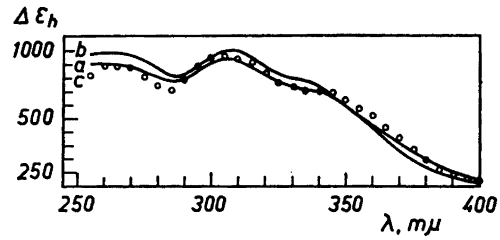

Fig. 5. Hydrogenation-$\Delta\varepsilon$ curves of Björkman lignin. *Curve a:* Difference between ε values of untreated lignin (*cf.* log ε curve *a* in Fig. 2) and ε values of lignin solution after 24 h hydrogenation according to Table 1, expt. 1. *Curve b:* Similar difference curve for hydrogenation expt. 5, Table 1. *Curve c:* Calculated for a mixture containing (mole per liter) 0.02 dehydrodi*iso*eugenol, 0.01 *iso*propylconiferyl alcohol (XVII), 0.04 ω-hydroxypropioveratrone, 0.01 α-guaiacoxypropioveratrone (XV), 0.03 *iso*propylconiferyl aldehyde (XVI), 0.003 coniferyl aldehyde. For $\Delta\varepsilon_h$ values of the model substances see Fig. 4 and Table 2.

reasonably close to the corresponding values obtained by Aulin-Erdtman [12] for Brauns lignin.

A "synthetic" $\Delta\varepsilon_h$ curve was constructed by summation of the $\Delta\varepsilon_h$ values for suitable amounts of model compounds, as given in the legend to Fig. 5. This curve (*c*) follows rather closely the $\Delta\varepsilon_h$ curves for Björkman lignin, which indicates that the interpretation of the latter curves and the choice of the model compounds in calculating the quantities of the various components was correct.

Evidently, the figures given above for the amounts of the chromophores VI—VIII in Björkman lignin can be reliable only if their hydrogenation has been complete. As shown by Fig. 6, this is actually the case. The curves represent the decrease of absorption, during the course of a hydrogenation experiment, at three different wave-lengths which are close to the $\Delta\varepsilon_h$ maxima characteristic of the three chromophore structures. Obviously, the hydrogenation of these structures approaches its end point within a period of 4—5 h.

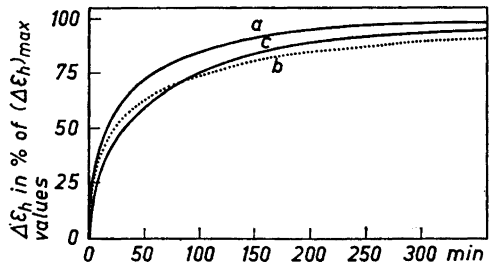

Fig. 6. Rate of hydrogenation of chromophores of Björkman lignin. Decrease of absorption at 270 mμ (*a*), 310 mμ(*b*) and 350 mμ(*c*). Reaction mixture: 0.3 g lignin, 1.5 g $PdCl_2$-$BaSO_4$, 50 ml of 93 % HOAc, H_2 at atmospheric pressure; room temperature. Extinction was measured in centrifuged samples and the $\Delta\varepsilon$ values obtained expressed as % of final $\Delta\varepsilon_h$, attained after 24 h hydrogenation.

The sum of cinnamaldehyde groups (type VII, 0.03—0.04 per OCH_3) and aryl-*a*-ketonic groupings (type VIII, 0.05 per OCH_3), determined as above, gives a total of 0.08—0.09 conjugated carbonyl groups per OCH_3. It represents somewhat less than half of all the carbonyl groups (about 0.20 CO/OCH_3) previously [3] found to be present in Björkman lignin by oximation. By the latter method, the catalytically hydrogenated lignin preparations (Table 1, expts. 1 and 5) were found to contain a residual number of 0.07 carbonyl groups per OCH_3. They can be assumed to be β-keto groups (IX), which in the model experiments [1] were found to be reduced extremely slowly, and which cannot be determined by the $\Delta\varepsilon_h$ method. Spectrochemical examination of lignin hydrogenation combined with the oximation of the hydrogenated lignin has thus revealed the presence of 0.09 + 0.07 = 0.16 CO groups per OCH_3. The difference, *i.e.* 0.20—0.16 = 0.04 CO/OCH_3, seems to be attributable to a fraction of the original amount of 0.10 β-keto groups [3], which has undergone hydrogenation.

The results regarding the various types of carbonyl groups reported above agree well with those obtained by means of the spectrochemical borohydride reduction and the oximation methods [3]. Gierer and Söderberg [16], on the basis of a volumetric borohydride reduction method, however, concluded that Björkman lignin contains a total of 0.41—0.44 CO/OCH_3, or twice the amount found by oximation (0.20). Since the number of conjugated CO groups now seems to be definitely limited to about 0.1 CO/OCH_3, the existing discrepancy might be supposed to be due to a failure of the oximation method in the determination of the isolated (β-)keto groups. As will be shown in the subsequent paper [17], however, the values obtained with the volumetric borohydride method under the conditions used by Gierer and Söderberg are too high. Support for this conclusion is also to be found in the results of hydrogenations with a nickel boride catalyst, part B of this paper.

B. HYDROGENATION OF BJÖRKMAN LIGNIN OVER A NICKEL BORIDE CATALYST

Model experiments [1] revealed that the nickel boride catalyst of Paul *et al.*[18] shows decreasing activity in the hydrogenation of the following series: C=C > β-CO groups > *p*-alkoxyaryl ketones > *p*-hydroxyaryl ketones > aryl carbinols. The ethylene groups were rapidly hydrogenated whereas the aryl carbinols were practically inert. The selectivity of the alkaline nickel boride system was rather different from that of the acidic Pd system. The β-CO groups, while largely resistant to hydrogenation over the Pd catalyst, where readily reduced in the presence of the boride catalyst. Conversely, aryl carbinols reacted with hydrogen when Pd was the catalyst but not when nickel boride was used.

When an alkaline solution of Björkman lignin was hydrogenated in the presence of the nickel boride catalyst, about 0.20 moles of H_2 per OCH_3 were consumed during 30 min., and the reaction practically ceased after 4—5 h, when 0.28 moles of H_2/OCH_3 had been consumed (Fig. 1, curve *b*).

UV and IR examination of the recovered hydrogenation product showed that the ethylenic bonds as well as the majority of the carbonyl groups had been reduced. Only about 0.01 phenolic aryl keto groups and traces of non-phenolic aryl keto groups (VIII, R = H or C) survived. The quinone monochloroimine colour reaction according to Gierer [19] was still positive, indicating that the phenolic aryl carbinol groupings (I, R = R′ = H) had not been affected. On treatment with methanolic hydrochloric acid at 20°, the hydrogenated product acquired 0.43 new OCH_3 groups per OCH_3 originally present, which is in harmony with the expectation that the benzyl alcohol and benzyl ether groupings would not undergo hydrogenolysis (*cf.* Ref.[6]).

Similar methylation introduces 0.56 OCH_3 (mean value) into untreated Björkman lignin, and 0.50 OCH_3 into borohydride-reduced Björkman lignin. The difference between these two figures may be due to the borohydride reduction of the ω-hydroxyguaiacylacetone structure, which may occur in lignin (the presence of about 0.1 β-keto groups has been demonstrated [3]) and which, in model experiments, was shown to undergo methylation. On hydrogenation over nickel boride these groups will also be reduced, but, in addition, coniferyl alcohol side-chains, which also react with $CH_3OH-HCl$ [6,7], will be saturated and thus be made resistant to methylation. In $NaBH_4$-lignin there will be present 0.03 original coniferyl alcohol groups (see p. 379) and a further 0.03 – 0.04 formed by reduction of coniferyl aldehyde groups. These relationships would explain the fact that the methylation of H_2/Ni boride-reduced lignin introduces 0.07 fewer methoxyl groups than the methylation of $NaBH_4$-reduced lignin. The 0.43 methylatable groups present in the former material then would mainly be aryl carbinol (ether) groupings.

In accordance with the hydrogenation experiments in the Pd—HCl system, the results obtained in the alkaline nickel boride system indicate that the sum of ethylenic and carbonyl groups in Björkman lignin does not exceed a value of 0.30 per OCH_3. Since the number of ethylenic groups is 0.06—0.08 (*i.e.*, 0.03—0.04 each present in cinnamaldehyde and in cinnamyl alcohol residues, *cf.* also Ref.[15]), the total amount of carbonyl groups is found to be 0.22—0.24 per OCH_3. This figure is close to the value of 0.20 total CO/OCH_3 previously found [3] by the oximation method.

EXPERIMENTAL

Björkman lignin (= "milled wood lignin", "M.W. lignin") was obtained from Norway spruce (*Picea abies*) [20].

Sodium borohydride-reduced Björkman lignin was prepared according to the procedure given by Adler, Hernestam and Walldén [2], with a few modifications. The lignin (3 g, OCH_3 15.23 %) was suspended in aqueous ethanol (1:1, 180 ml) and dissolved by the addition of 0.1 N sodium hydroxide (50 ml). Sodium borohydride (1.2 g) was added in portions. The initially red-brown colour of the solution slowly became a light yellow. Further portions of 0.1 g of sodium borohydride were added each of the following four days. The pH was adjusted to 4 with aqueous hydrochloric acid and the mixture was evaporated to dryness under reduced pressure. The residue was four times suspended in water and recovered by centrifuging. After four such washings it was dried in vacuum over P_2O_5 and NaOH. The light tan powder (2.6 g) was dissolved in 50 ml of a mixture of 1,2-dichloroethylene, abs. ethanol and dioxan (2:1:1); traces of undissolved material were removed by centrifugation. The solution was poured into 500 ml of a mixture of ether and petroleum ether (1:1), the lignin precipitate centrifuged off, washed twice with the latter solvent mixture and finally with petroleum ether. After drying in a stream of warm air, a cream coloured powder (2.5 g = 83 %; CH_3O 15.34 %) remained.

The preparation of the *catalysts* and the *hydrogenation procedure* have been described in the preceding paper [1]. For the experiments to Fig. 5, the reaction vessel was provided with a side-tube, which was covered by a rubber membrane. Samples were withdrawn from the reaction mixture by a syringe inserted through the rubber membrane. Experiments 5 and 6 (Table 1) were carried out in a Parr low pressure hydrogenation apparatus.

Isolation of the hydrogenated lignin products. a) After hydrogenation over Pd-$BaSO_4$. The catalyst was centrifuged off and washed with acetic acid, the washings being combined with the solution. The solvent was removed under reduced pressure (bath temp. not exceeding 45°). The residue was redissolved in 93 % acetic acid (5 ml for 0.1 g of lignin) and the solution was filtered and allowed to drop into a fifteenfold volume of water. The lignin precipitate was centrifuged off, washed with water and dried in a vacuum desiccator over P_2O_5 and NaOH. This material was dissolved in a mixture of 1,2-dichloroethylene and ethanol (2:1), reprecipitated by pouring the filtered solution into ether-petroleum ether (1:1) and washed and dried as described for the $NaBH_4$-lignin. Yield 90 %.

b) After hydrogenation over nickel boride. The centrifuged alkaline reaction mixture was acidified to pH 4 with hydrochloric acid, ethanol was removed under reduced pressure, and the lignin residue purified as above.

Methylation of Björkman lignin with methanolic hydrochloric acid. A solution of the lignin (150 mg) in abs. dioxan (15 ml) was mixed with 0.3 N methanolic hydrochloric acid (15 ml). After four days at room temperature the mixture was brought to pH 4 with 0.6 N methanolic sodium hydroxide, neutralised by the addition of a little solid sodium bicarbonate and evaporated under reduced pressure. The residue was kept for one day in a vacuum desiccator over P_2O_5, the lignin was dissolved in abs. dioxan (10 ml), and reprecipitated by pouring the filtered solution into ether-petroleum ether (1:1, 120 ml). The lignin was washed and dried as described above. Yield, 120—140 mg, ash content about 1 %.

The authors wish to thank Mrs. Terezia Marton for skilful experimental assistance and *Statens Tekniska Forskningsråd* for financial support.

REFERENCES

1. Adler, E. and Marton, J. *Acta Chem. Scand.* **15** (1961) 357.
2. Adler, E., Hernestam, S. and Walldén, I. *Svensk Papperstidn.* **61** (1958) 641.
3. Adler, E. and Marton, J. *Acta Chem. Scand.* **13** (1959) 75.
4. Adler, E. and Gierer, J. *Acta Chem. Scand.* **9** (1955) 84.
5. Adler, E. *Ind. Eng. Chem.* **49** (1957) 1377.
6. Adler, E. *4th Intern. Congr. Biochem.* Vol. II, Pergamon Press, 1959, p. 137.
7. Adler, E. and Delin, S. *To be published.*
8. Adler, E. and Yllner, S. *Svensk Papperstidn.* **57** (1954) 78.
9. Adler, E., Pepper, J. M. and Eriksoo, E. *Ind. Eng. Chem.* **49** (1957) 1391.
10. Freudenberg, K. *Angew. Chem.* **68** (1956) 84, 508.
11. Haworth, R. D. and Woodcock, D. *J. Chem. Soc.* **1939** 1054.
12. a) Aulin-Erdtman, G. *Svensk Kem. Tidskr.* **70** (1958) 145. b) Aulin-Erdtman, G. and Hegbom, L. *Svensk Papperstidn.* **61** (1958) 187.
13. Adler, E., Delin, S. and Lundquist, K. *Acta Chem. Scand.* **13** (1959) 2140.
14. Pew, J. C. *J. Am. Chem. Soc.* **73** (1951) 1678; **74** (1952) 5784.
15. Lindgren, B. O. and Mikawa, H. *Acta Chem. Scand.* **11** (1957) 826.
16. Gierer, J. and Söderberg, S. *Acta Chem. Scand.* **13** (1959) 127.
17. Marton, J., Adler, E. and Persson, K.-I. *Acta Chem. Scand.* **15** (1961) 384.
18. Paul, B., Buisson, P. and Joseph, N. *Compt. rend.* **232** (1951) 627; *Ind. Eng. Chem.* **44** (1952) 1006.
19. Gierer, J. *Acta Chem. Scand.* **8** (1954) 1319; *Chem. Ber.* **80** (1956) 257.
20. Björkman, A. *Svensk Papperstidn.* **59** (1956) 477.

Received October 3, 1960.

ACTA CHEMICA SCANDINAVICA 15 (1961) 384–392

Carbonyl Groups in Lignin

IV *. Infrared Absorption Studies and Examination of the Volumetric Borohydride Method **

JOSEF MARTON, ERICH ADLER and KARL-INGVAR PERSSON

Institutionen för organisk kemi, Chalmers Tekniska Högskola, Göteborg, Sweden

Infrared absorption studies have shown that a mixture of sodium borohydride-reduced Björkman lignin with *iso*propylconiferyl aldehyde (0.033 mole per OCH_3 of the mixture), arylpropanone-1 model substances (0.07 mole/OCH_3), and arylpropanone-2 models (0.11 mole/OCH_3), *i.e.*, a total of 0.21 carbonyl groups per OCH_3, gives an absorption pattern in the region of the carbonyl stretching vibration very similar to that given by untreated Björkman lignin.

Reduction of the latter lignin with sodium borohydride causes the hydroxyl content to increase by 0.20 hydroxyl groups per OCH_3.

An attempt has been made to explain the discrepancy between the carbonyl values obtained as above as well as by the oximation method (about 0.20 CO/OCH_3) and those found by Gierer and Söderberg with a volumetric borohydride method (about 0.40 CO/OCH_3). Reexamination of the latter method showed that values which are reasonably close to 0.20 are obtained if air is excluded from the apparatus.

Oximation of Björkman lignin with hydroxylamine hydrochloride at room temperature and titration of the hydrochloric acid liberated indicated the presence of 0.20 carbonyl groups per methoxyl [1]. (In the following, the abbreviation "CO" will be used for "carbonyl groups".) Examination of the spectral changes taking place on reduction of the lignin with sodium borohydride [2] showed that this total number of CO included, per OCH_3, about 0.01 coniferyl aldehyde and 0.01 aryl-*α*-ketone units with free phenolic 4-hydroxyl groups and, in addition, 0.03 coniferyl aldehyde and 0.05—0.06 aryl-*α*-ketone units, in which the 4-hydroxyl group was etherified. The difference between the

* Part III, see Ref.[3].

** Preliminary accounts of the results reported in Parts II—IV were given (by E.A.) at a colloquium at Chemisches Institut der Universität, Heidelberg, July 29, 1959 and (by J.M.) at Tionde Nordiska Kemistmötet, Stockholm, August 17—22, 1959; *cf. Svensk Kem. Tidskr.* **71** (1959) 439.

total number of CO (0.20) and that of the conjugated carbonyl structures mentioned, *i.e.*, about 0.10 CO, was attributed to isolated keto groups (in the β-position of the propane side-chains) [2]. Similar results regarding the number of carbonyl-containing chromophores were obtained by spectrochemical investigation of the hydrogenation of Björkman lignin over a palladium-barium sulphate catalyst [3]. Finally, the hydrogen consumption observed on hydrogenation over a nickel boride catalyst revealed [3] that the sum of carbonyl and ethylene groups in Björkman lignin does not exceed 0.30. Since the number of ethylene groups was found to be 0.06—0.08 (0.03—0.04 each present in coniferyl aldehyde and coniferyl alcohol groups, respectively) [3], a total number of 0.22—0.24 CO/OCH_3 was obtained by that method.

In contrast with these results, Gierer and Söderberg [4], using a volumetric borohydride method, arrived at values of 0.41—0.44 CO/OCH_3, *i.e.*, one carbonyl group per about 2.5 arylpropane units. Whereas the figures found in this laboratory more or less impart to the carbonyl groups the role of accessory structural elements — although possibly important in certain reactions of the lignin molecule — the values found by Gierer and Söderberg would imply that the carbonyl groups are of major structural importance in lignin. This situation prompted further investigation of the problem regarding the number of these groups.

The borohydride method was developed by Lindberg and co-workers [5] especially for the estimation of carbonyl groups in carbohydrates. In this method, the sample is allowed to react with an alkaline solution of sodium or potassium borohydride. During the reaction period some hydrogen is evolved by spontaneous decomposition of borohydride. Hydrogen is then liberated from the unconsumed borohydride with sulphuric acid, and the difference between the total amount of hydrogen obtained similarly in a blank and that found in the experiment yields the amount of carbonyl groups reduced. Applying this method to lignin, Gierer and Söderberg [4] allowed potassium borohydride to react for 5 h with an alcoholic alkaline solution of the lignin.

To explain the discrepancy between the CO values found by oximation (0.20) and by the volumetric borohydride method (0.41—0.44), Gierer and Söderberg made the following alternative suggestions.

1) The reaction between the carbonyl groups of lignin and hydroxylamine hydrochloride is incomplete, whereas their reduction by borohydride goes to completion.

2) A certain fraction of the carbonyl groups in lignin is present in a "masked" form, *e.g.*, as hemiacetals, which are unreactive towards hydroxylamine but reducible by borohydride.

Regarding possibility (1), it was actually found by Gierer and Söderberg [4] as well as in our laboratory [2] that certain aryl-α-ketones reacted very slowly with hydroxylamine but rapidly with borohydride. For instance, ketone V, when treated with hydroxylamine hydrochloride for 5 h at room temperature, gave only 3 % of the calculated amount of oxime, but was completely reduced on 5 h treatment with potassium borohydride. However, this pronounced difference regarding the reactivity of certain α-ketones in the two methods cannot be responsible for the difference in the lignin carbonyl values obtained. Being aware of the low reactivity of certain types of aryl α-ketones, we had used in our oximation experiments with lignin a reaction time of 500 h, which

yielded the value of 0.20 CO/OCH_3. Under these conditions the majority of the ketone model substances reacted completely, and the extremely "hindered" ketone V was converted to 60 % [2]. Furthermore, as mentioned above, the number of aryl *α*-ketones in Björkman lignin was shown by two independent methods [2,3] to be only 0.06—0.07 per OCH_3. Hence, the slow oximation of such ketones could not possibly explain the difference between the oximation and the volumetric borohydride values.

Gierer and Söderberg [4] found that ketone V, when oximated at reflux temperature, reacted almost completely within 5 h, and, furthermore, that Björkman lignin, under similar conditions, gave a CO value of 0.25 instead of the value of 0.20 obtained on oximation at room temperature. It must be pointed out, however, that the increased value observed after oximation of lignin in boiling solution, may well be due to the formation of new keto groups ("Hibbert ketones"), brought about by the hydrochloric acid liberated; *cf.* the acidolysis of guaiacylglycerol-*α*-aryl ether units studied by Adler, Pepper and Eriksoo [6,7].

Since the number of conjugated carbonyl groups, *i.e.*, the sum of aryl *α*-ketone groups and coniferyl aldehyde groups, has been shown to be limited to about 0.10 per OCH_3, a total CO content of 0.41—0.44 would require the presence of about 0.3 *β*-keto groups (concerning the occurrence of "masked" carbonyl groups, see below). This possibility, however, is eliminated by the weakness of the carbonyl absorption in the region of 5.8 *μ*, as shown in the IR spectrum of Björkman lignin (Fig. 1, *a*). Further evidence supporting the view that the carbonyl content of Björkman lignin is confined to about 0.1 each of conjugated and isolated carbonyl groups is provided by the following experiments.

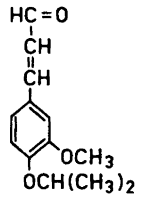

I

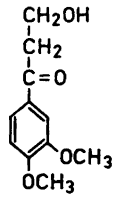

II

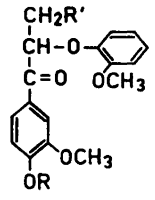

III: R = R' = H
IV: R = CH_3; R' = H
V: R = CH_3; R' = OH

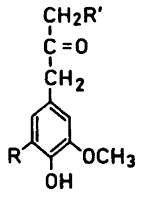

VI: R = OCH_3; R' = H
VII: R = H; R' = OH

In the IR spectrum of untreated Björkman lignin (Fig. 1, *a*) there is a comparatively strong absorption band near 6 *μ* (coniferyl aldehyde and aryl *α*-ketone groups, *cf.* also Refs.[2,8]) as well as a weaker band or shoulder at about 5.8 *μ* (isolated CO). The former band disappears when the lignin is reduced with sodium borohydride (Fig. 1, *b*). Some low-intensity absorption around 5.8 *μ* is left, probably due to minor amounts of carboxyl groups. The appearance of the carbonyl region of untreated lignin can be restored rather satisfactorily by adding model substances of the coniferyl aldehyde (I) and aryl *α*-ketone (II—V) as well as the *β*-ketone (VI—VII) type to the carb-

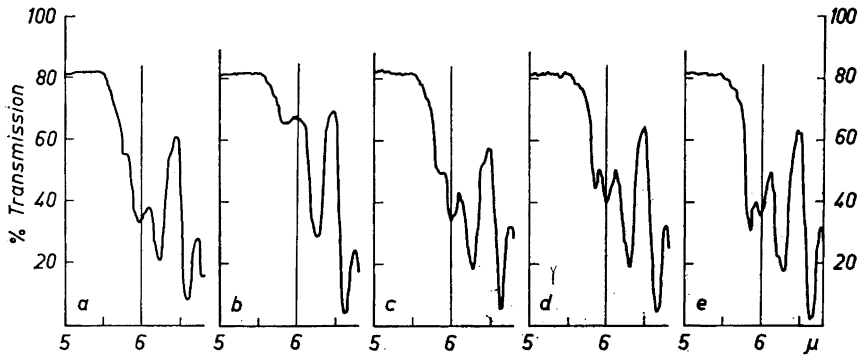

Fig. 1. Infrared absorption of Björkman lignin (*a*), $NaBH_4$-reduced Björkman lignin (*b*), and mixtures of the $NaBH_4$-reduced lignin with crystalline model substances, the concentrations of which are given in moles per mole of OCH_3 present in the mixture (for model compounds containing more than one OCH_3, only one OCH_3 group has been taken into consideration): *c*) $NaBH_4$-lignin plus 0.033 *iso*propylconiferyl aldehyde (I); α-ketones: 0.05 II, 0.01 III, 0.01 IV; β-ketones: 0.05 VI, 0.06 VII. Total CO added, 0.21. *d*) 0.04 *iso*propylconiferyl aldehyde (I); α-ketone: 0.07 V; β-ketones: 0.07 VI; 0.08 VII. Total CO added, 0.26. *e*) 0.04 *iso*propylconiferyl aldehyde (I); α-ketone: 0.07 V; β-ketones: 0.14 VI: 0.15 VII. Total CO added, 0.40.

onyl-free $NaBH_4$-lignin. Fig. 1, *c* shows the IR spectrum of a mixture of borohydride-reduced (CO-free) Björkman lignin with the following amounts of the model substances (given as moles per mole of total OCH_3 present in the mixture): 0.033 coniferylaldehyde, 0.07 aryl α-ketone, and 0.11 β-ketone (total, 0.21 CO/OCH_3). If the amount of the β-ketone models is increased to give 0.15 β-CO/OCH_3 (Fig. 1, *d*) or 0.30 β-CO/OCH_3 (Fig. 1, *e*), the latter mixture corresponding to a total of 0.40 CO/OCH_3, as claimed by Gierer and Söderberg [4], the shortwave carbonyl absorption becomes far stronger than that shown by Björkman lignin (1, *a*).

These results eliminate the possibility that the high carbonyl values of Gierer and Söderberg might be caused by the presence of (about 0.2) β-keto groups unable to react with hydroxylamine.

The alternative suggestion of Gierer and Söderberg postulated that oximation gave false low carbonyl values because of the presence of hemiacetal (hemiketal) groupings. However, an attempt by them to find experimental support for this idea was unsuccessful. They found that methylation of lignin with methanolic hydrochloric acid at room temperature did not diminish the number of "carbonyl" groups as determined by the borohydride method. Had hemiacetal groupings been present, they would have been methylated and become resistant to borohydride. For further clarification of the hemiacetalproblem, the change of the number of hydroxyl groups taking place on borohydride reduction of Björkman lignin has now been examined.

By acetylation (Verley-Boelsing, *cf.* also Ref.[9]), Björkman lignin was found to contain 1.40 OH/OCH_3 (uncorrected for small amounts of carbohydrates present [10]), whereas 1.60 OH/OCH_3 were found in the $NaBH_4$-lignin. The

increase by 0.20 OH/OCH_3 is in harmony with the presence of 0.20 CO/OCH_3 in the untreated lignin. If, in addition, 0.2 hemiacetal groupings had been present, these would have been reduced according to

$$HO-\underset{|}{\overset{|}{C}}-OR \xrightarrow{BH_4^-} HO-\underset{|}{CH} + HO-R,$$

and thus would have given rise to the formation of an additional amount of 0.2 OH groups. (This type of reduction is well-known from sugars as well as from other cases, *cf.* the reduction of the Wieland-Gumlich aldehyde [11]).

None of the results reported above provides any support for the presence, in lignin, of free or half-acetalised keto groups unreactive towards hydroxylamine, which might have explained the high carbonyl values obtained by Gierer and Söderberg. In fact, both the infrared absorption studies and the OH determination seem to constitute confirmative evidence for the correctness of the oximation value, *i.e.*, about 0.20 total CO/OCH_3.

The high borohydride consumption, indicating about 0.4 CO/OCH_3, as found by Gierer and Söderberg, then still required an explanation. The method was therefore reexamined.

REEXAMINATION OF THE VOLUMETRIC BOROHYDRIDE METHOD

In accordance with Gierer and Söderberg [4], a borohydride consumption corresponding to a value of about 0.4 CO/OCH_3 was found for Björkman lignin, if the experimental conditions given by these authors were used (Fig. 2, curve *a*; reaction time, 5 h). A considerably higher value, *viz.*, 0.55 CO/OCH_3, was obtained, if the reaction mixture was subject to magnetic stirring during the reduction period (Fig. 2, curve *b*; reaction time, 5 h). Under similar

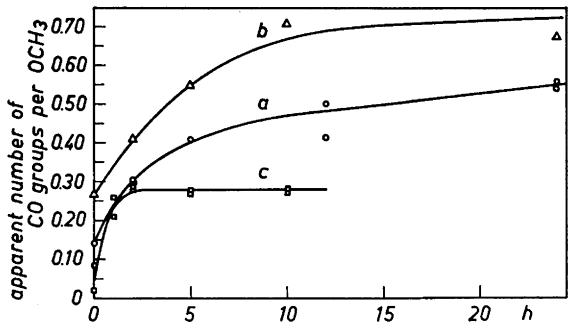

Fig. 2. Estimation of carbonyl groups by the volumetric borohydride method. Björkman lignin, 90—100 mg; 0.13 M KBH_4 in 0.1 N aqueous NaOH (3 ml), and 0.10 M H_3BO_3 in 96 % ethanol (4 ml). The reaction was stopped by the addition of 2 N H_2SO_4 (1 ml). Curve *a*: Air in the gas space, no stirring of the reaction mixture. Curve *b*: Air in the gas space, magnetic stirring of the reaction mixture. Curve *c*: Nitrogen in the gas space, no stirring of the reaction mixture. The values given at "zero time" were obtained on 5 h treatment of a $NaBH_4$-reduced Björkman lignin.

conditions, an appreciable "borohydride consumption", corresponding to a content of 0.26 CO/OCH_3 was also obtained with a $NaBH_4$-reduced, *i.e.*, carbonyl-free, lignin, and figures of 1.05 and 1.97 CO/OCH_3, which were quite obviously too high, were similarly found for Brauns lignin and a commercial kraft lignin, respectively. Furthermore, it was found that the end-point was not reached after a reaction time of 5 h, as used by Gierer and Söderberg, increasing CO values being obtained, if the reaction was carried on for prolonged periods of time. This was true whether the reaction mixture was stirred or not (Fig. 2, curves *a* and *b*).

Since the final gas mixture in the determination is a mixture of hydrogen and air, a reaction consuming either hydrogen or one of the constituents of air could produce such effects. Bearing in mind the method of preparing Björkman lignin three such reactions immediately come to mind, *viz.* (1) the reaction of some of the liberated hydrogen with the oxygen in the air, (2) oxidation of the lignin by the gaseous oxygen and (3) the hydrogenation of the ethylene groups in lignin (0.06—0.08 per OCH_3, see Ref.[3]). These reactions could be catalysed by contaminating traces of heavy metals or heavy metal ions present in the reaction mixtures. Emission spectrographic analysis * of the ash (about 0.1 %) obtained from Björkman lignin revealed a comparatively high content of heavy metals (Fe > Ni > Cr), probably originating from the grinding of the wood in a vibratory stainless steel ball mill.

In a volumetric borohydride experiment, the lignin was replaced by 25 mg of the wood powder residue which remains after the extraction of lignin from the milled wood with dioxan according to Björkman. (This wood powder has a gray colour due to the presence of contaminating metal.) After a reaction time of 5 h, 8 ml of gas (corresponding to 10 mg of carbonyl!) had been consumed as compared with a blank without wood meal. In a second experiment, the apparatus was filled with hydrogen before the components were mixed; the gas consumption was then only 1.3 ml (of H_2). This suggests that the major part of the gas consumption in the first experiment was due to catalytic oxidation, by air present in the apparatus, of hydrogen evolved from the borohydride (and, less probably, also of the wood meal).

The assumption that the procedure used by Gierer and Söderberg involves a consumption of hydrogen and of oxygen from the gas phase by the reactions mentioned above, would explain the effect of the reaction time as well as of the stirring of the reaction mixture.

Concerning the proper nature of the catalysts assumed to act in this system, it may be pointed out that heavy metal salts react with borohydride to form borides, which have shown to be excellent hydrogenation catalysts [12,13,3]. Also, such borides as well as heavy metals in a finely divided state will catalyse the combustion of hydrogen. Furthermore, they accelerate the decomposition of borohydrides with the formation of hydrogen [14].

If, in the borohydride reduction of Björkman lignin, the apparatus was filled with hydrogen or nitrogen rather than air, the values found for the borohydride consumption were considerably lower. Values of 0.27—0.29 CO/OCH_3 were then obtained after a reaction time of 2 h (the reaction mixture was not stirred). In contrast with the behaviour of the system in the presence of air, no further "borohydride consumption" was now observed after prolonged reaction times (Fig. 2, curve *c*).

* Kindly carried out by Metallografiska Institutet, Stockholm.

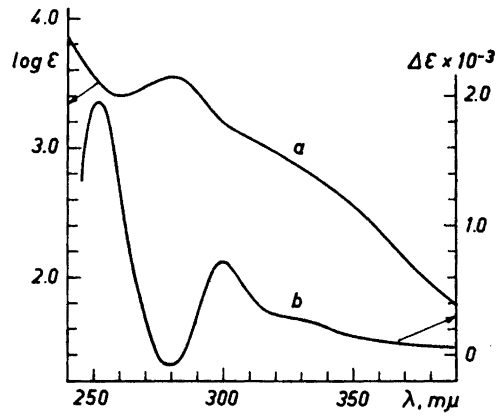

Fig. 3. Ultraviolet absorption (curve *a*) and ionisation-$\Delta\varepsilon$ curve (*b*) of Björkman lignin treated 1 h with KBH_4 under the conditions given for Fig. 2, curve *c*. (ε values based on OCH_3 concentration.) Neutral solvent, ethanol-ethylcellosolve (9:1); alkaline solvent, 0.1 N NaOH in ethanol-ethylcellosolve-water (4:1:5).

These results clearly show that the borohydride determination of carbonyl groups in Björkman lignin will yield erroneously high values if air is not excluded from the apparatus. Although the value obtained with the apparatus filled with N_2 or H_2 (mean, 0.28 CO/OCH_3) could be expected to be close to the actual carbonyl content of the lignin, it was still higher than that obtained by the oximation method (0.20). It was found, however, that a sodium borohydride-reduced lignin, although devoid of carbonyl groups, in the apparatus filled with H_2 or N_2, still gave apparent values of 0.04—0.08 CO/OCH_3, after a reaction period of 5 h. This may possibly be ascribed to incomplete removal of air from the apparatus. [The mean of these values has been taken in curve *c*, Fig. 2, as the "zero time" value. Similarly, the "zero time" values for curves *a* and *b* are those obtained in 5 h experiments in air with $NaBH_4$-lignin without stirring (*a*) and with stirring (*b*).] Correction of the final value obtained for Björkman lignin in hydrogen or nitrogen atmosphere (0.28 CO/OCH_2) for the corresponding 5 h value for $NaBH_4$-lignin (0.04—0.08 CO/OCH_3) would yield a value of 0.20—0.24 CO/OCH_3, with would be in accordance with the oximation value.

A lignin preparation which was recovered from a borohydride experiment after one hours' reduction time, exhibited the UV absorption and ionisation $\Delta\varepsilon$-curves shown in Fig. 3. Similar curves were obtained for products obtained after longer periods of reaction. Surprisingly enough, the $\Delta\varepsilon$-curve (Fig. 3, curve *b*) showed that the phenolic aryl-*a*-ketone groups were completely reduced already after one hour, no $\Delta\varepsilon$-maximum being found at 357 mμ (*cf.* the ionisation $\Delta\varepsilon$-curve of untreated Björkman lignin [3]). As shown in Part I [2], the borohydride reduction of 4-hydroxyphenyl ketones proceeds more slowly than that of the non-phenolic analogues, the half-time value for the reduction of ketone III, for instance, being 10 h at pH 12, and considerably higher at pH 13. The rapid reduction of phenolic aryl-*a*-ketone groupings in lignin, as observed in the volumetric experiments, seems to be attributable to the comparatively low pH (about 11.2) of the reaction mixture used. This finding also seems to indicate that the value of about 0.24 CO/OCH_3,

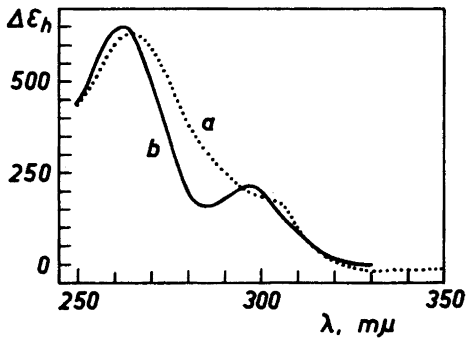

Fig. 4. Curve *a*: Hydrogenation-$\Delta\varepsilon$ curve of Björkman lignin pretreated 5 h with KBH_4 under N_2 (exptl. conditions as described for curve *c*, Fig. 2). Hydrogenation in 93 % HOAc over Pd-$BaSO_4$ (see Experimental). Curve *b*: Hydrogenation-$\Delta\varepsilon$ curve of 0.04 mole/l isopropylconiferyl alcohol (*cf.* Ref.[3]).

as obtained after one hour's reaction in a N_2 or H_2 atmosphere (Fig. 2, curve *c*) is closer to the actual CO content of the lignin than the final value (0.28), the gas-consuming side-reactions evidently proceeding more slowly than the borohydride reduction of the carbonyl groups.

By means of the borohydride reduction-$\Delta\varepsilon$ method [2], it could further be demonstrated that, as expected, the non-phenolic aryl-*a*-ketone groupings as well as the coniferyl aldehyde groupings had disappeared after on hour's reduction time.

As hydrogen is transferred to ethylenic bonds by the catalytic action of nickel boride [12,13,3], it could be suspected that, in the volumetric carbonyl analysis, some hydrogen might be consumed by similar reaction of double bonds in the lignin, thus contributing to the high apparent carbonyl values obtained. An attempt was therefore made to determine, in a recovered lignin product, the number of ethylenic groups conjugated with the aromatic nucleus. The product was hydrogenated over Pd-$BaSO_4$, as described in the preceding paper [3], and the hydrogenation-$\Delta\varepsilon$ curve ($\Delta\varepsilon_h$ curve) was constructed (Fig. 4, curve *a*). It indicated the presence of about 0.04 coniferyl alcohol groups per OCH_3. (For comparison, the wavelength curve of the $\Delta\varepsilon_h$ values, multiplied by 0.04, for *iso*-propylconiferyl alcohol [3], bas been given in Fig. 4, curve *b*.) For a borohydride-reduced lignin, a somewhat higher value for the coniferyl alcohol groups, *viz.*, 0.06—0.08, would be expected, 0.03—0.04 being present in untreated lignin and a similar number being formed by the reduction of the coniferyl aldehyde groups [3]. The value obtained (0.04) then would indicate that catalytic hydrogenation of 0.02—0.04 coniferyl alcohol side-chains has taken place under the conditions of the carbonyl determination method. Although the latter figures may be within the limits of error of this method, it seems possible that a minor fraction (0.02—0.04) of the CO values obtained after the exclusion of air actually should be ascribed to ethylene groups.

To summarise, the IR studies as well as the volumetric CO determination carried out with the exclusion of oxygen have confirmed that Björkman lignin contains about 0.20 CO/OCH_3, as found previously with the hydroxylamine hydrochloride method [1]. The IR studies have further provided new evidence for the correctness of the finding [2,3] that these carbonyl groups consist of 0.03—0.04 coniferyl aldehyde groups, about 0.07 aryl *a*-ketone groupings and about 0.10 β-ketone groupings. As shown by the spectrochemical borohydride ($\Delta\varepsilon_r$) and hydrogenation ($\Delta\varepsilon_h$) methods [2,3], only about 0.01 coniferyl aldehyde groups and about 0.01 aryl-*a*-ketone groups have free phenolic hydroxyl groups.

EXPERIMENTAL

Infrared spectra were recorded on a Perkin-Elmer model 21 instrument; KBr discs were used. The mixtures of model substances and $NaBH_4$-reduced lignin (Fig. 1) were made from the desired amounts of 1 % mixtures of the model substances in KBr and a lignin-KBr mixture, all mixtures being prepared by means of a vibrator. The total amount of organic material was 1.80 mg per 500 mg of KBr.

Ultraviolet absorption was measured with a Beckman DU spectrophotometer.

For the *isolation of the reduced lignin*, the potassium borohydride reaction mixture was acidified with acetic acid, the alcohol removed under reduced pressure and the lignin precipitate recovered as described in Part III [3] for similar preparation of $NaBH_4$-reduced lignin.

The *UV absorption of the reduced lignin* (Fig. 3) was measured in a neutral solution, obtained by dissolving 5.00 mg of the lignin in 5 ml of freshly distilled methylcellosolve and making up the mixture to 100 ml with 95 % ethanol (curve *a*), and in an alkaline solution containing 5.00 mg of the lignin in 100 ml of 0.1 N NaOH in 50 % aqueous ethanol. The difference values between the ε values of the latter absorption curve and curve *a* gave the ionisation-$\Delta\varepsilon$ curve (*b*).

The hydrogenation-$\Delta\varepsilon$ curve of the KBH_4-reduced lignin (Fig. 4, *a*) was obtained as follows. The recovered lignin preparation (0.1 g), dissolved in 93 % aqueous acetic acid, was hydrogenated for 6 h at room temperature over $PdCl_2$-$BaSO_4$ (0.5 g), as described before [3,13]. The catalyst was centrifuged off and washed, and the absorption was measured in a sample of the solution diluted with ethanol to contain about 0.05 g lignin/l. By subtracting the values obtained from those determined for the non-hydrogenated product, the $\Delta\varepsilon_h$ curve was constructed.

The volumetric borohydride method. The experiments for curve *a*, Fig. 2, were carried out according to Gierer and Söderberg [4]; in those for curve *b*, magnetic stirring of the solution was applied. If air had to be excluded, as in the experiments to curve *c*, the apparatus was evacuated by a water suction pump and refilled (five times) with nitrogen or hydrogen, before the borohydride and lignin solutions were mixed in the reaction vessel.

The authors wish to thank Mrs. Terezia Marton, who has carried out the infrared work and the hydroxyl group determinations. Financial support from *Statens Tekniska Forskningsråd* is gratefully acknowledged.

REFERENCES

1. Adler, E. and Walldén, I., quoted in Adler, E. and Gierer, J., in Treiber, E. *Die Chemie der Pflanzenzellwand*, Springer-Verlag, Berlin 1957, p. 446.
2. Adler, E. and Marton, J. *Acta Chem. Scand.* **13** (1959) 75. [Preliminary report, Marton, J. *Proc. IVth Intern. Congr. Biochem.*, Vienna 1958, vol. II (1959) 154.]
3. Marton, J. and Adler, E. *Acta Chem. Scand.* **15** (1961) 370.
4. Gierer, J. and Söderberg, S. *Acta Chem. Scand.* **13** (1959) 127.
5. Lindberg, B. and Misiorny, A. *Svensk Papperstidn.* **55** (1952) 13; Lindberg, B. and Theander, O. *Ibid.* **57** (1954) 83.
6. Adler, E., Pepper, J. M. and Eriksoo, E. *Ind. Eng. Chem.* **49** (1957) 1391.
7. Adler, E. and Walldén, I. *Unpublished.*
8. Pearl, J. *J. Org. Chem.* **24** (1959) 736.
9. Freudenberg, K. and Schlüter, H. *Chem. Ber.* **88** (1955) 617; note, p. 618.
10. Björkman, A. and Person, B. *Svensk Papperstidn.* **60** (1957) 158.
11. Anet, F. A. L. and Robinson, R. *J. Chem. Soc.* **1955** 2253; Fritz, H., Beach, E. and Wieland, Th. *Angew. Chem.* **71** (1959) 126.
12. Paul, R., Buisson, P. and Joseph, N. *Compt. rend.* **232** (1951) 627; *Ind. Eng. Chem.* **44** (1952) 1006.
13. Adler, E. and Marton, J. *Acta Chem. Scand.* **15** (1961) 357.
14. Gaylord, N. G. *Reduction with Complex Metal Hydrides*, Interscience Publ., New York 1956, pp. 60–61; Levy, A., Brown, J. B. and Lyons, C. J. *Ind. Eng. Chem.* **52** (1960) 211.

Received October 3, 1960.

ACTA CHEMICA SCANDINAVICA 15 (1961) 393–402

Studies in the Hydrolysis of Metal Ions 33

A Miniature Solubility Column and its Application to a Study of the Solubility of Red Mercury(II) Oxide in Acid 3 M $NaClO_4$ Solutions

DAVID DYRSSEN and VALENTINE TYRRELL*

Department of inorganic chemistry, Royal Institute of Technology, Stockholm 70, Sweden

A scaled-down version of a conventional solubility column which uses only about 2 g of solid material is described. It is well-adapted for handling radioactive materials, and has been used for radiochemical measurements of the solubility of red mercury(II) oxide in 3 M $NaClO_4$ solutions in the pH range 1–5.

Our results compare favorably with those of Garrett *et al.*[2,3], who obtained equilibrium by shaking for three weeks followed by settling for three to five days. Further improvements in the present method are proposed.

The presence of Hg^{2+}, $HgOH^+$, and $Hg(OH)_2$ as the only mercury-containing species is confirmed, and the following values for the equilibrium constants have been calculated:

$$\log {}^*K_1 + \log {}^*K_2 = -6.44 \pm 0.08$$
$$\log {}^*K_1 - \log {}^*K_2 = -0.30 \pm 0.30$$
$$\log K_{s2} = -3.75 \pm 0.01$$
$$\log {}^*K_{s0} = +2.69 \pm 0.10$$

where

$${}^*K_1 = [HgOH^+][H^+][Hg^{2+}]^{-1}; \quad {}^*K_2 = [Hg(OH)_2][H^+][Hg(OH)^+]^{-1};$$
$$K_{s2} = [Hg(OH)_2] \quad ; \quad {}^*K_{s0} = [Hg^{2+}][H^+]^{-2}.$$

Measurements of the solubility of sparingly soluble substances have traditionally been made by shaking samples of the solid and solvent together for periods long enough for equilibrium to be attained, and thereafter analysing the liquid phase, usually after separating it from the solid. Alternatively, and more conveniently, the solvent may be allowed to percolate slowly through a vertical column of the solid phase. The dimensions of this are not critical, but are usually chosen generously with a bed 20 cm or more in depth and perhaps 2 cm in diameter. Such a column requires a large amount of material, possibly too large if a radiometric method is to be used for the analysis of the

* On leave of absence from the University of Sheffield, England.

solution, since in some cases it may be essential to use a solid phase with a high specific activity. While smaller quantities are needed for the first method, manipulative difficulties in separating the phases may also become important. A method of avoiding these and other problems by precipitating the solid from an active solution and measuring the reduction in the activity of the latter has recently been described [1].

In this work, we have sought to adapt the column method for use with small quantities of active solid by reducing the dimensions of the solid bed. Because of the general interest of this laboratory in hydrolysis, attention has been directed towards the possibility of measuring the solubility of oxides by a radiochemical method in a column of small size, and, for the initial experiments described here, mercury(II) oxide has been selected. It has a convenient isotope, ^{203}Hg, half life 47 days, and the hydrolytic processes undergone by Hg(II) are of considerable interest.

The solubility of both red and yellow mercury(II) oxides as a function of the hydrogen ion concentration was the subject of a careful study by Garrett and Hirschler [2] (alkaline solutions) and by Garrett and Howell [3] (acid solutions) who used the first method mentioned above, and an electrometric method of analysis of the mercury content of the solution phase. The technique now usual in studies of equilibria, of using a medium of high and constant ionic strength as the solvent, was not used, and the interpretation of the results is therefore complicated by the necessity of allowing for changes in the activity coefficients of the ionic species present. They concluded that, in acid solutions, Hg^{2+}, $HgOH^+$ and $Hg(OH)_2$ only were present, that the neutral species predominated over a wide range of hydrogen ion concentrations on either side of neutrality, and that, in sufficiently alkaline solutions, $Hg(OH)_3^-$ was formed. There was no evidence for the formation of $Hg(OH)_4^{2-}$ even in 2 M sodium hydroxide solution. Any polymer species present of the type $Hg_m(OH)_{n+2m}$ would not, of course, be detected by solubility measurements alone, but the general correctness of this hydrolysis scheme in acid solutions was later confirmed by Hietanen and Sillén [4] for a 0.5 M sodium perchlorate medium. They used the potentiometric titration method and concluded that $*K_2$ was smaller than $*K_1$, these constants being defined as:

$$*K_1 = [HgOH^+][H^+][Hg^{2+}]^{-1} \quad (1)$$

$$*K_2 = [Hg(OH)_2][H^+][HgOH^+]^{-1} \quad (2)$$

Clearly, sufficient is known about the hydrolysis of Hg(II) to make it possible to decide whether the method adopted for measuring solubilities gives essentially reasonable results, while, at the same time, a fresh study of the variation of the solubility of mercury(II) oxide with hydrogen ion concentration in a medium of constant ionic strength is not undesirable. This paper describes the results of solubility measurements at 25°C on the red form of mercuric oxide in acid sodium perchlorate solutions of $I = 3$, carried out in a miniature solubility column, the mercury analyses being done radiochemically.

EXPERIMENTAL

Preparation of materials. Red mercury(II) oxide was prepared by dissolving redistilled mercury in concentrated nitric acid (Merck[1] p.a.), and evaporating the solution until a white "mercury(II) nitrate" precipitated. This was then heated at 400–500°C in an electric oven until all nitrogen oxides had been driven off. The resulting powder (dark red when hot, scarlet when cold) was washed by decantation with conductivity water at frequent intervals for about a week in an attempt to remove soluble matter and very fine particles of oxide (*cf.* Refs.[2,3]). It was then drained, dried over silica gel, and a 2 g sample sealed in a quartz tube for irradiation in the Swedish reactor R 1. As HgO is a rather soluble oxide it was only irradiated for 3 h in a flux of 5.5×10^{11} neutrons cm^2 sec^{-1}.

A concentrated solution of sodium perchlorate was prepared from chloride-free sodium carbonate (Merck p.a., selected sample) and perchloric acid (Kebo p.a.) by the method normally used in this laboratory. A stock solution of perchloric acid, about 1 M, was prepared from the concentrated acid, analysed with potassium bicarbonate, and used to prepare the following solutions:

a) 0.1 M perchloric acid, 2.90 M sodium perchlorate.
b) 0.01 M perchloric acid, 2.99 M sodium perchlorate.
c) 0.01 M sodium hydroxide, 2.99 M sodium perchlorate.

Solution (c) was prepared from the stock sodium perchlorate solution, and a carbonate-free solution of sodium hydroxide prepared from Kebo p.a. pellets. Solution (b) was used as a standard of hydrogen ion concentration, and, in mixtures with (c), for preparing solutions of suitable hydrogen ion concentrations down to about 10^{-5} M to feed into the solubility column. Solution (a) was used to prepare acid solutions with [H+] between 10^{-1} and 10^{-2}.

The solubility column. This was a conventional, scaled-down solubility column with the form and dimensions shown in Fig. 1. The column was immersed in a thermostated water-bath which also served as a radiation shield. The internal diameter of the column was made small enough to give a bed of mercury(II) oxide about 2 cm thick when a 2 g sample was used; it was felt that a further decrease in diameter might lead to flow along the walls rather than through the powder bed, and that, with a viscous medium like 3 M sodium perchlorate, the resistance to fluid flow would become unduly large. The height was chosen so that the closure at A lay above the level of the thermostat liquid when the bottom of the column rested on the bottom of the thermostat. The solid was held on a sintered glass pad, made in the laboratory and of uncertain pore size.

A novel feature of the column, particularly convenient when radioactive solutions are being handled, was the small lift-pump which was placed at such a level that the powder bed was never denuded of solution. Introduction of a slow stream of nitrogen at the point shown permitted the effluent from the column of solid to be transported without contamination to a suitable reservoir. Cylinder nitrogen freed from oxygen by passage over heated copper, and washed successively with 10 % sulphuric acid, 10 % sodium hydroxide, and then twice with 3 M sodium perchlorate solution, was used for this, and also to saturate all solutions with nitrogen before adding them to the column.

It was recognised that full equilibrium might well not be achieved by passing the solution once through such a shallow bed, and, in the earliest experiments, the solution was circulated from the column into an upper reservoir whence it dripped through the solid bed again. This continuous circulation was interrupted from time to time to take samples from the upper reservoir. These experiments showed clearly the excessively large amount of active mercury carried through the column when it was first used, but it proved more convenient in the main part of the work to collect a definite amount of solution which had passed through the column, and to analyse it before deciding whether further passage over the solid was necessary. To increase the head of liquid, and hence the rate of flow, the reservoir in these experiments was made from a 50 ml burette whose tip passed through the rubber stopper closing the column at A. This closure was gas-tight, and the contents of the reservoir dripped into the column at the same rate as the solution passed through the solid bed. Between 5 and 10 ml of solution were always above the solid bed in the column, and the solution coming in from the reservoir had ample time

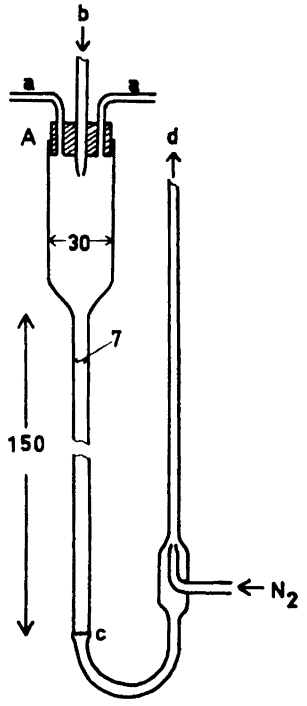

Fig. 1. Solubility column. All measures in mm.

a, a Inlet and outlet tubes for passing nitrogen through top of column, and for reducing the pressure at this point when re-packing the column. Closed during normal operation of column.
b End of reservoir-burette.
c Sintered glass pad.
d To collecting vessel

to reach temperature equilibrium with the thermostat since the flow rate amounted to only about 10 ml/h.

In the later experiments the following procedure was followed. A solution of the appropriate hydrogen ion concentration was prepared, and a stream of purified nitrogen passed through it for 20—30 min. It was then transferred to the burette reservoir and allowed to drip through the column. The first 10—15 ml coming over served to wash out the column and were discarded. The remaining contents of the system were collected, analysed, and returned to the column. Experiments at several different acidities (see below) showed that further small changes in concentration and acidity usually occurred up to and including the third pass through the column if this was working correctly, but that a fourth pass was not necessary. During the third and final run, at least two samples of 3—4 ml each were taken separately and analysed to check the homogeneity of the effluent and the reproducibility of the analyses.

The mercury content was found by taking a weighed sample of about 2 ml and counting the gamma radiation in a Tracerlab SC—57 low background well scintillation counter coupled to a SC—73 Versa/matic II Scaler. A standard mercury sample of known weight and of about the same volume was prepared from a solution made by dissolving about 0.04 g of the active oxide in approximately 1 ml of 3.5 M nitric acid and making up to 25 ml with solution (c). This was analysed chemically for mercury with potassium thiocyanate solution. This was itself standardised against a mercury standard prepared by dissolving an accurately known weight of pure mercury in 50 % nitric acid and diluting to a known volume. The mean of estimations was $6.35_2 \times 10^{-3}$ mole mercury per litre, with a standard deviation of 6×10^{-6}.

The acidity was measured with a Beckmann Red glass electrode connected to the silver-silver chloride reference electrode through a "Wilhelm" bridge, the complete cell being:

G.E. | Unknown solution | 3 M $NaClO_4$ | 2.99 M $NaClO_4$, 0.01 M $AgNO_3$ | AgCl, Ag

The e.m.f. of this was measured with a Radiometer pH meter, type 4. The reference electrode was prepared by Brown's method [5]. Hydrogen ion concentrations were calculated from the difference in e.m.f. observed when the glass electrode was immersed in solution (b) and in the solution under test; corrections for changes in the liquid junction potential with changing acidity were negligible in all solutions used.

To make these measurements, it was necessary to handle the solutions in the open laboratory which was not very desirable for solutions of low acidity since the buffer capacities were small, and it would be an improvement in future work of this kind to arrange to measure the acidity of the solution as soon after it leaves the solid as is possible. Another source of error in these acidity measurements was the small changes which occurred in the asymmetry potential of the glass electrode during the frequent washing and handling to which it was necessary to subject it. This, too, could be avoided by a modification of the kind suggested, and an improvement in the accuracy of this measurement would contribute appreciably to a reduction in the experimental scatter, and hence to an improvement in the precision with which the hydrolysis constants can be calculated.

RESULTS

Abnormally high "solubilities" in newly-prepared column. The column was filled by adding the dry active mercury(II) oxide to the dry clean column, and passing in a nitrogen saturated solution. This was made up to be 2.99 M in $NaClO_4$, 0.01 M in NaOH, and was chosen for the preliminary experiments mainly because of Garrett and Hirschler's observation [2] that the solubility was nearly independent of the acidity in this range. For the first five samples taken the solution was being circulated continuously through the system. If it is assumed that:

i) full solubility equilibrium is attained in one pass through the column,

ii) the rate of flow out of the reservoir is equal to that through the column,

it can be easily shown that the concentration C_t in the reservoir at any time t after the start of the experiment is related to the final steadystate value, C_∞, by the equation,

$$C_t = C_\infty(1—\exp.(—t/\Theta)) \qquad (3)$$

where $\Theta = v/V$. Here v is the rate of flow, and V the volume of the reservoir. The first of the above assumptions is not quite correct but this is not important for the present purpose. Table 1 shows some values of C_∞ calculated from (3) and observed values of C_t, t, and Θ. Samples 6—10 inclusive were obtained in subsequent experiments by direct sampling of the effluent from the column.

As can be seen, the apparent solubility of the oxide was highest for the earliest samples and fell as the total volume of liquid which had passed over the column increased. It was clear that the oxide sample was not completely uniform in spite of the prolonged washing it had received before irradiation. Had this been used in solubility measurements by the batch method, high and probably rather irregular values of the solubility would have been obtained, whereas by the column method it is easy to continue washing with a suitable solution until reproducible results are obtained.

Table 1. Apparent solubility of mercury(II) oxide in 0.01 M NaOH, 2.99 M $NaClO_4$ when the column is freshly packed.

Sample	t/Θ	$10^5\ C_\infty$ M Hg
1	0.2695	51.8
2	0.464	53.4
3	0.691	52.0
4	1.33	38.5
5	3.33	25.8
6	Direct sample	26.2
7	» »	25.2
8	» »	25.0
9	» »	22.9
10	» »	22.6

The attainment of equilibrium. After the preliminary conditioning made necessary by the high apparent solubilities observed with the freshly-packed column, it was found that the concentration of a solution which had passed once through the column could be increased slightly by passing it through a second time. Table 2 shows the changes in concentration of mercury and hydrogen ions when an initially mercury-free solution 0.01 M in perchloric acid and 2.99 M in $NaClO_4$ was passed four times through the column.

Table 2. Effect of repeated passages through the column of an initially mercury free solution, 0.01 M $HClO_4$, 2.99 M $NaClO_4$.

No. of passes through column	Mercury concentration M $\times 10^{-4}$	$-\log [H^+]$
1	41.3	2.57
2	42.0	2.58
3	43.4	2.57
4	43.0	(2.54)

In this case, and in several others which were studied, the third pass was necessary but not the fourth, and for this reason the experimental routine described earlier was adopted. From time to time, solubility values which were abnormally low compared with those expected from the provisional solubility curve drawn through the majority of experimental results, were obtained. These seemed to be due to some kind of mechanical defect such as channelling in the powder bed, since after reducing the pressure at the top of the column thereby sucking the powder back up it, and then allowing to settle again under gravity, normal results were obtained after two or three passes through the column. Some time would have been saved had this procedure been carried out more regularly.

A further point of practical importance is that it proved impossible to obtain satisfactory results by passing solutions through the column which

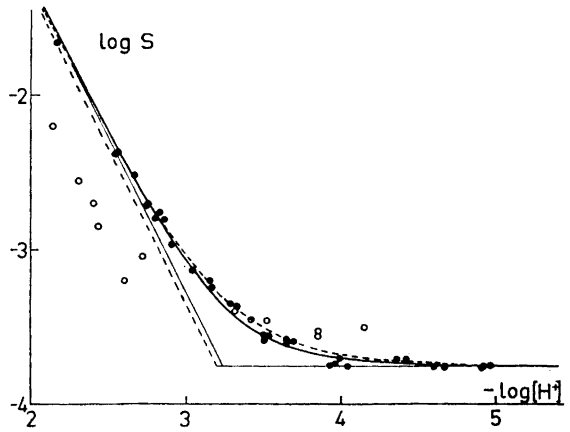

Fig. 2. Solubility results for red mercury(II) oxide in 3 M sodium perchlorate solutions. ● Experimental data reported in Table 3. O Garrett and Howell's data [3] in low and variable ionic strength medium.

Full curve: Normalised solubility curve with $p = 0.50$ fitted to data.
Broken curve: Normalised curve with $p = 1$ fitted to data. The thin lines are the asymptotes according to eqns. (7) and (8).

contained slightly more mercury than corresponded to their acidity. Repeated passages failed to change appreciably either the mercury content or the acidity. Two possible explanations are the presence of equilibria in the solution which were attained very slowly, or more probably, the presence in the supersaturated solution of mercury(II) oxide in a microcrystalline form which passed through the column unchanged, and was analysed as soluble mercury.

The solubility of mercury (II) oxide. The results of the solubility measurements, other than for those experiments in which solubility equilibrium was demonstrably not attained, are shown in Table 3. Fig. 2 is a plot of log S against log $[H^+]$ (filled circles) where S is the concentration of mercury in the solution, and $[H^+]$ is the free hydrogen ion concentration measured with the glass electrode. Garrett and Howell's [3] values (open circles) for the solubility of red mercury(II) oxide are also shown in this figure for comparison.

It can be seen that the change from a medium of very low ionic strength as used by Garrett and Howell [3] to a 3 M $NaClO_4$ medium produces a very large change in the solubility curve, while the reproducibility of the present results can fairly be claimed to be better than that attained in their carefully designed and executed experiments. It should be noted that their results as tabulated represent the means of several different experiments carried out under the same conditions, so that experimental variations have been smoothed out to some extent in their data plotted in Fig. 2. The lower solubility for the neutral species observed in the higher ionic strength medium is presumably a normal "salting-out" effect. The charged species are "salted-in".

Table 3. The variation of the solubility of red mercury(II) oxide with hydrogen ion concentration at 25°C in a 3M sodium perchlorate medium given as $-\log S$ ($-\log [H^+]$).

1.658(2.160), 1.657(2.165).
2.362(2.569), 2.366(2.544), 2.362(2.544), 2.371(2.544).
2.509(2.665).
2.701(2.751), 2.698(2.758).
2.752(2.845), 2.757(2.830), 2.767(2.835), 2.764(2.840).
2.799(2.865).
2.805(2.805), 2.799(2.802).
2.968(2.900), 2.964(2.910).
3.128(3.045), 3.124(3.045).
3.203(3.155), 3.196(3.160), 3.201(3.155), 3.199(3.155).
3.247(3.170), 3.246(3.170).
3.334(3.296), 3.341(3.299).
3.370(3.348), 3.360(3.339), 3.369(3.323).
3.582(3.510), 3.554(3.554), 3.551(3.510).
3.594(3.697), 3.603(3.658), 3.602(3.646), 3.603(3.660), 3.602(3.666), 3.605(3.646). 3.582(3.668), 3.588(3.660), 3.582(3.650).
3.761(4.050), 3.705(3.980), 3.705(3.950).
3.747(3.930), 3.737(3.970).
3.703(4.430), 3.701(4.375).
3.751(4.672), 3.753(4.605).
3.754(4.920), 3.761(4.920), 3.746(4.975).

Each group of results is derived from one independent experiment. They are included to show the degree of variation between samples taken from the column at successive times.

DISCUSSION

Both the earlier solubility work of Garrett and Howell [3], and the potentiometric study carried out by Hietanen and Sillén [4] could be interpreted on the basis of the following equilibria:

$$Hg^{2+} + H_2O \rightleftharpoons HgOH^+ + H^+ \quad (4)$$
$$HgOH^+ + H_2O \rightleftharpoons Hg(OH)_2 + H^+ \quad (5)$$

with equilibrium constants $*K_1$ and $*K_2$ defined by the eqns. (1) and (2) given earlier. The formation of anionic complexes does not occur until the solutions become strongly alkaline as can be seen from the solubility data of Garrett and Hirschler [2]. In view of these results it can be assumed that the total dissolved mercury S in the acid solutions studied here is given by

$$\log S = [Hg^{2+}] + [HgOH^+] + [Hg(OH)_2]$$

which, from the definitions (1) and (2), leads to the equation

$$S = [Hg(OH)_2](1 + *K_2^{-1}[H^+] + *K_1^{-1}*K_2^{-1}[H^+]^2)$$

or

$$\log S = \log [Hg(OH)_2] + \log(1 + *K_2^{-1}[H^+] + *K_1^{-1}*K_2^{-1}[H^+]^2) \quad (6)$$

Log $[Hg(OH)_2]$ is a constant if the solution is in equilibrium with the solid phase, and the plot of log S against $-\log [H^+]$ has two linear asymptotes.

When $*K_1^{-1}*K_2^{-1}[H^+]^2$ is large compared with $*K_2^{-1}[H^+]$ and unity, the asymptote has slope —2:

$$\log S = \log [Hg(OH)_2] - \log *K_1*K_2 + 2 \log [H^+] \quad (7)$$

When both terms involving $[H^+]$ are much less than 1 it has a slope zero:

$$\log S = \log [Hg(OH)_2] = \log K_{s2} \quad (8)$$

A standard curve-fitting technique, due to Sillén [6], has been used to determine the equilibrium constants. Plots of $\log (1 + pv + v^2)$ against $-\log v$ for values of the variable v lying between 0.01 and 100, with $p = 0$, 0.25, 0.50, 1 and 2, were drawn and compared with one of $\log S$ against $-\log [H^+]$ derived from the experimental data, all plots being drawn to the same scale. By comparison of eqn. (6) with the normalized variable $Y = \log (1 + pv + v^2)$ we find

$$p = \sqrt{*K_1/*K_2} \quad (9)$$

From values in Table 3 we calculated with eqn. (8)

$$\log S = -3.75 \pm 0.01 = \log K_{s2}$$

Using this value as the horizontal asymptote an acceptable fit to the experimental curve could be obtained with $p = 0.5$ and 1, $-\log [H^+]$ at the intersection point of the asymptotes being found as

$$-\log [H^+] = 3.22 \pm 0.04 = \tfrac{1}{2} \log *K_1*K_2$$

The deviation represents the limits within which this intersection could lie if the data are fitted to a curve with $p = 0.5$ or 1 (the curves are drawn in Fig. 2). Because of the experimental scatter, it is not possible to be very precise about the value of p. From Hietanen and Sillén's published constants [4], valid for a medium 0.5 M in sodium perchlorate, p can be calculated as 0.28 ± 0.05 and recently Ahlberg [7] has obtained the preliminary value $p = 0.39$ for 3 M $NaClO_4$. The present solubility data are therefore not quite consistent with the potentiometric measurements, but the difference is not too serious.

The solubility of the neutral species $Hg(OH)_2$ is $K_{s2} = (1.77 \pm 0.05) \times 10^{-4}$ M, and $\log *K_1 + \log *K_2 = -6.44 \pm 0.08$, both values referring to a 3 M sodium perchlorate medium at 25°C. The latter value is somewhat smaller than Ahlberg's potentiometric value [7] —6.22 (preliminary) and the value —6.30 determined for 0.5 M $NaClO_4$ by Hietanen and Sillén [4].

Separate values of $*K_1$ and $*K_2$ can be obtained by combining this sum with the difference derived from the values of p (eqn. (9)) which give the best fit to the curve. When $p = 1$, the two constants are equal, and when $p = 0.5$, $4*K_1 = *K_2$. We can therefore only obtain $\log *K_1$ and $\log *K_2$ separately with rather large errors: $\log *K_1 = -3.37 \pm 0.19$ and $\log *K_2 = -3.07 \pm 0.19$. Ahlberg [7] has obtained the preliminary values —3.52 and —2.70 and Hietanen and Sillén [4] —3.70 and —2.60. There is no doubt that at present a more accurate p value is obtained by the potentiometric method.

The solubility product $*K_{s0}$ of $Hg(OH)_2$ can also be calculated from the relation $K_{s2} = *K_{s0}*K_1*K_2$ as $\log *K_{s0} = 2.69 \pm 0.10$. In 3 M $NaClO_4$ at

25°C, Lagerström [8] found $pK_w = 14.03$, and hence, the solubility product of $Hg(OH)_2$ (pK_{s0}) for these conditions is 25.4.

No other study of the solubility of mercury(II) oxide in a 3 M sodium perchlorate medium has been reported. Some old solubility measurements of Grossman [9] in a variable ionic strength medium at 25°C gave a value for pK_{s0} of 25.4, and Latimer [10] calculated a value of 25.52 for an infinitely dilute solution. Garrett and Howell's [3] value for log $*K_{s0}$ at low ionic strength is 1.72 against the present one of 2.69 for 3 M $NaClO_4$. Their calculations of log$*K_1$ and log$*K_2$ were not done by curve-fitting methods, and they found —2.49 and —2.85, respectively, or log $*K_1*K_2 = -5.34$. These figures were based on solubility measurements of both red and yellow forms of mercury(II) oxide. Using only the data for the red oxide shown in Fig. 2, the curve fitting method gives a value for log$*K_1*K_2$ of about —5.6, but the values are too few to give any real estimate of the individual constants.

An important result of the present work is the conclusion that accurate solubility measurements can be obtained from the column method using a much smaller quantity of solid phase than is usually the case, the only penalties being the necessity of passing the solution through the column two or three times, and of frequent re-packing of the column by the simple technique described. This modified column method, with the technique of collecting samples using a small gas-lift pump, is well-adapted to handling radioactive materials, and could be safely used with a solid phase having a much higher specific activity than that employed here. This would be useful in studying substances of low solubility.

Acknowledgements. We are indebted to Professor Lars Gunnar Sillén for suggesting that further study of oxide solubilities would be timely and for his constant help and encouragement, and to Mr Frans Ericson for making the solubility column. The work was supported in part by the *Air Force Office of Scientific Research of the Air Research and Development Command, United States Air Force*, through its European Office.

REFERENCES

1. Duncan, J. F. *J. Inorg. & Nuclear Chem.* **11** (1959) 161.
2. Garrett, A. B. and Hirschler, A. E. *J. Am. Chem. Soc.* **60** (1938) 299.
3. Garrett, A. B. and Howell, W. W. *J. Am. Chem. Soc.* **61** (1939) 1730.
4. Hietanen, S. and Sillén, L. G. *Acta Chem. Scand.* **6** (1952) 747.
5. Brown, A. S. *J. Am. Chem. Soc.* **56** (1934) 646.
6. Sillén, L. G. *Acta Chem Scand* **10** (1956) 186.
7. Ahlberg, I. *Preliminary results to be published.*
8. Lagerström, G. *Acta Chem. Scand.* **13** (1959) 722.
9. Grossmann, H. *Z. anorg. Chem.* **43** (1905) 356.
10. Latimer, W. L. *Oxidation Potentials*, 2nd. Ed., Prentice-Hall, New York 1952.

Received October 1, 1960.

ACTA CHEMICA SCANDINAVICA 15 (1961) 403–406

The Crystal Structure of HfAl

LARS-ERIK EDSHAMMAR

Institute of Inorganic and Physical Chemistry, University of Stockholm, Stockholm, Sweden

The crystal structure of HfAl is of the B_f (CrB) structure type. The orthorhombic unit cell, space-group *Cmcm* (No. 63), has the dimensions $a = 3.25_3$ Å, $b = 10.83_1$ Å and $c = 4.28_2$ Å. A comparison between HfAl and other B_f structures is given.

Studies on arc-melted hafnium-aluminium alloys by means of X-ray powder methods have revealed the existence of the phases Hf_3Al_2, HfAl, Hf_2Al_3, $HfAl_2$ and $HfAl_3$. The structure types of Hf_3Al_2, $HfAl_2$ and $HfAl_3$ were reported in a previous note [1,2]. In the course of further studies on this system the crystal structure of HfAl has been derived.

EXPERIMENTAL

The alloy was prepared by arc-melting an equimolecular mixture of hafnium metal (98.5 % from I.C.I) and high-purity aluminium in an argon atmosphere. Crystals of HfAl were obtained by crushing the melt. They formed thin plates that could be cut down to dimensions suitable for single-crystal studies. A complete set of data was registered in a Weissenberg camera using CuK radiation and rotating the crystal around an axis situated in the plane of the crystal (a axis). The intensities of the reflexions were estimated visually.

Accurate unit cell dimensions were obtained from photographs taken in a Guinier focusing camera using stirctly monochromatized CuKa_1 radiation and applying a procedure described in a previous communication from this Institute [3].

DERIVATION OF THE STRUCTURE

The single crystal data obtained showed the structure to be orthorhombic. The unit cell dimensions derived from the Guinier powder photograph were:

$$a = 3.25_3 \text{ Å}, \qquad b = 10.83_1 \text{ Å}, \qquad c = 4.28_2 \text{ Å}.$$

The observed density of 8.97 indicated that the unit cell contains 4 formula units of HfAl, the calculated density being 9.07. The powder pattern of HfAl is given in Table 1.

Table 1. The Guinier powder pattern of HfAl ($CuK\alpha_1$ radiation)

hkl	$\sin^2\Theta_{obs}$	$\sin^2\Theta_{calc}$	I_{obs}	I_{calc}
020	0.02021	0.02023	m	7.0
021	0.05257	0.05259	vst	24.4
110	0.06109	0.06111	mw	4.8
040	0.08091	0.08091	w	3.1
111	0.09351	0.09347	vvst	30.3
130	0.10150	0.10156	st	16.9
041	0.11324	0.11327	st	12.6
002	0.12945	0.12944	m	7.5
131	0.13398	0.13392	vvw	0.6
022	0.14970	0.14967	vw	1.6
060	0.1823	0.18205	m	3.0
150		0.18248		2.4
112	0.19056	0.19055	w	2.2
042	0.21040	0.21035	w	2.1
061	—	0.21441	—	0.1
151	0.21486	0.21484	m	7.9
200	0.22418	0.22420	w	3.8
132	0.23101	0.23100	st	12.2
220	0.24444	0.24444	vw	0.9
221	0.27673	0.27679	mw	5.7
170	0.30400	0.30384	w	2.2
240	0.30504	0.30511	vw	1.5
023	0.3115	0.31147	mst	2.6
062		0.31149		3.4
152		0.31192		2.7
080	0.32358	0.32365	vvw	0.6
171	0.3370	0.33620	mw	5.7
241		0.33747	m	8.3
113	0.3530	0.35235	mw	7.3
202		0.35364	mw	5.5
081	0.35606	0.35601	w	4.1
043	0.37209	0.37215	w	4.1
133	—	0.39280	—	0.2
260	0.40626	0.40625	w	3.4
172	0.4335	0.43328	m	4.5
242		0.43455		3.1
082	0.45322	0.45309	vw	1.4
190	0.46557	0.46567	mw	4.5
063	0.4735	0.47329	mw	0.1
153		0.47372		7.0

Reflexions *hkl* were observed only for $h + k = 2n$, $0kl$ for $k = 2n$, $h0l$ for $h = 2n$ and $l = 2n$ and $hk0$ for $h + k = 2n$. The probable space-groups thus are *Cmcm* (No. 63), $Cmc2_1$ (No. 36) and *Ama*2 (No. 40). The symmetry, the unit-cell dimensions and the appearance of the Patterson projection along [100] suggested that the phase is isomorphous with CrB. Both the hafnium and aluminium atoms are thus in the point positions 4(*c*) of the space-group *Cmcm*:

$$\pm (0,\ y,\ \tfrac{1}{4}); \qquad \pm (\tfrac{1}{2},\tfrac{1}{2} + y,\ \tfrac{1}{4})$$

Approximate values of the y parameters were obtained from the Patterson projection and the signs of the $F(0kl)$ could be calculated. The projection of

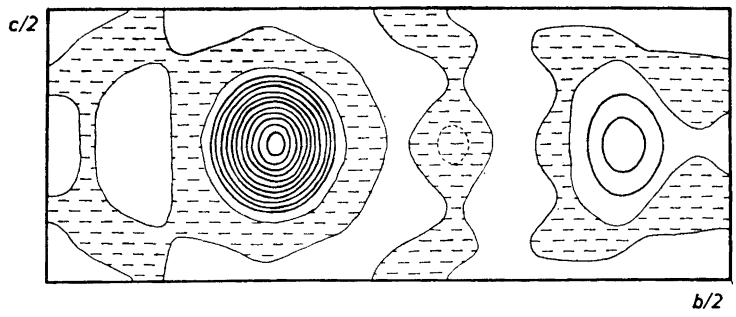

Fig. 1. a). Projection along [100] of the electron density of HfAl.

the electron density along [100] thus calculated (*cf.* Fig. 1a) gave the following parameter values:

$$y_{Hf} = 0.167 \qquad y_{Al} = 0.42_5$$

The difference synthesis ϱ $(F(0kl)_{obs} - F(0kl)_{Hf})$ gave the same value for the y_{Al} parameter (*cf.* Fig. 1b). However, the accuracy of the aluminium position is rather low due to the relatively low scattering power of this atom. The index of agreement

$$\Sigma \,||\, F(0kl)_{obs}\,| - |\, F(0kl)_{calc}\,|\,| \,/\, \Sigma \,|\, F(0kl)_{obs}\,|$$

corresponding to this structure is 0.11. Table 1 gives a comparsion between calculated and observed powder intensity data. The interatomic distances are given in Table 2.

DISCUSSION

Following Frank and Kasper [4], the structure of HfAl can be described as a $3^3 \cdot 4^2$ tessilation in the $z = \frac{1}{4}$-plane. This tessilation repated by the 2_1 axes parallel to [001] is demonstrated in Fig. 2. It is interesting to note that the zig-zag aluminium chains thus formed (A—B in Fig. 2) have quite normal

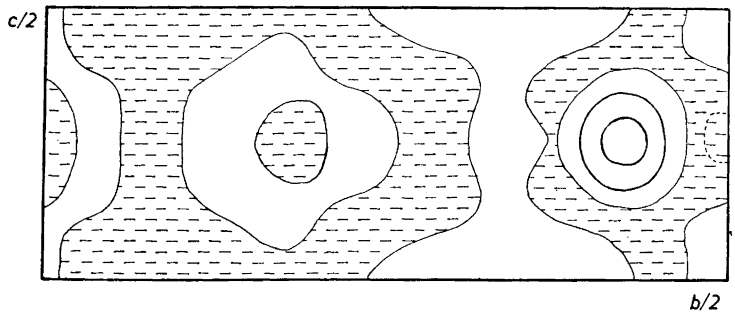

Fig. 1. b). The difference synthesis ϱ $(F(0kl)_{obs} - F(0kl)_{Hf})$. Shadowed areas indicate negative values.

Table 2. Interatomic distances in HfAl.

Hf	4 Hf	3.26 Å	Al	4 Hf	2.86 Å
	2 Hf	3.25		2 Hf	3.07
	4 Al	2.86		1 Hf	2.82
	2 Al	3.07		2 Al	3.25
	1 Al	2.82		2 Al	2.69

distances of about 2.69 Å. The corresponding boron-boron distances in CrB determined by Kiessling are extremely short and are probably due to boron-boron bonds of a covalent type [5,6].

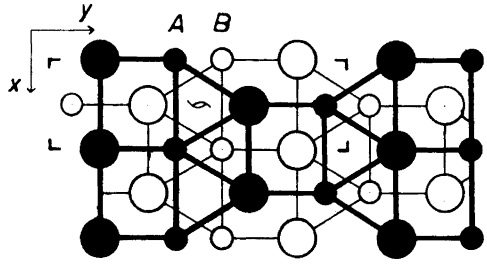

Fig. 2. The $3^3.4^2$ tessilation of HfAl. Large (Hf) and small (Al) black circles represent atoms at $z = \frac{1}{4}$ and open ones atoms at $z = \frac{3}{4}$. The unit cell is indicated by ⌊_.

The isomorphism between HfAl and ThAl (described by Braun [7] on a different system of axes) is also of considerable interest since the aluminium-aluminium distances along the zig-zag chains of the latter phase are reported to be as short as 2.46 Å. It might be that this is a matter of the relative size of the atoms, the ratios r_{Th}/r_{Al} and r_{Cr}/r_B being approximately the same and substantially higher than r_{Hf}/r_{Al}. However, the analogous crystal structure of ThCo does not support this assumption [8] since the cobalt-cobalt distances are 2.77 Å in spite of the atomic radius of cobalt being less than that of aluminium.

The atomic distances within the chains of several other phases of B_f structure, uncluding CaSi[9], CaGe [10], CaSn [10] and YSi [11], are throughout of the long "normal" type.

The author wishes to thank Dr. Arne Magnéli for his never failing support and many valuable discussions.

REFERENCES

1. Edshammar, L.-E. and Andersson, S. *Acta Chem. Scand.* **14** (1960) 223.
2. Edshammar, L.-E. *Acta Chem. Scand.* **14** (1960) 1220.
3. Westman, S. and Magnéli, A. *Acta Chem. Scand.* **11** (1957) 1587.
4. Frank, F. C. and Kasper, J. S. *Acta Cryst.* **12** (1959) 483.
5. Kiessling, R. *Acta Chem. Scand.* **3** (1949) 595.
6. Kiessling, R. *Acta Chem. Scand.* **4** (1950) 209.
7. Braun, P. B. and van Vucht, J. H. N. *Acta Cryst.* **8** (1955) 246.
8. Florio, J. V., Baenziger, N. C. and Rundle, R. E. *Acta Cryst.* **9** (1956) 367.
9. Hellner, E. *Z. anorg. Chem.* **261** (1950) 226.
10. Eckerlin, P., Mayer, H. I. and Wölfel, E. *Z. anorg. Chem.* **281** (1955) 322.
11. Parthé, E. *Acta Cryst.* **12** (1959) 559.

Received October 5, 1960.

ACTA CHEMICA SCANDINAVICA 15 (1961) 407–416

Structure of the Solid Compound Formed by Addition of Two Molecules of Iodine to One Molecule of Pyridine

O. HASSEL and H. HOPE

Universitetets Kjemiske Institutt, Blindern - Oslo, Norway

The crystal structure of the compound pyridine · $2I_2$ has been investigated. The crystals are *monoclinic*, space group $P2_1/c$, with the lattice constants

$a = 4.42$ $b = 15.37$ $c = 17.65$ $\beta = 103.8°$

The unit cell contains four molecules of pyridine and sixteen atoms of iodine. Centrosymmetrical cations — Py_2I^+ — are present which appear to be at least nearly planar.

The remaining iodine atoms form a network built up of centrosymmetrical triiodide ions with an I—I distance of 2.93 Å and of iodine molecules (I—I = 2.74 Å). Each of the "outer" atoms of the I^-_3 ions is linked to two iodine atoms belonging to iodine molecules by bonds of length 3.44 Å. The anionic arrangement closely resembles that found in tetraethyl-ammonium heptaiodide [7]. The N—I distance in the cation (2.16 Å) appears to be a little shorter than the N—I bond observed in simple addition compounds formed by tertiary amines and iodine.

The substance investigated may properly be regarded as dipyridineiodine heptaiodide.

Crystal structure determination of a number of 1:1 addition compounds formed by amines and halogens have been carried out during the last years [1]. The results are consistent and show that such compounds are true "charge transfer" compounds in which one particular halogen atom is linked to the donor (nitrogen) atom, the second halogen atom pointing away from the donor atom. The arrangement N-Hal-Hal has always been found to be *linear* or at least very nearly so. These findings thus contradict the suggestion put forward by Hantzsch [2] that the addition compounds in question should be regarded as salt-like compounds containing halogen substituted ammonium cations and halogen anions. However, no structure determinations of addition compounds formed by amines and halogen with a molar ratio other than 1:1 appears to have been carried out. It was felt that at least one compound containing more halogen molecules than amine molecules should be investigated. From state-

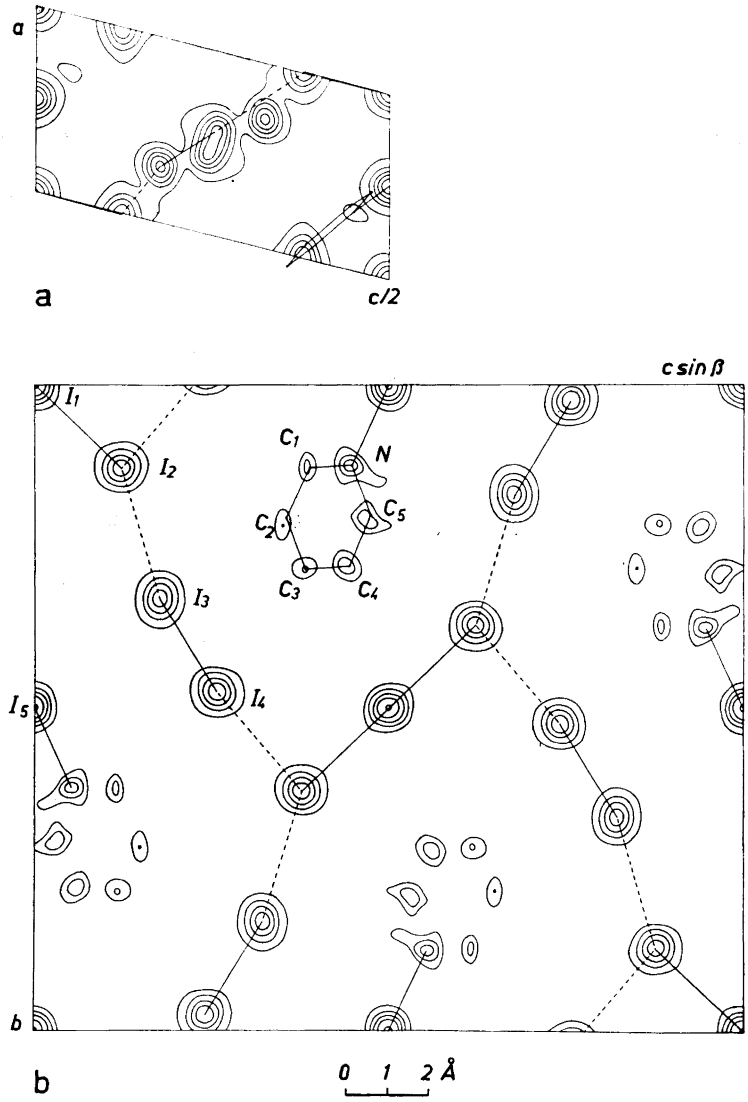

Fig. 1. Electron density maps a) projection along [010] b) projection along [100]. Contours at 10, 30, 50 . . . eÅ^{-2} (iodine) and 4, 6, 8 eÅ^{-2} (light atoms).

ments available in the literature we expected the compound pyridine · $2I_2$ to be sufficiently stable to allow single crystal work to be carried out. This substance was first prepared by Prescott and Trowbridge [3] by adding 1 mole of pyridine to an alcoholic solution containing two moles of iodine, whereby a crystalline substance having the composition $C_5H_5NI_4$ was formed. This sub-

stance may be recrystallized using different solvents, *e.g.* benzene, chloroform, or alcohol.

EXPERIMENTAL

The crystals used in the X-ray analysis were obtained from alcoholic solutions in the form of thin needles.

During the X-ray exposure, which was carried out at room temperature, the crystals were kept in sealed, thin-walled capillary tubes. The intensity data referring to the (0*kl*) zone were obtained using filtered Cu*Kα* radiation, and an integrating Weissenberg camera. The intensities were measured with a microphotometer. The cross section of the crystals was approximately 0.05 × 0.08 mm². The intensity data of the (*h*0*l*) zone were obtained from precession diagrams of crystals having a cross section of about 0.15 × 0.15 mm² using filtered Mo*Kα* radiation. The intensities were measured with a recording photometer. As the spots appeared to be of nearly the same shape, the peak heights were taken as the relative intensities.

248 independent (0*kl*) reflexions, and 97 (*h*0*l*) reflexions were observed. The maximum numbers compatible with the experimental conditions chosen are 331 and 119, respectively.

RESULTS

The crystals are monoclinic, with the space group $P2_1/c$. The unit cell containing four molecules of pyridine and sixteen iodine atoms has the following parameters:

$$a = 4.42 \text{ Å}; \qquad b = 15.37 \text{ Å}; \qquad c = 17.65 \text{ Å}; \qquad \beta = 103.8^0$$

A Patterson projection along [100] revealed that isolated iodine atoms were situated in centers of symmetry, and that centrosymmetric I_3 groups were also present. Approximate co-ordinates for the remaining two iodine atoms of the asymmetric unit could also be determined.

This interpretation of the Patterson projection indicated that the crystals are built up of centrosymmetrical Py_2I^+ resp. I^-_3 ions, the latter being connected by iodine molecules into a network.

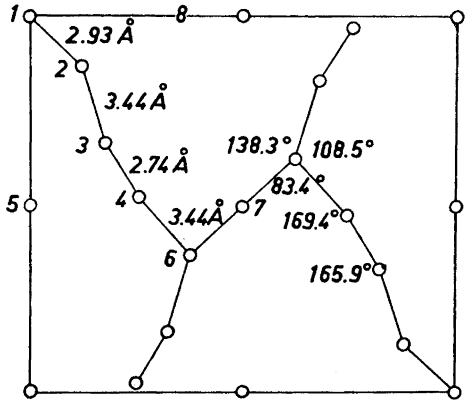

Fig. 2. Distances and angles within the anionic network (compare Fig. 1 b). Estimated standard deviations: I_1-I_2 0.01 Å, other I—I distances 0.02 Å.

Table 1. Final atomic parameters. The anisotropic temperature factor is $\exp(-uh^2-vhk-wk^2)$ (*h,k*, two-dimensional indices of the reflexions). The isotropic temperature factor is $\exp\left(-B\frac{\sin^2\Theta}{\lambda^2}\right)$. For iodine $B = \sqrt{B_{max} \cdot B_{min}}$.

	x	*y*	*z*	*B*	*u*	*v*	*w*
I_1		0	0	2.49	0.00205	0.00123	0.00290
I_1'	0		0	3.72	0.04362	0.01097	0.01449
I_2		0.1288	0.1219	2.99	0.00226	−0.00054	0.00360
I_2'	0.0078		0.3781	5.08	0.07591	0.00803	0.01503
I_3		0.3312	0.1776	3.86	0.00490	−0.00034	0.00274
I_3'	0.3010		0.1774	3.30	0.04704	0.00719	0.01039
I_4		0.4752	0.2581	3.27	0.00307	0.00062	0.00316
I_4'	0.4294		0.2419	3.80	0.04831	−0.00179	0.01304
I_5		0	0.5	2.14	0.00180	0.00078	0.00237
I_5'	0.5		0	3.26	0.04218	0.00713	0.01131
N	0.319	0.123	0.449	4.0			
C_1	0.069	0.126	0.389	4.5			
C_2	−0.067	0.202	0.354	4.5			
C_3	0.083	0.282	0.382	4.5			
C_4	0.342	0.278	0.444	4.5			
C_5	0.444	0.199	0.474	4.5			

In the corresponding Fourier map, obtained by using the signs derived from the Patterson synthesis, peaks due to the iodine atoms appeared near the expected positions, but the lighter atoms did not show up. With the help of the results from the [100] projection a sharpened Patterson projection along [010] was readily interpreted and the corresponding Fourier synthesis worked out (Fig. 1 a).

Using the coordinates obtained from the Fourier syntheses and a temperature factor with $B = 3$ Å^2, the *R* factors obtained for both projections were about 0.16. The coordinates were therefore considered sufficiently accurate to serve as starting values for least squares refinement. The Least Squares Programme used was designed by Curtis for the Ferranti Mercury Computer [4]. Two cycles of refinement of the coordinates and isotropic temperature factors of the [100] projection were first carried out. A Fourier map based on the structure factor signs thus derived revealed, beside the peaks corresponding to the iodine atoms, five additional peaks which clearly indicated the presence of atoms belonging to the pyridine ring. A sixth atom was also indicated, but the height of this peak was considerably lower.

Approximate coordinates of the light atoms were chosen from this Fourier synthesis combined with a model based on the structure of the pyridine molecule [5,6]. Keeping these coordinates fixed, three cycles of least squares refinement of the coordinates of the iodine atoms were carried out, introducing anisotropic temperature factors. The structure factor signs thus obtained served as a basis for the calculation of the Fourier map reproduced in Fig. 1 b. A $F_{obs}-F_I$ synthesis based on the final parameters was also computed. The pyridine ring was clearly brought out with reasonable peak heigths. The

Table 2. Calculated and observed structure factors in the (0*kl*) zone.

k	*l*	F_c	$\|F_o\|$	*k*	*l*	F_c	$\|F_o\|$
0	2	− 56	79		4	− 30	25
	4	110	113		5	252	243
	6	132	144		6	117	122
	8	266	255		7	− 90	93
	10	42	37		8	− 20	23
	12	127	125		9	−121	130
	14	− 69	65		10	− 54	51
	16	170	153		11	71	74
	18	53	51		12	− 28	25
	20	− 2	< 20		13	52	45
1	1	34	40		14	50	40
	2	−192	238		15	− 90	91
	3	− 29	20		16	− 15	< 25
	4	180	176		17	44	40
	5	−107	110		18	− 10	< 23
	6	64	68		19	− 45	40
	7	4	< 16		20	− 18	< 20
	8	− 32	23		21	26	< 20
	9	163	170	4	0	67	37
	10	44	37		1	− 20	20
	11	−127	127		2	72	74
	12	− 81	91		3	− 60	65
	13	18	< 24		4	468	430
	14	35	40		5	154	170
	15	− 8	< 25		6	4	< 15
	16	41	42		7	−185	184
	17	29	< 24		8	147	147
	18	− 56	51		9	126	127
	19	− 28	25		10	11	< 21
	20	1	< 20		11	− 14	< 22
	21	6	20		12	184	187
2	0	204	249		13	− 25	28
	1	49	51		14	81	79
	2	46	51		15	23	28
	3	−262	232		16	29	< 25
	4	389	345		17	13	< 24
	5	51	54		18	7	< 23
	6	− 58	68		19	− 34	40
	7	180	184		20	77	74
	8	290	289		21	30	28
	9	−100	102	5	1	− 90	93
	10	21	25		2	237	229
	11	−126	127		3	130	119
	12	133	125		4	−133	133
	13	115	116		5	11	28
	14	64	65		6	− 41	45
	15	− 12	< 25		7	−100	99
	16	72	62		8	− 5	< 19
	17	0	< 25		9	26	23
	18	15	< 23		10	17	< 21
	19	− 8	< 22		11	− 55	65
	20	66	57		12	25	34
	21	− 14	< 20		13	66	79
3	1	20	20		14	− 15	< 25
	2	−128	122		15	− 30	37
	3	−105	110		16	− 70	68

k	l	F_c	$\|F_o\|$	k	l	F_c	$\|F_o\|$
	17	− 15	< 24		13	88	91
	18	68	65		14	63	68
	19	4	< 20		15	− 47	51
	20	− 18	< 19		16	79	82
6	0	411	394		17	23	< 21
	1	252	246		18	44	42
	2	− 18	17		19	− 7	25
	3	20	25	9	1	86	91
	4	175	176		2	− 83	82
	5	27	25		3	−139	144
	6	168	176		4	− 38	40
	7	−176	190		5	25	28
	8	97	96		6	110	113
	9	110	122		7	23	23
	10	71	74		8	− 30	25
	11	10	< 23		9	− 14	25
	12	153	156		10	− 43	45
	13	7	< 25		11	22	31
	14	− 19	28		12	− 46	48
	15	− 89	88		13	− 35	40
	16	96	91		14	53	57
	17	33	< 23		15	− 17	< 24
	18	44	40		16	− 29	< 22
	19	13	25		17	49	48
	20	10	25		18	− 1	< 19
7	1	47	48		19	− 31	31
	2	− 7	< 17	10	0	72	76
	3	− 36	34		1	− 44	45
	4	68	76		2	132	130
	5	− 81	82		3	−158	153
	6	− 84	88		4	136	139
	7	38	40		5	188	190
	8	− 78	79		6	81	85
	9	107	119		7	− 74	85
	10	144	153		8	92	93
	11	− 79	82		9	52	54
	12	− 75	71		10	65	65
	13	− 10	< 25		11	− 87	88
	14	− 3	< 25		12	59	65
	15	5	< 25		13	24	28
	16	1	< 24		14	76	74
	17	12	< 22		15	32	31
	18	4	< 21		16	29	29
	19	− 18	< 19		17	4	< 20
	20	− 12	20		18	27	31
8	0	246	241	11	1	− 86	85
	1	178	178		2	18	23
	2	144	144		3	95	96
	3	−156	159		4	− 67	65
	4	52	51		5	25	25
	5	55	57		6	78	88
	6	9	< 21		7	− 43	48
	7	6	< 22		8	− 4	< 25
	8	249	263		9	− 25	< 25
	9	32	28		10	− 42	54
	10	72	79		11	− 3	< 25
	11	− 86	88		12	− 16	< 25
	12	2	< 25		13	40	42

k	l	F_c	$\|F_o\|$	k	l	F_c	$\|F_o\|$
	14	40	45		14	64	59
	15	— 8	< 21		15	— 52	42
	16	— 47	42	15	1	48	45
	17	— 40	40		2	37	37
12	0	25	28		3	— 71	68
	1	98	99		4	— 21	28
	2	69	65		5	— 26	28
	3	— 64	65		6	— 16	< 24
	4	138	136		7	36	34
	5	46	45		8	— 20	< 23
	6	161	164		9	2	< 22
	7	— 72	68		10	21	< 21
	8	— 50	48		11	15	< 20
	9	45	45		12	— 19	< 19
	10	82	85		13	— 45	45
	11	— 27	< 25	16	0	75	71
	12	117	116		1	— 14	< 24
	13	31	37		2	112	110
	14	39	42		3	— 42	40
	15	— 36	42		4	— 22	28
	16	17	23		5	54	54
	17	16	20		6	79	82
13	1	— 25	28		7	— 33	42
	2	27	< 25		8	73	68
	3	45	42		9	21	28
	4	29	< 25		10	77	71
	5	3	< 25		11	— 23	28
	6	— 66	68		12	— 13	20
	7	— 18	< 25	17	1	2	< 22
	8	— 59	57		2	— 34	45
	9	— 19	< 25		3	5	< 22
	10	89	85		4	— 30	28
	11	4	< 24		5	— 33	25
	12	— 41	48		6	51	54
	13	3	< 21		7	21	< 20
	14	— 16	< 20		8	1	< 19
	15	0	< 19		9	6	< 19
	16	— 16	< 18		10	— 42	37
14	0	45	42	18	0	19	23
	1	137	125		1	— 15	20
	2	136	127		2	75	79
	3	3	< 25		3	— 47	48
	4	22	< 25		4	32	40
	5	— 14	< 25		5	31	45
	6	72	68		6	96	85
	7	— 54	51		7	23	< 19
	8	76	76		8	— 11	< 19
	9	51	45	19	1	— 33	28
	10	80	79		2	— 25	25
	11	1	< 22		3	32	28
	12	6	< 20		4	12	< 18
	13	16	< 20				

Calculated and observed structure factors in the ($h0l$) zone. Half the absolute F values are given.

h	l'	F_c	$\|F_o\|$	h	l'	F_c	$\|F_o\|$
0	1	− 28	40		7	36	36
	2	54	62		8	6	10
	3	65	86		9	24	20
	4	129	148		10	6	< 6
	5	18	18	3	−11	15	12
	6	61	68		−10	− 24	23
	7	− 39	39		− 9	7	11
	8	80	75		− 8	22	20
	9	23	25		− 7	− 9	8
	10	− 5	12		− 6	− 42	40
	11	13	11		− 5	36	40
	12	13	12		− 4	− 32	35
1	−12	9	10		− 3	41	33
	−11	− 10	8		− 2	− 40	43
	−10	− 25	23		− 1	− 32	29
	− 9	− 38	36		0	64	65
	− 8	− 28	31		1	15	10
	− 7	41	46		2	− 57	58
	− 6	− 56	64		3	20	29
	− 5	3	< 6		4	7	8
	− 4	57	65		5	− 14	15
	− 3	63	75		6	16	12
	− 2	−286	261		7	− 27	20
	− 1	138	133		8	12	10
	0	− 16	21		9	4	< 5
	1	34	34	4	−11	0	< 4
	2	− 66	79		−10	2	< 7
	3	0	< 6		− 9	20	18
	4	12	21		− 8	20	18
	5	82	88		− 7	12	11
	6	− 88	95		− 6	36	35
	7	5	< 8		− 5	− 1	< 8
	8	21	22		− 4	55	54
	9	− 13	14		− 3	46	41
	10	− 2	< 7		− 2	− 18	22
	11	− 1	< 6		− 1	43	49
2	−12	12	11		0	46	46
	−11	− 4	< 7		1	16	15
	−10	30	30		2	24	26
	− 9	− 14	13		3	27	28
	− 8	64	68		4	3	< 8
	− 7	24	20		5	45	36
	− 6	− 7	< 7		6	− 10	10
	− 5	35	35		7	11	10
	− 4	183	171	5	− 9	− 3	< 6
	− 3	− 27	30		− 8	− 3	< 7
	− 2	108	98		− 7	11	11
	− 1	21	25		− 6	− 16	17
	0	121	125		− 5	− 4	8
	1	92	92		− 4	24	29
	2	3	< 6		− 3	− 17	22
	3	− 11	15		− 2	4	< 8
	4	129	141		− 1	− 1	< 8
	5	14	16		0	− 2	< 8
	6	8	10		1	0	< 8

h	l'	F_c	$\|F_o\|$	h	l'	F_c	$\|F_o\|$
5	2	8	< 8		− 3	15	18
	3	− 24	18		− 2	10	12
	4	22	20		− 1	8	8
6	− 5	19	22		0	8	10
	− 4	2	< 6				

final coordinates of the light atoms (given in Table 1) were derived from the difference synthesis combined with the pyridine model just mentioned.

Returning to the [010] projection three cycles of least squares refinement were carried out using the x coordinates of the iodine atoms obtained from the [010] Fourier projection and the final z coordinates derived from the [100] projection as initial values. Anisotropic temperature factors for the iodine atoms were introduced. From the pyridine model and the data from the [100] projection the x coordinates of the light atoms were estimated. These coordinates and the temperature factors with $B = 4.0$ Å^2 (nitrogen), and $B = 4.5$ Å^2 (carbon) were not refined. Due to overlapping the z coordinate of I_4 was not refined.

The final parameters listed in Table 1 were used in calculating F_c in Table 2, in which a comparison of calculated and observed F values is given. The R factor for the (100)-zone is 0.07. If the contribution from the light atoms is disregarded the R factor becomes 0.09. For the (010)-zone the R factor is 0.11. All R factors were computed excluding unobserved reflexions.

The I—I distances and I—I—I angles are given in Fig. 2 which corresponds to the [100] projection (Fig. 1 b). The I—I distance within the I^-_3 ion (2.93 Å) is approximately that previously found in other crystals. The distance between the two iodine atoms of the I_2 molecule (2.74 Å) is only slightly larger than in the free molecule. As would be expected the two distances between an iodine atom belonging to an I^-_3 ion and the two nearest iodine atoms belonging to I_2 molecules are considerably larger. These two I—I distances were both found equal to 3.44 Å.

The shortest distance between a C atom of the pyridine ring and an I atom is 4.3 Å. The whole anionic arrangement of I^-_3 ions connected by iodine molecules into a network very much resembles that found by Havinga in tetraethyl-ammonium heptaiodide [7].

The structure of the Py_2I^+ ion is of considerable interest. The present compound in which the iodine atoms contribute so heavily to the reflexion of X-ray is not very well suited for an accurate determination of the positions of the carbon and nitrogen atoms, but it appears certain from our results that the ion, besides having a center of symmetry, is nearly planar. The N—I distance cannot, however, be determined very accurately. The value deduced from the coordinates listed in Table 1 (2.16 Å) may therefore have an error of $\pm$ 0.1 Å. We think, however, that the N—I separation is probably shorter than that observed in simple addition compounds formed by tertiary amines and iodine (2.30 Å). The existence of the Py_2I^+ ion suggested by Carlsohn [8] has been confirmed by the present investigation. It would appear interesting to study the structure of this ion in a simple salt like the nitrate or perchlorate.

Structure determinations so far carried out seem to indicate that the ion PyI^+ is rather unstable.

This investigation has been sponsored by the *United States Air Force Development Command* under contract AF 61 (052)-71.

REFERENCES

1. Hassel, O. *Proc. Chem. Soc. London* **1957** 250; *Mol. Phys.* **1** (1958) 241.
2. Hantzsch, A. *Ber.* **38** (1905) 2161.
3. Prescott, A. B. and Trowbridge, P. F. *J. Am. Chem. Soc.* **17** (1895) 859.
4. Curtis, A. R. *A.E.R.E. Mercury Autocode Prog. No. 29*, Atomic Energy Research Div. Harwell, Berks.
5. Bak, B., Hansen, L. and Rastrup-Andersen, J. *J. Chem. Phys.* **22** (1954) 2013.
6. Almenningen, A., Bastiansen, O. and Hansen, L. *Acta Chem. Scand.* **9** (1955) 1306.
7. Havinga, E. E. *Thesis*, Groningen 1957.
8. Carlsohn, H. *Habilitationsschrift*, S. Hirzel, Leipzig 1932.

Received October 26, 1960.

ACTA CHEMICA SCANDINAVICA 15 (1961) 417–426

Optical Rotatory Dispersion Studies

XLII *. Disulfides and Diselenides **

CARL DJERASSI

Department of Chemistry, Stanford University, Stanford, Calif., U.S.A.

ARNE FREDGA and BERNDT SJÖBERG

Chemical Institute, University of Uppsala, Uppsala, Sweden

The rotatory dispersion of a number of disulfides and diselenides has been investigated and discussed. The steric relations of analogous disulfides and diselenides can be conveniently correlated by means of their dispersion curves, the same sign of the Cotton effects implying identical configuration.

Most of the optical rotatory dispersion work during the past five years (for reviews see Refs.[1–3]) has dealt with ketones and aldehydes. These compounds have their first ultraviolet absorption band in a readily accessible region of the spectrum (280—320 mμ) with such a low extinction ($\varepsilon < 100$) that it is usually possible to determine the optical rotation through this region and study the anomalous dispersion curves (for nomenclature see Refs.[3–4]). It has been clearly demonstrated that the shape of the anomalous dispersion curves can be correlated empirically to certain structural and steric features of the compounds, and in this way Cotton effect curves have found extensive use in the solution of various organic chemical problems [1–3]. It has also been shown [5,6] that the configurational relationship of some types of simple compounds, possessing only plain dispersion curves, can be deduced from the curves if the measurements are extended close to the anisotropic absorption region. It is evident, however, that plain curves cannot be as versatile as the more detailed Cotton effect curves, and the usefulness of optical rotatory dispersion in organic and theoretical chemistry lies principally in the area of Cotton effect curves.

* Paper XLI, C. Djerassi and J. Staunton. *In press.*

** Supported in part by grant No. CRTY-5061 from the *National Cancer Institute of the National Institutes of Health*, U.S. Public Service.

Some chromophores other than the carbonyl group may also give Cotton effects in a wavelength region currently accessible to spectropolarimetric work, and these chromophores have already been listed [3,7]. Because of the important biological functions of some organic disulfides, *e.g.* cystine and 6,8-thioctic acid, the disulfide group has recently attracted great interest, especially its energetics and spectral properties [8,9]. Despite this, however, prior to the present investigation the optical rotatory dispersion of disulfides has only been studied with cystine (I). This investigation [10] revealed a negative dispersion curve (Fig. 1) with a first extremum at 268 mμ, which seemed to be associated with a Cotton effect centered about the disulfide band at 255 mμ. Diselenides are closely analogous to disulfides in many respects and their ultraviolet absorption in particular is caused by similar electron excitations [11]. However, the diselenides absorb at longer wavelengths than the corresponding disulfides, hence it appeared likely that the optical rotatory dispersion curve of selenocystine (II) could be measured through the absorption region at 305 mμ. This proved to be the case and it was thus possible to demonstrate a Cotton effect centered about the low intensity absorption band (Fig. 1), showing that the diselenide band is optically active. These results suggest that the extremum in the dispersion curve of cystine is the through of a negative Cotton effect associated with the disulfide band. Similarly, (+)-*a*-dithio-*bis*propionic acid (III), (+)-dithio-*bis*phenylacetic acid (IV) and the corresponding diselenides (V and VII) exhibit very steep plain dispersion curves to the limit of the experimental measurements (Fig. 2), indicating imminent appearence of the first extrema of Cotton effects associated with the disulfide and diselenide absorption bands around 250 and 290 mμ, respectively. Although it was not possible to demonstrate any definite irregularities in the dispersion curves around the absorption bands of the diselenides V and VII, this may be due to the rather dilute solutions used and a weak positive Cotton effect may be hidden in a steep positive background curve.

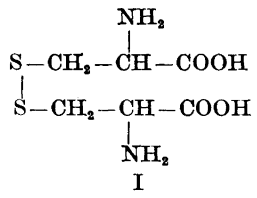

I

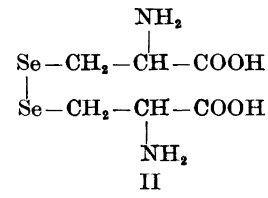

II

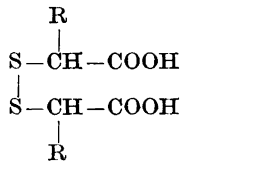

III R = CH_3
IV R = C_6H_5

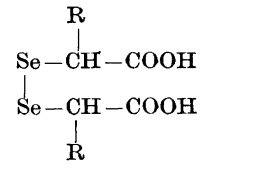

V R = CH_3
VI R = C_2H_5
VII R = C_6H_5

The location of the disulfide and diselenide absorption band varies considerably with the structure of the compounds [8,9], and a large bathochromic

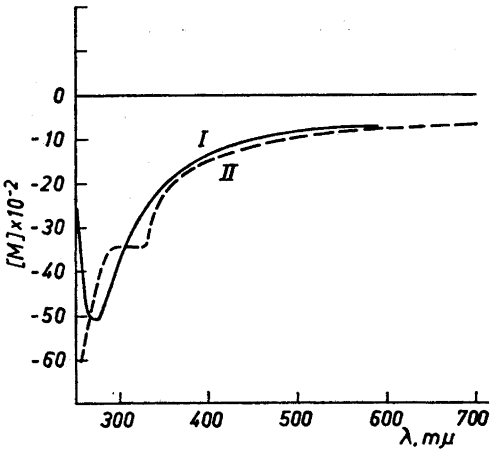

Fig. 1. Optical rotatory dispersion curves of (−)-cystine (I) and (−)-selenocystine (II).

shift is encountered when the disulfide or the diselenide group is incorporated in a six- and especially in a five-membered ring. The rotatory dispersion curves of (+)-1,2-dithiane-3,6-dicarboxylic acid (VIII) and (+)-1,2-diselenane-3,6-dicarboxylic acid (IX) are shown in Fig. 3. The disulfide shows an anomalous curve with a peak at 300 mμ, and the positive Cotton effect is definitely related to the absorption band, indicated by a shoulder at 280 mμ [12]. For the diselenide,

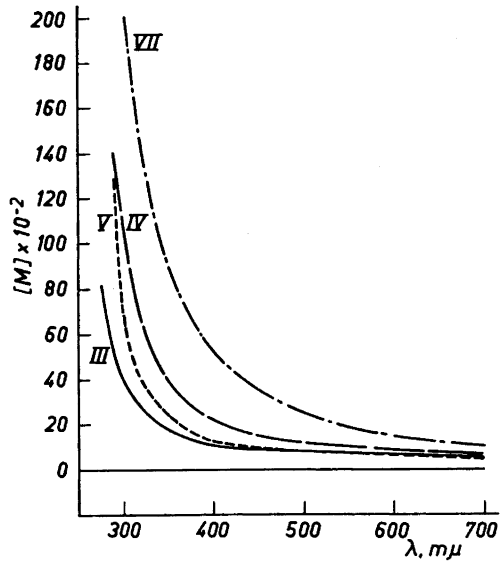

Fig. 2. Optical rotatory dispersion curves of (+)-α-dithio-*bis*propionic acid (III), (+)-dithio-*bis*phenylacetic acid (IV), (+)-α-diseleno-*bis*propionic acid (V) and (+)-diseleno-*bis*phenylacetic acid (VII).

which has its first absorption band at 341 mμ [11], it was possible to determine both the peak and the through of the Cotton effect.

The effect of moving the disulfide group away from the asymmetric center can be seen by comparing the dispersion curves of 1,2-dithiane-3,6-dicarboxylic acid (VIII) and 1,2-dithiane-4-carboxylic acid (X). The latter acid, which has the disulfide group in the β-position to the asymmetric center, also shows a strong Cotton effect (Fig. 3) related to the ultraviolet absorption found at 298 mμ [13]. The disulfide and diselenide groups apparently give rise to Cotton effects when they are both adjacent to the asymmetric center (as for III—IX) or one carbon atom removed from it (as for I, II and X). Whether this will be generally true is as yet impossible to say, since only β-compounds with a carboxyl group attached to the assymmetric center have been studied. The vicinal action from the carboxyl group may be important with respect to the anisotropy of the disulfide and diselenide groups.

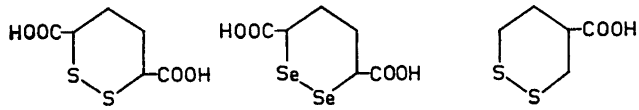

VIII IX X

A considerable bathochromic shift can be expected if the disulfide groups are conjugated with an aromatic system. The ultraviolet spectrum of 1,1'-dinaphthylene-2,2'-disulfide (XI) [14] is rather complex, with absorption bands at 238, 262, 318, 348 and 400 mμ (shoulder). It is likely that the low intensity, 400 mμ, band is related to an excitation at the conjugated system extended over the disulfide group, and a negative Cotton effect is also found in this wavelength region (Fig. 4).

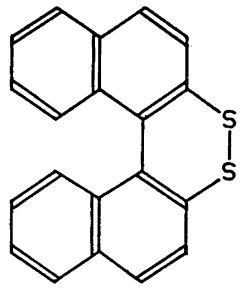

XI

The five-membered cyclic disulfide 6,8-thioctic acid (XII) has an important function in the decarboxylation of α-keto acids [15] and possibly also in photosynthesis [16]. It is therefore natural that special emphasis has been placed on studies of the chemistry of 1,2-dithiolane compounds [15,17]. Disulfides with a five-membered ring absorb at longer wavelengths than those with a six-membered ring, the values for 1,2-dithiolane and 1,2-dithiane being 334 and 295 mμ, respectively [18]; 1,2-dithiolane compounds should therefore be very suitable for spectropolarimetric studies. It was also found (Fig. 5) that the dispersion

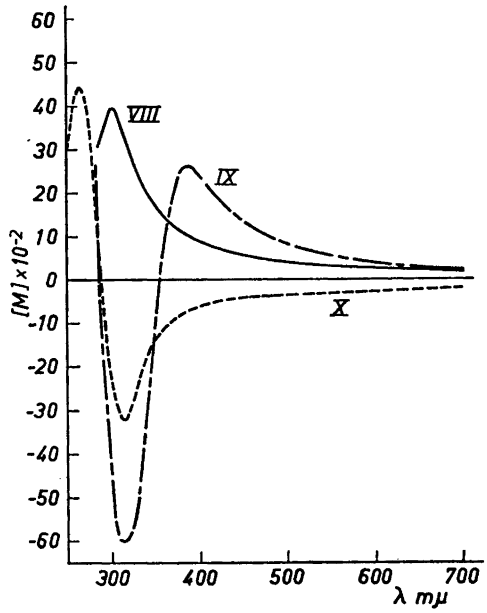

Fig. 3. Optical rotatory dispersion curves of (+)-1,2-dithiane-3,6-dicarboxylic acid (VIII), (−)-1,2-diselenane-3,6-dicarboxylic acid (IX) (−)-1,2-dithiane-4-carboxylic acid (X).

curve of 6,8-thioctic acid (XII) has a Cotton effect which is clearly related to the disulfide absorption band.

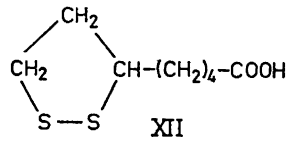

XII

The anisotropy of the disulfide group is even more strikingly demonstrated with some epidithio steroids. In Fig. 6 is shown the dispersion curve of 1*α*,5*α*-epidithioandrostane-3,17-dione (XIII). The curve has a negative Cotton effect with a trough at 405 mμ and a peak at 340 mμ superimposed on the strongly rotating positive Cotton effect [20] of androstane-3,17-dione. Selective reduction of the keto groups of XIII to 1*α*,5*α*-epidithioandrostane-3*α*,17*β*-diol (XIV) causes no appreciable changes in the negative Cotton effect, but the positive Cotton effect typical for androstane-3,17-dione disappears. Further reduction to 3*α*,17*β*-dihydroxyandrostane-1*α*,5*α*-dithiol (XV) affords a plain dispersion curve. The ultraviolet absorption of these three steroids has been investigated in detail [21], and a comparison between the absorption and dispersion curves shows an almost exact correspondence of the negative Cotton effect with the absorption maximum of the disulfide group. The very small irregularities in

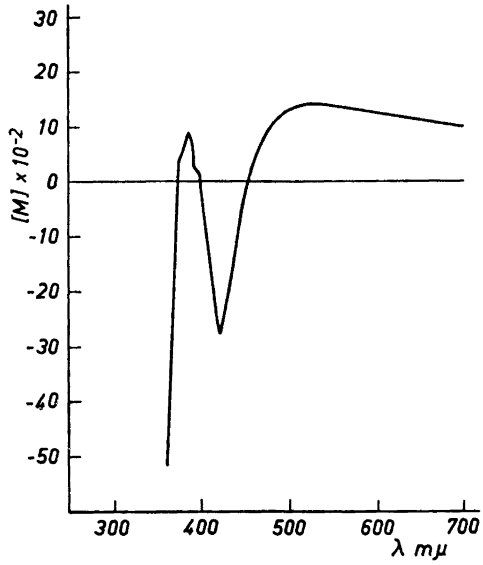

Fig. 4. Optical rotatory dispersion curve of (+)-1,1′-dinaphthylene-2,2′-disulfide (XI).

the rotatory dispersion curve of the dithiol XV at 340 and 405 mμ is most probably due to the presence of a trace of the disulfide XIV which can also be seen in the absorption curves [21] (Fig. 7).

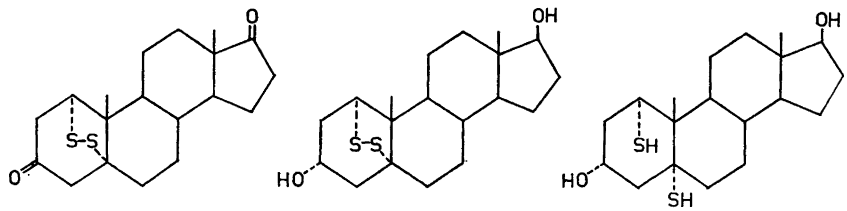

XIII XIV XV

Optically active selenocystine (II) has been prepared [22] from L-(—)-serine in a reaction sequence that did not involve the asymmetric center. The analogous configuration of cystine and selenocystine of the same sign of rotation (at the D-line) could in addition to this also be determined [22] by use of the quasi-racemate method [23]. As can be seen in Fig. 1 these two amino acids have both negative Cotton effect curves.

(+)-*a*-Dithio-*bis*propionic acid (III) and (+)-*a*-diseleno-*bis*propionic acid (V) have similar rotatory dispersion curves (Fig. 2), and the configuration of these two acids has also been shown to be the same [24]. The similarity in the rotational shifts of dithio-*bis*phenylacetic acid (IV) and diseleno-*bis*phenylacetic acid (VII) in different solvents at the D-line has been presented as evidence for the identical configuration of the acids with the same sign of rota-

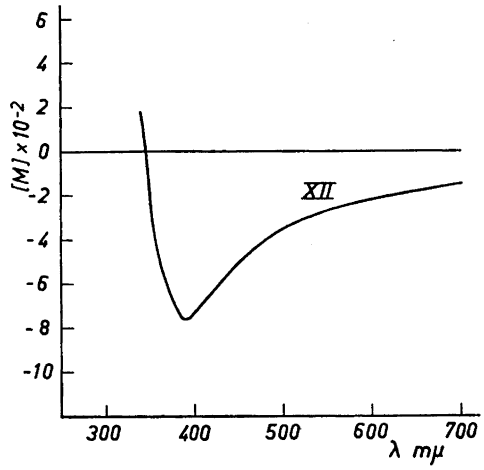

Fig. 5. Optical rotatory dispersion curve of (—)-6,8-thioctic acid (XII).

tion [25], and here too the dispersion curves are very similar (Fig. 2), the main difference being that the rotatory dispersion curves of the diselenides are relatively displaced towards higher wavelengths, due to the diselenides absorb-

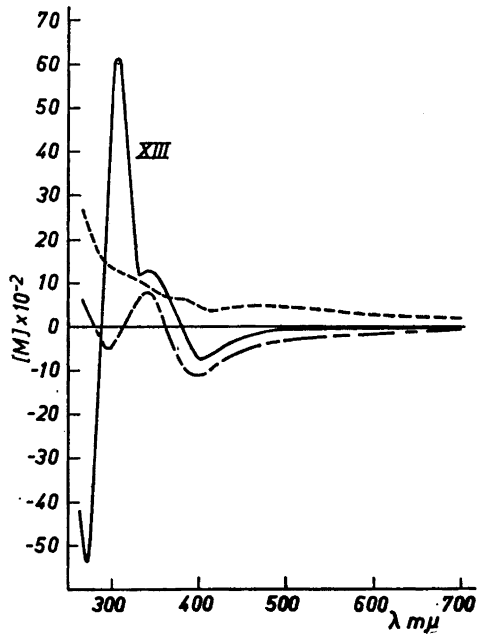

Fig. 6. Optical rotatory dispersion curves of 1α,5α-epidithioandrostane-3,17-dione (XIII), 1α,5α-epidithioandrostane-3α,17β-diol (XIV) ——— and 3α,17β-dihydroxyandrostane-1α,5α-dithiol (XV) - - - -.

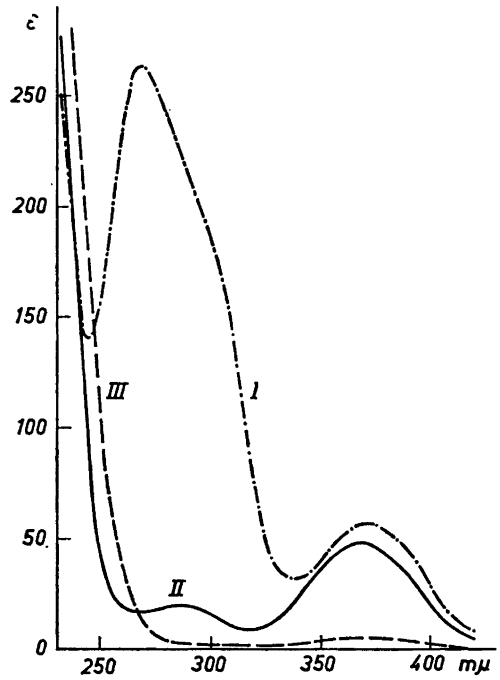

Fig. 7. Ultraviolet absorption spectra of 1α,5α-epidithioandrostane-3,17-dione (XIII) (curve I), 1α,5α-epidithioandrostane-3α,17β-diol (XIV) (curve II) and 3α,17β-dihydroxyandrostane-1α,5α-dithiol (XV) (curve III).

ing at higher wavelengths than the corresponding disulfides. The configurational identity of (+)-1,2-dithiane-3,6-dicarboxylic acid (VIII) and (+)-1,2-diselenane-3,6-dicarboxylic acid (IX) has been established by careful studies of the two-component mixtures of these acids [26,27]. It can be seen in Fig. 3 that the optical rotatory dispersion curves in this case also will give direct information about the steric relationship between the compounds.

The use of optical rotatory dispersion curves for the stereochemical correlations of disulfides and diselenides is well illustrated by the results outlined above. From these examples it is evident that the sterochemistry of analogous disulfides and diselenides can be correlated conveniently by means of their dispersion curves, the same sign of the Cotton effects implying identical configuration.

EXPERIMENTAL *

(−)-Cystine (I) R.D. (Fig. 1) in 0.1 N hydrochloric acid. The dispersion curve is reproduced from J. A. Schellman [10].

(−)-Selenocystine (II) [22] R.D. (Fig. 1) in 0.1 N hydrochloric acid (*c* 0.105): $[M]_{700}$ −650°, $[M]_{589}$ −770°, $[M]_{320}$ −3 460°, $[M]_{290}$ −3 450°, $[M]_{260}$ −6 060°.

* Several of the dispersion curves were measured by Mrs. T. Nakano to whom we express our thanks.

(+)-α-Dithio-bispropionic acid (III)[28] R.D. (Fig. 2) in methanol (*c* 0.150), temp 31°: $[M]_{700}$ + 480°, $[M]_{589}$ + 750°, $[M]_{400}$ + 1 040°, $[M]_{350}$ + 1 820°, $[M]_{300}$ + 4 230°, $[M]_{275}$ +8 120°.

(+)-Dithio-bisphenylacetic acid (IV)[29] R.D. (Fig. 2) in methanol (*c* 0.149), temp. 31°: $[M]_{700}$ + 690°, $[M]_{589}$ + 920°, $[M]_{400}$ + 2 200°, $[M]_{350}$ + 3 890°, $[M]_{300}$ + 10 100°, $[M]_{287.5}$ + 13 900°.

(+)-α-Diseleno-bispropionic acid (V)[25] R.D. (Fig. 2) in methanol (*c* 0.142), temp. 29°: $[M]_{700}$ + 380°, $[M]_{589}$ + 450°, $[M]_{400}$ + 880°, $[M]_{350}$ + 1 330°, $[M]_{300}$ + 4 050°; (*c* 0.028): $[M]_{270}$ + 9 780°.

(+)-α-Diseleno-bis-n-butyric acid (VI)[25] R.D. in methanol (*c* 0.095), temp. 29°: $[M]_{700}$ + 370°, $[M]_{589}$ + 510°, $[M]_{400}$ + 1 190°, $[M]_{350}$ + 2 600°, $[M]_{300}$ + 6 740°, $[M]_{290}$ + 12 900°.

(+)-Diseleno-bisphenylacetic acid (VII)[25] R.D. (Fig. 2) in methanol (*c* 0.190), temp. 26°: $[M]_{700}$ + 990°, $[M]_{589}$ + 1 510°, $[M]_{400}$ + 5 180°, $[M]_{350}$ + 9 540°; (*c* 0.038): $[M]_{300}$ + 19 700°, $[M]_{290}$ + 23 800°.

(+)-1,2-Dithiane-3,6-dicarboxylic acid (VIII)[26] R.D. (Fig. 3) in methanol (*c* 0.092), temp. 27°: $[M]_{700}$ + 190°, $[M]_{589}$ + 260°, $[M]_{400}$ + 920°; (*c* 0.018): $[M]_{305}$ + 3 920°, $[M]_{285}$ + 3 060°.

(+)-1,2-Diselenane-3,6-dicarboxylic acid (IX)[25] R.D. (Fig. 3) in methanol (*c* 0.091), temp. 28°: $[M]_{700}$ + 210°, $[M]_{589}$ + 400°, $[M]_{400}$ + 2 420°; (*c* 0.018): $[M]_{387.5}$ + 2 620°, $[M]_{315}$ −6 010°, $[M]_{282.5}$ + 2 660°.

(−)-1,2-Dithiane-4-carboxylic acid (X)[13] R.D. (Fig. 3) in methanol (*c* 0.148), temp. 25°: $[M]_{700}$ −230°, $[M]_{589}$ −280°, $[M]_{400}$ −590°, $[M]_{315}$ −3 200°, $[M]_{265}$ + 4 420°, $[M]_{250}$ + 2 920°.

(+)-1,1'-Dinaphthylene-2,2'-disulfide (XI)[14] R.D. (Fig. 4) in dioxane (*c* 0.090), temp. 25°: $[M]_{700}$ + 980°, $[M]_{589}$ + 1 270°, $[M]_{525}$ + 1 390°, (*c* 0.014): $[M]_{422.5}$ −2 750°, $[M]_{387.5}$ + 880°, $[M]_{360}$ −5 150°.

(−)-6,8-Thioctic acid (XII)[30] R.D. (Fig. 5) in methanol (*c* 0.136), temp. 27°: $[M]_{700}$ −150°, $[M]_{589}$ −220°, $[M]_{390}$ −760°; (*c* 0.034): $[M]_{340}$ +180°.

1α,5α-Epidithioandrostane-3,17-dione (XIII)[19] R.D. (Fig. 6) in methanol (*c* 0.095), temp. 24°: $[M]_{700}$ −30°, $[M]_{589}$ −30°, $[M]_{402.5}$ −730°, $[M]_{342.5}$ + 1 270°, $[M]_{322.5}$ + 1 190°; (*c* 0.019): $[M]_{307.5}$ + 6 110°, $[M]_{270}$ −5 360°, $[M]_{262.5}$ −4 220.

1α,5α-Epidithioandrostane-3α,17β-diol (XIV)[19] R.D. (Fig. 6) in methanol (*c* 0.100), temp. 23°: $[M]_{700}$ −60°, $[M]_{589}$ −170°, $[M]_{400}$ −1 120°, $[M]_{342.5}$ + 760°, $[M]_{295}$ −510°, $[M]_{265}$ + 600°.

3α,17β-Dihydroxyandrostane-1α,5α-dithiol (XV)[19] R.D. (Fig. 6) in methanol (*c* 0.095), temp. 25°: $[M]_{700}$ + 200°, $[M]_{589}$ + 230°, $[M]_{450}$ + 460°, $[M]_{415}$ + 330°, $[M]_{370}$ + 630° (infl.), $[M]_{300}$ + 1 350°, $[M]_{265}$ + 2 780°.

REFERENCES

1. Djerassi, C. *Bull. soc. chim. France* **1957** 741.
2. Djerassi, C. *Record Chem. Progr. Kresge-Hooker Sci. Lib.* **20** (1959) 101.
3. Djerassi, C. *Optical Rotatory Dispersion: Applications to Organic Chemistry*, McGraw-Hill Book Co. New York 1960.
4. Djerassi, C. and Klyne, W. *Proc. Chem. Soc.* **1957** 55.
5. Sjöberg, B. *Acta Chem. Scand.* **14** (1960) 273.
6. Sjöberg, B. *Arkiv Kemi* **15** (1960) 451.
7. Klyne, W. in Raphael, R. A., Taylor, E. C. and Wynberg, H. (Eds.) *Advances in Organic Chemistry: Methods and Results*, Interscience Publishers, Inc., New York 1960, Vol. 1, pp. 239–348.
8. Bergson, G. *Arkiv Kemi* **12** (1958) 233; Bergson, G. and Schotte, L. *Ibid.* **13** (1958) 43.
9. Bergson, G. *Arkiv Kemi. In press.*
10. Schellman, J. A. *Ref.*[3], p. 224.
11. Bergson, G. *Arkiv Kemi* **13** (1958) 11.
12. Schotte, L. *Arkiv Kemi* **8** (1955) 579.
13. Claeson, G. and Langsjoen, A. *Acta Chem. Scand.* **13** (1959) 840.
14. Amarego, W. L. F. and Turner, E. E. *J. Chem. Soc.* **1957** 13.
15. Reed, L. J. in Nord, F. F. (Ed.) *Advances in Enzymol.* **18** (1957) 319.

16. Calvin, M. and Barltrop, J. A. *J. Am. Chem. Soc.* **74** (1952) 6153.
17. Schotte, L. *Arkiv Kemi* **9** (1956) 441.
18. Barltrop, J. A., Hayer, P. M. and Calvin, M. *J. Am. Chem. Soc.* **76** (1954) 4348.
19. Tweitt, R. C. and Dodson, R. M. *J. Am. Chem. Soc.* **81** (1959) 4409.
20. Djerassi, C., Foltz, E. W. and Lippman, A. E. *J. Am. Chem. Soc.* **77** (1955) 4354.
21. Bergson, G., Sjöberg, B., Tweit, R. C. and Dodson, R. M. *Acta Chem. Scand.* **14** (1960) 922.
22. Fredga, A. *Svensk Kem. Tidskr.* **49** (1937) 124.
23. Fredga, A. *Tetrahedron* **8** (1960) 126.
24. Fredga, A. *Arkiv Kemi, Mineral Geol.* **12B** (1936) No. 22.
25. Fredga, A. *Uppsala Universitets Årsskrift* **1935:5**, 184.
26. Fredga, A. *Arkiv Kemi, Mineral Geol.* **12A** (1938) No. 27.
27. Rosenberg, A. and Schotte, L. *Arkiv Kemi* **8** (1955) 143.
28. Fredga, A. *Arkiv Kemi, Mineral Geol.* **12A** (1937) No. 13.
29. Fredga, A. *Acta Chem. Scand.* **4** (1960) 1307.
30. Walton, E., Wagner, A. F., Peterson, L. H., Holly, F. W. and Folkers, K. *J. Am. Chem. Soc.* **76** (1954) 4748.

Received October 4, 1960.

ACTA CHEMICA SCANDINAVICA 15 (1961) 427–455

Short Communications

Note on the Thermal Expansion of the Wolfram Bronzes of Potassium, Rubidium and Cesium

PER-ERIK WERNER, PEDER KIERKEGAARD and ARNE MAGNÉLI

Institute of Inorganic and Physical Chemistry, University of Stockholm, Stockholm, Sweden

The bronze samples used in this investigation were prepared by reducing mixtures of alkali carbonate and wolfram trioxide with hydrogen gas at about 600°C [1]. The products were purified by boiling alternately with concentrated alkali carbonate solution, concentrated hydrochloric acid and aqua regia. The chemical analysis was in most cases confined to a determination of the alkali content by heating the bronze in a stream of hydrogen chloride gas and oxygen at about 500°C for up to 5 h and titrating the residual alkali chloride according to Mohr. In some instances, the wolfram content was also determined [2].

X-Ray investigation of the preparations was carried out with powder methods using a Guinier camera with strictly monochromatized CuKa_1 radiation for the room temperature work and employing techniques described earlier [3]. The accuracy of the unit cell parameters thus obtained should be better than that previously reported by one of the present authors. The data given in Table 1 were thus obtained.

The studies at elevated temperatures were made using a Norelco diffractometer (CuK radiation) provided with a vacuum furnace producing a maximum temperature

Table 2. Coefficients of linear thermal expansion of wolfram bronzes.

Sample	Axis	Temperature region	β(/°C) × 10^6
$K_{0.30}WO_3$	*a*	20–545°C	(6 ± 1)
		545–750°C	−(12 ± 3)
	c	20–750°C	(15 ± 3)
$Rb_{0.27}WO_3$	*a*	20–500°C	(7 ± 2)
		700–900°C	0
		900–970°C	−(6 ± 3)
	c	20–970°C	(12 ± 3)
$Cs_{0.31}WO_3$	*a*	20–720°C	(2.0±0.7)
	c	20–720°C	(4 ± 1)
$K_{0.45}WO_3$	*a*	20–765°C	(4.8±0.5)
	c	20–765°C	(5 ± 2)
$K_{0.52}WO_3$	*a*	20–740°C	(4.8±0.5)
	c	20–740°C	(3 ± 1)

Table 1. Unit cell dimensions of wolfram bronzes.

Sample	Structural type	Unit cell dimensions at room temperature	
		a Å	*c* Å
$K_{0.30}WO_3$	hexagonal [5]	7.385 ± 0.002	7.513 ± 0.005
$Rb_{0.27}WO_3$	»	7.394 ± 0.002	7.516 ± 0.004
$Cs_{0.31}WO_3$	»	7.406 ± 0.002	7.608 ± 0.004
$K_{0.45}WO_3$	tetragonal [4]	12.297 ± 0.004	3.836 ± 0.002
$K_{0.52}WO_3$	»	12.308 ± 0.003	3.842 ± 0.001

of the specimen of more than 1 000°C [6]. The coefficients of linear thermal expansion β found for the various specimens are listed in Table 2.

Data on the thermal expansion of cubic sodium wolfram bronze specimens from room temperature to 600°C have been reported by Rosen, Post and Banks [7], who also studied the thermal expansion of wolfram trioxide within this interval [8]. They found that cubic sodium bronzes show expansion coefficients of $(11.8 \pm 0.4) \times 10^{-6}$/°C that vary with the content of sodium. The coefficients change sharply at the transition temperatures to values around 4.5×10^{-6}/°C which vary with the sodium content. Wolfram trioxide shows a similar transition near 330°C which manifests itself as a change in the low-temperature monoclinic structure to an orthogonal, very probably orthorhombic, form above this temperature. The coefficients of expansion of the *a* and *c* axes are both close to 13×10^{-6}/°C below 300°C and about 18×10^{-6}/°C for the high-temperature form. In the *b* direction, however, the transformation of low- to high-temperature structure is accompanied by a change in the expansion coefficient from 14×10^{-6}/°C to -1.3×10^{-6}/°C.

The present study has given results for the tetragonal potassium wolfram bronze samples which are of the same magnitude as those obtained by Rosen, Post and Banks [7] for the sodium bronze above the transition temperature.

The anomalous thermal expansion behaviour of hexagonal potassium wolfram bronze at 545°C is rather similar to those occurring in the cubic sodium bronzes and in wolfram trioxide. This may indicate similarities in the so far unknown transitional mechanisms.

It is obvious from Table 1 that the unit cell dimensions of the hexagonal potassium and rubidium wolfram bronzes are almost exactly the same and that the cesium bronze unit is only slightly larger. This indicates that the wolfram and oxygen atoms form a rather rigid threedimensional network, the interstices of which should be of appropriate size to accomodate the potassium or rubidium atoms while the cesium atoms cause a slight expansion of the holes [5]. These minor structure differences may be associated with the differences in thermal expansion shown by the three hexagonal bronzes (*cf.* Table 2). Thus the potassium and rubidium compounds behave analogously up to about 500°C. The change in the rubidium compound is certainly not an abrupt one as in the potassium bronze but extends over a wide temperature interval. However, above 900°C, the two bronzes again behave similarly. The cesium bronze on the other hand shows a thermal expansion which is substantially less than those of the potassium and rubidium compounds.

This investigation has been carried out within a research programme sponsored in part by the *Office, Chief of Research and Development, U.S. Department of Army* through its European Research Office.

1. Magnéli, A. and Blomberg, B. *Acta Chem. Scand.* **5** (1951) 372.
2. Magnéli, A. *Arkiv Kemi* **1** (1949) 273.
3. Westman, S. and Magnéli, A. *Acta Chem. Scand.* **11** (1957) 1587.
4. Magnéli, A. *Arkiv Kemi* **1** (1949) 213.
5. Magnéli, A. *Acta Chem. Scand.* **7** (1953) 315.
6. Kierkegaard, P. and Marinder, B.-O. *To be published.*
7. Rosen, C., Post, B. and Banks, E. *Acta Cryst.* **9** (1956) 477.
8. Rosen, C., Banks, E. and Post, B. *Acta Cryst.* **9** (1956) 475.

Received January 26, 1961.

Bromination and Subsequent Ozonisation of Ethyl 2,6-Dimethylbenzo [1.2-b, 4.5-b'] difuran-3,7-dicarboxylate

ERLING BERNATEK, TORE LEDAAL and SIGURD STEINSVIK

Universitetets Kjemiske Institutt, Blindern - Oslo, Norway

Ethyl 2,6-dimethylbenzo[1.2-b, 4.5-b'] difuran-3,7-dicarboxylate I was chlorinated by Ikuta in 1892 [1] and chlorine was found to attack the 4- and 8- position giving a dichloro compound II.

Ikuta found an independent synthesis of II through the reaction between chloranil and sodium acetoacetic ester. Two keto-ester groups were thus introduced in the quinone while subsequent reduction and ring-closure afforded II.

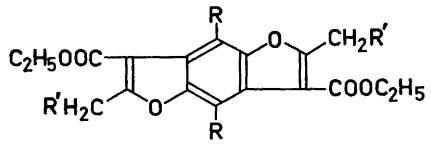

I R=R'=H
II R=Cl, R'=H
III R=Br, R'=H
IV R=R'=Br

Some years ago it was found [2] that compound I was able to form a very stable monozonide and an even more stable diozonide, and the interest for this class of compounds was thus to some extent revived.

We wish to report some experiments on the bromination of I and ozonisation of the brominated products. I was dissolved in chloroform and bromine added at room temperature in the presence of an iron bromide catalyst. One mole of bromine was absorbed and the dibromo compound III could be isolated in quantitative yield. If the bromine was added to the solution in absence of a catalyst and the reaction mixture irradiated with ultraviolet light, two moles of bromine was consumed and a tetrabromo compound IV was quantitatively formed. It could be transformed into III by reduction with zinc dust in glacia acetic acid.

On ozonisation in ethyl acetate III gave a diozonide $C_{18}H_{16}O_{12}Br_2$ which possessed a considerable stability. It could not be rearranged [3] by treatment with acetic anhydride and concentrated sulphuric acid. A probable monozonide could also be isolated. Reduction of the diozonide with sodium iodide in glacial acetic acid afforded a compound $C_{14}H_{12}O_8Br_2$ which evidently contained carbonyl and free hydroxyl groups. Most probably it has the structure V where the two expected acetyl groups have been lost during the working-up procedure. V could easily be acetylated to a diacetyl derivative, $C_{18}H_{16}O_{10}Br_2$.

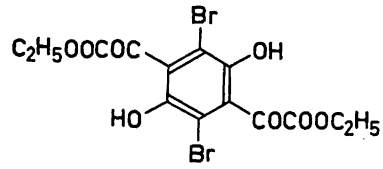

V

The tetrabromo compound IV also gave a stable diozonide, which proves that the additional two bromine atoms have not been added to any of the furan double bonds. On reduction with sodium iodide as before a compound $C_{14}H_{12}O_8Br_2$ was again isolated, which was found to be identical with V. It seems therefore likely that the tetrabromo compound has the proposed structure IV, where two bromine atoms sit in the aromatic nucleus while the other two are in the methyl groups. Also from IV a probable monozonide could be isolated.

Ikuta mentions that the dichloro compound II can form an oily "addition compound" with chlorine from which it can be regenerated by the action of zinc in glacial acetic acid, but he gives no analytical data. Also II has now been found to form a diozonide $C_{18}H_{16}O_{12}Cl_2$, which could not be rearranged by the usual method and which, by reduction with sodium iodide gave a product $C_{14}H_{12}O_8Cl_2$ probably analogous to V.

Experimental. Dibromo derivative III. I (5 g) was dissolved in chloroform (150 ml), some iron wool was added and bromine (40 g) added dropwise during 8 h. The mixture was kept at room temperature for 24 h whereafter it was washed with aqueous sodium bisulphite to remove unreacted bromine and with water.

After drying and evaporation of the chloroform fine crystals were left (7.5 g), (contained evidently a small amount of IV). Recrystallised from glacial acetic acid, m.p. 165°C. (Found: C 44.4; H 3.5; Br 32.4. Calc. for $C_{18}H_{16}O_6Br_2$: C 44.3; H 3.3; Br 32.7.)

Tetrabromo derivative IV. I (4 g) was dissolved in chloroform (150 ml) and bromine (60 g) added dropwise during 8 h. The mixture was kept for a total of 24 h and irradiated with ultraviolet light all the time. It was reduced to a volume of *ca.* 100 ml *in vacuo* and thereafter washed with aqueous sodium bisulphite, dried and evaporated. White needles remained (8 g), recrystallised from acetic acid the substance had m.p. 195°C. (Found: C 33.6; H 2.2; Br 49.8. Calc. for $C_{18}H_{14}O_6Br_4$: C 33.5; H 2.2; Br 49.5.)

Reduction of IV. Tetrabromo derivative (3 g) in glacial acetic acid (50 ml) was reduced with zinc dust at 30°C for 5 h with occasional shaking. The mixture was diluted with cold water (300 ml) and the separated substance collected and washed thoroughly. Dried and extracted at room temperature with ethyl acetate. Evaporation of the solvent gave white needles. M.p. alone and in mixture with III 166°C.

Ozonide of dibromo derivative. III (4.0 g) was dissolved in ethyl acetate (150 ml) and ozone (4 % in oxygen) was passed into the solution in about 10 % excess of the amount required for the formation of a diozonide. The ethyl acetate was evaporated and the remaining crystals washed with a small amount of ethanol and became then white (3.6 g). Recrystallised from dilute ethanol. M.p. 145°C. (Found: C 37.4; H 2.8; Br 27.4; act. O 5.5. Calc. for $C_{18}H_{16}O_{12}Br_2$: C 37.0; H 2.8; Br 27.4; act. O 5.5.) The ethanol used for washing the crude ozonide was concentrated and yellow crystals separated (0.5 g). These were extracted at room temperature with ethanol-water (3:1) and the extract slowly concentrated. Large yellow crystals were formed. M.p. *ca.* 90°C. (Found: Act. O 3.3. Calc. for $C_{18}H_{16}O_9Br_2$: Act. O 3.2.)

Reduction of the diozonide. The ozonide (3.5 g) was dissolved in chloroform (100 ml) and the solution cooled to −20°C. Twice the calculated amount of sodium iodide was dissolved in glacial acetic acid and the two solutions mixed. After about 1 h the liberated iodine was removed with aqueous sodium bisulphite and the acetic acid with sodium bicarbonate. After washing and drying the chloroform was evaporated. A dark viscous oil remained, which crystallised partly after several days in a vacuum desiccator. The crystals were washed with cold petrol ether and recrystallised from a mixture of petrol ether and benzene. Yellow needles m.p. 132°C. (Found: C 35.6; H 2.6; Br 35.1. Calc. for $C_{14}H_{12}O_8Br_2$: C 35.9; H 2.6; Br 34.2.) The substance gave a precipitate with 2,4-dinitrophenylhydrazine and a yellowish brown colour with ferric chloride. It dissolved easily in aqueous sodium hydroxide with a red colour. Acetylation was effected by dissolving it (1 g) in acetic anhydride (10 ml) to which anhydrous sodium acetate (1 g) had been added. The mixture was heated on a water-bath for 30 min and poured into ice-water (100 ml). A white, fluffy precipitate was formed, which, when recrystallised twice from ethanol formed light yellow needles, m.p. 141°C. (Found: C 39.1; H 2.9; Br 29.1. Calc. for $C_{18}H_{16}O_{10}Br_2$: C 39.1; H 2.9; Br 29.0.) The substance gave a precipitate with 2,4-dinitrophenylhydrazine, but did not dissolve in cold aqueous sodium hydroxide.

Ozonide of tetrabromo derivative. IV (0.7 g) was dissolved in ethyl acetate (100 ml) and ozonised as described above. The yellowish crude ozonide was washed with ethanol and became then white. It was dissolved in acetone, filtered and the solution was concentrated slowly. Colourless crystals separated. M.p. 131°C. (Found: Act. O 4.3. Calc. for $C_{18}H_{14}O_{12}Br_4$: Act. O 4.3.) The ozonide was reduced and worked up as described above. Yellow needles, m.p. and mixed m.p. with V 132°C. The ethanol used for washing the crude ozonide was concentrated and yellow crystals (0.6 g) were formed. These were washed with water, dissolved in acetone and filtered. A slow evaporation afforded a yellow substance m.p. *ca.* 70°C. (Found: Act. O 2.3. Calc. for $C_{18}H_{14}O_9Br_4$: Act. O 2.3.)

Ozonide of dichloro derivative. II (3.0 g) was dissolved in ethyl acetate (150 ml) and ozonised as described above. The ozonide (2.7 g) was recrystallised from aqueous acetone. M.p. 143°C. (Found: C 43.6; H 3.4; Cl 14.8; act. O 6.4; M (acetone) 507. Calc. for $C_{18}H_{16}O_{12}Cl_2$: C 43.7; H 3.3; Cl 14.3; act. O 6.5, M 495.)

The ozonide (3.0 g) was reduced with sodium iodide and worked up as already described. Yield 0.4 g of yellow needles. M.p. 120°C. (Found: C 43.8; H 3.3; Cl 18.6, Calc. for $C_{14}H_{12}O_8Cl_2$: C 44.3; H 3.2; Cl 18.7.) The substance gave a precipitate with 2,4-dinitrophenylhydrazine and a yellowish-brown colour with ferric chloride.

1. Ikuta, M. *J. prakt. Chem.* [2] **45** (1892) 65.
2. Bernatek, E. and Thoresen, F. *Acta Chem. Scand.* **9** (1955) 743.
3. Bernatek, E. and Thoresen, F. *Acta Chem. Scand.* **13** (1959) 342.

Received January 24, 1961.

Synthesis and Metabolism of Coprostane-7α-ol-3-one

Bile Acids and Steroids 109

HENRY DANIELSSON

Department of Chemistry, Karolinska Institutet, Stockholm, Sweden

Bergström and Lindstedt [1,2] have shown that both 7α-hydroxycholesterol and coprostane-3α,7α-diol are converted to cholic and chenodeoxycholic acid in the bile-fistula rat. Yamasaki and coworkers [3] have found that 7α-hydroxycholesterol is oxidized in rat liver homogenates to an α,β-unsaturated ketone which was suggested to be Δ^4-cholestene-7α-ol-3-one. This compound was proposed as an intermediate in the postulated formation of coprostane-3α,7α-diol from 7α-hydroxycholesterol. The identification of Δ^4-cholestene-7α-ol-3-one as a metabolite of 7α-hydroxycholesterol in mouse liver homogenates has recently been described [4]. This compound was found to be metabolized in the bile-fistula rat to cholic and chenodeoxycholic acid, but several unidentified acids were also formed [5]. The possibility that this compound might be an intermediate in the conversion of cholesterol to bile acids can, however, not be excluded. If Δ^4-cholestene-7α-ol-3-one were an intermediate one possible metabolite of this compound would be coprostane-7α-ol-3-one, *i.e.* the saturated compound with the rings A and B in *cis*-junction as in the normal bile acids.

In a communication published while this work was in progress, Yamasaki *et al.*[6] reported the synthesis of coprostane-7α-ol-3-one and suggested that this compound was an intermediate in the proposed conversion of 7α-hydroxycholesterol to coprostane-3α,7α-diol. In the present report an alternative and more simple synthesis of coprostane-7α-ol-3-one is described as well as the metabolism of tritium labeled coprostane-7α-ol-3-one in the bile-fistula rat.

Experimental. Coprostane-3α,7α-diol was synthesized according to Bergström and Krabisch[7] and had m.p. 78–79°, reported 84–86°. The infrared spectrum of the material of m.p. 78–79° was identical with that of m.p. 84–86°. Tritium-labeled coprostane-3α,7α-diol was prepared by exposure of part of above-mentioned material to tritium gas according to the method of Wilzbach[8] in the apparatus described by Bergström and Lindstedt[9] and purified by repeated chromatography [10]. Labeled coprostane-3α,7α-diol was also prepared by electrolytic coupling of *iso*valeric acid with chenodeoxycholic acid that had been labeled with tritium by the Wilzbach procedure. After purification by chromatography this labeled coprostane-diol was diluted with inactive material of m.p. 78–79°.

The method of synthesis of coprostane-7α-ol-3-one was based on the finding of Jones *et al.*[11] that cholic acid can be selectively oxidized at the 3-position by Oppenauer oxidation.

Synthesis I. 150 mg coprostane-3α,7α-diol randomly labeled with tritium, spec. act. 33 000 c.p.m./mg, were dissolved in 5 ml dry benzene and heated under reflux for 6 h with 200 mg aluminium *tert.*-butoxide in 3 ml acetone. The reaction mixture was acidified with 2 N sulfuric acid and the benzene layer washed with sodium carbonate and water and evaporated to dryness. The residue was chromatographed on a 15 g column of aluminum oxide (Woelm, Eschwege, Germany, grade III). After elution of coprostane-3,7-dione (42 mg) with benzene, coprostane-7α-ol-3-one (59 mg, spec.act. 19 800 c.p.m./mg) was eluted with 5 % ethyl acetate in benzene. Repeated crystallization from petroleum ether and methanol/water afforded 32 mg, m.p. 120–121°, reported m.p. 121–22°.

Synthesis II. 140 mg coprostane-3α,7α-diol labeled with tritium in the "chenodeoxycholic acid moiety" of the molecule, spec. act. 32 000 c.p.m./mg, were oxidized with same amounts of reagents as above, but only for 3 h. The reaction mixture was extracted and chromatographed as above. In this case little of the coprostane-dione was formed (8 mg) and the main product was coprostane-7α-ol-3-one (79 mg, spec.act. 23 000 c.p.m./mg). Crystallization as above afforded 47 mg, m.p. 121°.

Animal experiments. 2.6 mg of coprostane-7α-ol-3-one from synthesis I and 3.5 mg of material from synthesis II were injected intraperitoneally as emulsions with bovine serum albumin solution into two bile-fistula rats (RI and RII resp.). After saponification the first 24 h portions of bile were chromatographed with phase system F 1 [12] to separate the cholic and the chenodeoxycholic acid fractions. The cholic acid fractions were rechromatographed in phase system C 1 [12] and the chenodeoxycholic acid fractions in phase system F 1.

Results. When administered to bile-fistula rats coprostane-7α-ol-3-one was rapidly excreted in bile as bile acids (52 % of injected dose in R I and 25 % in R II during the first 24 h). The radioactivity

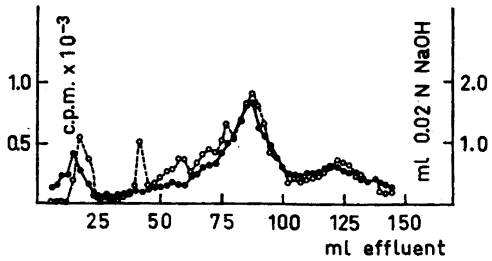

Fig. 1. Chromatography of the cholic acid fraction of hydrolyzed bile from Rat I. Column: 4.5 g hydrophobic Hyflo Supercel. Phase system C 1. Solid line: titration values. Broken line: radioactivity.

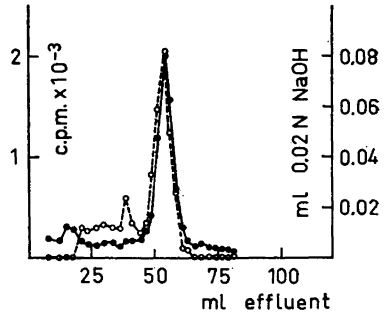

Fig. 2. Chromatography of the chenodeoxycholic acid fraction of hydrolyzed bile from Rat I. Column: 4.5 g hydrophobic Hyflo Supercel. Phase system F 1.

was distributed between the cholic and the chenodeoxycholic fractions in the proportion 6.5:3.5 (R I) and 6:4 (R II), resp. Rechromatography of the cholic acid fraction showed that a substantial part of the radioactivity coincided with the titration peak of cholic acid (Fig. 1) and the identity of the radioactive material with cholic acid was established by isotope dilution. The main part of the radioactivity in the chenodeoxycholic acid fraction was eluted as chenodeoxycholic acid (Fig. 2) and the identity was confirmed by isotope dilution.

Thus, coprostane-7α-ol-3-one is efficiently converted in the bile-fistula rat to both cholic and chenodeoxycholic acid. However, evidence for the formation of this compound from cholesterol, 7α-hydroxycholesterol or Δ^4-cholestene-7α-ol-3-one is lacking and it appears that discussions of coprostane-7α-ol-3-one as a possible intermediate in the formation of bile acids from cholesterol should await further experimentation.

Acknowledgments. The valuable technical assistance of Miss Birgitta Holmberg and Miss Marie-Louise Reinius is gratefully acknowledged.

This work is part of investigations supported by *The National Heart Institute*, Bethesda, Md., USA, and has also been supported by a grant from *Karolinska Institutets Reservationsanslag.*

1. Bergström, S. and Lindstedt, S. *Biochim. et Biophys. Acta* **19** (1956) 556.
2. Lindstedt, S. *Acta Chem. Scand.* **11** (1957) 417.
3. Yamasaki, K., Noda, F. and Shimizu, K. *J. Biochem. Tokyo* **46** (1959) 739, 747.
4. Danielsson, H. *Arkiv Kemi* **17** (1961). *In press.*
5. Danielsson, H. *Acta Chem. Scand.* **15** (1961) 242.
6. Yamasaki, K., Kawahara, T. and Shimizu, K. *Yonaga Acta Med.* **4** (1959) 37.
7. Bergström, S. and Krabisch, L. *Acta Chem. Scand.* **11** (1957) 1067.
8. Wilzbach, K. E. *J.Am. Chem. Soc.* **79** (1957) 1013.
9. Bergström, S. and Lindstedt, S. *Acta Chem. Scand.* **11** (1957) 1275.
10. Danielsson, H. *Biochim. et Biophys. Acta* **27** (1958) 401.
11. Jones, A. S., Webb, M. and Smith, F. *J. Chem. Soc.* **1949** 2164.
12. Norman, A. and Sjövall, J. *J. Biol. Chem.* **233** (1958) 872.

Received March 18, 1961.

Potentiometric Determination of Arylsulfinic Acids

L. GRINGRAS and G. SJÖSTEDT

The Laboratory of AB Ceaverken, Strängnäs, Sweden

Methods for the determination of benzenesulfinic acid and its salts have been published by Thomas [1], Krishna and Singh [2], Ackerman [3], Faerman and Simkina [4], and Alimarin and Kusnetsov [5]. Dale Nogare [6], reviewing known analytical methods, stated that attempts to determine various aromatic sulfinic acids failed: they gave only 80—90 % of the theoretical value. Alimarin and Sotnikov [7] stated that ceric sulfate in acid solution oxidizes the benzenesulfinic acid, the reaction products being dibenzenedisulfone, benzenesulfonic acid and an equivalent amount of cerous sulfate. No ceric benzenesulfinate was obtained. Forrest and Ryan [8] titrated benzenesulfinic acid with ceric sulfate. The endpoint of the titration, indicated by Ferroin, occurred at a molecular ratio of 1.8 Ce^{4+} to 1.0 benzenesulfinic acid. Dibenzenedisulfon was identified as a reaction product. Alimarin and Kusnetsov [5] attempted to use ceric sulfate for the determination of sulfinic acid but found that the reagent did not react stoichiometrically, the mole ratio being 1.1—1.2.

The aim of the present study has been to investigate the conditions under which ceric sulfate can be used as an analytica tool in the determination of arylsulfinic acids.

Ceric sulfate was chosen because of the stability of its solutions and the simple change of oxidation number from 4 to 3.

Experimental and results. The sodium and ammonium salts of *p*-toluenesulfinic acid were used as primary test substances. The acid itself is less suitable, being easily disproportionated and only slightly soluble in water.

The sodium salt was prepared from *p*-toluenesulfonyl chloride by reduction with zinc [9]. The salt is obtained as the dihydrate, the tetrahydrate was obtained by recrystallization from a saturated solution.

The ammonium salt was prepared in the following way. A cold saturated solution of the sodium salt was treated with ether, which removed traces of disulfides and mercaptans. The aqueous phase was filtered and the clear filtrate was acidified with 1:1 hydrochloric acid whilst being stirred and cooled. The precipitated *p*-toluenesulfinic acid was collected by suction on a Büchner funnel. The precipitate was washed with small portions of cold water which removed the very soluble *p*-toluenesulfonic acid. Without delay, the *p*-toluenesulfinic acid was dissolved in a small excess of ammonia and the clear solution was carefully evaporated on an infra-red heater to a volume small enough for cooling to initiate crystallization. Only the first crop of crystals of ammonium *p*-toluenesulfinate was collected; this was dried to constant weight at room temperature.

After drying for 2 h at 100°C the sodium salt decreased in weight by 27.6 %, which corresponds to the loss of four molecules of water of hydration. The dried salt gave a completely clear solution. The loss of weight for the ammonium salt was only 4.6 % and its solution in water was opaque, indicating that a disproportionation had taken place.

Surprisingly, the water of hydration could also be determined with the Karl-Fischer reagent (K-F stabilized, Pharmacia, Uppsala). The titration of the sodium *p*-toluenesulfinate in pre-titrated methanol gave the same figures for the water content as did the drying method. The titration of the ammonium salt indicated a water content of 10.2 % in good agreement with the theoretical value of 10.47 corresponding to one mole of hydration water. The ammonium salts of benzene and 2-naphthalenesulfinate also crystallize with one mole of water. The calcium *p*-toluenesulfinate crystallizes with four moles of water.

An approximately 0.1 N ceric sulfate solution (F. Smith, reagent grade) in 1.5 N sulfuric acid, was prepared and filtered. This solution was then carefully standardized against As_2O_3 with osmic acid as catalyst and Ferroin as indicator. The titer was checked every 8th day, but practically no change was observed. The titration was carried out potentiomertically with a Metrohm Potentiograph. The titrant was delivered from a 20 ml syringe buret synchronously driven by the recording unit. The solution to be titrated was stirred with a magnetic stirrer. A combined Pt-calomel electrode gave steady and reproducible readings. The end point was also very distinct at high dilution, and the very steep potential break indicated that the reaction was practically irreversible (Fig. 1). Of course, a simpler poten-

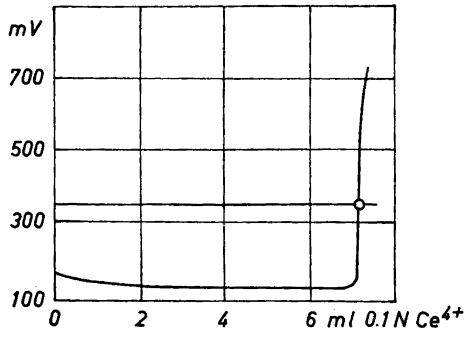

Fig. 1. Titration of 50 ml 0.01 N *p*-toluenesulfinic acid with 0.1 N Ce(IV) sulfate.

tiometer and a common buret may be used. The end of the titration was marked by a potential jump amounting to about 200 mV after the addition of only one drop.

Series of concentrations of *p*-toluenesulfinic acid ranging from 10^{-4} to 10^{-1} M were prepared by diluting aliquot portions of a 0.1 M standard solution to a volume of 100 ml. Prior to the dilution the solutions were acidified with 5 ml of 1 N sulfuric acid. In some experiments greater amounts of sulfuric acid up to 10 N were used, but the greater concentration of acid seemed to have no effect on the result of the titration.

In Fig. 2 the mole ratio, Ce^{4+}/RSO_2^-, obtained by the titration, is plotted as ordinate *versus* the concentration of the titrated solution in logarithmic units as abscissa. Within the limits of experimental error, this ratio is 1.5 in the concentration range above 5×10^{-3} M. At lower concentrations the mole ratio gradually decreases. For the range from 5×10^{-3} to 1×10^{-1} M, the overall reaction may be summed up as follows

$$4\ RSO_2^- + 6\ Ce^{4+} + 2\ H_2O \rightarrow (RSO_2)_2 + 2\ RSO_3^- + 6\ Ce^{3+} + 4\ H^+$$

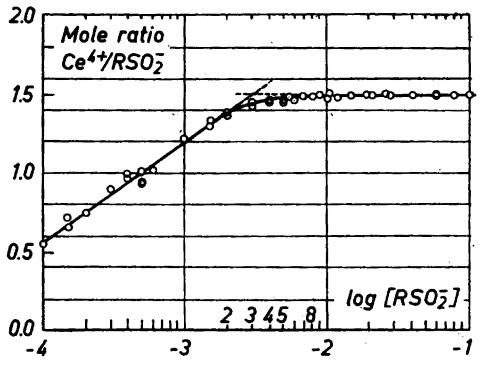

Fig. 2. The dependence of the Ce^{4+}/RSO_2^- mole ratio at the end point on the concentration of the solution to be titrated.

Some gravimetric experiments were performed to verify the stoichiometry of the reaction. The precipitated disulfone was collected by suction in a porcelain filter crucible, dried at 100°C for 2 h and weighed. The recovery was only 80—85 % of the theoretical value, possibly because of the solubility of the ditolyldisulfone.

Within the concentration limits indicated above, the following equation may be used in the calculation:

$$\frac{\text{ml of titrant} \times \text{normality}}{1\,000 \times 1.5} = \frac{\text{g of sample} \times \text{per cent purity}}{\text{mole-weight} \times 100}$$

For salts with divalent or tetravalent cations the factor 1.5 has to be replaced by 3.0 or 4.5.

The authors wish to thank the Directors of AB Ceaverken for permission to publish this investigation.

1. Thomas, J. *J. Am. Chem. Soc.* **95** (1909) 342.
2. Krishna, S. and Singh, H. *J. Am. Chem. Soc.* **50** (1928) 729.
3. Ackerman, L. *Ind. Eng. Chem. Anal. Ed.* **18** (1946) 243; Atkin, S. *Anal. Chem.* **19** (1947) 816.
4. Faerman, G. P. and Simkina, A. B. *Uspekki Nauch. Fot. Akad. Nauk S.S.S.R. Otdel. Khim. Nauk* **5** (1957) 76.
5. Alimarin, I. P. and Kusnetsov, D. I. *Vestnik Moskov. Univ. Ser. Fiz. Mat. i Estestven. Nauk* No. 3.
6. Dale Nogare, S. *Organic Analysis*, Vol. I, New York 1953.
7. Alimarin, I. P. and Sotnikov, V. S. *Doklady Akad. Nauk. S.S.S.R.* **113** (1957) 150.
8. Forrest, T. P. and Ryan, D. E. *Can. J. Chem.* **36** (1958) 1677.
9. *Organic Syntheses*, Coll. Vol. **I** (1947) 492.

Received January 28, 1961.

Paper Chromatography of Some Sulfinic Acids and Sulfonylchlorides

L. GRINGRAS and G. SJÖSTEDT

The Laboratory of AB Ceaverken, Strängnäs, Sweden

Feigl [1] used the orange-red insoluble iron(III) salt of benzenesulfinic acid as spot test. Gilman and Abbot [2] characterized *p*-toluenesulfinic acid by the melting point of thalliumdichloride-*p*-toluenesulfinate.

It has now been found that alkyl and arylsulfinic acids (or their salts) react with zinc chloride stabilized tetrazo-*o*-dianisidine

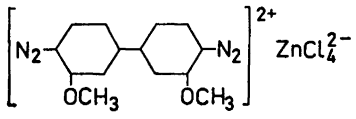

(Echtblau B Salz, E. Merck) to give a bright canary yellow dye, insoluble in water but soluble in benzene. Thus a drop of a solution of a sulfinic acid or a sulfinate absorbed on filter paper and dried, appears as a yellow spot when treated with a freshly prepared 0.5 % aqueous solution of the reagent. Thiosulfate, sulfite and thiocyanate react in the same way to give yellow dyes, but these dyes are easily soluble in cold water and can be completely removed from the spot by washing it. Aromatic sulfonic acids, sulfones, mercaptans, phenols and disulfides do not interfere.

It has also been found that solutions of sulfinic acids or their salts can be examined by ascending paper chromatography, using a mixture of equal volumes of *n*-butanol, *n*-propanol and water, as the solvent.

Essentially the same technique has been used for the analysis of alkyl and arylsulfonylchlorides except that the marked spot on the paper was pre-treated with an alkaline sodium sulfite solution before applying the sulfonylchloride. In this way the sulfonylchloride was converted to the sulfinic salt directly on the paper, before starting the chromatographic run.

Separation of mixtures of sulfinic acids or sulfonylchlorides was possible providing the R_F-values differed enough.

The following substances were investigated:

Sulfinic acids:
Benzenesulfinic acid and salts (Hoechst)
p-Toluenesulfinic acid (Bofors, Sweden)
2,6-Dichloro-*p*-toluenesulfinic acid (prepared according to Ref.[3])
Ethansulfinic acid, sodium salt (Hoechst)
2-Naphtalenesulfinic acid [3]
Sulfonylchlorides:
p-Toluenesulfonylchloride (Bofors, Sweden)
2,6-Dichloro-*p*-toluenesulfonylchloride (Bofors)
2-Naphthalenesulfonylchloride (Merck, Germay)
Methansulfonylchloride (Fluka, Switzerland)

Whatman No. 1 filter paper for chromatography, 24 × 40 cm in size was used. The chromatograms were developed in a suitably sized glass tank equipped with stainless steel racks from which the paper was suspended so as to dip into the solvent, which was placed at the bottom of the tank. The chromatograms were developed for 16 h at 20°C. The solvent consisted of chromatographically pure *n*-butanol, *n*-propanol and water (1:1:1).

Concentration standards, 5×10^{-3} and 5×10^{-2} M, were prepared from sulfinic acid salts in distilled water.

The sulfonylchlorides were dissolved in dioxan, ethanol or benzene. Liquid sulfonylchlorides were used directly, without dilution.

Detection of sulfinic acids. The standard solutions were applied from a glass capillary on a starting line 3 cm from the bottom edge of the paper sheet and 2 cm intervals between spots, by touching the end of the capillary to the paper and withdrawing it when the spot had attained the required size. The spots could be made visible after developing and drying the chromatogram, by spraying it with a dilute solution of potassium permanganate, when the sulfinic acid appeared as a white spot on the purple background. After some time, however, the purple background faded out. A spray

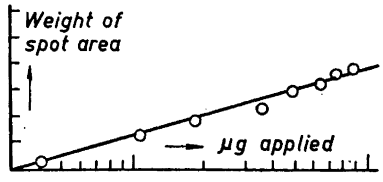

Fig. 1. Quantitative estimation of the amount of *p*-toluenesulfinic acid as a function of spot area.

Table 1.

Substance	R_F	Substance	R_F
Benzenesulfinic acid	0.58	2,6-Dichloro-*p*-toluenesulfinic acid	0.81*
p-Toluenesulfinic acid	0.65	Ethansulfinic acid	0.40
2-Naphtalenesulfinic acid	0.73	Methansulfinic acid	0.25**

* Practical grade salt gave a faint second spot (0.79).
** From reduced methansulfonyl chloride.

consisting of a solution of dinitrophenylindole gave white spots on a blue background. Neither of these reagents are specific for the sulfinic group. The insoluble yellow dye formed by spraying with a 0.25—0.5 % solution of the stabilized tetrazotized *o*-dianisidine, seems to be very specific. Darkening of the white background on storage can be prevented by washing the chromatogram with cold distilled water.

Detection of sulfonylchlorides. First a spot of a 20 % sodium hydroxide solution saturated with sodium sulfite was applied to a marked position on the starting line. This was dried and a spot of the solution of sulfonylchloride (or the mixture of sulfonylchlorides) was superimposed on it. By holding the paper for a short time over a dish containing hot or boiling water, or by conditioning it in a humidity cabinet for an hour, the sulfonylchloride was reduced to the parent sulfinic salt. If several spots were applied they were spaced at intervals of about 5 cm. After developing and spraying the chromatogram, the characteristic spots of the sulfinic group appeared. The sulfite spot, which had a rather large area due to the high sulfite concentration, disappeared when the chromatogram was washed.

The R_F-values obtained are reported in Table 1.

Weighed amounts of a standard solution of sodium *p*-toluenesulfinate were applied from a capillary pipet to the chromatographic paper. If necessary the loading was increased by multiple applications, each spot being dried before repeating the application. In this way series of spots corresponding to from 0.5 to 80 μg of the salt was obtained. The minimum quantity detectable after developing, drying and spraying the chromatogram as previously described was found to be 4 μg which is equal to 2.4×10^{-8} mole of sodium *p*-toluenesulfinate.

A quantitative estimation was carried out using the technique devised by Fisher *et al.*[4] The spots from a concentration series were circumscribed with a black pencil and copied on photographic document reflex paper or on transparent paper of uniform quality. The spots thus obtained are carefully cut out and weighed. By plotting on semi-logarithmic paper the weights of these "cut-outs" against the amounts of sulfinic salt applied on each spot, a straight calibration curve was obtained (Fig. 1), from which the content of an unknown sample could be determined.

The sulfonylchlorides could be examined in the same way provided the reduction was complete. Amounts as small as 100 μg could be detected without difficulty.

The authors wish to thank the Directors of AB Ceaverken for permission to publish this paper.

1. Feigl, F. *Laboratory Manual of Spot Tests.* New York 1943, p. 181—3; Feigl, F. *Quantitative Analysis of Spot Tests.* New York 1947, p. 366—7.
2. Gilman, H. and Abbot, R. K. *J. Am. Chem. Soc.* **71** (1949) 659.
3. *Organic Syntheses*, Coll. Vol. I (1947) 492.
4. Block, R. J., Durrum, E. L. and Zweig, G. *A Manual of Paper Chromatography and Electrophoresis.* New York 1955, p. 56.

Received January 28, 1961.

The Oxidation of Glycosides

XII *. Oxidation of Methyl 4,6-*O*-benzylidene-β-D-galactopyranoside with Chromium Trioxide

EILEEN BRIMACOMBE **, JOHN S. BRIMACOMBE **, BENGT LINDBERG and OLOF THEANDER

Träkemiska avdelningen, Svenska Träforskningsinstitutet, Stockholm Ö, Sweden

In previous investigations the formation of oxo-glycosides by chromium trioxide oxidation of the anomeric methyl glucopyranosides and some of their derivatives [1,2], and of methyl β-xylopyranoside [3] has been studied. The yield of a single oxo-glycoside has never exceeded *ca.* 5 %. The oxidation studies have now been extended to methyl β-D-galactopyranoside protected at $C_{(4)}$ and $C_{(6)}$ by a benzylidene group.

Two products predominated in the neutral oxidation mixture after removal of the benzylidene group. They showed characteristics of oxoglycosides: high mobility on hydrogen sulphite electrophoresis, strong reducing reaction with silver nitrate-sodium ethoxide reagent and characteristic colour reactions with anisidine hydrogen chloride and resorcinol-hydrochloric acid reagents. The two oxidation products and unreacted methyl galactoside, the main component in the reaction mixture, were eluted from a carbon-Celite column with similar ethanol concentration and the R_F-values of the three components were similar. This made preparative separation difficult.

The structure of the oxo-galactosides was proved by identifying the sugars obtained on reduction with Raney-nickel and hydrolysis. One of the oxo-galactosides (obtained in *ca.* 0.9 % yield) gave, on such treatment, talose and galactose thus proving it to be methyl β-2-oxo-galactoside (I). The other (*ca.* 0.7 %) gave gulose and galactose, thus proving it to be methyl β-3-oxo-galactoside (II). Both I and II were obtained in an amorphous state and could not be crystallised. The 3-oxo-compound had the lower R_F-value of the two and was also eluted somewhat more readily from the carbon column. Both gave elongated spots on paper chromatograms contrasting with the sharp round spots obtained with the corresponding oxo-glucosides. The oxo-galactosides were quite labile and a small amount of glucose was obtained in the products of II, after reduction and hydrolysis, possibly indicating that epimerisation took place.

In the fractions first eluted from the column were small amounts of a component chromatographically indistinguishable from lyxose. The presence of this sugar is analogous to the formation of arabinose in the oxidation of methyl glucoside [2] and indicates cleavage between $C_{(1)}$ and $C_{(2)}$.

Experimental. Melting points are corrected. Distillations were carried out under reduced pressure (bath temperature < 35°). Whatman 1 filter papers were used for paper chromatography and electrophoresis except for preparative separations, which were made on Whatman 3 MM filter papers previously washed with water.

Irrigants and buffer used:

A. Ethyl acetate — acetic acid — water, 3:1:3
B. Butanol — ethanol — water, 10:3:5
C. Butanol — pyridine — water, 6:2:5
D. Hydrogen sulphite buffer [4] (50°) pH 4.7, 0.1 M

Oxidation and fractionation of the products. Methyl 4,6-*O*-benzylidene-β-D-galactopyranoside (50 g) in acetone (3 l) was oxidised with chromium trioxide (26.5 g) and the reaction mixture worked up and fractionated essentially as previously described for the oxidation of methyl 4,6-*O*-ethylidene-β-D-glucopyranoside [2].

The neutral mixture obtained, after removal of the protecting benzylidene group, contained unreacted methyl galactoside as the main component. The majority of this was removed by crystallisation from ethanol. Of the expected reaction products 2-oxo-galactoside (I) and 3-oxo-galactoside (II) predominated. Of the minor components one was indistinguishable from lyxose. Two separations on carbon-Celite columns using gradient elution resulted in only partial fractionation of the unreacted methyl galactoside, I and II. The 3-oxo-compound was eluted at a somewhat lower concentration of ethanol than was the 2-oxo-compound. Subfractionation on thick filter paper (solvent A) was attempted but was rendered

* Part XI. *Acta Chem. Scand.* **14** (1960) 2236.

** Present address: Chemistry Department, The University of Birmingham, Birmingham 15, England.

difficulty by the fact that the compounds gave elongated spots and had similar migrations ($R_{Galactose}$-values: methyl β galactoside: 1.74, I ~ 2.0 and II ~ 1.6). After two fractionations on thick filter paper I and II were obtained *ca.* 80 % pure (most of the impurity being the unreacted methyl galactoside). The bulk of the two fractions was reduced, but further fractionation of aliquots of I and II on thick filter paper gave amorphous but chromatographically pure products. From these fractionations the total yield of I and II could be estimated as *ca.* 0.9 % and 0.7 %, respectively.

Characterisation of the oxo-galactosides. The oxo-galactosides gave strong reducing reactions with silver nitrate-sodium ethoxide reagent, characteristic orange-brown colourations with anisidine hydrogen chloride and orange-grey colourations with resorcinol-hydrochloric acid reagent.

The oxo-galactosides dissolved in 70 % aqueous ethanol were reduced by refluxing for 5 h with excess of Raney-nickel [5]. The product was hydrolysed with 0.5 N sulphuric acid for 17 h and the sugars obtained fractionated by chromatography on thick filter papers (solvent C). Talose and galactose only were obtained from I, and gulose and galactose from II, together with small amounts of glucose.

Part of the isolated gulose was reduced with sodium borohydride at pH 9.5. The product obtained, after deionisation, was chromatographically indistinguishable from D-gulitol. The acetylated (acetic anhydride/pyridine) product, after recrystallisation from aqueous ethanol, had the same R_F-value as authentic D-gulitol hexacetate on chromatographing on dimethylsulphoxide impregnated paper using *iso*propyl ether-light petroleum (1:1) as irrigant [6], and m.p. and mixed m.p. 98–99°.

Talose was characterised by paper chromatographic data (*e.g.*, $R_{Galactose}$-values in solvent C: talose: 1.52, gulose: 1.29 and glucose 1.15), and as its methylphenylhydrazone, m.p. 147–149° after recrystallisation from aqueous methanol (literature value [7], 154°).

The authors indebted are to Dr. H. G. Fletcher, Jr., Bethesda, U.S.A., for specimens of D-gulose and D-talose and to Mr. A. Assarsson for skilful assistance.

1. Theander, O. *Acta Chem. Scand.* **11** (1957) 1557.
2. Assarsson, A. and Theander, O. *Acta Chem. Scand.* **12** (1958) 1507.
3. Brimacombe, E., Brimacombe, J. S. and Lindberg, B. *Acta Chem. Scand.* **14** (1960) 2236.
4. Theander, O. *Acta Chem. Scand.* **11** (1957) 717.
5. Karabinos, J. V. and Ballun, A. T. *J. Am. Chem. Soc.* **75** (1953) 4501.
6. Wickberg, B. *Acta Chem. Scand.* **12** (1958) 615.
7. Levene, P. A. and Tipson, R. S. *J. Biol. Chem.* **95** (1931) 631.

Received February 1, 1961.

Alkaline Decomposition of Some Quaternary Phosphonium Compounds Containing Oxygen

GUNNAR AKSNES

Chemical Institute, University of Bergen, Bergen, Norway

The alkaline decomposition of aliphatic and aromatic quaternary phosphonium compounds with hydroxides and alkoxides results in the formation of hydrocarbons, ethers and phosphine oxides [1-3]. The alkaline decomposition of some oxygen-containing phosphonium compounds is reported in this paper.

The phosphorus analogs of choline(I) and choline acetate (II) were found to decompose in the following ways:

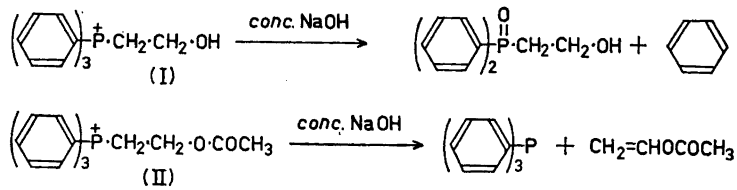

difficulty by the fact that the compounds gave elongated spots and had similar migrations ($R_{Galactose}$-values: methyl β galactoside: 1.74, I ~ 2.0 and II ~ 1.6). After two fractionations on thick filter paper I and II were obtained *ca.* 80 % pure (most of the impurity being the unreacted methyl galactoside). The bulk of the two fractions was reduced, but further fractionation of aliquots of I and II on thick filter paper gave amorphous but chromatographically pure products. From these fractionations the total yield of I and II could be estimated as *ca.* 0.9 % and 0.7 %, respectively.

Characterisation of the oxo-galactosides. The oxo-galactosides gave strong reducing reactions with silver nitrate-sodium ethoxide reagent, characteristic orange-brown colourations with anisidine hydrogen chloride and orange-grey colourations with resorcinol-hydrochloric acid reagent.

The oxo-galactosides dissolved in 70 % aqueous ethanol were reduced by refluxing for 5 h with excess of Raney-nickel [5]. The product was hydrolysed with 0.5 N sulphuric acid for 17 h and the sugars obtained fractionated by chromatography on thick filter papers (solvent C). Talose and galactose only were obtained from I, and gulose and galactose from II, together with small amounts of glucose.

Part of the isolated gulose was reduced with sodium borohydride at pH 9.5. The product obtained, after deionisation, was chromatographically indistinguishable from D-gulitol. The acetylated (acetic anhydride/pyridine) product, after recrystallisation from aqueous ethanol, had the same R_F-value as authentic D-gulitol hexacetate on chromatographing on dimethylsulphoxide impregnated paper using *iso*propyl ether-light petroleum (1:1) as irrigant [6], and m.p. and mixed m.p. 98–99°.

Talose was characterised by paper chromatographic data (*e.g.*, $R_{Galactose}$-values in solvent C: talose: 1.52, gulose: 1.29 and glucose 1.15), and as its methylphenylhydrazone, m.p. 147–149° after recrystallisation from aqueous methanol (literature value [7], 154°).

The authors indebted are to Dr. H. G. Fletcher, Jr., Bethesda, U.S.A., for specimens of D-gulose and D-talose and to Mr. A. Assarsson for skilful assistance.

1. Theander, O. *Acta Chem. Scand.* **11** (1957) 1557.
2. Assarsson, A. and Theander, O. *Acta Chem. Scand.* **12** (1958) 1507.
3. Brimacombe, E., Brimacombe, J. S. and Lindberg, B. *Acta Chem. Scand.* **14** (1960) 2236.
4. Theander, O. *Acta Chem. Scand.* **11** (1957) 717.
5. Karabinos, J. V. and Ballun, A. T. *J. Am. Chem. Soc.* **75** (1953) 4501.
6. Wickberg, B. *Acta Chem. Scand.* **12** (1958) 615.
7. Levene, P. A. and Tipson, R. S. *J. Biol. Chem.* **95** (1931) 631.

Received February 1, 1961.

Alkaline Decomposition of Some Quaternary Phosphonium Compounds Containing Oxygen

GUNNAR AKSNES

Chemical Institute, University of Bergen, Bergen, Norway

The alkaline decomposition of aliphatic and aromatic quaternary phosphonium compounds with hydroxides and alkoxides results in the formation of hydrocarbons, ethers and phosphine oxides [1-3]. The alkaline decomposition of some oxygen-containing phosphonium compounds is reported in this paper.

The phosphorus analogs of choline(I) and choline acetate (II) were found to decompose in the following ways:

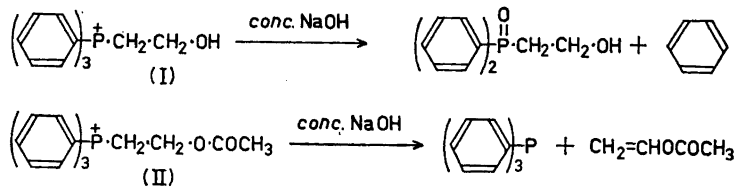

The reason for the different behaviour of (I) and (II) must be due to an easier ionization of the hydrogen in the hydroxyl group of (I) as compared with the hydrogen of the methylene group adjacent to the hydroxyl. A negative charge on the oxygen will thus prevent the attack of hydroxyl ion on the methylene hydrogen and the compound will therefore decompose according to the usual scheme for quaternary phosphonium compounds [1]. In the phosphonocholine acetate (II) the attack of the hydroxyl ion must be easier on the methylene hydrogen than on the carbonyl carbon or phosphorus.

Michaelis and Gimborn [4] and Worrall [5] have claimed that the betaine analogs of phosphorus can be obtained by treatment of the corresponding esters with strong alkali:

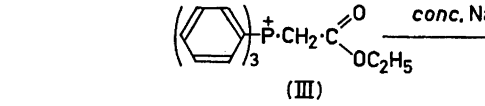

(III)

We have found that the compound isolated by Michaelis and Gimborn [4] does not correspond to the above formula. Its physical and chemical data show that the compound is a phosphorane and its formation is analogous to the formation of phosphoranes described by Ramirez and Dershowitz [6]:

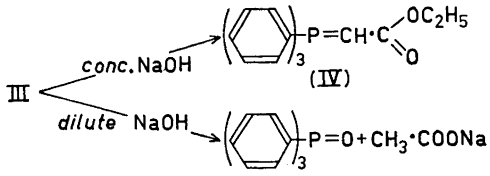

Treatment of (III) with dilute alkali or moist silver oxide in water gives phosphine oxide and acetic acid as already described by Michaelis and Gimborn [4]. The same authors have reported that chloroacetic acid does not react with triphenylphosphine. We have observed that bromoacetic acid reacts with triphenylphosphine but that the reaction does not give the expected betaine hydrobromide. Phosphine oxide and acetyl bromide are formed in nearly quantitative yields:

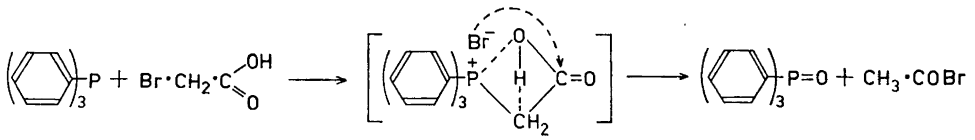

The phosphorus analogs of "propionbetaine" could be prepared from the corresponding ester by the use of moist silver oxide or dilute alkali. Treatment of the ester with concentrated sodium hydroxide gave on the other hand chiefly phosphine and the ester of acrylic acid. The "phosphonopropionbetaine" thus corresponds in its behaviour with the "propionbetaine"[7]. See p. 440.

Experimental. Phosphonocholine chloride (I). 10 g triphenylphosphine was added to 10 ml β-chloroethanol. The mixture was boiled for 2 h. The phosphonocholine chloride (I) crystallized by cooling of the reaction mixture. The compound was recrystallized from absolute ethanol. Yield 10 g; m.p. 233°. (Found: Cl 10.2. Calc. for $C_{20}H_{20}POCl$: Cl 10.4.)

Decomposition of (I) with conc. sodium hydroxide. 6 g of (I) was dissolved in 4 ml water. To the solution was added 5 ml conc. sodium hydroxide. Upon distillation 1.3 g benzene was recovered from the distillate (87 % of theory). The benzene was characterized as *m*-dinitrobenzene, m.p. 89°. Mixed melting point with pure *m*-dinitrobenzene showed no depression.

Acetylphosphonocholine chloride (II). 10 g triphenylphosphine and 6 g β-chloroethylacetate was boiled under reflux for 4 h. Upon diluting the reaction mixture with 5 ml acetone the chloride crystallized. The compound recrystallized from acetone-alcohol gave small needles, m.p. 287°. (Found: C 68.5; H 5.7. Calc. for $C_{22}H_{22}PO_2Cl$: C 69.2; H 5.6.)

Decomposition of (II) with conc. sodium hydroxide gave 95 % yield of triphenylphos-

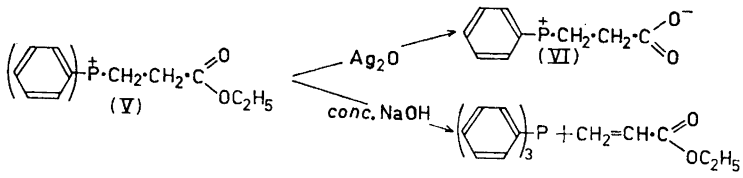

phine, m.p. 79–80°. Its infrared spectrum was identical with that of an authentic specimen.

Ethylester of phosphonobetaine bromide (III). 5 g bromoacetic acid ethylester was added to 10 g of triphenylphosphine. The mixture was heated to 80° and kept there for 5 min. The crystalline mass which separated upon cooling was recrystallized from alcohol-ether, m.p. 157°. (Found: Br 18.7. Calc. for $C_{22}H_{22}PO_2Br$: Br 18.7.)

Preparation of the phosphorane (IV). 4 g of (III) was dissolved in 4 ml water. Five ml cold conc. sodium hydroxide was added. The thick oil which immediately separated was extracted with ether. Upon evaporation of the ether the phosphorane (IV) solidified. It was crystallized from ether, m.p. 126–127° (Michaelis and Gimborn [4] 124–126°). (Found: C 75.7; H 6.06; P 9.15. Calc. for $C_{22}H_{21}PO_2$: C 76.2; H 6.05; P 8.79.)

Treatment of (IV) with HBr in ether solution gave a crystalline compound, m.p. 157° the infrared spectrum of which was identical with that of (III). Treatment of (IV) with excess ethyl iodide in alcohol gave a crystalline compound, m.p. 162° presumably:

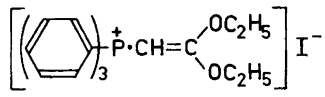

(Found: I 25.0. Calc. for $C_{24}H_{26}PO_2I$: I 25.1.

Ethylester of "phosphonopropionbetaine bromide" (V). 7 g β-bromopropionic acid ethylester was added to 9 g triphenylphosphine. The mixture was heated to 100° for 5 min. The product was washed with ether and acetone and recrystallized from 50 % water-alcohol mixture; small needles, m.p. 126°. (Found: Br 18.0. Calc. for $C_{23}H_{24}PO_2Br$: Br 18.0.)

Treatment of (V) with conc. sodium hydroxide gave triphenylphosphine, m.p. 79–80°. Its infrared spectrum was identical with that of an authentic specimen.

"Phosphonopropionbetaine" (VI). 2 g of (V) was dissolved in 50 ml of water. The solution was shaken with 3 g moist silver oxide. The silver bromide was filtered off and the solution concentrated to 5 ml in a vacuum. A small amount of triphenylphosphine formed during the hydrolysis was removed by shaking with 10 ml of ether. The phosphonopropionbetaine (VI) crystallizes from a concentrated water solution in white plates. The compound was dried at 140° for 1 h, m.p. 186°. (Found: C 75.2; H 5.7; P 9.5. Calc. for $C_{21}H_{19}PO_2$: C 74.5; H 5.5; P 9.0.)

The betaine (VI) was also formed on hydrolysis of (V) with hydrobromic acid followed by treatment of the betaine hydrobromide with moist silver oxide.

The reaction between triphenylphosphine and bromoacetic acid. 2.5 g bromoacetic acid and 5 g triphenylphosphine (1 equiv.) was heated to approximately 80°. The reaction started with evolution of acetyl bromide (characterized as ethyl acetate). An almost quantitative amount of triphenylphosphine oxide, m.p. 152° was recovered from the residue. Its infrared spectrum was identical with that of an authentic specimen of triphenylphosphine oxide.

My sincere thanks are due to the *Norwegian Defence Research Establishment* for financial support and to Senior Research Chemist Arnljot Nærland at the same institute for recording of the infrared spectra.

1. Fenton, G. W. and Ingold, C. K. *J. Chem. Soc.* **1929** 2342.
2. Hey, L. and Ingold, C. K. *J. Chem. Soc.* **1933** 531.
3. Grayson, M. and Keough, P. T. *J. Am. Chem. Soc.* **82** (1960) 3919.
4. Michaelis, A. and Gimborn, H. V. *Ber.* **27** (1894) 272.
5. Worrall, D. E. *J. Am. Chem. Soc.* **52** (1930) 2933.
6. Ramirez, F. and Dershowitz, S. *J. Org. Chem.* **22** (1957) 41.
7. Aksnes, G. and Prue, J. E. *J. Chem. Soc.* **1959** 103.

Received January 23, 1961.

Homogeneous Nucleation in Barium Sulfate Precipitation

ARNE E. NIELSEN

Universitetets fysisk-kemiske institut, Copenhagen, Denmark

From experiments reported previously we deduced [1] that the barium sulfate particles formed in 0.001 M aqueous solution start their growth on foreign nuclei (impurity particles). In the present work we have used much higher concentrations (up to 0.04 M) and we found that when the initial concentration is above 0.01 M most of the crystals originate from homogeneously formed nuclei.

The experiments were performed by mixing equivalent amounts of solutions of barium chloride and sodium sulfate. Analytical grade chemicals were dissolved in ordinary distilled water. The induction period was measured as the time between the mixing and the appearence of visible turbidity. At low concentrations, where the induction period was longer than about 1 second the solutions (usually 100 ml of each) were poured from 250 ml beakers into a 600 ml beaker; a stop watch was started in advance of the experiment and the solutions poured together at 5 seconds. When the first turbidity was observed in diffuse daylight near the window the watch was stopped and 5 seconds substracted from the reading. The times were reproducible within about 30 %. No special precautions were taken to avoid nucleating impurities, except that the 600 ml beaker was rinsed in concentrated sulfuric acid which dissolves the barium sulfate formed on the walls.

At the highest concentrations the solutions were mixed in a Roughton T tube [2] and the induction period t calculated from the rate of flow and the distance between the place where the solutions meet and the site of just visible turbidity. This was observed in diffuse daylight. The reproducibility is fair, but the precipitation zone is rather unsharp, corresponding to about 50 % of uncertainty. Because so wide a range of times is covered (almost seven decades) this uncertainty does not hide the phenomena to be studied. The solutions were sucked from two 200 ml measuring cylinders by opening a stopcock between the stem of the T tube and an evacuated 2 liter separating funnel acting as a recipient for the mixture.

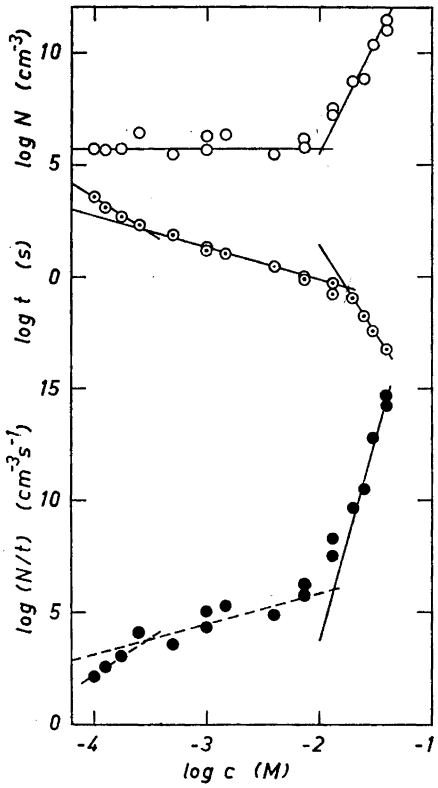

Fig. 1. The following quantities are shown as functions of the initial concentration c of barium sulfate. From above: 1, number concentration of crystals formed. 2, induction period. 3, quotient of the former two; for $c > 0.01$ M ($\log c > -2$) this is assumed to equal the rate of homogeneous nucleation.

In the end of each experiment the number of crystals formed per unit volume was determined by counting under the microscope. At the highest concentrations a peptizing agent had to be added to the sample to be put under the microscope, in order to prevent the coagulation of the particles. Gelatine, carboxymethylcellulose and sodiumpyrophosphate all were able to redisperse the precipitate when it had coagulated.

The same upper limit of the concentrations that can be used seems to arise from

the difficulty of observing the time in the T tube and by the impossibility of redispersing the precipitate by gentle means.

In Fig. 1 we see from the upper curve that within the reproducibility the number of crystals is independent of the initial concentration c when the latter is less than 0.01 M and proportional to c^{10} (the tenth power of the concentration) at $c > 0.01$ M. We do not know any other mechanism than homogeneous nucleation that can explain this phenomenon.

The second curve in Fig. 1 consists of three straight lines, corresponding to three different types of precipitation reaction. A similar curve (drawn from a compilation of different authors' data) has been published before [3], but without interpretation. Now we know that at $c < 0.0004$ M (log $c < -3.4$) the crystals grow by a fourth-order surface reaction, and at $c > 0.0004$ M the rate determining step is diffusion through the liquid [4]. The change of growth-controlling mechanism is the cause of the change of slope of the curve.

The other elbow is situated very close to the concentration where, as deduced from the upper curve, the precipitation process changes from being induced by foreign nuclei into development from spontaneously formed nuclei.

The bottom curve has been calculated as the number of crystals formed per unit volume, divided by the induction period. In case of homogeneous nucleation the induction period is supposed to be of the same order of magnitude as the effective nucleation period, and therefore we conclude that for $c > 0.01$ M the points of the curve show the rate of nucleation. This rate turns out to be proportional to c^{18} so that, in the language of chemical kinetics, the nucleation is an eighteenth order reaction.

A more detailed analysis of these results based on the Volmer-Becker-Döring theory of nucleation [5] will be published later. It leads to the conclusion that the interface tension between barium sulfate and aqueous solution is 90 ± 10 ergs/cm^2, both when it is calculated from the slope and from the position of the curve.

The surface tension of barium sulfate has never been measured before. Enüstün and Turkewich [7] recently found $\gamma = 84 \pm 8$ ergs/cm^2 for strontium sulfate against aqueous solution, and discovered the reason why all previous attemps to measure the surface tension of barium sulfate had failed. Enüstün and Turkewich calculate the surface tension of barium sulfate from the two assumptions, (1), the nucleus contains $3 \times 3 \times 3$ unit cells, and (2), the critical supersaturation ratio is 21.5. From the present work the most probable values are (1) 18 ions or 9 molecules of $BaSO_4$ = 775 Å^3, and (2) extrapolating the tangent to the right hand end of the bottom curve on Fig. 1 until log $(N/t) = 0$ we get the critical concentration for spontaneous nucleation, $c = 10^{-2.2}$ M. Thus $c/s = 10^{2.8} = 630$ when s = solubility of $BaSO_4 = 10^{-5}$ M. From these data, and eqn. (15) of Enüstün and Turkewich' paper, about 90 ergs/cm^2 is found for the surface tension, the exact value depending on the geometry assumed for the nucleus.

1. Nielsen, A. E. *Acta Chem. Scand.* **11** (1957) 1512.
2. Roughton, F. J. W. *Proc. Roy. Soc. (London)* **A 155** (1936) 258.
3. Nielsen, A. E. *J. Colloid Sci.* **10** (1955) 576.
4. Nielsen, A. E. *Acta Chem. Scand.* **12** (1958) 951.
5. Volmer, M. *Kinetik der Phasenbildung*, Steinkopff, Dresden and Leipzig 1939.
6. Nielsen, A. E. *Acta Chem. Scand.* **13** (1959) 784.
7. Enüstün, B. V. and Turkewich, J. *J. Am. Chem. Soc.* **82** (1960) 4502.

Received January 31, 1961.

Does Insulin Bind Hexokinase to Liver Mitochondria?

KARL-HEINZ KIESSLING and CARL-GÖRAN LUNDQUIST

Institute of Zoophysiology, University of Uppsala, Sweden

During the last years excellent progress has been made about the rôle of insulin in conjunction with the transport of sugars through cell membranes. There are, however, still a lot of effects of insulin on the cell metabolism which cannot be easily explained by an altered permeability only. This is especially evident in liver tissue, where insulin has no significant effect on the transport of glucose. The metabolism of glucose in liver is nevertheless strongly dependent on the presence of insulin.

the difficulty of observing the time in the T tube and by the impossibility of redispersing the precipitate by gentle means.

In Fig. 1 we see from the upper curve that within the reproducibility the number of crystals is independent of the initial concentration c when the latter is less than 0.01 M and proportional to c^{10} (the tenth power of the concentration) at $c > 0.01$ M. We do not know any other mechanism than homogeneous nucleation that can explain this phenomenon.

The second curve in Fig. 1 consists of three straight lines, corresponding to three different types of precipitation reaction. A similar curve (drawn from a compilation of different authors' data) has been published before [3], but without interpretation. Now we know that at $c < 0.0004$ M (log $c < -3.4$) the crystals grow by a fourth-order surface reaction, and at $c > 0.0004$ M the rate determining step is diffusion through the liquid [4]. The change of growth-controlling mechanism is the cause of the change of slope of the curve.

The other elbow is situated very close to the concentration where, as deduced from the upper curve, the precipitation process changes from being induced by foreign nuclei into development from spontaneously formed nuclei.

The bottom curve has been calculated as the number of crystals formed per unit volume, divided by the induction period. In case of homogeneous nucleation the induction period is supposed to be of the same order of magnitude as the effective nucleation period, and therefore we conclude that for $c > 0.01$ M the points of the curve show the rate of nucleation. This rate turns out to be proportional to c^{18} so that, in the language of chemical kinetics, the nucleation is an eighteenth order reaction.

A more detailed analysis of these results based on the Volmer-Becker-Döring theory of nucleation [5] will be published later. It leads to the conclusion that the interface tension between barium sulfate and aqueous solution is 90 ± 10 ergs/cm^2, both when it is calculated from the slope and from the position of the curve.

The surface tension of barium sulfate has never been measured before. Enüstün and Turkewich [7] recently found $\gamma = 84 \pm 8$ ergs/cm^2 for strontium sulfate against aqueous solution, and discovered the reason why all previous attemps to measure the surface tension of barium sulfate had failed. Enüstün and Turkewich calculate the surface tension of barium sulfate from the two assumptions, (1), the nucleus contains $3 \times 3 \times 3$ unit cells, and (2), the critical supersaturation ratio is 21.5. From the present work the most probable values are (1) 18 ions or 9 molecules of $BaSO_4$ = 775 Å^3, and (2) extrapolating the tangent to the right hand end of the bottom curve on Fig. 1 until log $(N/t) = 0$ we get the critical concentration for spontaneous nucleation, $c = 10^{-2.2}$ M. Thus $c/s = 10^{2.8} = 630$ when s = solubility of $BaSO_4 = 10^{-5}$ M. From these data, and eqn. (15) of Enüstün and Turkewich' paper, about 90 ergs/cm^2 is found for the surface tension, the exact value depending on the geometry assumed for the nucleus.

1. Nielsen, A. E. *Acta Chem. Scand.* **11** (1957) 1512.
2. Roughton, F. J. W. *Proc. Roy. Soc. (London)* **A 155** (1936) 258.
3. Nielsen, A. E. *J. Colloid Sci.* **10** (1955) 576.
4. Nielsen, A. E. *Acta Chem. Scand.* **12** (1958) 951.
5. Volmer, M. *Kinetik der Phasenbildung*, Steinkopff, Dresden and Leipzig 1939.
6. Nielsen, A. E. *Acta Chem. Scand.* **13** (1959) 784.
7. Enüstün, B. V. and Turkewich, J. *J. Am. Chem. Soc.* **82** (1960) 4502.

Received January 31, 1961.

Does Insulin Bind Hexokinase to Liver Mitochondria?

KARL-HEINZ KIESSLING and CARL-GÖRAN LUNDQUIST

Institute of Zoophysiology, University of Uppsala, Sweden

During the last years excellent progress has been made about the rôle of insulin in conjunction with the transport of sugars through cell membranes. There are, however, still a lot of effects of insulin on the cell metabolism which cannot be easily explained by an altered permeability only. This is especially evident in liver tissue, where insulin has no significant effect on the transport of glucose. The metabolism of glucose in liver is nevertheless strongly dependent on the presence of insulin.

Brain tissue, on the other hand, does not seem to require insulin to any larger extent. Recently it was shown by Johnson [1] that 75 % of the hexokinase of rat brain was present in the mitochondrial fractions, and was firmly attached to the particles. This firm binding of hexokinase to mitochondria does not exist in other tissues.

Lee and Wiseman [2], injecting insulin-^{131}I intravenously in rat, found that the major part of the intracellular ^{131}I in liver was bound to mitochondria and microsomes, and could not be removed merely by washing.

This observation by Lee and Wiseman together with the circumstances that on the one hand brain tissue, with its firmly bound hexokinase, has no obvious need for insulin, while using glucose almost exclusively, whereas on the other hand liver, with a more loosely bound hexokinase, shows a strong dependency on insulin for the metabolism of glucose, led us to the assumption that insulin might form a link between hexokinase and liver mitochondria *.

Experiments with alloxan diabetic rats which had shown glucosuria and polyurea for 2—10 days were used in an attempt of getting closer to this problem. They were treated in pairs, and for each experiment rats were chosen which had been injected with alloxan at the same time, and which as far as possible showed the same degree of diabetes. One rat was injected intravenously with 100 i.u. insulin together with a subcutaneous injection of the same quantity, the other rat remaining untreated. After varying times, from 30 min to 4 h, the rats were decapitated, and liver mitochondria prepared. Of the mitochondrial suspension, in 0.25 M sucrose, one half was mixed with hexokinase. Either was kept at 0°C with careful stirring for 15 min, centrifuged, washed once with sucrose, and recentrifuged. They were then incubated in Warburg vessels with glucose as a phosphate acceptor but without further addition of hexokinase. Glutamate was used as substrate. The oxygen consumption of the mitochondria from the insulin injected and from the untreated diabetic rats is seen in Table 1. As a comparison the oxygen consumption is given, when in addition hexokinase has been added to the vessels.

Table 1. Oxygen consumption of liver mitochondria from alloxan diabetic rats with and without addition of hexokinase. *Insulin* means that the diabetic rats have been injected with insulin before decapitation, *controls* that no insulin has been given. *Insulin + hexokinase* and *controls + hexokinase* denote the mitochondria pretreated with hexokinase as described in the text. Temp. 30°C. The figures are given as mm^3 O_2/20 min.

Treatment of the rats	No hexokinase added to the vessels	Hexokinase added to the vessels
Insulin	36	159
Insulin+hexokinase	42	160
Control	39	160
Control + hexokinase	44	171

The results seen in Table 1 are typical for all experiments, whether the rats were taken shortly after the diabetic symptoms or after ten days. Neither was the time which passed between the injection of insulin and the decapitation of any importance. It might be mentioned that alloxan diabetic rats exhibited convulsions only after very large doses of insulin as compared with normal animals. This indicates that alloxan in some way destroys insulin. On this account we had to use the relatively large quantities of the hormone.

The table shows that injected insulin had no effect on the respiration capacity of liver mitochondria from diabetic rats. The mitochondrial respiration is low in both insulin injected and untreated rats, and not until hexokinase is added directly to the vessels the respiration rises to normal values in either case. No indications of a function of insulin as a link between hexokinase and liver mitochondria could thus be obtained by this method.

* This hypothesis was also put forward recently by Bessman in connection with a lecture by R.B. Fisher and reproduced in print in *The Mechanism of Action of Insulin*, Blackwell Scientific Publications Ltd. 1960.

1. Johnson, M. K. *Biochem. J.* **77** (1960) 610.
2. Lee, N. D. and Wiseman, Jr., R. *Endocrinology* **65** (1959) 442.

Received February 15, 1961.

Crystalline Leghemoglobin

V. The N-Terminal Amino Acids of the Two Main Components

NILS ELLFOLK* and KLAS LEVIN

Medicinska Nobelinstitutet, Biokemiska Avdelningen, Karolinska Institutet, Stockholm, Sweden

Recent studies have shown that the two main components of leghemoglobin (Lhb) differ sligthly in respect to their molecular weights [1] and amino acid contents [2]. This indicates that they are individual proteins. Long-run electrophoresis at different pH values [3] showed them to be homogeneous. In order to get additional information on the homogeneity of the two components, it was decided to study their N-terminal amino acids using Sanger's 1-fluoro-2,4-dinitrobenzene (FDNB) method.

Experimental. The two main components of Lhb were prepared as described previously [3], and their homogeneity was electrophoretically checked. Different conditions of coupling with FDNB were tested, including the ethanol-bicarbonate and the ethanol-trimethyl-amine media, and it was decided to perform the coupling by stirring 0.2 μmoles of the dialyzed protein component in 3 ml of 0.1 M KCl solution with 100 μl FDNB at 40°C [4]. The pH of the solution was kept constant at 8.9 by successively adding 0.1 N NaOH from an Agla micrometer burett. The reaction was practically complete after 40 min, but was continued for still another 20 min during which the alkali consumption showed a linear course. The reaction mixture was then extracted with peroxide-free ether, after which the DNP-protein was precipitated by bringing the reaction mixture to pH 1.5 by adding 1 N HCl. A difference between the DNP-derivatives of the two components was observed in their ability to redissolve from the acid precipitate when the pH was increased. The DNP-derivate of the electrophoretically faster component went into solution easier than the derivative of the slower one. After the acid precipitation, the precipitates were washed with anhydrous ethanol and acetone, and stored in an evacuated desiccator over phosphorus pentoxide.

The DNP-proteins were hydrolyzed under varying conditions to meet the requirements for the detection of the more labile DNP-amino acids as well as those which are relatively stable. The hydrolyses were performed with HCl in the common way, as well as with a mixture of formic and perchloric acids in presence of acetic acid anhydride (1.0 : 015 : 055 by volume) according to Hanes *et al.*[5] Tubes with 0.2—0.3 ml of the acid and 0.2 μmoles of the DNP-protein were kept for varying times at 105° and 100°C for the HCl and formic-perchloric acid mixtures, respectively. The hydrolyzates were diluted with water and extracted in glass-stoppered test tubes with ether when the hydrolysis had been performed with HCl, and with benzene-*tert*-amyl alcohol (9:1 by volume) when it had been performed according to Hanes *et al.*[5] Each extract was washed with water to remove any acid-soluble material such as ε-DNP-lysine. The material which was soluble in ether or benzene-*tert*-amyl alcohol was transferred to Whatman No. 1 paper for two-dimensional chromatography according to Levy, as modified by Wallenfels and Arens [6]. The aqueous phase was examined by electrophoresis in 1 N NH_3, and by chromatography in *tert*-amyl alcohol — pH 6 phthalate [4].

For quantitative determination, the spots were eluted with 1 % sodium bicarbonate solution, and the amount of DNP-amino acid in the eluate determined spectrophotometrically. Readings of the optical densities were taken at 360 mμ, and the amounts of the amino acid derivatives were calculated using the extinction coefficient at 360 mμ of Wallenfels and Arens [6].

Results. In qualitative experiments, glycine was identified as the N-terminal amino acid for the electrophoretically faster component of Lhb, whereas valine was found to be the N-terminal group for the slower one. No other ether-soluble α-DNP-amino-acids could be identified on the chromatograms of the hydrolyzates of the DPN-derivatives of the two components. No positive evidence for the occurrence of histidine or arginine in the N-terminal position in the two components could be obtained.

Because of the well-known lability of DNP-glycine to hydrolysis, the DNP-derivative of the faster component was subjected to hydrolysis under various conditions. Short-time hydrolysis with formic and perchloric acids [5] was not found to be as quantitative with Lhb as was expected from the studies on the glycine peptides [5]. The hydrolysis is not complete under the conditions recommended (2 h at 100°C)

* Permanent address: Research Laboratories of the State Alcohol Monopoly, Helsinki, Finland.

since the extracts of hydrolyzates showed on chromatography a yellow streak which hardly moved in the phosphate-buffer system of Levy [4]. Chromatography of the aqueous phase in *tert*-amyl alcohol revealed the presence of ninhydrin-positive yellow spots which were obviously DNP-peptides of varying size. In addition, the yield of ε-DNP-lysine was very low. The incomplete hydrolysis was, therefore, one reason for the rather poor yield of glycine, which corresponded to 21 % of the total glycine present as an end group. The hydrolysis of the DNP-derivative of the faster component with 6 and 12 N HCl gave such low yields of DNP-glycine that it could not be measured. In comparison, the hydrolyzates of the DNP-derivative of the slower component showed on chromatography no derivatives which could be assumed to be DNP-peptides. The recovery of DNP-valine in the slower component was found to be 60 % after a 24 h hydrolysis at 105°C in 6 N HCl. According to Porter and Sanger [7], DNP-valine was 64 % unchanged in a 24 h hydrolysis in 5.7 N HCl. Using this value as a correction for the recovery of DNP-valine, a yield of 0.93 moles of valine was obtained for one mole of protein.

Discussion. The number of free α-amino groups gives the number of the open peptide chains present in the protein molecule. From the above findings it is evident that the electrophoretically-faster component of Lhb consists of one peptide with N-terminal glycine, whereas the slower one consists of one chain terminating in valine. These findings agree well with recent conclusions drawn from studies on the amino acid contents of the two components. The total lack of sulfur-containing amino acids, and accordingly the absence of S—S bonds that could form bridges between different peptide chains, led to the conclusion that the two components consist of one peptide chain only. Comparative studies on the N-terminal amino acids of normal and fetal human hemoglobin, as well as on the red cell pigments of various animal species, have shown that the number of peptide chains varies from two to six per molecule. It also seems that all hemoglobins contain at least one invariant chain terminating in valine [7,8]. In the case of myoglobins, which have a single peptide chain, the data are limited. Horse myoglobin has been found to terminate in glycine [7,9] in all the fractions (Mb I, Mb II and Mb III), while whale myoglobin [10] terminates in valine. The interchange of glycine and valine in the N-terminal position as found above in the two Lhb components gives additional support to the assumption recently put forward [2] that the synthesis of the two components is controlled by systems which are genetically different.

1. Ellfolk, N. *Acta Chem. Scand.* **14** (1960) 1819.
2. Ellfolk, N. *Ibid.* **15** (1961). *In press.*
3. Ellfolk, N. *Ibid.* **14** (1960) 609.
4. Fraenkel-Conrat, H., Harris, J. I. and Levy, A. L. *Methods of Biochemical Analysis* **2** (1955) 359.
5. Hanes, C. S., Hird, F. J. R. and Isherwood, F. A. *Biochem. J.* **51** (1952) 25.
6. Wallenfels, K. and Arens, A. *Biochem. Z.* **332** (1960) 217.
7. Porter, R. R. and Sanger, F. *Biochem. J.* **42** (1948) 287.
8. Ozawa, H. and Satake, K. *J. Biochem.* (Tokyo) **42** (1955) 641.
9. Åkeson, Å. and Theorell, H. *Arch. Biochem. Biophys.* **91** (1960) 319.
10. Anfinsen, C. B. and Redfield, R. R. *Advances in Protein Chem.* **11** (1956) 1.

Received February 2, 1961.

Derivatives of 4-Amino-2-hydroxybenzenesulfonic Acid

K. A. JENSEN and O. BUCHARDT

Chemical Laboratory of the University of Copenhagen, Copenhagen, Denmark

In connexion with researches [1-6] on derivatives of 4-amino-2-hydroxybenzoic acid (PAS) we wished to investigate the tuberculostatic activity of the analogous 4-amino-2-hydroxybenzenesulfonic acid and its derivatives. According to Lespagnol, Sevin and Beerens [7] the free acid is without tuberculostatic effect, but Youmans (*cf.* Doub *et al.*[8]) found both the acid and its amide to be slightly active. As the tuberculostatic effect of PAS is — at any rate in part — connected with an antagonism to *p*-aminobenzoic acid [1,9,10], it seemed not improbable that introduction of heterocyclic substituents into the sulfonamide group of 4-amino-2-hydroxybenzenesulfonamide might enhance the bacteriostatic activity of this compound very significantly just as it does with sulfanilamide. Our attempts to

since the extracts of hydrolyzates showed on chromatography a yellow streak which hardly moved in the phosphate-buffer system of Levy [4]. Chromatography of the aqueous phase in *tert*-amyl alcohol revealed the presence of ninhydrin-positive yellow spots which were obviously DNP-peptides of varying size. In addition, the yield of ε-DNP-lysine was very low. The incomplete hydrolysis was, therefore, one reason for the rather poor yield of glycine, which corresponded to 21 % of the total glycine present as an end group. The hydrolysis of the DNP-derivative of the faster component with 6 and 12 N HCl gave such low yields of DNP-glycine that it could not be measured. In comparison, the hydrolyzates of the DNP-derivative of the slower component showed on chromatography no derivatives which could be assumed to be DNP-peptides. The recovery of DNP-valine in the slower component was found to be 60 % after a 24 h hydrolysis at 105°C in 6 N HCl. According to Porter and Sanger [7], DNP-valine was 64 % unchanged in a 24 h hydrolysis in 5.7 N HCl. Using this value as a correction for the recovery of DNP-valine, a yield of 0.93 moles of valine was obtained for one mole of protein.

Discussion. The number of free α-amino groups gives the number of the open peptide chains present in the protein molecule. From the above findings it is evident that the electrophoretically-faster component of Lhb consists of one peptide with N-terminal glycine, whereas the slower one consists of one chain terminating in valine. These findings agree well with recent conclusions drawn from studies on the amino acid contents of the two components. The total lack of sulfur-containing amino acids, and accordingly the absence of S—S bonds that could form bridges between different peptide chains, led to the conclusion that the two components consist of one peptide chain only. Comparative studies on the N-terminal amino acids of normal and fetal human hemoglobin, as well as on the red cell pigments of various animal species, have shown that the number of peptide chains varies from two to six per molecule. It also seems that all hemoglobins contain at least one invariant chain terminating in valine [7,8]. In the case of myoglobins, which have a single peptide chain, the data are limited. Horse myoglobin has been found to terminate in glycine [7,9] in all the fractions (Mb I, Mb II and Mb III), while whale myoglobin [10] terminates in valine. The interchange of glycine and valine in the N-terminal position as found above in the two Lhb components gives additional support to the assumption recently put forward [2] that the synthesis of the two components is controlled by systems which are genetically different.

1. Ellfolk, N. *Acta Chem. Scand.* **14** (1960) 1819.
2. Ellfolk, N. *Ibid.* **15** (1961). *In press.*
3. Ellfolk, N. *Ibid.* **14** (1960) 609.
4. Fraenkel-Conrat, H., Harris, J. I. and Levy, A. L. *Methods of Biochemical Analysis* **2** (1955) 359.
5. Hanes, C. S., Hird, F. J. R. and Isherwood, F. A. *Biochem. J.* **51** (1952) 25.
6. Wallenfels, K. and Arens, A. *Biochem. Z.* **332** (1960) 217.
7. Porter, R. R. and Sanger, F. *Biochem. J.* **42** (1948) 287.
8. Ozawa, H. and Satake, K. *J. Biochem.* (Tokyo) **42** (1955) 641.
9. Åkeson, Å. and Theorell, H. *Arch. Biochem. Biophys.* **91** (1960) 319.
10. Anfinsen, C. B. and Redfield, R. R. *Advances in Protein Chem.* **11** (1956) 1.

Received February 2, 1961.

Derivatives of 4-Amino-2-hydroxybenzenesulfonic Acid

K. A. JENSEN and O. BUCHARDT

Chemical Laboratory of the University of Copenhagen, Copenhagen, Denmark

In connexion with researches [1-6] on derivatives of 4-amino-2-hydroxybenzoic acid (PAS) we wished to investigate the tuberculostatic activity of the analogous 4-amino-2-hydroxybenzenesulfonic acid and its derivatives. According to Lespagnol, Sevin and Beerens [7] the free acid is without tuberculostatic effect, but Youmans (*cf.* Doub *et al.*[8]) found both the acid and its amide to be slightly active. As the tuberculostatic effect of PAS is — at any rate in part — connected with an antagonism to *p*-aminobenzoic acid [1,9,10], it seemed not improbable that introduction of heterocyclic substituents into the sulfonamide group of 4-amino-2-hydroxybenzenesulfonamide might enhance the bacteriostatic activity of this compound very significantly just as it does with sulfanilamide. Our attempts to

Table 1.

Substance	Tuberculostatic effect			
	MA3	MA3(SM-res.)	MA3(PAS-res.)	MA3(INH-res.)
SM	6.8	5.8	6.8	6.9
PAS-Na	7.5	7.0	6.0	7.0
INH	7.8	7.8	7.5	5.3
II(amide)	<4	<4	<4	<4
IV(2-pyridylamide)	4.1	<4	4.0	4.3
V (anilide)	5.8	5.0	4.6	5.0

prepare the desired heterocyclic derivatives met with extraordinary difficulties, and at that time the problem was not pursued further. However, without the preparation of a PAS-analogue of sulfapyridine or sulfathiazole, *etc.*, we still considered our investigations on PAS-derivatives incomplete, and recently we succeeded in preparing the 2-pyridylamide of 4-amino-2-hydroxybenzenesulfonic acid in a pure state. Attempts to prepare derivatives of 2-aminothiazole, 2-amino-1,2,4-thiadiazole or 2-amino-4-methylpyrimidine by the same method yielded only small amounts of unidentified substances, which were not investigated further. It is remarkable that these difficulties are only met with when heterocyclic amines are used; the anilide of the sulfonic acid could be prepared without difficulty.

Recently Lora-Tamayo *et al.*[11] have prepared the hydrazide and some amides of 4-acetamido-2-hydroxybenzenesulfonic acid — also with a view to investigating their tuberculostatic activity — but have apparently not succeeded in deacetylating the amino group. A free amino group would, however, appear to be essential for any bacteriostatic effect.

By courtesy of Mr. L. Tybring, Bacteriological Department of the Leo Pharmaceutical Company, the bacteriostatic activity of 4-amino-2-hydroxybenzenesulfonic acid, its amide, anilide and 2-pyridylamide was tested against a *Mycobacterium tuberculosis* strain (MA 3) and against SM-resistant, INH-resistant and PAS-resistant variants of this strain in Dubos' medium (SM = streptomycin, INH = *iso*nicotinic hydrazide, PAS = *p*-aminosalicylic acid).

In Table 1 the tuberculostatic effect, a, is expressed as minus the logarithm of the dilution of the substance (1 g per 10^a g of the solution) that causes a definite but incomplete inhibition.

Accordingly 4-amino-2-hydroxybenzenesulfonic acid and its derivatives have a much less pronounced tuberculostatic effect than PAS, streptomycin, or *iso*nicotinic hydrazide, so the possibility of finding chemotherapeutics of practical importance in this group of substances seems to be excluded.

The activity of these substances against staphylococci, streptococci, gonococci, meningococci, and various Gram-negative bacteria was also found to be low (in most cases $a < 4$).

Experimental. 4-Amino-2-hydroxybenzenesulfonic acid. The acid was prepared by sulfonation of *m*-aminophenol (200 g) with conc. sulfuric acid (350 ml) containing a small amount of fuming sulfuric acid (1 ml), *cf.* Thorpe and Williams[12] and Miller *et al.*[13]. Yield 305 g of recrystallised product (88 %).

Pyridinium 4-acetylamino-2-acetoxybenzenesulfonate was prepared according to Thorpe and Williams[12] and recrystallised from ethanol. Yield 500 g from 330 g crude sulfonic acid (from 200 g *m*-aminophenol, *i.e.* 78 % calculated on a *m*-aminophenol basis).

4-Acetylamino-2-hydroxybenzenesulfonylchloride (I). The foregoing pyridinium salt (100 g) was finely powdered and placed in a roundbottom flask provided with a $CaCl_2$-tube. Phosphorus pentachloride (100 g) was added and the mixture shaken vigorously for 3—5 min and then warmed for 5—15 min on a water bath until a fairly homogeneous paste had formed. Then the flask was cooled rapidly and the mixture poured slowly, in small portions and with stirring, onto ice (*ca.* 700 g). The acid chloride separated as a crystalline white solid; it was filtered with suction and washed with water (100 ml). The product was spread on filter paper and dried at room temperature. The dry product was extracted with 500 ml of boiling chloroform, and filtered with suction. On cooling of the chloroform solution 10—15 g of pure chloride separated. The mother liquor was used again for extraction of the remaining product, *etc.*, until almost all the crude product had dissolved. Eventually the chloroform solu-

tion was concentrated to 100 ml and cooled. Total yield 52 g (63 %); m.p. 169°C. (Found: C 41.25; H 3.20; N 4.87. Calc. for $C_{10}H_{10}ClNO_5S$: C 41.17; H 3.43; N 4.80.)

4-Amino-2-hydroxybenzenesulfonamide (II), was prepared according to Thorpe and Williams [12] and recrystallised from propanol. M.p. 154–155°C. (Found: C 38.60; H 4.46; N 14.56. Calc. for $C_6H_8N_2O_3S$: C 38.30; H 4.28; N 14.89.)

2-(4'-Acetamido-2'-acetoxybenzenesulfonamido)-pyridine (III). The above acid chloride (5 g) and 2-aminopyridine (5 g) were dissolved in chloroform (50 ml), and the solution was refluxed for 10 min. The cooled solution was extracted three times with sodium carbonate solution. On acidification and cooling the sulfonamidopyridine separated as a white solid; yield 2 g. A better yield was obtained by the following procedure: The chloride (5 g) and 2-aminopyridine (2.1 g) were dissolved in pyridine (9 ml), and the solution was heated at 60–70°C for 10 min. The solution was diluted with 100 ml of water, acidified with acetic acid, and then neutralised with sodium bicarbonate. Yield 4 g (60 %). The product was recrystallised from glacial acetic acid; m.p. 247–249°C. (Found: C 51.05; H 4.20; N 11.68. Calc. for $C_{15}H_{15}N_3O_5S$: C 51.58; H 4.28; N 12.03.

2-(4'-Amino-2'-hydroxybenzenesulfonamido)-pyridine (IV). The foregoing compound (2 g) was dissolved in 2 N sodium hydroxide (10 ml), and the solution was refluxed for 4 h. On neutralisation of the cooled solution the deacetylated compound separated as a white solid. Yield 1.6 g. The compound was recrystallised from water with addition of carbon. It contained approximately half a molecule of water of crystallisation; it melted at 97–100°C, then solidified and melted again at 205°C. (Found: C 48.70; H 4.43; N 15.24, and after drying over phosphorus pentoxide: C 49.80; H 4.40; N 15.63. Calc. for $C_{11}H_{11}N_3O_3S.\frac{1}{2}H_2O$: C 48.20; H 4.80; N 15.15; and for $C_{11}H_{11}N_3O_3S$: C 49.81; H 4.18; N 15.84.)

4-Amino-2-hydroxybenzenesulfonanilide (V). The acetyl derivative was prepared in the same way as II. Yield 3.85 g from 5 g of the sulfonyl chloride (I). As analyses indicated a partial deacetylation, the compound was recrystallised from acetic anhydride. M.p. 208–213°C. (Found: C 54.80; H 4.70; N 7.98. Calc. for $C_{16}H_{16}N_2O_5S$: C 55.17; H 4.63; N 8.04.

The acetyl derivative (3 g) was dissolved in 1 N sodium hydroxide (20 ml) and refluxed for 2 h. On neutralisation and cooling the deacetylated compound separated. Yield 2.1 g; it was 1.3 g after three recrystallisations from water + ethanol. M.p. 175–176°C. (Found: C 54.60; H 4.66; N 10.27. Calc. for $C_{12}H_{12}N_2O_3S$: C 54.54; H 4.58; N 10.60.)

1. Jensen, K. A., Rosdahl, K.-G. and Ingvorsen, H. *Acta Chem. Scand.* **2** (1948) 220.
2. Jensen, K. A. and Ploug, J. *Ibid.* **3** (1949) 13.
3. Jensen, K. A. and Ingvorsen, H. *Ibid.* **6** (1952) 161.
4. Jensen, K. A. and Christensen, S. Å. K. *Ibid.* **6** (1952) 166.
5. Jensen, K. A. and Christensen, S. Å. K. *Ibid.* **6** (1952) 172.
6. Jensen, K. A. and Blok, G. *Ibid.* **6** (1952) 176.
7. Lespagnol, A., Sevin, A. and Beerens, H. *Compt. rend.* **229** (1949) 483.
8. Doub, L., Schaeffer, J. J., Bambas, L. L. and Walker, C. T. *J. Am. Chem. Soc.* **73** (1951) 903.
9. Youmans, G. P., Raleigh, G. W. and Youmans, A. S. *J. Bact.* **54** (1947) 409.
10. Lehmann, J. *Experientia* **5** (1949) 365.
11. Lora-Tamayo, M., Municio, A. M. and Ruiz, J. L. *Anales Fis. y quim. Madrid.* **55** (1959) 523; **56** (1960) 403.
12. Thorpe, W. V. and Williams, R. T. *Biochem. J.* **35** (1941) 63.
13. Miller, A. L., Mosher, H. S., Gray, F. W. and Whitmore, F. C. *J. Am. Chem. Soc.* **71** (1949) 3559.

Received February 23, 1961.

Derivatives of *p*-Chlorobenzenesulfonic Acid

K. A. JENSEN and O. BUCHARDT

Chemical Laboratory of the University of Copenhagen, Copenhagen, Denmark

In the course of investigations on compounds with potential diuretic or antidiabetic activity we had to use N-(β-chloroethyl)-*p*-chlorobenzenesulfonamide as a starting material. A product supposed to have this composition has been described by Kulka [1]. However, we found that the product prepared according to Kulka and having the indicated melting point contained no aliphatic chlorine, and it was soon shown actually to be di-β-(*p*-chlorobenzenesulfonylaminoethyl)-sulfite, $(ClC_6H_4SO_2NHCH_2CH_2O)_2SO$. Kulka gives no Cl analysis of his product, but only C, H, and N values, with respect to which the chloride does not differ very much from the sulfite. The desired chloride was prepared from the corresponding hydroxy compound

tion was concentrated to 100 ml and cooled. Total yield 52 g (63 %); m.p. 169°C. (Found: C 41.25; H 3.20; N 4.87. Calc. for $C_{10}H_{10}ClNO_5S$: C 41.17; H 3.43; N 4.80.)

4-Amino-2-hydroxybenzenesulfonamide (II), was prepared according to Thorpe and Williams [12] and recrystallised from propanol. M.p. 154–155°C. (Found: C 38.60; H 4.46; N 14.56. Calc. for $C_6H_8N_2O_3S$: C 38.30; H 4.28; N 14.89.)

2-(4'-Acetamido-2'-acetoxybenzenesulfonamido)-pyridine (III). The above acid chloride (5 g) and 2-aminopyridine (5 g) were dissolved in chloroform (50 ml), and the solution was refluxed for 10 min. The cooled solution was extracted three times with sodium carbonate solution. On acidification and cooling the sulfonamidopyridine separated as a white solid; yield 2 g. A better yield was obtained by the following procedure: The chloride (5 g) and 2-aminopyridine (2.1 g) were dissolved in pyridine (9 ml), and the solution was heated at 60–70°C for 10 min. The solution was diluted with 100 ml of water, acidified with acetic acid, and then neutralised with sodium bicarbonate. Yield 4 g (60 %). The product was recrystallised from glacial acetic acid; m.p. 247–249°C. (Found: C 51.05; H 4.20; N 11.68. Calc. for $C_{15}H_{15}N_3O_5S$: C 51.58; H 4.28; N 12.03.

2-(4'-Amino-2'-hydroxybenzenesulfonamido)-pyridine (IV). The foregoing compound (2 g) was dissolved in 2 N sodium hydroxide (10 ml), and the solution was refluxed for 4 h. On neutralisation of the cooled solution the deacetylated compound separated as a white solid. Yield 1.6 g. The compound was recrystallised from water with addition of carbon. It contained approximately half a molecule of water of crystallisation; it melted at 97–100°C, then solidified and melted again at 205°C. (Found: C 48.70; H 4.43; N 15.24, and after drying over phosphorus pentoxide: C 49.80; H 4.40; N 15.63. Calc. for $C_{11}H_{11}N_3O_3S.\frac{1}{2}H_2O$: C 48.20; H 4.80; N 15.15; and for $C_{11}H_{11}N_3O_3S$: C 49.81; H 4.18; N 15.84.)

4-Amino-2-hydroxybenzenesulfonanilide (V). The acetyl derivative was prepared in the same way as II. Yield 3.85 g from 5 g of the sulfonyl chloride (I). As analyses indicated a partial deacetylation, the compound was recrystallised from acetic anhydride. M.p. 208–213°C. (Found: C 54.80; H 4.70; N 7.98. Calc. for $C_{16}H_{16}N_2O_5S$: C 55.17; H 4.63; N 8.04.

The acetyl derivative (3 g) was dissolved in 1 N sodium hydroxide (20 ml) and refluxed for 2 h. On neutralisation and cooling the deacetylated compound separated. Yield 2.1 g; it was 1.3 g after three recrystallisations from water + ethanol. M.p. 175–176°C. (Found: C 54.60; H 4.66; N 10.27. Calc. for $C_{12}H_{12}N_2O_3S$: C 54.54; H 4.58; N 10.60.)

1. Jensen, K. A., Rosdahl, K.-G. and Ingvorsen, H. *Acta Chem. Scand.* **2** (1948) 220.
2. Jensen, K. A. and Ploug, J. *Ibid.* **3** (1949) 13.
3. Jensen, K. A. and Ingvorsen, H. *Ibid.* **6** (1952) 161.
4. Jensen, K. A. and Christensen, S. Å. K. *Ibid.* **6** (1952) 166.
5. Jensen, K. A. and Christensen, S. Å. K. *Ibid.* **6** (1952) 172.
6. Jensen, K. A. and Blok, G. *Ibid.* **6** (1952) 176.
7. Lespagnol, A., Sevin, A. and Beerens, H. *Compt. rend.* **229** (1949) 483.
8. Doub, L., Schaeffer, J. J., Bambas, L. L. and Walker, C. T. *J. Am. Chem. Soc.* **73** (1951) 903.
9. Youmans, G. P., Raleigh, G. W. and Youmans, A. S. *J. Bact.* **54** (1947) 409.
10. Lehmann, J. *Experientia* **5** (1949) 365.
11. Lora-Tamayo, M., Municio, A. M. and Ruiz, J. L. *Anales Fis. y quim. Madrid.* **55** (1959) 523; **56** (1960) 403.
12. Thorpe, W. V. and Williams, R. T. *Biochem. J.* **35** (1941) 63.
13. Miller, A. L., Mosher, H. S., Gray, F. W. and Whitmore, F. C. *J. Am. Chem. Soc.* **71** (1949) 3559.

Received February 23, 1961.

Derivatives of *p*-Chlorobenzenesulfonic Acid

K. A. JENSEN and O. BUCHARDT

Chemical Laboratory of the University of Copenhagen, Copenhagen, Denmark

In the course of investigations on compounds with potential diuretic or antidiabetic activity we had to use N-(β-chloroethyl)-*p*-chlorobenzenesulfonamide as a starting material. A product supposed to have this composition has been described by Kulka [1]. However, we found that the product prepared according to Kulka and having the indicated melting point contained no aliphatic chlorine, and it was soon shown actually to be di-β-(*p*-chlorobenzenesulfonylaminoethyl)-sulfite, $(ClC_6H_4SO_2NHCH_2CH_2O)_2SO$. Kulka gives no Cl analysis of his product, but only C, H, and N values, with respect to which the chloride does not differ very much from the sulfite. The desired chloride was prepared from the corresponding hydroxy compound

and thionyl chloride with the addition of a trace of pyridine. When the preparation is carried out without pyridine, only the sulfite is obtained.

We have further prepared *p*-chlorobenzenesulfonyl derivatives of some amino acids: glycine, *α*-alanine, *β*-alanine, and phenylglycine, and transformed them into the corresponding acid chlorides. From these some amides were prepared.

Some attempts were made to cyclise the above-mentioned hydroxy and chloro compounds to benzothiazine derivatives, but without success.

Experimental

1. N-(β-Hydroxyethyl)-p-chlorobenzenesulfonamide. To a stirred solution of 106 g of *p*-chlorobenzenesulfonylchloride (0.5 mole) in 200 ml of chloroform, 31 g of ethanolamine (0.5 mole) was added dropwise. Then a solution of 25 g NaOH in 250 ml of water was added dropwise with cooling and stirring. The ethanolamide which separated in crystalline form was filtered off, washed with water and dried. A little more amide was recovered by evaporation of the chloroform layer. Yield 105 g (90 %), after crystallisation from chloroform 76 g. M.p. 104–105°C. (Found: C 40.65; H 3.73; N 5.98. Calc for $C_8H_{10}ClNO_3S$: C 40.78; H 4.28; N 5.95.

2. Di-β-(p-chlorobenzenesulfonylaminoethyl)-sulfite. To N-(*β*-hydroxyethyl)-*p*-chlorobenzenesulfonamide (11.3 g) suspended in benzene (25 ml) was added 22 ml of freshly distilled thionyl chloride, and the mixture was heated under reflux for 3 h. Benzene and excess thionyl chloride were removed *in vacuo;* absolute ethanol (25 ml) was added and again distilled off *in vacuo*. The residue was recrystallised from ethyl acetate. White plates (4.7 g) of m.p. 150°C. (Found: C 37.25; H 3.57; Cl 13.67; S 18.60. Calc. for $C_{16}H_{18}Cl_2N_2O_7S_3$: C 37.14; H 3.50; Cl 13.70; S 18.59.)

3. N-(β-Chloroethyl)-p-chlorobenzenesulfonamide. N-(*β*-Hydroxyethyl)-*p*-chlorobenzenesulfonamide (45 g), thionyl chloride (90 ml) and pyridine (0.5 ml) were refluxed for 4 h. Excess thionyl chloride was removed *in vacuo;* 50 ml of absolute ethanol was added and subsequently removed *in vacuo*. The residue was recrystallised from ethyl acetate + petroleum ether. Yield 45 g (90 %). M.p. 84–85°C. (Found: C 38.00; H 3.42; Cl 27.55.Calc. for $C_8H_9Cl_2NO_2S$: C 37.82; H 3.57; Cl 27.90).

4. p-Chlorobenzene sulfonyl derivatives of amino acids. To a solution of the amino acid (0.1 mole) dissolved in 0.1 N sodium hydroxide (200 ml), a solution of *p*-chlorobenzenesulfonyl chloride (21.2 g, 0.1 mole) in chloroform (100 ml) was added, and the mixture was stirred vigorously for 2 h at room temperature and for an additional half hour at 40°C. The aqueous layer was separated and filtered. The acid was separated by addition of excess hydrochloric acid. The precipitate was filtered and recrystallised from water.

Yields: p-*Chlorobenzenesulfonylglycine.* M.p. 173°C. The compound has already been prepared by Nikolenko [2].

p-*Chlorobenzenesulfonyl-α-alanine.* M.p. 155°C. (Found: C 41.15; H 3.85; N 5.14. Calc. for $C_9H_{10}ClNO_4S$: C 41.19; H 3.81; N 5.30).

p-*Chlorobenzenesulfonyl-β-alanine.* M.p. 157.5°C. (Found: C 40.80; H 3.74; N 5.19. Calc. for $C_9H_{10}ClNO_4S$: C 41.19; H 3.80; N 5.30.)

p-*Chlorobenzenesulfonylaminophenylacetic acid.* M.p. 181–182°C. (Found: C 51.60; H 3.68; N 4.47. Calc. for $C_{14}H_{12}ClNO_4S$: C 51.62; H 3.71; N 4.30.)

p-*Chlorobenzenesulfonylaminoacetyl chloride.* The acid (12 g, 0.05 mole) was dissolved in thionyl chloride (50 ml) and the mixture refluxed for 2 h. Excess thionyl chloride was removed *in vacuo* and the residue crystallised from benzene. Yield 10 g (85 %). M.p. 130–131°C. (Found: C 36.10; H 2.79; N 5.54; Cl 25.80. Calc. for $C_8H_7Cl_2NO_3S$: C 35.85; H 2.63; N 5.23; Cl 26.45.)

In the same way were prepared:

α-(p-Chlorobenzenesulfonylamino)-propionyl chloride. Recrystallised from *n*-heptane. Decomp. at 100–120°C. (Found: C 38.90; H 3.15. Calc. for $C_9H_9Cl_2NO_3S$: C 38.50; H 3.20.)

β-(p-Chlorobenzenesulfonylamino)-propionyl chloride. Recrystallised from benzene + *n*-heptane. Decomp. at 100–120°C. (Found: C 39.10; H 3.79. Calc. for $C_9H_9Cl_2NO_3S$: C 38.50; H 3.20.)

The following amides were prepared by reaction of the acid chloride with an excess of the amine in benzene solution; they were recrystallised from water:

p-*Chlorobenzenesulfonylglycine isopropylamide.* M.p. 178°C. (Found: C 45.15; H 5.20. Calc. for $C_{11}H_{15}ClN_2O_3S$: C 45.13; H 5.20.)

p-*Chlorobenzenesulfonylglycine n-butylamide* M.p. 146°C. (Found: C 46.95; H 5.53. Calc. for $C_{12}H_{17}ClN_2O_3S$: C 47.28; H 5.62.)

p-*Chlorobenzenesulfonyl-β-alanine isopropylamide.* M.p. 143°C. (Found: C 47.50; H 5.68; N 9.10. Calc. for $C_{12}H_{17}ClN_2O_3S$: C 47.28; H 5.62; N 9.19.)

1. Kulka, M. *J. Am. Chem. Soc.* **72** (1950) 1215.
2. Nikolenko, L. N. *Zhur. Obshchei. Khim.* **26** (1956) 506.

Received February 23, 1961.

Separation of 2,4-Dinitrophenylhydrazones of Aliphatic Aldehydes by Liquid-Liquid Extraction

ERKKI HONKANEN

Laboratory of the Foundation for Chemical Research, Biochemical Institute, Helsinki, Finland

The easily prepared and stable 2,4-dinitrophenylhydrazones of carbonyl compounds are generally used for the isolation and characterization of the latter compounds. It is, however, very difficult to isolate hydrazones in pure form from their mixtures by crystallization because they readily form mixed crystals. Many good paper chromatographic methods have been developed, but they have only limited use in the separation of 2,4-dinitrophenyl-hydrazones. In this laboratory a cellulose powder column impregnated with dimethylformamide and the eluant *cyclo*hexane have been used for the separation of the 2,4-dinitrophenylhydrazones of the volatile carbonyl compounds of onion [1]. Good separations of the 2,4-dinitrophenylhydrazones of the lower aliphatic carbonyl compounds were effected by this technique, but it was not particularly effective for the higher homologs.

No counter-current method has been described for the separation of 2,4-dinitrophenylhydrazones. The selection of a suitable solvent system in which the 2,4-dinitrophenylhydrazones would be soluble enough and their partition coefficients sufficiently different is difficult. The best solvent system found was petroleum ether (b.p. 80—100°C): ethylene glycol monomethyl ether ("methyl oxitol", a product from the Shell Co.): water (10:10:2.5). The partition coefficients of the 2,4-dinitrophenylhydrazones of the normal aliphatic aldehydes (C_1—C_9) in this solvent system are given in Table 1.

The distribution studies were carried out in a countercurrent apparatus described by Hietala [2,3]. This apparatus (available from E. Hanslin & Co., Kaisaniemenk. 10, Helsinki, Finland) consists of 400 tubes

Table 1. Partition coefficients at 20°C of the 2,4-dinitrophenylhydrazones of normal aliphatic aldehydes (C_1—C_9) in the solvent system petroleum ether (b.p. 80—100°): ethylene glycol monomethyl ether: water (10:10:2.5).

Aldehyde	*K*
C_1	0.08
C_2	0.15
C_3	0.30
n-C_4	0.52
n-C_5	0.83
n-C_6	1.3
n-C_7	1.9
n-C_8	3.1
n-C_9	4.5

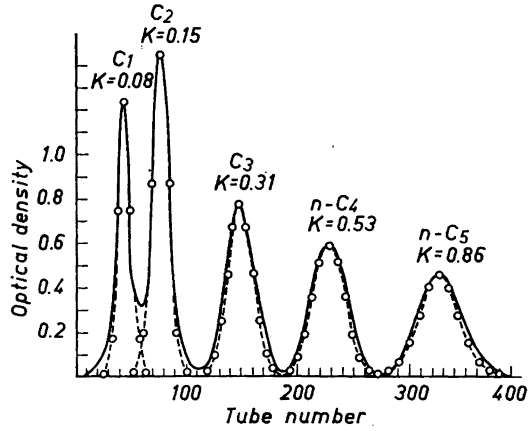

Fig. 1. Distribution of 2,4-dinitrophenylhydzones of normal aliphatic aldehydes (C_1—C_5) in the solvent system: petroleum ether: ethylene glycol monomethyl ether: water, (10:10:2.5). ——— experimental curve, optical density of the bottom phase at 360 mμ. O— —O theoretical curve.

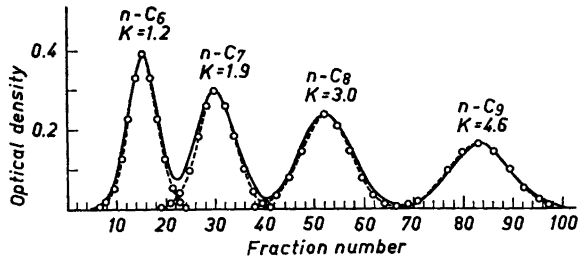

Fig. 2. Distribution of 2,4-dinitrophenylhydrazones of normal aliphatic aldehydes (C_6-C_9) in the solvent system: petroleum ether: ethylene glycol monomethyl ether: water (10:10:2.5). ——— experimental curve, optical density at 360 mμ. O——O theoretical curve. Volume of each fraction 96 ml.

and operates with continuous flow of either the top or the bottom phase.

A mixture of 2,4-dinitrophenylhydrazones of the normal C_1-C_5 aldehydes (0.1 mmole of each) was distributed first. Each tube was filled with 4.3 ml of the top phase (v_t) and 9.0 ml of the bottom phase (v_b). The run was made at about 20°C with the top phase mobile and the solvent flowing at a rate of 1.0 ml/min. The shaking mechanism was adjusted to make 36 complete strokes per minute and the tilting angle was about ± 55°. After 4 850 ml (V_t) of effluent had emerged, a sample of the bottom phase was taken from every fifth tube and the light absorptions of the samples measured at 360 mμ with a spectrophotometer.

The resulting distribution curves are shown in Fig. 1. A complete separation of the five 2,4-dinitrophenylhydrazones was obtained. The theoretical distribution curves (the normal error curves) were calculated from the extinction values at the maxima. The partition coefficients calculated from eqn. (1) [3] corresponded very well with those obtained using a separatory funnel (Table 1).

$$K = \frac{v_b x_t}{V_t - v_t x_t} \qquad (1)$$

V_t is the total volume (4 850 ml) of the effluent (top phase), v_t and v_b the volumes of the top and bottom phases, respectively, in one distribution tube, x_t the number of tubes through which the midpoint of the distribution of a substance has passed with the top phase.

For the separation of the higher homologs (C_6-C_9), a run was made with the bottom phase mobile. The phase volumes were now v_t = 4.75 ml and v_b = 8.55 ml and the other factors the same as before. After 4 220 ml of effluent had emerged, fractions 96 ml in volume were collected until the 2,4-dinitrophenylhydrazone of *n*-nonanal had come out. The distribution curves are shown in Fig. 2. By this procedure a good separation of the 2,4-dinitrophenylhydrazones of the C_6-C_9 aldehydes was effected. The separation would have been even better if the volume of the top phase in each distribution unit had been larger (and the volume of the bottom phase correspondingly smaller). The partition coefficients in Fig. 2 were calculated from eqn. (2) [3].

$$K = \frac{V_b - x_b v_b}{x_b v_b} \qquad (2)$$

V_b is the volume of the eluant needed to transport the midpoint of the distribution of a substance x_b (= 400) tubes.

Work on the separation of the 2,4-dinitrophenylhydrazones of the volatile carbonyl compounds of the flowers of red clover by the above liquid-liquid extraction technique is in progress.

This investigation is a part of a research project under U.S. Public Law No. 480, 83rd Congress.

1. Virtanen, A. I. and Spåre, C.-G. *Suomen Kemistilehti B* **34** (1961) 18; Spåre, C.-G. and Virtanen, A. I. *Acta Chem. Scand. In press.*
2. Hietala, P. K. *Acta Chem. Scand.* **14** (1960) 212.
3. Hietala, P. K. *Ann. Acad. Scient. Fennicae II A* **1960** No. 100.

Received January 19, 1961.

Diphosphides of the Group VIII Transition Metals

STIG RUNDQVIST

Institute of Chemistry, University of Uppsala, Uppsala, Sweden

The existence of phosphides with the composition MeP_2 (Me=transition metal) has been established for all Group VIII transition metals [1-7] except cobalt [8]. The unit cell dimensions and structure types have been determined [9-12] for FeP_2, RuP_2, OsP_2 and PtP_2, but no X-ray data have so far been published for RhP_2, IrP_2, NiP_2 and PdP_2.

During investigations of transition metal phosphides at this Institute, the above mentioned diphosphides have been synthesised by heating mixtures of metal powder and red phosphorus in evacuated and sealed silica tubes at temperatures between 800°C and 1 100°C. All attempts to grow single-crystals suitable for X-ray work were unsuccessful. However, an analysis of the X-ray powder patterns of RhP_2, IrP_2, NiP_2 and PdP_2 showed that the diffraction lines can be indexed on the basis of monoclinic unit cells. The powder data, taken with a Guinier-type focussing camera in Cr$K\alpha_1$ radiation (internal calibration standard silicon, a = 5.4305 Å) are collected in Tables 1 and 2. Variable unit cell dimensions indicating extended homogeneity

Table 1a. Powder data for RhP_2. (Cr$K\alpha_1$ radiation).

hkl	I_o	$\sin^2\Theta_o \times 10^4$	$\sin^2\Theta_c \times 10^4$
100	w−	468	468.4
011	w	843.8	843.8
11$\bar{1}$	v.st	953.0	953.3
020	st	1 561.4	1 561.6
10$\bar{2}$			1 564.3
111	m	1 670.8	1 671.2
002	st	1 813.1	1 813.8
200	st	1 873.9	1 873.6
11$\bar{2}$	v.w.	1 954	1 954.7
120	v.w.	2 030	2 030.0
12$\bar{1}$	m	2 125.2	2 124.5
012	w	2 203.2	2 204.2
20$\bar{2}$	w+	2 251.8	2 251.6
210	w	2 263.8	2 264.0
21$\bar{2}$	w	2 642.5	2 642.0
102	m−	3 000.1	3 000.1
12$\bar{2}$	w	3 125.6	3 125.8
022	m+	3 375.3	3 375.3
220	st	3 435.9	3 435.2
211			3 435.4
22$\bar{2}$	m+	3 812.8	3 813.2
113	st−	3 861.9	3 862.9
031	v.w	3 968	3 967.0
130	st	3 983.1	3 981.9
31$\bar{1}$			3 982.7
13$\bar{1}$	st	4 076.5	4 076.4
21$\bar{3}$	m	4 191.3	4 191.3
300	v.w	4 217	4 215.7
013	m	4 471.3	4 471.4
122	m−	4 561.5	4 561.6
131	st	4 795.3	4 794.3

Table 1b. Powder data for IrP_2. (Cr$K\alpha_1$ radiation).

hkl	I_o	$\sin^2\Theta_o \times 10^4$	$\sin^2\Theta_c \times 10^4$
100	w−	460	459.2
011	w+	833.9	833.9
11$\bar{1}$	v.st	961.3	961.0
020	st	1 564.2	1 563.4
10$\bar{2}$			1 567.0
111	st	1 625.5	1 625.2
002	st	1 772.4	1 772.0
200	st	1 836.9	1 836.9
11$\bar{2}$	v.w	1 959	1 957.9
120	v.w	2 023	2 022.7
12$\bar{1}$	w+	2 134.4	2 133.6
012	v.w	2 165	2 162.8
210	w	2 227.7	2 227.8
20$\bar{2}$	m+	2 280.9	2 280.6
21$\bar{2}$	v.w	2 673	2 671.4
102	m	2 895.0	2 895.4
12$\bar{2}$	w+	3 130.7	3 130.5
211	st	3 335.6	3 334.9
022			3 335.4
220	st	3 400.5	3 400.4
113			3 840.8
22$\bar{2}$	st+	3 843.0	3 844.0
031			3 960.7
31$\bar{1}$	st	3 970.8	3 970.7
130			3 977.0
13$\bar{1}$	st	4 087.8	4 087.9
21$\bar{3}$	m	4 222.4	4 222.2
013	m	4 377.7	4 377.8
122	m	4 458.3	4 458.8
131	st	4 752.2	4 752.0
202	m	4 937.5	4 937.2

Table 2a. Powder data for NiP_2. ($CrK\alpha_1$ radiation).

hkl	I_o	$\sin^2\Theta_o \times 10^4$	$\sin^2\Theta_c \times 10^4$
$11\bar{1}$	w	843.1	843.0
110	m	912.5	912.6
020	m	1 662.6	1 662.6
$20\bar{2}$	st	1 709.1	1 709.6
$11\bar{2}$	m	1 866.0	1 866.1
200	m	1 987.9	1 987.6
111	m	2 074.7	2 074.6
002	v.w	2 186	2 185.0
021	m	2 208.1	2 208.9
$22\bar{1}$	v.w	2 966	2 965.0
$22\bar{2}$	m	3 371.9	3 372.2
$31\bar{2}$			3 378.3
$31\bar{1}$	w	3 586.1	3 586.8
220	m	3 649.8	3 650.2
022	m	3 846.3	3 847.6
$11\bar{3}$	v.w	3 982	3 981.6
130	st	4 238.1	4 237.8
$31\bar{3}$	v.w	4 261	4 262.3
112	st	4 329.0	4 329.1
$22\bar{3}$	v.w	4 874	4 872.0
310	m	4 888.0	4 887.8

Table 2b. Powder data for PdP_2. ($CrK\alpha_1$ radiation).

hkl	I_o	$\sin^2\Theta_o \times 10^4$	$\sin^2\Theta_c \times 10^4$
$11\bar{1}$	v.w	778	776.9
110	v.st	823.0	822.9
020	m+	1 528.4	1 528.6
$20\bar{2}$	st	1 578.9	1 578.9
200	st	1 762.9	1 763.0
$11\bar{2}$	st	1 782.1	1 782.0
111	w	1 919.6	1 920.0
021	w	2 054.6	2 054.1
002	w	2 102.0	2 102.2
$31\bar{2}$	w	3 021.8	3 021.7
$22\bar{2}$	m	3 107.7	3 107.5
$31\bar{1}$	v.w	3 161	3 159.7
220	m	3 290.9	3 291.6
022	m	3 631.1	3 630.8
$13\bar{1}$	v.w	3 838	3 834.0
$11\bar{3}$			3 838.1
130	st	3 880.2	3 880.0
$31\bar{3}$	v.w	3 933	3 934.7
112	st	4 067.7	4 068.2
310	m	4 348.9	4 348.9
$40\bar{2}$	m	4 581.9	4 581.6
$22\bar{3}$	v.w	4 590	4 592.1
$13\bar{2}$	m	4 840.2	4 839.1
221	v.w	4 960	4 960.3

Table 3. Unit cell data for RhP_2, IrP_2, NiP_2 and PdP_2. (Estimated accuracy of the cell dimensions ± 0.02 %).

Phosphide	a(Å)	b(Å)	c(Å)	β°	U(Å^3)
RhP_2	5.742_9	5.794_2	5.837_0	112°.91$_9$	178.9
IrP_2	5.745_7	5.790_6	5.850_0	111.°60$_0$	181.0
NiP_2	6.365_9	5.615_2	6.071_5	126°.22$_4$	175.1
PdP_2	6.777_1	5.856_3	6.206_3	126.°42$_7$	198.2

ranges were not observed. The unit cell dimensions are given in Table 3.

It has been hinted that RhP_2 and IrP_2 are isostructural [3,4,10]. A comparison of the data in Tables 1a and 1b shows that this is undoubtedly true. Furthermore, it seems probable that these two phases are isostructural with $RhSb_2$, the unit cell dimensions of which are reported to be [13] $a = 6.6$ Å; $b = 6.4$ Å; $c = 6.7$ Å; $\beta = 117°$; probable space-group $P\ 2_1/c$ with four formula units in the cell.

NiP_2 and PdP_2 are also isostructural as seen from Tables 2a and 2b. The data indicate that the unit cells are face-centred, and this is not contradiacted by powder data taken with Cu$K\alpha$ radiation up to $\Theta = 45°$. The space-group might possibly be $C\ 2/c$ or Cc, and the unit cells contain four formula units.

Acknowledgements. This work has been supported by the *Air Force Office of Scientific Research of the Air Research and Development Command, United States Air Force* through its European Office under Contract No. AF 61(052)—40 and by the *Swedish State Council for Technical Research.*

1. Franke, W., Meisel, K., Juza, R. and Biltz, W. *Z. anorg. Chem.* **218** (1934) 346.
2. Biltz, W., Ehrhorn, H. J. and Meisel, K. *Ibid.* **240** (1939) 117.
3. Faller, F. E., Strotzer, E. F. and Biltz, W. *Ibid.* **244** (1940) 317.
4. Söffge, K. H., Heimbrecht, M. and Biltz, W. *Ibid.* **243** (1940) 297.
5. Biltz, W. and Heimbrecht, M. *Ibid.* **237** (1938) 132.
6. Wiehage, G., Weibke, F., Biltz, W., Meisel, K. and Wiechmann, F. *Ibid.* **228** (1936) 357.
7. Biltz, W., Weibke, F., May, E. and Meisel, K. *Ibid.* **223** (1935) 129.
8. Biltz, W., Heimbrecht, M. and Meisel, K. *Ibid.* **241** (1939) 349.
9. Meisel, K. *Ibid.* **218** (1934) 360.
10. Rundqvist, S. *Nature* **185** (1960) 31.

11. Thomassen, L. *Z. physik. Chem.* **B 4** (1929) 277.
12. Kjekshus, A. *Acta Chem. Scand.* **14** (1960) 1450.
13. Zhuravlev, N. N., Pak Gvan, O. and Kuz'min, R. N. *Vest. Mosk. Univ. Ser. mat., mekhan., astron., fiz., khim.*, **No. 5** (1958) 79. (See The Abstracts Journal for Metallurgy, **Part A**, Nr. 9/10 (**1959**) 50).

Received February 17, 1961.

Reactivity of Coordinated Substances

I. The Oxidation of EDTA Bound in the Cr(III)EDTA Complex by Permanganate Ion

M. T. BECK* and O. KLING**

Chemistry Department A, Technical University of Denmark, Copenhagen, Denmark

Earlier observations showed that free EDTA is oxidised by permanganate ion in acidic solution. Addition of Bi(III) in excess to EDTA results in a marked decrease of the reaction rate: the complex formation with Bi(III) protects the EDTA [1] against the oxidising effect of MnO_4^-.

This qualitative result suggests that it is possible to decide by a direct chemical method between the different types of coordination of EDTA to different metal ions. For this purpose we compared the oxidation of EDTA in the presence of excess Bi(III) and that of the inert Cr(III) EDTA complex by MnO_4^-. The reaction was studied in perchloric acid medium at $20 \pm 1-2°C$ by means of spectrophotometric investigations.

As is shown in Fig. 1, the Bi(III)EDTA complex is oxidised very slowly (curve 1), while the oxidation of Cr(III)EDTA takes place much faster (curve 2). Under similar conditions the reduction of MnO_4^- by free EDTA is completed within 30 sec. This characteristic behaviour may be explained most simply by the existence of at least one free functional group in the Cr(III)EDTA compound, *i.e.* the pentadentate nature of EDTA in this complex [2].

If Bi(III) is added to the Cr(III)EDTA the oxidation rate decreases (curve 3). This effect can be interpreted by an interaction of free Bi(III) and Cr(III)EDTA. It must be mentioned, however, that so far this interaction could not be demonstrated by other methods.

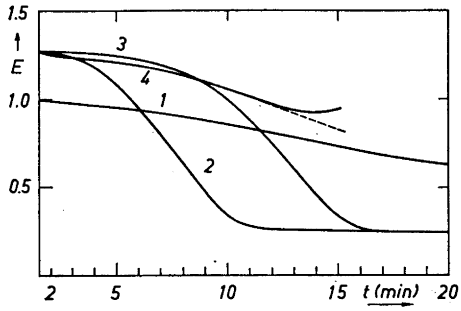

Fig. 1. Change of extinction (E) with time (t) of the following solutions: Curve 1. 2×10^{-3} M Bi(III), 10^{-3} M EDTA, 2.12×10^{-4} M MnO_4^-, 0.23 M $HClO_4$. Curve 2. 10^{-3} M Cr(III)EDTA, 2.12×10^{-4} M MnO_4^-, 0.23 M $HClO_4$. Curve 3. 10^{-3} M Cr(III)EDTA, 2×10^{-3} M Bi(III), 2.12×10^{-4} M MnO_4^-, 0.23 M $HClO_4$. Curve 4. 10^{-3} M Cr(III)EDTA, 2.12×10^{-3} M Mn(II), 2.12×10^{-4} M MnO_4^-, 0.23 M $HClO_4$. Wavelength 525 mμ, cell length 2 cm.

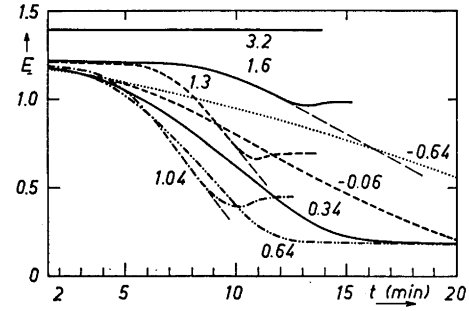

Fig. 2. The effect of pH on the reduction of MnO_4^- by Cr(III)EDTA complex. Numbers indicate pH values of solutions: 10^{-3} M Cr(III)EDTA, 2.12×10^{-4} M MnO_4^-. Wavelength 525 mμ, cell length 2 cm.

* Rask-Ørsted Fellow 1960/61, Permanent address: Institute of Inorganic and Analytical Chemistry, University of Szeged, Szeged, Hungary.

** Auslandsstipendium, Deutsche Forschungsgemeinschaft. Permanent address: Institut für physikalische Chemie, Universität Frankfurt a.M., Germany.

11. Thomassen, L. *Z. physik. Chem.* **B 4** (1929) 277.
12. Kjekshus, A. *Acta Chem. Scand.* **14** (1960) 1450.
13. Zhuravlev, N. N., Pak Gvan, O. and Kuz'min, R. N. *Vest. Mosk. Univ. Ser. mat., mekhan., astron., fiz., khim.*, **No. 5** (1958) 79. (See The Abstracts Journal for Metallurgy, **Part A**, Nr. 9/10 (**1959**) 50).

Received February 17, 1961.

Reactivity of Coordinated Substances

I. The Oxidation of EDTA Bound in the Cr(III)EDTA Complex by Permanganate Ion

M. T. BECK* and O. KLING**

Chemistry Department A, Technical University of Denmark, Copenhagen, Denmark

Earlier observations showed that free EDTA is oxidised by permanganate ion in acidic solution. Addition of Bi(III) in excess to EDTA results in a marked decrease of the reaction rate: the complex formation with Bi(III) protects the EDTA [1] against the oxidising effect of MnO_4^-.

This qualitative result suggests that it is possible to decide by a direct chemical method between the different types of coordination of EDTA to different metal ions. For this purpose we compared the oxidation of EDTA in the presence of excess Bi(III) and that of the inert Cr(III) EDTA complex by MnO_4^-. The reaction was studied in perchloric acid medium at $20 \pm 1-2°C$ by means of spectrophotometric investigations.

As is shown in Fig. 1, the Bi(III)EDTA complex is oxidised very slowly (curve 1), while the oxidation of Cr(III)EDTA takes place much faster (curve 2). Under similar conditions the reduction of MnO_4^- by free EDTA is completed within 30 sec. This characteristic behaviour may be explained most simply by the existence of at least one free functional group in the Cr(III)EDTA compound, *i.e.* the pentadentate nature of EDTA in this complex [2].

If Bi(III) is added to the Cr(III)EDTA the oxidation rate decreases (curve 3). This effect can be interpreted by an interaction of free Bi(III) and Cr(III)EDTA. It must be mentioned, however, that so far this interaction could not be demonstrated by other methods.

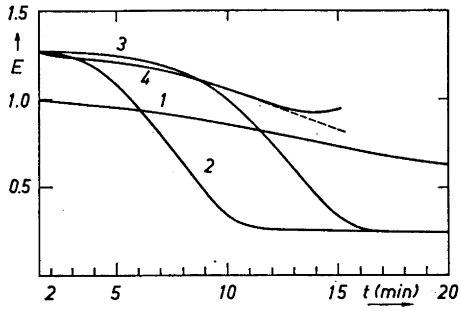

Fig. 1. Change of extinction (E) with time (t) of the following solutions: Curve 1. 2×10^{-3} M Bi(III), 10^{-3} M EDTA, 2.12×10^{-4} M MnO_4^-, 0.23 M $HClO_4$. Curve 2. 10^{-3} M Cr(III)EDTA, 2.12×10^{-4} M MnO_4^-, 0.23 M $HClO_4$. Curve 3. 10^{-3} M Cr(III)EDTA, 2×10^{-3} M Bi(III), 2.12×10^{-4} M MnO_4^-, 0.23 M $HClO_4$. Curve 4. 10^{-3} M Cr(III)EDTA, 2.12×10^{-3} M Mn(II), 2.12×10^{-4} M MnO_4^-, 0.23 M $HClO_4$. Wavelength 525 mμ, cell length 2 cm.

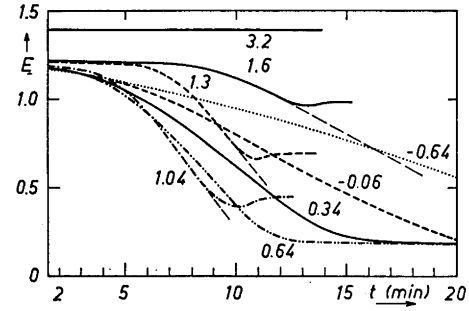

Fig. 2. The effect of pH on the reduction of MnO_4^- by Cr(III)EDTA complex. Numbers indicate pH values of solutions: 10^{-3} M Cr(III)EDTA, 2.12×10^{-4} M MnO_4^-. Wavelength 525 mμ, cell length 2 cm.

* Rask-Ørsted Fellow 1960/61, Permanent address: Institute of Inorganic and Analytical Chemistry, University of Szeged, Szeged, Hungary.

** Auslandsstipendium, Deutsche Forschungsgemeinschaft. Permanent address: Institut für physikalische Chemie, Universität Frankfurt a.M., Germany.

The shape of the curves shown in Fig. 1 is typical for autocatalytic processes, evidently due to the effect of Mn(II) formed during the reaction. Studying the influence of a large excess of Mn(II) it was observed that the reaction rate also decreases (curve 4). The Mn(II) ions have a double role, an accelerating one and a retarding one, the latter being presumably effected by an interaction with Cr(III) EDTA similar to that in the Bi(III) case.

It does not seem likely that the observed decrease of the reaction rates after addition of Bi(III) or Mn(II) is due only to a salt effect (cf. Ref.[3]). Any comparison with the permanganate-oxalate reaction is of course a very conditional one, it is found, however, that the influence of the ionic strength on the reaction rate may be either positive or negative [4]. Corresponding spectrophotometric investigations at 525 mμ made by Malcolm and Noyes [5] give the same qualitative shape of the curves as is shown in Figs. 1 and 2. They observed an increase of the reaction rate with increasing initial Mn(II) concentration. The permanganate-citrate oxidation [6,7] lead in the cases mentioned to opposite conclusions about the direction of the influence of added Mn(II). In any case, however, irrespective of the mechanism discussed, a direct association with the substance to be oxidised is proposed. Further investigations in this field will have to take account of these interferences.

The influence of hydrogen ion concentration on the oxidation of Cr(III)EDTA is shown in Fig. 2. Due to the complicated mechanism of the overall reaction it is difficult to find a definite measure of the reaction rate. But using either halftime or slope in the inflection point of the different curves the velocity of oxidation as a function of pH shows in every case a maximum at about pH 1. This sort of influence by hydrogen ions can hardly be explained otherwise than by the assumption that Cr(III)EDTA exists in acidic medium in two species of different reactivity. Although nothing is known about the molecularity of the oxidation reaction studied, it is very probable that the nonprotonated species is oxidised faster. Therefore on the basis of the results of the foregoing experiments, the following definite qualitative conclusions may be drawn:

The oxidation of complex bound EDTA by MnO_4^- depends primarily on the structure of the complex. The free functional groups are the most vulnerable.

Both protons and metal ions protect these groups against oxidation, the protective effect of the latter being greater.

Experimental. H[Cr EDTA (H_2O)] was prepared following Hamm [8] and three times recrystallised, the last recrystallisation under addition of HCl. The product proved to be free of Cl^-.

The extinction measurements were made in a 2 cm cell using an air thermostated CARY Spectrophotometer Model 11MS-50 at 525 mμ, *i.e.* the absorption maximum of MnO_4^- ion.

The solutions were made from stock solutions of 10^{-2} M H[Cr EDTA (H_2O)], 2.12×10^{-3} M MnO_4^-, 2.3 M $HClO_4$, and 10^{-2} M $Bi(NO_3)_3 \cdot 5H_2O$ in 10^{-1} M $HClO_4$.

The measurements of absorbancy were started 90 sec. after addition of MnO_4^-. At lower acidities (pH > 1) it was impossible to follow the reaction to completion, due to the transient formation of MnO_2 as it is indicated by a reincrease of extinction.

pH-Values were determined by means of a pH-Meter 3 (Radiometer, Copenhagen) or calculated with sufficient accuracy from the amount added of perchloric acid, using the pK-values given for H[Cr EDTA (H_2O)] by Furlani [2].

Acknowledgement. The authors wish to thank Professor Jannik Bjerrum for his kind interest and assistance and Professor J. A. Christiansen for helpful remarks. We are grateful for financial assistance from the *Rask-Ørsted Fondet* (M.T.B.) and the *Deutsche Forschungsgemeinschaft* (O.K.).

1. Beck, M. T. *Chem. Analyst* 1961. *In print.*
2. Schwarzenbach, G. and Biedermann, W. *Helv. Chim. Acta* **31** (1948) 459; Furlani, C., Morpurgo, G. and Sartori, G. *Z. anorg. u. allgem. Chem.* **303** (1960) 1.
3. Brønsted, J. N. *Z. physik. Chem.* **102** (1922) 169.
4. Fessenden, R. W. and Redmon, B. C. *J. Am. Chem. Soc.* **57** (1935) 2247.
5. Malcolm, J. M. and Noyes, R. M. *Ibid.* **74** (1952) 2772.
6. Bhale, V. M., Mohammad, S., Bhagwat, W.V. and Bafna, S. L. *J. Sci. Ind. Research (India)* **12B** (1953) 521; Bhale, V. M., Sant, P. G. and Bafna, S. L. *Ibid.* **15B** (1956) 45.
7. Cabrera, L. and Rio, C. Del, *Anales real soc. españ. fis. y quím. (Madrid)* **49B** (1953) 263.
8. Hamm, R. E. *J. Am. Chem. Soc.* **75** (1953) 5670.

Received February 14, 1961.

The Presence of Savinin in the Wood of *Juniperus communis* L. and *Juniperus thurifera* L.

J. B. BREDENBERG and J. RUNEBERG

Organisk-kemiska institutionen, Kungl. Tekniska Högskolan, Stockholm, Sweden

Some years ago a compound $C_{20}H_{16}O_6$, m.p. 142—144°, $[\alpha]_D^{20}$ −38° was isolated by one of us (J.B.B.) from the wood of the common juniper, *Juniperus communis*. Owing to the small amount obtained it could not be further investigated.

Recently a similar substance, "compound II", m.p. 156—157.5°, $[\alpha]_D^{20}$ −4°, was isolated from the wood of *Juniperus thurifera* [1]. The ultraviolet and infrared spectra of the two products were almost identical. It was noticed during the purification of "compound II", which involved repeated sublimations, that the melting point increased and the optical rotation decreased whilst the ultraviolet and infrared spectra remained almost unchanged. This appeared to indicate continuous racemisation and the product from *J. thurifera* was therefore subjected to purification by means of recrystallisation only. The resulting product had m.p. 143—145° and $[\alpha]_D^{20}$ −75°.

Both compounds have now been identified as slightly impure savinin (m.p. 145—146°, $[\alpha]_D^{20}$ −87°) a lignan previously isolated from the needles of *Juniperus sabina* [2,3].

The low optical rotation of the product from *J. communis* is probably due to the fact that strong alkali had been used during its isolation.

The product was obtained in the following way:

Ether-extracted wood of common juniper (9.4 kg) [4] was extracted with acetone for 60 h. The solvent was evaporated and the extraction residue poured into ether. The ether-soluble material was extracted with alkali and the neutral part steam distilled. The non-steam volatile part (13 g) was hydrolysed with 2 N KOH in ethanol for 30 min. The acidic extract (0.8 g) was chromatographed on alumina and gave in the ether eluate 24 mg of a slightly yellowish crystalline powder, m.p. 140—144°. One sublimation gave m.p. 142—144°, $[\alpha]_D^{20}$ −38° ($CHCl_3$, *c* 0.6, from 3 mg) mixed m.p. with authentic savinin, m.p. 145—146°, no depression. (Found: C 68.0; H 4.6; O 27.6. Calc. for $C_{20}H_{16}O_6$: C 68.2; H 4.6; O 27.3.) Ultraviolet spectrum: λ_{max} 238, 293 and 336 mμ (log ε 4.16, 4.10 and 4.23), λ_{min} 229, 268 and 307 mμ (log ε 4.11, 3.71 and 3.98). The infrared spectrum (in KBr) was identical with that of savinin.

For details of the isolation of "compound II" compare Ref.[1] When the crude compound was crystallised from benzene, absolute ethanol and from benzene again a product m.p. 143—145°, $[\alpha]_D^{20}$ −75° ($CHCl_3$, *c* 1), was obtained. Mixed m.p. with authentic savinin, no depression. The infrared spectrum (in KBr) was identical with that of savinin.

A sample of pure savinin $[\alpha]_D^{20}$ −80°, kindly supplied by Dr. A. Schrecker, was sublimed and the $[\alpha]_D^{20}$ was now found to be −84° and after another sublimation −78°.

Our thanks are due to professor H. Erdtman for drawing our attention to the similarity between our preparations and savinin.

1. Runeberg, J. *Acta Chem. Scand.* **14** (1960) 1985.
2. Hartwell, J. L., Johnson, J. M., Fitzgerald, D. B. and Belkin, M. *J. Am. Chem. Soc.* **75** (1953) 235.
3. Schrecker, A. W. and Hartwell, J. L. *J. Am. Chem. Soc.* **76** (1954) 4896.
4. Bredenberg, J. B. and Gripenberg, J. *Acta Chem. Scand.* **8** (1954) 1728.

Received February 3, 1961.

ACTA CHEMICA SCANDINAVICA 15 (1961) 457–462

Acid Hydrolysis of Organic Fluorophosphorus Compounds

GUNNAR AKSNES* and SVEIN IVAR SNAPRUD

Norwegian Defence Research Establishment, Toxicological Group, Kjeller pr Lillestrøm, Norway

The acid hydrolysis of dimethoxy-, methoxyethyl- and diethyl phosphoryl fluorides has been studied in different concentrations of hydrochloric acid at 0° and 25°C. By calculation of the specific rate constant, k_{H+} it is necessary to correct for the organophosphorus acid produced during the reaction. The pK-values of two of the organophosphorus acids have been measured. These values are in reasonable agreement with the values of the same acids reported by Hudson and Harper [1]. The activation energies, E_A have been calculated. The mechanisms of the acid hydrolysis of organic fluorophosphorus compounds are discussed.

In a previous publication [2], the connection between the ability of hydrogen bond formation with deuterium oxide of the phosphoryl group in organophosphorus compounds and the acid hydrolysis of corresponding phosphorus compounds was pointed out and discussed in some detail. In order to collect more information on the acid hydrolysis of organophosphorus compounds three organic fluorophosphorus compounds have been synthesized and their acid hydrolysis studied in different low concentrations of hydrochloric acid. The three compounds, dimethoxy-, ethylmethoxy- and diethylphosphoryl fluoride, are the same which previously have been used for the study of the nucleophilic reactions with hydroxyl ions and *iso*nitroso acetone [3]. Kilpatrick and Kilpatrick [4] have studied the acid hydrolysis of di*iso*propoxyphosphoryl fluoride (DFP) by using a dilatometric method. In the present paper we have used the ordinary titration method for determination of the acids produced during the reaction.

THE KINETICS OF THE ACID HYDROLYSIS OF ORGANIC FLUOROPHOSPHORUS COMPOUNDS

The acid hydrolysis of dimethoxy-, methoxyethyl- and diethyl phosphoryl fluorides was measured in hydrochloric acid in the concentration interval

* Present address: Chemical Institute, University of Bergen, Bergen, Norway.

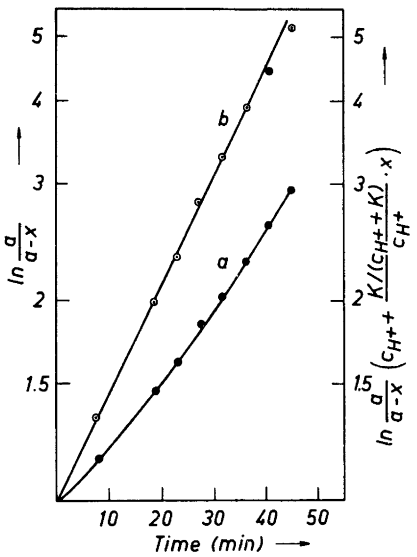

Fig. 1. The acid hydrolysis of dimethoxyphosphoryl fluoride in 0.04 N HCl. a) The plot of the experimental values according to the first order rate equation. b) The plot of the experimental values according to eqn. (6).

0.01—0.1 N. In such low concentration of hydrochloric acid it was necessary to correct for the increase of hydrogen ions in the reaction solution due to the formation of free acids during the reaction:

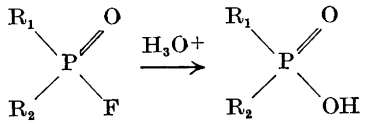

(1)

In Fig. 1a is plotted the experimental values of the hydrolysis of dimethoxyphosphoryl fluoride in 0.04 N HCl according to the first order rate equation, *i.e.* $\ln[a/(a-x)]$ as function of t. The curvature of the line is due to the catalysing effect of the organic phosphorus acid formed during the reaction. Hydrofluoric acid which has a pK of approximately 4.5 contributes so small amounts of hydrogen ions that its presence can be neglected. The three organophosphorus acids formed during the reaction have the following pK's: dimethoxyphosphorus acid, 1.29, methoxyethyl phosphorus acid, 2.0, and diethylphosphorus acid, 3.4[1].

If the amount of organic phosphorus fluoride hydrolysed after a time t is x the reaction can be described by the following equation:

$$\frac{dx}{dt} = k_{H+} \, (c_{H+} + c_h) \, (a-x) \qquad (2)$$

where k_{H+} = specific rate constant of hydrogen ions, c_{H+} = concentration of hydrogen ions due to the hydrochloric acid, c_h = contribution of hydrogen ions due to the organic phosphorus acid at the time t, and a = initial concentration of fluorophosphorus compound.

If the dissociation constant of the organic phosphorus acid is K the following equilibrium equation must be obeyed:

$$K = \frac{c_h(c_{H+} + c_h)}{x - c_h} \approx \frac{c_h \cdot c_{H+}}{x - c_h} \quad (3)$$

since in the present work $c_{H+} \gg c_h$. By rearrangement of eqn. (3) we get:

$$c_h = \frac{K}{c_{H+} + K} \cdot x \quad (4)$$

By inserting eqn. (4) in (2) we get for the rate of hydrolysis:

$$\frac{dx}{dt} = k_{H+}\left(c_{H+} + \frac{K}{c_{H+} + K} \cdot x\right)(a - x) \quad (5)$$

Upon integration of eqn. (5) the following rate equation is obtained:

$$k_{H+}\left(c_{H+} + \frac{K}{c_{H+} + K} \cdot a\right) = \frac{1}{t} \ln \frac{a}{a - x}\left(c_{H+} + \frac{K}{c_{H+} + K} \cdot x\right) \quad (6)$$

In Fig. 1b we have used the same experimental values as in Fig. 1a but in this case we have plotted

$$\ln \frac{a}{a - x}\left(\frac{c_{H+} + \frac{K}{c_{H+} + K} \cdot x}{c_{H+}}\right)$$

as function of t. The straight line which can be drawn through the calculated points shows that eqn. (6) can be used for the calculation of the specific rate constant k_{H+} when K is known. This was done in the case of dimethoxy — and methoxyethyl fluoride, but not diethylphosphoryl fluoride, since in the latter case the corresponding acid has as high a pK-value as approximately 3.4 [1], and the correction due to the formation of this acid during the reaction was found to be so small that the rate constants could be calculated according to the first order rate equation.

EXPERIMENTAL

Materials. The three organic fluorophosphorus compounds studied were synthesized according to previous descriptions [3]. All compounds are rather unstable in storage so freshly distilled products must always be used. The compounds are preferably kept in polyethylene bottles.

The hydrochloric acid solution used was prepared from constant boiling hydrochloric acid (B.D.H. Analar).

Kinetic measurements. These were performed in 250 ml Erlenmeyer flasks immersed in water of the desired temperature. A constant circulating water bath of ± 0.1°C accuracy was used for the measurements at 25°C; at 0°C the reaction flask was placed in water-ice mixture in a Dewar flask of 4 litres capacity.

The organic fluorophosphorus compound (0.5—0.9 g) was weighed into the Erlenmeyer flask. The flask was placed in the water bath for approximately 20 min, and the reaction started by quickly diluting the compound with 100 ml standardized hydrochloric acid which had been equilibrated beforehand in the same water bath.

After fixed intervals of time an aliquot of 10 ml of the reaction solution was transfered to an Erlenmeyer flask containing crushed ice. The total amount of acid was immediately titrated with standard 0.1 N sodium or barium hydroxide using cresol red as an

Table 1. Determination of dissociation constants of organic phosphorus acids. Temp 20°C.

Compound	Conc. of acid	Conc. of Na^+ present	Measured pH	K_a Calc.	pK_a Average
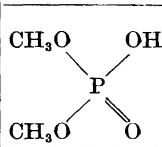	0.01806	0	1.87	0.068	1.22
	0.03612	0	1.65	0.049	
	0.07224	0	1.41	0.058	
	0.0903	0	1.33	0.065	
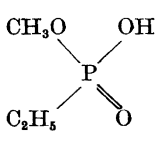	0.0355	0	1.82	0.0124	1.88
	0.0338	0.0047	1.91	0.0140	
	0.0323	0.0091	2.02	0.0137	
	0.0309	0.0131	2.15	0.0135	
	0.0296	0.0166	2.32	0.0128	
	0.0284	0.0200	2.54	0.0110	

indicator. Eight or nine individual titrations were made for every rate constant calculated. The average error of the rate constant is approximately ± 5 %.

DETERMINATION OF p*K*-VALUES OF THE ORGANIC PHOSPHORUS ACIDS

The organic phosphorus acids were made from the corresponding chloride by shaking with an equivalent amount of silver oxide in water. The silver chloride was filtered off and the clear water solution was directly used for the determination of the dissociation constants. The measurements were performed with a Metrohm Potentiometer Model E 187. With this instrument pH-values are reproducible to ± 0.02 pH units. In the case of methoxyethylphosphorus acid the pH in the acid solution was determined in the presence of varying amount of sodium hydroxide. From the measured pH the pK was calculated according to the following formula:

$$K = \frac{c_{H+}\left(c_{H+} + c_{Na+} - \frac{10^{-14}}{c_{H+}}\right)}{c_{HA} - \left(c_{H+} + c_{Na+} - \frac{10^{-14}}{c_{H+}}\right)}$$

where $c_{H+} = \frac{a_{H+}}{f_{H+}}$ = concentration of hydrogen ions and c_{HA} = total concentration of organic phosphorus acid. The values of f_{H+} were taken from the literature [5]. In Table I are summarized the calculated values of the dissociation constants of dimethoxy- and methoxyethyl phosphorus acids determined at different concentrations of acid and salt. The values are in reasonable agreement with the reported pK-values, 1.29 and 2.00, of the same compounds [1].

RESULTS AND AND DISCUSSION

In Table 2 are recorded the values of the rate constants at different acid concentrations of the acid hydrolysis of the three organic fluorophosphorus compounds studied. The values of k_{OH^-} are also included in the same table.

Table 2. Data from the acid hydrolysis of methoxy-, methoxyethyl- and diethylphosphoryl fluoride.

Compound	Specific rate constants, k_{H^+} l mole^{-1} min^{-1} in different concentrations of HCl							k_{OH^-} l mole^{-1} sec^{-1} 25.1°C	E_A kcal/mole
	Temperature: 25°C						Temp. 0°C		
	0.01 N	0.02 N	0.03 N	0.04 N	0.06 N	0.099N	0.099		
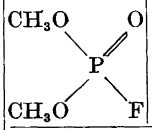	—	0.502	—	0.437	0.435	0.401	0.0618	18.2	12.1 ± 1
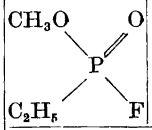	—	0.500	—	0.476	0.476	0.437	0.0518	49.1	13.8 ± 1
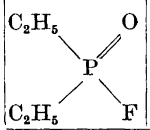	2.62	2.24	2.25	2.06	—	—	0.289 (in 0.02 N HCl)	726	13.2 ± 1

The substituents in these phosphorus compounds show a much smaller influence upon the rate of the acid catalysed hydrolysis than on the alkaline hydrolysis of the same compounds. In this respect the hydrolysis of organic fluorophosphorus compounds shows the same general tendency as the hydrolysis of esters of carboxylic acids [6]. From a theoretical point of view the acid catalysed reaction is more complex than the nucleophilic reaction with hydroxyl ions. The former involves an electrophilic attack of hydrogen ions probably on the oxygen of the phosphoryl group, and a nucleophilic attack of a water molecule on phosphorus. The rate determining step may be either the formation of a transition state with phosphonium structure:

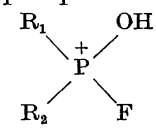

(I)

or this step includes a bifunctional simultaneous attack of both the hydrogen ion and the water molecule forming a transition state with pentavalent structure:

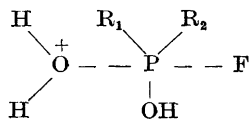

(II)

In the latter case we may expect that two opposing effects will contribute to the total picture of the reaction. The greater polarity of the phosphoryl group should favour a proton transfer from the water solution. If therefore the formation of the phosphonium structure (I) were the rate determining step, the rate of hydrolysis should be expected to increase steadily from the dimethoxy- to the diethyl phosphoryl fluoride in accordance with the increasing polarity of the P—O bond in the same series [3]. If on the other hand the pentavalent structure (II) is formed the stability of such a transition state may be expected to decrease from the dimethoxy to the diethyl compound in accordance with the decreasing negativity of the substituents in the same series [7]. The small differences in the rate constants of the acid hydrolysis of the three organic fluorophosphorus compounds thus seem to favour the hypothesis of a pentavalent structure of the transition state. In the same way if the phosphonium structure (I) represents the rate determining step, the acid hydrolysis of di*iso*propoxyphosphoryl fluoride ought to give a higher rate than the dimethoxy compound due to a stronger polarity of the P—O bond. From the measurements of Kilpatrick and Kilpatrick [4] we calculate that the k_{H+} of DFP at 25°C lies in the neighbourhood of 0.07 l mole^{-1} min^{-1}, and is thus approximately 1/7 of the k_{H+} of the dimethoxy compound. We therefore assume that the difference in k_{H+} is due to the entering of water in the rate determining step according to the pentavalent structure (II) of the transition state. In the case of DFP the bulky *iso*propoxy groups must be expected to give strong steric retardation during the formation of the transition complex.

As seen from Table 2 the specific rate constant, k_{H+}, decreases with increasing hydrogen ion concentration for the three organic fluorophosphorus compounds studied. The decrease can approximately be described by the equation: $k_{H+} = K \cdot [H^+]$ where K = constant. The magnitude of K in the hydrolysis of dimethoxy- and methoxyethyl phosphoryl fluoride is of the same order as observed for the K in hydrolysis of di*iso*propoxyphosphoryl fluoride (DFP) by Kilpatrick and Kilpatrick [4], but in the hydrolysis of diethylphosphoryl-fluoride K seems to be somewhat higher. This is in accordance with an explanation of the acid hydrolysis of phosphorus compounds put forward in a previous publication [2] according to which a stronger tendency of hydrogen bond formation of the substrate should favour a greater K-value.

REFERENCES

1. Hudson, R. F. and Harper, D. C. *J. Chem. Soc.* **1958** 1356.
2. Aksnes, G. *Acta Chem. Scand.* **14** (1960) 1526.
3. Aksnes, G. *Acta Chem. Scand.* **14** (1960) 1515.
4. Kilpatrick, M. L. and Kilpatrick, M. *J. Phys. & Colloid. Chem.* **53** (1949) 1371.
5. Harned, H. S. and Owen, B. B. *The Physical Chemistry of Electrolytic Solutions.* Reinhold., New York 1943.
6. Hammet, L. P. *Physical Organic Chemistry*, McGraw-Hill Book Co. New York 1940, pp. 211–213.
7. Pauling, L. *Nature of the Chemical Bond*, Cornell University Press, New York 1948, p. 93.

Received September 29, 1960.

ACTA CHEMICA SCANDINAVICA 15 (1961) 463–470

Free Radical Reactions Studied by Means of Luminescence

GUNNAR AHNSTRÖM

Institute of Organic Chemistry and Biochemistry, University of Stockholm, Sweden

Reactions of free radicals are accompanied by release of energy due to bond formation. Some of the energy quanta may primarily or secondarily be converted to light; therefore it is possible to study such radical reactions by luminescence measurements.

In the present study, Kolbe's synthesis of hydrocarbons, where radicals are expected to be involved, and the electrolysis of some aromatic amino acids in dilute salt solution, have been followed by light emission measurements.

The biological effects of ionizing radiation may be ascribed to ionized and possibly also to excited molecules which are the primary products formed on energy absorption. These molecules are subject to fast chemical and physical changes which arise partly in reactions with other molecules. Charged and uncharged free radicals seem to be important intermediates in the production of radiation effects [1].

The oxygen effect is believed to be due to reactions between oxygen and free radicals (or excited triplet states) leading to peroxy compounds.

Irradiated compounds have been shown to have radiomimetic effects in biological systems [2,3].

The reactions of the primarily changed molecules may be studied by physical and chemical methods. In solution, free radicals are extremely short-lived [4] because of rapid recombination, and hence the concentration of radicals is low. Further, if we study free radicals by means of their own properties (magnetic or optical), large amounts of energy must be introduced into the system to produce measurable amounts of radicals. However, if we measure a product of the reactions of radicals, we are independent of the lifetime of the radicals in the system.

The present investigation is an explorative study, employing luminescence measurements, of the reactions of electrolytically produced free radicals.

From a radio-chemical point of view, ionization means that a molecule (charged or uncharged) loses or gains electrons. In this process a free radical is formed (if charged, an ion radical). In principle, identical reactions, although somewhat more specific, occur at the anode and cathode, respectively, in electrolysis. This resemblance is not only valid from physical and chemical

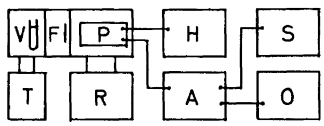

Fig. 1. Photon counting system: V—Reation vessel; F—Filter; P—Photomultiplier tube EMI 6255 A; H—High voltage supply; S—Scaler; T—Thermostat; R—Refrigerator; A—Amplifier; O—Oscilloscope.

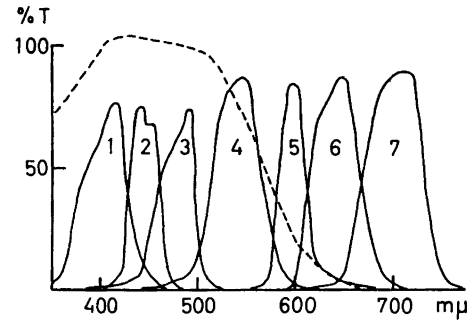

Fig. 2. Transmission curves for Balzers Broad-Band Interference filters Nos. 1—7. The broken curve shows arbitrary spectral sensitivity of EMI 6255 A.

points of view, in fact it has been shown that electrolytically produced reactive species are biologically active [5]. Electrolysis of tyrosine in diluted sodium acetate causes chromosome aberrations in barley root tips, thus resembling the indirect action of ionizing radiation.

Among the factors investigated was Kolbe's synthesis of hydrocarbons. For example, electrolysis of sodium acetate in water or methanol gives ethane and carbon dioxide in a reaction between methyl or acetoxyl radicals. In side reactions, some other substances are also formed, such as methane, methanol and methyl acetate [6]. The anode reaction was found to be accompanied by light emission in the visible range.

A few cases described earlier were reactions probably involving radical interaction and accompanied by light emission. In gas reactions of the type $H + NO = HNO$ and $H + Cl_2 = HCl + Cl$, chemiluminescence in the infra-red-visible range has been described [7]. In these cases the compound molecule is vibrationally excited in the ground state.

A luminescence has also been observed to be induced by ultrasonics in liquid systems such as H_2O—CCl_4, where the light emission has also been described as chemiluminescence occurring in the gas phase [8].

EXPERIMENTAL

A schematic diagram illustrating the equipment used for luminescence measurements is presented in Fig. 1.

In the thermostat-controlled vessel the electrolysis is performed in a small test-tube (1 ml) with 0.5 mm Pt-wire as electrodes. During electrolysis and/or luminescence measurements, different chemicals are injected when required into the reaction vessel with a syringe. To a circular plate was fixed a set of interference filters (Fig. 2). When the plate is rotated, these filters are introduced, one at a time, into a position between the test-tube and the photomultiplier tube.

The photomultiplier tube is cooled in a refrigerator to −30°C. The thermal background is hereby reduced by a factor of 100 to 20 counts per second. From the space angle and

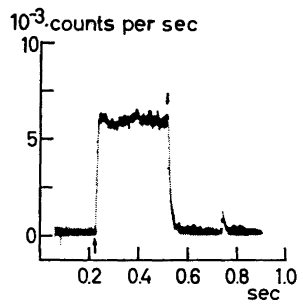

Fig. 3. Electrolysis of 1 M sodium acetate. The arrows show start and stop of electrolysis. The electrolysis current was 150 mA.

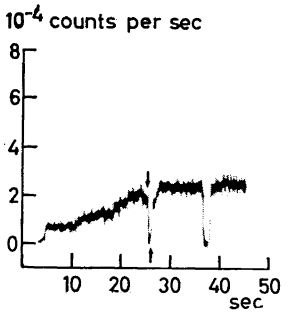

Fig. 4. Electrolysis of 0.001 M phenylalanine in 0.2 M Na_2SO_4. Arrows show stop and start of electrolysis. The current was 100 mA.

the quantum effectiveness of the photomultiplier tube (about 10 % in the range 350—550 mμ) it is calculated preliminarily that one photon is counted out of about 2 500 emitted. The photon pulses are either counted on a scaler or recorded on an oscilloscope with a simple rate metre. The time constant of the latter was 0.01 sec.

The following systems were studied.

1. Electrolysis of concentrated (≥1 M) sodium salts of carboxylic acids (Kolbe's synthesis)
2. Electrolysis of different organic compounds in an electrolyte.
3. Electrolysis of Grignard reagents.
4. Wurtz's synthesis (hydrocarbons from alkyl halides and sodium metal).

In the first mentioned type of systems 1 M solutions of for example acetate, propionate, citrate and tartrate were electrolysed. In all cases light emission was observed. In subsequent experiments, acetate was chosen as a model substance.

In series 2, among other substances tested, were several amino acids. Tyrosine and phenylalanine exhibited the brightest luminescence and were used in further experiments.

In the system types 3 and 4 the appearence of luminescence was observed. These experiments are still under progress and hence will not be discussed in the present communication.

RESULTS

Electrolysis of 1 M sodium acetate in water gives a light emission at the anode with maximum intensity in filter 2. When the electrolysis is performed in methanol solution the emission spectrum has its maximum in filter 3—4. At pH ~ 14 in water, the emission spectrum is broadened, the main emission being directed to filter 4. In the latter case, reactions presumably of $OH\cdot$ with $CH_3COO\cdot$ dominate in accordance with the known fact that electrolysis in alkaline solutions leads to alcohol formation. The species giving rise to light emission are formed immediately and are very short-lived as shown in Fig. 3. A time constant of 0.0001 sec. does not change the shape of the curve.

When Cl^- or Br^- is added to the system there is a great increase in the luminescence. The luminescence increases linearly by about 20 000 counts per second per mmole Cl^-. Paramagnetic and peroxide-decomposing ions such as Cu^{++}, Co^{++}, and $Fe^{++} + Fe^{+++}$ have no effect when added in moderate concentrations (<0.01 M). Temperature has little effect on the luminescence intensity.

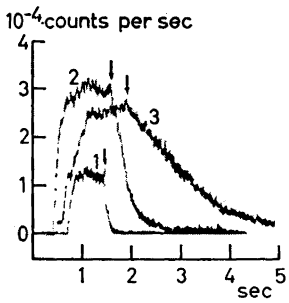

Fig. 5. Electrolysis of 0.001 M phenylalanine in 0.2 M Na_2SO_4 at different temperatures. The curves are from the point of maximum intensity in Fig. 4. Curve 1, 80°C; Curve 2, 25°C; Curve 3, 5°C.

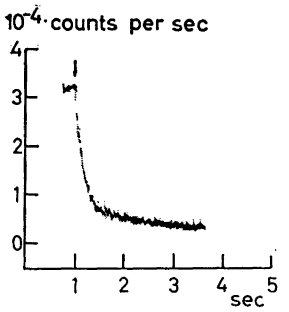

Fig. 6. Long lived luminescence in 0.001 M phenylalanine caused by prolonged electrolysis.

Electrolysis of tyrosine and phenylalanine in 0.2 M sodium sulphate exhibits a light emission having a maximum in filter 3. When electrolysis starts there is a slow increase in light emission intensity, the maximum being reached in about half a minute. As soon as the electrolysis current is broken the luminescence decays in less than one second. In a renewed electrolysis there is no slow build-up, the maximum intensity being reached in one second (Fig. 4). At this maximum intensity level the decay of phenylalanine luminescence was studied as a factor influenced by temperature and concentration of organic material, *etc.* Fig. 5 shows electrolysis of 0.001 M phenylalanine at 80, 25, and 5°C. The life length of the luminescence decreases at higher temperatures together with a decrease in light emission intensity at 80°C. The intensity and life length also decreases when an increase occurs in the concentration of organic material during electrolysis.

When phenylalanine in sodium sulphate solution is subject to a prolonged electrolysis a new, more long-lived luminescence appears, as shown in Fig. 6.

The effect of some inorganic ions were also studied. Cl^- and Br^-, which have an activating effect on the luminescence intensity in the Kolbe reaction, do not affect phenylalanine electrolysis. On the other hand ions such as Cu^{++}, Co^{++}, and $Fe^{++} + Fe^{+++}$ totally quench the last mentioned long-lived luminescence. Fig. 7 shows injection of 0.1 ml 0.01 M Cu^{++}. Renewed electrolysis resulted in the decay being the same as in curve 2, Fig. 5.

As a control experiment, oxygen free water was also injected, resulting in the unexpected increase of the luminescence shown in Fig. 8. The same effect could also be obtained by stirring the solution.

Addition of radical scavengers or radiation protectors (there may be no difference) has a noticeable effect on the intensity, the life length and the emission spectrum of the luminescence in the investigated systems, as shown by electrolysis of acetate in methanol. When the acetate solution contains I_2 or diphenylpicryl hydrazyl (a stable free radical), no luminescence is observed. Traces of hydroquinone, *p*-phenylenediamine and ascorbic acid have the same

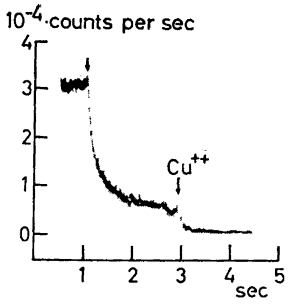

Fig. 7. Introduction of Cu^{2+} during long lived decay (*cf.* Fig. 6).

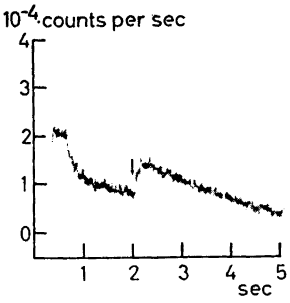

Fig. 8. Introduction of oxygen-free water during long lived decay(*cf.* Fig. 6).

effects, but when some amino acids (cysteine and methionine), known as radiation protectors, were introduced there was also a luminescence. However, a spectral analysis shows that the emission is thrown to longer wavelengths with maximum emission in filter 5—6.

DISCUSSION

The discussion of the luminescent reactions in the Kolbe's synthesis are to be based on available knowledge of possible products in this synthesis. As mentioned above the final main products from electrolysis of the acid $C_nH_{2n+1}COOH$ are the hydrocarbons $C_{2n}H_{4n+2}$. However, the Kolbe reaction is accompanied by many side-reactions, the extent to which these occur being governed both by experimental conditions and by the structure of the acid itself. In competing reactions, compounds such as olefins, esters and alcohols are produced, the formation of the latter being specially favoured by alkaline solution. Constituents other than hydroxyl ions may also participate, these being nitrates, nitrites and halogens.

Hydrocarbons of the first mentioned type are probably formed in a primary radical recombination [6], but the pathways involved in side reactions are not very well known. When radicals are formed at a low rate, immediate recombination is lowered and the radical might attack non-radical molecules by abstracting hydrogen. This seems to be the rule when aromatic compounds constitute the primary radicals. It is of interest to note that hydrogen abstraction seems to occur from C—H bonds and not from O—H bonds.[9] The rapid rise (without any build-up), and correspondingly rapid decay, of the luminescence as shown in Fig. 3 indicates a primary reaction, for example a radical recombination, in gas or liquid phase which gives a compound in an excited state (*cf.* H + NO = HNO) capable of emitting light. The available energy in bond formation, 80—100 kcal, in the Kolbe products, is not enough to give electronically excited states in simple molecules such as ethane or methyl chloride, but requires groups with more loosely bound electrons such as a carbonyl group.

Although the reaction $CH_3COO\cdot \rightarrow CH_3\cdot + CO_2$ is exothermic (12—14 kcal) and occurs spontaneously the possibility that recombination occurs before the splitting off of CO_2 should not be excluded, the compound molecule then containing carbonyl groups where the n—π transition energy might be of the same magnitude as the energy released in bond formation. Another possibility is that the energy released in a radical recombination might excite a third molecule which then emits light.

The Kolbe's synthesis applied to amino acids gives usually aldehydes together with H_3N liberation. This is also true of radiolysis.

The electrolysis of some amino acids in sodium sulphate solution was undertaken to study reactions similar to those occurring in the radiolysis of organic material in water, *i.e.*, where the primarily produced radicals originate from water.

The luminescence exhibited by electrolysis of phenylalanine or tyrosine is produced in a secondary reaction and depends on the production of a secondary product, as shown by the slow build-up of the luminescence intensity.

The effect of concentration and temperature may indicate that the luminescence occurs in different competing reactions with different quantum efficiency. As the increase in life length seems to be accompanied by increasing light emission, it is perhaps worthwhile to elucidate this problem by discussing possible reactions which might increase the life length of the reactive species.

The prolongation of the luminescence in phenylalanine electrolysis may be due either to a physical or to a chemical stabilization. A physical stabilization might consist of a conversion of an excited singlet state with a lifetime of about 10^{-8} seconds to a metastable triplet state with a lifetime that may exceed several seconds. The chemical stabilization may occur by radical chain reactions where the resulting radical is unreactive. The free radical may also combine with oxygen to form a peroxy radical which then may form a peroxide, a potent radical source. Physical and chemical stabilization is supposed to be combined in such a way that the above-mentioned triplet state reacts with oxygen to form a peroxide directly [10].

If oxygen has the above-mentioned effect on the lifetime of the products giving rise to the luminescent reaction, this does not necessarily mean that the light emission efficiency is increased by oxygen. However it is well-known that, in nearly all chemiluminescent reactions, oxygen or peroxides participate in some manner.

The effects of concentration, temperature and stirring may therefore be explained on the basis of oxygen competing with other participants in radical reactions. At a high radical concentration, radicals are expected to react with each other rather than with oxygen, and at high temperature the diffusion velocity of the radicals increases at the same time as the oxygen concentration is lowered in solution. Both effects make oxygen-radical reactions less frequent. Stirring of the solution probably increases the dissolving of oxygen from the oxygen bubbles formed at the anode.

The quenching effect of Cu^{++}, Co^{++}, and $Fe^{++} + Fe^{+++}$ may be ascribed both to their ability to react with radicals and peroxides as well as to their ability to affect the lifetime of the excited triplet state [11].

Information about the luminescent stage, from the shape of the decay curves, is made difficult by the fact that the luminescent species are not uniformly distributed in the solution due to their formation in an electrode process. This affects second and higher order reactions (*cf.* Fig. 8). However, the curves in Fig. 5 seem to be close to first order and this favours either an excited triplet state or an unimolecular decomposition of an unstable product as the rate determining step in the luminescent decay.

A radical recombination is probably the source of energy in the light emission studied here. It is then obvious that a radical scavenger should affect light emission either by recombination with the primary radical or by affecting the light emitting stage.

A radical scavenger may be a stable free radical such as diphenylpicryl hydrazyl, or NO, or a compound such as I_2 with a very weak bond which is easily attacked by a reactive free radical. Hence the energy released in the reaction of a reactive free radical and a scavenger molecule is usually considerably lower than when two reactive radicals react with each other. This lower energy release, together with the formation of an entirely new configuration, may cause the light emission to disappear. If light is still produced, the maximum of the emission spectrum is shifted to longer wavelengths, possibly out of the sensitive range of the photomultiplier tube. Therefore it is of interest that by introducing, in acetate electrolysis, some amino acids known as radiation protectors, this maximum is displaced to longer wavelengths (filter 5—6).

The above-mentioned method of studying free radical reactions should not unreservedly be transformed to radiation chemistry in solution. This is due to the difficulty in differentiating between the primarily produced excited states and excited states produced in radical reactions. However, by irradiation of a substance in the solid state, the energy is trapped in stable free radicals with a lifetime considerably longer than that of excited singlet and triplet states. By dissolving the irradiated substance in water the radicals are set free to react. This reaction is accompanied by light emission. Observations indicate that in this case at least two different light emitting reactions occur, one of which is short-lived (the lifetime probably shorter than the time necessary to dissolve the compound). This emission might be due to free radical reactions. In addition a rather slow reaction type occurs probably involving peroxides and other reaction products [12] (*cf.* also Westermark's investigations of irradiated inorganic compounds [13]).

Acknowledgment. The present investigation was supported by the *Swedish Natural Science Research Council.*

REFERENCES

1. Ehrenberg, L. *Radiation Research, Suppl.* **1** (1959) 102.
2. Natarajan, A. T. and Swaminathan, M. S. *Indian J. Gen. Plant Breed.* **18** (1958) 220.
3. Natarajan, A. T. *Risö Report* **16** (1960) 39.
4. Porter, G. *Radiation Research, Suppl.* **1** (1959) 479.
5. Ahnström, G. and Natarajan, A. T. *Nature* **188** (1960) 961.
6. Weedon, B. C. L. *Quart. Revs. London* **6** (1952) 380.
7. McKinley, J. D., Garvin, D. and Boudart, M. J. *J. Chem. Phys.* **23** (1955) 785.

8. Griffing, V. and Settle, D. *J. Chem. Phys.* **23** (1955) 503.
9. Clusius, K. and Schanzer, W. *Z. physik. Chem.* **A192** (1943) 273.
10. Reid, C. *Excited States in Chemistry and Biology*, Butterworths Scientific Publications, London 1957.
11. Porter, G. and Wright, M. R. *Discussions Faraday Soc.* **27** (1959) 18.
12. Ahnström, G. and v. Ehrenstein, G. *Acta Chem. Scand.* **13** (1959) 199.
13. Westermark, T. *Risö Report* **16** (1960) 28.

Received November 8, 1960.

ACTA CHEMICA SCANDINAVICA 15 (1961) 471–476

Ozonolysis of Phenols

I. Ozonolysis of Phenol in Ethyl Acetate

ERLING BERNATEK and CARLY FRENGEN

Universitetets Kjemiske Institutt, Blindern, Oslo, Norway

Phenol has been ozonised in ethyl acetate at 3—4°C. The ozonolysis fragments, carbon dioxide, formic and oxalic acids, and glyoxal, have been determined quantitatively. Possible reaction combinations are proposed to explain the experimental results. Classical formulae only are assumed in this connection.

The ozonolysis of phenols commands our interest for several reasons. There is for the present great interest in the mode of ozone attack on aromatic rings (and on olefinic double bonds). Aromatic systems and their reaction with ozone have been studied rather extensively, notably by Wibaut and collaborators. For references see Bailey [1]. Kinetic studies by the Wibaut group have, among other qualitative relationships, established that anisole reacts much faster than benzene. Phenol itself has, however, neither been investigated in this connection, nor seems any rigorous product analysis of its ozonolysis to have been carried out.

Industrial sewage and waste liqours commonly contain phenolic constituents. Due to their toxicity these compounds create a serious problem in river pollution and if they reach drinking water reservoirs they are due to cause objectionable tastes and odours. The usual chlorine-treatment would here only aggravate the situation as chlorinated phenols are formed. Ozone-treatment of drinking water is a method of long standing in few places only (*e.g.* Paris), but in later years with the advent of more economical "tonnage ozone" the problem has received a careful reconsideration by the responsible authorities. The oxidation of phenols with ozone was shown by Roth [2] to result in compounds of little or no odour and Patrick [3] demonstrated the nontoxicity of these oxidation products. Niegowski [4] has presented additional information on the ozone oxidation of phenol, cresols and phenolic wastes from coke plants, chemical plants and refineries. A facile reaction is indicated and by appropriate adjustment of the initial pH of the solution an almost complete elimination of phenolic compounds can be achieved. All the mentioned ozonisation experiments were conducted in dilute aqueous solution and

Table 1. Rate of absorption of ozone by phenol dissolved in ethyl acetate.

Mins. from start	Total absorbed O_3 (Mole O_3/mole phenol)	% absorbed O_3 in preceding interval
2	0.22	97
6	0.68	88
10	1.12	85
14	1.55	84
18	1.98	82
22	2.40	80
26	2.77	73
30	3.12	68
34	3.40	51
38	3.57	33
42	3.70	24

in no case the products were isolated and identified or their relative amounts determined.

Phenol, dissolved in ethyl acetate, absorbed fairly readily ozone at 3—4°C. With our experimental set-up some ozone always passed unreacted through the reaction mixture. The amounts of this unreacted ozone increased as the reaction proceeded, as will be seen from Table 1. In this run 6.7 mmole of phenol was ozonised with 5.8 % (wt.) ozone at an oxygen flow of 30 lh^{-1}. Somewhat more ozone than the three moles expected on the basis of a Kekulé structure is absorbed. On the other hand it is interesting to observe from Table 1 that when about three moles are absorbed the absorption curve dips rather steeply downwards. The ready consumption of ozone must be due to a facile reaction of the mono-ozonolysis products. This tendency is further shown by the determination of unreacted phenol when 1, 2 and 3 moles of ozone have been absorbed. The amounts of remaining phenol were, respectively, 60, 29, and 9 %. Consequently, when one mole of ozone had been absorbed only 0.4 mole of phenol had reacted corresponding to a consumption of 2.5 moles of ozone per mole of phenol. The immediate ozonolysis products seem therefore to react faster with ozone than phenol itself.

During the ozonolysis carbon dioxide was detected in the effluent gas. Since pure ethyl acetate only gives traces of carbon dioxide with ozone, it must result from the cleavage of phenol. The ozonised solution contained active oxygen and when left at room temperature it evolved carbon monoxide.

Decomposition of the reaction mixture was effected by stirring with cold water until the active oxygen had disappeared, and the ethyl acetate was extracted with further amounts of water. Also during the decomposition evolution of carbon dioxide could be noticed. In the aqueous decomposition solution several ozonolysis fragments were identified: Formaldehyde through its reaction with chromotropic acid, formic acid through its S-benzyl*iso*thiuronium salt, oxalic acid analogously by conversion to S-benzyl*iso*thiuronium oxalate, glyoxal through the *p*-nitrophenylosazone.

These findings point towards a fairly complete degradation of phenol by ozonolysis, but a better picture of this can only be gained through knowledge of the relative amounts in which the products occur.

Formaldehyde was not determined quantitatively as it was evident from the qualitative tests that the amount was very small. Further, it is known that ethyl acetate alone can give traces of formaldehyde with ozone and it is difficult to say whether all of it in our case stems from the solvent or from the phenol as well.

Formic acid was determined by distilling *in vacuo* aliquots of the aqueous decomposition solution into aqueous sodium hydroxide. The alkaline solution was then concentrated to half its original volume and oxidised with potassium permanganate. After acidification with dilute sulphuric acid, excess permanganate and the formed manganese dioxide were reduced with ammonium iron sulphate and the excess of this titrated with standard potassium permanganate. This somewhat roundabout method was necessary because some acetic acid from ethyl acetate always occurred in the decomposition solution.

Oxalic acid was determined gravimetrically as calcium oxalate in accordance with the standard analytical procedure.

Glyoxal was precipitated as *p*-nitrophenylosazone, dried and weighed. The method is not of highest accuracy, but due to the very slight solubility of the osazone in aqueous solutions it was considered adequate for our purposes.

Carbon dioxide was absorbed by soda asbestos after the necessary precautions to exclude volatile substances had been taken.

The beforementioned unreacted phenol was precipitated as tribromophenol and weighed.

The quantitative determinations were performed after absorption of 3 moles of ozone per mole of phenol and the results are given in Table 2.
About 86 % of the carbon in the starting material can thus be accounted for.

The aqueous decomposition solution was titrated directly with 0.1 N sodium hydroxide and was found to contain *ca.* 3.4 equivalents of acid per mole of phenol ozonised. The sum of formic and oxalic acids, on the other hand, is *ca.* 3.2 equivalents. Probably, the difference is due to acetic acid from the ethyl acetate and to glyoxal, which in the presence of alkali can undergo a Cannizzaro reaction.

Active oxygen in the ozonised solution (3 moles of ozone absorbed) was determined iodometrically to *ca.* 1.5 moles per mole of phenol. After decomposition with water at most a very small part of the active oxygen was retained as hydrogen peroxide since the aqueous decomposition solution gave only a faint yellow colour with titanium reagent.

Table 2. Ozonolysis products from phenol.

Product	Moles/mole phenol	Moles/mole reacted phenol	Recovered carbon, %
Carbon dioxide from the ozonolysis	0.33	0.36	5.5
Carbon dioxide from the decomposition	0.72	0.79	12.0
Formic acid	3.15	3.46	52.7
Oxalic acid	0.04	0.04	1.4
Glyoxal	0.14	0.15	4.7
Phenol	0.09		9.4

DISCUSSION

Even a brief examination of Table 2 gives some information regarding the ozonolysis of phenol: The degradation is of a certain complexity and more than one mode of reaction is indicated. The amount of formic acid seems somewhat low. The deficit in recovered carbon of 14.3 % is too large to be explained by analytical errors.

The latter point can be rationalised by carbon loss through the mentioned evolution of carbon monoxide. Probably this occurs already during the ozonisation and at the expense of formic acid, thereby explaining also the second of the above points.

Assuming thus that 14.3 % of the carbon is contained in the evolved carbon monoxide, we find that 0.94 mole of this compound is formed per mole of reacted phenol. On this basis the formation of the reaction products as well

Table 3. Reaction combinations in the ozonolysis of phenol. In the first column An. means anomalous ozonolysis, and Ac. means acid rearrangement.

Reaction combination	Moles of phenol reacted	Primary products	Secondary products	Moles of secondary products
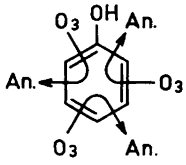	0.85	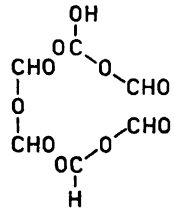	CO_2 5 [HCOOH or CO]	0.85 4.25
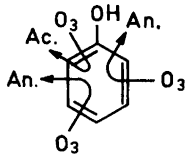	0.11	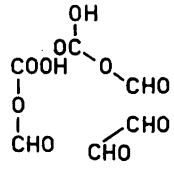	$2\,CO_2$ 2 [HCOOH or CO] CHO CHO	0.22 0.22 0.11
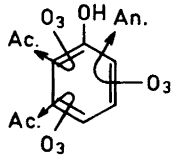	0.04	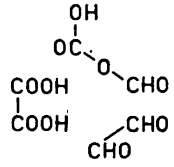	CO_2 [HCOOH or CO] CHO CHO COOH COOH	0.04 0.04 0.04 0.04

as their relative amounts can reasonably well be explained by a scheme comprising three reaction combinations. In all of these only two types of reaction are assumed: Anomalous ozonolysis (partly, in view of the content of active oxygen after ozonolysis, also ozonide formation with subsequent rearrangement) and acid rearrangement which is frequent in aldozonides.

In Table 3 the reaction combinations are given schematically. The primary reaction products consist largely of anhydrides of formic and carbonic acids. Such anhydrides are very unstable and break down rapidly to carbon monoxide and dioxide. In view of this, probably most of the formic acid found after hydrolysis is formed through a rearranged ozonide. It should, perhaps, be remarked that the immediate products from anomalous ozonolysis and ozonide rearrangement generally are identical.

Addition of the amounts of secondary products required by Table 3 gives: Carbon dioxide 1.11 mole (found 1.15 mole); oxalic acid 0.04 mole (found 0.04 mole); glyoxal 0.15 mole (found 0.15 mole); formic acid and carbon monoxide 4.51 mole (if assumed 0.94 mole carbon monoxide, found 4.40 mole).

Regarding the initial ozone attack on phenol and the sequence of bond cleavage the experimental evidence warrants no definite statement. One point might, however, be brought to attention. If in a Kekulé structure the double bond adjacent to the hydroxyl group is severed first, the two remaining double bonds, now in an aliphatic structure, will react rapidly and quantitatively with ozone. Assuming an initial attack on the 3,4 or 5,6 double bond, the resulting structure would be an aliphatic enol which most probably rapidly would be transformed to the keto form, thereby withdrawing one double bond from reaction with ozone contrary to experimental fact.

As will have been noted classical formulae alone are sufficient to explain the qualitative and quantitative course of the ozonolysis. A curious fact, however, is the absence of glyoxylic acid, a substance one would have expected to be formed in ample amounts.

EXPERIMENTAL

Ozonisation technique. The phenol (redistilled pure commercial product) was dissolved in pure ethyl acetate and the solution cooled in an ice-bath during the reaction. Ethyl acetate was chosen as a solvent preferably to chloroform because of the much higher distribution coefficient with respect to phenol of the system ethyl acetate-water than chloroform-water. It was thus possible to keep practically all the unreacted phenol in the organic phase during the decomposition with water. Ozone was produced by silent electrical discharge through dry oxygen and at an oxygen flow of 30 lh^{-1} there was formed *ca.* 2.5 g O_3/h. The ozone production was checked iodometrically before and after each run. As reaction vessel served a gas washing bottle with a sintered glass bottom which ensured a good distribution of the gaseous reactant. Connected to the reaction vessel was another gas washing bottle containing neutral aqueous potassium iodide where unreacted ozone would liberate iodine and be determined quantitatively by subsequent titration with sodium thiosulphate.

Determination of phenol. Unreacted phenol was determined after absorption of 1,2 and 3 moles of ozone. Phenol (629 mg, 6.7 mmoles) was dissolved in ethyl acetate and ozonised. To the reaction mixture was added water (50 ml) and the ethyl acetate evaporated off the heterogeneous mixture at room temperature. A 20 % solution of bromine in glacial acetic acid was added dropwise to the resulting aqueous solution until a light yellow colour persisted. The precipitate was washed and dried in a desiccator over phosphorus pentoxide until constant weight. Found after absorption of 1,2 and 3 moles of

ozone, respectively, (mean of three determinations): 1 320, 650, and 348 mg of the tribromo derivative.

Determination of carbon dioxide during ozonisation. Before entering the ozone generator the oxygen was led through a soda asbestos tube to remove traces of carbon dioxide. From the reaction vessel containing phenol (629 mg) in ethyl acetate (50 ml), the effluent gas was led through neutral potassium iodide to remove unreacted ozone which otherwise would have interfered with the determination. Thereafter the gas was led through a dry ice trap and concentrated sulphuric acid and finally into the soda asbestos tube. After the ozonisation a few ml dilute acetic acid was added to the potassium iodide solution and oxygen led through the apparatus for some minutes. Found in five determinations: 111, 99, 90, 95, and 91 mg. Mean 97 mg.

Decomposition of the ozonised solution. The ozonised solution was mixed with water (50 ml) and stirred in a closed vessel (magnetic stirrer) for 6 h. The ethyl acetate was then extracted four times with 30 ml portions of water and the aqueous extracts combined and made up to 250 ml. After evaporation of the ethyl acetate the residue weighed only *ca.* 4 mg. This is less than the amount of unreacted phenol which must, at least partly, have evaporated under the experimental conditions.

Determination of carbon dioxide during decomposition. The ozonised solution was transferred to a closed vessel fitted with gas inlet and outlet and a dropping funnel containing water. Through the vessel was led purified nitrogen and the water in the funnel (50 ml) added to the organic solution with continuous stirring with a magnetic stirrer. The effluent gas was led through a dry ice trap and through concentrated sulphuric acid before it entered a soda asbestos tube. Found in five determinations: 198, 216, 177, 236, 236 mg. Mean 213 mg.

Determination of formic acid. 25 ml aliquots of the decomposition solution were distilled to dryness *in vacuo* at a temperature of 28—30°C. The receiver contained aqueous sodium hydroxide (*ca.* 50 ml, 2 N). After the distillation the alkaline solution was evaported to half its original volume and mixed with a solution of potassium permanganate (0.1 N). The mixture was heated on a water-bath for one hour, acidified with dilute sulphuric acid and excess aqueous iron ammonium sulphate added. When all the manganese dioxide had dissolved, excess ferrous iron was titrated with standard potassium permanganate. Found in three ozonolyses: 933, 969, and 1 012 mg. Mean 971 mg.

Determination of oxalic acid. To 50 ml aliquots of the decomposition solution was added aqueous calcium chloride and the mixture heated to *ca.* 75°C. Dilute aqueous ammonia was then added until a yellow colour was formed with methyl red. The precipitate was filtered after 2 h, washed and dried. Found from three ozonolyses: 38.5, 37.0 and 35.0 mg. Mean 36.8 mg.

Determination of glyoxal. To the decomposition solution was added *p*-nitrophenylhydrazine dissolved in glacial acetic acid. A precipitate soon formed and was filtered off, washed and dried to constant weight. 288 mg. This is probably a maximum value for glyoxal *p*-nitrophenylosazone. The precipitate was recrystallised from glacial acetic acid and nitrobenzene and decomposed then at 298—300°C. Its infra-red spectrum was identical with that of authentic glyoxal *p*-nitrophenylosazone.

REFERENCES

1. Bailey, P. S. *Chem. Revs.* **58** (1958) 925.
2. Roth, W. *Ozonisation of Phenol in Water Solution*, Thesis, University, New York 1947.
3. Patrick, R. *Private communication* cited by Niegowski [4].
4. Niegowski, S. J. *Ind. Eng. Chem.* **45** (1953) 632.

Received October 17, 1960.

ACTA CHEMICA SCANDINAVICA 15 (1961) 477–482

A Thiamine Diphosphatase from Rat Liver

KARIN TILANDER and KARL-HEINZ KIESSLING

Institute of Zoophysiology, University of Uppsala, Sweden

An enzyme hydrolyzing thiamine diphosphate (cocarboxylase) to thiamine monophosphate has been partly purified from rat liver. The pH optimum is 9.3, and it requires the presence of Mg or Mn ions. Of inhibitors tested only fluoride strongly inhibits enzyme activity.

In previous work [1–2] the content of supernatant TDP * in liver has been shown to be lower in rats treated with CCl_4 as compared with untreated animals. The same was found also in the liver from rats given alcohol for a long time [3]. The low TDP content might be explained by an increase in the dephosphorylation rate of TDP found in liver homogenate. In a later investigation the thiamine diphosphatase (TDPase) activity was determined in the nuclear, supernatant, and mitochondrial fractions from normal and from CCl_4-treated rat liver [4]. TDP was found to be more rapidly dephosphorylated in the supernatant and mitochondrial fractions from CCl_4-treated rats than from normal. The pH-optimum of the TDPase was 9.3.

The present communication describes pH-optimum, activators, and inhibitors of the TDPase for rat liver, roughly purified by fractionation with ammonium sulphate.

EXPERIMENTAL

Materials. TDP and TMP were obtained from the Sigma Chemical Company and $^{32}P_i$ from the Radiochemical Centre, Amersham. TD ^{32}P and TM ^{32}P were synthesized according to Viscontini *et al.*[6] with the addition that also $^{32}P_i$ was present during the synthesis and paper chromatographically isolated in two subsequent solvents (*iso*butyric acid-versene-NH_3[7] followed by propanol-HAc-H_2O[8]).

Preparation and purification of enzyme. White rats, weighing about 200 g, were killed by decapitation, and the liver immediately removed and weighed in 0.02 M $KHCO_3$ at + 3°C. The liver was then homogenized in a Waring blendor for 2 min in 5 vol. 0.02 M $KHCO_3$ and incubated for 15 min with stirring. All operations were carried out at + 3°C. The homogenate was centrifuged for 10 min at 10 000 *g*, and the precipitate

* Abbreviations: TDP thiamine diphosphate, TMP thiamine monophosphate, ATP adenosine triphosphate, ADP adenosine diphosphate, AMP adenosine monophosphate, IDP inosine diphosphate, P_i inorganic phosphate, TDPase thiamine diphosphatase, ATPase adenosine triphosphatase.

Table 1. Fractionation of rat liver extract. Details about incubation conditions are given in the experimental part. Enzyme activity is given as units. One unit is that amount of enzyme which causes hydrolysis of 0.1 μmole of TDP to TMP in 45 min per ml of reaction mixture.

Enzyme preparation	Volume ml	Total protein, mg	Total activity units	Spec. activity, units/mg protein × 10^2
Original extract	29	1 030	79.3	7.7
0—15 % saturation	10	62	39.7	64
15—25 % saturation	10	74	41.3	56
25—30 % saturation	10	45	48.5	108
Supernatant	33	614	9.8	3

was discarded. To the supernatant saturated $(NH_4)_2SO_4$ solution was added with stirring to 15 % saturation. After standing for 15 min the precipitate was centrifuged 10 min at 10 000 *g*. The process was repeated, and the fractions at 15—25 and 25—30 % saturation were collected. The precipitates were dissolved in 0.02 M $KHCO_3$, and dialyzed against 0.02 M $KHCO_3$ for 18 h. The purification procedure is summarized in Table 1.

Enzyme test. Phosphatase activity was determined in a system containing 1.0 ml 2×10^{-3} M TD ^{31}P and traces of TD ^{32}P, 1.0 ml 0.1 M glycine buffer pH 9.3, 0.1 ml 0.1 M $MgCl_2$, and enzyme solution. Water was added to make a final volume of 2.5 ml. This system was incubated at 37°C for 45 min, and the reaction was stopped by the addition of 0.3 ml 5 M H_2SO_4.

After removal of the precipitate by centrifugation $^{32}P_i$ was determined in a 2 ml aliquot of the supernatant, as described elsewhere [9], and corrected for a blanc containing the same components as above, except enzyme, and incubated for the same time.

Protein content was estimated according to Warburg and Christian [10] by measuring light absorption at 260 and 280 mμ.

RESULTS

In the following experiments the fraction obtained between 25 and 30 % saturation with ammonium sulphate (Table 1) has been used. Deviations from the standard incubation as described in Methods are accounted for in detail for every special case.

Requirement for metal ions. The enzyme, like other phosphatases, needs the presence of divalent metal ions (Table 2).

As seen Mn^{2+} and Mg^{2+} were most active. At the rather high pH used in the experiments, Mn^{2+} was, however, partly oxidized and eliminated as a precipitation. For this reason we preferred Mg^{2+} in the following experiments.

Table 2. The influence of divalent metal ions on enzyme activity. Incubation was performed under standard conditions as described in Experimental, with addition of metal ions as seen in the table. The concentration of the metals was 4×10^{-3} M. 0.3 mg of enzyme protein was added.

Additions	% TDP hydrolyzed to TMP
None	2
Mg^{2+}	25
Mn^{2+}	35
Ni^{2+}	8

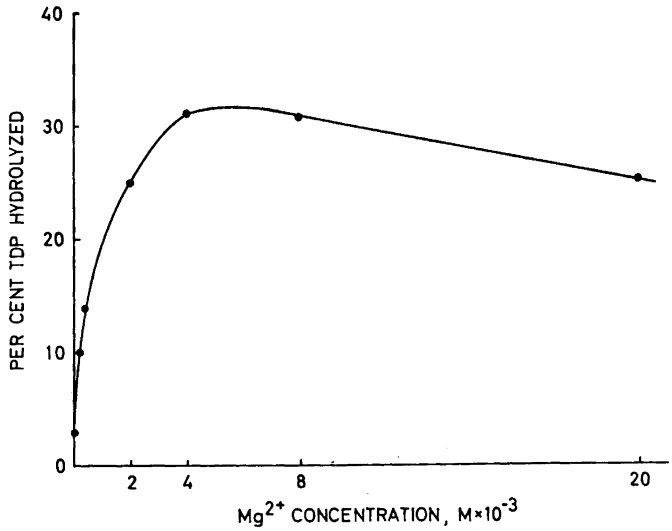

Fig. 1. The effect of Mg^{2+} on the enzymatic dephosphorylation of TDP. Incubation was performed under standard conditions for 45 min with Mg^{2+} additions as indicated. Enzyme fraction obtained between 25 and 30 % saturation with ammonium sulphate was used, corresponding to 0.3 mg protein.

Caffrey *et al.*[11], working with an adenosine triphosphatase from erythrocytes, found the metal ions to inhibit the reactions when concentrations of Mg^{2+} greater than that of the substrate were used. Fig. 1 shows the effect of

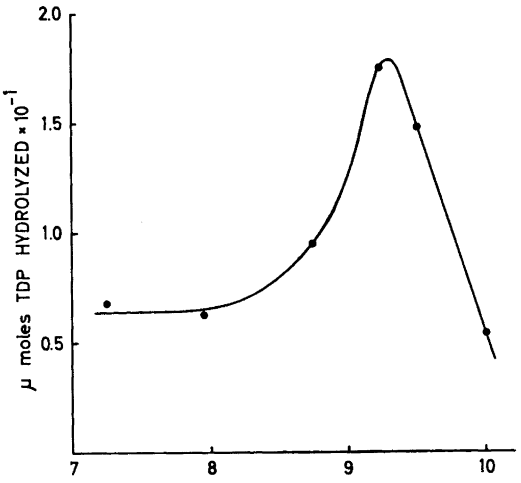

Fig. 2. Relation between pH and enzyme activity. Incubation was performed under standard conditions for 45 min. 0.2 ml Mg^{2+} 0.1 M was added.

Table 3. Effect of various inhibitors on TDPase activity. Incubations were performed as described in Experimental, but with optimal amounts of Mg^{2+} (0.2 ml 0.1 M). Enzyme was added corresponding to 0.3 mg protein.

Substance	Concentration M	% Inhibition
NaF	1×10^{-3}	17
	1×10^{-2}	66
	1×10^{-1}	92
KCN	1×10^{-3}	13
	1×10^{-2}	5
p-Chloromercuribenzoate	5×10^{-6}	0
	5×10^{-5}	0
	5×10^{-4}	0
N-Ethylmaleimide	1×10^{-4}	7
	1×10^{-3}	11
Iodoacetamide	5×10^{-4}	7
	5×10^{-3}	24

varying Mg^{2+} concentrations on the TDPase. Activation occurs up to a Mg^{2+} concentration ten times that of the substrate. Still higher concentrations are slightly inhibitory.

Relation between pH and enzyme activity. Previous experiments on TDPase activity in liver cell fractions [4] gave 9.3 as an optimal pH. The enzyme preparation obtained between 25 and 30 % saturation with ammonium sulphate (Table 1) was incubated in buffer solutions of the pH values indicated in Fig. 2. The pH optimum was found to be 9.3 also with this partly purified TDPase. Incubation of TDP at different pH without enzyme gave no hydrolysis.

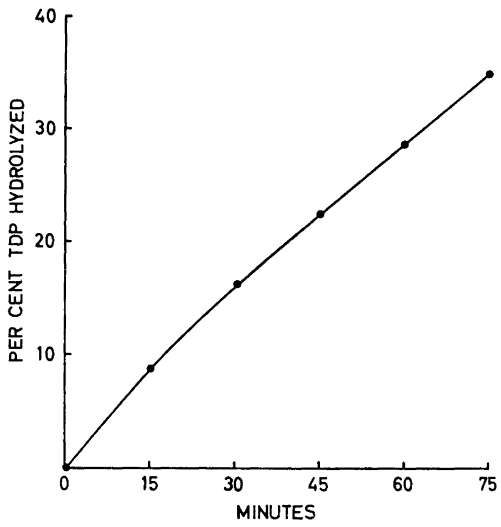

Fig. 3. Time course of hydrolysis of TDP. Incubation as in Fig. 2. Enzyme corresponding to 0.3 mg protein was added.

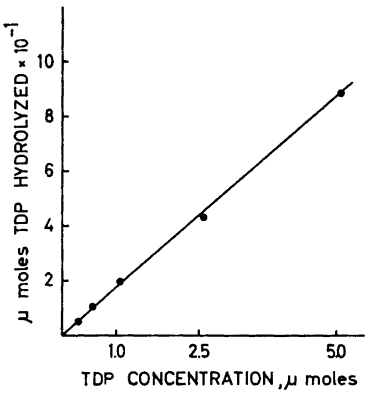

Fig. 4. Relation between substrate concentration and enzyme activity. Incubation as in Fig. 2 except that varying amounts of TDP have been added. The TDP concentration has been expressed as μmole TDP added per sample at the beginning of the incubation.

Inhibitors. The effect of several inhibitors on TDPase is summarized in Table 3. Fluoride is a powerful inhibitor, while cyanide and various SH inhibitors show no or little effect. Also TMP inhibits the hydrolysis of TDP. When added in the same concentration as TDP, it gives an inhibition of about 25 %.

Time course of hydrolysis of TDP. The progress of the hydrolysis of TDP with incubation time is seen in Fig. 3. Sometimes a slight bend on the line could be found after 30 min incubation. This we have ascribed to an inhibitory effect of TMP, formed during the incubation, as will be seen later. It is not seen on time curves at any other pH tested.

Relation between substrate concentration and enzyme activity. The hydrolysis of TDP at initial concentrations from 0.25 to 5 μM and constant concentration of enzyme during 45 min incubation was determined (Fig. 4). The values obtained plotted in the double reciprocal manner gave a K_m for TDP of about 1×10^{-3} M.

DISCUSSION

In previous papers we have shown that under certain conditions, as for example after intraperitoneal injection of CCl_4 or after forcing the animals to consume alcohol for a long time, the level of TDP in rat liver, especially in the supernatant fraction, is markedly lowered. In the same time an increase in the ability of the liver cell fractions to hydrolyse TDP to TMP could be shown [2-4]. The supernatant fraction contained most of the enzyme, here named TDPase, the activity of which could be increased more than 100 % by previous injections of CCl_4 into the rat. This increase, however, only implies a liberation or activation of the enzyme already present in the supernatant fraction (including microsomes and lyzosomes), as preparation of acetone extracts from supernatants from CCl_4-treated and normal rat livers gave no difference in the TDPase activity (unpublished data). The fact that an en-

zyme, hydrolyzing TDP, occurs latent, very likely hidden within subcellular particles, was already shown by Dianzani (personal communication) who treated the tissues with deterging agents, and supposed the enzyme to be liberated hereby from lyzosomes.

Enzymes transforming pyrophosphate groups into monophosphates are described among others by Gibson *et al.*[12], Plaut [13], Goldberg and Gilmour [14], Jones and Ernster [15]. In all cases nucleoside diphosphates were used as substrates, and only in the case with the ATPase, investigated by Goldberg and Gilmour, also TDP had been added without, however, being hydrolyzed.

Histochemically Naidoo and Pratt [16] have studied a thiamine pyrophosphatase in nervous tissue of normal and of thiamine deficient chickens. Their enzyme as well as the TDPase from liver, studied by us, was activated by Mg^{2+}, possessed optimal activity at a rather high pH as compared with the nucleoside diphosphates mentioned above, and did only split off one phosphate group from TDP. This indicates that their enzyme from chicken brain may be the same as that from rat liver studied by us.

Whether or not the TDPase examined by us also catalyzes the dephosphorylation of other phosphate esters, and then especially nucleoside diphosphates, has not been investigated in detail. Preliminary results indicate, however, that ADP is hydrolyzed by the same enzyme.

Acknowledgement. This work was supported by grants from the *Swedish Medical Science Research Council.*

REFERENCES

1. Dianzani, M. U. and Dianzani Mor, M. A. *Biochim. et Biophys. Acta* **24** (1957) 564.
2. Kiessling, K.-H. and Tilander, K. *Acta Chem. Scand.* **14** (1960) 841.
3. Kiessling, K.-H. and Tilahder, K. *Exptl. Cell. Research* **19** (1960) 628.
4. Kiessling, K.-H. and Tilander, K. *Biochim. et Biophys. Acta* **43** (1960) 335.
5. Dianzani, M. U. *Biochim. et Biophys. Acta* **14** (1954) 514.
6. Viscontini, M., Bonetti, G. and Karrer, P. *Helv. Chim. Acta* **32** (1949) 1478.
7. Kiessling, K.-H. *Acta Chem. Scand.* **10** (1956) 1356.
8. Siliprandi, D. and Siliprandi, N. *Biochim. et Biophys. Acta* **4** (1952) 479.
9. Kiessling, K.-H. *Biochim. et Biophys. Acta* **39** (1960) 412.
10. Warburg, O. and Christian, W. quoted by Layne in *Methods in Enzymology* II, p. 447.
11. Caffrey, R. W., Tremblay, R., Gabrio, B. W. and Huennekens, F. M. *J. Biol. Chem.* **223** (1956).
12. Gibson, D. M., Ayengar, P. and Sanadi, D. R. *Biochim. et Biophys. Acta* **16** (1955) 536.
13. Plaut, G. W. E. *J. Biol. Chem.* **217** (1955) 235.
14. Goldberg, M. and Gilmour, D. *Arch. Biochem. Biophys.* **51** (1954) 411.
15. Jones, L. C. and Ernster, L. *Acta Chem. Scand.* **14** (1960) 1839.
16. Naidoo, D. and Pratt, O. E. *Biochim. et Biophys. Acta* **16** (1958) 75.

Received October 27, 1960.

ACTA CHEMICA SCANDINAVICA 15 (1961) 483–486

Vibrational Mean-Square Amplitude Matrices

XIII. Remarks on Computing Mean-Square Amplitude Matrices

Y. MORINO* and S. J. CYVIN

Institutt for teoretisk kjemi, Norges tekniske høgskole, Trondheim, Norway

The previously evaluated secular equations involving the mean-square amplitude matrix (Σ) have been extended to

$$| \Sigma G^{-1} (GF)^m - \delta\lambda^m E | = 0$$

where m = 0, ± 1, ± 2, ... For the negative values of m, $(GF)^m$ must be interpreted as $(F^{-1} G^{-1})^{-m}$. It is pointed out that in cases where the F matrix is known, the extended secular equations give sufficient relations to compute the complete Σ matrix in the general case of polyatomic molecules.

The mean-square amplitude matrix Σ in the theory of small harmonic vibrations is defined in terms of its elements by

$$\Sigma_{ii} = \langle S_i^2 \rangle, \; \Sigma_{ij} = \langle S_i S_j \rangle \tag{1}$$

where S_i and S_j denote some arbitrary internal displacement coordinates. The following secular equations have previously been deduced for the Σ matrix.

$$| \Sigma G^{-1} - \delta E | = 0 \tag{2}$$

$$| \Sigma F - \delta\lambda E | = 0 \tag{3}$$

For details of the theory and further explanation of the symbols, see [1,2]. The applicability of these secular equations in practical computations has been discussed previously [2,3]. In the present article some additional remarks will be given as to the methods of computing the Σ matrix in the case when the force constants (F matrix elements) are known. In this connection an extension of the secular eqns. (2) and (3) will be communicated.

L MATRIX METHOD

The well-stablished method of computing mean-square amplitudes of vibration or Σ matrix elements in general may be termed the L matrix method. If

* Permanent address: Department of Chemistry, Faculty of Science, The University of Tokyo, Bunkyo-Ku, Tokyo, Japan.

the F matrix is known, the normal coordinate transformation matrix L ($S = LQ$) is obtainable according to

$$GFL = L\Lambda \tag{4}$$

by the generally adopted normal coordinate treatment proposed by Wilson [4]. Hence the Σ matrix may be computed according to [1-3]

$$\Sigma = L\Lambda\tilde{L} \tag{5}$$

SECULAR EQUATION METHOD

In the special case of linear triatomic molecules another method of calculating the mean-square amplitude quantities has been described [5]. In this case the relations obtained from the secular eqns. (2) and (3) were given. The four resulting equations contained three independent equations sufficient for calculating the three unknown quantities. This procedure of calculating mean-square amplitude quantities, which does not involve the computation of the L matrix, may be extended to the general case of polyatomic molecules. The extended secular equantions for the Σ matrix given in the next paragraph, must always provide a sufficient number of independent equations for computing all of the Σ matrix elements. The method involves namely completely the same information as regard to the vibrational problem as given alternatively by the L matrix.

EXTENSION OF THE SECULAR EQUATIONS

The two given secular eqns. (2) and (3) follow from the matrix relations

$$\Sigma G^{-1}L = L\Lambda \tag{6}$$

and

$$\Sigma FL = L\Lambda\Lambda \tag{7}$$

respectively. From eqn. (7) one has $\Sigma F = L\Lambda\Lambda L^{-1}$, which may be combined with $GF = L\Lambda L^{-1}$, obtained from eqn. (4). From the resulting relation $\Sigma FGF = L\Lambda\Lambda^2 L^{-1}$ it is obtained

$$\Sigma FGFL = L\Lambda\Lambda^2 \tag{8}$$

The procedure may be repeated and leads to the general equation

$$\Sigma F(GF)^n L = L\Lambda\Lambda^{n+1} \tag{9}$$

By putting $m = n + 1$ eqn. (9) may be written

$$\Sigma G^{-1}(GF)^m L = L\Lambda\Lambda^m \tag{10}$$

This equation contains (6) and (7) as special cases for $m = 0$ ($n = -1$) and $m = 1$ ($n = 0$), respectively. The secular equations corresponding to eqn. (10) read

$$|\Sigma G^{-1}(GF)^m - \delta\lambda^m E| = 0 \tag{11}$$

Negative values of m may also have a meaning, if eqn. (10) for m = —p is interpreted as

$$\Sigma G^{-1}(F^{-1}G^{-1})^{p}L = LA(A^{-1})^{p} \tag{12}$$

In the general case with the number of internal coordinates equal to N, the number of unknown Σ matrix elements is $\frac{1}{2}N(N+1)$. The number of equations obtained from one of the secular equations is N. Hence for computing the complete Σ matrix we must take so many of the secular equations (t) to make

$$tN \geqq \tfrac{1}{2}N(N+1) \tag{13}$$

From the tN equations it is possible to select a set being sufficient for computing the complete Σ matrix. The excess equations must evidently be dependent on the selected set. Consequently it is possible to calculate all of the Σ matrix elements without computing the L matrix.

EXAMPLE

The bent symmetrical XY_2 molecular model will be considered. The relations for the Σ matrix elements (based on symmetry coordinates) obtained from eqn. (2) or eqn. (11) with m = 0 have been reported previously [2,6]. For m = 1 one has with the same notation as used in Ref.[6]

$$\delta_1\lambda_1 + \delta_2\lambda_2 = \Sigma_1F_1 + \Sigma_2F_2 + 2\Sigma_{12}F_{12} \tag{14}$$

$$\delta_1\lambda_1\delta_2\lambda_2 = (\Sigma_1\Sigma_2 - \Sigma_{12}^2)(F_1F_2 - F_{12}^2) \tag{15}$$

$$\delta_3\lambda_3 = \Sigma_3F_3 \tag{16}$$

For m = 2 it has been found

$$\delta_1\lambda_1^2 + \delta_2\lambda_2^2 = \Sigma_1[F_1^2(2\mu_X\cos^2A + \mu_Y) + 2F_{12}^2(2\mu_X\sin^2A + \mu_Y) - 2\sqrt{2}F_1F_{12}\mu_X\sin 2A] + \Sigma_2[F_{12}^2(2\mu_X\cos^2A + \mu_Y) + 2F_2^2(2\mu_X\sin^2A + \mu_Y) - 2\sqrt{2}F_2F_{12}\mu_X\sin 2A] + 2\Sigma_{12}[F_1F_{12}(2\mu_X\cos^2A + \mu_Y) + 2F_2F_{12}(2\mu_X\sin^2A + \mu_Y) - \sqrt{2}(F_1F_2 + F_{12}^2)\mu_X\sin 2A] \tag{17}$$

$$\delta_1\lambda_1^2\delta_2\lambda_2^2 = 2(\Sigma_1\Sigma_2 - \Sigma_{12}^2)(F_1F_2 - F_{12}^2)(2\mu_X + \mu_Y)\mu_Y \tag{18}$$

$$\delta_3\lambda_3^2 = \Sigma_3F_3^2(2\mu_X\sin^2A + \mu_Y) \tag{19}$$

To establish these equations, only the F and G matrices have been employed, not the inverse G matrix. The Σ matrix elements of the A_1 species (*viz.* Σ_1, Σ_2 and Σ_{12}) may be calculated from eqns. (14), (15), and (17). Eqn. (18) is equivalent to eqn. (15). The identity of these equations is evident from the relation [*cf.* eqn. (6) of Ref.[6]]

$$\lambda_1\lambda_2 = 2(F_1F_2 - F_{12}^2)(2\mu_X + \mu_Y)\mu_Y \tag{20}$$

It should be noted too that the linear equation for Σ_1, Σ_2 and Σ_{12} corresponding to m = 0, *viz.* eqn. (8) of Ref.[6], is linearly dependent on eqns. (14) and (17).

CONCLUSION

The new method of computing the Σ matrix outlined in the present article is mainly of theoretical interest. For practical calculations the conventional L matrix method seems to be the most convenient one in the majority of special cases. But still the extended secular equations may give valuable relations of practical use between force constants and mean-square amplitude quantities, even in the cases where the secular equation method for computing the complete Σ matrix would be too complicated.

REFERENCES

1. Cyvin, S. J. *Spectrochim. Acta* **15** (1959) 828.
2. Cyvin, S. J. *Acta Polytechn. Scand.* (279/1960) Ph No. 6, Chapter 4.
3. Cyvin, S. J. *Acta Chem. Scand.* **13** (1959) 2135.
4. Wilson, E. B., Jr. *J. Chem. Phys.* **7** (1939) 1047; **9** (1941) 76; Wilson, E. B., Jr., Decius, J. C. and Cross, P. C. *Molecular Vibrations*, McGraw-Hill, New York 1955.
5. Cyvin, S. J. *Spectrochim. Acta* **15** (1959) 958.
6. Cyvin, S. J. *Acta Chem. Scand.* **13** (1959) 1400.

Received September 30, 1960.

ACTA CHEMICA SCANDINAVICA 15 (1961) 487–501

The Formation of Polynuclear Complexes

I. The Determination of the Composition and Formation Constants of Polynuclear Complexes

BROR SKYTTE JENSEN

Danish Atomic Energy Commission, Risø, Denmark

The composition and the formation constant of the primary polymerisation product in the reaction between a central atom B and ligand atom A are determined from log-log plots of the average number of ligands bound per central atom *versus* the free ligand concentration for different total concentrations C_B of central atom B.

The composition and the formation constant of the final product in the same reaction may under certain circumstances be obtained from a log-log plot of the average number of ligand atoms not bound to B *versus* the free ligand concentration for different total concentrations C_B of central atom B.

The method set forth in this paper is applied to available data on the hydrolysis of the vanadium(IV), vanadium(V) and aluminium(III) ions.

In recent years the formation of polynuclear complexes has been intensively investigated. Special and general methods for the treatment of the complex data have been published [1–8].

Most of the data obtained experimentally have been treated according to a "core-link" theory set forth by Sillén *et al.*[1–4] where complexes of composition $A_r(AB_t)_N$ or $B_s(A_tB)_N$ are assumed to be the most probable being formed.

Mainly the hydrolysis of metal salts has been investigated. An excellent review of this field has been presented recently [9].

In the present paper another approach to the problem of analysis of the experimental data will be presented. This approach is in some respects similar to those published previously; however, the solutions of the present set of formulas need not be presented in the "core-link" formulation of Sillén.

In the derivation of the formulas some simplifications had to be introduced as is almost always the case when very complex systems are considered. This naturally also introduces some restrictions with regard to the cases which can be treated by the method. The solutions to the equations will therefore only be approximate and their deviation from the true solutions are difficult to estimate.

In the derivation of the formulas real equilibria are assumed, *i.e.* the law of mass-action is assumed to apply.

LIST OF SYMBOLS

$[B]$ concentration of species B.
C_B total concentration of B.
$[A]$ concentration of free ligand.
A_b number per volume of moles of A bound in complexes with B.
C_A total concentration of species A.
$[B_rA_x]$, $[B_qA_y]$, concentrations of complexes of composition B_rA_x, B_qA_y.
$Z = A_b/C_B$ *i.e.* the average number of ligands bound to B.
Z_t The final value of Z corresponding to a defined product.

$$\beta_{rx} = \frac{[B_rA_x]}{[B]^r[A]^x}$$, the formation constant for the species B_rA_x

$\beta_{0,y} = 0$

$\beta_{1,0} = 1$

$$\varkappa_{rx} = \frac{[B_rA_x][H]^x}{[B]^r[HA]^x}$$

$K_w = [H][OH]$, the ion product of water.

$$n = \left(\frac{\partial \log Z)}{\partial \log [A]}\right)_{C_B}$$

$$n' = \left(\frac{\partial \log (Z_t - Z)}{\partial \log [A]}\right)_{C_B}$$

$$t = t' = \left(\frac{\partial \log C_B}{\partial \log [A]}\right)_Z$$

DERIVATION OF THE FORMULAS

In the solution the species B, A and B_iA_u ($i,u = 0,1,2,4 \ldots$) are assumed to exist.

The total concentration of B, C_B, can then be expressed as

$$C_b = \Sigma\Sigma i[B_iA_u] = \Sigma\Sigma i\beta_{i,u}[B]^i[A]^u \qquad (1)$$

where the summation include i and u equal to zero when $\beta_{1,0}$ is set equal to unity.

Similarly the concentration of A bound to B can be expressed as

$$A_b = \Sigma\Sigma u[B_iA_u] = \Sigma\Sigma u\beta_{i,u}[B]^i[A]^u \qquad (2)$$

with $\beta_{0,u}$ equal to zero. $\beta_{0,0}$ need not to be defined.

In eqns. 1 and 2 concentrations are used instead of activities, which is permissible if certain restrictions are put on the actual conditions under which the experiments are performed.

The expression for Z, the average ligand number per central atom then becomes

$$Z = \frac{\Sigma\Sigma u[B_iA_u]}{\Sigma\Sigma i[B_iA_u]} = \frac{\Sigma\Sigma u\beta_{i,u}[B]^i[A]^u}{\Sigma\Sigma i\beta_{i,u}[B]^i[A]^u} \quad (3)$$

To simplify eqn. 3 one may imagine certain concentration ranges where only two complexes exist simultaneously, *e.g.*, B_qA_y and B_rA_x where B_rA_x is considered the product in a reaction of B_qA_y with B and A, so that

$$x/r > y/q$$

This leads to

$$C_B = r[B_rA_x] + q[B_qA_y] \quad (4)$$

and

$$Z \simeq \frac{x[B_rA_x] + y[B_qA_y]}{C_B} \simeq \frac{x[B_rA_x]}{r[B_rA_x] + q[B_qA_y]} \quad (5)$$

From eqn. 5 is then derived

$$\frac{Z}{x/r - Z} = \frac{r[B_rA_x]}{q[B_qA_y]} \quad (6)$$

Two limiting cases are immediatedly discernible. The one that $Z \ll x/r$ and the other that $Z \simeq x/r$. In the former case we get

$$Z = \frac{x[B_rA_x]}{q[B_qA_y]} = \frac{x\beta_{r,x}[B]^r[A]^x}{q\beta_{q,y}[B]^q[A]^y} = \frac{x\beta_{r,x}}{q\beta_{q,y}}[B]^{r-q}[A]^{x-y} \quad (7)$$

As we have assumed C_B to be expressed as

$$C_B = q\beta_{q,y}[B]^q[A]^y \quad (8)$$

[B] can be found as a function of C_B and [A]. Thus

$$[B] = \sqrt[q]{C_B/q\beta_{q,y}[A]^y} \quad (9)$$

which when inserted into eqn. 7 gives

$$Z = \frac{x\beta_{r,x}}{(q\beta_{q,y})^{r/q}} C_B^{(r-q)/q}[A]^{(qx-ry)/q} \quad (10)$$

or

$$\log Z = \log\left(\frac{x\beta_{r,x}}{(q\beta_{q,y})^{r/q}}\right) + \left(\frac{r-q}{q}\right)\log C_B + \left(\frac{qx-ry}{q}\right)\log [A] \quad (11)$$

From this expression can be found

$$\left(\frac{\partial \log Z}{\partial \log C_B}\right)_{[A]} = \frac{r-q}{q} \quad (12)$$

$$\left(\frac{\partial \log Z}{\partial \log [A]}\right)_{C_B} = \frac{qx-ry}{q} = x - \frac{r}{q}y = n \quad (13)$$

$$\left(\frac{\partial \log C_B}{\partial \log [A]}\right)_Z = \frac{qx-ry}{q-r} = \frac{x-\frac{r}{q}y}{1-\frac{r}{q}} = t \tag{14}$$

If the above mentioned conditions are satisfied, *e.g.* that a complex B_rA_x dominates in the expression for A_b and at the same time a complex of composition B_qA_y dominates in the expression for C_B a linear relationship for a plot of log Z *versus* log [A] and in the same concentration range a linear relationship for a plot of, *e.g.*, log Z *versus* log C_B is to be expected, as in this case r, q, x, and y can be considered constants.

One may determine the slopes n and t defined by eqns. 13 and 14 from the linear parts of the experimental curves. From the two equations thus obtained only two independent ratios among the four variables r, q, x, and y can be determined.

From eqns. 13 and 14 are found

$$r = \frac{t-n}{t} q \tag{15}$$

and

$$x = \frac{t-n}{t} y + n \tag{16}$$

When Z approaches Z_f a new set of complexes $B_{r'}A_{x'}$ and $B_{q'}A_{y'}$ not necessarily identical with B_rA_x and B_qA_y might dominate in the expression 3.

In the case $Z \simeq x'/r'$ an equation similar to eqn. 10 is found from eqn. 6. Thus

$$(Z_f - Z) = \frac{x'q'\beta_{q'y'}}{r'(r'\beta_{r'x'})^{q'/r'}} C_B^{(q'-r')/r'} [A]^{(r'y'-q'x')/r'} \tag{17}$$

We next define the slopes n' and t'

$$\left(\frac{\partial \log(Z_f-Z)}{\partial \log [A]}\right)_{C_B} = \frac{r'y'-q'x'}{r'} = n' \tag{18}$$

$$\left(\frac{\partial \log C_B}{\partial \log [A]}\right)_Z = \frac{r'y-q'x'}{r'-q'} = t' \tag{19}$$

from which is found

$$r' = \frac{t'}{t'-n} q' \tag{20}$$

$$x' = \frac{t'}{t'-n'} (y'-n') \tag{21}$$

$$x'/r' = y'/q' - n'/q' = Z_f \tag{22}$$

DISCUSSION OF THE FORMULAS

The formulas 15, 16, 20, and 21 naturally determine an infinite number of sets of values (r,x), (q,y), (r',x'), and (q',y'). In order to chose among these sets, independent data are necessary. In the following will be shown how the data contained in a plot of $\log Z$ or $\log(Z_f - Z)$ *versus* $\log[A]$ can be applied.

Because of the following inequalities

$$Z = \frac{\Sigma\Sigma u[B_iA_u]}{C_B} = \frac{\Sigma\Sigma \frac{u}{i} i[B_iA_u]}{C_B} < \frac{x}{r} \frac{\Sigma\Sigma i[B_iA_u]}{C_B} = \frac{x}{r} \tag{23}$$

$$Z = \frac{A_b}{\Sigma\Sigma i[B_iA_\nu]} = \frac{A_b}{\Sigma\Sigma \frac{i}{u} u[B_iA_u]} > \frac{y}{q} \frac{A_b}{\Sigma\Sigma u[B_iA_u]} = \frac{y}{q} \tag{24}$$

$$\frac{y}{q} < Z < \frac{x}{r} \tag{25a}$$

$$\frac{y'}{q'} < Z < \frac{x'}{r'} \tag{25b}$$

the measured Z values must be near in magnitude to the u/i values of the compounds actually existing in the solution. By the use of this fact all but a few possible sets of values for (r,x), (q,y), (r',x'), (q',y') will usually be excluded.

In the case $Z < 0.1$, this must therefore mean

$$\frac{y}{q} < 0.1 \tag{26}$$

a very improbable case if y is not zero. Hence we must conclude that in the majority of cases y is equal to zero for Z smaller than 0.1.

The inserting of this value into eqn. 16 leads to

$$x = n \tag{27}$$

Therefore for $B_rA_x (= B_rA_n)$ to be a chemical entity we must have

$$n = \text{integer for } Z < 0.1 \tag{28}$$

As q most often is equal to unity for very low values of Z inspection of eqn. 15 shows that in this case the ratio n/t must also be an integer for r to be so. Thus

$$n/t = \text{integer for } Z < 0.1 \tag{29}$$

This fact often makes a choice of the exact value of a slope possible in cases where a slope is ill defined due to experimental error.

As the condition $Z < 0.1$ is easily realised experimentally the composition of the primary polymerisation product may very often be determined with great certainty.

Regarding the case where $Z - Z_f = x'/r'$ we find from eqns. 20 and 21

$$Z_f = x'/r' = \frac{y' - n'}{q'} \tag{30}$$

Here also an infinite number of sets (q',y') can be found which satisfy eqn. 30 within experimental error. If, however, the linearity of a log$Z$ and a log$(Z_f—Z)$ plot is approximately conserved for the same value of Z in the intermediate region, the only reasonable values of q' and y' are

$$q' = r \tag{31}$$

$$y' = x \tag{32}$$

If eqns. 31 and 32 are consistent with eqn. 30 with the experimentally determined values Z_f and n', the following main reactions can be considered identified.

$$r\mathrm{B} + x\mathrm{A} \rightarrow \mathrm{B}_r\mathrm{A}_x$$

and

$$\mathrm{B}_r\mathrm{A}_x—n'\mathrm{A} \rightarrow \mathrm{B}_r\mathrm{A}_{x-n'} = \frac{r}{r'}\,\mathrm{B}_{r'}\mathrm{A}_{x'}$$

where $\mathrm{B}_r\mathrm{A}_{x-n'}$ must not be considered a chemical entity.

To perform an analysis it is practical to identify the primary polymerisation product at first from a log$Z$ *versus* log [A] diagram. On the same plot it should be possible to estimate the magnitude of Z_f.

One next makes the plot of log $(Z_f—Z)$ *versus* log[A] and determines the slopes n' and t'.

The insertion of the values of Z_f and n' and substitution of r,x for q',y' into eqn. 30 is the next step. If the equation is consistent the values of q' and y' can be considered identified and r' and x' can be determined from eqn. 20 and 21.

THE DETERMINATION OF FORMATION CONSTANTS

If experimental data have allowed the determination of r, q, x, and y, the ratio $\beta_{r,x}/(\beta_{q,y})^{r/q}$ can be determined from eqn. 10.

The point where the line $Z = 1$ intersects the line described by eqn. 11 for a given value of C_B determines a corresponding log[A'] value.

The rearrangement of eqn. 10 leads to

$$\beta_{r,x}/(\beta_{q,y})^{r/q} = \frac{[\mathrm{A}']^{(ry-qx)/q}q^{r/q}}{xC_\mathrm{B}{}^{(r-q)/q}} = \left(\frac{[\mathrm{A}']^{-n}}{n\,C_\mathrm{B}{}^{-n/t}}\right)_{(q,y=1,0)} \tag{33}$$

In the case $\beta_{q,y} = \beta_{1,0} = 1$, $\beta_{r,x}$ can be determined immediately.

When considering hydrolysis equilibria the constants $\varkappa_{r,x}$ used by Sillén *et al.* are related to $\beta_{r,x}$ by the relation

$$\varkappa_{r,x} = \beta_{r,x}\ (K_\mathrm{w})^n \tag{34}$$

where K_w is the ion-product of water.

From eqn. 17 is similarly found for $Z_f—Z = 1$

$$(\beta_{r',x'})^{q'/r'}/\beta_{q',y'} = C_\mathrm{B}{}^{-n'/t'}[\mathrm{A}'']^{n'}\frac{q}{r^{q'/r'}}\frac{x'}{r'} \tag{35}$$

This can be considered the equilibrium constant for a reaction

$$B_{q'}A_{y'} + \frac{q'x'-r'y'}{r} A \rightarrow \frac{q'}{r'} B_{r'}A_{x'}$$

or

$$B_{q'}A_{y'} + (-n') A \rightarrow \frac{t'-n'}{t'} B_{r'}A_{x'} = B_{q'}A_{y'-n'}$$

Even in the case r' and x' are infinite can the formation constant of the repeating unit ($= B_{q'}A_{y'-n'}$) be found as the expression $r'^{q'/r'}$ in the denominator in eqn. 35 in this case can be replaced by unity.

Eqns. 33 and 35 have been used to determine the formation constants for several polymeric species in systems which will be discussed in the following pages.

THE EVALUATION OF EXPERIMENTAL ERRORS

The preceding discussion has shown that an analysis of experimental data by the present method is possible only when q and y are known with certainty. If we therefore presume that no uncertainties are connected with the magnitudes of q and y the effect of experimental errors in n and t on the magnitudes of r,x and $\beta_{r,x}$ can be estimated by means of eqns. 15, 16, and 33.

From eqns. 15 and 16 are obtained

$$r = \frac{t-n}{t}\left(1 \pm \sqrt{\left(\frac{n\,\Delta\, t}{t(t-n)}\right)^2 + \left(\frac{\Delta\, n}{t-n}\right)^2}\right) \tag{36}$$

and approximately

$$x = \left(\frac{t-n}{t} y + n\right)\left(1 \pm \sqrt{\left(\frac{n\,\Delta\, t}{t(t-n}\right)^2 + \left(\frac{\Delta\, n}{t-n}\right)^2}\right) \tag{37}$$

As r and x are known to be integers even data of moderate precision allow the determination of the most probable primary polymerisation product with great certainty.

From eqn. 33 is similarly found

$$\Delta\beta_{r,x} = \beta_{r,x}\left[\left(\frac{n\,\Delta\,[A']}{[A']}\right)^2 + \left(\frac{n\,\Delta\, C_B}{tC_B}\right)^2 + \left(\log[A'] + \frac{1}{t}\log\frac{q\beta_{qy}}{C_B} + \frac{1}{n}\right)^2 \Delta^2 n + \left(\frac{n}{t^2}\log\frac{q\beta_{qy}}{C_B}\right)^2 \Delta^2 t\right]^{\frac{1}{2}} \simeq \beta_{r,x}\left[(\log[A'] - \frac{1}{t}\log C_B)^2\Delta^2 n + \left(\frac{n}{t^2}\log C_B\right)^2 \Delta^2 t\right]^{\frac{1}{2}} = \beta_{r,x}\, k \tag{38}$$

The result will therefore be formulated as

$$\beta_{r,x}(1 \pm k) \simeq \beta_{r,x}(1 + k)^{\pm 1} = 10^{\log \beta_{r,x} \pm \log (1+k)} \tag{39}$$

Similar equations are found for r', x', and $\beta_{r',x'}$. Thus

$$r' = \frac{t'}{t'-n'} q'\left(1 \pm \sqrt{\left(\frac{n'\,\Delta\, t'}{t'(t'-n')}\right)^2 + \left(\frac{n'}{t'-n'}\right)^2}\right) \tag{40}$$

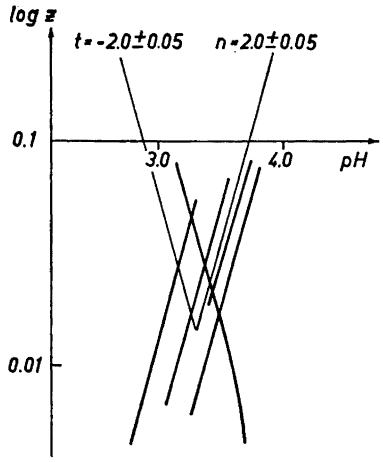

Fig. 1. A plot of log Z *versus* pH for the hydrolysis of the VO^{2+} ion. Data, Ref.[10]

and approximately

$$x' = \frac{t'}{t'-n'}(y'-n')\left(1 \pm \sqrt{\left(\frac{n'\,\Delta\, t'}{t'(t'-n')}\right)^2 + \left(\frac{\Delta\, n'}{t'-n'}\right)^2}\right) \qquad (41)$$

The uncertainty of $\beta^{q',r'}_{r',x'}/\beta_{q',y'}$ can be found from an equation similar to eqn. 38.

APPLICATION OF THE FORMULAS

The following hydrolysis equilibria will be discussed.

Species	Ref.
VO^{2+} ion	Rosotti and Rosotti [10]
VO_2^+ ion	Rosotti and Rosotti [11]
Al^{3+} ion	Brosset [12]

The vanadyl ion

In this case the function

$$Z = \frac{\Sigma\Sigma u[B_iA_u]}{C_B} = \frac{\Sigma\Sigma u[(VO^{2+})_i(OH^-)_n]}{C_{VO^{2+}}}$$

is being studied.

The data of Rosotti and Rosotti [10] are shown in Fig. 1 in a log$Z$ *versus* pH plot. In the range $0.005 < Z < 0.1$ the curves are parallel. The values for n and t in this range are

$$n = 2.0 \pm 0.05 \qquad t = -2.0 \pm 0.05$$

For low concentrations $t \to \infty$, and monomeric hydrolysis products may be assumed, as this means $r = q$. The data do not go to low enough concentrations to permit any conclusions about the monomeric hydrolysis.

The insertion of the values for n and t into eqn. 16 gives

$$x = (2.0 \pm 0.07)\ y + 2.0\ (\pm 0.05)$$

As $y = 0$ is the only value compatible with the low value of Z we immediately get

$$x = 2.0 \pm 0.05$$

From eqn. 15 is obtained

$$r = 2.0\ (\pm 0.07)q$$

Literature indicates a value for q equal to unity. We therefore obtain

$$r = 2.0 \pm 0.07$$

The linear curves can therefore be taken as representing the equilibrium

$$2\ VO^{2+} + 2\ OH^- \rightarrow (VO)_2(OH)_2^{2+}$$

as also proposed by Rosotti and Rosotti [10].

At $Z \simeq 0.1$ the curves bend slightly wherefore additional complexes are being formed, the exact nature of which cannot be ascertained.

For $C_B = 0.0207$ M and $C_B = 0.0515$ M the determination of $\beta_{2,2}$ gives

$$\beta_{2,2} = 10^{21.5 \pm 0.3}$$

and $\varkappa_{2,2} = 10^{-6.9 \pm 0.3}$ with $K_w = 10^{-14.22}$ Refs.[11,12].

From Ref.[10], $\varkappa_{2,2}$ was found to be

$$\varkappa_{2,2} = 10^{-6.88 \pm 0.05}$$

There is seen to be fair agreement between the two methods of analysis of the data in this case.

Rosotti and Rosotti were also able to determine the primary hydrolysis product at low concentrations as $(VO)OH^+$. An analogous determination cannot be made here with reasonable certainty as the true monomeric curve is not contained in the data.

The VO_2^+ ion in acid medium

In this case the function

$$Z = \frac{\Sigma\Sigma u[B_iA_n]}{C_B} = \frac{\Sigma\Sigma u[(VO_2^+)_i(OH^-)_u]}{C_{VO_2^+}}$$

is being studied.

The data from the publication of Rosotti and Rosotti [11] are shown in Fig. 2 in a log$Z$ *versus* pH plot. The data for $Z < 0.08$ are rather irregular and will not be considered in the analysis. The curves are linear for $0.08 < Z < 0.4$.

The values for n and t are estimated to

$$n = 7.0 \pm 0.6 \quad \text{and} \quad t = -1.4 \pm 0.05$$

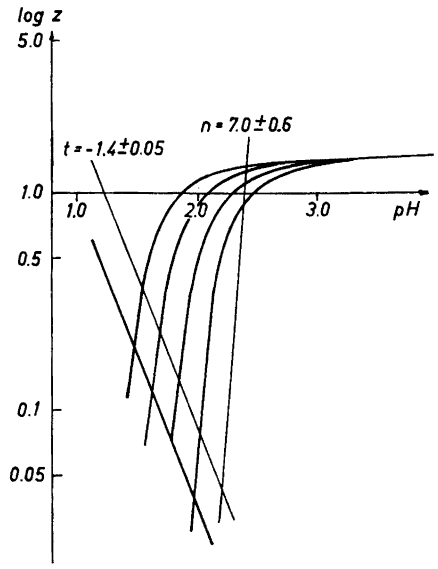

Fig. 2. A plot of log Z *versus* pH for the hydrolysis of the VO_2^+ ion. Data, Ref.[11]

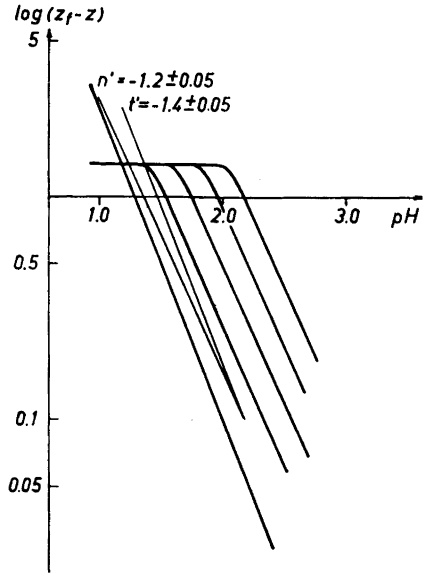

Fig. 3. A plot of log (1.41 − Z) *versus* pH for the hydrolysis of the VO_2^+ ion. Data, Ref.[11]

From these values we find

$$r = 6.0 \pm 0.6 \quad \text{and} \quad x = 5\ (\pm 0.5)\ y + 7\ (\pm 0.6)$$

The insertion of the values $y = 0$, which is reasonable for low values of Z, and $q = 1$ according to Ref.[11] leads to

$$r = 6.0 \pm 0.6 \quad \text{and} \quad x = 7.0 \pm 0.6$$

The following equilibrium can therefore be assumed to be responsible for the linear parts of the curves.

$$6\ VO_2^+ + 7\ OH^- = (VO_2)_6(OH)_7^-$$

The corresponding formation constant $\beta_{6,7}$ has been determined by means of eqn. 33 for $C_{VO_2^+} = 0.0025$ M and 0.02 M.

$\beta_{6,7} = 10^{94.6 \pm 0.5}$

$\varkappa_{6,7} = 10^{-2.0 \pm 0.5}$ with $K_w = 10^{-13.8}$ (Ref.[11])

The value of (x/r) does not satisfy the Z_f value of 1.40 ± 0.05 measured on the curves, for which reason further polymerisation must be supposed to occur.

In Fig. 3 the data are shown in a plot of $\log(Z_f - Z)$ *versus* pH.

From the curves we determine the best values of n' and t' as

$$n' = -1.2 \pm 0.05 \quad \text{and} \quad t' = -1.4 \pm 0.05$$

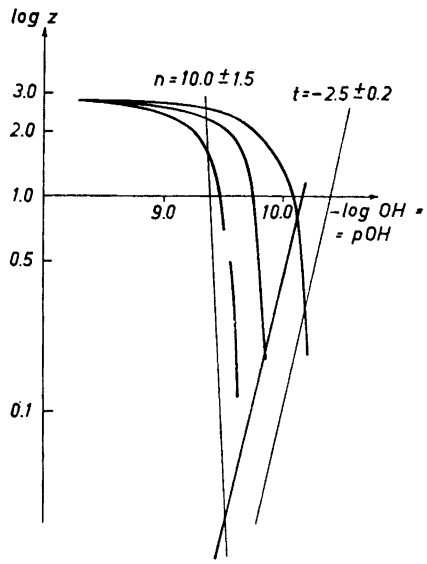

Fig. 4. A plot of log Z *versus* pOH (= −log[OH]) for the hydrolysis of the Al^{3+} ion. Data, Ref.[12]

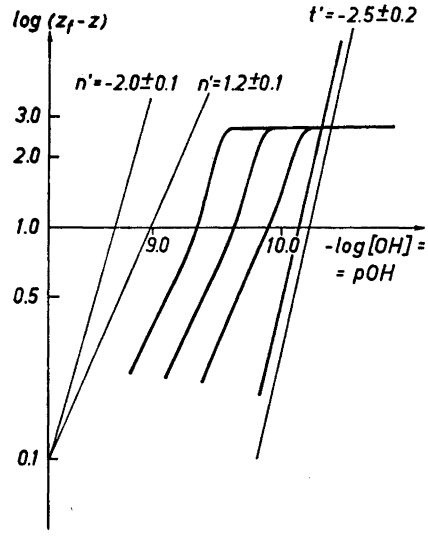

Fig. 5. A plot of log (2.75 − Z) *versus* pOH (= −log[OH]) for the hydrolysis of the Al^{3+} ion. Data, Ref.[12]

From eqns. 20 and 21 is seen that the final product obviously is highly polymerised. Thus.

$$r' = \frac{-1.4}{-0.2} q' = 7q'(1 \pm 0.5)$$

$$x' = \frac{-1.4}{-0.2} (y' - n') = 7(y' - n')(1 \pm 0.5)$$

The substitution of (6,7) for (q',y') in eqn. 30

$$Z_f = 1.40 = \frac{7 + 1.4}{6} = 1.40$$

shows that the final reaction can be formulated as

$$N(VO_2)_6(OH)_7^- + N\ 1.4\ OH^- = (VO_2)_{6N}(OH)_{8.4N}^{2.4N-}$$

where $N = 7 \pm 3$

The equilibrium constant for the final reaction has been determined by means of eqn. 35 in the case $N = 7$, for $C_{VO_2^+} = 0.02$ M

$$\beta_{42,59}/(\beta_{6,7})^6 = 10^{100 \pm 2}$$

The above conclusions are well in accord with experimental data.

As depolymerisation of the polyvanadates is known to occur for Z values larger than Z_f (= 1.4) an isohydric point is defined at $Z = Z_f$. This is known to correspond to the state of maximum polymerisation which from the present analysis seems to correspond to polymers containing from 24 to 60 VO_2 units.

The Al^{3+} ion in acid medium.

In this case the function

$$Z = \frac{\Sigma\Sigma u[B_i A_u]}{C_B} = \frac{\Sigma\Sigma u[Al^{3+}_i (OH^-)_u]}{C_{Al^{3+}}}$$

is being studied.

The data from the publication of Brosset [12] are shown in Fig. 4 in a log Z *versus* pOH plot. His paper contains data measured ½ h and 10—20 h after the mixing of the reagents. Only the last data will be considered.

The data for $Z < 0.1$ are rather irregular and will not be used in the analysis. The curves show the slopes

$$n = 10 \pm 1.5 \quad \text{and} \quad t = -2.5 \pm 0.2$$

and

$$Z_f = 2.75 \pm 0.03$$

For $(q,y) = (1,0)$, r and x are found to be

$$r = 5.0 \pm 0.7 \quad \text{and} \quad x = 10 \pm 1.4$$

The formation of the primary hydrolysis product of the Al^{3+} ion in a slow titration may therefore be formulated as

$$5\ Al^{3+} + 10\ OH^- \rightarrow Al_5(OH)_{10}^{5+}$$

The formation constant $\beta_{5,10}$ is found to be

$$\beta_{5,10} = 10^{107 \pm 1.5}$$

and

$$\varkappa_{5,10} = 10^{-28 \pm 1.5} \text{ with } K_w = 10^{-13.5} \text{ (Ref.}^{12}\text{)}$$

As the Z_f value is not satisfied with this product further polymerisation must be assumed.

From the log $(Z_f - Z)$ *versus* pOH plot (Fig. 5) two regions with linear curves are found.

For $(Z_f - Z) > 1.0$, n' and t' are found to be

$$n' = -2.0 \pm 0.1 \quad \text{and} \quad t' = -2.5 \pm 0.2$$

From eqns. 20 and 21 and $(q',y') = (1,0)$ are found

$$r' = 5.0 \pm 1 \quad \text{and} \quad x' = 10.0 \pm 2$$

in accord with the preceding analysis.

For very small values of $(Z_f - Z)$ are found

$$n' = -1.2 \pm 0.1 \qquad \text{and} \qquad t' = -2.5 \pm 0.2$$

The insertion of $n' = -1.2$ and the replacement of q' and y' with r and x (5,10) into eqn. 22 leads to

$$Z_f = 2.75 = \frac{y' - n'}{q'} \neq \frac{10 + 1.2}{5} = 2.24$$

which show that the final product cannot be formulated as a direct polymerisation product of $Al_5(OH)_{10}^{5+}$.

From eqns. 20 and 21 are found

$$r' = 1.9q(1 \pm 0.2) \qquad \text{and} \qquad x' = 1.9(y' + 1.2)(1 \pm 0.2)$$

which indicates that the last reaction is a dimerisation.

Recently Johansson [13] has investigated the crystalline basic sulphates and selenates of composition $Na_2O{:}13\ Al_2O_3{:}8\ SO_3{:}x\ H_2O$ and $Na_2O{:}13\ Al_2O_3{:}\ SeO_3{:}x\ H_2O$ and has identified a chemical entity of composition $Al_{13}O_4(OH)_{24}(H_2O)_{12}^{7+}$ $(= Al_{13}(OH)_{32}^{7+})$ in the crystals. The entity has a structure reminiscent of that of the heteropolyacids.

It seems reasonable to assume that the final product in the present analysis contains this Al_{13}-unit. A final product of structure

$$(Al_{13}(OH)_{36}^{3+})N \qquad x'/r' = 36/13 = 2.77$$

where N is unknown will therefore be proposed.

GENERAL DISCUSSION

The method presented seems well suited to treat titration data involving the formation of polynuclear complexes.

Because of the nature of the problem the principle of the method is somewhat similar to previously applied methods; however, it often leads to different results as shown in the examples.

It is obvious that a mathematical approach to the problem of polymer formation in itself offers no solution to the chemistry involved, but only the consequent use of the mass-action relationship connects the analysis to chemistry. Accordingly only data where this law is valid can be treated by the method, *i.e.* data involving real equilibria or apparent equilibria where the chemical reactions following the main reactions are very slow.

The present method is one by means of which the dominating terms in an unknown polynomium Z are identified and their coefficients determined. This is possible only under certain circumstances by the present method, but will almost always be the case for low values of the function Z.

Owing to experimental errors one can never be sure that the true term (or equivalent chemical entity) is identified with certainty, but within experimental error the term proposed by the present analysis will be as well suited to represent the experimental data as will results found by other methods of analysis.

A fit between curves calculated by means of constants found by the mathematical analysis with the experimental curves will eliminate large errors in the analysis but it will seldom allow a decision between two alternative polymerisation products proposed.

In principle any experimental curve can be approximated very closely by a polynomium when minor terms are included in the analysis. However, the magnitude of the experimental error often makes the inclusion of such minor terms of rather doubtful value.

The dominating term can, however, be identified with some certainty.

Other terms useful for the fitting of theoretical curves with experimental ones are preferably determined by identification of the corresponding chemical species if possible.

Alternatively one can propose a sort of mechanism for polymerformation as, *e.g.*, the "core-link" hypothesis where polymers are thought of as formed by the addition of links of constant composition one by one to a core usually being a single atom of B. Only terms corresponding to polymers of "core-link" composition are then taken into account when the theoretical curves are approximated to the experimental ones.

The success of this method in describing experimental data, however, does not prove that this is the actual mechanism of polymerformation.

An equally acceptable mechanism of polymer formation could be chemical reactions of polymers with each other to still larger aggregates — a sort of sequential dimerisations.

The actual mechanism of polymerformation might well be a "mixture" of those proposed above.

Which species actually are stable must depend very much on the geometrical pattern of the polymers and therefore on which atoms are involved, their radii, charge, electronegativity, *etc.* It seems reasonable to assume that the most stable ionic polymers (*i.e.* hydrolysis products of metal salts, *etc.*) in their structure should follow the rules set forth by Pauling [14] for the structure of ionic crystals.

As is seen, the analysis of the complex data obtained in the study of polymerisation reactions leaves much to chemical intuition. The present method cannot claim to be more exact or accurate than previous ones but has the advantage that it is more easy to apply. A distinct advantage is that the primary polymerisation product often can be determined with certainty.

The data [A] and A_b necessary for an analysis are usually (especially in the case of metal complexes) found by titrations where [A] is measured directly and A_b calculated.

Formally the equations 1, 2, 3... are symmetrical in A and B. The result of an analysis is therefore independent of which atom is considered central atom or ligand.

REFERENCES

1. Sillén, L. G. *Acta Chem. Scand.* **8** (1954) 299.
2. Sillén, L. G. *Ibid.* **8** (1954) 318.
3. Hietanen, S. and Sillén, L. G. *Ibid.* **8** (1954) 1608.

4. Biedermann, G. and Sillén, L. G. *Ibid.* **10** (1956) 1011.
5. Hedström, B. *Ibid.* **9** (1955) 613.
6. Simchen, A. E. *Bull. soc. chim. France.* **1951** 977.
7. Souchay, P. *Ibid.* **1949** 122.
8. Souchay, P. and Teyssédre, M. *Ibid.* **1949** 938.
9. Sillén, L. G. *Quart. Revs.* **13** (1959) 146.
10. Rosotti, F. J. C. and Rosotti, H. *Acta Chem. Scand.* **9** (1955) 1177.
11. Rosotti, F. J. C. and Rosotti, H. *Ibid.* **10** (1956) 957.
12. Brosset, C. *Ibid.* **6** (1952) 910.
13. Johansson, G. *Ibid.* **14** (1960) 771.
14. Pauling, L. *Nature of the Chemical Bond.* Cornell Univ. Press, London 1948.

Received September 9, 1960.

ACTA CHEMICA SCANDINAVICA 15 (1961) 502–520

The Kinetics of the Water Gas Conversion at Atmospheric Pressure

HANS BOHLBRO

The Haldor Topsøe Research Laboratory, Hellerup, Denmark

The kinetics of the water gas conversion $CO + H_2O \rightarrow CO_2 + H_2$ at atmospheric pressure over an iron oxide-chromium oxide catalyst has been investigated in the temperature range 330–500°C. The catalyst was "stabilized" by running for 10–14 days at working conditions before starting the measurements. It was found that the rate of the forward reaction could be expressed by an equation of the following exponential type, rate $= k\,(CO)^l(H_2O)^m(CO_2)^n$ where (CO), (H_2O) and (CO_2) are partial pressures of CO, H_2O and CO_2, respectively. The rate is independent of H_2 partial pressure. The exponents l, m, and n vary only slightly with temperature and are situated within the following ranges, $l = 0.80-1.00$, $m = 0.20-0.35$, and $n = -0.65$ to -0.50. Preliminary values of l, m, and n were obtained at relatively low conversions by a graphic method. For the final testing and for testing at higher degrees of conversion the rate expression has been integrated by means of an electronic digital computer. By application of an "average" rate expression for the whole temperature range the apparent energy of activation has been determined to be 27.4 kcal/mole.

The water gas conversion $CO + H_2O \rightarrow CO_2 + H_2$ over iron oxide based catalysts is of considerable industrial importance. Although a number of more or less conflicting rate equations [1–8] have been put forward, a generally accepted kinetic expression does not exist.

The present work was undertaken as part of a program aiming at establishing data for calculation of required amounts of catalyst for industrial plants. This work will later also include experiments at elevated pressure. During the work described here an electronic calculating machine has been used for establishing rate equations.

EXPERIMENTAL

Gases. All gases employed, CO, N_2, H_2, and CO_2, were taken from cylinders. CO was about 98.5 % pure, the rest being mainly N_2 (about 1 %), H_2 (about 0.5 %), and O_2 (about 0.2 %) Further, traces of iron carbonyl could be found. CO_2 was less than 0.1 %. CO was purified by passing over Cu-wire at 320°C (which removes traces of oxygen and

of iron carbonyl present), alumina, potassium hydroxide pellets, and active carbon. N_2 and H_2 were purified in the same way. CO_2 was used without further purification.

Catalyst. The catalyst used was a commercial iron oxide-chromium oxide catalyst. Particle size was 0.8—1.2 mm. The amount of catalyst used has been either 3.00 g (unreduced) diluted by 9.5 cm^3 inert material (quartz) of the same particle size, or 12.00 g diluted by 38.0 cm^3 inert material. The total volume of catalyst and diluting material was 12.0 cm^3 or 48.0 cm^3, respectively. The height of the catalyst bed was 5.2 cm or 21.0 cm, respectively. Before starting the measurements, the catalyst was reduced, and thereafter stabilized (or "aged") by running for 10—14 days at working conditions and at the temperature at which the measurements were intended to take place. Catalyst samples used for the runs at temperatures below 380°C, however, were stabilized at 380°C. During the stabilization period a decrease of the activity occurred accompanied by an increase in pore size and a decrease in surface area. Even the stabilized catalyst was not completely stable in activity, but after the stabilization period further loss of activity was so slow as to permit measurements which will be useful for the calculation of industrial performance during a considerable period of time.

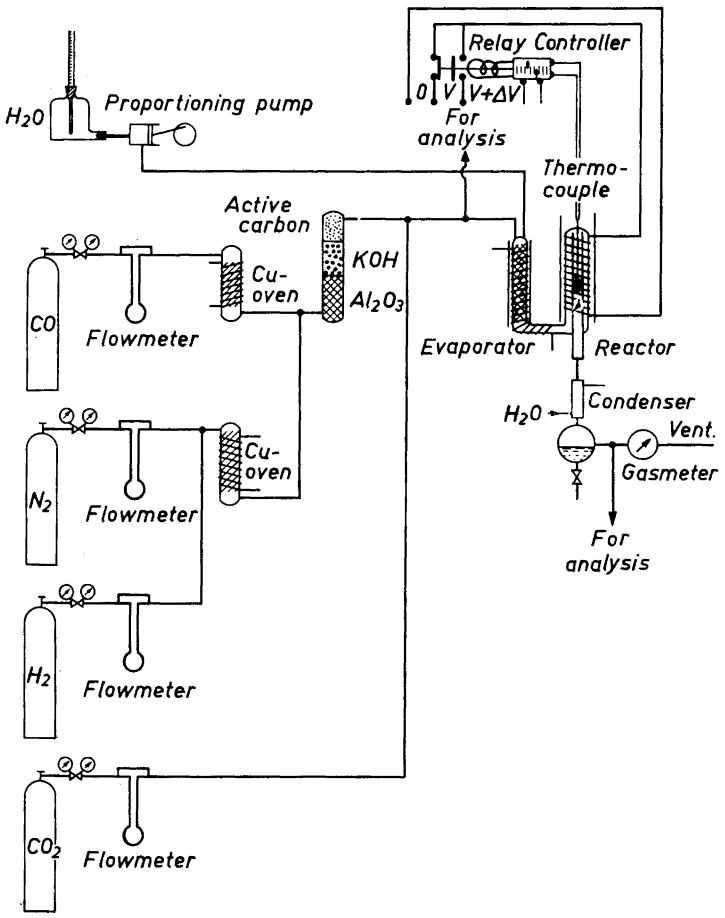

Fig. 1. Schematic drawing of experimental set-up.

Experimental set-up. A diagram of the experimental set-up is shown in Fig. 1. The gases were supplied through flowmeters and purification trains to the evaporator where liquid water was introduced by means of a proportioning pump. Mixture of water vapour and gases was passed through a heated tube to the glass reactor, which was constructed in the following way: The catalyst was placed in an inner tube, through which a thermocouple tube passed so that the temperature might be measured at any level of the catalyst layer. Incoming feed gas passed through an annular space in countercurrent flow with the gas in the catalyst tube. The outer wall of the annular space was provided with a Ni-chrome heating coil. Outside the heating coil was placed a glass mantle. By manipulating the insulation of this outer glass mantle it was possible to maintain almost isothermal conditions throughout the catalyst layer, the variation being at maximum 4°C between the warmest and the coldest spot. The thermocouple was ordinarily placed at a point having an average temperature. The temperature of the reactor was maintained by means of the thermocouple and a controller, which regulates the voltage of the heating coil. The calibration of the controller was controlled daily by means of a potentiometer.

Effluent gas passed through a condenser and a precision wet gas meter. Samples for analysis of exit gas could be taken out without changing the flow conditions in the reactor.

Analytical procedure. CO and CO_2 were determined in an Orsat apparatus by adsorption in KOH-solution and in CuCl-solution, respectively. H_2 was determined by gas chromatography. The rest of the gas was considered to be nitrogen. Between 3 and 6 analyses were made at each set of conditions. The figures given in the tables are average figures from these determinations.

LIST OF SYMBOLS

F = total feed rate (mole/h).
f = feed rate of CO (mole/h).
k = reaction rate constant for forward reaction.
K = equilibrium constant for the water gas conversion
K_1, K_2, K_3, K_4 = overall constants appearing in eqns. (4), (6), (8), and (10), respectively.
l, m, n, and q = exponents occurring in the reaction rate equation (1).
(CO), (H_2O), (CO_2), (H_2) = partial pressures (atm.) of CO, H_2O, CO_2, and H_2, respectively. Subscript zero indicates initial partial pressure.
r = net reaction rate (mole CO converted/(h) (g catalyst)).
r_f and r_b = forward and backward reaction rates, respectively.
x = degree of conversion of CO $\left(\frac{\text{moles CO converted}}{\text{moles CO in feed gas}}\right)$.
W = weight of catalyst (g).

DEVELOPMENT OF A RATE EQUATION

Past experience has shown [5,9,10] that it is generally possible to express the experimental results for a unidirectional rate by an equation of the type $r_f = k \cdot (A)^a \cdot (B)^b \cdot (C)^c \ldots$ where (A), (B), (C), *etc.* are partial pressures of reactants and products. An exponential equation of this type is more simple to use than an equation of the Langmuir-Hinshelwood-Hougen-Watson type. As discussed in Refs.[9,10] these two types of rate expressions can generally be approximated to each other.

For the present case a rate equation of the exponential type for the forward reaction is

$$f \cdot \frac{dx}{dw} = k \cdot (CO)^l \cdot (H_2O)^m \cdot (CO_2)^n \cdot (H_2)^q \quad (1)$$

Assuming the Horiuti stoichiometric number (*cf. e.g.* Ref.[5]) for the rate determining step to be one, the net rate is

$$r = r_f - r_b = k\ (CO)^l \cdot (H_2O)^m \cdot (CO_2)^n \cdot (H_2)^q \cdot (1-\beta) \quad (1a)$$

$$\text{where } \beta = (CO_2)(H_2)/K(CO)(H_2O)$$

The experiments rapidly showed the rate to be independent of the hydrogen partial pressure in the whole temperature range 330°—500°, *i.e.* $q = 0$.

By substituting this and $f = F\,(CO)_0$ in eqn. (1) we have

$$F \cdot \frac{dx}{dw} = k\,(CO)_0^{l-1}\,(1-x)^l\,[(H_2O)_0 - x \cdot (CO)_0]^m\,[(CO_2)_0 + x(CO)_0]^n \quad (2)$$

If $x \cdot (CO)_0$ is small in comparison with $(CO)_0$, $(H_2O)_0$, and $(CO_2)_0$ an approximate integration leads to

$$x = (kW/F) \cdot (CO)_0^{l-1}\left(1-\frac{x}{2}\right)^l [(H_2O)_0 - \frac{x}{2}(CO)_0]^m [(CO_2)_0 + \frac{x}{2}(CO)_0]^n \quad (3)$$

or, for constant F, $(CO)_0$ and $(H_2O)_0$,

$$\ln x = K_1 + n \cdot \ln\,[(CO_2)_0 + \frac{x}{2}(CO)_0] \quad (4)$$

i.e., by plotting

$$\ln x \textit{ vs. } \ln\,[(CO_2)_0 + \frac{x}{2}(CO)_0]$$

for varying $(CO_2)_0$ and small conversions n is obtained as the slope of a straight line if an equation of the type (1) is fulfilled. If $(CO_2)_0 = 0$ and $x \cdot (CO)_0$ is small in comparison with $(CO)_0$ and $(H_2O)_0$, (2) may be approximatively integrated to:

$$x^{-n+1} = (-n+1)(kW/F) \cdot (CO)_0^{n+l-1}\left(1-\frac{x}{2}\right)^l [(H_2O)_0 - \frac{x}{2}(CO)_0]^m \quad (5)$$

or for constant F and $(H_2O)_0$

$$(-n+1)\ln x = K_2 + (n+l-1)\ln\left[(CO)_0 \cdot \left(1-\frac{x}{2}\right)^{l/(n+l-1)}\right] \quad (6)$$

By applying the above value of n and choosing an approximate value of l (for calculation of the term $\left(1-\frac{x}{2}\right)^{l/(n+l-1)}$ which varies only slightly) and then plotting

$$\ln x \textit{ vs. } \ln\left[(CO)_0\left(1-\frac{x}{2}\right)^{l/(n+l-1)}\right]$$

for varying $(CO)_0$, a straight line should be obtained the slope of which is $(n + l—1)/(—n + 1)$ or

$$l = (1—n) + (1 — n) \times \text{slope} \tag{7}$$

If $(CO_2)_0 = 0$ and F and $(CO)_0$ are constant one obtains instead of (6)

$$(—n + 1)\ln x = K_3 + m\ln \left\{[(H_2O)_0 — \frac{x}{2}(CO)_0]\left(1—\frac{x}{2}\right)^{l/m}\right\} \tag{8}$$

By inserting an approximate value of m and making a logarithmic plot, a straight line should again be obtained, the slope of which is $m/(—n + 1)$ or

$$m = (—n + 1) \times \text{slope} \tag{9}$$

Finally it has also in some cases been of interest to determine l by varying the partial pressure of CO in feed gas while maintaining constant essential partial pressures of both CO_2 and H_2O. In this case eqn. (3) is transformed into

$$\ln\left[x/\left(1—\frac{x}{2}\right)^l\right] = K_4 + (l—1)\ln (CO)_0 \tag{10}$$

and $l—1$ is obtained as the slope of a straight line.

EVALUATION OF EXPERIMENTAL RESULTS

The procedure for obtaining the experimental data has been the following. At each of the temperatures 330°C, 380°C, 420°C, 460°C, and 500°C 4 or 5 series of runs have been made varying the partial pressure of one of the four components CO, H_2O, CO_2, and H_2 during each series without changing other variables. The balance partial pressure has been maintained by means of nitrogen, which is supposed not to influence the reaction.

At 360°C only a single series of runs has been made during which the CO-concentration has been varied while a constant CO_2-concentration has been maintained in the feed gas.

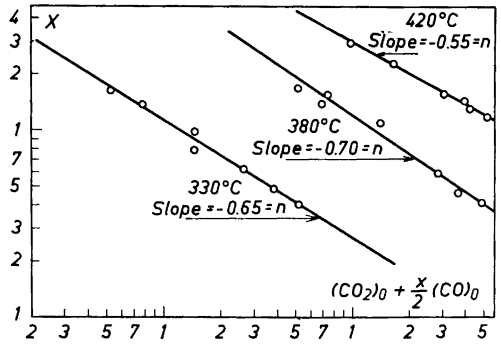

Fig. 2. Determination of n at 330°, 380°, and 420°C according to eqn. (4) by plotting $\ln x$ *vs.* $\ln ((CO_2)_0 + \frac{x}{2}(CO)_0)$. Experimental data are given in Tables 4, 8 and 13, respectively. The abscissa applied at 330°C is displaced one decade relatively to that applied at 380°C and 420°C.

The data obtained in this way at 330°C and 380°C have been plotted according to eqns. (4), (6), and (8) giving l,m, and n, respectively. Data obtained at 360°C, 380°C, and 420°C by varying the CO-concentration while keeping a constant CO_2-concentration have been plotted according to eqn. (10), giving l.

Further the data obtained at 420°C by varying the CO_2-concentration have been plotted according to eqn. (4), giving n. The other data obtained at 420°C and those obtained at higher temperatures have not been plotted, the conversions being too high.

The diagrams obtained by these plottings are shown in Figs. 2—5 and the values of l, m and n thus obtained are summarized in Table 1.

The correctness of the values of l, m, and n thus obtained has been controlled in the following way. An approximate value of k together with the above values of l, m, and n are inserted in the net rate equation (1a). This equation is then integrated for each set of the appropriate experimental conditions with the aid of an electronic digital computer (DASK) which directly prints the composition of the exit gas. The optimum values of the variables k, l, m, and n were found by trial and error in the following way. At the exit of the reactor an increase of the conversion Δx, is approximately proportional to an increase of the amount of catalyst ΔW for small values of Δx and ΔW. A fractional increase of W of $\Delta W/W$ is equal to a fractional increase of k of $\Delta k/k$. It is therefore possible by applying an approximate value of k and letting the computer print the gas composition at the exit and at a short distance before the exit to obtain by interpolation (or extrapolation) a value of k which makes the calculated value of x equal to the experimentally found value of x. l, m or n (depending upon which component is being varied) is varied until the values of k show no systematic variation within each series. If the average value of the k's thus obtained is essentially different from that applied for the electronic calculation the latter is repeated using the average value. l, m, and n have only been varied in steps of 0.05. The data used for Figs. 2—4 have been treated in this way. It appeared that the graphically found values of l, m, and n were very nearly correct.

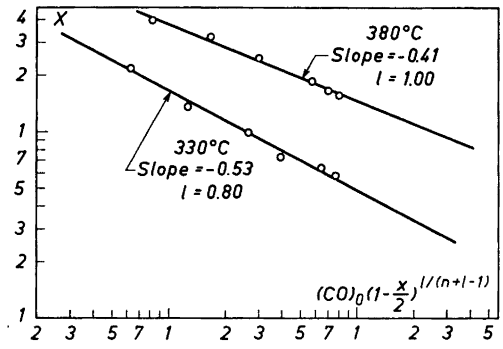

Fig. 3. Determination of l at 330° and 380° according to eqn. (6) by plotting $\ln x$ *vs* $\ln\left[(CO)_0\left(1-\frac{x}{2}\right)^{l/(n+l-1)}\right]$. Experimental data are given in Tables 2 and 6.

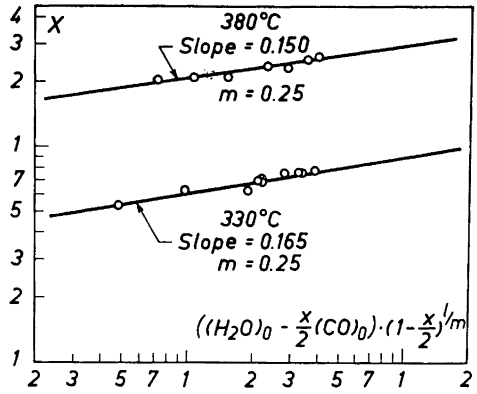

Fig. 4. Determination of m at 330° and 380° according to eqn. (8) by plotting $\ln x$ *vs.* $\ln \{[(H_2O)_0 - \frac{x}{2}(CO)_0]\left(1 - \frac{x}{2}\right)^{l/m}\}$. Experimental data are given in Tables 3 and 7.

At the conditions (higher temperatures) where the conversions obtained were too high to be plotted according to eqns. (4), (6), (8), and (10), it appeared, when applying the electronic computer, that only minor changes of the values obtained for l, m, and n at 380°C were necessary at these temperatures in order to obtain a constant value of k within each series.

In addition to the runs performed at constant space velocity and varying partial pressure of one of the components also a number of runs have been

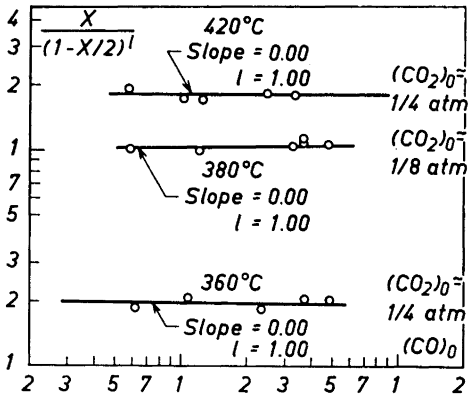

Fig. 5. Determination of l at 360°, 380°, and 420°C according to eqn. (10) by plotting $\ln\left[x/\left(1 - \frac{x}{2}\right)^l\right]$ *vs.* $\ln (CO)_0$. Experimental conditions at 360°C: $(H_2O)_0 \simeq (CO_2)_0 \simeq \frac{1}{4}$ atm., amount of catalyst 12.00 g, total feed gas $\simeq$ 2.4 mole/h. At 380°: $(H_2O)_0 \simeq \frac{3}{8}$ atm., $(CO_2)_0 \simeq \frac{1}{8}$ atm., amount of catalyst 3.00 g, total feed gas $\simeq$ 2.4 mole/h. At 420°: $(H_2O)_0 \simeq \frac{3}{8}$ atm., $(CO_2)_0 = \frac{1}{4}$ atm., amount of catalyst 3.00 g, total feed gas $\simeq$ 2.5 mole/h. The ordinate applied at 360° is displaced one decade relatively to that applied at 380° and 420°.

Table 1. The values of l, m, and n obtained from Figs. 2—5.

	330°C	360°C	380°C	420°C
l (eqn. 6)	0.80		1.00	
l (eqn. 10)		1.00	1.00	1.00
m (eqn. 8)	0.25		0.25	
n (eqn. 4)	−0.65		−0.70	−0.55

made with constant feed gas composition and varying space velocity so that the rate equation has been tested over a considerable range of degrees of conversion. Such series of runs have been performed at 330, 380, 400, and 420°C.

As the exponent n is negative the feed gas concentrations cannot be directly fed to the electronic computer when $(CO_2)_0 = 0$. In these cases the gas composition has been calculated by hand at a distance of ½—1 % of the total bed length from the top, and these data have then been applied to the computer. This calculation can be made fairly accurately by approximate methods.

The results of the calculations are shown in Tables 2—20. The rate equation given above each table is that which has been applied for calculating the degree of conversion shown in column 8 by means of the electronic digital computer. Column 9 gives the experimentally found degrees of conversion, and the last column gives the value of k which by means of the above described interpolation method makes the calculated conversion equal to the experimentally found conversion.

Finally a series of runs has been made during which the temperature has been varied. The catalyst was stabilized at 500°C, and measurements have been made at 500, 460, 420, 380, 360, 330, and again 500°C. The results of these runs are shown in Table 22.

DISCUSSION

It is of importance to ascertain whether the experimental results have been influenced by transport restrictions.

Table 2. 330°C. Variation of $(CO)_0$. Amount of catalyst 3.00 g. Rate equation for forward reaction $r_f = 0.0050 \cdot \frac{(CO)^{0.80} \cdot (H_2O)^{0.25}}{(CO_2)^{0.65}}$

No.	Total feed mole/h	Feed gas composition, %					Conv. calc. %	Conv. exptl. %	Rate constant k
		CO	CO_2	H_2	N_2	H_2O			
1	2.388	74.80	0	0.56	0.04	24.60	5.67	5.8	0.0052
2	2.388	62.80	0	0.47	12.13	24.60	6.21	6.45	0.0053
3	2.383	37.70	0	0.28	37.52	24.50	8.05	7.3	0.0042
4	2.383	25.20	0	0.19	50.11	24.50	9.86	10.0	0.0051
5	2.379	12.00	0	0.09	63.11	24.80	14.31	13.6	0.0046
6	2.363	5.60	0	0.04	63.86	24.50	20.71	22.0	0.0055
								Average	0.0050

Table 3. 330°C. Variation of $(H_2O)_0$. Amount of catalyst 3.00 g. Rate equation for forward reaction: $r_f = 0.0048 \cdot \frac{(CO)^{0.80} \cdot (H_2O)^{0.25}}{(CO_2)^{0.65}}$

No.	Total feed mole/h	Feed gas composition, %					Conv. calc. %	Conv. exptl. %	Rate constant k
		CO	CO_2	H_2	N_2	H_2O			
1	2.279	50.70	0	0.38	22.92	26.00	7.00	7.0	0.0048
2	2.413	48.20	0	0.36	12.24	39.20	7.41	7.6	0.0050
3	2.321	49.40	0	0.37	24.23	26.00	7.02	7.05	0.0048
4	2.254	48.40	0	0.37	4.43	46.80	7.91	8.0	0.0049
5	2.283	48.20	0	0.36	11.44	40.00	7.68	7.55	0.0047
6	2.317	47.60	0	0.36	18.44	33.60	7.45	7.6	0.0050
7	2.333	47.10	0	0.35	26.35	26.20	7.18	7.0	0.0046
8	2.363	49.40	0	0.37	27.63	22.60	6.79	6.4	0.0043
9	2.254	50.40	0	0.38	36.62	12.60	6.27	6.3	0.0048
10	2.296	50.20	0	0.38	42.72	6.70	5.54	5.4	0.0046
								Average	0.0048

A calculation by means of the method given by Hougen and Watson [11] shows that the external mass transfer to and from the geometrical surface is not of great importance at any of the experimental conditions used.

Internal diffusion in the catalyst pores is definitely not of importance at temperatures $\leq$ 380°C as shown by calculation as well as by experiment (comparison of conversion obtained by 1 mm and by 2 mm particles, respectively). At higher temperatures the situation is somewhat more complicated. For runs at 420°C without CO_2 in the feed gas calculations by the method of Hoogschagen [12] gave an effectiveness factor of at least 90 %, which, if correct, would be satisfactory. However, during these calculations certain assumptions have been made (*e.g.*, first order reaction, spherical catalyst particles) which are not correct. It would therefore be possible that the effectiveness factor actually were smaller. However, the agreement between the value of l (1.00) obtained

Table 4. 330°C. Variation of $(CO_2)_0$. Amount of catalyst 12.00 g. Rate equation for forward reaction: $r_f = 0.0054 \cdot \frac{(CO)^{0.80} \cdot (H_2O)^{0.25}}{(CO_2)^{0.65}}$

No.	Total feed mole/h	Feed gas composition, %					Conv. calc. %	Conv. exptl. %	Rate constant k
		CO	CO_2	H_2	N_2	H_2O			
1	2.329	24.70	0	0.18	50.12	25.00	23.1	22.8	0.0052
2	2.288	25.50	25.50	0.15	23.55	25.30	6.05	6.3	0.0056
3	2.283	24.80	13.20	0.13	36.37	25.50	8.92	7.9	0.0047
4	2.392	24.00	51.00	0.08	0.92	24.00	3.79	4.0	0.0057
5	2.288	24.80	38.10	0.08	12.82	24.20	4.72	4.9	0.0056
6	2.267	25.00	5.83	0.08	43.89	25.20	13.26	14.0	0.0058
7	2.333	24.80	3.09	0.08	45.73	26.30	16.40	16.5	0.0055
8	2.271	25.70	13.10	0.08	36.72	24.40	8.83	9.9	0.0061
								Average	0.0055

Table 5. 330°C. Variation of space velocity. Amount of catalyst 12.00 g. Rate equation for forward reaction $r_f = 0.0052 \cdot \frac{(CO)^{0.80} \cdot (H_2O)^{0.25}}{(CO_2)^{0.65}}$

No.	Total feed mole/h	Feed gas composition, %					Conv. calc. %	Conv. exptl. %	Rate constant k
		CO	CO_2	H_2	N_2	H_2O			
1	2.313	24.10	0	0.18	50.32	25.40	23.1	22.5	0.0050
2	1.125	23.90	0	0.18	49.22	26.70	34.2	33.3	0.0050
3	0.608	22.40	0	0.17	49.33	28.10	47.9	48.8	0.0054
4	4.704	24.70	0	0.19	48.91	26.20	15.45	15.6	0.0053
5	9.475	23.60	0	0.18	52.12	24.10	10.43	11.3	0.0059
								Average	0.0053

from runs containing a constant high concentration of CO_2 in the feed gas (Fig. 5 and Table 1) and from runs without CO_2 in the feed gas (Table 11) — the rate of reaction being much higher in the latter case — strongly indicates that diffusion restriction does not seriously influence the value of l. A possible influence of diffusion on m is even less likely as the conversion varies only slightly with $(H_2O)_0$. For the determination of n the feed gas has contained so much CO_2 that the rate has been sufficiently low. There is therefore good reason to believe that the values of l, m, and n obtained at 420°C have not been influenced by diffusion restriction. At 460°C and 500°C a constant high concentration of CO_2 has been superimposed in all runs. This results in the reaction rate being so low, especially at 460°C, that diffusion is not of importance.

As discussed later there is a linear relationship between ln k and $1/T$, which also shows that diffusion restriction over the entire temperature range 330—500°C has not been of importance.

It has been mentioned above that each catalyst sample has been "stabilized" by running for about 10 days at the temperature at which the measurements were going to be made (except the catalyst samples used for runs at temperatures below 380°C which have been stabilized at 380°C). In spite of

Table 6. 380°C. Variation of $(CO)_0$. Amount of catalyst 3.00 g. Rate equation for forward reaction: $r_f = 0.0290 \cdot \frac{(CO) \cdot (H_2O)^{0.20}}{(CO_2)^{0.65}}$

No.	Total feed mole/h	Feed gas composition, %					Conv. calc. %	Conv. exptl. %	Rate constant k
		CO	CO_2	H_2	N_2	H_2O			
1	2.262	24.60	0	0.18	49.62	25.60	24.4	24.8	0.0299
2	2.213	12.00	0	0.09	61.41	26.50	32.0	32.4	0.0297
3	2.267	70.80	0	0.53	1.97	26.70	16.4	15.6	0.0265
4	2.213	49.70	0	0.37	22.83	27.10	19.1	18.8	0.0282
5	2.246	61.40	0	0.46	11.44	26.70	17.4	16.8	0.0272
6	2.221	6.00	0	0.04	66.96	27.00	40.3	39.3	0.0276
								Average	0.0282

Table 7. 380°C. Variation of $(H_2O)_0$. Amount of catalyst 3.00 g. Rate equation for forward reaction $r_f = 0.0252 \cdot \frac{(CO) \cdot (H_2O)^{0.20}}{(CO_2)^{0.65}}$

No.	Total feed mole/h	Feed gas composition, %					Conv. calc. %	Conv. exptl. %	Rate constant k
		CO	CO_2	H_2	N_2	H_2O			
1	2.354	24.00	0	0.18	24.02	51.80	24.3	23.5	0.0237
2	2.238	23.00	0	0.17	0.93	75.90	26.5	26.8	0.0253
3	2.346	24.10	0	0.18	10.12	65.60	25.0	25.6	0.0263
4	2.192	24.10	0	0.18	34.52	41.20	24.6	23.9	0.0239
5	2.281	24.30	0	0.18	61.82	13.70	20.8	20.6	0.0248
6	2.263	25.20	0	0.19	54.91	19.70	21.7	21.1	0.0239
7	2.250	25.20	0	0.19	48.01	26.60	22.6	21.1	0.0222
								Average	0.0243

this "stabilization" (or ageing) the activity of the catalyst is not completely stable (especially at higher temperatures) which may be seen when running a sample over long periods. As only one set of conditions has been investigated per day, and as one catalyst sample generally has been used for several series (although only at one temperature) each sample has in fact been in constant use for a period of the order of a few months. For this reason the rate constant k obtained at constant temperature may be seen to vary slightly from one series to another in such a way that the lower constant is always obtained with the older sample. It should be added here that the constancy of the catalytic activity during a series of runs has often been controlled by repetition of selected runs, and in some cases it was found to be necessary to discard a number of runs due to an important drop in activity. The runs given in the tables are listed in chronological order within each series (table). The tables, however, are not placed in chronological order.

In connection with the ageing of the catalyst it should also be mentioned that a catalyst which has been aged at a higher temperature has a much

Table 8. 380°C. Variation of $(CO_2)_0$. Amount of catalyst 3.00 g. Rate equation for forward reaction: $r_f = 0.0290 \cdot \frac{(CO) \cdot (H_2O)^{0.20}}{(CO_2)^{0.65}}$

No.	Total feed mole/h	Feed gas composition, %					Conv. calc. %	Conv. exptl. %	Rate constant k
		CO	CO_2	H_2	N_2	H_2O			
1	2.438	24.60	49.20	0.17	0.93	25.10	4.13	4.1	0.0288
2	2.471	23.60	27.50	0.18	24.12	24.60	5.81	5.8	0.0290
3	2.367	24.00	12.70	0.22	37.88	25.20	9.45	11.0	0.0342
4	2.404	22.90	5.50	0.14	45.96	25.50	13.96	15.6	0.0332
5	2.363	24.70	5.11	0.19	44.10	25.90	14.45	14.0	0.0279
6	2.358	23.30	3.09	0.21	47.10	26.30	17.31	16.9	0.0281
7	2.308	24.20	35.80	0.23	12.87	26.90	5.38	4.6	0.0246
8	2.304	23.90	0	0.18	49.92	26.00	24.5	24.0	0.0279
								Average	0.0292

Table 9. 380°C. Variation of space velocity (and (CO_0) and $(H_2O)_0$). Amount of catalyst 3.00 g. Rate equation for forward reaction: $r_f = 0.0352 \cdot \frac{(CO) \cdot (H_2O)^{0.20}}{(CO_2)^{0.65}}$

No.	Total feed mole/h	Feed gas composition, %					Conv. calc. %	Conv. exptl. %	Rate constant k
		CO	CO_2	H_2	N_2	H_2O			
1	4.629	25.90	0	0.19	23.01	50.90	19.6	18.1	0.0304
2	0.781	13.10	0	0.10	10.00	76.80	61.5	63.6	0.0380
3	0.400	11.90	0	0.09	9.91	78.10	79.3	79.7	0.0357
4	1.667	12.10	0	0.09	12.81	75.00	45.1	45.0	0.0350
5	2.367	12.20	0	0.09	12.51	75.20	37.9	37.2	0.0339
6	3.100	12.30	0	0.09	13.31	74.30	32.9	31.8	0.0329
7	3.863	12.40	0	0.09	12.71	74.80	29.3	26.9	0.0298
8	1.750	31.00	0	0.23	34.57	34.20	29.4	32.4	0.0410
9	3.471	33.20	0	0.25	31.95	34.60	20.0	20.8	0.0376
10	5.192	34.30	0	0.26	32.24	33.20	15.7	16.3	0.0372
11	0.467	28.90	0	0.22	37.88	33.00	55.1	55.0	0.0350
12	2.325	36.50	0	0.27	37.83	25.40	23.0	23.1	0.0354
								Average	0.0352

lower activity when subsequently being used at a lower temperature than a catalyst which has been aged at this temperature. For instance if a catalyst sample has been aged at 500°C for two weeks its rate constant at 380°C will be less than ½ of that of a sample having been aged for the same period at 380°C. This phenomenon also contributes to the result that it has been possible to avoid diffusion restriction at relatively high temperatures.

It appears from the tables that a wider variation of partial pressures has been applied for the runs at temperatures of 380°C and below than at higher

Table 10. 400°C. Variation of space velocity (and $(CO)_0$ and $(H_2O)_0$). Amount of catalyst 3.00 g. Rate equation for forward reaction: $r_f = 0.054 \cdot \frac{(CO) \cdot (H_2O)^{0.20}}{(CO_2)^{0.65}}$

No.	Total feed mole/h	Feed gas composition, %					Conv. calc. %	Conv. exptl. %	Rate constant k
		CO	CO_2	H_2	N_2	H_2O			
1	2.358	35.50	0	0.27	37.43	26.80	29.0	30.2	0.058
2	1.200	34.80	0	0.26	38.84	26.10	40.1	41.7	0.058
3	0.613	35.80	0	0.27	38.73	25.20	51.3	51.3	0.054
4	1.213	34.90	0	0.26	38.34	26.50	39.9	42.2	0.062
5	4.696	37.60	0	0.28	36.62	25.50	19.6	19.6	0.054
6	1.225	23.90	0	0.18	25.02	50.90	49.2	54.0	0.065
7	2.267	23.00	0	0.17	24.03	52.80	37.4	39.0	0.058
8	0.613	22.60	0	0.17	25.53	51.70	66.1	69.0	0.060
9	0.317	26.00	0	0.20	23.80	50.00	77.9	79.6	0.058
10	3.604	24.80	0	0.19	25.61	49.40	28.6	29.0	0.055
								Average	0.058

Table 11. 420°C. Variation of $(CO)_0$. Amount of catalyst 3.00 g. Rate equation for forward reaction $r_f = 0.128 \cdot \frac{(CO) \cdot (H_2O)^{0.25}}{(CO_2)^{0.60}}$

No.	Total feed mole/h	Feed gas composition, %					Conv. calc. %	Conv. exptl. %	Rate constant k
		CO	CO_2	H_2	N_2	H_2O			
1	2.400	25.90	0	0.19	23.71	50.20	47.9	47.5	0.124
2	2.363	11.80	0	0.09	36.11	52.00	60.4	63.3	0.140
3	2.467	38.10	0	0.29	11.71	49.90	41.8	42.3	0.130
4	2.283	5.85	0	0.04	41.51	52.60	73.1	74.6	0.134
5	2.317	48.10	0	0.36	0.64	50.90	40.0	40.9	0.132
6	2.400	24.40	0	0.18	22.72	52.70	49.1	45.4	0.108
								Average	0.128

Table 12. 420°C. Variation of $(H_2O)_0$. Amount of catalyst 3.00 g. Rate equation for forward reaction: $r_f = 0.105 \cdot \frac{(CO) \cdot (H_2O)^{0.25}}{(CO_2)^{0.60}}$

No.	Total feed mole/h	Feed gas composition, %					Conv. calc. %	Conv. exptl. %	Rate constant k
		CO	CO_2	H_2	N_2	H_2O			
1	2.400	24.40	0	0.18	22.72	52.70	45.1	45.4	0.107
2	2.317	24.00	0	0.18	0.42	75.40	48.4	48.2	0.104
3	2.496	23.90	0	0.18	10.02	66.90	45.9	45.2	0.102
4	2.413	24.40	0	0.18	34.02	41.40	43.4	42.9	0.103
5	2.421	23.70	0	0.18	47.42	28.70	41.3	40.9	0.103
								Average	0.104

Table 13. 420°C. Variation of $(CO_2)_0$. Amount of catalyst 3.00 g. Rate equation for forward reaction: $r_f = 0.098 \cdot \frac{(CO) \cdot (H_2O)^{0.25}}{(CO_2)^{0.60}}$

No.	Total feed mole/h	Feed gas composition, %					Conv. calc. %	Conv. exptl. %	Rate constant k
		CO	CO_2	H_2	N_2	H_2O			
1	2.463	22.30	28.90	0.17	24.13	24.50	15.2	15.7	0.102
2	2.342	23.80	37.90	0.18	12.32	25.80	14.0	14.2	0.100
3	2.308	24.70	13.70	0.19	35.81	25.60	22.4	22.8	0.100
4	2.375	23.00	50.50	0.17	1.43	24.90	11.8	11.6	0.096
5	2.267	24.30	6.10	0.18	42.92	26.50	29.7	30.0	0.100
6	2.258	24.40	41.50	0.18	7.52	26.40	13.8	13.0	0.092
7	2.242	24.60	0	0.18	49.12	26.10	40.2	35.1	0.073
								Average	0.095

Table 14. 420°C. Variation of space velocity. Amount of catalyst 3.00 g. Rate equation for forward reaction $r_f = 0.080 \cdot \frac{(CO) \cdot (H_2O)^{0.25}}{(CO_2)^{0.60}}$

No.	Total feed mole/h	Feed gas composition, %					Conv. calc. %	Conv. exptl. %	Rate constant k
		CO	CO_2	H_2	N_2	H_2O			
1	1.346	19.80	0	0.15	42.05	38.00	52.5	57.1	0.096
2	0.629	18.80	0	0.14	45.76	35.30	70.3	71.8	0.086
3	2.533	22.80	0	0.17	44.13	32.90	36.6	37.6	0.084
4	4.304	22.60	0	0.17	46.63	30.60	27.6	28.5	0.085
5	1.371	15.50	0	0.13	33.27	51.10	58.1	59.3	0.084
6	5.446	22.20	0	0.17	41.93	35.70	25.0	24.4	0.077
								Average	0.085

Table 15. 460°C. Variation of $(CO)_0$. Amount of catalyst 3.00 g. Rate equation for forward reaction: $r_f = 0.104 \cdot \frac{(CO)^{0.80} \cdot (H_2O)^{0.30}}{(CO_2)^{0.60}}$

No.	Total feed mole/h	Feed gas composition, %					Conv. calc. %	Conv. exptl. %	Rate constant k
		CO	CO_2	H_2	N_2	H_2O			
1	2.279	25.20	25.40	0.07	23.73	25.60	21.7	22.8	0.110
2	2.321	12.70	24.20	0.04	36.26	26.80	25.9	25.9	0.104
3	2.250	30.60	24.80	0.10	18.60	25.90	21.1	21.7	0.108
4	2.325	19.50	24.70	0.07	28.33	27.40	23.4	23.7	0.106
5	2.304	6.18	24.10	0.02	41.50	28.20	30.6	28.6	0.096
6	2.254	36.80	24.40	0.13	11.47	27.20	20.5	19.7	0.099
7	2.308	24.60	24.10	24.10	0.10	27.10	19.0	17.6	0.092
8	2.333	24.10	25.30	0.07	23.53	27.00	21.9	21.4	0.101
9	2.288	9.13	25.00	0.02	38.35	27.50	27.8	27.6	0.103
10	2.275	37.90	24.90	0.12	9.98	27.10	20.0	19.7	0.102
								Average	0.102

In run No. 7 the feed gas contains an essential amount of H_2.

Table 16. 460°C. Variation of $(H_2O)_0$. Amount of catalyst 3.00 g. Rate equation for forward reaction: $r_f = 0.112 \cdot \frac{(CO)^{0.80} \cdot (H_2O)^{0.30}}{(CO_2)^{0.60}}$

No.	Total feed mole/h	Feed gas composition, %					Conv. calc. %	Conv. exptl. %	Rate constant k
		CO	CO_2	H_2	N_2	H_2O			
1	2.483	23.70	27.50	0.06	22.54	26.20	21.2	21.0	0.111
2	2.463	23.20	27.10	0.05	11.25	38.40	24.1	24.4	0.114
3	2.496	23.80	27.10	0.08	0.12	48.90	25.3	25.5	0.113
4	2.475	23.10	28.30	0.08	16.02	32.50	22.4	21.8	0.108
5	2.450	23.50	29.40	0.06	4.84	42.20	23.9	24.2	0.114
6	2.421	23.60	30.30	0.07	27.63	18.40	18.5	18.7	0.114
7	2.279	25.20	25.40	0.07	23.73	25.60	23.0	22.8	0.111
								Average	0.112

Table 17. 460°C. Variation of $(CO_2)_0$. Amount of catalyst 3.00 g. Rate equation for forward reaction: $r_f = 0.140 \cdot \frac{(CO)^{0.80} \cdot (H_2O)^{0.30}}{(CO_2)^{0.60}}$

No.	Total feed mole/h	Feed gas composition, %					Conv. calc. %	Conv. exptl. %	Rate constant k
		CO	CO_2	H_2	N_2	H_2O			
1	2.392	23.30	29.10	0.05	24.05	23.50	24.6	26.7	0.155
2	2.313	24.50	36.40	0.07	12.53	26.50	23.4	23.9	0.144
3	2.325	24.20	12.10	0.07	36.53	27.10	36.0	35.9	0.140
4	2.346	22.90	48.80	0.07	1.73	26.50	20.4	20.8	0.143
5	2.342	24.60	18.30	0.07	29.13	27.90	31.3	30.1	0.133
6	2.321	23.30	31.00	0.06	18.84	26.80	25.5	25.5	0.140
								Average	0.142

temperatures. This is due to two reasons. Firstly, at temperatures above 380°C the catalyst is quite easily reduced to elementary iron which catalyzes the decomposition of CO to C and CO_2, if the water partial pressure is reduced below a certain limit; this limit is not exactly known, it can, however, be mentioned that at 420°C this reduction does take place, if the water partial pressure is half that of the CO partial pressure. Secondly, as mentioned above, it was necessary to superimpose a constant CO_2-partial pressure at all runs performed at 460°C and 500°C. For this reason the results obtained at the higher temperatures may be less certain than those obtained at 380°C and below.

The tables containing data obtained at varying space velocities show that the rate formulas are valid over a quite large range of conversion. The fact that good agreement is obtained also at high conversions shows that the

Table 18. 500°C. Variation of $(CO)_0$. Amount of catalyst 3.00 g. Rate equation for forward reaction: $r_f = 0.244 \cdot \frac{(CO)^{0.80} \cdot (H_2O)^{0.35}}{(CO_2)^{0.50}}$

No.	Total feed mole/h	Feed gas composition, %					Conv. calc. %	Conv. exptl. %	Rate constant k
		CO	CO_2	H_2	N_2	H_2O			
1	2.133	12.10	24.80	0.03	31.77	31.30	45.9	47.6	0.258
2	2.163	5.01	25.60	0.02	39.27	30.10	52.0	52.0	0.244
3	2.183	26.30	23.50	0.08	19.42	30.70	38.1	38.7	0.251
4	2.358	29.50	24.00	0.09	10.51	35.90	36.9	35.9	0.234
5	2.558	16.00	22.80	0.06	29.34	31.80	39.7	39.9	0.246
6	2.292	17.50	23.80	0.06	25.34	33.30	41.8	40.0	0.228
7	2.304	8.57	23.60	0.02	34.01	33.80	48.6	49.7	0.252
8	2.404	23.00	23.70	21.60	0.20	31.50	30.2	28.5	0.222
9	2.288	35.20	25.10	0.11	6.59	33.00	34.3	32.8	0.227
								Average	0.240

In run No. 8 the feed gas contains an essential amount of H_2.

Table 19. 500°C. Variation of $(H_2O)_0$. Amount of catalyst 3.00 g. Rate equation for forward reaction: $r_f = 0.272 \cdot \frac{(CO)^{0.80} \cdot (H_2O)^{0.35}}{(CO_2)^{0.50}}$

No.	Total feed mole/h	Feed gas composition, %					Conv. calc. %	Conv. exptl. %	Rate constant k
		CO	CO_2	H_2	N_2	H_2O			
1	2.238	25.90	21.60	0.07	12.43	40.00	45.0	43.1	0.253
2	2.325	23.70	22.20	0.08	2.22	51.80	48.4	50.8	0.293
3	2.300	25.00	22.10	0.09	23.81	29.00	39.8	39.1	0.264
4	2.267	25.60	22.20	0.08	6.02	46.10	46.5	45.5	0.263
5	2.242	25.50	22.50	0.08	0.00	52.00	48.4	48.0	0.268
6	2.183	26.30	23.50	0.08	19.42	30.70	40.6	38.7	0.251
7	2.233	25.20	23.10	0.07	30.43	21.10	35.4	34.5	0.260
								Average	0.265

assumption concerning the stoichiometric number being equal to 1 is not contradicted by the experiments.

The values of the exponents l, m, and n, obtained at the different temperatures, are summarized in Table 21.

The value shown of l at 360°C has been obtained only from the graphic representation. The values shown at 400°C are those obtained at 380°C, and which have been applied for a series of runs of varying space velocity (Table 10).

It appears that the variation of l, m, and n over the whole temperature range is small, in most cases within the experimental uncertainty. It is perhaps surprising that the value of l both at low and high temperatures falls below 1. In this connection it should be mentioned that the runs at 330°C with varying $(CO)_0$ have been repeated three times with identical results. There is some indication that the value of m increases, whereas n decreases numerically when the temperature rises above 420°C; it must, however, be borne in mind that the values obtained at 460° and 500°C are less certain than those obtained at lower temperatures.

Table 20. 500°C. Variation of $(CO_2)_0$. Amount of catalyst 3.00 g. Rate equation for forward reaction: $r_f = 0.300 \cdot \frac{(CO)^{0.80} \cdot (H_2O)^{0.35}}{(CO_2)^{0.50}}$

No.	Total feed mole/h	Feed gas composition, %					Conv. calc. %	Conv. exptl. %	Rate constant k
		CO	CO_2	H_2	N_2	H_2O			
1	2.967	21.10	40.60	0.06	17.64	20.60	26.8	28.5	0.326
2	2.254	27.10	22.20	0.08	23.52	27.10	40.6	40.0	0.292
3	2.358	25.80	48.90	0.07	0.00	26.00	30.4	31.6	0.318
4	2.279	24.90	35.60	0.07	12.93	26.50	35.4	36.2	0.311
5	2.192	24.90	22.40	0.07	25.83	26.80	41.9	42.6	0.309
6	2.304	24.10	12.80	0.07	37.13	25.90	46.6	46.7	0.301
7	2.300	24.60	29.90	0.07	19.33	26.10	37.2	35.5	0.278
								Average	0.302

Table 21.

Temperature	l	m	n
330°C	0.80	0.25	−0.65
360°C	(1.00)	—	—
380°C	1.00	0.20	−0.65
400°C	(1.00)	(0.20)	(−0.65)
420°C	1.00	0.25	−0.60
460°C	0.80	0.30	−0.60
500°C	0.80	0.35	−0.50

As the variation of l, m, and n is small it is possible to establish a single rate expression which is valid with fairly good accuracy over the whole temperature range 330°—500°C. Such an expression would be

$$r_f = k(T) \cdot \frac{(CO)^{0.90} \cdot (H_2O)^{0.25}}{(CO_2)^{0.60}} \qquad (11)$$

where $k(T)$ varies with the temperature.

This expression is in essential agreement with the preliminary results reported by Stelling and Krusenstierna [5], but differs strongly from that proposed by Kul'kova and Temkin [1]. It differs more or less strongly from the other rate equations proposed.

Due to the dependence of the ageing effect upon the ageing temperature (and time) the data given in Tables 2—20 cannot be used for calculation of the apparent activation energy. For this reason a special series of runs at different temperatures was made with a catalyst which had been aged at 500°C. For the runs at 500°C and 460°C a CO_2-containing feed gas was used; for the runs at 380, 360 and 330°C a feed gas without CO_2 was used; at 420° runs with both kinds of feed gas have been used. The respective values of k were calculated according to the previously applied method using the "average" rate expression (eqn. 11) for the forward reaction (Table 22). By plotting ln k against $1/T$ a straight line is obtained (Fig. 6). This fact further

Table 22. Variation of reaction temperature. Amount of catalyst 3.00 g. Catalyst stabilized at 500°C. Rate equation for forward reaction $r_f = k \cdot \frac{(CO)^{0.90} \cdot (H_2O)^{0.25}}{(CO_2)^{0.60}}$

No.	Total feed mole/h	Feed gas composition, %					Conv. exptl. %	Rate constant k	Reaction temperature °C
		CO	CO_2	H_2	N_2	H_2O			
1	2.367	25.00	23.40	0.07	1.43	50.10	54.9	0.36	500
2	2.342	24.90	23.60	0.07	0.13	51.30	31.6	0.144	460
3	2.350	24.60	23.90	0.07	0.23	51.20	12.9	0.049	420
4	2.400	24.30	0	0.07	24.43	51.20	30.8	0.042	420
5	2.388	24.30	0	0.07	24.73	50.90	16.2	0.0134	380
6	2.379	24.00	0	0.07	24.63	51.30	11.2	0.0070	360
7	2.375	23.90	0	0.07	24.23	51.80	5.85	0.0024	330
8	2.371	23.50	24.30	0.07	1.43	50.70	54.3	0.35	500

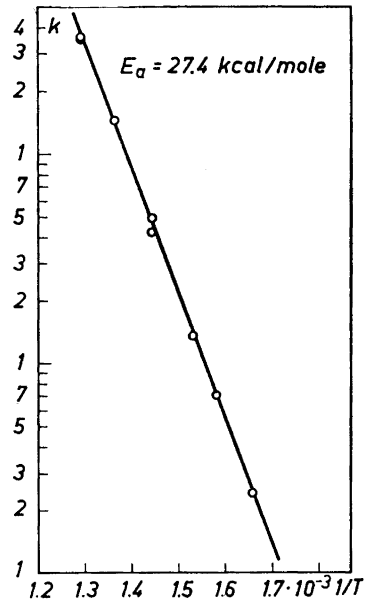

Fig. 6. log k *vs.* reciprocal absolute temperature. The "average" rate expression (eqn. 11) has been applied for the calculations.

confirms that diffusion restriction has not influenced the experimental results. From the slope of the straight line an apparent activation energy of 27.4 kcal per mole is calculated.

As often stated in the literature [5,9,10] it is necessary to apply the outmost caution when trying to deduce a mechanism from a rate expression as different mechanisms may very well yield rate expressions which are approximations of each other. Without going much into detail a reasonable mechanism for the above rate expression may seem to be the following: The rate determining step is reaction between gaseous CO and oxidized surface sites, or perhaps chemisorption of CO. CO_2 and H_2O are strongly adsorbed on the surface, whereas H_2 is not adsorbed.

Acknowledgement. The author wishes to express his thanks to Mr. Haldor Topsøe for permission and encouragement to publish the results. Thanks are also due to Dr. Jørgen Kjær for having performed the coding of the electronic calculations, and to Mr. C. Thomsen for assistance with the experiments.

REFERENCES

1. Kul'kova, N. V. and Temkin, M. I. *Zhur. Fiz. Khim.* **23** (1949) 695.
2. Atwood, K., Arnold, M. R. and Appel, E. G. *Ind. Eng. Chem.* **43** (1950) 1600.
3. Kodama, S., Fukui, K., Tame, T. and Kinoshita, M. *Catalyst (Japan)* **8** (1952) 50.
4. Kodama, S., Mazume, A., Fukuba, K. and Fukui, K. *Bull. Chem. Soc. Japan* **28** (1955) 318.
5. Stelling, O. and Krusenstierna, O. v. *Acta Chem. Scand.* **12** (1958) 1095.
6. Atroshchenko, V. J. and Bibr, B. *Zhur. Priklad. Khim.* **32** (1959) 997; *Chem. Abstr.* **53** (1959) 15735.

7. Kirillov, I. P. *Trudy Ivanovsk. Khim. — Teknol. Inst.* **1956** No. 5, p. 45; *Chem. Abstr.* **53** (1959) 11969.
8. Lebeder, A. T. and Popov, B. I. *Trudy Ivanovsk. Khim. — Teknol. Inst.* **1958** No. 7, p. 53; *Chem. Abstr.* **54** (1960) 8251.
9. Weller, S. *A. I. Ch. E. Journal* **2** (1956) 59.
10. Boudart, M. *A. I. Ch. E. Journal* **2** (1956) 62.
11. Hougen, O. A. and Watson, K. M. *Chemical Process Principles*, John Wiley & Sons, New York 1947, Part III, Chapter XX.
12. Hoogschagen, J. *Ind. Eng. Chem.* **47** (1955) 906.

Received October 24, 1960.

ACTA CHEMICA SCANDINAVICA 15 (1961) 521–524

The Action of Phenylmagnesium Bromide on Diphenylmethylenemalonic Ester

GUST.-AD. HOLMBERG

Institutet för organisk kemi, Åbo Akademi, Åbo, Finland

α-Benzoyl-β,β-diphenyl-β-ethoxypropionic ester is formed in the reaction between phenylmagnesium bromide and diphenylmethylenemalonic ester.

The action of Grignard reagents on alkylidenemalonic [1,2] and arylidenemalonic [3] esters usually results in 1,4-addition to the conjugated double bond system C=C—C=O:

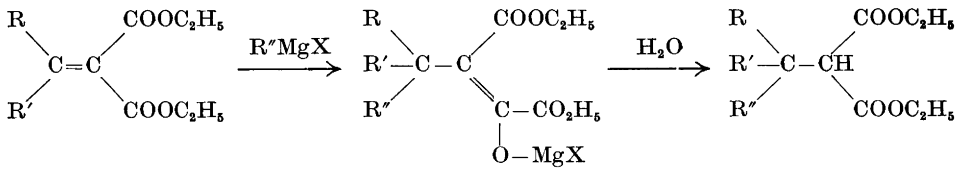

Reactions involving diphenylmethylenemalonic ester (R = R′ = phenyl) have not been studied, however. When the investigations were extended to the reaction between this substance and phenylmagnesium bromide, a compound melting at 164.5—165.5° was obtained in a low yield. A single 1,4-addition is not possible since this reaction would have resulted in triphenylmethylmalonic ester, m.p. 133°. Combustion analysis and molecular weight determination pointed to the composition $C_{26}H_{26}O_4$, *i.e.* one molecule of diphenylmethylenemalonic ester had taken up one phenyl group and one hydrogen atom.

In order to study the changes in structure, the IR spectra of diphenylmethylenemalonic ester and the reaction product dissolved in tetrachloromethane were compared with each other. The most dominant feature of the former spectrum is a strong and broad band at 1 750—1 700 cm^{-1} due to the conjugated double bond system $C=C(C=O)_2$. After the reaction with the Grignard reagent, this band is replaced by two bands at 1 755 and 1 720 cm^{-1}. Further, the bands in the neighbourhood of 3 000 cm^{-1} are slightly broadened and new,

distinct bands appear at about 1 640 (strong), 1 595—1 560 (strong), 1 140 (sharp), and 1 120 (sharp) cm^{-1}.

The change in the band at about 3 000 cm^{-1} and the new and strong band at 1 640 cm^{-1} implies an enolized β-keto ester containing a hydrogen bond (II) [4]. The additional absorption in the usual ketone region supports the hypothesis that even in this case an equilibrium between the keto form (I) and the enol form (II) exists.

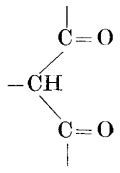

I

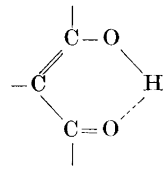

II

These circumstances and the composition $C_{26}H_{26}O_4$ suggest a 1,2-addition to the double bond between the carbon and oxygen atoms in one of the carbethoxy groups of the malonic ester followed by an allylic type rearrangement for the formation of the compound:

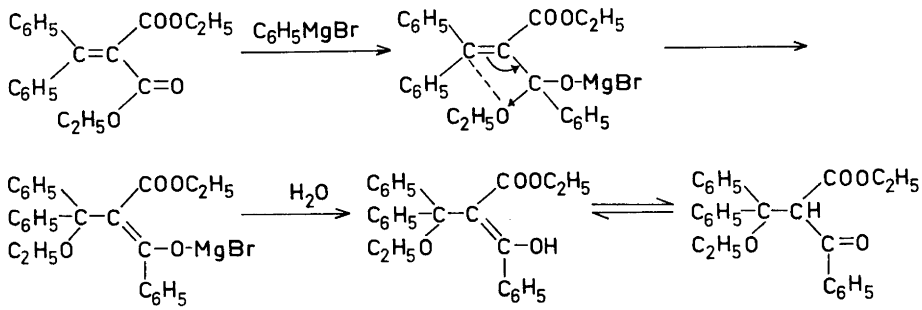

The two phenyl groups and the readily removed hydrogen atom in the vicinity should make the ethoxy group labile in both acid and alkaline solution. This prediction is in harmony with the experimental observations.

Further, asymmetrical C—O—C stretching vibrations of an open chain ether occur usually near 1 100 cm^{-1}. IR spectra of triphenylmethyl ethyl ether (III) and ethoxydiphenylacetic acid (IV) show absorption bands at 1 115 cm^{-1} which well correspond to the band of the present substance at 1 120 cm^{-1}.

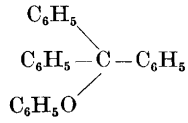

III

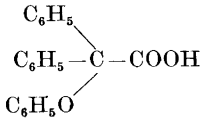

IV

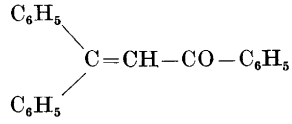

V

Owing to the instability of the substance, it was not possible to isolate in the pure state a simple fragment of the molecule containing the phenyl groups and the ethoxy group attached to the same carbon atom. The properties of the substance on saponification and oxidation may, however, be interpreted as proof of the suggested structure. When the substance is saponified with alkali, it may be expected that besides the reactions which occur with β-keto esters the ether group will be partly split off as ethanol. On oxidation of the alkaline solution, a part of the compound should therefore give benzophenone and a part a mixture of ethoxydiphenylacetic acid and benzoic acid. Experiments proved that benzophenone is formed (isolated as its 2,4-dinitrophenylhydrazone), and when the acids were chromatographed on paper, spots with the same R_F values as ethoxydiphenylacetic acid and benzoic acid were obtained in addition to spots with lower R_F values. When the ether group was split off by treating with hydrochloric acid before the saponification, the results were similar but the spot corresponding to ethoxydiphenylacetic acid was lacking.

It may be pointed out that even the reaction between phenylbenzylideneacetone (V) and phenylmagnesium bromide proceeds as a 1,2-addition [5].

EXPERIMENTAL

Diphenylmethylenemalonic ester was prepared according to Wideqvist [6].

Action of phenylmagnesium bromide on diphenylmethylenemalonic ester. To the Grignard reagent prepared from magnesium (3.60 g), bromobenzene (23.56 g) and dry ether (55 ml) a solution of diphenylmethylenemalonic ester (16.20 g) in dry ether (50 ml) was gradually added in the course of 15 min. After the brown mixture had been refluxed for one hour, it was cooled and poured into a mixture of ice and dilute hydrochloric acid. The ether phase was washed with water and a dilute solution of potassium carbonate. When it was dried with sodium sulphate, crystals began to separate on the surface of the drying agent. After standing overnight, the precipitate was filtered off and treated with warm water until free from sodium sulphate. When the ether filtrate was allowed to evaporate slowly, another smaller sample was obtained. The total yield of α-benzoyl-β,β-diphenyl-β-ethyoxypropionic ester was 25.5 % (5.12 g). After being dissolved in benzene and precipitated with ethanol it melted at 164.5—165.5°. (Found: C 77.53; H 6.46; Mol.wt. (Rast) 387 ± 15. Calc. for $C_{26}H_{26}O_4$: C 77.59; H 6.51; Mol.wt. 402).

Saponification and oxidation of the substance. A small sample (0.30 g) was dissolved in ethanol (30 ml). A solution of potassium hydroxide (0.80 g) in water (1 ml) was added and the mixture heated on a boiling water bath for 2 h. The alcohol was evaporated under reduced pressure and the residue dissolved in water. A 5 % potassium permanganate solution was then added until the red colour persisted. After the manganese dioxide had been dissolved by adding sodium hydrogen sulphite and dilute sulphuric acid, the organic substances were extracted with ether. Organic acids were removed by shaking with a dilute potassium hydroxide solution. From the residue (0.05 g) of the neutral ether solution, benzophenone was isolated as its 2,4-dinitrophenylhydrazone, m.p. 238—239°.

The alkaline aqueous solution containing the organic acids was acidified and extracted with ether. The residue (0.19 g) of the ether phase was examined chromatographically on paper (Schleicher & Schüll 2043 b Gl) and aqueous ammonium carbonate and propanol as the mobile phase. After spraying with an acid solution of bromophenol blue, spots with the following R_F values were obtained: 0.92, 0.77, 0.69 and 0.60. Under the same conditions ethoxydiphenylacetic acid and benzoic acid had R_F values of 0.92 and 0.76, respectively.

When a sample of the substance (0.55 g) was first boiled with a mixture of ethanol (125 ml), water (5 ml) and hydrochloric acid (6 ml) for 2 h and then treated as above after addition of potassium hydroxide (6 g) in water (6 ml), the spot with the R_F value 0.92 was absent.

The elementary analysis was carried out by Dr. A. Bernhardt, Mühlheim, and the IR spectra were taken by Mr. B. C. Fogelberg, Centrallaboratorium Ab., Helsingfors.

REFERENCES

1. Wideqvist, S. *Arkiv Kemi, Mineral. Geol.* **23 B** (1946) No. 4.
2. Holmberg, G. A. *Acta Chem. Scand.* **12** (1958) 229.
3. *e.g.* Kohler, E. P. *Am. Chem. J.* **34** (1905) 134.
4. Rasmussen, R. S. and Brattain, R. R. *J. Am. Chem. Soc.* **71** (1949) 1073.
5. Vorländer, D. and Siebert, C. *Ber.* **39** (1906) 1024.
6. Wideqvist, S. *Arkiv Kemi, Mineral. Geol.* **20 B** (1945) No. 7.

Received October 18, 1960.

ACTA CHEMICA SCANDINAVICA 15 (1961) 525–534

Microdetermination of Polyenoic Fatty Acids and Total Fatty Acids in Plasma and Tissue

JENS G. NØRBY

Biokemisk Institut, Århus Universitet, Århus, Denmark

A method for the isolation of fatty acids from 2 g plasma or tissue-homogenate prior to the determination of polyenoic acids is described. Total fatty acids are determined by titration. The polyenoic acids are determined by the method of Herb and Riemenschneider, the amount of fatty acids isomerized being 2 – 6 μequiv. This method gives highly reproducible results. The saponification step of the isolation procedure was investigated with respect to changes in composition and structure of the fatty acids during saponification. It was found that the degree of conjugation of double bonds was low, and that the proportions of the different polyenoic acids were not influenced by saponification.

Since Herb and Riemenschneider [1] published the micro-isomerization method for the determination of polyenoic fatty acids, their method has been used by several investigators [2–14] on extracts from biological materials and has proved to be a useful tool in lipid research.

The determination of polyenoic fatty acids in biological material necessitates the isolation of the fatty acids prior to their isomerization. Numerous methods for this purpose have been published, but only few authors [10–12] have given information with regard to changes in composition and structure of the polyenoic fatty acids during isolation of fatty acid mixtures from biological material. An important step is the saponification of the lipid extract since it is well known that conjugation of double bonds takes place when polyenoic fatty acids are treated with alkali. In order to avoid this, some workers [13,15] omit saponification and isomerize isolated esters. Nevertheless, for more accurate determinations on most biological materials, saponification seems to be necessary, since both Front and Daubert [16] and Holman and Hayes [15] have shown that cholesteryl esters are isomerized much more slowly than the free acids.

The present paper reports the result of an investigation on the extraction and saponification of lipids from 2 g plasma or tissue homogenate (*ca.* 1:10 in water), the polyenoic fatty acids being determined by the method of Herb

and Riemenschneider [1]. Simple and accurate methods for the isolation of fatty acids from biological material and for the determination of total fatty acids on the same sample as used for the determination of polyenoic fatty acids are described.

REAGENTS AND METHODS

Reagents

1. *Extraction and isolation of unsaponifiable and saponifiable fractions.*

Ethanol, aldehyde-free. 1.5 l 96 % ethanol is boiled for 12 h with 30 g KOH and 30 g Zn-powder and distilled.

Ethyl ether, peroxide-free. 1 l ethyl ether is stored for 2 days with 50 g KOH. The peroxide-free ether is obtained by decantation.

4 N ethanolic KOH (Merck p.a.). Should be prepared immediately before use.

Petroleum ether, b.p. 30—45°C, is prepared by fractional distillation of commercial petroleum ether, b.p. 50°C.

2. *Determination of polyenoic fatty acids.*

Isomerizing reagent. 21 % KOH in ethylene glycol (w/w), Merck p.a., is prepared as described by Pikaar and Nijhof [12]. The reagent is adjusted to 21.0 ± 0.1 % (after titration of a sample with 0.1 N HCl) with ethylene glycol.

Optically pure petroleum ether. 500 ml petroleum ether, b.p. 60—70°C, is stirred with 100 ml fuming H_2SO_4 for 30 min; the phases are allowed to separate and the petroleum ether is washed with water, 5 % NaOH and water. The whole procedure is repeated. The petroleum ether is dried over anhydrous Na_2SO_4 and distilled. Petroleum ether prepared in this way has a smooth, flat absorption curve (with water as the blank), the transmission being greater than 85 % in the region 220—400 mμ.

Lauryl alcohol, BDH.

Methanol, Merck, pure acetone-free.

3. *Titration of total fatty acids.*

0.025 N NaOH in water.

0.1 % thymol blue in 96 % ethanol.

Methods

1. *Preparation and extraction of plasma and tissue.*

1.1. Plasma. A 2 ml syringe provided with a blunt cannula (length 120 mm, inner diameter 1.5 mm) is filled with plasma and weighed. The plasma is added dropwise, with agitation, to 60 ml ethanol-ether 3:1 in a 100 ml volumetric flask (B 10 ground joint). The syringe is weighed again and the amount of plasma delivered is calculated. The extract is boiled for ½ min., cooled to 20°C and made up to volume with ethanol-ether 3:1. After mixing, the solution is filtered rapidly through a fat-free filter (Munktell No. 3, 9 cm, extracted with ether) and 40 ml extract is pipetted into a 100 ml flask provided with B 29 ground joint. Pumice is added and *ca.* 30 ml solvent is evaporated at 40°C in vacuum. Again 40 ml extract is transferred to the flask, the solvent is evaporated in vacuum until about 10 g (12 ml) is left, and the extract is ready for saponification (see 2).

1.2. Tissue. At least 0.5 g wet tissue is weighed into a beaker, 7—10 volumes of water is added and the beaker is weighed again. The tissue is homogenized for a few minutes with an Ultraturrax disintegrator, TP 18/2, and 2 g homogenate is treated as described for plasma. Homogenization in a Potter Elvehjem homogenizer was used in some experiments on liver.

2. *Saponification and extraction of the unsaponifiable and saponifiable fractions.*

To 12 ml extract prepared as described under 1, 1 ml H_2O and 4 ml 4 N ethanolic KOH is added. The mixture is boiled under reflux for 60 min. and after addition of 15 ml H_2O the flask is cooled to room temperature. The mixture, which should now contain 50 % ethanol, is extracted in the saponification flask with 4 × 10 ml petroleum ether, b.p. 30—45°C. After each extraction the extract is transferred by light suction to a 50 ml volumetric flask as shown in Fig. 1. Aliquots of this extract may be used for determination of total cholesterol. Now 4.5 ml 4 N HCl and 4.5 ml ethanol is added and

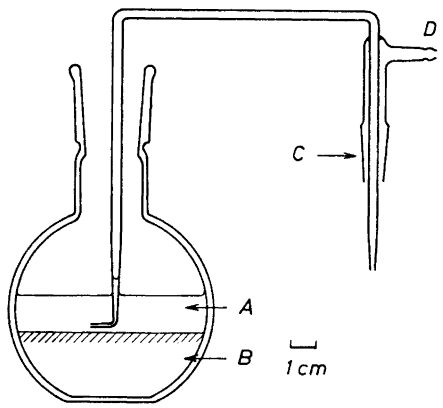

Fig. 1. Set-up for the extraction of unsaponifiable matter and fatty acids after saponification. A: petroleum ether, B: saponified mixture (50 % ethanol), C: B 10 ground joint connected to volumetric flask. By light suction at D the petroleum ether is transferred to the volumetric flask.

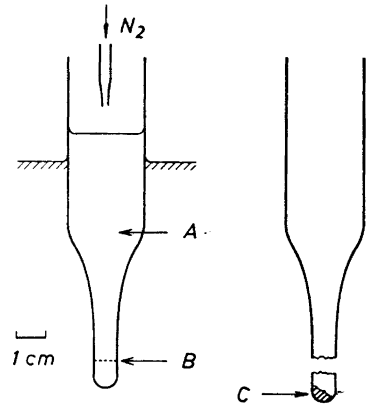

Fig. 2. Special tube used for the transfer of fatty acids from a petroleum ether aliquot to the isomerization tube. Left: tube with aliquot of fatty acid extract (A), B: scratch. Right: tube with bottom broken off, C: vial containing the fatty acids from the petroleum ether aliquot.

the fatty acids extracted as described for the unsaponifiable fraction. The volumetric flask containing the extract is made up to 50 ml with petroleum ether, b.p. 30—45°C, and aliquots of the extract are used for the determination of polyenoic fatty acids and total fatty acids.

3. *Determination of total fatty acids.*

For each determination a 5 ml aliquot of the fatty acid extract is transferred to a small test tube with flat bottom (70 × 14 mm) and the solvent is evaporated in vacuum. The fatty acids adhering to the sides of the tube are rinsed down with 0.5 ml solvent, which is evaporated. Now 1 ml ethanol containing 1 drop 0.1 % thymol blue per ml and 2 small stainless magnetic balls (diameter = 2—4 mm) are added, and the fatty acids are titrated with 0.025 N NaOH from the microburette described by Holm-Jensen [17] with magnetic stirring. CO_2-free N_2 is blown over the sample during titration. For each set of determinations 3 blanks (1 ml ethanol with thymol blue) and 3 standards (5 ml of a 0.36 mN solution of stearic acid in petroleum ether, treated as 5 ml fatty acid extract) are titrated.

4. *Determination of polyenoic fatty acids.*

4.1. Analysis for polyenoic fatty acids with non-conjugated double bonds is performed in duplicate on 20 ml fatty acid extract. 10 ml extract is placed in a special tube shown on Fig. 2. Two such tubes are easily made from an ordinary test tube (180 × 24 mm) from which the bottom has been removed. Before use, the special tubes are ringed with a scratch *ca.* 10 mm from the bottom. The tube containing the 10 ml aliquot is placed in a water bath at *ca.* 40°C, the solvent is evaporated under nitrogen, and during the evaporation the inner wall of the tube is rinsed 3—4 times with petroleum ether. By this procedure the fatty acids are concentrated in the bottom of the tube which can now be broken off by touching the scratch with a hot glass rod. The resulting small vial containing the fatty acids is transferred to an isomerization tube containing reagent preheated for 10 min. at 180°C and the isomerization performed at the conditions employed by Herb and Riemenschneider [1] (5 g 21 % KOH in ethylene glycol, 15 min., 180 ± 0.5°C under N_2). If the samples are not isomerized immediately after evaporation of the solvent, the dried fatty acids will easily oxidize. Covering the sample with a few drops of lauryl alcohol will protect against oxidation for at least 2 h.

After isomerization the sample is mixed with 2 ml methanol and the mixture is transferred by 3—4 washings with methanol to a 25 ml or 50 ml volumetric flask by a method similar to that shown in Fig. 1. Extinctions are determined with a Beckman DR at 400—230 mμ or with a Beckman DU at 375, 346, 315, 268, and 233 mμ with slit widths 0.2, 0.2, 0.3, 0.4, and 0.8 mm, respectively. The hydrogen lamp is used as light source at all wavelengths mentioned.

4.2. The spectra of the non-isomerized fatty acids are obtained from the residue of the fatty acid extract after aliquots have been drawn for determinations of polyenoic fatty acids and total fatty acids. The solvent is evaporated under N_2 and 10 ml optically pure petroleum ether is added. The extinctions are then determined with a Beckman as described for isomerized samples.

4.3. Calculations. Several authors have published spectral constants ($K = E^{1g/l}_{1cm}$) for pure samples of linoleic acid [1,18], linolenic acid [1,18], arachidonic acid [1,19], eicosapentaenoic acid [1,18-21,23], docosapentaenoic acid [1,20,21] and docosahexaenoic acid [18,20-23] isomerized by the method of Herb and Riemenschneider [1]. A critical examination of the purity criterions published for the above mentioned acids seems to justify the choice of the constants published by Herb and Riemenschneider [1] for linoleic, linolenic and arachidonic acids and those published by Holman [22] for eicosapentaenoic and docosahexaenoic acids. These constants are collected in Table 1 as $E^{1\,g/l}_{1\,cm}$ and $E^{1\,mequiv./l}_{1\,cm}$ ($= E^{1\,g/l}_{1\,cm} \times$ mol.wt. $\times 10^{-3}$) and are used in this investigation. The author has determined the spectral constant for linoleic acid at 233 mμ (K^{diene}_{233}) on a sample (Hormel) containing *ca.* 1.2 % triene and 0.5 % conjugated diene. The amount of diene (linoleic acid) in the sample was calculated as: % diene = 100 − % triene − % conjugated diene. After isomerization of samples from 0.1 mg to 12 mg, K^{diene}_{233} was calculated by the following equations:

$$k'_2 = K^{diene}_{233} \cdot \frac{\%\ diene}{100} + K^{triene}_{233} \cdot \frac{\%\ triene}{100}$$

$$K^{diene}_{233} = \frac{100 \cdot k'_2 - K^{triene}_{233} \cdot \%\ triene}{\%\ diene}$$

where k_2' is the increase in specific extinction coefficient at 233 mμ due to isomerization. K^{triene}_{233} was taken from Table 1 because this value was confirmed in a similar experi-

Table 1. Spectral constants for polyenoic fatty acids isomerized according to Herb and Riemenschneider [1].

Acid	Mol.wt.	K_{233}		K_{268}		K_{315}		K_{346}		K_{375}	
		$E^{1\,g/l}_{1\,cm}$	$E^{1\,mequiv./l}_{1\,cm}$	$E^{1\,g/l}_{1\,cm}$	$E^{1\,mequiv./l}_{1\,cm}$	$E^{1\,g/l}_{1\,cm}$	$E^{1\,mequiv./l}_{1\,cm}$	$E^{1\,g/l}_{1\,cm}$	$E^{1\,mequiv./l}_{1\,cm}$	$E^{1\,g/l}_{1\,cm}$	$E^{1\,mequiv./l}_{1\,cm}$
Linoleic *	280.44	91.6	25.69								
Linolenic *	278.42	47.5	13.22	90.5	25.20						
Arachidonic*	304.46	39.7	12.09	48.2	14.67	60.6	18.45				
Eicosapentaenoic **	302.44	37.0	11.19	32.9	9.95	71.1	21.50	74.1	22.41	4.37	1.322
Docosahexaenoic **	328.48	43.9	14.42	54.0	17.74	32.8	10.77	29.4	9.66	28.6	9.39

* Herb and Riemenschneider [1]
** Holman [22]

Table 2. Isolation of fatty acids from tissue and plasma. The samples were extracted with 60 ml ethanol:ether, the extract saponified and the fatty acids extracted with petroleum ether after acidification of the saponification mixture.

Sample	Weight of sample extracted g	Total fatty acids mequiv./100 g plasma or tissue
Human plasma 1.	1.046	1.01
	1.232	1.03
	1.681	1.04
	2.004	1.01
Human plasma 1. diluted 1:3 with 0.9 % NaCl	5.042	1.04
	5.067	1.06
Human plasma 2.	2.076	0.84
	2.181	0.80
Human plasma 3.	2.131	0.71
	2.145	0.69
Rat heart homogenate 1:10 in water	1.968	6.87
	2.111	6.73
	4.849	6.54
	5.146	6.43
Calf liver homogenate 1:10 in water	0.922	11.14
	0.957	11.10
	2.013	10.81
	2.062	10.88
	4.878	10.81
	5.101	10.34

ment with linolenic acid in the authors laboratory. In this way K^{diene}_{233} was found to be 91.2 ± 0.3 which is in close agreement with the value found by Herb and Riemenschneider [1].

By the following set of equations the content of the different types of polyenoic fatty acids is calculated as weight % of total fatty acids. These equations are used when the weight of the fatty acids isomerized is known, and are based on the $E^{1\,g/l}_{1\,cm}$ -values in Table 1. k'_2, k'_3, k'_4, k'_5, and k'_6 denote the increase induced by isomerization in the specific extinction coefficients of the sample ($E^{1\,g/l}_{1\,cm}$) at 233, 268, 315, 346, and 375 mμ, respectively. The k'-value is obtained as the difference between the specific extinction coefficient after (k'_{233}, k'_{268}, k'_{315}, k'_{346}, and k'_{375}) and before (k_{233}, k_{268}, k_{315}, k_{346}, and k_{375}) isomerization.

$$\text{Hexaene, } \% = k'_6 \cdot 3.722 - k'_5 \cdot 0.219$$
$$\text{Pentaene, } \% = k'_5 \cdot 1.437 - k'_6 \cdot 1.477$$
$$\text{Tetraene, } \% = k'_4 \cdot 1.65 - k'_5 \cdot 1.567 - k'_6 \cdot 0.282$$
$$\text{Triene, } \% = k'_3 \cdot 1.105 - k'_4 \cdot 0.879 + k'_5 \cdot 0.443 - k'_6 \cdot 1.534$$
$$\text{Diene, } \% = k'_2 \cdot 1.092 - k'_3 \cdot 0.573 - k'_4 \cdot 0.26 - k'_5 \cdot 0.026 - k'_6 \cdot 0.27$$

If the total fatty acids are determined by titration, the content of the different types of polyenoic fatty acids in equiv. per 100 equiv. total fatty acids is calculated by the following equations. These equations are based on the $E^{1\,\text{mequiv./l}}_{1\,cm}$-values in Table 1. k'_2, k'_3, k'_4, k'_5, and k'_6 are here given as $E^{1\,\text{mequiv./l}}_{1\,cm}$ of the sample instead of $E^{1\,g/l}_{1\,cm}$ as in the first set of equations.

$$\text{Hexaene, equiv./100 equiv.} = k'_6 \cdot 11.34 - k'_5 \cdot 0.669$$
$$\text{Petaene, equiv./100 equiv.} = k'_5 \cdot 4.75 - k'_6 \cdot 4.89$$
$$\text{Tetraene, equiv./100 equiv.} = k'_4 \cdot 5.42 - k'_5 \cdot 5.14 - k'_6 \cdot 0.921$$
$$\text{Triene, equiv./100 equiv.} = k'_3 \cdot 3.97 - k'_4 \cdot 3.16 + k'_5 \cdot 1.588 - k'_6 \cdot 5.52$$
$$\text{Diene, equiv./100 equiv.} = k'_2 \cdot 3.89 - k'_3 \cdot 2.04 - k'_4 \cdot 0.924 - k'_5 \cdot 0.961 - k'_6 \cdot 0.961$$

Table 3. Extraction of stearic acid from solutions with varying ethano concentration. 30 mg stearic acid.

Ethanol concentration % (v/v)	Number of determinations	ml pet.ether used for extraction	Recovery, %
25	6	20 + 10 + 10	90
40	2	20 + 10 + 10	94
50	5	20 + 10 + 10	98
50	12	10 + 10 + 10 + 10	99
62	3	20 + 10 + 10	97

RESULTS AND DISCUSSION

1. *Extraction.* Table 2 gives the results of experiments designed to show the reproducibility of the isolation of total fatty acids. It appears that the results are only slightly affected by variations in the sample size between 1 and 5 g. For a sample size of about 2 g the results can be reproduced within *ca.* ± 1 %. As the present experiments, besides extraction, include several other steps in the isolation of fatty acids, it can be concluded that the extraction method used is highly reproducible. It should be noted that ethanol:ether 3:1 in a volume 20—30 times that of the sample gives quantitative extraction of lipids [24]. In the experiments reported here the ratio between volume of ethanol:ether and sample varied from 12 to 60.

2. *Saponification and extraction of unsaponifiable and saponifiable fractions.* The experiments with stearic acid, the results of which are given in Table 3, indicate that the ethanol concentration of the saponification mixture should be about 50 % when the extraction of fatty acids is performed.

Other experiments showed that extraction of unsaponifiable matter before extraction of fatty acids results in a loss of about 0.5—2 % of stearic, oleic and linoleic acids, whereas linolenic acid is recovered 100 % in the fatty acid extract (*cf.* Table 4).

The results of recovery experiments, in which known amounts of fatty acids were saponified, extracted for unsaponifiable matter and extracted after acidification of the medium as described under methods, are given in Table 4. It appears that recovery is close to 100 % and that the methods used give highly reproducible results.

3. *The influence of saponification upon the determination of polyenoic fatty acids.* In order to determine the effect of saponification upon polyenoic fatty

Table 4. Recovery of fatty acids in acid extract after saponification and extraction of unsaponifiable fraction.

	Number of determinations	Recovery, %	SE	SD
Stearic acid	9	97.7	0.5	0.2
Oleic »	4	97.1	0.5	0.3
Linoleic »	2	98.1		
Linolenic »	6	100.5	1.0	0.4
Tristearin *	9	96.6	0.5	0.2
Olive oil *	5	98.0	0.7	0.3

* The recovery is calculated on a basis of a macrodetermination of the saponification number.

Table 5. The influence of saponification upon polyenoic fatty acids and soybean oil. All values are weight per cent of total fatty acids.

Fat	Saponification time, h.	% conj. diene before saponification	% conj. diene after saponification	% diene before saponification	% diene after saponification	% triene before saponification	% triene after saponification
Linoleic acid *	1	0.43	0.66	98.0	98.3	1.17	1.23
» »	1 ½	0.43	0.83	98.0	98.0	1.17	1.16
Linolenic acid **	1	1.29	2.86	−0.8	−1.7	99.6	98.2
» »	2	1.34	3.34	−0.8	−3.6	99.6	99.1
» »	2 ***	1.40	4.44	−0.8	−5.1	99.6	98.4
Soybean oil	1	0.27	0.60	51.9	52.2	7.73	7.78

* Hormel Foundation, containing only *cis*-isomers.
** Hormel Foundation, containing appreciable amounts of *trans*-isomers.
*** Allowed to stand hot for 1 ½ h after 2 h of saponification.

acids, different fats were saponified (see methods) for various length of time. The absorption spectra of non-isomerized as well as isomerized samples of the isolated fatty acids were determined and the composition was calculated. Table 5 gives the results of some experiments of this type with linoleic acid, linolenic acid and refined soybean oil. The content of conjugated constituents was calculated according to Brice and Swain [25] (see also Nørby [26]).

In another experiment (Table 6) six 2 g samples of calf liver homogenate (1:10 in water) were extracted, the extracts saponified for 1, 1 ½, or 2 h, and the proportion of conjugated and non-conjugated polyenoic fatty acids as well as total fatty acids determined as described. Besides the results given in Table 6 it was found that conjugated isomers with more than 3 double bonds were not present even after 2 h of saponification.

From Tables 5 and 6 it appears that small amounts of conjugated isomers are formed during saponification and that the degree of conjugation increases with increasing saponification time. The content of non-conjugated polyenoic fatty acids as determined by the isomerization method is, however, not signi-

Table 6. The influence of saponification time upon composition of fatty acids from calf liver.

Fatty acid *	Saponification time 1 hour		1 ½ hour		2 hours	
Conjugated dienoic	1.35	1.26	1.47	1.59	2.25	2.10
» trienoic	0.03	0.03	0.05	0.04	0.13	0.10
Dienoic	11.5	11.8	10.9	11.4	11.0	10.9
Trienoic	3.6	3.7	3.6	3.8	3.6	3.4
Tetraenoic	11.1	11.2	10.8	11.6	11.3	11.3
Pentaenoic	6.6	6.6	6.6	6.8	6.9	6.8
Hexaenoic	2.0	1.9	1.9	3.0	2.2	2.5
Total fatty acids **	8.78	8.72	8.65	8.51	8.28	8.45

* equiv./100 equiv. total fatty acids.
** mequiv./100 g liver (wet weight).

Table 7. Reproducibility of isomerization of pure acids and vegetable oils. Values for diene and triene are % of total fatty acids. Numbers in brackets are standard error of a single determination.

Sample	Sample weight * mg	No. det.	Diene %	Triene %
Linoleic acid	0.1—12	16	98.0 (1.2)	1.17 (0.07) **
Linolenic »	2.3— 3.5	9	—0.8 (0.4)	99.6 (0.6)
Soybean oil	1.7—40	19	51.8 (0.6)	7.68 (0.16)
Sunflower seed oil	3.3—17.8	5	59.1 (0.7)	0.106 (0.015) **

* The samples were weighed into small vials on a microbalance and isomerized. Samples weighing less than 0.5 mg were weighed as dilutions in lauryl alcohol.
** Determined according to Brice and Swain [25] and Nørby [26].

ficantly affected by saponification *. These observations agree well with that of Pikaar and Nijhof [12] who found that analysis of serum fatty acids after single and double saponification gave identical results.

From Fig. 2 in the paper of Pikaar and Nijhof [12] it appears that the absorbance at 233 mμ of serum fatty acids after saponification is about 15 % of that after isomerization. In a number of experiments on fatty acids from rat heart and rat plasma, which had a higher content of polyenoic fatty acids (see Table 8) than the fat analyzed by Pikaar and Nijhof [12], the author found the absorbance at 233 mμ after saponification to be 4—8 % of that after isomerization. The method of saponification and extraction of unsaponifiable and saponifiable fractions described here should probably be preferred to that of Pikaar and Nijhof [12] since it is more simple and produces less conjugation.

The results obtained in the experiments concerning the extraction and saponification step indicates that the methods used are well suited for the isolation of fatty acids from biological material prior to the determination of polyenoic fatty acids.

4. *Isomerization.* According to Herb and Riemenschneider [1] their microisomerization method requires only 1—10 mg of fat. In determinations on such a small amount of fat it is especially important that changes in the absorbance of the reagent itself are small and reproducible. In order to test the reproducibility of the blank (5.0 g reagent treated as described under methods), 8 series each consisting of 2 to 5 blanks were isomerized. After dilution to 25 ml with methanol the maximum difference in $E_{1\ cm}$ between the blanks in the same series was determined. The greatest difference between two blanks was 0.002, 0.003, 0.006, 0.016, and 0.035 at 375, 346, 315, 268, and 233 mμ. As extinction readings at 268 and 233 mμ usually are performed after dilution of the sample to 50 ml or more, the error introduced by variations in the reagent seems to be very small.

* The apparent decrease, with increasing saponification time, towards greater negative content of dienoic acid in the experiments with linolenic acid is an exception to this. If the specific extinction coefficient of the sample before saponification and before isomerization instead of that after saponification is used in the calculation of k_2', this decrease is not seen. This may indicate that the conjugated isomers formed by saponification of linolenic acid are unstable and during isomerization probably are converted to conjugated triene.

Table 8. Reproducibility of isomerization of fatty acids from egg yolk, rat plasma and rat heart. Numbers in brackets are standard error of a single determination.

Sample	Sample size	Number of duplicate det.	Content of polyenoic fatty acids * diene	triene	tetraene	pentaene	hexaene
			weight % of total fatty acids				
Egg yolk fatty acids	4—35 mg	10	10 (0.15)	0.8 (0.06)	2 (0.04)	0.4 (0.015)	1 (0.05)
			equiv./100 equiv. total fatty acids				
Rat plasma fatty acids	2—6 μequiv.	19	22 (0.55)	2 (0.27)	15 (0.42)	2 (0.21)	4 (0.28)
Rat heart fatty acids	*ca.* 3 μequiv.	21	20 (0.85)	0 (0.69)	16 (0.41)	2 (0.21)	11 (0.72)

* The composition of the fats analyzed is given in approximate values as a number of extracts from different yolks, plasmas and hearts were analyzed in duplicate.

The fatty acids were isolated and transferred to the isomerization tubes as described under methods p. 526.

The reproducibility of the isomerization method and the influence of sample size was tested in a number of experiments with pure fatty acids and vegetable oils (Table 7) and fatty acids from egg yolk, rat plasma and rat heart (Table 8). From the experiments with linoleic acid, vegetable oils (Table 7) and fatty

Table 9. Analysis of known mixtures of linoleic or linolenic acid and soybean oil by the method of Herb and Riemenschneider [1].

Expt. No. a)	Diene % calc.	found	Recovery, %	Triene % calc.	found b)	Recovery, %
1	88.5	88.1	99.5	2.59	2.55	98.5
2	85.6	85.9	100.4	2.98	2.87	96.3 c)
3	82.8	82.3	99.4	3.38	3.12	92.3 c)
4	82.4	82.2	99.8	3.44	3.40	98.8
5	77.1	76.0	98.6	4.14	4.17	100.7
6	76.8	76.3	99.3	4.21	3.96	94.1 c)
7	47.5	48.0	101.1	15.2	15.3	100.7
8	40.4	40.7	100.7	27.7	27.7	100.0
9	39.7	40.4	101.8	28.9	29.0	100.3
10	35.5	36.0	101.4	36.2	36.2	100.0
11	24.5	24.4	99.6	55.6	55.6	100.0
12	21.0	21.5	102.4	61.6	60.4	98.1
13	16.5	16.2	98.2	69.5	70.2	101.0
Average			100.2			99.8
SE			1.3			1.0
SD			0.4			0.3

a) 1—6: soybean oil + linoleic acid. 7—13: soybean oil + linolenic acid.

b) % triene in experiment 1—6 are calculated after correction for background absorption (Brice and Swain [25], Nørby [26]).

c) These samples, which were analyzed simultaneously, gave low triene values due to oxidation of the blank.

acids from egg yolk (Table 8) it is seen that the sample size may be varied over a wide range. Furthermore it appears from the results given in Table 8 that analysis of very small samples (*ca.* 3 μequiv. = *ca.* 1 mg) of complicated mixtures can be performed with considerable accuracy.

Results of experiments in which linoleic or linolenic acid were added to soybean oil and the mixtures analyzed are given in Table 9. Apart from experiments 2, 3, and 6, in which the blank was oxidized due to failure of the N_2-stream, the recovery was close to 100 %.

5. *Determination of total fatty acids.* The accuracy of the titration method described (p. 527) was determined by analysis of the results obtained in 19 duplicate titrations on 5 ml aliquots of fatty acid extracts from rat plasma and 21 duplicate titrations of fatty acids from rat heart. The standard error of a single titration was 1—3 %, the amount of fatty acid titrated being 2—6 μequiv.

It should be mentioned that titration of extracts from a saponification medium, to which pyruvic, lactic, β-hydroxybutyric, and citric acids had been added, gave values identical with the blank. This excludes these acids as sources of error in the determination of total fatty acids.

REFERENCES

1. Herb, S. F. and Riemenschneider, R. W. *Anal. Chem.* **25** (1953) 953.
2. Klein, P. D. and Johnson, R. M. *Arch. Biochem. Biophys.* **48** (1954) 172, 380.
3. Evans, J. D., Riemenschneider, R. W. and Herb, S. F. *Arch. Biochem. Biophys.* **53** (1954) 157.
4. Evans, J. D., Waldron, J. M. and Olekshyn, N. L. *J. Biol. Chem.* **218** (1956) 255.
5. Dam, H., Engel, P. and Nielsen, G. K. *Acta Physiol. Scand.* **37** (1956) 142.
6. Dam, H. and Nielsen, G. K. *Acta Physiol. Scand.* **37** (1956) 359.
7. Christensen, F., Dam, H. and Engel, P. F. *Acta Physiol. Scand.* **38** (1957) 373.
8. Mukherjee, S., Achata, K. T., Deuel jr., H. J. and Alfin-Slater, R. B. *J. Biol. Chem.* **226** (1957) 845.
9. Hallanger, L. E. *Proc. Soc. Exptl. Biol. Med.* **96** (1957) 473.
10. Tuna, N., Reckers, L. and Frantz jr., I. D. *J. Clin. Invest.* **37** (1958) 1153.
11. Dam, H. and Engel, P. F. *Acta Physiol. Scand.* **42** (1958) 28.
12. Pikaar, N. A. and Nijhof, J. *Biochem. J.* **70** (1958) 52.
13. Hauge, J. G. *Acta Physiol. Scand.* **45** (1959) 181, 375.
14. Peifer, J. *Arch. Biochem. Biophys.* **86** (1960) 302.
15. Holman, R. T. and Hayes, H. *Anal. Chem.* **30** (1958) 1422.
16. Front, J. S. and Daubert, B. F. *J. Am. Chem. Soc.* **67** (1945) 1509.
17. Holm-Jensen, I. *Scand. J. Clin. Lab. Invest.* **12** (1960) 247.
18. Antonis, A. in Sinclair, H. M. (ed.) *Essential Fatty Acids*, Butterworth, London 1958, p. 160.
19. Montag, W., Klenk, E., Hayes, H. and Holman, R. T. *J. Biol. Chem.* **227** (1957) 53.
20. Herb, S. F. *J. Am. Oil. Chemists' Soc.* **32** (1955) 456.
21. Abu-Nasr, A. M. and Holman, R. T. *J. Am. Oil Chemists' Soc.* **31** (1954) 41.
22. Holman, R. T. in Glick, D. (ed.) *Methods of Biochemical Analysis*, Interscience, New York **4** (1957) 121.
23. Hammond, E. G. and Lundberg, W. O. *J. Am. Oil Chemists' Soc.* **30** (1953) 433.
24. Sperry, W. M. in Glick, D. (ed.) *Methods of Biochemical Analysis*, Interscience, New York **2** (1955) 87.
25. Brice, B. A. and Swain, M. L. *J. Opt. Soc. Am.* **35** (1945) 532.
26. Nørby, J. G. *Acta Chem. Scand.* **14** (1960) 2057.

Received November 1, 1960.

ACTA CHEMICA SCANDINAVICA 15 (1961) 535–544

Spectral Changes during the Action of Myrosinase on Sinigrin

SIGMUND SCHWIMMER*

*Western Regional Research Laboratory, Albany 10, California**, and Organic Chemical Laboratory, Royal Veterinary and Agricultural College, Copenhagen, Denmark*

When myrosinase acts on sinigrin, the absorbancy at 227.5 mμ (maximum for the substrate) decreases linearly with time. On the basis of the observations a convenient, continuous method for estimation of enzyme activity has been developed. At 255 mμ, an isosbestic point for the spectra of the substrate sinigrin and allyl *iso*thiocyanate, presumably the only UV absorbing product of the enzyme reaction, there is observed an initial rapid rise in absorbance followed by a slower rise and still slower decrease to a final value somewhat above the initial absorbancy of the enzyme reaction mixture. The influence of enzyme and substrate concentration and of pH on the rate of change of absorbance at these two wavelengths was determined. K_M values obtained below neutrality were of the order of 0.1 mM, and the pH optimum was found to be between 6 and 7. At pH 7, the K_M values rose as much as one order of magnitude. The accelerating effect of ascorbic acid on the enzyme action was confirmed by the spectrophotometric method developed herein. The results indicate that the instability of ascorbic acid buffered at pH 6.0 is decreased during the action of the enzyme.

The structure and distribution of the naturally occurring derivatives of S-(glucosyl)-thiohydroximyl sulfates (mustard oil glucosides) have been elucidated in recent years, in large measure as a consequence of the investigations of Kjaer [1] and of Ettlinger and Lundeen [2]. As a result of this work and of more recent investigations of the properties of enzyme preparations responsible for the hydrolysis of these glucosides (myrosinase [2–4]) it has been suggested that the hydrolysis of these substances proceeds *via* simple thioglucosidase action accompanied by a Lossen rearrangement with concomitant sulfate displacement to yield *iso*thiocyanate derivatives. However, results published in the last year or so demonstrate a multiplicity of alternative pathways for the enzymatic breakdown. Thus, organic thiocyanate [5], thiocyanate ion [6], and

* Senior Postdoctoral Fellow, National Science Foundation, 1958–59.

** A laboratory of the Western Utilization Research and Development Division, Agricultural Research Service, U.S. Department of Agriculture.

nitrile [7] have been shown to be products of enzymatic action under appropriate conditions. Gaines and Goering [8], after separating the thioglucosidase and the sulfatase functions of myrosinase, have shown that both are necessary for the formation of *iso*thiocyanate. Furthermore, it has been found that ascorbic acid can influence both the rate of enzyme action and the nature of the products formed [4,7].

The present paper presents results of a spectroscopic investigation of the action of myrosinase on sinigrin, S-(glucosyl)-2-butenothiohydroximyl sulfate. These studies provide a basis for a convenient continuous method for the assay of myrosinase and show the effect of variations of substrate concentration, enzyme concentration, and pH. In addition, they show that a UV absorbing intermediate or side product is formed during the reaction and that added ascorbic acid and the enzymic reaction exert reciprocal effects; *i.e.*, the decomposition of sinigrin is accelerated by ascorbic acid, and ascorbic acid is protected from deterioration (as measured spectroscopically) in the presence of the enzyme reaction mixture.

MATERIALS AND METHODS

Sinigrin, purchased from Light & Co.* (London), was recrystallized twice from 90 % ethanol to yield sinigrin hydrate (m.p. = 124°–126°). Allyl *iso*thiocyanate was used as a fresh distillate of a commercial sample (Eastman). Ascorbic acid was also purchased from Eastman. The myrosinase preparation used in all these experiments was obtained from Coleman's yellow mustard powder according to the following procedure, carried out at 0°–4°. 100 g of the mustard powder was extracted 10 times with 300 ml portions of acetone. After drying *in vacuo*, the defatted powder was extracted two times with 300 ml of water. The residue was removed by centrifugation and the combined supernates were fractionated with acetone. The portion precipitating between 30 % and 70 % was dialyzed against distilled water for 41 h and the retentate, after removal of small amount of precipitate by centrifugation, was lyophilized to yield 2 g of white enzyme preparation. The spectra reported here were obtained with a Cary Recording Spectrophotometer, which was also used to determine the course and extent of enzyme action (*cf.* Fig. 2). For all the other experiments either a Beckman DU or Zeiss spectrophotometer was employed. Unless otherwise stated 10 mm and 1 mm light paths were used at 255 mμ and at 227.5 mμ, respectively.

RESULTS

Spectra of substrate and product. (Fig. 1). At the absorption maximum of the substrate sinigrin (227.5 mμ, $\varepsilon = 7\,800$) the molar extinction coefficient ε of the product, allyl *iso*thiocyanate, is 564 or 7.2 % of that of sinigrin. This suggests that one can conveniently follow the enzyme reaction at 227.5 mμ. The expected decrease in absorbancy at this wave length may be considered attributable to the disappearance of sinigrin. If one assumes that the only UV absorbing material formed is indeed allyl *iso*thiocyanate, then, $S_t = S_o - \Delta OD/\Delta\varepsilon$, and the % hydrolysis is $(\Delta OD/S_o\Delta\varepsilon) \times 100$; where S_t = molar concentration of substrate at time t, S_o is the initial substrate

* Mention of specific products does not imply recommendation by the Department of Agriculture over others of a similar nature not mentioned.

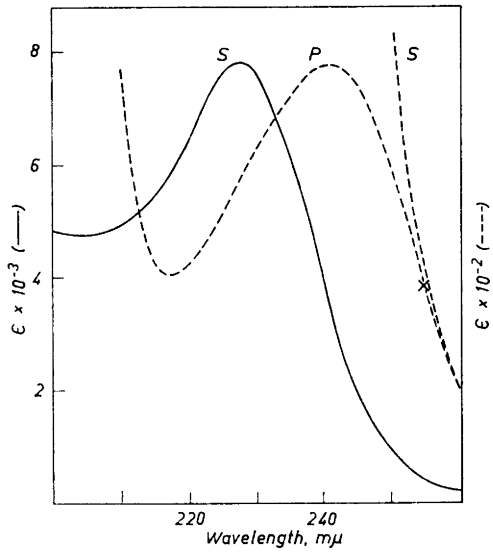

Fig. 1. Ultraviolet absorption spectra of aqueous solutions of 0.05 mM sinigrin (S) and 1 mM freshly prepared allyl *iso*thiocyanate (P); ε = molar extinction coefficient. Solid line (——————) is for $\varepsilon \times 10^{-3}$ and the broken lines (- - -) are for $\varepsilon \times 10^{-2}$. The two spectra are isosbestic at 255 mμ, ε = 380.

concentration, ΔOD the observed change in optical density and $\Delta\varepsilon$ the difference in molar extinction coefficients between that of the subtrate and that of the product. The ε value for allyl *iso*thiocyanate in dilute aqueous solution at its maximum of 240 mμ amounted to 770, and at this wavelength ε = 4 000 for sinigrin. It will be noted in Fig. 1 that the two spectra are isosbestic at 255 mμ (ε = 380). Therefore, if neither UV absorbing side products nor stable intermediates were formed during the course of the reaction there would be no change in optical density at this wavelength which could be attributed to enzyme action.

Dilute solutions of sinigrin were found to be spectroscopically stable for 3 h and over the pH range (3—9) used in the present studies. Small but significant changes did occur in allyl *iso*thiocyanate solutions. At room temperature, the absorbancy at 240 mμ of unbuffered solutions (pH 6) decreased 8 % in 2 h. Absorbancy at pH 8.65 (TRIS buffer) increased 10.9 %, 10.6 %, and 5.5 % at 227.5 mμ, 240 mμ, and 255 mμ, respectively. In addition to the 240 mμ peak, aqueous solutions of undistilled allyl *iso*thiocyanate exhibited a maximum at 298 mμ as well.

Enzyme-induced changes in absorbancy. Upon the addition of myrosinase to sinigrin at pH 6.0, a rapid decrease of absorbancy at 227.5 mμ was observed proceeding almost linearly during the first 50 % hydrolysis (Fig. 2). The rate of decrease in optical density then slowly decelerated until a minimum optical density was attained, corresponding to 96 % hydrolysis of sinigrin based on

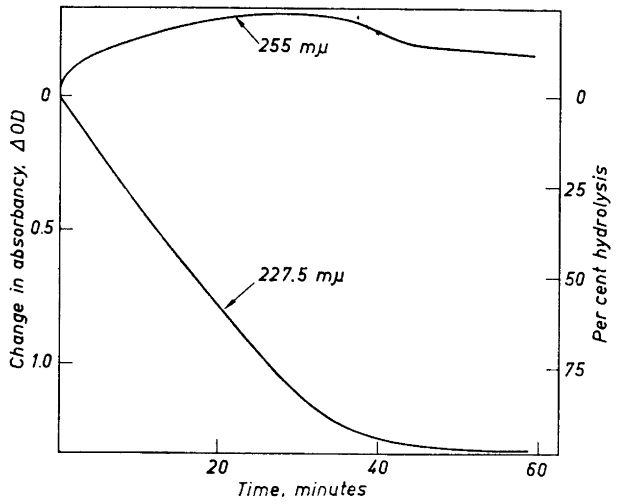

Fig. 2. Absorbancy changes with respect to time in a myrosinase-sinigrin reaction mixture. The curves were obtained with a Cary recording spectrophotometer, which began to record 12 sec. after the start of the reaction. The absorbancy values at zero-time used to calculate optical density change were obtained from the sum of the absorbancies of substrate and enzyme measured separately. One ml of enzyme reaction mixture at 25° contained; 1.9 μmoles substrate, 40 μmoles acetate buffer at pH 6.0, and 0.25 mg of myrosinase preparation. Percent hydrolysis of sinigrin is calculated on the assumption that allyl *iso*thiocyanate is the only stable material formed during the reaction absorbing at 227.5 mμ. Light paths at 227.5 mμ and at 255 mμ were 1 mm and 10 mm, respectively.

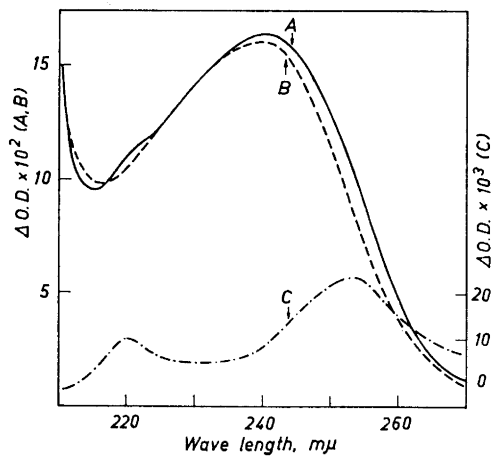

Fig. 3. Spectrum of enzyme reaction mixture described in Fig. 2 after 2.5 h. Points obtained after correction for protein (solid line, Curve A). Curve B (- - -) is the calculated spectrum of a mixture of 99 % allyl *iso*thiocyanate and 1 % sinigrin. Curve C (- · - · -) shows the difference spectrum between the two curves. All measurement made with 1 mm light path.

the assumptions outlined above. Instead of finding no change in absorbancy at the isosbestic point 255 mμ as expected, there was observed a very rapid initial rise in optical density followed by a slower increase until a maximum was reached. The optical density of the reaction mixture then decreased to an apparent minimum value somewhat higher than that at zero time.

The spectrum of the sinigrin-myrosinase digest (after correction for enzyme alone) at 2.5 h is shown in Fig. 3, Curve A. The spectrum of a mixture of 99 % allyl *iso*thiocyanate and 1 % sinigrin is shown for comparison, Curve B. The general shapes of the two spectra are similar. It will be noted that beyond 235 mμ, shift of the experimental spectrum in the bathochromic sense is observed. Also to be noted is the appearance of a slight shoulder in the experimental spectrum between 215 and 225 mμ. The difference spectrum, also shown in Fig. 3, indicates two relatively weak absorption bands at 220 and 253 mμ.

Influence of enzyme and substrate concentrations. Fig. 4 shows that there is a strict proportionality between rate of enzyme action, as measured by decrease of absorbancy at 227.5 mμ, and enzyme concentration. Applications of simple Michaelis kinetics to the curve describing the effect of substrate concentration on the initial rate yielded a value of $V_{max} = 0.033$ μmoles per ml per min. and a K_M value between 0.12 and 0.14 mM. An estimation of the turnover number as the number of molecules of sinigrin decomposed per min. by one molecule of enzyme (assumed mol.wt. = 100 000) yields a value of 181. This indicates that the enzyme is still in a very low state of purity.

The small but almost instantaneous increase of optical density at 255 mμ shown in Fig. 2 was too rapid to permit estimation of true initial rate. However, it was possible to measure a quasi-initial rate by plotting optical densities

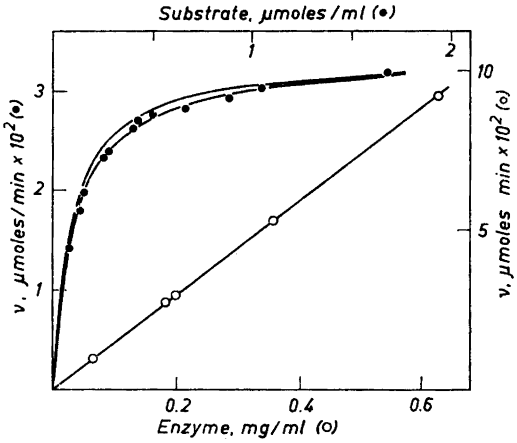

Fig. 4. Influence of enzyme and substrate concentration on the initial rate of decrease of absorbancy at 227.5 m*u*. This rate, *v* is expressed as moles of sinigrin disappearing per ml digest per min. The closed circles (●) are the experimentally found rates and the two curves are the theoretical curves for $V = 0.033$ μmoles/ml/min and $K_M = 0.12$ or 0.14 μmole/ml. Enzyme reaction mixture at pH 6.0 (acetate buffer) contained 0.83 μmole/ml of sinigrin for the enzyme concentration curve (O). The amount of enzyme for the plot of substrate *vs.* rate data was 0.185 mg/ml.

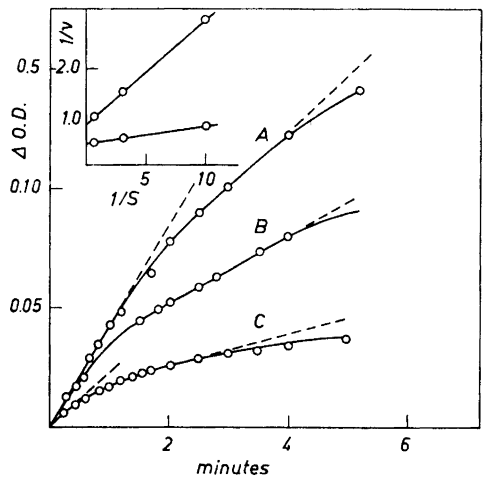

Fig. 5. Determination of "fast" and "slow" rates at 255 mμ as affected by substrate concentration. One ml of enzyme reaction mixture at 25° contained 33 μmoles of acetate buffer pH 4.0, 0.15 mg of enzyme preparation and the following μmoles of substrate: A, 1.67; B, 0.33; C, 0.10. The slopes of the broken straight lines (- - -) are estimated for determination of "fast" and "slow" rates. The insert shows reciprocal substrate-velocity plot used to determine K_M and V.

against time during the first half-minute of the reaction and extrapolating to zero time (Fast Reaction, Fig. 5). This "fast" reaction was followed by an interval in which the increase in optical density appeared to be linear with respect to time (Slow Reaction). Fig. 5 shows that plots of the reciprocal of these rates against reciprocal substrate concentrations yield straight lines, thus permitting calculation of quasi-kinetic constants.

Influence of pH. Table 1 summarizes the influence of pH on the kinetic constants for the decrease of absorbancy at 227.5 mμ and for the "fast" and "slow" increases at 255 mμ. It will be noted that the calculated maximum velocities (V relative) do not exhibit great changes with respect to pH. The value at pH 3 for the rate at 227.5 mμ is probably too low since the decrease in absorbancy due to sinigrin disappearance was counteracted by increase due to the formation of turbidity in the enzyme reaction mixture [7]. Above pH 7.0 the maximum rates for all three reactions decreased relatively rapidly. Below neutrality K_M values were of the order of 10^{-4} M and were fairly independent of pH. Perhaps the most remarkable feature observed was the rather dramatic increase in, and appearance of optimum K_M values at pH 6.96, amounting to a 10-fold increase for the "slow" reaction at 255 mμ. One effect of this remarkable increase is to create an apparent optimum pH of around 6.0 at substrate concentration below that required for saturation of the enzyme.

Influence of ascorbic acid. Fig. 6 and Table 2 show that the stoichiometric quantities of ascorbic acid used in these experiments appear to stimulate

Table 1. Influence of pH on kinetic constants V and K_M [1]

pH	Wave length, mμ					
	227.5	255 f	255 s	227.5	255 f	255 s
	V (relative)			K_M (μmole/ml)		
3.00	0.77	—	—	0.18	—	—
4.00	1.00	1.0	1.0	0.14	0.08	0.25
5.00	1.05	1.1	1.1	0.14	0.25	0.30
6.00	1.21	1.5	—	0.14	0.26	0.27
6.96	1.30	1.7	1.0	0.68	0.56	2.7
7.75	—	1.2	0.7	0.58	0.23	1.6
8.63	0.98	1.0	0.3	0.27	0.16	0.45

[1] Reaction mixture contained 0.15 mg/ml of enzyme preparation. Letters "f" and "s" represent "fast" and "slow" reactions as explained in text and Fig. 5. V's set at 1.00 at pH 4. Actual values for 227.5, 255 f and 255 s were, respectively: 0.028 μmole per min. per ml of digest; 0.22 optical density units per 5 min; and 0.11 optical density units per 5 min. The buffer used in final concentration of 0.033 M were as follows: malate for pH 3.0; acetate for pH 4.00, 5.00 and 6.00; TRIS for pH 6.96, 7.75 and 8.63. Other conditions are the same as in Fig. 5.

the action of the enzyme as measured by rate of decrease in optical density at 227.5 mμ. However, the results were complicated by the apparent spectroscopic instability of dilute ascorbic acid solution under the conditions of assay (Fig. 6, Curve A—I). This course of decrease of absorbancy was essentially the same as that of Curve A—I when either enzyme or substrate was added to the ascorbic acid separately (Table 2). The optical density at 227.5 mμ of the standard reaction mixture containing sinigrin and myrosinase (but no ascorbic acid) decreased linearly at a rate of 0.016 optical density units per min. (B—I). In the presence of ascorbic acid the rate of decrease of optical density was accelerated to 0.038 optical density units per min., over double that in the absence of ascorbic acid and the change was linear with respect to time (Curve C—I). It would thus appear that the increased rate did not include

Table 2. Absorbancy changes (ΔOD) in the presence of ascorbic acid [1]

Components [2]			ΔOD					
E	S	AA	227.5 mμ			255 mμ		
			2 min.	5 min.	10 min.	2 min.	5 min.	10 min.
+	+	+	−0.071	−0.184	−0.372	−0.001	−0.035	−0.072
+[3]	+	+	−0.064	0.162	−0.325	—	—	—
+	+	—	−0.030	−0.079	−0.157	+0.003	+0.006	+0.004
+	—	+	−0.027	−0.061	−0.059	−0.143	−0.368	−0.381
—	+	+	−0.024	−0.060	−0.060	—	—	—
—	—	+	−0.026	−0.058	−0.060	—	—	—

[1] Selected data from curves of Fig. 6.
[2] AA = Ascorbic acid; S = Substrate; E = Enzyme.
[3] E added 20 min after incubation of S + AA.

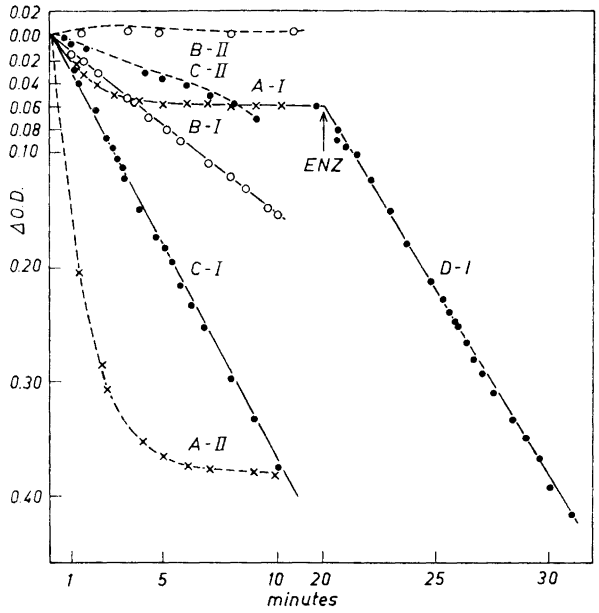

Fig. 6. Effect of ascorbic acid on change in absorbancy with time in a myrosinase-sinigrin reaction mixture. Broken lines (II) (- - -) represent date obtained at 255 mμ and smooth lines (I) (————) those obtained at 227.5 mμ (1 mm light path in both cases). Complete system contained per ml; 0.89 μmole of sinigrin, 0.90 μmole of ascorbic acid, 167 μmoles of pH 6.0 acetate buffer and 0.167 mg of enzyme preparation. Curves A (×) complete system less substrate and enzyme; Curves B, (●) complete system less ascorbic acid; Curves C, complete system (O); Curve D, complete system less enzyme at zero time; at 20 min. enzyme added (ENZ).

the decrease due to ascorbic acid. This suggestion is strengthened by the results obtained when enzyme was added to a sinigrin reaction mixture 20 min. after addition of ascorbic acid. The rate of decrease of optical density amounted to 0.032 per min., double that in the absence of ascorbic acid (Curve D—I).

Further substantiation of this conclusion is afforded by the results obtained at 255 mμ (Curves A—II, B—II, C—II, Fig. 6). The slight increase at 255 mμ in the presence of substrate and enzyme alone is shown in Curve B—II (The low values are the result of using a 1 mm light path instead of 10 mm as was used in the previous experiments at this wavelength). At 255 mμ under the conditions of the enzyme reaction, the optical density of ascorbic acid alone dropped precipitously in the first few minutes (Curve A—II). Curve C—II presents the results obtained with the complete system containing sinigrin, myrosinase and ascorbic acid. It will be noted that for the first minute there was practically no decrease in optical density after which the optical density decreased at a rate equal to 4 % of that in absence of enzyme plus substrate. (Comparison of Curve C—II and A—II). Absorbancy changes at 2.5 and 10 min. are shown in Table 2. These data were obtained by interpolation from the curves of Fig. 6.

DISCUSSION

The almost strict linearity between optical density changes at 227.5 mμ on one hand and both time and enzyme concentration on the other demonstrate the feasibility of a rapid convenient continuous method for assaying the overall activity of myrosinase preparations. In recent publications, one [3] and four [4] hour incubation periods have been used in assaying this enzyme. In the assay procedure proposed herein, easily measurable changes at the initial stages occur within 10 min.

The findings of optical density changes at 255 mμ, the isosbestic point of substrate and product during the action of the enzyme, suggest the formation of side reactions or of relatively stable intermediates. Alternatively, these changes might in fact be due to the spectrum of the enzyme-substrate complex. The extremely rapid initial rise, immeasurably fast with the equipment used in the studies, may be considered as tending to corroborate the latter hypothesis, at least for this very early stage of the reaction. The subsequent rise and fall of absorbancy may then be due to interaction of desulfurylated and/or desugared intermediates with the enzyme. In this connection, Gaines and Goering [8] in discussing the significance of their results on the separation of the sulfatase and glucosidase mixtures of myrosinase, suggest that in the presence of both enzymes (myrosinase), the residual structure from glucosidase action is bound to the sulfatase factor. In any case, the actual concentration of the components giving rise to this absorbancy must be very small in view of the data obtained at 227.5 mμ. If this is so, then the extinction coefficients of the components are very high indeed.

The enzymatic nature of the changes at 255 mμ are further corroborated by the finding that the rates of change obey simple enzyme kinetics and that the effect of pH on these constants are qualitatively the same as those obtained at 227.5 mμ.

In common with other hydrolytic enzymes, the dramatic change in K_M value in the neighborhood of neutrality (Table 1) suggests the involvement in the enzyme reaction of an ionizing group in the enzyme at pH 6.0 to 7.0.

The data of Fig. 6 corroborates previous reports that ascorbic acid accelerates the myrosinase-sinigrin reaction [4]. In addition, the data strongly suggest that in the presence of the enzyme-sinigrin reaction mixture, the break-down of ascorbic acid (as evidenced by decrease in absorbancy) is significantly retarded. The change in the optical density of the buffered solution of dilute ascorbic acid observed here are in agreement with the results of Mohler and Lohr [9].

Acknowledgements. The author wishes to thank Professor Anders Kjær, director of the Organic Chemical Laboratory, Royal Veterinary and Agricultural College, for his interest and advice and Mr. G. Bailey of this laboratory for help in the use of the Cary recording spectrophotometer.

REFERENCES

1. Kjær, A. *Fortschr. Chem. org. Naturstoffe* **18** (1960) 122.
2. Ettlinger, M. G. and Lundeen, A. J. *J. Am. Chem. Soc.* **79** (1957) 1764.
3. Reese, E. T., Clapp, R. C. and Mandels, M. *Arch. Biochem. Biophys.* **75** (1958) 228.
4. Nagashima, Z. and Uchiyama, M. *Bull. Agr. Chem. Soc. Japan* **23** (1959) 555; **24** (1960) A 11.
5. Gmelin, R. and Virtanen, A. I. *Acta Chem. Scand.* **13** (1959) 1474.
6. Gmelin, R. and Virtanen, A. I. *Acta Chem. Scand.* **14** (1960) 507.
7. Schwimmer, S. *Acta Chem. Scand.* **14** (1960) 1439.
8. Gaines, R. D. and Goering, K. J. *Biochem. Biophys. Research. Communs.* **2** (1960) 207.
9. Mohler, H. and Lohr, H. *Helv. Chim. Acta* **21** (1938) 485.

Received November 7, 1960.

ACTA CHEMICA SCANDINAVICA 15 (1961) 545–554

Crystalline Leghemoglobin

III. Amino Acid Composition of the Two Main Components

NILS ELLFOLK*

Medicinska Nobelinstitutet, Biokemiska avdelningen, Stockholm, Sweden

The amino acid composition of the two main components of leghemoglobin has been determined by the chromatographic technique of Stein and Moore. Separate determinations have been made for tryptophan and amide ammonia. The electrophoretically faster component is shown to contain the following amino acid residues: Asp_{12}, Thr_7, Ser_{11}, Glu_{14}, Pro_5, Gly_8, Ala_{21}, Val_{13}, $Ileu_6$, Leu_{12} Tyr_3, Phe_8, Lys_{13}, His_2, Arg_1, Try_3, $(-CONH_2)_8$ and the electrophoretically slower component: Asp_{11}, Thr_6, Ser_{10}, Glu_{12}, Pro_5, Gly_6, Ala_{24}, Val_{14}, $Ileu_4$, Leu_{12}, Tyr_3, Phe_7, Lys_{13}, His_2, Arg_2, Try_3, $(-CONH_2)_6$. Small but significant differences in the amino acid content of the two components involve: Ala, Arg, Glu, Gly, Ileu, and Val. No significant differences are found in the other amino acids of the two main components. The molecular weight of the faster component calculated on the basis of the amino acid content is 16 695 and for the slower one 15 429. The electrophoretic behavior of the two components can be satisfactorily explained on the basis of the amino acid composition. Leghemoglobin differs from other hemin proteins in showing a very low histidine content and the absence of methionine and cysteine. The results are discussed.

Information on the amino acid composition of leghemoglobin (Lhb) has been limited to one report on the histidine content of an unresolved preparation which was found to be one fourth of that of cow hemoglobin [7]. No other studies on the amino acid content of Lhb have been performed.

The present study reports the amino acid composition of the two main components of Lhb as evaluated mainly by the chromatographic method of ion exchange resin developed by Moore and Stein.

EXPERIMENTAL

Material. The two main components of Lhb used in these studies were prepared as described previously [2,3]. The electrophoretic homogeneity of the components were checked.

* Permanent address: Research Laboratories of the State Alcohol Monopoly, Helsinki, Finland.

Apoproteins of the two components of Lhb were prepared by adding one volume of cold, salt-free water solution of the two chromoproteins slowly with stirring to twenty volumes of acetone-hydrochloric acid solution (2 ml of N HCl/l of acetone) at −13°C. The precipitate was centrifuged in the cold (4 000 *g*, 5 min.) and dissolved in cold water and dialyzed in the cold against a dilute sodium bicarbonate solution (50 mg/l). A small amount of denaturated protein precipitated and was removed by high-speed centrifugation.

Amino acid analyses

Hydrolysis. 2.5 mg of the two main components of Lhb were hydrolyzed in sealed evacuated tubes in 1 ml 6 N HCl. The hydrolysis was conducted in an oven at 110°C for 20 and 70 h. The cooled tubes were opened and the contents evaporated over NaOH pellets *in vacuo* at room temperature. To complete the removal of hydrochloric acid, small portions of water were occasionally added.

Chromatography. The chromatographic separation of the amino acids in the hydrolysates were performed on columns of Amberlite IR 120 (< 200 mesh) with use of the 0.9 × 150 cm column for the acidic and neutral amino acids and 0.9 × 15 cm column for the basic ones as described by Moore *et al.*[4] The extent of recovery of amino acids from each column was determined by use of a synthetic mixture of amino acids (Schwarz Laboratories Inc) and hydrolysates of the following synthetic peptides: HCl·H·Leu—Phe—Pro·OMe, HCl·H·Gly—Gly—Phe·OEt, H·His—Leu—Leu·OH and HCl·H·Leu—Leu—Leu—Phe—Pro·OMe (Ciba Ltd.).

Determination of amino acids. The new photometric ninhydrin method of Moore and Stein [5] was used.

Determination of tryptophan [6] was carried out by the spectrophotometric analysis of a sample of the apoproteins of the two components in 0.1 N sodium hydroxide.

Determination of cyst(e)ine by oxidation to cysteic acid [7]. 5 mg freeze dried protein was dissolved in 1 ml of cold formic acid (98—100 %) and 0.06 ml of 30 % hydrogen peroxide was added. The reaction was terminated after one hour by addition of 2 ml of distilled water. The oxidized preparation was repeatedly dried *in vacuo* at room temperature over NaOH in order to remove traces of hydrogen peroxide, after which the preparation was hydrolyzed with HCl as above and analyzed for cysteic acid by the chromatographic procedure [4].

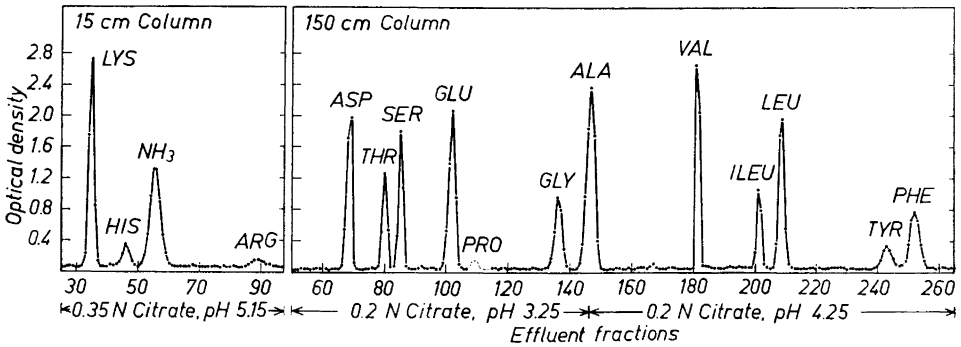

Fig. 1. Eluation patterns given by a 70 h hydrolysate of the electrophoretically faster component of leghemoglobin on Amberlite IR—120 columns. The data are given in optical densities at 570 mμ without corrections for base-line colors and for different color yields of the individual amino acids. The dashed curve for proline gives the optical density at 440 mμ with the base line corrected to that of the other amino acids. The abscissa shows the number of 2-ml fractions collected. The amount of hydrolysate put on the columns corresponded to 1.627 mg of protein.

Determination of amide ammonia. The procedure used was essentially the same as that described by Laki *et al.*[8] The Conway microdiffusion technique was employed and ammonia was determined by the photometric ninhydrin method of Moore and Stein [5]. The protein was heated in 2 ml of 1 N HCl for 4 h in a stoppered tube in a water bath at 100°C. From the hydrolysates, aliquots were added to Conway vessels containing 0.01 N H_2SO_4 in the inner chamber. Saturated sodium tetraborate solution was added to the outer chamber (200 ml sodium tetraborate and 50 ml 2 N NaOH). After standing over night, the solution of the inner chamber was analyzed for ammonia with the ninhydrin method. In order to get an accurate value for the traces of ammonium salts present in the protein sample, diffusion was allowed to continue as described above for periods of 5 to 24 h with the unhydrolysed protein. Under these conditions a slight liberation of amide ammonia occurred. Since the diffusion of ammonia was completed within 3 h, a linear correction for the liberation of amide ammonia could easily be applied.

RESULTS

Typical elution patterns, from the long and short ion exchange columns, obtained with 70 h hydrolysates of the two main components of Lhb are shown in Figs. 1 and 2. The most striking feature of these patterns is the absence of methionine or methionine sulfoxide as well as cysteine or cystine.

Table 1 lists the results of the duplicate experiments for the various amino acids in the hydrolysates of the two components which had been hydrolysed for 20 and 70 h. The variation is expressed as the average deviation. The data show that the recovery of the greater number of amino acids is independent of time of hydrolysis. Extensive decomposition with increasing time of hydrolysis occurred with tryptophan, threonine and serine only. The destruction of tryptophan was complete and therefore this amino acid was determined spectrophotometrically. The average molar ratio of tyrosine to tryptophan for the intact apoproteins of the two components was found to be 1.03 for the faster component and 0.98 for the slower one.

The concentration of serine and threonine were calculated by extrapolation to zero time of hydrolysis.

A comparison of lenghemoglobin with other proteins in regard to the destruction of various amino acids shows a slightly different behavior. Decreases in

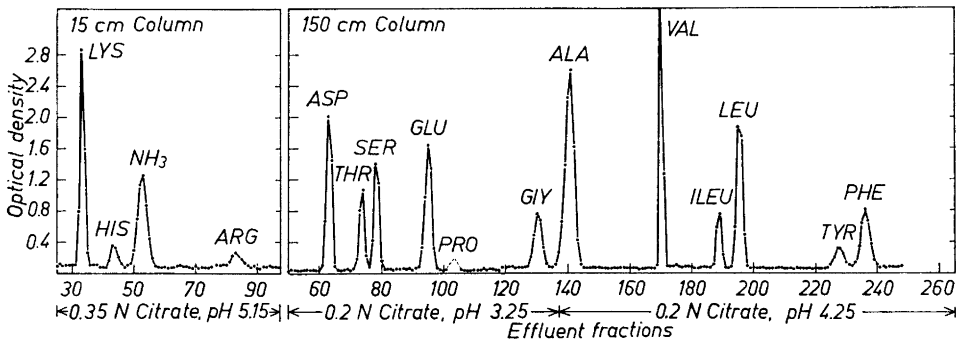

Fig. 2. Eluation patterns given by a 70 h hydrolysate of the electrophoretically slower component of leghemoglobin. The conditions are the same as in Fig. 1. The amount of hydrolysate put on the columns corresponded to 1.519 mg of protein.

Table 1. Amino acid recoveries from the two components of leghemoglobin. The results are in terms of grams of amino acid residue per 100 g of protein.

Amino Acid	Fast component			Slow component		
	Time of hydrolysis		Average or extrapolated value	Time of hydrolysis		Average or extrapolated value
	20 h	70 h		20 h	70 h	
Aspartic acid	8.03 ± 0.11	8.05 ± 0.09	8.04	7.98 ± 0.15	8.03 ± 0.07	8.03
Threonine	4.20 ± 0.05	3.74 ± 0.11	4.38 (a)	4.02 ± 0.00	3.79 ± 0.08	4.10 (a)
Serine	5.43 ± 0.07	4.64 ± 0.10	5.73 (a)	5.35 ± 0.13	4.79 ± 0.22	5.57 (a)
Glutamic acid	10.38 ± 0.11	10.62 ± 0.26	10.62 (b)	9.63 ± 0.32	9.84 ± 0.10	9.84 (b)
Proline	2.94 ±	2.79 ± 0.03	2.88	2.83 ± 0.11	3.04 ± 0.08	3.04 (b)
Glycine	2.61 ± 0.09	2.59 ± 0.00	2.60	2.28 ± 0.00	2.38 ± 0.04	2.38 (b)
Alanine	8.91 ± 0.08	9.04 ± 0.23	9.04 (b)	10.28 ± 0.12	10.89 ± 0.10	10.89 (b)
Valine	6.34 ± 0.14	7.45 ± 0.01	7.45 (b)	7.26 ± 0.05	8.74 ± 0.08	8.74 (b)
Methionine	0.00	0.00	0.00	0.00	0.00	0.00
Isoleucine	3.63 ± 0.07	3.97 ± 0.11	3.97 (b)	2.68 ± 0.05	2.85 ± 0.07	2.85 (b)
Leucine	8.18 ± 0.18	8.28 ± 0.15	8.28 (b)	8.11 ± 0.03	8.56 ± 0.03	8.56 (b)
Tyrosine	2.82 ± 0.04	3.07 ± 0.02	2.95	3.18 ± 0.51	3.25 ± 0.06	3.21
Phenylalanine	6.98 ± 0.25	7.24 ± 0.26	7.11	6.91 ± 0.11	7.10 ± 0.01	7.01
Lysine	9.74 ± 0.22	9.91 ± 0.24	9.83	10.50 ± 0.11	10.52 ± 0.09	10.51
Histidine	1.84 ± 0.09	1.7 ± 0.12	1.77	1.76 ± 0.06	1.95 ± 0.10	1.85
Arginine	0.76 ±	1.3 ± 0.02	1.03	2.13 ± 0.027	2.16	2.15
Cystine	0.00	0.00 (c)	0.00	0.00	0.00 (c)	0.00

(a) These values were obtained by extrapolation to zero time of hydrolysis.
(b) The 70 h value only.
(c) The same result was obtained when cyst(e)ine was determined as cysteic acid in a 50 h hydrolysate of performic acid oxidized protein.

aspartic acid, glutamic acid, arginine and lysine during the acid hydrolysis of carboxypeptidase and papain have been reported by Smith and coworkers [9,10]. Hirs, Stein and Moore have reported decreases in tyrosine, aspartic acid, glutamic acid, proline and arginine during acid hydrolysis of ribonuclease [11]. In the present study none of these amino acids were found to decrease during the period between 20—70 h of hydrolysis.

The yield of valine and *iso*leucine was slightly higher in the 70 h hydrolysates. From earlier work it was expected that the recovery of *iso*leucine and valine was incomplete on short hydrolysis. Peptides in which the carboxyl groups of *iso*leucine or valine are coupled in peptide linkages have shown a great resistance to hydrolysis [9–13]. This depends evidently on a steric hindrance through the branched alkyl residues [14,15]. This phenomenon is not known with leucine. Hence the increase of leucine yield on prolonged hydrolysis evidently depends on the formation of leucine peptides with valine and *iso*leucine. Only 70 h hydrolyses have been used in the final calculation of these amino acids.

Both components seem to lack the sulfur-containing amino acids, although traces of methionine could be detected on some chromatograms. No cystine or cysteic acid could be found in any of the unoxidized preparations. A single run, made after performate oxidation followed by hydrolysis for 50 h, was made

Table 2. Composition and molecular weight of the electrophoretically faster component of leghemoglobin.

Amino Acid	Grams of amino acid residue per 100 g of protein	Minimum molecular weight (d)	Assumed number of residues per molecule	Calculated molecular weight (e)	Calculated numbers of residues for $M = 16\,695$
Aspartic acid	8.04	1 431	12	17 172	11.7
Threonine	4.38 (a)	2 308	7	16 156	7.2
Serine	5.73 (a)	1 520	11	16 720	11.0
Glutamic acid	10.67	1 215	14	17 010	13.7
Proline	2.88	3 371	5	16 855	5.0
Glycine	2.60	2 193	8	17 544	7.6
Alanine	9.04	786	21	16 506	21.2
Valine	7.45	1 330	13	17 290	12.6
Methionine	0.00	—	—	—	—
Isoleucine	3.97	2 848	6	17 088	5.9
Leucine	8.28	1 366	12	16 392	12.2
Tyrosine	2.95	5 528	3	16 584	3.0
Phenylalanine	7.11	2 069	8	16 552	8.1
Lysine	9.83	1 303	13	16 939	12.8
Histidine	1.77	7 745	2	15 490	2.2
Ammonia (NH_2)	0.74 (b)	2 162	8 (b)	17 296	7.7 (b)
Arginine	1.03	15 153	1	15 153	1.1
Cystine	0.00	—	—	—	—
Tryptophan	3.27 (c)	5 691	3	17 073	2.9
Hemin	3.70	—	—	—	—
Totals	92.65		139	16 695	138.2

(a) These values were obtained by extrapolation to zero time of hydrolysis.
(b) These values omitted from the total.
(c) An estimated value based upon a tyrosine/tryptophan ratio of 1.03/1.
(d) (Molecular weight of amino acid residue × 100)/percent of amino acid residue in the protein.
(e) Minimal molecular weight × the nearest integral number of residues.

on both the components (hydrolysates of 2.1 mg of the faster component and 2.7 mg of the slower component were put on the column). No cysteic acid could be detected in these oxidized preparations. As a control, total sulfur was determined on dialysed preparations of the two components after passing them over a column of Lewatit in the OH form in order to remove traces of sulfate. The faster component showed an average sulfur content of 0.055 % S, corresponding to 0.28 atoms of sulfur per protein molecule. The slower component contained 0.15 % S, corresponding to 0.72 atoms of sulfur per protein molecule. In both cases the sulfur content is considerably lower than the minimum required for one sulfur-containing amino acid per molecule of the protein.

The amount of amide nitrogen of the two components was estimated by determining the release of ammonia at 100°C in 1 N HCl. An amide ammonia content of 0.79 % was found for the faster component and 0.66 % for the slower one. These values represent an amide residue content of 0.74 % for the faster

and 0.62 % for the slower component and correspond to 7.7 amide groups per mole for the faster component and 6.0 amide groups per molecule for the slower one.

The present estimates of the composition of the two main components of Lhb are summarized in Tables 2 and 3. For the most stable amino acids the values represent the average of four determinations.

The required limits of accuracy for the estimation of the number of residues of the amino acids in the minimum molecule depends upon the number of residues of any particular amino acid. For the purpose of calculation it has been assumed that if n is the number of residues of the amino acid in question then the maximum permitted variation would be $n \pm 0.4$ and accuracy therefore [16] $\pm 0.4/n$. The limits required for alanine, which is present in leghemoglobin in the largest molar amount, were calculated to be $\pm$ 1.90 % for the

Table 3. Composition and molecular weight of the electrophoretically slower component of leghemoglobin.

Amino Acid	Grams of amino acid residue per 100 g of protein	Minimum molecular weight (d)	Assumed number of residues per molecule	Calculated molecular weight (e)	Calculated number of residues for M = 15 429
Aspartic acid	8.03	1 433	11	15 763	10.8
Threonine	4.10 (a)	2 466	6	14 796	6.3
Serine	5.57 (a)	1 563	10	15 630	9.9
Glutamic acid	9.84	1 317	12	15 804	11.7
Proline	3.04	3 193	5	15 965	4.8
Glycine	2.38	2 398	6	14 388	6.4
Alanine	10.89	652	24	15 648	23.7
Valine	8.74	1 134	14	15 876	13.6
Methionine	0.00	—	—	—	—
Isoleucine	2.85	3 968	4	15 872	3.9
Leucine	8.56	1 321	12	15 852	11.7
Tyrosine	3.21	5 236	3	15 708	2.9
Phenylalanine	7.01	2 098	7	14 686	7.4
Lysine	10.51	1 219	13	15 847	12.7
Histidine	1.85	7 410	2	14 820	2.1
Ammonia (NH_3)	0.62 (b)	2 581	6 (b)	15 486	6.0 (b)
Arginine	2.15	7 260	2	14 520	2.1
Cystine	0.00	—	—	—	—
Tryptophan	3.57 (c)	5 212	3	15 636	3.0
	92.30				
Hemin	3.40				
Totals	95.70		134	15 429	133

(a) These values were obtained by extrapolation to zero time of hydrolysis.
(b) These values omitted from the total.
(c) An estimated value based upon a tyrosine/tryptophan ratio of 0.98/1.
(d) (Molecular weight of amino acid residue × 100)/percent of amino acid residue in the protein.
(e) Minimal molecular weight × the nearest integral number of residues.

faster component ($n = 21$) and $\pm$ 1.60 % for the slower one ($n = 24$). Lysine in the faster component ($n = 13$) requires an accuracy of $\pm$ 3.08 % and in the slower one ($n = 14$) requires an accuracy of $\pm$ 2.86 %. If the analytical data are accurate within 3 %, it should be possible to calculate with assurance the relative number of residues to the nearest integer of each of the amino acids except alanine.

The average molecular weight calculated from all the amino acid residues was found to be 16 695 for the faster component with a standard deviation of $\pm$ 651. For the slower component the average molecular weight was found to be 15 429 with a standard deviation of $\pm$ 548. The molecular weight of 16 800 for the faster component and 15 400 for the slower one obtained by the physical measurements [17] are in good agreement with the recoveries from the Amberlite IR 120 columns. The high degree of accuracy attending the determinations of several amino acids which have been used in the calculations of the minimum molecular weight, adds considerable support to these values. Moreover these estimations are independent of any complications arising from instability of these components, which evidently is the reason for the rather low iron content particularly for the slower component.

When the number as well as the dissociation constants of the various amino acids that make up the protein are known, the theoretical net charges can be calculated as a function of pH. It is assumed that all groups of a given type have the same intrinsic dissociation constant. Although along a peptide chain this may not be true, it nevertheless will provide a value of the proper order of magnitude. The pK values of Cohn and Edsall [18] have been used in this calculation. The terminal amino and carboxyl groups are not considered since they neutralize each other. By subtracting the amount of amide groups from the total amount of carboxyl groups, the theoretical titration curves for both the components could be calculated (Fig. 3). The isoionic point was at pH 4.5 for the apoprotein of the electrophoretically faster component and at pH

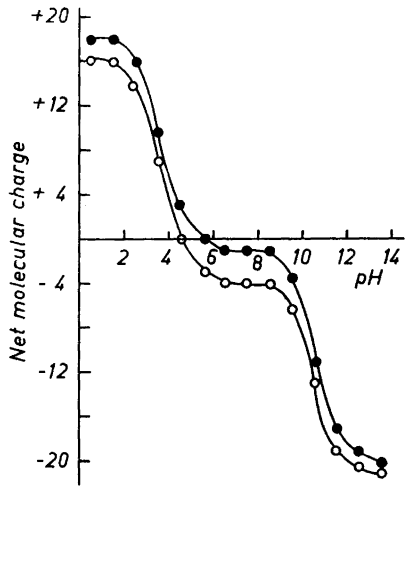

Fig. 3. Charge — pH relationship of the apoprotein of the electrophoretically faster (○) and slower (●) components of leghemoglobin (calculated from the amino acid content on the basis of the following pK's: γ- and δ-carboxyl 3.5, imidazole 5.6, phenol 9.5, ε-amino 10.5, and guanidinium 12.5).

Table 4. Comparative amino acid composition of the electrophoretically faster component of leghemoglobin and some other hemin proteins. The results are in terms of grams of amino acids per 100 g of protein.

Amino Acid	Human Hb A	Human Mb	*Aplysia* Mb	Japanese radish peroxidase	Lhb faster component
Aspartic acid	9.99	8.27	12.71	12.34	9.30
Threonine	5.48	2.85	1.70	5.93	5.16
Serine	4.77	4.43	8.29	9.83	6.93
Glutamic acid	6.89	16.17	9.58	7.06	12.11
Proline	5.22	5.40	0.98	6.58 *	3.42
Glycine	4.46	6.08	4.60	0.76	3.43
Alanine	9.33	5.82	11.66	10.43	11.30
Half cystine		0.00	0.00	2.18	0.00
Valine	10.44	4.64	6.00	4.30	8.81
Methionine	1.25	2.69	1.88	0.97	0.00
Isoleucine	0.02	5.27	4.89	3.62	4.61
Leucine	13.49	13.67	8.73	8.62	9.60
Tyrosine	3.05	2.19	1.48	1.07	3.27
Phenylalanine	7.33	8.22	11.75	5.51	7.80
Histidine	8.32	7.79	1.22	1.19	2.00
Lysine	9.00	19.09	6.89	1.78	11.22
Arginine	3.02	2.47	4.57	3.36	1.15
Tryptophan	2.0	3.40		0.92	3.59
Ammonia (NH_3)		1.22		1.55	0.79

* Proline + hydroxyproline.

5.6 for the apoprotein of the slower one. The two ferri porphyrin carboxyl groups present in the whole leghemoglobin components are omitted from the calculations. These carboxyl groups are expected to contribute somewhat to the acid character of these two proteins. The measured values for the isoelectric points 4.4 for the faster component and 4.7 for the slower one [19], are in good agreement with the isoionic points calculated above for the apoproteins of the two components.

A comparison of Lhb (represented by the electrophoretically faster component) and some other hemin proteins of rather low molecular weight is made in Table 4. These proteins are human (white) hemoglobin A [20] and human myoglobin [21], myoglobin from Mediterranean molluscs (*Aplysia Depilans* and *Aplysia Limacina*) [22] and Japanese radish peroxidase [23].

DISCUSSION

Comparison of the amino acid composition of Lhb with that of hemin proteins of various origins reveals a rather individual pattern of amino acid composition for Lhb (Table 4). Human myoglobin, *Aplysia* myoglobin and leghemoglobin are all in the same low molecular weight range. Lhb and *Aplysia* Mb are rather acidic proteins, whereas human Mb is a neutral protein. The differences in isoelectric points of these proteins are clearly correlated with the major differences in the arginine and lysine contents. In fact, in respect

to nearly all of the amino acids the relative composition of the four proteins are widely different. The most striking difference between Lhb and the other hemin proteins is the absence of the sulfur containing amino acids. This is of special interest because there is now much experimental evidence that all hemoglobins contain SH-groups and that these groups are related to the oxygenation process [24]. Lhb shows in this respect similarities to Mb which also contains no SH-groups.

The complete absence of disulfide bridges in these hemin proteins raises the question of the nature of the tertiary structure of these proteins. Present views ascribe to the α-helix a major role in maintaining coiled peptide chains. By its nature, however, the α-helix is rigid and straight. A molecule made up of the 134—139 amino acids in Lhb all in the form of a single α-helix would have an axial ratio of twenty, whereas in fact both components are nearly spherical. Smith [25] suggests that the covalent bonds involving thiol, imidazole, phenol and possibly other groups linked to carboxyl groups play an important role in maintaining the globular structure. In a protein like myoglobin, which is completely lacking in cysteine or cystine, it is suggested that histidine is implicated in maintaining the regular, globular structure [25].

Looking for some tentative hint of structural relationships among the different hemin proteins, their histidine content deserves special attention particularly as it is generally assumed that histidine functions as a hemelinked group in several hemin proteins. However, the histidine contents of the different proteins seem to vary considerably, even in the proteins containing only one heme per molecule. Lhb shows similarities to *Aplysia* Mb only, which also has a low histidine content.

It is apparent from the data on the amino acid analyses that the two main components definitely represent individual proteins. Several amino acids are present in equal concentrations, within experimental error. The differences in alanine, arginine, glutamic acid, glycine, threonine and valine, although not large, are considered significant. These differences in amino acid content of the two main components seem to satisfactorily explain the differences between the two components in electrophoretic mobility and their behavior on the ion exchange column.

The differences between the two components are rather small and are comparable to those observed in several biologically active proteins where certain amino acids from one species are replaced by other amino acids in another species, without changing the biological properties of the protein. The physical differences are slight because the replacements usually involve a pair of closely related amino acids. The amino acid exchanges most frequently encountered are those first observed in insulin from different species, namely the interchange of valine and *iso*leucine, of serine and glycine, and of alanine and threonine [26,27]. In the case of another peptide hormone, vasopressin, the molecules from the pig and ox are identical except for the presence of an arginine residue in the ox which is replaced by a lysine residue in the pig [28,29]. Of special interest are the amino acid interchanges in the hem-peptide fragments from partial hydrolysates of cytochrome c isolated from different species, namely the interchange of serine and alanine [30], of alanine and glutamic acid [31], and of alanine and leucine [32].

An examination of the differences in amino acid composition between the two main components of Lhb in light of the above examples on interchangeable amino acids suggests that some form of genetic control must be exerted over the synthesis of the globins of the two components.

Acknowledgements. The author wishes to express his thanks to Professor Hugo Theorell for continuous interest in the work. He is also indebted to Dr. Robert Schwyzer, Ciba Ltd., Basel for different samples of synthetic peptides used in this investigation. Able technical assistance has been given by Miss Anne-Marie Fridén. The investigation has been supported by a grant from *Finnish State Commission of Natural Sciences (Statens Naturvetenskapliga Kommission i Finland)* which is gratefully acknowledged.

REFERENCES

1. Ellfolk, N. and Virtanen, A. I. *Acta Chem. Scand.* **6** (1952) 411.
2. Ellfolk, N. *Acta Chem. Scand.* **13** (1959) 596.
3. Ellfolk, N. *Acta Chem. Scand.* **14** (1960) 609.
4. Moore, S., Spackman, D. H. and Stein, W. H. *Anal. Chem.* **30** (1958) 1185.
5. Moore, S. and Stein, W. H. *J. Biol. Chem.* **211** (1954) 907.
6. Bencze, W. L. and Schmid, K. *Anal. Chem.* **29** (1957) 1193.
7. Schram, E., Moore, S. and Bigwood, E. J. *Biochem. J.* **57** (1954) 33.
8. Laki, K., Kominz, D. R., Symonds, P., Lorand, L. and Seegers, W. H. *Arch. Biochem. Biophys.* **49** (1954) 276.
9. Smith, E. L. and Stockell, A. *J. Biol. Chem.* **207** (1954) 501.
10. Smith, E. L., Stockell, A. and Kimmel, J. R. *J. Biol. Chem.* **207** (1954) 551.
11. Hirs, C. H. W., Stein, W. H. and Moore, S. *J. Biol. Chem.* **211** (1954) 941.
12. Harfenist, E. J. *J. Am. Chem. Soc.* **75** (1953) 5528.
13. Wilcox, P. E., Cohen, E. and Tan, W. *J. Biol. Chem.* **228** (1957) 999.
14. Levenson, H. S. and Smith, H. A. *J. Am. Chem. Soc.* **62** (1940) 1556.
15. Newman, M. S. *J. Am. Chem. Soc.* **72** (1950) 4783.
16. Tristram, G. R. *Biochem. J.* **40** (1946) 721.
17. Ellfolk, N. *Acta Chem. Scand.* **14** (1960) 1819.
18. Cohn, E. J. and Edsall, J. F. *Proteins, Amino Acids and Peptides* Reinhold, New York 1943.
19. Ellfolk, N. and Virtanen, A. I. *Acta Chem. Scand.* **4** (1950) 1014.
20. Stein, W. H., Kunkel, H. G., Cole, R. D., Spackman, D. H. and Moore, S. *Biochim. et Biophys. Acta* **24** (1957) 640.
21. Rossi-Fanelli, A., Cavallini, D. and De Marco, C. *Biochim. et Biophys. Acta* **17** (1955) 377.
22. Rossi-Fanelli, A., Antonini, E. and Povoledo, D. in *Symposium on Protein Structure*, (Neuberger, A., Ed.) John Wiley and Sons, New York 1958, p. 144.
23. Morita, Y. and Kameda, K. *Bull Agr. Chem. Soc. Japan* **23** (1959) 1.
24. Riggs, A. in *Sulfur in Proteins*, (ed. R. Benesch, R. E. Benesch, P. D. Boyer, I. M. Kolz, W. R. Middlebrook, A. G. Szent-Györgyi, D. R. Schwarz) Academic Press, New York and London 1959, p. 173.
25. Smith, E. L. *J. Biol. Chem.* **233** (1958) 1392.
26. Brown, H., Sanger, F. and Kitai, R. *Biochem. J.* **60** (1955) 556.
27. Harris, J. I., Sanger, F. and Naughton, M. A. *Arch. Biochem. Biophys.* **65** (1956) 427.
28. Vigneaud, V. du, Lawler, H. C. and Popenoe, A. E. *J. Am. Chem. Soc.* **75** (1953) 4880.
29. Acher, R. and Chauvet, J. *Biochim. et Biophys. Acta* **12** (1953) 487.
30. Tuppy, H. and Paléus, S. *Acta Chem. Scand.* **9** (1955) 353.
31. Tuppy, H. and Dus, K. *Monatsh.* **89** (1958) 407.
32. Paléus, S. and Tuppy, H. *Acta Chem. Scand.* **13** (1959) 641.

Received October 14, 1960.

ACTA CHEMICA SCANDINAVICA 15 (1961) 555–564

Studies on the Hydrolysis of Metal Ions

Part 34. The Hydrolysis of the Indium(III)ion, In^{3+}, in 3 M (Na^+) Cl^- Medium

GEORGE BIEDERMANN, NORMAN C. LI and JUDY YU*

Department of Inorganic Chemistry, The Royal Institute of Technology, Stockholm 70, Sweden, and Department of Chemistry, Duquesne University, Pittsburgh 19, Pa., U.S.A.

The hydrolysis equilibria of In(III) have been studied at 25°C in the ionic medium 3 M$(Na^+)Cl^-$ by measuring the hydrogen ion concentration with a glass electrode. The [In(III)] ranged from 1×10^{-3} to 4×10^{-2} M, and the hydrogen ion concentration was varied from values high enough for the hydrolysis to be negligible to those low enough for a precipitate to be formed. The data could be explained by assuming the equilibria:

$$In^{3+} + H_2O \rightleftharpoons InOH^{2+} + H^+ \qquad \log k_{a1} = -6.9_5 \pm 0.1$$
$$2\,In^{3+} + 2\,H_2O \rightleftharpoons In_2(OH)_2^{4+} + 2\,H^+ \qquad \log \beta_{22} = -10.1_5 \pm 0.1$$

Comparison with the equilibrium constants for the formation of the species $InOH^{2+}$ and $In_2(OH)_2^{4+}$ in 3 M$(Na^+)ClO_4^-$ given in a previous work [1], indicates that in 3 M $(Na^+)Cl^-$ medium the species denoted by the collective formulas "$InOH^{2+}$" and "$In_2(OH)_2^{4+}$" are in reality mainly mixed $Cl^- - OH^-$-complexes (just as "In^{3+}" denotes mainly Cl^- complexes).

The hydrolysis equilibria of the In(III) ion at 25°C have been previously studied by Biedermann [1] who used 3 M $(Na^+)ClO_4^-$ as the ionic medium. The extensive data obtained were explained by assuming the formation of the mononuclear ions $InOH^{2+}$ and $In(OH)_2^+$, and of polynuclear species of the general composition $In(In(OH)_2)_n^{(3+n)+}$, where n is an integer which may take an unlimited series of values. The following equilibrium constants were determined:

* This investigation was started by N. Li and G. Biedermann who carried out a number of preliminary experiments in Stockholm. The main part of the experimental work was then done by N. Li and J. Yu in Pittsburgh. The theoretical interpretation is the responsibility of all the authors.

$$In^{3+} + H_2O \rightleftharpoons InOH^{2+} + H^+;\ \log k_{a1} = \log\{[InOH^{2+}]h[In^{3+}]^{-1}\} = -4.42 \quad (1)$$

$$In^{3+} + 2H_2O \rightleftharpoons In(OH)_2^+ + 2H^+;\ \log k_2 = \log(k_{a1}k_{a2}) =$$
$$\log\{[In(OH)_2^+]h^2[In^{3+}]^{-1}\} = -8.3 \quad (2)$$

$$(n+1)In^{3+} + 2nH_2O \rightleftharpoons In(In(OH)_2)_n^{(3+n)+} + 2nH^+;$$
$$\log K_n = \log\{[In(In(OH)_2)_n^{(3+n)+}]h^{2n}[In^{3+}]^{-(n+1)}\} = -0.52 - n4.69 \quad (3)$$

On the basis of these constants it can be shown that for [In(III)]$> 10^{-3}$M the predominant hydrolysis products are the polynuclear species.

In the present work, the hydrolysis equilibria of In(III) have been investigated in the ionic medium 3 M $(Na^+)Cl^-$. A study of the hydrolysis in this solvent seemed to be of interest for several reasons.

A number of investigators [2-4] have found evidence that In^{3+} forms strong mononuclear complexes with Cl^-. Thus, a comparison of the results obtained in Cl^- and ClO_4^- media may indicate the influence of chloride complex formation on the hydrolysis equilibria. It must be pointed out that, from equilibrium measurements in a constant ionic medium, one may only determine the number of those ions in the products formed whose concentrations are varied. However, no information can be obtained on the number of medium ions bound to the complexes because the concentration of the medium ions is always essentially constant. Thus, if we write $[In_p(OH)_q]$, the "concentration of the species $In_p(OH)_q$" in 3 M $(Na^+)Cl^-$, this symbol is really an abbreviation for the sum

$$[In_p(OH)_q] = \sum_r \sum_s \sum_t [In_p(OH)_qNa_rCl_s)(H_2O)_t] \quad (4)$$

A more detailed discussion on the limitations of the ionic medium method has been given by Sillén [5].

A study of indium solutions containing chloride also has some practical value. Metallic indium is dissolved most easily in a HCl solution, and therefore the starting material in many analytical and preparative methods is an ndium solution with an excess of chloride ions.

METHOD OF INVESTIGATION

All the indium solutions studied were made up to contain 3 M Cl^- by adding sodium chloride, so they had the general composition, B M In(III), H M H^+, (3.000 $-3B-H$) M Na^+, 3 M Cl^- = solution S, where B denotes the total concentration of indium and H is the hydrogen ion concentration assuming no hydrolysis. A series of B values ranging from 0.001 to 0.04 M were investigated. We have not been able to obtain sufficiently accurate data for $B<0.001$ M; this failure is explained by the very low buffer capacity of such dilute indium solutions. It has been of little interest to study solutions of $B>$ about 0.05 M, because the acidity range where appreciable hydrolysis occurs but no precipitate is formed becomes very narrow in concentrated indium solutions.

The hydrolysis equilibria were investigated by measuring the hydrogen ion concentration with the cell

$$-RE \mid \text{solution S} \mid GE + \quad (A)$$

where GE denotes a glass electrode and RE is the reference half-cell

$$\text{Ag, AgCl} \mid \text{3 M NaCl saturated with AgCl(s)} \mid \text{3 M NaCl} \mid$$

The emf of cell (A) may be written at 25°C

$$E = E_0 + 59.15 \log h + 59.15 \log f(H^+) - E_j \qquad (5)$$

where E_0 is a constant, h the hydrogen ion concentration at equilibrium, $f(H^+)$ the activity factor of hydrogen ions and E_j the liquid junction potential at the junction, solution S | 3 M NaCl. The standard state is defined so that $f(H^+)$ as well as the activity factors of the other reacting species tend to unity when the composition of the solution approaches 3 M NaCl. We have assumed that the activity factors may be regarded as constants. It is probable that no serious error is introduced by this assumption since the concentration of the reacting ions was always kept low in comparison with that of the medium ions.

By measuring the emf of the cell

$$\text{RE} \mid h \text{ M } H^+, (3.000 - h) \text{ M } Na^+, 3.000 \text{ M } Cl^- \mid \text{GE}$$

as a function of h, it was found that for, $h < 0.01$ M, E_j becomes less than 0.1 mV. Since the hydrolysis proved to be inappreciable for $\log h > -3$, E_j could be neglected in hydrolyzed solutions when h was calculated with eqn. (5).

Each series of measurements was performed, as is usual in the Stockholm laboratory, as a potentiometric titration. In each series B was kept constant and, by adding a NaOH solution (containing 3 M Cl^-), H was decreased from values where the hydrolysis is negligible to the point where a lasting precipitate was formed. The E data obtained in the region where $H = h$ served to calculate E_0. The analytical excess of hydrogen ions of the indium stock solution was calculated by the equation: $[H^+] = [Cl^-] - 3\,[In(III)]$.

In most cases E_0 was found to be constant within $\pm$ 0.2 mV when $\log H$ was decreased by one unit; this result indicates that the H value calculated from the analytical data is of sufficient accuracy.

In this way, for each series of measurements, we could calculate the average number of hydrogen ions set free per indium atom,

$$Z = \frac{h - H}{B} \qquad (6)$$

as a function of $\log h$. The composition of the hydrolysis products and the corresponding equilibrium constants were ascertained by the study of the family of functions $Z(\log h)_B$. This forms the subject of the "Results" section.

EXPERIMENTAL

Materials and analysis

Indium chloride solutions were prepared from indium metal of 99.93 % purity supplied by Kings Products Co. The metal was dissolved in an excess of a concentrated HCl solution which had been purified by distillation. A large part of the excess HCl, which was required to dissolve the metal rapidly, was then removed by evaporation using an infrared lamp.

In(III) in the indium chloride stock solution was determined by precipitating hydrous indium oxide with a slight excess of NH_3 aq; the precipitate was washed with hot water,

dried at 120°C and was finally ignited at 1 000°C until a constant weight was attained. Some current work by one of us (G. Biedermann) indicates that the precipitate ignited at 1 000°C contains some excess oxygen or water. An error of about 0.2 % is therefore introduced when the ignited oxide is assumed to have exactly the composition of In_2O_3. If rapid analyses are required In(III) may be determined as the oxide, but, for the most accurate work, the sulfide method [6] is to be preferred.

Cl^- in the indium stock solution was determined gravimetrically as AgCl. The analytical excess of the hydrogen ions, H, was calculated from $H = [Cl^-] - 3\,[In(III)]$.

It is essential for the proper functioning of Cl^- | AgCl, Ag half-cells that solutions containing less than 0.001 % Br^- should be used [7]. The *NaCl* solution used in the reference half-cell was therefore prepared from a batch of concentrated HCl and Na_2CO_3 of p.a. quality in which no Br^- ions could be detected using the test of Ref.[7]. The neutral 3 M NaCl solution made from these substances was shaken for several days with an excess of AgCl to attain a saturated solution.

The *NaCl stock solution* used to prepare solution S was made from NaCl p.a. Since this batch of NaCl proved to contain traces of HCl, the stock solution (about 4 M) was carefully neutralized with dilute NaOH using bromothymol blue as indicator.

The *hydrochloric acid* solution was standardized against $KHCO_3$, and the *NaOH* solution against potassium hydrogen phthalate. When the NaOH solution was titrated with the hydrochloric acid the equivalence point found by a Gran plot [8] has agreed within ± 0.1 % with the value calculated on the basis of the standardizations.

N_2 was taken from a cylinder and passed through 3 M NaCl to obtain the vapor pressure of solution S.

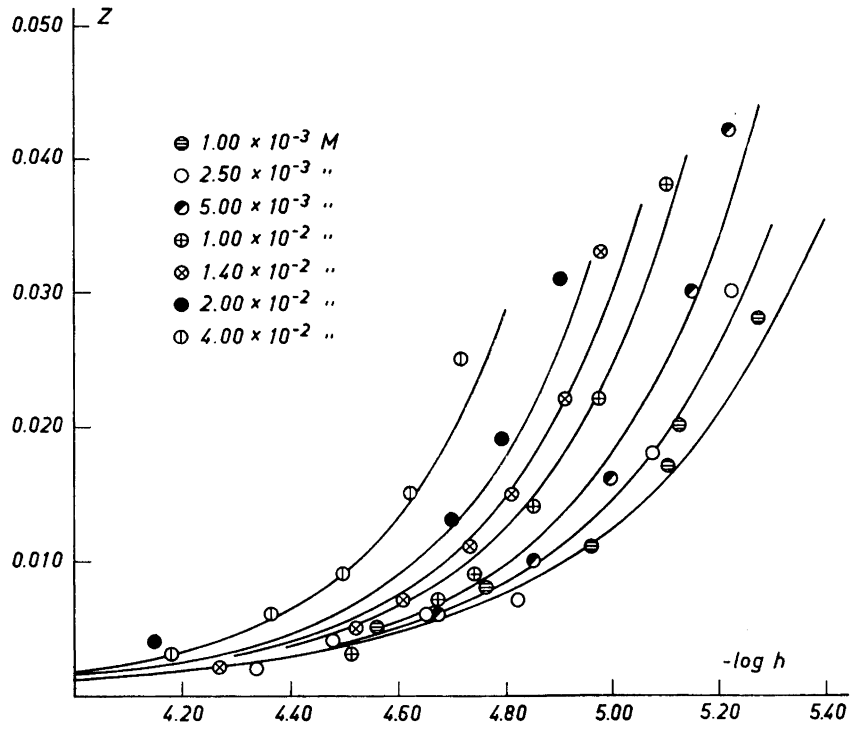

Fig. 1. Z, the average number of hydrogen ions set free by In(III), as a function of log h. The curves are calculated with $\log k_{a1} = -6.9_5$ and $\log \beta_{21} = -10.1_5$.

Emf measurements

All emf measurements were made in a thermostat at 25.0 ± 0.1°C. E was determined with a valve potentiometer Radiometer PHM3, Copenhagen. The reading accuracy of this instrument has been ± 0.1 mV.

The cell arrangement was that described by Forsling, Hietanen and Sillén [9]. Beckman glass electrodes of type No 40498 were employed. AgCl, Ag electrodes were prepared by the method normally used [1] in the Stockholm laboratory.

RESULTS

All the data are summarized in Table 1, and a graphical representation of the experimental results is given in Fig. 1. At Z values exceeding 0.04—0.05, this limit depending somewhat on B, no stable E values could be attained because of the slow formation of a colloidal precipitate which became visible in a couple of hours.

Since $Z(\log h)_B$ is seen in Fig. 1 to be a function of B as well as of h, polynuclear hydrolysis products must be present in considerable amounts. To find the composition of the polynuclear species and the corresponding equilibrium constants, Sillén's method [10] will be followed.

When smoothed curves were drawn through the $Z(\log h)_B$ data these were found for $B \geq 0.01$ M to be approximately parallel, and, for a constant value of Z, the spacing of the curves $\Delta \log B/\Delta \log h$ was about 2. Using the arguments given by Sillén [10], these results indicate that for $B \geq 0.01$ M the main products of the hydrolysis are polynuclear ions having the general composition $In(In(OH)_2)_n^{(3+n)+}$ (n = integer).

If these conclusions are correct, then Z should be a function of the single variable log B—2 log h. The plot $Z(\log B$—2 log $h)$ is shown in Fig. 2; clearly the data for $B \geq 0.01$ M form a single curve which represents the limiting curve for the polynuclear mechanism involving the formation of the species $In(In(OH)_2)_n$.

Table 1. Survey of measurements.

$B = 1.00 \times 10^{-3}$ M		$B = 2.50 \times 10^{-3}$ M		$B = 5.00 \times 10^{-3}$ M		$B = 1.00 \times 10^{-2}$ M		$B = 1.40 \times 10^{-2}$ M	
$-\log h$	Z	$-\log h$	Z	$-\log h$	Z	$-\log h$	Z	$-\log h$	Z
4.560	0.005	4.339	0.002	4.673	0.006	4.515	0.003	4.269	0.002
4.763	0.008	4.479	0.004	4.854	0.010	4.674	0.007	4.525	0.005
4.962	0.011	4.655	0.006	5.001	0.016	4.744	0.009	4.611	0.007
5.107	0.017	4.823	0.007	5.156	0.030	4.855	0.014	4.735	0.011
5.130	0.020	5.080	0.018	5.226	0.042	4.980	0.022	4.813	0.015
5.278	0.028	5.230	0.030			5.108	0.038	4.915	0.022
								4.981	0.033

$B = 2.00 \times 10^{-2}$ M		$B = 4.00 \times 10^{-2}$ M	
$-\log h$	Z	$-\log h$	Z
4.151	0.004	3.823	0.001
4.702	0.013	4.182	0.003
4.796	0.019	4.367	0.006
4.905	0.031	4.500	0.009
		4.624	0.015
		4.720	0.025

Plots of Z(log B—log h) and Z(log B—3 log h) were also tested, but in these cases no limiting curve could be obtained. Thus the accuracy of the data is sufficient to exclude the hypothesis that the polynuclear ions have the composition $In(InOH)_n$ or $In(In(OH)_3)_n$.

Next we made the assumption that a *single polynuclear* species is formed with $n = 1$, *i.e.* $In(In(OH)_2)^{4+}$. This seemed to be reasonable because only very low Z values could be studied. With this hypothesis, Z is given by the equation

$$Z = \frac{2\,\beta_{22}\,b\,h^{-2}}{1 + 2\,\beta_{22}\,b\,h^{-2}} \qquad \beta_{22} = \frac{[In_2(OH)_2^{4+}]\,h^2}{b^2} \qquad b = [In^{3+}] \tag{7}$$

and B, the total concentration of In(III), is equal to

$$B = b(1 + 2\,\beta_{22}\,b\,h^{-2}) \tag{8}$$

It can be seen from (7) and (8) that Z and Bh^{-2} are both functions of the same variable $b\,h^{-2}$, thus Z is a function of $B\,h^{-2}$. This conclusion is the basis of the arguments used above for the composition of the polynuclear species.

The correctness of the assumptions represented by (7) and (8) was tested by comparing the experimental data Z *versus* (log B—2 log h) with the normalized [11] form of (7), Z *versus* log X where

$$Z = \frac{2\,v}{1 + 2\,v} \qquad X = B\,h^{-2}\,\beta_{22} = v\,(1 + 2\,v) \tag{9}$$

and

$$v = \beta_{22}\,b\,h^{-2} \tag{10}$$

When the plot $Z = Z$ (log X) was superimposed on the data Z(log B—2 log h) a good agreement was found for $B \geq 0.01$ M, and the difference log X—(log B —2 log h) in the position of best fit gave log $\beta_{22} = -9.9 \pm 0.1$. The Z(log B —2 log h) curve calculated with log $\beta_{22} = -9.9$ is seen in Fig. 2 to represent, to a good approximation, the experimental data for $B \geq 0.01$ M.

To explain the positive deviations of the Z(log B —2 log h) data from the limiting polynuclear curve for $B \leq 0.005$ M it was assumed that in these dilute indium solutions the only important hydrolysis products are $In_2(OH)_2^{4+}$ and the mononuclear ion $InOH^{2+}$. Then B and Z will be given by the equations

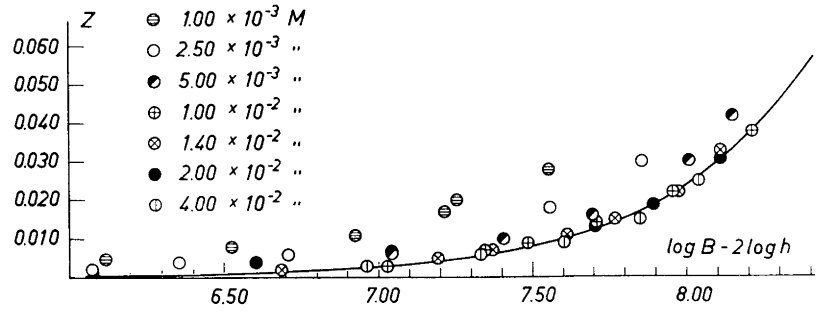

Fig. 2. Z as a function of log B − 2 log h. The limiting curve for the polynuclear mechanism is calculated with log $\beta_{22} = -9.9$.

$$Z = \frac{k_{a1}h^{-1} + 2\beta_{22}\, b\, h^{-2}}{1 + k_{a1}\, h^{-1} + 2\beta_{22}\, b\, h^{-2}};\ k_{a1} = [InOH^{2+}]\ h\ b^{-1} \qquad (11)$$

$$B = b\,(1 + k_{a1}\, h^{-1} + 2\,\beta_{22}\, b\, h^{-2}) \qquad (12)$$

which are the corrected forms of the approximate eqns. (7) and (8). The hypothesis represented by (11) and (12) was checked by calculating k_{a1} in the Z range 0.01 to 0.04 for each experimental point corresponding to B = 1, 2.5, and 5 × 10^{-3} M. The equation used was:

$$k_{a1} = \frac{Z\,h}{1 - Z} - 2\ \beta_{22}\ B\ (1-Z)\ h^{-1} \qquad (13)$$

which is obtained from (11) and (12) by eliminating b.

The calculated k_{a1} values have shown no trend with B or h and as the average value we have estimated log k_{a1} = — 6.9 ± 0.1.

The hypothesis that there are practically only In^{3+}, $In_2(OH)_2^{4+}$ and $In(OH)_2^{+}$ present was also tried. When $k_2 = k_{a1}k_{a2}$ was calculated from an equation corresponding to (13) a trend with h was found which greatly exceeded the experimental uncertainty.

The β_{22} value calculated with (7) and (8) must be regarded as a first approximation because we have neglected the mononuclear species. Similarly k_{a1} may be slightly in error since an approximate value for β_{22} has been used when applying (13). To refine these approximate results a method of calculation is needed which yields independent numerical values for β_{22} and k_{a1}. It would be preferable to apply the approach proposed by Biedermann and Sillén [12] but the low accuracy of the present data makes such a treatment too uncertain. Instead we have attempted to use the easily normalizable function:

$$a = Z\ h^2\ B^{-1}\ (1-Z)^{-2} = \beta_{22}\ (2 + k_{a1}\ \beta_{22}^{-1}\ h\ B^{-1}\ (1-Z)^{-1}) = \qquad (14)$$
$$= \beta_{22}\ (2 + k_{a1}\ \beta_{22}^{-1}\ w)$$

which is obtained from (11) and (12) by eliminating $b = B\,(1-Z)$, substituting it into (12) and rearranging the resulting equation. Thus if $InOH^{2+}$ and $In_2(OH)_2^{4+}$ are the sole products of hydrolysis a should be a function of the single variable w; both a and w may be calculated directly from the experimental data. To find the most probable values for the constants, the experimental log a (log w) data were compared with the normalized form of (14)

$$\log a_1 = \log\,(2 + w_1) = \log a_1\ (\log w_1) \qquad (15)$$

where $a_1 = a\ \beta_{22}^{-1}$ and $w_1 = w\ k_{a1}\ \beta_{22}^{-1}$. Superimposing (15) on the experimental data we have calculated from the differences (log a_1 — log a) and (log w_1 — log w) in the position of best fit the following values:

$$\log k_{a1} = -6.9_5 \pm 0.1$$
$$\log \beta_{22} = -10.1_5 \pm 0.1$$

which are, as would be expected, slightly lower than those found with the first approximation. Fig. 3 shows the log a (log w) data. All of them are seen to lie

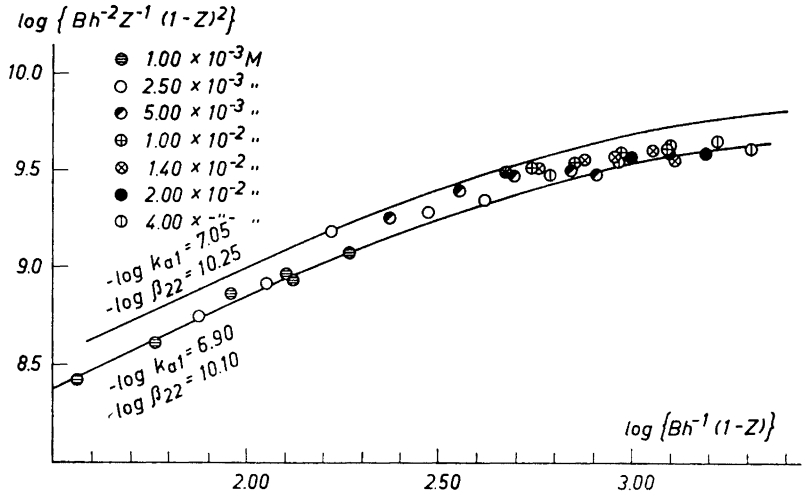

Fig. 3. $-\log a$ as a function of $-\log w$, see eqn. (14). The curves are calculated with the $\log k_{a1}$ and $\log \beta_{22}$ values given in the figure.

between the curves calculated by taking the upper and lower limits of the calculated $\log k_{a1}$ and $\log \beta_{22}$ values.

It should be added that variables as a and w containing the term $(1-Z)$ are to be avoided when Z values near to unity should be considered, because in such a case $1-Z$ is very sensitive to small experimental errors. In the present case $1-Z$ is practically equal to 1, therefore this factor has only a slight influence on the accuracy of a and w.

DISCUSSION

The main conclusion of the present work is that the hydrolysis equilibria in 3 M Cl^- can be interpreted in terms of species containing the same number of indium atoms and OH^- groups as those previously found [1] to be present in 3 M ClO_4^-. It seems that the hydrolysis products have a core built up from strongly bound In^{3+} ions and OH^- groups to which water and anions are attached. The absence of the higher members of the series $In(In(OH)_2)_n$ in 3 M Cl^- is understandable. At the very low Z values available the concentrations of complexes with $n > 1$ might not attain detectable values.

It is difficult to explain quantitatively the magnitude of the differences $k_{a1}(ClO_4^-) - k_{a1}(Cl^-)$ and $\beta_{22}(ClO_4^-) - \beta_{22}(Cl^-)$ because we are not able to estimate the variation of the activity factors of the reacting species when ClO_4^- is entirely replaced by Cl^-. Nevertheless the following arguments suggest that in 3 M $(Na^+)Cl^-$, Cl^- ions are bound to the main part of the hydrolysis products.

If we neglect the variation of the activity factors, and postulate that In^{3+} and its hydrolysis products do not form complexes with ClO_4^-, then we can write by taking into account the definition of $[In_p(OH)_q]$ given by eqn. (4).

$$\frac{k_{a1}\,(ClO_4^-)}{k_{a1}\,(Cl^-)} = \frac{1 + \Sigma\,\beta_n\,[Cl^-]^n}{1 + \Sigma\,\varkappa_m\,[Cl^-]^m} \tag{16}$$

$$\frac{\beta_{22}\,(ClO_4^-)}{\beta_{22}\,(Cl^-)} = \frac{(1 + \Sigma\,\beta_n\,[Cl^-]^n)^2}{1 + \Sigma\,\varkappa'_l\,[Cl^-]^l} \tag{17}$$

$$\beta_n = [InCl_n]\,[In^{3+}]^{-1}\,[Cl^-]^{-n} \tag{18}$$

$$\varkappa_m = [InOHCl_m]\,[InOH^{2+}]^{-1}\,[Cl]^{-m} \tag{19}$$

$$\varkappa'_l = [In_2(OH)_2\,Cl_l]\,[In_2(OH)_2^{4+}]^{-1}\,[Cl^-]^{-l} \tag{20}$$

and n, m, l may take a series of values.

Minimum values for (16) and (17) may be estimated by considering only β_1 and β_2, *i.e.* by assuming that the unknown β_n ($n > 2$) are negligible.

The complex formation at 20°C between In^{3+} and Cl^- has been extensively studied in 2 M $NaClO_4$ by Sundén [2] who was able to explain the data obtained at $[Cl^-]_{tot} \leq 0.5$ M in terms of two cationic complexes only with $\log \beta_1 = 2.15$ and $\log \beta_2 = 3.59$. At high $[Cl^-]_{tot}\,[In(III)]^{-1}$ Sundén [2], Carleson and Irving [3], Kraus *et al.* [4] have found evidence also for the presence of $InCl_3$ and $InCl_4^-$. Thus in our solutions where $[Cl^-]_{tot}[In(III)]^{-1}$ was always kept > 75, $\log(1 + \beta_1\,[Cl^-] + \beta_2[Cl^-]^2)$ is certainly much smaller than $\log\,(1 + \Sigma\,\beta_n[Cl^-]^n)$. As a consequence, we may estimate, using Sundéns β_1 and β_2 values that

$$\log \frac{k_{a1}\,(ClO_4^-)}{k_{a1}\,(Cl^-)} + \log\,(1 + \Sigma\,\varkappa_m\,[Cl^-]^m) \geq \log\,(1 + 3 \times 10^{2.15} + 9 \times 10^{3.59}) = 4.55 \tag{21}$$

and

$$\log \frac{\beta_{22}\,(ClO_4^-)}{\beta_{22}\,(Cl^-)} + \log\,(1 + \Sigma\,\varkappa'_l\,[Cl^-]^l) \geq 9.1 \tag{22}$$

On the other hand we find from our data

$$\log \frac{k_{a1}\,(ClO_4^-)}{k_{a1}\,(Cl^-)} = 2.5 \pm 0.3 \text{ and } \log \frac{\beta_{22}\,(ClO_4^-)}{\beta_{22}\,(Cl^-)} = 5.0 \pm 0.3 \tag{23}$$

Even if the fundamental assumptions leading to (16) and (17) may be regarded at best as crude approximations the difference between (23) and (21—22) indicates that the Σ terms are of the order of 10^2 to 10^4 so that species of the general composition $InOHCl_m$ and $In_2(OH)_2Cl_l$ would predominate in hydrolysed indium solutions containing 3 M Cl^-.

To determine the composition of the mixed complexes, one would have to study the hydrolysis equilibria in a series of solutions of varying $[Cl^-]_{tot}$, while $[Cl^-]_{tot}$ is to be kept at such low values that the influence of the activity factors may be negligible. Attempts should then be made to measure, besides h, the $[In^{3+}]$ and $[Cl^-]$ also.

Acknowledgements. We are indebted to Professor Lars Gunnar Sillén for his great interest in this work and for his valuable criticism. We would like to thank Dr. Helen S. Dunsmore for assistance in some experiments.

This work was financially supported by *Statens Naturvetenskapliga Forskningsråd (Swedish Natural Science Research Council)*, by the *Air Force Office of Scientific Research of the ARDC, USAF*, through its European Office on contract No AF 61 (052) 162 and by the *U.S. Atomic Energy Commission* through Contract No. AI—(30—1)—1922 with Duquesne University.

REFERENCES

1. Biedermann, G. *Arkiv Kemi* **9** (1956) 277.
2. Sundén, N. *Svensk Kem. Tidskr.* **66** (1954) 20, 173, 345.
3. Carleson, B. G. F. and Irving, H. *J. Chem. Soc.* **1954** 4390.
4. Kraus, K. A., Nelson, F. and Smith, G. W. *J. Phys. Chem.* **58** (1954) 11.
5. Sillén, L. G. *J. Inorg. & Nuclear Chem.* **8** (1958) 176.
6. Thiel, A. and Luckmann, H. *Z. anorg. Chem.* **172** (1928) 353.
7. Güntelberg, E. *Thesis*, Copenhagen 1938.
8. Gran, G. *Analyst* **77** (1952) 661.
9. Forsling, W., Hietanen, S. and Sillén, L. G. *Acta Chem. Scand.* **6** (1952) 901.
10. Sillén, L. G. *Acta Chem. Scand.* **8** (1954) 299, 318.
11. Sillén, L. G. *Acta Chem. Scand.* **10** (1956) 186.
12. Biedermann, G. and Sillén, L. G. *Acta Chem. Scand.* **10** (1956) 1011.

Received November 14, 1960.

ACTA CHEMICA SCANDINAVICA 15 (1961) 565–569

The Dimerization of Insulin

KJELD MARCKER and JOHN GRAAE

Universitetets fysisk-kemiske Institut and Universitetets hygiejniske Institut, Copenhagen, Denmark

The dimerization of insulin has been investigated by determinations of the molecular weight of insulin which has been treated with silver ions, and of insulin treated with cyanide. It is shown that silver ions prevent the formation of the dimer and that the addition of cyanide results in a reversal of the dimerization. In conclusion it is proposed that the dimerization of insulin proceeds by a disulfide interchange mechanism. The silver-insulin compound has been shown to be biologically active with a slightly prolonged effect.

It has long been known that insulin is polymerized in aqueous solution. From numerous investigations it is known that the polymerization depends upon the presence of metal ions, especially zinc, in the solution. Crystalline zinc-insulin containing two atoms of zinc per unit cell has been shown to be monodisperse in solution at basic and neutral pH having a molecular weight of 36 000 [1] which corresponds to six monomer units. It is generally believed that the structure of the zinc containing unit cell (*M.* 36 000) consists of three molecules having a molecular weight of 12 000 combined by means of the two zinc atoms. In a previous publication [1] it has been shown that the site of binding of the zinc is the N-terminal amino groups of insulin.

The behaviour of zinc-free insulin, however, is quite different. In the entire pH range zinc-free insulin is inhomogeneous with respect to molecular weight which depends on pH and insulin concentration [2]. While the association of insulin by means of zinc seems fairly well understood, nothing definite is known concerning the association of zinc-free insulin. It has been suggested that the latter may proceed by interactions of non-polar groups [3]. Anyhow it seems that the association monomer to dimer proceeds by a reaction which is different from the one leading to association of dimers to higher polymers, because the dimer is a rather stable unit. In fact it was for a long time believed that 12 000 was the minimum molecular weight of insulin. It should also be pointed out that the dimer is the building stone in the zinc-containing unit cell. It must be stressed, however, that the suggestions [4,5] hitherto reported concerning the difference between dimerization and subsequent polymerization have been of a purely speculative nature, but the results of a previous

experimental investigation [2] seemed to indicate that the difference actually exists.

In 1956 Fredericq [5] proposed that the dimerization proceeds by a disulfide interchange mechanism as shown in the following scheme:

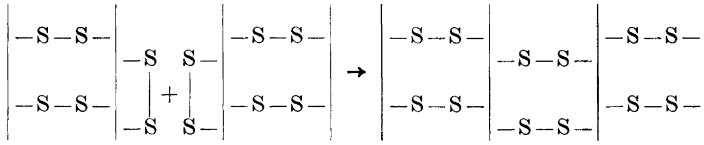

This suggestion was rejected when Sanger [5] pointed out that this structure by hydrolysis would lead to the formation of peptides other than those actually obtained by him. It was also stated that the outer disulfide bridge has a stability similar to the stability of the two other disulfide bridges. Sangers arguments, however, only hold if it is assumed that the two monomers have a parallel arrangement in the dimer, but assuming an antiparallel arrangement, having the following schematic formula:

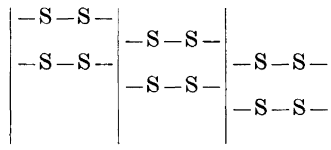

one would get exactly the same peptides as were isolated by Sanger. Concerning the question about the stability of the disulfide bridges Lindsey [6] has later shown that the outer disulfide bridge actually is more labile than the other two.

It is now generally accepted that sulfhydryl-disulfide reactions proceed by a cleavage of the disulfide bond induced by the mercaptide ion [7,8]:

$$R{-}S{-}S{-}R + R'S^- \rightarrow R{-}S{-}S{-}R' + RS^- \quad (1)$$

$$R{-}S{-}S{-}R' + R'S^- \rightarrow R'{-}S{-}S{-}R' + RS^- \quad (2)$$

It is to be expected that interchange reactions of this type would proceed at a more rapid rate as the pH and thus the mercaptide ion concentration is increased. In the case of compounds which contain no sulfhydryl group, the disulfide interchange reaction in neutral or basic solution appears to proceed by a similar mechanism [7,8], the initiating sulfhydryl group being produced by the hydrolysis of the disulfide bond:

$$R{-}S{-}S{-}R + H_2O \rightarrow RSOH + RSH \quad (3)$$

Most observations of sulfhydryl-disulfide interchange and disulfide interchange in proteins have been concerned with phenomena accompanying protein denaturation, chiefly those of aggregation, but these reactions have also been shown to participate in reversible protein association in the absence of denaturing agents, *e.g.* the dimerization of bovine plasma albumin [9] and the asso-

ciation of soluble feather keratin [10]. These associations have been shown to be freely reversible by such relatively mild manipulations as dilutions or changes in pH, which have the same effect upon insulin association [2]. The dimerization of bovine plasma albumin can be reversed or completely inhibited by addition of mercury chloride. In the experiments reported here silver nitrate is employed instead of mercury chloride since mercury ions have been shown to be involved in the formation of protein dimers under certain conditions [11].

The insulin preparations used were zinc-free insulin and crystalline zinc-insulin containing two atoms of zinc per unit cell. Determinations of the molecular weight were performed by means of the inverted microosmometer described by Christiansen and Jensen [12].

Zinc-free insulin was dissolved in 0.2 M KNO_3 at pH 8.6 to give a concentration of 0.1 %. Under these conditions insulin consists mainly of the monomer [2]. The calculated amount of $AgNO_3$ (one mole per monomer) was added and the solution was then acidified to pH 2. At this pH insulin mainly is present as the dimer [2]. Finally the molecular weight was determined.

From the results recorded in Table 1 it is clearly seen that the presence of silver ions effectively prevents the formation of the dimer. It is also seen that the addition of silver ions results in a breakdown of the hexamer unit into monomers. The solubility of the silver insulin differs from that of insulin itself. The range of the isoelectric precipitation of the silver-insulin is extended towards the acid region to about pH 2.

Treatment of zinc-free insulin with cyanide was also tried. Cyanide is known to cleave disulfides in the following manner [7,8]:

$$R-S-S-R' + CN^- \rightarrow RSCN + R'S^- \quad (4)$$

It was therefore expected that treatment of insulin with cyanide would lead to a splitting of the dimer into monomers. The result of this experiment is recorded in Table 2 from which it can be concluded that treatment of insulin with cyanide results in a reversal of the dimerization.

The simplest explanation of the results reported in this paper is that the dimerization of insulin proceeds by a disulfide interchange mechanism. These reactions proceed by the intermediate formation of a mercaptide ion by a hydrolytic cleavage of the disulfide:

Table 1. Apparent molecular weights of different insulin preparations treated as described in the text. All preparations dissolved at pH 8.6.

	Treatment	App.mol.wt.	pH
Zinc free insulin	Ag^+ added at pH 8.6	5.9×10^3	2
» » »	Ag^+ added at pH 2	9.3×10^3	2
» » »	No addition of Ag^+	10.5×10^3	2
Crystalline zinc insulin	Ag^+ added at pH 7	5.7×10^3	7

Table 2. Apparent molecular weight of insulin incubated with cyanide under a nitrogen atmosphere. 0.0110 mmole insulin (M 6 000) treated with 0.0120 mmole NaCN. pH = 7.5. 0.1 M barbiturate buffer.

Hours of incubation	0	20	40
App. mol. wt.	15×10^3	6.8×10^3	6.5×10^3

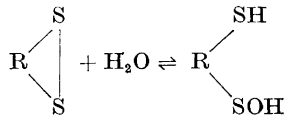

(5)

and the observed inhibition of the dimerization process by silver ions is then readily explained by the following reactions:

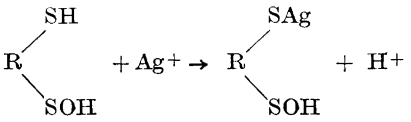

(6)

The reversal in the dimerization observed by cyanide treatment supports this point of view, since cyanide under the experimental conditions chosen has been shown to be highly specific for disulfides [7,8]. It is interesting to note in this connection that oxytocin [13] which has a disulfide bridge with the same configuration as the one present in the A chain in insulin has been shown to dimerize by the same mechanism as here proposed for insulin.

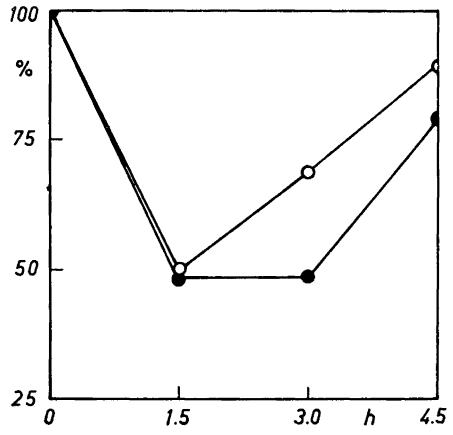

Fig. 1. The action of zinc-free insulin (—○—○—) and silver insulin (—●—●—) in fasting rabbits. Ordinate: Bloodsugar in per cent of initial bloodsugar. Abscissa: Hours after injection. Dose: 0.75 units per rabbit. Cross-over assay on 9 rabbits.

The biological activity of the silver insulin has been tested on rabbits. The result is shown in Fig. 1. Silver insulin is not able to polymerize but exists only as the monomer. Fig. 1 clearly illustrates that this unit is biologically active. The slightly prolonged effect might be due to an inhibition of one of the insulinases present in tissue.

The mentioned dimerization of oxytocin leads to inactivation, and if it is assumed that the dimerization of insulin has the same effect, the dimer would serve as a physiological storage product. Reactivation could then easily be accomplished by a simple dilution by which the monomer is produced. Whether or not the proposed disulfide interchange mechanism plays a role in the physiological action of insulin remains to be investigated, but it is of special interest in this connection that Klotz [14] has pointed out that such a mechanism could furnish a means of electron transport in oxidation-reduction involving sulfhydryl enzymes.

Acknowledgements. The authors thanks are due to Professor J. A. Christiansen, Professor P. Bonnevie, Professor D. Müller, and to Dr. J. Schlichtkrull for their help and advice. Financial support from *Statens Almindelige Videnskabsfond* and *Købmand i Odense Johann og Hanne Weimann født Seedorf's Legat* is gratefully acknowledged. The receipt of "Nordisk Forskningsstipendium" from the University of Oslo is acknowledged by J. G. The insulin preparations were kindly placed at our disposal by "Novo Terapeutisk Laboratorium".

REFERENCES

1. Marcker, K. *Acta Chem. Scand.* **14** (1960) 2071.
2. Marcker, K. *Acta Chem. Scand.* **14** (1960) 194.
3. Oncley, J. L., Ellenbogen, E., Gitlin, G. and Gurd, R. R. N. *J. Phys. Chem.* **56** (1952) 85.
4. Lindley, H. and Rollett, J. S. *Biochim. et Biophys. Acta* **18** (1955) 183.
5. Fredericq, E. *Ciba Foundation Colloquia on Endocrinology* **9** (1956) 119.
6. Lindsey, H. *J. Am. Chem. Soc.* **77** (1955) 4927.
7. Foss, O. *Kgl. Norske Videnskab. Selskab, Skrifter* **18** (1945) No. 2.
8. Parker, A. J. and Kharasch, N. *Chem. Revs.* **59** (1959) 583.
9. Bro, P., Singer, S. J. and Sturtevant, J. M. *J. Am. Chem. Soc.* **80** (1958) 389.
10. Woodin, A. M. *Biochem. J.* **57** (1954) 99.
11. Hughes, W. L. J. *J. Am. Chem. Soc.* **69** (1947) 1836.
12. Christiansen, J. A. and Jensen, C. E. *Acta Chem. Scand.* **7** (1953) 1247.
13. Ressler, C. *Science* **128** (1958) 1281.
14. Klotz, J. M., Ayers, J., Ho, J. Y. C., Horowitz, M. G. and Heiney, R. E. *J. Am. Chem. Soc.* **80** (1958) 2132.

Received October 19, 1960.

ACTA CHEMICA SCANDINAVICA 15 (1961) 570–574

Preliminary Notes on the Separation of Nucleic Acids and Proteins by Counter Flow Electrophoresis

R. ELIASSON, E. HAMMARSTEN, T. LINDAHL and H. PALMSTIERNA

Department of Bacteriology, Karolinska institutet, Stockholm, Sweden

A preliminary account is given of an electrophoretic method using the difference in the migration velocities between the nucleic acids and the most rapid acid proteins and *vice versa* from cell extracts.

It is based on a counter flow of buffer against the direction of the electric migration of the nucleic acids and the acid proteins.

Technical details and some results, including the finding of depolymerase activity in the nucleic acid fraction, are reported.

A separation of proteins and nucleic acids (NA) from cell extracts could be achieved by electrophoresis on long columns stabilized by ethanolized cellulose [1]. The length of the migration path needed to effectuate a separation was 300—320 cm. The diameter of the column was 35 mm, and in a few cases 80 mm (not published). Some material contained in the protein fractions was lost during the fractionation, *e.g.* a neurotoxin from *B. pertussis*. Such long columns gave a too high dilution of the fractions, too much occasion for enzymatic activity, and furthermore work with them was too time consuming.

For these reasons we have tried to replace the long migration path by a steady flow of buffer against the direction of anodically migrating compounds. We call this procedure [2] counter flow electrophoresis (CFE).

The purpose of the present experiments is to test the method especially on freshly made extracts from *E. coli* and to study the small amounts of protein that are met with in the NA. This protein shows depolymerase activity.

METHODS

One condition for a CFE separation is that the NA are in a state permitting them to migrate anodically with a velocity of at least 3 cm/h. It does not always occur in cell extracts, especially not when they contain structures (*e.g.* not disrupted microsomes or virus). Cell extracts that have been made by the use of detergents may cause difficulties due to aggregation, induced by the preparative measures.

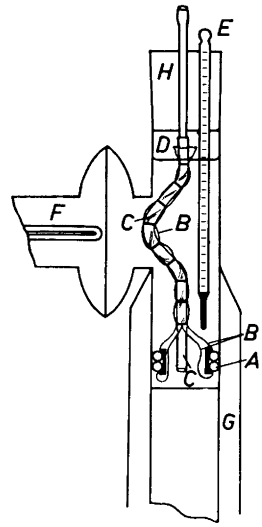

Fig. 1. A: Plastic ring and rubber bearings. B: Dialysis tubing. C: Suction tube. D: Surface of buffer solution and air bubble. E: Thermometer. F: Cooling finger in side tube. G: Cooling jacket. H: Rubber stopper.

The dimensions of the supported columns have been 450 × 35 mm and 33 × 10 mm. Ethanolized cellulose was used as support. The columns and fraction collectors were cooled with running water of + 1°C. The temperature at the top of the columns has been + 9°C during runs at 5 V/cm and 0.03 M M phosphate-0.01 M citrate of pH = 7.4. The electrolyte bathes were kept at + 4°C, and the buffer in them was continually exchanged between the bathes.

The proteins were continuously sucked off from a narrow space above the top of the columns. This space was limited by a plastic ring with rubber

Table 1. Column diameter = 10 mm. Length = 330 mm. Bed volume = 22–23 ml.

Experiment	Sample in mg: Serum albumin	NA	Sum of electrophoretic and counter flow velocities. cm/h.	Recovery in per cent. Protein calculated from the ninhydrin reaction.	NA
		DNA[1]			DNA
1	100	10	3.35	84	31
2	100	10	3.24	81	44
3	100	10	3.25	98	56
4	100	10	3.31	98	74
5	20	20	3.43	100	73
6	—	20	3.26	—	85
		RNA[2]			RNA
7	—	10	2.93	80	104
8		10	2.96	92	93

[1] From calf thymus.
[2] From yeast.

bearings tightly fitting against the ground inner glass wall and a tent of invaginated dialysis tubing (Fig. 1). This is tightly fixed by a plastic cord on the suction tube, the space in the invagination having first been filled with buffer. The suction was effected by micropumps.

In Table 1 some CFE runs are recorded on purified NA and protein. The sum of migration velocity and counter flow of course varies with the bed volume, and that can not be kept constant.

In more recent CFE runs on columns supported by plastic and in other cases by siliconed pyrex beads, where the bed volumes were only about half that of cellulose supports, the sum of velocities was about 6. In these cases the temperature was raised to about + 13°C.

Extracts of *E. coli* using 0.1 M phosphate, pH = 7.4 have been used. The cells were disrupted at −20°C at a pressure of 2.5 tons/cm (Ref. [3]). The cracked cells were extracted at 0°C for two min and immediately centrifuged at 0°C at 150 000 *g* for 30−60 min (horizontally). The pressure on the cracked cells against the bottom of the centrifuge tubes is squeezing out considerably more constituents than are diffusing out by mere extraction. Both DNA and RNA were present in the extracts in about the proportions characteristic for *E. coli* [4]. The supernatant was immediately subjected to CFE.

DISCUSSION AND RESULTS

The *NA* from CFE contains less than 0.1 mg of protein per 100 mg of NA as determined by the ninhydrin reaction after hydrolysis. Serum albumin or glycin were used as standards (Table 2).

Equimolar mixtures of ribose- and deoxyribose-mononucleotides were hydrolysed both in hydrochloric acid and in separate experiments in 88 % formic acid at 170°C. The mononucleotides gave ninhydrin reaction with identical light absorbtion as amino acids from protein. The reaction from proteins, however, was 300−400 times stronger per mg substance than that of the mononucleotides. It may be assumed that the content in the NA fractions of 0.1 % protein is not too low an estimate.

In some experiments $Na_2{}^{35}SO_4$ was included in the medium during the cultivation of *E. coli*. The NA fraction was highly labeled after dilution with inactive sodium sulfate, methionine, cysteine, cystine, and dialysis. Dilution was also made by hydrosulfate and evaporation. These preparations were carried out at + 4°C in 10 times 24 h. The activity in the CFE-protein fraction

Table 2. Column diameter = 10 mm. Length = 330 mm. Bed volume = 22−23 ml.

Experiment	Mg NA in *E. coli* extract. DNA + RNA	Sum of NA-migration and counter flow. cm/h	Protein in mg per 100 mg NA calculated from the ninhydrin reaction.
9	6.7	3.31	—
10	6.0	3.59	0.20
11	6.0	3.45	~0.1
12	6.1	3.37	~0.1

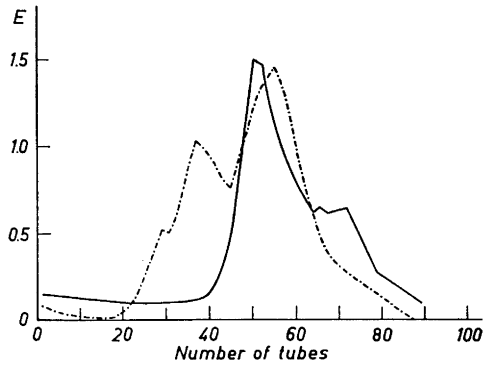

Fig. 2. DNA + serumalbumin. No counter flow. ——— Protein. Light absorbtion. Ninhydrin, 570 mμ. —·—·— DNA. Light absorbtion, 260 mμ. 4 ml per tube.

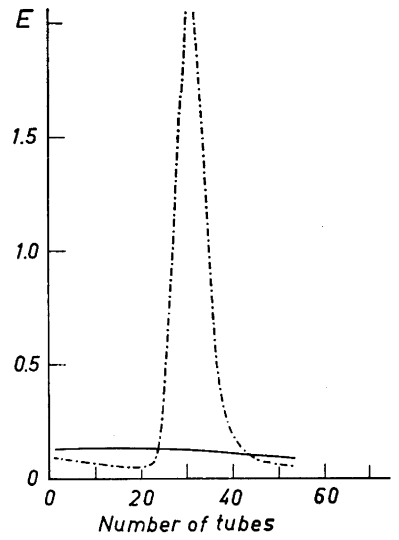

Fig. 3. DNA + serumalbumin. Counter flow. ——— Protein as the ninhydrin reaction at 570 mμ. —·—·— DNA as light absorbtion at 260 mμ. 4 ml per tube.

was about 2.2×10^6 c.p.m./mg protein. After the dilution with H_2S it dropped to 6×10^3 obviously by activation of proteolytic enzymes which have removed sulfur containing amino acids. During the same procedure the activity of the NA fraction was gradually reduced (Table 3).

The protein content in the NA fraction computed from the activities of protein- and NA-fraction has always been higher than the ninhydrin value and variable. In forthcoming experiments the isotope dilution will be made by precipitating the NA out of a mixture of adequate inactive compounds (autolysed NA fraction) (Table 3).

When, as the last step, base analysis was carried out on the assumed 2 700 μg of NA, no bases were found, although the ^{35}S activity was not correspondingly reduced, demonstrating the presence in the NA-fraction of active depolymerases that had not been removed by the CFE.

Table 3.

	Dilution with:		
	Na_2SO_4	S-amino acids	H_2S
$10^{-3} \times$ c.p.m./mg of NA	100	84	50

The reduction in the activity of the depolymerizing enzymes was not greatly less nor more than could be expected from the dilution procedure.

RNase and DNase are in *E. coli* more firmly bound to RNA and DNA than most or all other cell proteins. Considering the instability of NA-preparations a similar arrangement may possibly be expected in other cells. It remains to be seen if this arrangement is more or less general, and if it may have a biological significance.

These preliminary results indicate that the method should be supplemented by unsupported columns, and that lower temperatures are desirable.

The investigation has been supported by the *Research and Liaison Group, U.S. Department of Army*, European Office and by *Cernelle Ltd.*, Vegeholm, Sweden.

REFERENCES

1. Hammarsten, E., Palmstierna, H. and Meyer, E. *J. Biochem. and Microbiol. Technol. Engg.* **1** (1959) 273.
2. Eliasson, R., Hammarsten, E. and Palmstierna, H. *Acta Chem. Scand. In press.*
3. Edebo, L. *J. Bioch. Microbiol. Technol. Engg. In press.*
4. Eliasson, N. A., Hammarsten, E., Palmstierna, H. and Åqvist, S. *Acta Chem. Scand.* **11** (1957) 1381.

Received October 8, 1960.

ACTA CHEMICA SCANDINAVICA 15 (1961) 575–582

Further Studies on S-Substituted Phosphorothioic Acids *

Mixed Lithiumsodium Salts of S-(1-Carboxyethyl) Phosphorothioic Acid and S-(2-Carboxyethyl) Phosphorothioic Acid

STIG ÅKERFELDT

Biochemistry Section, Eastern Pennsylvania Psychiatric Institute, Philadelphia 29, Pennsylvania, U.S.A.

1. The two title compounds were prepared and their rate of hydrolysis as a function of pH was studied at 37°. *Ortho*phosphate and the corresponding thiol were formed and a maximum rate of hydrolysis was observed at about pH 4 for both compounds.
2. The reaction between iodine and the two title compounds was investigated.
3. Methods for the colorimetric determination of S-substituted phosphorothioic acids are described and discussed.

The S—P bond in S-substituted phosphorothioic acids has proven to be a very easily hydrolyzable one. Indeed, the lability of this bond in hot acid solutions places S-substituted phosphorothioic acids among the most labile phosphate esters known.

Only a few compounds of this category have previously been synthesized by others [5–10]. Several of these compounds, however, were obtained in a highly impure state [9,10].

The rate of hydrolysis of the S—P bond in S-substituted phosphorothioic acids seems to be markedly effected by the pH of the medium. Thus, both S-(*n*-butyl) phosphorothioate [8] and cysteamine S-phosphate [4] are hydrolyzed at a maximum rate around pH 3 at 37°.

Investigations of the properties of the S—P bond in S-substituted phosphorothioic acids has now been extended to include two new compounds, namely the mixed lithiumsodium salts of S-(1-carboxyethyl) phosphorothioic acid and S-(2-carboxyethyl) phosphorothioic acid.

* Previous work by the author on this subject has appeared in Refs.[1-4]

RESULTS AND DISCUSSION

Synthetic methods. The S-substituted phosphorothioic acids synthesized earlier by others were without exception prepared from the corresponding thiol with the aid of a phosphorylating agent ($POCl_3$[5–9] or dimorpholinophosphinic chloride [10]). This method, however, has several drawbacks: a) thiols containing certain additional functional groups (hydroxyl-, carboxyl-, amino-groups *etc.*) are liable to yield polyphosphorylated products (*cf.* Ref.[6]); b) the thiol group often reacts poorly with the phosphorylating agent; c) the presence of large amounts of phosphates derived from unreacted phosphorylating agent in the reaction mixture introduces purification problems (*cf.* Refs.[5–10]); d) the final yield of S-substituted phosphorothioic acid is usually small depending on the factors mentioned in a), b) and c).

It was demonstrated earlier that trisodium phosphorothioate is a convenient starting material for the preparation of several S-substituted phosphorothioic acids [1,2]. With the use of this compound well defined reaction products were obtained in good yields.

S-(1-carboxyethyl) phosphorothioate (I) was prepared from 2-bromopropionic acid and trisodium phosphorothioate. The reaction proceeded rapidly at room temperature in the presence of excess 2-bromopropionic acid, and a quantitative reaction of the phosphorothioate ion was obtained.

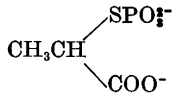

I

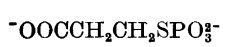

II

S-(2-carboxyethyl) phosphorothioate (II) was prepared in two ways: a) by reaction of 3-bromopropionic acid with trisodium phosphorothioate; and b) by addition of trisodium phosphorothioate to methyl acrylate followed by hydrolysis of the methoxycarbonyl group with strong alkali. Method b) is based on the earlier observation [2] that methyl acrylate adds trisodium phosphorothioate to the double bond forming S-[2-(methoxycarbonyl)ethyl] phosphorothioate. This reaction proceeds rapidly at room temperature, and with an excess of methyl acrylate a quantitative reaction of the trisodium phosphorothioate was obtained. Treatment of the resulting compound with strong alkali at low temperature results in the rapid hydrolysis of the methoxycarbonyl group, whereas the S—P bond in the molecule is virtually unaffected by this treatment.

3,3′-Dithiodipropionic acid was previously isolated as the product obtained after acid hydrolysis and subsequent iodine oxidation of the reaction product between methyl acrylate and trisodium phosphorothioate. From this result the conclusion was drawn that the phosphorothioate residue was attached to carbon No. 3 of the propionic acid part of the molecule. A search for S-(1-carboxyethyl) phosphorothioate as a contaminant of the major reaction product has now been undertaken. It has been concluded from the following that the presence of this substance, even in trace amounts, is unlikely: a) S-(1-carboxyethyl) phosphorothioate and S-(2-carboxyethyl) phosphorothioate

can be separated from each other (and from *ortho*phosphate) by paper chromatography in the solvent systems (Whatman No. 4 papers, ascending method): I. *iso*-propanol: *tert.*-butanol: NH_3 (29 %) : H_2O, 40:20:1:39 (R_F's 0.56 and 0.77, respectively); II. *iso*-propanol:N,N-dimethylformamide: *n*-butanol: NH_3(29 %): H_2O, 20:20:20:1:39 (R_F's 0.40 and 0.62, respectively). *Ortho*phosphate has an R_F of 0.43 in I and 0.28 in II. The reaction product from trisodium phosphorothioate and methyl acrylate was analyzed in the above solvent systems after hydrolysis in strong alkali. Only a spot corresponding in position to that of S-(2-carboxyethyl) phosphorothioate was found in this way. b) Paper chromatography according to Ref.[11] of acid hydrolysate of the reaction product, coupled to 2-chloromercuri-6-nitrophenol in alkaline solution *, gave only one spot, identical in position to MNP-3-mercaptopropionic acid in all four solvent systems listed in Ref.[11] No trace of MNP-2-mercaptopropionic acid was detected on the chromatograms. (The R_F's of MNP- 2-mercaptopropionic acid in these solvent systems are 110—124 % of those of MNP-3-mercaptopropionic acid).

Both the S-substituted phosphorothioic acids described in this paper were isolated as their mixed lithiumsodium salts. This affords a simple means of removing small amounts of *ortho*phosphate formed as trilithium phosphate. The preparations obtained in this way were considerably more pure than products isolated as barium or sodium salts.

Both the prepared compounds were found to contain methanol of crystallization. Similarily, Wieland and Lambert [7] found that S-(*n*-butyl) phosphorothioate has a strong affinity for ethanol.

There exists the possibility that the bromopropionic acids used in the preparation of the S-substituted phosphorothioic acids mentioned here could also react with the oxygen atom of the phosphorothioate ion and thus form O-substituted phosphorothioic acids as contaminants. This could also be the case in the methyl acrylate-trisodium phosphorothioate reaction. It is evident from the following, however, that no detectable amounts of such contaminants are present: a) acid hydrolysis of the prepared compounds gave a quantitative yield of thiols, as determined by iodine titration; b) hydrogen sulfide or phosphorothioic acid were not formed in detectable amounts during acid hydrolysis of the compounds (silver ions give a black precipitate or a brown coloring with phosphorothioic acid, which is easily detectable when the phosphorothioate concentration is above *ca.* 100 μM, *i.e.* 20 μg of trisodium phosphorothioate per ml. This test is practically independent of the pH of the solution tested.)

The available evidence therefore indicates that the S-atom is the sole reactive site of the phosphorothioate ion in this type of reactions. Indeed, this was also found to be true when 2-bromoethylammonium bromide and bromoacetic acid react with trisodium phosphorothioate [1,2].

Effect of pH on the hydrolysis of the prepared compounds. Fig. 1 describes the rate of hydrolysis of S-(1-carboxyethyl) phosphorothioate and S-(2-carboxyethyl) phosphorothioate as a function of pH at 37°. The products of hydrolysis

* Preparing the MNP-thiols [11] in alkaline medium prevents the formation of "ghost" spot on the chromatograms.

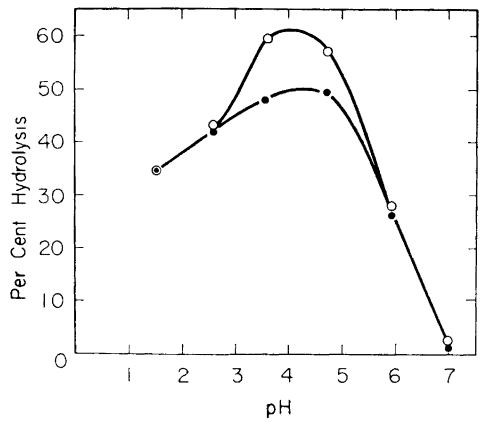

Fig. 1. Effect of pH on the hydrolysis of S-(1-carboxyethyl) phosphorothioate (2.2 mM; filled circles) and S-(2-carboxyethyl) phosphorothioate (2.1 mM; open circles) in 0.1 M citrate buffers. The samples were incubated for 15 min. at 37°C.

are *ortho*phosphate and the corresponding thiol. Both compounds show a maximum rate of hydrolysis at approximately pH 4. Only a very slow rate of hydrolysis is observed at pH 7. Similar hydrolysis curves were found earlier for S-(*n*-butyl) phosphorothioate [8] and for cysteamine S-phosphate [4]. In the case of S-(*n*-butyl) phosphorothioate a mechanism for the hydrolysis was proposed by Herr and Koshland to explain the observed effect of pH [8].

S-(1-carboxyethyl) phosphorothioate and S-(2-carboxyethyl) phosphorothioate are very rapidly hydrolyzed by heat in acid solution. Thus, 2 mM solutions of both compounds in 1 M HCl are completely hydrolyzed in about one minute at 100°, giving a quantitative yield of *ortho*phosphate and the corresponding thiol.

Reaction with iodine. One equivalent of iodine reacts instantaneously with one mole of the synthesized compounds at pH above *ca.* 2. During this process one mole of *ortho*phosphate is formed, and 2,2'-dithiodipropionic acid and 3,3'-dithiodipropionic acid, respectively, were isolated from the resulting solutions.

At pH's below *ca.* 1 the reaction between iodine and the two S-substituted phosphorothioic acids is very slow. Thus, 2 mmole of the compounds in 2 M HCl (50 ml) require more than 2.5 h to decolorize completely an equivalent amount of iodine at 25°C.

The effect of pH on the reaction between iodine and the two compounds described in this paper is similar to the one previously found in the reaction between cysteamine S-phosphate and iodine [4]. The mechanism suggested for the latter reaction [4] could apparently also be applied to explain the effect of pH on the reaction between iodine and the two S-substituted phosphorothioic acids described here.

Colorimetric determination of S-substituted phosphorothioic acids. The ease with which S-substituted phosphorothioic acids are hydrolyzed in hot acid

solutions offers a convenient means for their determination. Both *ortho*-phosphate and the liberated thiol can be determined colorimetrically in the hydrolysate (however, cysteine S-phosphate, as prepared by Binkley [6], seems to behave abnormally). Of these two methods, phosphate determination is the more accurate one (especially if a volatile thiol is formed).

Under certain circumstances it would be of value to have a method available for the liberation of *ortho*phosphate, which is more specific for S-substituted phosphorothioic acids than acid hydrolysis. It was previously shown [1] that cysteamine S-phosphate is rapidly hydrolyzed at room temperature by catalytic amounts of mercury(II) ions (or by 2-chloromercuri-6-nitrophenol), and this finding was utilized for the colorimetric determination of the phosphate residue in this substance. The hydrolysis of cysteamine S-phosphate by mercury(II) ions is not a unique property of this compound. Other phosphate esters, *e.g.* phosphoenolpyruvic acid [12], are known to be hydrolyzed by mercury(II) ions *. Coenzyme A S-phosphate is hydrolyzed by mercury(II) salts (in rather high concentrations [10]), and S-(*n*-butyl) phosphorothioate also appears to be hydrolyzed by this treatment [7].

The mercury method [1], when applied to the two S-substituted phosphorothioic acids described in this paper, gave satisfactory results with both compounds (it was found that S-(1-carboxyethyl) phosphorothioate is hydrolyzed quantitatively by the phosphate reagents alone). In the case of cysteamine S-phosphate and S-(2-carboxyethyl) phosphorothioate, copper(II) ions or silver ions can not substitute for the mercury(II) ions in similar concentrations. However, both copper(II) ions and silver ions (*e.g.* in concentrations of 0.5 mM) rapidly liberate *ortho*phosphate from the S-substituted phosphorothioic acids at pH 7.

Like iodine, bromine was found to liberate *ortho*phosphate rapidly and quantitatively from all S-substituted phosphorothioic acids studied by the author. The advantage of bromine over iodine in this respect is that bromine also seems to react rapidly with these compounds in strongly acid solution. Some results from experiments where *ortho*phosphate was determined after bromine treatment of S-substituted phosphorothioic acids are presented in

* However, with the small amounts of mercury(II) ions used in the authors method [1] phosphoenolpyruvate is only partially hydrolyzed.

Table 1. Recovery experiment for the determination of S-substituted phosphorothioic acids by the bromine method.

Substance	Added μmole	Found μmole	Error %
S-(2-Carboxyethyl) phosphorothioate	0.296	0.298	+ 0.7
	0.592	0.591	− 0.2
	0.888	0.885	− 0.3
Cysteamine S-phosphate	0.262	0.264	+ 0.8
	0.524	0.520	− 0.8
	0.786	0.787	+ 0.1

Table 1. Several other acid labile phosphate esters tested, *e.g.* adenosine-5'-triphosphate, do not liberate *ortho*phosphate by treatment with bromine water (*cf.* Ref.[14]). However, *e.g.* quinolphosphates [13] seem to be hydrolyzed by this treatment and phosphoenolpyruvate is hydrolyzed to some extent. Furthermore, Binkley [14] has reported that bromine liberates *ortho*phosphate quantitatively from the phosphorothioate ion.

EXPERIMENTAL

Materials. Trisodium phosphorothioate was prepared as described previously [4]. Methyl acrylate (stabilized with *p*-methoxyphenol) and the 2-resp. 3-bromopropionic acids used were purchased from Eastman Kodak Company.

General methods. Phosphate determinations were carried out using Gomori's [15] method, and thiols were determined according to Grunert and Phillips [16]. Standardization of the latter method was carried out with the use of acid-hydrolyzed solutions of the S-substituted phosphorothioic acids, the purity of which had been previously determined by iodine titrations and phosphate determinations. The hydrolysis rate experiments were performed by following the liberated thiols according to this method.

Methanol was determined using the method of Reid and Salmon [17] after passage of the sample through a double bed ion exchange column consisting of Dowex 50 W-X4 (H^+), top layer, and Dowex 21K (OH^-), bottom layer. Sodium and lithium were determined by flame spectrophotometry *. Lithium was also determined according to Thomason [18] after absorbtion on Dowex 50W-X4 (H^+) and subsequent eluation with 3 M HCl.

Determination of S-substituted phosphorothioic acids with the bromine method. To 0.10 ml of sample, containing 0—1 μmole of S-substituted phosphorothioic acid was added 0.20 ml of a saturated solution of bromine in water. The mixture was allowed to sit at room temperature for 10 min. 0.50 ml of "elon" [15], 1.00 ml of molybdate [15] and 3.20 ml of water were added. The color was developed for 1 h at room temperature and the absorbancy was read in a 1 cm cuvette at 660 mμ against a blank (containing water instead of sample). 1 μmole of S-substituted phosphorothioic acid in the sample gives an absorbancy of 0.712.

Lithiumsodium S-(1-carboxyethyl) phosphorothioate. 5.4 ml (60 mmole) of 2-bromopropionic acid in 30 ml of water were neutralized with 20 % lithium hydroxide under ice cooling. The cold bath was removed and 5.4 g (30 mmole) of trisodium phosphorothioate were added. The mixture was rapidly stirred at room temperature for 1 h, after which time all phosphorothioate had reacted (added silver ions give a clear yellow precipitate; a black or brownish precipitate indicates the presence of unreacted phosphorothioate).

7.0 g (170 mmole) of LiOH, H_2O were added and any precipitate (consisting of Li_3PO_4) was filtered off. 200 ml of N,N-dimethylformamide:methanol, 1:1, were then slowly added, the solution being cooled in an ice bath. The precipitate was filtered off, washed with methanol (100 ml), and redissolved in 30 ml of water. Any precipitate was filtered off and 200 ml of N,N-dimethylformamide:methanol, 1:1 were again added under ice cooling. The precipitate was filtered off and washed with methanol (100 ml). Yield **: 5.5 g (73 %; average of four prepns.). (Found: C 19.3; H 3.3; P 12.4. Calc. for $(PO_3SCH(CH_3)COO)Li_{2.1}Na_{0.9}$, CH_3OH (250): C 19.2; H 3.2; P 12.4. Found for ratios: Li/P = 2.10; Na/P = 0.91 and CH_3OH/P = 0.99.)

* These analyses were kindly performed by Miss Katherine Gallagher.

** All yields are calculated on the amount of Na_3SPO_3 used.

Synthesis of lithiumsodium S-(2-carboxyethyl) phosphorothioate

A. From methyl acrylate. 5.0 g (28 mmole) of trisodium phosphorothioate were dissolved in 50 ml of water and 5.0 ml (55 mmole) of methyl acrylate were added. The mixture was vigorously stirred for 5 min., after which time all the phosphorothioate had reacted (silver ion test; see above). The solution was extracted with 50 ml of benzene to remove excess methyl acrylate. 7.0 g (170 mmole) of $LiOH,H_2O$ were added and the solution was stirred in an ice bath for 30 min. The synthesized substance was precipitated with N,N-dimethylformamide:methanol, 1:1, and purified as described above. Yield: 5.1 g (80 %, average of four prepns.). The substance gave a completely negative hydroxylamine test for ester [20]. (Found: C 17.4; H 2.6; P 13.5. Calc. for $(PO_3SCH_2CH_2COO)$ $Li_{2.6}Na_{0.4}$ $(CH_3OH)_{0.3}(H_2O)_{0.5}$ (229): C: 17.3; H 2.8; P 13.5. Found for ratios: $Li/P = 2.63 \pm 0.04$; $Na/P = 0.37 \pm 0.02$ and $CH_3OH/P = 0.3 \pm 0.1$ (Average from two prepns. $\pm$ maximum deviation).

B. From 3-bromopropionic acid. 5.1 g (33 mmole) of 3-bromopropionic acid were dissolved in 45 ml of water. After neutralization under ice cooling with 20 % LiOH, 5.4 g (30 mmole) of trisodium phosphorothioate were added and the mixture was vigorously stirred for 1.5 h at room temperature, after which time all the phosphorothioate had reacted (silver ion test; see above). 7.0 g (170 mmole) of $LiOH,H_2O$ were added and after filtration the substance was isolated and purified as described under *A*. Yield: 5.7 g (84 %, average of four prepns.). (Found: C 17.3; H 2.6; P 13.6. Analysis for Li, Na and CH_3OH fell within the ranges given under *A*. For calculated values see under *A*.)

Acid hydrolysis and iodine titration of the compounds

1. Lithiumsodium S-(1-carboxyethyl) phosphorothioate. 1.98 mmole * of the substance were hydrolyzed in 30 ml of 5 % HCl at 90° for 5 min. H_2S or phosphorothioic acid were not detected as products of the hydrolysis. The hydrolysate consumed 1.99 matom of iodine as titrated with a standardized iodine solution. Extraction of iodine oxidized hydrolysate with ethylacetate (the water phase contained thiosulfate to reduce some oxidatively formed iodine) gave 2,2'-dithiodipropionic acid, m.p. 125—133° (unsharp, from benzene). Stoner and Dougherty [19] report 127—135° (from ethanol-water and then from benzene). Equiv. wt: found 106; calc. 105.

2. Lithiumsodium S-(2-carboxyethyl) phosphorothioate. The two substances from synthetic methods *A* and *B*, respectively, were hydrolyzed in 5 % HCl as described under *1*. H_2S or phosphorothioic acid were not detected as products of the hydrolysis. 2.18 mmole of substance from method *A* consumed 2.18 matom of iodine and 2.22 mmole of substance from method *B* consumed 2.21 matom of iodine. Extraction of iodine oxidized hydrolysates with ethylacetate (in the presence of thiosulfate) gave in both cases 3,3'-dithiodipropionic acid m.p. 154—155° (corr; from 4-methyl-2-pentanone), undepressed by admixture with an authentical sample.

Iodine treatment of the unhydrolyzed substances. 5.00 mmole each of the S-(1-carboxyethyl) phosphorothioate and the S-(2-carboxyethyl) phosphorothioate were dissolved in 30 ml of 20 % acetic acid. Titration with iodine showed a rapid reduction of 5 matom of iodine (endpoint not sharp; a slow further consumption of iodine was observed, probably indicating sulfoxide formation). Phosphate analysis of the resulting solutions showed the presence of 5.00 $\pm$ 0.04 mmole of *ortho*phosphate in both solutions, which were then acidified with conc. HCl, diluted with water and extracted with ethylacetate in the presence of thiosulfate. 2,2'-dithiodipropionic acid and 3,3'-dithiodipropionic acid were identified in the extracts as described above under *1* and *2*.

The author wishes to thank Miss Sarah Perry and Mrs. Mildred Gale for skillful assistance.

* The amounts taken are based on phosphate determinations.

Addendum. In his recent thesis [21], Ramsay has studied the effect of pH on the hydrolysis of S-(*n*-butyl) phosphorothioate and trisodium phosphorothioate. He finds a maximal rate of hydrolysis at pH 3.5 for the first compound and at pH 3.0 for the second. Jaenicke and Lynen [22] have recently elaborated on the chemistry of certain S-substituted phosphorothioic acids with special reference to coenzyme A S-phosphate.

REFERENCES

1. Åkerfeldt, S. *Acta Chem. Scand.* **13** (1959) 1479.
2. Åkerfeldt, S. *Acta Chem. Scand.* **13** (1959) 1897.
3. Åkerfeldt, S. *Acta Chem. Scand.* **14** (1960) 1019.
4. Åkerfeldt, S. *Acta Chem. Scand.* **14** (1960) 1980.
5. Walsh, E. O'F. *Nature* **169** (1952) 546.
6. Binkley, F. *J. Biol. Chem.* **195** (1952) 283.
7. Wieland, T. and Lambert, R. *Chem. Ber.* **89** (1956) 2476.
8. Herr, E. B. and Koshland, D. E. *Biochim. et Biophys. Acta* **25** (1957) 219.
9. Feuer, G. and Wolleman, M. *Acta Physiol. Acad. Sci. Hung.* **10** (1956) 1.
10. Smith, R. A. *Univ. Microfilms* No. 25286.
11. Åkerfeldt, S. *Acta Chem. Scand.* **13** (1959) 627.
12. Lohmann, K. and Meyerhof, O. *Biochem. Z.* **273** (1934) 60.
13. Todd, A. *Gazz. Chim. Ital.* **89** (1959) 126.
14. Binkley, F. *J. Biol. Chem.* **181** (1949) 317.
15. Gomori, G. *J. Lab. Clin. Med.* **27** (1942) 955.
16. Grunert, R. R. and Phillips, P. H. *Arch. Biochem. Biophys.* **30** (1951) 217.
17. Reid, V. W. and Salmon, D. G. *Analyst* **80** (1955) 704.
18. Thomason, P. F. *Anal. Chem.* **28** (1956) 1527.
19. Stoner, G. G. and Dougherty, G. *J. Am. Chem. Soc.* **63** (1941) 987.
20. Feigl, F. *Spot Tests in Organic Analysis*, Elsevier, Amsterdam 1956, p. 237.
21. Ramsay, O. B. *Univ. Microfilms* No. 60–3607.
22. Jaenicke, L. and Lynen, F. in Boyer, P. D., Lardy, H. and Myrbäck, K. *The Enzymes* (2nd Ed.), Academic Press, New York and London 1960, Vol. 3, p. 3.

Received November 21, 1960.

ACTA CHEMICA SCANDINAVICA 15 (1961) 583–591

Acid-Soluble Nucleotides during Early Embryonic Development of the Sea-Urchin *Paracentrotus lividus*

ROY NILSSON

Department of Zoophysiology, University of Lund, Sweden

Trichloroacetic acid extracts from unfertilized eggs and from different stages during the early development of the sea-urchin *Paracentrotus lividus* were analysed for nucleotides and for inorganic, acid-labile and acid-stable phosphates.

Fertilization was followed by a drop in the content of inorganic phosphate and a rise in the acid-labile and acid-stable phosphates. The acid-labile phosphate afterwards showed cycle variations during the first five divisions with an increase in the concentration during the early part of mitosis and a fall during the later part. The inorganic- and acid-stable phosphate fractions varied inversely with the acid-labile fraction.

The total nucleotide content did not vary appreciably during the first hours of development but showed an appreciable decrease 20 hours after fertilization. The individual compounds, however, varied, the greatest changes taking place in connexion with the fertilization and around the 16–32 cell stages.

During the last few decades the phosphorus metabolism of the sea-urchin embryo has been the subject of several investigations. Zielinski [1] found no change to occur in the inorganic phosphate content during the first cleavages of *P. lividus;* neither did he find any change in the amount of organic pyrophosphates. Similar results were obtained by Örström and Lindberg [2], who were unable to demonstrate any changes in inorganic and acid-labile phosphates following the fertilization of the sea-urchin egg. However, in 1949 Chambers and White [3], who used eggs of *Asteria forbesii* and *Strongylocentrotus dröbachiensis* found that inorganic phosphate disappeared and that acid-labile phosphate increased upon fertilization. According to Chambers and Mende [4], the reaction following fertilization was the incorporation of inorganic phosphate into arginine phosphate. Using enzymatic methods these authors [5] were unable to demonstrate any variation of the amounts of different adenosine nucleotides in various stages cf the first cell cleavage cycle. Recently

Hultin [6], who used chromatographic methods, measured the amounts of ATP *, AMP, UTP and UMP during the development of *Psammechinus miliaris*. He analyzed stages from the fertilization to the plutei stage and found a gradual decrease in the triphosphate content, while the monophosphates increased slightly.

This paper is concerned with determination of the amounts of different phosphate fractions, especially the different nucleotides, during the first 8 h of the embryonic life of the sea-urchin *P. lividus*. The occurrence of these substances in the unfertilized egg was reported in a previous paper [7].

MATERIAL AND METHODS

The sea-urchin species used was *Paracentrotus lividus* collected at *Station Biologique, Roscoff*. The eggs were shed in beakers containing sea water, freed from debris by filtering through gauze and washed four times by decanting with sea water. Dilute suspensions of the eggs were fertilized and allowed to develop in large glass vessels at 16°C. The culture was gently agitated by stirring with a motor driven glass rod. The development was followed by microscopic observation and only cultures with 100 % fertilization and which cleaved synhronously to at least the 32-cell stage were used for analysis. Aliquots were withdrawn from the cultures at different stages in the development, extracted with trichloroacetic acid in the way described previously [7]. A small part of the extract was used for phosphorus-analysis, the main part was freeze-dried and stored at −25°C until further analysis.

Analytical procedures, ion-exchange and paperchromatographic methods were the same as used before [7].

RESULTS

The main purpose of the investigation was to ascertain whether the amounts of the different nucleotides in the unfertilized sea-urchin egg underwent any variations during its development. However, the extract was also first analysed for its content of different phosphate fractions.

Only minor differences were found in the total amount of acid-soluble phosphates. But when the phosphate content was differentiated into phosphate determined as inorganic phosphate (P_i), acid-labile phosphates (P_2 and P_{10}) and acid-stable phosphate, variations were found within each group (Fig. 1). In agreement with the finding of Chambers and Mende [4], the amount of P_i decreased after fertilization, but it increased again before the first cleavage. Cyclic variations with a fall in the P_i content immediately after the cleavage and then an increase before next division recurred, at least during the first five cell divisions.

The fall in the P_i content following fertilization was compensated by an increase in the acid-labile phosphate fractions. Both the P_2- and P_{10} fractions increased after fertilization and afterwards varied inversely with the P_i content. The acid-stable phosphate content also increased upon fertilization, but then varied approximatively with the P_i content up to the 32-cell stage.

* ATP = 5′-adenosine triphosphate; GTP = 5′-guanosine triphosphate
ADP = 5′-adenosine diphosphate; GDP = 5′-guanosine diphosphate
AMP = 5′-adenosine monophosphate; GMP = 5′-guanosine monophosphate
UTP = 5′-uridine triphosphate; CTP = 5′-cytidine triphosphate
UDP = 5′-uridine diphosphate; CDP = 5′-cytidine diphosphate
UMP = 5′-uridine monophosphate; CMP = 5′-cytidine monophosphate
DPN = diphosphopyridine nucleotide; RNA = ribonucleic acid

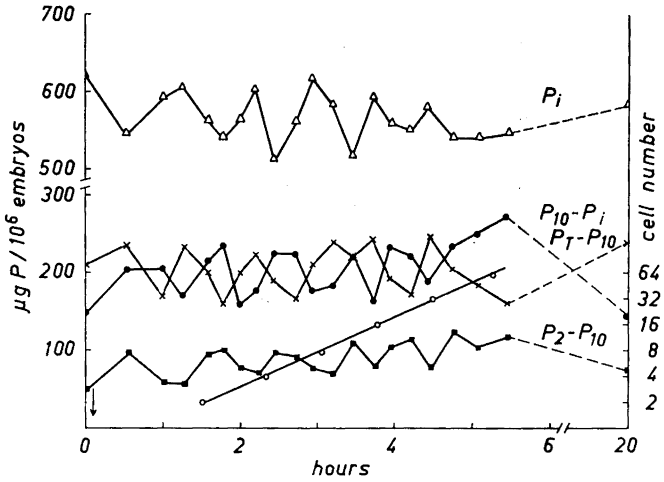

Fig. 1. Variation in the different phosphate fractions during the development of *P. lividus*. (△—△ P_i, ●—● $P_{10}—P_i$, ■—■ $P_2—P_{10}$, ×—× $P_T—P_{10}$, O—O cellnumber). The arrow indicates the time of fertilization.

After the 64-cell stage the synchronicity of the cultures began to disappear and the analysis was therefore not extended beyond this stage.

Like the total amount of the acid-soluble phosphates, the nucleotide content, as measured by the optical density at 260 mμ, did not vary to any greater extent during the period investigated. However, the ultraviolet absorption of the extract is not a true measure of the nucleotide content, as it has been shown [7] that about half of the optical density at 260 mμ in the extract of the unfertilized egg can be ascribed to non-nucleotide compounds. This also holds for the extract from the embryonic stages studied. However, when the amount of optical density at 260 mμ retained on Dowex-1, was taken as a measure of the nucleotide content there were only minor differences in the total nucleotide content of the embryo during the first 8—10 h (Table 1).

Fig. 2 shows a schematic picture of the main nucleotides in the unfertilized egg, in the embryo 8 h after fertilization when it contains about 300 cells, and in the early gastrula 20 h after fertilization. The unfertilized egg contained

Table 1. Amount of ultraviolet absorbing substances measured at 260 mμ in acid extracts from different embryonic stages of *P. lividus*, and the amount of the substances adsorbed on Dowex-1 from the same extracts.

	$E_{260}/10^6$ embryos									
Time in hours	0	1	2	3	4	5	6	7	8	10
Total extract	69	66	66	69	67	66	67	70	67	65
Adsorb.on Dowex-1	34	33	32	32	34	33	32	31	33	31

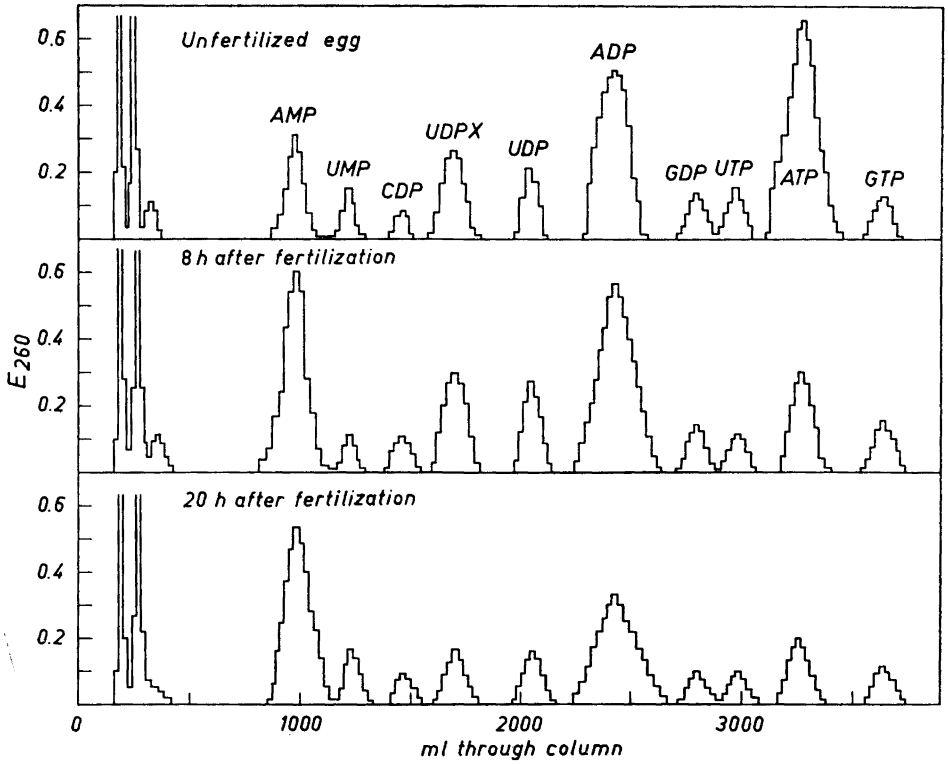

Fig. 2. A schematic picture of ion-exchange chromatograms of trichloroacetic acid extracts from unfertilized *P. lividus* eggs, from embryos 8 h, and 20 h after fertilization. Column: Dowex-1-formate (200—400 mesh, 1 × 20 cm). Elution solution: the formate system previously used [7].

appreciable amounts of ATP and ADP, but only a small amount of AMP. At 8 h after fertilization the ATP content was markedly reduced; the AMP content, increased; and the amount of ADP, largely unchanged. At the time of gastrulation 20 h after fertilization all fractions had diminished, but in relation to ATP and ADP the AMP content showed a further increase.

The other nucleotides demonstrated in the chromatograms were present in such small amounts that no variations in their concentrations could be seen in the figure. The three peaks in the beginning of the chromatograms contained several cytosine- and adenine derivatives some of which were not identified. They contained, amoung other substances, CMP and DPN.

A more detailed picture of the nucleotide content during the first hours of development of the sea-urchin embryo is shown in Fig. 3. The amounts of ATP, ADP, *etc.* were determined at different times up to the 64-cell stage 5.5 h after fertilization and then at 8 and 20 h after fertilization.

Regarding the adenine nucleotides (Fig. 3a), fertilization was followed by a considerable drop in the ATP content, which diminished from 6.5 to 4 μmoles

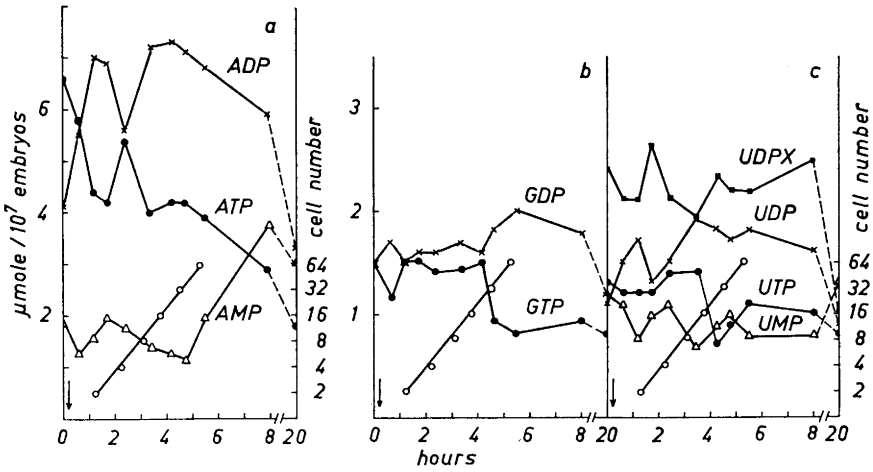

Fig. 3. Variation of adenosine-, guanosine- and uridine nucleotides during the development of *P. lividus*. The arrows indicate the time of fertilization. (O—O cellnumber.)

per 10^7 embryos, a concentration obtained at the time of the first cell division. Between the first and the second division the ATP content increased again to a value of 5.5 µmoles per 10^7 embryos. From the 4-cell stage to the 16-cell stage the amount of ATP then decreased to 4 µmoles. From this stage to the 64-cell stage the content remained fairly constant, but then slowly fell to 3 µmoles at 8 h after fertilization. In the gastrula the ATP content was further reduced to 2 µmoles per 10^7 embryos, *i.e.* a value less than a third of the initial concentration.

The ADP content varied inversely with the ATP content during the first cleavages. The concentration rose from 4 to 7 µmoles, then fell to 5.5 µmoles per 10^7 embryos and rose again to 7 µmoles per 10^7 embryos. After the 16-cell stage the ADP content showed a fall corresponding to that of the ATP content. The ADP content in the early gastrula was only slightly lower than in the unfertilized egg.

The AMP content of the unfertilized egg was low compared with ATP and ADP, and it did not vary appreciably during the first cleavages. However, after the 32-cell stage it showed a steady increase, and at 8 h after fertilization the AMP content was doubled. The amount was somewhat reduced in the early gastrula.

Of the guanine compounds, only GTP and GDP were estimated, the amount of GMP being too small to allow of a reliable analysis. Like ATP, the GTP content dropped in connexion with fertilization, but rose again to the initial value before the first cell division and then remained almost constant to the 32-cell stage. This stage was followed by a fall in the GTP content from 1.5 to 0.8 µmoles per 10^7 embryos. GDP varied roughly inversely with the GTP content (Fig. 3b).

Fig. 3c shows the variations in the uracil nucleotides. Besides the identified UTP, UDP and UMP fractions, a hitherto not completely identified frac-

tion, UDPX, was also estimated. It is an UDP derivative, which on hydrolysis yielded several amino acids including alanine, serine and glutamic acid.

Of the uracil compounds, UTP was affected least by fertilization, its concentration remaining nearly constant during the first cell-divisions. At the 16-cell stage the amount fell to 50 % of the initial value, but then slowly rose again. UMP showed rhythmic variations with the highest concentration in the unfertilized egg, in the 4-cell and 32-cell stages. The variations in the UDP and UDPX content showed a roughly inverse relationsship with a rise in the amount of UDP following fertilization. In connexion with the first cleavage the amount fell but increased again and reached a maxium immediately before the 16-cell stage. The UDP content then slowly decreased.

DISCUSSION

The fertilization of the sea-urchin egg starts a variety of chemical and metabolic reactions, which are the bases of embryonic development. The large number of different reactions make this process very complex and not easy to analyze. However, in the sea-urchin the problem is somewhat simplified by the fact that the embryo does not take up any food during the first period of its life. The changes found in the amounts of different substances can therefore be related entirely to reactions within the embryo. It should, however, be observed that the variations in the amount of a substance is not a measure of the rate of a single reaction but the resultant of both catabolic and anabolic reactions. The resultant may take the form of cyclic variations in the amount of a substance if the catabolic reaction is predominant at one time and the anabolic reaction at another time. The cycles may extend over several mitoses, as was shown by Kavanau [8] for free amino acids and by Bäckström [9,10] for some —SH containing substances and to some extent even for RNA. Fluctuations coinciding with the mitosis were shown by Saki and Dan [11] to be true for TCA-soluble —SH groups, but the best known examples of this type of variation is probably the rhythmic variations in oxygen-uptake found by Zeuthen[12,13] in marine eggs. In the present work both types of variations were found to occur during the early development of the embryo. The variations in the amounts of the different phosphate fractions coincided with phases of the mitotic cycle, while the nucleotide fractions showed cyclic variations covering several cell divisions.

The energy necessary for the development is generally assumed to be derived mainly from the oxidation of carbohydrates stored in the unfertilized egg [1,2]. Lindahl [14] has shown that the respiration, which in the unfertilized egg had a *RQ* of 0.73 indicating fat oxidation, increased after fertilization and further that the increment in respiration had a *RQ* of 1.0 suggesting a carbohydrate utilization. A decrease in the amount of carbohydrates following fertilization was found by Örström and Lindberg [2] and by Chambers and Mende [4].

The energy released on oxidation of carbohydrates is mediated to synthetic processes by means of phosphorylated metabolic intermediates. By determining the amount of the different acid-labile and acid-stable phosphates, it

should therefore be possible to obtain a picture of the energy expenditure during the development of the embryo.

However, as the embryo contains several phosphate esters, estimation of every one of them would be very time-consuming. Therefore, in this work a compromise was made; the acid-soluble phosphates were differentiated by phosphorus analysis into orthophosphate (including organic phosphates, which are hydrolysed to orthophosphate during the analytical procedure), acid-labile phosphates and acid-stable phosphates. One group of the phosphates, the acid-soluble nucleotides, was then analyzed in further detail.

Fertilization of the sea-urchin egg is accompanied by appreciable changes in the different phosphate fractions; a decrease in the orthophosphate content and an increase in the acid-labile phosphate fractions. This is in accordance with the work of Chambers and Mende [4], who showed that the labile phosphate formed was arginine phosphate. This substance is analysed as orthophosphate already after hydrolysis for 2 min. and is therefore easily distinguished from the acid-labile nucleotides, which need hydrolysis for 10 min. to split off inorganic phosphate.

The changes initiated by the fertilization were followed by rhythmic variations in the phosphate fractions for at least the first five mitoses (Fig. 2). The increase in acid-labile phosphate during the first stage of mitosis implies that during this period an energy depot is being built up to be used during the cleavage of the nucleus and the cytoplasm. The variations are synchronous with the variations in the oxygen uptake shown by Zeuthen [12,13] to be valid, at least during certain conditions, for the sea-urchin embryo. The oxygen uptake increased during the prophase and decreased during the later mitotic stages.

Among the nucleotides, the adenosine, guanosine and uridine compounds were studied for any variations in amount (Fig. 3). The adenosine derivatives occurred in the largest amount and they also showed the clearest picture during the development of the sea-urchin (Fig. 3a).

The adenosine nucleotides are generally thought to be connected with the conversion of energy in biological systems and variations in these substances may therefore indicate when substantial changes in energy are taking place. The first change in the nucleotide content was found to be related to the fertilization. This process was accompanied by a large and rapid fall in the ATP content and a corresponding rise in the ADP content. These changes may at least in part be attributed to the use of ATP for the synthesis of arginine phosphate.

$$\text{Arginine} + \text{ATP} \rightleftharpoons \text{Argininephosphate} + \text{ADP}$$

The fall in the concentration of inorganic phosphate depends then on the rephosphorylation of ADP by glycolysis and/or oxidative phosphorylation.

$$\text{ADP} + \text{P}_\text{i} \rightleftharpoons \text{ATP}$$

The fertilization and the first cleavage required a considerable amount of high energy compounds, as is seen from the large decrease in the ATP-content during this period.

This first period of expenditure of energy was followed by a short period — around the second and third divisions — with a net synthesis of ATP. However, the increase in the ATP-content was only temporary and during the rest of the period studied, the amount of ATP and of ADP showed a steady decrease indicating that the embryo is in a period requiring a large supply of energy with a maximal function of the ATP utilizing systems. The preponderance of the energy consuming reactions is not only seen in the decrease in the ATP- and ADP stores but also in the increase of the AMP content. When the ATP concentration is low enough, even the pyrophosphate bond in the ADP molecule can be utilized for energy transfers. For this purpose ADP is dismutated by adenylatekinase to ATP and AMP.

$$2\ \text{ADP} \rightleftharpoons \text{ATP} + \text{AMP}$$

Since ATP constantly being consumed the reaction is shifted to the right resulting in an increased AMP concentration.

The enhanced need for ATP is not only due to synthetic work for development, but also to the fact that after the hatching a large amount of energy is needed for ciliar movement in the swimming embryo.

Of the guanosine phosphates only GTP and GDP occurred in amounts large enough to allow of quantitative estimation. The largest changes in these compounds took place in connection with the fertilization and around the 16—32 cell stages, the early blastula. As mentioned above, the fertilization was followed by an increased respiration and a further increase occurred in the early blastula, as shown by Lindahl [15] and Borei [16]. According to Kavanau [8] the first intensive protein synthesis also begins at this stage. It is known that GTP is a cofactor in transphosphorylations in connexion with oxidation of some intermediates in Krebs' cycle [17,18] and that it is also required for some steps in protein synthesis [19]. One may therefore assume that the fall in the GTP concentration at the periods indicated are related to the increase in these activities.

The most complex picture was shown by the uridine derivatives. It is well known that these compounds are of greatest importance in the carbohydrate metabolism in which they take part as coenzymes and carrier of sugars and sugar fragments. Since the carbohydrate metabolism supplies the major part of the ultimate energy for the development [1,2,14] there should reasonably be wide variations in the different uridine compounds.

Immediately after fertilization, the UDP content increased, but as the UTP content did not change at that time, the increase was not caused by dephosphorylation as in the case of ATP—ADP. Instead, it seemed probable that UDP was released from some other type of nucleotide in connexion with the drop in reducible carbohydrates. The UDP content reached a maxium just before the first cell division was completed and then fell to the original value. A new maximum was, however, reached at the 16-cell stage. At this stage there also started a period of intensive metabolism, as judged by the steep increase in the oxygen consumption found by Lindahl [15]. The increase in the oxygen consumption lasted for about 3 h, and during approximatively the same time the UDP content persisted at a level nearly twice as high as the initial.

The compound from which UDP could be released or into which it could be incorporated may be the fraction called UDPX. This assumption is supported by the fact that the two compounds varied inversely indicating some sort of interaction. Unfortunately UDPX has not been fully identified. It might be a complex fraction containing several very similar nucleotide compounds, but which all contained UDP as the nucleotide moiety.

The UTP content did not show any appreciable change until the 16-cell stage was reached. At that stage, however, it rapidly dropped to half the amount originally present. The drop in the UTP content coincided with that of GTP and may be due to the increase in the metabolism at this stage. It may also be caused by incorporation of nucleotides into RNA, which, according to Bäckström [10], is rapidly synthesized at this time.

Cytidine nucleotides have not been discussed since only CMP occurred in amounts large enough for quantitative measurements. There were, however, also fractions which, judging from the positions in the ion-exchange chromatogram, should be CDP and CTP, respectively. Another cytidine derivative also obtained in too small an amount to allow of accurate measurement was CDP-choline. This compound probably plays a role in the lipid metabolism. Unfortunately the amount of embryonic material available was unsufficient to permit further analysis for this and other cytidine compounds.

I am indebted to Laborator A. Deutsch, Alnarp, for valuable and helpful comments on the manuscript. As part of the work was performed at the Laboratory for Dairy Chemistry and Bacteriology, Alnarp, I wish to thank the Director of the Laboratory, Professor G. Sjöström, for all the facilities put at my disposal. I also wish to thank Miss Christina Olsson for skilfull technical assistance.

This investigation was financially supported by the *Swedish Natural Science Research Council.*

REFERENCES

1. Zielinski, M. A. *Acta Biol. Exptl. (Lodz)* **13** (1939) 35.
2. Örström, A. and Lindberg, O. *Enzymologia* **8** (1940) 367.
3. Chambers, E. L. and White, W. E. *Biol. Bull.* **97** (1949) 225.
4. Chambers, E. L. and Mende, Th. *Exptl. Cell Research* **5** (1953) 508.
5. Chambers, E. L. and Mende, Th. *Arch. Biochem. Biophys.* **44** (1953) 46.
6. Hultin, T. *Exptl. Cell Reseach* **12** (1957) 413.
7. Nilsson, R. *Acta Chem. Scand.* **13** (1959) 395.
8. Kavanau, J. L. *Exptl. Cell Research* **7** (1954) 530.
9. Bäckström, S. *Exptl Cell Research* **16** (1959) 165.
10. Bäckström, S. *Arkiv Zool.* **12** (1959) 339.
11. Saki, H. and Dan, K. *Exptl. Cell Research* **16** (1959) 24.
12. Zeuthen, E. *Am. Naturalist* **83** (1949) 249.
13. Zeuthen, E. *Biol. Bull.* **108** (1955) 366.
14. Lindahl, P. E. *Wilhelm Roux' Arch. Entwicklungsmech. Organ.* **140** (1940) 168.
15. Lindahl, P. E. *Z. vergleich. Physiol.* **27** (1939) 233.
16. Borei, H. *Biol. Bull.* **95** (1948) 124.
17. Sanadi, D. R., Gibson, D. M., Ayengar, P. and Jacob, M. *J. Biol. Chem.* **218** (1956) 505.
18. Gibson, D. M., Ayengar, P. and Sanadi, D. R. *Biochim. et Biophys. Acta* **21** (1956) 86.
19. Keller, E. B. and Zamecnik, P. C. *J. Biol. Chem.* **221** (1956) 45.

Received October 21, 1960.

ACTA CHEMICA SCANDINAVICA 15 (1961) 592–598

Proton Magnetic Resonance Investigations on the Structure of Thujopsene and Hinokiic Acid

STURE FORSÉN and TORBJÖRN NORIN

Research Group for Nuclear Magnetic Resonance, Division of Physical Chemistry, and Division of Organic Chemistry, The Royal Institute of Technology, Stockholm 70, Sweden

The position of the *cyclo*propane ring in the sesquiterpene thujopsene and the corresponding acid, hinokiic acid, has been investigated by proton magnetic resonance (PMR) studies. The structure Ia for thujopsene and hinokiic acid has been confirmed.

On catalytic hydrogenation of the alkenyl-*cyclo*propane system in thujopsene and hinokiic acid, a conjugate addition of hydrogen takes place giving dihydroderivates which, as shown by the PMR spectra, have structure II.

The sesquiterpene thujopsene [1] occurs in the woods of many conifers [2]. It can be oxidised to an α,β-unsaturated carboxylic acid [3,4] identical with the naturally occurring hinokiic acid [2]. From the results of oxidative degradation and of earlier work on hinokiic acid [5] the structure Ib was tentatively suggested for thujopsene and hinokiic acid [2]. Kobayashi, Nagahama and Akiyoshi independently arrived at the same structure for the hydrocarbon [6]. However, further studies have shown that this structure requires modification.

The chemical investigations on the structure of thujopsene and hinokiic acid leading to structure Ia, R = CH_3 and R = COOH, respectively, have been published [7,8]. A simplified reaction scheme showing the relationships between thujopsene, hinokiic acid and some of their degradation products is given in Fig. 1.

On ozonisation thujopsene I gave the ketocarboxylic acid III which could be further oxidised to the C_{14}-dicarboxylic acid IV and easily transformed into the 5-membered ring ketone V. On treatment with potassium borohydride and then with acid the ketocarboxylic acid III furnished the corresponding lactone VII. The ketone V was oxidised to a C_{13}-dicarboxylic acid, which on heating gave a remarkably stable 6-membered ring anhydride VI. The C_{14}-dicarboxylic acid IV, however, gave a 7-membered ring anhydride VIII. The ketone V on reduction with potassium borohydride furnished the corresponding alcohol IX, which on dehydrogenation with selenium gave a-methylnaphthalene X. With methylmagnesium iodide the ketone V gave the alcohol XI, which on dehydrogenation with selenium gave 1,6-dimethylnaphthalene XII.

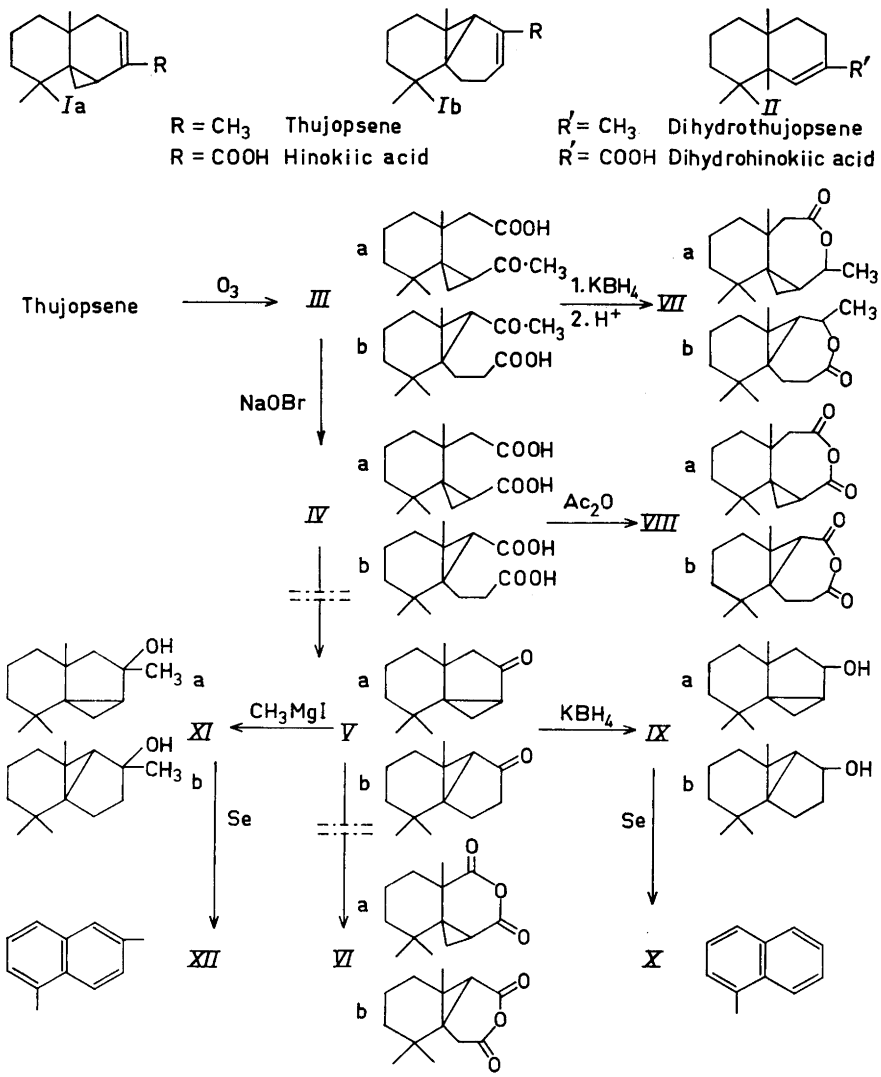

Fig. 1. Simplified reaction scheme showing relationships between thujopsene, hinokiic acid and their degradation products.

The dehydrogenation experiments established the carbon skeleton for the ketone V and located the position of the carbonyl function. UV- and IR-data for this ketone showed that the *cyclo*propane ring is "conjugated" with the carbonyl group. Structures Va and Vb are therefore both possible for the ketone. The keto group in the ketocarboxylic acid III was also shown to be "conjugated" with the *cyclo*propane ring. The problem was therefore to decide between structures Ia and Ib for thujopsene and hinokiic acid.

It was clear that if the number of hydrogens on the *cyclo*propane ring could be determined it would be possible to make a choice between the two structures Ia and Ib for thujopsene and hinokiic acid. The high PMR frequency of the protons on a *cyclo*propane ring (282 cps from benzene at a field of 9 400 gauss) [9] made a PMR approach to this problem seem feasible. It was found, however, that the signal from the hydrogens on the *cyclo*propane ring in thujopsene, hinokiic acid and many of their degradation products appeared at frequencies lower than 282 cps. As a consequence they interfered with signals from angular and geminal methyl groups thus making the interpretation of the PMR spectra difficult. The signals from the *cyclo*propane ring protons could be definitely distinguished in only a few compounds.

The PMR spectrum of thujopsene I is shown in Fig. 2. The signal at 90 cps is clearly due to the proton on the double bond; it may indicate coupling with two non-equivalent hydrogens in a methylene group. The peak at 266 cps is due to the angular methyl group. The shift is somewhat higher than is usually observed for methyl groups at junctions between 5- and 6-membered rings [10,11]. Methyl groups at double bonds in 6-membered rings are usually found at about 216 cps from benzene [9] and this suggests that the peak at 218 cps is due to the methyl group on the double bond in thujopsene I. The area is about that expected and the splitting found may be due to long range coupling with the hydrogen atom on the double bond. In the PMR spectrum of hinokiic acid I, in which this methyl group is oxidised, there is no signal near 218 cps.

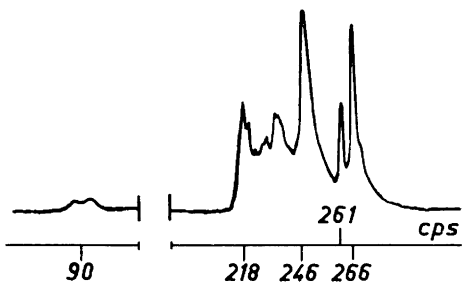

Fig. 2. The PMR spectrum of thujopsene, I, (R = CH_3). Solution in carbon tetrachloride, mole fraction 0.06. Benzene as internal refernece.

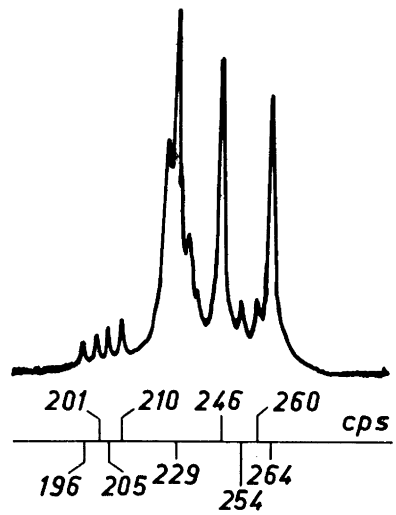

Fig. 3. The PMR spectrum of the C-13 anhydride, VI. Solution in carbon tetrachloride, mole fraction 0.05. Benzene as internal reference.

The signal at 261 cps and the unresolved signal at the base of the 266 cps signal are presumably due to protons on the *cyclo*propane ring. This interpretation favours structure Ia, since structure Ib cannot account for more than one PMR signal from the hydrogen on the *cyclo*propane ring.

The PMR spectrum of the C_{13}-dicarboxylic acid anhydride VI is shown in Fig. 3. Each of the three strong signals at 229 cps (on top of the methylene signals), 246 cps, and 264 cps corresponds to a methyl group. The geminal methyl groups are thus clearly non-equivalent. Models of the anhydride show that in structure VIa the CH_2 group of the *cyclo*propane ring comes very close to one of the geminal methyl groups and the non-equivalence of these two methyl groups may well be due to steric interactions. Inspection of the models indicates that structure VIb is not as crowded as structure VIa. The signals at 246 and 264 cps can be assigned to the geminal methyl groups and the signal at 229 cps to the angular methyl group (see below).

The four peaks at 196, 201, 205, and 210 cps could be due to the methylene group in the α-position to one of the anhydride carbonyl group in structure VIb. Two non-equivalent protons on this α-carbon should, however, give rise to an AB-spectrum (for nomenclature see Ref. [10]) with its characteristic small-large-large-small pattern and the spin coupling constant would be about 12—15 cps. This would not explain the two signals at 254 and 260 cps and is clearly not in agreement with the observed spectrum which is more consistent with structure VIa. As the two methylene protons on the *cyclo*propane ring can be expected to be non-equivalent the spectrum of the three *cyclo*propane ring hydrogens should be of the ABC- or, more likely, the ABX-type. Theoretically the X-part of the ABX-spectrum should consist of six lines. Two lines are however very weak and are not always observed (see Ref.[10] pp. 132—8) and the X-part of the ABX-spectrum can appear as a quartet with peaks of almost equal intensity (see Ref.[10] pp. 245 and 335). The signals at 254 and 260 cps can then be considered as a part of the AB-pattern. Unfortunately, the ABX-spectrum in Fig. 3 is not sufficiently distinct to permit a detailed analysis, but the X-part at about 200 cps can be described by $J_{AX} = 9.0$ cps and $J_{BX} = 5.0$ cps.

The proton on the *cyclo*propane ring and in α-position to one of the carbonyl groups in the C_{13}-anhydride VI has its resonance position at a comparatively low field which may be due to the fact that this proton lies in the C—C—O-plane of the carbonyl group. Jackman has given many examples of a carbonyl group causing shifts towards lower fields of neighbouring protons when these lie in this plane, and has discussed this in terms of the diamagnetic anisotropy of the carbonyl group [12].

Similarly the anisotropy of the other carbonyl group may account for the low resonance field (229 cps) assigned to the protons of the angular methyl group. In the C_{14}-anhydride VIIIa, where the angular methyl is in a β-position to the carbonyl group and thus where the shifts towards lower field should be considerably weaker, the angular methyl signal is at about 260 cps.

In the PMR spectra of the other degradation products containing carbonyl groups (V, VII, and VIII) the region around 200 cps is obscured by signals from the methylene groups in α-positions to the carbonyl group. The two protons on these methylene groups are clearly non-equivalent and give rise to

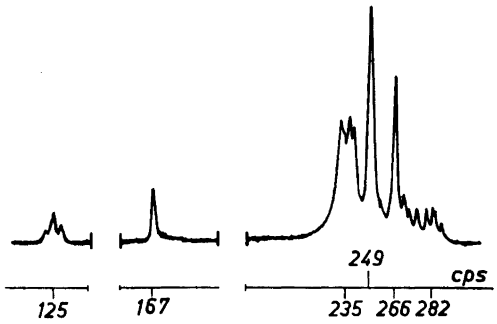

Fig. 4. The PMR spectrum of the alcohol, XI. Solution in carbon tetrachloride, mole fraction 0.06. Benzene as internal reference.

typical AB-patterns with a spin coupling constant J_{AB} = 15—15.5 cps. (For other examples of non-equivalent methylene protons see Refs.[11,13].)

The PMR spectrum of the alcohol IX is shown in Fig. 4. The position of the signal at 167 cps is sensitive to temperature and concentration and it is therefore assigned to the OH-group. The small triplet at 125 cps corresponds to the proton on the same carbon atom as the OH group. The pattern and the coupling constant J = 2.6 cps suggests spin coupling with equivalent or nearly equivalent methylene protons. According to this interpretation the coupling with the neighbouring *cyclo*propane proton is quite small. The disappearance of the spin coupling is not unexpected in the light of the dependence of the coupling on the dihedral angle between protons on adjacent carbon atoms [14,15]. Inspection of molecular models show the dihedral angle in this case to be close to 90° when the spin coupling should be very small. The strong signal at 249 cps corresponds to the geminal methyl groups and the signal at 266 cps to the angular methyl group. The pattern at about 280 cps

Table 1. Methyl group shifts in thujopsene, hinokiic acid and related compounds. (Solutions in carbon tetrachloride, mole fractions 0.04—0.06. Shifts in cps at 40 Mc/s relative to benzene as internal reference.)

Gem-dimethyls	Angular methyls	Compound
246	266	thujopsene (Ia, R = CH_3)
243 and 246	263.5	hinokiic acid (Ia, R = COOH)
253	253	dihydrothujopsene (II, R = CH_3)
250	250	dihydrohinokiic acid (II, R = COOH)
245 and 251	267.5	ketone (Va)
246 and 264 (tentative)	229	C-13 anhydride (VIa)
244 and 252	265	lactone (VIIa)
243 and 259 (tentative)	262	C-14 anhydride (VIIIa)
249	266	alcohol (IXa)

is due to the protons on the *cyclo*propane ring. The observed pattern can hardly be interpreted in terms of structure IXb but can well be part of an ABC-spectrum as would be expected from structure IXa.

The collected evidence from the PMR spectra in Figs. 2—4 leaves little doubt that thujopsene and hinokiic acid must have structure Ia.

As judged from models there seems to be a rough correlation between the non-equivalence of the *gem*-dimethyl groups expressed as difference in the PMR shifts and the degrees of steric interaction between the *cyclo*propane ring and the axial geminal methyl group. It is hoped to discuss this effect in a forthcoming paper. The observed positions of the PMR signals of the geminal methyl and angular methyl groups in the compounds studied in this work are listed in Table 1.

On hydrogenation of thujopsene and hinokiic acid (Ia) over palladised charcoal in methanol, a conjugate addition of hydrogen to the alkenyl*cyclo*propane system evidently takes place. From chemical and infrared evidence, structure II seemed to be correct for dihydrothujopsene and dihydrohinokiic acid [8]. This type of conjugate addition of hydrogen in catalytic hydrogenation has been observed in vinyl*cyclo*propane systems [16].

The PMR spectrum of dihydrothujopsene (Fig. 5) shows three signals, at 252, 253.5, and 254.5 cps, with areas corresponding to four methyl groups. The signal at 224 cps can be assigned to a methyl group on a double bond by comparison with the spectra of hinokiic acid and dihydrohinokiic acid. The signal at 235 cps corresponds to methylene groups.

The PMR spectrum of dihydrohinokiic acid shows a strong signal at 250 cps with an area corresponding to four fortuitously overlapping methyl groups.

The proton on the double bond in dihydrothujopsene II gives rise to a comparatively sharp line at 83 cps (Fig. 5) and the absence of spin splitting would suggest the grouping :C—CH=C:. The relative sharpness of the signal from the proton on the double bond in dihydrohinokiic acid II also suggests the presence of the same grouping.

The observed PMR spectra for dihydrothujopsene and dihydrohinokiic acid are thus in good agreement with structure II for these compounds.

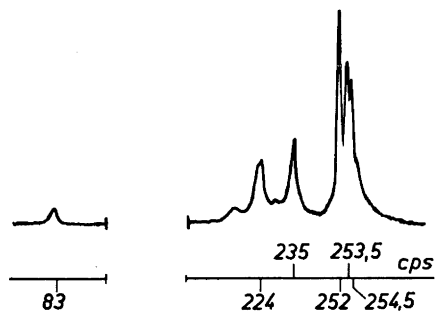

Fig. 5. The PMR spectrum of dihydrothujopsene, II. Solution in carbon tetrachloride, mole fraction 0.05. Benzene as internal reference.

EXPERIMENTAL

The PMR measurements were made with a Varian V-4300 Spectrometer operating at 40 Mc/s and equipped with a Varian V-K 3506 Stabilizer. The sample cells were thin-walled glass tubes with a good filling factor permitting studies at low concentrations. The spectra were recorded with comparatively dilute solutions in carbon tetrachloride (mole fractions 0.04—0.06). The proton chemical shifts in this work were obtained relative to benzene as internal standard. As, however, association between the small amounts of benzene used as internal standard and the substances under study could introduce large errors in the measured shifts, most shifts were also determined against an external benzene standard. The difference in the shifts determined with external and internal benzene standards were approximately constant and equal to 30 cps when no correction was made for macroscopic susceptibility effects. This seemed to justify the use of benzene as internal standard in the dilute carbon tetrachloride solutions.

The shifts were determined in cps by the audio frequency sideband method using a Hewlett-Packard 200 CD Audio Oscillator. The shift measurements were generally reproducible to within $\pm$ 1 cps.

Acknowledgements. The authors wish to thank Professor H. Erdtman and Dr. E. Forslind for their kind encouragement and interest. Thanks are also due to Dr. M. Nilsson for many stimulating discussions and to Dr. B. R. Thomas for revising the language of the manuscript. The cost of the NMR apparatus has been defrayed by grants from *Knut and Alice Wallenbergs Stiftelse.*

REFERENCES

1. Kawamura, J. *Bull. Imp. For. Exp. Stn. Japan* **30** (1930) 59.
2. Erdtman, H. and Norin, T. *Acta Chem. Scand.* **13** (1959) 1124.
3. Hirose, Y. and Nakatsuka, T. *J. Jap. Wood Research Soc.* **4** (1958) 26.
4. Erdtman, H. and Thomas, B. R. *Acta Chem. Scand.* **12** (1958) 267.
5. Okuda, O. *J. Pharm. Soc. Japan* **73** (1953) 9.
6. Kobayashi, H., Nagahama, S. and Akiyoshi, S. *Bull. Chem. Soc. Japan* **32** (1959) 203.
7. Erdtman, H. and Norin, T. *Chem. & Ind. London* **1960** 622.
8. Norin, T. *Acta Chem. Scand* **15** (1961). *In press.*
9. Brownstein, S. *Chem. Revs.* **59** (1959) 463.
10. Pople, J. A., Schneider, W. G. and Bernstein, H. J. *High Resolution Nuclear Magnetic Resonance.* McGraw Hill 1959, p. 292.
11. Shoolery, J. N. and Rogers, M. T. *J. Am. Chem. Soc.* **80** (1958) 5121.
12. Jackman, L. M. *Applications of Nuclear Magnetic Resonance Spectroscopy in Organic Chemistry,* Pergamon Press, London 1959, p. 112.
13. Shoolery, J. N. *Svensk Kem. Tidskr.* **69** (1957) 185.
14. Karplus, M. *J. Chem. Phys.* **30** (1959) 11.
15. Conroy, H. *Advances in Organic Chemistry. Vol. II,* Interscience Publishers, Inc., New York 1960.
16. Ullman, E. F. *J. Am. Chem. Soc.* **81** (1959) 5386.

Received November 4, 1960.

ACTA CHEMICA SCANDINAVICA 15 (1961) 599–606

The Conformational Analysis of Chloro*cyclo*hexane by Electron Diffraction

V. A. ATKINSON*

Universitetets Kjemiske Institutt, Blindern-Oslo, Norway

Chloro*cyclo*hexane has been rigorously re-examined using the latest techniques of gas-phase electron diffraction. A conformational equilibrium containing 45 ± 5 % of the form with chlorine in the axial position gives best agreement with the experimental results. This corresponds to an energy difference of less than 260 cal/mole between the two conformations.

The reliability of electron diffraction conformational assessments, past and present, is discussed.

An early electron diffraction investigation of chloro*cyclo*hexane [1] failed to detect any evidence for the existence of the conformation with chlorine in the axial position. Later Larnaudie [2] reported infra-red evidence for the co-existence of the axial and equatorial conformations, both in the liquid and in the vapour phase. Since that time there have been several attempts at conformational analysis. Klæboe, Lothe and Lunde [3] and Le Fèvre and his colleagues [4] independently calculate from infra-red data that there is 20 % of the axial form in the liquid phase, but these calculations are based on the assumption that the extinction coefficients of the characteristic equatorial and axial carbon-chlorine bond-stretching bands are equal. The latter group of workers also present alternative calculations, based on the molar Kerr constants, which lead to a value of 30 % for the proportion of the axial conformation present in the liquid phase. Chiurdoglu *et al.*[5] use a different approach to the infra-red data, and they conclude that there is an energy difference of 300 to 400 cal/mole between the two conformations in the liquid phase, which would correspond to an equilibrium containing 36 ± 2 % of the axial conformation. Kozima and Sakashita [6] have measured the infra-red spectra of gaseous chloro*cyclo*hexane at 117°C and 200°C and conclude that the energy difference between the two conformations is 340 cal/mole, which corresponds to an equilibrium containing over 40 % of the axial conformation at these temperatures.

* Present address: The British Council, 65 Davies Street, London W.1., England.

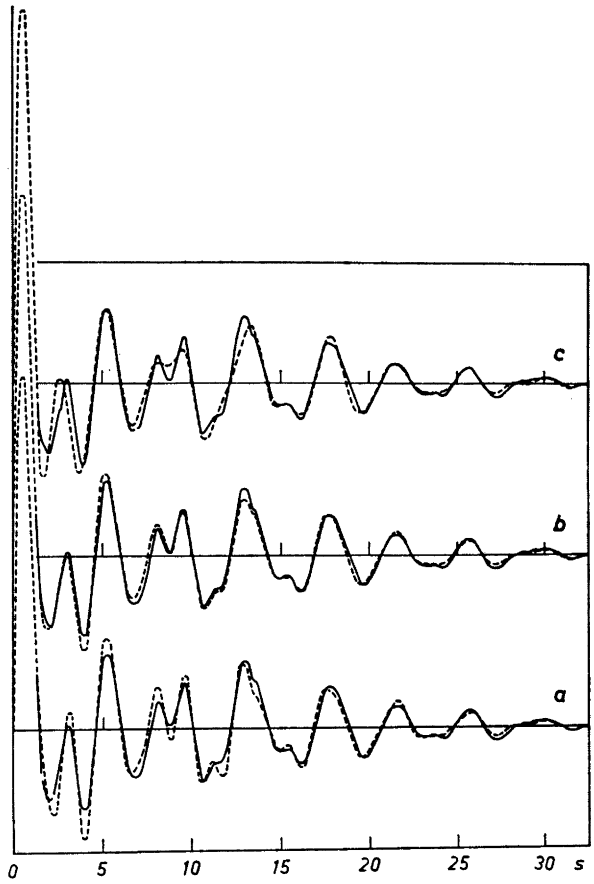

Fig. 1. The experimental intensity curve (full line) compared with the theoretical intensity curves (broken lines) for (a) the *e*-chloro conformation, (b) an equilibrium containing 55 % of the *e*-chloro form and 45 % of the *a*-chloro form, and (c) the *a*-chloro conformation. The heavily damped data for $s > 32.5$ has been omitted.

Since the weight of this evidence seemed to go against the conclusions of the original electron diffraction work, it was decided to re-investigate chloro-*cyclo*hexane using the latest electron diffraction procedure, which is very much in advance of the methods in use in 1943.

RESULTS

The electron diffraction measurements were made with the new Oslo apparatus [7], using distances of 19 cm and 48 cm between the nozzle and the photographic plates. The experimental data, extending from $s = 1.25$ to

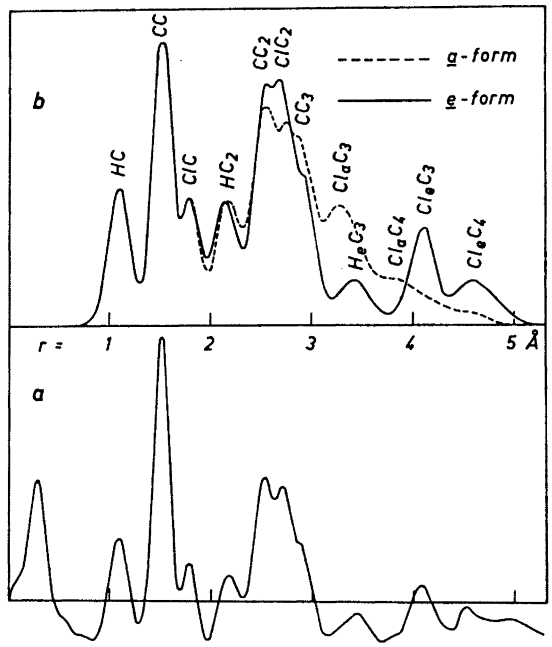

Fig. 2. Radial distribution curves: (a) initial experimental curve, and (b) theoretical curves for the two conformations. The internuclear distances responsible for the principal peaks are indicated.

$s = 45.0$, was subjected to the usual treatment [8] (including a damping factor of 0.0015), to give the intensity curve shown in Fig. 1. The Fourier transform of this curve is shown in Fig. 2a.

In electron diffraction work it is nowadays our practice to assume a model for the structure of the molecule being investigated, and to construct a theoretical radial distribution curve by summing Gauss curves, one for each internuclear distance r in the model. The area of each Gauss curve has to be proportional to the product of the atomic numbers of the two nuclei divided by the distance between them. Except in the simplest cases it is unrewarding to try and correlate the actual heights and widths of these Gauss curves with molecular vibrations, so the construction of the theoretical radial distribution curve is merely a matter of adjusting (within reasonable limits) the shape (but not the area) of the individual Gauss curves so that the sum curve agrees well with the experimental radial distribution curve. Despite this apparent flexibility in its construction the theoretical radial distribution curve is remarkably sensitive to the r values of the assumed model, and small errors in this model will give a theoretical curve with peaks perceptibly out of position when compared with experimental curve.

Since chloro*cyclo*hexane might exist in two conformations it was necessary to construct a theoretical radial distribution curve for each form (Fig. 2b).

The internuclear distances used were calculated from models in which the bond distances were: C—H = 1.102 Å, C—C = 1.530 Å and C—Cl = 1.810 Å (obtained from the initial experimental radial distribution curve), and the bond angles were C—C—C = 111.5°, C—C—X = 110.0° and X—C—X = 108.7° (obtained from the latest figures for the parent compound, *cyclo*hexane [9]). The model for the axial conformation included a distortion of the carbon-chlorine 6.3° outwards from the axial position (suggested by previous work on related compounds [10]).

Comparison between Figs. 2a and 2b shows good correlation between the positions of the peaks, so it may be taken that the models used are acceptable. It remains to analyse the sizes and shapes of the peaks in order to deduce the conformational equilibrium. This can not be done directly because the true sizes of the peaks in the initial experimental radial distribution curve are uncertain. This uncertainty is due to the omission from the Fourier transform of the inner peak of the intensity curve, which is experimentally unobtainable.

So instead of pursuing the correlation of the radial distribution curves, the two theoretical radial distribution curves were Fourier transformed back to give theoretical intensity curves, one for each conformation. Fig. 1 shows that neither the theoretical intensity curve for the equatorial conformation, nor that for the axial conformation, fits the experimental intensity curve particularly well. A number of composite theoretical intensity curves, representing different mixtures of the two conformations, were drawn and shown to give better agreement with the experimental curve. Table 1 shows that the mixture giving best agreement with the experimental curve would contain about 43 % of the axial conformation.

Final "experimental" radial distribution curves were then prepared using the experimental intensity data from $s = 1.25$ to $s = 45.0$, and theoretical intensity data for the experimentally unobtainable inner peak over $s = 0$ to $s = 1.25$, in the Fourier transform.

It has been suggested that the inclusion of this theoretical intensity data must affect the final "experimental" radial distribution curve and so invalidate

Table 1. Standard deviation of theoretical intensity curves from experimental intensity curve in the range $1.25 \leqslant s \leqslant 45.0$

Percentage of *a*-form in theoretical intensity curve.	Percentage dispersion of the standard error.
0	32.3
10	27.1
20	23.1
30	20.0
40	18.5
45	18.5
50	19.1
60	21.6
70	25.4
80	30.2
90	34.9
100	40.8

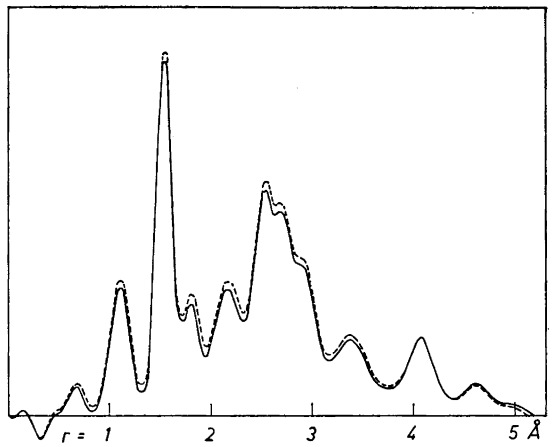

Fig. 3. Radial distribution curves: the full curve was calculated by including theoretical intensity data for the *e*-form, the broken curve by including it for the *a*-form, over the range $0 < s < 1.25$.

the subsequent analysis, but Fig. 3 shows that whichever theoretical intensity curve the additional data is taken from makes very little difference to the final "experimental" radial distribution curve obtained.

A factor having greater effect on the final analysis is the adjusting of the shapes of the individual Gauss curves which make up the theoretical radial distribution curves for the two conformations. It is possible by making some Gauss curves tall and slim, and others short and fat, to shift the apparent position of the equilibrium by up to 10 %.

In order to investigate this more closely a number of different theoretical curves were constructed for each of the two conformations, keeping the same molecular model and the same area for each Gauss curve, but varying the heights and widths of the Gauss curves within reasonable limits. These theoretical radial distribution curves were constructed in pairs, one for each confor-

Table 2. The correlation between some theoretical and experimental radial distribution curves.

Pre-selected equilibrium, *a*/*e*	30/70	40/60	45/55	50/50	60/40
Percentage dispersion of standard error for pre-selected equilibrium*	7.6	6.5	6.4	6.5	8.2
Best equilibrium, *a*/*e*, by least squares calculation	39/61	44/56	45/55	47/53	50/50
Shift from pre-selected to best equilibrium	+9	+4	0	−3	−10

* The great improvement of these errors over those in Table 1 is due more to the omission of the non-structural part of the radial distribution curve ($r < 0.8$ Å) than to the slight re-adjustment of the theoretical curves.

mation, so that the composite theoretical curve for a *pre-selected* conformational equilibrium should give *as good a fit as possible* with the final "experimental" radial distribution curve. The standard errors of these fits (Table 2) show that equilibria containing between 40 and 50 % of the axial form still give the best agreement with the experimental results.

A second, and perhaps more instructive, indication of the real position of the conformational equilibrium was obtained by using least squares procedure to calculate the equilibrium giving *the best fit* between the "experimental" curve and *any* composite curve based on each of the above biassed pairs of theoretical curves. These calculations showed (Table 2) that the equilibrium containing 45 % of the axial conformation gave the best and most consistent agreement with the experimental results. The size of the shift from the pre-selected equilibrium toward which the theoretical curves were biassed, to the best equilibrium seems to give a better indication of the possible error than does the standard deviation.

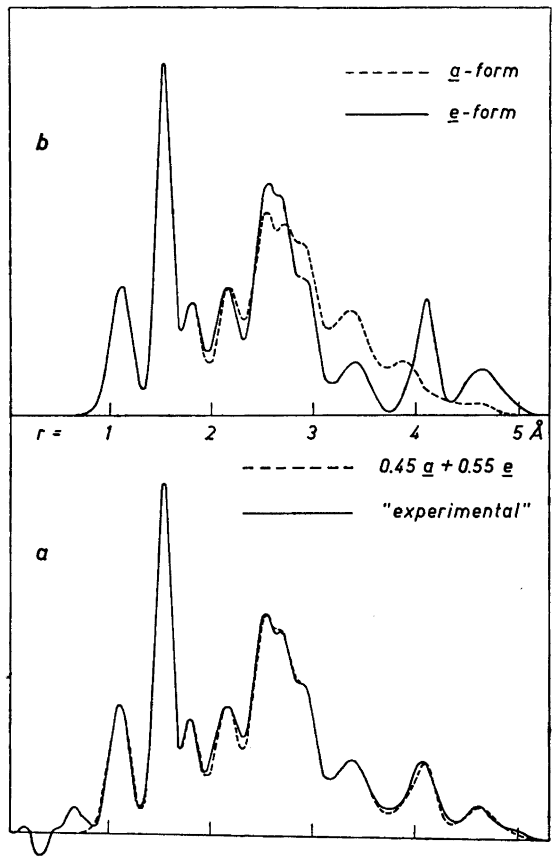

Fig. 4. Final radial distribution curves.

DISCUSSION

*Chloro*cyclo*hexane.* A conformational equilibrium containing 45 % of the compound in the form with chlorine in the axial position gives best agreement with the final "experimental" radial distribution curve (Fig. 4). The electron diffraction procedure is too complex to permit theoretical limits of error for the conformational analysis to be calculated, but the self-consistency of the results suggests that these might be confidently put at $\pm$ 5 %. An equilibrium containing 45 $\pm$ 5 % of the axial conformation corresponds to an energy difference of less than 260 cal/mole between the two conformations. This is in fair agreement with that infra-red work which involves no assumptions about extinction coefficients [5,6]. Moreover it is consistent with the results for *trans*-1,4-dichloro*cyclo*hexane, where both possible conformations were found in about equal proportions [10].

Conformational analysis by electron diffraction. At the time when Hassel and Viervoll [1] investigated chloro*cyclo*hexane the electron diffraction procedure did not give very good resolution of the radial distribution curve, so they made a differential radial distribution curve by subtracting the curve for *cyclo*hexane itself from that for chloro*cyclo*hexane, and then sought for evidence of the carbon-chlorine distances in this differential curve. Unfortunately, they had no accurate figures for the geometry of the *cyclo*hexane ring, so they had to assume that all the bond angles were tetrahedral. This theoretical model gave them values for the Cl_aC_3 and Cl_aC_4 distances which were appreciably smaller than those we now believe to be correct, and which coincided with troughs in their differential curve. If they had better figures for the bond angles they might have detected the presence of the axial conformation, but the method would still have been inadequate for determining the proportions in which the two forms were present.

Since that time the resolution obtainable from electron diffraction measurements has steadily improved, and during the last decade several substituted *cyclo*hexanes have been ascribed to one conformation or another on the basis of qualitative peak assignments made directly in the radial distribution curve. However, this sort of approach can still lead to errors, as can be seen from Fig. 2 where all the peaks of the experimental curve can be accounted for qualitatively by the conformation containing equatorial chlorine alone. It was only when the relative sizes of the peaks were considered that this assignment was found to be inadequate.

Modern electron diffraction procedure gives sufficiently well-resolved peaks in the radial distribution curve for the structures of single substances to be accurately determined. This can be extended to the conformational analysis of cyclic compounds provided (1) the structure of the parent cyclic compound is first accurately determined and (2) the areas under the radial distribution curves are treated quantitatively. A provisional result can be obtained by following the procedure outlined in this paper as far as the comparison of theoretical and experimental intensity curves, but it is probably safer to carry on to the correlation of theoretical and final "experimental" radial distribution curves because these curves are more readily interpreted in structural terms.

The author is grateful to Professor O. Hassel for his interest and encouragement, to A. Almenningen who kindly made the electron diffraction plates, to H. Viervoll and G. Eia for helpful discussion and to *Norges Teknisk-Naturvitenskapelige Forskningsråd* for their postdoctorate fellowship.

REFERENCES

1. Hassel, O. and Viervoll, H. *Tidsskr. Kjemi, Bergvesen Met.* **3** (1943) 35.
2. Larnaudie, M. *Compt. rend.* **235** (1952) 154; *J. Phys. Radium* **15** (1954) 650.
3. Klæboe, P., Lothe, J. J. and Lunde, K. *Acta Chem. Scand.* **10** (1956) 1465; **11** (1957) 1677.
4. Le Fèvre, C. G., Le Fèvre, R. J. W., Roper, R. and Pierens, R. K. *Proc. Chem. Soc.* **1960** 117.
5. Chiurdoglu, G., Kleiner, L., Masschelein, W. and Reisse, J. *Bull. soc. chim. Belges* **69** (1960) 143.
6. Kozima, K. and Sakashita, K. *Bull. Chem. Soc. Japan* **31** (1958) 796.
7. Bastiansen, O., Hassel, O. and Risberg, E. *Acta Chem. Scand.* **9** (1955) 232.
8. Almenningen, A. and Bastiansen, O. *Acta Chem. Scand.* **9** (1955) 815.
9. Davis, M. *To be published.*
10. Atkinson, V. A. and Hassel, O. *Acta Chem. Scand.* **13** (1959) 1737.

Received November 12, 1960.

ACTA CHEMICA SCANDINAVICA 15 (1961) 607–614

The Solubility of Silver Chloride and Silver Bromide in Aqueous Ammonia and the Formation of Mixed Silver-Ammonia-Halide Complexes

IDO LEDEN* and GÖRAN PERSSON

Department of Inorganic Chemistry, Chalmers Institute of Technology, Göteborg, Sweden

The silver ion does not take up more than two ammonia molecules as ligands in aqueous solutions, even if the solution is saturated with ammonia (J. Bjerrum [1]). It was of considerable interest to investigate, whether the diammine silver ion is coordinatively saturated, or if additional ligands other than ammonia, *e.g.* halide ions, can be coordinated. In this paper mixed complexes of the type $Ag(NH_3)_mX_n^{1-n}$, are reported where $(m;n) = (1;1)$, $(1;2)$ and $(2;1)$, if X = Cl, and $(m;n) = (1;1)$, $(1;2)$, $(1;3)$, $(2;1)$ and $(2;2)$, if X = Br. The measurements were performed at 25°C and a constant ionic strength of 1 M was maintained by adding ammonium perchlorate.

Few investigations of mixed silver ammonia halide complexes have been reported. Bodländer and Fittig [2] determined the solubility of silver chloride in aqueous ammonia and made some potentiometric measurements with silver electrodes. In both cases they found only one complex, *viz.* $Ag(NH_3)_2^+$. Derr, Stockdale and Vosburgh [3] measured the same solubility more accurately. They could not describe their measurements quantitatively as simply as Bodländer and Fitting, and they concluded that some mixed complex was also present in their solutions. They did not attempt, however, to identify any such species. Schigol [4] described his potentiometric measurements by means of the reaction $AgCl_2^- + 2\ NH_3 \rightleftharpoons Ag(NH_3)_2Cl_2^-$. The present authors were not able to confirm this particular mixed complex.

THE METHOD

The solubility of AgX was determined by shaking the respective halide in a solvent having the composition: c_{NH_3} M NH_3, c_{NH_4X} M NH_4X and $(1-c_{NH_4X})$ M NH_4ClO_4. The silver contents of the saturated solutions were determined by electroanalyses for silver chloride and by a tracer technique for silver bromide.

* Present address: Department of Inorganic and Physical Chemistry, University, Lund.

If only mononuclear species are involved, the solid AgX is dissolved according to the reactions (equilibrium constants $K_{s,m,n}$ M^{2-m-n})

$$AgX(s) + m\ NH_3 + (n-1)\ X^- \rightleftharpoons Ag(NH_3)_mX_n^{1-n} \qquad (1)$$

Some potentiometric measurements in this laboratory seem to support the view that polynuclear complexes are negligible in the range of concentration pertinent to the measurements of this paper. If M is the maximum number of ammonia molecules that can be attached to one silver ion, and N is the maximum coordination number of silver, the solubility, l M, may be written

$$l = \sum_{m=0}^{M} \sum_{n=0}^{N-m} Ag(NH_3)_mX_n^{1-n} = \sum_{m=0}^{M} \sum_{n=0}^{N-m} K_{s,m,n}\, a_{NH_3}^m\, [X^-]^{n-1} \qquad (2)$$

In practise the summations have to be carried out for values of m and n, corresponding to such species that exist in large enough concentrations to have a noticeable influence on the solubility. The total concentration, l_X M, of the pure halide complexes

$$l_X = \sum_{n=0}^{N} [AgX_n^{1-n}] \qquad (3)$$

can be determined independently by measuring the solubility of AgX in solutions free from ammonia. It turned out that l_{Cl} could be neglected compared with l in the whole range of concentrations used ($l_{Cl} < 10^{-5}$, *cf.* also Ref.[5]). On the other hand the solubility of silver bromide in ammonia is influenced by the presence of pure bromide complexes.

To analyse the results the function A is introduced

$$A = (l - l_X) \cdot [X^-] \cdot a_{NH_3}^{-2} \qquad (4)$$

A would be a constant, $K_{s,2,0}$, if no mixed complexes were formed.

Eqns. (2), (3) and (4) may be combined to

$$A = \sum_{m=1}^{M} \sum_{n=0}^{N-m} K_{s,m,n} \cdot a_{NH_3}^{m-2} \cdot [X^-]^n \qquad (5)$$

As $m \leqslant 2$ and $m + n \leqslant 4$, and as in the range of our measurements $[Ag(NH_3)_2^+] \gg [Ag^+] + [AgNH_3^+]$ (*vide* J. Bjerrum [1]), A is in practise simplified to

$$A = K_{s,2,0} + \left(\frac{K_{s,1,1}}{a_{NH_3}} + K_{s,2,1}\right) \cdot [X^-] + \left(\frac{K_{s,1,2}}{a_{NH_3}} + K_{s,2,2}\right) \cdot [X^-]^2 + \\ + \frac{K_{s,1,3}}{a_{NH_3}} \cdot [X^-]^3 = \sum_{i=0}^{3} B_i \cdot [X^-]^i \qquad (6)$$

From a series of measurements with almost constant ammonia activity and increasing halide ion concentration, A is obtained as a polynomial function of $[X^-]$. The coefficients, B_i, of this polynomial may be computed by the usual graphic methods. If the series is repeated at some other ammonia activities, the equilibrium constants $K_{s,m,n}$ may be calculated from the values of B_i for all such species, as exist in the solutions in sufficient concentrations. This method of calculation has been used for the chloride measurements, where

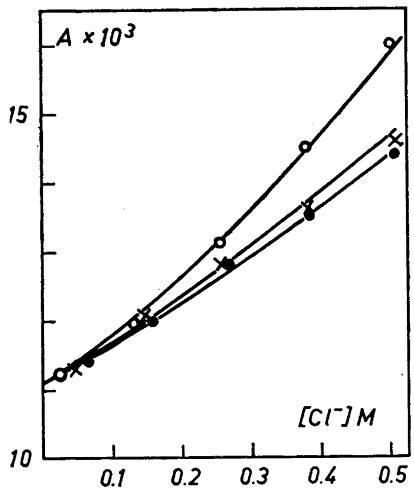

Fig. 1. The function $A(Cl^-)$. The points are calculated from eqn. (4). ○, × and ● denote ammonia activities 0.25, 0.5, and 0.74 M, respectively. The curves describe eqn. (6) with the constants from Table 4.

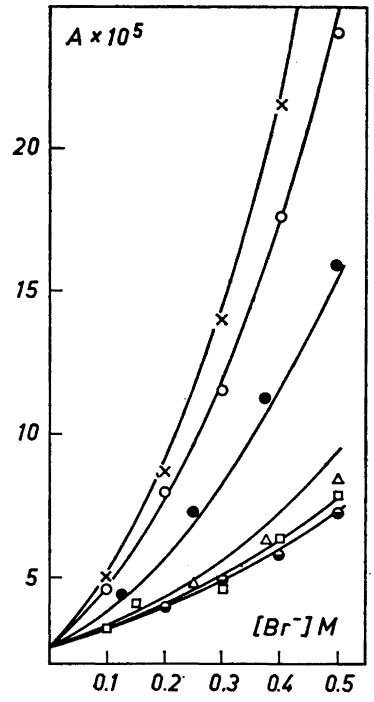

Fig. 2. $A(Br^-)$. The points are calculated from eqn. (4). ◒, □, △, ●, ○ and × denote ammonia concentrations 3.58, 3.05, 1.80, 0.70, 0.35, 0.259 M, respectively. The curves represent eqn. (6) with the constants from Table 4.

three equilibrium constants for mixed complexes were enough to describe the results.

In the bromide case the equilibrium constants were computed after a rearrangement of the terms in eqn. (6) in the following way

$$A = \sum_{i=0}^{2} K_{s,2,i} \cdot [X^-]^i + \sum_{i=1}^{3} K_{s,1,i} \cdot [X^-]^i \cdot a_{NH_3}^{-1} = A_0 + A_1 \cdot a_{NH_3}^{-1} \qquad (7)$$

(i) The family of curves $A(X^-)$ with a_{NH_3} as a parameter representing eqn. (6) is first drawn in a large scale diagram as accurate as possible through the experimental points.

(ii) The curves are cut with lines parallel to the ordinate axis for some values of $[X^-]$.

(iii) The ordinates for the points of intersection are plotted in a second diagram against $a_{NH_3}^{-1}$, which according to eqn. (7) should result in one straight line for every halide concentration, $[X^-]$, selected in (ii).

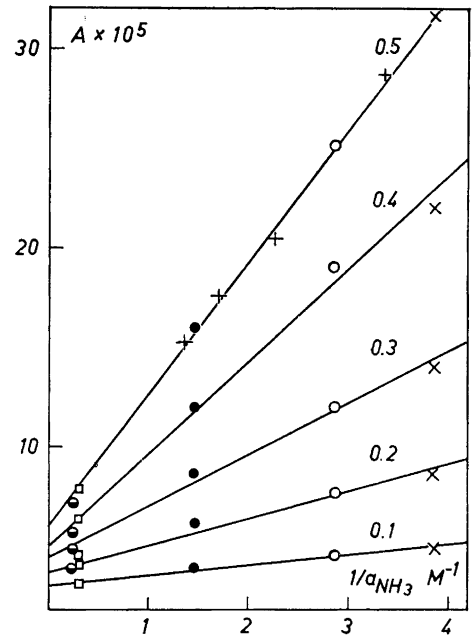

Fig. 3. The lines $A = A_0 + A_1 \cdot a_{NH_3}^{-1}$ at the bromide concentrations (M) given at each line. ◒, □, ●, O and × denote values of A, read in Fig. 2 for ammonia activities given there. + denotes values of A from Table 3.

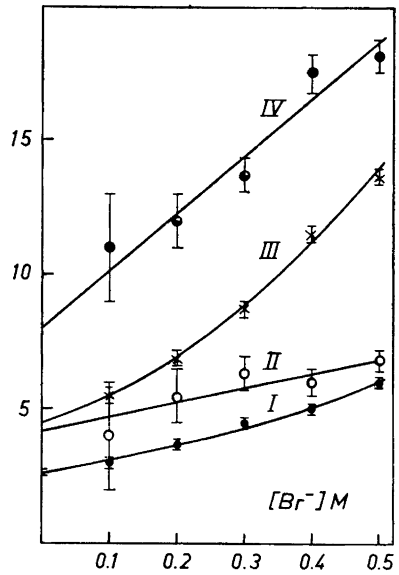

Fig. 4. Computation of the equilibrium constants for the bromide system. The curves are I: $A_0 \times 10^5$; II $(A_0 - 2.6) \times 10^5$ $[Br^-]^{-1}$ (M^{-1}); III: $A_1 \times 10^5$ $[Br^-]^{-1}$; IV: $(A_1 \cdot [Br^-]^{-1} - 4.5) \times 10^5$ $[Br^-]^{-1}$ (M^{-1}). The plotted values are calculated from the intercepts (A_0) and the slopes $(A_1$ M) of the lines in Fig. 3.

(iv) The intercept, A_0, of these straight lines are plotted in a third diagram as a function of $[X^-]$. From the resulting polynomial curve the equilibrium constants $K_{s,2,i}$ are obtained in the usual way, by drawing $(A_0 - K_{s,2,0})$ $[X^-]^{-1}$, which in our case is a straight line with the intercept $K_{s,2,1}$ and the slope $K_{s,2,2}$.

v) The slopes, A_1, of the straight lines in (iii) are finally used to calculate $K_{s,1,i}$ by plotting $A_1 \cdot [X^-]^{-1}$ with $[X^-]$ as the abscissa, which gives $K_{s,1,1}$ as the intercept. $K_{s,1,2}$ and $K_{s,1,3}$ are then obtained as intercept and slope from the straight line $(A_1 \cdot [X^-]^{-1} - K_{s,1,1})$ $[X^-]^{-1}$ plotted as a function of $[X^-]$.

The halide concentrations to be used in the eqns. (2)—(7) were calculated from

$$[X^-] = c_{NH_4X} + l \qquad (8)$$

In only one case was it necessary to correct eqn. (8) for those tiny amounts of halide ions, consumed by the complexes. In this case the concentration of free halide ion is also given (*vide* Table 1). The correction is easily computed by the aid of a preliminary $\bar{n}$-curve (*vide e.g.* Ref.[6]).

The ammonia activity a_{NH_3} is calculated from

$$a_{NH_3} = (c_{NH_3} - 2\ l) \cdot f_{NH_3} \qquad (9)$$

The activity factor f_{NH_3} is taken from Bjerrum [1, p. 148]. In most cases $2l \ll c_{NH_3}$. When this is not the case, the main part of the silver halide is dissolved as species containing two ammonia ligands. Hence, the first factor of the right hand member of eqn. (9) represents the ammonia concentration with sufficient accuracy.

The method of computation described above may be regarded as a special case of a general treatment of similar data given by Sillén [7] and used by Marcus [8] for mixed halide mercury complexes.

EXPERIMENTAL DETAILS

Ammonium perchlorate (Baker's Analyzed), ammonium chloride (Merck's *p.a.*) and ammonium bromide (The British Drug Houses Ltd) were used without further purification. The stock solutions were analyzed by allowing them to percolate through a hydrogen saturated cation exchanger and then titrating the eluate with sodium hydroxide. No foreign ions could be detected in any of these salts. The ammonia was Merck's *p.a.* It was standardised by titration with acid. The silver perchlorate used is described elsewhere [9]. The silver chloride was precipitated from hot dilute solutions of silver nitrate and hydrochloric acid. It was carefully washed with water and dried.

The saturation of the solutions with silver halide was carried out in brown or black painted glass bottles with paraffined glass or rubber stoppers. The bottles were rotated in a well controlled thermostat (25 ± 0.01°C) for about 20 h. Equilibrium was attained within a tenth of this time. A part (10—200 ml) of the saturated solution was drawn through a glass filter into a pipette. The silver bromide solutions were filtered through a membrane filter (*cf.* Ref.[7]).

The silver chloride solutions were electroanalyzed for silver after some sodium cyanide was added. A few analyses were also carried out by the tracer technique.

The silver bromide was labelled with ^{110}Ag (from Harwell). It was precipitated with ammonium bromide from silver nitrate solutions, prepared by dissolving labelled silver metal in nitric acid. It was thoroughly washed with 1 M NH_4ClO_4 before use. The activity of the two silver nitrate solutions used were determined as 5.21×10^8 and 1.74×10^{10} ipm/g-atom silver. Their silver contents were determined by electroanalysis and their activity — after dilution with inactive silver nitrate — by means of a scintillation spectrometer (NUKAB, Gothenburg). This apparatus was also used for the solubility determinations.

The solubility determinations were made in the following way. 1.00 ml solution containing 0.1 M inactive silver nitrate and 1 M sodium cyanide was poured into a measuring flask of 10.00 ml, which was then filled to the mark with the filtered saturated solution. From this solution 3.00 ml was taken for the activity determination, in which

Table 1. The solubility of silver chloride, l M, and the function A.

c_{NH_3} (M)	c_{NH_4Cl} (M)	$l \times 10^3$	$[Cl^-]$ (M)	$A \times 10^3$	c_{NH_4Cl} (M)	$c_{NH_3} = 0.494$ (M)		$c_{NH_3} = 0.247$ (M)	
						$l \times 10^3$	$A \times 10^3$	$l \times 10^3$	$A \times 10^3$
0.730	0.495	14.0	0.506	14.4	0.500	6.70	14.6	1.88	16.0
0.738	0.371	17.1	0.385	13.5	0.375	8.14	13.6	2.25	14.5
0.735	0.247	22.7	0.267	12.8	0.250	10.96	12.8	3.00	13.1
0.738	0.124	34.7	0.156	12.0	0.125	17.9	12.1	5.13	11.9
0.741	0	66.2	0.064	11.4	0	43.7	11.3	21.7	11.2

Table 2. The solubility of silver bromide, l M, and the function A.

c_{NH_3}; a_{NH_3} $\vec{M}$	0	3.58;	4.22	3.05;	3.48	1.80;	1.89	0.70;	0.71	0.35;	0.35	0.259;	0.259
c_{NH_4Br} M	$l_{Br} \times 10^6$	$l \times 10^3$	$A \times 10^5$	$l \times 10^3$	$A \times 10^5$	$l \times 10^4$	$A \times 10^5$	$l \times 10^4$	$A \times 10^5$	$l \times 10^5$	$A \times 10^5$	$l \times 10^5$	$A \times 10^5$
0.50	81.6	2.59	7.25	1.92	7.89	6.80	8.37	2.42	15.9	14.04	24.0	12.35	31.3
0.40	52.0	2.60	5.82	1.94	6.38					10.61	17.7	8.78	21.4
0.375	45.8					6.36	6.19	1.96	11.2				
0.30	29.3	2.87	4.89	1.87	4.64					7.63	11.5	16.05	14.0
0.25	20.7					7.01	4.76	1.69	7.35				
0.20	14.4	3.47	3.96	2.49	4.13					6.43	8.00	4.30	8.54
0.125	6.3							1.87	4.49				
0.10	4.47			3.73	3.14					6.11	4.62	3.79	4.98
0										189		123	

500 to 10^4 impulses were registered. At least 15 such determinations were made for each saturated solution.

The active silver nitrate solutions and the silver bromide were used as quickly as possible after their preparation to avoid difficulties with finely dispersed metallic silver, which was eventually formed because of the radioactivity.

THE SOLUBILITY OF SILVER CHLORIDE

The results of the chloride measurements are shown in Table 1.

$A(Cl^-)$ is plotted in Fig. 1. For the smallest ammonia concentration $A(Cl^-)$ is evidently curved, indicating a term of second degree. The curvature is obviously dependent on a_{NH_3}. The term $K_{s,1,2}/a_{NH_3}$ is essentially as large as the coefficient B_2, and therefore, $K_{s,2,2}$ cannot be determined.

The initial slope of the three lines is only slightly dependent on a_{NH_3}. Hence $K_{s,2,1}$ predominates in the coefficient B_1, and the value of $K_{s,1,1}$ becomes very uncertain. The curves are drawn with the constants $K_{s,m,n}$ of Table 4 ($B_3 = K_{s,2,2} = 0$).

THE SOLUBILITY OF SILVER BROMIDE

The solubility of silver bromide is shown in Tables 2 and 3. The values $A(Br^-)$ from Table 2 are plotted in Fig. 2. The intercepts between the curves $A(Br^-)$ and five vertical lines, $[Br^-] = 0.1$, 0.2, 0.3, 0.4, and 0.5 (M), are plotted against $a_{NH_3}^{-1}$ in Fig. 3., in which each value of $[Br^-]$ from Fig. 2 gives one straight line. For $[Br^-] = 0.5$ (M) the values of A from Table 3 are also plotted in Fig. 3. Finally the equilibrium constants, $K_{s,m,n}$, are obtained from A_0 and A_1 by the usual graphical methods as shown in Fig. 4. These constants have been used when drawing the curves in Fig. 2. The experimental points lie on these curves within fair accuracy. Hence the presented scheme describes the solubility over the range of concentrations, $a_{NH_3} < 4$ (M) and $[Br^-] < 0.5$ (M), covered by the experiments. Of course, some of the equilibrium constants can only be obtained with a rather small accuracy (*vide* Table 4), *viz.* those constants corresponding to complexes whose concentrations never exceed a

Table 3. The solubility of silver bromide, l M, at variated ammonia concentrations, c_{NH_3} M, in 1 M NH_4ClO_4 and in 0.5 M NH_4Br + 0.5 M NH_4ClO_4

$c_{NH_4Br} = 0$			$c_{NH_4Br} = 0.5$ (M)		
c_{NH_3}	$l \times 10^4$	$A \times 10^5$***	c_{NH_3}	$l \times 10^5$	$A \times 10^5$
6.20 *	449	2.62	0.739	24.9	15.3
2.07 **	117	2.73	0.591	20.5	17.6
0.61	31.2	2.62	0.443	16.2_2	20.5
0.366	18.8	2.64	0.296	13.1_6	28.7
0.244	12.5	2.61	0.148	10.2_7	48.3
0.122	6.3	2.67	0	8.1_6	—

* $a_{NH_3} = 8.74$. ** $a_{NH_3} = 2.21$. *** Mean of $A = 2.6_3 \times 10^{-5} = K_{s,2,0}$

Table 4. The equilibrium constants, $K_{s,m,n}$ M^{2-m-n}, for silver chloride (left column) and silver bromide (right column).

m, n	$K_{s,m,n} \times 10^3$	$K_{s,m,n} \times 10^5$
2 , 0	11.1 ± 0.1	2.6$_3$ ± 0.05
2 , 1	5 ± 1	4.3 ± 0.5
2 , 2		5 ± 2
1 , 1	0.4 ± 0.4	4.5 ± 0.5
1 , 2	1.5 ± 0.5	8 ± 4
1 , 3		20 ± 10

rather small part of the total silver concentration in the solution. The possible errors, also given in Table 4, can be estimated rather well from the trials to draw the "best" curves through the experimental points in Fig. 4.

THE EQUILIBRIUM CONSTANTS

From the constants in Table 4 the distribution of silver on the different species can easily be computed. The fraction $\alpha_{m,n}$ of silver, bound in $Ag(NH_3)_mX_n^{1-n}$, is

$$\alpha_{m,n} = \frac{K_{s,m,n} \cdot a_{NH_3}^m \cdot [X^-]^{n-1}}{l} \qquad (10)$$

where l is obtained from eqn. (2) in which all constants are now known. It follows that $Ag(NH_3)_2^+$ is highly predominant in the chloride solutions, since it never contains less than about two thirds of the total silver in the solutions within the range studied. In the bromide solutions, however, the silver is rather evenly distributed on several species at the highest bromide concentrations.

For the calculation of the gross complexity constants the solubility products of silver chloride and bromide must be known in 1 M NH_4ClO_4. These constants together with the constants for the stepwise formation of the complexes shall be discussed further elsewhere in connection with some potentiometric measurements in unsaturated solutions of silver halides.

Acknowledgements. Our thanks are due to Professor Cyrill Brosset, who put the facilities of his laboratory to our disposal for this work, and to Dr. Eric Berne for valuable advice for the tracer measurements. The English of this paper has been corrected by Dimitrios Karipides, Ph.D., Pennsylvania State University.

REFERENCES

1. Bjerrum, J. *Metal Ammine Formation in Aqueous Solution* (Diss.) Copenhagen 1941.
2. Bodländer, G. and Fittig, R. *Z. physik. Chem.* **39** (1902) 597.
3. Derr, P. F., Stockdale, R. M. and Vosburgh, W. C. *J. Am. Chem. Soc.* **63** (1941) 2670.
4. Schigol, M. B. *Zhur. Obschei Khim.* **22** (1952) 723.
5. Berne, E. and Leden, I. *Svensk Kem. Tidskr.* **65** (1953) 88.
6. Leden, I. *Acta Chem. Scand.* **10** (1956) 812.
7. Sillén, L. G. *Acta Chem. Scand.* **10** (1956) 803.
8. Marcus, Y. *Acta Chem. Scand.* **11** (1957) 811.
9. Leden, I. *Svensk Kem. Tidskr.* **64** (1952) 249.

Received November 17, 1960.

ACTA CHEMICA SCANDINAVICA 15 (1961) 615–620

Dissolution of Copper in Acidified Ferric Sulphate Solutions

TOR HURLEN

Central Institute for Industrial Research, Blindern, Oslo, Norway

Measurements have been made on the dissolution rate (i_c) and the mixed potential (E_c) of copper in unstirred sulphuric acid solutions of ferric sulphate at 21°C. These quantities have been found to be very nearly independent of time and to obey the following relationships:

$i_c = 0.011c$ A/cm²

$\mathrm{d}\,E_c/\mathrm{d}\log i_c = 2.303RT/2F$

where c is the ferric sulphate molarity. The mixed potential has moreover been found to be very nearly equal to the pure anodic dissolution potential of copper at equal dissolution rates.

1.0 INTRODUCTION

Following previous work [1,2] on the kinetics of the anodic dissolution and cathodic deposition of copper in acid sulphate solution under conditions of amperostatically applied currents, studies have been made on the depolarized dissolution of this metal in acidified ferric sulphate solutions.

In the former case, the dissolution reaction is electronically balanced by the applied current and is essentially the only reaction occurring at the copper anode. In the latter case, however, it is accompanied and electronically balanced by a simultaneous reduction of ferric ions at the same metal surface.

The main purpose of the present work is to compare the polarization characteristics of the dissolution reaction in these two different cases.

2.0 EXPERIMENTAL

The experimental work consists in the determination of the dissolution rate (corrosion rate) and the mixed potential (corrosion potential) of copper in unstirred 1 N and 0.1 N sulphuric acid solutions of ferric sulphate (0.001–0.2 M) at 21°C (room thermostated to ±0.5°C).

High purity copper (2 ppm Fe, 2 ppm Ag, 1 ppm Ni, 1 ppm Si, 1 ppm Na, and less than 1 ppm each of Ca and Mg, other metallic elements and the elements O, S, Se, Te, and P — if present — being below the limits of detection by the spectrographic, chemical, and metallographic methods applied) has been used in the form of sheets of thickness about 0.05 mm and apparent area (both sides) of 14 cm² for the rate measurements and about 2 cm² for the potential measurements. Prior to use, the sheets were vacuum annealed

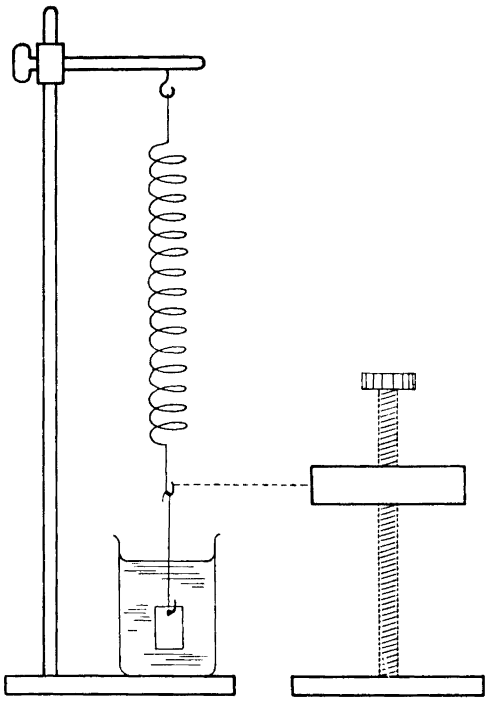

Fig. 1. The quartz helix technique for weight change measurements.

for about one hour at about 700°C, mechanically polished, etched in dilute nitric acid, and washed in running water, distilled water, and acetone (A.R.)

The solutions were prepared from A.R. quality ferric sulphate and sulphuric acid in water distilled from a "pure" and soft fresh water. No attempts were made to free these solutions of dissolved oxygen, and the experiments were performed with the solutions exposed to air.

The rate measurements were carried out by means of a semi-continuous quartz-helix technique as sketched in Fig. 1. This is standard technique for taking up rate curves in the field of high-temperature oxidation of metals. To our knowledge, however, it has not previously been used in the field of low-temperature electrochemical corrosion, even though this technique in many such cases has obvious advantages over the intermittent weighing usually applied. The quartz helix used in the present work, showed a linear extension of 0.505 mm per mg increase in load over a load range including and being much broader than the one covered by the actual experiments (about 0.2 to 0.3 g). It was calibrated for each run through weighings of the copper sheets on a Mettler semi-micro balance. The changes in the quartz helix extension were measured by means of a Fuess cathetometer allowing vertical displacements to be read to less than 0.01 mm. The whole set up was thus sensitive to weight changes of less than 5 μg and, for sheets of 14 cm^2, less than 0.36 μg/cm^2. The copper sheets were suspended by means of thin quartz hooks, which were cleaned in chromic acid and in a flame. The reaction took place in 600 ml beakers filled with the test solution. The experimental time varied from one hour to about one day depending on the reaction rate.

The potential measurements were carried out as sketched in Fig. 2 by means of a Cambridge pH-meter and saturated calomel electrodes. The copper electrodes were here exposed with an area of about 2 cm^2 to about 100 ml of the test solution. Potential readings

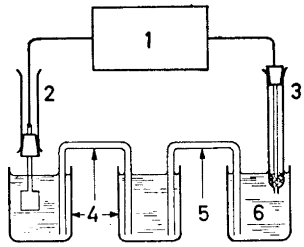

Fig. 2. The technique for potential measurements. 1, potentiometer; 2, test electrode; 3, saturated calomel electrode; 4, test solution; 5, potassium chloride saturated agar-agar bridge; 6, saturated potassium chloride solution.

were made over periods corresponding to those for the rate measurements. In transforming these readings to values on the normal hydrogen scale (NHS), a value of 0.244 V has been used for the saturated calomel electrode.

3.0 RESULTS

Examples of the rate curves and of the potential-time curves obtained are shown in Figs. 3 and 4, respectively. These curves apply to 0.1 N sulphuric acid solutions of ferric sulphate, but are representative also for the types of

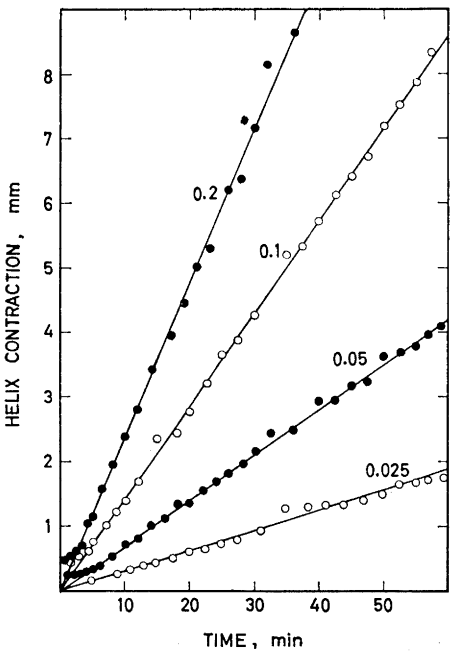

Fig. 3. Dissolution/time curves for copper in 0.1 N sulphuric acid solutions of ferric sulphate at various ferric ion molarities (21°C, helix sensitivity 0.505 mm/mg).

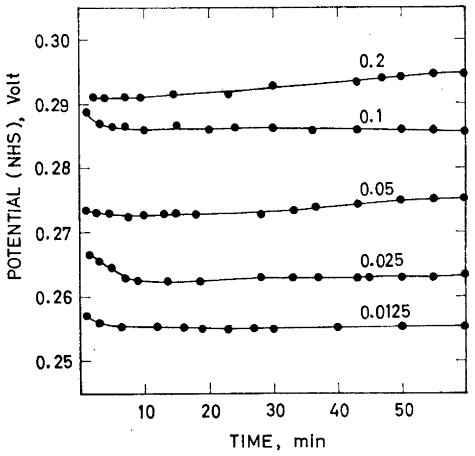

Fig. 4. Potential/time curves for copper in 0.1 N sulphuric acid solutions of ferric sulphate at various ferric ion molarities (21°C).

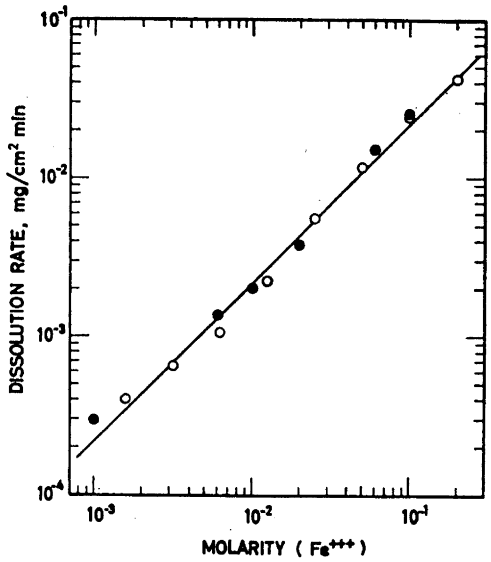

Fig. 5. Dissolution rate of copper in 1 N (closed circles) and 0.1 N (open circles) sulphuric acid solutions of ferric sulphate *versus* ferric ion molarity (21°C).

curves obtained in the 1 N sulphuric acid solutions. It was generally found that both the rate of dissolution and the corrosion potential of copper in any one of the solutions applied were quite nearly independent of time.

In Fig. 5, the average values found for the dissolution rate in the various solutions are plotted as a function of the ferric ion concentration. The results show that the dissolution rate is essentially independent of the sulphuric acid concentration and increases approximately linearly with the ferric sulphate concentration. The straight line drawn in Fig. 5 corresponds to the following relationship:

$$i_a = 0.22c \text{ mg(Cu)/cm}^2\text{min} \quad (1)$$

which on the basis of 100 % cupric ion formation and electronic balancing gives:

$$i_a = i_c = 0.011c \text{ A/cm}^2 \quad (2)$$

where i_a is the rate of copper dissolution, i_c the rate of ferric ion reduction, and c the ferric ion molarity.

In Fig. 6, the values obtained for the potential of copper in the various solutions are plotted as a function of the dissolution rate in the same solutions. No corrections have been made for possible liquid junction potentials between the test solutions and the saturated potassium chloride solution. In the same diagram (Fig. 6) is also given the *uncorrected* polarization curve previously [1] obtained from amperostatic measurements on the anodic dissolution of the

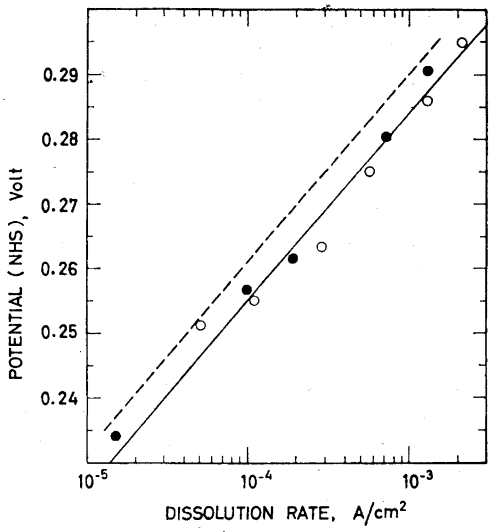

Fig. 6. Potential *versus* dissolution rate of copper in 1 N (closed circles) and 0.1 N (open circles) sulphuric acid solutions of ferric sulphate (21°C). The broken line represents the pure anodic dissolution potential of copper in 0.1 N sulphuric acid at 20°C (Ref.[1]). The potentials include liquid junction potentials between the test solutions and a saturated potassium chloride solution.

same type of copper in 0.1 N sulphuric acid at 20°C. The relatively small difference in position of these two curves may be due partly to the difference in temperature (20 and 21°C) and partly to possible differences in the liquid junction potential. The results do thus indicate that the anodic dissolution reaction of copper is nearly independent of it being electronically balanced by an impressed current or by a simultaneous reduction of ferric ions at the dissolving surface.

It is also of interest to note that the present results strongly support the amperostatically obtained ones [1,2] in showing a Tafel slope of:

$$b_a = 2.303\ RT/2F \qquad (3)$$

(0.029 V at 21°C) for the anodic dissolution of copper under stationary conditions.

4.0 DISCUSSION

The present finding that the rate of dissolution of copper in acidified ferric sulphate solution is proportional to the ferric ion concentration, is in agreement with previous results [3,4] and is analogous to what has been found for a number of other metals less noble than copper [3–7]. It is further qualitatively in accordance with what is to be expected for the rate when entirely controlled by diffusion of ferric ions to the metal surface. The rate data obtained are also quantitatively in agreement with this model, provided the diffusion coefficient of ferric sulphate under the present conditions is about 0.6×10^{-5} cm²/sec.

According to Kortüm and Bockris [8], namely, the limiting diffusion current for one electron exchanging ions with a diffusion coefficient of 1.3×10^{-5} cm^2/sec should be about $0.025c$ A/cm^2 in unstirred solutions (as compared to the here found rates of $0.011c$ A/cm^2). No direct data have been found for the diffusion coefficient of ferric sulphate, but the above value is probably not unreasonable. Zinc sulphate and magnesium sulphate, for instance, have diffusion coefficients of about 0.7×10^{-5} cm^2/sec in dilute solutions at 25°C [9].

The present results further show that the rate of dissolution of copper in acid sulphate solution is very nearly the same function of the electrode potential regardless of this being a pure copper dissolution potential (applied anodic current) or a mixed copper dissolution and ferric reduction potential. This indicates that the ferric/ferrous reaction does not interfere very much with the copper dissolution reaction, but tells nothing as to a possible interference of the latter with the former. An interference at the electrode surface will namely be of little importance for the rate of a diffusion controlled reaction. It is further known that an electrode reaction very well may interfere with another without this necessarily being mutual. An example is provided by the dissolution of iron under simultaneous hydrogen evolution in acid chloride solution [10]. Also in that case, the dissolution reaction is independent of whether it occurs alone or together with the cathodic reduction reaction. The latter reaction, however, is clearly stimulated by a simultaneous occurrence of the former.

The present results on copper are quite analogous to recent results of similar experiments on nickel [7].

Acknowledgement. The author is much indebted to Miss T. Tönderum for technical assistance, to various members of the staff at the Central Institute for Industrial Research for valuable discussions and other help, and to the *Royal Norwegian Council for Scientific and Industrial Research* and *the U.S.Department of Army, European Research Office,* for financial support.

REFERENCES

1. Hurlen, T. *Acta Chem. Scand.* **15** (1961) 630.
2. Hurlen, T. *Acta Chem. Scand.* **15** (1961) 621.
3. Van Name, E. A. and Hill, D. V. *Am. J. Sci.* **42** (1916) 307.
4. Salzberg, H. and King, C. V. *J. Electrochem. Soc.* **97** (1950) 290.
5. Makrides, A. C., Komodromos, N. M. and Hackerman, N. *J. Electrochem. Soc.* **102** (1955) 363.
6. Gatos, H. C. *J. Electrochem. Soc.* **103** (1956) 286; *Corrosion* **12** (1956) 32.
7. Kolotyrkin, Ja. M. and Bune, N. Ja. *Z. physik. Chem.* **214** (1960) 264.
8. Kortüm, G. and Bockris, J. O'M. *Textbook of Electrochemistry* (Volume II), Elsevier, Amsterdam/Houston/London/New York 1951, p. 405.
9. Robinson, R. A. and Stokes, R. H. *Electrolyte Solutions* (2nd Ed.), Butterworths, London 1959, p. 513.
10. Hurlen, T. *Acta Chem. Scand.* **14** (1960) 1533.

Received November 16, 1960

ACTA CHEMICA SCANDINAVICA 15 (1961) 621–629

Heats of Activation of the Cu/Cu_{aq}^{++} Electrode

TOR HURLEN

Central Institute for Industrial Research, Blindern, Oslo, Norway

From measurements of the effect of temperature (0–45°C) on the anodic polarization of copper in 0.1 N sulphuric acid and from known data on the temperature coefficient of the standard potential of this metal, a mean standard heat of activation of:

$$\Delta H_0^*(\text{mean}) = 15.2 \text{ kcal}$$

has been found for the Cu/Cu_{aq}^{++} electrode. On the basis of the kinetic stoichiometry and the heat of reaction of this electrode, this has been shown to indicate:

$$\Delta H_0^*(\text{anodic}) = 30.6 \text{ kcal (H-scale)}$$

$$\Delta H_0^*(\text{cathodic}) = -0.2 \text{ kcal (H-scale)}$$

The results further give an apparent Arrhenius factor of approximately:

$$A = 35\, nFT/\nu \text{ A/cm}^2$$

These values are compared with corresponding values for the Fe/Fe_{aq}^{++} electrode, and their accuracy and meaning are discussed.

The measurements support previous results in showing a Tafel slope of $2.303RT/2F$ for the anodic copper dissolution reaction under stationary conditions.

1.0 INTRODUCTION

In a previous work [1] on copper in acidified cupric sulphate solutions at 20 and 25°C, it has been shown that the Cu/Cu_{aq}^{++} electrode is symmetric and that its kinetic unit reaction [1,2] is:

$$2\,Cu = 2\,Cu^{++} + 4\,e^- \qquad (1)$$

It has further been shown [1] that the absolute rate of anodic dissolution of copper in 0.1 N sulphuric acid is not measurably affected by the addition of cupric sulphate to this electrolyte (the highest concentration tried being 0.3 M). Thereby, the standard exchange current (J_o) of the Cu/Cu_{aq}^{++} electrode in these solutions is given by its anodic polarization curve in 0.1 N sulphuric acid and its standard potential.

In the present work, advantage has been made of these findings in determining the heat of activation of the copper electrode reactions from measurements of the effect of temperature (0, 15, 35, and 45°C) on the *anodic* polarization curve in 0.1 N sulphuric acid and from known data on the effect of temperature on the standard potential of copper [3]. No corrections need here to be made for changes in the sulphuric acid activity and the water dissociation constant with temperature, as neither the sulphate (nor bisulphate) activity nor the pH have been found to affect the dissolution reaction very much [1].

Previous determinations [4-6] have invariably been made from *cathodic* overvoltage measurements at various temperatures in acidified cupric sulphate solutions of given composition. Seiter and Fischer [4] thereby obtained:

$$-R \text{ d}(\ln i_o)/\text{d}(1/T) = 12.3 \pm 2.0 \text{ kcal}$$

for the temperature effect (10—55°C) on the exchange current (i_o) in 1 N cupric sulphate + 1 N sulphuric acid. The results of Barnes, Storey, and Pick [5] (same electrolyte composition at 20—40°C) indicate a higher value (not explicitly given, but apparently 15 — 20 kcal) for the same relationship, whereas Mattsson and Lindström [6] report a corresponding value of 9.2 kcal. All these values, however, may include a possible effect of temperature on the cupric sulphate activity in the solutions applied (see eqns. (3) and (4) below). Such an effect is not encountered in the determinations made in the present work.

2.0 THEORETICAL BASIS

It has previously [7] been shown that the mean standard heat of activation of two mutually reverse and *symmetric* electrode reactions is given by

$$\Delta H_o^* \text{ (mean)} = -R \text{ d } \ln(J_o/T)/\text{d}(1/T) \qquad (2)$$

provided the pre-exponential factor (including the exponential activation entropy term) in the transition state equation for their rate constants is directly proportional to the Kelvin temperature. The mean standard heat of activation for symmetric reactions is defined by:

$$\Delta H_o^* \text{ (mean)} = \tfrac{1}{2} (\Delta H_{o,a}^* + \Delta H_{o,c}^*) \qquad (3)$$

where the subscripts a and c refer to the anodic and the reverse cathodic reaction, respectively. The standard exchange current (J_o) is defined by:

$$J_o = i_o [(\Pi a)_r^{1-\alpha} (\Pi a)_p^{\alpha}]^{-1} \qquad (4)$$

where i_o is the exchange current at the activity products $(\Pi a)_r$ and $(\Pi a)_p$ of the reactants and reaction products according to the kinetic unit equation (eqn.(1) in the present case), and α is the symmetry factor for the reaction from reactants to products. It is thus of no consequence in which direction a reaction is being considered to occur.

It has further been shown [7] that the standard heat of activation of any one symmetric electrode reaction for thermodynamic reasons must be given by:

$$\Delta H_o^* = \Delta H_o^* \text{ (mean)} + \tfrac{1}{2} (\Delta H_o/\nu) \qquad (5)$$

where ΔH_o is the standard heat of reaction and ν the stoichiometric number

of the reaction in question. The standard heat of reaction is here being referred to one "mole" of the thermodynamic overall reaction (in the present case: $Cu = Cu^{++} + 2e^-$ or its reverse). If it were referred to one "mole" of the kinetic unit reaction, the use of the stoichiometric number in (5) would have been avoided, just as this has been done in (4). If hydrogen scale (HS) values for the standard heat of reaction are applied, the values thereby obtained for the standard heat of activation are automatically also being referred to this arbitrary scale. So far, therefore, only relative values can be determined for the standard heat of activation of single electrode reactions, whereas absolute values can be determined for the mean standard heat of activation of mutually reverse reactions. In the present paper, this will be notified by writing (HS) in connection with relative values which refer to the hydrogen scale (*e.g.* $\Delta H^*_{o,a} = 2$ kcal (HS), $\Delta H^*_{o,c} = 44$ kcal (HS), and $\Delta H^*_o(\text{mean}) = 23$ kcal, which are the values previously found for the Fe/Fe^{++}_{aq} electrode reactions[7]). It is easily seen from (5) that the absolute values of the heat of activation of single electrode reactions are related to the corresponding hydrogen scale values by:

$$\Delta H^*_{o,a}(\text{absolute}) = \Delta H^*_{o,a}(\text{HS}) + (n/4\nu)\Delta H_{o,a}(H^+/H_2) \quad (6a)$$

$$\Delta H^*_{o,c}(\text{absolute}) = \Delta H^*_{o,c}(\text{HS}) + (n/4\nu)\Delta H_{o,c}(H^+/H_2) \quad (6b)$$

where n is the number of electrons in the thermodynamic reaction for the electrode reaction in question, ν is the stoichiometric number of this reaction (*not* the hydrogen electrode reaction), and the $\Delta H_o(H^+/H_2)$ terms are the absolute values of the standard heats of reaction of the hydrogen electrode.

This approach to the heat of activation of symmetric electrode reactions may easily be generalized to apply also to unsymmetric reactions (see Appendix).

3.0 EXPERIMENTAL

The materials and the method used in the present work, have been the same as described in the previous paper by the author [1] on the kinetics of the Cu/Cu^{++}_{aq} electrode at 20 and 25°C.

The present experiments have been carried out at approximately 0°C in an ice/water bath and at 15, 35, and 45°C in a water thermostat controlled to ± 0.1°C.

In all the experiments, the test electrolyte has been a hydrogen saturated 0.1 N sulphuric acid solution (made up at 20°C), and the potential measurements have been made against a saturated quinhydrone electrode in the same solution and of the same temperature as in the test cell.

The normal hydrogen scale (NHS) values of the reference electrode at the various temperatures were determined by measurements against a saturated quinhydrone electrode in 0.09 M potassium chloride + 0.01 M hydrochloric acid at the same temperatures. A saturated potassium chloride bridge was used in these measurements. The latter quinhydrone electrode has been ascribed the NHS-values:

0.605 V at 0°C
0.589 V at 15°C
0.566 V at 35°C
0.555 V at 45°C

These values have been estimated from the formula [8]:

$$V = 0.7181 - 0.00071t(°C) - (2.303\,RT/F)\,pH$$

for the potential of the quinhydrone electrode as a function of temperature and pH, and from known values of the pH of the solution in question at various temperatures [9].

4.0 RESULTS

The anodic potential-time curves obtained in the present work, are very much of the same type as those previously shown [1] for analogous experiments at 20°C. The lowest potentials shown by these curves (these potentials mostly being the stationary potentials reached after some time of electrolysis) have been plotted in the Tafel diagram in Fig. 1.

The Tafel lines shown in Fig. 1, have all been drawn with a slope of

$$b_a = 2.303\,RT/2F \tag{7}$$

which is in accordance with the previous results [1] at 20 and 25°C. The reasonable fit of the experimental points to these lines do therefore strongly support the previous conclusion of the anodic Tafel slope being given by eqn. (7).

The Tafel lines in Fig. 1 have moreover been placed so as to make the average experimental deviation from these lines a minimum. By an extrapolation of these lines to the standard potential of the Cu/Cu_{aq}^{++} electrode (see the introduction to this paper), which according to deBethune *et al.*[3] is given by:

$$E_o = 0.337 + 8 \times 10^{-6}\,(t - 25)V$$

where t is the temperature in °C, the following values are obtained for the standard exchange current (J_o) of this electrode in 0.1 N sulphuric acid solutions:

$$\begin{aligned} J_o &= (2.3 \pm 0.6)\,10^{-3}\ \text{A/cm}^2 \text{ at } 0°C \\ J_o &= (1.2 \pm 0.3)\,10^{-2}\ \text{A/cm}^2 \text{ at } 15°C \\ J_o &= (5.4 \pm 1.4)\,10^{-2}\ \text{A/cm}^2 \text{ at } 35°C \\ J_o &= (1.4 \pm 0.3)\,10^{-1}\ \text{A/cm}^2 \text{ at } 45°C \end{aligned} \tag{8}$$

The average deviations given, have been calculated from the average deviations of the experimental points in Fig. 1 from the Tafel lines. This implies the assumption that the Tafel slopes accepted (eqn. 7) are correct.

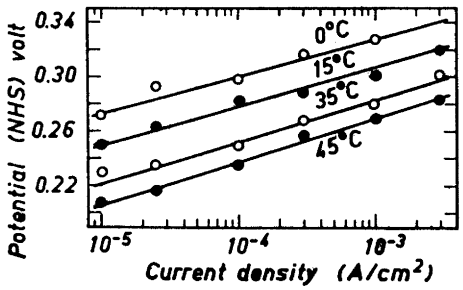

Fig. 1. Tafel diagram for anodic dissolution of copper in 0.1 N sulphuric acid at various temperatures.

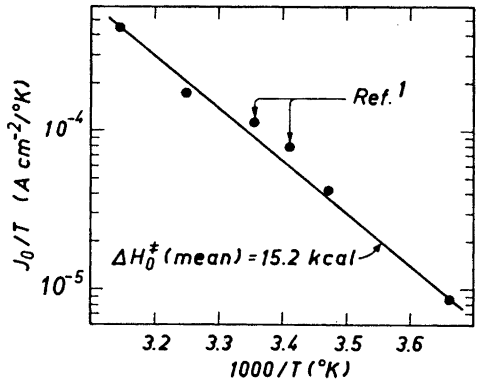

Fig. 2. Arrhenius plot for the standard exchange current (J_o) of the Cu/Cu_{aq}^{++} electrode.

The average values in (8) give the following equations for the temperature dependence of the standard exchange current:

$$-R \text{ d}(\ln J_o)/\text{d}(1/T) = 15.8 \pm 1.5 \text{ kcal} \quad (9)$$

$$-R \text{ d}(\ln J_o/T)/\text{d}(1/T) = 15.2 \pm 1.4 \text{ kcal} \quad (10)$$

The latter relationship is graphically illustrated by the Arrhenius plot in Fig. 2, where also previously data by the author [1] at 20 and 25°C have been included.

The accepted value for the standard heat of reaction of the Cu/Cu_{aq}^{++} electrode is [10]:

$$\Delta H_{o,a} = -\Delta H_{o,c} = 15.4 \text{ kcal (HS)} \quad (11)$$

As further this electrode has been found [1] to be symmetric and to have a stoichiometric number of 1/2, the data in (10) and (11), on the basis of (2) and (5), give:

$$\Delta H_o^* \text{ (mean)} = 15.2 \text{ kcal} \quad (12)$$

and the following hydrogen scale values:

$$\Delta H_{o,a}^* = 30.6 \text{ kcal (HS)} \quad (13a)$$

$$\Delta H_{o,c}^* = -0.2 \text{ kcal (HS)} \quad (13b)$$

for its standard heats of activation. The absolute values for the standard heat of activation of the two single electrode reactions should then be found by combining (13a) and (13b) with (6a) and (6b), when only the standard heat of reaction of the hydrogen electrode were reliably known.

The average values in (8) and (10) give the following Arrhenius equation for the Cu/Cu_{aq}^{++} electrode:

$$\log (J_o/T) = \log (nF/\nu) + (1.54 \pm 0.05) - 15200/2.303\ RT \quad (14)$$

showing the Arrhenius factor (A) to be given by:

$$\log (A/T) = 1.54 \pm 0.05 \quad (15)$$

where A is expressed in mole (activated complex)/cm^2 sec.

If the kinetics of the copper electrode reactions in this case is adequately covered by (1) and not dependent on factors representing the activity of surface sites, the present Arrhenius factor should, according to the transition state theory and the reasoning [7] leading to (2), be given by:

$$\log (A/T) = \log (k/h) + \Delta S_o^*(\text{mean})/R \qquad (16)$$

provided the transmission coefficient is equal to one. The mean standard entropy of activation, $\Delta S_o^*(\text{mean})$, which is defined analogous to (3), comes then out with a value of approximately -40 cal/°K.

5.0 DISCUSSION

From the present work on copper and previous work on iron [7], we have the following standard heat data:

Electrode :	Cu/Cu_{aq}^{++}	Fe/Fe_{aq}^{++}
$\Delta H_o^*(\text{mean})$:	15.2 kcal	23 kcal
$\Delta H_{o,a}^*$:	30.6 kcal(HS)	2 kcal(HS)
$\Delta H_{o,c}^*$:	-0.2 kcal(HS)	44 kcal(HS)
$\Delta H_{o,a} = -\Delta H_{o,c}$:	15.4 kcal(HS)	-21 kcal(HS)

The values for the heat of reaction have been taken from the compilation by Latimer [10] and refer to the reaction of one gramatom of the metal. The heats of activation refer to the formation of one mole of the "activated complex".

A most striking feature of these results is that, for both the copper and the iron electrode, the mean standard heat of activation and the standard heat of reaction have very nearly the same numerical value, even though the values of the former are absolute ones (see Chapter 2.0) whereas those of the latter are hydrogen scale values. Through eqn. (5), this approximate equality further makes the hydrogen scale value of the standard heat of activation in one direction near to naught and in the reverse direction near to twice the numerical hydrogen scale value of the standard heat of reaction (as shown in the above table). This could possibly mean:

a) that the reactions of these metal/metal ion electrodes do not pass through any state of much higher enthalpy than that of the highest end state (initial or final), and

b) that the standard heat of reaction of the hydrogen electrode on the metals concerned is near to zero.

In connection with a), one has to remember that the end states according to the kinetic unit equation encompass *two* gramatoms (or gramions) of the metal.

What is said under a) is just what is well known to be the case for reactions between a crystal and its vapour. It seems thus likely that the exchange be-

tween a metal and aqueous solutions of its ions in this respect is analogous to the exchange between a crystal and its vapour, and that in the former field we should have much to gain from a wider application of the important developments which have occurred in the latter field during the last decade. As an example can here be mentioned that the double metal ion mechanism, which now has been found to govern both the iron and the copper electrode reactions, is analogous to the parabolic growth predicted by Burton, Cabrera, and Frank [11] for cases in which the mean displacement of adsorbed molecules on the crystal surface is small compared to the circumference of the critical two-dimensional nucleus. This will be more thoroughly discussed in a subsequent paper.

What is said under b) is not unlikely. This may be seen from the following scheme:

Reaction	ΔH_o(kcal)
$\frac{1}{2}\,H_2(g) = H^+(g) + e^-(g)$	367.1
$H^+(g) = H^+(aq)$	−256.0
$e^-(g) = e^-(M)$	(−111.1)
$\frac{1}{2}\,H_2(g) = H^+(aq) + e^-(M)$	(0)

The symbols (g), (aq), and (M) refer the species to the gas phase, the aqueous phase, and the metal phase, respectively. The ionization and hydration enthalpy values have been adopted from Latimer [10] (p.35). The value of the electron transfer enthalpy corresponds to an electron work function of 4.85 eV, which is not far from many such data on copper and iron (according to the compilation by Michaelson [12]).

The present results on copper and previous results on iron [7] give the following apparent values of the mean standard entropy of activation:

Electrode:	Cu/Cu_{aq}^{++}	Fe/Fe_{aq}^{++}
ΔS_o^*(mean):	−40 cal/°K	+12 cal/°K

We call these values apparent because of the underlying assumptions i) that the rate constants from which they have been determined, are adequately given by the usual product of a frequency factor (kT/h) and an entropy factor (exp (ΔS_o^*(mean)/R)) without including any catalyst activity (*e.g.* the activity of special surface sites), and ii) that the transmission coefficient is equal to one.

The former assumption represents a matter of great importance for our understanding of heterogeneous reactions in general and of electrode reactions in particular. This matter seems little clarified, and the validity of the assumption may be questionable. It is nevertheless of interest to work out the apparent standard entropy of the activated state of the copper and iron electrode and to compare this with the standard entropy of their end states. This may be

done by using the absolute metal entropy values tabulated by Latimer [10] and the absolute ionic entropy values tabulated by Conway and Bockris [13]. The latter values are based on the standard entropy of electrons in metals being taken equal to zero, whereby we may ignore the electrons in the present treatment. On this basis, one arrives at the following standard entropy values at 15°C (cal/°K):

State	2Cu	(*)	$2Cu^{++}$	$2Fe + OH^-$	(*)	$2Fe^{++} + OH^-$
S_o	+16.0	−68.5	−73.0	+15.5	−14.9	−69.3

The values given for the activated states have been calculated from:

$$\Delta S^*_o(\text{mean}) = \tfrac{1}{2}\,(\Delta S^*_{o,a} + \Delta S^*_{o,c})$$

by the use of the end state entropies and the experimental values of the mean standard entropy of activation.

For the Cu/Cu^{++}_{aq} electrode, the entropy data strongly support the enthalpy data in showing the activated state of this electrode to be closely related to the *ionic* end state. For the Fe/Fe^{++}_{aq} electrode, the entropy data and the enthalpy data do not support each other that strongly, but are nevertheless mutually in agreement in indicating the activated state of this electrode to be relatively closely related to the *metallic* end state.

If some catalyst activities should be included in the experimental mean standard entropy of activation, the true value of this and thereby of the standard entropy of the activated state should be found by adding to the above values a term of:

$$-2.303\,R \log a$$

where a represents the product of the possibly included catalyst activities raised to the powers given by the stoichiometry of the catalyst interaction.

So far, it is difficult to say what a possibly might mean in the cases discussed here. However, it could have values down to about 10^{-8} for copper and about 10^{-7} for iron without the above mentioned correlation between the entropy and the enthalpy values being cancelled. It is also possible that such a correlation is not to be expected, whereby a may be even smaller. It could be of interest to compare this with step-lines in a crystal surface and kink sites on such step-lines. If the number of dislocations per cm^2 is 10^8, the number of atomic sites on the step-lines connecting them need not exceed 10^{-4} of all sites in the area. The relative number of kink sites must be smaller, but not necessarily very much smaller. It seems thus not impossible that the experimental activation entropy values obtained may include a catalyst activity term representing for instance i) the proportion of step sites or of kink sites in the surface or ii) the product of these proportions or iii) the square of the one or the other of them. This question will be more thoroughly dealt with elsewhere.

APPENDIX

From the general theory of activation controlled electrode reactions [14], we have:

$$\ln(J_0/T) = \ln(nFk/\nu h) + \Delta S_0^*/R - \Delta H_0^*/RT \pm \alpha nF\Delta\emptyset_0/\nu RT \quad (1')$$

when the transmission coefficient and the transition state activity coefficient are assumed equal to unity and all possible catalytic interactions are accounted for. In the last term, + and − apply to anodic and cathodic reactions, respectively.

For two mutually reverse reactions, the sum of the symmetry factors is equal to one ($\alpha_a + \alpha_c = 1$), and we have from (1'):

$$\ln(J_0/T) = \ln(nFk/\nu h) + \Delta S_0^*(\text{mean})/R - \Delta H_0^*(\text{mean})/RT \quad (2')$$

where:

$$\Delta H_0^*(\text{mean}) = \alpha_c \Delta H_{o,a}^* + \alpha_a \Delta H_{o,c}^* \quad (3')$$

$$\Delta S_0^*(\text{mean}) = \alpha_c \Delta S_{o,a}^* + \alpha_a \Delta S_{o,c}^* \quad (4')$$

These are more general equations which include those used above for the special case of $\alpha_a = \alpha_c = \frac{1}{2}$.

Acknowledgement. The author is much indebted to Miss E. Huseby and Mr. K. Trovaag for technical assistance, to various members of the staff at the Central Institute for Industrial Research for valuable discussions and other help, and to the *Royal Norwegian Council for Scientific and Industrial Research* and the *U.S. Department of Army, European Research Office,* for financial support.

REFERENCES

1. Hurlen, T. *Acta Chem. Scand.* **15** (1961) 630.
2. Hurlen, T. *Acta Chem. Scand.* **14** (1960) 1533.
3. deBethune, A. J., Licht, T. S. and Swendeman, N. *J. Electrochem. Soc.* **106** (1959) 616.
4. Seiter, H. and Fischer, H. *Z. Elektrochem.* **63** (1959) 249.
5. Barnes, S. C., Storey, G. G. and Pick, H. J. *Electrochim. Acta* **2** (1960) 195.
6. Mattsson, E. and Lindström, R. *CITCE VI* (1954), Butterworths, London 1955, p. 263.
7. Hurlen, T. *Acta Chem. Scand.* **14** (1960) 1564.
8. Harned, H. S. *J. Am. Chem. Soc.* **55** (1933) 4856.
9. Harned, H. S. and Owen, B. B. *The Physical Chemistry of Electrolyte Solutions* (3rd Ed.), Reinhold, New York 1958, p. 447.
10. Latimer, W. M. *Oxidation Potentials* (2nd Ed.), Prentice-Hall, New York 1952.
11. Burton, W. K., Cabrera, N. and Frank, F. C. *Phil. Trans. Roy. Soc. London* **A243** (1951) 299.
12. Michaelson, H. B. in *Handbook of Chemistry and Physics* (38th Ed.), Chemical Rubber Publishing Co., Cleveland 1956—1957, p. 2351.
13. Conway, B. E. and Bockris, J.O'M. in *Modern Aspects of Electrochemistry* (ed. J. O'M. Bockris), Butterworths, London 1954, Chapter 2.
14. Parsons, R. *Trans. Faraday Soc.* **47** (1951) 1332.

Received November 16, 1960.

ACTA CHEMICA SCANDINAVICA 15 (1961) 630–644

On the Kinetics of the Cu/Cu_{aq}^{++} Electrode

TOR HURLEN

Central Institute for Industrial Research, Blindern, Oslo, Norway

Investigations have been made on the anodic dissolution and cathodic deposition of copper in acid sulphate solution at 20 and 25°C by means of a slow amperostatic technique. The reactions have been found to obey the Tafel relationship, except for the occurrence of a cathodic limiting current, to have mutually symmetric Tafel lines with slopes of numerically 2.303 $RT/2F$, and to be little dependent on the pH and the sulphate concentration. The rate of deposition (in the Tafel region) is moreover found to be proportional to the square of the cupric ion activity, and the rate of dissolution to be independent of this activity. This indicates a mechanism covered by the equation:

$$2\,Cu = 2\,Cu_{aq}^{++} + 4\,e^-$$

For the exchange current (i_o) of the Cu/Cu_{aq}^{++} electrode in 0.1 N sulphuric acid solutions of cupric sulphate at 20 and 25°C, respectively, it is found:

$$i_o = 2.4\ a\ 10^{-2}\ A/cm^2$$
$$i_o = 3.4\ a\ 10^{-2}\ A/cm^2$$

where a is the cupric sulphate activity. The standard exchange current is by definition $J_o = i_o/a$.

1.0 INTRODUCTION

In a previous paper [1], it has been shown that the reactions of the Fe/Fe_{aq}^{++} electrode seem best represented by the "kinetic unit equation":

$$2Fe + OH^- = 2Fe^{++} + OH^- + 4e^-$$

indicating that two metal ions are transferred for each rate determining step in the electrode process, and that there is an interaction of one hydroxyl ion for every second metal ion reacting. It has further been suggested that the double metal ion mechanism might be a consequence of the steric relationship between water and metal, which for an iron/water interface of closest packing gives a relationship of very nearly 2:1 between the number of metal atoms and that of water molecules at this interface. However, it may be shown that this relationship does not suffice in explaining the occurrence of *two* metal ions in the kinetic unit equation.

Before attempting any further theoretical approach to this problem, it was assumed desirable to carry out the same type of slow amperostatic polarization measurements on other metals as those previously [1] performed on iron. The desirability of this is first of all due to the fact that (to our knowledge) no previous investigators in the field of metal/metal-ion electrode reactions have concluded on a kinetic unit equation involving *two* metal ions. This also necessitates a relatively thorough discussion of previous work.

The present work is confined to the behaviour of copper in sulphate solutions of various sulphuric acid and cupric sulphate concentrations. In these solutions, the cuprous ion is unstable [2] and can mainly be formed as a possible intermediate in the copper electrode reactions. The behaviour of copper in the presence of cuprous ion stabilizing anions (especially chloride ions) will be the subject of a subsequent paper.

2.0 PREVIOUS WORK

The anodic behaviour of metals in general has been reviewed by Hoar[3], and the cathodic deposition of metals by Fischer[4] and Bockris[5]. All these surveys include references to copper, but do not reveal any really good polarization data for anodic dissolution nor cathodic deposition of this metal.

More recently, however, these reactions have been studied by several investigators. Sroka and Fischer[6] found a Tafel slope of $b_c = -0.029$ V for the deposition of copper at low current densities (up to about 5×10^{-3} A/cm^2) from 1 N cupric sulphate + 1 N sulphuric acid at 22°C. At higher current densities, the polarization curve was steeper ($b_c = -0.232$ and -0.116 V), and they correlate this with changes in the crystallization habit (pyramidal to cubic to finely polycrystalline deposits with increasing current density). Analogous results are further reported by Seiter and Fischer[7], by Seiter, Fischer and Albert[8], and by Barnes, Storey and Pick[9]. Barnes[10] has moreover shown that the deposits formed at low current densities (up to about 15×10^{-3} A/cm^2) are extensions of the base, whereas twinning occurs at higher current densities (the twinning possibly initiating polycrystallinity). The low current density range seems thus to be of greatest interest for correlating studies on the mutually reverse reactions of the Cu/Cu_{aq}^{++} electrode. In the present work, therefore, special attention is paid to data obtained in this range (especially as far as the cathodic reaction is concerned). The polarization measurements of the above mentioned authors[6-9] do thus indicate that the proper cathodic Tafel slope is given by:

$$b_c = -2.303\ (RT/2F)$$

which is the same as previously obtained for iron[1]. These measurements have mainly been performed on polycrystalline cube-texture copper sheets of high purity.

Mattsson and Bockris[11], from galvanostatic short-pulse measurements on copper electrodes produced through electrodeposition (15×10^{-3} A/cm^2), found a linear V/i-relationship for both the anodic and the cathodic reaction at very low overpotentials (up to about 0.01 V) in acidified cupric sulphate solutions. This is in agreement with the theory of activation-controlled electrode reactions[5,13], but not with that of slow surface diffusion of adions[14] (which predicts a proportionality between the rate and the square of the overpotential at low overpotentials). Mainly from the relation between overpotential and time, Mattsson and Bockris nevertheless conclude that a surface diffusion is rate-controlling at low current densities, but also the assumptions on which this evaluation is based[15], have recently been criticised by Fleischmann and Thirsk[14].

At high current densities (above 15×10^{-3} A/cm^2), Mattsson and Bockris[11] (see also Mattsson and Lindström[12]) found the Tafel relationship to be obeyed and report $b_c = -0.12$ V and $b_a = 0.04$ V under steady state conditions at 30°C. They interprete this as indicating that the reactions under these conditions are controlled by the redox process between cupric and cuprous ions, whilst the latter ions exist in reversible equilibrium

with copper at the electrode surface. The correctness of this conclusion very much depends on the significance of the observed cathodic Tafel lines. All the above mentioned authors [6-9] (see especially Ref.[9]) observed a much stronger variation of potential with cathodic current density from about 15×10^{-3} A/cm² and upwards than did Mattsson and Bockris. The inconsistence in the results obtained by the various authors in this current density range (with nearly the same electrolyte composition), could perhaps mean that the conditions of stirring here are important, and that these conditions have been different in the various investigations. The limiting current to be expected for copper deposition from an unstirred 1 N cupric sulphate solution lies namely in the lower part of this current density range (see *e.g.* Ref.[16]).

The anodic Tafel slope value of about 0.04 V at 30°C reported by Mattsson and Bockris, may probably be somewhat too high. In drawing at least the two anodic Tafel lines shown in their paper (Figs. 7 and 8 in Ref.[11]), they have apparently ignored the appreciably lower-lying polarization points at high current densities. Gerischer and Rickert [17] have moreover given an anodic polarization curve for copper in an acidified cupric sulphate solution, and Piontelli *et al.*[18] some curves for copper single crystals in an acidified cupric perchlorate solution, all of which seem to indicate an anodic Tafel slope of about 0.03 V at 25°C. It may thus be that for the Cu/Cu_{aq}^{++} electrode we have:

$$b_a = -b_c = 2.303(RT/2F)$$

just as previously found for the Fe/Fe_{aq}^{++} electrode [1]. A symmetric behaviour of the Cu/Cu_{aq}^{++} electrode, when under activation control, is in accordance with the early results of Juza and Kopyl [19].

The exchange current (i_o) of the Cu/Cu_{aq}^{++} electrode has been determined by several investigators: Juza and Kopyl [19] (referred to by Bockris [5]) found $i_o = 2 \times 10^{-5}$ A/cm² from charging curves in 1 M cupric sulphate at room temperature. The cathodic Tafel lines given by Sroka and Fischer [6] in the low current density range (see above) indicate $i_o = 2 - 3 \times 10^{-4}$ A/cm² in 1 N cupric sulphate + 1 N sulphuric acid at 22°C. Seiter and Fischer [7], by calculations from cathodic $V - i$ slopes at low overpotentials in 0.1 to 1 N cupric sulphate + 1 N sulphuric acid at 25°C, found $i_o = 2 \times 10^{-3} \times c^{0.45}$ A/cm² (where c is the concentration of cupric ions in mole/l). Seiter, Fischer, and Albert [8] found in the same way $i_o = 1.6 \times 10^{-3}$ A/cm² and from morphologic data $i_o = 2.1 \times 10^{-3}$ A/cm² in 1 N cupric sulphate + 1 N sulphuric acid at 25°C. However, a Tafel extrapolation of their low current density polarization data (assuming $b_c = -2.303(RT/2F)$) indicates a value slightly below 1×10^{-3} A/cm². For the same temperature and electrolyte composition, Barnes, Storey, and Pick [9] also found $i_o = 1 \times 10^{-3}$ A/cm² by extrapolation of the cathodic Tafel line obtained at relatively low current densities. This value of i_o is also in good agreement with the data given by Piontelli *et al.*[18] for a corresponding perchlorate solution at 25°C. Mattsson and Bockris [11], from $V-i$ slopes at low overpotentials in 1 N sulphuric acid + 1 N, 0.15 N, and 0.022 N cupric sulphate at 30°C, give as mean values $i_o = 2.1 \times 10^{-3}$, 1.4×10^{-3}, and 0.9×10^{-3} A/cm² for helium prepared copper electrodes and, in the two strongest solutions, $i_o = 5.4 \times 10^{-3}$ and 2.7×10^{-3} A/cm² for electrodeposited copper electrodes. From impedance measurements on copper electrodes in 10^{-3} to 10^{-1} N cupric sulphate + 1 N sulphuric acid presumably at room temperature (not specified), Bockris and Conway [20] report $i_o = 0.6 \times c^{0.75}$ A/cm² (where c is the cupric sulphate concentration in mole/l). This is very much higher than the above quoted values. Similar impedance measurements have been made in 0.05 M cupric sulphate + 1 M H_2SO_4 by Lorenz [21], who reports an exchange between ad-atoms and cupric ions of $i_o = 3 \times 10^{-2}$ A/cm² and assumes a lower rate of exchange for lattice atoms. It does seem, however, that Lorenz in the evaluation of his results has ignored the possibility of a direct dissolution and deposition at lattice building sites (see Ref.[14]).

Neglecting the mutually and from the other data widely diverging i_o-values obtained from impedance measurements, and also the early results of Juza and Kopyl, the above results seem to agree relatively well in showing

$$i_o = 1 - 2 \times 10^{-3} \text{A/cm}^2$$

in 1 N cupric sulphate (or perchlorate) + 1 N sulphuric (or perchloric) acid at 25°C. It further seems that the i_o-values obtained by extrapolation of Tafel lines at relatively low current densities generally are lower than those obtained from $V - i$ slopes at very low overpotentials. The former values do not depend on any assumption as to the stoichiometry of the exchange reactions, whereas the latter do [5,13]. The above quoted determinations assume first order reactions. If these reactions should be second order (as has been found for the Fe/Fe_{aq}^{++} electrode reactions [1]), the above quoted i_o-values from $V - i$ slopes should be halved. This would give an even better agreement between the results.

The effect of cupric ion concentration on the rate of the Cu/Cu_{aq}^{++} electrode reactions has been little studied. As mentioned above, Seiter and Fischer [7] report

$$\text{d log } i_o/\text{d log } c = 0.45$$

and Bockris and Conway [20]:

$$\text{d log } i_o/\text{d log } c = 0.75$$

in 1 N sulphuric acid solutions of cupric sulphate.

The data of Mattsson and Bockris [11] indicate an exponent lower than any of these. Such data, however, do not directly give the specific effect of the cupric ion concentration on any of the two mutually reverse reactions of the electrode, but only a possible combination of these effects.

The effect of pH on the rate of these reactions does not seem to have been studied systematically. Seiter, Fischer, and Albert [8], however, have reported on the effect of pH on the electrocrystallization habit.

The crystallographic orientation of the copper surface has by several authors been shown to affect both the dissolution and the deposition reaction. Piontelli, Poli, and Paganini [18], Leidheiser and Gwathmey [22], and Glauner and Glocker [23] have all found the (111) plane to dissolve faster than the (100) plane. The differences in dissolution rate of these faces, however, seem to be relatively small (not more than some 20 %). Leidheiser and Gwathmey even found that the behaviour could be reversed by a hydrogen atmosphere anneal of the copper single crystals. The rate of deposition (at least at low overpotentials) has also been found [18,22] to be faster on (111) faces than on (100) faces, but the differences are here even smaller than on the anodic side. In accordance with these rate data, Tragert and Robertson [24] have shown that the (111) plane is in fact the only copper surface giving a stable, reversible Cu/Cu_{aq}^{++} half-cell. The exposure of other faces ((100), (110), and (210) to a cupric sulphate solution gives a slightly unstable potential which approaches that of the (111) face with time, the initial differences being approximately 0.005 V.

The effect of the crystallographic orientation of the base metal on the structure of electrodeposited copper has recently been studied by Pick *et al.* [9,25,26] (see also Wranglén [27]), and the role of dislocations in the electrocrystallization of copper by Vaughan and Pick [26] and by Economou, Fischer, and Trivich [28].

The reaction mechanism of the Cu/Cu_{aq}^{++} electrode is apparently far from clear as several distinctly different opinions exist on this matter. Mattsson and Bockris [11] arrived at the following consecutive reaction steps:

$$Cu^{++} + 2e^- = Cu^+ + e^- = Cu_{ad} = Cu$$

from left to right in deposition and oppositely in dissolution. They further conclude that the Cu^{++}/Cu^+ redox step is rate controlling at high current desities and the Cu_{ad}/Cu step at low current densities. As discussed above, however, these conclusions seem open to some criticism. Moreover, from impedance measurements on copper in acidified cupric sulphate solutions, Lorenz [21] could find no evidence for an intermediate formation of cuprous ions.

Bockris *et al.* [11,20,29], Fischer *et al.* [8], Lorenz [21], and Gerischer [30] seem otherwise to agree in suggesting the surface diffusion and crystallization process to be slower than the transfer reaction in cathodic deposition of copper. Gerischer [30] give a relationship of approximately 1:10 between these rates at equilibrium. Fleischmann and Thirsk [14], however, have shown that many of the kinetic data on copper deposition are in disagreement with the model of lattice growth being controlled by slow surface dissusion (see also the above

discussion of the *linear V/i*-relationship found by Mattsson and Bockris [11] at low overpotentials). The available anodic polarization data are moreover in disagreement with the anodic limiting current to be expected from the reverse of this model (Mattsson and Bockris [11]).

3.0 EXPERIMENTAL

Electrodes of high purity copper (2 ppm Fe, 2 ppm Ag, 1 ppm Pb, 1 ppm Ni, 1 ppm Si, 1 ppm Na, and less than 1 ppm each of Ca and Mg, other metallic elements and the elements O, S, Se, Te, and P either being not present or being below the limits of detection by the spectrographic, chemical, and metallographic methods applied) have been used in the form of circular sheets (about 4.5 cm diameter) punched from a cold-rolled strip (about 0.6 mm thick). Prior to use, the electrodes were vacuum annealed for about one hour at about 700°C, mechanically polished, etched in dilute nitric acid, washed in running water, distilled water, and acetone, dried and weighed. Each electrode was only used once in determining a single potential-time curve at constant applied current (see below).

The solutions were prepared from A. R. quality cupric sulphate and sulphuric acid in water distilled from a "pure" and soft fresh water. The solutions were presaturated with hydrogen which first was purified by passage through a palladium catalyst at about 250°C. The solutions were also stored under purified hydrogen and were further transferred to the test cell by hydrogen pressure. A sketch of the electrolyte preparation and storage unit is shown in Ref.[1].

The test cell was a cylindrical Pyrex glass cell (about 10 cm^2 internal cross section and about 15 cm long) carrying tubes for the ingress and egress of liquid and gas. The test electrodes are placed so as to form the two end walls of the cell. After having been clamped in position, the electrodes were covered around their outer edge with polystyrene (dissolved in chloroform) and paraffine wax. The cell further has two Haber-Luggin capillaries for electrolytic connections to two external reference electrodes, and copper wires for metallic connections to the potentiometer and to the current source. In this cell, a sketch of which is shown in Ref.[1], the electrolyte is exposed to the atmosphere in two capillaries of one millimeter diameter only.

The experiments were performed galvanostatically. The current was supplied from an assembly of four 12 V accumulators connected in series. It was read on a calibrated Avometer and controlled by a number of variable resistances in series with the cell. The electrode potential of each electrode as a function of time was measured against a saturated calomel electrode by means of a Cambridge pH-meter. Convection and diffusion between the test cell and the two reference electrodes were hindered by a closed stopcock in each of the connecting tubes.

The partial current density of the reactions was determined from the weight change of the electrodes over a considerable time at a constant applied current. A Mettler semimicro balance was used for these weighings. The duration of the runs varied from two days to one hour depending on the current applied, 10^{-5} — 10^{-2} A/cm^2 (apparent).

The experiments were carried out partly in a water thermostat at 25 ± 0.1°C and partly in a thermostated room at 20 ± 0.5°C. Except for one series of experiments with magnetic stirring in the cell, no stirring was applied.

The saturated calomel electrode has been ascribed the potentials 0.242 V and 0.245 V on the normal hydrogen scale (NHS) at 25 and 20°C, respectively.

4.0 RESULTS AND INTERPRETATIONS

Experiments of the above described type have been performed with the following nine electrolyte solutions:

H_2SO_4(1 N) + $CuSO_4$(0.5 M)
H_2SO_4(0.1 N) + $CuSO_4$ (0, 0.01, 0.03, 0.1, 0.3 M)
$CuSO_4$ (0.01, 0.1, 1 M)

These solutions have various pH-values in the range 0 to 5.

4.1 Reversible potentials, activities, and liquid junctions

In the not acidified cupric sulphate solutions at 25°C, the observed zero current potentials averaged to 0.268, 0.291, and 0.311 V (NHS) in the 0.01, 0.1 and 1 M solution, respectively. The values to be expected from the accepted [2,31] standard potential of 0.337 V and the activity coefficients (0.438, 0.154, and 0.043) tabulated by Parsons [31] are 0.267, 0.283, and 0.297 V. There may be several reasons for the discrepancies between these two sets of values, but they are easily accounted for by assuming the liquid junction potential between the saturated potassium chloride solution in the reference half-cell and the three cupric sulphate solutions to be 0.001, 0.008, and 0.014 V (+ $CuSO_4$/KCl—), respectively. This interpretation has here been accepted and corrections accordingly made in all the potential measurements in these solutions. The fact that these corrections bring the respective anodic Tafel lines (in a V(NHS)-log i diagram) to coincide mutually (see below), lends confidence to the above interpretation.

The potential measurements in the 0.1 N sulphuric acid solution have been corrected for a liquid junction potential of 0.004 V (—H_2SO_4/KCl +), a value tabulated by Milazzo [32].

The anodic Tafel lines obtained in the 0.1 N sulphuric acid solutions of cupric sulphate at 20°C coincide without corrections with the one obtained in pure 0.1 N sulphuric acid at the same temperature. This indicates that the liquid junction potential is negligible in these cases. The observed zero current potentials, which averaged to 0.263, 0.274, 0.285, and 0.296 V (NHS) at the cupric concentrations 0.01, 0.03, 0.1 and 0.3 M, respectively, may thus be regarded as the reversible potentials of copper in these solutions. According to de Bethune *et al.*[33] the isothermal temperature coefficient of the standard copper sulphate electrode is 8×10^{-6} V per degree centigrade, giving a standard potential of 0.337 V (NHS) also at 20°C. On this basis, the following activity coefficients of cupric sulphate in 0.1 N H_2SO_4 at 20°C are arrived at: 0.280 at 0.01 M, 0.224 at 0.03 M, 0.161 at 0.1 M and 0.129 at 0.3 M. The relationship between these and the corresponding coefficients in water seem to be in accordance (at least qualitatively) with what is to be expected from the dissociation constants of cupric sulphate and sulphuric acid [34].

In 1 N sulphuric acid + 0.5 M cupric sulphate, the average zero current potential was 0.306 V(NHS) at 25°C. No attempts have been made neither to evaluate the liquid junction potential encountered in these measurements, nor to determine the reversible potential and the cupric activity in this solution. Only overvoltage values (in which the liquid junction potential cancels out by difference) have been used in the below described kinetic studies in this solution.

The average deviation in the observed zero current potentials was generally about $\pm$ 0.002 V. The above evaluations moreover involve the approximation associated with the potential difference between the standard copper sulphate electrode and the saturated calomel electrode having been regarded the same on the *molal* as on the *molar* scale.

4.2 Current efficiencies

The weight change measurements on anodes used in 0.1 N sulphuric acid gave as an average of eighteen runs a current efficiency of 100.6 ± 1.8 % for the formation of cupric ions. There was no distinct trend in the results to indicate any variation in the efficiency with current density (10^{-5} to 10^{-2} A/cm^2).

In the acidified cupric sulphate solutions, a corresponding dissolution efficiency of 100.4 ± 2.3 % (34 runs) and a deposition efficiency of 100.8 ± 2.4% (28 runs) were obtained. At the highest current densities applied under conditions of no stirring, loosely adhering powdery deposits were formed on the cathodes. This gave rise to highly erratic (too low) cathodic efficiency values which have been neglected. This also applies to the not acidified cupric sulphate solutions. Except for its effect on the formation of powdery deposits, the stirring could not be found to have any effect on the current efficiency.

In the not acidified cupric sulphate solutions, the experimental efficiency values were far from 100 % (below for anodes and above for cathodes) at low current densities, approaching this value with increasing current density (except for the formation of powdery deposits). These results were found to be due to the formation of some solid compound on the copper surface. No attempts were made to identify this compound. According to the work of Miller and Lawless [35], however, it probably is cuprous oxide.

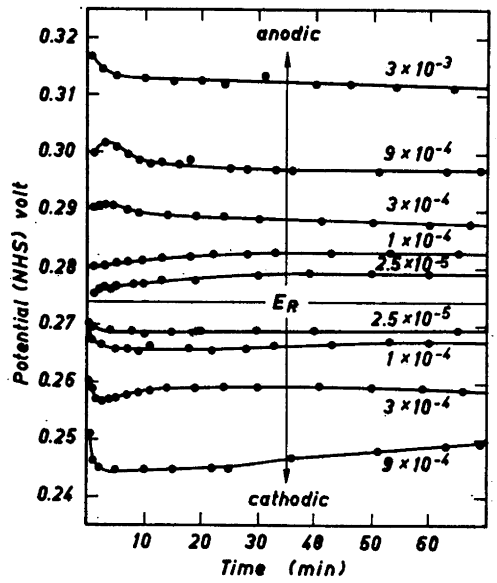

Fig. 1. Potential-time curves for copper at various anodic and cathodic current densities (A/cm^2) in 0.03 M cupric sulphate + 0.1 N sulphuric acid at 20°C.

4.3 Potential-time curves

Some examples of the potential-time curves obtained are shown in Fig. 1. These curves apply to 0.03 M cupric sulphate + 0.1 N sulphuric acid at 20°C, but are relatively representative for the time dependence generally found also in the other solutions. In some cases (especially in stirred solutions), the curves were almost straight horizontal all through the experimental time period, indicating a nearly time-independent potential. However, at those relatively high cathodic current densities at which powdery deposits were formed, the potential was always low (sometimes lower than the reversible hydrogen potential in the applied solution) and usually rather unstable. The current density above which this occurred, varied with the electrolyte composition and the stirring conditions just as is to be expected for a limiting current. The poorly adhering powdery deposits and the relatively low and rather unstable cathodic potentials appear thus to be due to the applied current exceeding the limiting current. This is further discussed below.

4.4 Polarization curves

In constructing polarization curves from the above described potential-time curves, it has in the case of time dependence been assumed that the potentials giving the lowest numerical overvoltage values are the most representative ones. This has most usually been the stationary potentials reached after some time of electrolysis (see Fig. 1).

The polarization data obtained in this way are given by the points in the Tafel diagrams presented in Figs. 2—5. The Tafel lines shown there have all been drawn with slopes of:

$$b_a = -b_c = 2.303(RT/2F) \quad (1)$$

per logarithmic unit in current density. The corresponding anodic and cathodic lines have moreover been drawn in such a way as to intersect at the reversible potential (which has been determined as described above).

The symmetric deviation from these Tafel lines in the vicinity of the reversible potential, is at least qualitatively in accordance with what is to be expected from the reverse reaction being appreciable. At higher overpotentials and especially in the 0.1 N sulphuric acid solution, the experimental *anodic* polarization points exhibit a reasonable fit to the lines drawn. Also the *cathodic* points mostly show a reasonable fit to the respective Tafel lines at medium current densities, but break relatively sharply away from the lines above a certain current density strongly dependent on electrolyte composition and stirring. This type of deviation is shown by the dashed curves in Figs. 4 and 5.

In unstirred 0.5 M cupric sulphate + 1 N sulphuric acid at 25°C, the unsymmetric deviation from the cathodic Tafel line seems to start even before the reverse anodic reaction has become negligible, whereby the polarization points do not even reach the line. This is shown in Fig. 2, where present results in an *unstirred* solution are compared with some previous results of Barnes, Storey, and Pick [9] in a *stirred* solution of the same composition and temperature. This comparison gives the first indication that the deviations observed from

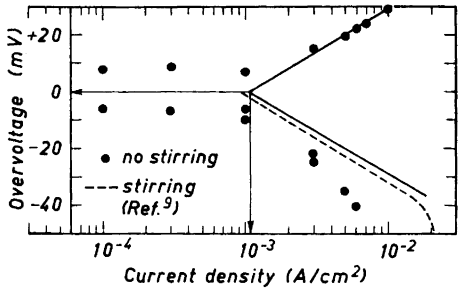

Fig. 2. Tafel diagram for the Cu/Cu^{++}_{aq} electrode in 0.5 M cupric sulphate + 1 N sulphuric acid at 25°C.

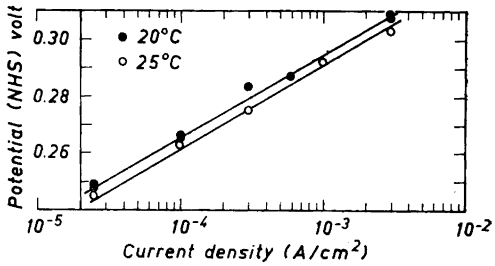

Fig. 3. Tafel curves for anodic dissolution of copper in 0.1 N sulphuric acid at 20 and 25°C.

the symmetrically drawn cathodic Tafel lines, are due to the deposition reaction becoming influenced by the rate of transport of cupric ions to the electrode surface.

This interpretation is further strongly supported by the effect of stirring shown in Fig. 4 (B), and the effect of increasing cupric sulphate concentration shown in Fig. 4 (A to D) and Fig. 5 (A to C), in counteracting the deviation by

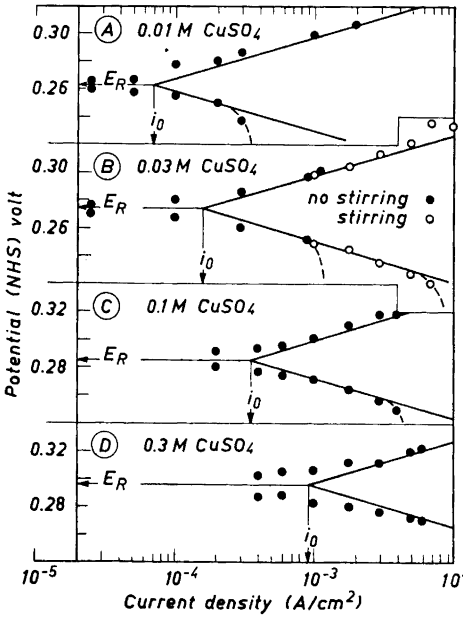

Fig. 4. Tafel diagrams for the Cu/Cu^{++}_{aq} electrode in 0.1 N sulphuric acid solutions of cupric sulphate at 20°C.

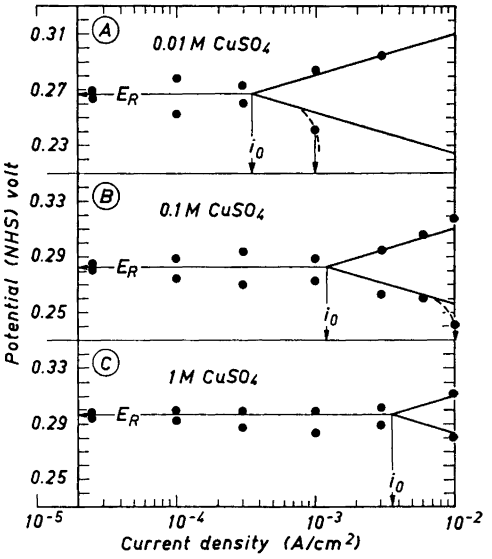

Fig. 5. Tafel diagrams for the Cu/Cu^{++}_{aq} electrode in solutions of cupric sulphate in water at 25°C.

transferring it to higher current densities. It is also of interest to note that analogous deviations occur at very nearly the same current densities in the deposition of iron from solutions of corresponding ferrous ion concentrations [1], and that these current densities coincide reasonably well with calculated approximate values of the limiting current [16].

It thus appears that the deviation from symmetry, as indicated by the dashed curves in Figs. 4 and 5, represents a transition from activation control to diffusion control in deposition, and that the symmetrically drawn Tafel lines are representative for the Cu/Cu_{aq}^{++} electrode reactions when under activation control. This is in agreement with the suggestions made in the above discussion of previous work, and indicates a symmetry factor (α) and a stoichiometric number (ν) of:

$$\alpha = 1/2 \tag{2}$$

$$\nu = 1/2 \tag{3}$$

for the Cu/Cu_{aq}^{++} electrode, just as has previously been found for the Fe/Fe_{aq}^{++} electrode [1].

4.5 Exchange currents

The exchange current (i_0) of the Cu/Cu_{aq}^{++} electrode in the various solutions applied (as given by the intersection of the Tafel lines at the reversible potential) is indicated by the vertical arrows in Figs. 2, 4, and 5. The values found at the various cupric sulphate concentrations and activities (as given above) in water at 25°C and in 0.1 N sulphuric acid at 20°C are moreover plotted in Fig. 6.

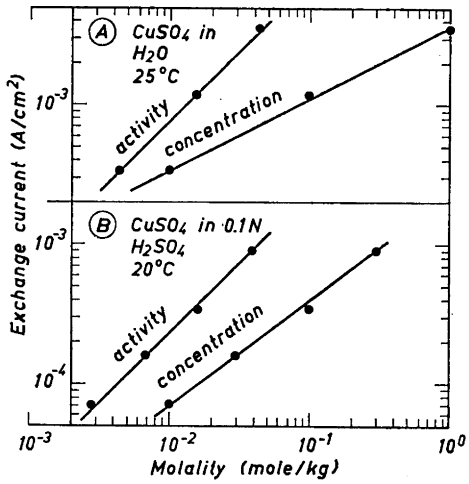

Fig. 6. Effect of cupric sulphate concentration and activity on the exchange current of the Cu/Cu_{aq}^{++} electrode in pure water solutions (25°C) and in 0.1 N sulphuric acid solutions (20°C) of cupric sulphate.

The straight lines drawn in Fig. 6 correspond to d log i_o/d log $c = 0.51$ (in water at 25°C) and 0.73 (in 0.1 N sulphuric acid at 20°C) and to:

$$\text{d log } i_o/\text{d log } a = 1 \tag{4}$$

in both cases. The results more explicitly give:

$$i_o = a(23.6 \pm 0.9)10^{-3} \text{ A/cm}^2 \tag{5}$$

$$i_o = a(80.5 \pm 2.1)10^{-3} \text{ A/cm}^2 \tag{6}$$

at 20 and 25°C, respectively. The values in the parentheses represent thus the *standard* exchange current in mA/cm² at the respective temperatures, provided the experimental data do not include any possible effects of the changes in pH and sulphate ion concentration accompanying the changes in the cupric sulphate concentration (see below).

In 0.5 M cupric sulphate + 1 N sulphuric acid at 25°C, the present results (Fig. 2) indicate an exchange current near to 1×10^{-3} A/cm². This is in excellent agreement with previous results (see above).

4.6 Effect of electrolyte composition

The effects to be discussed here, will only be those possibly exhibited by the components of pure and mixed solutions of cupric sulphate and sulphuric acid on the rate of copper dissolution and deposition when these reactions are under activation control. It has already been somewhat considered how the transition from activation control to diffusion control in deposition is affected by the composition of such solutions.

From Figs. 3 and 4 is seen that the anodic Tafel line has very nearly the same position in the Tafel diagram for the 0.1 N sulphuric acid solution as for any of its mixed solutions with cupric sulphate at 20°C. From Fig. 5 is further seen that the anodic Tafel lines obtained in the pure water solutions of cupric sulphate at 25°C, also have mutually the same position. This obviously means that neither the sulphate ions nor the cupric ions present in these solutions have any measureable effect on the dissolution reaction. As the sulphate ions are not components of the thermodynamic reaction equation of the Cu/Cu_{aq}^{++} electrode ($Cu = Cu^{++} + 2e^-$), it is thereby clear that they cannot directly interact in the deposition process either.

A comparison of the anodic data in Fig. 3—5 further indicates that the reactions also are very nearly pH independent in the pH-range concerned (approximately 0 to 5), but that there possibly is a slight tendency for the reaction rates to increase with increasing pH in the upper part of this pH-range (the anodic curves in Fig. 5 showing an approximately 2.2 times faster rate than the 25°C curve in Fig. 3 at corresponding potentials). This may be the reason for the relatively large difference shown by eqns. (5) and (6) in the standard exchange current for copper/cupric sulphate in water at 25°C and in 0.1 N sulphuric acid at 20°C, respectively.

As the cupric sulphate activity has not been found to have any effect on the rate of dissolution, the observed effect of this activity on the exchange current

(eqn. (4)) must be entirely due to its effect on the rate of deposition. On the basis of (1), (4), and the Nernst equation for the reversible potential, it is easily seen that this means:

$$(\mathrm{d}\ \log\ i_c/\mathrm{d}\ \log\ a)_{V,T} = 2 \qquad (7)$$

saying that the rate of deposition is proportional to the square of the cupric ion activity. According to the theory of activation controlled electrode reactions [5,13], the inverse of this exponent is equal to the stoichiometric number. The observed effect of activity is thereby in agreement with the observed effect of electrode potential in indicating this number to be 1/2 for the Cu/Cu_{aq}^{++} electrode reactions (see eqn. (3)).

Except for the absence of any pH-effect, this is quite analogous to what has previously been found for the Fe/Fe_{aq}^{++} electrode [1].

5.0 DISCUSSION

The results obtained in the present work, give the Tafel diagram shown in Fig. 7 (A) for the Cu/Cu_{aq}^{++} electrode at 25°C. For comparison, some representative Tafel diagrams for the Fe/Fe_{aq}^{++} electrode at the same temperature (constructed from the results discussed in Ref.[1]) are shown in Fig. 7 (B) and (C). The symbols pCu and pFe used there, mean the negative logarithm of the activity of cupric and ferrous ions, respectively. All these diagrams only apply as far as the reactions are under activation control and the metal surface is sufficiently active.

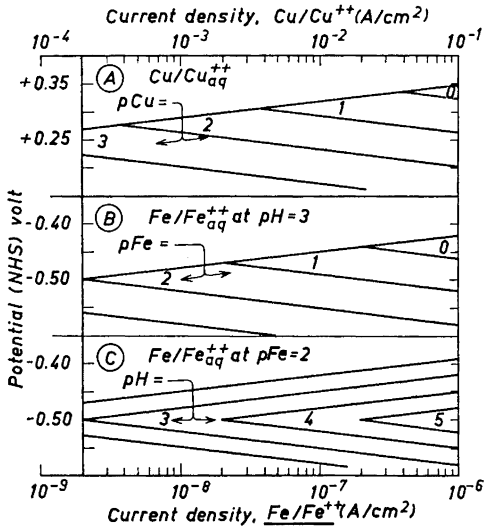

Fig. 7. Tafel diagrams for the Cu/Cu_{aq}^{++} and the Fe/Fe_{aq}^{++} electrode at 25°C when under activation control (effect of potential, metal ion activity, and pH on reaction rate).

The results clearly indicate that the kinetic unit reaction (the smallest repeating reaction unit) of the Cu/Cu_{aq}^{++} electrode in acid solution is:

$$2Cu = 2Cu^{++} + 4e^- \tag{8}$$

as compared to:

$$2Fe + OH^- = 2Fe^{++} + OH^- + 4e^- \tag{9}$$

for the Fe/Fe_{aq}^{++} electrode (see Ref.[1]). These reaction equations directly reflect the observed effects of metal ion activity, pH, and potential (the Tafel slope being numerically 1/4 of $2.303RT/\alpha F$) on the rate of the reactions in either direction.

The present results are not in agreement with the model of slow surface diffusion of ad-atoms, nor with the mechanism proposed by Mattsson and Bockris [11] of an intermediate formation of cuprous ions (see the above discussion of previous work). Both these models do namely seem to predict an unsymmetric behaviour of the electrode. Nevertheless, there obviously are several reasons to believe in the formation both of ad-atoms (see especially the work of Gerischer [30]) and of cuprous ions (see especially the work of Miller and Lawless [35]). A possible explanation of these apparent contradictions may be that the ad-atoms and the cuprous ions not are intermediates in the main reaction occurring under stationary conditions, but rather are components of some side reactions. As the reaction possibilities of the Cu/Cu_{aq}^{++} electrode are:

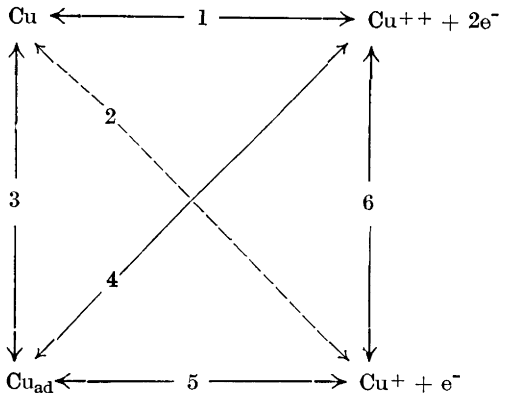

the above suggestion is equivalent to saying that the reactions 2 and 3 (or 4 and 6) are negligibly slow as compared to reaction 1, making the reactions 4, 5, and 6 (or 2, 3, and 5) an almost independent, non-interfering circuit of side reactions (the formal possibility mentioned in parenthesis being less likely). The present experiments do not reveal anything else as to the relative rates of these possible side reactions, nor anything about their kinetics. It is possible, however, that the available impedance data [20,21,36] and potentiostatic short-time transient data [30] may contain some clue to this question, when the model has been properly worked out.

A few remarks will finally be given to the crystallization habit by electro-deposition of copper. Both Fischer *et al.*[6-8] and Pick *et al.*[9,25,26] have shown that the crystal form of the deposit depends on either the current density (Fischer) or the overpotential (Pick) at which the deposition occurs. The main change is from a coherent pyramidal or ridged structure to an incoherent finely polycrystalline structure with increasing departure from equilibrium. In solutions rich enough in sulphuric acid, there appears an intermediate range in which a cubic or platelet type of structure is formed.

In the present work, poorly adhering powdery deposits (partly falling off the cathodes and thereby interfering with the cathodic current efficiency measurements) were obtained at current densities exceeding a limiting current dependent on both electrolyte composition and stirring. The limiting current is indicated by a steep deviation from the cathodic Tafel line (see Figs. 2, 4, and 5). These observations are essentially in accordance with those of Fischer *et al.* and Pick *et al.* However, with the additional information obtained in the present work through the observed effect of stirring (see especially Fig. 4B) it seems likely that the changes in crystallization habit simply are connected with the transition from activation control to diffusion control in deposition. All factors affecting this transition (*e.g.* electrolyte composition, temperature, stirring, inhibitors) must therefore be expected to be co-determining for the current densities (or overvoltages) at which the changes in crystallization habit occur. In the solutions of cupric sulphate in water (Fig. 5) and in 0.1 N sulphuric acid (Fig. 4), the transition seems to be distinctly sharper than in 1 N cupric sulphate + 1 N sulphuric acid (Fig. 2). It will at the present stage be refrained from going into the possible reasons for this, but only be pointed out that this trend is parallel to that of the occurrence of the cubic or platelet type of structure at intermediate current densities or overvoltages [8].

Acknowledgement. The author is much indebted to Miss E. Huseby and Miss T. Tönderum for technical assistance, to various members of the staff at the Central Institute for Industrial Research for valuable discussions and other help, and to the *Royal Norwegian Council for Scientific and Industrial Research* and the *U.S. Department of Army, European Research Office*, for financial support.

REFERENCES

1. Hurlen, T. *Acta Chem. Scand.* **14** (1960) 1533.
2. Latimer, W. M. *Oxidation Potentials* (2nd Ed.), Prentice-Hall, New York 1952, p. 185.
3. Hoar, T. P. in *Modern Aspects of Electrochemistry No. 2* (ed. J.O'M. Bockris), Butterworths, London 1959, Chapter 4.
4. Fischer, H. *Elektrokristallisation von Metallen*, Springer, Berlin/Göttingen/Heidelberg 1954.
5. Bockris, J. O'M. in *Modern Aspects of Electrochemistry No. 1* (ed. J. O'M. Bockris), Butterworths, London 1954, Chapter 4.
6. Sroka, R. and Fischer, H. *Z. Elektrochem.* **60** (1956) 109.
7. Seiter, H. and Fischer, H. *Z. Elektrochem.* **63** (1959) 249.
8. Seiter, H., Fischer, H. and Albert, L. *Electrochim. Acta.* **2** (1960) 97.
9. Barnes, S. C., Storey, G. G. and Pick, H. J. *Electrochim. Acta* **2** (1960) 195.
10. Barnes, S. C. *Acta Met.* **7** (1959) 700.
11. Mattsson, E. and Bockris, J. O'M. *Trans. Faraday Soc.* **55** (1959) 1586.

12. Mattsson, E. and Lindström, R. *CITCE VI* (1954), Butterworths, London 1955, p. 263.
13. Parsons, R. *Trans. Faraday Soc.* **47** (1951) 1332.
14. Fleischmann, M. and Thirsk, H. R. *Electrochim. Acta* **2** (1960) 22.
15. Mehl, W. and Bockris, J. O'M. *J. Chem. Phys.* **27** (1957) 818; *Can. J. Chem.* **37** (1959) 190.
16. Kortüm, G. and Bockris, J. O'M. *Textbook of Electrochemistry* (Volume II), Elsevier, Amsterdam/Houston/London/New York 1951, p. 405.
17. Gerischer, H. and Rickert, H. *Z. Metallk.* **46** (1955) 681.
18. Piontelli, R., Poli, G. and Paganini, L. *Nuovo cimento* **5** (1957) 1018.
19. Juza, V. A. and Kopyl, V. A. *Zhur. Fiz. Khim.* **14** (1940) 1074.
20. Bockris, J. O'M. and Conway, B. E. *J. Chem. Phys.* **28** (1958) 707.
21. Lorenz, W. *Z. physik. Chem. N. F.* **19** (1959) 377.
22. Leidheiser, H., Jr. and Gwathmey, A. T. *Trans. Electrochem. Soc.* **91** (1947) 95.
23. Glauner, R. and Glocker, R. *Z. Krist.* **80** (1931) 377.
24. Tragert, W. E. and Robertson, W. D. *J. Electrochem. Soc.* **102** (1955) 86.
25. Pick, H. J., Storey, G. G. and Vaughan, T. B. *Electrochim. Acta* **2** (1960) 165.
26. Vaughan, T. B. and Pick, H. J. *Electrochim. Acta* **2** (1960) 195.
27. Wranglén, G. *Electrochim. Acta* **2** (1960) 130.
28. Economou, N. A., Fischer, H. and Trivich, D. *Electrochim. Acta* **2** (1960) 207.
29. Conway, B. E. and Bockris, J. O'M. *Proc. Royal Soc. (London)* **A248** (1958) 394.
30. Gerischer, H. *Electrochim. Acta* **2** (1960) 1.
31. Parsons, R. *Handbook of Electrochemical Constants*, Butterworths, London 1959.
32. Milazzo, G. *Elektrochemie*, Springer, Wien 1952.
33. deBethune, A. J., Licht, T. S. and Swendeman, N. *J. Electrochem. Soc.* **106** (1959) 616.
34. Robinson, R. A. and Stokes, R. H. *Electrolyte Solutions*, Butterworths, London 1955.
35. Miller, G. T., Jr. and Lawless, K. R. *J. Electrochem. Soc.* **106** (1959) 854.
36. Hillson, P. J. *Trans. Faraday Soc.* **50** (1954) 385.

Received November 16, 1960.

ACTA CHEMICA SCANDINAVICA 15 (1961) 645–650

The Chemistry of the Natural Order Cupressales

XXXIII *. The Structure of Procerin

JARL RUNEBERG

Organisk-kemiska Institutionen, Kungl. Tekniska Högskolan, Stockholm, Sweden

A new C_{15}-tropolone, procerin, has been isolated from *Juniperus procera* Hochst. The structure of procerin was shown to be I by catalytic hydrogenation of procerin to nootkatin (III) and by cleavage of procerin glycol (II) to yield acetone. The proton magnetic resonance spectra of procerin and nootkatin are discussed.

The tropolones commonly found in the heartwoods of species of the natural order Cupressales, are nootkatin and α-, β- and γ-thujaplicin [1]. Recently, however, a number of new tropolones have been found including β-thujaplicinol (7-hydroxy-4-*iso*propyltropolone) isolated by Gardner [2] from western red cedar (*Thuja plicata*) and β-dolabrin (4-*iso*propenyltropolone) isolated by Nozoe and coworkers [3] from the japanese Hiba tree (*Thujopsis dolabrata*). Both of these compounds have since been found in other species of the Cupressales [4,5]. A methoxy thujaplicin, pygmaein, has been reported by Zavarin [6] to occur in *Cupressus pygmaea* and some related species.

As described in the present series of papers [7] (*cf.* Ref.[4]), the heartwoods of several junipers also contain nootkatin and thujaplicins. *Juniperus procera* Hochst., however, yielded a new C_{15}-tropolone which will be described in this paper. Other constituents of *J. procera* will be dealt with in a forthcoming publication.

Extraction of the light petroleum-soluble part of the acetone extract of *J. procera* with sodium carbonate, gave a partly crystalline product from which a compound, $C_{15}H_{18}O_2$, m.p. 71–72°, was obtained. It gave a chloroform-soluble copper salt and was evidently a tropolone as shown by its ultraviolet spectrum which was identical with that of nootkatin [8](III). It had almost the same R_F value as nootkatin [9] but its colour reaction with *bis*-diazotised benzidine was darker brown. The name procerin is proposed for this tropolone.

* Part XXXII. *Acta Chem. Scand.* **14** (1960) 2161.

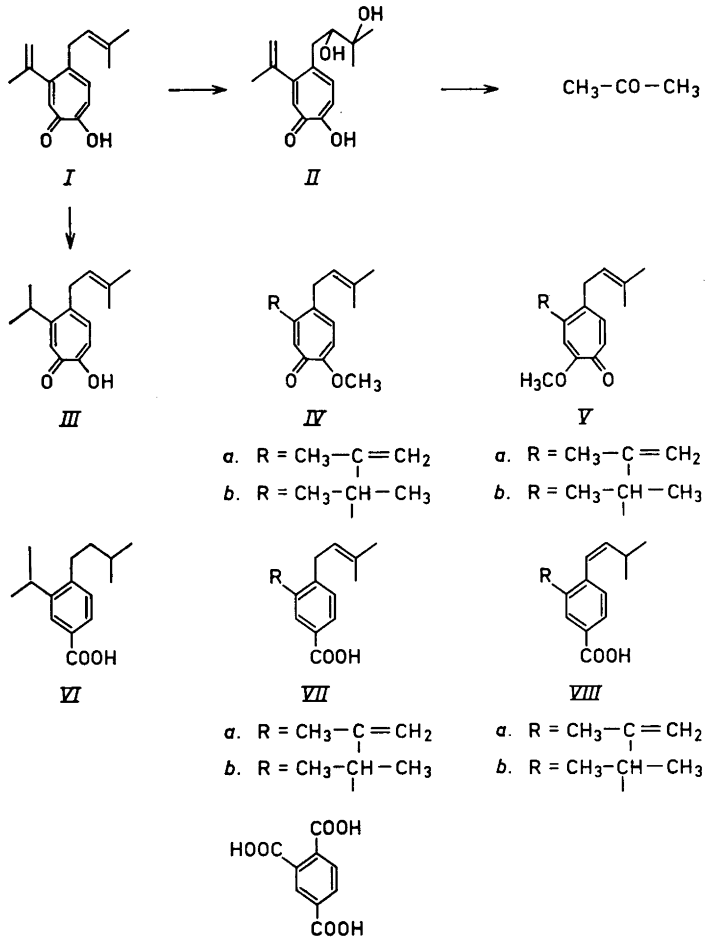

Fig. 1

Its infrared spectrum (*cf.* Fig 2) indicated that procerin differed from nootkatin in having an *iso*propenyl instead of an *iso*propyl group. On catalytic hydrogenation of procerin one mole of hydrogen was consumed and nootkatin (III) was obtained. The possibility of a diene system in the C_5-side chain undergoing 1,4-hydrogenation is very unlikely in view of the ultraviolet and infrared absorbtion of procerin.

During an attempt to determine the position of the side chain double bonds, procerin was treated with hydrogen peroxide in formic acid. Only one of the double bonds was attacked. The glycol monoformate obtained was readily hydrolysed to the corresponding glycol (II) which on treatment with periodic acid gave acetone in good yield. This proves the presence of an *iso*propylidene grouping in procerin and thus definitely eliminates the possibility that both

the double bonds are in the C_5-side chain. It follows that procerin must have the structure I.

Being unsymmetrically substituted, procerin on methylation gave two isomeric methyl ethers (IVa and Va). They could be separated into a crystalline and a liquid isomer. Both ethers on rearrangement with sodium methoxide [10] in methanol gave a mixture of the same two acids, the liquid isomer giving a much higher yield.

Oxidation of the acid mixture with dilute nitric acid afforded trimellitic acid (IX).

On catalytic hydrogenation the acid mixture absorbed two moles of hydrogen giving a single product, 4-*iso*pentyl-3-*iso*propyl-benzoic acid (VI) similarly obtained from nootkatin [10] (III).

The identity of the ultraviolet spectra of procerin and nootkatin appeared rather surprising in view of the distinct differences between the spectra of β-dolabrin [3] and β-thujaplicin (*cf.* Ref.[12]) which clearly indicate the effect of conjugation of the side chain double bond with the tropolone ring. A model of the procerin molecule shows, however, that the steric hindrance of the neighbouring *iso*pentenyl group forces the double bond of the *iso*propenyl group out of the plane of the tropolone ring, thus inhibiting conjugation. This is probably why only the C_5-side chain double bond reacted with performic acid.

A comparison of the proton magnetic resonance spectra of procerin and nootkatin indicated the presence in procerin of two protons of a $>C=CH_2$ group and the methyl protons of an *iso*propenyl group. Altogether three olefinic and three "aromatic" protons appeared to be present in this compound. The results are in full agreement with the proposed structure for procerin.

EXPERIMENTAL

Melting points were taken on a hot stage; melting and boiling points are uncorrected. Light petroleum refers to the fraction b.p. 40–60°.

Isolation of procerin. Air-dried heartwood of *Juniperus procera* Hochst. (24.4 kg, obtained from Kenya) was extracted with acetone for 24 h and the extract was fractionated as described in a previous paper in this series [13]. The fraction soluble in light petroleum and in sodium carbonate was an oil which, on standing for a month, yielded a crystalline precipitate (8.6 g). This was recrystallised from ligroin (b.p. 100–125°) and

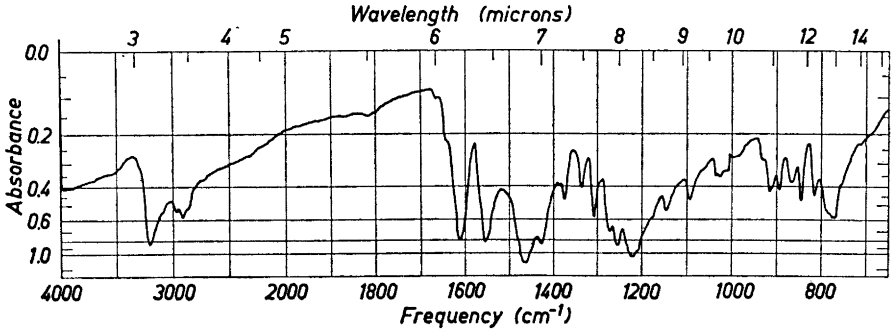

Fig. 2. Infrared spectrum of procerin in potassium bromide.

then from ethanol-water, m.p. 71—72°, $[\alpha]_D$ 0° (c, 3.4, $CHCl_3$). (Found: C 78.3; H 8.0; CH_3—(C) 9.7. $C_{15}H_{18}O_2$ requires C 78.2; H 7.9; CH_3—(C) (two) 12.9.) On further recrystallisation and sublimation in a high vacuum the melting point remained unchanged. A mixture of procerin and nootkatin melted at 67—91°. Infrared spectrum of procerin (in CCl_4): 3 075 w, 1 810 w, 1 640 m and 905 cm^{-1} s.

The copper complex, prepared by shaking a chloroform solution of procerin with a saturated aqueous solution of copper (II) acetate, was recrystallised from chloroform-ether, m.p. 203—204° (decomp.). (Found: C 68.9; H 6.5; ash 15.2. $C_{30}H_{34}O_4$ Cu requires C 69.0; H 6.6; ash (CuO) 15.2.)

Hydrogenation of procerin. Procerin (100 mg) was hydrogenated in ethanol (95 %) using a palladium (5 %)-charcoal catalyst. The reaction was interrupted after the absorption of one mole of hydrogen. The product was recrystallised from light petroleum and sublimed in a high vacuum, giving nootkatin [10] (III) m.p. 95—96° (mixed m.p., IR).

Procerin glycol monoformate. Procerin (900 mg) was treated with an ice-cooled solution of hydrogen peroxide (33 %, 860 mg) in formic acid (85 %, 9 ml). The mixture was kept at room temperature for 10 min and then heated at 40° for 2 h. Water (75 ml) and sulphuric acid (2 N, 5 drops) were then added and the solution was shaken vigorously. The product that crystallised out (720 mg) was recrystallised from ethanol (95 %), m.p. 181—183°. (Found: C 65.9; H 7.0; active H (Zerevitinoff) 0.72. $C_{16}H_{20}O_5$ requires C 65.7; H 6.9; active H (two) 0.69.) Infrared spectrum (in KBr): 1 810 w, 1 641 m, 905 cm^{-1} m.

Procerin glycol (II). Procerin glycol monoformate (400 mg) in aqueous potassium hydroxide (20 %, 16 ml) was heated in a nitrogen atmosphere on a boiling water bath for 2 h. The solution was cooled, diluted with water (40 ml), acidified with sulphuric acid (2 N) and extracted exhaustively with ether. The combined ether extracts were washed twice with a little water, dried and evaporated giving a glass which crystallised on treatment with light petroleum. The crystalline material was triturated with further amounts of light petroleum to remove traces of formic acid and repeatedly sublimed in a high vacuum, m.p. 120—121°. (Found: C 67.9; H 7.7; active H 1.22. $C_{15}H_{20}O_4$ requires C 68.2; H 7.6; active H (three) 1.14.) Infrared spectrum (in KBr): 1 815 w, 1 640 m and 904 cm^{-1} s.

Periodic acid oxidation of procerin glycol. An ice-cooled solution of procerin glycol (100 mg) in pure ethanol (95 %, 5 ml) was treated with sodium periodate (217 mg) in water (5 ml) at room temperature for 15 h. Water (20 ml) was then added and the solution was distilled (5 ml of distillate) into an excess of 2,4-dinitrophenylhydrazine in ethanolic phosphoric acid. The precipitate formed (48 mg, 53 %) was recrystallised from methanol-water, m.p. 124—125° and identified as acetone 2,4-dinitrophenylhydrazone (mixed m.p., IR). No acetone dinitrophenylhydrazone was obtained in a blank run.

Procerin methyl ethers (IVa and Va). Procerin (2.5 g) was treated with excess diazomethane in ether containing methanol (5 drops) and the mixture was kept over night in the refrigerator. The remaining diazomethane was then destroyed with acetic acid and the solution evaporated to dryness. The oily product (2.68 g) was chromatographed on silica gel (140 g). Ether-benzene (1:1) eluted a crystalline procerin methyl ether (1.31 g) which was recrystallised from light petroleum, m.p. 74—75°. (Found: C 78.3; H 8.0; CH_3O 12.7. $C_{15}H_{17}O$ (OCH_3) requires C 78.6; H 8.2; CH_3O 12.7.) Further elution with ether gave a liquid procerin methyl ether (1.08 g) which was distilled, b.p. 172—174°/0.3 mm. (Found: CH_3O 12.4. $C_{15}H_{17}O$ (OCH_3) requires CH_3O 12.7.)

Rearrangement of procerin methyl ethers. Liquid procerin methyl ether (880 mg) was dissolved in methanol (20 ml) containing sodium methoxide (from sodium, 1.8 g) and heated in a sealed tube for 15 h at 150°. The solvent was removed under reduced pressure and the residue dissolved in water. Extraction with ether gave an oil (36 mg) which was discarded. The aqueous solution was acidified and extracted with ether. The ether extract was washed with dilute sodium bicarbonate solution and then extracted with aqueous sodium carbonate. Acidification of the sodium carbonate solution, re-extraction with ether and evaporation gave a dark-brown resin (606 mg, 72 %). This was distilled in a high vacuum giving a product which crystallised immediately. On paper chromatography (dimethyl sulphoxide-impregnated paper, mobile phase: moist light petroleum [14]) the distillate gave two spots of about equal size (R_F 0.48 and 0.42), different from those of VIIb (R_F 0.56, λ_{max} 242 mμ) and VIIIb (R_F 0.45, λ_{max} 270 mμ) obtained by rearrangement of the nootkatin methyl ethers IVb and Vb [10]. The ultraviolet spectrum of the mixture of acids obtained from procerin showed maxima at 236 and 278 mμ. This mixture obviously consists of the acids VIIa and VIIIa.

Crystalline procerin methyl ether, when treated with sodium methoxide as described above, gave the same mixture of acids but in much lower yield (17 % of sodium carbonate-soluble material).

Oxidation of the acid mixture VIIa + VIIIa. The acids VIIa + VIIIa (100 mg) were heated with nitric acid (30 %, 12 ml) at 170° for 20 h in a sealed tube. The reaction mixture was concentrated to a small volume and the product that crystallised (IX, 54 mg) was heated briefly to 220° and then sublimed in a vacuum giving trimellitic acid anhydride, m.p. 164—165°, identified by mixed m.p. and IR.

Hydrogenation of the acid mixture VIIa + VIIIa. On hydrogenation in ethanol (95 %) over a palladium (5 %)-charcoal catalyst, the acid mixture VIIa + VIIIa rapidly absorbed two moles of hydrogen and then absorption ceased. The product, which was paperchromatographically homogeneous, was recrystallised from light petroleum and sublimed in a high vacuum, m.p. 124.5—126°, and identified as 4-*iso*pentyl-3-*iso*propylbenzoic acid (VI) obtained from nootkatin [10] (mixed m.p., IR).

Proton magnetic resonance measurements. The PMR spectra of procerin and nootkatin were run in dilute carbon tetrachloride solutions (mole fractions 0.04—0.12) with a Varian V-4 300 Spectrometer operating at 40 Mc/s. Measurements were made against an internal benzene standard.

The spectrum of procerin (I) showed a strong signal at 221 c/s and another of half its intensity at 208.5 c/s. The signal at 221 c/s can be assigned to the two equivalent methyl groups on the *iso*propylidene double bond. In the spectrum of nootkatin (III) the corresponding methyl peak occurred at 222 c/s. The signal at 208.5 c/s in the spectrum of procerin was assigned to the methyl protons of the *iso*propenyl group attached to the tropolone ring. (The signal from the methyl protons in α-methyl styrene occurs at 205 c/s.) In addition the spectrum of procerin showed peaks at 94 c/s and 84 c/s, respectively. In this region signals from olefinic hydrogens are expected. The peaks were rather broad and showed no fine structure. The total area of the olefinic signal group suggested that it was due to three protons.

In the spectrum of nootkatin the proton on the *iso*propylidene double bond appeared as a broad triplet with the central maximum at 88.5 c/s. A corresponding proton in procerin should absorb at about the same frequency and the two protons of the $\rangle C=CH_2$ group could also be expected to absorb in the 80—100 c/s region. By analogy with other compounds containing *iso*propenyl and vinyl groups the two protons of the $\rangle C=CH_2$ group in procerin should have slightly different chemical shifts and a comparatively small mutual spin-spin coupling constant (1—3 c/s) (*cf.* Ref.[15]). The combined effects of overlapping of the signals from two different olefinic proton groups and a small spin-spin coupling constant may explain the broadness and the lack of fine structure of the signals at 94 and 84 c/s in the spectrum of procerin.

This spectrum also contained another doublet with peaks at 153.7 and 161 c/s. These were assigned to the methylene group linking the tropolone ring with the *iso*propylidene double bond. The methylene protons should be spin-coupled with the neighbouring olefinic proton and the observed doublet was regarded as the A_2-part of an A_2X-spectrum (for nomenclature *cf.* Ref.[16]). The X-part evidently overlapped the signals from the olefinic protons of the *iso*propenyl group as was mentioned above. The spin-spin coupling constant J_{AX} was calculated to be 7.3 ± 0.2 c/s. (In the spectrum of nootkatin the corresponding methylene signals were found at 152 and 159.5 c/s, thus J_{AX} 7.5 ± 0.2 c/s.)

The spectrum of procerin showed additional peaks at 9 c/s and 5 c/s, respectively. The latter was apparently made up from two overlapping signals. These signals were assigned to the protons on the tropolone ring. The total area of the peaks at 9 and 5 c/s corresponded to three protons.

The procerin spectrum also showed a signal at −65 c/s which was assigned to the proton of the OH-group. The corresponding signal in the spectrum of nootkatin was found at −56 c/s.

Acknowledgements. The author is indebted to Professor H. Erdtman and Docent E. Forslind for their kind encouragement. My thanks are also due to the Tropical Products Institute, London, for a generous gift of wood of *J. procera*, to Dr. S. Forsén for the PMR spectra of procerin and nootkatin and for valuable discussions, to Miss G. Hammarberg for infrared and ultraviolet spectra and to the *Swedish Natural Science Research Council* for financial support.

REFERENCES

1. Erdtman, H. in Kratzl, K. and Billek, G. (Ed) *Biochemistry of Wood.* Pergamon Press, London 1958, p. 18.
2. Gardner, J. A. F., Barton, G. M. and MacLean, H. *Can. J. Chem.* **35** (1957) 1039.
3. Nozoe, T., Takase, K. and Ogata, M. *Chem. & Ind. London* **1957** 1070.
4. Zavarin, E., Smith, R. M. and Anderson, A. B. *J. Org. Chem.* **24** (1959) 1318.
5. Gardner, J. A. F. and Barton, G. M. *Can. J. Chem.* **36** (1958) 1612.
6. Zavarin, E., Smith, R. M. and Anderson, A. B. *J. Org. Chem.* **24** (1959) 1584.
7. Runeberg, J. *Acta Chem. Scand.* **14** (1960) 1995 and earlier publications.
8. Aulin-Erdtman, G. *Acta Chem. Scand.* **4** (1950) 1040.
9. Wachtmeister, C. A. and Wickberg, B. *Acta Chem. Scand.* **12** (1958) 1335.
10. Duff, S. R., Erdtman, H. and Harvey, W. E. *Acta Chem. Scand.* **8** (1954) 1073.
11. Aulin-Erdtman, G. and Theorell, H. *Acta Chem. Scand.* **4** (1950) 1493.
12. Aulin-Erdtman, G. *Acta Chem. Scand.* **4** (1950) 1036.
13. Runeberg, J. *Acta Chem. Scand.* **14** (1960) 1987.
14. Hammarberg, G. and Wickberg, B. *Acta Chem. Scand.* **14** (1960) 882.
15. Jackman, L. M. *Applications of Nuclear Magnetic Resonance Spectroscopy in Organic Chemistry.* Pergamon Press, London 1959, p. 85.
16. Pople, J. A., Schneider, W. G. and Bernstein, H. J. *High Resolution Nuclear Magnetic Resonance.* McGraw-Hill, New York 1959, sect. 5.2.

Received November 25, 1960.

ACTA CHEMICA SCANDINAVICA 15 (1961) 651–662

Lipid Formation in *Cryptococcus terricolus*

I. Nitrogen Nutrition and Lipid Formation

T. A. PEDERSEN*

Royal Institute of Technology, Division of Food Chemistry, Stockholm 70, Sweden

The yeast *Cryptococcus terricolus* was found to contain up to 70 % lipids on a dry weight basis. The lipid production was found to be independent of the quantities of nitrogen supplied. Even with 40 g $(NH_4)_2SO_4$ per litre of solution, corresponding to a carbon/nitrogen ratio of 1.9, the cells contained 55 % of lipids. Lipid production was also independent of the nature of the nitrogen source. The protein content amounted to 10–18 %.

Lipid production was closely connected with growth. In the logarithmic phase of growth, the production of lipids was at its maximum. Lipid respiration started when the carbohydrate of the medium had been consumed. This was indicated by the low R.Q. values found for starving yeast cells. The addition of glucose to starving cells caused a sudden increase in the R.Q. value.

The inverse relationship between lipids and proteins, usual in "fat" yeasts, does not occur in this organism. The protein content remains almost constant during growth, while the lipid content increases up to 65–70 %.

Numerous microorganisms have been shown to be capable of synthesizing large amounts of lipids from carbohydrates. As far as yeasts are concerned, many different species and strains have been tested for lipid production. As examples can be listed *Rhodotorula glutinis*, *R. gracilis*, *Lipomyces starkeyi*, and *Torulopsis lipofera*. These organisms are capable of accumulating 50 % or more of their dry weights as lipids. The conservative term "fat" yeast has been retained for these yeasts, but it is pointed out that "lipid" yeast would be the correct name.

The first isolations of *Cryptococcus terricolus* [1] revealed that the cells contained large globules, which after staining with Sudan III, could be said to contain lipids. The cells contained this lipid globule in all isolations and plate controls, independent of the medium used.

* Permanent address: Department of Microbiology, Agricultural College of Norway, Vollebekk, Norway.

Working with another soil yeast, now called *Lipomyces starkeyi*, Starkey [2] found that lipid formation occurred only on a nitrogen-deficient agar. His results were in accordance with the generally accepted view, that insufficient nitrogen supply leads to accumulation of lipids in "fat" yeast cells. The above-mentioned observations on *Cryptococcus terricolus* seemed to indicate that lipid formation was independent of the composition of the medium. An investigation of the influence of different sources of nitrogen in varying concentrations on the lipid synthesis of *C. terricolus* was therefore considered to be of interest. The results of this investigation are presented in this paper.

Microscopical examinations indicated that the lipid globule constituted as much as $^1/_2$—$^3/_4$ of the cell volume. Exact determinations of the lipid content should therefore be of interest.

EXPERIMENTAL

Strain No. 1 of *C. terricolus*, kept as a stock culture on vitamin-free synthetic agar [1], was used in this work. The strain was transferred to new slants at least fortnightly. In physiological experiments a two- or three-day-old culture was used as inoculum.

To obtain lipid formation the following substrate, used by Lundin and collaborators [3] in their work on *Rhodotorula gracilis*, was employed: glucose 40.0 g, $(NH_4)_2SO_4$ 1.0 g, KH_2PO_4 1.0 g, $MgSO_4 \cdot 7H_2O$ 1.0 g, NaCl 0.5 g, $CaCl_2 \cdot 6H_2O$ 0.5 g, and $FeCl_3 \cdot 6H_2O$ 0.005 g to one litre of distilled water. Beer wort was not added in these experiments, as it had been established previously[4] that optimal growth occurred in a synthetic, vitamin-free medium. Analytical grade chemicals were used.

The organism was grown in 750 ml conical E-flasks, containing 250 ml of nutrient solution. The flasks were placed at 25°C after inoculation and continuously shaken during the incubation period. The pH was controlled daily in all experiments by taking out aliquots. When necessary the culture fluid was adjusted to pH 4.5 — 6.0. All series were run at least in duplicate, and all experiments repeated.

The growth of the organism was determined as dry matter by centrifuging of 10 ml samples, followed by two washings of the precipitate, which was then dried over night at 80°C.

The ash content was determined by heating samples of dry matter in an electric muffle furnace at 550 to 650°C to constant weight.

The nitrogen contents of cells and culture solutions were determined according to the standard Kjeldahl procedure. The weight of yeast protein was calculated by multiplying the weight of the cell nitrogen by the factor 6.25.

The yeast carbohydrate content was determined by means of Dreywood's anthrone reagent [5]. The best reproducibility between the duplicates in these experiments was obtained by using the former method of Trevelyan and Harrison [6]. The determination was carried out as follows: 100 ml of yeast suspension were mixed with 10 ml of saturated mercuric chloride [7], and centrifuged at 4 000 r.p.m. for 15 min. The precipitate was washed twice and diluted with distilled water to a turbidity between 0.1 and 0.3, as measured by a Beckman spectrophotometer at 560 mμ. After colour development, the solutions were always clear, and the optical density was measured with the same spectrophotometer at 620 mμ. Only total carbohydrates were determined, and the results were referred to a glucose standard.

The decrease in the sugar content of the nutrient solutions during growth was followed by sugar determinations according to the modified Schoorl-method [8].

The determination of the lipid content was carried out according to the method of Steinberg and Ordal [9]. While these authors used 1.0 N hydrochloric acid for autoclaving the yeast material before extraction with petroleum ether, 1.2 N hydrochloric acid was used in this investigation. It should be mentioned that the lipid obtained by this procedure was a crude material. Possible contaminations were not removed, but re-extraction proved, in some cases, the amount of non-lipid components to be insignificant.

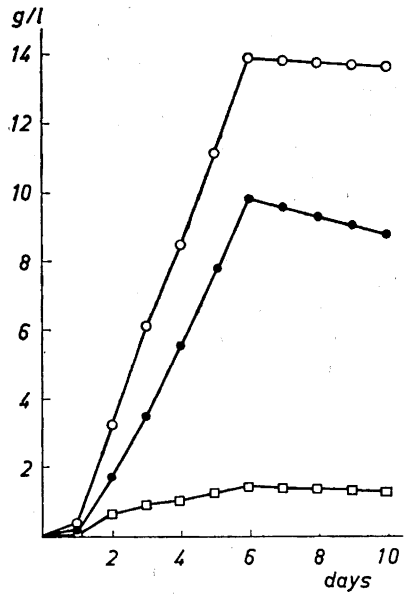

Fig. 1. Yield of yeasts, lipids, and proteins by *Cryptococcus terricolus* as functions of time. 1.0 g $(NH_4)_2SO_4$ added per litre. O yeast dry matter, ● lipids, □ proteins.

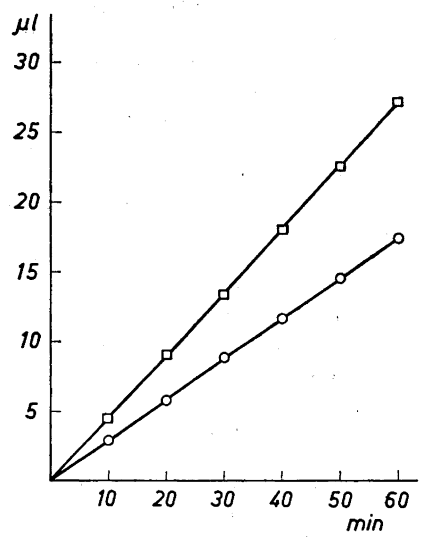

Fig. 2. Endogenous respiration of 5 day old *Cryptococcus terricolus* cells. Each vessel contained 11.7 mg of yeast material. Calculated R.Q. = 0.63. □ O_2 consumption, O CO_2 evolution.

The yeast material obtained after centrifuging followed by two washings was frozen and kept at −20°C. All analyses of the cell materials could then be performed within a few days.

Oxygen consumption was measured by the conventional Warburg technique. The washed cell suspension was added to the main compartment of the Warburg vessels, and the glucose solution, when used, to the side arm. The center well of the flasks contained 0.2 ml of 10 % KOH, absorbed on filter paper. The CO_2 evolution was measured according to the direct method of Warburg. All respiration measurements were made at 25°C and pH 4.8.

RESULTS

The ability of *Cryptococcus terricolus* cells to produce lipids was tested by means of the Rhodotorula medium mentioned previously. The high production of lipids shown by *Rhodotorula gracilis* in this medium was due to the low contents of nitrogen and phosphorus [10]. As these reductions are generally accepted to be necessary for obtaining yeasts with high lipid contents, this medium should also be expected to favour lipid production in *Cryptococcus terricolus*.

Fig. 1 shows the results for *C. terricolus* when grown in this medium. The amount of yeast increased rapidly between the first and the sixth day after which a weak autolysis set in. Maximum yield of dry matter was nearly 14 g per litre of solution; an amount comparable to that obtained for *Rhodotorula*

gracilis in solutions with the same sugar content. The production of lipids and proteins was closely associated with the growth of the organism. Maximum production of dry matter, lipids, and proteins occurred after six days. After the autolysis had started, the decrease in lipid content was evident. As, at that time, the sugar was shown to be completely consumed, this greater loss could perhaps be accounted for by lipid respiration. No unpleasant odours were produced during the relatively short autolysis period in this experiment.

The economic coefficient (g of yeast yield/100 g of sugar, in this case glucose) was about 35, and the "fat" coefficient (g of newly formed lipids/100 g of sugar consumed)[11] approximately 23. Consequently, the production of cells was of the order usually found in other "fat" yeast species, but the ability to convert carbohydrates to lipids was unusually high. After 4 days the protein constituted only *ca.* 12 % of the dry weight of the cells. This inverse proportionality between lipid and protein contents is always found in "fat" yeasts.

To verify that lipid respiration really occurred after the energy source had been consumed, investigations were made, using the Warburg technique. The R.Q. (Respiratory Quotient = CO_2 produced/O_2 consumed) indicates the nature of the metabolism taking place. In the oxidation of fatty acids, the amount of oxygen consumed must exceed that of CO_2 liberated, and the R.Q. will consequently be less than 1. Determinations of the endogenous respiration at different growth intervals of the organism always gave an R.Q. less than 0.9. Fig. 2 shows the endogenous respiration of a five-day-old culture. There

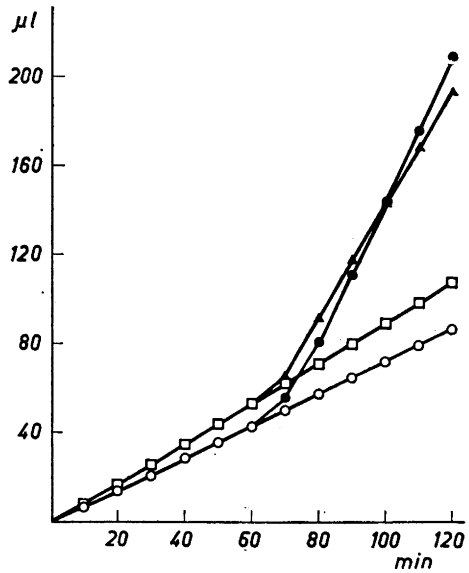

Fig. 3. Effect of addition of glucose on the respiration of starving 6-day-old *Cryptococcus terricolus* cells. Each vessel contained 39.9 mg of yeast material. Endogenous respiration, R.Q. = 0.85, respiration after addition of 5 mg of glucose per vessel, R.Q. = 1.20. □ endogenous O_2 consumption, ○ endogenous CO_2 evolution, ▲ O_2 consumption after glucose addition, ● CO_2 evolution after glucose addition.

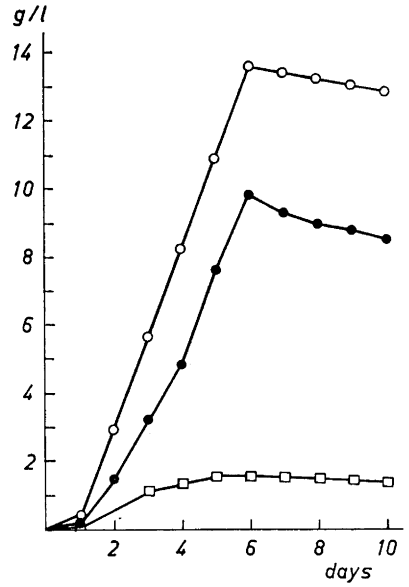

Fig. 4. Yield of yeasts, lipids, and proteins by *Cryptococcus terricolus* as functions of time. 10.0 g $(NH_4)_2SO_4$ added per litre. O yeast dry matter, ● lipids, □ proteins.

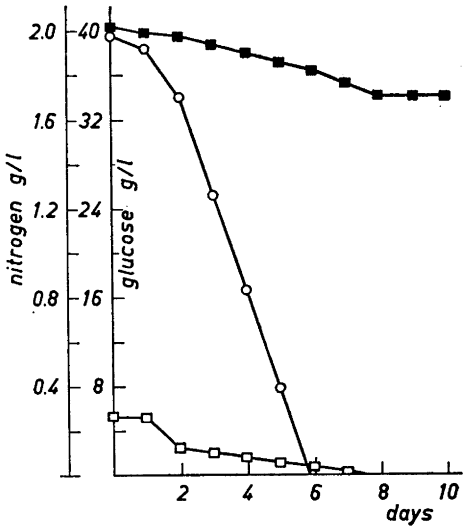

Fig. 5. Contents of glucose and nitrogen in a nitrogen-poor (I) and a nitrogen-rich (II) medium as functions of the growth time of *Cryptococcus terricolus*. I: 1.0 g $(NH_4)_2SO_4$ per litre, II: 10.0 g $(NH_4)_2SO_4$ per litre. O glucose content, both series I and II, □ nitrogen content in series I, ■ nitrogen content in series II.

is a significant difference between the volume of O_2 taken up and that of CO_2 given off. The R.Q. value of 0.63 can be explained only if lipids be the respiratory material.

A starving yeast culture, oxidizing lipids endogenously, was supplied with an energy source, in this case glucose. The results are shown in Fig. 3. After one hour of endogenous respiration, glucose was added to the yeast suspension in two flasks, while the endogenous respiration was going on in two other vessels. The respiratory activity increased rapidly after glucose addition. A higher CO_2 evolution than O_2 consumption was now established. The R.Q. increased from 0.85 to 1.20. This might indicate that lipid production started when glucose became available to the organism.

Effect of varying nitrogen concentrations on the lipid formation

As mentioned above. the isolated strains always contained a large lipid globule, regardless of the medium used for isolation. The different media, of course, contained varying amounts of nitrogen. An investigation of the effect

Table 1. Effect of varying concentrations of nitrogen on growth, lipid and protein formation in *Cryptococcus terricolus*. Results after 5 days' growth. Nitrogen contributed by the inoculum 0.04 g/l in all series. This amount is included in the C/N ratio.

Series	Nitrogen supply $(NH_4)_2SO_4$	N	Ratio C/N	Yeast dry matter	Lipid production		Protein production		Nitrogen content in protein
	g/l	g/l		g/l	g/l	%	g/l	%	g/l
1	40.00	8.48	1.9	0.48	0.26	55.0	0.09	18.2	0.01
2	20.00	4.24	3.7	6.04	3.40	56.3	0.98	16.2	0.16
3	10.00	2.12	7.4	6.86	3.88	56.6	1.04	15.1	0.17
4	5.00	1.06	14.5	7.07	4.16	58.8	1.07	15.1	0.17
5	2.50	0.53	28.1	7.41	4.47	60.3	1.17	15.8	0.19
6	1.25	0.27	51.6	7.86	4.77	60.7	1.27	16.1	0.20
7	0.63	0.13	94.1	7.74	4.74	61.3	1.17	15.1	0.19
8	0.32	0.07	145.4	7.00	4.59	65.6	0.87	12.4	0.14
9	0.16	0.03	228.6	5.71	3.88	67.9	0.88	15.4	0.14
10	0.00	0.00	400.0	5.03	3.49	69.3	0.73	14.6	0.12

of varying nitrogen concentrations on the lipid production therefore seemed to be of interest.

Fig. 4 shows the results obtained when the organism was grown in the usual Rhodotorula-medium, in which 10.0 g $(NH_4)_2SO_4$ were used instead of the original 1.0 g. A comparison of Figs. 1 and 4 shows the curves to be almost identical with respect to growth, lipid production, and protein production.

Fig. 5 gives the explanation to this conformity. The consumption of glucose followed the same pattern in both experiments. In the solution containing the least amount of nitrogen, all available nitrogen was assimilated. In the solution rich in nitrogen, however, only nitrogen from a little more than 1.0 g $(NH_4)_2SO_4$ was assimilated, the rest being left unassimilated in the medium.

As these results were highly unexpected, it was found worth while to investigate the effect of varying amounts of nitrogen on *C. terricolus*. The results are shown in Table 1. The concentrations of glucose and salts, except $(NH_4)_2SO_4$, were as before. From the table it will be seen that the yeast yield reached its maximum value between 0.32 and 10.0 g $(NH_4)_2SO_4$ per litre, with the best output at 0.63 and 1.25 g per litre. If the growth was prolonged to seven days, it was found that less than 0.63 g $(NH_4)_2SO_4$ per litre restricted the growth seriously. More than 10.0 g $(NH_4)_2SO_4$ per litre inhibited the growth, but with prolonged cultivation a certain adaptation occurred. Even with 40.0 g $(NH_4)_2SO_4$ per litre of nutrient solution, 55 % of lipids were found in the cells. With decreasing nitrogen supplies a slightly increased lipid content was found. A "fat" yeast, however, was produced in all cases. At optimal growth, the cells contained approximately 60 % of lipids. It was also found that the total lipid production reached its maximum under these conditions, whereas the lipid content of the cells increased to approximately 70 % with further decreasing nitrogen concentrations. The protein content constituted from 12 to 18 % of the dry weight. The highest protein value, however, was obtained under conditions causing a serious decrease in the growth of the organism. In series 7—10 the nitrogen values for the protein formed were higher than

expected from the amount of nitrogen supplied to the culture. This was probably due to the presence of assimilable nitrogen compounds in the air or in the chemicals used. As shown earlier [4] nitrogen fixation does not occur.

Effect of the nature of the nitrogen source on lipid formation

It was found earlier that *C. terricolus* could utilize ammonium-, nitrate-, amino-, and amido-nitrogen as sources of nitrogen [4]. In stationary cultures, the yeast yields were found to be almost the same with these various sources of nitrogen. A suboptimal growth found in the case of urea was perhaps due to a shift in pH during growth. In continuously shaken cultures with daily pH regulation, it was found that urea caused the most rapid growth. Concentrations of glucose and salts in the medium, except the nitrogen compounds, were as before. The yield of dry matter after 5 days was approximately 40 % higher with urea than with equivalent nitrogen quantities, supplied as $(NH_4)_2SO_4$, KNO_3, NH_4NO_3, or asparagine (Table 2). The lipid contents lay within the range of 58—64 % with the various nitrogen sources, except in the KNO_3 series where the lipid content was only 41 %. In preliminary experiments it was found that an additional supply of the quantity of potassium used here, had no effect on the lipid production. The results presented in Table 2 indicate a decrease in lipid production, possibly due to the presence of nitrate ions in the medium, without a corresponding increase in the protein content. The highest lipid output was found with urea as nitrogen source. This is in accordance with Kleinzeller [12] who found for *Torulopsis lipofera* that the conversion coefficient (percentage of carbon in substrate converted to carbon in lipids) was higher with urea than with NH_4Cl as the nitrogen source. Protein production was not promoted by any of the compounds, and nitrogen was left in all solutions.

Total cell composition

The composition of the *Cryptococcus terricolus* cells was primarily determined by analyzing the dry matter on lipids, proteins, and ash. A dry matter rest

Table 2. Influence of various sources of nitrogen (0.318 g N per litre) on growth, lipid and protein production in continuously shaken cultures of *Cryptococcus terricolus*. Results after 5 days' growth.

Addition per litre	Yeast dry matter	Lipid production		Protein production		Nitrogen in solution	
						Start	Rest
	g/l	g/l	%	g/l	%	g/l	g/l
1.500 g $(NH_4)_2SO_4$	7.93	4.91	61.9	1.17	14.7	0.32	0.15
2.288 g KNO_3	7.92	3.29	41.6	0.93	11.8	0.32	0.18
0.909 g NH_4NO_3	7.47	4.33	58.0	0.73	9.8	0.32	0.22
0.683 g urea	11.23	7.22	64.3	1.20	10.7	0.32	0.13
1.704 g asparagine	8.04	4.82	60.0	1.08	13.4	0.32	0.16

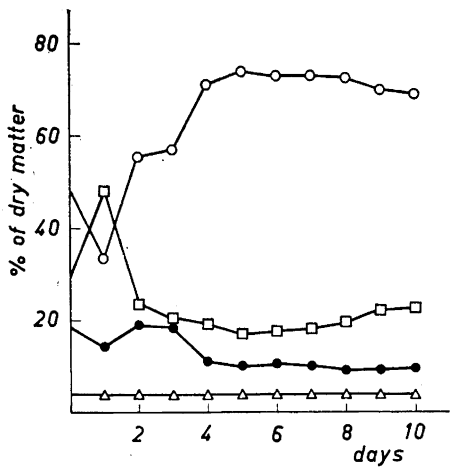

Fig. 6. Total composition of *Cryptococcus terricolus* cells as function of time. Grown in nitrogen-poor solution; 1.0 g $(NH_4)_2SO_4$ per litre. ○ lipids, ● proteins, △ ash, □ dry matter rest.

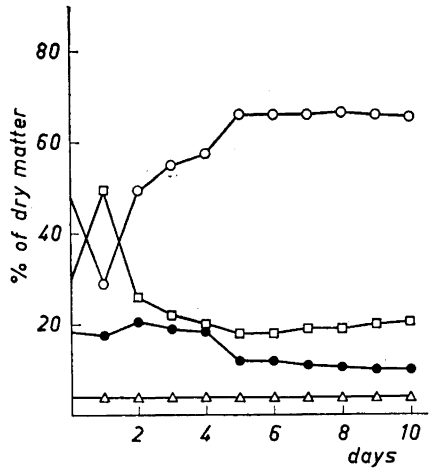

Fig. 7. Total composition of *Cryptococcus terricolus* cells as function of time. Grown in nitrogen-rich solution; 10.0 g $(NH_4)_2SO_4$ per litre. ○ lipids, ● proteins, △ ash, □ dry matter rest.

was calculated as the difference between the total cell content and the analyzed components.

Fig. 6 shows the total composition of the cells grown in nitrogen-poor solutions (1.0 g $(NH_4)_2SO_4$ per litre), and Fig. 7 the results in nitrogen-rich cultures (10.0 g $(NH_4)_2SO_4$ per litre). The ash content of the cells showed only minor variations, and 4 % was taken as the mean value throughout the experiment. The variations in lipid and protein amounts were almost identical in the two experiments. There were some indications that during the first days of growth, the lipid production was slightly increased by a low nitrogen content in the medium. From the fifth day the lipid content was about the same in both series. The protein content decreased from approximately 18 % in the start material to 10 % after more than five days' growth. Instead of the usual

Table 3. The content of carbohydrates, expressed as glucose, in *Cryptococcus terricolus* cells. Cells grown in a nitrogen-poor solution.

Days after incubation	Carbohydrates, as glucose mg/g	Days after incubation	Carbohydrates, as glucose mg/g
0	207	6	163
1	212	7	151
2	216	8	165
3	206	9	184
4	207	10	186
5	201		

inverse relationship between lipids and proteins in "fat" yeast cells, it seems in this case more correct to speak of an inverse relationship between the lipids and what so far can be called the dry matter rest.

As this rest includes the cell carbohydrates, analyses were performed to determine quantitatively the carbohydrate fraction. The results are shown in Table 3.

The carbohydrate content, as shown in the table, remained at a relatively constant level during the growth of the organism. If these results are compared with the curves for the dry matter rest in Figs. 6 and 7, the conclusion may be drawn that the carbohydrate content is possibly identical with the dry matter rest, with one distinct exception. The first day after inoculation a decrease in lipid content occurred in the cells. Simultaneously, a rapid increase in the dry matter rest without simultaneous increase in the carbohydrate content was noted. It seems very likely that an intermediary metabolite accumulated in the cells, as the lipid content on the second day showed an extremely rapid increase.

DISCUSSION

It has repeatedly been demonstrated that, in most "fat" yeasts and other lipid-forming organisms, growth and lipid production occur in the following order: When a medium, containing a small amount of assimilable nitrogen and a relatively great amount of sugar, is inoculated with a "fat" yeast, two cultural phases can be observed. During the first phase, *i.e.* the "protein" phase, the cells proliferate at logarithmic rate, and have a low lipid content. During the second phase, *i.e.* the "fattening" phase, beginning after the medium has been depleted of nitrogen, the cell population remains nearly constant, but the lipid content increases. This sequence has been clearly demonstrated by Enebo, Anderson and Lundin [10] in *Rhodotorula gracilis*. Later Steinberg and Ordal [9] separated the phase of fattening from that of growth or multiplication in this *Rhodotorula* yeast. This made it possible to study the lipid synthesis independent of the growth. Kleinzeller [12] found *Torulopsis lipofera* to be a suitable organism for a study of lipid synthesis, because of its rapid conversion of carbohydrates into lipids.

In *Cryptococcus terricolus* it seems impossible to separate growth and lipid production into two phases. Here, growth and lipid formation are closely connected. When the growth of the organism is in the logarithmic phase, the rate of lipid formation is simultaneously at its maximum. The fraction of lipids that forms part of the cell structure, follows, of course, the increase in cell number, but this fraction usually amounts to only a few per cent of the dry matter. In *C. terricolus*, the capacity for nitrogen assimilation seems to be very restricted, and this may be one of the reasons why this organism produces large quantities of lipids already in the early stage of its development. At present it is very difficult to account for this; however, one explanation may be found in connection with the ecology of the isolated strains. Living in carbohydrate-rich and nitrogen-poor spruce litter soil localities [1], the organism might have lost the power of high protein production. In any case, additional nitrogen, supplied as the compounds used in this investigation, does not

result in increased protein production. Investigations on the lipid-protein balance in this yeast are in progress.

The successful biotechnical production of yeasts depends on a rapid growth. For *Rhodotorula* yeast [10], three days were found to suffice for maximum yeast and lipid production, whereas in the experiments presented in this paper, the growth time had to be prolonged to six days. However, the great difference between the inocula used should be kept in mind. Enebo *et al.*[10] inoculated with an amount corresponding to *ca.* 1 g of dry substance per litre of final culture solution, while the inoculum in this work amounted to only 0.02 g. The generation time is a measure of growth; for *Rhodotorula gracilis* it was found to be 18.4 and 16.5 h, in two experiments. The calculated generation time for *Cryptococcus terricolus* was 15.9 h. In physiological experiments, it was found best to work with poor inocula, but, for biotechnical purposes, the inoculum should be of the magnitude used by Enebo *et al.*

When *Rhodotorula gracilis* was grown in solutions with a generous supply of nutrient salts, including nitrogen, for obtaining rapid growth, the generation time was shortened to only 2.8 h. In this case, however, the lipid content after 42 h was only 9.35 %. When *R. gracilis* was grown by continuous cultivation in a nitrogen-deficient medium to obtain high lipid formation, the generation time became 51 h[10]. In *Cryptococcus terricolus*, in which lipid formation is closely associated with growth, 15.9 h was the actual generation time for obtaining lipid-rich yeasts. For practical purposes it is essential to try to shorten this generation time. It should therefore be of interest to make a systematic investigation on the effect of varying growth conditions on the relationship between growth rate and lipid production.

The economic coefficient for *C. terricolus* was found to be 35. While this value is of the same order as that found in other "fat" yeasts [2,10], higher values have been found for protein yeasts [13]. The production of a certain amount of lipids, however, is a process requiring more energy than the production of the same quantity of proteins. One of the best food and fodder yeasts, *Torulopsis utilis*, has been found to contain maximally 60 % of protein, when grown in beet molasses [13]. Supposing the economic coefficient to be about 60 in this substrate, the calculated protein coefficient would be 36 (the economic coefficient based on the total sugar content was found to vary between 53.5 and 65.3 [14]). This means that *T. utilis*, under conditions favourable to protein production, would produce 36 g of protein from 100 g of sugar. However, if lipids are the desired product, *Cryptococcus terricolus* would produce 23 g of lipids from the same quantity of sugar. If the higher calorimetric value of lipids is taken into consideration, the calorific value of proteins produced by *Torulopsis utilis* under optimal conditions, is of the same order as the energy stored in the lipids produced by *Cryptococcus terricolus*.

In a recent review on microbiological lipids (Woodbine [15]), the lipid percentages and "fat" coefficients found in earlier experiments have been summarized. Of the different yeast species only *Endomyces vernalis*, *Lipomyces starkeyi*, and *Rhodotorula gracilis* were found to contain more than 50 % of lipids on a dry weight basis. *Lipomyces starkeyi* was reported to contain more than 60 %, and only *Rhodotorula gracilis* was found to contain more than 70 %. The 65—70 % content of lipids found in *Cryptococcus terricolus*

is, therefore, very high. It should be mentioned that this value refers to crude lipids. The content of purified lipids, however, is maximum only a few per cents lower. As far as could be controlled, the lipid values in the other publications mentioned also refer to crude lipids.

Blinc and Hočevar [16] found 74 % lipids in *Rhodotorula gracilis*. The economic coefficient was 28, and the "fat" coefficient consequently 21. If, as a mean value, it is calculated with 66 % lipids in *Cryptococcus terricolus*, the "fat" coefficient becomes 23. This high lipid content and effective lipid production is only possible if the protein content is very low. Rippel [11], in his theoretical calculations on lipid production, postulated 30 % proteins in the "fat" yeast. In fact, the protein content in *C. terricolus* was found to be only 12 %. Blinc and Hočevar [16] found 13.8 % proteins in *Rhodotorula gracilis*. With these low protein values the presence of reasonable amounts of carbohydrates and ash in the cell, can be explained.

The ash content of *Cryptococcus terricolus* lies within the limits usually found for yeasts [17]. The fraction of the cell content gathered under the name "dry matter rest" ranges from 17 to 50 % of the dry matter. The structural carbohydrates of brewer's and baker's yeast are a glucan and a mannan, constituting about 10 % of the dry weight [17]. The carbohydrate fraction of *C. terricolus*, at different stages of growth, was found to vary between 15 and 21 %, expressed as glucose.

The 50 % value for the dry matter rest after one day's growth, of which the carbohydrates constitute only *ca.* 2/5, is difficult to explain. The present picture of the fatty acid biosynthesis is represented by a cycle in which all steps are reversible, so that both a synthesis and a degradation of fatty-acid chains is possible, depending on the nutritional status of the cells. This reversibility between lipid production and oxidation is indicated also in *C. terricolus*. A lipid-oxidizing culture seems to start synthesizing lipids approximately 20 min after glucose has been added. The fatty acid composition of the lipids in a one-day-old culture will be investigated in a future work. By qualitative changes in the lipid composition in a young culture, which may lead to losses of lipids during the preparations of the extracts, the irregularities of the lipid and dry matter rest curves in Figs. 6 and 7 might be explained.

Our knowledge today of the direct link between the carbohydrate and the fatty acid metabolism, on the one hand, and the carbohydrate and the amino acid metabolism, on the other, both through the action of the citric acid cycle, might help us to explain the relationship between lipid and protein production. A protein yeast, supplied with nitrogen compounds, incorporates the nitrogen and forms amino acids and proteins. In a usual "fat" yeast, the products of the citric acid cycle, in the absence of nitrogen, are transformed into fatty acids. With regard to *C. terricolus*, a rich nitrogen supply does not result in an increased formation of amino acids and proteins. A supplement of different organic nitrogen compounds, such as peptone, does not alter this fact. The possible reason of this may be a block in the amino acid synthesis of the organism, causing the formation of fatty acids from the products of the citric acid cycle.

Acknowledgements. The author is greatly indebted to the *Royal Norwegian Council for Scientific and Industrial Research* for financial support through the Scandinavian Centres for Advanced Training, Growing Points Programme. He also wishes to express his thanks to Professor H. Lundin, Head of the Division of Food Chemistry, for placing laboratory facilities at his disposal.

REFERENCES

1. Pedersen, T. A. *Compt. rend. trav. lab. Carlsberg* **31** (1958) 93.
2. Starkey, R. L. *J. Bacteriol.* **51** (1946) 33.
3. Lundin, H. *J. Inst. Brewing* **56** (1950) 17.
4. Pedersen, T. A. *Physiol. Plantarum* **13** (1960) 64.
5. Trevelyan, W. E. and Harrison, J. S. *Biochem. J.* **63** (1956) 23.
6. Trevelyan, W. E. and Harrison, J. S. *Biochem. J.* **50** (1952) 298.
7. Fates, F. W. *J. Biol. Chem.* **193** (1951) 113.
8. Cellulosaindustriens Centrallaboratoriums Analyskommitté *Svenska pappers- och cellulosaingeniörsförenings tekniska meddelanden* CCA **11** (1942)
9. Steinberg, M. P. and Ordal, Z. J. *J. Agr. Food Chem.* **2** (1946) 383.
10. Enebo, L., Anderson, L. G. and Lundin, H. *Arch. Biochem.* **11** (1946) 383.
11. Rippel, A. *Arch. Mikrobiol.* **11** (1940) 271.
12. Kleinzeller, A. *Advances in Enzymol.* **8** (1948) 299.
13. Prescott, S. C. and Dunn, C. G. *Industrial microbiology*, McGraw-Hill, New York 1949.
14. Agarwal, P. N., Singh, K., King, P. S. and Peterson, W. H. *Arch. Biochem.* **14** (1947) 105.
15. Woodbine, M. *Progress in industrial microbiology* **1** (1959) 179.
16. Blinc, M. and Hočevar, B. *Monatsh.* **84** (1953) 1127.
17. Eddy, A. A. In Cook, A. H. *The chemistry and biology of yeasts*, Academic Press, New York 1958.

Received November 24, 1960.

ACTA CHEMICA SCANDINAVICA 15 (1961) 663–669

The Crystal Structure of $K_2Ti_2O_5$

STEN ANDERSSON* and A. D. WADSLEY

Chemistry Department, University of Melbourne, and
Division of Mineral Chemistry, C.S.I.R.O. Chemical Research Laboratories, G.P.O. Box 4331, Melbourne, Australia

The crystal structure of $K_2Ti_2O_5$ has been determined by Fourier projections and refined by a least squares analysis. The structure consists of layers of composition $(Ti_2O_5)^{2-}$, in which the titanium atoms have five coordination, separated by the potassium ions. The probable formation of a hydroperovskite $KHTiO_3$ as a hydration product is also discussed.

The alkali metals and earths form many ternary oxides with the metals of Groups IV, V, and VI of the periodic table, and much effort is at present directed towards certain structural types, notably the perovskite ABO_3, the pyrochlor $A_2B_2O_7$, and the tetragonal tungsten bronze AB_2O_6. We have noticed that the alkali metals form a composition series of compounds with titanium dioxide $A_2O \cdot nTiO_2$, where n has been given values from one to seven [1–3]. Of these, only the structure of Li_2TiO_3, which can exist in two forms, has been reported [4]. Several of the other phases with differing values of n are being examined by us, and the crystal structure determination of $K_2Ti_2O_5$, a brief account of which appeared elsewhere [5], is now reported in some detail.

EXPERIMENTAL

$K_2Ti_2O_5$ was readily prepared as colorless needles by melting K_2CO_3 and TiO_2 (anatase) in the molar ratio 1:2 at 1 300°C in a platinum crucible. Whilst the crystals could be kept for long periods in a desiccator, they decomposed on exposure to moist air and required protection during X-ray exposures. Despite a thick coating of cellulose acetate, an additional diffuse single crystal diffraction pattern appeared on the films which were well exposed for the intensity estimations, and the significance of this will be discussed at the end of this paper.

The crystallographic data are summarised in Table 1, the lattice dimensions having been determined from a Guinier film internally calibrated with KCl. These data agree with Schmitz-Dumont and Reckhard's brief description [1] but with two reservations. Firstly these authors gave the space group symbol *Cm* which was unsubstantiated by

* On leave from Department of Inorganic & Physical Chemistry, University of Stockholm, Sweden.

Table 1. Crystallographic data for $K_2Ti_2O_5$.

United cell dimensions:	$a = 11.37$ Å
	$b = 3.80$ Å
	$c = 6.62$ Å
	$\beta = 100.1°$
Systematic absent reflexions:	hkl with $h + k \neq 2n$
Possible space groups	Cm (No. 8)
	$C2$ (No. 5)
	$C2/m$ (No. 12)
D_{obs}	2.95 g.cm^{-3} (Ref.[1])
D_{calc}	2.99 g.cm^{-3}
z	2

additional evidence, whereas the absent reflexions lead to the alternatives $C2$ and $C2/m$ as well. The intensity distributions for $h0l$ and $h2l$ were observed by us to be virtually identical, and this was strong presumptive evidence for the centrosymmetrical space group $C2/m$ in which a satisfactory structure was subsequently found. Secondly their value for the length for the z axis was twice that in Table 1; whilst the diffuse reflexions caused by the decomposition of the phase could doubtless be misinterpreted, we do not dismiss the possibility that a second form of $K_2Ti_2O_5$, closely related in structure to the present one, can also exist.

The $h0l$ and $h1l$ intensities were recorded by multiple film Weissenberg photographs exposed with filtered copper radiation. The measurements, made by comparison with a standard intensity scale, were reduced to $|F|$ values by the usual methods. No corrections for absorption were made, although they would have been desirable in the latter part of the refinement. The scattering curve for titanium which was used had been derived by the self consistent field method [6] for Ti^{3+}. This was rounded off from the point $\sin\Theta = 0.3$ to a value of 18.0 at $\sin\Theta = 0$. Curves derived by Freeman [7] for K^+ and for O^{2-} by Suzuki [8] were also used. Fourier summations were made on SILLIAC, a high speed computer at the University of Sydney, and the structure factors and least squares calculations by hand.

STRUCTURE DETERMINATION

The derivation of the structure was a relatively simple matter. It was supposed that the space group was $C2/m$ for reasons given earlier, and because the y axis was short a minimum of overlap would occur. One oxygen could be placed in the special position 2(a), and the other atoms, one titanium, one potassium and two oxygens would then be in general positions 4(i). The Patterson function $P(u,w)$ was computed, and a model selected from it which refined by successive F_o and $F_o - F_c$ Fourier summations until the reliability factor was 18.9 %. Beyond this point this method proved troublesome and a least squares treatment was adopted. In this, the function

$$R = \Sigma\ w(h0l)\ [|F_o(h0l)| - |F_c(h0l)|]^2$$

was minimised, the observed and non-observed reflexions being weighted simply by $w = 1$ and 0, respectively. The positions of the atoms K and O_2 which, in the electron density projections were free of overlying atoms, were refined by neglecting the off-diagonal coefficients. The complete matrix expression was used for Ti and O_3 for which overlap occurs in projection down the y axis. Two cycles reduced the reliability to 13.4 %, and at this stage the estimated standard deviations for the atoms were in all cases greater than the

Table 2. Fractional atomic parameters and estimated standard deviations. Space group $C2/m$ ($\frac{1}{2}$ $\frac{1}{2}$ 0 +)

Atom	Point position	x	y	z
Ti	4(i)	0.1495 ±.0008	0	0.9072 ±.0017
K	4(i)	0.4022 ±.0010	0	0.6439 ±.0021
O_1	2(a)	0	0	0
O_2	4(i)	0.128 ±.003	0	0.664 ±.006
O_3	4(i)	0.325 ±.003	0	0.008 ±.007

corresponding changes to the positional parameters. The final values of these are given in Table 2 together with the deviations reduced to fractions of the cell edges.

There was some evidence from the F_o-F_c Fourier projections for anisotropic thermal motion, the maximum vibration being directed approximately normal to the (100) plane. However, no additional treatment of the data was considered. The crystal absorption and the overall temperature factor effectually cancel one another and the calculated structure factors, compared in Table 3 with the observations, contain no corrections of either kind. Despite considerable absorption, the $h1l$ terms gave a reliability of 17.9 % on comparison with the model for the space group $C2/m$ and this is considered to be adequate proof of the structure which is shown in Fig. 1.

DESCRIPTION

The principle feature of interest is the coordination of the titanium atom. It is bonded to five oxygens which are grouped in the form of a trigonal bipyramid, somewhat distorted. The metal-oxygen bond distances vary from 1.57 Å to 2.00 Å, and this is considered to be due to the repulsion between the nearest neighbour metal atoms. There is also a wide diversity of oxygen to oxygen distances, the shortest of 2.54 Å being an edge which is common to two of the bipyramids (Fig. 2(a)). The double unit formed in this way is an endless string extending in the y direction. Strings of a similar kind are joined

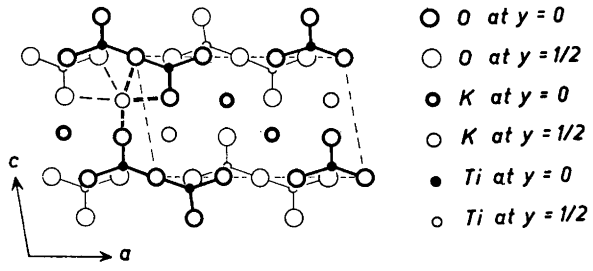

Fig. 1. Structure of $K_2Ti_2O_5$ projected on to (010). The $(Ti_2O_5)^{2-}$ sheets are parallel to the x direction. The bonds from one potassium atom to its eight oxygen neighbours are drawn as heavy broken lines. The unit cell is indicated by weaker broken lines.

Table 3. Comparison between observed and calculated structure factors.

hkl	F_o	F_c	*hkl*	F_o	F_c	*hkl*	F_o	F_c	*hkl*	F_o	F_c
001	10.0	12.8	605	7.8	$\bar{9}.\bar{2}$	$120\bar{1}$	12.0	14.8	$51\bar{2}$	7.5	8.8
2	9.1	10.1	4	< 7.4	$\bar{0}.\bar{5}$	$\bar{2}$	6.4	5.6	$\bar{3}$	16.7	19.4
3	21.6	22.2	3	11.8	$\bar{9}.\bar{8}$	$\bar{3}$	14.7	15.5	$\bar{4}$	< 6.6	2.5
4	17.9	$\bar{1}\bar{5}.\bar{9}$	2	< 6.1	2.7	$\bar{4}$	6.4	$\bar{8}.\bar{5}$	$\bar{5}$	< 6.8	2.9
5	8.6	$\bar{7}.\bar{2}$	1	17.4	17.6	$\bar{5}$	4.9	$\bar{3}.\bar{3}$	$\bar{6}$	< 7.5	4.3
6	< 7.4	$\bar{2}.\bar{9}$	0	10.8	8.8	1400	< 4.0	1.3	$\bar{7}$	9.9	$\bar{1}\bar{3}.\bar{4}$
7	13.7	$\bar{1}\bar{1}.\bar{4}$	$\bar{1}$	28.4	26.5	$\bar{1}$	6.4	10.8	716	10.8	$\bar{1}\bar{0}.\bar{4}$
8	< 4.6	$\bar{5}.\bar{6}$	$\bar{2}$	23.3	22.7	116	9.3	$\bar{8}.\bar{3}$	5	< 4.1	$\bar{0}.\bar{5}$
208	< 3.7	$\bar{1}.\bar{7}$	$\bar{3}$	< 6.1	1.1	5	13.5	$\bar{1}\bar{4}.\bar{1}$	4	15.0	$\bar{1}\bar{2}.\bar{7}$
7	9.6	$\bar{6}.\bar{1}$	$\bar{4}$	8.8	10.1	4	11.3	11.9	3	7.2	3.4
6	< 7.4	$\bar{3}.\bar{8}$	$\bar{5}$	7.3	$\bar{2}.\bar{3}$	3	6.6	7.1	2	17.0	16.5
5	11.8	12.9	$\bar{6}$	13.7	$\bar{1}\bar{4}.\bar{0}$	2	5.7	5.2	1	< 6.4	0.9
4	7.4	8.1	$\bar{7}$	< 6.1	2.4	1	25.6	32.1	0	25.7	21.2
3	17.2	14.4	806	< 4.2	2.7	0	5.3	2.3	$\bar{1}$	3.6	$\bar{4}.\bar{5}$
2	25.0	26.9	5	6.9	$\bar{9}.\bar{3}$	$\bar{1}$	3.6	$\bar{4}.\bar{5}$	$\bar{2}$	8.2	9.3
1	6.9	$\bar{4}.\bar{3}$	4	< 7.1	4.6	$\bar{2}$	3.2	4.5	$\bar{3}$	6.7	5.3
0	< 2.5	$\bar{0}.\bar{6}$	3	11.8	16.3	$\bar{3}$	14.0	$\bar{2}\bar{1}.\bar{5}$	$\bar{4}$	< 7.1	$\bar{7}.\bar{3}$
$\bar{1}$	15.2	$\bar{1}\bar{2}.\bar{7}$	2	< 7.1	$\bar{1}.\bar{2}$	$\bar{4}$	8.5	$\bar{1}\bar{1}.\bar{3}$	$\bar{5}$	14.6	$\bar{1}\bar{7}.\bar{8}$
$\bar{2}$	25.0	$\bar{2}\bar{6}.\bar{9}$	1	15.7	14.1	$\bar{5}$	< 6.9	$\bar{3}.\bar{5}$	915	10.9	11.1
$\bar{3}$	8.8	$\bar{6}.\bar{7}$	0	9.8	$\bar{8}.\bar{7}$	$\bar{6}$	8.4	$\bar{8}.\bar{5}$	4	14.0	15.7
$\bar{4}$	8.8	$\bar{9}.\bar{5}$	$\bar{1}$	14.5	$\bar{1}\bar{5}.\bar{2}$	$\bar{7}$	< 6.4	7.6	3	9.1	6.6
$\bar{5}$	8.6	$\bar{5}.\bar{0}$	$\bar{2}$	< 6.7	$\bar{1}.\bar{9}$	316	18.0	16.6	2	16.8	13.6
$\bar{6}$	11.0	13.5	$\bar{3}$	12.7	$\bar{1}\bar{2}.\bar{4}$	5	7.2	6.7	1	< 7.2	$\bar{3}.\bar{8}$
$\bar{7}$	7.8	4.6	$\bar{4}$	15.4	$\bar{1}\bar{8}.\bar{6}$	4	22.7	20.8	0	8.2	$\bar{7}.\bar{6}$
$\bar{8}$	< 4.9	4.6	$\bar{5}$	< 7.2	$\bar{1}.\bar{3}$	3	17.1	16.6	$\bar{1}$	< 7.0	$\bar{1}.\bar{2}$
407	12.5	14.6	$\bar{6}$	< 6.6	$\bar{3}.\bar{3}$	2	9.0	$\bar{7}.\bar{6}$	$\bar{2}$	11.7	$\bar{1}\bar{0}.\bar{9}$
6	< 7.0	$\bar{1}.\bar{6}$	$\bar{7}$	< 5.1	0.4	1	15.1	11.9	$\bar{3}$	7.3	$\bar{6}.\bar{6}$
5	11.5	12.6	1005	< 3.9	6.7	0	9.5	$\bar{7}.\bar{0}$	$\bar{4}$	< 7.2	6.0
4	7.8	$\bar{7}.\bar{2}$	4	< 5.8	2.3	$\bar{1}$	22.7	$\bar{2}\bar{1}.\bar{0}$	$\bar{5}$	< 6.8	$\bar{1}.\bar{2}$
3	17.9	$\bar{2}\bar{0}.\bar{0}$	3	8.6	9.7	$\bar{2}$	10.9	13.2	1113	10.9	$\bar{1}\bar{2}.\bar{8}$
2	< 5.1	$\bar{0}.\bar{9}$	2	< 7.2	$\bar{6}.\bar{9}$	$\bar{3}$	< 5.3	$\bar{1}.\bar{0}$	2	13.5	$\bar{1}\bar{1}.\bar{9}$
1	12.5	$\bar{1}\bar{3}.\bar{0}$	1	9.8	$\bar{9}.\bar{5}$	$\bar{4}$	< 6.2	3.2	1	< 6.8	$\bar{1}.\bar{2}$
0	30.9	$\bar{3}\bar{0}.\bar{0}$	0	< 7.4	$\bar{0}.\bar{4}$	$\bar{5}$	20.8	25.5	0	18.2	$\bar{1}\bar{6}.\bar{1}$
$\bar{1}$	15.9	13.3	$\bar{1}$	15.7	$\bar{1}\bar{6}.\bar{2}$	$\bar{6}$	< 7.3	6.9	$\bar{1}$	< 7.1	$\bar{0}.\bar{5}$
$\bar{2}$	< 4.0	1.3	$\bar{2}$	< 7.4	$\bar{0}.\bar{6}$	$\bar{7}$	< 6.4	$\bar{8}.\bar{3}$	$\bar{2}$	7.0	10.9
$\bar{3}$	< 5.4	1.4	$\bar{3}$	7.4	9.6	516	8.1	7.2	$\bar{3}$	< 7.4	$\bar{4}.\bar{9}$
$\bar{4}$	25.0	27.1	$\bar{4}$	< 7.1	$\bar{1}.\bar{4}$	5	< 7.2	1.0	$\bar{4}$	10.3	12.9
$\bar{5}$	7.3	6.7	$\bar{5}$	11.3	14.4	4	13.7	$\bar{1}\bar{6}.\bar{5}$	1311	8.1	10.2
$\bar{6}$	< 7.4	2.6	$\bar{6}$	14.0	13.3	3	9.2	6.0	0	9.7	9.6
$\bar{7}$	12.5	$\bar{8}.\bar{6}$	1203	6.1	7.5	2	16.6	$\bar{1}\bar{3}.\bar{0}$	$\bar{1}$	7.6	6.1
$\bar{8}$	10.0	$\bar{9}.\bar{8}$	2	< 5.8	$\bar{3}.\bar{2}$	1	22.6	$\bar{1}\bar{6}.\bar{9}$	$\bar{2}$	11.2	13.3
607	< 3.6	$\bar{0}.\bar{9}$	1	7.4	$\bar{6}.\bar{7}$	0	9.8	7.8			
6	6.2	$\bar{2}.\bar{9}$	0	6.4	6.9	$\bar{1}$	< 4.9	3.4			

together by having the oxygen atoms O_1 in common, leading to an infinite two dimensional sheet of composition $(Ti_2O_5)^{2-}$, the median of which is the plane (001) *.

Sheets are then separated from one another by the potassium ions, each having eight oxygens as near neighbours. Six are approximately at six of the eight corners of a cube, and the other two are on the same level as the potas-

* If each alternate string of bipyramids in a sheet is rotated through 180° in the plane normal to (001), the structure of it is identical with a single layer of the V_2O_5 structure [9].

sium, in a plane parallel to (010) which bisects the figure (Fig. 2(b)). It appears simply as if potassium occupies the best positions which can be created by the $(Ti_2O_5)^{2-}$ sheets when they are packed together (Fig. 1) and no other significance is attached to its coordination.

The trigonal bipyramid is rare in oxide structures but has been shown to occur in vanadium compounds; in V_2O_5 [9], for certain of the atoms in the alkali metal vanadium bronzes [10,11] as well as for the hydrated metavanadates $KVO_3 \cdot H_2O$ [12] and $Ca(VO_3)_2 \cdot 2H_2O$ [13] (the mineral metarossite). It has never before, to our knowledge, been demonstrated for titanium.

THE DECOMPOSITION PRODUCTS OF $K_2Ti_2O_5$

$K_2Ti_2O_5$ reacts readily with water. The diffuse single crystal diffraction pattern, which was recorded together with the reflexions of $K_2Ti_2O_5$, had pronounced pseudo cubic symmetry which could not be related to anatase, identified by Schmitz-Dumont and Reckhard [1] as one of the end products of the decomposition.

The unit cell was monoclinic, space group $P2_1$ or $P2_1/m$ with the dimensions

$$a = 9.6, \quad b = 3.8, \quad c = 10.8 \text{ Å}, \quad \beta = 112°.$$

The relationship between this and the sub cell is expressed by the axial transformation

$$\text{cubic} \rightarrow \text{monoclinic} = \bar{1}02/010/300$$

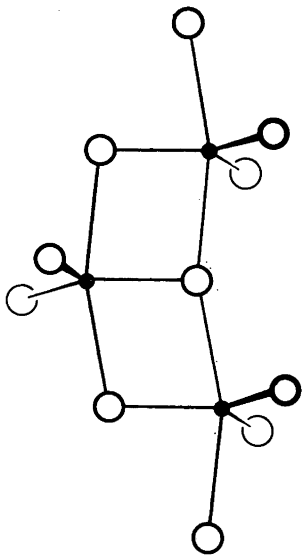

Fig. 2(a). Perspective drawing of the strings of double bipyramids formed by titanium (small black circles) and oxygen (larger open circles).

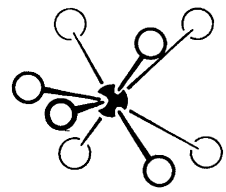

Fig. 2(b). The oxygen atom environment of a potassium atom (black circle) in a perspective drawing.

Table 4. Interatomic distances in Å.

	$Ti-O_1$	1.67 ± .02
	$Ti-O_2$	1.57 ± .04
	$Ti-O_3^1$	2.00 ± .04
(2)	$Ti-O_3$	2.00 ± .04
	O_1-O_2	2.86 ± .04
	$O_2-O_3^1$	2.90 ± .05
	$O_3^1-O_1$	3.69 ± .04
(2)	$O_3-O_3^1$	2.54 ± .08
(2)	O_3-O_1	2.76 ± .04
(2)	O_3-O_2	2.86 ± .05
	$Ti-Ti^1$	3.09 ± .02
	$K-O_2^{11}$	3.14 ± .04
	$K-O_3$	2.71 ± .04
(2)	$K-O_1$	3.08 ± .03
(2)	$K-O_2^1$	3.18 ± .04
(2)	$K-O_2$	2.76 ± .04
	$K-K^1$	3.17 ± .02

and this is shown in Fig. 3 which is also a possible interpretation of the crystal structure.

The sub cell reflexions were characteristic of the perovskite structure, and the true unit cell contains several of these units. Whilst it was obviously impossible to gain evidence of the chemical composition of this phase, it seemed not improbable that it was formed simply by the reaction

$$K_2Ti_2O_5 + H_2O \rightarrow 2KHTiO_3$$

to become a "hydroperovskite" containing hydrogen ions. On hydration, $K_2Ti_2O_5$ would be expected to undergo extensive rearrangement. The water molecules entering the lattice will undoubtedly change the titanium coordina-

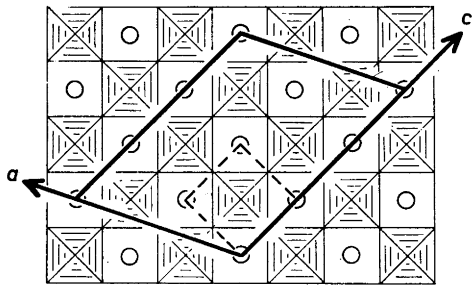

Fig. 3. The possible structure of the hydration product of $K_2Ti_2O_5$, seen in projection down the y axis. The titanium-oxygen octahedra are drawn as shaded squares, the potassium as open circles. The perovskite sub-cell is outlined by broken lines, the superstructure unit cell by the heavy lines, with the axial directions shown as arrows. Contraction, presumably the result of hydrogen bonding, occurs principally in the x direction.

tion from five to six, and can achieve this only at the expense of the original structure.

The superstructure could arise from the displacements of atoms from ideal cubic positions under the combined influence of polarisation effects and of hydrogen bonding. We had intended to attempt to solve the detailed structure of this phase, but were prevented from doing so by the too few reflexions which were recorded. In an attempt to increase the data, the original crystal, still with its heavy coating of cellulose acetate, was kept in moist air for several months, and again exposed in an X-ray camera. There was no trace of the structure of $K_2Ti_2O_5$, and the perovskite-like decomposition product also was no longer present. The crystal, still preserving its original form, was virtually amorphous. Attempts to prepare $KHTiO_3$ by heating together equimolar proportions of KOH and TiO_2, met with no success, the only product being $K_2Ti_2O_5$ identical with the former specimens. Whether or not this is the correct interpretation of the chemistry and structure of the decomposition product, the phase evidently has only a transitory existence.

The authors desire to thank Dr. B. Dawson and Mr. R. Grenfell Thomas for helpful comments.

REFERENCES

1. Schmitz-Dumont, O. and Reckhard, H. *Monatsh.* **90** (1959) 134. This contains references to the earlier literature.
2. Berry, K. L., Aftandilian, V. D., Gilbert, W. W., Meibohm, E. P. H. and Young, H. S. *Abstracts 136th Meeting Am. Chem. Soc. 1959* p. 39N.
3. Gulledge, H. C. *Ind. Eng. Chem. (Intern. Ed.)* **52** (1960), 117.
4. Jonker, G. H. *Trabajos de la Tercera Reunion Int. Sobre React. de los Solidos, Madrid* **1** (1957) 413.
5. Andersson, S. and Wadsley, A. D. *Nature* **187** (1960) 499.
6. Freeman, A. J. and Watson, R. E. *Quart. Progr. Rep. Solid State Mol. Str. Group,* M.I.T. Oct. 1959 p. 16.
7. Freeman, A. J. *Acta Cryst.* **12** (1959) 261.
8. Suzuki, T. *Acta Cryst.* **13** (1960) 279.
9. Byström, A., Wilhelmi, K-A. and Brotzen, O. *Acta Chem. Scand.* **4** (1950) 1119.
10. Wadsley, A. D. *Acta Cryst.* **8** (1955) 695.
11. Wadsley, A. D. *Acta Cryst.* **10** (1957) 261.
12. Christ, C. L., Clark, J. R. and Evans, H. T. *Acta Cryst.* **7** (1954) 801.
13. Kelsey, C. H. and Barnes, W. H. *Can. Mineralogist* **6** (1960) 448.

Received October 18, 1960.

ACTA CHEMICA SCANDINAVICA 15 (1961) 670–674

Direct Quantitation on Paper Chromatograms of Radioactivity From ^{14}C Labelled Fatty Acids

HEINZ J. M. HANSEN

The Danish Atomic Energy Commission, Research Establishment, Risö, Denmark

The present investigation is based on experiments using reversed phase chromatography with horizontal development. It is shown by varying spot size and type of fatty acid that the marginal distribution throughout the thickness of the paper of the molecules to be counted renders no bias to their quantitative evaluation. The said marginal distribution, however, influences the scanning error and it can be recommended to scan low energy labelled paper chromatograms from both sides of the paper and average the results.

The advantages of direct quantitation of radioactive substances separated by paper chromatography need hardly be stressed.

As long as the energy of the radiation from the isotopes used to label the substances in question remains above such a value that the absorption by the paper itself can be reasonably ignored, a simple scanning of the chromatogram with some sort of counting equipment should not offer any difficulties. However, when measuring low energy ^{14}C β-radiation and particularly when counting β-particles from ^{3}H, certain problems do need to be considered.

In the present investigation ^{14}C labelled fatty acids were separated by reverse-phase paper chromatography with horizontal development according to Kaufmann-Mohr [1]. The chromatographic paper used (Schleicher & Schüll 2040bM) had an average weight of 13 mg/cm^2. If one accepts a halving thickness for ^{14}C β-radiation of about 2.7 mg/cm^2 it is seen that in this case only about 4 % of the β-particles emitted from the side of the paper turning away from the counter window and only about 50 % of the β-particles emitted from the center of the paper will have a chance of being registered by the counter. This makes it clear that the geometrical distribution throughout the thickness of the paper of the molecules to be counted and thus the geometrical shape and density of the chromatographic spot to be evaluated, will be of major importance for the final result, while on the other hand self-absorption by the fatty acids will need no special consideration.

In their review article Giddings and Keller [2] point out that in case of an ideal model based partly on random diffusion (in the directions perpendicular

to the direction of flow of the mobile phase) and partly on both random and kinetic diffusion (in the direction of flow of the mobile phase) the shape of a chromatographic spot will be elliptic, with a Gauss-distribution of the molecules along any of the elliptic axes. In the same article reference is made to the experimental work of Åkerfeldt [3] who showed that while the pictured ideal case is often met with in practice, it also can happen that the molecular distribution along the elliptic axes resembles more a rectangular than a Gauss distribution, the latter case perhaps being due to "overloading" of the original spot of application. These considerations apply to the shape and density of the spot along the two coordinate axes (x, y) parallel to the surface of the paper. The marginal distribution of the molecules along the third dimension (z) perpendicular to the surface plane, which is of interest in the present investigation, is not discussed. However, one should not expect the latter distribution to vary from the random component of the x,y distributions except for the fact that the thickness of the paper being small in comparison to the x,y dimensions of the spot, the most probable marginal distribution function along the z axis in case of ideal diffusion will only be a segment of a Gauss curve placed symmetrically about the mean. In case of rectangular x,y distributions the z distribution should of course also be expected to be rectangular.

Based on the above considerations the problem in question can be put as follows:

A quantitative evaluation of the relative distribution of ^{14}C radioactivity between various spots on a paper chromatogram will only be free of bias if each of the spots shows the same geometrical marginal distribution throughout the thickness of the paper. If one accepts a model for the formation of the spots based on diffusion, this means in the present case that the diffusion coefficients should be independent of fatty acid concentrations.

On top of these considerations which refer to ^{14}C quantitation in general there is yet another question which might render a bias to the results in the present particular case, where use is made of reversed phase chromatography with horizontal development. It is the question whether the two liquid phases will have a tendency to separate according to their specific gravity, so that rising R_F values will mean an increasing probability of the mean of the spot to be found in the lower half of the paper, since in the present case the mobile phase is the heaviest one.

EXPERIMENTAL

All scanning was done with equipment constructed by the Health Physics Department at Risö.

The experiments were based on samples containing ^{14}C labelled palmitic and stearic acids. The ratio of measured palmitic activity (P) to measured stearic activity (S) expressed as % of the expected value was used as the dependent variable. Variation between the samples of the stearic and palmitic acid concentration ratios was achieved partly by varying the amount of each of the radioactive fatty acids added, partly by varying their specific activity; in total the concentration ratios of palmitic to stearic acid thus varied from $0.112 \times 1 = 0.112$ to $3.33 \times 8 = 26.7$ in accordance to a variation from 0.112 to 3.33 of the ratio

$$\frac{\text{added } ^{14}\text{C palmitic acid}}{\text{added } ^{14}\text{C stearic acid}} = \text{expected } P/S \text{ and a variation from 1.0 to}$$

Table 1.

Specific activity	Expected P/S 3.33 found P/S	3.33 % of expected	1.00 found P/S	1.00 % of expected	0.112 found P/S	0.112 % of expected	total average
Palmitic = 1.0 μC/mg	2.97	89.3	0.842	84.2	0.1066	95.3	89.4
Stearic = 1.0 μC/mg	3.15	94.6	0.847	84.7	0.0990	88.3	
Palmitic = 0.5 μC/mg	2.90	87.2	1.001	100.1	0.1113	99.5	87.4
Stearic = 2.0 μC/mg	2.53	76.0	0.761	76.1	0.0957	85.4	
Palmitic = 0.25 μC/mg	2.48	74.5	0.970	97.0	0.1083	96.8	95.4
Stearic = 2.0 μC/mg	3.21	96.5	1.064	106.4	0.1131	101.0	
Total average		86.4		91.4		94.4	90.7

8.0 of the ratio $\frac{\text{specific activity of added stearic acid}}{\text{specific activity of added palmitic acid}}$. Each sample was chromatographed twice. Results are given in Table 1.

Based on the above results one gets the following analysis of variance [4] (Table 2).

The question whether a bias owing to a separation of the two liquid phases could be expected was investigated by scanning both sides of each of 7 chromatograms. Results are given in Table 3.

Based on these results it can also be tested [4] whether the new estimate of s^2 derived from the mean of $\frac{1}{2}d^2$ differs from the result 87.2 found in the above analysis of variance:

$$t = \frac{-2.0}{(2 \times 87.2/7)^{\frac{1}{2}}} = -0.4; \; f = 17$$

$$v^2 = \frac{244.9}{87.2} = 2.81; \; f_1 = 7, \; f_2 = 17$$

Table 2.

Variation	SSD	f	s^2	test
Between columns	194.4	2	97.2	$v^2 = \frac{87.3}{87.1} = 1.00; f_1 = 8, f_2 = 9$
Between rows	208.2	2	104.1	
Residual	295.6	4	73.9	
Within sets	783.8	9	87.1	
Total	1 482.0	17	87.2	

Table 3.

% of expected P/S			
Scanning		d = deviation	$\frac{1}{2} d^2$
from top	from bottom	top − bottom	
94.6	106.1	−11.5	66.1
93.0	92.3	0.7	0.3
109.9	88.6	21.3	226.8
76.0	104.1	−28.1	394.8
76.1	111.3	−35.2	619.5
96.5	83.3	13.2	87.1
106.4	81.1	25.3	320.0
	mean	− 2.0	244.9

DISCUSSION

Tests in connection with the analysis of variance show that no bias is to be found from differences in fatty acid concentration, so that all spots will be scanned with the same efficiency independent of their size. Referring to the diffusion model of spot formation, this can be interpreted as proving the equality of the diffusion coefficients.

Also, there is no bias to be found from the location of the mean of the spot depending on the R_F value of the corresponding fatty acid. This is shown by the lack of significance of the t-test for $d \neq 0$ which makes it probable that the average location of the mean of any chromatographic spot will be in the same plane parallel to the surface of the paper. That the found total average of 90.7 % of expected P/S differs from 100 % must thus be due to errors in dilution of the two stock ^{14}C labelled fatty acid solutions used for sample preparations.

The influence of the geometrical marginal distribution of a chromatographic spot along a dimension perpendicular to the surface of the paper is first met with in connection with the scanning error or scanning variance. The mean of $\frac{1}{2}d^2$, where d refers to the deviation between the results of two opposite scannings of the same chromatogram, is significantly larger at the 95 % level than the corresponding value found as the final result of the analysis of variance. This would be in agreement with a theory claiming that the main source of scanning variance was a random difference between the geometrical distributions and with them the geometrical means of the palmitic and stearic spots scanned. The said deviation d would thus be a deviation between one value chosen at random within the general probability distribution of % of expected P/S and the corresponding value with the opposite probability. In this case the mean of $\frac{1}{2}d^2$ should be equal to $2s^2$. As a practical consequence of this explanation it can be recommended to scan low energy labelled paper chromatograms from both sides of the paper and average the results.

REFERENCES

1. Kaufmann, H. P. and Mohr, E. *Fette Seifen Anstrichsmittel* **60** (1958) 165.
2. Giddings, J. C. and Keller, R. A. *J. Chromatography* **2** (1959) 626.
3. Åkerfeldt, S. *Acta Chem. Scand.* **8** (1954) 521.
4. Hald, A. *Statistical Theory With Engineering Applications*. John Wiley and Sons Inc., New York 1957.

Received November 28, 1960.

ACTA CHEMICA SCANDINAVICA 15 (1961) 675–677

Nonaqueous Titration of Some Nitro Compounds Containing the Dinitrophenyl Group

BENGT SMITH and ÅKE HAGLUND

Institutionen för Organisk kemi, Chalmers Tekniska Högskola, Göteborg, Sweden

It is demonstrated that various types of nitro compounds obtained in the characterization of such organic compounds as alcohols, phenols, mercaptans and amines can be titrated quantitatively in acetone or pyridine using tetra-*n*-butylammonium hydroxide in benzene-methanol as titrant.

In the characterization of organic compounds various types of nitro derivatives have been utilized to a great extent. The reason for this is the excellent crystallization properties shown by the derivatives formed. The identification is generally based on melting point determination which method, however, is often hampered by the fact that the melting points of two or several compounds lie close together. Although other methods are available for the identification and analysis of the nitro derivatives, *e.g.* paper chromatography, absorption spectrophotometry and quantitative reduction, it is felt that a rapid titration method for determining the equiv. weight should be a useful adjunct to the existing methods.

Amoung organic compounds which are often characterized in the form of nitro derivatives are alcohols, phenols, thiols, amines, aldehydes and ketones. Thus to characterize alcohols and phenols they may be transformed into 2,4-dinitrophenyl ethers or 2,4-dinitrobenzoates and thiols into 2,4-dinitrophenyl thioethers. By reaction with 2,4-dinitrochlorobenzene, 2,4-dinitrobenzoyl chloride and 2,4-dinitrobenzaldehyde, amines may be transformed into N-substituted 2,4-dinitroanilines, 2,4-dinitrobenzamides and Schiff's bases, respectively, all of which are useful for characterization purposes. The transformation of aldehydes and ketones into 2,4-dinitrophenyl hydrazones is, perhaps, the most wellknown example of the utilization of nitro derivatives in the characterization of organic compounds.

The latter group was recently investigated by Sensabaugh *et al.*[1] and found to be titratable using tetra-*n*-butylammonium hydroxide in pyridine. The base consumption was believed to be due to the presence of an acidic hydrogen atom at nitrogen. The bulk of the derivatives mentioned above contain no

acidic hydrogen atoms. Nevertheless there seemed to be a good chance to analyse them using a titration procedure similar to that used by Sensabaugh *et al.* Meisenheimer [2] in 1902 showed that certain nonacidic nitro compounds, *e.g.* nitro derivatives of aromatic hydrocarbons and ethers, reacted with bases forming crystalline adducts. Later, Brockmann and Meyer [3] reported the titratability of aromatic nitro hydrocarbons and one nitro ether in nonaqueous solvents *, and recently nonaqueous titration was utilized by Fritz *et al.*[4] for the quantitative analysis of some aromatic nitro hydrocarbons. The background of the reaction will be given below.

The application of a nonaqueous titration procedure to the analysis of the nitro derivatives mentioned previously was found to give results accurate enough for the purpose, although the precision was not as good as in the titration of certain other acidic compounds, *e.g.* phenols, *cf.* Table 1. The titration was performed in acetone or pyridine using tetra-*n*-butylammonium hydroxide as the titrant. Acetone was found to be of more general utility than pyridine,

* No values were given, however.

Table 1. Titration of dinitrophenyl derivatives in acetone or pyridine using tetra-*n*-butylammonium hydroxide.

Compound		Base consumption, equiv. per mole		Derivative used for the characterization of
Type	Name	Solvent acetone	Solvent pyridine	
Ester	Methyl 3,5-dinitrobenzoate	1.03	1.02	Alcohols and Phenols
	Ethyl 3,5-dinitrobenzoate	1.02	1.04	
	n-Propyl 3,5-dinitrobenzoate	1.02	1.02	
	Phenyl 3,5-dinitrobenzoate *	1.00	1.01	
	Methyl 2,4,6-trinitrobenzoate	1.02	1.00	
Ether	2,4-Dinitrophenyl methyl ether	0.98	0.97	Alcohols and Phenols
	2,4-Dinitrophenyl ethyl ether	1.00	0.98	
	2,4-Dinitrophenyl phenyl ether **	1.04	0	
	2,4,6-Trinitrophenyl methyl ether	1.01	1.00	
Thioether	2,4-Dinitrophenyl *tert.*butyl thioether	1.05	1.35	Thiols
Amine	2,4-Dinitrophenyl N-*n*-propylamine	1.01	0.98	Amines
	2,4-Dinitrophenyl N-benzylamine	1.01	1.03	
	2,4-Dinitrophenyl N,N-dimethylamine	1.02	0	
Amide	N-*n*-Propyl 3,5-dinitrobenzamide	1.01	1.01	Amines
	N-Benzyl 3,5-dinitrobenzamide	1.03	0.99	
	N,N-Dimethyl 3,5-dinitrobenzamide	0.97	0.99	
Schiff's base	N-*n*-Propyl 3,5-dinitrobenzalamine	0.98	1.01	Amines
	N-Benzyl 3,5-dinitrobenzalamine	0.99	0.98	

* Two inflexion points were obtained.

** The base consumption of this compound was rather varying and appreciably higher values were sometimes obtained.

since certain compounds could not be titrated in the latter solvent or gave high values. The excess base consumption obtained for 2,4-dinitrophenyl *tert.* butyl thioether might be due to a partial splitting of the base adduct, *e.g.*

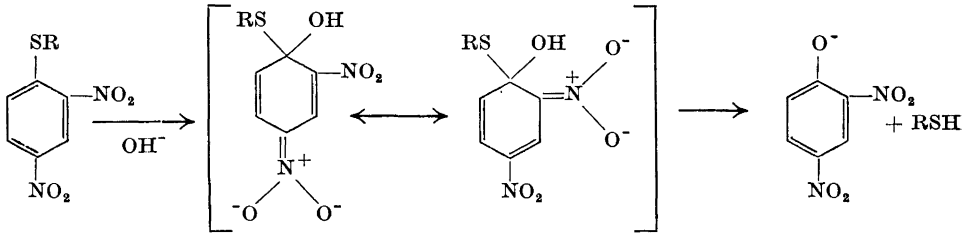

A similar explanation might be advanced in certain other cases, where a tendency to high values was observed, *e.g.* for 2,4-dinitrophenyl phenyl ether. For phenyl 3,5-dinitrobenzoate two inflexion points were obtained. The first one, which we believe is due to the addition of base, corresponded to a consumption of 1 equiv. of base per mole. The second inflexion point at about 1.6 equiv. of base per mole might be connected with the transesterification reaction which was recently [5] reported to take place with phenolic esters in the presence of the tetra-*n*-butylammonium base titrant. While the reaction of the esters, ethers, Schiff's bases and of the N,N-disubstituted amines and benzamides must involve addition of base to the molecule, the titratability of the N-monosubstituted amines and benzamides is most likely due to abstraction of an acidic hydrogen atom from the nitrogen atom.

EXPERIMENTAL

Materials. Most of the nitro compounds used in this investigation were prepared in this laboratory. Their purity was ascertained by melting point determination.

Titration procedure. The titrations were performed essentially as described by Fritz and Hammond [6] using 0.1 N tetra-*n*-butylammonium hydroxide in benzene-methanol as titrant and acetone or pyridine as solvent. The solvents were of reagent grade and the pyridine dried over potassium hydroxide and distilled before use. Glass calomel electrodes were used and the titration followed by means of a Radiometer Titrator model TTT 1.

Acknowledgement. The authors wishes to thank the *Town Council of Gothenburg* for financial support of this work.

REFERENCES

1. Sensabaugh, A. J., Cundiff, R. H. and Markunas, P. C. *Anal. Chem.* **30** (1958) 1445.
2. Meisenheimer, J. *Ann.* **323** (1902) 205.
3. Brockmann, H. and Meyer, E. *Naturwiss.* **40** (1953) 242.
4. Fritz, J. S., Moye, A. J. and Johnson Richard, M. *Anal. Chem.* **29** (1957) 1685.
5. Smith, B. and Haglund, Å. *Acta Chem. Scand.* **14** (1960) 1349.
6. Fritz, J. S. and Hammond, G. S. *Quantitative Organic Analysis*, J. Wiley and Sons, Inc., New York 1957, p. 266.

Received November 30, 1960.

ACTA CHEMICA SCANDINAVICA 15 (1961) 678–681

High Temperature X-Ray Study of the Thermal Expansion of $IrAs_3$ and $IrSb_3$

ARNE KJEKSHUS

Kjemisk Institutt A, Universitetet i Oslo, Blindern, Norway

$IrAs_3$ and $IrSb_3$ with the $CoAs_3$-type structure, have been studied by the X-ray powder method at temperatures in the range from 20 to 998°C. The average linear thermal expansion coefficient, β_a, is equal to 6.7×10^{-6} °C^{-1} for $IrAs_3$ (20–473°C), 5.7×10^{-6} °C^{-1} for $IrAs_3$ (600–998°C), 8.0×10^{-6} °C^{-1} for $IrSb_3$ (20–432°C), and 6.6×10^{-6} °C^{-1} for $IrSb_3$ (737–988°C). The volume expansion coefficient, α, is 20.2×10^{-6} °C^{-1} for $IrAs_3$ (20–473°C), 17.0×10^{-6} °C^{-1} for $IrAs_3$ (600–998°C), 24.1×10^{-6} °C^{-1} for $IrSb_3$ (20–432°C), and 20.0×10^{-6} °C^{-1} for $IrSb_3$ (737–988°C).

In recent high temperature X-ray studies [1,2] of thermal expansion the author found a departure from linearity in both linear and volume expansion at higher temperatures. The reasons for the different types of expansion found are not fully explained by the existing theories for the perfect lattice. Since a quantitative explanation might be possible when sufficient data are available to test a proposed theory, further expansion experiments are to be carried out.

The present paper is concerned with the thermal expansion of $IrAs_3$ and $IrSb_3$ which have structures of the $CoAs_3$-type [3]. A drawing of one unit cell of the $CoAs_3$-type structure is shown in Fig. 1. The atomic arrangement in terms of the space group $Im3$ (T_h^5) is as follows:

8 Co in (*e*) $\frac{1}{4}$ $\frac{1}{4}$ $\frac{1}{4}$ *etc.*

24 As in (*g*) 0 y z *etc.*

The two parameters y, z are 0.350 ± 0.002, 0.146 ± 0.002, and 0.343 ± 0.001, 0.157 ± 0.001 for $IrAs_3$ and $IrSb_3$, respectively, according to Kjekshus and Pedersen [3].

As $IrAs_3$ and $IrSb_3$ were formed peritectically [3,4], these compounds were also chosen to study the expansion below a decomposition point. A relationship of thermal expansion to transition-, decomposition- or melting-point is suggested to have important practical as well as theoretical significance [5,6].

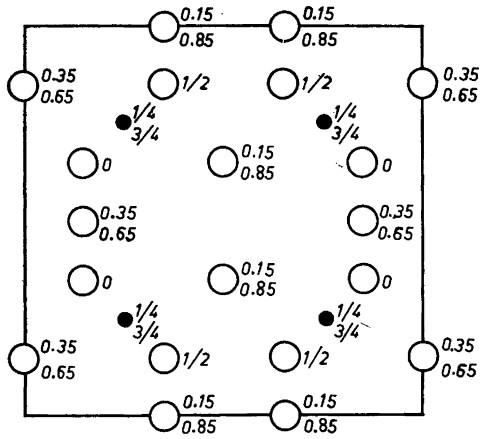

Fig. 1. Projection of one unit cell of the $CoAs_3$-type structure, with $y = 0.35$ and $z = 0.15$. Filled circles represent metal atoms and open circles represent metalloid atoms. Figures give the x-parameters of the atoms.

EXPERIMENTAL

The *iridium* metal used in this study was kindly placed at the disposal of Kjemisk Institutt by Falconbridge Nikkelverk A/S, Kristiansand S. A spectrographic analysis showed the presence of the following impurities: 0.1 % Ni, 0.01 % Rh, 0.01 % Pt, 0.001 % Ag, and 0.001 % Si.

The metallic *arsenic* was obtained from American Smelting and Refining Co. and reported to contain 99.999 % arsenic. The only reported impurities were a very faint trace of Cu and Pb. The high purity *antimony* from Brodley Mining Co., San Francisco, contained 0.001 % As, 0.0003 % Cu, 0.0003 % Fe, and 0.0002 % Pb.

According to Kjekshus and Pedersen [3] the $IrAs_3$ and $IrSb_3$ samples were made by heating stoichiometric quantities of iridium and arsenic or antimony, respectively, at about 850°C in pure alumina crucibles, placed inside silica tubes which were evacuated and sealed. The samples were heated at this temperature for one month and finally slowly cooled to room temperature.

X-Ray powder photographs of the compounds were taken in a 190 mm Unicam high-temperature camera, with the samples sealed in thin-walled quartz capillaries. The samples were studied at temperatures between 20 and 998°C.

By means of a voltage regulator, the registered temperature of the furnace surrounding the specimen was kept constant to within ± 5°C. The Pt/Pt−Rh thermocouples of the furnace had been calibrated with a standard couple located at the position of the specimen.

Lattice constants are given in Ångström units ($\lambda CuK\alpha_1 = 1.54050$ Å). The lattice constants were calculated by the extrapolation method of Nelson and Riley [7] using the

Table 1. Lattice constants and unit cell volumes of $IrAs_3$ at different temperatures.

t (°C)	a (Å)	V (Å^3)
20	8.4691	607.45
243	8.4818	610.19
306	8.4854	610.97
473	8.4947	612.98
600	8.5012	614.39
766	8.5096	616.21
903	8.5156	617.51
998	8.5208	618.64

Table 2. Lattice constants and unit cell volumes of $IrSb_3$ at different temperatures.

t (°C)	a (Å)	V (Å^3)
20	9.2495	791.33
179	9.2617	794.46
304	9.2703	796.68
432	9.2792	798.97
588	9.2878	801.20
737	9.2949	803.03
890	9.3042	805.45
988	9.3104	807.06

high angle reflection lines only. The probable error in the lattice constant determinations at temperatures above room temperature is estimated to be less than 0.01 %. Errors due to specimen contamination can be neglected, since the lattice constants at room temperature before and after the high temperature treatment were equal within the limit of the experimental error.

RESULTS

The lattice constant results and unit cell volumes are listed in Tables 1 and 2. The ratios $\frac{a_t - a_{20}}{a_{20}} = \frac{\Delta a}{a_{20}}$ and $\frac{V_t - V_{20}}{V_{20}} = \frac{\Delta V}{V_{20}}$ are calculated and plotted as $\frac{\Delta a_{20}}{a_{20}}$ *versus* t and $\frac{\Delta V}{V_{20}}$ *versus* t, respectively. The calculations of the expansion coefficients were based upon these data.

As shown in Fig. 2 the change in the length of the a-axis is similar. The a-axis increases linearly with increasing temperature for both compounds below 432 and above 737°C. The expansion coefficient, β_a, is equal to 6.7×10^{-6} °C^{-1} for $IrAs_3$ (20—473°C), 5.7×10^{-6} °C^{-1} for $IrAs_3$ (600—998°C), 8.0×10^{-6} °C^{-1} for $IrSb_3$ (20—432°C), and 6.6×10^{-6} °C^{-1} for $IrSb_3$ (737—988°C). At temperatures between 432 and 737°C the a-axis increases nonlinearly; this is most significant on the expansion-curve for $IrSb_3$.

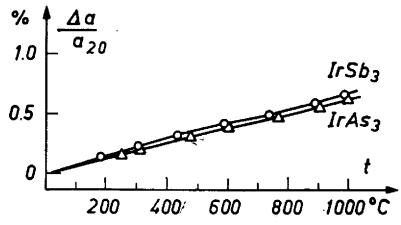

Fig. 2. Relative lattice constant variation as function of temperature.

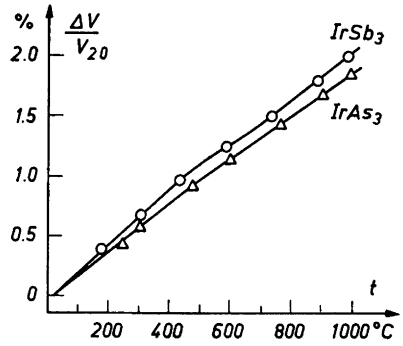

Fig. 3. Relative changes in volume with temperature.

The volume expansion is plotted as a function of temperature in Fig. 3. For both compounds the volume expansion has a similar temperature dependence as the a-axis. Since β_a is of the order of 10^{-6}, the average thermal volume expansion coefficient α is approximately $3\beta_a$. The numerical values for α are 20.2×10^{-6} °C^{-1} for $IrAs_3$ (20—473°C), 17.0×10^{-6} °C^{-1} for $IrAs_3$ (600—998°C), 24.1×10^{-6} °C^{-1} for $IrSb_3$ (20—432°C), and 20.0×10^{-6} °C^{-1} for $IrSb_3$ (737—988°C).

The intensities of the reflections on X-ray photographs taken at higher temperatures are almost equal to those of the corresponding photographs taken at room temperature. The parameters y and z must thus be nearly the same. The shortest interatomic distances between metal and metalloid atoms are

$$a \cdot 0.2887 \pm 0.0012 \text{ Å} \quad (IrAs_3)$$
$$a \cdot 0.2825 \pm 0.0006 \text{ Å} \quad (IrSb_3)$$

and between the metalloid atoms

$$a \cdot 0.292 \pm 0.034 \text{ Å} \quad (IrAs_3)$$
$$a \cdot 0.300 \pm 0.034 \text{ Å} \quad (IrAs_3)$$
$$a \cdot 0.314 \pm 0.018 \text{ Å} \quad (IrSb_3).$$

The thermal expansion is approximately equal to the expansion of the cell edge, *cf.* Fig. 2.

As the a-axis and the volume of $IrAs_3$ increase more slowly above 473°C than at lower temperatures the relative expansion is still on the upper part of the sigmoidal curve. The a-axis and the volume of $IrSb_3$ increase more slowly between 432 and 737°C than above 737°C and the relative expansion of this compound above 737°C is thus not on the sigmoidal part of the expansion curve. No large increase in the coefficient of thermal expansion for $IrAs_3$ and $IrSb_3$ is observed in the examined temperature range. A more rapid increase might well take place at higher temperatures.

The expected peritectical decomposition [3,4] of $IrAs_3$ and $IrSb_3$ is not observed at temperatures between 20 and approximately 1 000°C. Decomposition must accordingly take place in the range between approximately 1 000 and 1 200°C. For $IrSb_3$ this is higher than the range 800 to 950°C reported by Kuzmin *et al.*[4]

Acknowledgements. The author wishes to thank Professor Haakon Haraldsen for his kind interest in this study and for placing laboratory facilities at his disposal. Thanks are also due to Mr. Håkon Mohn for helpful technical assistance.

REFERENCES

1. Kjekshus, A. and Grønvold, F. *Acta Chem. Scand.* **13** (1959) 1767.
2. Kjekshus, A. *Acta Chem. Scand.* **14** (1960) 1623.
3. Kjekshus, A. and Pedersen, G. *To be published.*
4. Kuzmin, R. N., Zdanov, G. S. and Zuravlev, N. N. *Kristallografija* **2** (1957) 48.
5. Cartz, L. *Proc. Phys. Soc. (London)* **68** (1955) 957.
6. Lonsdale, K. *Z. Krist.* **112** (1959) 188.
7. Nelson, J. B. and Riley, D. P. *Proc. Phys. Soc. (London)* **57** (1945) 160.

Received October 24, 1960.

ACTA CHEMICA SCANDINAVICA 15 (1961) 682–712

Short Communications

The Identity of Cryptopimaric Acid and Sandaracopimaric Acid

V. P. ARYA, C. ENZELL, H. ERDTMAN

Organisk-Kemiska Institutionen, Kungl. Tekniska Högskolan, Stockholm, Sweden

and R. RYHAGE

Masspektrometrilaboratoriet, Kemiska Institutionen, Karolinska Institutet, Stockholm, Sweden

Sandaracopimaric acid has been isolated from the resin of *Tetraclinis articulata*, (Vahl) Masters, ("Sandarac resin") [1-3]. It belongs to the pimaric acid group of diterpenes [4] and its structure and configuration (I) has recently been settled [5-7]. The acid, on titration gave the pK^*_{MCS}-value [8] 7.92 which is in good agreement with the presence of a *trans* A/B ring junction and an equatorial carboxyl group [9].

Cryptopimaric acid * has been isolated from the resin [10] and heartwood [11] ** of *Cryptomeria japonica*, D. Don, and also shown to belong to the pimaric acid group[10]. Stenhagen *et al.*[12-14], on the basis of infra-red, mass spectrometric (*cf.* Ref.[15]) and surface-balance studies, have suggested a structure for cryptopimaric acid identical with that later proposed for sandaracopimaric acid [5-7]. The structure, however, has recently been questioned [16].

The mass spectrum of methyl sandaracopimarate, recorded in a mass spectrometric investigation of the diterpenes [17], was identical with that of methyl cryptopimarate [12]. The physical constants (Table 1) of the two acids show a striking similarity and indicate that they are in fact identical.

Sandaracopimaric acid and cryptopimaric acid showed an undepressed mixed melting point (168–170°) whilst the melting point of a mixture of sandaracopimaric acid and *iso*pimaric acid exhibited a large depression (*ca.* 30°). Similarly the mixed melting point of methyl sandaracopimarate and methyl cryptopimarate was not depressed (68–69°). The infra-red spectra of sandaracopimaric and cryptopimaric acids were superimposable.

It follows, therefore, that these acids are identical. The name sandaracopimaric acid has priority over cryptopimaric acid and the latter name may be deleted.

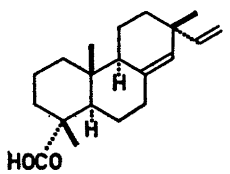

(I)

Acknowledgements. We thank Professors F. Petrů and V. V. Galík for samples of sanda-

* *Added in proof:* Apsimon et al. (*J. Chem. Soc.* **1961** 752) recently obtained a small amount (about 5 %) of dihydrosandaracopimaric acid as the only identifiable hydrogenation product of a cryptopimaric acid preparation (m.p. 160–162°, $[\alpha]_D$ −20°). From isomerisation experiments they conclude that, in spite of the high negative rotation, their acid contained mainly isopimaric and/or "Ukitas acid" and in addition a small amount of sandaracopimaric acid. We have found that a mixture of authentic sandaracopimaric and isopimaric acid (*ca.* 1:20) melts at 110–148°. "Ukitas acid" has not been available for comparison. It is possible that many cryptopimaric acid preparations have been impure.

** There referred to as *iso*pimaric acid.

Table 1. Physical constants of sandaracopimaric and cryptopimaric acids and their methyl esters.

Compound	m.p.	$[\alpha]_D$ (EtOH)	Reference
Sandaracopimaric acid	173°	−18.8°	2
» »	172°	−16.7°	3
» »	169°	−20°	7
» »	171°	−20°	Present work
Cryptopimaric acid	159−161°	−19°	10
» »	160−162°	−21.7°	12
» »	166−168°	−22°	11
» »	168−170° *	—	Present work
Methyl cryptopimarate	63−64°	−25.6°	11
» »	68−69°	—	Present work

* softening at 163°

racopimaric acid and its methyl ester, Professor H. H. Bruun for a sample of cryptopimaric acid and Dr. W. Simon for the titration of sandaracopimaric acid. Thanks are also due to the *Ciba Fellowship Trust* for a Post-doctoral fellowship (V.P.A.) and to the *Swedish Technical Research Council* for financial support.

1. Tschirch, A. and Wolff, M. *Arch. Pharm.* **244** (1906) 702: Henry, T. H. *J. Chem. Soc.* **79** (1901) 1144.
2. Balaš, Fr. and Brzák, J. *Collection Czechoslov. Chem. Communs* **1** (1929) 306, 352; from *Chem. Zentr.* **100** (1929) II, 990.
3. Petrů, F. and Galik, V. *Collection Czechoslov Chem. Communs* **18** (1953) 717.
4. Galík, V., Petrů, F. and Kuthan, J. *Tetrahedron* **7** (1959) 223.
5. Galík, V., Kuthan, J. and Petrů, F. *Chem. & Ind. London* **1960** 722.
6. Ireland, R. E. and Scheiss, P. W. *Tetrahedron Letters* **25** (1960) 37.
7. Edwards, O. E., Nicolson, A. and Rodger, M. N. *Can. J. Chem.* **38** (1960) 663.
8. Simon, W. *Helv. Chim. Acta* **41** (1958) 1835.
9. Sommer, P. F., Arya, V. P. and Simon, W. *Tetrahedron Letters* **20** (1960) 18.
10. Keimatsu, S., Ishiguro, T. and Fukuri, G. *J. Pharm. Soc. Japan* **57** (1937) 69; from *Chem. Abstr.* **31** (1937) 3932 [7].
11. Kondo, T., Imamura, H. and Suda, M. *Bull. Agr. Chem. Soc. Japan* **23** (1959) 233.
12. Bruun, H. H., Ryhage, R. and Stenhagen, E. *Acta Chem. Scand.* **12** (1958) 789.
13. Bruun, H. H., Fishmeister, I. and Stenhagen, E. *Acta Chem. Scand.* **13** (1959) 379.
14. Bruun, H. H. and Stenhagen, E. *Acta Chem. Scand.* **13** (1959) 832.
15. Enzell, C. *Acta Chem. Scand.* **15** (1961). *In the press.*
16. Bose, A. K. and Struck, W. A. *Chem. & Ind. London* **1959** 1628.
17. Enzell, C. and Ryhage, R. *To be published.*

Received February 21, 1961.

The Preparation of the Aldehyde of Kojic Acid (Comenaldehyde)

HANS-DIETER BECKER*

Institutionen för organisk kemi, Chalmers Tekniska Högskola, Göteborg, Sweden

Many derivatives of kojic acid (I) have been described but all attempts to synthesize its aldehyde (II, comenaldehyde, 2-formyl-5-hydroxy-γ-pyrone) have been unsuccessful.[1]

Both the oxidation of the hydroxymethyl group of kojic acid with mild oxidizing agents [2] and the reduction of comenyl chloride by Rosenmund's method [3] did not give the aldehyde II. Yabuta, who established the structure of kojic acid, concluded that comenaldehyde was a very unstable substance.[3]

* Present address: University of Wisconsin, Madison, Wis., U.S.A.

Table 1. Physical constants of sandaracopimaric and cryptopimaric acids and their methyl esters.

Compound	m.p.	$[\alpha]_D$ (EtOH)	Reference
Sandaracopimaric acid	173°	−18.8°	2
» »	172°	−16.7°	3
» »	169°	−20°	7
» »	171°	−20°	Present work
Cryptopimaric acid	159−161°	−19°	10
» »	160−162°	−21.7°	12
» »	166−168°	−22°	11
» »	168−170° *	—	Present work
Methyl cryptopimarate	63−64°	−25.6°	11
» »	68−69°	—	Present work

* softening at 163°

racopimaric acid and its methyl ester, Professor H. H. Bruun for a sample of cryptopimaric acid and Dr. W. Simon for the titration of sandaracopimaric acid. Thanks are also due to the *Ciba Fellowship Trust* for a Post-doctoral fellowship (V.P.A.) and to the *Swedish Technical Research Council* for financial support.

1. Tschirch, A. and Wolff, M. *Arch. Pharm.* **244** (1906) 702: Henry, T. H. *J. Chem. Soc.* **79** (1901) 1144.
2. Balaš, Fr. and Brzák, J. *Collection Czechoslov. Chem. Communs* **1** (1929) 306, 352; from *Chem. Zentr.* **100** (1929) II, 990.
3. Petrů, F. and Galik, V. *Collection Czechoslov Chem. Communs* **18** (1953) 717.
4. Galík, V., Petrů, F. and Kuthan, J. *Tetrahedron* **7** (1959) 223.
5. Galík, V., Kuthan, J. and Petrů, F. *Chem. & Ind. London* **1960** 722.
6. Ireland, R. E. and Scheiss, P. W. *Tetrahedron Letters* **25** (1960) 37.
7. Edwards, O. E., Nicolson, A. and Rodger, M. N. *Can. J. Chem.* **38** (1960) 663.
8. Simon, W. *Helv. Chim. Acta* **41** (1958) 1835.
9. Sommer, P. F., Arya, V. P. and Simon, W. *Tetrahedron Letters* **20** (1960) 18.
10. Keimatsu, S., Ishiguro, T. and Fukuri, G. *J. Pharm. Soc. Japan* **57** (1937) 69; from *Chem. Abstr.* **31** (1937) 3932 [7].
11. Kondo, T., Imamura, H. and Suda, M. *Bull. Agr. Chem. Soc. Japan* **23** (1959) 233.
12. Bruun, H. H., Ryhage, R. and Stenhagen, E. *Acta Chem. Scand.* **12** (1958) 789.
13. Bruun, H. H., Fishmeister, I. and Stenhagen, E. *Acta Chem. Scand.* **13** (1959) 379.
14. Bruun, H. H. and Stenhagen, E. *Acta Chem. Scand.* **13** (1959) 832.
15. Enzell, C. *Acta Chem. Scand.* **15** (1961). *In the press.*
16. Bose, A. K. and Struck, W. A. *Chem. & Ind. London* **1959** 1628.
17. Enzell, C. and Ryhage, R. *To be published.*

Received February 21, 1961.

The Preparation of the Aldehyde of Kojic Acid (Comenaldehyde)

HANS-DIETER BECKER*

Institutionen för organisk kemi, Chalmers Tekniska Högskola, Göteborg, Sweden

Many derivatives of kojic acid (I) have been described but all attempts to synthesize its aldehyde (II, comenaldehyde, 2-formyl-5-hydroxy-γ-pyrone) have been unsuccessful.[1]

Both the oxidation of the hydroxymethyl group of kojic acid with mild oxidizing agents [2] and the reduction of comenyl chloride by Rosenmund's method [3] did not give the aldehyde II. Yabuta, who established the structure of kojic acid, concluded that comenaldehyde was a very unstable substance.[3]

* Present address: University of Wisconsin, Madison, Wis., U.S.A.

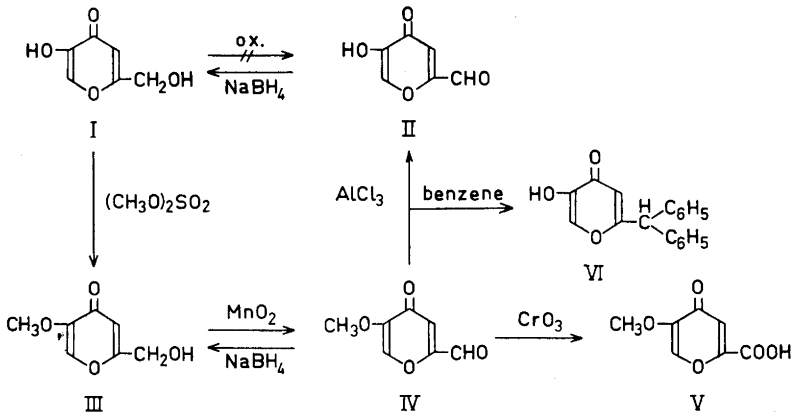

Previous oxidations of kojic acid monomethyl ether (III, 2-hydroxymethyl-5-methoxy-γ-pyrone) yielded comenic acid methyl ether (V). $KMnO_4$ in acetone solution [4], conc. HNO_3,[5] and air in the presence of catalysts [6] have been applied as oxidizing reagents. The 2-formyl-5-methoxy-γ-pyrone (IV) had not been obtained.

We recently [7] found that the γ-pyrone aldehyde IV can be prepared when a solution of III in benzene is refluxed for one hour in the presence of active manganese dioxide [8]. From the filtered solution IV crystallizes in colorless needles that sublime on heating (m.p. 202°C; Found: C 54.75; H 3.91; Calc. for $C_7H_6O_4$: C 54.55; H 3.92; IR spectrum: $\nu_{C=O}$ 1 705 cm^{-1}). The yield of IV was 50—70 %. With phenylhydrazine IV forms a phenylhydrazone (m.p. 205—206°C; Found: N 11.50; Calc. for $C_{13}H_{12}N_2O_3$ N 11.47).

When IV was oxidized by CrO_3/H_2SO_4 in acetone,[9] V was formed immediately (yield 90 %). Comenic acid methyl ether was also obtained by direct oxidation of III by CrO_3/H_2SO_4 in acetone (yield 70 %).

Reduction of IV by $NaBH_4$ in ethanol did not attack the γ-pyrone group but gave III in about 70 % yield.

Attempted demethylation of IV by the action of pyridine hydrochloride at 185°C resulted only in decomposition products. Treatment of IV in boiling benzene with an excess of $AlCl_3$ gave a colorless crystalline product, probably 2-(diphenylmethyl)-5-hydroxy-γ-pyrone, VI (m.p. 150—152°C; Found: C 77.24; H 5.17; Calc. for $C_{18}H_{14}O_3$: C 77.68; H 5.07; IR spectrum: ν_{OH} 3 200 cm^{-1}; red color with $FeCl_3$).

When the 2-formyl-5-methoxy-γ-pyrone (IV) was heated with $AlCl_3$ without a solvent at 120°C for 3 h, the hitherto unknown comenaldehyde was formed almost quantitatively. (Found: C 51.51; H 2.96; Calc. for $C_6H_4O_4$: C 51.44; H 2.88; IR spectrum: $\nu_{C=O}$ 1 718 cm^{-1}; ν_{OH} 3 230 cm^{-1}; red color with $FeCl_3$).

The comenaldehyde forms colorless prismatic needles, m.p. 162—163°C, and can easily be purified by sublimation or recrystallization from chloroform.

Formulation of the structure of II as 2-formyl-5-hydroxy-γ-pyrone was supported by its reduction with $NaBH_4$ in ethanol to kojic acid.

1. Beélik, A. *Advances in Carbohydrate Chem.* **11** (1956) 145.
2. Obata, Y. and Yamanishi, T. *J. Agr. Chem. Soc. Japan* **24** (1951) 334; *Chem. Abstr.* **46** (1952) 11474.
3. Yabuta, T. *J. Chem. Soc.* **125** (1924) 575.
4. Yabuta, T. and Kambe, K. *J. Agr. Chem. Soc. Japan* **6** (1930) 516; *Chem. Abstr.* **26** (1932) 1931.
5. Armit, J. W. and Nolan, T. J. *J. Chem. Soc.* **1931** 3023.
6. Heyns, K. and Vogelsang, G. *Chem. Ber.* **87** (1954) 13; Heyns, K. and Paulsen, H. *Angew. Chem.* **69** (1957) 600.
7. Becker, H.-D. *Svensk Kem. Tidskr.* **72** (1960) 608.
8. Attenburrow, J., Cameron, A. F. B., Chapman, J. H., Evans, R. M., Hems, B. A., Jansen, A. B. A. and Walker, T. *J. Chem. Soc.* **1952** 1094.
9. Curtis, R. G., Heilbron, I., Jones, E. R. H. and Weedon, B. C. L. *J. Chem. Soc.* **1953** 457.

Received March 21, 1961.

Sesquiterpenes from *Cedrus* Species *

J. B-SON BREDENBERG and H. ERDTMAN

Organisk-kemiska institutionen, Kungl. Tekniska Högskolan, Stockholm, Sweden

Rao, Dew and Guha isolated two bicyclic sesquiterpene hydrocarbons $C_{15}H_{24}$ called α- and β-himachalene from the wood of *Cedrus deodara* [1] and references to earlier work on sesquiterpenes from *Cedrus* species are given in this paper. α-Himachalene (b.p. 124°/10 mm, n_D^{27} 1.507, d^{27} 0.924, $[\alpha]_D^{27} - 86.5°$) as well as β-himachalene (b.p. 132°/10 mm, n_D^{27} 1.513, d^{27} 0.9264, $[\alpha]_D^{27} + 196.8°$, gave a dihydrochloride m.p. 118—119°, $[\alpha]_D \pm 0°$, and a monohydrochloride, m.p. 56—57°, $[\alpha]_D \pm 0°$. Selenium dehydrogenation gave mixtures of at least partly aromatic hydrocarbons. The authors concluded that the himachalenes probably belong to a new class of bicyclic sesquiterpenes.

We have obtained similar sesquiterpenes from the wood of *Cedrus atlantica* and *C. libani*. (Commercial essential oils and wood extracts.) However, our best α-himachalene preparation (according to gas-liquid chromatography (G.L.C.) about 96 % pure) obtained by careful fractional distillation followed by chromatography on alumina, had the following constants: b.p. 133°/15 mm, $[\alpha]_D^{20} - 198°$ ($CHCl_3$, $c = 2$), n_D^{25} 1.5073, d^{20}_4 0.9160 (according to its IR absorption it contained one exocyclic double bond). The quantitatively dominating β-himachalene, isolated in the same way, (G.L.C. purity, 99 %) had b.p. 138—139°/15 mm, $[\alpha]_D^{20} + 204°$ ($CHCl_3$, $c = 4$), n_D^{25} 1.5113, d^{20}_4 0.9244 (no exocyclic double bond in the I.R.). Both gave identical dihydrochlorides (HCl/HAc), m.p. (rapid heating) 115—117° (decomp.), $[\alpha]_D^{20} - 9°$ ($CHCl_3$, $c = 5$) immediately after dissolution, + 13° after 1 h and + 31° after 15 h (HCl liberated). Recrystallisation from methanol afforded the monohydrochloride containing one exocyclic double bond and having m.p. 55—57° but $[\alpha]_D^{20} + 106°$ ($CHCl_3$, $c = 3$).

Catalytic hydrogenation of α-himachalene gave mainly one dihydrocompound but hydrogenation of β-himachalene proceeded slowly and nonstoichiometrically. G. L. C. examination of the products indicated the formation of several compounds (2—6). One of these was an aromatic compound, "Ar III" ($C_{15}H_{22}$, (G.L.C. purity, 97 %), n_D^{25} 1.5257, inflexion 261 mμ (ε 342), λ_{max} 267, 276 mμ (ε 420, 380)) which could be isolated by low temperature (—70°) ozonisation followed by chromatography.

Selenium dehydrogenation of β-himachalene gave a large yield of a mixture of aromatic compounds "Ar I" (0—16 %), "Ar II" (27—35 %) and Ar III (56—70 %).

"Catalytic selenium dehydrogenation" (β-isomer:Se = 36:1) gave 40 % Ar II, 51 % Ar III and 9 % hydrogenated compounds. α-Himachalene gave similar results.

Ozonisation of the dehydrogenation mixture (1.1 g) followed by oxidation with NaOH + 30 % H_2O_2 furnished evil smelling volatile acids and non volatile acids (270 mg). The latter gave a *cyclo*hexylamine salt, m.p. 140—142°. The m.p. of the corresponding acid, 65—70°, (26 mg) was not depressed (68—71°) on admixture with 2,2,6-trimethylpimelic acid (m.p. 72—73)[2] kindly provided by Dr. G.F. Wright, Toronto. The I.R.- and mass spectra of the two acids were identical.

Chromic acid oxidation of the dehydrogenation mixture gave neutral products free from Ar III and acids which were chromatographed on silica gel. An acid, $C_{15}H_{20}O_2$, m.p. 135—137° (yield 30 %) was obtained. According to spectral data this was an aromatic acid. A strong "peak" of mass number 217 in the mass spectrum may indicate the loss of one CH_3 (232—15).

Fractional distillation of the dehydrogenation mixture (spinning band column) gave 12 fractions. Fraction 1 contained (G.L.C.) 28 % Ar I and 72 % Ar II and gave a large yield of terephthalic acid and some isophthalic acid on oxidation with 30 % HNO_3 at 170°. Fraction 4 contained 15 % Ar I, 82 % Ar II and 3 % Ar III. G.L.C. comparison with dihydro-*ar*-curcumene using 5 different columns conclusively demonstrated the identity of Ar II and dihydro-*ar*-curcumene and the comparison of the I.R.- and U.V.-spectra corroborated this. Fraction 12, b.p. 135—136°/14 mm, d^{20}_4 0.9212, n_D^{25} 1.5295 contained 1 % Ar II and 99 % Ar III and gave on nitric acid oxidation 3,3-dimethylphthalide-5-carboxylic acid (decarbonylation) m.p. 264—266°

* First presented at the Chemical Society symposium on terpene chemistry in London (23.2. 1961). *Proc. Chem. Soc.* **1961** 129.

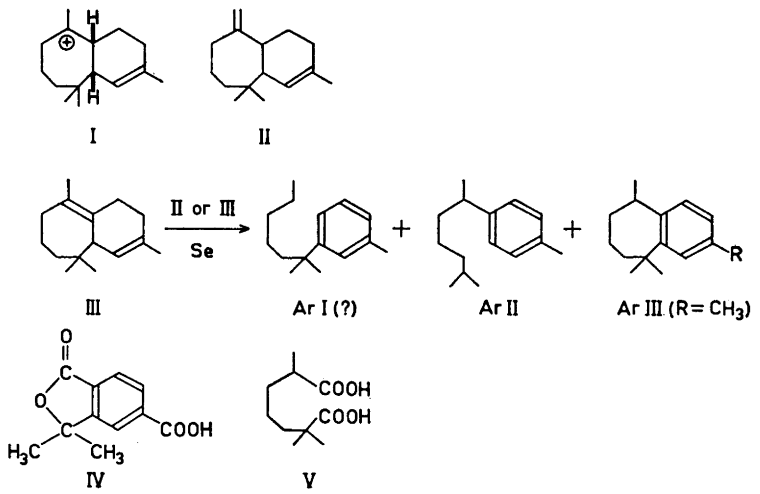

(I.R., mix. m.p.) and trimellitic acid (anhydride, m.p. 161–163°, I.R., mix. m.p.).

From the above results structure(II) and (III) may be tentatively proposed for *α*- and *β*-himachalene respectively.

Ar I could be the source of isophthalic acid, Ar II of terephthalic and Ar III (R = CH_3) of trimellitic acid, 3,3-dimethylphthalide-5-carboxylic acid (IV), 2,2,6-trimethylpimelic acid(V),and acid $C_{15}H_{20}O_2$, m.p. 135–137° (Ar III, R = COOH). The himachalenes would then appear to be formed by deprotonation of the cation (I) postulated by Hendrickson to be an intermediate in the transformation of *cis*-farnesol into longifolene [3] (and juniperol) [4]. If this assumption is correct the steric orientation of the hydrogen atoms at the assymmetric carbon atoms of (II) and (III) would be as in (I).

We thank *The Cellulose Industry Foundation* for economical support and Professor Dr. J. Kowalski, Poznan, Poland, who carried out much of the isolation work.

1. Rao, G. S. K., Dew, S. and Guha, P. C. *J. Indian Chem. Soc.* **29** (1952) 721.
2. Bell, A., Strickland, T. H. and Wright, G. F. *J. Org. Chem.* **16** (1951) 1742.
3. Hendrickson, J. B. *Tetrahedron* **7** (1959) 82.
4. Akiyoshi, S., Erdtman, H. and Kubota, T. *Tetrahedron* **9** (1960) 237.

Received March 7, 1961.

Synthetic Aminosugar Derivatives as Potential Antimicrobials; Oxazolidine Derivatives of 1-Arylamino-1-deoxy-D-fructopyranose

ALF WICKSTRÖM and JENS KRISTIAN WOLD

Universitetets farmasöytiske institutt, Blindern-Oslo, Norway

Amadori compounds such as 1-arylamino-1-deoxy-D-fructoses, which have interested the authors as potential antimicrobials (unpublished work), are known to be labile in solution because of their high reducing power. The first non-reducing derivative of an Amadori compound (1-(4-methylphenyl)-amino-1-deoxy-D-fructose) was prepared by condensation with benzaldehyde and tentatively described as 2,3-O-benzylidene-1-(4-methylphenyl)-amino-1-deoxy-D-fructopyranose [1]. Kuhn *et al.*[2] proved this condensation product to be 1,2-N,O-benzylidene-1-(4-methylphenyl)-amino-1-deoxy-D-fructopyranose (I), using methylation and degradation to 1,3,4,5-tetra-O-methyl-D-fructose. Formula (I) represents an aminosugar derivative in which the reducing function is blocked by ring formation and one of the parent sugar's

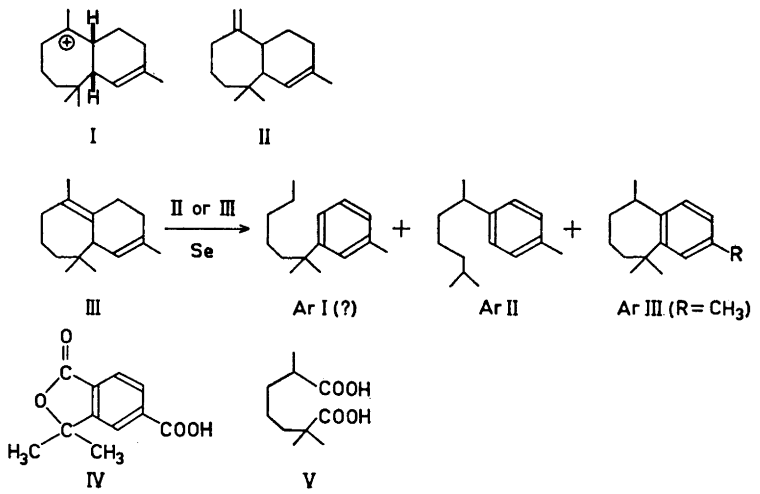

(I.R., mix. m.p.) and trimellitic acid (anhydride, m.p. 161–163°, I.R., mix. m.p.).

From the above results structure(II) and (III) may be tentatively proposed for *α*- and *β*-himachalene respectively.

Ar I could be the source of isophthalic acid, Ar II of terephthalic and Ar III (R = CH_3) of trimellitic acid, 3,3-dimethylphthalide-5-carboxylic acid (IV), 2,2,6-trimethylpimelic acid(V),and acid $C_{15}H_{20}O_2$, m.p. 135–137° (Ar III, R = COOH). The himachalenes would then appear to be formed by deprotonation of the cation (I) postulated by Hendrickson to be an intermediate in the transformation of *cis*-farnesol into longifolene [3] (and juniperol) [4]. If this assumption is correct the steric orientation of the hydrogen atoms at the assymmetric carbon atoms of (II) and (III) would be as in (I).

We thank *The Cellulose Industry Foundation* for economical support and Professor Dr. J. Kowalski, Poznan, Poland, who carried out much of the isolation work.

1. Rao, G. S. K., Dew, S. and Guha, P. C. *J. Indian Chem. Soc.* **29** (1952) 721.
2. Bell, A., Strickland, T. H. and Wright, G. F. *J. Org. Chem.* **16** (1951) 1742.
3. Hendrickson, J. B. *Tetrahedron* **7** (1959) 82.
4. Akiyoshi, S., Erdtman, H. and Kubota, T. *Tetrahedron* **9** (1960) 237.

Received March 7, 1961.

Synthetic Aminosugar Derivatives as Potential Antimicrobials; Oxazolidine Derivatives of 1-Arylamino-1-deoxy-D-fructopyranose

ALF WICKSTRÖM and JENS KRISTIAN WOLD

Universitetets farmasöytiske institutt, Blindern-Oslo, Norway

Amadori compounds such as 1-arylamino-1-deoxy-D-fructoses, which have interested the authors as potential antimicrobials (unpublished work), are known to be labile in solution because of their high reducing power. The first non-reducing derivative of an Amadori compound (1-(4-methylphenyl)-amino-1-deoxy-D-fructose) was prepared by condensation with benzaldehyde and tentatively described as 2,3-O-benzylidene-1-(4-methylphenyl)-amino-1-deoxy-D-fructopyranose [1]. Kuhn *et al.*[2] proved this condensation product to be 1,2-N,O-benzylidene-1-(4-methylphenyl)-amino-1-deoxy-D-fructopyranose (I), using methylation and degradation to 1,3,4,5-tetra-O-methyl-D-fructose. Formula (I) represents an aminosugar derivative in which the reducing function is blocked by ring formation and one of the parent sugar's

biochemically important terminal hydroxyl groups is replaced by a tertiary amino group. These structural features relate the compound (I) to the type of aminosugar derivatives previously studied by the authors as potential antimicrobials [3], and it seemed of interest to attempt the synthesis of a series of aminosugar derivatives analogous to (I) with a view to their use in microbiological tests.

The substances (I), (II), and (III) were obtained by refluxing the parent Amadori compounds with benzaldehyde in absolute ethanol. 1-(4-Ethoxyphenyl)-amino-1-deoxy-D-fructose reacted only to a minor degree and the corresponding 2-methylphenyl or 3,4-dimethylphenyl derivatives did not give oxazolidines under the experimental conditions employed. When benzaldehyde was replaced by monophenolic aldehydes (2-, 3-, or 4-hydroxybenzaldehyde, vanilline) substantial quantities of the various Amadori compounds were recovered unchanged. 4-Nitrobenzaldehyde, however, did react by prolonged reflux to give oxazolidines, *e.g.* substance (IV).

(IV) differs from the reference compound (I) only by the presence of a nitro group, and the size of the heterocyclic rings in this product (IV) could be determined by methylation followed by hydrolysis to 1 (4-methylphenyl)-amino-1-deoxy-3,4,5-tri-O-methyl-D-fructopyranose hydrochloride, obtained by Kuhn *et al.*[2] from (I).

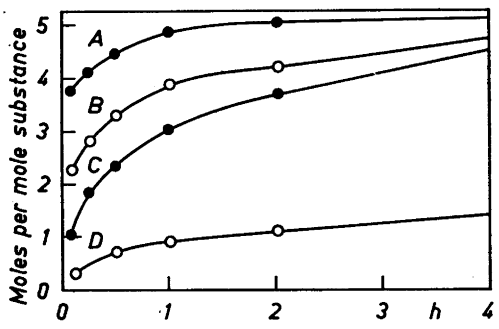

Fig. 1. Periodate oxidation of compounds I, II, and III. Curves A, B, and C represent the periodate uptake of the substances III, II, and I, respectively. Curve D represents the amount of monovalent acid liberated from each of the three compounds. Experimental conditions: test substance, 10^{-5} mole (5 ml, 50 % ethanol) + sodium metaperiodate, 5×10^{-5} mole (5 ml) at room temperature; periodate uptake by the arsenite method, acidity by direct titration after adding ethylene glycol.

To confirm the size of the heterocyclic rings constituting the substances (II) and (III) recourse was had to periodate oxidation, again using (I) as a reference compound, Fig. 1. Periodate first opens the pyranose ring, yielding one mole of monovalent acid and a product which upon reduction with potassium borohydride releases from all three substances ethylene glycol (C_5—C_6 of the sugar moiety), detected by paper chromatography. The periodate uptake (Fig. 1) was, especially under prolonged oxidation, higher than expected, probably because of a certain degree of hydrolytic opening of the oxazolidine ring, initiating secondary oxidation reactions which may also involve the aromatic amine components (coloured products). It should therefore be emphasized that the determination of the size of the rings in (II) and (III) is based upon a comparison with the well known compound (I).

The substances (I), (II) and (III) differ so little as to the character of the substituent R_1 that the uniformity of their molecular rotation (M_D) may be interpreted as corresponding to an identical steric configuration of all three compounds. The stereochemistry of oxazolidines formed by condensation of aminoalcohols with aldehydes has been reviewed by Bergmann [4]. It is seen from the formulas that the asymmetry of carbon 2 of the sugar moiety alone would account for the possibility of two diastereoisomers without considering the possible stereochemical contribution of the asymmetric carbon atom introduced in the oxazolidine ring by benzaldehyde. On examination in the polarizing microscope the crystalline reference compound (I) revealed no sign of being a mixture of diastereoisomers. The oxazolidine derivatives of the Amadori compounds probably result from an asymmetric synthesis intimately connected with the non-elucidated mechanism of the ring formation.

The aminosugar derivatives (I), (II), (III), and (IV) were tested as antimicrobials using the same techniques and the same pathogenic micro-organisms as previously described [3], but applying the substances as finely ground powder because of their extremely low solubility in water (less than 1:10 [4]). No antimicrobial activity could be observed.

Experimental. (All melting points are micro melting points, Kofler's hot-stage microscope. The various Amadori compounds were prepared and identified according to known methods [5].)

*1,2-N,O-benzylidene-1-(4-methylphenyl)-amino-1-deoxy-*D*-fructopyranose* (I). The following method was preferred to the direct condensation method without any solvent [1,2]. The parent Amadori compound (10^{-2} mole) was refluxed for 6—8 h with benzaldehyde (2×10^{-2} mole) dissolved in absolute ethanol (25 ml). The crude product separating on cooling was washed with light petroleum and suspended in water (50—60°) to dissolve unreacted Amadori compound. Recrystallizations from acetone-methanol 2:1 to constant m.p. 198—200°. Yield 30%. $[\alpha]_D^{20}$ −149.6 ($c = 0.4612$, pyridine). M_D −534. The product crystallizes in rods or needles with parallel extinction and elongation negative or positive. $\alpha = 1.567$ (20°) and $\gamma = 1.617$ (20°) measured on rods with negative elongation (flash figure in convergent polarized light). β not observable with accuracy. Crushed material with random orientation showed all indices between α and γ.

*1,2-N,O-benzylidene-1-(4-methoxyphenyl)-amino-1-deoxy-*D*-fructopyranose* (II). Preparation as above (yield 35 %), m.p. 210—212°. $[\alpha]_D^{20}$ −157.0° ($c = 0.4056$, pyridine) M_D −586. (Found: C 63.24; H 6.36; N 3.69. $C_{20}H_{23}O_6N$ requires C 64.33; H 6.21; N 3.75.)

*1,2-N,O-benzylidene-1-(4-hydroxyphenyl)-amino-1-deoxy-*D*-fructopyranose* (III). Preparation as above (yield 30 %), m.p. 204—206°. $[\alpha]_D^{20}$ −142.3° ($c = 0.288$, pyridine). M_D −511. (Found: C 63.59; H 5.87; N 3.89. $C_{19}H_{21}O_6N$ requires C 63.49; H 5.89; N 3.90.)

*1,2-N,O-4-nitrobenzylidene-1-(4-methylphenyl)-amino-1-deoxy-*D*-fructopyranose* (IV). Preparation as above (yield 40 %, reflux 14—16 h), m.p. 210—212°. $[\alpha]_D$ −79.7° ($c = 0.419$, pyridine). (Found: C 59.98; H 5.52; N 7.06. $C_{20}H_{22}O_7N_2$ requires C 59.70; H 5.51; N 6.96.) Methylation[2] introduced three methoxyl groups (syrupy product which crystallized when kept, m.p. 100—110°), (Found: MeO 20.7; $C_{23}H_{28}O_7N_2$ requires MeO 20.94). The methylated product was hydrolyzed in methanolic hydrochloric acid and the liberated 4-nitrobenzaldehyde removed (after dilution with water) by extraction with benzene-light petroleum. The remaining 1-(4-methylphenyl)-amino-1-deoxy-3,4,5-tri-O-methyl-D-fructopyranose hydrochloride [2] was recrystallized from methanol: m.p. 133—135° (decomp.). $[\alpha]_D^{20}$ −59.1° (initial) → −55.1° (constant, after 1 h), ($c = 0.843$, dmethylformamide). (Found: MeO 26.3; $C_{16}H_{25}O_5N$; HCl requires MeO 26.77).

Oxidation with periodate of the benzaldehyde condensation products (I) (II) (III). a) Experi-

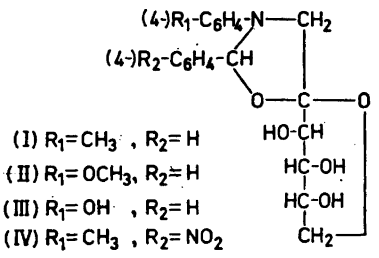

(I) $R_1 = CH_3$, $R_2 = H$
(II) $R_1 = OCH_3$, $R_2 = H$
(III) $R_1 = OH$, $R_2 = H$
(IV) $R_1 = CH_3$, $R_2 = NO_2$

mental conditions and results of the quantitative analyses are given in Fig. 1. b) 2.5×10^{-5} mole of the oxazolidine derivatives dissolved in ethanol (1 ml) + 10^{-4} mole of sodium metaperiodate (1 ml). After 2 h add potassium borohydride (30 mg) in water (1 ml) and leave overnight. Acidify with hydrochloric acid (0.5 N, 1.2 ml) and shake with silver carbonate (0.5 g). The filtrate is concentrated to dryness under reduced pressure, the residue extracted with ethanol (2 ml) and examined by paper chromatography (ethyl acetate:pyridine:water, 7:2:1 v/v) giving spots which could not be distinguished from those of ethylene glycol and of an intensity estimated to about one third of the amount of ethylene glycol corresponding to an opening of the pyranose ring not disturbed by secondary reactions. The technique employed is with some modification based upon the method given by Viscontini *et al.*[6].

The microbiological tests were carried out at the Department of Bacteriology (head: Dr. Ole G. Clausen) at Universitetets farmasöytiske institutt, Oslo, and the elementary micro analyses were performed by Mr. E. Manser, E.T.H., Zürich. Gratitude is expressed to *Norges almenvitenskapelige forskningsråd* for the award of a Research Fellowship to one of us (J.K.W.).

1. Micheel, F. and Frowein, A. *Chem. Ber.* **90** (1957) 1599.
2. Kuhn, R., Krüger, G. and Seeliger, A. *Ann.* **618** (1958) 82.
3. Wickström, A. and Wold, J. K. *Acta Chem. Scand.* **14** (1960) 1419.
4. Bergmann, E. D. *Chem. Revs.* **53** (1953) 309.
5. Hodge, J. E. *Advances in Carbohydrate Chem.* **10** (1955) 169.
6. Viscontini, M., Hoch, D. and Karrer, P. *Helv. Chim. Acta* **38** (1955) 642.

Received February 14, 1961.

Note on a Possible Dihydro-furofuran-(3,2-b) from *Chrysanthemum vulgare* Bernh.

ERLING GUDDAL*

Institutt for organisk kjemi, Norges tekniske høgskole, Trondheim, Norway

The recent appearance of a communication[1] concerning polyacetylenic compounds contained in the roots of *Chrysanthemum vulgare* Bernh. (= *Tanacetum vulgare* L.) prompts us to report preliminary data on a new compound isolated from the same plant some time ago [2], thereby extending our earlier reports on investigations in the same field [3-5].

The compound was isolated as colourless crystals from acetone extracts of the roots of *Chrysanthemum vulgare* Bernh. upon chromatography and subsequent countercurrent distribution. From deactivated alumina it is eluted by benzene:light petroleum (1:5), together with a complex mixture of polyacetylenes, the properties of which have been extensively investigated by Bohlmann *et al.*[1] When this fraction is distributed between light petroleum and 90 % aqueous alcohol over 50 cells in a Craig apparatus with a mobile upper phase, the compound is found in the cells Nos. 9—15, as indicated by the ultraviolet spectra. These fractions are combined, evaporated to dryness, and the residue dissolved in hexane. Upon cooling to —70°C, a complex mixture of polyacetylenes of the tri-yn-ene- and triyne-diene type is precipitated. The supernatant, upon concentration to a small volume and prolonged cooling to —10°C, deposits colourless crystals, which after two crystallisations from hexane melt at 64.5—66°C in an evacuated capillary. When heated in air the m.p. is 80—84°C (decomp). From 15 kg of fresh roots 32 mg of the new compound was obtained, the elementary analysis of which agrees with the formula $C_{14}H_{14}O_2$. The ultraviolet spectrum is shown in Fig. 1, and the infrared spectrum in Fig. 2. The spectrum contains no hydroxyl or carbonyl bands, but a band at 2 138 cm^{-1} indicates the presence of a triple bond. The double bond-stretching band at 1 637 cm^{-1} corresponds to a band reported to occurs in vinylethers [6-8]. The two high-frequency bands in the C—H-stretching region — appearing at 3 057 cm^{-1} and 3 101 cm^{-1} — would indicate the presence of two different olefinic hydrogen atoms, one aliphatic and one in an unsaturated five-membered ring, respectively.

The infrared spectrum is very complex, but throughout the spectral region there is a strong resemblance to that of 2,2,5,5-tetramethyldihydrofurofuran (3,2-b), the remarkable isomerization product of 2,7-dimethyl-2,7-dihydroxy-octa-3,5-diyne described by Audier [8]. This compound absorbs at 2 400 Å (ε = 6 900) and 3 030 Å (ε = 14 820), while the main absorbtion band of the compound isolated from *Chrysanthemum vulgare* Bernh. occurs at 3 225 Å (ε = 37 500). In this region, a red-shift of about 200 Å would be the normal effect of one double bond added to a poly-ene chromophore.

The isolated compound is optically active, $[\alpha]_D^{20} = -15.3°$ (0.2 %, $CHCl_3$). As all acetylenic compounds previously isolated from natural

* Present address: Leo Pharmaceutical Products, Ballerup, Denmark.

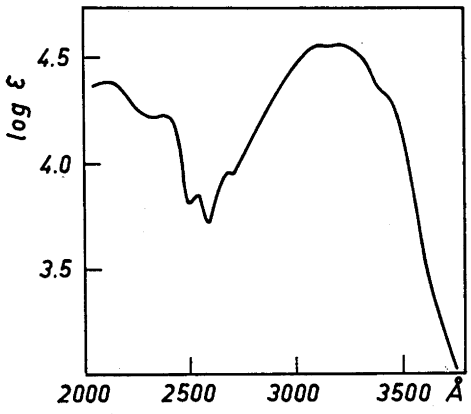

Fig. 1. Ultraviolet spectrum in hexane of compound from *Chrysanthemum vulgare* Bernh.

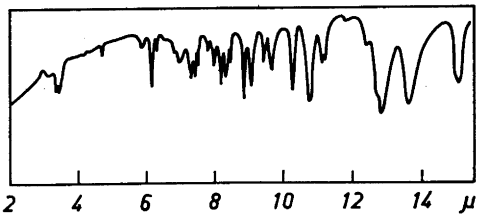

Fig. 2. Infrared spectrum in KBr of compound from *Chrysanthemum vulgare* Bernh.

Table 1.

	Pine Wood Test [10]	Ehrlich's Test [10]	Vanillin-HCl Test [9]
Isolated cpd.	Light green	Light yellow	Light orange
Perhydro cpd.	No reaction	No reaction	No reaction
Octahydro cpd.	Deep purple		Deep orange, turning brown on heating

sources may be derived from straight-chain compounds, the presence of an asymmetric carbon atom suggests that one of the ether oxygens is bound to a saturated carbon atom bearing two alkyl groups and one hydrogen. When hydrogenated over a $Pd/BaSO_4$-catalyst, the compound absorbs six moles of hydrogen, giving an oil which is transparent in the ultraviolet down to 2 200 Å, and in the infrared shows two ether bands at 1 115 cm^{-1} and 1 015 cm^{-1}. In addition to these two bands, the infrared spectrum shows only the normal CH, CH_2, and CH_3 absorption bands.

When hydrogenated over a deactivated Pd-catalyst [9], only four moles of hydrogen are absorbed. The octahydro-compound also shows unspecific absorption down to 2 200 Å, step-off beginning at 2 700 Å. Its infrared spectrum is quite complex, showing double-bond absorption and a strong band at 1 710 cm^{-1}, indicative of a saturated ketone. The formation of this grouping might be explained as the hydrogenolytic cleavage of a vinyl ether. This is in accordance with the formation of ketones upon catalytic hydrogenation of tetramethyldihydrofurofurane (3,2-b) [8]. Lack of substance prevented the isolation of the two hydrogenation products in a pure state, but the hydrogenation data together with the elementary analysis of the isolated compound suggests the presence of two rings in the molecule. Since the presence or absence of a furanoic structure could not be unequivocally stated from spectral studies, some colour tests [9,10] were made. The results are presented in Table 1.

According to Reichstein [10], a purple colour in the Pine Wood Test suggests the presence of a furan nucleus with at least two substituents. The isolated compound does not react with H_3CMgI at room temperature, but upon 5 min interaction in boiling benzene, followed by hydrolysis and chromatography on deactivated alumina, a compound with absorption maxima at 2 900 Å, 2 730 Å, and 2 590 Å is eluted by 10 % alcohol in ether. Seen in relation to the ultraviolet spectrum of 5-phenyl-pent-2-ene-4-yne-1-ol [11] — with absorption maxima at 2 890 Å, 2 720 Å, and 2 590 Å — this spectrum might well originate from the hitherto unknown chromophoric system furyl-yne-ene. Its infrared spectrum shows double bond and triple bond absorption, and indicates the presence of a saturated ketone group. With only one triple bond in the molecule, this must have a central position in the chromophoric system to produce acetylenic fine structure [12].

Based on these data — especially the similarities between the IR-spectra of the new compound and 2,2,5,5-tetramethyl-dihydrofurofuran (3,2-b) [5] — the compound from *Chrysanthemum vulgare* Bernh. is supposed to be a dihydrofurofuran with an exocyclic double bond and an isolated ene-yne chromophore. With the assumption that one oxygen atom is bound to carbon atom three as in *n*-tetradeca-6-ene-8,10, 12-triyne-3-one, a compound which occurs in the same plant, the tentative structure would be: 2(1-hex-1-yne-3-enyl)-5-ethylidene-dihydforurofuran-(3,2-b) (I).

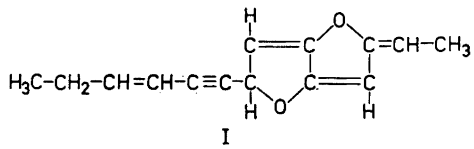

I

This work was carried out under the tenure of a research grant from *Norges tekniske høgskole*. Professor Dr. N. A. Sørensen is greatly acknowledged for his kind interest and helpful suggestions.

1. Bohlmann, F., Arndt, Chr. and Bornowski, H. *Chem. Ber.* **93** (1960) 1937.
2. Guddal, E. *Thesis, Norges tekniske høgskole*, May **1958**.
3. Sørensen, J. S. and Sørensen, N. A. *Acta Chem. Scand.* **12** (1958) 771.
4. Guddal, E. and Sørensen, N. A. *Acta Chem. Scand.* **13** (1959) 1185.

5. Guddal, E. *Acta Chem. Scand.* **13** (1959) 834.
6. Bohlmann, F. and Viehe, H. G. *Chem. Ber.* **88** (1955) 1017.
7. Christensen, P. K. *Norge Tekniske Vitenskapsakademi*, Serie 2 **Nr. 7** (1959) 74. *Chem. Abstr.* **54** (1960) 6531.
8. Audier, L. *Ann. chim. (Paris)* **13** (1957) 105.
9. Quilico, A., Piozzi, F. and Pavan, M. *Tetrahedron* **1** (1957) 177.
10. Reichstein, A. *Helv. Chim. Acta* **15** (1932) 1110; **16** (1933) 28, 37.
11. Haynes, L. J., Heilbron, I., Jones, E. R. H. and Sondheimer, F. *J. Chem. Soc.* **1947** 1585.
12. Dale, J. *Acta Chem. Scand.* **11** (1957) 265.

Received February 21, 1961.

Studies Related to Naturally Occurring Acetylene Compounds

XXVIII. A Note on the Occurrence of Pontica Epoxide in the Genus *Achillea* L.

E. HEMMER, E. TUXEN BORLAUG and NILS ANDREAS SÖRENSEN

Institutt for Organisk Kjemi, Norges Tekniske Högskole, Trondheim, Norway

In a recent paper Bohlmann, Arndt and Boronowski [1] have described the isolation of the polyacetylenic epoxide $C_{13}H_{10}O$ (I) from four different *Artemisia* species. After the first isolation from *A. pontica* L. the substance has been named "pontica epoxide". Some 100 members of the tribus *Anthemideae* of the *Compositae* are stated to have been investigated. Outside the genus *Artemisia* pontica epoxide was isolated only from three members of the genus *Chrysanthemum* (*viz. serotinum* L., *boreale* L. and *vulgare* Bernh.) and *Cladanthus arabicus* Cars.

A substance with the same properties as I had been isolated in our laboratory some years ago [2,3] from some members of the genus *Achillea*, also a member of the tribus *Anthemideae*. The m.p. and U.V. maxima are given below together with those of pontica epoxide.

	m.p.
Pontica epoxide	66°
Achillea ptarmica	60–63°
A. atrata * *clusiana*	62–62.5°

U.V.-maxima

3 335	3 115	2 920	2 755	2 505	(2 435)
3 335	3 112	2 928	2 756	2 510	(2 415)
3 345	3 130	2 930	2 765	2 500	2 400

The U.V. absorption curves are conform in height of all the 6 maxima and the 5 minima.

Bohlmann *et al.* have reported the infrared spectrum of pontica epoxide in carbon tetrachloride solution. Our measurements on the compound from the above mentioned *Achillea* species are in chloroform and in carbon disulfide. The small differences between the three spectra may be due to the effect of the solvents.

In five other *Achillea* species no I could be demonstrated. Besides some unknown polyacetylenes some members of this genus contained *cis*-and *trans*-dehydromatricaria-ester.

Details of our investigations will be presented in another contribution to this journal.

1. Bohlmann, F., Arndt, Chr. and Boronowski, H. *Chem. Ber.* **93** (1960) 1937.
2. Borlaug, E. Tuxen, *Graduation work*, N.T.H. 1953.
3. Hemmer, E. (née Vorvik), *Graduation work*, N.T.H. 1955.

Received February 9, 1961.

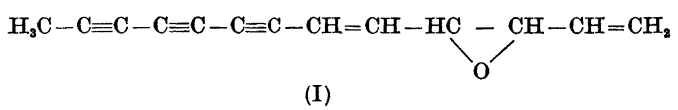

(I)

5. Guddal, E. *Acta Chem. Scand.* **13** (1959) 834.
6. Bohlmann, F. and Viehe, H. G. *Chem. Ber.* **88** (1955) 1017.
7. Christensen, P. K. *Norge Tekniske Vitenskapsakademi*, Serie 2 **Nr. 7** (1959) 74. *Chem. Abstr.* **54** (1960) 6531.
8. Audier, L. *Ann. chim. (Paris)* **13** (1957) 105.
9. Quilico, A., Piozzi, F. and Pavan, M. *Tetrahedron* **1** (1957) 177.
10. Reichstein, A. *Helv. Chim. Acta* **15** (1932) 1110; **16** (1933) 28, 37.
11. Haynes, L. J., Heilbron, I., Jones, E. R. H. and Sondheimer, F. *J. Chem. Soc.* **1947** 1585.
12. Dale, J. *Acta Chem. Scand.* **11** (1957) 265.

Received February 21, 1961.

Studies Related to Naturally Occurring Acetylene Compounds

XXVIII. A Note on the Occurrence of Pontica Epoxide in the Genus *Achillea* L.

E. HEMMER, E. TUXEN BORLAUG and NILS ANDREAS SÖRENSEN

Institutt for Organisk Kjemi, Norges Tekniske Högskole, Trondheim, Norway

In a recent paper Bohlmann, Arndt and Boronowski [1] have described the isolation of the polyacetylenic epoxide $C_{13}H_{10}O$ (I) from four different *Artemisia* species. After the first isolation from *A. pontica* L. the substance has been named "pontica epoxide". Some 100 members of the tribus *Anthemideae* of the *Compositae* are stated to have been investigated. Outside the genus *Artemisia* pontica epoxide was isolated only from three members of the genus *Chrysanthemum* (*viz. serotinum* L., *boreale* L. and *vulgare* Bernh.) and *Cladanthus arabicus* Cars.

A substance with the same properties as I had been isolated in our laboratory some years ago [2,3] from some members of the genus *Achillea*, also a member of the tribus *Anthemideae*. The m.p. and U.V. maxima are given below together with those of pontica epoxide.

	m.p.
Pontica epoxide	66°
Achillea ptarmica	60–63°
A. atrata * *clusiana*	62–62.5°

U.V.-maxima

3 335	3 115	2 920	2 755	2 505	(2 435)
3 335	3 112	2 928	2 756	2 510	(2 415)
3 345	3 130	2 930	2 765	2 500	2 400

The U.V. absorption curves are conform in height of all the 6 maxima and the 5 minima.

Bohlmann *et al.* have reported the infrared spectrum of pontica epoxide in carbon tetrachloride solution. Our measurements on the compound from the above mentioned *Achillea* species are in chloroform and in carbon disulfide. The small differences between the three spectra may be due to the effect of the solvents.

In five other *Achillea* species no I could be demonstrated. Besides some unknown polyacetylenes some members of this genus contained *cis*-and *trans*-dehydromatricaria-ester.

Details of our investigations will be presented in another contribution to this journal.

1. Bohlmann, F., Arndt, Chr. and Boronowski, H. *Chem. Ber.* **93** (1960) 1937.
2. Borlaug, E. Tuxen, *Graduation work*, N.T.H. 1953.
3. Hemmer, E. (née Vorvik), *Graduation work*, N.T.H. 1955.

Received February 9, 1961.

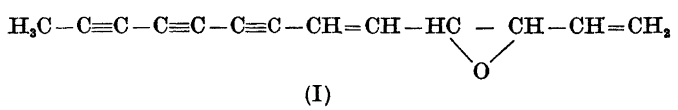

(I)

Infrared Studies of Some Phosphorus Ylids Containing Oxygen

GUNNAR AKSNES

Chemical Institute, University of Bergen, Bergen, Norway

Alkaline treatment of triphenyl-substituted phosphonium salts containing a reactive hydrogen atom attached to the α-carbon atom of the phosphonium compounds (α-position with respect to P) results in the formation of phosphorus ylids [1-4]. Due to the ability of phosphorus to expand its valence shell to a "ten electron shell" by utilization of one of its empty *d*-orbitals these compounds are most correctly described as resonance hybrids between the ylene form (Ia) and the ylid form (Ib): [2,5]

$$(Ph)_3P=CHR \longleftrightarrow (Ph)_3\overset{+}{P}-\overset{-}{C}HR$$

(Ia) (Ib)

When the substituent R contains a keto group which can participate in the resonance stabilization of the phosphorus ylid the stability of such compounds greatly increases [2]:

$$(Ph)_3P=CH\cdot C(=O)R \longleftrightarrow (Ph)_3\overset{+}{P}-CH=C(\overset{-}{O})R$$

(IIa) (IIb)

The "keto betaine" described by Michaelis and Köhler [6] which results from treatment of (III) with strong alkali was shown by Ramirez and Dershowitz [2] to be a phosphorus ylid:

$$(Ph)_3\overset{+}{P}CH_2\cdot COR \xrightarrow{NaOH} (Ph)_3P=CHCOR$$

(III) (IV)

In the same way the "phosphonium betaine" described by Michaelis and Gimborn [7] obtained from (V) with concentrated alkali was found by Aksnes [8] to be a phosphorus ylid:

$$(Ph)_3\overset{+}{P}CH_2\cdot COOC_2H_5 \xrightarrow{NaOH} (Ph)_3P=CHCOOC_2H_5$$

(V) (VI)

In this paper we have compared the infrared absorption spectra of some phosphorus ylids containing keto groups with closely related phosphonium and keto compounds in order to assign the absorption bands of the C=O groups in different phosphorus ylids.

Experimental. Triphenyl phosphine was a sample from L. Light & Co, recrystallized from alchohol, m.p. 79.5°.

The phosphonium compound No. 2 of Table 1 was prepared in the following way: 4.5 g of bromoacetone was added to 8.6 g of triphenyl phosphine (equivalent amount). 10 ml of alchohol was added and the mixture was boiled for 10 min. After cooling of the reaction mixture the phosphonium compound crystallized, m.p. 226° (Michaelis and Köhler [6], m.p. 226°).

The phosphorus ylid No. 3 was made by dissolving 4 g of No. 2 in 5 ml of cold water and adding 10 ml of cold concentrated sodium hydroxide solution. The white precipitate which immediately separated was filtered off and recrystallized from 60 % water-alcohol mixture, m.p. 203–204° (Michaelis and Köhler [6], m.p. 201°). (Found: C 79.3; H 5.8; P 9.6. Calc. for $C_{21}H_{19}OP$: C 79.0; H 6.0; P 10.0.)

The compound No. 4 was made from triphenyl phosphine (7.9 g) and chloroacetophenone (5 g) by heating the mixture to 80–90°C. The reaction was exothermic and a white crystalline mass separated upon cooling. The crystalline mass was washed several times with ether and recrystallized two times from water, m.p. 266° (decomp.).

Its corresponding phosphorus ylid, No. 5 of Table 1, was made from 4 g of No. 4 by dissolving it in 10 ml of water and adding 10 ml of cold concentrated sodium hydroxide solution. The compound which separated was recrystallized two times from 50 % alcohol-water mixture, m.p. 182° (Michaelis and Köhler, m.p. 183–84°). (Found: C 81.8; H 5.4; P 8.0. Calc. for $C_{26}H_{21}PO$: C 81.9; H 5.6; P 8.4.)

Compounds Nos. 6 and 7 of Table 1 were synthesized according to descriptions in a previous paper.[8]

Compounds Nos. 8, 10 and 12 were made according to descriptions of Ramirez and Dershowitz [10], Schönberg and Ismail [9] and Schönberg and Michaelis [14].

The infrared spectra were recorded on a Perkin-Elmer Spectrophotomer Model 21 using 1 mg of the compounds in KBr-briquets.

Compound	Frequencies (cm^{-1}) 1900 1800 1700 1600 1500 1400	$\nu_{C=O}$ cm^{-1}	$\Delta\nu_{C=O}$ cm^{-1}
1. $(Ph)_3P$			
2. $[(Ph)_3\overset{+}{P}-CH_2COCH_3]Br^-$		1719	177
3. $(Ph)_3P=CHCOCH_3$		1542	
4. $[(Ph)_3\overset{+}{P}-CH_2COPh]Cl^-$		1667	138
5. $(Ph)_3P=CHCOPh$		1529	
6. $[(Ph)_3\overset{+}{P}-CH_2COOC_2H_5]Br^-$		1740	120
7. $(Ph)_3P=CHCOOC_2H_5$		1620	
8. 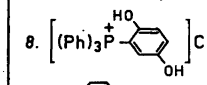			
9. 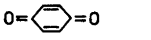		1662	135
10. 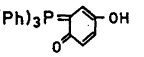		1527	
11. 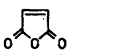		1788, 1845	86, 40
12. 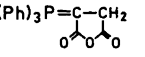		1702, 1805	

Table 1. The assignement of the stretching vibration frequencies of some oxygen containing phosphorus ylids.

Results and discussion. In Table 1 are recorded the main absorption bands between 1 900 and 1 400 cm^{-1} of the different phosphonium compounds, phosphorus ylids and keto compounds studied. The phosphorus compounds all contain the triphenyl phosphine residue and the characteristic bands of triphenyl phosphine at approx. 1 440 cm^{-1}, 1 490 cm^{-1}, and 1 590 cm^{-1} are found almost at the same positions in all of the phosphorus compounds.

The assignment of the carbonyl bands of the phosphorus ylids and their corresponding "parent compounds" containing the C=O group are shown in Table 1 where dotted lines combine the corresponding bands. The assigned C=O bands of the compounds Nos. 3 and 5 correspond with the bands of the carbonyl groups proposed by Wittig and Schöllkopf [4] and Ramirez and Dershowitz [2]. The very strong displacements of the C=O bands (so far the strongest ever known) upon formation of the phosphorus ylids show that the ionic structure (IIb) must contribute very strongly to the resonance hybrid of the phosphorus ylids. This is also in accordance with the dipole moments 5.45 *D* and 5.54 *D* observed for the compounds Nos. 3 and 5 in Table 1 [2]. The somewhat smaller displacements of the carbonyl bands of the phosphorus ylids Nos. 7 and 12 may be explained as due to the opposing inductive effect of the oxygen atoms adjacent to the carbonyl groups in these two compounds. The same argument is used by Hartwell *et al.*[11] to explain the higher carbonyl frequencies of esters as compared with ketones.

Schönberg and Ismail [9] have proposed the structure: 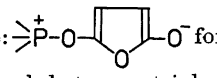 for the addition compound between triphenyl phosphine and maleic anhydride. Now it is known that all acid anhydrides give rise to two carbonyl bands in infrared due to the coupling between the following two types of stretching vibration: [13]



The two bands of maleic anhydride are found at 1 788 cm^{-1} and 1 845 cm^{-1}

(reported [12] 1 790 cm^{-1} and 1 850 cm^{-1}). The addition compound between triphenyl phosphine and maleic anhydride has two strong bands at 1 702 cm^{-1} and 1 805 cm^{-1}. We assume that these two bands are due to the coupling between two carbonyl groups and suggest therefore that the addition compound is a phosphorus ylid namely compound No. 12 in Table 1. This structure may also explain the unreactivity of 1,2-substituted maleic anhydrides [9].

My sincere thanks are due to *Norwegian Defence Research Establishment* for financial support and to Arnljot Nærland at the same institute for recording the infrared spectra.

1. Pinck, L. A. and Hilbert, G. E. *J. Am. Chem. Soc.* **69** (1947) 723.
2. Ramirez, F. and Dershowitz, S. *J. Org. Chem.* **22** (1957) 41.
3. Ford, Jr., J. A. *Org. Chem. Bull.* **31** (1959) No. 1.
4. Witting, G. and Schöllkopf, U. *Chem. Ber.* **87** (1954) 1318.
5. Wilson, B. D. *Org. Chem. Bull.* **32** (1960) No. 2.
6. Michaelis, A. and Köhler, E. *Ber.* **32** (1899) 1566.
7. Michaelis, A. and Gimborn, H. v. *Ber.* **27** (1894) 272.
8. Aksnes, G. *Acta Chem. Scand.* **15** (1961) 438.
9. Schönberg, A. and Ismail, A. F. A. *J. Chem. Soc.* **1940** 1374.
10. Ramirez, F. and Dershowitz, S. *J. Am. Chem. Soc.* **78** (1956) 5614.
11. Hartwell, E. J., Richards, R. E. and Thompson, H. W. *J. Chem. Soc.* **1948** 1436.
12. Norman Jones, R. and Sandorfy, C. in West, W. *Technique of Organic Chemistry* Volume IV p. 456. Interscience, New York 1956.
13. Davison, W. H. T. *J. Chem. Soc.* **1951** 2456.
14. Schönberg, A. and Michaelis, R. *Ber.* **69** (1936) 1080.

Received March 1, 1961.

"Pit-mapping" — a General Approach for Computer Refining of Equilibrium Constants

DAVID DYRSSEN, NILS INGRI and LARS GUNNAR SILLÉN

Department of Inorganic Chemistry, Royal Institute of Technology, Stockholm 70, Sweden

The problem of determining the equilibrium constants for a number of simultaneous equilibria in solution may be expressed as a special case of the following well-known general problem. Having measured a quantity y and assumed a functional relationship:

$$y = f(k_1, k_2..k_r..k_N; a_1, a_2...) \quad (1)$$

between y and some quantities a_1, a_2 ... that can be varied but whose values are assumed to be known accurately in each experiment, one seeks to determine the set of unknown constants, $k_1 \ldots k_N$.

Provided a) that the expression for f is correct, b) that there are no other errors (especially no systematic ones) except the random errors in y, c) that the errors in y are "normally" distributed around the correct value, and d) that the weight w_i given to each measurement y_i is inversely proportional to the square of its standard deviation; then the "best" values for $k_1 \ldots k_N$ would be those that minimize the error-square sum:

$$U = \sum_i w_i(y_i - f(k_1 \ldots k_N; a_{1i}, a_{2i} \ldots))^2 \quad (2)$$

Even though one can seldom hope that all these assumptions are correct, the "least-squares" condition, U = minimum, is often employed in calculations. It is "objective" in the sense that the same set of data, and the same assumptions, should give the same answer in the hands of different workers. Perhaps, however, one should not forget the risk of over-estimating the significance of the answer.

If f is a linear function of the k's, the "least-squares" condition leads to linear equations, which can be solved by straightforward methods. For instance, in studies of equilibria of step-wise complex formation, if one has measured the concentration of the central atom, or of one specific complex (as it is, for instance, usually done in extraction studies), this condition leads to

(reported [12] 1 790 cm^{-1} and 1 850 cm^{-1}). The addition compound between triphenyl phosphine and maleic anhydride has two strong bands at 1 702 cm^{-1} and 1 805 cm^{-1}. We assume that these two bands are due to the coupling between two carbonyl groups and suggest therefore that the addition compound is a phosphorus ylid namely compound No. 12 in Table 1. This structure may also explain the unreactivity of 1,2-substituted maleic anhydrides [9].

My sincere thanks are due to *Norwegian Defence Research Establishment* for financial support and to Arnljot Nærland at the same institute for recording the infrared spectra.

1. Pinck, L. A. and Hilbert, G. E. *J. Am. Chem. Soc.* **69** (1947) 723.
2. Ramirez, F. and Dershowitz, S. *J. Org. Chem.* **22** (1957) 41.
3. Ford, Jr., J. A. *Org. Chem. Bull.* **31** (1959) No. 1.
4. Witting, G. and Schöllkopf, U. *Chem. Ber.* **87** (1954) 1318.
5. Wilson, B. D. *Org. Chem. Bull.* **32** (1960) No. 2.
6. Michaelis, A. and Köhler, E. *Ber.* **32** (1899) 1566.
7. Michaelis, A. and Gimborn, H. v. *Ber.* **27** (1894) 272.
8. Aksnes, G. *Acta Chem. Scand.* **15** (1961) 438.
9. Schönberg, A. and Ismail, A. F. A. *J. Chem. Soc.* **1940** 1374.
10. Ramirez, F. and Dershowitz, S. *J. Am. Chem. Soc.* **78** (1956) 5614.
11. Hartwell, E. J., Richards, R. E. and Thompson, H. W. *J. Chem. Soc.* **1948** 1436.
12. Norman Jones, R. and Sandorfy, C. in West, W. *Technique of Organic Chemistry* Volume IV p. 456. Interscience, New York 1956.
13. Davison, W. H. T. *J. Chem. Soc.* **1951** 2456.
14. Schönberg, A. and Michaelis, R. *Ber.* **69** (1936) 1080.

Received March 1, 1961.

"Pit-mapping" — a General Approach for Computer Refining of Equilibrium Constants

DAVID DYRSSEN, NILS INGRI and LARS GUNNAR SILLÉN

Department of Inorganic Chemistry, Royal Institute of Technology, Stockholm 70, Sweden

The problem of determining the equilibrium constants for a number of simultaneous equilibria in solution may be expressed as a special case of the following well-known general problem. Having measured a quantity y and assumed a functional relationship:

$$y = f(k_1, k_2..k_r..k_N; a_1, a_2...) \quad (1)$$

between y and some quantities a_1, a_2 ... that can be varied but whose values are assumed to be known accurately in each experiment, one seeks to determine the set of unknown constants, $k_1 \ldots k_N$.

Provided a) that the expression for f is correct, b) that there are no other errors (especially no systematic ones) except the random errors in y, c) that the errors in y are "normally" distributed around the correct value, and d) that the weight w_i given to each measurement y_i is inversely proportional to the square of its standard deviation; then the "best" values for $k_1 \ldots k_N$ would be those that minimize the error-square sum:

$$U = \sum_i w_i(y_i - f(k_1 \ldots k_N; a_{1i}, a_{2i} \ldots))^2 \quad (2)$$

Even though one can seldom hope that all these assumptions are correct, the "least-squares" condition, U = minimum, is often employed in calculations. It is "objective" in the sense that the same set of data, and the same assumptions, should give the same answer in the hands of different workers. Perhaps, however, one should not forget the risk of over-estimating the significance of the answer.

If f is a linear function of the k's, the "least-squares" condition leads to linear equations, which can be solved by straightforward methods. For instance, in studies of equilibria of step-wise complex formation, if one has measured the concentration of the central atom, or of one specific complex (as it is, for instance, usually done in extraction studies), this condition leads to

linear equations which can be solved by means of the "least-squares" programs of various high-speed computers [1-3].

If the function f is not linear, the general trend has been to reduce it to a linear one, either by transformation (if possible), or, using the Gauss method, by expressing the derivatives of U by means of Taylor series, and using only the first terms. Programming a computer for the Gauss method is not always simple, and its performance is capricious [4].

In systems with polynuclear complexes between two reagents A and B, one usually meets with the two equations

$$B = b + \Sigma q\beta_{pq}a^p b^q;\ BZ = \Sigma p\beta_{pq}a^p b^q \quad (3)$$

In (3), B is the total concentration of B, a and b are the concentrations of free A and B, p and q are integers, β_{pq} are a set of equilibrium constants, and Z is the average number of A bound per B. The data are usually of the form $Z(B, a)$, so that B and a are known rather accurately. Since b must be eliminated from the equations, it seems hard to attack problems like this by straight-forward "least-squares" equations.

However, one can make oneself free from the condition that the equations should be linear, if one considers directly the error-square sum U in (2) and studies the function

$$U(k_1,\ k_2 \ldots k_N) \quad (4)$$

This is done in a family of computer programs "LETAGROP" which we are now developing, using the Ferranti-Mercury autocode.

The principle is as follows; it is so simple that it may have been used earlier by others without our being aware of it.

By means of graphical methods — which we consider as the most important part of the data treatment — we conclude which complexes are present or may be suspected to exist in appreciable amounts, and obtain a set of approximate equilibrium constants.

The computer then systematically varies each constant in turn, keeping the others constant, until it finds the value that gives the lowest value for U. Then it passes to another constant and etc; it can be made to return to a certain constant and readjust it later on. The procedure gives not only the lowest point:

$$U(\min = U_o = U(k_1'', k_2'' \ldots k_N'') \quad (5)$$

but also a map of the surroundings.

For linear expressions f in (1), in particular, $U(k_1 \ldots k_N)$ is a second-degree surface: if $N = 1$, it is a parabola, with $N = 2$ an elliptic paraboloid, for higher N it is a generalized elliptic paraboloid in $(N + 1)$-dimensional space. We shall for any value of N refer to the lowest point U_o and its immediate surroundings as the "pit":

A suitable measure of the spread of the data is the range around U_o enclosed by what we may call the "D boundary"

$$U = U_o + U_o(n-N)^{-1} \approx U_o + U_o/n \quad (6)$$

Here, U_o is the value of U at the lowest point (5) of the pit, and n is the number of experiments. In our experiments, as a rule, $n \gg N$. The projection of the D boundary along the U axis is two points if $N = 1$, an ellipse if $N = 2$, an ellipsoid if $N = 3$, and for higher N a generalized ellipsoid in N dimensional space $(k_1 \ldots k_N)$, with the "least-squares point" $(k_1'' \ldots k_N'')$ as its centre.

The range of values that each k_r can assume on the D boundary is identical with the range of its "standard deviation" $k_r'' \pm D[k_r]$, whatever connection this may have with chemical reality.

For non-linear cases it seems a permissible approximation to assume the "pit" to be a second-degree surface in the range close to U_o. By proper programming, the computer can be made to search for the lowest point of the "pit" within any reasonable precision; assuming the U surface to be of the second degree, one can calculate directly the position of the lowest point, and the extension of the D boundary, given a certain minimum number of U values (three for $N = 1$, six for $N = 2$, *etc*).*

If a certain k_r exerts an influence only in a limited region of the data field, the program allows one to screen out the other points, and then to consider the contribution to U from that part only.

The same main programs "LETAGROP" can be used for various non-linear problems. The special equations valid for each problem need only be stated in a short additional program and are then solved by the general method of our program "KUSKA" which forms a loop in LETAGROP. So, even though the machine may have to work several minutes more than in a straight-forward solution, great gains are made in the human programmer's time.

In the future we intend to apply these computer programs to a number of various chemical problems, especially the following:

* *Note added in proof.* This procedure has proved much faster than adjusting the constants one by one.

a) The refinement of the equilibrium constants in systems with polynuclear complexes, where approximate values have been found graphically.

b) Calculation of consecutive equilibrium constants in systems with mononuclear complexes, where only the ligand number has been determined: even if linear transformations can be made [3b] the pit-mapping method seems a worth-while alternative. Even spectrophotometric data, which commonly give non-linear expressions may be attacked by this method.

c) Calculation of the parameters in the "two parameters" approximation [5] for equilibria, where the available data are not accurate enough for determining, independently, the formation constants for all the complexes MA, MA_2, MA_3 ... MA_N. For such systems, two ways of approximate calculations have been proposed:

1) When the standard deviation of an individual equilibrium constant comes out as greater than the value of this constant, Sullivan, Rydberg and Miller [3b] eliminate that particular constant from their equations, which from a chemical point of view is equivalent to assuming that the concentration of the related species is equal to zero.

2) In the "two parameters" approximation [5], one assumes that all complexes exist and that the ratio between consecutive formation constants is a constant. — Neither of the approximations 1) or 2) can be completely true, but the second one may, we think, often come somewhat closer to chemical reality. Earlier, only the first approximation could be treated by computer programs [3].

Our results hitherto like, in our opinion, those of Sullivan *et al.*[3b] indicate that with good data, the "least-squares" approach gives no gain in real accuracy, as compared with adequate graphical methods, using the experimental data directly. In problems with many constants to be determined, considerable time may however be gained by making the final refinement of the constants by means of the computer.

The results and the full description of our program, will be published in due time.

This work is part of a program supported by the *Swedish Atomic Research Council* (AFR) and the *Swedish Natural Science Research Council* (NFR).

1. Panthaleon van Eck, C. *Thesis*, Amsterdam 1958.
2. McMaster, D. L. and Schaap, W. B. *Proc. Indiana Acad. Sci.* **67** (1958) 111.
3a. Rydberg, J. and Sullivan, J. C. *Acta Chem. Scand.* **13** (1959) 186.
3b. Sullivan, J. C., Rydberg, J. and Miller, W. F. *Acta Chem. Scand.* **13** (1959) 2023.
3c. Rydberg, J. and Sullivan, J. C. *Acta Chem. Scand.* **13** (1959) 2057.
3d. Rydberg, J. *Acta Chem. Scand.* **14** (1960) 157.
4. Moore, R. H. and Ziegler, R. K. *LA-2367*, 1960.
5. Dyrssen, D. and Sillén, L. G. *Acta Chem. Scand* **7** (1953) 663.

Received March 21, 1961.

Investigation of the Structure of Trifolirhizin, an Antifungal Compound from *Trifolium pratense* L.

J. B-SON BREDENBERG and PENTTI K. HIETALA

Laboratory of the Foundation for Chemical Research, Biochemical Institute, Helsinki, Finland

In an investigation of the antifungal substances in red clover (*Trifolium pratense* L.) the isolation of one of the main components, $C_{21}H_{24}O_{10}$, m.p. 139—140°, has been reported [1]. This compound has now been investigated more closely. Since it is apparently a new compound, isolated so far only from the roots, the name trifolirhizin is proposed for it.

Trifolirhizin crystallizes from methanol as rods, m.p. 142—144° (decomp.), $[\alpha]_D^{20}$ —183°, with one mole of methanol. The elementary composition of the compound has now been found to agree with $C_{22}H_{22}O_{10}$. It does not contain methoxyl or C-methyl groups and, according to the chemical and infrared data, is free from carbonyl and carboxyl groups. Upon catalytic hydrogenation it is recovered unchanged. It forms a tetraacetate, $C_{30}H_{30}O_{14}$, m.p. 188—189,° $[\alpha]_D^{20}$ —126° in which all the hydroxyl groups are acetylated. Upon acid hydrolysis it forms glucose and ether-soluble substances which could not be characterized. Alkaline hydrolysis probably also releases glucose. Trifolirhizin is thus a glucoside.

Taking the glucose molecule into account, the empirical formula for the agly-

a) The refinement of the equilibrium constants in systems with polynuclear complexes, where approximate values have been found graphically.

b) Calculation of consecutive equilibrium constants in systems with mononuclear complexes, where only the ligand number has been determined: even if linear transformations can be made [3b] the pit-mapping method seems a worth-while alternative. Even spectrophotometric data, which commonly give non-linear expressions may be attacked by this method.

c) Calculation of the parameters in the "two parameters" approximation [5] for equilibria, where the available data are not accurate enough for determining, independently, the formation constants for all the complexes MA, MA_2, MA_3 ... MA_N. For such systems, two ways of approximate calculations have been proposed:

1) When the standard deviation of an individual equilibrium constant comes out as greater than the value of this constant, Sullivan, Rydberg and Miller [3b] eliminate that particular constant from their equations, which from a chemical point of view is equivalent to assuming that the concentration of the related species is equal to zero.

2) In the "two parameters" approximation [5], one assumes that all complexes exist and that the ratio between consecutive formation constants is a constant. — Neither of the approximations 1) or 2) can be completely true, but the second one may, we think, often come somewhat closer to chemical reality. Earlier, only the first approximation could be treated by computer programs [3].

Our results hitherto like, in our opinion, those of Sullivan *et al.*[3b] indicate that with good data, the "least-squares" approach gives no gain in real accuracy, as compared with adequate graphical methods, using the experimental data directly. In problems with many constants to be determined, considerable time may however be gained by making the final refinement of the constants by means of the computer.

The results and the full description of our program, will be published in due time.

This work is part of a program supported by the *Swedish Atomic Research Council* (AFR) and the *Swedish Natural Science Research Council* (NFR).

1. Panthaleon van Eck, C. *Thesis*, Amsterdam 1958.
2. McMaster, D. L. and Schaap, W. B. *Proc. Indiana Acad. Sci.* **67** (1958) 111.
3a. Rydberg, J. and Sullivan, J. C. *Acta Chem. Scand.* **13** (1959) 186.
3b. Sullivan, J. C., Rydberg, J. and Miller, W. F. *Acta Chem. Scand.* **13** (1959) 2023.
3c. Rydberg, J. and Sullivan, J. C. *Acta Chem. Scand.* **13** (1959) 2057.
3d. Rydberg, J. *Acta Chem. Scand.* **14** (1960) 157.
4. Moore, R. H. and Ziegler, R. K. *LA-2367*, 1960.
5. Dyrssen, D. and Sillén, L. G. *Acta Chem. Scand* **7** (1953) 663.

Received March 21, 1961.

Investigation of the Structure of Trifolirhizin, an Antifungal Compound from *Trifolium pratense* L.

J. B-SON BREDENBERG and PENTTI K. HIETALA

Laboratory of the Foundation for Chemical Research, Biochemical Institute, Helsinki, Finland

In an investigation of the antifungal substances in red clover (*Trifolium pratense* L.) the isolation of one of the main components, $C_{21}H_{24}O_{10}$, m.p. 139—140°, has been reported [1]. This compound has now been investigated more closely. Since it is apparently a new compound, isolated so far only from the roots, the name trifolirhizin is proposed for it.

Trifolirhizin crystallizes from methanol as rods, m.p. 142—144° (decomp.), $[\alpha]_D^{20}$ —183°, with one mole of methanol. The elementary composition of the compound has now been found to agree with $C_{22}H_{22}O_{10}$. It does not contain methoxyl or C-methyl groups and, according to the chemical and infrared data, is free from carbonyl and carboxyl groups. Upon catalytic hydrogenation it is recovered unchanged. It forms a tetraacetate, $C_{30}H_{30}O_{14}$, m.p. 188—189,° $[\alpha]_D^{20}$ —126° in which all the hydroxyl groups are acetylated. Upon acid hydrolysis it forms glucose and ether-soluble substances which could not be characterized. Alkaline hydrolysis probably also releases glucose. Trifolirhizin is thus a glucoside.

Taking the glucose molecule into account, the empirical formula for the agly-

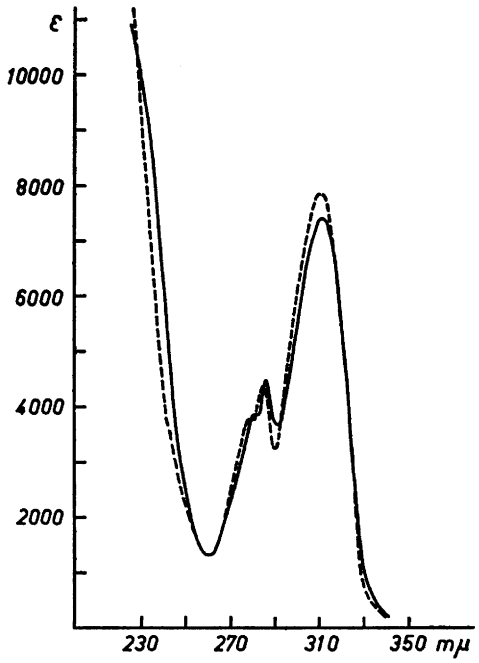

Fig. 1. Ultraviolet spectra in ethanol of pterocarpin (solid line) and trifolirhizin (broken line).

cone of trifolirhizin is $C_{16}H_{12}O_5$. One of the oxygen atoms is found in the glucoside bond. Since trifolirhizin contains four hydroxyl groups, all belonging to the glucose part, and since it does not have any carbonyl or carboxyl groups, the remaining four oxygen atoms in the aglycone must be of ether type. The infrared spectrum supports the presence of a methylenedioxy group [2]. The presence of glucose, however, makes the normal colour test [3] for this group of little value.

The low hydrogen content and resistance to hydrogenation can only be explained if two benzene rings are assumed to be present. The very peculiar ultraviolet spectrum (Fig. 1) can be interpreted according to this assumption: the maxima at 280 and

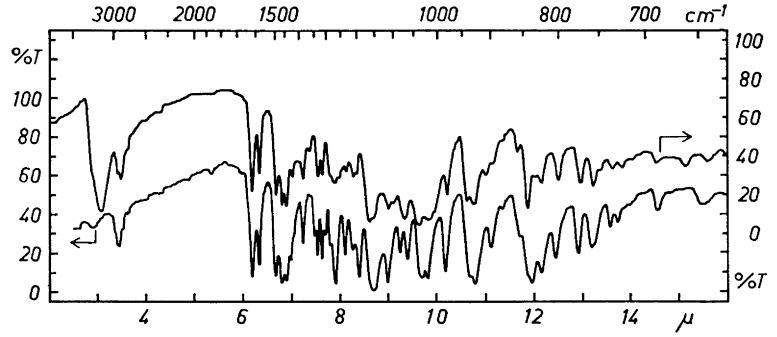

Fig. 2. Infrared spectra of trifolirhizin (above, right scale, 2.2 mg/300 mg KBr) and pterocarpin (below, left scale, 2.0 mg/300 mg KBr).

285 mμ are formed from a slightly substituted benzene ring and the maximum at 310 mμ from a strongly substituted benzene ring. The latter maximum, however, occurs at a surprisingly high wavelength.

Taking into account the occurrence of *iso*flavones in clover [4-6] and their antifungal properties [7-9] a compound of pterocarpin (I) [10] type could be assumed to be present. When the ultraviolet and infrared spectra of a sample of pterocarpin, kindly supplied by Dr. W. B. Whalley, of Liverpool, were compared with those of trifolirhizin, a striking similarity was observed (Figs. 1 and 2). The ultraviolet spectra show that the compounds have identical chromophores. Since pterocarpin is methylated at the 7-position and trifolirhizin does not contain any methoxyl group, the glucose is evidently bound to the aglycone at this point. This would also explain [11] the suspected alkali lability of trifolirhizin. On the basis of the above results the structure II is therefore tentatively suggested for trifolirhizin.

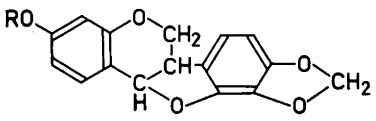

I: R=CH_3

II: R=Glucose

It is of interest to note the recent report [12,13] of the isolation of an antifungal compound from *Pisum sativum* L. which seems to bear a close relationship to the above-mentioned compounds. Lack of details, however, precludes further comparison.

Experimental. For details of the isolation, see Hietala [1]. A good concentrate of the compound can be obtained by analogous operation in a series of about ten separatory funnels. Trifolirhizin crystallizes well from methanol, forming rods, m.p. 142–144° (decomp.), $[\alpha]_D^{20}$ −183° (ethanol, *c* 1.5). (Found: C 57.89; H 5.58; O 35.96; O–CH_3 5.51, 7.35; C–CH_3 0.00. Calc. for $C_{22}H_{22}O_{10} \cdot CH_3OH$: C 57.73; H 5.48; O 36.78; O–CH_3 6.5. Crystallization from benzene gave C 59.46; H 5.23; O 33.52; O–CH_3 0.32. Calc. for $C_{22}H_{22}O_{10}$: C 59.19; H 4.97; O 35.84.) The compound is difficultly soluble in benzene, easily soluble in warm methanol. It does not react with 2,4-dinitrophenylhydrazine under normal conditions. Hydrogenation with platinum in ethanol or acetic acid at room temperature gave unchanged starting material (mixed m.p., IR). *Acetate:* The compound was acetylated with acetic anhydride and pyridine (30 min, water bath) and crystallized from methanol, cluster of needles, m.p. 188–189°, $[\alpha]_D^{20}$ −126° (acetone, *c* 1). (Found: C 58.49, 58.23; H 4.94, 5.07; O 35.76, 36.52; O–CH_3 0.00; Acetyl 27.74 %. Calc. for $C_{30}H_{30}O_{14}$: C 58.63; H 4.92; O 36.45; Acetyl (4–OH) 28.0 %.) The infrared spectrum had no absorption in the hydroxyl stretching range. *Hydrolysis experiments:* The compound (51 mg) was dissolved in acetic acid (10 ml) and conc. HCl (1 ml) was added. The solution was kept at room temperature for 20 h and was then warmed on a water bath for 30 min. After addition of water the solution was extracted with ether. The extracted aqueous solution was poured through a column of IR-120 in H-form and the column washed with water. The eluate was repeatedly evaporated to a small volume and rediluted with water; finally it was evaporated to dryness. The residue was extracted with hot ethanol and the ethanol solution evaporated. Paper chromatography of the evaporation residue in three different solvent systems (phenol-NH_3, butanol-acetic acid-water, ethyl acetate-pyridine-water) gave spots with the same R_F values as glucose. The osazone, prepared in the usual way, melted at 202–204° and gave no depression with authentic material. Upon evaporation the ether solution gave a dark, semisolid mass (27 mg), with a maximum in the ultraviolet at 286 mμ. No crystalline material could be obtained from this residue. Alkaline hydrolysis of trifolirhizin with boiling 1 N NaOH in methanol for 1.5 h yielded, after acidification and extraction as above, upon paper chromatography of the water phase, a spot with the same R_F value as glucose (butanol-acetic acid-water). No crystalline material could be obtained from the ether phase.

Our thanks are due to Professor Artturi I. Virtanen for his interest in this work. The investigation is a part of a research project under U. S. Public Law No. 480, 83rd Congress.

1. Hietala, P. K. *Ann. Acad. Sci. Fennicae, Series A II Chemica* **100** (1960) 61.
2. Briggs, L. H., Colebrook, L. D., Fales, H. M. and Wildman, W. C. *Anal. Chem.* **29** (1957) 904.
3. Stamm, O. A., Schmid, H. and Büchi, J. *Helv. Chim. Acta* **41** (1958) 2006.

4. Pope, G. S., Elcoate, P. V., Simpson, S. A. and Andrews, D. G. *Chem. & Ind. London* **1953** 1092.
5. Bate-Smith, E. C., Swain, T. and Pope, G. S. *Ibid.* **1953** 1127.
6. Pope, G. S. and Wright, H. G. *Ibid.* **1954** 1019.
7. Virtanen, A. I. and Hietala, P. K. *Suomen Kemistilehti B* **30** (1957) 99.
8. Virtanen, A. I. and Hietala, P. K. *Acta Chem. Scand.* **12** (1958) 579.
9. Bredenberg, J. B. *Suomen Kemistilehti B* **34** (1961) 23.
10. Robertson, A. and Whalley, W. B. *J. Chem. Soc.* **1954** 1440.
11. Ballou, C. E. *Advances in Carbohydrate Chem.* **9** (1954) 59.
12. Perrin, D. R. cited in *Angew Chem.* **72** (1960) 922.
13. Cruickshank, I. A. M. and Perrin, D. R. *Nature* **187** (1960) 799.

Received March 14, 1961.

A Physico-chemical Study on the Haemolytic Activities of *Staphylococcus aureus*

B. G. F. BERGRAHM

Dept. of Bacteriology, Royal Veterinary College, Stockholm 51; Dept. of Bacteriology, Karolinska Institutet, Stockholm 60; Dept. of Clinical Biochemistry, Royal Veterinary College, Stockholm 51, Sweden

In order to obtain good yields of haemolysins from *Staphylococcus aureus* (238) the cells have to be cultivated for rather long times. In the process heavily charged acid polyelectrolytes appear in the medium, most probably due to lysis of part of the cells. Whether the haemolytic activities are to be purified from the cells or, as in the following report, from the medium, these acid polyelectrolytes will interfere with the purification procedure [1,2]. Some results of a characterization by means of counter flow electrophoresis [2] and chromatography will be reported.

Materials and methods. Medium I. 1) Heat 1 800 g of freshly ground horse meat in 3 000 ml water to 75°C. 2) Add 3 000 ml 0.1 M sodium carbonate. 3) Allow to cool to 45–50°C. 4) 5 g pancreatine and 30 ml $CHCl_3$ are added. 5) Let stand for 3.5 h at 37°–40°C. 6) Add 40 ml conc. HCl. 7) Heat to boiling. 8) Filter through coarse filter paper (not cotton wool). 9) Adjust pH to 8.2–8.3 with 0.1 M HCl and 0.1 M NaOH. 10) Heat to boiling and filter again. 11) Add agar to 1.2 % W/v. 12) Autoclave for 30 min at 119°C. 13) Filter. 14) Autoclave for 20 min at 119°C. 15) Dissolve one part agar medium (I) in 1.34 parts broth medium (II, see below). This step gives a final agar concentration in medium I of 0.85 %. 16) Dispense and autoclave for 15 min at 119°C.

Medium II. 1) Autoclave together 2 500 g of freshly ground horse meat and 6 000 ml 0.25 M NaCl for one hour at atmospheric pressure and filter through cheese cloth and coarse filter paper. 2) Make up volume to 6 000 ml. 3) Add peptone (Merck) to give 4 % W/v. 4) Adjust pH to 7.4 (see step 9 for medium I). 5) Heat to boiling and filter through coarse filter paper. 6) Add 12 g KH_2PO_4 per litre. 7) Adjust pH to 7.4. 8) Boil the broth for 30 min, filter and autoclave for 20 min at 119°C. 9) Dispense and autoclave for 45 min at 100°C.

Cultivation technique. The cells were first cultivated on 10 % ox blood agar plates for 24 h at 37°C. No carbon dioxide was added to the air. The cells were transferred to a 10 % horse serum broth and cultivated for 24 h under the same atmospheric conditions.

From this culture 5 ml were inoculated into 400 ml of the semisolid medium I, contained in a 2 litre Fernbach bottle. After 72 h, 600 ml of medium II were added to the bottle, and the cultivation was continued for another 72 h. The temperature was 37°C and the gas phase consisted of CO_2:O_2 in the proportions 2:5. The gas phase was regulated by two narcose flowmeters (AGA 67827K and AGA 67828K, respectively) coupled in parallel.

Harvesting procedure. The culture was cooled rapidly to + 1°C and was centrifuged at + 1°C for 90 min at 7 000 × $g_{average}$.

Concentration of the medium. Different methods were tried. Freeze drying, pervaporation, the polyethylene glycol method of Kohn [3] and the technique of Palmstierna [4] were used. In our hands the last mentioned method gave the best results. Very small, if any, losses in haemolytic (*in vitro* [5]) and lethal activity (mice) were found. The lethal activity was tested on 12–14 g mice (Sigtuna strain) by giving 0.25 ml intraperitoneally. Serial dilutions were made in saline.

Chemical methods. In order to isolate the proteins from the acid polyelectrolytes under as mild conditions as possible, the counter flow electrophoresis (CFE) method of Eliasson *et al.*[2] was used. In this case the proteins were sucked off from the top of the column and pumped into a jacketed and cooled DEAE ion exchanger column [6] (2 × 20 cm) *via* a modified hose pressure micropump [2]. The electrophoresis

4. Pope, G. S., Elcoate, P. V., Simpson, S. A. and Andrews, D. G. *Chem. & Ind. London* **1953** 1092.
5. Bate-Smith, E. C., Swain, T. and Pope, G. S. *Ibid.* **1953** 1127.
6. Pope, G. S. and Wright, H. G. *Ibid.* **1954** 1019.
7. Virtanen, A. I. and Hietala, P. K. *Suomen Kemistilehti B* **30** (1957) 99.
8. Virtanen, A. I. and Hietala, P. K. *Acta Chem. Scand.* **12** (1958) 579.
9. Bredenberg, J. B. *Suomen Kemistilehti B* **34** (1961) 23.
10. Robertson, A. and Whalley, W. B. *J. Chem. Soc.* **1954** 1440.
11. Ballou, C. E. *Advances in Carbohydrate Chem.* **9** (1954) 59.
12. Perrin, D. R. cited in *Angew Chem.* **72** (1960) 922.
13. Cruickshank, I. A. M. and Perrin, D. R. *Nature* **187** (1960) 799.

Received March 14, 1961.

A Physico-chemical Study on the Haemolytic Activities of *Staphylococcus aureus*

B. G. F. BERGRAHM

Dept. of Bacteriology, Royal Veterinary College, Stockholm 51; Dept. of Bacteriology, Karolinska Institutet, Stockholm 60; Dept. of Clinical Biochemistry, Royal Veterinary College, Stockholm 51, Sweden

In order to obtain good yields of haemolysins from *Staphylococcus aureus* (238) the cells have to be cultivated for rather long times. In the process heavily charged acid polyelectrolytes appear in the medium, most probably due to lysis of part of the cells. Whether the haemolytic activities are to be purified from the cells or, as in the following report, from the medium, these acid polyelectrolytes will interfere with the purification procedure [1,2]. Some results of a characterization by means of counter flow electrophoresis [2] and chromatography will be reported.

Materials and methods. Medium I. 1) Heat 1 800 g of freshly ground horse meat in 3 000 ml water to 75°C. 2) Add 3 000 ml 0.1 M sodium carbonate. 3) Allow to cool to 45–50°C. 4) 5 g pancreatine and 30 ml $CHCl_3$ are added. 5) Let stand for 3.5 h at 37°–40°C. 6) Add 40 ml conc. HCl. 7) Heat to boiling. 8) Filter through coarse filter paper (not cotton wool). 9) Adjust pH to 8.2–8.3 with 0.1 M HCl and 0.1 M NaOH. 10) Heat to boiling and filter again. 11) Add agar to 1.2 % W/v. 12) Autoclave for 30 min at 119°C. 13) Filter. 14) Autoclave for 20 min at 119°C. 15) Dissolve one part agar medium (I) in 1.34 parts broth medium (II, see below). This step gives a final agar concentration in medium I of 0.85 %. 16) Dispense and autoclave for 15 min at 119°C.

Medium II. 1) Autoclave together 2 500 g of freshly ground horse meat and 6 000 ml 0.25 M NaCl for one hour at atmospheric pressure and filter through cheese cloth and coarse filter paper. 2) Make up volume to 6 000 ml. 3) Add peptone (Merck) to give 4 % W/v. 4) Adjust pH to 7.4 (see step 9 for medium I). 5) Heat to boiling and filter through coarse filter paper. 6) Add 12 g KH_2PO_4 per litre. 7) Adjust pH to 7.4. 8) Boil the broth for 30 min, filter and autoclave for 20 min at 119°C. 9) Dispense and autoclave for 45 min at 100°C.

Cultivation technique. The cells were first cultivated on 10 % ox blood agar plates for 24 h at 37°C. No carbon dioxide was added to the air. The cells were transferred to a 10 % horse serum broth and cultivated for 24 h under the same atmospheric conditions.

From this culture 5 ml were inoculated into 400 ml of the semisolid medium I, contained in a 2 litre Fernbach bottle. After 72 h, 600 ml of medium II were added to the bottle, and the cultivation was continued for another 72 h. The temperature was 37°C and the gas phase consisted of CO_2:O_2 in the proportions 2:5. The gas phase was regulated by two narcose flowmeters (AGA 67827K and AGA 67828K, respectively) coupled in parallel.

Harvesting procedure. The culture was cooled rapidly to + 1°C and was centrifuged at + 1°C for 90 min at 7 000 × $g_{average}$.

Concentration of the medium. Different methods were tried. Freeze drying, pervaporation, the polyethylene glycol method of Kohn [3] and the technique of Palmstierna [4] were used. In our hands the last mentioned method gave the best results. Very small, if any, losses in haemolytic (*in vitro* [5]) and lethal activity (mice) were found. The lethal activity was tested on 12–14 g mice (Sigtuna strain) by giving 0.25 ml intraperitoneally. Serial dilutions were made in saline.

Chemical methods. In order to isolate the proteins from the acid polyelectrolytes under as mild conditions as possible, the counter flow electrophoresis (CFE) method of Eliasson *et al.*[2] was used. In this case the proteins were sucked off from the top of the column and pumped into a jacketed and cooled DEAE ion exchanger column [6] (2 × 20 cm) *via* a modified hose pressure micropump [2]. The electrophoresis

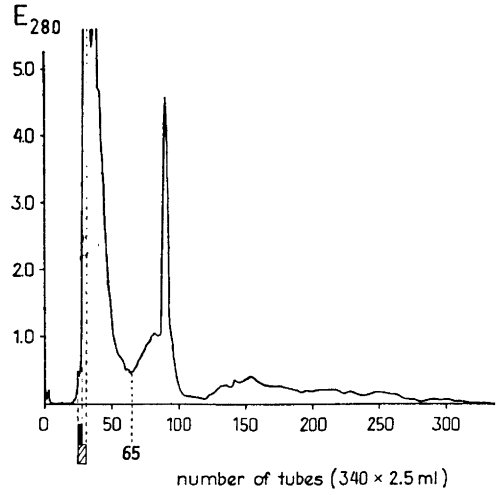

Fig. 1. Counter flow electrophoresis in combination with a DEAE column (2 × 20 cm, see text). The electrophoresis was finished at tube No. 65. Thereafter the DEAE was eluted with increasing concentration of NaCl in buffer. *Haemolytic activity* (tubenumbers: 25—28; black).

Lethal activity (tubenumbers: 25—31; striped).

was performed in 0.01 M Na-phosphate buffer (pH 6.85). The DEAE was in the phosphate form and equilibrated with the buffer mentioned.

The active fractions (*cf.* Fig. 1) were cut out and loaded on CMC-cellulose [6] or on cellulose esterified with succinic anhydride [7]. The pK in water of these exchangers were 3.8 and 7.6, respectively.

Concentrated medium was loaded on Sephadex G 25, G 50 and G 75 [8] jacketed and cooled columns, equilibrated with water. The columns were eluted at a rate of 1 ml per cm^2 and hour.

Paper chromatography for amino acids was performed on 18 h hydrolysates in 6 N HCl. In the first dimension butanol:glacial acetic acid:H_2O, 4:1:5 v/v, upper phase, was used. In the second dimension pyridine:H_2O, 8:2 v/v, was used.

Results and discussion. The haemolytic (*in vitro*) as well as the mouse lethal activity passed out from the top of the counter flow electrophoresis column in the front of the proteins. The toxins thus migrate like positively charged proteins.

The toxins are not retarded by DEAE at the pH and the ionic strength used (spec. conductivity: 1.18 × $10^{-3}\Omega^{-1}$ cm^{-1}). Since DEAE is an anion exchanger, the toxins are positively charged (or lacking ionic groups).

The toxic activities, purified by electrophoresis and passage through DEAE, were firmly fixed on cation cellulose exchangers. Succinate esterified cellulose (SEC) and CMC firmly fixed the toxins. They could not be eluted even with phosphate buffered 2 M NaCl, pH 6.85. The toxins were thus either destroyed or irreversibly fixed on these celluloses. Such a fixation indicates a high pK value of the toxins.

It is known that Sephadex retards basic materials under the conditions used [9]. Active material was retarded on Sephadex.

The toxins do not pass dialysis membranes. They migrate rapidly towards the cathode. They are not retarded on the DEAE-cellulose but they are retarded on Sephadex. They are almost irreversibly bound to CMC and SEC. Paper chromatography indicates that basic amino acids are represented in rather high proportion. The toxins may thus be associated to high molecular weight substances with dominating basic properties.

Work is continuing towards a better definition of these substances.

Acknowledgement. The author's thanks are due to Professor Hammarsten for the use of the CFE-apparatus at the Department of Bacteriology, Karolinska Institutet, Stockholm and to Dr. H. Palmstierna for advice.

The work has been performed with the aid of grants from the *Swedish Medical Research Council*, *Svenska Mejeriernas Riksförening*, the *Wallenberg Foundation* and *A. B. Cernelle.*

1. Hammarsten, E., Palmstierna, H. and Meyer, E. *J. Biochem. Microbiol. Technol. Eng.* **1** (1959) 273.
2. Eliasson, R., Hammarsten, E. and Palmstierna, H. *Acta Chem. Scand.* **14** (1960) 1212.
3. Kohn, I. *Nature* **183** (1959) 1055.
4. Palmstierna, H. *Biochem. Biophys. Research Communs* **2** (1960) 330.
5. Bergrahm, B. *To be published.*
6. Peterson, E. and Sober, H. *J. Am. Chem. Soc.* **78** (1956) 751.
7. Mc Intire, F. and Schenik, J. *J. Am. Chem. Soc.* **70** (1948) 1193.
8. Porath, J. and Flodin, P. *Nature* **183** (1959) 1657.
9. Gelotte, B. *J. Chromatography* **3** (1960) 330.

Received March 22, 1961.

Distribution and Excretion of Carnitine in the Rat

SVEN LINDSTEDT and GÖRAN LINDSTEDT

Department of Chemistry I, Karolinska Institutet, Stockholm 60, Sweden

Carnitine is widely distributed in Nature. The highest concentration — 35 mg/g dry weight — has been found in muscles of the horseshoe-crab (*Limulus polyphemus*) while mammalian muscle contains about 1 mg/g dry weight. The lack of a simple and specific quantitative method has hampered investigations on the distribution and excretion of carnitine. Available data have mostly been obtained with a bioassay using the meal worm (*Tenebrio molitor*) which has an absolute nutritional requirement for carnitine (See Ref.[1] for review). Strack has used a method in which carnitine is converted to the methyl ester of N-trimethylaminocrotonic acid which is assayed on frog rectus muscle. With this method he has determined the distribution of carnitine in rats up to 3 h after administration of 2—10 mg (lethal dose) per g body weight [2].

We have prepared (—)-carnitine-[methyl-^{14}C] and DL-carnitine-[carboxy-^{14}C] of high specific activity which has been used for a study on the distribution and excretion of carnitine administered in doses within the physiological range.

Experimental. DL-*Carnitine-[carboxy-^{14}C]*, 3.3 μC/mg, was prepared by methylation of DL-β-hydroxy-γ-aminobutyric acid-1-^{14}C.

(—)-*Carnitine-methyl-^{14}C*, 71.5 μC/mg, was made by the methylation of (—)-β-hydroxy-γ-aminobutyric acid prepared by resolution of the optically inactive acid *via* the strychnine and brucine salts. Details of these procedures will be published separately [3].

The labelled compounds were dissolved in 0.5 ml of water and given intraperitoneally to rats of the Sprague-Dawley strain. Total radioactivity in the expired carbon dioxide was determined by drawing the expiratory air through an ionization chamber (Frieseke & Hoepfner GmbH, FH 56/23) with continuous registration of the activity level. Urine and feces were collected daily and the activity determined by plating aliquots on aluminium planchets and counting in a windowless proportional counter (Frieseke & Hoepfner GmbH, FH 407 A). The rats were killed by a blow on the head, the tissues homogenized and extracted with 5 % trichloroacetic acid (TCA). Radioactivity was determined on aliquots after extraction of the TCA with ether.

Results and discussion. Data on the distribution of isotope after administration of labelled carnitine are given in Table 1. Paperchromatography of a TCA-extract (ethanol/ammonia/water, 90/5/5) from muscle after administration of (—)-carnitine-[methyl-^{14}C] showed only one labelled compound with the same mobility as carnitine. Carnitine was initially distributed over the whole animal with about the same

Table 1. Distribution of isotope after administration of (—)carnitine-[methyl-^{14}C] and DL-carnitine-[carboxy-^{14}C]

Tissue	% of administered dose per g tissue wet weight				
	(—) carnitine-[methyl-^{14}C]			DL-carnitine-[carboxy-^{14}C]	
	Rat 1. 223 g, 7 h after administration of 1.2 mg	Rat 2. 183 g, 7 d after administration of 1.1 mg	Rat 3. 156 g, 7 d after administration of 1.0 mg	Rat 4. 125 g, 36 h after administration of 2.2 mg	Rat 5. 225 g, 10 d after administration of 2.2 mg
Brain	0.05	0.03	0.04	—	0.03
Liver	0.64	0.06	0.07	0.54	0.09
Kidney	0.68	0.20	0.21	1.00	0.09
Spleen	0.55	0.15	0.14	0.44	0.12
Lung	—	0.18	0.13	—	—
Heart	0.58	0.67	0.45	1.45	0.28
Skeletal muscle	0.18	0.29	0.24	0.70	0.17

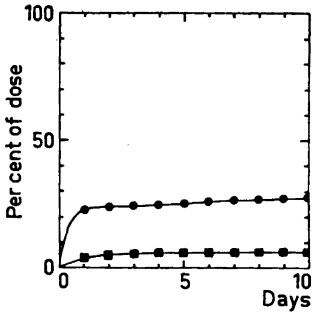

Fig. 1. Urinary excretion of isotope after administration of (−)-carnitine-[methyl-^{14}C] (1.1 mg) ■—■ and DL-carnitine-[carboxy-^{14}C] (2.2 mg) ●—●.

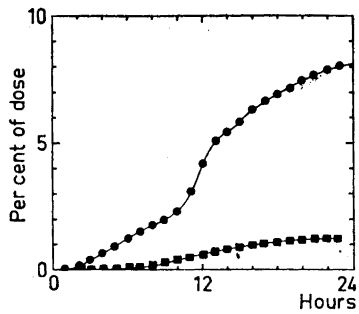

Fig. 2. $^{14}CO_2$ in expiratory air after administration of (−)-carnitine [methyl-^{14}C] (1.7 mg) ■—■ and DL-carnitine-[carboxy-^{14}C] (4.4 mg) ●—●.

concentration in all tissues except brain. After 7 and 10 days the highest concentration was found in heart muscle followed by skeletal muscle. Fritz [4] has shown that carnitine has a stimulatory effect on the oxidation of long chain fatty acids in muscle homogenates which is most pronounced with heart muscle preparation. The high uptake of administered carnitine by heart muscle may support his hypothesis that carnitine plays a role in the uptake of unesterified fatty acids by perifereal tissues, since heart is known to fill its energy requirements largely by oxidation of fatty acids.

The results obtained with (−)-carnitine showed that the amount present in the body after 7 days was approximately the same as after 7 h which indicates a slow biological turn-over of (−)-carnitine.

Figs. 1 and 2 illustrate the excretion of isotope in urine and expiratory CO_2 after administration of labelled carnitine. When (−)-carnitine-[methyl ^{14}C] was used 2−3 % was recovered as CO_2 in a 24 h period and less than 10 % in the urine in 10 days. After the first day the urinary excretion of activity remained at a fairly constant daily level of 0.1−0.2 % of the administered dose. When DL-carnitine-[carboxy-^{14}C] was given more of the isotope was recovered in the urine (30−40 %) and as $^{14}CO_2$ (10−15 %).

The experiments have demonstrated that when a small dose of natural carnitine is administered it is retained in the body over a long period. The slow biological turnover of carnitine may expain difficulties encountered in studies on the biosynthetic and degradative pathways of carnitine *.

This work has been supported by a grant from *Konung Gustaf V:s 80-årsfond.*

1. Fraenkel, G. and Friedman, S. *Vitamins and Hormones* **15** (1957) 74.
2. Strack, E., Rotzsch, W. and Lorenz, I. *Protides of the Biological Fluids, Proc. 7th Colloq. Bruges 1959*, p. 235.
3. Lindstedt, S. and Lindstedt, G. *Arkiv Kemi. To be published.*
4. Fritz, I. B. and Kaplan, E. *Protides of the Biological Fluids, Proc. 7th Colloq., Bruges 1959*, s. 252.

Received March 21, 1961.

* *Note added in proof.* Since completion of this work a paper has appeared in which the half-life of carnitine is estimated to 67 days in the rat. (Wolf, G. and Berger, C. R. A. *Arch. Biochem. Biophys.* **90** (1961) 360).

The Action of Trypsin on Casein

JOHN GRAAE and
E. SKIPPER RASMUSSEN

Universitetets Plantefysiologiske Laboratorium, Copenhagen, Denmark

The proteolytic enzymes from pancreas have been studied extensively ever since their discovery and several reaction mechanisms have been proposed to explain the observed kinetic data. Recently the mechanism of action of both trypsin and chymotrypsin have been shown to be more complex than was previously suggested [1,2]. Further data related to the mechanism of trypsin action are presented here.

Crystalline trypsin was kindly placed at our disposal by *Novo Terapeutisk Laboratorium*, Copenhagen, Denmark.

The substrate was a commercial »Casein nach Hammarsten». A stock solution was prepared according to Kunitz [3], except that instead of buffer the medium was 0.2 M KCl and KOH was added to adjust pH. This solution was diluted with 0.2 M KCl prior to experiment in order to give the desired concentration.

Table 1. The table gives the constants A and B. C is titration value after complete hydrolysis and can be taken as a measure of initial substrate concentration. Enzyme concentrations equals 6.5 mg/l in all experiments. (Calculations based on $\log_{10}$)

−A min	B min	C
29.2	140.0	1 080
16.4	83.4	620
8.0	44.4	340
4.75	26.1	180

The reaction was followed by continuous titration as previously described [2]. The pH was kept constant by the addition of KOH in minute quanta from a syringe; 1 titration unit equalled 0.0294 μequiv. The reaction mixture consisted of 30 ml casein solution and the reaction was initiated by the addition of 1 ml trypsin solution (20.1 mg/100 ml). Experiments were performed at pH = 7.00 and temperature = 25.3°C.

The reaction can be described by a combination of a zero order term and a first order term:

$$t = A \cdot a + B(-\log(1-a)),$$

Table 2. The table gives measured and calculated times, t_m and t_c, and degree of reaction, a. a is determined as the ratio between titration value at time t and titration value after complete hydrolysis. The calculations are based on the constants given in Table 1.

t_c	t_m	a	t_c	t_m	a	t_c	t_m	a	t_c	t_m	a
2.0	2	0.0593	1.7	2	0.0774	0.6	1	0.0471	0.8	1	0.1111
4.3	4	0.1213	3.7	4	0.1613	1.8	2	0.1412	1.8	2	0.2222
6.2	6	0.1657	6.1	6	0.2419	2.7	3	0.2000	2.8	3	0.3166
8.0	8	0.2065	8.5	8	0.3129	3.9	4	0.2706	4.0	4	0.4055
9.6	10	0.2389	9.9	10	0.3516	5.1	5	0.3324	5.1	5	0.4777
12.0	12	0.2843	12.2	12	0.4065	5.9	6	0.3676	6.0	6	0.5277
14.0	14	0.3175	14.4	14	0.4516	7.2	7	0.4205	7.4	7	0.5944
15.7	16	0.3453	16.6	16	0.4952	8.3	8	0.4617	8.4	8	0.6333
17.1	18	0.3667	18.3	18	0.5242	10.7	10	0.5412	9.3	9	0.6666
25.2	25	0.4731	20.7	20	0.5629	12.6	12	0.5941	10.0	10	0.6888
31.3	32	0.5380	25.7	25	0.6306	15.8	15	0.6647	12.6	12	0.7611
42.0	44	0.6296	30.7	30	0.6855	20.5	18	0.7471	14.2	14	0.7944
49.1	50	0.6778	35.2	35	0.7274	23.4	21	0.7853	16.0	16	0.8277
59.0	60	0.7333	41.0	40	0.7726	26.0	24	0.8147	17.5	18	0.8500
69.2	70	0.7796	46.3	45	0.8065	26.9	27	0.8235	18.7	20	0.8666
83.4	80	0.8296	55.1	55	0.8516	28.8	30	0.8412	21.8	22	0.9000
95.7	90	0.8630	60.3	65	0.8725	28.8	33	0.8412	25.4	24	0.9277
111.1	100	0.8954	68.6	75	0.9000	32.5	36	0.8706	26.3	26	0.9333

$$E \cdot t = \left(\frac{1}{k_2} - \frac{K_3}{k_1} - \frac{K_3 k_{-1}}{k_1 k_2}\right) \cdot a \cdot a - \left(\left(\frac{1}{k_1} + \frac{k_{-1}}{k_1 k_2}\right)(1 + K_3 \cdot a)\right) \log\,(1 - a)$$

where t is time, a is degree of reaction and A and B are constants. From graphs of t/a *versus* $\log\,(1-a)/a$ A and B are determined as the intercept on the ordinate and the slope, respectively. The constants A and B for four experiments with different initial concentrations of casein but with the same enzyme concentration are given in Table 1. In Table 2 the degrees of reaction are given together with measured and calculated values of t for the same four experiments.

As shown in Table 1 the constant A is negative, B is positive and both constants are proportional to the initial concentration of substrate. The tryptic action on casein thereby ressembles that on β-lactoglobulin, and the mechanism suggested for this reaction [1] could hold for the action on casein too. A mechanism involving an inhibition by the split products also could lead to a chronometric integral identical with that found empirically and so be a possible mechanism for the action of trypsin on casein and β-lactoglobulin.

The mechanism:

$$\begin{aligned} X_1 + C &\rightleftharpoons X_2 \qquad (\pm\ 1) \\ X_2 &\rightarrow X_1 + P \quad (+\ 2) \\ X_1 + P &\rightleftharpoons X_3 \qquad (\pm\ 3) \end{aligned}$$

gives the following chronometric integral by steady state treatment: (see eqn. above) which can give a negative coefficient to the zero order term and constants proportional to casein concentration if $K_3(k_2 + k_{-1}) > k_1$ and $K_3 \cdot a \gg 1$. (X_n might be an enzyme form, a combination of enzyme and substrate or a combination of enzyme and products, C is casein, P is reaction products, E is enzyme concentration, k_n is velocity constant for the n'th reaction and K_3 is the equilibrium constant for the reaction ($\pm$ 3)).

Acknowledgement. The authors thanks are due to professor dr D. Müller who kindly has permitted us to use the facilities of his laboratory. Financial support from *Statens Videnskabsfond, Købmand i Odense Johann og Hanne Weimann, født Seedorffs Legat* and *Carlsbergfondet* from Denmark, as well as the receipt of *Nordisk Forskningsstipendium* from the University of Oslo, Norway, is gratefully acknowledged by J. G.

1. Graae, J. *Biochim. et Biophys. Acta* **32** (1959) 510.
2. Graae, J. and Hansen, B. O. *Acta Chem. Scand.* **15** (1961). *In press.*
3. Kunitz, M. *J. Gen. Physiol.* **30** (1947) 291.

Received March 14, 1961.

Über die Rotationsdispersion von Tris-Diamin-Chrom(III)-Komplexen

O. KLING* und F. WOLDBYE

Chemisches Laboratorium A, Die Dänische Technische Hochschule, Kopenhagen, Dänemark

Bei der Messung der Absorptionsspektren von Chrom(III)-Komplexverbindungen wurde mehrfach festgestellt [1-3], dass das bei etwa 15 000 cm^{-1} ($\sim$ 650 mμ) liegende "Chromdublett", das auf Quartett-Dublett-Übergänge zurückzuführen ist [4,5], eine ausgeprägte Feinstruktur zeigt. Der Zusammenhang dieser schwachen Interkombinationsbanden mit gewissen Normalschwingungen des Moleküls [5] legte es nahe zu untersuchen, ob in diesem Spektralgebiet auch Beziehungen zwischen spektraler Absorption und Rotationsdispersion optisch aktiver Chrom(III)-Komplexe bestehen.

Für eine erste Untersuchung dieser Frage wurden die Luteochelate $[Cr\ en_3]^{3+}$ und $[Cr\ tn_3]^{3+}$ (en = Aethylendiamin, tn = Trimethylendiamin) ausgewählt, da bei ihnen die schwachen Dublettbanden noch nicht von den ersten hohen Zentralionenbanden überdeckt werden sondern frei liegen [1]. Rotationsdispersionskurven dieser beiden Verbindungen im Wellenzahlgebiet $\sim$ 17 000 – 28 000 cm^{-1} ($\sim$ 600 – 350 mμ) sind bereits seit längerem bekannt [6-8]. Mit Hilfe der in diesem Institut entwickelten Messeinrichtung [8,9] war es nun möglich,

* Derzeitige Anschrift: Institut für physikalische Chemie der Universität, Frankfurt a.M., Deutschland.

$$E \cdot t = \left(\frac{1}{k_2} - \frac{K_3}{k_1} - \frac{K_3 k_{-1}}{k_1 k_2}\right) \cdot a \cdot a - \left(\left(\frac{1}{k_1} + \frac{k_{-1}}{k_1 k_2}\right)(1 + K_3 \cdot a)\right) \log\,(1 - a)$$

where t is time, a is degree of reaction and A and B are constants. From graphs of t/a *versus* $\log\,(1-a)/a$ A and B are determined as the intercept on the ordinate and the slope, respectively. The constants A and B for four experiments with different initial concentrations of casein but with the same enzyme concentration are given in Table 1. In Table 2 the degrees of reaction are given together with measured and calculated values of t for the same four experiments.

As shown in Table 1 the constant A is negative, B is positive and both constants are proportional to the initial concentration of substrate. The tryptic action on casein thereby ressembles that on β-lactoglobulin, and the mechanism suggested for this reaction [1] could hold for the action on casein too. A mechanism involving an inhibition by the split products also could lead to a chronometric integral identical with that found empirically and so be a possible mechanism for the action of trypsin on casein and β-lactoglobulin.

The mechanism:

$$\begin{aligned} X_1 + C &\rightleftharpoons X_2 \qquad (\pm\ 1) \\ X_2 &\rightarrow X_1 + P \quad (+\ 2) \\ X_1 + P &\rightleftharpoons X_3 \qquad (\pm\ 3) \end{aligned}$$

gives the following chronometric integral by steady state treatment: (see eqn. above) which can give a negative coefficient to the zero order term and constants proportional to casein concentration if $K_3(k_2 + k_{-1}) > k_1$ and $K_3 \cdot a \gg 1$. (X_n might be an enzyme form, a combination of enzyme and substrate or a combination of enzyme and products, C is casein, P is reaction products, E is enzyme concentration, k_n is velocity constant for the n'th reaction and K_3 is the equilibrium constant for the reaction ($\pm$ 3)).

Acknowledgement. The authors thanks are due to professor dr D. Müller who kindly has permitted us to use the facilities of his laboratory. Financial support from *Statens Videnskabsfond, Købmand i Odense Johann og Hanne Weimann, født Seedorffs Legat* and *Carlsbergfondet* from Denmark, as well as the receipt of *Nordisk Forskningsstipendium* from the University of Oslo, Norway, is gratefully acknowledged by J. G.

1. Graae, J. *Biochim. et Biophys. Acta* **32** (1959) 510.
2. Graae, J. and Hansen, B. O. *Acta Chem. Scand.* **15** (1961). *In press.*
3. Kunitz, M. *J. Gen. Physiol.* **30** (1947) 291.

Received March 14, 1961.

Über die Rotationsdispersion von Tris-Diamin-Chrom(III)-Komplexen

O. KLING* und F. WOLDBYE

Chemisches Laboratorium A, Die Dänische Technische Hochschule, Kopenhagen, Dänemark

Bei der Messung der Absorptionsspektren von Chrom(III)-Komplexverbindungen wurde mehrfach festgestellt [1-3], dass das bei etwa 15 000 cm^{-1} ($\sim$ 650 mμ) liegende "Chromdublett", das auf Quartett-Dublett-Übergänge zurückzuführen ist [4,5], eine ausgeprägte Feinstruktur zeigt. Der Zusammenhang dieser schwachen Interkombinationsbanden mit gewissen Normalschwingungen des Moleküls [5] legte es nahe zu untersuchen, ob in diesem Spektralgebiet auch Beziehungen zwischen spektraler Absorption und Rotationsdispersion optisch aktiver Chrom(III)-Komplexe bestehen.

Für eine erste Untersuchung dieser Frage wurden die Luteochelate $[Cr\ en_3]^{3+}$ und $[Cr\ tn_3]^{3+}$ (en = Aethylendiamin, tn = Trimethylendiamin) ausgewählt, da bei ihnen die schwachen Dublettbanden noch nicht von den ersten hohen Zentralionenbanden überdeckt werden sondern frei liegen [1]. Rotationsdispersionskurven dieser beiden Verbindungen im Wellenzahlgebiet $\sim$ 17 000 – 28 000 cm^{-1} ($\sim$ 600 – 350 mμ) sind bereits seit längerem bekannt [6-8]. Mit Hilfe der in diesem Institut entwickelten Messeinrichtung [8,9] war es nun möglich,

* Derzeitige Anschrift: Institut für physikalische Chemie der Universität, Frankfurt a.M., Deutschland.

Tabelle 1. Bandenmaxima der Absorptionsspektren von $[Cr\ en_3]^{3+}$ und $[Cr\ tn_3]^{3+}$.

$[Cr\ en_3]^{3+}$			$[Cr\ tn_3]^{3+}$		
λ_{max} [mμ]	$\bar{\nu}_{max}$ [cm^{-1}]	ε	λ_{max} [mμ]	$\bar{\nu}_{max}$ [cm^{-1}]	ε
~ 677	~ 14 770	0.110	~ 677	~ 14 770	0.060
669	14 945	0.388	~ 671	~ 14 900	0.090
655	15 265	0.123	665	15 025	0.217
647	15 455	0.171	~ 659	~ 15 170	0.118
642	15 575	0.182	~ 656	~ 15 240	0.144
~ 639	~ 15 650	0.175	654	15 280	0.150
~ 632	~ 15 820	0.130	649	15 390	0.098
~ 627	~ 15 950	0.112	~ 646	~ 15 480	0.114
~ 619	~ 16 140	0.105	643	15 540	0.123
			636	15 725	0.157
			~ 631	~ 15 850	0.107
			627	15 935	0.105
			~ 622	~ 16 060	0.088
			620	16 115	0.090
			~ 616	~ 16 225	0.080
			~ 610	~ 16 390	0.066
			~ 606	~ 16 500	0.062

Tabelle 2. Extremwerte der Rotationsdispersion von D-$[Cr\ en_3](ClO_4)_3$ und L-$[Cr\ tn_3]Cl_3$ ([M] ist der molare Drehwert in Grad)

D-$[Cr\ en_3](ClO_4)_3$				L-$[Cr\ tn_3]Cl_3$			
λ_{max} [mμ]	λ_{min} [mμ]	$\bar{\nu}$ [cm^{-1}]	$[M]_{en}$	λ_{max} [mμ]	λ_{min} [mμ]	$\bar{\nu}$ [cm^{-1}]	$[M]_{tn}$
672		14 880	144	668		14 970	52
	668	14 970	85		665	15 035	73
644		15 530	182	659		15 175	65
	635	15 760	163		657	15 220	66
				654		15 290	63
					649	15 410	65
				640		15 615	57
					638	15 675	59.5
				636		15 725	59
					631	15 835	61
589	(Na D)	16 980	+308	589	(Na D)	16 980	−38
				565.5		17 685	0

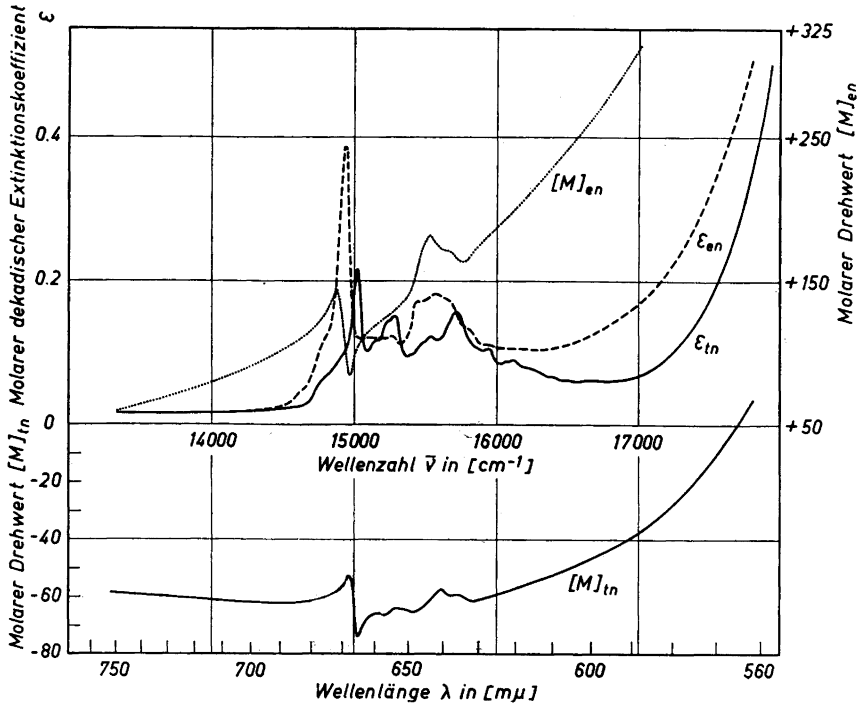

Abb. 1. Abhängigkeit des Extinktionskoeffizienten ε und des molaren Drehwertes [M] von der Wellenzahl $\bar{\nu}$. (Die Indizes en und tn beziehen sich auf die jeweiligen Messwerte von [Cr en_3] $(ClO_4)_3$ bzw. [Cr tn_3]Cl_3).

die Untersuchungen auch auf den Bereich von 13 500 – 18 000 cm^{-1} ($\sim$ 740 – 550 mμ), der bei früheren Messungen teilweise nicht erfasst worden war, auszudehnen und mit grosser spektraler Auflösung durchzuführen.

Die Messergebnisse sind in Abb. 1 dargestellt. Bei den Absorptionskurven ist der molare dekadische Extinktionskoeffizient ε gegen die Wellenzahl $\bar{\nu}$ aufgetragen. Die Rotationsdispersion ist als Funktion des molaren Drehwertes [M] in Abhängigkeit von $\bar{\nu}$ miteingezeichnet. Die Lage der Bandenmaxima der Absorptionsspektren mit ihren zugehörigen ε-Werten sind in Tab. 1 zusammengestellt (nicht genau lokalisierbare Schultern sind durch $\sim$ gekennzeichnet). Die Extremwerte der Rotationsdispersion sind in Tab. 2 angegeben.

Wie aus Abb. 1 und den Tabb. 1 und 2 zu ersehen ist, zeigen sowohl Absorptionsspektrum als auch Rotationsdispersion reiche Strukturen, die nur teilweise deutlich isoliert erscheinen. Die Verhältnisse beim Aethylendiamin-Komplex sind dabei einfacher und übersichtlicher als bei der Trimethylendiamin-Verbindung. Der isolierten langwelligen Bande bei λ_{max} = 669 mμ (en) bzw. 665 mμ (tn) entspricht je ein deutlicher Cotton-Effekt, dessen Wendepunkt mit dem entsprechenden Bandenmaximum zusammenfällt. Auch die anderen, aus mehreren Komponenten zusammengesetzten Banden zeigen sich überlagernde Cotton-Effekte, über deren jeweilige Zuordnung demnächst in einer quantitativen Analyse der erhaltenen Messergebnisse berichtet werden wird.

Experimentelles

1.) Die Darstellung von [Cr en_3]$^{3+}$ und [Cr tn_3]$^{3+}$ sowie die Trennung in ihre optischen Antipoden mit Hilfe von *d*-Nitrocampher erfolgte nach den bekannten Verfahren [1,8,10]. Die Nitrocampheronate wurden in die kristall-

wasserfreien Salze D-[Cr en_3] $(ClO_4)_3$ und L-[Cr tn_3]Cl_3 überführt [1], die im Vakuumexsikkator getrocknet und aufbewahrt wurden.

2.) Die Messungen der Absorptionsspektren erfolgten bei einer Schichtdicke von 10 cm mit 0.500 M wässrigen Lösungen der Komplexsalze an einem registrierenden Spektralphotometer CARY 11MS-50.

3.) Die Messung der Rotationsdispersion wurde mit Hilfe einer speziellen Messeinrichtung [9] ebenfalls am CARY 11MS-50 durchgeführt. Die Bestimmung des Analysatorwinkels Θ erfolgte mit einer Eichlösung von D-Sucrose (20 g/100 ml), deren spezifische Drehwerte bei 600, 625 und 650 mμ nach Angaben der Literatur [11] berechnet wurden. Die einzelnen Messdaten waren:

[Cr en_3]$(ClO_4)_3$: 0.300 M, $d = 5$ cm; $\Theta = 7.74 \pm 0.03°$, Schichtdicke der D-Sucrose-Lösung 5 cm.

[Cr tn_3]Cl_3: 0.500 M, $d = 5$ cm; $\Theta = 4.95 \pm 0.01°$, Schichtdicke der D-Sucrose-Lösung 1 cm.

Einer der Autoren (O.K.) dankt der Deutschen Forschungsgemeinschaft für ein Auslandsstipendium, in dessen Rahmen die vorliegende Arbeit durchgeführt wurde.

1. Schläfer, H. L. und Kling, O. *Z. anorg. u. allgem. Chem.* **302** (1959) 1.
2. Kling, O. *Unveröffentlicht.*
3. Schäffer, C. *Privatmitteilung.*
4. Schläfer, H. L. *Z. physik. Chem.* [*N.F.*] **11** (1957) 65.
5. Hartmann, H. und Schmidtke, H.-H. *Z. physik. Chem.* [*N. F.*] **19** (1959) 43.
6. Jaeger, F. M. *Rec. trav. chim.* **38** (1919) 204.
7. Mathieu, J.-P. *J. chim. phys.* **33** (1936) 78.
8. Woldbye, F. *Optical Rotatory Dispersion of Transition Metal Complexes*, European Research Office, US Army, Frankfurt a.M., 1959.
9. Woldbye, F. *Acta Chem. Scand.* **13** (1959) 2137.
10. Werner, A. *Ber.* **45** (1912) 863.
11. Lowry, T. M. und Richards, E. M. *J. Chem. Soc.* **125** (1924) 2523.

Eingegangen am 16. März 1961.

Note on the Crystal Structure of Niobium Dioxide

BENGT-OLOV MARINDER

Institute of Inorganic and Physical Chemistry, University of Stockholm, Stockholm, Sweden

The X-ray powder pattern of niobium dioxide was shown by Brauer [1] to contain the lines corresponding to a structure of rutile type and a considerable number of additional weak reflexions. Magnéli and coworkers [2] found that the pattern could be indexed assuming a tetragonal unit cell with $a = \sqrt{2}\ a_r = 13.71$ Å and $c = 2\ c_r = 5.985$ Å, where a_r and c_r represent the parameters of the subcell of rutile type. The unit cell should thus contain 32 formula units of NbO_2 which was confirmed by density measurements.

The present study has comprised a crystal structure determination on the basis of complete Weissenberg data registered with CuK radiation. The single crystals used were obtained from a sample prepared by melting a mixture of niobium metal and pentoxide in an electric are furnace in an argon atmosphere.

The structure determination was performed applying Fourier methods. All the atoms were found to occupy point positions 16(f) of the space-group $I4_1/a$ with the following parameter values corresponding to an R value of 0.165 for all observed reflexions.

	x	y	z
Nb_I	0.118	0.125	0.483
Nb_{II}	0.133	0.125	0.016
O_I	0.98_6	0.13_0	0.00_1
O_{II}	0.97_1	0.12_5	0.50_1
O_{III}	0.28_0	0.12_6	0.99_3
O_{IV}	0.26_6	0.11_8	0.50_3

The structure is built up of NbO_6 octahedra which are joined by edges and corners as in the rutile structure. However, within the strings of octahedra running in the c axis direction, the Nb—Nb distances are alternately shorter (2.80 Å) and longer (3.20 Å). The metal atom pairs thus present in the structure are likely to be associated with the remarkably low value of the magnetic susceptibility observed by Brauer [3]. The Nb—O and O—O distances have throughout normal values, being in

wasserfreien Salze D-[Cr en_3] $(ClO_4)_3$ und L-[Cr tn_3]Cl_3 überführt [1], die im Vakuumexsikkator getrocknet und aufbewahrt wurden.

2.) Die Messungen der Absorptionsspektren erfolgten bei einer Schichtdicke von 10 cm mit 0.500 M wässrigen Lösungen der Komplexsalze an einem registrierenden Spektralphotometer CARY 11MS-50.

3.) Die Messung der Rotationsdispersion wurde mit Hilfe einer speziellen Messeinrichtung [9] ebenfalls am CARY 11MS-50 durchgeführt. Die Bestimmung des Analysatorwinkels Θ erfolgte mit einer Eichlösung von D-Sucrose (20 g/100 ml), deren spezifische Drehwerte bei 600, 625 und 650 mμ nach Angaben der Literatur [11] berechnet wurden. Die einzelnen Messdaten waren:

[Cr en_3]$(ClO_4)_3$: 0.300 M, $d = 5$ cm; $\Theta = 7.74 \pm 0.03°$, Schichtdicke der D-Sucrose-Lösung 5 cm.

[Cr tn_3]Cl_3: 0.500 M, $d = 5$ cm; $\Theta = 4.95 \pm 0.01°$, Schichtdicke der D-Sucrose-Lösung 1 cm.

Einer der Autoren (O.K.) dankt der Deutschen Forschungsgemeinschaft für ein Auslandsstipendium, in dessen Rahmen die vorliegende Arbeit durchgeführt wurde.

1. Schläfer, H. L. und Kling, O. *Z. anorg. u. allgem. Chem.* **302** (1959) 1.
2. Kling, O. *Unveröffentlicht.*
3. Schäffer, C. *Privatmitteilung.*
4. Schläfer, H. L. *Z. physik. Chem.* [*N.F.*] **11** (1957) 65.
5. Hartmann, H. und Schmidtke, H.-H. *Z. physik. Chem.* [*N. F.*] **19** (1959) 43.
6. Jaeger, F. M. *Rec. trav. chim.* **38** (1919) 204.
7. Mathieu, J.-P. *J. chim. phys.* **33** (1936) 78.
8. Woldbye, F. *Optical Rotatory Dispersion of Transition Metal Complexes*, European Research Office, US Army, Frankfurt a.M., 1959.
9. Woldbye, F. *Acta Chem. Scand.* **13** (1959) 2137.
10. Werner, A. *Ber.* **45** (1912) 863.
11. Lowry, T. M. und Richards, E. M. *J. Chem. Soc.* **125** (1924) 2523.

Eingegangen am 16. März 1961.

Note on the Crystal Structure of Niobium Dioxide

BENGT-OLOV MARINDER

Institute of Inorganic and Physical Chemistry, University of Stockholm, Stockholm, Sweden

The X-ray powder pattern of niobium dioxide was shown by Brauer [1] to contain the lines corresponding to a structure of rutile type and a considerable number of additional weak reflexions. Magnéli and coworkers [2] found that the pattern could be indexed assuming a tetragonal unit cell with $a = \sqrt{2}\ a_r = 13.71$ Å and $c = 2\ c_r = 5.985$ Å, where a_r and c_r represent the parameters of the subcell of rutile type. The unit cell should thus contain 32 formula units of NbO_2 which was confirmed by density measurements.

The present study has comprised a crystal structure determination on the basis of complete Weissenberg data registered with CuK radiation. The single crystals used were obtained from a sample prepared by melting a mixture of niobium metal and pentoxide in an electric are furnace in an argon atmosphere.

The structure determination was performed applying Fourier methods. All the atoms were found to occupy point positions 16(f) of the space-group $I4_1/a$ with the following parameter values corresponding to an R value of 0.165 for all observed reflexions.

	x	y	z
Nb_I	0.118	0.125	0.483
Nb_{II}	0.133	0.125	0.016
O_I	0.98_6	0.13_0	0.00_1
O_{II}	0.97_1	0.12_5	0.50_1
O_{III}	0.28_0	0.12_6	0.99_3
O_{IV}	0.26_6	0.11_8	0.50_3

The structure is built up of NbO_6 octahedra which are joined by edges and corners as in the rutile structure. However, within the strings of octahedra running in the c axis direction, the Nb—Nb distances are alternately shorter (2.80 Å) and longer (3.20 Å). The metal atom pairs thus present in the structure are likely to be associated with the remarkably low value of the magnetic susceptibility observed by Brauer [3]. The Nb—O and O—O distances have throughout normal values, being in

the ranges 2.0—2.1 Å and 2.6—3.0 Å, respectively.

Full details on this study will be published elsewhere.

The work has been carried out within a research programme financially supported by the *Swedish Natural Science Research Council.*

1. Brauer, G. *Z. anorg. Chem.* **248** (1941) 1.
2. Magnéli, A., Andersson, G. and Sundkvist, G. *Acta Chem. Scand.* **9** (1955) 1402.
3. Brauer, G. *Z. anorg. Chem.* **256** (1948) 10.

Received March 28, 1961.

A High-Field Emission Ionization Detector for Gas Chromatography

ÖRN WAHLROOS

Laboratory of the Foundation for Chemical Research, Biochemical Institute, Helsinki

In addition to the various ways, reviewed by Lovelock [1], of providing primary electrons for ionization in gases, high field emission may be used. The detector tube constructed by Haahti and Nikkari [2,3], which obviously depends on field emission, is reported to function only at high temperatures [4]. A field emission-type ionization detector working at normal pressure and temperature with argon as carrier gas is described in this communication.

At normal temperature and pressure the current in commercial argon between electrodes 1 cm apart and at a potential difference of 1 000 V is about 10^{-12} to 10^{-11} A. This current is considerably higher than that between clean electrode surfaces in purified argon. This is explained by the fact that oxide or tarnish films on the electrode surfaces and impurities in the gas may greatly enhance the electron emission due to high fields [5].

If the voltage gradient is sufficiently high, there will be a small concentration of metastable argon atoms in the interelectrode space. At a certain concentration of vapour molecules with an ionization energy $\leq$ 11.6 eV, the probability of a collision leading to ionization between a vapour molecule and a metastable argon atom will be high. Because the rate of such a double impact ionization process is proportional to the square of the current [5], an electron avalanche will result, where collisions between vapour molecules and metastable argon atoms occur as intermediate stages. With such a mechanism it should be possible to make the ionization current dependent on the concentration of vapour molecules in the electric field [4].

On attempts to use the tube of Haahti and Nikkari at lower temperatures the tube was observed to work according to an "all-or-none" principle; the current impulse started by a minimum vapour concentration was limited by the associated circuit only. Because the too rapid current rise could be due to secondary processes at the cathode (liberation of secondary electrons due to positive ions, photons, or metastables), different geometries and cathode materials were tested.

The experiments were made with commercial argon led into the ionization tube under test through a short chromatographic column. The gas rates varied between 50 and 200 cm³/min. The temperature was + 18°C. The resistance in series with the ionization tube and the source of highvoltage (800—1 200 V) was 6×10^9 Ω. The potential difference across part of the series resistance was fed through a simple impedance converter into a potentiometric recorder.

With aluminium electrodes an increase of the interelectrode distance by ~100 % and/or a decrease of the surface-area of the cathode to ~ 1/20 of the dimensions reported by Haahti and Nikkari [3] led to a response roughly dependent on the concentration of organic vapour in the argon. The tube was observed to have a time lag of some seconds. With the aluminum electrodes a "dead period" was also observed; when the signal had passed, the sensitivity of the tube to the following samples of organic vapour was nil or greatly reduced during a time varying between 30 sec and several minutes. This "dead period" is suggested to be due to a transitory change of the emissive properties of the aluminum surface because of the local heating generated upon impact of positive ions. It is probable that when the tube constructed by Haahti and Nikkari is operated at an elevated temperature not only the concentration of metastables is higher because of the greater acceleration of electrons in the electric field, but also that tarnish films on the electrode surfaces are absent or differ structurally from those on the electrodes at low temperatures.

When the cathode was made of tungsten wire, a higher field was required to obtain the

the ranges 2.0—2.1 Å and 2.6—3.0 Å, respectively.

Full details on this study will be published elsewhere.

The work has been carried out within a research programme financially supported by the *Swedish Natural Science Research Council.*

1. Brauer, G. *Z. anorg. Chem.* **248** (1941) 1.
2. Magnéli, A., Andersson, G. and Sundkvist, G. *Acta Chem. Scand.* **9** (1955) 1402.
3. Brauer, G. *Z. anorg. Chem.* **256** (1948) 10.

Received March 28, 1961.

A High-Field Emission Ionization Detector for Gas Chromatography

ÖRN WAHLROOS

Laboratory of the Foundation for Chemical Research, Biochemical Institute, Helsinki

In addition to the various ways, reviewed by Lovelock [1], of providing primary electrons for ionization in gases, high field emission may be used. The detector tube constructed by Haahti and Nikkari [2,3], which obviously depends on field emission, is reported to function only at high temperatures [4]. A field emission-type ionization detector working at normal pressure and temperature with argon as carrier gas is described in this communication.

At normal temperature and pressure the current in commercial argon between electrodes 1 cm apart and at a potential difference of 1 000 V is about 10^{-12} to 10^{-11} A. This current is considerably higher than that between clean electrode surfaces in purified argon. This is explained by the fact that oxide or tarnish films on the electrode surfaces and impurities in the gas may greatly enhance the electron emission due to high fields [5].

If the voltage gradient is sufficiently high, there will be a small concentration of metastable argon atoms in the interelectrode space. At a certain concentration of vapour molecules with an ionization energy $\leq$ 11.6 eV, the probability of a collision leading to ionization between a vapour molecule and a metastable argon atom will be high. Because the rate of such a double impact ionization process is proportional to the square of the current [5], an electron avalanche will result, where collisions between vapour molecules and metastable argon atoms occur as intermediate stages. With such a mechanism it should be possible to make the ionization current dependent on the concentration of vapour molecules in the electric field [4].

On attempts to use the tube of Haahti and Nikkari at lower temperatures the tube was observed to work according to an "all-or-none" principle; the current impulse started by a minimum vapour concentration was limited by the associated circuit only. Because the too rapid current rise could be due to secondary processes at the cathode (liberation of secondary electrons due to positive ions, photons, or metastables), different geometries and cathode materials were tested.

The experiments were made with commercial argon led into the ionization tube under test through a short chromatographic column. The gas rates varied between 50 and 200 cm³/min. The temperature was + 18°C. The resistance in series with the ionization tube and the source of highvoltage (800—1 200 V) was 6×10^9 Ω. The potential difference across part of the series resistance was fed through a simple impedance converter into a potentiometric recorder.

With aluminium electrodes an increase of the interelectrode distance by ~100 % and/or a decrease of the surface-area of the cathode to ~ 1/20 of the dimensions reported by Haahti and Nikkari [3] led to a response roughly dependent on the concentration of organic vapour in the argon. The tube was observed to have a time lag of some seconds. With the aluminum electrodes a "dead period" was also observed; when the signal had passed, the sensitivity of the tube to the following samples of organic vapour was nil or greatly reduced during a time varying between 30 sec and several minutes. This "dead period" is suggested to be due to a transitory change of the emissive properties of the aluminum surface because of the local heating generated upon impact of positive ions. It is probable that when the tube constructed by Haahti and Nikkari is operated at an elevated temperature not only the concentration of metastables is higher because of the greater acceleration of electrons in the electric field, but also that tarnish films on the electrode surfaces are absent or differ structurally from those on the electrodes at low temperatures.

When the cathode was made of tungsten wire, a higher field was required to obtain the

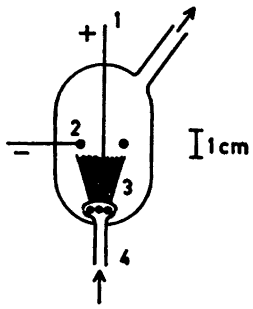

Fig. 1. Field emission ionization tube. 1. Platinum anode. 2. Tungsten cathode. 3. Diffusion net of 100 mesh metal gauze. 4. Gas inlet.

same sensitivity as with aluminum electrodes, but no "dead period" was observed. A platinum cathode behaved similarly, but a still higher field was required.

The smaller sensitivity but better correspondence to the concentration of dissociable vapour molecules in the carrier gas with the W and Pt cathodes could partly be due to the higher work function of these metals in comparison with aluminum. However, the work function of the cathode metal is considered to have little effect on the ionization of a gas at atmospheric pressures because the surface has an absorbed gas layer [5]. The view that gas or vapour layers sorbed on the cathode surface play an important role in the low-temperature field emission ionization detector is supported by the facts that (a) if the tungsten cathode has been heated to about 500°C by passing a current through it, the background ionization current in the tube is lowered and the sensitivity is nil until the cathode has been kept at room temperature in an argon stream for 1 or 2 h; (b) in nitrogen from a sample of organic vapours a signal current is obtained which over a wide range is independent of vapour concentration ($\sim 1{:}10^6$ to $\sim 1{:}10^3$). The signal current in this case is small, about 10 to 20 % of the background ionization current, because of the lack of gas amplification which occurs in argon through the production of metastables.

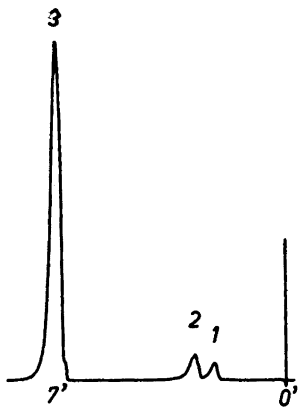

Fig. 2. Gas chromatogram obtained using the tube shown in Fig. 1 as detector. Anode- to cathode voltage: 1 000 V. Carrier gas: argon, 70 cm³/min. Column diam. 4 mm, length 20 cm, filling silicone M 550 on 40 – 60 mesh Firebrick. Column and detector temperature: + 18°C. Outlet pressure 1 atm. 1. Ethyl ether. 2. Ethyl formiate. 3. *Cyclo*hexane. About 1 μg mixture injected.

With all the cathode materials tested large oscillations of the signal current were frequently observed. This is thought to be due to disturbances caused by the gas stream of the space charge between the electrodes [1]. A stable signal current was obtained by inserting a diffusion net of fine metal gauze. A workable electrode arrangement for a field emission ionization detector working with argon at room temperature, and a gas chromatogram obtained with this detector are shown in Figs. 1 and 2. The tube has been tested with, and found to respond to hydrocarbons, alcohols, aldehydes, ethers, and esters. Its relative response to different compounds varies considerably. The background current of the tube is 5×10^{-12} A, and the noise level is about 5 % of this.

A more detailed report will be published elsewhere.

The author is greatly indebted to Professor A. I. Virtanen for his kind interest in this work. The investigation is a part of a research project under U. S. Public Law No. 480, 83rd Congress.

1. Lovelock, J. E. *Anal. Chem.* **33** (1961) 162.
2. Haahti, E. and Nikkari, T. *Acta Chem. Scand.* **13** (1959) 2125.
3. Haahti, E., Nikkari, T. and Kulonen, E. *J. Chromatogr.* **3** (1960) 372.
4. Lovelock, J. E. in R. P. W. Scott, *Gas Chromatography*, Butterworths, London 1960.
5. Llewellyn-Jones, F. *Ionization and Breakdown in Gases*, Methuen & Co., London 1957.

Received April 4, 1961.

A Method for the Determination of Reducing Disaccharides in the Presence of Aldohexoses

BIRGITTE B. JØRGENSEN and
O. B. JØRGENSEN

Department of Technical Biochemistry, The Technical University of Denmark, 14 Odensegade, Copenhagen, Denmark

This method is suitable for the study of glucosidases and especially those, *e.g.* isomaltases, which are difficult to determine [1] with the Tauber and Kleiner hexose sensitive reagent [2], and where a method is wanted that requires very little material. It seems possible also to use the method for determining higher oligosaccharides in mixtures with aldohexoses.

The principle of the method is an oxidation of the sugar mixture to the corresponding aldonic and aldobionic acids. The aldonic acid does not give any colour reaction when heated with anthrone in sulfuric acid, whereas the aldobionic acid — due to the non oxidized glucose residue that is liberated by the strong acid solution — will react with the anthrone reagent giving a blue-green colour reaction. The oxidation of the sugar mixture is performed at room temperature with an alkaline hypobromite solution. Keeping the hypobromite solution not too alkaline the over-oxidation of the aldobionic acid is negligible. After the oxidation excess hypobromite is destroyed with thiourea, and the determination proceeds using one of the anthrone methods.

Alkaline hypobromite reagent. 2.5 ml bromine is dissolved in 250 ml ice-cold 1 N NaOH and diluted to 400 ml with water. Kept in the refrigerator in a brown bottle this reagent is stable at least for 2 months. From this stock solution a hypobromite solution is prepared immediately before use by adding 5 ml 1.5 N H_2SO_4 to 20 ml of the stock solution.

Thiourea reagent. 7.5 g thiourea in 100 ml 0.5 N H_2SO_4.

Anthrone reagent. 0.2 g anthrone in 100 ml 95 % H_2SO_4 (prepared daily).

Procedure. Pipet 1 ml of each sample, having a disaccharide content $\leq 180 \times 10^{-3}$ mg, into a test tube. Include two blanks and two standards (see below). Add 0.5 ml of the diluted hypobromite reagent and mix carefully. The hypobromite reagent is added to each tube with intervals of, *e.g.*, 30 sec. After reaction for 20 min add 0.5 ml of the thiourea reagent and mix carefully after each of the additions, the thiourea beeing added with the same intervals as the hypobromite (constriction pipets are used). The analysis proceeds now using one of the modifications of the anthrone method, *e.g.* the conditions used by McCready *et al.*[3]: 4 ml of the anthrone reagent is added to the samples while cooling in a water bath. Mix thoroughly while cooling and heat the samples for 7.5 min at 100°C. Cool the tubes rapidly to 25° C and measure in a colorimeter at 625 mμ (or use a corresponding filter) in a 1 cm cell.

In each set of samples are included two blanks and two standards, the blanks containing 10^{-6} mole monosaccharide and the standards 0.5×10^{-6} mole disaccharide. Calculation of disaccharide (mole):

Table 1. Determination of some disaccharides in the presence of their corresponding monosaccharides.

Disaccharide mole × 10^6	Monosaccharide mole × 10^6	Disaccharide found mole × 10^6
Maltose	Glucose	Maltose
0.050	0.900	0.051
0.150	0.700	0.151
0.250	0.500	0.253
0.350	0.300	0.348
0.450	0.100	0.447
Isomaltose	Glucose	Isomaltose
0.050	0.900	0.051
0.150	0.700	0.151
0.250	0.500	0.252
0.350	0.300	0.352
0.450	0.100	0.451
Cellobiose	Glucose	Cellobiose
0.100	0.800	0.100
0.200	0.600	0.201
0.300	0.400	0.303
0.400	0.200	0.401
0.500	0.000	0.500
Lactose	Glucose/Galactose	Lactose
0.100	0.800	0.097
0.200	0.600	0.196
0.300	0.400	0.303
0.400	0.200	0.401
0.500	0.000	0.495

$$\frac{\text{Reading of sample} - \text{reading of blank}}{\text{Reading of standard} - \text{reading of blank}} \times 0.5 \times 10^{-6}$$

Normally the blank with monosaccharide will give nearly the same value as a water blank, and an extraordinarily high monosaccharide blank may be due to a too old hypobromite reagent.

In Table 1 are shown some examples of determinations. The amount of monosaccharide corresponds to different degrees of hydrolysis of the disaccharide. The blank corresponds to 100 % of hydrolysis. It is also possible to have greater amounts of monosaccharide (2—3 times the amounts used in the examples). In determining, *e.g.*, lactose the blank should contain half glucose and half galactose.

Ketohexoses will not be fully oxidized under the conditions given; *e.g.* fructose will need an oxidation time of at least 1 hour to give a negative anthrone reaction. This difference in oxidation rate has been used for the determination of fructose in the presence of glucose by Slein and Schneel [4].

Small amounts of protein and acetate and citrate buffers are without influence on the determination; if necessary the pH must be adjusted to about 10 before the addition of hypobromite.

If a faster method is wanted, one of the less accurate "heat of mixing" anthrone methods may be used [5].

Acknowledgements. We are gratefully indebted to Professor Holger Jørgensen for his interest of this work.

1. Dahlqvist, A. *Hog Intestinal α-Glucosidases* (Diss.), University of Lund 1960, p. 16.
2. Tauber, H. and Kleiner, I. S. *J. Biol. Chem.* **99** (1932) 249.
3. McCready, R. M., Guggolz, J., Silviera, V. and Owens, H. S. *Anal. Chem.* **22** (1950) 1156.
4. Slein, M. W. and Schnell, G. W. *Proc. Soc. Exptl. Biol. Med.* **82** (1953) 734.
5. Snell, F. D. and Snell, C. T. *Colorimetric Methods of Analysis*, 3rd Ed., D. van Nostrand Company, New York 1953, Vol. III, p. 199.

Received April 14, 1961.

Preliminary Results of an Electron Diffraction Reinvestigation of *Cyclo*butane and *Cyclo*pentane

A. ALMENNINGEN, O. BASTIANSEN and P. N. SKANCKE

Universitetets kjemiske institutt, Blindern-Oslo; Institutt for teoretisk kjemi, Norges tekniske høgskole, Trondheim, Norway

The molecular structure of *cyclo*butane and *cyclo*pentane have been reinvestigated by the electron diffraction sector method. However, further refinements and a more extensive analysis of the diffraction data have to be performed before the exact equilibrium conformation of the ring-formed carbon skeletons can be determined. Only some preliminary results therefore will be presented in this note.

As members of a group of molecules characterized by a strained conformation of the carbon skeleton, *cyclo*butane and *cyclo*pentane have been the object of a series of experimental and theoretical studies [1-16].

By this investigation we hope to be able to obtain results for the molecular structures which are more extensive and more accurate than those previously published. A comparison of the present results with unpublished structure data obtained by the same diffraction unit in 1956—1957, is also of great interest because it provides an opportunity for estimating the reproducibility of the results obtained by this method.

Cyclobutane. By an analysis of the intensity curve and of several radial distribution curves obtained by using different damping functions, the following values for the C—C and C—H bond distances have been obtained:

C—C: 1.548 ± 0.003 Å and C—H: 1.092 ± 0.010 Å.

The values found by the unpublished investigation in 1956—1957 are 1.547 Å and 1.089 Å, respectively.

These results demonstrate that the C—C bond distance in a saturated 4-membered ring is longer than the corresponding distance in the linear paraffins. For ethane the values 1.536 Å [17] and 1.534 Å [18] have been reported. Recent investigations of *n*-butane give the values 1.533 Å [19] and 1.539 Å [20]. Finally by an electron diffraction

$$\frac{\text{Reading of sample} - \text{reading of blank}}{\text{Reading of standard} - \text{reading of blank}} \times 0.5 \times 10^{-6}$$

Normally the blank with monosaccharide will give nearly the same value as a water blank, and an extraordinarily high monosaccharide blank may be due to a too old hypobromite reagent.

In Table 1 are shown some examples of determinations. The amount of monosaccharide corresponds to different degrees of hydrolysis of the disaccharide. The blank corresponds to 100 % of hydrolysis. It is also possible to have greater amounts of monosaccharide (2—3 times the amounts used in the examples). In determining, *e.g.*, lactose the blank should contain half glucose and half galactose.

Ketohexoses will not be fully oxidized under the conditions given; *e.g.* fructose will need an oxidation time of at least 1 hour to give a negative anthrone reaction. This difference in oxidation rate has been used for the determination of fructose in the presence of glucose by Slein and Schneel [4].

Small amounts of protein and acetate and citrate buffers are without influence on the determination; if necessary the pH must be adjusted to about 10 before the addition of hypobromite.

If a faster method is wanted, one of the less accurate "heat of mixing" anthrone methods may be used [5].

Acknowledgements. We are gratefully indebted to Professor Holger Jørgensen for his interest of this work.

1. Dahlqvist, A. *Hog Intestinal α-Glucosidases* (Diss.), University of Lund 1960, p. 16.
2. Tauber, H. and Kleiner, I. S. *J. Biol. Chem.* **99** (1932) 249.
3. McCready, R. M., Guggolz, J., Silviera, V. and Owens, H. S. *Anal. Chem.* **22** (1950) 1156.
4. Slein, M. W. and Schnell, G. W. *Proc. Soc. Exptl. Biol. Med.* **82** (1953) 734.
5. Snell, F. D. and Snell, C. T. *Colorimetric Methods of Analysis*, 3rd Ed., D. van Nostrand Company, New York 1953, Vol. III, p. 199.

Received April 14, 1961.

Preliminary Results of an Electron Diffraction Reinvestigation of *Cyclo*butane and *Cyclo*pentane

A. ALMENNINGEN, O. BASTIANSEN and P. N. SKANCKE

Universitetets kjemiske institutt, Blindern-Oslo; Institutt for teoretisk kjemi, Norges tekniske høgskole, Trondheim, Norway

The molecular structure of *cyclo*butane and *cyclo*pentane have been reinvestigated by the electron diffraction sector method. However, further refinements and a more extensive analysis of the diffraction data have to be performed before the exact equilibrium conformation of the ring-formed carbon skeletons can be determined. Only some preliminary results therefore will be presented in this note.

As members of a group of molecules characterized by a strained conformation of the carbon skeleton, *cyclo*butane and *cyclo*pentane have been the object of a series of experimental and theoretical studies [1-16].

By this investigation we hope to be able to obtain results for the molecular structures which are more extensive and more accurate than those previously published. A comparison of the present results with unpublished structure data obtained by the same diffraction unit in 1956—1957, is also of great interest because it provides an opportunity for estimating the reproducibility of the results obtained by this method.

Cyclobutane. By an analysis of the intensity curve and of several radial distribution curves obtained by using different damping functions, the following values for the C—C and C—H bond distances have been obtained:

C—C: 1.548 ± 0.003 Å and C—H: 1.092 ± 0.010 Å.

The values found by the unpublished investigation in 1956—1957 are 1.547 Å and 1.089 Å, respectively.

These results demonstrate that the C—C bond distance in a saturated 4-membered ring is longer than the corresponding distance in the linear paraffins. For ethane the values 1.536 Å [17] and 1.534 Å [18] have been reported. Recent investigations of *n*-butane give the values 1.533 Å [19] and 1.539 Å [20]. Finally by an electron diffraction

investigation of *n*-pentane, *n*-hexane and *n*-heptane Bartell *et al.*[21] have obtained the values 1.531 Å, 1.533 Å and 1.534 Å, respectively.

On the other hand our value for the C–C bond distance is significantly shorter than the corresponding value published by Dunitz and Schomaker [1].

The carbon ring is definitely found to be puckered. However, the magnitude of the deviation from planarity is not determined with any reasonable accuracy at this stage of the investigation. Furthermore, the question of the existence of an "inversion flopping" of the carbon ring has not yet been settled unambiguously.

The values for the bond distances reported here are not expected to be changed significantly by further refinements.

Cyclopentane. A study similar to that performed for *cyclo*butane gave the following values for the C–C and C–H bond distances:

C–C: 1.539 ± 0.003 Å and

C–H: 1.095 ± 0.010 Å.

The corresponding values obtained by the above mentioned unpublished investigation are 1.539 Å and 1.089 Å, respectively.

Within the limits of error the C–C bond length in *cyclo*pentane therefore is the same as that in the chain paraffins.

The ring system is found to deviate from planarity. The amplitude of the puckering, however, has not been determined. By further refinements we hope to solve this problem and also to study the claimed presence of a pseudo-rotation in the ring [10,13,15].

1. Dunitz, J. D. and Schomaker, V. *J. Chem. Phys.* **20** (1952) 1703.
2. Rathjens, G. W., Jr., Freeman, N. K., Gwinn, W. D. and Pitzer, K. S. *J. Am. Chem. Soc.* **75** (1953) 5634.
3. Rathjens, G. W., Jr. and Gwinn, W. D. *J. Am. Chem. Soc.* **75** (1953) 5629.
4. Hassel, O. and Viervoll, H. *Tidsskr. Kjemi, Bergvesen Met.* **6** (1946) 31.
5. Hassel, O. and Viervoll, H. *Acta Chem. Scand.* **1** (1947) 149.
6. Pauling, L. and Brockway, L. O. *J. Am. Chem. Soc.* **59** (1937) 1223.
7. Tschamler, H. and Voetter, H. *Monatsh.* **83** (1952) 1228.
8. Aston, J. G., Schumann, S. C., Fink, H. L. and Doty, P. M. *J. Am. Chem. Soc.* **63** (1941) 2029.
9. Aston, J. G., Fink, H. L. and Schumann, S. C. *J. Am. Chem. Soc.* **65** (1943) 341.
10. Pitzer, K. S. and Donath, W. E. *J. Am. Chem. Soc.* **81** (1959) 3213.
11. Miller, F. A. and Inskeep, R. G. *J. Chem. Phys.* **18** (1950) 1519.
12. McCullough, J. P. *J. Chem. Phys.* **29** (1958) 966.
13. McCullough, J. P., Pennington, R. E., Smith, J. C., Hossenloop, I. A. and Waddington, G. *J. Am. Chem. Soc.* **81** (1959) 5880.
14. Curnutte, B. and Shaffer, W. F. *J. Mol. Spectroscopy*, **1** (1957) 239.
15. Kilpatrick, J. E., Pitzer, K. S. and Spitzer, R. *J. Am. Chem. Soc.* **69** (1947) 2483.
16. Coulson, C. A. and Moffitt, W. E. *Phil. Mag.* **40** (1949) 1.
17. Almenningen, A. and Bastiansen, O. *Acta Chem. Scand.* **9** (1955) 815.
18. Allen, H. C., Jr. and Plyler, E. K. *J. Chem. Phys.* **31** (1959) 1062.
19. Bonham, R. A. and Bartell, L. S. *J. Am. Chem. Soc.* **81** (1959) 3491.
20. Kuchitsu, K. *Bull. Chem. Soc. Japan* **32** (1959) 748.
21. Bonham, R. A., Bartell, L. S. and Kohl, D. A. *J. Am. Chem. Soc.* **81** (1959) 4765.

Received April 7, 1961.

ACTA CHEMICA SCANDINAVICA 15 (1961) 713–720

The Chemistry of the Natural Order Cupressales

XXXIV.* Heartwood Constituents of *Juniperus procera* Hochst. and *Juniperus californica* Carr.

E. PETTERSSON and J. RUNEBERG

Organisk-kemiska Institutionen, Kungl. Tekniska Högskolan, Stockholm, Sweden

The heartwood of *Juniperus procera* contains a new sesquiterpene hydroxy acid, a diterpene phenol, the tropolone procerin, three other tropolones, carvacrol, α-cedrene, cuparene, cedrol, β-sitosterol and a C_{30}-compound previously isolated from *J. thurifera*.

The heartwood of *Juniperus californica* contains hinokiic acid, "Widdringtonia acid II", α-cedrene, thujopsene, cuparene, cedrol and widdrol.

Gas chromatography indicated the presence of several unidentified sesquiterpenes in both species.

With the exception of *J. procera* Hochst., a native of Kenya, all the species of the genus *Juniperus* are found in the northern hemisphere. *J. procera* is widespread in the equatorial highlands of Africa and in Abyssinia, thus occurring on both sides of the equator.

In Kenya it grows in the drier forests at altitudes of 5 000 to 6 800 ft. It is a big tree attaining 80—100 ft in height and sometimes 35 ft in girth.[1]

In the present series of papers [2] the heartwoods of a number of northern hemispheric junipers have been investigated. It was therefore of interest to investigate the pattern of heartwood constituents of *J. procera* which has probably spread from the north across the equator.

Cedrol, cedrene and *l*-limonene have previously been reported to occur in this species [3].

J. californica Carr. is a much branched shrub or small tree growing chiefly on the coastal mountains of Central and Southern California [4].

Both species were worked up essentially in the same way. The wood was extracted with acetone and the light petroleum-soluble part of the acetone extract was separated into sodium bicarbonate-, sodium carbonate-, potassium hydroxide-soluble and neutral fractions.

* Part XXXIII. *Acta Chem. Scand.* **15** (1961) 645.

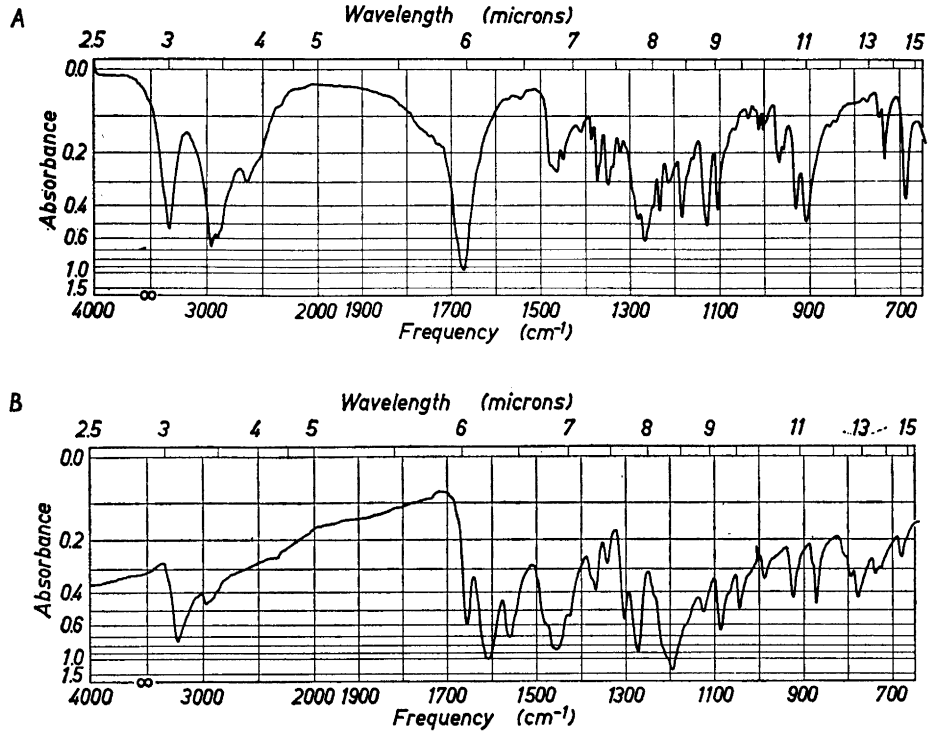

Fig. 1. Infrared spectra of hydroxy acid, m.p. 260—261° (A) and phenol, m.p. 149—151° (B) in potassium bromide.

J. procera. The wood used in this investigation was obtained from Kenya. The sodium bicarbonate-soluble material afforded a new sesquiterpene hydroxy acid, m.p. 260—261°, and a diterpene phenol, m.p. 149—151°. The infrared spectra of these compounds are shown in Fig. 1.

The sodium carbonate-soluble fractions of several junipers contain two sesquiterpene acids, hinokiic acid [5] and "Widdringtonia acid II" [6,2] (*cf.* below). The structure of the latter compound is still unknown. In the corresponding fraction from *J. procera* neither of these acids could be detected, but the fraction afforded a new C_{15}-tropolone which was named procerin. The elucidation of its structure has been described in a previous paper [7]. Chromatography of the rest of the sodium carbonate-soluble fraction gave three other compounds. These were isolated in such small amounts that analyses could not be obtained but spectroscopic evidence and paper chromatographic behaviour indicated that they were all new tropolones. According to infrared data two of the compounds contain an unsymmetrically substituted vinylidene group.

None of the tropolones common to other junipers investigated could be detected in *J. procera* by paper chromatography.

The tropolone fraction of *J. procera* thus differs remarkably from those of all other junipers investigated. The fungicidal properties of tropolones are well established [8] and most tropolone-producing conifers are known for the resistance of their heartwood to micro-organisms. The wood of *J. procera* is reported to be especially durable and to resist attack by insects [1]. This species, being adapted to the equatorial region, might well have developed a set of tropolones particularly effective against the attacks of micro-organisms and insects occurring in a tropical climate.

Further work on the tropolones of this species is in progress.

The neutral oil was distilled. Only traces of monoterpenes or compounds with similar boiling points could be detected in the lowest boiling material. The main constituent of the sesquiterpene hydrocarbon fraction was *α*-cedrene which was identified by conversion to *α*-cedrenic acid [9]. No thujopsene [5] could be detected. This was unexpected since all junipers examined in the present series of investigations [2] contained this compound. It is possible, however, that very small amounts of thujopsene occur in *J. procera*.

According to gas chromatography and infrared data the second largest component of the sesquiterpene hydrocarbon fraction could be identical with hydrocarbon X_2 from *J. thurifera* [10].

From the next higher boiling fraction a small amount of cuparene [11] was isolated.

The large crystalline sesquiterpene alcohol fraction that followed apparently consisted of cedrol only. The highest boiling neutral material remained liquid.

The neutral distillation residue yielded two crystalline compounds which were separated by sublimation.

These were *β*-sitosterol and a C_{30}-compound, the "triterpene diol", m.p. 243—244°, previously isolated from a similar fraction of *J. thurifera* [10].

According to its infrared spectrum, the remainder of the neutral distillation residue appeared to contain a complex mixture of alcohols and carbonyl compounds.

The compounds isolated are listed below with very approximate estimates of the amounts present (as percentages of the air-dried wood). Total acetone extract 9.4, ether-soluble acetone extract 2.9, light petroleum-soluble acetone extract 2.1, sodium bicarbonate-soluble 0.04, potassium hydroxide-soluble 0.5, neutral 1.6, sesquiterpene hydroxy acid 0.0004, diterpene phenol 0.0008, procerin 0.1, tropolone II 0.02, tropolone III 0.004, tropolone IV 0.0007, carvacrol 0.04, *α*-cedrene 0.5, cuparene 0.03, cedrol 0.5, *β*-sitosterol 0.001, "triterpene diol" 0.0007.

J. californica. The wood used in this investigation was collected in the Mohave Desert, California, USA.

The sodium carbonate-soluble fraction gave hinokiic acid [5] and "Widdringtonia acid II" [6]. Rather surprisingly, considering the close relationship of *J. californica* and *J. utahensis* [12,13], no known tropolones could be detected in the former species.

The neutral oil was distilled and the fractions analysed by infrared spectroscopy and gas chromatography. Thujopsene [5] was the major component of the sesquiterpene hydrocarbon fraction which also contained *α*-cedrene and cuparene [11] in addition to several unidentified compounds.

The crystalline sesquiterpene alcohol fraction that followed was separated into cedrol and widdrol [6] by chromatography.

The highest boiling fraction remained liquid, and from the distillation residue a small amount of a compound, m.p. 241—242°, was isolated. According to the infrared spectrum its carbon skeleton appeared to be very similar to that of the "triterpene diol", m.p. 243—244°, of *J. procera* and *J. thurifera* [10] (*cf.* above), but the hydroxyl absorbtion differed. The melting point of the former compound was depressed on admixture of the "triterpene diol".

The compounds isolated are listed below with very approximate estimates of the amounts present (as percentages of the air-dried wood). Total acetone extract 4.0, ether-soluble acetone extract 2.2, light petroleum-soluble acetone extract 1.3, sodium bicarbonate-soluble 0.05, potassium hydroxide-soluble 0.4, neutral 0.9, hinokiic acid 0.03, "Widdringtonia acid II" 0.02, α-cedrene 0.01, thujopsene 0.1, cuparene 0.004, cedrol 0.2 and widdrol 0.0006.

EXPERIMENTAL

Rotations were measured in chloroform unless otherwise specified; melting points, taken on a hot stage, and boiling points are uncorrected. Light petroleum refers to the fraction m.p. 40—60°.

Juniperus procera

The air-dried heartwood (24.4 kg) was extracted with acetone for 24 h and fractionated as described in a previous paper in this series [14]. Ether-insoluble acetone extract A (1 480 g), ether-soluble but light petroleum-insoluble acetone extract B (194 g), light petroleum- and sodium bicarbonate-soluble acetone extract C (9.8 g), light petroleum- and potassium hydroxide-soluble acetone extract D (117 g), light petroleum-soluble neutral acetone extract E (395 g).

Sodium bicarbonate-soluble fraction. The oil C was mixed with half its volume of light petroleum and on standing for several months deposited a small amount (324 mg) of crystalline material, which on fractional crystallisation from acetonitrile afforded a less soluble (101 mg) and a more soluble (210 mg) product. The less soluble material was recrystallised from acetonitrile and sublimed in a high vacuum to give a *hydroxy acid* (45 mg), m.p. 260—261°, $[\alpha]_D$ —30° (*c*, 1.9, pyridine). (Found: C 71.4; H 9.4; O 19.3; active H (Zerevitinoff) 0.81; CH_3—(C) 4.6. $C_{15}H_{24}O_3$ requires C 71.4; H 9.6; O 19.0; active H (two) 0.80; CH_3—(C) (one) 6.0.) The hydroxy acid did not exhibit any significant absorbtion in the 220—350 mμ range.

The more soluble material was recrystallised from ethanol (95 %) and sublimed in a high vacuum, giving pale greenish crystals of a *phenol* (120 mg), m.p. 149—151°, $[\alpha]_D$ +7° (*c*, 1.7). (Found: C 73.8; H 6.7; O 19.7; CH_3O—0.00; active H 0.69. $C_{20}H_{32}O_4$ requires C 73.6; H 6.8; O 19.6; active H (two) 0.62.) λ_{max} 230 mμ, log ε 4.37; λ_{max} 245 mμ, log ε 4.35; shoulder 265 mμ; λ_{max} 364 mμ, log ε 4.24; λ_{max} 398 mμ, log ε 4.26. The compound in methanol gave a greenish colour with methanolic ferric chloride.

Alkali-soluble fraction. The oil D was dissolved in ether and separated into a sodium carbonate-soluble fraction F (98.0 g) and a sodium carbonate-insoluble oil G (18.6 g). Fraction F partly crystallised on standing. This material was recrystallised from light petroleum and sublimed to give tropolone I (procerin [7], 8.6 g). On standing for several months fraction F yielded an additional amount (10.7 g) of crude procerin. The mother liquors from recrystallisation of procerin were evaporated and combined with the non-crystalline part of fraction F. A sample (1.85 g) of the combined material (H) was chromatographed on silica gel (120 g) impregnated with dimethyl sulphoxide (*cf.* Ref. [15]) using a mixture of light petroleum-dimethyl sulphoxide as eluent (light petroleum (1 part), light petroleum saturated with a solution of water (4 %) in dimethyl sulphoxide (4 parts)). The first 1 600 ml of solvent eluted procerin (410 mg), the next 500 ml eluted a crystalline

Table 1. Distillation of neutral fraction K. Total distillate 284 g or 86 %.

Fraction	Weight (g)	B.p./15 mm (°C)	Rotation ($[\alpha]_D$)	Refractive index (n_D^{25})
Ia	13.4	117–127	−51	1.4972
Ib	27.8	127–128	−75	1.4966
Ic	35.1	128	−74	1.4965
Id	27.4	128	−76	1.4967
Ie	21.1	128–135	−59	1.4981
If	22.2	135–158	5	—
Ig	53.8	158	12	—
Ih	57.4	158–159	8	—
Ii	25.9	159–166	−16	1.5186

substance (70 mg) which was repeatedly sublimed in a high vacuum to give tropolone II, (5 mg) m.p. 133–134°. λ_{max} 242 mμ, E 1 050 (for nomenclature *cf.* Ref. [16]); shoulder 290 mμ; shoulder 324 mμ; λ_{max} 334 mμ, E 305; λ_{max} 351 mμ, E 270; λ_{max} 367 mμ, E 370. Infrared spectrum (in KBr): 3 205 s, 1 645 m, 1 610 s, 1 554 s, 1 282 s, 1 217 s, 907 w, 888 cm^{-1} m. The next 500 ml of solvent eluted a bright yellow substance containing *tropolone III* (20 mg) which could not be obtained in a pure state, m.p. 119–127°. λ_{max} 228 mμ, E 880; λ_{max} 300 mμ, E 1 050; λ_{max} 313 mμ, E 1280; λ_{max} 327 mμ, E 790; λ_{max} 357 mμ, E 270; λ_{max} 370 mμ, E 340; λ_{max} 385 mμ, E 340; λ_{max} 410 mμ, E 220. Acetone-light petroleum (1:9) eluted *tropolone IV* (3 mg) which was sublimed in a high vacuum, m.p. 72–74°. λ_{max} 243; shoulder 334 mμ; λ_{max} 347 mμ; λ_{max} 369 mμ; shoulder 393 mμ. On paper chromatography [17] the following R_F values were obtained: procerin 0.72 (dark brown colour reaction with *bis*-diazotised benzidine), nootkatin 0.72, tropolone II 0.50 (brown), tropolone III 0.52 (brown, main spot) and 0.43 (violet, minor spot), tropolone IV 0.43 (light brown, weak colour), β-thujaplicin 0.39, γ-thujaplicin 0.30. In addition to these spots, the crude material H gave a fairly large spot with R_F 0.34 (orange red) and several minor spots with still lower R_F values.

The sodium carbonate-insoluble oil G had the characteristic smell of *carvacrol* and paper chromatography [17] indicated the presence of this compound (R_F 0.21).

Neutral fraction. By a fast preliminary distillation the neutral oil E was divided into fraction K, b.p. up to 140°/1 mm (330 g) and a residue L (61 g). The oil K was redistilled through a 1 m, vacuum-jacketed, packed column giving the fractions listed in Table 1.

Gas chromatographic analysis of the sesquiterpene hydrocarbon fractions. Gas chromatograms were run on a Pye Argon Chromatograph as described in a previous paper in this series [18] (temperature 150°, charge 0.025 μl).

In Table 2 the approximate areas of individual peaks of different retention times are given as percentages of total peak area.

Table 2. Gas chromatographic analysis of the sesquiterpene hydrocarbon fractions in Table. 1. Argon flow rate 20 ml/min.

Fraction	Retention time (min)								
	5.4	16.3	18.2	21.2	24.2	26.8	28.9	36.4	51.1
Ia	2	4	2	87	4			1	
Ib		2		91	7				
Ic				93	7				
Id				90	10				
Ie				78	16	3	3		
If (liquid part)									30

With the same argon flow rate the retention times of the following known compounds were: *α*-cedrene 21.2, thujopsene [5] 23.4 and cuparene [11] 51.1 min.

Identification of α-cedrene. Fraction Ie (6.0 g) was dissolved in ethanol (95 %, 80 ml), selenium dioxide (3.6 g) was added and the mixture was refluxed for 3 h. After filtering, the solution was evaporated and the oil obtained was distilled in a high vacuum giving a pale greenish distillate (4.6 g). This (2.0 g) was added to a solution of silver nitrate (3.1 g) in water-dioxane (1:6). A solution of sodium hydroxide (1.1 g) in water-dioxane (1:1) was added dropwise with stirring and the reaction mixture was then stirred for 1 h at room temperature followed by 21 h under reflux. After acidification (H_2SO_4, 2 N), water (500 ml) was added and the solution was extracted with ether. The ether solution was extracted with sodium carbonate (2 N), the alkaline solution was acidified and extracted with ether. The ether extract on evaporation gave a crystalline residue (1.5 g).

This residue (1.5 g) was chromatographed on silica gel impregnated with dimethyl sulphoxide [15]. *Iso*propyl ether-light petroleum (1:2) eluted a compound (1.1 g) which was repeatedly sublimed in a high vacuum, m.p. 124—125°, $[\alpha]_D$ −68° (*c*, 2.1), identified as *α*-cedrenic acid [9] (mixed m.p., I.R.). No other identifiable compound could be eluted and the rest of the chromatographed sample was a noncrystallisable gum.

Cuparene. The crystalline part of fraction If (Table 1) was filtered off and the filtrate (4.9 g) ozonised and treated as described in a previous paper [18]. The material unaffected by ozone (0.23 g), b.p. 119°/10 mm, $[\alpha]_D$ +59° (*c*, 2.5), n_D^{25} 1.5112 was identified as cuparene [10] by comparing its infrared spectrum and gas chromatographic data (see above) with those of an authentic sample.

Cedrol. The crystalline fraction Ih (Table 1, 2.0 g) was chromatographed on basic alumina (80 g). Ether-benzene (1:99) eluted a compound (1.9 g) which was recrystallised from ethanol (95 %), m.p. 85.5—86.0°, $[\alpha]_D$ +10° (*c*, 3.0) and identified as cedrol (mixed m.p., I.R.). The column was eluted with ether-benzene mixtures containing an increasing amount of the former solvent, and finally with methanol, but no further compounds were obtained.

β-Sitosterol. On standing for about 8 months the neutral distillation residue L deposited a small amount of crystals. These were washed with benzene and the remaining material (0.19 g) was separated into two compounds by repeated sublimation in a high vacuum along a temperature gradient. One of these (60 mg) was purified by further sublimation, m.p. 135—136°, and identified (mixed m.p., I.R.) as *β*-sitosterol.

C_{30}-compound. The other compound (40 mg) was recrystallised from benzene and sublimed in a high vacuum, m.p. 243—244°. It was identified (mixed m.p., I.R.) with "compound III" previously isolated from a similar fraction obtained from the heartwood of *Juniperus thurifera* [10].

Juniperus californica

The air-dried heartwood (4.78 kg) was extracted with acetone for 24 h and fractionated as previously described [14]. Ether-insoluble acetone extract A (88 g), ether-soluble but light petroleum-insoluble acetone extract B (42 g), light petroleum- and sodium bicarbonate-soluble acetone extract C (2.3 g), light petroleum- and potassium hydroxide-soluble acetone extract D (19.1 g), light petroleum-soluble neutral acetone extract E (41.1 g).

Alkali-soluble fraction. The potassium hydroxide-soluble oil D was dissolved in ether and extracted with sodium carbonate (2 N). The ether solution was washed with water, dried and evaporated to yield an oil F (4.6 g). On acidification and extraction with ether the sodium carbonate solution gave an oil G (14.0 g) which partly crystallised on standing. The crystals (1.27 g) were separated by filtration (mother liquor, H) and chromatographed on dried silica gel (15 g). The first 200 ml of light petroleum eluted oily material (28 mg), the next 200 ml eluted a compound (580 mg) which was repeatedly sublimed in a high vacuum, m.p. 164—166°, and identified (mixed m.p., I.R.) as *hinokiic acid* [5]. Ether-light petroleum (1:25) eluted another compound (450 mg) which was recrystallised from ethanol-water, sublimed in a high vacuum, m.p. 190—192°, and identified as the "*acid II*" isolated from *Widdringtonia* species [6]. When the column was stripped with methanol a small amount of an oil was obtained which was not further investigated.

Table 3. Distillation of neutral fraction K. Total distillate 20.2 g or 72 %.

Fraction	Weight (g)	B.p./15 mm (°C)	Rotation ($[\alpha]_D$)	Refractive index n_D^{25}
IIIa	1.59	115–126	−72	1.4988
IIIb	1.98	126–127	−90	1.5019
IIIc	1.83	127–128	−71	1.5047
IIId	3.28	128–147	7	1.5079
IIIe	2.02	147–159	10	—
IIIf	3.57	159	11	—
IIIg	2.35	159	15	—
IIIh	1.71	159–163	8	—
IIIi	1.85	163–166	7	1.5118

The oils F and H were analysed by paper chromatography [17] but no known tropolones were detected. The oil F gave a distinct spot with approximately the same R_F value as β-thujaplicin (0.39) but with a different colour reaction (bright red). Another major component of the oil gave a spot with an R_F value (0.24) slightly larger than that of carvacrol (0.21) and a similar colour reaction (orange red) but no carvacrol could be detected.

Neutral fraction. By a fast preliminary distillation the neutral oil E was divided into fraction K, b.p. up to 150°/1.3 mm (27.9 g) and a residue L (13.0 g). The oil K was redistilled through a 1 m spinning band column giving the fractions listed in Table 3.

Gas chromatographic analysis of the sesquiterpene hydrocarbon fractions. Gas chromatograms were run as described in a previous paper in this series [18] (temperature 150°, charge 0.025 μl).

In Table 4 the approximate areas of individual peaks of different retention times are given as percentages of total peak area.

With the same argon flow rate the retention times of the following known compounds were: *α-cedrene* 13.2, *thujopsene* [5] 14.3 and *cuparene* [11] 29.7 min. The presence of the above compounds in this species was confirmed by the infrared and ultraviolet spectra of the distillation fractions in Table 3.

Sesquiterpene alcohols. A sample of the crystalline fraction IIIg (1.0 g) was chromatographed on basic alumina (50 g). Ether-benzene (1:99) eluted a compound (970 mg) which was recrystallised from ethanol (95 %), sublimed in a high vacuum, m.p. 85–86°, and identified (mixed m.p. IR) as *cedrol*. Ether eluted another crystalline compound (3 mg) which was recrystallised from acetonitrile and sublimed, m.p. 92.5–94.5°, undepressed by an authentic sample of *widdrol* [6].

On standing for several months the neutral distillation residue L deposited a small amount of crystals (30 mg). This was recrystallised from benzene and sublimed in a high vacuum, m.p. 241–242°. Infrared spectrum (in KBr): 3 620 w, 3 500 m, 3 295 s, 1 275 m, 1 256 w, 1 236 w, 1 211 cm^{-1} w.

Table 4. Gas chromatographic analysis of the sesquiterpene hydrocarbon fractions in Table 3. Argon flow rate 34 ml/min.

Fraction	Retention time (min)									
	10.5	11.1	13.2	14.3	17.9	20.1	22.3	25.1	29.7	34.1
IIIa	1	4	13	82						
IIIb			9	91						
IIIc			4	83	2	2	6		3	
IIId			2	32	4	11	23	5	17	6

Acknowledgements. Our thanks are due to Professor H. Erdtman for his interest in this work, to the Tropical Products Institute, London, for generous gifts of wood of *J. procera*, to Docent O. Theander, Stockholm, for collecting the wood sample of *J. californica* used in this investigation, to Miss G. Hammarberg for infrared and ultraviolet spectra and to the *Swedish Natural Science Research Council* for financial support.

REFERENCES

1. Dallimore, W. and Jackson, A. B. *A Handbook of Coniferae including Ginkgoaceae.* Edward Arnold & Co, London 1948, p. 319.
2. Runeberg, J. *Acta Chem, Scand.* **14** (1960) 1995 and earlier publications.
3. Dumont, H. M. *Soap, Perfumery & Cosmetics* **13** (1940) 127; *Chem. Zentr.* **1940 I** 3717.
4. Ref. [1], p. 295.
5. Erdtman, H. and Norin, T. *Chem. & Ind. London* **1960** 622.
6. Erdtman, H. and Thomas, B.R. *Acta Chem. Scand.* **12** (1958) 267.
7. Runeberg, J. *Acta Chem. Scand.* **15** (1961) 645.
8. Erdtman, H. in Cohn (Ed.) *Progr. in Org. Chem.* **1** (1952) 47.
9. Treibs, W. *Ber.* **70** (1937) 2066.
10. Runeberg, J. *Acta Chem. Scand.* **14** (1960) 1985.
11. Enzell, C. and Erdtman, H. *Tetrahedron* **1958** 361.
12. Runeberg, J. *Acta Chem. Scand.* **14** (1960) 797.
13. Ref. [1], p. 330.
14. Runeberg, J. *Acta Chem. Scand.* **14** (1960) 1987.
15. Lindberg, B. and Wickberg, B. *Arkiv Kemi* **13** (1959) 447.
16. Gillam, A. E. and Stern, E. S. *An Introduction to Electronic Absorbtion Spectroscopy in Organic Chemistry*, Edward Arnold Ltd, London 1957, p. 7.
17. Wachtmeister, C. A. and Wickberg, B. *Acta Chem. Scand.* **12** (1958) 1335.
18. Runeberg, J. *Acta Chem. Scand.* **14** (1960) 803.

Received December 2, 1960.

ACTA CHEMICA SCANDINAVICA 15 (1961) 721–726

The Chemistry of the Natural Order Cupressales

XXXV *. Heartwood Constituents of *Juniperus foetidissima* Willd.

JARL RUNEBERG

Organisk-kemiska Institutionen, Kungl. Tekniska Högskolan, Stockholm, Sweden

The heartwood of *Juniperus foetidissima* contains two new sesquiterpene hydroxy acids, α-cedrene, calamenene, a new sesquiterpene oxide and the alcohols cedrol and widdrol. Positive evidence was obtained for the presence of δ-cadinene and an *iso*cadinene in addition to several unidentified sesquiterpene hydrocarbons.

In continuation of previous work on the constituents of the genus *Juniperus* [1], the heartwood of *J. foetidissima* Willd.[2] has been investigated. This species is a tree or shrub 10—12 ft high native to Greece and Asia Minor. The wood used in this investigation had been cut at an altitude of 5 000 ft in the Troodos Forest on the Island of Cyprus.

The heartwood was extracted with acetone and the light petroleum-soluble part of this acetone extract was separated into sodium bicarbonate-, sodium carbonate-, potassium hydroxide-soluble and neutral fractions.

The sodium bicarbonate-soluble material gave two new sesquiterpene hydroxy acids which were separated by chromatography. According to its ultraviolet absorption, hydroxy acid I, m.p. 166—168°, appeared to be an α,β-γ,δ-unsaturated acid or the cross-conjugated analogue. Hydroxy acid II, m.p. 152—153° is aromatic with the carboxyl group attached to a benzene ring. The infrared spectra of the two acids are shown in Fig. 1.

Hydroxy acid II was esterified with diazomethane and reduced to a diol which was dehydrogenated with selenium. The main product, according to its infrared spectrum, appeared to be an oxo-compound. Only traces of a compound giving a picrate were obtained.

Most junipers described in this series of investigations have contained carvacrol and tropolones [1] (*cf.* also Ref.[3]). Neither of these compounds could be detected in this species.

The neutral oil was distilled and the fractions analysed by gas chromatography. The first constant boiling fraction consisted mainly of α-cedrene which was identified as α-cedrenic acid [4].

---

* Part XXXIV. *Acta Chem. Scand.* **15** (1961) 713.

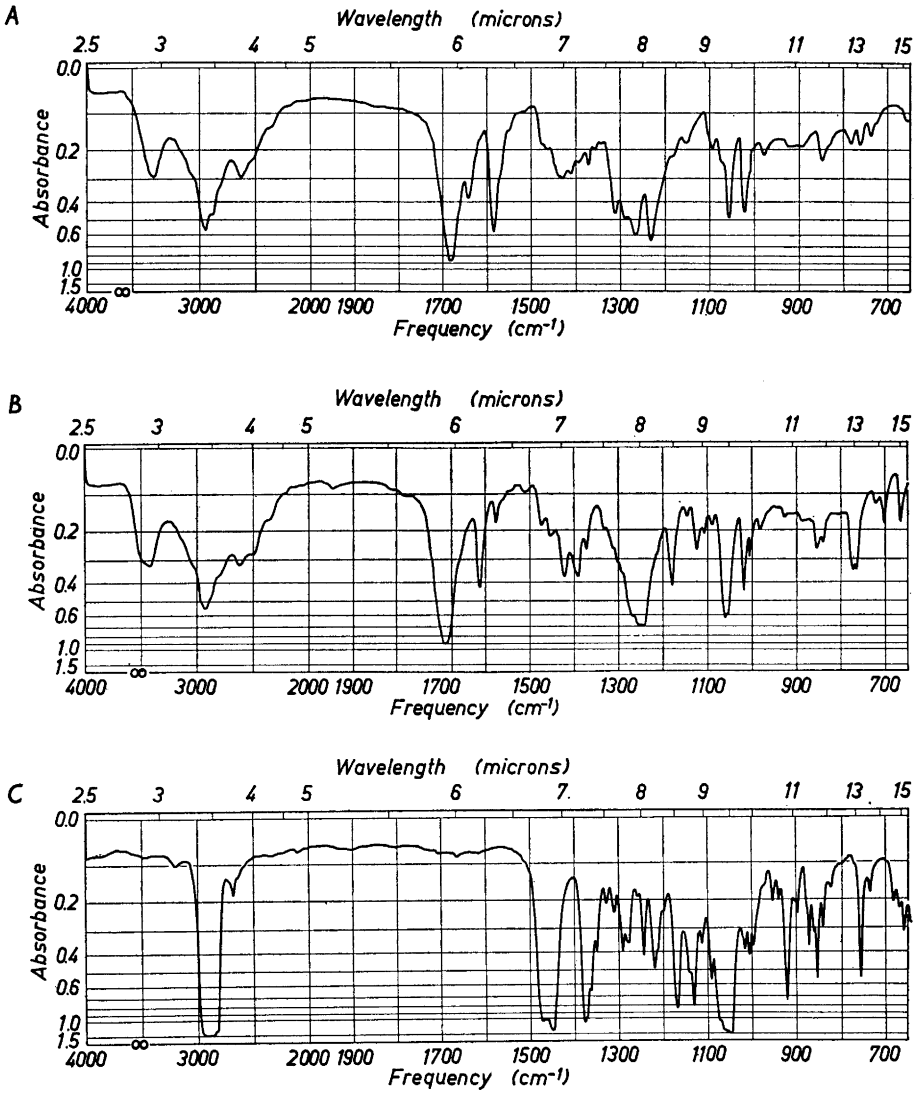

Fig. 1. Infrared spectra of hydroxy acid I, m.p. 166–168° (A), hydroxy acid II, m.p. 152–153° (B) (in KBr) and oxide, b.p. 131°/12 mm (C) (oil).

The slightly higher boiling material that followed gave a low yield of an adduct with maleic anhydride. On chromatography it was separated into three main fractions. The first, on selenium dehydrogenation, gave a good yield of cadalene. The infrared spectrum of this fraction was very similar to that of δ-cadinene [5] but the ultraviolet spectrum (λ_{max} 247 mμ) indicated the

presence of yet another compound. δ-Cadinene, isolated from three different sources was shown by Šorm and co-workers to contain an unknown *iso*cadinene with two conjugated double bonds [6]. The position of the ultraviolet absorption maximum due to this *iso*cadinene (λ_{max} 246 mμ) agrees well with that of the chromatographic fraction above. This therefore seems to consist of a mixture of δ-cadinene and an *iso*cadinene with conjugated double bonds.

The mixture was easily autoxidised and the infrared spectrum of even freshly isolated fractions showed some hydroxyl-absorption. This increased rapidly with time and in a few days the material, although stored in a sealed tube under nitrogen, became a viscous oil.

The next fraction eluted was identified as calamenene [5,7] by its infrared spectrum and physical constants. On selenium dehydrogenation it gave a good yield of cadalene.

The third fraction afforded an oil, b.p. 131°/12 mm, $[\alpha]_D$ −69°. According to elemental analysis, infrared absorption (strong triplet at 1 045—1 075 cm^{-1}, *cf.* Fig. 1.) and chromatographic behaviour, it appears to be a new sesquiterpene oxide.

Thujopsene, a constituent of most of the junipers investigated in this series [1], could not be detected. Small amounts of thujopsene may, however, occur in this species.

Previous papers in this series describe the heartwood constituents of junipers belonging to the section *Sabina* [1]. Several of the fractions containing sesquiterpene alcohols obtained from other members of this section, crystallised immediately. The corresponding fractions from *J. foetidissima* were oils with comparatively low viscosities and none of them crystallised on standing for a year. One of these sesquiterpene alcohol fractions on chromatography gave crystalline cedrol and widdrol [8].

According to its infrared spectrum, a fraction boiling slightly higher than the sesquiterpene alcohols appeared to contain an α,β-unsaturated oxo-compound.

The distillation residue appeared to contain rather large quantities of a lactone, but this material has not yet been investigated.

The compounds isolated are given below with very approximate estimates of the amounts present (as percentages of the air-dried wood). Total acetone extract 9.9, ether-soluble acetone extract 8.2, light petroleum-soluble acetone extract 6.0, sodium bicarbonate soluble 0.1, potassium hydroxide soluble 1.2, neutral 4.7, hydroxy acid I 0.002, hydroxy acid II 0.008, α-cedrene 0.7, δ-cadinene-*iso*cadinene mixture 0.2, calamenene 0.07, sesquiterpene oxide 0.6, cedrol 0.1 and widdrol 0.06.

EXPERIMENTAL

Rotations were measured in chloroform unless otherwise specified; melting points, taken on a hot stage, and boiling points are uncorrected. Light petroleum refers to the fraction b.p. 40—60°.

The air-dried heartwood (10.9 kg) was extracted with acetone for 40 h and fractionated as described in a previous paper in this series [9]. Ether-insoluble acetone extract A (182 g), ether-soluble but light petroleum-insoluble acetone extract B (238 g), light petroleum- and sodium bicarbonate-soluble acetone extract C (11.8 g), light petroleum- and potas-

sium hydroxide-soluble acetone extract D (126 g), neutral light petroleum-soluble acetone extract E (516 g).

Sodium bicarbonate-soluble fraction. The oil C was mixed with half its volume of light petroleum and after several months deposited crystals (1.3 g) which were chromatographed on silicagel (130 g) impregnated with dimethyl sulphoxide [10]. *Iso*propyl ether eluted *hydroxy acid I* (180 mg), recrystallised from ether-light petroleum and sublimed in a high vacuum, m.p. 166–168°, $[\alpha]_D$ + 26° (*c*, 2.2, ethanol (95 %)). (Found: C 72.2; H 9.1. $C_{15}H_{22}O_3$ requires C 72.0; H 8.9.) λ_{max} 298 mμ, log ε 4.1. Acetone eluted *hydroxy acid II* (820 mg), recrystallised from ether-light petroleum and sublimed, m.p. 152–153°, $[\alpha]_D$ + 14° (*c*, 1.7, ethanol (95 %)). (Found: C 72.3; H 8.1; O 19.5. $C_{15}H_{20}O_3$ requires C 72.6; H 8.1; O 19.3.) λ_{max} 237 mμ, log ε 4.2; shoulder 269 mμ; λ_{max} 279 mμ, log ε 2.8.

Selenium dehydrogenation. The methyl ester of hydroxy acid II (m.p. 67–68°) was prepared with diazomethane and reduced with lithium aluminium hydride to a diol (m.p. 156–157°). This was dehydrogenated with twice the amount of selenium at 280° for 36 h and the product was chromatographed on basic alumina. Light petroleum eluted only traces of a compound which gave an orange-red picrate. Ether eluted the main reaction product, λ_{max} 263 mμ, *E* 500; shoulder 280 mμ. Infrared spectrum (in KBr): 1 713 cm^{-1}s.

Alkali soluble fraction. The oil D was dissolved in ether and separated into a sodium carbonate-soluble oil F (85 g) and sodium carbonate-insoluble material G (40 g). The oil F gave no crystalline material on standing for a year. The oil G was dissolved in ligroin (100–125°) and shaken with a saturated solution of cupric acetate. The very small amount of copper salts formed was separated by filtration, washed with ligroin and water and decomposed with sulphuric acid (2 N). The acidic solution was extracted with ether and the ether solution was washed with water, dried and evaporated to give a reddish-brown oil (H, 16 mg). The ligroin filtrate was separated, washed with water, dried and evaporated to an oil (K).

The oils F, H and K were analysed by paper chromatography [11] but neither tropolones nor carvacrol could be detected in any of them.

Neutral fraction. By a fast preliminary distillation the neutral oil E was divided into a fraction L (297 g), b.p. up to 135°/1 mm, and a residue M. The oil L was redistilled through a 1 m, vacuum jacketed packed column giving the fractions listed in Table 1.

Table 1. Distillation of neutral fraction L. Total distillate 267 g or 90 %.

Fraction	Weight (g)	B.p./15 mm Hg (°C)	Rotation $[\alpha]_D$	Refractive index n_D^{25}
Ia	4.7	115–124	−29	1.4949
Ib	23.4	124–126	−64	1.4968
Ic	23.5	126	−78	1.4970
Id	18.7	126–127	−74	1.4970
Ie	23.3	127–139	−46	1.5019
If	19.2	139–142	−29	1.5094
Ig	24.6	142	−56	1.5089
Ih	24.6	142	−62	1.5061
Ik	23.5	142–145	−51	1.5047
Il	15.1	145–153	−42	1.5071
Im	13.7	153–155	0	1.5120
In	17.9	155–160	+11	1.5125
Io	19.1	160–166	−12	1.5155
Ip	15.9	166	−23	1.5155

Gas chromatographic examination of the sesquiterpene hydrocarbon fractions. Gas chromatograms were run on a Pye Argon Chromatograph as described in a previous paper [12].

In Table 2 the approximate areas of individual peaks of different retention times are given as percentages of total peak area.

Table 2. Gas chromatographic analysis of the sesquiterpene hydrocarbon fractions in Table 1. Argon flow rate 30 ml/min.

Fraction	Peak retention time (min)													
	4.3	7.7	10.7	11.6	14.1	15.9	20.4	23.8	27.3	33.9	36.4	41.2	45.4	52.7
Ia	1	9	31	4	52	3								
Ib		1	14		74	11								
Ic			3		81	16								
Id					78	22								
Ie					75	25								
If							10	54	2	1	8			25
Ig							4	30		2	10	2	2	50
Ih								20			9	2	2	67
Ik								4			4	4	3	85
Il											4	3	4	89

With the same flow rate the retention times of the following known compounds were: *a*-cedrene 14.1, *δ*-cadinene-*iso*cadinene mixture [6] (see below) 23.8, calamenene [7] 36.4, sesquiterpene oxide 52.7.

Identification of a-cedrene. Fraction Id (3.0 g) was oxidised with selenium dioxide (1.8 g) as described in a previous paper [14]. The crude aldehyde (2.52) was further oxidised with silver oxide (3.91 g silver nitrate, 1.84 g sodium hydroxide) to give acidic material (1.72 g). This was chromatographed on silica gel (50 g) impregnated with dimethyl sulphoxide [10]. *Iso*propyl ether-light petroleum (1:2) eluted *a-cedrenic acid* [4] (1.37 g) which was repeatedly sublimed in a high vacuum, m.p. 123.0—124.5° (identification by mixed m.p. and IR). The column was stripped with methanol but no other identifiable compound was obtained.

Maleic anhydride adduct. Fraction Ih (50 mg) in absolute benzene (5 ml) was treated with maleic anhydride (24 mg) giving an intensely yellow solution. This was refluxed for 3 h, the product was then precipitated by addition of light petroleum and recrystallised from benzene, m.p. 147—148° (13 mg).

Chromatography of the cadinene fraction. Fraction Ih (6.0 g) was chromatographed on basic alumina (600 g) which had been dried overnight at 150°. The first 460 ml of light petroleum eluted a *δ*-cadinene-*iso*cadinene [6] mixture (910 mg) which was distilled, n_D^{25} 1.5163, $[a]_D$ −80° (*c*, 2.2), λ_{max} 247 mμ, *ε* 3.9. On dehydrogenation with an equal amount of selenium in an atmosphere of nitrogen at 270° for 24 h, a 60 % yield of cadalene (isolated as the picrate) was obtained.

The next 280 ml of light petroleum eluted calamenene [7] (503 mg), which was distilled, n_D^{25} 1.5119, $[a]_D$ −46° (*c*, 1.7); λ_{max} 265 mμ, log *ε* 2.70; λ_{max} 269 mμ, log *ε* 2.75; λ_{max} 273 mμ, log *ε* 2.70; λ_{max} 278 mμ, log *ε* 2.72. Selenium dehydrogenation of this compound under the same conditions as above afforded a 76 % yield of cadalene.

Ether-light petroleum (1:1) eluted an *oxide* (3.73 g) which was distilled. The main fraction, b.p. 131°/12 mm, n_D^{25} 1.4967, $[a]_D$ −69° (*c*, 1.5) did not absorb above 220 mμ. (Found: C 81.6; H 10.9; CH_3O— 0.00; CH_3—(C) 5.6. $C_{15}H_{24}O$ requires C 81.8; H 11.0; CH_3—(C) (one) 6.8.) On attempted selenium dehydrogenation 85 % of the starting material was recovered unchanged.

Sesquiterpene alcohols. Fraction Im (2.0 g) was chromatographed on basic alumina (150 g). Benzene (750 ml) eluted an oil (150 mg) which was discarded. Ether-benzene (1:20, 750 ml) eluted *cedrol* (700 mg), recrystallised from ethanol (95 %), m.p. 85—86°. Ether-benzene (1:1) eluted *widdrol* [8] (340 mg) recrystallised from acetonitrile and sublimed in a high vacuum, m.p. 95—96° (identified by mixed m.p. and IR). Further elution with ether and with methanol gave oily fractions which have not been investigated.

Acknowledgements. The author is indebted to Professor H. Erdtman for his interest in this work, to the Tropical Products Institute, London, for kind assistance in obtaining a sample of *J. foetidissima*, to Miss G. Hammarberg for infrared and ultraviolet spectra and to the *Swedish Natural Science Research Council* for financial support.

REFERENCES

1. Pettersson, E. and Runeberg, J. *Acta Chem. Scand.* **15** (1961) 713 and previous publications.
2. Dallimore, W. and Jackson, A. B. *A Handbook of Coniferae including Ginkgoaceae.* Edward Arnold & Co, London 1948, p. 309.
3. Zavarin, E. and Anderson, A. B. *J. Org. Chem.* **21** (1956) 332; Zavarin, E., Smith, R. M. and Anderson, A. B. *J. Org. Chem.* **24** (1959) 1318.
4. Treibs, W. *Ber.* **70** (1937) 2066.
5. Šorm, F., Holub, M., Sýkora, V., Mleziva, J., Streibl, M., Plíva, J., Schneider, B. and Herout, V. *Collection Czechoslov. Chem. Communs.* **18** (1953) 514.
6. Ref.[5], p. 517.
7. Vonášek, F., Herout, V. and Šorm, F. *Collection Czechoslov. Chem. Communs.* **25** (1960) 919.
8. Erdtman, H. and Thomas, B. R. *Acta Chem. Scand.* **12** (1958) 267.
9. Runeberg, J. *Acta Chem. Scand.* **14** (1960) 1987.
10. Lindberg, B. and Wickberg, B. *Arkiv Kemi* **13** (1959) 447.
11. Wachtmeister, C. A. and Wickberg, B. *Acta Chem. Scand.* **12** (1958) 1335.
12. Runeberg, J. *Acta Chem. Scand.* **14** (1960) 803.
13. Runeberg, J. *Acta Chem. Scand.* **14** (1960) 1292.
14. Ref.[9], p. 1988.

Received December 6, 1960.

ACTA CHEMICA SCANDINAVICA 15 (1961) 727–734

Studies on the Hydrolysis of Metal Ions

Part 36. An Estimate of the Formation Constants of $CaOH^+$, $SrOH^+$ and $BaOH^+$ in 3 M $NaClO_4$

BIRGITTA CARELL and ÅKE OLIN

Department of Inorganic Chemistry, the Royal Institute of Technology, Stockholm 70, Sweden

The formation constants of $CaOH^+$, $SrOH^+$ and $BaOH^+$ have been estimated from measurements, at 25°C, of the emf, E, of the cells

$$Pt/H_2, B\ M\ B^{2+}, (3-2B)\ M\ Na^+, A\ M\ OH^-, (3-A)\ M\ ClO_4^-/Ref \quad (I)$$

$$Ag,AgCl(AgBr)/B\ M\ B^{2+}, (3-2B)\ M\ Na^+, X\ M\ Cl^-(Br^-), (3-X)\ M\ ClO_4^-/Ref \quad (II)$$

where B^{2+} stands for Ca^{2+}, Sr^{2+} or Ba^{2+} and the reference half-cell (Ref) was

$$/3\ M\ NaClO_4/2.99\ M\ Na^+, 0.01\ M\ Ag^+, 3\ M\ ClO_4^-/Ag, AgCl. \quad (III)$$

From the measured values of E, $[OH^-]$ was calculated using the relationship $E = E^\circ + 59.15\log[OH^-] - 9.3B - 8[OH^-]$.

The following formation constants were obtained.

$$Ca^{2+} + OH^- \rightleftharpoons CaOH^+ \qquad \log K_1 = 0.642 \pm 0.015$$
$$Sr^{2+} + OH^- \rightleftharpoons SrOH^+ \qquad \log K_1 = 0.225 \pm 0.015$$
$$Ba^{2+} + OH^- \rightleftharpoons BaOH^+ \qquad \log K_1 = 0.004 \pm 0.015$$

The determination of the equilibrium constants (K_1) for the association between the alkaline earth metal ions and OH^- has been the subject of a great number of investigations [1]. Since these constants are small the numerical values obtained are very sensitive to the assumptions made in deriving them. The difficulties met with when results from emf measurements are to be interpreted, are illustrated by the work of Bates, Bower, Canham and Prue [2]. From measurements with the cell Pt/H_2, $Ca(OH)_2$, KCl or $CaCl_2/AgCl$, Ag they found K_1 to be strongly dependent on the value chosen for f_{Cl^-}/f_{OH^-} and used in calculating $[OH^-]$.

SYMBOLS

A total concentration of OH^-
a $[OH^-]$, concentration of free OH^-

B total concentration of B^{2+}
b concentration of free B^{2+}
B^{2+} used to denote Ca^{2+}, Sr^{2+} or Ba^{2+}
K_1 equilibrium constant of the reaction $B^{2+} + OH^- \rightleftharpoons BOH^+$
$y(x)_v$ y as a function of x at constant v

All concentrations are expressed in M (moles/l) and equilibrium constants are given on the M scale.

EXPERIMENTAL

$HClO_4$, NaOH and $NaClO_4$ were prepared and analysed by the methods described in Refs. [3,4]

$Ca(ClO_4)_2$, $Sr(ClO_4)_2$ and $Ba(ClO_4)_2$ were prepared from the carbonates by the method described by Biedermann [5] for $NaClO_4$. The product was twice recrystallized from water and analysed by adding H_2SO_4, fuming off the $HClO_4$, and weighing as the sulphate.

Silver chloride and bromide electrodes were prepared according to Brown [6].

Hydrogen electrodes were prepared according to Bates [7].

ACTIVITY FACTOR OF OH^-, Cl^-, Br^-

In 1953 Biedermann and Sillén [8] published measurements on the cells

Ref/B M Me^{z+}, H M H^+, (3-H-zB) M Na^+, 3 M ClO_4^-/electrode reversible to Me^{z+}

Ref/H M H^+, (3—H) M Na^+, X M $Cl^-(Br^-)$, (3—X) M ClO_4^-/AgCl(AgBr), Ag

Their main conclusion was that as long as the anionic composition of the solution is kept constant, the activity factor of the cation is practically constant when its concentration is low compared to that of the added inert salt ($NaClO_4$).

The results from the second cell showed that when Na^+ was exchanged for H^+, log f_{Cl^-} or log f_{Br^-} varied linearly with $[H^+]$. Apparently a change in the composition of the counterions leads to changes in the activity factors. However, the interesting fact appears that the ratio $f_{Cl^-}/f_{Br^-} \simeq 1$, which suggests that in 3 M $NaClO_4$ it is a good approximation to set $f_{OH^-}/f_{Cl^-} = 1$.

In order to test this, measurements were made on the cell

$$\text{Ag, AgCl(AgBr)/3 M } Na^+, X \text{ M } Cl^-(Br^-), (3\text{-}X) \text{ M } ClO_4^-/\text{Ref} \qquad \text{(IV)}$$

$$E = E^\circ_{IV} + 59.15\log[X] + 59.15\log f_X + E_j \qquad (1)$$

where Ref = /3 M $NaClO_4$/ 2.99 M Na^+, 0.01 M Ag^+, 3 M ClO_4^-/Ag, AgCl (III) and on the cell

$$Pt/H_2, A \text{ M } OH^-, X \text{ M } Cl^-, (3-A-X) \text{ M } ClO_4^-, 3 \text{ M } Na^+/Ag, AgCl \qquad \text{(V)}$$

$$E = E^\circ_V + 59.15\log A/[X] + 59.15\log f_{OH^-}/f_{Cl^-} \qquad (2)$$

From these measurements, quantities E' were calculated, where for cell (IV)

$$E'_{IV} = E - 59.15\log[X] = E^\circ_{IV} + 59.15\log f_X + E_j \qquad (3)$$

and for cell (V)

$$E'_V = E - 59.15 \log A/[X] = E^\circ_V + 59.15\log f_{OH^-}/f_{Cl^-} \quad (4)$$

In the concentration range studied $0.005 < [X]$, $A < 0.025$ M, these quantities came out as constants. The simplest form of expression of these results is that, in 3 M $NaClO_4$, $f_{Cl^-} = f_{Br^-} = f_{OH^-} = 1$, and that E_j in cell (IV) is negligible.

Since a titration technique was used, cells involving liquid junctions were employed. They were

$$Pt/H_2, B\,M\,B^{2+}, (3-2B)\,M\,Na^+, A\,M\,OH^-, (3-A)\,M\,ClO_4^-/Ref \quad (I)$$

$$E = E^\circ_I + 59.15\log a + 59.15\log f_{OH^-} + E_j \quad (5)$$

$$Ag, AgCl(AgBr)/B\,M\,B^{2+}, (3-2B)\,M\,Na^+, X\,M\,Cl^-(Br^-), (3-X)\,M\,ClO_4^-/Ref \quad (II)$$

$$E = E^\circ_{II} + 59.15\log[X] + 59.15\log f_X + E_{jB} \quad (6)$$

and Ref = half-cell (III)

The important step in the evaluation of the formation constants (K_1) is the calculation of a from the emf of cell (I). To do this we shall make use of the following assumptions.

1. The liquid junction potential in cell (I), E_j, consists of two terms E_{jA} and E_{jB}.

$$E_j = E_{jA} + E_{jB} \quad (7)$$

E_{jB} is the liquid junction potential arising from the exchange of Na^+ for B^{2+}, and it is assumed to have the same value as in cell (II). E_{jA} is the liquid junction potential arising from the exchange of ClO_4^- for OH^- at constant B. It is assumed to have the value $E_{jA} = -8a$, which is the value in 3 M $NaClO_4$[9].

2. f_{OH^-} equals f_X. On this assumption we obtain from cell (II) ($59.15 \log f_{OH^-} + E_{jB}$) as a function of B.

Once numerical values for ($59.15\log f_{OH^-} + E_{jB}$) have been obtained, a can be calculated from eqn. (5).

B-DEPENDENT TERMS

Measurements on cell (II) were made with [X] ranging from 0.01 M to 0.025 M and B from 0 to 0.2 M. The results were plotted as

$$E - 59.15\log[X]\ (= E^\circ_{II} + 59.15\log f_X + E_{jB}) \quad (8)$$

as a function of B. In all cases, straight lines were obtained. The slopes of these lines, surprisingly enough, were the same ($= -9.3 \pm 0.3$ mV/M) for all the B—X pairs studied, *viz.* Ba—Cl, Ba—Br, Ca—Cl, Ca—Br and Sr—Cl.

The plot of (8) *versus* B reflects the variation of f_X with B. We shall assume then, that the same result would have been obtained for the hydroxides, had these been completely dissociated. On this assumption we have

$$59.15\log f_{OH^-} + E_{jB} = -(9.3 \pm 0.3)B \quad (9)$$

CHOICE OF A AND B RANGE

The values of the concentration of B^{2+} and OH^- used in cell (I) were chosen from the following reasons. If we assume that BOH^+ is the only complex formed (which leads to no contradiction of the data), then

$$A = a + [BOH^+] \tag{10}$$

$$B = b + [BOH^+] \tag{11}$$

$$K_1 = [BOH^+]\, f_{BOH^+}/abf_{OH^-}f_{B^{2+}} = [BOH^+]/abf \tag{12}$$

$$f = f_{B^{2+}}\, f_{OH^-}/f_{BOH^+} \tag{13}$$

which together with eqn. (5) give

$$E = E_I^\circ + 59.15\log A - 59.15\log(1 + K_1 fB/(1 + K_1 fa)) + 59.15\log f_{OH^-} + E_j \tag{14}$$

Choosing

$$Y = E - 59.15\log A \tag{15}$$

as the experimental variable and expanding the logarithm we get

$$Y \simeq E_I^\circ - 25.69K_1 fB(1 - K_1 fa) + 59.15\log f_{OH^-} + E_j \tag{16}$$

$$Y' = Y - E_j - E_I^\circ - 59.15\log f_{OH^-} \simeq -25.69K_1 fB(1 - K_1 fa) \tag{16a}$$

$$(\delta Y'/\delta B)_A \simeq -25.69K_1 f(1 - K_1 af) \tag{17}$$

$$(\delta Y'/\delta A)_B \simeq 25.69K_1^2 f^2 B \tag{18}$$

Y' is a measure of the association. K_1 is small, therefore it is necessary to use fairly large concentrations of B^{2+} and OH^- to get Y' values large enough for the value of K_1, subsequently calculated from Y', not to be seriously affected by errors in the measured emf. Large changes in the medium are unwanted even if allowance is made by the term $(59.15\log f_{OH^-} + E_j)$. We may therefore ask which of B^{2+} or OH^- leads to the largest change in Y', for the same change in concentration. From eqns. (17) and (18) we find

$$l = |(\delta Y'/\delta B)_A/(\delta Y'/\delta A)_B| \simeq 1/K_1 fB \tag{19}$$

Using provisional values of K_1 (M^{-1}) (4.39, Ca^{2+}; 1.68, Sr^{2+}; 1.01, Ba^{2+}) we find that $l > 1$ for moderate values of B. The titrations were therefore arranged so that B was varied (at the most to 0.2 M) whereas A was kept low.

PRELIMINARY MEASUREMENTS ON CELL (I) AND THE CORRECTION FOR THE LIQUID JUNCTION POTENTIAL

The preliminary titrations were carried out with $Ba(ClO_4)_2$ solutions. Initially cell (I) contained ca 0.025 M OH^- and no Ba^{2+}. A was then gradually decreased by the addition of $HClO_4$ and E_I° calculated from eqn. (5) with $E_j = -8A$. After E_I° had been determined, $Ba(ClO_4)_2$ in 3 M ($NaClO_4$) was added to attain the desired value of B, then A was increased gradually whilst B was kept constant by further additions of $Ba(ClO_4)_2$. The results were plotted in the form $Y(A)_B$ where $Y = E - 59.15\log A$. (15) The curves

were extrapolated to $A = 0$ in order to eliminate the liquid junction potential arising from the OH^- ions. On the basis of our assumptions (eqns. (7) and (9)) Y is given by

$$Y = E_I^\circ - 59.15\log(1 + K_1 fB/(1 + K_1 fa)) - 9.3B - 8a \qquad (20)$$

and the extrapolated value of Y ($= Y_0$), is given by

$$Y_0 = E_I^\circ - 59.15\log(1 + K_1 fB) - 9.3B \qquad (21)$$

It would have been more correct to plot $Y(a)_B$, however, the difference between A and a is small and the error introduced is negligible.

Support for the assumptions underlying eqn. (20) comes from the following results.

1. The lines $Y(A)_B$ were straight and, for $B < 0.1$ M, had slopes close to -8 mV/M, which is the value obtained with 3 M $NaClO_4$[9].

2. The points $(Y_0 - E_I^\circ)$ (B) fell on a straight line passing through the origin, as required by eqn. (21).

FINAL EXPERIMENTS AND CALCULATIONS

The simple relationship between $(Y_0 - E_I^\circ)$ and $[Ba^{2+}]$, led us to change the titration procedure. The measurements were started on a mixture of $Ba(OH)_2$ and $NaClO_4$, and $[Ba^{2+}]$ was then gradually increased by addition of $Ba(ClO_4)_2$ in 3 M $NaClO_4$. The initial values of A were between 0.015 M and 0.025 M. No OH^- was added during the titration so that A varied with the dilution only.

Y_0 was calculated from

$$Y_0 = E + 8A - 59.15\log A \qquad (21a)$$

and plotted as a function of $B = [Ba^{2+}]_{tot}$, and E_I° was found by fitting the data to a straight line by the method of least squares. With E_I° known, a was calculated from eqn. (5) using

$$59.15\log f_{OH^-} + E_{jB} = -9.3B;\ E_{jA} = -8A \qquad (9), (22)$$

The terms $[BaOH^+]$ and $[Ba^{2+}]$ were found from eqns. (10) and (11) and inserted into

$$K_1 = \frac{[BaOH^+]}{[Ba^{2+}]\,[OH^-]} \qquad (12a)$$

When K_1 had been determined a was calculated from eqns. (10), (11) and (12a) using the analytical data. E_I° was redetermined with the new value for E_{jA} $(-8a)$ and K_1 calculated for the new value of E_I° if the change exceeded 0.02 mV.

With Sr^{2+} the technique described above was used. For Ca^{2+}, however, the initial OH^- was provided by $Ba(OH)_2$ and $[Ba^{2+}]_{tot}$ was kept constant by adding $Ba(ClO_4)_2$ together with the $Ca(ClO_4)_2$. The additions of Ba^{2+} ranged between 0.007 and 0.012 M. Since we wanted to work with well buffer-

Table 1.

Ca^{2+}

E mV observed	A M $\times 10^3$	B M $\times 10^3$	K_1 M^{-1}	$E°$ mV calculated
1 390.46	15.21	3.092	4.15	1 498.74
1 388.91	14.52	5.092	4.44	1 498.70
1 387.47	13.88	8.475	4.57	1 498.68
1 386.12	13.29	10.84	4.39	1 498.71
1 384.83	12.76	13.01	4.41	1 498.72
1 383.61	12.26	15.00	4.33	1 498.73
1 382.44	11.80	16.86	4.33	1 498.75
1 381.31	11.38	18.58	4.33	1 498.74
1 380.19	10.98	20.19	4.37	1 498.71
1 379.22	10.61	21.68	4.37	1 498.75

Sr^{2+}

E mV observed	A M $\times 10^3$	B M $\times 10^3$	K_1 M^{-1}	$E°$ mV calculated
1 402.07	23.73	11.87	1.69	1 498.95
1 401.58	23.47	16.12	1.66	1 498.95
1 400.62	22.96	24.37	1.66	1 498.97
1 399.69	22.48	32.30	1.65	1 498.96
1 398.78	22.01	39.88	1.66	1 498.96
1 397.90	21.57	47.18	1.67	1 498.95
1 397.05	21.14	54.15	1.67	1 498.94
1 396.22	20.73	60.86	1.67	1 498.94
1 395.42	20.34	67.34	1.68	1 498.93
1 394.62	19.96	73.55	1.69	1 498.90
1 393.86	19.59	79.56	1.69	1 498.91
1 393.48	19.41	82.47	1.69	1 498.89

Ba^{2+}

E mV observed	A M $\times 10^3$	B M $\times 10^3$	K_1 M^{-1}	$E°$ mV calculated
1 403.90	25.59	18.83	0.949	1 498.90
1 402.94	25.04	30.24	1.003	1 498.87
1 402.01	24.51	41.23	1.017	1 498.87
1 401.13	24.01	51.71	1.020	1 498.85
1 400.30	23 52	61 81	0.988	1 498.89
1 399.47	23.06	71.47	1.003	1 498.87
1 398.65	22.61	80.75	1.009	1 498.85
1 397.93	22.18	89.72	0.978	1 498.90
1 397.13	21.76	98.31	0.996	1 498.87
1 396.38	21.36	100.6	1.000	1 498.86
1 396.00	21.17	110.7	1.004	1 498.83

ed solutions, the extrapolation of E_I° would have been quite long, had $Ca(OH)_2$ been used as the base. The ranges of B studied were:

$$Ca^{2+}, 0<B<0.025 \text{ M}; \quad Sr^{2+}, 0<B<0.1 \text{ M}; \quad Ba^{2+}, 0<B<0.125 \text{ M}.$$

The calculations with the data from the Sr^{2+} and Ca^{2+} titrations were carried out as described for Ba^{2+}; in the latter case this is permissible because $[Ba^{2+}]$ was kept constant.

Table 1 contains results typical of those obtained. One would expect the values of K_1 to show a trend since they relate to solutions in which Na^+ is increasingly replaced by B^{2+}. However, with Ca^{2+} and Ba^{2+} no such trend is observed; with Sr^{2+}, on the other hand, there is a small trend. As can be seen from the table the trend is only present at the highest Sr^{2+} concentrations. These values were excluded when taking the mean value of K_1. The following results were obtained:

$$Ca^{2+} + OH^- \rightleftharpoons CaOH^+ \qquad \log K_1 = 0.642 \pm 0.015$$
$$Sr^{2+} + OH^- \rightleftharpoons SrOH^+ \qquad \log K_1 = 0.225 \pm 0.015$$
$$Ba^{2+} + OH^- \rightleftharpoons BaOH^+ \qquad \log K_1 = 0.004 \pm 0.015$$

The last column in Table 1 shows the self-consistency of the treatment of the data. E_I° has been calculated from

$$E_I^\circ = E - 59.15 \log a + 9.3B + 8a \qquad (23)$$

with a found from the analytical data and the mean value of K_1 proper. For Ca^{2+} and Ba^{2+} E_I° comes out as a constant, as it should, whereas for Sr^{2+} there is a slight trend at the highest concentrations.

It is interesting to note that the ratios between K_1 (in 3 M $NaClO_4$) and K_1(in H_2O) for the different metals, are roughly the same, thus, Ca^{2+} $4.39/22.2 = 0.20$; Sr^{2+} $1.68/6.67 = 0.25$; Ba^{2+} $1.01/4.35 = 0.23$.

It is hard to say anything definite as to the physical significance of the formation constants. There is no theory which affords a means of calculating the properties of fully dissociated salts in solutions such as these. The simple results obtained with NaOH, NaBr, NaCl and the chlorides and bromides of Ca^{2+}, Sr^{2+} and Ba^{2+} in 3 M $NaClO_4$ seem to indicate that the thermodynamic properties of ions in an inert salt medium are, to a large extent, determined by the charge, and that size is of less importance. We may therefore have some confidence in taking the halides as "models" for the completely dissociated hydroxide. However, the formation constants obtained on this basis may be expected to give the upper limits for the true constants.

Acknowledgements. The authors are indebted to Professor Lars Gunnar Sillén for his continual interest in our work and to Mr. F. Ericson for construction of the apparatus. The English of this paper has been improved by Dr. Derek C. Lewis. This work has been supported by *Statens Tekniska Forskningsråd* (*Swedish Technical Research Council*).

REFERENCES

1. Bjerrum, J., Schwarzenbach, G. and Sillén, L. G. *Stability Constants*, Part II, The Chemical Society, London 1958. Chem. Soc. Spec. Publ. No. 7.

2. Bates, R. G., Bower, V. E., Canham, R. G. and Prue, J. E. *Trans. Faraday Soc.* **55** (1959) 2062.
3. Olin, Å. *Acta Chem. Scand.* **11** (1957) 1445.
4. Olin, Å. *Acta Chem. Scand.* **14** (1960) 126.
5. Biedermann, G. *Arkiv Kemi* **9** (1956) 277.
6. Brown, A. S. *J. Am. Chem. Soc.* **56** (1934) 646.
7. Bates, R. G. *Electrometric pH Determinations.* J. Wiley and Sons, New York, 1954.
8. Biedermann, G. and Sillén, L. G. *Arkiv Kemi* **5** (1953) 425.
9. Ingri, N., Lagerström, G., Frydman, M. and Sillén, L. G. *Acta Chem. Scand.* **11** (1957) 1034.

Received January 12, 1961.

ACTA CHEMICA SCANDINAVICA 15 (1961) 735–742

Steroid Xanthates and some Transformation Products thereof

POUL BORREVANG

Leo Pharmaceutical Products, Copenhagen, Denmark

Treatment of steroids containing a ketol side chain such as hydrocortisone, prednisone, and prednisolone with carbon disulphide and potassium hydroxide affords the corresponding 21-potassium xanthates, which are transformed into derivatives of 1,3-oxathiolane-2-thione-4-ol upon acidification. The xanthates react with alkyl halides to yield S-alkyl xanthates.

Testosterone, upon treatment with carbon disulphide and potassium hydroxide, yields smoothly the 17-potassium xanthate, which with alkyl halides is converted to the corresponding S-alkyl xanthates. Oxidation of the potassium xanthate with iodine leads to the di-xanthate.

The need for water soluble derivatives of certain corticosteroids made the synthesis of 21-alkali xanthates of these compounds desirable. In the steroid series alkali xanthates and some S-alkyl derivatives have been prepared from cholesterol and cholestanol by action of carbon disulphide on the steroid alcoholates in benzene or toluene [1–5]. For various reasons, however, this method was not suitable for corticosteroids, and a method, in which the reaction was performed in a two phase system consisting of dioxan and aqueous potassium hydroxide was therefore worked out.

A chilled solution of hydrocortisone (Ia) in dioxan was stirred with aqueous potassium hydroxide while adding carbon disulphide. After acidification and extraction with ether a substance of the composition $C_{22}H_{30}O_5S_2 \cdot 3H_2O$ could be isolated from the organic phase. This substance, the structure of which, as shown below, may be represented by formula IIa, was in alcoholic potassium hydroxide solution transformed into a potassium salt, to which the structure IIIa has been assigned for the following reasons: The ultraviolet spectrum (in water) showed besides the Δ^4-3-keto band at 245 mμ a maximum at 304 mμ, which gradually disappeared upon storage of the solution, and which is characteristic of simple alkali xanthates [6,7]. The infrared spectrum (KBr) contained bands at 1 615 and 1 655 cm^{-1} (Δ^4-3-keto) and at 1 717 cm^{-1} (20-keto). Reaction of the potassium salt with methyl iodide in acetone yielded a compound

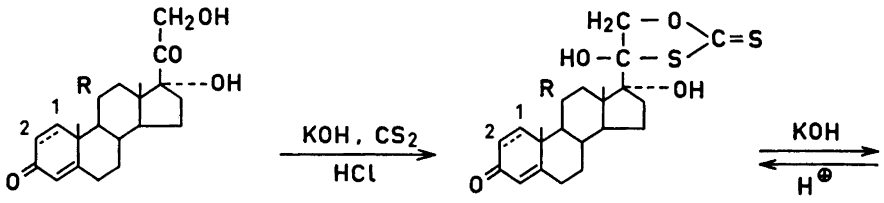

I a, b, c *II a, b, c*

a: R = H, OH(β)

b: Δ^1, R = O

c: Δ^1, R = H, OH(β)

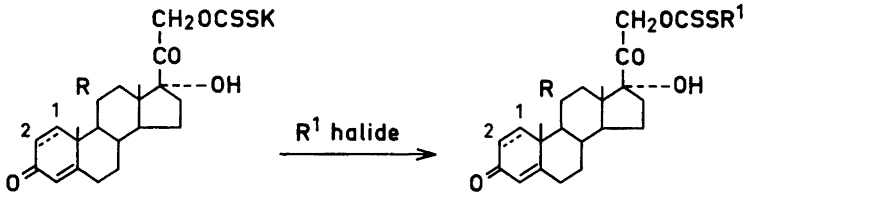

III a, b, c

IV a, c: $R^1 = CH_3, CH_3(CH_2)_{11}$

IV b: $R^1 = CH_2{=}CHCH_2$, $CH_3(CH_2)_3$ *and* $CH_3(CH_2)_{11}$

with an elementary analysis consistent with the 21-S-methyl xanthate formula (IVa, $R^1 = CH_3$) and an ultraviolet spectrum (ethanol) showing maxima at 239 mμ (Δ^4-3-keto) and 279 mμ. Simple S-alkyl xanthates are reported to absorb at the latter wave length [6,7]. The I.R. spectrum (KBr) contained bands at 1 617, 1 660 (Δ^4-3-keto), and 1 732 cm^{-1} (20-keto).

Upon acidification of an aqueous solution of IIIa followed by extraction with ether the above mentioned substance of the formula $C_{22}H_{30}O_5S_2 \cdot 3H_2O$ was obtained from the ether phase. The ultraviolet spectrum (λ_{max}^{EtOH} 240 mμ and 281 mμ *) was very similar to that of IVa, but in the infrared spectrum the 20-keto band was absent.

To obtain further information about the structure of this substance a similar series for reactions was performed with the simple α-ketol benzoin (V), in which the keto group constitutes a part of the chromophoric system. (λ_{max}^{EtOH} 245 mμ).

Treatment of a dioxan solution of V at room temperature with aqueous potassium hydroxide and CS_2 followed by acidification and extraction with

* Upon storage of the solution the maximum at 281 mμ gradually disappears.

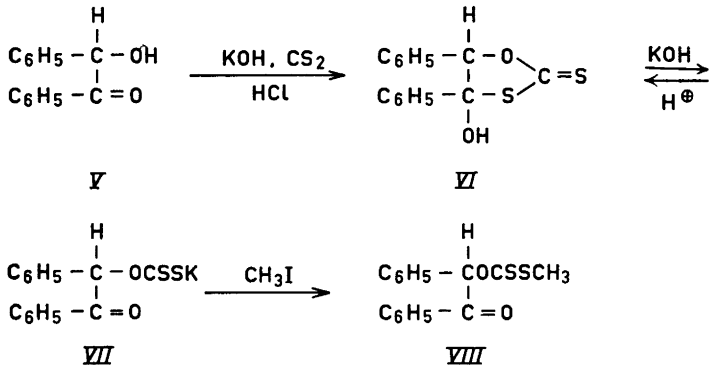

ether afforded a substance of the formula $C_{15}H_{12}O_2S_2$. The ultraviolet spectrum (ether) contained only one maximum at 282 mμ, which is characteristic of the chromophoric system RO · C(=S)—C— found in S-alkyl xanthates[6,7]. This finding in connection with the elementary analysis and the absence of a carbonyl band in the infrared suggested the structure VI.

A Zerewitinoff determination of active hydrogen was in accordance with this formulation. In alcoholic potassium hydroxide VI was converted into the potassium xanthate VII (U.V. $\lambda_{max}^{H_2O}$ 249 mμ and 304 mμ; I.R. (KBr) 1 690 cm^{-1}), which upon acidification was reconverted to VI. Alkylation of VII with methyl iodide yielded the S-methyl xanthate (VIII). (U.V. λ_{max}^{EtOH} 249 and 280 mμ; I.R. (KBr) 1 681 cm^{-1}).

It will be seen, that the reactions of hydrocortisone and benzoin described above as well as the spectral data of the two series of reaction products are completely analogous and the assignment of the structure IIa to the product obtained by acidification of a solution of the 21-potassium xanthate of hydrocortisone seems therefore justified.

The same series of reactions were performed with two other steroids containing the α-ketol side chain, namely prednisone (Ib) and prednisolone (Ic).

A number of 21-S-alkyl xanthates of Ia, b and c, prepared by action of an appropriate alkyl halide on the corresponding 21-potassium xanthates, are listed in Table 1.

The 21-potassium xanthate of hydrocortisone as well as other salts, e.g. the diethanolamine salt, are soluble in water (5—7 %). In aqueous solution, however, the xanthates are rapidly decomposed with the formation of hydrocortisone, the halflife value at 37°C and pH 7.2 being about 15 min.

Treatment of testosterone (IX) in dimethylformamide with aqueous potassium hydroxide and CS_2 leads to the potassium xanthate (X), which is rather stable in aqueous solution, but is decomposed with the formation of testosterone upon acidification.

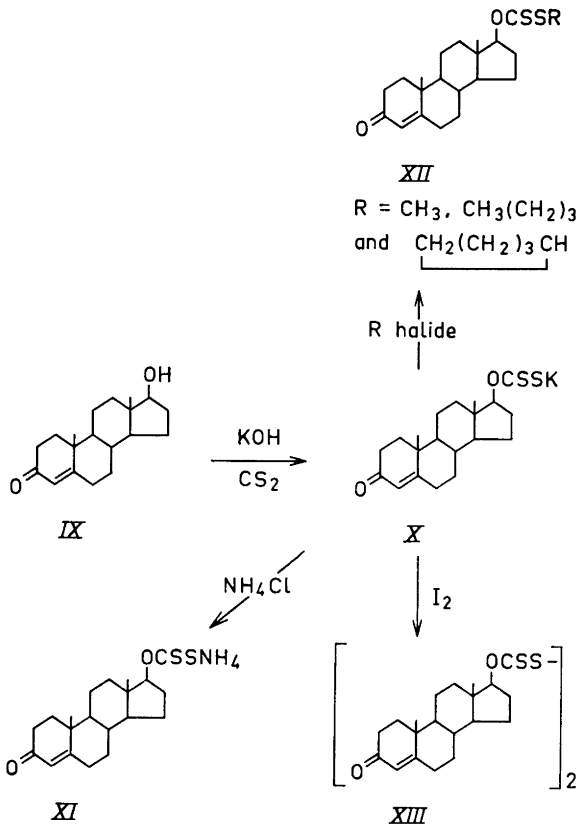

By action of alkyl halides on X the S-alkyl xanthates listed in Table 2 were obtained. Oxidation of X with iodine yielded the dixanthate XIII.

Biological properties. In adrenalectomized rats IIIa showed a glucocorticoid activity corresponding to that of hydrocortisone, when given intravenously *. The effect of intravenous administration of the corresponding diethanolamine salt in man has been investigated by Sprechler [8], and the topical use of these two salts in dermatology by Haxthausen [9,10]. X showed no androgenic activity in castrated male rats *.

EXPERIMENTAL

All melting points are uncorrected. Ultraviolet spectra were measured immediately after the preparation of the solutions.

17-(1,3-Oxathiolane-2-thione-4-ol-4-)androst-4-ene-3-one-11β,17α-diol (IIa). To a chilled solution of hydrocortisone (Ia) (3.0 g) in peroxide-free dioxan (90 ml) was added chilled 1.5 N aqueous potassium hydroxide (30 ml) with stirring. 5 min later a solution of carbon disulphide (3.0 g) in dioxan (5 ml) was added. After stirring of the chilled solution for 15 min ether (300 ml) followed by conc. hydrochloric acid (9 ml) were added

* These experiments were carried out in the endocrinological department of Leo Pharmaceutical Products.

with vigorous stirring. The two phases were separated, and the ether-phase washed with water. Hereby a precipitate separated, which was filtered off, washed with ether, and dried to yield 3.0 g of crude product. Recrystallization from aqueous acetone (10 % water) yielded the analytical specimen, which was decomposed at 118—120° (loss of CS_2) and melted at 215—17°C. Ultraviolet absorption spectrum: λ_{max}^{Ether} 233 mμ (ε 18 200) and 280 mμ (18 200). In 0.1 N aqueous NaOH: λ_{max} 245 mμ (ε 18 400) and 304 mμ (ε 18 800) *. (Found: C 53.63; H 7.42; S 12.84. Calc. for $C_{22}H_{30}O_5S_2,3H_2O$: C 53.63; H 7.37; S 13.02; H_2O 10.97). From acetone and methyl ethyl ketone solvated forms are obtained.

In the same way the following compounds were prepared:

17-(1,3-Oxathiolane-2-thione-4-ol-4-)androsta-1,4-diene-3,11-dione-17α-ol (IIb). The amount of ether was reduced to 60 ml. Yield: 58 %. From acetone a solvated product, which was decomposed at 134—135°C and melted at 232—233°C was obtained. Ultraviolet absorption spectrum: λ_{max}^{Ether} 229 mμ (ε 17 700) and 280 mμ (ε 18 000). In 0.1 N aqueous NaOH: λ_{max} 239 mμ (ε 21 000) and 304 mμ (ε 19 000). (Found: C 60.75; H 6.45; S 13.02. Calc. for $C_{22}H_{26}O_5S_2,C_3H_6O$: C 60.95; H 6.55; S 13.02).

17-(1,3-Oxathiolane-2-thione-4-ol-4-)androsta-1,4-diene-3-one-11β, 17α-diol (IIc). The amount of ether was reduced to 60 ml. Yield: 56 %. The substance crystallized from acetone in a solvated form, which was decomposed at 126—128°C and melted at 238—239°C. Ultraviolet absorption spectrum: λ_{max}^{Ether} 230 mμ (ε 18 100) and 280 mμ (ε 18 300). In 0.1 N aqueous NaOH: λ_{max} 241 mμ (ε 18 000) and 304 mμ (ε 18 200). (Found: C 60.64; H 6.97; S 12.89. Calc. for $C_{22}H_{28}O_5S_2$, C_3H_6O: C 60.70; H 6.93; S 12.96).

Corticosteroid-21-potassium xanthates (IIIa, b and c). These were prepared from IIa, b and c as follows: IIa (3.0 g) was dissolved in 2 % alcoholic potassium hydroxide (20 ml). Shortly afterwards crystals began to separate, which were collected and washed with ether to yield 2.7 g of IIIa. Ultraviolet absorption spectrum, $\lambda_{max}^{H_2O}$ 245 mμ (ε 17 500) and 304 mμ (ε 15 100).

Hydrocortisone-21-S-methyl xanthate (IVa, $R^1 = CH_3$). A mixture of IIIa (3.0 g), acetone (75 ml), and methyl iodide (6.0 ml) was stirred at room temperature for 1 h. Methyl *iso*butyl ketone (150 ml) was added, and the resulting solution was washed with water. After drying the solvent was removed *in vacuo*. The residue crystallized with ether to yield 1.7 g of crude product. After recrystallization from methanol the m.p. was 193—194°C. Ultraviolet absorption spectrum: λ_{max}^{EtOH} 239 mμ (ε 18 000) and 279 mμ (ε 12 300). (Found: C 61.07; H 7.00; S 14.08. Calc. for $C_{23}H_{32}O_5S_2$: C 61.03; H 7.13; S 14.17).

The 21-S-alkyl xanthates listed in Table 1 were prepared analogously.

4,5-Diphenyl-1,3-oxathiolane-2-thione-4-ol (VI). To a solution of benzoin (V) (10.0 g) in dioxan (300 ml) was added with stirring 1.5 N potassium hydroxide (100 ml) and carbon disulphide (10 ml). After stirring for 1 h ether (1 000 ml) and conc. hydrochloric acid (30 ml) were added. After separation the ether phase was washed three times with water. After drying and removal of the solvent *in vacuo* the residue was crystallized from chloroform-hexane to yield 9.4 g, which was decomposed at 111—113°C (loss of CS_2) and melted at 132—133°C. Ultraviolet absorption spectrum: λ_{max}^{Ether} 282 mμ (ε 16 400). (Found: C 62.52; H 4.10; S 22.32; "H" 0.37. Calc. for $C_{15}H_{12}O_2S_2$: C 62.47; H 4.20; S 22.23; "H" 0.35).

Potassium xanthate of benzoin (VII). To a solution of VI (5.0 g) in abs. ethanol (75 ml) was added 2 % alcoholic potassium hydroxide (50 ml). Upon scratching the potassium salt crystallized. After standing it was filtered off, washed with ethanol and ether, and dried. Yield: 4.5 g. Ultraviolet absorption spectrum: $\lambda_{max}^{H_2O}$ 249 mμ (ε 14 000) and 304 mμ (ε 11 400).

S-Methyl xanthate of benzoin (VIII). A mixture of VII (3.0 g), acetone (75 ml), and methyl iodide (6.0 ml) was stirred at room temperature for 1 h. Ether (200 ml) was added, and the solution was washed 2 times with water. After drying, the solvent was removed *in vacuo* and the residue recrystallized from ethanol to yield 2.1 g of a product with

* The bands at 233 mμ (ether) and 245 mμ (0.1 N NaOH) represent the sum of the Δ^4-3-keto band and a weaker band due to the xanthate group, which is reported to absorb near 226 mμ[6].

Table 1.

Compound	R [1]	Alkylhalide	Mole alkylhalide per mole K-salt	Yield %	M.p. °C	U.V. (ethanol) λ_{max} mμ	U.V. (ethanol) ε	Formula	C % Calc.	C % Found	H % Calc.	H % Found	S % Calc.	S % Found
IVa	$CH_3(CH_2)_{11}-$	Lauryl-bromide	2.4	42.4	135–36[c])	240 281	18 300 12 100	$C_{34}H_{54}O_5S_2$	67.28	67.22	8.97	9.12		
IVb[a])	$CH_2=CHCH_2-$	Allyl-bromide	3.3	60.0	188–89[b])	237 279	19 300 13 700	$C_{25}H_{30}O_5S_2$	63.26	63.23	6.37	6.24	13.51	13.20
	$CH_3(CH_2)_3-$	Butyl-bromide	5.4	67.3	118–20 and 173–75 [b])	237 281	18 700 13 700	$C_{26}H_{34}O_5S_2$	63.64	63.47	6.98	6.94	13.07	12.98
	$CH_3(CH_2)_{11}-$	Lauryl-bromide	2.4	31.3	124–26[b])	238 281	18 700 13 600	$C_{34}H_{50}O_5S_2$	67.73	67.62	8.36	8.55	10.64	10.62
IVc[a])	CH_3-	Methyl-iodide	10.7	52.6	220–21[c])	242 276	17 100 13 900	$C_{23}H_{30}O_5S_2$	61.30	61.38	6.71	6.79	14.23	13.58
	$CH_3(CH_2)_{11}-$	Lauryl-bromide	2.4	37.1	126–27[c])	240 279	16 900 13 500	$C_{34}H_{52}O_5S_2$	67.51	67.33	8.66	8.73	10.60	10.39

a) The reaction was performed in dimethylformamide and instead of methyl *iso*butyl ketone was used chloroform.
b) Recrystallized from ethanol.
c) Recrystallized from methanol.

Table 2.

R	Alkyl halide	Mole per 0.01 mole K-salt	Yield %	M.p., °C	U.V. (ethanol) λ_{max} mμ	U.V. (ethanol) ε	Formula	C % Calc.	C % Found	H % Calc.	H % Found	S % Calc.	S % Found
CH_3-	Methyl-iodide	0.13	63.8	121–22	236 278	22 600 10 700	$C_{21}H_{30}O_2S_2$	66.62	66.48	7.99	7.77	16.94	16.44
$CH_3(CH_2)_3-$	Butyl-bromide	0.013	35.9	77–78	237 282	23 300 11 000	$C_{24}H_{36}O_2S_2$	68.52	68.58	8.63	8.68	15.24	14.95
$CH_3(CH_2)_3CH-$ (cyclopentyl)	*Cyclo*pentyl-bromide	0.013	37.2	177–78	236 284	23 000 11 900	$C_{25}H_{36}O_2S_2$	69.39	69.20	8.39	8.48	14.82	14.73

m.p. 97–98°C. Ultraviolet absorption spectrum: λ_{max}^{EtOH} 249 mμ (ε 15 900) and 280 mμ (ε 14 000). (Found: C 63.45; H 4.70; S 21.15. Calc. for $C_{16}H_{14}O_2S_2$: C 63.55; H 4.67; S 21.20).

Potassium xanthate of testosterone (X). To a solution of testosterone (IX) (10.0 g) in dimethylformamide (50 ml) were added with stirring a solution of potassium hydroxide (10.0 g) in water (7.5 ml) and carbon disulphide (10 ml). After stirring for 1 h at room temperature the aqueous layer was removed by decantation and ether (800 ml) was added to the dimethylformamide phase. The oily precipitate, which formed, was crystallized from acetone-ether and thereafter recrystallized from ethanol-ether to yield 7.2 g of pure product. Ultraviolet absorption spectrum: λ_{max}^{EtOH} 235 mμ (ε 24 000) and 304 mμ (ε 15 200). (Found: S 15.78. Calc. for $C_{20}H_{27}KO_2S_2$: S 15.92).

Ammonium xanthate of testosterone (XI). To a solution of X (6.0 g) in water (225 ml) was added ammonium chloride (30.0 g) in water (100 ml). The precipitate was collected, washed with acetone followed by ether and dried to give 3.5 g of crude product. Recrystallization from methanol-ether yielded a product with m.p. 128–129°C (decomp.). (Found: C 62.87; H 8.16; N 3.73; S 16.43. Calc. for $C_{20}H_{31}NO_2S_2$: C 62.95; H 8.19; N 3.67; S 16.80).

S-Alkyl xanthates of testosterone XII (see Table 2). A mixture of 0.01 mole of the potassium xanthate (X), excess of the appropriate alkyl halide and acetone (200 ml) was stirred for 2–3 h. Ether (200 ml) was added, and the mixture was washed with water, dried, and evaporated to dryness *in vacuo*, whereafter the residue was recrystallized from abs. ethanol, combined, if necessary, with a treatment with decolorizing carbon.

Dixanthate of testosterone (XIII). The potassium xanthate (X) (5.0 g) was dissolved in water (300 ml). Iodine (1.58 g) in 10 % aqueous potassium iodide (50 ml) was added with stirring and the resulting suspension was extracted with methyl *iso*butyl ketone. The organic layer was separated, washed successively with water and aqueous sodium thiosulphate, and dried. After removal of the solvent *in vacuo* the residue crystallized with methanol. Yield of crude product: 3.5 g. Recrystallization from benzene-methanol yielded a product with m.p. 206–207°C (decomp.). Ultraviolet absorption spectrum: λ_{max}^{EtOH} 240 mμ (ε 55 000) and 286 mμ (ε 8 600). (Found: C 66.04; H 7.54; S 17.58. Calc. for $C_{40}H_{54}O_4S_4$: C 66.07; H 7.49; S 17.64).

Acknowledgement. The author wishes to thank Mr. O. Bremer for valuable discussions, Mr. P. Mørch for ultraviolet and infrared spectra, and Mr. G. Cornali for the microanalyses.

REFERENCES

1. Tschugaeff, L. and Gasteff, A. *Ber.* **42** (1909) 4631.
2. Tschugaeff, L. and Formin, W. *Ann.* **375** (1910) 288.
3. Bose, C. A. and Doran, W. *J. Chem. Soc.* **1929** 2244.
4. O'Connor, L. G. and Nace, R. H. *J. Am. Chem. Soc.* **74** (1952) 5454.
5. O'Connor, L. G. and Nace, R. H. *J. Am. Chem. Soc.* **75** (1953) 2118.
6. Treiber, E. *Monatsh.* **82** (1951) 53.
7. Schurz, J. *Mikrochim. Acta* **1955** 589.
8. Sprechler, M. *Ugeskrift Læger* **119** (1957) 1003.
9. Haxthausen, H. *Acta Dermato-Venereol.* **36** (1956) 381; *Ugeskrift Læger* **119** (1957) 554.
10. Haxthausen, H. *Acta Dermato-Venereol.* **37** (1957) 435; *Ugeskrift Læger* **120** (1958) 429.

Received September 30, 1960.

ACTA CHEMICA SCANDINAVICA 15 (1961) 743–749

Saccharopine, a New Amino Acid in Baker's and Brewer's Yeast

I. Isolation and Properties *

S. DARLING** and P. OLESEN LARSEN***

Biochemical Institute, University of Aarhus, Denmark

A new ninhydrin-positive substance, discovered by paper chromatography, has been isolated from hot water extracts of fresh baker's and brewer's yeast. By means of strongly acid and weakly basic ion exchange resins the amino acids of such extracts have been divided into one fraction containing the neutral and basic amino acids, and another containing the acid amino acids including the new compound, for which the name *saccharopine* is proposed.

Addition of ethanol to the eluate (pH 2) containing the acid amino acids, followed by recrystallization of the resulting precipitate from water (pH 3), affords pure saccharopine in amounts of 0.3 – 0.5 g from 2 kg batches of yeast. An anhydrous, analytical specimen possesses the composition $C_{11}H_{20}O_6N_2$ and contains three acid and two basic functions, the latter attributable to one primary and one secondary amino grouping.

On treatment at 125° with strong acid or base, saccharopine is partly transformed into a new compound, probably a lactam resulting from cyclodehydration involving the secondary amino grouping.

In the course of transamination studies in this laboratory, a ninhydrin-positive spot, which could not be assigned to any previously known amino acid, was observed on paper chromatograms of hot water extracts of baker's yeast (Fig. 1). The same amino acid pattern was found when extracts of mechanically disintegrated or freeze-dried yeast were utilized.

The unknown constituent may be identical with a component of dried baker's yeast, described by Lindan and Work [1] as 'No. 15', and with a substance in *Torulopsis utilis* indexed by Miettinen [2] as 'No. 30'. These authors reported

* A preliminary account of the present work was presented before The 9th Meeting of Scandinavian Chemists in Aarhus, Denmark, in 1956.

** Present address: Biochemical Department, The Royal Dental College, Aarhus, Denmark.

*** Present address: Organic Chemical Laboratory of the Royal Veterinary and Agricultural College, Copenhagen, Denmark.

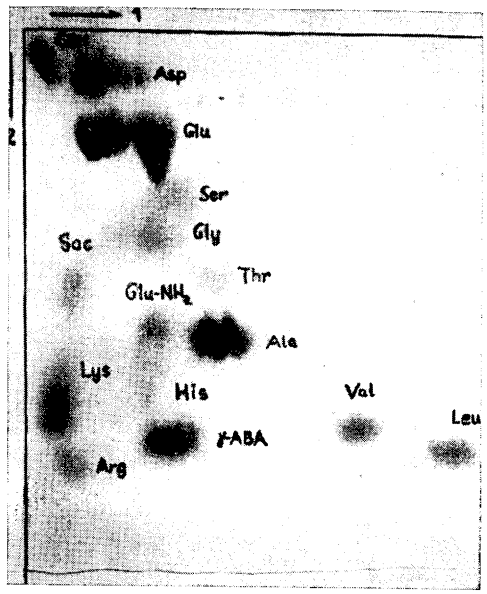

Fig. 1. Two-dimensional chromatogram of a hot water extract of baker's yeast after ion exchange on an acid resin and elution with ammonia. The applied volume is 5 μl, corresponding to 50 mg of fresh yeast. Solvent 1: butanol-pyridine-water (1:1:1). Solvent 2: phenol-water (3:1) with added NH_3 and cyanide. Spray-reagent: 0.2 % ninhydrin in acetone. Sac = saccharopine; other abbreviations are those commonly used. Glutamic acid appears as a double spot.

a remarkable acid stability of paperchromatographic isolates of the above-mentioned unknown compounds, though the treatment in both cases was accompanied by the production of minor amounts of a considerable number of the ordinary amino acids. Similarly, it was observed in this laboratory that a spot eluate of the unknown yeast constituent on acid hydrolysis gave mainly unchanged starting material, yet accompanied by a derivative thereof (*cf.* also Ref.[2]) besides small amounts of a number of the common amino acids. The presence in yeast extracts of a peptide, indistinguishable by paper chromatography from the unknown constituent, is consonant with the observed patterns. The present paper reports the isolation of the acid-stable compound, identified as an amino acid, for which the name *saccharopine* is proposed *.

Isolation experiments were initially performed on hot water extracts of baker's yeast. From such extracts the total amino acid fraction was absorbed on a strongly acid ion exchange resin. On standing, the acid effluent deposited

* This name is coined in accord with the biological origin of the amino acid and is furthermore in conformity with names such as octopine and lysopine, two naturally occurring amino acids with which the present compound is structurally related as demonstrated in a subsequent communication defining also the stereochemical specification [3].

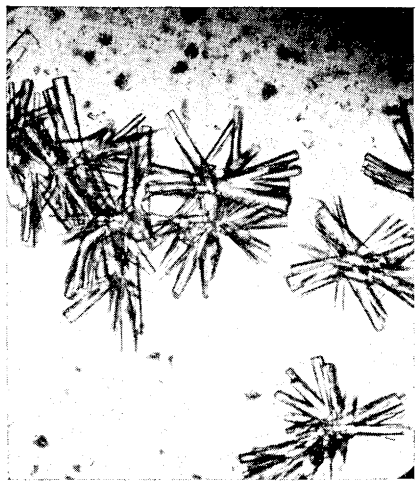

Fig. 2. Saccharopine from baker's yeast, recrystallized from an aqueous solution. 120 × natural size.

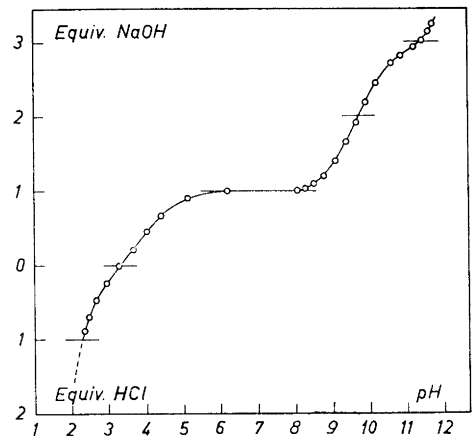

Fig. 3. Titration curve for saccharopine in water. Conditions are those outlined in the experimental part.

a precipitate which on basis of ultraviolet absorption data and its behaviour on acid hydrolysis appeared to be a nucleoprotein. Glutathione was the only detectable ninhydrin-positive substance in the effluent. The amino acids were displaced with ammonia, and the eluate subsequently passed through a weakly basic anion exchange resin in its acetate form, retaining all acid amino acids including saccharopine. The latter were then displaced from the column by hydrochloric acid, and the residue from the eluate was purified by repeated reprecipitations from aqueous solution at pH 2.0 with ethanol. Finally, adjusting of an ammonia solution to pH 3.5 caused saccharopine to separate in yields varying from 0.3 to 0.5 g per 2 kg of fresh yeast. Repetition of this purification procedure afforded a beautifully crystalline specimen of pure saccharopine (Fig. 2). When applied to extracts of brewer's yeast the above procedure yielded a crystalline compound which on basis of chromatographic properties and crystalline appearance proved identical with saccharopine from baker's yeast. Furthermore, no melting point depression was observed on admixture of the two preparations.

Direct isolation of saccharopine from the ammonia eluate of the acid ion exchange column was attempted by adjustment of the pH value to 2.00. However, addition of ethanol and reprecipitation with the same solvent resulted in a considerably smaller yield of a product, heavily contaminated with glutamic acid and lysine, both of which were difficult to remove by recrystallizations.

The new amino acid is sparingly soluble in water and ethanol but readily soluble in bases and strong acids. It gives off water over phosphorus pentoxide at 100°, and analysis of the hygroscopic, anhydrous preparation indicated its

elemental composition to be $C_{11}H_{20}O_6N_2$. Electrometric titration in water and titration in acetone revealed the presence of three acid and two basic functions in the amino acid. From the curve presented in Fig. 3 the following apparent dissociation constants were determined: pK_2 2.6, pK_3 4.1, pK_4 9.2 and pK_5 10.3.

The ninhydrin colour yield was determined according to Moore and Stein [4]. When calculated on molar basis, the colour yield was 90 %, relative to leucine. With acetaldehyde and sodium nitroprusside in alkaline solution, saccharopine produced an intensely blue colour, indicative of secondary amines [5]. Hence, the amino acid contains a primary as well as a secondary amino grouping.

On heating to 125° in 6 M hydrochloric acid, saccharopine was slowly but exclusively converted into a new compound. Even after a heating period of 16 days, however, the conversion was not complete. Similar treatment with saturated barium hydroxide likewise resulted in partial transformation of saccharopine into a compound, which is chromatographically indistinguishable from the product obtained on acid treatment. In accord with the strongly acid character of the new compound (*vide infra*), the paperchromatographically determined R_F-values are highly dependent on the pH-value of the applied solution in solvent systems devoid of buffering capacity towards acids (*e.g.* 0.26 in strongly acid solution, 0.15 in neutral or basic solution, in the solvent system *n*-butanol: acetic acid:water (4:1:5)). As expected, such variations are not encountered when phenol:water:ammonia or butanol:pyridine:water are used as solvent systems.

The first isolate of the transformation product was obtained from a one-dimensional chromatogram developed in butanol:acetic acid:water. Upon electrophoresis, the compound migrates towards the anode, both in citrate buffer (pH 2.5) and 0.1 M acetic acid (pH 3.3), whereas saccharopine travels towards the cathode. Consequently, the conversion product is a stronger acid than saccharopine. In 1 M acetic acid (pH 2.2) both substances migrate towards the cathode. By means of continuous paper electrophoresis at pH 3.8 about 15 mg of the transformation product, contaminated with ammonium chloride, was isolated from acid-treated, partially converted saccharopine. Upon electrometric titration with 1 M sodium hydroxide, a pK_2-value of 3.2 was determined for the conversion product, which proved to contain two acid and one basic groupings. The minimum molecular weights 268 and 258 were determined by electrometric titration and micro-Kjeldahl analysis, respectively, on the assumption that two nitrogen atoms are present. The latter molecular weight, which is considered to be the most reliable, indicates loss of the elements of water during the acid-induced transformation of saccharopine. The protolytic properties, together with the fact that acid-treated solutions of saccharopine give unchanged colour yield with ninhydrin, suggest that intramolecular cyclodehydration between a carboxylic group and the secondary amine function takes place, as further discussed in the subsequent communication [3].

Preliminary experiments on the influence of saccharopine on the growth of various strains of *B. subtilis* on agar showed a marked inhibitory action on four strains in concentrations as low as 10^{-5} M. In two cases, a growth-promoting effect of saccharopine was observed. No effects were observed, however, when liquid media were used.

EXPERIMENTAL

Melting points are determined in capillary tubes with the thermometer (Anschütz) fully immersed in the oil bath.

Ion exchange columns. The resin Zeo-Karb 225 (300 g) in H^+-form was packed wet into a glass tube with an internal diameter of 3.4 cm (the height of the resin bed was about 37 cm). The flow rate of the solutions was kept between 0.6 and 0.8 ml cm^{-2} min^{-1}. A column of the resin Amberlite IR-4B (analytical grade) in its acetate form was prepared as follows: a glass tube with an internal diameter of 3.7 cm was packed wet with 150 g of Amberlite IR-4B (OH^-). The resin was converted into its Cl^--form by passing 450 ml of 3 M HCl, followed by 3 l of water, through the column, which was then reconverted into its OH^--form with 1 200 ml of 1 M NH_3 followed by 1 500 ml of water. Finally, the resin was transformed into its acetate form by allowing 1 500 ml of 1 M acetic acid to pass through the column, followed by 300 ml of CO_2-free water. During all operations, the flow rates were not allowed to exceed 0.3 ml cm^{-2} min^{-1}.

Isolation of saccharopine from baker's yeast. Fresh baker's yeast obtained from *A/S Dansk Gæringsindustri* was used. The yeast was stored at + 4°, but never for more than a fortnight.

A suspension of 2 kg of yeast in 2 l of water was prepared and poured into 8 l of boiling water under constant stirring. The mixture was boiled for 60 min and then set aside at room temperature overnight. The sediment was filtered off on Büchner funnels with Hyflo-supercel as a filter aid. The filtrate was evaporated *in vacuo* to about 150 ml (with tributyl phosphate as an anti-foam agent), and the concentrate together with the rinsing water (150 ml) was centrifuged at 15 000 × *g* and 20° for 60 min. The supernatant was then diluted to 350 ml and passed through the cation exchange column, followed by 2 l of water. The first 100 ml of the effluent was transparent (pH 6). Then pH decreased to about 1, and the next 500 ml-fraction was turbid and of a greyish-brown colour. The pH-value now rose again to between 2 and 3, and the eluate became less cloudy. The last part of the yellowish effluent was perfectly clear (pH 5—6). All effluent fractions were discarded.

The entire amino acid fraction was now eluted with 2 l of 1 M ammonia, the first half of the eluate being slightly cloudy (pH 3—4). The pH-level then increased to 10, and the eluate became transparent and yellow. The solution was evaporated to dryness *in vacuo*, and the residue was redissolved in 100 ml of water. This solution was then passed through the anion exchange resin, and the column was washed with 500 ml of CO_2-free water. The first 100 ml was yellow (pH 6), while the remainder was colourless, with a final pH-value of about 3. This effluent, containing only neutral and basic amino acids, was discarded.

The acidic amino acids, including saccharopine, were now eluted with 800 ml of 3 M HCl, passed through from the bottom of the column. The first 600 ml of eluate were almost colourless (pH 6). Then the pH-level fell to below 1, and at the same time the solution acquired an intensely yellow colour. The eluate was evaporated to dryness *in vacuo* on a water bath kept at 40—45°. Excess HCl was removed by evaporating the residue twice with 100 ml-portions of water *in vacuo*, and the solid was dried over NaOH *in vacuo* at 40° for 6 h. It was then redissolved in 50 ml of water, the solution was treated with 5 g of acid-washed, activated charcoal (B.D.H.) and filtered. The combined filtrate and washing liquid was diluted to a volume of 65 ml. This solution, which was clear and faintly yellow, contained only saccharopine, glutamic acid, aspartic acid, and glutathione, as apparent from two-dimensional chromatograms.

The first ethanol precipitate was obtained by adjusting the concentrated eluate from the exchange column to pH 2.00 with conc. ammonia and then adding 8 volumes of 96 % ethanol. A crystalline precipitate began to appear after a few minutes. The suspension was kept at + 4° for 72 h, the crystals were collected and washed, first with ethanol-HCl (8 volumes of 96 % ethanol and 1 volume of 0.01 M HCl) and then with acetone. After drying over silica gel and potassium hydroxide *in vacuo*, the yield was 0.8—1.5 g. The product consisted mainly of saccharopine, contaminated with glutamic acid and traces of aspartic acid and glutathione. The solid was dissolved in 40 ml of water, the solution was clarified by centrifugation, pH was adjusted to 2.00 by addition of 3 M HCl, and 8 volumes of 96 % ethanol were added. After a few minutes, a crystalline sediment began to appear which was collected after 72 h at 4°, washed with ethanolic

HCl and acetone, and finally dried over silica gel and potassium hydroxide *in vacuo* (0.4—0.6 g). Paper chromatography of this product revealed a slight contamination with glutamic acid, aspartic acid and glutathione.

The partly purified material was redissolved in 5 ml of 1 M ammonia and pH was adjusted to 3.5 with 3 M HCl. After a few minutes, saccharopine crystallized in fine needles. After standing at 4° for 72 h, the crystals were filtered off and washed, first with ethanol-HCl and then with acetone. After drying over silica gel and potassium hydroxide *in vacuo*, the yield was 0.3—0.5 g. The product was still faintly yellow, hygroscopic and contaminated with traces of glutamic acid. After a new treatment with charcoal and reprecipitation, 1 g of this product yielded 700 mg of a colourless, homogeneous specimen, which was dried over phosphorus pentoxide at 100° and 0.1 mm for 4 h before analysis, m.p. 257—259° (decomp.). (Found: C 47.9; H 7.41; N 10.12 (Dumas). Calculated for $C_{11}H_{20}O_6N_2$: C 47.81; H 7.30; N 10.14), $[\alpha]_D^{23}$ + 33.6° (*c* 1.0, 0.5 N HCl); + 8.1° (*c* 2.2, 0.5 N NaOH).

Isolation of saccharopine from brewer's yeast. Following the above procedure the same amino acid was isolated from brewer's yeast grown on hop-free wort.

Electrometric titration of saccharopine. The titration curve in the pH-range below 7 (Fig. 3) was determined by titration with 0.5 M sodium hydroxide of 33.5 mg of saccharopine dissolved in 10 ml of 0.01 M hydrochloric acid. For the air-dried sample the equivalent weight 297 was determined. The remaining part of the curve was obtained by titration with 1 M sodium hydroxide of 7.584 mg of anhydrous saccharopine suspended in 250 µl of water (M 276). The titration values were converted into equivalents of sodium hydroxide per mole of saccharopine.

Acetone titration of saccharopine. Because the amino acid is slightly soluble in acetone, the original method [6] could not be used but was substituted by a modification of the procedure described by Zamecnik *et al.*[7]

From an approximately 0.01 M aqueous solution of saccharopine 0.40 ml was transferred to a test tube (3 1/8″ × 1/2″) designed for the "EEL" colorimeter. To this amount were added 6.3 µl of 0.1 % naphthyl red in 96 % ethanol and a known volume of 0.1 M HCl in 96 % ethanol, followed by 3.60 ml of acetone. The optical density (D) of the solution was immediately read in an "EEL"-colorimeter provided with filter (OGRI). It is important that the addition of acetone and the reading of D are done as rapidly as possible, since the acetone solution becomes turbid after a few minutes.

A blank value was determined as follows: a mixture of 0.40 ml of water, 3.60 ml of acetone and 6.3 µl of naphthyl red was titrated, and a curve constructed of the colorimetric reading as a function of the amounts of added HCl (in µl). This curve was used to estimate the blank acid consumption equivalent to the determined D-value. Determination on three 0.40 ml samples of a saccharopine-solution containing 0.27 N/ml gave titration values of 85 µl of 0.1 M HCl, corresponding to a content of 1.08 equivalent per equivalent of nitrogen.

Paper electrophoresis. Mixtures of saccharopine and its transformation product were studied on Whatman No. 1 paper in 0.1 N citrate buffers and 0.1 and 1 N acetic acid at 3 V per cm. The apparatus used was constructed as described by Kunkel and Tiselius [8].

Isolation of the transformation product. An amount of 100 mg of saccharopine was treated with 6 N HCl at 125° for 96 h. Saccharopine and its conversion product were separated from HCl by absorption on a Zeo-Karb 225 (H^+) column and eluted with 1 M NH_3. The eluate was evaporated to dryness *in vacuo*, and the residue dissolved in 25 ml of water. The mixture was then separated by continuous electrophoresis in an "Elphor V" apparatus at pH 3.8, utilizing an acetate buffer (ionic strength 0.05) at 170 V and 14 mA. Schleicher and Schüll paper No. 2040b was employed. The solution was applied to the paper at a rate of 0.36 ml/h. The fractions were collected in 22 tubes (No. 1 at the anode). The solution was applied above tube No. 21. The fractionation was controlled by paper chromatography in butanol:acetic acid:water. Saccharopine was found to be present in the tubes 17, 18 and 19, and its conversion product in 14 and 15. The latter fractions were pooled (26 ml) and applied to a Zeo-Karb 225 (H^+) column. The transformation product was eluted with ammonia solution and evaporated to dryness, and the residue was dissolved in 0.1 M HCl and precipitated with 10 volumes of acetone. Analyses of the contaminating ammonium chloride were performed by determination of ammonia by the Conway-method and chloride as described by Brun [9]. A content of 6.8 % of NH_4Cl was found.

Micro-Kjeldahl analyses were performed with selenium as a catalyst.

Baker's yeast was generously supplied by *A/S Dansk Gæringsindustri* and brewer's yeast by the *Research Laboratory of the Carlsberg Breweries.* Microanalyses for C, H and N (Dumas) were performed by Mr. P. Hansen, The Chemical Laboratory of the University of Copenhagen. The authors wish to thank Prof. A. Kjær for help during the preparation of the manuscript and Dr. P. J. Christensen for the determinations of the ninhydrin colour yields. The assistance of Dr. A. Stenderup in the microbiological studies is gratefully acknowledged.

This investigation was supported by *Statens Almindelige Videnskabsfond (The Danish State Research Foundation).*

REFERENCES

1. Lindan, O. and Work, E. *Biochem. J.* **48** (1951) 337.
2. Miettinen, J. K. *Ann. Acad. Sci. Fennicae Ser. AII* **58** (1954) 1.
3. Kjær, A. and Olesen Larsen, P. *Acta Chem. Scand.* **15** (1961) 750.
4. Moore, S. and Stein, W. H. *J. Biol. Chem.* **211** (1954) 907.
5. Feigl, F. *Spot Tests (II), Organic Applications* p. 189, Elsevier, 1954.
6. Linderstrøm-Lang, K. *Compt. rend. trav. Lab. Carlsberg, Ser. chim.* **174** (1927) 1.
7. Zamecnik, P. C., Lavin, G. I. and Bergmann, M. *J. Biol. Chem.* **158** (1945) 537.
8. Kunkel, H. G. and Tiselius, A. *J. Gen. Physiol.* **35** (1951) 89.
9. Brun, C. *Nord. Med.* **42** (1949) 1774.

Received December 1, 1960.

ACTA CHEMICA SCANDINAVICA 15 (1961) 750–759

Saccharopine, a New Amino Acid in Baker's and Brewer's Yeast

II. Structure and Synthesis

ANDERS KJÆR and P. OLESEN LARSEN

Organic Chemical Laboratory of the Royal Veterinary and Agricultural College, Copenhagen, Denmark

The combined chemical and biochemical data, presented in other communications of this series, suggest (I) or, less likely, (II), as plausible structures for the new yeast amino acid *saccharopine*. The former compound is synthesized as a mixture of diastereoisomerides by Strecker-reaction of N^2-(*p*-toluenesulphonyl)-L-lysine, potassium cyanide and 2-oxoglutaric acid. The route involves condensation of the three components, acid hydrolysis, decarboxylation and removal of the protecting group. Fractional crystallization affords synthetic material identical with natural saccharopine, and, in addition, its diastereoisomeride.

The synthetic route, together with rotation data for the two isomerides, unequivocally establishes (I), with L-centres in both the lysine and glutamic acid portions, as the structure of the new, natural amino acid, hence denoted L-saccharopine. The synthetic diastereoisomeride, possessing D-configuration at the glutamic acid centre, is accordingly named D-*allo*saccharopine. A synthetic by-product is tentatively formulated as a derivative of pyroglutamic acid.

The natural occurrence of related imino acids and the biogenesis of saccharopine are briefly discussed.

The combined chemical and biochemical evidence, presented in preceding communications [1,2], can be rationalized in terms of formula (I) or (II) as plausible expressions for the new amino acid, saccharopine, isolated from baker's yeast. The assay for α-monoamino monocarboxylic acids, developed in this laboratory [3], gave results favouring structure (I) rather than (II). Hence, efforts were directed towards synthesis of the former.

The rather few heretofore known N-carboxyalkylamino acids are almost all of the α,α′-type and have largely been synthesized by four different methods. (i) Reductive alkylation of amino acids with keto acids has been employed in, *e.g.*, the preparation of *allo*octopine from L-arginine and pyruvic

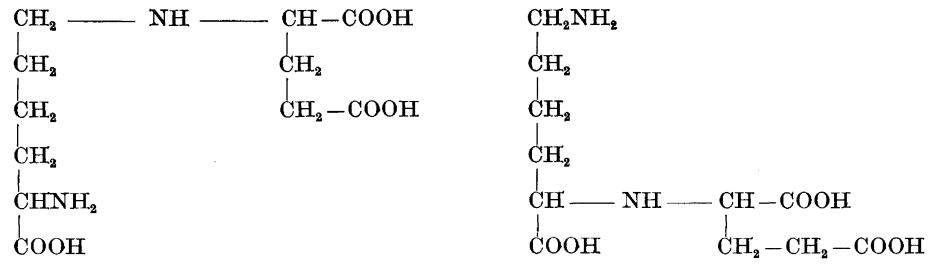

I II

acid [4], while attempts to produce octopine in a similar fashion from 2-oxo-5-guanidovaleric acid and alanine met with no success [5]; other failures to achieve similar reactions have been reported [6]. (ii) N-alkylation of amino acids with halo-acids has been repeatedly utilized in the syntheses of imino acids, *e.g.* optically active octopine [4,5] and N-(1-carboxyethyl)-substituted alanine [7], aspartic and glutamic acid [8]; (iii) Strecker-synthesis, involving the reaction between a carbonyl compound, cyanide and an amino acid, has yielded such amino acids as N-carboxymethyl-L-glutamic acid [9] and a mixture of diastereoisomeric N-(1-carboxyethyl)-glutamic acids [10]. (iv) Addition of an amino acid or ammonia to an unsaturated acid constitutes a known route to certain symmetric imino acids [11–13].

Common for the first and the two last methods is the introduction during synthesis of at least one asymmetric centre resulting in the formation of diastereoisomer mixtures of unpredictable compositions, whereas in the second method precise kinetic data are required for unequivocal prediction of the stereochemical course of the reaction.

In the synthetic approach to structure (I) various modifications of the first three of the above general methods were attempted. First, mixtures of 2-oxoglutaric acid and the copper complex of L-lysine or N^2-(*p*-toluenesulphonyl)-L-lysine [14,15] were subjected to hydrogenation over noble metal catalysts; in both cases, however, only reduction of the keto-acid to 2-hydroxyglutaric acid was observed. Subsequently, the synthesis of DL-5-(3-formylpropyl)-hydantoin, with a view to its application in reductive alkylation of L-glutamic acid, was unsuccessfully attempted. No better results attended experiments on the alkylation of ethyl L-glutamate with DL-5-(4-bromobutyl)-hydantoin [16]. However attractive for stereochemical reasons, further attempts to utilize optically active glutamic acid or esters hence were abandoned. As an obvious alternative, alkylation of N^2-(*p*-toluenesulphonyl)-L-lysine methyl ester [14,32] with ethyl DL-2-bromoglutarate [33], followed by saponification and detosylation, was attempted. A minute amount of a product, indistinguishable from saccharopine on paper chromatograms, was present in the reaction mixture, yet accompanied by considerable quantities of lysine and two nitrogen-free acids, probably 2-ethoxyglutaric acid and 1,2-cyclopropanedicarboxylic acid, both formed from the halo acid by metathetic and intramolecular cyclization reactions, respectively. The unsatisfactory course of this substitution reaction, together

with some uncertainty as to the structure of the resulting product *, made it natural at this stage to explore the merits of the Strecker-synthesis for the preparation of (I).

According to the following scheme, interaction between N^2-(*p*-toluenesulphonyl)-L-lysine (III, Ts = p-$CH_3C_6H_4SO_2$) and the cyanohydrin of succinaldehydic acid (IV, R = H) should provide a promising route to a mixture of diastereoisomerides of (I) (*cf.* foot-note, p. 754). The latter aldehyde has

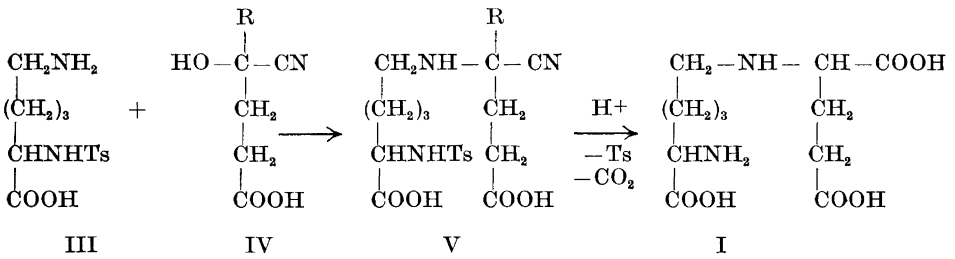

in fact been used previously in similar reactions with simple amines [18]. After a few preliminary experiments, however, it was found advantageous to replace the easily polymerizing succinaldehydic acid with the readily accessible 2-oxoglutaric acid in the above reaction scheme. In a model experiment, where the latter keto-acid was treated with ammonia and potassium cyanide, the formation of glutamic acid was paperchromatographically established. Subjected to similar conditions, (III) afforded a 65 % yield of the cyanohydrin (V, R = COOH) which, because of its rather labile character, was transformed without further purification into a semicrystalline product on acid hydrolysis.

After detosylation with hydrogen bromide in glacial acetic acid three ninhydrin-positive spots on the paper chromatograms could be tentatively assigned to lysine, saccharopine and its transformation product, discussed in a preceding communication [1]. Diastereoisomerides of the two last amino acids were later found to be inseparable upon paper chromatography. Probably, the notable quantity of lysine present in the reaction mixture originated from N^2-(*p*-toluenesulphonyl)-L-lysine, formed by concomitant acid fission of (V, R = COOH) during hydrolysis and decarboxylation of the latter. Attempts to suppress the quantities of lysine and the transformation product of saccharopine by employing alkaline hydrogen peroxide as a hydrolyzing agent and sodium in liquid ammonia for removal of the protecting group were unsuccessful.

On a preparative scale, the total amino acid fraction was isolated by means of a strongly acid ion exchange resin and subsequently freed of lysine by passage through a weakly basic resin in the acetate form. The acid eluate from the latter contained only the two amino acids, tentatively regarded as

* Cocker [17] actually utilized N-alkylation of N-benzenesulphonyl derivatives of α-monoamino acids as an intermediate stage in the preparation of sarcosine and simple homologues.

saccharopine and its transformation product. Repeated precipitations with ethanol from aqueous solutions of the mixture at pH 3.5 yielded a paperchromatographically homogeneous, crystalline product, possessing the same R_F-value and elemental composition as saccharopine isolated from yeast. However, considerable deviations in the infra-red spectra and optical rotations of this synthetic material clearly indicated its character as a mixture of two diastereoisomerides. Fractional crystallization of the latter was facilitated by seeding with saccharopine, and after a few recrystallizations from water a synthetic sample was obtained with correct elemental composition and pos-

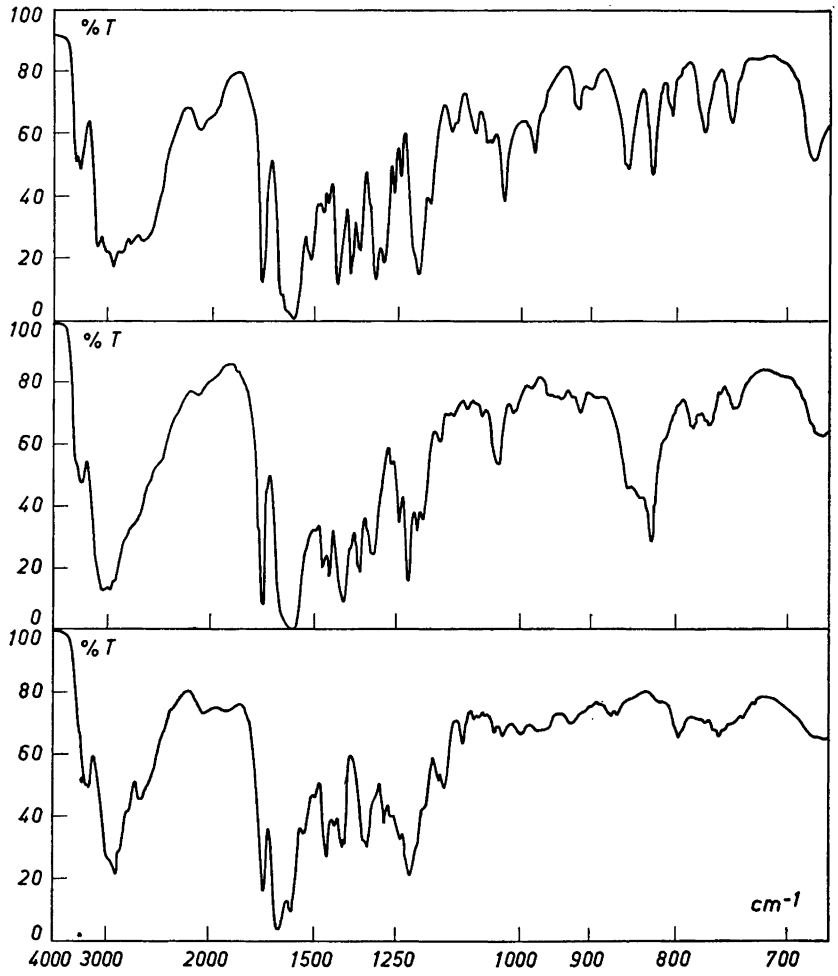

Fig. 1. Infra-red spectra (in KBr pellets). Upper curve: synthetic L-saccharopine (identical with that of the natural amino acid). Middle curve: synthetic D-*allo*saccharopine. Lower curve: cyclic by-product (VII), probably mixture of two diastereoisomerides.

sessing the same rotation, within experimental errors, as the natural amino acid. Furthermore, R_F-values, infra-red spectra (Fig. 1) and X-ray diffraction patterns of the two preparations were identical and no melting point depression was observed. Hence, apart from the absolute configuration around the second asymmetric centre, the above synthesis establishes (I) as the correct structure for the new amino acid saccharopine.*

Repeated recrystallizations of the mother liquor material afforded the more soluble diastereoisomeride with correct composition and a markedly different infra-red spectrum. Judged from the change in specific rotation on successive recrystallizations, this isomeride also was obtained in optically pure state.

Isolation of both synthetic diastereoisomerides rendered determination of their absolute configuration possible on basis of rotation data. By application of the principle of optical superposition to the two isomerides, the contribution of each asymmetric centre to the rotation was calculated. The values are presented in Table 1 together with rotation data for L-lysine and some appropriate derivatives of L-glutamic acid. From these considerations it can be safely concluded that saccharopine possesses L-configuration at both asymmetric centres as depicted in (VI), whereas the more soluble synthetic diastereoisomeride contains a D-centre in the glutamic acid portion of the molecule.

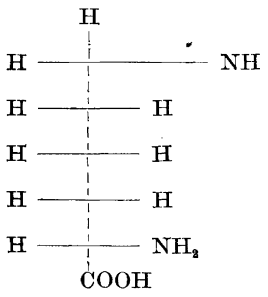

VI

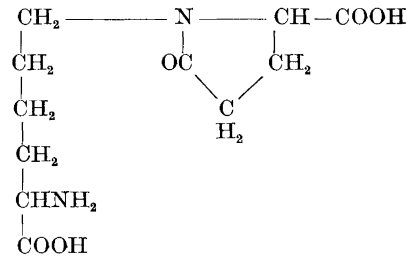

VII

According to the proposal of Vickery [34], the configurational designation in compounds given trivial names and containing two α-amino carboxylic acid groupings attached to dissimilar carbon chains shall be that of the α-carbon atom of the smaller of the two chains. Adopting this rule, the natural amino acid is to be denoted L-saccharopine, and the diastereoisomeride, differing in the configuration of the glutamic acid portion, is D-*allo*saccharopine.

* The possibility of the sterically unfavourable reaction between (III) and (IV) taking place at the ionized sulphonamido grouping, present in the strongly alkaline reaction mixture, in analogy with the reported reaction between sulphonamides and aliphatic aldehyde cyanohydrins [35], has been considered. In order to exclude the latter reaction in the present case, N^6-(*p*-toluenesulphonyl)-L-lysine was subjected to reaction with (IV) under conditions similar to those employed in the synthesis of saccharopine. No reaction occurred as evident from the presence of lysine as the sole amino acid, subsequent to hydrolysis and detosylation. Again, a Strecker-synthesis between (IV) and L-lysine furnished a moderate yield of the diastereoisomeric saccharopines.

Table 1. Optical rotation data for saccharopine and its diastereoisomeride, and contributions of the individual asymmetric centres to the rotation.

Compound	Measured $[M]_D$ in 0.5 N HCl	$[M]_D$ Lysine portion	$[M]_D$ Glutamic acid portion
L-Saccharopine	+ 93°	+ 45° *	+ 48° **
D-*allo*Saccharopine	−2°	+ 45°	− 48°

* For comparison: $[M]_D$ of L-lysine in 0.5 N HCl: + 38°; ** $[M]_D$ of L-glutamic acid: + 47° (0.5 N HCl), and for the following N-substituted L-glutamic acids: methyl + 40° (hydrochloride in H_2O) [19], ethyl + 38° [20], *n*-propyl + 41° [20], *n*-butyl + 39° [20] (the abstract of Ref.[20] does not state the character of the solvent).

During the present studies it was unsuccessfully attempted to prepare the isomeric compound (II) by Strecker-syntheses involving 2-oxoglutaric acid and N^6-benzyloxycarbonyl-L-lysine or N^6-(*p*-toluenesulphonyl)-L-lysine [21] (*cf*, footnote, p. 754). Attempts to effect reductive alkylation of the latter derivative with 2-oxoglutaric acid met with no better success.

From the combined mother liquors of the diastereoisomeric saccharopines the more soluble transformation product, invariably formed during the syntheses of saccharopine, was isolated in crystalline and paperchromatographically homogeneous form. Rotation data, however, suggested that the isolate was a difficultly separable mixture of diastereoisomerides. Earlier evidence [1], now supplemented with the elemental composition $C_{11}H_{18}O_5N_2$, ultra-violet absorption data, and a positive response to the assay for α-monoamino monocarboxylic acids [3], is consistent with a lactam structure such as (VII) for the by-product, comparable to that present in pyroglutamic acid. In analogy, heat treatment of N-(D-1-carboxypropyl)-L-glutamic acid has been shown elsewhere to cause conversion of the latter imino acid into an anhydride, formulated as the corresponding pyroglutamic acid derivative [8].

Upon heating in the dry state to temperatures close to the melting points, the diastereisomeric saccharopines were converted into cyclized products, indistinguishable from the lactams described above. Both isomerides were completely and irreversibly transformed into cyclic derivatives on heating with water at 125°, a behaviour deviating notably from the reversibility observed in strong acid or alkali (*cf.* Ref.[1]).

The structure of L-saccharopine does not preclude its biosynthesis from L-lysine and 2-oxoglutaric acid, but is, on the other hand, equally consistent with its biological formation from L-glutamic acid and L-2-amino-5-formylvaleric acid (α-aminoadipic-δ-semialdehyde). It is interesting in this connexion that the latter aldehyde most likely is an actual intermediate in the biosynthesis of lysine from α-aminoadipic acid in *Neurospora* and yeast [22,23].

Imino acids have occasionally been suggested as possible intermediates in transamination reactions [24] though the available experimental evidence is meagre. Apart from cyclic types and simple N-alkylated amino acids only a very limited number of imino acids have thus far been encountered in Nature. Octopine was isolated from *Octopus* muscle in 1927 [25] and its constitution as N^2-(D-1-carboxyethyl)-L-arginine established a decade later [26,27] (*cf.* also Ref.[5]).

Recently, a French group [28] established the structure of lysopine, an amino acid occurring in crown galls from several higher plants, as N^2-(D-1-carboxyethyl)-L-lysine.

EXPERIMENTAL

Melting points are uncorrected and determined in capillary tubes in an Anschütz-Hershberg apparatus with a rate of heating of about 2° per min. Rotations are measured in a 1 dm tube. Infra-red spectra are determined in potassium bromide pellets on a Perkin-Elmer "Infracord"-instrument.

N^6-Benzyloxycarbonyl-L-lysine. Although in principle the same as the published method (*cf. e.g.* Ref.[29]), the following synthetic procedure is believed to possess certain advantages. L-Lysine monohydrochloride (9 g) was boiled for 30 min with cupric carbonate (3.5 g) and water (100 ml). Magnesium oxide (6 g) was added to the filtrate, and a solution (13 ml) of benzyloxycarbonyl chloride (56 mequiv.) in toluene was added in small portions in the course of 30 min. to the ice-cooled and stirred suspension. After stirring for another 2 h at room temperature, the mixture was cooled in ice, filtered, and the precipitate was washed with water, ethanol and ether. A stirred suspension of the solid in 1 N HCl (325 ml) was saturated with hydrogen sulphide, whereupon the mixture was heated to boiling, filtered and adjusted to pH 5 with conc. NH_3. The resulting solid was recrystallized from water (1 700 ml) and dried at 80°. There resulted 11.2 g (80 %) of the pure compound, m.p. 240—244° (decomp.), $[\alpha]_D^{23}$ + 13.5° (*c* 1.4, 0.1 N HCl). Literature value: $[\alpha]_D$ + 14.4° (*c* 1.6, 2 equiv. HCl in H_2O) [29].

N^2-(p-Toluenesulphonyl)-N^6-benzyloxycarbonyl-L-lysine. This derivative was prepared as previously described [30,31] with the minor modifications that ether was used as a solvent for the sulphonyl chloride and chloroform for extraction of the reaction product. The latter was recrystallized from benzene and dried at 80°. A yield of 89 % of unsolvated (*cf.* Ref.[15]), pure product was obtained, m.p. 121—122°, $[\alpha]_D^{23}$ + 13.5° (*c* 2.2, CH_3OH). Lit. values: m.p. 123—124° [30], 126° [15]; no rotation reported.

N^2-(p-Toluenesulphonyl)-L-lysine. The preparation of this compound by hydrogenolysis of the foregoing derivative has previously been reported [14], yet without experimental details. In the present case, N^2-(*p*-toluenesulphonyl)-N^6-benzyloxycarbonyl-L-lysine (12 g) was dissolved in a mixture of acetone (125 ml) and conc. HCl (4.5 ml), and treated, in the presence of palladium black (0.85 g), at 50° with a stream of hydrogen until the evolution of CO_2 ceased. Then, 4 N HCl (10 ml) and water (60 ml) were added, the catalyst was filtered off and acetone removed from the filtrate, which was finally extracted twice with ether. After being adjusted to pH 6 with conc. NH_3, the aqueous phase deposited the somewhat impure reaction product (7.6 g or 91 %; Ref.[14] lists 90 %). A pure specimen was obtained in beautifully crystalline form from water, m.p. 262—265° (decomp.), $[\alpha]_D^{22}$ −50.9° (*c* 2.0, 0.5 N NaOH). Lit. values: 263—264° (decomp.)[14], $[\alpha]_D^{19}$ −51.6° (*c* 2.3, 0.5 N NaOH) [31].

N^2-(p-Toluenesulphonyl)-L-lysine methyl ester hydrochloride. As elsewhere described [14], treatment of the above amino acid derivative with anhydrous methanol and HCl afforded the methyl ester hydrochloride in a yield of 78 %. A correctly analyzing specimen was obtained from a mixture of methyl acetate and pentane, m.p. 143—144°, $[\alpha]_D^{22}$ + 9.5° (*c* 1.0, CH_3OH).* Lit. values: m.p. 146—147° [14], 148—150° [32]; $[\alpha]_D^{22}$ −10.2° (*c* 4.0, H_2O)[32]**.

Diethyl DL-2-bromoglutarate. This ester, used in preliminary attempts to synthesize saccharopine, was prepared in 94 % yield according to the directions given by Schwenk and Papa [33]. Redistillation of a center cut from the first distillation afforded a pure sample, b.p. 89—92° at 0.3 mm, n_D^{20} 1.4591. (Found: C 40.25; H 5.88; Br 29.76. Calc. for $C_9H_{15}O_4Br$: C 40.46; H 5.66; Br 29.92).

* This product proved identical with a specimen described [14] and kindly furnished by Dr. D. T. Elmore.

** The notable change in rotation with solvent has been verified in this laboratory.

Synthesis of a mixture of L-*saccharopine and* D-allo*saccharopine.* In order to determine the optimal conditions for the following synthesis, the dissociation constant for the cyanohydrin of 2-oxoglutaric acid was experimentally determined by electrometric titration of a mixture of the acid and potassium cyanide. The found value of ca. 10^{-3}, together with the acid dissociation constant of hydrogen cyanide, enabled calculations of the best conditions for the synthesis. To 2-oxoglutaric acid (730 mg), dissolved in water (15 ml) and 1.2 N NaOH (8.9 ml), potassium cyanide (2.5 g) was added and pH was adjusted to 11.3 with 4 N HCl. This solution was mixed with another, prepared by dissolving N^2-(*p*-toluenesulphonyl)-L-lysine (1.75 g) in water (15 ml), adding 1.2 N NaOH (5.25 ml) and adjusting the pH to 11.4 with 4 N HCl. The mixture was kept in a closed vessel for 18 h at 50° and after cooling acidified to pH 1.9 with conc. HCl, when the amino-cyanohydrin (V) separated in 65 % yield (1.5 g) as a colourless, crystalline product.

Without further purification, the latter (1.5 g) was dissolved in conc. HCl (25 ml) and set aside at room temperature for 16 h. Then water (25 ml) was added and the solution was refluxed for 2 h. After evaporation to dryness *in vacuo* and careful removal of the last traces of acid, the dry, semisolid mass was dissolved in liquid ammonia (100 ml), and sufficient metallic sodium (*ca.* 0.5 g) added to produce a persistent blue colour. Thirty min. later enough ammonium acetate was added to cause a change to yellow colour and the ammonia was allowed to evaporate. The residue was dissolved in water (10 ml), treated with charcoal, filtered, and pH in the filtrate adjusted to 3.8 with 4 N HCl. After two extractions with ether and dilution to a volume of 100 ml, the aqueous phase was applied to a column (36 cm × 1.5 cm) of a strongly acid ion exchange resin (Zerolit 225) in the hydrogen form. The column was washed with water and the entire amino acid fraction eluted with 1 N NH_3. The dry eluate residue (650 mg), dissolved in CO_2-free water (50 ml), was then applied to a weakly basic resin (Amberlite IR-4B, 24 cm × 1.5 cm) in acetate form, and after washing with water, 2 N HCl was used for elution. The eluate was concentrated to dryness *in vacuo* to give a semi-crystalline residue (470 mg), which on paper chromatography gave one spot attributable to the isomeric saccharopines, and another spot representing their transformation products.

A fraction (272 mg) of the above product was dissolved in water (2 ml) and treated with charcoal. After filtration and concentration to 0.8 ml, the addition of ethanol (0.5 ml) caused the precipitation of a finely crystalline product (65 mg). Four similar precipitations yielded a preparation (18 mg) of the diastereoisomer mixture which on paper chromatography was homogeneous and indistinguishable from authentic saccharopine, $[\alpha]_D^{25}$ + 14° (*c* 2.0, 0.5 N HCl, 0.5 dm tube) (Found (corrected for 0.77 % of ash): C 47.95; H 7.47; N 9.93. Calc. for $C_{11}H_{20}O_6N_2$: C 47.82; H 7.30; N 10.14).

Separation of diastereosiomerides. A solution in water (7.5 ml) of the above-described semi-crystalline residue from the HCl-eluate (1.25 g) was treated with charcoal, filtered, adjusted to pH 3.7 with 4 N ammonia and concentrated to a volume of 6 ml. Addition of ethanol (9 ml) caused the precipitation of a crystalline solid (340 mg), which according to paper chromatography was virtually free of the conversion products of the saccharopines. The solution of this product (230 mg) in water (6 ml), was treated with charcoal to give a colourless solution, which was concentrated to half of the volume, seeded with natural L-saccharopine, and kept at 4° for 6 days. The crystalline compound (77 mg, $[\alpha]_D^{23}$ + 25.7° (*c* 1.3, 0.5 N HCl)) was subsequently subjected to three similar recrystallizations to give a pure specimen (27 mg), m.p. 240–248° (decomp.), alone or in admixture with natural saccharopine, (Found: C 47.76; H 7.24; N 10.18) with $[\alpha]_D^{23}$ + 32.2° (*c* 1.0, 0.5 N HCl), compared to the value $[\alpha]_D^{23}$ + 33.6° (*c* 1.0, 0.5 N HCl) determined for pure, authentic L-saccharopine [1]. Furthermore, coinciding IR-spectra and X-ray diffraction patterns served to establish the identity of the two compounds.

On concentration to a small volume, the mother liquor from the first crystallization deposited a colourless solid (62 mg) with $[\alpha]_D^{24}$ + 4.2° (*c* 0.9; 0.5 N HCl). Once recrystallized from water the product had a specific rotation of −0.6°, and renewed recrystallizations afforded an end-product (17 mg), m.p. 235–250° (decomp., after preliminary sintering at 215–217°) with $[\alpha]_D^{23}$ −0.8° (*c* 0.4, 0.5 N HCl) (Found: C 47.51; H 7.46; N 10.28), and believed to represent pure or nearly pure D-*allo*saccharopine.

Isolation of a cyclic by-product. The combined mother liquors from the above described isolations of L- and D-*allo*-saccharopine were passed through a strongly acid ion exchange resin and eluted with ammonia to give a brownish glassy mass (600 mg). This was dissolved in water and decolourized by filtration through a small column of alumina. Addition of ethanol to the filtrate resulted in separation of the ammonium salt of the unknown by-product (180 mg). The filtrate was adjusted to pH 2.5 and acetone was added to induce crystallization of the cyclic by-product (230 mg), $[\alpha]_D^{21}$ + 7.0° (*c* 0.9, H_2O). Two additional recrystallizations from water and acetone gave material, m.p. 245–248° (decomp), with unchanged rotation ($[\alpha]_D^{23}$+6.8° (*c* 1.0, H_2O); $[\alpha]_D^{23}$+18.2° (*c* 0.9, 1 N HCl)) (Found: C 50.59; H 7.10; N 10.96. Calc. for $C_{11}H_{18}O_5N_2$: C 51.15; H 7.03; N 10.85). The infrared absorption curve is depicted in Fig. 1. The ultra-violet absorption spectrum had a molecular extinction of 4 200 at 205 mμ, compared to 200 for L-saccharopine, supporting the cyclic structure (VII).

The above rotation value, corresponding to molecular rotations of + 17.4° and + 46.5° in water and acid, on comparison with the $[M]_D$-values + 19.4° (H_2O) and + 37.9° (HCl) for L-lysine and −15.4° (H_2O) for L-pyroglutamic acid, suggest that the analyzed specimen may be a difficultly separable mixture of about equal parts of two diastereoisomerides.

The authors are grateful to Dr. K. Knakkergaard Møller for the determination of the X-ray diffraction patterns, and to Mr. G. Cornali for microanalyses.

Grants from *Det Teknisk-Videnskabelige Forskningsråd (The Research Council of the Technical Sciences)* and *Carlsbergfondets Legat for Den Kgl. Veternær- og Landbohøjskole (The Carlsberg Foundation Stipendium for The Royal Veterinary and Agricultural College)* for the acquisition of infrared and potentiometric equipment, respectively, are gratefully acknowledged.

REFERENCES

1. Darling, S. and Olesen Larsen, P. *Acta Chem. Scand.* **15** (1961) 743.
2. Darling, S. *To be published.*
3. Olesen Larsen, P. and Kjær, A. *Biochim. et Biophys. Acta* **38** (1960) 148.
4. Herbst, R. M. and Swart, E. A. *J. Org. Chem.* **11** (1946) 368.
5. Izumiya, N., Wade, R., Winitz, M., Otey, M. C., Birnbaum, S. M., Koegel, R. J. and Greenstein, J. P. *J. Am. Chem. Soc.* **79** (1957) 652.
6. Braunstein, A. E. *Enzymologia* **7** (1939) 25.
7. Karrer, P. and Appenzeller, R. *Helv. Chim. Acta* **25** (1942) 595.
8. Kögl, F., de Flines, J. and den Boer, D. H. W. *Rec. trav. chim.* **72** (1953) 1009.
9. Sugasawa, S. *J. Pharm. Soc. Japan* **1927** 54. *Chem. Zentr.* **1927 II** 932.
10. Stadnikoff, G. *Ber.* **40** (1907) 1014.
11. Stadnikoff, G. *Ber.* **44** (1911) 44.
12. Scheibler, H. *Ber.* **45** (1912) 2272.
13. Stadnikoff, G. *J. Russ. Phys.-Chem. Soc.* **41** (1909) 900; *Chem. Zentr.* **1909 II** 1988.
14. Barass, B. C. and Elmore, D. T. *J. Chem. Soc.* **1957** 4830.
15. Swallow, D. L., Lockart, I. M. and Abraham, E. P. *Biochem. J.* **70** (1958) 359.
16. Gaudry, R. *Can. J. Research* **26B** (1948) 387.
17. Cocker, W. *J. Chem. Soc.* **1937** 1693.
18. Sugasawa, S. *J. Pharm. Soc. Japan* **1927** 147; *Chem. Zentr.* **1928 I** 1646.
19. Knoop, F. and Oesterlin, H. *Z. physiol. Chem. Hoppe-Seyler's* **170** (1927) 206.
20. Kanao, S. *J. Pharm. Soc. Japan* **66** (1946) 4; *Chem. Abstr.* **45** (1951) 7956.
21. Stewart, F. H. C., Stedman, R. J. and duVignaud, V. *J. Am. Chem. Soc.* **78** (1956) 5883.
22. Work, E. In McElroy, W. D. and Glass, B. (Eds.) *Amino Acid Metabolism*, Johns Hopkins Press, Baltimore Md. 1955, p. 462.
23. Yura, T. and Vogel, H. J. *J. Biol. Chem.* **234** (1959) 339.
24. Karrer, P. and Brandenberger, H. *Helv. Chim. Acta* **34** (1951) 82.
25. Morizawa, K. *Acta Schol. Med. Univ. Imp. Kioto* **9** (1927) 285; *Chem. Zentr.* **1928 II** 2479.

26. Moore, E. and Wilson, D. W. *J. Biol. Chem.* **119** (1937) 573, 585.
27. Akasi, S. *J. Biochem. (Tokyo)* **25** (1937) 261, 281, 291.
28. Biemann, K., Lioret, C., Asselineau, J., Lederer, E. and Polonsky, J. *Bull. soc. chim. biol.* **42** (1960) 979.
29. Neuberger, A. and Sanger, F. *Biochem. J.* **37** (1943) 515.
30. Barras, B. C. and Elmore, D. T. *J. Chem. Soc.* **1957** 3134.
31. Kucherov, V. F. and Ivanov, A. I. *J. Gen. Chem. U.S.S.R.* **21** (1951)1248; *Chem. Abstr.* **46** (1952) 8006.
32. Irving, C. C. and Gutmann, H. R. *J. Org. Chem.* **24** (1959) 1979.
33. Schwenk, E. and Papa, D. *J. Am. Chem. Soc.* **70** (1948) 3626.
34. Vickery, H. B. *J. Biol. Chem.* **169** (1947) 237.
35. *Germ. Pat.* 847006 (1952); *Chem. Abstr.* **50** (1956) 2669.

Received December 1, 1960.

ACTA CHEMICA SCANDINAVICA 15 (1961) 760–768

The Action of α-Chymotrypsin on Tyrosine Ethyl Ester

JOHN GRAAE and B. O. HANSEN

Centrallaboratoriet, Kommunehospitalet, Copenhagen, Denmark

The splitting of tyrosine ethyl ester by α-chymotrypsin was studied by means of continuous titration in a pH-stat. The reaction was followed to about 99 % hydrolysis, and to explain the obtained results it is necessary to assume the simultaneous or consecutive uptake of 3 molecules of substrate before reaction takes place. This supports the view that transpeptidation is the first step in the splitting of this substrate.

Numerous investigations have been carried out on the action of α-chymotrypsin [1–3], and a good deal of these are made with phenylalanine derivatives as substrates, *e.g.* tyrosine ethyl ester (TEE). However, these investigators usually study the initial velocities of the reaction in order to analyse the results according to Michaelis and Menten [4]. If, however, the suggestion made by Kuk-Meiri and Lichtenstein [5] that the splitting of TEE should start with a transpeptidation is correct, a Michaelis-Menten analysis could very easily lead to misinterpretations. In order to distinguish between this and other suggested theories for the mechanism, the reaction was studied carefully and the results analysed according to the "steady state" method in the way suggested by Christiansen [6,7]; it is known that this method has given new information about the behaviour of the pancreatic enzymes on other substrates [8].

EXPERIMENTAL

Crystalline α-chymotrypsin was kindly placed at our disposal by *Novo Terapeutisk Laboratorium*, Copenhagen, Denmark.

TEE was a commercial product (L-tyrosine ethyl ester from Nutritional Biochemical Corporation, U.S.A.).

The experiments were carried out in 30 ml 0.2 M KCl, in which the desired amount of substrate was dissolved and adjusted to the desired pH by means of KOH. Substrate concentrations varied from 0.678 mmole/l to 9.50 mmole/l. The temperature, unless stated otherwise, was 27.09°C and the pH was 6.838. The hydrolysis was followed by continuous automatic titration with 0.10 M KOH + 0.2 M KCl in a selfrecording pH-stat. The degrees of reaction were calculated as the proportion between the titration value at the desired time and the titration value after complete hydrolysis.

The potassium hydroxide is added from a syringe in quanta corresponding to 1/100 mm movement of the piston. It should be noticed that at the highest degrees of reaction

Table 1. E = enzyme concentration in arbitrary units. t = times necessary to obtain the degrees of reaction, a, given in the first line. In order to confirm the $E \cdot t$ law the figures in the vertical columns $E \cdot t_n$ should be identical for each value of n, but different for different values of n. For further explanation see text.

a = 0.143			0.286		0.429		0.571		0.714		0.857	
E	t_1	$E \cdot t_1$	t_2	$E \cdot t_2$	t_3	$E \cdot t_3$	t_4	$E \cdot t_4$	t_5	$E \cdot t_5$	t_6	$E \cdot t_6$
8	0.95	7.6	2.1	16.8	3.4	27.2	4.0	32.0	6.0	48.0	8.1	64.8
6	1.2	7.2	2.8	16.8	4.2	25.2	5.0	30.0	7.7	46.2	10.5	63.0
4	2.0	8.0	4.1	16.4	6.4	25.6	7.6	30.4	12.5	50.0	18.6	74.4
2	3.8	7.6	8.0	16.0	12.7	25.4	15.4	30.8	26.0	52.0	38.7	77.4
1	8.3	8.3	17.3	17.3	27.2	27.2	32.8	32.8	56.5	56.5	87.0	87.0

the velocity was considerably lower than 1 quantum/min so that errors on calculated times of one or two minutes are to be expected in this area.

RESULTS

From Table 1 is seen that the chronometric integral, with acceptable accuracy, can be written in the form $E \cdot t = f(x_1 x_2 ... x_n)$ where E is enzyme concentration, t is time and x_1, x_2, ...x_n are the variables which determine the reaction rate, *e.g.* degree of reaction, pH and concentration of TEE. In a single experiment the only variable on the right side usually is the degree of reaction. In a series of experiments, where only the enzyme concentration is varied, the validity of writing the chronometric integral, as mentioned above, can be determined by comparing the times necessary to reach a given degree of reaction with different enzyme concentrations. Table 1 records the times necessary to obtain some different degrees of reaction for different enzyme concentrations and the products of these times and enzyme concentrations.

The dependence of activity on temperature and pH, as well as the pH optimum dependence on temperature, was investigated. The results are shown

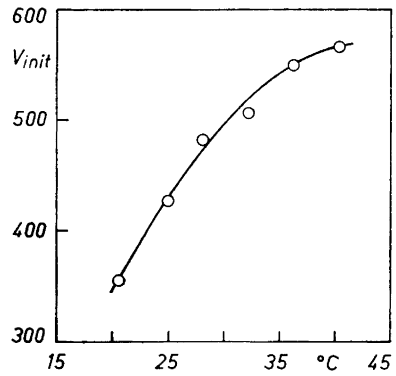

Fig. 1. Initial velocity as function of temperature. pH = 6.7.

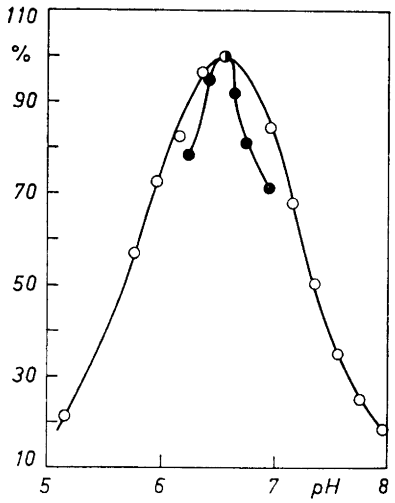

Fig. 2. A graph of initial velocity *versus* pH at two temperatures. ○, $t = 28.10°C$; ●, $t = 41.45°C$. Abscissa gives pH and ordinate gives the slope of the titration curve in per cent of the maximal slope at the same temperature. Substrate and enzyme concentrations are equal in all experiments at the same temperature. The dissociation of the amino group gives rise to a change in the fraction of the liberated acid that is titrated, this fraction being diminished in the pH range 6—8. The true optimum of the reaction is at pH 6.85.

in Figs. 1 and 2. It is interesting to compare these two figures with the same results obtained with subtilisin splitting the same substrate [9]. In the latter case, the changes of pH optimum with temperature clearly demonstrated that the enzyme attacked only the positively charged substrate mlecules; but the curves presented here in no way indicate that the same mechanism is the

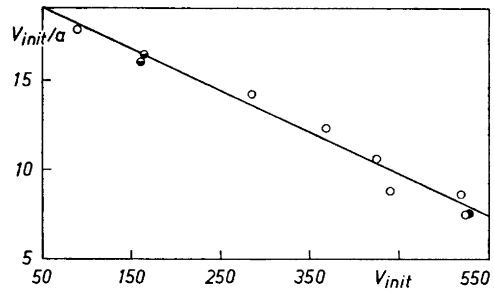

Fig. 3. The figure gives initial velocity divided by initial substrate concentration as ordinate and initial velocity as abscissa. Initial velocity is determined as the slope (in arbitrary units) at the origin of the lower concentrations and as the slope when d^2c/dt^2 is zero at the highest concentrations. (See: Discussion and Fig. 8 for further explanation). The two points marked ◒ are twin determinations at 10 mg/30 ml; ● is 70 mg/30 ml recrystallized from ethyl acetoacetate; the other points represent 5, 20, 30, 40, 50, 60, and 70 mg in 30 ml.

case with chymotrypsin, which suggests a fundamental difference in the action of the two enzymes on this substrate.

The reaction has often been described by a Michaelis-Menten function. From Fig. 3 it is seen that our results too satisfy the Michaelis-Menten equation. Using the method for graphical representation, suggested by Eadie [10], in which (initial velocity)/(substrate concentration) is plotted *versus* initial velocity, a reasonably straight line is obtained as seen in the figure. If, however, the reaction in its entire course should have a reaction scheme as the one suggested by Michaelis and Menten, the chronometric integral should consist of a zero order term and a first order term:

$$E \cdot t = A \cdot a - B \cdot \log(1-a) \qquad (1)$$

where a is the degree of reaction and A and B are constants. Indeed, this is not true for this reaction, which can easily be seen, for instance by plotting t/a *versus* $\log(1-a)/a$. If the reaction could be described by eqn. (1), this graph should be a straight line with the intercept on the ordinate axis being A and the slope B. With different initial substrate concentrations, A should be proportional to the initial substrate concentration and B should depend linearly on the same or be independent of this concentration.

In this way it can be clearly demonstrated that the experimental results recorded in Tables 2—7 in no way fit eqn. (1). It is further seen from such a

Tables 2—7. These tables give measured and calculated values of t together with corresponding values of a. The 6 tables represent 6 different concentrations of TEE and for every table is given a, A', B', C' and D'. (The B' values are based on calculations with $\log_{10}$.) The deviations between t_m and t_c at the highest degrees of reaction is understandable as the number of hydroxyl quanta from the titration outfit was below 1 quantum/min. The number of quanta for complete hydrolysis are given for every experiment as s_∞.

Table 2. a = 5 mg/30 ml; A' = 2.70; B' = 44.0; C' = −0.395; D' = 0.00170 and s_∞ = 224.

t_m	t_c	a
0	0.00	0.0000
5	4.61	0.1964
10	9.76	0.3750
15	15.28	0.5267
20	20.48	0.6383
25	25.78	0.7276
30	30.90	0.7946
35	36.18	0.8482
40	41.28	0.8883
45	45.58	0.9151
50	50.02	0.9375
55	54.37	0.9553
60	59.81	0.9732
65	63.16	0.9821
70	70.18	0.9910

Table 3. a = 10 mg/30 ml; A' = 5.50; B' = 46.6; C' = −0.189; D' = 0.00110 and s_∞ = 466.

t_m	t_c	a
0	0.00	0.0000
5	4.84	0.1759
10	10.07	0.3369
15	15.17	0.4678
20	20.35	0.5772
25	25.72	0.6795
30	30.67	0.7382
35	35.64	0.7940
40	40.37	0.8369
45	45.72	0.8755
50	50.21	0.9013
55	55.35	0.9249
60	59.42	0.9399
65	64.50	0.9549
70	69.18	0.9657
75	73.89	0.9742
80	78.63	0.9807
85	82.89	0.9850
90	89.40	0.9893
95	105.23	0.9936

graph that a negative term at the right side should be added to (1) and that this term should be relatively more important at low substrate concentrations than at high substrate concentrations, where it should be important only at the higher degrees of reaction. It is then reasonable to suggest that a second order term should be added to (1) making it:

$$E \cdot t = A'a - B'\log(1-a) + C'\left(\frac{1}{1-a} - 1\right) \qquad (2)$$

This equation is able to describe the obtained results with excellent accuracy except at the very highest degrees of reaction where calculated times will be too low as compared with those measured. It will be seen from the calculations below that the term which becomes significant at the highest degrees of reaction should be positive. Therefore a fourth term is added to the right side of (2) giving as chronometric integral:

$$E \cdot t = A'a - B'\log(1-a) + C'\left(\frac{1}{1-a} - 1\right) + D'\left(\frac{1}{(1-a)^2} - 1\right) \qquad (3)$$

We determined the best fitting values of A', B', C' and D' for six experiments with different TEE concentrations and the same enzyme concentration. These values are in Tables 2—7.

Table 4. a = 20 mg/30 ml; A' = 11.0; B' = 44.2; C' = — 0.080; D' = 0.00045 and s_∞ = 939.

t_m	t_c	a
0	0.00	0.0000
5	4.80	0.1512
10	10.00	0.2971
15	15.05	0.4207
20	20.14	0.5282
25	25.19	0.6187
30	30.29	0.6954
35	35.26	0.7572
40	40.40	0.8094
45	45.17	0.8488
50	50.12	0.8818
55	55.14	0.9084
60	60.22	0.9297
65	64.71	0.9446
70	69.56	0.9574
75	74.74	0.9680
80	78.72	0.9744
85	83.80	0.9808
90	88.35	0.9851
95	94.52	0.9893
100	102.25	0.9925
105	112.54	0.9947

Table 5. a = 30 mg/30 ml; A' = 16.2; B' = 46.5; C' = — 0.072; D' = 0.00027 and s_∞ = 1390.

t_m	t_c	a
0	0.00	0.0000
5	4.92	0.1302
10	10.10	0.2561
15	15.28	0.3698
20	20.28	0.4683
25	25.41	0.5576
30	30.54	0.6353
35	35.61	0.7014
40	40.53	0.7561
45	45.68	0.8043
50	50.49	0.8417
55	55.53	0.8741
60	60.46	0.9000
65	65.73	0.9223
70	68.84	0.9388
75	75.35	0.9518
80	79.94	0.9619
85	84.82	0.9705
90	89.46	0.9770
95	93.94	0.9820
100	99.96	0.9871
105	105.77	0.9906
110	111.00	0.9928
115	115.79	0.9942

Table 6. a = 40 mg/30 ml; A' = 20.2; B' = 46.5; C' = − 0.071; D' = 0.00022 and s_∞ = 1849.

t_m	t_c	a
0	0.00	0.0000
5	4.79	0.1152
10	9.87	0.2293
15	14.93	0.3342
20	19.98	0.4300
25	24.80	0.5127
30	29.87	0.5906
35	34.93	0.6593
40	40.05	0.7198
45	45.01	0.7701
50	49.97	0.8129
55	55.03	0.8496
60	60.18	0.8805
65	64.88	0.9037
70	70.27	0.9254
75	75.30	0.9416
80	80.08	0.9540
85	85.03	0.9643
90	89.93	0.9724
95	94.89	0.9789
100	100.22	0.9843
105	104.38	0.9876
110	108.71	0.9903
115	113.13	0.9924
120	120.00	0.9946

Table 7. a = 50 mg/30 ml; A' = 28.2; B' = 47.0; C' = − 0.045; D' = 0.00017 and s_∞ = 2298.

t_m	t_c	a
0	0.00	0.0000
5	4.31	0.0870
10	9.47	0.1867
15	14.70	0.2820
20	19.85	0.3703
25	24.77	0.4487
30	29.94	0.5248
35	35.01	0.5931
40	40.02	0.6540
45	45.15	0.7097
50	50.30	0.7597
55	55.44	0.8003
60	60.24	0.8359
65	65.17	0.8660
70	70.14	0.8916
75	74.91	0.9121
80	80.07	0.9304
85	84.86	0.9443
90	89.64	0.9556
95	94.66	0.9652
100	99.48	0.9726
105	104.47	0.9787
110	109.45	0.9835
115	113.92	0.9869
120	117.48	0.9891
125	122.96	0.9927
130	127.96	0.9935

REACTION MECHANISM

Assuming a steady state, we suggest the following reaction mechanism, based upon eqn. (3):

$$X_1 + 2\ TEE \rightleftharpoons X_2 \qquad (\pm 1)$$
$$X_2 + TEE \rightleftharpoons X_3 + P_1 \qquad (\pm 2)$$
$$X_3 \rightarrow X_1 + P_2 \qquad (+ 3)$$

In this scheme X_n means a form of the enzyme or a combination of enzyme and one or several substrate or product molecules. P_n is the reaction products; P_2 may represent either one or more molecules and nothing is assumed about their configuration.

Treating this reaction scheme according to the steady state method, in the way described by Christiansen [6,7], and using the following symbols: x_n = concentration of X_n; w_n = reaction probability for the n'th reaction; k_n = velocity constant for the same reaction; c = concentration of TEE; a = initial concentration of TEE; $s = -\mathrm{d}c/\mathrm{d}t$; E = enzyme concentration and t = time, we have:

$$s = x_1w_1 - x_2w_{-1}$$
$$s = x_2w_2 - x_3w_{-2}$$
$$s = x_3w_3$$

Remembering that $E = x_1 + x_2 + x_3$, we get by rearrangement and addition:

$$E/s = \frac{1}{w_1} + \frac{1}{w_2} + \frac{1}{w_3} + \frac{w_{-1}}{w_1 w_2} + \frac{w_{-2}}{w_2 w_3} + \frac{w_{-1} w_{-2}}{w_1 w_2 w_3}$$

Looking at the reaction scheme we see that we can introduce:

$$w_1 = k_1 c^2;\ w_{-1} = k_{-1};\ w_2 = k_2 c;\ w_{-2} = k_{-2}(a-c) \text{ and } w_3 = k_3,$$

if assuming that the concentration of $P_1 = (a-c)$. This changes the equation to:

$$E/s = \left(\frac{k_{-1}}{k_1 k_2} + a\frac{k_{-1}k_{-2}}{k_1 k_2 k_3}\right)\frac{1}{c^3} + \left(\frac{1}{k_1} - \frac{k_{-1}k_{-2}}{k_1 k_2 k_3}\right)\frac{1}{c^2} + \left(\frac{1}{k_2} + a\frac{k_{-2}}{k_2 k_3}\right)\frac{1}{c} + \left(\frac{1}{k_3} - \frac{k_{-2}}{k_2 k_3}\right)$$

Integrating this gives:

$$E \cdot t = Aaa - (B_1 + B_2 a)(\ln 10)\log(1-a) + C\frac{1}{a}\left(\frac{1}{1-a} - 1\right) + \tfrac{1}{2}(D_1 + D_2 a)\frac{1}{a^2}\left(\frac{1}{(1-a)^2} - 1\right)$$

a is the degree of reaction $= (a-c)/a$; $A = \frac{1}{k_3} - \frac{k_{-2}}{k_2 k_3}$; $B_1 = \frac{1}{k_2}$; $B_2 = \frac{k_{-2}}{k_2 k_3}$; $C = \frac{1}{k_1} - \frac{k_{-1}k_{-2}}{k_1 k_2 k_3}$; $D_1 = \frac{k_{-1}}{k_1 k_2}$ and $D_2 = \frac{k_{-1}k_{-2}}{k_1 k_2 k_3}$.

This calculated chronometric integral is identical with (3) if: $A' = A \cdot a$; $B' = B_1 + B_2 \cdot a$; $C' = C \cdot \frac{1}{a}$ and $D' \cdot 2a^2 = D_1 + D_2 \cdot a$.

From Figs. 4—7 it is seen that the dependence of A', B', C', and D' on a is in agreement with the calculated dependence.

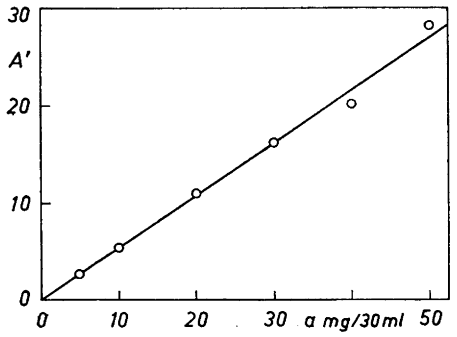

Fig. 4. A' from Tables 2—7 *versus* a.

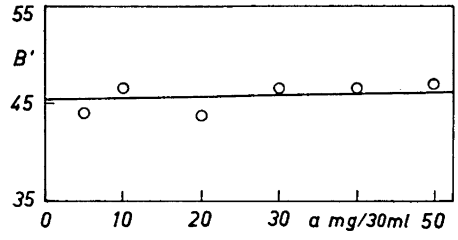

Fig. 5. B' from Tables 2—7 *versus* a.

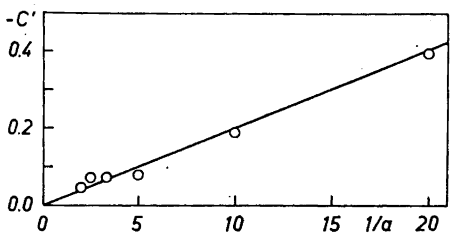

Fig. 6. C' from Tables 2—7 *versus* $1/a$.

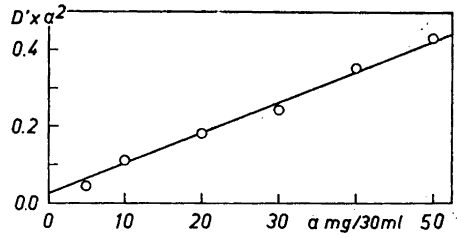

Fig. 7. D' from Tables 2—7 multiplied by a^2 as ordinate and as abscissa a.

DISCUSSION

The reaction mechanism suggested here differs from mechanisms, previously proposed, for the investigated reaction. A mechanism involving three steps has, however, been suggested before [2,3] and it has also been suggested that a crucial step should involve a transpeptidation [5]. Based on kinetical facts alone, it is not possible to conclude that the step involving two molecules of TEE is involving a transpeptidation; but it seems necessary to assume the participation of three molecules of TEE in order to explain the obtained results. Referring to the investigations by Kuk-Meiri and Lichtenstein [5], it seems reasonable to assume that the first two molecules form a dipeptide, and that the reaction thereafter takes place by substituting one of the molecules in the resulting tyrosyl-tyrosine ethyl ester (TTEE) with a third molecule of TEE. It seems reasonable to explain the kinetical data by assuming that the dipeptide synthesis is made directly from TEE so it can be written schematically:

$$2\ \text{TEE} \rightarrow \text{TTEE} + \text{EtOH}.$$

Another possibility, a reaction between tyrosine (T) and TEE:

$$\text{T} + \text{TEE} \rightarrow \text{TTEE}$$

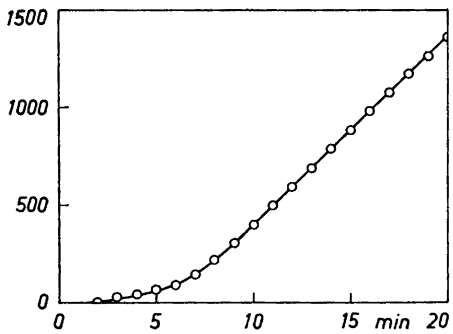

Fig. 8. Experiments with saturated TEE solutions. Note the obvious increase in reaction velocity in the first minutes.

as was suggested by Tauber [11] for the formation of phenylalanyl-phenylalanine ethyl ester does not seem to be supported by the kinetical data.

It should be noticed that the fourth term in the chronometric integral is needed for a second reason: It appears so that it is impossible to construct any reaction mechanism that gives a negative coefficient to the term corresponding to the highest reaction order. The necessity for this negative term is seen by plotting t/a *versus* $\log (1-a)/a$, especially at the lowest substrate concentrations.

The chronometric integral, suggested here, conforms with the experimental results to a very high extent, and it seems that the proposed reaction mechanism is one of the simplest that can explain the experimental facts. However, there is evidence which indicates that the reaction mechanism is in fact more complicated than the one proposed here. The deviation from the $E{\cdot}t$ law may not be large enough to disprove its validity but it might suggest the need for corrections. Secondly, a positive value of $\mathrm{d}s/\mathrm{d}t$ $(= -\mathrm{d}^2c/\mathrm{d}t^2)$ is seen in the first minutes for higher substrate concentrations and in solutions saturated with TEE, which indicates that under these circumstances the reaction does not attain a steady state immediately; that some reaction not identical with the overall reaction takes place in the first minutes (Fig. 8).

Further information on where hydrogen and hydroxyl ions enter in the reaction scheme, as well as whether several protolytic forms of substrate enter in the reaction, can probably be obtained by studying the four constants at different pH values. Experiments of that kind are in progress in this laboratory.

Acknowledgements. Financial support from *Statens Videnskabsfond*, *Carlsbergfondet* and *Købmand i Odense Johann og Hanne Weimann født Seedorffs Legat* from Denmark as well as the receipt of *Nordisk Forskningsstipendium* from the University of Oslo, Norway, is gratefully acknowledged by J. G.

REFERENCES

1. Goldenberg, H. and Goldenberg, V. *Arch. Biochem.* **29** (1950) 154.
2. Gutfreund, H. and Hammond, B. R. *Biochem. J.* **73** (1959) 526.
3. Spencer, T. and Sturtevant, J. M. *J. Am. Chem. Soc.* **81** (1959) 1874.
4. Michaelis, L. and Menten, M. *Biochem. Z.* **49** (1913) 333.
5. Kuk-Meiri, S. and Lichtenstein, N. *Biochim. et Biophys. Acta* **25** (1957) 182.
6. Christiansen, J. A. *Acta Chem. Scand.* **3** (1949) 493.
7. Christiansen, J. A. *Advances in Catalysis* **6** (1953) 311.
8. Graae, J. *Biochim. et Biophys. Acta* **32** (1959) 510.
9. Andersen, S. O. and Graae, J. *Acta Chem. Scand.* **13** (1959) 1109.
10. Eadie, G. S. *J. Biol. Chem.* **146** (1942) 85.
11. Tauber, H. *J. Am. Chem. Soc.* **74** (1952) 847.

Received December 5, 1960.

ACTA CHEMICA SCANDINAVICA 15 (1961) 769–774

The Crystal Structure of Calcium Carbide III

NILS-GÖSTA VANNERBERG

Institutionen för Oorganisk kemi, Chalmers tekniska högskola, Göteborg, Sweden

The crystal structure of CaC_2 III has been determined from three-dimensional X-ray data. The structure is built up of calcium and carbide ions arranged in a more complicated way than in the ordinary tetragonal calcium carbide structure.

The crystal structure of tetragonal face-centered calcium carbide, CaC_2 I, was determined by von Stackelberg [1]. The cell dimensions were found to be $a = 5.48$ and $c = 6.37$ Å. There are 4 formula units in the cell. The carbide (C_2^{2-}) ions have their length axis in the z-axis direction, see Fig. 2c. The distances between the carbon atoms in a carbide ion were found by v. Stackelberg to be 1.4 Å. However, in a recent investigation made by neutron diffraction, Atoji and Medrud [2] found the much more probable distance of 1.20 Å. This is in accordance with distances found in organic acetylidic compounds [3]. Earlier Dehlinger and Glockner [4] had described a cubic calcium-carbide structure. Their investigation was criticised by Herman [5] and v. Stackelberg [1]. This structure has nothing to do with the cubic face-centered high temperature modification found by Bredig [6]. The axes in the crystal structure of the latter compound were determined to be 5.92 Å. The structure is only stable above $450° \pm 20°$. On cooling according to Frank, Bredig and co-workers [7–9] and to Bredig [6], this structure may yield two modifications with low symmetry, CaC_2 II and CaC_2 III, which are both metastable in the temperature interval 0°—450°C. They are transformed into CaC_2 I by grinding. Below 0°C, CaC_2 II is said to be the stable modification. When the carbide is contaminated by sulphur, the modifications CaC_2 II and CaC_2 III are not formed when CaC_2 IV is cooled below 450°; instead CaC_2 I is obtained. When cyanamide and sulphur are present, CaC_2 II is formed. This structure is said to be able to incorporate about 5 mole % cyanamide ions at 450°C. When only cyanamide is present, CaC_2 III is formed. However, Bredig has earlier claimed that CaC_2 II and not CaC_2 III is formed in the presence of cyanamide [6]. While the actual investigation was still in progress, a similar view was presented by Bochert and Röder [10]. They found that CaC_2 IV was stable above 435°C. This phase was transformed into CaC_2 III when no impurities were present, into CaC_2 II when cyanamide and sulphur were present, and into CaC_2 I when sulphur

was the only contamination. They also found that III is transformed into I above 30°C under high pressure. Below 30°C, II is formed.

Later Nast and Pfab reported [11,12] a fifth modification of CaC_2, the X-ray pattern of which was very similar to that of Cu_2C_2. This work has been seriously criticised by Bredig [13,14], on good grounds according to this author's opinion.

According to Bochert and Röder [10] both CaC_2 II and CaC_2 III have tetragonal symmetry. CaC_2 II: $a = 23.40$ Å, $c = 22.31$ Å, and CaC_2 III: $a = 23.40$ Å, $c = 22.87$ Å.

PREPARATION OF THE COMPOUND

4 g calcium metal, granular, was mixed with 2 g graphite. The mixture was heated in an induction furnace of Philips' construction. A graphite crucible was used. The induction coil and the crucible were inserted in a glass flask (Fig. 1). The air was removed from the flask with the aid of a stream of argon gas. When the air had been carefully removed, the current was turned on and the temperature was gradually raised to about 1 800°C. This temperature was not enough to melt the carbide formed. The crystals obtained were rather small and had grown together in great aggregates. They were unsuitable for X-ray work. After many unsuccessful attempts it became clear that the temperature must be increased to the melting point in order to get better single crystals. In these experiments the radiation losses set the upper temperature limit. The radiation losses were considerably decreased by putting on a layer of zirconium oxide powder outside the induction coil. In this way the temperature was raised to above 2 200°, which was enough to melt the carbide. After a few attempts rather good crystals were obtained, suitable for single crystal work. The compound obtained consists of small transparent light-brown to colourless crystals. In addition there were black coloured grains, probably consisting of graphite.

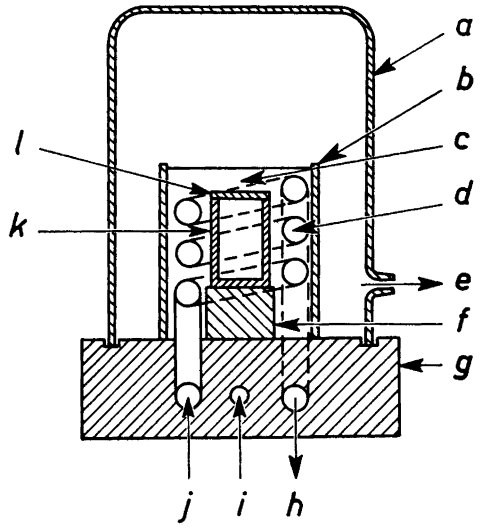

Fig. 1. Section through the induction furnace. Between the cover of zirconium oxide and the heating coil zirconium oxide powder is packed. a) Glass flask, b) cover of zirconium-oxide, c) zirconium oxide powder, d) heating coil, e) outlet for argon, f) cylinder of boron nitride, g) soap stone, h) water outlet, i) inlet for argon, j) water inlet, k) grafite crucible, l) cover of boron nitride.

Table 1. Chemical composition and density of CaC_2 III.

Sample	% Ca	% C_2^{2-}	density
I	60.8	36.8	2.16
II	61.2	36.9	2.15
Calculated	62.5	37.4	2.17

Analysis. The carbide content was determined by measuring the amount of gas liberated when a certain amount of water saturated with acetylene gas was added to a sample. The calcium content was determined volumetrically by titration of the precipitated oxalate with permanganate. The specific gravity was determined by a method given by Schrewelius [15].

THE DETERMINATION OF THE CRYSTAL STRUCTURE

The structural investigation was based on single crystal methods. The single crystals were rotated about the *c*-axes and Weissenberg photographs were taken for all zones detectable with Cu$K\alpha$ radiation. The reflexion intensities were estimated by visual comparison with known scales and corrected by Lorentz and polarization factors. The crystals were mounted inside capillary tubes in order to prevent atmospheric attack.

The unit cell was proved to be monoclinic with

$$\begin{aligned} a &= 8.36 \pm 0.02 \text{ Å} \\ b &= 4.20 \pm 0.01 \text{ Å} \\ c &= 11.25 \pm 0.03 \text{ Å} \\ \beta &= 96.3^\circ \pm 0.5 \end{aligned}$$

The space group is No 14 $B2_1/c$. A primitive cell could of course have been chosen by taking [101] and [$\bar{1}$01] as principal axes, but as this structure contains a cubic super-structure with $a = 5.9$ Å, the actual choice is easier to visualize. The single crystals, obtained from the melt at about 2 000°C, do not consist of CaC_2 III but of CaC_2 IV. These crystals are then transformed into CaC_2 III. It is obvious since the single crystals are not destroyed, that the crystal structure of CaC_2 IV and CaC_2 III must be very similar.

As the measured density is 2.15, there are eight formula units in the elementary cell.

The unit cell dimensions are not in accordance with those found by Bochert and Röder [10]. It is very probable that these authors have not used a perfect single crystal but a twin.

The calcium atom parameters were calculated from Patterson syntheses. The 2-dimensional synthesis gave too bad resolution to be used, so it was necessary to calculate a complete 3-dimensional synthesis. From the known calcium parameters the sign of every reflexion could be calculated. The positions of the atoms could now be calculated from a 3-dimensional Fourier synthesis.

In order to get better parameters for the carbon positions, a 3-dimensional difference synthesis was also performed.

Table 2. Observed and calculated structure factors for CaC_2 III

$h\ k\ l$	F_{obs}	F_{calc}	$h\ k\ l$	F_{obs}	F_{calc}
4 0 0	19.0	− 16.2	$\bar{9}$ 2 1	8.4	− 7.9
8 0 0	6.7	+ 7.4	2 2 2	9.0	− 4.6
2 0 2	9.5	+ 7.3	$\bar{2}$ 2 2	7.3	+ 5.5
$\bar{2}$ 0 2	6.6	− 10.3	6 2 2	8.4	+ 4.8
6 0 2	8.1	− 8.3	$\bar{6}$ 2 2	5.2	− 6.1
$\bar{6}$ 0 2	7.8	+ 11.4	1 2 3	8.5	+ 8.0
$\bar{10}$ 0 2	8.2	− 10.4	$\bar{3}$ 2 3	4.3	+ 4.7
4 0 4	15.0	+ 15.7	5 2 3	10.2	− 9.9
$\bar{4}$ 0 4	10.9	+ 10.2	$\bar{7}$ 2 3	2.6	− 4.6
$\bar{8}$ 0 4	4.4	− 5.2	0 2 4	4.3	+ 8.5
2 0 6	8.4	− 7.3	4 2 4	9.4	− 7.7
$\bar{2}$ 0 6	8.2	+ 11.6	8 2 4	5.6	+ 5.1
6 0 6	8.3	+ 5.6	$\bar{8}$ 2 4	4.3	− 3.3
$\bar{6}$ 0 6	7.8	− 12.2	$\bar{1}$ 2 5	15.0	+ 12.4
			3 2 5	8.8	+ 8.7
2 1 0	17.9	− 19.8	$\bar{5}$ 2 5	10.0	− 10.0
6 1 0	10.4	+ 9.3	7 2 5	5.7	− 4.3
10 1 0	6.8	− 4.5	$\bar{9}$ 2 5	—	—
1 1 1	5.3	+ 7.0	2 2 6	4.9	+ 4.5
$\bar{3}$ 1 1	8.1	− 8.7	$\bar{2}$ 2 6	5.6	− 6.1
5 1 1	2.1	− 2.8	6 2 6	4.3	− 3.6
$\bar{7}$ 1 1	5.1	+ 6.0	$\bar{6}$ 2 6	4.5	+ 6.4
9 1 1	2.2	+ 2.1			
0 1 2	7.0	+ 7.4	2 3 0	1.1	+ 1.5
4 1 2	12.8	− 6.8	6 3 0	1.8	− 1.5
$\bar{4}$ 1 2	8.0	+ 9.5	1 3 1	8.6	− 9.9
8 1 2	8.2	+ 7.8	$\bar{3}$ 3 1	11.8	+ 12.8
$\bar{8}$ 1 2	7.7	− 9.8	5 3 1	6.8	+ 5.7
1 1 3	2.7	− 3.6	$\bar{7}$ 3 1	13.4	− 11.0
3 1 3	6.3	+ 6.0	0 3 2	4.7	− 2.1
$\bar{5}$ 1 3	1.2	+ 2.5	4 3 2	4.5	+ 1.9
7 1 3	5.8	− 5.8	$\bar{4}$ 3 2	2.8	− 1.7
$\bar{9}$ 1 3	1.3	− 3.0	$\bar{1}$ 3 3	7.2	+ 6.9
2 1 4	14.7	+ 15.9	3 3 3	9.8	− 10.1
$\bar{2}$ 1 4	9.8	+ 12.6	$\bar{5}$ 3 3	5.2	− 5.2
6 1 4	10.8	− 10.8	7 3 3	10.6	+ 10.7
$\bar{6}$ 1 4	5.6	− 6.3	2 3 4	1.7	− 1.4
10 1 4	—	—	$\bar{2}$ 3 5	3.5	− 1.6
1 1 5	6.2	− 7.3	6 3 4	1.6	+ 1.2
$\bar{3}$ 1 5	6.8	+ 7.3	$\bar{6}$ 3 4	2.9	+ 1.6
5 1 5	3.6	+ 3.7	1 3 5	11.3	+ 11.8
$\bar{7}$ 1 5	3.6	− 4.6	$\bar{3}$ 3 5	12.9	− 12.5
0 1 6	8.1	− 8.5	5 3 5	9.0	− 7.2
4 1 6	7.6	+ 5.4	$\bar{7}$ 3 5	8.5	+ 8.6
$\bar{4}$ 1 6	7.1	− 10.6	0 3 6	—	+ 1.8
8 1 6	5.4	− 5.1	4 3 6	2.0	− 1.7
$\bar{8}$ 1 6	6.8	+ 9.6			
			0 4 0	3.2	− 4.7
0 2 0	7.8	− 10.6	4 4 0	1.6	+ 3.5
4 2 0	9.4	+ 7.5	$\bar{1}$ 4 1	11.7	+ 9.8
8 2 0	6.1	− 4.3	3 4 1	7.1	+ 6.7
$\bar{1}$ 2 1	11.4	− 12.3	$\bar{5}$ 4 1	12.5	− 10.3
3 2 1	7.9	− 6.7	7 4 1	2.2	− 4.4
$\bar{5}$ 2 1	12.4	+ 11.6	2 4 2	1.6	− 0.4
7 2 1	5.2	+ 3.9	6 4 2	2.4	+ 1.4

Table 2 (continued).

$h\ k\ l$	F_{obs}	F_{calc}	$h\ k\ l$	F_{obs}	F_{calc}
$\bar{6}\ 4\ 2$	2.1	− 2.7	$3\ 4\ 5$	8.9	− 8.2
$1\ 4\ 3$	6.2	− 7.5	$\bar{5}\ 4\ 5$	7.6	+ 9.1
$\bar{3}\ 4\ 3$	6.0	− 5.3			
$5\ 4\ 3$	9.5	+ 9.1	$2\ 5\ 0$	5.6	+ 7.7
$0\ 4\ 4$	3.4	+ 4.0	$1\ 5\ 1$	7.2	+ 5.5
$4\ 4\ 4$	3.0	− 4.1	$\bar{3}\ 5\ 1$	6.6	− 6.3
$\bar{4}\ 4\ 4$	1.9	− 1.9	$0\ 5\ 2$	2.5	− 2.5
$6\ 4\ 4$	—	—	$\bar{1}\ 5\ 3$	4.5	− 4.6
$\bar{1}\ 4\ 5$	7.8	− 10.6	$3\ 5\ 3$	3.7	+ 5.4

The parameters found were the following

	x	y	z
8 Ca	0.375	0.676	0.125
8 C	0.085	0.338	0.155
8 C	0.165	0.163	0.095

A comparison between observed and calculated structure factors can be found in Table 2. The R factor was found to be 0.20.

DISCUSSION

The distance between the carbon atoms was determined to be 1.24 Å, as compared with 1.20 in CaC_2 I. The difference is not significant. The distances (two in each case) between the calcium and carbon atoms are 2.46 Å, 2.69 Å, 2.78 Å, 2.86, Å, 3.72 Å, and 3.28 Å.

A picture of the coordination can be seen in Fig. 2.

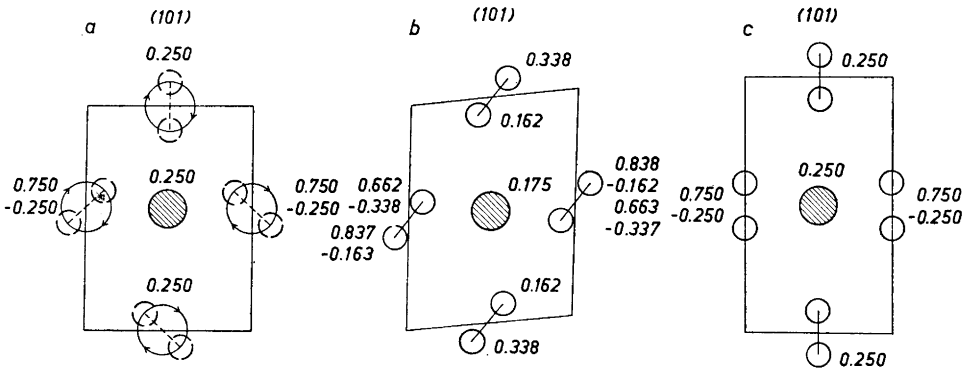

Fig. 2. The coordination of carbon atoms (small circles) about the calcium ions (shaded circles) in a) CaC_2 IV, b) CaC_2 III and c) CaC_2 I. In CaC_2 IV, each carbide ion is assumed to rotate freely about its centre main point. The locus of this point is fulldrawn.

The successive transformation

$$CaC_2\ IV \rightarrow CaC_2\ III \rightarrow CaC_2\ I$$

is illustrated in Fig. 2. The similarities between the three structures are very striking.

The observation by Bochert and Röder that CaC_2 III is transformed into CaC_2 I under high pressure is in accordance with the described structure. The calculated density for CaC_2 III is 2.17 g/cm^3, while that of CaC_2 I is 2.23 g/cm^3.

It will be of great interest to study the kind of disorder in CaC_2 IV. Such an investigation will be performed in a short time. The crystal structure of CaC_2 II has also been studied and is now under refinement. It appears to be very similar to that of CaC_2 III. When the two crystal structures mentioned have been determined, a further discussion of the calcium coordination will be performed.

Acknowledgements. The author is indebted to Professor Cyrill Brosset for his interest in this work and for the way he has facilitated its completion. Further the author's thanks are due to the *Swedish Natural Science Research Council* for financial support of this investigation.

REFERENCES

1. Stackelberg, M. v. *Z. physik. Chem. B* **9** (1930) 437; *Naturwiss.* **18** (1930) 305.
2. Atoji, M. and Medrud, C. *J. Chem. Phys.* **31** (1959) 332.
3. *Tables of Interatomic Distances and Configuration in Molecules and Ions.* London, Chemical Society 1958.
4. Dehlinger, U. and Glockner, R. *Z. Krist.* **64** (1926) 296.
5. Hermann, C. *Z. Krist.* **66** (1928) 314.
6. Bredig, M. A. *J. Phys. Chem.* **46** (1942) 801.
7. Franck, H. H., Bredig, M. A., Hoffmann, G. and Füldner, H. *Z. anorg. u. allgem. Chem.* **232** (1937) 61.
8. Franck, H. H., Bredig, M. A. and Kin-Hsing Kou *Z. anorg. u. allgem. Chem.* **232** (1937) 75.
9. Franck, H. H. Compt. rend. 17 congr. intern. chim. indust., Vol. 2 (1937) p. 1160.
10. Bochert, W. and Röder, M. *Z. anorg. u. allgem. Chem.* **302** (1959) 253.
11. Nast, R. and Pfab, W. *Z. anorg. u. allgem. Chem.* **292** (1959) 255.
12. Nast, R. and Pfab, W. *Z. anorg. u. allgem. Chem.* **304** (1960) 95.
13. Bredig, M. A. *Z. anorg. u. allgem. Chem.* **298** (1959) 255.
14. Bredig, M. A. *Z. anorg. u. allgem. Chem.* **304** (1960) 98.
15. Schrewelius, N. *Thesis.* Stockholm 1943.

Received December 9, 1960.

ACTA CHEMICA SCANDINAVICA 15 (1961) 775–782

An Application of the Jahn-Teller Theorem to the VCl_4 Molecule

C. J. BALLHAUSEN

Department of Physical Chemistry, University of Copenhagen, Copenhagen, Denmark

and

ANDREW D. LIEHR

Bell Telephone Laboratories, Incorporated, Murray Hill, New Jersey, U.S.A.

The tetrahedral molecule VCl_4 is expected to distort due to the implications of the Jahn-Teller theorem. Explicit calculations reveal that at temperatures above approximately 200° Kelvin the molecule undergoes a pseudo rotation in the sense that each chlorine atom is displaced from the regular tetrahedral position and rotates around the tetrahedral bond with a radius of 0.11 Å. However, at temperatures below 200° Kelvin VCl_4 assumes a static distortion in which two of the tetrahedral angles are closed 6°, and four of the angles are opened 3°. The consequences of the above distortions are enummerated, and paths for further experimental studies are indicated.

A great many papers [1–8] have in the past dealt with the theoretical consequences of the Jahn-Teller theorem [9], but only in a very few cases has it been possible to verify experimentally the predictions put forth [6,10]. Indeed, it often seems as if nature goes to great length in this matter in order to prevent us from obtaining any answers to our questions. The results arrived at here are no exception to this rule; however, it is hoped that they will stimulate experimentation designed toward clarifying this frustrating situation. We submit this note because it should be possible, in the special case to be discussed, either to prove or to disprove the theoretical predictions which we have recently derived.

We shall show that the compound VCl_4 should experience a configurational instability of the Jahn-Teller type. We shall further compare its behavior with that of the very closely related compound $TiCl_4$, a molecule unaffected by the implications of the Jahn-Teller theorem. Both VCl_4 and $TiCl_4$ are liquids at room temperature and both possess a tetrahedral structure [11,12] in the vapor

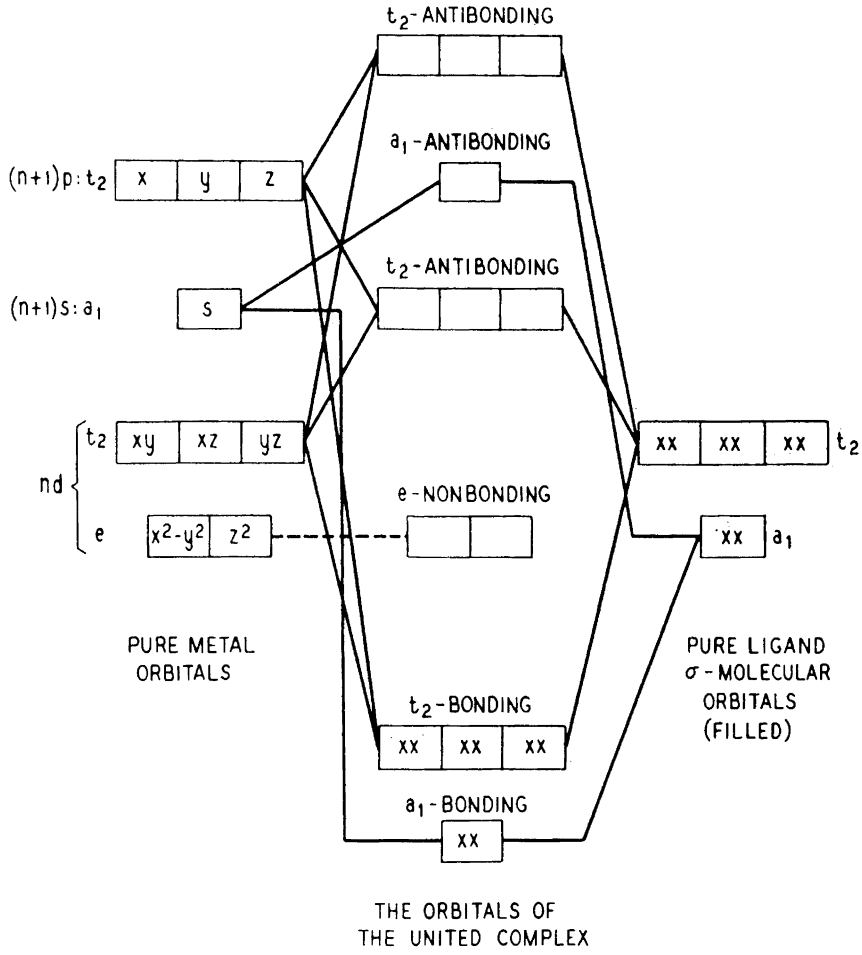

Fig. 1. Energy levels for the tetrahedral molecule VCl_4 in the σ-bonding approximation.

phase. The major difference between VCl_4 and $TiCl_4$ is that the former has one electron more than the latter. A comparison between them should therefore be of some interest.

THEORY

The electronic structure of V^{+4} is $[A]3d^1$, where [A] represents the closed, eighteen electron argon shell. A consideration of the bonding possible in a tetrahedral molecule reveals that the four ligands can produce σ-bonding orbitals of the symmetry a_1 and t_2. The 3d, 4s and 4p orbitals span the irreducible representations (t_2,e), a_1 and t_2, respectively. Thus if π bonding is neglected,

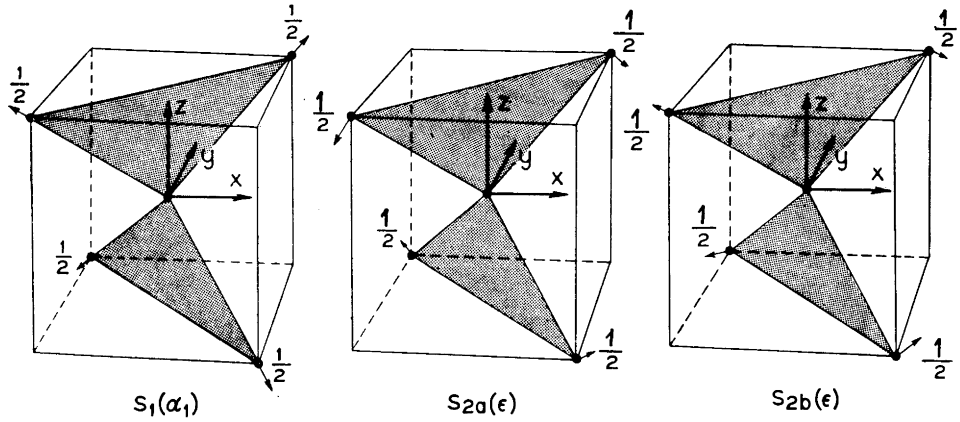

Fig. 2. The tetrahedral symmetry coordinates of species a_1 and ε.

the bonding scheme may be represented as in Fig. 1. The electronic structure of the molecule VCl_4 can then be written $(a_1^b)^2(t_2^b)^6(e)^1$, with the one unpaired electron present being placed in the σ-nonbonding, doubly degenerate, metal orbital.

In order for any molecule to possess a stable configuration it is obvious that the total energy of the system must be at a minimum. This means that the change in energy due to small displacements of the nuclei, must contain no terms linear in these displacements. Hence, it is necessary to minimize the total electronic energy with respect to all possible nuclear distortions of the molecular framework, if the equilibrium conformation is to be determined. After the removal of the translational and rotational degrees of freedom, it is found (by means of the usual methods[13]), that the nuclear symmetry coordinates span the irreducible representations a_1, ε and $2\tau_2$ of the point group T_d. The symmetry coordinates S_1 $(= a_1)$ and $S_{2a}, S_{2b} (= \varepsilon)$ are represented in Fig. 2.

By expanding the coulombic potential energy V around the equilibrium configuration in powers of the symmetry coordinates we obtain:

$$V = V_0 + \sum_i S_i V_i + \sum_{i,j} S_i S_j V_{ij} + \ldots \quad (1)$$

If at first only terms linear in the symmetry coordinates are retained, the change in the coulombic potential energy may be expressed

$$\Delta V = \sum_i S_i V_i \quad (2)$$

Here the expansion coefficients, V_i, are functions of the electronic coordinates only while the symmetry coordinates, S_i, are functions of the coordinates of the nuclei.

The energy change ΔE of the doubly degenerate ground state is given by first order perturbation theory as the solutions to the secular equation

$$\begin{vmatrix} \Delta V_{AA}-\Delta E & \Delta V_{AB} \\ \Delta V_{BA} & \Delta V_{BB}-\Delta E \end{vmatrix} = 0 \tag{3}$$

where

$$\Delta V_{AB} = \Delta V_{BA} = \int \psi_A \Delta V \psi_B d\tau \tag{4}$$
$$\Delta V_{AA} = \int \psi_A \Delta V \psi_A d\tau \tag{5}$$
$$\Delta V_{BB} = \int \psi_B \Delta V \psi_B d\tau \tag{6}$$

As our zero-order wavefunctions we take the two nonbonding orbitals $3d_{x^2-y^2}$ and $3d_{z^2}$. Hence (A,B) = ($d_{x^2-y^2}$,d_{z^2}). These two orbitals span the irreducible representation E in the point group T_d.

In order for the matrix elements (4)—(6) to be different from zero the direct product representation of the components must contain the identity representation A_1. The complete Hamiltonian for the system transforms like A_1; hence S_i and V_i must span the same representations in the point group T_d. The symmetric product of the representation E with itself is A_1 and E. Therefore, only the $S_{2a,b}$ symmetry coordinates are capable of mixing the $d_{x^2-y^2}$ and d_{z^2} like orbitals.

An actual (electrostatic) calculation of ΔV_{AA}, ΔV_{BB} and ΔV_{AB} then yields [14,15]

$$\Delta V_{x^2-y^2,x^2-y^2} = (2B_0 - \frac{2}{9}B_4)S_1 + \frac{a}{2}S_{2a} \tag{7}$$

$$\Delta V_{z^2,z^2} = (2B_0 - \frac{2}{9}B_4)S_1 - \frac{a}{2}S_{2a} \tag{8}$$

$$\Delta V_{x^2-y^2,z^2} = \Delta V_{z^2,x^2-y^2} = -\frac{a}{2}S_{2b} \tag{9}$$

where

$$a = \frac{8\sqrt{2}}{7r_0}(G_2 - \frac{5}{9}G_4) \tag{10}$$

with r_0 being the bond distance V—Cl. The radial integrals G_l and B_l are defined as [6]

$$G_l = \int_0^\infty R^2(r) f_l(r,r_0) r^2 dr \tag{11}$$

and

$$B_l = \frac{dG_l}{dr_0} \tag{12}$$

The quantities B_l and G_l are tabulated in Ballhausen and Ancmon.[16]

By inserting (7)—(9) into (3) and solving, ΔE is found to be

$$\Delta E = (2B_0 - \frac{2}{9}B_4)S_1 \pm \frac{a}{2}\sqrt{S_{2a}^2 + S_{2b}^2} \tag{13}$$

The total potential surface of VCl_4 is then given by

$$E = V_0 + \Delta E \tag{14}$$

We now assume that the potential surfaces of $TiCl_4$ and VCl_4 are the same, except for the terms due to ligand field effects, that is the terms in a and B_4. Making the substitutions

$$S_1 = q_1, \quad S_{2a} = q_2 \cos \varphi_2, \quad S_{2b} = q_2 \sin \varphi_2 \tag{15}$$

the potential surface for VCl_4 may be written

$$E = \tfrac{1}{2}k_1 q_1^2 - \frac{2}{9} B_4 q_1 + \tfrac{1}{2}k_2 q_2^2 \pm \frac{a}{2} q_2 \tag{16}$$

where k_1 and k_2 are the force constants for the harmonic vibrations of symmetry a_1 and ε, respectively.

In order to find the stable configuration of the molecule, (16) must be minimized with respect to q_1 and q_2. This is quite straightforward and leads to the results

$$\bar{q}_1 = \frac{\frac{2}{9} B_4}{k_1}, \quad \bar{q}_2 = \mp \frac{a}{2k_2} \tag{17}$$

DISCUSSION

A number of interesting conclusions can be inferred from (17). First if G_4 is defined as a positive quantity, ligand field theory demands [6,16] that B_4 must be a negative quantity. As a result $\bar{q}_1$ will be negative, and thus the V—Cl bond distance should be shorter than the Ti—Cl bond distance. This prediction is borne out by experiments, the reported values being 2.03 ± 0.02 Å, and 2.18 ± 0.04 Å for VCl_4 and $TiCl_4$, respectively [11,12]. Numerically the shortening of the bond distance is found to be $\simeq 0.02$ Å. The sign is seen to be correct, but not the order of magnitude. The discrepancy is, however, easily explained. When the derivative of the semiempirical potential, expressed by the parameters $G_l (l = 2,4)$, is taken, we cannot expect to get the correct slope of the potential since the bonding terms have not been properly included in the Hamiltonian. Since no splitting of the degenerate level takes place due to the influence of S_1 this term will be neglected in what follows.

The configurational instability of the Jahn-Teller type is apparent from the q_2 terms in (16). A positive a results in a splitting of the electronic degeneracy, and also in a continuous set of minima, found at $\bar{q}_2 = \frac{a}{2k_2}$. The energy gain ΔE is $-\frac{a^2}{8k_2}$. The apparent independence of φ_2 which this result show is due to the neglect of the second order terms in (1). If these are included a more refined potential surface of the form [14,15].

$$E = \tfrac{1}{2}k_1 q_1^2 - \frac{2}{9} B_4 q_1 + \tfrac{1}{2}k_2 q_2^2$$
$$\pm \tfrac{1}{2} q_2 \sqrt{a^2 + \beta^2 q_2^2 + \gamma^2 q_1^2 - 2\beta\gamma q_1 q_2 \cos 3\varphi_2 - 2a\beta q_2 \cos 3\varphi_2 + 2a\gamma q_1} \tag{18}$$

is obtained, where β and γ are constants involving further derivatives of the potential. The appearance of the cos $3\varphi_2$ term in (18) makes it clear that the molecule will have a threefold potential barrier.

The minimization of (18) with respect to φ_2 gives the condition

$$\sin 3\bar{\varphi}_2 = 0$$

$$\bar{\varphi}_2 = \frac{n\pi}{3} \quad (n = 0,\ 1,\ 2,\ 3,\ 4,\ 5) \tag{19}$$

Three of these points will give identical potential minima, the other three yielding identical saddle points. The identification of which is which can first be made once we know the sign of β. Now β is calculated to be positive in the molecular orbital approximation and negative in the electrostatic limit [14,15], and hence, the minima are found at $\bar{\varphi}_2 = \frac{n\pi}{3}$ $(n = 1,\ 3,\ 5)$ for the covalent case and at $(n = 0,\ 2,\ 4)$ in the electrostatic case. A positive β further indicates that the stable configuration takes the shape of an *elongated* tetrahedron. For VCl_4 we expect that β is greater than zero.

In order to obtain a crude numerical estimate of the effect, we place β equal to zero. Now G_4 may be estimated from the absorption spectra [17] of VCl_4, and G_2 may be found in the tables of Ballhausen and Ancmon [16]. We find a to be about 0.20×10^{-3} dyne. If for illustrative purposes $k_2 = 0.47 \times 10^5$ dyne/cm, corresponding to [18] $\nu_2 = 150$ cm^{-1}, $\bar{q}_2$ will equal 0.21 Å. The stable configuration then corresponds to an closing of $\simeq 6°$ of two of the tetrahedral angles, the four others being opened each $\simeq 3°$. The height of the threefold barrier has further been estimated to be ≈ 150 cm^{-1} [14]. The value of $\bar{q}_2$ corresponds to a Jahn-Teller Energy gain, ΔE, of 250 cm^{-1}. Note that the ordinary zero point amplitude, $\sqrt{\langle q_2^2 \rangle_0}$, is roughly one-fourth (0.055 Å) of the Jahn-Teller amplitude $\bar{q}_2$.

The situation can thus be described as follows: At low temperatures the molecule will be frozen into one of the three potential traps, and it will assume the shape of an *elongated* tetrahedron. At temperatures so high that the molecule has sufficient energy to override the barriers, the complex will exhibit a sort of pseudo rotation: all of the Cl^- nuclei are forced to perform a coupled rotation about the (regular) tetrahedral bond angles, each one rolling upon a cone with an apex angle of 6° (See Fig. 3).

We must now ask ourselves: are there any experimental proofs as to this rather remarkable behavior of VCl_4? Unfortunately there are none at the time of writing. The existing electron diffraction data [12] cannot, without refinement, decide whether the predicted behavior is true *.

Three other methods of substantiating these predictions are possible however. One would be an investigation of the Raman spectrum. By this tech-

* This is due to the fact that the molecule librates freely at the temperature at which the diffraction measurements are performed. Hence the measured Cl—Cl distance is an average distance, *i.e.*, the bond distance found for a strictly tetrahedral molecule. The Jahn-Teller motions may yet be detected, however, by their production of an anomalous temperature dependent scattering factor. This possibility should be investigated.

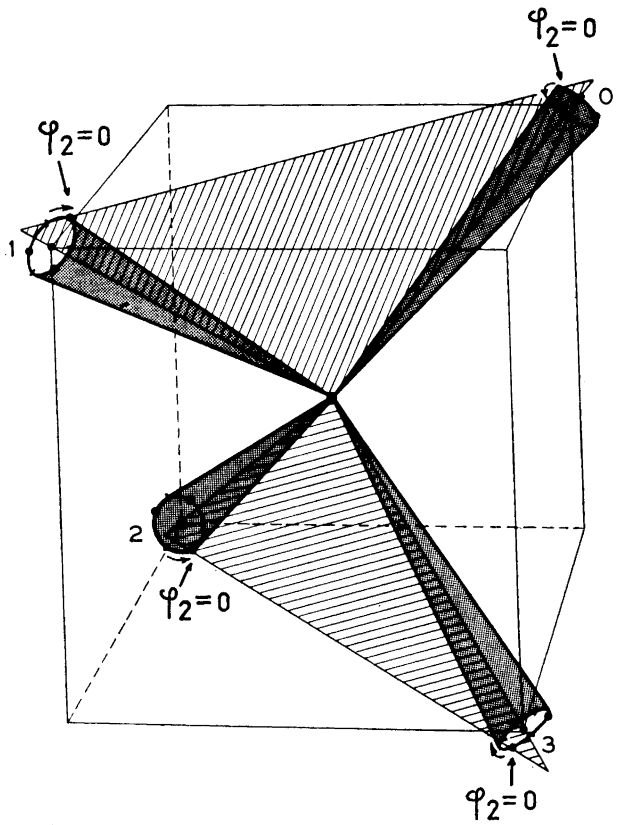

Fig. 3. Jahn-Teller motions in the VCl_4 molecule, $\beta > 0$..

nique one could decide whether the symmetry of the molecule is instantaneously lower than T_d.[15] Furthermore, an investigation of the paramagnetic resonance spectrum should yield results identical to those found [6,10] for $Cu(H_2O)_6SiF_6$, that is, an isotropic g-factor is expected when the molecule can interconvert freely. On the other hand we would get an anisotropic g-factor if the molecule is trapped in one of the potential holes. As pointed out previously by the authors [6], it would furthermore be possible to estimate the sign of β by using the result of such a measurement. Lastly, optical measurements at low temperatures should exhibit anomalously intense vibrational progressions in the ε mode *. It seems to the authors that these three experiments are well worth doing. Such work is now in progress [19,20,22].

* This last experiment is difficult to interpret for VCl_4, but has been performed [21] and analyzed [15] for Cu++:ZnO.

The work reported in this note is being continued in two mutually complementary directions by the authors. One direction is an attempt to include the molecular orbital approach in the calculation of the Jahn-Teller configurational instability for tetrahedral molecules in both their ground- and excited-states [14], and the second is an attempt to mathematically describe the concomitant Jahn-Teller nuclear motions in these self-same systems without regard to any specific model [15].

Acknowledgements. The authors should like very much to thank Drs. J. C. W. Chien, R. Pappalardo, M. Robin and G. E. Walrafen for informing them of their current experimental researches on related topics, and for undertaking further experimental work to prove or disprove the theoretical speculations here outlined.

REFERENCES

1. Van Vleck, J. H. *J. Chem. Phys.* **7** (1939) 72.
2. Moffitt, W. and Liehr, A. D. *Phys. Rev.* **106** (1957) 1195.
3. Öpik, U. and Pryce, M. H. L. *Proc. Roy Soc. London* **A238** (1957) 425.
4. Moffitt, W. and Thorson, W. *Phys. Rev.* **108** (1957) 1251.
5. Longuet-Higgins, H. C., Öpik, U., Pryce, M. H. L. and Sack, R. A. *Proc. Roy Soc. London* **A244** (1958) 1.
6. Liehr, A. D. and Ballhausem, C. J. *Ann. of Physics* [N.Y.] **3** (1958) 304.
7. Van Vleck, J. H. *Physica* **26** (1960) 544.
8. Liehr, A. D. *Revs. Modern. Phys.* **32** (1960) 436.
9. Jahn, H. A. and Teller, E. *Proc. Roy. Soc. London* **A161** (1937) 220.
10. Abragam, A. and Pryce, M. H. L. *Proc. Phys. Soc. London* **A63** (1950) 409.
11. Lister, M. W. and Sutton, L. E. *Trans. Faraday Soc.* **37** (1941) 393.
12. Lipscomb, W. N. and Whittaker, A. G. *J. Am. Chem. Soc.* **67** (1945) 2019.
13. Wilson, E. B., Decius, J. C. and Cross, P. C. *Molecular Vibrations*, McGraw-Hill, New York 1955.
14. Ballhausen, C. J. (*to be published*) and *Advances in Chemical Physics* (Ed. I. Prigogine), Interscience Publishers Inc., Vol. 4 (1961).
15. Liehr, A. D. (*to be published*), and *Progress in Inorganic Chemistry* (Ed. F. A. Cotton), Interscience, Vol. 4, (1961).
16. Ballhausen, C. J. and Anemon, E. M., *Mat. Fys. Medd. Dan. Vid. Selsk.* **31** (1958) No. 9.
17. Ballhausen, C. J. *Kgl. Danske Videnskab. Selskab. Mat. Fys. Medd.* **29** (1954) No. 4.
18. Herzberg, G. *Infrared and Raman Spectra of Polyatomic Molecules*, D. Van Nostrand, New York 1945.
19. Walrafen, G. E. *To be published.*
20. Chien, J. C. W. *To be published.*
21. Pappalardo, R. *To be published.*
22. Robin, M. *To be published.*

Received December 16, 1960.

ACTA CHEMICA SCANDINAVICA 15 (1961) 783–790

The Determination of α-Tocopherol in Animal Tissues by Column Chromatography

J. G. BIERI*, C. J. POLLARD**, I. PRANGE and H. DAM

Department of Biochemistry and Nutrition, Polytechnic Institute, Copenhagen, Denmark and the
National Institute of Arthritis and Metabolic Diseases, National Institutes of Health, Bethesda, Maryland. U.S.A.

A rapid method for the chromatographic separation and quantitative determination of small amounts of α-tocopherol in the unsaponifiable matter of animal tissue is described. The unsaponifiable material from 0.5—1.5 g of tissue, containing 1—20 μg of α-tocopherol, is put on a 0.5 × 5 cm column packed with a mixture of activated alumina, zinc carbonate and Celite. Twenty per cent benzene in *cyclo*hexane is passed through the column and eight fractions of 1 ml are collected. The Emmerie-Engel reaction is performed on each fraction. α-Tocopherol separates sharply in 3—4 fractions free of other reducing substances.

Although many procedures have been described for the determination of α-tocopherol, there appeared to be a need for a rapid method applicable to small quantities of animal tissues. Many methods which are suitable for materials with a relatively high content of α-tocopherol fail when applied to samples of animal origin. The molecular distillation [1,1a,2,14] of α-tocopherol, which is perhaps the most specific method currently used, requires preliminary removal of interfering materials; a specialized apparatus is also necessary. Paper chromatographic procedure [3–5], which separate some of the tocopherols in plant lipids, require a preliminary removal of sterols when extracts of animal unsaponifiable material with low tocopherol content are analyzed. The procedure described recently [6] which adapts previous paper chromatographic techniques to the analysis of animal tissues appears to require excessive amounts of mate-

* Fulbright Research Scholar in Denmark, 1959—1960. Permanent address: National Institute of Arthritis and Methabolic Diseases, National Institutes of Health, Bethesda, Maryland, U.S.A.

** Present address: Division of Biology, California Institute of Technology, Pasadena, California, U.S.A.

rial and also involves prolonged steps which greatly lengthen the time required for the analysis.

Column chromatographic methods which have been used for analyzing plant and feed materials [7,8] have not been adapted to small samples containing less than 20 μg of α-tocopherol. The use of floridin earth columns [2,9] for animal tissues in our experience is unsatisfactory because reducing substances other than α-tocopherol frequently appear in the eluate, especially when liver is analyzed [10]. Furthermore, it was felt that a method should be devised in which readily available adsorbents, not requiring special treatment, could be utilized.

Because of these various limitations in existing procedures, the present method was developed as an aid to studies of the metabolism and function of α-tocopherol. The procedure involves saponification of the sample, extraction of the unsaponifiable material and its chromatography on a column consisting of a mixture of alumina and zinc carbonate. The α-tocopherol is collected in the eluate free of other reducing substances and is quantitatively determined colorimetrically. Although the method has been used primarily for tissues from rats and chicks fed purified type diets, it should be applicable to other species under natural feeding conditions.

EXPERIMENTAL

Chemicals

1. Ethanol, 96 %, refluxed over KOH for 30 min and distilled.
2. Potassium hydroxide, 50 %. Dissolve 100 g of KOH in 100 ml water.
3. Hexane, purified. Although some commercial hexanes are pure enough after distillation, others have had to be washed with concentrated sulfuric acid, then with saturated potassium permanganate and finally distilled. *Cyclo*hexane may be used in place of hexane. This solvent from several sources has been found satisfactory without distillation.
4. Bipyridyl, 0.5 %, in ethanol.
5. Ferric chloride (hexahydrate), 0.2 %, in ethanol (kept in brown glass bottle).
6. Celite No. 545, John-Manville Corp., New York, N.Y. Celite Analytical Filter Aid also may be used.
7. Zinc carbonate, powdered, analytical reagent. Two brands which have been found to be satisfactory were: J. T. Baker Chemical Co., Phillipsburg, N. J., and May and Baker, Ltd., Dagenham, England (labelled approx. $ZnCO_3 - 2\ ZnO,3H_2O$). The product "Basic Zinc Carbonate" of Mallinkrodt Chemical Works, St. Louis, Mo., also was satisfactory but gave a very slow flow rate.
8. Activated alumina. Only alkaline aluminas have been found suitable. Merck & Co., Inc., Rahway, N. J. "Aluminum oxide, suitable for chromatography"; May and Baker, Ltd., "Aluminium Oxide, for chromatography". Aluminum Co. of America, Pittsburgh, Pa., "Activated Alumina F-20". All of these products gave satisfactory results. Several other activated aluminas gave recoveries of α-tocopherol below 90 %.
9. Pyrogallol, reagent grade.
10. Anhydrous sodium sulfate, reagent grade.
11. Benzene, reagent grade.

Apparatus

1. Chromatographic tubes. These are made from 19 cm lengths of glass tubing with an inside diameter of 4.5—5 mm. A constriction in the tube, to hold a cotton plug, is made about 5 cm from one end. A glass rod slightly smaller than the tube is used for tamping the column.
2. Glassware: 500 ml suction flasks, 50 and 100 ml Erlenmeyer flasks, separatory funnels.
3. Nitrogen gas.
4. A photoelectric colorimeter in which volumes of 3—4 ml of solution may be used. The Beckman model C colorimeter, the Coleman Jr. spectrophotometer, and the Klett-Summerson photoelectric colorimeter have been used. The Beckman DU spectrophotometer is also satisfactory.

PROCEDURE

Saponification and extraction of tissues. 0.5 to 3 g of tissue is homogenized in a tissue grinder with 5 to 10 ml of water and transferred to a 50 or 100 ml Erlenmeyer flask. To this are added an equal volume of ethanol, 50—100 mg pyrogallol and a few boiling stones. The flask is fitted with a reflux condensor (an air condensor is also satisfactory), placed on a hot plate or steam bath, and when the mixture is boiling, a volume of freshly boiled 50 % KOH which is equal to one-half the weight of the tissue is added through the condensor (very fatty tissues may require more). Gentle boiling is continued for 15—25 min, depending on the size and fat content of the sample.

An alternate procedure is to chop the tissue, preferably when frozen, into small pieces and saponify in 15—25 ml of ethanol without the addition of water.

When saponification is complete, the flask is cooled rapidly and the contents transferred to a separatory funnel, containing 10—15 ml hexane. If no water had been added previously, a volume equal to the saponified mixture is now added. This order of mixing reduces the tendency to form emulsions. The mixture is extracted by moderate shaking for one min; the extraction is repeated with 8 and 5 ml of hexane. The extract is washed five times with water, dried over anhydrous sodium sulfate, filtered or decanted and made to a convenient volume with hexane.

An aliquot of the extract equivalent to 0.5—1.5 g of tissue is evaporated to dryness in a conical centrifuge tube, using nitrogen and a warm water bath. Large volumes of solvent may be removed by a flash evaporator. The residue is dissolved in 0.05—0.1 ml of hexane and is ready for the column.

Chromatography. The three aluminas we have used required weakening by the addition of 4—12 % of water immediately before use. The actual amount needed is determined by observing the rate of migration of 10—50 μg of vitamin A alcohol on the mixed column. When 8—10 ml of the developing solvent (below) is passed through the column the vitamin A should move about 1 cm down the column. Usually, it will lie in a band 2—12 mm from the top. To check this, the column is sucked practically dry and the packing gently blown out by light air pressure. (A finger is held loosely over the end of the tube and compressed air applied at the bottom. When the column moves to the top of the tube, remove the air supply and blow on the end gently to push the packing out of the tube.) Antimony trichloride in chloroform (25 %) is then dropped onto the column from a pipet to locate the vitamin A.

To 0.3 g of alumina in a mortar is added the requisite volume of water (as indicated above) from a micro pipet and the two mixed by grinding gently with a pestle. 0.3 g of zinc carbonate and 0.15 g of Celite are added and mixed in. The mixed adsorbent must then be packed into the glass tube *within 10 minutes*, since on standing it becomes more strongly adsorptive. Once the column has been wet with hexane, it may stand for several hours.

The glass column, in a rubber stopper, is mounted on a suction flask connected to a water pump or to the house vacuum. A cotton or glass wool plug is inserted into the constriction in the tube and the adsorbent is added in portions of about 1.5 cm with the aid of a small funnel, using *very weak* suction. The top of the tube is tapped 2—3 times (not more) with a glass rod to facilitate settling of the adsorbent which is finally packed

firmly, but *lightly*, with the rod. The column is packed to a height of 5 cm; usually the adsorbent is put into the tube in 4—5 portions. A small amount of anhydrous sodium sulfate may be placed on top of the column.

Two or three ml of hexane are then passed through the column and the suction is increased until the flow rate is 1 ml per 2—2 1/2 min. With the vacuum off, the sample in 50—100 μl hexane is placed on the column using a micro pipet. Suction is reapplied and another 50—100 μl of hexane is used to rinse the sample tube. As soon as this has gone onto the column, 1 ml of the developing solvent, benzene in hexane (1:4 by volume), is added. The surface of the column is never permitted to become dry.

One ml fractions are collected in colorimeter tubes placed in the flask under the column. Seven to ten fractions are usually taken. As a check on the behavior of the column, after a liver sample has been run through, the column is extruded and treated with antimony trichloride. The vitamin A should be about one-half to two-thirds of the way down the column. If above or below this, then the column is too slow or too fast, and the water content of the alumina must be changed. This check is only necessary when a new batch of alumina is being used for the first time.

Colorimetric determination of α-tocopherol. The fractions are evaporated under nitrogen and the residue dissolved in 3 ml of ethanol. Then 0.2 ml of bipyridyl followed by 0.2 ml of ferric chloride are added and the density at 520 mμ determined 30 sec. after the addition of the ferric chloride. A room with artificial light should be used. The reagent blank is subtracted from the reading of the fractions containing α-tocopherol (see Table 1). Calculations are made from a standard curve employing pure α-tocopherol. These volumes may be varied depending on the instrument used. With the volumes indicated, the working range is 1—20 μg α-tocopherol.

To speed up the procedure, if the colorimeter tubes are marked at the 3 or 4 ml volume, the ethanol can be added to the mark without evaporating the solvent. This proportion of hexane-benzene solvent does not alter the Emmerie-Engel reaction.

COMMENTS AND RESULTS

Saponification. In agreement with other investigators [7,8,11], we have found α-tocopherol to be recovered quantitatively, as determined by the Emmerie-Engel reaction, after saponification if caution is used in the exclusion of air and pyrogallol is added as an antioxidant. When 5—60 μg of *dl*-α-tocopherol were saponified 20 min as described, recoveries were always above 93 %. However, we consistently found that with one source of potassium hydroxide the saponified tocopherol underwent a 10—15 % loss when put through the column. Since unsaponified tocopherol did not show this loss (below), it is apparent that the saponification procedure changed some of the tocopherol so that it was still reducing but would not pass through the column.

Packing the column. When properly packed, the α-tocopherol will come off sharply in two to four fractions. If the activity of the adsorbent is correct and not too much unsaponifiable matter is put on, the α-tocopherol should begin to appear in the 2nd, 3rd or 4th fractions. Two typical elution patterns are shown in Table 1. If the column is not packed uniformly the tocopherol will spread out over 5 or more fractions.

We have tried packing the column wet, *i.e.*, suspending the adsorbent in hexane and pouring the mixture into the tube. This procedure was found to give considerable variation in behavior of the column. Because of the different density and particle size of the three components in the adsorbent mixture, there was an uneven settling as the particles fell through the solvent.

Table 1. Typical elution patterns of unsaponified fractions from tissues.

Fraction *	Chick liver, 0.33 g			Rat muscle, 1 g		
	$A_{520m\mu}$	μg Tocopherol		$A_{520m\mu}$	μg Tocopherol	
1	0.059	—		0.062	—	
2	0.058	—		0.083	1.6	
3	0.063	—		0.143	6.0	10.5 μg/g
4	0.117	4.1	5.1 = 15.3 μg/g	0.101	2.9	
5	0.076	1.0		0.063	—	
6	0.062	—		0.064	—	
7	0.062	—		0.062	—	
8	0.058	—		0.058	—	
Reagent blank	0.062			0.062		

* Eluate fractions of 1 ml collected.

Recovery of α-tocopherol from the column. Samples of pure *dl*-α-tocopherol ranging from 8—30 μg were put through the column and the recovery in the eluate fractions determined. With the sources of alumina and zinc carbonate listed above, recoveries were from 94—99 % in fifteen tests. Other sources of activated aluminas gave recoveries from 76—85 %. When small amounts of α-tocopherol were added to the unsaponifiable material from rat or chick tissues which were either adequate or devoid of vitamin E, the recovery was quantitative (Table 2). If impure hexane is used, losses during chromatography can be appreciable.

When 15 to 60 μg of α-tocopherol were added to 0.5 g of vitamin E-free lard, or to 1.0 g of muscle from a vitamin E-depleted chick, and carried through the entire procedure, the recoveries were above 90 %.

Table 2. Recovery of α-tocopherol from the chromatographic column when added to tissue unsaponifiable fractions.

Expt.	Weight of tissue * (g)	Tocopherol present ** (μg)	Tocopherol added (μg)	Total tocopherol found (μg)	Recovery of added tocopherol (%)
1	0.5, rat liver	8.7	3.3	12.1	103
2	1.0, rat muscle	10.5	3.3	13.7	97
3	1.0, rat liver	0.0	14.6	13.1	90
4	1.0, rat liver	0.0	11.5	11.0	96
5	1.0, chick liver	0.0	14.6	13.9	95

* The hexane extract put onto the column was equivalent to this weight of tissue.
** Determined on a aliquot of the hexane extract.

Table 3. Comparison of column eluates with and without molecular distillation.

Tissue	Weight of tissue chromatographed (g)	α-Tocopherol content of tissue (μg/g)	
		Direct eluate	Distilled eluate
Rat A, liver	0.5	18.7	19.5
Rat B, testes	0.5	18.4	18.5
Rat B, muscle	1.0	10.5	9.4
Rat C, depot fat	0.5	8.8	7.8
Chick A, liver	0.5	18.7	19.4
Chick B, heart	0.5	26.6	23.3

Amount of unsaponifiable material put on the column. This has varied from less than 1 mg to 6 mg, representing the unsaponifiable matter from 0.4—1.5 g of tissue. No attempt was made to determine the upper limit of capacity. Before chromatographing the unsaponifiable matter from brain, it was necessary to desterolize the extract first by low-temperature freezing in methyl alcohol. The only interference encountered was from excessive vitamin A in livers from chicks dosed heavily with the vitamin. The column was found to be capable of holding 100 μg of vitamin A. If more than this amount is present in liver samples, a larger column can be used. It is desirable to use as small a sample as possible since better separation of the α-tocopherol is achieved. Thus, if the tocopherol content of a tissue exceeds 30 μg/g, a sample of 0.25—0.5 g is sufficient for the chromatography.

Separation of other unsaponifiable materials. β-Carotene passes through the column rapidly and appears in the first fraction. The only other substance which comes through in eight fractions is ubiquinone (coenzyme Q). This migrates at about the same rate as α-tocopherol but with the amounts present in tissues no significant color is given in the Emmerie-Engel Reaction. β-, δ- and γ-tocopherols stay on the column as do vitamin A and cholesterol. Reduced ubiquinone, prepared with $LiAlH_4$, is strongly adsorbed on the top of the column. Ubichromenol[13] did not come through the column even after 12 ml of developing solvent were used.

The reducing material in *Torula* yeast, which also occurs in the livers of animals fed the yeast, and which passes readily through Florex columns prepared with stannous chloride, was strongly adsorbed on the alumina-zinc carbonate column and did not appear after 16 ml of developing solvent were passed through.

Molecular distillation of the eluate. In order to determine if substances which might either enhance or inhibit the Emmerie-Engel reaction were coming through the column, eluates of a variety of tissues were molecularly distilled in the apparatus of Glavind, Heslet and Prange[14]. For this study, duplicate aliquots of tissue extracts were chromatographed and the Emmerie-Engel reaction run on the eluate fractions from one sample. The corresponding 3 or 4 fractions containing vitamin E, of the duplicate sample, were combined and

distilled for one hour at 100°C and 10^{-4} mm and the tocopherol content of the distillate determined. The results, shown in Table 3, indicate that no significant amount of interfering material comes through the column. As mentioned above, ubiquinone comes off the column with the α-tocopherol. We have found, as reported by Pudelkiewicz and Matterson [12], that ubiquinone does not distill under these conditions. (Reduced ubiquinone and ubichromenol similarly did not distill). The data in Table 3 provide evidence that ubiquinone in the amounts present normally in tissues does not interfere in the Emmerie-Engel reaction.

Analysis of tissues from vitamin E-deficient animals. Further evidence that the column effectively separates α-tocopherol from other Emmerie-Engel reducing substances was provided by analyzing tissues from young rats and chicks which had been fed purified diets, devoid of α-tocopherol, for 5—8 weeks. When the unsaponifiable matter from 1—2 g of tissue was analyzed there was no reducing material in the eluate fractions where α-tocopherol should appear. If the vitamin was added to such samples prior to chromatography quantitative recovery was achieved (Table 2). In several vitamin E-depleted rat and chick liver samples of one g, a small amount of reducing material, equivalent to 1—3 μg of tocopherol, came off the column in three fractions immediately after those containing the added α-tocopherol.

Application of the method. The following rat tissues have been analyzed satisfactorily: liver, kidney, spleen, heart, testes, lung, intestine, muscle and depot fat. When brain was analyzed, it was necessary to remove sterols prior to chromatography, as indicated above. Liver, heart and muscle from chicks also have been analyzed.

In the early development of the method, a column of adsorbent 1 × 6 cm was used with tissue samples from 1 to 3 g. Eluate fractions of 2—3 ml were collected. Results were similar to those found with the smaller column. Presumably, even larger columns could be adapted for isolation work or for problems involving interest in unsaponifiable constituents other than α-tocopherol. The eluate fractions may also be used for determining the ubiquinone (coenzyme Q) content of the sample. The solvent is evaporated, the residue dissolved in 3 ml ethanol, and the adsorbancy at 275 mμ before and after reduction with KBH_4 determined [15]. If the tocopherol content of the sample is sufficiently high, 6 ml of ethanol may be added to the colorimeter tubes; 3 ml are then removed for ubiquinone estimation while the Emmerie-Engel reaction is performed on the remaining 3 ml.

Acknowledgement. The authors wish to thank F. Hoffmann-La Roche, Inc., for supplying ubiquinone-50 and Professor R. A. Morton for a sample of ubichromenol isolated from human kidneys.

REFERENCES

1. Dam, H., Glavind, J., Prange, I. and Ottesen, J. *Kgl. Danske Videnskab. Selskab., Biol. Medd.* **16** (1941) 7 (p. 1—39).
1a. Quaife, M. L. and Harris, P. L. *Ind. Eng. Chem., Anal. Ed.* **18** (1946) 707.
2. Pudelkiewicz, W. J., Matterson, L. D., Potter, L. M., Webster, L. and Singsen, E. P. *J. Nutrition* **71** (1960) 115.
3. Brown, F. *Biochem. J.* **52** (1952) 523.

4. Eggitt, P. W. R. and Ward, L. D. *J. Sci. Food Agr.* **4** (1953) 176.
5. Green, J., Marcinkiewicz, S. and Watt, P. R. *J. Sci. Food Agr.* **6** (1955) 274.
6. Edwin, E. E., Diplock, A. T., Bunyan, J. and Green, J. *Biochem. J.* **75** (1960) 450.
7. Tosic, J. and Moore, T. *Biochem. J.* **39** (1945) 498.
8. Bro-Rasmussen, F. and Hjarde, W. *Acta Chem. Scand.* **11** (1957) 34.
9. Swick, R. W. and Baumann, C. A. *Anal. Chem.* **24** (1952) 758.
10. Bieri, J. C., Briggs, G. M., Pollard, C. J. and Fox, M. R. S. *J. Nurtition* **70** (1960) 47.
11. Mervyn, L. and Morton, R. A. *Biochem. J.* **72** (1959) 106.
12. Pudelkiewicz, W. J. and Matterson, L. D. *J. Biol. Chem.* **235** (1960) 496.
13. Laidman, D. L., Morton, R. A., Paterson, J. Y. F. and Pennock, J. F. *Biochem. J.* **74** (1960) 541.
14. Glavind, J., Heslet, H. and Prange, I. *Z. Vitaminforsch.* **13** (1943) 266.
15. Lester, R. L., Hatefi, Y., Widmer, C. and Crane, F. L. *Biochim. et Biophys. Acta* **33** (1959) 169.

Received December 16, 1960.

ACTA CHEMICA SCANDINAVICA 15 (1961) 791–802

Radiation Induced Free Radicals in Alanine and Some Related Amino Acids

Electron Spin Resonance Studies *

SVEIN PRYDZ** and THORMOD HENRIKSEN***

Norsk Hydro's Institute for Cancer Research, The Norwegian Radium Hospital, Oslo, Norway

Free radicals induced by ionizing radiation in polycrystalline samples of α-alanine and some related amino acids have been studied by electron spin resonance techniques. The results show that the observed spectra very often represent the composite pattern of more than one radical. Qualitative changes occur in the electron spin resonance spectra, demonstrating that secondary processes take place at a fairly slow rate in the solid state.

The number of induced radicals has been measured as a function of the radiation dose as well as of the time after the end of the exposure. The dose effect curves are straight lines up to a certain dose level and then flatten out. This occurs before any saturation effects are to be expected. Time studies demonstrate the surprisingly high stability of radicals induced and trapped within solid amino acids.

For the amino acids studied, 5–50 electron volts were found necessary to induce one primary radical with lifetime long enough to be observed. These low values seem to imply that the radicals originate not only from ionizations, but also from excitation processes which are subsequently followed by rupture of chemical bonds. Conceivably the radical fragments induced may take part in reactions with intact neighbour molecules, a circumstance which may explain the observed qualitative changes in the resonance patterns.

Radiation induced free radicals trapped in the solid state or in frozen solutions can be studied by electron spin resonance techniques (ESR) [1–5]. Since the work of Combrisson and Uebersfeld in 1954 [11], unpaired spins in solid amino acids have been studied by a number of investigators [6–10]. Thus, Shields and Gordy [6] have presented qualitative resonance spectra for different amino acids which have been exposed to high X-ray doses, but no quantitative

* Supported by *National Institute of Health, U.S. Public Health Service.*

** Present address: Institute of Physics, University of Oslo, Blindern, Norway.

*** Fellow of the *Norwegian Cancer Society.*

results were given. Box and Freund [7] have measured radiation yields for some amino acids. Usually *G*-values (number of unpaired spins produced per 100 eV of absorbed energy) less than 1 were found. These results seem to be in agreement with those of Randolph and Parrish [8], but differ from the result of Zimmer *et al.*[9] on glycine. In a recent work Randolph and Parrish [10] have also studied the stability of the induced radicals. They found a very slow decay of spins in *a*-alanine and glutamic acid during the first 6 months.

In a previous study of thiols and disulphides [12–14] we found that the qualitative and quantitative ESR measurements are influenced by parameters such as the radiation dose, the temperature, the oxygen pressure and the time elapsed between the end of the exposure and the measurements. The results indicated that secondary processes take place at a fairly slow rate in the solid state. These findings are somewhat in conflict with the above mentioned works, and the purpose with the present paper is therefore mainly to extend our work on sulphur compounds to ordinary amino acids. *a*-Alanine and some related amino acids have been chosen for this purpose. Special attention has been given to the above mentioned parameters. Extensive time studies have been made in order to see if secondary processes take place in these substances as well.

The results show that radicals are induced in these amino acids with surprisingly high yields, a finding which seems to be of considerable interest with regard to the mechanism of radical production.

MATERIALS AND METHODS

The spectrometer. The spectrometer which is described in a previous paper by Henriksen and Pihl [14] operates at a frequency of 9 200 Mc/sec. The magnetic field is modulated at a frequency of 110 kc/sec. In the present experiment the microwave frequency is measured with a wavemeter with an accuracy of about 0.1 %, and the magnetic field is measured with a proton resonance field meter. The sweep rate of the magnetic field is 19 gauss/min. The microwave power was small and no saturation effects were observed.

The substances. DL-Alanine, DL-serine, L-cysteine, L-glutamic acid, DL-glutamic acid monohydrate, L-glutamic acid monohydrochloride, L-phenylalanine, L-histidine, L-tryptophane, were purchased from Nutritional Biochemical Corporation. The *β*-alanine was purchased from Hoffmann-la Roche, and L-aspartic acid from Sigma Chemical Co. The compounds were all of the highest analytical grade. The samples were prepared by grinding the amino acids in a mortar, and each sample consisted of about 10—40 mg dry powder.

The samples were evacuated by a high vacuum diffusion pump and sealed off at a vacuum of 10^{-4}—10^{-5} mm Hg.

Irradiation conditions. A 220 kV Siemens X-ray tube externally filtered by 0.7 mm glass was used. The dose rate was 7 700 r/min. The total doses varied between 1×10^4 r and 6×10^6 r. In most cases the dose was about 1.5×10^5 r with an exposure time of 20 min. The doses were measured with an ionization chamber.

The samples were irradiated and measured at room temperature. The first spectrum was usually recorded 10 min after the end of the exposure. Some of the samples were heat treated at controlled temperatures between the exposure and the measurements.

Quantitative procedures. It is generally assumed that the number of radicals are proportional to the area of the absorption curves [1]. Since this spectrometer gives the first derivative of the actual spectra, the desired area was obtained by double integration which was performed graphically. In order to obtain the absolute number of free radicals per gram of irradiated compound, the spectra were compared with those of reference samples measured under the same conditions.

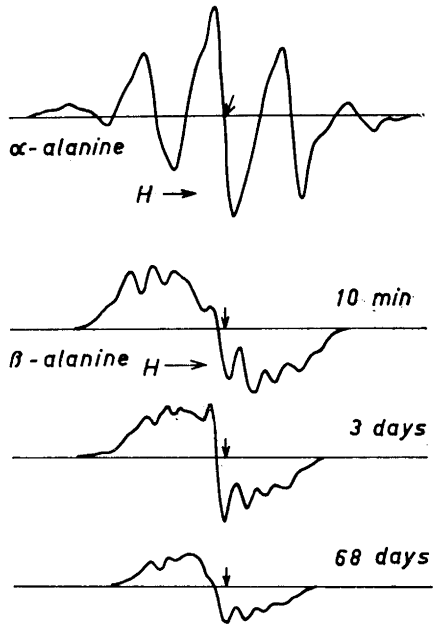

Fig. 1. The upper curve is the spectrum of α-alanine observed 10 min after irradiation, and the 3 lower spectra represent β-alanine observed at different times after the exposure. All spectra in this paper represent the first derivative of the actual absorption curves. The arrows indicate the position of the resonance of DPPH ($g = 2.0036$). The spectra may only be compared qualitatively since different gains were used. The samples were irradiated and stored in vacuum, at room temperature (20°C).

The free radical 1,1-diphenyl-2-picryl-hydrazyl (DPPH) is frequently used as a reference system. When DPPH is crystallized from CS_2 both the line shape and the measured area vary with the oxygen pressure [15]. Correct areas are observed when the samples are measured in high vacuum. This oxygen effect is much smaller when the compound is crystallized from benzene or chloroform, but the addition complex now obtained must be chemically analysed [16]. Because of the above mentioned effects we found it inconvenient to use DPPH, and anthracite carbon powder was used in this work. This secondary standard was calibrated against DPPH which was recrystallized from CS_2 and measured in high vacuum. The absolute number of spins thus obtained may be off by as much as about 50 %.

The energy absorbed by the compound in question was calculated on the assumption that the radiation is absorbed predominantly by Compton scattering [17].

RESULTS

Qualitative measurements. α- and β-Alanine, when exposed to X-rays, give resonance patterns which are shown in Fig. 1.

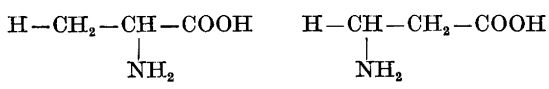

(I) (II)

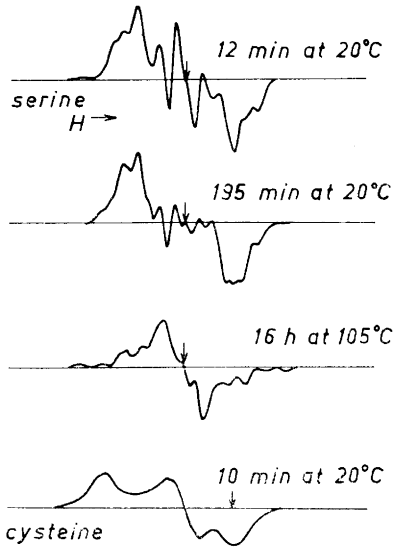

Fig. 2. The qualitative spectra of serine and cysteine. The lower serine pattern is observed after heat treatment at 105°C for 16 h. Otherwise conditions as in Fig. 1.

α-Alanine (I), shows a nearly symmetrical 5-line spectrum with an unresolved pattern superimposed. This resonance spectrum which is nearly the same as that observed by Gordy *et al.*[2,6] was found to be independent of the radiation dose and the time after the end of the exposure. Also, it was unchanged upon heat treatment for several hours at about 110°C. These findings suggest that only one single radical is induced in α-alanine. From work with single crystals Miyagava and Gordy [18] presume the radical to be $CH_3-\dot{C}HR$ where the unpaired electron interacts with 4 protons, and R is a group which has no detectable coupling.

The resonance pattern of β-alanine (II), on the other hand, is not stable and shows qualitative changes with time (Fig. 1). The initial pattern seems to be more resolved than previously observed by Shields and Gordy [6], and by Randolph and Parrish [8]. The central peak with a g-value of 2.0056 increases gradually during the first days, reaches a maximum and then decays slowly and finally becomes smeared out.

It seems to be quite clear that the position of the amino group in alanine modifies the resonance pattern, and in order to get more information about the influence of different chemical groups a number of derivatives of α-alanine were studied. Thus we have studied serine were OH is substituted for one of the methyl protons; (R = OH), cysteine (R = SH),

$$\begin{array}{c} R-CH_2-CH-COOH \\ \quad\quad\quad\quad\;\; | \\ \quad\quad\quad\quad\;\; NH_2 \end{array}$$

(III)

aspartic acid (R = COOH), different types of glutamic acid (R = CH_2—COOH) and a few amino acids with aromatic rings like phenylalanine, histidine, and tryptophane.

In Fig. 2 the spectra of cysteine and serine are compared. The cysteine spectrum which remains unchanged with time is displaced to a lower magnetic field strength than ordinary hydrocarbon radicals. This increase in g-value (g = 2.025 for the central peak) is consistently found for thiols [13] and other sulphur compounds [19,20], and the spectrum most likely represents one single radical where the unpaired electron is localized on the sulphur atom as proposed by Gordy and Shields [21]. When the sulphur atom is replaced by oxygen, a completely new resonance pattern is observed. Thus Fig. 2 shows that DL-serine gives a pattern which initially consists of at least 10 lines, and is about 125 gauss wide. This resonance is quite unstable and after few hours at room temperature qualitative changes are observed. Heat treatment for about 16 h at 105°C completely changes the resonance, and this spectrum does not show further changes. The spectrum, which is now about 140 gauss wide, resembles that found by Shields and Gordy [6] for L-serine. The g-value for the center of the resonance is close to that of DPPH (g = 2.0036). The reason for the great difference between serine and cysteine is not immediately obvious. Whereas the unpaired electron in cysteine seems to be localized on the sulphur atom, no evidence is found from the serine spectra that the unpaired electron is localized on the oxygen atom in this compound.

In Fig. 3 the spectra of aspartic acid and of different types of glutamic acid are shown. The resonance pattern of aspartic acid shows only moderate changes with time, and even heat treatment at 105°C for several hours intro-

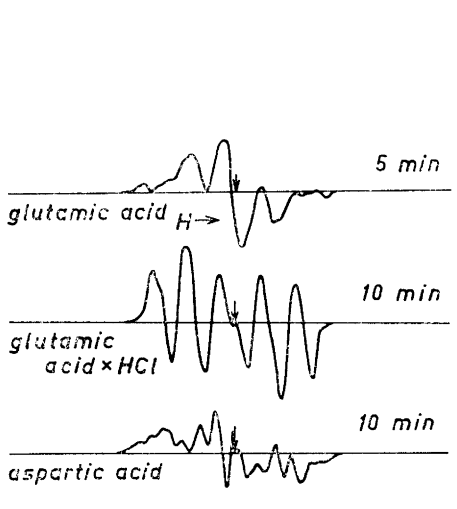

Fig. 3. The qualitative resonance patterns of aspartic acid, glutamic acid, and glutamic acid hydrochloride. Otherwise conditions as in Fig. 1.

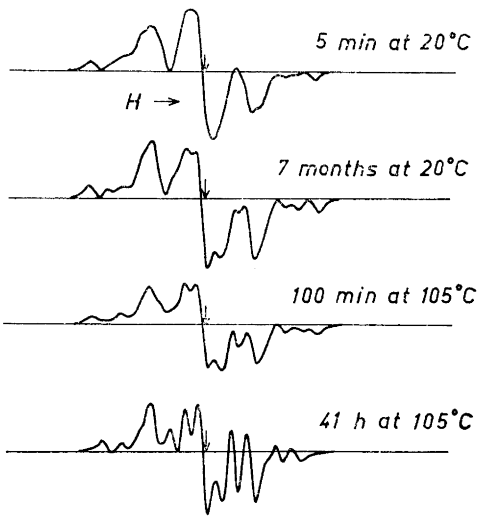

Fig. 4. The qualitative spectra of glutamic acid observed under different conditions. All samples were irradiated at room temperature.

duces only minor changes in the spectrum. The initial spectrum which is about 140 gauss wide consists of 13 unresolved peaks, but after 20 h at 105°C only 10 peaks are observable.

For glutamic acid, which contains one CH_2 group more than aspartic acid, we have studied glutamic acid monohydrate and glutamic acid hydrochloride as well as free glutamic acid. Approximately the same qualitative resonance pattern was found for glutamic acid and glutamic acid · H_2O, whereas a different spectrum was found for glutamic acid · HCl (Fig. 3). The resonance pattern of glutamic acid · HCl was found to be very stable. Thus, after heat treatment at 105°C for 2 days the spectrum remained unchanged. On the other hand, the radicals induced in glutamic acid · H_2O decay rapidly and no spectrum was detectable after 60 min at 105°C. This rapid decay possibly means that the added water acts as bridges for recombination processes.

The initial pattern of free glutamic acid is about 130 gauss wide and shows 7 unresolved hyperfine lines. This resonance is relatively stable, but upon prolonged storage at room temperature the resonance becomes more resolved, and after 7 months the 7-lined spectrum is changed into at least 12 lines (Fig. 4). The qualitative changes which take place very slowly at room temperature, proceed more rapidly but in much the same way at elevated temperatures. In Fig. 4 is shown that the same qualitative changes which are obtained after 7 months at room temperature are reached in the course of 100 min at 105°C. Further heat treatment gives a final spectrum of 13 lines, and it is interesting to notice that this spectrum of glutamic acid shows many similarities to that of aspartic acid (Fig. 3).

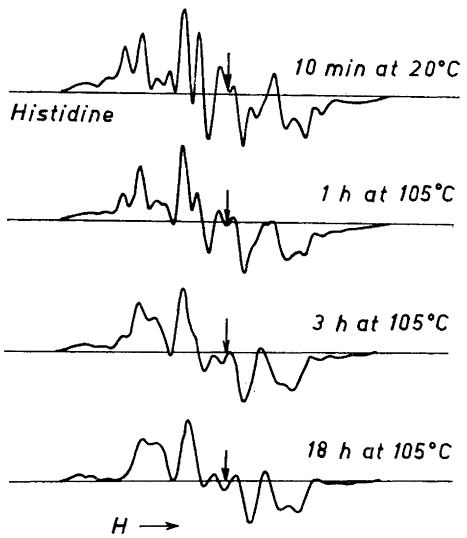

Fig. 5. The qualitative spectra of histidine observed after different treatments. Otherwise conditions as in Fig. 1.

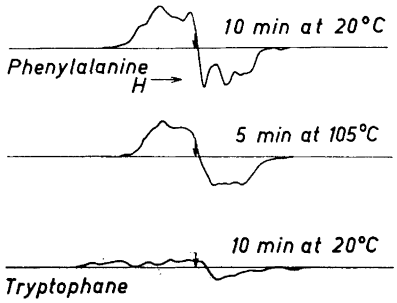

Fig. 6. The qualitative resonance pattern of phenylalanine and tryptophane. The dose for tryptophane was 9×10^5 r.

Amino acids with aromatic rings have also been examined (Figs. 5 and 6). Both phenylalanine and histidine show a much more resolved hyperfine structure than that observed by Shields and Gordy [6]. The initial resonance pattern of histidine is about 155 gauss wide, a little unsymmetrical, and about 16 hyperfine lines are observable. Fig. 5 shows the spectra of histidine after heat treatment. The resonance becomes symmetrical and with a g-value like that of DPPH for the central peak. After 18 h at 105°C only 9 peaks are observable. The initial pattern of histidine shows many similarities with aspartic acid and glutamic acid after heat treatment.

Table 1. Summary of qualitative data.

Compound	R in formula III	Total with in gauss[a]	Number of peaks initially observed	Qualitative changes with time at 20°C	Qualitative changes with time at 105°C
β-Alanine	—	95	10 unresolved	small and slow	small
DL-α-Alanine	—H	145	5	none	none
L-Aspartic acid	—COOH	140 ↓ [b] 125	13 unresolved	very small	small, 10 peaks after 20 h
L-Glutamic acid	$-CH_2-COOH$	130	7	large, but very slow (months)	large, 13 peaks after 41 h
DL-Glutamic acid, monohydrate	$-CH_2-COOH \cdot H_2O$	125	7	small during the first 14 days	no resonance after 1 h
L-Glutamic acid, monohydrochloride	$-CH_2-COOH \cdot HCl$	140	6	none (3 months)	small during the first 41 h
DL-Serine	—OH	125 ↓ [b] 140	≥10 unresolved	large, 12 peaks after 3 hours	very large
L-Cysteine	—SH	140	3 unresolved	none	none
L-Phenylalanine	$-C_6H_5$	120 ↓ [b] 90	≥7 unresolved	small	the hyperfine structure is smeared out after 1 h
L-Histidine	imidazolyl	155 ↓ [b] 145	16	none (3 days)	great but slow, 9 peaks after 18 h
L-Tryptophane	indolyl	120	probably 10 (smeared out)	—	—

[a] The error in these values is about ± 10 %.

[b] The upper figure represents the initial spectrum. The arrow and the lower figure mean that the total width of the spectrum is changed after heat treatment.

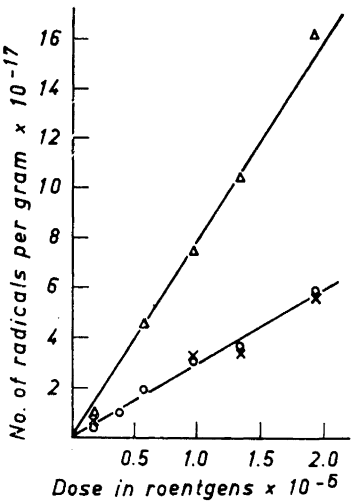

Fig. 7. The number of induced radicals in glutamic acid as a function of the radiation dose in the range 0—2.5 × 10^5 r. △ = glutamic acid hydrochloride, ○ = glutamic acid, and × = glutamic acid monohydrate.

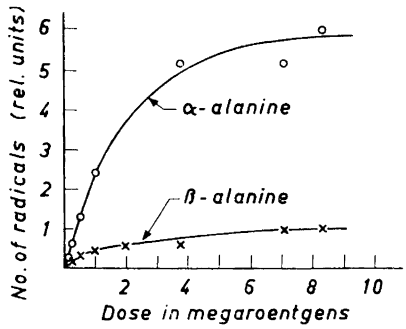

Fig. 8. The total number of radicals in *a*- and *β*-alanine, respectively, as a function of the radiation dose in the megaröntgen range.

The spectrum of phenylalanine is about 120 gauss wide and 7 hyperfine lines are observable (Fig. 6). This resonance shows many similarities with the spectrum of *β*-alanine. Upon heat treatment the hyperfine structure is smeared out and the final spectrum is only 90 gauss wide.

Tryptophane gives a very faint resonance even upon prolonged irradiation (Fig. 6). No definite resonance structure can be ascribed to this compound. Both the qualitative and quantitative results show that the radicals are not so easily stabilized in aromatic compounds. The qualitative data here presented are summarized in Table 1.

Quantitative measurements. The total number of radiation induced free radicals was measured as a function of the radiation dose (dose-effect curve). In Fig. 7 dose-effect curves are given for the three types of glutamic acid in the dose range up to 2 × 10^5 r. The exposure time was 25 min throughout and all spectra were recorded 10 min after exposure. The dose-effect curves are straight lines in the relatively low dose range, a result which agrees with that found for glycine by Zimmer *et al.*[9] However, when exposed to doses in the mega-röntgen range, it was found that the dose-effect curves flatten out as exemplified for *a*- and *β*-alanine in Fig. 8. This flattening out which we have previously found for a number of sulphur compounds [12–13], is difficult to explain. Saturation can hardly account for this effect since it can be calculated that less than 1 out of 1 000 molecules is hit at the dose of 1 × 10^6 r. In experiments with doses in the mega-röntgen range, the exposure time varied and one possible explanation for the observed flattening out of the dose-effect curves is therefore that decay processes may occur during exposure.

Extensive studies were made in order to obtain information on the stability of the induced radicals. The total number of observable spins was plotted against the time elapsed after the end of the exposure. The results in Fig. 9 demonstrate the surprisingly high stability of radicals induced in α- and β-alanine. After a slight initial increase in the observable number of free spins, the decay may be described by a straight line in this semilogaritmic plot. In a previous study of sulphur compounds [12–13] we found that the decay of the total number of spins (N) was best described by the formula $N = a \ln t + b$, where a and b are constants. Interestingly, this formula may also be used for amino acids as shown in Figs. 9 and 10. Even decay at elevated temperatures may be described in this way as shown for glutamic acid in Fig. 11. The results for the three types of glutamic acid (Fig. 7 and Table 2) show that three times more radicals are induced in glutamic acid · HCl than in the two other types of glutamic acid. The data in Figs. 10 and 11 also demonstrate that these radicals are more stable than those induced in free glutamic acid and glutamic acid monohydrate.

The results presented in Fig. 9 clearly demonstrate that the above mentioned flattening out of the dose-effect curves (Fig. 8) cannot be explained by a simple decay process during the exposure. This flattening out may therefore be the result of other processes during irradiation. The possibility should be considered that during exposure the new radicals formed may combine with radicals already formed, and that this process competes with the trapping process. A similar explanation has been proposed by Atherton *et al.*[22] for the copolymerization of methyl methacrylate by UV irradiation.

The quantitative data from our experiments are summarized in Table 2. In this table the observed yields for radical production are given. Since different parameters influence the ESR measurements, the yields are values extrapolated to the conditions of zero dose, room temperature (20°C), high vacuum (10^{-4}—10^{-5} mm Hg), and measurements obtained 10 min after the end of the exposure. Presented in Table 2 are the inverse values of the yield, *i.e.* electron volts per radical.

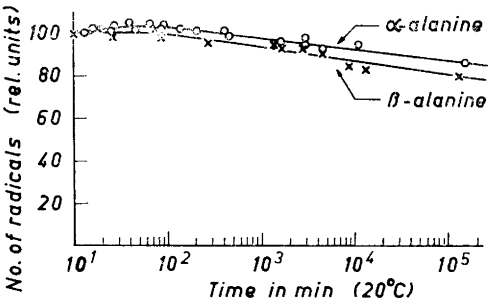

Fig. 9. The decay of radiation induced radicals in α- and β-alanine at 20°C. O = α-alanine and × = β-alanine. The data are given in per cent of that observed 10 min after irradiation.

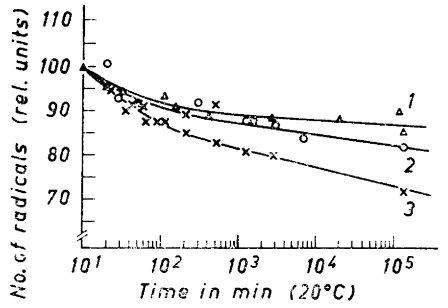

Fig. 10. The decay of radiation induced radicals in the 3 types of glutamic acid at 20°C. △ = glutamic acid hydrochloride, O = glutamic acid, and × = glutamic acid monohydrate. The data are given in per cent of that observed 10 min after irradiation.

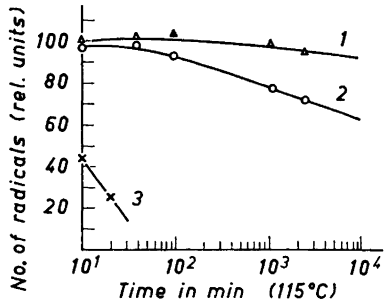

Fig. 11. The decay of radicals in the 3 types of glutamic acid after heat treatment for varying periods of time at 115°C. The number before heat treatment was set equal to 100 in all 3 cases. The first measurement was made after heat treatment for 10 min. △ = glutamic acid hydrochloride, ○ = glutamic acid, and × = glutamic acid monohydrate.

Table 2. Summary of quantitative data.

Compound	R in formula III	Inverse yields in [a] eV/rad.	Decay (in %) after storage for 1 h at 20°C	Decay (in %) after storage for 1 day at 20°C	Decay (in %) after storage for 1 h at 105°C
β-Alanine	—	25	1	6	24
DL-α-Alanine	—H	13	— 3 [c]	2	4
L-Aspartic acid	—COOH	17	3	17	22
L-Glutamic acid	$-CH_2-COOH$	15	8	12	— [d]
DL-Glutamic acid, monohydrate	$-CH_2-COOH \cdot H_2O$	15	10	18	— [d]
L-Glutamic acid, monohydrochloride	$-CH_2-COOH \cdot HCl$	5	7	11	— [d]
DL-Serine	—OH	14	— 4 [c]	19	23
L-Cysteine	—SH	34	— 2 [c]	2	>20
L-Phenylalanine	$-C_6H_5$	36	2	6	12
L-Histidine	imidazolyl	52	— 8 [c]	— 1	15
L-Tryptophane	indolyl	265 [b]	—	—	—

[a] The error in these values may be as much as 50 %.
[b] The value observed at 9×10^5 r.
[c] The total number of observable ESR centers for these compounds increased slightly during the first minutes after irradiation.
[d] See Fig. 11.

DISCUSSION

The results here presented clearly demonstrate that qualitative changes with time occur in the ESR spectra of irradiated amino acids. Such qualitative changes could be explained if several primary radicals with different rates of decay were induced. The results for serine, glutamic acid and histidine also demonstrate that the initial spectrum represents the composite pattern of more than one radical. However, when the quantitative results are compared with the qualitative changes in the ESR spectra, it seems that other processes than simple decay take place. In a previous work on glutathione [14], we found that by such secondary processes the unpaired electron spins may even migrate to one specific group, the sulphur atom of the cysteine residue. However, the nature of these secondary processes is at the moment obscure. The results here presented demonstrate that these processes can be speeded up by heat treatment.

In Table 2 the number of electron volts needed to induce one primary radical is given. The values, ranging from 5 to 50 eV per radical, differ greatly from the results of Box and Freund [7], and Randolph and Parrish [8]. The values in this work refer to zero dose. When the flattening out of the dose-effect curves is considered, these differences in yield may probably be explained.

The high yields (low values in Table 2) observed may be of interest with regard to the mechanism for the radical production. Up to now it has usually been assumed that the radicals observed are formed from ionization processes [23] and that the observed spins represent positive holes [2,24]. The negative ions formed from the trapped electrons are assumed to give too broad spectra to be observed [2].

Very little is known about the primary radiation processes in the solid state. Thus, the energy necessary to induce one ion pair (W) is measured only for some semiconductors like Ge [25] and Si [26], for a few silver halide crystals [27] and for diamond [28,29]. Surprisingly low values, ranging from 3 eV to 10 eV have been reported. No such data are reported for solid organic compounds. In hydrocarbon gases W has been found to be about 26 eV [30]. In the gaseous state the ratio W/I is usually about 2 (I is the ionization potential) [30]. It seems therefore reasonable that the ratio W/E for solids (E is the minimum energy to liberate an electron in a solid) will be about 2.

In view of these facts no conclusive statement can be given to the theory that the ESR spectra represent positive holes. However, the radiation yields here presented seem to indicate that also other processes with the formation of radicals may take place. One possible mechanism is that some of the ionized molecules which are in an excited state may undergo a homolytic dissociation and thus give molecular fragments with unpaired spins. In a previous paper [14] we have also proposed the possibility that some of the primary excitation processes are subsequently followed by rupture of chemical bonds with the formation of fragment radicals. Magee and Funabashi [31] have proposed a similar dissociation of excited molecules as one possible mechanism for radical production.

Some of the radical fragments produced by rupture of chemical bonds may have enough kinetic energy to escape an immediate recombination. These

radicals may then be stabilized within a cage of intact neighbouring molecules. It is likely that the radical fragments take part in secondary reactions inside the cage. These reactions are assumed to be rapid and temperature independent. Also reactions outside the cage may occur, but since the radicals now must escape from the cage, these processes are assumed to be slower and influenced by temperature. The results in this work are consistent with such a mechanism.

Acknowledgements. The authors are grateful for technical advice and assistance from Mr. Otto Sörensen. Thanks are due to Dr. A. Pihl for valuable discussions.

REFERENCES

1. Ingram, D. J. E. *Free Radicals as Studied by Electron Spin Resonance*, Butterworths Scientific Publications, London, 1958.
2. Gordy, W., Ard, W. B. and Shields, H. *Proc. Natl. Acad. Sci. u.s.* **41** (1955) 983.
3. Gibson, J. E., Ingram, D. J. E., Symons, M. C. R. and Townsend, M. G. *Trans. Faraday Soc.* **53** (1957) 914.
4. Smaller, B. and Matheson, M. S. *J. chem. Phys.* **28** (1958) 1169.
5. Conger, A. D. and Randolph, M. L. *Radiation Research*, **11** (1959) 54.
6. Shields, H. and Gordy, W. *J. Phys. Chem.* **62** (1958) 789.
7. Box, H. C. and Freund, H. G. *Nucleonics* **17** (1959) 66.
8. Randolph, M. L. and Parrish, D. L. *Radiation Research* **9** (1958) 170.
9. Zimmer, K. G., Ehrenberg, A. and Ehrenberg, L. *Strahlentherapie* **103** (1957) 3.
10. Randolph, M. L. and Parrish, D. L. *Radiation Research* **11** (1959) 462.
11. Combrisson, J. and Uebersfeld, J. *Compt. rend.* **238** (1954) 1397.
12. Henriksen, T. and Pihl, A. *Nature* **185** (1960) 307.
13. Henriksen, T. in Blois, M. S. (Ed.) *Free Radicals in Biological systems*, Academic Press, New York, 1961 Chap. 21, p. 278.
14. Henriksen, T. and Pihl, A. *Intern. J. Rad. Biol.* **3** (1961) 351.
15. Bennet, J. E. and Morgan, E. J. H. *Nature* **182** (1958) 199.
16. Lothe, J. and Eia, G. *Acta Chem. Scand.* **12** (1958) 1535.
17. Hine, G. and Brownell, G. L. *Radiation Dosimetry*, Academic Press, New York, 1956, p. 12.
18. Miyagawa, I. and Gordy, W. *J. Chem. Phys.* **32** (1960) 255.
19. Gardner, D. M. and Fraenkel, G. K. *J. Am. Chem. Soc.* **78** (1956) 3279.
20. Ingram, D. J. E. and Symons, M. C. R. *J. Chem. Soc.* **1957** 2437.
21. Gordy, W. and Shields, H. *Radiation Research* **9** (1958) 611.
22. Atherton, N. M., Melville, H. W. and Whiffen, D. H. *Trans. Faraday Soc.* **54** (1958) 1300.
23. Kirby-Smith, J. S. and Randolph, M. L., In Buzzati-Traverso, A. A. (Ed.). *Immediate and Low Level Effects of Ionizing Radiation*, Taylor and Francis, London, 1960 pp. 11–24.
24. Blumenfeld, L. A. and Kalmanson, E. A. *Biophysics (U.S.S.R.) (English Translation)* **3** (1958) 87.
25. McKay, K. G. *Phys. Rev.* **84** (1951) 829.
26. Vavilov, V. S., Smirnov, L. S. and Patskevitch, V. M. *Intern. J. Appl. Radiation and Isotopes* **2** (1957) 255.
27. Hofstadter, R. *Nucleonics* **4** (1949) 29.
28. Ahearn, A. J. *Phys. Rev.* **73** (1948) 1113.
29. McKay, K. G. *Phys. Rev.* **77** (1950) 816.
30. Platzman, R. In Claus, W. D. (Ed.) *Radiation in Biology and Medicine*, Addison-Wesley Publishing Company, Inc., Reading, Mass., U.S.A., 1958 Chap. 2.
31. Magee, J. L. and Funabashi, K. *Radiation Research* **12** (1960) 454.

Received November 28, 1960.

ACTA CHEMICA SCANDINAVICA 15 (1961) 803–807

Zur Spaltung von β-Hydroxy-alkyl-aryläthern durch Alkali

JOSEF GIERER und ISA KUNZE

Die Holzchemische Abteilung des Schwedischen Holzforschungsinstituts, Stockholm, Schweden

Am Beispiel der beiden Glycerin-monoguajacyläther (I und III) wird gezeigt, dass die alkalische Spaltung von β-Hydroxyalkyl-aryläthern über die Zwischenstufe der entsprechenden Epoxyde verläuft.

Die Spaltung von Alkyl-aryläthern durch Alkali erfordert im allgemeinen radikale Reaktionsbedingungen [1]. So wird Anisol von 20 %iger alkoholischer Kalilauge durch 7-stündiges Erhitzen auf 200° nur zu 7 % gespalten [2]. Alkyläther mehrwertiger Phenole, wie z.B. Veratrol und Pyrogallol-trimethyläther, zeigen zwar ein grösseres Reaktionsvermögen, doch sind auch für ihre Spaltung (zu Guajakol [3], bzw. zu Pyrogallol-1,3-dimethyläther [4]) sehr hohe Alkalikonzentrationen erforderlich.

Eine seit langem bekannte Ausnahme der Stabilität der Alkyl-aryläther gegenüber Alkali bilden Verbindungen, bei denen die Ätherbindung durch elektronegative Substituenten am aromatischen Rest aufgelockert wird [5]. Die Spaltbarkeit von Alkyl-aryläthern durch Alkali kann aber auch durch Substitution im Alkylrest erleichtert werden. Im Zusammenhang mit einem Studium der strukturellen Voraussetzungen des alkalischen Abbaues von Lignin [6] wurde nämlich eine weitere Kategorie verhältnismässig leicht spaltbarer Verbindungen in den β-Hydroxy-alkyl-aryläthern gefunden, deren alkalische Hydrolyse die vorliegende Arbeit am Beispiel zweier einfacher Vertreter (*o*-Methoxy-phenyl-glycerinäther I und III) näher behandelt.

Es zeigte sich, dass die beiden Guajacyl-glycerinäther I und III durch 2-stündiges Erhitzen in 2 N Natronlauge auf 170°C weitgehend gespalten werden (siehe Tabelle 1). Da unsubstituierte Alkyläther des Guajakols, wie z. B. das oben erwähnte Veratrol, unter diesen Bedingungen praktisch stabil sind (Spal-

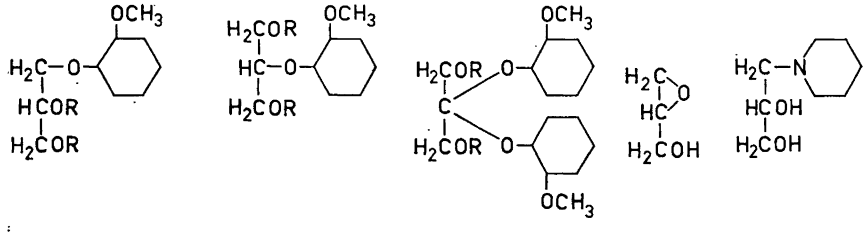

I R=H II R=CH_3 III R=H IV R=CH_3 V R=H VI R=CH_3 VII VIII

tungsgrad 3 %), darf die Alkalilabilität der Verbindungen I und III auf ihre Hydroxylgruppen zurückgeführt werden. Diese sind der Arylätherbindung benachbart und daher befähigt, die Aroxygruppe durch nukleophile Substitution unter Ausbildung intermediärer Epoxygruppen zu verdrängen:

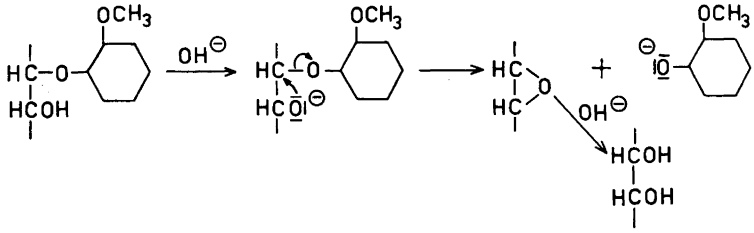

Für die Gültigkeit dieser Annahme spricht die Tatsache, dass die Spaltbarkeit der Verbindungen I und III durch Methylierung ihrer Hydroxylgruppen fast vollkommen aufgehoben wird (siehe die Verbindungen II und IV in Tab. 1).

Eine weitere Stütze für die Annahme, dass die Spaltung der Verbindungen I und III über das Epoxyd VII (Glycid) als (gemeinsame) Zwischenstufe verläuft, konnte dadurch erbracht werden, dass die Reaktion mit einer Mischung aus Piperidin (9 Teile) und 2 N Natronlauge (1 Teil) als spaltendes Agenz durchgeführt wurde. Aus dem Reaktionsansatz liess sich sowohl im Falle des *α*-Guajacyl-glycerinäthers (I), als auch im Falle des *β*-Guajacyl-glycerinäthers (III) die *α*-Piperidinoverbindung VIII (1-Piperidino-propandiol-2,3) gewinnen

Tabelle 1. Spaltung der Substanzen I—VI.

Substanz (500 mg)	Spaltendes Agenz (15 ccm)	Reaktionsdauer bei 170°C (Aufheizperiode 2 St.)	Zurückgewonnenes Ausgangsmaterial (mg)	Isoliertes Guajakol (Rohausb. in mg)	% Spaltung ber. aus Guajakolausbeute
I	2 N NaOH	2 Stdn.		272	86.9
III	»	»		265	84.5
V	»	»		356	92.0
II	2 N alkohol. NaOH	2 Stdn.	295	23	8.3
IV	»	»	334	24	8.7
VI	»	»	350	31	8.7
			Isolierte Piperidin-Verbindung		
I	Piperidin-2 N NaOH (9:1)	17 Stdn.	180 (45 % d. Th.)	149	47.6
III	»	»	155 (39 % d. Th.)	132	42.1

und durch Schmelzpunkt und Misch-Schmelzpunkt identifizieren. Die Ausbeute (in % d. Th.) entsprach ungefähr der Menge des nach der Spaltung isolierten Guajakols (siehe Tabelle 1). Die Piperidinoverbindung VIII wurde auch bei gleicher Behandlung des angenommenen Zwischenproduktes VII (Glycid) in guter Ausbeute erhalten, und es konnte durch Papierchromatographie gezeigt werden, dass sich bei der Reaktion kein Glycerin gebildet hatte. Behandelt man hingegen Glycerin unter den gleichen Bedingungen mit der Mischung aus Piperidin und 2 N Natronlauge, lässt sich im Reaktionsansatz papierchromatographisch keine Piperidinoverbindung VIII nachweisen.

Der Verlauf der durch Alkali bewirkten Spaltung von β-Hydroxy-alkyl-aryläthern ist demnach dem der alkalischen Spaltung von Arylacetalbindungen in Phenyl β-D-glykosiden analog. Bei dieser werden aufgrund der Abhängigkeit von der anomeren Konfiguration [7] und vom Vorhandensein einer freien Hydroxylgruppe am Kohlenstoffatom 2 [8,9] ebenfalls Epoxyde als Zwischenstufen angenommen [7–11]. Die alkalische Spaltung von Alkylglykosiden wird nach dem Ergebnis einer neueren Untersuchung [12] durch β-ständige Hydroxylgruppen im Aglykon erleichtert. Auch dieser Sachverhalt lässt sich am besten mit der Annahme erklären, dass sich bei der Reaktion intermediär Epoxyde bilden [12].

Um die Analogie im Verhalten von β-Hydroxy-alkyl-aryläthern und von entsprechenden Arylacetalen zu bekräftigen, wurde die alkalische Spaltung auch mit dem Diguajacylketal des 1,3-Dihydroxypropanons-2 (V) durchgeführt. Wie bei den Guajacyläthern I und III wurde bei dem Ketal V unter den oben angegebenen Bedingungen eine fast vollständige Spaltung erzielt, während der entsprechende 1,3-Dimethyläther (VI), wie die Verbindungen II und IV, unverändert zurückgewonnen werden konnte (siehe Versuchsteil).

EXPERIMENTELLES

Darstellung der *o*-Methoxy-phenoxy-propandiole (I, III, V)

1-(o-Methoxy-phenoxy)-propandiol-2,3 (I) aus Glycerin-α-monochlorhydrin und Natriumguajakolat (vgl. Ref.[13]). Schmp. 79°. Ausb. 72 % d. Th. ($C_{10}H_{14}O_4$ (198.1): Ber. C 60.62; H 7.06. Gef. C 60.64; H 7.21).

2-(o-Methoxy-phenoxy)-propandiol-1,3 (III) wurde durch Lithium-aluminiumhydrid—Reduktion von *o*-Methoxy-phenoxy-malonsäure-diäthylester (siehe unten) und Zersetzung des Aluminates durch Alkali (vgl. Ref.[14]) hergestellt. Aus 52 g *o*-Methoxy-phenoxy-malonsäure-diäthylester wurden 15.2 g (41.6 % d. Th.) 2-(*o*-Methoxy-phenoxy)-propandiol-1,3 erhalten. Das Produkt wurde im Vakuum (0.4 Torr) destilliert und ging zwischen 144 und 148° als farbloses Öl über, das bei Kühlung erstarrte. Umkristallisieren aus Benzol ergab Prismen vom Schmp. 61—62°. ($C_{10}H_{14}O_4$ (198.1); Ber. C 60.62; H 7.06; O 32.36. Gef. C 60.53; H 7.24; O 32.40).

o-Methoxy-phenoxy-malonsäure-diäthylester aus Monochlor-malonsäurediäthylester ($Sdp._{16}$ 117—119°) und Natriumguajakolat in absolutem Äthanol durch Erhitzen unter Rückfluss bis zur neutralen Reaktion [15,16]. $Sdp._{0.4}$ 144—146°.

2,2-Bis-(o-methoxy-phenoxy)-propandiol-1,3 (V) wurde durch Lithium-aluminiumhydrid—Reduktion von Bis-(*o*-methoxy-phenoxy)-malonsäure-diäthylester (siehe unten) und Zersetzung des Aluminates durch Alkali (vgl. Ref.[14]) hergestellt. 15 g des Esters ergaben 5.5 g (46 % d. Th.) krist. 2,2-Bis-(*o*-methoxy-phenoxy)-propandiol-1,3 (V), das aus Chloroform — Hexan umkristallisiert wurde. Schmp. 126.5°. ($C_{17}H_{20}O_6$ (320.2): Ber. C 63.76; H 6.25; OCH_3 19.37. Gef. C 63.65; H 6.14; OCH_3 19.36).

Diacetat von V durch Acetylierung von V mit Acetanhydrid-Pyridin und Umkristallisieren aus Äthylacetat — Hexan. Nadeln vom Schmp. 118—119°. ($C_{21}H_{24}O_8$ (404.2): Ber. C 62.39; H 5.94. Gef. C 62.40; H 6.09).

Bis-(o-methoxy-phenoxy)-malonsäure-diäthylester aus Monobrom-malonsäure-diäthylester (Sdp.$_{16}$ 121—126°) und Natriumguajakolat in absol. Äthanol neben der Mono-*o*-methoxy-phenoxy — Verbindung durch "Disproportionierung"[16]. Nach Abdestillieren des Lösungsmittels kristallisierte das Produkt aus dem öligen Rückstand aus. Es wurde abfiltriert, mit Äthanol gewaschen und aus Äthanol umkristallisiert. Schmp. 71—72°.

Darstellung der *o*-Methoxy-phenoxy-dimethoxy-propane (II, IV, VI)

Die *o*-Methoxy-phenoxy-dimethoxy-propane II, IV und VI wurden durch 3-malige Methylierung mit Methyljodid-Silberoxyd in Dimethylformamid[17] aus den entsprechenden *o*-Methoxy-phenoxy-propandiolen I, III bzw. V gewonnen.

1-(o-Methoxy-phenoxy)-2,3-dimethoxy-propan (II): Aus 2.0 g I wurden 1.1 g II als farbloses Öl vom Sdp.$_{0.2}$ 106—108° erhalten. Ausb. 48 % d. Th. ($C_{12}H_{18}O_4$ (226.1): Ber. C 63.74; H 7.96; O 28.30. Gef. C 63.71; H 7.90; O 28.59).

2-(o-Methoxy-phenoxy)-1,3-dimethoxy-propan (IV): 2 g III ergaben 1.5 g (= 66 % d. Th.) IV als farbloses Öl vom Sdp.$_{0.8}$ 108—110°. ($C_{12}H_{18}O_4$ (226.1): Ber. C 63.74; H 7.96; O 28.30. Gef. C 63.68; H 8.04; O 28.46).

2,2-Bis-(o-methoxy-phenoxy)-1,3-dimethoxy-propan (VI): 2.0 g V lieferten 1.8 g (= 83 % d. Th.) VI. Blättchen aus Äthanol—Wasser. Schmp. 81—82° ($C_{19}H_{24}O_6$ (348.2); Ber. C 65.53; H 6.89; O 27.57; OCH_3 35.62. Gef. C 65.21; H 6.88; I 27.89; OCH_3 35.34).

Darstellung des 1-Piperidino-propandiols-2,3 (VIII) durch Umsetzung äquimolarer Mengen von Glycid (VII) und Piperidin bei Zimmertemperatur. Das Reaktionsprodukt kristallisierte beim Anreiben mit Petroläther. Umkristallisieren aus Benzol. Schmp. 79.5—80.5°. Die gleiche Verbindung wurde auch durch Behandlung von Glycid mit der Mischung aus Piperidin und 2 N Natronlauge unter den unten angegebenen Bedingungen erhalten.

Spaltung der Substanzen I—VI mit Natronlauge

Je 500 mg Substanz wurden in 15 ccm 2 N wässriger — bzw. bei den methylierten Substanzen II, IV und VI in 15 ccm 2 N wässrig — alkoholischer (1:3) — Natronlauge gelöst und in einen Autoklaven aus rostfreiem Stahl übergeführt. Der Autoklav wurde hierauf mit lose aufgeschraubter Verschlusskappe in einen Vakuumexsikkator gestellt und dieser dreimal evakuiert und dazwischen mit Stickstoff gefüllt. Nach der letzten Stickstoff-Füllung wurde der Exsikkator rasch geöffnet, die Verschlusskappe festgeschraubt und der Autoklav in einem Polyglykolbad unter Rotation 2 Stdn. lang auf 170° gehalten (Aufheizungszeit 2 Stdn.). Nach Erkalten wurde die Lösung wenn erforderlich (bei Substanzen II, IV und VI), durch Einengen und Aufnehmen in Wasser von Äthanol befreit, hierauf schwach angesäuert und mit Äther dreimal ausgeschüttelt. Den vereinigten Ätherextrakten wurde das Guajakol mit 2 %iger Natronlauge entzogen und die wässrige Lösung nach Ansäuern erneut ausgeäthert. Die Menge des nach Trocknung der Ätherlösung und Abdestillieren des Äthers zurückbleibenden Roh-Guajakols ergab den in Tab. 1 angegebenen Spaltungsgrad in % d. Th. Diese Arbeitsweise liefert natürlich nur angenäherte Werte, da einerseits der Rückstand Verunreinigungen enthalten kann und da andererseits geringe Verluste beim wiederholten Ausschütteln unvermeidlich sind. In der wässrigen Lösung (nach Ansäuern und Ausschütteln mit Äther) wurde im Falle der Substanzen I und III Glycerin zunächst papierchromatographisch (siehe unten) nachgewiesen und hierauf als Tribenzoat isoliert. Schmp. 76°, keine Schmp.-Depression mit aus Glycerin hergestelltem Tribenzoat.

Die Ätherextrakte der angesäuerten Spaltungsansätze enthielten im Falle der Substanzen II und IV nach Entfernung der geringen Guajakolmengen (siehe Tab. 1) die unveränderten Ausgangsmaterialien, die isoliert und ohne weitere Reinigung durch Analyse identifiziert wurden.

II rückgewonnen, $C_{12}H_{18}O_4$ (226.1): Ber. C 63.74; H 7.96; O 28.30. Gef. C 63.48; H 8.00; O 28.73.

IV rückgewonnn $C_{12}H_{18}O_4$ (226.1): Ber. C 63.74; H 7.96; O 28.30. Gef. C 63.43; H 8.00; O 28.76.

Die Substanz VI kristallisierte nach der Kochung beim Verdünnen der äthanolischen Lösung mit Wasser direkt aus und wurde durch Umkristallisieren aus Äthanol-Wasser gereinigt. Schmp. 80—81°. Der Misch-Schmp. mit dem Ausgangsmaterial ergab keine Depression.

Spaltung der Substanzen I und III mit Piperidin—2N Natronlauge

Je 500 mg der Substanzen I und III wurden in 15 ccm einer Mischung aus 9 Tln. Piperidin und 1 Tl. 2 N Natronlauge gelöst und die Lösung, wie bei den Spaltungen mit Natronlauge beschrieben, behandelt. Die Reaktionszeit wurde auf 17 Stdn. verlängert. Nach Abkühlung wurde das Piperidin abdestilliert und die letzten Reste durch wiederholtes Aufnehmen in Äthanol und Abdestillieren im Vakuum entfernt. Die rotviolette Lösung des Rückstandes wurde mit verd. Salzsäure schwach angesäuert, mit Äther ausgeschüttelt und durch Zusatz von Aktivkohle fast vollkommen entfärbt. Die vereinigten Ätherextrakte lieferten, wie oben beschrieben, das Roh-Guajakol. Nach dreimaligem Einengen der sauren wässrigen Lösung und Aufnehmen des Rückstandes in Wasser wurde mit verd. Natronlauge alkalisch gemacht und hierauf erneut zur Trockne eingeengt. Der Rückstand wurde mit Benzol erschöpfend extrahiert und die Benzollösung nach Trocknung und Filtration auf kleines Volumen gebracht. Bei Impfung mit aus Glycid (VII) und Piperidin hergestellter Vergleichssubstanz (siehe oben) kristallisierte sowohl im Falle der Substanz I, als auch im Falle der Substanz III die Piperidinoverbindung VIII in schönen rhombischen Blättchen aus. Die Rohausbeuten sind in Tab. 1 angegeben. Schmp. nach einmaligem Umkristallisieren aus wenig Benzol 79—80°. Misch-Schmp. mit oben erwähnter Vergleichssubstanz ergab in beiden Fällen (I und III) keine Depression (78.5—80°).

Papierchromatographie: Es wurde Whatman No. 1 Filtrierpapier und als Lösungsmittelgemisch Butanol: Äthanol: Wasser (4:1:5) verwendet. Die Entwicklung der Chromatogramme erfolgte durch Silbernitrat (in Aceton) und Natriumhydroxyd (in Äthanol)[18]. R_F-Wert des Glycerins: 0.36, R_F-Wert der Piperidinoverbindung (VIII): 0.28.

LITERATUR

1. Übersichtsreferate über Ätherspaltungen siehe Lüttringhaus, A. und Sääf, G. *Angew. Chem.* **51** (1938) 915; Burwell, jr., R. L. *Chem. Revs.* **54** (1954) 615.
2. Hughes, G. K. und Thompson, E. O. P. *J. Proc. Roy. Soc. N. S. Wales* **83** (1950) 269.
3. Merck, Dtsch. Reichs-Pat. 78.910., *Chem. Zentr.* **1895**, I, 719.
4. Basler Chemische Fabrik, Dtsch. Reichs-Pat. 162.658., *Chem. Zentr.* **1905**, II, 1061.
5. Klemenc, A. *Monatsh.* **33** (1912) 375; Oliverio, A. *Chem. Zentr.* **1939**, II, 3977; Kolhatkar, G. B. und Bapat, V. V. *J. Univ. Bombay* **7** (1938) Tl. 3, 157,; *Chem. Abstr.* **33** (1939) 5268; *Chem. Zentr.* **1940**, II, 2000; Ogata, Y. und Okano, M. *J. Am. Chem. Soc.* **71** (1949) 3211.
6. Gierer, J. und Kunze, I. *Unveröffentlicht.*
7. Montgomery, E. M., Richtmyer, N. K. und Hudson, S. S. *J. Am. Chem. Soc.* **65** (1943) 3.
8. McCloskey, C. M. und Coleman, G. H. *J. Org. Chem.* **10** (1945) 184.
9. Bardolph, M. P. und Coleman, G. H. *J. Org. Chem.* **15** (1950) 169.
10. Dyfverman, A. und Lindberg, B. *Acta Chem. Scand.* **4** (1950) 878.
11. Umfassendes Übersichtsreferat über Alkali-labile Glykoside siehe Ballou, C. E. *Advances in Carbohydrate Chem.* **9** (1954) 59.
12. Janson, J. und Lindberg, B. *Acta Chem. Scand.* **13** (1959) 138.
13. Wheeler, T. S. und Willson, F. G. *Org. Syntheses* **6** (1926) 48.
14. Chaikin, S. W. *J. Am. Chem. Soc.* **70** (1948) 3522.
15. Bischoff, C. A. *Ber.* **33** (1900) 1396.
16. Niederl, J. B. und Roth, R. T. *J. Am. Chem. Soc.* **62** (1940) 1154.
17. Kuhn, R., Trischmarn, H. und Löw, I. *Angew. Chem.* **67** (1955) 32.
18. Trevelyan, W. E., Procter, D. P. und Harrison, J. S. *Nature* **166** (1950) 444.

Eingegangen am 14. Dezember 1960.

ACTA CHEMICA SCANDINAVICA 15 (1961) 808–816

Hydrolysis of Palatinose (Isomaltulose) by Pig Intestinal Glycosidases

ARNE DAHLQVIST

Department of Physiological Chemistry, University of Lund, Lund, Sweden

Homogenates of intestinal mucosa from adult pigs hydrolyze palatinose (6-(α-D-glucopyranosyl)-D-fructose).

The palatinase activity is caused by a mixture of three separate enzymes, namely *specific isomaltase*, *maltase II* and *maltase III*.

These three enzymes also hydrolyze isomaltose, but the relative rates of hydrolysis of isomaltose and palatinose during the conditions used for glycosidase activity determination are different for the three enzymes.

Maltase III alone exerts about 50 % of the total palatinase activity of crude homogenates of pig intestinal mucosa.

The isolation of a new disaccharide, *palatinose* (isomaltulose, (6-(α-D-glucopyranosyl)-D-fructose), formed by a bacterium isolated from sugar beets, was recently described by Weidenhagen and Lorenz [1–3]. This disaccharide is hydrolysed by some species of yeast. The hydrolysis seems not, however, to be caused by maltase (α-glucosidase), as might have been expected, but by a specific *palatinase* [4].

It is not known whether the glycosidases of the *intestinal mucosa* are able to hydrolyze palatinose or not. This question is of interest as the effect of orally administered palatinose on intestinal flora is currently under study [5]. It is also important for the further characterization of the specificity of the different pig intestinal α-glucosidases recently separated [6]. Professor Weidenhagen kindly supplied the author with a sample of palatinose for the study of the action of pig intestinal glycosidases on this sugar.

MATERIALS AND METHODS

Intestinal glycosidase preparations

The mucosa and the contents of the small intestine of adult pigs were obtained by pressing the intestine between two rollers immediately after the slaughter. The whole length of the small intestine was used. In the first experiments the preparation obtained was homogenized in an Ultra-Turrax homogenizer for 2 min [7], and after centrifugation

in an ordinary laboratory centrifuge for 5 min the opalescent supernatant was analyzed immediately. Later preparations were used which had been solubilized and thereafter purified by ethanol precipitation as described earlier [6].

Substrates

Sucrose (2-(*a*-D-glucopyranosyl)-*β*-D-fructofuranoside) (cryst.) was obtained from Baker Co. (U.S.A.) and *maltose* (4-(*a*-D-glucopyranosyl)-D-glucose) (cryst., monohydrate) from Merck A.G. (Germany). *Isomaltose* (6-(*a*-D-glucopyranosyl)-D-glucose) and *phenyl-a-D-glucopyranoside* were prepared by the methods described earlier [8,9]. *Palatinose* (isomaltulose, 6-(*a*-D-glucopyranosyl)-D-fructose) (cryst., monohydrate) was kindly supplied by Professor R. Weidenhagen (Neuoffstein, Germany).

Glycosidase activity determinations

Methods for the determination of *invertase, maltase, isomaltase* and *phenyl-a-D-glucopyranosidase* activities have been described in a previous paper [10].

Palatinase activity was determined by the use of glucose oxidase in the same way as has been described earlier for *turanase* and *lactase* activity determinations [10]. The substrate solution was prepared by dissolving 1.90 g of palatinose in 0.10 M maleate buffer pH 6.5 to a final volume of 100 ml* (*cf.* Table 5 in Ref.[10]). In accordance with the other glycosidase activities one unit of palatinase activity is defined as the activity causing 5 % of hydrolysis in 2.0 ml of reaction mixture in 60 min at 37°C.

Protein determinations

The determination of protein was performed with the method of Lowry *et al.*[11] using the modified reagent B introduced by Eggstein and Kreutz [12]. A standard curve was prepared with human serum albumin, kindly supplied by A. B. Kabi.

Mutual displacement chromatography

The mutual displacement technique as applied to the chromatography of glycosidases upon TEAE-cellulose columns has been described in a previous paper [13]. The TEAE-cellulose was prepared in the laboratory from Solkafloc cellulose powder SW 40 A [13]. The ion exchanger was stored and used in its bromide form. Commercial TEAE-cellulose (from Serva Entwicklungslabor, Germany) was found unsuitable for columns of the dimensions used (1 × 100 cm) since the flow rate became too low.

RESULTS AND DISCUSSION

Palatinase activity of crude intestinal preparations

Fresh intestinal mucosa homogenates from adult pigs hydrolyzed palatinose with a rate that was 0.3—0.5 times the rate for the hydrolysis of isomaltose; 0.1—0.2 times that for sucrose; and 0.02—0.05 times that for maltose during the conditions used for glycosidase activity determination.

* Since palatinose did not decrease in weight on storage *in vacuo* over P_2O_5 at 50°C it was believed to be anhydrous. The sugar contains, however, one mole of crystal water which is difficultly removed [5]. The substrate solution therefore should contain 2.0 g of palatinose per 100 ml [10]. The activity measured at the somewhat lower substrate concentration used here is, however, only about 2 % too low.

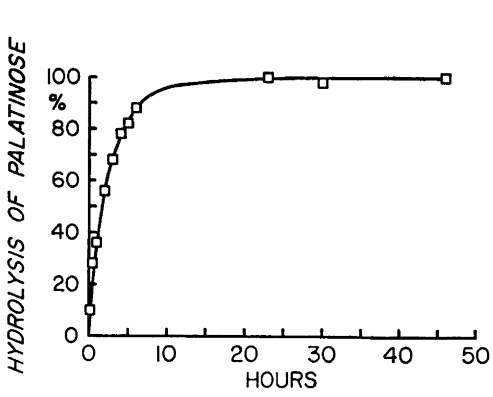

Fig. 1. Hydrolysis of palatinose by a crude extract of pig intestinal mucosa at 0.027 M substrate concentration in 0.05 M maleate buffer pH 6.5 at 37°C. Toluene was used as a preservative. The hydrolysis proceeded to completion.

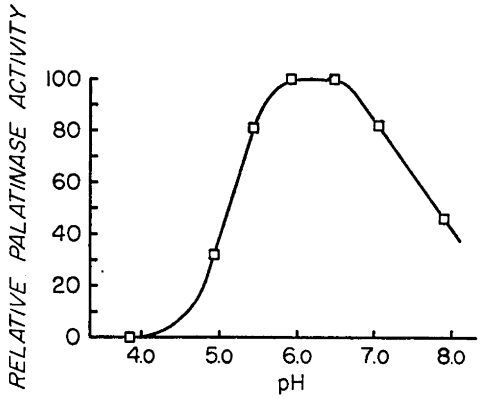

Fig. 2. Influence of pH on the palatinase activity of a crude extracts of pig intestinal mucosa. Substrate concentration 0.027 M. Temperature 37°C. Buffers: 0.05 M acetate buffer pH 4—5, 0.05 M maleate buffer pH 5.5—6.5, and 0.025 M veronal buffer pH 7—8.

Solubilization of the preparation by the method described earlier [6], and precipitation of the solubilized preparation with ethanol [6,7], did not alter the ratio of palatinase activity to the isomaltase, invertase or maltase activity. Like these activities, therefore, the palatinase activity is undamaged by solubilization and ethanol precipitation, and for the experiments described below preparations treated in this way were used.

The hydrolysis of palatinose by crude intestinal glycosidase preparations proceeded to completion (Fig. 1). The palatinase activity had its optimum pH at 6.0—6.5 (Fig. 2).

Experiments were then performed to determine whether the intestinal palatinase activity was exerted by a specific palatinase, as in yeast [4], or by one or several of the intestinal *a*-glucosidases previously separated [6].

Separation of palatinase from trehalase

The fact that the palatinase activity was undamaged by ethanol precipitation seemed to indicate that intestinal *trehalase* was without palatinase activity, since this enzyme is inactivated by ethanol [7]. This also became evident from the analysis of a purified intestinal trehalase preparation, obtained as described elsewhere [14]. Intestinal trehalase had no detectable palatinase activity under conditions such that hydrolysis of palatinose with a rate only 1/250 of that of trehalose would have been detected.

The remaining intestinal *a*-glucosidases to be considered were: *invertase* (=maltase I), *maltase II*, *maltase III*, *specific isomaltase* and *specific phenyl-a-*D*-glucopyranosidase* [6,9].

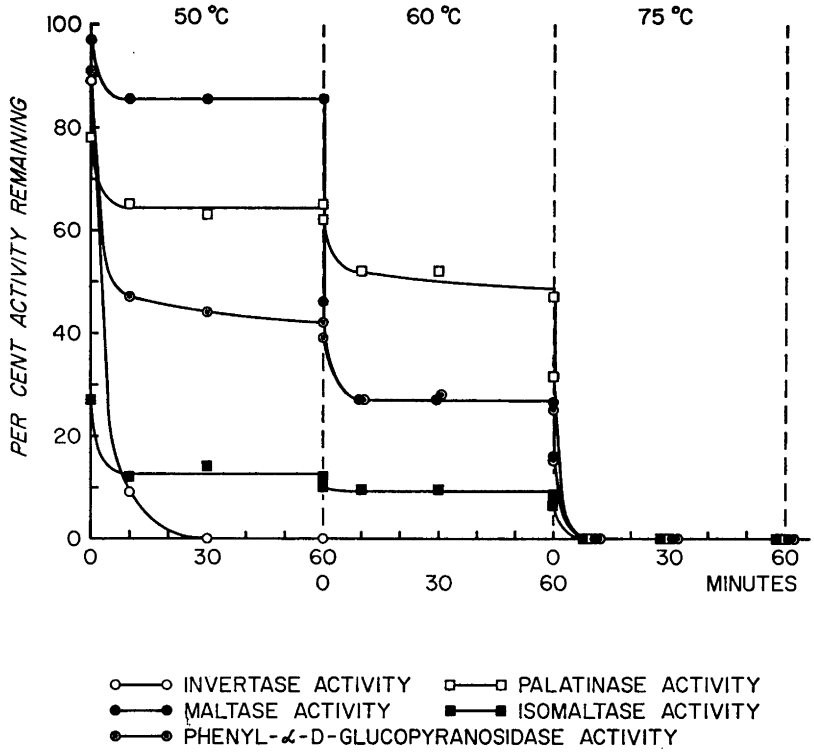

Fig. 3. Heat inactivation of intestinal α-glucosidases in three separate steps. The enzyme preparation contained 2.0 mg/ml of protein in 0.01 M phosphate buffer pH 7.0.

Step-wise heat inactivation of a crude intestinal glycosidase preparation

It has been demonstrated earlier that the differences between pig intestinal invertase (= maltase I), maltase II and maltase III, with regard to their sensitivity to heat, is so great that these enzymes may be heat-inactivated in three separated steps under appropriate conditions [13]. The results of such an experiment, in which also the palatinase, isomaltase, and phenyl-α-D-glucopyranosidase activities were followed are seen in Fig. 3.

The solubilized crude intestinal glycosidase preparation used for this experiment contained 2.0 mg of protein per ml in 0.01 M phosphate buffer pH 7.0. The α-glucosidase activities of the preparation were as follows; invertase 93 units/ml, maltase (total) 350 units/ml, palatinase 10.8 units/ml, isomaltase (total) 30 units/ml and phenyl-α-D-glucopyranosidase (total) 13.5 units/ml. The technique used for heat inactivation has been described earlier [13,15].

The heat inactivation experiment illustrated in Fig. 3 was performed at pH 7.0 at all temperatures. In the experiments previously reported, the pH

was lowered to 6.0 before heating at 60°C [13]. Later this precaution was found to be unnecessary.

A. Inactivation at 50°C. During heating at 50°C the invertase activity (93 units/ml) was completely abolished, together with 60 units/ml of maltase activity (this fraction amounting to 17 % of the total maltase activity of the preparation), (Fig. 3). This fraction of the maltase activity is known to be exerted by the invertase (=maltase I) [16]. The maltase/invertase activity quotient for this enzyme as calculated from the present experiment is 0.65, which agrees well with the figure reported earlier [10].

At this temperature 26 units/ml (87 % of the total) of the isomaltase activity and 7.5 units/ml (56 %) of the phenyl-*a*-D- glucopyranosidase activity were inactivated (Fig. 3). Since purified intestinal invertase (= maltase I) previously has been obtained which exerted neither isomaltase nor phenyl-*a*-D-glucopyranosidase activity [8], these activities are caused by one or two other enzymes (specific isomaltase and specific phenyl-*a*-D-glucopyranosidase [6,9]).

Of the palatinase activity 3.8 units/ml (35 %) was inactivated at 50°C (Fig. 3). This fraction of the palatinase activity may be caused by any of the different enzymes inactivated at this temperature.

B. Inactivation at 60°C. During heating at 60°C the maltase activity decreased by further 198 units/ml (57 % of the original maltase activity of the preparation), this fraction corresponding to the maltase II present in the preparation [6,8,13]. In the same time the isomaltase activity decreased by 1.5 units/ml (5 % of the original value) and the phenyl-*a*-D-glucopyranosidase by 2.5 units/ml (19 %). These activities are known to be exterted by the maltase II *per se* [8]. The isomaltase/maltase and phenyl-*a*-D-glucopyranosidase/maltase activity quotients for this enzyme were both calculated to be about 0.01. As was to be expected [10] these quotients are somewhat lower than those earlier obtained with the use of more concentrated substrate [8].

The palatinase activity decreased by 2.0 units/ml (19 % of the original value) during heating at 60°C. There seems to be reason to suppose that this part of the palatinase activity is caused by the maltase II *per se*. Under this assumption the palatinase/maltase activity quotient for maltase II may be calculated to be 0.01, *i.e.* palatinose and isomaltose, which are structurally very similar to each other, are hydrolyzed at about the same rate by this enzyme during the conditions used for glycosidase activity determination.

C. Inactivation at 75°C. All the glycosidase activities hitherto remaining were completely abolished during heating at 75°C. The fraction of the maltase activity which was inactivated in this step amounted to 92 units/ml (26 % of the original activity); isomaltase, 2.5 units/ml (8 %); phenyl-*a*-D-glucopyranosidase, 3.5 units/ml (26 %), and palatinase 5.0 units/ml (46 %).

The fractions of the maltase, isomaltase and phenyl-*a*-D-glucopyranosidase activities inactivated in this step are known to be exerted by one single enzyme, maltase III [8,17]. The isomaltase/maltase activity quotient (0.03) and the phenyl-*a*-D-glucopyranosidase/maltase activity quotient (0.04) calculated from the present experiment are comparable with the figures earlier obtained [10].

Using the assumption that the fraction of the palatinase activity inactivated in this step is that caused by maltase III *per se*, (for further evidence for this assumption, see below), the palatinase/maltase activity quotient for this enzyme may be calculated to be 0.05.

Palatinase activity of purified invertase and maltase III preparations

Purified invertase (= maltase I) and maltase III were obtained by mutual displacement chromatography on TEAE-cellulose columns of a solubilized intestinal glycosidase preparation as described in a previous paper [13]. The concentrated phosphate buffer present in the fractions obtained was removed by dialysis, before heat inactivation experiments were performed.

A. Purified invertase (= maltase I). The invertase preparation obtained by mutual displacement chromatography contained 930 units/ml of invertase and 6.1 mg/ml of protein. It had maltase/invertase activity quotient 0.7, and thus contained no maltase II or maltase III. The preparation had palatinase activity, 72 units/ml. It had, however, also isomaltase activity, 352 units/ml, and phenyl-α-D-glucopyranosidase activity, 124 units/ml, *i.e.* the preparation contained, in addition to invertase, specific isomaltase and specific phenyl-α-D-glucopyranosidase.

On earlier occasions invertase preparations have been obtained by this method which had neither isomaltase nor phenyl-α-D-glucopyranosidase activities [8]. It has also been observed that the specific isomaltase is rapidly inactivated during adsorption to anion exchange cellulose [9]. In the present experiment it was therefore somewhat astonishing to find that the specific isomaltase activity had survived the mutual displacement chromatography which involved adsorption of the enzymes to TEAE-cellulose at room temperature (20°C) for about 24 h. As far as the author is aware the only difference between this experiment and that described earlier is that in the present case a solubilized intestinal glycosidase preparation was used, which had been stored in the frozen state (−16°C) for several months, while in the eaerlier case a fresh preparation was used. Storage in the frozen state is known to affect the specific isomaltase in a complicated way, causing an initial decrease, followed by a slower increase of the activity of this enzyme [9], and may also alter the stability of the enzyme during adsorption to TEAE-cellulose.

To reveal which enzyme in the preparation was responsible for the palatinase activity, attempts were made to separate the activities by heat inactivation. At pH 7.0 (in 0.01 M phosphate buffer) the palatinase and isomaltase activities were found to be more sensitive to heat than the invertase and phenyl-α-D-glucopyranosidase activities. The course of the inactivation at 32°C is seen in Fig. 4. At this temperature the palatinase and isomaltase activities were slowly inactivated, and the inactivation of these activities ran parallel, while the invertase and phenyl-α-D-glucopyranosidase activities were only very slightly affected. It seems justifiable, therefore, to suppose that the most heat-labile fraction of the palatinase activity (*i.e.* the fraction inactivated at 50°C in the experiment with the crude preparation described above) is exerted by the specific isomaltase. The palatinase/isomaltase activity quotient for this enzyme may be calculated to be 0.2. The experiment also shows that specific isomaltase and specific phenyl-α-D-glucopyranosidase are two separate enzymes.

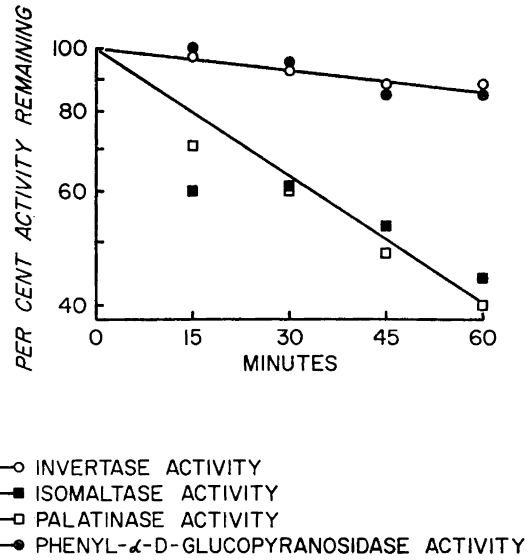

Fig. 4. Heat inactivation of a purified invertase preparation (obtained by mutual displacement chromatography) at 32°C in 0.01 M phosphate buffer pH 7.0. The preparation contained specific isomaltase and specific phenyl-α-D-glycopyranosidase as contaminants (see text). The enzyme solution used for heat inactivation contained 0.2 mg/ml of protein, 37 units/ml of invertase, 12.4 units/ml of isomaltase, 4.0 units/ml of phenyl-α-D-glucopyranosidase and 2.5 units/ml of palatinase.

Inactivation at so low temperature as 32°C occurs only with purified preparations at low salt concentration. When a homogenate of intestinal mucosa was heated at 37°C for 2 h, no inactivation of the glycosidase activities investigated was observed. There is therefore no reason to suppose any heat inactivation of intestinal glycosidases to occur *in vivo* at body temperature. Nor does inactivation occur during the conditions for glycosidase activity determinations (at 37°C) even with purified preparations. Experiments with varying incubation time showed the amount of monohexoses formed during the last half hour of the incubation to be the same as the amount formed during the first half hour.

B. Purified maltase III. The purified maltase III preparation obtained by mutual displacement chromatography contained 304 units/ml of maltase and 0.8 mg/ml of protein. It had no invertase activity. The preparation contained 13 units/ml of isomaltase, 15 units/ml of phenyl-α-D-glucopyranosidase and 22 units/ml of palatinase. The isomaltase and phenyl-α-D-glucopyranosidase activities of the preparation are known to be caused by the maltase III *per se* [8,10,17].

During heating of the preparation at 71°C (in 0.01 M phosphate buffer pH 6.0) the maltase and palatinase activities of this preparation were inactivated in a parallel manner, indicating the palatinase activity of this preparation to be also caused by the maltase III *per se* (Fig. 5). The palatinase/maltase activity quotient for this enzyme was calculated to be 0.06.

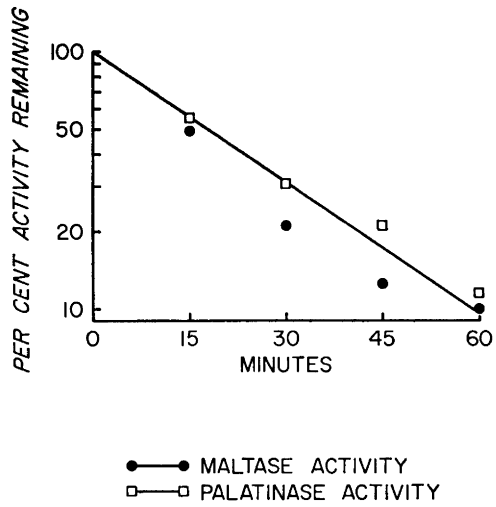

Fig. 5. Heat inactivation of a purified maltase III preparation at 71°C in 0.01 M phosphate buffer pH 6.0. The enzyme solution used for heat inactivation contained 0.15 mg/ml of protein, 55 units/ml of maltase and 2.6 units/ml of palatinase.

Relations between palatinase and isomaltase activity

From the experiments described above, it appears that palatinose is hydrolyzed by the same intestinal glycosidases as hydrolyze isomaltose, *i.e. specific isomaltase, maltase II* and *maltase III*. This is in harmony with the structural similarity between the two substrates. It is apparent that none of the enzymes is absolutely specific for the structure around the 1st and 2nd carbon atom of the *aglycon* of the substrate.

Nevertheless the structural difference between isomaltose and palatinose causes marked differences in the relative rates of hydrolysis of the two substrates by the different enzymes. During the conditions used for glycosidase activity determinations *specific isomaltase* hydrolyzes palatinose with a rate that is only one fifth of the rate for hydrolysis of isomaltose by the same enzyme. *Maltase II* hydrolyzes the two substrates at approximately the same rate, and *maltase III* hydrolyzes palatinose nearly twice as fast as isomaltose.

These differences make maltase III the most important enzyme for the hydrolysis of palatinose by crude extracts of intestinal mucosa, for this enzyme causes about 50 % of the total palatinase activity of such preparations, although it causes only about 10 % of the total isomaltase activity.

Acknowledgement. This investigation has been supported by grants from the *Swedish Medical Research Council*. Mrs. K. Hagebris and Miss A. Hansson are acknowledged for skillful technical assistance.

REFERENCES

1. Weidenhagen, R. and Lorenz, S. *Z. Zuckerind.* **7** (1957) 533.
2. Weidenhagen, R. and Lorenz, S. *Angew. Chem.* **69** (1957) 641.
3. Lorenz, S. *Z. Zuckerind.* **8** (1958) 535.
4. Emeis, C. C. and Windisch, S. *Z. Zuckerind.* **10** (1960) 248.
5. Weidenhagen, R. *Personal communication.*
6. Dahlqvist, A. *Hog Intestinal α-Glucosidases.* Diss. Lund 1960.
7. Borgström, B. and Dahlqvist, A. *Acta Chem. Scand.* **12** (1958) 1997.
8. Dahlqvist, A. *Acta Chem. Scand.* **14** (1960) 1.
9. Dahlqvist, A. *Acta Chem. Scand.* **14** (1960) 72.
10. Dahlqvist, A. *Acta Chem. Scand.* **14** (1960) 1797.
11. Lowry, O. H., Rosebrough, N. J., Farr, A. L. and Randall, R. J. *J. Biol. Chem.* **193** (1951) 265.
12. Eggstein, M. and Kreutz, F. H. *Klin. Wochschr.* **33** (1955) 879.
13. Dahlqvist, A. *Acta Chem. Scand.* **13** (1959) 1817.
14. Dahlqvist, A. *Acta Chem. Scand.* **14** (1960) 9.
15. Dahlqvist, A. *Acta Chem. Scand.* **13** (1959) 945.
16. Dahlqvist, A. *Acta Chem. Scand.* **14** (1960) 63.
17. Dahlqvist, A. *Acta Chem. Scand.* **13** (1959) 2156.

Received December 8, 1960.

ACTA CHEMICA SCANDINAVICA 15 (1961) 817–822

O-Substituted Pyridine-N-oxide Derivatives

1. N-Trimethylammoniumethoxy-Pyridinium Compounds, a New Type of Choline Derivatives

KLAS-BERTIL AUGUSTINSSON and HANS HASSELQUIST

Institute of Organic Chemistry and Biochemistry, University of Stockholm, Sweden

The synthesis of a series of O-substituted pyridine-*N*-oxides containing an *N*-trimethylammoniumethoxy substituent is described. This new type of choline derivatives was obtained by a reaction between the *N*-oxide and bromocholine.

The reaction of amine oxides with alkyl halogenides to form C-alkyl compounds, known since the classical experiments of Meisenheimer in 1913 [1], has also been studied with pyridine-*N*-oxides [2,3]. Particular interest in the quaternary salts formed arose when it was demonstrated that these compounds are decomposed by alkali to tertiary amine and aldehyde [4]. This is a suitable method for preparing aromatic aldehydes and for deoxygenating pyridine-*N*-oxides under non-reducing conditions [3,5].

In the following report is described the synthesis of a series of O-substituted pyridine-*N*-oxides containing an *N*-trimethylammoniumethoxy substituent. This new type of choline derivatives was obtained by a reaction between the *N*-oxide and bromocholine. The biological properties of these compounds are under investigation.

In the cases of pyridine-*N*-oxide and its monomethyl derivatives, the *N*-oxide and bromocholine reacted readily when heated at about 120°C in the absence of any solvent. When the technique was applied to the dimethylpyridine-*N*-oxides, degradation of these compounds occurred, giving rise to a brownish mass of unknown composition. The reaction between these N-oxides and bromocholine was therefore carried out in a solvent, acetonitrile giving the best results except in the case of 2,6-lutidine-*N*-oxide.

The reaction between the two components, being used in concentrated solutions, probably proceeds as a S_N1 reaction according to the following sequence of reactions:

$$R\text{-}CH_2\text{-}Br \longrightarrow R\text{-}CH_2^+ + Br^-$$

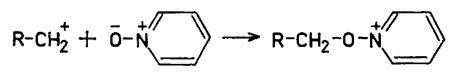

The more readily Br is split off as anion, the higher is the reaction velocity. This splitting is determined by the polarisation of the C—Br bond, being increased both by the inductive effect of the quaternary ammonium group in bromocholine and by the polar *N*-oxide present. The carbenium cation formed reacts with the electron-donating oxygen in the *N*-oxide. This reaction is obviously dependent also on the polarity of the N—O bond in the *N*-oxide, which in its turn is regulated by the inductive and hyperconjugation (Baker-Nathan) effects of the methyl groups in the ring.

With two exceptions the reaction proceeded without complications. In the case of 4-methylpyridine-*N*-oxide (4-picoline-*N*-oxide) a violent exothermic reaction started when it was melted with bromocholine. The boiling mass resulted in a viscous dark-brown product. Part of the original *N*-oxide was degraded to 4-picoline by the high temperature of the reaction mixture. The brown mass consisted of a polymerisation product, probably being formed according to the following reaction:

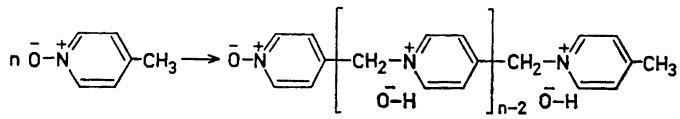

This process is analogous with the thermic polymerisation shown by 4-chloropyridine [6].

Bromocholine and 2,6-lutidine-*N*-oxide (in contradistinction to the other dimethyl derivatives used) reacted only in aqueous solution; no reaction occurred in acetonitrile or by melting the two compounds together. We suggest, as a possible explanation for this phenomenon, that weak H-bonds block the oxygen in the *N*-oxide (I), thus preventing it from reacting with the carbenium ion. A similar idea was proposed recently by Jerchel and Melloh[7] for 2-substituted

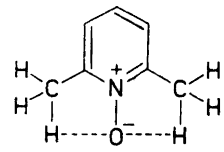

(I)

pyridine-*N*-oxides with active hydrogen atoms in the substituents (OH, NH_2, CH_3), for which hydrogenation (deoxygenation) proceeds at a much lower rate than for 3- and 4-substituted *N*-oxides. Steric hindrance may also partly be a determining factor for the lower reactivity of 2,6-dimethylpyridine-*N*-oxide. The fact that the reaction proceeds in aqueous solution, but not in acetonitrile, may be due to the much higher dielectric constant of water.

EXPERIMENTAL

2,5- and 3,5-Lutidine-*N*-oxides

The *N*-oxides used (with two exceptions) were either synthesised according to previously described methods (Table 1) or purified from commercial grade products. The synthesis of the 2,5- and 3,5-lutidine-*N*-oxides, not previously described in the literature, was performed according to a general method described by Thomas and Jerchel [8].

Table 1. *N*-Oxides of the pyridine-series used and references to methods for their synthesis.

N-oxide	b.p. or m.p.*	Authors	Ref.
Pyridine-*N*-oxide	138–140/15	Ochiai 1953; see also Thomas and Jerchel 1958	4,8
2-Picoline-*N*-oxide	123–124/15	Boekelheide and Linn 1954	9
3-Picoline-*N*-oxide	146–149/15	*Idem*	9
4-Picoline-*N*-oxide	185–186 *	*Idem*	9
2,4-Lutidine-*N*-oxide	148/13	*Idem*	9
2,5-Lutidine-*N*-oxide	149/23	Present authors	
2,6-Lutidine-*N*-oxide	115–119/18	Boekelheide and Linn 1954	9
3,5-Lutidine-*N*-oxide	166–168/23	Present authors; picrate, see Shindo 1956	10

A mixture of lutidine (10 g, 93 mmoles), glacial acetic acid (25 ml) and 30 % hydrogen peroxide (12.5 ml) was refluxed for 8 h on a water bath at 80°C; an addition of another 9 ml H_2O_2 was made after 3 h. The mixture was left for 15 h at 35°C, evaporated under vacuum to half its volume and mixed with the same volume of water. After evaporation under vacuum in a boiling water bath to completely remove all water, an equal volume of chloroform and dry Na_2CO_3 was added until no more CO_2 was evolved. After 24 h at room temperature, the crystals formed were treated with three volumes of chloroform under stirring. Sodium acetate and Na_2CO_3 were filtered off, and the clear chloroform solution was evaporated under vacuum in a boiling water bath.

2,5-Lutidine-N-oxide and its picrate. The residue was fractionated under vacuum on an oil bath. The *N*-oxide (b.p. 149°C) was obtained as a colourless liquid in 62 % yield (7.15 g); 0.3 g (2.4 mmoles) was dissolved in 1 ml water, and 30 ml of a saturated aqueous solution of picric acid was added. The *N*-oxide picrate was precipitaed immediately, isolated by filtration after 3 h at room temperature and washed carefully with water. The pure product in the form of yellow blades, recrystallised three times from absolute ethanol, had m.p. 128–129°C. Yield 46.5 % (0.4 g). Because the m.p. found was close to that of picric acid (122–123°C), the mixed m.p. of the two compounds was measured and found to be 95–108°C; the m.p. of 2,5-lutidine picrate was 169°C. Analyses of 2,5-lutitine-*N*-oxide picrate, calc. for $C_{13}H_{12}O_8N_4$ (352.16): C 44.33; H 3.44; N 15.91. Found: C 44.62; H 3.47; N 15.94.

3,5-Lutidine-N-oxide and its picrate. The residue (from above), a hygroscopic almost colourless crystalline mass, was distilled by fractionation under vacuum over an open flame; steam was introduced into outer jacket of the condenser, since the *N*-oxide easily solidified there at lower temperature. The pure product, b.p. 166–168°C/23, was a colourless liquid which solidified immediately in the receiver and was very hygroscopic. It can, if desired, be recrystallised from a small amount of benzene and washed with benzene-petrol ether (1:1). The picrate was made in the same way as described for 2,5-lutidine-*N*-oxide picrate (see above) and was isolated as small yellow needles, m.p. 135–136°C. Yield 65.2 % (0.56 g). This picrate has been described previously by Shindo [9] who reported m.p. 138–139°C.

Table 2. Melting points, analytical data and yield of the compounds synthesised

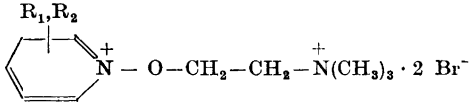

Derivative	Code	Mol. formulae	Mol. wt.	m.p. °C	% C		% H		% N		% Br		Yield	
					calc.	found	calc.	found	calc.	found	calc.	found	g	% of theor.
Pyridinium (R_1, R_2 = H)	AH 7	$C_{10}H_{18}ON_2Br_2$	342.09	198	35.11	35.07	5.34	5.44	8.19	8.00	46.7	46.9	1.04	75
Picolinium (R_1= CH_3, R_2= H):														
2–	AH 6	$C_{11}H_{20}ON_2Br_2$	356.12	196	37.10	37.11	5.66	5.63	7.87	7.65	44.9	44.8	0.45	51
3–	AH 8	$C_{11}H_{20}ON_2Br_2$	356.12	175	37.10	37.42	5.66	5.75	7.87	7.57	44.9	44.5	0.20	14
4–	AH 18	$C_{11}H_{20}ON_2Br_2$	356.12	190 *	37.10	36.82	5.66	6.06	7.87	8.03	44.9	44.5	0.25	50
Lutidinium (R_1, R_2= CH_3):														
2,4–	AH 21	$C_{12}H_{22}ON_2Br_2 \cdot H_2O$	388.16	195–195.5	37.13	36.50	6.23	6.43	7.22	7.21	41.2	40.9	0.31	67
2,5–	AH 22	$C_{12}H_{22}ON_2Br_2 \cdot H_2O$	388.16	191	37.13	37.59	6.23	6.47	7.22	7.17	41.2	40.9	0.23	49
2,6–	AH 24	$C_{12}H_{22}ON_2Br_2 \cdot 2H_2O$	406.18	175–175.5	35.48	35.37	6.45	6.19	6.90	6.86	39.4	40.4	0.16	9.5
3.5–	AH 20	$C_{12}H_{22}ON_2Br_2$	370.14	196.5–197	38.94	38.52	5.99	6.15	7.57	7.66	43.2	42.0	0.45	100

* See text for comments on this melting point.

N-Trimethylammoniumethoxy-pyridinium aibromides

General techniques used in preparing the choline derivatives. A mixture of the *N*-oxide and finely powdered bromocholine bromide (BrCh) was heated for various periods of time. After completion of the reaction, the product was isolated in crystalline form and recrystallised. All compounds synthesised were readily soluble in water and methanol, and decomposed on melting. Table 2 summarises melting points (uncorrected), analytical data and yield.

N-Trimethylammoniumethoxy-pyridinium dibromide (AH 7). A mixture of 1.0 g (4.1 mmoles) of BrCh and 3.0 g (31.6 mmoles) of pyridine-*N*-oxide was heated on a paraffin bath at 140°C for 5 min. After 1 min, the BrCh had dissolved and the reaction product had begun to crystallise out; some *N*-oxide was decomposed during the reaction (smell of pyridine). After cooling, 50 ml of benzene was added to the reaction mixture; the insoluble crystals were isolated by filtration and recrystallised from methanol-acetone. The product was obtained as colourless prisms which were soluble in hot methanol and slightly soluble in acetone. This synthesis was also carried out with acetonitrile as solvent, the constituents being boiled for 6 h, which gave the same yield.

N-Trimethylammoniumethoxy-2-picolinium dibromide (AH 6). BrCh (0.61 g, 2.5 mmoles) was suspended in 1.2 g (11 mmoles) of 2-picoline-*N*-oxide and heated on a paraffin bath at 140°C until all BrCh had dissolved (about 5 min). After cooling the reaction product crystallised as small needles. The crystalline mass was treated with benzene, filtered off and washed with the same solvent. The colourless needles were readily soluble in glacial acetic acid and slightly soluble in acetone and benzene.

N-Trimethylammoniumethoxy-3-picolinium dibromide (AH 8). 3-Picoline-*N*-oxide (1.1 g, 10 mmoles) and BrCh (1.0 g, 4 mmoles) were heated with stirring on a paraffin bath at 130°C, giving after 5 min a homogeneous dark-brown mass. After heating for another 2 min and cooling, ethanol (3 ml) was added followed by acetone until crystallization began. The reaction product was extremely hygroscopic, and special precautions were therefore undertaken during filtration. The crystalline mass was transferred to a glass filter (No. 3); during sucking care was taken to keep the mass moist with solvent. Washing was performed with acetonitrile in the same way, and the crystalline mass, still wet with acetonitrile, was rapidly transferred to a test tube and dissolved in as small an amount of methanol as possible. Three volumes of acetonitrile were added, and the brown solution treated with active carbon and filtered. Methanol was evaporated by heating the colourless filtrate on a water bath, when the product crystallised. After complete crystallisation in a closed bottle, the colourless needles were filtered off and washed with acetonitrile in the way described. The final product in the glass filter was transferred to a desiccator, which was evacuated; the product was slightly soluble in acetone and acetonitrile.

N-Trimethylammoniumethoxy-4-picolinium dibromide (AH 18). A mixture of 0.35 g (1.4 mmoles) BrCh and 0.35 g (3.2 mmoles) 4-picoline-*N*-oxide was refluxed with 1 ml acetonitrile in a boiling water bath for 10 h. BrCh was slowly dissolved with simultaneous crystallisation of the reaction product as brownish grey prisms. After completions of the reaction and the addition of 4 ml of acetonitrile, the crystals were filtered off and washed with acetonitrile and acetone. The crude product melted at 182—184°C (decomp.) Recrystallisation from *n*-butanol gave the pure compound as light brown prisms which were slightly soluble in acetone, *iso*propanol and ethyl acetate. Depending on the rapidity of heating, the compound melted at 182—190°C (melting occurred within one degree in this region). The brownish colour could not be removed with active carbon.

N-Trimethylammoniumethoxy-2,4-lutidinium dibromide (AH 21). BrCh (0.3 g, 1.2 mmoles), 2,4-lutidine-*N*-oxide (0.3 g, 2.4 mmoles) and 1 ml acetonitrile were refluxed for 18 h on a boiling water bath. The crystals formed were filtered off and washed with acetonitrile and acetone. The crude product (brown prisms, m.p. 193—194°C, decomp.) was dissolved in 1 ml methanol and 1.5 ml *n*-butanol, the solution treated with active carbon and filtered. Methanol was evaporated by gently heating on a boiling water bath. On cooling, small colourless prisms crystallised out and the product, readily soluble in ethanol and slightly soluble in aceton, *iso*propanol and ethyl acetate, was shown to be chromatographically pure.

N-Trimethylammoniumethoxy-2,5-lutidinium dibromide (AH 22). The synthesis was carried out in the same way as described for AH 21. The compound formed crystallised from *n*-butanol as rhombic crystals which were hygroscopic and had the same solubilities in various solvents as was reported for AH 21.

N-Trimethylammoniumethoxy-2,6-lutidinium dibromide (AH 24). BrCh (1.0 g, 4.1 mmoles), 2,6-lutidine-N-oxide (1.0 g, 8.1 mmoles) and 2 ml water were heated in a bomb tube at 100°C for 18 h. Part of the *N*-oxide was decomposed during the reaction, and some BrCh was left unchanged, as could be demonstrated by a paper chromatographic analysis. Because the reaction product and BrCh showed similar solubility in various organic solvents, and consequently, recrystallisation of the reaction mixture resulted in an appreciable loss of the *N*-substituted lutidinium derivative, the mixture was treated in the following way. The remaining BrCh was forced to react by pouring out the reaction mixture in a petri dish kept on a boiling water bath until all water had evaporated. The same volume of water was then added and evaporated in the same way. The brownish crystalline mass was shown chromatographically to be free of BrCh. The lutidine formed was removed by two extractions with 50 ml chloroform. The remaining product was treated with absolute ethanol, filtered off, washed carefully with the same solvent, and dried in a desiccator over KOH under vacuum. The crude product (260 mg) melted at 170—172°C (decomp.). The greyish crystalline powder was dissolved in as small an amount of boiling ethanol as possible, was treated with active carbon, and the solution filtered. On cooling the pure compound crystallised as hygroscopic colourless prisms, soluble in ethanol and slightly soluble in chloroform and acetone.

N-Trimethylammoniumethoxy-3,5-lutidinium dibromide (AH 20). The synthesis was carried out in the same way as was described for AH 21, except that the reaction was completed after 8 h. Acetonitrile (2 ml) was added to the reaction mixture, the crystals were filtered off and washed with acetonitrile and acetone. Recrystallisation from *n*-butanol gave the pure product as colourless blades, which were somewhat hygroscopic, and showed solubility properties similar to those of the other compounds in this series.

This investigation has been supported by a grant from *Magn. Bergvalls Stiftelse*. Dr. Lennart Larsson is gratefully acknowledged for valuable comments to the presentation of the results obtained.

REFERENCES

1. Meisenheimer, J. *Ann.* **397** (1913) 373.
2. Ochiai, E., Kutada, M. and Waito, T. *J. Pharm. Soc. Japan* **64** (1944) 210.
3. Katritsky, A. R. *J. Chem. Soc.* **1956** 2404.
4. Ochiai, E. *J. Org. Chem.* **18** (1853) 534.
5. Feely, W., Lehn, W. L. and Boekelheide, V. *J. Org. Chem.* **22** (1957) 1135.
6. Wibaut, J. P. and Broekman, F. W. *Rec. trav. chim.* **58** (1939) 885.
7. Jerchel, D. and Melloh, W. *Ann.* **613** (1958) 144.
8. Thomas, K. and Jerchel, D. *Angew. Chem.* **70** (1958) 719.
9. Boekelheide, V. and Linn, W. J. *J. Am. Chem. Soc.* **76** (1954) 1286.
10. Shindo, H. *Pharm. Bull. (Japan)* **4** (1956) 460.

Received November 30, 1960.

ACTA CHEMICA SCANDINAVICA 15 (1961) 823–838

Studies on the Microbiological Determination of Niacin in Some Marine Algae

ARNE E. BOLINDER and BJØRN LARSEN

Division of Food Chemistry, Royal Institute of Technology, Stockholm 70, Sweden, and Norwegian Institute of Seaweed Research, N.T.H., Trondheim, Norway

1. The microbiological determination of niacin in marine algae has been carried out with three different test organisms: *Streptococcus faecalis* ATCC 8043, *Lactobacillus arabinosus* ATCC 8014, and *Lactobacillus casei* ATCC 7469. A single basal medium, with minor changes, was used for the three test organisms.

2. A cup plate assay method for niacin with *S. faecalis* as the test organism is described in detail. In the concentration range of 0.05 to 100 μg of niacin per ml, well defined zones of dense growth were obtained.

3. Comparative assays for niacin on eight selected algal samples were carried out in both laboratories using the cup plate method with *S. faecalis* and also the turbidimetric tube assay method with *S. faecalis* and *Lb. arabinosus*. The most favourable conditions for the extraction of niacin were determined. Recovery tests with added niacin were also performed.

The highest niacin assay values were obtained by hydrolysing the samples with N sulfuric acid for 1 h at 120°C and assaying by the *Lb. arabinosus* tube method. For the purpose of screening a large number of algal samples, hydrolysing with 3 N sulfuric acid at 120°C for 1 h and assaying by the *S. faecalis* cup plate method is recommended. This assay method generally gives 0–20 % lower niacin assay values than the *Lb. arabinosus* tube method.

4. Bioautography of extracts of the eight selected algal samples was made with *Lb. arabinosus* plates. In extracts prepared by hydrolysing with N or 3 N sulfuric acid, only niacin was found. However, in extracts prepared by hydrolysing with 0.1 N sulfuric acid, niacinamide was predominant while niacin was either absent or found only in trace amounts.

5. A simple method for the bioautographic detection of "bound" niacin (an alkali-labile complex containing niacin) was developed. Bioautographic tests for the presence of "bound" niacin in the algal samples were negative.

6. Comparative assays for niacin on another set of selected algal samples were carried out by the turbidimetric tube assay method with *Lb. arabinosus*, *Lb. casei* and *S. faecalis*. The results with *Lb. arabinosus* and *Lb. casei* agreed very well although the former test organism in some cases gave slightly higher assay values than the latter. The *S. faecalis* tube method gave considerably lower niacin assay values.

Numerous reports have been published on the determination of niacin in various natural materials. However, the only report concerning the determination of niacin in marine algae has been published by Ericson [1]. His determinations were made microbiologically by the cup plate method using *Lactobacillus arabinosus* ATCC 8014 as the test organism. Apart from testing several extraction procedures for the liberation of niacin, no attempt was made to ascertain the validity or accuracy of the assay method used, *e.g.* by recovery tests, comparative assays with the tube method or assays with other test organisms.

The most commonly used assay method for the microbiological determination of niacin is the tube assay method with *Lb. arabinosus* as the test organism [2–8], the response of which is measured either turbidimetrically or by titration of the acid produced. Other organisms have also been used for the tube assay of niacin (*cf.* Ref. [3]), notably lactobacilli, *e.g.* *Lactobacillus casei* [9–13] and *Leuconostoc mesenteroides* [14–16], but these methods have not been investigated so thoroughly as the assay with *Lb. arabinosus*. Microbiological assays for niacin by the plate assay method with *Lb. arabinosus* as the test organism have also been published [1,17–25]. Compared to the tube method, the plate assay method is simpler to carry out and less time-consuming, although the sensitivity is lower [26,27]. The plate assay method is particularily suitable when a great number of samples are to be assayed.

This paper deals with the comparative assays for niacin in marine algae carried out by several assay methods. The most favourable conditions for the extraction of niacin from algae were investigated and bioautographic studies were made. Values for the niacin contents of marine algae obtained by utilizing the assay procedures given in this paper have already been published [28,29].

EXPERIMENTAL*

Samples. Eight different samples of marine algae from the Norwegian coast were selected for a collaborative investigation on comparative assays for niacin carried out according to the cup plate method with *S. faecalis* and the turbidimetric tube assay method with *Lb. arabinosus* and *S. faecalis*. The species used are listed in Table 1 together with habitat and date of harvest for each sample. In a separate investigation, where the turbidimetric tube assay methods for niacin with *S. faecalis*, *Lb. arabinosus* and *Lb. casei* were compared, another set of algal samples was used (see Table 8).

Each algal sample consisted of at least fifty plants. After drying at room temperature, the samples were ground in a Wiley laboratory mill and stored in air-tight tins. A sample of wheat bran was used as a source of "bound" niacin. It was purchased in a local store and ground in a Wiley laboratory mill.

All niacin assay values are given as μg per g dry weight of sample.

Preparation of extracts. Extraction of the algal samples for niacin assays was carried out with N or 3 N sulfuric acid. The following procedure was used: 1 g of dried sample was throughly mixed with 15 ml sulfuric acid (N or 3 N) in a small beaker covered with aluminium foil and the mixture was autoclaved for 1 h at 120°C. After cooling, 3 ml sodium hydroxide (5 N or 15 N) was added. After cooling once again, the pH of the mixture was adjusted to 6.7 ± 0.2 with sulfuric acid or sodium hydroxide. The slurry was transferred quantitatively to a volumetric flask and diluted with distilled water to

* If not otherwise stated in the text, exactly the same experimental procedures were used in laboratory I (Division of Food Chemistry, Stockholm) and laboratory II (Norwegian Institute of Seaweed Research, N.T.H., Trondheim).

Table 1. Algal samples selected for the collaborative investigation of assay methods for niacin.

Algae	Sample	Locality	Date of harvest
Ascophyllum nodosum	An 1	Reine	27.2.1956
» »	An 2	»	30.8.1956
Fucus serratus	Fs 1	Trondheimsfjord	19.3.1956
» »	Fs 2	»	10.8.1956
Laminaria hyperborea	Lh 1	Reine	25.2.1955
» »	Lh 2	»	22.8.1955
Rhodymenia palmata	Rp 1	Trondheimsfjord	7.2.1955
» »	Rp 2	»	25.4.1955

Table 2. Composition of assay media used for the microbiological assay of niacin. The amounts refer to 500 ml double strength medium. The pH of each medium was adjusted to 6.5.

Component	Acetate medium	Citrate medium
Bacto vitamin free casamino acids (Difco)	5 g	5 g
Sodium acetate (3 aq)	20 g	1 g
Trisodium citrate (2 aq)	—	20 g
Glucose	20 g	20 g
DL-Alanine	100 mg	100 mg
L-Asparagine	100 mg	100 mg
L-Cysteine hydrochloride	100 mg	100 mg
L-Cystine hydrochloride	100 mg	100 mg
DL-Tryptophan	200 mg	200 mg
Adenine sulfate	10 mg	10 mg
Guanine hydrochloride	10 mg	10 mg
Uracil	10 mg	10 mg
Xanthine	10 mg	10 mg
Thiamine hydrochloride	1 mg	1 mg
Riboflavin	1 mg	1 mg
Calcium pantothenate	1 mg	1 mg
Pyridoxine hydrochloride	1 mg	1 mg
Pyridoxal hydrochloride	1 mg	1 mg
Pyridoxamine dihydrochloride	1 mg	1 mg
p-Aminobenzoic acid	500 μg	500 μg
Biotin	20 μg	20 μg
Folic acid	20 μg	20 μg
Dipotassium phosphate	1 g	3 g
Sodium chloride	1 g	1 g
Ammonium sulfate	1 g	1 g
Magnesium sulfate (7 aq)	100 mg	500 mg
Manganese sulfate (4 aq)	30 mg	150 mg
Ferrous sulfate (7 aq)	10 mg	50 mg
Tween 80 (Atlas)	0.5 ml	0.5 ml

25 ml (laboratory II) or to 50 ml (laboratory I). After centrifuging, the supernatant was stored in small flasks at −20°C.

Extracts used for bioautography were prepared by autoclaving 1 g of dried algal sample with 15 ml 0.1 N sulfuric acid for 30 min at 120°C. After cooling, the pH was adjusted to 6.7 ± 0.2 and the slurry centrifuged. The supernatant was stored at −20°C.

Test organisms. Stab cultures of *Streptococcus faecalis* ATCC 8043, *Lb. arabinosus* ATCC 8014, *Lb. casei* ATCC 7469, *Lb. fermenti* ATCC 9338 and *Leuconostoc mesenteroides* ATCC 9135 were maintained on Bacto micro assay culture agar (Difco)*. The organisms were transferred at least once every month. After incubation overnight at 37°C, the cultures were stored in a refrigerator.

Measurement of bacterial growth in the tubes. For the standardization of the inocula used for the plate and the tube assays, as well as for the measurement of the bacterial growth in the tube assays, turbidimetric measurements were made at 640 mμ and expressed as percent light transmittance. The measurements in laboratory I were made with optically calibrated rimless test tubes (19 × 180 mm) in a Coleman Model 11 Universal spectrophotometer and in laboratory II with optically calibrated rimless test tubes (16 × 150 mm) in a Unicam Model DG spectrophotometer. Since test tubes of larger diameter were used in laboratory I, the same bacterial suspension will give a lower reading for percent light transmittance in laboratory I than in laboratory II.

Assay media. One single basal medium, with minor changes, was used in the assays for niacin with the different test organisms. Two variants of this basal medium, the acetate medium and the citrate medium, were used and the composition of these media is given in Table 2. These basal media have the same general composition as the commonly used B-vitamin assay media recommended for lactobacilli.[3-5] Adjustment of the pH of the media was made with sodium hydroxide or sulfuric acid. The acetate medium was used for the assays with *Lb. arabinosus* and *Lb. casei* (and for the preliminary cup plate tests with *Lb. fermenti* and *L. mesenteroides*) and the citrate medium for the assays with *S. faecalis*. Solutions of the components of the assay media were made according to procedures published earlier.[2-8] All chemicals used for preparing the media were of at least "puriss" quality in laboratory I and mostly of "analytical grade" in laboratory II. Distilled water from a commercial laboratory scale metal distillation apparatus was used for all work in both laboratories. The unsterilized double strength media were stored at −20°C. Media stored for 3−4 months have been successfully used.

Inoculum media. Bacto inoculum broth (Difco) was used as the inoculum medium for *S. faecalis*. However, this inoculum medium was not satisfactory for obtaining a good and rapid growth of the other test organisms. We therefore also used a fortified Bacto micro inoculum broth, the composition of which is given in Table 3. This inoculum medium promoted a rapid growth of the remaining test organisms as well as of other test organisms commonly used for microbiological assays, *e.g. Lb. acidophilus, Lb. leichmannii* and *Pediococcus cerevisiae* (*Leuconostoc citrovorum*).

Centrifuge tubes (16 × 110 mm) were filled with 5 ml portions of inoculum medium and a glass bead was added to each tube. The cotton-plugged tubes were sterilized for 15 min at 120°C.

Preparation of inocula. Broth subcultures were incubated at 37°C, in laboratory I for 10−12 h and in laboratory II for 16−20 h. To prepare the inocula, the subcultures were centrifuged, washed two times with 5 ml portions of sterile 0.9 % sodium chloride solu-

* Difco Laboratories, Inc., Detroit, Michigan, USA.

Table 3. Composition of the fortified Bacto micro inoculum broth (Difco). The amounts refer to 1 000 ml single strength medium.

Bacto micro inoculum broth (Difco)	37 g
Double strength acetate medium[a]	10 ml
Niacin	20 μg
Leucovorin (synthetic folinic acid)	0.5 μg
Vitamin B_{12}	0.05 μg

[a] See Table 2 for composition.

tion, and then resuspended and diluted with sterile 0.9 % sodium chloride solution to the desired turbidity. When adjusting the inocula, a tube containing distilled water and set at 100 % transmittance was used as the blank.

For making plates with the test organisms, 5 ml of an inoculum with a light transmittance of 50 % was used for each plate. Since the instruments and tubes for adjusting the inocula were different in the two laboratories, this inoculum density corresponds in laboratory I to 60—80 μg and in laboratory II to 220—280 μg dry weight of cell material per ml inoculum.

For the tube assays, a dilute inoculum was employed. One ml of a washed cell suspension of each test organism having a light transmittance of 50 % was mixed with 50 ml sterile sodium chloride solution and, after shaking thoroughly, two drops of this dilute suspension was used to inoculate each tube.

Preparation of plates. For the cup plate assays and the bioautography, large plates were used, each containing 150 ml of agar medium inoculated with the test organism. Each plate consisted of a chromium-plated brass frame, 20 × 40 cm, laid between two sheets of 3 mm thick glass. The plates were sterilized in a drying oven. For each plate, 150 ml of single strength medium together with 3.0 g Bacto agar (Difco) in a 500 ml flask was sterilized by autoclaving for 10 min at 120°C. The flasks were then placed in a water bath thermostated at 47°C for 0.5—1 h. The contents of each flask were mixed with 5 ml of washed and optically standardized inoculum (see above) and then poured into the plate and allowed to cool. Before pouring the agar media, the plates had been placed on a carefully levelled surface (using oil levels) in order to obtain a uniform thickness in the agar layer.

Cup plate assays. For the cup plate assays, 60—80 cups, 6 mm in diameter were bored in the solid agar medium of each plate. In laboratory I, a specially designed apparatus for making the cups was used. [30] Standard and test solutions in 0.03 ml aliquots were pipetted into the cups. In order to minimize the effect of time [31] on the assay results (*i.e.* to reduce the tendency of those solutions first applied to give larger zones than those last applied), the cups in each plate were filled in the shortest time possible and the plate was then left at room temperature for at least 10—15 min prior to incubation at 37°C. An experienced worker can fill the cups of one plate in 10—15 min. After incubation overnight at 37°C in a thermostated room, the diameters of the growth zones were measured.

The following concentrations of niacin standard were used: in laboratory I, 0.05, 0.1, 0.3, 1, and 3 μg per ml and, in laboratory II, 0.1, 0.3, 1, 3, and 10 μg per ml. At least four cups per plate were used for each standard concentration. The twenty standard cups were spread over the plate in a systematic way in order to eliminate the effect of variations in the thickness of the agar layer.

The algal extracts were assayed undiluted and at two different dilutions in laboratory I. In laboratory II only undiluted extracts were assayed. At least three cups per plate were used for each concentration of extract.

Both laboratories normally used plates with 68 cups. Since twenty cups were used for the standards, the remaining 48 cups could be used for the assay of 16 different test solutions. The growth zones were measured to the nearest 0.5 mm with a transparent ruler.

Bioautography. For bioautography, paper chromatography by means of the descending technique was carried out on large sheets (19 × 57 cm) of Whatman No. 1 filter paper whereby 6—8 samples could be run simultaneously. The chromatograms were run in a mixture of *iso*propanol-water (75:25 v/v) at 21°C. When the solvent front had advanced to about 40 cm from the starting line, the chromatograms were dried in a stream of warm air and cut to fit the agar plates. The dried chromatograms were placed on *Lb. arabinosus* plates, and the plates were incubated overnight at 37°C. *S. faecalis* plates can also equally well be used.[32]

Usually 1—5 μl of each algal extract — applied as a small spot — was used for the bioautographic investigation. Niacin and niacinamide were employed as standards and had R_F values of 0.46 and 0.70, respectively, in the solvent system used. As little as 0.03—0.05 μg of either niacin or niacinamide could be easily detected bioautographically.

For the bioautographic detection of "bound" niacin, the following procedure was used: After the paper chromatogram was run in the *iso*propanol-water mixture and dried, the upper part was sprayed with conc. ammonia. While still wet, it was laid between two

glass plates and placed in a drying oven at 50°C for 10 min. The chromatogram was then dried in a stream of warm air and developed on a *Lb. arabinosus* plate.

Tube assays. A final volume of 10 ml per tube was used. For information about test tubes, turbidity measurements and instruments, see section entitled "Measurement of bacterial growth in the tubes". A 5 ml aliquot of standard or sample was added to the test tubes, followed by 5 ml of double strength medium and a glass bead. The tubes were then covered (see below) and sterilized by autoclaving at 120°C for 5 min. After cooling to room temperature under running tap water and inoculating (see above), the tubes were incubated at 37°C in a thermostated water bath. Both laboratories used an incubation time of 24—26 h for the *Lb. arabinosus* and *Lb. casei* tube assay. For *S. faecalis*, an incubation time of 18—22 h was used in laboratory I whereas 30—36 h was used in laboratory II due to the somewhat slower growth.

In laboratory I, the test tubes were covered with aluminium caps. To four series of tubes, standard niacin solution was added to give the following amounts of niacin per tube: 0, 0,01, 0.025, 0.05, and 0.1 μg. In laboratory II, the test tubes in each rack were covered with a metal cover lined with a thick layer of cotton. To six series of tubes, standard solution was added to give the following amounts of niacin per tube: 0, 0.02, 0.04, 0.06, 0.10, and 0.20 μg.

In both laboratories, the test extracts were, after appropriate dilution, set up in triplicate and each assay was carried out at three concentration levels. Uninoculated tubes containing distilled water and medium were used as blanks.

For cleaning the test tubes, a washing powder consisting of polymer phosphates and neutral surface active agents was used. When a tube series was finished, the tubes were emptied and rinsed twice with tap water. After soaking overnight in a solution of the washing powder, the tubes were cleaned by means of a brush and rinsed several times with tap water followed by one rinsing with distilled water. The tubes were than filled with distilled water, autoclaved at 120°C for 10 min, emptied and rinsed twice with distilled water and finally dried overnight in an oven.

RESULTS AND DISCUSSION

Extraction procedures for niacin. The extraction of niacin from natural materials generally offers little difficulty because of the stability of this compound. The extraction procedures mostly used involve autoclaving the finely divided sample for 15—30 min at 120°C in either N sulfuric acid [4,7,8,12,16,21] or N hydrochloric acid [2,5,17]. Of the several extraction procedures tested by Ericson in his investigation on the determination of niacin in marine algae, autoclaving in N sulfuric acid for 1 h at 120°C was found to be the best [1].

In the preliminary experiments of this investigation, the *S. faecalis* cup plate method was used as assay procedure for establishing the most favourable conditions for the extraction of niacin from algal samples. In order to ascertain the completeness of the extraction, we first of all compared autoclaving in N and 3 N sulfuric acid for 1 h at 120°C and found that 3 N acid gave 20—50 % higher niacin assay values than did N acid. We also compared autoclaving in 3 N sulfuric acid at 120°C for 0.5 h and for 1 h, and found that in some instances somewhat higher niacin assay values were obtained with the longer autoclaving time. Extracting the same sample twice with 3 N sulfuric acid for 1 h at 120°C revealed that the second extract contained less than 5 % of the amount of niacin found in the first one. The extraction procedures finally chosen involved autoclaving the samples with N or 3 N sulfuric acid for 1 h at 120°C (for details, see Experimental).

Cup plate assays for niacin. Plate assays for the microbiological determination of niacin with *Lb. arabinosus* as the test organism have been published

by Ericson [1], Morris and Jones [17–18], Simpson [19,20], Karkun and De [21] and Kojima *et al.* [22–25]. The three major variants of the plate assay method [26] have been used, *viz.* the cup plate method [1,17–20], the cylinder plate method [21] and the paper disc method [22–25]. Although the use of large plates instead of petri dishes has the advantage of improved precision and increased through-put of samples [19,20,26,31], only Ericson [1] and Simpson [19,20] have employed large plates for the microbiological assay of niacin. Kojima *et al.* [22–25] have performed a very thorough investigation of the paper disc method for the microbiological determination of niacin as well as several other B-vitamins and amino acids. [22–25] They also used *Lb. casei* and *L. mesenteroides* as test organisms in the plate assay for niacin but found *Lb. arabinosus* to be superior.

We started with *Lb. arabinosus* as the test organism in the cup plate assay for niacin and employed the acetate medium (Table 2). However, we did not find this method to be sufficiently reliable and sensitive. Only occasionally were good cup plates with well defined growth zones obtained, although several variations in the assay medium and the inoculum were tried. The lowest standard concentration that gave readable growth zones was 0.5 or 1.0 μg of niacin per ml which is in agreement with the findings of previous workers [17,19,22–25]. We also tested *Lb. casei* ATCC 7469, *Lb. fermenti* ATCC 9338 and *L. mesenteroides* ATCC 9135 with the acetate medium but without success. *Lb. fermenti* at first seemed very promising since zones of heavy growth were obtained in clear plates without any background growth. However, the edges of the dense growth zones were always too fuzzy for accurate work.

The cup plate assay for niacin with S. faecalis. In laboratory I, *S. faecalis* ATCC 8043 had been used for several years in the cup plate assay and bioautography of folic and folinic acid factors [33–35]. Tube assays for niacin with *S. faecalis* had been suggested earlier in the literature [36,37]. We therefore decided to try this test organism in the cup plate assay for niacin. With the citrate medium given in Table 2, *S. faecalis* never failed to give very good, sensitive and reproducible cup plate assays. In the concentration range of 0.05 to 100 μg of niacin per ml, well defined zones of dense growth were obtained. In Fig. 1, the mean values for the diameters of the growth zones obtained from ten arbitrarily chosen plates from each laboratory are plotted against the logarithm of the standard concentration. As can be seen, the straight-line relationship between the logarithm of the concentration and the mean zone diameter norm-

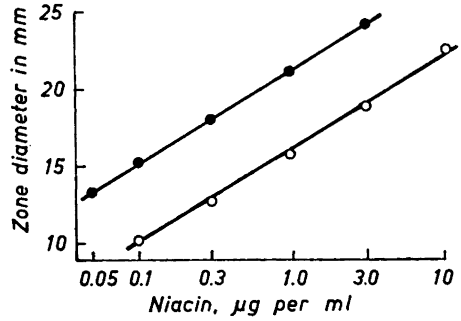

Fig. 1. Growth response of *S. faecalis* to niacin in the cup plate assay method; ● standard of Laboratory I; O standard of Laboratory II.

ally found in plate assays [26,31] was obtained in both laboratories for the niacin standards. For the same concentration, the growth zones obtained in laboratory I were about 5 mm larger than those in laboratory II. This is due to the lighter inoculum used for preparing the *S. faecalis* plates in laboratory I since, for a given standard concentration, the size of the growth zone is inversely related to the density of the plate inoculum [31].

The growth zones were measured to the nearest 0.5 mm with a transparent ruler. The mean value of the zone diameters from cups with identical solutions was calculated to the nearest 0.1 mm. The niacin assay value for each algal sample, obtained from each plate, was calculated to the nearest μg. This was also the case when several dose levels of the same algal extract were assayed simultaneously with the undiluted extract on the same plate. Some investigators recommend the reading of the zone diameters to the nearest 0.1 mm with slide calipers modified by the addition of needle points [19,31,38]. We also tested this measuring procedure but, apart from being more time consuming, we found that it did not significantly alter the assay results. Furthermore, the sharpness of the niacin growth zones could not justify a more precise measurement than to the nearest 0.2 mm.

The sensitivity of our *S. faecalis* plate method is about ten times higher than that of the plate methods with *Lb. arabinosus* previously described [17,19,22–25]. Thus, with the techniques used in both laboratories, the lower assay limit for the cup plate method corresponded to 2—3 μg of niacin per g dry weight of the test material.

The reproducibility of the cup plate assay for niacin with *S. faecalis* as test organism compares favourably with that usually obtained in plate assays of growth factors, *viz.* ± 15—20 % [26]. Both laboratories made three extracts (one with N and two with 3 N sulfuric acid) of each of the eight algal samples listed in Table 1. A detailed record of the cup assays for three of the algal samples (18 extracts) is given in Table 4 and a summarized record for all algal samples in Table 7. A very good agreement was obtained between the assays carried out in both laboratories as well as between the two 3 N sulfuric acid extracts prepared from each sample. In order to obtain a reliable determination of niacin, we employed a minimum of three separate cup plate assays, made on three different days, for each extract. As a rule, each extract was assayed with 5—6 plates in laboratory I and with 3—5 plates in laboratory II (Tables 4, 6, and 7). Of the about 220 separate assay values obtained for the 48 algal extracts, made in both laboratories, there were only ten instances where the separate assay values differed from the mean assay value of the extract in question by ± 20—25 %; 18 separate assay values were found to differ by ± 15—20 % whereas the remaining 190 assay values differed by less than ± 15 %.

The validity of the cup plate assay method for niacin with *S. faecalis* was investigated by recovery tests (see Table 6). Recoveries of 90—100 % were obtained.

When assaying for niacinamide in the *S. faecalis* plates, zones of dense growth were obtained but the edges were very fuzzy and ill-defined. Mixtures of niacin and niacinamide also gave ill-defined growth zones. The reason for this is not known. The appearance of the growth zones in the cup plate assay

Table 4. Reproducibility of the cup plate assay for niacin with *S. faecalis*. The assay values are given as μg niacin per g dry weight.

Algal sample[a]	Sulfuric acid used for extraction[b]	Laboratory I		Laboratory II	
		Separate assay values[c]	Mean value	Separate assay values	Mean value
Fs 1	N	18 14 20 15 15	16.4	14 14 16 19 19	16.4
	3 N	20 23 23 25 25 22	23.0	22 22 25	23.0
	3 N	23 20 22 20 18	20.6	19 21 21	20.3
Lh 2	N	11 10 10 13 10	10.8	9 11 11 12	10.8
	3 N	11 16 17 13 11	13.6	11 12 13 14 13	12.6
	3 N	15 12 12 12 11	12.4	13 13 17	14.3
Rp 1	N	19 18 18 21 19	19.0	20 18 17 20 21 21	19.5
	3 N	24 26 28 25 26 24	25.5	26 28 28 30	28.0
	3 N	23 21 21 27 23	23.0	26 27 29	27.3

[a] See Table 1.

[b] In both laboratories two extracts were made with 3 N sulfuric acid, and the assay values for each extract are recorded separately. Only one extract was made with N sulfuric acid.

[c] Each assay value recorded was obtained from a separate plate.

could, within certain limits, be used as a check of the bioautography results for the presence or absence of niacinamide in the test preparations. The algal extracts prepared for bioautographic tests (extraction with 0.1 N sulfuric acid) and shown to contain mainly niacinamide, all gave ill-defined growth zones in the cup plates. Thus, in order to be able to use *S. faecalis* in the cup plate assay for niacin, the samples must be hydrolyzed so that they contain only niacin. This condition is easily fullfilled by the use of N or 3 N sulfuric acid for the extraction. In these extracts, only niacin was found by bioautography.

In laboratory I, severe infections of the *S. faecalis* plates sometimes occurred. All work with *S. faecalis* plates (citrate medium) was therefore carried out in a sterile room and special care was taken to avoid infection of the plates. This difficulty was not met with in laboratory II. No similar difficulties were experienced in either laboratory when using *Lb. arabinosus* plates (acetate medium) for bioautography. No infection occurred within the first 24 h and these plates could therefore be used and handled anywhere in the laboratories without any special precautions. This is also the case with other acetate medium plates used for cup plate assays and bioautography with other test organisms, *e.g. Lactobacillus leichmannii* 313 ATCC 7830 used for vitamin B_{12} (factors), deoxyribonucleosides and deoxyribonucleotides, and *Pediococcus cerevisiae* ATCC 8081 used for folinic acid factors and thymidine [35,39].

Tube assays for niacin. The most commonly used assay method for the microbiological determination of niacin is the tube assay method with *Lb.*

arabinosus ATCC 8014 as the test organism [2-8], and this method has also reached an official status in some countries [2,4,7,8]. Tube assay methods for niacin with *Lb. casei* ATCC 7469 [9-13], *L. mesenteroides* ATCC 9135 [14-16], and *S. faecalis* ATCC 6057 [40] have been published but these have not been investigated so thoroughly as the assay with *Lb. arabinosus*. *S. faecalis* ATCC 8043 has also been suggested for use as test organism in tube assays for niacin [36,37] and standard curves (or tables) were given, but this assay method has never been tested in practice.

Since a reliable cup plate assay method for niacin with *S. faecalis* could be developed, we also wanted to test this organism in the tube assay for niacin. In this investigation, both laboratories have assayed a certain number of algal samples (see Table 1) for niacin with the *S. faecalis* cup plate assay method and with the *S. faecalis* turbidimetric tube assay method, and these two assay methods have been compared with the *Lb. arabinosus* turbidimetric tube assay procedure. Moreover, in an investigation performed on some other algal samples, a comparison was made between the niacin assay values obtained by the turbidimetric tube assay method with *Lb. arabinosus*, *Lb. casei* and *S. faecalis*.

The dose response curves obtained with *Lb. arabinosus* and *S. faecalis* are given in Fig. 2. The percent light transmittance readings in each response curve were obtained from ten arbitrarily chosen tube series. The relatively high blank of 83 % light transmittance obtained in the *Lb. arabinosus* assay in laboratory I is in agreement with the findings of Loy *et al.* [41] They obtained a blank of 80 % light transmittance and found that, in turbidimetric tube assays, more growth occurred in the blanks for the niacin assays than in the assays of other B-vitamins.

The duration of the incubation period used for the different test organisms was determined by the time required for the tube series to obtain maximum turbidity. That maximum turbidity had been reached was proved by the observation that no significant increase occurred during an additional two hour period of incubation in the tubes containing the highest level of standard vitamin solution [41-43]. The niacin assay value obtained for each extract in a tube assay was calculated to the nearest 0.5 μg per g dry weight (see Table 5).

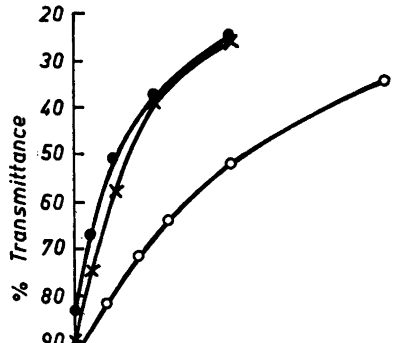

Fig. 2. Growth response of *Lb. arabinosus* and *S. faecalis* to niacin in turbidimetric tube assays; ● *Lb. arabinosus* standard curve of Laboratory I; ○ *Lb. arabinosus* standard curve of Laboratory II; × *S. faecalis* standard curve of Laboratory I.

Table 5. Reproducibility of the turbidimetric tube assay method for niacin with *S. faecalis* and *Lb. arabinosus*. The assay values are given as μg niacin per g. dry weight. The extracts were made by autoclaving in 3 N sulfuric acid for 1 h at 120°C [a]

Algal sample[b]	Test organism	Laboratory I		Laboratory II	
		Separate assay values	Mean value	Separate assay values	Mean value
Fs 1	*S. faecalis*	21.5 24.0 22.0 21.0 19.0 18.5	22.5[a] 19.5[a]	23.0 21.5 21.0	21.8[c]
Lh 2		11.0 12.5 9.5 11.0 10.5 13.5	11.0 11.7	12.0 10.5 10.5	11.0[c]
Rp 1		22.5 25.0 21.5 22.0 24.0	23.0 23.0	25.5 23.5 26.0	25.0[c]
Fs 1	*Lb. arab.*	23.5 23.0 21.0 23.0 23.0 25.5	22.5 23.8	31.0 29.0 27.0 26.0	30.0 26.5
Lh 2		13.5 15.0 14.5 12.0 15.0 13.5	14.3 13.5	15.5 15.5 16.0 15.0	15.5 15.5
Rp 1		28.0 21.5 26.0 25.0 24.5 28.0	25.2 25.8	30.0 30.5 27.0 28.0	30.3 27.5

[a] In both laboratories two extracts were made with 3 N sulfuric acid, and the assay values for each extract are recorded separately.

[b] See Table 1.

[c] Only one of the two extracts was assayed by the *S. faecalis* tube method in Laboratory II.

A detailed record of the tube assays for three of the algal samples is given in Table 5 and a summarized record of all algal samples is shown in Table 7. The assay values given in Tables 6, 7, and 8 are the mean values obtained from two or three separate tube assays. A very good agreement was obtained between the assays carried out in both laboratories as well as between the two 3 N sulfuric acid extracts prepared from each sample. The reproducibility of the turbidimetric tube assay for niacin with *S. faecalis* and *Lb. arabinosus* compares favourably with that usually obtained in tube assays of growth factors, *i.e.* ± 10 % [6,27]. The validity of the tube assays for niacin was also investigated by recovery tests (see Table 6). Somewhat lower recoveries were obtained with the *S. faecalis* tube method (77—89 %) than with the *Lb. arabinosus* tube method (85—107 %).

Comparative determinations of niacin carried out by the cup plate method with S. faecalis *and by the tube method with* Lb. arabinosus *and* S. faecalis. Comparative niacin assay values obtained by these three assay methods for the eight algal samples are given in Table 7. A very good agreement was obtained between the assays carried out in both laboratories. When comparing the assay values of the N and 3 N sulfuric acid extracts of each algal sample obtained with the three assay methods, the following *descending* order of niacin assay

Table 6. Recovery of niacin added to algal samples. The extracts were made by autoclaving in 3 N sulfuric acid for 1 h at 120°C. The niacin assays were carried out by the cup plate method with *S. faecalis* and by the tube method with *Lb. arabinosus* and *S. faecalis*.

Extract No.[a]	Algal sample[b]	Addition of niacin, μg per g sample	Assay method	Niacin in μg per g		Recovery %
				Measured before addition of niacin[c]	Measured after addition of niacin	
1	An 2	10.0	*S.f.* cup	9.8	18.8	91
			S.f. tube	8.2	16.5	83
			*Lb.arab.*tube	9.8	18.2	84
2	Fs 1	20.0	*S.f.* cup	21.8	41.8	100
			S.f. tube	21.0	36.3	77
			*Lb.arab.*tube	23.2	43.2	100
3	Rp 2	40.0	*S.f.* cup	34.4	71.3	92
			S.f. tube	35.2	70.8	89
			*Lb.arab.*tube	38.5	76.3	95
4	An 2	10.0	*Lb.arab.*tube	11.0	21.7	107
5	Fs 2	20.0	»	18.2	38.7	103
6	Rp 2	35.0	»	41.4	77.3	103

[a] Extracts No. 1, 2, and 3 were made and assayed in Laboratory I and extracts No. 4, 5, and 6 in laboratory II.
[b] See Table 1.
[c] These assay values are also given in Table 7.

values was generally obtained: 1) N sulfuric acid extract assayed by the *Lb. arabinosus* tube method, 2) 3 N sulfuric acid extract assayed by the *Lb. arabinosus* tube method, 3) 3 N sulfuric acid extract assayed by the *S. faecalis* cup method, 4) and 5) N and 3 N sulfuric acid extracts assayed by the *S. faecalis* tube method, and 6) N sulfuric acid extract assayed by the *S. faecalis* plate method.

This study shows that the generally adopted method employing extraction with N sulfuric acid and assaying with the *Lb. arabinosus* tube method gives the highest results also for algal samples. However, for the purpose of assaying a large number of samples, the *S. faecalis* cup method carried out on extracts prepared with 3 N sulfuric acid can be recommended. The *S. faecalis* cup plate method generally gives 0—20 % lower assay values than the *Lb. arabinosus* tube method. Only in one instance, sample Fs2, was a nearly 40 % lower assay value obtained. Furthermore, control assays with the *Lb. arabinosus* tube method on the 3 N sulfuric acid extracts used in the *S. faecalis* cup method will give assay values 0—10 % lower than those obtained by the best assay method, *viz.* by the *Lb. arabinosus* tube method with N sulfuric acid extracts. Only for sample Fs 2 was a nearly 20 % lower assay value obtained.

The *S. faecalis* tube method for the assay of niacin in algal samples is hardly of any practical value since the *Lb. arabinosus* tube method in most instances

Table 7. Comparative assays for niacin in algal samples carried out by the cup plate method with *S. faecalis* and by the tube assay method with *Lb. arabinosus* and *S. faecalis*. The assay values are given as μg niacin per g dry weight.

Algal sample[a]	Sulfuric acid used for extraction[b]	Laboratory I			Laboratory II		
		S.faecalis cup	*S.faecalis* tube	*Lb.arab.* tube	*S.faecalis* cup	*S.faecalis* tube[c]	*Lb.arab.* tube
An 1	N	13.0	13.7	15.3	12.0	—[d]	—[d]
	3 N	15.5	11.7	14.1	15.6	10.3	15.4
An 2	N	6.7	8.0	10.2	6.6	—	—
	3 N	9.8	8.2	9.8	10.3	8.5	11.0
Fs 1	N	16.4	22.0	22.7	16.4	—	—
	3 N	21.8	21.0	23.2	21.7	21.8	28.3
Fs 2	N	12.8	15.8	22.5	15.5	—	—
	3 N	16.4	13.9	18.5	15.7	14.2	18.2
Lh 1	N	14.2	16.7	20.7	11.5	—	—
	3 N	17.3	15.8	20.5	17.5	15.2	19.2
Lh 2	N	10.8	12.5	14.8	10.8	—	—
	3 N	13.0	11.4	13.9	13.5	11.0	15.5
Rp 1	N	19.0	24.2	26.0	19.5	—	—
	3 N	24.3	23.0	25.5	27.7	25.0	28.9
Rp 2	N	29.2	36.8	40.5	32.2	—	—
	3 N	34.4	35.2	38.5	37.2	42.0	41.4

[a] See Table 1.

[b] In both laboratories two extracts were made with 3 N sulfuric acid, and the mean value from the assays of these two extracts is given. Only one extract was made with N sulfuric acid.

[c] Only one of the two extracts made with 3 N sulfuric acid was assayed by the *S. faecalis* tube method in Laboratory II.

[d] The N sulfuric acid extracts were not assayed by the tube method with *S. faecalis* and *Lb. arab.* in Laboratory II.

gave considerably higher assay values. Furthermore, a lower recovery was obtained with the *S. faecalis* tube method (Table 6). Upon comparing the cup and tube assay methods with *S. faecalis*, it is seen that, with the N sulfuric acid extracts, the tube method gave higher assay values than the cup method whereas the opposite result was obtained with the 3 N sulfuric acid extracts. This suggests that the stronger acid liberated substances from the algal samples which interfered in the *S. faecalis* tube method. Morris and Jones [17] used N hydrochloric acid for the extraction of niacin from several samples and *Lb. arabinosus* as the test organism. They obtained a variable agreement between the niacin assays carried out by the cup plate and tube assay methods and concluded that alterations in the method of extraction are presumably necessary for different materials. The cup plate method gave in most cases lower assay values than the tube method.

Table 8. Comparative assays for niacin in algal samples carried out by the tube assay metod with *Lb. arabinosus, Lb. casei* and *S. faecalis*. The extracts were prepared by autocloaving in 3 N sulfuric acid for 1 h at 120°C. The assay values are given as μg niacin per g dry weight.[b]

Algal sample[a]		Test organism		
		Lb. arabinosus	*Lb. casei*	*S. faecalis*
Laminaria hyperborea	5/52	29.0	27.5	24.0
» »	5/53	29.0	27.5	24.0
» »	4/55	37.0	34.5	23.0
Laminaria digitata	5/52	35.0	37.5	30.0
» »	7/52	32.5	33.0	24.0
Ascophyllum nodosum	5/53	30.0	26.5	21.5
Fucus serratus	5/52	21.0	21.5	14.0
Rhodymenia palmata	4/51	83.0	59.0	45.0

[a] A separate set of samples, not included in Table 1.
[b] Each figure is the mean of at leas+ two tube assays.

Comparative determinations of niacin carried out by the tube assay method with Lb. arabinosus, Lb. casei *and* S. faecalis. This comparison was made as a further test of the validity of the *Lb. arabinosus* tube assay. A separate set of algal samples, not included in Table 1, was used for this investigation. The results of these comparative assays are given in Table 8. It will be seen that the results obtained by the tube assay method with *Lb. arabinosus* and *Lb. casei* agree very closely although the former test organism gave as a rule somewhat higher assay values than the latter. Only in one instance, *viz.* the red alga *Rhodymenia palmata*, did the results differ considerably thus indicating the presence of either specific stimulatory or inhibitory substances. Hence, the tube assay values obtained with *Lb. casei* on the whole support the validity of the *Lb. arabinosus* tube assay values. In accordance with the results obtained above, considerably lower niacin assay values were obtained with the *S. faecalis* tube method.

Bioautography. In algal extracts used for niacin assays, only niacin was found. In order to avoid deamination of the niacinamide, the extracts for bioautography were prepared by autoclaving in 0.1 N sulfuric acid (see Experimental). Furthermore, if the algal samples contained any "bound" niacin similar to that occurring in various cereal brans, extraction with 0.1 N acid would liberate this "bound" niacin without hydrolysing the complex [44–49]. Strong acid hydrolysis or treatment with 0.1 N alkali at room temperature are necessary for the liberation of niacin from "bound" niacin (an alkali-labile complex containing niacin). The "bound" form of niacin is generally a poor source of the vitamin for lactobacilli. Of the lactobacilli used for niacin assays, *Lb. arabinosus* can best utilize the "bound" form of niacin from various cereal brans. [44,46,48] Previous investigators have also shown that "bound" niacin does not move on paper chromatograms developed with certain organic solvent systems (mostly mixtures of lower alcohols and water). A chemical spray has been used to locate its position (exposure to CNBr vapour and spraying with *p*-aminobenzoic acid reagent). [46,48,50] The possibility that the algal samples

Table 9. Results of bioautographic studies with *Lb. arabinosus* as the test organism. Extracts were prepared by autoclaving in 0.1 N sulfuric acid for 30 min at 120°C.[a]

Sample[b]	Niacin	Niacinamide	"Bound" niacin
An 1	+[c]	+++	0
An 2	+	+++	0
Fs 1	0	+++	0
Fs 2	0	+++	0
Lh 1	0	+++	0
Lh 2	+	+++	0
Rp 1	+	+++	0
Rp 2	+	+++	0
Wheat bran	+	++	++[d]

[a] For further details, see Experimental.
[b] For algal samples, see Table 1.
[c] +++ Predominant component.
++ Component but, not predominant.
+ Detectable.
0 Not detectable.
[d] Only detectable after treatment with ammonia; see Experimental and the text.

contained "bound" niacin (*cf* Refs. [6,44]), as is the case with bran from wheat, barley, corn and rice, was excluded by bioautographic tests. In any case, extraction of algal samples with alkali is impracticable because of the highly gelatinous nature of the extracts obtained.

In this investigation, bioautographic studies with *Lb. arabinosus* as the test organism were made on extracts of the eight algal samples of Table 1 and on a sample of wheat bran which was used as a source of "bound" niacin. A simple method for the detection of "bound" niacin on paper chromatograms was developed. It involved spraying the upper part of the developed and dried paper chromatogram with conc. ammonia in order to liberate niacin from the "bound" niacin (for details, see Experimental). This method was used to test for the presence of "bound" niacin in the algal samples but the tests were all negative. In the sample of wheat bran as well as in the algal samples, no "bound" niacin was found bioautographically when the spraying with ammonia was omitted.

The results of these bioautographic studies are given in Table 9. In the algal samples, niacinamide predominated, and traces of niacin were only found in An 1, An 2, and Lh 2. No other active factors were detected in the extracts. The same bioautographic results were obtained in both laboratories.

Acknowledgements. The authors are very grateful to Professor H. Lundin and Dr. L.-E. Ericson for their encouraging interest in this work. Thanks are also due to Mr. D. Knutson, Miss M. Ahrens, and Miss K. Malvig for skilled technical assistance.

REFERENCES

1. Ericson, L.-E. and Carlson, B. *Arkiv Kemi* **6** (1953) 511.
2. Analytical Methods Committee, Society of Public Analysts and other Analytical Chemists, *Analyst* **71** (1946) 397.
3. Snell, E. E. In György, P. (Ed.) *Vitamin Methods*, Academic Press, New York 1950, Vol. I, p. 327.

4. Association of Vitamin Chemists, *Methods of Vitamin Assay*, 2nd Ed., Interscience, New York 1951, p. 180.
5. Barton-Wright, E. C. *The Microbiological Assay of the Vitamin B-Complex and Amino Acids*, Sir Isaac Pitman & Sons, Ltd., London 1952, p. 46.
6. Snell, E. E. In Sebrell, W. H. and Harris, R. S. (Eds.) *The Vitamins*, Academic Press, New York 1954, Vol. II, p. 538.
7. *National Formulary*, 10th Ed., J. B. Lippincott Co., Philadelphia, Pa. 1955, p. 693.
8. *Official Methods of Analysis*, 8th Ed., Association of Official Agricultural Chemists, Washington 4, D.C. 1955, p. 826.
9. Landy, M. and Dicken, D. M. *J. Lab. Clin. Med.* **27** (1942) 1086.
10. Roberts, E. C. and Snell, E. E. *J. Biol. Chem.* **163** (1946) 499.
11. Clegg, K. M., Kodicek, E. and Mistry, S. P. *Biochem. J.* **50** (1951) 326.
12. Hoff-Jörgensen, E., Moustgaard, J. and Möller, P. *Acta Agr. Scand.* **2** (1952) 305.
13. Banerjee, S., Rohatgi, K. and Lahiri, S. *Food Research* **19** (1954) 134.
14. Johnson, B. C. *J. Biol. Chem.* **159** (1945) 227.
15. Krehl, W. A., De la Huerga, J., Elvehjem, C. A. and Hart, E. B. *J. Biol. Chem.* **166** (1946) 53.
16. Gupta, P. N. S. *Indian J. Appl. Chem.* **21** (1958) 45.
17. Morris, S. and Jones, A. *Analyst* **78** (1953) 15.
18. Jones, A. *Analyst* **79** (1954) 586.
19. Simpson, J. S. *J. Med. Lab. Technol.* **13** (1956) 474.
20. Simpson, J. S. and Harris, D. F. *Analyst* **82** (1957) 210.
21. Karkun, J. N. and De, S. P. *Indian J. Med. Research* **40** (1952) 257.
22. Kojima, H., Matsuya, Y., Ozawa, H., Konno, M. and Uemura, T. *J. Agr. Chem. Soc. Japan* **32** (1958) 33.
23. Kojima, H. and Matsuya, Y. *Ibid.* **32** (1958) 38.
24. Kojima, H. and Matsuya, Y. *Ibid.* **32** (1958) 100.
25. Kojima, H. and Matsuya, Y. *Ibid.* **32** (1958) 189.
26. Gavin, J. J. *Appl. Microbiol.* **5** (1957) 25.
27. Gavin, J. J. *Ibid.* **5** (1957) 235.
28. Haug, A. and Larsen, B. *Nature* **181** (1958) 1225.
29. Larsen, B. *Norweg. Inst. Seaweed Research Rept.* **No. 19** (1958) 13 pp.
30. Callieri, D. A. *Acta Chem. Scand.* **12** (1958) 2045.
31. Lees, K. A. and Tootill, J. P. R. *Analyst* **80** (1955) 95.
32. Ovenfors, C. *Science Tools* **7** (1960) 1.
33. Bolinder, A., Widoff, E. and Ericson, L.-E. *Arkiv Kemi* **6** (1953) 487.
34. Ericson, L.-E. *Ibid.* **6** (1953) 503.
35. Bolinder, A., Kurz, W. and Lundin, H. *J. Inst. Brewing* **62** (1956) 497.
36. Luckey, T. D., Briggs, G. M. and Elvehjelm, C. A. *J. Biol. Chem.* **152** (1944) 157.
37. Rabinowitz, J. C. and Snell, E. E. *Ibid.* **163** (1947) 631.
38. Harrison, E., Lees, K. A. and Wood, F. *Analyst* **76** (1951) 696.
39. Bolinder, A. E. and Kurz, W. G. *Acta Chem. Scand.* **14** (1960) 1173.
40. McCoy, T. A. and Snyder, J. Q. *Proc. Oklahoma Acad. Sci.* **31** (1950) 100.
41. Loy, H. W., Jr., Parrish, W. P. and Schiaffino, S. S. *J. Assoc. Offic. Agr. Chemists* **39** (1956) 172.
42. Ref. 8, p. 837.
43. *United States Pharmacopeia*, 15th Revision, Mack Publishing Co., Easton, Pa. 1955, p. 888.
44. Sweeney, J. P. and Parrish, W. P. *J. Assoc. Offic. Agr. Chemists* **37** (1954) 771.
45. Chaudhuri, D. K. and Kodicek, E. *Nature* **165** (1950) 1022.
46. Reddi, K. K. *Ibid.* **170** (1952) 745.
47. Guha, B. C. and Das, M. L. *Ibid.* **180** (1957) 1285.
48. Kodicek, E., Braude, R., Kon, S. K. and Mitchell, K. G. *Brit. J. Nutrition* **10** (1956) 51.
49. Kodicek, E. and Wilson, P. W. *Biochem. J.* **76** (1960) 27 P.
50. Kodicek, E. and Reddi, K. K. *Nature* **168** (1951) 475.

Received December 2, 1960.

ACTA CHEMICA SCANDINAVICA 15 (1961) 839–848

The Structure of Phloropyron

ANERI PENTTILÄ and JACOBUS SUNDMAN

The Research Laboratories, Medica Ltd., Helsinki, Finland

Phloropyron (X), a phloroglucinol derivative isolated from *Dryopteris* fern, has been shown to be a dimerous compound wherein 3-butyrylfilicinic acid is tied to 6-propyl-2,3-dihydropyran-2,4-dione by means of a methylene bridge.

The structures of the following naturally occurring phloroglucinol derivatives from *Dryopteris* species have been reported and described by several investigators:

aspidinol (I) — Boehm [1], Robertson and Sandrock [2]
albaspidin (II) — Boehm [3]
aspidin (III) — Riedl and Mitteldorf [4]
flavaspidic acid (IV) — McGookin, Robertson and Simpson [5], Riedl [6]
desaspidin (V) — Büchi, Aebi and Kapoor [7]
filixic acid (VI) — Riedl [6], Chan and Hassall [8].

A new compound, for which we suggest the name phloropyron, has now been isolated and its structure has been proved by identifying its decomposition products and by synthesis.

In earlier reports concerning phloroglucinol derivatives from *Dryopteris* species two other substances are of interest, *i.e.* aspidinin and polystichinin. No attempts to explain the structures of these compounds have been made.

In 1897, Boehm [9] described aspidinin as a colourless crystalline substance, m.p. 110°, slightly soluble in alcohol and petroleum ether, soluble in sodium carbonate, the solution first being colourless and then turning dark red in a few hours. The addition of dilute ferric chloride to an alcoholic solution of aspidinin gives a green colour which rapidly changes to dark brown.

In 1898, Poulsson [10] isolated from *Aspidium spinulosum* a substance melting at 110.5°, for which he proposed the name polystichinin. The properties of his compound agree, in part fairly well with those of aspidinin. However, minor differences in crystal form and ferric chloride reaction forced him to doubt the identity of polystichinin with aspidinin.

About forty years later Maizite [11] isolated from *Nephrodium austriacum* a substance melting at 112—113°. On the basis of its physical and chemical

properties he assumed it to be identical with aspidinin and polystichinin mentioned above.

In more recent investigations, Mühlemann [12], Widén [13], Büchi, Aebi and Kapoor [7] and Aho [14] report that they have not been able to find aspidinin. According to Büchi [7] the existence of aspidinin is highly doubtful; he supposed that the earlier investigators actually dealt with a stable mixture of aspidin and albaspidin, melting sharp at 110—112°, rather than with a genuine compound.

The properties of our phloropyron, including melting point, solubility and colour reactions, agree to such an extent with those of Boehm's aspidinin that there seems to be little doubt of their identity. In spite of this we have chosen a new name in order to emphasize the wide structural differences between phloropyron and the other phloroglucinols mentioned above. The impossibility of phloropyron being a mixture of aspidin and albaspidin is evidenced by our results and can, moreover, easily be proved by paper chromatographic separation [15], the R_F-values being: aspidin 0.73, albaspidin 0.56 and phloropyron 0.28.

That also the polystichinin of Poulsson is identical with phloropyron was found out by preparing an aniline derivative of phloropyron. According to Poulsson [10] the aniline derivative of polystichinin had a m.p. of 110—113°; the corresponding compound derived from phloropyron melted at 111—112°. Though the analytical data of polystichinin as reported by Poulsson [10] are in rather poor agreement with our data on phloropyron there is, however, no reason to question the identity of these two substances.

Phloropyron was found in *Dryopteris austriaca* (Jacq.) Woynar in amounts of 0.2 % as calculated on air dried rhizomes. In *Dryopteris filix mas* (L.) Schott it could not always be detected, but when present, it amounted to 0.10—0.15 %. The figures mentioned are based on semiquantitative paper chroma-

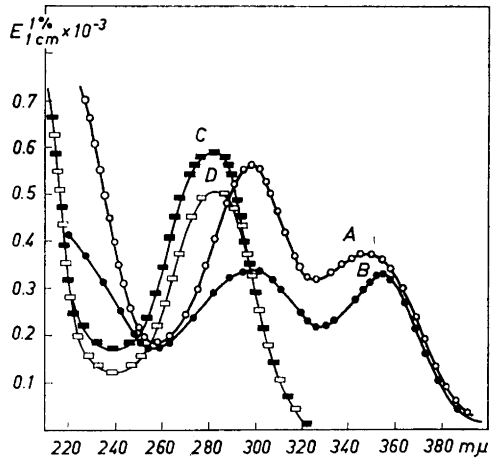

Fig. 1. Ultraviolet absorption spectra of flavaspidic acid (A), phloropyron (B), triacetic lactone (C) and 6-propyl-2,3-dihydropyran-2,4-dione (D) in ethanol (99.5 %).

tographic analyses of non-alkali treated phloroglucinol concentrates. At their best the amounts of phloropyron actually isolated from the rhizomes rise to one half of the figures above.

Phloropyron, together with other phloroglucinol substances, was obtained from *Dryopteris* species by extraction, the extract was freed of lipid material and phloropyron was separated from the other phloroglucinols by reextraction. After several recrystallisations from ethanol, phloropyron was obtained in a pure state as white needles melting at 111—112°. It was a monobasic acid the analytical data of which agreed with the formula $C_{21}H_{26}O_7$. Molecular weight determinations confirmed it as 390. Phloropyron failed to give the methoxyl group reaction. In chloroform solution it proved to be optically inactive. The ultraviolet spectrum of phloropyron resembled that of flavaspidic acid (IV) (Fig. 1.); it did not supply further information.

The alkaline cleavage [16] of phloropyron yielded butyric acid, propionic acid, acetic acid and filicinic acid (VII); other phloroglucinols could not be found. If the alkaline degradation was carried out under very mild conditions [14] butyrylfilicinic acid (VIII) could be identified by paper chromatographic separation [15].

The amount of fatty acids, calculated as butyric acid, obtained by the alkaline decomposition was about 45 % of phloropyron. Paper chromatographic separation of the fatty acids [17] indicated that the major part consisted of butyric acid, but small amounts of acetic acid and propionic acid could always be found.

Rather different results were obtained by the acidic degradation of phloropyron. When warmed with conc. sulphuric acid only butyric acid could be identified, the same amounting to about 22 %. A new crystalline compound could also be isolated from the sulphuric acid solution. The analytical data for this compound agreed with the formula $C_{17}H_{20}O_6$, indicating that it probably is a product resulting from phloropyron by removal of the butyric acid moiety. This new compound, desbutyrophloropyron (IX), had a m.p. of 161—162°.

When desbutyrophloropyron (IX) and 3-butyrylfilicinic acid (VIII) were dissolved in potassium hydroxide (1 %) and the solution was treated with formaldehyde, phloropyron (X) could be identified by paper chromatography [15] among the products formed. Consequently, butyrylfilicinic acid partly replaced the filicinic acid component in the desbutyrophloropyron molecule. The reaction can be interpreted as evidence in support of phloropyron being a methylene compound with butyrylfilicinic acid as one member. Further investigations were concentrated on the isolation of the second half of the phloropyron molecule.

By gentle alkaline treatment with dilute sodium carbonate, phloropyron was broken up and the expected new compound isolated from the solution by extraction. In order to obtain this substance, hereinafter designated as PPD, in a pure state, a chromatographic separation through a column filled with perlon powder [18] proved to be effective. After recrystallisations PPD had a melting point of 93—94°. It is a monobasic acid forming long white needles, soluble in hot water, very soluble in ethanol and acetone and slightly soluble in ether. The ferric chloride reaction is yellowish brown.

The formula of PPD, $C_8H_{10}O_3$, satisfied the requirements of an isomer of filicinic acid (VII) but its properties differed widely from those typical of phloroglucinols [19].

By catalytic hydrogenation of PPD carried out in the Warburg apparatus [20] one mole of hydrogen was absorbed indicating one double bond. The hydrogenation product was not isolated. By diazomethane treatment PPD gave a methoxyl compound containing one methoxyl group. With diazoaminobenzene yellow needles were obtained, m.p. 134—135°.

Boiling of PPD with dilute sodium hydroxide resulted in total decomposition of the molecule. By steam distillation a mixture of ketonic compounds could be isolated. After acidifying the product the volatile acids were distilled off. The ketones were converted to the corresponding dinitrophenylhydrazones, from the mixture of which the derivatives of acetone and methyl propyl ketone were identified. The volatile acids were separated by a paper chromatographic analysis [17]. Butyric acid and acetic acid were identified and, furthermore, the butyric acid was proved by gas chromatography to be the *n*-isomeric one.

When boiled with dilute acids PPD decomposed to carbon dioxide and a volatile compound which could be isolated by steam distillation. This compound gave a greyish blue copper complex, m.p. 167—169°, which easily hydrolysed to give the decomposition products already mentioned, namely butyric acid, acetic acid, acetone and methyl propyl ketone. It was, consequently, a β-diketone and was identified as heptane-2,4-dione [21] by melting point and mixed melting point determinations of the copper complex of synthetic heptane-2,4-dione.

Considering the instantaneous decarboxylation on acidic hydrolysis of PPD it is believed that the carboxy group is in β-position to either oxo-group in heptane-2,4-dione, this obviously leading to an enol lactone structure for PPD. The relatively high stability of PPD permitted us to ignore the possibilities arising from a β-lactone structure, thus leaving only the δ-lactones to be

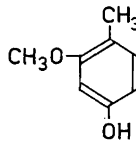

I

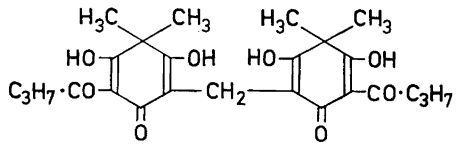

II

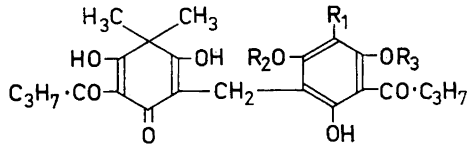

III $R_1 = R_3 = CH_3$; $R_2 = H$

IV $R_1 = CH_3$; $R_2 = R_3 = H$

V $R_1 = R_3 = H$; $R_2 = CH_3$

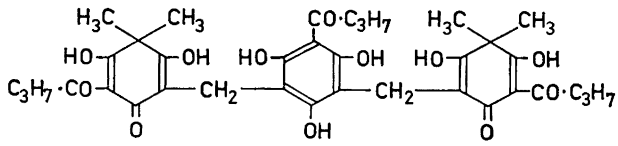

VI

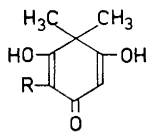

VII R = H
VIII R = CO·C_3H_7

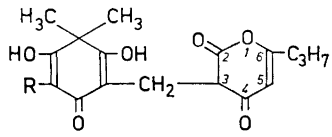

IX R = H
X R = CO·C_3H_7

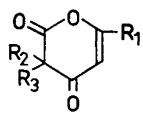

XI $R_1 = C_3H_7$; $R_2 = R_3 = H$
XII $R_1 = CH_3$; $R_2 = R_3 = H$
XIII $R_1 = CH_3$; $R_2 = CO·CH_3$; $R_3 = H$

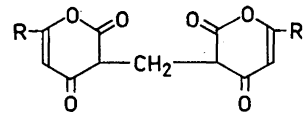

XIV R = C_3H_7
XV R = CH_3

taken into consideration. Of the two possibilities, the δ-lactone derived from heptane-2,4-dione with the carboxy group in position 5 had a m.p. of 185—188° [22–24] and, consequently, was out of question.

The facts thus obtained seemed to be sufficient for formulating PPD as the δ-lactone of 3-oxo-5-hydroxy-4-octenoic acid (XI). Its synthesis as 6-propyl-2,3-dihydropyran-2,4-dione (XI) is reported by Kögl and Salemink [25]. The identity of PPD with the compound reported by these authors was confirmed by mixed m.p. determination of the synthetic 6-propyl-2,3-dihydropyran-2,4-dione. PPD was thus shown to be a homolog of triacetic lactone (XII), the compound easily obtained from dehydroacetic acid (XIII) [24,26].

Phloropyron (X) was synthetised by dissolving 3-butyrylfilicinic acid (VIII) and 6-propyl-2,3-dihydropyran-2,4-dione (XI) in dilute alkali and treating the solution with formaldehyde. The m.p. of the synthetic phloropyron was 111—112° showing no depression on mixing with natural phloropyron. Desbutyrophloropyron, synthetised correspondingly from filicinic acid and 6-propyl-2,3-dihydropyran-2,4-dione, was shown to have the structure (IX).

As already mentioned, propionic acid could be identified among the volatile acids obtained by alkaline cleavage of phloropyron. This acid, however, could not be found when 6-propyl-2,3-dihydropyran-2,4-dione was treated similarly. Likewise, methyl ethyl ketone could be identified in phloropyron decomposi-

tion but was lacking when 6-propyl-2,3-dihydropyran-2,4-dione was the starting material. These facts can be explained by the primary cleavage of phloropyron which yields both 6-propyl-2,3-dihydropyran-2,4-dione and 3-methyl-6-propyl-2,3-dihydropyran-2,4-dione, the latter producing the decomposition compounds mentioned.

There is every probability that the methylene bridge in the phloropyron molecule is attached to the carbon 3 of 6-propyl-2,3-dihydropyran-2,4-dione as shown in (X) leaving the carbon 5 as the less plausible one. To confirm this the condensation products of 6-propyl-2,3-dihydropyran-2,4-dione (XIV) and triacetic lactone (XV) with formaldehyde, called methylene-bis- compounds, were synthesised. Both were obtained in good yields by the method described before. This is in full agreement with earlier reports concerning methylene-bis-triacetic lactone condensed by slightly different methods [27,28]. Dehydroacetic acid (XIII), however, totally failed to form any methylene-bis-compound [27], which confirms the position of the methylene bridge in (X).

The ultraviolet absorption curve of 6-propyl-2,3-dihydropyran-2,4-dione closely resembles that of triacetic lactone (Fig. 1) showing an abnormal hypsochromic shift in alkaline solution, $\lambda_{max}^{EtOH-NaOH}$ 277 mμ (log ε 3.89), which earlier has been observed in the case of 4-hydroxy-2-pyrones and their enol tautomers [34,35].

The ultraviolet absorption has been shown to differentiate between the 2- and 4-pyrone structures in the absence of additional chromophoric groups [36,37]. From this it follows that 6-propyl-2,3-dihydropyran-2,4-dione exhibiting λ_{max} 283 mμ (log ε 3.88) and λ_{min} 242 mμ (log ε 3.28) clearly exists as a 2-pyrone tautomer in ethanol solution [36,37].

The infrared spectrum of 6-propyl-2,3-dihydropyran-2,4-dione (Fig. 2), however, considerably varies from that reported for triacetic lactone, for which a strong carbonyl absorption band at 1 720 cm^{-1} and further bands at about 1 650 cm^{-1} and 1 250 cm^{-1} indicate a typical 2-pyrone structure [37,38]. 6-Propyl-2,3-dihydropyran-2,4-dione has no absorption band at 1 720 cm^{-1}, the first carbonyl band occurring at 1 677 cm^{-1} which is close to the carbonyl absorption band reported for 4-pyrones (1 660—1 670 cm^{-1}) [37,38] and therefore a 4-pyrone structure for this compound in the solid state appears to be the most probable one. 6-Phenyl-2,4-pyronone is reported to behave similarly [37].

To our knowledge the case of phloropyron is unique among the naturally occurring phloroglucinol derivatives, formulated as dimerous methylene compounds, since a phloroglucinol group is substituted by a pyronic group.

EXPERIMENTAL

The ultraviolet spectra were measured on a Unicam SP.500 instrument. The infrared recording was carried out in the Finnish Pulp and Paper Research Institute, Helsinki, using a Perkin-Elmer model 21 instrument fitted with a sodium chloride prism. The microanalyses were done partly in the laboratory of Dr. A. Bernhardt, Mühlheim, Germany and partly in the Department of Chemistry, University of Helsinki. The gas chromatographic analysis was done on a Perkin-Elmer model 154-B gas chromatography set in the Research Laboratories of the State Alcohol Monopoly, Helsinki.

Isolation of phloropyron. The finely ground rhizomes of *Dryopteris austriaca* (Jacq.) Woynar were extracted with ether for 8 hours. The solvent was distilled off and the resi-

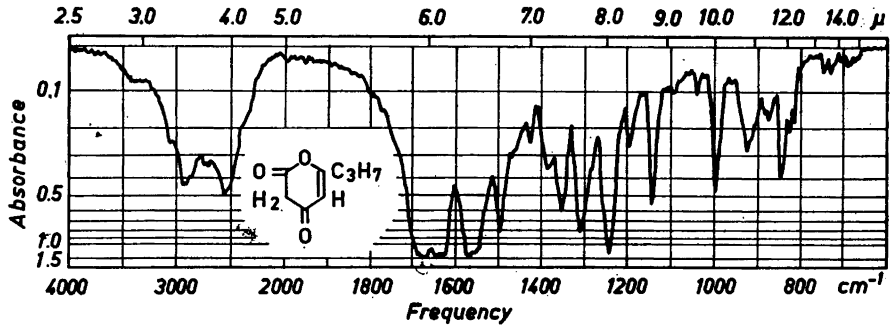

Fig. 2. Infrared absorption spectrum of 6-propyl-2,3-dihyropyran-2,4-dione (KBr-disc)

due freed of fatty materials by MgO treatment [29]. The "raw aspidin" so obtained was dissolved in ether and extracted with sodium carbonate (2 %) and this solution was reextracted with ether. The ether residue and the ethereal extracts were rejected. The sodium carbonate solution was acidified with dilute hydrochloric acid, the obtained precipitate filtered off, dried in vacuum and dissolved in methanol. The first substance which crystallised from methanol at 4° was flavaspidic acid and was rejected. The following crystallisations contained phloropyron together with flavaspidic acid and small amounts of desaspidin. Phloropyron was recrystallised from ethanol and light petroleum. The pure product had a m.p. of 111—112°. (Found: C 64.54; H 6.70. Calc. for $C_{21}H_{26}O_7$ C 64.60; H 6.67).

The aniline derivative of phloropyron. 10 g of phloropyron and 8 g of aniline, redistilled b.p. 184°, were mixed on a steam bath and 25 ml of absolute ethanol was added [10]. The mixture was kept in the refrigerator for some days and the crystals filtered off. Recrystallisations from ethanol yielded white crystals, m.p. 111—112°. (Found: C 69.25; H 6.53; N 3.28. Calc. for $C_{27}H_{31}O_6N$ C 69.67; H 6.66; N 3.01).

Phloropyron and its aniline derivative have widely different R_F-values, 0.28 and 0.95, respectively [15]. Treated with dilute alkali the aniline derivative of phloropyron yielded unchanged phloropyron.

Alkaline cleavage of phloropyron. Phloropyron (300 mg) was dissolved in aqueous sodium hydroxide (2 M, 50 ml), zinc dust (600 mg) was added and the mixture boiled for 8 h. After addition of water (100 ml) the solution was acidified with sulphuric acid (10 %) and the volatile acids were distilled off and collected in a measured volume of standard alkali. The excess of alkali was determined by potentiometric titration. The amount of fatty acids, calculated as butyric acid, was about 45 % of phloropyron. For qualitative analysis of the fatty acids the titrated solution was made alkaline and evaporated to dryness. 5 ml of water was added and the solution made acidic with sodium hydrosulphate and extracted with *n*-butanol. The butanol solution was neutralised with ethylamine and the volatile acids chromatographed as their ethylamine salts [17]. Butyric acid and minor amounts of acetic acid and propionic acid could be identified.

The sulphuric acid solution was extracted with chloroform and filicinic acid (VII) was identified in the chloroform solution by paper chromatographic separation (R_F-value in *n*-butanol:acetic acid:water (5:1:4) was 0.83, which is identical with the R_F-value obtained for authentic filicinic acid, m.p. 215—220° (decomp.).

In the alkaline cleavage of phloropyron for obtaining butyrylfilicinic acid (VIII) as the degradation product, phloropyron was added to a boiling solution of sodium hydroxide (1 M) containing zinc dust [14]. The mixture was boiled for 5 min and after cooling and filtering the solution was acidified with diluted sulphuric acid. Butyrylfilicinic acid was extracted with ether and identified in the ethereal residue by paper chromatography [15].

Acidic cleavage of phloropyron. Phloropyron (800 mg) was dissolved in conc. sulphuric acid (10 ml) and heated on a steam bath for 10 min. The mixture was diluted with 100 ml of water, cooled and the precipitate filtered off. The volatile acids were steam distilled

and determined as before. A yield of about 22 % was obtained; by paper chromatographic analysis [17] only butyric acid could be identified.

The precipitate was dried in vacuum and crystallised from benzene and aqueous ethanol (60 %). M.p. 161—162°. (Found: C 63.76; H 6.37. Desbutyrophloropyron (IX) $C_{17}H_{20}O_6$ requires C 63.75; H 6.25).

Isolation of PPD. Phloropyron was dissolved in sodium carbonate (2 %) and boiled for some minutes. The cooled solution was made acidic with hydrochloric acid (10 %) and kept at room temperature over night. The clear liquid was poured off and extracted with chloroform. The solvent was evaporated and the residue dissolved in water on a steam bath. The filtered solution was chromatographed through a column of perlon powder [18] with water as an eluent. Use was made of the ferric chloride reaction in fractionation and PPD was finally located by condensing an aliquot of each fraction with butyrylfilicinic acid and formaldehyde in dilute alkali. Phloropyron thus obtained was identified by paper chromatography [15]. PPD once isolated by this technique was subsequently prepared by omitting the perlon chromatography step and instead continuing directly with the crystallisations from water and carbon tetrachloride. The pure product had a m.p. of 93—94°. (Found: C 62.33; H 6.67. Calc. for $C_8H_{10}O_3$ C 62.34; H 6.49).

Hydrogenation. PPD (1 mg) in ethanol solution was hydrogenated in a Warburg apparatus [20] over palladised charcoal (10 %) at 35°. The uptake, 1 mole of hydrogen, was completed in 3 h.

Methoxylation of PPD. PPD (50 mg) was methoxylated in ethereal solution with diazomethane. The obtained product was analysed without further purification. (Found: C 61.92; H 7.05; OCH_3 18.19. Calc. for $C_9H_{12}O_3$ C 64.25; H 7.14; OCH_3 18.45).

Diazoaminobenzene derivative of PPD. To PPD (154 mg) dissolved in ethanol (5 ml) was added diazoaminobenzene (197 mg) in ethanol (5 ml). The solution was heated on a steam bath for some minutes and then kept at room temperature overnight. The precipitate as recrystallised from ethanol had a m.p. of 134—135°. (Found: C 65.64; H 5.44; N 11.30. Calc. for $C_{14}H_{14}O_3N_2$ C 65.12; H 5.42; N 10.85).

Alkaline cleavage of PPD. PPD was refluxed with sodium hydroxide (5 %) for 2 h. After adding water the solution was distilled and the distillate treated with dinitrophenylhydrazine in hydrochloric acid (10 %). Using paper chromatographic analysis [30] as a guide the dinitrophenylhydrazone mixture was separated by repeated recrystallisations into two main ketonic compounds: the one with acetone, m.p. 125—127° and the other with methyl propyl ketone, m.p. 145—146°. No depression was observed in mixed m.p. determinations with pure dinitrophenylhydrazones of acetone and methyl propyl ketone. (Found: C 45.49; H 4.42; N 23.8. The acetone derivative $C_9H_{10}O_4N_4$ requires C 45.38; H 4.20; N 23.6. Found: C 49.74; H 5.30; N 22.1. The methyl propyl derivative $C_{11}H_{14}O_4N_4$ requires C 49.62; H 5.25; N 21.05.)

The reaction product resulting from the alkaline cleavage was acidified with sulphuric acid and then steam distilled for volatile acids and the distillate was collected in sodium hydroxide. The salt solution was evaporated to dryness and the liberated acids extracted with *n*-butanol. Paper chromatographic analysis [17] indicated butyric acid and acetic acid. In order to distinguish between *n*-butyric and *iso*butyric acids the salt mixture was evaporated and the acids liberated as before. Now the mixture was extracted with ether. The ethereal solution was gas chromatographed. Found: retention time 7.0. Authentic specimens of *n*-butyric acid, b.p. 163° and *iso*butyric acid, b.p. 154° had retention times of 7.0 and 5.3, respectively.

Acidic cleavage of PPD. PPD was boiled with dilute sulphuric or phosphoric acid for one hour. The determination of the liberated carbon dioxide resulted in 1 mole CO_2 [31]. In order to isolate heptane-2,4-dione, the acidic decomposition mixture was steam distilled and the distillate extracted with ether. The ethereal extract was evaporated and the residue dissolved in methanol and treated with aqueous copper acetate. A greyish blue copper complex was obtained, m.p. 167—169°. (Found: C 52.97; H 6.94; Cu 19.9. Calc. for $C_{14}H_{22}O_2Cu$ C 52.90; H 6.93; Cu 20.0.)

Synthesis of heptane-2,4-dione. Acetone was acylated with butyric acid ethyl ester by means of sodium amide yielding heptane-2,4-dione [32] which was converted to its copper complex as described before. M.p. 168—169°, and mixed m.p. 167—169°. (Found: C 52.82; H 6.87; Cu 20.1. Calc. for $C_{14}H_{22}O_2Cu$ C 52.90; H 6.93; Cu 20.0.) The copper contents were determined by a complexometric titration [33].

Synthesis of 6-propyl-2,3-dihydropyran-2,4-dione (XI). According to Kögl and Salemink [25] PPD was prepared synthetically as follows: *n*-butyryl chloride and sodium enolate of acetyl acetic acid ethyl ester were condensed forming butyryl acetyl acetic acid ethyl ester. After splitting off the acetyl chain the resulting butyryl acetic acid ethyl ester was self condensed giving butyryl PPD. This was converted to PPD by splitting off the butyryl group. The product obtained had a m.p. of 93—94°. Mixed m.p. with isolated PPD was 93—94°. (Found: C 62.28; H 6.46. Calc. for $C_8H_{10}O_3$: C 62.34; H 6.49.)

Synthesis of phloropyron (X). Butyrylfilicinic acid (224 mg) and PPD (154 mg) were dissolved in potassium hydroxide (10 ml, 1 %) and formaldehyde (0.75 ml, 4 %) was added. The mixture was kept at room temperature for 15 min and made acidic with hydrochloric acid (10 %). The precipitate was filtered off, washed with water and dried. After several recrystallisations from ethanol the product had a m.p. of 111—112° and with natural phloropyron a mixed m.p. of 111—112°. (Found: C 64.92; H 6.74. Calc. for $C_{21}H_{26}O_7$: C 64.60; H 6.67.)

Synthesis of desbutyrophloropyron (IX). Filicinic acid (154 mg) and PPD (154 mg) were dissolved in potassium hydroxide (10 ml, 1 %) and formaldehyde (0.75 ml, 4 %) was added. The mixture was kept at room temperature for 15 min and made acidic with hydrochloric acid (10 %). The precipitate was filtered off, washed with water and dried. The identification was made by paper chromatographic analysis [15]. The R_F-value was identical with that of desbutyrophloropyron, m.p. 161—162°, obtained by acidic cleavage of isolated phloropyron.

Synthesis of methylene-bis-PPD (XIV). PPD (308 mg) was dissolved in potassium hydroxide (20 ml, 1 %) and formaldehyde (0.75 ml, 4 %) was added. The mixture was kept at room temperature for 24 h and acidified with hydrochloric acid (10 %). The precipitate was collected, washed with water and dried in vacuum. Recrystallisation from light petroleum yielded a product with a m.p. of 67—69°. (Found: C 64.09; H 6.34. Calc. for $C_{17}H_{20}O_6$: C 63.75; H 6.25.)

Synthesis of methylene-bis-triacetic lactone (XV). Triacetic lactone, m.p. 188—189°, was prepared from dehydroacetic acid, m.p. 110—112°, by the method of Collie [26].

Triacetic lactone (2.52 g) was dissolved in potassium hydroxide (200 ml, 1 %) and treated with formaldehyde (0.75 ml, 40 %). After standing at room temperature for 15 min the solution was acidified and the product recrystallised from ethanol, m.p. 250—251°. (Found: C 59.19; H 4.54. Calc. for $C_{13}H_{12}O_6$ C 59.07; H 4.58.)

REFERENCES

1. Boehm, R. *Ann.* **318** (1901) 245.
2. Robertson, A. and Sandrock, W. F. *J. Chem. Soc.* **1933** 819.
3. Boehm, R. *Ann.* **318** (1901) 253.
4. Riedl, W. and Mitteldorf, R. *Ber.* **89** (1956) 2595.
5. McGookin, A., Robertson, A. and Simpson, T. H. *J. Chem. Soc.* **1953** 1828.
6. Riedl, W. *Ann.* **585** (1954) 32.
7. Büchi, J., Aebi, A. and Kapoor, A. *Sci. Pharm.* **25** (1957) 248.
8. Chan, W. R. and Hassall, C. H. *Experientia* **13** (1957) 349.
9. Boehm, R. *Arch. exptl. Pathol. Pharmakol. Naunyn-Schwiedeberg's* **38** (1897) 35.
10. Poulsson, E. *Arch. exptl. Pathol. Pharmakol. Naunyn-Schwiedeberg's* **41** (1898) 246.
11. Maizite, J. *Arch. Pharm.* **280** (1942) 173.
12. Mühlemann, H. *Pharm. Acta Helv.* **8—9** (1943) 494.
13. Widén, B. *Untersuchungen über die Phloroglucinderivate finnischer Farnarten (Diss.) University Helsinki 1944.*
14. Aho, E. *Ueber Isolierung und tautomere Formen der Flavaspidsäure und anderer Filixphloroglucinabkömmlinge (Diss.) University Turku 1958.*
15. Penttilä, A. and Sundman, J. *J. Pharm. Pharmacol.* **13** (1961) 531.
16. Boehm, R. *Ann.* **318** (1901) 230.
17. Lindqvist, B. and Storgårds, T. *Acta Chem. Scand.* **7** (1953) 87.
18. Grassmann, W., Endres, H., Pauckner, W. and Mathes, H. *Ber.* **90** (1957) 1125.
19. Boehm, R. *Ann.* **302** (1898) 171.
20. Umbreit, W. W., Burris, R. H. and Stauffer, J. F. *Manometric Techniques,* Burgess Publishing Co, Minneapolis, Minn. Revised ed. 1957 p. 105.

21. *Beilstein's Handbuch der Organischen Chemie* IV Ed. 1918, I Band, 792.
22. Oppenheim, A. and Precht, H. *Ber.* **9** (1876) 1101.
23. Malachowski, R. and Wanczura, T. *Bull. intern. acad. polon.* **1933** A 547.
24. Berson, J. A. *J. Am. Chem. Soc.* **74** (1952) 5172.
25. Kögl, F. and Salemink, C. A. *Rec. trav. chim.* **71** (1952) 779.
26. Collie, J. N. *J. Chem. Soc.* **59** (1891) 607.
27. Dieckmann, W. and Breest, F. *Ber.* **37** (1904) 3387.
28. Borsche, W. and Blount, B. K. *Ber.* **65** (1932) 820.
29. Ackermann, M. and Mühlemann, H. *Pharm. Acta Helv.* **21** (1946) 157.
30. Meigh, D. F. *Nature* **170** (1952) 579.
31. Houben-Weyl, *Methoden der organischen Chemie*, Band II, Ed. by Eugen Müller, Stuttgart 1953, IV Ed. p. 769.
32. Adams, J. T. and Hauser, C. R. *J. Am. Chem. Soc.* **66** (1944) 1220.
33. Lucchesi, C. A., Stearns, J. A. and Hirn, C. F. *Chemist-Analyst* **48** (1959) 9.
34. Berson, J. A. *J. Am. Chem. Soc.* **74** (1952) 5172.
35. Berson, J. A., Jones, W. M. and O'Callaghan, S. L. F. *J. Am. Chem. Soc.* **78** (1956) 622.
36. Chmielewska, I., Cieślak, J. and Kraczkiewicz, T. *Roczniki Chem.* **30** (1956) 1009.
37. Herbst, D., Mors, W. B., Gottlieb, O. R. and Djerassi, C. *J. Am. Chem. Soc.* **81** (1959) 2427.
38. Wiley, R. H. and Jarboe, C. H. *J. Am. Chem. Soc.* **78** (1956) 624.

Received December 20, 1960.

ACTA CHEMICA SCANDINAVICA 15 (1961) 849–852

Zur selektiven Oxydation von Benzylalkoholen

ERICH ADLER und HANS-DIETER BECKER

Institutionen för organisk kemi, Chalmers Tekniska Högskola, Göteborg, Schweden

Wie an einigen Veratrylcarbinolen gezeigt wird, gelingt mit Hilfe von aktivem Mangandioxyd bei Zimmertemperatur in neutralem Lösungsmittel die selektive Oxydation der Benzylalkoholgruppe. 1-Veratrylpropan-1,2-diole und -1,2,3-triole unterliegen hierbei der Glykolspaltung.

Seit 1946 wird "aktives Mangandioxyd" zur selektiven Oxydation α,β-ungesättigter primärer und sekundärer Alkohole verwendet [1]. Zahlreiche Beispiele aus der Chemie der Polyene [2], Terpene [3] und Steroide [4] sind beschrieben worden. Die Reaktion verläuft bei Zimmertemperatur in den meisten Fällen glatt unter Bildung α,β-ungesättigter Aldehyde oder Ketone.

Die bisher in der Literatur mitgeteilten Erfahrungen über das Verhalten von Benzylalkoholen gegenüber aktivem Mangandioxyd sind nicht eindeutig. Nach einer Angabe von Ball, Goodwin und Morton [5] wird Benzylalkohol durch MnO_2 nicht angegriffen. Turner [6] berichtet, dass Benzylalkohol bei der Behandlung mit MnO_2 in Benzol unverändert blieb, während Methylphenylcarbinol unter den gleichen Bedingungen nach 12-tägigem Stehen Acetophenon in einer Ausbeute von 34 % lieferte. Nach Harfenist, Bawley und Lacier [7] dagegen wurde Benzylalkohol von einem durch Pyrolyse von Manganoxalat erhaltenen Mangandioxyd oxydiert. Ferner wurde die Überführung von Veratrylalkohol in Veratrumaldehyd beschrieben [8]. Über die Oxydation von 1-Hydroxy-4,4-paracyclophan zum entsprechenden 1-Keto-4,4-paracyclophan mit MnO_2 berichteten kürzlich Cram und Dewhurst [9].

Als Vorarbeit zu ligninchemischen Studien untersuchten wir nun das Verhalten einer Reihe substituierter Benzylalkohole. Da sich zeigte, dass Phenole durch MnO_2 angegriffen werden, sahen wir von der Untersuchung der an sich interessanten 3-Methoxy-4-hydroxybenzylalkohole (Guajacylcarbinole) zunächst ab und beschränkten uns auf 3,4-Dimethoxybenzylalkohole (Veratrylcarbinole). Unter den im experimentellen Teil angegebenen Bedingungen wurden sämtliche untersuchten Veratrylcarbinole oxydiert (siehe Tabelle 1). Die Carbinole I und II sowie V—VIII lieferten in guten Ausbeuten die entsprechenden Ketone. Dem aromatischen Kern nicht benachbarte Carbinolgruppen, wie in den Diolen VI und VIII, wurden dabei nicht angegriffen.

Tabelle 1. Oxydation von Veratrylcarbinolen mit aktivem Mangandioxyd. R = 3,4-Dimethoxyphenyl; R′ = 2-Methoxyphenyl.

Alkohol	Oxydations-produkt	Ausbeute %	Reaktions-zeit (Stunden)	g MnO_2 / g Alkohol
R-CH(OH)-CH_3 I	R-CO-CH_3	89	3	10
R-CH(OH)-CH_2-CH_3 II	R-COCH_2CH_3	90	15	10
R-CH(OH)-CH(OH)-CH_3 III *	R-CHO	81	19	10
		98	1	10
R-CH(OH)-CH(OH)-CH_2OH IV **	R-CHO	99	17	10
R-CH(OH)-CO-CH_3 V [17]	R-CO-CO-CH_3	91	1	6.6
R-CH(OH)-CH_2-CH_2OH VI	R-CO-CH_2-CH_2OH	94	5	11
R-CH(OH)-CH(OR′)-CH_3 VII [18]	R-CO-CH(OR′)-CH_3 [18]	91	5	10
R-CH(OH)-CH(OR′)-CH_2OH VIII [19]	R-CO-CH(OR′)-CH_2OH [19]	91	17	7.5

* Das von Kolokoloff [14] als *α*-Form bezeichnete Racemat vom Schmp. 123° wurde verwendet. Es erwies sich als die D,L-*erythro*-Form [15].

** Das nach Adler und Björkquist [16] dargestellte Racemat (Schmp. 109—110°) hat sich als die D,L-*threo*-Form erwiesen [15].

Freudenberg und Mitarb.[10] konnten zeigen, dass Coniferylalkohol in Methanol oder Aceton beim Behandeln mit MnO_2 (in Gegenwart von Luft) dimere und oligomere Dehydrierungsprodukte liefert. Diese Reaktion illustriert den dehydrierenden Angriff des MnO_2 auf das Phenolhydroxyl. Das 2,4-Dinitrophenylderivat *a* wurde durch MnO_2 in Aceton an der *α,β*-ungesättigten Alkoholgruppe unter Bildung des entsprechenden Zimtaldehyds *b* oxydiert [11]; im Gegensatz zu den von uns gemachten Erfahrungen blieb in diesem Falle die sekundäre Arylcarbinolgruppe intakt.

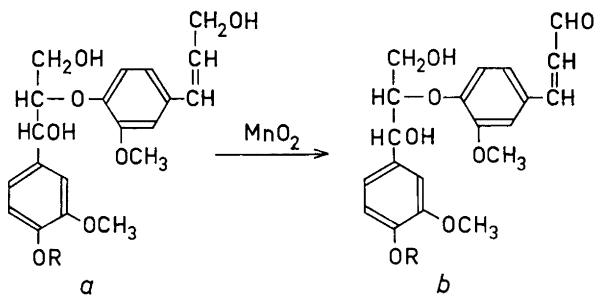

R = 2,4-Dinitrophenyl

Die Spaltung von Glykolen durch aktives MnO_2 ist bisher nur bei höherer Temperatur beobachtet worden [12]. Um so überraschender war die glatte Bildung von Veratrumaldehyd aus den Verbindungen III und IV bei Zimmertemperatur. Eine Ketolspaltung, wie sie bei höherer Temperatur (siedendes

Chloroform) aus der Steroidchemie [13] bekannt ist, wurde in unseren Versuchen nicht beobachtet; Acetylveratrylcarbinol (V) lieferte das entsprechende Diketon.

Neben Mangandioxyd haben auch andere Reagenzien zur selektiven Oxydation von Benzylalkoholen Verwendung gefunden. So berichteten z.B. Lecomte und Dufour [20] über die Oxydation von Benzylalkoholen mit N-Bromacetamid. Eine interessante Variante hiervon ist die von Lecomte und Gault [21] beschriebene oxydative Spaltung eines Benzyläthers. Auf die ligninchemische Anwendung dieser Reaktionen wollen wir später zurückkommen. Die Oxydation von Benzylalkoholen mit Chinonen ist in der Literatur ebenfalls beschrieben worden [22]. Eigene Versuche in dieser Richtung wurden gesondert veröffentlicht [23].

EXPERIMENTELLER TEIL

Methylveratrylcarbinol (I). 8.7 g Methylveratrylketon (4-Acetoveratron) wurden in 55 ml Äthanol gelöst und mit 0.4 g $NaBH_4$ reduziert. Nach 3-stündigem Schütteln blieb die Lösung weitere 4 Stunden stehen. Anschliessend wurde mit 100 ml Wasser verdünnt und 3 mal mit je 70 ml Chloroform ausgeschüttelt. Die vereinigten Chloroformlösungen wurden mit Na_2SO_4 getrocknet, das Chloroform wurde abdestilliert und der ölige Rückstand der Vakuumdestillation unterworfen. Kp. 103°/5 × 10^{-2} mm Hg (Lit.[24] 156–160°/9 mm Hg). Ausbeute 7.9 g, entspr. 90 % d.Th. Das IR-Spektrum zeigte keine Carbonylbande; die Hydroxylbande lag bei 3 400–3 480 cm^{-1}.

Äthylveratrylcarbinol (II). 10 g Äthylveratrylketon (4-Propioveratron) wurden in Äthanol mit 1 g $NaBH_4$ bei 60° reduziert. Nach 24 Stunden wurde mit Wasser verdünnt und mit Äther extrahiert. Nach Abdestillieren des Äthers hinterblieb ein wasserklares Öl, das mit Äther-Hexan nadelformige Kristalle vom Schmp. 35–36° lieferte. Ausbeute 9 g, entspr. 90 % d.Th. (Gef.: OCH_3 31.70. Ber. für $C_{11}H_{16}O_3$: OCH_3 31.63.)

Die Verbindung wurde bereits von Roberti, York und MacGregor [25] durch Grignard-Synthese dargestellt, jedoch nicht kristallin erhalten.

1-Veratrylpropandiol-(1,3) (VI). 2 g β-Hydroxypropioveratron wurden in 40 ml Äthanol mit 0.3 g $NaBH_4$ reduziert. Nach 3-stündigem Schütteln blieb die Lösung noch 15 Stunden stehen, wurde dann mit 50 ml Wasser verdünnt und 3 mal mit je 30 ml Chloroform ausgeschüttelt. Die vereinigten Chloroformlösungen wurden mit Na_2SO_4 getrocknet und im Vak. eingeengt. Destillation des öligen Rückstandes bei 150°/5 × 10^{-2} mm Hg gab ein farbloses Öl (600 mg, entspr. 30 % d.Th.), das nach mehrerenMonaten kristallisierte. Tafeln aus Benzol oder Isopropyläther, Schmp. 58–59°. Das IR-Spektrum der Substanz zeigte keine CO-Bande; das UV-Spektrum ihrer äthanolischen Lösung hatte λ_{max} = 279 mμ, log ε = 3.48. (Gef.: C 62.41; H 7.66; OCH_3 28.75. Ber. für $C_{11}H_{16}O_4$: C 62.25; H 7.60; OCH_3 29.26.)

Aktives Mangandioxyd wurde nach der Vorschrift von Attenburrow und Mitarb.[26] hergestellt. Als Lösungsmittel gelangte ausschliesslich über K_2CO_3 getrocknetes frisch destilliertes Aceton zur Verwendung. Die Oxydationen wurden bei Zimmertemperatur durchgeführt. Übrige Versuchsdaten ergeben sich aus Tabelle 1.

Die Durchführung der *Oxydationen* sei an einem Beispiel beschrieben.

Eine Lösung von 300 mg Äthylveratrylcarbinol (II) in 12 ml Aceton wurde mit 3 g MnO_2 15 Stunden bei Zimmertemperatur unter N_2 geschüttelt. Das MnO_2 wurde hierauf abgesaugt und 3 mal mit je 20 ml Aceton gewaschen. Die vereinigten Acetonlösungen hinterliessen nach dem Abdestillieren des Lösungsmittels 4-Propioveratron, identifiziert durch Schmp. (60°, Lit.[27] 59–60°) und IR-Spektrum. Ausbeute 270 mg, entspr. 90 % d.Th.

Auch in den übrigen Fällen wurden die Oxydationsprodukte durch Schmelzpunkt und Mischschmelzpunkt sowie IR-Spektrum identifiziert.

Für die Gewährung eines Forschungsbeitrages sind wir *Statens Naturvetenskapliga Forskningsråd* zu Dank verpflichtet.

LITERATUR

1. Ball, S., Goodwin, T. W. und Morton, R. A. *Biochem. J.* **40** (1946) Proc. Biochem. Soc. LIX.
2. Evans, R. M. *Quart. Revs. (London)* **13** (1959) 61 (Übersichtsartikel).
3. Ohloff, G. *Ann.* **617** (1958) 134.
4. Sondheimer, F. und Rosenkranz, G. *Experientia* **9** (1953) 62.
5. Ball, S., Goodwin, T. W. und Morton, R. A. *Biochem. J.* **42** (1948) 516.
6. Turner, D. L. *J. Am. Chem. Soc.* **76** (1954) 5175.
7. Harfenist, M., Bawley, A. und Lacier, W. *J. Org. Chem.* **19** (1954) 1608.
8. Highet, R. J. und Wildman, W. C. *J. Am. Chem. Soc.* **77** (1955) 4399.
9. Cram, D. J. und Dewhurst, K. C. *J. Am. Chem. Soc.* **81** (1959) 5963.
10. Freudenberg, K. und Grion, G. *Chem. Ber.* **92** (1959) 1355. — Freudenberg, K. und Friedmann, M. *Chem. Ber.* **93** (1960) 2138.
11. Freudenberg, K. und Lehmann, B. *Chem. Ber.* **93** (1960) 1354.
12. Barakat, M. Z., Abdel-Wahab, M. F. und El-Sadr, M. M. *J. Chem. Soc.* **1956** 4685.
13. Padilla, J. und Herran, J. *Bol. inst. quim. univ. nacl. auton. Méx.* **8** (1956) 3; *Chem. Abstr.* **51** (1957) 8124.
14. Kolokoloff, M. *J. Russ. phys.-chem. Ges.* **29** (1896) 23; *Chem. Zentr.* **1897** I, 915.
15. Adler, E. und Gustafsson, B. *Unveröffentlicht.*
16. Adler, E. und Björkquist, K. J. *Acta Chem. Scand.* **5** (1951) 241.
17. Eastham, A. M., Fisher, H. E., Kulka, M. und Hibbert, H. *J. Am. Chem. Soc.* **66** (1944) 26.
18. Adler, E. und Delin, S. *Unveröffentlicht.*
19. Adler, E., Lindgren, B. O. und Saedén, U. *Svensk Papperstidn.* **55** (1952) 245.
20. Lecomte, J. und Dufour, C. *Compt. rend.* **234** (1952) 1887.
21. Lecomte, J. und Gault, H. *Compt. rend.* **238** (1954) 2538.
22. Braude, E. A., Linstead, R. P. und Wooldridge, K. R. *J. Chem. Soc.* **1956** 3070.
23. Becker, H.-D. und Adler, E. *Acta Chem. Scand.* **15** (1961) 218.
24. Mannich, C. *Arch. Pharm.* **248** (1910) 139.
25. Roberti, P. C., York, R. F. und MacGregor, W. S. *J. Am. Chem. Soc.* **72** (1950) 5760.
26. Attenburrow, J., Cameron, A. F. B., Chapman, J. H., Evans, R. M., Hems, B. A., Jansen, A. B. A. und Walker, T. *J. Chem. Soc.* **1952** 1094.
27. Cramer, A. B., Hunter, M. J. und Hibbert, H. *J. Am. Chem. Soc.* **61** (1939) 515.

Eingegangen am 19. Dezember 1960.

ACTA CHEMICA SCANDINAVICA 15 (1961) 853–855

Micro Determination of Cysteine plus Cystine in Proteins

JOHN GOA

Department of Medical Biochemistry, University of Gothenburg, Sweden *

A method is described for microdetermination of the total amount of cysteine and cystine in proteins. By means of hydrazinolysis the cysteine and cystine sulphur is transformed to hydrogen sulphide which is subsequently measured colorimetrically as bismuth sulphide. Quantities of 20–200 μg cysteine plus cystine can be determined. Neither methionine nor ammonium sulphate interfere with the reaction.

The method of Kuratomi, Ohno and Akabori [1] for the determination of cysteine plus cystine in proteins is very convenient. The procedure involves reduction of cysteine- and cystine-sulphur by hydrazine hydrate to hydrogen sulphide which is determined by Caro's reaction (dimethyl-*p*-phenylendiamine + H_2S → methylene blue) followed by colorimetry.

The method works with amounts of 10 to 50 μmole of cystine or 2 to 10 mg. With smaller amounts the Caro reaction does not give quantitative results. Thus with proteins containing 2 % cysteine plus cystine at least 100 mg are required for a single determination. In protein work such amounts are not always available and it is necessary to analyse much smaller quantities.

The aim of this work was therefore to find a method 50 to 100 times more sensitive. This was obtained by leading the hydrogen sulphide formed by hydrazinolysis into a solution of bismuth tartrate whereby bismuth sulphide was formed. When held in colloidal form the bismuth sulphide could be measured colorimetrically [2].

REAGENTS

Hydrazine hydrate, 99–100 per cent (British Drug Houses LTD).

Bismuth reagent. Dissolve 2.2 g $Bi(NO_3)_3 \cdot 5H_2O$ in 250 ml of a 3.2 per cent solution of mannitol in water. Add 80 ml redistilled glycerol (Merck) and 360 ml of a 2.5 per cent solution of gum arabic in water. Dilute to 1,000 ml with 0.2 N acetate buffer pH = 5.2 (11 vol. 0.2 N NaAc + 3 vol. 0.2 N HAc) and filter. The reagent is stable for at least one month.

Cystine standard. Dissolve 40 mg recrystallized cystine in a small amount of 0.1 N hydrochloric acid in a 100 ml volumetric flask and dilute to the mark with distilled water.

6 N sulphuric acid.

---

* Present address: Central Laboratory, Rikshospitalet, Oslo, Norway.

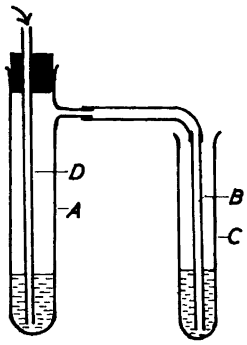

Fig. 1. Arrangement for transferring the hydrogen sulphide into the bismuth reagent. Explanation is given in the text.

PROCEDURE

From the standard cystine solution amounts of 50 to 500 μl (= 0.02 to 0.20 mg cystine) are pipetted into small ampullas or tubes and an equal volume of hydrazine hydrate is added. Into another series of tubes the protein to be analysed are placed in amounts equal to 0.02 to 0.2 mg cystine, *i.e.* at least 1 mg of a protein containing 2 % cysteine plus cystine. The protein can be placed in the tubes either in dry form or in solution. Hydrazine hydrate is then added in such amounts that the final concentration will be 50 to 100 %. The tubes are sealed and heated for 18 h at 120°C. After cooling the tubes are opened and the contents quantitatively transferred by means of 1—2 ml water to a test tube fitted with a side arm (tube A in fig. 1). The side arm of tube A is connected to a glass tube B by polyethylene tubing. B is placed into another test tube C containing 4 ml of bismuth reagent. The top of tube A is closed by a rubber stopper through which a glass tube D is inserted. Through D is added 2 ml 6 N sulphuric acid and nitrogen gas is immediately passed through the system at a rate of about three bubbles per second. The nitrogen gas is first washed by passing it through a 10 % solution of sodium hydroxide. Tube A is placed in a water bath at 60°C. The liberated hydrogen sulphide is under these conditions quantitatively transferred to the bismuth reagent within 15 min. The brown colour of the bismuth sulphide formed is read in a spectrophotometer at 400 mμ. Bismuth reagent serves as blank.

From a standard curve the cysteine + cystine content of the analysed protein sample is read. In our laboratory the equation of the standard curve was found to be:

$$\text{mg cysteine + cystine in the sample} = A^{1\,\text{cm}}_{400\,\text{m}\mu} \times 0.32 + 0.008.$$

EXPERIMENTAL

Hydrazinolysis. The final concentration of hydrazine hydrate during hydrolysis was varied between 40 and 99 % and time of hydrolysis was varied between 12 and 24 h without change in the results. A concentration of about 50 % and hydrolysis for 18 h was chosen for convenience.

Aeration of hydrogen sulphide. Nitrogen gas was allowed to pass the system for varying times. An aeration time of 5 min gave a yield of 80 %, after 10 min the yield was close to 100 % and after 15 min or longer the yield was constant 100 %. It was observed that when new polyethylene tubings were used there was a considerable loss of hydrogen

Table 1. Analyses with the given method on different combinations of sulphur containing substances.

Analysed	$A^{1\,cm}_{400\,m\mu}$	mg found mg = A × 0.32 + 0.008	Per cent of theoretical
0.1 mg methionine	0.002	0.0	
0.2 mg »	0.000	0.0	
1 mg ammonium sulphate	0.000	0.0	
2 mg » »	0.000	0.0	
0.051 mg cystine	0.135	0.051	100
0.077 mg »	0.215	0.077	100
0.077 mg » + 0.1 mg methionine	0.225	0.080	104
0.077 mg » + 0.2 mg »	0.211	0.075	98
0.077 mg » + 1 mg ammonium sulphate	0.210	0.075	98
0.077 mg » + 2 mg » »	0.220	0.079	103
1.87 mg β-lactoglobuline	0.170	0.063	
1.87 mg »	0.176	0.065	
1.87 mg » + 0.1 mg methionine	0.178	0.065	102
1.87 mg » + 0.2 mg »	0.178	0.065	102
1.87 mg » + 1 mg amm. sulphate	0.178	0.065	102
1.87 mg » + 2 mg » »	0.180	0.066	103
1.87 mg » + 0.051 mg cystine	0.330	0.114	99
1.87 mg » + 0.077 mg »	0.425	0.146	104

sulphide and small amounts of sulphur could be seen inside the tubing. However, if a surplus amount of hydrogen sulphide was allowed to pass the tubing before use, no further loss could be measured.

Colorimetry. The brown colour of bismuth sulphide has no absorption maximum, the absorption increases with decreasing wavelength. Thus at 400 mμ the absorption is twice that read at 475 mμ and five times that read at 575 mμ. In this work a Beckman spectrophotometer model B was used with 1 cm cells and readings at 400 mμ.

Specificity of the method. This was investigated by analysing different combinations of cystine, methionine, ammonium sulphate and protein in the following way: (see also Table 1).

1. Methionine or ammonium sulphate gave no absorbancy after hydrolysis.
2. Addition of methionine or ammonium sulphate to cystine standards gave no increase in absorbancy.
3. Addition of methionine or ammonium sulphate to protein samples gave no increase in absorbancy.
4. Addition of cystine to protein samples gave full recovery.

With the described method the content of cysteine plus cystine in crystalline β-lactoglobuline was found to 3.4 % and in crystalline insulin to 11.7 %. Tristam [3] gives the respective values to 3.39 and 12.0—12.5. The cysteine plus cystine content in pea albumin was found to be 5.5 %, in vicilin 0.0 % and in legumin 0.9 % [4]. In orosomucoid the value 1.7 % was found.

The method works with an accuracy within ± 5 %.

REFERENCES

1. Kuratomi, K., Ohno, K. and Akabori, S. *J. Biochem. (Tokio)* **44** (1957) 183.
2. Koren, H. and Gierlinger, W. *Mikrochim. Acta* **1953** 220.
3. Tristram, G. R. *Advances in Protein Chem.* **5** (1949) 83.
4. Goa, J. and Strid, L. *Arch. Mikrobiol.* **33** (1959) 253.

Received December 10, 1960.

ACTA CHEMICA SCANDINAVICA 15 (1961) 856–860

Biosynthesis and Excretion of Vitamin B_6 by *Escherichia coli* during the Lag and Acceleration Phases of Growth

VEIKKO NURMIKKO and RAIMO RAUNIO

Department of Biochemistry, University of Turku, Turku, Finland

The biosynthesis and excretion of vitamin B_6 has been followed during the initial growth phases of *Escherichia coli*. The determination of vitamin B_6 has been carried out by the biological method using *Saccharomyces carlsbergensis* 4228 (ATCC 9080), *Lactobacillus casei* (ATCC 7469) and *Streptococcus faecalis* R (ATCC 8043) as test organisms. The biosynthesis of vitamin B_6 takes place at a significant rate already during the lag phase and rises to a maximum during the acceleration phase. After this the rate of biosynthesis slowly decreases to the initial level at the end of the exponential growth phase. No excretion of vitamin B_6 was observed under the experimental conditions during any of these growth periods.

In two previous communications [1,2] it was reported that *Escherichia coli* excretes certain vitamins of the B-complex in quite remarkable amounts especially during the earlier growth phases. Very little is known about the rate of biosynthesis of the B vitamins which function as coenzymes during the lag and exponential phases of bacterial growth. The present investigations were undertaken to obtain information on the rate of biosynthesis and on the excretion of vitamin B_6 by *E. coli* especially during the first phases of cell growth. The results reported here show that this organism synthesizes unusually large amounts of vitamin B_6 during the lag phase between cell divisions.

RESULTS

In the experiments the inoculum was prepared by harvesting the cells during the exponential growth phase in order to obtain rapidly growing cells and thus to shorten the lag phase. As can be seen from Fig. 1, the rate of synthesis of vitamin B_6 increases during the lag phase which in this experiment lasted 30 min. At the beginning of the lag phase, the vitamin B_6 content of the cells was 70 mμg per mg (dry weight of the cells) but the contents increased to 105 mμg per mg during the 30 min, the increase being approximately 30 % of the

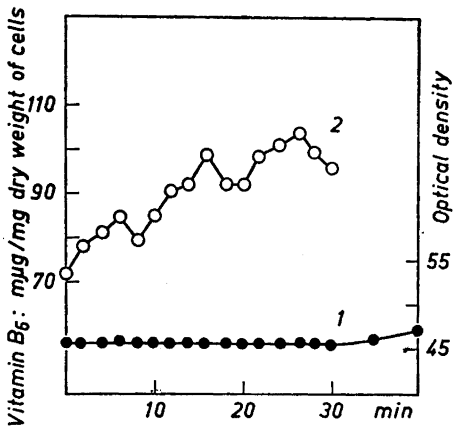

Fig. 1. Formation of vitamin B_6 by *Escherichia coli* cells during the lag phase of growth.
1. Growth curve (right-hand scale).
2. Vitamin B_6 content of cells.

original content. The test organism in this experiment was *S. carlsbergensis* 4228.

The results of the experiments on the synthesis and excretion of vitamin B_6 during the acceleration and exponential phases, and also during the early retardation phase, are shown in Fig. 2. *E. coli* did not excrete vitamin B_6 into the medium during any of these growth phases. Remarkable variations are noted in the synthesis of vitamin B_6 during the different periods of growth. The rate of formation of vitamin B_6 is high already in the lag phase and it

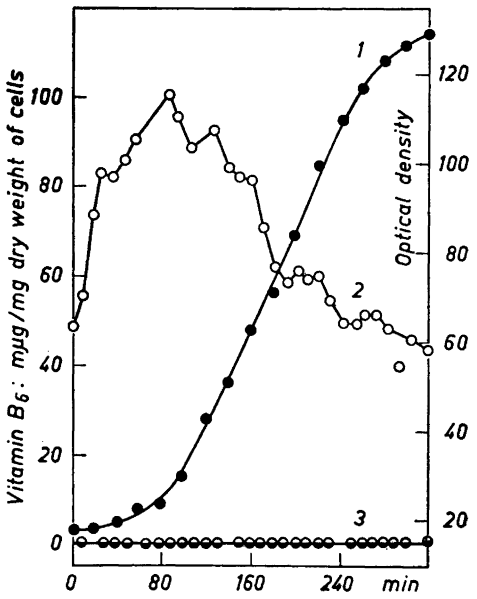

Fig. 2. Formation and excretion of vitamin B_6 by *Escherichia coli* cells during the growth cycle.
1. Growth curve (right-hand scale).
2. Vitamin B_6 content of cells.
3. Excretion of vitamin B_6 into the growth medium.

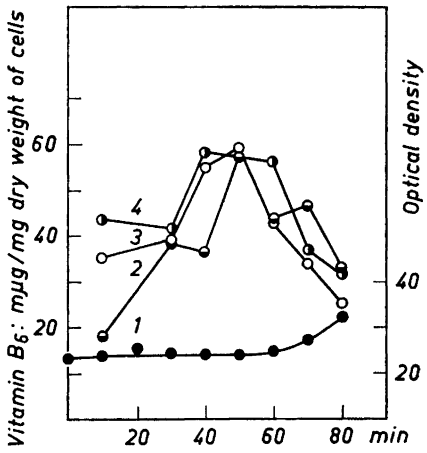

Fig. 3. Formation of pyridoxine, pyridoxamine and pyridoxal by *Escherichia coli* cells during the lag and early acceleration phases of growth.

1. Growth curve (right-hand scale).
2. Pyridoxal content of cells. *Lactobacillus casei* (ATCC 7469) used as test organism.
3. Pyridoxamine content of cells. *Streptococcus faecalis R* (ATCC 8043) used as test organism.
4. Pyridoxine, pyridoxal and pyridoxamine content of cells. *Saccharomyces carlsbergensis* (ATCC 9080) used as test organism.

reaches its maximal value during the acceleration phase. This peak was reached after the content had increased to 150 % of the original. During the exponential phase the rate of synthesis decreased steadily, and during the retardation phase the cells again contained the same amount of vitamin B_6 as at the beginning of the lag phase (50 mμg of vitamin B_6 per mg of dry weight). The results shown in this figure were obtained by using *S. carlsbergensis* 4228 as test organism.

Fig. 3 shows the results of experiments where the synthesis and excretion of vitamin B_6 in *E. coli* was followed using *Str. faecalis* R and *Lb. casei* in addition to *S. carlsbergensis* 4228 as test organisms. As the results show, the rate of synthesis of vitamin B_6 increased until the maximum content was reached during the acceleration phase, in other words, 50 min after the experiment was started. It is of interest to note that with all the test organisms used the content of vitamin B_6 was a maximum at about the same stage of the acceleration phase. No excretion of vitamin B_6 was established in these experiments. All the experiments described above were repeated at least three times.

DISCUSSION

In this paper Monod's definitions of the phases of bacterial growth have been followed [5]. The results of the experiments show that the formation of vitamin B_6 started already at the beginning of the lag phase and that generally the rate of formation rose to a maximum in the middle of the acceleration phase. As is well known, the vitamin B_6 enzymes (*e.g.* transaminases, deaminases, decarboxylases) participate in the metabolism of amino acids. The fact that cells synthesize amino acids and proteins before their division explains why the biosynthesis of vitamin B_6 should take place early in the lag phase and why the rate of biosynthesis is so high during the acceleration phase. The rate of synthesis of vitamin B_6 decreased throughout the exponential growth phase. This can probably be attributed to a more rapid formation of the vitamin B_6

enzyme systems during the acceleration growth phase than during the other phases. If this were true, the decrease in the rate of formation of vitamin B_6 would be understandable. No excretion of the vitamin into the medium was observed and therefore it can be assumed that the whole amount of vitamin B_6 synthesized was used quantitatively by the cells in the formation of vitamin B_6 enzyme systems. It should be noted that the results shown in Figs. 1 and 2 were obtained using *S. carlsbergensis* 4228 as the test organism. Therefore it cannot be said with certainty what member of the vitamin B_6 complex is formed first. However, the results of the experiments shown in Fig. 3 indicate that pyridoxal is formed in larger quantities than the other members of the vitamin B_6 complex. This is supported by the finding that the activity of vitamin B_6 was highest when *Lb. casei* was used as test organism. Snell [6] has found that of the three known forms of vitamin B_6, only pyridoxal is highly active in supporting growth of *Lb. casei*, whereas pyridoxamine and pyridoxine have negligible activity.

Under the essay conditions employed, *E. coli* did not produce any inhibiting or any growth promoting factors as no upward or downward drifts were noted in the microbiological determinations.

In a previous report from this laboratory [1], it was demonstrated that, when a very complex growth medium is used, *E. coli* cells excrete large amounts of vitamin B_6 into the medium,particularly during the exponential growth phase. In the present study the medium had a more simple composition. This is, no doubt, the reason why no excretion of vitamin B_6 was observed during the growth cycle.

EXPERIMENTAL

Organism and media. *Escherichia coli*, strain U5-41, was cultured with monthly transfers in an agar medium which contained 2.0 g of glucose, 1.4 g of KH_2PO_4, 100 mg of trisodium citrate, 200 mg of ammonium sulphate, 220 mg of Casamino acids (Difco), 20 mg of $MgSO_4 \cdot 7\ H_2O$, 10 mg of tryptophan, and 2.0 g of agar (Difco) in 100 ml of distilled water and which had previously been adjusted to pH 6.7—6.8 and autoclaved 10 min at 105°C.

The inoculated agar slant was incubated 24 h at 3°C and then stored in a refrigerator.

The inoculum medium contained 1.0 % of glucose, 1.0 % of trisodium citrate, 0.5 % of Bacto-tryptone (Difco), and 0.5 % of yeast extract (Difco). The pH of the medium was adjusted to 6.7—6.8 and the medium autoclaved 10 min at 115°C.

The growth medium of *E. coli* contained 1.0 g of glucose, 700 mg of KH_2PO_4, 50 mg of trisodium citrate, 100 mg of $(NH_4)_2SO_4$, 100 mg of NH_4Cl, 10 mg of $MgSO_4 \cdot 7H_2O$ and 20 mg of L-glutamic acid in 100 ml of distilled water. The medium was neutralized with 1 N NaOH to pH 6.7—6.8 and boiled shortly before the experiment was started.

Determination of vitamin B_6. The total pyridoxine, pyridoxamine and pyridoxal content was determined with *Saccharomyces carlsbergensis* 4228 (ATCC 9080) according to Atkin *et al.*[3], the pyridoxamine and pyridoxal content with *Streptococcus faecalis* R (ATCC 8043) by the method of Rabinowitz and Snell [4], and pyridoxal with *Lactobacillus casei* (ATCC 7469) according to Rabinowitz *et al.*[5]

Procedure. At the beginning of each experiment 2 l of the growth medium of *E. coli* was inoculated with a strong inoculum which was prepared as follows. *E. coli* was transferred from the agar slant to 100 ml of the inoculum medium. After overnight incubation at 37°C, the cells were harvested by centrifuging (3 500 rpm), transferred into 200 ml of the same medium, and again incubated 10—15 h at 37°C. The cells were then centrifuged (3 500 rpm) 15 min and washed three times with 0.9 % NaCl solution. Immediately after washing, this inoculum was placed in a refrigerator (+ 2°C) for at least 30 min. All the

cells were used as inoculum and the resulting growth medium contained approximately 0.05 mg of *E. coli* cells (calculated as dry weight) per millilitre. Before inoculation the temperature of the growth solution was raised to 37° on a water bath, and after this adjustment continually mixed with an electric stirrer. After the incubation, specimens were taken at intervals of 2 min. during the lag phase and at intervals of 10—15 min during the other growth phases. Each specimen taken from the medium was cooled in ice-water with continuous stirring. The turbidities of the cooled specimens were measured with a Klett-Summerson photometer employing a 620 mμ filter. The cells were harvested from 10 ml of the suspension by centrifuging (3 500 rpm) 15 min and the medium was completely removed with a pipette. The cells were washed three times with 0.9 % NaCl and then autoclaved together with 5 ml of 0.005 N HCl at 120°C for 3 h. After the hydrolysis, the pH was adjusted to 4.5—5.0 and the volume made up to 20 ml. When vitamin B_6 was determined with *Lb. casei* the cells were hydrolyzed in 3 ml of the 0.5 % acetate buffer, pH 4.5, to which about 1 mg each of papaine and diastase had been added, under toluene at 37°C for 24 h and the specimen to be analyzed was added aseptically before the inoculation.

REFERENCES

1. Nurmikko, V. *Fifth Intern. Congr. Nutrition*, Abstracts (1960) 45.
2. Nurmikko, V. and Laaksonen, S. *Suomen Kemistilehti* **B34** (1961) 7.
3. Atkin, L., Schultz, A. S., Williams, W. L. and Frey, N. C. *Ind. Eng. Chem. Anal. Ed.* **15** (1943) 141.
4. Rabinowitz, J. C. and Snell, E. E. *J. Biol. Chem.* **169** (1947) 631.
5. Monod, J. *Ann. Rev. Microbiol.* **3** (1949) 371.
6. Snell, E. S. in György, P. *Vitamin Methods*, Academic Press, N.Y. Vol. I (1950) 327.

Received December 8, 1960.

ACTA CHEMICA SCANDINAVICA 15 (1961) 861–870

The Crystal Structures of Pd_5B_2, (Mn_5C_2) and Pd_3B

ERIK STENBERG

Institute of Chemistry, University of Uppsala, Uppsala, Sweden

The crystal structures of Pd_5B_2 and Pd_3B have been determined by single-crystal methods.

Pd_5B_2 has a monoclinic unit cell with the following dimensions: $a = 12.786$ Å, $b = 4.955$ Å, $c = 5.472$ Å, $\beta = 97°2'$. There are four formula units in the unit cell and the space-group is $C2/c$. The twenty palladium atoms are situated in two eightfold positions 8(*f*) with $x_I = 0.0958$, $y_I = 0.0952$, $z_I = 0.4213$ and $x_{II} = 0.2127$, $y_{II} = 0.5726$, $z_{II} = 0.3138$ and one fourfold position 4(*e*) with $y_{III} = 0.5727$. The boron atoms are situated in an 8(*f*) position with $x = 0.106$, $y = 0.311$, $z = 0.077$. Pd_5B_2 is isomorphous with Mn_5C_2.

Pd_3B has the cementite (Fe_3C) structure. The space-group is *Pnma* with $a = 5.463$ Å, $b = 7.567$ Å, $c = 4.852$ Å and the unit cell contains eight palladium atoms in 8(*d*) with $x_I = 0.1798$, $y_I = 0.0700$, $z_I = 0.3276$ and four palladium atoms in 4(*c*) with $x_{II} = 0.0372$, $z_{II} = 0.8446$. Four boron atoms are situated in 4(*c*) with $x = 0.884$, $z = 0.433$.

The literature on the Pd-B system is very scanty. Buddery and Welch [1] report a hexagonal compound occurring at 6.33 wt % B (Pd_3B_2). However, there are reasons to believe that their product, which was obtained by heating palladium and boron in silica tubes, might have been Pd_2Si [2,3]. Recently, Lehrer [4] made a thermal and microscopic analysis in the range 0—6 wt % (0—39 atomic %) B. However, the examination did not yield any definite information on the composition of the intermediate phases.

An X-ray investigation of the Pd-B system has been started at this Institute. In sintered alloys three intermediate phases have been identified. The structures of two of them, Pd_5B_2 and Pd_3B, are described in this paper. Although the structure of the third phase (containing more boron than Pd_5B_2) has not yet been determined, it has been found that it is certainly not identical with the phase reported by Buddery and Welch.

EXPERIMENTAL

The samples were prepared by heating mixtures of palladium powder (claimed purity ca. 99.8 % from Heraeus, Hanau, Germany) and boron powder (claimed purity 99.0—99.7 %, kindly donated by Borax Consolidated, London) in evacuated, sealed silica tubes at temperatures between 800° and 1 100°C. The alloys were prevented from coming into

contact with the walls of the silica tube by placing them in small crucibles of pure aluminium oxide. No appreciable reaction between Al_2O_3 and the palladium borides was detected. However, the compositions of the alloys did not correspond to the nominal compositions, since varying amounts of boron were unavoidably lost during the reactions.

Chemical analyses were made at the Department of Analytical Chemistry of this Institute. For analyses two alloys were chosen in which only the powder diffraction lines of Pd_5B_2 and Pd_3B respectively could be detected.

Results of the chemical analyses.

Phase detected in powder photograph.	Chemical analysis (weight per cent) Pd	B	Formula according to the analysis
Pd_5B_2	93.97	5.84	$Pd_{3.28}B_2$
Pd_3B	96.05	3.44	$Pd_{2.85}B$

The analyses show that no other elements than palladium and boron were present. The large boron contents of the Pd_5B_2-alloy are probably due to unreacted boron.

X-Ray powder photographs were taken with Guinier-type focussing cameras using Cu$K\alpha$ radiation ($\lambda_{CuK\alpha} = 1.5418$ Å). Each powder film used for lattice parameter measurements was calibrated with either silicon ($a = 5.4306$ Å) or calcium fluoride ($a = 5.4630$ Å) as an internal standard.

For the structure determinations, Weissenberg photographs were taken of small single-crystal fragments selected from the crushed alloys with niobium-filtered MoK radiation. The multiple-film technique was used with thin iron foils between successive films, and the intensities were estimated visually by comparison with a standard intensity scale. Fourier series and structure factor calculations were made on the electronic digital computer BESK with programmes (available at BESK) devised by Edstrand and Åsbrink *et al.*[5] In the structure factor calculations the atomic scattering factors were approximated to the following expression:

$$f_i = A_i \exp\left(-\frac{a_i}{\lambda^2}\sin^2\Theta\right) + B_i \exp\left(-\frac{b_i}{\lambda^2}\sin^2\Theta\right) + C_i \exp\left(-\frac{c_i}{\lambda^2}\sin^2\Theta\right) + D_i$$

Appel [6] has calculated the following constants on the basis of the scattering factor tables by Tomas and Umeda [7] (palladium) and Ibers [8] (boron).

	A	B	C	a	b	c
Palladium	15.865	17.354	12.288	0.233	2.565	19.828
Boron	1.644	0.406	2.878	0.6069	4.5832	33.019

The real part of the dispersion correction, (D_i in the above expression), for palladium was taken from the table of Dauben and Templeton [9].

RESULTS

Pd_5B_2 was found to be monoclinic with the unit cell dimensions $a = 12.786$ Å, $b = 4.955$ Å, $c = 5.472$ Å, $\beta = 97°2'$, $U = 344.1$ Å^3. Pd_3B was found to have an orthorhombic unit cell with $a = 5.463$ Å, $b = 7.567$ Å, $c = 4.852$ Å, $U = 200.6$ Å^3.

Neither of these phases displays appreciable variations of lattice parameter, this indicates that both have narrow homogeneity ranges. It should be pointed out that the composition has not been accurately established for either phase, and it is accordingly possible that they show departures from stoichiometry.

For Pd_5B_2 the following conditions for possible reflexions were found: (hkl) only for $h + k = 2n$ and ($h0l$) only for $l = 2n$. This gives Cc or $C2/c$ as possible space-groups. The Patterson section $P(x0z)$ was calculated from the three-dimensional intensity data (700 reflexions). This section contained several large maxima and gave strong indications that the space-group is $C2/c$. Therefore, an attempt was made to interpret the Patterson section in accordance with this space-group.

Large maxima were situated at the following approximate positions: (0, 0, 0); ± (0.21, 0, 0.07); ± (0.19, 0, 0.35); ± (0.19,0, 0.76); ± (0.40, 0, 0.83); ± (0.39, 0, 0.11). The last maximum was unsymmetrically extended in the a direction. It was assumed that all these maxima corresponded mainly to Pd-Pd vectors. Since no maxima were found at ($\frac{1}{2}$, 0, 0), (0, 0, $\frac{1}{2}$) or ($\frac{1}{2}$, 0, $\frac{1}{2}$) the positions 4(a), 4(b), 4(c) and 4(d) were ruled out. Thus 4(e) and 8(f) are the only possible positions. An evaluation of the three-dimensional Patterson function along $P(0, y, \frac{1}{2})$ showed a broad maximum at y 0.16, indicating that the y parameter in the positions 4(e) or 8(f) should be about ± 0.08 or 0.50 ± 0.08. From packing considerations a structure model with the following approximate palladium positions was proposed:

8 Pd_I	in 8(f):	x_I	= 0.10	y_I	= 0.09	z_I	= 0.42
8 Pd_{II}	in 8(f):	x_{II}	= 0.21	y_{II}	= 0.58	z_{II}	= 0.32
4 Pd_{III}	in 4(e):	x_{III}	= 0	y_{III}	= 0.59	z_{III}	= 0.25

With this model all the peaks in the Patterson section $P(x0z)$ could be explained. As atoms belonging to different positions had approximately the same y parameters, vectors between them gave maxima in $P(x0z)$.

The signs of the $F(h0l)$ and the $F(hk0)$ values were computed from the model, and the electron density projections $\varrho(xz)$ and $\varrho(xy)$ were calculated using the intensity data from the zero layer lines around the b and c axes. The coordinates of the palladium atoms were refined from successive difference syntheses. An empirical temperature factor was applied with $B = 0.40$ Å^2 for the $F(h0l)$-values and with $B = 0.42$ Å^2 for the $F(hk0)$-values. In the $(F_o - F_c)$-synthesis, in which only the contribution from the palladium atoms was included for the F_c terms, boron maxima corresponding to one 8(f) position became visible. However, the maxima were too diffuse for an accurate determination of the coordinates, so the boron atoms were placed in the centres of the triangular prisms of palladium atoms. These parameter values were wholly compatible with the experimental intensity data. The final R values obtained were 0.077 for 92 non-equivalent observed $h0l$ reflexions and 0.053 for 52 non-equivalent observed $hk0$ reflexions *. In the final stages of refinement the F_o values of the three strongest $hk0$ reflexions, which were obviously weakened because of extinction, were replaced by the corresponding F_c values.

The final atomic parameters of Pd_5B_2 are:

* A list of calculated and observed structure factors can be obtained from this Institute on request.

Table 1. Interatomic distances in Pd_5B_2 (in Å).

			Average
Pd_I	— 4 Pd_I : 2.85, 2.89 (2), 2.90		
	— 5 Pd_{II} : 2.81, 2.90, 2.90, 2.96, 3.08		2.90
	— 3 Pd_{III}: 2.77, 2.83, 2.97		
	— 4 B : 2.18, 2.18, 2.80, 3.06		
Pd_{II}	— 5 Pd_I : 2.81, 2.90, 2.90, 2.96, 3.08		
	— 5 Pd_{II} : 2.77 (2), 2.77, 2.83 (2)		2.85
	— 1 Pd_{III}: 2.70		
	— 3 B : 2.18, 2.19, 2.60		
Pd_{III}	— 6 Pd_I : 2.77 (2), 2.83 (2), 2.97 (2)		
	— 2 Pd_{II} : 2.70 (2)		2.82
	— 2 Pd_{III}: 2.83 (2)		
	— 4 B : 2.18 (2), 2.19 (2)		
B	— 4 Pd_I : 2.18, 2.18, 2.80, 3.06		
	— 3 Pd_{II} : 2.18, 2.19, 2.60		2.18
	— 2 Pd_{III}: 2.18, 2.19		(six shortest)

(Space-group $C2/c$—(C_{2h}^6); $Z = 4$.)

		x	y	z
8 Pd_I	in 8(f):	0.0958 ± 0.0002	0.0952 ± 0.0003	0.4213 ± 0.0003
8 Pd_{II}	in 8(f):	0.2127 ± 0.0002	0.5726 ± 0.0003	0.3138 ± 0.0003
4 Pd_{III}	in 4(e):	—	0.5727 ± 0.0003	—
8 B	in 8(f):	0.106	0.311	0.077

The standard deviations were calculated from Cruickshank's [10] formula. Interatomic distances are listed in Table 1.

Pd_5B_2 appears to be isomorphous with Mn_5C_2 ($a = 11.66$ Å, $b = 4.573$ Å, $c = 5.086$ Å, $\beta = 97.75°$), reported by Kuo and Persson [11], and with a double carbide of iron and manganese found by Öhman [12] in ferromanganese alloys. In Table 2 the powder data for Mn_5C_2 with observed intensities, reported by Kuo and Persson, are shown together with intensities, calculated assuming the atomic parameters in Mn_5C_2 to be the same as those in Pd_5B_2. Owing to the good agreement it seems quite certain that the two phases are isomorphous.

The powder diffraction lines of Pd_3B, which could be indexed with an orthorhombic unit cell, showed close resemblance to the powder pattern of Pd_3Si [13], which is isostructural with cementite (Fe_3C). Therefore the signs of the $F(h0l)$ and the $F(hk0)$ values were computed from the cementite structure, and the intensity data from the zero layer lines around the b and c axes were used for the refinement of the palladium coordinates with successive difference syntheses. As in the structure determination described above the boron maxima in the difference synthesis were too diffuse to allow any accurate determination of their coordinates. The boron atoms were placed in the centres of the palladium prisms. The final R values obtained were 0.069 for 67 observed $h0l$ reflexions and 0.058 for 54 observed $hk0$ reflexions *; an empirical temperature

* A list of calculated and observed structure factors can be obtained from this Institute on request.

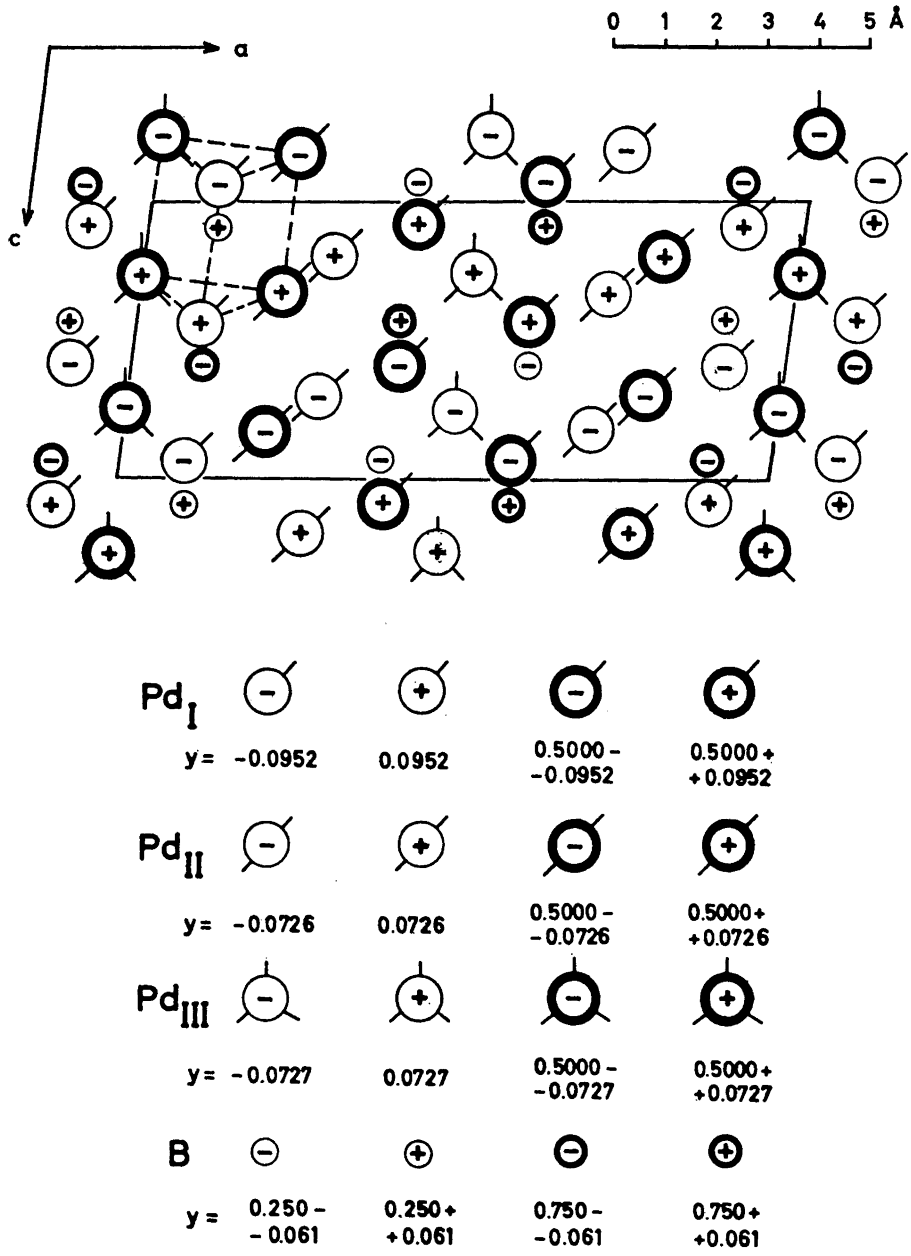

Fig. 1. The structure of Pd_5B_2 projected on the *ac*-plane.

Table 2. Powder data for Mn_5C_2 (CrKa radiation)

hkl	d_{obs} (Å)*	$\sin^2\Theta_{calc}$	I_{obs}*	I_{calc}	$pF^2_{calc} \times 10^{-4}$
200		0.0393		<0.01	0.002
110		0.0726		0.01	0.01
11$\bar{1}$	3.325	0.1182	vw	<0.01	0.001
111		0.1303		0.02	0.04
310	2.938	0.1512	vw	<0.01	0.01
400	2.881	0.1573	vw	0.12	0.23
31$\bar{1}$	2.659	0.1846	m	0.80	1.86
002	2.514	0.2067	m	0.56	1.39
311	2.431	0.2211	m	0.98	2.59
20$\bar{2}$	2.427	0.2217		0.67	1.80
020	2.282	0.2510	st-	2.04	5.67
11$\bar{2}$	2.212	0.2671	st	3.60	10.59
202	2.198	0.2703	st-	2.36	6.94
220		0.2903		0.05	0.14
112	2.117	0.2914	st-	1.37	4.14
021	2.078	0.3026	vst	5.71	17.31
510	2.058	0.3085	st	9.91	30.98
40$\bar{2}$	2.035	0.3153	st-	2.11	6.39
31$\bar{2}$	2.016	0.3214	st	3.65	11.40
51$\bar{1}$	1.990	0.3297	st	1.92	5.81
22$\bar{1}$**		0.3298		1.85	5.60
600	1.972	0.3538	st	0.50	1.46
221**		0.3541		2.82	8.29
511	1.829	0.3905	st-	2.15	5.80
312	1.820	0.3943	st-	3.22	8.69
420		0.4082		0.59	1.52
402	1.779	0.4125	st-	2.66	6.82
42$\bar{1}$	1.732	0.4356	st	2.00	4.76
51$\bar{2}$	1.695	0.4543	st-	1.57	3.57
022	1.690	0.4576	vw	0.93	2.07
22$\bar{2}$	1.663	0.4726	w	0.52	1.10
421		0.4842		0.11	0.23
60$\bar{2}$	1.636	0.4876	m	2.61	5.22

* As reported by Kuo and Persson.

** The 22$\bar{1}$ and 221 reflexions, which have large I_{calc} values, are not reported by Kuo and Persson, but probably they have been overlooked because of the overlap with the 51$\bar{1}$ and 600 reflexions, respectively.

factor with $B = 0.53$ Å^2 was applied in both cases. The final atomic parameters of Pd_3B are as follows:

(Space-group $Pnma$ — (D^{16}_{2h}); $Z = 4$.)

		x	y	z
8 Pd_I	in 8(d):	0.1798 ± 0.0003	0.0700 ± 0.0002	0.3276 ± 0.0003
4 Pd_{II}	in 4(c):	0.0372 ± 0.0005	—	0.8446 ± 0.0005
4 B	in 4(c):	0.884	—	0.433

Interatomic distances are listed in Table 3.

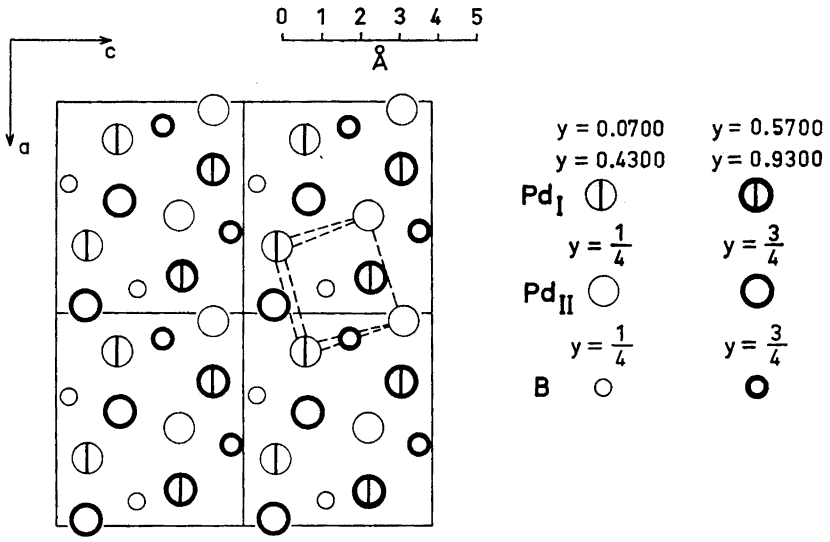

Fig. 2. The structure of Pd_3B projected on the *ac*-plane.

DESCRIPTION OF THE STRUCTURES AND DISCUSSION

Projections of the Pd_5B_2 and the Pd_3B structures are shown in Figs. 1 and 2, respectively.

In both Pd_5B_2 and Pd_3B the palladium atoms are densely packed, and the palladium — palladium contacts are on the average only about 0.10 Å longer than in pure palladium, where they are 2.75 Å.

The Pd_5B_2 structure can be described in terms of corrugated layers of palladium atoms parallel with {010}. The layers are composed of interconnected squares and triangles with metal atoms at the corners (Fig. 3). Similar layers can be found in other borides, as for example in the Me_2B-borides with the $CuAl_2$ structure [14].

The environments of the boron atoms in Pd_5B_2 and Pd_3B are shown in Figs. 4 and 5. The boron atoms are situated in triangular prismatic 'holes' in

Table 3. Interatomic distances in Pd_3B (in Å).

		Average
Pd_I	— 6 Pd_I : 2.72, 2.76 (2), 2.79, 2.83 (2)	2.82
	— 5 Pd_{II} : 2.82, 2.82, 2.86, 2.87, 2.96	
	— 3 B : 2.17, 2.17, 2.71	
Pd_{II}	—10 Pd_I : 2.82 (2), 2.82 (2), 2.86 (2), 2.87 (2), 2.96 (2)	2.87
	— 2 Pd_{II} : 2.88 (2)	
	— 3 B : 2.17, 2.18, 2.97	
B	— 6 Pd_I : 2.17 (2), 2.17 (2), 2.71 (2)	2.17 (six shortest)
	— 3 Pd_{II} : 2.17, 2.18, 2.97	

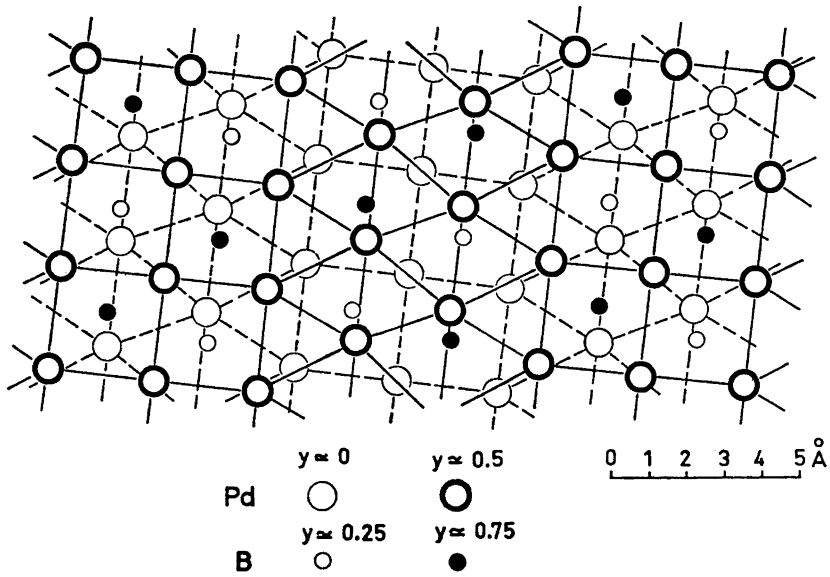

Fig. 3. A schematic picture of the Pd_5B_2 structure as seen along the *b*-axis.

the metal atom lattice, with six metal atoms at the corners of the prism, and three metal atoms, outside each four-sided side of the prism, forming a triangle around the boron atoms. There are no boron-boron contacts in Pd_5B_2 and Pd_3B. The type of non-metal atom coordination found in these borides is shared with many other transition metal borides as well as with several transition metal silicides, carbides and phosphides. The average of the shortest

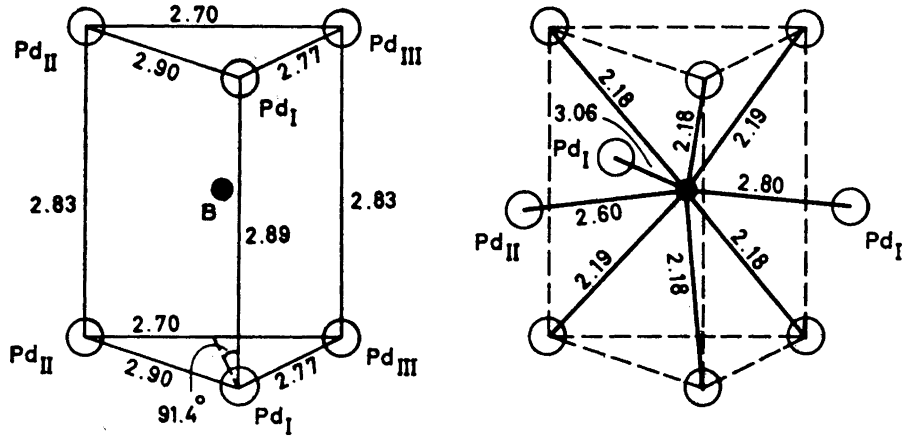

Fig. 4. The environment of the boron atoms in Pd_5B_2.

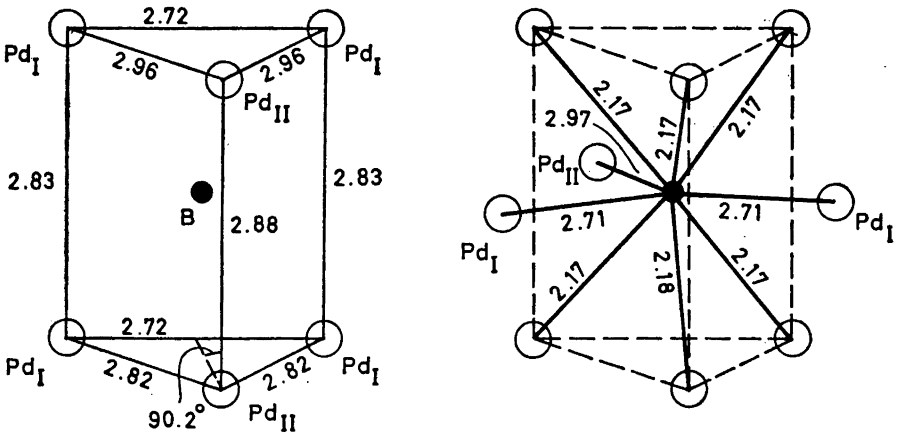

Fig. 5. The environment of the boron atoms in Pd_3B.

palladium-boron distances is 2.18 Å in Pd_5B_2 and 2.17 Å in Pd_3B. If r_{Pd} = 1.38 Å, r_B will be about 0.80 Å. This boron radius is rather small but is in accordance with the Me-B distances found in some other transition metal borides with the same boron environment, *e.g.* Ru_7B_3 (B — 6 Ru 2.16 Å) [15].

Pd_5B_2 and Pd_3B are two new examples of borides which are isostructural with carbides. It has previously been shown that Ni_3B and Co_3B [16], as well as Pd_3B, crystallize with the cementite (Fe_3C) structure and that Ru_7B_3 [15], Rh_7B_3 [17] and Re_7B_3 [17] are structurally very closely related to Cr_7C_3 and Mn_7C_3.

Acknowledgements. I wish to thank Professor G. Hägg for his kind interest and for all facilities put at my disposal.

I also want to thank Drs. B. Aronsson and S. Rundqvist for introducing me to this interesting field of science.

Thanks are also due to Mr. J. Åselius for many stimulating discussions.

Financial support is gratefully acknowledged from the *Air Force Office of Scientific Research and Development Command, United States Air Force*, through its European Office under Contract No. AF 61(052)—40 and from the *Swedish Technical Science Research Council*. Facilities for use of the electronic digital computer BESK were given by the *Swedish Board for Computing Machinery*.

REFERENCES

1. Buddery, J. H. and Welch, A. J. E. *Nature* **167** (1951) 362.
2. Rundqvist, S. and Jellinek, F. *Acta Chem. Scand.* **13** (1959) 425.
3. Anderko, K. and Schubert, K. *Z. Metallk.* **44** (1953) 307.
4. Lehrer, W. M. *Trans. AIME* **215** (1959) 168.
5. Åsbrink, S., Blomqvist, G. and Westman, S. *Arkiv Kemi* **14** (1959) 545.
6. Appel, K. *Technical Note from the Quantum Chemistry Group, University of Uppsala.*
7. Tomas, L. H. and Umeda, K. *J. Chem. Phys.* **26** (1957) 293.
8. Ibers, J. A. *Acta Cryst.* **10** (1957) 86.
9. Dauben, C. H. and Templeton, D. H. *Ibid.* **8** (1955) 841.
10. Cruickshank, D. W. J. *Ibid.* **2** (1949) 65.

11. Kuo, K. and Persson, L. E. *J. Iron Steel Inst. London* **178** (1954) 39.
12. Öhman, E. *Jernkontorets Ann.* **128** (1944) 13.
13. Aronsson, B. and Nylund, A. *Acta Chem, Scand.* **14** (1960) 1011.
14. Black, P. J. *Acta Met.* **4** (1956) 172.
15. Aronsson, B. *Acta Chem. Scand.* **13** (1959) 109.
16. Rundqvist, S. *Ibid.* **12** (1958) 658.
17. Aronsson, B., Stenberg, E. and Åselius, J. *Acta Chem. Scand.* **14** (1960) 733.

Received December 1, 1960.

ACTA CHEMICA SCANDINAVICA 15 (1961) 871–878

The Hydrolysis of 1,3-Dioxolan and Its Alkyl-Substituted Derivatives. Part I. The Structural Factors Influencing the Rates of Hydrolysis of a Series of Methyl-Substituted Dioxolans

PENTTI SALOMAA and ALPO KANKAANPERÄ

Department of Chemistry, University of Turku, Turku, Finland

The acid-catalysed hydrolysis reactions of 1,3-dioxolan and its 2-methyl, 4-methyl, 2,2-dimethyl, 2,4-dimethyl (*cis* and *trans* forms), 2,2,4-trimethyl, 4,4,5,5-tetramethyl and 2,4,4,5,5-pentamethyl derivatives have been studied kinetically at different temperatures using dilatometric and titrimetric methods. The results are discussed in the light of the mechanism of acetal hydrolysis and it is shown that the rates of hydrolysis of the compounds are mainly influenced by structural factors of two types, polar factors that are similar to those observed in acyclic acetals, and steric strain due to the methyl substituents that enters the picture when the transition state is approached.

By considering the possible influence of the above factors on the rates of hydrolysis of the two isomeric 2,4-dimethyl-1,3-dioxolans, it is concluded that the low-boiling isomer, which hydrolyses about four times as fast as the high-boiling isomer, is the *cis* form. This conclusion is in agreement with that based on a comparison of the properties of the isomers with those of the known 1,3-dimethyl*cyclo*pentane isomers.

1,3-Dioxolan and its derivatives are acetals which undergo hydrolysis in acid media.

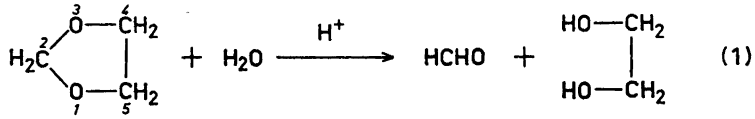

(1)

The hydrolysis reactions of these compounds have been studied kinetically to only a limited extent. Leutner [1,2] measured the rates of hydrolysis of dioxolan and several of its methyl derivatives, but only at one temperature; one of the compounds he studied was 2,4-dimethyldioxolan, but he did not take into

consideration that *cis* and *trans* forms of this compound exist. Laurent *et al.*[3] recently measured the rates of hydrolysis of unsubstituted 1,3-dioxolan at several temperatures. More extensive studies of the rates of hydrolysis of dioxolan derivatives containing aryl substituents in position 2 have been carried out by Ceder [4].

The purpose of the present investigation was to obtain a more detailed picture of the influence of structural factors, in particular the stereochemical configurations of the molecules, on the kinetics of hydrolysis of alkyl-substituted 1,3-dioxolans. A further aim was to find out whether kinetic data can be used to decide the configurations of geometric isomers that cannot readily be determined by other methods.

EXPERIMENTAL

Chemicals. 1,3-Dioxolan was synthesised from ethylene glycol and paraformaldehyde by the method of Delepine [5] in which concentrated sulphuric acid is employed as the catalyst. The layer containing the acetal was dried with potassium carbonate before it was distilled by fractionation to isolate the desired dioxolan from other higher-boiling formals present. The dioxolan was then treated with sodium bisulphite to remove any formaldehyde present and distilled once again from metallic sodium. The final product boiled at 74.2–74.7°C/756 torr and had the following physical properties: $d_4^{20} = 1.0624$, $n_D^{20} = 1.3992$, $[R]_D = 16.87$ (*calc.* 16.97).

2-Methyl-1,3-dioxolan was prepared by the same method from ethylene glycol and paraldehyde. B.p. 81.3–81.8 °C/767 torr, $d_4^{20} = 0.9814$, $n_D^{20} = 1.3972$, $[R]_D = 21.63$ (*calc.* 21.59). The compound has been synthesised by the same method by Hibbert and Timm [6].

4-Methyl-1,3-dioxolan was prepared from propylene glycol and paraformaldehyde as described by Clarke [7]. B.p. 83.7–84.2°C/756 torr, $d_4^{20} = 0.9906$, $n_D^{20} = 1.3989$, $[R]_D = 21.51$ (*calc.* 21.59).

2,2-Dimethyl-1,3-dioxolan was prepared according to Leutner [1] from ethylene glycol and acetone. B.p. 91.1–91.5°C/762 torr, $d_4^{20} = 0.9443$, $n_D^{20} = 1.3980$, $[R]_D = 26.10$ (*calc.* 26.22).

The *cis* and *trans* forms of 2,4-dimethyl-1,3-dioxolan were prepared by heating an acidified mixture of acetaldehyde di-*n*-amyl acetal and propylene glycol and distilling the two isomers from the reaction mixture. The method was the same as that employed by Lucas and Guthrie [8] except that the mixture of isomers obtained was heated under reflux in the presence of *p*-toluenesulphonic acid before the two components were separated by fractionation under alkaline conditions (a Todd precise fractionation assembly was employed). This was done because the method of preparing the two isomers by distilling an acidified mixture of the di-*n*-amyl acetal and propylene glycol undoubtedly favours the formation of the low-boiling isomer. The following physical constants were obtained for the two isomers:

Isomer I, b.p. 90.3–90.5°C/757 torr, $d_4^{20} = 0.9280$, $n_D^{20} = 1.3940$, $[R]_D = 26.33$ (*calc.* 26.22).

Isomer II, b.p. 93.2–93.3°C/759 torr, $d_4^{20} = 0.9322$, $n_D^{20} = 1.3956$, $[R]_D = 26.31$ (*calc.* 26.22).

2,2,4-Trimethyl-1,3-dioxolan was prepared by the same method as 2,2-dimethyl-1,3-dioxolan from acetone and propylene glycol. B.p. 99.6–100.0°C/761 torr, $d_4^{20} = 0.9011$, $n_D^{20} = 1.3946$, $[R]_D = 30.88$ (*calc.* 30.84). This compound has been previously described by Böeseken and Hermans [9].

4,4,5,5-Tetramethyl-1,3-dioxolan was prepared from pinacol and paraformaldehyde as described by Leutner [2]. B.p. 123.8–124.2°C/755 torr, $d_4^{20} = 0.9146$, $n_D^{20} = 1.4120$, $[R]_D = 35.42$ (*calc.* 35.47).

2,4,4,5,5-Pentamethyl-1,3-dioxolan was prepared by the same method from pinacol and paraldehyde. B.p. 133.2–134.0°C/760 torr, $d_4^{20} = 0.8957$, $n_D^{20} = 1.4110$, $[R]_D = 39.98$ (*calc.* 40.09).

Table 1. Dilatometrically determined mean rate coefficients (and their standard deviations) for various derivatives of 1,3-dioxolan at different temperatures.

	10^3k l mole^{-1} s^{-1}		
	10°C	20°C	30°C
2-Methyl-1,3-dioxolan	1.87 ± 0.012	7.13 ± 0.04	25.4 ± 0.1
2,2-Dimethyl-1,3-dioxolan	21.1 ± 0.05	75.5 ± 0.4	264 ± 3
2,4-Dimethyl-1,3-dioxolan (the low-boiling form)	3.02 ± 0.01	11.1 ± 0.1	34.0 ± 0.1
2,4-Dimethyl-1,3-dioxolan (the high-boiling form)	0.793 ± 0.010	2.68 ± 0.02	9.26 ± 0.02
2,2,4-Trimethyl-1,3-dioxolan	22.3 [a] ± 0.3	86.4 ± 0.5	255 [b] ± 1
2,4,4,5,5-Pentamethyl-1,3-dioxolan	0.295 ± 0.003	1.08 ± 0.009	3.36 [b] ± 0.02

[a] temperature 10.06°C [b] temperature 30.13 °C

Kinetic measurements. The rates of the reactions were followed by two procedures. A dilatometric method was employed when following the rates of dioxolan derivatives with one or two methyl groups at position 2 (*i.e.* acetals derived from acetaldehyde and ketals derived from acetone) and a titrimetric method based on the analysis of formaldehyde when following the reactions of dioxolan and its derivatives that did not have substituents at position 2 (*i.e.* acetals derived from formaldehyde).

A) Dilatometric method. The thermostats employed were heated by electricity and cooled with water and equipped with sensitive mercury-toluene regulators that maintained the temperature constant within ± 0.002°C during the experiments. The dilatometers, about 15 ml in capacity, had two capillary tubes of equal diameter (inside diameter about 0.2 mm) and were of the type *C* of Benford and Ingold [10]. After the reaction mixture had been introduced into the dilatometer, one of the capillary tubes was closed with a mercury lock because it was found that the liquid in the two capillary arms did not remain exactly at the same level during the experiments. The reaction mixture was prepared by mixing equal volumes of an aqueous hydrochloric acid solution and an aqueous solution of the dioxolan under study. The mixture was then immediately transferred to the dilatometer by suction. The first reading was taken when temperature gradients had disappeared, about 10 min after the solutions had been mixed. About ten readings were taken during the course of the reaction, generally from 15 to 80 % change, and several readings of the final level. The rate coefficients were computed from the first-order rate equation, which the data for the reactions satisfied fairly well. In some cases the method of Guggenheim [11] for the evaluation of rate coefficients was also applied, in which cases the number of readings taken during the course of the reaction was much larger. Both methods of calculation yielded identical values for the rate coefficients of the compounds examined.

The distilled water employed in preparing the solutions for the dilatometric rate measurements was boiled with potassium permanganate and sulphuric acid to remove

Table 2. The influence of the initial acetal concentration on the dilatometrically measured rate of hydrolysis of 2-methyl-1,3-dioxolan.

°C	20.00	20.00	19.88	19.88	20.00
Initial concn. mole/l	0.069	0.136	0.136	0.265	0.507
10^3k l mole^{-1} s^{-1}	6.83	7.13	6.93	7.25	7.51

Table 3. Mean rate coefficients (and their standard deviations) derived from data obtained by the titrimetric method for the hydrolysis of 1,3-dioxolan and its 4- and 5-substituted methyl derivatives.

	°C	10^4k l mole^{-1} s^{-1}
1,3-Dioxolan	51.34	0.850 ± 0.005
—»—	66.84	5.54 ± 0.04
—»—	82.80	27.9 ± 0.3
4-Methyl-1,3-dioxolan	51.34	1.14 ± 0.008
—»—	66.79	7.26 ± 0.05
—»—	82.82	33.6 ± 0.3
4,4,5,5-Tetramethyl-1,3-dioxolan	67.44	1.49 ± 0.01
—»—	82.80	8.69 ± 0.05
—»—	98.21	37.8 ± 0.3

any organic impurities and distilled after being made alkaline. The hydrogen chloride concentrations of the reaction mixtures varied between 0.002 – 0.05 M depending on the rate of the reaction in question. The initial acetal concentrations were approximately 0.13 M except in the experiments that were carried out to determine the effect of the initial acetal concentration on the rate. Mean values obtained for the rate coefficients of the reactions that were followed dilatometrically at different temperatures are given together with their standard deviations in Table 1. Table 2 shows the results of the study of the effect of the initial acetal concentration on the rate of its hydrolysis. The rate coefficients are seen to have increased with the acetal concentration. As, however, the majority of the experiments was carried out employing relatively low initial acetal concentrations which in addition were approximately equal, this variation with concentration could not appreciably influence the conclusions drawn in a comparison of the rates of reaction of the different acetals.

B) Titrimetric method. This method was based on the titration of the aldehyde liberated in the reaction as in a study of the aliphatic acetals of formaldehyde [12]. In the experiments carried out at temperatures above 50°C, samples of the reaction mixture were sealed in small ampoules employing the same technique as in an earlier study of the hydrolysis of alkyl formates at high temperatures [13]. The mean rate coefficients computed from the titrimetric data are presented in Table 3. Table 4 shows data for three reactions obtained by both the dilatometric and titrimetric methods.

DISCUSSION

Values of the Arrhenius parameters computed by the method of least squares for the hydrolysis of the dioxolan derivatives and the values of the activation entropy at 25°C computed from these are given together with the rate coefficients at 25°C in Table 5. The dioxolan derivatives are grouped according to the parent aldehyde or ketone.

Table 4. Dilatometrically and titrimetrically measured rate coefficients for various derivatives of 1,3-dioxolan. 25°C.

	10^2k l mole^{-1} s^{-1} dilat.	titrim.
2-Methyl-1,3-dioxolan	1.36	1.41
2,4-Dimethyl-1,3-dioxolan (low-boil. form)	1.95	2.08
2,4-Dimethyl-1,3-dioxolan (high-boil. form)	0.507	0.497

Table 5. Values of the parameters of the Arrhenius equation, activation entropies at 25°C and rate coefficients at 25°C for the hydrolysis of 1,3-dioxolan and its methyl-substituted derivatives.

	E kcal/mole	log A	ΔS^* E.U.	$10^4 k$ l mole^{-1}s^{-1}
(*I*) 1,3-Dioxolan	25.48	13.10	− 0.57	0.0265
(*II*) 4-Methyl-1,3-dioxolan	24.68	12.69	− 2.43	0.0402
(*III*) 4,4,5,5-Tetramethyl-1,3-dioxolan	26.43	13.14	− 0.38	0.00592
(*IV*) 2-Methyl-1,3-dioxolan	22.25	14.44	+ 5.57	136
(*V*) 2,4-Dimethyl-1,3-dioxolan (*a*)	20.66	13.43	+ 0.96	195
(*VI*) 2,4-Dimethyl-1,3-dioxolan (*b*)	20.95	13.06	− 0.74	50.7
(*VII*) 2,4,4,5,5-Pentamethyl-1,3-dioxolan	20.63	12.40	− 3.77	18.9
(*VIII*) 2,2-Dimethyl-1,3-dioxolan	21.54	14.95	+ 7.88	1440
(*IX*) 2,2,4-Trimethyl-1,3-dioxolan	20.74	14.37	+ 5.24	1460

[a]) The low-boiling isomer [b]) The high-boiling isomer

If the rate coefficients at 25°C given in Table 5 for the dioxolans studied by Leutner [1,2] are compared with the rate coefficients reported by the latter author, it is found that the values for the compounds *IV* and *VIII* are in good agreement, but the values for the compounds *I* and *III* differ by 10—15 %. The rate coefficients for the compounds *V*, *VI* and *VII* show very poor agreement. An obvious reason for the dicrepancy in the case of the compounds *V* and *VI* is that Leutner considered these isomers to be a single compound; actually, his rate coefficients decreased some 80 % in value toward the end of the reaction, evidently owing to the different rates of hydrolysis of the two component isomers present.

The activation entropies given in Table 5 are nearly of the magnitude generally found for unimolecular *A-1* reactions [14]. It is thus highly probable that the dioxolans hydrolyse by essentially the same mechanism as acyclic acetals [15]. More reliably this is seen from the observed structural effects although in some respects the latter deviate from those found for the acyclic acetals (*vide infra*).

From the values of Table 5 it is seen that the introduction of a methyl substituent at the carbon 2 of the 1,3-dioxolan ring effects a great increase in the rate of hydrolysis, the rate coefficients of the 2-methyl-substituted dioxolans being from 1 200 to 5 000 times the rate coefficients of the dioxolans with no substituent on carbon 2. The higher rates of hydrolysis of the the 2-methyl dioxolans are primarily due to low activation energies. This parallels the increase in rate by a factor of about $10^{3.5}$ when a methyl substituent is introduced into an aliphatic formal to give the corresponding acetal of acetaldehyde [15]. A rate increase of the same order is observed when a second methyl substituent is added to the same carbon atom as shown by the rates of hydrolysis of the acyclic acetals of acetaldehyde and the ketals of acetone. However, as seen from Table 5, the introduction of a second methyl group into 2-methyl-substituted dioxolans at position 2 leads to an increase in the rate that is of the order of one power of ten. The rates of hydrolysis of 2,2-dimethyldioxolans

are thus exceptionally low; also the activation energies do not decrease in a uniform manner as in the case of the dioxolans derived from formaldehyde and acetaldehyde. Furthermore, it is seen from Table 5 that the introduction of one or more methyl groups at the carbons 4 and 5 in the dioxolan ring has an even more complex effect on the rate of hydrolysis, for in some cases the rate increases slightly, while in other cases, when there are several methyl substituents in the molecule, the rate decreases clearly. A possible explanation for these observations which is based on the stereochemistry of the reaction is presented below.

According to the widely accepted mechanism of acetal hydrolysis [15], the slow, rate-determining stage that follows the proton uptake in the hydrolysis of dioxolans may be written as follows:

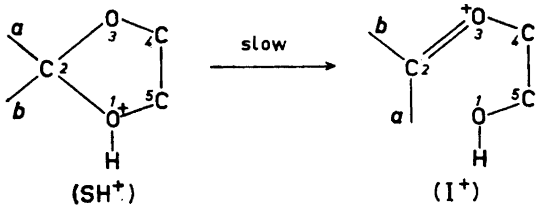

(2)

The reaction intermediate I^+ that is formed from the conjugate acid SH^+ of the substrate has a mesomeric structure resonating between the carbonium and oxonium ion structures. As a consequence the 2,3-bond in this intermediate has a partial double-bond character.

As to polar factors, electron-releasing substituents such as alkyl groups should greatly increase the rate when they are located at the reaction centre, the carbon atom 2. Alkyl groups on the carbon atoms 4 and 5 should also increase the rate, although to a much lesser extent. The polar influence of these groups should facilitate the reaction when they are on either side of the bond that is broken in reaction (2) as indicated by the observation that alkyl groups promote the hydrolysis of dialkyl formals both when they are substituents in the stem of the molecule and when they are a part of the leaving group [16]. There is, however, an essential difference between the structural factors that have an influence on the key stage of the hydrolysis in the case of acyclic acetals and the 1,3-dioxolan derivatives. Owing to the partial double-bond character of the 2,3-bond in the ion I^+, the nuclei that are joined by the 2,3-, 3,4-, *a*- and *b*-bonds tend to be in the same plane. From this it follows that in the attainment of the transition state of reaction (2) the bonds *a* and *b* must be bent to a certain extent toward the plane of the dioxolan ring. This cannot be achieved without a certain amount of steric strain whose magnitude depends upon the substituents attached to the ring.

This steric strain readily explains the anomalies observed in the reactions of the 2-methyl-substituted derivatives of 1,3-dioxolan. When a methyl group is introduced into dioxolan at position 2, the increase in the rate of hydrolysis is almost as great as the difference in the rates of an acyclic acetal of formaldehyde and the corresponding acetal of acetaldehyde. In the case of 2-methyldioxolan, it is obviously the bond joining the hydrogen atom to carbon

atom 2 that is bent toward the centre of the dioxolan ring in reaction (2) because this produces much less strain than the bending in this direction of the bond joining the methyl group to the carbon atom 2. The steric strain is thus of the same magnitude as in the reaction of unsubstituted dioxolan and a "normal" rate of hydrolysis is observed. In the case of 2,2-dimethyl-1,3-dioxolan, however, one of the bonds joining a methyl group and carbon atom 2 must be bent toward the dioxolan ring and owing to the size of the methyl group this leads to a much greater steric strain than in the case of a hydrogen atom. Consequently 2,2-dimethyl-1,3-dioxolan hydrolyses at a much lower rate than if only polar effects were decisive as in the case of the corresponding acyclic compounds.

The steric strain effect of methyl substitution at positions 4 and 5 in 1,3-dioxolan may be expected to be quite small compared to the effect of the substitution at position 2 owing to the greater distance from the reaction centre, but even this effect can be distinguished in the data of Table 5. For example, 4,4,5,5-tetramethyl-1,3-dioxolan hydrolyses more slowly than unsubstituted 1,3-dioxolan and 2,4,4,5,5,-pentamethyl-1,3-dioxolan hydrolyses at a lower rate than 2-methyl-1,3-dioxolan. Thus the steric strain effects of the methyl groups overweigh their polar rate-increasing effects that are based on their electron-releasing character. The steric effect of the methyl group does not become evident in the case of 4-methyl-1,3-dioxolan because the reaction may primarily take place by the less demanding of two alternative routes: that of the bonds *a* and *b* which is on the side opposite the 4-methyl group bends toward the ring and this bending does not produce any more strain than that produced in unsubstituted 1,3-dioxolan. As a result the rate is slightly higher than that of 1,3-dioxolan in accordance with the polar character of the methyl group.

The rates of hydrolysis of the geometric isomers of 2,4-dimethyl-1,3-dioxolan provide an interesting illustration of the structural effects just discussed. As the steric strain is more pronounced when substituents are located at carbon atom 2 than when they are in other positions, it is the carbon to hydrogen bond in the above isomers (and in general, in the dioxolans derived from acetaldehyde) that is bent toward the middle of the dioxolan ring in reaction (2). If, now, the 4-methyl group is on the same side of the ring as this bond (*i.e.* in the *trans* form of 2,4-dimethyl-1,3-dioxolan) the 4-methyl group should retard the reaction by its steric influence; in the opposite case (the *cis* form of 2,4-dimethyl-1,3-dioxolan), the steric conditions are similar to those prevailing in the absence of the 4-methyl substituent (*i.e.* in 2-methyl-1,3-dioxolan). As the polar effects may be expected to be similar in both cases, it follows that the *cis* form of 2,4-dimethyl-1,3-dioxolan should hydrolyse faster than the *trans* form. The values of the rate coefficients for the isomers in Table 5 thus lead to the same conclusion about the configurations of these isomers as Barker, Bourne, Pinkard, Stacey and Whiffen [17] arrived at when they compared the properties of these compounds with those of the isomeric dimethyl*cyclo*pentanes whose configurations had been established by another method. The assignment of the *cis* structure to the low-boiling isomer of 2,4-dimethyl-1,3-dioxolan is also in agreement with the results of a study of the *cis-trans* isomerization reactions of these compounds [18].

Acknowledgement. One of us (*A.K.*) wishes to record his indebtedness to the *Finnish State Council for Natural Sciences (Valtion Luonnontieteellinen Toimikunta)* for financial aid.

REFERENCES

1. Leutner, R. *Monatsh.* **60** (1932) 317.
2. Leutner, R. *Monatsh.* **66** (1935) 222.
3. Laurent, P. A., Garras da Silva Pinto, A. and Cardoso Pereira, J. L. *Bull. soc. chim. France* **1960** 926.
4. Ceder, O. *Arkiv. Kemi* **6** (1954) 523.
5. Delepine, M. *Compt. rend.* **131** (1900) 745.
6. Hibbert, H. and Timm, J. A. *J. Am. Chem. Soc.* **46** (1924) 1286.
7. Clarke, H. T. *J. Chem. Soc.* **1912** 1804.
8. Lucas, H. J. and Guthrie, M. S. *J. Am. Chem. Soc.* **72** (1950) 5490.
9. Boeseken, J. and Hermans, P. H. *Rec. trav. chim.* **42** (1923) 1104.
10. Benford, G. A. and Ingold, C. K. *J. Chem. Soc.* **1938** 931.
11. Guggenheim, E. A. *Phil. Mag. (7)*, **2** (1926) 538.
12. Salomaa, P. *Suomen Kemistilehti B* **33** (1960) 11.
13. Salomaa, P. *Acta Chem. Scand.* **14** (1960) 577.
14. Taft, Jr., R. W., Purlee, E. L., Riesz, P. and DeFazio, C. A. *J. Am. Chem. Soc.* **77** (1955) 1584.
15. Ingold, C. K. *Structure and Mechanism in Organic Chemistry*, G. Bell and Sons Ltd., London 1953, pp. 333–335.
16. Salomaa, P. *Ann. Acad. Sci. Fennicae*, **Ser. A II** (1961) No. 103.
17. Barker, S. A., Bourne, E. J., Pinkard, R. M., Stacey, M. and Whiffen, D. H. *J. Chem. Soc.* **1958** 3232.
18. Salomaa, P. *Ann. Univ. Turkuensis*, **Ser. A I** (1961) No. 46.

Received December 14, 1960.

ACTA CHEMICA SCANDINAVICA 15 (1961) 879–887

Bisbenzyltetrahydro*iso*quinoline Alkaloids

I. A General Method for Determining Partition Coefficients and Testing Homogeneity

ESKIL HULTIN*

Department of Pharmacology, University of California Medical Center, Los Angeles 24, California, U.S.A.

Partition coefficients can be computed from solute concentrations measured in a series of extracts obtained in such a way that one portion of a phase of two immiscible solvents is extracted with several portions of the other phase. The logarithms of the concentrations are plotted *versus* the numbers of the corresponding extractions. If the solute is homogeneous, and if the partition coefficient is independent of the concentration, the points lie about a straight line, the inclination of which equals the logarithm of the fraction q of the solute remaining in the extracted phase after an extraction. If the partition coefficient is defined as the ratio of the concentration in the less polar phase to that in the more polar phase, and if the volumes of the phases are V_l and V_m, respectively, then the partition coefficient equals $(V_m/V_l)\ (1-q)/q$ when the more polar phase is extracted with the less polar phase, and $(V_m/V_l)q/(1-q)$ when the less polar phase is extracted with the more polar phase. If the solute is a mixture of two components, the partition coefficient of one component can be computed by using the asymptote of the points from one experimental series in which the less polar phase is extracted, and the partition coefficient of the other can be similarly obtained from another experimental series in which the more polar phase is extracted. Both partition coefficients can also be computed from one series by using the differences between the concentrations observed and those computed for one component from the asymptote, for making another plotting, valid for the other component.

Although tertiary bisbenzyltetrahydro*iso*quinoline alkaloids have been investigated extensively, efficacious methods still have not been adopted for the separation of many naturally occurring mixtures of these alkaloids nor for the separation of such mixtures of their isomers as are obtained by partial methylation or demethylation. A study of these alkaloids was taken

* Present address: Institutionen för organisk kemi, Tekniska högskolan, Stockholm 70, Sweden.

up in this laboratory, and the importance of working out counter current separation methods for them soon became obvious. It may be pointed out here that the separation problem arising at the beginning of this investigation and dealt with in this paper only concerns separation of substances whose partition coefficients differ by a factor of about 3 or more. It was highly desirable that the separation procedure be suitable for amounts varying at least between 0.1 and 100 g, and that the separation could be done by hand with separatory funnels.

For planning a counter current separation of a mixture of two substances it is of some importance to know the partition coefficients for each of the substances, both for choosing the best volume ratio and for choosing the appropriate number of transfers.

A general equation for the relation between optimum volume ratio and partition coefficients was derived by Baker [1]. He found that a symmetrical counter current separation of two substances is most efficacious, if the ratio of the volume of the less polar phase of two immiscible solvents to the volume of the more polar phase equals the inverse value of the square root of the product of the partition coefficients of the two substances.

The number of transfers necessary to give a certain degree of separation depends [2,3] on the ratio of the two distribution coefficients.

When the partition ocefficients of the two components in a mixture are not known and the components are not available separately as pure substances, it is usually recommended [4–6] that the value obtained from a simple determination of the distribution of the mixture between the two solvent phases be used for the counter current distribution separation. This may work fairly well if the amounts of the two substances are about equal, but if one of the substances is in considerable excess, the value found for the partition coefficient of the mixture will be near the value valid for the substance in excess and differ considerably from the geometric mean of the values for the two substances. Hence, the separation will not be as efficient as would otherwise be possible. If an apparatus permitting a large number of transfers is available this may not be a serious problem in most cases. However, if the separation is carried out by hand with a few separatory funnels and with the convenient method [7] for finally obtaining two fractions called "diamond separation" and "completion of squares", a large amount of the substance in excess in the original mixture will still be found in the fraction containing most of the substance present only in small amounts, and hence a second determination of the partition coefficient of this mixture may give a value still too near that of the substance originally in excess.

Another fairly common difficulty in determining distribution coefficients in a conventional way is that the two solvent phases may contain other substances, *e.g.*, buffer salts, which may complicate the analysis of the two phases.

In the case of bisbenzyltetrahydro*iso*quinoline alkaloids the concentration can easily be determined spectrophotometrically. However, these alkaloids decompose readily, partly to substances with strong absorption. Most of these substances have partition coefficients which are considerably lower than those of the pure alkaloids. Hence, partition coefficients computed from a simple determination of the light absorption in both phases may be highly erroneous.

These difficulties can, however, in many cases be overcome by a simple procedure which will be described here, and by which it is possible to determine the partition coefficients of each of two substances in a mixture. This procedure is also useful in the determination of the distribution coefficient of a pure substance and of a substance with some impurities. It is also useful for checking the purity of a preparation and for determining whether or not a partition coefficient is independent of the concentration of the substance.

Stevenson [8] independently found the same general method carrying out another investigation in this laboratory.

THEORETICAL

In this procedure for determining partition coefficients appropriate volumes of the two phases are used for dissolving the preparation. These volumes do not need to be equal. One of these phases is extracted successively with portions of the other phase. The volumes of each portion must be the same. Either the phase which is extracted or the extracts are analyzed for their content of the preparation, and the values obtained are used for computing the partition coefficients, checking the purity, *etc.*

In this paper the two phases of the solvent system are referred to as the more polar phase and the less polar phase instead of the upper and the lower phase. This is advantageous for comparing partition coefficients, *e.g.*, between ether and buffer and between chloroform and buffer. Partition coefficients are consequently calculated as concentration in the less polar phase divided by concentration in the more polar phase.

The following symbols are used.

K partition coefficient (distribution constant)
V_l volume of the less polar phase
V_m volume of the more polar phase
c_{l1} concentration of preparation in the less polar phase after the first equilibration
c_{m1} concentration of preparation in the more polar phase after the first equilibration
c_{l2} concentration of preparation in the less polar phase after the second equilibration
c_{m2} concentration of preparation in the more polar phase after the second equilibration
q fraction of the solute remaining in the extracted phase after equilibration

With these symbols the distribution law [9,10] can be written

$$K = c_{l1}/c_{m1} = c_{l2}/c_{m2} \qquad (1)$$

Depending on the value of the partition coefficient (if considerably larger or smaller than 1) it may be advantageous either to extract one portion of the more polar phase with several portions of the less polar phase or *vice versa*. In many cases it is not too inconvenient to run both extraction series. Methods for calculation of distribution coefficients of pure substances and of a two-component mixture will be presented.

The more polar phase is extracted with several portions of the less polar phase

It is assumed in the following method that the concentration of the substance is measured in the more polar phase. However, there will be no difference in the final result if the substance is measured in the other phase because the concentration in one phase is proportional to the concentration in the other.

After the first equilibration the amount of solute in the more polar phase is $V_m c_{m1}$. If this phase is extracted with a second portion of the less polar phase, the amounts of solute present in the two phases are $V_m c_{m2}$ and $V_l c_{l2}$, respectively. Thus,

$$V_l c_{l2} + V_m c_{m2} = V_m c_{m1} \tag{2}$$

Because the concentration is not measured in the less polar phase, c_{l2} must be eliminated, which is done as follows. According to eqn (1), $c_{l2} = Kc_{m2}$, and eqn (2) can thus be written

$$V_l K c_{m2} + V_m c_{m2} = V_m c_{m1} \tag{3}$$

Hence,

$$c_{m2} = \frac{V_m}{V_l K + V_m} c_{m1} \tag{4}$$

and, generally,

$$c_{mn} = \left(\frac{V_m}{V_l K + V_m}\right)^n \cdot c_{m1} \tag{5}$$

This equation is equivalent to Craig and Craig's [11] eqn (8), but a corresponding equation was first published by Herz [12].

By writing this equation in logarithmic form

$$\log c_{mn} = n \cdot \log \frac{V_m}{V_l K + V_m} + \log c_{m1} \tag{6}$$

we arrive at the main improvement suggested in this paper for the calculation of partition coefficients *.

This equation implies that if the logarithms of the values for the solute concentration in successive extracts are plotted in a graph *versus* the numbers of the extractions, the points are expected to lie about a straight line, the inclination of which is $\log V_m/(V_l K + V_m)$, provided the substance is homogeneous and provided no reaction occurs which is not accounted for in the method of calculation (association or dissociation).

The partition coefficient is computed from the value of the inclination of the line which is measured. The fraction of substance remaining after equilibration is c_{m2}/c_{m1}, if we consider the amounts present in the more polar phase before and after the second extraction, and this quotient is in our denotation called q. Eqn (4) can then be written

* After this manuscript was prepared, a similar equation has been published by Rudstam [13].

$$\frac{V_m}{V_l K + V_m} = q \tag{7}$$

In the procedure of computing the value of the partition coefficient, q is the antilogarithm of the inclination of the line fitted as just described. By solving eqn (7) we get

$$K = \frac{V_m}{V_l} \frac{1 - q}{q} \tag{8}$$

It would, of course, be possible to compute K from two extractions, as eqn (4) can be written

$$K = \frac{V_m}{V_l} \frac{c_{m1} - c_{m2}}{c_{m2}} \tag{9}$$

but the use of more than two extractions makes it possible to check the solute for homogeneity. If the solute is homogeneous, and if there is no association or dissociation, the points fit a straight line; then several extractions make the assay of the partition coefficient more accurate.

If the points do not fit a straight line, and if this is caused by the presence in the substance of some impurity or by the presence in the substance of two components with different partition coefficients, one may fit an asymptote, from which it is possible to compute the partition coefficient of the component which is less readily extracted from the more polar phase.

The less polar phase is extracted with several portions of the more polar phase

It is assumed also in the following method that the concentration of the solute is measured in the more polar phase, but the result of the computation of the partition coefficient will be the same if the concentration is measured in the less polar phase, as the concentration in one phase is proportional to the concentration in the other.

After the first equilibration the amount of substance present in the less polar phase is $V_l c_{l1}$. The more polar phase is removed, and the less polar phase is extracted with a fresh portion of the more polar phase. After equilibration the amount of solute present in the less polar phase is $V_l c_{l2}$ and in the more polar phase $V_m c_{m2}$. Thus,

$$V_l c_{l2} + V_m c_{m2} = V_l c_{l1} \tag{10}$$

Because the concentration is measured in the more polar phase, c_{l1} and c_{l2} must be eliminated. Considering eqn (1), we can rewrite eqn (10) in the following form

$$V_l K c_{m2} + V_m c_{m2} = V_l K c_{m1} \tag{11}$$

Hence,

$$c_{m2} = \frac{V_l K}{V_l K + V_m} c_{m1} \tag{12}$$

and, generally,

$$c_{mn} = \left(\frac{V_l K}{V_l K + V_m}\right)^n c_{m1} \tag{13}$$

This equation is rewritten in logarithmic form

$$\log c_{mn} = n \cdot \log \frac{V_l K}{V_l K + V_m} + \log c_{m1} \tag{14}$$

This equation implies that if the logarithms of the concentrations of a homogeneous solute in a series of extracts are plotted *versus* the numbers of the extractions, the points lie about a straight line, the inclination of which is log $V_l K/(V_l K + V_m)$. Here $V_l K/(V_l K + V_m)$ can be identified as the fraction q of a substance remaining after an extraction in the phase which is extracted. Thus, q is the antilogarithm of the inclination of the line fitted as described, and we get

$$K = \frac{V_m}{V_l} \frac{q}{1 - q} \tag{15}$$

If the solute is impure or is a mixture of two components, the partition coefficients of which differ noticeably, an asymptote may be fitted to the points. The partition coefficient of the component which is less readily extracted from the less polar solvent phase can be computed from the inclination of this line.

Computation of two partition coefficients for a mixture of two components

There are obviously two ways for determining the two partition coefficients for a mixture consisting of two components. One way, already intimated, is to run two distribution series, one series in which the more polar phase is extracted with the less polar, and another series, in which the less polar phase is extracted with the more polar, and then to compute the partition coefficients from the two asymptotes plotted as described in the previous sections. Another way to determine the two partition coefficients is to compute them from one series of extractions in the following way.

The logarithms of the concentrations of the solute in the extracts are plotted *versus* the numbers of the corresponding extracts, and an asymptote is fitted as described. The logarithms of the concentrations of the component, for which the asymptote is valid, are calculated for the various extracts. The corresponding antilogarithms give the concentrations of this compound. The differences between the concentrations actually measured and the concentrations thus computed are the concentrations of the other substance in the series of extracts. The logarithms of these values are plotted *versus* the numbers of the extracts, and a straight line is fitted. The inclination of this line is read, and its antilogarithm q is used for computing the partition coefficient, using eqn (8) or (15), depending on whether the more polar or less polar solvent phase was extracted.

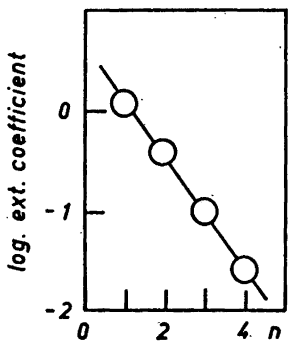

Fig. 1. A preparation of pure *d*-chondrocurine gives points, all of which lie closely about a straight line even over a wide concentration range. The logarithms of the extinction coefficients are plotted *versus* the numbers of the corresponding extracts.

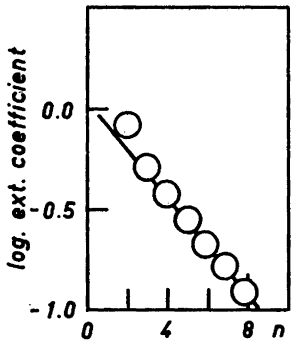

Fig. 2. A preparation of monodemethylated *l*-curine (not crystallized); the diethyl ether phase was extracted with buffer. The points indicate the presence of an impurity with considerably lower partition coefficient but do not indicate any heterogeneity of the monodemethylated *l*-curine.

EXPERIMENTAL

A few examples will be given to illustrate the suggested method. The examples have been chosen from various determinations of partition coefficients for some bisbenzyltetrahydro*iso*quinoline alkaloids: *d*-chondrocurine, and monomethyl and monodemethylated derivatives of *l*-curine. The results from more determinations will be reported in forthcoming publications [14,15].

Determination of the partition coefficient for d-*chondrocurine between diethyl ether and water at pH 11.6.* The water phase consisted of a buffer solution containing 2 g of potassium metabisulfite $K_2S_2O_5$ and 0.5 g of K_3PO_4 and somewhat more than 1 g of KOH in 100 ml of water. The amount of KOH was chosen so that the pH value of the buffer was 11.6. A high concentration of sodium ions was avoided because a glass electrode was used for measuring the pH values. The solution was equilibrated with diethyl ether. 25 ml of the ether phase and 10 ml of the water phase were added to a separatory funnel, and a few drops of a solution of *d*-chondrocurine in a mixture of equal parts of chloroform and methanol were added. The ether phase was successively extracted with 10 ml portions of the water phase, and the extinction coefficient at 289 mμ was read for each extract. The following values were obtained: 1.20, 0.365, 0.098, and 0.027. The measurements thus were extended over a wide range of concentrations. The logarithms of the values were plotted (Fig. 1) *versus* the numbers of the extractions, and a straight line was fitted to the points. The inclination of the line, log q, was read as -0.56; hence $q = 0.275$. The values of the volumes and of q were substituted in eqn (15).

$$K = \frac{10}{25} \cdot \frac{0.275}{0.725} = 0.15$$

Determination of the partition coefficient of one of the isomers of monodemethylated l-*curine for diethyl ether and water at pH 10.3.* The water phase consisted of 1 g of $K_2S_2O_5$, 3 g of $Na_2CO_3 \cdot H_2O$ and 1.5 g of K_3PO_4 in 100 ml of water, with pH adjusted to 10.3, and equilibriated with diethyl ether. The experiment was done both by extracting 25 ml of the ether phase with 10 ml portions of the water phase and by extracting 15 ml of the water phase with 25 ml portions of the ether phase. The following extinction values were obtained when the ether phase was extracted: 0.835, 0.496, 0.363, 0.273, 0.209, 0.161, and 0.120. A straight line was fitted, the inclination of which was -0.12 (Fig. 2). The corresponding value of the partition coefficient was 1.24, computed according to

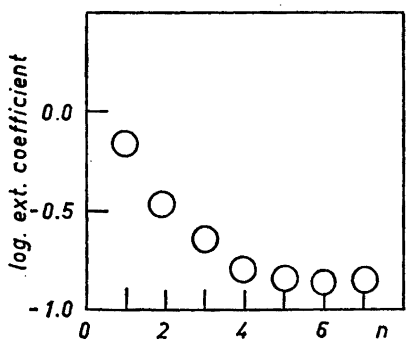

Fig. 3. A preparation of monodemethylated *l*-curine as in Fig. 2; the water phase was extracted with diethyl ether. The points indicate the presence in the water phase of an impurity with considerably lower partition coefficient.

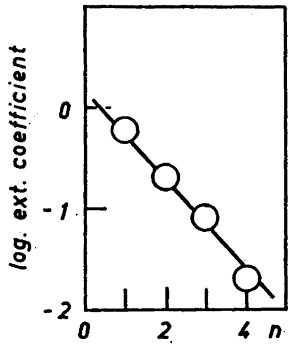

Fig. 4. Monodemethylated *l*-curine. The same experiment as in Fig. 3 but with the extinction coefficient of the impurity subtracted from the measured values.

eqn (15). When the water phase was extracted, the values obtained were the following: 0.690, 0.333, 0.218, 0.156, 0.145, 0.138, and 0.140. The logarithms of these values are plotted in Fig. 3. It is obvious that one light absorbing impurity with very low partition coefficient is present in the water phase. Assuming that the extinction caused by this impurity is 0.140, and subtracting this value from the measured values, we get an estimate of the extinction caused by the monodemethylated *l*-curine. The logarithms of these values were plotted *versus* the numbers of the corresponding extractions (Fig. 4), and a straight line was fitted. Its inclination, −0.45, corresponded to the value 1.09 of the partition coefficient.

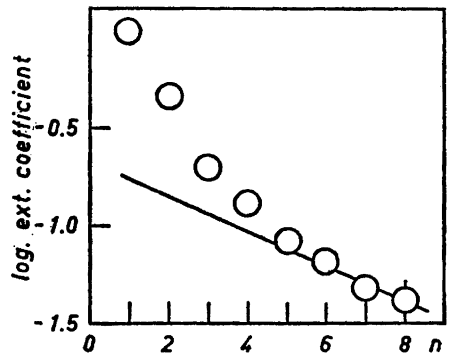

Fig. 5. A mixture of the *d*-chondrocurine monomethyl ethers. The distribution coefficient for one of them is computed from the asymptote.

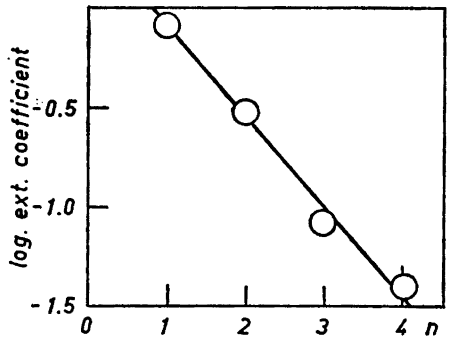

Fig. 6. The same experiment as in Fig. 5. The partition coefficient of the other *d*-chondrocurine monomethyl ether is computed from the difference between the observed values for the extinction coefficient and the values computed from the asymptote The logarithms of the differences are plotted *versus* the numbers of the corresponding extracts.

Preliminary determination of the partition coefficients of the two d-*chondrocurine monomethyl ethers in a solvent system containing benzene, heptane, methanol, and water (2, 4, 3, and 3 volumes, respectively).* The water phase contained 0.5 % $K_2S_2O_5$ and 0.5 % Na_2CO_3, and the pH-value of this solution was adjusted to 8.0. A preparation of partly methylated *d*-chondrocurine had been separated [14] into three fractions, one of which consisted of the monomethyl ethers of *d*-chondrocurine. A few milligrams were dissolved in a few drops of a mixture of chloroform and methanol (1:1) and added to a separatory funnel containing 10 ml of the lower phase and 15 ml of the upper phase of the solvent system. The lower phase was changed. The extinction readings at 280 mμ for the extracts were 0.995, 0.440, 0.198, 0.131, 0.085, 0.065, 0.047, and 0.041. The logarithms of the values are plotted in Fig. 5, and an asymptote fitted to the tail values. The partition coefficient value corresponding to this line is 2.7. The antilogarithms of the ordinata values of this line at abscissa values corresponding to the numbers of the successive extractions give the calculated concentrations of the substance with the partition coefficient 2.7 in the various extracts. These values were subtracted from the original readings, and the logarithms of the remainders for the first four extracts were plotted *versus* the number of the corresponding extractions (Fig. 6). A straight line was fitted to the points, and its inclination read. The corresponding partition coefficient was 0.35. This value is somewhat too low; the value 0.5 was later obtained from a crystallized preparation of this substance. The values found are, however, sufficiently accurate to enable a rational planning of a counter current separation. It can be concluded from these figures, that one should use about equal volumes of the two solvent phases for a counter current separation, and that the ratio of the partition coefficients is so large that a fair separation of the two *d*-chondrocurine monomethyl ethers can be carried out, using a conveniently small number of separatory funnels. Such a separation was also carried out, using five funnels. The separation can be considerably improved by repeating the separation with each fraction.

The author wishes to express his sincere thanks to *Sverige Amerika Stiftelsen, American Scandinavian Foundation* and *Astra Pharmaceutical Products, Inc.* for fellowships, and to Professor Dermot B. Taylor for the privilege of joining his alkaloid research team and for supplying various *Chondrodendron* alkaloids and partly methylated preparations of them.

REFERENCES

1. Bush, M. T., Goth, A. and Dickison, H. L. *J. Pharmacol. Exp. Therap.* **84** (1945) 262, footnote 6.
2. Hecker, E. *Verteilungsverfahren im Laboratorium*, Verlag Chemie, Weinheim/Bergstr. 1955, p. 78.
3. Rauen, H. M. and Stamm, W. *Gegenstromverteilung*, Springer-Verlag, Berlin-Göttingen-Heidelberg 1953, p. 4.
4. Hecker, E. Ref.[2], p. 140.
5. Rauen, H. M. and Stamm, W. Ref.[3], p. 22.
6. Jübermann, O. in Müller, E. *Methoden der organischen Chemie* I/1, Georg Thieme Verlag, Stuttgart 1958, p. 303.
7. Bush, M. T. and Densen, P. M. *Anal. Chem.* **20** (1948) 121.
8. Stevenson, G. *To be published.*
9. Riecke, E. *Z. physik. Chem.* **7** (1891) 97.
10. Nernst, W. *Z. physik. Chem.* **8** (1891) 110.
11. Craig, L. C. and Craig, D. in Weissberger, A. *Technique of organic Chemistry* III:I, Interscience Publishers, Inc., New York 1956, p. 162.
12. Herz, W. *Sammlung chemischer und chemisch-technischer Vorträge* **15** (1910) 1.
13. Rudstam, G. *Anal. Chem.* **32** (1960) 1664.
14. Hultin, E. *Acta Chem. Scand.* **15** (1961). *In press.*
15. Hultin, E. *Acta Chem. Scand. In press.*

Received December 21, 1960.

ACTA CHEMICA SCANDINAVICA 15 (1961) 888–892

Die Quantenausbeute des Schwärzungsprozesses von photoaktiven Kuproverbindungen

JAN WOJTCZAK*

Physikalisch-Chemisches Institut der Universität Uppsala, Schweden

Der Verfasser hat die Oxydation eines kolloidalen Systems von Cu_2O und Cu_{met} unter Einwirkung von Licht studiert. Dieser Artikel beschreibt einen Versuch, die Quantenausbeute des Prozesses zu bestimmen. Diese war sehr hoch, sie variierte zwischen 2,5 und 16 in dem Wellenlängenbereich 280 nm bis 640 nm, wo sie bestimmt wurde.

In einer früher publizierten Arbeit wurden die phototropen Eigenschaften eines neuen lichtempfindlichen Systems beschrieben. Die Methoden zur Bereitung der Suspensionen und der Schwärzungsmechanismus dieses Systems wurden angegeben und erklärt. Ausserdem wurden die Geschwindigkeitkonstanten der Schwärzungsreaktion im Lichte und der Entfärbungsreaktion im Dunkeln dieses Systems bestimmt und auch die Lichtempfindlichkeit im Violetten und sichtbaren Licht wurde näherungsweise geschätzt [1].

Das System, das in Ref.[1] beschrieben wird, ist eine kolloidale gelbe Suspension von Cu_2O und Cu_{met}. Diese oxydiert sich sehr leicht im Lichte zu braunschwarzem CuO, was zu intensiver Schwärzung des Systems führt. Die Berechnung der Quantenausbeute der CuO-Bildung unter der Strahlungswirkung von Licht verschiedener Wellenlängen war das Ziel dieser Arbeit.

Da es schwierig ist, Lichtmengen, die von einem kolloidalen System absorbiert werden, quantitativ zu bestimmen, sind die Ergebnisse in Tabelle 1 mit beträchtlichen Fehlern behaftet. Da die Quantenausbeuten unter der Annahme vollständiger Absorption des einfallenden Lichtes berechnet sind, sind sie als Mindestwerte anzusehen. Die gebildete Menge von CuO wurde spektrophotometrisch bestimmt.

Es ist sehr auffallend, dass die Quantenausbeuten so hoch sind. Im ganzen Gebiet 280 nm** bis 640 nm sind sie grösser als 1 und bei etwa 400 nm sind sie grösser als 10.

---

* Gegenwärtige Adresse: Katedra Chemii Fizycznej, Coll. Chemicum, Poznań Polen,

** nm = nanometer.

1. Bereitung des Systems

Das untersuchte lichtempfindliche System war aus den selben Verbindungen und in analoger Weise hergestellt wie in der oben genannten Arbeit [1] beschrieben wurde. Doch wurden in diesem Fall verdünntere Systeme verwendet, weil sie für photometrische Messungen bequemer waren.

Die Systeme wurden folgendermassen bereitet: zu 6,5 ml 0,5 % wässriger Kupferacetatlösung gibt man 1 ml 1 % Ascorbinsäurelösung und nachher 0,3 ml 45 % Essigsäure. Es bildete sich unter diesen Bedingungen eine kolloidale gelbe Suspension. Die Herstellung der Präparate und die Messungen wurden bei Zimmertemperatur durchgeführt, d.h. zwischen 18° und 20°C.

2. Belichtungsapparatur

Die untersuchten Präparate wurden in einem grossen Monochromator belichtet, der von Professor Dr. Stig Claesson, dem Direktor des phys.chem. Inst. der Universität Uppsala, zu Verfügung gestellt wurde. Die genaue Beschreibung dieses Instruments kann man in separaten Veröffentlichungen finden [2]. Die Lichtquelle in diesem Gerät war eine Philips Hochdruck-Quecksilberlampe Typ "SP" von 500 W Leistung. Die Möglichkeit, in diesem Gerät zwischen Glasprisma und Wasserprisma zu wechseln, hat die Messtätigkeit im ganzen Spektralbereich der obengenannten Lampe, d.h. von etwa 250 nm bis etwa 650 nm, ermöglicht.

3. Messapparatur

Der Schwärzungsgrad belichteter Präparate wurde mit Hilfe des Beckmanspektrophotometer Model B bestimmt. Die Messungen wurden bei 650 nm, in 1 cm Schichtdicke und mit einer rotempfindlichen Photozelle gemacht. Diese Messwellenlänge wurde ausgewählt, da die rote Strahlung durch das heterogene untersuchte System verhältnismässig stark absorbiert und zugleich am wenigsten zerstreut wurde, was auf die Genauigkeit und Reproduzierbarheit der Ergebnisse einen günstigen Einfluss hatte.

4. Bestimmung der gebildeten CuO-Menge bei Belichtung mit monochromatischem Licht verschiedener Wellenlängen

Die gebildete CuO-Menge wurde spektrophotometrisch bestimmt. Um die Messungen gegen die gebildete CuO-Menge zu eichen, wurden einige belichtete Systeme chemisch analysiert.

Das belichtete System wird zuerst mit H_2SO_4 bis pH = 1 angesäuert. Bei diesen Bedingungen verschwinden die reversiblen Eigenschaften der photoempfindlichen Suspension, aber ihre Konzentration und Zusammensetzung bleiben eine Weile (ungefähr 1 St.) praktisch unverändert. Unmittelbar nachher wird die Suspension abzentrifugiert und der erhaltene Niederschlag in HCl gelöst. Bei diesen Bedingungen werden die Kupferoxyde (Cu_2O, CuO) gelöst und das metallische Kupfer bleibt ungelöst. Dies wird wieder abzentrifugiert und in HNO_3 gelöst.

Tabelle 1. Die Abhängigkeit des Schwärzungsgrades des Systems, (ΔS), Cu_{met} und CuO-Menge von der Belichtungszeit.

t Belicht. Zeit in Min.	λ = 435 nm			λ = 600 nm		
	Schwärzung ΔS	Cu_{met}-Menge in %	CuO-Menge in %	Schwärzung ΔS	Cu_{met}-Menge in %	CuO-Menge in %
0	0,00	100	0,0	0,00	100	0,0
1	0,10	73	26	0,035	91	9
2	0,19	49	52	0,065	83	17
3	0,28	25	77	0,095	75	25

Zu den erhaltenen Kupferlösungen wird Ammoniaklösung im Überschuss zugegeben und danach wird das Kupfer photometrisch quantitativ bestimmt. In dieser Weise kann man die Kupfermenge und die Gesamtmenge der Kupferoxyde bestimmen. Wenn man die Gesamtmenge von Cu_{met} kennt, kann man die Menge von CuO in Präparaten verschiedenen Schwärzungsgrades im Niederschlag nach Zusatz von H_2SO_4 auf trockenem Wege bestimmen. Die oben angegebene Analyse muss man so schnell wie möglich ausführen, weil eine langsame Ausführung und auch die Luftsauerstoffwirkung auf die Reproduzierbarkeit der Ergebnisse eine ungünstige Wirkung haben.

Quantitative Daten: Auf 10 ml des photoaktiven Systems werden 2 ml 0,25 M H_2SO_4 zugegeben. Der gesamte Niederschlag wird in 4 ml 0,5 M HCl und das zurückgebliebene Kupfer in 2 ml 1 M HNO_3 gelöst.

Die Ergebnisse für λ = 435 nm und 600 nm sind in Tabelle 1 zusammengestellt. Im unbelichteten System (t = 0) ist die relative Extinktion S = 0,00 und die CuO-Menge in der Suspension = 0. Die totale Kupfermenge im abzentrifugierten Niederschlag wird zu 100 % gesetzt. Die in der Tabelle 1 angegebenen Zahlen sind Mittelwerte von 3 bis 5 einzelnen Messungen.

Der mittlere Fehler dieser Bestimmungen ist 5—10 %. Aus den Werten der Tabelle 1 ergibt sich, dass unter den beschriebenen Versuchsbedingungen eine relativ gute Proportionalität zwischen ΔS, gebildeter CuO-Menge und Belichtungszeit vorliegt. Diese Proportionalität wird bei grösseren Lichtmengen nicht mehr erfüllt. In diesem Fall kann man entsprechend die Belichtungszeit verkürzen. Die genaue Bestimmung der Maximumlagen der Intensität auf der Trommelskala des Monochromators wurde mit Hilfe einer Selenphotozelle ermittelt. Bei Messungen im U-violetten war die Photozelle mit fluoreszierenden Plättchen bedeckt.

Unmittelbar nach der Herstellung wurde das zu untersuchende System in eine Küvette aus Quarz eingegossen und je nach Strahlungsintensität von 1 bis 3 Minuten (± 1 Sek.) belichtet. Die Küvette, von 3,5 ml Volumen, drehte sich mit einer Geschwindigkeit von 1 Umdrehung/Min.

Die Breite von Eintritt- und Austrittspalte war 0,5 mm.

Bei 365 nm und 406 nm wurden Messungen mit Glasprisma und mit Wasserprisma gemacht.

Tabelle 2. Sp. 1: Wellenlänge in nm. Sp. 2: Lichtstrom durch die Austrittspalte des Monochromators, Quanten $sek^{-1} \times 10^{-15}$. Sp. 3: Geschw. der Bildung von CuO, Molekeln $sek^{-1} \times 10^{-15}$. Sp. 4: Quantenausbeute. Sp. 5: Methode der Lichtmessung: a mit Aktinometer bestimmt, p mit Photozelle bestimmt, a(p) wurden zur Eichung der Photozelle benutzt. Sp. 6: Dispergierendes Medium: w = Wasser, g = Glas.

1	2	3	4	5	6
280	1,45	3,9	2,7	a	w
295	2,96	15,6	5,3	a	w
302	4,03	20,3	5,0	a	w
312	6,10	31,2	5,1	a	w
334	3,10	18,0	4,9	a	w
365	23,8	281	11,8	a	w
365	1,88	28,8	15,3	a	g
406	25,0	277	11,1	a(p)	w
406	3,68	60,0	16,3	a(p)	g
435	5,95	72,5	12,2	a(p)	g
485	2,2	19,5	8,9	p	g
547	13,9	46,8	3,3	p	g
579	9,7	41,4	4,3	p	g
600	7,2	23,4	3,3	p	g
620	5,3	23,4	4,4	p	g
640	10	25,8	2,6	p	g

5. Bestimmung der Lichtintensität in dem Monochromator

Die Lichtintensität im Wellenlängenbereich 280 nm bis 435 nm wurde mit dem chemischen Aktinometer nach Hatchard und Parker [3] bestimmt.

Eine aktinometrische Bestimmung der Lichtintensität oberhalb 435 nm ist nicht mehr praktisch wegen Mangel von passenden Aktinometern. Darum

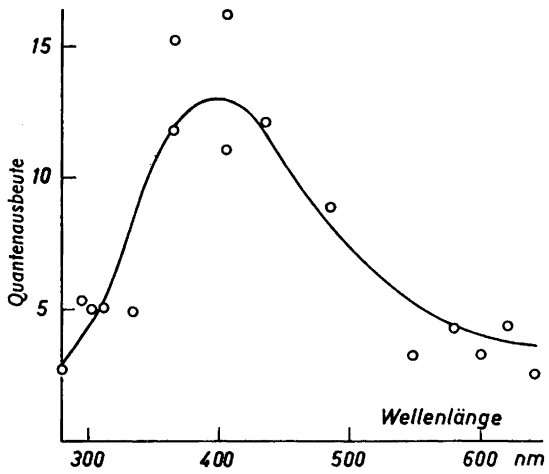

Fig. 1. Quantenausbeute als Funktion der Wellenlänge.

wurde die Lichtintensität in diesem Gebiet mit einer Selenphotozelle bestimmt. Die relative Empfindlichkeit der Photozelle wurde mit einer Standardwolframlampe [4] bekannter Spektralverteilung und einem Zeiss-Monochromator "Mess 262 B" [5] mit einer bekannten reziproken linearen Dispersion bestimmt. Die Transmission im Monochromator war im Messgebiet praktisch konstant. Die absolute Empfindlichkeit wurde durch vergleich mit aktinometrischen Messungen bei 350 nm — 435 nm bestimmt. Die relative Eichung wurde bei der Lampenfadentemperatur 2 600°K durchgeführt. Die Spaltbreiten des Monochromators waren 0,2 mm, und der Abstand des Lampenfadens von der Eintrittspalte war ungefähr 4 cm.

Die Resultate der Untersuchung sind in Tabelle II zusammengefasst. In Fig. 1 wird die Quantenausbeute als Funktion der Wellenlänge gezeigt.

Ich spreche Herrn Professor Dr. Stig Claesson, dem Direktor des Phys.-chem. Institutes der Universität in Uppsala, meinen herzlichsten Dank dafür aus, dass er mir die Möglichkeit gegeben hat, diese Forschungen mit Hilfe der modernsten Apparatur durchzuführen und für die fruchtbare Diskussion der erhaltenen Ergebnisse.

Ich danke auch Herrn Lic. G. Wettermark für die freundliche Hilfe beim Aufbau mancher Messapparaturen.

LITERATUR

1. Wojtczak, J. *Roczniki Chem.* **32** (1958) 553.
2. Claesson, S. *Arkiv Kemi. In Druck.*
3. Hatchard, C. G. und Parker, C. A. *Proc. Roy. Soc. (London)* **A 220** (1953) 104; **A 235**, (1956) 519.
4. Barbrow, L. E. *J. Opt. Soc. Am.* **49** (11), (1959) 1122.
5. Czerny, M. und Plettig, V. *Z. Physik* **63** (1930) 590.
6. Wojtczak, J. *Poznańskie Towarzystwo Przyjaciół Nauk, Prace Komisji Mat.-Przyr.Ser.* **A 7** (2) (1954); **7** (6) (1956).

Eingegangen am 12. December 1960.

ACTA CHEMICA SCANDINAVICA 15 (1961) 893–902

The Crystal Structure of Ni_3Si_2 with some Notes on Ni_5Si_2

GUNVOR PILSTRÖM

Institute of Chemistry, University of Uppsala, Uppsala, Sweden

The crystal structure of Ni_3Si_2 has been determined from single crystal data. The unit cell is orthorhombic and contains 16 formula units. The space-group is $Cmc\,2_1$. The unit cell dimensions determined by powder diffraction techniques are: $a = 12.229$ Å, $b = 10.805$ Å and $c = 6.924$ Å. The nickel atoms are situated in four eight-fold and four four-fold positions and the silicon atoms are situated in three eight-fold and two four-fold positions.

The single crystal data have also been used to determine the symmetry and unit cell dimensions of Ni_5Si_2 for which a trigonal unit cell has been found. This phase has a small homogeneity range. Thus Ni_5Si_2 in equilibrium with δ-Ni_2Si has the cell dimensions, $a = 6.670$ Å and $c = 12.267$ Å whereas in equilibrium with Ni_3Si the dimensions are $a = 6.670$ Å and $c = 12.332$ Å.

The existence of Ni_3Si_2 was first established in 1906 by Guertler and Tammann[1] who made a thermal and microscopic investigation of the Ni-Si system. They found that Ni_3Si_2 is formed by a peritectoid reaction at 830°C. Iwasé and Okamoto [2], who revised the Ni-Si diagram in 1936, found that the peritectoid reaction takes place at 845°C. In 1939 Ôsawa and Okamoto [3] published an X-ray analysis of the Ni-Si system. The unit cell of Ni_3Si_2 was stated to be orthohexagonal with the unit cell dimensions $a = 6.605$ kX, $b = 7.627$ kX and $c = 9.574$ kX, and a cell content of 45 atoms.

Ni_5Si_2 was also stated to be orthohexagonal with the unit cell dimensions $a = 13.29$ kX, $b = 7.672$ kX and $c = 9.752$ kX, and a cell content of 90 atoms. In the present investigation single crystal examinations show that the unit cell of Ni_5Si_2 is in fact trigonal. The cell dimensions, determined by the powder method, vary slightly with composition. Ni_5Si_2 in equilibrium with δ-Ni_2Si gives values for a and c of 6.670 and 12.267 Å, respectively, compared with values of 6.670 and 12.332 Å obtained for the phase in equilibrium with Ni_3Si.

EXPERIMENTAL

The materials used for alloy preparations were: Nickel sponge (98.2 %) obtained from Johnson Matthey Co., Ltd, London and silicon (99.9 %) obtained from Pechiney & C:ie Paris.

Table 1. Powder data for Ni_3Si_2. ($CrKa_1$ radiation).

hkl	$\sin^2\Theta_{obs} \times 10^4$	$\sin^2\Theta_{calc} \times 10^4$	I_{obs}	I_{calc}	*hkl*	$\sin^2\Theta_{obs} \times 10^4$	$\sin^2\Theta_{calc} \times 10^4$	I_{obs}	I_{calc}
110	200	200	m	138	023	2 912	2 909	w	65
200	350	351	w	32	422	[a]	2 945	w−	27
020	449	449	w−	13	600	3 156	3 155	st+	625
111	—	473		4	151	—	3 167	[b]	22
021	—	722		0.1	440	—	3 198	[b]	122
220	—	800		10	530	—	3 201	[b]	73
310	—	901		3	242	3 241	3 241	st+	1170
221	1 073	1 073	w+	52	223	—	3 260	[b]	51
002	—	1 094		0.3	313	3 361	3 362	st+	989
130	—	1 098		0.1	512	3 396	3 397	st	493
311	1 174	1 174	w−	18	441	—	3 472		8
112	1 294	1 294	m+	294	531	3 476	3 475	m+	312
131	1 372	1 372	m	120	133	3 555	3 558	[c]	120
400	1 403	1 402	w--	18	350	3 593	3 596	st	613
202	1 442	1 444	w−	32	602	—	3 604	[b]	44
022	1 544	1 543	w	42	351	3 873	3 869	w+	54
040	—	1 796		0.1	621	—	3 877		12
330	1 798	1 799	w+	138	152	—	3 988		6
420	1 848	1 851	w	45	060	—	4 041		2
222	1 889	1 893	w−	27	620	—	4 165		1
312	[a]	1 995	w−	17	043	4 257	4 256	w+	79
041	—	2 069		0.2	333	—	4 259		9
331	[a]	2 072	w−	29	442	} 4 294	4 292		542
421	—	2 125		0.1	532		4 295	st	38
240	—	2 147		11	423	—	4 312	[b]	22
132	[a]	2 191	w−	23	061	—	4 314	[b]	27
510	—	2 303		0.1	004	4 378	4 374	m+	331
241	—	2 420		3	260	—	4 392		4
402	—	2 496		17	710	—	4 407		7
511	[a]	2 577	w−	21	114	—	4 574		10
113	—	2 660		0	243	—	4 607		4
042	} 2 897	2 890		151	261	—	4 665		18
332		2 893	m	23	352	[a]	4 689	w−	23
150	—	2 894		3	204	—	4 725		6
					024	—	4 823		25

[a] The line is too diffuse to be measured accurately.
[b] The line is too near a strong line to be discernible.
[c] This line is overlapped by a line of the calibration standard.

An arc melted alloy with the nominal composition Ni_3Si_2 was annealed at 830°C for 30 days. X-Ray powder photographs were taken in a Guinier-type focusing camera with $CrKa_1$ radiation. Si was used as an internal standard ($\lambda_{CrKa_1} = 2.2896$ Å, Si: $a = 5.4306$ Å). The accuracy of the lattice parameter values is estimated to be 0.03 %. For the structure determination a small fragment was selected from the annealed alloy. Photographs were taken in a Weissenberg camera with $MoKa$ radiation. Intensity data were obtained using a multiple film technique with iron foil interleaved between the films. The *c*-axis was used as the rotation-axis and the layer-lines 0 – 6 were recorded. The intensities of 367 non-equivalent reflexions were estimated visually. The calculations of Fourier series and structure factors were made with the aid of the electronic digital computer BESK using programmes devized by Westman *et al.*[4] and by Åsbrink *et al.*[5]. The constants A_i, B_i, C_i, a_i, b_i, c_i in the expression for the atomic scattering factors f_i (given by Åsbrink *et al.*[5]) have been determined by Appel [6] as follows:

	A_i	B_i	C_i	a_i	b_i	c_i
Ni	9.664	10.559	7.537	0.321	3.479	25.262
Si	2.8315	6.8065	4.5870	0.3235	2.2965	51.770

THE DETERMINATION OF THE STRUCTURE OF Ni_3Si_2

From single crystal and powder photographs the unit cell of Ni_3Si_2 was found to be orthorhombic with the dimensions: $a = 12.229$ Å, $b = 10.805$ Å, $c = 6.924$ Å. Powder data are given in Table 1. Ôsawa and Okamoto [3] found the density (D_m) to be 6.32 g cm^{-3} and from this the unit cell was assumed to contain 16 formula units, giving the calculated X-ray density 6.74 g cm^{-3}. (Densities given by these authors for other compounds show that they have usually obtained values that are in fact too low.)

The Weissenberg films showed the systematic extinctions: $F(hkl)$ for $h + k = 2n + 1$ and $F(h0l)$ for $l = 2n + 1$. The possible space-groups were $Cmcm$, $Ama2$ and $Cmc2_1$. The Patterson section $P(X0Z)$ showed that $Cmc2_1$ was the most probable space-groups. During the refinement of the structure there was nothing which indicated that another space-group should be chosen.

The Patterson sections $P(X0Z)$ and $P(XY\frac{1}{2})$ gave rough x and y parameters. As the electron density projection $\varrho\ (xy)$ was the only centrosymmetric one this projection was first refined. There were no Harker peaks to give the z-coordinates. As the x and y-coordinates obtained from $\varrho\ (xy)$ were good apart from some overlapping and the measured density shows that the structure must be fairly densely packed it was possible to get rough z-parameters from spatial considerations. The z-coordinate of Ni_5 was arbitrarily put at 0. The whole of the three-dimensional intensity data was finally used for refining all the parameters. The refinement was made by calculating $\varrho(F_{obs})$ and $\varrho(F_{calc})$ and was taken to a point at which all shifts were smaller than the standard deviations. The standard deviations were calculated using the formula given by Cruickshank [7]. As only one electron density projection is centrosymmetric the values of standard deviations given are twice those calculated for a centrosymmetric space-group. For final parameters and standard deviations see

Table 2. Atomic parameters for Ni_3Si_2.

	x	y	z
8 Ni_1 in 8(b)	0.1732	0.1177	0.518
8 Ni_2 in 8(b)	0.1723	0.1189	0.900
8 Ni_3 in 8(b)	0.1972	0.2467	0.217
8 Ni_4 in 8(b)	0.1824	0.4975	0.225
4 Ni_5 in 4(a)		0	0
4 Ni_6 in 4(a)		0.2345	0.024
4 Ni_7 in 4(a)		0.2330	0.400
4 Ni_8 in 4(a)		0.3814	0.714
8 Si_I in 8(b)	0.120	0.059	0.214
8 Si_{II} in 8(b)	0.152	0.344	0.506
8 Si_{III} in 8(b)	0.151	0.343	0.920
4 Si_{IV} in 4(a)		0.157	0.712
4 Si_V in 4(a)		0.409	0.218

Table 2a. Standard deviations of the atomic parameters [a] of Ni_3Si_2.

σ_x(Ni)	= 0.0003
σ_y(Ni)	= 0.0005
σ_z(Ni)	= 0.002
σ_x(Si)	= 0.001
σ_y(Si)	= 0.001
σ_z(Si)	= 0.006

[a] The standard deviation for Ni_4 is 0 as this atom defines the origin.

Tables 2 and 2a. An isotropic temperature factor with $B = 0.22$ Å^2 was applied. The reliability index $R = \frac{\Sigma \, | \, |F_o| - |F_c| \, |}{\Sigma \, |F_o|}$ was 0.118 after the last refinement.

DESCRIPTION OF THE STRUCTURE OF Ni_3Si_2

The structure of Ni_3Si_2 is very complicated and thus difficult to describe. It may be visualized, however, as consisting of flat and puckered layers perpendicular to the a-axis. The flat layers lie in the mirror planes $x = 0$ and $x = \frac{1}{2}$. The puckered layers, which are at $x \simeq \pm 1/6$ and $x \simeq \pm 1/3$ are symmetrically equivalent. Fig. 1 shows the nickel atoms in these layers projected on the bc-plane. Fig. 2 shows a flat layer and Fig. 3 a puckered layer in which both nickel and silicon atoms are present.

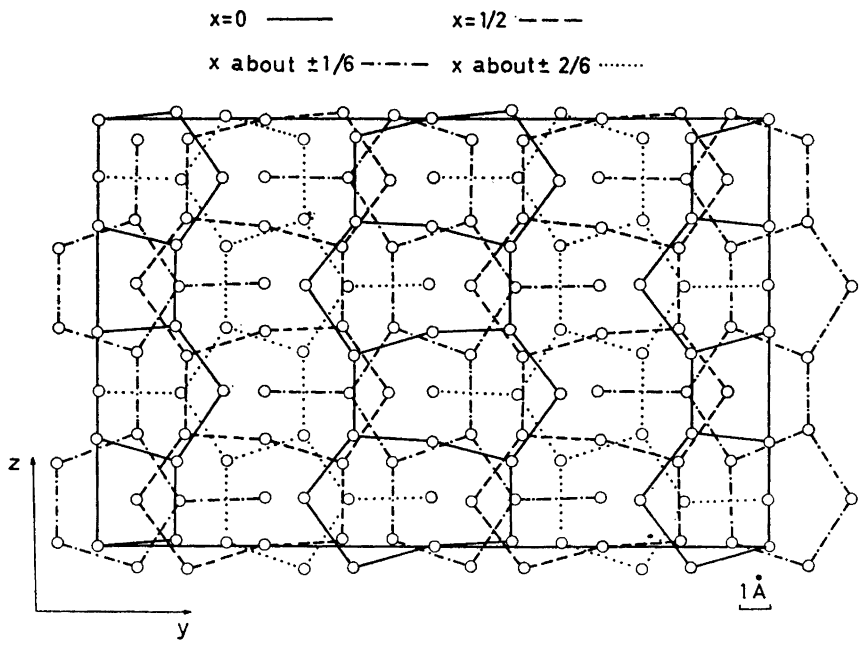

Fig. 1. The nickel atoms projected on the b c plane. Four unit cells are shown.

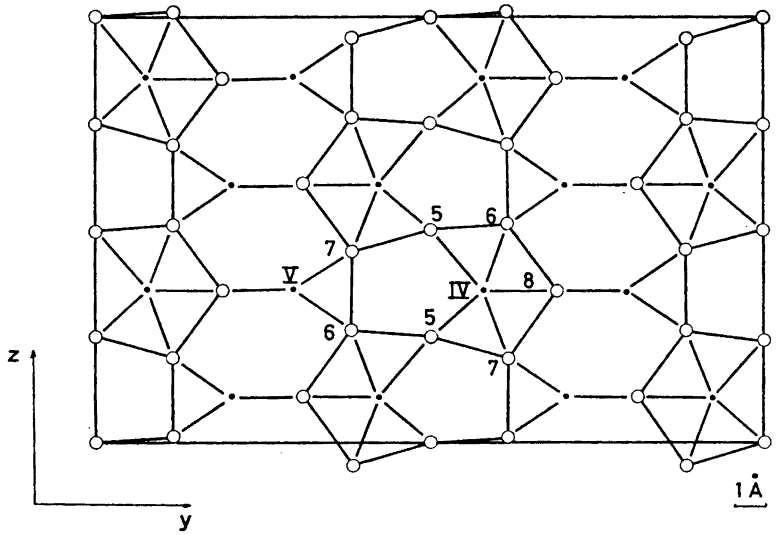

Fig. 2. The pattern of atoms in the mirror plane $x = 0$ (or $x = \frac{1}{2}$). The circles are nickel atoms, the dots are silicon atoms. The Arabic figures are the indices of the nickel atoms and the Roman figures those of the silicon atoms. Four unit cells are shown.

Table 3 gives interatomic distances and Table 4 and Figs. 4 (a) — (m) show the environments of each atom. Most of the Ni-Ni distances lie in the range 2.47—2.76 Å and in particular, there are a number with values of about

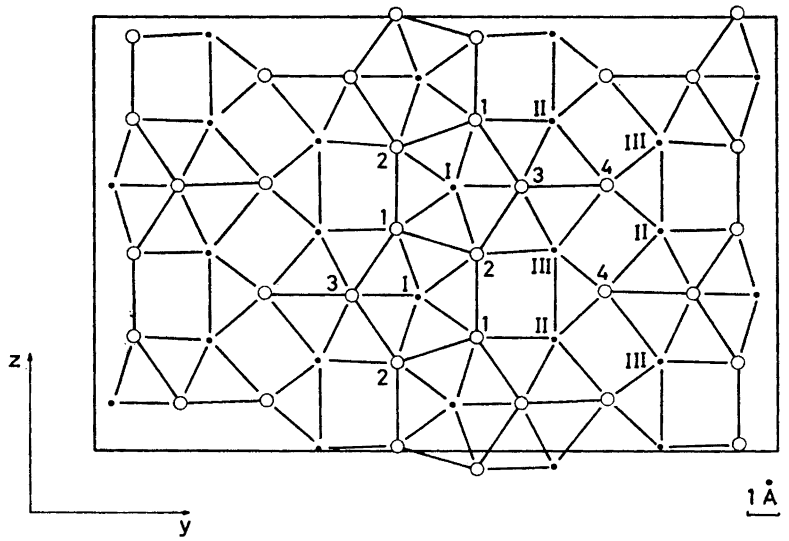

Fig. 3. The figure corresponds to Fig. 2 for the puckered layer. Unit cell is outlined with respect to x near 1/6.

Table 3. Interatomic distances in Ni_3Si_2 (Å) <3.3.

	$-Ni_1$	$-Ni_2$	$-Ni_3$	$-Ni_4$	$-Ni_5$	$-Ni_6$	$-Ni_7$	$-Ni_8$	$-Si_I$	$-Si_{II}$	$-Si_{III}$	$-Si_{IV}$	$-Si_V$
Ni_2-		2.65 2.68	2.53 2.56	2.59 2.99	2.47		2.59		2.29 2.43	2.46	2.30	2.54	
Ni_2-	2.65 2.68		2.50 2.61	2.49 3.15	2.56	2.60			2.35 2.40	2.31	2.44	2.51	
Ni_3-	2.53 2.56	2.50 2.61		2.72		2.76	2.73		2.24	2.33 2.55	2.37 2.53		2.98
Ni_4-	2.59 2.99	2.49 3.15	2.72 3.07					2.59	2.50	2.32 2.58	2.22 2.72		2.43
Ni_5-	2.47(2)	2.56(2)				2.54	2.61		2.18(2) 2.55(2)			2.24 2.61	
Ni_6-		2.60(2)	2.76(2)		2.54		2.60	2.67	2.74(2)		2.30(2)	2.32	2.32
Ni_7-	2.59(2)		2.73(2)		2.61	2.60		2.70	2.72(2)	2.33(2)		2.31	2.29
Ni_8-				2.59(2)		2.67	2.70			2.38(2)	2.37(2)	2.43	2.26
Si_I-	2.29 2.43	2.35 2.40	2.24	2.50	2.18 2.55	2.74	2.72		2.94			2.75	
$Si_{II}-$	2.46	2.31	2.33 2.55	2.32 2.58			2.33	2.38			2.87 3.20	3.10	2.81
$Si_{III}-$	2.30	2.44	2.37 2.53	2.22 2.72		2.30		2.37		2.87 3.20		3.09	2.86
$Si_{IV}-$	2.54(2)	2.51(2)			2.24 2.61	2.32	2.31	2.43	2.75(2)	3.10(2)	3.09(2)		
Si_V-			2.98(2)	2.43(2)		2.32	2.29	2.26		2.81(2)	2.86(2)		

Table 4. Coordinations of the atoms of Ni_3Si_2.

Atom	Ni neighbours		Si neighbours	
	No.	mean distance (Å)	No.	mean distance (Å)
Ni_1	8	2.63	5	2.41
Ni_2	8	2.65	5	2.40
Ni_3	7	2.63	6	2.50
Ni_4	7	2.80	6	2.46
Ni_5	6	2.54	6	2.39
Ni_6	7	2.65	6	2.45
Ni_7	7	2.65	6	2.45
Ni_8	4	2.64	6	2.37
Si_I	10	2.44	2	2.85
Si_{II}	8	2.41	4	3.00
Si_{III}	8	2.41	4	3.01
Si_{IV}	9	2.45	6	2.98
Si_V	7	2.53	4	2.84

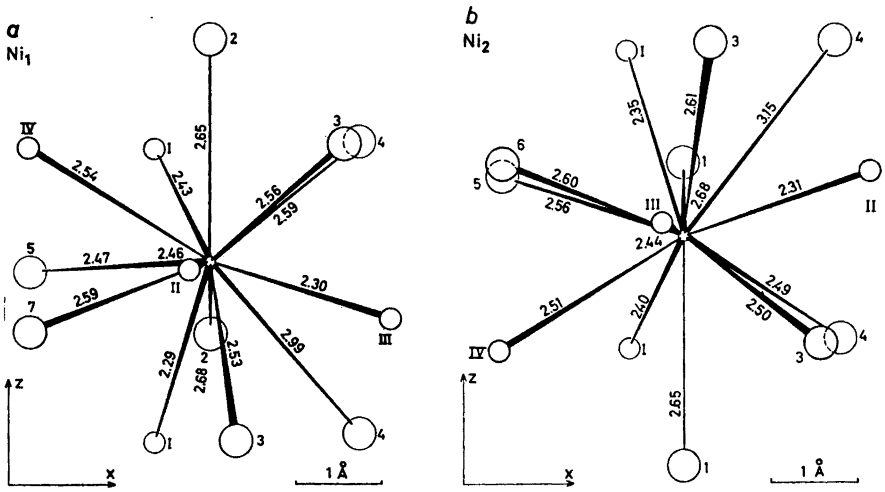

2.60 Å. This value corresponds to $2r_{Ni} + 0.1$ Å. A similar investigation of the Ni-Si distances shows that most of them lie between 2.20 and 2.55 Å and in particular, there are a number with values in the range 2.30—2.33 Å. This corresponds to $r_{Ni} + r_{Si} - 0.10 = 2.32$ Å.

The environments of the individual atoms are very irregular and dissimilar. It may be observed that the coordination of Ni_1 is practically identical with

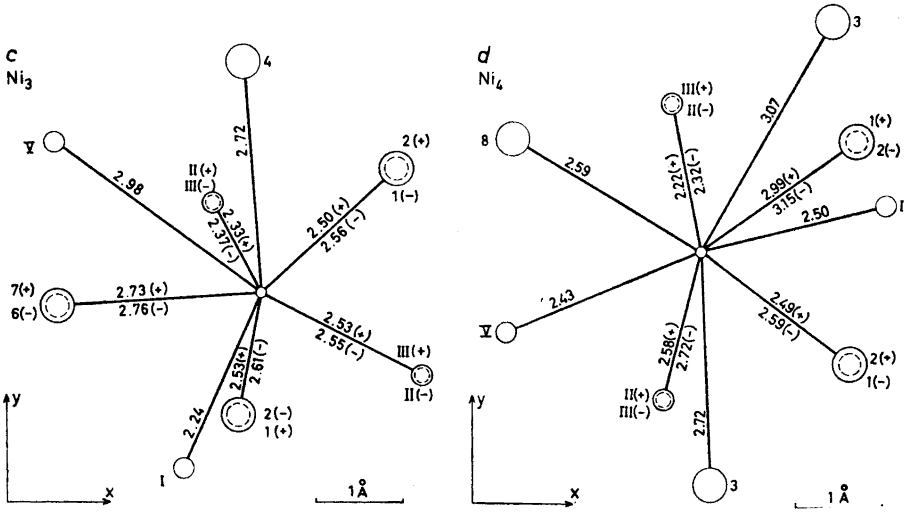

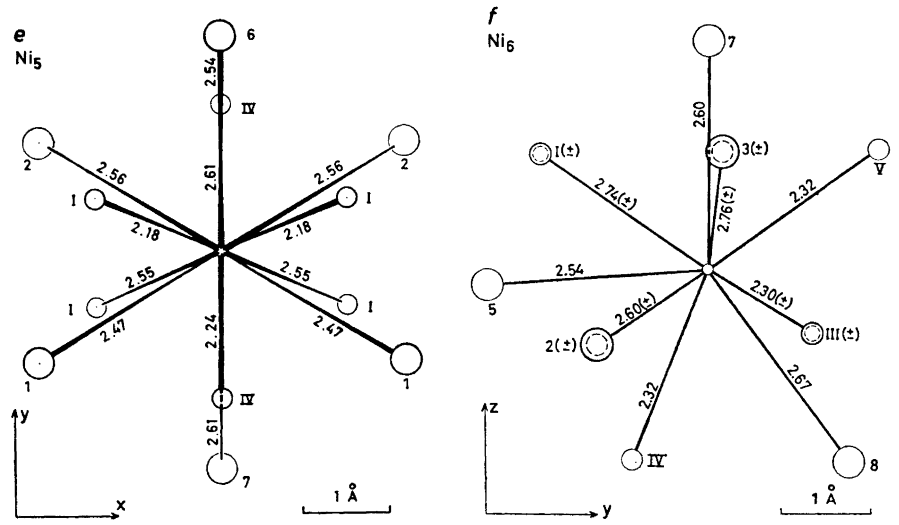

that of Ni_2. The same is true for Ni_6 and Ni_7 and for Si_{II} and Si_{III}. Ni_5 and Ni_8 have the most regular coordinations of all atoms. Ni_5 is surrounded by a fairly regular icosahedron of six nickel and six silicon atoms and Ni_8 coordinates a tetrahedron of nickel atoms and an octahedron of silicon atoms. The six silicon neighbours of Ni_4, Ni_6 and Ni_7 may also be described as forming a distorted octahedron.

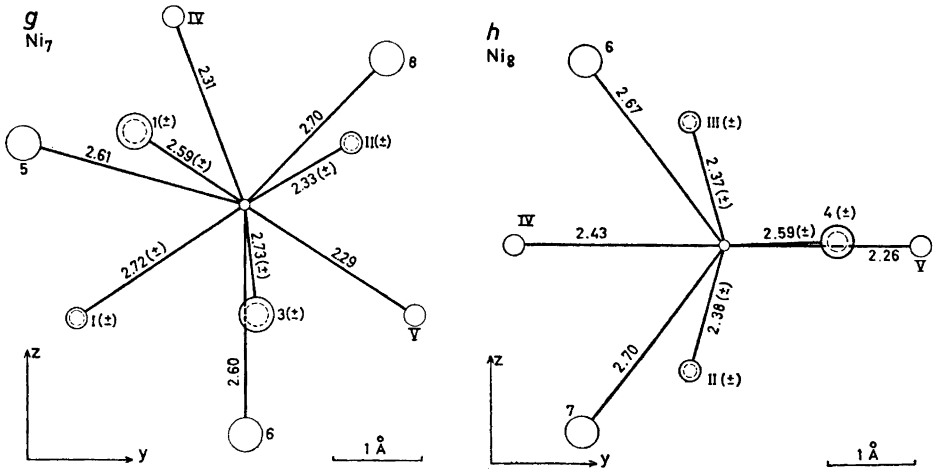

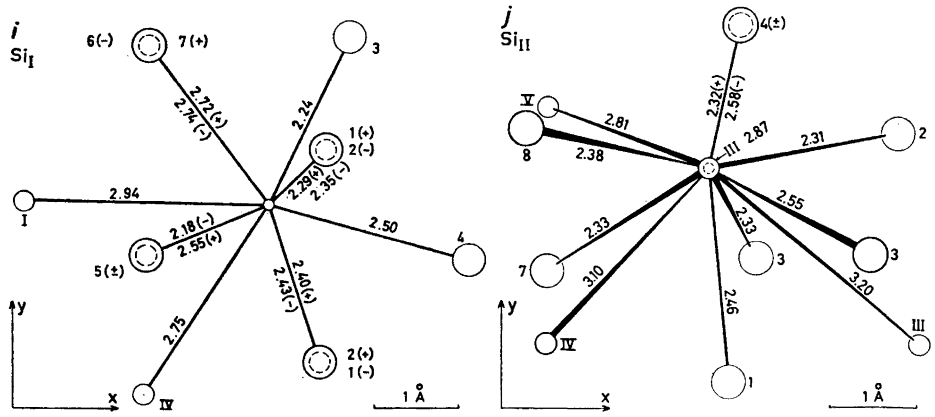

It is of interest to compare this structure with those of NiSi and δ-Ni_2Si. The nickel atoms in NiSi coordinate a nickel tetrahedron and a silicon octahedron (Toman)[8] analogously to the environment of Ni_8 in Ni_3Si_2, The mean distance between each nickel atom and its four nickel neighbours is 2.67 Å in NiSi and 2.64 Å in Ni_3Si_2. The corresponding mean distance to the six silicon atoms is 2.37 Å in both structures. In δ-Ni_2Si the nickel atoms are surrounded

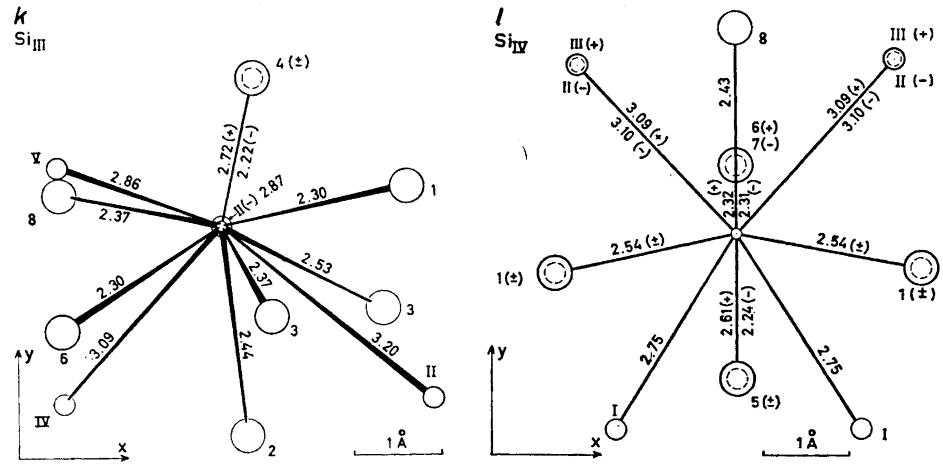

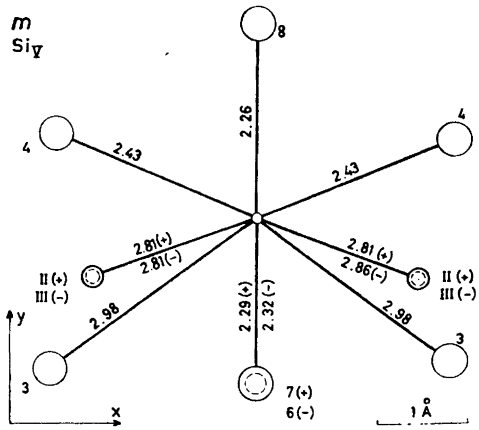

Fig. 4. (a)—(h) show the surroundings of the nickel atoms and (i)—(m) the surroundings of the silicon atoms. A large circle is a nickel atom, a small circle a silicon atom. Double circles refer to superimposed atoms. Atoms connected to the central atom by lines of uniform thickness are coplanar (within ± 0.1 Å). Arabic figures denote the indices of the nickel atoms and Roman figures those of silicon atoms. The minus signs refer to atoms below the median plane and plus signs to atoms above this plane. Distances from the central atom to the neighbours are given (in Å).

by eight nickel and five silicon atoms (Toman)[9] like Ni_1 and Ni_2 in Ni_3Si_2 but the environments are dissimilar.

Acknowledgements. This work has been financially supported by the *Swedish State Council of Technical Research* and by the *Air Force Office of Scientific Research of the Air Research and Development Command, United States Air Force,* yh ough its European Otfice under Contract No. AF 61(052)-40. Facilities for the use of the electronic digital computer BESK were granted by the *Swedish Board for Computing Machinery.*

The author wishes to thank professor G. Hägg for his kind interest. Thanks are also due to Dr. B. Aronsson and Dr. S. Rundqvist for valuable advice and stimulating discussions.

REFERENCES

1. Guertler, W. and Tammann, G. *Z. anorg. Chem.* **49** (1906) 93.
2 Iwasé, K. and Okamoto, M. *Sci. Repts Tôhoku Imp. Univ., K. Honda Anniv. Vol.* (1936) 777.
3 Ôsawa, A. and Okamoto, M. *Sci. Repts Tôhoku Imp. Univ.* **27** (1939) 326.
4. Westman, S., Blomqvist, G. and Åsbrink, S. *Arkiv Kemi* **14** (1959) 535.
5. Åsbrink, S., Blomqvist, G. and Westman, S. *Ibid* **14** (1959) 545.
6. Appel, K. Technical Note from the *Quantum Chemistry Group, University of Uppsala.*
7. Cruickshank, D. W. J. *Acta Cryst.* **2** (1946) 65.
8. Toman, K. *Ibid* **4** (1951) 462.
9. Toman, K. *Ibid* **5** (1952) 329.

Received December 7, 1960.

ACTA CHEMICA SCANDINAVICA 15 (1961) 903–912

Optical Rotatory Dispersion Studies

XLVI *. Stereochemical Assignments through Anomalous Rotatory Dispersion Curves of α-Amino Acid Derivatives. 3-Phenyl-2-Thiohydantoins and N-Thionocarbethoxy Amino Acids

CARL DJERASSI and KJELL UNDHEIM

Department of Chemistry, Stanford University, Stanford, California, U.S.A.,

R. C. SHEPPARD and W. G. TERRY

Department of Organic Chemistry, University of Liverpool, Liverpool, England,

BERNDT SJÖBERG

Department of Organic Chemistry, Chemical Institute, University of Uppsala, Sweden **

Some derivatives of α-amino acids, whose optical rotatory dispersion curves can be used for establishing their absolute configurations, have been investigated. In particular, derivatives have been studied which are also employed in the sequential degradation of peptides, and the present paper is mainly concerned with the optical rotatory dispersion of 3-phenyl-2-thiohydantoins and N-thionocarbethoxy amino acids.

The use of optical rotatory dispersion measurements [1,2] for stereochemical assignments and conformational problems is now well established. The applicability of anomalous rotatory dispersion curves is, however, usually limited to optically active chromophores (*e.g.* carbonyl groups [3], disulfides [4], *etc.*), which absorb in a suitable spectral range with relatively low extinction. A number of important functional groups, however, do not satisfy these requirements. In order to circumvent this difficulty, we have been investigating the preparation of "chromophoric" derivatives which would exhibit Cotton effect curves in contrast to the plain curves [5] of the "non-chromophoric"

* Paper XLV, Djerassi, C., Records, R. and Bach, B. *Chem. & Ind. London. In press.*
** Present address, AB Astra, Södertälje, Sweden.

parent. Obviously, such an approach would enormously increase the scope of rotatory dispersion applications in the field of organic chemistry and several recent publications have demonstrated the feasibility of such studies. Dithiocarbamates (I)[6], xanthates (II)[6], thioureas (III)[7] and osmates [8] have proved to be useful in yielding Cotton effect curves for the otherwise transparent amino, hydroxy, carboxylic acid or olefinic groups. While N-dithiocarbalkoxy (dithiocarbamate) derivatives of α-amino acids (I) have proved to be very suitable [6] for establishing the absolute configuration of the α-asymmetric center — a positive Cotton effect corresponding to the L-configuration, and a negative one corresponding to the D-configuration — we have nevertheless felt that it would be profitable to examine other derivatives of α-amino acids for the same purpose. In particular, it seemed appropriate to study derivatives which are also employed in the sequential degradation of peptides, and the present paper is concerned with two such derivatives.

3-PHENYL-2-THIOHYDANTOINS

One of the generally accepted chemical methods [9] for the stepwise degradation of a peptide sequence is due to Edman [10] and proceeds through the 5-substituted 3-phenyl-2-thiohydantoins (IV) [11]. These derivatives show strong ultraviolet absorption maxima near 267 mμ [12], whose intensity (log $\varepsilon > 4.2$) precludes rotation measurements through this absorption band. However, as shown in Fig. 1, for two typical cases (3-phenyl-2-thiohydantoins derived from alanine and tyrosine), there is also present a low intensity shoulder around 310 mμ and it is this absorption feature which prompted us to prepare the phenylthiohydantoins of several optically active α-amino acids for rotatory dispersion measurements. Edman [11] has called attention to the fact that in those instances where he examined optically active amino acids, the specific

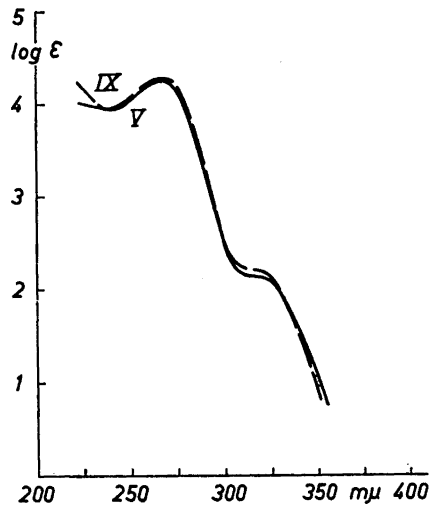

Fig. 1. Ultraviolet absorption in methanol of 5-methyl-3-phenyl-2-thiohydantoin (V) and 5-*p*-hydroxybenzyl-3-phenyl-2-thiohydantoin (IX).

rotation of the phenylthiohydantoins at the sodium D-line was either 0° or very low, indicating complete or partial racemization. If the electronic transition responsible for the 310 mμ absorption is "optically active", one could expect rather high rotations near the extrema of its Cotton effect and even partially racemized phenylthiohydantoins should yield measurable Cotton effects. As we have already pointed out elsewhere [13–15], for purposes of absolute configurational assignments the sign only (rather than the amplitude as well) of the Cotton effect is required and even partially racemized substances lend themselves to this approach [15].

In Fig. 2 are reproduced the optical rotatory dispersion curves of the 3-phenyl-2-thiohydantoins derived from L-alanine (V), L-valine (VI) and L-proline (VII). All three show positive Cotton effects, suggesting that the earlier generalization [6] concerning the N-dithiocarbalkoxy α-amino acids (I), namely, that a positive Cotton effect is attributable to the L-configuration of the α-asymmetric center, applies here too. The location of the Cotton effect, with the first extremum appearing near 340 mμ, shows quite clearly that the 310 mμ ultraviolet band (Fig. 1) is responsible for the anomalous character of the dispersion curve. The amplitudes of the Cotton effects are quite small and this may possibly be due to partial racemization, as has been suggested by Edman [11].

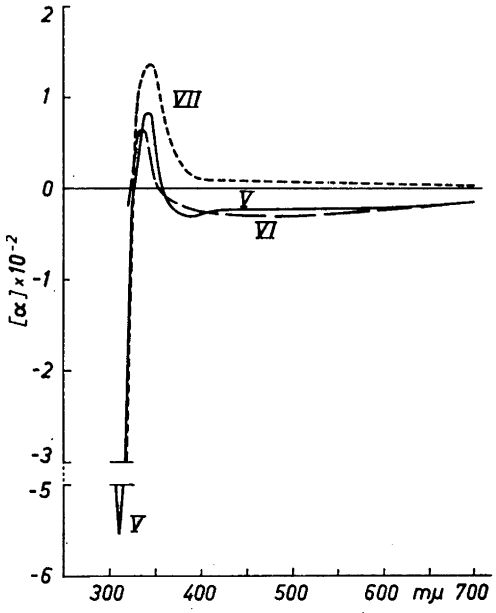

Fig. 2. Optical rotatory dispersion curves of 5-methyl-3-phenyl-2-thiohydantoin (V), 5-*iso*propyl-3-phenyl-2-thiohydantoin (VI) and 1,5-*cyclo*trimethylene-3-phenyl-2-thiohydantoin (VII).

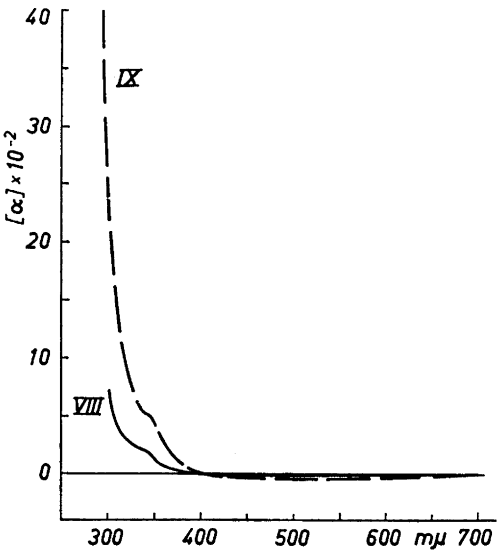

Fig. 3. Optical rotatory dispersion curves of 5-benzyl-3-phenyl-2-thiohydantoin (VIII) and 5-*p*-hydroxybenzyl-3-phenyl-2-thiohydantoin (IX).

When an aromatic ring is present in the *a*-amino acid, the situation is altered. The phenylthiohydantoins of L-phenylalanine (VIII) and L-tyrosine (IX) exhibit rotatory dispersion curves (Fig. 3) which are characterized by a very steep rise in rotation below 350 mμ, this being particularly pronounced with the tyrosine derivative (IX). The Cotton effect associated with the 310 mμ absorption band can now only be seen as a slight irregularity in the dispersion curves, the dominant factor presumably being the second ultraviolet absorption maximum through which rotation measurements cannot be conducted with the currently available instruments. It would appear, however, that the positive sign of these dispersion curves can be utilized for stereochemical purposes in an analogous manner to the plain curves of simpler carboxylic acids [14].

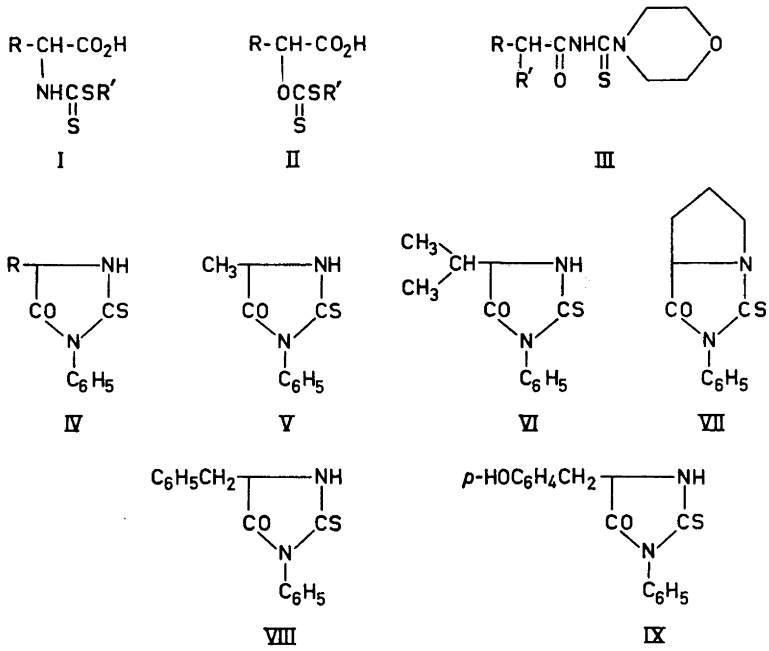

N-THIONOCARBETHOXY *a*-AMINO ACIDS

Kenner and Khorana [16] have pointed out that N-thionocarbethoxy derivatives of peptides, readily prepared by the action of dialkylxanthates, constitute useful intermediates for peptide degradation. In spite of its promise, this approach does not appear to have been widely used in peptide chemistry and the British workers limited their model experiments to optically inactive substrates. In order to examine the suitability of N-thionocarbethoxy derivatives (X) of *a*-amino acids for rotatory dispersion work, it was first necessary to determine whether the C=S grouping in this moiety possessed a suitable ultraviolet absorption band. Careful ultraviolet measurements showed that

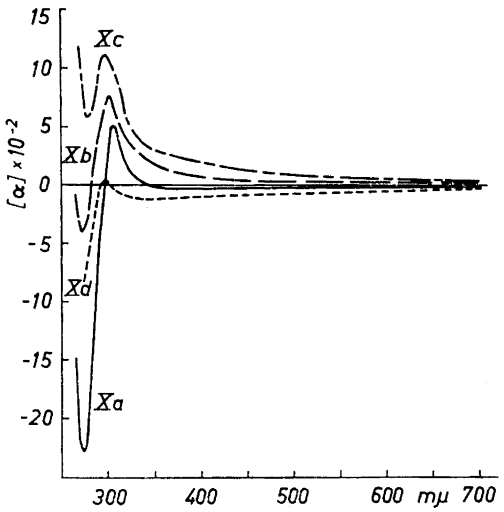

Fig. 4. Optical rotatory dispersion curves of N-thionocarbethoxy L-alanine (Xa), N-thionocarbethoxy L-methionine (Xb), N-thionocarbethoxy L-phenylalanine (Xc) and N-thionocarbethoxy S-benzyl-L-cysteine (Xd).

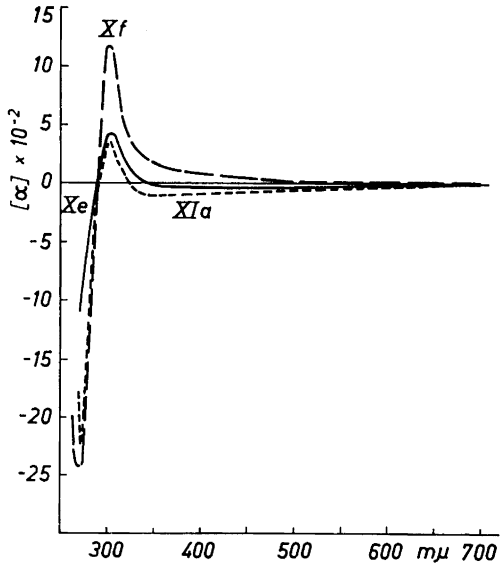

Fig. 5. Optical rotatory dispersion curves of N-thionocarbethoxy L-valine (Xe), N-thionocarbethoxy L-leucine (Xf) and N-thionocarbethoxy L-proline (XIa).

while the principal ultraviolet absorption band of such derivatives occurs at 247 mμ (log $\varepsilon \sim 4.2$) *, there is present in the spectrum a very slight shoulder between 280—285 mμ. If "optically active", the low extinction (log $\varepsilon \sim 2.2$) of this absorption band would lend itself to experimentally measurable Cotton effects and this prompted us to synthesize a number of optically active N-thionocarbethoxy α-amino acids (X).

The rotatory dispersion results are summarized in Figs. 4—6 and demonstrate clearly that the inflection in the ultraviolet absorption spectrum near 280 mμ is responsible for the observed Cotton effects. The rotatory dispersion curves of N-thionocarbethoxy L-alanine (Xa), L-methionine (Xb), L-phenylalanine (Xc) and S-benzyl-L-cysteine (Xd) shown in Fig. 4, as well as those of N-thionocarbethoxy L-valine (Xe), L-leucine (Xf) and L-proline (XIa) collected in Fig. 5, are unexceptional. All of them exhibit positive Cotton effect curves in accordance with expectation [6] for members of the L-series. The only exception from this generalization is found in Fig. 6 in which are shown the rotatory dispersion curves of N-thionocarbethoxy allohydroxy-L-proline (XIb) and hydroxy-L-proline (XIc). The former again shows a positive Cotton effect, as did the corresponding derivative XIa of L-proline (Fig. 5),

* This strong absorption maximum may prove useful in some analytical applications involving N-thionocarbethoxy intermediates.

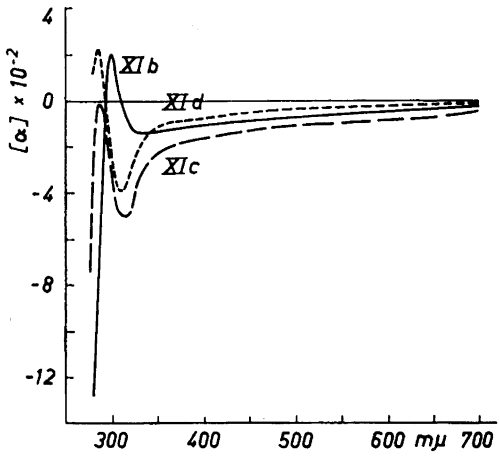

Fig. 6. Optical rotatory dispersion curves of N-thionocarbethoxy allohydroxy-L-proline (XIb), N-thionocarbethoxy hydroxy-L-proline (XIc) and N-thionocarbethoxy acetoxy-L-proline (XId).

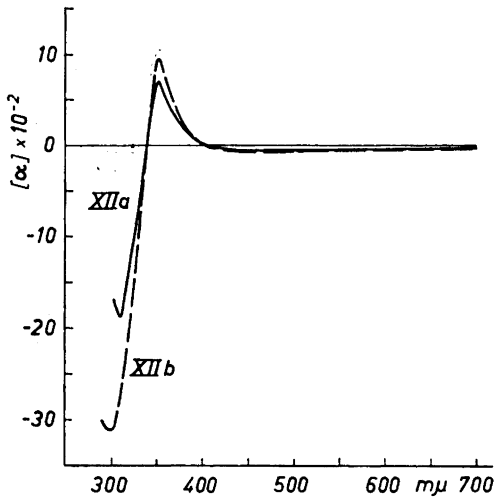

Fig. 7. Optical rotatory dispersion curves of N-dithiocarbethoxy hydroxy-L-proline (XIIa) and N-dithiocarbethoxy allohydroxy-L-proline (XIIb).

but the hydroxy-L-proline analog (XIc) exhibits a negative Cotton effect. This anomaly cannot be ascribed to the free hydroxy function, since N-thionocarbethoxy acetoxy-L-proline (XId) behaved similarly (see Fig. 6). No uncertainty can be attached to the structure of the derivative obtained from hydroxy-L-proline, since the analytical and spectroscopic properties are in agreement with formulation XIc. Furthermore, the identical product was obtained by direct treatment of hydroxy-L-proline with O-ethyl methyl-xanthate, as well as from acetoxy-L-proline *via* the derivative XId followed by saponification.

In order to examine further the anomalous behaviour of N-thionocarbethoxy hydroxy-L-proline (XIc), we have now synthesized the corresponding dithiocarbamate, N-dithiocarbethoxy hydroxy-L-proline (XIIa), as well as N-dithiocarbethoxy allohydroxy-L-proline (XIIb), as these two amino acid derivatives were not included in our earlier study. As shown in Fig. 7, both XIIa and XIIb exhibit positive Cotton effect curves, in accordance with the earlier enunciated [6] generalization that N-dithiocarbalkoxy *a*-amino acids of the L-series possess positive Cotton effects.

The Cotton effects associated with the dispersion curves of N-dithiocarbalkoxy (I) or N-thionocarbalkoxy (X) derivatives of *a*-amino acids are due to interaction of the electrons involved in the appropriate transition of the C=S chromophore (which give rise to the low-intensity ultraviolet absorption band) with the partially unshielded nuclei of other substituents in the asymmetric environment. It seems likely that a given "rotometer" of the substituent attached to the nitrogen predominates in the amino acid derivatives

under discussion, so that the disposition in space of the other substituents with respect to the C=S chromophore is always similar. This explains why the same sign of the Cotton effect is observed for members of identical absolute configuration and why this generalization applies to the dithiocarbalkoxy (I) as well as to the thionocarbalkoxy (X) derivatives. In view of this apparently systematic behaviour, the exception of N-thionocarbethoxy hydroxy-L-proline (XIc), (Fig. 6), when contrasted with the "normal" behaviour of the corresponding N-dithiocarbethoxy derivative XIIa (Fig. 7), suggests that the C=S chromophore of the former has in some way been forced into an unusual spatial position.

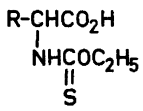

Xa R = CH_3
b R = $CH_3SCH_2CH_2$
c R = $C_6H_5CH_2$
d R = $C_6H_5CH_2SCH_2$
e R = $(CH_3)_2CH$
f R = $(CH_3)_2CHCH_2$

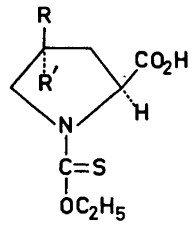

XIa R = R′ = H
b R = OH; R′ = H
c R = H; R′ = OH
d R = H; R′ = OAc

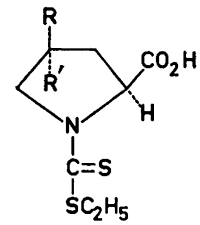

XIIa R = H; R′ = OH
b R = OH; R′ = H

The amplitudes of the Cotton effects of the N-dithiocarbalkoxy (I) and N-thionocarbalkoxy (X) derivatives were found to be relatively large, and it seemed likely that only little racemization, if any, had occurred during the preparation of these derivatives. In order to determine the extent of racemization, we performed lithium aluminum hydride reductions of the crude N-dithiocarbethoxy L-alanine and N-thionocarbethoxy L-alanine. Reduction of carbamates usually yield N-methylamines [17] and accordingly we obtained N-methylalaninol. The specific rotations were found to be +35.8° for the reduction product of N-dithiocarbethoxy L-alanine and +36.6° for that of N-thionocarbethoxy L-alanine. Authentic N-methyl-L-alaninol, obtained from a purified sample of N-dithiocarbethoxy L-alanine which was undoubtedly optically pure [18], had a specific rotation of 38.0°. Apparently, at least for the alanine derivatives, there is little racemization in the preparation of the dithiocarbethoxy and thionocarbethoxy derivatives, in contrast to the situation obtaining with Edman's phenylthiohydantoins.

CONCLUSION

Of the three α-amino acid derivatives (I, IV, X) which lend themselves to stereochemical assignments by consideration of their anomalous optical rotatory dispersion, the dithiocarbamates (I)[6] appear to be the most useful

ones, particularly since their relevant absorption band (*ca.* 330 mμ) occurs in a more convenient region. Furthermore, no exceptions have been noted to the generalization that L-amino acid derivatives show positive Cotton effect curves, this being true even of N-dithiocarbethoxy hydroxy-L-proline (XIIa). In terms of ease of preparation, N-thionocarbethoxy derivatives (X) are equally satisfactory and since their rotatory dispersion curves have proved to be quite instructive (Figs. 4—6), the actual choice of derivative may well depend on other factors (ease of crystallization or preparation incidental to peptide degradation). The reduced amplitude of the Cotton effect of the phenylthiohydantoins (IV) makes them less desirable for the purposes described in this paper.

EXPERIMENTAL

All rotatory dispersion measurements were determined in methanol solution (22—25°) by Mrs. R. Records and Mrs. T. Nakano, by means of an automatically recording Rudolph spectropolarimeter. The data are reported below in the manner outlined in Ref.[5]

3-Phenyl-2-thiohydantoins (IV)

These were prepared by the method of Edman [11] by dissolving the amino acid in 50 % aqueous pyridine, adjusting the pH to 9 with 1 N sodium hydroxide and stirring with phenyl*iso*thiocyanate at 40° until alkali consumption stopped (the pH being maintained at 9 by addition of alkali). After extraction with benzene (discarded), the aqueous solution containing the phenylthiocarbamate derivative was adjusted to pH 2.5 by means of hydrochloric acid and left at room temperature for two days. The thiohydantoin was then filtered and recrystallized, the melting points agreeing in every instance with those reported by Edman [11].

5-Methyl-3-phenyl-2-thiohydantoin (V), R.D. (Fig. 2), *c*, 0.105: $[a]_{700}$ −8°, $[a]_{589}$ −19°, $[a]_{342.5}$ +84°, $[a]_{310}$ −553°, $[a]_{290}$ −36°.

5-Isopropyl-3-phenyl-2-thiohydantoin (VI), R.D. (Fig. 2), *c*, 0.100: $[a]_{700}$ −8°, $[a]_{589}$ −18°, $[a]_{335}$ +64°, $[a]_{322.5}$ −20°.

1,5-Cyclotrimethylene-3-phenyl-2-thiohydantoin (VII), R.D. (Fig. 2), *c*, 0.102: $[a]_{700}$ +4°, $[a]_{589}$ +6°, $[a]_{342.5}$ +137°, $[a]_{310}$ −311°.

5-Benzyl-3-phenyl-2-thiohydantoin (VIII), R.D. (Fig. 3), *c*, 0.105: $[a]_{700}$ −15°, $[a]_{589}$ −25°, $[a]_{340}$ +200° (inflect.), $[a]_{295}$ +866°.

5-p-Hydroxybenzyl-3-phenyl-2-thiohydantoin (IX), R.D. (Fig. 3), *c*, 0.102: $[a]_{700}$ −31°, $[a]_{589}$ −39°, $[a]_{340}$ +520° (inflect.), $[a]_{292.5}$ +4040°.

N-Thionocarbethoxy *a*-amino acids (X)

These were prepared according to the procedure of Kenner and Khorana [16], except that the L-amino acid was used in each instance. All of the derivatives showed the typical ultraviolet absorption maximum at 247 mμ (log. ε ~4.2) with a slight shoulder in the 280—285 mμ region.

N-Thionocarbethoxy-L-alanine (Xa), m.p. 80° (from chloroform/light petroleum). (Found: C 40.84; H 6.27; N 8.04; S 18.27. $C_6H_{11}NO_3S$ requires C 40.68; H 6.26; N 7.91; S 18.06.)

R.D. (Fig. 4), *c*, 0.195 (0.039 below 290 mμ): $[a]_{700}$ −10°, $[a]_{589}$ −22°, $[a]_{305}$ +512°, $[a]_{275}$ −2 305°, $[a]_{264}$ −1 460°.

N-Thionocarbethoxy L-methionine (Xb), viscous oil, R.D. (Fig. 4), *c*, 0.115 (0.057 below 290 mμ): $[a]_{700}$ 0°, $[a]_{589}$ +2°, $[a]_{302.5}$ +758°, $[a]_{272.5}$ −402°, $[a]_{267.5}$ −105.

N-Thionocarbethoxy L-phenylalanine (Xc), m.p. 87° (from ether/light petroleum). (Found: C 57.14; H 5.98; N 5.65; S 12.31. $C_{12}H_{15}NO_3S$ requires C 56.91; H 5.97; N 5.53; S 12.64.)

R.D. (Fig. 4), *c*, 0.410 (0.082 below 350 mμ): $[a]_{700}$ +30°, $[a]_{589}$ +55°, $[a]_{298}$ +1 116°, $[a]_{277.5}$ +578°, $[a]_{270}$ +1 200°.

N-Thionocarbethoxy S-benzyl-L-cysteine (Xd), viscous oil, R.D. (Fig. 4), *c*, 0.098: $[a]_{700}$ −41°, $[a]_{589}$ −55°, $[a]_{300}$ +21°, $[a]_{275}$ −775°.

N-Thionocarbethoxy L-valine (Xe), m.p. 65° (from benzene/light petroleum). (Found: C 46.97; H 7.38; N 6.81; S 15.33. $C_8H_{15}NO_3S$ requires C 46.82; H 7.37; N 6.83; S 15.59.)

R.D. (Fig. 5), *c*, 0.510 (0.102 below 300 mμ): $[a]_{700}$ −16°, $[a]_{589}$ −23°, $[a]_{302.5}$ +441°, $[a]_{275}$ −1 080°.

N-Thionocarbethoxy L-leucine (Xf), m.p. 79° (from benzene/light petroleum). (Found: C 49.62; H 7.73; N 6.44; S 14.90. $C_9H_{17}ON_3S$ requires C 49.34; H 7.82; N 6.39; S 14.62.)

R.D. (Fig. 5), *c*, 0.290 (0.058 below 290 mμ): $[a]_{700}$ 0°, $[a]_{589}$ 0°, $[a]_{302.5}$ + 1 175°, $[a]_{270}$ −2 440°, $[a]_{265}$ −1 995°.

N-Thionocarbethoxy L-proline (XIa), m.p. 69° (from ether/light petroleum). (Found: C 47.15; H 6.51; N 6.94; S 16.12. $C_8H_{13}NO_3S$ requires C 47.29; H 6.45; N 6.89; S 15.75.)

R.D. (Fig. 5), *c*, 0.113: $[a]_{700}$ −23°, $[a]_{589}$ −42°, $[a]_{302.5}$ + 375°, $[a]_{271}$ −2 220°, $[a]_{269}$ −1 785.

N-Thionocarbethoxy allohydroxy-L-proline (XIb), m.p. 107−8° (from chloroform/light petroleum). (Found: C 43.84; H 6.16; N 6.13; S 14.86. $C_8H_{13}NO_4S$ requires C 43.83; H 5.98; N 6.39; S 14.60.)

R.D. (Fig. 6), *c*, 0.121: $[a]_{700}$ −27°, $[a]_{589}$ −53°, $[a]_{325}$ −136°, $[a]_{300}$ +207°, $[a]_{280}$ −1 270°.

N-Thionocarbethoxy hydroxy-L-proline (XIc), m.p. 124° (from chloroform/light petroleum). (Found: C 43.98; H 5.88; N 6.42; S 14.62. $C_8H_{13}NO_4S$ requires C 43.83; H 5.98; N 6.39; S 14.60.)

R.D. (Fig. 6), *c*, 0.096: $[a]_{700}$ −37°, $[a]_{589}$ −79°, $[a]_{312.5}$ −507°, $[a]_{285}$ −10°, $[a]_{275}$ −729°.

N-Thionocarbethoxy acetoxy-L-proline (XId). O-Acetylhydroxy-L-proline [19] (1.8 g) was dissolved in water (15 ml) and 2-methoxyethanol (60 ml) containing O-ethyl methyl xanthate (5 ml) added. The solution was kept for 24 h at pH 8.5 (glass electrode) by the gradual addition of N sodium hydroxide (autotitrator). Isolation of the product in the usual manner afforded the N-thionocarbethoxy derivative (1.81 g) as a viscous oil.

R.D. (Fig. 6), *c*, 0.116; $[a]_{700}$ −14°, $[a]_{589}$ −21°, $[a]_{310}$ −382°, $[a]_{285}$ +217°.

A sample was hydrolysed at pH 12 (autotitrator) in 80 % 2-methoxy-ethanol for 24 h, and furnished N-thionocarbethoxy hydroxy-L-proline, m.p. and mixed m.p. 123−4°.

N-Dithiocarbethoxy α-amino acids (XII)

These were prepared in the same manner as previously described [6,17]. The derivatives showed the typical ultraviolet absorption maxima at 333, 278, and 251 mμ. ($\log \varepsilon \sim 1.8$, 4.0 and 4.0).

N-Dithiocarbethoxy hydroxy-L-proline (XIIa), m.p. 89−91° (from ether/light petroleum). (Found: N 5.90; S 26.90. $C_8H_{13}NO_3S_2$ requires N 5.95; S 27.25.

R.D. (Fig. 7), *c*, 0.18: $[a]_{700}$ −38°, $[a]_{589}$ −51°, $[a]_{352.5}$ +690°, $[a]_{310}$ −1 780°, $[a]_{300}$ −1 585.

N-Dithiocarbethoxy allohydroxy-L-proline (XIIb), m.p. 115−117° (from ether/light petroleum). (Found: N 5.87; S 27.52. $C_8H_{13}NO_3S_2$ requires N 5.95; S 27.25.)

R.D. (Fig. 7), *c*, 0.083 (0.017 below 350 mμ): $[a]_{700}$ −41°, $[a]_{589}$ −48°, $[a]_{352.5}$ +945°, $[a]_{300}$ −3 140°, $[a]_{295}$ −3 010°.

N-Methyl-L-alaninol

N-Dithiocarbethoxy-L-alanine was prepared according to Fredga [18]. The product was recrystallized four times from carbon tetrachloride, m.p. 107, $[a]^{23}_D$ −27.3° (*c*, 1.9 in benzene). Fredga reported for the optically pure product, m.p. 106−107°, $[a]^{25}_D$ −27.2° (c, 1.9 in benzene).

A solution of the N-dithiocarbethoxy-L-alanine (2.0 g) in dry tetrahydrofuran (50 ml) was added dropwise to a solution of lithium aluminum hydride (2 g) in tetrahydrofuran (200 ml). After the addition was complete, the mixture was heated under reflux for about 20 h, cooled, and excess hydride decomposed with saturated aqueous sodium sulphate solution. The dried (Na_2SO_4) solution was filtered, evaporated and the residue distilled,

to yield 0.70 g of N-methyl-L-alaninol, b.p. 64–65°/11 mm, $[\alpha]^{23}_D$ +38.0° (*c*, 2.0 in ethanol). (Found: C 53.85; H 12.40; N 15.80. $C_4H_{11}NO$ requires C 53.89; H 12.44; N 15.71.

Reduction of crude N-dithiocarbethoxy-L-alanine

L-alanine (1.8 g) was converted to the N-dithiocarbethoxy derivative in the usual manner, and the crude product reduced without prior purification. The reduction and work-up procedures were as described above. $[\alpha]^{22}_D$ +35.8° (*c*, 2.1 in ethanol). (Found: C 53.72; H 12.45; N 15.75. $C_4H_{11}NO$ requires C 53.89; H 12.44; N 15.71.

Reduction of crude N-thionocarbethoxy-L-alanine

L-alanine (1.8 g) was converted to the N-thionocarbethoxy derivative in the usual manner, and the crude product reduced without prior purification. The reduction and work-up procedures were as described above. $[\alpha]^{18}_D$ +36.6° (*c*, 4.9 in ethanol). (Found: C 53.52; H 12.45; N 15.73. $C_4H_{11}NO$ requires C 53.89; H 12.44; N 15.71.

Acknowledgement. We are indebted to the *National Cancer Institute* of the National Institutes of Health, U.S. Public Health Service for a grant (CYTR-5061), to Dr. B. Witkop for a gift of allohydroxy-L-proline and to Prof. G. W. Kenner for his interest.

REFERENCES

1. Djerassi, C. *Optical Rotatory Dispersion: Applications to Organic Chemistry*, McGraw-Hill Book Co., New York 1960.
2. Djerassi, C. *Bull. soc. chim. France* **1957** 741; Djerassi, C. Record Chem. Progr. *Kresge-Hooker Sci. Lib.* 20 (1959) 101; Klyne, W. in Raphael, R. A., Taylor, E. C. and Wynberg, H. Advances in Org. Chem. **1** (1960) 239. Leemann, H. G. *Chimia* **14** (1960) 1; Nakanishi, K. *Kagaku no Ryoiki* **13** (1959) 2.
3. For leading references see chapter 4–13 in Ref.[1]
4. Djerassi, C., Fredga, A. and Sjöberg, B. *Acta Chem. Scand.* **15** (1961) 417.
5. For nomenclature see chapter 2 in Ref. [1]
6. Sjöberg, B., Fredga, A. and Djerassi, C. *J. Am. Chem. Soc.* **81** (1959) 5002.
7. Djerassi, C. and Undheim, K. *J. Am. Chem. Soc.* **82** (1960) 5755.
8. Bunnenberg, E. and Djerassi, C. *J. Am. Chem. Soc.* **82** (1960) 5953.
9. Thompson, E. O. P. in Raphael, R. A., Taylor, E. C. and Wynberg, H. *Advances in Org. Chem.* **1** (1960) 149.
10. Edman, P. *Acta Chem. Scand.* **4** (1950) 283.
11. Edman, P. *Acta Chem. Scand.* **4** (1950) 277.
12. Dahlerup-Peterson, B., Linderstrøm-Lang, K. and Ottesen, M. *Acta Chem. Scand.* **6** (1952) 1135; Fraenkel-Conrat, H. and Harris, J. I. *J. Am. Chem. Soc.* **76** (1954) 6058.
13. See Ref.[1] pp. 135 and 206.
14. Sjöberg, B. *Acta Chem. Scand.* **14** (1960) 273.
15. Sjöberg, B. *Arkiv Kemi* **15** (1960) 473.
16. Kenner, G. W. and Khorana, H. G. *J. Chem. Soc.* **1952** 2076.
17. Gaylord, N. G. *Reduction with Complex Metal Hydrides*, Interscience Publ., New York 1956.
18. Fredga, A. *Svensk Kem. Tidskr.* **54** (1942) 26.
19. Sakami, W. and Toennies, G. *J. Biol. Chem.* **144** (1942) 203.

Received December 19, 1960.

ACTA CHEMICA SCANDINAVICA 15 (1961) 913–918

Potentiometric Determination of the Solubility Product of Lead Carbonate

REINO NÄSÄNEN, PAAVO MERILÄINEN and KAARINA LEPPÄNEN

Department of Chemistry, University of Helsinki, Helsinki, Finland

A simple potentiometric pH method has been employed in the determination of the solubility product of lead carbonate. The method gave consistent values for the solubility product on both precipitation and dissolution of lead carbonate. The effect of added potassium nitrate on the solubility equilibrium was also investigated. The results are discussed on the assumption that the complex ion $PbNO_3^+$ is formed. Values of the first acid dissociation constant of carbonic acid in potassium nitrate solutions were determined. Extrapolation to zero ionic strength gave the value $10^{3.55}$ (25°C; $I = 0$) for the equilibrium constant of the reaction: $PbCO_3$ (s) + $2H^+ \rightleftharpoons Pb^{2+} + CO_2$ (aq) + H_2O. Solubility product of lead carbonate was calculated to be $10^{-13.13}$ (25°C; $I = 0$).

The determinations of the solubility product of lead carbonate are relatively few in number and the conditions to which the results refer are mostly poorly specified [1]. This concerns especially the partial pressure of carbon dioxide in equilibrium with the solution. A redetermination of the solubility product seemed therefore justified.

The reaction primarily studied is

$$PbCO_3(s) + 2H^+ \rightleftharpoons Pb^{2+} + CO_2(aq) + H_2O \qquad (1)$$

Two methods were followed when carrying out the determinations. In the first method, a weighed amount of lead carbonate was allowed to stand in water through which carbon dioxide was passed. In some experiments, small amounts of strong acid were present in the solution. In the second method, carbon dioxide was passed through a lead nitrate solution to which some sodium hydroxide had been added. In both cases the pH of the solutions was measured after 2—4 days. The equilibrium constant of reaction (1)

$$K = [Pb^{2+}][CO_2]/[H^+]^2 \qquad (2)$$

can be evaluated from the equations:

$$[HCO_3^-] = [CO_2]K_1/[H^+] \qquad (3)$$

and

$$[Pb^{2+}] = \tfrac{1}{2}\{[HCO_3^-] + c_A + 2c_{Pb} - c_B - [H^+]\} \quad (4)$$

where K_1 is the apparent first acid dissociation constant of carbonic acid, c_A the total molarity of the added perchloric acid, c_{Pb} that of the added lead nitrate and c_B that of the added sodium hydroxide.

Some of the measurements were carried out without added neutral salt present and some with potassium nitrate present. This salt was chosen because the solubility of carbon dioxide in potassium nitrate solutions is known. Randall and Failey [2] have found that at 25°

$$\log \gamma = 0.0265 \mu \quad (5)$$

where γ is the activity coefficient of carbon dioxide and μ the ionic strength, both on the molality scale. Conversion to the molarity scale gives

$$\log y = 0.0458 I \quad (6)$$

As values of the apparent first acid dissociation constant of carbonic acid

$$K_1 = [H^+] [HCO_3^-]/[CO_2] \quad (7)$$

in potassium nitrate solutions have not been determined previously, the values of the constant in 0.25, 1.00 and 2.00 molar solutions were determined. The method was as follows. Carbon dioxide was passed into a potassium nitrate solution and the solution was titrated with sodium hydroxide solution, the hydrogen ion concentration being measured after each addition of sodium hydroxide. The acid dissociation constant can be evaluated from

$$K_1 = [H^+](c_B + [H^+])/[CO_2] \quad (8)$$

where c_B is the total molarity of the added sodium hydroxide. The concentration $[CO_2]$ is obtained from

$$[CO_2] = p_{CO_2} S_o/y \quad (9)$$

where p_{CO_2} is the partial pressure of carbon dioxide in atm., S_o the Henry's law constant for carbon dioxide in pure water and y the activity coefficient. The value $3.44 \cdot 10^{-2}$ was used for the Henry's law constant S_o at 25°C [3] and the value of y was computed from eqn. (6).

EXPERIMENTAL

Purified carbon dioxide gas was passed first through a spiral bubbling saturator into the solution in the titration vessel. The cover of the titration vessel had holes for tubes through which the gas entered and left the vessel, for the electrodes and for the buret. The partial pressure of carbon dioxide was obtained by subtracting the vapour pressure of the potassium nitrate solution [4] from the barometric pressure.

The hydrogen ion concentration was measured with a Beckman 4990–83 glass electrode in combination with a calomel electrode. Two types of calomel electrode were used. When the solution under study contained no added neutral salt, the usual "saturated" electrode was used. When the solution contained potassium nitrate, the electrode vessel was filled with sodium chloride solution and the bridge with potassium nitrate solution, both equal in concentration to that of the salt in the test solution. In the former case, a 0.05 M solution of potassium hydrogen phthalate (pH = 4.01) served as the standard buffer solution. The conventional pH values obtained were converted to values

Table 1. Acetate buffers 0.005 M in acetic acid and sodium acetate at 25°C.

	$-\log [H^+]$
0.250 M KNO_3	4.535
1.000 » »	4.567
2.000 » »	4.688

of $-\log[H^+]$ by means of apparent pf_{H+} values [5]. When the test solutions contained potassium nitrate, acetate buffers 0.005 M in acetic acid and 0.005 M in sodium acetate served as standards. The three standard buffer solutions used are described in Table 1. The hydrogen ion concentrations of these buffers were determined by comparing them with the hydrogen ion concentrations of 0.005 M hydrochloric acid solutions containing the same concentrations of potassium nitrate. The values obtained were in good agreement with the values calculated from the acid dissociation constants of acetic acid determined by Ellilä [6].

All chemicals used were of analytical grade. Several commercial preparations of lead carbonate were used and in addition a lead carbonate prepared by a method described by Centnerszwer, Falk and Awerbuch [7]. Identical results were obtained with all preparations. The analysis of the solid phase after equilibrium was reached showed it to be normal lead carbonate.

RESULTS

The accuracy obtained in the determination of the apparent first acid dissociation constant of carbonic acid in potassium nitrate solution is seen from Table 2 where data from an individual titration are shown. The values obtained for the constant K_1 are collected in Table 3. As seen from this table these values are satisfactorily represented by the equation

$$pK_1 = 6.35 - \frac{1.018\sqrt{I}}{1 + 1.40\sqrt{I}} + 0.055\,I. \qquad (10)$$

The value of pK_1 at zero ionic strength was taken to be 6.35. Harned and Bonner [8] have obtained the value 6.352 and Näsänen [9] the value 6.349, for this constant at 25°C.

The results of the determinations of the equilibrium constant of reaction (1) when no potassium nitrate was added are summarized in Table 4. The values given are means of several individual values. When dissolving lead carbonate, a small amount of perchloric acid was added since the pH measurement was then more accurate, probably because of the higher buffer capacity of the solution. The value of constant K at zero ionic strength given in Table 4 was calculated from the expression

$$\log K^\circ = \log K - 1.018\sqrt{I}. \qquad (11)$$

Table 2. Data from a titration for the determination of the apparent first acid dissociation constant of carbonic acid in a 2 M potassium nitrate solution at 25°C. $S_0 = 3.44 \times 10^{-2}$.

$c_B \times 10^3$	$-\log [H^+]$	p_{CO_2} (atm)	$1/y$	pK_1
5.00	5.232	0.982	0.810	5.976
7.00	5.381	0.982	0.810	5.973
10.00	5.537	0.982	0.810	5.974

Table 3. Values of the apparent first acid dissociation constant of carbonic acid in potassium nitrate solutions at 25°C.

I	pK_1(exptl.)	pK_1(eqn. 10)
0.257	6.059	6.064
1.007	5.991	5.982
2.007	5.973	5.979

The results of a series of measurements in a 2 M potassium nitrate solution are given in Table 5. In this case mineral acid was not added since the pH could be measured very well even without the addition. The results for potassium nitrate solutions are summarized in Table 6. The results are very satisfactorily represented by the expression

$$\log K = 3.55 + \frac{2.036\sqrt{I}}{1+\sqrt{I}} - \frac{1.018\sqrt{I}}{1+2.20\sqrt{I}} + 0.33\,I \qquad (12)$$

where the second term on the right is due to the activity coefficient of the lead ion and the third term to that of the hydrogen ion. The third term was taken somewhat arbitrarily from a previously reported equation for "the apparent activity coefficient" of the hydrogen ion [5]. The other parameters were adjusted so that eqn. (12) conformed to the experimental results as well as possible. The results could be represented satisfactorily by the following simple expression:

$$\log K = 3.55 + 1.018\sqrt{I} + B\,I \qquad (13)$$

but not quite so well as by expression (12).

DISCUSSION

The solubility product of lead carbonate

$$K_{sp} = [Pb^{2+}][CO_3^{2-}] \qquad (14)$$

can be calculated from the expression

$$K_{sp} = K\ K_1K_2 \qquad (15)$$

where K is the equilibrium constant of reaction (1), K_1 the first and K_2 the second acid dissociation constant of carbonic acid. The value obtained for

Table 4. Equilibrium constant of reaction $PbCO_3(s) + 2H^+ \rightleftharpoons Pb^{2+} + CO_2(aq) + H_2O$ in dilute solutions at 25°C.

Conditions	Number of separate measurements	$\sqrt{I}$	log K	log $K°$
185.4 mg $PbCO_3$; a small amount of strong acid added.	6	0.037	3.60	3.56
$Pb(NO_3)_2$ solution titrated with alkali hydroxide.	4	0.078	3.62	3.54
	5	0.102	3.64	3.54
	4	0.104	3.67	3.56
				mean 3.55

Table 5. Values of the equilibrium constant of reaction $PbCO_3(s) + 2H^+ \rightleftharpoons Pb^{2+} + CO_2$ (aq.) + H_2O in a 2 M potassium nitrate solution at 25°C.

$PbCO_3$, mg	Standing period, h	$-\log[H^+]$	p_{CO_2}, atm.	$1/y$	log K
140.2	23	4.820	0.989	0.810	5.063
135.2	52	4.825	0.965	0.810	5.055
101.7	26	4.825	0.968	0.810	5.059
130.0	23	4.823	0.968	0.810	5.053

the solubility product at zero ionic strength when the above value log $K^0 = 3.55$, the value [8,9] $pK_1^0 = 6.35$ and the value $pK_2^0 = 10.33$ determined by Harned and Scholes [10] were substituted in (15) was $pK_{sp}^0 = 13.13$. ($I = 0$, 25°C). For the second acid dissociation constant pK_2^0 of carbonic acid, Näsänen [11] obtained the value 10.32 at 25°C.

Recently Uggla [12] determined the solubility product of lead carbonate conductometrically and obtained the value $pK_{sp}^0 = 13.23$ (25°C). From the data in a compilation of the National Bureau of Standards [13] one can calculate the value $pK_{sp}^0 = 13.0$ (25°C). The partial pressure of carbon dioxide in equilibrium with the solution has not been specified in the earlier determinations and the older data for the solubility product must therefore be regarded as unreliable [1,14].

The effect of neutral salt additions on the solubility equilibrium of lead carbonate has not been studied before. In Fig. 1 the equilibrium constant K of reaction (1) is plotted as a function of ionic strength. The limiting slope according to the Debye-Hückel theory is also drawn in the figure. As is seen log K is always higher than expected from Debye's limiting law. This is not, however, at variance with the Debye-Hückel theory since log K is given very satisfactorily by eqn. (12). On the other hand, it is likely, as has been claimed [15], that lead and nitrate ions form a complex as follows:

$$Pb^{2+} + NO_3^- \rightleftharpoons PbNO_3^+. \qquad (16)$$

If this reaction is considered to take place, one obtains for the "true" constant of reaction (1) the expression

$$K' = K/(1 + \tfrac{1}{2}\beta_1[NO_3^-]) \qquad (17)$$

where K is the above apparent equilibrium constant of reaction (1) and β_1 is defined by

$$\beta_1 = [PbNO_3^+]/[Pb^{2+}][NO_3^-] \qquad (18)$$

Table 6. Values of the equilibrium constant of reaction $PbCO_3(s) + 2H^+ \rightleftharpoons Pb^{2+} + CO_2$ (aq) + H_2O in potassium nitrate solutions at 25°C.

I	log K (exptl.)	log K (eqn. 12)
0.251	4.076	4.070
1.002	4.581	4.581
2.002	5.058	5.053

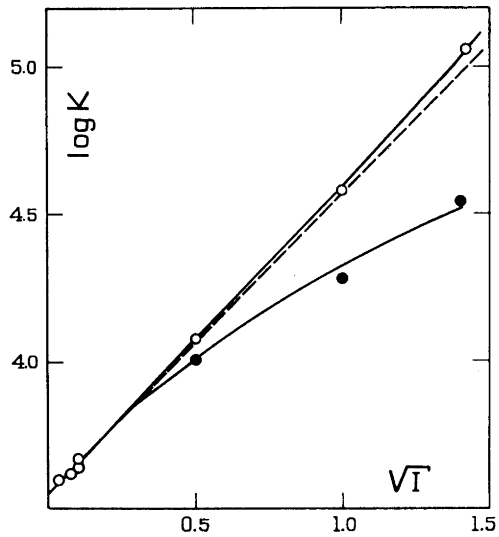

Fig. 1. Equilibrium constant of reaction (1) as a function of ionic strength. O, apparent constant; ●, "true" constant; — — —, limiting Debye-Hückel plot.

The "true" constant K' can be calculated from eqn. (17) if the stability constant β_1 is known. Using the values log $\beta_1 = 0.25$ in 0.5 M, log $\beta_1 = 0.31$ in 1 M, and log $\beta_1 = 0.36$ in 2 M perchloric acid solution, determined by Biggs, Parton and Robinson [16], the values plotted in Fig. 1 were obtained for the "true" constant. These values of the "true" constant are approximate and reveal only the direction of the effect of reaction (16).

REFERENCES

1. *Cf.* Kelley, K. K. and Andersson, C. T. *U.S. Bur. Mines Bull.* **384** (1934).
2. Randall, M. and Failey, C. F. *Chem. Revs.* **4** (1927) 281.
3. Harned, H. S. and Davis, R. *J. Am. Chem. Soc.* **65** (1943) 2030.
4. Timmermans, J. *The Physico-chemical Constants of Binary Systems in Concentrated Solutions*, New York 1960, Vol. **3**, p. 554.
5. Näsänen, R., Lumme, P. and Mukula, A.-L. *Acta Chem. Scand.* **5** (1951) 1199.
6. Ellilä, A. *Ann. Acad. Sci. Fennicae A II* **1954** No. 51.
7. Centnerszwer, M., Falk, G. and Awerbuch, A. *Z. physik. Chem.* **115** (1925) 29.
8. Harned, H. S. and Bonner, T. *J. Am. Chem. Soc.* **67** (1945) 1026.
9. Näsänen, R. *Acta Chem. Scand.* **1** (1947) 204.
10. Harned, H. S. and Scholes, S. R. *J. Am. Chem. Soc.* **63** (1941) 1706.
11. Näsänen, R. *Suomen Kemistilehti* B **19** (1946) 90.
12. Uggla, R. *Ann. Acad. Sci. Fennicae A II* **1959** No. 79.
13. Rossini, F. D., Wagman, D. D., Evans, W. H., Levine, S. and Jaffe, I. *Natl. Bur. Standards*, Circ. **500** (1952).
14. Bjerrum, J., Schwarzenbach, G. and Sillén, L. G. *Stability Constants of Metal-ion Complexes.* Part II: *Inorganic Ligands.* London 1958, p. 46.
15. Ibid. p. 56.
16. Biggs, A. I., Parton, H. N. and Robinson, R. A. *J. Am. Chem. Soc.* **77** (1955) 5844.

Received December 21, 1960.

ACTA CHEMICA SCANDINAVICA 15 (1961) 919–925

X-Ray Studies on Solid Solutions of Oxygen in α-Zirconium

BO HOLMBERG and TORE DAGERHAMN

Institute of Inorganic and Physical Chemistry, University of Stockholm, Stockholm, Sweden

The solubility of oxygen in α-zirconium in the temperature region, 400°–800°C, has been investigated by X-ray methods. The solubility, which is independent of temperature, is 28.6 at % ($ZrO_{0.40}$). With increasing oxygen content, the length of the *c* axis increases over the entire solubility range while that of the *a* axis passes through a maximum at the composition $ZrO_{0.25}$. In the solubility range there exist two phases, *viz.* ZrO_{0+x}, with randomly distributed oxygen atoms, and Zr_3O_{1+y}, with partly ordered oxygen atoms. At the limiting composition ($ZrO_{0.33}$), the oxygen atoms are completely ordered (Zr_3O).

Previous studies on the solubility of oxygen in the hexagonal, close-packed α-modification of zirconium have shown that oxygen can enter into solid solution up to the composition $ZrO_{0.395}$ (28.3 at% O)[1]. The solubility mechanism deduced has been thought to imply that the oxygen atoms occupy the major interstices of the metal structure, *i.e.* the octahedral holes, in a perfectly random way[2]. The incorporation of the oxygen atoms in the α-structure has been reported to be accompanied by a considerable expansion of the *c* axis and by only a slight change in the *a* axis[3].

EXPERIMENTAL

The starting materials for the syntheses were zirconium metal and zirconium dioxide. Two series of alloys were prepared, one with metal from A. D. Mackay Inc. (lump, low in hafnium) and the other with metal from the Foote Mineral Comp. (crystal bar, 99.9 % Zr with 260 ppm O, the principal impurity, and 70 ppm Hf). For the first set of alloy preparations, a Mackay "hafnium free" dioxide was used and, for the second, a dioxide obtained by heating the Foote metal in a stream of oxygen.

The preparation of the alloys was carried out by arc melting the appropriate mixtures of the starting materials in an argon atmosphere as described earlier[4]. After pulverisation, the samples were homogenized by heat-treatment in sealed, evacuated silica capsules. The heat-treatment was always abruptly stopped by quenching in water. The Mackay alloys were heat-treated at 400°C for 1 month and thereafter at 600°C or at 800°C for 1 week and the Foote alloys at 600°C for 1 month. At these temperatures, no reaction was found to occur between the silica and the specimens.

Table 1. Comparison between analytically found (x_a) and starting composition (x_s), their differences and the corrected composition (x_c) for samples ZrO_x heat-treated at 600°C and 400°C for 1 month.

x_a	x_s	$x_a - x_s$	x_c
Foote alloys			
0.148	0.100	0.048	0.118
0.225	0.200	0.025	0.195
0.263	0.240	0.023	0.233
0.351	0.320	0.031	0.321
0.366	0.340	0.026	0.336
0.378	0.350	0.028	0.348
0.400	0.370	0.030	0.370
0.427	0.400	0.027	0.397
0.443	0.420	0.023	0.413
0.475	0.450	0.025	0.445
0.547	0.500	0.047	0.517
Mackay alloys			
0.275	0.240	0.035	0.245
0.314	0.280	0.034	0.284
0.361	0.320	0.041	0.331
0.382	0.340	0.042	0.352
0.409	0.350	0.059	0.379
0.447	0.400	0.047	0.417
0.463	0.420	0.043	0.433
0.492	0.450	0.042	0.462
0.551	0.500	0.051	0.521

The oxygen contents of the heat-treated samples were determined by chemical analysis. Weighed samples of about 0.2 g were heated in silica boats in an oxygen stream at 950°C for some hours, admixed with a known amount of TiO_2 (rutile form) to avoid spitting and reduce sintering. The compositions of the preparations were thus determined from the increase in weight upon oxidation to dioxide.

The analytically found compositions differ slightly from the starting compositions (*cf.* Table 1). The difference amounts for Foote samples to about 0.03 units and for the Mackay samples to about 0.04 units in the ratio O to Zr. These differences depend most likely on a systematic error in the analysing method rather than on composition changes caused by the syntheses and heat-treatments. So with pure Foote metal a result was obtained corresponding to an oxygen content of about 1 % which is much higher than the correct one of 260 ppm. The somewhat higher difference for the Mackay samples can be explained by the fact that the starting metal contained oxygen. The hafnium content of the Mackay starting materials has been found spectrographically to be 220—250 ppm.

Table 2. Observed densities of samples ZrO_x heat-treated at 600°C for 1 month and calculated densities for interstitial solutions.

x	d_{obs}	d_{calc}
0	6.49 [5]	6.50 [6]
0.118	6.52	6.55
0.195	6.60	6.60
0.233	6.64	6.63
0.321	6.76	6.73
0.336	6.76	6.75
0.348	6.75	6.77
0.370	6.79	6.80
0.397	6.82	6.83

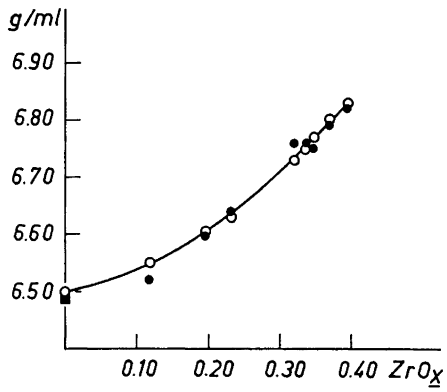

Fig. 1. Observed density of samples ZrO_x heat-treated at 600°C for 1 month (filled circles) and calculated density for interstitial solutions (open circles).

The results of the analyses have therefore been corrected, using a constant equal to 0.030 units, to give the ratios of oxygen to zirconium in the alloys.

Density determinations have been carried out by measuring the weight of the samples in air and benzene. Table 2 and Fig. 1 show the observed densities for samples heat-treated at 600°C for 1 month and the calculated densities for interstitial solutions.

X-Ray powder photographs were taken of all the samples using a Guinier set-up with monochromatized CuKa_1 radiation. Potassium chloride (a = 6.2919 Å at 20°C [7]) was always added to the specimens as an internal standard. Details about the techniques employed in the X-ray powder work have been given elsewhere [8].

Table 3. Lattice parameters of specimens ZrO_x heat-treated at various temperatures.

x	a Å		c Å		
0	3.2323 [7]		5.1477 [7]		
Foote alloys	600°C	~ 1 800°C	600°C	~ 1 800°C	
0.118	3.2470	3.2455	5.1689	5.1703	
0.195	3.2528	3.2518	5.1790	5.1776	
0.233	3.2540	3.2542	5.1825	5.1813	
0.321	3.2527	3.2532	5.1875	5.1864	
0.336	3.2510	3.2515	5.1937	5.1889	
0.348	3.2485	3.2495	5.1954	5.1940	
0.370	3.2470	3.2487	5.1987	5.1974	
0.397	3.2448	3.2448	5.2014	5.1985	
0.413	3.2437	3.2439	5.2043	5.2017	(two-phase region)
0.445	3.2436	3.2445	5.2046	5.2014	—»—
0.517	3.2434	3.2441	5.2043	5.2006	—»—

Mackay alloys	400°C	600°C	800°C	400°C	600°C	800°C	
0.245	3.2562	3.2541	3.2548	5.1854	5.1837	5.1858	
0.284	3.2557	3.2536	3.2548	5.1903	5.1861	5.1889	
0.331	3.2518	3.2497	3.2509	5.1941	5.1920	5.1941	
0.352	3.2503	3.2480	3.2494	5.1975	5.1983	5.1985	
0.379	3.2504	3.2456	3.2474	5.2023	5.2010	5.2005	
0.417	3.2458	3.2441	3.2437	5.2031	5.2019	5.2021	—»—
0.433	3.2463	3.2447	3.2444	5.2065	5.2045	5.2038	—»—
0.462	3.2454	3.2438	3.2447	5.2044	5.2073	5.2020	—»—
0.521	3.2469	3.2442	3.2442	5.2045	5.2040	5.2041	—»—

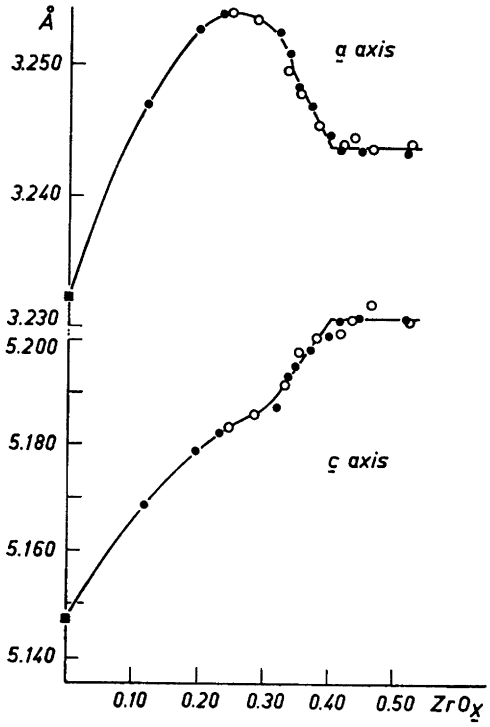

Fig. 2. Lattice parameters of samples ZrO_x heat-treated at 600°C for 1 month (filled circles) and 1 week (open circles).

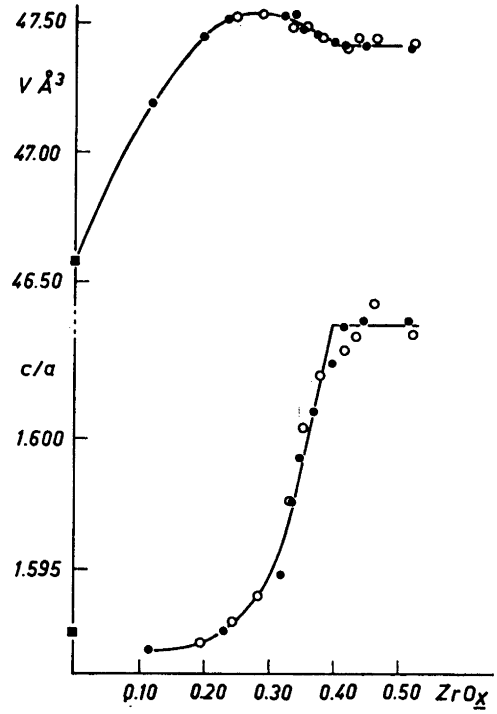

Fig. 3. Unit cell volume and axial ratio of samples ZrO_x heat-treated at 600°C for 1 month (filled circles) and 1 week (open circles).

The single-crystal photographs were taken in a Weissenberg camera using CuK radiation.

RESULTS

The dependence of the metal lattice parameters of preparations $ZrO_{0-0.52}$ on the oxygen content is shown in Table 3.

For each composition the lattice parameters are, within the experimental error, independent of the heat-treatment. Fig. 2 gives the a and c axes as functions of the oxygen contents for both sets of alloys heat-treated at 600°C. The agreement between the two series is good.

The incorporation of oxygen atoms in the α-zirconium lattice causes a considerable increase in the c axis over the entire range of solid solubility. A marked change in the rate of increase of the c axis is observed at the composition $ZrO_{\sim 0.32}$. The length of the a axis is less affected by the oxygen content but passes through a pronounced maximum at the composition $ZrO_{0.25}$.

Table 4. Unit cell volume and c/a of samples ZrO_x heat-treated at 600°C for 1 month (Foote alloys) and 1 week (Mackay alloys).

	x	V Å^3	c/a	
	0	46.58 [7]	1.5926 [7]	
Foote alloys	0.118	47.19	1.5919	
	0.195	47.45	1.5922	
	0.233	47.52	1.5927	
	0.321	47.53	1.5948	
	0.336	47.54	1.5976	
	0.348	47.48	1.5993	
	0.370	47.46	1.6011	
	0.397	47.43	1.6030	
	0.413	47.42	1.6044	(two-phase region)
	0.445	47.42	1.6046	—»—
	0.517	47.41	1.6046	—»—
Mackay alloys	0.245	47.53	1.5930	
	0.284	47.54	1.5940	
	0.331	47.49	1.5977	
	0.352	47.49	1.6005	
	0.379	47.45	1.6025	
	0.417	47.41	1.6035	—»—
	0.433	47.45	1.6040	—»—
	0.462	47.45	1.6053	—»—
	0.521	47.43	1.6041	—»—

The changes in the values of the lattice parameters are such that the c/a ratio is almost constant up to the composition $ZrO_{0.25}$ but thereafter, increases rapidly — this is shown in Table 4 and Fig. 3 together with values for the volume of the unit cell.

From the measurements of the metal lattice parameters, the solubility limit of oxygen in α-zirconium was found to be close to the composition $ZrO_{0.40}$ (28.6 at % O) and to be independent of the heat-treatment in good agreement with earlier result [1].

Preparations with oxygen contents below $ZrO_{0.34}$ give powder patterns substantially identical to that of the pure metal, which indicates that the oxygen atoms are randomly distributed in the octahedral interstices of the metal structure (ZrO_{0+x}).

However, the powder photographs of all samples with compositions corresponding to the composition $ZrO_{0.35}$ and higher contain extra lines independent of the previous heat-treatment. This powder pattern can be hexagonally indexed using a unit cell three times the size of the unit cell of the metal.

This superstructure has been determined from single-crystal data using crystals from samples with the compositions $ZrO_{0.35}$ and $ZrO_{0.42}$ which had been heat-treated at 400°C for 1 month.

Table 5 gives the powder pattern of the former sample and Table 6 the observed and calculated intensities of the superstructure reflexions. The following structure, slightly modified during the process of structural refinement from that preliminarily reported [9], was thus derived for the ideal composition $ZrO_{0.33}$:

Table 5. Powder pattern of the sample $ZrO_{0.352}$ heat-treated at 400°C for 1 month. Dimensions of the hexagonal unit cell:

$a = \sqrt{3} \cdot 3.2503$ Å $= 5.6295$ Å $\qquad c = 5.1975$ Å

I	$\sin^2\Theta_{obs}$	hkl	$(hkl)_{\alpha\text{-Zr}}$	$\sin^2\Theta_{calc}$
vw	0.02508	100		0.02496
w	0.04686	101		0.04692
m	0.07487	110	100	0.07488
m	0.08787	002	002	0.08785
vst	0.09682	111	101	0.09684
vw	0.12170	201		0.12180
m	0.16274	112	102	0.16273
vw	0.19674	211		0.19668
m	0.22466	300	110	0.22463
m	0.27249	113	103	0.27253
w	— *	220	200	0.29951
m	0.31250	302	112	0.31248
m	0.32147	221	201	0.32147

* Line overlaps line of KCl.

Space group: $P6_322$ (No. 182)
Unit cell content: 2 Zr_3O
2 O in 2(*c*): $\frac{1}{3},\frac{2}{3},\frac{1}{4}$; $\frac{2}{3},\frac{1}{3},\frac{3}{4}$
6 Zr in 6(*g*): $\frac{1}{3},0,0$; $0,\frac{1}{3},0$; $\frac{2}{3},\frac{2}{3},0$; $\frac{2}{3},0,\frac{1}{2}$; $0,\frac{2}{3},\frac{1}{2}$; $\frac{1}{3},\frac{1}{3},\frac{1}{2}$

The metal atoms in this structure have the same packing as in the pure metal. The oxygen atoms occupy a certain number of the octahedral interstices of the metal lattice in an ordered way (*cf.* Fig. 4). Thus the superstructure arises from the ordering of the oxygen atoms to give, at this composition, a

Table 6. Observed and calculated intensities of the superstructure reflexions.

	Guinier		Weissenberg	
hkl	I_{obs}	I_{calc}	I_{obs}	I_{calc}
001	—	0	—	0
100	vw	3	— *	10
101	w	10	26	28
200	—	0.6	— *	4
102	—	0.9	2	3
201	vw	2	11	8
210	—	0.4	—	1
202	—	0.3	—	1
211	vw	2	3	4
003	—	0	—	0
103	—	0.8	3	3
301	—	0	—	0
212	—	0.4	—	0.7
203	—	0.5	—	2
310	—	0.1	—	0.5
311	—	0.9	—	1
213	—	0.7	—	1

* covered by the $h00$ continuous radiation streak.

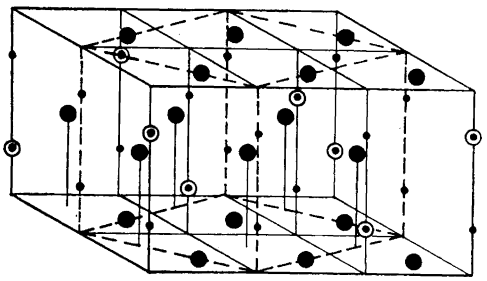

Fig. 4. The structure of Zr_3O. Large filled circles indicate zirconium atoms, small filled circles the center of the octahedral interstices and open circles oxygen atoms. The unit cell is indicated with dashed lines and the basic α-Zr with full lines.

completely ordered solid solution, indicated by Zr_3O and isostructural with the Ni_3N type.

Preparations richer in oxygen give powder patterns which are entirely analogous to that of Zr_3O. No intensity differences could be observed for different contents of oxygen. This implies that the excess oxygen atoms are randomly distributed in the empty interstices of the Zr_3O structure. This region of a partly ordered solid solution (Zr_3O_{1+y}) exists up to the solubility limit ($ZrO_{0.40}$).

A discussion of the results obtained for the solid solutions of small non-metal atoms in titanium, zirconium and hafnium will be published elsewhere.

Acknowledgements. This investigation has been sponsored in part by the *AB Atomenergi* and in part by the *Office, Chief of Research and Development, U.S. Department of Army*, through its European Research Office.

The authors wish to express their sincere gratitude to Dr. Arne Magnéli, for his never-failing interest and for many valuable discussions.

Thanks are due to Mrs. Stina Nord and to Mr. Georg Kruuse for valuable experimental assistance.

The work has been greatly promoted by the support of Dr. Roland Kiessling, Mr. Gustaf Östberg (civ.ing.) and their co-workers at the AB Atomenergi.

REFERENCES

1. Domagala, R. F. and McPherson, D. J. *J. Metals* **6** (1954) 238.
2. Fast, J. D. *Metallwirtschaft* **17** (1938) 641.
3. Domagala, R. F. and McPherson, D. J. *U.S.A.E.C. Publ.* COO-181 (1953).
4. Andersson, S , Collén, B., Kuylenstierna, U. and Magnéli, A. *Acta Chem. Scand.* **11** (1957) 1641.
5. Adenstedt, H. K. *Trans. Am. Soc. Metals* **44** (1952) 949.
6. Treco, R. M. *J. Metals Trans.* **5** (1953) 344.
7. Humbling, P. G. *Acta Cryst.* **6** (1953) 98.
8. Westman, S. and Magnéli, A. *Acta Chem. Scand.* **11** (1957) 1587.
9. Holmberg, B. and Magnéli, A. *Acta Chem. Scand.* **12** (1958) 1341.

Received December 17, 1960.

ACTA CHEMICA SCANDINAVICA 15 (1961) 926–960

Short Communications

Action of the Bacterial Proteinase, Subtilisin B, on "Native" Hemoglobin A

M. OTTESEN and W. A. SCHROEDER

Chemical Department, Carlsberg Laboratory Copenhagen, Denmark

The commonly held opinion that "native" or "undenatured" proteins are not digested by enzymes is difficult to document by investigations that have used sensitive modern methods. Indeed, many proteins require such complex and protracted methods of isolation that the identity of the molecule with its native state may truly be questioned. The present investigation was designed to study the effect of enzymes on "native" or "undenatured" hemoglobin A through the medium, first, of the pH-stat.[1] Hemoglobin may be isolated under milder conditions than most proteins (conditions, at least, which do not alter its most vital property of reversible dissociation with oxygen) and, hence, presumably it is in a state near to that of the native or undenatured protein. The most significant results were obtained with subtilisin A [2] and its near relative, subtilisin B,[3,4] (previously designated as Novo bacterial proteinase) from a related strain of *Bacillus subtilis*.

Whole oxyhemoglobin A was prepared by the method [5] except that the preparation was dialyzed against distilled water. Subtilisin B (Lot Ch31C) was a preparation from the Novo Pharmaceutical Company, Copenhagen. Subtilisin A was taken from a preparation that had been made by methods previously described [2]. Conditions of the reaction were: pH 8.00, temperature 31.5°C, a specific gaseous atmosphere in the reaction vessel, 118 mg of hemoglobin in 5 ml of water, and 1 mg of subtilisin B unless subtilisin A is specified. The specific gaseous atmosphere was achieved by passing a gas over the reaction mixture at a rate of 10 ml per min under one of three conditions: (1) nitrogen for 2 h at pH 8.00 prior to the addition of enzyme and throughout the reaction period, (2) nitrogen, but the pH was brought to 8.00 immediately and enzyme was added, and (3) a mixture of oxygen and nitrogen in the proportions in air to exclude carbon dioxide. A Radiometer pH-stat with a Dich recorder [1] was used to record the uptake of base as a function of time after the addition of enzyme. After the reaction had reached the desired state of completion, any remaining protein was precipitated by the addition of an equal volume of 20 % trichloroacetic acid. The precipitate was filtered off and selected samples were dinitrophenylated. The non-protein material

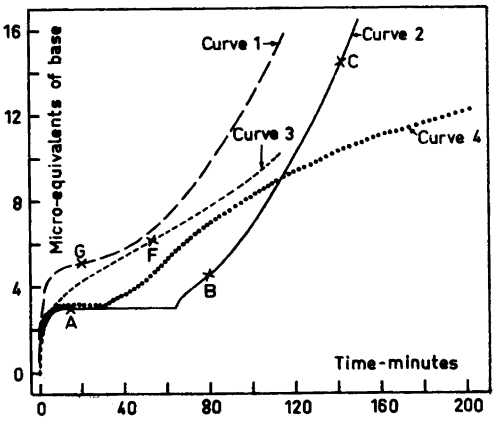

Fig. 1. Action of subtilisin B on hemoglobin A. The figure reproduces the uptake of base as a function of time as recorded by the pH-stat. In some experiments, the action of the enzyme was continued for longer periods: thus, point D on Curve 2,26.6 μequiv. at 165 min; point E on Curve 2, 145 μequiv. at 665 min; point H on Curve 1, 21.0 μequiv. at 140 min. For further details, see text.

in the filtrate was investigated by Kjeldahl analysis in order to determine the quantity, by unidimensional paper electrophoresis, and by "fingerprinting"[6].

Fig. 1 depicts typical pH-stat tracings, which have been superimposed at the point of addition of enzyme. The uptake of base described by Curve 1 resulted under condition (1) above, in which the enzyme is acting on deoxygenated hemoglobin.[7] Curve 2 shows the uptake under condition (2); oxyhemoglobin is first present but deoxygenates in the course of the experiment. Under condition (3), which produces Curve 3, oxyhemoglobin is maintained in this form during the experiment.

In the initial stages the curves follow rather different courses, but later all show an increasing rate. The enzyme under conditions (1) and (3) is acting on a definite derivative of hemoglobin, but under condition (2) the form of the derivative changes in the course of the reaction. The cessation of uptake in Curve 2 between 10 and 65 min results because the deoxygenating oxyhemoglobin is acting as its own pH-stat: because reduced hemoglobin is a weaker acid than oxyhemoglobin [7], the molecule itself combines with the hydrogen ions that normally would be titrated. The differences in Curves 1 and 3 presumably reflect a difference in the attack of the enzyme on the two derivatives. The results shown in Fig. 1 may be obtained reproducibly with samples of oxyhemoglobin that have been stored at 5° C for periods of one to two weeks. Older samples may show more bizarre effects. Presumably, older solutions would have had greater opportunity to denature, and hence the action of the enzyme should be more rapid. The reverse is the case. For example, Curve 4 resulted to a greater or lesser degree under essentially condition (2) when old samples were studied: the rate of reaction actually fell off in the later stages. The explanation of this type of behavior is not obvious.

In order to gain an insight into the nature of the reaction, the material not precipitated by trichloroacetic acid was further studied. The reaction was stopped at various points that are indicated by the point on the curve and the letter adjacent in Fig. 1. The non-precipitable nitrogen is essentially a linear function of the uptake of base; at point C, about 10 % was non-precipitable. A sample corresponding to point B, as expected from the above explanation of this curve, contains more nitrogen in solution than would be expected from the uptake of base. Portions which contained equivalent quantities of non-precipitable nitrogen were taken from available samples and submitted to paper electrophoresis at pH 3.5 in pyridine-acetic acid buffer. The results from all samples noted in Fig. 1 (except E, which was not then available) were identical both in movement of the spots and in the relative amounts of the various spots; indeed, the same results were obtained with a sample from the action of subtilisin A. Samples from points B, D, E were selected for more extensive investigation by »fingerprinting»[6]. The fingerprints of samples D and E were essentially indistinguishable and that of sample B differed only in small details. Fig. 2a is representative of the results. In a further comparison, a sample of heat-denatured [6] hemoglobin was treated with enzyme until the uptake of base approximated that of sample D; the time required to achieve the same uptake of base was 4 min with the heat-denatured sample as compared to 165 min with sample D. A comparison of the fingerprints of sample D and of heat-denatured hemoglobin is presented in Fig. 2. Appreciable differences are apparent.

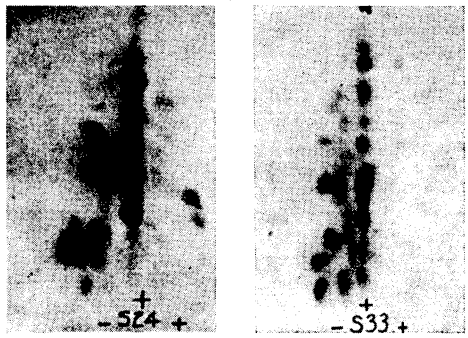

Fig. 2. "Fingerprints" of non-precipitable material from the action of subtilisin B on (a) undenatured and (b) heat-denatured hemoglobin A.

The trichloroacetic acid precipitate from sample D was dinitrophenylated. The DNP-protein was hydrolyzed for 15 min in refluxing 6 N hydrochloric acid as previously described[8]. The N-terminal DNP-peptides were extracted, identified, and quantitatively estimated. The DNP-pep-

tides agreed both in kind and quantity with those [8,9] that would be obtained from hemoglobin that had not been treated with enzyme.

The results of the present investigation bear upon several as yet unanswered questions about the action of proteolytic enzymes on proteins. (1) They show that certain enzymes act vigorously on hemoglobin, a protein which is probably as "native" or "undenatured" as any. (2) They indicate that the type of reaction is the so-called "one-by-one" type [10]; that is, at any time after the action of the enzyme has begun, a molecule has either reacted to the fullest possible extent or it has not reacted at all. The identity of the non-precipitable products at various stages of reaction and the normal nature of the N-terminal DNP-peptides of the trichloroacetic acid precipitate are strong evidence for this conclusion. (3) They show that, if an enzyme must denature a protein prior to cleaving it or if it reacts only with the denatured protein of a reversible equilibrium between denatured and undenatured protein [11], then, the denaturation is of a different type than that produced by heat because the products from "undenatured" and heat-denatured hemoglobin differ.

We wish to thank Mrs. Kirsten Mikkelson for nitrogen determinations and Mrs. Joan Shelton for the determination of the N-terminal DNP-peptides. This investigation was carried out during the tenure of a Guggenheim Fellowship of one of us (W.A.S.).

1. Jacobsen, C. F., Léonis, J., Linderstrøm-Lang, K. and Ottesen, M. *Methods of Biochemical Analysis*, **4** (1957) 171.
2. Güntelberg, A. V. and Ottesen, M. *Compt. rend. Lab. Carlsberg, Sér. chim.* **29** (1954) 36.
3. Ottesen, M. and Spector, A. *Ibid.* **32** (1960) 63.
4. Hunt, J. and Ottesen, M. *Biochim. et Biophys. Acta. In press.*
5. Clegg, M. D. and Schroeder, W. A. *J. Am. Chem. Soc.* **81** (1959) 6065.
6. Ingram, V. M. *Biochim. et Biophys. Acta* **28** (1958) 539.
7. Wyman, J., Jr. *Advances in Protein Chem.* **4** (1948) 460.
8. Rhinesmith, H. S., Schroeder, W. A. and Pauling, L. *J. Am. Chem. Soc.* **79** (1957) 4682.
9. Rhinesmith, H. J., Schroeder, W. A. and Martin, N. *Ibid.* **80** (1958) 3358.
10. Linderstrøm-Lang, K. *Lane Medical Lectures, Stanford University Press*, Stanford, Calif. 1952, p. 65.
11. *Ibid.* pp. 58 and 59.

Received April 7, 1961.

Kinetics of the Reaction between β-Sulfinylpropionic Acids and Iodide Ion in Acid Solution

STIG ALLENMARK

Department of Organic Chemistry, Chemical Institute, University of Lund, Lund, Sweden

The rate of the reaction: $RSOR' + 2\,H^+ + 2\,I^- \rightarrow RSR' + I_2 + H_2O$ where $R = HOCOCH_2CH_2$-, $R' = HOCOCH_2CH_2$-, and $CH_3CH_2CH_2$-, has been studied at 25°C in solutions of perchloric acid and perchloric acid-sodium perchlorate. With hydrogen- and iodide ions in excess the reaction is kinetically of the first order, *i.e.*, one obtains the rate expression:

$$k = \frac{1}{t} \ln \frac{a}{a-x}$$

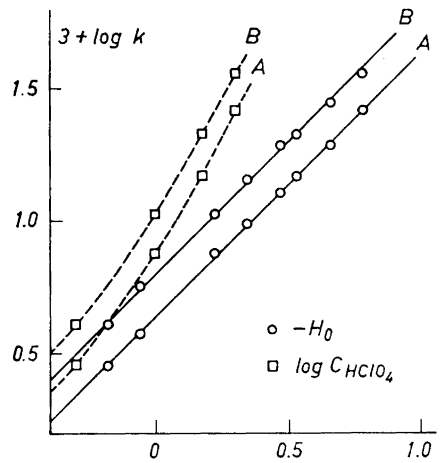

Fig. 1. Log k as a function of $-H_0$ (unbroken lines) and of log C_{HClO_4} (dashed lines) for the reaction for A and B, respectively, with iodide ion in acid solution at 25°C. (The dashed curves refer to perchloric acid solutions without any added sodium perchlorate.)

tides agreed both in kind and quantity with those [8,9] that would be obtained from hemoglobin that had not been treated with enzyme.

The results of the present investigation bear upon several as yet unanswered questions about the action of proteolytic enzymes on proteins. (1) They show that certain enzymes act vigorously on hemoglobin, a protein which is probably as "native" or "undenatured" as any. (2) They indicate that the type of reaction is the so-called "one-by-one" type [10]; that is, at any time after the action of the enzyme has begun, a molecule has either reacted to the fullest possible extent or it has not reacted at all. The identity of the non-precipitable products at various stages of reaction and the normal nature of the N-terminal DNP-peptides of the trichloroacetic acid precipitate are strong evidence for this conclusion. (3) They show that, if an enzyme must denature a protein prior to cleaving it or if it reacts only with the denatured protein of a reversible equilibrium between denatured and undenatured protein [11], then, the denaturation is of a different type than that produced by heat because the products from "undenatured" and heat-denatured hemoglobin differ.

We wish to thank Mrs. Kirsten Mikkelson for nitrogen determinations and Mrs. Joan Shelton for the determination of the N-terminal DNP-peptides. This investigation was carried out during the tenure of a Guggenheim Fellowship of one of us (W.A.S.).

1. Jacobsen, C. F., Léonis, J., Linderstrøm-Lang, K. and Ottesen, M. *Methods of Biochemical Analysis*, **4** (1957) 171.
2. Güntelberg, A. V. and Ottesen, M. *Compt. rend. Lab. Carlsberg, Sér. chim.* **29** (1954) 36.
3. Ottesen, M. and Spector, A. *Ibid.* **32** (1960) 63.
4. Hunt, J. and Ottesen, M. *Biochim. et Biophys. Acta. In press.*
5. Clegg, M. D. and Schroeder, W. A. *J. Am. Chem. Soc.* **81** (1959) 6065.
6. Ingram, V. M. *Biochim. et Biophys. Acta* **28** (1958) 539.
7. Wyman, J., Jr. *Advances in Protein Chem.* **4** (1948) 460.
8. Rhinesmith, H. S., Schroeder, W. A. and Pauling, L. *J. Am. Chem. Soc.* **79** (1957) 4682.
9. Rhinesmith, H. J., Schroeder, W. A. and Martin, N. *Ibid.* **80** (1958) 3358.
10. Linderstrøm-Lang, K. *Lane Medical Lectures, Stanford University Press*, Stanford, Calif. 1952, p. 65.
11. *Ibid.* pp. 58 and 59.

Received April 7, 1961.

Kinetics of the Reaction between β-Sulfinylpropionic Acids and Iodide Ion in Acid Solution

STIG ALLENMARK

Department of Organic Chemistry, Chemical Institute, University of Lund, Lund, Sweden

The rate of the reaction: $RSOR' + 2\,H^+ + 2\,I^- \rightarrow RSR' + I_2 + H_2O$ where $R = HOCOCH_2CH_2$-, $R' = HOCOCH_2CH_2$-, and $CH_3CH_2CH_2$-, has been studied at 25°C in solutions of perchloric acid and perchloric acid-sodium perchlorate. With hydrogen- and iodide ions in excess the reaction is kinetically of the first order, *i.e.*, one obtains the rate expression:

$$k = \frac{1}{t} \ln \frac{a}{a-x}$$

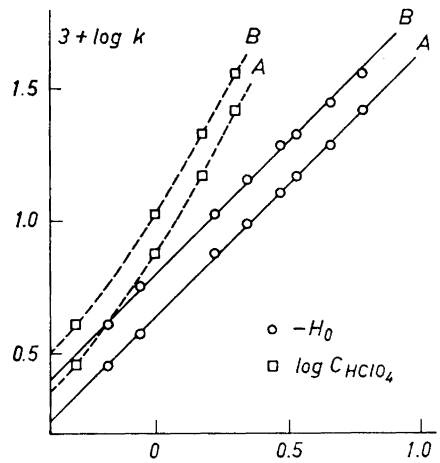

Fig. 1. Log k as a function of $-H_0$ (unbroken lines) and of log C_{HClO_4} (dashed lines) for the reaction for A and B, respectively, with iodide ion in acid solution at 25°C. (The dashed curves refer to perchloric acid solutions without any added sodium perchlorate.)

Table 1. The rate of the reaction for $HOCOCH_2CH_2SOCH_2CH_2COOH$ (A) and $CH_3CH_2CH_2SOCH_2CH_2COOH$ (B), respectively, with iodide ion in acid solution at 25°C.

C_{HClO_4} M	C_{NaClO_4} M	10^3k min^{-1}		$-H_0$	$-(\log k + H_0)$	
		A	B		A	B
2.00	0	26.2	36.2	0.78	2.36	2.22
1.50	0	14.8	21.1	0.53	2.36	2.21
1.00	0	7.56	10.6_5	0.22	2.34	2.19
0.50	0	2.86	4.07	−0.18	2.36	2.21
1.50	0.50	19.4	27.8	0.66	2.37	2.22
1.00	1.00	12.7	19.2	0.47	2.37	2.19
1.00	0.50	9.76	14.4	0.34_5	2.36	2.19
0.50	0.50	3.73	5.67	−0.06	2.37	2.19

where a and $a-x$ are the concentrations of the sulfinyl compound at the start of the experiment and after t minutes, respectively [1]. In Table 1 the observed rate constants k (in min^{-1}) are correlated to the acidity function H_0 as definied by Hammett [2,3]. Hereby a fairly good linearity between log k and $-H_0$ with unit slope has been obtained (Fig. 1), which according to the Zucker-Hammett hypothesis [4] means that the first step of the reaction consists of a rapid proton transfer to the oxygen atom in the sulfinyl group:

$$\rangle SO + H^+ \rightleftharpoons \rangle SOH^+ \quad \text{rapidly}$$

$$\rangle SOH^+ \rightarrow \overset{*}{M}{}^+ \quad \text{rate determining}$$

The activated complex $\overset{*}{M}{}^+$ then reacts rapidly with a nucleophilic reagent such as an iodide ion.

Materials and method. The sulfinyl acids have been obtained through oxidation of the corresponding sulfide acids in acetone solution with perhydrol in an excess of 10 %. The sulfide acids were prepared in the following manner:

(*a*) β-Thiodipropionic acid from β-chloropropionic acid and sodium sulfide in water solution [1].

(*b*) β-Propylmercaptopropionic acid from β-mercaptopropionic acid, sodium hydroxide and *n*-propylbromide in water-ethanol solution [5]. By using 70 g β-mercaptopropionic acid 89.5 g (91 %) β-propylmercaptopropionic acid was obtained, b.p. 154°/20 mm Hg, $n^{20}{}_D = 1.4803$, $d_4^{20} = 1.0735$. (Found: C 48.3; H 8.07; S 21.4; $MR_D = 39.24$. Calc. for $C_6H_{12}O_2S$: C 48.6; H 8.16; S 21.6; $MR_D = 39.41$.)

The sulfinyl acids could easily be purified through recrystallization from water. The melting point of β-propylsulfinylpropionic acid (about 75°) was not sharp, probably due to a disproportionation at this temperature. (Found: C 43.9; H 7.40; S 19.4; equiv. wt 164.6. Calc. for $C_6H_{12}O_3S$: C 43.9; H 7.37; S 19.5; equiv. wt 164.2.)

The kinetic experiments have been made at 25.0 ± 0.05°C. An oxygen-free solution containing known quantities of sodium iodide, sodium perchlorate and perchloric acid was pre-heated to the temperature mentioned. At the time $t = 0$ a certain quantity of a solution composed of sulfinyl acid, perchloric acid and sodium perchlorate was rapidly put down into it. This quantity had been carefully measured by means of an injection syringe. Thus the reaction mixture at this time had the following composition: $C_{\text{sulfinyl acid}} = 5.00$ mM, $C_{\text{iodide}} = 200$ mM, C_{HClO_4} and C_{NaClO_4} according to Table 1.

At the time t the reaction was stopped in such a way that the reaction mixture was rapidly cooled by addition of finely crushed ice. After that the liberated iodine could be titrated with sodium thiosulfate.

The author's thanks are accorded to Professor Erik Larsson for his kind interest in this work.

1. Larsson, E. *Svensk Kem. Tidskr.* **45** (1943) 29.
2. Hammett, L. P. and Deyrup, A. J. *J. Am. Chem. Soc.* **54** (1932) 2721.
3. Paul, M. A. and Long, F. A. *Chem. Revs.* **57** (1957) 1, 935.
4. Zucker, L. and Hammett, L. P. *J. Am. Chem. Soc.* **61** (1939) 2791.
5. Larsson, E. *Trans. Chalmers Univ. Technol., Gothenburg* **87** (1949) 23.

Received May 2, 1961.

Separation of Human Skin Waxes by Gas Chromatography

E. O. A. HAAHTI* and E. C. HORNING

Laboratory of Chemistry of Natural Products, National Heart Institute, Bethesda, Maryland, U.S.A.

Wax esters occur widely in both plants and animals. They were among the first natural products to be studied in modern times (cetyl alcohol was obtained from sperm oil by Chevreul in 1817 [1]), but they have received very little attention in recent years. Their study is difficult because the isolation and identification of pure compounds has required prolonged fractionation procedures.

The development of gas chromatographic methods for the separation of steroids [2] suggested, that related techniques might be developed for work with wax esters. However, waxes usually have a wide molecular weight range, and under isothermal conditions this leads to unduly long retention times for higher members of the series. Further, for many studies compounds containing up to about forty carbon atoms must be separated. Preliminary studies indicated, that suitable methods could be developed by employing a relatively thin film of thermostable liquid phase in the column, and by using a temperature-programmed procedure. Phases with sufficient thermal stability for this work were found to be silicone polymer SE-30 (General Electric Co.), ethylene glycol *iso*phthalate (EGIP), neopentyl glycol succinate (NGS) and fluoroalkyl silicone polymer *Q*F-1 (Dow-Corning Corp.). Of these, SE-30 was the most useful because of its ability to separate monoene and diene esters from saturated esters. With temperature programming from 100° to 280° and with a 1 % SE-30 column it was found possible to scan a wide molecular weight range, and to separate unsaturated and saturated esters from about C_{10} to the C_{40-42} level. Two applications were examined.

Fig. 1 shows a separation of the wax esters of a commercial sample of spermaceti. It is known, that cetyl palmitate is the major component of this material [3]. This is clearly indicated by the analytical record; the presence of even and odd-numbered homologs is also indicated. The absence of unsaturated esters was confirmed by analytical gas chromatographic examination of the acid and alcohol fractions resulting from hydrolysis of the wax.**

Fig. 2 shows a separation of the human wax esters of the skin surface lipid film. Skin surface lipids were collected by acetone washing, and a wax fraction containing both wax esters and cholesterol esters was separated by chromatography on silicic

* Visiting Scientist of the National Heart Institute from the University of Turku, Turku, Finland.

** Early studies on sperm oil indicate that unsaturated compounds are present; these are evidently lost in the commercial isolation process used for spermaceti.

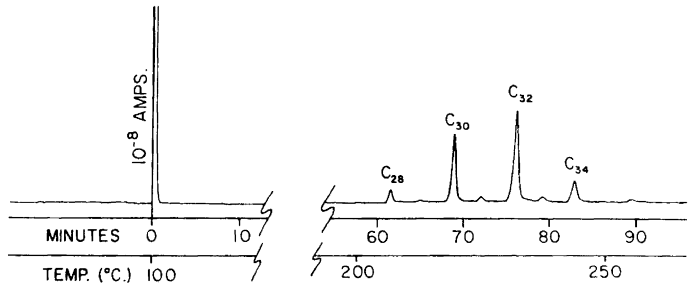

Fig. 1. Separation of components of spermaceti. Conditions: 6 ft. × 3.4 mm glass coil column; 1 % SE-30 (General ElectricCo.) on 100–140 mesh Gas-Chrom P; argon inlet pressure 30 psi.; argon ionization detector. Heating rate, 1.73°C/min. The sample was introduced in benzene solution. Carbon numbers refer to total carbon content of wax esters; full scale deflection as shown is 1×10^{-8} amp.

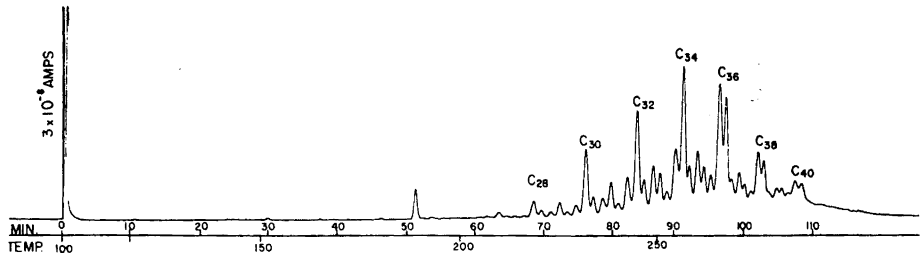

Fig. 2. Separation of components of human skin surface waxes. The conditions were the same as for Fig. 1. Carbon numbers refer to total carbon content of wax esters.

acid [4]. The major wax esters were recognized as a monene and a diene C_{36} ester by comparison with authentic (synthetic) samples of saturated and unsaturated wax esters. Homologs differing by a $-CH_2CH_2-$ group are also indicated in the figure. This separation, while giving a precise definition of the molecular weight range of waxes of the human skin surface, indicates only the combined chain length present in the esters; it does not indicate the individual acid or alcohol chain lengths. The ester fraction was saponified, and the distribution of individual acids and alcohols was determined by analytical gas chromatography (the acids were separated as methyl esters, and the alcohols were separated both free and as acetates). The major alcohols were found to be eicosanyl alcohol and a monoene C_{20} alcohol. The occurrence of saturated and unsaturated C_{20} alcohols is in agreement with mass spectroscopic work carried out in a study of human hair fat.[5] The "*iso*" C_{20} alcohol reported in an earlier study of sebum alcohols [6] was found only as a relatively minor component. The major acid was found to be palmitoleic acid. These results suggested, that the two chief C_{36} wax components were eicosanyl palmitoleate and eicosenyl palmitoleate (unsaturated bond position unspecified in the alcohol). To confirm this finding, a preparative separation on a milligram scale was carried out for the major C_{36} ester. An analytical examination of the acids and alcohols in the isolated fraction showed, that this material was in fact almost entirely derived from an eicosenyl alcohol and palmitoleic acid. Small amounts of branched chain acids and alcohols were also present, indicating that some branched chain esters as well as straight chain esters were present originally.

As far as we can determine, unsaturated waxes of the structure found here have not been reported previously, in spite of the almost universal occurrence of long chain wax esters in biological systems.

The gas chromatographic techniques used for this work should prove useful for studying many other natural products.

1. Chevreul, M. E. *Ann. Chim.* [2] **7** (817) 155.
2. VandenHeuvel, W. J. A., Haahti, E. O. A. and Horning, E. C. *J. Org. Chem.* **26** (1961) 626, and references cited therein.
3. Heintz, W. *Ann.* **80** (1851) 293; **92** (1854) 299; Krafft, F. *Ber.* **17** (1884) 1627; Warth, A. H. *The Chemistry and Technology of Waxes*, Reinhold Publ. Co., New York 1947.
4. Horning, M. G., Williams, E. A. and Horning, E. C. J. *Lipid Research* **1** (1960) 482.
5. Brown, R. A., Young, W. S. and Nicolaides, N. *Anal. Chem.* **26** (1954) 1653.
6. Boughton, B. and Wheatley, V. R. *Biochem. J.* **73** (1959) 144.

Received April 21, 1961.

Correction to "The Stability of Metal Halide Complexes in Aqueous Solution III. The Chloride, Bromide and Iodide Complexes of Bismuth" *

STEN AHRLAND AND INGMAR GRENTHE

Department of Inorganic and Physical Chemistry, Chemical Institute, University of Lund, Lund, Sweden

An error has crept into the calculations of the last column of Table 3B, where the head should read $X_5 \cdot 10^{-6}$ M^{-5} instead of $X_5 \cdot 10^{-7}$ M^{-5}. As a consequence, the values of β_5 and β_6 for the chloride system have come out one power of ten too high. In Table 11, the correct values of log β_5 and log β_6 should therefore read 6.72 and 6.56 (instead of 7.72 and 7.56, respectively).

This correction means that the complex formation curve of the chloride system is much less steep in its upper part than was reported before. It is gratifying however that the new course, presented in the Fig. 1, fits much better

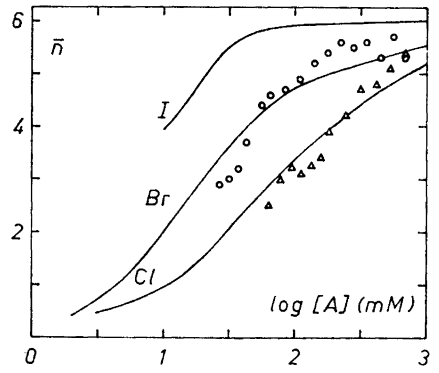

Fig. 1.

than the previous one to the experimental values of $\bar{n}$ which are found from the slope of the C_M, C_A lines of constant E_M. In spite of their considerable random error, these values are therefore on the whole much more reliable than was once believed.

The correction also implies that the range of existence of the third and, especially, the fourth complex is in reality wider and that of the fifth complex narrower than was reported in Fig. 3 of the original paper.

We are indebted to Dr G. A. Wright, University of Auckland, New Zealand, who kindly informed us of the error revealed by his careful reading.

Received May 12, 1961.

* *Acta Chem Scand.* **11** (1957) 1111.

A Convenient Synthetic Route to ^{36}Cl-labelled Aromatic Compounds

BO LAMM

Nobel Institute of Chemistry, Stockholm 50, Sweden

The method generally applied [1] for introducing isotopically labelled chlorine into aromatic compounds is based on the well-known reaction

$$ArH + Cl_2 \rightarrow ArCl + HCl \qquad (1)$$

which has been carried out with chlorine gas containing the isotope in question, generally ^{36}Cl (ArH meaning, in general, any suitable aromatic compound). It is evident from formula (1) that half the amount of chlorine taking part in the reaction is lost as hydrochloric acid. For the sake of economy, it is generally necessary to recover the hydrochloric acid when working with ^{36}Cl in view of the high price [2] of this isotope, the recovered material being used in subsequent runs.

In the present communication, an alternative method of introducing ^{36}Cl into aromatic compounds will be described. This method has the advantage of utilizing in a single step almost all of the radioactive starting material (hydrochloric acid-^{36}Cl) taking part in the reaction, albeit at the price of dilution with inactive chlorine. In the author's work, the latter circumstance does not cause any inconvenience, as the starting material obtained from The Radiochemical Centre, Amersham, England, has a sufficiently high specific activity to allow for about a tenfold dilution with inactive chlorine. Another advantage of the method suggested below is that the somewhat intricate preparation and handling of radioactive chlorine gas is completely circumvented, the aqueous solution of hydro-

chloric acid-^{36}Cl obtained from the supplier being used as such.

The method of chlorination adopted was developed by Orton *et al.*[3,4] An aromatic compound and a corresponding amount of dichloramine T (N,N-dichloro-*p*-toluenesulphonamide) are dissolved together in a suitable solvent. Upon addition of a catalytic amount of hydrochloric acid, a reaction sequence starts that may be formulated in the following way.

$$TsNCl_2 + HCl \xrightarrow{\text{rapid}} TsNHCl + Cl_2 \quad (2a)$$

$$TsNHCl + HCl \xrightarrow{\text{rapid}} TsNH_2 + Cl_2 \quad (2b)$$

$$ArH + Cl_2 \xrightarrow{\text{slow}} ArCl + HCl. \quad (3)$$

In the reaction scheme above, Ts denotes the *p*-toluenesulphonyl, "tosyl", group, and ArH means any aromatic compound. The relative significance of steps (2a) and (2b) is of no interest in the present case, since both reactions are rapid ones as compared to step (3). It simply bears a reference to the stoichiometrically stipulated fact that each mole of dichloramine T liberates two moles of chlorine and, in consequence, suffices for two moles of ArH, if monosubstitution is achieved.

The kinetic behaviour of the reaction sequence formulated above has been established from ^{38}Cl tracer experiments carried out by Olson *et al.*[5] In fact, if labelled hydrochloric acid is added as the catalyst, there will be isotopic equilibrium between the hydrochloric acid and the molecular chlorine that is postulated as the chlorinating agent in step (3) above. Now, it was thought that this circumstance might serve as the theoretical foundation for a synthetic method in which the isotopic chlorine is introduced as hydrochloric acid-^{36}Cl in the above-mentioned reaction sequence. If the molar amount of hydrochloric acid-^{36}Cl is appreciably smaller than that of dichloramine T, a correspondingly high radiochemical yield of ^{36}Cl-labelled organic substance may be expected. In actual fact, this turned out to be true. The chlorination of acetanilide could be performed in 90 % radiochemical yield, the theoretically attainable value being 92 %. The chemical yield was 99 %. Indeed, practially quantitative chemical yields were also reported by Orton *et al.*[4] The product resulting after hydrolysis of the chloroacetanilides initially formed, an isomeric mixture of chloroanilines, had the following composition (found by the isotope dilution technique): *o* 26 ± 2 %, *m* 2 ± 1 %, *p* 72 ± 2 %. These values are in fair agreement with those found by Orton *et al.*[4], *o* 35 ± 5 %, *p* 65 ± 5 % (the *o*/*p*-ratio depending somewhat on the solvent employed).

Finally a few words might be said about the scope of the reaction. The "Orton" chlorination with dichloramine T and hydrochloric acid is generally applicable for compounds having a high reactivity, similar to that of acetanilide. Benzene itself failed to react in chloroform solution, and other solvents also gave negative results. On the other hand, the product of monochlorination of benzene, chlorobenzene-^{36}Cl, may be prepared indirectly from an isomeric mixture of ^{36}Cl-labelled chloroanilines by diazotisation and reduction with hypophosphorous acid. The *ortho* and *para* isomers of chloroaniline-^{36}Cl may each be isolated in the pure state from the isomeric mixture resulting from the synthesis in accordance with a procedure employed by Jones *et al.*[6], which involves preferential steam-distillation of the *ortho* isomer from an acid solution of the amines. The *para* isomer is recovered from the nonvolatile part by acetylation, recrystallization of the anilide and hydrolysis.

A full experimental account will be published later.

Financial support from the *Swedish Natural Science Research Council* is gratefully acknowledged.

1. Murray, A. and Williams, D. L. *Organic Syntheses with Isotopes*, Interscience, New York and London 1958, Part II, pp. 1178—1194.
2. Sørensen, P. *Isotopfortyndingsanalyser* (Diss.) DTH, Copenhagen 1957, p. 34.
3. Orton, K. J. P. and King, H. *J. Chem. Soc.* **99** (1911) 1185.
4. Orton, K. J. P. and Bradfield, A. E. *J. Chem. Soc.* **1927** 986.
5. Olson, A. R., Porter, C. W., Long, F. A. and Halford, R. S. *J. Am. Chem. Soc.* **58** (1936) 2467.
6. Jones, W. J. and Orton, K. J. P. *J. Chem. Soc.* **95** (1909) 1056.

Received May 3, 1961.

Correction to "The Stability of Metal Halide Complexes in Aqueous Solution III. The Chloride, Bromide and Iodide Complexes of Bismuth" *

STEN AHRLAND AND INGMAR GRENTHE

Department of Inorganic and Physical Chemistry, Chemical Institute, University of Lund, Lund, Sweden

An error has crept into the calculations of the last column of Table 3B, where the head should read $X_5 \cdot 10^{-6}$ M^{-5} instead of $X_5 \cdot 10^{-7}$ M^{-5}. As a consequence, the values of β_5 and β_6 for the chloride system have come out one power of ten too high. In Table 11, the correct values of log β_5 and log β_6 should therefore read 6.72 and 6.56 (instead of 7.72 and 7.56, respectively).

This correction means that the complex formation curve of the chloride system is much less steep in its upper part than was reported before. It is gratifying however that the new course, presented in the Fig. 1, fits much better

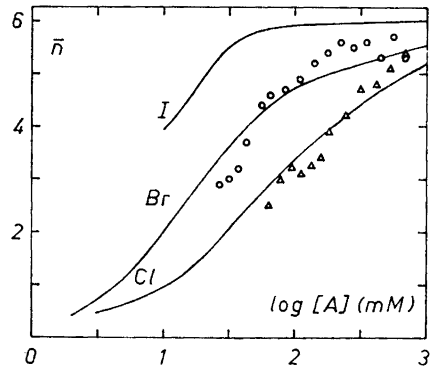

Fig. 1.

than the previous one to the experimental values of $\bar{n}$ which are found from the slope of the C_M, C_A lines of constant E_M. In spite of their considerable random error, these values are therefore on the whole much more reliable than was once believed.

The correction also implies that the range of existence of the third and, especially, the fourth complex is in reality wider and that of the fifth complex narrower than was reported in Fig. 3 of the original paper.

We are indebted to Dr G. A. Wright, University of Auckland, New Zealand, who kindly informed us of the error revealed by his careful reading.

Received May 12, 1961.

* *Acta Chem Scand.* **11** (1957) 1111.

A Convenient Synthetic Route to ^{36}Cl-labelled Aromatic Compounds

BO LAMM

Nobel Institute of Chemistry, Stockholm 50, Sweden

The method generally applied [1] for introducing isotopically labelled chlorine into aromatic compounds is based on the well-known reaction

$$ArH + Cl_2 \rightarrow ArCl + HCl \qquad (1)$$

which has been carried out with chlorine gas containing the isotope in question, generally ^{36}Cl (ArH meaning, in general, any suitable aromatic compound). It is evident from formula (1) that half the amount of chlorine taking part in the reaction is lost as hydrochloric acid. For the sake of economy, it is generally necessary to recover the hydrochloric acid when working with ^{36}Cl in view of the high price [2] of this isotope, the recovered material being used in subsequent runs.

In the present communication, an alternative method of introducing ^{36}Cl into aromatic compounds will be described. This method has the advantage of utilizing in a single step almost all of the radioactive starting material (hydrochloric acid-^{36}Cl) taking part in the reaction, albeit at the price of dilution with inactive chlorine. In the author's work, the latter circumstance does not cause any inconvenience, as the starting material obtained from The Radiochemical Centre, Amersham, England, has a sufficiently high specific activity to allow for about a tenfold dilution with inactive chlorine. Another advantage of the method suggested below is that the somewhat intricate preparation and handling of radioactive chlorine gas is completely circumvented, the aqueous solution of hydro-

On the Crystal Structure of Hydrated Sodium Peroxoborate

ARNE HANSSON

Institute of Chemistry, University of Uppsala, Uppsala, Sweden

There is some controversy about the nature of the compound that crystallizes from a water solution of sodium borate and hydrogen peroxide. Thus it has been described both as $NaBO_2.H_2O_2.3H_2O$ and as $NaBO_3.4H_2O$.

The author obtained crystals of the compound from a solution of 3.5 g borax, 0.35 g NaOH and 9 ml 30 % H_2O_2 in 125 ml water. Analyses of the sodium, boron and active oxygen contents of the crystals were in agreement with the composition given by the above formulae. Weissenberg photographs were taken of two single crystals rotated around different axes. Comparison of single crystal photographs and powder photographs established that only one substance had crystallized from the solution. The intensities of 500 independent reflexions were estimated. The triclinic unit cell contains one formula unit $Na_2B_2(O_2)_2(OH)_4.6H_2O$ and has the dimensions $a = 7.34$ Å, $b = 6.81$ Å, $c = 8.15$ Å, with $\alpha = 101°$, $\beta = 110°$ and $\gamma = 120°$. The space group is P $\bar{1}$.

The structure has been determined by means of Harker-Kasper inequalities and three dimensional Patterson functions and has been verified by comparison of one calculated and one observed three dimensional electron density function. The unrefined parameters are given in Table 1.

There is one centrosymmetrical anion in the unit cell. The arrangement of the atoms is shown in Fig. 1. The bond distances and the bond angles in the negative ion are given in Tables 2 and 3. The B—O distances are in agreement with those reported earlier for tetrahedrally coordinated boron atoms [1]. The bond angles at the oxygen atoms and the bond distance within the peroxo group agree with the values reported for H_2O_2 [2]. The dihedral angle is 64° (Fig. 2).

Table 1. The unrefined parameters of Na, O and B atoms.

		x	y	z
1 Na_1	in	0	0	0
1 Na_2	in	0	½	0
2 O_1	in	0.240	0.445	0.245
2 O_2	in	0.205	0.950	0.265
2 O_3	in	0.295	0.620	0.895
2 O_4	in	0.200	0.065	0.830
2 O_5	in	0.235	0.810	0.635
2 O_6	in	0.235	0.105	0.530
2 O_7	in	0.140	0.250	0.520
2 B	in	0.120	0.930	0.615

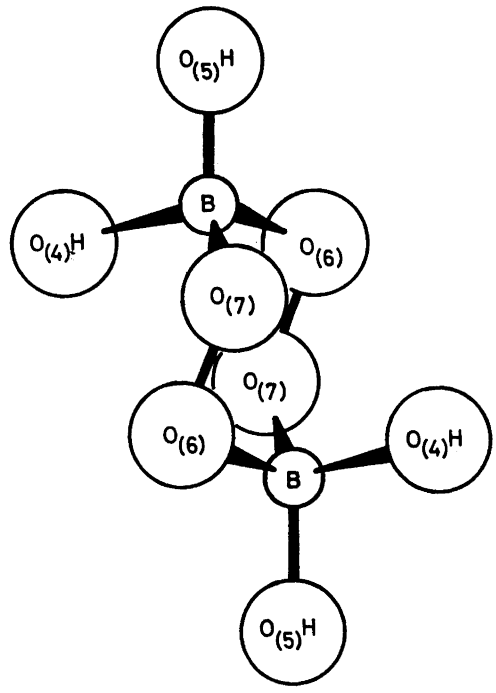

Fig. 1. The shape of the $B_2(O_2)_2(OH)_4^{2-}$ ion.

The sodium ions are at symmetry centres of oxygen octahedra which share opposite edges. A part of the octahedral chains is shown in Fig. 3. Relevant bond distances are given in Table 4. The chains are parallel to the b-axis. The shared oxygen atoms

Table 2. Bond distances within the peroxoborate ion.

B — O_4	1.54 Å
B — O_5	1.44 Å
B — O_6	1.52 Å
B — O_7	1.42 Å
O_6 — O_7	1.47 Å

Table 3. Bond angles within the peroxoborate ion.

O_4-B-O_5	101°
O_4-B-O_6	116°
O_4-B-O_7	115°
O_5-B-O_6	104°
O_5-B-O_7	112°
O_6-B-O_7	108°
$B-O_6-O_7$	107°
$B-O_7-O_6$	107°

belong to water molecules. The sodium ions link the negative ions in the following way. In alternate octahedra in each chain, the two unshared oxygen atoms are incorporated in $O_{(4)}H$-groups from two negative ions. In every other octahedron each unshared oxygen atom forms part of a water molecule which is linked in turn by a hydrogen bond to an $O_{(5)}H$-group in a different negative ion.

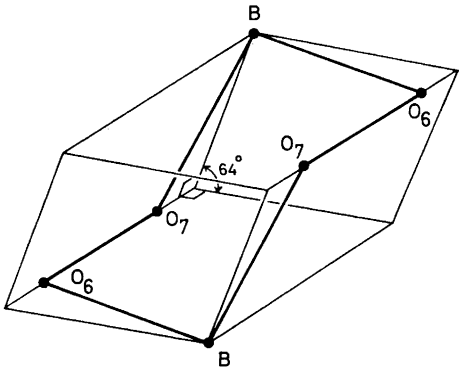

Fig. 2. The double peroxo bridge connecting two boron atoms.

The complete structure determination will be published when the refinement of the parameters has been completed.

Table 4. Bond distances between sodium and oxygen atoms.

Na_1-O_1	2.46 Å
Na_1-O_2	2.37 Å
Na_1-O_4	2.29 Å
Na_2-O_1	2.40 Å
Na_2-O_2	2.61 Å
Na_2-O_3	2.42 Å

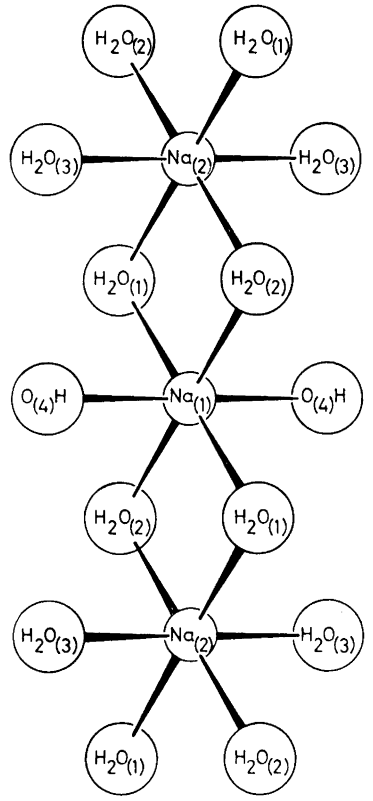

Fig. 3. Part of the chains of octahedra.

The author wishes to express his thanks to Prof. G. Hägg for all the facilities placed at his disposal, to Dr. I. Lindqvist for suggesting the problem and to Mr. Allan Brown for linguistic corrections of the manuscript. This investigation has been sponsored by grants from the *Nobel Foundation* and from *Anslaget till främjande av ograduerade forskares vetenskapliga verksamhet.* Facilities for the use of the digital computer BESK were granted by the Swedish Board for Computing Machinery.

1. Pauling, L. *The Nature of the Chemical Bond.* Cornell University Press, Ithaca, N. Y. 1960.
2. *Tables of Interatomic Distances and Configuration in Molecules and Ions,* The Chemical Society, London 1958.

Received May 12, 1961.

Confirmation of the Structure of Trifolirhizin

J. B-SON BREDENBERG AND PENTTI K. HIETALA

Laboratory of the Foundation for Chemical Research, Biochemical Institute, Helsinki, Finland

In a recent communication [1], structure I was tentatively suggested for trifolirhizin, an antifungal glucoside of red clover. Since the structure of pterocarpin, on which the tentative structure was based, now has been revised to II[2], the corresponding change has to be made in the structure of trifolirhizin (III). This structure has now been confirmed by the isolation of the aglycone (IV) and its methylation to pterocarpin.

Acid hydrolysis of trifolirhizin probably releases the aglycone. Unfortunately, the small amount of starting material available and the instability of the aglycone to acid treatment made its isolation difficult. The low solubility of trifolirhizin in water also hindered the enzymatic cleavage of the pure compound. It was therefore decided to isolate the aglycone from the plant after enzymatic cleavage *in situ*. The whole roots of red clover were crushed in water and left for the enzymatic reaction to take place. The ethanol-soluble part was distributed between light petroleum — *n*-butanol/1 N ammonia. When the extracts were worked up, no trifolirhizin was found. Instead, the aglycone m.p. 179.5—180° $[\alpha]_D^{20}$ −214°, was obtained at the expected place. The infrared spectrum of the aglycone resembled that of pterocarpin but showed hydroxyl band absorption in the stretching range. The ultraviolet spectrum in ethanol was almost identical in shape with those of pterocarpin and trifolirhizin [1].

Methylation of the compound with diazomethane gave, in high yield, a neutral compound identified as pterocarpin, thus confirming structure IV for the aglycone and III for trifolirhizin.

When the ultraviolet spectrum of the aglycone is taken in alkaline solution, a bathochromic shift to about 300 mμ is observed for the maxima at 281 and 287 mμ, which shows that these maxima belong to ring A. The maximum at 310 mμ is not influenced and thus belongs to ring B. This is essentially in agreement with the previously made interpretation of the ultraviolet spectrum of trifolirhizin [1].

Application of Klyne's method [3] for steroid glycosides shows that trifolirhizin is a β-glucoside. (The molecular rotation difference between trifolirhizin and the aglycone is −209; phenyl glucosides [4]: *a*-form + 402, β-form −182. The acetates give −166 for trifolirhizin, and + 688 and −123 for the respective phenyl glucosides.)

Biogenetical considerations would make structure V an attractive formula for the newly found antifungal substance pisatin [5].

Experimental. All m.p.'s are corrected. The ultraviolet spectra were measured with a Beckman DU apparatus. The infrared spectra were measured with a Perkin-Elmer No. 21 spectrometer.

Isolation of the aglycone. 550 g of roots of red clover were sliced and homogenised in a Waring Blendor apparatus with addition of 300 ml of water. The pulp was left at room temperature for 18 h, after which ethanol was added until a concentration of 70 % was reached. The next day the solution was filtered and the residue exhaustively extracted with 2 liter of 96 % ethanol. The extracts were filtered cold and evaporated *in vacuo*. The residue was suspended in 100 ml of 1 N ammonia and extracted with three portions of 100 ml of light petroleum (40—60°). The light petroleum extract was checked for the absence of the aglycone by ultraviolet spectrophotometry, and

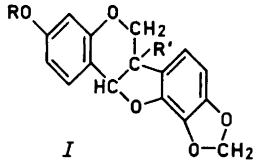

I

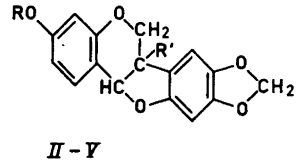

II–V

I and III: R = Glucose, R' = H; *II:* R = CH_3, R' = H;
IV: R = H, R' = H; *V:* R = CH_3, R' = OH.

discarded. A Craig countercurrent distribution in six tubes was performed between 1 N ammonia and a mixture of light petroleum and *n*-butanol (v/v 3:1) (after the fundamental distribution, all upper phases were withdrawn and combined, extract A) followed by a distribution in the same way with the solvent mixture 1 N ammonia — mixture of light petroleum and *n*-butanol (v/v 1:3) (extract B). Extract B yielded 40 mg of pratol (IR, m.p.) but no trifolirhizin could be isolated. Extract A was evaporated *in vacuo* and the residue again distributed between the former solvent system as before. The upper phase was evaporated *in vacuo*, the residue dissolved in 200 ml of methanol and 20 ml of water and the solution filtered.The filtrate was extracted with a small amount of light petroleum, which was discarded. Upon addition of 200 ml of water, an oil slowly separated out and after a time crystallised as tiny needles. The crystals were filtered, washed with aqueous methanol and water, and dried, yield 204 mg, m.p. 167–172°. Crystallisation from light petroleum gave a fine crystalline powder which sublimed at 150°/0.1 mm as long, fine needles, m.p. 179.5–180°, $[\alpha]_D^{20}$ −214° (ethanol, *c* 1 %). (Found C 66.84, H 4.11, O–CH_3 0.00; Calc. for $C_{16}H_{12}O_5$ C 67.59, H 4.26.) The compound is sparingly soluble in light petroleum and readily soluble in methanol. Ultraviolet spectra: ethanol, λ_{max} 281, 287, 310 mμ (log ε 3.58, 3.63, 3.83), λ_{min} 260, 283, 291 mμ (3.18, 3.575, 3.57); 0.1 N sodium hydroxide in 50 % ethanol, λ_{max} 249, 300–303 mμ (log ε 4.11, 3.92), inflexion 309 mμ (3.89), λ_{min} 233, 270 mμ (3.93, 3.43). Infrared spectrum: KBr, 3 530, 3 330, 1 628, 1 598, 1 506 cm^{-1}. *Methylation.* The aglycone (20 mg) was methylated with an excess of diazomethane in dry ether for three days at + 4°. The excess of diazomethane was decomposed by a drop of acetic acid and the solution was extracted with 1 N sodium hydroxide solution. The extracted ether solution was evaporated and the residue (18 mg) crystallised from light petroleum and sublimed in a high vacuum. The sublimate, m.p. 162–163°, $[\alpha]_D^{20}$ −200° (ethanol, *c* 0.2 %) gave no depression with authentic pterocarpin, m.p. 163–164°, ($[\alpha]_{5461}^{20}$ −207.5° (chloroform)) [6], kindly provided by Dr. W. B. Whalley, Liverpool. The ultraviolet and infrared spectra were identical. There was no change in the ultraviolet spectrum upon addition of alkali.

Our thanks are due to Professor A. I. Virtanen for his interest in this work. We also wish to express our thanks to Professor Holger Erdtman for facilities for taking the infrared spectra. This investigation is a part of a research project under U.S. Public Law No. 480, 83rd Congress.

1. Bredenberg, J. B. and Hietala, P. K. *Acta Chem. Scand.* **15** (1961) 696.
2. Bredenberg, J. B. and Shoolery, J. N. *Tetrahedron Letters* **1961**. *In press.*
3. Klyne, W. *Biochem. J.* **47** (1950) xli.
4. Vogel, H. and Georg, A. *Tabellen der Zucker und ihrer Derivate* Julius Springer, Berlin 1931.
5. Cruickshank, I. A. M. and Perrin, D. R. *Nature* **187** (1960) 799.
6. McGookin, A., Robertson, A. and Whalley, W. B. *J. Chem. Soc.* **1940** 787.

Received May 8, 1961.

A Qualitative Chemical Method for the Demonstration of "Pauly-positive" Bases in Rumen Contents

W. THORSELL

Department of Chemistry, Royal Veterinary College, Stockholm, Sweden

Many methods have been described for the demonstration of physiologically active amines in biological material. Few methods have been applied to rumen contents [1]. Since histamine and tyramine, so-called Pauly-positive bases, are among compounds of interest in ruminant metabolism [2], a relatively simple chemical method was developed for demonstrating these substances in rumen contents, care being taken to avoid secondary processes during the course of the analysis.

To one volume rumen contents, with and without added histamine, tyramine, and histidine, were momentarily added 4 volumes of a 99:1 (volume) mixture of ethanol and acetic acid [3]. The mixture was centrifuged at 2 000 *g* for 15 min, and the supernatant adjusted to pH 7.0 with sodium hydroxide. Any precipitate formed was removed by centrifugation. The clear solution was treated with 2.5 volumes Amberlite IRC 50 and the bases adsorbed were eluted with 0.1 N hydrochloric acid [4]. The eluate was evaporated to dryness in a water bath and the residue was washed

discarded. A Craig countercurrent distribution in six tubes was performed between 1 N ammonia and a mixture of light petroleum and *n*-butanol (v/v 3:1) (after the fundamental distribution, all upper phases were withdrawn and combined, extract A) followed by a distribution in the same way with the solvent mixture 1 N ammonia — mixture of light petroleum and *n*-butanol (v/v 1:3) (extract B). Extract B yielded 40 mg of pratol (IR, m.p.) but no trifolirhizin could be isolated. Extract A was evaporated *in vacuo* and the residue again distributed between the former solvent system as before. The upper phase was evaporated *in vacuo*, the residue dissolved in 200 ml of methanol and 20 ml of water and the solution filtered.The filtrate was extracted with a small amount of light petroleum, which was discarded. Upon addition of 200 ml of water, an oil slowly separated out and after a time crystallised as tiny needles. The crystals were filtered, washed with aqueous methanol and water, and dried, yield 204 mg, m.p. 167–172°. Crystallisation from light petroleum gave a fine crystalline powder which sublimed at 150°/0.1 mm as long, fine needles, m.p. 179.5–180°, $[\alpha]_D^{20}$ −214° (ethanol, *c* 1 %). (Found C 66.84, H 4.11, O–CH_3 0.00; Calc. for $C_{16}H_{12}O_5$ C 67.59, H 4.26.) The compound is sparingly soluble in light petroleum and readily soluble in methanol. Ultraviolet spectra: ethanol, λ_{max} 281, 287, 310 mμ (log ε 3.58, 3.63, 3.83), λ_{min} 260, 283, 291 mμ (3.18, 3.575, 3.57); 0.1 N sodium hydroxide in 50 % ethanol, λ_{max} 249, 300–303 mμ (log ε 4.11, 3.92), inflexion 309 mμ (3.89), λ_{min} 233, 270 mμ (3.93, 3.43). Infrared spectrum: KBr, 3 530, 3 330, 1 628, 1 598, 1 506 cm^{-1}. *Methylation.* The aglycone (20 mg) was methylated with an excess of diazomethane in dry ether for three days at + 4°. The excess of diazomethane was decomposed by a drop of acetic acid and the solution was extracted with 1 N sodium hydroxide solution. The extracted ether solution was evaporated and the residue (18 mg) crystallised from light petroleum and sublimed in a high vacuum. The sublimate, m.p. 162–163°, $[\alpha]_D^{20}$ −200° (ethanol, *c* 0.2 %) gave no depression with authentic pterocarpin, m.p. 163–164°, ($[\alpha]_{5461}^{20}$ −207.5° (chloroform)) [6], kindly provided by Dr. W. B. Whalley, Liverpool. The ultraviolet and infrared spectra were identical. There was no change in the ultraviolet spectrum upon addition of alkali.

Our thanks are due to Professor A. I. Virtanen for his interest in this work. We also wish to express our thanks to Professor Holger Erdtman for facilities for taking the infrared spectra. This investigation is a part of a research project under U.S. Public Law No. 480, 83rd Congress.

1. Bredenberg, J. B. and Hietala, P. K. *Acta Chem. Scand.* **15** (1961) 696.
2. Bredenberg, J. B. and Shoolery, J. N. *Tetrahedron Letters* **1961**. *In press.*
3. Klyne, W. *Biochem. J.* **47** (1950) xli.
4. Vogel, H. and Georg, A. *Tabellen der Zucker und ihrer Derivate* Julius Springer, Berlin 1931.
5. Cruickshank, I. A. M. and Perrin, D. R. *Nature* **187** (1960) 799.
6. McGookin, A., Robertson, A. and Whalley, W. B. *J. Chem. Soc.* **1940** 787.

Received May 8, 1961.

A Qualitative Chemical Method for the Demonstration of "Pauly-positive" Bases in Rumen Contents

W. THORSELL

Department of Chemistry, Royal Veterinary College, Stockholm, Sweden

Many methods have been described for the demonstration of physiologically active amines in biological material. Few methods have been applied to rumen contents [1]. Since histamine and tyramine, so-called Pauly-positive bases, are among compounds of interest in ruminant metabolism [2], a relatively simple chemical method was developed for demonstrating these substances in rumen contents, care being taken to avoid secondary processes during the course of the analysis.

To one volume rumen contents, with and without added histamine, tyramine, and histidine, were momentarily added 4 volumes of a 99:1 (volume) mixture of ethanol and acetic acid [3]. The mixture was centrifuged at 2 000 *g* for 15 min, and the supernatant adjusted to pH 7.0 with sodium hydroxide. Any precipitate formed was removed by centrifugation. The clear solution was treated with 2.5 volumes Amberlite IRC 50 and the bases adsorbed were eluted with 0.1 N hydrochloric acid [4]. The eluate was evaporated to dryness in a water bath and the residue was washed

several times with an 80 %, v/v, ethanol-water mixture. The procedure of evaporation and washing with ethanol-water was repeated to free the solution from contaminants. The final alcohol solution was centrifuged, if cloudy, and the solution investigated by paper chromatography [4]. The so-called Pauly-reagent [5] was used to visualize the bases.

Controls were performed with pure histamine, tyramine and histidine.

Fig. 1 represents a paper chromatogram for samples corresponding to 1.5 ml of rumen contents.

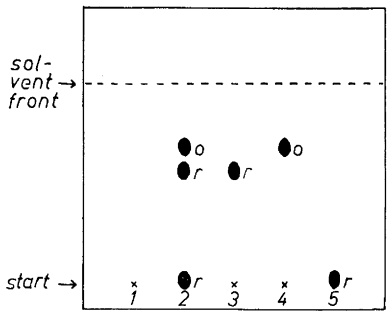

Fig. 1. Paper chromatographic separation of "Pauly-positive" bases. 1, Rumen contents; 2, Rumen contents + histamine, tyramine, and histidine; 3, histamine, sensitivity 0.5–1.0 × 10^{-7} g; 4, tyramine, the same sensitivity; 5, histidine, the same sensitivity; r = red; o = orange.

The method thus affords the possibility of demonstrating "Pauly-positive" bases present in rumen contents without resorting to dialysis [1].

Thanks are due to the Head of the Department, Professor K. Sjöberg, and to Mrs. K. Rönn for her assistance.

1. Dain, J. A., Neal, A. L. and Dougherthy, R. W. *J. Animal. Sci.* **14** (1955) 930.
2. Annison, E. F. and Lewis, D. *Metabolism in the rumen.* Methuens monographs on biochemical subjects. London 1959.
3. Schwyzer, R. *Acta Chem. Scand.* **6** (1952) 219.
4. Pénau, H., Saïas, E. and Andreetti, C. *Ann. pharm. franç.* **10** (1952) 514.
5. Hais, I. M. and Mazek, K. *Handbuch der Papierchromatographie.* Bd. 1, Jena 1958, p. 743.

Received June 19, 1961.

Selena-hexanoic and Selena-pentanoic Acids

ARNE FREDGA and ARILD LINDGREN

Organic Department, Chemical Institute, University of Uppsala, Sweden

In recent years, organoselenium compounds have attracted attention from biochemical viewpoints [1,2]. Earlier, selenium was regarded primarily as a toxic element; if present in soils, for example, it can be taken up by plants and cereals, thus causing injury to grazing animals. It is now known that it may also have a positive effect and that certain dietary diseases of sheep, cattle and rats may be cured by minute amounts of certain selenium compounds. At different times organoselenium compounds have also been tested for chemotherapeutical effects. Very little is known, however, about the metabolism of selenium and its compounds.

In the course of current investigations in selenium chemistry, we have started a programme to study long-chain fatty acids with a selenium atom incorporated in the chain. The biological and pharmacological properties of the acids are being investigated. In this connection the position of the selenium atom in the chain may be important. Long-chain acids with a heavy heteroatom may also be used as model substances in X-ray crystallographic investigations. Furthermore, their physico-chemical properties, *e.g.* their behaviour in monolayers, may be of interest.

The acids are easily obtained by reduction of ω-diseleno-di-alkanoic acids to ω-selenol acids (not isolated) and subsequent reaction of these compounds with alkyl bromides:

$$[\text{-Se-(CH}_2)_m\text{-COOH}]_2 \rightarrow \text{HSe-(CH}_2)_m\text{-COOH} \xrightarrow{\text{CH}_3\text{-(CH}_2)_n\text{-Br}} \text{CH}_3\text{-(CH}_2)_n\text{-Se-(CH}_2)_m\text{-COOH}$$

In our experiments the reduction has been performed with Rongalite in aqueous ammonia, but other reductants will be tested. As the selenol acid is easily oxidised, the solution must be protected against atmospheric oxygen. The reaction is best performed in an ordinary flask, closed by a cork stopper, and opened only momentarily when the reactant is added. About

several times with an 80 %, v/v, ethanol-water mixture. The procedure of evaporation and washing with ethanol-water was repeated to free the solution from contaminants. The final alcohol solution was centrifuged, if cloudy, and the solution investigated by paper chromatography [4]. The so-called Pauly-reagent [5] was used to visualize the bases.

Controls were performed with pure histamine, tyramine and histidine.

Fig. 1 represents a paper chromatogram for samples corresponding to 1.5 ml of rumen contents.

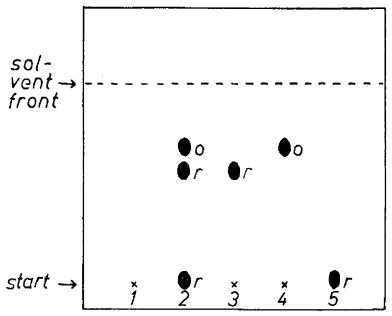

Fig. 1. Paper chromatographic separation of "Pauly-positive" bases. 1, Rumen contents; 2, Rumen contents + histamine, tyramine, and histidine; 3, histamine, sensitivity 0.5–1.0 × 10^{-7} g; 4, tyramine, the same sensitivity; 5, histidine, the same sensitivity; r = red; o = orange.

The method thus affords the possibility of demonstrating "Pauly-positive" bases present in rumen contents without resorting to dialysis [1].

Thanks are due to the Head of the Department, Professor K. Sjöberg, and to Mrs. K. Rönn for her assistance.

1. Dain, J. A., Neal, A. L. and Dougherthy, R. W. *J. Animal. Sci.* **14** (1955) 930.
2. Annison, E. F. and Lewis, D. *Metabolism in the rumen.* Methuens monographs on biochemical subjects. London 1959.
3. Schwyzer, R. *Acta Chem. Scand.* **6** (1952) 219.
4. Pénau, H., Saïas, E. and Andreetti, C. *Ann. pharm. franç.* **10** (1952) 514.
5. Hais, I. M. and Mazek, K. *Handbuch der Papierchromatographie.* Bd. 1, Jena 1958, p. 743.

Received June 19, 1961.

Selena-hexanoic and Selena-pentanoic Acids

ARNE FREDGA and ARILD LINDGREN

Organic Department, Chemical Institute, University of Uppsala, Sweden

In recent years, organoselenium compounds have attracted attention from biochemical viewpoints [1,2]. Earlier, selenium was regarded primarily as a toxic element; if present in soils, for example, it can be taken up by plants and cereals, thus causing injury to grazing animals. It is now known that it may also have a positive effect and that certain dietary diseases of sheep, cattle and rats may be cured by minute amounts of certain selenium compounds. At different times organoselenium compounds have also been tested for chemotherapeutical effects. Very little is known, however, about the metabolism of selenium and its compounds.

In the course of current investigations in selenium chemistry, we have started a programme to study long-chain fatty acids with a selenium atom incorporated in the chain. The biological and pharmacological properties of the acids are being investigated. In this connection the position of the selenium atom in the chain may be important. Long-chain acids with a heavy heteroatom may also be used as model substances in X-ray crystallographic investigations. Furthermore, their physico-chemical properties, *e.g.* their behaviour in monolayers, may be of interest.

The acids are easily obtained by reduction of ω-diseleno-di-alkanoic acids to ω-selenol acids (not isolated) and subsequent reaction of these compounds with alkyl bromides:

$$[\text{-Se-(CH}_2)_m\text{-COOH}]_2 \rightarrow \text{HSe-(CH}_2)_m\text{-COOH} \xrightarrow{\text{CH}_3\text{-(CH}_2)_n\text{-Br}} \text{CH}_3\text{-(CH}_2)_n\text{-Se-(CH}_2)_m\text{-COOH}$$

In our experiments the reduction has been performed with Rongalite in aqueous ammonia, but other reductants will be tested. As the selenol acid is easily oxidised, the solution must be protected against atmospheric oxygen. The reaction is best performed in an ordinary flask, closed by a cork stopper, and opened only momentarily when the reactant is added. About

90 % of the Rongalite is added in one portion and the rest in small amounts until the yellow colour of the diselenide has completely disappeared, but some care must be taken since the reaction is not quite instantaneous. Often the solution assumes a yellow colour during the reaction owing to slight oxidation by the alkyl bromide. In such cases, the solution is decolourised by a little more Rongalite after which a corresponding quantity of the alkyl bromide is added. This should always be done if the diseleno acid is sparingly soluble and is likely to interfere with the purification of the product.

Table 1. Selena-hexadecanoic acids $C_{15}H_{30}O_2Se$: Se calc. 24.57 %.

Position of Se	m.p.	% Se found
4	62.5—63.5°	24.61
5	51—52°	24.51
6	45.5—47°	24.62
7	46.5—47.5°	24.70
9	42—43°	24.51
12	43—44°	24.61

Table 2. Selena-pentadecanoic acids $C_{14}H_{28}O_2Se$: Se calc. 25.69 %

Position of Se	m.p.	% Se found
3	52.5—53.5°	25.50
4	57.5—58.5°	25.64
5	40—40.5°	25.60
6	44—45°	25.61
7	36.5—37.5°	25.56
12	42.5—43.5°	25.54

The acids are recrystallised from petrol ether or dilute methanol. Owing to the rather high solubility and the low melting-points of the acids, it is appropriate and in some cases even necessary to let the crystallisation take place at 0—5°. The acids form glistening flakes or plates, very similar to those formed by ordinary long-chain acids.

A list of the acids prepared so far is given in Tables 1 and 2. The preparation of two of them is described in detail in the experimental part.

Experimental. 4-Selena-hexadecanoic acid. 7.60 g (0.025 mole) of β,β′-diseleno-dipropionic acid [3] were dissolved in 75 ml of 2 N aqueous ammonia and reduced with Rongalite as indicated above. A solution of 12.5 g (0.05 mole) of dodecyl bromide in 200 ml of ethanol was then added, the flask was shaken for 12 h and left to stand for one day. The solution was then poured into twice its volume of water, filtered and acidified with excess of 4 N sulphuric acid. The readily crystallising precipitate was filtered off, dried and recrystallised three times from dilute (80 %) methanol and once from petrol ether. Yield of crude product 7.8 g (48 %), after recrystallisation 6.9 g (43 %). The acid forms glistening leaves with m.p. 62.5—63.5°. (Found: Se 24.61; equiv. wt. 320.7, 321.0. Calc. for $C_{15}H_{30}O_2Se$: Se 24.57; equiv. wt 321.4).

A quantity of β,β′-diseleno-dipropionic acid could be regenerated from the acidified solution.

12-Selena-hexadecanoic acid. 10.56 g (0.02 mole) of ω,ω′-diseleno-diundecanoic acid (prepared from commercial ω-bromoundecanoic acid) [4] was dissolved in 150 ml of 2 N ammonia + 100 ml of ethanol; if no ethanol was added, a sparingly soluble ammonium salt separated. The solution was reduced with Rongalite, 5.50 g (0.04 mole) of *n*-butyl bromide, dissolved in 100 ml of ethanol were added, the flask was shaken for 12 h and left to stand over-night. The acid was liberated as described above and recrystallised once from dilute methanol and three times from petrol ether. Yield of crude product 11.2 g (87 %), after recrystallisation 9.1 g (71 %). Glistening leaves or plates with m.p. 43—44°. (Found: Se 24.61; equiv. wt. 321.4, 321.8. Calc. for $C_{15}H_{30}O_2Se$: Se 24.57; equiv. wt. 321.4).

A grant from *AB Astra* is gratefully acknowledged.

1. Schwarz, K. and Foltz, C. M. *J. Am. Chem. Soc.* **79** (1957) 3292.
2. Schwarz, K. *Vitalstoffe-Zivilisationskrankheiten* **4** (1959) 1.
3. Fredga, A. *Uppsala Univ. Årsskr.* **1935**; 5, p. 106.
4. Fredga, A. and Lindgren, A. *To be published.*

Received May 17, 1961.

Fluorometrische Untersuchungen des Glutaminsäuredehydrogenase-DPNH-Komplexes

HORST SUND

Medicinska Nobelinstitutet, Biokemiska avdelningen, Stockholm, Schweden

Boyer und Theorell beobachteten 1956 die Erhöhung der Fluoreszenz des DPNH * und eine Verschiebung seines Fluoreszenzmaximums nach kürzeren Wellenlängen in Gegenwart von Alkoholdehydrogenase aus Pferdeleber [1]. Analoge Ergebnisse wurden mit den binären Komplexen des DPNH oder TPNH und Hefe-Alkoholdehydrogenase [2], Milchsäuredehydrogenase [3], Äpfelsäuredehydrogenase [4], Isocitronensäuredehydrogenase [5] sowie Glu-DH [6] erhalten. Glu-DH aus Rinderleber wird durch DPNH sehr stark gehemmt [8,9] und verschiedene Verbindungen, unter anderem Adenosin, Adeninnucleotide und Derivate des Glycins können diese Hemmung verhindern [8-10]. Ausserdem erhöht DPNH die Dissoziation der Glu-DH, während TPNH einen gegenteiligen Effekt ausübt und keine Hemmwirkung besitzt [11]. Um festzustellen, ob Glu-DH für DPNH verschiedene Arten von Bindungsstellen besitzt, wurde mit Hilfe der Fluoreszenztechnik der binäre Komplex Glu-DH—DPNH studiert.

Experimenteller Teil. Die Fluoreszenzmessungen wurden mit einem registrierenden Spektrofluorophotometer vorgenommen, das früher bereits beschrieben wurde [12]. Für die Berechnung von $K_{E,R}$ und der Bindungsstellen dienten die von Theorell und Winer angegebenen Gleichungen [12]. Sämtliche Messungen wurden bei 20° in Na-Phosphat-Puffer ($\mu = 0{,}1$) pH 7,5 vorgenommen. Die Titration des Enzyms mit DPNH erfolgte durch Messen der Fluoreszenzemission bei 440 mμ, die Anregung bei 350 mμ. Die Maxima der Emissions- und Anregungsspektren sind unkorrigiert für die durch die Intensität des Anregungslichtes und der Empfindlichkeit der Fotozelle bei Änderung der Wellenlänge auftretenden Abweichungen. Für das benutzte Instrument ergibt die Korrektur eine Verschiebung der Maxima um etwa 15 mμ nach kürzeren Wellenlängen. Glu-DH aus Rinderleber wurde von der Firma C. F. Boehringer und Soehne, Mannheim, Deutschland *, erhalten und in Gegenwart von Na_2SO_4 zweimal umkristallisiert, Wechselzahl 6 500 [13]. Das Enzym war in der Elektrophorese (Wanderungsgeschwindigkeit bei pH 7,4: $4{,}8 \times 10^{-5}$ $cm^2.sec^{-1}.V^{-1}$) und in der Ultrazentrifuge einheitlich. Proteinbestimmung auf Grund der Absorption bei 280 mμ ($\varepsilon_{280} = 0{,}95$ $cm^2 \cdot mg^{-1}$) und des Kjeldahl-Stickstoffs (15,5 %). Verhältnis der Absorption bei 280 und 260 mμ: 1,97—2,00. Vor der Titration wurde die Glu-DH ohne Aktivitätsverlust zwei Tage gegen Na-Phosphat-Puffer ($\mu = 0{,}1$) pH 7,5 dialysiert. DPNH war ein Präparat der Sigma Chemical Co., St. Louis, Missouri, USA, (Reinheit bezogen auf die Absorption bei 340 mμ 89 %, davon 95 % enzymatisch aktiv). Glutaminsäure wurde von E. Merck, Darmstadt, Deutschland, bezogen (Reinheit auf Grund des Kjeldahl-Stickstoffs 98,5 %, papierchromatographisch einheitlich). $ZnSO_4 \cdot 7H_2O$ war durch Extraktion mit 8-Hydroxychinolin und Acetylaceton von allen Schwermetallspuren befreit.

Ergebnisse und Diskussion. Das Maximum der Fluoreszenzemission des DPNH bei 478 mμ (korrigiert 462 mμ) wird bei gleichzeitiger Erhöhung der Fluoreszenz in Gegenwart von Glu-DH nach 468 mμ verschoben, Glutaminsäure erhöht die Fluoreszenz des ER-Komplexes ohne dessen Maximum zu verschieben [6]. Abb. 1 zeigt nebeneinander die Emissions- und Anregungsspektren von DPNH, ER, der ternären Komplexe ERS und ERZn sowie des quaternären Komplexes ERSZn. Aus der fluorometrischen Titrationskurve der Glu-DH mit DPNH wird bei einer Enzymkonzentration von 1,09 mg/ml ein Äquivalentgewicht von 59 000 pro DPNH-Bindungsstelle gefunden, $K_{E,R}$ besitzt den Wert 0,49 μM. Erniedrigung der Enzymkonzentration führt zu einer Abnahme des Äquivalentgewichtes, Q nimmt ebenfalls etwas ab, während $K_{E,R}$ ansteigt (Tabelle 1). Anzeichen für das Vorhandensein verschiedenartiger DPNH-Bindungsstellen bei den jeweiligen Enzymkonzentrationen konnten wir nicht finden, die mit den in der Tabelle 1 angegebenen Werten berechneten Titrationskurven stimmen mit den experimentell gefundenen gut überein (Abb. 2). Die Messungen anderer Autoren ergaben bei der

* *Abkürzungen:* DPNH, R: reduziertes Diphosphopyridinnucleotid; Glu-DH, E: Glutaminsäuredehydrogenase; Q: Fluoreszenz ER/R; S: Glutaminsäure; TPNH: reduziertes Triphosphopyridinnucleotid; $K_{E,R} = [E][R]/[ER]$.

* Der Firma C. F. Boehringer und Soehne danken wir sehr für die grosszügige Überlassung der Glu-DH.

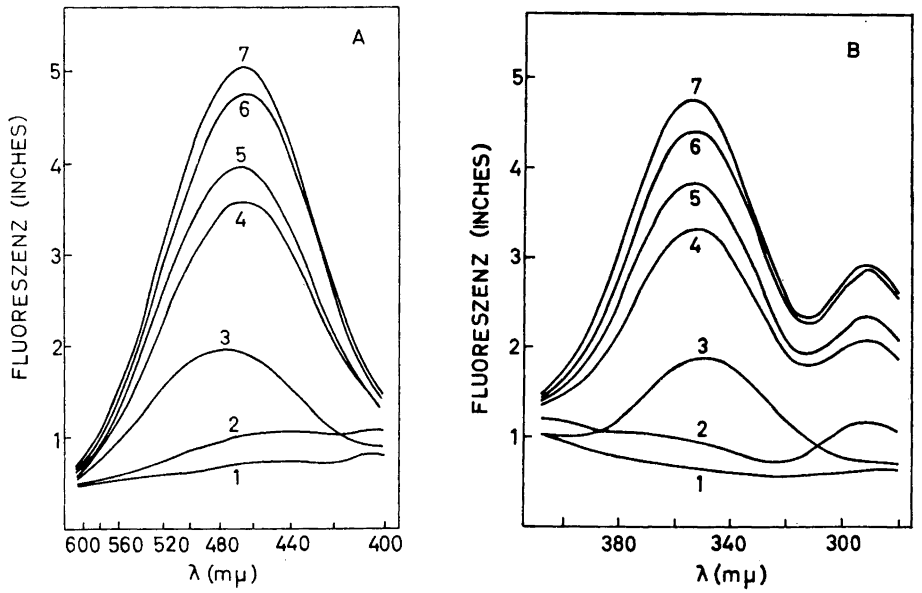

Abb. 1. Fluoreszenzspektren der Komplexe von Glu-DH aus Rinderleber mit DPNH, Glutaminsäure und Zn^{++} in Na-Phosphat-Puffer (μ=0,1) pH 7,5 bei 20°. A: Emissionsspektren (Anregung bei 350 mμ), B: Anregungsspektren (gemessen bei 468 mμ). 1: Puffer; 2: 0,64 mg/ml Glu-DH; 3: 0,90 μM DPNH; 4: 0,64 mg/ml Glu-DH, 0,90 μM DPNH; 5: 0,64 mg/ml Glu-DH, 0,90 μM DPNH, 254 μM Glutaminsäure; 6: 0,64 mg/ml Glu-DH, 0,90 μM DPNH, 47,7 μM $ZnSO_4$ 7: 0,64 mg/ml Glu-DH, 0,90 μM DPNH, 254 μM Glutaminsäure, 47,7 μM $ZnSO_4$.

direkten Bestimmung in der Ultrazentrifuge in Gegenwart von 5,1 mg/ml Glu-DH ein Äquivalentgewicht von 66 000 [14], bei der fluorometrischen Titration mit TPNH oder DPNH in Gegenwart von 1 mg/ml einen Wert von etwa 100 000 [7]. Bemerkenswert ist die Erhöhung der Fluoreszenz des ER-Komplexes in Gegenwart von Zn-Ionen (Q etwa 3,1) und bei der Bildung des quaternären Komplexes ERSZn (Q etwa 3,4), bei der das Maximum des binären

Tabelle 1. Abhängigkeit der DPNH-Bindungsstellen und $K_{E,R}$ von der Glu-DH-Konzentration.

[Glu-DH] mg/ml	Äquivalentgewicht pro DPNH-Bindungsstelle	$K_{E,R}$ (μM)	Q
1,09	59 000	0,49	2,3
0,60	45 000	1,42	2,1
0,31	31 000	1,96	1,8

Komplexes ER nicht verändert wird (Abb. 1). Das Maximum des Anregungsspektrum von DPNH bei 350 mμ wird nur unwesentlich nach 353 mμ verschoben, wenn der binäre ER-Komplex oder die höheren Komplexe gebildet werden (Abb. 1). Imidazol (4,8 × 10^{-2} M), das mit Leber-Alkoholdehydrogenase Komplexe bildet [15], und NH_4Cl (2,0 × 10^{-3} M) verändern die Fluoreszenz des ER-Komplexes nicht. Zn-Ionen haben unter den angegebenen Bedingungen keinen Einfluss auf die Fluoreszenz des Enzyms oder DPNH.

Aus Diffusionsmessungen geht hervor, dass die durch Dissoziation der Glu-DH beim Verdünnen entstehenden Untereinheiten symmetrischer sind als die Assoziate [16]. Die Ergebnisse der Fluoreszenzmessungen zeigen, dass Dissoziation und Formveränderung der Glu-DH zu einer Vermehrung der Bindungsstellen für DPNH führen. Möglicherweise sind die hierbei auftretenden neuen Bindungstellen verantwortlich für die starke Hemmung der En-

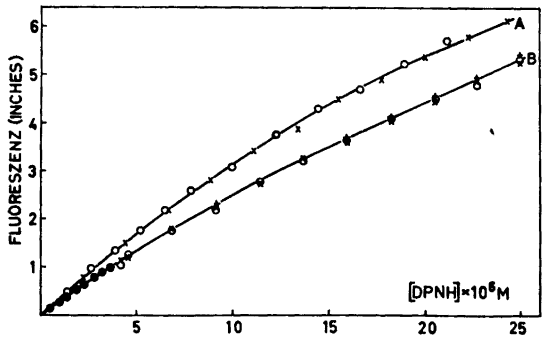

Abb. 2. Titration von Glu-DH mit DPNH. [Glu-DH] = 0,60 mg/ml (A) und 0,31 mg/ml (B). Ausgezogene Kurven berechnet mit den in der Tabelle 1 angegebenen Werten. O, ×, +, experimentelle Werte verschiedener Titrationen.

zymaktivität durch DPNH. Dieser Befund ist von Bedeutung für die Betrachtung der Verhältnisse *in vivo*, da die Konzentrationen der Glu-DH in der Leber und in unseren Versuchen etwa gleich sind. Über die Natur der Enzym-Coenzym-Bindung kann noch nichts ausgesagt werden, doch ist der Zinkgehalt [17] zu niedrig, um eine Beteiligung des Zinks an der Bindung zwischen DPNH und Glu-DH annehmen zu dürfen. Die Untersuchungen werden fortgesetzt und später in dieser Zeitschrift in extenso publiziert und diskutiert.

Herrn Professor Hugo Theorell danke ich sehr für wertvolle Diskussionen und Hinweise und für die mir gewährte Gastfreundschaft. Der *Deutschen Forschungsgemeinschaft* danke ich für ein Auslandsstipendium.

1. Boyer, P. D. und Theorell, H. *Acta Chem. Scand.* **10** (1956) 447.
2. Duysens, L. N. M. und Kronenberg, G. H. M. *Biochim. et Biophys. Acta* **26** (1957) 437.
3. Winer, A. D., Novoa, W. B. und Schwert, G. W. *J. Am. Chem. Soc.* **79** (1957) 6571.
4. Theorell, H. und Langan, T. A. *Acta Chem. Scand.* **14** (1960) 933.
5. Langan, T. A. *Acta Chem. Scand.* **14** (1960) 936.
6. Winer, A. D. und Schwert, G. W. *Biochim. et Biophys. Acta* **29** (1958) 424.
7. Frieden, C. *Biochim. et Biophys. Acta* **47** (1961) 428.
8. Wallenfels, K. und Summ, H. D. *Klin. Wochschr.* **35** (1957) 849.
9. Wallenfels, K. und Sund, H. *Arzneimittelforsch.* **9** (1959) 81.
10. Sund, H. und Müller-Hill, B. *Biochem. Z. In Vorbereitung.*
11. Frieden, C. *J. biol. Chem.* **234** (1959) 809.
12. Theorell, H. und Winer, A. D. *Arch. Biochem. Biophys.* **83** (1959) 291.
13. Wallenfels, K., Sund, H. und Diekmann, H. *Biochem. Z.* **329** (1957) 48.
14. Kubo, H., Yamano, T., Iwatsubo, M., Wateri, H., Soyama, T., Shiraishi, J., Sawada, S., Kawashima, N., Mitani, S. und Ito, K. *Bull. soc. chim. biol.* **40** (1958) 431.
15. Theorell, H. und McKinley McKee, J. S. *Acta Chem. Scand.* **15** (1961). *Im Druck.*
16. *Unveröffentlichte Versuche.*
17. Vallee, B. L., Adelstein, S. J. und Olson, J. A. *J. Am. Chem. Soc.* **77** (1955) 5196.

Eingegangen am 19. Mai 1961.

Polarographic Determination of Molybdenum in Rocks and Ores

C. H. HOLTEN.*

Kryolitselskabet Øresund A/S, Copenhagen Ø, Denmark

Several methods for colorimetric determination of molybdenum in rocks and ores by means of thiocyanate have been published [1-5]. In our experiments, we found it difficult to obtain a stable colour; the extinction tended to grow with the time. The method of Winterstein [5] has been tried here, but very often an extremely stable emulsion was formed during the extraction with *n*-butyl acetate, preventing the completion of the analysis.

Therefore, an investigation was carried out to find a polarographic method for the determination. According to Kanevskiĭ and Shvartsburd [6], the sample is fused with potassium hydroxide and sodium peroxide, and leached with hot water. To an aliquot of the filtrate a large amount of phosphoric acid is added, and the polarogram is recorded and measured. Meites [7] has described a method for polarographic determination of molybdenum in sodium tungstate. The supporting electrolyte is a neutral solution of sodium citrate, and a rather broad single wave is obtained with half-wave potential of −1.111 V and −0.927 V *vs.* S.C.E. in 0.1 M, and 1 M sodium citrate, respectively.

The investigation showed that it is possible to determine molybdenum in rocks and ores using a modification of the polarographic method of Meites [7]. The modification consists in a fusion with peroxide and hydroxide; indifferent salts coming from the sample or introduced for the fusion remain in the solution. The range of molybdenum content covered by the method is 0.01 % to several per cent. No interfering elements are found.

Experimental

Apparatus. The polarograms were obtained with a Polariter, type PO4, from Radiometer, Copenhagen. Diffusion currents were measured, using the extrapolation method, described by Meites [8].

Measuring of pH and automatic titrations were performed with a titrator, type TTT1, from Radiometer, Copenhagen.

Reagents. All reagents were analytical grade and were used without further purification.

Standard solutions of molybdenum containing 1 mg/ml or 0.2 mg/ml were prepared as follows. A weighed amount of molybdenum trioxide was dissolved in the minimum amount of 1 N sodium hydroxide, and neutralised with 1 N perchloric acid to pH 6−7; the volume was adjusted to make the content 1.0 mg/ml, and then this solution was further diluted with water to make 0.2 mg/ml.

Sodium citrate (50 %) was prepared by dissolving 500 g of trisodium citrate in water and diluting to 1 liter.

Procedure. Grind the sample to pass mesh 100 (to the inch) and mix well. Wigh 1 g in a nickel crucible and mix with 4 g of sodium peroxide and 1 g of sodium hydroxide. Place the crucible in an oven and heat to 500°C for 30 min. After cooling dissolve in water and adjust the volume to 50 ml in a volumetric flask. Filter the solution through a dry paper, the first 5 ml of filtrate being discarded. Boil an aliquot of 10 ml for 15 min to destroy peroxide. After cooling add 20 ml of 50 % sodium citrate and titrate the mixture potentiometrically with 4 N perchloric acid, added slowly to pH = 6.0. Transfer the resulting solution to a volumetric flask and adjust the volume to 50 ml with water. If a copious amount of silica-gel is formed, allow the solution to stand overnight to complete the coagulation, and filter through a dry paper, the first 5 ml of filtrate being discarded.

The solution is now ready for recording the polarogram. Each 10 ml corresponds to $\frac{10}{50} \cdot \frac{10}{50} = \frac{1}{25}$ of the original sample weight. No addition of maximum depressant agent is needed.

Place 10 ml solution in the cell, deaerate with nitrogen (freed from oxygen), and record the polarogram. The molybdenum wave appears at $E_{1/2} = -1.0$ V. The diffusion current is about 6 μA/mg Mo/10 ml. Assess the content of molybdenum according to this; add a corresponding amount of standard solution of molybdenum, and record the new polarogram.

Measure the two diffusion currents using the geometric extrapolation [8] shown in Fig. 1. The length of the line MN at $E_{1/2}$ is a measure for the diffusion current. Calculate the content of molybdenum:

$$\% \text{ Mo} = 2500s[i_1/(i_2(1 + v/10) - i_1)]/W$$

* Present address: Danmarks Ingeniørakademi, Department of Chemistry, Copenhagen K.

Table 1. Molybdenum content in ore samples.

No.	Mo polarographic determination %	Mo colorimetric determination %
8	0.18	0.17
9	0.16	0.16
32	0.16	0.15 −0.16
42	0.14	0.125−0.14
44	0.11	0.115−0.13
standard ore	0.30	0.31

Colorimetric determinations of samples Nos. 32, 42 and 44 by Nordisk Mineselskab, performed according to the method of Winterstein [5]. Samples Nos. 8 and 9 were analysed simultaneously by Dr. Christoph Winterstein, Staatshüttenlaboratorium, Hamburg, and here, whereupon the results were exchanged. Standard ore prepared by American Metal Climax Inc.

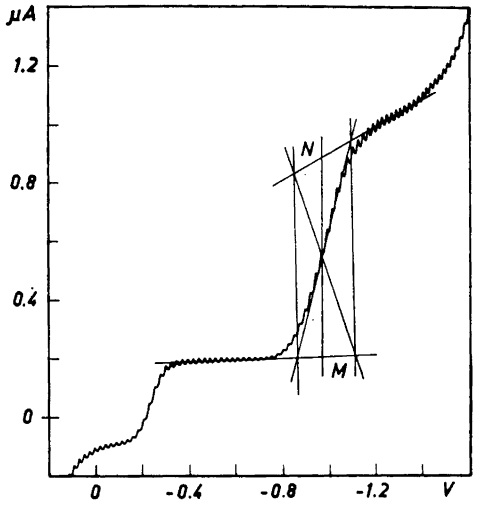

Fig. 1. Typical polarogram, obtained with the standard ore from American Metal Climax Inc.; Mo content: 0.31 %. The geometric extrapolation used to measure diffusion currents is shown; the length MN at $E_{½}$ gives the diffusion current.

where W is the sample weight, s and v the molybdenum content and volume of the standard solution, i_1 and i_2 the diffusion currents of the original solution and of the solution after the standard addition.

Results. The method was used to determine the molybdenum content of 54 samples containing molybdenite (MoS_2). The molybdenum content ranged from 0 to 0.8 %. Five analysed samples from the Mestersvig area, Greenland, and a standard ore prepared by American Metal Climax Inc. were placed at our disposal by Nordisk Mineselskab. The molybdenum content of these samples are found in Table 1, which shows the close agreement between the polarographic and the colori-

Table 2. Polarographic waves in citrate electrolyte.

Element	$E_{½}$	Notes	Effect of fusion.
Cu^{II}	−0.17 V.	W.-d.	Wave disappears
Zn^{II}	−1.3 V.	Ill-d.[b]	
Cd^{II}	−0.68 V.	W.-d.	Wave diminished
Tl^{III}	−0.48 V.	Small wave	Wave disappears
Zr^{IV}	*ca.* −0.7 V.	Ill-d.[c]	Wave disappears
Pb^{II}	−0.51 V.	W.-d.	Wave diminished
V^{V}	>0 V.	W.-d.	
Bi^{III}	−0.33 V.	W.-d.	Wave disappears
Cr^{VI}	>0 V.	W.-d.[d]	
Mo^{VI}	−1.00 V.	W.-d.	
W^{VI}	−1.5 V.[a]	Ill-d.[b]	
U^{VI}	*ca.* −0.7 V.	Ill-d.[e]	Wave diminished

W.-d. = Well-determined plateau of the wave.
Ill-d. = Ill-determined wave.
a: Meites [7].
b: Interfering with the final reduction of the electrolyte.
c: Very broad wave, extending from −0.5 to −0.9 V.
d: Large maximum, eliminated on fusion.
e: Very broad, apparantly composed wave, extending from −0.5 to −0.9 V.

metric methods. Molybdenum contents down to 0.01 % can be determined. This corresponds to about 0.004 mg of molybdenum in 10 ml of the final solution or to a diffusion current of 0.02—0.03 μA. The error of the analysis is assessed at about ± 5 % (rel.), or ± 0.01 % (abs.), whichever is the larger.

A typical polarogram is shown in Fig. 1. The molybdenum wave is found at −1.00 or −1.01 V; Meites [7] found $E_{½}$ −1.111 V or −0.927 V, depending on the concentration of the electrolyte. Most of the samples produced a wave with $E_{½}$ about −0.3 V. It has not been possible to identify the substance producing this wave; it is not bismuth.

Interferences. With the purpose of finding any interfering substances, and of identifying, if possible, the substance producing the wave at −0.3 V, a series of metals were examined. Cerium IV, titanium IV, thorium VI, tin IV, niobium V, tantalum V, arsenic V, antimony V, cobalt II, and nickel II did not produce any wave. Solutions of copper II, thallium III, zirconium IV, bismuth III, and uranium VI, in the electrolyte were reduced, but these metals were eliminated by the fusion. Zinc II, cadmium II, lead II, vanadium V, chromium IV and tungsten VI produced polarographic waves, persisting after fusion, but none of these waves interfered with the molybdenum wave. The values of $E_{½}$ are shown in Table 2.

Acknowledgements. Thanks are due to Nordisk Mineselskab, A/S, for the analysed samples of molybdenum ore, to Kryolitselskabet Øresund A/S for permission to publish this paper, to H. Pauly, Ph. D., J. Bjerrum, professor, Ph.D., and H. Buchwald, chief analyst, for valuable discussions and good advice.

1. Sandell, E. B. *Ind. Eng. Chem. Anal. Ed.* **8** (1936) 336.
2. Grimaldi, F. S. and Wells, R. C. *Ind. Eng. Chem. Anal. Ed.* **15** (1940) 315.
3. Dobritskaya, Yu. I., *Pochvovedenie* **1957** No. 3, 91; *cf. Anal. Abstr.* **5** (1958) No. 3931.
4. Hope, R. P. *Anal. Chem.* **29** (1957) 1053.
5. Winterstein, C. *Erzmetall* **10** (1957) 549.
6. Kanevskiĭ, E. A. and Shvartsburd, L. A. *Zavodskaya Lab.* **7** (1940) 283; *cf. Chem. Abstr.* **34** (1940) 5782 [8].
7. Meites, L. *Anal. Chem.* **25** (1953) 1752.
8. Meites, L. *Polarographic Techniques*, New York 1955, p. 65.

Received May 3, 1961.

The Structure of Cedrolic Acid

JARL RUNEBERG

Organisk-kemiska Institutionen, Kungl. Tekniska Högskolan, Stockholm, Sweden

Recently a saturated, tricyclic hydroxy acid, $C_{15}H_{24}O_3$, was isolated from the heartwood of the American desert juniper, *Juniperus utahensis* Lemm.[1]. The name cedrolic acid and the structure 2 are proposed for this compound, which appears to be the first naturally occurring sesquiterpene hydroxy acid described. Small amounts of three other compounds of the same class have since been isolated from heartwood of *Juniperus* species [2,3].

Cedrolic acid melts over a wide range (m.p. 181—187°). The sharp-melting methylester (3, m.p. 98.0—98.5) was reduced to a diol [1] (4, m.p. 130—131°). This diol has now been oxidised with chromic acid in pyridine to the hydroxy aldehyde 5, which on reduction by the Huang-Minlon procedure gave cedrol (6) in good yield.

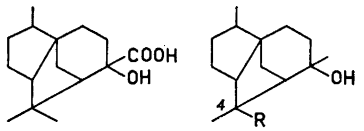

1 2 R=−COOH 3 R=−COOCH$_3$
4 R=−CH$_2$OH 5 R=−CHO
6 R=−CH$_3$

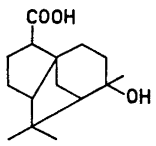

7

Of the possible structures 1, 2 and 7 for cedrolic acid, 1 can be eliminated because the acid formed on dehydration from cedrolic acid is not α,β-unsaturated [1]. Evidence against 7 is obtained from the infrared spectra of cedrolic acid, its methylester, the diol 4 and the hydroxy aldehyde 5. These spectra have only a single peak in the 1 375 cm^{-1} region, indicating the absence of a *gem*-dimethyl group in the above compounds.

metric methods. Molybdenum contents down to 0.01 % can be determined. This corresponds to about 0.004 mg of molybdenum in 10 ml of the final solution or to a diffusion current of 0.02—0.03 μA. The error of the analysis is assessed at about ± 5 % (rel.), or ± 0.01 % (abs.), whichever is the larger.

A typical polarogram is shown in Fig. 1. The molybdenum wave is found at −1.00 or −1.01 V; Meites [7] found $E_{½}$ −1.111 V or −0.927 V, depending on the concentration of the electrolyte. Most of the samples produced a wave with $E_{½}$ about −0.3 V. It has not been possible to identify the substance producing this wave; it is not bismuth.

Interferences. With the purpose of finding any interfering substances, and of identifying, if possible, the substance producing the wave at −0.3 V, a series of metals were examined. Cerium IV, titanium IV, thorium VI, tin IV, niobium V, tantalum V, arsenic V, antimony V, cobalt II, and nickel II did not produce any wave. Solutions of copper II, thallium III, zirconium IV, bismuth III, and uranium VI, in the electrolyte were reduced, but these metals were eliminated by the fusion. Zinc II, cadmium II, lead II, vanadium V, chromium IV and tungsten VI produced polarographic waves, persisting after fusion, but none of these waves interfered with the molybdenum wave. The values of $E_{½}$ are shown in Table 2.

Acknowledgements. Thanks are due to Nordisk Mineselskab, A/S, for the analysed samples of molybdenum ore, to Kryolitselskabet Øresund A/S for permission to publish this paper, to H. Pauly, Ph. D., J. Bjerrum, professor, Ph.D., and H. Buchwald, chief analyst, for valuable discussions and good advice.

1. Sandell, E. B. *Ind. Eng. Chem. Anal. Ed.* **8** (1936) 336.
2. Grimaldi, F. S. and Wells, R. C. *Ind. Eng. Chem. Anal. Ed.* **15** (1940) 315.
3. Dobritskaya, Yu. I., *Pochvovedenie* **1957** No. 3, 91; *cf. Anal. Abstr.* **5** (1958) No. 3931.
4. Hope, R. P. *Anal. Chem.* **29** (1957) 1053.
5. Winterstein, C. *Erzmetall* **10** (1957) 549.
6. Kanevskiĭ, E. A. and Shvartsburd, L. A. *Zavodskaya Lab.* **7** (1940) 283; *cf. Chem. Abstr.* **34** (1940) 5782 [8].
7. Meites, L. *Anal. Chem.* **25** (1953) 1752.
8. Meites, L. *Polarographic Techniques*, New York 1955, p. 65.

Received May 3, 1961.

The Structure of Cedrolic Acid

JARL RUNEBERG

Organisk-kemiska Institutionen, Kungl. Tekniska Högskolan, Stockholm, Sweden

Recently a saturated, tricyclic hydroxy acid, $C_{15}H_{24}O_3$, was isolated from the heartwood of the American desert juniper, *Juniperus utahensis* Lemm.[1]. The name cedrolic acid and the structure 2 are proposed for this compound, which appears to be the first naturally occurring sesquiterpene hydroxy acid described. Small amounts of three other compounds of the same class have since been isolated from heartwood of *Juniperus* species [2,3].

Cedrolic acid melts over a wide range (m.p. 181—187°). The sharp-melting methylester (3, m.p. 98.0—98.5) was reduced to a diol [1] (4, m.p. 130—131°). This diol has now been oxidised with chromic acid in pyridine to the hydroxy aldehyde 5, which on reduction by the Huang-Minlon procedure gave cedrol (6) in good yield.

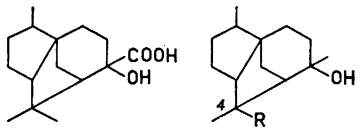

1 2 R=−COOH 3 R=−COOCH$_3$
4 R=−CH$_2$OH 5 R=−CHO
6 R=−CH$_3$

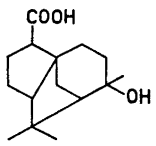

7

Of the possible structures 1, 2 and 7 for cedrolic acid, 1 can be eliminated because the acid formed on dehydration from cedrolic acid is not α,β-unsaturated [1]. Evidence against 7 is obtained from the infrared spectra of cedrolic acid, its methylester, the diol 4 and the hydroxy aldehyde 5. These spectra have only a single peak in the 1 375 cm^{-1} region, indicating the absence of a *gem*-dimethyl group in the above compounds.

The carbon-methyl value for cedrolic acid and its dehydration product [1] is in better agreement with structure 2 for cedrolic acid than with 7.

The proton magnetic resonance spectrum of cedrolic acid methylester was compared with that of cedrol [4] and agrees with structure 2 for the acid but not with 1 or 7.

The absolute configuration of cedrol was elucidated by Stork and Clarke [5] in connection with the total synthesis of this compound. Büchi and co-workers [6] have recently confirmed the absolute configuration of cedrene.

So far it has not been possible to determine the configuration at C_4 in cedrolic acid (2). On attempted lactonisation (acetic anhydride, pyridine) the formation of a strained 5-membered ring lactone in very low yield was indicated (IR).

The PMR spectrum of cedrolic acid methylester and a comparison between the infrared spectra of this compound in a polar and a nonpolar solvent (*cf.* Ref.[7]) gave no indication of any hydrogen bonding between the ester carbonyl and the alcoholic hydroxyl group. The pK^*_{MCS}-values [8,9] of cedrolic acid ($pK^*_{MCS} = 8.37$) and that of its dehydration product [1] ($pK^*_{MCS} = 8.23$) are close to one another.

Experimental. Melting points, taken on a hot stage, are uncorrected.

The carbon-methyl value of cedrolic acid (m.p. 181–187°, $[\alpha]_D$ −47°) was redetermined (*cf.* Ref.[1]. Found: CH_3–(C) 9.9; 10.9. $C_{15}H_{24}O_3$ requires CH_3–(C) (one) 6.0).

Hydroxy aldehyde (5). A solution of the diol 4 (0.50 g, prepared as described previously [1]) in dry pyridine (7 ml) was added to chromic acid (1.00 g) in the same solvent (20 ml) and left for 11 h at room temperature. Methanol (10 ml) was then added, and after an additional hour the reaction mixture was diluted with ice-cold sodium hydroxide (20 ml) and extracted with ether. The ether solution was first washed with ice-cold hydrochloric acid (2 N) to remove pyridine and then with water, dried (Na_2SO_4), and evaporated to dryness. The residue (401 mg) was recrystallised from light petroleum and from methanol-water yielding the hydroxy aldehyde 5, m.p. 62–64°, $[\alpha]_D$ −77° (*c*, 2.2, $CHCl_3$). (Found: C 75.9; H 10.2. $C_{15}H_{24}O_2$ requires C 76.2; H 10.2.) Infrared spectrum (in KBr): 3 480 m, 2 695 m, 1 721 cm^{-1} s. 2,4-Dinitrophenylhydrazone, m.p. 172–174°. (Found: N 13.9. $C_{21}H_{28}O_5N_4$ requires N 13.5.)

Cedrol from the hydroxy aldehyde. The hydroxy aldehyde 5 (102 mg) was refluxed for 1 h with a mixture of potassium hydroxide (280 mg), hydrazine hydrate (99–100 %, 0.31 ml) and ethylene glycol (3.5 ml, redistilled). The temperature of the reaction mixture was then raised to 200° while some water was removed by distillation. The mixture was then refluxed (at about 230°) under oxygen-free nitrogen for 4 h, cooled, diluted with water (25 ml) and extracted with light petroleum. The extract was washed with water, dried (Na_2SO_4), and evaporated, leaving a crystalline residue (89 mg). This was chromatographed on basic alumina (Brockmann, Grade II), eluting with benzene containing an increasing amount of ether. Pure ether eluted the main product (74 mg) which was recrystallised from ethanol (95 %), m.p. 85–86°, $[\alpha]_D$ 10° (c, 3.1). The product was identified (mixed m.p., IR) as cedrol.

Acknowledgements. My thanks are due to Professor H. Erdtman for his interest in this work, to Miss G. Hammarberg for spectral measurements and to the *Swedish Natural Science Research Council* for financial support.

1. Runeberg, J. *Acta Chem. Scand.* **14** (1960) 797.
2. Pettersson, E. and Runeberg, J. *Acta Chem. Scand.* **15** (1961) 713.
3. Runeberg, J. *Acta Chem. Scand.* **15** (1961) 721.
4. Forsén, S. and Runeberg, J. *To be published.*
5. Stork, G. and Clarke, F. H., Jr. *J. Am. Chem. Soc.* **77** (1955) 1072.
6. Büchi, G., Erickson, R. E. and Wakabayashi, N. *J. Am. Chem. Soc.* **83** (1961) 927.
7. Åkermark, B. *Acta Chem. Scand.* **15** (1961). *In the press.*
8. Simon, W. *Helv. Chim. Acta* **41** (1958) 1835.
9. Arya, V. P., Erdtman, H. and Kubota, T. *Tetrahedron* **1961**. *In the press.*

Received June 22, 1961.

The Position of the Aromatic Methoxyl Group in Falcatine

KURT TORSSELL

Institute of Organic Chemistry and Biochemistry, University of Stockholm, Sweden

Degradative studies by Wildman *et al.*[1,2] have revealed structures I aor Ib for the alkaloid. The position of the methoxyl is still uncertain. Based on studies of ultra violet spectra of a number of *Amaryllidaceae* alkaloids Warnhoff and Wildman [3] assigned the aromatic methoxyl in undulatine II to position C_{10}. In the biogenetic scheme for the *Amaryllidaceae* alkaloids proposed by Barton and Cohen [4] falcatine and undulatine can be derived from a common precursor III. One would therefore predict that formula Ia is the most probable for falcatine.

From falcatine a degradation product IVa or IVb has been isolated [2]. Synthesis of one of these compounds will give conclusive evidence on the complete structure [5].

Methyl 2-hydroxy-3,4-methylenedioxy benzoate V is easily obtainable according to a recent method by Dallacker [6,7]. Methylation with dimethyl sulphate, hydrolysis and nitration gave VI. The isomeric acid VII seemed to be more difficult to prepare and therefore it was decided to synthesize IVb despite the fact that it was more likely that the other isomer IVa was the one derived from the natural product. The amide VIII, prepared *via* the acid chloride, was reduced catalytically, diazotized and cyclized. Chromatography on alumina of the crude product gave as a

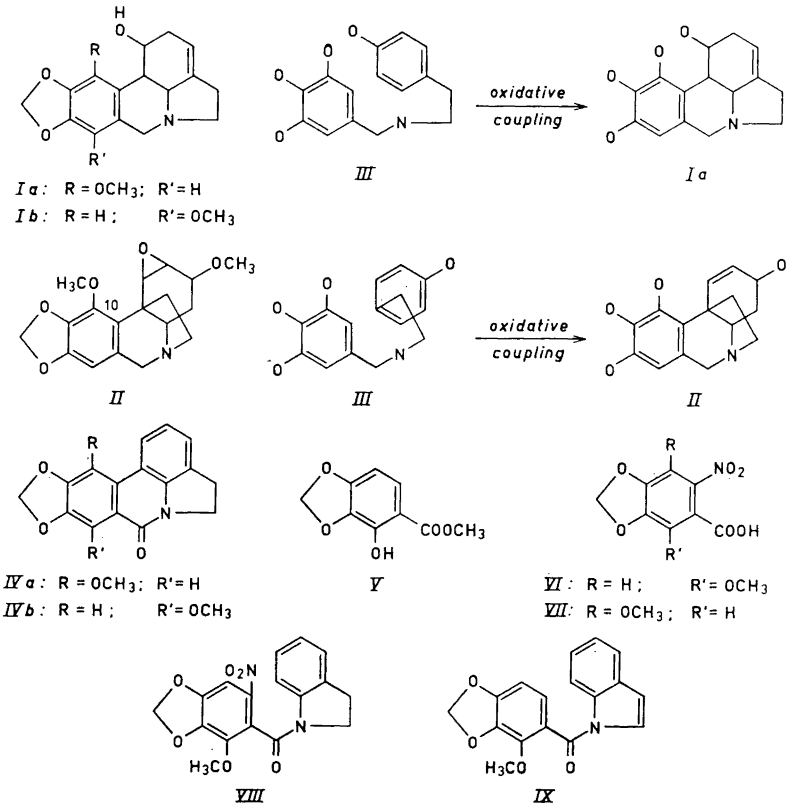

first fraction the indole derivative IX and as a second fraction the phenanthridone IVb. Its melting point, 272–274°, differed markedly from the melting point reported in the literature, 198–201°, for the degradation product [2] and its UV spectrum, though essentially the same as the spectrum of the degradation product, showed around 300–350 mμ a slight shift to longer wave lengths (λ_{max} 251, 273 sh, 288 sh, 301 sh, 337 and 350; UV maxima for the degradation product [2]:λ_{max} 256, 273, 300 sh, 332 and 347). The compounds are obviously not identical. The structures Ia and IVa can therefore be assigned to falcatine and its degradation product, respectively. The assignment of the methoxyl in undulatine to C_{10} is further supported by this evidence.

Experimental. 2-Methoxy-3,4-methylenedioxy-6-nitro benzoic acid IV. Methyl 2-hydroxy-3,4-methylenedioxy benzoate [7] V (2.8 g) was dissolved in boiling 6 % sodium hydroxide (50 ml). The solution was cooled to room temperature and dimethyl sulphate (4 ml) was added slowly so that after every addition no unreacted dimethyl sulphate remained. The acid was precipitated with conc. hydrochloric acid, filtered, washed with cold water and dried. The finely divided crude product was added in portions to conc. nitric acid (28 ml) at 5–10° with stirring. 10 min after the last addition the mixture was poured into ice water (130 ml). The precipitate was filtered and crystallized from water-methanol (10:1). Yield 1.2 g. M.p. 190–193° (softening at 184°), lit.[8] 190–92°.

2,3-Dihydro-1-(2-methoxy-3,4-methylenedioxy-6-nitro benzoyl)indole VIII. The acid VI (1.35 g) was dissolved in thionyl chloride (3 ml). The excess was evaporated in vacuum. The yellow oil, which crystallized on cooling, was dissolved in chloroform (10 ml) and slowly added to a stirred water-cooled mixture of chloroform (5 ml), pyridine (0.7 ml) and indoline (1.4 g). After 15 min water was added, the aqueous phase was acidified with hydrochloric acid. The organic layer was separated, dried and the solvent evaporated. The residue was crystallized from ethanol. Yield 1.2 g, m.p. 156–158°. (Found: C 59.45; H 4.30. Calc. for $C_{17}H_{14}O_6N_2$(342.3): C 59.65; H 4.12).

2,3-Dihydro-1-(2-methoxy-3,4-methylenedioxy-6-amino benzoyl) indole. The corresponding nitro compound VIII (0.38 g) was catalytically reduced with Raney-Ni in ethyl acetate. The residue after evaporation of the solvent, was crystallized from ethanol. Yield 0.35 g, m.p. 190–191°. (Found: C 65.35; H 5.38. Calc. for $C_{17}H_{16}O_4N_2$ (312.3): C 65.37; H 5.16).

Pschorr cyclisation of the amine. The amine was cyclized according to the method of Humber *et al.*[9] The chloroform extract from the reaction mixture (0.30 g amine) was chromatographed over alumina. The first fraction (benzene) yielded 60 mg of pale yellow crystals, which proved to be 1-(2-methoxy-3,4-methylenedioxy benzoyl) indole, m.p. 133°, from ethanol, λ_{max} 246, 302 (log ε 3.99, 4.36). (Found: C 69.06; H 4.45; N 4.91. Calc. for $C_{17}H_{13}O_4N$ (295.3): C 69.14; H 4.43; N 4.75). With chloroform-benzene (1:1) a reddish band was eluted, which gave 13 mg of the phenanthridone IVb, m.p. 272–274°, from nitromethane, pale yellow prisms. λ_{max} 251, 273sh, 288sh, 301, 337, 350 (log ε 4.53, 4.23, 3.98. 3.89, 3.85, 3.87). (Found: C 68.50; H 4.27. Calc. for $C_{17}H_{13}O_4N$ (295.3): C 69.14; H 4.43).

Added in proof. Recently Wildman *et al.* (*Tetrahedron Letters* **1961** p. 105) reinvestigated the structure of undulatine. They revised its structure and assigned the methoxyl group to C_7, which is in disagreement with the biogenetic scheme and also with the conclusion drawn above. This prompted us to synthesize the other isomer IVa. Dallacker *et al.* (*Monatsh. Ch.* **91** (1960) 1089) recently prepared the methylester of VII and they very kindly provided us with a sample of this compound. After hydrolysis with aqueous sodium hydroxide it was transformed into IVa according to the methods outlined above for VI. Our compound analyzed correctly for IVa and its physical constants agree excellently with the data reported for the degradation product. M.p. 196–199° (from ethanol-water); λ_{max} 256, 273, 295sh, 332, 347 mμ. Found: C 69.34; H 4.44; Calc. for $C_{17}H_{13}O_4N$ (295.3): C 69.14; H 4.43. It is therefore no doubt that Ia represents the correct structure for falcatine.

This work has been supported by a grant from the *Swedish Natural Science Research Council.* Experimental assistance has been given by Messrs. U. Selberg and K. Dahlqvist.

1. Wildman, W. C. and Kaufman, C. J. *J. Am. Chem. Soc.* **77** (1955) 4807.
2. Fales, H. M. and Wildman, W. C. *Ibid.* **80** (1958) 4395.
3. Warnhoff, E. W. and Wildman, W. C. *Ibid.* **82** (1960) 1472.
4. Barton, D. H. R. and Cohen, T. *"Festschrift Arthur Stoll"*, Birkhäuser, Basel 1957, p. 117.
5. Wildman, W. C. in Manske, R. H. F. (ed.) *The Alkaloids*, Vol. VI, p. 289.
6. Dallacker, F. *Ann.* **633** (1960) 14.

7. Dallacker, F. *Ibid.* **633** (1960) 23.
8. Wagner, A. F., Walton, E., Wilson, A. N., Rodin, J. O., Holly, F. W., Brink, N. G. and Folkers, K. *J. Am. Chem. Soc.* **81** (1959) 4983.
9. Humber, L. G., Kondo, H., Kotera, K., Tagaki, S., Takeda, K., Taylor, W. I., Thomas, B. R., Tsuda, Y., Tsukamoto, K., Uyeo, S., Yajima, H. and Yanaihara, N. J. *Chem. Soc.* **1954** 4622.

Received May 30, 1961.

Preparation of Benzonitrile, Isotopically Labelled in the Cyanide Group

BØRGE BAK, JØRGEN TORMOD NIELSEN and LEIF LIPSCHITZ

Chemical Laboratory V, University of Copenhagen, Copenhagen, Denmark

As a pre-requisite for the study of infrared and microwave spectra of benzonitrile(I), species isotopically labelled in the cyanide group were prepared.

$C_6H_5{}^{13}CN$. 2.65 g (0.0134 mole) of commercial $BaCO_3$ (52 % enriched in ^{13}C) was converted to carbon dioxide(II), which was distilled at −80°C for purification. Bromobenzene (2.62 g, 0.0167 mole) was converted to phenylmagnesium bromide and afterwards to benzoic acid (III) by addition of (II), roughly following Ref.[1] For the present purpose it was found useful to omit the prescribed extraction of (III) by ether. The yield of (III), contaminated by a small amount of inorganic substance, was 1.70 g. Refluxing for 3 h of (III) with 13 ml dry benzene and 2.3 ml $SOCl_2$ produced a quantity of benzoyl chloride (IV), mixed with traces of benzene and $SOCl_2$ after its distillation. (IV) was converted to benzamide (V), following the indications by Swan and Kelly [2], but using concentrated ammonium hydroxide in excess instead of NH_4NO_3 and base. Yield 1.02 g (0.0084 mole). The infrared absorption curve showed the substance to be pure. Following Ref.[1], (V) was converted to (I). The problem of removing the last traces of HCl in samples of the present magnitude was solved by pumping off the vapors in equilibrium with the liquid phase at room temperature six times with 2 h intervals after which the vapor pressure became normal. The infrared absorption curve of the undiluted sample showed that it consisted of the expected mixture of 52 % $C_6H_5{}^{13}CN$ and 48 % C_6H_5CN as evidenced by the relative intensity of the bands at 2 180 cm^{-1}($C_6H_5{}^{13}CN$) and at 2 230 cm^{-1}(C_6H_5CN). This disclosed that the weak line observed in non-enriched benzonitrile at 2 180 cm^{-1} is due to the presence of 1 % $C_6H_5{}^{13}CN$. The yield of (I) obtained was 0.566 g (0.0055 mole) or 41 % with respect to the enriched $BaCO_3$ applied.

$C_6H_5C^{15}N$. Following Ref.[2], 720 mg (0.0090 mole) of commercial NH_4NO_3 (33 % enriched in ^{15}N), dissolved in 30 ml of water, was treated with 1.35 g benzoyl chloride (0.0096 mole), dissolved in 70 ml chloroform, and 0.0190 mole of 1 N NaOH aq. for 1 h at room temperature under vigorous shaking. On evaporation of the chloroform layer and the small portions of chloroform used for extraction of the aqueous phase, a residue of 860 mg (0.0071 mole) enriched benzamide (VI) was obtained. The infrared spectrum showed (VI) to be pure. Hence, the suggested extraction by petrol ether is unnecessary, at least for the present purpose. (VI) was converted to ^{15}N-enriched benzonitrile(VII) by the same procedure as above, the yield being 540 mg (0.0052 mole) or 58 % with respect to enriched NH_4NO_3. The infrared absorption curve of the undiluted sample showed it to consist of the expected mixture of 33 % $C_6H_5C^{15}N$ (absorbing at 2 200 cm^{-1}) and 67 % C_6H_5CN (absorbing at 2 230 cm^{-1}). The spectral isotope effect of ^{15}N as compared to ^{13}C in benzonitrile is only 2/3. In natural abundance (1/3 %), ^{15}N in benzonitrile may still give rise to observable absorption at 2 200 cm^{-1}, if sufficient spectroscopic power of resolution is available.

1. Murray, A. and Williams, D. L. *Organic Syntheses with Isotopes I, Interscience Publishers N.Y.* 1958.
2. Swan, G. A. and Kelly, P. *J. Chem. Soc.* **1954** 416.

Received May 19, 1961.

7. Dallacker, F. *Ibid.* **633** (1960) 23.
8. Wagner, A. F., Walton, E., Wilson, A. N., Rodin, J. O., Holly, F. W., Brink, N. G. and Folkers, K. *J. Am. Chem. Soc.* **81** (1959) 4983.
9. Humber, L. G., Kondo, H., Kotera, K., Tagaki, S., Takeda, K., Taylor, W. I., Thomas, B. R., Tsuda, Y., Tsukamoto, K., Uyeo, S., Yajima, H. and Yanaihara, N. J. *Chem. Soc.* **1954** 4622.

Received May 30, 1961.

Preparation of Benzonitrile, Isotopically Labelled in the Cyanide Group

BØRGE BAK, JØRGEN TORMOD NIELSEN and LEIF LIPSCHITZ

Chemical Laboratory V, University of Copenhagen, Copenhagen, Denmark

As a pre-requisite for the study of infrared and microwave spectra of benzonitrile(I), species isotopically labelled in the cyanide group were prepared.

$C_6H_5{}^{13}CN$. 2.65 g (0.0134 mole) of commercial $BaCO_3$ (52 % enriched in ^{13}C) was converted to carbon dioxide(II), which was distilled at −80°C for purification. Bromobenzene (2.62 g, 0.0167 mole) was converted to phenylmagnesium bromide and afterwards to benzoic acid (III) by addition of (II), roughly following Ref.[1] For the present purpose it was found useful to omit the prescribed extraction of (III) by ether. The yield of (III), contaminated by a small amount of inorganic substance, was 1.70 g. Refluxing for 3 h of (III) with 13 ml dry benzene and 2.3 ml $SOCl_2$ produced a quantity of benzoyl chloride (IV), mixed with traces of benzene and $SOCl_2$ after its distillation. (IV) was converted to benzamide (V), following the indications by Swan and Kelly [2], but using concentrated ammonium hydroxide in excess instead of NH_4NO_3 and base. Yield 1.02 g (0.0084 mole). The infrared absorption curve showed the substance to be pure. Following Ref.[1], (V) was converted to (I). The problem of removing the last traces of HCl in samples of the present magnitude was solved by pumping off the vapors in equilibrium with the liquid phase at room temperature six times with 2 h intervals after which the vapor pressure became normal. The infrared absorption curve of the undiluted sample showed that it consisted of the expected mixture of 52 % $C_6H_5{}^{13}CN$ and 48 % C_6H_5CN as evidenced by the relative intensity of the bands at 2 180 cm^{-1}($C_6H_5{}^{13}CN$) and at 2 230 cm^{-1}(C_6H_5CN). This disclosed that the weak line observed in non-enriched benzonitrile at 2 180 cm^{-1} is due to the presence of 1 % $C_6H_5{}^{13}CN$. The yield of (I) obtained was 0.566 g (0.0055 mole) or 41 % with respect to the enriched $BaCO_3$ applied.

$C_6H_5C^{15}N$. Following Ref.[2], 720 mg (0.0090 mole) of commercial NH_4NO_3 (33 % enriched in ^{15}N), dissolved in 30 ml of water, was treated with 1.35 g benzoyl chloride (0.0096 mole), dissolved in 70 ml chloroform, and 0.0190 mole of 1 N NaOH aq. for 1 h at room temperature under vigorous shaking. On evaporation of the chloroform layer and the small portions of chloroform used for extraction of the aqueous phase, a residue of 860 mg (0.0071 mole) enriched benzamide (VI) was obtained. The infrared spectrum showed (VI) to be pure. Hence, the suggested extraction by petrol ether is unnecessary, at least for the present purpose. (VI) was converted to ^{15}N-enriched benzonitrile(VII) by the same procedure as above, the yield being 540 mg (0.0052 mole) or 58 % with respect to enriched NH_4NO_3. The infrared absorption curve of the undiluted sample showed it to consist of the expected mixture of 33 % $C_6H_5C^{15}N$ (absorbing at 2 200 cm^{-1}) and 67 % C_6H_5CN (absorbing at 2 230 cm^{-1}). The spectral isotope effect of ^{15}N as compared to ^{13}C in benzonitrile is only 2/3. In natural abundance (1/3 %), ^{15}N in benzonitrile may still give rise to observable absorption at 2 200 cm^{-1}, if sufficient spectroscopic power of resolution is available.

1. Murray, A. and Williams, D. L. *Organic Syntheses with Isotopes I, Interscience Publishers N.Y.* 1958.
2. Swan, G. A. and Kelly, P. *J. Chem. Soc.* **1954** 416.

Received May 19, 1961.

Dissociation of Alginic Acid

ARNE HAUG

Norwegian Institute of Seaweed Research, N.T.H., Trondheim, Norway

The dissociation of alginic acid has been studied by a number of authors [1-5]. All these investigations were carried out on the assumption that alginic acid is a homogeneous and well-defined compound. Recently, however, it has been shown that alginates are chemically heterogeneous compounds [6,7], and that alginates from different sources may vary considerably in chemical composition [8,9]. It has also been shown that ion exchange properties of alginates depend on the proportion of D-mannuronic and L-guluronic acid present in the alginate. The present note reports an investigation on the correlation between acid strength and uronic acid composition of alginates.

Materials and methods. The sampling of seaweed and preparation of alginate and alginate fractions have been described earlier [7,8]. Alginic acid was prepared by shaking sodium alginate with a large volume of 0.1 N hydrochloric acid over-night. The alginic acid was washed thoroughly several times with distilled water and dried *in vacuo*.

As alginic acid is insoluble in water, part of the titration curve must be determined for a two-phase system. To obtain equilibrium, it was found necessary to shake the alginate suspension for at least one hour after the addition of alkali. The following procedure was therefore adopted: Small samples (25 mg) of alginic acid were suspended in water or sodium chloride solution and the chosen amount of 0.1 N sodium hydroxide solution added. When the measurements were carried out in the presence of sodium chloride, the amounts of sodium was kept constant throughout the titration curve (mequiv. NaCl + mequiv. NaOH = const.). The volume was chosen so that the alginate concentration was 0.025 N. The suspension was shaken over-night and the pH was determined by a Beckman Zeromatic pH-meter. As a standard buffer, a 0.05 M potassium-hydrogenphthalate solution was used. When measurements were carried out in sodium chloride solution, salt was added to the buffer solution to obtain the same strength as in the test solution.

The pH of half neutralized alginic acid was determined in the following way: Alginic acid was suspended in water, and sodium hydroxide added in slight excess. By titrating with 0.1 N hydrochloric acid the amount of alkali consumed by the alginic acid was determined. To another sample of alginic acid half the determined amount of alkali was added, and the pH was measured after equilibrium was obtained.

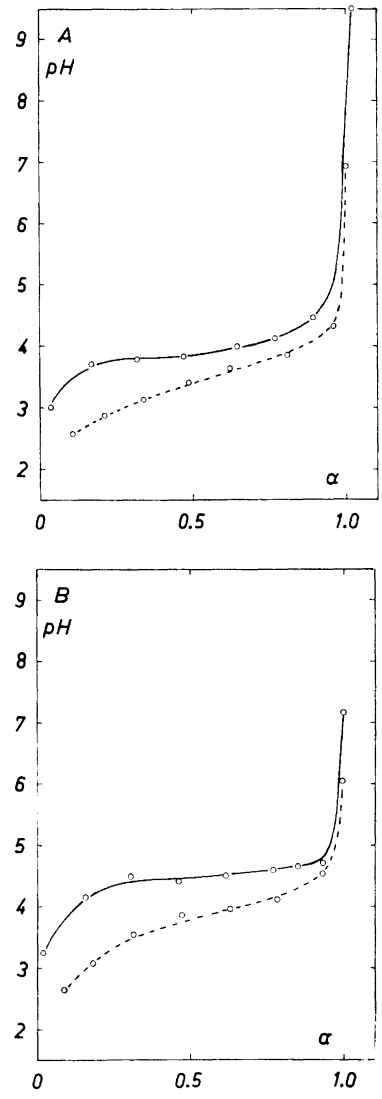

Fig. 1. A) *L. digitata*, Kråkvågøy, 3/7; ---- water and —— 0.1 N NaCl. B) *L. hyperborea* stipes, Hustad, 12/2; —— water and ---- 0.1 N NaCl.

Table 1.

Source of alginate	Medium	n	pK_s'
L. hyperborea, stipes, Hustad, 26/2	Water	0.40	4.36
» » » » 12/2	»	0.34	4.41
» » » » 12/2	(NaCl + NaOH) = 0.1 N	0.87	3.74
L. digitata, Kråkvågøy, 3/7	Water	0.44	3.93
» » » 3/7	(NaCl + NaOH) = 0.1 N	0.92	3.42
» » Espevær, 4/7	Water	0.70	3.87
» » » 4/7	(NaCl + NaOH) = 0.025 N	0.98	3.70
» » » 4/7	(NaCl + NaOH) = 0.1 N	0.90	3.42
» » » 8/1	Water	0.60	3.94
» » » 8/1, K_iMn_s	»		3.75*
» » » 8/1, K_sMn_i	»		4.00*
» » Tarva, 3/7	»		3.84*
» » » 3/7, K_iMn_s	»		3.72*
» » » 3/7, K_sMn_i	»		4.10*

Concentration of alginate in all cases was 0.025 N.

* pH for half neutralized samples.

Fig. 1 shows typical titration curves of alginic acid from *Laminaria digitata* and *Laminaria hyperborea* stipes, in water and in 0.1 N sodium chloride solution. If the results are calculated according to the modified Henderson equation $pH = pK_s' + n \log \frac{a}{1-a}$, the values given in Table 1 are obtained for the constants pK_s' and n. The degree of neutralization a is corrected for the presence of free hydrogen ions. The table also shows the pH of half neutralized samples of alginate fractions prepared by precipitation with potassium chloride and manganous sulphate [9]. If necessary, the observed pH has been corrected for the presence of free hydrogen ions to give the pK_s' value.

Both n and pK_s' vary with varying amounts of sodium chloride in the solution. With increasing ionic strength n increases towards 1, while the normal behaviour for polyacids is that n is higher than 1 at low ionic strength and decreases towards 1 when the ionic strength is increased. The abnormal behaviour may, at least partly, be due to the fact that part of the titration is carried out in a two-phase system, where the Donnan equilibrium will cause a considerable difference between the pH in the external solution and the pH in the gel, particularly when the ionic strength is low. As normal for polyacids the pK_s' decreases with increasing ionic strength. The concentration of alginic acid markedly influenced the value of the pK_s' of alginic acid in water. When the alginate concentration was varied from 0.06 to 0.006 N the pH of half neutralized samples increased by approximately 0.4 units, while no significant variation with dilution was observed when the medium was 0.1 N sodium chloride solution.

Alginate from *L. hyperborea* stipes contains more guluronic than mannuronic acid [9], while the opposite is the case for alginate from *L. digitata*. The fraction which is soluble in potassium chloride solution and precipitated by manganous ions (K_iMn_s) is enriched in guluronic acid residues, while the opposite fraction (K_sMn_i) is enriched in mannuronic acid residues. The results in Table 1 thus clearly indicate that there exists a correlation between the pK_s' values and the uronic acid composition of alginates, so that alginates rich in guluronic acid residues have a higher pK_s' value than alginates containing more mannuronic acid.

Samples of mannuronic and guluronic lactones were prepared from hydrolysates of alginic acid according to the method of Fischer and Dörfel [8]. The lactones were transformed to salts by adding alkali, and the acids liberated by running the solutions through a column of Dowex 50 ion exchange resin. The uronic acid solutions were immediately titrated with 0.1 N

sodium hydroxide solution, and the pK_s values of 3.38 and 3.65 were found for mannuronic and guluronic acid, respectively. The differences observed in the pK_s' values for polymers with different uronic acid composition are thus in good agreement with the pK_s values found for the monomeric units.

1. Pauli, W. and Sternbach, L. *Kolloid-Z.* **84** (1938) 291.
2. Saric, S. P. and Schofield, R. K. *Proc. Roy Soc. (London)* **A 185** (1946) 431.
3. Unruh, C. C., McGee, P. A., Fowler, W. T. and Kenyon, W. O. *J. Am. Chem. Soc.* **69** (1947) 349.
4. Seiyama, T. *J. Chem. Soc. Japan, Ind. Chem. Sect.* **52** (1948) 298, **53** (1950) 122, 157, 222, 244.
5. Sobue, H. and Tabata, Y. *J. Chem. Soc. Japan, Ind. Chem. Sect.* **56** (1933) 638.
6. McDowell, R. H. *Chem. & Ind. (London)* **1958** 1401.
7. Haug, A. *Acta Chem. Scand.* **13** (1959) 601.
8. Fischer, F. G. and Dörfel, H. *Z. physiol. Chem. Hoppe-Zeyler's* **302** (1955) 186.
9. Haug, A. *Acta Chem. Scand.* **13** (1959) 1250.

Received April 20, 1961.

Experimental Determination of Br *f* Values by Electron Diffraction

HAROLD P. HANSON*

Universitetets Kjemiske Institutt, Avd. C. Blindern, Oslo, Norway

A study of the electron diffraction pattern of the Br_2 molecule was carried out in conjuntion with a Fulbright research grant to Norway. From data taken on the Oslo diffraction unit, it had appeared that there existed an anomaly in the intensity of the electron scattering from bromine compounds. For the compounds ordinarily studied, usually hydrocarbons and chlorine substituted hydrocarbons, it was always possible to bring the observed atomic scattering into almost exact coincidence with that calculated theoretically [1]. This could not be done for bromine containing compounds. Since the Br_2 molecule is the simplest of bromine compounds, and since it also exhibits the apparent anomaly, the diffraction pattern from this molecule was studied in detail.

Except for constants, the total intensity observed in electron scattering by a diatomic molecule is given by

$$I \, a \, \frac{1}{s^4}\left[g^2(s) + ZS + g^2(s)e^{-ds^2}\,\frac{\sin sr}{sr}\right]$$

where the first two terms in brackets constitute the atomic scattering, and the third term is the molecular effect. The term ZS is the incoherent atomic scattering which is usually relatively small; s is equal to $(4\pi/\lambda)\sin\Theta/2$; d is the damping factor; and $g(s)$ is the amplitude of the coherently scattered wave. Within the limits of the Born approximation, $g(s)$ is equal to $(Z-f)$, where f is the ordinary X-ray atomic form factor. The data is recorded photographically, and since a flat plate plus a rotating sector are employed, suitable correction must be made. Since the sector effectively compensates for the well known $\csc^4\Theta/2$ effect, the over-all variation in intensity is sufficiently small that recording the intensity photographically introduces little error.

It was established that the difficulty of calculating the atomic scattering lay mainly in the use of the bromine f values obtained from statistical atomic models. For small values of s, the intensity is highly sensitive

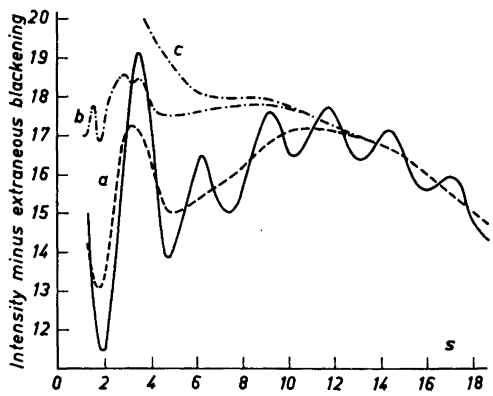

Fig. 1. Intensity in electron diffraction pattern from Br_2: (a) Observed atomic scattering; (b) predicted atomic scattering from Thomas-Fermi atom with exchange; (c) predicted atomic scattering for Thomas-Fermi atom without exchange.

* Fulbright Senior Research Scholar. Permanent address: The Department of Physics University of Texas, Austin, Texas, U.S.A.

sodium hydroxide solution, and the pK_s values of 3.38 and 3.65 were found for mannuronic and guluronic acid, respectively. The differences observed in the pK_s' values for polymers with different uronic acid composition are thus in good agreement with the pK_s values found for the monomeric units.

1. Pauli, W. and Sternbach, L. *Kolloid-Z.* **84** (1938) 291.
2. Saric, S. P. and Schofield, R. K. *Proc. Roy Soc. (London)* **A 185** (1946) 431.
3. Unruh, C. C., McGee, P. A., Fowler, W. T. and Kenyon, W. O. *J. Am. Chem. Soc.* **69** (1947) 349.
4. Seiyama, T. *J. Chem. Soc. Japan, Ind. Chem. Sect.* **52** (1948) 298, **53** (1950) 122, 157, 222, 244.
5. Sobue, H. and Tabata, Y. *J. Chem. Soc. Japan, Ind. Chem. Sect.* **56** (1933) 638.
6. McDowell, R. H. *Chem. & Ind. (London)* **1958** 1401.
7. Haug, A. *Acta Chem. Scand.* **13** (1959) 601.
8. Fischer, F. G. and Dörfel, H. *Z. physiol. Chem. Hoppe-Zeyler's* **302** (1955) 186.
9. Haug, A. *Acta Chem. Scand.* **13** (1959) 1250.

Received April 20, 1961.

Experimental Determination of Br *f* Values by Electron Diffraction

HAROLD P. HANSON*

Universitetets Kjemiske Institutt, Avd. C. Blindern, Oslo, Norway

A study of the electron diffraction pattern of the Br_2 molecule was carried out in conjuntion with a Fulbright research grant to Norway. From data taken on the Oslo diffraction unit, it had appeared that there existed an anomaly in the intensity of the electron scattering from bromine compounds. For the compounds ordinarily studied, usually hydrocarbons and chlorine substituted hydrocarbons, it was always possible to bring the observed atomic scattering into almost exact coincidence with that calculated theoretically [1]. This could not be done for bromine containing compounds. Since the Br_2 molecule is the simplest of bromine compounds, and since it also exhibits the apparent anomaly, the diffraction pattern from this molecule was studied in detail.

Except for constants, the total intensity observed in electron scattering by a diatomic molecule is given by

$$I \, a \, \frac{1}{s^4}\left[g^2(s) + ZS + g^2(s)e^{-ds^2}\,\frac{\sin sr}{sr}\right]$$

where the first two terms in brackets constitute the atomic scattering, and the third term is the molecular effect. The term ZS is the incoherent atomic scattering which is usually relatively small; s is equal to $(4\pi/\lambda)\sin\Theta/2$; d is the damping factor; and $g(s)$ is the amplitude of the coherently scattered wave. Within the limits of the Born approximation, $g(s)$ is equal to $(Z-f)$, where f is the ordinary X-ray atomic form factor. The data is recorded photographically, and since a flat plate plus a rotating sector are employed, suitable correction must be made. Since the sector effectively compensates for the well known $\csc^4\Theta/2$ effect, the over-all variation in intensity is sufficiently small that recording the intensity photographically introduces little error.

It was established that the difficulty of calculating the atomic scattering lay mainly in the use of the bromine f values obtained from statistical atomic models. For small values of s, the intensity is highly sensitive

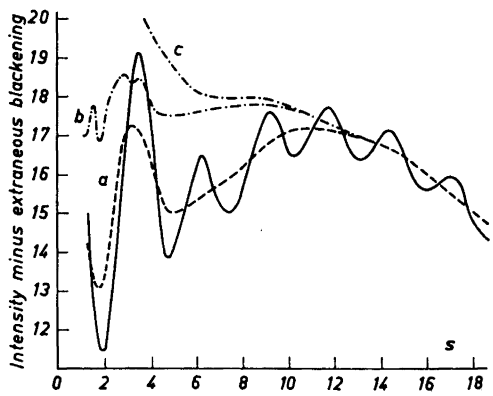

Fig. 1. Intensity in electron diffraction pattern from Br_2: (a) Observed atomic scattering; (b) predicted atomic scattering from Thomas-Fermi atom with exchange; (c) predicted atomic scattering for Thomas-Fermi atom without exchange.

* Fulbright Senior Research Scholar. Permanent address: The Department of Physics University of Texas, Austin, Texas, U.S.A.

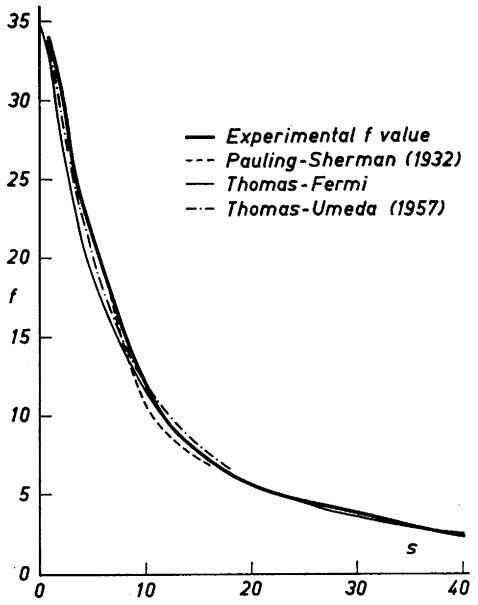

Fig. 2. Experimental f values for bromine with various theoretical curves.

to the f values employed as is shown by the easily obtained approximate relation,

$$\frac{dI}{I} = \frac{2df}{Z-f}$$

When f approaches Z, as it does for small s, one sees that a small error in f will produce a large discrepancy between the calculated and the observed intensity. One can observe the effect of this sensitivity in Fig. 1. The observed intensity is plotted with the atomic scattering to the expected on the basis of the Thomas-Fermi and Thomas-Fermi-Dirac models. In addition, the obvious relation that exists between the molecular scattering and the total atomic scattering makes it possible to determine the amount of the noise that comes with the signal, and thus to establish what the atomic scattering actually must be; the latter is also shown in Fig. 1.

The sensitivity of the calculated atomic scattering to the f values implies that one possesses a suitable technique for measuring the f values experimentally. One knows, however, that the Born approximation is inadequate to describe the scattering at the voltages commonly employed in electron diffraction [2]. By making the reasonable assumption that the relation between $g(s)$ and $(Z-f)$ in a Thomas-Fermi atom is preserved in the bromine atom proper, one obtains the f values shown in Fig. 2. Several theoretical curves are also shown.

The question still remains as to the reliability of the results. The general shape of the curve is quite reasonable; it retains vestigial features of the curves of lighter elements and it has much in common with the f values of Rb^+ for which Hartree calculations exist [3]. By normalization to a computed value of $f = 2.42$ at $s = 40$, where the hydrogen-like inner orbitals play the major role [4], one finds good agreement with the Thomas-Fermi results for $s = 11$ to $s = 23$. A hump in the region of $s = 4$ to $s = 11$ is predicted by Pauling-Sherman as is the slight hump at $s = 30$. The high values for $s < 4$ may be due to (1) the enhanced possibility for error due to the sector correction, (2) the failure to consider the polarization of the atom and the uncertainty of the incoherent scattering term, or (3) a real effect. If the latter is the case, it indicates that the charge cloud due to the outer electrons is held somewhat closer to the nucleus than the statistical models predict. This would be consistent with the fact that the f values found here are the effective values for a bonded atom. In any event, electron diffraction techniques offer a sensitive method for obtaining f values. By considering the scattering from sufficiently simple molecules, it should be possible to compile experimental f values which are superior to the theoretical values which are known to be in error.

I am particularly indebted to four people: Professor O. Hassel for permission to work in his department at the University of Oslo; Professor O. Bastiansen for pointing out the apparent anomaly in bromine; Cand. real. A. Almenningen for the extremely careful experimental work on which these results must depend; and especially to Cand. real. Per Andersen for his co-operation and assistance in all phases of this work.

1. Bastiansen, O. *Acta Cryst.* **10** (1957) 861.
2. Ibers, J. A. and Hoerni, J. A. *Acta Cryst.* **7** (1954) 405.
3. James, R. W. and Brindley, G. W. *Z. Krist.* **78** (1931) 470.
4. Pauling, L. and Sherman, J. *Z. Krist.* **81** (1932) 1.

Received May 10, 1961.

On the Occurrence of Biotin in Different Fractions of Municipal Sewage

HALINA Y. NEUJAHR and JOHAN HARTWIG

Royal Institute of Technology Division of Food Chemistry, Stockholm 70, Sweden

The microbial activities which take place in sewage and wastes result in a considerable synthesis of a number of vitamins [1]. The occurrence of vitamin B_{12} and its analogues in municipal sewage sludge has been extensively studied in this laboratory [2] and by others [3,4]. It has also been found in a previous study [5,6] that certain fractions of sewage can satisfy the growth requirements of *Propionibacterium shermannii*, an organism which is known to require biotin for its growth. The occurrence of this vitamin in different fractions of municipal sewage was therefore studied. Biotin occurs in animal and plant tissues mainly in combined forms. Vigorous acid hydrolysis is necessary to release the vitamin from such forms before a microbiological assay can be made. The sewage fractions studied in this investigation were assayed for biotin activity both before and after acid hydrolysis in order to investigate the "free" forms of the vitamin which may possibly occur.

Experimental. The sewage fractions investigated were those previously studied in experiments with *Mb. omelianskii* [7] and *Propionibacterium shermannii* [5]. They are listed in Table 1. The pretreatment of the samples for the biotin determination was as follows.

Hydrolyzed samples: 50 ml sample + 10 ml 18 N sulphuric acid were autoclaved for 30 min at 121°C. 7.2 g NaOH was dissolved in each sample, 2 ml 2.5 M NaAc solution added, the pH adjusted to 4.5 and the volume to 75 ml. The samples were centrifuged for 20 min, 25 ml of the supernatant was removed, its pH adjusted to 6.8 and the resulting precipitate centrifuged off. The final supernatants were stored at −20°C until being assayed for biotin activity.

Non-hydrolyzed samples: The non-hydrolyzed samples were treated in a similar way, water being substituted for sulphuric acid and room temperature for autoclaving. All biotin values obtained were corrected for the volume changes due to pH adjustments, etc.

Biotin was determined using *Lb. arabinosus 17—5* in the turbidimetric assay method (Difco's Biotin Assay Medium). The results obtained are given in Table 1.

In Table 2, the results of experiments concerning the recovery of added biotin are recorded. The samples with added biotin were treated similarly and assayed simultaneously with the samples without added biotin in order to check the reliability of the method. In certain experiments, the samples were subjected to paper chromatography using the *sec.* butanol: water:

Table 1. Biotin content of different fractions of municipal sewage.

Sewage fraction [a]	Dry solids content [b] g/l	Biotin content μg/l [c] Non-hydrolyzed samples	Hydrolyzed samples [d]	Average biotin content μg/g dry solids
A	20	5	20	1.0
B	20	30	30	1.5
C	100	50	50	0.5
D	3.0	30	30	10.0
E	15	0	10	0.7
F	≤1	not determined	0.3	
G	≤1	» »	0.3	
H	≤1	» »	0.2	

[a]) A, raw sludge; B, sludge after one-step digestion; C, digested sludge; D, supernatant from digestion tanks; E, activated sludge; F incoming sewage; G, supernatant from sedimentation tanks; H, effluent from activated sludge tanks (= highly purified sewage).

[b]) average values of several determinations.

[c]) average values of six determinations by the turbidimetric method using *L. arabinosus* 17—5 and Difco's Biotin Assay Medium.

[d]) 3 N H_2SO_4, 30 min at 121°C.

Table 2. Typical biotin assay results using internal biotin standards.

Sewage fraction [a]	Biotin added mμg/ml	Biotin content found μg/l Non-hydrolyzed samples	Hydrolyzed samples	Recovery % Non-hydrolyzed samples	Hydrolyzed samples
C	no	47.5	49.3		
C	20	72.5	74.1	125	124
D	no	32.5	33.2		
D	20	53.0	56.2	102	111
E	no	0	9.3		
E	20	16.9	24.5	85	76

[a] *cf.* explanations to Table 1.

acetic acid system (75:25:1). The spots were located by incubating pieces of the chromatograms with the assay medium.

Results and discussion. It can be seen in Table 1 that most of the sewage fractions investigated contained considerable amounts of biotin, *viz.* 10—50 μg/l. Exceptions are of course the very dilute or purified fractions F, G, and H. In raw sewage (fraction A), about 75 % of the vitamin content occurs in a bound form. The values in Table 1 indicate that practically all of the vitamin in sewage fractions which have undergone methane fermentation occurs in a form directly available to the test organism. Further, digested sludge (sediment) contains only 0.5 μg biotin/g dry solids whereas the corresponding value for the supernatant from digestion tanks is as high as 10 μg/g. This strengthens the impression that biotin is released from the bacterial cells as the methane fermentation proceeds and the great difference between the two figures makes it hardly possible to explain this release by mere autolysis.

Activated sludge which is a product of aerobic fermentation differs markedly from the digested sludges and also to a great extent from raw sludge. All biotin in activated sludge is bound and has to be released by vigorous hydrolysis in order to become available to the test organism.

Table 2 shows recovery values for biotin added to certain sewage fractions assayed by the method used in this investigation. It can be seen in Table 2 that the recovery values varied between 76 and 125 %. However, with sewage fractions which had undergone methane fermentation, the recovery values obtained were consistently higher than 100 % whereas activated sludge always gave values lower than 90 %.

Paper chromatography of the hydrolyzed samples gave only one spot with an R_F value equal to that of crystalline biotin.

1. Kocher, V. and Corti, U. A. *Schweiz. Z. Hydrol.* **14** (1912) Fasc. 2.
2. Neujahr, H. Y. *On Vitamin B_{12} Factors in Sewage Sludge*, Thesis, Almqvist & Wiksell, Uppsala 1960.
3. Friedrich, W., Dellweg, H., Gross, G., Becher, E., Spande, S. and Bernhauer, K. *Vitamin B_{12} and Intrinsic Factor* (H.C. Heinrich, Ed.) Enke, Stuttgart 1957, p. 62.
4. Friedrich, W. and Bernhauer, K. *Biologie und Biochemie der natürlichen Vitamin B_{12}-Analoga*, Thieme, Stuttgart 1959.
5. Neujahr, H. Y. *Acta Chem. Scand.* **13** (1959) 2158.
6. Neujahr, H. Y., Kurz, W. G. and Rossi-Ricci, G. C. *Arkiv Kemi* **15** (1960) 363.
7. Neujahr, H. Y. and Callieri, D. *Acta Chem. Scand.* **12** (1958) 1153.

Received May 27, 1961.

A Simple Apparatus for Controlled-Potential Electrolysis

C. H. HOLTEN*

Kryolitselskabet Øresund A/S, Copenhagen Ø, Denmark

Electrolysis at controlled potential has proved to be a valuable tool in polarographic work. Sand[1] introduced the method in electrogravimetric work, and Lingane[2] showed its utility for separations prior to polarography. In Lingane's first apparatus the control of the cathode potential was performed manually, and to eliminate this tedious work several varieties of automatic apparatus have been constructed [3-9].

The purpose of this paper is to show the construction of an easily built apparatus for the performance of controlled-potential electrolysis. The reference voltage supply and zero-galvanometer relay in the potentiostats constructed by Lingane [4,5] are replaced by a line-operated pH-meter, working as a voltmeter. This pH-meter is provided with a recorder connection which can be used to operate the control circuit.

Apparatus. The construction of the apparatus is shown in Fig. 1. Direct current is supplied from a voltage divider, connected to 110 V, d.c., or from any other convenient d.c. supply.

* Present address: Department of Chemistry, Danmarks Ingeniørakademi, Copenhagen K.

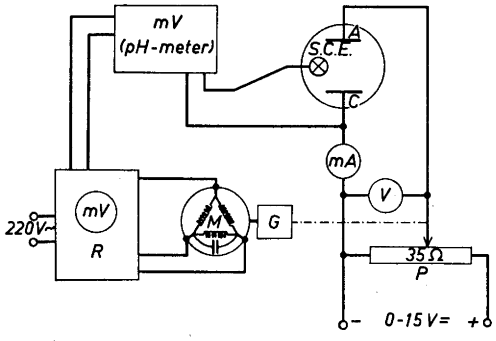

Fig. 1. Electrical circuit for electrolysis at controlled potential. A: Anode. C: Cathode. S.C.E.: Saturated calomel reference electrode. R: Contact meter with double electronic relay. M: Reversible condenser motor. G: Triple worm gear. P: Potentiometer (electrolysis current supply).

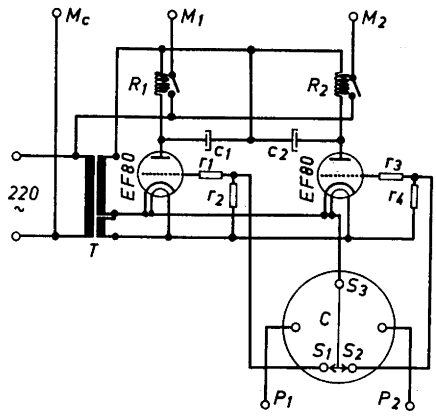

Fig. 2. Contact meter with double electronic relay. C: Contact meter (10 mA, 500 Ω). P_1, P_2: pH-meter recorder connection. S_1, S_2: Adjustable contacts, closed by the pointer, S_3. T: Transformer, 220 V/180 + 6.3 V. r_1, r_2, r_3, r_4: 100 000 Ω. c_1, c_2: 50 μF. R_1, R_2: Magnetic relay, 4700 Ω. M_C, M_1, M_2: Motor connection, M_C: common lead. Valves EF 80.

This voltage which can be coarsely adjusted between 0 and 15 V is connected to a potentiometer, P (35 Ω, 100 W), used as a voltage divider. The electrolysis current is then conducted from the sliding contact and from one end of P to the working electrodes. Suitable meters are connected to this circuit to follow the progress of the electrolysis.

The electrolysis cell recommended by Lingane [2] has been used. The potential of the mercury cathode with respect to a saturated calomel electrode is measured with a pH-meter, type PHM 22 (Radiometer, Copenhagen), working as a voltmeter (range 0–2.2 V). The recorder connection of this pH-meter supplies through a resistance of 500 Ω a current proportional to the pointer deflection. This current amounts to 10 mA for full deflection. The recorder current is led to a 500 Ω ammeter, constructed to give the same pointer deflections as the pH-meter. This dependent instrument is provided with two adjustable limiting contacts, closing when the pointer passes above, respectively below the adjusted limits. The limiting contacts control a double electronic relay which in turn activates a reversible motor to revolve in one direction or the other, depending on which one of the limiting contacts has been closed. The contact instrument and the joined double relay (Fig. 2) has been constructed by Mr. Tynell, Jensen Electric

I/S, Copenhagen. The reversible motor (condenser motor, type 15GK, from Hans Heidolph, Ohg., Schwabach by Nürnberg) is connected to the shaft of the potentiometer, P, by means of a triple worm gear (from Hans Heidolph). The worm gear is constructed to move the potentiometer contact from one end to the other within one minute.

When the cathode potential differs from the desired value, adjusted at the limiting contacts, the electronic relay and the motor are activated to alter the electrolysis voltage from P in the appropriate direction, until the desired potential is reached.

The apparatus may be used to perform automatic potentiometric titrations when the relay is used to operate a magnetic valve for the standard solution. The magnetic valve must be connected at M_C and M_1 or M_2 (Fig. 2).

Experimental. To show the effectiveness of the apparatus the following experiment was performed: Copper sulfate (0.05 M) and lead nitrate (10^{-4} M) were dissolved in an ammonium acetate-acetic acid supporting electrolyte containing hydroxylamine as depolarisator (2 M CH_3COONH_4, 2 M CH_3COOH, 0.5 M $(HO)NH_3Cl$). The hydroxylamine is necessary to avoid loss of lead deposited as PbO_2 on the anode. This solution was electrolysed using the apparatus. The cathode was a mercury pool kept in rapid motion by a glass propellor at the surface, and the anode was a platinum wire wrapped as a helix on the stirrer shaft. The cathode potential was controlled at −0.3 V *vs.* a saturated calomel electrode (Radiometer, type K4311). In the course of about 90 min the electrolysis current decreased from the initial 255 mA to less than 1 mA while the voltage between the anode and the cathode during the first 25 min decreased from 3.0 V to about 1.6 V and was then almost constant or slightly increasing. The effect of the electrolysis is shown in Fig. 3. Polarogram A is obtained from the electrolysed solution; a copper wave at −0.22 V and a lead wave at −0.50 V are observed. Polarogram B is obtained from a solution containing 10^{-4} Pb ion in the same electrolyte. It is obvious that the two lead waves are of the same magnitude, which indicates that no loss of lead ion has occurred. At the same time the copper ion concentration has decreased to the same order of magnitude as the lead ion concentration or to about 1/500 of its original concentration.

In the original solution the copper ion concentration was too large (0.05 M) to admit the recording of a polarogram. After 100-fold dilution with the electrolyte a polarogram showed a clean copper wave, but the lead wave was hardly visible, even when the diffusion current compensation technique was used.

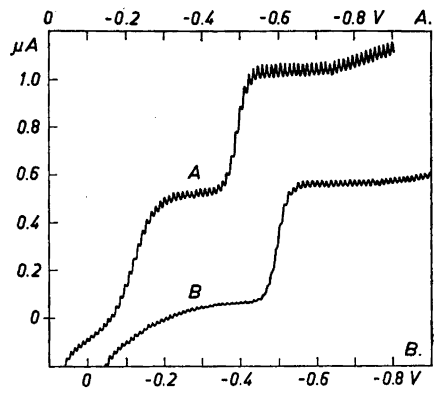

Fig. 3. Effect of electrolysis: Original solution contained 0.05 M Cu++ and 10^{-4} Pb++ (electrolyte: 2M CH_3COONH_4, 2 M CH_3COOH, 0.5 M $(HO)NH_3Cl$). Polarogram A (abscissa at the top) obtained after electrolysis at cathode potential −0.3 V *vs.* S.C.E. Polarogram B (abscissa at the bottom) obtained from a solution containing 10^{-4} M Pb++ (no Cu++ added).

Acknowledgements. Thanks are due to Kryolitselskabet Øresund for the permission to publish this paper, to Mr. O. Tynell, Jensen Electric I/S, for the construction of the contact instrument with electronic relay, to professor J. Bjerrum, Mr. N. Brems, Radiometer, and to Mr. H. Buchwald, for valuable discussions and good advice.

1. Sand, H. J. S. *Trans. Chem. Soc.* **91** (1907) 373.
2. Lingane, J. J. *Ind. Eng. Chem., Anal. Ed.* **16** (1944) 147.
3. Caldwell, C. W., Parker, R. C. and Diehl, H. *Ind. Eng. Chem., Anal. Ed.* **16** (1944) 532.
4. Lingane, J. J. *Ind. Eng. Chem., Anal. Ed.* **17** (1945) 332.
5. Penther, C. J. and Pompeo, D. J. *Ind. Eng. Chem., Anal. Ed.* **21** (1949) 178.
6. Lingane, J. J. and Jones, S. L. *Anal. Chem.* **22** (1950) 1169.
7. Greenough, M. L., Williams, W. E. and Taylor, J. K. *Rev. Sci. Instruments* **22** (1951) 484.
8. Lamphere, R. W. and Rodgers, L. B. *Anal. Chem.* **22** (1950) 463.
9. Lamphere, R. W. *Anal. Chem.* **23** (1951) 258.

Received May 20, 1961.

Partial Desulphurisation of Sugar Thioacetals

BENGT LINDBERG and LARS NORDÉN

Institutionen för träkemi, Kungl. Tekniska Högskolan, Stockholm, Sweden

Reductive desulphurisation of sugar thioacetals with Raney nickel, as devised by Wolfrom and Karabinos [1], is a convenient method for the preparation of deoxyalditols. In the course of the study of a natural deoxyheptitol [2], we used this method to prepare the 1-deoxyheptitols from some heptose diethyl dithioacetals. Chromatographic examination of the reaction products sometimes revealed the presence of a component with an R_F-value intermediate between those of the starting material and the desired product. On further treatment with Raney nickel this component disappeared. It therefore seemed probable that the component was the 1-deoxy-1-thioethyl-heptitol and that 1-deoxy-1-thioalkyl-alditols in general could be prepared by controlled reductive desulphurisation of the corresponding sugar thioacetals with Raney nickel. This reduction has now been studied with two more easily available substances, the diethyl dithioacetals of D-galactose and D-mannose.

Different preparations of Raney nickel may differ in activity and this also decreases with the age of the preparation. Furthermore it is difficult to estimate the amount of Raney nickel used in a reaction accurately. The preferred procedure was therefore to treat the thioacetal with an insufficient quantity of Raney nickel, characterise the reaction products by paper chromatography and continue the treatment with fresh amounts of Raney nickel until the starting material had just disappeared on the chromatograms. In the two examples studied, the 1-deoxy-1-thioethyl-hexitol could then be isolated by crystallisation, and further amounts obtained by fractionation of the mother liquors on a cellulose column.

The 1-deoxy-1-thioethyl-hexitols prepared gave correct analyses and on further treatment with Raney nickel yielded the expected 1-deoxy-hexitols. This, together with their mode of preparation, should prove their structures. It is believed that the described reductive desulphurisation of sugar thioacetals is a general reaction and might find synthetic applications.

Experimental. Chromatograms were run on Whatman No. 1 filter papers, using 95 % aqueous acetone (v/v) as irrigant. A satisfactory separation was obtained in 30 min. The spots were developed with silver nitrate-sodium hydroxide [3]. Butan-1-ol, saturated with water, was used as irrigant in the cellulose column separations.

1-Deoxy-1-thioethyl-D-galactitol. A solution of D-galactose diethyl dithioacetal (10 g), in 70 % aqueous ethanol (150 ml) was refluxed on the steam bath. Successive amounts of Raney nickel W-2, prepared according to *Org. Syntheses* [4] were added as slurries in anhydrous ethanol and the mixture was characterised by paper chromatography 15 min after each addition. When the starting material had disappeared, the mixture was cooled, the nickel removed by filtration and washed with ethanol and water. The combined filtrate and washings were concentrated to dryness and crystallised from water, yielding 1-deoxy-1-thioethyl-D-galactitol (2.48 g), m.p. 148–149°, $[\alpha]_D^{20}$ −3° (*c*, 2.0 in pyridine) (Found: C 42.4; H 7.94; S 14.0. Calc. for $C_8H_{18}O_5S$: C 42.5; H 8.01; S 14.2).

Fractionation of the mother liquors on a cellulose column yielded further 1-deoxy-1-thioethyl-D-galactitol (1.08 g) and 1-deoxy-D-galactitol (1.20 g), m.p. 153–154°.

1-Deoxy-1-thioethyl-D-mannitol. D-Mannose diethyl dithioacetal (10 g) was treated as described above for the corresponding D-galactose derivative. The reaction product, on crystallisation from ethanol, yielded the 1-deoxy-1-thioethyl-D-mannitol (3.06 g) of m.p. 107–108°. An analytical sample melted at 114–115° and showed $[\alpha]_D^{20}$ + 32° (*c*, 2.0 in water). (Found: C 42.8; H 8.06; S 14.0. Calc. for $C_8H_{18}O_5S$: C 42.5; H 8.01; S 14.2).

Further amounts of the same substance (1.25 g) and 1-deoxy-D-mannitol (0.98 g) m.p. 121–122°, were obtained from the mother liquors after fractionation on a cellulose column.

1. Wolfrom, M. L. and Karabinos, J. V. *J. Am. Chem. Soc.* **66** (1944) 909.
2. Lindberg, B. and Meier, H. *Acta Chem. Scand. In press.*
3. Trevelyan, W. E., Procter, P. P. and Harrison, J. S. *Nature* **166** (1950) 444.
4. Org. Syntheses, Coll. Vol. **3** (1954) 181.

Received June 6, 1961.

The Rate of Decomposition of Urethane in Acid Solution II

KAI JULIUS PEDERSEN

Chemical Laboratory, Royal Veterinary and Agricultural College, Copenhagen, Denmark

In an earlier paper [1] the rate of decomposition of urethane was studied at 37.0°C in concentrated solutions of hydrochloric and sulphuric acids (c M). The first-order rate constant k (in sec^{-1}) could, up to $c = 6$, be expressed for solutions of hydrochloric acid by

$$\log(k/c) = 0.705 - 8 + 0.063\,c$$

and for solutions of sulphuric acid by

$$\log(k/c) = 0.801 - 8 + 0.0895\,c$$

It was suggested that the rate-determining step is a bimolecular reaction between a urethane molecule and a hydrated hydrogen ion (probably $H(H_2O)_4^+$, but here for simplicity written as H^+) on which reaction the strong acids exert a kinetic salt effect. In the earlier paper it was for both acids assumed that $[H^+] = c$. For sulphuric acid this is only a very rough approximation. The values of $[H^+]$ given in Table 1 are presumably more accurate. They were computed from estimates of the two dissociation constants of sulphuric acid made by Young and Blatz [2] mainly on the basis of measurements of intensities of Raman-lines carried out by Rao [3]. In Fig. 1 is shown that, when $\log(k/[H^+])$ is plotted against c, the points fall (up to $c = 7$) very close to a straight line with the equation

$$\log(k/[H^+]) = 0.768 - 8 + 0.094\,c$$

By extrapolation to $c = 0$ is obtained $k/[H^+] = 5.86 \times 10^{-8}$, a value that is higher than that found for hydrochloric acid (5.07×10^{-8}), possibly due to catalysis by hydrogen sulphate ions.

Measurements were also carried out on solutions of perchloric acid (prepared by dilution of Merck's Perchloric Acid, 60 %, pro analysi). The results are given in Table 1, and in Fig. 1 is shown a plot of $\log(k/[H^+])$ against c (where $[H^+] = c$). Instead of a straight line is obtained a curve with a minimum for a value of c between 2 and 3. By extrapolation to $c = 0$ is, however, found nearly the same value of $k/[H^+]$ as for hydrochloric acid.

Table 1. Rate of decomposition of urethane at 37.0°C.

Sulphuric acid			Perchloric acid	
c	$[H^+]$	$k \times 10^7$	c	$k \times 10^7$
1.00	1.07	0.78	1.00	0.497
2.00	2.11	1.90	2.00	0.968
3.00	3.13	3.55	3.00	1.44
4.00	4.14	5.70	4.00	2.05
5.00	5.11	8.98	5.00	2.94
6.00	6.01	12.86	6.00	4.23
6.96	6.68	17.6	7.00	6.03
8.00	7.15	22.2	8.00	7.69
8.97	7.48	24.9		
10.00	7.11	24.2		

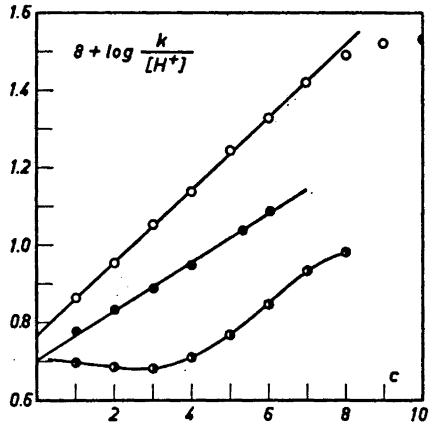

Fig. 1. Plot of $\log(k/[H^+])$ against c for the decomposition of urethane in solutions of sulphuric acid (open circles), hydrochloric acid (closed circles), and perchloric acid (semi-closed circles).

1. Pedersen, K. J. *Acta Chem. Scand.* **14** (1960) 1448.
2. Young, T. F. and Blatz, L. A. *Chem. Revs.* **44** (1949) 102.
3. Rao, N. R. *Indian J. Phys.* **14** (1940) 143.

Received June 3, 1961.

The Triamide of Methane-tricarboxylic Acid

ARNE FREDGA and LARS PILSTRÖM

Organic Department, Chemical Institute, University of Uppsala, Sweden

In connection with work on compounds with adamantoid structure (urotropine structure), we were interested in preparing the triamide I. Earlier attempts to obtain this substance had failed. Philippi *et al.*[1], who treated ethyl methane-tricarboxylate with dry liquid ammonia in sealed tubes at room temperature, could only isolate malonamide (II) and urethane (III). This indicates a direct cleavage of the molecule, effected by ammonia.

The present authors attempted to perform the reaction in aqueous or alcoholic ammonia at various concentrations, but malonamide was in every case obtained. On treatment with gaseous ammonia in nonpolar solvents, the ammonium salt of the ester separated. The desired compound was at last obtained in moderate yield by converting the ester into the ammonium salt, which was left to stand in an ammonia atmosphere for several days. The product was then treated with concentrated aqueous ammonia as described in the experimental part.

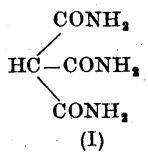

(I)

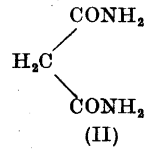

(II)

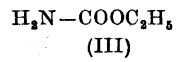

(III)

Once formed, the compound is fairly stable and can be recrystallised from hot water. It melts with decomposition at about 203°.

Attempts to prepare compounds of adamantoid structure from the triamide have so far been unsuccessful. Substitution of the "acid" hydrogen by a more or less bulky alkyl group might perhaps favour the ring closure and we plan to extend the work in this direction. Experiments with a triester without "acid" hydrogen might also throw some light on the mechanism of the formation of the triamide and the cleavage of the ester molecule. It should be mentioned, however, that the ethyl ethane-hexacarboxylate (IV), investigated by Philippi *et al.*[1], seems quite inert towards ammonia. Even after long treatment with dry liquid or concentrated aqueous ammonia, the ester was recovered unchanged.

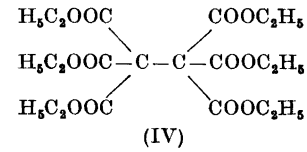

(IV)

Experimental. A 50 ml two-necked flask is filled with gaseous ammonia, taken from a bomb and dried with solid potassium hydroxide. 20 ml (22.2 g) of ethyl methane-tricarboxylate [2] are introduced into the flask and a slow current of dry ammonia is passed through the apparatus. When all the ester has been converted into the dry ammonium salt (which requires about 30 min.), the flask is closed with rubber stoppers and left to stand for at least three days. 15 ml of concentrated aqueous ammonia are then added and the flask is shaken from time to time until a homogeneous solution is obtained. On further standing, the triamide gradually separates; after three days it is filtered off, washed with water, alcohol and ether and recrystallised from hot water. In some cases, the crude product was contaminated by the lower-melting malonamide, which could be removed by extraction with cold water. The triamide is much less soluble.

The triamide forms needles with m.p. 203° (decomp.). Yield 1–2 g (7–14 %). (Found: C 33.03; H 4.76; N 28.85. Calc. for $C_4H_7O_3N_3$: C 33.10; H 4.86; N 28.96.)

The ester may be diluted with 5–10 ml of dry ether during the reaction, but this modification has no favourable effect on the yield.

The triamide can also be prepared from methyl methane-tricarboxylate. In this case, addition of ether is appropriate since the methyl ester melts at 43°.

A grant from the University (*Nycanderska fonden*) is gratefully acknowledged.

1. Philippi, E., Hanusch, J. and von Wacek, H. *Ber.* **54** (1921) 901.
2. Lund, H. and Voigt, A. *Org. Syntheses, Coll. volume II*, New York 1946, p. 594.

Received June 21, 1961.

ACTA CHEMICA SCANDINAVICA 15 (1961) 961–966

The Chemistry of the Natural Order Cupressales

XXXVI. The Ethereal Oil of the Wood of *Juniperus communis* L.

JOHAN B-SON BREDENBERG

Organisk-kemiska Institutionen, Kungl. Tekniska Högskolan, Stockholm, Sweden

From the ethereal oil of the wood of *Juniperus communis* L. thujopsene, cuparene, humulene, cedrol, widdrol, and an α,β-unsaturated aldehyde have been isolated. Chromatographic and spectroscopic evidence has been obtained for the presence of calamenene, δ-cadinene, an *iso*cadinene, α- and β-thujaplicin and nootkatin.

The non-volatile part of the extract from the wood of the common juniper (*Juniperus communis* L.) has been earlier investigated and found to contain several diterpene phenols [1–4]. The steam volatile part was briefly investigated a few years ago [5] and cedrene and cedrol were supposed not to occur in this material.

Through the courtesy of Professor and Mrs. Sörensen, Trondheim, a large sample of the steam volatile oil of the wood of *J. communis* was put at our disposal. The oil was extracted with alkali and the neutral part subjected to fractional distillation. The hydrocarbon fractions were analysed by gas chromatography. The main fraction was identified as thujopsene [6]. The fractions boiling below thujopsene were complex mixtures giving seven peaks in the gas chromatograms in addition to some minor ones. One of the major peaks (C_1) corresponded to that of the tricyclic sesquiterpene hydrocarbons Z and U from *Juniperus thurifera* L [7]. Another peak (E) corresponded to that of cedrene or longifolene (junipene) but neither compound could be identified.

The fractions in the boiling range 117—136°/9 mm gave ten peaks. By redistillation of the proper fractions and chromatography on alumina one substance could be isolated in a reasonably pure state and was identified as humulene by means of its infrared spectrum and that of its hydrogenation product [8,9]. Similarly, a fraction giving a single peak on gas chromatography was obtained which on dehydrogenation with selenium furnished a large yield of cadalene and on treatment with hydrogen chloride a low yield of (—)-cadinene dihydrochloride. The infrared spectrum was, except for an additional band at 1 615 cm^{-1} and some minor differences in the finger-print region, identical with that reported for δ-cadinene [10]. The ultraviolet spectrum, however,

showed a maximum at 248 mμ (ε about 5 000). The freshly isolated fractions exhibited optical rotations ranging from −47° to −10°. These fractions were easily autoxidised and when the non-oxidised part of them was isolated it always had a lower negative rotation, sometimes even weakly positive.

From the above results this gas chromatographically homogeneous fraction appears to be a mixture of δ-cadinene and the *iso*cadinene, reported to occur in small amounts in several oils together with δ-cadinene [11,12]. The wood oil of the common juniper, however, seems to contain unusually large amounts of *iso*cadinene that prevent the isolation of δ-cadinene in a pure state. The position of the UV absorption maximum (248 mμ) for the *iso*cadinene indicates that the double bonds are heteroannular and highly substituted. The infrared spectrum of the cadinene mixture possesses the same bands in the CH out-of-plane deformation range as pure δ-cadinene. These observations together with the structure proposed for δ-cadinene [13] (I) enable the tentative structures II or III to be proposed for the *iso*cadinene.

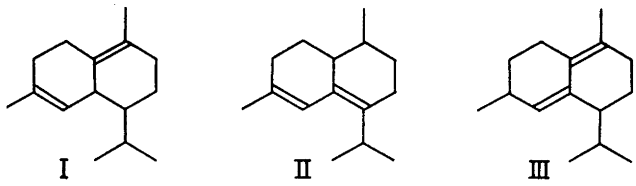

The presence of cuparene was indicated by gas chromatography and infrared spectra and pure cuparene could be isolated by ozonisation [14]. One peak (N) in the gas chromatograms was found to correspond to that of calamenene [15] and the maxima at 1 500 and 1 615 cm^{-1} in the IR spectra of the fractions giving this peak further supports [11] the assumption of the presence of this compound. It could, however, not be separated from cuparene.

The approximate amounts of the hydrocarbons, as percentage of the oil, calculated from the peak areas of the gas chromatograms, were as follows: "peak C_1" 1.5, "peak E" 1.5, thujopsene 37, humulene 4, δ-cadinene + *iso*-cadinene 12, cuparene 3, "peak N" 2. All the other peaks corresponded to compounds occurring in amounts less than 1 %. The amount of monoterpenes was very low, below 0.1 %.

The higher boiling fractions, containing alcohols and oxo-compounds, failed to crystallise. From the fractions, b.p. 142—147°/9 mm, cedrol and widdrol [16] could be isolated by chromatography. The estimated amounts of cedrol and widdrol were 2 and 1 % of the oil, respectively. The alcohol, m.p. 75—76°, isolated during the previous investigation [5] was not found in this oil but a direct comparison of the infrared spectra and a mixed m.p. kindly carried out by Dr. O. Motl, has shown it to be identical with the cadinol, m.p. 75°, from juniper berry oil [17].

Oxo-compounds were isolated with Girard reagents from several of the "alcohol fractions". The infrared spectra of the products from the lower boiling fractions showed that they were complex mixtures and no crystalline semicarbazone could be obtained from them. From a high-boiling fraction a small

amount of a crystalline semicarbazone, $C_{16}H_{25}ON_3$, was obtained, m.p. 237—239° (decomp.). The infrared spectrum of the compound, m.p. 32—35°, obtained by hydrolysis of the semicarbazone and the ultraviolet spectrum of the semicarbazone indicated that the compound was an α,β-unsaturated aldehyde.

Zavarin, Smith and Anderson [18] reported the presence of α-thujaplicin, nootkatin, pygmaein, and an unknown compound in a specimen of *Juniperus communis*, grown in California. The acidic fraction of our oil was therefore distilled but the distillates did not exhibit the spectral characteristics of tropolones. Since the oil investigated had been stored for a long time a sample of juniper wood was subjected to distillation with steam. The ultraviolet spectrum of the acidic fraction from the volatile products clearly showed the presence of tropolones and paper chromatography indicated the presence of α- and β-thujaplicin and nootkatin.

It has previously been suggested that cedrene and cedrol occur only in the Section *Sabina* of the junipers [5]. This, however, has now been shown to be incorrect since not only does *J. communis* contain cedrol but also *J. cedrus* [19] and *J. rigida* [20], all belonging to the Section *Oxycedrus*. The amount of cedrol in the wood of the latter junipers is small, however, and it is a matter of some difficulty to isolate it.

EXPERIMENTAL

All m.p.'s were determined with a Kofler microscope and are corrected. The microanalyses were performed by Dr. A. Bernhardt, Mülheim. The infrared spectra were recorded with a Perkin-Elmer No. 21 instrument, and the ultraviolet spectra with a Beckman DK-2 instrument. The gas chromatograms were made on a Pye Argon Chromatograph and, when not otherwise stated, with a dinitrophenyl naphthyl ether column described elsewhere [21]. Light petroleum refers to b.p. 40—60°.

The juniper wood oil (4.1 kg), obtained in several batches had been stored for over ten years in an ice chest in well stoppered, dark flasks. The different batches, except one with the strongest negative rotation (I) were combined. The oil was extracted with 2 N NaOH and the acid extracts combined (13.5 g, 0.3 %). Two thirds (2.6 kg) of the combined neutral fractions were distilled in a column packed with metal spirals (diameter 5 cm, length 150 cm). All the following distillations were made in a 1 m LKB-column. Since the physical constants and relative amounts of the fractions in the distillation of the oil were essentially identical with the results earlier recorded [5] they will not be mentioned here. The fractionation of the hydrocarbons was followed by gas chromatography and gave the following peaks, relative retention volumes, thujopsene = 1: several small peaks (monoterpenes) 0.09—0.22, A 0.50, B 0.61, C_1 0.73, C_2 0.78, D 0.85, E 0.89, F (thujopsene) 1, G 1.09, H 1.22, I 1.42, K 1.53, L 1.65, M 2.18, N 2.36, O 2.97, P 3.32.

Fractions b.p. 95—117°/9 mm. These fractions showed the peaks A—F. In the first fraction, b.p. 95—112°/9 mm, the peaks R_{rel} 0.09—0.22 were observed but only in a very low amount. They corresponded to monoterpenes. The fraction was yellow in colour. Upon chromatography on alumina neither the infrared nor the ultraviolet spectra of the yellow eluates showed the presence of thymoquinone, but a small amount of carvacrol methyl ether might have been present in this fraction. Some of the eluates had a strong odour of citronellol.

Peak C_1 corresponded to the peak obtained from the tricyclic sesquiterpene hydrocarbons Z and U from *J. thurifera* [7]. Peak E had the same retention volume as cedrene and longifolene. It always occurred together with peaks B, C, and D in small amounts in admixture with large amounts of peak F. Chromatography on alumina did not increase the relative amount of the substance corresponding to peak E but partial low-temperature ozonisation increased it slightly until an amount of about 12 % was attained. An infrared spectrum did, however, not show any of the bands of cedrene. This does not disprove the presence of cedrene since infrared spectra of known mixtures of thujopsene and

cedrene did not give any indication of the presence of cedrene when present in amounts below 15 %. Gas chromatograms of the E-enriched fractions were run on several different columns, the best results being obtained on Apiezon L. The results could not, however, give any decisive answer as to the presence or absence of either cedrene or longifolene. Peak F corresponded to thujopsene. One of the distillates, b.p. 116.5°/8 mm, n_D^{20} 1.5049, $[\alpha]_D^{20}$ −99° (oil), from batch I was gas chromatographically homogeneous. Its infrared spectrum was identical with that of thujopsene and selenium dioxide oxidation [16] gave widdrenal, m.p. 74—75°, identified by mixed m.p. determination with authentic material.

Fractions b.p. 117—136°/9 mm. These fractions showed the peaks F—P. Attempts to isolate the substance corresponding to peak G by distillation and chromatography on alumina did not give the substance in a purity higher than 35 %. Peak I was more enriched in the fractions b.p. 122—126°/9 mm, which were redistilled. Chromatography with light petroleum on a hundredfold amount of alumina (Merck, nach Brockmann, activated at 170° for 24 h) of the distillates having the highest content of I gave the compound in the end fractions, a behaviour earlier found by Šorm *et al.*[10] for humulene. The purest fraction obtained, n_D^{25} 1.5045, $[\alpha]_D^{20}$ −5.7° ($CHCl_3$, *c* 10), had a purity of about 85 % (gas chromatography). Its infrared spectrum was identical with that of humulene [8], except for a small band at 1 525 cm^{-1} possibly due to the presence of small amounts of cuparene. Upon hydrogenation with PtO_2 in acetic acid the product consumed 3.1 moles H_2/mole. The hydrogenated material was chromatographed on alumina giving an oil, n_D^{25} 1.4760, $[\alpha]_D^{20}$ −0.9° ($CHCl_3$, *c* 10), purity about 85 % (gas chromatography). The infrared spectrum was in good agreement with the spectra published for humulane [8,9].

The compound corresponding to the peak K was enriched in the fractions b.p. 131—132°/9 mm. Chromatography on activated alumina gave in the first eluates gas chromatographically homogeneous "product" K. These eluates gave, upon selenium dehydrogenation, an 85 % yield of cadalene, picrate m.p. 116—117°, mixed m.p. with authentic material, no depression, and with hydrogen chloride in 20 % yield (−)-cadinene dihydrochloride, m.p. 117—118.5°, $[\alpha]_D^{20}$ −36.5° ($CHCl_3$, *c* 2), mixed m.p. with authentic material, no depression. The very first eluate had a rotation of $[\alpha]_D$ −47° which fell to about −10° in the later fractions. All fractions had an ultraviolet maximum at 248 mμ. The highest extinction value observed was ε 5 700. The fractions were very sensitive to autoxidation, *e.g.* one fraction stored for a week in a refrigerator gave upon chromatography on alumina only one fourth of the original amount in the light petroleum eluate. The rotation had at the same time decreased from −28° to −4°.

Peak M corresponded to cuparene. A distillate of batch I with a low content of peak N (see below) was ozonised at low temperature [14] and cuparene isolated by chromatography and distillation. The distillate, b.p. 117°/7 mm, n_D^{20} 1.5238, $[\alpha]_D^{20}$ + 67° ($CHCl_3$, *c* 2), was gas chromatographically homogeneous and the infrared spectrum was identical with that of cuparene. Peak N had the same retention volume as calamenene [15]. The fractions showing this peak had maxima in the infrared at 1 615 and 1 500 cm^{-1}. They could not be freed from cuparene.

Fractions b.p. 136—150°/9 mm. These fractions contained mainly alcohols. Upon fractionation with Girard D reagent small amounts of oxo-compounds were isolated. The infrared spectra showed that they were complex mixtures and no crystalline semicarbazones could be obtained from them. The carbonyl-free fractions were chromatographed on a fortyfold amount of alumina (Merck, nach Brockmann). Benzene-benzene + 1 % ether eluted crude cedrol, m.p. 45—70°. This was difficult to obtain pure by crystallisation, but gradient sublimation ultimately gave pure cedrol, m.p. 85—86°, $[\alpha]_D^{20}$ + 9° ($CHCl_3$, *c* 2), mixed m.p., IR. Benzene + ether (10:1 to 1:1) eluted widdrol, crystallised from acetonitrile, m.p. 97.5—98°, $[\alpha]_D^{20}$ + 103° ($CHCl_3$, *c* 2), mixed m.p., IR. No further crystalline compounds could be isolated.

In order to make sure that no other alcohols were present in the crude cedrol a preparation of m.p. 65—67° was subjected to dehydration with formic acid. The hydrocarbon fraction was isolated by chromatography on alumina and investigated by gas chromatography. It showed the cedrene peak as well as a few peaks due to very small

amounts of contaminating hydrocarbons. Similarly pure widdrol gave rise to a hydrocarbon mixture exhibiting three major peaks and four minor ones and *α*-, *β*-, *δ*- and *iso*-cadinol to a mixture showing thirteen peaks of different magnitude. The "impurity peaks" from cedrol cannot be correlated with certainty with any of these peaks.

Fractions b.p. 130—135°/2 mm. These fractions did not give any crystalline substance after chromatography. The benzene eluate from the fraction, b.p. 134—135°/2 mm, gave an infrared spectrum which indicated that this eluate probably contained a rather homogeneous oxo-compound. Fractionation with Girard D reagent of the whole fraction (13 g) gave 1.6 g of oxo-compounds from which a crystalline semicarbazone was obtained in the usual way. It gave, after crystallisation from ethanol, 0.30 g of leaflets, m.p. 237—239° (decomp.), $[\alpha]_D^{20}$ −31° (pyridine, *c* 2). λ_{max} 271 mμ (log ε 4.45). (Found: C 69.4; H 8.8; N 15.3. Calc. for $C_{16}H_{25}ON_3$: C 69.8; H 9.15; N 15.3.) From the mother liquors 0.30 g of crystals, $[\alpha]_D^{20}$ −25°, separated. The last crystals were steam distilled in the presence of phthalic anhydride yielding 0.14 g of steam-volatile oil which, after distillation, crystallised partly, m.p. 32—35°. The compound showed strong bands in infrared at 2 810, 2 720, 1 680, and 1 630 cm^{-1} (in CCl_4). Comparison of the spectrum with that of synthetic cedrenal showed that they were not identical.

Acidic fraction. The acidic fraction was distilled and ultraviolet spectra were taken from the distillates. No selective absorption was detected above 300 mμ.

Steam distillation of wood. 1.13 kg milled juniper wood was steam distilled until 12 litres of distillate had been collected. Salt was added and the water exhaustively extracted with ether. The ether extract was shaken with 1 N NaOH and the acidic part (0.27 g, λ_{max} 335 mμ, *a* 9.2) recovered from the alkaline solution in the usual way. The ultraviolet spectrum of the neutral part exhibited no absorption above 300 mμ. The acidic part was dissolved in 100 ml ether and extracted successively with 2 × 50 ml of the following solutions: (A) 5 % $NaHCO_3$, saturated with CO_2, (B) 5 % $NaHCO_3$, (C) 2.5 % $NaHCO_3$ +2.5 % Na_2CO_3, and (D) 5 % Na_2CO_3, leaving a residue (E). Ultraviolet spectra and paper chromatograms [22] were run on each fraction giving the following results: (A) 77 mg, no selective absorption, *β*-thujaplicin (+); (B) 20 mg, inflexion 310 mμ (*a* 2.8), *β*-thujaplicin (+); (C) 52 mg, max. 330 mμ (*a* 4.0), *β*-thujaplicin ++, *α*-thujaplicin (+); (D) 61 mg, max. 333 mμ (*a* 5.9), *β*-thujaplicin +++, *α*-thujaplicin +, nootkatin +; (E) 58 mg, max. 337 mμ (*a* 23.2), *β*-thujaplicin +, *α*-thujaplicin +, nootkatin +++.

The author is deeply indebted to Professor Holger Erdtman for his encouraging interest. Thanks are also due to Fil.lic. Jarl Runeberg for valuable discussions, Miss Gurli Hammarberg for the infrared and ultraviolet spectra and Dr. Ian Wellings for checking the English. The work has been financially supported by *Cellulosaindustrins stiftelse för teknisk och skoglig forskning och utbildning* which is gratefully acknowledged.

REFERENCES

1. Bredenberg, J. B. and Gripenberg, J. *Acta Chem. Scand.* **8** (1954) 1728.
2. Bredenberg, J. B. and Gripenberg, J. *Acta Chem. Scand.* **10** (1956) 1511.
3. Bredenberg, J. B. *Acta Chem. Scand.* **11** (1957) 932.
4. Bredenberg, J. B. *Acta Chem. Scand.* **14** (1960) 385.
5. Bredenberg, J. B. *Acta Chem. Scand.* **11** (1957) 98.
6. Erdtman, H. and Norin, T. *Chem. & Ind. London* **1960** 622.
7. Runeberg, J. *Acta Chem. Scand.* **14** (1960) 1985.
8. Herout, V., Streibl, M., Mleziva, J. and Šorm, F. *Collection Czechoslov. Chem. Communs.* **14** (1949) 716.
9. Dev, S. *Tetrahedron* **8** (1960) 171.
10. Pliva, J., Herout, V., Schneider, B. and Šorm, F. *Collection Czechoslov. Chem. Communs.* **18** (1953) 500.
11. Šorm, F., Holub, M., Šykora, V., Mleziva, J., Streibl, M., Pliva, J., Schneider, B. and Herout, V. *Collection Czechoslov. Chem. Communs.* **18** (1953) 512.
12. Herout, V., Motl, O. and Šorm, F. *Chem. listy* **48** (1954) 589.
13. Herout, V. and Santavy, F. *Collection Czechoslov. Chem. Communs.* **19** (1954) 118.

14. Enzell, C. and Erdtman, H. *Tetrahedron* **4** (1958) 361.
15. Runeberg, J. *Acta Chem. Scand.* **15** (1961) 721.
16. Erdtman, H. and Thomas, B. R. *Acta Chem. Scand.* **12** (1958) 267.
17. Herout, V. and Šykora, V. *Tetrahedron* **4** (1958) 255.
18. Zavarin, E., Smith, R. M. and Anderson, A. B. *J. Org. Chem.* **24** (1959) 1318.
19. Runeberg, J. *Acta Chem. Scand.* **14** (1960) 1991.
20. Nakatsuka, T. *Private communication.*
21. Runeberg, J. *Acta Chem. Scand.* **14** (1960) 797.
22. Wachtmeister, C. A. and Wickberg, B. *Acta Chem. Scand.* **12** (1958) 1335.

Received December 14, 1960.

ACTA CHEMICA SCANDINAVICA 15 (1961) 967–974

Crystal Structure of the 1:1 Addition Compound Formed by 4-Picoline and Iodine

O. HASSEL, CHR. RØMMING and T. TUFTE

Universitetets Kjemiske Institutt, Blindern-Oslo, Norway

The crystal structure of an equimolecular addition compound of 4-picoline and iodine has been determined by X-ray methods at temperatures about −40°C. The space group is $P2_1/c$, the lattice parameters: $a = 4.72$ Å; $b = 9.05$ Å; $c = 21.55$ Å; $\beta = 101°$. The I-I-N arrangement is linear with the I-I distance 2.83 Å and the I-N distance 2.31 Å.

Glusker and Miller [1] have examined two different solid compounds formed by 4-picoline and iodine. One compound (I), $(C_6H_7N)_2I_2$, is water-soluble, alcohol-insoluble, and has a melting point of 244°C. The second compound (II), $C_6H_7N.I_2$ is insoluble in water and its melting point is 83°C. For both substances radial distribution functions were worked out, based on intensities collected from X-ray powder experiments. The conclusions drawn from the radial distribution curves were that compound I contains no I-I distance shorter than 3 Å and that compound II contains one I-I distance botween 1.9 Å and 3.0 Å per molecule picoline. They were thus led to the conclusion that the compound I has an ionic structure while the compound II is a molecular addition compound.

Recently Hassel and Hope [2] by carrying out a structure determination of a reaction product of pyridine and iodine demonstrated the existence of a centrosymmetric $(C_6H_5N)_2I^+$ ion. It appears very probable that the cation of compound I has a similar structure:

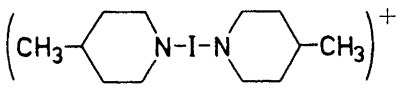

rather than the *a*-addition arrangement proposed by Glusker and Miller.

We also found Glusker and Miller's argument regarding the structure of compound II somewhat inconclusive. One alternative explanation of the radial distribution curve might, *e.g.*, be given by assuming the presence of (4-picoline)$_2$I$^+$ and I_3^- ions.

A single crystal X-ray investigation of the 1:1 compound (II) has now been carried out in order to determine the spatial arrangement of the atoms.

EXPERIMENTAL

A solution of iodine in ethyl ether was added to an equimolecular amount of 4-picoline and the solvent slowly evaporated at −30°C. The crystals thus obtained were either plates or needles, those having the latter habit were preferred for use in the X-ray examination. They were kept in sealed, thin-walled capillary tubes. Also during the preparation and mounting of the crystals care was taken to avoid moisture, and during the X-ray exposure they were cooled to temperatures below −40°C.

The melting point of the compound was found equal to 83°C and the density measured by the flotation method 2.4 g/cm^3. This is in good agreement with the figures reported by Glusker and Miller for compound II.

Oscillation and Weissenberg photographs (Cu*Ka* radiation) with rotation about two crystallographic axes were taken in order to determine the unit cell dimensions and the space groups. The 0*kl* and *h*0*l* intensities were estimated partly from Weissenberg diagrams by visual comparison with a standard scale and partly from measurements on a microphotometer of films taken with an integrating Weissenberg camera. 128 0*kl* reflexions and 116 *h*0*l* reflexions were recorded, the maximum numbers obtainable with Cu*Ka*-radiation are 230 and 128, respectively. The intensities were corrected for Lorentz and polarization effects and eventually for secondary extinction using a method given by Pinnock, Taylor and Lipson [3]. No absorption corrections were applied.

The computations involved in the present investigation were carried out on a Ferranti Mercury computer; the least squares programme used has been designed by Curtis [4]. The atomic scattering factors used to suit this programme are given as an analytical approximation by Forsyth and Wells [5].

RESULTS

The crystals were found to be monoclinic, space group $P2_1/c$ with the unit cell dimensions:

$a = 4.72$ Å; $b = 9.05$ Å; $c = 21.55$ Å; $\beta = 101°$

With four molecules per unit cell the calculated density is 2.55 g/cm^3.

Patterson syntheses based on the 0*kl* and *h*0*l* intensities were worked out and the parameters of the two independent iodine atoms determined. The corresponding electron density Fourier maps were evaluated from experimental structure factors with signs based on the iodine parameters. From the Fourier maps more accurate iodine parameters could be determined and indications regarding the position of the light atoms were also obtained. The organic part of the compound was well resolved in the projection along the *a* axis. In the projection along the *b* axis, however, overlapping occurred for two pairs of carbon atoms of the six-membered ring. A normal series of Fourier refinements could then be performed. At the stage at which no further structure factor signs changed, the reliability index *R* for the two zones were 0.17 and 0.18, respectively. The intensities were corrected for secondary extinction, and the refinement of the parameters was continued with the method of least squares.

Table 1. Atomic coordinates as fractions of the cell-edges.

Atom	x	y	z
I_1	0.1821	0.1388	0.0837
I_2	0.5456	0.1431	0.2040
N	0.875	0.144	0.299
C_2	0.003	0.005	0.320
C_3	0.003	0.275	0.326
C_4	0.250	0.019	0.373
C_5	0.250	0.019	0.373
C_6	0.372	0.141	0.408
C_7 (methyl)	0.630	0.153	0.458

The atomic coordinates eventually arrived at using this method are listed in Table 1, the z-coordinate being in each case the mean of values derived from the two projections. The mean B values in the temperature factor expression were 2.2 Å^2 for the "outer" iodine atom, 1.1 Å^2 for the iodine atom linked to the nitrogen atom and 2.7 Å^2 for nitrogen and carbon atoms. The final R values were 0.12 and 0.16 in the $0kl$ and the $h0l$ zones, respectively. A compari-

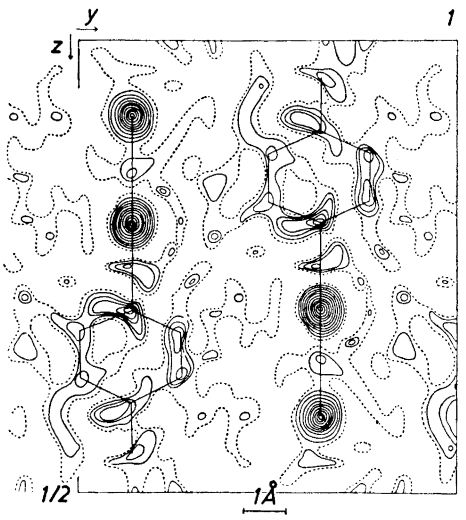

Fig. 1. Projection along the a-axis. Contours at intervals of 10 e · Å^{-2} in the iodine peaks and of 2 e · Å^{-2} in the rest of the map. The 2 e · Å^{-2} is dotted.

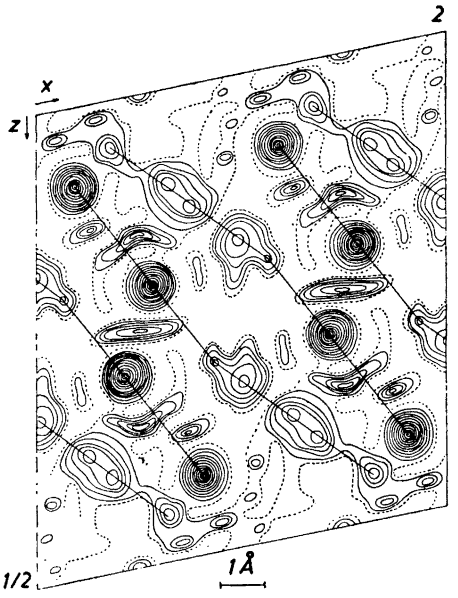

Fig. 2. Projection along the b-axis. Contour lines as in Fig. 1.

Table 2.

h	k	l	F_{obs}	F_{calc}
0	0	2	5.0	− 9.4
		4	7.0	− 6.8
		6	12.0	−12.1
		8	18.6	−21.0
		10	22.2	22.6
		12	1.4	− 2.4
		14	12.8	11.0
		16	7.4	− 3.8
		18	15.2	−12.4
		20	5.4	3.2
		22	6.4	− 4.4
		24	13.0	11.2
		26	1.8	0.0
		28	< 0.2	0.4
1	0	$\bar{2}8$	< 0.3	0.6
		$\bar{2}6$	4.4	4.2
		$\bar{2}4$	2.8	− 2.6
		$\bar{2}2$	5.8	4.0
		$\bar{2}0$	19.0	−16.8
		$\bar{1}8$	5.4	2.6
		$\bar{1}6$	6.8	5.2
		$\bar{1}4$	6.6	6.0
		$\bar{1}2$	14.6	16.2
		$\bar{1}0$	20.0	−23.2
		$\bar{8}$	3.8	− 4.2
		$\bar{6}$	3.8	− 3.8
		$\bar{4}$	9.4	8.0
		$\bar{2}$	22.0	22.0
		0	8.8	− 7.6
		2	7.0	6.0
		4	24.8	−28.2
		6	6.8	− 6.6
		8	9.4	11.6
		10	4.8	3.2
		12	17.6	18.6
		14	18.0	−14.8
		16	7.0	− 4.4
		18	2.8	− 0.6
		20	7.4	− 3.4
		22	14.2	12.4
		24	4.4	− 3.2
		26	< 0.5	0.1
2	0	$\bar{2}6$	1.8	1.8
		$\bar{2}4$	2.2	− 2.2
		$\bar{2}2$	11.2	−10.0
		$\bar{2}0$	7.8	6.8
		$\bar{1}8$	4.0	− 2.8
		$\bar{1}6$	12.4	13.8
		$\bar{1}4$	5.2	2.0
		$\bar{1}2$	10.0	−11.2
		$\bar{1}0$	2.0	1.4
		$\bar{8}$	22.0	−23.6
		$\bar{6}$	18.4	20.6
		$\bar{4}$	12.4	12.2
		$\bar{2}$	4.2	− 2.4
		0	5.6	3.4
		2	33.6	−31.6
		4	11.4	10.0
		6	7.6	5.0
		8	10.4	8.6
		10	10.8	11.8
		12	14.6	−15.0
		14	< 1.4	− 1.5
		16	11.8	− 9.2
		18	9.2	5.4
		20	12.4	8.6
		22	4.4	− 4.4
		24	3.4	3.4
3	0	$\bar{2}6$	6.8	− 5.6
		$\bar{2}4$	4.2	− 4.8
		$\bar{2}2$	2.8	4.0
		$\bar{2}0$	5.4	− 3.6
		$\bar{1}8$	13.4	−15.2
		$\bar{1}6$	5.6	− 3.8
		$\bar{1}4$	8.0	− 8.0
		$\bar{1}2$	5.8	− 4.2
		$\bar{1}0$	10.6	− 9.0
		$\bar{8}$	16.8	18.0
		$\bar{6}$	1.8	0.8
		$\bar{4}$	7.6	6.8
		$\bar{2}$	7.0	− 5.4
		0	16.0	−16.2
		2	9.4	8.0
		4	3.4	− 4.4
		6	17.8	17.0
		8	< 1.3	− 0.6
		10	13.0	−11.6
		12	2.0	1.8
		14	11.0	−10.2
		16	12.4	9.4
		18	4.8	2.8
		20	< 0.6	0.9
		22	< 0.2	1.8
4	0	$\bar{2}2$	1.8	2.6
		$\bar{2}0$	5.8	7.2
		$\bar{1}8$	5.8	− 7.0
		$\bar{1}6$	5.0	4.0
		$\bar{1}4$	8.2	−10.2
		$\bar{1}2$	< 1.4	− 0.3
		$\bar{1}0$	9.0	11.6
		$\bar{8}$	< 1.4	0.6
		$\bar{6}$	10.6	11.4
		$\bar{4}$	12.4	−13.2
		$\bar{2}$	7.0	− 7.4
		0	3.4	3.4
		2	< 1.4	− 0.9
		4	15.4	14.2
		6	5.8	− 4.8
		8	2.4	− 1.4
		10	5.8	− 5.2
		12	4.8	− 5.2
		14	11.4	10.2

Table 2. Continued.

h	k	l	F_{obs}	F_{calc}
		16	< 0.6	1.3
5	0	$\bar{18}$	1.8	1.6
		$\bar{16}$	5.8	− 9.0
		$\bar{14}$	3.4	4.0
		$\bar{12}$	2.4	3.6
		$\bar{10}$	1.8	2.0
		$\bar{8}$	4.2	4.4
		$\bar{6}$	9.8	−11.8
		$\bar{4}$	1.8	1.8
		$\bar{2}$	4.8	− 4.6
		0	3.4	4.8
		2	7.8	10.6
		4	4.6	− 7.6
		6	1.6	3.0
		8	6.4	− 4.0
		10	< 0.9	0.6
6	0	$\bar{8}$	< 0.2	− 0.1
		$\bar{6}$	< 0.3	0.2
		$\bar{4}$	< 0.3	0.1
		$\bar{2}$	< 0.2	− 0.1
0	0	2	7.4	− 9.2
		4	8.3	7.4
		6	12.9	−12.5
		8	20.3	−21.0
		10	25.2	23.5
		12	< 4.0	0.9
		14	12.3	11.0
		16	6.5	− 4.7
		18	16.0	−14.1
		20	5.2	3.9
		22	4.0	− 2.5
		24	11.7	13.2
		26	< 3.7	0.6
0	1	1	8.6	8.9
		2	13.9	−14.4
		3	6.2	− 5.4
		4	< 2.1	− 0.2
		5	< 2.4	0.8
		6	10.8	−12.5
		7	15.1	−17.6
		8	16.3	20.5
		9	4.0	5.4
		10	5.5	5.2
		11	6.2	6.7
		12	3.4	− 2.4
		13	3.4	2.8
		14	< 4.5	− 2.2
		15	4.6	5.8
		16	15.1	−14.5
		17	10.8	−10.9
		18	7.1	8.3
		19	< 4.8	− 3.3
		20	< 5.2	2.2
		21	< 5.2	− 0.8
		22	4.0	2.4
		23	< 4.9	1.9
		24	< 4.3	2.3
		25	4.0	5.0
		26	5.2	− 6.4
0	2	0	8.6	− 8.0
		1	27.7	−30.8
		2	3.1	2.2
		3	7.4	− 8.6
		4	< 2.4	− 0.4
		5	11.1	−11.9
		6	< 3.0	1.7
		7	< 3.7	1.2
		8	< 3.4	3.6
		9	22.5	28.0
		10	< 3.7	− 3.5
		11	8.3	− 8.7
		12	< 4.3	0.9
		13	4.3	4.0
		14	< 4.6	− 2.3
		15	14.5	−13.6
		16	< 4.9	1.1
		17	7.7	− 5.8
		18	< 5.5	1.9
		19	13.5	12.3
		20	< 5.2	− 1.1
		21	< 5.2	− 0.3
		22	< 4.9	1.0
		23	8.6	8.8
		24	< 4.0	− 2.2
		25	5.8	− 8.1
0	3	1	16.9	−16.7
		2	10.8	−10.8
		3	15.7	14.2
		4	< 3.0	0.9
		5	< 3.0	− 1.4
		6	5.2	− 4.8
		7	20.3	20.4
		8	7.7	8.4
		9	6.2	− 7.3
		10	2.5	2.7
		11	8.0	− 9.0
		12	< 4.6	− 1.6
		13	< 4.6	− 2.3
		14	< 4.6	− 0.9
		15	8.0	− 8.5
		16	6.8	− 6.8
		17	14.2	13.6
		18	< 5.2	2.4
		19	< 5.2	1.5
		20	< 5.2	1.5
		21	< 4.9	1.1
		22	< 4.6	2.8
		23	< 4.3	− 3.3
		24	< 3.7	0.9
		25	6.2	− 7.6
0	4	0	28.9	−26.8
		1	8.9	8.2

Table 2. Continued.

h k l	F_{obs}	F_{calc}
2	5.2	3.5
3	< 3.4	0.1
4	< 3.7	− 0.7
5	3.7	4.0
6	14.2	12.4
7	< 4.0	0.9
8	17.5	15.8
9	8.0	− 8.2
10	18.2	−17.6
11	3.7	4.0
12	< 4.0	− 0.5
13	< 4.6	− 2.5
14	10.2	− 9.9
15	< 4.9	4.2
16	8.0	7.0
17	< 5.2	1.6
18	12.6	11.4
19	< 5.2	− 3.8
20	6.5	− 6.7
21	< 5.2	1.2
22	4.3	3.5
23	< 4.6	− 3.0
24	7.1	− 8.7
0 5 1	6.2	− 3.6
2	20.6	18.5
3	< 4.0	2.4
4	4.6	2.8
5	< 4.3	0.7
6	11.1	9.6
7	5.5	3.5
8	18.2	−17.3
9	< 4.6	− 1.2
10	5.5	− 3.9
11	< 4.9	− 2.2
12	4.0	3.3
13	< 5.2	− 0.9
15	< 5.2	− 1.8
16	14.2	14.4
17	< 5.2	3.1
18	7.7	− 6.5
19	< 4.9	1.1
20	< 4.6	− 2.5
21	< 4.3	0.2
22	7.1	− 4.7
0 6 0	14.2	12.8
1	16.0	15.1
2	5.8	− 4.2
3	4.6	3.0
4	< 4.6	0.8
5	6.8	5.7
6	4.6	− 3.0
7	< 4.9	− 0.4
8	6.5	− 7.3
9	17.5	−16.7
10	8.0	8.2
11	5.2	4.5
12	< 5.2	− 1.6
13	< 5.2	− 1.0
14	< 5.2	4.5
15	6.8	8.4
16	< 5.2	− 1.9
17	4.0	3.4
18	4.0	− 4.1
19	7.7	− 7.9
0 7 1	9.5	9.7
2	< 4.8	− 0.9
3	8.6	− 6.8
4	< 4.9	1.4
5	< 5.2	− 0.2
6	< 5.2	0.3
7	16.6	−16.1
8	< 5.2	− 0.8
9	6.2	6.2
10	< 5.2	− 1.0
11	6.8	6.2
12	< 5.2	− 0.2
13	< 5.2	2.6
14	< 5.2	0.7
15	6.5	6.9
16	< 4.6	0.8
17	11.4	−13.4
0 8 0	15.7	14.4
1	13.2	−10.6
2	5.2	− 2.5
3	< 5.2	− 0.8
4	< 5.2	− 1.8
5	< 5.2	− 2.9
6	< 5.2	− 4.7
7	5.2	− 1.0
8	6.8	− 5.9
9	9.2	9.4
10	6.8	8.2
11	5.8	− 5.4
12	< 4.9	0.8
13	4.0	4.3
14	< 4.6	4.0
15	4.3	− 3.4
16	< 4.0	− 2.3
17	< 3.7	− 2.3
0 9 1	< 5.2	− 0.5
2	9.9	− 9.0
3	< 5.2	1.4
4	< 5.2	− 0.3
5	< 5.2	− 1.1
6	9.5	− 8.2
7	< 4.9	1.2
8	11.7	11.8
9	< 4.6	− 1.1
10	< 4.6	4.0
11	< 4.3	− 0.3
12	< 4.3	− 2.1
13	< 4.0	0.6

Tale 2. Continued.

h k l	F_{obs}	F_{calc}	h k l	F_{obs}	F_{calc}
14	< 3.7	− 1.8	8	4.0	5.7
15	< 3.4	− 1.0	9	3.1	5.0
16	< 3.0	− 8.3	10	8.0	− 6.8
17	4.0	3.6	0 11 1	4.0	− 6.6
0 10 0	11.7	−10.5	2	< 3.4	1.9
1	4.6	− 5.0	3	4.9	5.1
2	3.7	4.7	4	< 3.4	− 1.3
3	< 4.6	− 2.2	5	< 3.4	0.2
4	< 4.6	− 0.1	6	< 3.0	1.7
5	< 4.3	− 2.0	7	< 2.8	7.4
6	< 4.3	3.4	8	4.3	− 4.3
7	< 4.3	1.2			

son between observed and calculated structure factors is given in Table 2. The two electron density maps are reproduced in Figs. 1 and 2.

The structure determination proves that the compound II is a molecular addition compound. The atoms I_1-I_2-N form, within the accuracy of the measurements, a straight line. The I_1-I_2 distance is 2.83 Å (standard deviation [6] 0.003) Å which implies a lengthening of about 0.17 Å compared with the distance in the free iodine molecule. The I_2-N distance is 2.31 Å (standard deviation 0.02 Å). These results are in good agreement with measurements on similar compounds already investigated as may be seen from Table 3.

The distance between the light atoms deduced from the atomic coordinates given in Table 1 are certainly not very accurate in a structure like the present one containing atoms as heavy as iodine. The greatest deviations from the corresponding figures in the pyridine molecule are as large as 0.08 Å.

A line drawn through I_1, I_2, and N is forming an angle of 13° with the plane of the picoline ring and the plane defined by this line and the C_4-atom is approximately normal to the plane containing the light atoms. One would perhaps have expected the line to pass through the C_4-atom, but intermolecular forces are evidently strong enough to distort the planar configuration.

This investigation has been sponsored by the *United States Air Force Development Command* under contract AF 61 (052)−71.

Table 3. A comparison of bond lengths in various addition compounds containing iodine.

Compound	Ref.	I-I (Å)	I-N (Å)
Trimethylamine · I_2	7	2.83	2.27
Dithiane · I_2	8	2.79	
Benzylsulphide · I_2	9	2.82	
Pyridine · ICl	10		2.26
Trimethylamine · ICl	11		2.30
4-Picoline · I_2	present examination	2.83	2.31

REFERENCES

1. Glusker, D. L. and Miller, A. *J. Chem. Phys.* **26** (1957) 331.
2. Hassel, O. and Hope, H. *Acta Chem. Scand.* **15** (1961) 407.
3. Pinnock, P. R., Taylor, C. A. and Lipson, H. *Acta Cryst.* **9** (1956) 175.
4. Curtis, A. R. *A.E.R.E. Mercury Autocode Program No. 29.*
5. Forsyth, J. B. and Wells, M. *Acta Cryst.* **12** (1959) 412.
6. Cruickshank, D. W. J. *Acta Cryst.* **2** (1949) 65.
7. Strømme, K. O. *Acta Chem. Scand.* **13** (1959) 268.
8. Chao, G. Y. and McCullough, J. D. *Acta Cryst.* **13** (1960) 727.
9. Rømming, C. *Acta Chem. Scand.* **14** (1960). 2145.
10. Hassel, O. and Rømming, C. *Acta Chem. Scand.* **10** (1956) 696.
11. Hassel, O. and Hope, H. *Acta Chem. Scand.* **14** (1960) 391.

Received January 13, 1961.

ACTA CHEMICA SCANDINAVICA 15 (1961) 975–984

Crystalline Leghemoglobin

IV. Spectroscopic Studies of the Two Main Metleghemoglobin Components and Some of their Fatty Acid Complexes

NILS ELLFOLK*

Medicinska Nobelinstitutet, Biokemiska avdelningen, Stockholm, Sweden

The transition from acid to alkaline metleghemoglobin follows a monovalent dissociation curve. The pK values (at an ionic strength of 0.1) were determined spectrophotometrically and were found to be 8.16 for the electrophoretically faster moving component, and 8.34 for the slower one. No other hem linked groups were spectrophotometrically demonstrable between the pH values of 5.35 and 10.45. Acetate, propionate, butyrate and valerate were found to form reversible complexes with the two main metleghemoglobin components. The isosbestic points for the complexes were at 583 and 500–490 mμ. The pK values of the fatty acid complexes at pH 4.8 were $pK_{acetate} = 2.9$, $pK_{propionate} = 2.8$, $pK_{butyrate} = 2.4$ and $pK_{valerate} = 2.6$. The pK values were essentially independent of the sizes of the alkyl groups. This has led to the conclusion that the hem is not buried within the folds of the apoprotein, but is attached to the surface of it.

In 1939 Kubo [1] for the first time examined spectrophotometrically the pigment from soy bean root nodules and determined the positions of its absorption bands under different conditions. The oxygenated pigment showed absorption bands at 575 and 540 mμ, which on reduction were replaced by one band at 555 mμ. In the carbon monoxide compound, the bands were shifted to 570 and 535 mμ. The oxidized ferri-compound had bands at 625, 563, and 530 mμ. This compound was found to react with cyanide or fluoride to give compounds with bands at 540 or 610 mμ, respectively.

These original observations have been essentially confirmed in several laboratories. Keilin and Wang [2] found the absorption maxima of the oxygenated compound at 574 and 540 mμ. Little and Burris [3] found exactly the same maxima as Kubo, whereas Sternberg and Virtanen [4] reported maxima at 573 and 540 mμ. The maxima of the reduced leghemoglobin was found to be at 557 mμ by Keilin and Wang [2], whereas Little and Burris as well as Sternberg

* Permanent address: Research laboratories of the State Alcohol Monopoly, Helsinki, Finland.

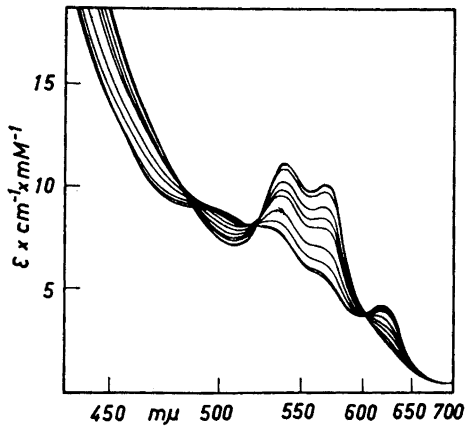

Fig. 1. The effect of pH upon the absorption spectra in the visible (700—450 mμ) of the electrophoretically faster component of metleghemoglobin in solutions of 0.1 μ ionic strength at + 20°C. The absorption curves corresponding to different pH values may be distinguished in the spectral region between 570—540 mμ, where the absorption increases with increasing basicity. At the pH values in parenthesis the spectral curves are superimposed: (5.35, 5.80, 6.40, 6.80), 7.47, 7.89, 8.31, 8.44, 8.75, 9.06, 9.50 (10.00, 10.45).

and Virtanen confirmed the value of Kubo. The maximum of the cyanide compound at 540 mμ, as determined by Kubo, was confirmed by Sternberg and Virtanen as well as by Little and Burris, with only a slight deviation (541 mμ). Greater differences were found between Kubo's values for the maxima of the carbon monoxide compound and those values determined by Keilin and Wang [2] (564 and 538 mμ), by Little and Burris [3] (565 and 539 mμ) and by Sternberg and Virtanen (565 and 538 mμ). The maximum of the fluoride compound was found to be at 605 mμ by Little and Burris as well as by Sternberg and Virtanen, and thus differed slightly from Kubo's value of 610 mμ.

The pK value for the transitation from acid to the alkaline form of metleghemoglobin of the unresolved material was determined for the first time by Sternberg and Virtanen, and was found to be equal to 8.254, $\mu = 0.1$. Later, Thorogood [5,6] made determinations of the pK values of the two main components isolated by paper electrophoresis, and found them to be equal to 8.02 for the electrophoretically faster component, and 8.22 for the slower one at an ionic strength of 0.1.

In the present investigation, the pK's for the transition from the acid to alkaline forms of the two metleghemoglobins were determined. The reversible formation of acetate, propionate, butyrate and valerate complexes with the two metleghemoglobins was also investigated.

EXPERIMENTAL

Methods. Spectrophotometric measurements were made with a Beckman model DK 2 in the most experiments. The pH's of the solutions were measured with the glass electrode which was standardized against phthalate and borate solutions.

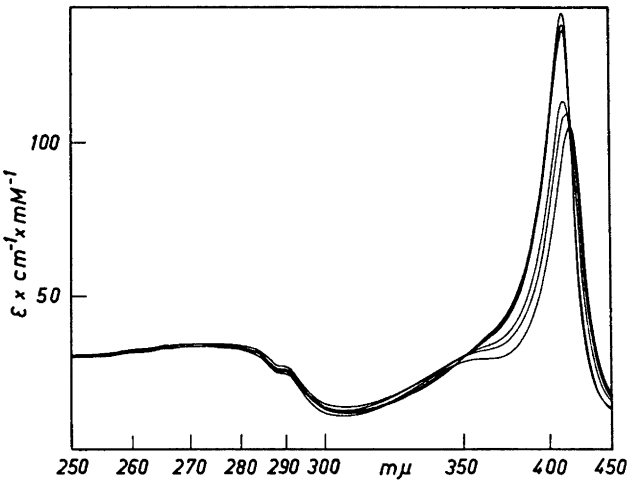

Fig. 2. The effect of pH upon the absorption spectra in the ultraviolet (450—250 mμ) of the electrophoretically faster component of metleghemoglobin in solutions of 0.1 ionic strength at + 20°C. The pH order may be followed in the spectral region between 403.5—412 mμ. The curves were obtained at pH: 5.35, 6.80, 7.47, 8.31, 8.75 and 9.50. The Soret band increases in intensity with increasing acidity.

Material. The two components of metleghemoglobin (metLhb or Lhb^+) were prepared as described previously [7,8]. Their electrophoretic homogeneity was always checked. Horse myoglobin I was prepared chromatographically [9].

RESULTS

Studies of the absorption spectra of the two main metLhb components in the visible and ultraviolet regions of the spectrum were carried out on solutions of the proteins in phosphate, veronal, and glycine-NaOH buffers of 0.1 ionic strength. Figs. 1 and 2 show the molecular extinction coefficients (250 to 700 mμ) of the faster component as a function of pH. In the visible region, all the curves intersect at four isosbestic points, which were found for both of the main metLbh components at 604—606, 523—525, 483—495 and 410 mμ. In the ultraviolet region, an isosbestic point was found for the two components at about 355—353 mμ. The Soret band was situated at 403.5 mμ at acid pH, and the height of the band decreased at alkaline pH with a concomitant shift to 412 mμ. From the figures, it can be concluded that only one hem linked acid group is demonstrable by spectrophotometric analysis between pH 5.35 and 10.45. Thorogood [5,6] has, however, reported the presence of a second porphyrin linked acid group which was titrable spectrophotometrically below pH 7. Thorogood found the isosbestic points of the dissociation in the acid range at 582, 503, and 484 mμ.

Since the changes in light absorption were maximal at 575 mμ, a series of determinations were made at this wave length and at different pH values for both of the two components. By plotting

$$\log \left[\frac{\varepsilon_{acid} - \varepsilon_{obs}}{\varepsilon_{obs} - \varepsilon_{alk}} \right]$$

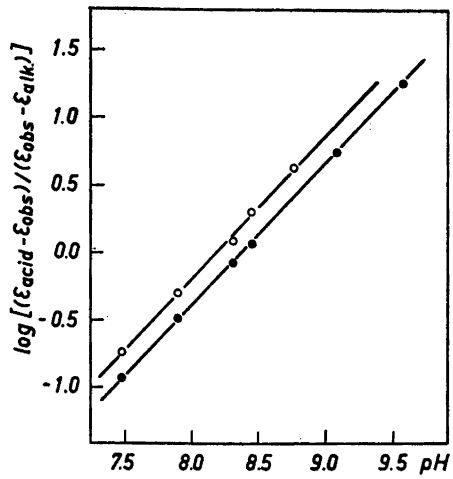

Fig. 3. Graphical determination of the pK-values of the transition from acid to alkaline metLhb's of the two metLhb components at an ionic strength of 0.1 and +20°C. ε_{acid} is the absorption of the total acid forms of the metLhb's when increased acidity caused no further change in absorption, and ε_{alk} the absorption of the total alkaline forms of the metLhb's, when increased alkality caused no further change in absorption, and ε_{obs} the absorption of the metLhb's at different pH values. All solutions contained buffers of ionic strength 0.1; (○) electrophoretically faster component of metLhb, pK = 8.16 (●) electrophoretically slower component of metLhb, pK = 8.34. The slopes of the lines equalled 1.

against pH a straight line was obtained with $n_{H^+} = 1$ (Fig. 3) for the two metLhb components. The equilibrium is illustrated by the equation

$$Lhb^+ \cdot H_2O \rightleftharpoons Lhb \cdot OH + H^+ \qquad (1)$$

The pH values when $[Lhb^+ \cdot H_2O] = [Lhb^+ \cdot OH^-]$, is equal to the p$K$, and was determined to be 8.16 for the electrophoretically faster component of

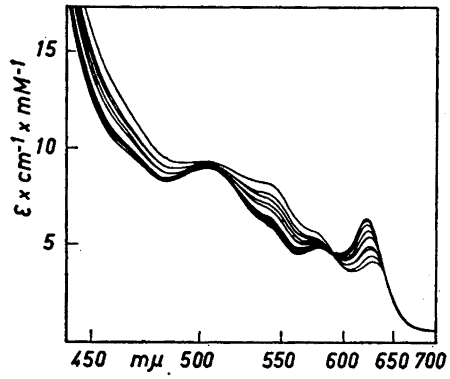

Fig. 4. Absorption spectra in the visible (700—450 mμ) of the electrophoretically faster component of metLhb at pH 5.50 in acetic acid buffers showing the effect of acetate concentration from 0 to 0.16 M at + 20°C.

metLhb and 8.34 for the electrophoretically slower one, both at an ionic strength of 0.1.

The pK values of the separated components agree well with the value of 8.254 determined by Sternberg and Virtanen [4] for the unresolved material. The pK values for the transition from acid to alkaline form of methemoglobins from different sources have values of 8.1—8.6 [10–15], and differ slightly from the values of 8.8—8.9 reported for the myoglobins [16,17].

When an acetic acid buffer is added to a solution of metleghemoglobin, a color change to the green is noticeable [8]. The spectral changes are illustrated in Fig. 4 with the electrophoretically faster component of metLhb in acetate buffers of different concentrations at pH 5.50, a pH where no hem linked groups are spectrophotometrically demonstrable in a phosphate buffer. The metleghemoglobin band at 625 mμ is increased in intensity and shifted to 618 mμ. The curves of the different concentrations of acetate intersect at two isosbestic points, one at 583 mμ and the other one at 500—490 mμ. From these findings it is evident that the acid dissociation reported by Thorogood [5,6] is caused by complex formation between metLhb and the acetate buffer used. Since changes in light absorption were maximal at 555 mμ, a series of determinations at this wavelength were carried out at different acetate concentrations but at constant pH. By plotting

$$\log \left[\frac{\varepsilon_0 - \varepsilon_{obs}}{\varepsilon_{obs} - \varepsilon_\infty} \right]$$ against $-\log$ [acetate], a straight line was obtained

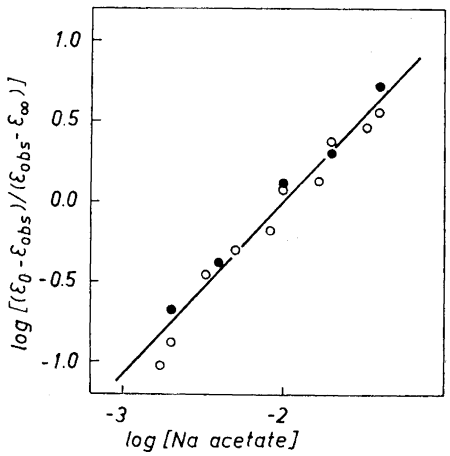

Fig. 5. Graphical determination of the average pK values for the acetate complexes from the absorption at 555 mμ of the two metLhb components in presence at varying concentrations of acetate. ε_0 is the absorption of metLhb in absence of acetate in phosphate buffer at pH 5.50. ε_{obs} is the absorption of metLhb at different concentrations of acetate, shown in the abscissa, and ε_∞ the absorption of metLhb when further addition of acetate did not cause further change in absorption. All solutions had the pH of 5.50 and temperature + 20°C. (●) electrophoretically faster component and (O) electrophoretically slower one; pK = 2.0. The slope of the line equalled 1.

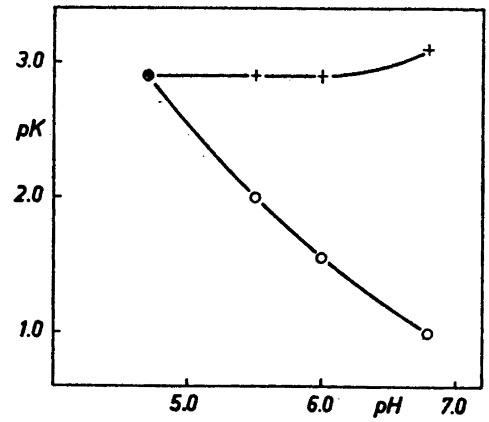

Fig. 6. The pH-dependence curve of the average pK values of the acetate or acetic acid complexes of the two metLhb components. Ordinate: pK value equal to -logarithm of the acetate (O) and acetic acid (+) concentrations, when [Lhb$^+$ acetate$^-$] or [Lhb$^+$ acetic acid] is equal to [Lhb$^+$H$_2$O]. Abscissa: pH.

for the two metLhb components with $n_{acetate} = 1$. This equilibrium is illustrated by the equation

$$Lhb^+ \cdot H_2O + CH_3COO^- \rightleftharpoons Lhb^+ \cdot CH_3COO^- + H_2O \qquad (2)$$

The value for $-\log$ [acetate] when [Lhb$^+$ · acetate$^-$] = [Lhb$^+$ · H$_2$O], is equal to the pK, and was determined to be 2.0 for the two metLhb components at pH 5.50 (Fig. 5).

In order to learn whether the complex involves acetate or undissociated acetic acid, the pH-dependence of the pK was investigated. The ligand concentration was calculated both as acetate and as undissociated acetic acid (Fig. 6). When the pK was calculated from acetate concentration it was found to vary with pH from 4.8 to 7, a region in which no hem-linked dissociation occurs. This behavior is not in accordance with eqn. (2) and is similar to that noted by Agner and Theorell [18] for catalase. On the other hand when the pK was calculated on the basis of undissociated acetic acid concentration it was found to be essentially pH independent. It therefore can be assumed that the formation of the complex below pH 7 involves the undissociated acetic acid molecule according to the following reaction:

$$Lhb^+ \cdot H_2O + CH_3COOH \rightleftharpoons Lhb^+ \cdot CH_3COOH + H_2O \qquad (3)$$

Several other fatty acids were examined for their ability to form complexes with both metLhb components. The experiments were conducted at pH 4.8, which is close to the pK_a values for the fatty acids studied. At this pH, the apparent pK calculated for the complex is the same whether one assumes that it is the fatty acid or the fatty acid anion, which is involved in the complex. The spectra of the acetate, propionate, butyrate and valerate complexes were

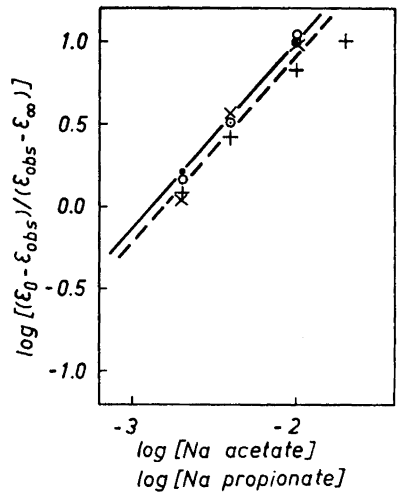

Fig. 7. Graphical determination of the average pK values of acetate and propionate complexes of the two metLhb components at pH 4.8 and + 20°C. The determinations were performed in a similar way as in Fig. 5 Acetate complex: electrophoretically faster component (●), electrophoretically slower component (○). The average pK value was 2.9 for the two components.
Propionate complex: electrophoretically faster component (×), electrophoretically slower component (+). The average pK value was 2.8 for the two components. In both cases the slopes of the lines equalled 1.

all similar (Fig. 5). The isosbestic points for these complexes were the same as those found for the acetate complex. By plotting

$$\log \left[\frac{\varepsilon_0 - \varepsilon_{obs}}{\varepsilon_{obs} - \varepsilon_\infty} \right] \textit{ versus } -\log [\text{ligand}]$$

at pH 4.8, a straight line was obtained (Figs 7 and 8). In all cases, the number of ligand groups involved in the complex was one. The average pK values for complexes with both of the Lhb components was 2.9 for the acetate complex, 2.8 for the propionate, 2.4 for the butyrate, and 2.6 for the valerate complexes.

As a comparison, horse myoglobin I was examined for its ability to form complexes with the fatty acids used above. No complex formation was observed under identical conditions of pH and concentrations.

DISCUSSION

In the trivalent state, the iron in hemoglobin as well as in myoglobin is able to combine with certain compounds, mainly anions. The compounds formed, are assumed to be complexes with the ferric iron. The iron in the center of the prophyrin nucleus has its six co-ordination valences occupied. Four of the valences lie in one plane, and link the iron atom to the nitrogen atoms of the pyrrol nuclei of the porphyrin. The remaining two valences, the fifth and sixth, are perpendicular to each side of the flat hem molecule and are pro-

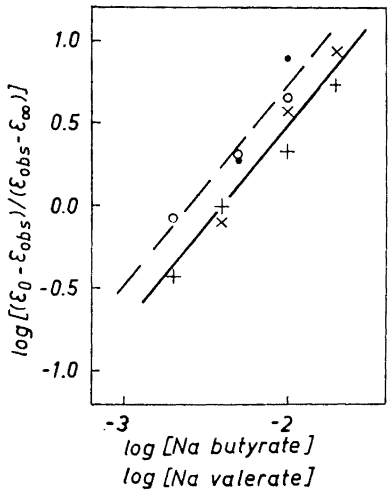

Fig. 8. Graphical determinations of the average pK-values of butyrate and valerate complexes of the two metLhb components at pH 4.8 and 20°C. The determinations were performed as described in Fig. 5. Butyrate complex: electrophoretically faster component (+), electrophoretically slower component (×). The average pK value was 2.4 for the two components. Valerate complex: electrophoretically faster component (O), electrophoretically slower component (•). The average pK value was 2.6 for the two components. In both cases the slopes of the lines equalled 1.

bably linked to an imidazole [19–23] moiety of a histidine residue of the protein molecule (position 5), and to a water molecule [22–25] (position 6).

At alkaline pH, a proton is dissociated from the water molecule (position 6) leaving the hydroxyl group bond to the iron. The dissociation of the water proton in the hemoglobins is found to occur within very narrow pH limits. The corresponding pK values for the fast and slow components of metLhb are very similar to these pK values, thereby indicating that the hem bound groups in hemoglobin and leghemoglobin probably are identical. The small differences between the pK's of the two main components is not necessarily an indication of differences in the hem bound group, but more probably reflect small differences in the protein structure close to the hemin ring, since amino acid analyses of the two main components do show small differences in their amino acid composition [26].

As to the position of the hemin ring in hemoglobin, St. George and Pauling [27] assumed it to lie within a fold or crevice of the globin. This assumption was based on the fact that hemoglobin combines more strongly with ethyl*iso*cyanide than with *tert*-butyl*iso*cyanide corresponding to a factor of 200 in equilibrium constants. Keilin [28] disagreed with this theory and proposed that the hem is situated on the surface of the globin. Recently, Lein and Pauling [29] arrived at the conclusion that the hem in myoglobin is also buried within the protein molecule. Strong additional support in favor of the view that the hem is buried within a fold of the peptide chains was obtained from X-ray analyses of crystals of hemoglobin [22] and myoglobin [23].

The experiments carried out in this study on the combination of different fatty acids with metleghemoglobin provide support for a picture of leghemoglobin which differs from that of myoglobin. Acetic, propionic, butyric and valeric acids combine almost equally tightly with metleghemoglobin, but at the same concentrations do not combine with myoglobin. It is evident, therefore, that the hem in leghemoglobin is much more accessible to ligands than

the hem in myoglobin, and forms equally strong complexes with fatty acids regardless of the size of the groups attached to the fatty acid carboxyl.

Although it has been well known that hemoglobin and myoglobin combine reversibly with molecular oxygen, it appears that no satisfactory explanation has yet been proposed to account for the remarkable property of combining reversibly with molecular oxygen, while at the same time protecting its divalent iron from oxidation. The mere formation of a co-ordination bond between a donor group of globin and the ferrous iron in hem is clearly inadequate to prevent the irreversible oxidation of the latter by molecular oxygen.

Wang *et al.*[30] have recently put forward a plausible theory which explains how the globin acts in order to let the hem combine reversibly with molecular oxygen. It is assumed that the hemin groups in hemoglobin and myoglobin are not completely exposed to water because of the low dielectric environment of the individual binding sites in the protein. Hydrophobic groups of the globin cover them at least partially. As a result, the average dielectric constant of the local environment of each binding site is much lower than that of freely exposed hem. This effectively retards the irreversible oxidation process without interferring with the reversible binding and release of molecular oxygen. Wang [31] has devised a synthetic model of hemoglobin to substantiate the picture of the binding sites. A film was prepared with a derivative of hem, 1-(2-phenylethyl)-imidazole carbonmonoxy hem diethylester, imbedded in a matrix of an amorphous mixture of polystyrene and 1-(2-phenylethyl)-imidazole. After a complete removal of the bound carbon monoxide by flushing with nitrogen, the film was exposed to air. A rapid combination with oxygen occurred, giving a product which displayed an oxyhemoglobin type of spectrum. The oxygenation was found to be reversible because oxygen was again removed by flushing the film with nitrogen. This cycle could be carried out repeatedly. Another film, in which the diethyl ester derivative of the hem was replaced with free hem, was immediately oxidized to the ferric state after exposure to air. This seemed to suggest that in contrast to the ester, free hems are not imbedded in the hydrophobic matrix but are quite exposed. The theory of Wang for the basis of oxygenation of hemoglobin and myoglobin is in good agreement with the concept of the imbedded position of the hem group as proposed by Pauling.

The strong autooxidizability of leghemoglobin may be explained satisfactorily by the uncovered position of the hem ring in a similar way as in Wang's model when the free hem on the surface of the polystyrene film was irreversibly oxidized but not oxygenated.

It has been established that the capacity of the leguminous root nodules to fix atmospheric nitrogen is parallel to the concentration of the hem proteins found in the nodules [32,33]. The action of leghemoglobin may be due to its ability to store oxygen and thereby promote the respiration of the nodule bacteria. However, the properties of Lhb make it less suited to function as an oxygen carrier only. Other functions for leghemoglobin have also been proposed. Hamilton *et al.*[34] reported recently an oxidation of leghemoglobin to metleghemoglobin when an extract of soybean root nodules had been exposed to nitrogen gas. The opposite reaction was observed with hydrogen gas.

Leghemoglobin was therefore suggested to act as an oxidoreduction catalyst in the symbiotic nitrogen fixation.

Bauer and Mortimer [35-37] recently proposed that the secondary attachment of N_2 to the hem group in Lhb is the first step in the symbiotic N_2-fixation. This hypothesis was based on the fact that a small amount of N_2 can be taken up by Lhb. This confirms the observation of van Slyke *et al.*[38] that oxygenated Hb takes up N_2 to a small extent.

Acknowledgements. The author wishes to express his thanks to Professor Hugo Theorell for encouraging interest in the work and to Mr. Å. Åkeson for a sample of myoglobin I. The investigation has been supported by a grant from the *Finnish State Commission of Natural Sciences* (*Statens Naturvetenskapliga Kommission i Finland*) which is gratefully acknowledged.

REFERENCES

1. Kubo, H. *Acta Phytochim. (Japan)* **11** (1939) 195.
2. Keilin, D. and Wang, Y. L. *Nature* **155** (1945) 227.
3. Little, H. N. and Burris, R. H. *J. Am. Chem. Soc.* **69** (1947) 838.
4. Sternberg, H. and Virtanen, A. I. *Acta Chem. Scand.* **6** (1952) 1342.
5. Thorogood, E. *Chromoproteins from Soy bean Nodules.* Diss. University of Pennsylvania, Philadelphia, 1955.
6. Thorogood, E. *Science* **126** (1957) 1011.
7. Ellfolk, N. *Acta Chem. Scand.* **13** (1959) 596.
8. Ellfolk, N. *Acta Chem. Scand.* **14** (1960) 609.
9. Åkeson, Å. and Theorell, H. *Arch. Biochem. Biophys.* **91** (1960) 319.
10. Austin, J. H. and Dabkin, D. L. *J. Biol. Chem.* **112** (1935) 67.
11. Coryell, C. D., Stitt, F. and Pauling, L. *J. Am. Chem. Soc* **59** (1937) 633.
13. Theorell, H. *Arkiv Kemi, Mineral Geol.* **A16** (1943) No. 14.
14. George, P. and Hanania, G. *Biochem. J.* **55** (1953) 236.
15. Havemann, R. and Mahling, A. *Z. physik. Chem.* **204** (1955) 60.
16. Theorell, H. and Ehrenberg, A. *Acta Chem. Scand.* **5** (1951) 823.
17. George, P. and Hanania, G. *Biochem. J.* **52** (1952) 517.
18. Agner, K. and Theorell, H. *Arch. Biochem.* **10** (1946) 321.
19. Wyman, J. *Advances in Protein Chem.* **4** (1948) 407.
20. Coryell, C. D. and Pauling, L. *J. Biol. Chem.* **132** (1940) 769.
21. Keilin, J. *Nature* **187** (1960) 365.
22. Perutz, M. F., Rossmann, M. G., Cullis, A. F., Muirhead, H., Will, G. and North, A. C. T. *Nature* **185** (1960) 416.
23. Kendrew, J. C., Dickerson, R. E., Strandberg, B. E., Hart, R. G., Davies, D. R., Philips, D. C. and Shore, V. C. *Nature* **185** (1960) 422.
24. Haurowitz, F. *J. Biol. Chem.* **193** (1951) 443.
25. Keilin, D. and Hartree, E. F. *Nature* **170** (1952) 161.
26. Ellfolk, N. *Acta Chem. Scand.* **15** (1961) 545.
27. St. George, R. C. C. and Pauling, L. *Science* **114** (1951) 629.
28. Keilin, D. *Nature* **171** (1953) 922.
29. Lein, A. and Pauling, L. *Proc. Natl. Acad. Sci. U.S.* **42** (1956) 51.
30. Wang, J. H., Nakahara, A. and Fleischer, E. B. *J. Am. Chem. Soc.* **80** (1958) 1109.
31. Wang, J. H. *J. Am. Chem. Soc.* **80** (1958) 3168.
32. Virtanen, A. I., Jorma, J., Linkola, H. and Linnasalmi, A. *Acta Chem. Scand.* **1** (1947) 90.
33. Virtanen, A. I., Erkama, J. and Linkola, H. *Acta Chem. Scand.* **1** (1947) 861.
34. Hamilton, P. B., Shug, A. L. and Wilson, P. W. *Proc. Natl. Acad. Sci. U.S.* **43** (1957) 297.
35. Mortimer, R. G. and Bauer, N. *J. Phys. Chem.* **64** (1960) 387.
36. Bauer, N. and Mortimer, R. G. *Biochim. et Biophys. Acta* **40** (1960) 170.
37. Bauer, N. *Nature* **188** (1960) 471.
38. van Slyke, D. D., Dillon, R. T. and Margaria, R. *J. Biol. Chem.* **105** (1934) 571.

Received December 23, 1960.

ACTA CHEMICA SCANDINAVICA 15 (1961) 985–990

A Method for Distinguishing between Inter- and Intramolecular Hydrogen Bonding

BJÖRN ÅKERMARK

Organisk-kemiska Institutionen, Kungl. Tekniska Högskolan, Stockholm, Sweden

A method has been investigated for distinguishing between inter- and intramolecular hydrogen bonding in hydroxy-carbonyl compounds with the aid of infra-red measurements. It is based on the fact that compounds containing intermolecular hydrogen bonds exhibit considerably higher carbonyl frequencies in dioxan solution than in the pure state and that compounds capable of intramolecular hydrogen bonding show only small differences. This method has been applied to pannaric acid, giving support for the structure previously proposed. The infra-red results were also confirmed by ultraviolet absorption data.

During studies on the lichen constituents pannaric acid [1] and calycin [2] it became desirable to determine the type of hydrogen bonding present in these compounds.

It is sometimes difficult to decide if a compound contains intramolecular hydrogen bonds or whether hydrogen bonds are formed between neighbouring molecules.

A common method is to study the stretching frequency of a hydrogen bonded hydroxy or amino group at various concentrations in an inert solvent such as carbon tetrachloride. In a similar way the shift in the nuclear magnetic resonance of a hydrogen bonded proton can be investigated. However, the type of hydrogen bonding in compounds, which are only slightly soluble in carbon tetrachloride, for example pannaric acid and calycin, cannot be determined with these methods. For compounds containing hydrogen bonded carbonyl groups a simple infra-red method has been developed using dioxan as solvent.

Dioxan and similar solvents form complexes with hydroxy groups [3–8], effectively disrupting even strong intermolecular hydrogen bonds. Compounds containing such bonds should thus exhibit considerably higher carbonyl stretching frequencies in dioxan solution than in the pure state. Strong intramolecular hydrogen bonds, on the other hand, are almost unaffected by dioxan (*cf.* Ref.[9]). Compounds forming intramolecular hydrogen bonds there-

Table 1. Infra-red carbonyl absorption of hydrogen bonded compounds in the pure state and in solution.

Compound		ν_{CO} (pure compound)	ν_{CO} (solution)	Shift cm^{-1}
o-Hydroxybenzaldehyde	(ch)	1 662 [c]	1 665 [d]	3
p-Hydroxybenzaldehyde	(i)	1 665 [a]	1 688 [d]	23
		1 670 [b]		18
o-Hydroxyacetophenone	(ch)	1 640 [c]	1 640 [d] (1 640 [e])	0 (0)
p-Hydroxyacetophenone	(i)	1 658 [a]	1 678 [d] (1 672 [e])	20 (14)
		1 663 [b]		15
Methyl *o*-hydroxybenzoate	(ch)	1 675 [c]	1 677 [d] (1 675 [e])	2 (0)
Methyl *p*-hydroxybenzoate	(i)	1 680 [a]	1 720 [d] (1 710 [e])	40 (30)
		1 682 [b]		38
2-Hydroxy-1-naphtaldehyde	(ch)	1 635 [a]	1 645 [d]	10
		* 1 637 [b]		8
Acetylacetone	(ch)	** 1 616 [c]	1 617 [d]	1
Dimedone	(i)	‡ 1 618—1 610 [a]	1 655 [d]	41 (av)
		‡ 1 615 [b]		40
Salicylic acid	(ch)	‡‡ 1 665 [a]	1 680 [d] (1 675 [e])	15 (10)
p-Hydroxybenzoic acid	(i)	‡‡ 1 687 [a]	1 718 [d] (1 707 [e])	31 (20)
Pannaric acid (I)	(ch)	1 662 [a]	1 658 [e]	−4
	(i)	1 690 [a]	1 710 [e]	20
Dimethyl pannarate (II)	(ch)	1 657 [a]	1 660 [e]	3
	(i)	1 688 [a]	1 715 [e]	27

Infra-red absorption in KBr (a), in nujol (b), as liquid (c), in dioxan (d) and in THF (e). i = intermolecular hydrogen bonding; ch = chelation; av = average; * Ref.[19] ** Ref.[20] ‡ Ref.[21] ‡‡ Ref.[22]

fore show approximately the same carbonyl frequency in dioxan solution and in the pure state. It should thus be possible to establish the type of hydrogen bonding by measuring the carbonyl frequencies of a compound in the pure state and in dioxan solution. To test this, a number of simple compounds capable of either inter-or intramolecular hydrogen bonding were investigated.

The infra-red measurements on pure solid compounds were done in potassium bromide discs or nujol mulls. Different results are sometimes obtained with these two techniques but in our case only small differences were observed (Table 1).

INFRA-RED ABSORPTION MEASUREMENTS

The results of the measurements are listed in Table 1. As expected, compounds containing only intermolecular hydrogen bonds showed considerably higher carbonyl frequencies in dioxan solution than in the pure state. The difference varied from 20 cm^{-1} for *p*-hydroxyacetophenone to 41 cm^{-1} for dimedone. The intramolecularly hydrogen bonded compounds behaved quite differently, showing comparatively small shifts (0—10 cm^{-1}). The only exception was salicylic acid which exhibited a shift of 15 cm^{-1}. This is probably due to the fact that the carboxyl group in salicylic acid can take part in both inter- and intramolecular hydrogen bonding as indicated by X-ray data [10]. Methyl salicylate behaved normally (Table 1). It might thus be advisable to esterify carboxyl groups prior to measurements.

In some cases, the more polar tetrahydrofuran (THF) was used as solvent in place of dioxan. The difference between the carbonyl frequency of the compound in the pure state and in solution was then decreased. *p*-Hydroxyacetophenone and *p*-hydroxybenzoic acid, for example, showed shifts of 14 and 20 cm^{-1} respectively. However, inter- and intramolecular hydrogen bonding could still be distinguished since for *o*-hydroxyacetophenone no shift was observed and for salicylic acid a shift of 10 cm^{-1} only.

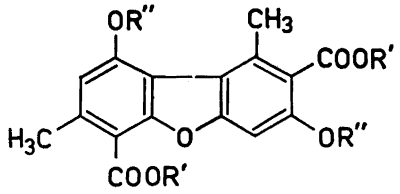

I R'=R''=H
II R'=CH_3, R''=H
III R'=R''=CH_3

Pannaric acid which has been assigned structure (I) was also investigated. THF was used as solvent since both pannaric acid and its dimethyl ester were only slightly soluble in dioxan. In the pure state, pannaric acid and dimethyl pannarate showed two overlapping carbonyl bands. In THF one band was considerably shifted to a higher frequency (Table 1). Pannaric acid must therefore contain one inter- and one intramolecularly hydrogen bonded carbonyl group in agreement with the proposed structure (I).

ULTRAVIOLET ABSORPTION MEASUREMENTS

An attempt was also made to correlate infra-red and ultraviolet absorption data.

Table 2. Ultraviolet absorption of hydrogen bonded compounds and their methyl ethers.

Compound		UV absorption in dioxan	UV absorption of O-methyl derivative in dioxan	Shift on methylation (mμ)
o-Hydroxybenzaldehyde	(ch)	325	313	−12
p-Hydroxybenzaldehyde	(i)	269	270	+ 1
o-Hydroxyacetophenone	(ch)	322	301	−21
p-Hydroxyacetophenone	(i)	265	266	+ 1
Methyl *o*-hydroxybenzoate	(ch)	306	292	−14
Methyl *p*-hydroxybenzoate	(i)	252	253, 255	+ 2 (av)
Methyl 3-hydroxy-2-naphtoate	(ch)	* 366	* 338	−28
Acetylacetone	(ch)	273	251	−22
Dimedone	(i)	** 244	243	− 1
Dimethyl pannarate	(ch)	335 (sh)	299	−36
	(i)	302 (sh)	299	− 3

i, ch, av, see Table 1. sh = shoulder. * Ref.[23] ** Ref.[21]

The type of hydrogen bonding in a phenolic compound can often be determined by measuring the difference in wavelength between corresponding ultraviolet absorption peaks in the compound and its O-methyl derivative A red-shift on methylation indicates intermolecular hydrogen bonding, whereas a blue-shift is observed for compounds which form intramolecular hydrogen bonds [11–13]. These measurements have generally been made in non-polar solvents which are often unsuitable for hydroxyl compounds (*cf.* however Refs. [13,23]). Dimedone, for example, has been shown to exist almost exclusively in the diketo form in carbon tetrachloride [14]. In our measurements dioxan was therefore used as solvent.

The results of the measurements are shown in Table 2. The closest correlation between the type of hydrogen bonding and the wavelength shift on methylation was found for the strong absorption ($\varepsilon > 10^3$) which appeared at 250–325 mμ in the simple phenolic compounds investigated. Only these shifts are therefore listed.

Both hydrogen bonding with dioxan and methylation of a hydroxyl group which is part of a chromophoric system, seem to have similar effects on the ultraviolet absorption of this system. Thus in dioxan solution compounds containing intermolecular hydrogen bonding showed absorption maxima at approximately the same wavelength as the corresponding methyl ethers. Since strong intramolecular hydrogen bonds, on the other hand, are unaffected by dioxan, the chelates investigated exhibited large blue-shifts on methylation ($\geq$ 14 mμ).

The measurements were also extended to dimethyl pannarate (Table 2) but the conclusions are somewhat uncertain owing to the complexity of the absorption spectrum in the relevant region.

Although the interpretation may be difficult, ultraviolet absorption data can undoubtedly often be used to support the results from infra-red measurements.

Table 3. Infra-red carbonyl absorption of non hydrogen bonded compounds in the pure state and in solution.

Compound	ν_{CO} (pure)	ν_{CO} (dioxan solution)	Shift cm^{-1}
o-Methoxybenzaldehyde	1 685 [c]	1 690	5
p-Methoxybenzaldehyde	1 685 [c]	1 675	−10
o-Methoxyacetophenone	1 675 [c]	1 665	−10
p-Methoxyacetophenone	1 677 [a]	1 682	5
Methyl *o*-methoxybenzoate	1 720 [c]	1 730	10
Methyl *p*-methoxybenzoate	1 710 [a]	1 717	7
Benzophenone	1 655 [a]	1 662	7
Anthraquinone	1 677 [a]	1 677	0
Fluorenone	1 710 [a]	1 720	10
Permethyl pannarate (III)	1 722 [a]	1 727	5

a, c, i, ch, see Table 1.

CONCLUSIONS

The close dependence of the hydroxyl stretching frequency on both the O—H distance of the hydrogen bonded group and on the O—O distance of the O—H...O bond has been demonstrated [15]. In both solid and liquid compounds the shift in hydroxyl frequency on hydrogen bonding and the strength of the bond are also closely related [16]. Although the changes in carbonyl frequency are generally smaller, they show the same trend as the shifts in hydroxyl frequency [17]. It therefore seems probable that other intermolecular effects are negligible in comparison with strong hydrogen bonding. For some carbonyl compounds containing no hydroxyl groups, the difference in carbonyl frequency in the pure state and in solution was generally small (Table 3; *cf.* also Ref.[18]).

The comparison between the carbonyl frequencies of a hydroxy-carbonyl compound in pure liquid or solid state and in dioxan solution thus offers a simple method for distinguishing between strong inter- and intramolecular hydrogen bonds. It seems likely that a similar method can be applied also to other hydrogen bonded systems.

EXPERIMENTAL

Melting points were determined on a Kofler micro hot stage. Infra-red measurements were done on a Perkin-Elmer spectrophotometer Nr 21, fitted with a sodium chloride prism. The absorption of the solvent was compensated. Solids were investigated in potassium bromide discs or in nujol mull and oils as liquid films. The concentration of the solutions measured varied between 0.2 and 0.05 M depending on the solubility. Spectra were taken in a 0.1 mm cell.

Ultraviolet absorption spectra were recorded with a Beckman DK-2 spectrophotometer.

Dioxan was purified according to Hess *et al.*[24] THF was refluxed 96 h with sodium wire prior to distillation. No carbonyl absorption was detected in the pure solvents.

The materials used were generally commercial samples, purefied to the literature constants.

o-Methoxyacetophenone (b.p.$_{20}$ 131—132°) and methyl *o*-methoxybenzoate (b.p.$_{13}$ 127°) were prepared from *o*-hydroxyacetophenone and methyl salicylate, respectively, by methylation (dimethyl sulfate and potassium carbonate in acetone).

Acknowledgements. The author would like to thank Professor H. Erdtman for his encouragement and kind interest in this work. Thanks are also due to Miss G. Hammarberg and Mr. E. Pettersson for infra-red and ultraviolet absorption measurements and to Dr. I. Wellings for checking the English.

Financial support from *Statens Tekniska Forskningsråd* is gratefully acknowledged.

REFERENCES

1. Åkermark, B., Erdtman, H. and Wachtmeister, C. A. *Acta Chem. Scand.* **13** (1959) 1885.
2. Åkermark, B. *To be published in Acta Chem. Scand.*
3. Lindberg, J. J. *Soc. Sci. Fennica Commentationes Phys. Math.* **20** (1957) 3.
4. Flett, M. St. C. *J. Soc. Dyers Colourists* **68** (1952) 59.
5. Nagakura, S. and Baba, H. *J. Am. Chem. Soc.* **74** (1952) 5693.
6. Nagakura, S. *J. Chem. Soc. Japan, Pure Chem. Sect.* **74** (1953) 153.
7. Tsuboi, M. *J. Chem. Soc. Japan, Pure Chem. Sect.* **72** (1951) 146.

8. Searles, S. and Tamres, M. *J. Am. Chem. Soc.* **73** (1951) 3704.
9. Bellamy, L. J. and Hallam, H. E. *Trans. Faraday Soc.* **55** (1959) 220.
10. Cochran, W. *Acta Cryst.* **6** (1953) 260.
11. Lippert, E. in Hadzi (ed.) *Hydrogen Bonding*, Pergamon, London 1959, p. 217.
12. Burawoy, A. *Ibid.* p. 259.
13. Dearden, J. C. and Forbes, W. F. *Can. J. Chem.* **38** (1960) 1837.
14. Angell, C. L. and Werner, R. L. *Austr. J. Chem.* **6** (1953) 294.
15. Pimentel, G. C. and McClellan, A. L. *The Hydrogen Bond*, Freeman, San Francisco 1960, p. 85.
16. *Idem, Ibid.* p. 82.
17. *Idem, Ibid.* p. 136.
18. Bellamy, L. J. and Williams, R. L. *Trans. Faraday Soc.* **55** (1959) 14.
19. Hunsberger, I. M. *J. Am. Chem. Soc.* **72** (1950) 5626.
20. Landolt-Börnstein, 6 Aufl. Band I, 2. Berlin 1951, p. 427.
21. Tamm, C. H. and Albrecht, R. *Helv. Chim. Acta* **43** (1960) 68.
22. Flett, M. St. C. *J. Chem. Soc.* **1948** 1441.
23. Bergman, E. D., Hirshberg, Y. and Pinchas, S. *J. Chem. Soc.* **1950** 2351.
24. Hess, K. and Frahm, H. *Ber.* **71** (1938) 2627.

Received January 10, 1961.

ACTA CHEMICA SCANDINAVICA 15 (1961) 991–1002

On the Constitution of the Products Formed in the Reaction between 5-Aminotetrazole and Arenesulfonyl Chlorides

KAI ARNE JENSEN and CHRISTIAN PEDERSEN

Chemical Laboratory of the University of Copenhagen, Copenhagen, Denmark

The primary reaction products of acetylsulfanilyl chloride, *p*-toluenesulfonyl chloride, and other arenesulfonyl chlorides with 5-aminotetrazole have been shown to be arenesulfonylguanyl azides and not 5-sulfonamidotetrazoles. Under the influence of strong bases the sulfonylguanyl azides are rearranged to the isomeric 5-sulfonamidotetrazoles.

Three isomeric *p*-toluenesulfonylaminoguanidines have been prepared. 1-*p*-Toluenesulfonyl-3-aminoguanidine forms with nitrous acid an azide identical with the product of the reaction between *p*-toluenesulfonyl chloride and 5-aminotetrazole in pyridine. 1-Methyl-5-aminotetrazole does not react with *p*-toluenesulfonyl chloride, indicating that the point of attack of the sulfonyl chloride on 5-aminotetrazole is not the amino group, but the NH-group in the ring.

In 1941–1942 three compounds (A, B, and C) with the composition of an acetylsulfanilylaminotetrazole were described:

Compound A was obtained by Jensen [1] and by Tappi [2] by the reaction of 5-aminotetrazole with *p*-acetamidobenzenesulfonyl chloride in pyridine solution.

Compound B was obtained by Veldstra and Wiardi [3] by carrying out the condensation between 5-aminotetrazole and *p*-acetamidobenzenesulfonyl chloride in aqueous sodium carbonate solution.

Compound C was obtained by Tappi [2] and by Veldstra and Wiardi [4] by dissolution of compound A in 0.1 N sodium hydroxide and precipitation by acidification.

The mixed melting point of compounds B and C showed no depression, and only very small differences in crystal form and titration curves were noted, but Veldstra and Wiardi nevertheless considered the products to be different compounds. It should, however, be pointed out at once that we have found that compound A is the primary product also when the reaction is carried out in sodium carbonate solution; only by treatment with sodium

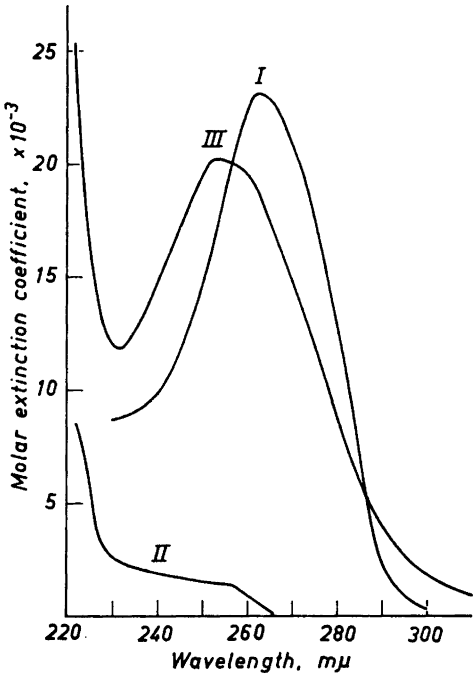

Fig. 1. Absorption spectra of *p*-acetamidobenzenesulfonylguanyl azide in methanol (I), 0.1 N methanolic HCl (II), and 0.1 N methanolic KOH (III).

hydroxide, which was used by Veldstra and Wiardi for purification, is it transformed into the higher melting compound. There is therefore no reason to assume that compounds B and C should be different, and actually we have found the infrared spectra of the two products to be completely identical. It may therefore be concluded that we need only consider the constitution of two compounds, A and B = C.

Jensen [1] found that alkaline hydrolysis of compound A resulted in a complete breakdown of the molecule with the formation of hydrazoic acid, HN_3. Mainly on this evidence the compound was formulated as the true 5-(acetylsulfanilamido)tetrazole (I; R = *p*-$CH_3CONHC_6H_4$), because from experience with other heterocyclic sulfanilyl derivatives it might be expected that a compound with the sulfanilyl group bound to one of the nitrogen atoms in the ring would easily hydrolyse into sulfanilic acid and 5-aminotetrazole, which is not transformed further under the conditions of the experiment.

Jensen and Hansen [5] formulated compound B as 1-acetylsulfanilyl-5-aminotetrazole (II), but Veldstra and Wiardi [4] adduced convincing evidence that their compound B was actually 5-(acetylsulfanilamido)tetrazole. In electrometric titrations this compound behaves as a dibasic acid, which is only compatible with formula I, the acidic groupings being $-SO_2NH-$ and $-NH-$ in the tetrazole ring.

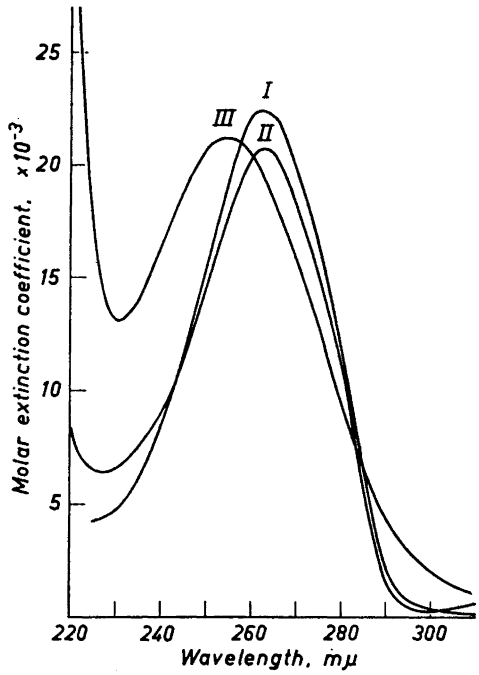

Fig. 2. Absorption spectra of 5-(*p*-acetamidobenzenesulfonamido)tetrazole in methanol (I), 0.1 N methanolic HCl (II), and 0.1 N methanolic KOH (III).

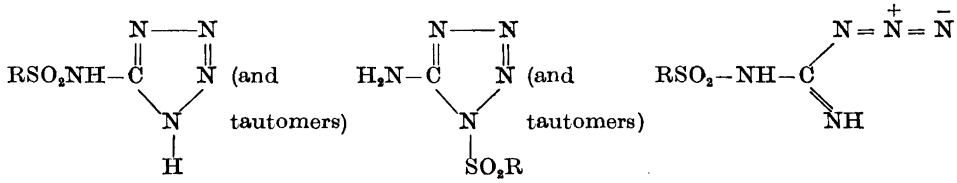

I II III

In 1952 Jensen and Hansen [6] showed that compound A could also be prepared from acetylsulfanilylaminoguanidine and nitrous acid. Although the compound was still tentatively formulated as 5-acetylsulfanilamidotetrazole, it was announced that a closer examination of the isomeric compounds was in progress. This soon led us to the conclusion that compound A is actually an azide (III). These experiments were mainly carried out with *p*-toluenesulfonyl derivatives instead of the acetylsulfanilyl derivatives because the latter are more difficult to purify and have poorly defined melting points.

The conclusion that the product formed from 5-aminotetrazole and sulfonyl chlorides in pyridine solution are sulfonylguanyl azides is based on the following arguments: 1) The infrared spectra of these compounds show the characteristic absorption band at 4.67 μ characteristic of the azide group. 2) The

compounds are formed from guanyl hydrazides and nitrous acid. 3) Their properties are those characteristic of azides; especially, they may be hydrolysed to give hydrazoic acid or reduced by hydrogen sulfide or catalytically to give sulfonylguanidines. The reducibility by hydrogen sulfide is a common property of guanylazides [7]. The substances formed from the azides by treatment with bases have quite different properties: They can neither be hydrolysed nor reduced, and in contrast to the azides they form slightly soluble silver salts, a characteristic property of tetrazoles which are unsubstituted in the 1-position. They are weak acids without basic properties, whereas the azides are weak bases without acid properties, as shown by the change of the ultraviolet spectra by addition of hydrochloric acid or potassium hydroxide (Figs. 1 and 2). A comparison of the properties of the azides and tetrazoles is shown in Table 1.

These results show that compounds obtained by condensation of 5-aminotetrazole with sulfonyl chlorides in pyridine are sulfonylguanyl azides and not sulfonylaminotetrazoles. This does not only apply to the acetylsulfanilyl derivative, but also to a *p*-toluenesulfonyl derivative prepared by Dahlbom and Ekstrand [8] and to a *p*-nitrobenzenesulfonyl derivative prepared by Roblin *et al.*[9], who by catalytic hydrogenation of their product obtained sulfanilylguanidine instead of the expected sulfatetrazole. We have now shown that in both cases are the true 5-sulfonamidotetrazoles obtained by treatment of the azide with sodium hydroxide. We have further studied the reaction between β-napthalenesulfonyl chloride and 5-aminotetrazole in pyridine. Also in this case the primary product is the azide, which by treatment with sodium hydroxide is rearranged to the isomeric tetrazole. We encountered, however, difficulties in obtaining analytically pure preparations, and therefore the naphthalenesulfonyl derivatives were not investigated further.

Table 1.

Azides (III)	*Tetrazoles (I)*
1. Formed as primary products from 5-aminotetrazole and sulfonyl chlorides or from aminoguanidines and nitrous acid.	1. Formed by rearrangement of the azides by means of bases, therefore also by the reaction of 5-aminotetrazole with sulfonyl chlorides in the presence of strong bases.
2. Have basic properties and are dissolved in strong acids with salt formation (titration, UV-spectra), but are transformed into tetrazoles by bases.	2. Have no basic properties (insoluble in aqueous acids, UV-spectra of an alcoholic solution not changed by addition of hydrochloric acid).
3. No precipitate with Ag^+.	3. White precipitate with Ag^+.
4. Form sulfonylguanidines on catalytic hydrogenation.	4. Unchanged by catalytic hydrogenation.
5. Reduced by hydrogen sulfide to sulfonylguanidines with precipitation of sulfur.	5. Not reduced by hydrogen sulfide.
6. Concentrated hydrochloric acid slowly splits off the sulfonyl group with the formation of a sulfonyl chloride or sulfonic acid.	6. Not changed on standing with concentrated hydrochloric acid.
7. Hydrazoic acid is formed by hydrolysis with a strong base.	7. Unchanged by boiling with a strong base.

The compound 1-acetylsulfanilyl-3-aminoguanidine, which forms acetylsulfanilylguanyl azide on reaction with nitrous acid, has been prepared in several different ways [6,10,11]. We have prepared the corresponding 1-*p*-toluenesulfonyl-3-aminoguanidine in the following unambiguous way:

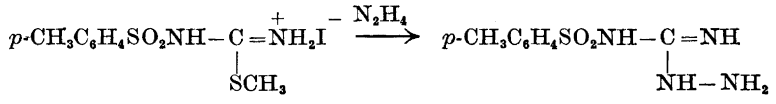

IV

With nitrous acid this hydrazide gives *p*-toluenesulfonylguanyl azide identical with the product of the reaction between *p*-toluenesulfonyl chloride and 5-aminotetrazole in pyridine solution.

Greer *et al.*[11] have prepared the three possible structural isomers of sulfanilylaminoguanidine. Similarly, three structural isomers of *p*-toluenesulfonylaminoguanidine are possible, *viz.* in addition to the above-mentioned isomer, IV, the following two:

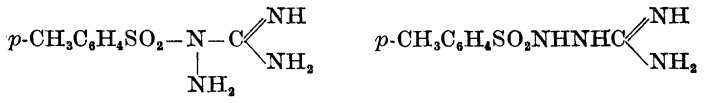

V VI

The isomer V was prepared from nitroguanidine in a way analogous to that in which Greer *et al.* prepared the corresponding sulfanilylaminoguanidine;

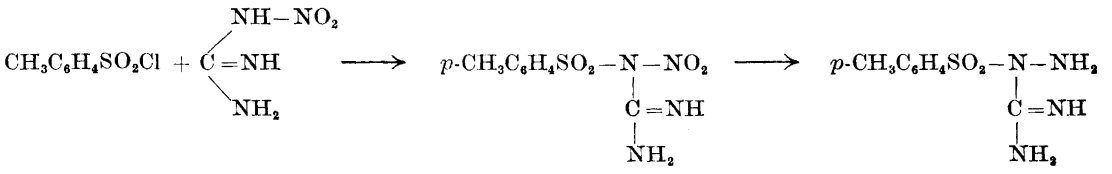

VII V

This isomer reacts with nitrous acid with formation of *p*-toluenesulfonylguanidine:

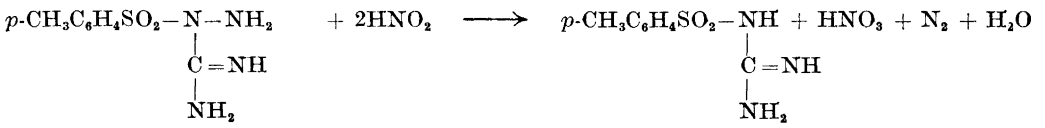

The third isomer, VI, was obtained by sulfonylation of aminoguanidine in aqueous solution at pH 6, *i.e.* by sulfonylation of the aminoguanidinium ion:

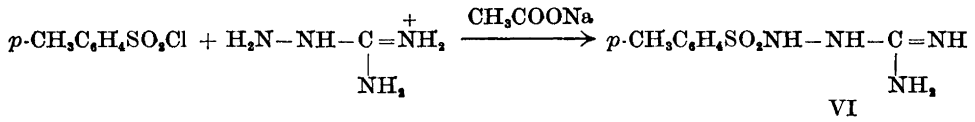

VI

The *p*-toluenesulfonylaminoguanidine is a much weaker base than aminoguanidine and is mainly present in the uncharged state at pH 6; it crystallises from the solution on cooling.

From the reaction between *p*-toluenesulfonyl chloride and aminoguanidine in pyridine solution, or in aqueous solution with the addition of sodium carbonate, we did not succeed in obtaining a pure substance. Analyses indicated that the products always contained a considerable amount of a disulfonyl derivative. With nitrous acid, however, the reaction products gave a certain amount of pure *p*-toluenesulfonylguanyl azide and so must have contained the monosulfonylderivative IV. As would be expected, sulfonylation of *free* aminoguanidine therefore takes place first in the =NH group, followed probably by sulfonylation in the hydrazine group.

We tried to prepare the isomer VI also by treatment of *p*-toluenesulfonyl-*S*-methylisothiosemicarbazide [XI] with ammonia. However, instead

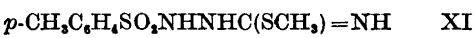

XI

of the formation of an aminoguanidine a McFadyen-Stevens reaction took place with formation of *p*-toluenesulfinic acid. This reaction has been subjected to a closer examination which will be published in another paper.

The formation of azides in the reaction between hydrazides and nitrous acid is, of course, well known, and the ring closure of guanyl azides to tetrazoles is a general way of preparing tetrazoles. The splitting of the tetrazole ring to give guanyl azides under the influence of sulfonyl chlorides is, however, a remarkable reaction, although it is not quite unprecedented. Hart [12] found, *e.g.*, that cyanogen bromide and 5-aminotetrazole react to give the following azide:

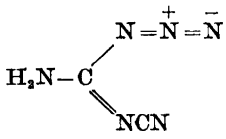

The reaction between 5-aminotetrazole and acetyl chloride or benzoyl chloride in pyridine solution gives the known compounds 5-acetamidotetrazole and 5-benzamidotetrazole, prepared by Thiele and Ingle [13] in another way. These compounds are true tetrazoles: They are neither hydrolysed by concentrated hydrochloric acid nor reduced by hydrogen sulfide or catalytically. With silver nitrate solution they give a white precipitate. Thus carboxylic acid chlorides are not able to split aminotetrazole in contrast to sulfonyl chlorides.

We have further studied the reaction of *p*-toluenesulfonyl chloride with the following aminotetrazoles:

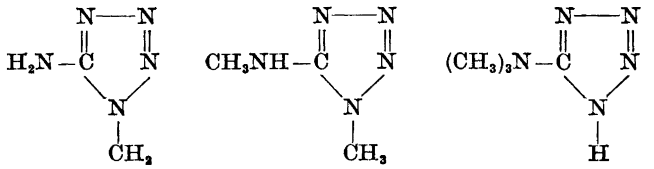

VIII IX X

1-Methyl-5-aminotetrazole (VIII) was prepared from 5-aminotetrazole and diazomethane or from 1-methyl-3-aminoguanidine and nitrous acid by ring closure of the azide formed. It has earlier been prepared by methylation of aminotetrazole [14,15], from methylthiourea, sodium azide and lead oxide [16], and from methyl *iso*thiocyanate and hydrazoic acid [17]. In all these ways the same methyltetrazole is obtained. The assignment of structure VIII to this compound is undoubtedly correct because it has no acidic character and gives no precipitate with silver nitrate solution.

The two dimethyl derivatives of 5-aminotetrazole (IX and X) were prepared from the appropriate dimethylaminoguanidines in the same way as 5-aminotetrazole from aminoguanidine. The structures of the two dimethyl derivatives follow unambiguously from their mode of preparation. Compound X gives a precipitate with silver nitrate, whereas IX does not, in accordance with their formulae.

1-Methyl-5-aminotetrazole and 1-methyl-5-methylaminotetrazole are unaffected by *p*-toluenesulfonyl chloride in pyridine solution. Both could be recovered unchanged. In contrast 5-dimethylaminotetrazole reacted with *p*-toluenesulfonyl chloride with the formation of *NN*-dimethylhydrazine. A study of this reaction will be published in another paper.

These results seem to indicate that the point of attack of the sulfonyl chloride is the NH-group in the tetrazole ring. Probably the primary reaction product is the 1-sulfonyltetrazole (II), which is immediately rearranged to an azide because of the strong electrophilic character of the sulfonyl group. The presence of the 5-amino group is necessary to produce a sufficiently high electron density in the tetrazole ring. Tetrazole itself does not react with *p*-toluenesulfonyl chloride in pyridine — neither could its silver salt be induced to react with *p*-toluenesulfonyl chloride. With the less electrophilic acyl group, RCO, no opening of the ring takes place. If a 1-acyl derivative is formed also in this case as the primary product, it is rearranged into a 5-acylamino derivative by an acyl migration.

This work was completed in the year 1952. In a recent publication [18], Nagy *et al.* have come to the same conclusion concerning the structure of the product formed in the reaction between 5-aminotetrazole and acetylsulfanilyl chloride in pyridine.

EXPERIMENTAL

p-*Acetamidobenzenesulfonylguanyl azide.* (III; R = p-$CH_3CONHC_6H_4$) Prepared by condensation of anhydrous 5-aminotetrazole and p-acetamidobenzenesulfonyl chloride in pyridine according to Jensen [1] and Jensen and Hansen [5], this compound was obtained as a colourless powder with m.p. 166°C after recrystallisation from acetone + water. (Found: C 38.28; H 3.73; N 29.54; S 11.20. Calc. for $C_9H_{10}N_6O_3S$: C 38.29; H 3.57; N 29.78; S 11.36.)

This compound is also obtained from 5-aminotetrazole and p-acetamidobenzenesulfonyl chloride in sodium carbonate solution according to the directions of Veldstra and Wiardi [3], but *without* treatment with sodium hydroxide. From 2 g of 5-aminotetrazole we obtained 3.45 g of crude product with m.p. *ca.* 156°C. Recrystallisation from ethanol raised the melting point to 165–166°C; no depression on admixture of the foregoing product.

The same compound is finally obtained from 4-acetylsulfanilylaminoguanidine and nitrous acid (*cf.* Jensen and Hansen [6], who give a slightly higher m.p., which was determined on a preheated block).

The compound does not yield a precipitate with silver nitrate; it is insoluble in 4 N hydrochloric acid, but dissolves in concentrated hydrochloric acid; when this solution was evaporated after standing for three days, a solid residue was obtained, and when this was recrystallised from water, colourless crystals formed; they were identified as sulfanilic acid. An aqueous solution of the compound is reduced by hydrogen sulfide with formation of sulfur, and it is reduced catalytically to acetylsulfanilylguanidine: A solution of 0.20 g in 30 ml ethanol to which was added 20 mg of PtO_2 was hydrogenated at room temperature and 1 atm. until the calculated amount of hydrogen had been absorbed. The solution was filtered and evaporated to dryness. Yield 0.18 g acetylsulfanilguanidine with m.p. 255°C; after recrystallisation from water m.p. 263–265°C; no depression on admixture of an authentic sample of acetylsulfanilylguanidine. (Found: C 39.41; H 5.14; N 20.42. Calc. for $C_9H_{12}N_4O_3S{\cdot}H_2O$: C 39.16; H 5.41; N 20.52.)

5-Acetylsulfanilamido tetrazole (I; R = p–$CH_3CONHC_6H_4$). Prepared according to Veldstra and Wiardi [3,4] by condensation of p-acetylaminobenzenesulfonyl chloride (16.8 g) with a solution of 5-aminotetrazole (6 g) and sodium carbonate (7.4 g) in water (70 ml). The crude product was dissolved in 0.2 N sodium hydroxide, precipitated with hydrochloric acid, and recrystallised from water. M.p. 205–206°C. Prepared in this way the compound contains approximately 1.5 moles water of crystallisation, which is given off by storage over phosphorus pentoxide or by heating to 170–180°C. (Found: C 35.11; H 4.26; N 27.25; S 10.30; H_2O 8.93. Calc. for $C_9H_{10}N_6O_3S.1\frac{1}{2}H_2O$:C 34.94; H 4.24; N 27.17; S 10.36; H_2O 8.73.)

The same compound was obtained by dissolving p-acetamidobenzenesulfonylguanyl azide in sodium hydroxide and precipitating with hydrochloric acid or by prolonged treatment of the azide with sodium carbonate: 0.3 g of the azide was stirred with a solution of 2 g of sodium carbonate in 20 ml of water; after 12 h the mixture was heated slowly to 50°C and kept at this temperature until practically all had dissolved. The solution was filtered and acidified with hydrochloric acid. The precipitate which separated was recrystallised from water. M.p. 215–216°C, mixed m.p. on addition of the foregoing product 204–206°C. The product was analysed after drying to constant weight over phosphorus pentoxide. (Found: C 38.72; H 3.66; N 28.91; S 11.26. Calc for $C_9H_{10}N_6O_3S$: C 38.29; H 3.57; N 29.78; S 11.36.)

In contrast to the azide, this compound gives a precipitate with silver nitrate, is insoluble in concentrated hydrochloric acid, and is not reduced by hydrogen sulfide or catalytically: 0.2 g was dissolved in 50 ml of ethanol, 20 mg of PtO_2 was added, and the solution was treated with hydrogen for 24 h. The compound was recovered unchanged, m.p. 214–216°C, 210–211°C after mixing with the starting product. (Found: S 10.34. Calc. 10.36.)

p-*Toluenesulfonylguanyl azide* (III; R = p–$CH_3C_6H_4$). Prepared by condensation of p-toluenesulfonyl chloride with 5-aminotetrazole in pyridine [6]. M.p. 150–151°C after recrystallisation from ethanol. (Found: N 29.31. Calc. for $C_8H_9N_5O_2S$: N 29.27.) The compound is not precipitated by silver nitrate in aqueous solution. By hydrogenation with PtO_2 as catalyst it is transformed into p-toluenesulfonylguanidine. Yiel d0.16 g from 0.20 g of the azide; m.p. 207–208°C after recrystallisation from water, m.p. 206–

208°C on admixture of an authentic sample of *p*-toluenesulfonylguanidine (m.p. 205–206°C). Analysed after drying for 24 h at 100°C over phosphorus pentoxide. (Found: N 19.72; S 14.83. Calc. for $C_8H_{11}N_3O_2S$; N 19.70; S 15.03.) By reduction with hydrogen sulfide, *p*-toluenesulfonylguanidine is similarly formed: 0.5 g of the azide was dissolved in 25 ml of warm ethanol, and hydrogen sulfide was bubled through the solution. After an hour, 10 ml of water was added, and hydrogen sulfide was let in for another hour. The solution was filtered from the free sulfur which had separated and was concentrated somewhat and cooled. A white powder separated. Yield 0.37 g; m.p. 204–206°C, no depression occurring on admixture of *p*-toluenesulfonylguanidine.

The azide is transformed into *p*-toluenesulfonyl chloride by treatment with concentrated hydrochloric acid; 1 g of the azide was shaken with 25 ml of concentrated hydrochloric acid. After three days all the azide had dissolved, and instead colourless, needlelike crystals had separated. Yield 0.72 g with m.p. 63–65°C, no depression on admixture of an authentic sample of *p*-toluenesulfonyl chloride.

5-(p-Toluenesulfonamido)tetrazole (I; R = $p-CH_3C_6H_4$). *p*-Toluenesulfonyl azide (0.20 g) was dissolved in 0.2 N sodium hydroxide (15 ml); the solution was filtered and acidified with hydrochloric acid. A white crystalline product separated. Yield 0.09 g. M.p. 189–191°C after two crystallisations from water. (Found: C 40.11; H 3.99; N 29.22; S 13.29. Calc for $C_8H_9N_5O_2S$: C 40.15; H 3.74; N 29.27; S 13.40.)

The same compound was obtained by treatment of the azide (0.50 g) with a solution of sodium carbonate (4 g) in water (40 ml) for 24 h and heating for a short time at 50°C. Most of the azide had then dissolved. The solution was filtered and acidified with hydrochloric acid. The white precipitate was recrystallised three times from water. M.p. 195–196°C; it was 189–191°C after mixing with the foregoing product. (Found: C 40.16; H 3.75; N 29.27; S 13.40. Calc. for $C_8H_9N_5O_2S$: C 40.15; H 3.79; N 29.27; S 13.40.)

Ring closure also took place when the azide was treated with hydrazine or dissolved in boiling xylene.

The tetrazole was insoluble in concentrated hydrochloric acid and remained unchanged after treatment for three days with this acid. It was not changed by boiling for one hour with 1 N sodium hydroxide. It is neither reduced with hydrogen sulfide nor catalytically. With an aqueous solution of silver nitrate it gives a white precipitate.

5-p-Nitrobenzenesulfonylguanyl azide (III; R = $p-NO_2C_6H_4$). Prepared by condensation of *p*-nitrobenzenesulfonyl chloride with 5-aminotetrazole in pyridine. M.p. 185–186°C after recrystallisation from acetone + water. (Found: C 30.44; H 2.43. Calc. for $C_7H_6N_6O_4S$: C 31.12; H 2.24.) As found by Roblin *et al.*[9], this compound forms sulfanilylguanidine on catalytic hydrogenation and also shows the other properties characteristic of an azide.

5-(p-Nitrobenzenesulfonylamido)tetrazole (I; R = $p-NO_2C_6H_4$). The azide (1 g) was stirred with 0.2 N NaOH (50 ml) for half an hour; the solution was filtered and acidified with hydrochloric acid. A white precipitate separated (0.35 g). M.p. 204–205°C after recrystallisation from water. (Found: C 30.90; H 2.24. Calc. for $C_7H_6N_6O_4S$: C 31.12; H 2.24.) The compound shows the properties characteristic of a tetrazole. By catalytic hydrogenation it is transformed into 5-sulfanilamidotetrazole, m.p. 202–203°C in accord with Veldstra and Wiardi[4].

5-Acetylaminotetrazole. To an ice-cold solution of anhydrous 5-aminotetrazole (2 g) in pyridine (15 ml), acetyl chloride (2 g) is added dropwise. The solution is then warmed for one hour on a steam bath, and after cooling poured into water (200 ml). After addition of concentrated hydrochloric acid (20 ml) to the cooled solution a white powder separates. Yield 0.8 g with m.p. 271–273°C after recrystallisation from ethanol. (Found: N 55.16. Calc. for $C_3H_5N_5O$:55.12.) The compound is soluble in sodium hydroxide, but is recovered unchanged on acidification. It is not changed by treatment with sodium hydroxide or concentrated hydrochloric acid, and it is not reduced by hydrogen sulfide or catalytically.

5-Benzoylaminotetrazole. Prepared in the same way as the acetyl derivative, but precipitated with 4 N hydrochloric acid. Yield 2.3 g from 2 g of 5-aminotetrazole. M.p. 277–282°C after recrystallisation from ethanol. (Found: C 51.06; H 3.92; N 36.97. Calc. for $C_8H_7N_5O$: C 50.78; H 3.73; N 37.02.) Like the foregoing compound it is recovered unchanged after treatment with sodium hydroxide, hydrochloric acid, or hydrogen sulfide, or by catalytic hydrogenation.

1-Methyl-5-aminotetrazole (VIII). This compound was prepared in two ways:

a) Anhydrous 5-aminotetrazole (1 g) was dissolved in methanol, and a solution of diazomethane in ether was added; the solution attained a yellow colour. The solvent was removed by evaporation, and the residue (0.38 g) was recrystallised from water. M.p. 220–223°C. (Found: C 24.18; H 5.29. Calc. for $C_2H_5N_5$: C 24.25; H 5.08.)

b) An aqueous solution of 2-methyl-1-aminoguanidinium iodide [19] (7.3 g) was shaken with an excess of silver chloride until negative iodine reaction. The filtered solution was cooled in ice, and sodium nitrite (2.3 g) and 1 N hydrochloric acid (34 ml) were added. After 15 min sodium acetate (10 g) was added, and the solution was evaporated to dryness. The residue was extracted repeatedly with boiling acetone. The acetone solution was evaporated and the residue recrystallised from water. Yield 0.77 g. M.p. 223–228°C, no depression on admixture of the foregoing preparation. (Found: N 70.49. Calc. for $C_2H_5N_5$: 70.66.)

By the same method the two following dimethylaminotetrazoles were prepared. They form colourless crystals which are slightly soluble in cold water. The preparation of the necessary dimethylaminoguanidines is described below. After completion of our work these compounds have been described by Finnegan, Henry and Lieber [20].

1-Methyl-5-methylaminotetrazole (IX). Yield 60 %; m.p. 172–174°C (recrystallised from ethanol). (Found: C 31.68; H 6.01; N 61.94. Calc. for $C_3H_7N_5$: C 31.85; H 6.24; N 61.93.)

5-Dimethylaminotetrazole (X). Yield 34 %; m.p. 235–240°C (recrystallised from water). (Found: 32.16; H 6.50; N 61.70. Calc. for $C_3H_7N_5$: C 31.85; H 6.24; N 61.93.)

2,3-Dimethyl-1-aminoguanidinium iodide. *S*-Methyl-4-methylthiosemicarbazidium iodide (7 g) was dissolved in an excess of 30 % aqueous methylamine solution. After standing overnight the solution was evaporated to dryness, and the residue was recrystallised from ethanol. Yield 5.6 g (75 %), m.p. 299–300°C. (Found: C 15.86; H 4.63; I 54.91. Calc for $C_3H_{11}IN_4$: C 15.66; H 4.82; I 55.16.)

2,2-Dimethyl-1-aminoguanidinium iodide. Prepared in the same way as the foregoing compound from *S*-methylthiosemicarbazidium iodide (20 g) and dimethylamine (yield 16.6 g, 84 %). Recrystallised from abs. ethanol; m.p. 185–187°C. (Found: C 15.59; H 4.90; I 55.12. Calc. for $C_3H_{11}IN_4$: C 15.66; H 4.82; I 55.16.)

3-(p-Toluenesulfonyl)-1-aminoguanidine (IV). A suspension of *p*-toluenesulfonyl-*S*-methylisothiourea [21] (10 g) in water (100 ml) to which had been added an excess of hydrazine hydrate (5 ml) was kept for 3–4 h with shaking and warming now and then, until the evolution of methanethiol had ceased and the solid had dissolved. The solution was evaporated to dryness and the residue crystallised from water. Yield 3.9 g (41 %) with m.p. *ca.* 160°C. After four more recrystallisations from water the product showed a constant m.p. of 185–186°C. (Found: N 24.63; S 14.12. Calc. for $C_8H_{12}N_4O_2S$: N 24.55; S 14.04.)

This compound reacts with nitrous acid with the formation of *p*-toluenesulfonylguanyl azide: 0.59 g of IV was dissolved in 15 ml of 4 N sulfuric acid, and a solution of sodium nitrite (0.3 g) in water (2 ml) was slowly added. The solution was heated to 80°C for a moment and then cooled in ice. The crystals which separated were recrystallised from ethanol. Yield 0.25 g. M.p. 150–151°C, not depressed on admixture of III. (Found: S 13.33. Calc. for $C_8H_9N_5O_2S$: S 13.40.)

1-(p-Toluenesulfonyl)-1-nitroguanidine. (VII). Nitroguanidine (10.4 g) was suspended in acetone (150 ml), and a solution of potassium hydroxide (12.3 g) in water (25 ml) was added. When the nitroguanidine had dissolved, 20 g of *p*-toluenesulfonyl chloride were added in small portions to the stirred solution while the temperature was kept at 18°C. When all the sulfonyl chloride had been added a white precipitate separated; 50 ml of water was added, and the stirring was continued for 3 h. Then the suspension was neutralised with acetic acid and filtered. The isolated product was the potassium salt of VII. Yield 19.5 g (66 %). It is easily soluble in hot water, slightly soluble in cold water and in ethanol. After three recrystallisations from water the m.p. was 230–231°C. (Found: C 32.32; H 3.00. Calc. for $C_8H_9KN_4O_4S$: C 32.43; H 3.06.) On addition of dilute hydrochloric acid to an aqueous solution of the potassium salt, 1-(*p*-toluenesulfonyl)-1-nitroguanidine separated as a white solid, which was recrystallised from water. M.p. 181–183°C. (Found: N 21.60; S 12.73. Calc. for $C_8H_{10}N_4O_4S$: N 21.69; S 12.40.)

1-(p-Toluenesulfonyl)-1-aminoguanidine (V). A solution of the nitro compound (VII) in ethanol was hydrogenated (catalyst PtO_2); the solution was filtered and evaporated to dryness and the residue recrystallised from water. Yield almost quantitative.

M.p. 159—161°C, strongly depressed on admixture of the isomer (IV). (Found: C 41.95; H 5.56; S 14.06. Calc. for $C_8H_{12}N_4O_2S$: C 42.09; H 5.30; S 14.04.)

Treatment of this compound with sodium nitrite as described for IV yielded *p*-toluenesulfonylguanidine, m.p. 206—207°C, not depressed on admixture of an authentic sample.

p-*Toluenesulfonylamidoguanidine (VI).* *p*-Toluenesulfonyl chloride (3.8 g) was added to a solution of aminoguanidinium sulfate (3.4 g) and sodium acetate (6 g) in 15 ml of water. The mixture was boiled until the sulfonyl chloride had dissolved completely. On cooling, a white crystalline solid separated. Yield 4.0 g (75 %). It was recrystallised three times from ethanol. M.p. 204—205°C. (Found: C 39.15; H 5.66; N 22.63. Calc. for $C_8H_{12}N_4O_2S.H_2O$: C 39.02; H 5.73; N 22.76).

The compound is easily soluble in hot water and quite soluble also in cold water, but slightly soluble in cold ethanol and insoluble in benzene.

p-*Toluenesulfonylthiosemicarbazide* was prepared in two ways:

a) 2.9 g of $Ba(SCN)_2 \cdot 2H_2O$ was dissolved in 10 ml water, and 5 ml of 4 N sulfuric acid was added. The barium sulfate was filtered off, 1.9 g of *p*-toluenesulfonic hydrazide was added, and the solution was heated on a steam bath for one hour. After cooling, the white solid which had formed was filtered off, washed with water, and recrystallised from ethanol. Yield 1.3 g (60 %). M.p. 214—215°C. (Found: N 17.10; Calc. for $C_8H_{11}N_3O_2S_2$: N 17.13.)

b) The same compound was obtained from *p*-toluenesulfonyl chloride and thiosemicarbazide under the conditions described for VI, but only in slight yield (6—16 %). From the reaction between *p*-toluenesulfonyl chloride and thiosemicarbazide in pyridine solution no pure compound could be obtained, but the product seemed mainly to consist of di-*p*-toluenesulfonylthiosemicarbazide.

p-*Toluenesulfonyl*-S-*methyl-isothiosemicarbazide (XI).*

a) A solution of *p*-toluenesulfonylthiosemicarbazide (210 mg) and methyl iodide (150 mg) in ethanol (10 ml) was refluxed for one hour. The ethanol was removed *in vacuo* and the residue dissolved in water; on addition of sodium carbonate, XI separated. Yield 175 mg (80 %). When recrystallised from water it formed colourless needles with m.p. 175—177°C. (Found: N 16.24. Calc. for $C_9H_{13}N_3O_2S_2$: N 16.21.)

b) *S*-Methyl*iso*thiosemicarbazidium iodide (2.3 g) was dissolved in pyridine (8 ml), *p*-toluenesulfonyl chloride (1.9 g) was added, and the solution was heated to boiling and cooled in ice. On addition of water an oil separated; it soon crystallised. Yield 0.7 g (27 %). After recrystallisation from water it had m.p. 175—176°C. (Found: S 24.89; Calc. for $C_9H_{13}N_3O_2S_2$: S 24.73.)

The molten substance gives off methanethiol and soon solidifies to a substance melting at about 250°C. On boiling a solution of XI in aqueous ammonia, methanethiol is similarly formed; on acidification of the cooled solution, *p*-toluenesulfinic acid separates; m.p. 84—86°C (litt. 87°C).

Infrared spectra. Characteristic of the infrared spectra of the sulfonylguanyl azides (III) is a relatively strong band at 4.66 μ, which was also found in the spectra of benzazide and guanyl azide. The spectra of the sulfonylguanyl azides exhibit most of the bands of acetylsulfanilamide and *p*-toluenesulfonamide except a strong band in the 11 μ range; the azides have a band at 12.7 μ not found in the spectra of the sulfonamides or of aminotetrazole and tetrazole. Samples of *p*-acetaminobenzenesulfonamidotetrazole, prepared in pyridine solution and in aqueous solution containing sodium carbonate, yielded identical spectra.

The infrared spectra of the 5-sulfonamidotetrazoles lack the band at 4.66 μ. Bands which could be atributed to the tetrazole ring could not be identified with certainty, because acetylsulfanilamide and *p*-toluenesulfonamide have strong bands overlapping the bands of tetrazole and 5-aminotetrazole. 5-(*p*-Acetamidobenzenesulfonamido)tetrazole has a band at 9.5 μ, at the same place where 5-aminotetrazole has a strong band, but this band is lacking in the spectrum of 5-(*p*-toluenesulfonamido)tetrazole; more likely it corresponds to a band at 9.6 μ in the spectrum of acetylsulfanilamide. The products obtained from *p*-toluenesulfonylguanyl azide by treatment with sodium hydroxide and by heating in xylene, respectively, yielded identical spectra.

REFERENCES

1. Jensen, K. A. *Dansk Tidsskr. Farmaci* **15** (1941) 299.
2. Tappi, G. and Migliardi, C. *Arch. sci. biol. Ital.* **27** (1941) 170. Tappi, G. *Rec. trav. chim.* **62** (1943) 207.
3. Veldstra, H. and Wiardi, P. W. *Rec. trav. chim.* **61** (1942) 627.
4. Veldstra, H. and Wiardi, P. W. *Rec. trav. chim.* **62** (1943) 661.
5. Jensen, K. A. and Rosenlund Hansen, O. *Rec. trav. chim.* **62** (1943) 658.
6. Jensen, K. A. and Rosenlund Hansen, O. *Acta Chem. Scand.* **6** (1952) 195.
7. Hantzsch, A. and Vagt, A. *Ann.* **314** (1900) 354.
8. Dahlbom, R. and Ekstrand, T. *Sv. Kem. Tidskr.* **55** (1943) 122.
9. Roblin, R. O., Williams, J. H., Winnek, P. S. and English, J. P. *J. Am. Chem. Soc.* **62** (1940) 2002.
10. Winnek, P. S., Anderson, G. W., Marson, H. W., Faith, H. E. and Roblin, R. O. *J. Am. Chem. Soc.* **64** (1942) 1682.
11. Greer, A. H., Kertesz, D. L. and Smith, G. B. L. *J. Am. Chem. Soc.* **71** (1949) 3005.
12. Hart, C. V. *J. Am. Chem. Soc.* **50** (1928) 1922.
13. Thiele, J. and Ingle, H. *Ann.* **287** (1895) 234.
14. Thiele, J. and Ingle, H. *Ann.* **287** (1895) 249, 252.
15. Henry, R. A. and Finnegan, W. G. *J. Am. Chem. Soc.* **76** (1954) 923
16. Stollé, R. *J. prakt. Chem* [2] **134** (1932) 285.
17. Oliveri-Mandalà, E. *Gazz. chim. Ital.* **52** (1922) 103.
18. Nagy, H. K., Tomson, A. J. and Horwitz, J. P. *J. Am. Chem. Soc.* **82** (1960) 1609.
19. Kirsten, G. W. and Smith, G. B. L. *J. Am. Chem. Soc.* **58** (1936) 800.
20. Finnegan, W. G., Henry, R. A. and Lieber, E. *J. Org. Chem.* **18** (1953) 779.
21. Bergmann, F. *J. Am. Chem. Soc.* **68** (1946) 761.

Received January 23, 1961.

ACTA CHEMICA SCANDINAVICA 15 (1961) 1003–1006

The Chemistry of the Natural Order Cupressales

XXXVII. * Monoterpenes from the Bark of *Juniperus communis* L.

H. ERDTMAN and T. KUBOTA

Organisk-kemiska Institutionen, Kungl. Tekniska Högskolan, Stockholm, Sweden

The monoterpene fraction of the essential oil from the bark of the common juniper has been investigated.

The steam volatile oil from the bark of the common juniper was first investigated by Hellström [1] and this work was reported by Mattson [2] in 1913. Two sesquiterpenes, juniperene and juniperol, were isolated. As the result of a recent reinvestigation [3] of the sesquiterpene fraction it was shown that juniperene is identical with kuromatsuene and with longifolene and that juniperol is identical with kuromatsuol and with the longiborneol obtained from longifolene by Naffa and Ourisson. The identity of juniperol and macrocarpol had been demonstrated earlier [4].

Mattson also reported the occurrence of *l*-α-pinene and sylvestrene (Δ^3-carene) in this essential oil. They were characterised as their hydrochlorides. Evidence was also obtained for the presence of camphene, phellandrene and dipentene.

We have now examined a low-boiling, neutral fraction of the essential oil from the bark of *Juniperus communis* and found it to contain about 30 % longifolene. 16 % consisted of a higher boiling sesquiterpene mixture. The monoterpene fractions were subjected to a gas chromatographic investigation [5] and the following monoterpenes were detected (approximate yields in parenthesis): α-pinene (22), Δ^3-carene (14), terpinolene (2), *cis*-menthane (1), β-pinene (1), limonene (1), myrcene (1), camphene (0.5), α-terpinene (0.5), γ-terpinene (0.5), β-phellandrene (0.5) and cymene (0.5 %).

It is interesting to note that Hendrickson [6] recently suggested that longifolene is derived from *cis*-farnesol. The same seems to apply to the sesquiterpenes hitherto isolated from the wood of several *Juniperus* species investigated in this laboratory by Runeberg [7] and by Bredenberg [8], *e.g.* cadinenes, cedrene, cuparene and thujopsene [9].

* Part XXXVI. *Acta Chem. Scand.* **15** (1961) 961.

Šorm *et al.*[10] investigated the berry oil of *Juniperus communis* in considerable detail and found sesquiterpenes derivable both from *cis*- and *trans*-farnesol (*e.g.* cadinane and selinane derivatives). Bark and wood are relatively simple organs contrary to the berries that consist of the united, fleshy cone scales and the seeds. A separate investigation of the two components of the berries would therefore seem to be a matter of interest. Apart from *J. sabiniana* little is known about the composition of the needle oils of junipers. In most cases commercial oils from conifer "needles" include volatile constituents of the twigs. For taxonomic purposes it is important that the constituents of as simple organs as possible are compared[11]. Results from investigations of complex organs or products from non-homogeneous starting materials must be used with care.

EXPERIMENTAL

The neutral part of the steam volatile oil from juniper bark was subjected to a preliminary rough vacuum-distillation to remove the highest boiling products. The fraction b.p. <120°/3 mm (A) was then fractionally distilled using a vacuum jacketed, packed column (LKB). The results are given in Table 1.

Table 1. Fractional distillation of the essential oil from the bark of *J. communis*.

Fraction	b.p./mm	Colour	n_D		$[\alpha]_D$	Yield (%)
I	64–70/33	Colourless	n_D^{21}	1.4670	−49.7°	22.7
II	70–74.5/33	»	n_D^{21}	1.4729	+9.63°	17.7
III	98–108/7	Slightly yellow	n_D^{21}	1.4892	−2.62°	4.4
IV	108–110/7	Slightly yellow	n_D^{22}	1.5031	+37.1°	25.5
V	110/7	Colourless	n_D^{23}	1.5033	+36.9°	4.5
VI	110–114/7	Very slightly yellow	n_D^{20}	1.5051	+13.5°	10.0
VII	107–110/3	Slightly yellow	n_D^{20}	1.5082	+4.16°	2.3
VIII	110–112/3	Yellow	n_D^{20}	1.5150	+10.02°	4.2
IX	Residue	Dark orange		—	—	8.9
						100.2

Fractions IV and V were almost pure longifolene (juniperene). Fractions I, II, and III were analysed by gas chromatography. A Perkin-Elmer Vapor Fractometer Model 154 in conjunction with a Speedmax Type G recorder (Leeds, Northrup Co) was used. The aluminium column was 4 m long and had an internal diameter of 5 mm. The stationary

Table 2. Constituents of fraction I.

Terpene	Relative retention volume	Yield (%)	% of A
α-Pinene	1.00	89.8	20.4
cis-Menthane	1.16	3.5	0.8
Camphene	1.24	1.7	0.4
β-Pinene	1.52	2.4	0.5
Δ^3-Carene	1.79	1.9	0.4
α-Terpinene	2.16	0.6	0.1
		99.9	22.6

phase was 60—80 mesh celite impregnated with 2,4-dinitrophenyl-2-naphthyl ether (m.p. 95°, 15 % by weight). The temperature was kept at 110° and the flow of helium 44 ml/min. The results are given in Tables 2, 3, and 4. In these tables the retention volumes of the various components are given in relation to α-pinene = 1. The amounts of the components were determined by measuring the area of the peaks with a planimeter.

Table 3. Constituents of fraction II.

Terpene	Relative retention volume	Yield (%)	% of A
α-Pinene	1.00	6.9	1.2
cis-Menthane	1.16	0.8	0.15
Camphene	1.24	0.4	0.08
β-Pinene	1.53	3.3	0.6
Myrcene	1.69	4.2	0.7
Δ^3-Carene	1.80	75.8	13.4
α-Terpinene	2.16	1.4	0.25
Limonene	2.34	2.6	0.46
β-Phellandrene	2.64	1.1	0.2
γ-Terpinene	2.85	0.2	0.04
Terpinolene	3.28	0.5	0.09
p-Cymene	3.55	2.7	0.7
		99.9	17.9

Table 4. Constituents of fraction III.

Terpene	Relative retention volume	Yield (%)	% of A
Δ^3-Carene	1.80	10.2	0.45
α-Terpinene	2.21	1.3	0.05
Limonene	2.38	16.0	0.70
β-Phellandrene	2.66	8.9	0.4
γ-Terpinene	2.88	13.5	0.6
Terpinolene	3.42	50.0	2.2
p-Cymene	3.60	trace	trace
		99.9	4.4

Our thanks are due to Professor and Mrs. Sörensen, Trondheim, for the bark-oil, to Dr A. Groth for his kind assistance during the gas chromatographic investigation and to the *U.S. Army and Development Liaison Group* through its European Office (Contract number DA-91-591-EUC-1113 OI-1376—59) for financial support.

REFERENCES

1. *Cf.* Hellström, A. *Östra Nyland-Kotka Nyheter*, Febr. 5th and 8th 1955.
2. Mattson, G. *Bidrag till kännedom af Finlands natur och folk.* Utgifna av Finska Vetenskapssocieteten. H. 72. No. 1. Helsingfors 1913.
3. Akiyoshi, S., Erdtman, H. and Kubota, T. *Tetrahedron* **9** (1960) 237.
4. Erdtman, H. and Thomas, B. *Chem. and Ind. London* **1955** 384.

5. *Cf.* Groth, A. *Svensk Papperstidn.* **61** (1958) 311 and forthcoming publication.
6. Hendrickson, J. B. *Tetrahedron* **7** (1959) 82.
7. Runeberg, J. *Acta Chem. Scand.* **14** (1960) 1288 and earlier and forthcoming papers.
8. Bredenberg, J. B-son. *Acta Chem. Scand. In the press.*
9. *Not published.* Reported at the Third Organic Chemistry Conference on The Chemistry of Natural Products and Organic Reaction Mechanisms held at Natick, Mass., October 1959.
10. *Cf.* Herout, V. and Sýkora, V. *Tetrahedron* **4** (1958) 247; Motl, O., Herout, V. and Šorm, F. *Collection Czechoslov. Chem. Communs.* **22** (1957) 785; **23** (1958) 1293.
11. Erdtman, H. In Todd, A. *Perspectives in Organic Chemistry.* Interscience 1956, p. 453; *Experientia*, Suppl. II, **1955** 156.

Received January 16, 1961.

ACTA CHEMICA SCANDINAVICA 15 (1961) 1007–1016

On the Crystal Structure of Sn_2OSO_4

GUNNAR WERNFORS

Department of Inorganic Chemistry, Royal Institute of Technology, Stockholm 70, Sweden; Department of Inorganic and Physical Chemistry, Chemical Institute, University of Lund, Lund, Sweden

A crystalline basic tin(II)sulfate, Sn_2OSO_4, has been prepared, and powder, rotation and Weissenberg photographs have been taken. The crystals proved to be tetragonal with $a = 10.930$ Å, $c = 8.931$ Å, and $V = 1\,067$ Å^3. The systematically absent reflections are characteristic of space group No. 114 $P\bar{4}2_1c$. In the unit cell there are 8 formula units. The tin positions have been found from Patterson projections and sections. The results show that the 16 tin atoms of the unit cell are arranged in two 8-fold positions, and that they form isolated groups, each containing 8 atoms, see Fig. 7.

Many investigations have been made on the hydrolysis of tin(II)salts in solution. Perhaps the most thorough recent work concerning this problem is that of Tobias [1], who studied the hydrolysis of tin(II) in a constant ionic medium using emf titrations. He concluded that the main product of the hydrolysis reaction is the polynuclear complex $Sn_3(OH)_4^{2+}$ and that small amounts of $Sn_2(OH)_2^{2+}$ and $SnOH^+$ are also formed. Tobias also gives an extensive survey of earlier work on the hydrolysis of tin(II) in aqueous solutions.

In connection with investigations of equilibria of complex ions in solution it is often of value to study the results of investigations of the structures of the corresponding solid substances. Thus, studies of the crystal structures of basic tin(II)salts are of value in relation to those of the hydrolysis of tin(II). Now, as is also pointed out by Tobias [1], no such studies have been published in the literature and therefore it seemed worthwhile to determine the structures of some basic tin(II) salts.

A number of basic tin(II) salts are described in Mellor's comprehensive treatise on inorganic and theoretical chemistry [2]. No new compounds of this type seem to have been described since 1927, when Mellor's book was printed.

From the present point of view, the most interesting of these compounds are some basic chlorides and sulfates which were reported by Ditte [3,4,6] and Carson [5,7] to be fairly easy to prepare in the crystalline form. They are the chlorides $Sn_2OCl_2(H_2O)_4$, $Sn_5O_3Cl_4(H_2O)_6$ [3,4] and $Sn_8O_5Cl_6(H_2O)_3$[5], and the sulfates $Sn_3O_2SO_4(H_2O)_n$ where $n = 1.5-3$ [6], and Sn_2OSO_4[7].

The investigation was started with the sulfates because they were reported to crystallize better than the chlorides, and one of the basic tin(II)sulfates has the same Sn:OH (or Sn:O) ratio as the hydrolyzed complexes in aqueous solutions, described by Tobias.

Attempts were made to prepare $Sn_3O_2SO_4(H_2O)_n$ and Sn_2OSO_4 by the methods described by Ditte [6] and Carson [7] (by treating SnO with hot dilute sulfuric acid or by precipitating the compounds from a boiling, acidic tin(II) sulfate solution with dilute sodium or potassium hydroxide solutions) but no crystals suitable for X-ray investigations were obtained in this way. However, by using hydrothermal methods, which often are of great value in the preparation of crystals, it was possible to get good crystals of Sn_2OSO_4 for structure determinations. The investigation is continuing and at lower temperatures it may perhaps be possible to prepare crystals with other Sn:O or Sn:OH ratios.

PREPARATION OF Sn_2OSO_4

Crystals of Sn_2OSO_4 were prepared in the following way: A stock solution of tin(II) sulfate was prepared by slowly passing a saturated solution of copper(II) sulfate through a column of granular tin metal so that complete reduction of copper(II) to copper metal occurred. The use of this method eliminates the oxidation of tin(II) by air.

Series of solutions with different tin(II) ion concentrations and different values of pH were then prepared. Portions of the stock solution were diluted and were made slightly acidic with sulfuric acid. For some of the solutions the pH was increased by adding small amounts of ammonia or freshly precipitated and washed tin(II) hydroxide. The solutions were then sealed in thick-walled Pyrex tubes and heated in an oven at temperatures ranging from 100°C to 150°C for periods of from one day to three or four weeks. On completion of the period of heating the tubes were quickly cooled and opened, and the crystals were filtered off, washed with water several times and dried in air.

In all cases the same sort of crystals was formed in spite of the great variations in pH and concentration. The crystals proved to have the formula Sn_2OSO_4 (see below). They were octahedral (not quite regular) and were sometimes rather large (1 cm in diameter or more).

Analysis

Tin was determined as *tin (II) oxide*. Concentrated nitric acid was added to a sample of the crystals, contained in a platinum crucible, and the whole was evaporated to dryness under a heating lamp. This process was repeated several times. The crucible was then ignited, cooled and weighed, and the amount of tin(II) in the crystals was calculated from the weight of tin(IV)oxide formed.

Sulfur trioxide was determined by the formation of barium sulfate. A sample of the crystals was dissolved in strong perchloric acid (solutions in dilute acid are opalescent, and precipitation occurs in solutions in water) and the solution was passed through a cation exchange column. The eluate was treated with barium perchlorate solution and the precipitated barium sulfate was filtered off, washed, ignited, cooled and weighed.

Water was determined by Penfield's method, modified after Hartwig-Bendig [8,9]. The water content of the crystals was found to be negligible.

The density of the crystals was determined from their loss of weight in benzene.

	Found		Calculated for Sn_2OSO_4
% SnO	77.8	77.5	77.1
% SO_3	22.2	22.2	22.9
% H_2O	0	0	0
Density	4.26	4.27	4.35

Table 1. Powder photograph of Sn_2OSO_4. Guinier camera. Cu$K\alpha_1$ radiation. Cu$K\alpha_1$ = 1.54050 Å.

hkl	$10^5\sin^2\Theta$ calc	$10^5\sin^2\Theta$ obs	*I* obs	*hkl*	$10^5\sin^2\Theta$ calc	$10^5\sin^2\Theta$ obs	*I* obs
110	993	994	st	412	11 420	11 411	w
101	1 241	1 242	st	313	11 662	11 649	vvw
200	1 987	1 993	vvw	510	12 914		
210	2 484	2 491	vvw	422	12 910	12 903	st
201	2 731	2 728	st	114	12 896		
002	2 976	2 974	m	501	13 162	13 159	st
211	3 228	3 226	w	323	13 152		
102	3 473	3 480	vvw	511	13 658	13 660	vw
112	3 969	3 970	st	224	13 890	13 883	vw
220	3 974			403	14 642	14 619	vvw
202	4 963	4 963	m	521	15 148	15 155	vvw
310	4 967			413	15 139		
301	5 214	5 213	w	440	15 895		
212	5 460	5 459	st	512	15 890	15 871	m
311	5 711	5 716	vst	224	15 877		
222	6 950	6 952	st	423	16 629	16 629	m
321	7 201	7 201	st	530	16 888	16 870	m
103	7 192			314	16 870		
302	7 446	7 444	st	522	17 380	17 358	w
400	7 947	7 945	m	531	17 632	17 633	st
312	7 943			600	17 881	17 871	m
410	8 444	8 440	vvw	324	18 360	18 340	vvw
401	8 691	8 685	st	601	18 625	18 616	vvw
203	8 682			611	19 122		
330	8 941	8 939	vvw	503	19 113	19 108	st
411	9 188	9 185	vvw	105	19 096		
213	9 179			513	19 609	19 575	vvw
322	9 433	9 435	w	620	19 868		
420	9 934	9 932	m	532	19 864	19 838	w
421	10 678	10 681	st	404	19 850		
402	10 923	10 925	m				

The powder photograph was measured and interpreted to $\sin^2\Theta = 0.50$, but only reflections with $\sin^2\Theta < 0.20$ have been given in the table.

UNIT CELL AND SPACE GROUP

Crystals (0.1 mm in diameter) were set with [001], [010] and [110] as rotation axes and Weissenberg photographs (*hk*0 —*hk*4, *h*0*l* — *h*5*l*, *hhl* — *h*, *h* + 7, *l*) were taken with CuK radiation. The reflections were recorded photographically using the multiple film technique, and the intensities were estimated visually. The $|F|^2$-values were calculated from the intensities using polarization and Lorentz ' factors given by Lu [10]. No correction was applied for absorption.

From the rotation and Weissenberg photographs it was concluded that the crystals are tetragonal with the following approximate cell dimensions: $a = 11.0$ Å and $c = 8.98$ Å. More accurate values of the cell dimensions were calculated from powder photographs (see Table 1), taken with Cu$K\alpha_1$ radiation ($\lambda = 1.54050$ Å) in a Guinier type focusing camera:

$$a = 10.930 \pm 0.002 \text{ Å}; \; c = 8.931 \pm 0.002 \text{ Å}; \; V = 1\,067 \text{ Å}^3$$

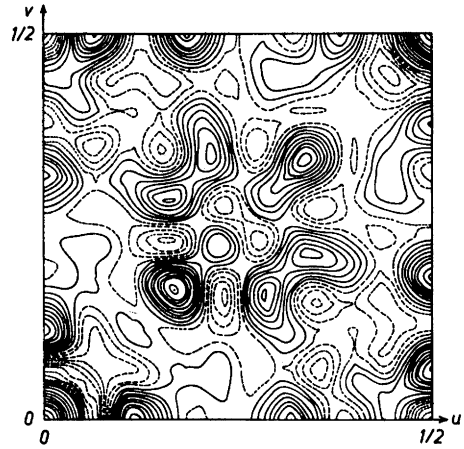

Fig. 1. The Patterson projection $P(uvp)$ for Sn_2OSO_4. Dashed lines indicate negative values. For the maximum (0, 0) only every fourth and for the maximum (½, ½) only every second contour has been drawn.

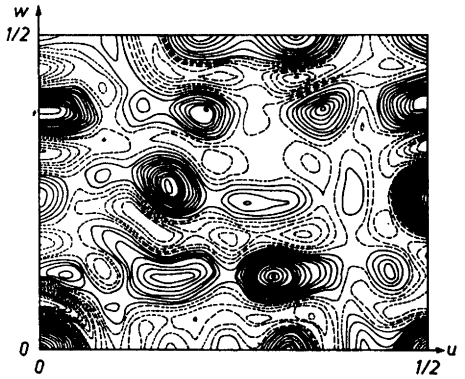

Fig. 2. The Patterson projection $P(upw)$ for Sn_2OSO_4. For the maximum (0, 0) only every fourth and for the double maximum $u = 0.20-0.35$ $w = ½$ only every second contour has been drawn. Dashed lines indicate negative values.

From the observed density and the volume of the unit cell, the number of formula units in the cell was calculated to be $7.83 \approx 8$. The following reflections were systematically absent from the Weissenberg photographs: *hhl* with *l* odd; *h*00 with *h* odd. This is characteristic of space group $P\bar{4}2_1c$, No. 114 in the International Tables [11].

POSITIONS OF THE TIN ATOMS

To determine the parameters of the tin atoms the Patterson projections $P(uvp)$ and $P(upw)$ were at first calculated (see Figs. 1 and 2).

The interatomic vectors within a point position 8(*e*) in $P\bar{4}2_1c$ are:

	u	*v*	*w*	weight
I	$\pm 2x$	$\pm 2y$	0	1
II	$\pm (x + y)$	$\pm (x-y)$	$2z$	1
III	$\frac{1}{2} \pm 2x$	$\frac{1}{2}$	$\frac{1}{2} \pm 2z$	1
IV	$\frac{1}{2} \pm 2y$	$\frac{1}{2}$	$\frac{1}{2} \pm 2z$	1
V	$\frac{1}{2} \pm (x + y)$	$\frac{1}{2} \pm (x + y)$	$\frac{1}{2}$	2
VI	$\frac{1}{2} \pm (x-y)$	$\frac{1}{2} \pm (x-y)$	$\frac{1}{2}$	2

Moreover, for each vector *uvw* there is also one *vuw*.

The interatomic vectors between two different point positions $8(e)_1$ and $8(e)_2$ are:

	u	*v*	*w*	weight
A	$\pm (x_1-x_2)$	$\pm (y_1-y_2)$	z_1-z_2	1
B	$\pm (x_1 + x_2)$	$\pm (y_1 + y_2)$	z_1-z_2	1
C	$\pm (x_1 + y_2)$	$\pm (y_1-x_2)$	$z_1 + z_2$	1
D	$\pm (x_1-y_2)$	$\pm (y_1 + x_2)$	$z_1 + z_2$	1
E	$\frac{1}{2} \pm (x_1 + x_2)$	$\frac{1}{2} \pm (y_1-y_2)$	$\frac{1}{2}-z_1-z_2$	1
F	$\frac{1}{2} \pm (x_1-x_2)$	$\frac{1}{2} \pm (y_1 + y_2)$	$\frac{1}{2}-z_1-z_2$	1
G	$\frac{1}{2} \pm (x_1-y_2)$	$\frac{1}{2} \pm (y_1-x_2)$	$\frac{1}{2} + z_1-z_2$	1
H	$\frac{1}{2} \pm (x_1 + y_2)$	$\frac{1}{2} \pm (y_1 + x_2)$	$\frac{1}{2} + z_1-z_2$	1

For a vector *uvw* there is also one vector *vuw*.

The 16 tin atoms in the unit cell should be arranged in one of the following ways:

a. 8(*e*) + 8(*e*)
b. 8(*e*) + 4(*d*) + 4(*d*)
c. 8(*e*) + 4(*c*) + 4(*c*)
d. 8(*e*) + 4(*d*) + 4(*c*)
e. 8(*e*) + 4(*d*) + 2(*a*) + 2(*b*)
f. 8(*e*) + 4(*c*) + 2(*a*) + 2(*b*)
g. combinations of four fourfold positions 4(*c*) or 4(*d*)
h. 2(*a*) + 2(*b*) + combinations of three fourfold positions 4(*c*) or 4(*d*).

Of these g. and h. should give maxima in $P(uvp)$ at $u = 0, \frac{1}{2}$; $v = 0, \frac{1}{2}$ only. Since $P(uvp)$ in Fig. 1 shows very pronounced maxima outside these points, there should be at least one eightfold tin position in the unit cell and arrangements according to g. and h. above can be ruled out.

For the determination of the tin parameters we compared at first the vectors I—VI with $P(uvp)$ and $P(upw)$ in Figs. 1 and 2. III and IV gave the following possible x and y parameters from $P(uvp)$ and possible z parameters from $P(upw)$:

$x =$	0;	0.06;	0.16;	0.22;	0.28;	0.34;	0.44;	0.50
$y =$	0;	0.06;	0.16;	0.22;	0.28;	0.34;	0.44;	0.50
$z =$	0;	0.05;	0.13;	0.25;	0.37;	0.45;	0.50	

The different x, y, and z values were then combined and those, not belonging to the same point position, were tested with the vectors I—VI and A—H above.

For the parameters of Sn_1 the relations $0 \leq x \leq \frac{1}{4}$, $0 \leq y \leq \frac{1}{2}$, $0 \leq z \leq \frac{1}{4}$, $x \leq y$ and $x \leq \frac{1}{2} - y$ also hold, since every arrangement of Sn_1 with parameters outside these limits may be transformed by a change of the origin or the direction of the axes of the unit cell, to an arrangement obeying the inequalities above.

Many alternatives were ruled out, but the result of the calculations was not completely satisfactory. The great overlapping of the vectors in both projections made it difficult to distinguish accurately between some of the possibilities. In order to facilitate the determination of the parameters it was decided therefore to calculate the following sections in $P(uvw)$:

$$P(uv0) = \sum_h \sum_k [\sum_l |F_{hkl}|^2] \cos 2\pi(hu + kv)$$

$$P(uv\tfrac{1}{2}) = \sum_h \sum_k [(\sum_{l=\text{even}} |F_{hkl}|^2 - \sum_{l=\text{odd}} |F_{hkl}|^2)] \cos 2\pi(hu + kv)$$

$$P(u0w) = \sum_h \sum_l [\sum_k |F_{hkl}|^2] \cos 2\pi(hu + lw)$$

$$P(u\tfrac{1}{2}w) = \sum_h \sum_l [(\sum_{k=\text{even}} |F_{hkl}|^2 - \sum_{k=\text{odd}} |F_{hkl}|^2)] \cos 2\pi(hu + lw)$$

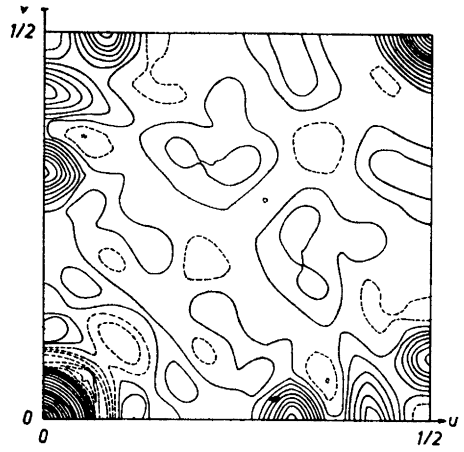

Fig. 3. The Patterson section $P(uv0)$ for Sn_2OSO_4. For the maximum (0, 0) only every fifth contour has been drawn. Dashed lines indicate negative values.

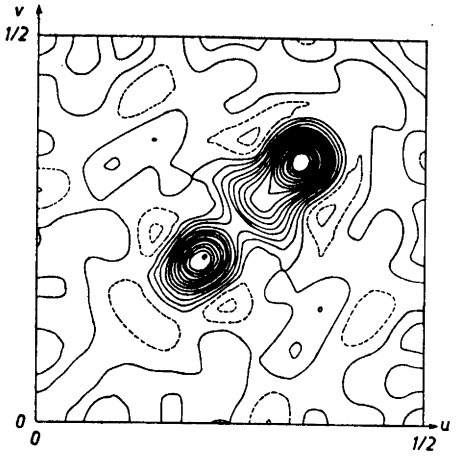

Fig. 4. The Patterson section $P(uv\,1/2)$ for Sn_2OSO_4. Dashed lines indicate negative values.

The results are shown in Figs. 3, 4, 5, and 6.

Now, it is seen from the section $P(uv1/2)$ that the alternatives above with 2-fold positions must be ruled out since there is no maximum at $00\,1/2$, thus e. and f. are ruled out. Moreover, within the 4-fold position $4(d)$ there should be a vector $00\,1/2$ and consequently b. and d. also are ruled out, and only a. and c. remain to be taken into account.

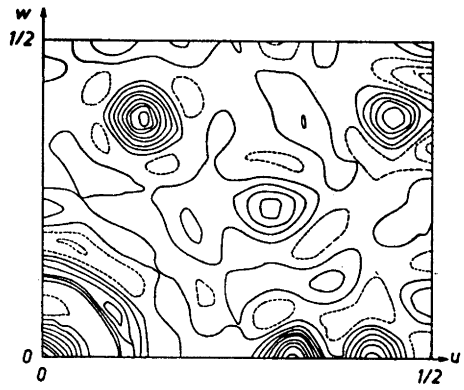

Fig. 5. The Patterson section $P(u0w)$ for Sn_2OSO_4. For the maximum (0, 0) and the negative region close to it only every tenth contour has been drawn. Dashed lines indicate negative values.

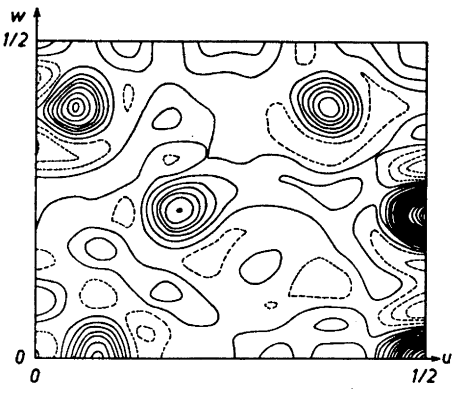

Fig. 6. The Patterson section $P(u\,1/2w)$ for Sn_2OSO_4. Dashed lines indicate negative values.

From $P(uv0)$ the possible values of x and y were calculated (vector I). Similarly, from $P(u\frac{1}{2}w)$ the values of z (vectors III, IV) were calculated. The result should be better than that from the projections alone, because all the data are used and overlapping is diminished. The following parameters were found:

x	0.039	0.160	0.212	0.250	0.289	0.340	0.461
y	0.039	0.160	0.212	0.250	0.289	0.340	0.461
z	0.052	0.136	0.250	0.364	0.448		

All these possibilities were combined and tested first with the vectors V and VI and then also with II and all the vectors A—H. The latter vectors could only be tested in the Patterson projections. In this way all possibilities except one were ruled out. Thus it may be concluded that the 16 tin atoms in the unit cell are arranged in the following way:

8 Sn_1 in 8(e) with $x_1 \approx 0$ $y_1 \approx 0.160$ $z_1 \approx 0.136$
8 Sn_2 in 8(e) with $x_2 \approx 0.289$ $y_2 \approx 0$ $z_2 \approx 0.241$

During the tests it was found that the first accepted value of $z_2(0.250)$ had to be changed a little to make the vectors C, D, G and H fall on the top of maxima in $P(u0w)$ and $P(u\frac{1}{2}w)$.

However, both x_1 and y_2 could not be exactly 0, since with $x_1 = y_2 = 0$ the tin contributions to the structure factors $hk0$ should be 0 if $h + k$ is odd [11]. This is contradicted by the intensity data, which show some fairly strong reflections $hk0$ with $h + k =$ odd.

An attempt was made to determine more exact values of x_1 and y_2, by calculating five new sections of $P(uvw)$, namely $P(uv\ 0.105)$, $P(uv\ 0.123)$, $P(uv\ 0.272)$, $P(uv\ 0.377)$, and $P(uv\ 0.395)$ which should contain the vectors II (for Sn_1) and A—H above, but it was not successful. Overlappings made it impossible to find the exact values of x_1 and y_2, though the sections at some points (concerning z_2) verified the results already found.

When the Patterson calculations failed to give more exact x_1 and y_2 values, some preliminary "trial and error" calculations were started, in which x_1 and

Table 2. Vectors in the Patterson sections.

u	v	w	observed height (arbitrary units)	weight
0	0.320	0	4 500	1
0.422	0.040	0	3 000	1
0.309	0.269	0.482	4 000	1
0.500	0.500	0.228	9 000	2
0.180	0.500	0.228	3 000	1
0.078	0.500	0.018	3 500	1
0.480	0.500	0.018	7 500	2
0.340	0.340	0.500	9 000	2
0.191	0.191	0.500	6 500	2
0.231	0.231	0.500	6 500	2
0.020	0.129	0.377	4 000	1
0.020	0.449	0.377	2 750	1
0.480	0.371	0.395	3 200	1
0.480	0.051	0.395	4 000	1

Table 3. Vectors in $P(uvp)$.

u	v	observed height (arbitrary units)	weight
0	0.320	700	1
0.422	0.040	200	1
0.309	0.269	300	1
0.160	0.160	1 100	2
0.500	0.500	2 500	4
0.180	0.500	850	1
0.078	0.500	1 000	2
0.340	0.340	850	2
0.191	0.191	900	2
0.231	0.231	350	2
0.289	0.140	700	1
0.289	0.180		1
0.020	0.129	600	1
0.020	0.449	300	1
0.211	0.360	600	1
0.211	0.320		1
0.480	0.371	400	1

Table 4. Vectors in $P(upw)$.

u	w	observed height (arbitrary units)	weight
0.320	0	900	1
0.422	0	400	1
0.309	0.482	1 000	1
0.269	0.482	400	1
0.160	0.272	1 200	2
0.500	0.228	1 800	3
0.180	0.228	700	1
0.500	0.018	1 300	2
0.480	0.018		1
0.078	0.018	—	1
0.340	0.500	2 300	2
0.191	0.500	1 400	2
0.231	0.500	1 400	2
0.289	0.105	1 500	2
0.140	0.105	650	1
0.180	0.105	650	1
0.020	0.377	1 200	2
0.129	0.377	300	1
0.449	0.377	500	1
0.211	0.123	600	2
0.360	0.123	1 400	1
0.320	0.123		1
0.480	0.395	1 100	2
0.371	0.395	700	1
0.051	0.395	400	1

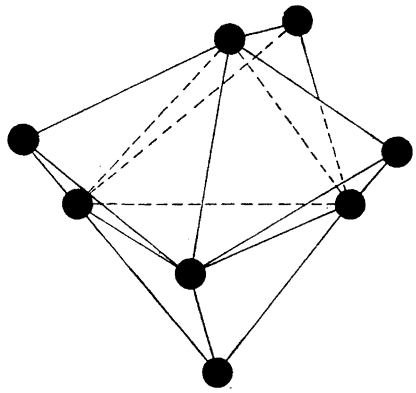

Fig. 7. The group of 8 Sn-atoms occurring in the crystals of Sn_2OSO_4.

y_2 were varied within the limits -0.04 and $+ 0.04$, and the calculated tin contributions to the structure factors [12,13] were compared with the observed structure factors. A full investigation of this kind can not be expected to give good results until the positions of the sulfur and oxygen atoms in the unit cell are known, at least approximately. The results of the preliminary "trial and error" calculations seem, however, to indicate that $x_1 = 0$ and $y_2 = 0.020$. The following arrangement is thus proposed for the tin atoms in the unit cell:

8 Sn_1 in $P\bar{4}2_1c$ with $x_1 \approx 0$ $y_1 \approx 0.160$ $z_1 \approx 0.136$
8 Sn_2 in $P\bar{4}2_1c$ with $x_2 \approx 0.289$ $y_2 \approx 0.020$ $z_2 \approx 0.241$

In the Tables 2—4 the vectors Sn—Sn calculated with these parameters are given and compared to the sections and projections of $P(uvw)$ which were calculated. The agreement is quite good, but in the projections there are some small discrepancies, the most obvious one being the vector $u = 0.078$; $w = 0.018$ in $P(upw)$, which falls in a negative region. However, its weight is low it is situated close to the large maximum at the origin and is consequently heavily influenced by diffraction effects. Moreover, the vector appears with the expected height in $P(u\frac{1}{2}w)$.

The agreement between the calculated and observed vectors in $P(uvw)$ can thus be considered as satisfactory.

DISCUSSION

The present investigation has led so far to the determination of the tin positions. It is hoped to publish later a determination of the positions of the sulfur and oxygen atoms and also a refinement of the whole structure.

The tin atoms form groups, each containing eight atoms (*cf.* Fig. 7). Four atoms Sn_1 form an almost regular tetrahedron, with a $Sn_1—Sn_1$ distance of 3.5 Å. Four atoms Sn_2 are situated so that four new tetrahedra are formed, each of them having one face in common with the Sn_1 tetrahedron. The top

atoms (= Sn_2) of the new four tetrahedra are situated 3.6—3.8 Å from the three tin atoms (= Sn_1) in the central tetrahedron. The shortest Sn—Sn distances between the groups are 4.5 Å.

Acknowledgements. The author wishes to thank Professor Sture Fronæus and Professor Lars Gunnar Sillén for their kind encouragement. The author is also much indebted to Dr Georg Lundgren for his introducing me in the methods of X-ray crystallography and for many helpful discussions during this work.

My thanks are also due to my wife, Mrs. Margareta Wernfors, to Miss Gunilla Bergström, Mr. Arne Jonsson, Mr. Rudolf Tholin, and Mr. Frans Ericson, who all have helped me in the practical work.

I am also very thankful to Dr. Derek Lewis for correcting the English text of this paper.

The support given to the work by the *Faculty of Mathematics and Natural Science, University, Lund*, Sweden and by the *Swedish Natural Science Research Council* is gratefully acknowledged.

This work has been sponsored in part by the *Air Force Office of Scientific Research of the ARDC, USAF*, through its European Office on contract number AF 61(052)—162.

The author is also indebted to the *Swedish Board for Computing Machinery* and to the University of Lund, Lund, Sweden, for the opportunity to make the calculations on the computers BESK and SMIL.

REFERENCES

1. Tobias, S. *Acta Chem. Scand.* **12** (1958) 198.
2. Mellor, J. W. *A comprehensive treatise on inorganic and theoretical chemistry*, Vol. VII, p. 478. Longmans, Green and Co. London 1927.
3. Ditte, A. *Ann. Chim. Phys.* **27** (1882) 145.
4. Ditte, A. *Compt. rend.* **97** (1883) 42.
5. Carson, C. M. *J. Am. Chem. Soc.* **41** (1919) 1969.
6. Ditte, A. *Ann. Chim. Phys.* **27** (1882) 159.
7. Carson, C. M. *J. Am. Chem. Soc.* **48** (1926) 906.
8. Kolthoff, I. M. and Sandell, E. B. *Textbook of Quantitative Inorganic Analysis*, Macmillan, New York 1943, p. 753.
9. Hartwig-Bendig, M. *Z. angew. Mineral.* **3** (1941)195.
10. Lu, C. S. *Rev. Sci. Instr.* **14** (1943) 331.
11. *International Tables for X-ray Crystallography*, Vol. I, The Kynoch Press, Birmingham, 1952.
12. Vand, V., Eiland, P. F. and Pepinsky, R. *Acta Cryst.* **10** (1957) 303.
13. Åsbrink, S., Blomqvist, G. and Westman, S. *Arkiv. Kemi* **14** (1959) 545.

Received January 13, 1961.

ACTA CHEMICA SCANDINAVICA 15 (1961) 1017–1020

Separation of Nucleotides on Ecteola Cellulose

ROY NILSSON and MARGOT SJUNNESSON

Department of Zoophysiology, University of Lund and State Dairy Research Station, Alnarp, Sweden

A chromatographic method is described for separating nucleotides. The method is based on ion-exchange on ecteola cellulose. The nucleotides are separated by elution with a linear gradient of triethylammonium acetate at pH 6.

The method is suitable for the analysis of solutions or extracts containing labile compounds, since the separation is performed at a pH not far from neutrality and since the eluent is easily removed by freeze-drying.

Determination of the nucleotide content of different organs and organisms is chiefly based upon separation of the nucleotides by ion-exchange chromatography on different anion-exchange resins.

In 1950 Cohn [1] developed a method in which the nucleotide components of nucleic acid were separated by elution from Dowex-2 columns with hydrochloric acid. In 1953 Cohn and Volkin [2] extended the versatility of the method by introducing formic acid — formate mixtures as eluents. Several authors have since modified this method in various respects. For example Bergkvist and Deutsch [3] and Hurlbert *et al.*[4] developed different formic acid — formate elution systems and Pontis and Blumson [5] a system with a gradient of calcium chloride and dilute hydrochloric acid.

Very complex nucleotide mixtures can be resolved with these methods. However, there remain two major problems; the quantitative recovery of the components and the recovery of labile compounds in intact form.

The compounds can be recovered in two different ways from the dilute solution in which they are obtained from the column; the eluent can be removed or the eluted nucleotides can be removed selectively. In some cases the eluent is easily removed, *e.g.* formic acid by freeze-drying and ammonium formate by sublimation, but in other cases, *e.g.* sodium formate, it is difficult to remove the eluent.

The best method for removing the nucleotides from the eluates is the procedure developed by Crane and Lipmann [6]. The nucleotides are adsorbed on charcoal from acid solution and can then be eluted with ammoniacal ethanol. However, even if the removal of the nucleotides is quantitative the method has a drawback in that the elution is not quantitative and in some cases only little of the compounds is recovered.

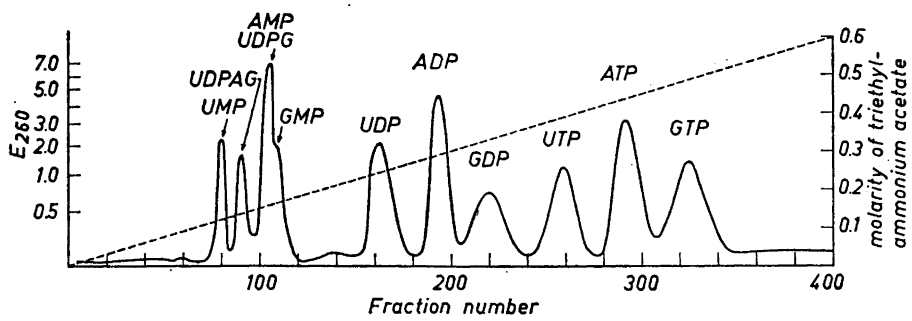

Fig. 1. Ion-exchange chromatography of nucleoside polyphosphates. Column: ecteola cellulose, 1 cm × 25 cm. Eluent: a linear gradient of triethylammonium acetate, pH 6. The adsorbed material had a total optical density $E_{260} = 825$. Recovery 98 %.

Furthermore, in most of the methods used, the nucleotides are exposed to rather extreme acid and alkaline conditions which may destroy labile compounds. The advantages gained by using a mild extracting agent such as phenol or ethanol are therefore more or less lost on exposing of the extract to drastic changes in pH either during the ion-exchange chromatography or in the concentration step by the charcoal method.

To avoid the difficulties mentioned, the ion-exchange chromatography of extracts containing acid or alkali labile compounds should be performed at a pH around pH 7 and one should use an eluent that can be quantitatively removed at low temperatures. The method described below appears largely to satisfy these requirements.

The ion-exchange material which promised to give the best results was the weakly basic ecteola cellulose, which has been used by several authors [7–11] for fractionation of oligonucleotides and nucleic acids. Michelson [11] also used ecteola columns for separation of different adenosine monophosphates.

In previous investigations, sodium chloride or lithium chloride were used as eluents. In preliminary experiments we have also found a good separation of AMP *, ADP and ATP by using a gradient of lithium chloride at pH 6. But since it was difficult to remove the lithium chloride — even if it can be done by extraction with absolute ethanol after freeze-drying — we sought an eluent more suitable for our purposes.

We found triethylammonium acetate to serve the purpose well. It gives good separations, it is easily removed by freeze-drying, and since it has a very low light absorption at wavelengths over 250 mμ it does not interfere with the measurements of the fractions.

Fig. 1 shows the separation of 11 nucleotides on an ecteola column using a linear gradient of triethylammonium acetate at pH 6 as eluent. The gradient

* A = adenosine
G = guanosine
C = cytidine
U = uridine
UDPG = UDP-glucose
UDPAG = UDP-acetylglucosamine
MP = 5′-monophosphate
DP = 5′-diphosphate
TP = 5′-triphosphate
DPN = diphosphopyridine nucleotide

was applied in two steps. The first step running from 0 to 0.3 M triethylammonium acetate eluted the nucleoside mono- and diphosphates with the exception of GDP; in the next step a gradient from 0.3 to 0.6 M eluted the remaining compounds.

In each group of nucleotides, *viz.* the different mono-, di- and triphosphates, the substances were eluted in the order uridine, adenosine and guanosine compounds. As judged from the elution position for CTP between ADP and UTP, the cytidine derivatives are eluted before the corresponding uridine derivatives. DPN is eluted before UMP. Bases and nucleosides are only weakly retained on the column; part of them runs straight through the column and the rest is eluted in the first fractions.

Very complex mixtures of nucleotides are not completely resolved by this method. The overlapping of UDPG, AMP and GMP is seen in Fig. 1, and with an increased number of components in the solution to be chromatographed there should be still more chances for overlapping. However, heterogeneous fractions can be resolved into individual components by rechromatography of the freeze-dried fraction, using a less steep gradient.

The method is very useful for the separation of extracts containing only a few components. The nucleotides in extracts from the rabbit's vagina [12] were thus well and rapidly separated. The method has also been used for resolving complex fractions obtained by chromatography on Dowex-1. The uric acid peak from human milk [13] was thus resolved into three components when rechromatographed on ecteola [14].

The recovery of each of the compounds is quantitative. However, the ecteola cellulose seemed rapidly to alter its exchange properties in that respect. The first four or five runs gave a recovery of 95—105 %, but in the following runs it decreased and after eight runs only 65 % of the adsorbed optical density was eluted. The irreversible adsorption might be due to the accumulation of metal ions on the column, as was reported by Lipkin *et al.*[15] to occur on Dowex-1. However, treatment of the ecteola columns with ethylenediaminetetraacetic acid did not restore the original ion-exchange properties as it did with Dowex-1.

Triethylammonium acetate is easily removed by freeze-drying, but the formate is still better in that respect and should therefore presumably be more suitable as eluent. However, substituting formate for acetate impaired the separation; therefore the acetate was preferred.

The advantages of the present method can be summarized as follows: (1) the separation is performed under mild conditions, at almost neutral pH, (2) the eluent is easily removed also under mild conditions, as *e.g.* by freeze-drying, (3) the separation is very rapid, a complete run not taking more than 24—36 h and (4) the individual compounds appear as sharp and high peaks, which make it possible to use rather small samples.

EXPERIMENTAL

Nucleotides were obtained from Sigma Chemical Co. Some samples of UMP, UDPG, UDPAG and UDP were, however, substances isolated from cow's colostrum [16].

Triethylamine was obtained from Eastman Kodak Co. It contained a component with high absorption in the ultraviolet range but could be purified by distillation through a 35 cm Vigreux column.

Acetic acid and *formic acid* were of Merck's analytical grade.

Chromatography. Ecteola cellulose (Whatman) in powder form was suspended in water and freed from fines by decantation. A dilute suspension of the ecteola powder was poured into a column and allowed to settle under gravity. The column (1 cm × 25 cm) was washed with 200 ml of M triethylammonium acetate pH 6 and then with water to remove the excess triethylammonium acetate.

The substances to be separated were adsorbed from a dilute water solution at a pH between 6 and 7. After adsorption the column was washed with three bed volumes of water; the optical density of the effluent at 260 mμ was then usually below 0.05.

The elution was performed with a linear gradient of triethylammonium acetate with the following composition: 500 ml of distilled water (in a flask, No. 1, fitted with a magnetic stirrer and connected to the column) and 500 ml of 0.3 M triethylammonium acetate, pH 6 (in another flask, No. 2, connected with flask No. 1 by a siphon). The two flasks were placed at the same level. If the separation was not finished by this solution it was continued with 500 ml of 0.3 M triethylammonium acetate in flask No. 1 and 500 ml of 0.6 M solution in flask No. 2.

The flow rate was 1—2 ml per min.

The optical density of the eluate was continuously read at 254 mμ in a LKB Uvicord Ultraviolet Absorptiometer. The eluate was then collected in 5 ml fractions in a fraction collector.

The identification of the components was based on ultraviolet spectra and R_F-values in several paper chromatographic solvent systems. Appropriate fractions from the ion-exchange were pooled and freeze-dried; the residue was taken up in a small volume of water and used for paper chromatography before and after hydrolysis.

The purine or pyrimidine part of the nucleotides was identified after hydrolysis for 1 h in N hydrochloric acid at 100°C by paper chromatography in *iso*butyric acid — ammonia (*d* 0.880) — water (66:1:33).

The sugar moiety was identified after hydrolysis in N hydrochloric acid for 10 min at 100°C, by chromatography in ethylacetate — pyridine — water (20:7:5) and butanol — pyridine — water (6:4:3). The carbohydrate spots were detected by spraying with aniline hydrogen phthalate and with the Elson-Morgan reagent.

The identification was finally checked by chromatography in *iso*butyric acid — ammonia (*d* 0.880) — water (66:1:33) and ethanol — M ammonium acetate, pH 7.5 (70:30).

This work has been supported by the *Swedish Natural Science Research Council* and *Kungl. Fysiografiska Sällskapet, Lund.*

REFERENCES

1. Cohn, W. E. *J. Am. Chem. Soc.* **72** (1950) 1471.
2. Cohn, W. E. and Volkin, E. *J. Biol. Chem.* **203** (1953) 319.
3. Bergkvist, R. and Deutsch, A. *Acta Chem. Scand.* **8** (1954) 1877.
4. Hurlbert, R. B., Schmitz, H., Brumm, A. F. and Potter, V. R. *J. Biol. Chem.* **209** (1954) 23.
5. Pontis, H. G. and Blumson, N. L. *Biochim et Biophys. Acta* **27** (1958) 618.
6. Crane, R. K. and Lipmann, F. *J. Biol. Chem.* **201** (1953) 235.
7. Bendich, A., Fresco, J. R., Rosenkranz, H. S. and Beiser, S. M. *J. Am. Chem. Soc.* **77** (1955) 3671.
8. Bradley, D. F. and Rich, A. *J. Am. Chem. Soc.* **78** (1956) 5898.
9. Bendich, A., Pahl, H. B., Korngold, G. C., Rosenkranz, H. S. and Fresco, J. R. *J. Am. Chem. Soc.* **80** (1958) 3949.
10. Tener, G. M., Khorana, H. G., Markham, R. and Pol, E. H. *J. Am. Chem. Soc.* **80** (1958) 6233.
11. Michelson, A. M. *J. Chem. Soc.* **1959** 3655.
12. Bengtsson, L. Ph., Deutsch, A. and Nilsson, R. *To be published.*
13. Deutsch, A. and Nilsson, R. *Z. physiol. Chem. Hoppe-Seyler's* **321** (1960) 246.
14. Deutsch, A. and Lundqvist, K. *To be published.*
15. Lipkin, D., Markham, R. and Cook, W. H. *J. Am. Chem. Soc.* **81** (1959) 6075.
16. Deutsch, A. and Mattsson, S. *Milk and Dairy Research (Alnarp Sweden)* Report No. 63 (1960).

Received January 7, 1961.

ACTA CHEMICA SCANDINAVICA 15 (1961) 1021–1025

On the Alkylation of Diphenylpyridylmethanes

O. MÅRTENSSON and E. NILSSON

Pharmacia Research Laboratories, Uppsala, Sweden

The 2-, 3-, and 4-isomers of diphenylpyridylmethane have been alkylated in an inert solvent (generally toluene) by using commercial, ground sodamide as basic agent. The diphenyl-3-pyridylmethane reacts definitely slower than the 2- and 4-isomers in forming sodium compounds when treated with sodamide in the refluxing solvent. The yields of alkylated compounds also proved to be lower in this case. Attempts to prepare the sodium compound of the 3-isomer by using sodamide in liquid ammonia or by using phenylsodium did not improve the yield of alkylation product.

The present authors have previously reported the result of their studies of the alkylation at the *a*-position of N,N-disubstituted arylacetic acid carbonamides [1] and of N,N-disubstituted toluene(*a*)sulphonamides and diphenylmethane(*a*)sulphonamides [2]. In these cases, the activation of the hydrogen atom at the *a*-position is caused by the phenyl group(s) and the carbonamide or sulphonamide group. In connection with these studies, we found it to be of interest to look somewhat at the alkylation conditions of the diphenylpyridylmethanes. The trend of this work, like the preceding ones, has been to find out the simplest, least laborious alkylation method. The reaction can be represented by the formula:

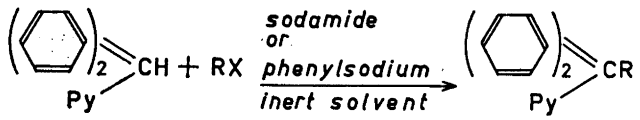

Py = 2-, 3- and 4-pyridyl. R = *neo*hexyl, *n*-octyl and *p*-chlorobenzyl. X = halogen.

It is well known, that the *a*-hydrogen of triphenylmethane is very active and can be fairly easily replaced by sodium or other alkali metals. The sodium compound, generally named tritylsodium, is, however, generally not prepared from the hydrocarbon but from trityl chloride and sodium amalgam [3,4] or, as we have found most convenient, from trityl chloride and sodium dispersion. Its preparation from the hydrocarbon requires a fairly strong basic agent, *e.g.* phenylsodium. It can presumably also be prepared from tolylsodium or diphenylmethylsodium, but since these compounds are most easily prepared *via* phenylsodium, these routes are of less interest. Of interest in this context is that tritylsodium cannot be prepared merely from sodamide and the hydro-

carbon in boiling toluene. In contrast to triphenylmethane and not quite unexpectedly, all the three diphenylpyridylmethanes form sodium compounds under this reaction condition. Metalations of diphenylpyridylmethanes have been reported earlier but, as far as we can find, not with this simple procedure. These metalations have been carried out by means of butyllithium or the phenylsodium — phenyllithium complex [5].

2-Pyridyldiphenylmethane and the 4-isomer react easily when refluxed with sodamide in toluene, giving, respectively, brick red and bright red solutions from which the sodium compounds begin to precipitate after a fairly short time of reflux. Benzene can even be used as solvent but in most cases toluene is to be preferred. The strong evolution of ammonia ceases after one or two hours reflux but the formation of sodium compound is not complete since parts of the sodamide remain enclosed in the precipitate. A second "ammonia peak" is therefore observed after the alkylating agent has been added and the precipitated sodium compound has reacted and disappeared. The sodium compounds are fairly stable and some alkylating agents such as ordinary alkyl chlorides react slowly with them even at the reflux temperature of the reaction mixture. Unless the chlorides are rather reactive, bromides are to be preferred. For further details, we refer to the experimental part.

It is obvious that at least the 2- and 4-pyridyldiphenylmethanes can be alkylated generally by this simple procedure. Of course, the groups intended to be introduced must not contain hydrogen atoms more mobile than the *a*-hydrogen atom of the parent methane, or groups which may rearrange as to form such active hydrogen. However, the reaction mixtures often are difficult to work up. When bulky groups are introduced, the alkylation product can be separated from the parent methane and some tarry products by distillation *in vacuo* but this separation method demands fairly bulky groups. Indeed, even the *neo*hexyl derivative is difficult to isolate from the parent methane by mere distillation. Moreover, in most cases the alkylation product is more soluble in most organic solvents than is the parent methane, a fact which leads to considerable losses during repeated recrystallization. Therefore, in this paper, we have selected *p*-chlorobenzyl chloride and octyl bromide as alkylating agents. We have also included the results from attempts with *neo*hexyl bromide, but the alkylation products proved to be difficult to isolate in yields which are representative of how the alkylation had proceeded.

As expected, 3-pyridyldiphenylmethane behaves somewhat differently compared with the 2- and 4-isomers. It reacts definitely slower with sodamide in boiling inert solvents than do the 2- and 4-isomers. In boiling benzene, the formation of the dark brown to almost black sodium compound proceeds very slowly and the yields of alkylation products are very low even after prolonged reflux. Toluene and xylene give better results and the yields calculated on the parent methane seem to increase to some extent with the temperature in alkylations with *n*-octyl bromide. On the other hand, the amounts of tarry remainders increase when higher temperatures are used. Yields somewhat higher than 40 % have only rarely been obtained. We have also tried to get a more complete sodium compound formation by using liquid ammonia and sodamide in this step but this procedure does not seem to give any improvement. Nor did another attempt in which phenylsodium was used as metalation agent

improve the yield. In these two last attempts, *n*-octyl bromide was used as alkylating agent.

Briefly, one can say that the difference between the diphenylpyridylmethanes on one side and triphenylmethane on the other is caused by the higher degree of electron attraction power of the pyridine nucleus compared with the phenyl nucleus (as the picolines are stronger acids than toluene). Within the diphenylpyridylmethane series, the 2- and 4-pyridyl compounds are the most active ones as is also the case within the picoline series.

Whether or not any side-reactions occur during the sodamide treatment or during the alkylation itself is difficult to decide. In addition to the alkylation product and limited amounts of the parent methane (in the case of the 3-isomer, considerable amounts), only reddish brown tarry oils or semisolid products seem to occur in the reaction mixture or seem to have been formed during the distillation. Amination of the pyridine nucleus (Chichibabin reaction) and/or metalation of the aromatic nuclei may be mentioned as examples of side-reactions which cannot be excluded as completely improbable.

EXPERIMENTAL

The diphenylpyridylmethanes used as starting materials have been prepared by the conventional route *via* the carbinols. The improved method of reduction of diphenylpyridylcarbinols recently reported in a paper by Otto *et al.*[5] has been used for the preparation of diphenyl-3-pyridylmethane but the 2- and 4-compounds had been prepared before the appearance of this paper. Since the earlier reported synthesis of diphenyl-3-pyridylcarbinol from 3-bromopyridine [6] is fairly troublesome, we have instead prepared this carbinol from the easily available 3-benzoylpyridine [7] and phenyllithium in excellent yield. Attempts to prepare the carbinol from 3-benzoylpyridine or ethyl nicotinate and phenyl magnesium bromide by the conventional procedure have given very unsatisfactory yields, As has been reported recently by Fuson and Miller [8], 3-benzoylpyridine reacts with phenylmagnesium bromide under formation of 45 % of dihydro-3-benzoyl-4-phenylpyridine and only 22 % of 3-pyridyl-diphenylcarbinol.

Diphenyl-3-pyridylcarbinol hydrochloride. A solution of phenyllithium in ether, prepared from 13.2 g (1.88 mole) of lithium, is cooled to −5°. While stirring, a solution of 140 g (0.76 mole) of 3-benzoylpyridine in 400 ml of dry ether is added by means of a dropping funnel during the course of 20−25 min. and during intermittent cooling with a dry ice-ethanol bath in order to keep the temperature at about −5°. When the addition is finished, the cooling bath is removed and the reaction mixture is left at room temperature and stirred for 1.5 h. 500 ml of 10 % hydrochloric acid is added as rapidly as possible, while cooling with the cooling bath. The temperature in the flask is kept at 20−25° during the addition of the acid. The mixture is now left at room temperature, while stirring, for about 30 min. The precipitated hydrochloride is filtered off, washed with ether and dried at room temperature. It is then washed by dispersing in 500 ml of acetone and is filtered off again, washed with ether and dried. The yield is about 225 g or approximately quantitative (calculated on 3-benzoylpyridine). The product melts at 226−229° and is sufficiently pure to be used in the reduction step.

Diphenyl-n-octyl-2-pyridylmethane. 17.2 g (0.07 mole) of diphenyl-2-pyridylmethane, 3.0 g of commercial, ground sodamide and 100 ml of dry toluene are refluxed in a flask equipped with stirrer, reflux condensor, and thermometer. A strong evolution of ammonia begins and the contents become brick red. After about one hour's reflux, a thick precipitate of the sodium compound has been formed in the flask and the ammonia evolution has almost ceased. The contents in the flask are cooled somewhat (to about 100°), and 15.5 g (theoretically 14.5 g) of *n*-octyl bromide are added dropwise by means of a dropping funnel *via* the condensor. During the course of the addition, the precipitate disappears almost completely and evolution of ammonia begins again. The dropping funnel and the condensor are rinsed with a small amount of dry toluene and the flask is heated to reflux and is maintained at this temperature for 5 h. The contents in the flask are cooled to

room temperature, water is added and the toluene layer is washed with water in a separatory funnel. The toluene layer is dried with anhydrous sodium sulphate and the toluene is driven off. The remaining reddish oil is distilled *in vacuo*. After a fore-run of a few grams, the main part distils at 185—195°/0.1 mm (20.4 g). Redistillation gives 19.5 g (77 %) of an almost colourless, viscous oil with b.p. 190—195°/0.1 mm. (Found: C 87.11; H 9.04; N 3.79. Calc. for $C_{26}H_{31}N$ (357.5): C 87.34; H 8.74; N 3.92.) Picrate: M.p. 178—179° (from alcohol).

After standing some weeks, the oil solidifies. Two recrystallizations from small amounts of petroleum ether give colourless crystals with m.p. 41—42.5°.

Diphenyl-n-octyl-4-pyridylmethane. This synthesis is carried out analogously to the preceding one. The colour of the sodium salt of the 4-isomer, however, is blood red. The final product is redistilled at 200—202°/0.1 mm. The *n*-octyl derivative is a viscous almost colourless oil. Yield 56.5 %. (Found: C 86.90; H 8.87; N 3.85.) Picrate: M.p. 139—141° (from alcohol).

Diphenyl-n-octyl-3-pyridylmethane. The sodium compound, used in the preparation of this compound, is prepared in three different ways:

a) With sodamide. A mixture of 24.5 g (0.1 mole) of diphenyl-3-pyridylmethane, 4.2 g of sodamide and 125 ml of dry toluene is refluxed for about 2 h. The ammonia evolution is fairly strong at the beginning of the reflux and the contents of the flask become intensely dark brown. The heating is interrupted and *n*-octyl bromide is added by means of a dropping funnel at about 100° until the colour of the contents lightens. About 10 g or half the total amount of bromide (20.0 g, theoret. 19.3 g), are consumed in this step. The temperature is raised and the mixture is refluxed for about half an hour. The evolution of ammonia is fairly strong immediately after the addition of the bromide. This procedure is repeated again and the remainder of the bromide added, followed by reflux for 4 h. The reaction mixture is worked up in the usual way, and the remaining oil distilled. A fore-run at 155—160°/0.2 mm consists of 14.5 g (64 %) of the parent methane. Another fraction at 185—200°/0.2—0.5 mm consists of fairly pure *n*-octyl derivative, 10.0 g (28 %). After redistillation, 7.0 g (20 %) is obtained as a viscous, colourless oil. B.p. 187—190°/0.1 mm. (Found: C 86.80; H 8.82; N 3.87.) Picrate: M.p. 117—118° (from alcohol).

The above method can be modified and xylene used as solvent: The mixture is refluxed for 2 h, cooled to about 120° and the bromide is added. After the addition of the bromide, which gives definitely exothermic reaction with decolourization of the flask contents, the temperature is increased and the mixture refluxed for 3 h. The recovered amount of parent methane is in this case 7.0 g (28 %). The yield of *n*-octyl derivative with b.p. 194—200°/0.1 mm is 15.0 g (42 %). The amount of tarry remainder in the distillation flask is definitely larger in this case than in the preceding one.

b) Sodamide in liquid ammonia. Sodamide in liquid ammonia is prepared in conventional manner from 2.7 g of sodium. 24.5 g (0.1 mole) of the methane, dissolved in 100 ml of dry toluene is added by means of a dropping funnel. The temperature is kept at about 35° by intermittent cooling of the flask. The ammonia is allowed to evaporate while the flask is flushed slowly with nitrogen. The contents are now warmed gently to 70—80°. 20.0 g (theoret. 19.3 g) of octyl bromide, diluted with 25 ml of dry toluene are added slowly, during which procedure the dark brown colour becomes pale. After the addition of the bromide, the contents are refluxed for 2 h. The reaction mixture is worked up in the usual way. Distillation gives two main fractions: the first one at 150—165°/0.1 mm consisting of 15.0 g (61 %) of parent methane; the second one at 195—200°/0.2 mm consisting of 11.0 g (31 %) of the *n*-octyl derivative.

c) With phenylsodium. Description of the metalation procedure has been given earlier [2]. The solution of 24.5 g (0.1 mole) of the methane in 50 ml of dry toluene is added to the phenylsodium suspension (from 5.0 g of sodium) while stirring at a temperature of about 30° (intermittent cooling). After the addition the stirring is continued for 15 min. The *n*-octyl bromide (20.5 g), diluted with 10 ml of dry toluene, is added drop by drop. During this procedure the dark colour becomes paler and disappears at the end of the addition. The stirring is continued for 1 h after the addition. A few ml of alcohol are added to the reaction mixture before the addition of water but, otherwise, the mixture is worked up in the usual way. At distillation, 12.5 g (15 %) of the parent methane is recovered (b.p. 165—170°/0.3—0.4 mm). The octyl derivative distils at 200—205°/0.3—0.4 mm with a yield of 13.0 g (36 %). The remainder in the distillation flask is small (2 g).

p-*Chlorobenzyl-diphenyl-2-pyridylmethane.* 22.1 g (0.09 mole) of diphenyl-2-pyridylmethane, 3.7 g of sodamide and 125 ml of dry xylene are refluxed for 3 h. The *p*-chlorobenzyl chloride (15.0 g, theoret. 14.5 g) dissolved in 50 ml of dry xylene is added during the course of 15 min. The mixture is refluxed for 2.5 h at which time the evolution of ammonia has ceased. The reaction mixture is worked up in the usual way. A main fraction (210—215°/0.1—0.2 mm) gives 16.5 g or 49.5 %. Recrystallization from a mixture of methanol and cyclohexane gives 14.8 g (44.5 %). M.p. 148—151.5°.

With toluene as solvent the yields have been lower (about 20 %), but we think that this yield may be improved. A sufficiently pure product melts at 151—152.5°. (Found: C 81.40; H 5.34; N 3.72. Calc. for $C_{25}H_{20}NCl$ (369.9): C 81.17; H 5.45; N 3.79).

p-*Chlorobenzyl-diphenyl-4-pyridylmethane* is prepared in toluene by the conventional method but the mixture is kept at a temperature of about 80° throughout the synthesis. 0.1 mole of the parent methane is used. The after-heating lasts for 9 h. The reaction mixture is worked up as above. The remaining oil, on distillation, gives two main fractions: at 160—165°/0.2 mm, 5.5 g (22.5 %) of the parent methane; at 230—240°/0.2—0.3 mm, 23.0 g (62 %) of the desired *p*-chlorobenzyl compound. After recrystallization from methanol the yield is 17.0 g (46 %) with m.p. 154—156°. (Found: C 81.51; H 5.45; N 3.82; Cl 9.46. (Calc. Cl 9.58).

p-*Chlorobenzyl-diphenyl-3-pyridylmethane.* A mixture of 24.5 g (0.1 mole) of diphenyl-3-pyridylmethane, 4.2 g of sodamide and 125 ml of dry toluene is refluxed for about 2 h. The evolution of ammonia is fairly strong at the beginning of the reflux and the contents soon become dark brown. The contents of the flask are cooled to about 80° and a solution of 17.0 (theoret. 16.1) g of *p*-chlorobenzyl chloride in 50 ml of dry toluene is added by means of a dropping funnel until the dark brown colour becomes pale and the contents appear clear (about half the amount of the solution is consumed for this purpose). The flask is now heated and the contents are refluxed for about half an hour. The contents are now cooled to about 80° again and the remaining chloride solution added by means of the dropping funnel. The flask is heated again and kept at reflux for one hour, after which time the evolution of ammonia has almost completely ceased. The reaction mixture is cooled to room temperature. The toluene layer is washed with water, dried and the toluene driven off. After a fore-run, giving 9.0 g of the parent methane, the *p*-chlorobenzyl derivative distils at 157—160°/0.1 mm. After recrystallization from a mixture of chloroform and methanol, 6.5 g (17.5 %) of white crystals with m.p. 174—175° are obtained. (Found: C 80.99; H 5.74; N 3.79).

3',3'-Dimethylbutyl-diphenyl-2-pyridylmethane was prepared from 0.05 mole of diphenyl-2-pyridylmethane as described for the *n*-octyl compound but with 9.0 (theoret. 8.25) g of *neo*hexyl (3,3-dimethylbutyl) bromide as alkylating agent. It was isolated after several recrystallizations from petroleum ether of the semisolid remainder from the toluene layer. Yield 6.5 g (39.5 %) of colourless crystals with m.p. 70.5—71.5°. (Found: C 87.73; H 8.31; N 4.28. Calc. for $C_{24}H_{27}N$ (329.5): C 87.49; H 8.26; N 4.25.)

3',3'-Dimethylbutyl-diphenyl-4-pyridylmethane was prepared analogously to the 2-isomer. It proved to be difficult to separate from the parent methane. After many recrystallizations from petroleum ether, a compound with m.p. 92—93.5° was obtained in low yield. (Found: C 87.78; H 8.36; N 4.26.)

The authors are indebted to Mr. W. Kirsten and his assistants for elementary analyses and to Mr. H. Andersson for the preparation of diphenyl-3-pyridylmethane.

REFERENCES

1. Mårtensson, O. and Nilsson, E. *Acta Chem. Scand.* **14** (1960) 1129.
2. Mårtensson, O. and Nilsson, E. *Ibid.* **14** (1960) 1151.
3. Hauser, C. H. and Hudson, Jr., B. E. *Org. Reactions* **1** (1942) 248.
4. *Org. Syntheses Coll. Vol.* **II** (1944) 607.
5. Otto, P. Ph. H. L., Wibaut, J. P. and Groenendaal, G. W. J. M. *Rec. trav. chim.* **78** (1959) 446.
6. French, H. E. and Sears, K. *J. Am. Chem. Soc.* **73** (1951) 469.
7. *Org. Syntheses* **37** (1957) 6.
8. Fuson, R. C. and Miller, J. J. *J. Am. Chem. Soc.* **79** (1957) 3477.

Received December 23, 1960.

ACTA CHEMICA SCANDINAVICA 15 (1961) 1026–1038

On the "Second Alkylation" at the α-Position of Some N,N-disubstituted Arylacetic Acid Amides

O. MÅRTENSSON and E. NILSSON

Pharmacia Research Laboratories, Uppsala, Sweden

The authors have previously given a survey of the alkylation at the α-position of N,N-disubstituted arylacetic acid amides by using sodamide as basic agent and toluene or benzene as inert solvents. In this paper we report some of the results from our investigation of the introduction of a second substituent at the α-position by means of alkylation, a procedure which we briefly call the second alkylation. In contrast to the first alkylation, the second one is less general as to its application and practical use. The mobility of the remaining α-hydrogen seems to vary definitely with the group introduced during the first alkylation. In all probability also steric effects are involved in and complicate the alkylation reaction. Some of the parent α-substituted amides proved to be somewhat unstable against the basic agent when treated with it alone in toluene or when the alkylation procedure was carried out. The use of phenylsodium as salt forming agent in most cases did not improve the method.

It is known [1–4] that N,N-disubstituted diphenylacetic acid amides can be alkylated at the α-position by the simple method of using sodamide or lithium amide as basic agent in the presence of an inert solvent such as toluene or benzene. This procedure is often carried out so that the diphenylacetic acid amide (when no confusion can arise, we omit the epithet N,N-disubstituted) first is more or less completely converted to its alkali metal compound by heating with the alkali metal amide in the inert solvent. The appropriate alkylating agent is then added and the mixture is refluxed for some hours. Actually the amides of diphenylacetic acid react fairly easily with ordinary, commercial, ground sodamide. The activation of the α-hydrogen is fairly pronounced in these compounds, since, in addition to the amide group, not less than two phenyl groups contribute to the activation. The present authors [5] have recently given an account of the application of the same substitution method to many simple arylacetic acid amides. In this case, in addition to the amide group, only one aryl group (phenyl, 1-naphthyl or 3-phenanthryl) contributes to the activation of the α-hydrogen. We have also shown [6] that the

method can be used in alkylation of at least some N,N-disubstituted toluene-(*a*)sulphonamides and diphenylmethane(*a*)sulphonamides.

In this paper we intend to collect the main results of our investigation of the alkylation reaction

$$\mathrm{Ar{-}\underset{\displaystyle R}{\underset{|}{CH}}{-}COY} + R_1X \xrightarrow[\text{inert solvent}]{\text{basic agent}} \mathrm{Ar{-}\overset{\displaystyle R_1}{\overset{|}{\underset{\displaystyle R}{\underset{|}{C}}}}{-}COY}$$

where Ar is an aryl group (mostly phenyl), R is a group (actually ethyl, 2,2-dimethylbutyl, *cyclo*hexyl, allyl, benzyl, 2-pyridyl, 2-thenyl or 2-thiazolyl) which has been (or can be) introduced by the alkylation procedure described by us earlier, R_1 is the alkyl or other group which we intend to introduce in this step, and X is halogen (mostly chlorine). In our investigation, Y in the carbonamide group is a dimethylamino, diethylamino, di*iso*propylamino, *n*-propylbenzylamino, pyrrolidino, piperidino or morpholino group. The diphenyl case (Ar = R = phenyl) is excluded as sufficiently known by other investigations. Since, as pointed out above, the parent amides used in this alkylation reaction can be prepared by alkylation, in order to be brief, we call the alkylation reaction we intend to treat in this paper the second alkylation. The second alkylation is less general as to its practical application than the first one, the yields often are considerably lower and side-reactions may in some cases be important. In some cases where the conventional sodamide procedure has failed to work out satisfactorily (yields of expected substitution product lower than 40 %) we have tried phenylsodium as salt forming agent. Also potassium amide in liquid ammonia has been used. Since this last, more laborious method did not prove to give definitely better results, we did not apply it in more than one case (the alkylation of *a*-benzyl-phenylacetic acid benzyl-propyl-amide). These efforts will be commented on below.

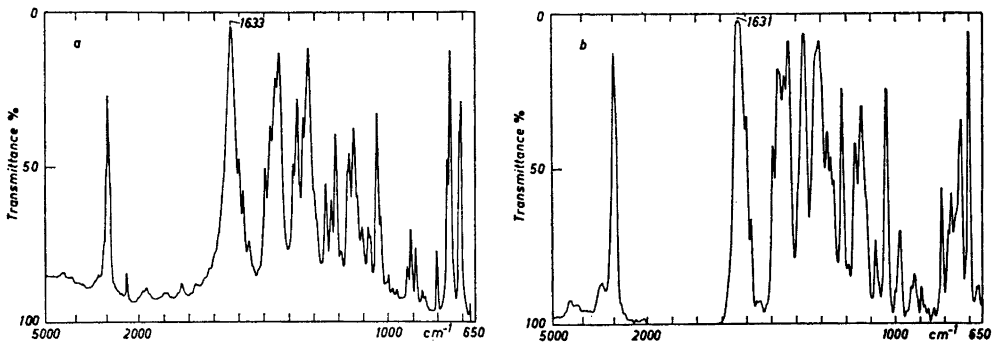

Fig. 1. Infrared spectrum of the parent amide, ethylphenylacetic acid N,N-di*iso*propylamide (a) and its *a*-(3,3-dimethylbutyl) derivative (b), showing that the frequency and intensity of the C=O bond of the amide group at about 1 630 cm^{-1} remain practically unchanged. All spectra are drawn with KBr pellet technique on a Unicam SP 100 IR instrument. The experimental error is ± 2 cm^{-1}.

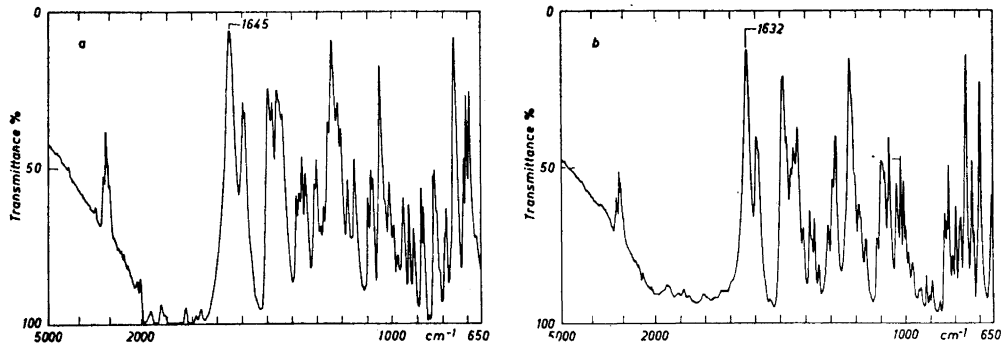

Fig. 2. Infrared spectrum of the parent amide, α-phenoxy-phenylacetic acid N,N-diethylamide (a), and its α-(*p*-chlorobenzyl) derivative (b), showing, that frequency and intensity of the C=O bond (at about 1 640 cm^{-1}) remain almost unchanged. All spectra are drawn with KBr technique on a Unicam SP 100 IR instrument. The experimental error is ± 2 cm^{-1}.

Some tentative efforts have also been made to extend the alkylation method to cases in which R is connected with the α-carbon atom *via* a heteroatom (N or O). The results of these efforts will be mentioned in the last chapter.

When substitution takes place, the reaction, as expected, leads to an alkylation at the α-carbon atom. This is indicated by the fact that the frequency and the intensity of the C=O bond of the amide group are practically unchanged after alkylation. In Figs. 1—3 the infrared spectra of three parent amides can be compared with alkylated compounds derived from them. Figs. 2 and 3 include the cases when R is phenoxy and diethylamino groups, respectively. Moreover, acid hydrolysis and decarboxylation of, for example, the expected compound γ-dimethylamino-α-(*p*-chlorophenyl)-α-(2′-pyridyl)-butyric acid di-

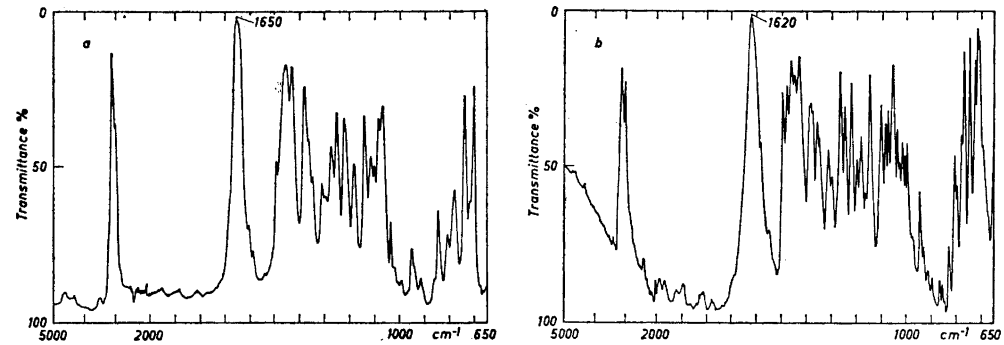

Fig. 3. Infrared spectrum of the parent amide, α-(diethylamino)-phenylacetic acid N,N-diethylamide (a), and its α-benzyl derivative (b), showing, that frequency and intensity of the C=O bond (at about 1 650 cm^{-1}) remain almost unchanged. All spectra are drawn with KBr pellet technique on a Unicam SP 100 IR instrument. The experimental error is ± 2 cm^{-1}.

methylamide gives 1-dimethylamino-3-(*p*-chlorophenyl)-3-(2′-pyridyl)-propane in excellent yield.

Tentative efforts indicate that, in contrast to the parent amides, the amide group of the alkylated products cannot be reduced by lithium aluminium hydride. This behaviour is to be expected, since there remains no hydrogen at the *a*-position (or at the amide nitrogen).

As mentioned earlier by us, in most cases the introduction of a second *a*-substituent in the arylacetic acid amides (the general discussion below is confined to phenylacetic acid amides, *i.e.* with Ar = phenyl), is more difficult than the introduction of the first one. Exceptions are formed by those cases where the earlier introduction of R includes an increase in the activation of the remaining *a*-hydrogen. When R is, for example, ethyl, *cyclo*hexyl or benzyl the reactivity against sodamide in toluene is definitely less than for the parent phenyl acetic acid amides, and it seems as if phenylsodium is to be preferred to sodamide in some of these cases (see below). The amides of phenyl-(2-pyridyl)-acetic acid form a group of compounds which can be advantageously alkylated by using sodamide (Table 1). Their sodium salts generally precipitate during their formation in boiling toluene. They react easily with tertiary 2-aminoethyl chlorides[7] but fairly slowly with ordinary alkyl chlorides. It seems as if bromides are to be preferred unless the alkylating halide is very reactive. Then the corresponding chloride can be used. The mobility of the *a*-hydrogen of these amides is at least as great as in the corresponding amides of diphenylacetic acid. That such is the case is not surprising, since the methyl hydrogen of 2-picoline is already highly active as is well known from the use of picolyllithium in synthetic work. However, too detailed conclusions about the reactivity of the amides against ordinary, commercial sodamide must not be drawn. The particle size of the ground sodamide may vary from one experiment to another, for example due to layer formation in the vessel in which the sodamide is preserved. Corrosion of the surface of the particles due to moisture during even short air exposure may decrease the reactivity even when it is stoichiometrically unimportant.

The dependence of Y of the amide group on the alkylation is more difficult to survey. Judging from the case where R = 2-pyridyl, we tentatively assume that the influence of the amide group is mainly steric, which means that amides of phenyl-(2-pyridyl)-acetic acid can be alkylated fairly independent of the nature of the substituents of the amide group, provided that R_1 is not too bulky. This is in agreement with our experience from the first alkylation procedure, in which case the substituents of the amide group are of minor importance for the applicability of the method.

From the above it follows, that when one intends to replace the two *a*-hydrogen atoms of an arylacetic acid amide, it is not unimportant in what order one tries to introduce the two groups. It seems to be a general rule, that the strongest activating (or least desactivating) group should be introduced first in order to secure a sufficient mobility of the remaining *a*-hydrogen atom for the next alkylation step.

The phenylsodium method has some advantages. Provided that the amide is stable against strong basic agents, it gives a more complete and rapid salt formation at a lower temperature than the conventional sodamide procedure.

Table 1. Compounds prepared by the "second alkylation" at the α-position of N,N-disubstituted phenyl-(2-pyridyl)-acetic acid amides *.

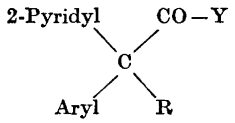

Aryl	Y	R	Yield %	B.p.°C/mm Hg M.p.°C	Formula	Analyses %					
						Calc.			Found		
						C	H	N	C	H	N
Cl-	$-N(CH_3)_2$	Cl- $-CH_2-$	62.5	134 —135 [d]	$C_{22}H_{20}Cl_2N_2O$	66.17	5.05	7.02	65.80	4.91	6.96
—"—	—"—	$-CH_2CH_2N$ H O	50	125 —126.5 [ab]	$C_{21}H_{26}ClN_3O_2$	65.02	6.76	10.83	64.98	6.80	10.70
—"—	—"—	$-CH_2CH_2N(CH_3)_2$	65	177 —180/0.2	$C_{19}H_{24}ClN_3O$	65.98	6.99	12.15	65.62	6.91	12.11
	$-N(C_2H_5)_2$	—"—	73	183 —188/0.5							
				80 — 82 [b]	$C_{21}H_{29}N_3O$	74.30	8.61	12.38	74.30	8.60	12.40
Cl-	—"—	—"—	62	190 —194/0.2							
			25	86 — 88 [c]	$C_{21}H_{28}ClN_3O$	67.45	7.55	11.24	67.48	7.65	11.03

Table 1. Continued.

Aryl	Y	R	Yield %	B.p.°C/mm Hg M.p. °C	Formula	Analyses %					
						Calc.			Found		
						C	H	N	C	H	N
	$-N[CH(CH_3)_2]_2$	$-CH_2CH_2N(C_2H_5)_2$	61 44	170 –172/0.2 66.5– 67.5 [b]	$C_{25}H_{37}N_3O$	75.90	9.43	10.62	75.83	9.57	10.56
— " —		$-CH_2CH_2N(CH_3)_2$	72 40	84 – 87 93.5– 95 [e]	$C_{21}H_{27}N_3O$	74.74	8.07	12.45	74.91	8.07	12.59
— " —			55 32	220 –227/0.2 89 – 91.5[ab]	$C_{24}H_{31}N_3O_2$	73.25	7.94	10.68	73.52	7.96	10.54
— " —	— " —	— " — , HCl		187– 88.5							
— " —		$-CH_2CH_2N(C_2H_5)_2$	65	205 –207/0.3	$C_{23}H_{31}N_3O_2$	72.41	8.19	11.01	72.14	8.00	10.85

* Method I has been applied. The yields are the total ones and refer to the parent amide. When more than one yield figure is given, the compound prepared has been further purified by recrystallization. — Melting points and boiling points are uncorrected. The former have been read from short normal thermometers covering intervals of 50°. The alkylations have been carried out with 0.1—0.05 mole of parent amide. Unless otherwise stated, X in the compound RX is chlorine.

a—e) Recrystallization from a) benzene; b) petroleum ether; ab) a mixture of benzene and petroleum ether; c) *cyclo*hexane; bc) a mixture of *cyclo*hexane and petroleum ether; d) methanol; e) acetone.

Table 2. Compounds prepared by the "second alkylation" at the α-position of some N,N-disubstituted aryl acetic acid amides.

$$\begin{matrix}\mathrm{Ar}\\ \mathrm{R}\end{matrix} > \mathrm{C} < \begin{matrix}\mathrm{R_1}\\ \mathrm{CO\text{-}Y}\end{matrix}$$

Parent amide	R_1	Method	Yield %	B.p.°C/mm Hg M.p.°C	Formula	Analyses					
						Calc.			Found		
						C	H	N	C	H	N
Ph-CHCON(CH$_3$)$_2$ | CH$_2$CH$_2$C(CH$_3$)$_3$	$-CH_2CH_2CH_2N(C_2H_5)_2$	I II	17 47	136 −138/0.05 146 −150/0.1	$C_{23}H_{40}N_2O$	76.61	11.18	7.77	76.88	11.13	7.46
Ph-CHCON(CH$_3$)$_2$ | Ph-CH$_2$	$-CH_2CH_2N(CH_3)_2$	I II	39 24 32	165 −170/0.3 92 − 93 [b] 89 − 92	$C_{21}H_{28}N_2O$	77.73	8.70	8.64	77.85	8.76	8.64
Ph-CHCON(CH$_3$)$_2$ 	$-CH_2CH_2CH_2N[CH(CH_3)_2]_2$	I	31 15	ca 65 75 − 77 [bc]	$C_{22}H_{33}N_3OS$	68.17	8.58	10.84	67.80	8.40	10.78
Ph-CHCON(C$_2$H$_5$)$_2$ | CH$_2$CH=CH$_2$	$-CH_2CH_2C(CH_3)_3$	I	41	130 −135/0.2	$C_{21}H_{33}NO$	79.94	10.55	4.44	80.09	10.64	4.59
— " —	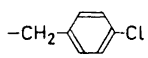	I	76	165 −167/0.1	$C_{22}H_{26}ClNO$	74.24	7.36	3.94	74.37	7.29	3.95
— " —	$-CH_2CH_2N(CH_3)_2$	I	64	124 −130/0.15	$C_{19}H_{30}N_2O$	75.45	10.00	9.26	74.65	10.00	9.23

Table 2. Continued.

Parent amide	R_1	Method	Yield %	B.p.°C/mm Hg M.p.°C	Formula	Analyses					
						Calc.			Found		
						C	H	N	C	H	N
— II —	$-CH_2CH_2CH_2N(C_2H_5)_2$	I	57	170 —174/0.4	$C_{22}H_{36}N_2O$	76.69	10.53	8.13	76.12	10.55	8.20
Ph–CHCON(C_2H_5)$_2$ | $CH_2CH_2C(CH_3)_3$	$-CH_2CH_2N(CH_3)_2$	I	54	140 —142/0.2	$C_{22}H_{38}N_2O$	76.22	11.05	8.08	76.13	11.03	8.13
— II —	$-CH_2CH_2-N$ (H) O	I	19	168 —173/0.05							
		II	25 13	172 —178/0.1 86 — 89 [b]	$C_{24}H_{40}N_2O_2$	74.18	10.38	7.21	74.04	10.15	7.31
Ph–CHCON(C_2H_5)$_2$ (H)	$-CH_2CH_2-N$ (H) O	I	15	117 —118 [b]	$C_{24}H_{38}N_2O_2$	74.56	9.91	7.25	74.31	9.92	7.38
Ph–CHCON(C_2H_5)$_2$ | Ph–CH_2	$-CH_2CH_2N(C_2H_5)_2$	I	62	190 —205/0.5	$C_{25}H_{36}N_2O$	78.90	9.54	7.36	78.82	9.20	7.14
Ph–CHCON(C_2H_5)$_2$ | CH_2 (S)	$-CH_2CH_2N(CH_3)_2$	I II	14 25 21	77.5 — 79.0 70 — 73 76 — 78 [b]	$C_{21}H_{30}N_2OS$	70.35	8.43	7.82	70.11	8.44	7.51

Parent amide	R_1	Method	Yield %	B.p.°C/mm Hg M.p.°C	Formula	Analyses					
						Calc.			Found		
						C	H	N	C	H	N
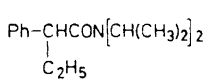	$-CH_2CH_2C(CH_3)_3$	I	50	125 —127/0.1	$C_{22}H_{37}NO$	79.70	11.25	4.23	79.47	10.87	4.35
— " —	$-CH_2CH_2N(C_2H_5)_2$	I	58	153 —155/0.8	$C_{22}H_{38}N_2O$	76.24	11.05	8.09	75.89	11.03	8.19
— " —	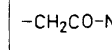	I	16 5	200 —210/0.5 125.5—127.0[ab]	$C_{23}H_{36}N_2O_2$	74.15	9.74	7.52	74.40	9.60	7.57
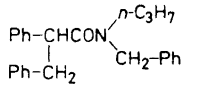	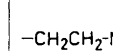	KNH_2 in liq. NH_3 I	48 24 34 30	122 —136 137.5—139.0[c] 135 —138[c] 138.5—140	$C_{31}H_{38}N_2O_2$	79.11	8.14	5.95	79.09	8.23	6.12
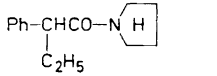	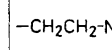	I	23	185 —187/0.2	$C_{20}H_{30}N_2O_2$	72.69	9.15	8.48	72.66	9.12	8.63
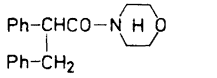	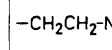	I	34	138 —139.5[c]	$C_{25}H_{32}N_2O_3$	73.50	7.90	6.86	73.85	7.89	6.85
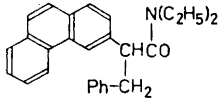	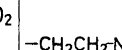	I	52 40	165 —168.5[d] 170.5—171.5	$C_{33}H_{39}N_2O_2$	79.96	7.93	5.65	80.16	7.86	5.66

Notes: Method I refers to the sodamide method; method II to the phenylsodium method. The yields are the total ones and refer to the parent amide. When more than one yield figure is given under a certain method the compound prepared according to this method has been further purified by recrystallization. — Melting points and boiling points are uncorrected. The former have been read from short normal thermometers covering intervals of 50°. With a few exceptions the alkylations have been carried out with 0.1—0.05 mole of parent amide. Unless otherwise stated, X in the compound RX is chlorine. — a—e) Recrystallization from a) benzene; b) petroleum ether; ab) a mixture of benzene and petroleum ether; c) *cyclo*hexane; bc) a mixture of *cyclo*hexane and petroleum ether; d) methanol; e) acetone.

Reaction which may occur between the more reactive halides and the sodamide can thus be avoided. On the other hand, the preparation of phenylsodium involves a further step in the alkylation procedure. The transference of small amounts (0.05—0.1 mole) from one vessel to another involves some difficulties apart from the generally hazardous properties associated with the suspensions of phenylsodium.

In addition to the mobility of the *a*-hydrogen, steric factors probably are of importance. As mentioned above, bulky groups in at least two of the variables R, Y and R_1 appear to decrease the practical applicability of the method. In several cases, side-reactions have proved to occur and may predominate with low or almost no yield of the expected substitution product. To some extent these undesired results can be explained by the fact that some of the parent amides may be more or less unstable against a mere refluxing with sodamide in toluene. Thus, from the reaction mixture of 0.05 mole of the morpholide of phenylethylacetic acid (which belongs to those amides which proved to be difficult to alkylate), refluxed with sodamide for 4.5 h, only a very small amount of the morpholide could be recovered, but 42 % of a compound with the boiling point of propylbenzene could be isolated. Several of the dimethylamides show a definite tendency to split off the dimethylamide group during the alkylation procedure. This is the case when either sodamide or phenylsodium is used in the salt formation step, and the side-reaction seems to be very pronounced in some cases. When *neo*hexylphenylacetic acid dimethylamide (0.1 mole) was alkylated with 3-dimethylaminopropyl chloride and with sodamide as basic agent, the yield of *a*-substitution product was only 17 %. From the non-basic part of the reaction mixture, *neo*heptylbenzene and the parent amide could be isolated in yields of 48 % and 10 %, respectively. When phenylsodium was used the corresponding amounts were 47 %, 25 % and 5 % (0.1 mole of amide used). Since mere refluxing of the parent dimethylamide (0.05 mole) with sodamide in toluene for 5 h gives only traces of any product with the distillation temperature of *neo*heptylbenzene and since 66 % of dimethylamide could be recovered, it seems that, at least in this case, the cleavage of the parent amide is more pronounced when the alkylating agent is present. In the same way, benzylphenylacetic acid dimethylamide (0.6 mole) by alkylation with 2-dimethylaminoethyl chloride gave 39 % of the expected *a*-substitution product, 36.5 % of 1,2-diphenylethane and 14.5 % of recovered dimethylamide. In the phenylsodium case (with 0.1 mole of parent amide) the corresponding amounts were 32 %, 38.5 %, and 16 %, respectively. We have not studied these side-reactions in detail but we mention them here since they form an important limitation in the use of the second alkylation.

Presumably an exchange of a carbon atom adjacent to the *a*-carbon atom with an atom more electronegative than carbon ought to increase the activity of the *a*-hydrogen atom. We have therefore investigated two cases, R = phenoxy and R = diethylamino (both with Ar = phenyl and Y = diethylamino). These amides react easily with sodamide. The activity of their *a*-hydrogen atoms seems to be comparable with that of the amides of diphenylacetic acid or phenyl-2-pyridylacetic acid. The description of the alkylation of these two amides having phenoxy or diethylamino groups in *a*-position together with other data is given under Experimental.

EXPERIMENTAL

Most of the parent amides used have been prepared by the first alkylation procedure described by us earlier. The di*iso*propylamide of α-ethylphenylacetic acid (b.p. 112—116°/0.9 mm; m.p. 70—72°) and the diethylamide of α-allylphenylacetic acid (b.p. 120—122°/0.1—0.2 mm) have been prepared from the commercially available acids by conventional route *via* their acid chlorides.

α-Diethylamino-phenylacetic acid diethylamide has been obtained in good yield directly from the α-bromoacid chloride and diethylamine in benzene. B.p. 112—113°/0.1 mm.

α-Phenoxy-phenylacetic acid diethylamide has been prepared in good yield from the α-bromoacid chloride, which first has been converted to the diethylamide. This and sodium phenolate gave the desired α-phenoxy compound. In both cases benzene has been used as solvent. M.p. 101—102° (from benzene and petroleum ether). (Found: C 76.43; H 7.53; N 5.05. Calc. for $C_{18}H_{21}NO_2$ (283.4): C 76.29; H 7.47; N 4.94.)

α-Benzyl-α-(2-dimethylaminoethyl)-phenylacetic acid N,N-dimethylamide. Method I (with sodamide). 151.8 g (0.6 mole) of α-benzylphenylacetic acid N,N-dimethylamide, 24.2 g of commercial, ground sodamide and 600 ml of dry toluene are refluxed while stirring for about 2 h. After that time, the strong evolution of ammonia has decreased and a yellow precipitate of the sodium compound has been formed. The mixture is cooled to about 60°, a dried solution of 2-dimethylaminoethyl chloride (0.65 mole) in 200 ml of toluene is added and the mixture is warmed gently to reflux. Ammonia is evolved and the precipitate disappears. The reflux is continued for about 3 h. The reaction mixture is cooled to room temperature and then water is added carefully. The toluene layer is washed with water and extracted with dilute hydrochloric acid. The basic parts are precipitated by alkalisation of the united acid extracts and taken up in benzene. The benzene solution is dried, the benzene if driven off and the remaining oil is distilled. After a small fore-run, the desired α-(2-dimethylaminoethyl) compound distils at 160°/0.1 mm within an interval of a few degrees. It forms a viscous, faintly yellowish oil which crystallizes on standing. Yield 63 g (32.5 %). Recrystallization from petroleum ether gives 48.5 g (25 %) with m.p. 91—92°. For analyses, see Table 2. The remainder in the distilling flask is unimportant and scarcely more than the hold up volume.

By working up the toluene solution, a fraction, boiling at about 105°/1—2 mm, is received. It solidifies and gives after recrystallization from petroleum ether 40 g of 1,2-diphenylethane with m.p. 48—50°. (Found: C 92.06; H 7.93. Calc. C 92.26; H 7.74) It corresponds to 36.5 % of the parent amide.

22 g (14.5 %) of the parent amide could be isolated from a higher boiling fraction.

Method II (with phenylsodium). A solution of 38.0 g (0.15 mole) of α-benzylphenylacetic acid N,N-dimethylamide in 100 ml of dry toluene is dropped rapidly, while stirring, into a mixture of phenylsodium in toluene containing a slight excess of phenylsodium. The temperature of the contents increases from room temperature to about 50°. The mixture is now warmed to about 80°, and a dried solution of 2-dimethylaminoethyl chloride (from 27 g of the hydrochloride) in toluene is added while stirring during the course of about 15 min. The temperature rises somewhat (to about 95°), the brownish, precipitated salt is consumed but the colour remains almost unchanged. The mixture is now heated to 105—110° for about 1 h. The contents of the flask are cooled to room temperature, water is added carefully, and the toluene layer is washed with water. It is poured, while stirring, into dilute hydrochloric acid. The precipitated hydrochloride is taken on a filter, and washed with a small amount of cold water and ether. The yield of hydrochloride is 17.5 g (32 %). The base is liberated in a yield of 91.5 % from a warm water solution of the hydrochloride by means of dilute ammonia. M.p. 89—92°.

From the extracted toluene solution 10.5 g of 1,2-diphenylethane is obtained by distillation (b.p. 80—85°/0.2 mm), corresponding to 38.5 % of the parent amide. Another fraction (b.p. 140—145°/0.2 mm) consists of 6.0 g (16 %) of the parent amide.

α-(2-Dimethylaminoethyl)-α-(2'-pyridyl)-phenylacetic acid pyrrolidide.

Method I. A mixture of 53.3 g (0.2 mole) of α-(2-pyridyl)-phenylacetic acid pyrrolidide, 8.2 g of commercial, ground sodamide and 200 ml of dry toluene is refluxed for about 1 h or until the strong evolution of ammonia has decreased and a yellowish precipitate has been formed in the flask. The contents are cooled to about 50° and a dried solution of 2-dimethylaminoethyl chloride (from 33 g of the hydrochloride) in about 100 ml

of toluene is added. The mixture is heated to reflux. After about 1 h reflux, the precipitate has disappeared and the second strong evolution of ammonia has decreased. After a total reflux of about 3 h, the contents are cooled to room temperature, water is added and the toluene layer washed with water. The toluene is driven off from the dried solution and the remaining oil is distilled. After a very small fore-run the main part distils at 192—195°/0.1 mm. This fraction, a reddish viscous oil, crystallizes on scratching with petroleum ether. Since it is soluble in this solvent cooling with dry ice decreases the losses. Yield 49 g (72 %). M.p. about 87°. Recrystallization from *cyclo*hexane raises the m.p. to 90—93°. After another two recrystallizations from acetone the m.p. is 93.5—95°, but the total yield has now decreased to 40 %. For analytical data see Table 1.

α-Benzyl-α-(2-morpholinoethyl)-phenylacetic acid N-benzyl-N-propyl-amide. (With KNH_2). A solution of 53.6 g (0.15 mole) of α-benzyl-phenylacetic acid N-benzyl-N-propyl-amide in 100 ml of dry toluene is added while stirring to a suspension of potassium amide in liquid ammonia (prepared from 5.9 g of potassium, about 200 ml of liquid ammonia and traces of ferric nitrate by conventional procedure). The cooling bath (dry ice and alcohol) is removed and the ammonia is allowed to evaporate through the reflux condensor. This process is facilitated by gently warming the flask by means of a heating lamp until the contents have reached room temperature. The colour of the contents is now brownish black. A solution of 22.5 g of recently distilled 2-morpholinoethyl chloride in 50 ml of dry toluene is added directly by means of a dropping funnel. The flask contents are heated to boiling and the reflux is continued for 2 h. Strong evolution of ammonia takes place during the first part of the heating, the colour of the mixture becomes paler and is yellowish white after 2 h. The mixture is cooled to room temperature, water is added and the toluene layer is washed with water. The basic components are extracted with dilute hydrochloric acid and the united acid solutions are treated with dilute sodium hydroxide. The precipitated oil is taken up in ether. When the ether is removed, the remaining oil solidifies, giving 33.5 g (47.5 %) of crystalline crude product with m.p. 122—136°. Recrystallization from *cyclo*hexane yields 16.5 g (24 %) of the α-morpholinoethyl compound. M.p. 137.5—139°. For analytical data see Table 2.

α-n-Octyl-α-diethylamino-phenylacetic acid N,N-diethylamide. A mixture of 26.2 g (0.1 mole) of α-diethylamino-phenylacetic acid N,N-diethylamide, 4.2 g of sodamide and 125 ml of dry toluene is refluxed for 1—2 h while stirring. The strong evolution of ammonia has then ceased but no precipitate has been formed in the brown-coloured contents of the flask. 20.0 g (theoret. 19.3 g) of *n*-octyl bromide is now slowly added (to the refluxing flask contents) by means of a dropping funnel and the reflux is continued for 6 h. After cooling to room temperature, water is added and the toluene layer is washed with water. The separated toluene layer is dried with anhydrous sodium sulphate, the toluene is driven off and the remaining oil is distilled in vacuo. After a fore-run of 4.0 g, consisting mainly of unreacted bromide and parent amide, a main fraction is collected at 165—168°/0.2 mm (28.7 g or 77 %) as an almost colourless, viscous oil. (Found: C 76.98; H 11.15; N 7.60. Calc. for $C_{24}H_{42}N_2O$ (374.6); C 76.95; H 11.30; N 7.48).

α-Benzyl-α-diethylamino-phenylacetic acid N,N-diethylamide. The alkylation was carried out in the same manner as in the preparation of the *n*-octyl compound described above. The benzyl compound distils as a viscous, faintly yellowish oil at 172—175°/0.1—0.2 mm. Yield 50 %. Recrystallizations from small amounts of petroleum ether give white crystals with m.p. 109.5—110.5°. (Found: C 78.47; H 9.24; N 8.00. Calc. for $C_{23}H_{32}N_2O$ (352.6): C 78.34; H 9.17; N 7.95).

α-n-Octyl-α-phenoxy-phenylacetic acid N,N-diethylamide. A mixture of 28.4 g (0.1 mole) of α-phenoxy-phenylacetic acid N,N-diethylamide, 4.2 g of sodamide and 125 ml of dry toluene is refluxed while stirring. After about 1 h reflux, the strong evolution of ammonia has ceased and the flask is filled with a grayish green precipitate. 20.0 g (theoret. 19.3 g) of *n*-octyl bromide is added to the refluxing mixture by means of a dropping funnel during the course of 15—30 min and the precipitate disappears. The reflux is continued for about 8 h. The reaction mixture is worked up in the usual manner. After a fore-run of 6.6 g, mainly consisting of unreacted parent amide, the *α-n*-octyl compound distils at 165—170°/0.1 mm as a viscous, faintly yellowish oil. Yield 26.0 g or 66 %. Redistillation gives 20.1 g (51 %). (Found: C 78.58; H 9.36; N 3.65. Calc. for $C_{26}H_{37}NO_2$ (395.6): C 78.93; H 9.43; N 3.54).

α-Neohexyl-α-phenoxy-phenylacetic acid N,N-diethylamide. This compound is prepared analogously with the preceding one, but 17.0 g (theoret. 16.5 g) of *neo*hexyl bromide is

used instead of octyl bromide. After a fore-run of 2.0 g, a main fraction (25.0 g or 68 %) distils at 150—152°/0.05—0.1 mm. In spite of the narrow interval, this fraction contains amounts of the parent amide of which about 5 g could be recovered by scratching the oil with petroleum ether. The mother liquor gave by cooling in a dry ice-alcohol bath 6.0 g of a compound with m.p. 71—73°. (Found: C 78.39; H 8.94; N 3.83. Calc. for $C_{24}H_{33}NO_2$ (367.5): C 78.43; H 9.05; N 3.81).

α-(p-Chlorobenzyl)-α-phenoxy-phenylacetic acid N,N-diethylamide is synthetized in the same way as the *n*-octyl derivative from 14.2 g (0.05 mole) of α-phenoxy-phenylacetic acid diethylamide. The *p*-chlorobenzyl chloride, dissolved in 25 ml of dry toluene, is added at a temperature of about 80°, followed by reflux for 3.5 h. A fore-run (up to 180°/0.1 mm) gives 5.0 g. The main fraction, 180—205°/0.1—0.2 mm (11.2 g or 55 %), gives, on recrystallization from small amounts of petroleum ether, 7.0 g (35 %) of *p*-chlorobenzyl compound, m.p. 101—102°. From the fore-run 0.8 g of parent amide and 1.0 g of *p*-chlorobenzyl derivative are isolated. (Found: C 73.70; H 6.46; N 3.43. Calc. for $C_{25}H_{26}ClNO_2$ (407.9): C 73.60; H 6.43; N 3.43).

The authors are indebted to Mr. W. Kirsten and his assistants for elementary analyses and to Dr. B. Nygård for infrared analyses.

Errata: In the tables in our preceding papers (this journal **14** (1960) 1129 and 1151) in this series treating the "first alkylation" of carbonamides and the alkylation of sulphonamides, the following misprints occur:

p. 1137,	column	Formula, line 3: for $C_{16}H_{25}NO$	read	$C_{16}H_{25}NO_2$
pp. 1138—39,	»	Y: for $-[CH(CH_3)_2]_2$	»	$-N[CH(CH_3)_2]_2$
p. 1139,	»	R: for $-CH_2CH_2N_3(C_2H_5)$	»	$-CH_2CH_2N(C_2H_5)_2$
p. 1140,	»	R: for $-CH_2CH_2CH_2N[CH(CH_2)_3]_2$	»	$-CH_2CH_2CH_2N[CH(CH_3)_2]_2$
p. 1158,	»	R: (line 1): for phenyl	»	H

REFERENCES

1. Bockmuhl, M. und Ehrhardt, G. Germ. P. 731 560; Danish P. 61 654.
2. Cheney, L. C., Wheatley, W. R., Speeter, M. E. *et al. J. Org. Chem.* **17** (1952) 770.
3. Moffett, R. B. and Aspegren, B. D. *J. Am. Chem. Soc.* **79** (1957) 4462.
4. Janssen, P. *J. Am. Chem. Soc.* **78** (1956) 3862.
5. Mårtensson, O. and Nilsson, E. *Acta Chem. Scand.* **14** (1960) 1129.
6. Mårtensson, O. and Nilsson, E. *Acta Chem. Scand.* **14** (1960) 1151.
7. Brändström, A. E., Hjelte, N. S. and Mårtensson, O. Brit. P. 771, 814; U.S.P. 2, 841, 589; Can. P. 573, 771.

Received December 13, 1960.

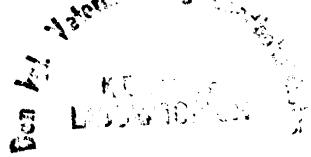

ACTA CHEMICA SCANDINAVICA 15 (1961) 1039–1063

Polarographische Untersuchungen organischer Selenverbindungen. I. Das polarographische Verhalten der Diselen-diessigsäure (Diselen-diglykolsäure)

BENGT NYGÅRD*

Institut für Physikalische Chemie der Universität Bonn, Deutschland, und Chemisches Institut der Universität Uppsala, Schweden

Diselen-diessigsäure dient als Modellsubstanz für polarographische Untersuchungen organischer Diselen-Verbindungen. Im Gegensatz zu der entsprechenden Dithio-diessigsäure gibt die Selenverbindung sehr gute Polarogramme im ganzen untersuchten pH-Bereich. Diselendiessigsäure ($Se_2R_2H_2$) und Selenoglykolsäure (HSeRH) stellen an der Quecksilberelektrode ein reversibles System dar, in dem der entscheidende Elektrodenprozess auf folgenden Einelektronenvorgang bezogen ist.

$$HgSeRH + H^+ + e \rightleftharpoons HSeRH + Hg$$

Dieser Mechanismus setzt eine schnell eintretende homolytische Radikaldissoziation der -Se-Se- Brücke an der Elektrodenoberfläche als vorgelagerte Reaktion voraus und schliesst somit eine direkte Reduktion des Diselenides zum entsprechenden Selenol an der Quecksilberelektrode aus. Die Reversibilität der angeführten Elektrodenreaktion wird auf verschiedenen Wegen bewiesen. Aus der pH-Abhängigkeit des Halbstufenpotentials ergibt sich die Dissoziationskonstante $1{,}0 \times 10^{-7}$ der SeH-Gruppe der im reinen Zustand nicht bekannten Selenoglykolsäure. Die Polarographie öffnet damit die Möglichkeit unter Benutzung der entsprechenden Diselenide Messungen von Dissoziationskonstanten bisher nicht fassbarer Selenole durchzuführen. Die Brückenstabilität der -Se-Se- und -S-S- Gruppen ist für das polarographische Verhalten von ausschlaggebender Bedeutung.

Organische Thiol-Verbindungen und Disulfide sind Gegenstand zahlreicher polarographischer Originalarbeiten gewesen. Besonderes Interesse ist dabei den vom biochemischen Standpunkt wichtigen Systemen Cystein-Cystin und Glutathion (im reduzierten und oxydierten Zustand) geschenkt worden, was damit zusammenhängt, dass man auch mit Hilfe der tropfenden Quecksilber-

* Neue Anschrift: Pharmacia, Uppsala, Schweden.

elektrode versucht hat, die Redoxpotentiale derartiger Systeme festzustellen. Der stark komplexbildende Charakter des Quecksilbers den Schwefelverbindungen gegenüber hat jedoch zur Folge, dass bei den entsprechenden mehrstufigen Polarogrammen erhebliche Schwierigkeiten bei der Deutung auftreten. Dadurch wird eine Beurteilung der Redoxeigenschaften der betreffenden Systeme im gleichen Mass erschwert. Auch wenn man keine in thermodynamischer Hinsicht wohlbegründeten Redoxpotentiale der angeführten Schwefelsysteme erhalten kann, hat man dennoch durch die Polarographie weitgehende Einblicke in das Verhalten ihrer Quecksilberverbindungen gewonnen.

Um neue Gesichtspunkte über das polarographische Verhalten einiger Disulfide zu erhalten, sind vor einigen Jahren polarographische Untersuchungen der entsprechenden Diselen-Verbindungen in Angriff genommen worden. In der polarographischen Literatur sind bisher keine Untersuchungen organischer Diselenverbindungen zu finden gewesen, was auch ein Grund für die Aufnahme eines derartigen Arbeitsthemas war. In dieser Arbeit wird das polarographische Verhalten der Diselen-diessigsäure * eingehend beschrieben, weil diese Säure als erstes und einfachstes Glied der homologen Reihe $HOOC-(CH_2)_n-Se-Se-(CH_2)_n-COOH$ auch als polarographisches Vorbild dieser Verbindungen aufgefasst werden kann. In kommenden Veröffentlichungen werden die darauffolgenden Homologen mit n = 2, 3 und 4 sowie die Polarographie der *aa'*-Diamino-diselen-dihydrakrylsäure (Selenocystin) behandelt.

Für die folgende Darstellung dürfte zwecks Vergleich eine kurze Übersicht der Polarographie der in der Einleitung erwähnten Schwefelsysteme von Wert sein.

Kolthoff und Barnum [1] haben Cystein untersucht und erklären die anodische Hauptstufe als eine oxydative Mercaptidbildung gemäss

$$RSH + Hg \rightarrow RSHg + H^+ + e$$

wobei das Elektroden-Quecksilber oxydiert wird. Cystin [2] dagegen wird an derselben Elektrode irreversibel zu Cystein reduziert nach

$$RSSR + 2H^+ + 2e \rightarrow 2\,RSH$$

Im Hinblick auf spätere Arbeiten über dieses Thema von Grubner und Mitarbeiter [3,4], Kolthoff, Stricks und Tanaka [5] sowie von Biegler und Breyer [6] sind die polarographischen Effekte auch in den Einzelheiten weitgehend aufgeklärt worden.

Gluthathion ist von Stricks und Kolthoff [7] sowie von Tachi und Koide [8] eingehend untersucht worden. Diese konnten feststellen, dass die anodische Oxydation der reduzierten Form wie beim Cystein mit einer Mercaptidbildung reversibel verläuft. Im oxydierten Zustand wird Gluthathion irreversibel zum Thiol reduziert. Für die vorliegende Untersuchung sind die Arbeiten

* Nygård, B. Im Auszug beim Polarographischen Kolloquium, Bonn 1958, vorgetragen; *Z. anal. Chem.* Sonderheft **173** (1960) 112.

über Mercaptoessigsäure-Dithiodiessigsäure * von besonderem Interesse. So haben u.a. Leussing und Kolthoff [9] gefunden, dass die Mercaptoessigsäure nach demselben Mechanismus wie Cystein und Gluthathion oxydiert wird, während die Polarogramme der kathodischen Stufen der Dithio-diessigsäure zweifelsohne eine irreversible Elektrodenreaktion andeuten.

Zusammenfassend kann festgestellt werden, dass der anodische Elektrodenvorgang der drei erwähnten Schwefelsysteme an der Quecksilbertropfelektrode in analoger Weise verläuft. Die kathodische Reduktion dagegen kann nicht durch einen gemeinsamen Reaktionsmechanismus erklärt werden. Die erschwerenden Umstände liegen dabei in dem ausgeprägt irreversiblen Charakter der entsprechenden Elektrodenreaktionen der Disulfide.

Fredga [10,11] hat die Beobachtung gemacht, dass Reaktionen zwischen Quecksilber oder Quecksilbersalzen und gewissen Diselenverbindungen sehr glatt verlaufen. So ist es möglich aus Diselen-diessigsäure (I) und Quecksilber schon bei Zimmertemperatur eine Merkuri-bis-selenoglykolsäure (II) herzustellen. Eine entsprechende Reaktion der Dithio-diessigsäure findet nicht statt, was auf einen entscheidenden Unterschied in der Brückenstabilität der Diselenid- und der Disulfidbindung hindeutet.

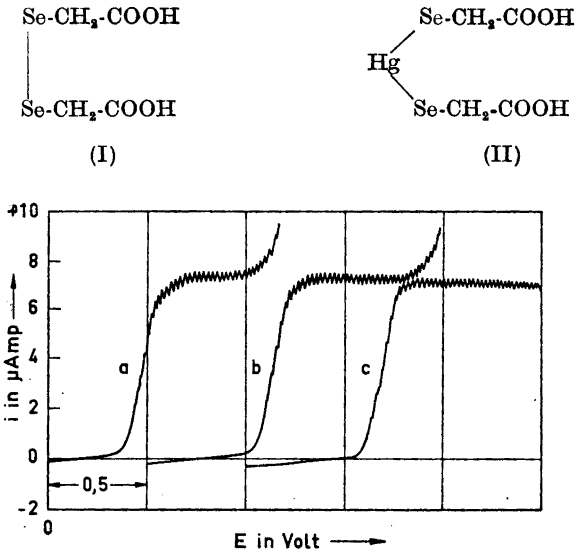

Abb. 1. Polarogramme von 1 × 10^{-3} M Diselen-diessigsäure in drei verschiedenen Pufferlösungen. Kurve (a) entspricht pH = 3,06, (b) pH = 5,80 und (c) pH = 9,14. Jedes Polarogramm ab 0 Volt aufgenommen.

* In der folgenden Darstellung werden gemäss in jüngster Zeit gemachten Vorschlägen die Namen Mercaptoessigsäure und Dithio-diessigsäure statt Thioglykolsäure bzw. Dithio-diglykolsäure benutzt. Demzufolge wird auch Diselen-diglykolsäure durch Diselen-diessigsäure ersetzt. Seleno-glykolsäure und Merkuri-bis-selenoglykolsäure, die in vorliegender Arbeit auch diskutiert werden, lassen sich leider nicht auf einfache Weise in terminologischen Einklang mit den angeführten Verbindungen bringen und die Namen werden deswegen beibehalten. Der Verfasser ist sich der dadurch entstandenen Inkonsequenz bewusst.

Die beiden genannten Diselenverbindungen (I) und (II) lassen sich, in gewissen Konzentrationsbereichen, polarographisch gut untersuchen. Abb. 1 und 2 geben einige typische Polarogramme wieder, aus denen man schliessen kann, dass in beiden Fällen wahrscheinlich derselbe Elektrodenvorgang für die gut ausgebildeten kathodischen Stufen verantwortlich sein muss. Diese Annahme wird auch durch Messung der entsprechenden Halbstufenpotentiale bestätigt. Von den theoretisch denkbaren Wegen einer kathodischen Reduktion muss derjenige ausgewählt werden der mit den erwähnten experimentellen Ergebnissen vereinbar ist. Weiter ist unter allen Umständen mit Selenoglykolsäure als Endprodukt des Reduktionsvorganges zu rechnen. Folgende schematische Aufstellung gibt mögliche Reaktionswege wieder.

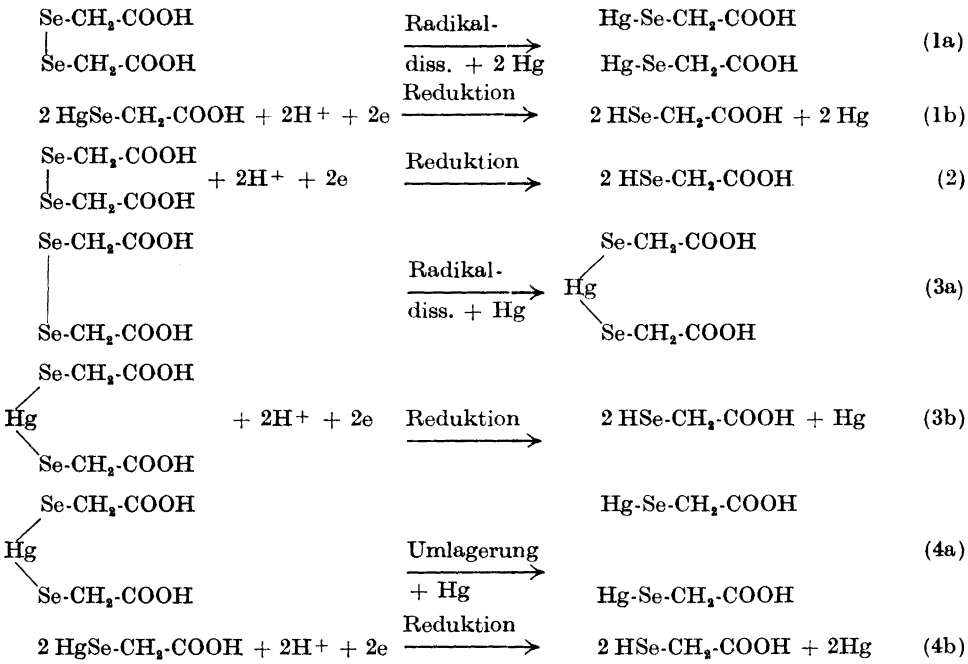

Die Reaktionsfolgen 1 und 4 können mathematisch als Einelektronenprozesse betrachtet werden im Gegensatz zu den zwei übrigen, die in dieser Beziehung Zweielektronencharakter besitzen. Ohne der folgenden Darstellung zu viel vorzugreifen, kann schon hier erwähnt werden, dass nur der Einelektronenvorgang es ermöglicht, die Theorie in Übereinstimmung mit den experimentellen Ergebnissen zu bringen. Die Diselen-diessigsäure und die Merkuribis-selenoglykolsäure müssen dann beide in der Form einer Merkuroverbindung an dem Elektrodenprozess teilnehmen. Diese Annahme setzt eine Radikaldissoziation der Se-Se Bindung bzw. eine Umlagerung der Se-Hg-Se Brücke in dieselbe Hg(I)-Verbindung als vorgelagerte Reaktion an der Elektrodenoberfläche voraus. Fredga hat schon früher auf die Möglichkeit einer mit Quecksilber schnell eintretenden Radikaldissoziation der Diselenbindung hingewiesen.

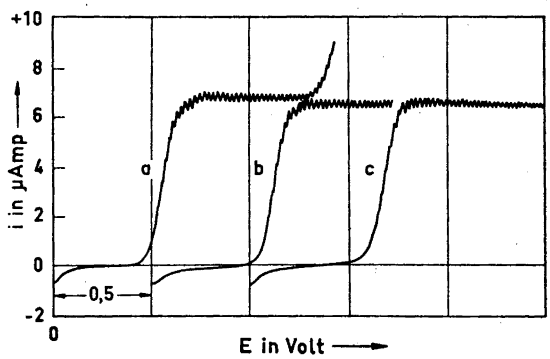

Abb. 2. Polarogramme von 1 × 10^{-3} M Merkuri-bis-selenoglykolsäure in drei verschiedenen Pufferlösungen. Kurve (a) entspricht pH = 4,64, (b) pH = 5,90 und (c) pH = 9,18. Jedes Polarogramm ab 0 Volt aufgenommen.

Wenn für die kathodische Reduktion an der Tropfelektrode die Gleichungen (1) und (4) massgebend sind, ist ganz analog den entsprechenden Reaktionen bei den Thiolen folgende anodische Oxydation der Selenoglykolsäure zu berücksichtigen.

$$HgSe\text{-}CH_2\text{-}COOH + H^+ + e \xleftarrow{\text{Oxydation}} HSe\text{-}CH_2\text{-}COOH + Hg \qquad (5)$$

Die theoretische Überlegung wird nun demgemäss das vollständige Redoxsystem (6) behandeln, und zwar unter der Voraussetzung eines *reversiblen* Verhaltens gemäss

$$HgSe\text{-}CH_2\text{-}COOH + H^+ + e \rightleftharpoons HSe\text{-}CH_2\text{-}COOH + Hg \qquad (6)$$

Folgende Abkürzungen werden zur Vereinfachung eingeführt.

$$\begin{matrix} Se\text{-}CH_2\text{-}COOH \\ | \\ Se\text{-}CH_2\text{-}COOH \end{matrix} = Se_2R_2H_2$$

$$\begin{matrix} Se\text{-}CH_2\text{-}COOH \\ | \\ Se\text{-}CH_2\text{-}COO^- \end{matrix} = Se_2R_2H^- \qquad \begin{matrix} Se\text{-}CH_2\text{-}COO^- \\ | \\ Se\text{-}CH_2\text{-}COO^- \end{matrix} = Se_2R_2^{2-}$$

$$HSe\text{-}CH_2\text{-}COOH = HSeRH \longrightarrow \text{Dissoziationskonstante } K_1$$

$$HSe\text{-}CH_2\text{-}COO^- = HSeR^- \longrightarrow K_2$$

$$^-Se\text{-}CH_2\text{-}COO^- = SeR^{2-}$$

$$HgSe\text{-}CH_2\text{-}COOH = HgSeRH \longrightarrow K_3$$

$$HgSe\text{-}CH_2\text{-}COO^- = HgSeR^-$$

Wir setzen weiter voraus, dass auf der Oberfläche der Elektrode gebildetes HgSeRH bzw. $HgSeR^-$ sowie ihre Reduktionsprodukte zum grössten Teil

durch Diffusion in die Lösung von der Quecksilberoberfläche beseitigt worden sind. Die folgenden Ableitungen sind nur für die in Lösung an der Elektrodenoberfläche befindlichen, nicht adsorbierten Komponenten gültig.

Betrachtet man das Redoxsystem bei einem pH-Wert, bei dem eine primäre Dissoziation stattgefunden hat, so kann die Gleichung (6) geschrieben werden

$$HgSeR^- + H^+ + e \rightleftharpoons HSeR^- + Hg \tag{7}$$

Wendet man auf die Redoxreaktion (7) die *Nernst-Peterssche* Gleichung an, so gilt für das Potential (E) des Systems

$$E = E_0 + \frac{RT}{nF} \ln \frac{a^\circ_{HgSeR^-}\, a^\circ_{H^+}}{a^\circ_{HSeR^-}\, a^\circ_{Hg}} \tag{8}$$

Durch die Zeichen a° ist angedeutet, dass es sich um die Aktivitäten an der Elektrodenoberfläche handelt.

E° ist das Normalpotential des Redoxsystems.

$a^\circ_{Hg} = 1$ an der Oberfläche der Quecksilberelektrode.

$n = 1$ für einen Einelektronenvorgang.

Die Aktivitätskoeffizienten der einwertigen Ionen $HgSeR^-$ und $HSeR^-$ können approximativ einander gleichgesetzt werden.

Unter der Voraussetzung, dass die Pufferkapazität der Lösung genügend ist, kann man $a^\circ_{H^+} = a_{H^+}$ setzen, wo a_{H^+} die Wasserstoffionenaktivität in der Lösung angibt.

Für eine Temperatur $T = 25°C$ kann dann die Gleichung (8) geschrieben werden.

$$E = E_0 + 0{,}059 \log \frac{C^\circ_{HgSeR^-}}{C^\circ_{HSeR^-}} + 0{,}059 \log a_{H^+} \tag{9}$$

Ferner ist

$$C_{HSeRH} = C_{HSeR^-} \frac{a_{H^+}}{K_1} \tag{10}$$

$$C_{SeR^{2-}} = C_{HSeR^-} \frac{K_2}{a_{H^+}} \tag{11}$$

$$C_{HgSeRH} = C_{HgSeR^-} \frac{a_{H^+}}{K_3} \tag{12}$$

Ausser der Beeinflussung durch geringe Variationen der Diffusionskoeffizienten (D) ist der Diffusionstrom (i_d) unabhängig von dem Ionisationszustand der Selenoglykolsäure bzw. der Diselen-diessigsäure. Approximativ ist dann D gleich einem Durchschnittswert aller Ionisationszustände der betreffenden Säure zu setzen. Unter der Voraussetzung, dass in der Lösung sowohl Selenoglykolsäure als auch Diselen-diessigsäure vorliegen, die beide eine depolarisierende Wirkung an der Tropfelektrode ausüben, lassen sich die Ausdrücke des *anodischen* Grenzstromes i^a_d und des *kathodischen* Grenzstromes i^k_d berechnen. Es sei nochmals betont, dass diese Grenzströme nur dem Anteil

der Elektrodenreaktion entsprechen, an der gelöste Stoffe teilnehmen. Für den anodischen Diffusionsstrom i_d^a gilt

$$i_d^a = k\,(C_{HSeRH} + C_{HSeR^-} + C_{SeR^{2-}}) \tag{13}$$

wo nach der Ilkovič-Gleichung

$$k = 607\, D^{1/2}\, m^{2/3}\, t^{1/6}$$

und C (ohne Index "O") die Konzentrationen im Innern der Lösung bezeichnen. In jedem Punkt der Strom-Spannungskurve ist die Stromstärke i proportional der Differenz der Depolarisatorkonzentration in der Lösung und an der Tropfenoberfläche. Es gilt also für den anodischen Elektrodenvorgang

$$-(i_d^a - i) = k\,(C^\circ_{HSeRH} + C^\circ_{HSeR^-} + C^\circ_{SeR^{2-}}) \tag{14}$$

Die Ausdrücke (10) und (11) für C_{HSeRH} bzw. $C_{SeR^{2-}}$ welche in gleicher Form auch für C°_{HSeRH} und $C^\circ_{SeR^{2-}}$ gültig sind, in Gleichung (14) eingesetzt geben

$$C^\circ_{HSeR^-} = \frac{i - i_d^a}{k\left(1 + \frac{a_{H^+}}{K_1} + \frac{K_2}{a_{H^+}}\right)} \tag{15}$$

Der kathodische Diffusionsstrom i_d^k der Hg(I)-selenoglykolsäure ist durch folgenden Ausdruck bestimmt

$$i_d^k = 2k'(C_{Se_2R_2H_2} + C_{Se_2R_2H^-} + C_{Se_2R_2^{2-}}) \tag{16}$$

wo $k' = 607\ (D')^{1/2} m^{2/3} t^{1/6}$

Für die Stromstärke i (ehe der Grenzstrom erreicht ist) gilt in analoger Weise

$$i_d^k - i = 2k'(C^\circ_{Se_2R_2H_2} + C^\circ_{Se_2R_2H^-} + C^\circ_{Se_2R_2^{2-}}) \tag{17}$$

Wir setzen voraus, dass eine Radikaldissoziation der Se-Se Bindung als vorgelagerte Reaktion ohne kinetische Hemmung an der Tropfelektrode stattfindet. Dann ist

$$i_d^k - i = k'(C^\circ_{HgSeRH} + C^\circ_{HgSeR^-}) \tag{18}$$

Wird (12) in Gleichung (18) eingesetzt ergibt sich

$$C^\circ_{HgSeR^-} = \frac{i_d^k - i}{k'\left(1 + \frac{a_{H^+}}{K_3}\right)} \tag{19}$$

Unter Berücksichtigung der Gleichungen (15) und (19) kann (9) geschrieben werden

$$E = E_0' + 0{,}059 \log \frac{\left(1 + \frac{a_{H^+}}{K_1} + \frac{K_2}{a_{H^+}}\right) a_{H^+}}{1 + \frac{a_{H^+}}{K_3}} + 0{,}059 \log \frac{k}{k'} - 0{,}059 \log \frac{i - i_d^a}{i_d^k - i} \tag{20}$$

In (20) ist E_0 (= das thermodynamische Normalpotential) durch E_0' ersetzt worden, um zu bezeichnen, dass es sich um ein Normalpotential im engeren Sinne (u.a. abhängig von der Ionenstärke der Lösung) handelt.

Die Dissoziationskonstanten K_1 und K_3 sind unbekannt und auch schwer messbar, weil die entsprechenden Säuren in reinem Zustand nicht vorhanden sind. Durch vergleichende Messungen der primären und sekundären Dissoziationskonstanten der Diselen-diessigsäure und der Hg(II)-bis-selenoglykolsäure scheint es wohlberechtigt die Approximation $K_1 = K_3$ einzuführen *.

Die Konstanten k und k' nach der Ilkovič-Gleichung sind $\sqrt{D}$ bzw. $\sqrt{D'}$ proportional. D und D' sind die der Selenoglykolsäure bzw. der Diselendiessigsäure entsprechenden Diffusionskoeffiziente wo $D > D'$. Im Vergleich mit beispielsweise dem System Mercaptoessigsäure-Dithiodiessigsäure ($D = 9{,}5 \times 10^{-6}$ bzw. $D' = 6 \times 10^{-6}$ cm^2 sek^{-1}) dürfte in diesem Falle das Verhältnis D/D' nicht viel grösser als 1,5 sein. Das Glied $0{,}059 \log \frac{k}{k'}$ ist dann wahrscheinlich kleiner als 6 mV und weil es ausserdem ziemlich konstant bleibt wird es im folgenden vernachlässigt.

Beim Halbstufenpotential $E_{\frac{1}{2}}$ gilt $i = \frac{i_d^k + i_d^a}{2}$

Aus der Gleichung (20) kann damit und mit $K_1 = K_3$ abgeleitet werden

$$E_{\frac{1}{2}} = E_0' + 0{,}059 \log \left(a_{H^+} + \frac{K_2}{1 + \frac{a_{H^+}}{K_3}} \right) \tag{21}$$

Insbesondere ergibt sich

$$a_{H+} \gg K_2 \qquad E_{\frac{1}{2}} = E_0' - 0{,}059 \text{ pH} \tag{22}$$

$$a_{H+} \ll K_2 \qquad E_{\frac{1}{2}} = E_0' - 0{,}059 \text{ p}K_2 \tag{23}$$

Die graphische Darstellung der Gleichung (22) ist eine Gerade mit dem Winkelkoeffizient $-0{,}059$ während $E_{\frac{1}{2}}$ nach (23) konstant ist. Der Schnittpunkt der Geraden gibt den pK_2-Wert der Selenolgruppe an.

Die Gleichungen (20) und (21) geben

$$E = E_{\frac{1}{2}} - 0{,}059 \log \frac{i - i_d^a}{i_d^k - i} \tag{24}$$

Für eine rein kathodische Stufe ist $i_d^a = 0$, und

$$E = E_{\frac{1}{2}} - 0{,}059 \log \frac{i}{i_d^k - i} \tag{25}$$

* Die prim. und sek. Dissoziationskonstanten, $4{,}86 \times 10^{-4}$ bzw. $6{,}40 \times 10^{-5}$, der Diselendiessigsäure sind auf potentiometrischem Wege erstmals von Fredga [12] gemessen worden. Mit derselben Methode wurde in der vorliegenden Untersuchung $4{,}70 \times 10^{-4}$ bzw. $7{,}25 \times 10^{-5}$ gefunden. Im Hinblick auf die verschiedenen Ionenstärken der Lösungen sowie auf pH-Standarde zeigen die Messergebnisse eine genügende Übereinstimmung. Für die Hg(II)-bis-selenoglykolsäure wurden in dieser Arbeit die Konstanten $2{,}55 \times 10^{-4}$ bzw. $4{,}40 \times 10^{-5}$ gefunden.

Mit Hilfe der Gleichungen (24) und (25) wird die genaue Analyse der Form der entsprechenden polarographischen Kurven durchgeführt. Polarogramme von Lösungen, die gleichzeitig Selenoglykolsäure und Diselen-diessigsäure enthalten, werden Gleichung (24) bestätigen. Insbesondere wird das reversible Verhalten dadurch angezeigt, dass die polarographische Kurve ohne Verzerrung die Galvanometer-Nullinie hindurchgeht.

Die Reaktionsfolgen (2) und (3) sind als alternative Möglichkeiten in Betracht zu ziehen. Mathematische Ableitungen können ganz analog durchgeführt werden. Für eine kathodische Reduktion werden in beiden Fällen E und i durch folgende Gleichung bestimmt

$$E = E_{\frac{1}{2}} - \frac{0{,}059}{2} \log \frac{i^2}{i_d^k - i} \tag{26}$$

Im Falle einer anodischen Oxydation ist analog

$$E = E_{\frac{1}{2}} + \frac{0{,}059}{2} \log \frac{i^2}{i_d^a - i} \tag{27}$$

EXPERIMENTELLES

Chemikalien

Diselen-diessigsäure war nach Behaghel [13] hergestellt. Reinheit (alkalimetrisch geprüft) 99,8 %.

Merkuri-bis-selenoglykolsäure wurde nach Fredga [10] bereitet. Nur frisch hergestellte Präparate (99,5 % oder besser, iodometrisch bestimmt) wurden benutzt, weil ältere Produkte eine Tendenz haben dunkel zu werden. Durch Zerfall der Säure bildet sich langsam HgSe.

Selenoglykolsäure ist wegen ihrer Leichtoxydierbarkeit in reinem Zustand nicht beschrieben worden. In verdünnter Lösung und in Mischung mit Merkuri-bis-selenoglykolsäure bzw. Diselen-diessigsäure kann jedoch die betreffende Säure nach zwei Methoden dargestellt werden.

Methode 1. Aus Hg(II)-bis-selenoglykolsäure und einer äquivalenten Menge Natriumsulfid in alkalischer Lösung nach Fredga [14]. Die Ausbeute der Reaktion ist von dem Gleichgewicht abhängig und steigt im alkalischen Gebiet. Bei dem Umsatz fällt HgS kolloidal aus, was jedoch ohne Einfluss auf die polarographische Analyse ist. Dagegen wirkt ein Überschuss von Natriumsulfid störend, weil eine anodische Oxydation der S^{2-}-Ionen im aktuellen Untersuchungsbereich stattfindet. Die anodische Stufe entspricht dann der Entstehung einer HgS-Schicht an der Tropfelektrode. In saurer Lösung ist es möglich durch Einleiten von H_2 (H_2S entweicht) dieser Schwierigkeit zu entgehen. Im alkalischen Bereich dagegen muss man mit etwas weniger als der äquivalenten Menge an Natriumsulfid arbeiten.

Methode 2. Durch elektrolytische Reduktion der Diselen-diessigsäure an einer Platinelektrode unter Wasserstoffatmosphäre. Die Elektrolyse wurde in einem H-Gefäss mit 0,1 N H_2SO_4 zur Erhöhung der Leitfähigkeit ausgeführt. Ungefähr 20 Stunden Elektrolysenzeit mit einer Stromstärke von 25 mA zeigten sich als günstige Bedingungen um eine Ausbeute von etwa 50 % an Selenoglykolsäure zu erhalten. Bei neuen Versuchen mit anderen Diselen-dikarbonsäuren ist diese Ausbeute erheblich verbessert worden. Spuren von Selenwasserstoff können auftreten, was aus den entsprechenden Polarogrammen klar hervorgeht. Freies Selen scheint auch bei zu hohen Stromstärken oder zu langen Zeiten ausreduziert zu werden.

Mercaptoessigsäure und Dithio-diessigsäure (Reinheit 98,5 % bzw. 99,6 %) wurden zum vergleichenden Zweck gebraucht.

Die übrigen Chemikalien, KCl und KNO_3 sowie die Puffersubstanzen, waren alle Merck p.a. Sämtliche Pufferlösungen wurden nach Sörensen bereitet.

Apparatives

Die normalen Polarogramme wurden zum grössten Teil mit dem Leybold-Polarographen 54 aufgenommen. Einige ergänzenden Messungen wurden ausserdem mit Hilfe des LKB-Polarographen 3266 B durchgeführt. Diese Instrumente ermöglichen eine Messgenauigkeit von etwa ± 1 mV in der Bestimmung der Halbstufenpotentiale. Für die polarometrischen Präzisionsmessungen wurde ein Polarometer nach Hans [15] verwendet.

Als Elektrolysengefäss diente eine thermostatierte Zelle nach Schwabe und Berg [16]. Diese Zelle scheint u.a. für Selen-Untersuchungen besonders geeignet zu sein, weil das angesammelte Boden-Quecksilber sehr schnell aus dem Gefäss entfernt werden kann. Damit vermeidet man, mindestens zum grössten Teil, eine Reaktion zwischen Depolarisator und Boden-Quecksilber. Eine Herabsetzung der Depolarisatorkonzentration durch eine derartige Nebenreaktion wurde nie beobachtet. Die Bezugselektrode (gesättigte Kalomelelektrode) war durch eine Glasfritte mit Agarfüllung von der Lösung getrennt. Um polarographische Untersuchungen im positiven Spannungsbereich zu ermöglichen, wo Cl^- störend wirkt, war die Agarbrücke mit KNO_3 hergestellt. Die dadurch bedingte Spannungskorrektur (Veränderung des Diffusionspotentials) betrug −15 mV. Der Ohmsche Widerstand der Zelle wurde mit einer Philip Messbrücke GM 4249 kontrolliert. Die iR-Korrekturen des Spannungsabfalls wurden nach Ilkovič berechnet und bei der Auswertung der Halbstufenpotentiale berücksichtigt.

Die pH-Messungen wurden mit der Glaselektrode und einem pH-Meter Beckman G durchgeführt.

Zur Aufnahme von Elektrokapillarkurven, oszillographischen Spannung-Zeit-Kurven sowie Stromstärke-Zeit-Kurven wurden spezielle Apparaturen benutzt, die im Zusammenhang mit den entsprechenden Ergebnissen kurz erwähnt werden.

Die spurenweise Bildung von HgSe, das die Kapillaren verstopfen kann, ist schwierig ganz zu vermeiden. Trotz sorgfältiger Handhabung wurden für die ausgeführten Untersuchungen drei Kapillaren benötigt, deren Konstanten häufig kontrolliert wurden. Die Kapillarenkonstanten $m^{2/3}t^{1/6}$ (mit 0,1 M KNO_3, offenem Stromkreis und 50 cm Hg-Druck) betrugen:

2,018, 1,983 und 2,463 $mg^{2/3}$ $sek^{-1/6}$.

Durchführung der Messungen. Die gesamten Messungen wurden in gepufferten Wasserlösungen ausgeführt. Als Leitsalz diente in der Mehrzahl der Versuche 0,1 M KNO_3. Damit wurde die Ionenstärke der Lösungen auf etwa 0,2 festgelegt. 0,005 % Gelatine in den Lösungen wurde als Maximadämpfer verwendet. Als Normalwert der Depolarisatorkonzentration ist $1{,}0 \times 10^{-3}$ M anzusehen. Die Temperatur wurde in den zu untersuchenden Lösungen auf 25°C einreguliert und konnte mittels eines Höppler Ultra-Thermostates auf ± 0,1° konstant gehalten werden. Die Entfernung des Luftsauerstoffs wurde mit reinem Wasserstoff vorgenommen und die Tropfelektrode wurde erst nach dem Entlüften in die Lösung eingeführt. Nach Aufnahme der Stromspannungskurve mit dem Schreiber-Polarographen wurde durch ein manuelles Verfahren das entsprechende Halbstufenpotential auf ± 1 mV gemessen.

Alle Potentialangaben beziehen sich auf die gesättigte Kalomelelektrode. Weil die Selenverbindungen stark kapillaraktiv wirken, sind die Stufenhöhen — nach Verlängern von Grund- und Grenzstrom — bei $E_{\frac{1}{2}}$ gemessen. Bei polarometrischer Auswertung ist nach der Differenzmethode verfahren worden.

ERGEBNISSE

1. Untersuchungen an der Quecksilbertropfelektrode mit registrierenden Gleichspannungspolarographen. Eine grössere Anzahl Polarogramme wurde unter verschiedenen Bedingungen von Diselen-diessigsäure, Hg(II)-bis-selenoglykolsäure und Selenoglykolsäure (in Gemisch mit den beiden ersterwähnten) aufgenommen. Etwa dreissig Polarogramme, die für die genaue Analyse der Stufenform nach den Gleichungen (24), (25) und (26) zur Anwendung kamen, wurden zur Kontrolle auf manuellem Weg punktweise gemessen. In Abb. 3 wird die pH-Abhängigkeit der Halbstufenpotentiale für Diselen-diessigsäure

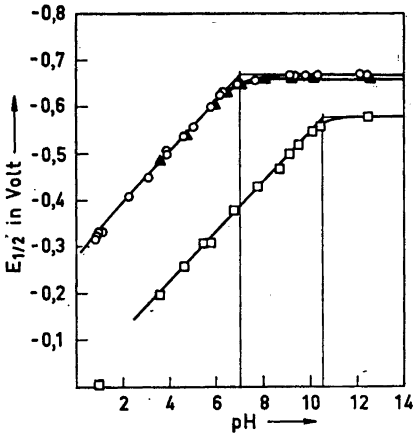

Abb. 3. Abhängigkeit des Halbstufenpotentials $E_{\frac{1}{2}}$ vom pH der Lösung.
(○) 1 × 10^{-3} M Diselen-diessigsäure
(▲) 1 × 10^{-3} M Merkuri-bis-selenoglykolsäure
(□) 1 × 10^{-3} M Mercaptoessigsäure (nach Leussing und Kolthoff)

und Hg(II)-bis-selenoglykolsäure graphisch dargestellt. Die entsprechenden Messwerte sind, um einen Einblick in die Messgenauigkeit zu geben, in Tab. 1 und 2 zusammengefasst. Wegen der Schwerlöslichkeit war es nicht möglich die Hg(II)-bis-selenoglykolsäure in stark saurem Bereich zu untersuchen.

Tabelle 1. Diselen-diessigsäure 1 × 10^{-3} M in verschiedenen Pufferlösungen. $E_{\frac{1}{2}}$ *vs.* ges. Kalomelelektrode gemessen. Leitsalz 0,1 M KNO_3 oder 0,1 M KCl. 0,005 % Gelatine.

pH	Puffer	$-E_{\frac{1}{2}}$ gemessen Volt	Korrektur mV		$-E_{\frac{1}{2}}$ korrigiert Volt
			$\frac{4}{3} R \frac{i_d}{2}$	Diff. pot.	
0,80	Perchlorat	0,330	+ 10		0,320
0,84	»	0,323	+ 9	− 15	0,329
1,05	»	0,326	+ 9	− 15	0,332
2,25	Citrat-Phosphat	0,403	+ 9	− 15	0,409
3,06	»	0,460	+ 10		0,450
3,83	Biphthalat	0,500	+ 11	− 15	0,504
3,90	»	0,506	+ 9		0,497
4,60	Acetat	0,543	+ 9		0,534
5,01	Citrat-Phosphat	0,564	+ 9		0,555
5,80	»	0,612	+ 10		0,602
6,20	Phosphat	0,618	+ 9	− 15	0,624
6,22	»	0,627	+ 10	− 15	0,632
6,90	»	0,655	+ 10		0,645
7,60	»	0,665	+ 9		0,656
9,10	Borax	0,674	+ 9		0,665
9,16	»	0,660	+ 8	− 15	0,667
9,75	Borax-NaOH	0,676	+ 9		0,667
10,25	»	0,676	+ 9		0,667
12,10	NaOH	0,661	+ 9	− 15	0,667
12,40	»	0,661	+ 9	− 15	0,667

Tabelle 2. Hg(II)-bis-selenoglykolsäure 1 × 10^{-3} M in verschiedenen Pufferlösungen. $E_{\frac{1}{2}}$ *vs.* ges. Kalomelelektrode. Leitsalz 0,1 M KNO_3. 0,005 % Gelatine.

pH	Puffer	$-E_{\frac{1}{2}}$ gemessen Volt	Korrekture mV		$-E_{\frac{1}{2}}$ korrigiert Volt
			$\frac{4}{3} R \frac{i_d}{2}$	Diff. pot.	
3,57	Acetat	0,476	+ 8	− 15	0,483
4,64	»	0,530	+ 8	− 15	0,537
5,90	Citrat-Phosphat	0,597	+ 8	− 15	0,604
6,42	Phosphat	0,621	+ 8	− 15	0,628
7,00	»	0,641	+ 8	− 15	0,648
8,02	»	0,652	+ 8	− 15	0,659
9,12	Borax	0,652	+ 8	− 15	0,659
10,15	Borax-NaOH	0,654	+ 8	− 15	0,661
12,50	NaOH	0,652	+ 8	− 15	0,659

Im ganzen untersuchten pH-Bereich erhält man gut ausgebildete kathodische Stufen, die für die vorliegenden Säuren einen fast identischen Verlauf aufweisen. Daher lässt sich vermuten, dass in allen Fällen die gleiche Elektrodenreaktion vorliegen muss. Damit sollte auch die Möglichkeit ausgeschlossen sein, dass eine Reduktion der -Se-Se-Brücke für die kathodischen Effekte verantwortlich ist. Zwischen pH = 1 und 6 beträgt die Neigung der Geraden

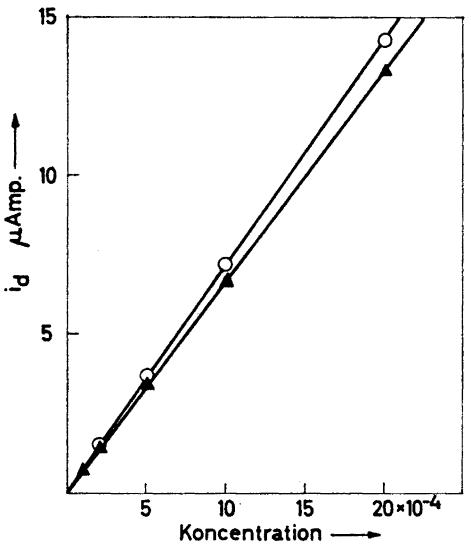

Abb. 4. Diselen-diessigsäure. Beziehung zwischen Konzentration und Diffusionsstrom. (O) Perchloratlösung pH = 1,0; (▲) Acetatpuffer pH = 4,60.

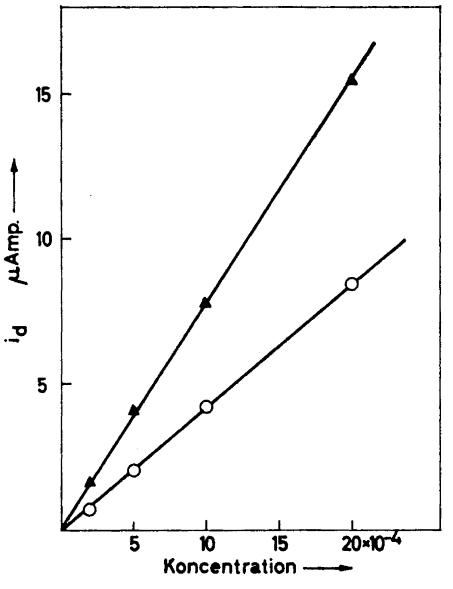

Abb. 5. Merkuri-bis-selenoglykolsäure. Beziehung zwischen Konzentration und Grenzstrom im Phosphatpuffer pH = 6,35. (▲) Kathodische Stufe; (O) Anodische Stufe.

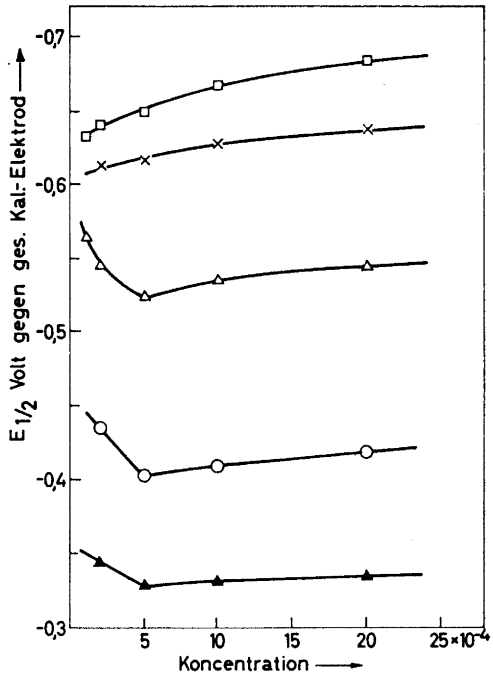

Abb. 6. Abhängigkeit des Halbstufenpotentials $E_{\frac{1}{2}}$ von der Konzentration des Depolarisators in verschiedenen Puffern.
Diselen-diessigsäure: (▲) pH = 1,0 (○) pH = 2,2;
(△) pH = 4,6 (□) pH = 9,2;
Merkuri-bis-selenoglykolsäure: (×) pH = 6,35.

$-0{,}055$ V/pH-Einheit, ab pH = 9 ist $E_{\frac{1}{2}}$ von pH unabhängig. In Abb. 3 ist zum Vergleich die von Leussing und Kolthoff [9] gefundene $E_{\frac{1}{2}}$/pH-Kurve der Mercaptoessigsäure auch eingetragen. Die Einzelheiten der Diagramme werden im Diskussionsabschnitt näher erörtert. Die genaue Auswertung der Polarogramme nach den Gleichungen (25) und (26) deutet auf eine bessere Linearität nach (25) hin. Die Steilheit der Stufen beträgt im Durchschnitt im sauren Gebiet etwa 0,061 und im alkalischen 0,068 (mit den in (25) gewählten Einheiten). Somit ist der kathodische Elektrodenvorgang als ein Einelektronenprozess anzusehen, weil die Abweichungen vom theoretischen Wert 0,059 innerhalb der experimentellen Fehlergrenzen liegen.

Abb. 4 und 5 geben bei einigen pH-Werten die Beziehungen zwischen Konzentration und Grenzstrom der beiden Säuren wieder. Im gesamten pH-Bereich ist dabei für Konzentrationen bis zu 2×10^{-3} M eine gute Linearität zu finden. Die kathodischen Grenzströme weisen also in dieser Hinsicht diffusionsbedingte Eigenschaften auf.

Die in Abb. 6 wiedergegebene Abhängigkeit des Halbstufenpotentials von der Konzentration scheint sich teilweise ganz anomal zu verhalten. Durch eine

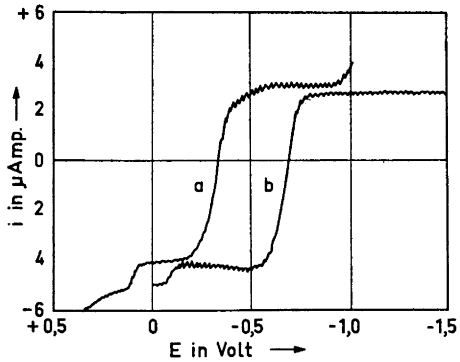

Abb. 7. Polarogramme von Selenoglykolsäure (in Mischung mit Hg(II)-bis-selenoglykolsäure) nach Methode 1 hergestellt und in zwei verschiedenen Pufferlösungen. Ausgangskonzentration der Merkuri-bis-selenoglykolsäure 1×10^{-3} M. Kurve (a) entspricht pH = 0,85, (b) pH = 9,20.

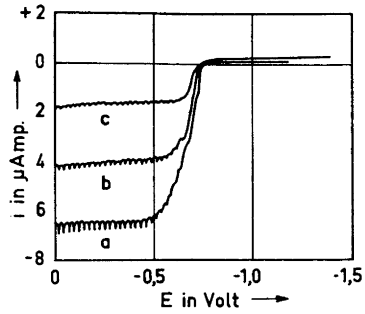

Abb. 8. Polarogramme von 1×10^{-3} M (Ausgangskonzentration) Natriumsulfid im Boratpuffer. H_2-Einleitungszeiten: (a) 10, (b) 20 und (c) 40 Min.

genaue Analyse der Stufenform ist klargelegt worden, dass die diffusionsbedingte Stufe aus zwei Teilen besteht und zwar einer Hauptstufe (A) (bei einer Depolarisatorkonzentration 1×10^{-3} M zu etwa 80—90 % der Höhe der Gesamtstufe) die von einer kleineren Stufe (B) überlagert ist, deren Halbstufenpotential etwas negativer als das der Hauptstufe liegt. Die beiden Stufen A och B lassen sich im ganzen untersuchten pH-Gebiet schlecht trennen, weshalb auf eine genauere Aussage über die Eigenschaften der wenig hervortretenden Stufe B vorläufig verzichtet werden muss. Weil aber die Stufe B eine innerhalb gewissen Konzentrationsgrenzen konstante Höhe besitzt, ist es höchst wahrscheinlich, dass die gefundenen Desorptionserscheinungen auf der Elektrodenoberfläche mit dieser Stufe zusammenhängen. B könnte also die Eigenschaften einer Desorptionsstufe besitzen. Infolgedessen bleibt das Halbstufenpotential der Gesamtstufe nicht konstant. Wie Abb. 6 zeigt, geht $E_{\frac{1}{2}}$ bei kleinen Depolarisatorkonzentrationen in saurer Lösung durch ein Minimum. Eine approximative Korrektion des Einflusses der Stufe B gibt für die Hauptstufe ein von der Konzentration in saurer Lösung recht unabhängiges Halbstufenpotential, was im Einklang mit dem angegebenen Mechanismus (25) steht. Die Desorptionsstufen treten bei den höheren Homologen und in Wasser-Äthanollösung etwas besser hervor, werden deshalb in einer folgenden Veröffentlichung näher berücksichtigt und diskutiert.

Die Ionenstärke der Lösung wirkt wenig auf das Halbstufenpotential und die Stufenform ein. Beispielsweise kann für 1×10^{-3} M Diselen-diessigsäure in Boratpuffer (pH = 9,12) mit $\mu = 0{,}2$ und $\mu = 1{,}1$ eine Differenz der Halbstufenpotentiale von 4 mV gemessen werden. (Mit steigendem μ-Wert verschiebt sich $E_{\frac{1}{2}}$ in positivier Richtung.)

Der Einfluss der Temperatur auf die Stufenhöhen (A + B) der Diselendiessigsäure und der Hg(II)-bis-selenoglykolsäure beträgt im untersuchten

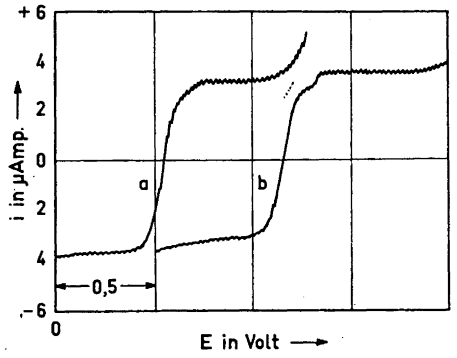

Abb. 9. Polarogramme von Selenoglykolsäure (in Mischung mit Diselen-diessigsäure) nach Methode 2 hergestellt und in zwei verschiedenen Puffern. Ausgangskonzentration der Diselen-diessigsäure 1×10^{-3} M. Kurve (a) entspricht pH = 4,58, (b) pH = 6,93.

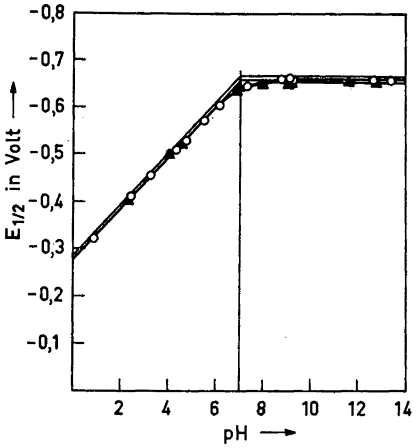

Abb. 10. Abhängigkeit des Halbstufenpotentials $E_{\frac{1}{2}}$ vom pH der Lösung.
(O) Selenoglykolsäure (in Mischung mit Hg(II)-bis-selenoglykolsäure) nach Methode 1.
(▲) Selenoglykolsäure (in Mischung mit Diselen-diessigsäure) nach Methode 2.

Intervall 18° — 45°C im Durchschnitt 1,62 % bzw. 1,56 % pro Grad. Nach von Stackelberg [17] hat man für einen diffusionsbedingten Strom ohne Nachregulierung der Tropfgeschwindigkeit mit einer Erhöhung von i_d um 1,6 % pro Grad zu rechnen. Die Übereinstimmung ist also befriedigend.

Die Einwirkung der Gelatine auf die Stufen ist besonders untersucht worden. Ohne Dämpfer treten, spez. im Perchlorat- und Acetatpuffer, typische Strömungsmaxima auf. Bei der Depolarisatorkonzentration 1×10^{-3} M werden diese Maxima durch 0,005 % Gelatine ganz unterdrückt. Auf die Halbstufenpotentiale der Diselen-diessigsäure und der Hg(II)-bis-selenoglykolsäure scheint eine derartige Gelatinekonzentration ohne Einfluss zu sein. Eine Verschiebung der Halbstufenpotentiale durch die Anwesenheit von Campher (0,035 %) konnte auch nicht beobachtet werden.

Selenoglykolsäure, im Gemisch mit Hg(II)-bis-selenoglykolsäure bzw. Diselen-diessigsäure wie früher erwähnt, wurde im gesamten pH-Bereich unter denselben Bedingungen wie die behandelten Säuren untersucht. In Abb. 7 und 9 sind einige Polarogramme wiedergegeben, die den beiden Herstellungsmethoden entsprechen. Es geht deutlich hervor, dass die der Selenoglykolsäure entsprechende anodische Stufe *direkt* in eine kathodische übergeht. Somit ist die Reversibilität der Elektrodenreaktion sichergestellt.

Die hier erhaltenen Polarogramme können nicht ohne Vorsicht für quantitative Auswertungen benutzt werden. Nach der Methode 1 wirkt sich nämlich ein Überschuss von Natriumsulfid störend aus, was besonders in alkalischer Lösung trotz erheblich erhöhten H_2-Einleitungszeiten schwer zu beseitigen ist (Abb. 8). Bei der Herstellung von Selenoglykolsäure nach der Methode 2

sind gewisse Verluste (Selenwasserstoff und freies Selen können sich langsam bilden) nicht zu vermeiden. Beispielsweise ist in Abb. 9 (Kurve b) eine kleine kathodische Stufe ersichtlich, die die etwas positivere Hauptstufe überlagert. In der Tat liegt hier eine maskierte anodische Welle vor, die auf kleine Mengen von Selenwasserstoff zurückzuführen ist. Das Halbstufenpotential der Stufe stimmt nämlich mit dem von Lingane [18] gefundenen Wert der Se^{2-}-Ionen überein.

Die gemessenen anodisch-kathodischen Halbstufenpotentiale sind in Abb. 10 graphisch dargestellt. Bei kleinen pH-Werten überlagern sich die beiden Kurven ganz. Der im alkalischen Bereich gefundene Unterschied von im Durchschnitt 6 mV ist sicher von der gerade erörterten Störung von Natriumsulfid abhängig. Der allgemeine Verlauf der Kurven ist mit dem früher für die Diselen-diessigsäure und die Hg(II)-bis-selenoglykolsäure gefundenen (Abb. 3) identisch. Zum Vergleich ist die der Diselen-diessigsäure entsprechende Kurve auch in Abb. 10 eingezeichnet.

Die Stufenform lässt sich in diesem Falle nach der Gleichung (24) untersuchen. Die linearen Beziehungen geben eine zwischen 0,060 (pH = 4,58) und 0,064 (pH = 7,30) wechselnde Steilheit der Stufen, in Übereinstimmung mit dem theoretischen Wert 0,059 V.

Es ist somit wohlbegründet die Schlussfolgerung zu machen, dass die Selenoglykolsäure sowohl mit der Diselen-diessigsäure als auch mit der Merkuri-bis-selenoglykolsäure an der tropfenden Quecksilberelektrode innerhalb der experimentellen Fehlergrenzen reversible Systeme darstellen. Der entscheidende Elektrodenprozess ist auf einen Einelektronenvorgang bezogen. Grundsätzlich gibt dann eine Durchtrittsreaktion nach der Gleichung (6) die einzige Möglichkeit, diese Ergebnisse zu vereinen.

Im Folgenden zielt diese Untersuchung darauf hin, mit spez. dafür geeigneten Methoden den Reaktionsmechanismus genauer fassbar zu machen, um den Elektrodenvorgang endgültig beweisen zu können. Auch werden einige wesentliche Konstanten des Systems mittels Präzisionsmessungen bestimmt.

2. Elektrokapillarkurven. Zur Aufnahme von Elektrokapillarkurven wurde eine Apparatur nach Hans und Hauck [19] verwendet, die die Tropfzeit automatisch auf dem Lichtschirm eines Kathodenstrahloszillographen registriert. Die von der Tropfzeit abhängige Ablenkung des Lichtpunktes des Kathodenstrahles wird mit einem sehr langsam laufenden Hellige-Kymographion photographiert. Im Vergleich zu der üblichen Methode der Tropfzeitbestimmung mit der Stoppuhr, die sehr zeitraubend ist, kann hier eine vollständige Elektrokapillarkurve (Kapillarogramm) in etwa 6 Min. erhalten werden. Nebenreaktionen zwischen Bodenquecksilber und Diselen-Verbindungen im Gefäss konnten in der kurzen Zeit praktisch ganz vermieden werden. Die beschriebene Methode ist besonders für stark kapillaraktive Substanzen geeignet, zu welcher Kategorie die Diselenverbindungen ganz allgemein gehören. Originalaufnahmen von automatisch registrierten Kapillarkurven sind in Abb. 11 und 12 zu finden. Von Absolutwerten der Tropfzeiten wird abgesehen, weil uns in diesem Zusammenhang hauptsächlich die Konturen der individuellen Kapillarogramme interessieren. Die Kurven (b) und (c) in Abb. 11 zeigen deutlich wie

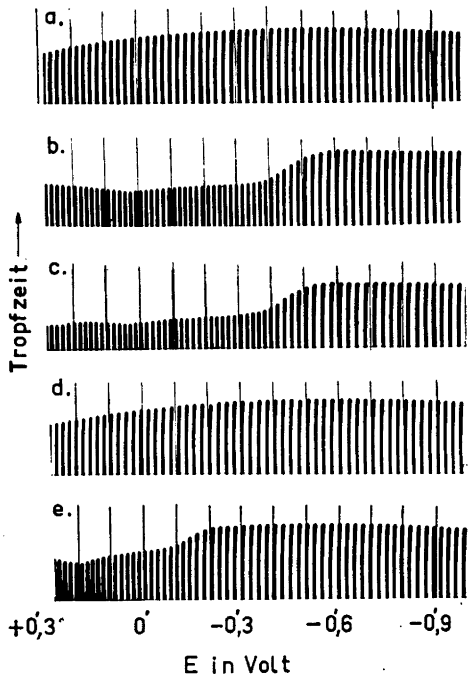

Abb. 11. Elektrokapillarkurven (willkürliche Höhe) mit Perchlorat als Leitsalz (0,1 M $HClO_4$, 0,1 M $NaClO_4$, 0,005 % Gelatine) pH = 1,0.

(a) Ohne Depolarisator
(b) Diselen-diessigsäure 1 × 10^{-3} M
(c) Merkuri-bis-selenoglykolsäure 1 × 10^{-3} M
(d) Dithio-diessigsäure 1 × 10^{-3} M
(e) Mercaptoessigsäure 1 × 10^{-3} M

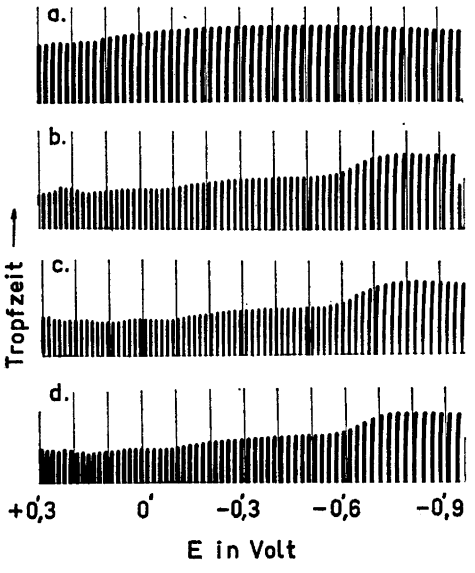

Abb. 12. Elektrokapillarkurven im Acetatpuffer aufgenommen (0,1 M KNO_3, 0.005 % Gelatine) pH = 4,60.

(a) Ohne Depolarisator
(b) Diselen-diessigsäure 1 × 10^{-3} M
(c) Hg(II)-bis-selenoglykolsäure 1 × 10^{-3} M
(d) Hg(II)-bis-selenoglykolsäure 1 × 10^{-3} M + Na_2S 2 × 10^{-3} M

stark kapillaraktiv die Selenverbindungen wirken. Ferner zeigt sich, dass die Dithio-diessigsäure im Gegensatz zu der Mercaptoessigsäure keine Depression der Elektrokapillarkurve aufweist. Die Kapillarogramme (b), (c) und (d) in Abb. 12 können als Beweis dafür vorgelegt werden, dass in allen drei Fällen die gleiche kapillaraktive Verbindung auf dem Quecksilbertröpfchen die Adsorptionserscheinungen bewirkt. Dabei muss es sich dann um eine Quecksilberverbindung der Selenoglykolsäure handeln, die als dünne Adsorptionsschicht an der Tropfenoberfläche gebildet wird. Eine derartige Hg-Verbindung kann sich auch mit der Mercaptoessigsäure bilden, aber nicht mit der entsprechenden Dithio-diessigsäure. Bemerkenswert ist ferner, dass die Desorption der Selenverbindungen in den Kapillarogrammen in demselben Spannungsbereich angezeigt wird, in dem die normale polarographische Stufe auftritt. Auch das kann als Beweis dafür angesehen werden, dass die Reduktion einer Quecksilberverbindung die kathodischen Stufen hervorruft.

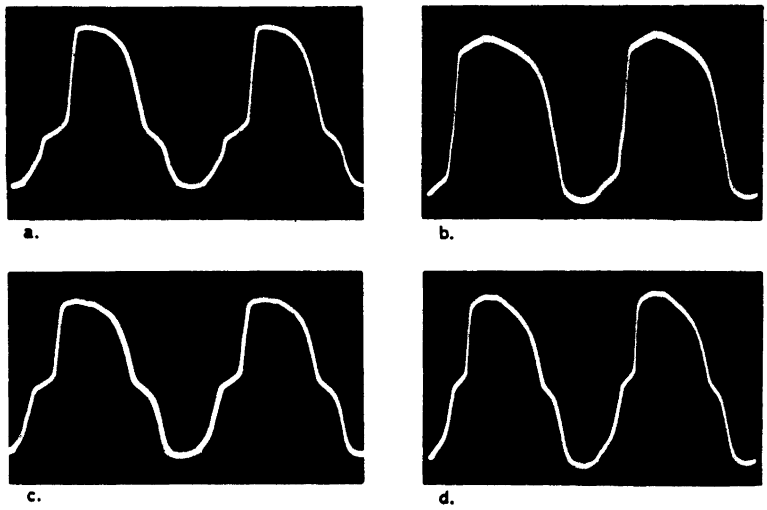

Abb. 13. V-t-Oszillogramme bei verschiedenen pH-Werten 0,1 M KNO_3 und 0,005 % Gelatine. Strömende Quecksilberelektrode. 0,15 mA. Frequenz 30 Hz.

(a) Mercaptoessigsäure 4×10^{-3} M. pH = 5,78
(b) Dithio-diessigsäure 2×10^{-3} M. pH = 5,76
(c) Diselen-diessigsäure 2×10^{-3} M. pH = 9,04
(d) Diselen-diessigsäure 2×10^{-3} M. pH = 5,70.

3. Oszillographische Wechselstrompolarographie nach Heyrovský. Die Reversibilität der Elektrodenreaktionen bei verschiedenen pH-Werten wurde mit einer strömenden Quecksilberelektrode und einer oszillographischen *V-t*-Apparatur nach Heyrovský und Forejt [20] untersucht. Die *V-t*-Kurven (Abb. 13 und 14), wo die Einschnitte auf dem kathodischen und anodischen Ast deutlich zu sehen sind, zeigen bei den Selenverbindungen im gesamten untersuchten pH-Bereich eine vollkommene Reversibilität. Ausserdem ist diese Reversibilität unabhängig davon, ob man von der Diselen-diessigsäure, der Hg(II)-bis-selenoglykolsäure oder der Selenoglykolsäure ausgeht. Diese Befunde können nur in Übereinstimmung mit einem Elektrodenmechanismus nach der Gleichung (6) erklärt werden. Es sei noch erwähnt, dass die Mercaptoessigsäure im Gegensatz zu der Dithio-diessigsäure an der strömenden Elektrode ein reversibles System darzustellen vermag (Abb. 13(a) und (b)). Wie bei den entsprechenden Elektrokapillarkurven ist diese Tatsache auch hier auf die Bildung einer Merkuroverbindung der Mercaptoessigsäure zurückzuführen.

4. Stromstärke-Zeit-Kurven. Mit einem schnellstschwingenden Galvanometer (T_0 = 0,03 sek.) wurden *i-t*-Kurven von Einzeltropfen aufgenommen und mittels eines Hellige-Kymographions photographisch registriert. Durch eine automatische Schaltapparatur [21] war es möglich, die Spannung genau im Moment des Abfallens eines Tropfens anzulegen. Damit konnte der polaro-

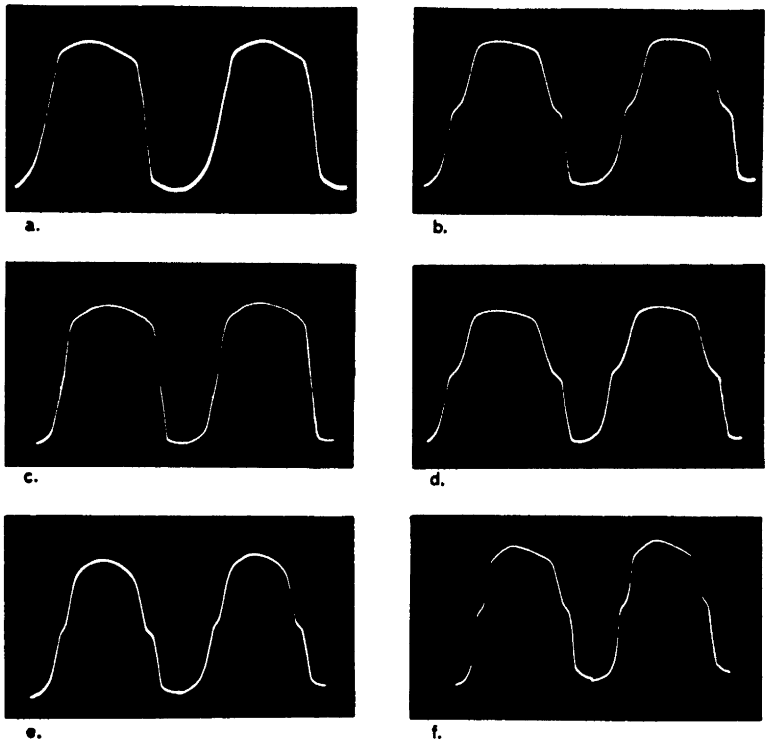

Abb. 14. V-t-Oszillogramme wie in Abb. 13.

(a) Phosphatpuffer ohne Depolarisator pH = 6,98
(b) Selenoglykolsäure nach Methode 2. Ausgangskonzentration der Diselen-diessigsäure 2×10^{-3} M. pH = 6,94.
(c) Phthalatpuffer ohne Depolarisator pH = 4,00
(d) Hg(II)-bis-selenoglykolsäure 1×10^{-3} M. pH = 6,96
(e) Selenoglykolsäure nach Methode 2 wie (b). pH = 3,90 und
(f) pH = 9,12.

graphische Verarmungseffekt ausgeschaltet werden. Mit Diselen-diessigsäure als Depolarisator wurden *i-t*-Kurven bei konstanter Spannung in mehreren Puffern an verschiedenen Stellen der entsprechenden Stufen registriert. Abb. 15 gibt ein Beispiel wieder, wo das erste und zweite Tröpfchen ganz und das dritte teilweise erscheinen. Der Exponent x dieser parabelförmigen Kurven $i \sim t^x$ beträgt bei diffusionsbegrenzten Strömen $x = 1/6$, für reaktionsbegrenzten Ströme dagegen $x = 2/3$. Mehrere Kurvenanalysen der ersten Tröpfchen bestätigen eine Übereinstimmung mit dem Parabelexponentenwert $x = 1/6$. Eine mit dieser Methode feststellbare kinetische Hemmung kann also nicht vorliegen, was für die Theorie der Elektrodenreaktion von wesentlicher Bedeutung ist. Damit ist nämlich bewiesen, dass die der kathodischen Reduktion vorgelagerte Radikalspaltung ohne merkliche kinetische Hemmung verläuft.

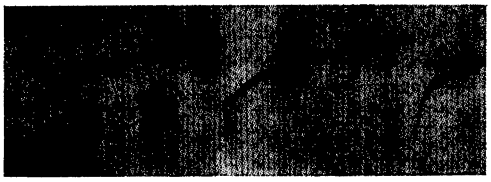

Abb. 15. Stromstärke-Zeit-Kurven der Diselen-diessigsäure in Phosphatpuffer (pH = 6,22) aufgenommen.

0,1 M KNO_3 und 0,005 % Gelatine. Kathodenpotential −1,0 Volt. Tropfzeit 3,43 Sek.

Diese grundsätzlich wichtige Frage werde ich in einer kommenden Veröffentlichung näher behandeln.

5. Polarometrische Messungen. Auf polarometrischem Wege sind Diselen-diessigsäure und Hg(II)-bis-selenoglykolsäure mit grösster Genauigkeit untersucht worden. Die Werte der Diffusionskonstante D wurden aus den gemessenen Polarogrammen berechnet (Tabelle 3). Dabei wurde die korrigierte Ilkovič-Gleichung [22] in folgender Form angewendet

$$i_d = 607nD^{1/6}Cm^{2/3}t^{1/6}\left(1 + \frac{39D^{1/6}t^{1/6}}{m^{1/3}}\right)$$

Die polarometrischen Kurven sind auch nach den Gleichungen (25) und (26) ausgewertet worden. Die Ergebnisse mit Diselen-diessigsäure zeigt Abb. 16. Frühere Beobachtungen über die Linearität werden bestätigt. Die nach (25) berechneten Kurven zeigen im unteren Teil eine befriedigende Linearität, im oberen dagegen eine kräftige Abbeugung, die in saurer Lösung ausgeprägter ist. Diese Erscheinung ist eine direkte Folge der entsprechenden Stufenform (Abb. 1 und 2): Die oben anormale Abrundung der Stufen, besonders bei kleinen pH-Werten, wird durch die schon erwähnte überlagerte Stufe (B) bedingt.

Tabelle 3. Die Diffusionskonstante D in verschiedenen (Biphthalat, Phosphat, Borax) Pufferlösungen 25°C. Leitsalz 0,1 M KNO_3. 0,005 % Gelatine. Ionenstärke μ = 0,2.

pH	D cm² sek⁻¹	
	Diselen-diessigsäure	Hg(II)-bis-selenoglykolsäure
3,85	$6{,}75 \times 10^{-6}$	—
6,30	$6{,}65 \times 10^{-6}$	$5{,}70 \times 10^{-6}$
9,10	$6{,}45 \times 10^{-6}$	$5{,}55 \times 10^{-6}$

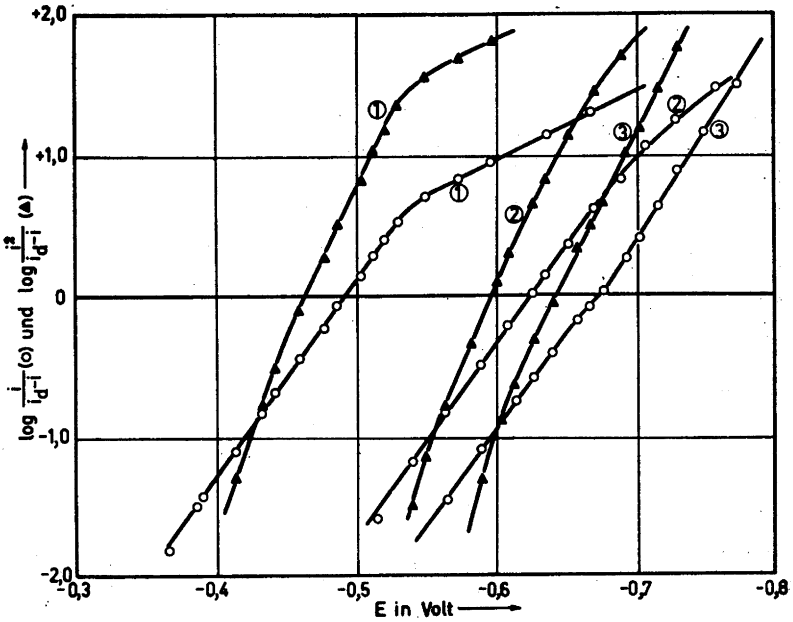

Abb. 16. Diselen-diessigsäure 1 × 10^{-3} M bei verschiedenen pH-Werten. Analyse der Kurven nach den logarithmischen Gleichungen (25) und (26).

(1) Phthalatpuffer pH = 3,85 (2) Phosphatpuffer pH = 6,30 (3) Boratpuffer pH = 9,10.

6. Untersuchung der anodischen Stufen. Die kathodische Stufe der Diselen-diessigsäure sowie der Hg(II)-bis-selenoglykolsäure ist diffusionsbegrenzt, was auch aus der linearen Abhängigkeit von der Wurzel ($\sqrt{h}$) der Hg-Niveauhöhe hervorgeht. Zusätzlich treten kleine anodische Stufen im positiveren Spannungsbereich auf, die andere Eigenschaften besitzen. Bei den Schwefelverbindungen kommen derartige Stufen oft vor. Auch wenn es noch nicht ganz klar ist, aus welcher Elektrodenreaktion sie entstanden sind, ist ihre wahre Natur als adsorptionsbedingte Stufen bei den Schwefelverbindungen festgestellt worden. Die Potentiale der anodischen Stufen der Diselen-diessigsäure und der Hg(II)-bis-selenoglykolsäure sind relativ pH-unabhängig. Während die Höhen der anodischen Stufen der ersten Säure bei einer Konzentrationsvariation einer Adsorptionsisothermen gehorchen, sind die der zweiten Säure mehr konzentrationsproportional (Abb. 5.). Der Temperaturkoeffizient der ersten Gruppe schwankt im Intervall 18°—45°C zwischen 3,2 und 5,1 % pro Grad. Für die anodische Stufe der Hg(II)-bis-selenoglykolsäure ist dagegen der Koeffizient konstant 3,1 % pro Grad. Weiter ist der Adsorptionscharakter dieser Stufen der Diselen-diessigsäure durch die Abhängigkeit der Stufenhöhen von der Quecksilberniveauhöhe (h) bewiesen worden (Abb. 17 und 18). Die Frage, welcher elektrochemische Vorgang für diese anodischen Stufen ver-

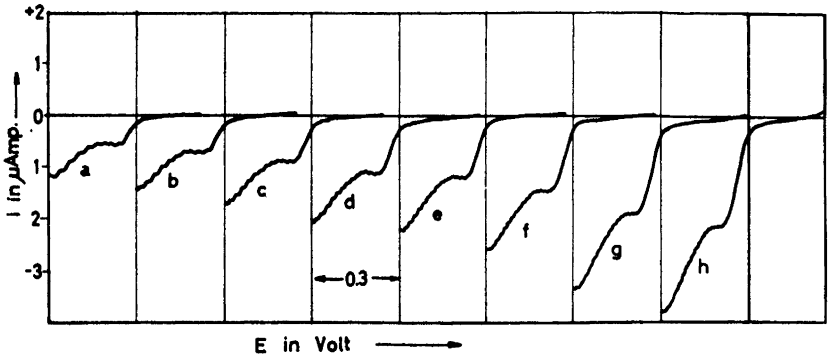

Abb. 17. Anodische Adsorptionsstufen der Diselen-diessigsäure bei verschiedenen Quecksilberniveauhöhen h. Konzentration 1 × 10^{-3} M pH = 2,25. Jedes Polarogramm bei +0,3 Volt begonnen. (a) h = 33,5 cm (b) 43,5 (c) 53,5 (d) 63,5 (e) 73,5 (f) 88,5 (g) 115,5 (h) 136,0.

antwortlich ist, muss vorläufig offen gelassen werden. Möglich ist, dass intermediäre Komplexe vom Typ Se — CH_2 — COO oder wahrscheinlicher Polymere davon entstehen. Es ist schliesslich hinzuzufügen, dass in dem Bereich wo diese Stufen auftreten, die entsprechenden Kapillarkurven eine bemerkenswerte Depression zeigen (Abb. 11 und 12).

DISKUSSION

Trotz der scheinbaren Reversibilität des Systems Diselendiessigsäure-Selenoglykolsäure an der tropfenden Quecksilberelektrode ist durch die vorliegende Untersuchung eindeutig dargelegt worden, dass nur das Redoxsystem Hg(I)-selenoglykolsäure-Selenoglykolsäure nach Gleichung (6) in einer befriedigenden Weise alle experimentellen Befunde erklären kann. Diese Schluss-

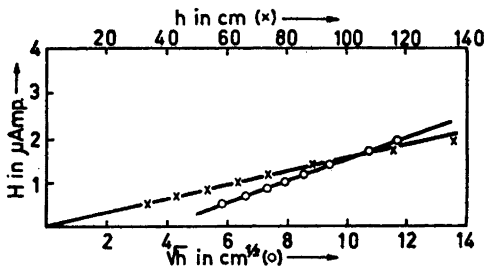

Abb. 18. Adsorptionsstufen wie in Abb. 17. Beziehung zwischen Stufenhöhe in μAmp und Quecksilberniveauhöhe h (×) oder $\sqrt{h}$ (○).

folgerung setzt weiter als etwas sehr Wichtiges eine homolytische Radikalspaltung der -Se-Se- Brücke als vorgelagerte Reaktion voraus. Eine dabei auftretende kinetische Hemmung konnte bischer nicht durch i-t-Kurven gezeigt werden.

Die Beziehungen zwischen Halbstufenpotential und pH verhalten sich gemäss den in (22) und (23) abgeleiteten Gleichungen. Der kleine Unterschied der Halbstufenpotentiale der beiden Selensäuren in Abb. 3 lässt sich durch die Differenz der entsprechenden Diffusionskonstanten erklären (Tab. 3). Durch das Glied 0,059 $\log(k/k')$in Gleichung (20), das bisher vernachlässigt wurde, tritt ein Unterschied von etwa 6 mV (berechnet) auf, was mit den experimentellen Ergebnissen sehr wohl übereinstimmt.

Aus dem Knickpunkt der Geraden (Abb. 3) berechnet sich $pK_2 = 7{,}00$ der Selenoglykolsäure mit einer Genauigkeit in der K_2-Bestimmung von etwa $K_2 = (1{,}0 \pm 0{,}1) \times 10^{-7}$. Somit liegt hier die Messung der Dissoziationskonstante einer Säure vor, die in reinem Zustand nicht charakterisiert worden ist. Die beschriebene Methode eröffnet also eine Möglichkeit, unter Benutzung der entsprechenden Diselenide Dissoziationskonstantmessungen bisher nicht fassbarer Selenolgruppen durchzuführen. Derartige Untersuchungen sind im Gange, wobei auch versucht wird den Einfluss der früher erwähnten Desorptionsstufe (Stufe B) auf die Genauigkeit der K_2-Werte festzustellen. Korrekturen für diesen Einfluss sind hier nicht durchgeführt worden.

In diesem Zusammenhang ist zu bemerken, dass die in der vorliegenden Arbeit durchgeführten Berechnungen der Stufenneigung nach (24), (25) oder (26) alle einen kleinen systematischen Fehler aufweisen und zwar weil die Auswertungen sich auf die Gesamtstufe (A + B) beziehen. Dadurch ist auch i_d gleich $i_d^A + i_d^B$ gesetzt. Die Gesamtstufe weist im Konzentrationsbereich 1×10^{-3} M diffusionsbedingte Eigenschaften auf, welche höchst wahrscheinlich auf die dominierende Teilstufe A zurückzuführen sind, während die hier kleine Teilstufe B offenbar mit den Desorptionerscheinungen an der Elektrodenoberfläche zusammenhängt. Eine Parallelle würde dann gewissermassen mit den von Zuman und Mitarbeitern [23] untersuchten anodischen Stufen des 2,3-Dimercaptopropanols vorliegen. Wie wohlbegründet diese Anschauung bei den kathodischen Selenstufen ist, kann erst durch weitere Versuche entschieden werden, unter Bedingungen wo die beiden Stufen besser getrennt sind. Weil die Ableitungen nur für die in Lösung befindlichen Stoffe gültig sind, müsste die genaue Stufenanalyse sich auf die Stufe A beschränken. Aus oben angeführten Gründen kann nur eine ungefährliche Schätzung von i_d^A in Frage kommen. Es zeigt sich dann, dass bei diesen verhältnismässig hohen Depolarisatorkonzentrationen die ursprunglichen Berechnungen geringfügig so korrigiert werden müssen, dass die Resultate dem theoretischen Wert 0,059 etwas näher kommen. Auf derartige Korrektionen wird in dieser Untersuchung verzichtet, weil die grundsätzlichen Ergebnisse dadurch nicht beeinflusst werden können.

Es ist interessant die Konstante $K_2 = 1{,}0 \times 10^{-7}$ mit dem entsprechenden Wert der Mercaptoessigsäure zu vergleichen. Für diese Säure ist $K_2 = 2{,}95 \times 10^{-11}$ auf potentiometrischem Wege gemessen worden. Die Selenolgruppe weist,

wie aus den Grössen der Selen- und Schwefel-Atome zu erwarten ist, erheblich stärkere Säureeigenschaften als die entsprechende Mercaptogruppe auf.

Leussing und Kolthoff [9] geben in ihrer Arbeit über die Mercaptoessigsäure als eine mögliche Erklärung für die Abweichungen der experimentell gefundenen Halbstufenpotentiale von den theoretisch abgeleiteten die im sauren Gebiet auftretenden anodischen Adsorptionsstufen an. Unter Berücksichtigung dessen, dass auch die Hg(I)-Verbindung eine Säure ist, dürfte die theoretische Kurve auch bei kleinen pH-Werten ziemlich geradlinig verlaufen, wie das bei der Selenverbindung der Fall ist.

Mit $pK_2 = 7{,}0$ in Gleichung (20) und dem Korrektionsglied $-0{,}006$ V $[0{,}059 \log (k/k')]$ ergibt sich $E_0 = -0{,}260$ V (*vs.* ges. Kal.-Elektrode).

Die Brückenstabilitäten der -Se-Se- und -S-S- Gruppen sind durch diese Untersuchung hauptsächlich vom qualitativen Standpunkt her beleuchtet worden. Da bei den Diseleniden die Reduktion an der Tropfelektrode über eine Merkuroverbindung vor sich geht, können die elektrochemischen Messwerte nicht für eine unmittelbare Berechnung der Bindungsenergien der -Se-Se-Brücke benutzt werden.

Aus den bisherigen auf polarographischem Wege gewonnenen Ergebnissen über die Quecksilberverbindungen der Diselenide lässt sich schliessen, dass nur die grössere Brückenstabilität der -S-S- Gruppe gegenüber der -Se-Se-Gruppe für die ausgeprägte polarographische Irreversibilität der in der Einleitung erwähnten Disulfide massgebend ist. Diese Schlussfolgerung wird von den Arbeiten von Stricks und Kolthoff [24,25] gestützt, wo gezeigt wird, dass die drei Thiole Mercaptoessigsäure, Cystein und Gluthathion im Stande sind, u.a. Mercaptide des einwertigen Quecksilbers zu bilden, die an der Quecksilberelektrode als Redoxsysteme auftreten können. Die in vorliegender Untersuchung gefundenen *V-t*-Kurven der Mercaptoessigsäure und Dithio-diessigsäure bestätigen diese Tatsache. Eine weitere Stütze der hier vorgebrachten Theorie der Brückenstabilität als entscheidendem Faktor sind die von Nygård und Schotte [26,27] ausgeführten polarographischen Untersuchungen gewisser zyklischer Disulfide. Die Ringspannung der fünf-, sechs- und siebengliedrigen Disulfide ist für die Redoxeigenschaften von grosser Bedeutung. Während die weniger gespannten Sechs- und Siebenringe in polarographischer Hinsicht den ausgeprägt irreversiblen Disulfiden wie Dithio-diessigsäure gleichen, zeigen die Fünfringe ein den Diseleniden analoges Verhalten an der Tropfelektrode auf.

Ich möchte an dieser Stelle Prof. Dr. M. von Stackelberg, Bonn, für seine wertvollen Hinweise und das fördernde Interesse an dieser Untersuchung meinen herzlichsten Dank aussprechen.

Prof. Dr. A. Fredga, Uppsala, bin ich für die Überlassung eines Präparates der Diselendiessigsäure sowie für viele Diskussionen auf dem Gebiet der Selenchemie zu grossem Dank verpflichtet.

Prof. Dr. G. Hägg danke ich für die mir im Chemischen Institut, Uppsala, gegebenen apparativen Möglichkeiten für die Durchführung elektrochemischer Arbeiten.

Dem *Schwedischen Naturwissenschaftlichen Forschungsrat (Statens Naturvetenskapliga Forskningsråd)* danke ich für die finanzielle Unterstützung. Mit dem Beitrag konnte die vorliegende Untersuchung zum grössten Teil im Institut für Physikalische Chemie der Universität Bonn ausgeführt werden.

LITERATUR

1. Kolthoff, I. M. und Barnum, C. *J. Am. Chem. Soc.* **62** (1940) 3061.
2. Kolthoff, I. M. und Barnum, C. *J. Am. Chem. Soc.* **63** (1941) 520.
3. Grubner, O. *Collection Czechoslov. Chem. Communs.* **19** (1954) 444.
4. Kaloušek, M., Grubner, O. und Tockstein, A. *Collection Czechoslov. Chem. Communs.* **19** (1954) 1111.
5. Kolthoff, I. M., Stricks, W. und Tanaka, N. *J. Am. Chem. Soc.* **77** (1955) 4739.
6. Biegler, Th. und Breyer, B. *Rev. Polarography (Japan)* **7** (1959) 31.
7. Stricks, W. und Kolthoff, I. M. *J. Am. Chem. Soc.* **74** (1952) 4646.
8. Tachi, I. und Koide, S. *Intern. Polarographic Congr. Prague* **1** (1951) 386.
9. Leussing, D. L. und Kolthoff, I. M. *J. Electrochem. Soc.* **100** (1953) 334.
10. Fredga, A. *Arkiv Kemi, Mineral. Geol.* **11 B** (1934) No. 44.
11. Fredga, A. *Ber.* **71** (1938) 286.
12. Fredga, A. *Studien über Selen-di-Karbonsäuren und Diselen-di-Karbonsäuren* (Diss.) Universität, Uppsala 1935.
13. Behaghel, O. und Rollmann, M. *Ber.* **62** (1929) 2696.
14. Fredga, A. *Svensk Kem. Tidskr.* **48** (1936) 91.
15. Hans, W. *Chem.-Ing.-Tech.* **23** (1951) 428.
16. Schwabe, K. und Berg, H. *Z. Elektrochem.* **56** (1952) 952.
17. v. Stackelberg, M. *Polarographische Arbeitsmethoden*, Berlin 1950, p. 292.
18. Lingane, J. J. und Niedrach, L. W. *J. Am. Chem. Soc.* **71** (1949) 196.
19. Hans, W. und Hauck, G. *Unveröffentlicht.*
20. Heyrovský, J. und Forejt, J. *Z. physik. Chem.* **193** (1943) 77.
21. Hans, W., Henne, W. und Meurer, E. *Z. Elektrochem.* **58** (1954) 836.
22. Lingane, J. J. und Loveridge, B. A. *J. Am. Chem. Soc.* **72** (1950) 438.
23. Zuman, P., Zumanova, R. und Teisinger, J. *Collection Czechoslov. Chem. Communs.* **20** (1955) 139.
24. Stricks, W., Kolthoff, I. M. und Heyndrickx, A. *J. Am. Chem. Soc.* **76** (1954) 1515.
25. Stricks, W. und Kolthoff, I. M. *J. Am. Chem. Soc.* **75** (1953) 5673.
26. Nygård, B. und Schotte, L. *Acta Chem. Scand.* **10** (1956) 469.
27. Nygård, B. *In Vorbereitung.*

Eingegangen am 22. Dezember 1960.

ACTA CHEMICA SCANDINAVICA 15 (1961) 1064–1066

Estimation of Dithionate

HANNE CROSSLAND and NIELS HOFMAN-BANG

Chemistry Department A, Technical University of Denmark, Copenhagen, Denmark

An improved method for the estimation of dithionate has been developed. The method is based on rapid oxidation with ammonium vanadate in a medium of hot, fairly concentrated sulfuric acid. The vanadyl ions formed are titrated with permanganate. The effects of the concentrations of sulfuric acid and of vanadate are discussed.

Quantitative determination of dithionate has always been a problem due to the exceptional stability of dithionate ions in aqueous solution. Kurtenacker *et al.*[1] describe a direct method; in earlier methods the content of dithionate has usually been calculated as a difference. Kurtenacker uses ammonium vanadate in 4 N sulfuric acid as the oxidizing agent, and he then titrates the vanadyl ions formed with permanganate. However, complete oxidation of dithionate requires at least 20 min. boiling. Vasudeva Murthy [2] uses dichromate in 10 N sulfuric acid as the oxidizing agent. About 1 hour's boiling is necessary to secure complete oxidation. It is further necessary to run a blank and subtract the amount of cromic ions formed. Yost and Pomeroy [3] have made an investigation of the decomposition and oxidation of dithionic acid. They have measured the rate of decomposition of dithionic acid into sulfurous and sulfuric acids in the presence of various concentrations of hydrochloric acid and perchloric acid. The rate was found to be proportional to the concentration of the dithionate and to that of the total acid, provided its concentration does not exceed 0.6 N; but at higher acid concentrations the rate increases more rapidly. The rate of oxidation of dithionic acid by dichromate, bromate and iodate was found to be about the same for these three oxidizing agents, to be independent of their concentrations, and to be nearly identical with the rate of the decomposition of the acid into sulfurous and sulfuric acids. This shows that the first step in the oxidation of dithionic acid presumably is its hydrolysis, which is catalyzed by hydrogen ions.

The investigation mentioned above combined with the observed fact that moistening of a solid dithionate with conc. sulfuric acid causes immediate liberation of sulfur dioxide, led us to the conclusion that the oxidation of dithionate to sulfate by means of vanadate could be brought about in a very short time in a rather concentrated sulfuric acid solution. This turned out to be the case.

EXPERIMENTAL

As dithionate standard $Na_2S_2O_6,2H_2O$ was used. This was controlled by igniting it to sodium sulfate (99.85 and 99.95 % was found).

A vanadate solution was made by dissolving 20 g ammonium vanadate, p.a., in a cold mixture of 40 ml conc. sulfuric acid and 190 ml distilled water. This solution is about 0.7 M with respect to vanadate.

The method used for the estimation of dithionate is as follows: *Ca.* 0.3 g of sodium dithionate dihydrate is dissolved in 5 ml of distilled water in a 300 ml Erlenmeyer flask. 7 ml of vanadate solution is added, after which 12 ml of conc. sulfuric acid is poured into the mixture. The flask is rotated a little, so that complete mixing takes place. Under these conditions (heat of mixing and considerable concentration of sulfuric acid) the oxidation is complete after 1 min. The solution is now diluted with water to *ca.* 200 ml and heated to about 50°C. It is then titrated with standard permanganate solution. Colour change from green yellow to brown yellow.

In Table 1 the first four experiments show the accuracy of the method. Expts. Nos. 5 to 12 show the influence of varying amounts of conc. sulfuric acid. It is clearly seen that a considerable volume of conc. sulfuric acid must be added to give enough heat of mixing and a fairly small concentration of water. However, 12 ml of conc. sulfuric acid is sufficient, and more than 12 ml does not seem to be of any use. If the oxidation is carried out in a 50 ml beaker, after which it is transferred into a larger flask for titration, it is sufficient with 8 ml of conc. sulfuric acid due to the smaller loss of heat to the glass. Expts. Nos. 13 and 14 are carried out in a 50 ml beaker, for which reason the error is less than in Nos. 11 and 12, which experiments are carried out in a 300 ml flask.

The necessary excess of oxidizing agent (vanadate) has also been investigated. About 100 % in excess must be present, but more in excess does not give better results.

The temperature of a vanadyl ion solution, which has to be titrated with permanganate seems to be subject to much disagreement. Czudnowicz [4] performs the titration in hot solution, while Wegelin [5] claims room temperature gives the best results. Rieman, Neuss and Naiman's *Quantitative Analysis* [6] claims 50°C to be a convenient temperature of the titrand, because this temperature gives a sufficiently rapid reaction near the endpoint. This is in accordance with our experience.

It has been tried if dichromate may be used instead of vanadate. This is not the case, because a small percentage of Cr(VI) under the conditions used, will become reduced with the evolution of oxygen.

Table 1. Estimation of dithionate. For each experiment is given the weighed amount of sodium dithionate, the volume of water in which it is dissolved, the volume of vanadate solution added, the volume of conc. sulfuric acid added, the amount of sodium dithionate, which corresponds to the volume of standard decinormal permanganate used for the titration, and finally the percentage error.

Expt. No.	$Na_2S_2O_6,2H_2O$ taken g	Water ml	Vanadate solution ml	Conc. sulfuric acid ml	$Na_2S_2O_6,2H_2O$ found g	Error %
1	0.3090	5	7	12	0.3088	−0.06
2	0.3037	5	7	12	0.3028	−0.30
3	0.3006	5	7	12	0.2986	−0.66
4	0.3133	5	7	12	0.3125	−0.25
5	0.3057	5	7	16	0.3050	−0.23
6	0.3029	5	7	16	0.3023	−0.20
7	0.3127	5	7	10	0.3090	−1.18
8	0.3186	5	7	10	0.3183	−0.09
9	0.3086	5	7	8	0.3071	−0.49
10	0.3073	5	7	8	0.3021	−1.68
11	0.3108	5	7	6	0.2995	−3.65
12	0.3098	5	7	6	0.2984	−3.70
13	0.3494	5	7	6	0.3435	−1.69
14	0.3099	5	7	6	0.3061	−1.23

REFERENCES

1. Lang, R. and Kurtenacker, H. *Z. anal. Chem.* **123** (1942) 81.
2. Vasudeva Murthy, A. R. *Current Sci (India)* **22** (1953) 371.
3. Yost, D. M. and Pomeroy, R. *J. Am. Chem. Soc.* **49** (1927) 703.
4. Czudnowicz, C. *Ann. Physik.* **120** (1863) 17.
5. Wegelin, G. *Z. anal. Chem.* **53** (1914) 81.
6. Rieman, W., Neuss, I. D. and Naiman, B. *Quantitative Analysis*, 3rd Ed., McGraw-Hill Book Company, New York 1951, p. 333.

Received January 23, 1961.

ACTA CHEMICA SCANDINAVICA 15 (1961) 1067–1070

Studies of Thioacids and Their Derivatives

I. General Programme of the Investigation

KAI ARNE JENSEN

Chemical Laboratory of the University of Copenhagen, Copenhagen, Denmark

As an introduction to ten papers on thioacids and their derivatives a short review has been given of the approach to the problem and the main results.

Until 1944 only rather special types of thiohydrazides were known. Thiosemicarbazides have, of course, been known for a long time, and ethylxanthogenhydrazide, $C_2H_5OCSNHNH_2$, was prepared, in 1934, by Jensen [1], who also tried without success to prepare thioacethydrazide. Further some phenylhydrazides of thioacids have been prepared by Wuyts [2], who also mentions, that he had obtained a small amount of *p*-methylthiobenzhydrazide [3]. However, the first example of the more general type of thiohydrazides to be studied in detail was thiobenzhydrazide, prepared in 1943 by Holmberg [4], who carried out an extensive investigation on this compound and its derivatives [5].

In 1952 Jensen and Miquel [6] found that thiobenzhydrazide forms chelate nickel complexes of the same type as are formed by thiosemicarbazides [7] and on the basis of this observation and the hypothesis that antibacterial effects of organic compounds are often in some way connected with an ability to form chelates [8], Jensen and Jensen [9] prepared several new thiohydrazides and observed that these compounds in general possess a rather pronounced tuberculostatic and fungistatic effect. As these compounds show some similarity to two well-known tuberculostatic agents, *p*-acetamidobenzaldehyde-thiosemicarbazone (TBl) and *iso*nicotinic hydrazide(INH), it was hoped to find still more active compounds belonging to this class. A large number of thiohydrazones were prepared, and several experiments were carried out to obtain heterocyclic thiohydrazides. The thiohydrazones are rather similar to *p*-acetamidobenzaldehyde-thiosemicarbazone, but most of these compounds were very slightly soluble in water and showed no tuberculostatic activity *in vitro*. The activity of some of these compounds, especially *p*-acetamidobenzaldehyde-2-furanthiocarbohydrazone, was also tested in animal experiments, but they showed only slight activity. In our experiments the preparation of hetero-

cyclic thiohydrazides met with unusual difficulties, and in the meantime *iso*-nicotinic thiohydrazide was prepared by König *et al.*[10], but it turned out to be less active than *iso*nicotinic hydrazide against tubercle bacilli.

Thus the attempts to find new chemoterapeutics of practical importance within this class of compounds had not been too promising. On the other hand their more or less pronounced bacteriostatic effect is almost certainly connected with their ability to combine with metal ions, and we decided to investigate this property from a more fundamental point of view. The influence of thiohydrazides on the growth rate of *Aerobacter aerogenes* in the presence of various metal ions was investigated, and it was shown that certain metal ions, especially the zinc ion, show a very pronounced synergistic effect on the bacteriostatic effect of the thiohydrazides. It was also found that *NN*-dimethylthiohydrazides of certain acids, especially salicylic acid and its derivatives, had a much stronger effect than the unsubstituted thiohydrazides, and this was found also to be the case with their effect on tubercle bacilli *in vitro*. This led us to prepare a series of N-substituted thiohydrazides of salicylic acid and of *o*-alkoxysubstituted benzoic acids. At the same time the successful introduction of certain thioamides and thioureas, which are active against INH-resistent tubercle bacilli, in the therapy of tuberculosis [11] led us to some extent to consider not only thiohydrazides but also thioamides. Certain of the compounds prepared showed *in vitro* an effect which was at least as great as the effect of INH, but unfortunately their effect in animal experiments was negligible, probably because of rapid transformation of the compounds *in vivo*.

In parallel with the investigation of the antibacterial effect of the compounds prepared their complex-forming ability has been investigated. Our interest in co-ordination compounds also led us to prepare a large number of new thiosemicarbazides, although the antibacterial effect of this class of compounds was found to be much less pronounced than that of the regular thiohydrazides (with a carbon radical attached directly to the $-CSNHNH_2$ group).

Our interest in the thiohydrazides and thioamides has not only been dictated by their potential effect as antitubercular substances and their ability to form co-ordination compounds. Also from a purely organic chemical point of view these compounds are most interesting, and at the beginning of our investigation very little was known of the chemical properties of thiohydrazides. Although the chemical reactions of thiobenzhydrazide and of dithiocarbohydrazides (*i.e.* compounds of the type $RSCSNHNH_2$) have later been investigated very carefully and extensively by Holmberg [12] and by Sandström [13], our results are of a more general character, in that we have studied thiohydrazides of aliphatic, aromatic and heterocyclic acids and N-substituted thiohydrazides with many different substituents in the hydrazide group.

Accordingly our researches consist of the following parts:

1. An extensive investigation of the preparation of carboxymethyl dithioates, which are the most convenient intermediates for the preparation of the thiohydrazides (paper No. II). In connection with the preparation of these new compounds their infrared spectra have been investigated; this work has already been published [14].

2. The preparation of a large number of new thiohydrazides and thiosemicarbazides, derived not only from unsubstituted hydrazine but also from several monoalkyl- and dialkylhydrazines (papers No. III, V, and IX). Especially it was shown that the steric influence of the alkyl group determines whether monoalkylhydrazines form thiohydrazides of the type $RCSNR'NH_2$ or of the type RCSNHNHR' or a mixture of both.

3. Investigation of certain transformations of thiohydrazides and thioamides. It was found that aromatic and heterocyclic thiohydrazides can be transformed into compounds of the type $RCSN_3$, and these were proved to be thiatriazoles and not thioazides (paper No. IV). The transformation of thiohydrazides into tetrazines and thiadiazoles was investigated (paper No. VI), and during these investigations we prepared the basic 1,3,4-thiadiazole, which was prepared almost at the same time by Goerdeler [15] in a different way. The previously unknown 2-phenyl-5-thiazolone was prepared, and it was shown that it easily polymerises giving a product hitherto considered to be the thiazolone (paper No. VII). By oxidation of malonic dithiamide, salts of the dithiolenium ion were prepared [16], and it was shown that this ion constitutes a new aromatic system (paper No. VIII).

4. The ability of thiohydrazides to form co-ordination compounds, especially with metals of the first transition group, was investigated (paper No. X).

5. The antibacterial effect of the thiohydrazides and related compounds, especially as shown by the growth rate of bacteria in presence of thiohydrazides and metal ions, was investigated (paper No. XI).

Most of this work has been carried out in the years 1952—1957, but other work has delayed publication.

The researches have been supported by grants from *Statens Almindelige Videnskabsfond*.

The microanalyses were performed by Albert Grossmann (1952—53), Walther Egger (1953—54), and Preben Hansen (since 1954).

REFERENCES

1. Jensen, K. A. *Z. anorg. allgem. Chem.* **221** (1934) 11.
2. Wuyts, H. *Bull soc. chim. Belges* **39** (1930) 58. Wuyts, H. and Lacourt, A. *Bull. soc. chim. Belges.* **42** (1933) 1.
3. Wuys, H. *2me Congrés National des Sciences*, Bruxelles *1935 Compt. rend.* p. 497.
4. Holmberg, B. *Arkiv Kemi, Mineral Geol.* **17 A** (1944) No. 23.
5. Holmberg, B. *Arkiv Kemi, Mineral. Geol.* **25 A** (1947) No. 18.
6. Jensen, K. A. and Miquel, J. F. *Acta Chem. Scand.* **6** (1952) 189.
7. Jensen, K. A. and Rancke Madsen, E. *Z. anorg. allgem. Chem.* **219** (1934) 243.
8. Carl, E. and Marquardt, P. *Z. Naturforsch.* **4b** (1949) 280; Liebermeister, K. *Ibid.* **5b** (1950) 79; Hagelloch, G. and Liebermeister, K. *Ibid.* **6b** (1951) 147; Sorkin, E., Roth, W. and Erlenmeyer, H. *Helv. Chim. Acta* **35** (1952) 1736; Erlenmeyer, H., Bäumler, J. and Roth, W. *Ibid.* **36** (1953) 941; Albert, A. *Experientia* **8** (1952) 298; *Nature* **177** (1956) 525; Albert, A. *Metal-binding Agents in Chemotherapy. The Strategy of Chemotherapy*, p. 112—138. Cambridge Univ. Press 1958; Cymerman-Craig, J., Willis, D., Rubbo, S. D. and Edgar, J. *Nature* **176** (1955) 34. Foye, W. O. *J. Am. Pharm. Assoc.* **44** (1955) 415. Foye, W. O. and Duvall, R. N. *Ibid.* **47** (1958) 282, 285. Weinberg, E. D. *Bacteriol. Rev.* **21** (1957) 46.
9. Jensen, K. A. and Jensen, C. L. *Acta Chem. Scand.* **6** (1952) 957. Jensen, K. A. *Det 8. Nord. Kemikermøde*, Oslo 1954. *Beretning og Foredrag*, p. 240.
10. König, H. B., Siefken, W. and Offe, H. A. *Chem. Ber.* **87** (1954) 825.

11. Gardner, T. S., Wenis, E. and Lee, J. *J. Org. Chem.* **19** (1954) 753. Meltzer, R. I., Lewis, A. D. and King, J. A. *J. Am. Chem. Soc.* **77** (1955) 4062. Libermann, D., Rist, N. and Grumbach, F. *Bull. soc. chim. biol.* **38** (1956) 231. Libermann, D., Rist, N., Grumbach, F. and Cals, S. *Ibid.* **39** (1957) 1195. Libermann, D., Rist, N., Grumbach, F., Cals, S., Moyeux, M. and Rouaix, A. *Bull. soc. chim.* **1958** 687.
12. Holmberg, B. *Arkiv Kemi* **4** (1952) 33, 105; **7** (1954) 501, 513, 517, 529; **9** (1956) 47, 65.
13. Sandström, J. *Arkiv Kemi* **4** (1952) 297; **7** (1954) 249; **8** (1955) 487; 523; **9** (1956) 127, 255; **15** (1960) 195. Sandström, J. *Sv. Kem. Tidskr.* **68** (1956) 131.
14. Bak, B., Hansen-Nygaard, L. and Pedersen, Chr. *Acta Chem. Scand.* **12** (1958) 1451.
15. Goerdeler, J., Ohm, J. and Tegtmeyer, O. *Chem. Ber.* **89** (1956) 1534.
16. Jensen, K. A. *Kgl. Danske Videnskab. Selskab, Overs. Selskab. Virksomhed* 1957–58, p. 61. København 1958.

Received January 23, 1961.

ACTA CHEMICA SCANDINAVICA 15 (1961) 1071–1080

Magnetic Properties of Iron and Copper in Cytochrome Oxidase

ANDERS EHRENBERG and TAKASHI YONETANI

Biokemiska avdelningen, Medicinska Nobelinstitutet, Karolinska Institutet, Stockholm, Sweden, and Johnson Research Foundation, University of Pennsylvania, Philadelphia, Pennsylvania, USA

The paramagnetic susceptibilities of the transition metal components (cytochromes *a* and a_3 and copper) of cytochrome oxidase, oxidized, reduced and in the presence of cyanide and carbon monoxide, have been determined. Assuming that reduced cytochrome a_3 is the only component responsible for the volume magnetic susceptibility changes of the reduced enzyme preparation upon the addition of cyanide or carbon monoxide, the results obtained with a densitive volume magnetic susceptometer and electron spin resonance spectrometers are analyzed. Cytochrome a_3 in the oxidized form has a molar susceptibility of 7 900 $\times$ 10^{-6} cgs emu, which is intermediate between known data of oxidized hemoproteins of the low and high spin types, whereas cytochrome *a* is a hemoprotein of the low spin type magnetically similar to cytochrome *c*. Although copper is found to be responsible for part of the susceptibility changes in some part of the results, no evidence in favour of a role of copper in the oxidase mechanism is found.

Purified preparations of cytochrome oxidase contain two different cytochromes designated *a* and a_3[1,2]. Cytochrome *a* is inert to cyanide, carbon monoxide and oxygen, whereas cytochrome a_3 reacts with these compounds. In addition, since the carbon monoxide compound of reduced cytochrome a_3 is photodissociable [3] and its absorption spectrum is identical with the photochemical action spectra of the carbon monoxide-inhibited cellular inhibition [4], cytochrome a_3 is considered to be *Atmungsferment* of mammalian tissues [1–3]. Purified preparations of cytochrome oxidase also contain copper in an atomic ratio to the iron of haemin *a* which according to different investigators varies from 1 to 2 [5–8]. Although it was demonstrated that the copper in the oxidized preparation is in the cupric state and can be partially reduced by various reducing systems [6,7], it has been suggested that the rapid electron donation to oxygen is accountable in terms of the heme and not the copper portion of the oxidase preparation [9,10]. It has further been proved that most of the copper is not required for the enzyme activity of cytochrome oxidase [11]. The magnetic susceptibility change during the reaction of cytochrome oxidase was

previously investigated [10] by using a sensitive magnetic susceptometer combined with a regenerative rapid flow system [12] in which an increase in volume magnetic susceptibility was observed in the reaction of reduced cytochrome oxidase with oxygen.

The present investigation of the magnetic properties of a cytochrome oxidase preparation was undertaken to measure more accurately the magnetic susceptibility of the preparation with the aim to elucidate the properties and mode of action of the iron of cytochromes *a* and a_3 and of the copper in connection with the previous magnetic study [10]. Because of the complexity of the system it was important that determination of the bulk magnetic susceptibility in solution could be combined with a study of the electron spin resonance (ESR) absorption due to the copper to monitor changes of the copper valency as described by Malmström *et al.*[13]

EXPERIMENTAL

Material. Purified cytochrome oxidase was prepared from beef heart as described by Yonetani [8] and was dialysed for 72 h against 0.05 M phosphate buffer, pH 7.2, containing 1 % Emasol 4130 [14]. Aliquots of this buffer were taken and used as reference solutions throughout the work. In every case the reference solution was given the same additions and treated in the same way as the sample. The dry weight of cytochrome oxidase in the stock solution was determined to be 94.0 mg/ml. The partial specific volume was measured to be 0.81 (± 0.02) ml/g by weighing several samples of the stock solution, of the buffer and of water, taken by a micropipet. The iron content was found to be 510 μM by a modification of Lorber's method with sulfosalicylic acid [15]. Based on this analysis the extinction coefficient at 605 mμ was found to be 21.0 (mM Fe)$^{-1}$ cm^{-1} [8]. Copper was determined from the colour (measured at 450 mμ) developed by addition of diethyldithiocarbamate to the sample, after previous digestion with H_2SO_4 and H_2O_2, and additions of pyrophosphate and ethyl alcohol according to a slight modification of the standard procedure [16]. The stock solution contained 1025 μM Cu which means that the atomic ratio Cu/Fe of the sample was 2:1. No part of this copper could be removed by dialysis against 0.5 mM KCN for 48 h. The ratio of the increase in optical density at 445 and 605 mμ upon reduction with dithionite was 6.1. The cytochrome c used was made by Sigma Type III, from horse heart.

Methods. The volume susceptibility of the samples was investigated at 20°C by means of the sensitive susceptometer balance constructed by Theorell and Ehrenberg [17] and equipped with an improved temperature control. The instrument was calibrated with a carefully analyzed solution of $NiCl_2$ assuming $\chi_{NiCl_2} = 4434 \times 10^{-6}$ cgs emu.

The measurements of ESR absorption were made at the temperature of liquid nitrogen and at room temperature. The low temperature measurements were made with an X-band spectrometer with 70 cycles field modulation, constructed by one of the authors (A.E.), and with the Varian X-band spectrometer V-4500 equipped with a 100 kc field modulation unit. The room temperature experiments could only be made at the higher sensitivity obtained with the latter instrument. Quartz sample tubes with 3 mm inner diameter were used at liquid nitrogen temperature and with 1 mm inner diameter at room temperature. Diphenylpicrylhydrazyl with g = 2.0036 was used as a g-value reference.

All samples were made anaerobic by rapid evacuation in Thunberg tubes and twice flushing with nitrogen or argon. Reduction was achieved by the addition of 10 μl 15 % $Na_2S_2O_4$ per ml sample, reaction with cyanide by the addition of 10 μl 0.3 M KCN per ml sample, and reaction with CO by flushing the Thunberg tube with this gas. Any contact with air was avoided as far as possible during the filling of the sample tube of the susceptometer balance or of the ESR spectrometer. When necessary, complete anaerobiosis was achieved in the ESR experiments by attaching the sample tube *via* a tygon tubing to a separate outlet of the Thunberg tube, and washing the argon with pyrogallol.

Table 1. Experimental susceptibility data on the investigated cytochrome oxidase samples, and tentative molar susceptibilities of the transition metal components. The errors given are estimated maximal deviations. For comparison data on haem *a* treated as a single haemoprotein, cytochrome *A*, have been included. A correction of 290×10^{-6} cgs emu has to be added to the susceptibilities of *a*, a_3 and *A* according to Griffith.[24]

Sample No.	Additions made to oxidized cytochrome oxidase	Instrument reading Scale divisions	χ mean $\times 10^6$ cgs emu $a + a_3 + Cu$ (1 535 μM)	$\chi_M \times 10^6$ cgs emu			
					haem *a*		
					as two different cytochromes		as a single haemoprotein
				Cu (1 025 μM)	*a* (330 μM)	a_3 (180 μM)	Cytochrome *A* (510 μM)
1	None	− 4 (± 2)	2 470 (± 50)	1 500 (Cu″)	2 400(*a*‴)	7 900(a_3‴)	4 300 (*A*‴)
2	KCN	− 48 (± 2)	1 840 (± 50)	1 500 (Cu″−CN)	2 400(*a*‴)	2 400(a_3‴−CN)	2 400 (*A*‴−CN)
3	$Na_2S_2O_4$	− 79 (± 10)	1 400 (± 50)	0 (Cu′)	0 (*a*″)	12 000(a_3″)	4 200 (*A*″)
4	KCN + $Na_2S_2O_4$	−169 (± 10)	130 (± 150)	0 (Cu′) or (Cu′−CN)	0(*a*″)	2 400(a_3‴−CN)	0 (*A*″−CN)
5	$Na_2S_2O_4$+ KCN	−171 (± 2)	100 (± 50)	0 (Cu′) or (Cu′−CN)	0(*a*″)	0(a_3″−CN)	0 (*A*″−CN)
6	$Na_2S_2O_4$ + CO	−178 (± 2)	0	0 (Cu′) or (Cu′−CO)	0(*a*″)	0(a_3″−CO)	0 (*A*″−CO)

RESULTS AND DISCUSSION

The readings on the susceptometer balance for the six different samples are given in column 3 of Table 1.

The interpretation of the experimental data on cytochrome oxidase is difficult (a) because multiple components are involved and (b) because the separate molar magnetic susceptibilities of the components have not yet been determined. In order, however, to make a preliminary interpretation of the data, it is desirable to make a series of assumptions and to determine what conclusions can be made concerning the nature of cytochrome oxidase on the basis of such assumptions. The first assumption with regard to the data of Table 1 is that Cu′ * and its hypothetical CO compound in samples 3 and 6 (*cf.* column 5) are diamagnetic, since other cuprous compounds are known to be diamagnetic [18,19]. Secondly, it is assumed that haem-*a*-CO compounds are diamagnetic, since this is a property common to all hitherto investigated haem-CO compounds. The experimental observation that there is a great difference of magnetic susceptibility between samples 3 and 6 indicates that a high spin haem is involved. If one computes the molar magnetic susceptibility from the data on samples 3 and 6 on the basis of the total haem content of the preparation (510 mM) a value of $4\,200 \times 10^{-6}$ cgs emu is obtained for A'' (*cf.* column 8). This value differs from that of any known ferro-haemoprotein (haemoglobin, [20], myoglobin [21], leghaemoglobin [22] and horse radish peroxidase [23]). It is, therefore, more appropriate to consider (a) that only a part of the total reduced haem-*a* is in the high spin state and this part can combine with CO, and (b) that this part has a molar magnetic susceptibility of $12\,000 \times 10^{-6}$ cgs emu in common with other known ferrohaemoproteins [20–23], which can combine with CO. Thus the magnetic susceptibility of the cytochrome oxidase will be analyzed in accordance with the concept that cytochromes *a* and a_3 are separate identities [1–3]. On the basis of the assumed susceptibility of $12\,000 \times 10^{-6}$ cgs emu for a_3 we are able to compute the concentration of cytochrome a_3, and obtain a value of 180 μM, *i.e.* 35 % of the total haem *a*. It is further possible to compute a series of values for the molar magnetic susceptibilities of Cu and cytochromes *a* and a_3 as illustrated by columns 5, 6 and 7 on the basis of the results of Keilin and Hartree [1] and Yonetani [2].

The above arguments do not include any assumption concerning the magnitude of the susceptibility of a''. However, all the three transition metal components of sample 6 are likely to be diamagnetic. From the instrument reading obtained for this sample we calculate, after correction for the diamagnetism of the buffer constituents and for the residual, orbital paramagnetism of the metal atoms [24], a value of -0.63×10^{-6} cgs emu for the mass susceptibility of the cytochrome oxidase. This is of the magnitude to be expected for a lipoprotein with a lipid content of about 20 %, a figure estimated from the partial specific values of 0.81 ml/g. If, however, a'' is paramagnetic with four unpaired electrons, the diamagnetic mass susceptibility of the oxidase would

* Abbreviations used: Cu″ and Cu′: oxidized and reduced copper; a''' and a'': oxidized and reduced cytochrome *a*; a_3''' and a_3'': oxidized and reduced cytochrome a_3; A''' and A'': oxidized and reduced cytochrome *A*, representing cytochrome *a* in a single haemoprotein concept of cytochrome oxidase.

have to be -0.67×10^{-6} cgs emu which is difficult to reconcile with a lipid content of only 20 %. A similar argument cannot be applied to the case that a'' has two unpaired electrons, since the necessary correction of the diamagnetism would be too small. This case must, however, be considered improbable for theoretical reasons [25]. The most reasonable assumption to make is, therefore, that a'' is diamagnetic. For a more precise conclusion on this point it would be necessary to determine more accurately the lipid content and the diamagnetism of cytochrome oxidase. The partial specific volume is of special importance with respect to the latter, since its value has a great influence on the calculated diamagnetism.

The mean susceptibility of the oxidized sample treated with cyanide (sample 2 in Table 1) is $1\,840 \times 10^{-6}$ cgs emu. The ESR absorption data to be described below indicate that practically all the copper in the oxidized samples is present in the paramagnetic cupric form with one unpaired electron. a''' and a_3'''—CN must, therefore, both be low spin forms with one unpaired electron in the iron. A mean value of the susceptibility of haem compounds of this type is $2\,400 \times 10^{-6}$ cgs emu. If this figure is assumed to be valid in the present case the susceptibility of Cu''—CN calculates to $1\,500 \times 10^{-6}$ cgs emu, which is about the maximal value of the known data for cupric compounds [18,19,26].

The increase in susceptibility when going from the cyanide treated oxidized sample to the untreated oxidized sample must be due to the susceptibility difference between a_3'''—CN and a_3''', since a''' does not react with cyanide, and the susceptibility of Cu'' can hardly be larger than the $1\,500 \times 10^{-6}$ cgs emu of Cu''—CN. If this value is taken also for the susceptibility of Cu'', the susceptibility of a_3''' is found to be $7\,900 \times 10^{-6}$ cgs emu. The susceptibility of Cu'' might possibly be as much as 250×10^{-6} cgs emu lower, corresponding to $9\,400 \times 10^{-6}$ cgs emu for a_3'''.

From the data in Table 1 it is seen that the magnetic properties of cytochrome a are similar to those of cytochrome c [27]. This is in accord with the similarity in response of the two haemoproteins to CN and CO, and also with their similar function, *i.e.* transporting electrons on the same level in the electron transporting system [28]. Cytochrome a_3, on the other hand, seems to be different from most other haemoproteins. The reduced form a_3'' is of the high spin type also found for haemoproteins which transport oxygen or have hydroperoxidatic activity. The susceptibility of the oxidized form a_3''', however, is intermediate between the 2 000 and 13 000—15 000 $\times 10^{-6}$ cgs emu usually found for oxidized haemoproteins of the low and high spin forms, respectively. The hydroxides of oxidized myoglobin and haemoglobin have also been found to have similar intermediate susceptibility values [29,30]. These compounds have been shown to be thermally balanced equilibrium mixtures between high and low spin forms [31]. We have recently found that the acid form of leghaemoglobin with a susceptibility of $9\,500 \times 10^{-6}$ at 20°C also must be considered as an equilibrium mixture of this type [22]. The similarity in susceptibility of cytochrome a_3 and leghaemoglobin might be more than coincidental and since the function of the latter is still obscure it might perhaps pay to test it for functional similarities with cytochrome a_3.

The records of ESR spectra of Fig. 1 show that cytochrome oxidase at 77°K gives only a very faint absorption at the magnetic field, where the acid

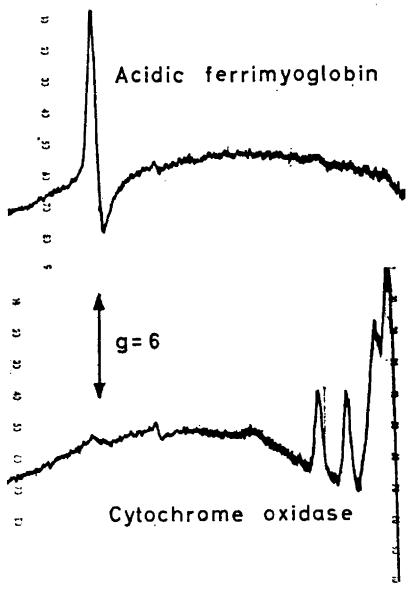

Fig. 1. Derivative records of ESR absorption from acidic ferrimyoglobin (250 μM) and cytochrome oxidase (510 μM in Fe) at 77°K. Field modulation 100 kc, 6 gauss peak to peak. Magnetic field increases from left to right. Microwave power *ca.* 1 mW.

form of ferrimyoglobin has an intense absorption of g-value 6. Derivatives of ferriprotoporphyrin of the high spin type are known to give an ESR absorption with this g-value [32]. The hydroxide of ferrimyoglobin also gives this absorption in aqueous solution at room temperature [33] under which conditions it has been shown to be an equilibrium mixture between high and low spin forms [31]. At 77°K, however, the absorption is to a large extent abolished, which has been interpreted as due to a shift of the equilibrium in favour of the low spin form [33]. Even if high spin derivatives of ferriporphyrin *a* are likely to give an ESR absorption of g-value 6, in analogy with high spin ferriprotoporphyrin derivatives, this absorption has not yet been demonstrated experimentally. Due to lack in sensitivity in the present experiments with aqueous solutions it was not possible to test for a possible analogy between a_3''' and ferrimyoglobin hydroxide.

The ESR spectrum of oxidized cytochrome oxidase recorded at 77°K is presented in Fig. 2. The same spectrum, but with a much smaller signal to noise ratio, was obtained at room temperature. The asymmetric shape of record A is typical for cupric compounds of tetragonal structure in glasses [34] and frozen solutions [35], or even in aqueous solutions at room temperature, if the copper is bound to a macromolecule [35]. The integrated intensity of the absorption at room temperature was compared with that of 1 mM cupric ions bound to myoglobin [36]. A ratio of 1:1 of the intensities was found, which indicates that all the copper of the oxidized cytochrome oxidase is in the cupric form.

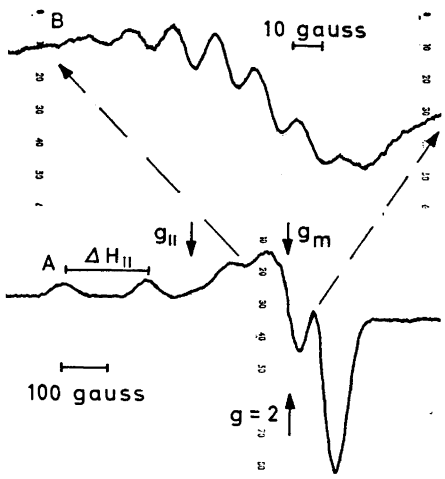

Fig. 2. Derivative records of ESR absorption from copper in cytochrome oxidase (1.025 mM in Cu) at 77°K. Field modulation 100 kc, 12 and 3 gauss peak to peak for A and B, respectively. Magnetic field increases from left to right. Microwave power *ca.* 0.25 mW.

This is in agreement with the result of Takemori [6] and Yonetani [10], who used specific chelating agents to determine the valency of the copper. The ESR absorption completely disappeared after reduction with dithionite, justifying our conclusion that all the copper is in the diamagnetic cuprous form in reduced cytochrome oxidase. Reduction with cytochrome *c* plus ascorbate, or ascorbate alone, likewise removed the absorption to a large extent in the presence or absence of cyanide. This is in accord with the results of Sands and Beinert [7]. Contrary to these authors, however, we have not been able to observe any reduction of the copper in presence of an excess of reduced cytochrome *c* devoid of any additional reducing agent. In one experiment cytochrome oxidase (300 μM in Cu) and cytochrome *c* (3 mM in Fe^{++} and 0.5 mM in Fe^{+++}) were mixed under complete anaerobiosis. After 5 min the sample was frozen and measured in the ESR spectrometer. No reduction of the copper could be observed. Spectroscopic observation of the thawed solution revealed strong absorption bands at 605 and 550 mμ showing that cytochromes *a* and a_3 were reduced and that the excess of reduced cytochrome *c* still persisted. New observations after that the sample had been stored for 20 h at + 3°C gave identical results, both in the ESR spectrometer and in the spectroscope. The cytochrome *c* was immediately oxidized when the sample was exposed to the atmospheric oxygen. These results demonstrate that the copper of the cytochrome oxidase preparation used does not change valence at the same time as the cytochromes *a* and a_3 are reduced by cytochrome *c*.

The g-value in a direction perpendicular to the tetragonal symmetry axis is approximated by g_m, measured at maximum absorption [35]. We obtain $g_m = 2.042$. For the direction parallel to the symmetry axis we find that $g_{||} = 2.185$. $\Delta H_{||}$, the hyperfine spacing due to the copper and valid for the

latter direction, is measured to be 184 gauss. In Fig. 2, record B is a magnification of a portion of curve A. Several, at least 9, additional hyperfine lines are visible and are centered close to g_m. The spacing between the lines is uniform and equals 15.6 gauss.

The shape of the ESR-spectrum is slightly changed when KCN is present, which demonstrates that CN^- in fact is bound to the copper, in agreement with our previous result [11]. The main peak centered close to g_m is decreased and somewhat broadened. g_m and $g_{||}$ are decreased to 2.036 and 2.160, respectively. $\Delta H_{||}$ remains unchanged, but the spacing between the additional hyperfine lines is increased to 17.7 gauss.

Well resolved hyperfine structures due to interaction with nitrogen and hydrogen nuclei in the chelating agent have been observed by Maki and McGarvey for cupric chelates in crystals [37]. The additional hyperfine structure observed here for cytochrome oxidase is no doubt correspondingly caused by an interaction with atoms of the groups of the protein that are coordinated to the copper. This implies a certain degree of delocalisation of the unpaired electron, or, which is equivalent, the associated unpaired hole. The increased splitting when CN^- is bound indicates that the strong field from CN^- enhances this delocalisation. Several cupric complexes have been investigated and similar but not identical hyperfine structures have been found when nitrogen is present among the coordinating atoms but not when there is only oxygen. Imidazole and/or amino groups are hence likely to be involved in the binding of copper to cytochrome oxidase.

The hyperfine spacing $\Delta H_{||} = 184$ gauss corresponds to a splitting constant of 0.019 cm^{-1}, which is of the magnitude ordinarily found for cupric complexes [35]. Malmström and Vänngård recently found the uniquely low value of 0.008 cm^{-1} for two oxidative copper enzymes, laccase and ceruloplasmin, in which copper has been shown to change valence during the enzymatic reaction [35]. They suggested that there is a relation between the enzymatic activity and the high degree of delocalisation of the unpaired hole as evidenced by the small splitting constant. The normal splitting constant of the ESR absorption from the copper of cytochrome oxidase can thus be taken as a further support of our conclusion that this copper does not take part in the enzymatic reaction by changing valence.

From the previous it is seen that the measurement of the magnetic susceptibility of a reduced sample of cytochrome oxidase offers a possibility to estimate the amount of cytochrome a_3 separately. Cytochromes a and a_3 have been demonstrated to contribute 65 and 35 percent of the total a of the present preparation, respectively. The accuracy of the tentative susceptibilities of the derivatives of cytochromes a and a_3 of Table 1 might be improved by measurements on cytochrome oxidase samples devoid of copper. Our experiments with a new copper specific chelating agent, Bathocuproine sulfonate [11] have shown that it should be possible to remove the copper under mild chemical conditions. It has been possible through the use of spectrophotometric and chemical methods [9-11] to obtain evidence that the main portion of the copper of cytochrome oxidase does not take part in the electron transfer of cytochrome oxidase which is in accord with the data presented here. The discrepancy between our results and those of Sands and Beinert [7] concerning the reducibility

of the cytochrome oxidase copper by reduced cytochrome *c* remains to be explained. Since most of the copper probably is an impurity it might be bound differently depending on the method of preparation and hence also respond differently to reducing agents. The observation by Sands and Beinert [7], that added cupric ions were not reduced by ascorbate at the same time as the original copper changes valency, lends some support for this hypothesis.

The previous magnetic titration of cytochrome oxidase [10] was carried out during the reaction of reduced cytochrome oxidase with oxygen in the presence of reducing agents. Hence the observed magnetic susceptibility changes were due to a difference in susceptibility between the reduced and aerobic steady state oxidized preparations while the present results are due to differences between the reduced and completely oxidized preparations. Therefore further experiments are required to interpret the discrepancy between the two results.

Acknowledgements. The work has been supported by *Statens Naturvetenskapliga Forskningsråd, Statens Medicinska Forskningsråd* and a grant of *National Science Foundation.* The authors wish to thank Professors Hugo Theorell and Britton Chance for their valuable advice and criticism. One of the authors (T.Y.) also appreciates the varm hospitality of Professor Hugo Theorell.

REFERENCES

1. Keilin, D. and Hartree, E. F. *Proc. Roy. Soc. London*, **B 127** (1939) 167.
2. Yonetani, T. *J. Biol. Chem.* **235** (1960) 845.
3. Chance, B. *J. Biol. Chem.* **202** (1953) 397.
4. Warburg, O. *Angew. Chem.* **45** (1932) 1.
5. Wainio, W. W., Wende, C. V. and Shimp, N. F. *J. Biol. Chem.* **234** (1959) 2433.
6. Takemori, S. *J. Biochem. Tokyo* **47** (1960) 382.
7. Sands, R. H. and Beinert, H. *Biochem. Biophys. Res. Communications* **1** (1959) 175.
8. Yonetani, T. *J. Biol. Chem.* **236** (1961) 1680.
9. Chance, B. and Yonetani, T. *Fed. Proc.* **18** (1959) 202.
10. Yonetani, T. *Fed. Proc.* **19** (1960) 32.
11. Yonetani, T. *Biochem. Biophys. Res. Communications* **3** (1960) 549.
12. Brill, A. S., den Hartog, H. and Legallais, V. *Rev. Sci. Instr.* **29** (1958) 383.
13. Malmström, B. G., Mosbach, R. and Vänngård, T. *Nature* **183** (1959) 321.
14. Yonetani, T. *J. Biochem. Tokyo* **46** (1959) 917.
15. Paul, K. G. *Acta Chem. Scand.* **2** (1948) 430.
16. McFarlane, W. *Biochem J.* **26** (1932) 1022.
17. Theorell, H. and Ehrenberg, A. *Arkiv Fysik* **3** (1951) 299.
18. Selwood, P. W. *Magnetochemistry*, Interscience Publishers New York (1956).
19. Nakamura, T. *Biochim. et Biophys. Acta* **30** (1958) 640.
20. Taylor, D. S. and Coryell, C. D. *J. Am. Chem. Soc.* **60** (1938) 1177.
21. Taylor, D. S. *J. Am. Chem. Soc.* **61** (1939) 2150.
22. Ehrenberg, A. and Ellfolk, N. *To be published.*
23. Theorell, H. *Arkiv Kemi, Mineral. Geol.* **16A** (1942) No. 3.
24. Griffith, J. S. *Biochim. et Biophys. Acta* **28** (1958) 439.
25. Orgel, L. E. in Falk, J. E., Lemberg, M. R. and Morton, R. K. *Proceedings of the Haematin Enzyme Symposium, Canberra*, Pergamon Press, London (in press).
26. Ray, P. and Sen, D. N. *J. Indian Chem. Soc.* **25** (1947) 473.
27. Theorell, H. *J. Am. Chem. Soc.* **63** (1941) 1820.
28. Yonetani, T. *J. Biol. Chem.* **235** (1960) 3138.
29. Theorell, H. and Ehrenberg, A. *Acta Chem. Scand.* **5** (1951) 823.
30. Coryell, C. D., Stitt, F. and Pauling, L. *J. Am. Chem. Soc.* **59** (1937) 633.
31. George, P., Beetlestone, J. and Griffith, J. S. in Falk, J. E., Lemberg, M. R., and Morton, R. K. *Proceedings of the Haematin Enzyme Symposium, Canberra*, Pergamon Press, London (in press).

32. Gibson, J. F., Ingram, D. J. E. and Schonland, D. *Discussions Faraday Soc.* **26** (1958) 72.
33. Ehrenberg, A. *To be published.*
34. Sands, R. H. *Phys. Rev.* **99** (1955) 1222.
35. Malmström, B. G. and Vänngård, T. *J. Mol. Biol.* **2** (1960) 118.
36. Ehrenberg, A. and Henderson, R. *To be published.*
37. Maki, A. H. and McGarvey, B. R. *J. Chem. Phys.* **20** (1958) 35.

Received January 28, 1961.

ACTA CHEMICA SCANDINAVICA 15 (1961) 1081–1086

The Reaction between Vanillyl Alcohol and Sulphite

LENNART IVNÄS and BENGT LINDBERG

Institutionen för träkemi, Kungl. Tekniska Högskolan, Stockholm, Sweden

A kinetic study of the reaction between vanillyl alcohol and sulphite in aqueous solutions of various pH values has been made. The results indicate that the formation of sulphonic acid proceeds *via* the methylenequinone formed from vanillyl alcohol by elimination of one molecule of water. This hypothetical intermediate also explains the high reactivity of *p*-hydroxybenzyl alcohols compared to that of analogous *p*-alkoxybenzylalcohols.

The suggestion that benzyl alcohol and benzyl ether groupings in the lignin are responsible for several of the latter's characteristic reactions (*e.g.* sulphonation on the reaction with sulphite) was originally made by Berg and Holmberg [1]. Further studies on the reactions of lignin and model substances have corroborated this hypothesis; it is also in agreement with the conception of the lignin molecule obtained from biogenetic studies. (*cf.* Ref.[2]).

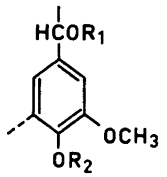

I

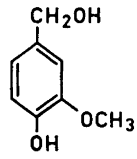

II

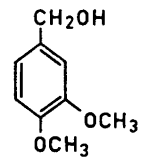

III

a. $R_1 = R_2 = H$
b. $R_1 = alkyl$, $R_2 = OH$
c. $R_1 = H$, $R_2 = alkyl$
d. $R_1 = R_2 = alkyl$

The generalised structure for a benzyl alcohol or ether grouping in coniferous lignin (I) can be divided into four alternative structures (a, b, c and d). Model substances, representative of these types, show differences in reactivity which are especially pronounced in models which carry a hydroxyl group (a and b) and an alkoxyl group (c and d) in a *p*-position to the benzyl group. It is belie-

ved that important lignin reactions, such as sulphonation, and etherification with methanolic hydrogen chloride, can be rationalised, at least to a considerable degree, as being due to the presence of these four structural elements.

Lindgren [3] made a qualitative study of the reaction of some model substances, among them vanillyl alcohol (II) and veratryl alcohol (III), in sulphite solutions of different pH at 135°. He found that vanillyl alcohol was sulphonated rapidly in both alkaline and acid solutions. Veratryl alcohol, however, was rapidly sulphonated only in acid solutions; in neutral or alkaline solutions, the reaction was slow. Groupings which show analogous reactivities are also present in lignin. Migita *et al.* [4] made a kinetic study of the reaction between vanillyl alcohol and sulphite and found that the velocity was rather independent of pH in the pH range studied.

Results from the present study have shown that vanillyl alcohol reacts with sulphite at 80° and pH 6.9 about 1 000 times faster than veratryl alcohol does at the same pH and 135°. The difference in σ-values [5] in Hammet's equation for p-OH (−0.357) and p-OCH_3 (−0.268) can not possibly account for this disparity and it must be assumed that the reactions proceed according to different mechanisms. In the present paper a kinetic study of the reaction between vanillyl alcohol and sulphite is reported. Most of the reactions were performed at 80° but some were conducted at 50° in order to obtain an approximation of the activation energy. The solutions were buffered at pH 3.4, 4.1, 5.1, 6.1, and 6.9; the ionic strength was about 1.0 in all experiments. The initial concentration of vanillyl alcohol was about 0.02 M and three runs were made at each pH with the initial concentrations of sulphite equal to 0.04, 0.02, and 0.01 M. The reactions were followed by iodometric titration of the sulphite.

The values were analysed assuming a first and a second order reaction, according to eqns. 1 and 2.

$$\frac{d[VS]}{dt} = k_I [V] \qquad (1) \qquad\qquad \frac{d[VS]}{dt} = k_{II}[V][S] \qquad (2)$$

VS = vanillyl sulphonic acid
V = vanillyl alcohol
S = total sulphite

The sulphite is present as $SO_3^=$, HSO_3^- and H_2SO_3, but as the solutions were strongly buffered, the relative concentrations of these three species at each pH were constant throughout the reaction. It is justified, therefore, to consider the total sulphite concentration only in eqns. 1 and 2. The results of these calculations are summarised in Table 1. At pH 4.1 and 5.1 the reaction is approximately first order, but at higher and lower pH-values the deviations from this order are considerable. On the other hand, the deviations from the second order at the highest and the lowest pH-values studied (3.4 and6.9) are smaller.

Thus, it is obvious that the reaction is no simple first or second order reaction but must follow a more complicated course. As will be demonstrated below, the assumption that the reaction proceeds *via* the unstable methylene-

Table 1. Values for the velocity constants obtained when the reaction between vanillyl alcohol and sulphite is treated as a first and second order reaction. $t = 80.7°$, $[V_o] = 0.02M$. Time in min.

pH	$[S_o] : [V_o]$	$10^3 \times k_I$	$10 \times k_{II}$
3.4	2	7.2 ± 0.5	2.1 ± 0.4
3.4	1	5.3 → 3.6	2.8 → 3.5
3.4	0.5	2.6 → 1.5	2.9 → 3.6
4.1	2	3.2 ± 0.3	0.5 → 1.0
4.1	1	3.4 ± 0.2	1.7 → 2.3
4.1	0.5	2.6 ± 0.3	2.9 → 5.5
5.1	2	3.1 ± 0.4	0.95 ± 0.15
5.1	1	2.7 ± 0.3	1.0 → 2.2
5.1	0.5	2.7 ± 0.2	1.8 → 8.7
6.1	1.7	5.3 ± 0.2	1.8 ± 0.2
6.1	0.6	3.6 ± 0.1	3.3 → 6.2
6.1	0.3	2.5 ± 0.2	5.5 → 9.8
6.9	2	9.5 ± 2.0	2.9 ± 0.6
6.9	1	5.7 ± 0.7	3.3 → 4.4
6.9	0.5	3.8 ± 0.6	6.3 → 9.1

quinone (IV) intermediate is in agreement with the observed results. This possibility was also discussed by Migita *et al.*[4]

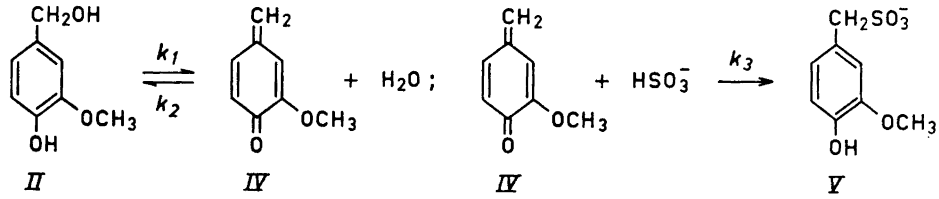

II IV IV V

Using the method of the unstable intermediate, the velocity is expressed by eqn. 3.

$$\frac{d[VS]}{dt} = \frac{k_1 \cdot k_3}{k_2 + k_3[S]} [V][S] \qquad (3)$$

p-Methylenequinones are easily formed by the reaction of *p*-hydroxybenzyl halogenides with alkali. A similar reaction of *p*-hydroxybenzyl alcohols does not seem improbable, nor does the fact that the latter react with acids to give methylenequinones and not carbonium ions. Methylenequinones are also known to be highly reactive,[6] easily adding the elements of water.

The reversible transformation of vanillyl alcohol into methylenequinone is catalysed both by acids and bases. This is possibly an example of general acid-base catalysis which is also dependent upon the components and their concentrations in the buffering system. At high and low pH-values, k_2 may be expected to be high compared to k_3 [S] and eqn. 3 then approaches that of a

second order reaction. On the other hand, k_2 may be much smaller than k_3 [S] at some intermediate pH-values, and then the reaction approaches a first order reaction, as happens at pH 4.1 and 5.1 in the concentration range studied. The assumption of a methylenequinone derivative as intermediate also accounts for the great difference in reactivity between vanillyl alcohol and veratryl alcohol in neutral and alkaline solutions, as only the former substance can give this reactive intermediate. At lower pH-values, veratryl alcohol probably reacts *via* the carbonium ion (VI), while vanillyl alcohol (as discussed above) may also form the methylenequinone in this pH-region.

$$k_1 = \frac{k_2}{k_3} \cdot k_{II} + k_I \qquad (4)$$

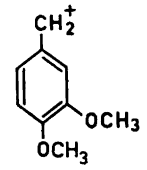

VI

Integration of eqn. 3 gives eqn. 4, in which k_I and k_{II} are variables; the latter values can be calculated from eqns. 1 and 2. k_1 and k_2/k_3 were calculated from eqn. 4. The values obtained, which must be regarded only as approximate, are given in Table 2.

As is evident from Figs. 1 and 2, the experimentally observed values lie reasonably close to the theoretical concentration *versus* time curves constructured from the values of k_1 and k_2/k_3 in Table 2.

Some experiments were performed at 50° and pH 6.9 and the same concentrations used at 80°. From these experiments the apparent energy of activation was determined to be 24 kcal · mole^{-1}.

A similar reaction, the formation of sulphonate from epinephrin (VII) and sulphite, has recently been studied by Higuchi and Schroeter [7].

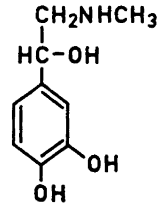

VII

At pH values above 5 the reaction was of second order and at pH 4 it approached first order, being independent of the sulphite concentration. The authors suggest that the reaction is of the *SN* 2 type, in competition with a *SN* 1 reaction with a carbonium ion intermediate. The first order reaction accounts for the fact that an optically inactive sulphonic acid is obtained from optically active epinephrin; the latter substance is also racemised at a comparable rate at pH 4.0 in the absence of sulphite. At higher pH-values when the reaction

Table 2. k_1 and k_2/k_3 calculated from the observed values, using eqn. 4.

pH	$k_1 \times 10^{-3}$ min^{-1}	$k_2/k_3 \times 10^3$ moles
3.4	13	30
4.1	4	—
5.1	4	—
6.1	9	13
6.9	11	9

is of second order, optically inactive sulphonic acid is also obtained and the authors assume that the initially-formed, optically active sulphonic acid is rapidly racemised. Alternatively, the results of Higuchi and Schroeter may be explained by the assumption of a methylenequinone intermediate. Epinephrin occurs as an ammonium ion in the pH-range studied, 4—7. It seems reasonable to assume that by an inductive effect the base catalysed formation of methylenequinone is facilitated and the acid catalysed is hindered. Consequently, the apparent order should be second at higher pH values and first at

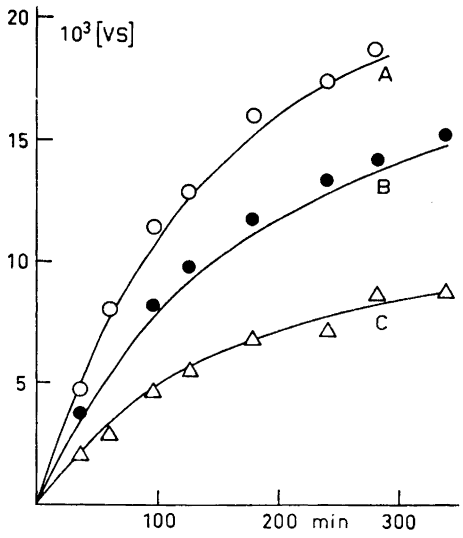

Fig. 1. Concentration of reaction product *versus* time at pH 3.4. The curves are calculated from the initial concentrations and the values of k_1 and k_2/k_3 given in Table 2. The symbols represent the observed values.

Curve A, ○ $[V_o] = 0.0219$, $[S_o] = 0.0416$
Curve B, ● $[V_o] = 0.0219$, $[S_o] = 0.0209$
Curve C, △ $[V_o] = 0.0219$, $[S_o] = 0.0102$

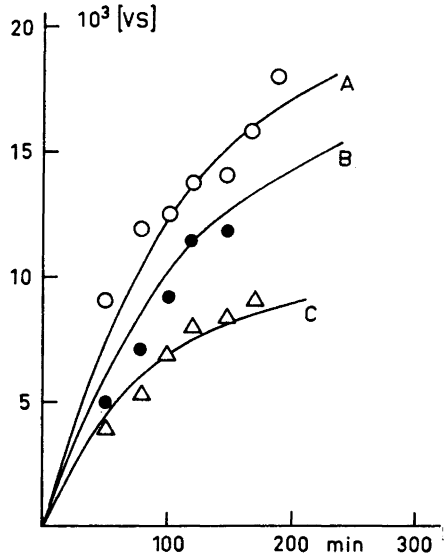

Fig. 2. Concentration of reaction product *versus* time at pH 6.9. The curves are calculated from the initial concentrations and the values of k_1 and k_2/k_3 given in Table 2. The symbols represent the observed values.

Curve A, ○ $[V_o] = 0.0213$, $[S_o] = 0.0409$
Curve B, ● $[V_o] = 0.0213$, $[S_o] = 0.0197$
Curve C, △ $[V_o] = 0.0213$, $[S_o] = 0.0095$

lower ones. With the uncharged vanillyl alcohol, however, it seems reasonable to find a second order reaction both at high and low pH-values and first order at intermediate levels.

The hypothesis of methylenequinones as intermediates in the reactions of *p*-hydroxybenzyl alcohols is not restricted to the reaction with sulphite. It seems possible that several other reactions which proceed with great ease, such as the etherification on treatment with alcohol and acid and the reactions with various thiols, also proceed *via* this intermediate.

EXPERIMENTAL

Solutions Vanillyl alcohol, 0.085 M, in water

Sodium sulphite, 0.17—0.042 M, in water
M Citrate buffer, pH 3.4
M Acetate buffer, pH 4.1
M Acetate buffer, pH 5.1
0.2 M Phosphate buffer, pH 6.1
0.2 M Phosphate buffer, pH 6.9

Sodium chloride was added to the buffers to an ionic strength of 2.0. The solutions were flushed with and stored under nitrogen.

Kinetic experiments. The solutions of vanillyl alcohol (1 part), sulphite (1 part) and buffer (2 parts) were added to test tubes which were flushed with nitrogen and sealed. The test tubes, 10 in each run, were placed in a water bath maintained at 80.7°. The variation was about 0.1°. At intervals tubes were removed, cooled in icewater, opened under water and the amount of sulphite determined iodometrically. Three blanks without vanillyl alcohol were run simultaneously.

The three series at pH 5.1 were repeated. The average values for k_I were 2.6 and $2.8 \cdot 10^{-3}$ in the two runs.

REFERENCES

1. Berg, G. A. and Holmberg, B. *Svensk Kem. Tidskr.* **47** (1935) 257.
2. Adler, E. and Gierer, J. in Treiber, E. *Die Chemie der Pflanzencellwand*, Springer Verlag 1957.
3. Lindgren, B. O. *Acta Chem. Scand.* **3** (1949) 1011.
4. Migita, N., Mitsukawa, R., Nakano, J. and Ichino, M. *J. Japan Tech. Assoc. Pulp and Paper Ind.* **8** (1954) 2; [*C.A.* **49** (1955) 1324b].
5. Joffe, H. H. *Chem. Rev.* **53** (1953) 191.
6. Hultzsch, K. *Chemie der Phenolharze.* Springer Verlag 1950, p. 63.
7. Higuchi, T. and Schroeter, L. C. *J. Am. Chem. Soc.* **82** (1960) 1904.

Received February 1, 1961.

ACTA CHEMICA SCANDINAVICA 15 (1961) 1087–1096

Studies of Thioacids and Their Derivatives

II. Carboxymethyl Dithioesters

KAI ARNE JENSEN and CHRISTIAN PEDERSEN

Chemical Laboratory of the University of Copenhagen, Copenhagen, Denmark

As intermediates for the preparation of thiohydrazides a number of new carboxymethyl dithioates have been synthesized. Three different routes to these compounds have been studied in detail: I. The reaction between chloroacetic acid and crude dithioacids, prepared by the Grignard reaction. II. The reaction between chloroacetic acid and crude dithioacids, prepared from aldehydes and ammonium polysulfide. III. Thiohydrolysis of *S*-carboxymethylthiopiperididium bromides, prepared from thiopiperidides and bromoacetic acid. Methods I and II are essential in special cases, but Method III is more generally applicable, and the yields obtained by this method are much higher than those obtained by Methods I and II (*cf.* Table 1).

In the synthesis of thiohydrazides carboxymethyl dithioates have proved to be very suitable starting materials. Apart from being good thioacylating agents these compounds have the advantage over ordinary dithioesters of being crystalline solids forming water-soluble sodium salts. Two of these compounds, *viz.* carboxymethyl dithiobenzoate and dithiophenylacetate, were prepared by Holmberg [1] and Kjær [2,3]. Both authors have shown that these compounds are powerful thioacylating agents [2–5].

For the preparation of the carboxymethyl dithioesters we used three methods of which a description is given in the following.

Method I. According to this method the magnesium halide salts of dithioacids were prepared by the well-known reaction of Grignard compounds with carbon disulfide [6–9] and were subsequently esterified with chloroacetic acid,

$$RMgX + CS_2 \longrightarrow RCSSMgX \xrightarrow{ClCH_2COONa} RCSSCH_2COONa$$

Using this procedure, Kjær [2,3] obtained good yields of carboxymethyl dithiobenzoate * and dithiophenylacetate. We have applied the method to the pre-

* The first of these compounds has been prepared almost a hundred times by different workers in this laboratory, but it has not been possible again to obtain the yield given by Kjær; generally 50–55 g instead of 77 g, *i.e.* 36–40 % instead of 56 % is obtained, and often the yield is much lower. Several experiments have been carried out to find the cause of this discrepancy, but without positive result. It can only be said that the lower the yields are, the more is formed of an insoluble by-product. The conditions given by Kjær are not very critical, and it seems to be unnecessary to use a nitrogen atmosphere and "reversed addition".

paration of several carboxymethyl dithioesters with varying yields (Table 1). In addition to the compounds listed in Table 1, we have without success tried to prepare carboxymethyl esters of the following dithioacids: dithiopropionic acid (even authentic dithiopropionic acid did not give the expected carboxymethyl ester on reaction with sodium chloroacetate), dithiopivalic acid, β-phenyldithiopropionic acid, 8-quinolinedithiocarboxylic acid, 3-pyridinedithiocarboxylic acid and α-thiophenedithiocarboxylic acid. The lack of success in the first three cases is in accord with the low yields generally obtained in the preparation of aliphatic dithioacids from Grignard compounds [9]. The lack of success in the last case is remarkable because α-thiophenedithiocarboxylic acid is obtained in good yield by method II.

Aromatic dithioacids may also be prepared from trichlorocompounds, *e.g.* Holmberg [1] prepared carboxymethyl dithiobenzoate from benzotrichloride. This method may also be used to prepare certain heterocyclic dithioacids, *e.g.* König *et al.*[10] prepared dithio*iso*nicotinic acid in this way. Furthermore potassium dithioformate has been prepared from chloroform [11], but we were unable to prepare dithioacetic acid from 1,1,1-trichloroethane. Potassium dithioformate reacts with sodium chloroacetate with formation of a compound having the composition of carboxymethyl dithioformate, but it is colourless and does not show any thioacylating properties. It is possibly a trimeric compound [12].

Method II. According to this method the dithioacids were prepared from aldehydes by reaction with ammonium polysulfide, the esterification being performed as above:

$$RCHO \xrightarrow{(NH_4)_2S_x} RCSSH \xrightarrow{ClCH_2COONa} RCSSCH_2COOH$$

For the preparation of the dithioacids we followed the directions given by Bost and Shealey [13], but since we did not extract the dithioacids from the resinous material produced in the course of the reaction, we generally got lower yields than these authors. This method has the advantage of being fast and convenient, but the yields are rather low and they are very dependent on the structure of the aldehyde used. The best results are obtained with aromatic hydroxyaldehydes and non-nitrogenous heterocyclic aldehydes. The method is especially valuable for the preparation of dithioesters derived from thiophene carboxaldehyde, furfural, salicylaldehyde, and *p*-hydroxybenzaldehyde. *o*-Methoxybenzaldehyde gave nothing, and anisaldehyde only 3—4 % of a product which was difficult to purify. *o*-Chlorobenzaldehyde gave only a trace of the dithioester, the *m*- and *p*-compound 3—4 %. The last two compounds could, however, be obtained in excellent yields by method III, but this method also failed with the *o*-compound. Bruni and Levi [14] report on the preparation of dithiocinnamic acid from cinnamic aldehyde and ammonium polysulfide, but we were unable to duplicate this result. Nor could we obtain dithioacids from 3- and 4-pyridinealdehydes or from pivalaldehyde.

Method III. Since Sakurada [15] prepared a large number of dithioesters by treating thioimidoesters in ether solution with hydrogen sulfide, this method was tried for the preparation of the carboxymethyl esters of dithioacetic and dithiobenzoic acids according to the following scheme:

Table 1. Carboxymethyl dithioates, $RCSSCH_2COOH$.

R	Yield, %, by method of preparation			M.p., °C	Colour	Formula	Analyses							
							Carbon		Hydrogen		Sulfur		Nitrogen	
	I	II	III				Found	Calc.	Found	Calc.	Found	Calc.	Found	Calc.
Phenyl [a]	40		82	126–127	red	$C_9H_8O_2S_2$								
Benzyl [b]			50	77– 78	yellow	$C_{10}H_{10}O_2S_2$								
β-Phenylethyl [b]			55	92– 93	yellow	$C_{11}H_{12}O_2S_2$	55.20	54.97	5.17	5.03	26.71	26.68		
o-Tolyl [a]	46			122–124	orange	$C_{10}H_{10}O_2S_2$	53.05	53.07	4.66	4.45	28.14	28.33		
p-Tolyl [a]	34			118–119	red	$C_{10}H_{10}O_2S_2$	53.35	53.07	4.59	4.45	28.46	28.33		
o-Hydroxyphenyl [a]		16		124–125	yellow	$C_9H_8O_3S_2$	47.10	47.35	3.49	3.54	28.50	28.09		
p-Hydroxyphenyl [c]		32		194–197	orange	$C_9H_8O_3S_2$	47.50	47.35	3.58	3.54	27.80	28.09		
o-Methoxyphenyl [d]		0	38	96– 98	red	$C_{10}H_{10}O_3S_2$	49.70	49.57	4.20	4.16	26.48	26.46		
p-Methoxyphenyl [a]		4	67	124–125	or.-yel.	$C_{10}H_{10}O_3S_2$	49.75	49.57	4.18	4.16	26.59	26.46		
o-Propoxyphenyl [d]			46*	93– 94	orange	$C_{12}H_{14}O_3S_2$	53.25	53.30	5.24	5.22				
o-*Iso*propoxyphenyl [e]			40	145–146	orange	$C_{12}H_{14}O_3S_2$	53.50	53.30	5.40	5.22	23.58	23.73		
o-Butoxyphenyl [d]			58*	108–109	orange	$C_{13}H_{16}O_3S_2$	54.85	54.90	5.86	5.67				
p-Butoxyphenyl [d]			96*	113–115	salmon	$C_{13}H_{16}O_3S_2$	55.00	54.90	5.60	5.67				
o-*Iso*butoxyphenyl [f]			20**	104–105	orange	$C_{13}H_{16}O_3S_2$	54.60	54.90	5.32	5.67	22.96	22.55		
o-*sec*-Butoxyphenyl [f]			16**	94– 95	orange	$C_{13}H_{16}O_3S_2$	55.05	54.90	5.71	5.67	22.32	22.55		
m-Chlorophenyl [a]		3	85	124–126	or.-red	$C_9H_7ClO_2S_2$	44.00	43.81	2.98	2.86	26.25	26.02		
p-Chlorophenyl [b]	4		82	115–117	or.-red	$C_9H_7ClO_2S_2$	44.10	43.81	2.95	2.86	26.20	26.02		
m-Nitrophenyl [a]			71	145–147	red	$C_9H_7NO_4S_2$	42.60	42.01	2.97	2.74			5.15	5.45
p-Acetamidophenyl [g]		8	94*	206–208	red	$C_{11}H_{11}NO_3S_2$	49.25	49.05	4.27	4.12			5.35	5.20
α-Naphthyl [a]	54			142–144	or.-yel.	$C_{13}H_{10}O_2S_2$	59.60	59.50	3.89	3.84	24.36	24.44		
β-Naphthyl [a]	15			147–148	pink	$C_{13}H_{10}O_2S_2$	59.53	59.50	3.74	3.84	24.50	24.44		
2-Furyl [a]		21		132–133	or.-red	$C_7H_6O_3S_2$	41.80	41.57	3.17	2.99	31.65	31.70		
2-Thienyl [a]	0.7	26		123–124	red	$C_7H_6O_2S_3$	38.45	38.48	2.94	2.77	44.16	44.10		
2-Pyrryl [a]	21			140–141	yellow	$C_7H_7NO_2S_2$	41.85	41.77	3.64	3.51			6.76	6.96
3-Indolyl [h]	22			163–166	yellow	$C_{11}H_9NO_2S_2$	52.60	52.57	3.57	3.61			5.44	5.57
Methyl [i]	0		60	80– 81	yellow	$C_4H_6O_2S_2$	32.15	31.98	4.24	4.03	42.80	42.67		
Ethyl [i]	0		60	51– 52	yellow	$C_5H_8O_2S_2$	36.65	36.56	5.03	4.91	39.20	39.04		
*Iso*propyl [i]	70***			48– 49	yellow	$C_6H_9O_2S_2$	40.30	40.45	5.80	5.66	36.29	35.95		

* Yield based on the thiopiperidide. ** Plus 50–60 % of oily ester; the *o*-ethoxy-, *o*-pentyloxy- and *o*-hexyloxydithiobenzoates were only obtained as red oils. *** From pure dithio*iso*butyric acid. Solvents used for recrystallisation: a) benzene; b) light petroleum (b.p. 100–140°C); c) water; d) benzene-light petroleum (b.p. 60–100°C); e) methylcellosolve-water; f) *n*-heptane; g) ethanol; h) benzene-ethanol; i) light petroleum (b.p. 60–100°C).



However, the reaction produced none of the desired products.

While this work was in progress a paper by Marvel *et al.*[16] appeared describing a modification of Sakurada's method in which the thioimidoester salt was treated with hydrogen sulfide in dry pyridine. We also tried this method and obtained a low yield (24 %) of impure carboxymethyl dithioacetate, whereas the attempted preparation of carboxymethyl dithiobenzoate was unsuccessful, yielding thiobenzamide (20 %) as the only product. Similarly, attempts to prepare methyl trichlorodithioacetate or pyridine dithiocarboxylates from the corresponding nitriles *via* the thioimidic esters gave negative results.

The poor results of these experiments may be partly ascribed to decomposition of the thioimidoester upon liberation from its salt by dissolution in pyridine, since Holmberg [17] has shown that the reaction

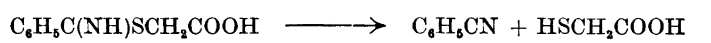

takes place when the thioimidoester is liberated from its salt in aqueous solution. Furthermore, any dithioester formed may react with ammonia and give the thiobenzamide

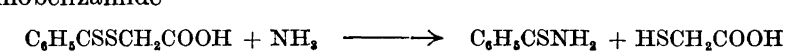

The formation of thiobenzamide from benzonitrile and hydrogen sulfide is unlikely as it has been shown [18] that this reaction does not take place in pyridine solution unless a strong base is present. Finally, the thioimidoester may undergo ring closure with formation of thiazolones (*cf.* number VII in this series).

Since Marvel *et al.*[16] described only the preparation of aliphatic dithioesters we tried to prepare methyl and ethyl dithiobenzoate by their method. Ethyl dithiobenzoate was obtained from *S*-ethylthiobenzamidium bromide in 75 % yield. It was contaminated with thiobenzamide, from which it could be separated by extraction with light petroleum. However, when *S*-methylthiobenzamidium iodide was treated with hydrogen sulfide in pyridine, only traces of methyl dithiobenzoate was produced, the main product being thiobenzamide. *O*-Methyl thiobenzoate was prepared in 90 % yield from *O*-methylbenzamidium chloride (methyl benzimidate hydrochloride).

Peak and Stansfield [19] obtained good yields of dithiocarboxylic esters by thiohydrolysis of *S*-methylthiomorpholidium iodides in absolute ethanol. In the same way Doyle *et al.*[20] prepared methyl indole-3-dithiocarboxylate by thiohydrolysis of the corresponding *S*-methylthiomorpholidium iodide. We investigated the analogous thiohydrolysis of several *S*-carboxymethylthiopiperididium bromides in absolute ethanol

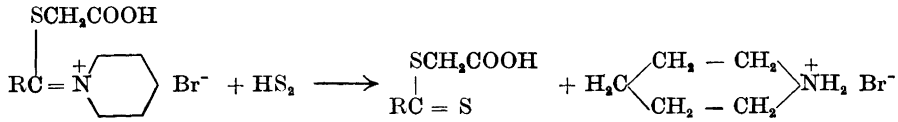

Table 2. Thiopiperidides. 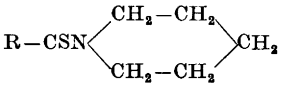

R	Yield %	M.p., °C	Formula	Analyses					
				Carbon		Hydrogen		Nitrogen	
				Found	Calc.	Found	Calc.	Found	Calc.
β-Phenylethyl [a]	37	67 – 68	$C_{14}H_{19}NS$	72.15	72.05	8.11	8.21	6.01	6.00
o-Methoxyphenyl [b]	70	92 – 93	$C_{13}H_{17}NOS$	66.15	66.34	7.06	7.28	5.87	5.95
p-Methoxyphenyl [a]	90	107 – 108	$C_{13}H_{17}NOS$	66.50	66.34	7.27	7.28	5.89	5.95
o-Ethoxyphenyl [c]	84	102 – 103	$C_{14}H_{19}NOS$	67.40	67.44	7.25	7.68	5.47	5.62
o-Propoxyphenyl [c]	73	60 – 61	$C_{15}H_{21}NOS$	68.45	68.41	7.82	8.04	5.20	5.32
p-Butoxyphenyl [c]	88	59 – 60	$C_{16}H_{23}NOS$	69.03	69.27	8.27	8.36	5.21	5.05
m-Chlorophenyl [b,c]	72	63 – 64	$C_{12}H_{14}ClNS$	60.35	60.11	5.83	5.89	5.93	5.84
p-Chlorophenyl [b,c]	84	108 – 109	$C_{12}H_{14}ClNS$	60.30	60.11	6.19	5.89	5.68	5.84
m-Nitrophenyl [b]	51	91 – 92	$C_{12}H_{14}N_2O_2S$	57.80	57.58	5.60	5.64	11.20	11.19
p-Nitrophenyl [d]	50	176 – 178	$C_{12}H_{14}N_2O_2S$	57.50	57.58	5.62	5.64	11.20	11.19
p-Acetamidophenyl [b]	82	201 – 202	$C_{14}H_{18}N_2OS$	64.00	64.09	7.03	6.91	10.53	10.68
Ethyl	57	b.p.111/1 mm	$C_8H_{15}NS$	61.30	61.09	9.47	9.61	8.86	8.91
*Iso*propyl [e]	71	b.p.130/3 mm	$C_9H_{17}NS$	62.40	63.11	9.86	10.01		
tert-Butyl [e]	97	81 – 82	$C_{10}H_{19}NS$	64.90	64.81	10.45	10.34	7.40	7.56

Solvents used for recrystallisation: a) light petroleum (b.p. 100 – 140°C); b) ethanol; c) light petroleum (b.p. 60 – 100°C); d) benzene; e) ethanol-water.

Thiopiperidides with R = *o-Iso*propoxyphenyl, *o*-butoxyphenyl, *o-iso*butoxyphenyl, *o-sec*-butoxyphenyl, *o*-pentyloxyphenyl and *o*-hexyloxyphenyl were isolated as oils and were not purified, the crude products being used directly for the preparation of the dithioesters.

Table 3. S-Carboxymethyl-thiopiperidium bromides,

R	Yield %	M.p., °C	Formula	Analyses					
				Carbon		Hydrogen		Nitrogen	
				Found	Calc.	Found	Calc.	Found	Calc.
Benzyl	95	137–138	$C_{15}H_{20}BrNO_2S$	50.30	50.28	5.53	5.63	3.83	3.91
β-Phenylethyl	81	131–132	$C_{16}H_{22}BrNO_2S$	51.90	51.61	6.07	5.96	3.69	3.76
o-Methoxyphenyl	98	167–169	$C_{15}H_{20}BrNO_3S$	48.20	48.13	5.56	5.39	3.60	3.74
p-Methoxyphenyl	84	156–159	$C_{15}H_{20}BrNO_3S$	48.10	48.13	5.51	5.39	3.65	3.74
*o-Iso*propoxyphenyl	95	165 (d.)	$C_{17}H_{24}BrNO_3S$	50.60	50.75	5.96	6.02	3.59	3.48
*o-Iso*butoxyphenyl	90	146–148(d.)	$C_{18}H_{26}BrNO_3S$	51.68	51.92	6.14	6.30	3.37	3.36
o-sec-Butoxyphenyl	90	160 (d.)	$C_{18}H_{26}BrNO_3S$	51.70	51.92	6.17	6.30	3.40	3.36
m-Chlorophenyl	70	170–173	$C_{14}H_{17}BrClNO_2S$	44.40	44.40	4.63	4.53	3.61	3.70
p-Chlorophenyl	80	161–164	$C_{14}H_{17}BrClNO_2S$	44.55	44.40	4.57	4.53	3.54	3.70
m-Nitrophenyl	78	157–159	$C_{14}H_{17}BrN_2O_4S.\frac{1}{2}H_2O$	42.25	42.21	4.66	4.55	6.78	7.03
Methyl	95	168–169	$C_9H_{16}BrNO_2S$	38.30	38.30	5.47	5.72	4.84	4.96
Ethyl	86	121–122	$C_{10}H_{18}BrNO_2S$	40.45	40.54	6.15	6.12	4.65	4.73
*Iso*propyl	60	83– 84	$C_{11}H_{20}BrNO_2S$	41.70	42.57	7.05	6.50	4.42	4.51

and obtained excellent yields in all the cases tried (Table 1). The thiopiperidides, in our experience, showed definite advantages over the thiomorpholides.

The thiopiperidides (Table 2) were prepared by the Willgerodt-Kindler method or from piperidides and phosphorus pentasulfide.

The *S*-carboxymethyl-thiopiperididium bromides were prepared from the thiopiperidides and bromoacetic acid with benzene as solvent (Table 3). This is the method which Holmberg [21] used for the preparation of *S*-carboxymethyl-thiobenzpiperididium bromide.

p-Nitrothiobenzpiperidide and thiopivaloylpiperidine reacted very incompletely with bromoacetic acid, and we were therefore unable to prepare the corresponding carboxymethyl dithioesters. Thiopivaloylpiperidine, however, reacted well with methyl iodide in boiling acetone, and the resulting *S*-methyl-thiopivaloylpiperidinium iodide, on thiohydrolysis, afforded methyl dithiopivaloate. In principle there seems to be no difficulty in obtaining the higher homologues of the aliphatic carboxymethyl dithioesters, but they are waxy substances which are difficult to purify. Carboxymethyl hexanedithioate was prepared, but it was not obtained in a completely pure state.

EXPERIMENTAL *

Method I

Carboxymethyl α-dithionaphthoate. To a solution of α-naphthylmagnesium bromide, prepared from α-bromonaphthalene (53.4 g) and magnesium (6.5 g) in 300 ml of ether, was added, with ice-cooling and stirring, 23.8 ml of carbon disulfide. The mixture was kept overnight, thus acquiring room temperature. Ice was added and the ether layer separated. To the aqueous layer was added a solution of chloroacetic acid (24.4 g) neutralised with sodium carbonate. After standing for 24 h at room temperature the mixture was acidified with conc. hydrochloric acid. The carboxymethyl ester separated as brownish crystals, which were washed with water and dried. The product (57 g) on recrystallisation from benzene gave 35 g (54 %) of yellow crystals with m.p. 136—138°C. After two additional recrystallisations from benzene the substance was pure.

The other compounds shown in Table 1 (Method I) were prepared in the same way. 2-Pyrryl- and 3-indolylmagnesium bromides were made from pyrrole and indole with ethylmagnesium bromide [22,23]. It was found convenient to purify 3-indole-dithiocarboxylic acid *via* its sodium salt, which is only slightly soluble.

Method II

Carboxymethyl 2-furandithioate. A solution of furfural (25 ml) in ethanol (90 ml) was heated to 65°C, and 135 ml of an ammonium polysulfide solution (prepared according to Bost and Shealy [13]) was added in 10 ml portions during 10 min, the temperature being kept at 65°C by heating now and then. The resulting mixture was boiled for 10 min, immediately cooled in ice, and acidified with conc. hydrochloric acid. The dithioacid, which separated as a red oil, was extracted with ether (3 × 150 ml). The ether solution was extracted with 1 N NaOH (3 × 100), and to this solution was added a solution of chloroacetic acid (28 g) neutralised with sodium carbonate. The pH of the resulting mixture was adjusted to 7. After standing overnight at room temperature the dark solution was acidified with conc. hydrochloric acid. The carboxymethyl ester separated

* Some preliminary experiments were carried out in this laboratory in 1951—53 by P. Nedenskov and I. Crossland. The *o*-alkoxydithiobenzoates were prepared by H. R. Baccaro and O. Buchardt.

as an oil, which crystallised on cooling. It was filtered off and recrystallised from water. Orange-red crystals, yield 12.6 g (21 %), m.p. 130–132°C. After two recrystallisations from benzene the substance was pure.

The substances shown in Table 1 (Method II) were prepared in the same way.

Method III

p-*Methoxythiobenzpiperidide.* Anisaldehyde (24 ml, 0.2 mole), piperidine (30 ml, 0.3 mole), and sulfur (9.6 g, 0.3 mole) were refluxed for one hour. After cooling, water was added and the mixture acidified with conc. hydrochloric acid. The brown oil rapidly solidified to a hard cake, which was crushed, filtered off, and washed with water. Recrystallisation from ethanol (200 ml) gave 43 g (90 %) of yellow crystals with m.p. 104–106°C. After two recrystallisations from light petroleum (b.p. 100–140°C) the substance was pure, forming pale yellow crystals.

The other aromatic thiobenzpiperidides shown in Table 2 were prepared in the same way. They all formed yellow to pale yellow crystals.

β-Phenylthiopropionylpiperidine. Propiophenone (22 ml), piperidine (25 ml, 1.5 equiv.) and sulfur (8 g, 1.5 equiv.) were refluxed for 7 h. Excess piperidine was removed *in vacuo*, and the oily residue was extracted with ether; the ether solution was washed with dilute hydrochloric acid and water and dried (Na_2SO_4). After evaporation of the ether a brown, crystalline solid remained. It was recrystallised from light petroleum (b.p. 100–140°C). Yield 14 g (37 %), m.p. 66–68°C. After two additional recrystallisations from light petroleum the substance was pure, forming pale yellow crystals.

Thiopropionylpiperidine. Propionylpiperidine (40 g), dry pyridine (75 ml), and phosphorus pentasulfide (31 g) were refluxed for 2 h. After removal of the pyridine *in vacuo*, water and HCl were added, and the dark, oily layer was extracted with ether. The ether solution was dried (Na_2SO_4) and the ether removed. The residue was distilled, the fraction boiling at 110–115°C (2–3 mm) being collected. Yield 25 g (56 %). Before analysis the substance was redistilled, and the fraction boiling at 111–112°C (2–3 mm) collected. The pure product was a yellow oil.

Thiopivaloylpiperidine and thio*iso*butyrylpiperidine were prepared in the same way (Table 2). Thioacetylpiperidine was obtained in 65 % yield, m.p. 55–56°C (Russel [24] reports m.p. 60–61°C).

S-*Carboxymethyl*-p-*methoxythiobenzpiperididium bromide.* *p*-Methoxythiobenzpiperidide (10 g) was dissolved in dry benzene (50 ml), and bromoacetic acid (6.5 g, 1.1 equiv.) was added. After a few minutes at room temperature a colourless oil began to separate. After 24 h at room temperature dry ether (150 ml) was added to precipitate the product completely. A little of the oily product was induced to crystallise by scratching and washing with dry ether, and the main portion was seeded with the crystals. The mixture was cooled to 0°C and the product filtered off and washed carefully with dry ether. Colourless crystals, yield 13.4 g (84 %), m.p. 150–152°C (decomp.). A sample was purified by dissolving it in absolute ethanol followed by precipitation with dry ether.

The other *S*-carboxymethyl-thiopiperididium bromides shown in Table 3 were prepared in the same way. They were all recrystallised from ethanol-ether and formed colourless crystals melting with decomposition. The *p*-acetamido compound was very hygroscopic, and purification was therefore not attempted. The *o*-propoxy and *o*- and *p*-butoxythiobenzpiperididium bromides were not isolated, but were transformed directly into the corresponding dithioesters.

Carboxymethyl p-*methoxydithiobenzoate.* *S*-carboxymethyl-*p*-methoxythiobenzpiperididium bromide (13.4 g) was dissolved in absolute ethanol (40 ml), and the solution was cooled in ice while hydrogen sulfide was passed through it for 3–4 h (2–3 bubbles per second). The red solution was kept overnight at 0°C and the ethanol then removed *in vacuo*. The residue was repeatedly extracted with ether until it became colourless (piperidinium bromide). The red ether solution was evaporated to dryness *in vacuo* and the residue recrystallised from benzene. Orange-yellow crystals, yield 5.9 g (67 %), m.p. 120–122°C.

The same procedure was used for the preparation of the other carboxymethyl dithioesters except in two cases, *viz.* the *p*-chloro- and the *p*-acetamidodithiobenzoates, which were too insoluble in ether to be easily extracted with this solvent. Instead they were

isolated by adding water to the residue which was obtained after evaporation of the ethanol. The product was then filtered off, washed with water, and dried. This procedure is easier and could possibly be used generally, but if any unreacted thioimidic ester is present it will be hydrolysed to an *S*-thioester ($RCOSCH_2COOH$), which will be very difficult to separate from the dithioester.

Ethyl dithiobenzoate. *S*-Ethylthiobenzamidium chloride [25] (30 g) was dissolved in pyridine (120 ml); the solution was cooled in ice, and hydrogen sulfide was passed through it for 3 h. After standing overnight at 0°C, the mixture was diluted with water and acidified with conc. hydrochloric acid. The red oil that separated was extracted with ether, the ether solution was dried (Na_2SO_4) and the ether removed *in vacuo*. The residue was distilled, the fraction boiling at 153–158°C (14 mm) being collected. During the distillation crystals of thiobenzamide began to separate in the distillate, wherefore this was mixed with 500 ml of light petroleum (b.p. 40–60°C), in which thiobenzamide is insoluble. After cooling, the thiobenzamide was filtered off and the light petroleum evaporated. Distillation of the residue gave 20.3 g (75 %) of material boiling at 153–154°C (13 mm). Gilman *et al.*[26] report the boiling point 155–160°C (15 mm).

S-Methylthiobenzamidium iodide (78.7 g) (prepared from thiobenzamide and methyl iodide) was treated with hydrogen sulfide in pyridine. The product that separated when water and hydrochloric acid was added to the pyridine solution was a solid contaminated with drops of a red oil (methyl dithiobenzoate); the mixture smelled strongly of methanethiol. The solid, when filtered off, dried, and washed with light petroleum, gave 16.4 g (47 %) of thiobenzamide. From *S*-methylthiobenzpiperididium iodide methyl dithiobenzoate was obtained in 99 % yield.

S-*Methylthiopivaloylpiperidinium iodide.* Thiopivaloylpiperidine (40 g) and methyl iodide (65 g) were dissolved in dry acetone (250 ml), and the solution was refluxed for one hour. Acetone and excess methyl iodide were removed *in vacuo*, and ether (400 ml) was added to the residual oil, causing it to crystallise. Yield 63 g (90 %), of m.p. 112–120°C. The product was purified by recrystallisation from absolute ethanol-ether. The pure compound formed colourless crystals of m.p. 129–130°C. (Found: C 40.40; H 6.78; N 4.19. Calc. for $C_{11}H_{22}INS$: C 40.37; H 6.76; N 4.27.)

S-*Methylthio*iso*butyrylpiperidinium iodide* was prepared analogously. M.p. 106–107°C. (Found: I 40.4. Calc. for $C_{10}H_{20}INS$: I 40.6.)

Methyl dithiopivaloate. *S*-Methylthiopivaloylpiperidinium iodide (45.6 g) in absolute ethanol (250 ml) was cooled in ice and treated with hydrogen sulfide for three hours. The mixture was kept overnight at 0°C, and a large volume of ether was added. The precipitated piperidinium iodide was filtered off, and the yellow ethanol-ether solution was distilled through a column packed with glass helices. The fraction boiling at 65–65.5°C (12 mm) was collected. Yellow oil, yield 13.9 g (68 %). (Found: C 48.62; H 8.38; S 43.12. Calc. for $C_6H_{12}S_2$: C 48.65; H 8.16; S 43.24.)

*Methyl dithio*iso*butyrate* was prepared by the same procedure. Yield 66 %. B.p. 86/50 mm. (Found: C 44.95; H 7.66. Calc. for $C_5H_{10}S_2$: C 44.74; H 7.50.)

In a similar way methyl *p*-butoxydithiobenzoate was prepared from *p*-butoxythiobenzpiperidide (2.77 g). The ethereal solution left on evaporation a red crystalline residue, which was recrystallised from methanol. Yield 1.5 g (63 %); m.p. 38–38.5°C. (Found: C 59.99; H 6.71. Calc. for $C_{12}H_{16}OS_2$: C 60.05; H 6.87.)

REFERENCES

1. Holmberg, B. *Arkiv Kemi, Mineral. Geol.* **17 A** (1943) No. 23.
2. Kjær, A. *Acta Chem. Scand.* **4** (1950) 1347.
3. Kjær, A. *Acta Chem. Scand.* **6** (1952) 327.
4. Holmberg, B. *Arkiv Kemi, Mineral. Geol.* **25 A** (1947) No. 18.
5. Holmberg, B. *The Svedberg Memor. Vol.* (1944) 299.
6. Houben, J. and Kesselkaul, L. *Ber.* **35** (1902) 3695.
7. Houben, J. *Ber.* **39** (1906) 3219.
8. Houben, J. and Pohl, H. *Ber.* **40** (1907) 1303.
9. Houben, J. and Pohl, H. *Ber.* **40** (1907) 1725.
10. König, H. B., Siefken, W. and Offe, H. A. *Chem. Ber.* **87** (1954) 825.

11. Levi, T. G. *Atti accad. nazl. Lincei* (5) **32 I** (1923) 569.
12. Levi, T. G. *Atti accad. nazl. Lincei* (6) **9** (1929) 170.
13. Bost, R. W. and Shealy, O. L *J. Am. Chem. Soc.* **73** (1951) 25.
14. Bruni, G. and Levi, T. G. *Gazz. chim. ital.* **54** (1924) 389.
15. Sakurada, Y. *Mem. Coll. Sci. Kyoto Imp. Univ.* **10** (1926–27) 79.
16. Marvel, C. S., Radzitzky, P. de and Brader, J. J. *J. Am. Chem. Soc.* **77** (1955) 5997.
17. Holmberg, B. *Arkiv Kemi, Mineral. Geol.* **20 A** (1945) No. 1.
18. Fairfull, A. F. S., Lowe, J. L. and Peak, D. A. *J. Chem. Soc.* **1952** 743.
19. Peak, D. A. and Stansfield, F. *J. Chem. Soc.* **1952** 4067.
20. Doyle, F. P. *et al. J. Chem. Soc.* **1956** 2853.
21. Holmberg, B. *Arkiv Kemi, Mineral. Geol.* **24 A** (1947) No. 3.
22. Oddo, B. and Mingoia, Q. *Gazetta chim. ital.* **56** (1926) 782.
23. McCay, C. M. and Schmidt, C. L. A. *J. Am. Chem. Soc.* **48** (1926) 1933.
24. Russel, W. F. *J. Chem. Soc.* **97** (1910) 953.
25. Bernthsen, A. *Ann.* **197** (1879) 341.
26. Gilman, H., Robinson, J. and Beaber, N. J. *J. Am. Chem. Soc.* **48** (1926) 2715.

Received January 23, 1961.

ACTA CHEMICA SCANDINAVICA 15 (1961) 1097–1103

Studies of Thioacids and Their Derivatives

III. Methods for the Preparation of Thiohydrazides

KAI ARNE JENSEN and CHRISTIAN PEDERSEN

Chemical Laboratory of the University of Copenhagen, Copenhagen, Denmark

Several new thiohydrazides (see Table 1) have been prepared from carboxymethyl dithioates and hydrazine or from dithioacids and hydrazine. A number of other potential methods for the preparation of thiohydrazides were tried without success. An excess of carboxymethyl dithioate leads generally to the formation of thiadiazoles; in two cases, however, dithioacylated hydrazines were obtained.

For the preparation of thiohydrazides the reaction between carboxymethyl dithioates and hydrazine, originally used by Holmberg [1] for the preparation of thiobenzhydrazide, has proved to be most convenient. The carboxymethyl esters of dithioacids, dissolved in aqueous sodium hydroxide, react rapidly with hydrazine at 0°C. The methyl and ethyl esters may also be used, but the higher alkyl esters seem to be rather unreactive: amyl dithiobenzoate reacts only slowly with hydrazine even at 100°C.

The hydrazides may also be prepared directly from dithioacids. The hydrazinium salts of these acids are rapidly transformed into hydrazides in dilute aqueous solution:

$$RCSS^{-}N_2H_5^{+} \longrightarrow RCSNHNH_2 + H_2S$$

This reaction is accompanied by a decolorization of the red or brown solution. The method is mainly of importance when the dithioacids can be obtained by the reaction of aldehydes with ammonium polysulfide. The preparation of a number of new thiohydrazides by these methods has already been announced (Jensen and Jensen [2]); they are included in Table 1, and details of their preparation are given in the experimental part.

Thiohydrazides with the $-CSNHNH_2$ group attached to an aromatic or a non-basic heterocyclic nucleus can in most cases be prepared without difficulties. Sometimes, however, a thiadiazole is formed as the main product (see No. VI of this series), and we were unable to prepare *m*-nitrothiobenzhydrazide. In this case the carboxymethyl dithioate reacts rapidly with hydrazine with the formation of hydrogen sulfide, and no thiohydrazide could be isolated. Most aliphatic dithioacids and dithioesters react in the same way with hyd-

Table 1. Thiohydrazides, $RCSNHNH_2$.

R	Yield, %, by procedure		M.p., °C	Formula	Analyses							
					Carbon		Hydrogen		Sulfur		Nitrogen	
	I [a]	II [b]			Found	Calc.	Found	Calc.	Found	Calc.	Found	Calc.
Benzyl [d]		55	70— 71	$C_8H_{10}N_2S$	57.52	57.82	5.95	6.07	19.25	19.26	16.96	16.86
β-Phenylethyl [e]		78	105—106	$C_9H_{12}N_2S$	59.80	60.00	6.68	6.72			15.69	15.52
o-Tolyl [c]												
p-Tolyl [d]		63	137—138	$C_8H_{10}N_2S$	57.75	57.80	5.85	6.07			17.10	16.83
o-Hydroxyphenyl [e]	40	67	101—102	$C_7H_8N_2OS$	49.98	50.00	4.85	4.80	18.92	19.07	16.95	16.66
m-Hydroxyphenyl [f]	10		146—147	$C_7H_8N_2OS$	49.80	50.00	4.89	4.80			16.64	16.66
p-Hydroxyphenyl [f]	26	77	200—201	$C_7H_8N_2OS$	50.25	50.00	4.73	4.80			16.83	16.66
o-Methoxyphenyl [e]		50	34— 35	$C_8H_{10}N_2OS$							15.30	15.38
p-Methoxyphenyl [d]		80	125—126	$C_8H_{10}N_2OS$	52.85	52.72	5.48	5.53	17.30	17.59	15.31	15.38
o-Propoxyphenyl [e]		78	52— 53	$C_{10}H_{14}N_2OS$	57.22	57.13	6.79	6.71			13.43	13.33
o-*Iso*propoxyphenyl [e]		70	58— 59	$C_{10}H_{14}N_2OS$	57.20	57.13	6.70	6.71			13.33	13.33
o-Butoxyphenyl [e]		70	66— 67	$C_{11}H_{16}N_2OS$	59.10	58.91	7.10	7.19			12.42	12.49
o-Hexyloxyphenyl [e]		29	56— 57	$C_{13}H_{20}N_2OS$	62.05	61.86	8.18	7.99			11.22	11.10
3-Methoxy-4-hydroxyphenyl [f]	13		147—148	$C_8H_{10}N_2O_2S$	48.68	48.48	5.18	5.09			14.06	14.14
m-Chlorophenyl [d]		83	118—119	$C_7H_7ClN_2S$	44.75	45.05	3.87	3.78			15.25	14.99
p-Chlorophenyl [d]		62	123—124	$C_7H_7ClN_2S$	45.00	45.05	3.60	3.78			15.14	14.99
p-Acetamidophenyl [g]	6	70	235—240(d.)	$C_9H_{11}N_3OS$	51.71	51.67	5.38	5.30			20.41	20.09
α-Naphthyl [d]		82	96— 98	$C_{11}H_{10}N_2S$	65.30	65.30	4.93	4.99	15.93	15.84	13.82	13.86
β-Naphthyl [e]		65	163—165	$C_{11}H_{10}N_2S$	65.15	65.30	5.08	4.99			13.85	13.86
2-Furyl [d]	40	55	130—131	$C_5H_6N_2OS$	42.28	42.25	4.44	4.26	22.45	22.52	19.84	19.71
2-Thienyl [h]	56	60	155—156	$C_5H_6N_2S_2$	38.11	37.98	3.58	3.83	40.42	40.53	17.83	17.72
2-Pyrryl [d]		77	121—122	$C_5H_7N_3S$	42.66	42.55	5.29	5.00	22.56	22.67	29.82	29.78
3-Indolyl [h]		75	173—174	$C_9H_9N_3S$	56.97	56.54	5.02	4.75	16.85	16.77	22.16	21.98
tert-Butyl [i]		60	93— 94	$C_5H_{12}N_2S$	45.35	45.40	8.99	9.16			21.24	21.20

a. From 10 g of the aldehyde, b. From 0.01 mole of the carboxymethyl dithioate. c. Isolated as the benzylidene derivative (see text). Solvents used for recrystallisation. d) benzene; e) benzene-light petroleum (b.p. 60—100°C); f) ethanol-water; g) ethanol; h) benzene-ethanol; i) light petroleum (b.p. 60—100°C). In most cases the compounds may also be recrystallised from hot water.

razine. We have tried to prepare the benzylidene derivatives of such thiohydrazides by reaction of dithioesters with benzalhydrazone, but without success. The only purely aliphatic thiohydrazide we have been able to prepare is trimethylthioacethydrazide (thiopivalic hydrazide). Phenylthioacetic hydrazide and β-phenylpropionic thiohydrazides were prepared in good yields but the former is decidedly less stable than aromatic thiohydrazides. *N*-Substituted thiohydrazides could be prepared in all cases (see No. V of this series).

The thiohydrazides are colourless substances which are easily soluble in ethanol or benzene and somewhat soluble in water. They are amphoteric substances and therefore soluble in dilute aqueous solutions of strong acids or bases. Their pK_a values are about 10.5 and their pK_b values about 8.5 as determined from titration curves.

A number of other potential methods for the preparation of thiohydrazides have also been tried, but without success.

a. The reaction of hydrazides with phosphorus pentasulfide generally seems to give a thiadiazole instead of a thiohydrazide. However, Profft *et al.*[3] obtained a small yield of picolinic thiohydrazide in this way. We were unable to prepare nicotinic or *iso*nicotinic thiohydrazide by this procedure, but obtained a 6 % yield of thiobenzhydrazide from benzhydrazide and phosphorus pentasulfide.

b. Thioamides react with hydrazine with evolution of hydrogen sulfide, and dihydrotetrazines or thiadiazoles, but no thiohydrazides, are formed. Junghahn [4] obtained dibenzyldihydrotetrazine from phenylthioacetamide and hydrazine, and McMillan *et al.*[5] obtained a thiadiazole from *iso*nicotinic thiamide and hydrazine; we have qualitatively shown that many other thiamides react in a similar way. It seemed, however, possible that the reaction would be different with a hydrazinium salt instead of free hydrazine (*cf.* Galat and Elion [6]), but attempts to prepare thiohydrazides in this way also gave a negative result.

c. *O*-Alkyl monothioates react with hydrazine with evolution of hydrogen sulfide, and no thiohydrazide is formed. From the reaction product of *O*-ethyl thiobenzoate and hydrazine we have isolated diphenyldihydrotetrazine and diphenyltriazole, *i.e.* the same products which are formed by the reaction of hydrazine with ethyl imidobenzoate (Pinner [7]) or with *N*-phenylthiobenzhydrazide (Wuyts [8]). The preparation of *iso*nicotinic thiohydrazide from *O*-ethyl thio*iso*nicotinate has been described in a Japanese patent [9], but we were unable to duplicate this result.

d. At an early stage of this investigation we tried to prepare thioacethydrazide from acethydrazidine and hydrogen sulfide. The lack of success in this case is understandable because it later became evident that thioacethydrazide is not a stable substance. That thiohydrazides may in principle be prepared from hydrazidines has, however, been shown by Zemplén [10], who has prepared a number of *N*-phenyl-thiohydrazides in this way.

e. Some attempts were made to prepare thiohydrazides from *a*-chlorobenzalazine:

$$\begin{array}{l} C_6H_5C=N-N=CHC_6H_5 \\ \quad\quad | \\ \quad\quad Cl \end{array}$$

Table 2. Thioacylhydrazones, RCSNHN=CHR'

R	R'	M.p., °C	Colour	Formula	% N	
					Found	Calc.
Phenyl	*o*-Hydroxyphenyl	155	yellow	$C_{14}H_{12}N_2OS$	11.09	10.93
Phenyl	*m*-Hydroxyphenyl	158	white	$C_{14}H_{12}N_2OS$	11.08	10.93
Phenyl	*o*-Methoxyphenyl	145	white	$C_{15}H_{14}N_2OS$	10.54	10.37
Phenyl	*p*-Methoxyphenyl	84	white	$C_{15}H_{14}N_2OS$	10.36	10.37
Phenyl	*p*-Nitrophenyl	109	pale yellow	$C_{14}H_{11}N_3O_2S$	14.66	14.73
Phenyl	*p*-Acetamidophenyl	187	white	$C_{16}H_{15}N_3OS$	14.19	14.14
Phenyl	*p*-Succinylamino-phenyl	176	white	$C_{18}H_{17}N_3O_3S$	11.88	11.83
Phenyl	*p*-Dimethylamino-phenyl	125	red	$C_{16}H_{17}N_3S$	14.68	14.83
Phenyl	1-Naphthyl	126	white	$C_{18}H_{14}N_2S$	9.74	9.65
Phenyl	2-Naphthyl	132	white	$C_{18}H_{14}N_2S$	9.76	9.65
Phenyl	2-Quinolyl	138	white	$C_{17}H_{13}N_3S$	14.10	14.42
Phenyl	8-Quinolyl	159	white	$C_{17}H_{13}N_3S$	14.14	14.42
Phenyl	1-Phenyl-pyrryl (2)	118	white	$C_{18}H_{15}N_3S$	13.88	13.76
o-Hydroxyphenyl	*p*-Acetamidophenyl	195	white	$C_{16}H_{15}N_3O_2S$	13.50	13.41
o-Hydroxyphenyl	8-Quinolyl	180	white	$C_{17}H_{13}N_3OS$	13.89	13.68
p-Methoxyphenyl	*p*-Acetamidophenyl	172	white	$C_{17}H_{17}N_3O_2S$	12.94	12.84
p-Acetamidophenyl	*p*-Acetamidophenyl	160 (d.)	yellow	$C_{18}H_{18}N_4O_2S$	15.61	15.81
Benzyl	Phenyl	140	white	$C_{15}H_{14}N_2S$	10.95	11.02
Benzyl	*p*-Methoxyphenyl	152	white	$C_{16}H_{16}N_2OS$	9.76	9.85
Benzyl	2,4-Dichlorophenyl	152	white	$C_{15}H_{12}Cl_2N_2S$	8.80	8.66
Benzyl	*p*-Nitrophenyl	171	pale yellow	$C_{15}H_{13}N_3O_2S$	14.13	14.04
Benzyl	*p*-Acetamidophenyl	207	white	$C_{17}H_{17}N_3OS$	13.20	13.50
Benzyl	*o*-Carboxyphenyl	167	white	$C_{16}H_{14}N_2O_2S$	9.56	9.40
Benzyl	1-Naphthyl	160	white	$C_{19}H_{16}N_2S$	9.36	9.21
Benzyl	2-Furyl	98	white	$C_{13}H_{12}N_2OS$	11.55	11.47
2-Furyl	2-Furyl	138	yellow	$C_{10}H_8N_2O_2S$	12.60	12.72
2-Furyl	*p*-Acetamidophenyl	197	yellow	$C_{14}H_{13}N_3O_2S$	14.63	14.63
2-Thienyl	2-Thienyl	138	yellow	$C_{10}H_8N_2S_3$	11.27	11.11
2-Thienyl	*p*-Acetamidophenyl	205	yellow	$C_{14}H_{13}N_3OS_2$	13.89	13.86
2-Pyrryl	2-Quinoxalyl	250 (d.)	brownish yellow	$C_{14}H_{11}N_5S$	24.84	24.90

No reaction could be induced between this compound and hydrogen sulfide, but with potassium xanthate *a*-ethylxanthylbenzalazine was formed:

$$C_6H_5C(S-CS-OC_2H_5)=N-N=CHC_6H_5$$

It was expected that this compound would be split by ammonia with formation of benzaldehyde-thiobenzhydrazone, but no reaction took place. With hydrazine it reacted rapidly with formation of hydrogen sulfide and diphenyldihydrotetrazine; no thiohydrazide could be isolated.

An excess of carboxymethyl dithioate generally leads to formation of a thiadiazole, but in two cases we obtained dithioacylated hydrazines, *viz.* in

the reaction between hydrazine and carboxymethyl *o-iso*butoxydithiobenzoate or *o*-pentyloxydithiobenzoate.

With the purpose of testing them for antibacterial activity, a number of thioacylhydrazones were prepared by condensation of thiohydrazides with aldehydes in aqueous-alcoholic solution [2]. These hydrazones are listed in Table 2.

EXPERIMENTAL

2-Furanthiocarboxhydrazide. a. From carboxymethyl 2-furancarbodithioate. Carboxymethyl 2-furancarbodithioate (2.0 g) was dissolved in 1 N NaOH (10 ml, 1 equiv.) + 10 ml of water. The solution was cooled in ice and hydrazine hydrate (0.5 g, 1 equiv.) was added. The product separated almost immediately and the orange colour of the solution disappeared. A little 1 N HCl was added to bring the pH to 5—6, and the mixture was kept in ice for one hour. The product was then filtered off, washed with water and dried. The crude product (1.15 g) was recrystallised from benzene, yielding 0.75 g (55 %) of colourless crystals with m.p. 128—29°C. After an additional recrystallisation the compound was pure, m.p. 132—133°C.

Most of the other thiohydrazides shown in Table 1 were prepared in the same way. In two cases, *viz.* the *o*-methylthiobenzhydrazide and the *a*-thionaphthoic hydrazide, the reaction between hydrazine and the carboxymethyl ester was rather slow, 1—2 h being needed. In all the other cases the reaction took place in 1—2 min as seen from the disappearance of the colour of the carboxymethylester and the precipitation of the product.

Phenylthioacethydrazide is rather unstable, and prolonged heating should be avoided during recrystallisation. The compound decomposes in a few months when kept at room temperatur (see No. VI of this series).

b. From furfural. A solution of furfural (10 g) in ethanol (30 ml) is heated to 60°C and 44 ml of a solution of ammonium disulfide, prepared according to the directions of Bost and Shealy [11], are added. The solution is heated to boiling for 10 min, decanted from a precipitate and cooled in ice. After addition of 50 ml of ether, concentrated hydrochloric acid is added with stirring until all the dithioacid has been liberated. The dark red ethereal solution is separated and washed with water and then several times with an aqueous solution of hydrazine hydrate (*ca.* 10 %), totalling about 50 ml. The strongly red-brown coloured solutions of the hydrazinium salt are combined and kept for ½—1 h, in the course of which time the colour of the solution fades and a greyish, crystalline product separates. The solution is acidified with acetic acid and filtered. The thiohydrazide is recrystallised from benzene or from water with the addition of active carbon. The thiohydrazide is rather soluble in boiling water, only slightly in cold water. Yield 5.5 g (40 %).

In the same way were prepared (from 10 g of the aldehyde): 4-hydroxythiobenzhydrazide (3.6 g; 26 %), 3-hydroxythiobenzhydrazide (1.2 g; 9 %), 4-acetamidothiobenzhydrazide (0.7 g; 6 %) and 2-thiophenethiocarboxhydrazide (8.0 g; 56 %). No thiohydrazide could be prepared in this way from benzaldehyde, *p-iso*propylbenzaldehyde, *o*-alkoxybenzaldehydes, chlorobenzaldehydes, cinnamic aldehyde, pyridine aldehydes, quinoline aldehydes, *etc.*

o-*Hydroxythiobenzhydrazide.* a. From carboxymethyl *o*-hydroxydithiobenzoate. Attempts to prepare this compound in the same way as furanthiocarboxhydrazide gave an almost quantitative yield of 2,5-di-(*o*-hydroxyphenyl)-1,3,4-thiadiazole (see No. VI of this series). The following procedure was used for the preparation of *o*-hydroxythiobenzhydrazide:

Carboxymethyl *o*-hydroxydithiobenzoate (1.0 g) was dissolved in 1 N NaOH (4.4 ml. 1 equiv.) and water (10 ml). The solution was cooled in ice and added with stirring to hydrazine hydrate (0.44 g, 2 equiv.). The thiohydrazide separated immediately and the mixture became colourless. The pH was brought to 6 with dilute hydrochloric acid and the solution was extracted with ether. The ethereal solution was dried (Na_2SO_4) and the ether removed *in vacuo*. The residue was recrystallised from benzene-light petroleum (b.p. 60—100°C), giving 0.50 g (67 %) of salicylic thiohydrazide, m.p. 95—97°C. After two additional recrystallisations the compound was pure, m.p. 101—102°C.

b. From salicylaldehyde. A solution of hydrazinium 2-hydroxydithiobenzoate, prepared from salicylaldehyde in the same way as described for the dithiofuroate, does not separate crystals because the thiohydrazide is rather soluble in water (on prolonged standing a precipitate consisting of various transformation products of the thiohydrazide separates). After ½ h the solution was acidified with acetic acid and extracted with ether. The thiohydrazide left after evaporation of the ether was recrystallised as above or from tepid water, from which it separates as large colourless crystals. Yield *ca.* 2 g from 10 g salicylaldehyde (14 %).

In the same way 3-methoxy-4-hydroxythiobenzhydrazide was prepared from vanillin.

o-*Methylthiobenzhydrazide.* This hydrazide was obtained as an oil which could not be brought to crystallisation. When the crude thiohydrazide (from 2.26 g of carboxymethyl dithio-*o*-toluate) was treated with benzaldehyde (0.8 g) in ethanol-water 1.9 g (75 %) of the benzylidene derivative was obtained. Two recrystallisations from petroleum ether gave the pure compound as yellow crystals, m.p. 63—65°C. (Found: C 70.80; H 5.21; N 11.03; Calc. for $C_{15}H_{14}N_2S$: C 71.00; H 5.56; N 11.02.)

Thiopivalic hydrazide. Methyl dithiopivaloate (1.0 g) was dissolved in methanol (5 ml). and hydrazine hydrate (0.35 ml) was added. Methanethiol was formed at once, and after 5 min the yellow colour of the dithioester had disappeared. The solvent was removed *in vacuo*, leaving an oil which crystallised on scratching. The product was stirred with water, the pH was brought to 6 with dilute hydrochloric acid, and the crystals were filtered off and recrystallised from petroleum ether. Yield 0.53 g (60 %). This thiohydrazide is rather soluble in water.

The benzylidene derivatives was obtained from thiopivalic hydrazide (0.2 g) dissolved in 1 N hydrochloric acid (5 ml) and a solution of benzaldehyde (0.15 g) in ethanol (5 ml). The compound separated as an oil which crystallised on cooling (0.31 g, 93 %); it was recrystallised from ethanol-water and then from petroleum ether. Colourless crystals, m.p. 100—102°C. (Found: C 65.40; H 7.40; N 12.52. Calc. for $C_{12}H_{16}N_2S$: C 65.50; H 7.35; N 12.72).

Thiobenzhydrazide from methyl dithiobenzoate. Methyl dithiobenzoate (1.0 g) was dissolved in methanol (10 ml), and hydrazine hydrate (0.3 g) was added. After 15 min at room temperature the red colour of the dithioester had disappeared, and the solution smelled strongly of methanethiol. On addition of water and cooling, the thiohydrazide separated as colourless crystals (0.62 g, 70 %).

When ethyl dithiobenzoate was used the reaction was slower and only a 39 % yield of thiobenzhydrazide was obtained. The products were identical with thiobenzhydrazide prepared from carboxymethyl dithiobenzoate (m.p. 72—73°C).

*N,N'-Di-(*o-iso*butyloxythiobenzoyl)hydrazine* and *N,N'-di(*o-*pentyloxythiobenzoyl)-hydrazine.* In attempts to prepare the hydrazides of *o-iso*butyloxythiobenzoic acid and *o*-pentyloxythiobenzoic acid from the carboxymethyl dithioates the hydrazides separated as colourless oils; the reaction mixture was left in an ice box for crystallisation. In the course of three weeks most of the oily products were transformed into intensively yellow crystals, which were separated and recrystallised from ethanol and hexane. Analyses show that these compounds are the dithioacylated hydrazines. (*Iso*butyloxy derivative, Found: C 63.58; H 6.73; N 6.68; S 15.16. Calc. for $C_{22}H_{28}N_2O_2S_2$: C 63.44; H 6.78; N 6.73; S 15.38. Pentyloxy derivative, Found: C 65.30; H 7.13; N 6.64. Calc. for $C_{24}H_{32}N_2O_2S_2$: C 64.84; H 7.26; N 6.30).

a-Ethylxanthylbenzalazine. *a*-Chlorobenzalazine [12] (4.6 g) and potassium xanthate (6.3 g) were dissolved in ethanol (10 ml) and refluxed for 5 h. The solution was filtered hot from the potassium chloride formed in the reaction and cooled in ice. Yield: 4.5 g of colourless crystals which were recrystallised from ethanol-water (4:1). M.p. 80—81°C. (Found: C 61.93; H 4.97, S 19.58, EtO 13.57. Calc.: C 62.14, H 4.91, S 19.51, EtO 13.72)

The compound was recovered unchanged after refluxing an ethanolic ammoniacal solution of it for several hours Addition of hydrazine to an alcoholic solution at room temperature resulted in formation of hydrogen sulfide and diphenyldihydrotetrazine (m.p. 156—157°C; formation of red diphenyltetrazine on exposure to air).

REFERENCES

1. Holmberg, B. *Arkiv Kemi, Mineral. Geol.* **17 A** (1943) No. 23.
2. Jensen, K. A. and Jensen, C. L. *Acta Chem. Scand.* **6** (1952) 957.
3. Profft, E., Schneider, F. and Beyer, H. *J. prakt. Chem.* [4] **2** (1955) 166.
4. Junghahn, A. *Ber.* **31** (1898) 312.
5. McMillan, F. H., Leonard, F., Meltzer, R. I. and King, J. A. *J. Am. Pharm. Assoc.* **42** (1953) 457.
6. Galat, A. and Elion, G. *J. Am. Chem. Soc* **65** (1943) 1566.
7. Pinner, A. *Ann.* **297** (1897) 256.
8. Wuyts, A. and Lacourt, A. *Bull. soc. chim. Belges* **45** (1936) 685.
9. Nori Sugimoto and Susumu Shigematsu *Jap. Pat.* 7481 (1954); *Chem. Abstr.* **50** (1956) 4236.
10. Zemplén, G., Mester, L. and Messmer, A. *Chem. Ber.* **86** (1953) 697.
11. Bost, R. W. and Shealy, O. L. *J. Am. Chem. Soc.* **73** (1951) 25.
12. Stollé, R. *J. prakt. Chem.* [2] **85** (1912) 386.
13. Stollé, R. and Helwerth, Fr. *Ber.* **47** (1914) 1135.

Received January 23, 1961.

ACTA CHEMICA SCANDINAVICA 15 (1961) 1104–1108

Studies of Thioacids and Their Derivatives

IV. On 1,2,3,4-Thiatriazoles

KAI ARNE JENSEN and CHRISTIAN PEDERSEN

Chemical Laboratory of the University of Copenhagen, Copenhagen, Denmark

Aromatic and heterocyclic thiohydrazides react with nitrous acid to give compounds which according to their infrared spectra and chemical reactions are thiatriazoles and not thioazides. The same compounds can, in most cases, also be obtained by reaction of carboxymethyl dithioates with sodium azide.

Few compounds containing the 1,2,3,4-thiatriazole ring have hitherto been described in the literature (Freund *et al.*[1], Oliveri-Mandalà [2]). In 1952 Crossland, in this laboratory, observed (unpublished) that the sodium salt of carboxymethyl dithiobenzoate reacted with sodium azide in aqueous solution to form a compound with the composition $C_6H_5CSN_3$, which was shown by its infrared spectrum not to be an azide and therefore probably was the isomeric thiatriazole.

This reaction has proved to be a rather general one. We have tried the reaction of all the carboxymethyl dithioates we have prepared with sodium azide. Most of the dithioates reacted well with sodium azide at room temperature (approximate reaction times are given in Table 1) with formation of the corresponding thiatriazoles:

$$RCSSCH_2COO^- + N_3^- \rightarrow RCSN_3 + {}^-SCH_2COO^-$$

In most cases good yields were obtained (Table 1, Method 1, see also the experimental part). Some of the dithioates did not react with sodium azide after several days of standing at room temperature (see further below).

In a number of cases the same compounds were prepared by the reaction of thiohydrazides with nitrous acid (Table 1, Method 2):

$$RCSNHNH_2 + HONO \rightarrow RCSN_3 + 2\ H_2O$$

This reaction seems to be the most general one since it gives thiatriazoles in some cases where the dithioates do not react with sodium azide, *viz.* *o*-hydroxyphenyl-, *a*-naphthyl-, 2-pyrryl-, and 3-indolyl-1,2,3,4-thiatriazole.

Table 1. 1,2,3,4-Thiatriazoles, R—C(=N—N)—S—N

R	Yield %		M.p. °C	Formula	Analyses					
					Carbon		Hydrogen		Nitrogen	
	Dithio-ester + NaN_3	Thiohydrazide +HONO			Found	Calc.	Found	Calc.	Found	Calc.
Phenyl [a,b]	80 (24 h)	65	95— 96	$C_7H_5N_3S$					25.76	25.75
o-Tolyl [c]	56 (72 h)		45— 46	$C_8H_7N_3S$	53.85	54.21	4.26	3.98	24.08	23.71
p-Tolyl [d]	95 (24 h)		97— 98	$C_8H_7N_3S$	54.15	54.21	3.92	3.98	23.74	23.70
p-Hydroxyphenyl [e]		88	152—153	$C_7H_5N_3OS$	47.00	46.91	2.88	2.81	23.86	23.45
o-Methoxyphenyl [d]	77 (24 h)		104—105	$C_8H_7N_3OS$	49.85	49.72	3.78	3.65	21.82	21.75
p-Methoxyphenyl [d]	90 (60 h)		104—105	$C_8H_7N_3OS$	49.85	49.72	3.65	3.65	21.90	21.75
m-Chlorophenyl [a,d]	75 (1 h)		83— 85	$C_7H_4ClN_3S$	42.90	42.53	2.50	2.04	21.50	21.26
p-Chlorophenyl [c]	82 (24 h)		101—102	$C_7H_4ClN_3S$	42.60	42.53	2.12	2.04	21.46	21.26
m-Nitrophenyl [b]	66 (½ h)		95— 97	$C_7H_4N_4O_2S$	40.55	40.38	1.93	1.94	27.20	26.92
p-Acetamidophenyl [f]	83 (60 h)		141—142	$C_9H_8N_4OS$	49.30	49.07	3.70	3.66	25.30	25.44
α-Naphthyl [a]	traces	75	46— 47	$C_{11}H_7N_3S$	62.10	61.95	3.40	3.31	19.95	19.71
β-Naphthyl [b]	50 (24 h)	70	96— 97	$C_{11}H_7N_3S$	61.95	61.95	3.37	3.31	19.97	19.71
2-Furyl [a]	43 (3-4 h)	83	63— 64	$C_5H_3N_3OS$	39.00	39.21	1.95	1.97	27.44	27.44
2-Thienyl [d]	67 (72 h)	95	100—102	$C_5H_3N_3S_2$	35.68	35.49	1.93	1.78	24.90	24.84
2-Pyrryl [b]		83	130—131	$C_5H_4N_4S$	39.16	39.46	2.79	2.65	36.74	36.82
3-Indolyl [b]		83	135—136	$C_9H_6N_4S$	53.80	53.45	3.22	2.99	27.73	27.71

Solvents used for recrystallisation: a) ethanol-water; b) benzene-light petroleum (b.p. 60—100°C); c) ether-light petroleum (b.p. 40—60°C); d) light petroleum (b.p. 60—100°C); e) ethanol; f) acetone-water.

The evidence for the structure proposed by Freund *et al.* for the compounds obtained by nitrosation of thiosemicarbazides has hitherto not been quite unambiguous, the possibility that these compounds are azides not being definitely excluded. In fact Oliveri-Mandalà considered the compounds he prepared to be azides (I):

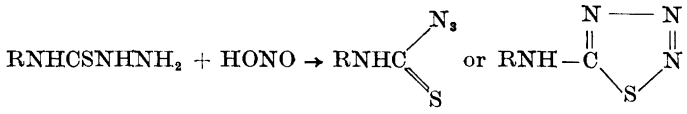

I II

That this possibility has to be considered seriously is shown by the observation that after reaction of aminoguanidines with nitrous acid often both tetrazoles and the isomeric azides can be isolated (Thiele [3], Jensen and Pedersen [4]).

To decide between the two structures I or II we have studied the infrared spectra of six of the compounds. In all cases these showed complete absence of the characteristic azide band in the 4.5—5 μ range [5]. This eliminates structure I for our compounds and probably also for the compounds of Freund *et al.* For comparison we also took infrared spectra of the nitrosation products of thiosemicarbazide and aminoguanidinium nitrate. The thiosemicarbazide product has no azide band, in accordance with formula II, whereas "diazoguanidinium nitrate", to which Thiele [3] has ascribed the structure III, had a strong band at 4.66 μ. After the completion of this work three papers by Lieber [6] have appeared, confirming structure II for the thiosemicarbazide nitrosation product by infrared and degradative studies.

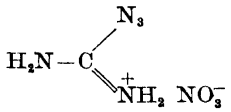

III

The thiatriazoles do not give colour reaction with iron(III) chloride and are not reduced by hydrogen sulfide, in contrast to the behaviour of azides. Furthermore these compounds do not have thioacylating properties. Thioazides have been proposed as thioacylating agents, but attempts to prepare them were unsuccesful (Mc Omie [7]). It now seems certain that the reactions attempted will only give thiatriazoles without thioacylating properties.

Most of the thiatriazoles prepared were stable at room temperature, but decomposed vigorously when heated to the melting point (and in some cases already during recrystallisation) with formation of a nitrile, sulfur, and nitrogen (see the experimental part). This is in agreement with the finding of Freund and Lieber *et al.* and also does not support structure I, which on heating might be expected to give an *iso*thiocyanate in accordance with the well known behaviour of the corresponding oxygen compounds.

In no cases could thiatriazoles with aliphatic substituents be prepared. Potassium dithioformate and carboxymethyl dithioacetate did not react with sodium azide. Thiopivalic hydrazide, which is the only known aliphatic thiohydrazide (*cf.* Paper No. III of this series), gave an oil on reaction with nitrous acid. This is probably the 5-*tert*-butyl-1,2,3,4-thiatriazole; it is, however, very unstable and decomposes in a few minutes at 0°C with nitrogen evolution and formation of sulfur. Reaction of thiophenylacethydrazide, and thio-β-phenylpropionic hydrazide with nitrous acid also gave oily products which decomposed rapidly. Carboxymethyl dithiophenylacetate and dithio-β-phenylpropionate did not react with sodium azide. Thiosalicylic hydrazide on reaction with nitrous acid gave a solid of melting point 86—88°C (decomp.), it was, however, too unstable to be purified. Carboxymethyl dithiosalicylate reacted slowly with sodium azide with evolution of gas.

EXPERIMENTAL

1,2,3,4-Thiatriazoles from carboxymethyl dithioates and sodium azide

5-Phenyl-1,2,3,4-thiatriazole. Carboxymethyl dithiobenzoate (2.1 g, 0.01 mole) was dissolved in 1 equiv. (10 ml) of 1 N NaOH, and a solution of sodium azide (1.3 g, 0.02 mole) in 10 ml of water was added. After 15 min crystals began to separate, and after 24 h at room temperature the red colour of the carboxymethyl ester had disappeared. The product was filtered off and washed with water. Colourless crystals, yield: 1.3 g (80 %), m.p. 94—95°C. After two recrystallisations from benzene-light petroleum (b.p. 60—100°C) the product was pure. The compound could also be obtained from methyl dithiobenzoate and sodium azide. It is insoluble in water and in aqueous solutions of strong acids or bases and reacts neither with methyl iodide nor with bromine.

In this way all the reactions between carboxymethyl dithioesters and sodium azide were performed. In a few cases it was necessary to add more water to prevent separation of the sodium salt of the carboxymethyl ester. The completion of the reactions was easily seen from the disappearance of the colour of the carboxymethyl ester. Prolonged heating should be avoided during recrystallisations to prevent decomposition. Further data are given in Table 1.

1,2,3,4-Thiatriazoles from thiohydrazides and nitrous acid

5-Phenyl-1,2,3,4-thiatriazole. Thiobenzhydrazide (0.5 g) was dissolved in 7.2 ml (2 equiv.) of 1 N hydrochloric acid. The solution was cooled in ice and stirred, and a solution of 0.25 g (1.1 equiv.) of sodium nitrite in 5 ml of water was added during 5 min. The product separated immediately and was filtered off and washed with water. Recrystallisation from ethanol-water gave 0.35 g (65 %), m.p. 92—94°C.

The same procedure was used in all the other cases where thiatriazoles were prepared from thiohydrazides (Table 1).

Formation of nitriles

p-*Hydroxybenzonitrile.* 5-(*p*-Hydroxyphenyl)-1,2,3,4-thiatriazole (0.46 g) was added in portions to a test tube, which was kept at 150°C in an oil bath. Each addition caused a vigorous evolution of nitrogen. The product was recrystallised from benzene-light petroleum (b.p. 60—100°C) giving 0.24 g (78 %) of colourless crystals with m.p. 103—

106°C. After three additional recrystallisations pure *p*-hydroxybenzonitrile was obtained, m.p. 107—109°C (lit.[8] 113°C). (Found: C 70.40; H 4.20; N 11.62. Calc. for C_7H_5NO: C 70.58; H 4.23; N 11.76).

p-*Acetamidobenzonitrile*. 5-(*p*-Acetamidophenyl)-1,2,3,4-thiatriazole (0.19 g) was heated to 190°C for *ca.* 10 min, until the nitrogen evolution had ceased. The product was recrystallised from water. Yield 0.08 g (58 %), m.p. 201—202°C. An additional recrystallisation gave pure *p*-acetamidobenzonitrile, m.p. 202—203°C (lit.[9] 200°C). (Found: C 67.40; H 4.99; N 17.88. Calc. for $C_9H_8N_2O$: C 67.48; H 5.04; N 17.49).

p-*Methoxybenzonitrile*. 5-(*p*-Methoxyphenyl)-1,2,3,4-thiatrazole (0.35 g) was added in portions to a test tube kept at 130°C in an oil bath. The residue was recrystallised from light petroleum (b.p. 60—100°C) giving 0.16 g (66 %) of colourless crystals with m.p. 54—56°C. Two more recrystallisations provided an analytical sample, m.p. 61—62°C (lit.[10] 59—61°C). (Found: C 72.20; H 5.45; N 10.49. Calc. for C_8H_7NO: C 72.16; H 5.30; N 10.52).

Benzonitrile (isolated as thiobenzamide). 5-Phenyl-1,2,3,4-thiatriazole (1 g) was decomposed at 130°C as described above. The product was dissolved in 1 ml of pyridine + 1 ml of triethylamine. Hydrogen sulfide was passed through the solution for 2 h, and the mixture was then kept overnight. Addition of dilute hydrochloric acid precipitated a yellow solid, which, after two recrystallisations from benzene-light petroleum (b.p. 60—100°C) gave 0.45 g (54 %) of thiobenzamide with m.p. 115—117°C. The mixed melting point with an authentic sample of thiobenzamide showed no depression.

REFERENCES

1. Freund, M. and Hempel, H. *Ber* **28** (1895) 74; Freund, M. and Schwarz, H. P. *Ber.* **29** (1896) 2491; Freund, M. and Schander, A. *Ber.* **29** (1896) 2500.
2. Oliveri Mandalà, E. *Gazz. chim. ital.* **44** (1914) 670.
3. Thiele, J. *Ann* **270** (1892) 54.
4. Jensen, K. A. and Pedersen, Chr. *Acta Chem. Scand.* **15** (1961) 991.
5. Lieber, E., Rao, C. N. R., Chao, T. S. and Hoffman, C. W. W. *Anal. Chem.* **29** (1957) 916.
6. Lieber, E., Rao, C. N. R., Pillai, C. N., Ramachandran, J. and Hites, R. D. *Can. J. Chem.* **36** (1958) 801; Lieber, E., Oftedahl, E., Pillai, C. N. and Hites, R. D. *J. Org. Chem.* **22** (1957) 441; Lieber, E. and Pillai, C. N. *J. Org. Chem.* **22** (1957) 1054.
7. Mc Omie, J. F. N. *Ann. Repts. on Progr. Chem. (Chem. Soc. London)* **45** (1948) 198.
8. Hartmann, O. *J. prakt. Chem.* [2] **16** (1877) 54.
9. Bogert, M. T. and Kohnstam, L. *J. Am. Chem. Soc.* **25** (1903) 478.
10. Bamberger, E. and Pemsel, W. *Ber.* **36** (1903) 370.

Received January 23, 1961.

ACTA CHEMICA SCANDINAVICA 15 (1961) 1109–1123

Studies of Thioacids and Their Derivatives

V. *N*-Substituted Thiohydrazides

KAI ARNE JENSEN, HANS RUEDI BACCARO, OLE BUCHARDT, GERT E. OLSEN, CHRISTIAN PEDERSEN and JENS TOFT

Chemical Laboratory of the University of Copenhagen, Copenhagen, Denmark

A large number of new thiohydrazides derived from mono-and dialkylhydrazines have been prepared. It is generally not possible to prepare thiohydrazides of the type RCSNR′NH_2 when the radical R′ is an aryl radical or a secondary or tertiary aliphatic radical; in these cases only thiohydrazides of the type RCS–NHNHR′ are formed. As a consequence of this rule, symmetric dialkyl hydrazines, R′NH–NHR′, do not react with carboxymethyl dithioates when the radical R′ is secondary or tertiary. Symmetric dialkylhydrazines with primary radicals react without difficulty, and asymmetric dialkylhydrazines, R'_2NNH_2, react in all cases with carboxymethyl dithioates. Monoalkylhydrazines with a primary alkyl group yield generally a mixture of the two isomeric thiohydrazides, but the N^2-alkylthiohydrazide, RCS–NHNHR′, is formed almost exclusively when R = *tert*-butyl.

With the exception of N^1- and N^2-methylthiobenzhydrazides, *N*-alkylthiohydrazides were hitherto unknown. They may in general be prepared in the same way as the unsubstituted thiohydrazides by reaction of carboxymethyl dithioates with the free hydrazine. Apart from certain symmetric dialkylhydrazines, the hydrazines are not less reactive than hydrazine itself.

Wuyts [1] prepared some *N*-arylthiohydrazides by heating a mixture of an arylhydrazine with a dithioacid, but in this reaction also hydrazones are formed, often as the only isolable products. Some thioformylarylhydrazines have been prepared by Baker *et al.*[2] and by Sato and Ohta [3]. In a few cases Wuyts [4] also tried the reaction of dithioacids with methylhydrazine and obtained the arylhydrazone of an N^1-methylthiohydrazide.

An *N*-methylthiobenzhydrazide was prepared by Jensen and Miquel [5], who considered their product to be N^2-methylthiobenzhydrazide because it forms an innercomplex nickel compound. It was, however, pointed out by Holmberg [6] and by Bähr and Schleitzer [7], that this thiohydrazide must be the N^1-methylthiohydrazide (I) because it has no acid character. This is very remarkable from a complex-chemical point of view, because from our experiences

with thiosemicarbazides [8] only compounds with a potential HS-group would be expected to form innercomplex compounds. We even considered the possibility of an isomerisation of the methylthiobenzhydrazide during complex formation; but the methylthiobenzhydrazide isolated from nickel complex was shown to be identical with the starting material (m.p. 91—92°C, mixed m.p. 90—92°C).

Holmberg [9] prepared the isomeric N^2-methylthiobenzhydrazide (II) by hydrolysis of the reaction product of *l*-arabinose-thiobenzhydrazone with

Table 1. Comparison of yields (%) of N^1- and N^2-alkyl (or aryl) thiohydrazides, RCS—NR'NH_2 and RCS—NHNHR', formed in the reaction between dithioates and monoalkyl- or monoarylhydrazines. Numbers in parenthesis: The compounds were isolated in a crystalline state, but in such small amounts that no purification was attempted. In the cases where the yield is given as ~0, the ethereal solution became turbid with hydrogen chloride and a minute amount of an oil separated, but it is uncertain whether this contained the isomeric thiohydrazide or other by-products.

R / R'		Methyl	*Iso*-propyl	*tert*-Butyl	Benzyl	β-Phenylethyl	Phenyl	*p*-Tolyl	2-Furyl
Methyl	N^1	65	53	~0	77		82	87	93
	N^2	0	35	42	14		10	(5)	~ 0
Ethyl	N^1						43		
	N^2						32		
Propyl	N^1						60		
	N^2						34		
*Iso*propyl	N^1				0		(2)		0
	N^2				87		90		76
Butyl	N^1	72			50	51	66	70	82
	N^2	~ 0			47	36	17	(12)	~ 0
*Iso*butyl	N^1						25		
	N^2						63		
sec-Butyl	N^1				0		0		0
	N^2						70		
tert-Butyl	N^1	~ 0					0		
	N^2	77					94		
Hexyl	N^1		(3)	(0.8)	(14)		44	16	
	N^2		37	59	59		48	56	
*Cyclo*hexyl	N^1	0			0		0		0
	N^2	82			73		85		78
Benzyl	N^1	69	(9)	8	(20)		22		52
	N^2	18	25	58	68		72		37
α-Phenylethyl	N^1			0			0		
	N^2			74			97		
β-Phenylethyl	N^1	43			17		41		
	N^2	18			52		34		
γ-Phenylpropyl	N^1						29		
	N^2						65		
Phenyl	N^1	0			0		0		0
	N^2	57			90		96		83

Table 2. N^1-Alkylthiohydrazides, R—CSNR′NH_2.

R	R′	Yield %	M.p., °C	Formula	Analyses					
					Carbon		Hydrogen		Nitrogen	
					Found	Calc.	Found	Calc.	Found	Calc.
Methyl	Methyl	65	79 – 80	$C_3H_8N_2S$	34.50	34.50	7.70	7.74	26.78	26.90
Methyl	Butyl	72	120 – 121	$C_6H_{14}N_2S.HCl$					15.17	15.32
Methyl	Benzyl	69	64 – 65	$C_9H_{12}N_2S$	60.00	59.98	6.89	6.71	15.70	15.55
Methyl	β-Phenylethyl	43	81 – 82	$C_{10}H_{14}N_2S$	61.90	61.83	7.32	7.27	14.34	14.42
Ethyl	Methyl	60	134 – 137	$C_4H_{10}N_2S.HCl$	30.90	31.05	7.13	7.18	18.15	18.13
*Iso*propyl	Methyl	53	170 – 172	$C_5H_{12}N_2S.HCl$	35.50	35.60	7.64	7.70		
tert-Butyl	Benzyl	8	108 – 110	$C_{12}H_{18}N_2S.HCl$	55.65	55.69	6.95	7.40		
Benzyl	Methyl	77	65 – 66	$C_9H_{12}N_2S$	60.10	60.00	6.50	6.72	15.48	15.53
Benzyl	Butyl	50	117 – 118	$C_{12}H_{18}N_2S.HCl$					10.63	10.82
Benzyl	β-Phenylethyl	17	65 – 67	$C_{16}H_{18}N_2S$	71.00	71.09	6.70	6.71	10.35	10.36
β-Phenylethyl	Butyl	51	138 – 140	$C_{13}H_{20}N_2S.HCl$					10.39	10.28
Phenyl	Methyl	82	91 – 92	$C_8H_{10}N_2S$					16.91	16.86
Phenyl	Ethyl	43	62.5 – 63	$C_9H_{12}N_2S$	60.05	59.98	6.76	6.71	15.32	15.55
Phenyl	Propyl	60	46 – 47	$C_{10}H_{14}N_2S$					14.57	14.42
Phenyl	Butyl	66	115 – 118	$C_{11}H_{16}N_2S.HCl$					11.28	11.43
Phenyl	*Iso*butyl	25	157 – 159	$C_{11}H_{16}N_2S.HCl$					11.58	11.43
			57 – 58	$C_{11}H_{16}N_2S$					13.57	13.45
Phenyl	Hexyl	44	137 – 140	$C_{13}H_{20}N_2S.HCl$					10.42	10.27
Phenyl	Benzyl	22	85.5 – 86	$C_{14}H_{14}N_2S$	69.40	69.40	6.00	5.83	11.57	11.56
Phenyl	β-Phenylethyl	41	66 – 67	$C_{15}H_{16}N_2S$	70.25	70.29	6.20	6.29	10.94	10.93
Phenyl	γ-Phenylpropyl	29	146 – 148	$C_{16}H_{18}N_2S.HCl$					9.24	9.13
p-Tolyl	Methyl	87	92 – 92.5	$C_9H_{12}N_2S$	59.90	59.98	6.72	6.71	15.52	15.55
p-Tolyl	Butyl	70	123 – 126	$C_{12}H_{18}N_2S.HCl$					10.89	10.82
p-Tolyl	Hexyl	16	57 – 57.5	$C_{14}H_{22}N_2S$	67.20	67.17	8.98	8.86	11.07	11.19
o-Hydroxyphenyl	Hexyl	83	123 – 124	$C_{13}H_{20}N_2OS$					11.10	11.10
p-Hydroxyphenyl	Methyl	70	116 – 117	$C_8H_{10}N_2OS$	52.90	52.74	5.55	5.53	15.50	15.38
p-Butoxyphenyl	Allyl	50	76 – 77	$C_{14}H_{20}N_2OS$					10.82	10.61
p-Butoxyphenyl	Propyl	70	57 – 58	$C_{14}H_{22}N_2OS$					10.51	10.53
p-Butoxyphenyl	Butyl	65	52 – 53	$C_{15}H_{24}N_2OS$					10.05	10.00
2-Furyl	Methyl	93	142 – 144	$C_6H_6N_2OS.HCl$	37.20	37.40	4.73	4.72	14.52	14.53
2-Furyl	Butyl	82	134 – 137	$C_9H_{14}N_2OS.HCl$					11.77	11.93
2-Furyl	Benzyl	52	80 – 81	$C_{12}H_{12}N_2OS$	62.20	62.06	5.31	5.21	12.02	12.06

formaldehyde. We have found that this isomer is formed in 5—10 % yield together with N^1-methylthiobenzhydrazide in the reaction between methylhydrazine and carboxymethyl dithiobenzoate or methyl dithiobenzoate.

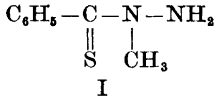

I

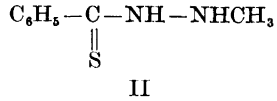

II

Methylhydrazine also reacts with most other carboxymethyl dithioates with predominant formation of N^1-methylthiohydrazides. In some cases, however, it was shown that the N^2-isomer is formed as a by-product, and methyl dithiopivaloate forms the N^2-isomer almost exclusively (Table 1).

All the N^1-methylthiohydrazides are obtained in crystalline form, but the reaction of carboxymethyl dithioates with higher monoalkylhydrazines in most cases results in the formation of oils. This is partly due to the fact that a mixture of the two isomeric hydrazides is formed, but it also seems that many of the N^2-alkylthiohydrazides with primary alkyl groups actually are liquids at room temperature. Even N^2-methylthiobenzhydrazide could not be induced to crystallise. In some cases these hydrazides crystallised by cooling below zero, but melted again beneath room temperature. Alkylthiobenzhydrazides with substituents in the *para*-position in the benzene nucleus are more liable to crystallise than the unsubstituted thiobenzhydrazides; this is the reason why some *p*-methyl- and *p*-butoxythiobenzhydrazides were prepared (Table 2). In most cases, however, crystalline primary alkylthiohydrazides could not be obtained directly from the reaction mixture; *N-iso*propyl-, and *N-tert*-butylthiohydrazides on the other hand crystallise readily.

The separation of the isomeric *N*-alkylthiobenzhydrazides was attained in the following way: The crude hydrazides were extracted with ether and the ether solution extracted with 1 N sodium hydroxide. From the alkaline solution the base-soluble hydrazides were set free with acetic acid and extracted with ether. The two ether solutions were dried and precipitated with dry hydrogen chloride. In most cases crystalline hydrochlorides of sufficient purity were obtained directly, so that a comparison of the yields of the two isomers could be obtained directly by weighing the crude hydrochlorides (Table 1). When crystalline thiohydrazides could be obtained from the hydrochlorides, the recrystallised thiohydrazides were analysed; in the cases where the thiohydrazide was an oil, the hydrochloride was recrystallised from ethanol or ethanol + ether.

A glance at Table 1 suffices to show that phenylhydrazine only forms N^2-substituted hydrazides. Also from *o*- and *p*-tolylhydrazine only one isomer was obtained, and Wuyts obtained from *p*-bromophenylhydrazine 71 % of N^2-*p*-bromophenylthiobenzhydrazide and 27 % of the corresponding hydrazone. It therefore seems safe to conclude that aromatic hydrazines never form N^1-arylthiohydrazides. It should be mentioned, by the way, that the formation of hydrazones by elimination of sulfur from thiohydrazides, which in many of Wuyts' experiments resulted in the predominant and often exclusive formation of hydrazones instead of hydrazides, has never been met with in our preparations of thiohydrazides from carboxymethyl dithioates.

Table 3. N^2-Alkylthiohydrazides, R—CSNHNHR′.

R	R′	Yield %	M.p., °C	Formula	Analyses					
					Carbon		Hydrogen		Nitrogen	
					Found	Calc.	Found	Calc.	Found	Calc.
Methyl	*tert*-Butyl	77	166–171	$C_6H_{14}N_2S.HCl$					15.37	15.34
			85– 86	$C_6H_{14}N_2S$					19.23	19.17
Methyl	*Cyclo*hexyl	82	90– 91	$C_8H_{16}N_2S$	55.75	55.70	9.40	9.36	16.19	16.25
Methyl	Benzyl	18	165–166	$C_9H_{12}N_2S.HCl$					12.72	12.92
Methyl	β-Phenylethyl	18	116–117	$C_{10}H_{14}N_2S.HCl$					11.76	11.63
Methyl	Phenyl	57	95–96 [a]	$C_8H_{10}N_2S$					16.80	16.86
			80–81 [a]						16.93	16.86
*Iso*propyl	Methyl	35	177–178	$C_5H_{12}N_2S.HCl$	35.70	35.60	7.65	7.70		
*Iso*propyl	Hexyl	37	120–121	$C_{10}H_{22}N_2S.HCl$					11.76	11.73
*Iso*propyl	Benzyl	25	155–156	$C_{11}H_{16}N_2S.HCl$					11.30	11.45
tert-Butyl	Methyl	42	118–120	$C_6H_{14}N_2S$	49.45	49.27	9.56	9.66	19.22	19.17
			158–160	$C_6H_{14}N_2S.HCl$					15.49	15.34
tert-Butyl	Hexyl	59	100–101	$C_{11}H_{24}N_2S.HCl$	52.25	52.25	9.90	10.01	11.19	11.08
tert-Butyl	Benzyl	58	60– 61	$C_{12}H_{18}N_2S$	64.70	64.72	8.09	8.16	12.60	12.60
tert-Butyl	α-Phenylethyl	74	190–191	$C_{13}H_{20}N_2S.HCl$	57.05	57.22	7.92	7.76	10.53	10.37
Benzyl	Methyl	14	121–122	$C_9H_{12}N_2S.HCl$					12.81	12.93
Benzyl	*Iso*propyl	87	46– 47	$C_{11}H_{16}N_2S$					13.52	13.45
Benzyl	Butyl	47	166–168	$C_{12}H_{18}N_2S.HCl$					10.66	10.82
Benzyl	Hexyl	59	140–143	$C_{14}H_{22}N_2S.HCl$					9.96	9.77
Benzyl	*Cyclo*hexyl	73	70–70.5	$C_{14}H_{20}N_2S$					11.32	11.28
Benzyl	Benzyl	68	81– 82	$C_{15}H_{16}N_2S$	70.30	70.29	6.31	6.29	10.90	10.93
Benzyl	β-Phenylethyl	52	102–103	$C_{16}H_{18}N_2S$	71.10	71.09	6.69	6.71	10.29	10.36
Benzyl	Phenyl	90	91.5–92 [b]	$C_{14}H_{14}N_2S$					11.51	11.56
β-Phenylethyl	Butyl	36	117–120	$C_{13}H_{20}N_2S.HCl$					10.37	10.28
Phenyl	Methyl	10	169–170	$C_8H_{10}N_2S.HCl$	47.50	47.45	5.41	5.48	14.05	13.83
Phenyl	Ethyl	32	50– 52	$C_9H_{12}N_2S$	60.00	59.98	6.63	6.71	15.36	15.55
Phenyl	Propyl	34	144–147	$C_{10}H_{14}N_2S.HCl$					12.30	12.16
Phenyl	*Iso*propyl	90	112–112.5	$C_{10}H_{14}N_2S$					14.55	14.42
Phenyl	Butyl	17	44– 45	$C_{11}H_{16}N_2S$					13.32	13.45
Phenyl	*Iso*butyl	63	79– 80	$C_{11}H_{16}N_2S$					13.60	13.45
Phenyl	*sec*-Butyl	70	66.5–67.5	$C_{11}H_{16}N_2S$					13.51	13.45
Phenyl	*tert*-Butyl	94	119–120	$C_{11}H_{16}N_2S$					13.58	13.45

Table 3. Continued.

R	R'	Yield %	M.p., °C	Formula	Analyses					
					Carbon		Hydrogen		Nitrogen	
					Found	Calc.	Found	Calc.	Found	Calc.
Phenyl	Hexyl	48	109–113	$C_{13}H_{20}N_2S.HCl$					10.39	10.27
Phenyl	*Cyclo*hexyl	85	106–107	$C_{13}H_{18}N_2S$	66.75	66.74	7.75	7.74	11.87	11.96
Phenyl	Benzyl	72	147–148	$C_{14}H_{14}N_2S$	69.52	69.75	5.93	5.68	11.57	11.56
Phenyl	α-Phenylethyl	97	103–104	$C_{15}H_{16}N_2S$					11.01	10.93
Phenyl	β-Phenylethyl	34	90– 91	$C_{15}H_{16}N_2S$	70.15	70.29	6 18	6.29	10.89	10.93
Phenyl	γ-Phenylpropyl	65	76–77.5	$C_{16}H_{18}N_2S$	71.00	71.09	6.70	6.71	10.28	10.36
			152–154	$C_{16}H_{18}N_2S.HCl$					9.02	9.13
Phenyl	Phenyl	96	69.5– 70 [c]	$C_{13}H_{12}N_2S$					12.38	12.27
			90– 91 [c]						12.35	12.27
Phenyl	*o*-Tolyl	83	125–127	$C_{14}H_{14}N_2S$	69.35	69.40	5,81	5.83	11.60	11.56
Phenyl	*p*-Tolyl	60	98–99 [d]	$C_{14}H_{14}N_2S$	69.35	69.40	5.81	5.83	11.59	11.56
m-Nitrophenyl	Phenyl	75	122–123	$C_{13}H_{11}N_3O_2S$	57.30	57.14	3.91	4.06	15.50	15.38
p-Tolyl	Hexyl	56	54.5– 55	$C_{14}H_{22}N_2S$	67.10	67.15	8.82	8.90	11.26	11.19
2-Furyl	*Iso*propyl	76	84– 85	$C_8H_{12}N_2OS$					15.12	15.21
2-Furyl	*Cyclo*hexyl	78	176–179	$C_{11}H_{16}N_2OS.HCl$					10.70	10.74
2-Furyl	Benzyl	37	85– 86	$C_{12}H_{12}N_2OS$	62.30	62.06	5.12	5.21	11.97	12.02
2-Furyl	Phenyl	83	107–108	$C_{11}H_{10}N_2OS$					12.70	12.84

a) Dimorphous; m.p. in lit.[1] 82°C. b) Lit.[1] 89°C. c) Dimorphous; the low-melting form is transformed into the high-melting by seeding. M.p. in lit. 88 [1], 87–88[5], and 89–90[20]°C. d) Lit.[1] 96°C.

Table 4. Benzalhydrazones of N^1-Alkylthiohydrazides,

$$R-CSN(R')-N=CHC_6H_5$$

R	R′	Yield, %	M.p., °C	Formula	Analyses					
					C		H		N	
					Found	Calc.	Found	Calc.	Found	Calc.
H	CH_3	80	82–82.5	$C_9H_{10}N_2S$	60.55	60.70	5.65	5.66	15.80	15.69
CH_3	CH_3	65	115–116	$C_{10}H_{12}N_2S$	62.35	62.50	6.36	6.29	14.42	14.56
C_2H_5	CH_3	65	37– 38	$C_{11}H_{14}N_2S$	64.15	64.20	6.95	6.85	13.55	13.58
C_6H_5	CH_3	82	127–128	$C_{15}H_{14}N_2S_4$	71.10	70.90	5.46	5.56	10.94	11.07

The different behaviour of phenylhydrazine and methylhydrazine might be ascribed to the electrophilic character of the phenyl radical. A glance at Table 1 shows, however, that the difference is rather due to a steric influence; *tert*-butylhydrazine, like phenylhydrazine, gives exclusively the N^2-isomer. Also, alkylhydrazines with a secondary alkyl group, like *cyclo*hexylhydrazine, *a*-phenylethylhydrazine, and *sec*-butylhydrazine, give exclusively, or almost exclusively, the N^2-isomer (Table 3). An N^1-isomer could only be isolated in the case of *iso*propylhydrazine, and only in minute amount. In contrast, alkylhydrazines with primary alkyl groups generally form both isomers. As mentioned above, methylhydrazine only forms a small amount of the base-soluble isomer. With the higher alkylhydrazines the two isomers were formed in amounts of the same order of magnitude. A larger primary alkyl group favours the formation of a larger amount of the N^2-isomer, but even with rather bulky alkyl groups the N^1-isomer is formed in appreciable amount (*cf.* Table 1). When R of the acid radical RCS- is a secondary or tertiary alkyl group, however, the N^2-isomer is formed almost exclusively.

Table 5. *NN*′Dialkylthiohydrazides, R–CSNR′NHR′.

R	R′	Yield, %	M.p., °C	Formula	Analyses					
					C		H		N	
					Found	Calc.	Found	Calc.	Found	Calc.
C_6H_5	CH_3	81	135–145	$C_9H_{12}N_2S.HCl$	50.15	49.90	6.06	6.06	12.66	12.92
$C_6H_5CH_2$	CH_3	57	46– 47	$C_{10}H_{14}N_2S$	62.05	61.80	7.30	7.26	14.45	14.41
C_6H_5	$C_6H_5CH_2$	40	113–114	$C_{21}H_{20}N_2S$					8.50	8.43

It is a striking consequence of the difference between primary and secondary alkylhydrazines that symmetric di-secondary-alkylhydrazines, like di-*iso*propylhydrazine and di*cyclo*hexylhydrazine, are quite unreactive towards carboxymethyl dithioates. After 24 h the dithioates could be recovered unchanged. In contrast, *NN'*-dipropylhydrazine and *NN'*-dibenzylhydrazine react in the same way as the monoalkylhydrazines.

NN'-Diphenylhydrazine (hydrazobenzene) does not react, whereas *NN*-diphenylhydrazine reacts in the normal way. *NN'*-Di-*tert*-butylhydrazine is at present unknown, but would undoubtedly be unreactive.

The effect of the acid radical on the relative amounts of the two isomers is not so clear as the effect of the alkyl group (Table 1). It should be pointed out that the numbers represent yields in actual preparations and not the results of physico-chemical measurements. Considerable variation in the yields may therefore be expected in different preparations, although duplication of the preparations in several cases showed that the yields were quite reproducible. The reaction proceeds rapidly already during adjustment of the pH of the solution or during the mixing of the solutions of the dithioate and the hydrazine, so no constancy of pH or temperature during reaction can be claimed. It is, however, evident that carboxymethyl dithioacetate is more liable to give the N^1-isomer than dithioates of higher molecular weight whereas methyl dithiopivaloate and methyl dithio*iso*butyrate show the opposite behaviour. It also seems that carboxymethyl dithiophenylacetate and β-phenyldithiopropionate give higher yields of the N^2-isomers than do aromatic and heterocyclic dithioates. This difference may not be real, but it would be quite understandable from steric reasons.

The asymmetric *NN*-dialkylhydrazines react easily with carboxymethyl dithioates in the normal way, irrespective of the nature of the alkyl groups. A large number of such hydrazides were prepared (Table 6) since we observed that *NN*-dimethyldithiobenzhydrazide had a much higher bacteriostatic effect than the unsubstituted thiohydrazides.

NN'-Dimethylhydrazine reacts with carboxymethyl dithioates in the normal way giving N^1N^2-dimethylthiohydrazides (Table 5). The behaviour of some higher symmetric dialkylhydrazines was discussed above.

Most of the alkylthiohydrazides are colourless (white). The phenylthioacethydrazides are easily obtained as dazzling white, crystalline powders, but the thiobenzhydrazides are often more difficult to purify. N^1-Methylthiobenzhydrazide has been described in the literature [5,6] as yellowish or chamois but is actually colourless. Some thiohydrazides of benzoic and furoic acid have a genuine yellow colour: the phenylthiohydrazides are sulfur-yellow, *o*- and *p*-tolylthiobenzhydrazide, and *N*-(thiobenzoyl)-aminomorpholin have a slightly more intensive colour. Alkylhydrazides are generally colourless; some of them were at first obtained with a slight yellow colour, but in most cases they became colourless on repeated recrystallisation with addition of Darco G 60. The hydrochlorides are more often yellow; thus all the hydrochlorides of alkyl-2-furanthiocarboxyhydrazides have an intensive yellow colour. The hydrochloride of N^2-γ-phenylpropylthiobenzhydrazide is yellow, whereas the hydrochloride of the isomer is white; both the free thiohydrazides are, however, colourless.

Table 6. N^3-Dialkylthiohydrazides, R—CSNHNR′R″.

R	R′	R″	Yield, %	M.p., °C	Formula	Analyses					
						Carbon		Hydrogen		Nitrogen	
						Found	Calc.	Found	Calc.	Found	Calc.
H	Methyl	Methyl	61	84— 86	$C_3H_8N_2S$	34.80	34.60	7.73	7.74	26.56	26.90
Methyl	Methyl	Methyl	57	96— 97	$C_4H_{10}N_2S$	40.80	40.60	8.48	8.53	23.50	23.65
Phenyl	Methyl	Methyl	80	106—107	$C_9H_{12}N_2S$	59.85	60.00	6.83	6.72	15.45	15.52
Phenyl	Ethyl	Ethyl	20	64— 65	$C_{11}H_{16}N_2S$	63.20	63.42	7.68	7.74	13.29	13.45
Benzyl	Methyl	Methyl	56	99—100	$C_{10}H_{14}N_2S$	61.90	61.80	7.13	7.26	14.52	14.41
o-Hydroxyphenyl	Methyl	Methyl	74	165—166	$C_9H_{12}N_2OS$	55.25	55.09	6.25	6.17	14.13	14.28
o-Hydroxyphenyl	Methyl	Ethyl	70	145—146	$C_{10}H_{14}N_2OS$	57.25	57.13	6.60	6.71	13.54	13.33
o-Hydroxyphenyl	Ethyl	Ethyl	71	98— 99	$C_{11}H_{16}N_2OS$	58.80	58.91	7.01	7.19	12.69	12.49
o-Hydroxyphenyl	Butyl	Butyl	28	139—140	$C_{15}H_{24}N_2OS$	64.20	64.26	8.76	8.63	9.84	9.99
o-Hydroxyphenyl	*Iso*butyl	*Iso*butyl	93	105—106	$C_{15}H_{24}N_2OS$	64.10	64.26	8.54	8.63	9.76	9.99
o-Hydroxyphenyl	Methyl	Allyl	68	109—111	$C_{11}H_{14}N_2OS$	59.45	59.45	6.39	6.35	12.50	12.60
o-Hydroxyphenyl	Methyl	Propyl	71	107—108	$C_{11}H_{16}N_2OS$	58.85	59.91	7.02	7.19	12.46	12.49
o-Hydroxyphenyl	Methyl	Butyl	50	102—103	$C_{12}H_{18}N_2OS$	60.55	60.48	7.69	7.61	11.71	11.76
o-Hydroxyphenyl	Methyl	Benzyl	73	121—122	$C_{15}H_{16}N_2OS$	66.05	66.16	5.80	5.92	10.23	10.29
o-Hydroxyphenyl	Methyl	*Cyclo*hexyl	60	137—138	$C_{14}H_{20}N_2OS$	63.60	63.61	7.38	7.63	10.48	10.60
o-Methoxyphenyl	Methyl	Methyl	65	135—136	$C_{10}H_{14}N_2OS$	57.30	57.13	6.67	6.71	13.14	13.33
o-Propoxyphenyl	Methyl	Methyl	38	92— 93	$C_{12}H_{18}N_2OS$	60.60	60.47	7.57	7.60	11.28	11.76
o-*Iso*propoxyphenyl	Methyl	Methyl	30	92— 93	$C_{12}H_{18}N_2OS$	60.65	60.47	7.51	7.60	11.54	11.76
o-Butoxyphenyl	Methyl	Methyl	42	90— 91	$C_{13}H_{20}N_2OS$	62.00	61.88	8.00	7.99		
o-Hexyloxyphenyl	Methyl	Methyl	13	83— 84	$C_{15}H_{24}N_2OS$	63.70	64.24	8.38	8.63		
p-Hydroxyphenyl	Methyl	Methyl	53	157—158	$C_9H_{12}N_2OS$	54.95	55.09	6.21	6.17	14.12	14.28
p-Methoxyphenyl	Methyl	Methyl	77	125—126	$C_{10}H_{14}N_2OS$	57.15	57.13	6.66	6.71	13.22	13.33
p-Methoxyphenyl	Butyl	Butyl	24	68— 69	$C_{16}H_{26}N_2OS$	65.15	65.28	8.80	8.90	9.48	9.52
p-Butoxyphenyl	Methyl	Methyl	32	95— 97	$C_{13}H_{20}N_2OS$	62.00	61.88	7.97	7.99	11.00	11.10
p-Acetamidophenyl	Methyl	Methyl	90	167—168	$C_{11}H_{15}N_3OS$	55.60	55.67	6.26	6.36	17.76	17.72
m-Nitrophenyl	Methyl	Methyl	65	135—136	$C_9H_{11}N_3O_2S$	48.15	48.00	4.93	4.93	18.65	18.65
2-Furyl	Methyl	Methyl	60	81— 82	$C_7H_{10}N_2OS$	49.80	49.40	6.09	5.92	16.24	16.47
2-Thienyl	Methyl	Methyl	63	94— 95	$C_7H_{10}N_2S_2$	45.00	45.15	5.36	5.37	15.16	15.05
2-Thienyl(hydrochloride)	Ethyl	Ethyl	45	155—156	$C_9H_{14}N_2S_2.HCl$					11.08	11.17
										Cl 14.18	14.14

The higher *NN*-dialkylhydrazides are very photosensitive and rapidly turn yellow on exposure to daylight. The chemistry of this colour change has not been investigated.

The acid and base strengths of the thiohydrazides were determined by potentiometric titration of the hydrochlorides with 0.1 N NaOH in 50 % aqueous-alcoholic solution. In their pK_a values the monoalkylthiohydrazides, R—CSNHNHR′, do not differ significantly from the unsubstituted thiohydrazides, but the phenylthiohydrazides (R′ = C_6H_5) are somewhat stronger acids and weaker bases. The unsubstituted thiohydrazides have the following pK_a values: pK_{a1} = 5.0—6.0 (hydrazinium ion), and pK_{a2} = 10.2—11.2 (—CSNH— grouping). For the N^2-substituted thiohydrazides the following values were found:

R	R′	pK_{a1}	pK_{a2}
Alkyl or Aralkyl	Alkyl or Aralkyl	5.6—6.2	10.7—11.1
	Phenyl	4.4—4.7	9.3—10.1
Phenyl or 2-Furyl	Alkyl or Aralkyl	4.9—5.7	9.9—10.4
	Phenyl	4.2—4.3	9.2— 9.6

The N^2-dialkylthiohydrazides are somewhat stronger bases (pK_{a1} = 6.5—6.7) and weaker acids than the monoalkylthiohydrazides. Although they form salts with 1 N NaOH, the titration curves of the hydrochlorides with 0.1 N NaOH exhibit only one break. Naturally N^2-dialkylthiohydrazides containing phenolic hydroxyl groups, such as the *o*-hydroxy- and *p*-hydroxythiobenzhydrazides, form an exception. For these the values pK_{a1} = 4.9—5.7 and pK_{a2} = 10.6—11.2 were found.

The N^1-alkylthiohydrazides exhibit no acid function; they are somewhat stronger bases than the N^2-alkylthiohydrazides (pK_{a1} = 7.2—7.5).

EXPERIMENTAL

Monoalkylhydrazines

With the exception of methylhydrazine [10] and ethylhydrazine [11], all the monoalkylhydrazines were prepared by alkylation of hydrazine with the alkyl chloride or bromide [12,13]. Ethylhydrazine was also obtained, instead of the expected *NN′*-diethylhydrazine, by reduction of acetaldazine with sodium boron hydride. The following hydrazines were prepared: methylhydrazine, ethylhydrazine, allylhydrazine, propylhydrazine, *iso*propylhydrazine, butylhydrazine, *iso*butylhydrazine, *sec*-butylhydrazine, *tert*-butylhydrazine, hexylhydrazine, *cyclo*hexylhydrazine, benzylhydrazine, *α*-phenylethylhydrazine (b.p. 99—100°/2.2 mm), *β*-phenylethylhydrazine (b.p. 135°/12 mm), and *γ*-phenylpropylhydrazine (b.p. 265—267°/760 mm, and 142°/13 mm).

The following compounds are not mentioned in the literature: Benzylhydrazine, sulfate (m.p. 156—157°C; Found: N 12.76. Calc.: N 12.73). *α*-Phenylethylhydrazine (Found: C 71.10; H 8.83; N 22.37. Calc. C 70.45; H 8.88; N 20.57). *β*-Phenylethylhydrazine, sulfate (m.p. 166.5—167.5°C; Found: N 12.09. Calc. N 11.97). *γ*-Phenylpropylhydrazine, sulfate (m.p. 153—154°C; Found: N 11.32. Calc. N 11.29).

Dialkylhydrazines

The following *NN*-dialkylhydrazines were prepared by reduction of the corresponding nitrosamines with lithium aluminium hydride [14-16]: dimethylhydrazine, dipropylhydrazine, di*iso*propylhydrazine, dibutylhydrazine, di*iso*butylhydrazine, di-*sec*-butylhydrazine, dipentylhydrazine, methylethylhydrazine, methylpropylhydrazine, methyl*iso*propyl-

hydrazine, methylbutylhydrazine, methylallylhydrazine, methyl*cyclo*hexylhydrazine, methylbenzylhydrazine, ethylpropylhydrazine, and ethylbutylhydrazine. For the *NN*-dialkylhydrazines with two different radicals, boiling points, yields and analyses are given below. Most of these hydrazines are new.

	Boiling point	Yield, %	Analyses, % N. found	calc.
NN-Methylethylhydrazine	83– 84°/760 mm	50	38.10	37.80
NN-Methylpropylhydrazine	106–108°/760 mm	45	31.80	31.78
NN-Methyl*iso*propylhydrazine	104–106°/760 mm	45	31.87	31.78
NN-Methylbutylhydrazine [17]	130–132°/760 mm	55	28.15	27.42
NN-Methylallylhydrazine	110–112°/760 mm	40	32.46	32.53
NN-Methyl*cyclo*hexylhydrazine	68– 69°/9 mm	65	21.58	21.85
NN-Methylbenzylhydrazine [18]	87– 88°/6 mm	65	20.58	20.57
NN-Ethylpropylhydrazine	125–126°/760 mm	55	27.44	27.42
NN-Ethylbutylhydrazine	146–148°/760 mm	70	24.16	24.11

Most of the amines used for the preparation of the nitrosamines were prepared in the following way:

Benzylidine derivatives of primary amines were prepared by stirring the amine with benzaldehyde at room temperature. They were dried with $CaCl_2$ and distilled *in vacuo:* benzylideneethylamine (b.p. 93°/9 mm; 85 %), benzylidenepropylamine (b.p. 94°/8 mm; 83 %), benzylidene*iso*propylamine (b.p. 88–90°/10 mm; 81 %), benzylidenebutylamine (b.p. 113°/17 mm; 65 %), benzylidene*tert*butylamine (b.p. 91–93°/12 mm; 95 %), benzylideneallylamine (b.p. 96°/10 mm; 90%).

These benzylidene derivatives were alkylated with dimethyl or diethyl sulfate: A mixture of the benzylideneamine (1 mole), dimethyl or diethyl sulfate (1.05 mole) and benzene (50 ml) is heated carefully to 80°C, when a vigorous reaction sets in (it may be necessary to cool). The mixture is then refluxed for 15 min. or one hour, depending on whether dimethyl or diethyl sulfate was used for the reaction. After refluxing, the red or brown reaction mixture, which has separated into two layers, is extracted once with benzene (100 ml) and twice with light petroleum (100 ml). The residue is mixed with its own volume of ethanol and boiled with reflux for one hour. Then an equal volume of water is added, and the solution is evaporated *in vacuo*. A volume of 250 ml of 4 N hydrochloric acid is added, and the solution is again evaporated as far as possible *in vacuo*. The residue, a thick oil, is mixed with potassium hydroxide pellets, and the amine is distilled off, dried with potassium hydroxide and fractionated. In this way the following secondary amines were prepared: methylethylamine (58 %), methylpropylamine (40 %), methyl*iso*propylamine (55 %), methylallylamine (50 %), methylbutylamine (50 %), methyl-*tert*-butylamine (25 %), ethylpropylamine (65 %), ethyl*iso*propylamine (43 %), and ethylbutylamine (60 %). Methylbenzylamine was prepared from benzyl chlorid and methylamine. Methyl*cyclo*hexylamine was a commercial product.

The nitrosamines were prepared by the conventional method. The following nitrosamines are not mentioned in the literature: methyl-*tert*-butylnitrosamine, b.p. 70°/10 mm, m.p 22-24°C. (Found: N 24.10. Calc.: N 24.12). Ethylbutylnitrosamine, b. p. 98-100°/18 mm. (Found: N 21.20. Calc.: N 21.52).

NN′-Di*iso*propylhydrazine, and NN′-di*cyclo*hexylhydrazine, and NN′-dibenzylhydrazine, were prepared by hydrogenation of the corresponding azines. *NN′*-Dipropylhydrazine and *NN′*-dibutylhydrazine (b.p. 78–80°/12 mm) were obtained from the corresponding azines by reduction with lithium aluminium hydride [19].

Monoalkylthiohydrazides

The monoalkylthiohydrazides were in most cases obtained by the following general procedure: The carboxymethyl dithioate (0.01 mole) was dissolved in the equivalent amount of 1 N NaOH (10 ml), and to the cooled solution, a slight excess (10 %) of the free hydrazine (or in some cases a solution of a hydrazinium salt in the equivalent amount of sodium hydroxide) was added. The reaction proceeded almost instantaneously with

slight heat evolution and separation of the hydrazide, generally as an oil. If necessary, a few drops of sodium hydroxide was added to bring the pH of the solution to 9—10. After standing for half an hour the solution was acidified with acetic acid and extracted three times with ether. The ether solution was extracted repeatedly with 1 N NaOH, until no turbidity appeared on acidification of the alkaline extract with acetic acid. The combined acidified alkaline extracts were extracted with ether. The two ether solutions, containing the two isomers of the monoalkylthiohydrazide, were dried with sodium sulfate. To each, an equal volume of light petroleum was added, and the hydrochloride of the thiohydrazide was precipitated with dry hydrogen chloride.

The alkylthiohydrazides of pivalic acid and the *N*-benzyl and *N*-hexylthiohydrazides of *iso*butyric acid were prepared from methyl dithiopivaloate and methyl dithio*iso*butyrate, respectively (the methylthiohydrazides of *iso*butyric acid were prepared in the usual way from the carboxymethyl ester). The reaction between hydrazines and methyl dithioates proceeds much slower than the reaction between carboxymethyl dithioates, and the yields are lower. The methyl ester and the hydrazine were dissolved in ethanol and kept for ca. 40 h; then the solvent was removed *in vacuo* and the residue was dissolved in ether and treated as above. The relative yields of the two isomers seem not to be greatly influenced by application of methyl dithioates instead of carboxymethyl dithioates. From methyl dithiobenzoate (17 g) and methylhydrazine we obtained 1.5 g of N^2-methylthiobenzhydrazide hydrochloride (7 %) and 11 g of N^1-methylthiobenzhydrazide (66 %).

The extents to which the two isomers were formed with different alkylhydrazines are seen from Table 1. The thiohydrazides were liberated by treatment of the hydrochlorides with dilute sodium hydroxide and neutralisation with acetic acid. When a thiohydrazide separated as an oil, the hydrochloride was used as such and recrystallised from ethanol + ethyl ether. The hydrochlorides can be isolated in a beautiful crystalline form, but they are somewhat unstable and soon begin to smell of hydrogen sulfide. On melting, the hydrochlorides split off some hydrogen chloride; melting points determined on a hot stage are therefore very ill-defined. The melting points of the hydrochlorides listed in Tables 2 and 3 were determined on substances contained in a sealed capillary tube; even then the melting points were not very sharp. The Kofler microscope hot-stage melting-point apparatus was used for melting point determination in all other cases.

The thiohydrazides were as a rule recrystallised from more or less dilute ethanol; the methylthiohydrazides could be recrystallised from water (N^2-*tert*-butylthioacethydrazide was easily soluble even in cold water), or water with a slight addition of ethanol; for the higher alkylhydrazides less dilute ethanol, and in a few cases ethanol without addition of water, was used. The phenylhydrazides were recrystallised from benzene + hexane, and this solvent was also used for recrystallisation in a few other cases. The thiohydrazides are generally very soluble in ethanol or benzene. Most of the thiohydrazides prepared were colourless, but some of the hydrazides of aromatic or heterocyclic thioacids had a distinct yellow colour. Properties and analyses of all the thiohydrazides prepared are listed in Tables 2 and 3. When one of the isomers is prevailing, or when both isomers are crystalline, the procedure may be somewhat simplified as shown in the following detailed descriptions:

N^1-*Methylthiophenylacethydrazide.* Carboxymethyl dithiophenylacetate (2.26 g) was dissolved in 1 N sodium hydroxide (10 ml); the yellow solution was cooled in ice, and a cold solution of methylhydrazinium sulfate (1.44 g) in 20 ml of 1 N sodium hydroxide was added together with a small excess quantity of sodium hydroxide solution to bring the pH to 9—10. Colourless crystals separated in a few minutes, and after standing for one hour the product was filtered off, washed with water and dried. The crude product (1.4 g) was recrystallised twice from benzene + light petroleum. Yield 1 g (55 %) of m.p. 65—66°C.

N^2-*Isopropylthiobenzhydrazide. Iso*propylhydrazine (0.85 g) was added with shaking and cooling to a solution of carboxymethyl dithiobenzoate (2.15 g) in 1 N NaOH (10 ml). After half an hour's standing at room temperature the pH of the solution was brought to 5 by addition of acetic acid. The crystalline precipitate was filtered off and dried. Yield 1.70 g (88 %). M.p. 112—112.5°C after recrystallisation from benzene + hexane.

N^2-*Benzylthiopivalic hydrazide.* A solution of methyl dithiopivaloate (3.00 g) and benzylhydrazine (2.44 g) in ethanol (5 ml) was kept for 40 h at room temperature. The ethanol was removed *in vacuo;* the residue was dissolved in ether (30 ml) and the solution was extracted with 1 N NaOH (10 + 5 × 5 ml). On acidification of the combined aqueous

solutions with acetic acid the hydrazide separated in a crystalline state; it was filtered off and recrystallised from dilute (70 %) ethanol (15 ml). Yield 2.1 g (47 %); m.p. 60—61°C.

N^1-*Methylthioacethydrazide*. Carboxymethyl dithioacetate (1.5 g) was dissolved in 10 ml 1 N sodium hydroxide, and a solution of methylhydrazine sulfate (1.6 g) in 10 ml 2 N NaOH was added. After 2 h at room temperature, the solution was neutralised and the reaction product extracted with ether. The ether solution was dried (Na_2SO_4) and the ether evaporated *in vacuo*. A residue of colourless crystals was obtained; yield after crystallisation from benzene-light petroleum: 0.68 g (65 %) with m.p. 79—80°C. The compound is very soluble in water as opposed to the corresponding aromatic compounds.

N^1-*Methylthioformhydrazide* and N^1-*methylthiopropionic hydrazide* were prepared in a similar way from potassium dithioformate and carboxymethyl dithiopropionate, respectively. Both compounds are liquids at room temperature; the thiopropionyl derivative was isolated as the hydrochloride and the thioformyl derivative as the benzalhydrazone. This and other benzalhydrazones prepared from hydrochlorides of N^1-alkylthiohydrazides and benzaldehyde are listed in Table 4.

N^2-*Cyclohexylthiobenzhydrazide*. On addition of *cyclo*hexylhydrazine to a solution of carboxymethyl dithiobenzoate (1 g) in sodium hydroxide, an oil, which soon crystallised, separated. The solid product was stirred with 1 N NaOH (10 ml) and filtered. The undissolved residue (0.17 g; 15 %) had m.p. *ca.* 135°C, after recrystallisation from light petroleum 139—140°C. This product was not a hydrazide, but 2,5-diphenylthiadiazole (m.p. 139—141°C), formed from hydrazine which was contained as an impurity in the *cyclo*hexylhydrazine. (Found: C 71.25; H 4.20; N 11.86. Calc. for $C_{14}H_{10}N_2S$: C 70.58; H 4.23; N 11.76). The solution gave, on neutralisation, N^2-*cyclo*hexylthiobenzhydrazide as a precipitate (0.76 g; 69 %) with m.p. 105—106°C, after recrystallisation from light petroleum m.p. 106—107°.

NN'-Dialkylthiohydrazides

NN'-Dimethylhydrazine reacts easily with neutralised aqueous solutions of carboxymethyl dithioates. *NN'*-Dimethylthiobenzhydrazide separated as an oil and was extracted with ether and isolated as the hydrochloride. *NN'*-Dimethylthiophenylacethydrazide also separated as an oil, but was obtained crystalline on evaporation of the ethereal solution. *NN'*-Dipropylhydrazine, *NN'*-dibutylhydrazine, and *NN'*-dibenzylhydrazine react much slower (in the course of some hours); only *NN'*-dibenzylthiobenzhydrazide was isolated.

From *NN'*-di*iso*propylhydrazine, *NN'*-di*cyclo*hexylhydrazine and *NN'*-diphenylhydrazine (hydrazobenzene) no thioacylated derivatives could be obtained (a large number of carboxymethyl dithioates were tested).

Melting points and analyses of the compounds prepared are listed in Table 5.

NN-Dialkylthiohydrazides

Each dialkylthiohydrazide was prepared from a neutralised aqueous solution of the carboxymethyl dithioate and a slight excess (10—20 %) of the hydrazine. The reaction proceeded almost instantaneously with slight heat evolution, separation of the hydrazide and disappearance of the colour of the solution. The higher alkylhydrazines are somewhat liable to give oily reaction products, but crystalline products could in most cases be obtained by addition of ethanol to the solution. In a few cases the oily hydrazide was extracted with ether and isolated as the hydrochloride.

The dialkylthiohydrazides were in most cases recrystallised from dilute ethanol (70 %) and then from benzene + hexane. N^2-Dimethylthioacethydrazide and the corresponding thioformyl compound are rather soluble in water. They were isolated by extraction of the neutralised reaction mixture with chloroform.

The dialkylthiohydrazides form colourless crystals. With the exception of the thioformyl derivatives they are quite stable in darkness, but they are more or less photosensitive. Especially the higher dialkylthiohydrazides are very sensitive to light and rapidly turn yellow on exposure to daylight.

Melting points and analyses of the dialkylthiohydrazides prepared are listed in Table 6. In the following a few typical preparations are described:

N^2-*Dimethylthioformhydrazide.* To a solution of potassium dithioformate (1.16 g) in water (10 ml) a solution of dimethylhydrazinium chloride (0.96 g) was added, and the pH of the solution was brought to 8. After standing overnight the solution was extracted with chloroform. The chloroform layer was dried with sodium sulfate and evaporated *in vacuo*, and the colourless crystals were recrystallised from benzene + hexane. Yield 0.55 g (61 %). The compound is rather unstable; already after two days a lower melting point was found. The corresponding N^2-dimethylthioacethydrazide was prepared in the same way.

N^2-*Dimethylthiobenzhydrazide.* To a solution of carboxymethyl dithiobenzoate (2.1 g) in 1 N NaOH (10 ml) dimethylhydrazine (0.7 g) was added. After standing for one hour the solution was neutralised and the precipitate filtered. Yield 1.4 g (80 %) with m.p. 100–104°C; after recrystallisation from water or from benzene + hexane the m.p. was raised to 106–107°C. This compound was also prepared from methyl dithiobenzoate and dimethylhydrazine.

N^2-*Methylethyl*-o-*hydroxythiobenzhydrazide.* Carboxymethyl dithiosalicylate (5.7 g) was dissolved in the equivalent amount of 1 N NaOH, and methylethylhydrazine (2 g) was added. After cooling in ice, the crystalline thiohydrazide was filtered and recrystallised from dilute ethanol. Yield 3.7 g (70 %). M.p. 145–146°C.

N^2-*Diisobutyl*-o-*hydroxythiobenzhydrazide.* Carboxymethyl dithiosalicylate (1.14 g) was dissolved in 5 ml 1 N NaOH + 5 ml ethanol, and to the solution 0.9 g of *NN*-di*iso*-butylhydrazine was added. Next day beautiful colourless crystal needles had formed. Yield 1.3 g (93 %). After recrystallisation from ethanol (70 %) and then from benzene + hexane, 0.80 g (57 %) with m.p. 105–105.5°C. The filtrate on addition of water and neutralisation gave only a small amount of an oily product.

N-*(Thiobenzoylamino)morpholin*, $C_6H_5CSNHN\begin{matrix} CH_2CH_2 \\ \diagup \quad \diagdown \\ \diagdown \quad \diagup \\ CH_2CH_2 \end{matrix}O$. Prepared in the general way from carboxymethyl dithiobenzoate and *N*-aminomorpholin. Yield 62 %. Recrystallisation from water. M.p. 147–148°C. (Found: C 59.55; H 6.42; N 12.65. Calc. for $C_{11}H_{14}N_2OS$: C 59.60; H 6.37; N 12.62).

N^2-*Dimethylthiopivalic hydrazide.* Methyl dithiopivaloate (3.00 g) and *NN*-dimethylhydrazine (1.20 g) were dissolved in ethanol (5 ml). After standing for four days the solution was evaporated to dryness and the residue was recrystallised from ethanol. Yield 0.10–0.12 g (3–4 %) of m.p. 119–120°C. (Found: N 17.49. Calc. for $C_7H_{16}N_2S$:N 17.48). According to these findings the reaction proceeds only to a very limited extent. No better yield was obtained by refluxing the solution.

REFERENCES

1. Wuyts, H. *Bull. soc. chim. Belges.* **38** (1929) 195; **39** (1930) 58; Wuyts, H. and Goldstein, M. *Bull. soc. chim. Belges.* **40** (1931) 497; Wuyts, H. and Lacourt, H. *Bull. soc. chim. Belges* **42** (1933) 1.
2. Baker, W., Ollis, W. D. and Poole, W. D. *J. Chem. Soc.* **1950** 3392.
3. Sato, T. and Okta, M. *Bull. Chem. Soc. Japan* **27** (1954) 624.
4. Wuyts, H. and Li Chia Kuang, *Bull. soc. chim. Belges.* **42** (1933) 153.
5. Jensen, K. A. and Miquel, J. F. *Acta Chem. Scand.* **6** (1952) 189.
6. Holmberg, B. *Arkiv Kemi* **9** (1955) 47.
7. Bähr, G. and Schleitzer, G. *Angew. Chem.* **68** (1956) 375.
8. Jensen, K. A. and Madsen, E. Rancke *Z. anorg. u. allgem. Chem.* **219** (1934) 243.
9. Holmberg, B. *Arkiv Kemi* **4** (1952) 105.
10. Hatt, H. H. *Organic Syntheses. Coll. Vol.* **2** (1959) 395.
11. Gever, G. and Hayes, K. *J. Org. Chem.* **14** (1949) 813.
12. Brit. Pat. 695,513 (1953).
13. Westphal, O. *Ber.* **74** (1941) 759.
14. Hanna, C. and Schueler, F. W. *J. Am. Chem. Soc.* **73** (1951) 4996; **74** (1952) 3693.

15. Zimmer, H., Andrieth, L. F., Zimmer, M. and Rowe, R. A. *J. Am. Chem. Soc.* **77** (1955) 790.
16. Vogel, A. I., Cresswell, W. T., Jeffery, G. H. and Leicester, J. *J. Chem. Soc.* **1952** 538.
17. Franchimont, A. P. N. and van Erp, H. *Rec. trav. chim.* **14** (1895) 318.
18. Hinman, R. L. *J. Am. Chem. Soc.* **78** (1956) 2463.
19. Renaud, R. and Leitch, L. C. *Can. J. Chem.* **32** (1954) 545.
20. Holmberg, B. *Arkiv Kemi* **7** (1954) 519.

Received January 23, 1961.

ACTA CHEMICA SCANDINAVICA 15 (1961) 1124–1129

Studies of Thioacids and Their Derivatives

VI. Formation of Thiadiazoles and Tetrazines in the Preparation of Thiohydrazides

KAI ARNE JENSEN and CHRISTIAN PEDERSEN

Chemical Laboratory of the University of Copenhagen, Copenhagen, Denmark

Some by-products and transformation products obtained in the preparation of thiohydrazides have been shown to be thiadiazoles and tetrazines. The formation of these compounds in some cases proceeds at such a rate that no thiohydrazides can be isolated. 2,5-Disubstituted thiadiazoles are generally obtained in good yields from thiohydrazides and carboxymethyl dithioates.

Thiohydrazides are easily transformed into heterocyclic compounds. Such reactions are well known in the case of thiosemicarbazides and thiosemicarbazones, and similar reactions with phenylhydrazides of thioacids and thiobenzhydrazide have been extensively investigated by Wuyts [1,2] and Holmberg [3–6], respectively.

The main purpose of the present paper is to prove the identity of some by-products obtained in the preparation of thiohydrazides, but at the same time it demonstrates the general character of the reactions studied by Wuyts and Holmberg. Besides, some new thiadiazoles have been prepared, among these the basic 1,3,4-thiadiazole, which in the meantime has been prepared by Goerdeler *et al.*[7] in a different way.

In the preparation of thiohydrazides, the formation of tetrazines and thiadiazoles sometimes proceeds at such a rate that no thiohydrazides can be isolated. It has already been mentioned (No. III of this series) that no thiohydrazides could be obtained from the reaction of aliphatic thioacids or thioesters with at least one hydrogen atom at the α-carbon atom. When for instance dithiopropionic acid reacts with hydrazine, a white sulfur-free compound with 34—38 % nitrogen is formed. This compound turns red in air, and this property together with its high nitrogen content shows that it mainly consists of diethyldihydrotetrazine (calc. 40.0 % N), although this was not obtained in a pure state. Also dithioformic acid gives a product which turns red in air, but from which no definite compound could be isolated. On the other hand, from the reaction of potassium dithioformate or carboxymethyl dithiopro-

pionate with hydrazine, 1,3,4-thiadiazole and 2,5-diethyl-1,3,4-thiadiazole could be isolated in good yields.

Phenylthioacethydrazide often decomposes on standing with evolution of hydrogen sulfide, and from this product 2,5-dibenzyl-1,3,4-thiadiazole could be isolated. This decomposition is catalysed by impurities and proceeds only slowly in pure samples of the thiohydrazide. It was shown that the much more stable furanthiocarboxhydrazide on heating is similarly transformed into 2,5-di-(2′-furyl)-1,3,4-thiadiazole.

Jensen and Miquel [8] noticed that thiobenzoylthiosemicarbazide on heating is transformed into another substance. This has now been shown to be the expected 2-phenyl-5-amino-1,3,4-thiadiazole.

Thiadiazoles are also formed by oxidation of thiohydrazides [6] and by the reaction of thiohydrazides with carboxymethyl dithioates (see below).

In the preparation of phenylthioacethydrazide, the corresponding dihydrotetrazine is a frequent contaminant of the crude product, which often assumes a red colour when exposed to air. In one case when we tried the preparation of phenylthioacethydrazide on a larger scale (100 g) we obtained no thiohydrazide at all. Instead, a colourless substance with a higher melting point was formed, and when this product was exposed to air it rapidly assumed the characteristic red-violet colour of a tetrazine. From this product we succeeded in obtaining pure 3,6-dibenzyl-1,2,4,5-tetrazine (m.p. 74°C). The formation of the tetrazine was probably caused by a local excess of hydrazine, since Wuyts [2] has shown that tetrazines are formed in the reaction of *N*-phenylthiohydrazides with hydrazine.

When phenylthioacethydrazide reacts with methyl iodide, 3,6-dibenzyl-dihydro-1,2,4,5-tetrazine is formed:

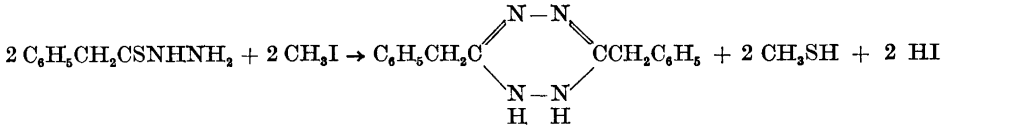

Similarly 3,6-(2′-furyl)-dihydro-1,2,4,5-tetrazine was obtained from 2-furanthiocarboxhydrazide. Holmberg [4,5] has obtained 3,6-diphenyldihydro-1,2,4,5-tetrazine in a similar reaction. All three compounds were already prepared by Pinner [9] from the corresponding imidoesters.

The thiohydrazides in most cases react easily with carboxymethyl dithioates with formation of thiadiazoles. This reaction undoubtedly proceeds *via* dithioacylated hydrazine, which spontaneously splits off hydrogen sulfide:

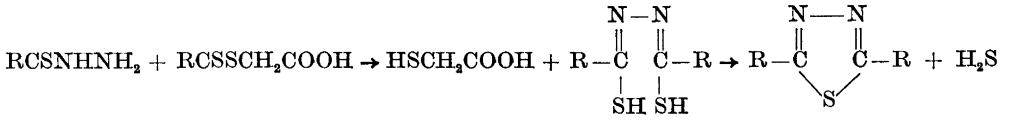

This reaction was observed by Holmberg [3] in the case of thiobenzhydrazide (R = C_6H_5), and we have observed similar reactions with phenylthioacethydrazide, phenylthiopropionic hydrazide, 2-furanthiocarboxhydrazide, 2-thio-

phenethiocarboxhydrazide, salicylic thiohydrazide and *p*-hydroxythiobenzhydrazide. It is generally not possible to isolate the intermediate dithioacylated hydrazines. However, as mentioned in our paper No. III, such compounds were formed from carboxymethyl *o-iso*butoxydithiobenzoate or carboxymethyl *o*-pentyloxydithiobenzoate and hydrazine. They are transformed into the corresponding thiadiazoles on heating.

When carboxymethyl dithiobenzoate is added to a solution of N^1-methylthiobenzhydrazide, $C_6H_5CSN(CH_3)NH_2$, hydrogen sulfide is similarly formed, but the reaction product is of course not a thiadiazole. There are two possible formulae for the reaction product, of which II has been shown to be the correct one by comparison with the authentic compounds I and II prepared by benzoylation of N^1-methylthiobenzhydrazide and by thiobenzoylation of N^1-methylbenzhydrazide, respectively.

$C_6H_5CSN(CH_3)NHCOC_6H_5$ or $C_6H_5CON(CH_3)NHCSC_6H_5$

I II

By reaction of potassium dithioformate with thiobenzhydrazide, 2-phenyl-1,3,4-thiadiazole [6,10,11] is formed:

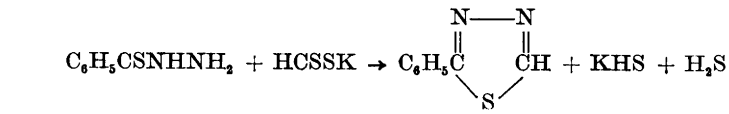

Similarly, 2-benzylthiadiazole was obtained from phenylthioacethydrazide.

The reaction between thiobenzhydrazide and carbon disulfide gives 2-phenyl-5-mercapto-1,3,4-thiadiazole (prepared by Sandström [12] in a different way):

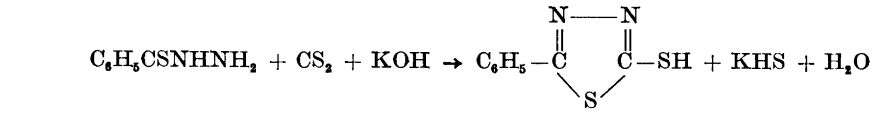

EXPERIMENTAL

1,3,4-Thiadiazole. To an ice-cooled solution of potassium dithioformate (2.3 g) in 10 ml of water was added 0.5 ml (0.5 equiv.) of hydrazine hydrate. The mixture was then allowed to warm up to room temperature and was kept overnight. The solution was adjusted to pH 7 and extracted continuously with ether for 6 h. The ether solution was dried with sodium sulfate and concentrated to *ca.* 10 ml. Addition of light petroleum (b.p. 40–60°C) and cooling caused the 1,3,4-thiadiazole to crystallise. Yield 0.45 g (52 %) with m.p. 38–41°C; after two crystallisations from benzene-light petroleum the m.p. was 41–42°C (analyses see Table 1).

2,5-Dimethyl-1,3,4-thiadiazole was prepared in the same way in 44 % yield from 2 equiv. of carboxymethyl dithioacetate to 1 of hydrazine (Table 1); when the molar ratio was 1:1 the yield was only 10 %; a small amount of tetrazine (red colour) and a brown tarry product were formed.

2,5-Di-(β-phenylethyl)-1,3,4-thiadiazole. To 0.3 g of carboxymethyl dithio-β-phenylpropionate dissolved in the equivalent amount of 1 N NaOH was added a solution of β-phenylthiopropionic hydrazide (0.23 g) in 5 ml of ethanol. Hydrogen sulfide was formed

Table 1. 2,5-Disubstituted-1,3,4-thiadiazoles:

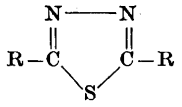

R	Yield %	M.p., °C	Formula	Analyses					
				Carbon		Hydrogen		Nitrogen	
				Found	Calc.	Found	Calc.	Found	Calc.
H [7]	52	41 – 42	$C_2H_2N_2S$	28.00	27.90	2.56	2.35	32.40	32.55
Methyl [16]	44	65 – 67	$C_4H_6N_2S$	42.00	42.05	5.42	5.28	24.35	24.55
Benzyl [17]	85	100 – 102	$C_{16}H_{14}N_2S$					10.28	10.52
β-Phenylethyl	75	72 – 74	$C_{18}H_{18}N_2S$	73.20	73.40	5.87	6.17	9.38	9.52
o-Hydroxyphenyl	88	231 – 232	$C_{14}H_{10}N_2O_2S$	62.20	62.30	3.68	3.74	10.50	10.36
*o-Iso*butoxyphenyl	90	85 – 86	$C_{22}H_{26}N_2O_2S$	69.20	69.09	6.76	6.85		
o-Pentyloxyphenyl	90	115 – 116	$C_{24}H_{30}N_2O_2S$	70.40	70.22	7.40	7.37	7.79	7.79
p-Hydroxyphenyl	75	>300	$C_{14}H_{10}N_2O_2S$	62.15	62.30	3.95	3.74	10.31	10.36
2-Furyl	72	118 – 119	$C_{10}H_6N_2O_2S$	55.25	55.01	2.91	2.77	12.66	12.86
2-Thienyl	69	157 – 158	$C_{10}H_6N_2S_3$	48.05	48.00	2.57	2.42	11.19	11.18

immediately. After 24 h at room temperature 20 ml of water was added; an oily product separated, but it soon crystallised. It was filtered off and washed with water. The substance was recrystallised from light petroleum (b.p. 60 – 100°C). It forms colourless crystals of m.p. 72 – 74°C (Table 1).

Most of the other 2,5-disubstituted 1,3,4-thiadiazoles with aromatic or heterocyclic substituents were prepared in the same way. The reaction between 2-hydroxythiobenzhydrazide and carboxymethyl dithiosalicylate is completed in a few minutes; for this reason it is difficult to prepare the thiohydrazide by the usual method, the thiadiazole being obtained instead (see No. III of this series). The corresponding *p*-hydroxythiobenzhydrazide reacted rather slowly, 72 h being necessary to complete the formation of thiadiazole. In the other cases the reaction time was less than 24 h.

The 2,5-(dialkoxyphenyl)-1,3,4-thiadiazoles were prepared by melting the corresponding dithioacylated hydrazines (*cf.* our paper No. III) and keeping them in a molten state for half an hour. The yellow substances then turned colourless with evolution of hydrogen sulfide. The reaction products were recrystallised from hexane. Further data are given in Table 1.

The formation of the thiadiazoles by heating the thiohydrazides was demonstrated in the case of 2-furanthiocarboxhydrazide: 0.5 g of the thiohydrazide was melted and kept at 140 – 150°C for a quarter of an hour. Hydrogen sulfide and ammonia were evolved, and a black mass was formed; it was extracted with ether. The ether was evaporated and the residue dissolved in benzene; the solution was treated with decolourising carbon and filtered. On addition of light petroleum a yellowish substance crystallised. The substance was crystallised once more from ethanol-water. M.p. 119 – 120°C, no depression on mixing with an authentical sample of 2,5-di(2′-furyl)-1,3,4-thiadiazole.

The rather unstable phenylthioacethydrazide is transformed into a thiadiazole already at room temperature: An old preparation of phenylthioacethydrazide, which had m.p. 83 – 90°C (originally 68 – 69°C), was recrystallised from ethanol + water, and the product was extracted with ether; from the ether solution a yellow crystalline substance separated on addition of light petroleum. After one crystallisation from ethanol + water this product had m.p. 98 – 100°C and showed no depression on mixing with an authentical sample of 2,5-dibenzyl-1,3,4-thiadiazole.

2-Phenyl-1,3,4-thiadiazole. To a solution of thiobenzhydrazide (0.5 g) in water (5 ml) + ethanol (5 ml) was added a solution of potassium dithioformate (0.38 g) in water (5 ml).

The mixture was kept over night at room temperature. The ethanol was then removed *in vacuo*, dilute hydrochloric acid was added to bring the solution to pH 7, and the solution was extracted with ether (3 × 10 ml). The ether solution was dried (Na_2SO_4), and the ether was removed *in vacuo* leaving an oil which crystallised on cooling. The crystals were washed with light petroleum and recrystallised from benzene-light petroleum. M.p. 40–41°C, in accord with Holmberg [6]. (Found: C 59.50; H 3.84; N 17.07. Calc. for $C_8H_6N_2S$: C 59.23; H 3.73; N 17.27).

2-Benzyl-1,3,4-thiadiazole was prepared by the same procedure from phenylthioacethydrazide. The product was recrystallised from light petroleum (b.p. 40–60°C). Yield 56 %. Colourless crystals of m.p. 28–29°C. (Found: C 61.45; H 4.28; N 16.00. Calc. for $C_9H_8N_2S$: C 61.30; H 4.58; N 15.91).

2-Phenyl-5-mercapto-1,3,4-thiadiazole. To a solution of thiobenzhydrazide (0.5 g) in 1 N alcoholic KOH (6.6 ml; 2 equiv.) was added 0.5 g of carbon disulfide in 5 ml of ethanol. The mixture was kept overnight at room temperature. Ethanol and excess carbon disulfide were removed *in vacuo* and enough water was added to dissolve the potassium salt which had separated. Acidification with dilute hydrochloric acid precipitated the thiadiazole as colourless crystals, which were filtered off and washed with water. Yield 0.6 g (94 %). After recrystallisation from 70 % ethanol the m.p. was 215–216°C in accord with Sandström [12]. (Found: N 14.54. Calc. for $C_8H_6N_2S_2$: N 14.40).

2-Benzyl-5-mercapto-1,3,4-thiadiazole was prepared in the same way from phenylthioacethydrazide in 75 % yield. The product was recrystallised from benzene-light petroleum. (b.p. 60–100°C). Colourless crystals with m.p. 115–116°C. (Found: C 52.05; H 3.90; N 13.58. Calc. for $C_9H_8N_2S_2$: C 51.90; H 3.87; N 13.46).

2-Phenyl-5-amino-1,3,4-thiadiazole. Thiobenzoylthiosemicarbazide (1.5 g) was heated to 140°C for half an hour and then dissolved in hot 1 N hydrochloric acid. The filtered solution was neutralised with NaOH and the white solid which separated was filtered, washed with water and recrystallised twice from ethanol. M.p. 222–223°C, in accord with the literature [13,14]. (Found: N 23.72. Calc. for $C_8H_7N_3S$: N 23.71).

N^1-*Methyl*-N^2-*thiobenzoylbenzhydrazide.* N^1-Methyl-benzhydrazide [15] (0.5 g) was added to a neutralised aqueous solution of carboxymethyl dithiobenzoate (0.7 g). In the course of two days a yellow substance separated. The solution was brought to pH 7 and filtered. Yield 0.75 g (83 %) with m.p. *ca.* 160°C. The compound was purified by dissolving in 1 N NaOH, filtering, precipitation with hydrochloric acid and recrystallisation, first from benzene + light petroleum and then from ethanol. M.p. 166–168°C. (Found: C 66.80; H 5.23; N 10.24. Calc. for $C_{15}H_{14}N_2OS$: C 66.60; H 5.22; N 10.36).

This compound was also prepared from N^1-methylthiobenzhydrazide (0.5 g), which was dissolved in ethanol (2 ml) and added to a neutral solution of carboxymethyl dithiobenzoate (0.64 g) in 1 N NaOH. A precipitate separated; it was filtered, dried, extracted with light petroleum, which removed some unchanged methylthiobenzhydrazide, and recrystallised from benzene. Yield 0.20 g (25 %) with m.p. 165–166°C, unchanged on mixing with the above mentioned preparation, but strongly depressed on mixing with the isomer. (Found: C 67.00; H 5.22; N 10.60; S 11.85. Calc. for $C_{15}H_{14}N_2OS$: C 66.60; H 5.22; N 10.36; S 11.85).

N^2-*Methyl*-N^2-thiobenzoylbenzhydrazide. N^1-Methylthiobenzhydrazide (0.5 g) was dissolved in dry pyridine (5 ml), and with cooling in ice benzoyl chloride (0.35 ml) was added. After 24 h the solution was diluted with water, hydrochloric acid was added, and the precipitate was filtered and washed with water. The substance was purified by solution in 1 N NaOH, filtering, precipitation with acid, and recrystallisation from benzene + light petroleum and then from ethanol + water. M.p. 166–167°C. (Found: C 66.80; H 5.18; N 10.36. Calc. for $C_{15}H_{14}N_2OS$: C 66.60; H 5.22; N 10.36).

3,6-Dibenzyl-dihydro-1,2,4,5-tetrazine. Phenylthioacethydrazide (0.5 g) was dissolved in 3 ml 1 N NaOH + 3 ml ethanol, and 0.5 ml of methyl iodide was added. The solution soon became turbid and smelled of methanethiol. After *ca.* 12 h the mixture was diluted with water, the precipitate filtered and recrystallised from ethanol. M.p. 162–164°C (Pinner [9]: 158–160°). (Found: C 72.75; H 6.04. Calc. for $C_{16}H_{16}N_4$: C 72.70, H 6.10).

The same procedure was used for the preparation of 3,6-di-(2′-furyl)-dihydro-1,2,4,5-tetrazine. M.p. 214–216° (Pinner [9]: 208°). (Found: C 55.65; H 4.07; N 25.02. Calc. for $C_{10}H_8N_4O_2$: C 55.55; H 3.73; N 25.92).

REFERENCES

1. Wuyts, H. and Lacourt, A. *Bull. soc. chim. Belges* **42** (1933) 376.
2. Wuyts, H. and Lacourt, A. *Ibid.* **45** (1936) 685.
3. Holmberg, B. *Arkiv Kemi, Mineral. Geol.* **17 A** (1944) No. 23.
4. Holmberg, B. *Arkiv Kemi, Mineral. Geol.* **25 A** (1947) No. 18.
5. Holmberg, B. *Arkiv Kemi* **9** (1955) 47.
6. Holmberg, B. *Arkiv Kemi* **9** (1955) 65.
7. Goerdeler, J., Ohm, J. and Tegtmeyer, O. *Chem. Ber.* **89** (1956) 1534.
8. Jensen, K. A. and Miquel, J. *Acta Chem. Scand.* **6** (1952) 189.
9. Pinner, A. *Ann.* **298** (1897) 1, 24, 31.
10. Ohta, M., Hagiwara, R. and Mizushima, Y. *J. Pharm. Soc. Japan* **73** (1953) 701.
11. Ainsworth, C. *J. Am. Chem. Soc.* **77** (1955) 1150.
12. Sandström, J. *Arkiv Kemi* **4** (1952) 297; **8** (1955) 487.
13. Young, G. and Eyre, W. *J. Chem. Soc.* **79** (1901) 54.
14. Hoggarth, E. *J. Chem. Soc.* **1949** 1164.
15. Hinman, R. L. *J. Am. Chem. Soc.* **78** (1956) 2466.
16. Stollé, R. *Ber.* **32** (1899) 798; *J. prakt. Chem.* [2] **69** (1904) 152.
17. Stollé, R. *J. prakt. Chem.* [2] **69** (1904) 381.

Received January 23, 1961.

ACTA CHEMICA SCANDINAVICA 15 (1961) 1130–1140

Bisbenzyltetrahydro*iso*quinoline Alkaloids

II. * Methods for Preparing the Two Monomethyl Ethers of *d*-Chondrocurine

ESKIL HULTIN**

Department of Pharmacology, University of California Medical Center, Los Angeles 24, California, U.S.A.

Partly methylated *d*-chondrocurine *** can easily be separated into one unmethylated and one methylated fraction with a counter current procedure, using four separatory funnels and three volumes of ether and one volume of buffer pH 11.9. The dimethyl ether of *d*-chondrocurine is likewise easily separated from the fraction of monomethyl ethers at pH about 13.3, using four volumes of buffer and one volume of ether. One of the monomethyl ethers, but not the other, can easily be crystallized from methanol.

Chondrocurine was first discovered by Wintersteiner and Dutcher [1] in an authenticated concentrated extract of *Chondrodendron tomentosum* Ruíz and Pavon, prepared in Peru. Soon thereafter King [2] found *d*-chondrocurine to be present in a commercial curare from Peru. Kondo, Satome and Odera [3] have identified this alkaloid in another commercial preparation, and Bick and Clezy [4] have recently isolated it in plant material from commercial sources, from which tubocurarine chloride had been extracted.

Wintersteiner and Dutcher [1,5] prepared the dimethochloride of *d*-chondrocurine, and this synthesis was repeated by Marsh and Herring [6] and by Marsh [7] for their investigation of the curariform activity of the menispermaceous alkaloids. Dutcher [8] found that this compound, *d*-chondrocurarine † chloride, also occurs naturally and can be found, *e.g.*, in mother liquors from which *d*-tubocurarine has been crystallized. Preparations of crystalline *d*-tubocurarine chloride have shown different physiological potencies, and Dutcher [9]

---

* Part I. *Acta Chem. Scand.* **15** (1961) 879.

** Present address: Institutionen för organisk kemi, Tekniska högskolan, Stockholm 70, Sweden.

*** The spelling chondo . . . occurs but should be regarded as an orthographic error [13].

† The quaternary compounds corresponding to curine *etc.* are called curarine *etc.*

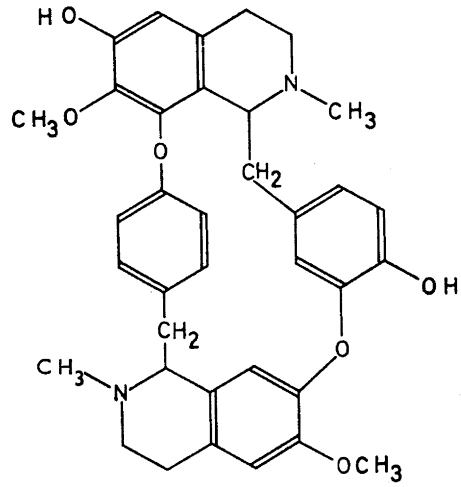

Fig. 1. Chondrocurine.

proved that this could be explained by the presence of *d*-chondrocurarine in sufficient amounts to have a noteworthy effect.

Dutcher [10] also studied the structure of chondrocurine. He found that the dimethyl ether of *d*-chondrocurarine iodide is identical with the dimethyl ether of *d*-tubocurarine iodide. Dutcher [10] further found that *d*-chondrocurine gives a positive Millon reaction. He concluded [8], considering King's [11] commonly accepted [12] inference on the Millon reaction, that *d*-chondrocurine has a hydroxyl group and not a methoxyl group on one of its central benzene rings and that the hydroxyl group and the methoxyl group in *ortho* position on one of the tetrahydro*iso*quinoline rests have reversed positions in *d*-chondrocurine and *d*-tubocurarine. It had been shown previously by King [14,15] that these groups are so located that tubocurarine is a 7-hydroxy-6-methoxy-tetrahydro-*iso*quinoline derivative, and hence chondrocurine is a 6-hydroxy-7-methoxy-tetrahydro*iso*quinoline derivative (Fig. 1).

Bick and Clezy [16] prepared the amorphous dimethyl ether of *d*-chondrocurine and carried out a reductive fission with sodium in liquid ammonia, as was first done for structure determinations in this group of alkaloids by Tomita, Fujita and Murai [17]. The results of the investigation was that the asymmetric center in that tetrahydro*iso*quinoline rest which has a substituted phenoxy rest in 7-position is dextrorotatory, and that the asymmetric center in the other tetrahydro*iso*quinoline rest, which has its substituted phenoxy rest in 8-position, is levorotatory.

The natural occurrence of a monoquaternary bisbenzyltetrahydro*iso*-quinoline alkaloid, N-monomethyl *d*-chondrocurine, has been reported by Bodendorf and Scheibe [18]. They crystallized this substance as nitrate and called it *d*-protochondrocurarine nitrate. Also chondrocurarine (which had previously [8,9] been crystallized only as iodide with halogenated hydrocarbons as solvent of crystallization) was crystallized as nitrate and, thus purified, could be crystallized as chloride [18].

A new, important achievment in this field has recently been reported by Voronin, Tolkachev and Preobrazhenskii [19,20]: the synthesis of isomers of curare alkaloids.

After this review of work on *d*-chondrocurine by others, an account will be given of the results in the present investigation, which was carried out mainly in the early part of 1959.

SEPARATION METHODS

The purpose of this work was to prepare the two monomethyl ethers of *d*-chondrocurine. A similar problem, preparing the two monomethyl ethers of *l*-curine, has previously been partly solved by Späth and Kuffner [21] as one proof among several others for the correctness of the opinion that curine consists not of one but of two benzyltetrahydro*iso*quinoline rests. The methods suggested here for preparing the two monomethyl ethers of *d*-chondrocurine have some resemblance to Späth and Kuffner's method in the general approach: the alkaloid is partly methylated with diazomethane, and the reaction products are separated — more or less efficiently — by a distribution procedure between two immiscible solvents, whereupon they are crystallized. Both processes make use of the property of the completely methylated compounds to be almost insoluble in a strong potassium hydroxide solution but fairly easily soluble in ether, in order to accomplish their separation from substances which are not completely methylated and which as a consequence thereof are soluble in a strong potassium hydroxide solution due to the formation of a salt. The main difference between the principles for separation described here and the separation carried out by Späth and Kuffner is that whereas they had no efficacious procedure, based on distribution between two immiscible solvents, for separating the unmethylated compound from the two monomethyl ethers (but tried a simple fractionated extraction as a support to fractionated crystallization), the present work includes an investigation of the conditions for such a separation. A simple and efficacious method has been worked out, which can be generally used for this kind of separation problems. The value of this method lies in the fact that both in the case of chondrocurine and its monomethyl ethers, and in the case of curine and its monomethyl ethers, the unmethylated alkaloid otherwise has to be separated by a series of fractionated crystallizations, and in both cases methanol is the solvent of choice for crystallizing both the original alkaloid and one of its monomethyl ethers.

Group separation with ether and buffer

The best way to separate mixtures obtained from partial methylation of a bisbenzyltetrahydro*iso*quinoline alkaloid is to start by separating the mixture into groups of isomers according to the number of free hydroxyl groups in the molecule. In the case of *d*-chondrocurine Fig. 2 contains the partition coefficients successively obtained during the work by a procedure described in the preceding paper [22] in this series. The partition coefficients were computed from extinction values at maximum absorption at about 280—290 mμ (the

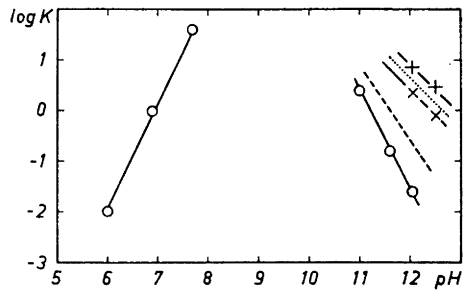

Fig. 2. The influence of pH on the partition coefficient K for *d*-chondrocurine (O) and its monomethyl ethers ($\times$ and $+$) between diethyl ether and buffer. The dashed line gives the optimum relationship between volume ratio and pH for separation of *d*-chondrocurine from its monomethyl ether with partition coefficient closest to that of *d*-chondrocurine, and the dotted line gives the optimum relationship between volume ratio and pH for separation of the two monomethyl ethers of *d*-chondrocurine.

optimum wave length depending on pH and degree of methylation) in the more polar solvent in a series of extractions.

Fig. 2 gives the conditions for a separation between the group of *d*-chondrocurine monomethyl ethers and *d*-chondrocurine. In a distribution system the best separation is obtained when the ratio of the volumes of the two solvent phases equals the inverse value of the geometric mean between the partition coefficients for the two substances [23]. If this is applied to a diagram which gives the logarithms of the partition coefficients for two substances as curves (Fig. 2), a curve drawn midway between them gives the negative value of the logarithm for the best ratio between the volumes of the two solvent phases. Thus, for a separation of *d*-chondrocurine and that of its monomethyl ethers whose partition coefficient is nearer to that of *d*-chondrocurine, we can read from Fig. 2 that the pH value at which equal volumes of buffer and ether give the best separation (abscissa value zero) is 11.6. At pH 11.9 the ordinate value for the line is -0.5, and hence the logarithm for the optimum ratio of the volumes of the less polar (ether) and more polar (buffer) phase is $+0.5$, *i.e.*, 3 volumes of ether for 1 volume of buffer. (The partition coefficients were computed for the solvents in the same order: the quotient obtained by dividing the concentration in the less polar phase by the concentration in the more polar phase.)

We can also see from the diagram that if we start the separation procedure using 3 volumes of ether and 1 volume of buffer pH 11.9, the *d*-chondrocurine will distribute itself in such a way that there will be about 10 times as much in the water phase as in the ether phase, because the difference in abscissa values for the line from which we read the best separation conditions and the line giving the distribution coefficients for *d*-chondrocurine is one unit in the logarithmic scale. One of the monomethyl ethers will distribute in such a way that there will be about 10 times as much in the ether phase as in the water phase, and as to the other monomethyl ether, there will be about 30 times more present in the ether phase than in the water phase. The dimethyl ether of *d*-chondrocurine will be present almost entirely in the ether phase.

One simple distribution at a correctly chosen combination of volume ratio and pH thus gives a fair separation. The result can easily be greatly improved by using a few more separatory funnels in the way described by Bush and Densen [24]. For an example, say three separatory funnels are used, numbered 1, 2, and 3. All funnels contain the proper volume of the upper solvent phase. An equal number of portions, in this case consequently three, of the proper volume of the lower solvent phase are successively transferred through the series, starting with funnel No. 1, into which the mixture to be separated is also introduced at the beginning of the separation. After equilibration and adjustment of pH (because of the formation of a phenolate) the lower phase in the first funnel is transferred to the second, and a second portion of the lower solvent phase is introduced into the first funnel. After new equilibration the lower phase in the second funnel is transferred into the third funnel and so on till all batches of the lower solvent phase have passed the funnels. These portions are pooled and contain the fraction consisting mainly of the substance or substances with a partition coefficient lower than that which corresponds to the separation condition (volume ratio) chosen. Likewise, the portions of the upper solvent phase left in the funnels are pooled and contain the fraction consisting mainly of the substance or substances with a distribution constant higher than that which corresponds to the separation condition. In the separation problem considered here the situation is, as mentioned, that *d*-chondrocurine distributes itself so that 10 times as much substance is in the lower phase as in the upper phase. Thus, by a separation procedure using one funnel we can theoretically recover 90.9 % of the *d*-chondrocurine from the lower phase. It can easily be worked out that by using two funnels in a separation as described we can recover 97.7 %; three funnels give 99.0 %, and four funnels give 99.8 % recovery.

When preparations of partly methylated *d*-chondrocurine, which were larger than about 0.5 g, were separated, it was found convenient to introduce the solute in several portions according to the principle described by O'Keeffe, Dolliver and Stiller [25]. From their description of the procedure, it actually is a superimposition of two simultaneously and independently run separation series, whereas a scheme for the procedure in a single series is given by Jübermann [26].

From the example given in a previous paragraph, with three separatory funnels, the separation could be expanded in the following way. After the procedure has been carried out so far that all three portions of the upper solvent phase are in the funnels, a new portion of the solute is introduced into funnel No. 2, and the phases are equilibrated under adjustment of pH. As one new portion of solute is introduced, one more portion of each of the two solvent phases should be used (one may, of course, use more portions to get a better final separation). This is done as follows. The lower phase of funnel No. 3 is collected in a container for the bottom phase fraction, and the bottom phase in funnel No. 2 is poured into No. 3. The bottom phase in funnel No. 1 is poured into funnel No. 2, and the top phase in funnel No. 1 is collected in a container for the top phase fraction. The contents of funnel No. 2 are poured into No. 1, and the contents of funnel No. 3 are poured into No. 2, and the phases are equilibrated (one may instead remove fun-

nel No. 1 and add a funnel No. 4 for the continuation of the separation). A fresh portion of the upper phase solvent is added to No. 3. The bottom phase in funnel No. 2 is poured into No. 3, and that of No. 1 is poured into No. 2. A fresh portion of the lower phase solvent is added to No. 1. The separation is continued either by introducing a new portion of solute into funnel No. 2 or by continuing the transferring of the phases till all portions of the phases have passed each other. Any number of funnels may be used; when the series is expanded, solute is introduced successively into funnels Nos. 1, 2, 3, *etc.* till the funnel in the middle of the series is used for this introduction of the solute, if the number of funnels is odd; or till the last funnel in the first half of the series is used, if the number is even.

In a similar way, the two monomethyl ethers can be efficiently separated from the dimethyl ether. A suitable procedure can be derived from the values given in Fig. 2, although the distribution coefficient is not given for the *d*-chondrocurine dimethyl ether. It is very reasonable to presume that the logarithm for the distribution constant for this substance between ether and an alkaline buffer is not less than 1.5 but sooner larger than 2, and the results from actual separations have not been contradictory to this presumption. If we want to run the separation in such a way that the *d*-chondrocurine monomethyl ether with the higher distribution constant is present in 10 times as large quantities in the water phase as in the ether phase, we may use 4 volumes of a buffer solution pH 13.3 and 1 volume of ether (Fig. 2). Then the percentage of this *d*-chondrocurine monomethyl ether recovered in the pooled water phases after a counter current separation for various number of funnels will be the same as the percentage of *d*-chondrocurine recovered in the previously described separation, where 10 times as much substance was also present in one phase as in the other. The fraction recovered in the case of that *d*-chondrocurine monomethyl ether which has the lower distribution constant will obviously be better, and the recovery of *d*-chondrocurine dimethyl ether in the pooled ether phases can also reasonably be expected to be about equally good or better.

Separation of the *d*-chondrocurine monomethyl ethers with diethyl ether and buffer

The prospect and conditions for a counter current separation of the two monomethyl ethers of *d*-chondrocurine can also be read from Fig. 2. In this figure, two lines represent the logarithms of the distribution constants for these substances as functions of pH. A line drawn midway between these two lines gives the condition for best separation. The abscissa value for this line is zero at a pH value about 12.7, which means that equal volumes of the two solvent phases give the best separation at this pH value. The difference in pH values (abscissa values for equal ordinate values) between this line and one of the lines giving the logarithm of the partition coefficient of a *d*-chondrocurine monomethyl ether is about 0.25. This implies that even such a small deviation in the pH value from the optimum value as say 0.1 would have a considerable influence on the separation. Considering that in ordinary simple pH determinations uncorrected results obtained with various appa-

ratus differ noticeably at high pH values, and that the time response for various glass electrodes may differ considerably [27], it is recommended that when a separation of this kind is intended, the influence of possible differences in pH determinations be taken into account by checking the value of the partition coefficient of one of the substances for a suitable pH value.

As the difference in ordinate values between the line for best separation and the line for one of the *d*-chondrocurine monomethyl ethers is also about 0.25, the amount of the monomethyl ether with lower partition coefficient will be only about 1.5 times as large in the lower phase as in the upper phase. This implies that a counter current distribution with a small number of funnels cannot give a very good separation but that a considerable number of transfers or theoretical plates would be required. However, a fairly acceptable separation can be achieved by again fractionating the fractions obtained after using only a small number of transfers.

Recovery of the fractions

The various fractions can be recovered in the following way. In the case of a water phase solution, so much fairly strong hydrochloric acid (say 6 N) is added to the solution that its pH value is adjusted to about 8.5, whereby the substance appears as a precipitate. The final adjustment of pH is made easier if sodium bicarbonate is added to the mixture and a more dilute solution of hydrochloric acid (say 1 N) is used at the end. It is recommended that the precipitate not be directly filtered off but first extracted with diethyl ether because ether leaves various impurities undissolved, whereas it rather easily dissolves *d*-chondrocurine and its methyl ethers. Chloroform, however, dissolves all or almost all those impurities which usually appear and hence is not recommended for this step. A mixture of one volume of ether and two volumes of chloroform leaves much of the impurities undissolved. This mixture was used in some cases. — Ether solutions are filtered through cotton if they contain impurities in suspension and are then extracted with several portions of dilute hydrochloric acid (0.05 N HCl is suitable) till the pH value of the extract is small, say about 2. When a mixture of chloroform and ether was used, the hydrochloric acid extracts were washed with ether because otherwise small droplets of the mixture of chloroform and ether appeared in the bottom of the container when the alkaloid was precipitated and disturbed the recovery considerably. Potassium hydroxide (*e.g.*, a 25 % solution) or sodium hydroxide is carefully added to the hydrochloric acid extract till the pH value of the mixture is slightly above 8.5. The final adjustment of pH is facilitated, if some sodium bicarbonate is added to the mixture. If the alkali solution is added too quickly, part of it may be included in ball-shaped particles and cause considerable disturbances in the recovery procedure by slowly making the mixture more alkaline than was intended. The precipitate is filtered off and dried. It turned out that using silica gel for drying the preparation in a desiccator was very convenient, and if the desiccator was evacuated with an oil pump to a sufficiently low pressure, it worked as freeze-drying. The bisbenzyltetrahydro*iso*quinoline alkaloids slowly deteriorate if left in

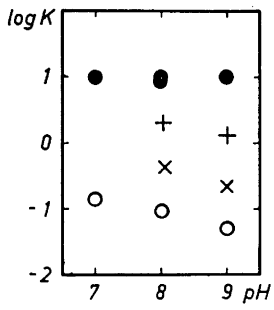

Fig. 3. The influence of pH on the partition coefficient K for *d*-chondrocurine (O), its monomethyl ethers (× and +) and its dimethyl ether (●) between two solvent phases consisting of a mixture of benzene (1/3) and heptane (2/3) in equilibrium with a mixture of equal volumes of methanol and water containing buffer salts (volume ratios 1:2:4:4 or 2:4:3:3).

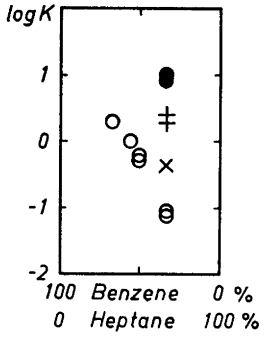

Fig. 4. The influence of the ratio of the volumes of benzene and heptane on the partition coefficient K for *d*-chondrocurine (O), its monomethyl ethers (× and +) and its dimethyl ether (●) between two solvent phases consisting of benzene and heptane in equilibrium with a mixture of equal volumes of methanol and water containing buffer salts.

the open air at room temperature; they can, however, be kept in a closed container in a refrigerator.

The water phase contained potassium sulfite because sulfites prevent the formation of coloured matter in solutions of these alkaloids; it further contained potassium phosphate and potassium hydroxide. Potassium salts were chosen because they do not have the same disturbing effect on ordinary glass electrodes for pH determinations as sodium salts have.

A conveniently flexible four component solvent system

Benzene, heptane, methanol, and water constitute a conveniently flexible solvent system especially for checking the identity and purity of bisbenzyltetrahydro*iso*quinoline alkaloids, including their methylated and demethylated derivatives, by determination of their partition coefficients. Paper chromatography [9] proved less satisfactory; among the solvents tested ethyl methyl ketone with about 4 % methanol and almost saturated with water (which depresses tailing and increases R_F values) was best.

As part of the procedure for working out separation methods, partition coefficients of *d*-chondrocurine and its methyl ethers were measured for various compositions of the four component system. The results are given in Figs. 3 and 4. Most preparations used for these measurements were not yet completely separated. A procedure previously described [22] was used for computing the partition coefficients.

It appears from these figures that the partition coefficient increases about 10 times for every hydroxyl group methylated, whereas in the case of

ether and buffer, the value of the partition coefficient increases about 100 times for every hydroxyl group methylated in the pH range in which a separation can be carried out conveniently. Thus, the mixture of benzene, heptane, methanol, and water is not as suitable as ether and alkaline water for a counter current separation of a mixture into one fraction with no hydroxyl groups, one fraction with one hydroxyl group, and one fraction with two hydroxyl groups in the molecule.

Counter current separation of isomers with the four component system

It has previously been described in this paper how one can easily obtain a pure preparation consisting of a mixture of the two *d*-chondrocurine monomethyl ethers. A few attempts were made to separate them, using the four component solvent system and five separatory funnels. The fractions obtained consisted of mixtures, in which one and the other of the monomethylated ethers, respectively, had been considerably concentrated as can be expected from the moderately favourable difference in partition coefficients. However, the separation experiments according to this method were not continued because a way to separate the monomethyl ethers by crystallization was found at that time. Nevertheless, it is obvious that this method is valuable in those cases in which one or several components in a mixture of isomers related to the groups of alkaloids considered here must be concentrated before one can crystallize them. It may be added here that Engel, Alexander, Carter, Elliott and Webster [28] have described a general method for determining which composition of a quaternary system is most suitable for specific separation problems.

The possibility of using the four component system for separating such isomers as, *e.g.*, *d*-chondrocurine and *l*-curine has been considered. The distribution coefficient of *l*-curine is about 3.5 times as large as that of *d*-chondrocurine for various compositions of the less polar phase of the mixture as shown in Fig. 4 for *d*-chondrocurine.

It is certainly possible to use ether and buffer for separation of several kinds of mixtures of isomers, but there is one advantage in using the four component solvent system: the influence of pH on the value of the distribution constant is small. However, there is also one inconvenience: the solubility of the alkaloids in this solvent is so low that one would have a concentration of only a few tenths of a per cent, whereas the larger solubility in ether and alkaline water makes it possible to have a concentration of a few per cent. Both these solvent systems have the advantage that one can make use of the absorption peak at 280—290 mμ to measure the alkaloid concentration, and that it is easy to recover the alkaloids. In the case of the four component solvent system the organic components of the fractions are first evaporated in a rotating evaporator under vacuum, whereupon the residue is treated as previously described.

Separation of the *d*-chondrocurine monomethyl ethers by crystallization

Both *d*-chondrocurine and one of its monomethyl ethers can easily be crystallized from methanol, whereas the other monomethyl ether so far has resisted all attempts to crystallize it from methanol. A convenient way to prepare a pure preparation of that *d*-chondrocurine monomethyl ether which crystallizes from methanol is hence to partly methylate *d*-chondrocurine, isolate the *d*-chondrocurine monomethyl ether fraction by means of two counter current separations using diethyl ether and buffer, dissolve one part of the fraction in a few parts of methanol and, after the crystallization is completed, separate the crystals from the mother liquor. The crystalline *d*-chondrocurine monomethyl ether so obtained may be recrystallized from methanol. The mother liquor contains the other *d*-chondrocurine monomethyl ether. This substance long resisted all attempts to crystallize it, including cold treatments of its solutions [29]. Experiments using benzene were not successful, but the substance was finally obtained in what is believed to be crystalline form from diethyl ether. However, this solvent cannot be looked upon as very satisfactory for the crystallization of this *d*-chondrocurine monomethyl ether.

EXPERIMENTAL

Separating d-*chondrocurine, its monomethyl ethers, and its dimethyl ether.* 565.4 mg of crude, partly methylated *d*-chondrocurine (from 500 mg of *d*-chondrocurine and diazomethane) were dissolved in 4 ml of a mixture of equal parts of chloroform and methanol and poured into a separatory funnel containing 30 ml of diethyl ether phase and 10 ml of buffer phase, containing 2 % of $K_2S_2O_5$, 0.5 % of K_3PO_4 and about 1.2 % of KOH (pH 12.1), and pH was adjusted to 12.1 after equilibration. A counter current separation with 4 funnels and four portions of each solvent phase was carried out. The pH value of the pooled water phase solutions was adjusted with HCl to 8.5, and the *d*-chondrocurine fraction was extracted with a mixture of 1 volume of ether and 2 volumes of chloroform. This solution was extracted with portions of about 0.05 N HCl (till pH was below 3 in the extract), and the extract was washed with ether, whereupon the alkaloid was precipitated with KOH (pH 8.5; $NaHCO_3$ added), filtered off and dried *in vacuo*. The batches of ether phase, containing the methyl ethers of *d*-chondrocurine, were extracted with 20 ml of water, to which a sufficient number of drops of HCl (1:1) were added. For the separation of the monomethyl ether from the dimethyl ether, pH of the buffer solution was adjusted to 13.2 with KOH. The extract was mixed with an equal volume of buffer, and KOH pellets were added so that the pH value in the water phase was 13.2 when the solution was in equilibrium with 10 ml of the diethyl ether phase. A counter current distribution was carried out with four funnels and four portions of each phase (40 ml of water phase and 10 ml of ether phase). Thereafter, the water phases were adjusted with HCl (1:1) to pH 8.5 ($NaHCO_3$ added), the monomethyl ether fraction was extracted with ether, and this solution was extracted with hydrochloric acid (0.05 N) in portions till the pH of the extract was below 3. The monomethyl ether fraction was again precipitated with KOH, filtered off, washed with distilled water (pH adjusted to 8.5) and dried *in vacuo*. The *d*-chondrocurine dimethyl ether fraction was extracted from the portions of ether phase with hydrochloric acid, precipitated with KOH, filtered off, and dried *in vacuo*. Yield: *d*-chondrocurine 163.1 mg, *d*-chondrocurine monomethyl ethers 188.8 mg, *d*-chondrocurine dimethyl ether 78.7 mg.

Separating the two d-*chondrocurine monomethyl ethers by crystallization.* 5.4 g of *d*-chondrocurine monomethyl ethers were dissolved in 21 ml of hot methanol. Crystals formed over night. The mother liquor was separated and evaporated. Yield: crystals 2.1 g, m.p. 166°C, amorphous rest 3.3 g. A solution was made up consisting of 0.77 g of this amorphous material, 8 drops of HCl 1:1 and 25 ml of water. The solute was precipitated

with KOH at pH 8.5 and extracted with 25 ml of diethyl ether. This solution was washed with water containing some $NaHCO_3$ (pH 8) and filtered through cotton into an Erlenmeyer flask, which was placed in the cold room (+4°C). Part of the solute appeared as an amorphous sediment, part of it on the walls of the flask in a seemingly crystalline state. The sediment and the mother liquor were replaced by a warm, saturated ether solution of a preparation of this *d*-chondrocurine monomethyl ether, and the flask with its contents was left to cool down slowly in a water bath. After a few hours the mother liquor was poured off and the flask dried. No seemingly amorphous substance appeared, but 0.758 g of substance were recovered from the walls of the flask; m.p. 137–138°C. Part of this material was dried in a drying pistol at 63°C without appreciable loss in weight. When thereafter the temperature was increased to 109°C, the material blew around. (Analysis of the *d*-chondrocurine monomethyl ether crystallized from methanol: C 72.3, H 7.2; N 4.3; CH_3O 15.2. Analysis of the *d*-chondrocurine monomethyl ether which crystallized from ether: C 71.4; H 6.6; N 4.6; CH_3O 15.2. Calc. for $C_{37}H_{40}O_6N_2$: C 73.0; H 6.6; N 4.6; CH_3O 15.3).

The author wishes to express his sincere thanks to *Sverige Amerika Stiftelsen, American Scandinavian Foundation,* and *Astra Pharmaceutical Products, Inc.* for fellowships, and to Professor Dermot B. Taylor for the privilege of joining his alkaloid research team and for supplying various *Chondrodendron* alkaloids and partly methylated preparations of them.

REFERENCES

1. Wintersteiner, O. and Dutcher, J. D. *Science* **97** (1943) 467.
2. King, H. *J. Chem. Soc.* **1948** 1945.
3. Kondo, H., Satome, M. and Odera, T. *Ann. Rept. ITSUU Lab. (Tokyo)* **4** (1953) 59.
4. Bick, I. R. C. and Clezy, P. S. *J. Chem. Soc.* **1960** 2402.
5. Wintersteiner, O. and Dutcher, J. D. *U.S. Patent* 2,440,708.
6. Marsh, D. F. and Herring, D. A. *Experientia* **6** (1950) 31.
7. Marsh, D. F. *J. Pharmacol. Exptl. Therap.* **105** (1952) 299.
8. Dutcher, J. D. *J. Am. Chem. Soc.* **74** (1952) 2221.
9. Dutcher, J. D. *Ann. N.Y. Acad. Sci.* **54** (1951) 326.
10. Dutcher, J. D. *J. Am. Chem. Soc.* **68** (1946) 419.
11. King, H. *J. Chem. Soc.* **1940** 737.
12. Bick, I. R. C., Ewen, E. S. and Todd, A. R. *J. Chem. Soc.* **1949** 2767.
13. King, H. *J. Chem. Soc.* **1935** 1381.
14. King, H. *J. Chem. Soc.* **1939** 1157.
15. King, H. *J. Chem. Soc.* **1948** 265.
16. Bick, I. R. C. and Clezy, P. S. *J. Chem. Soc.* **1953** 3893.
17. Tomita, M., Fujita, E. and Murai, F. *J. Pharm. Soc. Japan* **71** (1951) 226.
18. Bodendorf, K. and Scheibe, W. *Arch. Pharm.* **287/59** (1954) 555.
19. Voronin, V. G., Tolkachev, O. N. and Preobrazhenskii, N. A. *Doklady Akad. Nauk S.S.S.R.* **121** (1958) 455.
20. Voronin, V. G., Tolkachev, O. N. and Preobrazhenskii, N. A. *Doklady Akad. Nauk S.S.S.R.* **122** (1958) 77.
21. Späth, E. and Kuffner, F. *Ber.* **67** (1934) 55.
22. Hultin, E. *Acta Chem. Scand.* **15** (1961) 879.
23 Bush, M. T., Goth, A. and Dickison, H. L. *J. Pharmacol. Exptl. Therap.* **84** (1945) 262, footnote 6.
24. Bush, M. T. and Densen, P. M. *Anal. Chem.* **20** (1948) 121.
25. O'Keeffe, A. E., Dolliver, M. A. and Stiller, E. T. *J. Am. Chem. Soc.* **71** (1949) 2452.
26. Jübermann, O. in Müller, E. *Methoden der organischen Chemie* Band I/1, Georg Thieme Verlag, Stuttgart 1958, p. 256.
27. Perley, G. A. *Anal. Chem.* **21** (1949) 559.
28. Engel, L. L., Alexander, J., Carter, P., Elliott, J. and Webster, M. *Anal. Chem.* **26** (1954) 639.
29. Lüttringhaus, A. in Müller, E. *Methoden der organischen Chemie* Band I/1, Georg Thieme Verlag, Stuttgart 1958, p. 341.

Received February 2, 1961.

ACTA CHEMICA SCANDINAVICA 15 (1961) 1141–1150

A Potentiometric Study of the Reaction of the Diammine Silver Ion with Chloride and with Bromide

IDO LEDEN* and GÖRAN PERSSON

Department of Inorganic Chemistry, Chalmers Institute of Technology, Göteborg, Sweden

Measurements of the solubility of silver chloride and silver bromide in ammonia have indicated that the saturated solutions contain several complexes other than the diammine silver ion (*vide* Ref.[1]). Potentiometric measurements in unsaturated solutions reported below indicate mixed complexes of the type, $Ag(NH_3)_mX_n^{1-n}$, where $(m,n) = (1,1)$ and $(2,1)$, if X = Cl, and $(m,n) = (2,1)$ and $(2,2)$, if X = Br. The equilibrium constants computed from the measurements are given in Table 3. They are valid at 25°C and for the ionic strength 1 M (NH_4ClO_4).

The e.m.f. of the following cell (I) was measured at 25°C. X represents Cl or Br.

$$-\mathrm{Ag}\;\left|\begin{array}{l} c_{NH_3}\ \mathrm{M\ NH_3} \\ c_X\ \mathrm{M\ NH_4X} \\ c_{Ag}\ \mathrm{M\ AgClO_4} \\ (1-c_X-c_{Ag})\ \mathrm{M\ NH_4ClO_4} \end{array}\right|\;\; 1\ \mathrm{M\ NH_4ClO_4}\;|\;\mathrm{Hg, Hg_2SO_4}\;+ \qquad \text{(I)}$$

No change of the mercury, mercurous sulfate electrode could be detected during the time used for the measurements. Its drift was less than 1 mV a month. The main investigation consisted of a series of potentiometric titrations. In each titration the concentrations of ammonia and silver were kept constant, while the concentration of ammonium halide was increased from 0 to 0.5 M. The e.m.f. of the cell (I), E mV, is given by

$$E = E_0 - 59.16 \log [Ag^+] - E_j \qquad (1)$$

The sign [] denotes concentrations, in M, of species in the left hand solution of cell I.

The standard potential E_0 mV (standard state: 1 M NH_4ClO_4) was determined from solutions, in which $c_X = c_{NH_3} = 0$, and $0.002 < c_{Ag} = [Ag^+] < 0.01$. This gave

$$E_0 = 61.0 \pm 0.2 \qquad (2)$$

* Present address: Department of Inorganic and Physical Chemistry, University, Lund, Sweden.

In the bromide case no correction was made for the liquid junction potential, E_j. For the chloride measurements, E_j (mV) was calculated from the equation

$$E_j = 1.7\ c_{Cl} \tag{3}$$

This equation, valid for $c_{Cl} < 0.5$ (M), results approximately (accuracy 0.05 mV) from Henderson's formula (Büchi [2]). The ionic mobilities used for NH_4^+, Cl^- and ClO_4^- were taken for zero ionic strength as tabulated by Landolt-Börnstein (Eg III c, p. 2059). This method of computing E_j was supported by measurements of the following cell (II), e.m.f. E_{Cl} mV.

$$-\text{Ag, AgCl} \;\Big|\; \begin{matrix} c_{Cl}\ \text{M}\ NH_4Cl \\ (1-c_{Cl})\ \text{M}\ NH_4ClO_4 \end{matrix} \;\Big|\; 1\ \text{M}\ NH_4ClO_4 \mid \text{Hg, } Hg_2SO_4 + \tag{II}$$

$$E_{Cl} = E^\circ_{Cl} - E_j + 59.16\ \log\ c_{Cl} \tag{4}$$

E_{Cl} was measured for $0 < c_{Cl} < 0.5$. If E_j from eqn. (3) is inserted, one value of E°_{Cl} can be computed from each E_{Cl} measured. All these values of E°_{Cl} (mV) lay within the limits

$$E^\circ_{Cl} = 489.9 \pm 0.05 \tag{5}$$

This perfect constancy also indicates that the activity factor of the chloride ions is not affected, even though as much as half of the perchlorate ions is exchanged for chloride ions. A cell corresponding to (II) but with bromide instead of chloride was also measured. This gave

$$E^\circ_{Br} = 644.4 \pm 0.3 \tag{6}$$

The concentration of the ammonia was kept sufficiently high in all the series of the main investigation to avoid any precipitation of silver halide. The silver in the solution is to be found in the species $Ag(NH_3)_mX_n^{1-n}$. That no polynuclear complexes are present follows from the fact that the function F_0, defined below, is independent of c_{Ag}. The equilibrium constant $\beta_{m,n}$ $M^{-(m+n)}$ for the formation of the complex from its $m + n + 1$ constituents is

$$\beta_{m,n} = [Ag(NH_3)_mX_n^{1-n}] \cdot [Ag^+]^{-1} a_{NH_3}^{-m}\ [X^-]^{-n} \tag{7}$$

Hence

$$c_{Ag} = \sum_{m=0}^{M} \sum_{n=0}^{N-m} Ag(NH_3)_mX_n^{1-n} = [Ag^+] \sum_{m=0}^{M} \sum_{n=m}^{N-m} \beta_{m,n} a_{NH_3}^m [X^-]^n \tag{8}$$

M is the maximum number of ammonia molecules bound in one complex, and N is the maximum coordination number of the silver ion. We define F_0 as

$$F_0 = \frac{c_{Ag}}{[Ag^+]} = \sum_{m=0}^{M} \sum_{n=0}^{N-m} \beta_{m,n}\, a_{NH_3}^m [X^-]^n \quad (\beta_{0,0} = 1) \tag{9}$$

In practice, the summations have to be carried out for all values of m and n corresponding to species which are present in high enough concentrations to

influence the measurements noticeably. For the calculation of F_0 eqn. (1) may be rewritten as

$$E = E_0 - E_j + 59.16(\log F_0 - \log c_{Ag}) \quad (10)$$

Every titration series begins with a measurement of the potential $E = E_1$ in a solution free from chloride. Practically all of the silver in this solution is present as diammine silver ions for the range of ammonia concentrations taken (*vide* Bjerrum [3]). Hence for these initial solutions, $c_{Ag} = [Ag(NH_3)_2^+]$ and $F_0 = \beta_{2,0} \times a_{NH_3}^2$, which changes eqn. (10) to

$$E_1 = E_0 + 59.16 \log (\beta_{2,0} \cdot a_{NH_3}^2) - 59.16 \log c_{Ag} \quad (11)$$

During a titration c_X increases from 0 and E from E_1. We write

$$E = E_1 + \Delta E \quad (12)$$

Combination of eqns. (10), (11) and (12) gives

$$\Delta E = 59.16 \log (F_0 \cdot \beta_{2,0}^{-1} \cdot a_{NH_3}^{-2}) - E_j \quad (13)$$

Finally we introduce a function φ_0, from which some equilibrium constants can be easily computed.

$$\varphi_0 = F_0 \beta_{2,0}^{-1} a_{NH_3}^{-2} = \beta_{2,0}^{-1} \sum_{m=0}^{M} \sum_{n=0}^{N-m} \beta_{m,n} a_{NH_3}^{m-2} [X^-]^n \quad (14)$$

For each titration series with constant a_{NH_3} a plot of φ_0 against $[X^-]$ shows all sufficiently large terms in the double sum. Each such term corresponds to a detectable complex species in the solution. φ_0 is calculated from

$$\log \varphi_0 = \frac{\Delta E + E_j}{59.16} \quad (15)$$

ΔE (mV) is determined directly in the experiments as a difference between two e.m.f.'s. E_j is calculated from eqn. (3) for the chloride measurements. For the bromide case $E_j = 0$.

EXPERIMENTAL DETAILS

The chemicals used were the same as previously described (Ref.[1]).

The solutions were kept free from air by bubbling nitrogen through them during the titration. The nitrogen was passed over hot copper wires to remove traces of oxygen, and then through two washing flasks containing 1 M ammonium perchlorate and ammonia of the same concentration as in the electrode vessel. In this way, changes in concentration due to the nitrogen stream could be avoided in the electrode vessel. The ammonia concentration was standardised against hydrochlorid acid after each potentiometric titration.

The silver electrodes were silver plated platinum wires sealed in glass tubes.

The potentiometer set up was from N. C. Jensen, Copenhagen, type 10 A, with a light spot galvanometer from Norma Fabrik, Wien. Its sensibility was 2×10^{-9} A/mm. The Weston cell, type D-402-B (saturated), was from Muirhed & Co Ltd.

All the measurements were carried out in a well controlled water thermostat at 25 ± 0.01°C.

The electrode vessel for the reference electrode was of the simple type with a side tube dipping into a test tube with 1 M NH_4ClO_4. The vessel for the main titrations was

Table 1. The e.m.f., $E_I + \Delta E$ mV, of cell (I). X = Cl.

c_{NH_3} (M) →	0.5	1.00	1.94	2.92	3.90
f_{NH_3} →	1.00	1.02	1.07	1.14	1.21
E_I*(mV) →		492.5	529.2	551.3	570.5
$10^{-7}\beta_{2,0}$ →	2.2	2.2	2.2	2.1	2.2
$10^3 \cdot c_{Cl}$	ΔE (mV)				
32	1.1	0.9	0.7	0.8	0.7
167	3.1	3.1	2.7	2.6	2.4
286	4.8	4.3	4.2	3.9	3.7
444	6.9	6.0	6.2	5.5	5.1
500	7.6	6.5	6.9	6.0	5.7
Uncertainty →	± 0.4	± 0.3	± 0.1	± 0.1	± 0.2

* These values are for $c_{Ag} = 0.01$. With $c_{NH_3} = 0.5$ and 1.00, E_I was measured for $c_{Ag} = 5.10^{-3}$ which gave $E_I = 474.7$ and 509.2 respectively. With $c_{NH_3} = 0.5$ and $c_{Ag} = 2.5.10^{-3}$, E_I became 490.8. All these values give $\beta_{2,0} = 2.2 \times 10^7$. ΔE was independent of c_{Ag} in all cases.

connected to this test tube by means of a bent stopcock tube containing 1 M NH_4ClO_4. The electrode vessel was closed with a stopper with holes for a connection tube, electrodes, tube for inlet of nitrogen and burette tip.

COMPUTATION OF THE COMPLEXITY CONSTANTS

The results of the measurements are shown in Table 1 for the chloride and in Table 2 for the bromide.

The ammonia activity a_{NH_3} M was calculated from

$$a_{NH_3} = f_{NH_3} \cdot (c_{NH_3} - 2\, c_{Ag}) \qquad (16)$$

where the activity factors, f_{NH_3}, are those used by Bjerrum [3].

In all cases, ΔE was independent of c_{Ag}. φ_0, calculated from eqn. (15), is plotted against c_{Cl} in Fig. 1 for the chloride case. The total chloride concentration c_{Cl} and the concentration, $[Cl^-]$, of f r e e chloride ions agree as closely as the former can be used at the calculations instead of the latter. φ_0 is represented by a straight line, which is almost the same for all the titration series. Hence the predominating complexes are $Ag(NH_3)_2^+$ and $Ag(NH_3)_2Cl$ (*vide* eqn. (14)). The difference between the lines for the titration series with different a_{NH_3} is not much greater than the experimental uncertainty. If it is real, it may be caused by any or both of the following reasons: (i) Changes of activity

Table 2. The e.m.f., $E_I + \Delta E$ mV, for cell (I). X = Br.

c_{NH_3}(M) →	10	8	6
f_{NH_3} →	1.9	1.6	1.4
$10^3 \cdot c_{Ag}$ →	10	8	6
E_I (mV) →	632	617	604
$10^{-7} \cdot \beta_{2,0}$ →	1.4	1.4	1.5
$10^3 \cdot c_{Br}$	ΔE (m)V		
48	3.5	3.4	3.5
91	5.9	5.6	5.8
167	9.9	9.6	9.4
231	13.2	12.9	12.6
310	17.1	17.0	16.6
375	20.2	20.1	19.7
444	23.3	23.3	22.9
500	25.3	25.6	25.5
Uncertainty	± 0.2	± 0.2	± 0.3

factors caused by different a_{NH_3}. (ii) The presence of the complexes $AgNH_3Cl_n^{1-n}$ in small amounts, though increasing with decreasing ammonia concentrations. Since φ_0 is represented by straight lines $n = 1$ is selected. Probably species with other values of n also exist [1], even though the accuracy of the measurements does not permit us to conclude anything about an eventual curvature of φ_0. Hence it can be expected that the calculated complexity constant, $\beta_{1,1}$, of $AgNH_3Cl$ becomes too high (*cf.* Table 4). If (ii) is assumed to be valid, φ_0 is simplified to

$$\varphi_0 = 1 + (\beta_{2,1} \cdot \beta_{2,0}^{-1} + \beta_{1,1} \cdot \beta_{2,0}^{-1} \cdot a_{NH_3}^{-1}) \cdot [Cl^-] \qquad (17)$$

The straight lines in Fig. 1 are drawn with $\beta_{2,1} \cdot \beta_{2,0}^{-1} = 0.52 \pm 0.05$ (M^{-1}) and $\beta_{1,1} \cdot \beta_{2,0}^{-1} = 0.1_1 \pm 0.05$, which gives the slope of each line. The intercept of the lines is 1.02 instead of 1 corresponding to an e.m.f. error of 0.5 mV. This difference cannot be caused by some effect of complex formation or change of activity factors. This means that the silver electrode does not function very well in the ammonia solutions. It seems to us that the electrode potentials are more stable in those solutions where a part of the ammonium perchlorate has been exchanged for ammonium chloride.

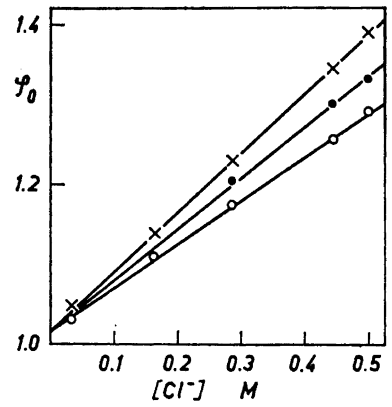

Fig. 1. The function $\varphi_0(Cl^-)$. Each line represents eqn. (17) at one ammonia concentration, 0.5 M (×), 1 M (●) and 3.9 M (○), respectively. The points are calculated from the ΔE values of Table 1 by means of eqn. (15).

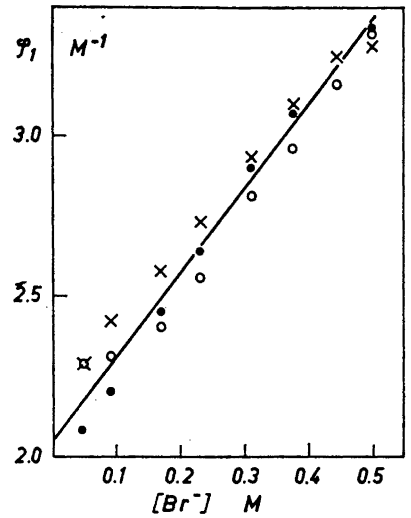

Fig. 2. The function $\varphi_1(Br^-)$ M^{-1}. The line represents the equation $\varphi_1 = (\beta_{2,1} + \beta_{2,2}[Br^-]) \cdot \beta_{2,0}^{-1}$. The points are calculated from the ΔE values of Table 2 by means of eqns. (15) and (18). Points from series with different ammonia concentrations, 10 M (×), 8 M (●) and 6 M (○), coincide approximately on the the same line.

For the bromide solutions, φ_0 could be determined only for rather high ammonia concentrations because of the low solubility of silver bromide. ΔE, and hence, φ_0, are independent of the ammonia concentration within the uncertainty of the experiments. Also in this case, φ_0, plotted against $[X^-]$, gave a value for the intercept which was too high, *viz.* 1.04 instead of the theoretical value 1. To determine the complexity constants, φ_1 (M^{-1}) is plotted in Fig. 2 against $[Br^-]$.

$$\varphi_1 = (\varphi_0 - 1.04) \times [Br^-]^{-1} \tag{18}$$

The difference between c_{Br} and $[Br^-]$ is small and easily computed, *e.g.* with the aid of an $\bar{n}$-curve and the equation $c_{Br} - [Br^-] = \bar{n} \cdot c_{Ag}$. Since φ_1 is independent of a_{NH_3}, only species with two ammonia molecules are involved. In addition, since φ_1 is a straight line, the only mixed complexes in the solutions are $Ag(NH_3)_2Br$ and $Ag(NH_3)_2Br_2^-$ (*cf.* eqns. (14) and (18)). φ_1 in Fig. 2 gives $\beta_{2,1}/\beta_{2,0} = 2.0_5$ (M^{-1}) as the intercept, and $\beta_{2,2}/\beta_{2,0} = 2.7$ (M^{-2}) as the slope of the line.

The solubility products, L_{AgX} M^2, of silver chloride and silver bromide may be obtained from

$$E_x^0 - E_0 = 59.16 \,.\, \log L_{AgX} \tag{19}$$

Table 3. Complexes and equilibrium constants. 1 M NH_4ClO_4. 25°C.

$L_{AgCl} = 4.9 \times 10^{-10}$ (M^2) $L_{AgBr} = 1.2 \times 10^{-12}$ (M^2)
$Ag(NH_3)_2Cl$: $\beta_{2,1} = 1.2 \times 10^7$ (M^{-3}) $Ag(NH_3)_2Br$: $\beta_{2,1} = 4.4 \times 10^7$ (M^{-3})
$AgNH_3Cl$: $\beta_{1,1} = 2 \times 10^6$ (M^{-2}) $Ag(NH_3)_2Br_2^-$: $\beta_{2,2} = 5.8 \times 10^7$ (M^{-4})
$Ag(NH_3)_2^+$: $\beta_{2,0} = 2.2 \times 10^7$ (M^{-2})

where the values of E_x^0 and E_0 are from eqns. (2), (5) and (6). The values of $\beta_{2,0}$ M^{-2}, computed in Table 1 and 2, were obtained from eqn. (11), where E_1 mV is the first e.m.f. measured in each titration.

The complexes that were found and their equilibrium constants are given in Table 3.

DISCUSSION

Equilibrium constants, $K_{s,m,n}$ M^{2-n-m} for dissolving solid silver halide in ammonia have recently been determined (Ref.[1]). These constants are connected by the equilibrium constants reported in the present paper by the equation

$$K_{s,m,n} = L_{AgX} \cdot \beta_{m,n} \qquad (20)$$

The two sets of constants, which are computed from two quite independent methods, are compared in Table 4. They all agree within the experimental uncertainty.

The existence of mixed bromide complexes containing only one ammonia molecule could not be demonstrated by the potentiometric measurements. This was due to the high ammonia concentration, which is necessary to keep the silver concentrations as high as is essential for obtaining stable e.m.f.'s.

Table 4. Comparision of the equilibrium constants, $K_{s,m,n}$ M^{2-m-n}, from the potentiometric measurements with those from the solubility determinations (Ref.[1]).

(m,n)	$K_{s,m,n} \times 10^3$ (chloride)		$K_{s,m,n} \times 10^5$ (bromide)	
	Ref.[1]	This paper	Ref.[1]	This paper
(2,0)	11.1 ± 0.1	11 ± 0.5	2.6_3 ± 0.05	2.6 ± 0.2
(2,1)	5 ± 1	5.7 ± 0.5	4.3 ± 0.5	5.3 ± 0.5
(2,2)			5 ± 2	7.0 ± 1
(1,1)	0.4 ± 0.4	1* ± 0.5	4.5 ± 0.5	
(1,2)	1.5 ± 0.5		8 ± 4	
(1,3)			20 ± 10	

* This value is probably too high, because the existence of other monammine species had to be disregarded in the calculations (*cf.* p. 1145).

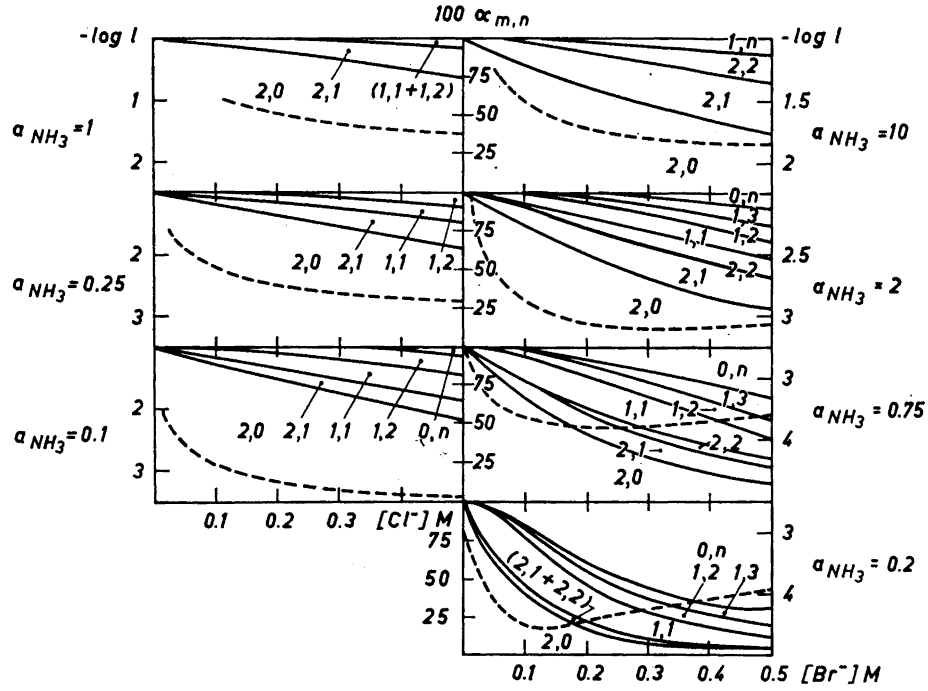

Fig. 3. The distribution, $a_{m,n}$ of silver on the species $Ag(NH_3)_mX_n^{1-n}$ for some ammonia activities, a_{NH_3}, M. m and n are given in each field. The solubility, l M, of AgX. The dashed curve gives $-\log l$. X = Cl to the left, X = Br to the right.

At these high ammonia concentrations the monoammine species would be quite negligible, if their complexity constants, computed from the solubility measurements, are true (*cf.* Fig. 3).

The distribution of the silver on the different complexes is shown in Fig. 3, which also shows the solubility calculated from the constants in Table 4. Since no polynuclear species are formed, the distribution is independent of the total silver concentration of the solutions. The fraction, $a_{m,n}$, of silver present as $Ag(NH_3)_mX_n^{1-n}$ is

$$a_{m,n} = \frac{\beta_{m,n} \cdot a_{NH_3}^m \cdot [X^-]^n}{\sum_{m=1}^{2} \sum_{n=0}^{4-m} \beta_{m,n} \cdot a_{NH_3}^m [X^-]^n} \qquad (21)$$

In practise, the summation is carried out for the values of (m,n) in Table 4. It is quite obvious from the figures that the mixed complexes are far from negligible in systems containing ammonia, silver ions and halide ions.

A survey of the results is shown in Table 5. For each species $\log \beta_{m,n}$ is also given. Let $K_{m,n}$ M^{-1} be the equilibrium constant for the stepwise uptake of ammonia, described by the reaction

$$Ag(NH_3)_mX_n^{1-n} + NH_3 \rightleftharpoons Ag(NH_3)_{m+1}X_n^{1-n}$$

Then $\log K_{m,n} = \log (\beta_{m+1,n}/\beta_{m,n})$ can be read off directly as the difference between two consecutive numbers in a horizontal line in Table 5. Correspondingly, the logarithm of the equilibrium constant $k_{m,n} = \beta_{m,n+1}/\beta_{m,n}$ (M^{-1}) for the stepwise uptake of halide ions by the reaction

$$Ag(NH_3)_mX_n^{1-n} + X^- \rightleftharpoons Ag(NH_3)_mX_{n+1}^{n}$$

is obtained as differences between consecutive numbers in a vertical line of the table. The differences mentioned are a measure of the affinity of the complex for taking up a further ligand, since they are proportional to $-\Delta G_0$ for the reaction.

From these differences it is obvious that in all cases shown in the table a (linear) species already containing two ligands has a rather low affinity for a third ligand. Using Bjerrum's [3] terminology, this means that the silver ion has a characteristic coordination number of two.

Silver(I) species bind ammonia molecules stronger than chloride ions, since $\log (K_{m,n}/k_{m,n}) = \log (\beta_{m+1,n}/\beta_{m,n+1}) = 1 \pm 0.3$ for all but two species in the chloride system. This is seen from those diagonal rows of Table 5, in which $m + n$ is a constant. In these rows the value of $\log \beta$ increases with about one unit for each substitution of a chloride ion for an ammonia molecule. The one exception is $Ag(NH_3)_2^+$, which does not take up ammonia at all in aqueous solution, although it binds chloride ions to form $Ag(NH_3)_2Cl$. The other is the silver ion, for which $\log (K_{0,0}/k_{0,0})$ is as low as 0.3. This may mean that the negative residual effect (Bjerrum [3]) in the silver ammonia system, depends on an abnormal unstability of $AgNH_3^+$ rather than on an extra stability of $Ag(NH_3)_2^+$.

Bromide ions and ammonia molecules have about the same strength as complexing agents for silver ions, *i.e.* the values of $\beta_{m,n}$, for which $m + n$ is constant, are of the same order of magnitude. For example, when $m + n = 3$, $\log \beta_{m,n}$ is 7.9, 7.8 or 7.6 (*vide* the corresponding diagonal row in Table 5). From statistical reasons we cannot expect $\beta_{m,n}$-values, for which $m + n =$ constant $= i$, to be quite equal, even if $\beta_{i,0}$ were exactly equal to $\beta_{0,i}$. If statistical reasons alone determined the equilibrium constants, the following relations would be valid for $\beta_{1,1}$, if the "stop" of the complex formation after the uptake of two ligands is sufficiently pronounced (*cf.* Bjerrum [3], Fronæus [4], Marcus [5]).

$$\beta_{1,1} = \beta_{1,0} \cdot \beta_{01}/2 \quad \text{and} \quad \beta_{1,1}^2 = \beta_{2,0} \cdot \beta_{0,2}/4$$

ble 5. Silver(I) species in the ammonia-chloride-silver and ammonia-bromide-silver system together with $\log \beta_{m,n}$. $\beta_{m,n}$ in $M^{-(m+n)}$.

+	$AgNH_3^+$ (3.3)[3]	$Ag(NH_3)_2^+$ (7.3)	Ag^+	$AgNH_3^+$ (3.3)[3]	$Ag(NH_3)_2^+$ (7.3)
)l (3.0)[4]	$AgNH_3Cl$ (6.3)	$Ag(NH_3)_2Cl$ (7.1)	$AgBr$ (4.3)[5]	$AgNH_3Br$ (7.6)[1]	$Ag(NH_3)_2Br$ (7.6)
$)l_2^-$ (5.0)[4]	$AgNH_3Cl_2^-$ (6.5)[1]		$AgBr_2^-$ (7.2)[5]	$AgNH_3Br_2^-$ (7.8)[1]	$Ag(NH_3)_2Br_2^-$ (7.7)
$)l_3^{2-}$ (5.3)[4]			$AgBr_3^{2-}$ (7.9)[5]	$AgNH_3Br_3^{2-}$ (8.2)[1]	
$)l_4^{3-}$ (5)[4]			$AgBr_4^{3-}$ (8.0)[5]		

Since the pure ammonia and halide systems are not themselves statistical, both the relations cannot be expected to hold true. The second, however, corresponds to the experimental values within their limits of uncertainty. This means that the reaction

$$Ag(NH_3)_2^+ + AgX_2^- \rightleftharpoons 2\ AgNH_3X$$

has an equilibrium constant, $\beta_{1,1}^2 \cdot \beta_{0,2}^{-1} \cdot \beta_{2,0}^{-1}$, close to the statistical value 4.

From the table it is also obvious that the affinity for X^- is the same for Ag^+ and $AgNH_3^+$. Then the affinity for NH_3 is also the same for Ag^+ and AgX. This follows from the nonstatistical relation $\beta_{1,1} = \beta_{1,0} \cdot \beta_{0,1}$ between the experimental values in Table 5.

Silver complexes with more than two ligands should probably not be regarded as species with some of the ligand atoms in an "outer sphere". This is known directly for the saturated pure iodide complex, in which the iodide ions are tetrahedrally arranged around the silver ion (Nilsson[6]). If $Ag(NH_3)_2X$ did contain its halide ion in an outer sphere, it should also be expected that the species would be more stable with X = Cl than with X = Br, because of the minor radius and greater electronegativity of the chloride ion. As is seen from Table 5, the opposite is true. For $Co(NH_3)_6^{3+}$ Evans and Nancollas [9] have found that the strength of its outer halide complexes decreases in the order $Cl^- > Br^- > I^-$. From Table 5 we also learn that compared with other three-ligand-species $Ag(NH_3)_2X$ is only a little weaker than would be expected from statistical reasons. The strength of $Ag(NH_3)_2Br_2^-$ is also comparable with the other four-ligand-species. Hence, there does not seem to be much reason why $Ag(NH_3)_2X$ and $Ag(NH_3)_2X_2^-$ would be examples of outer complexes in contrast to other silver complexes with more than two ligands, even if the entrance of a halide ligand into $Ag(NH_3)_2^+$ is slightly less favoured than into other silver species already containing two ligands. In this connection it would be interesting to know the structure of solids like $Ag(NH_3)_2X$ and $MeAg(NH_3)_2X_2$.

Acknowledgements. Our thanks are due to Professor Cyrill Brosset for all the facilities put at our disposal for this work and to Ragnar Larsson, Lund, for valuable discussions. The English of this paper has been corrected by Dimitrios Karipides, Ph.D., Pennsylvania State University.

REFERENCES

1. Leden, I. and Persson, G. *Acta Chem. Scand.* **15** (1961) 607.
2. Büchi, P. *Z. Elektrochem.* **30** (1924) 443.
3. Bjerrum, J. *Metal Ammine Formation in Aqueous Solution* (Diss.), Copenhagen, 1941, pp. 135, 141, 73, 57, 41.
4. Berne, E. and Leden, I. *Svensk Kem. Tidskr.* **65** (1953) 88.
5. Berne, E. and Leden, I. *Z. Naturforsch.* **8a** (1953) 720.
6. Fronæus, S. *Acta Chem. Scand.* **5** (1951) 148.
7. Marcus, Y. *Ibid.* **11** (1957) 811.
8. Nilsson, R. *Arkiv Kemi* **12** (1958) 513.
9. Evans, M. G. and Nancollas, G. H. *Trans. Faraday Soc.* **49** (1953) 363.

Received January 7, 1961.

ACTA CHEMICA SCANDINAVICA 15 (1961) 1151–1164

Electrochemical Methods in Kinetic Studies of Isotopic Exchange Reactions. I. Application to Systems of the Type $RI + I^{*-} \rightleftharpoons RI^{*} + I^{-}$

PER BERONIUS

Division of Physical Chemistry, The Royal Institute of Technology, Stockholm 70, Sweden

A new method for the measurement of the isotopic exchange between organic and inorganic iodides has been investigated. The procedure used is as follows. From a mixture of the organic and inorganic components in the solvent used, small fractions of the iodide ions (I^{-}-131) are deposited anodically on silver electrodes at certain times. The radioactivity of the thin layers of radioactive silver iodide is measured. From the activity values, and from the concentration of the components, it is possible to calculate the rate constant.

The anodic formation of silver iodide was performed at constant current. To prevent discharging of any other component than the iodide ions, it is necessary to keep the current density below the limiting current density for the discharge of iodide ions. The limiting current density was measured, at sharply defined conditions, for sodium iodide in water, methanol and an ethanol-water mixture. Linearity was found between the concentration of sodium iodide and the limiting current density.

The method described was used to study the reaction $CH_3I + NaI^{*} \rightarrow$ $\rightarrow CH_3I^{*} + NaI$ in dry methanol. The value of the second order rate constant was found to be 33.5×10^{-4} l · mole^{-1}sec^{-1} at 25.0°C.

The application of this method to the study of rapid reactions is discussed.

Even at moderate concentrations, the isotopic exchange between some organic iodides and alkali iodides is rapid in certain solvents. From the value of the rate constant for the isotopic exchange between methyl iodide and sodium iodide [1] in acetone at 25°C, *viz.* 6 l.mole^{-1}sec^{-1}, it can be calculated that, with an equal concentration for both components of 0.05 mole.l^{-1}, the half-life of the reaction is about 1 sec. For benzyl iodide, under the same conditions, the half-life is of the same order of magnitude [2].

With the separation methods hitherto used for the reacting components, *viz.* extraction, which is most frequently used, distillation and precipitation, it is clear that one is restricted to the study of isotopic exchange under such conditions that the half-life of the reaction is rather long, say at least 10 sec,

in order to obtain accurate results. Otherwise the time of separation becomes too long in comparison with the time of reaction. Hence it would be of value to extend the time range available for the study of isotopic exchange reactions of the type discussed.

The purpose of this investigation was to develop an electrolytical separation method which, after certain improvements, may make it possible to study reactions with half-lives as short as a few thousands of a second.

The method has been described briefly in a previous paper [5]. The present article gives a more detailed account of the work. The electrolytic deposition reaction has been studied in some respects and the method has been applied to the investigation of the system, methyl iodide + sodium iodide in dry methanol, at such concentrations of the reacting species that the half-life of the reaction was longer than 10 min.

GENERAL PRINCIPLES OF THE METHOD

The course of the reaction, which can be written

$$RI + I^{*-} \rightleftharpoons RI^{*} + I^{-} \qquad (1)$$

where RI is an organic iodide * and the asterisk indicates a radioactive iodine atom, is followed by depositing small fractions, about 1 ‰, of the total amount of iodide ions electrolytically on silver anodes at different times of the reaction. Thin layers of radioactive silver iodide are thereby formed. If the amount of current is equal for all the anodes, their radioactivity will be proportional to the specific activity of the iodide ions in the reaction mixture at the time in question. From the change in radioactivity of the anodes with the time of reaction and from the known concentrations of the reactants, it is then possible to calculate the rate constant.

In the conventional methods the iodides are completely separated and the distribution of radioactivity between the organic and inorganic iodides is determined. Since the amount of electrodeposited iodine can be made very small, the sample is almost unaltered even after several depositions have been carried out. In this respect the method can be compared with non-destructive analytical ones, *e.g.* spectrophotometric, thermal *etc.*

If a number of electrode pairs are placed at various points in the observation tube of a flow apparatus of the type used by Hartridge and Roughton [3], it would be possible to perform measurements a few thousands of a second after the reactants have been mixed. This means that the method would permit an extension of the observable time range [4] for exchange reactions of this type by a factor of about 10 000.

Reactions which are too slow for the Hartridge-Roughton technique but too rapid for ordinary analytical work might be studied by anyone of the following methods.

---

* There is no reason why the method could not be extended to systems involving bromides or chlorides or other systems where it is possible to precipitate one of the reactants electrolytically without affecting the other one.

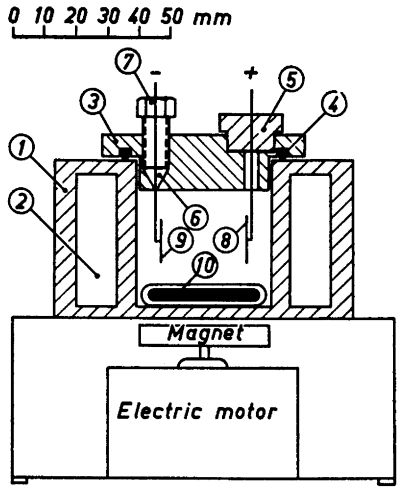

Fig. 1. Electrolysis cell,

1. Aluminium vessel;
2. Water jacket (the tangential inlet and outlet for water from a thermostat bath are not shown in the figure);
3. Teflon lid;
4. Gasket;
5. Teflon holder for the anode;
6. Teflon cone for tightening the silver wire inlet. The tightening cone is pressed downwards by a screw, 7;
8. Silver anode soldered to a copper wire;
9. Silver cathode attached to a silver wire;
10. Rotating magnetic bar.

The vessel was thermally insulated.

If a silver anode, in the form of a band, is drawn with a constant speed through the reaction mixture during electrolysis, the specific activity of the iodide ions could be continuously registered as a function of the time of reaction. The activity at various points of the band, together with information concerning the concentrations of the reactants, would then make it possible to calculate the rate constant.

It might also be possible to use a method in which the electrolytic precipitation is performed between stationary electrodes during such a long time that the composition of the reaction mixture alters appreciably. This method, in the following referred to as "the integral method", will receive a more detailed account at the end of the article.

Another possibility is the capacity flow method [13] in which a uniform and steady state is created in a reactor vessel. After the steady state has been attained, electrolysis could be performed between electrodes mounted in the vessel.

EXPERIMENTAL DETAILS

The reaction vessel. The cylindrical electrolysis cell shown in Fig. 1 was used for determining the limiting current density and for the kinetic experiments. It consisted of a water-jacketed aluminium vessel of 50 ml volume. The inside of the vessel was covered with the plastic fluorocarbon material [14] Kel-F to prevent any contamination of the reaction mixture due to corrosion of the vessel. The teflon lid was provided with a gasket which made the vessel tight. The lid was kept in position by six screws. Stirring was provided by means of a magnetic stirrer. The cylindrical, teflon-covered stirring rod was 38 mm long and 8 mm in diameter. Its rate of revolution was measured using a stroboscope.

The electrodes. The circular electrodes were symmetrically located in the vessel at a distance of 30 mm from each other. The silver cathode, which had an area of 1.5 cm^2, was attached to a silver wire by spot welding. The wire was inserted in a hole in the lid and was kept in position by a teflon cone which was forced down by means of a screw.

The anode * was stamped from thin sheet-silver (0.1 mm) which had been previously polished with emery paper ("Emery Polishing Paper 3/0"). It was soldered to a copper

* Each anode was used for only one deposition and was then replaced by a new one.

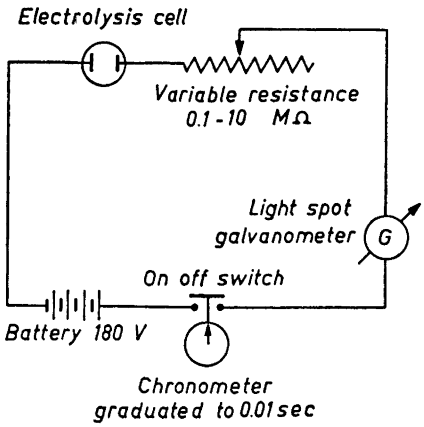

Fig. 2. Circuit used for accurate measurement of the amount of current.

wire. This wire was inserted in a narrow hole in a holder made out of teflon. When the holder was put in the lid, as Fig. 1 indicates, the anode was kept in its correct position and was easily exchangeable.

The back of the anode, the sharp edges along its periphery and the copper wire were covered with paraffin wax to prevent electrodeposition on these parts.

It is of extreme importance that the surface of the anode should be perfectly clean. Otherwise reproducible results are not obtained. Washing with liquid detergent and thorough rinsing with distilled water gave a satisfactorily clean electrode surface.

The circuit. The radioactivity of the anode is proportional to the amount of current and the specific activity of the iodide ions. To get reproducible results it is thus necessary to determine the amount of current very exactly. The circuit used for this is shown in Fig. 2. By means of a large series resistance, which compensated for the change in the cell resistance due to polarization, the current strength could be kept practically constant during the electrolysis.

The time of electrolysis, which varied between 1 and 30 sec, was measured by a chronometer graduated to 0.01 sec. A switch was attached to the starting button of the chronometer and was adjusted so that the latter was started and stopped at the instant when the circuit was closed and broken respectively. This device permitted the time of electrolysis to be determined with an accuracy of $\pm$ 0.02 sec (checked against a rapid recorder (Mingograf 230)).

The counting equipment. The activity of the anodes was measured by a proportional flow-counter provided with a mylar window. Propane was used as counting gas. The counting equipment consisted of a University Series Proportional Counting System which comprises a Scaler Assembly 4125 and a Model 821 B Flow Counter in a Model 800 D Low Background Shield.

Calculation of the electrode activity. The activities measured by the flow counter were corrected for the background and the decay of the iodine (half-life 8.07 days) [16]. The corrected activity values were then converted to equal amounts of current.

Reagents for the kinetic experiments. "Analytical reagent" methanol was refluxed for 2 h with magnesium methoxide [15] and was then distilled in an atmosphere of dry nitrogen. Merck's purest methyl iodide was distilled over silver foil in a 450 mm high Vigreux Column. "Analytical reagent" sodium iodide was dried at 110°C. Carrier-free NaI−131 in a dilute solution of sodium thiosulphate was obtained from The Radiochemical Centre, Amersham, England. The solution was evaporated to dryness and the radioactive sodium iodide was dissolved in dry methanol.

Reagents for the other experiments. Sodium nitrate, of analytical reagent grade, was used as supporting electrolyte in the measurements of limiting current density in water, methanol and an ethanol-water mixture. The distilled water had a specific conductivity of 1.0×10^{-6} $ohm^{-1}cm^{-1}$. The methanol was of analytical reagent grade and was not

further purified. To the commercial ethanol used, water was added to make the supporting electrolyte sufficiently soluble. The ethanol-water mixture contained 10 % water by volume.

Preparations of solutions and methods of analysis. Stock solutions (about 0.01 M) of sodium iodide in the different solvents were prepared. The concentration was determined by titration with standard silver nitrate solution with eosin as indicator. From the stock solutions, 10 ml portions were transferred to volumetric flasks, sodium nitrate was added, in the cases where a supporting electrolyte was necessary, and the solvent in question was added to the correct volume. The solutions used for the kinetic experiments were made up at 25.0°C in volumetric flasks which had been calibrated at this temperature. The other solutions were made up at room temperature.

Methyl iodide was added to the sodium iodide solution just before the kinetic experiments were carried out. The concentration of methyl iodide was determined by accurately weighing the liquid into a known volume of the sodium iodide solution, and the concentration was checked by gravimetric analysis (precipitation of the iodine with silver nitrate).

DETERMINATION OF LIMITING CURRENT DENSITY FOR THE ANODIC DEPOSITION OF IODIDE IONS

General remarks. A prerequisite for a successful application of the electrolytic method is that the anodic precipitation reaction, which is written

$$Ag + I^{*-} \rightarrow AgI^{*} + e^{-}, \tag{2}$$

is able to occur with a 100 % current efficiency. That this is the case, provided that the anode potential is kept within a certain range, was demonstrated by Lingane [6] who determined halide ions by coulometric techniques.

When the electrolytic precipitation is performed according to the "constant current" technique, which is the case in this investigation, it is necessary to keep the current density below a limiting value. Otherwise the anode potential will exceed the oxidation potential for some other electrode reaction. It is therefore necessary to determine this limiting current density. To be of the greatest value, the determination must be carried out under accurately defined conditions.

Definition of the stirring efficiency. The stirring efficiency will be specified here by stating the following data: The size and shape of the stirring rod and electrolysis vessel, the number of revolutions of the rod and the location of the anode. The dimensions of the electrolysis vessel and stirring rod and the location of the anode have been given under "Apparatus".

Factors governing the limiting current. If diffusion is the current-controlling factor, it can be shown [7] that the limiting current, i_l, is given by the expression:

$$i_l = \frac{n \cdot F \cdot D \cdot A \cdot C}{\delta} \tag{3}$$

where

n = number of electron equivalents per molar unit of the reaction
F = Faraday's constant
D = diffusion coefficient
A = electrode area
C = concentration in the bulk of the solution
δ = thickness of the diffusion layer.

Eqn. (3) has been deduced on the assumption that the concentration in the diffusion layer is a linear function of the distance from the surface of the electrode. If, for a given solvent, the electrode area, stirring rate and temperature are kept constant but the concentration is varied, then eqn. (3) can be written

$$i_l = \text{const} \cdot C \tag{4}$$

In eqn. (4), the variation in the value of the diffusion coefficient with concentration is neglected.

The limiting current density for a certain electrode process is for different solvents, if all other conditions are constant, a function of the diffusion coefficient and the thickness of the diffusion layer. In this case, eqn. (3) becomes

$$i_l = \text{const} \cdot \frac{D}{\delta} \tag{5}$$

Eqn. (3) is valid for the case where diffusion is the current-controlling factor. If (electrical) migration contributes to the current, then the limiting current, for anion oxidation, is given by the expression [9,11]

$$i_l = \frac{n \cdot F \cdot D \cdot A \cdot C}{(1-t)\,\delta} \tag{6}$$

where t = transport number of the anions.

Experimental determination of the limiting current density. The limiting current density was determined under various conditions by measuring the current density as a function of the applied cell voltage [8]. When the limiting current has been reached, a further increase in the cell voltage does not cause any increase in the current until the decomposition potential of another component has been attained.

Determinations were performed for sodium iodide in three solvents, *viz.* water, methanol and an ethanol-water mixture, at 25.0°C and at two stirring rates, *viz.* 400 and 1 000 rpm. Sodium nitrate was used as a supporting electrolyte at such concentrations that the transport number of the iodide ions was effectively reduced to zero. The vessel was completely filled with the solution. The anode was made comparatively small (area 0.48 cm^2) to keep down the total deposition of iodide ions. The amount deposited never exceeded 1 % of the total quantity. After taking each current-cell voltage curve, both the solution and the anode were replaced by fresh samples.

The temperature, which was determined with an accuracy of $\pm$ 0.05°C, was measured using a calibrated thermometer obtained from "Deutsches Amt für Mass und Gewicht".

The circuit employed is shown in Fig. 3. The cell voltage, which was measured by a vacuum tube voltmeter with an internal resistance of 11 MΩ, was increased stepwise by means of a variable resistance. The electrolysis current could be read off directly on the galvanometer because practically no current passed through the voltmeter.

When a supporting electrolyte was not added to the electrolyte, an almost straight line was obtained upon plotting the current against the cell voltage

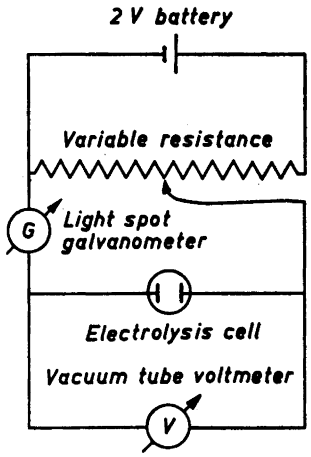

Fig. 3. Circuit used for measurement of limiting current density.

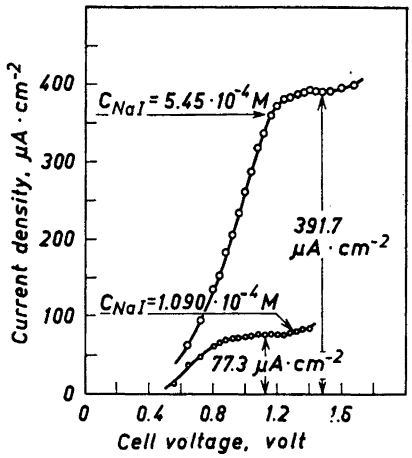

Fig. 4. Current-cell voltage curves obtained for anodic deposition, of I^- from a solution of NaI in methanol. Supporting electrolyte, 0.10 M $NaNO_3$; Stirring rate, 400 rpm; Temp. 25.0°C; Anode area, 0.48 cm^2.

and it was thus not possible to read off the limiting current from the diagram. The fact that the current efficiency for reaction (2) becomes less than 100 % when the limiting current is exceeded was used to determine this quantity in a pure sodium iodide solution by means of a radioactive method. This method, which is comparatively laborious, was restricted to one experiment only for the purpose of demonstration, and was carried out as follows.

From 250 ml of a solution of sodium iodide in methanol containing 5 μC NaI—131, 50 ml portions were transferred to the electrolysis cell. Depositions were performed on a number of anodes (area 1.50 cm^2) at different current densities. Each 50-ml portion of the electrolyte was used for three depositions. On each anode, 0.4 % of the total amount of iodide was deposited. Thus the maximum reduction was 1.2 %. The electrolysis times were adjusted so that the amount of current was nearly equal for all the anodes. After the usual corrections, the electrode activities were plotted against the current density (Fig. 6).

Results. In Fig. 4, the current density has been plotted against cell voltage for two concentrations of sodium iodide in methanol. The height of the steps represents the magnitude of the limiting current densities. According to eqn. (4), these should be proportional to the concentration of the iodide ions. From the data given in the diagram, it can be calculated that the ratio between the two concentrations is 5:1.00 and that the ratio between the corresponding limiting current densities, which should theoretically be the same, is 5:0.99. Thus there is good agreement between the theoretical and experimental values.

Fig. 5 shows a plot of the limiting current density against the concentration of sodium iodide in three solvents and at two stirring rates. According

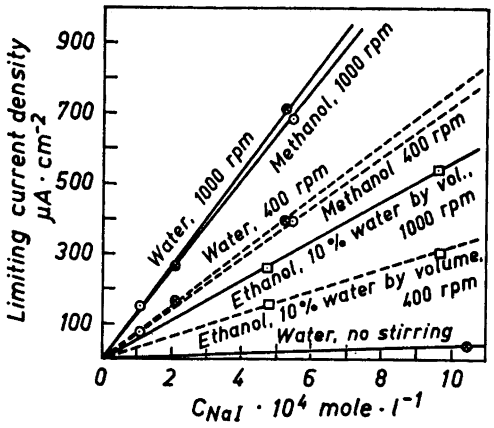

Fig. 5. Limiting current density as function of NaI concentration in different solvents at 25.0°C and two stirring rates. The concentration of the supporting electrolyte (sodium nitrate) is 0.1 M in water and methanol and 0.05 M in ethanol.

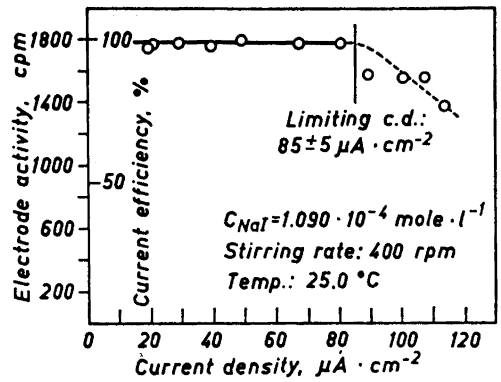

Fig. 6. Current efficiency as function of current density for anodic formation of silver iodide.

to eqn. (4), the points should fall on straight lines passing through the origin. This was in fact the case to within rather small errors.

The thickness δ of the diffusion layer at the electrode surface, for the various solvents used, can be calculated by eqn. (3) and the data given in Fig. 5. The results are summarized in Table 1.

Table 1. Estimated thickness of the diffusion layer for anodic deposition of iodide ions from solutions of sodium iodide in different solvents at 25°C and at various stirring efficiencies.

Solvent	Supporting electrolyte	$D°_{I^-} \times 10^5$ cm². sec⁻¹	δ cm (no stirring)	δ cm (400 rpm)	δ cm (1 000 rpm)	Temp °C
Water	0.1 M $NaNO_3$	2.05	0.050	0.0026	0.0015	25.0
Methanol	0.1 M $NaNO_3$	1.68	—	0.0022	0.0013	25.0
Ethanol (10 % water by vol.)	0.05 M $NaNO_3$	0.81	—	0.0024	0.0014	25.0

The diffusion coefficients used in the calculations have been estimated [12] by the formula $D° = \frac{RT}{nF^2} \cdot \lambda°$. The $\lambda°$-values used were: 76.8 for water [18], 62.8 for methanol [19] and 30.4 for the ethanol-water mixture [20]. The last value was computed by interpolation between values given for pure ethanol and for ethanol containing 25 % water by volume.

Eqn. (5) indicates that the difference in magnitude of the limiting current density for different solvents is due to differences in the quotient D/δ. From Table 1 one can see that, at a given stirring rate, the difference in thickness of the diffusion layers for the solvents used is not very great and that the limiting current density is mainly determined by the value of the diffusion coefficient. The magnitude of δ is in agreement with previous experience that the thickness of the diffusion layer tends to a minimum value [10] of about 0.001 cm in well-stirred solutions. The calculated value for δ in an unstirred solution of sodium iodide in water is 0.05 cm. This is also a plausible value.

In Fig. 6, the current efficiency for the anodic formation of radioactive silver iodide from a solution of sodium iodide in methanol has been plotted against the current density. From this curve, the limiting current density 85 ± 5 $\mu A \cdot cm^{-2}$ can be read off. This is to be compared with the value 77 $\mu A \cdot cm^{-2}$ which, according to Figs. 4 and 5, is obtained when a supporting electrolyte is present. The higher value obtained for the pure sodium iodide solution is due to the contribution of a migration current to the diffusion current according to eqn. (6). This positive effect is, however, counteracted by a decrease in the value of the diffusion coefficient * so that the overall net effect is only a slight increase in the limiting current density.

ELECTROLYSIS TIME

When the kinetic experiments are performed by electrolytic deposition on a number of electrodes at stated intervals, the electrolysis time should be short compared with the total observable time range. Otherwise the composition of the reaction mixture changes too much during the deposition. It is therefore of interest to know how short one can make the electrolysis time without causing a serious deterioration is the reproducibility. This was investigated as follows. From a radioactive solution of sodium iodide in methanol, depositions were carried out on a number of anodes under the same experimental conditions and the activities were measured. The mean value was computed, after the usual corrections and recalculation of the individual activity values to equal amounts of current. The electrolysis times were then successively shortened to a minimum value of 1 sec, but the current density was kept unchanged.

In Table 2, the results obtained are given together with the experimental conditions. All activities are converted to 6 000 μQ which was approximately the total amount of current after 30 sec. electrolysis. The discrepancy in the individual activities, from the mean value, is after 30 sec. electrolysis in most cases less than 1 %. The accuracy is acceptable down to an electrolysis time as short as about 5 sec. This minimum may probably be shortened still more after further development of the method.

* The diffusion coefficient, estimated to be 1.68×10^{-5} $cm^2.sec^{-1}$ at 25°C for iodide ions in the presence of a supporting electrolyte, is reduced to about 1.2×10^{-5} $cm^2.sec^{-1}$ for the pure sodium iodide solution. This latter value has been estimated from the value [17] 1.0×10^{-5} $cm^2.sec^{-1}$ given at 14°C whereby it has been assumed that the temperature coefficient [12] for the diffusion coefficient is 2 % deg^{-1}.

Table 2. Influence of electrolysis time on reproducibility of anodic deposition of radioactive silver iodide.

Electrolysis time, sec.	Activity, cpm, after recalculation to 6 000 μQ		Deviation (in %) of the activity from the mean value (12 647)	Experimental conditions
30.06	12 570		−0.6	Initial composition of the electrolyte: 0.000272 M NaI in methanol.
30.12	12 486		−1.3	
30.45	12 654		+ 0.1	
30.13	12 690	Mean	+ 0.4	4 μC NaI * in 50 ml sample.
30.48	12 564	value	−0.6	
30.16	12 690	12 647	+ 0.4	
30.17	12 402		−1.9	Temp.: 25.0°C
30.13	12 684		+ 0.3	
29.98	12 906		+ 2.1	Stirring rate: 400 rpm.
30.20	12 822		+ 1.4	
				Current density:
20.18	12 606		−0.3	130 $\mu A \cdot cm^{-2}$
7.03	12 120		−4.2	
5.06	12 618		−0.2	Anode area: 1.50 cm^2
3.08	11 784		−6.8	
2.06	11 610		−8.2	
1.07	13 800		+ 9.1	

HETEROGENEOUS EXCHANGE BETWEEN THE SILVER IODIDE-COVERED ELECTRODE SURFACE AND THE REACTION MIXTURE

If heterogeneous exchange occurs between the silver iodide-covered surface of the anode and the methyl iodide in the reaction mixture, an error will be introduced. On the other hand, an exchange between the electrode and the iodide ions in the solution will cause no error because the ratio between the number of active and inactive iodine atoms is equal * for the silver iodide layer and for the sodium iodide in the solution. Thus any heterogeneous exchange between these components will not change the radioactivity of the electrode.

To find out whether there is any heterogeneous exchange between the methyl iodide in the solution and the electrode, the following experiment was carried out. A silver electrode, with a thin layer of electrolytically formed inactive silver iodide, was dipped into a solution of radioactive methyl iodide ** in methanol which was kept at 25.0°C and stirred at a rate of 400 rpm. After 5 min, the electrode was removed, rinsed and counted. No activity above the background activity was found. Thus there was no measurable exchange between the methyl iodide and the silver iodide-covered electrode under the conditions in question.

* A condition for this is however that the time of deposition is so short that the change in composition of the reaction mixture can be neglected.

** The radioactive methyl iodide was prepared by adding 1 μC carrier-free NaI−131 to 50 ml 0.03 M methyl iodide + 0.0002 M NaI in methanol. The solution was allowed to stand until equilibrium had been reached.

INVESTIGATION OF THE ISOTOPIC EXCHANGE BETWEEN METHYL IODIDE AND SODIUM IODIDE IN METHANOL

The experimental technique. The kinetic experiments were performed as follows. The electrolysis cell was completely filled with a solution of inactive sodium iodide and methyl iodide in dry methanol. When the reaction mixture had reached the thermostat temperature, the exchange reaction was started by adding carrierfree NaI—131 in 0.2 ml of the dry solvent. The radioactive solution was added rapidly by means of a syringe. At pre-determined times of reaction, different anodes were dipped into the reaction mixture and electrolysis was carried out. The times of reaction, taken at the middle of the electrolysis, were measured by a stop-watch. After the electrolytic deposition, the anode was immediately removed and replaced by a new one. The silver iodide-covered anode was then treated as follows: After a thorough rinsing with alcohol, the paraffin wax was removed by petroleum ether. The copper wire was cut off near the silver plate. The latter was then mounted in a reproducible manner on a source holder and counted in the flow counter. If counting could not be performed immediately, the electrodes were kept in the dark to prevent any loss of activity due to photochemical decomposition of the radioactive silver iodide.

The rate equation. If the reaction,

$$CH_3I + NaI^* \underset{k}{\overset{k}{\rightleftharpoons}} CH_3I^* + NaI,$$

is of the second order, then the rate equation can be deduced as follows: Let the concentrations of the reacting species at times 0 and t be:

	CH_3I	NaI^*	CH_3I^*	NaI
$t = 0$	a_o	b_o	0	c_o
$t = t$	$(a_o - x)$	$(b_o - x) = b$	x	$(c_o + x)$

Then the reaction rate is given by the expression:

$$\frac{dx}{dt} = k(a_o - x)(b_o - x) - kx(c_o + x) \tag{7}$$

which after integration becomes

$$\log_e \frac{a_o b_o - x(a_o + b_o + c_o)}{a_o b_o} = -k(a_o + b_o + c_o) \cdot t \tag{8}$$

If the organic iodide is used in great excess, c_o can be neglected in comparison with a_o, and since b_o is negligibly small, eqn. (8) reduces to

$$\log_e \frac{b_o - x}{b_o} = \log_e \frac{b}{b_o} = -k \cdot a_o \cdot t \tag{9}$$

Eqn. (9) can be written in the simple form

$$b = b_o \cdot e^{-k't} \tag{10}$$

where $k' = k \cdot a_o$ is the pseudo-first order rate constant.

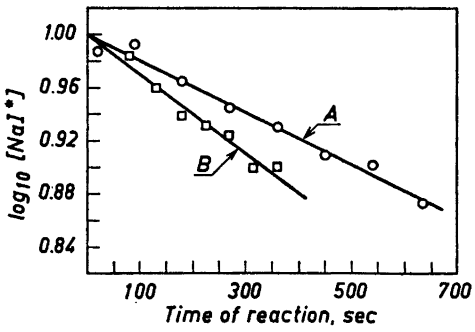

Fig. 7.

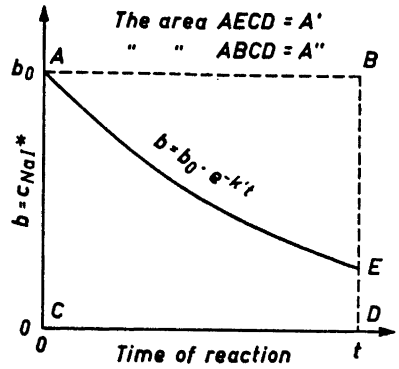

Fig. 8.

Since the radioactivity of the electrodes, at equal amounts of current, is proportional to b, a straight line should be obtained when the logarithm of the electrode activities is plotted against the time of reaction. The slope of the line is equal to $-k'/2.303$.

Results. In Fig. 7 the logarithm of the electrode activities has been plotted against time for two runs. The straight lines have been fitted to the points according to the method of least squares. The experimental conditions and results are summarized in Table 3.

Table 3. Results of exchange experiments between CH_3I and NaI in dry methanol. Experimental conditions, which were equal for A and B: Spec. activity of NaI: 1 μC/50 ml sample. Current density: 130 $\mu A.cm^{-2}$. Electrolysis time: 12 sec. Stirring rate *: 400 rpm. Anode area: 1.50 cm^2. Total reduction of iodide ions: 1.3 %. Radioactivity of the anodes: 850—1 200 cpm.

Expt.	A	B	Previous expts.[5]	
Temp. °C	25.0	25.0	25.0	25.0
a_0 mole·l^{-1}	0.1291	0.2174	0.00736	0.01508
c_0 mole·l^{-1} × 10^4	2.80	2.80	2.00	2.00
Rate constant × 10^4 l·$mole^{-1}$·sec^{-1}	34.8	31.5	34.2	33.4
		Mean value	33.5	

* The solution was stirred only during the course of the electrolysis.

In experiment A, the total observation time was 10 min. The scattering of the points is not very great and the k-value is in good agreement with the values reported in a preliminary account of this work [5]. In experiment B, the scattering of the points is greater, though the k-value could be accepted.

From the fact that straight lines are obtained when log b is plotted against time and from the fact that a 30-fold change in the concentration of the methyl iodide does not alter the k-value, it is clear that the reaction is of first order with respect to the inorganic iodide as well as the organic iodide. Thus the overall reaction is second order. The k-value obtained by Swart and Le Roux [1], 80×10^{-4} l·mole^{-1}·sec^{-1}, at the same temperature, 25°C, must be too high.

RAPID REACTIONS

It is evident that kinetic measurements can be performed, with good accuracy, by electrodeposition on a number of different electrodes provided that the observable time range is at least about 10 min. At shorter times it is necessary to modify the method. This case will now be discussed. For simplicity, the discussion will refer to pseudo-first order exchange reactions in which the organic iodide is used in great excess.

Without any special modifications the Hartridge-Roughton technique is applicable to reactions with halflives up to 10 sec. This technique could certainly be combined with the electrolytic method in a useful way.

Reactions which are too slow for the Hartridge-Roughton method but too rapid for common work might be studied either by a moving silver band anode, by the integral method or by the capacity flow method. The last method is undoubtly realizable in practice but is, unfortunately, rather laborious and requires comparatively large amounts of liquid since a steady state has to be created before electrolysis can be performed. It would thus be advantageous if one of the other methods proposed could be made successful.

The principle of the integral method will be described using Fig. 8. The curve in the diagram represents a pseudo-first order exchange reaction, $b = b_0 \cdot e^{-k't}$, in which the organic iodide is in great excess. If an electrolytic deposition is carried out with a constant current strength during t sec from the very moment when the exchange reaction is started, the resulting radioactivity, A', of the anode can be represented by the area AECD between the curve and the t-axis. Consequently:

$$A' = \int_0^t b_0 \cdot e^{-k't}\, dt = \frac{b_0}{k'} [1 - e^{-k't}] \tag{11}$$

If another deposition from an iodide ion solution of specific activity equal to the initial specific activity of the iodide ions in the reaction mixture is then carried out on a new anode, the electrode activity, A'', obtained after t sec. electrolysis can be represented by the rectangle ABCD. Hence

$$A'' = b_0 \cdot t \tag{12}$$

After elimination of b_0 between eqns. (11) and (12), one obtains:

$$\frac{A'}{A''} = \frac{1 - e^{-k't}}{k't} \tag{13}$$

This equation can thus be used for calculation of k'.

From the experimental data in Table 2, it is obvious that electrode activities of the order of magnitude 1 000 cpm can be obtained after a deposition time of a few seconds, even with a rather low specific activity for the sample. Provided that the mixing time can be made short enough, it appears to be possible to study exchange reactions of this type with halflives as short as a few seconds by means of the integral method. This, and the other methods proposed, will be studied in further investigations.

Acknowledgements. The author wishes to thank Professor Ole Lamm, Head of this Division, for suggesting and supporting this work. Grateful acknowledgement is likewise due to Dr. Stig Ljunggren for valuable discussions and to the *Swedish Atomic Research Council* for the instrumental support.

REFERENCES

1. Swart, E. R. and Le Roux, L. J. *J. Chem. Soc.* **1957** 406.
2. Leary, J. A. *Diss. Abstr.* **17** (1957) 47.
3. Hartridge, H. and Roughton, F. J. W. *Proc. Roy. Soc. London* **A 104** (1923) 376.
4. Weissberger, A. *Rates and Mechanisms of Reactions.* Interscience Publishers Inc. 1953, p. 669.
5. Beronius, P. and Lamm, O. *Trans. Faraday Soc.* **56** (1960) 1793.
6. Lingane, J. J. and Small, L. A. *Anal. Chem.* **21** (1949) 1119.
7. Lingane, J. J. *Electroanalytical Chemistry,* Interscience Publishers Inc. 1958, p. 225–227.
8. *Ibid.* p. 198–201.
9. Potter, E. C. *Electrochemistry, Principles and Applications.* Cleaver-Hume Press Ltd., London 1956, p. 146.
10. *Ibid.* p. 146.
11. Kolthoff, I. M. and Lingane, J. J. *Polarography,* Interscience Publishers Inc. 1952, p. 122.
12. *Ibid.* p. 52–53.
13. Denbigh, K. G. and Page, F. M. *Discussions Faraday Soc.* **17** (1954) 145.
14. *Materials & Methods,* **38** (1953) 102.
15. Fieser, L. F. *Experiments in Organic Chemistry,* D. C. Heath and Co. Boston 1955, p. 289.
16. Slack, L. and Way, K. *Radiations from Radioactive Atoms in Frequent Use,* USAEC, February 1959.
17. *International Critical Tables* **V** p. 72.
18. Robinson, R. A. and Stokes, R. H. *Electrolyte Solutions,* Butterworths Scientific Publications, London 1955, p. 452.
19. *Ibid.* p. 163.
20. Asunmaa, S. *Ann. Acad. Sci. Fennicae* **A 53** (1940) No. 11, p. 84.

Received December 23, 1960.

ACTA CHEMICA SCANDINAVICA 15 (1961) 1165–1176

Methods for the Paper Chromatographic and Paper Electrophoretic Separation of Iodide, Iodotyrosines, Iodothyronines and their Derivatives

F. BJÖRKSTÉN, R. GRÄSBECK and B.-A. LAMBERG

The Minerva Foundation Institute for Medical Research, Apollogatan 5 B, Helsingfors, Finland

The authors present new techniques and a critical review of the techniques currently used for the separation and identification of thyroid hormones and related compounds. The solvent systems considered potentially useful were first classified into six groups and the general properties of these groups investigated. New chromatographic and electrophoretic systems were developed and these are described in detail. Special attention was paid to two-dimensional techniques. Solvent systems which continuously changed their composition were used, their action being analogous to the gradient elution employed in column chromatography. Staining methods are discussed.

Paper chromatography and paper electrophoresis, often in combination with isotope techniques, are widely used for the separation and identification of thyroid hormones and related compounds *. The methods have been reviewed by Roche, Lissitzky and Michel [2] and by Taurog and Chaikoff [3].

In spite of the large number of such techniques described, some of the analytical problems encountered in the authors' studies on the metabolic transformations of thyroid hormones could not be solved with the existing methods. For instance, no effective two-dimensional system seemed to have been evolved. A systematic investigation of the current techniques was therefore undertaken, and efforts were made to devise new and more satisfactory methods.

* Abbreviations: The abbreviations are those used by Solomon and Dowling [1]: DIT diiodotyrosine, MIT monoiodotyrosine, T_2 diiodothyronine, T_3 triiodothyronine, T_4 thyroxine, T_2A diiodothyroacetic acid, T_3A triiodothyroacetic acid, T_4A tetraiodothyroacetic acid, T_3F triiodothyroformic acid, T_4F tetraiodothyroformic acid, T_3P triiodothyropropionic acid, T_4P tetraiodothyropropionic acid.

PREPARATION OF SAMPLES

In nature, thyroid hormones and related compounds occur in very low concentrations. This frequently makes it necessary to purify samples before chromatography or electrophoresis, since only a limited amount of substance can be applied to the paper. Purification procedures have been discussed in the reviews mentioned [2,3] and many other articles [4,5]. A useful and widely employed method is extraction of the compounds with *n*-butanol, which is then concentrated to a suitable volume under reduced pressure. This simple technique has been used in our laboratory prior to the chromatography and electrophoresis of the iodine compounds contained in plasma, tissue homogenates, urine, faeces, bacterial incubation media [6], *etc.*

SOLVENT SYSTEMS FOR CHROMATOGRAPHY

For the paper chromatography of thyroid hormones and related compounds many different solvent systems have been recommended. It was found useful to classify these systems into groups (Table 1). The systems of each group are similar both in composition and resolving properties.

The results reported were obtained with Whatman No. 1 paper for chromatography. Unless otherwise stated, the ratios of the solvents in solvent mixtures are volume ratios (v/v).

Alkaline organic systems. Usually the solvent systems of this group are made up of the following two or three components:

1. An aliphatic C_3—C_5 alcohol is the main constituent.
2. Occasionally a smaller amount of an aliphatic C_1—C_4 alcohol or some other solvent of similar polarity, *e.g.* acetone or dioxane, is added.
3. The organic solvent(s) is (are) saturated with aqueous ammonia. The molarities of the ammonia solutions used vary within wide limits.

Other alkaline organic systems have also been used. A frequently utilized system is composed of collidine and aqueous ammonia.

In preparing the solvent systems the components are first mixed by shaking, and the two phases formed are then separated. The organic phase is used for chromatography, and the aqueous phase may be used for the saturation of the atmosphere in the chromatography tank.

All systems of this group separate the compounds in a similar manner. Thus the relative mobilities of the compounds in the different systems are fairly similar. The relative mobilities indicated by the R_F values given for two systems (Table 4) are typical. It was noted that the resolving efficiency and the R_F values are highly dependent on the ammonia concentration in the atmos-

Table 1. Grouping of chromatography solvent systems.

1. Alkaline organic systems
2. Neutral organic systems
3. Acidic organic systems
4. Alkaline aqueous systems
5. Neutral aqueous systems
6. Acidic aqueous systems

phere of the tank. Since ammonia readily escapes from the tank, accurate reproduction of conditions and results is difficult, and R_F values can only be taken as indicators of relative mobilities. In order to minimise variations in mobility, we found it necessary, immediately before each run, to check and adjust the ammonia content of the aqueous phase kept in the tank.

The following two empirical rules proved helpful when new systems were being developed and when it was found difficult to reproduce results reported in the literature:

1. An increase in the concentration of component No. 2 will counteract trailing and increase the R_F values. Particularly the R_F values for highly iodinated compounds like DIT and T_4 will increase.

2. An increase in the ammonia concentration has effects similar to an increase of component No. 2.

The chromatograms reproduced in Figs. 1 and 2 show how variations in ethanol and ammonia concentrations influence the results.

The alkaline organic system group is the most useful one in the separation of compounds of the present type. It is particularly well suited for the separation of different iodothyronine derivatives from each other and from iodide



Fig. 1. One-dimensional chromatogram run with the *n*-butanol — 0.5 M ammonia — ethanol — water system. Some pure compounds and a mixture of MIT, DIT, T_3 and T_4 were applied to the paper. The positions of the iodine substituents in the compounds are given in Table 4.

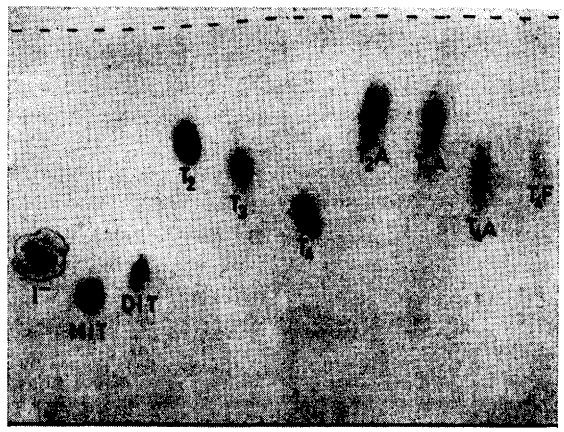

Fig. 2. One-dimensional chromatogram run with *n*-butanol — ethanol — 2 M ammonia (10:3:10). Some pure compounds were applied to the paper. The positions of the iodine substituents in the compounds are given in Table 4.

and the iodotyrosines. Some of the most popular systems are listed in Table 2. The best single system seems to be *tert*-amyl alcohol — 2 M ammonia.

Unfortunately this valuable group also has its shortcomings. As the relative mobilities of the compounds are similar in the different systems, it is difficult to check the results obtained with one system with the aid of another belonging to the same group. It is also inadvisable to use a combination of two alkaline

Table 2. Solvent systems generally used for the paper chromatographic separation of iodotyrosines, iodothyronines and their derivatives.

Group according to Table 1	Solvent system	References	Uses
Alkaline organic systems	*tert*-Amyl alcohol — 2 M ammonia (1:1)	3, 7	Particularly efficient for the separation of thyronine derivatives from each other and from iodide and iodotyrosines
»	*n*-Butanol — dioxane — 2 M ammonia (4:1:5)	2, 3, 8	General use
»	*n*-Butanol — ethanol — 2 M ammonia (5:1:2)	9	» »
»	Collidine — water (100:35) with ammonia in the atmosphere	2,3	» »
Acidic organic systems	*n*-Butanol — acetic acid — water (78:5:17)	2, 10	Separation of I^-, MIT and DIT from each other and from the iodothyronine group

organic systems for two-dimensional chromatography (see section on two-dimensional systems). Further, most alkaline organic systems fail to separate MIT and DIT efficiently. A few of the solvents have some drawbacks. Dioxane is said to cause the formation of artefacts [5]. This can to some extent be prevented by purification of the dioxane by distillation and by the addition of cyanide or some other reducing agent [5]. Collidine has an unpleasant odour.

We have felt the need for a simple system which would effectively separate the chief compounds found in the thyroid and the blood, *i.e.* I^-, MIT, DIT, T_3 and T_4. For this purpose we have modified [6] the *n*-butanol — ethanol — 2 M ammonia system listed in Table 2. 20 volumes of *n*-butanol are added to 20 volumes of 0.5 M ammonia and shaken, whereupon the phases are separated. To the organic phase are added 2 volumes of 94 % (w/w) ethanol and 1 volume of water. The entire aqueous phase and 40 % of the organic phase are used for the saturation of the atmosphere. The water phase must be 0.3—0.4 M in respect to ammonia. Note that the organic phase used in the run is not completely in equilibrium with the phases saturating the atmosphere. The solvent migrating into the paper will therefore undergo a gradual change until it is equilibrated with the atmosphere. Fig. 1 shows a paper run with the *n*-butanol — 0.5 M ammonia — ethanol — water system. For R_F values see Table 4. A fault of the system is that thyronine derivatives show moderate trailing which more or less precludes its use for two-dimensional chromatography. The system *n*-butanol — ethanol — 2 M ammonia (10:3:10) gives rounder and sharper spots but poorer separation (Fig. 3 and Table 4). This system is better suited for two-dimensional chromatography.

Acidic organic systems. The systems of this group in general use all have as their basis *n*-butanol to which varying amounts of acetic acid and water are



Fig. 3. One-dimensional chromatogram run with toluene — formic acid — ethanol (10:3:3). Some pure compounds and a mixture of T_4 and T_4A were applied to the paper. The positions of the iodine substituents in the compounds are given in Table 4.

added. In Table 2 a popular system is given as an example. The *n*-butanol — acetic acid — water systems are usually employed for the separation of I^-, MIT, DIT and the iodothyronines. The iodothyronines and their derivatives are not separated from each other.

Many authors have pointed out the risk of artefact formation when acidic systems are used [3,5,11,12]. Small amounts of iodide may be oxidised into iodine, and the free iodine may exchange with the bound iodine of the iodothyronine molecules [7]. The following equations show schematically how labelled T_4 may appear as an artefact:

$$*I^- + I^- \longrightarrow *I{-}I\,(=I_2) + 2\,e^-$$

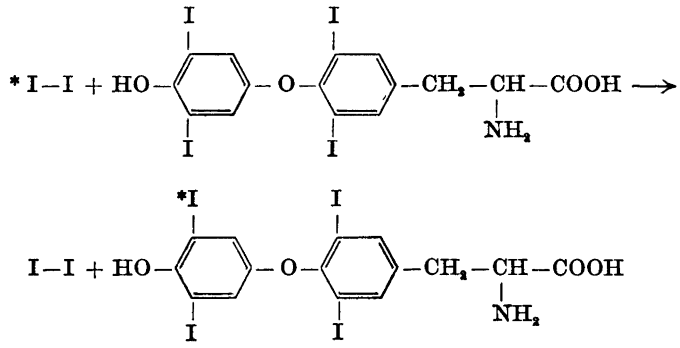

Thus radioactive iodine may cause the labelling of non-labelled T_4. Previously non-iodinated substances may also be iodinated and labelled by the free iodine[11]. Attempts have been made to prevent the formation of artefacts by addition of reducing agents, such as sodium thiosulphate [5, 12], which keep the iodine in reduced iodide form. Dilution of the radioactive iodide with carrier will also decrease the formation of artefacts.

The acidic systems are poorly suited for quantitative separation of iodide from other compounds, since some iodide, in the form of hydrogen iodide, will evaporate from the paper.

The following new acidic organic system has been found useful: Just before use, 10 volumes of toluene are mixed with 3 volumes of formic acid and 3 volumes of 94 % (w/w) ethanol containing 1.5 g/l sodium thiosulphate. No phases separate. Ascending chromatography is used. The running time is 2 h, in which time the solvent front travels about 20 cm. Since the ethanol and the formic acid are rapidly esterified, the composition of the system changes during the run. At the end, about 50 % of the formic acid is esterified. The products formed in the reaction cause the appearance of two phases. The toluene — formic acid — ethanol system is a second example of a continuously changing chromatographic system. Deaminated thyronine analogues, *e.g.* T_4A and T_4P, move close to the solvent front and are not separated from each other. Iodide, iodotyrosines and iodothyronines have different R_F values, but the differences are too small to produce effective separation. (Fig. 2 and Table 4). The system may profitably be used for detecting deaminated thyronine analogues in a

Table 3. New solvent systems for paper chromatography. For details concerning preparation, see text.

Group according to Table 1	Solvent system	References	Uses
Alkaline organic systems	*n*-Butanol – 0.5 M ammonia – ethanol – water	6	Particularly suitable for the separation of I^-, MIT, DIT, T_3 and T_4
»	*n*-Butanol – ethanol – 2 M ammonia (10:3:10)		Two-dimensional chromatography
Acidic organic systems	Toluene – formic acid – ethanol (10:3:3)		Separation of deaminated thyronine derivatives, *e.g.* T_4A and T_4P, from other compounds
Acidic aqueous systems	Water – formic acid (5:1)		Particularly suitable for two-dimensional chromatography in combination with an alkaline organic system

preparation. The formation of artefacts is minimised by the addition of sodium thiosulphate and by the unusually short running time.

Acidic aqueous systems. As far as we know this type of chromatography system has not previously been used for the separation of thyroid hormones and related compounds. However, an investigation of this group showed that the system water – formic acid (5:1) with 0.3 g/l sodium thiosulphate added had many valuable properties. It is very rapid; the solvent front travels 35 cm in 3 h. The compounds are also well separated, and the R_F values are quite different from those obtained with other systems. This makes the water – formic acid system particularly well suited for two-dimensional chromatography in conjunction with an alkaline organic system (Fig. 4).

In the first experiments with acidic aqueous systems some difficulty was experienced because of the low solubility of many of the iodinated compounds. In particular, the tetraiodothyronine derivatives showed poor solubility. However, good results were obtained when the compounds were applied to the paper in sufficiently small quantities. An amount of the order of 0.1 μg of each compound is usually suitable. Such quantities are still easily detected with the sensitive colour reagents available [13,14].

The main disadvantage of the water – formic acid system is its acidity, as acidic systems may cause the formation of artefacts and evaporation of some iodide (see section on acidic organic systems). The undesirable tendencies are minimised by the short running time needed and by addition of sodium thiosulphate to the solvent system and carrier iodide to the sample.

Neutral organic, alkaline aqueous and neutral aqueous systems. These systems proved less useful for our purposes. Neutral organic systems have been employed by some investigators. Two such systems are mentioned as examples 95 % ethanol – 0.2 M ammonium carbonate (2:1) [3,15] and *n*-butanol – ethanol

Table 4. R_F values and electrophoretic mobilities of iodide, iodotyrosines, iodothyronines and their derivatives. R_F values are given for the new solvent systems listed in Table 3. The electrophoretic mobilities were obtained in paper electrophoresis with a diethylbarbiturate buffer with a pH of 8.0 and an ionic strength of 0.06. Serum albumin was used as reference in the electrophoresis, and its mobility was given the value 1.

Compound	R_F values				Electrophoretic mobilities
	n-butanol — 0.5 M ammonia — ethanol — water	*n*-butanol — ethanol — 2 M ammonia (10:3:10)	toluene — formic acid-ethanol (10:3:3)	water — formic acid (5:1)	
I^-	0.27	0.44	0.03	0.79	3.4
3-MIT	0.17	0.34	0.14	0.77	0.59
3,5-DIT	0.10	0.40	0.17	0.67	1.09
3,5-T_2	0.71	0.72	0.18	0.68	0.23
3,5,3'-T_3	0.70	0.65	0.22	0.54	0.10
3,5,3',5'-T_4	0.54	0.53	0.29	0.35	0.20
3,5-T_2A	0.80	0.78	0.94	0.57	0.96
3,5,3'-T_3A	0.79	0.75	0.98	0.36	0.88
3,5,3',5'-T_4A	0.64	0.63	0.98	0.14	1.34
3,5,3'-T_3F	0.81	0.74	0.98	0.20	0.74
3,5,3',5'-T_4F	0.70	0.67	0.99	0.12	1.16
3,5,3'-T_3P	0.79	0.75	0.97	0.28	0.80
3,5,3',5'-T_4P	0.66	0.72	0.98	0.08	1.15

— water (4:1:5) [16]. A few experiments with alkaline aqueous systems indicated that the compounds travel close to the solvent front and are not separated from each other. Some systems belonging to the neutral aqueous group have been employed. The best known is methanol — 0.2 M ammonium acetate (2:5) [3,13]. This system separates iodide and the iodotyrosines from each other and from the iodothyronine group.

PAPER ELECTROPHORESIS

Paper electrophoresis has frequently been used by French workers [17–19] and occasionally by others [20–23]. Both high-voltage and low-voltage techniques have been employed. Although buffers within the pH range 5.8—9.5 have been used, in our experience the best separation is obtained with a pH of about 8. Diethylbarbiturate [18,20,22] and ammonium carbonate [17] buffers are commonly used. At pH 8, most of the compounds move towards the anode. Only the amines, *e.g.* thyroxamine, remain stationary or have cathodic mobility. Iodide migrates much faster than the organic compounds and can be separated from these by applying the current for a short time only. The other compounds separate when electrophoresis is continued for a longer time. The quality of the separation is similar to that obtained with paper chromatography. Since the electrophoretic mobilities differ from the chromatographic ones, the two techniques supplement each other, and may be combined into two-dimensional chromatography-electrophoresis [17,19]. Electrophoresis is particularly to be recommended because of its mild conditions.

A few experiments conducted with different buffers led to the use of a diethylbarbiturate buffer with a pH of 8.0 and an ionic strength of 0.06. A voltage gradient of 7 V/cm was applied. The relative mobilities of some compounds in this system are given in Table 4. Fig. 5 shows a two-dimensional chromato-electropherogram.

TWO-DIMENSIONAL TECHNIQUES

As the number of naturally occuring thyroid hormone analogues has turned out to be great, the necessity of resorting to two-dimensional techniques has become apparent. It is doubtful, for instance, whether the acetic acid analogues can be identified with the sole aid of one-dimensional chromatography [24]. Many combinations of the numerous existing systems have been employed for two-dimensional runs.

Practically all the chromatographic systems in general use belong to either the alkaline organic or the acidic organic group. The acidic organic solvent systems do not separate thyronine derivatives and their application is therefore limited to some special purposes. An alkaline organic system may profitably be utilised for chromatography in one direction, but it is not very advisable to use systems from this group for both directions, since the relative mobilities of the compounds are similar in all alkaline organic systems. When a combination of such systems is used, a chromatogram is produced on which all the compounds lie approximately along a straight line, and the separation is not much better than on a one-dimensional strip.

Two methods were found to give good results: The first one consists of two-dimensional chromatography with *tert*-amyl alcohol — 2 M ammonia (1:1) in one direction and water — formic acid (5:1) containing 0.3 g/l sodium thiosulphate in the other (Fig. 4).

The second method is a slight modification of the technique employed by the French school [17,19]. First, chromatography with *tert*-amyl alcohol — 2 M ammonia (1:1), then electrophoresis with a diethylbarbiturate buffer of pH 8.0 and an ionic strength of 0.06 in the second direction (Fig. 5). Care must be taken not to disturb the spot pattern on the paper when it is moistened with the electrophoresis buffer. The best way to apply the buffer is to place the dry paper on a glass plate and spray the buffer evenly over it with an atomiser operated with compressed air from an electric pump. The amount of buffer applied is not very critical.

COLOUR REAGENTS

Several colour reagents are suitable for the detection of thyroid hormones and related compounds on filter paper.

An alkaline solution of diazotised sulphanilic acid (Pauly's reagent) gives characteristic red and violet colours with phenolic compounds, and is useful for the detection of tyrosine and thyronine derivatives. The reagent may be conveniently applied by spraying the paper with a freshly prepared solution of diazotised sulphanilic acid and sodium carbonate in water [3]. Its principal disadvantage is the comparatively low sensitivity; 5—50 μg of the compound to be coloured is needed.

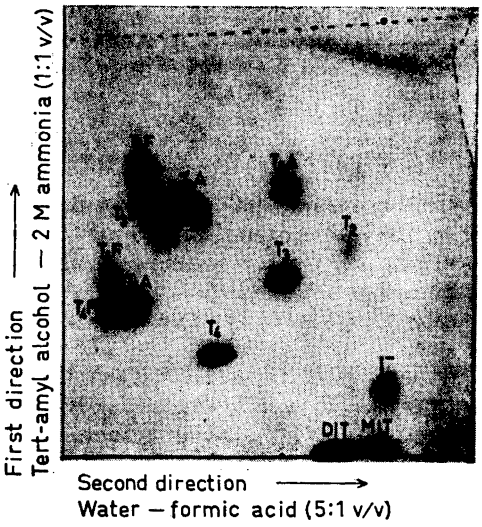

Fig. 4. Two-dimensional chromatogram run in the first direction with *tert*-amyl alcohol — 2 M ammonia (1:1) and in the second with water — formic acid (5:1). The positions of the iodine substituents in the compounds applied to the paper are given in Table 4.

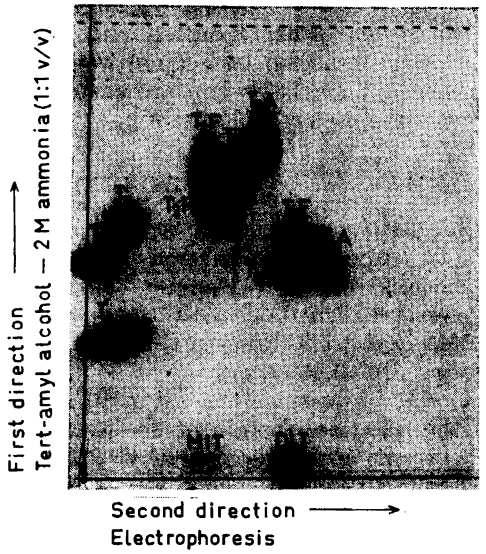

Fig. 5. Two-dimensional chromato-electropherogram. Chromatography in the first direction with *tert*-amyl alcohol — 2 M ammonia (1:1) and electrophoresis in the second, a diethylbarbiturate buffer with a pH of 8.0 and an ionic strength of 0.06 being used. The positions of the iodine substituents in the compounds applied to the paper are given in Table 4.

Iodide and many iodine containing compounds can be detected with a ceric sulphate — arsenious acid colouring agent. The original reagent [25] has been modified by several investigators [14,26-28]. It is fairly specific and highly sensitive; 0.005 μg of organic iodine can be detected [14]. Neither this reagent nor the following one is completely specific for iodine; some reducing substances also give the colour reactions.

A second spraying reagent based on the catalytic properties of iodine has been described by Gmelin and Virtanen [13], who use an acidic solution of ferric chloride, potassium ferricyanide and sodium arsenite. The limit of detection is 0.001 μg of iodide and 0.002 μg of thyroxine [13]. In our laboratory this reagent has been found very useful for the location of minute amounts of iodine containing compounds. The reagent is an important supplement to the water — formic acid chromatography system, which permits the application of only small amounts of the compounds on the paper. The high sensitivity necessitates cleanliness in the handling of the papers. The paper itself may contain impurities which cause undesirable background colouring. The impurities can be removed before the paper is used by descending "chromatography" with water — formic acid (5:1). This solvent is permitted to drip off the lower edge of the paper for 1—2 h.

Ninhydrin is suitable for the detection of iodotyrosines and iodothyronines [2], which are amino acids.

Palladous chloride is a specific reagent for iodide. A solution containing 0.1—1 % palladous chloride in dilute hydrochloric acid is suitable for the staining of paper chromatograms [29,30].

DISCUSSION

The purpose of this investigation was to develop effective chromatographic and electrophoretic techniques for a research program which requires reliable identification of thyroid hormone metabolites. In the course of the work it was found helpful to group all conceivably useful chromatographic solvent systems into six groups (Table 1). The systems in each group are similar in composition and separation properties. For instance, the relative mobilities of the compounds are usually similar in different systems belonging to the same group. After this systematisation, a study of the general properties of the different groups could be undertaken. Such a systematic approach would also be useful when solvent systems for other kinds of compounds are developed. In our case the alkaline organic, acidic organic and acidic aqueous systems were found to have the most useful properties.

Alkaline organic solvent systems are particularly efficient. A dependable system belonging to this group was developed for the one-dimensional resolution of the chief iodine compounds of the thyroid and blood, *i.e.* I^-, MIT, DIT, T_3 and T_4. Most acidic organic systems separate thyronine derivatives poorly. They are, however, useful for certain special purposes. There seemed to be a particular need for an efficient solvent system with properties different from those of the alkaline organic group. This gap has been filled by a system belonging to the previously unused acidic aqueous group.

A good two-dimensional separation procedure should resolve the compounds analysed into small, well-defined spots, distributed over a large area of paper. This can be accomplished with a combination of two good one-dimensional systems in which the compounds have different relative mobilities. When thyroid hormones and related compounds are analysed, an alkaline organic system, e.g. *tert*-amyl alcohol — 2 M ammonia, can be recommended for use in the first direction. For the second direction two acceptable methods are available. One consists of chromatography with the new acidic aqueous system water — formic acid. The second possibility is electrophoresis with a buffer having a pH of approximately 8.

Carefully stabilised solvent systems are usually employed in paper chromatography. However, it was found that continuously changing solvent systems sometimes offer advantages. Such systems can be produced by using solvent systems in which a reaction occurs during the run or which are not in equilibrium with the atmosphere of the chromatography tank. The process is to some extent analogous to the gradient elution technique used in column chromatography.

Acknowledgments. The skilled technical assistance of Mrs. Leena Kivistö is gratefully acknowledged. The authors wish to thank Glaxo Laboratories Ltd., Greenford, Middlesex, England, Dr. R. I. Meltzer of the Warner-Lambert Research Institute, Morris Plains,

N.J., U.S.A., and Drs. R. Pitt-Rivers and J. R. Tata of the National Institute of Medical Research, London, England, for gifts of pure thyroid hormone analogues. Mrs. Jean Margaret Perttunen kindly revised the English language. The study was aided by grants from the *Sigrid Juselius Stiftelse*, *Medicinska Understödsföreningen Liv och Hälsa* and *Statens Naturvetenskapliga Kommission*.

REFERENCES

1. Solomon, D. H. and Dowling, J. T. *Ann. Rev. Physiol.* **22** (1960) 615.
2. Roche, J., Lissitzky, S. and Michel, R. in Glick, D. *Methods of Biochemical Analysis*, Interscience, New York 1954, Vol. 1, p. 243.
3. Taurog, A. and Chaikoff, I. L. in Colowick, S. P. and Kaplan, N. O. *Methods in Enzymology*, Academic Press Inc., New York 1957, Vol. 4, p. 856.
4. Block, R. J., Werner, S. C., Mandl, R. H., Row, V. V. and Radichevich, I. *Arch. Biochem. Biophys.* **88** (1960) 98.
5. Shaw, E. I. and Goldsby, R. *Intern. J. Appl. Radiation and Isotopes* **3** (1958) 161.
6. Gräsbeck, R., Lamberg, B.-A. and Björkstén, F. *Acta Endocrinol.* **34** (1960) 113.
7. Gleason, G. I. *J. Biol. Chem.* **213** (1955) 837.
8. Gross, J., Leblond, C. P., Franklin, A. E. and Quastel, J. H. *Science* **111** (1950) 605.
9. Taurog, A., Wheat, J. D. and Chaikoff, I. L. *Endocrinology* **58** (1956) 121.
10. Roche, J., Jutisz, M., Lissitzky, S. and Michel, R. *Biochim. et Biophys. Acta* **7** (1961) 257.
11. Acland, J. D. *Nature* **170** (1952) 32.
12. Dobyns, B. M. and Barry, S. R. *J. Biol. Chem.* **204** (1953) 517.
13. Gmelin, R. and Virtanen, A. I. *Acta Chem. Scand.* **13** (1959) 1469.
14. Mandl, R. M. and Block, R. J. *Arch. Biochem. Biophys.* **81** (1959) 25.
15. Roche, J., Michel, R. and Nunez, J. *Bull. soc. chim. biol.* **37** (1955) 809.
16. Fletcher, K. *Biochem. J.* **67** (1957) 140.
17. Michel, R. *Am. J. Med.* **20** (1956) 670.
18. Roche, J., Michel, R., Closon, J. and Michel, O. *Biochim. et Biophys. Acta* **38** (1960) 325.
19. Lissitzky, S., Bénévent, M.-T., Roques, M. and Roche, J. *Bull. soc. chim. biol.* **41** (1959) 1329.
20. Taurog, A., Tong, W. and Chaikoff, I. L. *J. Biol. Chem.* **227** (1957) 759.
21. Matsuura, T. and Cahnmann, H. J. *J. Am. Chem. Soc.* **81** (1959) 871.
22. Tata, J. R., Rall, J. E. and Rawson, R. W. *Endocrinology* **60** (1957) 83.
23. Lybeck, H. *Acta Med. Scand.*, Suppl. 327 (1957).
24. Pitt-Rivers, R. and Tata, J. R. *The Thyroid Hormones*, Pergamon Press, London 1959, p. 157.
25. Bowden, C. H., Maclagan, N. F. and Wilkinson, J. H. *Biochem. J.* **59** (1955) 93.
26. Fletcher, K. and Stanley, P. G. *Nature* **175** (1955) 730.
27. Dragúnová, I. and Langer, P. *Nature* **178** (1956) 537.
28. Štolc, V. *Nature* **182** (1958) 52.
29. Gross, J. and Leblond, C. P. *Endocrinology* **48** (1951) 714.
30. Feigl, F. *Qualitative Analysis by Spot Tests*, Elsevier, New York 1947, p. 197.

Received February 27, 1961.

ACTA CHEMICA SCANDINAVICA 15 (1961) 1177–1208

Short Communications

Preparation of Furan from *cis*-2-Butene-1,4-diol

NIELS CLAUSON-KAAS

Centrallaboratoriet, Sadolin & Holmblad A/S, Copenhagen, Denmark

According to Reppe *et al.*[1] catalytic dehydrogenation of *cis*-2-butene-1,4-diol (I) gives butyrolacton together with "appreciable amounts of furan". Apart from the reaction temperature (120°) and the composition of the catalyst no experimental data and no yields are reported.

Oxidation of butenediol with an aqueous solution of chromic acid-sulfuric acid gives a 62 % yield of furan. Evidently the reaction goes through the intermediate 4-hydroxy*iso*crotonaldehyde (II), the cyclic semiacetal form of which (III) rapidly undergoes 1,4-elimination of water to give furan. Since the reaction takes place at 90°, furan distills off immediately, thereby evading the destructive influence of the acidic and oxidizing reaction mixture. Thus the first part of the reaction is a usual chromic acid oxidation of an allylic alcohol, while the following furanization reaction is similar to Quennehen and Normant's [2] quantitative transformation of 2-ethoxy-2,5-dihydrofuran into furan and ethanol under the influence of acidic reagents.

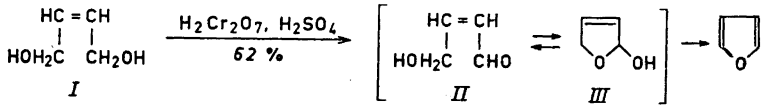

Experimental. Butenediol (purified product from General Aniline and Film Corporation, U.S.A., contains maximally 93 % of *cis*-butenediol) (20.0 g) and water (40 ml) are placed in a 250 ml reaction flask. The mixture is heated rapidly to 90°. Heating is discontinued and a solution of sodium dichromate (30.0 g of the dihydrate) in aqueous sulfuric acid (20 g of concentrated sulfuric acid in 70 ml of water) added dropwise with efficient stirring at such a rate, that the temperature is kept at 90–92°. A mixture of furan and water distills off immediately at a distillation temperature of 75–85°. Addition is complete after about 10 min. The mixture is then heated during 2–5 min to 100° (distillation temperature maximally 95°) to complete the reaction. The distillate consists of water (about 2 g) and impure furan (about 10 g). An impurity of the furan layer, detectable by its odor, is acrolein, which evidently has been formed by oxydation of allyl alcohol present as an impurity in butenediol. A 50 % aqueous solution of hydrazine (0.50 ml) is added to the distillate, and the resulting mixture shaken for 10 min at room temperature. All acrolein present in the furan layer is hereby removed. The mixture is now cooled to −20°, and the furan layer removed from the frozen aqueous layer by decantation and distilled from powdered potassium hydroxide (2.5 g). Furan (8.94 g, b.p. 31°, n_D^{20} 1.4208) is obtained as the only fraction. The yield, based upon pure *cis*-butenediol, is 62 %, or higher.

1. Reppe, W. *et al. Ann.* **596** (1955) 159, 182.
2. Quennehen, F. and Normant, H. *Compt. rend.* **228** (1949) 1301.

Received June 7, 1961.

The Crystal Structure of Cr_3B_4

MATS ELFSTROM

Institute of Chemistry, University of Uppsala, Uppsala, Sweden

A number of borides isostructural with Ta_3B_4 have already been investigated by Andersson and Kiessling [1-3]. From his data on Mn_3B_4 Kiessling [4] concluded that there are boron-boron distances as short as 1.50 Å in this phase and he believed these short boron-boron distances to be present also in the other Me_3B_4 phases [3]. The value 1.5 Å is considerably shorter than any boron-boron distance previously reported. However, the atomic parameters are very uncertain. A reinvestigation of these compounds is therefore being undertaken in order to achieve greater accuracy. The present communication deals with the results obtained for the alloy Cr_3B_4.

Table 1. Atomic parameters in Cr_3B_4

Cr_I	in 2(c)	
Cr_{II}	in 4(*g*)	with $y = 0.1861 \pm 0.0000_6$
B_I	in 4(*g*)	with $y = 0.3607 \pm 0.0003$
B_{II}	in 4(*h*)	with $y = 0.4351 \pm 0.0003$

Experimental. The alloys were prepared by arc-melting mixtures of boron (99.0 %) and chromium (99.9 %) in an atmosphere of purified argon. X-Ray photographs were taken in a Guinier camera with Si as internal standard (aSi = 5.4306 Å) and with Cr$K\alpha$-radiation. The atomic parameters were determined from single crystal data, obtained in a Weissenberg camera with Mo$K\alpha$-radiation. The relative intensities were estimated visually using the multiple film technique and a calibrated intensity scale. The electron density projection $\varrho(xy)$, the structure factors and the scale- and temperature factors were computed and refined on the digital electronic computer BESK with programs available at BESK. The scattering factors according to Watson and Freeman [5] for chromium and Ibers [6] for boron were used.

Results. Within the limits of the experimental errors (estimated to be ± 0.04 %) no lattice parameter variations were observed. The lattice parameters of Cr_3B_4 obtained in this investigation (a = 2.986 Å, b = 13.02$_0$ Å, c = 2.952 Å) are in excellent agreement with Anderson's and Kiessling's [1] values (a = 2.984 Å, b = 13.02 Å, c = 2.953 Å).

The space group *Immm* derived by Kiessling in his study of Ta_3B_4 was confirmed. The atomic parameters obtained in this investigation for Cr_3B_4 are given in Table 1 with standard deviations calculated from Cruickshank's formula [7]. The final R-value for the 94 independent $hk0$ reflexions was 7.6 %.

Interatomic distances are given in Table 2. Of particular interest are the shortest boron-boron distances, which have a standard deviation of 0.02 Å. The difference between the two shortest non-equivalent boron-boron distances is not significant. Thus it has been shown that in Cr_3B_4 there exist no such abnormally short boron-boron distances as suggested by Kiessling [3].

Table 2. Interatomic distances in Cr_3B_4 shorter than 3 Å.

Cr_I	–	Cr_I	2.952	(2),	2.986	(2)	B_I	–	Cr_I	2.35	(2)
Cr_I	–	Cr_{II}	2.83$_7$	(4)			B_I	–	Cr_{II}	2.19	(4), 2.27 (1)
Cr_I	–	B_I	2.35	(4)			B_I	–	B_I	2.952	(2), 2.986 (2)
Cr_I	–	B_{II}	2.26	(8)			B_I	–	B_{II}	1.77	(2)
Cr_{II}	–	Cr_I	2.83$_7$	(2)			B_{II}	–	Cr_I	2.26	(4)
Cr_{II}	–	Cr_{II}	2.67$_6$	(4),	2.952	(2), 2.986 (2)	B_{II}	–	Cr_{II}	2.17	(2)
Cr_{II}	–	B_I	2.19	(4)	2.27	(1)	B_{II}	–	B_I	1.77	(2)
Cr_{II}	–	B_{II}	2.17	(2)			B_{II}	–	B_{II}	1.69	(1), 2.952 (2), 2.986 (2)

Acknowledgements. The author wishes to thank Professor G. Hägg for the facilities put at his disposal. This work has been supported by the *Air Force Office of Scientific Research of the Air Research and Development Command, US Air Force*, through its European Office under contract No. AF 61(052)-40. Facilities for use of the digital computer BESK were granted by the *Swedish Board for Computing Machinery.*

1. Andersson, L.-H. and Kiessling, R. *Acta Chem. Scand.* **4** (1950) 160.
2. Kiessling, R. *Ibid.* **3** (1949) 90.
3. Kiessling, R. *Ibid.* **4** (1950) 209.
4. Kiessling, R. *Ibid.* **4** (1950) 146.
5. Watson, R. E. and Freeman, A. J. *Acta Cryst.* **14** (1961) 27.
6. Ibers, J. A. *Ibid.* **10** (1957) 86.
7. Cruickshank, D. W. J. *Ibid.* **2** (1949) 65.

Received May 16, 1961.

Tautomeric Cyclic Thiones

I. "Mercapto-thiadiazolyl-hydrazones"

KRISTINA ARVIDSSON and JAN SANDSTRÖM

Department of Organic Chemistry, University of Lund, Lund, Sweden

Stollé and Fehrenbach [1] have prepared a compound, which they isolated as hydrochloride and benzylidene derivative and described as 2-mercapto-5-hydrazino-1,3,4-thiadiazole. Sandström [2,3] has prepared compounds described as acetone and *cyclo*hexanone mercapto-thiadiazolylhydrazones. The mercapto-thiadiazolylhydrazones can exist in the tautomeric forms (Ia) and (Ib). In recent years the tautomerism of cyclic thionamides has been the subject of several investigations, and in most cases (*e.g.* Refs.[4,5]) the thione form has been found to preponderate. However, in some bifunctional thiadiazole derivatives [6,7] the thiol form is found to dominate, and therefore it was considered worthwile to investigate the tautomeric structure of the so called mercapto-thiadiazolylhydrazones. Because of the strongly chromophoric properties of the thione group, the form (Ia) can be expected to absorb light at longer wavelengths than (Ib).

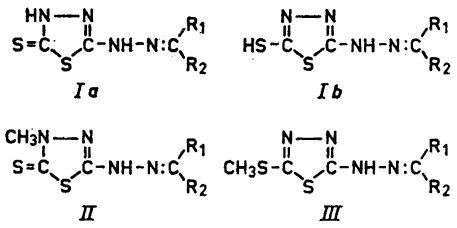

Ia *Ib*

II *III*

Since the exchange of the mobile hydrogen atom for a methyl group does not greatly affect the π electron system, a comparison of the spectrum of the parent compound with those of the N- and S-methyl derivatives (II) and (III) might allow a qualitative estimation of the position of the tautomeric equilibrium. Since suitably substituted derivatives were available, the *cyclo*hexanone mercapto-thiadiazolylhydrazone

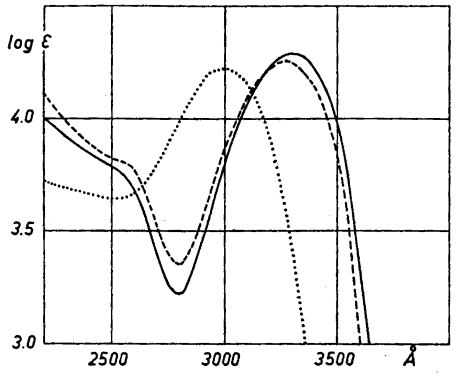

Fig. 1.

——— *Cyclo*hexanone 1,3,4-thiadiazol-5(4)-thion-2-yl-hydrazone (I)

– – – – – *Cyclo*hexanone 4-methyl-1,3,4-thiadiazol-5(4)-thion-2-yl-hydrazone (II)

. . . . . *Cyclo*hexanone 5-methylthio-1,3,4-thiadiazol-2-yl-hydrazone (III).

(I, $R_1R_2 = (CH_2)_5$) was chosen for investigation. The parent compound (I) was prepared according to Ref.[3], and when it reacted with diazomethane, a mixture of (II) and (III) was obtained. The S-methyl derivative (III) was prepared in an unambigous way by reaction between methylthio-thiadiazolylhydrazine [2] and *cyclo*hexanone. The UV spectra of (I—III) were recorded in absolute ethanol solution (Fig. 1) and the close similarity of the spectra of (I) and (II) shows that (I) is predominantly in the thione form (Ia) in absolute ethanol. It should therefore be called *cyclo*hexanone 1,3,4-thiadiazol-5(4)-thion-2-yl-hydrazone. The possibility of an amidine type of tautomerism in (I—III) will be discussed in a forthcoming publication.

Experimental. Cyclo*hexanone methylthio-thiadiazolylhydrazone (III).* Methylthio-thiadiazolylhydrazine [2] (0.36 g) was dissolved in hot water (10 ml), and *cyclo*hexanone (0.2 g) in ethanol (5 ml) was added. A precipitate of yellow rods was formed, which crystallized from toluene-heptane as pale yellow rods, m.p. 176—176.5°. (Found: C 44.7; H 5.82; N 23.0; S 26.5. $C_9H_{14}N_4S_2$ (242.35) requires C 44.6; H 5.82; N 23.1; S 26.5).

Cyclo*hexanone 4-methyl-1,3,4-thiadiazol-5(4)-thion-2-yl-hydrazone (II)*.*Cyclo*hexanone 1,3,4-thiadiazol-5(4)-thion-2-yl-hydrazone (I, R_1R_2= $(CH_2)_5$, 2.3 g) was added to a solution of diazomethane (0.45 g) in ether (15 ml). A slow evolution of gas ensued, and on the following day the undissolved material (1.4 g) was removed by filtration. It crystallized from a mixture of toluene and heptane as pale yellow rods, m.p. 176–176.5°, not depressed on admixture with the *cyclo*hexanone methylthio-thiadiazolylhydrazone (III) described above.

The ether solution was examined by chromatography on paper, impregnated with dimethyl sulphoxide according to Wickberg [8]. Three spots were located by photographing the paper in UV light, one with R_F *ca.* 0.33, one with R_F *ca.* 0.45, corresponding to (III), and one with R_F *ca.* 1. The solution was evaporated to dryness, and the residue was dissolved in benzene and subjected to chromatography on alumina. Benzene eluted first an orange solid (0.04 g), corresponding to the spot with R_F 1, which was not further investigated. Then a second fraction appeared as a pale yellow solid (0.22 g) with R_F 0.33, which crystallized from benzene-heptane as pale yellow needles, m.p. 182–183°, of cyclo*hexanone 4-methyl-1,3,4-thiadiazol-5(4)-thion-2-yl-hydrazone (II)*. (Found: C 44.6; H 5.65; N 23.0; S 26.4. $C_9H_{14}N_4S_2$ (242.35) requires C 44.6; H 5.82; N 23.1; S 26.5).

Finally ether eluted a third fraction as a pale yellow solid (0.23 g), which crystallized from toluene-heptane as pale yellow rods, m.p. 176–176.5°, not depressed by admixture with (III).

1. Stollé, R. and Fehrenbach, K. *J. prakt. Chem.* [2] **122** (1929) 289.
2. Sandström, J. *Acta Chem. Scand.* **14** (1960) 1939.
3. Sandström, J. *Acta Chem. Scand.* **15** (1961). *In press.*
4. Ettlinger, M. S. *J. Am. Chem. Soc.* **72** (1950) 4699.
5. Albert, A. and Barlin, G. *J. Chem. Soc.* **1959** 2384.
6. Sheinker, Yu. N., Postovskii, I. Ya. and Voronina, N. M. *Zhur. Fiz. Khim.* **33** (1959) 302.
7. Thorn, G. D. *Can. J. Chem.* **38** (1960) 1439
8. Wickberg, B. *Acta Chem. Scand.* **12** (1958) 615.

Received June 13, 1961.

Resolution of α-*n*-Propylamino-2-methylpropioanilide and the Absolute Configuration of its Stereoisomers

CLAËS TEGNÉR and NILS-ERIK WILLMAN

Research Laboratories, AB Astra, Södertälje, Sweden

During recent years, much attention has been drawn to the influence of stereoisomerism on biological activity [1,2]. It is generally held that local anesthetics, as well as narcotics, act by pure physical-chemical influence on nervous structures, and that chemical binding to specific "receptors" is of minor importance. The differences in anesthetic activity observed earlier in stereoisomers of compounds containing ester linkages and acting as local anesthetics have been interpreted by Schaumann [1] to be due to the contact of the substances with esterases which break down the different stereoisomers of the anesthetic at different rates.

As the surface of the membrane of the nerve cell consists of a protein network, it is of interest to study the effect of stereoisomers of anesthetics containing peptide linkages. Af Ekenstam *et al.*[3] studied the toxicity and the anesthetic effect in wheal tests of the isomers of N-methylpipecolinoyl-2,6-xylidine but no statistic differences could be established. However, Kudrjashowa *et al.*[4] and Motovilov [5] report the observation of different anesthetic effects produced by the different stereoisomers of three diethylaminopropioanilides.

The observation of different activity of stereoisomers of compounds acting as local anesthetics may not only be due to differences in "intrinsic anesthetic potency" or in the speed of enzymatic breakdown but may also depend on side effects such as vasomotor activity.

In view of these facts, it is interesting to study the behaviour of the stereoisomers of a local anesthetic in different pharmacological tests.

The present paper describes the resolution of α-*n*-propylamino-2-methylpropioanilide [6] with the aid of D- and L-di-*p*-toluoyltartaric acid. By reductive alkylation of L-alanine with *n*-propanal and subsequent reaction of the L-*n*-propyl-

Cyclo*hexanone 4-methyl-1,3,4-thiadiazol-5(4)-thion-2-yl-hydrazone (II)*.*Cyclo*hexanone 1,3,4-thiadiazol-5(4)-thion-2-yl-hydrazone (I, R_1R_2= $(CH_2)_5$, 2.3 g) was added to a solution of diazomethane (0.45 g) in ether (15 ml). A slow evolution of gas ensued, and on the following day the undissolved material (1.4 g) was removed by filtration. It crystallized from a mixture of toluene and heptane as pale yellow rods, m.p. 176–176.5°, not depressed on admixture with the *cyclo*hexanone methylthio-thiadiazolylhydrazone (III) described above.

The ether solution was examined by chromatography on paper, impregnated with dimethyl sulphoxide according to Wickberg [8]. Three spots were located by photographing the paper in UV light, one with R_F *ca.* 0.33, one with R_F *ca.* 0.45, corresponding to (III), and one with R_F *ca.* 1. The solution was evaporated to dryness, and the residue was dissolved in benzene and subjected to chromatography on alumina. Benzene eluted first an orange solid (0.04 g), corresponding to the spot with R_F 1, which was not further investigated. Then a second fraction appeared as a pale yellow solid (0.22 g) with R_F 0.33, which crystallized from benzene-heptane as pale yellow needles, m.p. 182–183°, of cyclo*hexanone 4-methyl-1,3,4-thiadiazol-5(4)-thion-2-yl-hydrazone (II)*. (Found: C 44.6; H 5.65; N 23.0; S 26.4. $C_9H_{14}N_4S_2$ (242.35) requires C 44.6; H 5.82; N 23.1; S 26.5).

Finally ether eluted a third fraction as a pale yellow solid (0.23 g), which crystallized from toluene-heptane as pale yellow rods, m.p. 176–176.5°, not depressed by admixture with (III).

1. Stollé, R. and Fehrenbach, K. *J. prakt. Chem.* [2] **122** (1929) 289.
2. Sandström, J. *Acta Chem. Scand.* **14** (1960) 1939.
3. Sandström, J. *Acta Chem. Scand.* **15** (1961). *In press.*
4. Ettlinger, M. S. *J. Am. Chem. Soc.* **72** (1950) 4699.
5. Albert, A. and Barlin, G. *J. Chem. Soc.* **1959** 2384.
6. Sheinker, Yu. N., Postovskii, I. Ya. and Voronina, N. M. *Zhur. Fiz. Khim.* **33** (1959) 302.
7. Thorn, G. D. *Can. J. Chem.* **38** (1960) 1439
8. Wickberg, B. *Acta Chem. Scand.* **12** (1958) 615.

Received June 13, 1961.

Resolution of α-*n*-Propylamino-2-methylpropioanilide and the Absolute Configuration of its Stereoisomers

CLAËS TEGNÉR and NILS-ERIK WILLMAN

Research Laboratories, AB Astra, Södertälje, Sweden

During recent years, much attention has been drawn to the influence of stereoisomerism on biological activity [1,2]. It is generally held that local anesthetics, as well as narcotics, act by pure physical-chemical influence on nervous structures, and that chemical binding to specific "receptors" is of minor importance. The differences in anesthetic activity observed earlier in stereoisomers of compounds containing ester linkages and acting as local anesthetics have been interpreted by Schaumann [1] to be due to the contact of the substances with esterases which break down the different stereoisomers of the anesthetic at different rates.

As the surface of the membrane of the nerve cell consists of a protein network, it is of interest to study the effect of stereoisomers of anesthetics containing peptide linkages. Af Ekenstam *et al.*[3] studied the toxicity and the anesthetic effect in wheal tests of the isomers of N-methylpipecolinoyl-2,6-xylidine but no statistic differences could be established. However, Kudrjashowa *et al.*[4] and Motovilov [5] report the observation of different anesthetic effects produced by the different stereoisomers of three diethylaminopropioanilides.

The observation of different activity of stereoisomers of compounds acting as local anesthetics may not only be due to differences in "intrinsic anesthetic potency" or in the speed of enzymatic breakdown but may also depend on side effects such as vasomotor activity.

In view of these facts, it is interesting to study the behaviour of the stereoisomers of a local anesthetic in different pharmacological tests.

The present paper describes the resolution of α-*n*-propylamino-2-methylpropioanilide [6] with the aid of D- and L-di-*p*-toluoyltartaric acid. By reductive alkylation of L-alanine with *n*-propanal and subsequent reaction of the L-*n*-propyl-

aminopropionic acid with *o*-tolylphosphazo-*o*-toluidide the absolute configuration of the isomers was shown to be L-(+)- and D-(−)-*α*-*n*-propylamino-2-methylpropioanilide, respectively.

The results of the pharmacological investigations of the isomers will be published elsewhere.

The D- and L-di-*p*-toluoyltartaric acids used were prepared and purified as described by Stoll and Hofmann [7].

(−)-α-n-Propylamino-2-methylpropioanilide hydrochloride — I. To a hot solution of 0.15 mole (62 g) of D-di-*p*-toluoyltartaric acid in 180 ml of 95 % ethanol was added 0.15 mole (33 g) of *α*-*n*-propylamino-2-methylpropioanilide [6] dissolved in 100 ml of hot 95 % ethanol. On cooling, first to room temperature and then in a refrigerator, crystals separated. After three recrystallisations from ethanol a constant rotation was obtained. The tartrate thus obtained was dissolved in water, the base liberated by the addition of 1 N sodium hydroxide, extracted with ether and the ethereal solution dried over sodium sulphate. The hydrochloride was then precipitated by the addition of ethereal hydrogen chloride. On recrystallisation from ethanol colourless crystals were obtained, m.p. 192−194°; $[\alpha]_D = -13.8° \pm 0.1°$ ($c = 1.0$ in glac. acetic acid). Yield 10.2 g (53 %).

(+)-α-n-Propylamino-2-methylpropioanilide hydrochloride — II. The mother liquids from the crystallisations of compound I were combined, the solvent evaporated to dryness and the residue dissolved in water. The base was liberated by the addition of 1 N sodium hydroxide and then taken up in ether. After drying the solution over sodium sulphate and evaporating the ether, 0.084 mole (18.4 g) of *α*-*n*-propylamino-2-methylpropioanilide was obtained. It was dissolved in 100 ml of hot ethanol (95 %) and was added to a hot solution of 0.084 mole (34.8 g) of L-di-*p*-toluoyltartaric acid in 180 ml of 95 % ethanol. On cooling, crystals separated, which were recrystallised and treated as described above for compound I. The hydrochloride had a melting point of 192−194°; $[\alpha]_D = +13.8° \pm 0.1°$ ($c = 1.0$ in glac. acetic acid). Yield 9.5 g (50 %). The mixed melting point of equal quantities of compounds I and II melted at 167−169° in agreement with that of the racemate [6].

L-(+)-α-n-Propylaminopropionic acid — III. L-*α*-Propylaminopropionic acid was obtained by reductive alkylation of L-alanine with *n*-propanal using the method described by Bowman [8] for the preparation of the corresponding N-butyl derivative. M.p. 290° (decomp.) from aqueous acetone; $[\alpha]_D = +6.9°$ ($c = 1.0$ in water). Yield 34 % (Found: N 10.7. Calc. for $C_6H_{13}NO_2$ (131.2): N 10.7).

L-(+)-α-n-Propylamino-2-methylpropioanilide hydrochloride — IV. *o*-Tolylphosphazo-*o*-toluidide was prepared as described by Grimmel *et al.*[9] for the preparation of the corresponding *para* derivative. The product obtained contained 77 % of phosphazo compound and was used in the next step without further purification.

A mixture of 0.007 mole(2.2 g) of the phosphazo compound and 0.014 mole (2.3 g) of the hydrochloride of compound III was heated to 130−140° for 1 h. The reaction mixture was dissolved in water and the pH of the solution was adjusted to 5.9. The mixture was extracted with ether to remove *o*-toluidine. The aqueous layer was then made strongly alkaline with sodium hydroxide and the toluidide was extracted with ether. The ethereal solution was dried over sodium sulphate and the hydrochloride of the toluidide was precipitated by the addition of ethereal hydrogen chloride. On recrystallisation twice from ethanol-isopropyl ether colourless crystals were obtained. M.p. 191−193°; $[\alpha]_D = +13.1°$ ($c = 1.0$ in glac. acetic acid). Yield 0.8 g (22 %).

The mixed melting point of compound IV and II showed no depression whereas that of compound IV and I gave a considerable depression.

1. Schaumann, O. *Sci Pharm.* **21** (1953) 342.
2. Beckett, A. H. *Angew. Chem.* **72** (1960) 686.
3. af Ekenstam, B., Egnér, B. and Pettersson. G. *Acta Chem. Scand.* **11** (1957) 1183.
4. Kudrjaschowa, N. I., Remisov, A. L. and Khromov-Borisov, N. V. *J. Gen. Chem. USSR* **29** (1959) 1240; Kudrjaschowa, N. I. and Khromov-Borisov, N. V. *J. Gen. Chem. USSR* **30** (1960) 4035.
5. Motovilov, P. E. *Farmakol. i Toksikol.* **24** (1961) 113.
6. Löfgren, N. and Tegnér, C. *Acta Chem. Scand.* **14** (1960) 486.
7. Stoll, A. and Hofmann, A. *Helv. Chim. Acta* **26** (1943) 922.
8. Bowman, R. E. *J. Chem. Soc.* **1950** 1346.
9. Grimmel, H. W., Guenther, A. and Morgan, J. F. *J. Am. Chem. Soc.* **68** (1946) 539.

Received June 30, 1961.

Bacterial Carotenoids

VIII.* A Structural Scheme for the Biosynthesis of Coloured Carotenoids in the Photosynthetic Bacterium *Rhodospirillum rubrum*

SYNNØVE LIAAEN JENSEN

Institutt for Organisk Kjemi, Norges Tekniske Høgskole, Trondheim, Norway

In the present paper the chemical structures of some bacterial carotenoids, already discussed in a series of papers (Bacterial Carotenoids I—VII) in this journal [1-7], are correlated with the results of biosynthetic studies.

By kinetic studies of the carotenoid biosynthesis in the photosynthetic purple bacterium *Rsp. rubrum* performed by Stanier and his associates [8], it was demonstrated that spirilloxanthin was formed at the expense of the lycopene group (lycopene and OH-lycopene) and the P481 group (P481 and OH-P481) in a manner strongly suggesting the sequence:

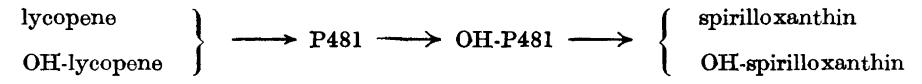

When the present work was started the following structures for three of these carotenoids, namely for lycopene (I), OH-lycopene assumed to be identical with lycoxanthin (II)[9,10], and spirilloxanthin (III),[11,12] were largely accepted.

The transformation from lycopene (I) to spirilloxanthin (III) through a reasonable number of simple chemical reactions *via* lycoxanthin (II) and the unknown components P481 and OH-P481 is not easily envisaged. The aim of the present investigation therefore was to check the correctness of the previously assigned structures and to establish the structures of the unknown components of this series. Recent work has led to the establishment of chemical structures for spirilloxanthin (IV)[2,13], monodemethylated spirilloxanthin (OH-spirilloxanthin) (V)[7], rhodovibrin (OH-

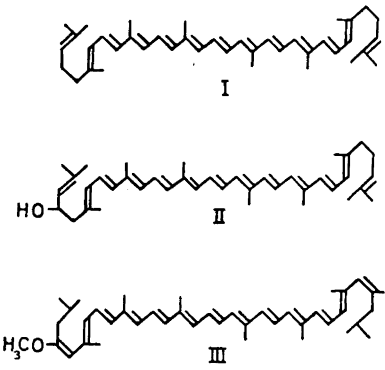

P481) (VI or VII)[1,5] and rhodopin (OH-lycopene) (VIII)[3,4]. The available data for P481 [9,1,8,14] indicate the structures (IX) or (X) for this carotenoid. From the formal relationship between rhodovibrin (VI or VII) and P481 (IX or X), the denomination anhydro-rhodovibrin is suggested for P481. Additional evidence for the identity of lycopene from *Rsp.rubrum* and authentic lycopene (I) has been provided by a quantitative comparative study of the iodine catalyzed equilibrium mixtures of the two carotenoids [14].

A structural interpretation of the biochemical reactions leading from lycopene to spirilloxanthin has been attempted by Barber, Jackman and Weedon [13]. Some of the structures favoured by these authors, however, were later shown to be incorrect [3-5].

The establishment of chemical structures for the carotenoids participating in these transformations, makes possible a more definite interpretation in chemical terms of the reactions involved in later steps of carotenoid biosynthesis in *Rsp. rubrum*.

From the chemical structure of rhodopin (VIII) compared to that of lycopene (I) and anhydro-rhodovibrin (IX or X), the position of rhodopin in the biosynthetical sequence can be settled with reasonable assurance. A similar inference can be made for monodemethylated spirilloxanthin (V), which is obviously an intermediate between rhodovibrin (VI or VII) and spirilloxanthin

* No. VII of this series *Acta Chem. Scand.* **14** (1960) 952.

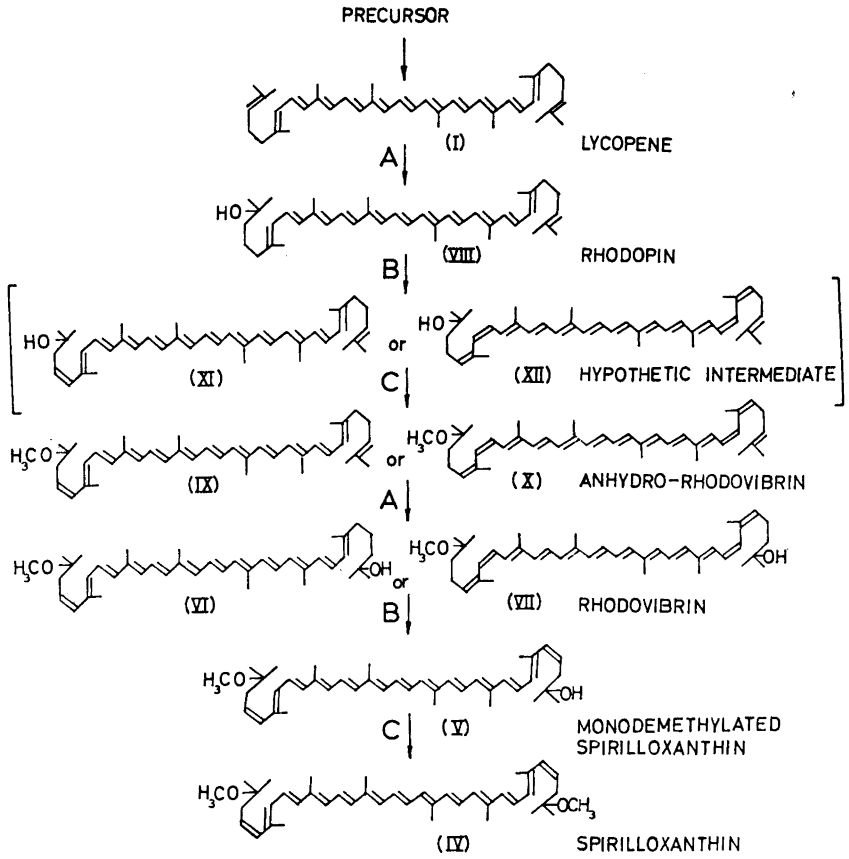

(IV). The final biosynthetic sequence can then be represented in the manner given above.

The intermediate (XI or XII) is hypothetic, and has not been isolated.

Based on the scheme depicted above the biochemical events leading from lycopene to spirilloxanthin can be envisaged in terms of three simple reactions, the sequence of which reflects the relative rates with which they proceed:

A. Addition of H_2O to an *iso*propylidene double bond with the formation of a tertiary alcohol.

B. Introduction of an additional double bond either in conjugation with the double bond chain at the same side as the hydroxyl group, or as an α,ω-dehydrogenation.

C. Methylation of the tertiary hydroxyl group.

To explain the formation of rhodopin, it is assumed that reaction A is faster than reaction B. The kinetic evidence [8] further reveals that the reactions B and C proceed with very similar rates. Thus neither products of the type (XI or XII), expected as intermediates if reaction B were faster than reaction C, nor a methylated rhodopin (XIII) or methylated rhodovibrin (XIV or XV), predicted as intermediates in the opposite case, have been isolated. Moreover, monodemethylated spirilloxanthin (V) has been isolated only in very small amounts.

The compounds (XI or XII), (XIII), and (XIV or XV) would, however, in the non-

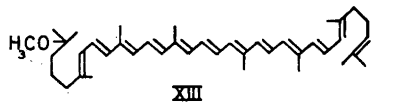

XIII

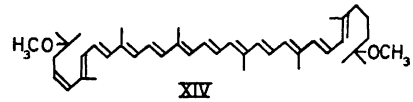

XIV

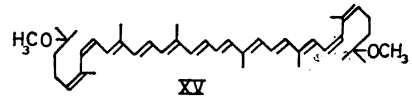

XV

crystalline state be difficult to distinguish from rhodovibrin, lycopene and anhydro-rhodovibrin respectively. The given sequence of the successive steps B and C is based on the isolation of monodemethylated spirilloxanthin. The suggestion that the methylation reaction C, which is dependent on the availability of intracellular methyl donors is slower than the oxidation reaction B, seems also the more plausible.

Biological hydroxylation mechanisms have been discussed by Hunt, Hughes and Lowenstein [15] and by Massart and Vercauteren [16]. Analogies for the net reaction (addition of H_2O to a carbon-carbon double bond) involved in the hydroxylation of lycopene and anhydro-rhodovibrin can be found among the common metabolites such as the transformation of fumaric to malic acid and the conversion of *cis*-aconitic acid to citric acid or *iso*citric acid. Another example is the hydroxylation of nicotinic acid in *Pseudomonas fluorescens* [15]. In the cases mentioned as examples above the oxygen atom of the hydroxyl group is derived from water (another possibility is gaseous oxygen), and at least in the two first cases well characterized enzymes [17] are responsible for the transformation.

It can be concluded that the supernumerary carbon atoms in the methoxyl groups of anhydro-rhodovibrin, rhodovibrin, monodemethylated spirilloxanthin and spirilloxanthin are introduced by methylation of preceding hydroxy intermediates. It is of interest in this respect to note that transmethylation is a well-known and widespred biological reaction [18], contrary to transmethoxylation which apparently has not been demonstrated. Recent investigations using labelled carbon have revealed that the methyl moiety of the methoxyl groups in the alkaloid ricinin (*Ricinus communis*) [19], in the lignin of tobacco leaves and barley [20] and also in mycophenolic acid (*Penicillium brevi-compactum*) [21] are synthesized *in vivo* by transmethylation. These observations are taken to indicate a rather universal occurrence of this type of reaction in living organisms. Braithwaite and Goodwin [22] have also favoured the view that the methoxyl groups of spirilloxanthin were introduced by transmethylation.

The establishment of chemical structures for the carotenoids participating in the biochemical transformation of lycopene to spirilloxanthin, unfortunately does not give any hint to the general mechanism for extension of the conjugated double bond chain. The oxidation reaction B seems to proceed rapidly, leaving no detectable intermediates behind.

A discussion of the path of carotenoid biosynthesis in *Athiorhodaceae* in general will be published elsewhere.

Maintenance grants from *Norges Tekniske Högskole* and *Norges Teknisk Naturvitenskaplige Forskningsråd* are gratefully acknowledged.

1. Liaaen Jensen, S. *Acta Chem. Scand.* **12** (1958) 1698.
2. Liaaen Jensen, S. *Acta Chem. Scand.* **13** (1959) 381.
3. Liaaen Jensen, S. *Acta Chem. Scand.* **13** (1959) 842.
4. Liaaen Jensen, S. *Acta Chem. Scand.* **13** (1959) 2142.
5. Liaaen Jensen, S. *Acta Chem. Scand.* **13** (1959) 2143.
6. Liaaen Jensen, S. *Acta Chem. Scand.* **14** (1960) 950.
7. Liaaen Jensen, S. *Acta Chem. Scand.* **14** (1960) 952.
8. Liaaen Jensen, S., Cohen-Bazire, G., Nakyama, T. O. M. and Stanier, R. Y. *Biochim. et Biophys. Acta* **29** (1958) 477.
9. Goodwin, T. W. and Land, D. G. *Arch. Mikrobiol.* **24** (1956) 305.
10. Zechmeister, L. and Cholnoky, L. v. *Ber.* **69** (1936) 422.
11. Karrer, P. and Koenig, H. *Helv. Chim. Acta* **23** (1940) 460.
12. Polgàr, A., van Niel, C. B. and Zechmeister, L. *Arch. Biochem.* **5** (1944) 243.
13. Barber, M. S., Jackman, L. M. and Weedon, B. C. L. *Proc. Chem. Soc.* **1959** 96.
14. Liaaen Jensen, S. *To be published.*

15. Hunt, A. L., Hughes, D. E. and Lowenstein, J. M. *Biochem. J.* **69** (1958) 170.
16. Massart, L. and Vercauteren, R. *Ann. Rev. Biochem.* **28** (1959) 527.
17. Ochoa, S. in Summer, J. B. and Myrbäck, K. *The Enzymes.* Vol. I. Part 2, p. 217. Acad. Press, New York 1951.
18. Cantoni, G. L. *Proc. 3rd Intern. Congr. Biochem.* **1955** 233.
19. Dubeck, M. and Kirkwood, S. *J. Biol. Chem.* **199** (1952) 307.
20. Byerrum, R.U., Flokstra, J.H., Dewey, L.J. and Ball C.D. *J. Biol. Chem.* **210** (1954) 633.
21. Birch, J. A., English, R. J., Massy-Westropp, R. A., Slayton, M. and Smith, H. *J. Chem. Soc.* **1958** 365.
22. Braithwaite, G. D. and Goodwin, T. W. *Nature* **182** (1958) 1304.

Received June 3, 1961.

Moss Anthocyanins

GERD BENDZ and OLLE MÅRTENSSON

Chemical Institute, University of Uppsala, and Pharmacia, Research Laboratories, Uppsala, Sweden

From the red moss, *Bryum cryophilum* O. Mårt. (*B. obtusifolium* Lindb.) two crystalline anthocyanins have been isolated and by means of cellulose column chromatography separated from each other. One of these anthocyanins occurs in about 0.5 % of the dry weight of the moss whereas the other one occurs in a much smaller concentration, hence the latter has been investigated mainly chromatographically.

On acid hydrolysis, the two anthocyanins yield the same aglycone (identical absorption spectra, chromatographic data and colour reactions) and, according to the paper chromatogram, only one sugar, *viz.* glucose. The aglycone has been identified as luteolinidin (3′,4′,5,7-tetrahydroxyflavylium chloride) [1,2], by comparing its spectral and chromatographic data as well as its characteristic colour reactions with those of a synthetic sample [3].

By treating the anthocyanin occurring most abundantly with hydrochloric acid for a few minutes, a mixture of pigments is obtained. When this mixture is chromatographed on paper in 1 % of hydrochloric acid it gives three spots, one of which has the same R_F-value as the unchanged pigment (0.44) and another the same as the anthocyanidin (0.03). The third spot has the same R_F-value (0.13) and the same colour as those of the other isolated anthocyanin. Furthermore, this latter gives on partial hydrolysis only two spots having R_F-values of 0.13 and 0.03, corresponding to the unchanged pigment and to the aglycone, respectively. These facts indicate that the first anthocyanin is a bioside and the second one is the corresponding monoside [4].

According to Harborne [5], anthocyanins with a free hydroxyl group in the 5-position have higher absorption intensity in the region 410—450 mμ than those having a substituted hydroxyl group in this position. Since the ratios of the optical density at 440 mμ compared to that at the wavelength of maximal absorption (E_{440}/E_{max}) for the isolated anthocyanins are only half those of the corresponding anthocyanidins, the two anthocyanins ought to be luteolinidin-5-diglucoside and luteolinidin-5-monoglucoside.

A detailed report will appear later elsewhere.

A grant from the *Swedish Natural Science Research Council* is gratefully acknowledged. We are also indebted to fil.stud. Lars Terenius for valuable assistance.

1. Pratt, D. D. and Robinson, R. *J. Chem. Soc.* **127** (1925) 1128.
2. Harborne, J. B. *John Innes Ann. Rept.* **1957** 25.
3. León, A. and Robinson, R. *J. Chem. Soc.* **133** (1931) 2732.
4. Harborne, J. B. and Sherratt, H. S. A. *Experientia* **13** (1957) 486.
5. Harborne, J. B. *Biochem. J.* **70** (1958) 22.

Received June 28, 1961.

15. Hunt, A. L., Hughes, D. E. and Lowenstein, J. M. *Biochem. J.* **69** (1958) 170.
16. Massart, L. and Vercauteren, R. *Ann. Rev. Biochem.* **28** (1959) 527.
17. Ochoa, S. in Summer, J. B. and Myrbäck, K. *The Enzymes.* Vol. I. Part 2, p. 217. Acad. Press, New York 1951.
18. Cantoni, G. L. *Proc. 3rd Intern. Congr. Biochem.* **1955** 233.
19. Dubeck, M. and Kirkwood, S. *J. Biol. Chem.* **199** (1952) 307.
20. Byerrum, R.U., Flokstra, J.H., Dewey, L.J. and Ball C.D. *J. Biol. Chem.* **210** (1954) 633.
21. Birch, J. A., English, R. J., Massy-Westropp, R. A., Slayton, M. and Smith, H. *J. Chem. Soc.* **1958** 365.
22. Braithwaite, G. D. and Goodwin, T. W. *Nature* **182** (1958) 1304.

Received June 3, 1961.

Moss Anthocyanins

GERD BENDZ and OLLE MÅRTENSSON

Chemical Institute, University of Uppsala, and Pharmacia, Research Laboratories, Uppsala, Sweden

From the red moss, *Bryum cryophilum* O. Mårt. (*B. obtusifolium* Lindb.) two crystalline anthocyanins have been isolated and by means of cellulose column chromatography separated from each other. One of these anthocyanins occurs in about 0.5 % of the dry weight of the moss whereas the other one occurs in a much smaller concentration, hence the latter has been investigated mainly chromatographically.

On acid hydrolysis, the two anthocyanins yield the same aglycone (identical absorption spectra, chromatographic data and colour reactions) and, according to the paper chromatogram, only one sugar, *viz.* glucose. The aglycone has been identified as luteolinidin (3′,4′,5,7-tetrahydroxyflavylium chloride) [1,2], by comparing its spectral and chromatographic data as well as its characteristic colour reactions with those of a synthetic sample [3].

By treating the anthocyanin occurring most abundantly with hydrochloric acid for a few minutes, a mixture of pigments is obtained. When this mixture is chromatographed on paper in 1 % of hydrochloric acid it gives three spots, one of which has the same R_F-value as the unchanged pigment (0.44) and another the same as the anthocyanidin (0.03). The third spot has the same R_F-value (0.13) and the same colour as those of the other isolated anthocyanin. Furthermore, this latter gives on partial hydrolysis only two spots having R_F-values of 0.13 and 0.03, corresponding to the unchanged pigment and to the aglycone, respectively. These facts indicate that the first anthocyanin is a bioside and the second one is the corresponding monoside [4].

According to Harborne [5], anthocyanins with a free hydroxyl group in the 5-position have higher absorption intensity in the region 410—450 mμ than those having a substituted hydroxyl group in this position. Since the ratios of the optical density at 440 mμ compared to that at the wavelength of maximal absorption (E_{440}/E_{max}) for the isolated anthocyanins are only half those of the corresponding anthocyanidins, the two anthocyanins ought to be luteolinidin-5-diglucoside and luteolinidin-5-monoglucoside.

A detailed report will appear later elsewhere.

A grant from the *Swedish Natural Science Research Council* is gratefully acknowledged. We are also indebted to fil.stud. Lars Terenius for valuable assistance.

1. Pratt, D. D. and Robinson, R. *J. Chem. Soc.* **127** (1925) 1128.
2. Harborne, J. B. *John Innes Ann. Rept.* **1957** 25.
3. León, A. and Robinson, R. *J. Chem. Soc.* **133** (1931) 2732.
4. Harborne, J. B. and Sherratt, H. S. A. *Experientia* **13** (1957) 486.
5. Harborne, J. B. *Biochem. J.* **70** (1958) 22.

Received June 28, 1961.

Structure of Xanthan Hydride

ASBJØRN HORDVIK *

University College of Addis Abeba, Ethiopia

So far X-ray structure determinations of three unsaturated five-membered cyclic disulphides have been reported [1-3]. The relatively high stability of these compounds as contrasted with unsaturated ones, seems to be due to some aromatic character of the ring. This idea may be tested by a structure determination of the 1,2,4-dithiazolidine derivatives, rhodan hydrate [3] and xanthan hydride.

According to Hantzsch and Wolvekamp [4], xanthan hydride has structure I.

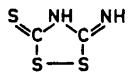

I

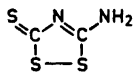

II

The unit cell and space group of xanthan hydride have been reported by Foss [5]. The crystals are monoclinic prismatic, $a = 4.05$ Å, $b = 10.59$ Å, $c = 12.78$ Å, $\beta = 97°$. The space group is $P2_1/c$.

The structure was solved by means of Harker-Kasper inequalities and systematic use of the "multiplication rule" [6]. This led to 8 sets of signs for the 45 strongest reflections in the a-axis projection. The molecule

Table 1. Atomic coordinates, in fractions of corresponding cell edges.

	y	z
S_1	0.349	0.051
S_2	0.342	0.199
S_3	0.118	0.299
C_1	0.187	0.030
C_2	0.177	0.190
N_1	0.141	−0.055
N_2	0.125	0.105

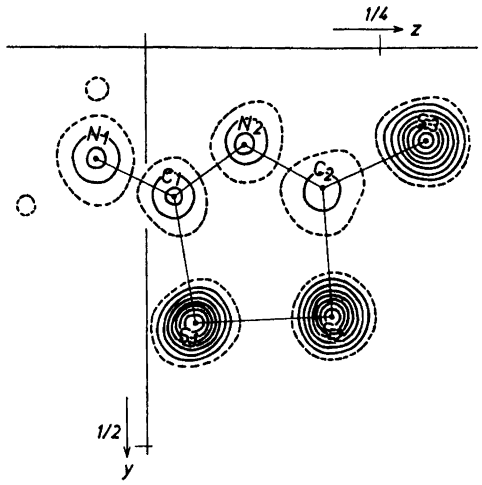

Fig. 1. Electron density projection of xanthan hydride along the a-axis showing one asymmetric unit. Plane group *pgg* and origin in center of symmetry. Contours at arbitrary but equal intervals.

was recognised in one of the corresponding Fourier maps, and after three Fourier refinements the reliability factor R was 0.18. The electron density map is reproduced in Fig. 1. Two small maxima near to the exocyclic nitrogen atom are most likely hydrogen peaks. The heights correspond approximately to 1 e.Å^{-2}, and the distance from nitrogen is about 1 Å if the hydrogen atoms are assumed to lie in the plane of the molecule, thus making possible a π orbital overlap C—N as in thiuret hydroiodide [1]. The bond angles H—N—H and H—N—C would be *ca.* 120°, and the peaks are both situated between atoms where hydrogen bonding may be expected. Further refinement of the rhodan hydrate structure [7] also strongly indicates that the two hydrogen atoms in the molecule belong to the exocyclic nitrogen atom. It may therefore be more correct to assign both rhodan hydrate and xanthan hydride a structure of type II.

Refinement of the xanthan hydride structure will be continued by means of $(F_o - F_c)$-technique.

I wish to thank *Fr. Meltzers Høyskolefond* for a grant.

* On leave from Chemical Institute, University of Bergen, Bergen, Norway.

1. Foss, O. and Tjomsland, O. *Acta Chem. Scand.* **12** (1958) 1799.
2. Kehl, W. L. and Jeffrey, G. A. *Acta Cryst.* **11** (1958) 813.
3. Hordvik, A. *Acta Chem. Scand.* **14** (1960) 1218.
4. Hantzsch, A. and Wolvekamp, M. *Ann.* **331** (1904) 265.
5. Foss, O. *Acta Chem. Scand.* **10** (1956) 868.
6. Zachariasen, W. H. *Acta Cryst.* **5** (1952) 68.
7. Hordvik, A. *Work in progress.*

Received June 3, 1961.

On Molybdenum Oxide Hydroxides Genotypic with MoO_3

LARS KIHLBORG, GÖRAN HÄGERSTRÖM and AXEL RÖNNQUIST

Institute of Chemistry, University of Uppsala, Uppsala, Sweden

A series of molybdenum oxide hydroxides, which may be assigned the general formula $MoO_{3-x}(OH)_x$ have been prepared by Glemser *et al.*[1-4] by the reduction of crystalline MoO_3 with (*a*) Zn and HCl, (*b*) Mo powder in the presence of water, (*c*) atomic hydrogen, or (*d*) $LiAlH_4$. Four members of this series were prepared, namely those with $x = 0.5$, 1.0, 1.6, and 2.0, and in addition a compound $Mo_5O_8(OH)_8$, which may be formulated $MoO_{1.6}(OH)_{1.2}(H_2O)_{0.2}$. The close connection existing between these reduced phases and MoO_3, demonstrated by the possibility for stepwise reduction and oxidation, has led Glemser and Lutz to describe them as *genotypic with* MoO_3 and to suppose that this chemical relationship would be reflected in their crystal structures [1].

Preliminary X-ray investigations have been made by the present authors in order to study the structural relationships within this genotypic series. Samples of MoO_3 were subjected to different degrees of reduction by methods (*a*), (*b*), and (*c*) above and the X-ray powder patterns of the products were recorded in Guinier focusing cameras with Cu$K\alpha$ radiation using KCl as an internal standard ($a = 6.2921$ Å).

The existence of a number of different crystalline phases was verified. Their powder patterns, which are all very similar to that of MoO_3, could be interpreted in most cases, and the unit cell dimensions thus derived were seen to differ only slightly from those of MoO_3, *viz.* within 5 % for the *a* and *b* axes and within 10 % for the *c* axis. In some cases the cell is slightly monoclinically deformed, the *a* axis being the unique axis. It is thus evident, that the term "genotypic with MoO_3" is also appropriate when considering the structural relationships between these compounds.

Although no data for chemical analysis were available, one phase could be identified as the compound $Mo_4O_{10}(OH)_2$ ($x = 0.5$) described by Glemser and Lutz, since it could be prepared by method (*b*) above, specific for this compound, and its powder pattern (Table 1) was seen to agree with the data given by these authors. The orthorhombic unit cell has the dimensions: $a = 3.888$ Å, $b = 14.082$ Å, $c = 3.734$ Å, which may be compared with the values for MoO_3[5]: $a = 3.963$ Å, $b = 13.855$ Å, $c = 3.696$ Å.

Table 1. X-Ray powder pattern of $MoO_{2.5}(OH)_{0.5}$. Cu$K\alpha$ radiation.

I	$\sin^2\Theta_{obs}$	*hkl*	$\sin^2\Theta_{calc}$
m	0.01195	020	0.01199
v st	0.04219	110	0.04231
m	0.04797	040	0.04795
v st	0.05453	021	0.05460
w	0.06626	130	0.06628
st	0.08488	111	0.08492
v w	0.09059	041	0.09057
m	0.10802	060	0.10789
m	0.10895	131	0.10890
w	0.11430	150	0.11423
w	0.15066	061	0.15051
m	0.15719	200	0.15724
st	0.17051	002	0.17046
w	0.20519	240	0.20519
m	0.21173	221	0.21184
m	0.21276	112	0.21277
w	0.21846	042	0.21842
w	0.22885	171	0.22888
v w	0.23460	081	0.23442
v w	0.23677	132	0.23675
v w	0.24794	241	0.24780
v w	0.26509	260	0.26513
w	0.27846	062	0.27836
w	0.28474	152	0.28470

v = very, st = strong, m = medium, w = weak.

1. Foss, O. and Tjomsland, O. *Acta Chem. Scand.* **12** (1958) 1799.
2. Kehl, W. L. and Jeffrey, G. A. *Acta Cryst.* **11** (1958) 813.
3. Hordvik, A. *Acta Chem. Scand.* **14** (1960) 1218.
4. Hantzsch, A. and Wolvekamp, M. *Ann.* **331** (1904) 265.
5. Foss, O. *Acta Chem. Scand.* **10** (1956) 868.
6. Zachariasen, W. H. *Acta Cryst.* **5** (1952) 68.
7. Hordvik, A. *Work in progress.*

Received June 3, 1961.

On Molybdenum Oxide Hydroxides Genotypic with MoO_3

LARS KIHLBORG, GÖRAN HÄGERSTRÖM and AXEL RÖNNQUIST

Institute of Chemistry, University of Uppsala, Uppsala, Sweden

A series of molybdenum oxide hydroxides, which may be assigned the general formula $MoO_{3-x}(OH)_x$ have been prepared by Glemser *et al.*[1-4] by the reduction of crystalline MoO_3 with (*a*) Zn and HCl, (*b*) Mo powder in the presence of water, (*c*) atomic hydrogen, or (*d*) $LiAlH_4$. Four members of this series were prepared, namely those with $x = 0.5$, 1.0, 1.6, and 2.0, and in addition a compound $Mo_5O_8(OH)_8$, which may be formulated $MoO_{1.6}(OH)_{1.2}(H_2O)_{0.2}$. The close connection existing between these reduced phases and MoO_3, demonstrated by the possibility for stepwise reduction and oxidation, has led Glemser and Lutz to describe them as *genotypic with* MoO_3 and to suppose that this chemical relationship would be reflected in their crystal structures [1].

Preliminary X-ray investigations have been made by the present authors in order to study the structural relationships within this genotypic series. Samples of MoO_3 were subjected to different degrees of reduction by methods (*a*), (*b*), and (*c*) above and the X-ray powder patterns of the products were recorded in Guinier focusing cameras with Cu$K\alpha$ radiation using KCl as an internal standard ($a = 6.2921$ Å).

The existence of a number of different crystalline phases was verified. Their powder patterns, which are all very similar to that of MoO_3, could be interpreted in most cases, and the unit cell dimensions thus derived were seen to differ only slightly from those of MoO_3, *viz.* within 5 % for the *a* and *b* axes and within 10 % for the *c* axis. In some cases the cell is slightly monoclinically deformed, the *a* axis being the unique axis. It is thus evident, that the term "genotypic with MoO_3" is also appropriate when considering the structural relationships between these compounds.

Although no data for chemical analysis were available, one phase could be identified as the compound $Mo_4O_{10}(OH)_2$ ($x = 0.5$) described by Glemser and Lutz, since it could be prepared by method (*b*) above, specific for this compound, and its powder pattern (Table 1) was seen to agree with the data given by these authors. The orthorhombic unit cell has the dimensions: $a = 3.888$ Å, $b = 14.082$ Å, $c = 3.734$ Å, which may be compared with the values for MoO_3[5]: $a = 3.963$ Å, $b = 13.855$ Å, $c = 3.696$ Å.

Table 1. X-Ray powder pattern of $MoO_{2.5}(OH)_{0.5}$. Cu$K\alpha$ radiation.

I	$\sin^2\Theta_{obs}$	*hkl*	$\sin^2\Theta_{calc}$
m	0.01195	020	0.01199
v st	0.04219	110	0.04231
m	0.04797	040	0.04795
v st	0.05453	021	0.05460
w	0.06626	130	0.06628
st	0.08488	111	0.08492
v w	0.09059	041	0.09057
m	0.10802	060	0.10789
m	0.10895	131	0.10890
w	0.11430	150	0.11423
w	0.15066	061	0.15051
m	0.15719	200	0.15724
st	0.17051	002	0.17046
w	0.20519	240	0.20519
m	0.21173	221	0.21184
m	0.21276	112	0.21277
w	0.21846	042	0.21842
w	0.22885	171	0.22888
v w	0.23460	081	0.23442
v w	0.23677	132	0.23675
v w	0.24794	241	0.24780
v w	0.26509	260	0.26513
w	0.27846	062	0.27836
w	0.28474	152	0.28470

v = very, st = strong, m = medium, w = weak.

The space group of MoO_3 is *Pbnm* (No. 62 of *Int. Tab.* in a different orientation) with the atoms in 4-fold positions 4(*c*):x, y, $\frac{1}{4}$; $\frac{1}{2}-x$, $\frac{1}{2}+y$, $\frac{1}{4}$; $\frac{1}{2}+x$, $\frac{1}{2}-y$, $\frac{3}{4}$; $\bar{x},\bar{y},\frac{3}{4}$. The atomic parameter values are [6]:

	x	y
Mo	0.0847	0.0998
O_1	−0.025	0.935
O_2	−0.060	0.600
O_3	0.015	0.230

The intensity distribution in the powder pattern of $MoO_{2.5}(OH)_{0.5}$ is remarkably similar to that of MoO_3, with the important exception that all reflections with $h + k = 2n + 1$ are missing. This indicates a *C*-centering of the lattice, which can be achieved if the four x coordinates above are put equal to zero. The atomic positions are thereby moved to exactly half-way between the glide-planes, and can be described as positions 4(*c*): 0, y, $\frac{1}{4}$; $\frac{1}{2}$, $\frac{1}{2}+y$, $\frac{1}{4}$; $\frac{1}{2},\frac{1}{2}-y$, $\frac{3}{4}$; 0, $\bar{y}$, $\frac{3}{4}$; of the space group *Cmcm* (No. 63), which is a super-group to the preceding one. Structure factors based on this structure model with the same y parameters as above were calculated.

It is probable that the intensities of the powder lines of the hydroxide will be seriously modified by orientation effects, as in the case of MoO_3. It was therefore not possible to obtain very reliable observed $|F|$-values for the hydroxide from intensity measurements. However, the assumption that these effects have the same influence on the intensities in both cases, produced relatively good agreement between calculated and observed values. The y coordinates of the molybdenum atoms are thus evidently fairly close to the values in MoO_3. The corresponding oxygen parameters are of course approximate, as they effect the intensities to a much smaller extent. Single crystal studies appear to be necessary if the precise oxygen positions are to be evaluated.

It is clear that the substitution of two OH groups for one O atom per unit cell of MoO_3 causes a transition to a more ideal structure, at least as regards the metal atom arrangements. The same effect has been observed in the tungsten oxide hydroxides studied by Glemser and Naumann [7]. It is also in accordance with Magnéli's observation on molybdenum and tungsten compounds containing structural elements of ReO_3- or perovskite type, that a lower valency for the metal atom favours a less distorted arrangement [8].

Acknowledgements. We wish to thank Professor G. Hägg and Professor A. Magnéli for all facilities put at our disposal and for their continued interest in this investigation. The studies form a part of a research program on transition metal oxides and related compounds financially supported by the *Swedish Natural Science Research Council.*

1. Glemser, O. and Lutz, G. *Z. anorg. u. allgem. Chem.* **264** (1951) 17.
2. Glemser, O., Hauschild, U. and Lutz, G. *Z. anorg. u. allgem. Chem.* **269** (1952) 93.
3. Glemser, O. *Nachr. Akad. Wiss. Göttingen, Math.-physik.-Kl., Abt. IIa* **1955** 121.
4. Glemser, O., Lutz, G. and Meyer, G. *Z. anorg. u. allgem. Chem.* **285** (1956) 173.
5. Westman, S. and Magnéli, A. *Acta Chem. Scand.* **12** (1958) 363.
6. Andersson, G. and Magnéli, A. *Acta Chem. Scand.* **4** (1950) 793.
7. Glemser, O. and Naumann, Ch. *Z. anorg. u. allgem. Chem.* **265** (1951) 288.
8. Magnéli, A. *J. Inorg. & Nuclear Chem.* **2** (1956) 330.

Received June 21, 1961.

Mimosaceen-Aminosäuren. Teil VII *

Isolierung von Willardiin (3-(1-Uracyl)-L-Alanin) aus den Samen von *Acacia millefolia, Acacia lemmoni* und *Mimosa asperata*

ROLF GMELIN

Aus dem Laboratorium der Stiftung für Chemische Forschung, Biochemisches Institut, Helsinki, Finnland

In einer früheren Mitteilung wurde die Isolierung von Willardiin, einer neuen pflanzlichen Aminosäure, aus den Samen von *Acacia Willardiana* Rose (*Mimosaceae*)

* Teil VI: R. Gmelin. *Z. Physiol. Chem. Hoppe-Seyler's. In Vorbereitung.*

The space group of MoO_3 is *Pbnm* (No. 62 of *Int. Tab.* in a different orientation) with the atoms in 4-fold positions 4(*c*):x, y, $\frac{1}{4}$; $\frac{1}{2}-x$, $\frac{1}{2}+y$, $\frac{1}{4}$; $\frac{1}{2}+x$, $\frac{1}{2}-y$, $\frac{3}{4}$; $\bar{x},\bar{y},\frac{3}{4}$. The atomic parameter values are [6]:

	x	y
Mo	0.0847	0.0998
O_1	−0.025	0.935
O_2	−0.060	0.600
O_3	0.015	0.230

The intensity distribution in the powder pattern of $MoO_{2.5}(OH)_{0.5}$ is remarkably similar to that of MoO_3, with the important exception that all reflections with $h + k = 2n + 1$ are missing. This indicates a *C*-centering of the lattice, which can be achieved if the four x coordinates above are put equal to zero. The atomic positions are thereby moved to exactly half-way between the glide-planes, and can be described as positions 4(*c*): 0, y, $\frac{1}{4}$; $\frac{1}{2}$, $\frac{1}{2}+y$, $\frac{1}{4}$; $\frac{1}{2},\frac{1}{2}-y$, $\frac{3}{4}$; 0, $\bar{y}$, $\frac{3}{4}$; of the space group *Cmcm* (No. 63), which is a super-group to the preceding one. Structure factors based on this structure model with the same y parameters as above were calculated.

It is probable that the intensities of the powder lines of the hydroxide will be seriously modified by orientation effects, as in the case of MoO_3. It was therefore not possible to obtain very reliable observed $|F|$-values for the hydroxide from intensity measurements. However, the assumption that these effects have the same influence on the intensities in both cases, produced relatively good agreement between calculated and observed values. The y coordinates of the molybdenum atoms are thus evidently fairly close to the values in MoO_3. The corresponding oxygen parameters are of course approximate, as they effect the intensities to a much smaller extent. Single crystal studies appear to be necessary if the precise oxygen positions are to be evaluated.

It is clear that the substitution of two OH groups for one O atom per unit cell of MoO_3 causes a transition to a more ideal structure, at least as regards the metal atom arrangements. The same effect has been observed in the tungsten oxide hydroxides studied by Glemser and Naumann [7]. It is also in accordance with Magnéli's observation on molybdenum and tungsten compounds containing structural elements of ReO_3- or perovskite type, that a lower valency for the metal atom favours a less distorted arrangement [8].

Acknowledgements. We wish to thank Professor G. Hägg and Professor A. Magnéli for all facilities put at our disposal and for their continued interest in this investigation. The studies form a part of a research program on transition metal oxides and related compounds financially supported by the *Swedish Natural Science Research Council.*

1. Glemser, O. and Lutz, G. *Z. anorg. u. allgem. Chem.* **264** (1951) 17.
2. Glemser, O., Hauschild, U. and Lutz, G. *Z. anorg. u. allgem. Chem.* **269** (1952) 93.
3. Glemser, O. *Nachr. Akad. Wiss. Göttingen, Math.-physik.-Kl., Abt. IIa* **1955** 121.
4. Glemser, O., Lutz, G. and Meyer, G. *Z. anorg. u. allgem. Chem.* **285** (1956) 173.
5. Westman, S. and Magnéli, A. *Acta Chem. Scand.* **12** (1958) 363.
6. Andersson, G. and Magnéli, A. *Acta Chem. Scand.* **4** (1950) 793.
7. Glemser, O. and Naumann, Ch. *Z. anorg. u. allgem. Chem.* **265** (1951) 288.
8. Magnéli, A. *J. Inorg. & Nuclear Chem.* **2** (1956) 330.

Received June 21, 1961.

Mimosaceen-Aminosäuren. Teil VII *

Isolierung von Willardiin (3-(1-Uracyl)-L-Alanin) aus den Samen von *Acacia millefolia, Acacia lemmoni* und *Mimosa asperata*

ROLF GMELIN

Aus dem Laboratorium der Stiftung für Chemische Forschung, Biochemisches Institut, Helsinki, Finnland

In einer früheren Mitteilung wurde die Isolierung von Willardiin, einer neuen pflanzlichen Aminosäure, aus den Samen von *Acacia Willardiana* Rose (*Mimosaceae*)

* Teil VI: R. Gmelin. *Z. Physiol. Chem. Hoppe-Seyler's. In Vorbereitung.*

beschrieben [1]. Die für Willardiin vorgeschlagene Struktur ist inzwischen von Kjær *et al.*[2] durch Synthese bewiesen worden. Eine Synthese von DL-Willardiin wurde kürzlich durch Shaw und Dewar [3] beschrieben. Da diese Aminosäure wegen ihrer biogenetischen Verwandtschaft zu Albizziin [4,5] (L-2-Amino-3-ureidopropionsäure) [6] und zu L-2,3-Diaminopropionsäure [5], zwei weiteren Mimosaceen-Aminosäuren, und wegen ihres, für Aminosäuren ungewöhnlichen, Uracil-Rests von gewissem biochemischem Interesse ist, erschien es lohnend, ihre Verbreitung in der Mimosaceen-Familie näher zu untersuchen. Die vorliegende Notiz soll kurz über Ergebnisse entsprechender Untersuchungen berichten.

Für eine papierchromatographische Vorprüfung, bei der die UV-Absorption des Willardiins bei 262 mμ in Verbindung mit dem Ninhydrin-Farbtest von diagnostischem Wert war, standen Samen von etwa 100 verschiedenen Mimosaceen-Arten zur Verfügung. Lediglich bei den Arten *Acacia millefolia* *, *Acacia lemmoni* * und *Mimosa asperata* * waren sichere Anhaltspunkte für das Vorkommen von Willardiin vorhanden. Zur Bestätigung der papierchromatographischen Befunde wurde Willardiin aus den genannten Arten isoliert. Da die Isolierungsmethoden sich an früher beschriebene Methoden anlehnen, seien sie hier nur kurz aufgeführt. Durch Ionenaustausch an *Amberlite* IR 120 (H-Form) wurden aus den methanolisch-wässrigen Auszügen der Samen zunächst die gesamten Aminosäuren angereichert. In einem bei Hietala [7] beschriebenen Versuch wurde das Aminosäurengemisch aus *Acacia millefolia* durch kontinuierliche Gegenstromverteilung aufgetrennt. Hierbei wurde eine Albizziin und Willardiin enthaltende Fraktion erhalten. Durch fraktionierte Kristallisation konnte daraus Willardiin abgetrennt werden. Ausbeute etwa 120 mg Willardiin aus 65 g Samen, Fp. 204–205°.

Das Aminosäuren-Gemisch aus *Acacia lemmoni* wurde einer fraktionierten Kristallisation unterworfen wie sie für *Acacia Willardiana* beschrieben worden war. Aus 12 g Samen wurden dabei 18 mg Willardiin gewonnen, Fp. 202–204°.

Das Aminosäuren-Gemisch aus *Mimosa asperata* wurde auf einer Zellulose-Säule (4,5 cm × 24 cm) mit der Oberphase des Lösungsmittelsystems Butanol-Äthanol-Wasser 4:1:3 chromatographisch aufgetrennt. Willardiin erschien in den Fraktionen 62 bis 80 (1 Fraktion = 20 ml). Aus 32 g Samen wurden 54 mg Willardiin erhalten, Fp. 204–205°.

Die Identität dieser drei Präparate mit dem ursprünglichen Willardiin-Präparat aus *Acacia Willardiana* konnte auf Grund ihrer Schmelzpunkte, ihrer identischen UV-Spektren bei pH 1 und pH 12, ihrer identischen IR-Spektren sowie ihres papierchromatographischen Verhaltens in verschiedenen Lösungsmittelsystemen sichergestellt werden.

Willardiin liess sich somit bisher in zwei verschiedenen Triben der Mimosaceen-Familie antreffen: in den *Acacieae* und *Eumimoseae*. In ersteren ist es stets von Albizziin begleitet, das als biogenetische Vorstufe von Willardiin vermutet werden kann. In letzteren wurde L-2,3-Diaminopropionsäure gefunden [5], das wiederum biogenetisch verwandt mit Albizziin sein dürfte.

Herrn Prof. Dr. A. I. Virtanen danke ich für sein Interesse an diesen Untersuchungen und für die Förderung dieser Arbeit. Herrn P. Garnier, Bouaké, Côte d'Ivoire, und Herrn Dr. Q. Jones, United States Department of Agriculture, New Crops Research, Beltsville, Maryland, danke ich für die freundliche Beschaffung des Pflanzenmaterials, Herrn Prof. Dr. A. Kjær, Kopenhagen, für die Aufnahme der IR-Spektren.

1. Gmelin, R. *Z. Physiol. Chem. Hoppe-Seyler's* **316** (1959) 164.
2. Kjær, A., Knudsen, A. und Olesen Larsen, P. *Acta Chem. Scand.* **15** (1961) 1193.
3. Shaw, G. und Dewar, J. H. *Proc. Chem. Soc. (London)* **1961** 216.
4. Gmelin, R., Strauss, G. und Hasenmaier, G. *Z. Naturforsch.* **13 b** (1958) 252.
5. Gmelin, R., Strauss, G. und Hasenmaier, G. *Z. Physiol. Chem. Hoppe-Seyler's* **314** (1959) 28.
6. Kjær, A., Olesen Larsen, P. und Gmelin, R. *Experientia* **15** (1959) 253.
7. Hietala, P. *Ann. Acad. Sci. Fennicæ* **A II**, 100 (1960).

Eingegangen am 1. August 1961.

* Die erhaltenen Samenproben waren ohne Angabe der Autoren-Namen, genaue Standortangaben und Herbarmaterial liegen jedoch vor.

X-Ray Crystal Data on Some Methyl-Pentofuranosides

SVEN FURBERG and HANS HAMMER

Institute of Chemistry, University of Oslo, Blindern-Oslo, Norway

A great deal of information on the conformations of pyranose sugars has been collected during latter years and the structure of several of these compounds has been determined by X-ray crystallographic methods [1,2]. Much less is known about the furanose structures of the sugars and we thought it therefore of interest to examine a simple compound of this type in detail. In this note the unit cell dimensions and space groups of five methyl pentofuranosides are reported.

The compounds were prepared by Professor Dr. E. Berner and collaborators [3,4], whom we would like to thank for placing samples at our disposal. The unit cell dimensions (which are accurate to about 0.5 %) were derived from oscillation and Weissenberg diagrams taken with Cu$K\alpha$-radiation (λ = 1.542 Å). The space groups were determined from systematic absences, taking also into account that the substances are optically active. Densities were measured by flotation in mixtures of carbon tetrachloride and benzene.

Methyl β-ribofuranoside, m.p. 80°C, specific rotation in water $[\alpha]^{20}_D = -49.8°$. The compound crystallizes from ethyl acetate in well-developed crystals elongated along *c*, bounded by {100} and {010}. They are orthorhombic, with unit cell dimensions a = 12.87 Å, b = 24.07 Å and c = 4.86 Å. Reflexions $h00$, $0k0$ and $00l$ are absent for odd values of the indices, and the space group is $P2_12_12_1$. The density was found to be 1.43 g·cm^{-3}, and there are eight (calc. 7.90) molecules in the unit cell. The asymmetric unit in the crystal thus consists of two molecules.

Methyl α-xylofuranoside, m.p. 84°C, $[\alpha]^{20}_D = +182°$. The crystals are monoclinic, elongated along *c*, with cell dimensions a = 8.81 Å, b = 8.11 Å, c = 6.24 Å and $\beta = 123°$. The space group is $P2_1$. The measured density of 1.43 g·cm^{-3} corresponds to two (calc. 1.96) molecules in the unit cell.

The reflexion $20\bar{1}$ is by far the strongest one in the $h0l$ zone and the molecules are probably lying roughly in these planes.

Methyl α-arabofuranoside, m.p. 51°C, $[\alpha]^{20}_D = +126°$. The crystals are very hygroscopic and were kept in glass capillaries during the examination. They were needle- or rod-shaped, in general poorly developed, and showed straight extinction, or nearly so, under the polarizing microscope. The diagrams obtained were rather poor, but indicated that the crystals probably are triclinic (pseudo-monoclinic). Space group $P\bar{1}$. The following lattice parameters were derived: d_{100} = 12.09 Å, b = 6.87 Å, c = 4.61 Å, $\beta = 100°$, $\gamma = 93°$. Two molecules in the unit cell correspond to a density of 1.42 g·cm^{-3}. This value is somewhat smaller than those of the other three simple pentofuranosides, for which values 1.45—1.46 g·cm^{-3} are calculated. The melting point is also lower.

Methyl α-lyxofuranoside, m.p. 97°C, $[\alpha]^{20}_D = +129°$. The crystals were needle-shaped, elongated along *c*, with forms {100} and {010} developed. The cell dimensions are a = 10.34 Å, b = 15.56 Å and c = 4.63 Å and the space group is $P2_12_12_1$. The density calculated on the basis of four molecules per unit cell is 1.46 g·cm^{-3}.

Methyl α-fucofuranoside, m.p. 126°C, $[\alpha]^{20}_D = -111.4°$. The crystals occur either as nicely developed pyramids or as needles. They are trigonal, with space group $P3_1$, and cell dimensions $a = b$ = 9.21 Å and c = 8.98 Å. The density was found to be 1.33 g·cm^{-3} and there are three (calc. 2.97) molecules in the unit cell.

Discussion. The unit cell dimensions and space groups of a great number of sugar derivatives have been determined by Cox [5]. He found that one of the axes frequently had a length of about 4.5 Å, indicating a molecular "thickness" of this order of magnitude, with the ring "plane" roughly perpendicular to the short axis. As will be seen, three of the compounds described above have an axis of this type.

Amongst the compounds studied, the lyxoside derivative clearly is the most suitable one for a detailed structure analysis. We have collected three-dimensional intensity data, and tried to solve the structure by Patterson syntheses, inequalitites and other methods, but so far without success. We believe that the "centre" of the molecule lies in the neighbourhood of

either (0, 1/4, 1/4) or (1/4, 0,0). The Patterson syntheses show that there are layers of molecules $c/2$ apart approximately parallel to the *ab*-plane. Correspondingly, the 002 reflexion is extremely strong. It is interesting that the corresponding hexose sugar, methyl *α*-mannofuranoside, has the same space group and very similar unit cell dimensions, namely 4.64 Å, 11.73 Å and 15.87 Å. These two sugars have the same furanose configuration, the mannoside being derived by substituting a hydrogen at C_5 in the lyxoside with $-CH_2OH$. This increases the length of the *a* axis from 10.34 Å to 11.73 Å, whereas the other axes remain nearly unchanged. This indicates, as is seen from models, that the methyl lyxoside molecule is most extended in the direction of *b*.

Further attempts to solve the structure are being carried out.

1. McDonald, T. R. R. and Beevers, C. A. *Acta Cryst.* **5** (1952) 654.
2. Hordvik, A. *Acta Chem. Scand.* **15** (1961) 16.
3. Augestad, I. and Berner, E. *Acta Chem. Scand.* **8** (1954) 251.
4. Augestad, I. and Berner, E. *Acta Chem. Scand.* **10** (1956) 911.
5. Cox, E. G., Goodwin, T. H. and Wagstaff, A. I. *J. Chem. Soc.* **1935** 1495.
6. Cox, E. G. and Goodwin, T. H. *J. Chem. Soc.* **1932** 1844.

Received June 28, 1961.

The Structures of Widdrol * and the Alcohol, $C_{15}H_{26}O_2$, Isolated from *Widdringtonia juniperoides* (L.) Endl.

C. ENZELL

Organisk-kemiska Institutionen, Kungl. Tekniska Högskolan, Stockholm, Sweden

Erdtman and Thomas [1] isolated the sesquiterpene alcohol widdrol, $C_{15}H_{26}O$, (m.p. 98°) and a further alcohol, $C_{15}H_{26}O_2$, (m.p. 154°; $[\alpha]_D$ −9°) from the heartwood of *Widdringtonia* species. These authors suggested that widdrol was a dicyclic, tertiary alcohol containing one double bond and they obtained 1,7-dimethyl-4-*iso*propylnaphthalene (1) on selenium dehydrogenation. Recently Nagahama [2] has shown that widdrol is formed on hydration of thujopsene [3] (2) with oxalic acid. The following experimental evidence shows that widdrol has structure (3).

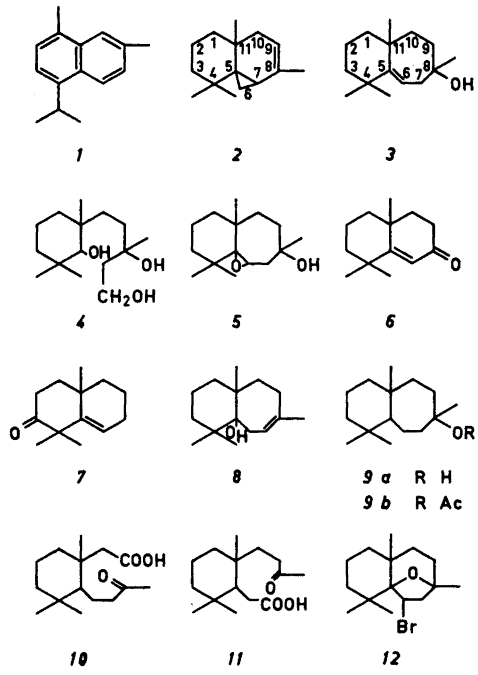

Widdrol [I.R.: $\nu_{max}^{CHBr_3}$ 839, 1635 cm^{-1}; PMR: τ 4.50 ($CR_2 = CRH$)] on ozonolysis, followed by reduction with lithium aluminium hydride, gave a triol (4) (m.p. 97–98°) together with minor amounts of an epoxyalcohol (5) (m.p. 153–154°).

The triol (4) on oxidation (chromium trioxide-sulphuric acid-acetone) furnished a hydroxyketoaldehyde ($\nu_{max}^{CCl_4}$ 2 720, 1 717, 1 690 cm^{-1}), which on treatment with alkali yielded an *α,β*-unsaturated ketone (6)[λ_{max}^{EtOH} 240 mμ (ε 13 000); 2,4-dinitrophenylhydrazone m.p. 204–205°] and acetaldehyde. The DL-octalone (6) was synthesised from the ketone (7) [4] by Huang-

* Presented by H. Erdtman at the Chemical Society symposium on terpene chemistry in London (23.2.1961). *Proc. Chem. Soc.* **1961** 129.

either (0, 1/4, 1/4) or (1/4, 0,0). The Patterson syntheses show that there are layers of molecules $c/2$ apart approximately parallel to the *ab*-plane. Correspondingly, the 002 reflexion is extremely strong. It is interesting that the corresponding hexose sugar, methyl *α*-mannofuranoside, has the same space group and very similar unit cell dimensions, namely 4.64 Å, 11.73 Å and 15.87 Å. These two sugars have the same furanose configuration, the mannoside being derived by substituting a hydrogen at C_5 in the lyxoside with $-CH_2OH$. This increases the length of the *a* axis from 10.34 Å to 11.73 Å, whereas the other axes remain nearly unchanged. This indicates, as is seen from models, that the methyl lyxoside molecule is most extended in the direction of *b*.

Further attempts to solve the structure are being carried out.

1. McDonald, T. R. R. and Beevers, C. A. *Acta Cryst.* **5** (1952) 654.
2. Hordvik, A. *Acta Chem. Scand.* **15** (1961) 16.
3. Augestad, I. and Berner, E. *Acta Chem. Scand.* **8** (1954) 251.
4. Augestad, I. and Berner, E. *Acta Chem. Scand.* **10** (1956) 911.
5. Cox, E. G., Goodwin, T. H. and Wagstaff, A. I. *J. Chem. Soc.* **1935** 1495.
6. Cox, E. G. and Goodwin, T. H. *J. Chem. Soc.* **1932** 1844.

Received June 28, 1961.

The Structures of Widdrol * and the Alcohol, $C_{15}H_{26}O_2$, Isolated from *Widdringtonia juniperoides* (L.) Endl.

C. ENZELL

Organisk-kemiska Institutionen, Kungl. Tekniska Högskolan, Stockholm, Sweden

Erdtman and Thomas [1] isolated the sesquiterpene alcohol widdrol, $C_{15}H_{26}O$, (m.p. 98°) and a further alcohol, $C_{15}H_{26}O_2$, (m.p. 154°; $[\alpha]_D$ −9°) from the heartwood of *Widdringtonia* species. These authors suggested that widdrol was a dicyclic, tertiary alcohol containing one double bond and they obtained 1,7-dimethyl-4-*iso*propylnaphthalene (1) on selenium dehydrogenation. Recently Nagahama [2] has shown that widdrol is formed on hydration of thujopsene [3] (2) with oxalic acid. The following experimental evidence shows that widdrol has structure (3).

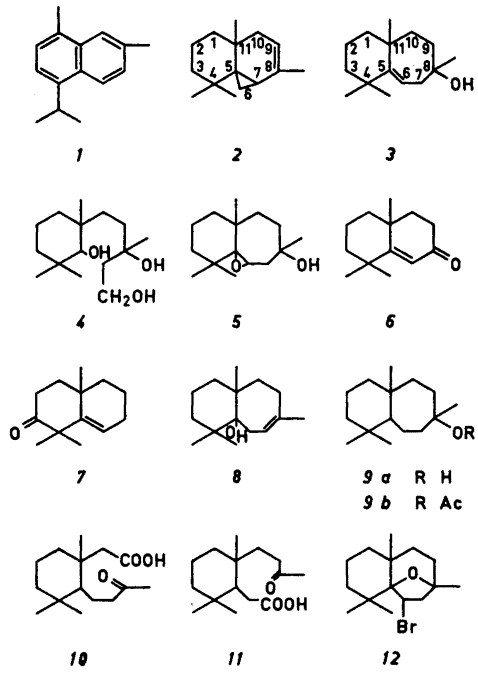

Widdrol [I.R.: $\nu_{max}^{CHBr_3}$ 839, 1635 cm^{-1}; PMR: τ 4.50 ($CR_2 = CRH$)] on ozonolysis, followed by reduction with lithium aluminium hydride, gave a triol (4) (m.p. 97–98°) together with minor amounts of an epoxyalcohol (5) (m.p. 153–154°).

The triol (4) on oxidation (chromium trioxide-sulphuric acid-acetone) furnished a hydroxyketoaldehyde ($\nu_{max}^{CCl_4}$ 2 720, 1 717, 1 690 cm^{-1}), which on treatment with alkali yielded an *α,β*-unsaturated ketone (6)[λ_{max}^{EtOH} 240 mμ (ε 13 000); 2,4-dinitrophenylhydrazone m.p. 204–205°] and acetaldehyde. The DL-octalone (6) was synthesised from the ketone (7) [4] by Huang-

* Presented by H. Erdtman at the Chemical Society symposium on terpene chemistry in London (23.2.1961). *Proc. Chem. Soc.* **1961** 129.

Minlon reduction followed by oxidation with sodium dichromate in acetic acid. It furnished a 2,4-dinitrophenylhydrazone (m.p. 204–205°), which gave ultra-violet, infra-red and mass spectra identical with those of the corresponding derivative of widdrol.

The epoxyalcohol (5), also obtained from widdrol on oxidation with perphthalic acid, was recovered unchanged after treatment with chromium trioxide-sulphuric acid in acetone. Its formation on ozonisation was taken as an indication of the presence of a sterically hindered double bond [5] in widdrol.

The above results favour structure (3) for widdrol. The alternative structure (8) is excluded by the following reactions. Hydrogenation of widdrol with Adams catalyst in acetic acid gave dihydrowiddrol (9a) and a small amount of a saturated hydrocarbon, $C_{15}H_{28}$. On pyrolysis dihydrowiddrol acetate (9b) gave a mixture of unsaturated hydrocarbons, containing, according to its infra-red absorption, minor amounts of the exocyclic isomer. This hydrocarbon mixture on ozonolysis and subsequent steam distillation gave a low yield of formaldehyde and a non-volatile product which, on oxidation with silver oxide, furnished a keto acid (10 or 11), (2,4-dinitrophenylhydrazone m.p. 232–236°) as the main product. This keto acid gave iodoform on treatment with sodium hypoiodite.

Structure (3) for widdrol is also in good agreement with the mass spectrometric and PMR results. The strongest peak in the mass spectrum of widdrol is found at *m/e* 151 and corresponds to an ion formed by rupture of the C(7)–C(8) and C(10)–C(11) bonds [6]. The PMR spectrum of dihydrowiddrol shows the presence of the angular methyl group (τ 9.01), the geminal dimethyl group (τ 8.90 and 8.96) and the methyl group at C(8) (τ 8.83); the latter is found at somewhat lower field (τ 8.53) in the spectrum of dihydrowiddrol acetate.

The configuration at C(11) in widdrol remains unclear. Comparison of the positive R.D. curve of ketone (6) with the negative curve for 3β-acetoxy-Δ^5-lanosten-7-one [7] indicates that the angular methyl group is α-oriented. This is unexpected since on similar grounds it has been suggested that the angular methyl group in thujopsene is β-oriented. This problem is being further investigated and additional evidence of the α-orientation will be communicated in the full paper.

The low yield of the exocyclic isomer obtained on pyrolysis of dihydrowiddrol acetate and the formation of a bromoether, probably (12), on bromination of widdrol indicates that the hydroxyl group is quasi-axial.

The alcohol, $C_{15}H_{26}O_2$ (m.p. 154°), was found to be identical with widdrol epoxide (5). This compound has been encountered in two conifers of the natural order Cupressales, while widdrol has been found in many.

Acknowledgements. I express my gratitude to Dr. W. Klyne, Post Graduate Medical School, London, for the R.D. determinations, to Dr. R. Ryhage, Karolinska Institutet, Stockholm, for the mass spectrometric determinations, to Dr. S. Forsén for measuring and interpreting the PMR-spectra and to Professor H. Erdtman for his kind interest. Thanks are also offered to the *Swedish Technical Research Council* for financial support.

1. Erdtman, H. and Thomas, B. R. *Acta Chem. Scand.* **12** (1958) 267.
2. Nagahama, S. *Bull. Chem. Soc. Japan.* **33** (1960) 1467.
3. Norin, T. *Acta Chem. Scand.* **15** (1961). *In press.*
4. Mukherjee, S. L. and Dutta, P. C. *J. Chem. Soc.* **1960** 67.
5. Bailey, P. S. *Chem. Revs.* **58** (1958) 925.
6. Enzell, C. *Acta Chem. Scand.* **15** (1961). *In press.*
7. Djerassi, C., Halpern, O., Halpern, V. and Riniker, B. *J. Am. Chem. Soc.* **80** (1958) 4001.

Received July 3, 1961.

Amino Acid Studies

Part IV.* Structure and Synthesis of the Plant Amino Acid Willardiine [3-(1-Uracyl)-L-alanine]

ANDERS KJÆR, ALLAN KNUDSEN and P. OLESEN LARSEN

Department of Organic Chemistry. The Royal Veterinary and Agricultural College, Copenhagen, Denmark

In 1959, Gmelin [1] reported the isolation of several non-protein amino acids from *Acacia Willardiana* Rose (*Mimosaceae*). One of these, named *willardiine*, was formulated as 3-(1-uracyl)L-alanine (I) on basis of its elemental composition, spectroscopic properties and stability towards strong acid. The formal similarity of (I) to L-albizziine (II) [2,3], present in the same seed material, was adduced in support of the proposed structure, particularly its steric configuration [1]. In order to provide an unambiguous proof of the structure of willardiine, the following synthetic work was undertaken.

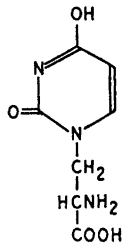

I

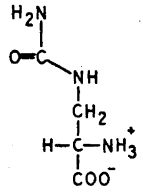

II

The elegant procedure developed by Shaw *et al.*[4] for the synthesis of uracil, 1-methyl-, 1-ethyl- and 1-phenyl-uracil was adopted as the most promising synthetic approach. β-Ethoxyacryloyl chloride [5] was converted into β-ethoxyacryloyl isocyanate [4] (III) and the latter, in turn, combined with the methyl ester of L-2-(*p*-toluenesulphonamido)-3-aminopropionic acid (IV), prepared by Fischer esterification of the acid, which is readily accessible from L-asparagine [6,7].

On alkali treatment, the intermediately formed, linear urea (V) was transformed, without isolation, into L-*2-(p-toluenesulphonamido)-3-(1-uracyl)-propionic acid* (VI), a beautifully crystalline compound, which proved to be identical with a specimen of *N*-(p-*toluenesulphonyl*)-*willardiine*, produced by tosylation of the natural amino acid. Hence, willardiine possesses the structure (VII).*

Attempts to remove the protecting group from (VI) to furnish L-willardiine were only partly successful. Detosylation experiments with sodium in liquid ammonia resulted in destruction of the uracil ring and production of at least five ninhydrin positive components, one of which was presumably diaminopropionic acid. Treatment of (VI) with anhydrous hydrogen bromide in glacial acetic acid [8] at 70° for 3 h resulted in complete removal of the protecting group. However, the reaction under these conditions seemed to be accompanied by complete racemization. Gmelin[1] proved willardiine to be stable towards hot 48 % hydrogen bromide, yet without controlling the rotation subsequent to the acid treatment. It appears likely that racemization occurred also under these conditions.

Hence, N-tosyl-L-willardiine was subjected to the same conditions as above but for only one hour. From the reaction mixture, a low yield of willardiine could be isolated, indistinguishable from the natural product with regard to rotation and infra-red spectra. In addition, some starting material was recovered as well as partly racemized fractions of willardiine. Again, it appears likely that the detosylation was accompanied by a certain decomposition, because small amounts of foreign ninhydrin positive substances were observable upon paper chromatography of the mother liquors.

Experimental. Microanalyses were performed by Mr. G. Cornali. Rotations were measured in a 1 dm tube. Infra-red spectra were

* Part III: *Acta Chem. Scand.* **14** (1960) 961.

* *Added in proof:* After this communication was submitted to publication, Shaw and Dewar [9] independently reported a synthesis of DL-willardiine. According to a private communication from Dr. G. Shaw, the racemic modification has now been resolved to give (−)-willardiine, identical with a specimen of natural origin. Clearly, this synthetic approach provides no information as to the absolute configuration of natural willardiine.

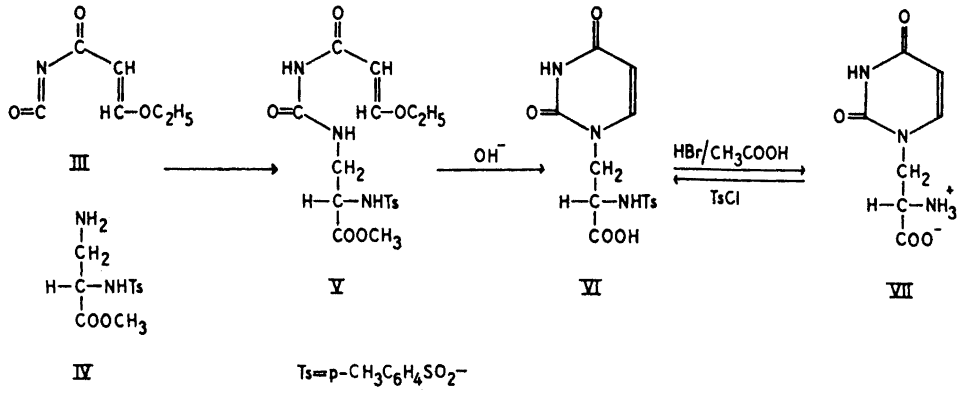

determined in potassium bromide pellets on a Perkin-Elmer "Infracord"-instrument. Melting points were determined in capillary tubes in an Anschütz-Hershberg apparatus equipped with fully immersed thermometers. The standard rate of heating was 2° per min.

L-2-(p-*Toluenesulphonamido*)-3-(*1-uracyl*)-*propionic acid* (VI). (*a*) L-2-(*p*-Toluenesulphonamido)-3-aminopropionic acid (5 mequiv.) was dissolved in anhydrous methanol, and dry HCl was introduced until the acid had dissolved. After 16 h at room temperature, the solution was evaporated to dryness and the oily residue was dried over P_2O_5 at 0.1 mm Hg for 24 h. The ester was liberated on addition of triethylamine (20 mequiv.) in anhydrous benzene (20 ml), and triethylammonium chloride filtered off. β-Ethoxyacryloyl chloride [5] (5.3 mequiv.) was shaken with dry AgOCN (7.6 mequiv.) and anhydrous benzene (20 ml) for 3 h at room temperature, and the filtered solution was introduced directly into the above ester solution. A slight evolution of heat was noticed. The solution was shaken for 4 h at room temperature, gradually depositing a slight precipitate of crystalline material. The entire mixture was taken to dryness and boiled up with NaOH (15 ml, 1 N), causing the major part of the oil to dissolve. After 15 h at 70°, subsequent cooling and ether extraction, HCl was added to bring the pH-value to 1 – 2. Crystalline L-2-(*p*-toluenesulphonamido)-3-(1-uracyl)-propionic acid thereby separated in a yield of 1.02 g (58 %). Two recrystallizations from water afforded an analytically pure specimen m.p. > 250° (decomp.), $[\alpha]_D^{25}$ −67.1° (*c* 1.0, 0.1 N NaOH), λ_{max} 264 mμ, ε 7 000; λ_{max} 227 mμ, ε 15 900; λ_{max} 207 mμ, ε 15 400; (solvent: 0.08 N NH_3). (Found: C 47.45; H 4.41; N 11.77. Calc. for $C_{14}H_{15}N_3O_6S$: C 47.58; H 4.28; N 11.90).

(*b*) Willardiine of natural origin (0.24 mequiv.) was dissolved in NaOH (6.9 ml, 0.1 N) and shaken with a solution of *p*-toluenesulphonyl chloride (0.32 mequiv.) in ether for 3 h. The ether phase was discarded and the aqueous phase was adjusted to pH 1 – 2 with HCl, when L-2-(*p*-toluenesulphonamido)-3-(1-uracyl)-propionic acid (28.8 mg) separated. Retosylation of the mother liquor afforded an additional crop (18.7 mg), thereby increasing the total yield to 57 %. Recrystallization from water afforded a pure specimen, $[\alpha]_D^{26}$ −66.0° (*c* 1.0, 0.1 N NaOH) (Found: C 47.38; H 4.43 N 11.78). The infra-red spectrum was indistinguishable from that of the specimen prepared as described under (*a*).

3-(1-Uracyl)-L-alanine (willardiine) (VII). L-2-(*p*-Toluenesulphanomido)-3-(1-uracyl)-propionic acid (1 mequiv.) was dissolved in glacial acetic acid (12 ml) saturated with HBr. After 1 h at 70°, anhydrous ether was added to the cooled solution and a spongy precipitate was obtained. After decantation and thorough washing with dry ether, the precipitate was dissolved in a small volume of water; the pH-value was adjusted to 6 with NH_3 and ethanol added, causing a light brown solid (33 mg) to separate. Reprecipitation from water-ethanol, followed by recrystallization from water, afforded 3.9 mg of a nearly colourless product, $[\alpha]_D^{26}$ −11° (*c* 0.25, 1 N HCl), comparable to the value $[\alpha]_D^{22}$ −12.1° (*c* 1.16, 1 N HCl) reported

for the natural product [1]. The two specimens gave identical R_F-values and infra-red spectra. The mother liquors from the purification gave crystalline fractions presumably representing partly racemized willardiine as estimated from infrared data.* Unchanged, crystalline L-2-(*p*-toluenesulphonamido)-3-(1-uracyl)-propionic acid (120 mg) separated from the original reaction mixture.

The authors are indebted to Dr. R. Gmelin for a specimen of natural willardiine. The present work is part of investigations supported by *Kai Hansen's Fond.*

1. Gmelin, R. *Z. physiol. Chem. Hoppe-Seyler's* **316** (1959) 164.
2. Gmelin, R., Strauss, G. and Hasenmaier, G. *Z. Naturforsch.* **13b** (1958) 252.
3. Kjær, A. and Olesen Larsen, P. *Acta Chem. Scand.* **13** (1959) 1565.
4. Shaw, G. and Warrener, R. N. *J. Chem. Soc.* **1958** 157.
5. Shaw, G. and Warrener, R. N. *J. Chem. Soc.* **1958** 153.
6. Zaoral, M. and Rudinger, J. *Collection Czechoslov. Chem. Communs.* **24** (1959) 1993.
7. Kjær, A. and Vesterager, E. *Acta Chem. Scand.* **14** (1960) 961.
8. Poduška, K., Rudinger, J. and Šorm, F. *Collection Czechoslov. Chem. Communs.* **20** (1955) 1174.
9. Shaw, G. and Dewar, J. H. *Proc. Chem. Soc.* **1961** 216.
10. Dewar, J. H. and Shaw, G. *J. Chem. Soc. (in preparation).*

Received July 8, 1961.

* *Added in proof:* On comparison of the infra-red spectra with one of authentic, synthetic DL-willardiine, kindly furnished by Dr. G. Shaw, these fractions in fact appeared to be racemic willardiine. The infra-red spectrum of the latter deviated notably from that of the L-isomeride in the solid state.

Studies on the Occurrence of Cholesterol in Water-Containing Liquid-Crystalline Form

I. The Minimum Fatty Acid Anion Concentrations Able to Transform Cholesterol Crystals into a Water-Containing Mesomorphous Form

PER EKWALL, HERRICK BALTSCHEFFSKY and LEO MANDELL

Institute of Physical Chemistry, Åbo Akademi, Åbo, Finland

Information about the different forms in which cholesterol separates from aqueous solutions and in which cholesterol can occur in aqueous systems is of both physical-chemical and biological interest.

It has long been known that certain derivatives of cholesterol undergo a transformation into the liquid-crystalline state on heating (thermotropic mesomorphism). Cholesterol is also known to be transformed into the liquid-crystalline state by the action of solvents (lyotropic mesomorphism). Thus, for example, Steiger stated that cholesterol is transformed into a myelinic mesomorphous phase by water containing fatty acids and alkali [1]. Dervichian reported the formation of myelinic figures in the presence of water by mixtures of cholesterol with a number of biologically active long-chain substances, such as lysolecithin, alkylcholine chlorides, fatty acid salts, alkyl sulphates and alkyl phosphates [2]. Lawrence recently reported a series of observations on the transformation of solid crystalline cholesterol into a water-containing mesomorphous phase by the action of relatively concentrated association colloid solutions [3]. The liquid-crystalline substance that is formed in a 20 % sodium dodecyl sulphate solution containing an equimolar amount of cholesterol is stable on heating up to 195°C, where it separates into two isotropic liquids. When a solution of an association colloid such as sodium dodecyl sulphate flows over a cholesterol crystal, a gelatinous membrane composed of doubly-refracting matter is seen under the microscope to be formed immediately when the two phases come into contact. The membrane gradually increases in thickness and the solid crystal decreases in size, while at the same

for the natural product [1]. The two specimens gave identical R_F-values and infra-red spectra. The mother liquors from the purification gave crystalline fractions presumably representing partly racemized willardiine as estimated from infrared data.* Unchanged, crystalline L-2-(*p*-toluenesulphonamido)-3-(1-uracyl)-propionic acid (120 mg) separated from the original reaction mixture.

The authors are indebted to Dr. R. Gmelin for a specimen of natural willardiine. The present work is part of investigations supported by *Kai Hansen's Fond.*

1. Gmelin, R. *Z. physiol. Chem. Hoppe-Seyler's* **316** (1959) 164.
2. Gmelin, R., Strauss, G. and Hasenmaier, G. *Z. Naturforsch.* **13b** (1958) 252.
3. Kjær, A. and Olesen Larsen, P. *Acta Chem. Scand.* **13** (1959) 1565.
4. Shaw, G. and Warrener, R. N. *J. Chem. Soc.* **1958** 157.
5. Shaw, G. and Warrener, R. N. *J. Chem. Soc.* **1958** 153.
6. Zaoral, M. and Rudinger, J. *Collection Czechoslov. Chem. Communs.* **24** (1959) 1993.
7. Kjær, A. and Vesterager, E. *Acta Chem. Scand.* **14** (1960) 961.
8. Poduška, K., Rudinger, J. and Šorm, F. *Collection Czechoslov. Chem. Communs.* **20** (1955) 1174.
9. Shaw, G. and Dewar, J. H. *Proc. Chem. Soc.* **1961** 216.
10. Dewar, J. H. and Shaw, G. *J. Chem. Soc. (in preparation).*

Received July 8, 1961.

* *Added in proof:* On comparison of the infra-red spectra with one of authentic, synthetic DL-willardiine, kindly furnished by Dr. G. Shaw, these fractions in fact appeared to be racemic willardiine. The infra-red spectrum of the latter deviated notably from that of the L-isomeride in the solid state.

Studies on the Occurrence of Cholesterol in Water-Containing Liquid-Crystalline Form

I. The Minimum Fatty Acid Anion Concentrations Able to Transform Cholesterol Crystals into a Water-Containing Mesomorphous Form

PER EKWALL, HERRICK BALTSCHEFFSKY and LEO MANDELL

Institute of Physical Chemistry, Åbo Akademi, Åbo, Finland

Information about the different forms in which cholesterol separates from aqueous solutions and in which cholesterol can occur in aqueous systems is of both physical-chemical and biological interest.

It has long been known that certain derivatives of cholesterol undergo a transformation into the liquid-crystalline state on heating (thermotropic mesomorphism). Cholesterol is also known to be transformed into the liquid-crystalline state by the action of solvents (lyotropic mesomorphism). Thus, for example, Steiger stated that cholesterol is transformed into a myelinic mesomorphous phase by water containing fatty acids and alkali [1]. Dervichian reported the formation of myelinic figures in the presence of water by mixtures of cholesterol with a number of biologically active long-chain substances, such as lysolecithin, alkylcholine chlorides, fatty acid salts, alkyl sulphates and alkyl phosphates [2]. Lawrence recently reported a series of observations on the transformation of solid crystalline cholesterol into a water-containing mesomorphous phase by the action of relatively concentrated association colloid solutions [3]. The liquid-crystalline substance that is formed in a 20 % sodium dodecyl sulphate solution containing an equimolar amount of cholesterol is stable on heating up to 195°C, where it separates into two isotropic liquids. When a solution of an association colloid such as sodium dodecyl sulphate flows over a cholesterol crystal, a gelatinous membrane composed of doubly-refracting matter is seen under the microscope to be formed immediately when the two phases come into contact. The membrane gradually increases in thickness and the solid crystal decreases in size, while at the same

time the outer parts of the mesomorphous layer dissolve in the surrounding solution until finally a homogeneous solution results. Since 1956 similar observations have been made in our laboratory on the behaviour of cholesterol crystals in contact with solutions of sodium dodecyl sulphate, fatty acid soaps and albumin-dodecyl sulphate and albumin-soap complexes. We were first mainly interested in determining the lowest concentrations of these substances that interact and reported briefly a few years ago that the interaction between solid cholesterol crystals and aqueous solutions of various alkali metal salts of fatty acids can be observed until the solutions are diluted down to the limiting association concentrations (LAC) of the soaps [4]. In the first two papers of this series we present experimental data that define the limiting conditions necessary for the conversion of cholesterol into the mesomorphous state. In later papers the results of a more systematic study of the processes in question will be reported.

The cholesterol employed (Hoffmann-La Roche) melted at 148–149°C. The cholesterol was used partly in the anhydrous form and partly as the crystalline monohydrate. The salts of the fatty acids were prepared by dissolving the pure fatty acids in absolute ethanol and neutralising them with a solution of sodium ethylate in ethanol. The isolated dried soaps were dissolved in twice distilled water to obtain solutions of known concentrations. The interaction between the solid cholesterol crystals and soap solutions was followed with a microscope between crossed nicols and in ordinary (unpolarized) light with or without using a phase contrast condenser. The solutions were usually allowed to enter between the object and cover slides from one end until they came into contact with the cholesterol crystals. As the observations were made over long periods the cholesterol crystals were placed in thin plane-parallel cuvettes which were tightly sealed to prevent any evaporation.

The cholesterol crystals underwent no change when they were immersed in water, alkaline solutions containing sodium hydroxide or sodium carbonate, and sufficiently dilute aqueous soap solutions, but a strong interaction was observed when the crystals came into contact with soap solutions whose concentrations exceeded the respective critical micelle concentrations (CMC). In the latter experiments a layer of mesomorphous matter rapidly formed on the surfaces of the cholesterol crystals and increased in thickness until the whole crystal was transformed. The mesomorphous phase is, however, also produced in soap solutions with concentrations below the CMC, but the process slows down as the soap concentration decreases until it ceases altogether. Table 1 gives the concentration ranges where the formation of the mesomorphous phase definitely did not occur at 20°C. A weak formation of mesomorphous substance was still noted at the upper concentration limit, but no signs of the transformation were noted at the lower concentration limit although the crystals and solutions were in contact for long periods (24 h).

From the standpoint of the phase rule, this means that in the phase diagram of the three-component system cholesterol-soap-water one of the corners of a three-phase triangle lies in the given concentration range of homogeneous soap solutions, whereas the two other corners represent solid crystalline cholesterol and the mesomorphous cholesterol-soap-water phase in equilibrium with the soap solution in question. The triangle separates two two-

Table 1.

Association colloid	Concentration range below which no mesomorphous matter was formed.	LAC
Sodium nonylate	0.11 –0.14 M	0.06 M
Sodium caprate	0.020 –0.033 »	0.025 »
Sodium laurate	0.005 –0.0068 »	0.006 »
Sodium myristate	0.001 –0.0013 »	0.0011 »
Sodium oleate	0.00004–0.0003 »	0.00025 »

phase regions, one consisting of aqueous solutions of low concentration in equilibrium with solid crystalline cholesterol and the other of more concentrated aqueous solutions in equilibrium with the mesomorphous cholesterol-containing phase.

Values of the so-called limiting association concentrations (LAC) for the soaps in question are also given in Table 1. These have been determined by studying the interactions between aqueous solutions containing fatty acid salts and the respective undissociated fatty acids or these salts and liquid paraffin chain alcohols and represent the lowest fatty acid anion concentrations where such interactions are observed. The interaction of fatty acid anions and cholesterol referred to above which leads to formation of an aqueous mesomorphous phase containing cholesterol thus takes place down to approximately the same concentrations as these other processes.

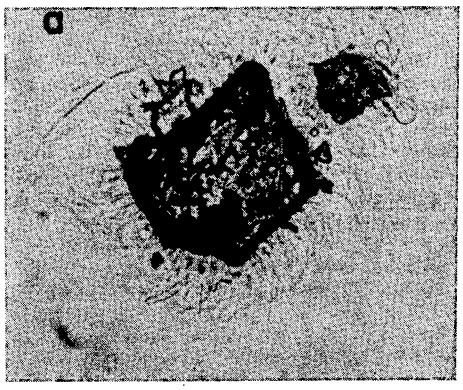

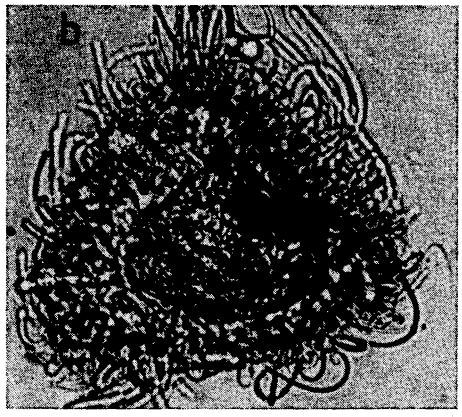

Fig. 1. Ordinary (unpolarized) light. 200 ×.

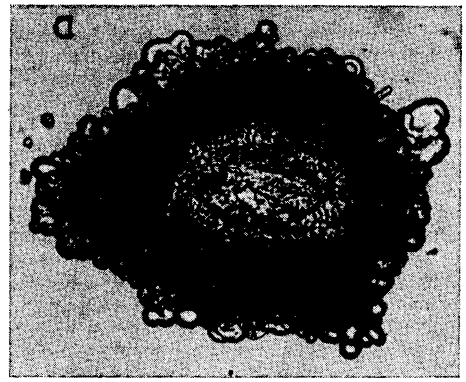

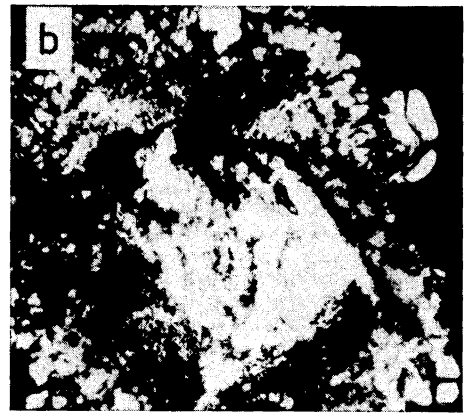

Fig. 2. a) Ordinary (unpolarized) light. 200 ×. b) Crossed nicols. 200 ×.

The microphotographs in Fig. 1 illustrate the formation of the mesomorphous phase on cholesterol crystals immersed in 0.052 M (a) and 0.103 M (b) sodium caprate solutions. The mesomorphous phase grows out forming myelin-like figures, sausage- and thread-like formations. In Figs. 2a and 2b relating to a 0.30 M sodium caprate solution the mesomorphous phase occurs in the form of doubly-refracting spheres with characteristic black crosses. The mesomorphous phase formed at low concentra-

tions just above the LAC differs somewhat in appearance from the phase formed at higher concentrations.

It may be of biological significance that the lowest concentrations at which fatty acid salts are capable of transforming solid crystalline cholesterol into the mesomorphous state varies from acid to acid and decreases regularly with increasing chain length of the parent acid. This means that aqueous solutions containing fatty acid anions in very low concentrations (only about 2.5×10^{-4} M in the case of oleate, for example) are able to effect the transformation of solid cholesterol into the mesomorphous state. If cholesterol separates from an aqueous biological medium in which the fatty acid anion concentration exceeds the LAC, it is thus probable that the cholesterol does not separate in the usual crystalline form, but rather as a water-containing mesomorphous phase.

We have found that cholesterol occurring in the mesomorphous state is not stained by oil-soluble dyes such as Sudan Red III and IV, Oil Blue N and Oil Red 4B, which are employed to detect cholesterol in tissue specimens. This was established in experiments where the dye was initially dissolved in the solid cholesterol crystals or in the micelles of the soap solutions. It therefore is doubtful whether cholesterol that occurs in the mesomorphous state in tissues can be identified by the customary staining methods.

1. Steiger, A. *Microcosmos* **35** (1941/1942) 54.
2. Dervichian, D. *Bull. soc. chim. biol.* **28** (1946) 419.
3. Lawrence, A. S. C. *Discussions Faraday Soc.* **25** (1958) 51; Durham, K. (Ed.) *Surface Activity and Detergency*, Macmillan, London 1961, p. 158.
4. Ekwall, P. *Proc. 2nd Intern. Congr. Surface Activity*, London (1957) Vol. I, 405. Butterworths 1957.

Received July 26, 1961.

Studies on the Occurrence of Cholesterol in Water-Containing Liquid-Crystalline Form

II. The Formation of Cholesterol-Containing Mesomorphous Phases in the Presence of Protein-Association Colloid Complexes, Serum Albumin and Bile Acid Salts

PER EKWALL and HERRICK BALTSCHEFFSKY

Institute of Physical Chemistry, Åbo Akademi, Åbo, Finland

We have previously established that aqueous solutions containing protein-association colloid complexes are able to solubilize compounds such as polycyclic aromatic hydrocarbons, steroid hormones, fat-soluble vitamins and other substances which possess marked lipophilic properties [1]. When, however, cholesterol is added to these solutions, a mesomorphous water-containing phase separates in many cases. We have found that this occurs with solutions containing complexes formed by serum albumin and sodium dodecyl sulphate or fatty acid soaps, but not with solutions containing complexes formed by serum albumin and sodium taurocholate. As it is known that both sodium dodecyl sulphate and fatty acid soaps as such in aqueous solutions down to very low concentrations (as low as the LAC) are able to transform solid crystalline cholesterol into a mesomorphous phase composed of cholesterol, water and association colloid [2], it seems probable that the reason for the separation of the mesomorphous phase from solutions containing protein-association colloid complexes is the presence also in these solutions of free dodecyl sulphate and fatty acid anions in sufficiently high concentrations. The concentrations of these anions in the last-mentioned solutions, however, have not yet been determined. No formation of a mesomorphous cholesterol-containing phase has been observed to result from the interaction of cholesterol with aqueous solutions of taurocholate or other bile acid salts, and hence it seems natural that neither are their protein complexes able to effect a similar transformation of cholesterol. In these latter cases the interaction is limited to a solubilisa-

tions just above the LAC differs somewhat in appearance from the phase formed at higher concentrations.

It may be of biological significance that the lowest concentrations at which fatty acid salts are capable of transforming solid crystalline cholesterol into the mesomorphous state varies from acid to acid and decreases regularly with increasing chain length of the parent acid. This means that aqueous solutions containing fatty acid anions in very low concentrations (only about 2.5×10^{-4} M in the case of oleate, for example) are able to effect the transformation of solid cholesterol into the mesomorphous state. If cholesterol separates from an aqueous biological medium in which the fatty acid anion concentration exceeds the LAC, it is thus probable that the cholesterol does not separate in the usual crystalline form, but rather as a water-containing mesomorphous phase.

We have found that cholesterol occurring in the mesomorphous state is not stained by oil-soluble dyes such as Sudan Red III and IV, Oil Blue N and Oil Red 4B, which are employed to detect cholesterol in tissue specimens. This was established in experiments where the dye was initially dissolved in the solid cholesterol crystals or in the micelles of the soap solutions. It therefore is doubtful whether cholesterol that occurs in the mesomorphous state in tissues can be identified by the customary staining methods.

1. Steiger, A. *Microcosmos* **35** (1941/1942) 54.
2. Dervichian, D. *Bull. soc. chim. biol.* **28** (1946) 419.
3. Lawrence, A. S. C. *Discussions Faraday Soc.* **25** (1958) 51; Durham, K. (Ed.) *Surface Activity and Detergency*, Macmillan, London 1961, p. 158.
4. Ekwall, P. *Proc. 2nd Intern. Congr. Surface Activity*, London (1957) Vol. I, 405. Butterworths 1957.

Received July 26, 1961.

Studies on the Occurrence of Cholesterol in Water-Containing Liquid-Crystalline Form

II. The Formation of Cholesterol-Containing Mesomorphous Phases in the Presence of Protein-Association Colloid Complexes, Serum Albumin and Bile Acid Salts

PER EKWALL and HERRICK BALTSCHEFFSKY

Institute of Physical Chemistry, Åbo Akademi, Åbo, Finland

We have previously established that aqueous solutions containing protein-association colloid complexes are able to solubilize compounds such as polycyclic aromatic hydrocarbons, steroid hormones, fat-soluble vitamins and other substances which possess marked lipophilic properties [1]. When, however, cholesterol is added to these solutions, a mesomorphous water-containing phase separates in many cases. We have found that this occurs with solutions containing complexes formed by serum albumin and sodium dodecyl sulphate or fatty acid soaps, but not with solutions containing complexes formed by serum albumin and sodium taurocholate. As it is known that both sodium dodecyl sulphate and fatty acid soaps as such in aqueous solutions down to very low concentrations (as low as the LAC) are able to transform solid crystalline cholesterol into a mesomorphous phase composed of cholesterol, water and association colloid [2], it seems probable that the reason for the separation of the mesomorphous phase from solutions containing protein-association colloid complexes is the presence also in these solutions of free dodecyl sulphate and fatty acid anions in sufficiently high concentrations. The concentrations of these anions in the last-mentioned solutions, however, have not yet been determined. No formation of a mesomorphous cholesterol-containing phase has been observed to result from the interaction of cholesterol with aqueous solutions of taurocholate or other bile acid salts, and hence it seems natural that neither are their protein complexes able to effect a similar transformation of cholesterol. In these latter cases the interaction is limited to a solubilisa-

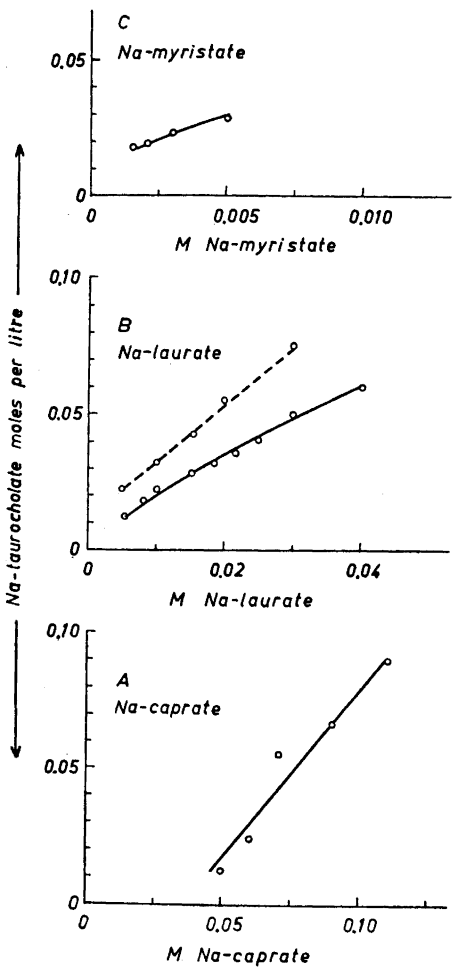

Fig. 1.

tion of cholesterol, whereupon homogeneous isotropic solutions are formed [3].

We have considered it of interest to study whether protein (serum albumin) or bile acid salts (sodium taurocholate) are able to promote or prevent the development of mesomorphous phases containing cholesterol, soap, and water by interaction with fatty acid ions. By microscope observations the minimum concentrations of fatty acid soaps that are required to transform cholesterol crystals into the mesomorphous state in the presence of various concentrations of the mentioned compounds were determined.

We have found that aqueous solutions of bovine serum albumin (Armour Laboratories) alone (0.5—2.0 %, pH 9.3) are unable to transform cholesterol into the mesomorphous state. Neither was bovine serum albumin in the mentioned concentrations found to have any effect on the interaction between sodium laurate and cholesterol; as in pure laurate solutions, the mesomorphous cholesterol-containing phase was in these cases formed as soon as the sodium laurate concentration exceeded 0.005—0.006 M.

Sodium taurocholate, on the other hand, was found to suppress the formation of the mesomorphous phase by interaction between cholesterol and fatty acid anions to some extent and necessitated an increase of the minimum concentration of soap anions to a higher value. The approximate minimum concentrations of sodium taurocholate that are sufficient to prevent the formation of the mesomorphous phase in various soap solutions are plotted in Fig. 1. The presence of 2 % serum albumin decreases the effect of taurocholate to some extent as shown by the broken line in Fig. 1 B.

It may be of biological significance that a protein such as serum albumin does not influence the separation of cholesterol as a mesomorphous phase. It is also of interest that an association colloid that does not cause such a separation to take place can obviously alter the conditions that promote the separation, but cannot completely prevent the latter from occurring.

1. Ekwall, P. *Proc. 2nd Intern. Conf. Biochem. Problems of Lipids*, Ghent 1955, 121. Butterworths, 1955.
2. Part I of this series. *Acta Chem. Scand.* **15** (1961) 1195.
3. Ekwall, P. *Proc. 1st Intern. Conf. Biochem. Problems of Lipids*. Brussels 1953, 103. *Koninkl. Vlaamse Acad. Wetenschap. Belgie*, 1953.

Received July 26, 1961.

A Convenient Method for Reduction of α,β-Unsaturated Carboxylic Acids

NILS S. HJELTE

Research Laboratories, Aktiebolaget Pharmacia, Uppsala, Sweden

There are many methods for reduction of α,β-unsaturated carboxylic acids. The most commonly used is the catalytic hydrogenation, especially with Raney-Ni as the catalyst. In an interesting paper Schwenk *et al.*[1] have shown that cinnamic acid among other acids can be reduced in strongly alkaline water solution at atmospheric pressure by means of Raney-Ni/Al alloy, where the aluminium by reaction with sodium hydroxide gives the desired hydrogen. However, the method has some disadvantages as aluminium hydroxide often contaminates the reduced acid in the final separation from the mother liquor. The mixture of the reduced acid and aluminium hydroxide is difficult to separate, especially when the acid is a solid.

In order to avoid these difficulties the author looked for other systems having a reducing power, without the disadvantages mentioned above. Such a system is hydrazine hydrate and Raney-Ni in ethanol which, however, is said to reduce only nitro groups, leaving α,β-unsaturated carboxylic acids unaffected. For example, *p*-nitrocinnamic acid is reduced to *p*-aminocinnamic acid [2]. From the work of Schwenk *et al.* one might presume that as a rule the sodium salts of α,β-unsaturated acids are more readily reduced than the corresponding free acids. Therefore, reduction of these acids in the form of their sodium salts might be achieved by hydrazine and Raney-Ni in water.

Experiments have shown that reduction is achieved in this way if the hydrazine is added slowly. Experimental data are given for the reduction of cinnamic acid to 3-phenylpropionic acid.

In Table 1 are summarized further examples of the reduction. Physical data of the acids prepared are in good agreement with those known from the literature.

Table 1.

Acid reduced	Acid isolated	Yield %	B.p. °C/mm Hg M.p. °C
α-Methyl-cinnamic [a]	2-Methyl-3-phenyl-propionic	93	152–154°/8
Maleic	Succinic	70 [b]	188–189
Fumaric	Succinic	71 [b]	188–189

a. Trans isomer.

b. Isolated by filtration from the acidified and chilled water solution.

Preparation of 3-phenylpropionic acid. 300 g (2.02 moles) of *trans*-cinnamic acid is dissolved in a solution of 85 g (2.12 moles) of sodium hydroxide in 2 liters of water. A teaspoonful of Raney-Ni W6 is added. The mixture is agitated and heated to 90°C, at which temperature 260 ml (4.5 moles) of 85 % hydrazine hydrate is added within 2 h. When all the hydrazine hydrate has been added the temperature is held at 90°C until no more gas is evolved. The catalyst is then filtered off and the solution is acidified. The liberated acid is extracted from the water layer with two portions of chloroform. The chloroform layer is dried with magnesium sulfate and the chloroform is evaporated. The residue is distilled under reduced pressure. A fraction is collected boiling at 146–148°C/8 mm Hg, weighing 257 g (85 %) with a m.p. of 47.5°–48.5°C. No melting point depression was observed when the acid was mixed with an authentic sample of 3-phenylpropionic acid.

The author is indebted to Mr. R. Lindblom for valuable assistance and to Dr. K. Skagius for kind interest.

1. Schwenk, E., Papa, D., Whitman, B. and Ginsburg, H. F. *J. Org. Chem.* **9** (1944) 175.
2. Balcom, D. and Furst, A. *J. Am. Chem. Soc.* **75** (1953) 4334.

Received July 17, 1961.

Proton Magnetic Resonance of Thiophenes. X. On the Mechanism of Side-chain Couplings in Methylthiophenes *

SALO GRONOWITZ, BO GESTBLOM and RAGNAR A. HOFFMAN

Institute of Chemistry and Institute of Physics, University of Uppsala, Uppsala, Sweden

It has earlier been shown that a methyl group in the 2-position of thiophene couples with the hydrogen in the 3-position with a coupling constant of 1.00—1.15 c/s and to the 4-hydrogen with 0.2—0.5 c/s [1], these two couplings being of opposite sign [2]. Likewise a methyl group in the 3-position couples with hydrogen 2 with 0.9—1.25 c/s and to the 4- and 5-hydrogens with 0.4—0.5 c/s [1]. These side-chains couplings have been ascribed to hyperconjugation [1,3,4] and on this assumption one would expect [5] a coupling between the methyl groups of 2,3-dimethylthiophene of about 1 c/s as it has been demonstrated that the attenuation factor of the π-electron contribution to the couplings in going from an aromatic proton to a methyl group proton is approximately minus one.

Corio and Weinberg [4] studied the spectrum of 2,3-dimethylthiophene at 60 Mc/s and found no coupling between the α-hydrogen and either of the two methyl groups. The greater broadening of the β-hydrogen as compared to that of the α-hydrogen was ascribed to coupling of the former with the 3-methyl group [4]. The present authors have reinvestigated the spectrum of 2,3-dimethylthiophene and found in addition that the methyl group bands were appreciably broadened due to unresolved fine-structure, which was ascribed to a coupling $J_{CH_3-CH_3}$ [1].

As the magnitude of this latter coupling is a measure of the π-electron contribution to the side-chain couplings in methylthiophenes we have investigated the spectra of 2,3-dimethylthiophenes, substituted in the 4- and 5-positions with non-coupling substituents in order to avoid the additional broadening of the methyl group peaks caused by coupling to the ring hydrogens.

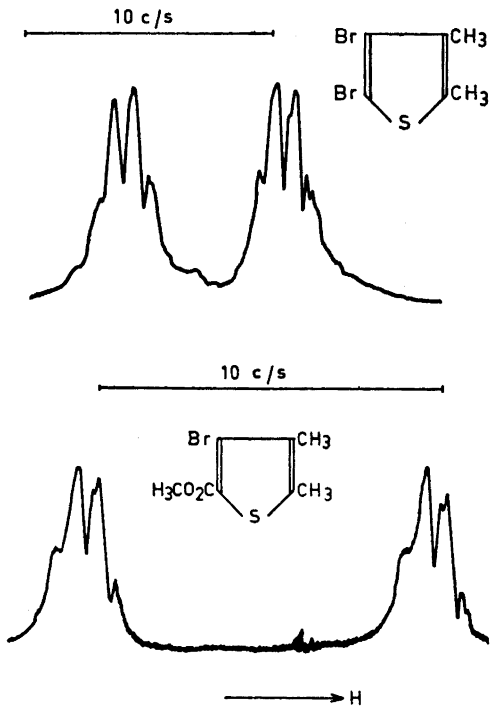

Fig. 1. Methyl group resonance in the 40 Mc/s NMR-spectrum a) of liquid 2,3-dimethyl-4,5-dibromothiophene; b) of methyl 2,3-dimethyl-4-bromo-5-thiophenecarboxylate in *cyclo*-hexane (27 wt%).

2,3-Dimethyl-4,5-dibromothiophene was prepared through bromination of 2,3-dimethylthiophene [7] in CS_2 solution. Through halogen-metal interconversion with *n*-butyllithium followed by carbonation the 2,3-dimethyl-4,5-dibromothiophene was converted to 2,3-dimethyl-4-bromo-5-thiophenecarboxylic acid, the methyl ester of which was obtained through reaction with diazomethane.

The spectrum of 2,3-dimethyl-4,5-dibromothiophene (Fig. 1a) displays two 1:3:3:1 quartets due to the coupling $J_{CH_3-CH_3}$ equal to 0.75 ± 0.10 c/s. The splitting of the two largest peaks in each quartet has the value of 0.73 ± 0.10 c/s, and one-third of the separation between the two outermost components equals to 0.68 ± 0.04 c/s. The difference between these two values can be ascribed to the

* Part IX. *Arkiv Kemi* **17** (1961) 237.

partial overlapping of the quartet components, which reduces the separation of the overlapping lines, thereby introducing a systematic error of the order of 0.05 c/s. Similarly in methyl 2,3-dimethyl-4-bromo-5-thiophenecarboxylate (Fig. 1b) a coupling $J_{CH_3-CH_3} = 0.60 \pm 0.10$ c/s is observed. Due to the low solubility of 2,3-dimethyl-4-bromo-5-thiophenecarboxylic acid in non-polar solvents the spectrum was recorded in dimethyl sulphoxide solution (37 wt %). The methyl group spectrum so obtained consists of two bands in which the splitting only of the central lines of the quartets were resolved. The lower resolution obtained in this case might be due to strong intermolecular association. From the resolved splitting we obtain $J_{CH_3-CH_3} = = 0.55 \pm 0.10$ c/s.

We have earlier used the method of methyl substitution to demonstrate that the coupling between the thiol and ring protons in thiophenethiols is dominated by a π-electron contact mechanism [1] and that this mechanism does not account for the sidechain couplings of 2-thiophenealdehydes [1,6]. The fact that the coupling $J_{CH_3-CH_3}$ in substituted 2,3-dimethylthiophenes is only slightly smaller than J_{CH_3-2} in 3-methylthiophene or J_{CH_3-3} in 2-methylthiophene proves that the largest contribution to the side-chain couplings in the methylthiophenes is also due to π-electron interactions.

Experimental. *2,3-Dimethyl-4,5-dibromothiophene.* To an ice-cold solution of 22.4 g (0.20 mole) of 2,3-dimethylthiophene [7] in 120 ml of dry carbon disulphide was added dropwise 64 g (0.20 mole) of bromine in 40 ml of carbon disulphide. After standing over-night the solvent was distilled off, the residue refluxed for 4 h with 12 g of potassium hydroxide in 15 ml of methanol and then steam-distilled. The organic layer of the distillate was taken up in ether, dried and fractionated, yielding 30.3 g (56 %) of 2,3-dimethyl-4,5-dibromothiophene, b.p. 129–130°/15 mm Hg, $n^{20}D = 1.6030$. (Found: C 26.50; H 2.15; Br 58.94. Calc. for $C_6H_6Br_2S$ (270.0): C 26.69; H 2.24; Br 59.23). Though this preparation analysed correctly, the NMR-spectrum revealed the presence of small amounts of impurity which, however, did not cause any complication in the interpretation.

2,3-Dimethyl-4-bromo-5-thiophenecarboxylic acid. 37 ml of 1.35 N *n*-butyllithium was added to 12.0 g (0.044 mole) of 2,3-dimethyl 4,5-dibromo-thiophene in 50 ml of dry ether at −70° in the usual nitrogen-swept four-necked flask. After 10 min, the mixture was poured onto solid carbon dioxide covered with ether. The reaction mixture was hydrolyzed with water and the ether phase extracted with 2 N sodium hydroxide. On acidification with 2 N hydrochloric acid, the combined aqueous phase yielded 8.2 g (79 %) of crude acid which was recrystallized from aqueous methanol. M.p. 222–224°. (Found: C 35.90; H 3.00; Br 33.67. Calc. for $C_7H_7BrO_2S$ (235.1): C 35.76; H 3.00; Br 33.99;)

Methyl 2,3-dimethyl-4-bromo-5-thiophenecarboxylate. An ethereal solution of diazomethane was added drop-wise to an ice-cooled solution of 1.09 g (0.0046 mole) of 2,3-dimethyl-4-bromo-5-thiophenecarboxylic acid in 40 ml of ether until the yellow diazomethane colour persisted. Removal of the ether gave 0.9 g (78 %) of the methyl ester which crystallized from petrol-ether in needles, m.p. 64–65°. (Found: C 38.37; H 3.79; Br 31.84. Calc. for $C_8H_9Br_2S$ (249.1): C 38.57; H 3.64; Br 32.07.)

The NMR-spectra were obtained with a Varian Associates model V 4300B high resolution spectrometer operating at 40.00 Mc/s and a flux-stabilized 12 in magnet equipped with shim-coils from the same company. The magnet sweep was calibrated with the modulation sideband technique.

Acknowledgements. The authors wish to express their thanks to Prof. Arne Fredga and to Prof. Kai Siegbahn for their interest in this work and for all facilities put at their disposal. The elementary analyses were carried out by Dr A. Bernhardt, Mülheim (Ruhr). Grants from the *Swedish Natural Science Research Council* to S.G. and from the *Swedish Technical Research Council* to R.A.H. are gratefully acknowledged.

1. Hoffman, R. A. and Gronowitz, S. *Arkiv Kemi* **16** (1960) 563.
2. Hoffman, R. A. and Gronowitz, S. *Arkiv Kemi* **16** (1960) 501.
3. Hoffman, R. A. *Mol. Phys.* **1** (1958) 326.
4. Corio, P. L. and Weinberg, L. *J. Chem. Phys.* **31** (1959) 569.
5. Hoffman, R. A. and Gronowitz, S. *Arkiv Kemi* **16** (1960) 471.
6. Hoffman, R. A. *Arkiv Kemi* **17** (1961) 1.
7. Gronowitz, S., Moses, P., Hörnfeldt, A.-B. and Håkansson, R. *Arkiv Kemi* **17** (1961) 165.

Received July 17, 1961.

Beiträge zur Chemie α-substituierter Sulfide

VIII *. Die Einführung der Trichlormethylmerkaptogruppe in die 3-Stellung zyklischer Äther

ALEXANDER SENNING und SVEN-OLOV LAWESSON

Laboratorium für Organische Chemie, Chemisches Institut der Universität Uppsala, Uppsala, Schweden

2,3-Dihydrofuran (I) addiert in Gegenwart einer katalytischen Menge Chlorwasserstoff Trichlormethansulfenylchlorid. Während bei der durch Chlorwasserstoff katalysierten Addition von Alkoholen und Karbonsäuren RO^- bzw. $RCOO^-$ in 2-Stellung und H^+ in 3-Stellung eintritt [1,2], geht bei der Addition von Sulfenylchloriden das Spaltstück RS^+ in 3-Stellung und Cl^- in 2-Stellung. Dass das Additionsprodukt, 2-Chlor-3-trichlormethylmerkaptotetrahydrofuran (II), ein zum Äthersauerstoffatom α-ständiges Chloratom besitzt, beweist die Reaktivität dieser Verbindung (vgl. die Reaktionen des 2,3-Dichlortetrahydrofurans bei Reppe und Mitarbeitern [3]). Versucht man, die Substanz zu destillieren, wird in exothermer Reaktion Chlorwasserstoff abgespalten, wobei neben Teerprodukten 3-Trichlormethylmerkapto-4,5-dihydrofuran erhalten wird. Es ist uns noch nicht gelungen, diese Verbindung analysenrein zu destillieren.

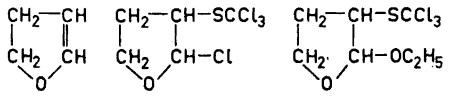

I II III

Setzt man 2-Chlor-3-trichlormethylmerkaptotetrahydrofuran mit Äthanol um, erhält man das stabile 2-Äthoxy-3-trichlormethylmerkaptotetrahydrofuran (III). Infolge der Reaktivität des Chloratoms in 2-Stellung gelingt die Umsetzung bereits bei 0°.

Diese unseres Wissens neuartige Reaktion zur Einführung von Alkyl- bzw. Arylmerkaptogruppen in die 3-Stellung zyklischer Äther ist von grossem präparativem Wert, da alle drei Reaktionsteilnehmer (α,β-ungesättigter zyklischer Äther + Sulfenylchlorid + Alkohol, Merkaptan, Karbonsäure usw.) innerhalb weiter Grenzen variiert werden können. Wir werden die präparativen Möglichkeiten dieser Reaktion weiter untersuchen und zu gegebener Zeit darüber berichten.

Versuchsbeschreibung. 28,0 g (0,4 Mol) 2,3-Dihydrofuran werden bei 0° unter Rühren mit einem Tropfen konz. Salzsäure und dann langsam mit 37,2 g (0,2 Mol) Trichlormethansulfenylchlorid versetzt. Nach einer weiteren Viertelstunde werden 18,4 g (0,4 Mol) Äthanol zugetropft und danach noch zwei Stunden gerührt. Das Reaktionsprodukt wird mit Äther aufgenommen, zweimal mit Natriumbikarbonatlösung und zweimal mit Wasser ausgeschüttelt und über Magnesiumsulfat getrocknet. Nach Abziehen des Lösungsmittels gehen zwischen 135°/15 mm und 142°/15 mm 35,1 g (66 % der Theorie) über, n_D^{20} 1,5105. Die analysenreine Substanz siedet bei 138°/20 mm, n_D^{20} 1,5101. (Gef. C 31,73; H 4,24; Cl 39,90; S 11,58; 12,15. Ber für $C_7H_{11}Cl_3O_2S$: C 31,66; H 4,17; Cl 40,05; S 12,07).

Wir sind Herrn Professor A. Fredga für die Überlassung des Arbeitsplatzes und *Jordbrukets Forskningsråd* für die finanzielle Unterstützung unserer Arbeit zu Dank verpflichtet. Der Badischen Anilin- und Soda-Fabrik, Ludwigshafen, Deutschland danken wir für die kostenlose Überlassung von 2,3-Dihydrofuran.

1. Normant, H. *Compt. rend.* **228** (1949) 102.
2. Lawesson, S.-O. und Berglund, C. *Arkiv Kemi* **17** (1961) 475.
3. Reppe, W. und Mitarbeiter *Ann.* **596** (1955) 80.

Eingegangen am 31. Juli 1961.

* VI. Mitteilung: Senning, A. und Lawesson, S.-O. *Arkiv Kemi* **18** (1961) 95; VII. Mitteilung: Senning, A. und Lawesson, S.-O. *Acta Chem. Scand. Im Druck.*

Electron Spin Resonance in Solid State Samples of Phenothiazine and Oxazine Dyes

CARL LAGERCRANTZ and MARGARETA YHLAND

Department of Medical Physics, University of Göteborg

It has been shown by Chernyakovskii *et al.*[1] that several compounds from the series of triphenylmethane dyes exhibit electron spin resonance (ESR) in the solid state. The intensity of the signal varied from compound to compound and amounted to $10^{16}-10^{18}$ paramagnetic particles per gram sample. In all cases a narrow solitary absorption line without any hyperfine structure was observed. It was suggested that the ESR-signal of the triphenylmethane dyes was not related to the structure of the molecule itself but to the crystalline state as the signal disappeared on solution and reappeared when the sample was dried. The hypothesis was expressed that the presence of unpaired electrons depended on a highly conjugated system which extended through the crystal structure, and which permits a high degree of delocalization of the π-electrons.

It this laboratory we have found that the phenothiazine dyes methylene blue, thionine and toluidine blue, and the oxazine dyes capri blue, resazurin and nile blue have an ESR-absorption in the solid state.

(i). The intensity of the ESR-absorption was within the same limits as those reported for the triphenylmethane dyes, *i.e.* 10^{15} to 10^{18} spins per gram substance corresponding to about one paramagnetic particle per 10^4 and 10^2 molecules respectively.

(ii). The spectra exhibited a single line of a width about 15 gauss except of nile blue sulphate. The g-value was close to that of DPPH.

(iii). The intensity of the ESR-signal increased when the samples were kept at a moderately elevated temperature. Thus, powdered sample of methylene blue chloride recrystallized from water was found to have about 10^{16} spins per gram. Kept in an open vessel overnight at 75°C, this sample had lost about 5 molecules of crystal water. At the same time the intensity of the ESR-signal had increased by a factor of 100. The high signal was found to persist unchanged for many days. Further treatment at a pressure of 0.05 mm Hg at 75°C for an hour involved an increase of the ESR-signal by a factor about two and a simultaneous reduction of the line width from 16 to 6 gauss. Evacuation of the sample at room temperature did not change the line width.

(iv). Nile blue chloride was found to have an ESR-signal corresponding to about 10^{15} spins per gram substance. After being kept at 75°C for two days, the signal increased about 10 times. No crystal water is present in nile blue chloride. Evacuation at 75°C reduced the line width as described for methylene blue.

Nile blue chloride exhibits polymorphism and has a melting point at about 159°C, where the dark-green substance transforms to a brown-red modification with an almost metallic lustre. At the same time the signal increases by a factor of 100 as compared with an unheated sample.

(v). Nile blue sulphate recrystallized from cold diluted sulphuric acid * has a signal corresponding to about 5×10^{15} spins per gram. The signal strength seems to be rather unaffected by heat treatment. Contrary to the other compounds here investigated the spectrum of nile blue sulphate exhibits an asymmetrical shape with four incompletely resolved lines (Fig. 1).

(vi). The ESR-signals of the compounds here studied seem to be mainly a solid state phenomenon as only a small signal ($< 10^{14}$ spins per gram substance) could be detected in concentrated water solutions.

Discussion. The presence of unpaired electrons in solid state specimens of phenothiazine and oxazine dyes is not wholly understood. It is possible that the mechanism of the origin is similar to that suggested for the triphenylmethane dyes [1]. Considering the primary process of unpairing the electrons involved, it may be pointed out that the phenothiazine and oxazine dyes constitute redox systems in aqueous solution. A possible mechanism is that an

* Due to their high solubility the nile blue compounds are difficult to crystallize from aqueous solutions. Nile blue sulphate A (G. T. Gurr, London) was crystallized as follows. 0.5 g substance was dissolved in 10 ml water. To the chilled solution 1 ml concentrated H_2SO_4 was slowly added under vigourous stirring. After being kept at + 4°C overnight the crystals (dark-green small needles) were collected and washed with cold diluted H_2SO_4 and finally with ether in order to remove H_2SO_4.

intermediate free radical is formed and trapped at the crystallization process.

As regards the increase of the signal when heating the samples a carbonization process is ruled out as the temperatures used are low compared with those necessary to obtain charred products. It is possible that the increase to a minor extent is due to removal of paramagnetic oxygen. Another factor of importance seems to be an increase of some kind of lattice imperfections. This suggestion is supported by the increase of the signal in connection with the removal of crystal water (methylene blue) and a phase transition (nile blue chloride). In both cases there is a change in the original arrangement with breaking of intermolecular bonds.

The spectrum of nile blue sulphate has certain features in common with that obtained from phenothiazine radicals when adsorbed on a cation exchanger [2]. Both spectra are highly asymmetrical and exhibit four incompletely resolved lines. The asymmetrical shape of the phenothiazine spectrum was suggested to depend on a g-value anisotropy and a hindered rotation of the adsorbed radical. The four lines were interpreted as a hyperfine structure due to the combined interaction of one nitrogen and one hydrogen nucleus in the central ring of the phenothiazine radical. It is possible that a similar interpretation is valid also for the spectrum of nile blue sulphate. The hyperfine interaction is not wholly understood, however, as the formula given for nile blue compounds (Fig. 1) does not involve a hydrogen attached to the ring nitrogen as in phenothiazine. The presence of more than one radical species or the possibility of different g-values in different parts of the crystal structure could not be excluded without an ESR-investigation at another frequency than that used here (9 500 Mc). A hyperfine interaction in the spectrum of nile blue sulphate would indicate that the unpaired electrons are more localized and trapped in this compound than in the other dyes investigated.

Besides in the triphenylmethane dyes[1] and the compounds here concerned, an ESR-absorption has recently been reported

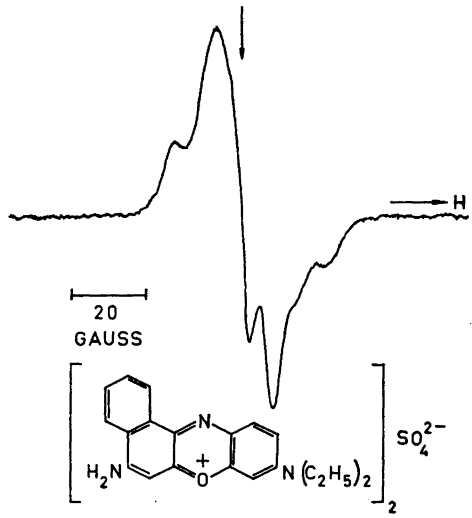

Fig. 1. The ESR-spectrum of a polycrystalline sample of nile blue sulphate (unheated). The vertical arrow gives the position of the g-value of a polycrystalline sample of DPPH.

in phthalocyanine complexes of diamagnetic metals by Neiman and Kivelson [3]. It is possible that the presence of varying amounts of unpaired electrons in solid state specimens is a common phenomenon in organic dyes. If this phenomenon is restricted to dyes only is unknown so far.

The ESR-spectra were obtained at room temperature using a Varian 100 kc spectrometer.

1. Chernyakovskii, F. P., Kalmanson, A. E. and Blyumenfel'd, L. A. *Optics and Spectroscopy* **9** (1960) 414.
2. Lagercrantz, C. *Acta Chem. Scand.* **15** (1961). *In press.*
3. Neiman, R. and Kivelson, D. *J. Chem. Physics* **35** (1961) 162.

Received July 31, 1961.

Comparison of the Albumins of Different Cereal Grains

TOR-MAGNUS ENARI and JUHANI MIKOLA

Laboratory of Brewing, Helsinki, Finland

We have recently described the fractionation of the albumins of barley grains by ion-exchange chromatography on diethylaminoethyl-cellulose (DEAE-cellulose) [1,2]. About 30 % of the proteins were basic and went unretarded through the column in 5 mM sodium phosphate pH 7.5. The neutral and acid proteins adsorbed were resolved into about 15 peaks by gradient elution with descending pH and ascending molarity of phosphate (Fig. 1). There were significant differences between the elution patterns corresponding to different varieties and different places of growth.

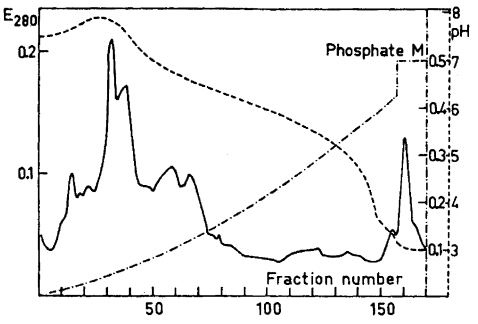

Fig. 1. Elution diagram of barley (Pirkka).

We have now compared the albumin fractions of barley, rye, oat, and summer and winter wheat with the technique developed. The experimental details are exactly as described before [1,2]. The elution diagrams are shown in Fig. 2. They are generally rather similar. However, the total amount of albumin is greater in wheat and oat and smaller in rye when compared to barley. Wheat contains a smaller proportion of acid albumins and oat contains a greater

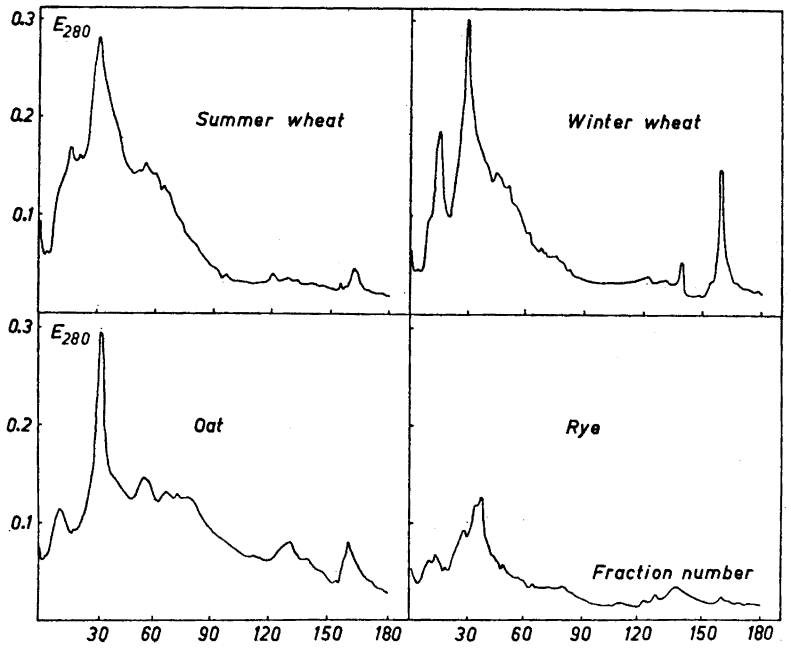

Fig. 2. Elution diagrams of summer wheat (Tammi), winter wheat (Varma), oat (Tammi) and rye (Ensi). Gradients of phosphate and pH as in Fig. 1.

proportion of moderately acid albumins than the other species. The proportion of basic, non-adsorbing proteins is smaller in oat (20 %) than in the other species (winter wheat 36 %, summer wheat 33 %, rye 32 % and barley 32 %).

1. Enari, T.-M. and Mikola, J. *Suomen Kemistilehti* **B 33** (1960) 206.
2. Enari, T.-M. and Mikola, J. *European Brewery Conv. Proc.*, Wien 1961.

Received July 22, 1961.

Synthesis of an Oxime Analogue to Atropin

L.-E. TAMMELIN and A. FLORMARK

Research Institute of National Defence, Dept. 1, Sundbyberg 4, Sweden

Atropin is the drug of choice in treatment of organophosphorus anticholinesterase poisoning. Very promising results have also been obtained with oximes such as pyridine-aldoxime methiodide or mono-*iso*-nitrosoacetone [1]. It seemed thus, without any pretention of strict pharmacological thinking, tempting to prepare an oxime closely analogous to atropin such as phenyl-glyoxylic acid tropylester oxime, see formulae I—III.

Iso-nitrosation by butyl nitrite was used as a final step in the synthesis. This method may result in *iso*-nitrosation of other groups than the methylene group of the phenyl-acetic acid. Thus the structure of the final product was studied by infrared spectroscopy.

Results. Phenyl-glyoxylic acid tropylester oxime has been prepared and the structure of the compound has been confirmed by the following results from IR-spectra.

Phenyl-glyoxylic acid ethylester oxime. The 3 500—2 500 cm^{-1} region: An absorption band at 3 220 cm^{-1} can be ascribed to intramolecular bonded OH. Between 3 180 and 2 990 cm^{-1} the CH absorption bands are found.

The 1 800—1 600 cm^{-1} region: At 1 725 cm^{-1} a strong absorption band can be ascribed to C=O and at 1 685 cm^{-1} a weaker band may indicate presence of C=N.

The 1 600—1 400 cm^{-1} region: At 1 575 cm^{-1} and 1 490 cm^{-1} weak absorption bands characteristic of the benzene ring in a conjugated system are found.

The 1 400—1 100 cm^{-1} region: At 1 300 cm^{-1} an absorption band occurs which might be ascribed to OH and at 1 195 a strong band indicates ester C—O.

Phenyl-glyoxylic acid tropylester oxime. The 3 500—1 800 cm^{-1} region: An absorption band at 2 990 can be ascribed to CH. At 2 800—2 200 cm^{-1} and 2 100—1 800 two broad bands occur which can be ascribed to $\equiv\overset{+}{N}H$.

The 1 800—1 600 cm^{-1} region: At 1 710 a strong absorption band can be ascribed to C=O and at 1 665 a weak band may be ascribed to C=N.

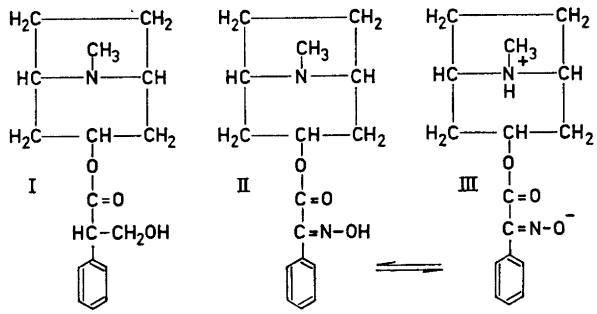

Fig. 1. I is atropin. II and III are protomeric forms of phenyl-glyoxylic acid tropylester oxime.

proportion of moderately acid albumins than the other species. The proportion of basic, non-adsorbing proteins is smaller in oat (20 %) than in the other species (winter wheat 36 %, summer wheat 33 %, rye 32 % and barley 32 %).

1. Enari, T.-M. and Mikola, J. *Suomen Kemistilehti* **B 33** (1960) 206.
2. Enari, T.-M. and Mikola, J. *European Brewery Conv. Proc.*, Wien 1961.

Received July 22, 1961.

Synthesis of an Oxime Analogue to Atropin

L.-E. TAMMELIN and A. FLORMARK

Research Institute of National Defence, Dept. 1, Sundbyberg 4, Sweden

Atropin is the drug of choice in treatment of organophosphorus anticholinesterase poisoning. Very promising results have also been obtained with oximes such as pyridine-aldoxime methiodide or mono-*iso*-nitrosoacetone [1]. It seemed thus, without any pretention of strict pharmacological thinking, tempting to prepare an oxime closely analogous to atropin such as phenyl-glyoxylic acid tropylester oxime, see formulae I—III.

Iso-nitrosation by butyl nitrite was used as a final step in the synthesis. This method may result in *iso*-nitrosation of other groups than the methylene group of the phenyl-acetic acid. Thus the structure of the final product was studied by infrared spectroscopy.

Results. Phenyl-glyoxylic acid tropylester oxime has been prepared and the structure of the compound has been confirmed by the following results from IR-spectra.

Phenyl-glyoxylic acid ethylester oxime. The 3 500—2 500 cm^{-1} region: An absorption band at 3 220 cm^{-1} can be ascribed to intramolecular bonded OH. Between 3 180 and 2 990 cm^{-1} the CH absorption bands are found.

The 1 800—1 600 cm^{-1} region: At 1 725 cm^{-1} a strong absorption band can be ascribed to C=O and at 1 685 cm^{-1} a weaker band may indicate presence of C=N.

The 1 600—1 400 cm^{-1} region: At 1 575 cm^{-1} and 1 490 cm^{-1} weak absorption bands characteristic of the benzene ring in a conjugated system are found.

The 1 400—1 100 cm^{-1} region: At 1 300 cm^{-1} an absorption band occurs which might be ascribed to OH and at 1 195 a strong band indicates ester C—O.

Phenyl-glyoxylic acid tropylester oxime. The 3 500—1 800 cm^{-1} region: An absorption band at 2 990 can be ascribed to CH. At 2 800—2 200 cm^{-1} and 2 100—1 800 two broad bands occur which can be ascribed to $\equiv\overset{+}{N}H$.

The 1 800—1 600 cm^{-1} region: At 1 710 a strong absorption band can be ascribed to C=O and at 1 665 a weak band may be ascribed to C=N.

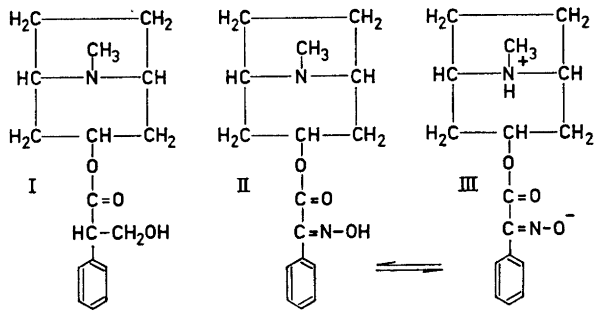

Fig. 1. I is atropin. II and III are protomeric forms of phenyl-glyoxylic acid tropylester oxime.

The 1 600 – 1 400 cm^{-1} region: At 1 575 cm^{-1} and 1 500 cm^{-1} weak absorption bands characteristic of the benzene ring in a conjugated system are found.

The 1 400 – 1 100 cm^{-1} region: At 1 290 cm^{-1} an absorption band occurs which might be ascribed to OH and at 1 205 a strong band indicates ester C – O.

The IR-spectra and earlier findings [2] strongly support the structure given in the preceding formulae. The absorption bands between 2 800 and 1 800 cm^{-1} show that formula III is dominating. Preliminary pharmacological tests indicate that phenyl-glyoxylic acid tropylester oxime has a weak atropin effect.

Experimental. The syntheses were performed as follows.

Phenyl-glyoxylic acid ethylester oxime was prepared as described by Wislicenus and Grützner [2]. Found m.p. 112°C.

Phenyl-acetic acid tropylester was prepared as described by Barrowcliff and Tutin [3]. Found m.p. of picrate 171°C[4].

Phenyl-glyoxylic acid tropylester oxime was prepared as follows. 4.4 g of phenyl-acetic acid tropylester and 1.75 g butyl nitrite in 100 ml sodium distilled ether at −20°C were added to potassium ethoxide in 50 ml of ether at −20°C, prepared from 0.66 g potassium. The mixture was stirred for 45 min and temperature rose to 0°C. After cooling 30 ml of icecooled water were added. After shaking, the aqueous phase was separated and treated with carbon dioxide while cooling. After 3 min a yellow red precipitate was formed. The precipitate was filtered off and washed with water and ether. Yield 0.75 g. The compound was recrystallized twice from ethyl acetate. M.p. 196°C. (Found: C 66.8; H 7.0; N 9.8. Calc. for $C_{16}H_{20}N_2O_3$ (288.3): C 66.7; H 7.0; N 9.7).

Infrared spectra of phenyl-glyoxylic acid tropylester oxime and phenyl-glyoxylic acid ethylester oxime were recorded using potassium bromide pellets.

1. Holmstedt, B. *Pharmacol. Revs.* **11** (1959) 567.
2. Wislicenus, W. and Grützner, R. *Ber.* **42** (1909) 1930.
3. Barrowcliff, M. and Tutin, F. *J. Chem. Soc.* **95** (1909) 1966.
4. Jowett, H. A. D. and Pyman, F. L. *J. Chem. Soc.* **95** (1909) 1020.

Received July 17, 1961.

ACTA CHEMICA SCANDINAVICA 15 (1961) 1209–1214

The Preparation of α-Halogeno-*sec.*-alkyl Esters of Aliphatic Acids

ERKKI EURANTO and TAUNO KUJANPÄÄ

Department of Chemistry, University of Turku, Turku, Finland

α,β-Dichloro-*sec.*-propyl acetate (b.p. 27–28°C/1.4 torr), α,β-dichloro-*sec.*-propyl *n*-butyrate (b.p. 48–50°C/1.3 torr), and α,β,β′-trichloro-*sec.*-propyl acetate (b.p. 55–56°C/2.5 torr) have been prepared by allowing acetyl or *n*-butyryl chloride to react with chloroacetone or *sym.*-dichloroacetone in the presence of anhydrous zinc chloride. The reaction is a new one for ketones. α-Chloro-*sec.*-propyl acetate was not found among the products of the reaction between acetone and acetyl chloride. α,β,β′-Trichloro-*sec.*-propyl acetate was probably also produced when 3-chloropropen-(1)-yl-(2) acetate (b.p. 150–152°C/754 torr) was chlorinated. Other attempts to synthesize the above or other α-halogeno-*sec.*-alkyl esters by treating saturated or unsaturated esters with halogens or hydrogen halides did not lead to the expected compounds, the products being always an acid halide and a ketone.

It might be expected that α-halogeno-*sec.*-alkyl esters RCOOCXR′R″ (R′ and R″ ≠ H) could be prepared by the following methods which are similar to those by which primary α-halogenoalkyl esters have been synthesized (for references, see Euranto [1–3]): (1) the reaction between a ketone and an acid halide in the presence of anhydrous zinc chloride, (2) the halogenation of *sec.*-alkyl esters, (3) the addition of halogen to the double bonds of α,β-unsaturated *sec.*-alkyl esters, and (4) the addition of hydrogen halide to α,β-unsaturated *sec.*-alkyl esters. Three reports on the preparation of α-halogeno-*sec.*-alkyl esters have been published. Bruylants, Tits, Dieu, and Gauthier [4] have claimed having prepared α-chloro-*sec.*-propyl acetate by chlorinating *sec.*-propyl acetate in the gaseous state. On the basis of experimental data presented below, however, it seems probable that the compound evidently produced in the first stage of the reaction reacted further in the described reaction conditions to chloroacetone and acetyl chloride *. On the other hand, Utermohlen [5], has reported on the synthesis of α,β-dihalogeno-*sec.*-alkyl and arylalkyl esters of the type RCOOCXR′CH_2X (X = Cl or Br, R and R′ are aryl, alkyl, or aryl-

* Bruylants *et al.* report the boiling point of the ester to be 64–68°C/100 torr. This boiling point seems too low to be that of the ester, but would better represent that of chloroacetone. These authors state that the compound is unstable and lachrymatory; the latter property is typical of chloroacetone. See the experimental part of the present paper.

alkyl groups) by halogenation of the corresponding unsaturated esters. Physical constants for the 1,2-dichloro- and 1,2-dibromo-*sec.*-propyl acetates were given. On the basis of the reported values of the constants, it is obvious that the compound first formed decomposed into the acid halide and the halogenoacetone during the treatment.* One *α*-halogeno-*sec.*-alkyl ester has evidently been prepared, for Gayler and Waddle [9] obtained a compound which they reported to be *α*-chloro-*sec.*-propyl trichloroacetate in 25 % yield by the action of chlorine on *sec.*-propyl trichloroacetate at 120°C under exposure to light.

The cases mentioned above refer to reactions (2) and (3). In the case of *sec.*-propenyl acetate, reaction (4) leads to the formation of acetone and acetyl chloride [10]. Also here the initially formed *α*-halogeno-*sec.*-alkyl ester decomposes into an acid halide and a ketone by a reaction that is the reverse of reaction (1). On the other hand, it has been found that *α,β*-unsaturated *sec.*-alkyl esters are formed when acetoacetic ester and acetyl or benzoyl chloride react in the presence of pyridine [11] and when aliphatic ketones with a relatively long chain are boiled with benzoyl or valeryl chloride [12]. The intermediate compounds have been assumed to be *α*-chloro-*sec.*-alkyl esters, which lose hydrogen halide by a reaction which is the reverse of reaction (3). The reaction between acetone and acetyl chloride has been reported to yield the compounds

$(CH_3)_2CCl-CH_2-CO-CH_3$ and $(CH_3)_2CCl-CH_2-CO-CH_2-CCl(CH_3)_2$,

which react further to mesityl oxide and phorone [13].

In the following the results of experiments are described which were carried out to prepare *α*-halogeno-*sec.*-alkyl esters for kinetic studies.

EXPERIMENTAL

Analytical

The indices of refraction of the isolated compounds were determined with an Abbe refractometer and the densities with a Sprengel-Ostwald pyknometer. The molar refractions calculated from these values were compared with the theoretical molar refractions derived from refraction equivalents [14]. For analysis, the esters were hydrolysed in water or in an excess of sodium hydroxide solution. The total amount of acids liberated on hydrolysis was determined by acid-base titration and the amount of halide ion formed by titration with silver nitrate. The titrations were performed with a Radiometer titrator TTT 1 employing glass and calomel or silver and mercury/mercury(I) sulphate electrodes.

The progress of the reaction in the syntheses was followed by a kinetic method. Samples withdrawn from the reaction mixture were added to a water-acetone mixture (containing 50 or 75 % acetone by weight). After a period of time sufficient for the remaining acid halide to hydrolyse completely, the hydrolysis reaction was followed by conductometry or by titrating the halide ion produced (*cf.* Refs.[1-3]). In this way it was found whether *α*-halogenoalkyl esters had been formed and in what amounts. In some cases the acid halides were identified kinetically by determining conductometrically the rate of hydrolysis in water-acetone mixtures containing about 5 % water.

* The boiling point reported for the former compound was 45–46°C/41 torr and that reported for the latter compound 62–63.5°C/40 torr. The following boiling points have been reported for chloro- and bromoacetone: CH_3COCH_2Cl, 35°C/29 torr [6]; CH_3COCH_2Br, 63.5–64°C/50 torr [7]. The boiling point obtained in the present study for 1,2-dichloro-*sec*-propyl acetate is much higher (see the experimental part). The reaction products were used to prepare 2-amino-4-alkylthiazoles by allowing them to react with thiourea and treating the products with potassium hydroxide. It has long been known that 2-amino-4-methylthiazole can be prepared by the same procedure from chloroacetone and thiourea [8].

Syntheses by method 1

α,β,β'-Trichloro-sec.-*propyl acetate.* 9 g (0.11 mole) of freshly distilled acetyl chloride and 14.5 g (0.11 mole) of *sym.*-dichloroacetone, which was obtained as a by-product in an attempt to prepare *α,β*-dichloro-*sec.*-propyl acetate and which was recrystallized several times, were mixed and a small amount of anhydrous zinc chloride added to the mixture. Heat was evolved and the mixture slowly became dark brown in colour. After the reaction mixture had stood at room temperature about 24 h, it was heated at 50—60°C for one hour. The mixture was then washed with ice water, dried with calcium chloride and distilled twice under reduced pressure. The yield of *α,β,β'*-trichloro-*sec.*-propyl acetate (b.p. 55—56°C/2.5 torr) was 6 g (26 % of theory). A small amount of unreacted *sym.*-dichloroacetone was also recovered. Physical data for the ester: n_D^{20} 1.4705, d_4^{20} 1.3905, $[R]_D$ 41.27 (calc. 41.27). Analytical data: On hydrolysis in water 0.738 mmole of the ester yielded 1.328 mmoles of acid and 0.680 mmole of chloride ion. On hydrolysis in sodium hydroxide solution, 0.607 mmole of the ester yielded 2.812 mmoles of acid and 1.780 mmoles of chloride ion. A possible explanation for the analytical results obtained is the following. On hydrolysis in water one equivalent each of hydrogen chloride, acetic acid, and *sym.*-dichloroacetone is formed whereas on hydrolysis by sodium hydroxide the last-mentioned compound decomposes further giving two equivalents of chloride ion and, in addition, some organic acid.

α,β-Dichloro-sec.-*propyl acetate.* 44 g (0.56 mole) of acetyl chloride and 38.5 g (0.42 mole) of chloroacetone (b.p. 119.0—119.5°C/748 torr), the latter prepared by chlorinating acetone in the presence of marble chips and purified by washing with water and distilling [15], were mixed. The mixture was cooled in ice before anhydrous zinc chloride was added to it. The reaction mixture first turned green and gradually dark brown. After the mixture had stood several hours at room temperature, it was analysed kinetically and found to contain about 40 % α-chloroalkyl ester. Heating of the reaction mixture to 30—40°C decreased the yield of ester. The reaction mixture was stored about 24 h at room temperature and about 5 days at —6°C. After this treatment, the mixture was washed with a small quantity of ice water, dried with calcium chloride, and distilled under reduced pressure. In addition to unreacted chloroacetone, acetic acid, *etc.*, 45 g (62 % of theory) of pure, colourless *α,β*-dichloro-*sec.*-propyl acetate (b.p. 27—28°C/1.4 torr) was obtained. Physical data for the ester: n_D^{25} 1.4442, d_4^{25} 1.2474, $[R]_D$ 36.43 (calc. 36.43). Analytical data: On hydrolysis in water 0.637 mmole of the ester gave 1.250 mmoles of acid and 0.623 mmole of chloride ion. On hydrolysis in sodium hydroxide solution 0.596 mmole of ester gave 1.950 mmoles of acid and 1.180 mmoles of chloride ion (*cf.* preceding paragraph).

α,β-Dichloro-sec.-*propyl* n-*butyrate.* 65 g (0.61 mole) of *n*-butyryl chloride and 45.5 g (0.49 mole) of chloroacetone (see above) were mixed and cooled in ice water and a small quantity of anhydrous zinc chloride was added to the mixture. The mixture became first yellow and later dark brown. The mixture was kept at room temperature for 16 h, washed with ice water, dried with calcium chloride and distilled under reduced pressure. In addition to *n*-butyryl chloride, chloroacetone, and *n*-butyric acid, 24 g (25 % of theory) of pure, colourless *α,β*-dichloro-*sec.*-propyl *n*-butyrate (b.p. 48—50°C/1.3 torr) was isolated. Physical data: n_D^{25} 1.4432, d_4^{25} 1.1523, $[R]_D$ 45.82 (calc. 45.74). Analytical results: On hydrolysis in water, 1.017 mmoles of the ester gave 2.009 mmoles of acid and 0.986 mmole of chloride ion. An attempt that was made to distill the crude reaction mixture without washing it with water to remove the zinc chloride led to the complete decomposition of the ester, evidently into the original reactants.

The reaction between acetone and acetyl chloride. A small quantity of anhydrous zinc chloride was added to a mixture of 44 g of acetyl chloride and 32.5 g of acetone. The temperature of the mixture rose and the mixture became first green and later dark brown. Kinetic experiments revealed that possibly a small amount (at most 5 % of theory) of the α-chloroalkyl ester had formed. The amount of ester did not increase when the reaction mixture was allowed to stand at room temperature and at about —6°C. α-Chloro-*sec.*-propyl acetate was not isolated from the mixture, the distillation products containing, besides other compounds, mesityl oxide and phorone.

Syntheses by method 2

The chlorination of sec.-*propyl acetate. sec.*-Propyl acetate was prepared from acetic acid and *sec.*-propanol employing sulphuric acid as catalyst [16]. The ester boiled at 88.2—88.8°C/761.0 torr. The chlorination of the ester was carried out in three different ways: (a) equimolar amounts of *sec.*-propyl acetate and sulphuryl chloride were dissolved in a small volume of carbon tetrachloride and 0.2 mole-% of benzoyl peroxide was added to the mixture (*cf.* Brown and Ash [17]); (b) chlorine gas was led into cold *sec.*-propyl acetate under exposure to ultraviolet light [4] (mercury vapour lamp Philips No. 93 110); (c) chlorine was led into a reaction vessel which contained the gaseous ester and which was irradiated with ultraviolet light [18]. The reaction mixture was in each case distilled in a fractionation assembly. The distillation yielded, in addition to unreacted ester, β-chloro-*sec.*-propyl acetate (b.p. 69—70°C/40 torr) and a fraction boiling in the range 40—60°C/40 torr from which a substance was isolated which according to its boiling point [6] (118—120°C/751 torr), odour [19], and dye reaction [20] was evidently chloroacetone. A kinetic study of the low-boiling part of the fraction in 95 % acetone-water at 15°C gave a rate coefficient of hydrolysis equal to about 1.5×10^{-2} s^{-1}. The rate coefficient of the hydrolysis of acetyl chloride under the same conditions was found to be 2.5×10^{-3} s^{-1}. These experimental data show that the fraction in question probably contained chloroacetyl chloride (b.p. 104.8—104.9°C/743 torr) and dichloroacetyl chloride (b.p. 107.9—108.1°C/766 torr) which solvolyse at a somewhat higher rate than acetyl chloride [21].

Syntheses by method 3

The chlorination of sec.-*propenyl acetate. sec.*-Propenyl acetate was obtained by passing ketene into warm acetone to which sulphuric acid had been added [22]. The compound was chlorinated in the dark either by leading chlorine gas into the ice-cold ester or by adding the ester at about —60°C dropwise to liquid chlorine. The reaction products were distilled under reduced pressure. The distillates were found to contain primarily acetyl chloride and chloroacetone and a small amount of *sym.*-dichloroacetone. Some of the fractions were found kinetically to contain small amounts of some α-chloroalkyl ester, but this compound could not be isolated. The reaction products resulting from the chlorination at —60°C were not found kinetically even before warming and distillation to contain any other compound than acetyl chloride that underwent solvolysis.

The bromination of sec.-*propenyl acetate.* An equimolar amount of bromine was slowly added dropwise to ice-cold *sec.*-propenyl acetate with which it reacted readily. Only bromoacetone and acetyl bromide were isolated from the reaction products.

The chlorination of 3-chloropropen-(1)-yl-(2) acetate. 3-Chloropropen-(1)-yl-(2) acetate was prepared by leading ketene [23] into chloroacetone (see preceding paragraph) which contained 3 mole-% sulphuric acid. The reaction mixture was stirred with a magnetic stirrer and its temperature held at 80—90°C. The mixture was then cooled, the sulphuric acid neutralised with sodium bicarbonate, and the product distilled under ordinary pressure. The fraction boiling in the range 136—160°C was washed with water, dried with calcium chloride and redistilled. A small amount (about 8 ml from 100 g of chloroacetone) of pure, colourless 3-chloropropen-(1)-yl-(2) acetate (b.p. 150—152°C/754 torr, n_D^{20} 1.4378, d_4^{20} 1.1333, $[R]_D$ 31.16 (calc. 31.16)) was isolated. On hydrolysis in sodium hydroxide solution, 0.867 mmole of the ester gave 1.680 mmoles of acids and 0.817 mmole of chloride ion.

The ester was chlorinated in the dark as described above. On distilling the reaction mixture, there was obtained in addition to highly chlorinated matter and substances that had been produced by other reactions (see Discussion) a small amount of matter that probably contained trichloro-*sec.*-propyl acetate identical with that obtained from *sym.*-dichloroacetone and acetyl chloride, which shows that the initial product was actually 3-chloropropen-(1)-yl-(2) acetate. A kinetic study of the product of the chlorination yielded values of the rate coefficient that decreased during the hydrolysis from an initial value that was about 60 % of the value of the rate coefficient obtained for α,β,β'-trichloro-*sec.*-propyl acetate. This result must evidently be ascribed to the presence of some slowly reacting ester whose presence was also indicated by the poorer solubility of the reaction product in 40 % acetone-water (see below).

Syntheses by method 4

The addition of hydrogen chloride to sec.*-propenyl acetate.* Hydrogen chloride gas was directed into *sec.*-propenyl acetate that had been cooled with a mixture of ice and salt. A reaction was observed but no α-chloro-*sec.*-propyl acetate was isolated by distilling the reaction mixture under reduced pressure, probably because the ester had decomposed during the reaction or during the distillation into acetone and acetyl chloride which could not be condensed at the pressure employed.

DISCUSSION

Of the attempted syntheses of α-halogeno-*sec.*-alkyl esters RCOOCXR'R'', only those of α,β-dichloro-*sec.*-propyl acetate, α,β-dichloro-*sec.*-propyl *n*-butyrate and α,β,β'-trichloro-*sec.*-propyl acetate were successful. At least one of the groups R' and R'' in these compounds contains an electronegative chlorine atom. Of these, the dichloro-substituted compounds where R'' is a methyl group are relatively unstable because heating of the reaction mixture to about 30°C lowered the yield of the ester and distillation of the reaction mixture with zinc chloride led to a complete decomposition of the ester already at pressures so low that the distillation temperature did not exceed 30—40°C. In addition to the α-halogeno-*sec.*-alkyl esters prepared in this study, only α-chloro-*sec.*-propyl trichloroacetate, which has the highly electronegative trichloromethyl group as the acyl group R, has been prepared previously [9], using a temperature as high as 120°C. Aldehydes (R'' = H) react with halogen halides almost quantitatively to α-halogenoalkyl esters at room temperature, but already at about 80°C α-chloroethyl acetate and butyrate and α,β-dichloroethyl acetate and at about 110°C α-chloroethyl chloroacetate decompose into acid chloride and aldehyde in the presence of zinc chloride [24]. The anhydrous zinc chloride obviously only catalyses the reactions, and hence the success of the above distillations in the absence of zinc chloride is due to the fact that the equilibrium did not have time enough to shift during the distillation.

It is hence obvious that the equilibrium

$$RCOX + R'R''CO \rightleftharpoons RCOOCXR'R''$$

is farther on the left the higher the temperature (the reaction to the right is exothermic) and the more electropositive the groups R, R' and R''. The polarities of these groups do not, however, alone determine the equilibrium state, since, *e.g.*, α-chloroethyl acetate (R' = CH_3, R'' = H) is more stable than α,β-dichloro-*sec.*-propyl acetate (R' = CH_3, R'' = CH_2Cl) although the electronegativity of the chloromethyl group is greater than that of the hydrogen atom (Taft's polar substituent constants σ* are 1.050 for chloromethyl and 0.490 for the hydrogen atom ($\sigma^*_{CH_3} = 0$)) [25].

α-Halogeno-*sec.*-alkyl esters could be more easily prepared from ketones and carboxylic acid halides than by chlorinating α,β-unsaturated *sec.*-alkyl esters, although the reaction products revealed that the following reaction evidently does take place in the latter case:

$$RCOOC(R')=CH_2 + X_2 = RCOOCXR'CH_2X$$

It may be noted that α,β-dichloro-*sec.*-propyl acetate ($R' = CH_3$, $X = Cl$) was not found in the reaction mixture even when *sec.*-propenyl acetate was chlorinated at $-60°C$. The reason may be that the chlorination reaction is so exothermic that the ester $RCOOCXR'CH_2X$ first formed decomposes immediately to RCOX and CH_2XCOR', *i.e.* before the energy has dissipated from the reacting molecule. It seems furthermore possible on the basis of the observations made that at least in the chlorination of 3-chloropropen-(1)-yl-(2) acetate a reaction of the type [26]

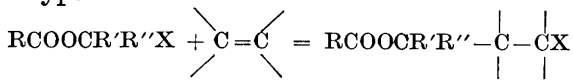

which leads to high-molecular halogenoalkyl compounds, takes place between the α-halogenoalkyl ester already formed and the unsaturated ester that has not reacted.

Acknowledgement. The authors wish to thank the *State Commission for Natural Sciences (Valtion Luonnontieteellinen Toimikunta)* for financial aid in support of their work.

REFERENCES

1. Euranto, E. *Ann. Univ. Turkuensis A I* **31** (1959).
2. Euranto, E. *Suomen Kemistilehti B* **33** (1960) 41.
3. Euranto, E. *Ann. Univ. Turkuensis A I* **42** (1960).
4. Bruylants, A., Tits, M., Dieu, C. and Gauthier, R. *Bull. soc. chim. Belges* **61** (1952) 366.
5. Utermohlen, Jr., W. O. *U.S. Pat.* 2 404 416 (1946); *Chem. Abstr.* **40** (1946) 7238; *cf.* also Hagemeyer and Hull [10].
6. Herbst, H. *Kolloidchem. Beih.* **23** (1927) 313.
7. Catch, J. R., Elliott, D. F., Hey, D. H. and Jones, E.R.H. *J. Chem. Soc.* **1948** 272.
8. Traumann, V. *Ann.* **249** (1888) 31; *cf.* also *Org. Syntheses* **19** (1939) 10 and *Coll. Vol.* **2** (1943) 31.
9. Gayler, C. W. and Waddle, H. M. *J. Am. Chem. Soc.* **63** (1941) 3358.
10. Hagemeyer, Jr., H. J. and Hull, D. C. *Ind. Eng. Chem.* **41** (1949) 2920.
11. Claisen, L. and Haase, E. *Ber.* **33** (1900) 1242.
12. Lees, F. H. *J. Chem. Soc.* **83** (1903) 145.
13. Descudé, M. *Ann. chim. Paris* [7] **29** (1903) 486.
14. Vogel, A. I. *J. Chem. Soc.* **1948** 1833.
15. Ellinger, L. P. and Goldberg, A. A. *J. Chem. Soc.* **1949** 263.
16. Vogel, A. I. *A Text-book of Practical Organic Chemistry*, Longmans, Green and Co., London 1948, p. 377.
17. Brown, H. C. and Ash, A. B. *J. Am. Chem. Soc.* **77** (1955) 4019.
18. Bruylants, A., Tits, M. and Dauby, R. *Bull soc. chim. Belges* **58** (1949) 310.
19. Bertrand, G. *Compt. rend.* **171** (1920) 965.
20. Mulder, E. *Ber.* **5** (1872) 1007.
21. Leimu, R. *Ann. Univ. Turkuensis A IV* (1935) No. 3.
22. Gwynn, B. H. with Degering, Ed. F. *J. Am. Chem. Soc.* **64** (1942) 2216.
23. Williams, J. W. and Hurd, C. D. *J. Org. Chem.* **5** (1940) 122.
24. German Patent 527 874 (1931); *Fortschritte der Teerfarbenfabrikation und verwandter Industriezweige* **18** (1933) 796.
25. Taft, Jr., R. W. in Newman, M. S. *Steric Effects in Organic Chemistry*, John Wiley & Sons, Inc., New York 1956, p. 619.
26. Colonge, J. and Robert, H. *Bull. soc. chim. France* **1960** 463.

Received February 1, 1961.

ACTA CHEMICA SCANDINAVICA 15 (1961) 1215–1222

An X-Ray Crystallographic Study of Some Racemates and Quasi-racemates

STEINAR HUSEBYE

Chemical Institute, University of Bergen, Bergen, Norway

Unit cells and space groups of some racemates and quasi-racemates have been determined. The following data were found: Quasi-racemate of (−)-1,2-dithiane-3,6-dicarboxylic acid and (+)-1,2-diselenane-3,6-dicarboxylic acid, a = 9.75 Å, b = 9.38 Å, c = 9.80 Å, β = 103 ½°; space group $C_2^3 - I2$ with Z = 4. *Racem-a*-(1-naphthyl)-propionic acid, a = 7.89 Å, b = 9.04 Å, c = 15.01 Å, β = 96 ½°; space group C_{2h}^5-$P2_1/c$ with Z = 4. *Racem-a*-(3-thianaphthenyl)-propionic acid, a = 8.71 Å, b = 10.45 Å, c = 11.01 Å, β = 96°; space group C_{2h}^5-$P2_1/c$ with Z = 4. Quasi-racemate of *a*-(1-naphthyl)-propionic acid and *a*-(3-thianaphthenyl)-propionic acid, a = 8.86 Å, b = 29.00 Å, c = 8.07 Å, Z = 8, space group probably D_2^4-$P2_12_12_1$. *Racem-a*-(3-indolyl)-propionic acid, a = 16.00 Å, c = 7.79 Å; space group C_{4h}^4-$P4_2/n$ with Z = 8.

The unit cell and space group of the quasi-racemate of dithiane-dicarboxylic acid and diselenane-dicarboxylic acid are closely related to those of the parent, true racemates, the major difference being the lack of the centre of symmetry and the glide planes which transform one antipode into the other. The similarity in structure has been confirmed through Fourier analysis of the *b*-axis projection of this quasi-racemate. The result is in agreement with views concerning the constitution of quasi-racemates put forward by Fredga and Hägg. No corresponding relation seems to exist between the structure of the other quasi-racemate and those of the parent, true racemates.

About sixty years ago, racemate-like compounds showing optical activity were reported by Centnerzwer [1]. During the last 20—30 years especially Fredga and co-workers have made comprehensive studies of such compounds, which by Fredga were termed quasi-racemates [2,3].

A quasi-racemate can be derived from a corresponding, true racemate by a not too extensive change in one of the antipodes [3,4]. True antipodes can be brought to coincide by means of the symmetry elements $\bar{1}$,*m*,*c* and $\bar{4}$. In a quasi-racemate, the components are not true enantiomorphs; by means of the

above-mentioned symmetry elements they can be brought to coincide approximately [2], but not exactly, because at least one atom or atom group is different in the two molecules. If the lack of these symmetry elements is the only difference from the space group of a parent racemate, there will, as pointed out by Hägg [5], be a simple relation between the space groups of the two. Where this rule is valid and the cell dimensions are similar, the (+) and (−) components in racemate and quasi-racemate will probably be distributed on roughly the same positions. The only possibility for all symmetry elements of a true racemate to remain in a quasi-racemate would be through a statistical distribution of the molecules.

CRYSTAL DATA

Unit cell and space group data were obtained from single-crystal oscillation and Weissenberg photographs. Cu$K\alpha$ radiation with $\lambda = 1.542$ Å was used. Axial lengths are believed to be accurate within $\pm$ 0.5 %. Densities were determined by a flotation method.

Quasi-racemate of (−)-1,2-dithiane-3,6-dicarboxylic acid and (+)-1,2-diselenane-3,6-dicarboxylic acid (III)[6]. For comparison with the parent racemates, *racem*-1,2-dithiane-3,6-dicarboxylic acid (I)[6-8] and *racem*-1,2-diselenane-3,6-dicarboxylic acid (II)[6,7,9], the unit cell and space group data of all three are listed below:

	C-centered setting		*I*-centered setting					
	a	*β*	*a*	*β*	*b*	*c*	*Z*	Space group
I	12.09 Å	129°	9.62 Å	102 ½°	9.26 Å	9.70 Å	4	C_{2h}^6-2/*c*
II	9.97 Å	105°	12.01 Å	127°	9.43 Å	9.78 Å	4	C_{2h}^6-2/*c*
III	12.11 Å	128 ½°	9.75 Å	103 ½°	9.38 Å	9.80 Å	4	C_2^3-2

The most orthogonal cells have been chosen for further work. The crystals of III were yellow prisms, monoclinic sphenoidic, with density, calc. 1.94, found 1.96 g/cm³. There are two molecules of each type in the unit cell.

Racem-*a-(1-naphthyl)-propionic acid (IV)*. Flat colourless prisms, monoclinic prismatic, extended along the *b*-axis with forms {100} and apparently {001}, {110} and {011} were developed on some crystals. There are four molecules in a unit cell of dimensions $a = 7.89$ Å, $b = 9.04$ Å, $c = 15.01$ Å, and $\beta = 96\frac{1}{2}°$. Density, calc. and found 1.25 g/cm³. Systematic absences, $h0l$ when l is odd and $0k0$ when k is odd. The space group is then C_{2h}^5-$P2_1c$.

Racem-*a-(3-thianaphthenyl)-propionic acid (V)*. Large irregular crystals with $a = 8.71$ Å, $b = 10.45$ Å, $c = 11.01$ Å, and $\beta = 96°$. There are four molecules in a unit cell; density, calc. 1.37, found 1.34 g/cm³. Systematic absences are $0k0$ when k is odd and $h0l$ when l is odd. The space group is thus C_2^5-$P2_1c$.

Quasi-racemate of a-(1-naphthyl)-propionic acid and a-(3-thianaphthenyl)-propionic acid. (VI). Irregular prisms and needles elongated along the *c*-

axis, bounded by {110} and, less developed, {010}; {011} was seen on some crystals. Unit cell data are, $a = 8.86$ Å, $b = 29.00$ Å, and $c = 8.07$ Å. 4 molecules of each kind per unit cell. Density, calc. 1.30, found 1.29 g/cm^3. Systematic absences, $h00$ when h is odd, $0k0$ when k is odd. Even after long exposure, no $00l$ reflections could be observed. Possible space groups: D_2^4-$P2_12_12_1$ or D_2^3-$P2_12_12$.

Racem-*a*-(*3-indolyl*)-*propionic acid* (*VII*). Small orange needles and prisms extended along the *c*-axis, bounded by {110} and {001}. From the symmetry of the photographs, the crystals are tetragonal. Unit cell data were $a = 16.00$ Å, $c = 7.79$ Å. Density, calc. 1.26, found 1.24 g/cm^3. Systematic absences are $hk0$ when $h + k$ are odd, and $00l$ when l is odd. The space group is therefore C_{4h}^4-$P4_2/n$.

It appears that the true racemates crystallize in non-enantiomorphous space groups. This is not the case with the space groups of the two quasi-racemates, which are lacking the symmetry elements $\bar{1}$,*m*,*c* and $\bar{4}$; one or more of which are found in true racemates. The unit cells of I, II and III are very similar; this is not unexpected because of the small difference in covalent radius between sulphur and selenium. The quasi-racemate III does not possess the glide planes and symmetry centres of I and II. As this is the only difference between their space groups, the rule of Hägg [5] is valid here, and the positions in the crystal lattice of III should be occupied in the same manner as in I and II.

The racemates IV and V are not isomorphous, nor is there any relation between the unit cell and space group of any of these and that of the corresponding quasi-racemate VI. This must be the result of the relatively great structural difference between the components of the quasi-racemate, which apparently require quite another packing of the molecules than in the parent, true racemates.

To confirm the similar arrangement in III and its parent, true racemates, the projection of the structure of III along the *b*-axis was worked out. The detailed crystal structures of I[8] and II[9] have already been determined in this laboratory.

A FOURIER ANALYSIS OF THE QUASI-RACEMATE OF (−)-1,2-DITHIANE-3,6-DICARBOXYLIC ACID AND (+)-1,2-DISELENANE-3,6-DICARBOXYLIC ACID

The intensities of the $h0l$ reflections were estimated visually from zero layer Weissenberg photographs. Ni-filtered CuK radiation with $\lambda = 1.542$ Å was used. 90 out of 117 reflections within the range of $\sin \Theta = 0.980$ were observed and measured. The intensities were corrected for Lorentz and polarization factors. They were then converted to relative structure amplitudes and ultimately brought to an approximately absolute scale by comparison with the calculated values. Because of the similarity in cell dimensions and the simple relation between the space groups of I, II and III, the atomic positions were assumed to be little different in the three compounds. In the true racemates I[8] and II[9], with space group [7] C_{2h}^6-$2/c$, the systematic absences of $h0l$ when h is odd and l is odd, are caused by the axial and diagonal glide

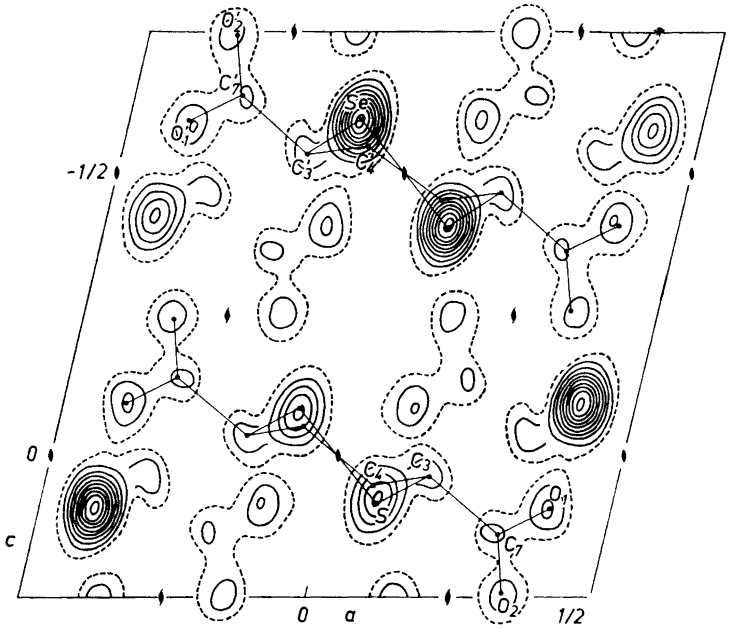

Fig. 1. Electron density projection of the quasi-racemate of (−)-1,2-dithiane-3,6-dicarboxylic acid and (+)-1,2-diselenane-3,6-dicarboxylic acid along the *b*-axis. One unit cell (four asymmetric units) are shown. Lines are drawn to indicate one molecule of each kind. The contour intervals are 5 e/Å² for sulphur and selenium, 3 e/Å² for oxygen and carbon, and the 5-electron line is dashed.

planes. These glide planes do not exist in III, but are replaced by pseudo glide planes, which transform a dithiane-dicarboxylic acid molecule into a diselenane-dicarboxylic acid molecule. This will as observed on the photographs, cause the *h*0*l* reflections with odd indices to be weak and the other reflections to be intermediates between the corresponding ones in I and II. The assumption was therefore made, that where corresponding reflections with both *h* and *l* even had the same sign in I and II, they probably had that sign in III too. In this way, signs of 30 relatively strong reflections were found. The resulting Fourier map showed a clear resemblance to the *h*0*l* maps from I[8] and II[9], with an asymmetric unit of half the real one and a well resolved average S-Se peak and peaks for the lighter atoms. Sulphur and selenium were then placed in the real asymmetric unit in positions corresponding to the heavy atoms in (+) and (−) molecules in I[8], with twofold axes in the middle of the rings. With the heavy atoms placed, the structure was solved and refined through succesive Fourier and difference syntheses.

Beevers-Lipson strips were used for summation at intervals of 6°. The atomic coordinates from the final structure factor calculation were corrected for gradients still present in several atomic positions in the last difference map. C_4 and C_4' overlap with sulphur and selenium and were placed so as to obtain

C-C bonds of 1.54 Å. The final coordinates for half a molecule of each type are listed in Table 1, and indicated through dots in the final electron density map in Fig. 1. A prime is used to denote the lighter atoms in the diselenane-dicarboxylic acid molecule. For comparison, the final atomic coordinates of I[8] and II[9] are also listed in Table 1.

The observed and calculated structure factors are listed in Table 2. Atomic scattering curves used were those of Viervoll and Øgrim [10] for sulphur, of Berghuis *et al.*[11] for carbon and oxygen and of Thomas and Umeda [12] for selenium. The Se-curve was corrected for dispersion and anomalous diffraction [13,14]. In the temperature factors, exp $[-B(\sin^2\Theta/\lambda^2)]$, used in calculation of structure factors, the final values of B, chosen on basis of the difference maps, were 4.0 Å^2 and 5.0 Å^2 for carbon and oxygen, respectively, and $(2 + 6\cos^2\varphi)$ Å^2 for sulphur and $(2.5 + 4\cos^2\varphi)$Å^2 for selenium, where φ is the angle between the normal of the reflecting plane and the direction of maximum vibration of the atoms. The latter direction made an angle of 15° with the c-axis in the acute angle in both cases.

Table 1. Atomic coordinates of the quasi-racemate III in fractions of cell edges. Origin on twofold axis in the dithiane-dicarboxylic acid molecule.

The dithiane-dicarboxylic acid molecule			The diselenane-dicarboxylic acid molecule		
	x	z		x	z
S	0.0871	0.0846	Se	0.4030	−0.0957
C_3	0.168	0.036	C_3'	0.323	−0.034
C_4	0.073	0.052	C_4'	0.425	−0.047
C_7	0.312	0.139	C_7'	0.186	−0.137
O_1	0.391	0.094	O_1'	0.104	−0.092
O_2	0.342	0.246	O_2'	0.153	−0.243

Atomic coordinates of corresponding molecules in the true racemates I[9] and II[9], respectively, in fractions of cell edges.

Racem-dithiane-dicarboxylic acid			*Racem*-diselenane-dicarboxylic acid		
	x	z		x	z
S	0.0885	0.0825	Se	0.3976	−0.0896
C_3	0.171	0.042	C_3	0.330	−0.037
C_4	0.072	0.052	C_4	0.428	−0.045
C_7	0.313	0.129	C_7	0.188	−0.125
O_1	0.396	0.092	O_1	0.090	−0.092
O_2	0.348	0.248	O_2	0.171	−0.248

The relatively strong reflection $10\bar{1}$, has markedly lower observed than calculated value, probably due to secondary extinction, and was therefore omitted from the difference syntheses and scale factor calculation, and included in the final Fourier synthesis with calculated instead of observed value. The final reliability index $R = \Sigma||F_o| - |F_c||/\Sigma|F_o|$ with non-observed reflections included when $|F_c|$ exceeded the observable limit, and $10\bar{1}$ excluded, was 0.086.

Table 2. Observed and calculated *h0l* structure factors for the quasi-racemate of (−)-1,2-dithiane-3,6-dicarboxylic acid and (+)-1,2,diselenane-3,6-dicarboxylic acid.

h	F_o	F_c	h	F_o	F_c
	*h*00			*h*04	
2	41	29			
4	160	−160	0	62	− 63
6	67	− 67	2	108	−110
8	15	− 12	4	7	1
10	43	40	6	59	54
			8	26	28
	*h*01		10	11	− 9
1	14	− 16			
3	50	53		*h*0$\bar{4}$	
5	31	32	2	48	54
7	18	− 16	4	61	63
9	27	− 23	6	50	55
11	< 4	− 1	8	30	− 29
			10	55	− 47
	*h*0$\bar{1}$		12	< 5	3
1	48	− 63			
3	15	− 16			
5	35	37		*h*05	
7	28	26	1	28	29
9	14	− 12	3	16	− 16
11	16	− 15	5	30	− 30
			7	< 8	− 2
	*h*02		9	13	16
0	97	94			
2	46	− 37		*h*0$\bar{5}$	
4	118	−112	1	30	33
6	35	− 25	3	13	− 9
8	42	41	5	28	− 31
10	36	33	7	< 8	− 3
			9	15	13
	*h*0$\bar{2}$		11	< 6	5
2	120	130			
4	50	55		*h*06	
6	72	− 74	0	82	− 93
8	55	− 54	2	32	− 31
10	< 8	4	4	65	66
12	16	18	6	26	27
			8	12	− 11
	*h*03				
1	44	48		*h*0$\bar{6}$	
3	34	34	2	14	− 15
5	18	− 17	4	40	44
7	31	− 27	6	53	53
9	< 7	− 3	8	< 8	− 1
			10	29	− 22
	*h*0$\bar{3}$				
1	13	− 16		*h*07	
3	41	− 48	1	11	− 11
5	12	− 13	3	23	− 24
7	23	24	5	< 8	3
9	20	15	7	13	15
11	8	− 7			

h	F_o	F_c	h	F_o	F_c
	$h0\bar{7}$			$h010$	
1	17	19	0	< 7	4
3	19	20	2	14	14
5	< 8	− 7	4	< 5	− 5
7	15	− 13			
9	< 7	− 1			
11	5	4		$h0\bar{1}\bar{0}$	
			2	< 8	4
	$h08$		4	12	− 9
0	< 8	4	6	17	− 15
2	< 8	6	8	10	11
4	16	18			
6	9	2			
				$h011$	
	$h0\bar{8}$		1	< 6	− 1
2	26	− 23	3	< 4	6
4	19	− 18			
6	17	18		$h0\bar{1}\bar{1}$	
8	20	16	1	8	− 9
10	< 6	0	3	< 7	− 2
			5	< 6	4
	$h09$		7	< 5	2
1	14	− 14			
3	< 7	− 3			
5	8	11		$h012$	
			0	< 4	3
	$h0\bar{9}$				
1	< 8	− 6			
3	11	10		$h0\bar{1}\bar{2}$	
5	11	8	2	8	8
7	< 7	− 3	4	6	− 8
9	7	− 4	6	< 4	− 4

The standard deviation of the electron density is 0.53 e/Å^2, estimated from the last difference map. The s. d. of the atomic coordinates were found from the root-mean-square gradients of the same map and the curvatures of the peaks in the final Fourier map [15]. For overlapped atoms, the standard deviations were taken as about twice those which would otherwise have applied. The following values were found: $\sigma(x) = 0.007$ Å, $\sigma(z) = 0.009$ Å for S; $\sigma(x) = 0.003$ Å, $\sigma(z) = 0.004$ Å for Se. For the other atoms, the s. d. varied between 0.02 and 0.07 Å.

STRUCTURE OF THE QUASI-RACEMATE OF (−)-1,2-DITHIANE-3,6-DICARBOXYLIC ACID AND (+)-1,2-DISELENANE-3,6-DICARBOXYLIC ACID AS COMPARED WITH THE CORRESPONDING TRUE RACEMATES

With only one projection, the true distances which can be calculated are those over twofold axes and screw axes. These distances together with some of the corresponding distances of the parent racemates [8,9] are listed in Table 3 below.

The S-S and the Se-Se bond lengths show good agreement in the three compounds. As the atoms also have approximately the same x and z coordinates in I, II and III, as shown in Table 1, it is clear that the constitution of

this quasi-racemate and its parent racemates is very similar. The unit cells of I and III are very like, both having *I*-centered settings with twofold screw axes and twofold axes in the same positions. As seen from Table 3, some distances across these axes show good agreement.

Table 3. Bond lengths in Å.

	I	II	III
S-S	2.069 ± 0.014		2.078 ± 0.016
Se-Se		2.321 ± 0.012	2.332 ± 0.007
C_4-C_5			1.55 ± 0.13
C_4'-C_5'			1.54 ± 0.12

Non-bonded intermolecular distances in Å.

Shortest distances over twofold screw axes		Shortest distances over twofold axes	
S-S in I	6.12	O_1-O_1 in I	2.94
S-S in III	6.15	O_1-O_1 in III	3.12
Se-Se in III	5.99	O_1'-O_1' in III	3.01

In the *C*-centered racemate II, the packing of the molecules is a little different from that in the *I*-centered I and III, there being an interchange of locations of screw axes and symmetry centres at $x = 1/4$ and $x = 3/4$. This allows a closer non-bonded approach of the selenium atoms in II and is also reflected in the orientation of the carboxyl group, which is different in II as compared with I and III. The difference in packing is probably caused by the difference in van der Waals radius between sulphur and selenium, together with a tendency of minimum distance between heavy atoms [9].

The *b*-axis projection of the structure of this quasi-racemate thus confirms the conclusions from space group data that the (+) and (−) molecules are distributed on the same positions as in the parent, true racemates.

The author wishes to express his thanks to Professor Arne Fredga, University of Uppsala, for his kindness in placing samples of the compounds at his disposal.

REFERENCES

1. Centnerzwer, M. *Z. physik. Chem.* **29** (1899) 715.
2. Fredga, A. *Arkiv Kemi Mineral. Geol.* **18B** (1945) No. 4.
3. Fredga, A. *Svensk Kem. Tidsskr.* **67** (1955) 343.
4. Fredga, A. "*The Svedberg 1884 30/8 1944*", Uppsala 1944, p. 261.
5. Hägg, G. "*The Svedberg 1884 30/8 1944*", Uppsala 1944, p. 145.
6. Fredga, A. *Arkiv Kemi Mineral. Geol.* **12A** (1938) No. 27.
7. Foss, O. and Schotte, L. *Acta Chem. Scand.* **11** (1957) 1424.
8. Foss, O. and Reistad, T. *Acta Chem. Scand.* **11** (1957) 1427, and unpublished work.
9. Foss, O. and Johnsen, K. Unpublished work.
10. Viervoll, H. and Øgrim, O. *Acta Cryst.* **2** (1949) 277.
11. Berghuis, J., Haanappel, I. M., Potters, M., Loopstra, B. O., MacGillawry, C. H. and Veenendaal, A. L. *Acta Cryst.* **8** (1955) 478.
12. Thomas, L. H. and Umeda, K. *J. Chem. Phys.* **26** (1957) 293.
13. Dauben, C. and Templeton, D. H. *Acta Cryst.* **8** (1955) 841.
14. James, R. W. *The Optical Principles of the Diffraction of X-Rays* Bell and Sons Ltd, London 1954, p. 149.
15. Jeffrey, G. A. and Cruickshank, D. W. J. *Quart. Revs. (London)* **7** (1953) 335.

Received January 13, 1961.

ACTA CHEMICA SCANDINAVICA 15 (1961) 1223–1230

Gas-Liquid Chromatographic Retention Data for Some *iso*Thiocyanates

AAGE JART

Organisk-kemisk Laboratorium, Royal Technical University, Copenhagen, Denmark

The gas-chromatographic behaviour of 32 *iso*thiocyanates on various stationary phases has been studied. The investigation comprises saturated and unsaturated, branched and unbranched aliphatic *iso*thiocyanates, aromatic *iso*thiocyanates, ω-methylthio-substituted compounds of the type $CH_3S(CH_2)_nNCS$ and *iso*thiocyanates containing ester- or sulfone-groupings. The results are mainly presented in retention time/reciprocal temperature diagrams.

As pointed out in a preliminary communication [1] the occurrence in higher plants of mixtures of mustard oil glucosides, enzymically hydrolyzed to mixtures of *iso*thiocyanates, renders the analytical separation of the latter a matter of considerable interest. But also from a gaschromatographic point of view considerable interest is associated with a study of this group of organic compounds.

It is the purpose of the present communication to present gas-liquid chromatographic retention data for a rather wide selection of *iso*thiocyanates, chromatographed on various stationary phases. Those employed include polar phases (dinonyl phthalate and tritolyl phosphate) as well as unpolar phases (squalane, Apiezon L, silicone grease and elastomer). The results are given as plots of logarithm of retention times *vs.* reciprocal values of the absolute temperature.

APPARATUS

The apparatus used in the present investigation was a Griffin & George gas chromatograph (mark II), equipped with a katharometer detector of limited sensitivity. As many of the *iso*thiocyanates investigated are difficultly accessible, small quantities had to be used, requiring the highest obtainable sensitivity of the detector. The electrical current through the katharometer was fixed at 150 mA, which is near the upper limit of the detector. Furthermore, it was necessary to use a reduced outlet pressure on the column, though this arrangement results in lower efficiency. The outlet pressure was fixed at 40 mm by means of the manostat previously described [2].

Table 1. Summary of the columns used.

Column	Stationary phase	character	Solid support	Column lenght
A	Apiezone L	unpolar	Celite	1.8 m
B	Silicone elastomer	unpolar	Celite	1.8 m
C	Silicone grease	unpolar	firebrick	1.8 m
D	Squalane	unpolar	Celite	1.8 m
E	Dincnyl phthalate	polar	firebrick	0.9 m
F	Tritolyl phosphate	polar	Celite	1.8 m

Initially the samples were introduced by means of a micro syringe through a rubber cap. This system, however, was unsatisfactory and was exchanged with an ampoule breaker of stainless steel placed in a rubber stopper (Fig. 1). A sealed capillary tube provided with a little bulb (4—5 mm Ø) serves as the vessel and is placed at the bottom of the ampoule breaker. After temperature equilibrium has been attained the vessel is crushed by turning the piston. The heating element (30 Watt) is regulated by means of a variable transformer and compensates for the heat loss through the ampoule breaking system.

Some of the compounds investigated (*e.g.* many of the aliphatic *iso*thiocyanates) have so high vapour pressures that heating could be omitted. With the less volatile compounds it was impossible to get satisfactory chromatograms without heating. In all cases it was important to break the ampoule totally. If only the capillary was broken too long a time was required to force the sample completely into the column resulting in tailing.

For the present purpose the described procedure proved satisfactory. It was possible to work practically without any loss of material and a precise weighing of the samples thus was practicable. As an additional convenience, the air in the ampoule gives rise to a reliable zero point on the chromatograms (the air peak).

STATIONARY PHASES ETC.

All columns were made of glass and had a diameter of 6 mm. They were available in U-shaped sections of 90 cm length. In most cases a total column length of 1.8 m was used. As stationary phases polar as well as unpolar systems were employed. In four of the columns, Celite 545, from which most of the finest material had been eliminated, served as the solid support, whereas two other columns were packed with firebrick, sieved to a definite particle size. The properties of the individual columns are listed in Table 1.

Helium was used throughout as a carrier gas at a rate of 1 litre per hour, measured at the column inlet. The standard sample size was 2—5 mg.

ALIPHATIC *iso*THIOCYANATES

The chromatographic behaviour of aliphatic five-component mixtures was studied on six different columns, specified in Table 1. The mixtures had the following compositions:

Methyl *iso*thiocyanate	(1— 3 %)
Ethyl *iso*thiocyanate	(16 %)
*Iso*propyl *iso*thiocyanate	(18—21 %)
Allyl *iso*thiocyanate	(31—32 %)
*Iso*butyl *iso*thiocyanate	(29—33 %)

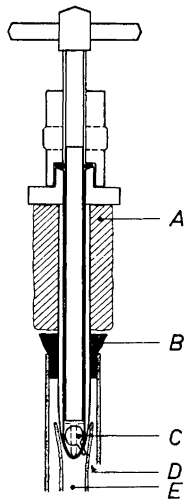

Fig. 1. Ampoule breaker. A, Heating element. B, Rubber stopper. C, Ampoule, D, Carrier gas inlet. E, To the column.

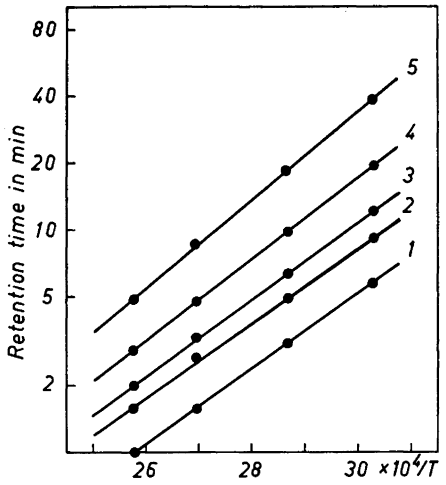

Fig. 2. Effect of temperature on retention of aliphatic *iso*thiocyanates. 1, Methyl. 2, Ethyl. 3, *Iso*propyl. 4, Allyl. 5, *Iso*butyl. Column: Apiezon grease L/Celite.

An expression of column efficiency in terms of theoretical plate number n can be calculated by the equation: $n = 16 \cdot l^2/d^2$, in which l represents the retention time and d the peak width, the last quantity being determined as the segment of base line intercepted by tangents to the inflection points on either side of the peak.

Under the conditions used the squalane column proved to be the most efficient of the unpolar columns employed. But silicone grease on firebrick also appeared to be a good stationary phase for aliphatic *iso*thiocyanates. It should be mentioned that all the employed stationary phases produced well-shaped, symmetric peaks. The components of the above mentioned mixtures emerged from the columns in the same order as listed, *i.e.* according to increasing boiling points.

Although the columns used had only a rather limited number of theoretical plates (100—800), good separation of the components was achieved. The order of appearance of the individual components was not always the same, as apparent from Figs. 2—5. The ordinate is a logarithmic scale giving the retention time in minutes whereas the abscissa represents 10^4 divided by the absolute temperature.

In addition to the above mustard oils, chromatographic runs of propyl, α-methallyl, β-methallyl, *iso*pentyl and 4-pentenyl *iso*thiocyanate were made on the *silicone grease/firebrick column* (Fig. 4). It appears that allyl, propyl and α-methallyl *iso*thiocyanate migrate at almost the same rate. Hence, this column is not suited for their separation. *Iso*butyl and β-methallyl *iso*thiocyanate also run closely together on the column.

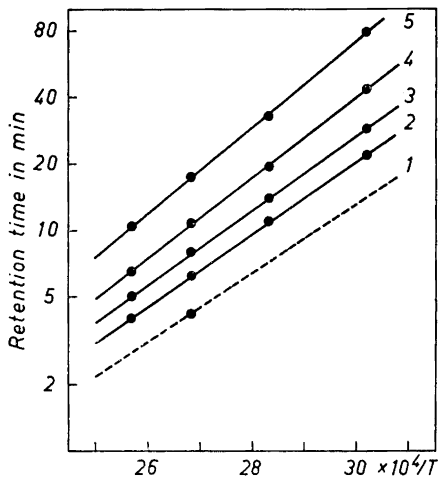

Fig. 3. Effect of temperature on retention of aliphatic *iso*thiocyanates. 1, Methyl (The curve has been estimated from only one point!). 2, Ethyl. 3, *Iso*propyl. 4, Allyl. 5, *Iso*butyl. Column: Silicone elastomer/Celite.

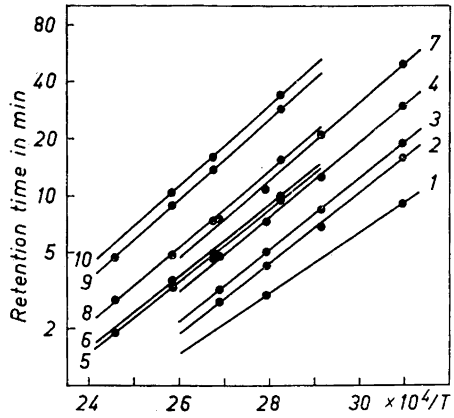

Fig. 4. Effect of temperature on retention of aliphatic *iso*thiocyanates. 1, Methyl. 2, Ethyl. 3, *Iso*propyl. 4, Allyl. 5, Propyl. 6, *α*-Methallyl. 7, *Iso*butyl. 8, *β*-Methallyl. 9, *Iso*pentyl. 10, 4-Pentenyl. Column: Silicone grease/firebrick.

All isothiocyanates mentioned were investigated on the *squalane column*. In this case the investigation was extended to include 3-butenyl, *n*-butyl and *trans*-crotyl *iso*thiocyanate as well as methyl 4-*iso*thiocyanatobutyrate (Fig. 5). It was not possible to distinguish between *iso*butyl and *β*-methallyl *iso*thiocyanate. The *n*-butyl isomeride and *trans*-crotyl *iso*thiocyanate also run at about the same rate with this filling, but between the three compounds: allyl, propyl and *α*-methallyl *iso*thiocyanate a better separation was achieved on the squalane column than on the silicone grease column. Under the conditions used the components emerged from the squalane column in the following order:

Methyl, Ethyl, *Iso*propyl, Allyl, Propyl,
α-Methallyl, *Iso*butyl and *β*-Methallyl,
3-Butenyl, *n*-Butyl, *trans*-Crotyl, *Iso*pentyl,
4-Pentenyl *iso*thiocyanate, and
Methyl 4-*iso*thiocyanatobutyrate.

The above five-component mixture was also investigated on the polar phases dinonyl phthalate (Fig. 6) and tritolyl phosphate (Fig. 7). It appears from the diagrams that the separation on the phthalate of ethyl and *iso*propyl *iso*thiocyanate is not as good as on the unpolar phases. On the tritolyl phosphate column the peaks of the two *iso*thiocyanates actually coincidide. The tritolyl column was used also in experiments with propyl, *α*-methallyl, *β*-methallyl, *n*-butyl, 3-butenyl, *trans*-crotyl, *iso*pentyl and 4-pentenyl *iso*thiocyanate. On a polar stationary phase there will be a tendency for a compound contain-

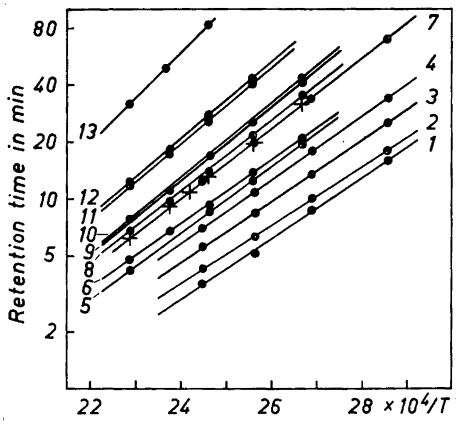

Fig. 5. Effect of temperature on retention of aliphatic *iso*thiocyanates. 1, Methyl. 2, Ethyl. 3, *Iso*propyl. 4, Allyl. 5, Propyl. 6, *a*-Methallyl. 7, *Iso*butyl and *β*-methallyl (+). 8, 3-Butenyl. 9, *n*-Butyl. 10, *trans*-Crotyl. 11, *Iso*pentyl. 12, 4-Pentenyl. 13, Methyl 4-*iso*thiocyanatobutyrate. Column: Squalane/Celite.

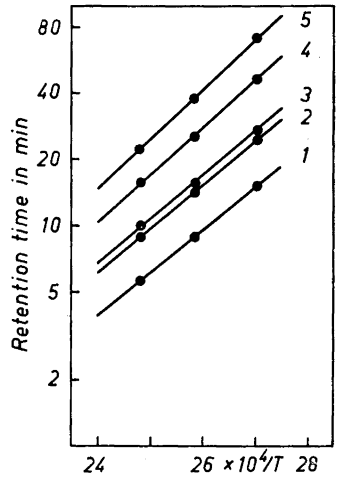

Fig. 6. Effect of temperature on retention of aliphatic *iso*thiocyanates. 1, Methyl. 2, Ethyl. 3, *Iso*propyl. 4, Allyl. 5, *Iso*butyl. Column: Dinonyl phthalate/firebrick.

ing double bonds to be retarded. This also applies to the tritolyl phosphate column where different retention times are observed for *n*-butyl and 3-butenyl *iso*thiocyanate (Fig. 7). In the case of the allyl-propyl system, however, the result is not comparable. According to boiling points, the allyl compound should be expected to emerge before the propyl compound, and this is in fact the case with an unpolar phase. With a polar system, however, the two tendencies will be opposite, and under the present conditions no separation of the two *iso*thiocyanates occurred. The compounds investigated on the tritolyl phosphate column emerged in the following order:

Methyl, Ethyl and *iso*propyl,
Allyl and propyl, *a*-Methallyl, *Iso*butyl,
β-Methallyl, *n*-Butyl, 3-Butenyl,
trans-Crotyl, *Iso*pentyl, and 4-Pentenyl *iso*thiocyanate.

AROMATIC *iso*THIOCYANATES

Some aromatic *iso*thiocyanates were chromatographed on the silicone elastomer column under the conditions already described. The compounds were phenyl, benzyl, 1-phenylethyl, 2-phenylethyl, *o*-methoxybenzyl, *m*-methoxybenzyl, *p*-methoxybenzyl and 3-benzoyloxypropyl *iso*thiocyanate, and they emerged from the column in the above order (Fig. 8). The benzyl and the 1-phenylethyl compounds run closely together, and the

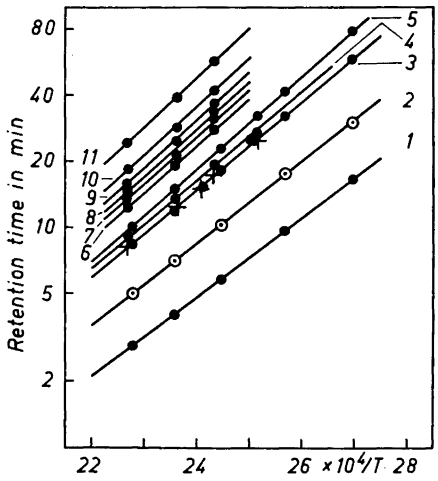

Fig. 7. Effect of temperature on retention of aliphatic *iso*thiocyanates. 1, Methyl. 2, Ethyl and *iso*propyl (o). 3, Allyl and propyl (+). 4, *α*-Methallyl. 5, *Iso*butyl. 6, *β*-Methallyl. 7, *n*-Butyl. 8, 3-Butenyl. 9, *trans*-Crotyl. 10, *Iso*pentyl. 11, 4-Pentenyl. Column: Tritolyl phosphate/Celite.

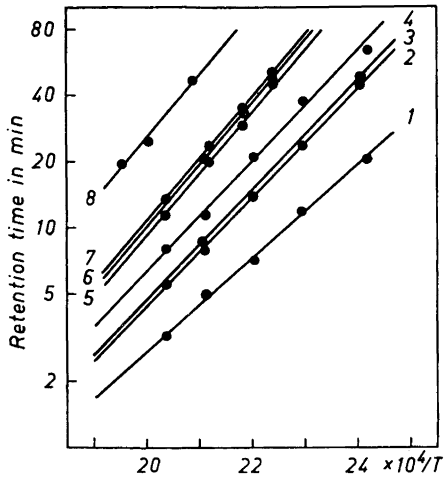

Fig. 8. Effect of temperature on retention of aromatic *iso*thiocyanates. 1, Phenyl. 2, Benzyl. 3, 1-Phenylethyl. 4, 2-Phenylethyl. 5, *o*-Methoxybenzyl. 6, *m*-Methoxybenzyl. 7, *p*-Methoxybenzyl. 8, 3-Benzoyloxypropyl. Column: Silicone elastomer/Celite.

same applies to the three methoxybenzyl *iso*thiocyanates. Difficulties may arise in connection with 3-phenylpropyl *iso*thiocyanate (which is not included in this investigation) as it probably runs closely to *o*-methoxybenzyl *iso*thiocyanate. The next number in this series (4-phenylbutyl *iso*thiocyanate) would be expected to emerge later than all the methoxybenzyl compounds.

METHYLTHIOALKYL *iso*THIOCYANATES

This type of isothiocyanates, characterized by containing a terminal methylthio-grouping in a straight alkyl chain, have the general formula $CH_3S(CH_2)_nNCS$. The eight homologues from 2-methylthioethyl *iso*thiocyanate (n = 2) to 9-methylthiononyl *iso*thiocyanate (n = 9) were chromatographed on the silicone elastomer column (Fig. 9). This column allowed good separations of all the *iso*thiocyanates in eight-component mixtures.

In Fig. 10 the retention times (on a logarithmic scale) of some eight-component mixtures at different temperatures are given as functions of n in the above general formula. As in similar cases (*e.g.* fatty acid methyl esters [2]) straight lines are obtained. This can be of diagnostic value in connection with the identification of *ω*-methylthioalkyl *iso*thiocyanates.

SULFONE *iso*THIOCYANATES

Chromatographic runs in the range 200—240° of the two sulfone *iso*thiocyanates *cheirolin*, $CH_3SO_2(CH_2)_3NCS$, and *erysolin*, $CH_3SO_2(CH_2)_4NCS$, were performed on the silicone elastomer column. It appeared that under these

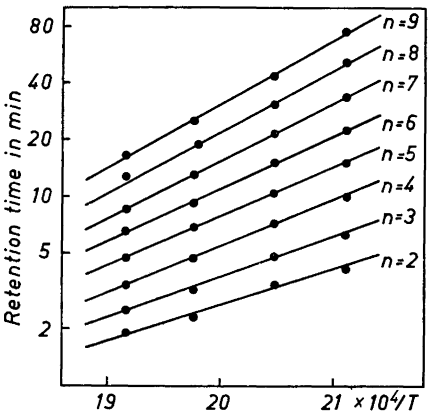

Fig. 9. Effect of temperature on retention of ω-methylthio-substituted *iso*thiocyanates. 2-Methylthioethyl (n = 2). 3-Methylthiopropyl (n = 3). 4-Methylthiobutyl (n = 4). 5-Methylthiopentyl (n = 5). 6-Methylthiohexyl (n = 6). 7-Methylthioheptyl (n = 7). 8-Methylthioöctyl (n = 8). 9-Methylthiononyl (n = 9). Column: Silicone elastomer/Celite.

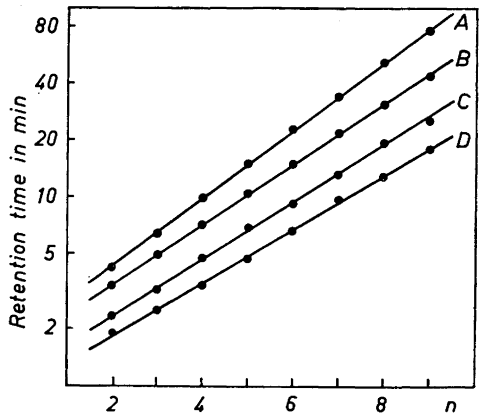

Fig. 10. Retention for methylthioalkyl *iso*thiocyanates as function of n in the general formula: $CH_3S(CH_2)_nNCS$ at different temperatures. A, 201°. B, 215.5°. C, 233°. D, 249°. Column: Silicone elastomer/Celite.

conditions the two sulfones almost coincided with the curves, n = 6 and n = 7, respectively, of Fig. 9. Further work on the gaschromatographic behaviour of the sulfones is planned.

APPLICATION

The present investigation has demonstrated that gas chromatography is a very useful method for separation, quantitative determination and identification of *iso*thiocyanates. Even with columns of a rather low efficiency — as in the present work — it is possible to solve many analytical problems. Under such conditions it is important to employ a stationary phase, which is well suited for the problem in question; perhaps the use of more than one column would be advantageous.

EXPERIMENTAL

Iso*thiocyanates*. The purity of the *iso*thiocyanates used in the present investigation ranged from 90 % to above 99 %. They were all supplied by professor A. Kjær, and references to their syntheses and properties may be found in a recent comprehensive survey [3].

Column A. The stationary phase consisted of 20 % Apiezon grease L on Kieselguhr, prepared as follows: 300 g of Celite 545 (Johns Manville Co., Ltd.) was size-graded by repeated suspension in water in a 5 l beaker and all the material that did not settle out in less than 2 min was discarded. The procedure was repeated twice, and the product was oven-dried for 3—4 h at 150°. The powder was treated in vacuum with sufficient amounts of a solution of Apiezon grease L in chloroform to produce a slurry. The solvent was then slowly

evaporated and the last traces were removed by oven-drying at 110° for 30 min. The material was carefully packed into U-shaped column sections. The pressure drop over the column with a rate of carrier gas of 1.0 l He per hour was 405 mm at 24° and 490 mm at 124°.

Column B. The stationary phase consisted of 25 % silicone elastomer (E 301) on Celite. In this case the suspension procedure was performed only once, and the material was heated in a muffle oven for 3 h at 300° and then washed with conc. hydrochloric acid and with water. After drying for 1 h at 145° the material was treated with the stationary phase as described for column A. The pressure drop over the column with a rate of carrier gas of 1.0 l He per hour was 755 mm at 24°, 935 mm at 124° and 1 130 mm at 224°.

Column C. The stationary phase consisted of 25 % silicone grease on firebrick. The silicone grease was "Dow Corning" from wich a great part of the low-molecular constituents had been removed by precipitation from a 15 % solution in ethyl acetate by adding the same volume of 96 % ethanol. The firebrick was prepared by crushing a brick and sieving the material; the 40 – 50 mesh fraction was used for the preparation of this column. The pressure drop over the column with a rate of carrier gas of 1.0 l He per hour was 405 mm at 24° and 525 mm at 124°.

Column D. The stationary phase consisted of 25 % squalane on Celite, pretreated as described for column B. The squalane was a commercial product (B.D.H.), the purity of which was first controlled by gas chromatography on column C at 270°. The pressure drop over the column with a rate of carrier gas of 1.0 l He per hour was 565 mm at 24° and 690 mm at 124°.

Column E. The stationary phase consisted of 30 % dinonyl phthalate on firebrick. In this case the 60 – 80 mesh fraction was selected for preparation of the column. The pressure drop over the column with a rate of carrier gas of 1.0 l He per hour was 890 mm at 24° and 1 070 mm at 124°.

Column F. The stationary phase consisted of 25 % tritolyl phosphate on Celite. The solid support was pretreated as described for column B, and the stationary phase was prepared by distillation of a technical grade tri-*o*-tolyl phosphate, the fraction boiling over the range 190 – 230° at 0.2 mm being used. The pressure drop over the column with a rate of carrier gas of 1.0 l He per hour was 685 mm at 24° and 850 mm at 124°.

Acknowledgement. I am grateful to prof. Anders Kjær for the generous gift of the *iso*-thiocyanates investigated and for continuous interest in this investigation. The permission of *The Danish Fat Research Institute* to utilize its gaschromatographic apparatus is gratefully acknowledged.

REFERENCES

1. Kjær, A. and Jart, Aa. *Acta Chem. Scand.* **11** (1957) 1423.
2. Jart, Aa. *Fette, Seifen, Anstrichmittel* **61** (1959) 541.
3. Kjær, A. *Fortschr. Chem. org. Naturstoffe* **18** (1960) 122.

Received February 14, 1961.

ACTA CHEMICA SCANDINAVICA 15 (1961) 1231–1238

Electrochemical Behaviour of Copper in Acid Chloride Solution

TOR HURLEN

Central Institute for Industrial Research, Blindern, Oslo, Norway

It has been verified that the anodic dissolution of copper in chloride solutions goes to the monovalent state. This reaction and its reverse cathodic deposition reaction have been studied in various acid chloride solutions by means of a slow galvanostatic technique. The reactions are under all conditions found to obey the relationship

$$V = E_R + (RT/nF)\ln(1 \pm i/i_{lim})$$

for pure concentration polarization and, by stirring experiments, shown to be under diffusion control.

From the effect of the chloride molality on the reversible potential and on the dissolution rate at given potentials, a value of 0.6 is found for the ratio β_2/β_3 between the stability constants of the 1:2 and the 1:3 cuprous chloride complex. On a somewhat uncertain activity estimate, the same data indicate $\beta_2 = 2.9 \cdot 10^5$ and $\beta_3 = 4.8 \cdot 10^5$.

1.0 INTRODUCTION

It has long been known [1,2] that the dissolution of copper in some solutions (*e.g.* perchlorate, sulphate, phosphate, acetate) mainly leads to the cupric state and in other solutions (*e.g.* chloride, bromide, cyanide) mainly to the cuprous state. It is now further well known that the anions involved in the latter case are typical cuprous ion stabilizing complexing agents [3,4].

In a recent series of papers [5], the electrochemical behaviour of copper in solutions of the former type (especially sulphate solutions) has been described. It is there concluded that the transfer between the metallic and the cupric state most probably is a direct one, and that the reaction of the Cu/Cu_{aq}^{++} electrode under stationary conditions are represented by the "kinetic unit equation":

$$2Cu = 2Cu^{++} + 4e^-$$

indicating a double metal ion mechanism which also has been found to govern the Fe/Fe_{aq}^{++} electrode reactions (with the addition of a catalytic hydroxyl ion interaction) [6].

In the present work, analogous studies have been made on the behaviour of copper in chloride solutions, being representative for the latter of the above mentioned solution types. The main purpose of this work is to elucidate the mechanism of the copper/cuprous reactions at *active* copper electrodes, to compare this with what has been found for the copper/cupric reactions, and to determine the effect of the complexing chloride ions on the rate of the former reactions.

2.0 EXPERIMENTAL

The experimental work consists in determinations of current efficiency and potential-time curves for anodic dissolution and cathodic deposition of copper at constant current densities ($10^{-5}-10^{-2}$ A/cm^2) in various pure and mixed solutions of hydrochloric acid, sulphuric acid, potassium chloride, and cuprous chloride.

Some introductory measurements were first made at 25°C with the solutions:

KCl(1 M) + HCl(0 and 0.1 M)

Some more comprehensive series of experiments were then made at 20°C with the solutions:

H_2SO_4(0.1 N) + KCl(0.3, 0.6, 1, 2 and 3 M)

in which the chloride content varies, and with the solutions:

HCl(0.1 M) + KCl(1.899 M) + CuCl(0.001 M)
HCl(0.1 M) + KCl(1.89 M) + CuCl(0.01 M)
HCl(0.1 M) + KCl(1.87 M) + CuCl(0.03 M)
HCl(0.1 M) + KCl(1.8 M) + CuCl(0.1 M)

in which the total chloride content is kept constant at 2 M.

The experimental technique and equipment have been exactly the same as previously described [5,6]. This also applies to the type and the pretreatment of the high purity copper electrodes used [5]. The electrolytes were prepared from Analar quality acids and salts in water distilled from a "pure" fresh water. They were further presaturated with hydrogen [6]. The experiments at 20°C were performed in a thermostated room (± 0.5°C) and those at 25°C in a water thermostat (± 0.1°C). In most experiments, no stirring was applied in the cell. When stirring was applied (this is notified in the text), this was performed with a magnetic stirrer which was placed close to the electrode studied.

The potentials were measured against saturated calomel electrodes, which have been ascribed the potentials [7] 0.245 and 0.242 V on the normal hydrogen scale (NHS) at 20 and 25°C, respectively. No attempts have been made to correct for liquid junction potentials between the test solutions and the saturated potassium chloride solution. According to values tabulated by Milazzo [8], however, these potentials are assumed very low and probably negligible in the present cases.

3.0 RESULTS

The weight measurements clearly show that the anodic dissolution of copper under the present conditions goes to the *cuprous* state. The current efficiency found for this process was in most cases close to 100 %. In some cases, however, the weight loss gave an apparent efficiency slightly higher than 100 %. This mainly occurred at low current densities (long experimental time) in the solutions richest in cuprous chloride, and was found to be due to corrosion. The corrosion correspondingly gave an apparent deposition efficiency slightly lower than 100 %, the anodic and cathodic deviations from this figure mostly being mutually symmetric.

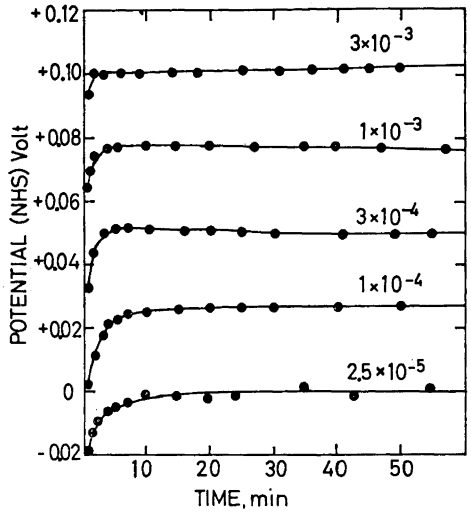

Fig. 1. Anodic potential/time curves for copper at various current densities (A/cm²) in unstirred 0.1 N sulphuric acid + 1 N potassium chloride at 20°C.

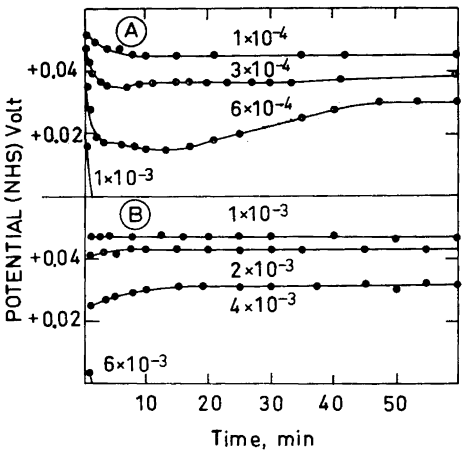

Fig. 2. Cathodic potential/time curves for copper at various current densities (A/cm²) in unstirred (A) and stirred (B) 0.03 M cuprous chloride + 0.1 M hydrochloric acid + 1.87 M potassium chloride at 20°C.

At cathodic current densities exceeding the limiting diffusion current for deposition (see below), loosely adherent powdery deposits (of the type also obtained in sulphate solutions [5]) were formed. This resulted in erratic efficiency values. In these cases, however, there also was hydrogen evolution at the cathodes, whereby the actual deposition efficiency certainly must have been lower than 100 %.

At the highest anodic current densities in the solution of lowest chloride content (0.3 M), the anodic efficiency values obtained were lower than 100 %. This was found to be due to a precipitation of cuprous chloride on the anode surface, making the experimental weight loss too small.

The potential-time curves obtained in the present work are exemplified in Figs. 1 and 2. The initial rise in the anodic potential to a stationary value, as shown by the curves in Fig. 1, is typical for the anodic behaviour observed in the present work with unstirred solutions of no or low copper content. In solutions of higher copper content, this initial rise was usually not observed, the stationary potential mostly prevailing from the very first reading (1/2 or 1 min). This also applies in the case of initially copper free solutions when stirring was applied at the anode, the stirring lowering the stationary potential (see below). This is indicative of a diffusion controlled polarization. The observed potential rise, therefore, is most likely due to an increased concentration of reaction products being built up in the anolyte.

The cathodic potential-time curves shown in Fig. 2, are typical for those obtained under conditions giving nearly 100 % deposition efficiency. These

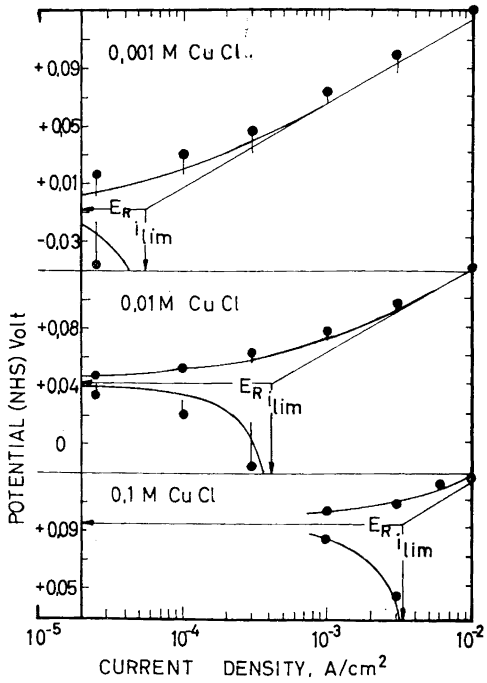

Fig. 3. Tafel diagrams for anodic dissolution and cathodic deposition of copper in unstirred x M cuprous chloride + 0.1 M hydrochloric acid + (1.9−x) M potassium chloride at 20°C.

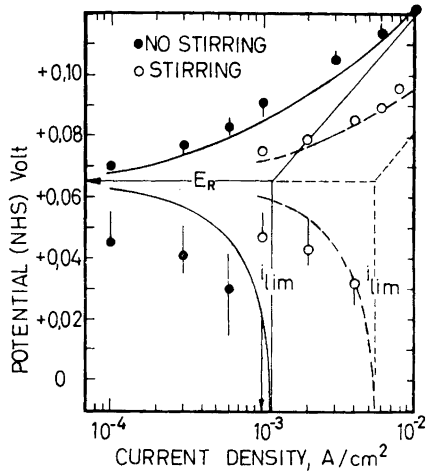

Fig. 4. Tafel diagram for anodic dissolution and cathodic deposition of copper in 0.03 M cuprous chloride + 0.1 M hydrochloric acid + 1.87 M potassium chloride at 20°C (effect of stirring).

curves clearly show the generally observed increasing instability of the deposition potential with increasing current density and the effect of stirring in transferring the onset of this instability to higher current densities. At sufficiently high current densities (dependent on the stirring conditions and the cuprous chloride content of the solution), the cathode potential falls down to values comparable to those for hydrogen evolution on copper at the same current densities in cuprous free solutions of the same pH. This is just what is to be expected when the applied current exceeds the limiting current for deposition.

The polarization data obtained for the anodic dissolution and cathodic deposition of copper under some of the conditions studied, are presented in the from of Tafel diagrams in Figs. 3—6. The various points in these diagrams represent the most stationary potentials observed, and the vertical lines extending from most of these points, indicate the range over which the potential has varied.

The anodic Tafel lines suggested in these diagrams have all been drawn with slopes of:

$$b_a = 2.303\ RT/F \qquad (1)$$

and those in Figs. 3 and 4 have moreover been placed so as to intersect with the corresponding limiting current lines for deposition (i_{lim}) at the observed reversible potential (E_R). Both this intersection and the suggested Tafel slope value are what to be expected for a monovalent metal/metalion electrode when its reactions are under diffusion control. In that case, the polarization behaviour should namely with good approximation be given by [9]:

$$V = E_R + (RT/nF)\ln(1 \pm i/i_{lim}) \quad (2)$$

where, in the double sign, + and − apply to anodic and cathodic reactions, respectively. This equation shows not only the approach to a Tafel line of the above type at high anodic reaction rates ($i >> i_{lim}$), but also how the anodic and cathodic polarization theoretically should be at lower reaction rates. The curves drawn in Figs. 3 and 4 have been constructed from (2) by applying the E_R and i_{lim} values given in the respective diagrams, and they show reasonable agreement with the experimentally obtained polarization data.

The limiting current (i_{lim}) given in Figs. 3 and 4 for the deposition reaction in unstirred solutions of x M cuprous chloride + (1.9 − x) M potassium chloride + 0.1 M hydrochloric acid (x being in the range 0.001—0.1), seems best represented by the formula:

$$i_{lim} = 0.027(\mathrm{Cu})^{0.9} \text{ A/cm}^2 \quad (3)$$

where (Cu) is the total cuprous molality in the solution. This is of the right magnitude for limiting diffusion currents in unstirred solutions, but one should perhaps have expected a somewhat larger concentration exponent [9].

The results in Fig. 4 further show that the limiting current is greatly increased by stirring. It is increased by a factor of about 5 by the stirring applied in the present work. On the basis of (2), one should thus also expect an equal

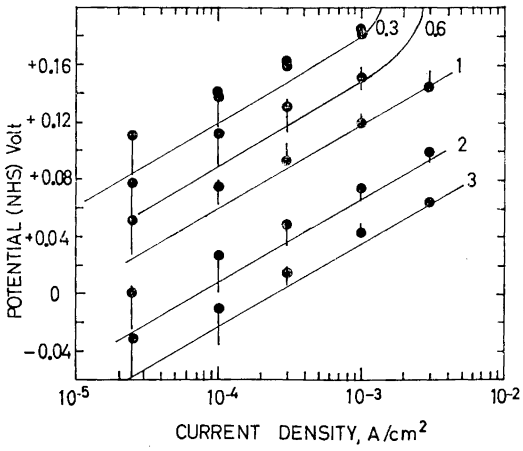

Fig. 5. Tafel diagram for anodic dissolution of copper in unstirred 0.1 N sulphuric acid solutions of potassium chloride at various chloride molalities at 20°C.

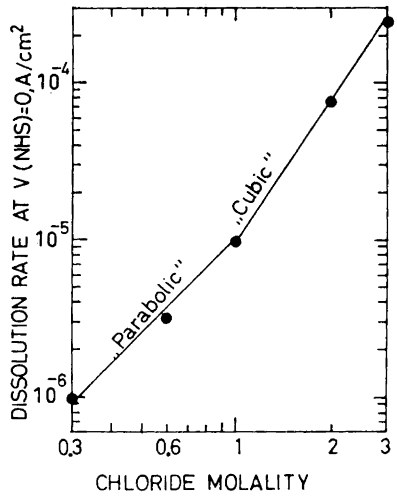

Fig. 6. Effect of the chloride molality on the anodic dissolution of copper in unstirred 0.1 N sulphuric acid solutions of potassium chloride at 20°C.

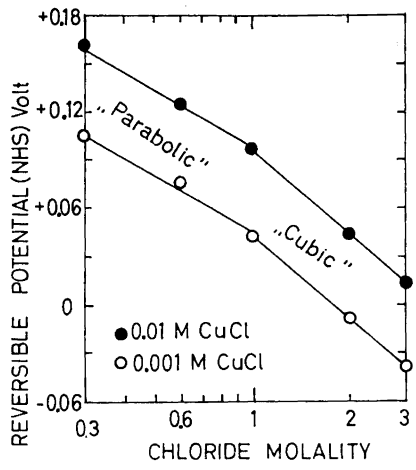

Fig. 7. Effect of the total chloride and cuprous molality on the reversible potential of copper in 0.1 N sulphuric acid solutions of cuprous chloride and potassium chloride at 20°C.

stirring at anodes to shift the anodic polarization curve towards higher current densities by the same factor. That it really is so, is satisfactorily verified by the results in Fig. 4, and also by results obtained in initially cuprous free solutions. This effect of stirring verifies that the reactions are under diffusion control.

The acidity of the electrolyte was found to have no effect on the anodic polarization of copper in 1 M chloride solutions of pH from about 1 to about 7.

The chloride content greatly affects the anodic dissolution reaction. This is demonstrated for unstirred solutions by the results in Fig. 5 and more explicitly shown in Fig. 6, where the rate of anodic dissolution at the standard hydrogen potential (as found by interpolation and extrapolation of the Tafel lines in Fig. 5) is plotted *versus* the chloride molality. The straight lines in Fig. 6 correspond to a parabolic and a cubic relationship at low and high chloride concentrations, respectively. When also (1) is considered, these relationships may be written (20°C, no stirring):

$$i = 9.9 \cdot 10^{-6}(\mathrm{Cl})^2 \exp(FV/RT) \text{ A/cm}^2 \text{ at } (\mathrm{Cl}) < 1 \text{ M} \quad (4a)$$

$$i = 9.9 \cdot 10^{-6}(\mathrm{Cl})^3 \exp(FV/RT) \text{ A/cm}^2 \text{ at } (\mathrm{Cl}) > 1 \text{ M} \quad (4b)$$

where V is the electrode potential referred to the normal hydrogen scale, and (Cl) is the total chloride molality. That the numerical factors in these two equations are mutually equal, is a simple consequence of the transition between the two relationships occurring very near to a chloride molality of 1 (Fig. 6).

The reversible potential (E_R) of copper in a series of hydrogen saturated 0.1 N sulphuric acid solutions of cuprous and potassium chloride at 20°C (in addi-

tion to those described above) has been measured as described in the third paper of Ref.[5]. The results are presented in Fig. 7, where the straight lines correspond to the relationships:

$$E_R = 0.200 + (RT/F)\ln \frac{(Cu)^{0.9}}{(Cl)^2_i} \text{ Volt at } (Cl) < 1 \text{ M} \quad (5a)$$

$$E_R = 0.200 + (RT/F)\ln \frac{(Cu)^{0.9}}{(Cl)^3} \text{ Volt at } (Cl) > 1 \text{ M} \quad (5b)$$

where (Cu) and (Cl) mean the total cuprous and chloride molality, respectively. The cuprous molality exponent of 0.9 is first of all found from the reversible potential data in Figs. 3 and 4.

The results in (5) show a quite analogous chloride dependence to those in (4). They further indicate the transition in this dependence at the chloride molality of 1 to be due to a reversal in the mutual activity relationship of the complexes $CuCl_2^-$ and $CuCl_3^{--}$ at this chloride concentration. As the activity of potassium chloride in a 1 M solution is about 0.6 (Ref.[10]), this means that we for the stability constants of these complexes should have:

$$\beta_2/\beta_3 = 0.6 \quad (6)$$

where β_n is defined by the activity relationship $(CuCl_n^{(n-1)-})/(Cu^+)(Cl^-)^n$. By further assuming the activity coefficients of the complexes also to be 0.6 in the 1 M chloride solution, and adopting the value 0.521 V for the standard Cu/Cu^+_{aq}-potential, we have from (5a) and (6), when neglecting the exponent of 0.9 : $\beta_2 = 2.9 \cdot 10^5$ and $\beta_3 = 4.8 \cdot 10^5$. This is not far from many values previously given for these stability constants [3,4], but the rough activity estimate makes the values somewhat uncertain.

The results in (3), (4), and (5) may be used for a further check of the validity of the theoretical equation (2) for pure concentration polarization in the present cases. By combining these results, we easily have:

$$V = (E_R - 0.001) + (RT/F)\ln(i/i_{lim}) \text{ Volt} \quad (7)$$

Remembering that the polarization data in (4) apply to cases where $i/i_{lim} \gg 1$, this result must be regarded an excellent confirmation of the anodic dissolution of copper in all the applied chloride solutions obeying (2) and, thereby of it exhibiting pure concentration polarization.

4.0 DISCUSSION

The weight changes, the anodic Tafel slopes, the reversible potentials, and the chloride ion effect observed in the present work, are mutually in agreement in showing that copper in acid (and neutral) chloride solutions behaves as a copper/cuprous electrode, the cuprous ions being complexed by chloride ions. The anodic and cathodic polarization data, the cathodic limiting current data, and the reversible potential data obtained, combine excellently with

each other to show that the reactions of this electrode in unstirred solutions give rise to a pure concentration polarization. This is further supported by the observed effect of stirring on the polarization. The stirring experiments indicate this type of polarization to be due to slow diffusion and to be predominant even at stirring rates giving a five-fold increase of the limiting current.

These results obviously mean that the electrode reactions themselves and their possibly accompanying chemical reactions are fast compared to the transport of cuprous species in the electrolyte to (cathodic) and from (anodic) the electrode surface. In such a case, the polarization is independent of the mechanism of the electrode reactions (as demonstrated by the absence of kinetic parameters as i_o, a, and ν in eqn. (2) above) and does, therefore, not reveal anything exact of their kinetics. The only conclusion one in this respect can draw from the above results, is:

$$i_o > 5i_{lim,o} \tag{8}$$

where i_o is the exchange current, and $i_{lim,o}$ is the cathodic limiting current in unstirred solution. This is contrary to what is found for the copper/cupric electrode [5], and it is easily seen by comparison that this is mainly due to the immensely stimulating effect of the chloride ions on the anodic dissolution of copper, and of this stimulation being more pronounced than the possible retardation in deposition ability when going from cupric ions to complex cuprous chloride species.

To the author's knowledge, this is the first example in which the reactions of a solid metal/metalion electrode has been proved to be under diffusion control and thereby to exhibit pure concentration polarization. Several examples of such a behaviour exist for amalgam electrodes [9], however, and a quite analogous behaviour has recently been found in our laboratory for copper in bromide solutions [11].

Acknowledgement. The author is much indebted to Miss E. Huseby and Miss T. Tönderum for technical assistance, to various members of the staff at the Central Institute for Industrial Research for valuable discussions, and to the *U.S. Department of Army, European Research Office,* for financial support.

REFERENCES

1. Bolton, W. *Z. Elektrochem.* **2** (1895) 185.
2. Abel, E. and Redlich, O. *Z. Elektrochem.* **34** (1928) 323.
3. Latimer, W. M. *Oxidation Potentials (2nd ed.)*, Prentice-Hall, New York 1952.
4. Bjerrum, J., Schwarzenbach, G. and Sillén, L. G. *Stability Constants (Part II)*, The Chemical Society, London 1958.
5. Hurlen, T. *Acta Chem. Scand.* **15** (1961) 630, 621, and 615.
6. Hurlen, T. *Acta Chem. Scand.* **14** (1960) 1533.
7. deBethune, A. J., Licht, T. S. and Swendeman, N. *J. Electrochem. Soc.* **106** (1959) 616.
8. Milazzo, G. *Elektrochemie*, Springer, Wien 1952, p. 98.
9. Vetter, K. J. *Elektrochemische Kinetik*, Springer, Berlin/Göttingen/Heidelberg 1961.
10. Robinson, R. A. and Stokes, R. H. *Electrolyte Solutions (2nd ed.)*, Butterworths, London 1959.
11. Hurlen, T. *Acta Chem. Scand. In the press.*

Received February 3, 1961.

ACTA CHEMICA SCANDINAVICA 15 (1961) 1239–1245

Dissolution of Copper by Oxidation Agents in Acid Chloride Solution

TOR HURLEN

Central Institute for Industrial Research, Blindern, Oslo, Norway

Investigations have been made on the dissolution of copper by cupric, ferric, and permanganate ions in unstirred acid chloride solutions. Except at relatively low chloride concentrations, where precipitation of cuprous chloride on the metal surface complicates the matter, the corrosion rate is determined by the limiting reduction rate of the oxidation agent and the corrosion potential (E_c) varies with this rate (i_c) and the chloride concentration (Cl) according to:

$$\mathrm{d}\, E_c/\mathrm{d} \ln i_c = RT/F \text{ at constant (Cl)}$$

$$\mathrm{d}\, E_c/\mathrm{d} \ln (\mathrm{Cl}) = nRT/F \text{ at constant } i_c$$

where n is 2 at chloride concentrations below about 1 M and 3 at higher concentrations. This is independent of the oxidation agent applied, whereas the actual values of the corrosion potential at given corrosion rates and chloride concentrations to some extent depend on the properties of the oxidation agent. All results are well accounted for by a mixed potential treatment of the red/ox and $Cu/CuCl_n^{(n-1)-}$ electrode, regarding the former to operate at its cathodic limiting current and the latter to exhibit pure concentration polarization.

1.0 INTRODUCTION

Following previous work [1] on the behaviour of the copper/cuprous electrode under galvanostatic conditions in non-oxidizing acid chloride solutions, studies have been made on the dissolution of this metal by cupric, ferric, and permanganate ions in otherwise the same type of solutions. This work is a continuation of analogous studies on copper in acid sulphate solutions [2] and on iron in acid solutions [3] and is aiming at contributing to the elucidation of metal dissolution reactions and their possible interactions with cathodic reduction reactions simultaneously occurring at the same metal surface.

Much data are available on the rate of dissolution of copper in chloride solutions of oxidation agents. A comprehensive study has recently been made by Ferrari [4], who also gives an excellent survey of the literature on the subject. However, it does not seem to be much data on the correlation between the dissolution rate and the mixed potential of copper in such solutions, data which are necessary for the evaluation aimed at in the present work.

2.0 EXPERIMENTAL

The experimental work consists in determinations of the dissolution rate (corrosion rate) and the mixed potential (corrosion potential) of copper in unstirred solutions of cupric chloride (0.005 to 0.1 M), ferric chloride (0.005 to 0.3 M), and potassium permanganate (0.001 to 0.03 M), respectively, in 0.1 N sulphuric acid + potassium chloride to various total chloride concentrations (0.1—3 M) at 20°C (room thermostated to ± 0.5°C).

The solutions were prepared from A.R. quality acid and salts in water distilled from a "pure" fresh water and the experiments were performed with the solutions exposed to air. The high purity copper sheets used, were of the same type and were given the same pretreatment as previously described [2].

The rate measurements were performed partly by the continuous quartz helix technique previously described [2], and partly by determining the weight change of copper sheets over given experimental periods (mostly from 1 to 3 hours). Sheets of 14 cm^2 geometrical surface area were used in these experiments and each of them were exposed to 600 ml test solution.

The potential measurements were carried out as previously described [2] (sheets of 2 cm^2 geometrical surface area in 100 ml test solution). The saturated calomel electrode used has been ascribed the potential [5] 0.245 V on the normal hydrogen scale (NHS) at 20°C. No attempts have been made to correct for the (possibly negligible [6]) liquid junction potentials between the test solutions and the saturated potassium chloride solution.

3.0 RESULTS

The rate curves obtained were mostly linear and the potential-time curves usually showed very nearly time independent stationary potentials (as in Figs. 3 and 4 of Ref.[2]) except at the higher ox-ion concentrations in the solutions of low chloride content. This deviating behaviour, which was strongest in the cupric chloride solutions, was found to be accompanied by a precipitation of cuprous chloride on the copper surface. In some cases, this precipitation even resulted in a weight gain instead of a weight loss of the copper sheets. More detailed investigations are now being made on this matter, which will be more thoroughly discussed in a separate paper, whereby we here mainly will deal with the dissolution occurring under entirely active conditions.

In Figs. 1—3, values obtained for the dissolution rate and the mixed potential of copper at various ox-ion (Cu^{++}, Fe^{+++}, and MnO_4^-, respectively) and chloride ion concentrations are presented in the form of Tafel diagram plots. The dissolution rate is there expressed in A/cm^2, the current density values having been calculated from the weight loss data on the basis of the dissolution being solely to the monovalent state [1]. Solid curves are drawn through points applying to given total chloride ion concentrations, and dashed curves through points applying to given ox-ion concentrations. Except for the above mentioned deviations in the upper part of these diagrams (see especially Fig. 1), it is obvious that these curves essentially represent Tafel lines for the anodic dissolution reaction and limiting current curves for the cathodic ox-ion reduction, respectively.

The anodic Tafel lines in Figs. 1—3 have all been drawn with a slope of

$$b_a = 2.303\ RT/F \qquad (1)$$

i.e. 58 mV per logarithmic unit in dissolution rate at 20°C. This is the same as

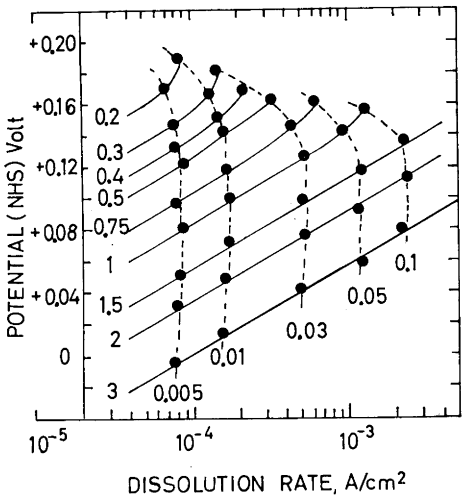

Fig. 1. Dissolution rate and corrosion potential of copper in unstirred 0.1 N sulphuric acid solutions of cupric sulphate (0.005—0.1 M) and potassium chloride (0.2—3 M) at 20°C.

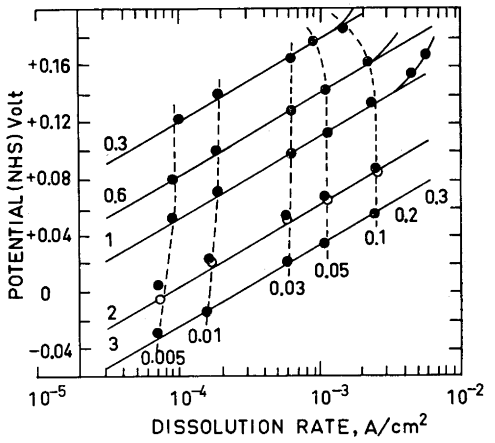

Fig. 2. Dissolution rate and corrosion potential of copper in unstirred 0.1 N sulphuric acid solutions of ferric chloride and potassium chloride at various ferric ion (0.005—0.3 M) and chloride ion (0.3—3 M) concentrations. 20°C.

has previously been found for the anodic dissolution of copper in chloride solutions by amperostatically applied currents [1].

From the position of the anodic Tafel lines is further seen that the rate of the anodic dissolution reaction at given potentials distinctly increases with increasing chloride ion concentration. This effect of the chloride ions is more explicitly shown in Fig. 4, where the rate of the anodic dissolution reaction at the potential of the standard hydrogen electrode is plotted as function of the chloride ion molality in solutions of any of the three oxidation agents applied. The straight lines drawn in this diagram correspond to a parabolic and a cubic relationship:

$$i_a = k_p(Cl^-)^2 \exp(FV/RT) \quad (2)$$

$$i_a = k_c(Cl^-)^3 \exp(FV/RT) \quad (3)$$

at low and high chloride concentrations, respectively. This is analogous to what has previously been obtained from experiments with amperostatically applied currents [1]. In (2) and (3), regard is also made of (1).

The results in Fig. 4 further clearly show that the rate of the anodic dissolution reaction is not only a function of the chloride concentration and the electrode potential, but that it to some extent also depends on how the electrode-potential is obtained. Thus, at equal chloride ion concentrations and potentials, the rate is slightly higher in the permanganate solutions and appreciably lower in the cupric solutions than in the ferric solutions, in which it is nearly

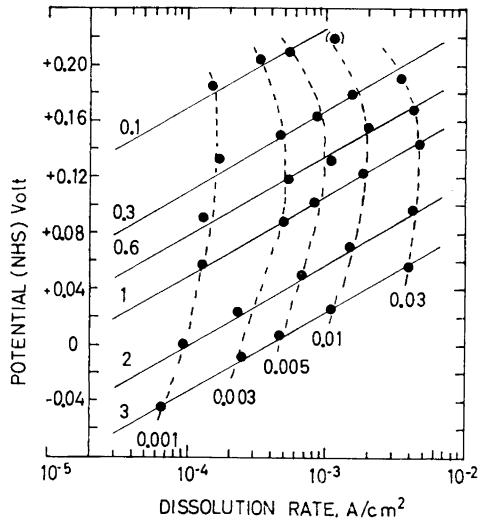

Fig. 3. Dissolution rate and corrosion potential of copper in unstirred 0.1 N sulphuric acid solutions of potassium permanganate (0.001—0.03 M) and potassium chloride (0.1—3 M) at 20°C.

equal to what is found for the pure anodic dissolution by applied current in non-oxidizing chloride solutions [1]. This is quantitatively expressed by the values given in Table 1 for the anodic rate constants k_p and k_c defined by (2) and (3). These data refer to *concentration* values (molality) and not activity values for the chloride ions, and to hydrogen scale values for the potential.

Table 1. Values of the anodic rate constants k_p and k_c under various conditions at 20°C (in $\mu A/cm^2$).

Condition	Mixed potentials Cu++	Fe+++	MnO_4^-	Pure dissolution potentials (Ref.[1])
k_p	2.5	10	13	9.9
k_c	3.4	10	13	9.9

The limiting rate of the various cathodic reduction reactions, as given by the dashed curves in Figs. 1—3, shows a tendency to decrease with increasing chloride ion concentration. This tendency is weak for the cupric and the ferric reduction (Figs. 1—2), but appreciable for the permanganate reduction (Fig. 3). From the same diagrams is further seen that the limiting rates are nearly proportional to the ox-ion concentration. This is more explicitly shown in Fig. 5, where the maximum dissolution rate at various ox-ion concentrations is plotted *versus* the ox-ion concentration. The straight lines drawn there correspond to the following relationships:

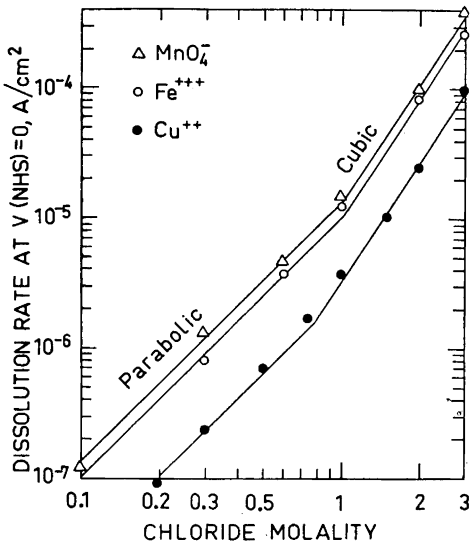

Fig. 4. Effect of the chloride ion concentration and various balancing cathodic reduction reactions on the rate (at given potential) of the simultaneous anodic dissolution reaction of copper.

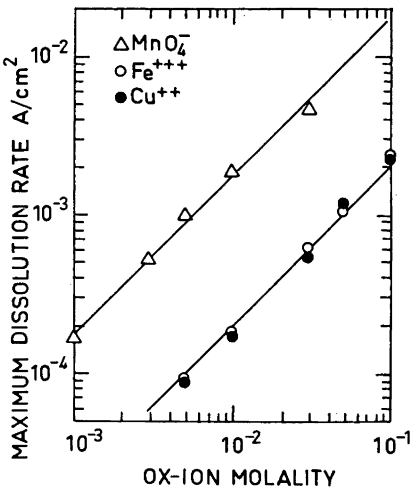

Fig. 5. Maximum dissolution rate of copper by various oxidation agents as function of their concentration in the applied unstirred solutions. (Equivalent to the limiting reduction rate of the oxidation agents).

$$i_{lim} = 0.020 \cdot 1 \cdot (Cu^{++}) \quad A/cm^2 \tag{4}$$
$$i_{lim} = 0.020 \cdot 1 \cdot (Fe^{+++}) \quad A/cm^2 \tag{5}$$
$$i_{lim} = 0.036 \cdot 5 \cdot (MnO_4^-) \quad A/cm^2 \tag{6}$$

for the three cathodic reduction processes under the present conditions. Quite similar equations are also valid at various constant chloride concentrations. The first numerical factor in these equations, especially the one in (6), varies somewhat with the chloride ion concentration, however. It is further possible that the results would be better represented by functions having an ox-ion concentration exponent slightly higher than 1 (see Fig. 5).

The results in (4)—(6) are of the right type and magnitude for limiting diffusion currents in unstirred solutions. For such cases, Kortüm and Bockris [7] give as an average at 25°C:

$$i_{lim} = 0.025 \cdot n \cdot c \ A/cm^2 \tag{7}$$

based on an average diffusion coefficient of $1.3 \cdot 10^{-5}$ cm²/sec for the reacting species. The above results may thus be explained simply by assuming other values for the actual diffusion coefficients. On the basis of what is known about diffusion of electrolytes [8–10], it is not surprising that the permanganate diffusion is appreciably faster than the cupric and the ferric diffusion, and that the

latter two are mutually equal. It is namely likely that $FeCl^{++}$ is the main ferric species present in these relatively strong chloride solutions [11]. The present results in ferric chloride solutions and the previous results in ferric sulphate solutions [2] further show that the limiting rate of the ferric reduction is almost twice as high in the former as in the latter case (0.020 : 0.011). There does not seem to be any direct diffusion data available for checking this relationship. However, in dilute solutions at 25°C, magnesium chloride and magnesium sulphate have diffusion coefficients [8-10] of 1.2 and $0.7 \cdot 10^{-5}$ cm^2/sec, respectively. The ratio between these values is not far from that indicated above for the corresponding ferric compounds.

4.0 DISCUSSION

The correlating rate and potential measurements made in the present work, reveal cathodic limiting curves for the reduction of the oxidation agents applied and anodic polarization curves for the dissolution of copper under the applied conditions.

The cathodic limiting curves obtained clearly show that the rate of dissolution of copper by permanganate, ferric, and cupric ions in unstirred chloride solutions of sufficiently high chloride content is controlled by the diffusion of the oxidation agent from the solution to the metal surface. This is in accordance with what is to be expected (at least for the permanganate and the ferric solutions) from previous results on metal dissolution processes of this type in general (recently reviewed by Hoar [12]) and on copper in ferric sulphate solutions in particular [2].

The anodic polarization curves obtained show exactly the same Tafel slope and the same type of chloride dependence as previously found for the anodic dissolution of copper by applied currents in unstirred, non-oxidizing chloride solutions [1]. Together with the values obtained for the anodic rate constants k_p and k_c (see Table 1), this strongly supports the previous conclusion that the complex copper/cuprous-chloride electrode exhibits pure concentration polarization in unstirred solutions. On this basis, it is further easily understandable why the above mentioned rate constants are appreciably lower in the cupric solutions than in the other oxidizing and corresponding non-oxidizing solutions. This may simply be due to the extra amount of cuprous species produced and chloride ions consumed (by complex formation) at the copper surface by the cupric reduction. At given dissolution rates, this reduction reaction should namely be expected to make the potential determining activity relationship $(CuCl_n^{(n-1)-})/(Cl^-)^n$ at the copper surface more han twice as high as in the case of pure anodic dissolution in non-oxidizing solutions, and thereby to lower the anodic rate constant by the same factor. The values of 3 to 4 obtained for this factor (see Table 1) do therefore not seem unreasonable, and it seems logical that this factor should be slightly higher for the parabolic (low chloride concentrations) than for the cubic (high chloride concentrations) rate constant. The slightly higher value found for these rate constants by the permanganate reaction than by applied current, may similarly be due to the concentration polarization being lowered by a possible homogeneous reaction of cuprous chloride complexes with permanganate ions in the diffusion layer.

As a conclusion, it may thus merely be said that all the observations made in the present work on the dissolution of copper by oxidation agents in unstirred acid chloride solutions, are well accounted for by regarding it a mixed $Cu,nCl^-/CuCl_n^{(n-1)-}$ ($n = 2$ above and 3 below chloride concentrations of about 1 M) and red/ox electrode, the latter operating at its cathodic limiting current and the former exhibiting pure concentration polarization. In cases like this, both the corrosion rate and the corrosion potential are independent of the exact mechanism of the electrode reactions occurring, and can therefore reveal neither their kinetics nor their possible interaction at the metal surface.

Acknowledgement. The author is much indebted to Miss E. Huseby and Miss T. Tönderum for technical assistance, to various members of the staff at the Central Institute for Industrial Research for valuable discussions, and to the *U.S. Department of Army, European Research Office*, for financial support.

REFERENCES

1. Hurlen, T. *Acta Chem. Scand.* **15** (1961) 1231.
2. Hurlen, T. *Acta Chem. Scand.* **15** (1961) 615.
3. Hurlen, T. *Acta Chem. Scand.* **14** (1960) 1555.
4. Ferrari, H. M. *Thesis* University of Michigan, 1958.
5. deBethune, A. J., Licht, T. S. and Swendeman, N. *J. Electrochem. Soc.* **106** (1959) 616.
6. Milazzo, G. *Elektrochemie*, Springer, Wien 1952, p. 98.
7. Kortüm, G. and Bockris, J. O'M. *Textbook of Electrochemistry*, Elsevier, Amsterdam/Houston/London/New York 1951, p. 405.
8. Harned, H. S. and Owen, B. B. *The Physical Chemistry of Electrolytic Solutions* (*3rd ed.*), Reinhold, New York 1958.
9. Robinson, R. A. and Stokes, R. H. *Electrolyte Solutions* (2nd ed.), Butterworths, London 1959.
10. Parsons, R. *Handbook of Electrochemical Constants*, Butterworths, London 1959.
11. Bjerrum, J., Schwarzenbach, G. and Sillén, L. G. *Stability Constants* (*Part II*), The Chemical Society, London 1958.
12. Hoar, T. P. in *Modern Aspects of Electrochemistry No. 2* (ed. J.O'M Bockris), Butterworths, London 1959, Chapter 4.

Received February 3, 1961.

ACTA CHEMICA SCANDINAVICA 15 (1961) 1246–1254

Film Growth on Copper in Acidified Cupric Chloride Solutions

TOR HURLEN

Central Institute for Industrial Research, Blindern, Oslo, Norway

The reaction of copper with cupric ions in chloride containing acid solutions is accompanied by a precipitation of cuprous chloride on the metal surface when the chloride concentration is below a certain limit depending on the cupric concentration. This precipitation and its effect on the above reaction have been studied mainly in 0.1 N sulphuric acid + 0.1 M cupric sulphate + x M potassium chloride by means of rate measurements (quartz helix, intermittent weighing, dissolution of precipitated layers) and potential measurements (corrosion potential). In these solutions, the reaction of copper with cupric ions to cuprous species becomes noticeable at x-values above about 0.01 and gives cuprous chloride precipitation at all x-values up to about 1.5. The reaction rate goes through a maximum around $x = 0.05$ and a minimum around $x = 0.125$ and becomes essentially independent of x at x-values above 1.5. Also the amount of cuprous chloride precipitated on the surface in given times shows a maximum at about $x = 0.05$. These transitions in chloride ion dependence are further reflected in the corrosion potential.

1.0 INTRODUCTION

It is well known that copper in cupric ion containing chloride solutions does not act as a reversible copper/cupric electrode, but as an irreversible and mixed copper/cuprous and cupric/cuprous electrode, the cuprous ions being complexed with chloride ions [1–3]. When copper is immersed in such a solution, therefore, it will react with the cupric and the chloride ions to form various cuprous chloride species.

In a previous work [4], this reaction has been studied mainly under conditions of negligible cuprous chloride precipitation. The pure anodic dissolution reaction in corresponding cupric free solutions has also been studied [5]. The former investigations show that cuprous chloride is precipitated on the copper surface when the cupric concentration is high enough (dependent on the chloride concentration). The present work is aiming at elucidating this cuprous chloride precipitation and its effect on the reaction of copper with cupric ions in chloride solutions. To avoid a concurrent cuprous oxide formation, the investigations have been performed with acid solutions of pH about 1.

Previous work related to this matter is especially due to Cooper *et al.*[6,7], who have studied the formation of cuprous chloride films on copper anodes in hydrochloric acid solutions.

2.0 EXPERIMENTAL

The main part of the experimental work consists in determinations of the weight change of copper sheets in various cupric ion containing chloride solutions (specified below) and of their successive weight loss in 1 N hydrochloric acid. The latter weight loss represents the dissolution of the cuprous chloride layer formed on the sheets during their immersion in the former solutions.

The weight change measurements have been performed both by the semi-continuous quartz helix technique previously described [8] and by intermittent weighing. From quartz helix measurements, it was found that even the thickest cuprous chloride layers encountered were completely dissolved in the 1N hydrochloric acid solution in less than 15 min. A duration of 15 min was therefore chosen for these dissolution runs, whereas the duration of the actual reaction experiments has varred mostly from 2 to 120 min. The dissolution runs were accompanied by blank tests, none of which showed any noticeable dissolution of the copper metal itself. All these experiments have been performed with sheets of 14 cm^2 total surface area (geometrical) exposed to 500 ml solution. The quartz helix used had a sensitivity of 0.505 mm/mg. Because of buoyancy, no attempts have been made to transfer the helix readings to actual weight changes, whereby these measurements only give semiquantitative indications of the weight changes occurring.

A few corrosion potential measurements have been made in the way previously described [8], and also a few preliminary radio-tracer experiments. The latter experiments have been performed partly with neutron activated copper sheets in chloride solutions of inactive cupric salts and partly under opposite activation conditions. This type of measurements is now being continued and extended and will only be touched upon in the present work. A more complete description of the tracer technique will therefore be postponed.

The same type of annealed and etched sheets of high purity copper as previously described [8] have been used, and the solutions have been made from A.R. quality acids and salts in water distilled from a rather pure tap water. All the experiments have been performed at room temperature (about 22°C) and no stirring have been applied.

3.0 RESULTS

From X-ray diffraction measurements directly on the surface of copper sheets having been immersed in some of the solutions to be mentioned below, clear evidence is found for the presence of cuprous chloride. The diffractograms do not show reflections from any other compound.

The total weight change. The weight change of copper sheets as indicated by quartz helix measurements during their immersion in various cupric and chloride containing acid solutions is shown in Figs. 1 and 2. The zero point position of the quartz helix has in these cases been determined by a somewhat uncertain free hand extrapolation of the readings to zero time in a linear plot. The same uncertainty is thus attached to the ordinate position of the "helix extension"/time curves, but not to the variations shown by these curves from the first reading on.

The curves in Fig. 1 apply to solutions of 0.1 N hydrochloric acid + x M cupric chloride (x = 1, 0.3, and 0.1). In all these solutions, the reaction of copper with cupric ions is accompanied by a precipitation of cuprous chloride on the metal. During a first stage, this gives rise to a weight increase of the

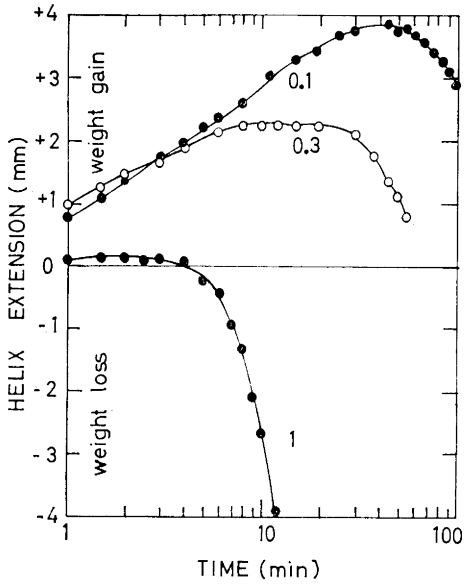

Fig. 1. Helix extension curves for copper (14 cm²) in 0.1 N hydrochloric acid + x M cupric chloride at $x = 1$, 0.3, and 0.1.

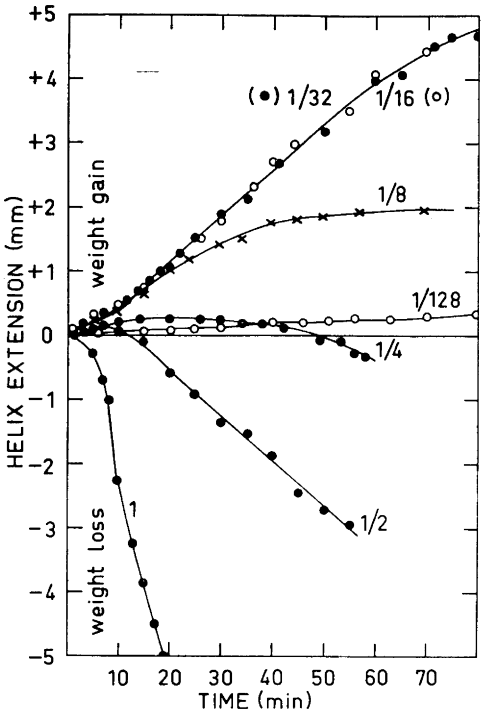

Fig. 2. Helix extension curves for copper (14 cm²) in 0.1 N sulphuric acid + 0.1 M cupric sulphate + x M potassium chloride at various values of x.

copper sheets, a weight increase which apparently is not far from obeying a direct logarithmic time dependence. Successively, however, the weight increase comes to an end, whereafter the further reaction makes the sheets loose in weight. In the solutions applied, the initial weight gain is less distinct and the weight loss starts earlier the higher is the cupric chloride concentration.

The curves in Fig. 2 apply to solutions of 0.1 N sulphuric acid + 0.1 M cupric sulphate + x M potassium chloride $x = 1$, 1/2, 1/4, 1/8, 1/16, 1/32, and 1/128). Also in these solutions it is quite clear that a weight influencing precipitation of reaction products occurs on the copper surface. The film growth seems most pronounced at some intermediate chloride concentrations (1/32—1/16 M) and becomes less pronounced to both sides of this chloride range. At the lower side, there still is a weight increase all over the experimental time applied, but this increase becomes very slow at low chloride concentrations (see the curve for $x = 1/128$). At the higher side, the helix extension curves are essentially of the same type as described above for the hydrochloric acid solutions of cupric chloride. The initial weight gain becomes here less and less distinct with increasing chloride concentration and is not observable at chloride

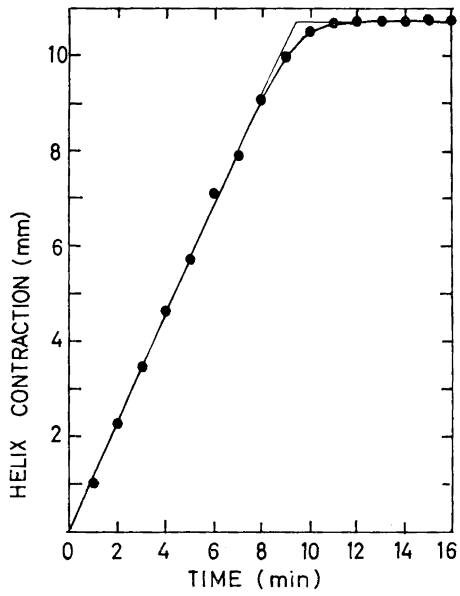

Fig. 3. Helix contraction curve for the dissolution in 1 N hydrochloric acid of the cuprous chloride layer formed on a copper sheet (14 cm²) during one hours immersion in 0.1 N sulphuric acid + 0.1 M cupric sulphate + 0.05 M potassium chloride.

concentrations above 1 M. Even at 1 M, however, there probably is a rate affecting precipitation on the copper surface. The dissolution rate is here distinctly slower than at higher chloride concentrations at which it becomes independent of the chloride concentration [4]. As is evident from previous results (see especially Fig. 1 in Ref.[4]), the chloride concentration range in which there is a rate affecting precipitation increases with the cupric sulphate concentration in solutions of the type discussed here.

The film growth. Fig. 3 shows a typical example of the weight change of a cuprous chloride covered copper sheet in 1 N hydrochloric acid, as this is indicated by quartz helix measurements. It is there seen that the dissolution rate is essentially constant until it relatively sharply drops to zero. This obviously represents the complete dissolution of the cuprous chloride layer, the weight of which may be determined by weighings before and after the dissolution process.

Results of determinations of this type of the cuprous chloride layer formed on copper during various lengths of immersion in 0.1 N sulphuric acid + 0.1 M cupric sulphate + x M potassium chloride (x = 0.25, 0.125, and 0.05) are given in Fig. 4. It is there seen that, in all these solutions, the layer grows rapidly in the first few minutes of immersion. At the lowest chloride concentration (0.05 M), laying in the above described chloride range of most pronounced film formation, the layer continues to grow relatively rapidly, but the growth rate decreases somewhat with time. This decrease, however, is less than what would correspond to a parabolic time dependence. At the two higher chloride concentrations applied, there is a relatively sharp fall in the growth rate after the

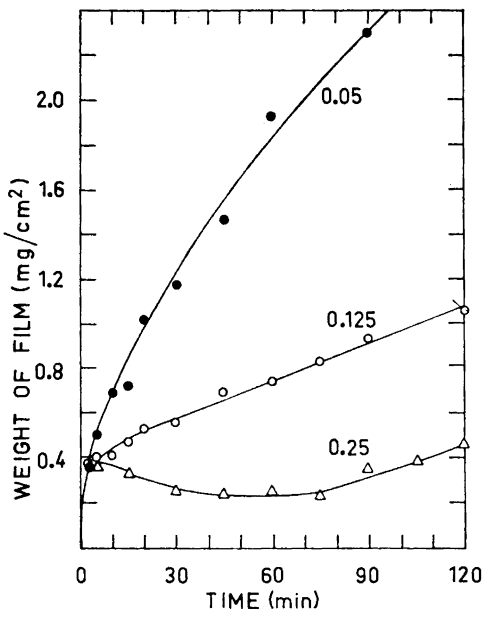

Fig. 4. Growth of cuprous chloride on copper in 0.1 N sulphuric acid + 0.1 M cupric sulphate + x M potassium chloride at x = 0.25, 0.125, and 0.05.

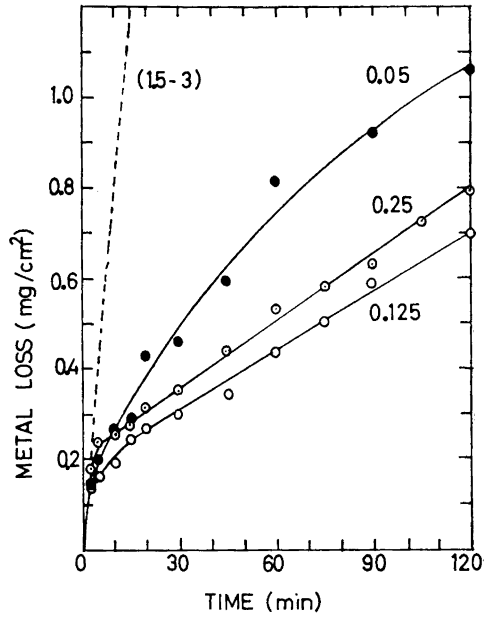

Fig. 5. Total reaction of copper in 0.1 N sulphuric acid + 0.1 M cupric sulphate + x M potassium chloride at x = 0.25, 0.125, and 0.05.

first few minutes, a fall which in the strongest chloride solution goes practically to zero.

Each of the experimental points in Fig. 4 represents the average of at least four experiments. The reproducibility has not always been very good, however. This applies especially to the strongest chloride solution.

The reaction rate. The reaction of copper with cupric ions in the solutions applied does certainly not only lead to cuprous chloride precipitated on the surface, but also to cuprous species in the solution. Besides being obvious, this is also verified by tracer experiments (neutron activated copper sheets). If we by w_0, w_1, and w_2 designate the weight of a copper sheet at the start of the experiment, after immersion in the test solution, and after removal of the cuprous chloride layer, respectively, the metal loss $w_0 - w_2$ should represent the total amount of copper that has reacted with the test solution. Results of such measurements for various lengths of time in solutions of 0.1 N sulphuric acid + 0.1 M cupric sulphate + x M potassium chloride (x = 0.25, 0.125, and 0.05) are given in Fig. 5. The slope of the curves there drawn is a measure of the reaction rate.

In the solution of the lowest chloride content (0.05 M), the reaction rate decreases with time qualitatively in the same way as the rate of growth of

the cuprous chloride layer. Within the experimental times applied, however, the weight increase of the layer (Fig. 4) is always faster than the metal loss (Fig. 5) whereby the total weight of the specimen increases all the time. This is in accordance with the results of the quartz helix measurements in analogous solutions of similar chloride content (Fig. 2).

Also in the solution of medium chloride content (0.125 M), the reaction rate varies with time in very much the same way as does the growth rate of the cuprous chloride layer. A comparison of the rate curve for film growth (Fig. 4) and for metal loss (Fig. 5), shows also in this case reasonable agreement with the quartz helix measurements in the same solution (Fig. 2). It is here further interesting to note that, after an initial period, both the reaction rate and the growth rate becomes essentially independent of time. This may indicate that the increase in thickness of the cuprous chloride layer, when above a certain limit, does not mean very much for the reaction rate. There is at least no inverse proportionality and no other simple relationship between the layer thickness and the reaction rate. This may also be seen by comparing the results in the solutions of 0.125 and 0.05 M potassium chloride, respectively. Even though the cuprous chloride layer (Fig. 4) becomes appreciably thicker in the latter than in the former case, the reaction rate (Fig. 5) remains higher, at least over most of the time period covered.

Also in the solution of the highest chloride content (0.25 M), there is a relatively sharp fall in the reaction rate to a steady value after a short initial period. The steady value is slightly higher than in the 0.125 M chloride solution. There is also in this case relatively good agreement between the specific results in Figs. 4 and 5 with the composite results in Fig. 2.

For comparison, previous results [4] on the reaction of copper with cupric ions in solutions of the same sulphuric acid and cupric sulphate concentration as given above and of high enough potassium chloride content (1.5 — 3 M) to avoid any rate influencing cuprous chloride precipitation, are reproduced by the stipulated line in Fig. 5. This line applies to all chloride concentrations within (and probably above) the range mentioned. The results in Fig. 5 further indicate that the reaction follows this line for a short initial period also at the lower chloride concentrations at which it is accompanied by a cuprous chloride precipitation on the metal surface. It may seem, therefore, that the precipitation does not affect the reaction very much until the surface is covered by an appreciable amount of precipitated cuprous chloride, about 0.3 mg/cm^2 when judged from the results in Figs. 4 and 5. This amount corresponds to a layer of average thickness around 10^4 Å.

The results in Fig. 5 further show that the steady reaction rate in the 0.125 and the 0.25 M chloride solution is about 5 to 6 percent of the initial rate, and that the reaction rate seems to slow down to a similar value also in the 0.05 M chloride solution during the time period covered.

The corrosion potential. The corrosion potential of copper in solutions of the above described type, 0.1 N sulphuric acid + 0.1 M cupric sulphate + x M potassium chloride with x in the range 10^{-2} — 1, have been measured over periods of about one hour. In all the solutions applied, the corrosion potential was found to be stationary almost from the beginning. Some variation some-

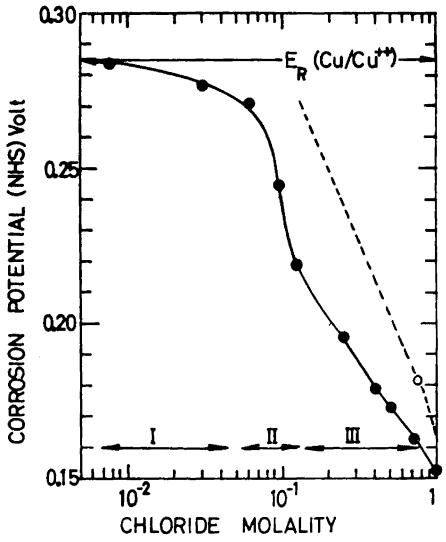

Fig. 6. Corrosion potential of copper in 0.1 N sulphuric acid + 0.1 M cupric sulphate + x M potassium chloride as a function of x.

times observed in the very first minutes of immersion, could very well simply be due to disturbancies introduced by the starting operations. Stirring, for instance, was found to affect the potential.

In Fig. 6, the stationary potentials found are plotted *versus* the chloride concentration of the respective solutions. In the same diagram are also given the value found for the reversible potential of copper at the extreme of no potassium chloride in the solution (horizontal line), and values to be expected for the corrosion potential in the imaginary case of no cuprous chloride precipitation (the stipulated line with a break at a chloride molality of about 0.8). These "expected" potentials are estimated by extrapolation of previous results [4] obtained under conditions of no cuprous chloride precipitation in solutions of the same type as here applied, but partly at higher chloride concentrations and partly at lower cupric sulphate concentrations.

The results in Fig. 6 thus show that the potential of copper in the solutions concerned is essentially determined by the reversible copper/cupric exchange reactions at chloride concentrations below about 10^{-2} M, and by the irreversible and mixed copper/cuprous and cupric/cuprous reactions and the effect of the cuprous chloride precipitation on these reactions at chloride concentrations higher than this. That the precipitation on the surface also affects the potential (and not only the rate) is indicated by the distinct deviation of the experimental curve from the "expected" one in Fig. 6. It is further interesting that this deviation shows a maximum very nearly at that chloride concentration at which the reaction rate (see Fig. 5) shows a minimum (*i.e.* at about 0.125 M).

The experimental potential curve is clearly composed of three main sections applying to three successive chloride concentration regions. These regions are indicated in Fig. 6, but their boundaries are not well established. In region I (low chloride concentrations), the potential falls somewhat and the reaction

rate increases with increasing chloride concentration. In region II, the potential fall is much steeper and the reaction rate has turned over to decrease with increasing chloride concentration. In region III, the potential fall is again lower and the reaction rate again increases with increasing chloride concentration. Region III terminates at a chloride concentration somewhere between 1 and 1.5 M, above which there is no (or only a negligible) cuprous chloride precipitation and the reaction rate is essentially independent of the chloride concentration (see Ref.[4]). What here is said about the reaction rate is based on the data in Figs. 2 and 5.

Tracer studies. Only a few preliminary tracer experiments have so far been made in some mixed sulphate and chloride solutions of the above type (partly with neutron activated copper sheets and partly with neutron activated cupric sulphate). These measurements show essentially the same features as already mentioned in the above description of the film growth and the reaction rate. They further indicate that the cuprous ions in the precipitated layers originate about half and half from the metal and from the cupric ions in the solution. This work is now being continued, and the detailed description will therefore be postponed until a more complete set of measurements has been made.

4.0 DISCUSSION

The present work clearly shows that the reaction of copper with cupric ions in acid chloride and mixed chloride and sulphate solutions, over a large chloride concentration range (dependent on the cupric concentration [4]), leads to a precipitation of cuprous chloride on the metal surface. It further shows that this precipitation (after an initial period) affects both the potential and the rate of the further reaction, and thereby also the further growth of the cuprous chloride layer. These effects are rather strange, however, as they seem more determined by the conditions (electrolyte composition) under which the reaction (and the precipitation) occurs than of the actual amount of precipitated cuprous chloride on the surface. This is also indicated by the observed constancy in potential and partly also in reaction rate (Fig. 5) even under conditions of relatively rapid growth of the cuprous chloride layer (Fig. 4). It is further interesting to note that the observed potentials are on the *active* side of those to be expected (from extrapolation) for the imaginary case of no precipitation (see Fig. 6). This is the opposite of what is encountered in the formation of passivity films on metals.

The present experiments have mainly been performed in solutions of 0.1 N sulphuric acid + 0.1 M cupric sulphate with various amounts of potassium chloride, and the results indicate three successive chloride concentration regions of different chloride ion effects on the reaction and the precipitation. In the low region, the reaction seems first of all determined by the small amount of chloride ions available, and its rate increases therefore with the chloride ion concentration. The cuprous chloride layers formed in this region, apparently have relatively low protecting properties. However, the protecting properties may seem to increase with the chloride ion concentration at which the layers are formed, successively resulting in a reversal of the chloride concentration

dependence into that encountered in the medium chloride concentration region. The solubility and also the dissolution rate [9] of cuprous chloride increases with the chloride concentration, and the chloride dependence found in the third region is qualitatively what to be expected from these effects to become appreciable. In this region, the precipitation is increasingly diminished and the reaction rate increases with increasing chloride concentration, until no precipitate is formed at all. The reaction rate then becomes independent of the chloride concentration and entirely determined by the cupric ion diffusion [4].

The present work is just comprehensive enough to suggest the above trend, and more work is needed before a more complete account can be given of the cuprous chloride precipitation and its role in the reaction of copper with cupric chloride in acid solutions.

In closing this discussion, it might be appropriate to point out some consequences of the reaction of and precipitation on copper in cupric chloride and bromide [9] solutions. Such solutions have previously been used by several investigators in radiochemical studies on the exchange of copper between the metal phase and aqueous solutions of cupric salts and on the effect of anions on this exchange (see, *e.g.*, Ref.[10]). Some strange conclusions have also been drawn from such measurements as to the exchange reaction [10,11]. It should now be clear, however, that these measurements have little to do with the reversible copper/cupric exchange reaction, but are reflecting partly the irreversible dissolution of and partly the cuprous halide precipitation on copper in these solutions.

Acknowledgement. The author is much indebted to Miss T. Tönderum and Miss K. Storström for technical assistance, to various members of the staff at the Central Institute for Industrial Research for valuable discussions, and to the *U.S. Department of Army, European Research Office,* for financial support.

REFERENCES

1. Latimer, W. M. *Oxidation Potentials,* 2nd Ed., Prentice-Hall, New York 1952.
2. Pourbaix, M. *Thermodynamics of Dilute Aqueous Solutions,* Arnold, London 1949.
3. Bjerrum, J., Schwarzenbach, G. and Sillén, L. G. *Stability Constants. Part II: Inorganic Ligands,* The Chemical Society, London 1958.
4. Hurlen, T. *Acta Chem. Scand.* **15** (1961) 1239.
5. Hurlen, T. *Acta Chem. Scand.* **15** (1961) 1231
6. Cooper, R. S. *J. Electrochem. Soc.* **105** (1958) 506.
7. Cooper, R. S. and Bartlett, J. H. *J. Electrochem. Soc.* **105** (1958) 109.
8. Hurlen, T. *Acta Chem. Scand.* **15** (1961) 615.
9. Hurlen, T. *To be published.*
10. Haissinsky, M. *La Chimie Nucleaire et Ses Applications,* Masson, Paris 1957, pp. 490–94.
11. Haissinsky, M., Cottin, M. and Varjabédian, B. *J. chim. phys.* **45** (1948) 212.

Received February 3, 1961.

ACTA CHEMICA SCANDINAVICA 15 (1961) 1255–1258

The Action of Phenylmagnesium Bromide on Ethyl 3-Coumarincarboxylate

GUST.-AD. HOLMBERG

Institutet för organisk kemi, Åbo Akademi, Åbo, Finland

Ethyl 4-phenyl-3,4-dihydro-3-coumarincarboxylate is formed through 1,4-addition of phenylmagnesium bromide to the conjugated double bond system of ethyl 3-coumarincarboxylate. This rapid reaction is followed by a much slower one in which another molecule of phenylmagnesium bromide reacts with the product of the first reaction.

Reactions between Grignard reagents and different alkylidene and arylidenemalonic esters have previously been investigated in this laboratory. A natural continuation of this work is the study of the reactions between a Grignard reagent and ethyl 3-coumarincarboxylate (I) because this latter substance can be considered an intramolecular arylidenemalonic phenyl ester.

Ethyl 3-coumarincarboxylate was, therefore, brought to react with phenylmagnesium bromide. In the first experiment, in which the molecular ratio of ester and Grignard reagent was 1:2.5, the reaction mixture was worked up after it had been warmed for 15 min. The yield of the main product, ethyl 4-phenyl-3,4-dihydro-3-coumarincarboxylate (II), was 68.2 %. Owing to the solubility of this substance in ethanol, the rest of it had to be isolated after saponification as 4-phenyl-3,4-dihydrocoumarin; the yield was 9.7 %. Also 3-(*o*-hydroxyphenyl)-3-phenylpropiophenone (III) was isolated from the reaction products of the saponification in a yield of 5.8 %.

However, when, in a second experiment, the reaction product mixture was decomposed after a reaction period of 1.5 h, the yield of the 4-phenyl-3,4-dihydrocoumarincarboxylic ester decreased to 58.4 %, while the yields of 4-phenyl-3,4-dihydrocoumarin and 3-(*o*-hydroxyphenyl)-3-phenylpropiophenone increased to 12.0 and 12.5 %, respectively. When the molecular ratio of ethyl 3-coumarincarboxylate and phenylmagnesium bromide was changed to 1:3.5 and the reaction time increased to 24 h, the respective yields were 38.0, 18.8, and 19.9 %.

Ethyl 4-phenyl-3,4-dihydro-3-coumarincarboxylate was evidently formed through a 1,4-addition of phenylmagnesium bromide to the conjugated double bond system of ethyl 3-coumarincarboxylate. The substance, which gives

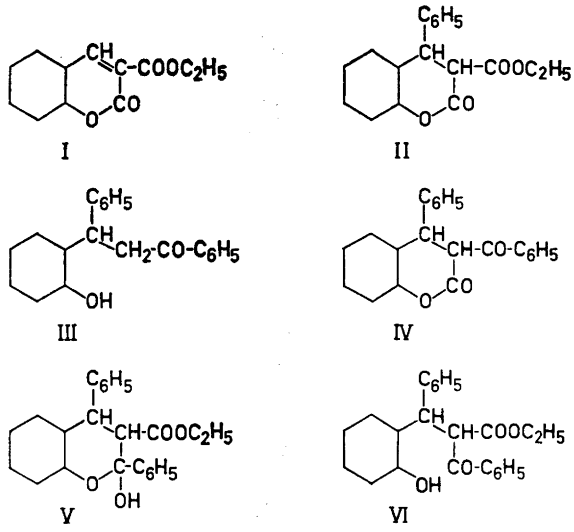

3-(*o*-hydroxyphenyl)-3-phenylpropiophenone on saponification, has apparently its origin in the reaction between phenylmagnesium bromide and the initially formed magnesium compound of ethyl 4-phenyl-3,4-dihydro-3-coumarincarboxylate. However, this reaction can lead to three compounds, *viz.* 3-benzoyl-4-phenyl-3,4-dihydrocoumarin (IV), ethyl 2-hydroxy-2,4-diphenyl-3-chromanecarboxylate (V), and ethyl *α*-benzoyl-*β*-(*o*-hydroxyphenyl)-*β*-phenylpropionate (VI). It is not possible to state which of them is formed on the basis of the present experimental data.

In order to estimate the lowest extent to which 1,4-addition has occurred in an experiment, the yields of ethyl 4-phenyl-3,4-dihydro-3-coumarincarboxylate, 4-phenyl-3,4-dihydrocoumarin, and 3-(*o*-hydroxyphenyl)-3-phenylpropiophenone should be summed. Thus, the total yield of the 1,4-addition was about 80 % in each of the three experiments. This reaction is a relative fast one since it went to completion within 15 min.

On the other hand, the yield of 3-(*o*-hydroxyphenyl)-3-phenylpropiophenone in an experiment expresses the extent to which ethyl 3-coumarincarboxylate has reacted with two moles of phenylmagnesium bromide. This value increases slowly with reaction time. This second reaction is, therefore, much slower than the first.

The reaction products were identified by degradation and synthesis. Ethyl 4-phenyl-3,4-dihydro-3-coumarincarboxylate was transformed into 4-phenyl-3,4-dihydrocoumarin by saponifying it and heating the saponification products for a short time. The identity of the last-mentioned substance was established by its synthesis according to Simpson and Israelstam [1]. Further, when the potassium salt, formed in the saponification, was methylated, dimethyl *o*-methoxybenzhydryl malonate was obtained. By saponification of this substance and decarboxylation of the reaction product, an acid was obtained which was identical with the previously [2] known *β*-*o*-anisyl-*β*-phenylpropionic acid.

3-(Hydroxyphenyl)-3-phenylpropiophenone was converted to 4-phenyl-2-chromene according to Löwenbein, Pongrácz, and Spiess [3] and was also in other respects identical with a sample prepared by the procedure of these authors.

The question whether the 3-(*o*-hydroxyphenyl)-3-phenylpropiophenone is an open ketone or a cyclic semiketal, 4-phenyl-2-chromanol, has not yet been definitely answered. Löwenbein, Pongrácz, and Spiess [3] consider it to be cyclic, whereas Geissman [4] denies this. For the present the author has chosen to call the compound a ketone and hopes to return to the question later.

EXPERIMENTAL

The action of phenylmagnesium bromide on ethyl 3-coumarincarboxylate. A solution of ethyl 3-coumarincarboxylate (10.90 g) in benzene (50 ml) was gradually added to a Grignard reagent prepared from bromobenzene (19.63 g), magnesium (3.00 g), and dry ether (100 ml). The reaction mixture was gently warmed on a water bath for 15 min and then poured into a mixture of hydrochloric acid (30 ml), water (60 ml), and ice (about 200 g). After adding more ether and shaking, the organic phase was separated and washed with water and dilute potassium hydrogen carbonate solution. The acid aqueous phase was extracted once more with ether and this ether was also washed with water and dilute potassium hydrogen carbonate solution before it was combined with the main portion. After drying with sodium sulphate, the ether was evaporated and the residue dissolved in hot ethanol. Ethyl 4-phenyl-3,4-dihydro-3-coumarincarboxylate (10.10 g) m.p. 101—102° after recrystallization from ethanol, separated on cooling. (Found: C 73.07; H 5.53. Calc. for $C_{18}H_{16}O_4$: C 72.96; H 5.44).

The ethanolic filtrate was evaporated under reduced pressure and the residue (6.81 g) dissolved in ethanol (150 ml). A solution of potassium hydroxide (7.00 g) in water (7 ml) and ethanol (25 ml) was added and the mixture heated on a boiling water bath for 2 h. After the mixture had cooled overnight, the precipitated potassium salt was filtered off and dissolved in water. The solution was acidified with hydrochloric acid and extracted with ether. The ether phase was dried with sodium sulphate and the ether was evaporated. The residue was heated at 160—170° for 10 min and after cooling the substance was treated with ligroin. In this way 4-phenyl-3,4-dihydrocoumarin (1.18 g), m.p. 82—83° after recrystallization from a mixture of benzene and ligroin, was obtained. The substance was identical with a sample prepared according to Simpson and Israelstam [1].

The filtrate, obtained when the potassium salt was separated, was evaporated under reduced pressure and water was added to the residue. The oil that separated was taken up in ether. The solution was dried and the solvent evaporated. The residue was treated with ethanol and the separated crystals (0.87 g) of 3-(*o*-hydroxyphenyl)-3-phenylpropiophenone, m.p. 167.5—168.5° after recrystallization from ethanol, were filtered off. A sample of this ketone was dehydrated to 4-phenyl-2-chromene, m.p. 109—110°, by the method of Löwenbein, Pongrácz, und Spiess [3]. The substance was also in other respects identical with a sample prepared according to the same authors.

When the experiment was repeated but the reaction mixture warmed for 15 min and then kept at room temperature for 1.5 h before it was worked up, the yield of 4-phenyl-3,4-dihydro-3-coumarincarboxylic ester decreased (to 8.65 g) while the yields of 4-phenyl-3,4-dihydrocoumarin and 3-(*o*-hydroxyphenyl)-3-phenylpropiophenone increased (to 1.34 g and 1.88 g, respectively).

When more bromobenzene (27.48 g), magnesium (4.20 g), and dry ether (140 ml) were used in the preparation of the Grignard reagent and the reaction time at room temperature extended to 24 h, the yield of ethyl 4-phenyl-3,4-dihydro-3-coumarincarboxylate was still lower (5.62 g) and the yields of 4-phenyl-3,4-dihydrocoumarin and 3-(*o*-hydroxyphenyl)-3-phenylpropiophenone were still higher (2.10 g and 3.01 g, respectively).

Saponification of ethyl 4-phenyl-3,4-dihydro-3-coumarincarboxylate. A sample (3.56 g) of ethyl 4-phenyl-3,4-dihydro-3-coumarincarboxylate was dissolved in ethanol (80 ml), a solution of potassium hydroxide (3.50 g) in water (3.5 ml) and ethanol (15 ml) was added, and the reaction mixture heated on a boiling water bath for 2.5 h. While the solution was kept in a refrigerator overnight, crystals of a potassium salt separated. The salt was

filtered off and dissolved in water. The aqueous solution was acidified and extracted with ether. The organic phase was dried with sodium sulphate and the solvent evaporated. The residue was heated to 160—170° for 10 min, the melted substance cooled and treated with ligroin. The separated crystals (2.58 g) of 4-phenyl-3,4-dihydrocoumarin, m.p. 82—83° after recrystallization from a mixture of benzene and ligroin, were filtered off.

Ethyl 4-phenyl-3,4-dihydro-3-coumarincarboxylate (5.44 g) was saponified in ethanol (125 ml) as above with a solution of potassium hydroxide (5.50 g) in water (5.5 ml) and ethanol (15 ml). The precipitated potassium salt was dissolved in water (75 ml) and the solution shaken with dimethyl sulphate (7.00 g) for half an hour. A solution of potassium hydroxide (3.10 g) an water (15 ml) was added and the mixture shaken with dimethyl sulphate (7.00 g) another half an hour. The substance (5.45 g) that had separated during the shaking was filtered off, washed with ether and then dissolved in a large quantity of ether. When the solvent had been partly evaporated, the substance separated again and was filtered off. After another similar treatment, dimethyl *o*-hydroxybenzhydrylmalonate, melting at 113.5—144.5°, was isolated. (Found: C 69.77; H 6.15. Calc. for $C_{19}H_{20}O_5$: C 69.50; H 6.14.)

A solution of potassium hydroxide (3.00 g) in water (3 ml) and ethanol (25 ml) was added to a solution of dimethyl *o*-methoxybenzhydrylmalonate (2.38 g) in ethanol (100 ml) and the mixture heated on a boiling water bath for 3 h. The potassium salt that separated when the reaction mixture was kept overnight in a refrigerator was filtered off and dissolved in water. The aqueous solution was acidified and after some time crystals (1.86 g) of impure *o*-methoxybenzhydrylmalonic acid formed. A sample (1.42 g) of this substance was heated in an oil bath at 190° for 5 min. The residue (1.20 g) was teated with benzene and the precipitated substance, m.p. 132—133°, was filtered off. It was identical with β-*o*-anisyl-β-phenylpropionic acid [2].

The elementary analyses were carried out by Dr. Alfred Bernhardt, Mühlheim.

REFERENCES

1. Simpson, J. D. M. and Israelstam, S. S. *J. S. African Chem. Inst.* **2** (1949) 165 as reviewed in *Chem. Abstr.* **45** (1951) 6196.
2. Holmberg, G. A. *Acta Chem. Scand.* **6** (1952) 421.
3. Löwenbein, A., Pongrácz, E. and Spiess, E. A. *Ber.* **57 B** (1924) 1517.
4. Geissman, T. A. *J. Am. Chem. Soc.* **62** (1940) 1363.

Received February 20, 1961.

ACTA CHEMICA SCANDINAVICA 15 (1961) 1259–1262

Biosynthesis and Excretion of Folic Acid during the Growth Cycle of *Lactobacillus arabinosus*

VEIKKO NURMIKKO and JUHANI SOINI

Department of Biochemistry, University of Turku, Turku, Finland

The folic acid content of *Lactobacillus arabinosus* cells and the excretion of the compound during the active growth phases of the cells have been studied. Marked variations occurred in the folic acid content of the cells as early as during the lag phase (between cell divisions). The folic acid content of the cells increased during the early exponential growth phase, rose to a maximum when one-third of the phase had elapsed, and then decreased rather sharply to the original level. *Lb. arabinosus* did not excrete any folic acid during the lag phase, but did so during the acceleration and retardation phases.

It is a well-known fact that certain microbes are able to synthesize and excrete folic acid. In connection with investigations concerning symbiosis phenomena in lactobacilli it has been found that certain strains, for instance, *Lactobacillus arabinosus* 17—5 (ATCC 8014), both synthesize folic acid and excrete it into the growth medium [1,2]. Whether variations occur in the biosynthesis and excretion of folic acid during the different growth phases has not been investigated in greater detail and we have therefore undertaken a study of the amounts of folic acid synthesized and excreted by *Lactobacillus arabinosus* 17—5 during the active growth phases. In addition, we especially wanted to find out whether *Lb. arabinosus* synthesizes or excretes folic acid already in the lag phase. Monod's definitions of the bacterial growth phases have been followed in this paper, and according to these definitions we have taken the lag phase to extend over the period when cell division is not taking place before the growth[3].

EXPERIMENTAL

Organisms. Lactobacillus arabinosus 17—5 (ATCC 8014) and *Streptococcus faecalis* R (ATCC 8043) were used in this study. The bacteriological technique for maintaining stock cultures has been described in an earlier paper.[4]

Preparation of inoculum. In the experiments concerning the exponential growth phase the preparation of the inoculum was conducted as follows. *Lb. arabinosus* cells were transferred from the stock cultures to 7 ml of a glucose-citrate-tryptone-yeast extract medium and incubated at 37° for 16—18 h. The cells were then centrifuged, isola-

ted and washed 4—5 times with 0.9 % sterile saline. After washing the cell mass was dispersed in 100 ml of the saline solution. The turbidity of the suspension was so low that a Klett-Summerson colorimeter did not give any reading. Two drops of this weak suspension was used to inoculate 20 ml of the final growth medium.

The inoculum used in the study of folic acid synthesis and excretion during the lag phase of growth was prepared in the same way except that the bacteria were cultured first in ten tubes each containing 7 ml of the glucose-citrate-tryptone-yeast extract medium and the washed cells were mixed with saline solution to give suspensions with optical density readings of 150—200 (using filter 62), equivalent to 0.4—0.5 mg dry weight of cells per ml of the suspension. One ml of this thick suspension was used to inoculate 20 ml of the final growth medium.

Procedure. The basal medium employed was the one described by MaciasR [5] except that the folic acid was left out and thiamine (1 μg per ml of basal medium) added. The pH was adjusted to 6.8.

In the experiments relating to the lag phase, 10 ml of the basal medium and 9 ml of water were added to large test tubes (20 × 180 mm). After they had been autoclaved at 112° for 10 min, the tubes were cooled to 37° and 1 ml of the heavy inoculum was added to each. The tubes were then transferred to an incubator at 37°. At intervals of 15 min single tubes were removed from the incubator and cooled in ice-water.

The experiments relating to the exponential phase were conducted in the same way as those relating to the lag phase except that a light inoculum suspension was used and the tubes were removed only after several hours of incubation (Fig. 2). In all experiments the growth was followed turbidimetrically with a Klett-Summerson colorimeter employing filter No. 62. The calibration curve plotting bacterial density (mg dry wt. of cells per ml) against turbidity proved to be valid both for the inoculum and for the cultures.

Preparation of samples for folic acid assay. When the turbidities of the suspensions had been measured, the cells were centrifuged down (10 min at 3 500 rpm) and washed four times with 0.9 % saline. For the folic acid assay an enzymatic hydrolysis was performed by the method of Snell [6] modified as follows. The washed cells were suspended in 5 ml of 0.5 % acetate buffer solution (pH 4.5) to which 1 mg each of papain and diastase and 5 ml of toluene had been added. The solution was then incubated at 37° for 24 h. The enzymes were then destroyed by heating the suspension in an autoclave at 120° for 10 min. The cooled suspension was centrifuged. The clear supernatant was neutralized to pH 6.8 and diluted with distilled water to a volume of 50 ml.

The culture filtrate was also diluted with distilled water to 40 ml and preserved at + 1° until assayed.

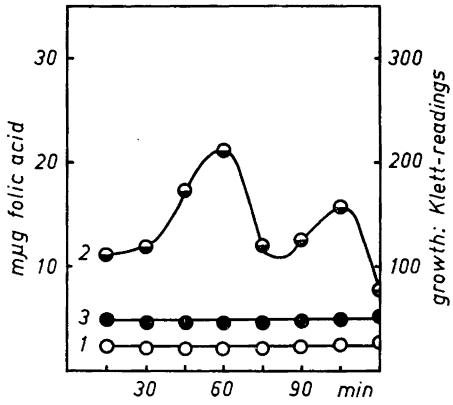

Fig. 1. Formation and excretion of folic acid by *Lb. arabinosus* during the lag phase of growth. 1, Growth curve (right-hand scale); 2, Content of folic acid in the cells (mμg per mg of dry matter); 3, Amount of folic acid excreted by 1 mg (dry wt.) of cells per 20 ml of growth medium.

Assay of folic acid. The folic acid assay was performed according to the standard procedure [7] using *Str. faecalis* R (ATCC 8043). Pteroylglutamic acid was used as standard. No upward or downward drifts were noted. In this connection it should be noted that in addition to pteroylglutamic acid also pteroic acid, 10-formylpteroic acid, 10-formylfolic acid and reduced folic acid derivatives are equally active for this organism (reviewed recently by Rabinowitz [8]).

RESULTS AND DISCUSSION

In the first stage of the present work the experiments aimed at clarifying whether *Lb. arabinosus* is able to synthesize folic acid and possibly excrete it into the growth medium already in the lag phase. A heavy inoculum was used in these experiments but in the experiments relating to the exponential phase the inoculum was a light one. The advantage of using a heavy suspension lies in the large number of cells available for study. The lag phase lasted 2 h at most.

Two maxima were observed in the curve plotting the folic acid content of the cells against time during the growth of *Lb. arabinosus*. The first maximum occurred when half the lag phase had passed. At this point the cells contained 22 mμg of folic acid per mg of dry matter. At the beginning of the lag phase they contained 11 mμg/mg, which value was obtained also when two-thirds of the phase (82 min) had passed. The second maximum occurred when 87 % of the lag phase had passed; the concentration of folic acid in the cells was then 14 mμg per mg of dry matter. No folic acid was excreted into the medium during the lag phase.

In the experiments relating to the exponential growth phase the folic acid content of the cells increased already from the beginning of the phase (the expo-

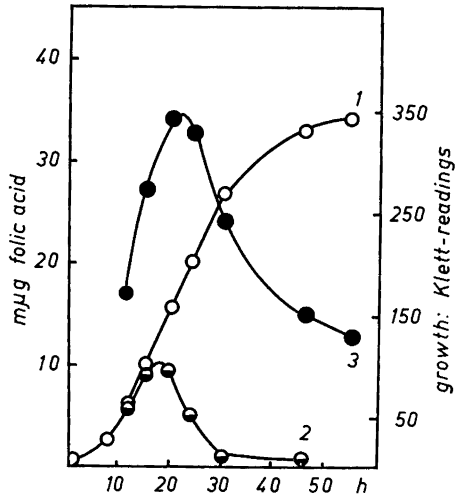

Fig. 2. Formation and excretion of folic acid by *Lb. arabinosus* during the exponential and retardation phases of growth. 1, Growth curve (right-hand scale); 2, Content of folic acid in the cells (mμg per mg of dry matter); 3, Amount of folic acid excreted by 1 mg (dry wt.) of cells per 20 ml of growth medium.

nential growth phase was taken to have begun 11.5 h after the inoculation) and attained a maximum level after 17 h. Thus the maximum occurred at a point where 30 % of the exponential phase had passed. The folic acid content of the cells was at this point 11 mμg/mg (5 mμg/mg at the beginning of the phase).

The folic acid content then decreased relatively rapidly to a point 30 h after the inoculation, when the cells contained 1 mμg of folic acid per mg dry weight of cells. The content then remained practically constant. It should be noted that the exponential growth phase ended at this same point, 30 h after the inoculation. The content of folic acid in the cells thus remained constant during the retardation phase.

As Fig. 2 shows, *Lb. arabinosus* excreted folic acid into the growth medium during both the exponential and the retardation growth phases. In the experiment in question the exponential phase began 11.5 h after the inoculation. At this point of growth each mg of cells (dry wt.) had excreted 1.2 mμg of folic acid per ml of growth medium. The amount of folic acid excreted then rose sharply, reaching a maximum (2.3 mμg/ml medium excreted by 1 mg cells) at the mid-point of the exponential growth phase. After this the excretion decreased, and at the end of the exponential phase 1 mg of cells excreted 1.6 mμg of folic acid per ml of growth medium. During the retardation phase, the folic acid excretion decreased further to a minimum of 0.9 mμg/mg. All the experiments were repeated three times; the same results were obtained in all replications.

The most interesting finding of this study is the marked variation in the folic acid content of the cells during the lag phase, but it is very difficult to draw any definite conclusions as to why such variations occur on the basis of the experiments carried out hitherto. As folic acid derivatives participate in the biosynthesis of nucleotides [8] the increases in the folic acid content may be considered to reflect a very active metabolism of nucleic acid components within the cell.

This work is a part of a more extensive study in progress in this laboratory which is connected with the biosynthesis of folic acid and related compounds and coenzymes during early phases of cell growth.

Acknowledgement. This work has been supported by a grant from the *State Commission for Natural Sciences (Valtion Luonnontieteellinen Toimikunta).*

REFERENCES

1. Nurmikko, V. *Acta Chem. Scand.* **6** (1952) 1258.
2. Nurmikko, V. *Proc. 4th Intern. Congr. Biochem.* Vienna 1958. Pergamon Press, 1959, Vol. XIII, 395.
3. Monod, J. *Ann. Rev. Microbiology* **3** (1949) 371.
4. Nurmikko, V. *Ann. Acad. Sci. Fennicae A II* **1954** No. 54.
5. MaciasR, F. M. *Appl. Microbiol.* **5** (1957) 249.
6. Snell, E. E. in György, P. *Vitamin Methods* **1** (1950) 327, p. 396.
7. Mücke, D. *Einführung in mikrobiologische Bestimmungsverfahren,* Thieme Verlag, Stuttgart 1955, p. 89.
8. Rabinowitz, J. C. in Boyer, P. D., Lardy, H. and Myrbäck, K. *The Enzymes* **2** (1960) 185.

Received January 14, 1961.

ACTA CHEMICA SCANDINAVICA 15 (1961) 1263–1270

Variations in the Transaminase Activity of *Escherichia coli* Cells during the Lag Phase of Growth

VEIKKO NURMIKKO and RAIMO RAUNIO

Department of Biochemistry, University of Turku, Turku, Finland

Variations in transaminase activity during the lag growth period of *Escherichia coli* have been investigated using α-ketoglutaric acid and eight amino acids as transaminase reactants. A rise was observed in the activities of the following transaminases: valine-glutamic, leucine-glutamic, *nor*valine-glutamic, *nor*leucine-glutamic and *iso*-leucine-glutamic. The transaminase activities rose to a maximum after approximately 40 min of lag growth and remained constant or, in a few cases, decreased slightly during the remaining part of the lag phase. Under the experimental conditions the lag phase lasted 50 min. During this time no variations were observed in the activities of the aspartic-, phenylalanine-, and tryptophan-glutamic transaminases.

A recent study carried out in this laboratory revealed that the rate of synthesis of vitamin B_6 in *Escherichia coli* cells rises to a maximum during the acceleration growth phase and then decreases slowly to the initial level towards the end of the exponential phase of growth [1,2]. It is a well-known fact that pyridoxal phosphate and pyridoxamine phosphate act as coenzymes of vitamin B_6 and participate in, for instance, transaminase reactions. With these facts in mind, it seems probable that variations should occur also in the transaminase activity during the growth phases in question. However, we find no published information on variations in the transaminase activity of bacterial cells during the early growth phases; in fact, there seems to be very little information about variations in enzyme activity in general during the lag and acceleration phases of growth. There is, however, a paper by Mc Carty [3] on the variations in dehydrogenase and deaminase activity during bacterial growth, and hence also during the lag phase. The present study was undertaken to determine whether any variations take place in the transaminase activity during the lag phase of growth of *E. coli*. It constitutes a part of a more extensive study on variations in enzyme activity and in rates of biosynthesis of the vitamin B complex and vitamin B coenzymes during the early growth phases of *E. coli* cells.

EXPERIMENTAL

Growth organism. The *Escherichia coli* strain U5-41 isolated as reported earlier [2] was used in all the experiments.

Culture methods. The *E. coli* strain was transferred monthly and incubated for inoculation of the media described in the previous report [2]. The growth medium contained 2.0 g of glucose, 1.4 g of dihydrogenpotassium phosphate, 100 mg of trisodium citrate, 200 mg of ammonium sulphate, 200 mg of ammonium chloride and 20 mg of magnesium sulphate heptahydrate in 100 ml of distilled water. The medium was neutralized with sodium hydroxide to pH 6.7—6.8 and briefly heated before the inoculation.

Procedure. E. coli was transferred from the agar slant into approximately 5 ml of the inoculum medium and incubated for 6—9 h. The cell suspension was then poured aseptically into one litre of the same inoculum medium and again incubated 12—14 h at 37°. The cells were centrifuged 15 min in a Wifug centrifuge at 2 500 rpm and washed three times with 0.9 % saline. Before transfer to the growth medium, the cells were stored in a refrigerator for not more that 30 min. All the cells were added as inoculum and one millilitre of the growth medium contained approximately 0.2 mg of *E. coli* cells, calculated as dry weight. The growth medium was heated to 37° on a water bath and mixed with an electric stirrer during the whole experiment. The first sample was taken 5 min after the inoculation in order to ensure a homogeneous suspension. After this, samples were taken at intervals of 3—5 min into tubes which were immediately immersed in an ice bath. After cooling, the turbidities of the samples were measured with a Klett-Summerson colorimeter using filter 62. After this the samples were centrifuged 15 min at 3 500 rpm.

Preparation of extracts. The centrifuged cells were treated with cold acetone (−20°) for 10—20 min, the precipitate was centrifuged down and the acetone poured out. The remaining acetone was removed in a vacuum and the cell powder transferred to a refrigerator. Before the enzyme assays the cell powder was suspended in a 0.01 M tris-buffer of pH 8.0, and stored overnight in the refrigerator. This suspension was used in all enzyme assays.

Transaminase assay. For the determination of enzyme activity, 0.050 ml volumes of a substrate solution containing 5 μmoles of L-amino acid (or 10 μmoles of DL-amino acid) and 10 μmoles α-ketoglutaric acid in a 0.05 M tris-buffer of pH 8.0 were pipetted into 60 × 7 mm test tubes and neutralized with potassium hydroxide. When pyridoxal-5-phosphate was added as activator, the amount was 2.5 μg per 0.050 ml of the substrate solution. The substrate solution was prepared some time before the assay and the tubes were stored in ice water. A 0.050 ml volume of the cell extract containing 0.25—0.30 mg (dry wt.) of the cells was pipetted into the tubes and they were shaken. After an incubation period of 60 min at 37°, the reaction was stopped by pipetting 0.020 ml volumes of 70 % trichloroacetic acid solution into the test tubes. The precipitated protein was removed by centrifuging 5-10 min at 3500 rpm.

Glutamic acid formed in the reaction was determined chromatographically. For this purpose samples (0.020 ml) of the clear supernatant were pipetted onto Whatman No. 1 paper. The glutamic acid was separated from the substrate amino acids by the ascending technique in a 17 × 68 × 62 cm tank. For the separation of threonine, alanine, serine, and glycine, an ethanol-water-ammonia (18:1:1) mixture was used as solvent system. For aspartic acid, a pyridine-acetic acid-water (10:7:3) mixture was used. In the first case the development time was 40—50 h and in the latter 20—30 h. In other cases an *n*-butanol-glacial acetic acid-water (120:30:50) mixture was used as solvent system. After the runs, the chromatograms were dried in a hood and sprayed with 0.5 % ninhydrin in acetone containing 5 % pyridine as color intensifier. After the chromatograms had been sprayed, the color was allowed to develop at room temperature for several hours and finally at 60° for 30 min in a moist oven. Pieces of paper, all of the same size, containing the glutamic acid spots were cut out and the color extracted with 4.0 ml of methanol for 2 h. The density was measured with a Beckman DU spectrophotometer at wavelength 570 mμ. The assays were carried out in duplicate on the same paper. The average density was calculated from the two values. In each assay one of the following substances was omitted from one specimen: cell extract, α-ketoglutaric acid, and amino acid, or one of the two substrates. A standard curve for glutamic acid (shown in Fig. 1) was used to determine the amount of glutamic acid formed.

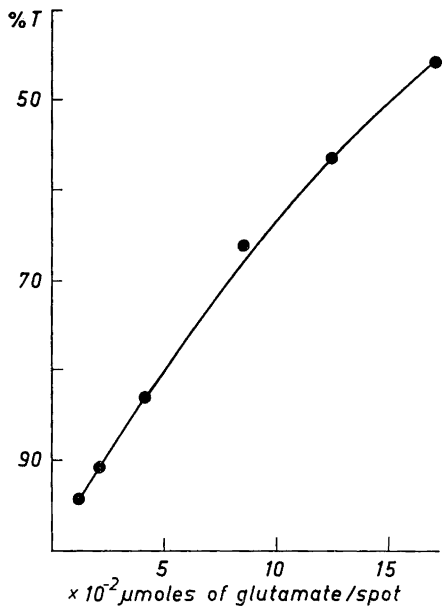

Fig. 1. Standard curve for glutamic acid determination.

The transaminase activity is expressed as the number of μmoles of glutamic acid formed per mg (dry weight) of the cells in one hour. Fig. 2 shows the progress curves obtained under the assay conditions with leucine, *iso*leucine, aspartic acid, tryptophan, phenylalanine, valine, *nor*leucine, and *nor*valine, as amino group donors to α-ketoglutaric acid.

As can be seen from Fig. 2, the reaction time employed, 60 min, was not too long a time for revealing variations in the activity under the experimental conditions.

Chemicals. DL-Ornithine and α-ketoglutaric acid were obtained from L. Light & Co Ltd, DL-tryptophan, glycine, DL-methionine, L-proline and DL-*iso*leucine from British Drug Houses Ltd, DL-lysine, DL-valine, DL-phenylalanine, DL-serine, L-tyrosine, L-leucine,

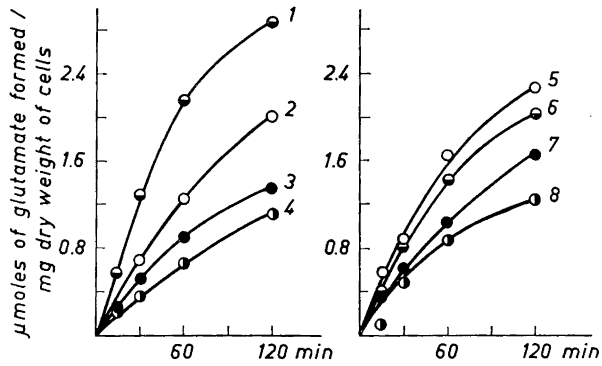

Fig. 2. Progress curves for transaminase reactions between α-ketoglutaric acid and certain amino acids. 1,aspartic acid; 2,tryptophan; 3,*nor*valine; 4,*nor*leucine; 5,*iso*leucine; 6,leucine; 7,phenylalanine; 8,valine.

Table 1. Transamination between α-ketoglutaric acid and amino acids. Crude *E. coli* cell extracts have been used in all experiments.

Amino acid	Feldman and Gunsalus[4], μmoles glutamate formed in one hour	Rudman and Meister[5], μmoles glutamate formed in two hours	Our experiments, glutamate formed in one hour: percentage from the aspartic acid activity (= 100)
D-Alanine			0
L-Alanine	0	w *	6
Arginine		w	5
Asparagine			94
Aspartic acid	25	41.0	100
Cysteine			0
Cystine		w	12
Glutamine			16
Glycine	10	w	0
Histidine	10	w	0
Hydroxyproline			0
*Iso*leucine	10	16.4	61
Leucine	20	16.9	47
Lysine	10		6
Methionine	15	12.5	42
*Nor*leucine	20	15.9	42
*Nor*valine		17.3	48
Ornithine		w	12
Phenylalanine	15	15.3	56
Proline	0	w	0
Serine		w	0
Threonine	8	w	0
Tryptophan	15	29.8	48
Tyrosine	12	10.3	22
Valine	25	12.3	52

* w = weak or not detectable.

L-cystine, L-cysteine, L-arginine, L-asparagine, and L-glutamic acid from E. Merck AG, DL-threonine, L-glutamine, L-histidine, DL-homocystine, L-hydroxyproline, DL-*nor*valine, L-aspartic acid, L-alanine, and D-alanine from Hoffman La Roche & Co Ltd, and DL-*nor*-leucine from General Biochemicals, Inc. Pyridoxal-5-phosphate was obtained from Hoffman La Roche & Co Ltd. In enzyme assays the buffer used was prepared from Sigma 7 — 9 reagent and obtained from Sigma Chemical Co. All other chemicals used in the experiments were AnalaR reagents obtained from E. Merck AG and British Drug Houses Ltd.

RESULTS

The first aim of the study was to find out what transaminase reactions involving the transaminase systems formed by α-ketoglutaric acid and the 25 different amino acids take place in *E. coli* cells. Pyridoxal phosphate was added as coenzyme to all these transaminase systems. The *E. coli* cells were harvested in the middle of the exponential growth phase. The results obtained are shown in Table 1. Under the experimental conditions used, the following amino acids transaminated weakly or not at all: DL-threonine, L-alanine, D-alanine, DL-serine, L-cysteine, L-histidine, L-hydroxyproline, L-proline, L-cystine, DL-orni-

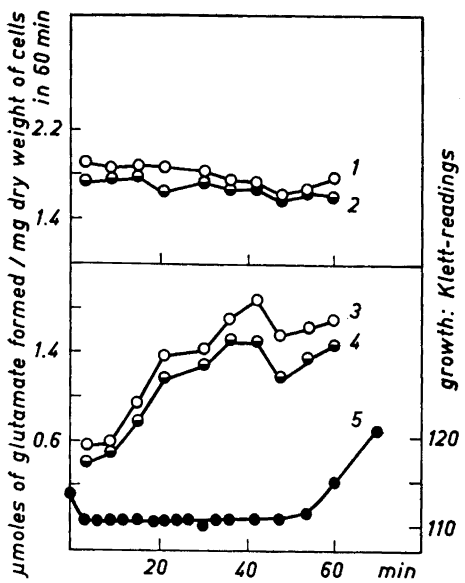

Fig. 3. Transaminase activity during the lag phase of growth of *E. coli*. 1,glutamic-aspartic transaminase (pyridoxal phosphate was added); 2,glutamic-aspartic transaminase; 3,glutamic-leucine transaminase (pyridoxal phosphate was added); 4,glutamic-leucine transaminase, 5,growth curve (right-hand scale).

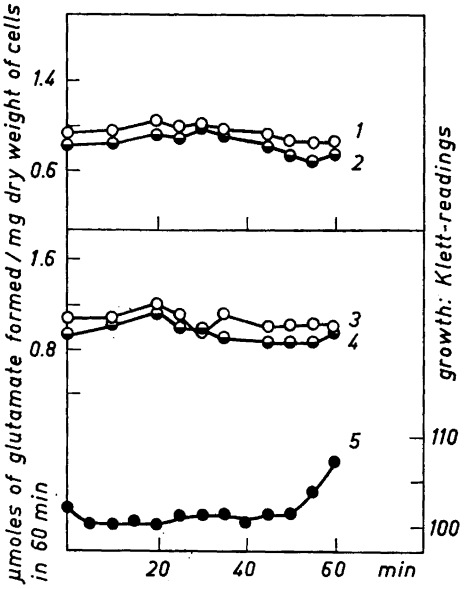

Fig. 4. Transaminase activity during the lag phase of growth of *E. coli*. 1,glutamic-phenylalanine transaminase (pyridoxal phosphate was added); 2,glutamic-phenylalanine transaminase; 3,glutamic-tryptophan transaminase (pyridoxal phosphate was added); 4,glutamic-tryptophan transaminase; 5, growth curve (right-hand scale).

thine, L-arginine, L-glutamine, and DL-lysine. Amino acids which definitely exhibited transamination activity were DL-*nor*leucine, DL-phenylalanine, DL-tryptophan, DL-*nor*valine, DL-valine, L-tyrosine, DL-*iso*leucine, DL-methionine, L-leucine, and L-aspartic acid. All the amino acids of this latter group except tyrosine and methionine were included in the experiments in which the variations in transaminase activity were studied during the lag phase of growth. In the transamination reaction of asparagine and α-ketoglutaric acid, glutamic acid was synthesized in large amounts, but also aspartic acid was produced in quite considerable amounts. The results of the determinations of transaminase activity are shown in Figs. 3—6.

The length of the lag phase varied between 30 and 50 min in these transamination experiments. The initial culture contained 0.20—0.22 mg (dry wt.) of cells per ml of growth medium, and had an optical density of 100—195 with filter 62. The values of the optical density at the beginning of the lag phase were higher than those measured later because the culture suspensions could not be made homogeneous at once with the experimental procedure used. The high values thus do not indicate any increase in bacterial count as compared to the count in the later part of the lag phase. In order to ensure an accurate determination of the length of the lag phase, the growth was followed into the acceleration phase; as seen from the figures, the transaminase activities were

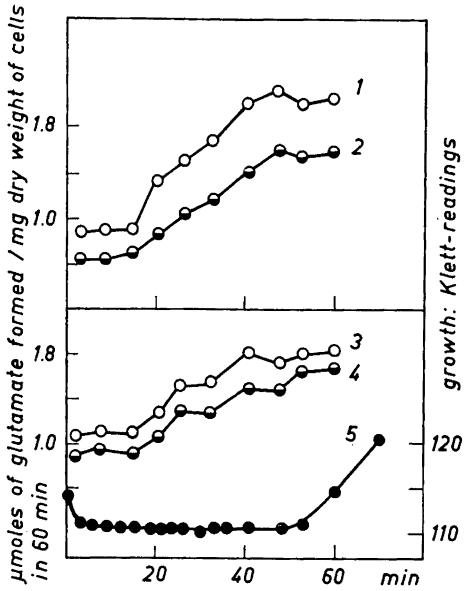

Fig. 5. Transaminase activity during the lag phase of growth of *E. coli*. 1,glutamic-*iso*-leucine transaminase (pyridoxal phosphate was added); 2,glutamic-*iso*leucine transaminase; 3,glutamic-valine transaminase (pyridoxal phosphate was added); 4,glutamic-valine transaminase; 5,growth curve (right-hand scale).

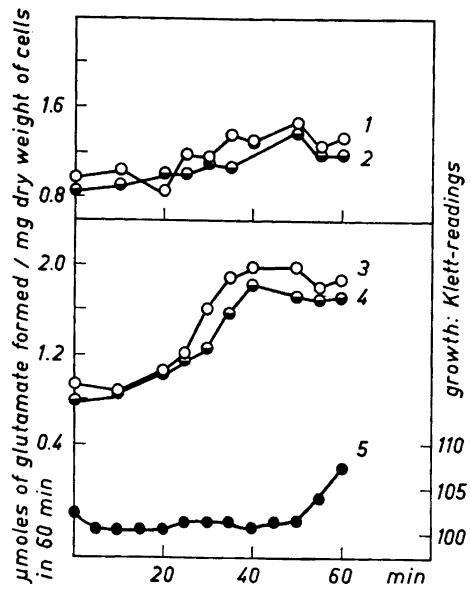

Fig. 6. Transaminase activity during the lag phase of growth of *E. coli*. 1,glutamic-*nor*-leucine transaminase (pyridoxal phosphate was added);2, glutamic-*nor*leucine transaminase; 3,glutamic-*nor*valine transaminase (pyridoxal phosphate was added); 4, glutamic-*nor*valine transaminase; 5, growth curve (right-hand scale).

also determined during the early acceleration growth phase. In the following, however, only the results pertaining to the lag phase are presented.

As can be seen from Fig. 3 the aspartic-glutamic transaminase activity remained constant throughout the lag phase. As seen from the same figure, the leucine-glutamic transaminase activity underwent a fourfold increase from the beginning of the lag phase.

No variations were noted in the activities of the phenylalanine-glutamic and tryptophan-glutamic transaminases (Fig. 4), but Fig. 5 demonstrates that the activities of the *iso*leucine-glutamic and the valine-glutamic transaminases increased considerably, nearly three times and one and a half times, respectively.

Fig. 6 shows that a 1.5-fold increase occurred in the activity of *nor*leucine-glutamic transaminase, and a twofold increase in the activity of the *nor*valine-glutamic transaminase.

Figs. 3—6 show data obtained in experiments where pyridoxal phosphate was present in the medium and in experiments where it was absent. As the results demonstrate, the transaminase activities were slightly higher when pyridoxal phosphate was present than when it was absent. In a few cases this difference was quite considerable, for instance, for the *iso*leucine-glutamic transaminase and for the valine-glutamic transaminase.

DISCUSSION

The present investigation has revealed that variations occur in certain transaminase activities during the lag phase of growth of *E. coli*. The study of the abilities of 25 amino acids to function in transamination reactions gave the same results as were obtained by Feldman and Gunsalus [4] and by Rudman and Meister [5] (Table 1).

On the basis of the results, those transaminases which clearly are present in *E. coli* cells can be divided into two groups. The transaminases (Group A) exhibiting clear variations in activity are the following: *iso*leucine-glutamic, valine-glutamic, leucine-glutamic, *nor*valine-glutamic, and *nor*leucine-glutamic. Those transaminases (Group B) for which no variations in activity were observed were the aspartic-glutamic, phenylalanine-glutamic, and tryptophan-glutamic transaminases.

Perhaps the most interesting result of this work is that the activities of certain transaminases, those included in Group A, increase during the lag phase. In these cases the length of the lag phase was approximately 50 min. As Figs. 5 and 6 show, the activities of the transaminases of Group A increased already at the beginning of the lag phase and reached a maximum about 40 min later. From this point onwards, the activities remained practically constant. With the leucine-glutamic transaminase, the activity decreased after the maximum had been reached. In this connection it is interesting to note that Rudman and Meister [5] obtained two fractions, A and B, when they fractionated an extract of *E. coli* cells. In fration B these authors found *iso*leucine-glutamic transaminase, valine-glutamic transaminase, and leucine-glutamic transaminase. In the present work the activities of these same transaminases were observed to increase during the lag phase, while the other transaminase systems that we found to undergo no change in activity are the same as those which Rudman and Meister found in their fraction A.

The variations we found in the transaminase activities were not caused by changes in the pH of the medium, because no changes in pH were observed during the experiments. Thus they cannot be explained by the finding of Gale and Epps [6] that the amount of enzyme per cell increases when the pH becomes unfavourable.

An interesting comparison can be made between the increases in the transaminase activities observed in this work and the increase in the rate of biosynthesis of vitamin B_6 demonstrated in one of our previous studies [2]. The rate of biosynthesis of vitamin B_6 increased throughout the lag phase of growth and reached a maximum during the acceleration phase, while the activities of the transaminases of Group A reached their maximal values already during the lag phase (providing that no other maxima occur during the later part of the growth cycle). These activities either remained constant or decreased when the growth progressed to the acceleration phase, where the rate of biosynthesis of vitamin B_6 seemed to be especially high.

At the present stage of our studies, the observation that the activities of certain transaminases increase while those of others remain practically constant cannot be easily explained. However, a plausible explanation may lie in the accepted fact that glutamic acid and glutamine are the first amino

acids synthesized by the assimilation of inorganic nitrogen (ammonia) [7], and that the other amino acids are synthesized from these. It may be that during the lag phase of growth the organism needs three branched-chain amino acids, *iso*leucine, leucine, and valine, in increasing amounts (*e.g.* for protein synthesis) before cell division can occur. If these amino acids are synthesized from glutamic acid by transaminase reactions, the rise in the enzyme activity of *iso*leucine-glutamic, leucine-glutamic, and valine-glutamic transaminases would be understandable.

Our opinion is that a close study of the variations in enzyme activity, especially during the first growth phase of an organism, will throw new light on the mechanism regulating the growth of cells. Experiments in this field are therefore being continued in this laboratory.

Acknowledgement. This work has been supported by a grant from the *State Commission for Natural Sciences (Valtion Luonnontieteellinen Toimikunta).*

REFERENCES

1. Nurmikko, V. and Laaksonen, S. *Suomen Kemistilehti. In press.*
2. Nurmikko, V. and Raunio, R. *Acta Chem. Scand.* **15** (1961) 856.
3. Mc Carty, B. J. *Proc. Roy. Soc. London* B **150** (1959) 410.
4. Feldman, L. I. and Gunsalus, J. C. *J. Biol. Chem.* **187** (1951) 821.
5. Rudman, D. and Meister, A. *J. Biol. Chem.* **200** (1953) 591.
6. Gale, E. F. and Epps, H. M. R. *Biochem. J.* **36** (1942) 600.
7. Roine, P. *Ann. Acad. Sci. Fennicae A II* **1947** No. 26.

Received January 14, 1961.

ACTA CHEMICA SCANDINAVICA 15 (1961) 1271–1279

The Interaction of Cystine and Cysteine with Beef Liver Catalase *

ALEXANDER PIHL, ROLF LANGE** and ANDERS EVANG

Norsk Hydro's Institute for Cancer Research, The Norwegian Radium Hospital, Montebello, Norway

A study has been made of the interaction of crystalline beef liver catalase with cystine and with the thiols, cysteine, cysteamine, and penicillamine.

Native beef liver catalase contains 8 SH-groups readily titratable with *p*-chloromercuribenzoate. The catalase SH-groups interact with ^{35}S-cystine to form mixed disulphide groups. A maximum of 4 moles of cysteine residues are bound to the enzyme while concurrently 4 enzyme SH-groups are oxidized to SS-groups.

Incubation of catalase with thiols is associated with the formation of the inactive catalase hydrogen peroxide complex II, confirming the report of Keilin and Nicholls. The inhibition of catalase by thiols is spontaneously reversible. The degree of inhibition obtained under different experimental conditions is proportional to the amount of complex II formed. The data provide evidence that the thiol inhibition of catalase can be quantitatively accounted for by formation of the inactive catalase complex II formed from hydrogen peroxide generated in the oxidation of the thiols.

The inhibition of catalase by cystine is prevented by prior blocking of the enzyme SH-groups with *p*-chloromercuribenzoate. It is spontaneously reversible and, like the cysteine inhibition, it is prevented by ethylenediaminetetraacetate or ethanol. The data indicate that the inhibiting effect of cystine is due to its interaction with catalase SH-groups with the consequent liberation of cysteine, which in turn inhibits the enzyme according to the mechanism outlined above.

It has been known since many years [1,2] that catalase is inhibited by cysteine and various other thiols. More recently it has been shown that cystine as well exerts a moderate inhibiting effect [3,4]. Several mechanisms have been suggested for the thiol inhibition of catalase, but none of these has been generally accepted, and no explanation seems to have been offered to account for the inhibition of catalase by cystine.

* Supported by *The Norwegian Research Council for Science and the Humanities* and by *The Norwegian Cancer Society.*

** Fellow of *The Norwegian Cancer Society.*

The present investigation was prompted by the observation in this laboratory [5] that catalase possesses SH-groups which interact with cystamine to form mixed disulphide groups with the concomitant liberation of cysteamine. This finding suggested the possibility that the inhibition by cystine might be due to an interaction with catalase SH-groups with the consequent liberation of the inhibiting thiol, cysteine. The data here presented provide evidence in support of this hypothesis. Furthermore, the results strongly indicate that the inhibition of catalase by cysteine and other thiols is due to the formation of the inactive catalase hydrogen peroxide complex II, as suggested by Keilin and Nicholls [6].

EXPERIMENTAL

Materials. Catalase was purchased from Boehringer & Soehne G.m.b.H., Mannheim, Germany (Kat. I). The preparation had a Kat. F (Katalase Fähigkeit) = 80 000 and the ratio [7] $D_{276\ m\mu} / D_{404\ m\mu}$ was found to be 1.14.

^{35}S-cystine ($C^{35}S^{35}SC$) was obtained from the Radiochemical Centre, Amersham, England.

Hydrogen peroxide as well as the other reagents used were of highest analytical grade. The water used was glass distilled and de-ionized by passage through a mixed bed ion exchange column.

Procedure. Catalase was incubated with ^{35}S-cystine in M/15 phosphate buffer, pH 7.4, containing 0.02 M disodium ethylenediaminetetraacetate (EDTA). The buffer was made from water boiled under a stream of nitrogen and the incubation was carried out in a nitrogen atmosphere. After incubation the labelled components were separated by electrophoresis at pH 2 in paper pretreated with mercuric acetate [8]. The radioactivity on the strips was located and measured by a strip counter. Three radioactive peaks were obtained corresponding to the location of catalase, cysteine ($C^{35}SH$), and cystine, respectively. In some experiments the incubation mixture was extensively dialyzed, and the number of labeled residues bound to the catalase was determined by direct plating of the solution and measurement of the radioactivity in a flow-counter. Paper electrophoresis and strip counting established that after dialysis all remaining radioactivity was bound to the catalase.

In the inhibition experiments the solutions were in equilibrium with air. The thiols were brought in solution immediately before they were added to the enzyme solution. The details of the experimental conditions are given below.

The catalase activity was determined at 0°C according to the rapid titration technique of Bonnichsen *et al.*[9]. The catalase stock solution (Kat. I) was diluted to the desired concentration with M/15 phosphate buffer, pH 7.0, and the enzyme concentration was determined spectrophotometrically using the molar absorption coefficient $E_{404} = 6.36 \times 10^5$ (Tauber and Petit [7]).

The SH-determinations were carried out in M/15 phosphate buffer at pH 7.0, according to the method of Boyer [10]. Because of the high absorption of catalase at 255 mμ, catalase was used in the blank solution.

The spectrophotometric measurements were carried out in a Zeiss spectrophotometer.

RESULTS AND DISCUSSION

The SH-groups of catalase. The existence of reactive SH-groups in catalase does not seem to have been demonstrated until it was found by Pihl and Eldjarn [5] that catalase interacts with cystamine to form mixed disulphides. Later the presence of SH-groups in catalase has been confirmed by Schütte and Nürnberger [11]. These authors reported that beef liver catalase contains 6

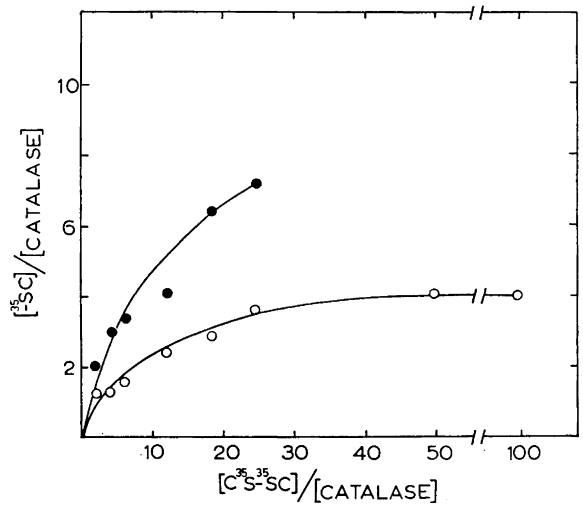

Fig. 1. Binding of cystine radioactivity to catalase and the concomitant liberation of cysteine as a function of the initial molar ratio of cystine to catalase. Catalase was incubated in nitrogen atmosphere at 37°C and with ^{35}S-cystine in M/15 phosphate buffer, pH 7.4, containing 1×10^{-2} M EDTA. After 60 min incubation the reaction products were separated by paper-electrophoresis at pH 2, and the radioactivity was measured in a strip-counter.
O—O Catalase bound ^{35}S; ●—● ^{35}S cysteine liberated.

SH-groups titratable with *p*-chloromercuribenzoate (pCMB). Upon denaturation with 8 M guanidine hydrochloride, 4 additional SH-groups became titratable.

When catalase was incubated with increasing concentrations of ^{35}S-cystine, increasing amounts of radioactivity were bound to the enzyme (Fig. 1). The maximum radioactivity bound corresponded to approximately 4 thiol residues. It can be seen that the radioactivity of the cysteine liberated was approximately twice the radioactivity bound to the protein. The data are in excellent agreement with those previously obtained with labeled cystamine [5].

On the basis of the previous cystamine data it was suggested [8] that catalase possesses a total of 8 reactive SH-groups, 4 of which may form stable mixed disulphides, whereas 4 are arranged in pairs with the consequence that the mixed disulphides initially formed react subsequently with adjacent protein SH-groups to form disulphide groups as depicted below:

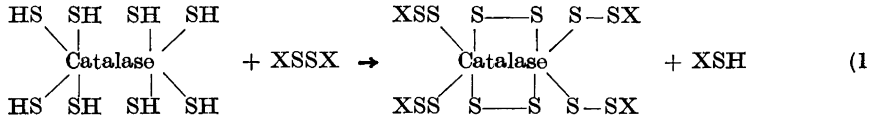

(1)

Quantitative evidence supporting this reaction scheme has been obtained here in experiments where the binding of cysteine residues to catalase was

correlated with the concomitant disappearance of protein SH-groups. In the native catalase a total of 8 SH-groups was titrated with pCMB (Table 1). Upon incubation of catalase with increasing concentrations of cystine, more protein SH-groups disappeared than can be accounted for by the concurrent binding of cysteine residues, in agreement with eqn. 1. Thus it can be seen that the sum of the cysteine residues bound and the number of remaining titratable SH-groups was close to 4 in all instances, indicating that the interaction of the catalase SH-groups with excess cystine results in the oxidation of 4 protein SH-groups to SS-groups.

Table 1. The titratable SH-groups of native and cystine treated catalase. Catalase (2.3×10^{-5} M) was incubated for 60 min in M/15 phosphate buffer, pH 7.4, with different concentrations of ^{35}S-cystine. After incubation the solution was dialyzed for 48 h. The radioactivity was determined after plating in cups.

Conditions	$\frac{(C^{35}S\ ^{35}SC)}{(\text{catalase})}$	$C^{35}S$ bound in moles per mole of catalase [a]	Titratable catalase SH-groups
Catalase	—	—	8 (10) [b]
Catalase + $C^{35}S^{35}SC$ + dialysis	10	1.7	1.8
» » »	25	2.8	1.1
» » »	50	3.6	0.5

a) A comparison of the data with those given in Fig. 1 reveals that during dialysis some of the labelled residues were released from the protein.
b) After incubation for 24 h with *p*CMB.

The inhibition of catalase by thiols. The inhibition of catalase by cysteine, reduced glutathione and other thiols was studied by Stern [1], Waldschmidt-Leitz *et al.*[2] and later by Boeri and Bonnichsen [12], Dale and Russell [3] and by Ceriotti [4]. It was established by the early workers that the inhibition increases slowly with time [1,2], and it was suggested that the inhibition is due to a slow formation of an inactive complex between the enzyme and the thiol [1,2]. This mechanism seemed to receive support by the findings of Boeri and Bonnichsen [12] and of Aebi and Frei [13] that blood and liver catalase is capable of catalyzing the oxidation of thiols in the presence of oxygen. However, in the oxidation of cysteine by oxygen, hydrogen peroxide will be formed (eqn. 2). Chance [14] has demonstrated that when H_2O_2 is continuously generated, as in the oxidation of glucose in the presence of oxygen and glucose oxidase, the inactive catalase peroxide complex II which is slowly formed from the active complex I (eqn. 4), will accumulate to an appreciable extent.

$$2\ CSH + O_2 \longrightarrow CSSC + H_2O_2 \qquad (2)$$

$$\text{Catalase} + H_2O_2 \longrightarrow \text{Catalase peroxide-I} \qquad (3)$$

$$\underset{\text{(Active)}}{\text{Catalase peroxide—I}} \xrightarrow{\text{slowly}} \underset{\text{(Inactive)}}{\text{Catalase peroxide —II}} \qquad (4)$$

Recently Keilin and Nicholls [6] in a preliminary note reported that catalase in the presence of cysteine undergoing auto-oxidation changes its characteristic absorption spectrum to that of catalase hydrogen peroxide complex II, and they concluded that the inhibitory effect of cysteine on the catalatic destruction of hydrogen peroxide may be due to the formation of this inactive complex. They also suggested that the increase in the rate of the auto-oxidation of thiol compounds in the presence of catalase is brought about not by catalase itself but by non-haematin iron and possibly some degradation products of haematin present in catalase preparations.

Since the paper of Keilin and Nicholls was not supported by experimental data, experiments have been carried out to study whether or not the inhibition of catalase by thiols can be accounted for by complex II formation. In Fig. 2 the changes in the absorption spectrum occurring when catalase was incubated with a thousand fold molar excess of cysteamine, is shown. The spectrum shows features characteristic of the catalase peroxide complex II [15]. Thus, the absorption at the Soret band at 405 mμ is decreased, while the absorption at 435 mμ is increased. The absorption band of catalase at 625 mμ disappeared and an absorption maximum typical of catalase hydrogen peroxide complex II appears at 568 mμ.

At 435 mμ catalase and catalase complex I have an isosbestic point [15]. The absorption at this wave-length can therefore be taken as a measure of the amount of catalase complex II formed. In Table 2 data are given on the enzyme inhibition and the concurrent increase in optical density at 435 mμ when

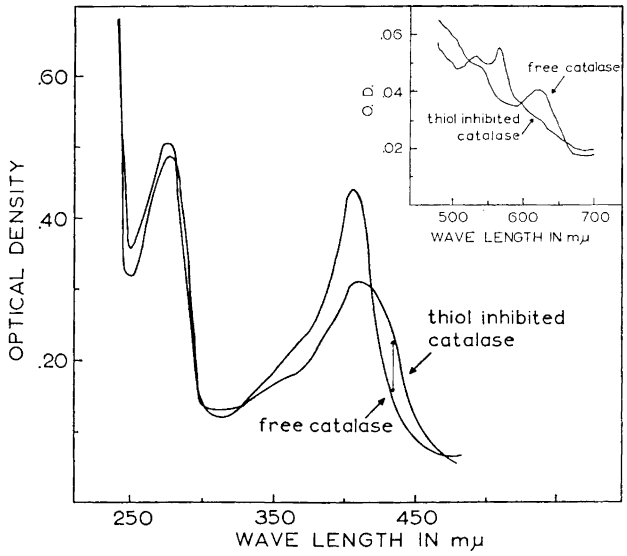

Fig. 2. The spectra of free catalase and thiol inhibited catalase. Catalase (6.92×10^{-7} M) was incubated for 1 h in M/15 phosphate buffer, pH 7.0, at 23°C with a thousand fold molar excess of cysteamine. The spectrum of the thiol inhibited catalase was recorded when the enzyme inhibition was maximal (70 per cent).

Table 2. The inhibition of catalase by various thiols and the concomitant increment in optical density at 435 mμ. Catalase (7×10^{-7} M) was incubated at 20°C in M/15 phosphate buffer, pH 7.0, with the thiols. The solutions were in equilibrium with air.

Conditions	(Thiol)/(Catalase)	Incubation time in min.	A = inhibition in per cent	B = $\Delta D_{435\ m\mu}$	$\frac{A}{B} \times 10^2$
Catalase + cysteine	10^2	21	36	0.037	9.7
	10^2	41	32	0.036	8.9
	10^2	380	4.5	0.006	7.5
Catalase + cysteine	10^3	5	0	0	—
	10^3	20	12	0.021	5.7
	10^3	25	18	0.024	7.5
	10^3	30	21	0.028	7.5
	10^3	40	34	0.043	5.9
	10^3	50	39	0.045	6.5
	10^3	60	41	0.060	6.8
	10^3	70	49	0.064	7.7
	10^3	80	54	0.076	7.1
Catalase + cysteamine	2.5×10^2	25	7.5	0.009	8.3
	2.5×10^2	35	10	0.012	8.3
	2.5×10^2	45	14	0.016	8.7
	2.5×10^2	60	16.5	0.019	8.7
	2.5×10^2	90	21	0.028	7.5
	2.5×10^2	180	13	0.022	5.9
Catalase + cysteamine	10^3	25	13	0.015	8.6
	10^3	35	19	0.022	8.6
	10^3	45	22	0.030	7.4
	10^3	60	23	0.027	8.5
	10^3	70	34	0.049	7.0
	10^3	110	60	0.078	7.7
Catalase + penicillamine	10^3	13	21	0.030	7.0
	10^3	39	48	0.069	7.0
	10^3	170	73	0.101	7.2

catalase was incubated for different lengths of time with various thiols. It should be noted that the inhibition was rather variable from experiment to experiment. However, the significant fact is that under experimental conditions giving enzyme inhibition varying from 4.5 to 73 %, the extent of inhibition was, within experimental error, proportional to the amount of complex II formed. These data provide evidence that the catalase inhibition by thiols can be quantitatively accounted for by catalase complex II formation. The fact that the inhibition data were variable and somewhat erratic is consistent with the view [6] that a spontaneous oxidation is an essential step in the inhibition mechanism inasmuch as such processes are notoriously difficult to reproduce [16].

It can be seen from Table 2 that when a hundred fold molar excess of cysteine was used, the inhibition of catalase was spontaneosuly reversed. With a greater excess of cysteine (thousand fold) the inhibition was not reversed in the course of the observation time when the reaction was carried out in phosphate

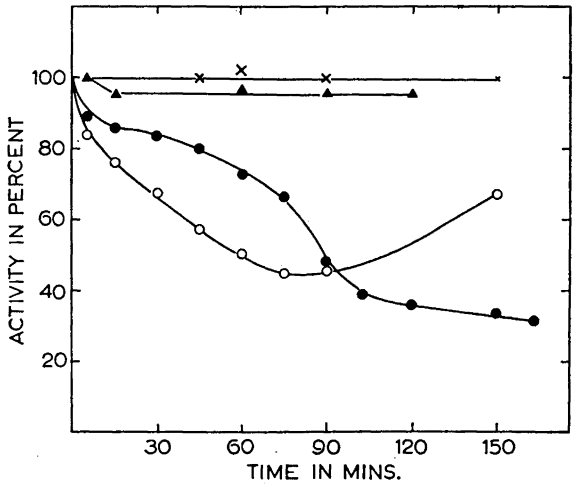

Fig. 3. The reversible inhibition of catalase by cysteine. The effect of EDTA and of ethanol. Catalase (7.0×10^{-7} M) was incubated at pH 7.0 with cysteine (7×10^{-4} M) at 20°C.
O—O Tris buffer (M/20).
● —● Phosphate buffer (M/15).
× — × » » » containing EDTA (1×10^{-2} M).
▲—▲ » » » » ethanol (7×10^{-4} M).

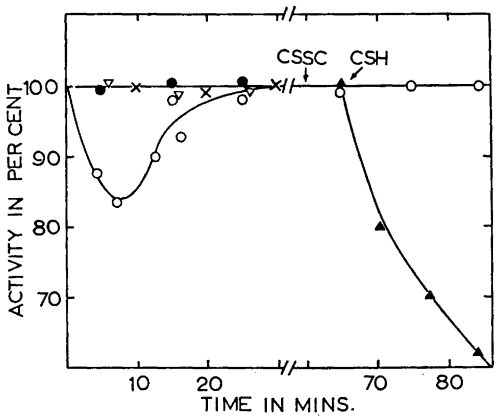

Fig. 4. Inhibition of catalase by cystine (CSSC). Catalase (7.4×10^{-7} M) was incubated at 37°C in M/15 phosphate buffer, pH 7.0, with cystine (3.7×10^{-5} M).
O—O An additional amount of CSSC (3.7×10^{-5} M) added at the time indicated by the arrow.
▲—▲ CSH (7×10^{-4} M) added at the time indicated.
● —● Catalase pretreated with 10 equiv. of pCMB.
× — × EDTA (1×10^{-2} M) present.
△—△ Ethanol (7×10^{-4} M) present.

buffer, but the reversibility was readily demonstrated when tris-(hydroxymethyl)aminomethane (Tris) buffer was used (Fig. 3). The data are clearly consistent with the inhibition mechanism represented in eqns. 2—4. Appreciable amounts of complex II are only formed and maintained when H_2O_2 is continuously generated [14], and if the H_2O_2 production ceases, reaction 4 is reversed. The spontaneous reversal of the inhibition may therefore be ascribed to the eventual exhaustion of the supply of thiols in solution with consequent decline in the H_2O_2 production. The finding that the inhibition of catalase by cysteine is completely abolished in the presence of EDTA (Fig. 3) supports the above reaction mechanism as EDTA blocks the oxidation of thiols in the absence as well as in the presence [6] of catalase. The fact that the cysteine inhibition of catalase is virtually abolished in the presence of ethanol (Fig. 3) in agreement with an early observation of Waldschmidt-Leitz *et al.*[2], is readily explained in terms of the above mechanism, as catalase complex I reacts with ethanol according to the following equation [14]:

$$\text{Catalase peroxide I} + CH_3CH_2OH \rightarrow \text{Catalase} + CH_3CHO + H_2O \qquad (5)$$

Accordingly, in the presence of ethanol the steady state concentration of catalase complex I will be kept low and the formation of the inactive complex II will be negligible.

The inhibition of catalase by cystine. The fact that cystine interacts with catalase SH-groups with liberation of cysteine opened the possibility that the inhibition of catalase by cystine might be due to the sequence of reactions 1 to 4. In that event, the cystine inhibition would be expected to be reversible, and it should be influenced by the same factors which influence the thiol inhibition. The data in Fig. 4 demonstrate that the inhibition of catalase by cystine is indeed reversible, and that it is abolished by EDTA and by ethanol. These findings seem to provide strong evidence in support of the mechanism proposed. It was therefore highly unexpected that the cystine inhibition could not be shown to be associated with an increase in the optical density at 435 mμ (Table 3). However, when the catalase was preincubated for 5 min with a hund-

Table 3. The inhibition of catalase by cystine. Catalase (7×10^{-7} M) was incubated at 20°C with cystine (7×10^{-5} M) in M/15 phosphate buffer, pH 7.0.

Conditions	Incubation time in min.	A = inhibition in per cent	B = $\Delta D_{435\ m\mu}$	$\frac{A}{B} \times 10^2$
Catalase + cystine	6	11	0	—
	16	8	0	—
	25	1	0	—
Catalase + hydrogen peroxide * + cystine	20	12	0.021	6.3
	25	15	0.019	8.3
	30	11	0.017	6.5

* The catalase was preincubated for 5 min with a 100 fold excess of hydrogen peroxide.

red fold excess of hydrogen peroxide prior to the addition of cystine, the expected optical density increase at 435 mμ did occur. It should be clear that preincubation with hydrogen peroxide without subsequent addition of cystine gave no enzyme inhibition and no optical density change at this wavelength. No adequate explanation can be offered for the effect of the preincubation, but the fact that the optical density increase showed the same quantitative relationship to the inhibition as in the experiments with cysteine, is hardly fortuitous.

Further evidence in support of the suggested mechanism was obtained in experiments where the effect of blocking the catalase SH-groups was tested. When catalase was pretreated with 10 equivalents of pCMB, no cystine inhibition was observed (Fig. 4). In agreement with this fact is was found that when catalase had been reversibly inhibited by incubation with excess cystine, a procedure which presumably removed all free protein SH-groups (Table 1), the addition of a second portion of cystine gave no inhibition. On the other hand, the addition of cysteine resulted in a prompt inhibition, as expected. Blocking of the enzyme SH-groups had no effect on the enzyme activity in the absence of cystine. The above data establish that the SH-groups of catalase play an essential role in the inhibition of catalase by cystine.

Altogether the results presented in this paper provide strong evidence that the inhibition of catalase by cystine is caused by cysteine liberated in the interaction of the disulphide with the enzyme SH-groups.

REFERENCES

1. Stern, K. G. *Z. physiol. Chem. Hoppe-Seyler's* **209** (1932) 176.
2. Waldschmidt-Leitz, E., Scharikova, A. and Schäffner, A. *Z. physiol. Chem. Hoppe-Seyler's* **214** (1933) 75.
3. Dale, W. M. and Russell, C. *Biochem. J.* **62** (1956) 50.
4. Ceriotti, G., Spandrio, L. and Berti, E. *Biochim. et Biophys. Acta* **23** (1957) 362.
5. Pihl, A. and Eldjarn, L. *Proc. 4th Intern. Congr. Biochem.*, Pergamon Press, London 1959, Vol. XIII, p. 43.
6. Keilin, D. and Nicholls, P. *Biochim. et Biophys. Acta* **28** (1958) 225.
7. Tauber, H. and Petit, E. L. *J. Biol. Chem.* **195** (1952) 703.
8. Eldjarn, L. and Pihl, A. *J. Am. Chem. Soc.* **79** (1957) 4589.
9. Bonnichsen, R. K., Chance, B. and Theorell, H. *Acta Chem. Scand.* **1** (1947) 685.
10. Boyer, P. D. *J. Am. Chem. Soc.* **76** (1954) 4331.
11. Schütte, H. R. and Nürnberger, H. *Z. physiol. Chem. Hoppe-Seyler's* **315** (1959) 13.
12. Boeri, E. and Bonnichsen, R. K. *Acta Chem. Scand.* **6** (1952) 968.
13. Aebi, H. and Frei, E. *Helv. Chim. Acta* **41** (1958) 361.
14. Chance, B. *Nature* **161** (1948) 914.
15. Chance, B. *Biochem. J.* **46** (1950) 387.
16. Waters, W. D. *Oxidation Processes* in Gilman, H. *Organic Chemistry*, John Wiley & Sons, New York 1953, Vol. IV, p. 1120.

Received February 9, 1961.

ACTA CHEMICA SCANDINAVICA 15 (1961) 1280–1284

The Volatile Carbonyls and Alcohols in the Flavour Substances of Onion (*Allium cepa*)

C.-G. SPÄRE and ARTTURI I. VIRTANEN

Laboratory of the Foundation for Chemical Research, Biochemical Institute, Helsinki, Finland

When the volatile substances in the onion were studied, two unknown carbonyl compounds were found in addition to acetaldehyde and propionaldehyde. One of the unknown substances was chemically characterized as 2-methyl-2-pentenal. The other carbonyl compound, which was present in very small amounts, has not yet been identified. On the basis of its UV-spectrum and behaviour on the paper chromatogram, it may be a saturated aldehyde. 2-Methyl-2-pentenal is formed enzymatically in crushed onion. The only alcohols found were methanol and ethanol.

In our studies on the flavour substances of crushed onion (*Allium cepa*), our attention was also drawn to the carbonyl compounds. When air was sucked through a homogenized onion mass with the aid of a vacuum pump and the airborne vapours were led into a dilute solution of 2,4-dinitrophenylhydrazine, a number of 2,4-dinitrophenylhydrazones (DNPHones) were precipitated. Acetaldehyde DNPHone and propionaldehyde DNPHone could be identified by paper chromatography. In addition, a spot containing an unknown aldehyde DNPHone was found.

In order to identify the unknown compound, the experiment was repeated on a larger scale and the precipitate of DNPHones was divided into fractions on a cellulose powder column. In addition to the unknown aldehyde DNPHone, another unknown DNPHone was detected in small amounts in the first fractions collected. DNPHones of the following carbonyl compounds were thus separated:

a) the minor unknown, designated as Y
b) the major unknown, designated as X
c) propionaldehyde
d) acetaldehyde

Acetaldehyde (d) DNPHone was identified by its m.p., by its mixed m.p with an authentic specimen, by paper chromatography, and by its UV-spectrum. The UV-spectra of the DNPHones are not very specific, but they can be

used to divide the DNPHones into classes, *e.g.* into saturated aldehydes, 2-en-1-als, 2,4-dien-1-als, and methylketones [1].

Propionaldehyde (c) DNPHone was identified by the same criteria as acetaldehyde DNPHone.

The unknown X, which was crystallized twice from methanol and then formed red, rhombohedral crystals, was investigated more closely in order to determine its structure. Elementary analysis of the X—DNPHone (Found C 51.91; H 5.04; N 20.00; O 23.21) gave the empirical formula $C_6H_{10}O$ for the carbonyl compound (Calc. for its DNPHone: C 51.79; H 5.07; N 20.14; O 23.00). The compound took up two atoms of bromide and accordingly contained one double bond. The unknown carbonyl compound might thus have been 2-hexenal, which is also called leaf aldehyde. This compound was synthesized [2]. The m.p. of its DNPHone was 143°C, in agreement with the m.p. reported in the literature; the m.p. of the X—DNPHone was 155°C, and the mixed m.p. 120°C. The nonidentity of the two compounds was thus established.

On the basis of the IR-spectra of different hexenals and the unknown DNPHone, it appeared that X is not 2-, 5-, or 3-hexenal. Regarding the identity of X and 4-hexenal, the IR-spectra gave no conclusive proof.

In order to establish the identity or nonidentity of the X—DNPHone and 4-hexenal DNPHone definitely, the latter was synthesized. The m.p. of the synthetic compound was 120°C. The bromine addition products of 4-hexenal DNPHone and X—DNPHone had different melting points, the former melting at 90—92°C and the latter at 105—110°C. They also separated on paper chromatograms. Geometric isomerism was not hence the cause of the difference in the melting points. The isolated compound X was not therefore 4-hexenal.

On the basis of these results it was obvious that the unknown X was not a hexenal. It seemed probable that the compound X had a branched carbon chain.

The unknown carbonyl compound X was liberated from its DNPHone by transderivation with levulinic acid by a modification of the method of Keeney [3] which seemed to increase the yield. The resulting solution of the free carbonyl in methylene chloride was ozonized, and the ozonide split with an alkaline silver oxide suspension. A test for keto acid was positive. The keto acid formed was identified as pyruvic acid by paper chromatography. In addition, acetic acid and a small amount of propionic acid were formed. For comparison, 2-hexenal liberated from its DNPHone was ozonized in a similar way. The test for keto acid was negative. Butyric acid and small amounts of propionic and acetic acids were formed. The ozonization of 2-hexenal thus seems to proceed as expected (with the formation of butyric acid), although small amounts of other products, including acetic and propionic acids are produced.

The formation of pyruvic acid as an ozonization product of X suggested that the structure of the carbonyl compound might be $CH_3—CH_2—CH = C(CH_3)—CHO$. A study of the literature revealed that the m.p. of 2-methyl-2-pentenal DNPHone is close to that of the isolated X—DNPHone. 2-Methyl-2-pentenal was synthesized by the method of Häusermann [4]. After being crystallized several times from methanol, the compound formed beautiful, red, rhombohedral crystals similar to those of the isolated X—DNPHone.

The m.p. and the mixed m.p. with the isolated compound were both 155°C (uncorr.). The UV-spectra were identical and the compounds were not separated on a paper chromatogram. On the basis of all known facts, the hitherto unknown aldehyde in onion vapour may safely be considered as 2-methyl-2-pentenal.

Niegisch and Stahl [5] concluded from mass-spectrometric evidence that the higher aldehyde present in onion vapour is 4-hexenal and not a condensation product of propionaldehyde which they erroneously assumed to be α-methyl-β-methyl-acrolein.

The minor unknown carbonyl Y was isolated in an amount so small that we have not had enough of its DNPHone for a more detailed study. The UV-spectrum, however, corresponds to that of a saturated aldehyde DNPHone. On the paper chromatogram it is inseparable from authentic hexenal DNPHone.

In order to elucidate the origin of 2-methyl-2-pentenal, the enzymes of onion were destroyed with trichloroacetic acid (TCA), and the volatile carbonyls distilled with steam into an ice-chilled DNPH solution .The DNPHones formed were separated on a cellulose powder column. The other aldehydes were present as usual, but at most only traces of 2-methyl-2-pentenal. In another experiment the onion was homogenized with water and the resulting pulpy mass was left to stand for one hour before TCA was added. After steam distillation, the DNPHones were fractionated as above. 2-Methyl-2-pentenal DNPHone was present in normal amounts. The results suggest that this carbonyl may be formed enzymatically in crushed onion. Because the compound was also formed in an oxygen-free solution, oxygen may not be needed for the reaction. As the amount of propionaldehyde in onion is comparatively large, it is possible that 2-methyl-2-pentenal is formed from propionaldehyde by a condensation reaction.

The volatile alcohols among the flavour substances of onion were converted into their 3,5-dinitrobenzoates as described below and chromatographed on paper. By comparison with known derivatives, they were found to be methanol and ethanol. No other volatile alcohols were isolated.

EXPERIMENTAL

Air was sucked through a homogenate of 9.5 kg of onions and 12 l of water with the aid of a vacuum pump. The vapours were trapped in a dilute 2,4-dinitrophenylhydrazine solution. After four days 595 mg of crude DNPHone mixture was collected.

Paper chromatography of DNPHones. Sheets (24 × 24 cm) of chromatographic filter paper were immersed in a 25 % solution of dimethylformamide in ethanol for 5 min and blotted between two filter papers. The unknowns were applied in chloroform solution (10—20 μl contained 5—10 μg) to the still moist paper. The paper was immediately rolled into a cylinder and development effected with *cyclo*hexane saturated with dimethylformamide employing upward flow.

Cellulose powder column chromatography of DNPHones. A cellulose powder column (7.5 × 60 cm) was prepared in the "wet" way by suspending the powder in ethanol. The column was then saturated with dimethylformamide by percolating a 15 % ethanolic solution of the latter through it and washed with *cyclo*hexane saturated with dimethylformamide until the effluent contained only one phase. The crude DNPHone mixture was dissolved, added to the column, and eluted with the same solvent.

Determination of the number of double bonds. The determinations were made according to the method of Rossmann [6] on the unknown and on synthetic 2-hexenal DNPHone. Four determinations on 2-hexenal DNPHone gave a mean double bond number of 1.27,

and four determinations on the unknown a mean double bond number of 1.03. The unknown DNPHone contained accordingly one double bond in the carbonyl part of the molecule.

Preparation of 4-hexenal DNPHone. 4-Hexenol was synthesized by the method of Brandon *et al.*[7] The corresponding aldehyde, 4-hexenal, was prepared by rapid low-temperature dichromate oxidation of this alcohol according to the method of Delaby and Guillot-Allègre [8]. After the resulting ether solution had been shaken with a dilute solution of DNPH and then washed with 2 N HCl and water, it was evaporated to dryness in vacuum and the residue crystallized from methanol. The crystals were sublimed in vacuum, crystallized from methanol and dried. The product consisted of beautiful, yellow-brown needles melting at 120°C (uncorr.). (Found: C 50.69; H 4.93; N 20.64; O 23.97. Calc. for $C_{12}H_{14}N_4O_4$: C 51.79; H 5.07; N 20.14; O 23.00).

Preparation of 4,5-dibromo-hexenal DNPHone. Bromine was rapidly added to 5 ml of 4-hexenal until a permanent colour remained. The excess bromine was destroyed by shaking the mixture with a solution of sodium hydrogen sulphite and the product washed. The oxidation and preparation of the DNPHone were carried out as above. The product consisted of oily, yellow crystals melting at 90 – 92°C.

Preparation of dibromo-X-DNPHone. 12.8 mg of the X-DNPHone was dissolved in chloroform. A solution of bromine (1 ml in 20 ml of chloroform) was added until a permanent bromine colour remained. The excess bromine was destroyed as above and the solution evaporated to dryness in vacuum. When crystallized, the residue yielded yellow crystals melting at 105 – 110°C.

Transderivation of DNPHone. 25 mg of the DNPHone and 25 ml of levulinic acid reagent (levulinic acid: N HCl = 9:1 (v/v)) were placed in a test tube provided with a vertical condenser tube. The test tube was warmed on a steam bath for 25 min and the contents washed into a separatory funnel with 60 ml of water and extracted with three 15 ml portions of methylene chloride. The methylene chloride solution was extracted with a halfsaturated sodium bicarbonate solution until no more colour could be extracted and then washed with water. The resulting methylene chloride solution, the colour of which indicated the transderivation to be incomplete, was transferred to a small distillation flask together with an equal volume of distilled water. The methylene chloride was distilled off first, and subsequently water, both into the same flask. Water was distilled until the small stream in the condenser was observed to consist of only one phase. The distillates were shaken and the aqueous layer discarded. The methylene chloride solution of the parent carbonyl was dried.

Ozonization of the free carbonyl. Ozone in approximately 5-fold excess was bubbled through the ice-cold carbonyl solution. The solution was evaporated to dryness in vacuum within one hour, and the residue treated in the usual way with alkaline silver oxide suspension and filtered (80 ml).

Preparation of keto acid DNPHone. 20 ml of a dilute solution of DNPH in hydrochloric acid was added to 10 ml of the above filtrate and warmed for 20 min on a water bath. The mixture was extracted with methylene chloride until the coloured matter had been transferred into the methylene chloride. The methylene chloride solution was then extracted with a saturated bicarbonate solution, acidified with sulphuric acid, and again extracted with methylene chloride. The resulting methylene chloride solution was subjected to paper chromatography.

Paper chromatography of the keto acid DNPHones. The keto acid DNPHones were chromatographed on Whatman No. 1 paper which was developed through downward displacement with butanol-ethanol-water (5:1:4). The chromatogram of the keto acid DNPHones derived from X showed spots which did not separate from authentic pyruvic acid DNPHone spots over a distance of 50 cm and an unidentified minor spot near the solvent front.

Enzymatic experiments. An onion (80 g fresh wt.) was chilled in dry ice, crushed, and homogenized in 150 ml of 10 % TCA. The homogenate was distilled with steam into 100 ml of a dilute DNPH solution until about 200 ml had been collected. After overnight storage, the distillate was extracted with methylene chloride. The methylene chloride solution was extracted with hydrochloric acid in order to remove excess DNPH, washed, and evaporated to dryness. The residue, 25 mg in all, consisted of oily, red crystals with a dungy odour. Fifteen milligrams of crystals were fractionated on a cellulose powder column (1.5 × 75 cm). Only one fraction contained tracesof 2-methyl-2-pentenal DNPHone.

Another onion (44 g fresh wt.) was homogenized with 150 ml of water and the homogenate left to stand for one hour. Fifteen grams of TCA was then added, the homogenate steam-distilled, and the distillate worked up and fractionated as above. 2-Methyl-2-pentenal DNPHone appeared in nine fractions in an amount far exceeding that recovered in the preceding experiment.

In a third experiment an onion (131 g fresh wt.) was homogenized in 150 ml of oxygen-free water in an oxygen-free atmosphere (purified nitrogen) in a special apparatus and the homogenate left to stand in this atmosphere under a low pressure for one hour. 18 g of TCA dissolved in 30 ml of boiled, warm water was added through a stopcock and mixed with the homogenate. The homogenate was removed with a low pressure to the steam distillation apparatus and worked up as above. Eleven fractions contained 2-methyl-2-pentenal DNPHone in an amount approximately equal to that recovered in the preceding experiment.

The volatile alcohols. 194 g of onions were homogenized in a Waring blendor with 450 ml of distilled water and immediately transferred to a flask and steam distilled. The distillation was discontinued when 600 ml of distillate had been collected. The distillate was then exhaustively percolated with peroxide-free ether and the ether solution (250 ml) dried ($CuSO_4$) and filtered. One gram of 3,5-dinitrobenzyl chloride was then added and the solution was shaken until all had dissolved. After standing for 24 h, the ether was distilled off in vacuum. The residue was heated on a steam bath for a few minutes and dissolved in peroxide-free ether. The ether solution was extracted with water and distilled to dryness in vacuum. The residue (41 mg) was dissolved in 2 ml of chloroform and subjected to paper chromatography.

Paper chromatography of alkyl 3,5-dinitrobenzoates. Sheets (24 × 24 cm) of chromatographic filter paper (Whatman No. 4) were immersed in a 25 % ethanolic solution of dimethylformamide for 5 min and blotted between two filter papers. The compounds were applied in chloroform solution (3 – 15 μl) to the still moist paper and the paper immediately rolled into a cylinder and developed with decaline saturated with dimethylformamide by the ascending technique. The spots on the dried paper were visible in ultraviolet light.

This investigation is a part of a research project under U.S. Public Law No. 480, 83rd Congress.

REFERENCES

1. Gaddis, A. M., Ellis, R. and Currie, G. T. *Food Research* **24** (1959) 283.
2. Houben-Weyl *Methoden der Organischen Chemie* **7** (1954) 1, p. 120.
3. Keeney, M. *Anal. Chem.* **29** (1957) 1489.
4. Häusermann, M. *Helv. Chim. Acta* **34** (1951) 1482.
5. Niegisch, W. D. and Stahl, W. H. *Food Research* **21** (1956) 657.
6. Rossmann, E. *Ber.* **65** (1932) 1847.
7. Brandon, R. C., Derfer, J. M. and Boord, C. E. *J. Am. Chem. Soc.* **72** (1950) 2120.
8. Delaby, R. and Guillot-Allègre, S. *Bull. soc. chim. France* IV **54** (1933) 301.

Received January 12, 1961.

ACTA CHEMICA SCANDINAVICA 15 (1961) 1285–1288

Polarographic Reduction of Aliphatic Esters

MILDA PRYTZ and TH. ØSTERUD

Yrkeshygienisk Institutt, Blindern - Oslo, Norway

Reaction mixtures of pure esters with hydroxylamine have been polarographed in ethanol-water solutions of tetra-*n*-butylammonium iodide, buffered with tetraethylammonium hydroxide. The resulting hydroxamic acid curves gave direct polarographic determinations of the aliphatic esters in question.

A series of esters were treated with an excess of hydroxylamine and sodium hydroxide in methanol solutions. After the reaction mixtures had been heated for fixed periods they were polarographed at room temperature and at different pH's with ethanol-water solutions of tetra-*n*-butylammonium iodide and tetraethylammonium hydroxide as supporting electrolyte.

We got distinct polarographic waves showing constant half wave potentials. These were for nearly related esters practically corresponding. Parallels without any addition of esters gave no analogous waves, *i.e.* the above mentioned curves have to be ascribed to the hydroxamic acid produced by the interaction of esters and hydroxylamine.

Esters have previously been determined colorimetrically as hydroxamic acids by Thompson [1]. Our reaction mixtures did not differ essentially from his.

EXPERIMENTAL

A recording polarograph from Radiometer, Copenhagen (new model) was used. A mixture of nitrogen and hydrogen was passed through a chromochloride solution before it was bubbled through the electrolytic cell. For the heating of the reaction mixtures a water bath was used. Various concentrations of esters and of hydroxylamine as well as different lengths of time for heating of the reaction mixtures were tried. We fixed on a solution of ester in methanol, which was refluxed with a solution of hydroxylamine hydrochloride and sodium hydroxide in methanol in a water bath. The concentrations were as regards esters 0.04 M, as regards hydroxylamine hydrochloride 0.7 M and as to sodium hydroxide 3 M. Blank parallels without esters were also run. As supporting electrolyte was used a 0.1 M solution of $(n\text{-}C_4H_9)_4NI$ from A. Frederick Smith, Columbus, Ohio, in a mixture of 50 parts of 95 % ethyl alcohol to 45 parts of water. In the electrolytic cell was added 9 drops of reaction mixture and some drops of tetraethylammonium hydroxide to 10 ml of the supporting electrolyte, and the pH was controlled. The tetraethylammonium hydroxide was either self prepared or obtained from the British Drug Houses. We found that a pH of about 12 gave the best curves. We had earlier found that the first hydroxamic

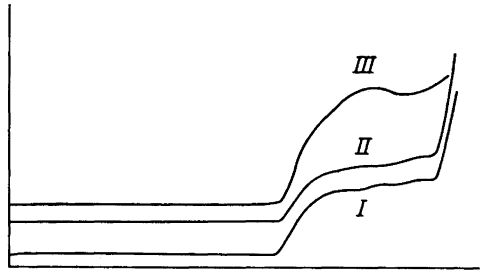

Fig. 1. Polarographic waves of acetic acid ethyl ester and of butyric acid ethyl ester at pH 12.6. Mercury anode.

I. Acetic acid ethyl ester. Reaction mixture heated 1 h. Sens. 1.5 × 1 000.
II. Acetic acid ethyl ester. Reaction mixture heated 2 h. Sens. 1.5 × 1 000.
III. Butyric acid ethyl ester. Reaction mixture heated 1 h. Senc. 2 × 1 000.

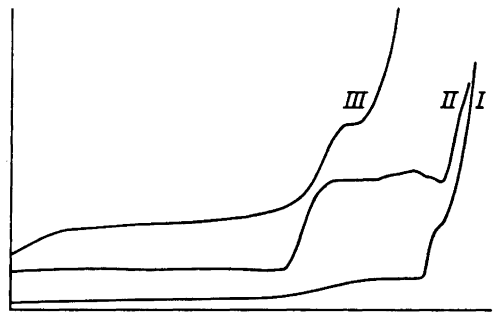

Fig. 2. Polarographic curves of:

I. Blank test, heated for 1 h. Sens. 1.5 × 1 000, pH 12.6.
II. Acetic acid *iso*propyl ester. Reaction mixture heated for 2 h. Sens. 1.5 × 1 000, pH 12.6.
III. Propionhydroxamic acid. Sens. 7 × 10, pH 12.6.
Mercury anode.

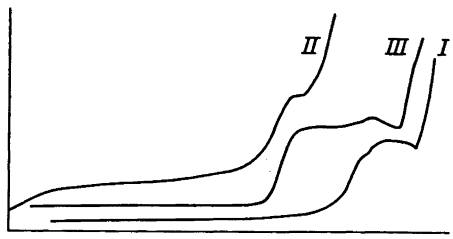

Fig. 3. Polarographic curves at pH 12.5 of:

I. Acetaldoxime. Sens 5 × 100.
II. Propionhydroxamic acid. Sens. 7 × 10.
III. Acetic acid *iso*propyl ester. Sens. 1.5 × 1 000. Mercury anode.

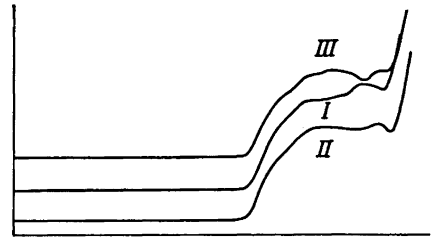

Fig. 4. Polarographic curves with S.C.E. anode of reaction mixtures heated for 1.5 h.

I. Acetic acid *iso*propyl ester.
II. Propionic acid ethyl ester.
III. Butyric acid ethyl ester.

wave was most suitable for analytical purposes [2] and consequently we concentrated on that. For control some pure hydroxamic acids were polarographed in our present supporting electrolyte. In our polarographic investigation of oximes [3] we used McIlvaine buffers. We therefore also determined the half-wave potentials of oximes in the above mentioned supporting electrolyte. We found that a mercury anode gave more reliable curves than a S.C.E. anode, as with use of the latter the cathode was apt to run. We therefore found the mercury pool anode more suited for practical analytical purposes in this connection, and only used the S.C.E. anode for recording of half wave potentials.

As a maximum depressor was used tylose, about 0.005 %.

RESULTS

Earlier investigations [4] have shown that polarographic waves for hydroxamic acids in alkaline solutions were not affected, within reasonable limits, by time and heating, whereas polarographic waves for hydroxylamine in alkaline solutions decrease if the solutions stand for some time, and the decrease was greatly accelerated by heating. We therefore polarographed a series of reaction mixtures at different pH's, with varying excess of hydroxylamine, and with diverse lengths of time for heating, until we found the most favourable conditions for obtaining unmistakable and good waves. We decided on alkaline solutions with an excess of hydroxylamine of about 1 part of ester to 17.5 parts of hydroxylamine (molar conc.), and a time of heating of the reaction mixture between the limits 1 h and 2 h.

In Fig. 1 some curves are given for acetic acid ethyl ester (ethyl ethanoate) corresponding to acethydroxamic acid and of butyric acid ethyl ester (ethyl butanoate). In Fig. 2 are given curves for acetic acid *iso*propyl ester, corresponding to propionhydroxamic acid, as well as for a blank test.

Comparisons between oximes, pure hydroxamic acids and those produced in a reaction mixture seem to be indicated. A grouping of polarographic waves

Table 1. Polarographic half wave potentials of oximes and of pure hydroxamic acids and of converted esters at different pH's. Supporting electrolyte was $(n\text{-}C_4H_9)_4NI + (C_2H_5)_4NOH$ in equal parts of ethanol and water.

a. Mercury anode			b. S.C.E. anode		
Compound	pH	Half wave potential, V	Compound	pH	Half wave potential, V
Acetaldoxime	8.8	2.00	Acetaldoxime	8.5	2.25
Acetaldoxime	11.6	2.04	Acetaldoxime	9.6	2.26
Propionhydroxamic acid	8.6	1.79			
Propionhydroxamic acid	10.8	1.79			
Acetic acid ethyl ester	12.6	1.67→1.70	Acetic acid ethyl ester	12.6	1.76
Acetic acid *iso*propyl ester	12.6	1.68→1.70	Acetic acid *iso*propyl ester	12.6	1.80
Butyric acid ethyl ester	12.6	1.69			

of an oxime, a hydroxamic acid and a reaction mixture in the supporting electrolyte used for this investigation is therefore given in Fig. 3. A mercury pool anode has been used.

As it might be of interest to record the half wave potentials with regard to the S.C.E. some determinations were made of ethyl esters of acetic acid and of propionic acid. Curves are given in Fig. 4.

Values of half wave potentials (under as similar conditions as possible as regards pH, supporting electrolyte and concentrations, and for esters time of heating) for oximes, for pure hydroxamic acids, and for reaction mixtures *i.e.* the corresponding esters are given in Table 1.

DISCUSSION

Our earlier observations that hydroxamic acids may be determined polarographically in alkaline solutions even if these originally contained some hydroxylamine [4] have been the basis of the present investigation.

We have now been able to verify our assertions, even when hydroxamic acids are present in solution as a direct result of interaction between esters and hydroxylamine. As the reaction mixture was very simple to prepare, the excess of hydroxylamine was very easy to destroy without affecting the hydroxamic acid, and the polarographic curves were unmistakable, we dare claim to have found a serviceable method for direct polarographic qualitative determination of aliphatic esters.

Experiments of a more quantitative nature will be undertaken. The method will also be tested on ester-containing herbs.

The authors are greatly indebted to Dr. Karl Wülfert for giving us working facilities at Yrkeshygienisk Institute, likewise to Cand. mag. Nicolay Soteland for the recording of the polarograms.

REFERENCES

1. Thompson, Adrienne R. *Australian J. Sci Research Ser. A* **3** (1950) 128.
2. Prytz, M. and Østerud, Th. *Acta Chem. Scand.* **11** (1957) 1530.
3. Østerud, Th. and Prytz, M. *Acta Chem. Scand.* **10** (1956) 451.
4. Østerud, Th. and Prytz, M. *Acta Chem. Scand.* **13** (1959) 2114.

Received February 24, 1961.

ACTA CHEMICA SCANDINAVICA 15 (1961) 1289–1294

Vibrational Mean-Square Amplitude Matrices

XIV. Treatment of Linear Symmetrical X_2Y_2 Molecules with Application to Cyanogen

S. J. CYVIN and E. MEISINGSETH

Institutt for teoretisk kjemi, Norges tekniske høgskole, Trondheim, Norway

A theoretical treatment of the vibrational mean-square amplitude quantities for linear symmetrical X_2Y_2 molecules is presented. The evaluation of the generalized (parallel and perpendicular) mean-square amplitudes for the four types of interatomic distances is included. Numerical computations for cyanogen are reported, *viz.* those of the mean amplitudes of vibration, and the mean-square parallel and perpendicular amplitudes, the latter ones having been used for calculating the "shrinkage" effects.

The mean-square amplitude matrices [1] have proved to be very useful in spectroscopic calculations, especially those associated with electron-diffraction investigations. In the present paper some studies on cyanogen are reported, which have been actuated by recent electron-diffraction work on this molecule, to be communicated later. The theoretical treatment here presented may also be adapted to butatriene [2], if this molecule is considered as a linear four-particle structure ($CH_2{=}C{=}C{=}CH_2$).

THEORETICAL TREATMENT

The treatment is based on the assumption of small harmonic vibrations.[3]

Symmetry coordinates. The chosen symmetry coordinates are specified below.

Symmetry species Σ_g^+:	S_1	$= 2^{-\frac{1}{2}}(r_1 + r_2)$
	S_2	$= d$
» » Σ_u^+:	S_3	$= 2^{-\frac{1}{2}}(r_1 - r_2)$
» » Π_g:	S_{4a}	$= 2^{-\frac{1}{2}}(RD)^{\frac{1}{2}}(\alpha_1 - \alpha_2)$
» » Π_g:	S_{4b}	$= 2^{-\frac{1}{2}}(RD)^{\frac{1}{2}}(\alpha_1' - \alpha_2')$
» » Π_u:	S_{5a}	$= 2^{-\frac{1}{2}}(RD)^{\frac{1}{2}}(\alpha_1 + \alpha_2)$
» » Π_u:	S_{5b}	$= 2^{-\frac{1}{2}}(RD)^{\frac{1}{2}}(\alpha_1' + \alpha_2')$

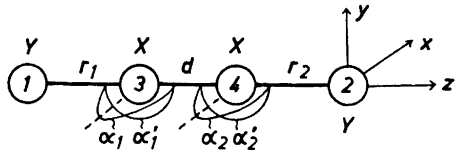

Fig. 1. Notation and orientation used for the linear symmetrical X_2Y_2 molecular model. Notice the numbering of atoms.

Here r_1 and r_2 designate the X—Y stretching coordinates, d designating the X—X stretchings. a_1 and a_2 designate the XXY angle bendings in the xz plane, a_1' and a_2' designating those in the yz plane (see Fig. 1). R and D are used to identify the X—Y and X—X equilibrium distances, respectively.

Cartesian displacement coordinates. With the chosen orientation of the Cartesian coordinate axes and numbering of the atoms (see Fig. 1) the following expressions have been found for the Cartesian displacement coordinates in terms of the symmetry coordinates.

$$x_1 = 2^{-\frac{1}{2}}(D/R)^{\frac{1}{2}}m_X K^{-1}S_{4a} + 2^{-\frac{1}{2}}(R/D)^{\frac{1}{2}}m_X(m_X + m_Y)^{-1}S_{5a}$$
$$y_1 = 2^{-\frac{1}{2}}(D/R)^{\frac{1}{2}}m_X K^{-1}S_{4b} + 2^{-\frac{1}{2}}(R/D)^{\frac{1}{2}}m_X(m_X + m_Y)^{-1}S_{5b}$$
$$z_1 = -2^{-\frac{1}{2}}S_1 - \tfrac{1}{2}S_2 - 2^{-\frac{1}{2}}m_X(m_X + m_Y)^{-1}S_3$$
$$x_2 = -2^{-\frac{1}{2}}(D/R)^{\frac{1}{2}}m_X K^{-1}S_{4a} + 2^{-\frac{1}{2}}(R/D)^{\frac{1}{2}}m_X(m_X + m_Y)^{-1}S_{5a}$$
$$y_2 = -2^{-\frac{1}{2}}(D/R)^{\frac{1}{2}}m_X K^{-1}S_{4b} + 2^{-\frac{1}{2}}(R/D)^{\frac{1}{2}}m_X(m_X + m_Y)^{-1}S_{5b}$$
$$z_2 = 2^{-\frac{1}{2}}S_1 + \tfrac{1}{2}S_2 - 2^{-\frac{1}{2}}m_X(m_X + m_Y)^{-1}S_3$$
$$x_3 = -2^{-\frac{1}{2}}(D/R)^{\frac{1}{2}}[1 + 2(R/D)]m_Y K^{-1}S_{4a} - 2^{-\frac{1}{2}}(R/D)^{\frac{1}{2}}m_Y(m_X + m_Y)^{-1}S_{5a}$$
$$y_3 = -2^{-\frac{1}{2}}(D/R)^{\frac{1}{2}}[1 + 2(R/D)]m_Y K^{-1}S_{4b} - 2^{-\frac{1}{2}}(R/D)^{\frac{1}{2}}m_Y(m_X + m_Y)^{-1}S_{5b}$$
$$z_3 = -\tfrac{1}{2}S_2 + 2^{-\frac{1}{2}}m_Y(m_X + m_Y)^{-1}S_3$$
$$x_4 = 2^{-\frac{1}{2}}(D/R)^{\frac{1}{2}}[1 + 2(R/D)]m_Y K^{-1}S_{4a} - 2^{-\frac{1}{2}}(R/D)^{\frac{1}{2}}m_Y(m_X + m_Y)^{-1}S_{5a}$$
$$y_4 = 2^{-\frac{1}{2}}(D/R)^{\frac{1}{2}}[1 + 2(R/D)]m_Y K^{-1}S_{4b} - 2^{-\frac{1}{2}}(R/R)^{\frac{1}{2}}m_Y(m_X + m_Y)^{-1}S_{5b}$$
$$z_4 = \tfrac{1}{2}S_2 + 2^{-\frac{1}{2}}m_Y(m_X + m_Y)^{-1}S_3$$

Here it has been made use of the abbreviation

$$K = (D/R)(m_X + m_Y) + 4[1 + (R/D)]m_Y$$

m_X and m_Y denote the X and Y atomic masses, respectively.

F and G matrices. The set of equations connecting force constants and normal frequencies are given in the book of Herzberg [4] and shall not be repeated here. The Wilson G matrix elements may be evaluated by the standard methods [3,5–7]. For some aspects of the GF matrix treatment of the linear symmetrical X_2Y_2 molecular model in particular, see [8]. For the linear vibrations, see also Ref.[9]

Σ matrix. The six non-vanishing elements of the symmetrized mean-square amplitude matrix ($\Sigma = \langle S \tilde{S} \rangle$) are defined by

$$\Sigma_1 = \langle S_1^2 \rangle,\ \Sigma_2 = \langle S_2^2 \rangle,\ \Sigma_{12} = \langle S_1 S_2 \rangle,$$
$$\Sigma_3 = \langle S_3^2 \rangle,\ \Sigma_4 = \langle S_{4a}^2 \rangle = \langle S_{4b}^2 \rangle,\ \Sigma_5 = \langle S_{5a}^2 \rangle = \langle S_{5b}^2 \rangle$$

One has the following relations for the normal frequencies in terms of the Σ matrix elements.

$$\begin{aligned} \Delta_1 + \Delta_2 &= m_Y\Sigma_1 + \tfrac{1}{2}(m_X + m_Y)\Sigma_2 + 2^{\frac{1}{2}}m_Y\Sigma_{12} \\ \Delta_1\Delta_2 &= \tfrac{1}{2}\, m_X m_Y(\Sigma_1\Sigma_2 - \Sigma_{12}^2) \\ \Delta_3 &= m_X m_Y(m_X + m_Y)^{-1}\Sigma_3 \\ \Delta_4 &= m_X m_Y K^{-1}\Sigma_4 \\ \Delta_5 &= (R/D)m_X m_Y(m_X + m_Y)^{-1}\Sigma_5 \end{aligned}$$

The normal frequencies are implied according to

$$\Delta_k = (h/8\pi^2\nu_k)\, \coth(h\nu_k/2kT)$$

where h is Planck's constant, k Boltzmann's constant, and T the absolute temperature.

Additional mean-square amplitude quantities. Further mean-square amplitude quantities will be introduced for the parallel vibrations of the considered molecular model, viz.:

$$\sigma_r = \langle r_1^2 \rangle = \langle r_2^2 \rangle,\ \sigma_{rr} = \langle r_1 r_2 \rangle,$$
$$\sigma_d = \langle d^2 \rangle,\ \sigma_{rd} = \langle r_1 d \rangle = \langle r_2 d \rangle$$

For these quantities in terms of the Σ matrix elements introduced above, one finds

$$\sigma_r = \tfrac{1}{2}(\Sigma_1 + \Sigma_3),\quad \sigma_{rr} = \tfrac{1}{2}\,(\Sigma_1 - \Sigma_3),$$
$$\sigma_d = \Sigma_2,\qquad \sigma_{rd} = 2^{-\frac{1}{2}}\Sigma_{12}$$

The quantities σ_r and σ_d represent the mean-square amplitudes of vibration for the (bonded) X—Y and X—X distances, respectively, σ_{rr} and σ_{rd} being the interaction mean-square amplitudes.

For the mean-square amplitudes of vibration for the (non-bonded) X...Y and Y...Y distances one finds

$$\sigma_{r+d} = \sigma_r + \sigma_d + 2\sigma_{rd} = \tfrac{1}{2}\Sigma_1 + \Sigma_2 + 2^{\frac{1}{2}}\Sigma_{12} + \tfrac{1}{2}\Sigma_3$$

and

$$\sigma_{r+d} = 2\sigma_r + 2\sigma_{rr} + \sigma_d + 4\sigma_{rd} = 2\Sigma_1 + \Sigma_2 + 8^{\frac{1}{2}}\Sigma_{12}$$

respectively.

Mean-square perpendicular amplitudes and the "shrinkage" effect. The shrinkage effect in linear molecules, which has been observed from electron-diffraction by Bastiansen *et al.*[2,10,11] may be calculated spectroscopically by means of the mean-square perpendicular amplitudes [12], as has been pointed out by Morino [13]. In the present case of the symmetrical X_2Y_2 molecular model, the following two independent shrinkage effects, given to the first approximation (valid for small harmonic vibrations), will be encountered:

$$-\delta^g_{r+d} = \frac{\tau_{r+d}}{R+D} - \frac{\tau_r}{R} - \frac{\tau_d}{D}$$

$$-\delta^g_{2r+d} = \frac{\tau_{2r+d}}{2R+D} - \frac{2\tau_r}{R} - \frac{\tau_d}{D}$$

Here

$$\tau_r = \langle(x_1-x_3)^2\rangle = \langle(x_2-x_4)^2\rangle = \langle(y_1-y_3)^2\rangle = \langle(y_2-y_4)^2\rangle$$

$$\tau_d = \langle(x_3-x_4)^2\rangle = \langle(y_3-y_4)^2\rangle$$

$$\tau_{r+d} = \langle(x_1-x_4)^2\rangle = \langle(x_2-x_3)^2\rangle = \langle(y_1-y_4)^2\rangle = \langle(y_2-y_3)^2\rangle$$

$$\tau_{2r+d} = \langle(x_1-x_2)^2\rangle = \langle(y_1-y_2)^2\rangle$$

Evaluation of the generalized mean-square amplitudes. Let and arbitrary atom pair ij be considered. The corresponding generalized mean-square amplitudes may be expressed as $\langle(\xi_i-\xi_j)\,(\eta_i-\eta_j)\rangle$, where $\xi,\eta = x, y$ or z. In the present case the given expressions of the Cartesian displacement coordinates make it possible to detect the transformation coefficients in any expression of the type

$$\xi_i-\xi_j = \sum_n A^{\xi}_{ijn} S_n = \widetilde{A^{\xi}_{ij}}\, S$$

or

$$\eta_i-\eta_j = \sum_n A^{\eta}_{ijn}\, S_n = \widetilde{A^{\eta}_{ij}} S$$

Hence the generalized mean-square amplitudes may be evaluated in terms of the Σ matrix elements according to

$$\langle(\xi_i-\xi_j)(\eta_i-\eta_j)\rangle = \widetilde{A^{\xi}_{ij}}\,\Sigma\, A^{\eta}_{ij}$$

For the mean-square parallel amplitudes, corresponding to $\xi = \eta = z$, the above given expressions for σ_r, σ_d, σ_{r+d} and σ_{2r+d} are obtained. These expressions, referred to as the mean-square amplitudes of vibration, are identical with the mean-square parallel amplitudes to the first approximation.

As to the mean cross product in the present case, all of them vanish because of symmetry.

The results obtained for the mean-square perpendicular amplitudes are given in the following.

Table 1. Mean-square parallel (σ) and perpendicular (τ) amplitudes for $^{12}C_2{}^{14}N_2$ at $T = 0$ and 298°K.

Distance	Symbol	Generalized mean-square amplitudes (Å² units)	
		$T = 0$	298°K
C≡N	σ_r	0.001215	0.001217
	τ_r	0.007590	0.012955
C−C	σ_d	0.001730	0.001758
	τ_d	0.004948	0.005885
C···N	σ_{r+d}	0.002055	0.002102
	τ_{r+d}	0.006006	0.011082
N···N	σ_{2r+d}	0.002381	0.002452
	τ_{2r+d}	0.000507	0.000603

Table 2. Mean amplitudes of vibration for $^{12}C_2{}^{14}N_2$ at $T = 0$ and 298°K.

Distance	Symbol	Mean amplitude of vibration (Å units)	
		$T = 0$	298°K
C≡N	u_r	0.0349	0.0349
C—C	u_d	0.0416	0.0419
C···N	u_{r+d}	0.0453	0.0458
N···N	u_{2r+d}	0.0488	0.0495

$$\tau_r = \tfrac{1}{2}(D/R)\{m_X + [1 + (R/D)]m_Y\}^2K^{-2}\Sigma_4 + \tfrac{1}{2}(R/D)\Sigma_5$$

$$\tau_d = 2(D/R)[1 + 2(R/D)]^2m_Y{}^2K^{-2}\Sigma_4$$

$$\tau_{r+d} = \tfrac{1}{2}(D/R)\{m_X - [1 + 2(R/D)]m_Y\}^2K^{-2}\Sigma_4 + \tfrac{1}{2}(R/D)\Sigma_5$$

$$\tau_{2r+d} = 2(D/R)m_X{}^2K^{-2}\Sigma_4$$

For the meaning of K, see the above section of Cartesian displacement coordinates.

NUMERICAL COMPUTATIONS FOR CYANOGEN

The adopted values for the equilibrium interatomic distances are $R = 1.157$ Å for C≡N [14,15] and $D = 1.380$ Å for C—C [15], which are not much different from the values used by Langseth and Møller [16] in their calculations of the potential constants for cyanogen. In the present calculations the interaction force constant value $F_{12} = 0.08485$ mdyne/Å (referred to the symmetry coordinate system) was taken from Langseth and Møller [16]. To determine the remaining force constants, the $^{12}C_2{}^{14}N_2$ vibrational frequencies taken from the same paper [16] were applied, *viz.* Raman frequencies from the investigation of the mentioned authors [16], together with some earlier infrared frequencies [17]. The final values showed only slight deviations from those of Langseth and Møller [16], mainly due to the different equilibrium parameters employed.*

Table 3. Shrinkage effect for $^{12}C_2{}^{14}N_2$ at $T = 0$ and 298°K.

Distance	Symbol	Shrinkage effect (Å units)	
		$T = 0$	298°K
C···N	δ^g_{r+d}	0.008	0.011
N···N	δ^g_{2r+d}	0.017	0.024

* The present values are $F_1 = 15.654$, $F_2 = 7.308$, $F_{12} = 0.08485$ and $F_3 = 17.582$ for the linear vibrational force constants, all in mdyne/Å. It should be noticed that Langseth and Møller [16] uses different symmetry coordinates from the present ones. In terms of their notation for the potential constants, one has: $F_1 = 4a_{11}$, $F_2 = 2(a_{11} + a_{22} + 2a_{12})$, $F_{12} = 8\frac{1}{2}(a_{11} + a_{12})$, and $F_3 = 4a_{33}$.

The Σ matrix elements were calculated according to [1]

$$\Sigma = L \Delta \tilde{L}$$

where L is the normal coordinate transformation matrix ($S = LQ$) and has been determined by the standard method of characteristic vectors [3]. The final results, obtained by means of the Σ matrix elements, are presented in Tables 1—3. Table 1 shows the mean-square parallel and perpendicular amplitudes for the four types of interatomic distances. Table 2 shows the mean amplitudes of vibration for the same types of distances, viz. $u_{X-Y} = \sigma_r^{\frac{1}{2}}$, $u_{X-X} = \sigma_d^{\frac{1}{2}}$ $u_{X\cdots Y} = \sigma_{r+d}^{\frac{1}{2}}$ and $u_{Y\cdots Y} = \sigma_{2r+d}^{\frac{1}{2}}$. Finally, in Table 3 the calculated shrinkage effects are shown.

It is intended to compare the presently calculated mean amplitudes of vibration and shrinkage effects with the results from an electron-diffraction investigation now in progress.

REFERENCES

1. Previous articles of this series: Cyvin, S. J. *Spectrochim. Acta* **15** (1959) 828, 835, 958; *Acta Chem. Scand.* **13** (1959) 1397, 1400, 1809; *J. Mol. Spectroscopy* **5** (1960) 38.
2. Almenningen, A., Bastiansen, O. and Trætteberg, M. *Acta Chem. Scand. In press.*
3. Wilson, E. B., Jr., Decius, J. C. and Cross, P. C. *Molecular Vibrations*, McGraw-Hill Book Co., New York 1955.
4. Herzberg, G. *Infrared and Raman Spectra of Polyatomic Molecules*, D. van Nostrand Co. New York 1945.
5. Wilson, E. B., Jr. *J. Chem. Phys.* **9** (1941) 76.
6. Decius, J. C. *J. Chem. Phys.* **11** (1948) 1025.
7. Ferigle, S. M. and Meister, A. G. *J. Chem. Phys.* **19** (1951) 982.
8. Cleveland, F. F. and Meister, A. G. *J. chim. phys.* **46** (1949) 108.
9. Cyvin, S. J. *Spectrochim. Acta* **15** (1959) 341.
10. Almenningen, A., Bastiansen, O. and Munthe-Kaas, T. *Acta Chem. Scand.* **10** (1956) 261.
11. Almenningen, A., Bastiansen, O. and Trætteberg, M. *Acta Chem. Scand.* **13** (1959) 1699.
12. Morino, Y. and Hirota, E. *J. Chem. Phys.* **23** (1955) 737.
13. Morino, Y. *Private communications.*
14. Westenberg, A. A. and Wilson, E. B., Jr. *J. Am. Chem. Soc.* **72** (1950) 109.
15. Møller, C. K. and Stoicheff, B. P. *Can. J. Phys.* **32** (1954) 635.
16. Langseth, A. and Møller, C. K. *Acta Chem. Scand.* **4** (1950) 725.
17. Bailey, C. R. and Carsons, S. C. *J. Chem. Phys.* **7** (1939) 859.

Received February 7, 1961.

ACTA CHEMICA SCANDINAVICA 15 (1961) 1295–1302

Cyclizations of Thiocarbohydrazide and its Mono-hydrazones

Part III *. Reactions with Carbon Disulphide in Pyridine

JAN SANDSTRÖM

Department of Organic Chemistry, University of Lund, Lund, Sweden

When thiocarbohydrazide reacts with carbon disulphide in boiling pyridine, the pyridinium salts of 3,5-dimercapto-4-amino-4,1,2-triazole and 2,4-dimercapto-[4,1,2]-triazolo-[3,4-b]-[1,3,4]-thiadiazole are formed. The dimercapto-amino-triazole has been described as "dithio-*p*-urazine" by previous authors. — Under the same conditions mono-thiocarbohydrazones give 5-mercapto-1,3,4-thiadiazol-2-yl-hydrazones.

In 1923, Arndt and Bielich [1] reported the synthesis of 3,5-dimercapto-4-amino-4,1,2-triazole (Ia) from hydrazindithiocarboxamide and hydrazine. They reported the m.p. 228° and prepared a dibenzyl derivative (Ib) with m.p. 147° and a benzylidene derivative with m.p. 136°. This synthesis has been confirmed by Hoggarth [2]. In 1924, Guha and De [3,4] described the preparation of "dithio-*p*-urazine" (II) in a variety of ways, one of which was by heating thiocarbohydrazide and carbon disulphide in a sealed tube. They reported the m.p. 203—204° and prepared a dibenzyl derivative with m.p. 142°, but they were unable to obtain a benzylidene derivative. In the same communication [4] Guha and De claim to have prepared the triazole (Ia) by treatment of 1-thiocarbamoyl-thiocarbohydrazide with hydrochloric acid, but Scott and Audrieth [5] and Beyer and Kröger [6] have shown that the starting material of Guha and De was not 1-thiocarbamoyl-thiocarbohydrazide, which reacts quite differently with hydrochloric acid. Therefore, this statement of Guha and De is open to doubt.

Their evidence in favour of the structure (II) has recently been critically examined by Wiley [7], who supported their conclusion. The preparation of (II) has also been reported by Beckett and Dyson [8] and more recently by Wangel [9], who also prepared a monobenzyl and a dicarboxymethyl derivative.

* Part II. *Acta Chem. Scand.* 14 (1960) 1939.

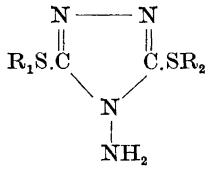

I

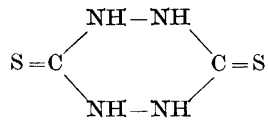

II

a, $R_1 = R_2 = H$
b, $R_1 = R_2 = PhCH_2$
c, $R_1 = PhCH_2$, $R_2 = H$
d, $R_1 = R_2 = CH_2CO_2H$
e, $R_1 = CH_3$, $R_2 = H$
f, $R_1 = R_2 = CH_3$

However, it has been known for a long time that the compound first described as the oxygen analogue of (II)[10–12], and several compounds first given similar structures [11,13] are in fact 4-aminotriazoles, and there is ample reason to suspect that the alleged dithio-*p*-urazine of Guha and De is identical with the 4-amino-dithiourazole (Ia) of Arndt and Bielich.

Both preparations have now been repeated, and the products obtained gave the same melting points (222°) after several recrystallizations, and they gave identical ultraviolet and infrared spectra. The dibenzyl derivatives were also identical with m.p. 148—149°. The monobenzyl and dicarboxymethyl derivatives (Ic) and (Ie) were also prepared and were found to have melting points close to those reported by Wangel [9].

The 4-amino-triazole structure was demonstrated by deamination of the dibenzyl derivative (Ib) with nitrous acid. 3,5-Dibenzylthio-1,2,4-triazole was formed, which has already been described by Arndt and Milde [14] and by Fromm [15]. The dibenzyl derivative (Ib) also gave a Schiff base with benzaldehyde, contrary to the statement of Arndt and Bielich [1].

The 4-aminotriazoles (Ia-f) all show a fairly strong infrared band in the region 1 600—1 620 cm^{-1}, and a similar band is found in 3-mercapto-4-amino-4,1,2-triazole [16] and in 3-mercapto-4-amino-5-methyl-4,1,2-triazole [17] at 1 610 cm^{-1}. This band is missing in corresponding triazoles without 4-amino group. The band is very likely due to the scissoring vibration of the primary amino group, which is listed by Randall *et al.*[18] in the region 1 560—1 640 cm^{-1}. Brown *et al.*[19] have found a band at 1 590 cm^{-1} in the spectrum of 3-amino-rhodanine, which is ascribed to a N—H bending mode in the N-amino group. The N—H stretching modes are obscured by strong hydrogen bonding, and no useful information has been obtained from this region. For solubility reasons all spectra had to be recorded with the samples in potassium bromide disks.

A convenient synthesis of (Ia) was found in the reaction between thiocarbohydrazide and two equivalents of carbon disulphide in boiling pyridine. From the boiling solution a pyridine salt of (Ia) separates in high purity in 50 % yield. The free acid (Ia) is rapidly oxidized to the disulphide in the air, and it is therefore conveniently stored as the pyridinium salt, from which it is easily prepared by acidification of an aqueous solution with hydrochloric acid. For a spectrophotometric investigation of the structure of (Ia), the results of which will be reported in a later communication, the mono- and dimethyl thioethers (Ie) and (If) were prepared.

From the mother liquor of the pyridinium salt of (Ia) the pyridinium salt of 2,4-dimercapto-[4,1,2]-triazolo-[3,4-b]-[1,3,4]-thiadiazole (IIIa) is obtained in 40 % yield together with a small amount of the pyridinium salt of 2,5-dimercapto-1,3,4-thiadiazole. As the latter compound is formed in excellent yield when hydrazine reacts with carbon disulphide in boiling pyridine, its formation can probably be explained by a slight decomposition of the thiocarbohydrazide in the boiling pyridine with liberation of hydrazine. The thiols (Ia) and IIIa) are fairly strong acids, and the pyridinium salt of (IIIa) crystallizes unchanged from N hydrochloric acid. To obtain the free thiol, 5 N HCl had to be used to decompose the salt.

The following tentative scheme is proposed to explain the formation of (Ia) and (IIIa) in the present reaction: (Py = C_5H_5N):

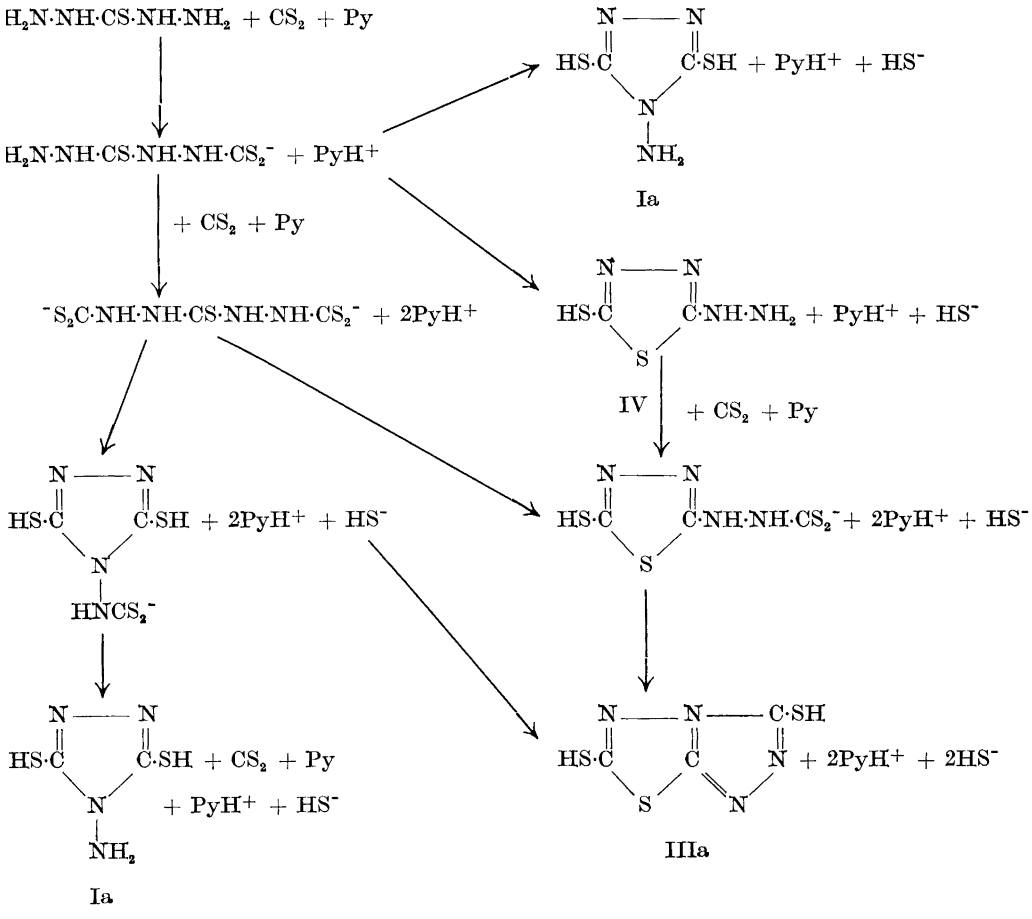

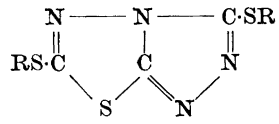

a, R = H
b, R = CH_3
c, R = CH_2CO_2H
d, R = CH_2Ph

III

Bicyclic compounds with the same ring system as (III) have been prepared by Kanaoka by dehydration of 4-acylamino-5-mercapto-4,1,2-triazoles with phosphorus oxychloride [20] and by cyclization of 1,3,4-thiadiazolylhydrazines with orthoesters and imino esters [21].

Attempts to isolate the 5-mercapto-1,3,4-thiadiazol-2-yl-hydrazine [22] (IV) by reaction between thiocarbohydrazide and carbon disulphide in the proportion 1:1 were in vain. Only unreacted thiocarbohydrazide was obtained together with (Ia) and (IIIa). However, (IV) may be an intermediate, since it reacts with carbon disulphide in pyridine to give (IIIa). On the other hand, (Ia) cannot be an intermediate, since it does not react with carbon disulphide under the conditions employed. The proportion of (IIIa) relative to (Ia) increases with the proportion of carbon disulphide relative to thiocarbohydrazide.

The thiol (IIIa) reacts readily with organic halides in alkaline solution, and the bis-thioethers (IIIb—d) have been prepared.

The course of cyclization of thiocarbohydrazide with carbon disulphide was somewhat unexpected, since thiosemicarbazide under the same conditions gave a high yield of 2-amino-5-mercapto-1,3,4-thiadiazole:

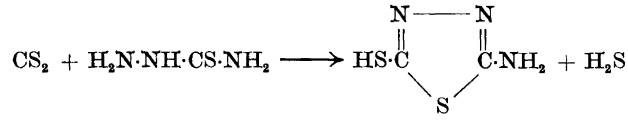

When mono-thiocarbohydrazones react with carbon disulphide in boiling pyridine, the directing influence of the azomethine group, discussed in Ref.[23], comes into play, and the main products are 5-mercapto-1,3,4-thiadiazol-2-yl-hydrazones:

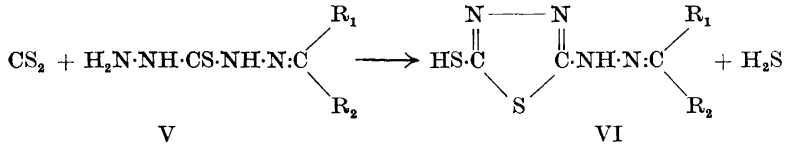

V VI

a, $R_1 = R_2 = CH_3$
b, $R_1R_2 = (CH_2)_5$
c, $R_1 = H$, $R_2 = Ph$

However, with acetone and *cyclo*hexanone monothiocarbohydrazones 14 % and 3 %, respectively, of (Ia) are formed. This by-product may have its origin in thiocarbohydrazide, formed by disproportionation of (V) to thiocarbohydrazide and bisthiocarbohydrazone, but it may also have been formed by direct cyclization of (V) to the Schiff base of (Ia), followed by reaction with a

further mole of (V) to give (Ia) and bis-thiocarbohydrazone. To prove the structure of the thiadiazolylhydrazones (VI) they were also prepared from 5-mercapto-1,3,4-thiadiazol-2-yl-hydrazine (IV), prepared according to Stollé and Fehrenbach [22], and the appropriate carbonyl compounds, and the respective products were found to be identical. Methylation of (VIa) and (VIc) gave the corresponding methylthio-thiadiazolylhydrazones, described in Part II of this series.

As has been shown in numerous cases, cyclic thioamides, capable of thione-thiol tautomerism, preferentially exist in the thione form. Spinner [24] has proposed that these compounds for convenience should be referred to as thiols, even in cases where the thione structure is proved. This convention may be questionable, but it has been applied in the present work. The fine structure of (Ia) and (IIIa) will be discussed in a forthcoming communication.

EXPERIMENTAL

Reaction between thiocarbohydrazide and carbon disulphide

Thiocarbohydrazide (10.6 g) and carbon disulphide (14.4 g) were refluxed in pyridine (100 ml) for one hour. From the boiling solution a precipitate was formed, and after cooling pale yellow prisms (11.1 g, 50 % yield) were obtained, m.p. 200°, which crystallized from water as long, pale yellow rods of unchanged m.p. The product was the pyridinium salt of (Ia). (Found: C 36.9; H 4.11; N 31.0; S 28.1. Calc. for $C_7H_9N_5S_2$ (227.31): C 37.0; H 3.99; N 30.8; S 28.2).

This salt (4.6 g) was dissolved in hot water (20 ml), and conc. HCl (3 ml) was added. Colourless rods separated (2.8 g, 92 % yield), m.p. 216–217° (decomp.). The product was recrystallized three times from N HCl, and the m.p. rose to 222° (decomp.). The product, which was considerably more soluble in water than in strong dilute acids, was *3,5-dimercapto-4-amino-4,1,2-triazole* (Ia). (Found: C 16.4; H 2.84; N 37.9; S 43.0. Calc. for $C_2H_4N_4S_2$ (148.20): C 16.2; H 2.72; N 37.8; S 43.3). λ_{max} 2 600 Å with ε 23 400.

The pyridine mother liquor from the pyridinium salt of (Ia) was evaporated to dryness *in vacuo*. The residue was ground with water (15 ml) to remove the pyridinium salt of 2,5-dimercapto-1,3,4-thiadiazole. The undissolved material (9.0 g, 33 % yield) crystallized from water as pale yellow needles, m.p. 212° (decomp.), consisting of the pyridinium salt of (IIIa). (Found: C 35.7; H 2.60; N 26.0; S 35.4. Calc. for $C_8H_7N_5S_3$ (269.36): C 35.7; H 2.62; N 26.0; S 35.7).

This salt (2.7 g) was dissolved in boiling water (25 ml), and conc. HCl (25 ml) was added. A colourless precipitate was formed, which still contained some pyridine, but after a second precipitation colourless rods were formed (1.2 g, 63 % yield), m.p. 193–193.2° (decomp.), consisting of pure *2,4-dimercapto-[4,1,2-]-triazolo-[3,4-b]-[1,3,4]-thiadiazole* (IIIa). (Found: C 19.0; H 1.19; N 29.4; S 50.4. Calc. for $C_3H_2N_4S_3$ (190.27): C 18.9; H 1.06; N 29.5; S 50.6). λ_{max} 3 035 Å with ε 16 700, and 2 705 Å with ε 12 500.

The aqueous extract of the pyridinium salt of (IIIa) was added to a solution of benzyl chloride (1 g) in ethanol (30 ml) and N NaOH (10 ml). A colourless precipitate was formed (0.65 g) which crystallized from ethanol as colourless plates, m.p. 86–87°, and which did not depress the m.p. of authentic *2,5-bis-benzylthio-1,3,4-thiadiazole* [25]. (Found: C 58.2; H 4.30; N 8.58; S 29.3. Calc. for $C_{16}H_{14}N_2S_3$ (330.47): C 58.2; H 4.27; N 8.48; S 29.1).

When the experiment was repeated as above but with 21.6 g of carbon disulphide instead of 14.4 g, the yield of the pyridinium salt of (Ia) decreased to 33 % and that of the pyridinium salt of (IIIa) rose to 48 %. When 7.2 g of carbon disulphide was employed, a 45 % yield of the salt of (Ia) was obtained. The mother liquor was distilled *in vacuo* to remove the pyridine, and the residue was ground and stirred over night with N HCl (100 ml). The undissolved material (4.9 g, 18 % yield) was identified by its m.p. and by formation of the dimethyl derivative (IIIb) described below as the pyridinium salt of (IIIa). The hydrochloric acid extract was added to a solution of benzaldehyde (5 g) in

ethanol (100 ml). A flocculent precipitate (6.2 g, 22 % yield) of dibenzaldehyde thiocarbohydrazone [16] was obtained, m.p. and mixed m.p. 193—194° (decomp.). (Found: C 63.6; H 4.94. Calc. for $C_{15}H_{14}N_4S$ (282.35): C 63.8; H 5.00).

Reaction between thiosemicarbazide and carbon disulphide

Thiosemicarbazide (9.3 g) and carbon disulphide (12 g) were refluxed with pyridine (75 ml) for 2 h. Then the pyridine was removed *in vacuo*, and the residue was crystallized from water (400 ml) as long, pale yellow rods (10.8 g, 82 % yield), m.p. 233.8—234.0° (decomp.) of *2-amino-5-mercapto-1,3,4-thiadiazole* [26]. (Found: C 18.3; H 2.35; N 31.7; S 48.2. Calc. for $C_2H_3N_3S_2$ (133.18): C 18.0; H 2.27; N 31.6; S 48.2).

Reaction between hydrazine and carbon disulphide

Hydrazine hydrate (100 %, 5.0 ml) and carbon disulphide (18 g) were refluxed in pyridine (50 ml) for one hour. The clear, yellow solution was evaporated in a stream of air to about half of the original volume, when spontaneous crystallization occurred. The product (22.0 g, 96 % yield), crystallized from a small volume of water as pale yellow rods, m.p. 176—177°, consisting of the pyridinium salt of 2,5-dimercapto-1,3,4-thiadiazole. (Found: C 36.6; H 3.12; N 18.3; S 41.7. Calc. for $C_7H_7N_3S_3$ (229.23): C 36.7; H 3.08; N 18.3; S 41.9).

This salt (2.3 g) was dissolved in water (25 ml), and conc. HCl (5 ml) was added. Colourless rods were obtained (1.36 g, 90 % yield), m.p. 169—169.5°, consisting of *2,5-dimercapto-1,3,4-thiadiazole* [25]. (Found: C 15.8; H 1.38; N 18.6; S 63.5; equiv. wt. 152. Calc. for $C_2H_2N_2S_3$ (150.24): C 16.0; H 1.34; N 18.7; S 64.0; equiv. wt. 150).

3-Alkylthio-4-amino-5-mercapto-4,1,2-triazoles

The mono-alkylthioethers of (Ia) were prepared by dissolving the pyridinium salt of (Ia) in water and adding one equivalent of the appropriate organic halide in sufficient ethanol to give a homogeneous solution. Crystallization soon started, and the products were found to be pure after one recrystallization.

3-Benzylthio-4-amino-5-mercapto-4,1,2-triazole (Ic) was obtained in 85 % yield and crystallized from toluene as colourless, irregular prisms, m.p. 158—158.5°. Wangel [9] reports m.p. 155.5—158.2°. (Found: C 45.5; H 4.41; N 23.7; S 27.0. Calc. for $C_9H_{10}N_4S_2$ (238.33): C 45.4; H 4.23; N 23.5; S 26.9).

3-Methylthio-4-amino-5-mercapto-4,1,2-triazole (Ie) was obtained in 80 % yield and crystallized from water as colourless hairs, m.p. 182—182.5°. (Found: C 22.4; H 3.63; N 34.5; S 39.7. Calc. for $C_3H_6N_4S_2$ (162.24): C 22.2; H 3.73; N 34.5; S 39.5). λ_{max} 2 580 Å with ε 15 400.

3,5-Dialkylthio-4-amino-4,1,2-triazoles

The pyridinium salt of (Ia, 2.3 g) was dissolved in N NaOH (20 ml), and a solution of monochloroacetic acid (2.5 g) in N NaOH (26.0 ml) was added. On the following day the mixture was acidified with 5N HCl (10 ml), and after scratching crystallization began. The product (2.45 g. 92 % yield) was recrystallized twice from water to give colourless rods of *3,5-dicarboxymethylthio-4-amino-4,1,2-triazole* (Id), m.p. 180—180.6° (decomp.). Wangel [9] reports m.p. 183.5—184°. (Found: C 27.3; H 3.07; N 21.0; S 24.3; equiv. w: 134.8. Calc. for $C_6H_8N_4O_4S_2$ (264.28): C 27.3; H 3.05; N 21.2; S 24.3; equiv. w: 132.1).

The pyridinium salt of (Ia, 2.3 g) was dissolwed in N NaOH (20 ml), and methyl iodide (3 g) in ethanol (20 ml) was added. After 24 h the clear solution was evaporated to about one third of the original volume, and colourless rods then separated (1.35 g, 77 % yield), which were recrystallized twice from *n*-butanol to give colourless plates, m.p. 148—148.6°, of 3,5-dimethylthio-4-amino-4,1,2-triazole (If). (Found: C 27.6; H 4.65; N 31.9; S 36.3. Calc. for $C_4H_8N_4S_2$ (176.26): C 27.3; H 4.57; N 31.8; S 36.4). λ_{max} 2 250 Å with ε 8 660.

The pyridinium salt of (Ia, 2.3 g) was dissolved in N NaOH (20 ml), and benzyl chloride (2.7 g) in ethanol (40 ml) was added. Crystallization started almost at once, and the product (3.0 g, 90 % yield) crystallized from ethanol as colourless plates, m.p. 148—149°, of *3,5-dibenzylthio-4-amino-4,1,2-triazole* (Ib). (Found: C 58.6; H 4.86; N 17.1; S 19.6. Calc. for $C_{16}H_{16}N_4S_2$ (328.44): C 58.5; H 4.91; N 17.1; S 19.5).

This aminotriazole (0.66 g) was ground with glacial acetic acid (5 ml), and a solution of sodium nitrite (0.4 g) in water (3 ml) was added dropwise. When the evolution of gas had ceased, the undissolved material was collected (0.55 g, 95 % yield). It crystallized from toluene as colourless, irregular prisms, m.p. 116—117°, consisting of *3,5-dibenzylthio-1,2,4-triazole*. (Found: C 61.3; H 4.92; N 13.5; S 20.2. Calc. for $C_{16}H_{15}N_3S_2$ (313.43): C 61.3; H 4.82; N 13.4; S 20.5). For this triazole the m.p. has previously been reported as 111° [14] and 112° [15].

The aminotriazole (Ib, 0.66 g) was dissolved in ethanol (5 ml), and benzaldehyde (0.25 g) and one drop of 5 N HCl were added. After some hours crystallization began, and the product (0.74 g, 89 % yield) crystallized from ethanol as colourless rods of *3,5-dibenzylthio-4-benzylidenamino-4,1,2-triazole*, m.p. 146—147°, strongly depressed by the starting material. (Found: C 66.2; H 4.89; N 13.6; S 15.2. Calc. for $C_{23}H_{20}N_4S_2$ (416.55): C 66.3; H 4.84; N 13.5; S 15.4). λ_{max} 2 820 Å with ε 13 500.

2,4-Dialkylthio-[4,1,2]-triazolo-[3,4-b]-[1,3,4]-thiadiazoles

These compounds were prepared from the pyridinium salt of (IIIa) in the same way as the corresponding 4-aminotriazoles (I). The dimethyl derivative (IIIb) was obtained in 75 % yield and crystallized from absolute ethanol as colourless rods, m.p. 168—169°. (Found: C 27.7; H 2.90; N 25.8; S 44.3. Mol. weight 230 (Rast). Calc. for $C_5H_6N_4S_3$ (218.31): C 27.5; H 2.77; N 25.7; S 44.1). λ_{max} 2 620 Å with ε 12 900.

The dicarboxymethyl derivative (IIIc) was obtained from the aqueous solution in 70 % yield and crystallized from absolute ethanol in colourless plates as the monohydrate, m.p. 174—174.5° (decomp.). (Found: C 26.0; H 2.52; N 17.2; S 29.5; equiv. wt. 163. Calc. for $C_7H_6O_4N_4S_3 \cdot H_2O$ (324.35): C 25.9; H 2.49; N 17.3; S 29.7; equiv. wt. 162).

The dibenzyl derivative (IIId) was obtained in 95 % yield and crystallized from absolute ethanol as colourless plates, m.p. 131—132°. (Found: C 55.1; H 3.88; N 15.1; S 26.2. Calc. for $C_{17}H_{14}N_4S_3$ (370.50): C 55.1; H 3.81; N 15.1; S 26.0). λ_{max} 2 660 Å with ε 13 200.

Reaction between 5-mercapto-1,3,4-thiadiazol-2-yl-hydrazine (IV) and carbon disulphide

Mercapto-thiadiazolylhydrazine hydrochloride [22] (0.37 g) and carbon disulphide (0.3 ml) were refluxed for one hour in pyridine (5 ml). The solution was evaporated to dryness *in vacuo*, and the residue was dissolved in N NaOH (6 ml). Methyl iodide (0.5 ml) in ethanol (5 ml) was added, and crystallization soon set in. The product (0.33 g, 76 % yield) crystallized from absolute ethanol as colourless rods, m.p. 168—169°, which did not depress the m.p. of the 2,4-dimethylthio-triazolo-thiadiazole (IIIb) described above. (Found: N 25.7; S 44.2. Calc. for $C_5H_6N_4S_3$ (218.31): N 25.7; S 44.1).

Reactions between mono-thiocarbohydrazones (V) and carbon disulphide

Monoacetone thiocarbohydrazone [23] (Va, 4.5 g) and carbon disulphide (3.6 g) were refluxed in pyridine (40 ml) for 6 h. A pale yellow precipitate was formed (1.0 g, 15 % yield), which was identified as the pyridinium salt of (Ia) by its m.p. and by formation of the dibenzyl derivative (Ib). The filtrate was evaporated to about half of the original volume, and the residue was poured into water (50 ml). A crystalline product was obtained (1.9 g, 32 % yield), which crystallized from ethanol as colourless rods, m.p. 216—217°, identified by its infrared spectrum with the *acetone 5-mercapto-1,3,4-thiadiazol-2-yl-hydrazone* (VIa) described in Part II, p. 1942. Reaction with methyl iodide in alkaline solution gave the acetone methylthio-thiadiazolylhydrazone described in the same place.

When monocyclohexanone thiocarbohydrazone [23] (Vb) and carbon disulphide reacted as in the preceding experiment, a 3 % yield of the pyridinium salt of (Ia) was obtained, and when the filtrate was poured into water, *cyclohexanone 5-mercapto-1,3,4-thiadiazol-2-yl-hydrazone* (VIb) separated in 60 % yield. It was purified by dissolution in N sodium bicarbonate solution followed by precipitation with acetic acid and it was then recrystallized from *n*-butanol to give colourless rods, m.p. 216–219° (decomp.). (Found: C 42.1; H 5.37; N 24.7; S 27.9. Calc. for $C_8H_{12}N_4S_2$ (228.25): C 42.1; H 5.30; N 24.5; S 28.1).

When monobenzaldehyde thiocarbohydrazone (Vc) reacted as above, no pyridinium salt of (Ia) was obtained, but *benzaldehyde 5-mercapto-1,3,4-thiadiazol-2-yl-hydrazone* [22] (VIc) separated in 85 % yield when the reaction mixture was poured into water. The product was dissolved in N sodium carbonate solution and precipitated with acetic acid and finally recrystallized from methanol to give long, colourless plates with m.p. 246–246.5° (decomp.). (Found: C 45.9; H 3.50; N 23.5; S 27.0. Calc. for $C_9H_8N_4S_2$ (236.30): C 45.8; H 3.41; N 23.7; S 27.1).

Reaction with methyl iodide in alkaline solution gave the benzaldehyde methylthiothiadiazolylhydrazone described in Part II. p. 1943.

The mercapto-thiadiazolylhydrazones (VIa–VIc) have also been prepared by reaction between mercaptothiadiazolylhydrazine hydrochloride [22] and the appropriate carbonyl compounds in 50 % aqueous ethanol. The products were obtained in good yields and were recrystallized as above, and the identities of the products were confirmed with infrared spectra.

UV-Spectra were recorded with a Beckman DU spectrophotometer in absolute ethanol solution.

My thanks are due to the *Swedish Natural Science Research Council* for financial aid, to Miss Ingeborg Leutiger for valuable experimental assistance and to Miss Kerstin Kulle for recording the infrared spectra.

REFERENCES

1. Arndt, F. and Bielich, F. *Ber.* **56** (1923) 809.
2. Hoggarth, E. *J. Chem. Soc.* **1952** 4818.
3. Guha, P. C. and De, S. C. *J. Chem. Soc.* **125** (1924) 1215.
4. Guha, P. C. and De, S. C. *Quart. J. Indian Chem. Soc.* **1** (1924) 141.
5. Scott, E. S. and Audrieth, L. F. *J. Org. Chem.* **19** (1954) 742.
6. Beyer, H. and Kröger, C.-F. *Ann.* **637** (1960) 126.
7. Wiley, P. F. in Weissberger, *The chemistry of heterocyclic compounds: The 1,2,3- and 1,2,4-triazines, tetrazines and pentazines.* Interscience, New York 1956, p. 195.
8. Beckett, T. and Dyson, G. M. *J. Chem. Soc.* **1937** 1362.
9. Wangel, J. *Kem. Maanedsblad* **39** (1958) 73.
10. Busch, M. *Ber.* **34** (1901) 2311.
11. Stollé, R. *J. prakt. Chem.* [2] **75** (1907) 416.
12. Diels, O. *Ber.* **47** (1914) 2183.
13. Bülow, C. *Ber.* **39** (1906) 4106.
14. Arndt, F and. Milde, E. *Ber.* **54** (1921) 2109.
15. Fromm, E. *Ann.* **426** (1922) 340.
16. Stollé, R. and Bowles, P. E. *Ber.* **41** (1908) 1099.
17. Beyer, H. and Kröger, C.-F. *Ann.* **637** (1960) 135.
18. Randall, H. M., Fowler, R. G., Fuson, N. and Dangl, J. R. in *Infrared determination of organic structures.* Van Nostrand, New York 1949, p. 20.
19. Brown, F. C., Bradsher, C. K., Moser, B. and Forrester, S. *J. Org. Chem.* **24** (1959) 1056.
20. Kanaoka, M. *J. Pharm. Soc. Japan* **76** (1956) 1133.
21. Kanaoka, M. *Pharm. Bull. Tokyo* **5** (1957) 385.
22. Stollé, R. and Fehrenbach, K. *J. prakt. Chem.* [2] **122** (1929) 289.
23. Sandström, J. *Acta Chem. Scand.* **14** (1960) 1037.
24. Spinner, E. *J. Chem. Soc.* **1960** 1237.
25. Busch, M. *Ber.* **27** (1894) 2520.
26. Busch, M. and Lotz, H. *J. prakt. Chem.* [2] **90** (1914) 257.

Received February 23, 1961.

ACTA CHEMICA SCANDINAVICA 15 (1961) 1303–1312

The Chemistry of the Natural Order Cupressales *38* *

The Structures of the Diterpenes Torulosol, Torulosal and Agatholic Acid **

C. ENZELL

Organisk-kemiska Institutionen, Kungl. Tekniska Högskolan, Stockholm, Sweden

Torulosol (*1*) and torulosal (*2*), occurring in *Cupressus torulosa*, have been correlated with manool and agathic acid and shown to be a hydroxy- and an oxo-manool, respectively.

Agatholic acid (*7*), isolated from Manila copal, has been correlated with the substances mentioned and prepared therefrom.

The mass-spectra of these and some related compounds are discussed.

Two new diterpenes, torulosol, $C_{20}H_{34}O_2$ (*1*) † and torulosal, $C_{20}H_{32}O_2$ (*2*), were isolated during a recent investigation of the heartwood constituents of *Cupressus torulosa* [1]. They occur in the heartwood in comparatively large amounts together with a number of other substances of which manool, from biogenetic and chemotaxonomic points of view, is perhaps the most interesting. The structures assigned to torulosol and torulosal are based on the following evidence.

Torulosol (*1*) on hydrogenation with a Raney-nickel catalyst gave dihydrotorulosol (*3*) and with a palladium catalyst tetrahydrotorulosol. This indicated that the compound was dicyclic since the two oxygen atoms were present as hydroxyl groups.

Oxidation of torulosol with chromium trioxide in pyridine gave torulosal (*2*), which had also been isolated from the wood of *Cupressus torulosa* [1]. The aldehyde group of torulosal, (1 716 and 2 720 cm^{-1}; −97 c/s from an internal benzene ref. at 40 Mc/s) did not react with silver oxide or Schiff's reagent and

* Part *37 Acta Chem. Scand.* **15** (1961) 1003.

** The present names, being less confusing or shorter, are preferred to torulol, torulal and agathadienecarbinolcarboxylic acid, used when part of this work was presented at "De tredje kemistdagarna i organisk kemi", Stockholm 9–11 June 1960, *Svensk Kem. Tidskr.* **9** (1960) 602; the name agathadienecarbinolcarboxylic acid has been used once previously [14].

† Numbering system: Cocker, J. D and Halsall, T. G. *J. Chem. Soc.* **1956** 4262.

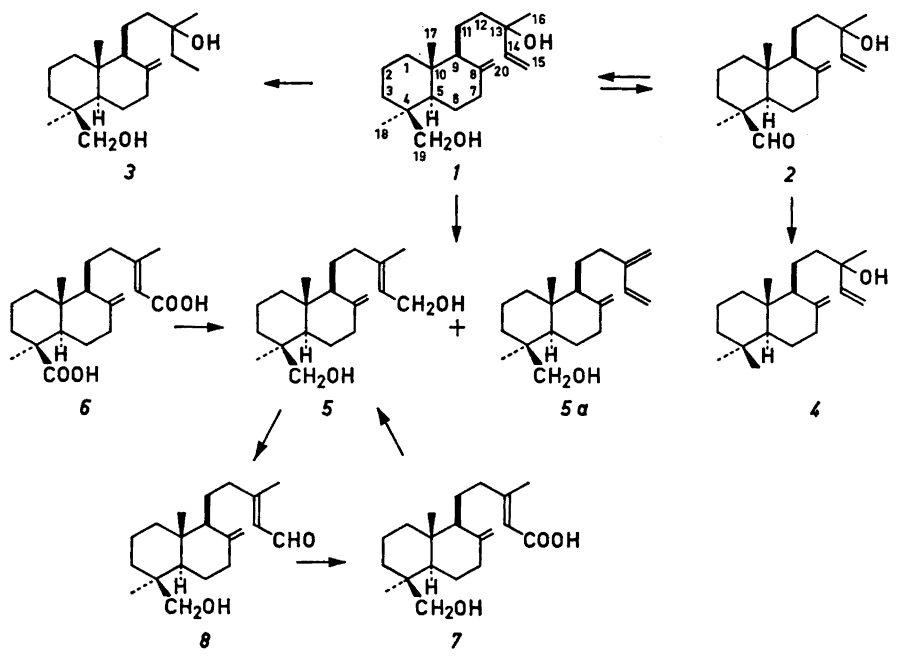

this was attributed to steric hindrance. It crystallised together with carbon-tetrachloride, possibly as an "inclusion compound" [2]. Torulosal, not being completely stable, is best characterised by conversion to torulosol with potassium borohydride or as the semicarbazone.

These results and a comparison of the infrared and mass spectra of manool and torulosol indicate that the latter is a hydroxy manool. The infrared spectrum of torulosol (Fig. 1) shows considerable similarity to that of manool and differs mainly in the presence of an additional hydroxyl band (1 020 cm^{-1}). The mass spectra of manool (Fig. 4) and torulosol (Fig. 5) show a series of strong peaks in common and a series of strong peaks differing by the

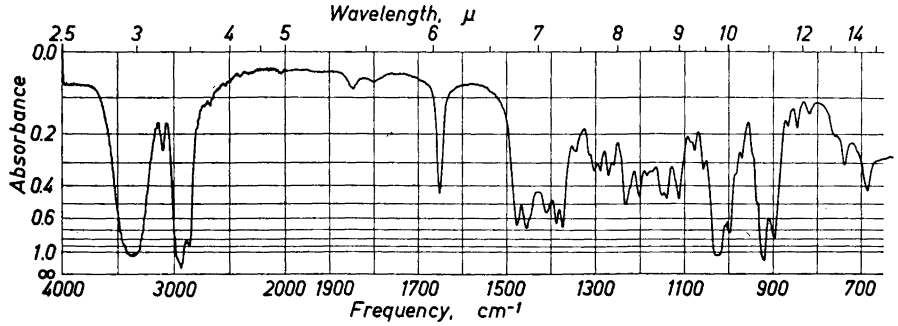

Fig. 1. Infra-red spectrum of torulosol (KBr).

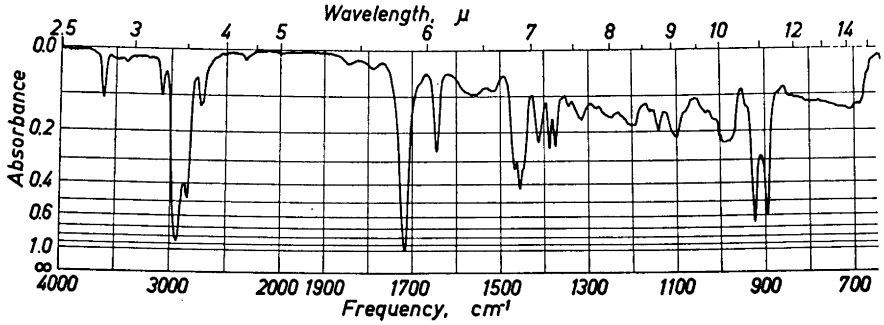

Fig. 2. Infra-red spectrum of torulosal (CCl_4).

atomic weight of oxygen. Of the peaks in common those at *m/e* 71 are probably due to the ion (CH_3—C(OH)—CH=CH_2) obtained by rupture of the C(12)—C(13) bond [3], since they occur at *m/e* 73 in the spectra of the dihydrocompounds, and indicate that these parts of the two compounds are identical. Further comparison indicates a common *A*,*B*-ringcarbon skeleton and that the primary carbinol group is located on ring *A*. The reasons for these conclusions are given below.

Huang-Minlon reduction of torulosal (*2*) gave manool (*4*), for which the structure and absolute configuration at C(5), C(9) and C(10) are known [4-6] and that at C(13) has been suggested [7]. This correlation therefore established the structure and stereochemistry at these centres of torulosal and torulosol except for the position of the extra oxygen atom.

The position of the extra oxygen atom was determined by subjecting torulosol to an allylic rearrangement [8,9] yielding, the triene alcohol (*5a*) and the diol (*5*). The latter was identical with a synthetic specimen obtained from the dimethyl ester of agathic acid (*6*) by lithium aluminium hydride reduction. Since the tertiary carboxyl group of agathic acid has been shown [10] to be in the 4*β*-position, it follows that torulosol (*1*) and torulosal (*2*) are oxygenated at C(19). The triene alcohol (*5a*) and its dihydroproduct, obtained on reduction with sodium in alcohol, were used to establish the structure of communic acid [11].

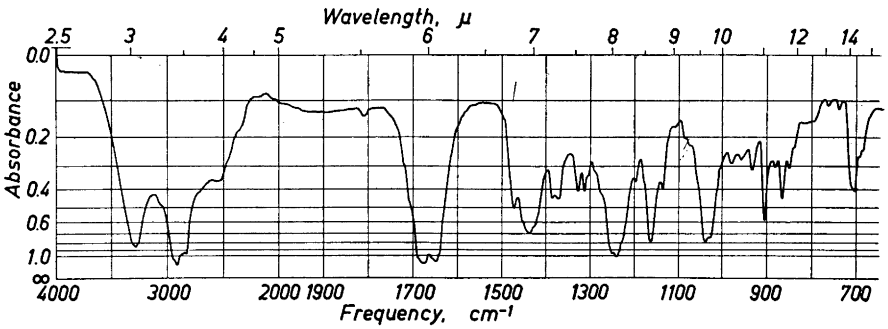

Fig. 3. Infra-red spectrum of agatholic acid (KBr).

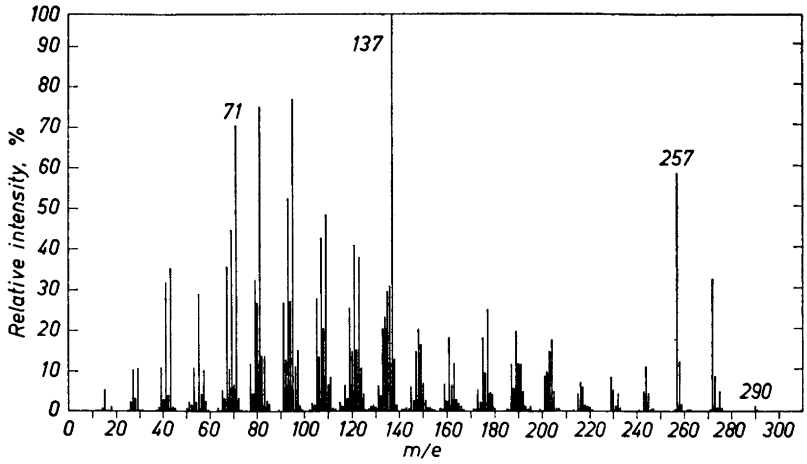

Fig. 4. Mass spectrum of manool.

The correlation of agathic acid (*6*) with manool (*4*) *via* torulosol proves that the side chain at C(9) is β-oriented in agathic acid.

The PMR spectrum of torulosol supports structure (*1*) and provides additional evidence for the β-orientation of the primary carbinol group. It showed, in addition to a C(4)-methyl band (254 c/s), an angular methyl band (268.5 c/s) and a side chain methyl band (244 c/s), a quartet (about 154 c/s) typical of an AB-spectrum [12] (J_{AB} 12 c/s). The position and splitting of this band suggest that it is due to the two non-equivalent methylene hydrogen atoms of the CH_2OH group. The most probable cause of non-equivalence of these two hyd-

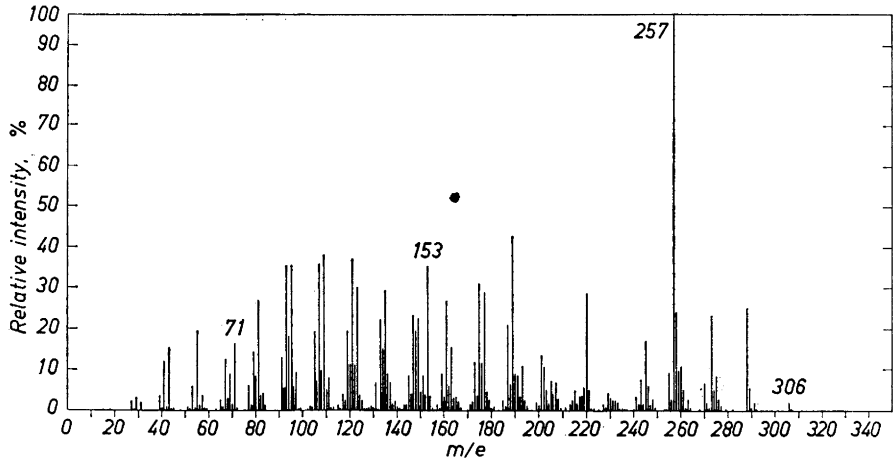

Fig. 5. Mass spectrum of torulosol.

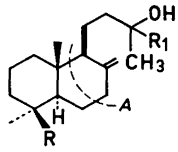

9 (R CH_3; R_1 C_2H_5)
10 (R CDHOH; R_1 $CH{=}CH_2$)

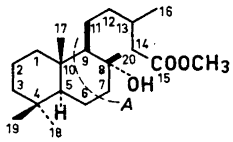

11

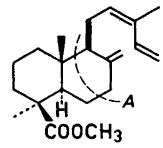

12

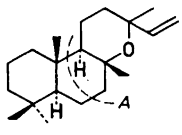

13

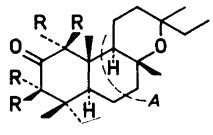

14 (R H)
15 (R D)

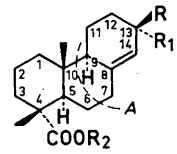

16 (R $CH{=}CH_2$; R_1 CH_3; R_2 CH_3)
17 (R $CH{=}CH_2$; R_1 CH_3; $R_2C_2H_5$)
18 (R CH_3; R_1 $CH{=}CH_2$; R_2 CH_3)

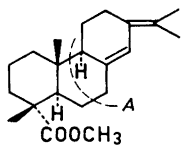

19

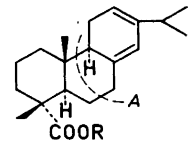

20 (R CH_3)
21 (R C_2H_5)

rogen atoms is restricted rotation of the group. Examination of molecular models indicates that this should only occur if the primary carbinol group is in the 4β-position where its rotation can be hindered by the 10β-angular methyl group.

Simultaneously with the isolation of agathic acid from a hard grade of Manila copal, attempts were also made to obtain this acid from a softer grade. The main product from this softer copal, when worked up largely according to the method given by Ruzicka and Hosking [13], was not agathic acid but a new acid, $C_{20}H_{32}O_3$, named agatholic acid. The infrared (Fig. 3), ultraviolet and mass spectra of this acid indicate that it is α,β-unsaturated and that it differs from torulosol only with respect to the side chain at C(9). Agatholic acid on esterification with diazomethane followed by reduction with lithium aluminium hydride gave the diol (*5*). This correlation together with the spectral data established the structure and absolute configuration of agatholic acid (*7*). The diol (*5*) on oxidation with manganese dioxide gave the hydroxy aldehyde (*8*) which on further oxidation with silver oxide gave agatholic acid.

The mass spectra of the new compounds and of several related known compounds show a point of interest. Peaks corresponding to ions obtained from ring *A* by rupture of the C(6)—C(7) and C(9)—C(10) bonds and removal of hydrogen — fragmentation A (see *9*, *etc.*) — were found to occur in the mass spectra of dicyclic as well as tricyclic diterpenes (*cf.* Table 1). In order to ascer-

Table 1. Peaks corresponding to fragmentations A in the mass spectra of some diterpenes. The figures within brackets give the peak intensities as percentages of the strongest peak in the spectrum.

Compound	Peaks corresponding to fragmentation A at *m/e*	
Manool (*4*)	137	(100)
Dihydromanool (*9*)	137	(100)
Torulosol (*1*)	153	(37)
Dihydrotorulosol (*3*)	153	(8)
Deuterotorulosol (*10*)	154	(13)
Torulosal (*2*)	151	(14)
Agatholic acid (*7*)	153	(24)
Methyl labdanolate * (*11*) [5]	137	(45)
Methyl communate (*12*) [11]	181	(15)
Manoyl oxide * (*13*) [15]	137	(43)
Dihydroketomanoyl oxide (*14*)	151	(20)
Deuterodihydroketomanoyl oxide (*15*)	155	(16)
Methyl pimarate (*16*) [16,17]	181	(24)
Ethyl pimarate (*17*) [17]	195	(11)
Methyl sandaracopimarate (*18*) [16,17,18]	181	(22)
Methyl neobietate (*19*) [17]	181	(10)
Methyl levopimarate (*20*) [17]	181	(17)
Ethyl levopimarate (*21*) [17]	195	(3)

tain the origin of these ions the mass spectra of deuterodihydroketomanoyl oxide [14] (*15*) and deuterotorulosol (*10*), prepared by reduction of torulosal with sodium and deuterium oxide in dioxan, were recorded. The peaks, corresponding to fragmentation A, were shifted in the expected manner.

The heights of the peaks resulting from fragmentation A were found to increase with the absence of polar substituents in ring *A* and with the presence at C(8) of a double bond exocyclic to ring *B* or of an 8 *a*-oxygen atom, which has been shown to be easily eliminated giving this double bond [6].

EXPERIMENTAL

Melting points were determined on a Kofler micro hot stage, unless stated to the contrary, and are corrected. Infrared spectra were recorded on a Perkin-Elmer No. 21 instrument (NaCl prism), ultraviolet spectra on a Beckman DK 2 recording spectro-photometer, mass spectra on an instrument [19] with an all glass heated inlet system (energy of electrons 70 eV) and PMR spectra (in $CDCl_3$; benzene internal standard) on a Varian V-4300 instrument operating at 40 Mc/s equiped with a Varian VK-3506 stabiliser. Microanalyses by Dr. A. Bernhardt, Mühlheim.

Torulosol (1) *and torulosal* (2) were isolated from the heartwood of *Cupressus torulosa* [1]: Torulosol, m.p. 110—111°, $[a]_D$ + 31° ($CHCl_3$, *c* 2.0), (Found: C 78.5; H 10.9; O 10.6. $C_{20}H_{34}O_2$ requires C 78.4; H 11.2; O 10.4 %). Torulosal, n_D^{25} 1.521, $[a]_D$ + 29° ($CHCl_3$, *c* 1.8), was not completely stable (about one half had changed on keeping in methanol solution for one week in stoppered pyrex tube at room temperature) and did not analyse well. (Found: C 78.4; H 10.2. $C_{20}H_{32}O_2$ requires C 78.9; H 10.6 %). It gave with carbon tetrachloride a compound, m.p. 80—85° (Pyrex tube), $[a]_D$ + 24° ($CHCl_3$, *c* 2.0), which even after drying (30°/0.001 mm) contained carbon tetrachloride (Found: C 59.4; H 7.7; O 12.9; Cl 19.6 %). The carbon tetrachloride was only partly removed on recrystallisation

* I am grateful to Professors S. Bergström and E. Stenhagen for allowing me to see these spectra prior to their publication.

from solvents such as methanol and *iso*propyl ether giving crystals of lower melting point and lower chlorine content (*e.g.*, after two recrystallisations from *iso*propylether followed by drying under high vacuum to constant weight. Found: C 72.8; H 9.6; Cl 6.5 %). Torulosal was characterised by conversion to torulosol or to the semicarbazone, m.p. 195—197° (decomp.), $[\alpha]_D$ −9° (pyridine, *c* 1.0), (Found: C 69.5; H 9.3; N 11.5. $C_{21}H_{35}O_2N_3$ requires C 69.8; H 9.8; N 11.6), which was prepared by a procedure used for O-methylpodocarpinal [20] and was purified by repeated recrystallisation from ethanol, chloroform and acetone.

The mass spectrum of torulosal includes major peaks at $m/e = 32$ (10), 49 (13), 55 (17), 57 (20), 61 (21), 69 (17), 71 (3), 85 (13), 89 (13), 99 (26), 100 (25), 111 (20), 125 (19), 135 (100), 137 (97), 151 (15; fragmentation A), 165 (13), 179 (13), 193 (10), 205 (11), 236 (13), 261 (11), 271 (6; loss of H_2O and CH_3), 275 (19; loss of CHO); 286 (5; loss of H_2O), 289 (10; loss of CH_3), 304 (10; molecular ion).

The figures within brackets give peak intensities as percentages of the strongest peak (135).

Tetrahydrotorulosol. Torulosol (150 mg, 0.49 mmole) was dissolved in ethanol (95 %, 15 ml) and hydrogenated over a pre-reduced palladium on charcoal catalyst (10 %, 20 mg) at room temperature and atmospheric pressure. It took up hydrogen in two steps; the first (11.6 ml) was completed in 20 min and the second (23.2 ml) in 30 hrs. The catalyst was filtered off, the solvent evaporated and the crystalline residue recrystallised from isopropyl ether and acetonitrile to give tetrahydrotorulosol, m.p. 119—124°, $[\alpha]_D$ + 16°, ($CHCl_3$, *c* 2.0), (Found: C 77.5; H 12.3; O 10.5. $C_{20}H_{38}O_2$ requires C 77.4; H 12.3; O 10.3 %).

Dihydrotorulosol (*3*). Torulosol (306 mg, 1 mmole) dissolved in absolute ethanol and in the presence of a Raney-nickel catalyst (50 mg) took up 0.9 mmole of hydrogen in 3 min whereafter the hydrogenation ceased. Filtration, evaporation of the solvent and recrystallisation of the crystalline residue from *iso*propyl ether and aqueous methanol followed by sublimation at reduced pressure gave dihydrotorulosol, m.p. 120—122°, $[\alpha]_D$ + 27° ($CHCl_3$, *c* 2.0) (Found: C 77.9; H 11.7. $C_{20}H_{36}O_2$ requires C 77.9; H 11.8 %) $\nu_{max}^{CCl_4}$ 3 660, 3 510, 1 127, 1 023; 3 100, 1 785, 1 648, 893 cm^{-1}.

When the hydrogenation, under the conditions described for tetrahydrotorulosol, was stopped after 1.1 mole of hydrogen per mole of torulosol had been consumed, the resulting material showed an infrared spectrum similar to that of torulosol, though the intensities of some bands (3110, 1847, 1651, 1410, 917, 894 cm^{-1}) were lower.

The mass spectrum of dihydrotorulosol (*3*) includes major peaks at m/e = 41 (87), 55 (100), 67 (55), 73 (35; $CH_3-C(OH)-CH_2CH_3$), 81 (83), 95 (48), 107 (25), 121 (19), 135 (16), 149 (11), 153 (8; fragmentation A), 161 (9), 177 (9), 189 (13), 203 (4), 220 (4), 243 (3), 259 (27; loss of CH_2OH and H_2O), 275 (7; loss of CH_3 and H_2O), 290 (4; loss of H_2O).

The figures within brackets give peak intensities as percentages of the strongest peak (55).

Chromium trioxide oxidation of torulosol. A solution of torulosol (500 mg) in pyridine (7 ml) was added to chromium trioxide-pyridine complex [21], prepared by adding chromium trioxide (500 mg) to pyridine (10 ml), and left 12 h at room temperature. Methanol (5 ml) was added and after an additional hour the reaction mixture was diluted with ice-cold aqueous sodium hydroxide (5 %, 100 ml) and extracted with ether. The ether solution was extracted with ice-cold hydrochloric acid (10 %) to remove pyridine, washed with water and dried (Na_2SO_4). The residue (430 mg), on recrystallisation from carbon tetrachloride, gave the torulosal-carbon tetrachloride compound, m.p. and mixed m.p. 80—85° (pyrex tube), $[\alpha]_D$ + 24° ($CHCl_3$, *c* 2.0). Infrared spectra identical. Semicarbazone, m.p. and mixed m.p. 195—197° (decomp.), $[\alpha]_D$ −11° (pyridine, *c* 1.5).

Potassium borohydride reduction of torulosal. Torulosal (200 mg), isolated from a heartwood extract of *Cupressus torulosa* [1], was added to a solution of potassium borohydride (200 mg) and sodium hydroxide (5 mg) in aqueous methanol (1:9, 10 ml) and left overnight. The reaction mixture was diluted with water (200 ml) and extracted with ether. The ether extract was dried (Na_2SO_4) and the solvent was removed to give a crystalline residue (170 mg), which on recrystallisation from *iso*propyl ether and sublimation gave pure torulosol, m.p. and mixed m.p. with the natural product 110—111°, $[\alpha]_D$ + 31° ($CHCl_3$, *c* 2.1). Infrared spectra identical.

Huang-Minlon reduction of torulosal. Crude torulosal (360 mg), obtained on oxidation of torulosol with chromium trioxide-pyridine complex, potassium hydroxide (550 mg) and hydrazine hydrate (99—110 %, 0.62 ml) in diethylene glycol (7 ml, redistilled) were refluxed for 1 h. The apparatus was changed to distillation and the internal temperature raised to 200° whereafter the mixture was refluxed (220—240°) under oxygen-free nitrogen for 4 h. The reaction product was diluted with water (50 ml) and extracted with light petroleum (b.p. 35—60°). The extract was dried (Na_2SO_4) and the solvent removed leaving an oil (310 mg) which was chromatographed on alumina (10 g, Merck stand., activity II). Light petroleum (b.p. 35—60°)-ether eluated an oil (260 mg), which immediately started to crystallise when seeded with manool. Recrystallisation from light petroleum gave pure manool (*4*), m.p. and mixed m.p. 53—55°, $[\alpha]_D$ + 33° ($CHCl_3$, *c* 1.2). Infrared spectrum identical with that of authentic material.

Torulosol, diethylene glycol (7 ml) and potassium hydroxide (550 mg) on refluxing under oxygen-free nitrogen for 4 h gave an almost quantitative yield of unchanged starting material, m.p. and mixed m.p. 110—111°, $[\alpha]_D$ + 31° ($CHCl_3$, *c* 1.3). Infra-red spectra identical.

Rearrangement[8] *of torulosol.* Torulosol (1.04 g) was boiled under reflux with a mixture of acetic anhydride (1.2 ml) and glacial acetic acid (1.2 ml) for 6 h. The reaction mixture was poured onto ice, made alkaline (10 % aq. NaOH) and extracted with ether. The ether solution was concentrated and the residue boiled under reflux with ethanolic potassium hydroxide (5 %, 15 ml) for 6 h. The reaction mixture was diluted with water (200 ml) and extracted with ether. The extract on drying (Na_2SO_4) and removal of the solvent gave a very thick oil (1.00 g), which was adsorbed on alumina (30 g; Merck neutral, activity II) and eluated with a light petroleum (b.p. 35—60°)-ether gradient.

The first fraction (0.46 g) was according to paper chromatographic results (hexadecane impregnated glass fibre paper and an aqueous methanol solution of silver fluoroborate as mobile phase)[22] and its ultra-violet absorption, λ_{max}^{EtOH} 227 mμ (ε 22 000), a mixture of a tricyclic compound and the triene alcohol (*5a*). The triene alcohol (*5a*), 3,5-dinitrobenzoate m.p. 71—72°, and its dihydroderivate, 3,5-dinitrobenzoate m.p. 105—106°, obtained on reduction with sodium and propanol, are discussed elsewhere[14]. The second fraction (0.40 g) was crystalline and recrystallisation from *iso*propyl ether gave pure agathadiol (*5*), m.p. 107—108°, $[\alpha]_D$ + 31° ($CHCl_3$, *c* 2.0). The mixed m.p. with the corresponding synthetic specimen from agathic acid dimethyl ester was undepressed, 107—108°. The infrared spectra of the two compounds were superimposable.

Agathic acid (*6*), m.p. 202—203°, $[\alpha]_D$ + 58° (EtOH, *c* 2.0), λ_{max}^{EtOH} 207 mμ (ε 12 000), 216 (ε 11 000), isolated from a hard grade of Manila copal (m.p. 135°) by a method described by Ruzicka and Hosking[12], gave on treatment with diazomethane followed by filtration through alumina (Merck, neutral, activity III) and quick distillation at low pressure (0.5 mm) agathic acid dimethyl ester, $[\alpha]_D$ + 63° (EtOH, *c* 2.0), n_D^{25} 1.5139, λ_{max}^{EtOH} 220 mμ (ε 13 000).

Agathadiol (*5*). Agathic acid dimethyl ester (1.1 g) dissolved in dry ether (7 ml) was added to a suspension of lithium aluminium hydride in dry ether (20 ml) and the mixture boiled under reflux for 6 h. Addition of ethyl acetate followed by icecold dilute sulphuric acid (5 %, 100 ml) and extraction with ether gave on evaporation of the solvent a crystalline residue (1.0 g), which was recrystallised from *iso*propyl ether-methanol to give pure agathadiol, m.p. 107—108°, $[\alpha]_D$ + 31° ($CHCl_3$, *c* 2.0) ν_{max}^{KBr} 3 290, 1 025, 992 1 666, 845; 1 647, 1 411, 897 cm^{-1}. (Found: C 78.1; H 11.1; O 10.5. $C_{20}H_{34}O_2$ requires C 78.4; H 11.2; O 10.4 %).

Isolation of agatholic acid (*7*). Finely divided Manila copal (250 g, m.p. 95—105°) was added to a well stirred suspension of Celite (20 g) in ether (750 ml) and the resulting suspension was stirred for 20 h. After filtration, the solid material was extracted in the same way with a further amount of ether (750 ml). The combined ether solutions were diluted with more ether (1 500 ml) and, after addition of activated charcoal, filtered. The ether solution was extracted twice with alcoholic potassium hydroxide (5 %, 250 ml each time), to which a sufficient amount of water was added to effect separation

into two layers, and then three times with water. The combined aqueous solutions were diluted with water to a total volume of 2 l and acidified with carbon dioxide. The solid material was removed by filtration and the filtrate acidified with ice cold dilute sulphuric acid (10 %) to give crystalline material (10 g), which was removed by filtration and washed repeatedly with water. Recrystallisation from methanol and ethyl acetate gave pure agatholic acid, m.p. 184—186°, $[\alpha]_D$ + 42° (EtOH, *c* 2.0), λ_{max}^{EtOH} 208 mμ (ε 13 000) (Found: C 78.4; H 10.0; O 15.1; equiv. wt. 335. $C_{20}H_{32}O_3$ requires C 75.0; H 10.1; O 15.0; equiv. wt. 320). Agatholic acid methyl ester, m.p. 77—79°, [α] + 44° ($CHCl_3$, *c* 1.0), λ_{max}^{EtOH} 219 mμ (ε 13 000), $\nu_{max}^{CCl_4}$ 1 721 cm^{-1} was obtained in the same way as described for agathic acid dimethyl ester. The mass spectrum of agatholic acid (*7*) includes major peaks at *m/e*: 18 (7), 29 (9), 31 (4), 43 (57), 55 (56), 67 (41), 71 (11), 81 (100), 95 (91), 100 (18), 107 (79), 121 (61), 135 (59), 149 (40), 153 (24; fragmentation A), 163 (24), 175 (20), 189 (27), 203 (16), 245 (46), 261 (17), 275 (7), 289 (27; loss of CH_2OH), 302 (4; loss of H_2O), 305 (4; loss of CH_3), 320 (2; molecular ion).

The figures within brackets give peak intensities as percentages of the strongest peak (81).

Agatholal (*8*). Agathadiol (1.5 g) was dissolved in dry acetone (210 ml) and after addition of manganese dioxide [23] (22 g) the resulting mixture was shaken at room temperature for 10 h. The solid material was filtered off, washed three times with acetone and the combined acetone solutions taken to dryness. The crystalline residue (1.3 g) on recrystallisation from *iso*propyl ether gave agatholal, m.p. 70—72°, $[\alpha]_D$ + 40° ($CHCl_3$, *c* 2.0), λ_{max}^{EtOH} 239 mμ (ε 15 000), $\nu_{max}^{CCl_4}$ 3 655, 3 510, 1 025; 3 090, 1 786, 1 645, 895; 2 770, 1 688; 1 615 cm^{-1}, (Found: C 78.9; H 10.5. $C_{20}H_{32}O_2$ requires C 78.9; H. 10.6) Semicarbazone m.p. 199—201°.

Silver oxide oxidation [8] *of agatholal* (*8*). Agatholal (0.30 g) and finely divided silver nitrate (0.65 g) were dissolved in absolute ethanol (6 ml) and a solution of sodium hydroxide (0.36 g) in aqueous ethanol (1:9, 10 ml) was added dropwise with good stirring. After 24 h at room temperature the mixture was diluted with water, acidified with ice-cold dilute sulphuric acid (5 %) and extracted with ether. The ether solution on drying and evaporation of the solvent gave a crystalline residue (0.30 g) which on sublimation (150°/0.1 mm) and recrystallisation gave pure agatholic acid (*7*), m.p. and mixed m.p. with the natural product 184—186°, $[\alpha]_D$ + 50°. The infrared spectra were superimposable.

Deuterotorulosol (*10*). Torulosal (250 mg) was dissolved in a mixture of dry dioxan (5 ml) and deuterium oxide (2 ml). Sodium (2 g) was added in small pieces to the refluxing solution during 4 h. Deuterium oxide (2 ml) was added to destroy remaining sodium and the reaction mixture was then diluted with water (200 ml) and extracted with ether. After removal of the ether the residue was sublimed at reduced pressure (0.5 mm Hg) and chromatographed on alumina (10 g, activity IV). Elution with a light petroleum (b.p. 35—60°)-ether gradient followed by sublimation gave deuterotorulosol (90 mg), m.p. 110—111°.

The mass spectrum of deuterotorulosol (*10*) includes major peaks at *m/e* = 18 (35), 29 (34), 31 (24), 32 (16; CHDOH), 43 (100), 55 (69), 67 (43), 71 (68; $CH_3C(OH)CH=CH_2$), 81 (76), 95 (57), 107 (40), 121 (34), 133 (20), 147 (17) 154 (13; fragmentation A), 161 (19), 175 (13), 189 (21), 221 (6) 229 (2), 246 (4), 257 (26; loss of CHDOH and H_2O), 274 (4; loss of CH_3 and H_2O), 275 (2; loss of CHDOH), 289 (3; loss of H_2O), 292 (0.8; loss of CH_3), 307 (0.4; molecular ion).

The figures within brackets give peak intensities as percentages of the strongest peak (43).

Acknowledgements. I thank Prof. H. Erdtman for his kind interest, Dr. R. Ryhage, Karolinska Institutet, Stockholm, for the mass spectrometric determinations, Dr. S. Forsén for measuring and interpreting the PMR-spectra, Mrs. S. Strand for skilful assistance and Dr. E. Forslind for putting the PMR-equipment at our disposal. Thanks are also due to the *Swedish Technical Research Council* for financial support.

REFERENCES

1. Barreto, H. and Enzell, C. *Acta Chem. Scand.* **15** (1961) 1313.
2. Cramer, F. *Einschlussverbindungen*, Springer-Verlag, Heidelberg 1954.
3. Beynon, J. H. *Mass Spectrometry and its Application to Organic Chemistry*, Amsterdam 1960, p. 325, 347.
4. Simonsen, J. and Barton, D. H. R. *The Terpenes* (*2nd Ed.*) Vol. III Cambridge 1951, p. 333, 350.
5. Cocker, J. D. and Halsall, T. G. *J. Chem. Soc.* **1957** 4401.
6. Ohloff, G. *Helv. Chim. Acta* **41** (1958) 845.
7. Barltrop, J. A. and Bigley, D. B. *Chem. & Ind. (London)* **1959** 1378; Bigley, D. B., Rogers, N. A. J. and Barltrop, J. A. *J. Chem. Soc.* **1960** 4613.
8. Ohloff, G. *Ann.* **617** (1958) 134.
9. Simonsen, J. and Owen, L. N. *The Terpenes* (2nd Ed.) Vol. I, Cambridge 1947; p. 59; Simonsen, J. and Barton, D. H. R. *The Terpenes* (2nd Ed.) Vol. III, Cambridge 1951, p. 364.
10. Simonsen, J. and Barton, D. H. R. *The Terpenes* (2nd Ed.), Vol. III, Cambridge 1951, p. 469.
11. Arya, V. P., Enzell, C., Erdtman, H. and Kubota, T. *Acta Chem. Scand.* **15** (1961) 225.
12. Jackman, L. M. *Applications of Nuclear Magnetic Resonance in Organic Chemistry*, London 1959, p. 89.
13. Ruzicka, L. and Hosking, J. R. *Ann.* **469** (1929) 147.
14. Enzell, C. *Acta Chem. Scand.* **14** (1960) 2053.
15. Hodges, R. and Reed, R. I. *Tetrahedron* **10** (1960) 71.
16. Bruun, H. H., Ryhage, R. and Stenhagen, E. *Acta Chem. Scand.* **12** (1958) 789.
17. Bruun, H. H. and Gåsland, S. *Acta Acad. Aboensis, Math. et Phys.* **22**; No. 185 Bruun, H. H., Ryhage, R. and Stenhagen, E. *Acta Chem. Scand.* **12** (1958) 1355.
18. Arya, V. P., Enzell, C., Erdtman, H. and Ryhage, R. *Acta Chem. Scand.* **15** (1961) 682.
19. Ryhage, R. *Arkiv Kemi* **16** (1960) 19.
20. Campbell, W. P. and Todd, D. *J. Am. Chem. Soc.* **64** (1942) 928.
21. Poss, G. I., Arth, G. E., Beyler, R. E. and Sarett, L. H. *J. Am. Chem. Soc.* **75** (1953) 422.
22. Wickberg, B. *Private communication* (*Cf.* Ref.[1]).
23. Houben-Weyl-Müller, *Methoden der Organischen Chemie*, (4. Aufl.) Stuttgart 1954, Bd 7/1, p. 178.

Received March 7, 1961.

ACTA CHEMICA SCANDINAVICA 15 (1961) 1313–1318

The Chemistry of the Natural Order Cupressales 39 *

Heartwood Constituents of *Cupressus torulosa* Don.

H. S. BARRETO** and C. ENZELL

Organiska-kemiska Institutionen, Kung. Tekniska Högskolan, Stockholm, Sweden

The heartwood of *Cupressus torulosa*, Don contains carvacrol, carvacrol methyl ether, α-thujaplicin, β-thujaplicin, β-thujaplicinol, nootkatin, ferruginol, hinokiol, hinokione, manool and the new diterpenes torulosal and torulosol. Paper and gas chromatographic evidence was obtained for the presence of cuparene, humulene and thujopsene and paper chromatographic and spectroscopic evidence for the presence of β-dolabrin.

Cupressus torulosa, the Bhutan or Nepal cypress, belongs to the comparatively large genus *Cupressus*, which is being subjected to a systematic chemotaxonomic study [1,2] in this laboratory. This species grows wild in the outer ranges of the western Himalayas and in western Szechwan, China, but the material used in this investigation was obtained from a tree grown in Switzerland and was kindly made available to us by Professor A. U. Däniker, Zürich. The first preliminary investigation of this material was carried out by one of us (H.B.) in 1958. Ahluwalia and Seshadri [3] have already shown that the heartwood contains nootkatin.

Cupressus torulosa heartwood was extracted with acetone and the light petroleum-soluble part of this extract was separated into acidic and neutral fractions. The neutral oil was chromatographed on alumina giving nine main fractions.

The first fraction was very small and its infrared spectrum and the results of gas-liquid and liquid-liquid partition chromatography showed that it was a mixture of at least nine hydrocarbons. The main component of this fraction was identified as humulene [4] and two other components as thujopsene [5] and cuparene [6]. The liquid-liquid partition chromatography was carried out with a silver fluoborate-hexadecane system [7].

The very small second fraction was partly crystalline. The crystalline material, according to its infrared spectrum, was a mixture of straight chain hydro-

* Part *38*, *Acta Chem. Scand.* **15** (1961) 1303.

** Present address: Rural University, Rio de Janeiro, Brazil.

carbons; the non-crystalline part was mainly carvacrol methyl ether, which was identified by conversion to carvacroxyacetic acid.

Fraction three, by far the largest fraction, was practically pure manool [8].

Fraction four also contained manool and was shown by paper chromatography to be a mixture of ferruginol and manool.

Fraction five was a mixture of ferruginol and a second component. It was separated on a light petroleum-impregnated polyvinyl chloride column, using aqueous methanol as the mobile phase [7], into ferruginol and its main component, a new hydroxyaldehyde which was named torulosal [9]. Ferruginol was identified by conversion to the crystalline acetate. The ultra-violet spectrum and the optical rotation of the acetate showed that, within the limits of error, it was free from the Δ^6-dehydrocompound (steroid numbering) which apparently [10] often accompanies ferruginol.

Fractions six and seven, in addition to ferruginol, contained a new diol which was named torulosol. The structures of torulosol and torulosal have been discussed in a preceding paper [9].

Fraction eight was largely crystalline and contained torulosol as the main component. On fractional crystallisation it gave hinokione and a mixture of hinokione and hinokiol, which was separated by preparative paper chromatography on dimethyl sulphoxide-impregnated paper. The structures of these two substances have recently been discussed by Chow and Erdtman [11].

Fraction nine, the end fraction, was subjected to a quick distillation at low pressure. The distillate contained, according to paper chromatography, the same components as the previous fraction.

The acidic fraction from *Cupressus torulosa* contained nootkatin as the main component. The remaining material was separated into eight fractions by preparative chromatography on paper impregnated with dimethyl sulphoxide and ethylenediaminetetraacetic acid [12]. The compounds obtained on extraction of the strips were purified by sublimation and, where possible, by crystallisation. It was possible to identify carvacrol (after conversion to carvacroxyacetic acid), hinokiol, hinokione, β-thujaplicinol [13], nootkatin, α-thujaplicin and β-thujaplicin by mixed melting points and infra-red spectra. One of the zones, in addition to hinokione, contained a more volatile material, which, according to paper chromatographic results obtained by two methods and in agreement with the spectroscopic data, contained β-dolabrin [14] as the main component.

Though wide variations are possible in biological material approximate estimates of the amount of each compound are given in the annexed table as percentages of air-dry heartwood.

Total acetone extract 5.7 %

Light petroleum-soluble acetone extract 3.1 % (acidic 0.3 %, neutral 2.8 %)

Carvacrol	0.003 %	Cuparene	0.002 %	Ferruginol	0.2 %
Carvacrol methyl ether	0.007 %	Humulene	0.02 %	Hinokiol	0.03 %
β-Dolabrin	0.0004 %	Nootkatin	0.2 %	Hinokione	0.09 %
α-Thujaplicin	0.008 %	Thujopsene	0.003 %	Manool	1.4 %
β-Thujaplicin	0.004 %			Torulosal	0.4 %
β-Thujaplicinol	0.004 %			Torulosol	0.4 %

Simonsen [15] in 1923 investigated the leaf oil of *Cupressus torulosa* and found that this, unlike the heartwood we investigated here, was very rich in monoterpenoids.

A comparison of the different types of compounds isolated in the present investigation with those previously isolated from other conifers is of some interest. Tropolones are present in many conifers of the *Cupressaceae* and, in a recent paper-chromatographic survey [16] on their occurrence, they have been used to illuminate certain taxonomic relationships in this family. The sesquiterpenes and the tricarbocyclic diterpenes isolated during this investigation occur in several genera of the *Cupressaceae* and some of the diterpenes have also been found in a number of genera of the *Podocarpaceae;* however the chemotaxonomic value of these compounds is at present less clear. The dicarbocyclic diterpenes seem to offer an interesting chemotaxonomic peculiarity in that they have so far only been found [1] within the genus *Cupressus* of the family Cupressaceae, but whether this difference will survive more careful examination of other genera remains to be seen. General relationships among these conifers have been fully discussed by Erdtman [17] in the light of recent results.

EXPERIMENTAL

Melting points were taken on a Kofler micro hot stage, unless otherwise stated. Infrared spectra were recorded on a Perkin-Elmer No. 21 instrument (NaCl prism). Ultra-violet spectra were measured in ethanol on a Beckman recording spectrophotometer, model DK-2. Light petroleum refers to a fraction b.p. 35—60°, unless stated to the contrary. Micro-analyses by Dr. A. Bernhardt, Mülheim.

Extraction. Finely milled air-dry heartwood of *Cupressus torulosa* (5.7 kg) was extracted with acetone for 24 h. The extract was filtered, the acetone was evaporated and the residue was poured with vigorous stirring into a tenfold volume of light petroleum. The precipitate obtained was filtered off, dissolved in a small volume of acetone and the solution was poured into a fivefold volume of light petroleum and filtered. The precipitation was repeated. The combined light petroleum solutions were concentrated to a small volume, poured with vigorous stirring into a tenfold volume of light petroleum and filtered. The light petroleum insoluble precipitates (160 g) were not further investigated. The clear light-petroleum solution was concentrated to 1 litre, extracted repeatedly with aqueous potassium hydroxide (10 %) until it gave no colour reaction with bis-diazotized benzidine and then washed with water. The alkaline solutions were combined, washed with light petroleum, acidified with dilute sulphuric acid (10 %) and extracted with light petroleum. The combined neutral solutions, after drying (Na_2SO_4) and evaporation of the solvent, gave a yellow-brown oil (160 g, 2.2 % of the wood). The acidic solution, on drying (Na_2SO_4) and evaporation of the solvent, gave a solid residue (16 g, 0.5 % of the wood).

The neutral oil. Part (77 g) of the neutral oil, diluted with light petroleum (100 ml), was adsorbed on a column of alumina (2.2 kg, Merck, activity II). It was eluted with solvents of increasing polarity and collected in 1 litre fractions. These were combined according to the results of paper chromatography on hexadecane-impregnated (10 % hexadecane in light petroleum, b.p. 60—71°) glass fibre paper (Schleicher and Schüll, 0.17—0.23 mm) using methanol-water (7:3—9:1) as mobile phase and dipping the dried paper (100°, 2—3 min) in antimony pentachloride-chloroform (1:9) solution for detection of the spots [7]. The results are summarised in Table 1.

Fraction 1, according to its infra-red absorption and the results of gas-liquid and liquid-liquid partition chromatography, was a mixture of at least 9 different hydrocarbons. The gas-liquid chromatographic examination was made with a Pye instrument (one metre column; 2,4-dinitrophenyl-2-naphthyl ether (20 %) on Celite [18]; column temp. 150°; flow rate 25.5 ml/min of argon; charge 0.025 μl). Nine peaks were found, with the following elution times and areas (as percentages of the total area): A 4.2 min (2 %), B 8.6 (1 %), C 15.0 (2 %), D 17.6 (9 %), E 19.9 (3 %), F 25.2 (50 %), G 26.2 (25 %), H 30.4

Table 1.

Fraction No.	Weight of fraction in g	Volume of fraction in l	Eluent
1	0.9	1	Light petroleum
2	0.2	1	» »
3	37.0	14	Benzene and then ether-light petroleum (1:99—1:9)
4	3.0	1	Ether-light petroleum (1:1)
5	16.8	4	Ether-light petroleum (1:1—1:0)
6	1.4	2	Ether
7	1.7	1	Ether-ethanol (99:1)
8	13.2	2	Ether-ethanol (97:3)
9	2.3	6	Ether-ethanol (95:5—0:1)

(3 %), I 43.1 (5 %). The elution times of the peaks D, F and I are identical with those found for thujopsene, humulene and cuparene, respectively, under identical conditions. Paper chromatography on hexadecane-impregnated glass fibre paper (Schleicher and Schüll, 0.17—0.23 mm) with a solution of silver fluoborate (30 % w/v) in aqueous methanol (1:9) as mobile phase gave spots with R_F-values 0.04, 0.08, 0.17, 0.24, 0.42, 0.54 and 0.80 after drying and treatment with an antimony pentachloride-chloroform (1:9) solution. R_F-values 0.08, 0.17, and 0.80 are the same as those found for cuparene, thujopsene and humulene under the conditions mentioned. A further indication of the presence of cuparene is found in the infrared spectrum of the fraction, which showed a band at 1 518 cm^{-1}.

Fraction 2 was partly crystalline. The solid material was filtered off and washed with a small amount of acetone giving a white crystalline material (0.02 g) which after repeated recrystallisation from acetone had m.p. 58—61°, $[\alpha]_D$ 0° ($CHCl_3$, *c* 0.7). The infra-red spectrum of this substance was extremely simple ν_{max}^{KBr} 2 935 (s), 2 865 (s), 1 477 (m), 1 462 (m), 1 386 (w), 731 (w), 716 (m), indicating a mixture of saturated straight chain hydrocarbons. The non-crystalline part, according to its infrared spectrum, was largely carvacrol methyl ether. Demethylation with hydrogen bromide (30 %, 1.5 h) followed by etherfication with ethyl chloracetate and saponification of the ester gave carvacroxyacetic acid, m.p. and, mixed m.p. 151—152°.

Fraction 3, according to its infra-red spectrum, was manool which started to crystallise immediately on seeding. Recrystallisation from light petroleum gave pure manool, m.p. and mixed m.p. 52—53°, $[\alpha]_D$ + 33° ($CHCl_3$, *c* 2.0), with an infrared spectrum identical with that of authentic material.

Fraction 4, on recrystallisation from light petroleum, gave manool (1.1 g), which was identified as above. The mother liquors, according to paper chromatographic results, contained a mixture of manool and ferruginol in about a 3:1 ratio.

Fraction 5 was a mixture of two components. These were separated on an impregnated polyvinyl chloride (PVC) column [7]. The column was prepared as follows: PVC-powder (Wackerchemie, Germany, purified, 350 g) was washed with aqueous ethanol (2 l, 2:1) and ethanol (2 l), sucked dry on a Büchner funnel and finally air-dried at room temperature. The dry PVC-powder was suspended in aqueous methanol (2.4 l, 3:7), saturated with light petroleum (b.p. 60—71°) and then further light petroleum (245 ml, b.p. 60—71°) was added with stirring. The suspension was added, in portions, to a tube (5 × 100 cm) partly filled with the same solvent mixture. After the first addition the bottom tap was opened and the PVC-powder packed with a stopper as it settled from the flowing suspension. As the flow became slower with increasing length of the column it was speeded up by applying pressure. The last few centimetres of the column of adsorbent (5 × 50 cm) were packed by placing a cottonwool disc followed by a porcelain filter disc on the top of the column and applying pressure with the stopper. The material to be chromatographed was extracted with 5 portions (200 ml each) of aqueous methanol (1:3), which were added successively to the top of the column. The fractions (150 ml) obtained on elution with

aqueous methanol (3 l of 1:3 and thereafter 3:17) saturated with light petroleum were combined according to paper chromatographic results into two fractions. These were diluted with water (twice the amount of the eluate) and extracted with ether. The ether extracts were dried (Na_2SO_4) and the solvent was evaporated leaving torulosal (11 *g*, fract. 2—9) and ferruginol (2.9 g, fract. 16—25, identified by I.R.).

Torulosal, n_D^{25} 1.521, $[a]_D$ + 29° ($CHCl_3$, *c* 1.8) was paper chromatographically pure. It was characterised as the carbon tetrachloride "inclusion compound", m.p. 80—85° (Pyrex tube), $[a]_D$ + 24° ($CHCl_3$, *c* 2.0), and the semicarbazone, m.p. 195—197° (decomp.), $[a]_D$ −9° (pyridine, *c* 1.0) and by conversion into torulosol [9], m.p. and mixed m.p. 110—111°, $[a]_D$ + 31°.

A part (0.50 g) of the ferruginol was dissolved in pyridine (6 ml) and acetic anhydride (2 ml) and kept for two days at room temperature and then for one hour on the water bath. The product was diluted with water, extracted with ether and after extraction with aq. NaOH (10 %) the ether solution was taken to dryness. Recrystallisation from ethanol gave pure ferruginol acetate (0.39 g), m.p. and mixed m.p. 81—83°, $[a]_D$ + 59° (EtOH, *c* 2.0), λ_{max}^{EtOH} 268 mμ (ε 1 240), 278 mμ (ε 1 330). The infra-red spectrum was identical with that of authentic material.

Fraction 6 was shown by paper chromatography to be a mixture of about equal amounts of ferruginol and torulosol.

Fraction 7 on repeated recrystallisation from *iso*propyl ether gave pure torulosol (0.7 g), m.p. 110—111°, $[a]_D$ + 31° ($CHCl_3$, *c* 2.0). The combined mother liquors, according to paper chromatographic results, were a mixture of ferruginol and torulosol in about a 3:1 ratio.

Fraction 8 was partly crystalline and on repeated recrystallisation from *iso*propyl ether gave pure torulosol (8.7 g). Concentration of the mother liquors gave two fractions with melting points higher than that of torulosol. One fraction, (m.p. 110- 170°, 2.5 g), on repeated recrystallisation from methanol, gave pure hinokione, m.p. and mixed m.p. 186—188° (slight decomp. from just above 180°), $[a]_D$ + 113° ($CHCl_3$, *c* 2.0). The infrared spectrum was identical with that of authentic material.

A part (0.090 g) of the second fraction (m.p. 186—202°, 0.13 g) was separated by chromatography on two sheets of paper (24 × 56 cm, Whatman 3MM) impregnated with dimethyl sulphoxide using *iso*propyl ether as the mobile phase. The two zones were detected by spraying strips with bisdiazotised benzidine and had R_F-values corresponding to those of hinokiol and hinokione. The slow-moving zone was cut out and extracted with ether. The ether solution, after washing with water, drying (Na_2SO_4) and removal of the solvent, gave a crystalline residue (42 mg), which was sublimed along a temperature gradient under reduced pressure (0.2 mm). This crystalline sublimate (10 mg) was resublimed twice and then showed a m.p. of 232—235° which was raised to 236—239° on admixture with hinokiol (m.p. 236—239°). The infrared spectra of the two compounds were superimposable.

A part (0.3 g) of *fraction 9* was distilled under reduced pressure (0.5 mm) and the distillate (0.2 g) was shown by paper chromatography to contain the same components as fraction 8.

The acidic fraction. A part (11 g) of the acidic fraction was recrystallised from light petroleum to give pure nootkatin (6 g), m.p. and mixed m.p. 95—96°, infrared spectrum identical with that of authentic material. The mother liquors were combined and the solvent evaporated giving a residue (5 g), a part (1.5 g) of which was separated by preparative paper chromatography. A concentrated solution in light petroleum (b.p. 60—71°, 6 ml) was applied to ten sheets of paper (Whatman 3MM, 24 × 56 cm), which had previously been impregnated with ethylenediaminetetraacetic acid and dimethyl sulphoxide [12]. The chromatograms were run in light petroleum (b.p. 60—71°) and the different zones (8), detected by ultraviolet light, were cut out and extracted with ether. These ether solutions were shaken with water and dried (Na_2SO_4). The residues, obtained on removal of the ether, were purified by sublimation or distillation along a temperature gradient and where possible by crystallisation. The results obtained are given in Table 2. The compounds identified (carvacrol after conversion to carvacroxyacetic acid) all showed undepressed mixed melting points and correct infrared spectra.

Table 2.

Fraction	R_F-value	Weight of extracted material in mg	Compound isolated
1	0.69	66	unidentified
2	0.66	500	nootkatin
3	0.55	100	α-thujaplicin
4	0.37	12	unidentified
5	0.29	46	β-thujaplicin
6	0.22	88	hinokione + β-dolabrin
7	0.14	88	β-thujaplicinol + carvacrol
8	0.02	360	hinokiol

Fraction 1, on sublimation and repeated crystallisation from methanol, gave a small amount (3 mg) of a compound, m.p. 60—63° which, according to infrared and ultraviolet spectra, seemed to be an oxoalcohol. Fraction 4 on distillation gave an easily volatile oil which according to its infrared and U.V. spectra was an α,β-unsaturated acid. Fraction 6 on sublimation gave, together with hinokione, a small amount (5 mg) of a much more volatile oil. This, according to further paper chromatographic results, using the method of Zavarin and Anderson [19], and according to its infrared and ultraviolet absorption was largely β-dolabrin [16,14,13].

Acknowledgements. We thank Prof. H. Erdtman for his kind interest in this work and Mrs. S. Strand for skilful assistance.

Thanks are also due to the *Swedish Technical Research Council* (C.E.) and the *U.S. Army and Development Liason Group* (contract number DA-91-508-EUC-288) (H.B.) for financial support.

REFERENCES

1. Enzell, C. and Erdtman, H. *Acta Chem. Scand.* **11** (1957) 902.
2. Enzell, C. and Krolikowska, M. *To be published.*
3. Ahluwalia, V. K. and Seshadri, T. R. *Current Sci. (India)* **23** (1954) 154.
4. Dev, S. *Tetrahedron Letters* **1959**, No. 7, 12.
5. Erdtman, H. and Norin, T. *Chem. & Ind. (London)* **1960** 622.
6. Enzell, C. and Erdtman, H. *Tetrahedron* **4** (1958) 361.
7. Wickberg, B. *Private communication.*
8. Barltrop, J. A. and Bigley, D. B. *Chem. & Ind. (London)* **1959** 1378.
9. Enzell, C. *Acta Chem. Scand.* **15** (1961) 1303.
10. Bredenberg, J. B. *Acta Chem. Scand.* **11** (1957) 932.
11. Chow, Y. L. and Erdtman, H. *Proc. Chem. Soc.* **1960** 174.
12. Wachtmeister, C. A. and Wickberg, B. *Acta Chem. Scand.* **12** (1958) 1335.
13. Gardner, J. A. F. and Barton, G. M. *Canad. J. Chem.* **36** (1958) 1612.
14. Nozoe, T., Takase, K. and Ogata, M. *Chem. & Ind. London* **1957** 1070.
15. Simonsen, J. L. *Indian Forest Records* **10** (1923) 1; from *Chem. Abstr.* **18** (1924) 881.
16. Zavarin, E., Smith, R. M. and Anderson, A. B. *J. Org. Chem.* **24** (1959) 1318.
17. Erdtman, H. *4th Intern. Congr. Biochem.* Vol. II — *Biochemistry of Wood* (1958).
18. Groth, A. B. *Svensk Papperstidn.* **61** (1958) 311.
19. Zavarin, E. and Anderson, A. B. *J. Org. Chem.* **21** (1956) 332.

Received March 7, 1961.

ACTA CHEMICA SCANDINAVICA 15 (1961) 1319–1326

Kinetics of the Carbon Dioxide Hydration under Conditions of Enforced Stationarity

JØRGEN KOEFOED and KNUD ENGEL

Universitetets Fysisk-Kemiske Institut, Copenhagen, Denmark

The hydration of carbon dioxide has been investigated in a new way. A solution of sodium bicarbonate is kept saturated with carbon dioxide. When the pH of the solution has attained its equilibrium value, pH_0, a motor driven syringe is started, and strong acid or base is supplied at a constant rate, s. After a few minutes the pH is again stationary at $pH_0 + \Delta pH$. ΔpH is plotted against s.

From the kinetic equations is derived the theoretical dependence of ΔpH on s corresponding to the various possible routes of the reaction, and the experimental curves are analysed accordingly.

For the "spontaneous" reaction between CO_2 and H_2O and for the base reaction, $CO_2 + OH^-$, our experiments gave results which are in agreement with those of Faurholt and others. Since we were able to measure under other conditions than previous workers we could also detect an acid catalysis and catalysis by HCO_3^- and by H_2CO_3, the latter to a high power of the H_2CO_3-concentration, indicating the existence of a polymeric carbonic acid intermediate.

In spite of the physiological and technical importance of the carbon dioxide hydration and in spite of the numerous studies which have been made on the kinetics of this reaction, our knowledge of its details is still not quite satisfactory. In particular no quantitative information is available in the literature regarding the catalytic influence of acid, presumably because the techniques of previous authors have not been well suited to investigate this question.

In our experiments we have enforced stationary conditions upon the system through the steady supply of base or acid to a solution which is kept saturated with carbon dioxide. By varying the concentration of sodium bicarbonate in the solution, we can thus measure at different pH, and get the velocity of the reaction directly under controlled circumstances and without addition of buffer substances other than bicarbonate-carbonic acid.

EXPERIMENTAL

Three sets of experiments at 0°C are reported here with solutions, which were 1) 0.25 M $NaHCO_3$ + 0.50 M NaCl, 2) 0.50 M $NaHCO_3$ + 0.25 M NaCl and 3) 0.75 M $NaHCO_3$.

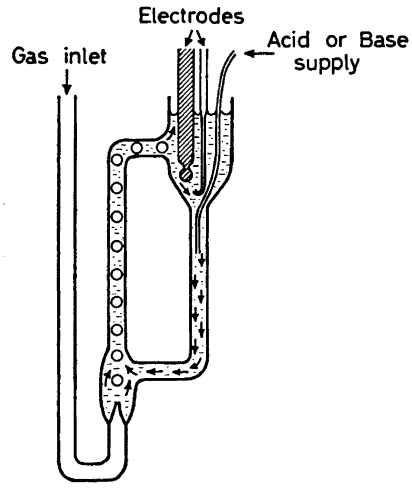

Fig. 1. The Pyrex glass apparatus. Contains 8 ml of solution.

8 ml of the solution is placed in the Pyrex apparatus drawn in Fig. 1. Carbon dioxide is washed in two bubble flasks in an ice bath and is blown through the solution to saturate it and to stir it vigorously by the Cottrell circulation pump arrangement. Circulation time is about one second.

pH is measured with a standardized glass electrode and a battery operated pH-meter (PHM4, Radiometer, Copenhagen) which reads to 0.002 in pH. Standard buffer was: 0.025 M KH_2PO_4 + 0.025 M Na_2HPO_4; pH = 6.98 at 0°C (NBS).

2 M NaOH or HCl is supplied from a calibrated polythene syringe which is driven by a worm gear operated through a torsion cable from an AC asynchrous motor with a variable friction gear. The motor is placed about one meter from the electrodes and is well screened to eliminate the influence of electrical noise on the pH-meter. A telephone-counter counts the number of rotations of the cable.

When the pH after some 10—15 min has attained its equilibrium value, pH_0, the syringe is started at some selected speed. pH and the telephone counter are read at regular intervals. After a few minutes the pH attains a stationary value, $pH_0 + \Delta pH$, because hydrogen ions are produced or used by the hydration reaction at exactly the same rate as they are consumed or supplied through the chemicals from the syringe.

After running for an interval of time sufficient to control steadiness of supply and of pH, the syringe is stopped. pH is followed until it has returned to pH_0 or to a somewhat different value corresponding to a "secular" change caused by the change in bicarbonate concentration from the added chemicals.

In the high speed experiments this variation becomes appreciable and the true ΔpH value must be found by extrapolation.

From the readings on the counter we calculate the reaction rate s in moles of hydrogen ions produced by the reaction per second and per liter. The values are in the range of 0 to 5 $\times$ 10^{-4} M l^{-1} sec^{-1}.

At low values of s a few runs can be made with the same filling, otherwise a new solution must be used for each run; that is, for each determination of a set of (s, ΔpH) values.

THEORETICAL

The total turnover, s, in a net process which can take place by several routes is obviously the sum of the reaction rates by each of the routes:

$$s = s_A + s_B + s_C + \ldots \quad (1)$$

Now, for each reaction scheme, X, we can design, we can calculate an expression for the dependence of the reaction rate s_X on ΔpH. The eventual analysis of the experimental curves will consist of producing from such s_X-functions a linear combination which will reproduce the results with a satisfactory degree of accuracy.

For the present experiments it has turned out that we must combine five different reaction schemes: the Spontaneous reaction, the Base reaction, the Acid catalyzed reaction, the biCarbonate catalyzed reaction and the Fivefold acid catalyzed reaction:

S: $CO_2 + H_2O \rightleftharpoons H_2CO_3 = HCO_3^- + H^+$

B: $CO_2 + OH^- \rightleftharpoons HCO_3^-$

A: $CO_2 + H_2O + H^+ = HCO_2^+ + H_2O \rightleftharpoons H_3CO_3^+ = HCO_3^- + 2H^+$

C: $CO_2 + H_2O + HCO_3^- \rightleftharpoons HC_2O_5^- + H_2O = 2HCO_3^- + H^+$

F: $CO_2 + H_2O + 4HCO_3^- + 5H^+ = CO_2 + H_{11}C_4O_{13}^+ \rightleftharpoons H_{11}C_5O_{15}^+ = 5HCO_3^- + 6H^+$

In these schemes proton exchanges, polymerisations and depolymerisations are assumed to be very rapid reactions and are indicated by an equals mark (=), whereas the rate determining steps involving the establishment of a chemical bond to C in CO_2 are marked with double arrows. We control the concentrations of the first and the last combinations of molecular and ionic species in each scheme. In between we have suggested such hypothetical intermediates as we find the most probable — or the least improbable. The velocity expressions refer exclusively to the first kind of species.

It is convenient to introduce the equilibrium velocities, v_X°, which are the velocities of the forward reactions at equilibrium and hence also of the back reactions at equilibrium, $v_{-X}^\circ = v_X^\circ$. Equilibrium values of the concentrations are marked $[OH^-]_o$ and $[H^+]_o$ and water concentration is taken into the constants. We derive the following:

$$s_S = v_S - v_{-S} = k_S[CO_2] - k_{-S}[HCO_3^-][H^+] = v_S^\circ\ (1 - 10^{-\Delta pH})$$

since $\quad v_S^\circ = k_S[CO_2] = v_{-S}^\circ = k_{-S}[HCO_3^-][H^+]_o$

and $\quad [H^+]/[H^+]_o = 10^{-\Delta pH};\ [HCO_3^-] = [HCO_3^-]_o;\ [CO_2] = [CO_2]_o$

In the same way we derive

$$s_B = v_B - v_{-B} = k_B[CO_2][OH^-] - k_{-B}[HCO_3^-] = v_B^\circ\ 10^{\Delta pH}\ (1 - 10^{-\Delta pH})$$
$$v_B^\circ = k_B[CO_2][OH^-]_o = k_{-B}[HCO_3^-]$$
$$s_A = v_A - v_{-A} = k_A[CO_2][H^+] - k_{-A}[HCO_3^-][H^+]^2 = v_A^\circ\ 10^{-\Delta pH}\ (1 - 10^{-\Delta pH})$$
$$v_A^\circ = k_A[CO_2][H^+]_o = k_{-A}[HCO_3^-][H^+]_o^2$$
$$s_C = v_C - v_{-C} = k_C[CO_2][HCO_3^-] - k_{-C}[HCO_3^-]^2[H^+] = v_C^\circ(1 - 10^{-\Delta pH})$$
$$v_C^\circ = k_C[CO_2][HCO_3^-] = k_{-C}[HCO_3^-]^2[H^+]_o$$
$$s_F = v_F - v_{-F} = k_F[CO_2][HCO_3^-]^4[H^+]^5 - k_{-F}[HCO_3^-]^5[H^+]^6 = v_F^\circ\ 10^{-5\Delta pH}\ (1 - 10^{-\Delta pH})$$
$$v_F^\circ = k_F[CO_2][HCO_3^-]^4[H^+]_o^5 = k_{-F}[HCO_3^-]^5[H^+]_o^6$$

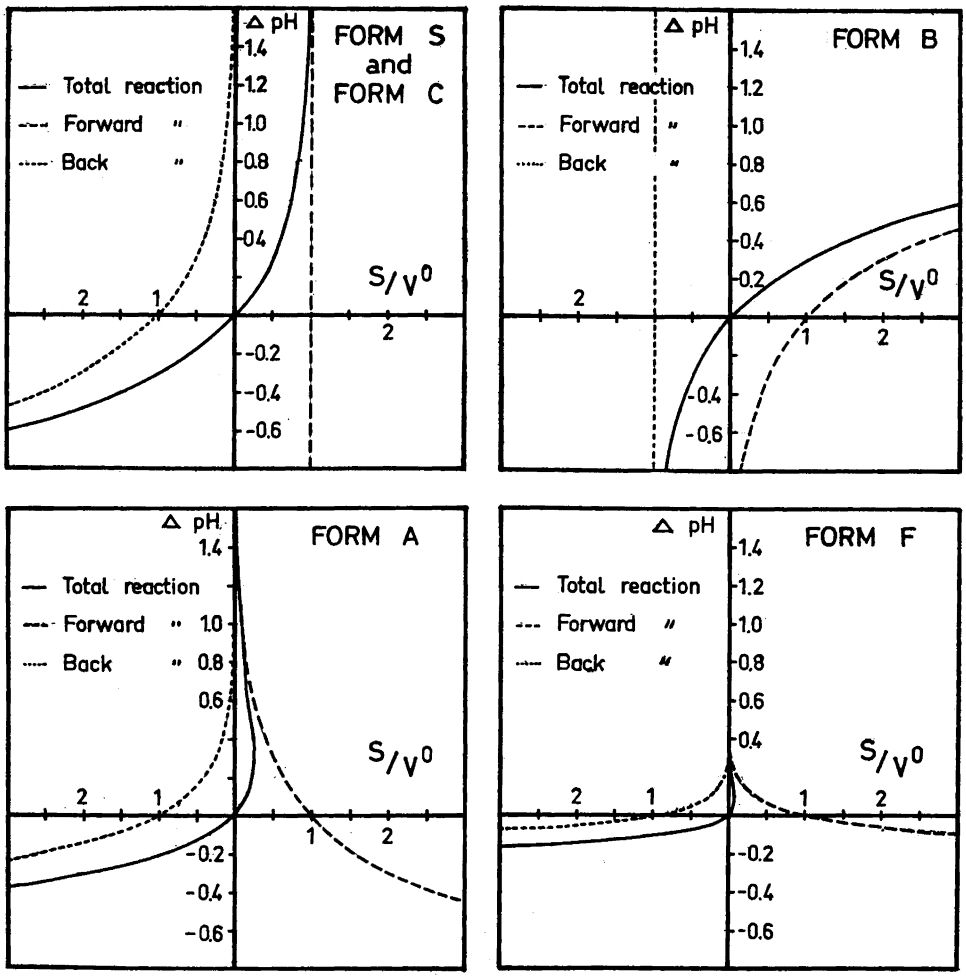

Fig. 2. The general patterns of the ΔpH *versus* s curves that would be shown if each of the reactions could proceed separately. Drawn to such scales that forward and back reactions proceed with unit velocity at equilibrium (ΔpH = 0).

The patterns of the curves are shown on Fig. 2. For each of the schemes are plotted v_X, v_{-X} and s_X to such a scale that v_X° is put equal to one. Reactions S and C have the same form of curves, but v_C° is proportional to bicarbonate concentration whereas v_S° is independent of it.

Incidentally we notice that these plots are also affinity-velocity plots for these reactions, since for all the reactions:

$$A = -\Delta G = \mu(CO_2) + \mu(H_2O) - \mu(HCO_3^-) - \mu(H^+) = (RT\ln 10)\ \Delta\text{pH}$$

since $\mu(CO_2) + \mu(H_2O) = \mu(HCO_3^-) + \mu_o(H^+)$

and $\mu(H^+) - \mu_o(H^+) = -(RT\ln 10)\ \Delta\text{pH}$

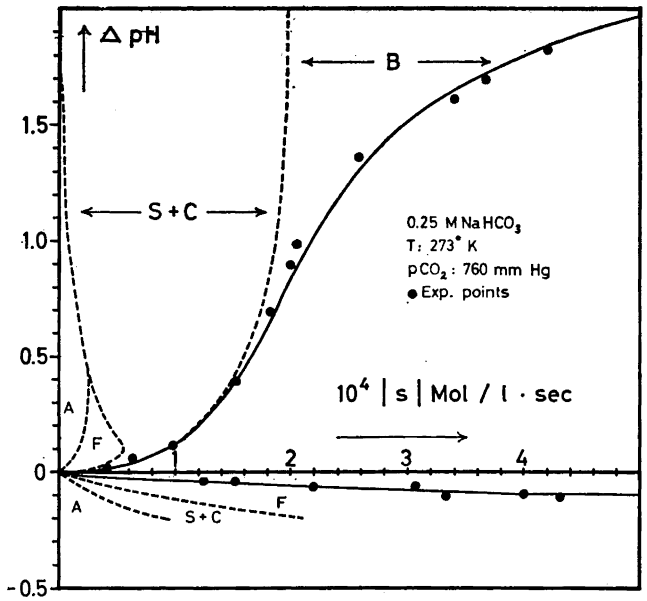

Fig. 3. Experimental results, series 1. Solution: 0.25 M $NaHCO_3$ + 0.50 M NaCl. CO_2 gas saturated with H_2O at 0°C. pH_0 = 6.75. NaOH supplied at positive ΔpH, HCl at negative ΔpH. Full curve represents calculated values, dotted lines indicate contributions from the various reactions according to the chosen parameters (see Table 1).

In accordance with De Donder's theory we find, therefore, that all the curves go through the origin as continuous and differentiable functions; but proportionality between velocity and affinity is for reaction F certainly restricted to infinitesimal intervals. This curve is reminiscent of a voltage *versus* current plot for an electrical rectifier.

RESULTS

The measured values are plotted in Figs. 3—5. To save space the numerical value of s has been chosen as abscissa, so that negative ΔpH corresponds to acid supply by the syringe and acid consumption by the reaction, which in the theoretical section were counted as negative values of s.

The full curves in these figures represent calculated values, derived from the above expressions with the choice of v° values shown in Table 1 together with the corresponding values of the velocity constants. Values of v° are estimated to about one significant figure only, and no attempt has been made to improve the fit by fine adjustment of the constants.

Also shown in the figures are the contributions from each of the reactions. Each abscissa value on the full curve is a sum of contributions from the five reactions and these contributions are represented by the length between consecutive pairs of the dotted lines, as indicated by the corresponding letters.

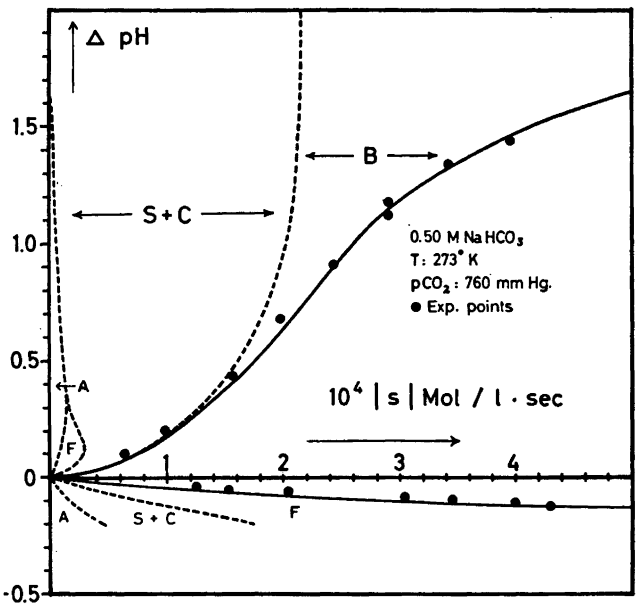

Fig. 4. Experimental results, series 2. Solution: 0.50 M $NaHCO_3$ + 0.25 M NaCl. pH_o = 7.05. Otherwise as Fig. 3.

It is clear that all of the reactions are necessary to make up the total rate, each having its main influence in one particular range of ΔpH with some variation according to bicarbonate concentration. It is the very unsymmetrical

Table 1. Experimental results. 0°C, ionic strength 0.75 M. Parameters used in drawing the curves in Figs. 3—5.

$NaHCO_3$	NaCl	pH_o	$10^4 v_S^o$	$10^4 v_B^o$	$10^4 v_C^o$	$10^4 v_A^o$	$10^4 v_F^o$
0.25	0.50	6.75	1.8	0.033	0.2	1.0	6.0
0.50	0.25	7.05	1.8	0.066	0.4	0.5	3.0
0.75	0	7.23	1.8	0.10	0.6	0.33	2.0

$[CO_2]$ = 0.062 M (Harned and Davies [6])
$-\log K_w$ = 14.94 (Harned and Owen [7])
$-\log f_\pm$ = 0.18 (estimated)

$k_S = v_S^o/[CO_2] = 0.003$

$k_B = v_B^o/[CO_2][OH^-]_o = 5\,500$
$(\log [OH^-]_o = \log K_w + pH_o - \log f_\pm)$

$k_C = v_C^o/[CO_2][HCO_3^-] = 0.0013$

$k_A = v_A^o/[CO_2][H^+]_o = 6\,000$

$k_F = v_F^o/[CO_2][HCO_3^-]^4[H^+]_o^5 = 1.7 \cdot 10^{33}$

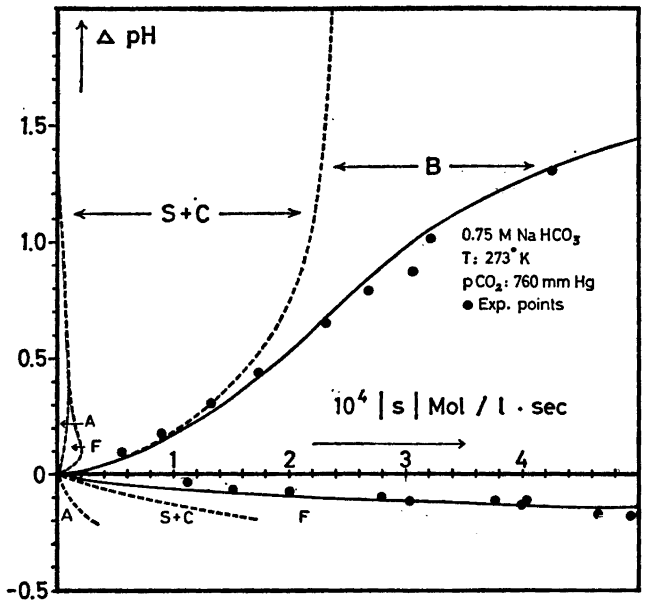

Fig. 5. Experimental results, series 3. Solution: 0.75 M $NaHCO_3$. $pH_o = 7.23$. Otherwise as Figs. 3 and 4.

behaviour towards acid and base that makes necessary the high power of hydrogen ion concentration in s_F, but if bicarbonate did not enter also to some high power, it would not be possible to fit the acid branches of the three curves with the same function. The contributions from reactions A and C are the least important and it would be possible to make a reasonable fit without them. That we have included these two reactions and not taken any further possible reactions into account is the result of a somewhat arbitrary estimate regarding what is reasonable in view of our experimental accuracy.

DISCUSSION

The method we have applied seems in many respects to be very well suited for the purpose, and from the results we have obtained it is not difficult to see why previous methods have been less satisfactory. All previous methods have allowed a drift of pH over a certain range during the reaction, and too many parameters are therefore changed at the same time.

The value of our k_S is in excellent agreement with Faurholt's [1] value ($0.0013 \times 2.3 = 0.0030$) and with Ljunggren and Lamm's [2] value at 4°C (0.0044). The agreement with Roughton's [3] value (0.0021) is not quite so good.

Our value of k_B is about six times that of Faurholt [1]. Experiments at lower carbon dioxide pressures must be made before this peculiar fact can be discussed.

In the acid reaction we have proposed the intermediate HCO_2^+, because this structure should be favourable for a bond formation to the carbon atom.

The base strength of CO_2 has not been measured. pK is probably between -3 and -6 (*cf.* Hammett [4]).

The most remarkable feature in our results is the necessity of assuming a reaction like F. Whether the exponent to hydrogen ion activity is really five, or whether it might as well be four, six or seven cannot be said with certainty. We only know that it must be high and that it must be about one higher than that of the bicarbonate concentration.

The only reasonable explanation for this peculiar behaviour is that some polymeric carbonic acid is present and acts as a powerful catalyst. Tentatively we suggest that it might be structures like the following that describe the changes involved in the rate determining step of reaction F.

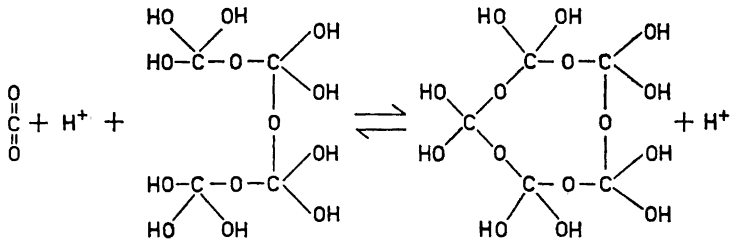

The existing evidence for polymerization of carbonic acids has been summarized by Rosotti [5]. Whether polymerization occurs through hydrogen bonds or through addition to the C—O double bond as assumed above cannot be decided. That boric acid, silicates and many other similar compounds polymerize in aqueous solution is too well known to need discussion.

Faurholt [1] has pointed out the difficulty in understanding why H_2CO_3 is not a considerably stronger acid than formic acid. If most of the hydrated carbon dioxide exists in the form of very weak monomeric or polymeric orthoacids, true H_2CO_3 may still be some ten to a hundred times stronger than it is now believed to be.

It is difficult, however, to tell through what kind of experiments crucial evidence could be obtained for these molecular species. We plan some measurements at reduced CO_2 pressure, which will necessitate modification of the apparatus. Although we can only hope to provide circumstantial evidence in this way, it may still be worth while to learn more about this important reaction.

REFERENCES

1. Faurholt, C. *Diss.* Copenhagen 1924.
2. Ljunggren, S. and Lamm, O. *Acta Chem. Scand.* **12** (1958) 1834.
3. Pinsent, B. R. W. and Roughton, F. J. W. *Trans. Faraday Soc.* **47** (1951) 263.
4. Hammett, L. P. *Physical Organic Chemistry*, New York 1940.
5. Rosotti, F. J. C. *Nature* **188** (1960) 936.
6. Harned, H. S. and Davis, R. *J. Am. Chem. Soc.* **65** (1943) 2030.
7. Harned, H. S. and Owen, B. B. *The Physical Chemistry of Electrolytic Solutions.* New York 1943, p. 485.

Received March 3, 1961.

ACTA CHEMICA SCANDINAVICA 15 (1961) 1327–1332

The Mixing of $3d^n$ and $3d^{n-1}4s$ States in Crystalline Field Theory

HARRY B. GRAY* and C. J. BALLHAUSEN

Universitetets fysisk-kemiske Institut, Copenhagen, Denmark

The effect upon the crystalline field energies of mixing $3d^n$ and $3d^{n-1}4s$ states under the $1/r_{12}$ term present in the Hamiltonian is investigated. It is shown that the inclusion of higher states will improve the agreement with theory and experiment somewhat, especially that some of the apparent term reduction $^3P-{}^3F$ found, *e.g.*, in Ni^{++} complexes is explained in this way. However, due to the approximations of the theory it is impossible to assert just how much a full configuration interaction will affect the levels in question.

The crystalline field theory has been remarkably successful in explaining the visible spectra of complexes of transition metal ions, by representing the energy states of interest with pure d^n wave functions [1,2]. No doubt a better approximation of the energy states is one in which all permissible configuration interaction is included. The purpose of this note is to investigate in detail the effect of including one important such interaction, $3d^74s$ with $3d^8$, in the "weak" octahedral field calculation of Ni^{2+}. It is well known [1] that the states $(3d)^n$ and $(3d)^{n-1}(4s)^1$ cannot mix under an octahedral field V_0. However, the term $1/r_{12}$ present in the full Hamiltonian is capable of performing a mixing of these atomic configurations. Consequently we first perform a scrambling of the various states under $1/r_{12}$, and then proceed to evaluate their crystal field energies.

THEORY

Proper wave functions in the SLM_LM_S scheme for $3d^8$ and $3d^74s$ terms were obtained using angular momentum operators, as outlined in Condon and Shortley [3]. The energy states of greatest interest in determining the visible spectra of Ni^{2+} compleces are the ground state ^3F and the excited ^3P level. For the configuration $3d^8$ there is one ^3F and one ^3P; for $3d^74s$, there are two ^3F's and two ^3P's.

* National Science Foundation Postdoctoral Fellow, 1960–61.

The secular determinants of electrostatic interaction mixing these levels are

$$
{}^3F \quad \begin{vmatrix} 1.\ a3d^8 & 2.\ b3d^74s & 3.\ c3d^74s \\ -E & 0 & \frac{2}{35}\sqrt{15}\,R^2 \\ 0 & \Delta_{12}-E & 0 \\ \frac{2}{35}\sqrt{15}\,R^2 & 0 & \Delta_{13}-E \end{vmatrix} = 0 \qquad (1)
$$

and

$$
{}^3P \quad \begin{vmatrix} 1.\ a3d^8 & 2.\ b3d^74s & 3.\ c3d^74s \\ -E & 0 & \frac{\sqrt{210}}{35}\,R^2 \\ 0 & \Delta_{12}-E & 0 \\ \frac{\sqrt{210}}{35}\,R^2 & 0 & \Delta_{13}-E \end{vmatrix} = 0 \qquad (2)
$$

where Δ_{12} and Δ_{13} are the energy separations between repsective $3d^74s$ levels and $3d^8$, and R^2 is the radial integral defined as

$$
\mathrm{R}^2(3d,3d;\ 3d,4s) = e^2 \int_0^\infty \int_0^\infty \frac{r_<^2}{r_>^3} R_1(3d)R_2(3d)R_1(3d)R_2(4s)\mathrm{d}r_1\mathrm{d}r_2 \qquad (3)
$$

Δ's were taken as the experimental energy separations of the terms as given by Shenstone [4]. Term energies for some important states in the $3d^74s$ configuration were calculated using the Slater-Condon F_k and G_k parameters [3], and are given in the Table. A reasonable fit of terms is obtained by taking $F_2(3d,3d) = 1\,770$ cm^{-1}, $F_4(3d,3d) = 135$ cm^{-1} and $G_2(3d,4s) = 1\,900$ cm^{-1}. A value is needed for R^2 $(3d,3d;\ 3d,4s)$. It should reasonably lie between $F^2(3d,3d)$

Table 1. Energies of some important terms in the $3d^74s$ configuration of the free Ni^{2+} ion. All energies are given in cm^{-1}.

Term	Energy expressed in Slater-Condon parameters *	Predicted energy with $F_2 = 1\,770$ cm^{-1} $F_4 = 135$ cm^{-1} and $G_2 = 1\,900$ cm^{-1}	Experimental term energy **
^5F	$-5G_2-43F_2-324F_4$	55 406	55 406 (3)
$b\,^3F$	$-G_2-43F_2-324F_4$	63 006	62 606 (3)
^5P	$-5G_2-28F_2-399F_4$	71 816	71 384 (2)
^3G	$-4G_2-39F_2-239F_4$	75 857	75 647 (4)
$b\,^3P$	$-G_2-28F_2-399F_4$	79 416	78 483 (1)
$c\,^3P$	$-4G_2-34F_2-264F_4$	81 327	82 277 (1)
^3H	$-4G_2-34F_2-264F_4$	81 327	82 194 (5)
$c\,^3F$	$-4G_2-19F_2-339F_4$	97 761	97 996 (3)

* See Ref.[3] Each term also has common parameters $7F_0(3d,4s) + 21F_0(3d,3d)$.
** From Ref.[4]; J values in parentheses.

and $G^2(3d,4s)$ as it does in calculations made by Ufford [5] on configuration interaction among $3d^3$, $3d^24s$ and $3d4s^2$. Ufford calculated R^2 in order to obtain the best fit of the free ion spectrum involved, but in our case there are less data available, so it is estimated as the geometric mean of G^2 and F^2, giving $R^2 = 28\,700$ cm^{-1} *.

The solutions of determinants (1) and (2) yield the following "best" wave-functions for ^3F and ^3P in this approximation:

$$(^3F) = \lambda_1[a\ ^3F(3d^8)] + \lambda_2[c\ ^3F(3d^74s)] \tag{4}$$

$$(^3P) = \lambda_3[a\ ^3P(3d^8)] + \lambda_4[c\ ^3P(3d^74s)] \tag{5}$$

$$\lambda_1 = 0.9978, \quad \lambda_2 = 0.0656; \quad \lambda_3 = 0.9827, \quad \lambda_4 = 0.1852.$$

In an octahedral crystal field the ^3F state splits into three levels, $^3T_{1g}$, $^3T_{2g}$ and $^3A_{2g}$ with energies calculated in the weak field approximation as follows **:

$$\begin{aligned} E(^3T_{1g}) &= (\lambda_1)^2(^3T_{1g}(a3d^8) \mid V_0 \mid {}^3T_{1g}(a3d^8)) \\ &\quad + (\lambda_2)^2(^3T_{1g}(c3d^74s) \mid V_0 \mid {}^3T_{1g}(c3d^74s)) \end{aligned} \tag{6}$$

$$\begin{aligned} E(^3T_{2g}) &= (\lambda_1)^2(^3T_{2g}(a3d^8) \mid V_0 \mid {}^3T_{2g}(a3d^8)) \\ &\quad + (\lambda_2)^2(^3T_{2g}(c3d^74s) \mid V_0 \mid {}^3T_{2g}(c3d^74s)) \end{aligned} \tag{7}$$

$$\begin{aligned} E(^3A_{1g}) &= (\lambda_1)^2(^3A_{2g}(a3d^8) \mid V_0 \mid {}^3A_{2g}(a3d^8)) \\ &\quad + (\lambda_2)^2(^3A_{2g}(c3d^74s) \mid V_0 \mid {}^3A_{2g}(c3d^74s)) \end{aligned} \tag{8}$$

and with

$$\begin{aligned} &(^3T_{1g}(a3d^8) \mid V_0 \mid {}^3T_{1g}(a3d^8)) = 6Dq,\ (^3T_{1g}(c3d^74s) \mid V_0 \mid {}^3T_{1g}(c3d^74s)) = -Dq \\ &(^3T_{2g}(a3d^8) \mid V_0 \mid {}^3T_{2g}(a3d^8)) = -\ 2Dq,\ (^3T_{2g}(c3d^74s) \mid V_0 \mid {}^3T_{2g}(c3d^74s)) = \tfrac{1}{3}Dq \\ &(^3A_{2g}(a3d^8) \mid V_0 \mid {}^3A_{2g})a3d^8)) = -12Dq,\ (^3A_{2g}(c3d^74s) \mid V_0 \mid {}^3A_{2g}(c3d^74s)) = 2Dq \end{aligned}$$

we obtain

$$\begin{aligned} E(^3T_{1g}) &= 5.97\ Dq \\ \mathrm{E}(^3T_{2g}) &= -1.99\ Dq \\ E(^3A_{2g}) &= -11.94\ Dq \end{aligned} \tag{9}$$

The ^3P state is not split and gives a $^3T_{1g}$ level in the octahedral field. The secular determinant mixing $^3T_{1g}(F)$ and $^3T_{1g}(P)$ under V_0 is ***

$$\begin{array}{c|cc|} & 1.\ {}^3T_{1g}(F) & 2.\ {}^3T_{1g}(P) \\ {}^3T_{1g} & 5.97\ Dq - E & 3.99\ Dq \\ & 3.99\ Dq & 15\,617 - E \end{array} = 0 \tag{10}$$

* Recall, as defined in Ref.[3], $G^2 = 5G_2$ and $F^2 = 49F_2$; in this case $G^2 = 9\,500$ cm^{-1} and $F^2 = 86\,730$ cm^{-1}.

** Details of the calculation of levels in the weak field approximation are given in Refs.[1,2]

*** The off-diagonal element, $(^3T_{1g}(F)|V_0|^3T_{1g}(P)$ is equal to $(\lambda_1)(\lambda_3)(^3T_{1g}(F)(a3d^7)|V_0|^3T_{1g}(P)(a3d^8)) + (\lambda_2)(\lambda_4)\ (^3T_{1g}(F)(c3d_74s)|V_0|^3T_{1g}(P)(c3d^74s))$ with $(^3T_{1g}(F)(3d^8)|V_0|^3T_{1g}(P)(3d^8)) = 4Dq$ and $(^3T_{1g}(F)(c3d^74s)|V_0|^3T_{1g}(P)(c3d^74s)) = \frac{11}{7}\sqrt{14}\ Dq$. The $^3F-{}^3P$ term interval, 15 617 cm^{-1}, is the value from Ref.[4] for the Ni^{2+} free ion.

The value of Dq is determined from the ${}^3A_{2g} \rightarrow {}^3T_{2g}$ transition, which for $Ni(H_2O)^{2+}$ gives [6] $Dq = 854$ cm^{-1}. Solving (10) we obtain

Transition	Predicted energy (cm^{-1}) for $3d^8 + 3d^74s$	Predicted energy for $3d^8$ only	Spectral maxima found * (cm^{-1})
${}^3A_{2g} \rightarrow {}^3T_{1g}(F)$	14 288	14 297	13 500 ** 15 400
${}^3A_{2g} \rightarrow {}^3T_{1g}(P)$	26 820	26 820	25 300

DISCUSSION

It is apparent from these results that the calculated energies are only very slightly affected by the inclusion of $3d^74s$ with $3d^8$, suggesting that no serious error is involved in the $3d^8$ approximation of the states. On the other-hand, in the pure $3d^8$ case the predicted energy of the ${}^3A_{2g}$—${}^3T_{1g}(P)$ transition is too large by approximately 1 500 cm^{-1}. This discrepancy has been attributed by some authors [8,9] to be a reduction in the ${}^3F$—${}^3P$ term interval in going from a free to a complexed ion, as a result of the delocalization of metal ion electrons in the latter (covalent bonding). However, the molecular orbital treatment of chrome alum carried out by Tanabe and Sugano [10] has cast some doubt on this interpretation, since the calculation did not lead to smaller values for the electron repulsion integrals (F_k's).

It is however significant that a more complete calculation than the above, mixing ${}^3T_{1g}(F)$ and ${}^3T_{1g}(P)$ with higher ${}^3T_{1g}$'s arising from pure $3d^74s$ terms will result in an improvement of the predicted energy of the ${}^3A_{2g} \rightarrow {}^3T_{1g}(P)$ transition, since the ${}^3T_{1g}(P)$, with more $3d^74s$ character (eqn. 5), will be depressed relative to ${}^3T_{1g}(F)$. The magnitude of this depression of ${}^3T_{1g}(P)$ can be roughly estimated at about 30 cm^{-1} by looking at the various off-diagonal elements and term separations involved. For the same reason the extension of configuration interaction to include the two ${}^3F$'s and the two ${}^3P$'s in the $3d^64s^2$ configuration will result in another improvement, but it is difficult to estimate the magnitude interaction since the $3d^64s^2$ levels haven't been located experimentally for Ni^{2+}.

Interaction with states of the configuration $3d^74d$ may also be of importance, since there are seven ${}^3F$'s and five ${}^3P$'s in $3d^74d$. A calculation which included all these possibilities would be quite tedious to perform, but to get an idea of the effect we carried out a calculation similar to the one above for Ti^{2+} ion,

* From Ref.[6]

** These two maxima are now believed to result from spin-orbit splitting of the ${}^3T_{1g}(F)$. See Ref.[7] for details.

mixing the $^3F(3d^2)$ and $^3P(3d^2)$ levels with the one $^3F(3d4d)$ and one $^3P(3d4d)$, respectively. This gives a result in the right direction, "moving" the $^3T_{1g}(P)$ some 50 cm^{-1} closer to the ^3F levels.

By summing the expected contributions from the inclusion of $3d^74s$, $3d^64s^2$ and $3d^74d$ levels, a definite improvement in the predicted energy of the $^3A_{2g}$—$^3T_{1g}(P)$ transition for Ni^{2+} complexes results. Thus it is tempting to suggest that it may be possible to resolve the apparent ^3F—^3P term interval reduction in the limits of crystalline field theory by inclusion of all possible configuration interaction. Furthermore, this explanation would of course be consistent with the experimental observation that the apparent reduction in the ^3F—^3P term interval is larger as the Dq value becomes larger, since the magnitude of the depression of $^3T_{1g}(P)$ with respect to the ^3F levels increases with increasing Dq. In any case, we see that by the inclusion of configuration interaction in the crystalline field theory a result is obtained which if extended to its limits could possibly account for the apparent reduction of the ^3F—^3P term interval. Although some degree of covalent bonding must of necessity exist in metal complexes it is not at all clear at present just how this interval is affected by this type of bonding.

APPENDIX

Some other examples in which inclusion of $3d^{n-1}4s$ and $3d^{n-2}4s^2$ with $3d^n$ levels might be of interest in crystalline field calculations are the following:

1. $3d^3$. Ground state ^4F. There is a ^4F state for the configuration $3d^24s$ but it doesn't mix with the $3d^3$ ^4F state [5].

2. $3d^6$. Ground state ^5D. There are ^5D's for both $3d^54s$ and $3d^44s^2$ configurations. Complete matrices of electrostatic interaction are given by Trees and Harvey [11]. This case is of little practical interest in an octahedral field calculation since the ^5D splits into only two levels, with the splitting parameter Dq taken from experiment. The configuration interaction calculation would only change the Dq value.

3. $3d^7$. Ground state ^4F, with an excited ^4P state approximately 14 500 cm^{-1} above it [12]. This case is somewhat analogous to the $3d^8$ case, there being two ^3F's and two ^3P's in both $3d^64s$ and $3d^54s^2$ configurations. The electrostatic matrix elements have not been worked out.

4. $3d^9$. Ground state ^2D. There are ^2D's in both $3d^84s$ and $3d^74s^2$ configurations, but the electrostatic matrix elements have not been calculated. As in ^5D, the octahedral field calculation would only change the Dq value.

REFERENCES

1. Moffitt, W. and Ballhausen, C. J. *Ann. Rev. Phys. Chem.* **7** (1956) 107.
2. Dunn, I. M. in Lewis, J. and Wilkins, R. G. *Modern Coordination Chemistry*, Interscience, New York 1960, Chap. 4.
3. Condon, E. U. and Shortley, G. H. *The Theory of Atomic Spectra*, Cambridge University Press 1955.
4. Shenstone, A. G. *J. Opt. Soc. Am.* **44** (1954) 749.
5. Ufford, C. W. *Phys. Rev.* **44** (1933) 732.

6. Jørgensen, C. K. *Acta Chem. Scand.* **9** (1955) 1362.
7. Liehr, A. D. and Ballhausen, C. J. *Annals of Physics.* **6** (1959) 134.
8. Owen, J. *Proc. Roy. Soc. London* **A 227** (1955) 183.
9. Dunn, T. M. *J. Chem. Soc.* **1959** 623.
10. Tanabe, Y. and Sugano, S. *J. Phys. Soc. Japan* **11** (1956) 864.
11. Trees, R. E. and Harvey, M. M. *J. Research NBS* **49** (1952) 397.
12 Moore, C. E. *Atomic Energy Levels*, NBS Circular No. 467, Vol. II (1952).

Received February 17, 1961.

ACTA CHEMICA SCANDINAVICA 15 (1961) 1333–1336

Molecular Orbitals for the Protonated Sandwich Compounds

C. J. BALLHAUSEN and J. P. DAHL

Universitetets fysisk-kemiske Institut, Copenhagen, Denmark

A set of orbitals for a "twisted" sandwich compound is proposed. These new orbitals explain the behaviour of sandwich compounds when protonated.

The recent discovery [1] of the existence of protonated "sandwich" compounds [2] has motivated the modified molecular orbitals given below. Whereas in ferrocene for instance the two rings in $Fe(C_5H_5)_2$ are found to be parallel, we propose here that in $Fe(C_5H_5)_2H^+$ the two rings are not parallel any more (Fig. 1). The two rings are twisted in such a way that the radius vectors from the metal atom to the center of the rings make an angle, ω.

a) The Cp rings. When the rings are placed as in Fig. 1 we treat the bonds to the two rings as being independent of each other. With $\varphi_r^{(S)}$ being the r'th $2p_z$-orbital on ring S (S = A or B) we write as usual [3] the orbitals on the rings as follows, neglecting overlap:

$$\mathrm{CpS}(a_2) = \sqrt{\tfrac{1}{5}}\,(\varphi_1^S + \varphi_2^S + \varphi_3^S + \varphi_4^S + \varphi_5^S)$$

$$\mathrm{CpS}(e_1') = \sqrt{\tfrac{2}{5}}\,(\varphi_1^S + \cos\frac{2\pi}{5}\,(\varphi_2^S + \varphi_5^S) + \cos\frac{4\pi}{5}\,(\varphi_3^S + \varphi_4^S))$$

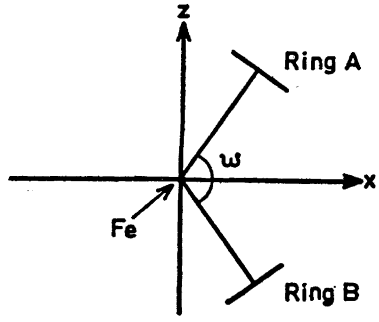

Fig. 1. Molecular structure of a twisted sandwich. The rings are drawn perpendicular to the xz plane, the radius vectors in the xz plane.

$$\mathrm{CpS}(e_1'') = \sqrt{\tfrac{2}{5}}\ (\sin\frac{2\pi}{5}\ (\varphi_2^S - \varphi_5^S) + \sin\frac{4\pi}{5}\ (\varphi_3^S - \varphi_4^S))$$

$$\mathrm{CpS}(e_2') = \sqrt{\tfrac{2}{5}}(\varphi_1^S + \cos\frac{4\pi}{5}\ (\varphi_2^S + \varphi_5^S) + \cos\frac{2\pi}{5}\ (\varphi_3^S + \varphi_4^S))$$

$$\mathrm{CpS}(e_2'') = \sqrt{\tfrac{2}{5}}(\sin\frac{4\pi}{5}\ (\varphi_2^S - \varphi_5^S) - \sin\frac{2\pi}{5}\ (\varphi_3^S - \varphi_4^S))$$

The energies are found [3] to be:

$$\mathrm{CpS}(a_2) = a + 2\beta$$

$$\mathrm{CpS}(e_1) = a + 2\beta\cos\frac{2\pi}{5}$$

$$\mathrm{CpS}(e_2) = a - 2\beta\cos\frac{\pi}{5}$$

With β negative the order is $E(a_2) < E(e_1) < E(e_2)$. As the e_2 orbital is antibonding we shall not use it in the bonding scheme.

b) The metal atom. The following valence orbitals will be used for the metal atom; all $3d$ orbitals, all $4p$ and the $4s$ orbitals. Utilizing these nine orbitals we now construct hybrid orbitals guided by the following principles:

We want to construct 3 hybrids $\psi_A(a_2)$, $\psi_A(e_1')$ and $\psi_A(e_1'')$ of which $\psi_A(a_2)$ only overlaps with $\mathrm{CpA}(a_2)$. This can be done in a unique way. Then we construct a hybrid $\psi_A(e_1')$ which is orthogonal upon $\psi_A(a_2)$, and which only overlaps with $\mathrm{CpA}(e_1')$ and in the same way $\psi_A(e_1'')$ is made up, only having overlap with $\mathrm{CpA}(e_1'')$. Then we construct the corresponding three orthogonal hybrids $\psi_B(a_2)$, $\psi_B(e_1')$ and $\psi_B(e_1'')$, only overlapping with $\mathrm{CpB}(a_2)$, $\mathrm{CpB}(e_1')$ and $\mathrm{CpB}(e_1'')$, respectively.

We now demand that the two sets of hybrids should be orthogonal upon each other, and transform into each other by reflection in the xy-plane. A necessary condition for this to take place turns out to be that the angel ω should lie between 135° and 180°.

Finally we construct three new hybrids, which are orthogonal upon each other and upon the six ring-hybrids. Of these ψ_O is cylindrical around the x-axis, and ψ_y and ψ_{-y} go into each other by reflection in the xz plane.

For ω equal to 135° these three non-bonding hybrids look as follows, calling

$$\mathrm{tg}\frac{\pi}{8} = a$$

$$\psi_O = a\,\psi(4s) - \sqrt{1-a^2}\ \psi\ (4p_x)$$

$$\psi_y = \frac{1}{\sqrt{2}}\ a\ \psi\ (4p_y) - \frac{1}{\sqrt{2}}\sqrt{1-a^2}\,\psi\,(3d_{xy}) - \sqrt{\tfrac{1}{8}}\ \psi\ (3d_{z^2}) - \sqrt{\tfrac{3}{8}}\,\psi(3d_{x^2-y^2})$$

$$\psi_{-y} = -\frac{1}{\sqrt{2}}\ a\ \psi\ (4p_y) + \frac{1}{\sqrt{2}}\sqrt{1-a^2}\ \psi\ (3d_{xy}) - \sqrt{\tfrac{1}{8}}\,\psi\ (3d_{z^2}) - \sqrt{\tfrac{3}{8}}\ \psi\ (3d_{x^2-y^2})$$

All of the nine possible hybrids are very strongly space directed. The ring hybrids are directed straight against the rings. ψ_O is directed towards the

negative end of the x-axis, while ψ_y and ψ_{-y} are directed, respectively, in between the positive and negative ends of the y-axis and the negative end of the x-axis (Fig. 2).

c. Molecular orbitals. Using the orbitals of the (Cp) rings given in a) and the metal hybrids given in b) we construct the six bonding molecular orbitals:

$$\begin{aligned} \Phi_S(a_2) &= \cos\varphi\ \psi_S(a_2) + \sin\varphi\ \mathrm{CpS}(a_2) \\ \Phi_S(e_1') &= \cos\chi\ \psi_S(e_1') + \sin\chi\ \mathrm{CpS}(e_1') \qquad (S = A,B) \\ \Phi_S(e_1'') &= \cos\xi\ \psi_S(e_1'') + \sin\xi\ \mathrm{CpS}(e_1'') \end{aligned}$$

Of course we get six antibonding molecular orbitals as well, but their energy must be so high that we need not consider them.

These six bonding molecular orbitals contain twelve electrons. This electronic structure is common for all sandwich compounds and we will look apart from them in what follows [4]. We remark in passing that the total overlap of these twelve bonding electrons with the rings is nearly equal both in the "straight" and "twisted" form of the sandwiches. We get for instance for $\omega = 150°$, $S_{\text{twisted}} = 1.87$ and for $\omega = 180°$, $S_{\text{straight}} = 2.00$. This indicates that the bonding of the rings to the metal-atom is not very dependent upon whether the molecule is "straight" or "twisted".

The remaining electrons in the sandwich compound are treated as "chemically active" electrons [4], and furthermore the hybrids ψ_O, ψ_y and ψ_{-y} are supposed to have a lower energy than the non-bonding ring orbitals $\mathrm{CpS}(e_2')$ and $\mathrm{CpS}(e_2'')$.

The number of electrons in surplus of the twelve used already are

3 in $(C_2H_5)_2$ Ta
4 in $(C_2H_5)_2$ W
5 in $(C_2H_5)_2$ Re
6 in $(C_2H_5)_2$ Fe

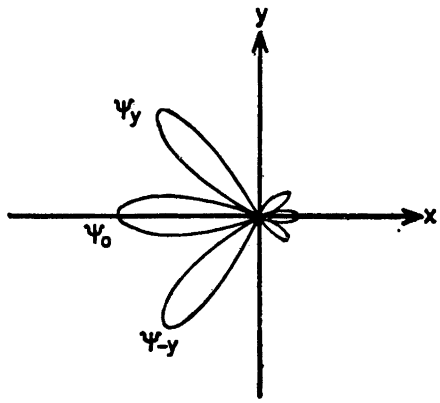

Fig. 2. Hybrid orbitals not used for ring bonding in a "twisted" sandwich molecule.

These electrons are then placed in the ψ_0, ψ_y and ψ_{-y} orbitals. These hybrids can now be used for further bonding purposes, *e.g.* ferrocene can take one proton up, presumably in ψ_0.

If we suppose that the maximum number of protons and hydrogens which can be bonded is determined by the condition that we can only have one positive charge on the hydrides we should be able to make the following compounds, of which the majority have already been prepared [1]:

$(Cp)_2TaH$	$(Cp)_2TaH_2$	$(Cp)_2TaH_3$
$(Cp)_2WH$	$(Cp)_2WH_2$	$(Cp)_2WH_3^+$
$(Cp)_2ReH$	$(Cp)_2ReH_2^+$	
$(Cp)_2FeH^+$		

Notice that in $(Cp)_2TaH_3$ and $(Cp)_2WH_3^+$ one of the hydrogen atoms is bonded differently from the other two. The latter two on the other hand are bonded equivalently. This again is confirmed by experiments [1]. It is furthermore remarkable that in order to obtain these results no f-orbitals need to be used.

Some suggestions. We suggest that the two Cl^-'s in $(Cp)_2TiCl_2$ are bonded to ψ_y and ψ_{-y}, and hence that the two rings are not planar. Furthermore in the compound 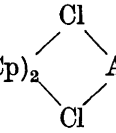 the molecule will probably use the new orbitals ψ_y and ψ_{-y} for the chlorine bonds since it is known that the rings are not planar [5].

Acknowledgement. We want to thank Professor G. Wilkinson for having drawn our attention to this problem, and for many stimulating discussions.

REFERENCES

1. Wilkinson, G. *Private Communication.*
2. Wilkinson, G. and Cotton, F. A. *Progr. Inorg. Chem.* Vol. **1** Interscience, New York 1959
3. Moffitt, W. *J. Am. Chem. Soc.* **76** (1954) 3386.
4. Dahl, J. P. and Ballhausen, C. J. *Kgl. Danske Videnskab. Selskab, Mat.-fys. Medd.* **33** (1961) No. 5.
5. Natta, G., Corradini, P. and Bassi, I. W. *J. Am. Chem. Soc.* **80** (1958) 755.

Received February 21, 1961.

ACTA CHEMICA SCANDINAVICA 15 (1961) 1337–1346

Studies of Hydrogen Bonding

Part II *. Intermolecular Hydrogen Bond Association between Organophosphorus Compounds and Methanol, α-Naphthol and Pentachlorophenol, respectively

THOR GRAMSTAD

Norwegian Defence Research Establishment, Division for Toxicology, Kjeller, Lillestrøm, Norway

The K_{ass}, ΔH, ΔF and ΔS values of the equilibrium reaction between sixteen organophosphorus compounds and methanol, α-naphthol and pentachlorophenol, respectively, have been determined. It has been found that for each system the ΔH, ΔF and ΔS values form linear relationships with the hydrogen bond frequency shift. The effect of solvent interaction on the hydrogen bond association is considered.

The ability of organophosphorus compounds to form intermolecular hydrogen bonds has been observed earlier. Gordy and Stanford [2,3] have shown that *n*-butyl phosphate causes a much greater O—D bond frequency shift with heavy methanol than does any other ester except *n*-butyl borate. Further it has been shown by using heat of mixing as a criterion, that organophosphorus compounds form hydrogen bonds with chloroform [4–6]. These results have also been confirmed by an infrared study [7] of the frequency shifts of the phosphoryl group and determination of the changes in the integrated absorption intensities of the C—H bond of chloroform and other solvents. However, very few systematic determinations of hydrogen bond energies have hitherto been made, and the spectroscopic evidence already available presents a somewhat confused picture. Badger and Bauer [8] have pointed out that there appears to be a linear relationship between the energy of the hydrogen bond and the shift in frequency of the OH-bond which accompanies the formation of the bond. More recently, Badger [9] reports that there exists a fairly strong indication that the relation between frequency shift and energy is not linear. Pimentel and Brown [10] have also reported data which do not substantiate the first proposed relation of Badger.

* First paper in this series: Ref.[1]

In a previous publication [1] it was shown that organophosphorus compounds containing the P=O group form very strong intermolecular hydrogen bonds with phenol. Furthermore, it was shown that the ΔH, ΔF, ΔS and the half band width of the equilibrium reaction varied lineary with the hydrogen bond O—H frequency shift. It was also shown [1,11] that when sufficiently low concentrations of phenol and organophosphorus compound were used, the only association complex formed is the dimeric intermolecular hydrogen bond complex. The inductive and mesomeric effects of the substituents in phosphorus compounds upon hydrogen bond association were also discussed.

Since we possessed a variety of bases which formed well defined hydrogen bonded complexes, which could be readily determined by spectroscopy, it was of interest to study the thermodynamic properties of the hydrogen bond equilibrium reaction with acidic compounds other than phenol.

EXPERIMENTAL

Materials. The physical data and methods of preparation of the organophosphorus compounds used, have been published elsewhere [1]. However, in all cases the phosphorus compounds were purified by fractional distillation or recrystallisation just before use. The following materials were used without further purification: "Merck Guaranteed Reagent" phenol, *a*-naphthol and carbon disulphide, "Merck Spectroscopic Grade" methanol and carbon tetrachloride, "Fluka puriss." pentachlorophenol.

Infrared measurements. The infrared spectroscopic measurements were made with a Perkin-Elmer Model 21 Spectrophotometer with sodium chloride optics. This instrument was used for the determination of the frequency shift of the ground state stretching vibration of the OH-band which accompanies the formation of hydrogen bond. The same instrument was used for the determination of the stretching frequencies of the P=O group, the half band width, $\nu_{1/2}$, and the intensity, $\varepsilon_{max} \times \nu_{1/2}$ of the O—H band. Instrumental conditions were as follows: Resolution, 975; gain, 5.5; response, 1:1; speed, 3.5; suppression, 2. The cell was calibrated by the interference fringe method and was found to be of 1.00 mm thickness. For all spectra the *a*-naphthol or pentachlorophenol concentration was kept at 0.006 M, and the concentration of organophosphorus compound was, with few exceptions, 0.012 M. For the system organophosphorus compounds-methanol, the concentrations were, due to the smaller amount of hydrogen bond formation, 0.03 and 0.06 M, respectively.

The spectra were run in the following way: A solution of the organophosphorus compound in carbon tetrachloride was first run using the instrumental conditions given above, compensated with carbon tetrachloride in a reference cell of the same thickness. Secondly, the mixture of organophosphorus compound and proton donor in carbon tetrachloride was run on the same sheet and compensated with the same reference cell containing CCl_4. Thirdly, still on the same sheet, the mixture was run again, but this time compensated with a reference cell containing the same concentration of organophosphorus compound as in the mixture.

Near-infrared measurements. The near-infrared measurements were carried out with a Beckman Ratio Recording Spectrophotometer Model DK-2. Instrumental conditions were as follows: Scanning time, full scale, 5 min; range, 0—100, sensitivity, 50; time constant, 0.6; per cent transmittance. This instrument was used for the determination of the association constants. The concentration of free proton donor was determined from the first overtone band of the stretching vibration of the hydroxyl group. These appear, with carbon tetrachloride as solvent, at 7 119 cm^{-1}, 7 098 cm^{-1}, and 6 860 cm^{-1} for methanol, *a*-naphthol and pentachlorophenol, respectively. K_{ass} is calculated as shown below:

$$A{-}H + B \rightleftharpoons A{-}H\ldots B$$

$$K_{ass} = \frac{(A{-}H\ldots B)}{[A{-}H]\,[B]} = \frac{x}{(a-x)\,(b-x)}$$

where x is the concentration in mole/l of the hydrogen bonded complex, calculated from the free OH-band; a and b are the formal concentrations in mole/l of proton donor and proton acceptor, respectively. The quartz absorption cell of 10 cm path length used, was the same as that described earlier. The spectra were run immediately after preparing the solutions, at temperatures of 20°C and 50°C (when carbon disulphide was used as solvent, the measurements were carried out at 20°C and 40°C). For all spectra the proton donor concentration was kept at 0.006 M to prevent self-association. The values of the association constants recorded in Table 2 are the mean values of three or four separate determinations. In Table 1 are recorded the experimental results from the determination of K_{ass} for one of the compounds studied. The concentration range shown in Table 1 was used for the systems OPC-pentachlorophenol and OPC-α-naphthol, whereas for the system OPC-methanol, the following concentrations of OPC were used, 0.012, 0.024, 0.036 and 0.06 mole/l.

RESULTS

Association constant and free energy. In a previous publication [1] it was shown that, within experimental error, the logarithms of the association constants K_{ass} between organophosphorus compounds (OPC) and phenol form a linear relation with the shift in frequency, $\Delta\nu$, of the OH-band of phenol which accompanies the formation of the hydrogen bond. The same relation has now been found to be valid for the systems, OPC-methanol, OPC-α-naphthol and OPC-pentachlorophenol (see Fig. 1). It can easily be seen from this figure that it would be impossible by taking K_{ass} values from different systems to maintain the linear relationship between frequency shift and the logarithms of the association constants. Grunwald and Coburn [12] have collected values of

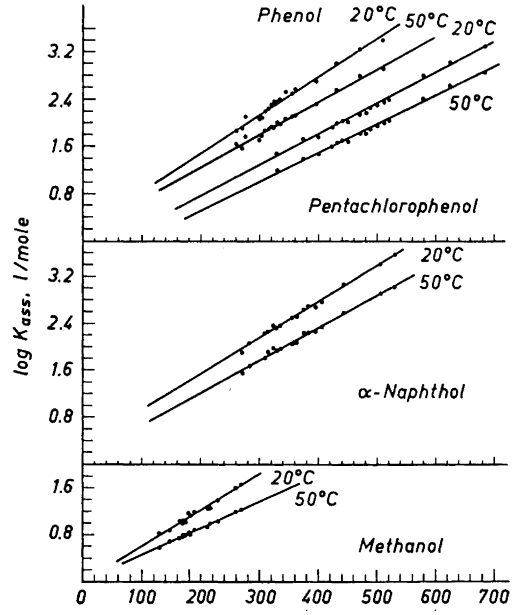

Fig. 1. The relation between the logarithms of the association constants and the frequency shifts for the hydrogen bonded complexes between organophosphorus compounds and phenol, pentachlorophenol, α-naphthol and methanol, respectively.

Table 1. Determination of the association constant between pentachlorophenol and trimethylphosphate in carbon tetrachloride. Cell length, 10 cm. Temperature 20°C.

Concentration mole/l		Optical density for free O—H band	Concentration of free pentachlorophenol mole/l	Concentration of complex mole/l	K_{ass} l/mole	K_{ass} mean value
Pentachlorophenol	Trimethylphosphate					
0.006	0	0.1367	0.006	0	0	
0.006	0.003	0.1135	0.004983	0.001017	102.9	103.0
0.006	0.006	0.0958	0.004207	0.001793	101.4	
0.006	0.012	0.0701	0.003077	0.002923	104.7	

$\Delta\nu$ and K_{ass} for hydrogen bond association and have shown that the sequence of the ΔF values (or log K_{ass} values) does not follow that of $\Delta\nu$. However, they also indicate that there may exist a monotonic relationship between $\Delta\nu$ and ΔF at least for those compounds in which the hydrogen bond donors and acceptors have some common electronic feature.

In Fig. 1 our results for log K_{ass} are plotted as a function of the frequency shift of the ground state stretching vibration of the OH-bands. The straight lines drawn through the calculated log K_{ass} values (see Table 1) at 20°C and 50°C, are all within experimental error. For each system the two lines at 20°C and 50°C possess different slopes. The sequence, as can be seen in Fig. 1, is, in order of decreasing divergence, OPC-methanol > OPC-phenol > OPC-*a*-naphthol > OPC-pentachlorophenol. The thermodynamic significances of the observations indicated above are, a) the free energy, ΔF, of the hydrogen bond equilibrium reaction can be fairly accurately described as a linear function of the frequency shift as shown in Fig. 2, b) as a consequence of this linear relationship together with the thermodynamic equation $\Delta F = \Delta H - T\Delta S$,

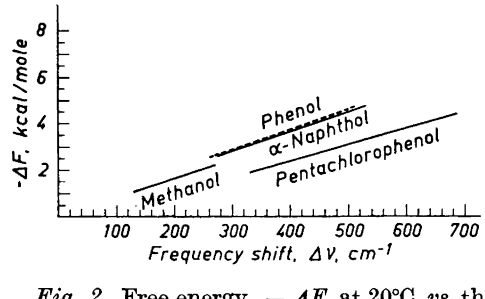

Fig. 2. Free energy, $-\Delta F$, at 20°C, *vs.* the frequency shift, $\Delta\nu$, for O—H bond, for hydrogen bonded systems.

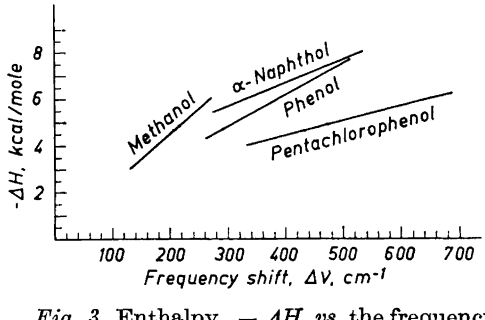

Fig. 3. Enthalpy, $-\Delta H$, *vs.* the frequency shift, $\Delta\nu$, for O—H bond, for hydrogen bonded systems.

Table 2. Data of dimeric hydrogen bond association between organophosphorus compounds and phenol, methanol, α-naphthol and pentachlorophenol, respectively. Solvent: carbon tetrachloride.

Compound	$\nu P=O$ cm^{-1}	Phenol [a]				Methanol				α-Naphthol				Pentachlorophenol			
		$\Delta\nu OH$ cm^{-1}	K_{ass} 20°C	K_{ass} 50°C	$\Delta\nu P=O$ cm^{-1}	$\Delta\nu OH$ cm^{-1}	K_{ass} 20°C	K_{ass} 50°C	$\Delta\nu P=O$ cm^{-1}	$\Delta\nu OH$ cm^{-1}	K_{ass} 20°C	K_{ass} 50°C	$\Delta\nu P=O$ cm^{-1}	$\Delta\nu OH$ cm^{-1}	K_{ass} 20°C	K_{ass} 50°C	$\Delta\nu P=O$ cm^{-1}
$CCl_3PO(OC_2H_5)_2$	1282	260	73.2	44.8		130	6.8	3.8		273	81.8	36.2	16	330	29.7	15.7	32
$CHCl_2PO(OC_2H_5)_2$	1279	275	133.1	60.7		148	7.5	5.0		283	117.6	47.5	41	374	56.3	24.7	38
$HPO(OCH_3)_2$	1265	300	123.1	53.4		169	9.8	5.8		310	167.7	64.0	23	400	61.2	29.0	27
$HPO(OC_2H_5)_2$	1258	310	161.9	76.8	35	170	10.8	6.2		316	187.7	83.3	26	425	85.5	40.7	26
$CH_3OPO(OCH_3)_2$	1274	315	182.9	78.9	31	175	10.6	6.2		323	238.7	97.4		433	103.0	46.7	34
$CH_2ClPO(OC_2H_5)_2$	1270	325	239.0	84.2		165	10.9	5.6		330	217.3	88.1	34	440	110.3	50.3	32
$HPO[OCH(CH_3)_2]_2$	1256	330	237.3	99.9	34	180	14.7	6.8	10	336	236.1	93.4	22	450	107.3	48.3	23
$CH_3PO(OCH_2CH_2CH_2Cl)_2$	1245	335	247.0	95.7	28	182	13.6	6.3	7	356	307.8	114.2	27	473	145.3	67.0	21
$C_2H_5OPO(OC_2H_5)_2$	1263	345	350.5	121.1	30	189	15.5	7.7		363	323.5	115.9	29	481	153.1	67.1	33
$C_2H_5PO(OCH_3)_2$	1231	355	329.7	126.5	20	—	—	—	—	383	482.4	179.7	24	488	186.6	80.6	—
$CH_3PO(OC_2H_5)_2$	1243	360	381.0	141.0	23	211	18.1	8.5	8	376	435.0	178.6	25	500	214.0	92.5	21
$C_2H_5PO(OC_2H_5)_2$	1228	—	—	—	—	211	17.5	8.4	5	396	476.5	180.9	23	511	234.8	101.0	—
$(C_2H_5)_2N-PO(OC_2H_5)_2$	1254	395	518.2	211.8	28	217	17.6	9.8	14	406	581.9	221.8	26	519	257.7	111.0	24
$C_6H_5PO(C_6H_5)_2$	1202	430	1055.4	365.5	21	231	24.3	10.6	16	443	1166.0	384.5	18	578	673.6	269.6	42
$CH_3PO(CH_3)_2$	1198	470	1836.0	639.4	30	260	40.1	15.5	18	506	2575.0	802.4	23	623	1136.0	440.7	48
$C_2H_5PO(C_2H_5)_2$	1178	510	2522.0	858.0	23	270	45.9	16.7	12	530	3763.0	1085.0	20	685	2095.5	727.9	35

[a] Data from Part 1, Ref.[1]

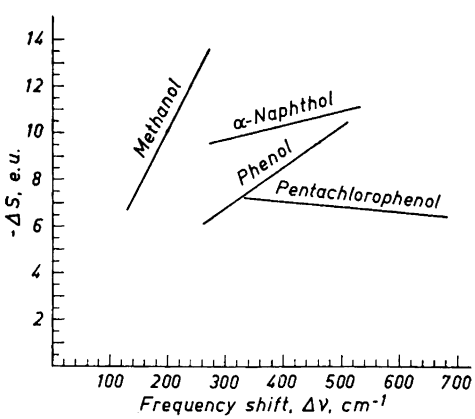

Fig. 4. Entropy, $-\Delta S$, *vs.* the frequency shift, $\Delta\nu$, for O—H bond, for hydrogen bonded systems.

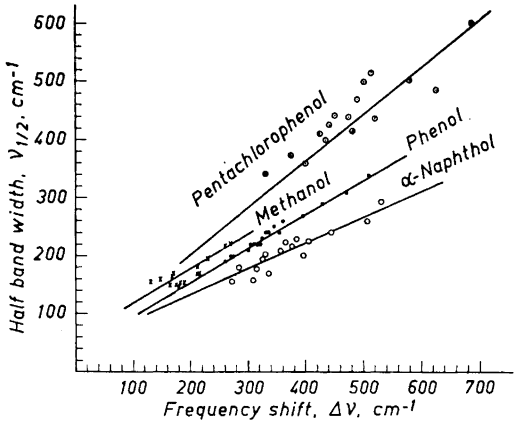

Fig. 5. Frequency shift, $\Delta\nu$, *vs.* half band width, $\nu_{1/2}$, of O—H bond, for hydrogen bonded systems.

both the enthalpy ΔH and the entropy ΔS must also vary linearly with the frequency shift $\Delta\nu$ (see Figs. 3 and 4), c) the difference in slope between the K_{ass} *vs.* $\Delta\nu$ plots for 20°C and 50°C for each system is strongly reflected in the ΔH *vs.* $\Delta\nu$ and ΔS *vs.* $\Delta\nu$ plots.

The hydrogen donors studied show an increasing tendency to form intermolecular hydrogen bonds with the organophosphorus compounds used in the order *a*-naphthol > phenol > pentachlorophenol > methanol (see Table 2). There is a reasonable amount of evidence to suggest that the drop in association constants for pentachlorophenol compared with those for phenol and *a*-naphthol is due to solvent interactions.

Enthalphy and entropy. Figs. 3 and 4 show that the displacement of the frequency of the associated band from that of the free hydroxyl band varies in an inverse linear manner with the enthalpy and entropy. The values used are calculated from the smoothed values of log K_{ass} found from the straight lines in Fig. 1. It should be noted that the ΔH and ΔS curves flatten with increasing acidity of the proton donors, the sequence of decreasing slope being, methanol > phenol > *a*-naphthol > pentachlorophenol. Table 3 shows the range of ΔH and ΔS values, and the slope for each system. As can be seen the increase in enthalpy is compensated by a decrease in entropy, except for the system OPC-pentachlorophenol.

Half band width and intensity. In Fig. 5 the displacement $\Delta\nu$ is plotted as a function of the observed half band width $\nu_{1/2}$ for the O—H bond. The straight lines drawn through the observed values cut the $\nu_{1/2}$-axis at 47, 51, 66, and 83 cm^{-1}, which correspond approximately to the half band widths of the hydroxyl groups, in carbon tetrachloride, of phenol, pentachlorophenol, *a*-naphthol and methanol, respectively. As can be seen a fairly good linear relationship is found between $\Delta\nu$ and $\nu_{1/2}$ for each system. Furthermore, there is for each of the proton donors studied, a systematic increase in $\Delta\nu$ and $\nu_{1/2}$ as the base

Table 3. Maxima and minima values of hydrogen bonding energies and entropy changes together with the slopes for different systems. Solvent, carbon tetrachloride.

System	ΔH kcal/mole		ΔS e. u.		Slope [a]	
	from	to	from	to	ΔH-curve	ΔS-curve
OPC *-methanol	−3.0	−6.2	−6.7	−13.6	0.91	1.97
OPC-phenol	−4.3	−7.8	−6.2	−10.5	0.55	0.70
OPC-α-naphthol	−5.5	−8.1	−9.6	−11.2	0.40	0.25
OPC-pentachlorophenol	−4.1	−6.4	−7.3	− 6.5	0.26	−0.0086

* OPC means the series of organophosphorus compounds shown in Table 2.
[a] see Figs. 3 and 4.

strength increases, while on the other hand there are deviations from a simple progression for $\Delta\nu$ and $\nu_{1/2}$ as the acid strength increases. This is in agreement with the results reported by Huggins and Pimentel [13], although these authors found a linear relation applicable to a wide variety of systems. In this connection it should be pointed out that Huggins and Pimentel [13] studied binary and the present author ternary solutions. Another dependence which seems to be more empirical is the relationship between pK_a of the proton donors used and the O—H bond frequency shift, as shown in Fig. 6, where only three of sixteen systems are plotted. A linear relation between pK_a and $\Delta\nu$ which seems to be of general validity has also been found by Henry [14] using a variety of alcohols.

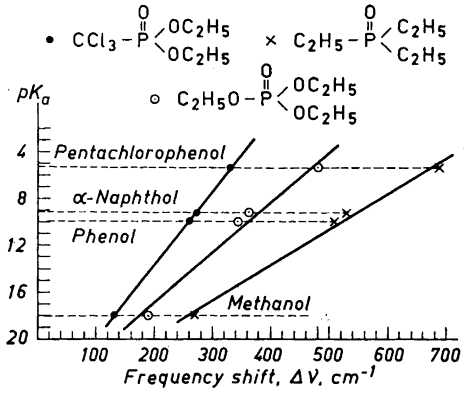

Fig. 6. The relation between pK_a values of the proton donors and the frequency shift, $\Delta\nu$, for some hydrogen bonded systems.

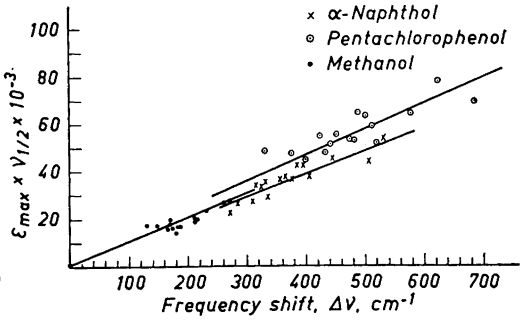

Fig. 7. IR frequency shift, $\Delta\nu$, *vs.* intensity, $\varepsilon_{max} \times \nu_{1/2}$, of O—H bond, for hydrogen bonded systems.

We have found as shown in Fig. 7 that the correlation between intensity expressed in terms of $\nu_{1/2} \times \varepsilon_{max}$ and O—H bond freuqency shift is surprisingly close to a linear relation. The straight lines drawn cut the ordinate at 4.00, 1.54 and 0.89 which correspond to the $\varepsilon_{max} \times \nu_{1/2} \times 10^{-3}$ values of pentachlorophenol, *a*-naphthol and methanol, respectively. ε_{max} is the molecular extinction coefficient at the absorption maximum, and is calculated by using the association constant from the smoothed line in Fig. 1, as follows:

$$\varepsilon_{max} = \frac{D}{X \cdot l}$$

$$X = \frac{(KC + 1) - \sqrt{(KC + 1)^2 - 4K^2 ab}}{2K}$$

X = concn., mole/l of hydrogen bonded complex.
K = association constant, l/mole, at 20°C.
a = concn., mole/l of proton donor.
b = concn., mole/l of proton acceptor.
$C = a + b$, total concn., mole/l.
D = optical density.
l = cell length, cm.

DISCUSSION OF RESULTS

When a polar molecule is placed in a polarisable medium it produces polarisation in the medium. The magnitude of this induced polarisation (μ) is given by the familiar equation, $\mu = aF$, where F is proportional to the dipole moment of the solute molecule and a is the polarisability of the medium. Now it has been shown [16] that the dipole moment and the shift of the absorption spectrum in near ultraviolet are anomalously large when hydrogen bond is formed. Furthermore, Sutton and collaborators [17,18] have shown that there appears to be an additional dipole moment about 1.0 D when trimethylamine forms complexes with weakly acidic substances in *cyclo*hexane solution. From the equation above it can easily be seen that the additional dipole moment is due to an increase of F, *i.e.*, there is an increase of dipole moment from the reactants to the hydrogen bonded complex. In a previous publication [1] it has been pointed out that this increase of dipole moment will contribute to a negative entropy of reaction due to a greater orientation of the solvent molecules around the complex. The contribution of negative entropy difference between reactants and hydrogen bonded complex was found to be greatest for the strongest hydrogen bond.

The present investigation on ternary systems has established the following facts: Firstly, the absorption bands due to hydrogen bonding are for each system progressively lowered in frequency, broadened in contour, and enhanced in integrated intensity (or $\varepsilon_{max} \times \nu_{1/2}$) as the base strength of the proton acceptor increases. The same is also the case with increasing acid strength, although deviations may occur. Secondly, the ease with which the hydrogen donors studied form hydrogen bonds in carbon tetrachloride solution with the organophosphorus compounds used is in order of decreasing association constant as follows: *a*-naphthol > phenol > pentachlorophenol > methanol.

Table 4. A comparison of thermodynamic data of hydrogen bonds in different solvents.

Compound	$\Delta\nu$OH cm^{-1}	K_{ass} 20°C	K_{ass} 50°C	ΔH kcal	ΔF kcal	ΔS e.u.	νP=O cm^{-1}	$\Delta\nu$P=O cm^{-1}	$\nu_{1/2}$ cm^{-1} for O–H bond	Solvent
$C_6H_5OH...O=P(C_6H_5)_3$	416	1372.0	576.6*	−7.9	−4.2	−12.6	1204	27	286	CS_2
	430	1055.4	356.5	−6.7	−4.1	− 8.9	1202	21	290	CCl_4
$C_6Cl_5OH...O=P(C_6H_5)_3$	620	1071.7	453.1*	−7.8	−4.1	−12.9	1203	43	600	CS_2
	578	673.6	269.6	−5.7	−3.8	− 6.7	1202	42	502	CCl_4
$C_6H_5OH...O=C(CH_3)(OC_2H_5)$ [a]				−5.7		−13.7				naphtha
				−4.8		−11.9				CCl_4

* Measured at 40°C.
[a] Data from Ref.[13]

Thirdly, the sequence of the variation of ΔH and ΔS with $\Delta\nu$ for each system is, in order of decreasing slope, methanol > phenol > α-naphthol > pentachlorophenol (see Figs. 3 and 4). The reason for these anomalies, especially with regard to pentachlorophenol, is not yet clear, but the following reasons may be taken into consideration: solvent interaction on the proton donor, on the acceptor, on the hydrogen bonded complex, and steric factors. As a consequence of the fact that a linear relation between K_{ass} and $\Delta\nu$ exists, the conclusion has been drawn that the solvent interaction on the proton acceptors and *vice versa* is constant or nearly constant for the whole series of organophosphorus compounds studied. Steric factors are also excluded, due to the fact that K_{ass} and ΔH for the system pentachlorophenol-triphenylphosphine oxide are increased enormously by replacing carbon tetrachloride with carbon disulphide as can be seen in Table 4. This again supports the view that the anomalies are due to interaction between the solvent molecules and the proton donor and the hydrogen-bonded complex. Nagakura [15] has shown that for the system phenol-ethylacetate, the enthalpy is increased by approximately 1 kcal by replacing the solvent carbon tetrachloride with naphtha. He concludes that the reason for this increase may be that the dielectric constant of carbon tetrachloride is evidently larger than that of naphtha. It has been shown in Table 4, however, that by replacing carbon tetrachloride with carbon disulphide which possesses a larger dielectric constant (2.24 $^{20°C}$ and 2.63 $^{20°C}$, respectively), the reverse is the case. The association constant and enthalpy are increased, particularly with respect to pentachlorophenol. It should also be

noted that the increase in enthalpy is accompanied by a decrease in entropy. As a consequence of this we suggest that the anomalies observed are at least partly due to hydrogen bond formation between the proton donor and the solvent, such as $-OH\ldots Cl-\overset{|}{\underset{|}{C}}-$. This explanation is also in accordance with the observation that the solvent interaction becomes more pronounced with increasing acidity of the proton donor. In carbon disulphide, however, the hydrogen bond formed, $-OH\ldots .S=C=S$, is much weaker, hence the solvent interaction is less pronounced. According to this one should expect that the shape of the absorption bands in these two solvents should differ. Actually, however, the half band width as can be seen in Table 4, does not differ very much in the two solvents. A rather small tendency for the bands to broaden is found by replacing carbon tetrachloride with carbon disulphide. In the first overtone region the half band widths of phenol in carbon tetrachloride and in carbon disulphide are approximately 21 mμ and 36 mμ, and of pentachlorophenol 25 mμ and 32 mμ, respectively.

Our conclusions concerning the effect of solvent interaction on hydrogen bonding are thus that for the system OPC-methanol, the solvent interaction is predominantly due to the solvation effect around the hydrogen bonded complex. As the proton-donating power increases the solvent interaction with the proton donor becomes more pronounced. For the systems OPC-phenol and OPC-*a*-naphthol both the solvation and the solvent-proton donor effects come into play. For the system OPC-pentachlorophenol the solvent-proton donor effect predominates. These views may also explain the systematic change of the slopes for the ΔH- and ΔS-curves as shown in Figs. 3 and 4. Furthermore, we conclude that the linear relations between frequency shift and ΔH, ΔF, ΔS, $\nu_{1/2}$ and $\nu_{1/2} \times \varepsilon_{max}$, respectively, are only valid when kept to one system.

REFERENCES

1. Aksnes, G. and Gramstad, T. *Acta Chem. Scand.* **14** (1960) 1485.
2. Gordy, W. and Stanford, S. C. *J. Chem. Phys.* **8** (1940) 170.
3. Gordy, W. and Stanford, S. C. *J. Chem. Phys.* **9** (1941) 204.
4. Marvel, C. S., Copley, M. J. and Ginsburg, E. *J. Am. Chem. Soc.* **62** (1940) 3109.
5. Andrieth, L. F. and Steinman, R. *J. Am. Chem. Soc.* **63** (1941) 2115.
6. Kosolapoff, G. M. and McCullough, J. F. *J. Am. Chem. Soc.* **73** (1951) 5392
7. Halpern, E., Bouck, J., Finegold, M. and Goldenson, J. *J. Am. Chem. Soc.* **77** (1955)4472.
8. Badger, R. M. and Bauer, S. H. *J. Chem. Phys.* **5** (1937) 839.
9. Badger, R. M. *J. Chem. Phys.* **8** (1940) 288.
10. Pimentel, G. C. and McClellan, A. L. *The Hydrogen Bond*, Reinhold Publishing Co., New York 1960, p. 85.
11. Aksnes, G. *Acta Chem. Scand.* **14** (1960) 1475.
12. Grundwald, E. and Coburn, W. C. *J. Am. Chem. Soc.* **80** (1958) 1322.
13. Huggins, C. M. and Pimentel, G. C. *J. Phys. Chem.* **60** (1956) 1615.
14. Lippert, E. in Hadzi, D. and Thompson, H. N. (Eds.) *Hydrogen Bonding*, Papers presented at the Symposium of Hydrogen Bonding held at Ljubljana, 29 July – 3 August 1957, Pergamon Press, London 1959, p. 163.
15. Nagakura, S. *J. Phys. Chem.* **76** (1954) 3070.
16. Nagakura, S. and Baba, H. *J. Phys. Chem.* **74** (1952) 5693.
17. Sutton, L. E. *J. chim. phys.* **46** (1949) 435.
18. Hulett, J. R., Pegg, J. D. and Sutton, L. E. *J. Chem. Soc.* **1955** 3901.

Received February 28, 1961.

ACTA CHEMICA SCANDINAVICA 15 (1961) 1347–1366

Studies on the Hydrolysis of Metal Ions

Part 35. The Hydrolysis of the Lanthanum Ion, La^{3+}

GEORGE BIEDERMANN and LIBERATO CIAVATTA

Department of Inorganic Chemistry, Royal Institute of Technology, Stockholm 70, Sweden

The hydrolysis equilibria of the La(III) ion have been studied at 25°C by hydrogen ion concentration measurements, using a glass electrode. The total [La(III)] was varied between 0.1 and 1.0 M, whilst the concentration of the ClO_4^- ion was held constant at 3 M by the addition of $LiClO_4$. The data, which indicate a slight hydrolysis in the log h range −6.5 to −8.1, can be explained by assuming the equilibria

$$La^{3+} + H_2O \rightleftharpoons LaOH^{2+} + H^+ \qquad \log \beta_{1,1} = -10.1 \pm 0.1 \qquad (1)$$

$$2La^{3+} + H_2O \rightleftharpoons La_2OH^{5+} + H^+ \qquad \log \beta_{1,2} = -9.9_5 \pm 0.1 \qquad (2)$$

$$5La^{3+} + 9H_2O \rightleftharpoons La_5(OH)_9^{6+} + 9H^+ \qquad \log \beta_{9,5} = -71.4_5 \pm 0.1 \qquad (3)$$

Equally good agreement with the data (see Fig. 1) is obtained by replacing equilibrium (3) with

$$6La^{3+} + 10\,H_2O \rightleftharpoons La_6(OH)_{10}^{8+} + 10\,H^+ \qquad \log \beta_{10,6} = -78.7_5 \pm 0.1 \qquad (4)$$

No other mechanism, involving the formation of only three hydrolysed species, could be found which would explain the experimental data.

The experimental conditions necessary for accurate results to be obtained, when the hydrolysis equilibria must be studied in poorly buffered solutions, are discussed in some detail.

The first quantitative study on the hydrolysis equilibria of the La(III) ion was carried out in 1916 by Vesterberg [1], who measured the distribution ratio of acetic acid between lanthanum acetate solutions and ether. By taking into account the acidity and distribution constants of acetic acid, Vesterberg was able to calculate the hydrogen ion concentration in the lanthanum acetate solutions from the distribution data. The results were explained by assuming the equilibrium

$$La^{3+} + H_2O \rightleftharpoons LaOH^{2+} + H^+ \qquad \beta_{1,1} = [LaOH^{2+}]\,h\,[La^{3+}]^{-1} \qquad (1)$$

and Vesterberg found $\beta_{1,1}$ to be approximately equal to the acidity constant of the NH_4^+ ion (thus the value of log $\beta_{1,1}$ is around −9.4).

During the last fifteen years interest in the chemistry of the rare earths has revived and several attempts have been made to find the composition of the hydrolysis products of La(III).

In 1946 Moeller [2] measured the acidity of a series of purified lanthanum sulfate solutions at 25°C using a glass electrode. The data for [La(III)] $\leq$ 0.01M could be well explained by equilibrium (1) with log $\beta_{1,1} = -10$. At higher concentration of La(III), however, the calculated $\beta_{1,1}$ values showed a tendency to increase, from which Moeller concluded that additional hydrolysis products become important at high values of [La(III)].

In 1953 Wheelwright, Spedding and Schwarzenbach [3] titrated with NaOH, using a glass electrode, a 0.01 M $LaCl_3$ solution containing an excess of HCl at 25°C. On the basis of these measurements they have estimated log $\beta_{1,1} = -8.4$. Similar measurements were also made in 1953 by Busey and Cowan [4], and Kraus [4] has used their data to estimate log $\beta_{1,1} = -8.3$.

In 1957 Lewis [5] measured the solubility of La_2O_3 in solutions of log h varying between -7.5 and -10.5 and concluded that extensive hydrolysis occurs in this acidity range.

Symbols often used in the text

h = hydrogen ion concentration at equilibrium
H = analytical excess of hydrogen ions = $[ClO_4^-] - 3B - [Li^+]$
B = total concentration of La(III)
Z = average number of hydrogen ions set free per lanthanum atom = $(h-H)\,B^{-1}$
p = number of OH groups bound to hydrolysed species
q = number of La atoms present in hydrolysed species
b = concentration of La^{3+}
K_p = equilibrium constant for formation of all species containing p OH groups
$\beta_{p,q}$ = equilibrium constant for formation of $La_q(OH)_p$

CHOICE OF EXPERIMENTAL CONDITIONS

Preparation of the solutions. In the present work the hydrolysis equilibria were studied at 25°C by measuring the hydrogen ion concentration in a series of lanthanum perchlorate solutions of varying acidity. Preliminary experiments have indicated that the hydrolysis becomes appreciable at log $h < -6.5$, and that only a small part of La^{3+} can be transformed to hydrolysis products before precipitation starts. It was found that in clear solutions the highest value of Z cannot exceed 0.02, thus we must confine our work to solutions of a very low buffer capacity. Under such experimental conditions great care is required to avoid contamination of the solutions to be studied by foreign protolytes, *e.g.* those inevitably present at small concentrations in strong base solutions (carbonate, borate, silicate and aluminate).

In favorable cases, when the hydrolysis equilibria can be studied in solutions of log $h > -5$, the preparation of hydrolysed solutions is simple. One

may start with a solution of such a high h that the hydrolysis is negligible, and add successively increasing amounts of a strong base solution. If log $h > -5$, then the impurities, most likely to be introduced with a strong base solution, do not cause an appreciable error because all of them are present in the unhydrolysed form. For this reason also $NaHCO_3$ can be used, instead of NaOH, as was suggested by Hedström [6].

On the other hand, when the hydrolysis becomes appreciable at log $h < -5$ and only low Z values can be attained, the measured value of h may be seriously in error if the hydrolysed solution is prepared by adding a strong base, because at these low acidities the impurities are protolysed to a considerable extent. Clearly the lower the values of Z and h that are studied, the greater becomes the error caused by the protolysis of the contaminants.

We have made a number of attempts to purify $Ba(OH)_2$ (which is to be preferred to NaOH) by repeated recrystallizations in a N_2 atmosphere. The carbonate content could be much reduced by three recrystallizations (though it was still too high for our purposes), but the concentration of the other impurities (silicates, *etc.*) was thereby increased somewhat, because of prolonged contact with glass surfaces.

It should be added, that at log $h < -11$ the impurities present in a strong base solution again have a negligible influence on h, because all of them, with the exception of silicates, are mainly present in the completely hydrolysed form.

The method finally adopted for preparing hydrolysed lanthanum solutions does not require a strong base. We have started from a slightly acid lanthanum perchlorate solution (log $h \sim -4$, measured with an indicator paper) which was freed of CO_2 by passing purified nitrogen through it. The hydrogen ion concentration of this initial solution was decreased by adding an excess of freshly ignited La_2O_3; rapid equilibration was ensued by stirring for several hours at 90°C. Finally the excess La_2O_3 was removed by careful filtration. All the operations were carried out in an atmosphere of nitrogen.

Using this method, the introduction of foreign substances is avoided and the maximal value of Z in the final solution can be approached closely, by stirring with the solid for a sufficiently long time. (In the cases studied hitherto equilibrium was attained within 24 h). Moreover, since log h never becomes less than -8 (see Fig. 1) no significant amounts of impurities are brought into the solution by contact with glass surfaces. Nevertheless, Jena glass is to be preferred to Pyrex to diminish dissolution of boric acid.

Methods similar to that described above have proved to be of great value for the preparation of hydrolysed solutions of a number of metal ions, as Ag^+ (Ref.[7]), Cd^{2+}, Ni^{2+}, Ce^{3+} and Y^{3+}, in a state of high purity.

The composition of the solutions. The main prerequisite for obtaining accurate data on hydrolysis equilibria is to work in solutions of appreciable buffer capacity. This requirement could be realized in the present case by studying rather concentrated lanthanum solutions: values of B ranging from 0.1 to 1 M have been investigated. In each series of experiments (except two which were done for special purposes) the $[ClO_4^-]$ was kept constant at 3 M by adding the inert salt $LiClO_4$.

On the basis of measurements made by one of us (G.B.) it may be concluded that when the ratio $r = z_i c_i/[ClO_4^-]$ exceeds about 0.1 (z_i = charge of reacting cation, c_i = concentration of the reacting cation) the deviation of the activity factors of the reacting ions from constancy becomes appreciable. Consequently, the methods of calculation worked out for treating data obtained in an inert medium ($r < 0.1$) cannot be applied to our measurements which were made in solutions for which r had high values.

One can, however, use the "self-medium" approach proposed by Hietanen and Sillén [8]. The principle of this method is that data obtained at different values of B are regarded separately. In each series of measurements, where B is kept constant and low values of Z are studied, the variation of the activity factors is negligible because the composition of the solution changes only slightly. In consequence, the law of mass action expressed in terms of concentrations can be applied to the data to evaluate the number of OH groups bound to the reaction products, p. Obviously, the number of metal ions present in the reaction products, q, cannot be obtained straightforwardly by the self-medium method, because in each series of experiments the concentration of the free (unhydrolysed) metal ions, b, is very close to B.

The self-medium method is used generally to detect the formation of species $Me_q(OH)_p$ (Me = metal ion) with a high value of q/p, whereas the main body of information is obtained with the inert medium method. For such an unfavorable case as the La(III) ion an exact treatment of the data is possible, at present, only by the self-medium method.

It will be shown in the "Composition of the hydrolysis products" section that, although the unknown variation of the activity factors introduces some uncertainty, plausible arguments can be given for estimating the probable values of q.

THE METHOD OF MEASUREMENTS.

In each series of measurements, which were carried out as potentiometric titrations, B was kept constant; the B values studied ranged from 0.0973 to 1.111 M. The measurements were performed by starting with a solution ("S_0") containing an initially unknown deficit of hydrogen ions ($-H_0$) and adding to it successively increasing volumes (V_T ml) of another solution ("T") containing about 0.02 to 0.10 M $HClO_4$ ($= H_T > -H_0$).

Since the hydrolysis of La^{3+} proved to be quite negligible for $\log h > -5$ the hydrogen ion concentration in solution T is equal to the analytical excess of hydrogen ions. Both S_0 and T were prepared from a partially hydrolysed lanthanum perchlorate stock solution which was itself prepared as described in the previous section.

The concentration of ClO_4^- in all the solutions studied (except two, see below) was made up to 3.00 M by the addition of $LiClO_4$. $LiClO_4$ was chosen as the "solvent salt" because, in contrast to $NaClO_4$, it can be purified easily by recrystallisation. In the lanthanum stock solution $[ClO_4^-]$ was set approximately equal to 3 [La(III)] which is near to the true $[ClO_4^-] = 3.000 + H_0$. The maximal value of H_0 was -0.017 M (at $B = 1$ M), therefore the deviation of $[ClO_4^-]$ from 3 M has never exceeded 0.6 %.

The solutions thus had the general composition

B M La(III), H_s M H^+, $(3.000 - 3B - H_s + H_0)$ M Li^+, $(3.000 + H_0)$ M ClO_4^- = solution S

where H_s, the analytical excess of hydrogen ions, is equal to

$$H_s = \frac{V_0 H_0 + V_T(H_T + H_0)}{V_0 + V_T} = H_0 + \frac{V_T H_T}{V_0 + V_T} \qquad (2)$$

In (2) H_T denotes the hydrogen ion concentration in solution T, calculated by assuming H_0 to be negligible, V_0 is the volume of S_0 and V_T is the volume of T added.

A few series of measurements were made with solutions in which B was 0.1 M and $[Li^+]$ was 0.01 M. The purpose of these measurements was to check whether any appreciable amounts of impurities were introduced by adding $LiClO_4$. A number of additional measurements were also made with solutions in which B was 1.111 M and $[Li^+]$ was 0.1 M, in order to get some idea on the influence of the counter ion concentration on the numerical values of the equilibrium constants. The solutions containing 0.31 M and 3.43 M ClO_4^- were studied in the same way as solutions S.

The hydrogen ion concentration of solutions S was measured by means of the cell

$$- \text{ GE / solution S / SE } + \qquad (A)$$

where GE denotes a glass electrode and SE is the reference half-cell

$$/3.000 \text{ M } LiClO_4/2.990 \text{ M } LiClO_4, 0.010 \text{ M } AgClO_4/AgCl, Ag$$

The emf of cell (A) at 25°C can be written

$$E = E_0 - 59.15 \log h - 59.15 \log f(H^+) + E_j(h,B) \qquad (3)$$

where E_0 is a constant and h is the hydrogen ion concentration at equilibrium. $f(H^+)$ denotes the activity factor of H^+. The standard state is defined so that $f(H^+)$, as well as the activity factors of the other reacting species, tend to unity when the composition of the solution approaches 3 M $LiClO_4$. For each series of measurements, when B was kept constant, it is certainly a good approximation to assume that $f(H^+)$ = constant, consequently we may write

$$E = E_0' - 59.15 \log h + E_j(h,B) \qquad (4)$$

where E_0' is a function of B.

In (3) and (4) $E_j(h,B)$ denotes the liquid junction potential at the junction solution S/3 M $LiClO_4$. $E_j(h,B)$ was determined by measuring the emf of the cells

GE and H_2(Pt)/h M H^+, $(3.000 - h)$ M Li^+, 3.000 M ClO_4^-/SE (B)

and

GE/0.967 M La^{3+}, h M H^+, $(0.100 - h)$ Li^+, 3.000 M ClO_4^-/SE (C)

in the h range 0.01 to 0.1 M.

From the emf data with cell (B) we have calculated $E_j(h,0) = -15.8\,h$ mV, and from those with cell (C) $E_j(h, 0.967) = -20.0\,h$ mV. Thus up to $h = 0.01$

M no appreciable error is made when $E_j(h,0)$ is used for the entire B range 0.1—1.0 M.

It was necessary to use the two cells (B) and (C), because in solutions where $[La^{3+}] \geq 0.1$ M the hydrogen electrode was found to give potentials which drifted at the rate of several mVs per hour. Moreover, when two hydrogen electrodes were immersed in the same lanthanum solution they differed by 40 to 60 mV. A similar difficulty was encountered previously in solutions of other tervalent ions such as In^{3+} and Sc^{3+}. The failure of hydrogen electrode in these solutions may be caused by the strong adsorption of tervalent ions on the platinized platinum surface, which thus looses its catalytic activity.

The hydrolysis of La(III) could not be studied by the quinhydrone electrode, because quinone is not stable in solutions of $\log h < -7$. The glass electrodes were calibrated against the quinhydrone electrode. When a glass and a quinhydrone electrode were immersed in the same solution and $\log h$ was varied from -2 to -7, the difference between the potentials of the glass and the quinhydrone electrode was found to be constant within $\pm$ 0.2 mV.

Each of the potentiometric titrations may be divided into two parts. The measurements in the low acidity range ($\log h < -5$, part I) were made to determine h in hydrolysed solutions, whereas the E data at higher acidities (part II) served to calculate H_o and E_o'. The value of H_o was obtained by means of a Gran plot [9], which was constructed on the basis of the E values

Table 1. A series of measurements with $B = 0.0973$ M

$[La(III)] : 9.73 \times 10^{-2}$ M, $[Li^+] : 2.700$ M, $[ClO_4^-] : 3.00$ M = S_o, $V_o = 50.00$ ml
$[La(III)] : 9.73 \times 10^{-2}$ M, $H_T : 2.000 \times 10^{-2}$ M, $[Li^+] : 2.680$ M, $[ClO_4^-] : 3.00$ M = T

V_T ml	E mV	$-\log h$	$BZ \times 10^3$ M	E_o' mV	
0.00	421.4	8.056	1.718		
0.70	420.5	8.040	1.442		
1.20	419.6	8.025	1.249		
1.70	418.2	8.001	1.060		
2.20	416.1	7.966	0.875_1		part I
2.60	413.1	7.915	0.729_5		
2.90	409.2	7.850	0.621_7		
3.10	405.5	7.787	0.550_6		
3.40	398.7	7.672	0.444_8		
3.70	392.2	7.562	0.340_0		
4.00	383.3	7.412	0.236_7		
4.20	366.5	7.128	0.168_4		
5.00	178.7	4.000		119.5	
5.50	156.2	3.579		122.0	
6.00	144.2	3.372		122.2	
7.00	130.2	3.136		122.2	part II
8.00	121.4	2.983		122.4	
9.00	115.0	2.875		122.4	
10.00	110.1	2.792		122.4	

$E_o' = 122.3 \pm 0.1$ mV
$H_o = -(1.718 \pm 0.005) \times 10^{-3}$ M

obtained in part II by taking into account (2) and (4). Then we could calculate E_o' for each experimental point of part II with (4). E_o' proved to be constant at least within $\pm$ 0.2 mV, typical results are shown in Table 1. Finally, the values of H_o and E_o' thus obtained, were used for the calculation of log h and Z corresponding to the experimental points of part I.

MATERIALS AND ANALYSIS

Lanthanum perchlorate solutions were made from La_2O_3 of 99.997 % purity supplied by Lindsay Chemical Division, West Chicago, USA. According to the manufacturer the maximum amount of rare earth impurities in this material is 0.0025 %, consisting mainly of praseodymium oxide. No Fe(III)-, heavy metal-, Cl^- or SO_4^{2-} ions could be detected in the batches of La_2O_3 used, each of these batches, however, contained some carbonate.

The method employed to prepare partially hydrolysed lanthanum perchlorate solutions has been described in the "Preparation of the solutions" section. We shall discuss here only two important experimental details: 1) the preparation of carbonate-free La_2O_3 and 2) the removal of excess La_2O_3.

1) It was found that a La_2O_3 preparation, which has been kept in contact with air, must be ignited to 1 100°C to expel the last traces of carbonate. In materials ignited at 900°C, the temperature generally recommended for analytical purposes, appreciable amounts of carbonate could be detected. The ignition should be made preferably in a porcelain crucible, because the carbonate in La_2O_3 seems to react with platinum at high temperature. Avoidance of platinum is especially important if La_2O_3 is prepared by decomposing lanthanum oxalate.

2) It is essential to add some filter paper pulp before filtering the lanthanum perchlorate solution which contains suspended La_2O_3, because (if this precaution is not taken) the finest La_2O_3 particles are likely to go through a sintered glass filter of porosity G4. We have used each time, one half of a "Whatman ashless tablet" (Balstone Ltd, England).

To test the filter paper pulp for impurities a suspension was made containing one tablet in 10 ml distilled water. No Cl^- or heavy metal ions could be detected in the filtrate from this suspension, and the filtrate, which had the same pH as the distilled water, did not contain acidic or alkaline impurities in significant amounts.

The filtered lanthanum perchlorate solutions were regularly examined for turbidity during several weeks (in one case during three months) but no suspended La_2O_3 particles could be detected. In order to detect turbidity the solution was illuminated by an intense and thin light beam in a dark room.

The [La(III)] in the stock solutions was determined by precipitating lanthanum oxalate, then dissolving this in 1 M H_2SO_4 and oxidizing it with $KMnO_4$. Essentially the procedure proposed by Kolthoff and Elmquist [10] was followed. The results were reproducible within $\pm$ 0.1 %. The $KMnO_4$ solution was standardised (*via* a $Na_2S_2O_3$ solution) against KIO_3, which serves as a primary standard in this laboratory.

An approximate value for the deficit of hydrogen ions ($[ClO_4^-]-3$ [La(III)]) in the stock solution was found by adding a measured volume of a standardised $HClO_4$ to a weighed amount of the lanthanum solution and titrating this mixture with NaOH using methyl-red as indicator.

$LiClO_4$ solutions were made from Li_2CO_3 and $HClO_4$, both of p.a. quality, supplied by Baker Chemical Corporation. First a saturated solution of $LiClO_4$ was prepared at room temperature, and to it was added a small excess of Li_2CO_3. The slightly alkaline solution (pH $\sim$ 8) was left to stand overnight and then the precipitate that formed, which consisted mainly of FeOOH and $SiO_2(H_2O)_n$, was removed by filtration. The pH was then decreased to 3 by the addition of dilute $HClO_4$, the solution was boiled to expel CO_2 and to concentrate it further. Then, the slightly acidic solution was slowly cooled to 0°C and the crystals of $LiClO_4$ which formed were filtered off. The $LiClO_4$, which contained traces of $HClO_4$, was twice recrystallized from water. No Cl^-, SO_4^{2-} or Fe(III) could be detected in a 4 M $LiClO_4$ stock solution.

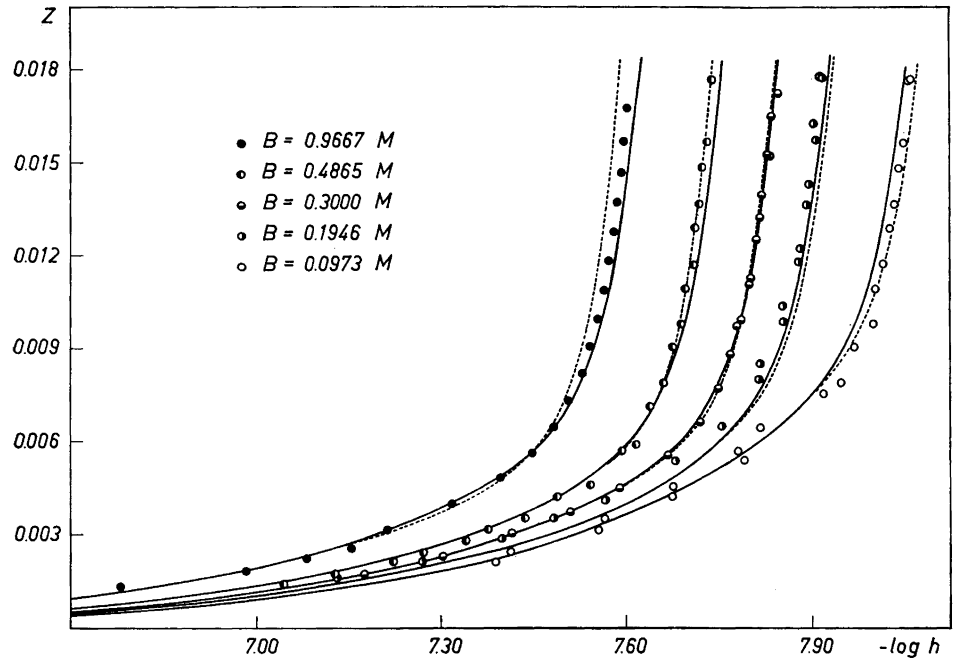

Fig. 1. Z, the average number of hydrogen ions set free per lanthanum, as a function of $-\log h$. The full-drawn curves have been calculated with $-\log \beta_{1,1} = 10.1$, $-\log \beta_{1,2} = 9.95$ and $-\log \beta_{9,5} = 71.45$. The dotted curves have been calculated with the same $\beta_{1,1}$ and $\beta_{1,2}$ values and $-\log \beta_{10,6} = 78.75$.

A series of experiments was made with $LiClO_4$ which had been recrystallized a third time using platinum vessels. The $Z(\log h)_B$ data found with this preparation coincided with those obtained when twice recrystallized $LiClO_4$ was used. We may thus conclude that no appreciable amounts of protolytes were dissolved from glass surfaces when the $LiClO_4$ was prepared.

The concentration of the stock solution was determined by passing a weighed amount through a cation exchanger in the hydrogen form and titrating the eluate with standardised NaOH.

$AgClO_4$ solutions were made using Merck p.a. $AgNO_3$. A great excess of 11 M $HClO_4$ was added to a concentrated solution of $AgNO_3$, and HNO_3 was expelled, together with a large part of the excess $HClO_4$, by evaporating the mixture nearly to dryness. $[Ag^+]$ was determined potentiometrically with a NaCl solution made from a Br^- and water-free NaCl preparation.

$HClO_4$ solutions were standardised against $KHCO_3$ and Tl_2CO_3. The results obtained with these standard substances agreed within $\pm$ 0.1 %.

NaOH solutions were titrated with standardised $HClO_4$.

Experimental details of the emf measurements. All emf measurements were carried out at 25.00 $\pm$ 0.01°C in a paraffin oil thermostat. The cell arrangement was similar to that described by Forsling, Hietanen and Sillén [11]. The titration vessel was filled with N_2 before the starting solution was introduced, and a vigorous stream of N_2 was passed through solution S during the measurements. The nitrogen, which was taken from a cylinder, was purified and presaturated by passing it through 2 M NaOH, then water and finally 3 M $LiClO_4$.

Table 2. Survey of measurements.

$B = 0.967\ M$

$Z \times 10^3$, $-\log h$. 16.69, 7.604; 15.66, 7.599; 14.66, 7.594; 13.68, 7.587; 12.71, 7.581; 11.77, 7.572; 10.84, 7.564; 9.91, 7.554; 9.03, 7.542; 8.15, 7.528; 7.29, 7.506; 6.47, 7.483; 5.61, 7.447; 4.79, 7.395; 3.99, 7.315; 3.20, 7.211; 2.55, 7.153; 2.27, 7.079; 1.82, 6.981; 1.36, 6.778.

$B = 0.486_8\ M$

$Z \times 10^3$, $-\log h$. Series a. 17.66, 7.738; 15.63, 7.731; 13.63, 7.719; 11.68, 7.709; 9.76, 7.689; 7.89, 7.664; 6.03, 7.616; 4.57, 7.544; 3.50, 7.435; 2.79, 7.341; 2.08, 7.222; 1.38, 7.043.

Series b. 17.66, 7.738; 14.82, 7.723; 12.84, 7.711; 10.90, 7.696; 9.00, 7.674; 7.13, 7.638; 5.66, 7.594; 4.21, 7.488; 3.14, 7.374; 2.44, 7.265; 1.73, 7.126.

$B = 0.300_0\ M$

$Z \times 10^3$, $-\log h$. Series a. 16.45, 7.834; 15.24, 7.827; 13.95, 7.819; 12.52, 7.811; 10.99, 7.797; 9.87, 7.785; 8.76, 7.770; 7.65, 7.750; 6.56, 7.721; 5.48, 7.672; 4.42, 7.591; 3.71, 7.510; 3.01, 7.415; 2.32, 7.302; 1.63, 7.173. Series b. 17.21, 7.836; 15.18, 7.829; 13.18, 7.817; 11.23, 7.799; 9.69, 7.778.

$B = 0.194_6\ M$

$Z \times 10^3$, $-\log h$. Series a. 17.73, 7.917; 15.69, 7.907; 13.69, 7.893; 11.74, 7.878; 9.83, 7.853; 7.94, 7.814; 6.46, 7.755; 5.36, 7.680; 4.28, 7.566; 3.57, 7.481; 2.86, 7.396; 2.15, 7.268.

Series b. 17.75, 7.915; 16.22, 7.905; 14.22, 7.896; 12.20, 7.881; 10.33, 7.854; 8.44, 7.814; 2.09, 7.127.

$B = 0.097_3\ M$

$Z \times 10^3$, $-\log h$. Series a. 17.66, 8.061; 15.62, 8.049; 13.63, 8.034; 11.67, 8.015; 9.76, 7.991; 7.86, 7.946; 5.30, 7.790; 4.21, 7.674; 3.14, 7.554; 2.08, 7.378;

Series b. 17.66, 8.056; 14.82, 8.040; 12.84, 8.025; 10.89, 8.001; 8.99, 7.966; 7.50, 7.915; 6.39, 7.850; 5.66, 7.787; 4.57, 7.672; 3.49, 7.562; 2.43, 7.412.

$B = 1.11_1\ M$, $[ClO_4^-] = 3.43_3\ M$

$Z \times 10^3$, $-\log h$. Series a. 17.87, 7.579; 16.98, 7.577; 16.10, 7.572; 14.40, 7.562; 12.77, 7.552; 11.20, 7.542; 9.68, 7.527; 8.23, 7.508; 6.81, 7.481; 5.46, 7.444; 4.13, 7.369; 3.49, 7.309; 2.86, 7.222; 2.24, 7.112; 1.64, 6.977; 1.04, 6.683.

Series b. 17.81, 7.586; 16.50, 7.581; 15.19, 7.576; 13.53, 7.564; 11.93, 7.552; 10.38, 7.538; 8.90, 7.552; 7.46, 7.501; 6.09, 7.471; 4.74, 7.417; 3.95, 7.361; 3.32, 7.293; 2.81, 7.217; 2.44, 7.155; 2.07, 7.089; 1.70, 7.008, 1.34, 6.881; 0.98, 6.626; 0.74, 6.296.

$B = 0.100_0\ M$, $[ClO_4^-] = 0.31\ M$

$Z \times 10^3$, $-\log h$. 17.92, 8.039; 17.26, 8.033; 16.41, 8.023; 15.36, 8.012; 14.33, 7.996; 13.32, 7.978; 12.33, 7.959; 11.36, 7.939; 10.41, 7.910; 9.66, 7.883; 8.92, 7.853; 8.38, 7.831; 8.02, 7.809; 7.48, 7.783; 6.77, 7.743; 5.90, 7.699; 5.56, 7.665; 5.05, 7.619; 4.55, 7.565; 4.05, 7.503; 3.55, 7.434, 3.06, 7.332; 2.58, 7.183; 1.93, 6.997; 1.62, 6.644.

Type 1190—80 Beckman glass electrodes were used; in our solutions, these came to a steady state within 10 min, and gave potentials constant within ± 0.2 mV.

A number of lanthanum stock solutions were prepared from different batches of La_2O_3; the $Z(\log h)_B$ data obtained with solutions of different origin have agreed within the limits of experimental uncertainty (± 0.003 log h units).

Ag, AgCl electrodes were prepared according to Brown [12].

E was measured with a Radiometer PHM 4 valve potentiometer, this instrument was calibrated against a Leeds & Northrup type K_3 compensator.

THE COMPOSITION OF THE HYDROLYSIS PRODUCTS

The $Z(\log h)_B$ data, which form the basis of the following calculations, are summarized in Table 2 and are represented graphically in Fig. 1.

The determination of the composition of the hydrolysis products and the evaluation of the corresponding equilibrium constants will be carried out in three steps. In the first (section I), each set of data pertaining to a particular value of B will be treated by the self-medium method. Using this method we can calculate for each value of B studied, the number of OH groups bound to the hydrolysis products, p, and the formation constants of species having a common p, $K_p = K_p(B)$.

In the second step (section II), probable values are derived for the number of lanthanum atoms present in the hydrolysed species, q, by analysing the $K_p(B)$ functions. Lastly all the $Z(\log h, B)$ data are considered simultaneously and as a final check they are compared with normalised model functions.

I. The calculation of p. Treatment of the data by the self-medium method

When we consider a set of data obtained at a constant B and take into account that in our solutions the maximal value of Z never exceeds 0.02, then, without introducing any appreciable error, we may simplify the *preliminary* calculations by using the approximation

$$[La^{3+}] = b \simeq B = \text{constant} \tag{5}$$

Assuming the formation of a series of reaction products with the general composition $La_q(OH)_p^{(3q-p)+}$, the concentration of hydrogen ions set free by hydrolysis, BZ, is expressed by the equation

$$BZ = \sum_p \sum_q p\,[La_q(OH)_p] = \sum_p \sum_q p\beta'_{p,q}\, b^q h^{-p}\, f^{-1}(p,q) f^q(La^{3+}) f^{-p}(H^+) \tag{6}$$

where the formation constant of $La_q(OH)_p$ is denoted by

$$\beta'_{p,q} = [La_q(OH)_p] h^p b^{-q} f(p,q) f^p(H^+) f^{-q}(La^{3+}) \tag{7}$$

p and q represent integers, and f is the symbol for the activity factors.

In each series of measurements (B = constant) the activity factors may be regarded as constants and we may use approximation (5), thus (6) can be written

$$BZ \simeq \sum_p \sum_q p h^{-p} B^q \beta_{p,q} = \sum_p p h^{-p} K_p \tag{8}$$

where

$$\beta_{p,q} = \beta_{p,q}(B) = [La_q(OH)_p] h^p b^{-q} \tag{9}$$

and

$$K_p = K_p(B) = \sum_q B^q \beta_{p,q} \tag{10}$$

K_p is the formation constant of the species containing p OH groups. Complexes having the same value of p but different values of q may be called homoligandic complexes.

We first tried to explain our data in the simplest way by assuming that all hydrolysed species are homoligandic. To test this hypothesis we compared

the experimental data $BZ(\log h)_B$ with the normalised[13] form of (8), $\varphi_p(\log w)$, calculated for the case where p has a single value, P

$$\varphi_p = BZ = PK_P h^{-P} = Pw^P;\ \log w = \frac{\log K_P}{P} - \log h \qquad (11)$$

Values of P ranging from 1 to 12 were inserted in (11), but, over the entire BZ range studied, no satisfactory agreement with any set of values of $Z(\log h)_B$ was found. When $Z \leq 0.01$, however, the data for each value of B seemed to fit the function φ_1, indicating the predominance of species $La_q(OH)$. No certain conclusions concerning the composition of the species which become important when $Z > 0.01$ can be drawn on the basis of (11).

The predominance of monoligandic species at $Z < 0.01$ can be shown very clearly by calculating (using approximation (5)) the average number of OH groups bound to the reaction products, $\bar{p}$.

$$\bar{p} = \frac{\Sigma p[La_q(OH)_p]}{\Sigma[La_q(OH)_p]} = BZ\ [2.303 \int_{\log h}^{\infty} BZ\ \mathrm{d}\log h]^{-1} \qquad (12)$$

Eqn. (12) is derived from (8) by considering that $Z \to 0$ as $\log h \to \infty$. The value of $\int_{\log h}^{-7} BZ\ \mathrm{dlog}\ h$ was calculated by means of the trapezoidal formula, using a plot of BZ *versus* $-\log h$. Smooth curves were drawn through the experimental points and the integration was done with intervals of 0.05 log h unit. In order to eliminate errors introduced by drawing smooth curves, another integration was also performed taking the experimental points directly (*i.e.* with unequal intervals). The results of the two integrations coincided within the limits of experimental uncertainty.

The evaluation of the residual integral $2.303 \int_{-7}^{\infty} BZ\ \mathrm{dlog}\ h$ was carried out by extrapolation. The three lowest experimental $Z(\log h)_B$ values were fitted to φ_1 (*cf.* (11)), which was assumed to represent the experimental points at those high acidities where no data were available. Another extrapolation was also made by using φ_2 instead of φ_1. The areas under the curves were calculated by

$$\int_0^{w_0} \varphi_p \frac{\mathrm{d}w}{w} = \int_0^{w_0} Pw^{(P-1)}\ \mathrm{d}w = {w_0}^P$$

where w_0 is the value of w corresponding to $h = 10^{-7}$. The magnitude of the residual integral was, of course, influenced to some extent by the choice of the extrapolation function, but at $\log h < -7.3$ the values of $\int_{\log h}^{\infty} BZ\ \mathrm{dlog}\ h$ calculated with φ_1 and φ_2 agreed within 3 %.

The results of our calculations are shown in Fig. 2 where $\bar{p}$ is plotted *versus* $-\log h$. It can be seen that, for each value of B, a range of $\log h$ of considerable width can be found where $\bar{p}$ is equal to 1.00 ± 0.05. In this range of $\log h$, $K_1 \cong BZh$ was calculated for each experimental point. The calculated K_1 values have shown no appreciable trend with h. The probable values of the constants are summarised in Table 3.

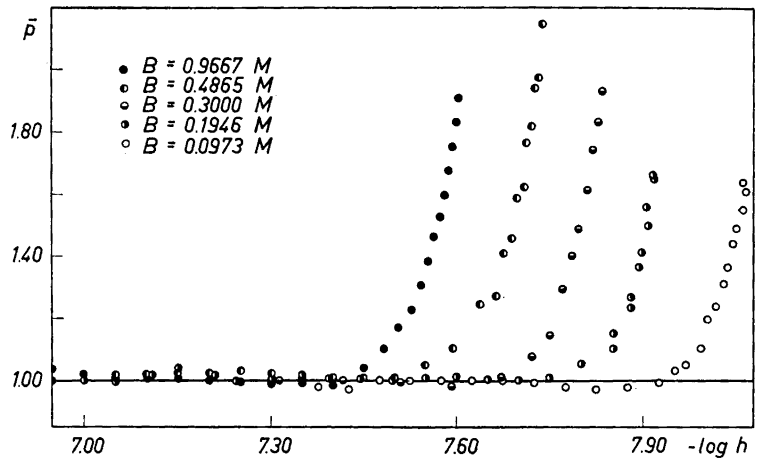

Fig. 2. $\bar{p}$ (eqn. (12)), the average number of OH groups bound to the complexes, as a function of $-\log h$.

Fig. 2 shows moreover that, as log h approaches the value where precipitation starts, $\bar{p}$ increases steeply and attains values exceeding 2. This suggests that species with $p > 2$ are also formed in appreciable amounts at each of the values of B studied.

In order to explain the data obtained at higher values of Z the hypothesis was made that, in addition to La^{3+} and La_qOH, a further species $La_{q'}(OH)_{p'}$ is present in our solutions (in these formulas p' denotes a constant whereas q and q' may take a series of values). This hypothesis was tested by comparing the experimental data, recalculated to the form log (BZh) *versus* $(-\log h)_B$, with a group of functions obtained by normalizing (8). Assuming the formation of two species with $p = 1$ and $p = p'$ (8) can be written

$$BZ = K_1 h^{-1} + p' K_{p'} h^{-p'} \qquad (13)$$

Table 3. Survey of the calculated K_1 and p' values.

B M	K_1 M²	p' eqns. (5) and (16)	p' eqn. (17)
1.11_1*	$(19.0 \pm 0.5)\ 10^{-11}$	8.5 ± 0.5	9.0 ± 0.5
$0.967_{\cdot}$	$(18.5 \pm 1.0)\ 10^{-11}$	9.2 ± 0.5	9.7 ± 0.5
0.486_5	$(6.2_5 \pm 0.4)\ 10^{-11}$	9.5 ± 0.5	10.0 ± 0.5
0.300_0	$(3.41 \pm 0.3)\ 10^{-11}$	10.0 ± 0.5	10.4 ± 0.5
0.194_6	$(2.3_5 \pm 0.2)\ 10^{-11}$	—	—
0.097_3	$(0.9 \pm 0.1)\ 10^{-11}$	—	—
0.100_0**	$(1.3_2 \pm 0.1)\ 10^{-11}$	—	—

* $[ClO_4^-] = 5.43$ M ** $[ClO_4^-] = 0.31$ M

A normalized form of (13), log $W(\log u)_{p'}$, was chosen which allows the simultaneous determination of p', K_1 and $K_{p'}$:

$$\log W(p') = \log (1 + p'u^{(p'-1)}) \tag{14}$$

where

$$W = BZhK_1^{-1} \text{ and } \log u = \frac{1}{p'-1} \log (K_{p'}K_1^{-1}) - \log h \tag{15}$$

If hypothesis (13) is valid then the data log (BZh) *versus* $(\log h)_B$ can be fitted to that member of the group of functions $W(p')$ which represents the correct value of p'. The most probable values of K_1 and $K_{p'}$ may be obtained by reading off, in the position of best fit, the displacement along the X axis, log u + log h, and that along the Y axis, log W − log (BZh). Values of p', ranging from 2 to 12, were inserted into eqn. (14). For each value of B studied a satisfactory agreement could be found between the set of experimental points, log (BZh) *versus* $(\log h)_B$, and the functions $W(9)$ and $W(10)$; whereas successively increasing systematic deviations were obtained when p' was lower than 9 or higher than 10. The uncertainty of the data does not allow to make a distinction between $W(9)$ and $W(10)$.

We may thus conclude that our data may be explained by the formation of La_qOH and either $La_{q'}(OH)_9$ or $La_{q'}(OH)_{10}$ but not with any other mechanism involving only two values of p. The most probable log K_1, log K_9 and log K_{10} values, calculated with (14), are summarised in Table 4. With both pairs of constants (K_1, K_9) and (K_1, K_{10}) an excellent agreement could be attained with all sets of data.

Table 4. Homoligandic equilibrium constants calculated with self-medium method.

B M	$-\log K_1$	$-\log K_9$	$-\log K_{10}$
1.11_1*	9.72	71.10	78.69
0.967	9.73	71.45	79.08
0.486_5	10.20	72.87	80.61
0.300_0	10.47	74.06	81.87
0.194_6	10.63	74.95	81.90
0.097_3	11.03	76.66	84.81
0.100_0**	10.90	76.63	—

* $[ClO_4^-] = 3.43$ M. ** $[ClO_4^-] = 0.31$ M.

It is not easy to give, on the basis of curve-fitting, a numerical estimate for the uncertainty of the calculated p' value, because, only a very narrow Z range is accessible, and the slope of the W curves becomes exceedingly high for $p' > 5$. An attempt was made therefore to examine systematically, how the calculation of p' is affected by the uncertainty of the data and by that of the numerical value of K_1.

Eqn. (13) may be put in the form

$$\log (BZ - K_1h^{-1}) = \log p' + \log K_{p'} - p' \log h \tag{16}$$

where the left-hand side contains quantities directly known from the experiments, BZ and h, and K_1, which was calculated with reasonable accuracy previously. Two methods were employed for the estimation of p'. The first was a graphical method based on (16); p' was evaluated from the slope of the straight line which, according to the principle of least squares, best fitted a plot of log $(BZ-K_1h^{-1})$ *versus*(log $h)_B$. The second was a numerical method; an even number of points $(2n)$ were considered for each value of B, and p' was calculated by

$$p' = \frac{\sum_{1}^{n} y_i - \sum_{n+1}^{2n} y_i}{\sum_{1}^{n} x_i - \sum_{n+1}^{2n} x_i}$$

where y_i and x_i denote a pair of corresponding values of $\log(BZ-K_1h^{-1})$ and $\log h$. Both the upper and the lower limit of K_1, as given in Table 3, was used to calculate $(BZ-K_1h^{-1})$ from the experimental data. The effect of random experimental error was taken into account by varying the number of points $(2n)$ considered for a given value of K_1.

The measurements at $B = 0.1$ and 0.2 M could not be used to get a reliable value of p' by means of (16) because $(BZ-K_1h^{-1})$ becomes too small at these low lanthanum concentrations.

The p' values calculated using (16) (see Table 3) clearly indicate that, in complete agreement with the results found by curve-fitting, the most probable values of p' are 9 and 10. Moreover, the accuracy of the data seems to be sufficient to exclude the hypothesis that complexes with p' greater than 10 or less than 9 would be present in appreciable amounts.

Data of much higher accuracy than those we have been able to attain are required to decide between $La_{q'}(OH)_9$ and $La_{q'}(OH)_{10}$. It may be added, that the present accuracy would be quite sufficient to get more complete information concerning the composition of the hydrolysis products, if Z values up to, say, 0.1 could have been studied.

All the calculations in this section were made using approximation (5). The magnitude of the error introduced by this approximation was estimated by repeating the curve-fitting and the calculation of p' on the assumption that the species formed have the composition LaOH and $La_{p'}(OH)_{p'}$ *i.e.*

$$b = B(1-Z) \qquad (17)$$

The results of the next section indicate that for those values of Z where the difference between (5) and (17) is of any importance, b is not likely to be significantly lower than $B(1-Z)$, thus (17) is a good approximation.

Functions corresponding to W (eqn. (14)) were calculated by assuming (17) and these were compared with the data. A satisfactory fit could be found only for $p' = 9$ and 10, and the K_1, K_9 and K_{10} values calculated using (17) coincided within the limits of experimental uncertainty with those obtained using (5).

The p' values calculated on the basis of (17) by an equation corresponding to (16) are given in Table 3. They are seen to be slightly higher than those found with (5), but the differences hardly exceed the experimental uncertainty.

Summarising these arguments we may infer that, for the low Z values in question, no appreciable error was introduced by using approximation (5). The main conclusions were not affected by the approximations employed in this section (eqns. (5) and (17)), since the final constants were obtained using the exact formulas (cf. section III).

II. The calculation of q, the number of lanthanum atoms present in the hydrolysis products

To find q, we must compare data obtained at different values of B, because in our solutions b is always practically equal to B. Such a comparison involves some uncertainty, since we are not able to estimate the variation of the activity factors caused by the replacement of a large part of the inert cations (Li^+) by the reacting ions. In the following calculations the rough approximation was made that the changes in the activity factors are negligible when B varies from 0.097 to 0.967 M while $[ClO_4^-]$ is kept constant at the value $3B + [Li^+] + H$.

The calculations are based on the analysis of the functions $K_1(B)$, $K_9(B)$ and $K_{10}(B)$ which form power series; values of these functions, as obtained by the self-medium method, are tabulated in Table 3. According to (10) K_1 is equal to

$$K_1 = B\,\beta_{1,1} + B^2\,\beta_{1,2} + \ldots . \qquad (18)$$

As Fig. 3 shows, a plot of K_1B^{-1} approximates closely to a straight line. This fact indicates according to (18) that the species $LaOH^{2+}$ and La_2OH^{5+} are formed. From the intercept and slope of the best line, obtained by the method of least squares, we have calculated the equilibrium constants

$$\log\,\beta_{1,1} = \log\{[LaOH^{2+}]\,h\,b^{-1}\} = -10.1 \pm 0.1$$

and

$$\log\,\beta_{1,2} = \log\{[La_2OH^{5+}]\,h\,b^{-2}) = -10.0 \pm 0.3$$

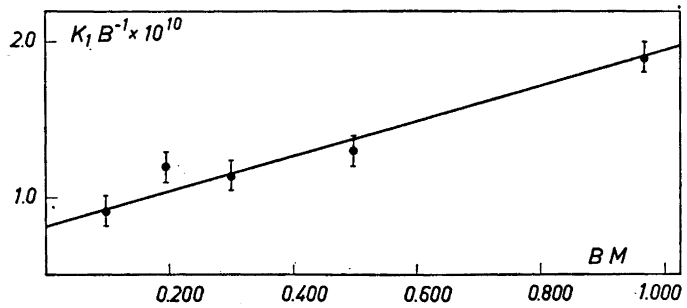

Fig. 3. K_1B^{-1} (eqn. (18)) as a function of B. The straight line represents the equation $K_1B^{-1} = 8.2 \times 10^{-11} + 1.14 \times 10^{-10}\,B$.

The uncertainties of the log $\beta_{1,1}$ and log $\beta_{1,2}$ values given represent the maximal deviations. Since the self-medium data could be equally well interpreted with K_9 and K_{10}, we have to consider both of the two functions

$$K_9 = \Sigma B^{q_i}\beta_{9,q\,i} \text{ and } K_{10} = \Sigma B^{q_k}\beta_{10,q_k} \quad (19)$$

where q_i and q_k may take a series of values.

Each of the plots log K_9(log B) and log K_{10}(log B) could be well represented with a straight line, which had a slope of 5 for log K_9(log B) and of 6 for log K_{10}(log B). These results can be explained in the simplest way by assuming the formation of $La_5(OH)_9^{6+}$ (for $p = 9$) and $La_6(OH)_{10}^{8+}$ (for $p = 10$). The calculations are illustrated in Fig. 4a where (log $K_9 - q_i$ log B) is plotted against B for $q_i = 4$, 5 and 6, and in Fig. 4b where (log $K_{10} - q_k$ log B) is plotted against B for $q_k = 5$, 6 and 7. It is seen, that log $\beta_{9,5}$ and log $\beta_{10,6}$ prove to be constant within the limits of experimental uncertainty, whereas a great systematic trend is found for the adjacent q values. Moreover, the deviation from constancy changes sign when q passes through 5 and 6. We can read off from the figures the values

$$\log \beta_{9,5} = \log \{[La_5(OH)_9]h^9b^{-5}\} = -71.4 \pm 0.2$$

or

$$\log \beta_{10,6} = \log \{[La_6(OH)_{10}]\ h^{10}b^{-6}\} = -78.8 \pm 0.2$$

which may be regarded as first approximations.

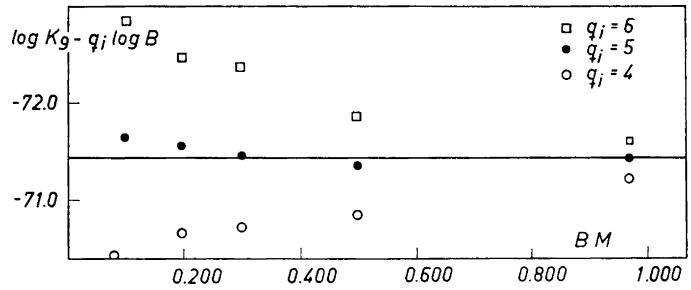

Fig. 4a. log $K_9 - q_i$ log B (eqn. (19)) as a function of B for $q_i = 4$, 5 and 6. The points for $q_i = 4$ have been shifted vertically by + 0.2 and those for $q_i = 6$ by −0.2 units.

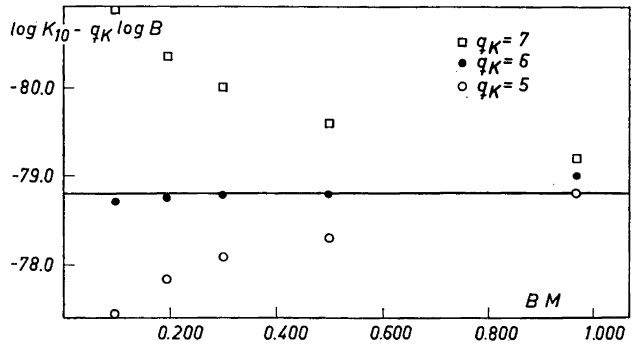

Fig. 4b. log $K_{10} - q_k$ log B (eqn. (19)) as a function of B for $q_k = 5$, 6 and 7. The points for $q_k = 5$ have been shifted vertically by + 0.2 and those for $q_k = 7$ by −0.2 units.

III. Comparison of the data with normalised projection maps

In the preceding section probable values for the q—s and the $\beta_{p,q}$—s were derived by analysing the dependence of the overall equilibrium constants, K_p, on B. The conclusions drawn on the basis of these calculations must be regarded as preliminary ones, because they are appreciably influenced by the uncertainty of the numerical values of the K_p—s. Moreover, the results of section II are in such a remote contact with the data, that it is difficult to estimate the effect of the experimental uncertainty.

In order to check the previously estimated q and $\beta_{p,q}$ values a plot covering the complete set of the experimental data was compared with groups of normalised functions. Since the same plot may be compared with groups of functions representing different hypotheses, it may be inferred whether the experimental accuracy is sufficient to make a decision between these different hypotheses. This highly effective way to analyze experimental data when three variables must be considered, has been proposed by Sillén [14]. The method of calculation described in a previous work [15] was followed closely.

First, the experimental $Z(\log h)_B$ data were recalculated to the form $\log B\ (\log B - 2 \log h)_Z$, by interpolation. A plot of $\log B\ (\log B - 2 \log h)_Z$ was then compared with two groups of normalised functions, both of which were calculated by assuming the formation of three species. For the first group the hypothesis was made that the species have the composition $LaOH^{2+}$, La_2OH^{5+} and $La_5(OH)_9^{6+}$ (hypothesis 5,9), whereas for the second the combination $LaOH^{2+}$, La_2OH^{5+} and $La_6(OH)_{10}^{8+}$ was chosen (hypothesis 6, 10).

The essential steps of the calculation will be described in some detail for the first hypothesis only; a closely analogous method was followed for the second.

We started with the fundamental equations

$$B = b(1 + \beta_{1,1}h^{-1} + 2\,\beta_{1,2}bh^{-1} + 5\,\beta_{9,5}b^4h^{-9}) \tag{20}$$

and

$$BZ = b(\beta_{1,1}h^{-1} + \beta_{1,2}bh^{-1} + 9\,\beta_{9,5}b^4h^{-9}) \tag{21}$$

Introducing the new variables

$$\beta_{1,1}h^{-1} = a,\ (\beta_{9,5}\beta_{1,1}^{-1})^{1/4}bh^{-2} = u \tag{22}$$

and

$$\beta_{1,2}(\beta_{1,1}^{5}\beta_{9,5}^{-1})^{1/4} = \gamma \tag{23}$$

eqns. (20) and (21) can be written

$$B = (\beta_{1,1}^{9}\beta_{9,5}^{-1})^{1/4}a^{-2}u(1 + a + 2\gamma ua^{-1} + 5u^4a) \tag{24}$$

$$Z = \frac{a + \gamma ua^{-1} + 9\,u^4a}{1 + a + 2\gamma ua^{-1} + 5\,u^4a} \tag{25}$$

Eliminating a from (24) and (25), and keeping Z and γ constant, B can be expressed as a function of the single variable u

$$B = B(u)_{Z,\gamma} \tag{26}$$

We then constructed, on the basis of (26), (25) and (24), the normalised functions $Y(u)_Z$ and $X(u)_Z$; the calculations were made with the aid of a Ferranti-Mercury high-speed computer.

$$Y = \log u - 2 \log a + \log (1 + a + 2\gamma u a^{-1} + 5u^4 a) = \log B - \tfrac{9}{4} \log \beta_{1,1} + \tfrac{1}{4} \log \beta_{9,5} \quad (27)$$

and

$$X = Y + 2 \log a = \log B - 2 \log h - \tfrac{1}{4} \log \beta_{1,1} + \tfrac{1}{4} \log \beta_{9,5} \quad (28)$$

Y and X, which represent the normalised form of $\log B$ and $(\log B - 2 \log h)$, were calculated for a series of Z values ranging from 0.003 to 0.015. Log γ values ranging from -4.20 to -4.90 were considered. Each group of functions calculated with a particular γ value was superimposed on the plot $\log B(\log B - 2 \log h)_Z$. The best agreement was obtained with $\log \gamma = -4.70$. The differences $X - (\log B - 2 \log h)$ and $Y - \log B$ were read off, in the position of best fit, and then the most probable values of the constants $\log \beta_{1,1}$, $\log \beta_{1,2}$ and $\log \beta_{9,5}$ could be calculated using (23), (27) and (28). The results are given in Table 5.

Table 5. Survey of the calculated equilibrium constants, $\beta_{p,q}$.

Method	$-\log \beta_{1,1}$	$-\log \beta_{1,2}$	$-\log \beta_{9,5}$	$-\log \beta_{10,6}$
Projection map Hypothesis (5,9) $LaOH^{2+}$, La_2OH^{5+} and $La_5(OH)_9^{6+}$	10.1 ± 0.1	$9.9_2 \pm 0.1$	$71.4_4 \pm 0.1$	–
Hypothesis (6,10) $LaOH^{2+}$, La_2OH^{5+} and $La_6(OH)_{10}^{6+}$	10.1 ± 0.1	$9.9_7 \pm 0.1$	–	$78.7_5 \pm 0.1$
$K_p(B)$ Eqn. (18)	10.1 ± 0.15	10.0 ± 0.3	–	–
Eqn. (19)	–	–	$71.4_5 \pm 0.2$	78.8 ± 0.2
Probable value	10.1 ± 0.1	$9.9_5 \pm 0.1$	$71.4_5 \pm 0.1$	$78.7_5 \pm 0.1$

When the data were compared with normalised curves representing hypothesis (6, 10) the best agreement was found for the $\log \beta_{1,1}$, $\log \beta_{1,2}$ and $\log \beta_{10,6}$ values shown in Table 5.

The results of all these calculations are illustrated in Fig. 5, which shows that the experimental data can be represented equally satisfactorily by hypothesis (5,9) or (6,10), using the constants given in Table 5. It is seen that the values of the equilibrium constants obtained in section II (shown in Table 5) are in good agreement with those calculated on the basis of the normalised functions (27) and (28).

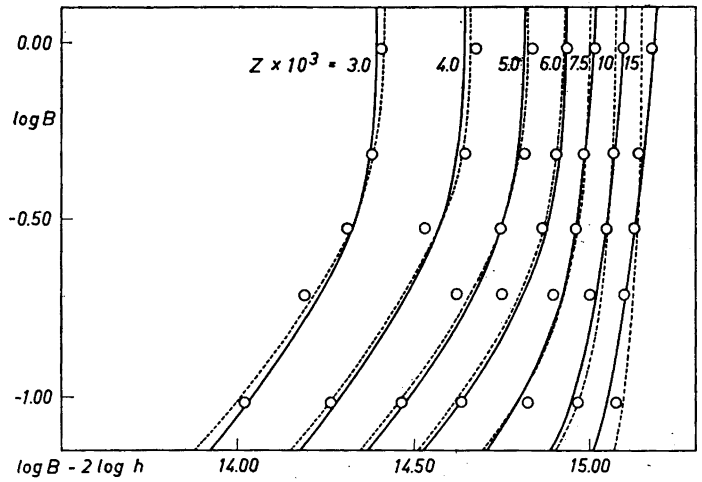

Fig. 5. log B as a function of (log B − 2 log h) for Z values 0.003 to 0.015. Circles: experimental points. The full-drawn curves have been calculated with hypothesis (5,9), the dotted curves with hypothesis (6, 10). The constants given in Table 5 were used.

Finally we may consider Fig. 1. The full-drawn curves represent hypothesis (5,9), the dotted curves hypothesis (6,10). Both of them seem to describe satisfactorily the experimental data of present accuracy.

It must be pointed out that our conclusions concerning the number of lanthanum atoms present in the hydrolysed species, q, include the uncertainty caused by the unknown variation of the activity factors, whereas this complication is of no importance for the determination of p (the number of OH groups bound to the hydrolysis products). We are inclined to believe that the proposed values of q are not far from the correct ones, and that the main effect of the variation of the activity factors is an increased uncertainty in the numerical values of the equilibrium constants $\beta_{p,q}$. There is some experimental evidence [16] which suggests that when the inert cation is largely replaced by the reacting cation, in solutions where $[ClO_4^-] = 3$ M, the individual activity factors of the reacting ions change considerably, but certain combinations of them vary only slightly, *e.g.* $f(In^{3+})f(H^+)^{-3}$.

Acknowledgements. We are indebted to Professor Lars Gunnar Sillén for his great interest in this work and for his valuable criticism. We thank Dr. Clara Berecki-Biedermann for many helpful suggestions. We thank Dr. Derek C. Lewis for improving the English text. Mr Frans Ericson has been of great help by making many parts of our equipment.

One of the authors (L.C.) would like to take the opportunity to thank Professor Arnaldo Liberti, Messina, Italy, for introducing him to the interesting field of coordination chemistry.

This work was financially supported by *Statens Naturvetenskapliga Forskningsråd (Swedish Natural Science Research Council)* and the *Air Force Office of Scientific Research of the ARDC, USAF*, through its European Office, on contract no. AF 61(052)—162.

The financial support of the *Italian Foreign Office* for an interchange grant with *Svenska Institutet för Kulturellt Utbyte med Utlandet* to L.C. is gratefully acknowledged.

REFERENCES

1. Vesterberg, K. A. *Z. anorg. Chem.* **94** (1916) 371.
2. Moeller, T. *J. Phys. Chem.* **50** (1946) 242.
3. Wheelwright, E. J., Spedding, F. H. and Schwarzenbach, G. *J. Am. Chem. Soc.* **75** (1953) 4196.
4. Busey, H. M. and Cowan, H. D. *USAEC, LAMS-1105* (1950), quoted by Kraus, K. A. in *Proc. Intern. Conf., Geneva* **7** (1955) 245.
5. Lewis, D. C. *Chem. & Ind. (London)* **1957** 1238.
6. Hedström, B. O. A. *Arkiv Kemi* **6** (1953) 1.
7. Biedermann, G. and Hietanen, S. *Acta Chem. Scand.* **14** (1960) 711.
8. Hietanen, S. and Sillén, L. G. *Acta Chem. Scand.* **13** (1959) 533.
9. Gran, G. *Analyst* **77** (1952) 661.
10. Kolthoff, I. M. and Elmquist, R. *J. Am. Chem. Soc.* **53** (1931) 1225.
11. Forsling, W., Hietanen, S. and Sillén, L. G. *Acta Chem. Scand.* **6** (1952) 901.
12. Brown, A. S. *J. Am. Chem. Soc.* **56** (1934) 646.
13. Sillén, L. G. *Acta Chem. Scand.* **10** (1956) 186.
14. Sillén, L. G. *Acta Chem. Scand.* **10** (1956) 803.
15. Biedermann, G. and Sillén, L. G. *Acta Chem. Scand.* **10** (1956) 1011.
16. Biedermann, G. *To be published.*

Received January 4, 1961.

ACTA CHEMICA SCANDINAVICA 15 (1961) 1367–1371

Piperazine Compounds Containing a 2,6-Dimethylphenyl Residue

RICHARD DAHLBOM* and ALFONS MISIORNY

Research Laboratories, AB Astra, Södertälje, Sweden

A number of piperazine compounds containing a 2,6-dimethylphenyl residue were prepared and tested for local anesthetic, ataractic and sedative properties. No appreciable effects were found.

In connection with investigations on local anesthetics of the aminoacylanilide type a series of compounds were prepared using an N-substituted piperazine as the amine component (type I, X = $-NHCOCH_2-$ or $-NHCOCH(C_2H_5)-$). As an extension of this work a number of compounds were prepared in which the 2,6-dimethylphenyl and piperazine residues were joined by a carbamoyl (II, X = $-NHCO-$) or a carbonyl (III, X = $-CO-$) group.

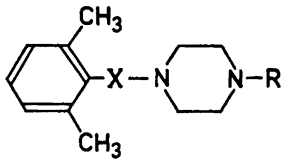

I. X = $-NHCOCH_2-$, $-NHCOCH(C_2H_5)-$

II. X = $-NHCO-$

III. X = $-CO-$

R = CH_3, $-CH_2CH=CH_2$, $-CH_2C_6H_5$, $-CH_2CH_2OH$, $-COOC_2H_5$, $-CH_2COOC_2H_5$

The new compounds were synthesized by treating an N-substituted piperazine derivative with the following: halogenoacyl-2,6-dimethylaniline (method A); 2,6-dimethylphenyl*iso*cyanate (method B); or 2,6-dimethylbenzoyl chloride (method C).

The N-methylpiperazine derivatives (R = $-CH_3$) could also be smoothly prepared from the corresponding urethanes (R = $-COOC_2H_5$) according to

* Present address: Department of Chemistry, Kungl. Farmaceutiska Institutet, Stockholm, Sweden.

Table 1. Piperazines containing a 2,6-dimethylphenyl group.

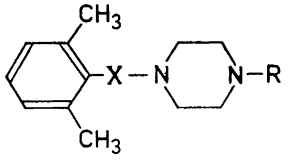

No.	X	R	Method	Yield %	Derivative	M.p. °C	Recryst. Solvent [a]	Formula	Calc. % C	Calc. % H	Calc. % N	Found % C	Found % H	Found % N
1	$-NHCOCH_2-$	$-COOC_2H_5$	A	92	Base	94–95	L	$C_{17}H_{25}N_3O_3$	63.9	7.89	13.2	63.9	7.82	13.3
2	»	$-CH_3$	A	70	2 HCl	267–268 (d)	E-Aq	$C_{15}H_{23}N_3O \cdot 2\,HCl$	53.9	7.54	21.2	54.0	7.54	21.0
			D	66	2 HCl	267–268 (d)	E-Aq							
3	»	$-CH_2C_6H_5$	A	73	Base	145–146	M	$C_{21}H_{27}N_3O$	74.7	8.07	12.45	74.6	7.99	12.3
4	»	$-CH_2COOC_2H_5$	A	62	Base	83– 84	L	$C_{18}H_{27}N_3O_3$	64.8	8.16	12.6	64.7	8.27	12.6
5	»	$-CH_2CH_2OH$	D	99	Base	111–112	L-B	$C_{16}H_{25}N_3O_2$	65.9	8.65	14.4	65.7	8.52	14.4
			A	84	Base	111–112	L-B							
6	»	$-CH_2CH=CH_2$	A	52	Base	88– 89	L	$C_{17}H_{25}N_3O$	71.0	8.77	14.6	71.0	8.40	14.4
7	$-NHCOCH(C_2H_5)-$	$-COOC_2H_5$	A	45	Base	127–128	L-B	$C_{19}H_{29}N_3O_3$	65.6	8.41	12.1	65.5	8.21	11.8
8	»	$-CH_2COOC_2H_5$	A	31	Base	91– 92	L	$C_{20}H_{31}N_3O_3$	66.5	8.64	11.6	66.5	8.64	11.6
9	$-NHCO-$	$-COOC_2H_5$	B	98		231–232	M	$C_{16}H_{23}N_3O_3$	62.9	7.59	13.7	63.1	7.66	13.9
10	»	$-CH_3$	D	86	Base	198–199	B	$C_{14}H_{21}N_3O$	68.0	8.56	17.0	68.0	8.32	16.8
11	»	$-CH_2C_6H_5$	B	97	Base	235–236	M	$C_{20}N_{25}N_3O$	74.3	7.79	13.0	74.6	7.77	13.2
12	»	$-CH_2COOC_2H_5$	B	91	Base	132–134	B	$C_{17}H_{25}N_3O_3$	63.9	7.89	13.2	64.2	7.68	13.2
13	»	$-CH_2CH_2OH$	D	63	Base	164–165	B	$C_{15}H_{23}N_3O_2$	64.9	8.36	15.2	65.1	8.37	15.2
			B	97	Base	164–165	B							
14	»	$-CH_2CH=CH_2$	B	89	Base	171–172	E-Aq	$C_{16}H_{23}N_3O$	70.3	8.48	15.4	70.5	8.47	15.5
15	$-CO-$	$-CH_3$	D[b]	92	HCl	267–268 (d)	E	$C_{14}H_{20}N_2O \cdot HCl$	62.6	7.88	10.4	62.2	7.83	10.3
			C	62	HCl	267–268 (d)	E							
16	»	$-CH_2C_6H_5$	C	56	HCl	257–259	E	$C_{20}H_{24}N_2O \cdot HCl$	69.6	7.30	8.12	69.6	7.63	7.98
17	»	$-CH_2COOC_2H_5$	C	93	Base	206–207	E-Et	$C_{17}H_{24}N_2O_3 \cdot HCl$	59.9	7.39	8.22	59.3	7.35	7.99
18	»	$-CH_2CH_2OH$	D	90	HCl	184–185	E-Et	$C_{15}H_{22}N_2O_2 \cdot HCl$	60.5	7.78	9.41	60.2	7.59	9.69
19	»	$-CH_2CH=CH_2$	C	69	HCl	222–224	E-Et	$C_{16}H_{22}N_2O \cdot HCl$	65.2	7.86	9.50	64.9	7.97	9.43

a E, ethanol; Et. ether; Aq, water; B, benzene; M, methanol; L, ligroin.

b The starting material for this reduction, 1-(2,6-dimethylbenzoyl)-4-ethoxycarbonylpiperazine, was prepared by method C but could not be obtained in crystalline form. Therefore it was used without further purification.

Table 2. Piperazinoacylbenzhydrylamines and phenothiazines.

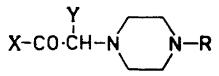

No.	X	Y	R	Method	Yield %	Derivative	M.p. °C	Recryst. Solvent[a]	Formula	Calc. %			Found %		
										C	H	N	C	H	N
20	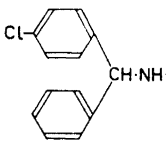	H	$-COOC_2H_5$	A	90	$HClO_4$	214–216 (d)	E-Aq	$C_{22}H_{26}ClN_3O_3 \cdot HClO_4$	51.2	5.27	8.14	51.4	5.34	8.02
21	»	»	$-CH_3$	A	73	Base	143–144	M-Aq	$C_{20}H_{24}ClN_3O$	67.1	6.76	11.7	66.8	6.84	11.4
22	»	»	$-CH_2COOC_2H_5$	A	77	2 HCl	201–203 (d)	E	$C_{23}H_{28}ClN_3O_3 \cdot 2\ HCl$	54.9	6.01	8.36	55.2	6.13	8.11
23	»	»	$-CH_2CH_2OH$	A	69	2 HCl	254–256 (d)	E-Aq	$C_{21}H_{26}ClN_3O_2 \cdot 2\ HCl$	54.7	6.12	9.12	54.5	6.32	9.07
24	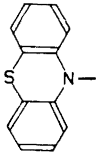	»	$-CH_2C_6H_5$	A	72	Base 2 HCl	141–142 227–229 (d)	E-Aq M-Et	$C_{25}H_{25}N_3OS$ $C_{25}H_{25}N_3OS \cdot 2\ HCl$	72.3 61.5	6.06 5.57	10.1 8.60	72.4 61.1	6.06 5.75	10.0 8.73
25	»	$-CH_3$	»	A	80	Base 2 HCl	135–136 213–214	E-Aq M-Et	$C_{26}H_{27}N_3OS$ $C_{26}H_{27}N_3OS \cdot 2\ HCl$	72.7 62.1	6.34 5.82	9.79 8.36	72.8 61.9	6.28 6.06	9.62 8.22

a See Table 1.

the excellent method of Dannley *et al.*[1] (method D). (This method involves preparation of methylamines from urethanes by reduction with lithium aluminium hydride). The β-hydroxyethyl compounds (R = $-CH_2CH_2OH$) were alternatively prepared by reduction of the corresponding ethoxycarbonylmethyl derivative (R = $-CH_2COOC_2H_5$).

The compounds and their properties are listed in Table 1. The new compounds were tested for local anesthetic action on rabbit cornea, using Xylocaine as standard. The observed effects were slight and it is evident that the piperazine residue decreases the anesthetic potency in the aminoacylanilide type of local anesthetics.

Toxicity tests showed some compounds to have a sedative effect; attempts were therefore made to enhance this effect by replacing the 2,6-dimethylphenyl group by a *p*-chlorobenzhydryl or a phenothiazine residue (compounds 20—25 in Table 2). However, these compounds had little or no ataractic and sedative properties in pharmacological tests.

EXPERIMENTAL

The melting points were determined in an electrically heated metal block using calibrated Anschütz thermometers.

All compounds were dried at 50°/0.01 mm for 4 h before analysis.

1-Methylpiperazine and *1-(β-hydroxyethyl)-piperazine* are commercially available. *1-(Ethoxycarbonyl)-piperazine* [2], *1-benzylpiperazine* [3] and *ethyl 1-piperazineacetate* [4] were prepared by published methods. *1-Allylpiperazine* was prepared in 35 % yield from allylchloride and piperazine hexahydrate following the method for preparation of 1-benzylpiperazine given by Baltzly *et al.*[3]; b.p. 62—64°/11 mm.

α-Chloro-2,6-dimethylacetanilide [5], *α-bromo-2,6-dimethylbutyranilide* [6], *10-chloroacetylphenothiazine* [7], *10-(α-bromopropionylphenothiazine* [7], *2,6-dimethylphenylisocyanate* [8] and *2,6-dimethylbenzoylchloride* [9] were prepared according to procedures described in the literature.

N-(Chloroacetyl)-p-chlorobenzhydrylamine was prepared from chloroacetyl chloride and *p*-chlorobenzhydrylamine [10] in 64 % yield according to the method of Löfgren [5] for the chloroacetylation of amines. M.p. 116—117° after recrystallisation form ligroin-benzene. (Found: C 61.7; H 4.66; N 4.99. Calc. for $C_{15}H_{13}Cl_2NO$: C 61.2; H 4.45; N 4.76).

Piperazinoacylamines (*Method A*). A solution of the appropriate piperazine compound (0.125 mole) and a halogenoacylamine (0.05 mole) in benzene (50 ml) was refluxed. The reflux time was 2 h for compounds 1—4 and 5—6 h for compounds 5—8 and 20—25. Toluene was used as solvent in the preparation of compounds 24 and 25. After cooling to room temperature the amine hydrohalogenide was filtered and the filtrate extracted thoroughly with 2 N hydrochloric acid. The extract was made alkaline with 5 N sodium hydroxide. The reaction product usually separated as an oil which soon crystallised and was purified by recrystallisation. When the base failed to crystallize, it was extracted with ether and converted to the *hydrochloride* by the addition of an ethereal solution of hydrogen chloride.

2,6-Dimethylphenylcarbamoylpiperazines (*Method B*). A solution of 2,6-dimethylphenyl-*iso*cyanate (0.1 mole) and the appropriate piperazine derivative (0.12 mole) in benzene (50 ml) was refluxed for 2 h. On cooling, the reaction product separated in practically pure form.

2,6-Dimethylbensoylpiperazines (*Method C*). A solution of 2,6-dimethylbenzoyl chloride (0.05 mole) and the appropriate piperazine derivative (0.12 mole) in benzene (100 ml) was refluxed for 2 h. The reaction mixture was then worked up as described for method A.

Reductions of ethoxycarbonyl- and ethoxycarbonylmethylpiperazines by lithium aluminium hydride (*Method D*). The piperazine compound (0.02 mole) was added in small portions to a solution of lithium aluminium hydride (0.05 mole) in ether (200 ml). The mixture was

refluxed for 2 h and 2 N sodium hydroxide (10 ml) was added. The ether layer was separated, dried over sodium sulphate and evaporated. The residue was recrystallised or converted to the hydrochloride.

Physical constants and analytical data are collected in Tables 1 and 2.

REFERENCES

1. Dannley, R. L., Lukin, M. and Shapiro, J. *J. Org. Chem.* **20** (1955) 92.
2. More, T. S., Boyle, M. and Thorn, V. M. *J. Chem. Soc.* **1929** 39.
3. Baltzly, R., Buck, J. S., Lorz, E. and Schön, W. *J. Am. Chem. Soc.* **66** (1944) 263.
4. Braker, W. and Christiansen, W. G. *J. Am. Pharm. Assoc.* **22** (1933) 1950.
5. Löfgren, N. *Studies on Local Anesthetics.* (Diss.) Stockholm 1948, p. 25.
6. Dahlbom, R., Tegner, C., Willman, N.-E. and Löfgren, N. *To be published.*
7. Dahlbom, R. and Ekstrand, T. *Acta Chem. Scand.* **5** (1951) 102.
8. Dahlbom, R. and Österberg, L.-E. *Acta Chem. Scand.* **9** (1955) 1553.
9. Lock, G. and Schmidt, K. *J. prakt. Chem.* **140** (1934) 229.
10. Clemo, G. R., Gardner, C. and Raper, R. *J. Chem. Soc.* **1939** 1958.

Received February 20, 1961.

ACTA CHEMICA SCANDINAVICA 15 (1961) 1372–1380

On the Action of Human Whole Blood and Serum on β-Dimethylaminoethyl *p*-(*n*-amylamino)-Benzoate and Some Homologues

KAJ Ö. U. PERSSON

Research Laboratories, Draco, Lunds Farmaceutiska AB, Lund, Sweden

Blood and serum are shown to hydrolyze β-dimethylaminoethyl *p*-(*n*-amylamino)-benzoate and three homologues, *viz.* the *n*-butyl (tetracaine), *n*-hexyl, and *n*-heptyl derivatives. Simple spectrophotometric methods for the determination of the enzymic hydrolysis of β-dimethylaminoethyl *p*-(*n*-alkylamino)-benzoates by serum are described. The velocities of hydrolysis of the four esters are determined in different normal sera. The reaction is shown to be independent of substrate concentration within a concentration range of 1 to 1 000 μg/ml but strongly dependent on pH. Plasma and serum have the same hydrolytic activity towards the esters, whereas blood is only 60 % as active as serum or plasma. The low activity of whole blood depends on the contents of erythrocytes, which do not possess hydrolytic activity towards the present esters. The relative velocities of hydrolysis of the *n*-butyl, *n*-amyl, *n*-hexyl, and *n*-heptyl derivatives are found to be 0.45, 1.00, 0.92, and 0.74, respectively. The absolute values of reaction velocity of the *n*-amyl derivative in different sera range from 5.4 to 11.5 μmole/l · min at 37°C and pH 7.4. Conclusions regarding the relative toxicity of the esters are drawn.

This investigation was undertaken in order to learn about the fate and toxicity of the above-mentioned local anaesthetic esters in blood. Their hydrolysis velocities in blood and serum may give this information, since the hydrolytic products are β-dimethylaminoethanol[1], which is a normal metabolite and *p*-(*n*-alkylamino)-benzoic acids, which are relatively nontoxic. Thus, a high velocity of hydrolysis implies low toxicity. The suggestion that the toxicity of the esters is concerned with the velocity of their enzymic hydrolysis in blood is supported by the work of Foldes [2], which indicates that the toxicity of local anaesthetic agents depends on their plasma concentration, whatever their route of administration. Because of the goal of the investigation no fractionation of the serum to obtain a purified enzyme preparation was performed, nor was the identity of the enzyme with procaine esterase and/or serum choline esterase confirmed [3]. A survey of analytical methods suitable for analysis of substances rela-

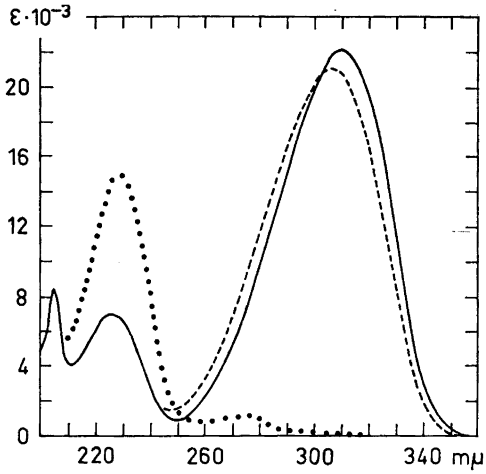

Fig. 1. Molecular extinction *vs.* wave length for β-dimethylaminoethyl *p*-(*n*-amylamino)-benzoate at three different pH values: . . . pH = 0.2; ——— pH = 6.8; — — — pH = 10.5. Temp. 23°C.

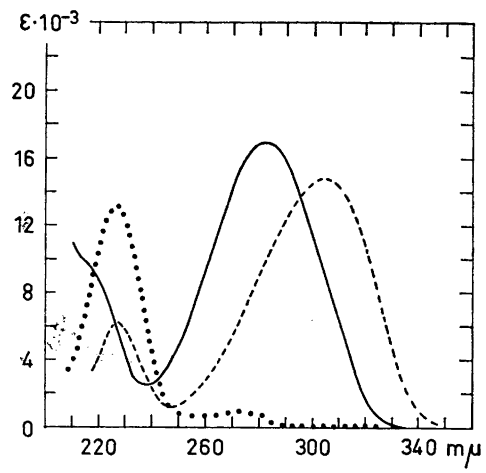

Fig. 2. Molecular extinction *vs.* wave length for *p*-(*n*-amylamino)-benzoic acid at three different pH values: . . . pH = 0.2; — — — pH = 3.7; ——— pH = 6.8. Temp. 23°C.

ted to β-dimethylaminoethyl *p*-(*n*-amylamino)-benzoate suggested that spectrophotometry would probably be the simplest and most accurate method for the determination of the enzymic hydrolysis of the *n*-butyl (tetracaine), *n*-amyl, *n*-hexyl, and *n*-heptyl derivatives (subsequently to be referred to as compounds 4-R, 5-R, 6-R, and 7-R, respectively). Measurements of the spectrophotometric data of the esters confirmed this suggestion. However, the strongly U.V. light-absorbing proteins of the sera interfered with the absorption measurements of the esters. Two methods were worked out to avoid this interference. One method employed spectrophotometric measurements directly on the incubation mixtures, which consisted of extensively diluted sera and substrates. In this case the possibility of the influence of enzyme-substrate complex formation and U.V. light radiation on the accuracy of the method had to be investigated. The other method involved measurements on deproteinized samples of the incubation mixtures which were then moderately diluted. The two methods were used to elucidate the influence of substrate concentration and pH on the hydrolysis velocities of the esters in human serum, plasma, and blood. In order to obtain information about the normal differences of the hydrolytic activity

Table 1. Spectrophotometric data and pK_a values for the esters and their hydrolytic products.

	Molar ext. × 10^{-3} at 310 mμ and pH 7.4	pK_a for aniline group	pK_a for tert. amine group	pK_a for carboxyl group
Tetracaine, 5-R, 6-R, and 7-R	22.0	2.2	8.5	—
The corresponding *p*-(*n*-alkylamino)-benzoic acids	6.1	2.5	—	4.5

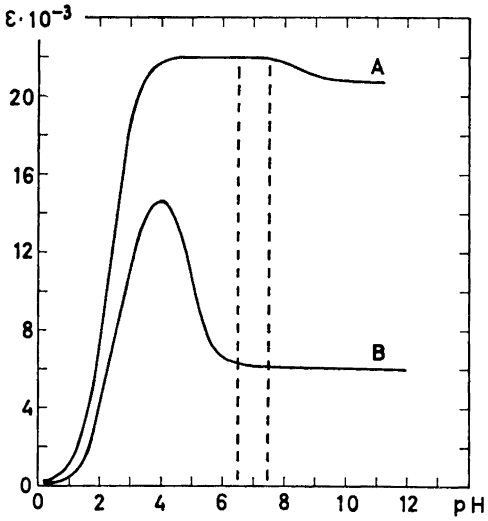

Fig. 3. Molecular extinction *vs.* pH at 310 mμ. *A* = β-dimethylaminoethyl *p*-(*n*-amylamino)-benzoate. B = *p*-(*n*-amylamino)-benzoic acid. Temp. 23°C.

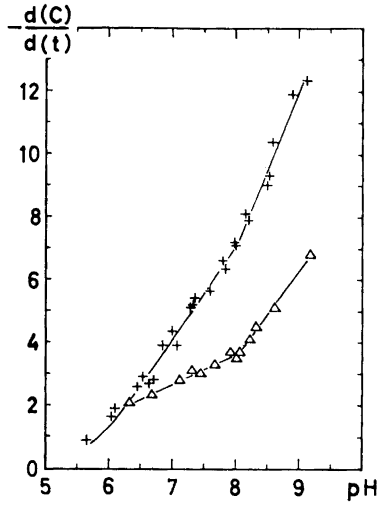

Fig. 4. Velocity of hydrolysis of β-dimethylaminoethyl *p*-(*n*-amylamino)-benzoate (5-R) *vs.* pH for two sera with different esterase activity. The ordinate refers to μg of the hydrochloride of 5-R hydrolyzed per ml per min at 37°C.

twelve samples of sera from different healthy persons of both sexes were investigated.

To ensure that the enzymic process was a hydrolysis the esters were incubated at 37°C with serum. The U.V. light-absorbing reaction products were isolated (see the experimental part) and identified in three different ways: 1, U.V. absorption spectra were measured at three different pH values and showed to be identical with those obtained with authentic *p*-(*n*-alkylamino)-benzoic acids (Fig. 2); 2, The melting points of the isolated acids coincided with the melting points of the corresponding authentic samples and so did the mixed

Table 2. Extinction ratios at 23°C. The figures are valid at pH 5—7.5 for tetracaine, 5-R, 6-R, and 7-R, and at pH 6.5 and upwards for their hydrolytic products.

	E_{270}/E_{280}	E_{300}/E_{280}	E_{310}/E_{280}	E_{280}/E_{310}
Tetracaine, 5-R, 6-R, and 7-R	—	2.03	2.26	0.44
The corresponding *p*-(*n*-alkylamino)-benzoic acids	0.85	0.66	0.36	2.78

	E_{300}/E_{310}	E_{320}/E_{310}	E_{330}/E_{310}
Tetracaine, 5-R, 6-R, and 7-R	0.89	0.88	0.52
The corresponding *p*-(*n*-alkylamino)-benzoic acids	1.87	—	—

melting points; 3, The paper-ionophoretic mobilities of the isolated substances were the same as for the authentic samples.

The U.V. absorption spectra measurements of tetracaine [4], 5-R, 6-R, and 7-R showed that the extinction coefficients were identical at different pH values throughout the range tested and thus the pK_a values of the ionizable groups (the aniline and tertiary amine groups). (See Figs. 1 and 2, and Tables 1 and 2.) This is also the case with the U.V. light-absorbing hydrolytic products, the *p*-(*n*-alkylamino)-benzoic acids. (Figs. 2 and 3, and Tables 1 and 2.) β-Dimethylaminoethanol has practically no absorption in the region above 260 mμ. As is evident from Figs. 1, 2, and 3, 310 mμ is a suitable wave length for concentration measurements if the pH value lies between 6.5 and 7.5. Thus, the spectrophotometric data provide a sound basis for the determination of the rates of hydrolysis of the four esters.

However, the difficulty of getting rid of the very strongly U.V. light-absorbing proteins of the sera also had to be overcome. (Too high background extinction will cause great uncertainty in the extinction readings originating from the esters or even make extinction measurements impossible.) This difficulty was overcome in two ways. The first included use of dilute sera (dilution 1:50). The second involved denaturation of the interfering protein material with 7 % perchloric acid, subsequent centrifugation and absorption measurements at 23°C on the appropriately diluted and buffered supernatants.

By using dilute sera it was possible to measure the absorption changes of the incubation mixtures directly in the cuvettes, which in this case were held at 37°C by means of a thermostatically controlled cuvette housing. (All incubations were performed at 37°C.) In this way the rates of hydrolysis were measured at starting concentrations of the esters ranging from 1—10 μg/ml. The second method had to be used at higher ester concentrations. The lowest limit of substrate concentration, 1 μg/ml, is given by the magnitude of the extinction coefficients, the upper limit by the solubility of the hydrolytic products (the *p*-(*n*-alkylamino)-benzoic acids). The solubility of the amyl-, hexyl-, and heptylaminobenzoic acids at 25°C and pH 7.5 are about 1 000, 500, and 330 μg/ml, respectively.

Enzyme-substrate complex formation sometimes interferes with the measurement of the absorption of the substrate. Therefore it is necessary to consider this possibility whenever spectrophotometry is carried out directly on an incubation mixture. Such disturbances were without significance in the first case described above, as the extrapolated "starting" extinctions of the incubation mixtures and the extinctions at the end of the hydrolysis followed the calculated values well within the limits of the accuracy of the method.

It is well known that U.V. radiation denatures proteins. However, any influence of the light of the spectrophotometer on the enzyme activity was not detected, presumably due to the short exposure time and the low intensity of the light beam.

In the second case the values of the "starting" extinctions (extrapolated) and the "end" extinctions did not reach the calculated values as in the first case (for tetracaine, however, they did). The obtained values were too low; 5-R gave 3—7 %, 6-R 7—13 %, and 7-R about 20 % too low values. These findings may be explained to be due to some kind of linking between the dena-

tured protein and the substrates. Corrections for the discrepancies were simply made for every determination by extrapolation of the extinctions to zero time and comparison with the calculated value. Moreover, the obtained correction factors were the same in different experiments with the same substrate, provided that the relation between serum concentration and perchloric acid concentration was identical.

The determinations of the reaction velocities were in most cases performed with serum as the enzyme source. However, to get a correlation between the rates of hydrolysis in serum and whole blood additional determinations on blood were necessary. As the whole blood was heparinized the action of heparin on the reaction velocity was also investigated. The heparinized and nonheparinized blood (from which serum was obtained after coagulation) was taken from the same individuals on the same occasion. Blood from three different persons was investigated to obtain a sure correlation. Serum, plasma (from centrifugation of heparinized blood) and serum + heparin (0.5 mg/ml) hydrolyzed each of the esters with identical velocities. The pH was carefully controlled (*cf.* Fig. 4). Thus heparin did not affect the hydrolysis. In blood the hydrolysis proceeded with velocities which were only 60 % of those obtained with serum or plasma. Temperature, pH, and substrate concentration were identical in the different cases, *viz.* 37°C, 7.4, and 0.25 mM. As 40—45 % of the blood volume is occupied by erythrocytes, it may be concluded that these do not possess hydrolytic activity towards the present esters. This was confirmed through experiments with washed erythrocytes, hemolysate, and erythrocyte cell membranes ("ghosts" which contain the specific acetylcholinesterase of erythrocytes). The reason why whole blood was not chosen as the enzyme source in all determinations was that its high protein content (about 20 % whereas serum has about 7 %) made greater dilution necessary and hence the reaction time much longer. Moreover, direct spectrophotometry at low substrate concentrations was impossible to perform due to the strong absorption and the heterogeneity of blood.

Dilution of serum did not affect the activity of the hydrolytic enzyme(-s) if the dilution was not very great. In these experiments the pH was in each case carefully adjusted to that of the undiluted serum *i.e.*, between 7.6 and 7.8. A fivefold dilution of the serum decreased the reaction velocity to 20 % of the original value as expected, whereas a fiftyfold dilution decreased the reaction velocity to 1.70—1.75 % of the original value (expected value 2 %). The buffer system used in these experiments was 0.05 M trishydroxymethylaminomethane-HCl. The possibility of increasing the enzyme activity to the expected value by using other ionic strengths of the buffer solution or other buffer systems was not investigated.

RESULTS AND DISCUSSION

The relation between reaction velocity and pH was determined at a substrate concentration of 0.25 mM (the starting value) and a serum to buffer ratio of 1:1. Acetate buffers, 0.1 M, were used at pH 7 and below, 0.05 M "tris" buffers between pH 7 and 8.5 and glycine buffers above pH 8.5. As the buffering capacity of serum is rather great, the pH of the serum-buffer mixtures

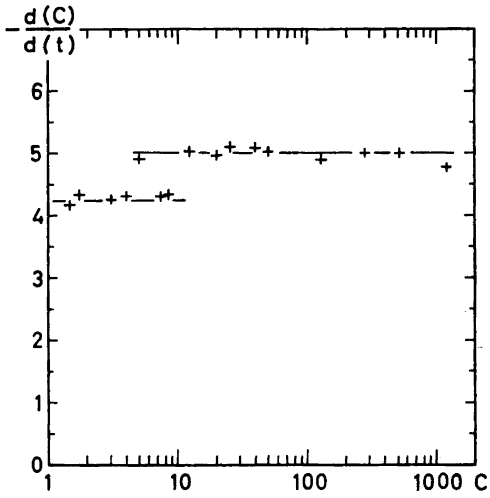

Fig. 5. Velocity of hydrolysis of β-dimethylaminoethyl *p*-(*n*-amylamino)-benzoate (5-R) at pH 7.4 and 37°C *vs.* substrate concentration. C = μg of the hydrochloride of 5-R per ml. $-\frac{d(C)}{d(t)}$ = μg of the hydrochloride of 5-R hydrolyzed per ml per min. The two parts of the diagram correspond to experiments at different dilutions of the serum used. The right part was performed at a serum to buffer ratio of 1:1, the left part at a ratio of 1:49. The obtained values have been converted to those assumed for undiluted serum and plotted. See text.

had to be controlled at 37°C (the incubation temperature) before every experiment. The buffer systems used were without influence on the reaction velocity. This was shown for the "tris" buffer (see above) and then for the other buffers by comparison with the "tris" buffers in the pH regions where both "tris", acetate, and glycine buffers, respectively, were utilizable. Two characteristic curves of the reaction velocity-pH dependence for 5-R (two different sera) are shown in Fig. 4. Two other sera were investigated in the same way. Intermediate values of the slopes were obtained. The differences of the slopes are hard to explain, however, similar results were obtained with the other esters. Some considerations may be made. As the reaction apparently follows zero order kinetics (see below), the variation of the ion species of the substrates ($pK_a = 8.5$) cannot be responsible for the great pH dependence of the reaction velocity. It is more adequate to ascribe this dependence to ionization phenomena of groups at the active site of the enzyme (*cf.* Krupka and Laidler [5]). In this connection it is important to stress that nonenzymic hydrolysis is entirely negligible in the pH-range investigated [4], which was shown by experiments performed at 37°C in plain buffer solutions and in sodium arsenite-poisoned sera. More definite explanations of the strong pH dependence may not be given until highly purified and homogeneous enzyme preparations are available for investigation. The practical consequence is quite obvious: pH has to be carefully controlled in order to get a satisfactory comparison of the velocity of hydrolysis between different sera and with different substrate concentrations.

The correlation between reaction velocity and substrate concentration for 5-R is shown in Fig. 5. The left part of the curve was obtained according to the first method described above (*i.e.*, direct spectrophotometry on mixtures with diluted sera), the right part according to the second method. The influence of extensive dilution on the reaction velocity is obvious. The shape of the curves for tetracaine, 6-R, and 7-R was exactly the same as for 5-R. These curves are not plotted in Fig. 5 for the sake of clarity. The reaction follows "zero" order

Table 3. Velocity of hydrolysis of tetracaine (4-R), 5-R, 6-R, and 7-R at 37°C and pH 7.4. The figures refer to μg of substrate (hydrochloride) hydrolyzed per ml of undiluted serum per min. The velocity is independent of substrate concentration.

Serum No.	4-R	5-R	6-R	7-R
1	1.44	2.98	2.82	2.3
2	1.40	3.10	2.56	2.2
3	1.70	3.84	3.46	2.5
4	1.72	3.88	3.76	2.9
5	1.94	4.18	4.06	3.0
6	2.08	4.54	4.20	3.0
7	2.26	5.32	4.54	4.0
8	2.58	5.70	5.60	4.0
9		2.90		
10		3.10		
11		5.00		
12		5.30		

kinetics throughout the substrate concentration range investigated. This range extends from 1—1 200 μg/ml for tetracaine and 5-R, from 1—500 μg/ml for 6-R, and from 1—20 μg/ml for 7-R. (The figures refer to μg of the hydrochlorides of the substances.) Thus, the Michaelis-Menten constant cannot be calculated from the obtained data. It is possible, however, to establish that the value of the constant is less than 2×10^{-6} mole/litre which indicates a great affinity of the substrates for the enzyme.

In Table 3 are summarized the results from experiments with different sera and substrates. It is seen from the table that tetracaine was hydrolyzed at a speed of about 45 % of that of 5-R. The corresponding figures for 6-R and 7-R were 92 % and 74 %. The velocities of hydrolysis in whole blood are 60 % of those in sera (see above) and thus the ranges of these velocities in blood for tetracaine, 5-R, 6-R, and 7-R are 0.8—1.6 μg/ml · min, 1.7—3.5 μg/ml · min, 1.6—3.2 μg/ml · min, and 1.3—2.6 μg/ml · min, respectively.

Due to the high decomposition rates of these esters in the vascular system they do not accumulate and hence they are assumed to be comparatively non-toxic if not given in massive doses. Evidently toxicity also concerns the varying influence on relevant enzyme systems. In this connection it is of interest to consider the strongly decreased activity of the specific acetylcholinesterase caused by the esters. The ester concentrations that cause 50 % inhibition of the activity of this enzyme are 0.32×10^{-3} M, 0.18×10^{-3} M, 0.95×10^{-4} M, and 0.55×10^{-4} M for tetracaine, 5-R, 6-R, and 7-R, respectively [6]. If these figures are assumed to be representative for the potencies of the esters with regard to their action and toxicity, some conclusions may be drawn. Tetracaine is hydrolyzed half as rapidly as 5-R and is about half as active as an enzyme inhibitor. Therefore the toxicity may presumably be the same for these two esters. LD_{50} has been determined to 0.683 ± 0.019 g/kg for tetracaine and to 0.672 ± 0.028 g/kg for 5-R (oral administration to rat). In regard to the above assumption 6-R ought to be twice and 7-R four times as toxic as 5-R or tetracaine. Experiments on intravenous administration of tetracaine to homo for the purpose of comparing the toxicity of some local anaesthetics have revealed that doses of 35—60 mg given at a rate of 0.125 mg/kg · min involve no danger [2]. Most probably these figures also apply to 5-R when administered in the same way.

EXPERIMENTAL

Materials. The blood was taken from the antecubital vein of healthy persons of both sexes. Plasma was obtained through centrifugation of heparinized blood and serum from coagulated blood. When stored at 0°C the esterase activities of the sera were unchanged for at least 14 days provided the preparations were performed aseptically. The esters were synthesized in this laboratory according to the methods described in Swed. pat. 5561/59 and 5339/60. The *p-n*-alkylaminobenzoic acids were formed through boiling slightly alkaline sodium *p*-aminobenzoate solutions with *n*-alkylbromide under reflux. The acids were isolated as precipitates since the pH had been adjusted to 3.8 and the temperature to about 0°C. (Fig. 3, curve B). The washed precipitate was recrystallized from ethanol-water. (*Cf.* the above-mentioned patents.) The melting points were 135°—137°C, 122°—124°C, and 107°—109°C for *p-n*-amyl-, *p-n*-hexyl-, and *p-n*-heptylaminobenzoic acid respectively.

The acids were also prepared through enzymic hydrolysis. Mixtures of 50 ml serum and 50 ml 0.05 M "tris"-buffer (pH of the mixtures was 7.4) were shaken with the esters (100 mg) at 37°C for suitable lengths of time. The incubation mixtures were poured into vigorously stirred 100 ml portions of 7 % perchloric acid and the denaturated protein centrifuged off. The pH of the clear supernatants was adjusted to 3.8 with sodium hydroxide. The precipitates were collected after cooling, washed and recrystallized as above. The recoveries were 80 to 90 %. The melting points and mixed melting points coincided with those given above.

Other substances used were commonly available *p.a.* reagents.

Extinction measurements were performed with the Beckman model DU spectrophotometer provided with a cuvette housing whose bottom and walls were attachable to a water thermostat. It was possible to hold the desired temperature in the cell compartment within ± 0.05°C with this arrangement.

A pH-meter (Radiometer, Copenhagen) with glass electrode was used for pH determinations.

Continuous shaking of the incubation mixtures (the second case) was obtained with a "Microid" flask shaker (Griffin and George, London) provided with a suitably designed simple attachment.

Centrifugations were performed with a MSE Minor centrifuge (London).

The incubation temperature was held at 37.0° ± 0.05°C by means of an open water bath in which the reaction flasks were dipped (the second case).

All volumes were measured with calibrated pipettes. Voll pipettes were used for volumes greater than 2 ml and constriction pipettes ("Carlsberg pipettes") for 2 ml and smaller volumes. The error of one measurement of volume therefore was within ± 0.1 %.

Appropriate considerations were taken of the differences in temperature of the fluids to be measured.

Procedure for the first method. One part of serum was diluted to 50 parts with 0.05 M trishydroxymethyl aminomethane buffer and the pH was controlled at 37°C. 3 ml of this mixture were transferred to a 10 ml conical flask which was then shaken at 37.0°C for 10 min. 0.1 ml of the desired ester solution (in *aq. dest.*) was now added, the time was noted ("zero time"), and the mixture was quickly transferred into the cuvette (which was held at 37.0°C in the thermostatically controlled cuvette housing) with a suitable, prewarmed pipette. The extinction was read at 310 mμ against a similarly treated blank (water instead of ester solution) at intervals. The correctness of the blank was controlled at 360 mμ. The extinction readings at this wavelength ought to be zero (see Figs. 1 and 2). If they were not, the readings at 310 mμ were corrected according to the values obtained at 360 mμ.

Procedure for the second method. One part of buffer was mixed with one part of serum and the pH was controlled at 37.0°C. 3 ml of the mixture were transferred to a 10 ml small-necked conical flask which was stoppered and brought to 37.0°C as above. At zero time 0.1 ml ester solution were added. Aliquots of 0.5 or 0.2 ml (depending on substrate concentration) were withdrawn at intervals and denaturated through pouring into 0.5 ml portions of chilled (0°C) 7 % perchloric acid in small test tubes which were stored in an ice bath. Every withdrawal of a sample from the incubation mixture did not last more

than 20 sec. The times when half the parts of the aliquots had been denaturated were noted. The samples were shaken vigorously for 8 min and centrifugated. Then 0.5 or 0.8 ml of the supernatants were transferred to suitable volumes of 0.3 M phosphate buffer pH 7.5 and measured against a blank prepared in the same way. In this case the accuracy of the blank had to be controlled at 360 mμ for every sample and corrections had to be made if deviations from zero were found (see above).

Example: At a substrate concentration of 76.2 μg/ml of 5-R, 0.5 ml aliquots of the incubation mixture were denaturated with 0.5 ml of 7 % perchloric acid. Thereafter 0.5 ml of the supernatants of the denaturated samples were buffered with 3 ml phosphate buffer each. A dilution of 1:14 was thus obtained. The plot of extinction *versus* time gave a fall in extinction of 0.261 in 36 min. The calculated extinction at the beginning of the experiment was 0.379, the obtained value 0.365. Thus the correction factor was 0.379: 0.365 = 1.04. The molecular weight of 5-R (hydrochloride) is 314.8 and the molar extinction 22.0×10^3. The molar extinction of the hydrolysis product is 6.1 and hence the "molar extinction change" due to hydrolysis 15.9×10^3 at 310 mμ. The velocity of hydrolysis was $14 \times 0.261 \times \frac{1}{36} \times \frac{1}{15.9} \times 1.04 \times 314.9 = 2.09$ μg/ml · min. (The molecular weights of the hydrochlorides of tetracaine, 6-R, and 7-R are 300.8, 328.9, and 342.9, respectively.) In the undiluted serum the reaction velocity at the same pH ought to be $2.09 \cdot \frac{3.10}{1.50} = 4.32$.

Estimation of errors. An estimation of the maximal error of a single extinction determination involves the following points:

1: Dilution errors	± 1 %
2: Accuracy of spectrophotometry	± 2 %
3: Blank error	± 1 %
4: Time error (depends on time for complete hydrolysis)	± 0.5 – ± 3 %
5: Error due to uncertainty in pH determination (See Fig. 4)	± 2 %

A value of reaction velocity was obtained from the slope of the straight line: Extinction = f(time). This line was drawn by means of at least six different points and every value of reaction velocity was the average of two determinations. Hence, the error of the reported reaction velocities most probably is considerably below ± 7 %.

Determination of acetylcholinesterase activity. In these experiments the specific acetylcholinesterase of human erythrocyte cell walls ("ghosts") was used as enzyme and acetylcholine chloride as substrate. The esterase activity was determined with common Warburg technique [7]. The inhibitor concentrations that effected 50 % inhibition of the enzyme activity were determined at a substrate concentration of 3.30×10^{-3} M and at an enzyme concentration such that 44 % of the substrate was hydrolyzed in 30 min. Further details will be published elsewhere.

Acknowledgement. The author gratefully acknowledges the assistance of Miss B. Olsson and Mr. B. Bunke.

REFERENCES

1. Pepen, G., Freedman, D. X. and Giarman, N. J. *J. Pharmacol. Exptl. Therap.* **129** (1960) 291.
2. Foldes, F. F., Molloy, R., McNall, P. G. and Koukal, L. R. *J. Am. Med. Assoc.* **172** (1960) 89/1493.
3. Kalow, W. *J. Pharmacol. Exptl. Therap.* **104** (1952) 122.
4. Karlén, B. and Ågren, A. *Acta Chem. Scand.* **14** (1960) 197.
5. Krupka, R. M. and Laidler, K. J. *Trans. Faraday Soc.* **56** (1960) 1477.
6. Persson, K. Ö. U. *Unpublished paper.*
7. Augustinsson, K. B. *Acta Physiol. Scand.* Suppl. 52 (1948).

Received February 6, 1961.

ACTA CHEMICA SCANDINAVICA 15 (1961) 1381–1385

Isolation and Characterisation of an Acetylated Glucomannan from Pine (*Pinus silvestris* L.)

HANS MEIER

Träkemiska avdelningen, Svenska Träforskningsinstitutet, Stockholm Ö, Sweden

A mixture of polysaccharides isolated from pine holocellulose has been fractionated under conditions where acetyl groups are stable. A pure glucomannan was obtained with an acetyl content of 5.95 %, corresponding to a DS of 0.24. Periodate oxidation studies on the glucomannan showed that almost all of the acetyl groups are linked to carbon atoms 2 or 3 of the mannose residues. An almost pure glucurono-arabinoxylan isolated from the holocellulose dimethyl sulfoxide extract contained only traces of acetyl groups. It seems likely therefore, that most of the acetyl groups in pine wood are linked to the glucomannan fraction.

Hägglund *et al.*[1] reported that the hemicelluloses extracted from a spruce holocellulose with dimethyl sulfoxide had an acetyl content of 5.0 %. Among other sugars a hydrolysate of the extract contained 23.4 % mannose and 58.6 % xylose. After extraction with dimethyl sulfoxide, the holocellulose was treated with hot water, thereby affording a hemicellulose fraction with an acetyl content of 10.1 %. The hydrolysate of this fraction contained 66.4 % mannose and 14.4 % xylose. These results suggest that the acetyl groups in spruce wood hemicelluloses are linked principally to the glucomannan fraction; this is in contrast to birch wood where they are linked to the xylans [1,2].

The main difficulty in the investigation of partially acetylated polysaccharides lies in their isolation and their fractionation into pure components under conditions where the acetyl groups are retained. In the present investigation a partially acetylated glucomannan has been isolated in a pure state by using two new separation methods [3,4], and the position of the acetyl groups has been demonstrated by periodate oxidation studies.

A pine chlorite-holocellulose was extracted with dimethyl sulfoxide and then with hot water. The hemicelluloses from the hot water extract (Table 1) were dissolved in water and CTA-Br (cetyl-trimethylammonium bromide) was added [3]. The precipitate (fraction A, Table 1) was enriched in xylan whereas the supernatant (fraction B) was enriched in glucomannan. However carbohydrate analysis of fraction B showed, that all of the acidic polysaccharides

Table 1. Carbohydrate and acetyl analyses.

	Galactose %	Glucose %	Mannose %	Arabinose %	Xylose %	Acetyl %
Pine wood, extracted with acetone	3.0	65.6	18.9	2.8	9.7	0.85
Holocellulose (yield 70.1 %)	2.0	73.0	14.6	1.5	8.9	1.06
Water extract (after dimethyl sulfoxide extraction)	9.7	15.8	49.0	7.9	17.5	3.31
fraction A	20.3	5.2	14.2	16.0	44.3	1.40
fraction B	8.4	16.5	60.8	2.8	11.5	4.51
fraction B 1	4.8	18.0	77.2	—	—	5.95
Pulp after dimethyl sulfoxide and water extraction	1.8	75.3	13.5	1.0	8.4	0.91

(xylans, galactans) were not removed with CTA-Br. Further fractionation of fraction B was accomplished on a DEAE-cellulose (diethylaminoethyl-cellulose) column in the phosphate form [4]. The first two fractions from the column, eluted with water and 0.05 M monosodium phosphate (adjusted to pH 5.5) respectively, had a similar composition and were combined to give fraction B 1 (Table 1), completely free from glucuronoarabinoxylans. Furthermore the acidic galactans [5], obviously present in fraction B, had been removed. Fraction B 1 therefore represents a pure glucomannan containing a small number of galactose residues most probably linked terminally to mannose (and possibly glucose) residues through carbon atom 6 [6,7]. The later fractions from the DEAE-cellulose column (eluted with 0.5 M monosodium phosphate (pH 5.5), followed by 0.1 M sodium hydroxide) contained increasing amounts of arabinose and xylose residues.

Fraction B 1 had an acetyl content of 5.95 % corresponding to a DS (degree of substitution) of 0.24. Both B 1 and a deacetylated sample of this fraction were subjected to periodate oxidation. The periodate-oxidised polysaccharides where reduced with sodium borohydride and the polyalcohols so obtained hydrolysed [8]. Glucose, mannose, erythritol and glycerol were identified chromatographically and determined quantitatively (Table 2). No galactose was detected in either of the two samples. In the acetylated sample, a large quantity of mannose survived periodate oxidation whereas only a small amount of glucose was present. The acetyl groups therefore appear to be linked mainly to carbon atoms 2 and 3 of the mannose residues. The small amount of glucose which survived does not necessarily indicate that some glucose residues are also acetylated but may result from incomplete oxidation, or from the presence of a branch point in the glucomannan molecule [9]. Deacetylated fraction B 1 yielded very small amounts of both glucose and mannose possibly due to underoxidation, incomplete deacetylation or a small number of anomalous linkages (units linked 1 → 3 in the main chain, or branch points) in the glucomannan molecule. The glycerol contents of the two B 1 samples (7.4 and 6.8 % for the acetylated and the deacetylated sample, respectively) agree well with the amount of non-reducing end groups in the polysaccharide. Such groups

Table 2. Composition (in mole %) of hydrolysates of fraction B 1 after periodate oxidation and reduction.

	Glucose %	Mannose %	Erythritol %	Glycerol %
B 1 (acetylated)	0.9	21.9	69.9	7.3
B 1 (deacetylated)	1.5	1.7	90.0	6.8

consist principally of galactose residues (4.8 %) and to a minor extent of glucose and mannose units (about 2 % if the polysaccharide with DP 100 has one branch point).

The percentage of surviving mannose residues in the acetylated B 1 sample (21.9 %) indicates a DS of approximately 0.22. The DS which has been calculated from the acetyl analysis of B 1 is 0.24. This close agreement strongly indicates that virtually all of the acetyl groups are linked to carbon atoms 2 or 3 of the mannose residues and that a few, if any, mannose residues carry two acetyl groups, or an acetyl group at carbon atom 6.

The low acetyl content of fraction A (Table 1) suggests that the glucurono-arabinoxylans and other minor hemicellulose components (*e.g.* galactans and arabinogalactans which may be present in this fraction) contain no acetyl groups. In a separate experiment only traces of acetyl were found in an essentially pure glucurono-arabinoxylan. The latter was obtained by CTA-Br fractionation of the dimethyl sulfoxide extract of a pine holocellulose.

Present methods permit the isolation of only a small portion of the glucomannans from softwoods under conditions where the acetyl groups are not cleaved. If all the acetyl groups in pine are assumed to be bound to the glucomannan (which represents about 16 % of the dry weight of the wood) and if the glucomannan has a mean acetyl content of 6 %, the wood should contain 1 % acetyl groups. The pine wood used in this study had an acetyl content of 0.9 % (Table 1), a value lower than those previously reported in the literature [10]. The acetyl contents reported in this study were determined by gas-liquid chromatography (described in the experimental section). Although these values were considerably lower than those obtained by conventional acetyl determinations on wood, the method gives correct results with model substances of known composition. However, the variation of the acetyl content in wood from different locations and in stems of different ages, and the changes which might occur under storage, are not well known. It may be that the stem used in this study had a relatively low acetyl content. It is also possible that by other methods which are not specific for acetic acid, acidic degradation products are formed thus giving high values for the acetyl content.

During the course of the present investigation, Koshijima [11] reported a study on the acetyl groups in hemicelluloses from *Pinus densiflora*. Without isolating a pure acetylated glucomannan fraction, he obtained good evidence

that at least part of the acetyl groups were linked to glucomannans in the 2 or 3 positions of the mannose residues, in good agreement with the results of the present investigation.

EXPERIMENTAL

The quantitative analysis of sugars by paper chromatography was conducted according to the method of Saeman *et al.*[12]

Acetyl analyses. The method of Spingler and Markert [13] (somewhat modified) was employed. A sample (20—100 mg) of the polysaccharide was placed in a glass tube, N anhydrous methanolic hydrochloric acid (1 ml) and methanol (1 ml) containing a known amount of methylene chloride (5—10 mg) as internal standard, were added. The tube was sealed and heated for 30 min in a boiling water bath. The reaction product was analysed by gas-liquid chromatography, using an apparatus, recently described by Selleby [14], which was built at this Institute by I. Cedergren. The stationary phase was carbowax 1 500 (Perkin Elmer column K) and the length of the column was 3 m. Helium was used as the carrier gas with a flow rate of 25 ml/min at a temperature of 65°. Samples of about 40 µl were injected into the column. The procedure was calibrated using penta-*O*-acetyl-D-galactose as standard. The areas of the methyl acetate and methylene chloride peaks were cut out and compared by weighing.

Isolation and fractionation of the polysaccharides. Pine wood meal (0.5—2.0 mm) was extracted with acetone and the residue delignified by the chlorite method at 60° and pH 4.7. The holocellulose was obtained in a yield of 70.1 %. A sample (450 g) was treated for one hour in a Valley beater and twice extracted overnight with dimethyl sulfoxide (2 × 10 l). The residue was filtered, washed thoroughly with cold water and extracted twice with water (2 × 10 l) at 100° for 30 min. The aqueous extracts were combined and concentrated to about 2 l, adjusted to pH 4 with hydrochloric acid and the polysaccharides, precipitated with 8 l of ethanol, were centrifuged and washed several times with ethanol and acetone (yield 14.5 g). A sample (13 g) was dissolved in water (200 ml), a small insoluble fraction centrifuged and a 5 % aqueous solution of CTA-Br added until no further precipitate was formed. After centrifugation the polysaccharides were recovered by dissolving the precipitate in very dilute hydrochloric acid and precipitating with ethanol (yield 1.7 g, fraction A, Table 1). The supernatant was acidified with a small amount of hydrochloric acid and the polysaccharides precipitated with ethanol, washed and dried (yield 7.8 g, fraction B, Table 1).

A sample of fraction B (3 g) was dissolved in water (20 ml) and added to the top of a diethylaminoethyl-cellulose column (4 × 40 cm), which had been saturated with 0.5 M monosodiumphosphate (adjusted to pH 5.5) and washed with water. The polysaccharides were then eluted successively with water (2 l), 0.05 M monosodiumphosphate (2 l), 0.5 M monosodiumphosphate (2 l), and 0.1 N sodium hydroxide (2 l). The fractions were recovered by freeze drying, the second, third and fourth after deionization (Amberlite IR 120 and IR 4B, mixed bed). The hydrolysates of the water and 0.05 M monosodiumphosphate eluates had similar compositions and therefore were combined (fraction B 1, yield 770 mg). The fractions eluted with 0.5 M monosodiumphosphate (yield 960 mg) and 0.1 N sodium hydroxide (yield 350 mg) contained glucurono-arabinoxylan in addition to glucomannan as indicated by the composition of their hydrolysates.

Periodate oxidation. A sample of B 1 (40 mg) was dissolved in water (10 ml), 0.1 M sodium metaperiodate (10 ml) added and the solution kept in the dark at room temperature. Another sample was deacetylated by treating overnight with 10 % sodium hydroxide. The solution was deionized and the polysaccharide precipitated with ethanol, washed, dried and then treated in a manner similar to the first sample. The consumption of periodate, determined spectrophotometrically [15], reached an almost constant value after 300 h. This amounted to 0.85 and 1.10 moles per anhydrohexose unit for the acetylated and deacetylated samples, respectively. After precipitation of the periodate and the iodate with barium carbonate, an aliquot of both samples (10 ml) was reduced with sodium borohydride (30 mg). Sulfuric acid was added to a concentration of 4 % and the samples were hydrolysed by heating at 120° for one hour. After neutralisation with barium hydroxide, the solutions were passed through a cation exchange resin (IR 120) and the residual boric acid was removed by codistillation with methanol. An aliquot (containing approxi-

mately 0.4 mg) of each of the samples was applied to chromatographic paper (Schleicher and Schüll No. 2043 a) and the chromatograms irrigated with ethyl acetate-pyridine-water (8:2:1). Glucose, mannose, erythritol and glycerol, localised with the aid of guide strips, were well separated and were eluted from the paper. The reducing sugars were determined quantitatively according to the method of Saeman *et al.*[12] and erythritol and glycerol according to the procedure of Lambert and Neish [16]. The determinations were performed in triplicate, the results being in good agreement.

Acknowledgement. The author is much indebted to Professor Bengt Lindberg for his interest in this work and to Miss Hillevi Svensson for skilful assistance.

REFERENCES

1. Hägglund, E., Lindberg, B. and McPherson, J. *Acta Chem. Scand.* **10** (1956) 1160.
2. Bouveng, H. O., Garegg, P. J. and Lindberg, B. *Acta Chem. Scand.* **14** (1960) 742.
3. Scott, J. E. *Chem. & Ind. London* **1955** 168.
4. Neukom, H., Deuel, H., Heri, W. J. and Kündig, W. *Helv. Chim. Acta* **43** (1960) 65.
5. Bouveng, H. O. and Meier, H. *Acta Chem. Scand.* **13** (1959) 1884.
6. Hamilton, J. K., Partlow, E. V. and Thompson, N. S. *J. Am. Chem. Soc.* **82** (1960) 451.
7. Meier, H. *Acta Chem. Scand.* **14** (1960) 749.
8. Hamilton, J. K. and Smith, F. *J. Am. Chem. Soc.* **78** (1956) 5907.
9. Croon, I., Lindberg, B. and Meier, H. *Acta Chem. Scand.* **13** (1959) 1299.
10. Hägglund, E. *Chemistry of Wood.* Academic Press Inc., New York 1951, p. 350.
11. Koshijima, T. *J. Japan Wood Research Soc.* **6** (1960) 194.
12. Saeman, J. F., Moore, W. E., Mitchell, R. L. and Millet, M. A. *Tappi* **37** (1954) 336.
13. Spingler, H. and Markert, F. *Mikrochim. Acta* **1959** 122.
14. Selleby, L. *Svensk Papperstidn.* **63** (1960) 81.
15. Aspinall, G. O. and Ferrier, R. J. *Chem. & Ind. London* **1957** 1216.
16. Lambert, M. and Neish, A. C. *Can. J. Research* **28** (1950) 83.

Received March 7, 1961.

ACTA CHEMICA SCANDINAVICA 15 (1961) 1386–1390

Inhibition of Cholinesterases by Tetrahydroaminacrin

EDITH HEILBRONN

Research Institute of National Defence, Department 1, Sundbyberg 4, Sweden

The influence of tetrahydroaminacrin upon acetylcholinesterase and butyrylcholinesterase is described. The compound acts as a reversible inhibitor, partly competitive with the substrate. It is a more potent inhibitor of BuChE than of AChE.

Tetrahydroaminacrin, 1,2,3,4-tetrahydro-5-aminoacridine, also called Tacrin or THA, has been described in 1953 by Shaw and Bentley [1]. They mentioned that the substance inhibits cholinesterase [2]. A short time ago the compound gained new interest as a substance able to prolong *in vivo* the muscle relaxing effect of succinylcholine [3,4]. This prolongation is supposed to be connected with the ability of tetrahydroaminacrin to inhibit cholinesterase. Cholinesterase, especially butyrylcholinesterase, is considered to be responsible for the *in vivo* breakdown of succinylcholine. However, it has not yet been settled, whether the synergism of cholinesterase inhibitors with succinylcholine depends upon an acetylcholine action or on inhibition of the breakdown of succinylcholine.

The present paper describes the result of a study of the effect of Tacrin upon acetylcholinesterase and of a more detailed investigation of the butyrylcholinesterase inhibition.

EXPERIMENTAL

An automatic recording titrator [5] was employed in all experiments except in the determination of the pI_{50}-values and the *in vivo* experiments, where an electrometric method [6] was used. Both methods were used at pH 8.0, $t = 25°C$. pI_{50}-Determinations were made with human erythrocytes and human plasma. Studies on the type of inhibition were made with a butanol-washed preparation of stroma from bovine blood and on a horse serum fraction prepared according to Strehlitz [7]. Substrates were acetylcholine iodide, butyrylcholine iodide and acetyl-β-methylcholine iodide. In one experiment sarin was used as inhibitor. Values obtained in *in vitro* experiments and used for calculations were corrected for spontaneous hydrolysis of the substrate. The compound was tested in a dog.

RESULTS

In vitro experiments. The pI_{50}-value (incubation time 30 min) for acetylcholinesterase (AChE) was found to be 6.2 and for butyrylcholinesterase (BuChE) 7.6. The inhibition was controlled during 0—30 min and found to be constant during this interval.

Table 1. Incubation of butyrylcholinesterase with 1.5×10^{-8} M Tacrin in the presence or absence of 10^{-2} M acetylcholine iodide.

	% inhibition
Acetylcholine present	66, 65, 67
Acetylcholine absent	77, 77, 76
Acetylcholine and Tacrin added together	66, 66, 67

Incubation of the enzyme with the inhibitor in the presence or absence of the substrate [10^{-2} M] showed only a small difference in the degree of inhibition as is seen in Table 1. It was therefore expected that Tacrin might not act as a competitive inhibitor. This was studied in the usual way [8], *i.e.* the concentration quotient substrate/inhibitor was varied and the activity determined. The results are seen in Figs. 1 and 2 and in Table 2. They indicate that the inhibition is of the "mixed" type [8], with a tendency towards competitive inhibition at higher substrate concentration and towards noncompetitive inhibition at lower substrate concentration. The curves seen in Fig. 1 could be reproduced in other experiments. K_I calculated from the competitive part of the curve seen in Fig. 1 is 1.5×10^{-9}, which fits in Table 2.

Experiments with 1.25×10^{-7} M (final solution) sarin in the presence or absence of Tacrin (7.5×10^{-9} M, final solution) and in the presence of the substrate gave k_2-values for the reaction between BuChE and sarin of 3.5×10^3 l mole^{-1} sec^{-1}, respectively 8.9×10^3 l mole^{-1} sec^{-1}. If sarin was added to the enzyme before the substrate, but in the presence of Tacrin, a protective effect of Tacrin was observed.

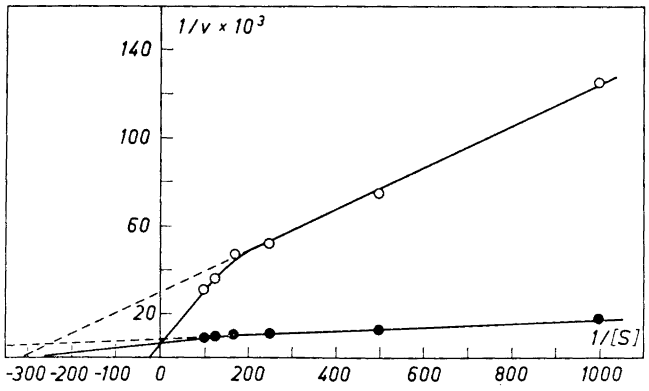

Fig. 1. Reciprocal of butyrylcholinesterase activity plotted against reciprocal of substrate concentration. ● = uninhibited enzyme, O = enzyme inhibited by 1.5×10^{-8} M Tacrin. All points represent mean values of two determinations.

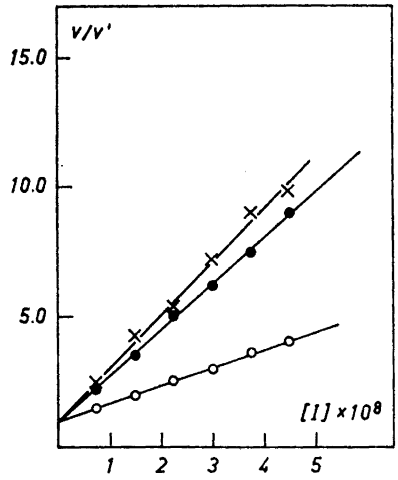

Fig. 2. Ratio of activity of uninhibited enzyme to inhibited enzyme plotted against the concentration of Tacrin. Concentration of acetylcholine iodide: ○ = 5×10^{-2} M, ● = 1×10^{-2} M, × = 5×10^{-3} M. All points represent mean values of two determinations.

The reversibility of the Tacrin inhibition was studied in dialysis experiments. The enzymes were dissolved in 0.1 M potassium chloride and inhibited with Tacrin (BuChE: 3×10^{-7} M, AChE: 5×10^{-7} M, final solution). The degree of inhibition was measured after a varying time of dialysis at + 4°C against 0.1 M potassium chloride. As is seen in Table 3, dialysis restored the enzyme activities. The activities were checked with uninhibited controls.

In vivo experiments. 1 mg Tacrin/kg body weight was injected *i.v.* in a dog. Bloodsamples were taken before the injection and 5, 15, 30, 120, 1 200 and 3 000 min after the injection. Plasma and erythrocytes were separated and the cholinesterase activity determined with three substrates. The result is seen in Fig. 3.

Table 2. Calculation of K_I according to $v/v' = 1 + [I] \frac{K_M}{K_I([S] + K_M)}$ (competitive inhibition), and $v/v' = 1 + [I] \frac{1}{K_I}$ (noncompetitive inhibition)

Series	[S]	K_I comp.	K_I noncomp.
1	5×10^{-2}	1.0×10^{-9}	14.8×10^{-9}
	1×10^{-2}	1.5×10^{-9}	5.6×10^{-9}
	5×10^{-3}	2.1×10^{-9}	5.0×10^{-9}
2	5×10^{-2}	0.95×10^{-9}	14.4×10^{-9}
	1×10^{-2}	1.4×10^{-9}	5.0×10^{-9}
	5×10^{-3}	2.0×10^{-9}	4.6×10^{-9}

Table 3. Dialysis of Tacrin-inhibited cholinesterase against 0.1 M potassium chloride.

Time of dialysis	Relative enzyme activity of			
	BuChE		AChE	
	control	inhibited enzyme	control	inhibited enzyme
Before dialysis	86, 86	0, 0	49, 45	13, 11
24 h of dialysis	83, 83	44, 45	—	—
48 h —,,—	81, 81	89, 91	35, 36	30, 30
96 h —,,—	—	—	25, 26	25, 25

It was observed that the dog 2 min after the injection salivated and showed increased lacrymation. Respiration was also increased. The pronounced respiration came and went several times during 20 min. After 30 min the dog was released and walked without difficulties.

DISCUSSION

In studies on the structure of the active center of the cholinesterases several results can be interpreted by assuming the presence of an anionic group in acetylcholinesterase but not in butyrylcholinesterase, or it can at least be assumed, that the anionic group is of more importance for the binding of substrates and inhibitors to AChE than to BuChE [9,10]. It is, *e.g.*, known that quaternary ammonium compounds have a greater inhibitory effect upon AChE than upon BuChE. Tacrin has no cationic group and is a better inhibitor of BuChE than AChE. This seems to be another confirmation of the above mentioned theory.

The experiments described in this paper show that Tacrin *in vivo* as well as *in vitro* acts as a reversible inhibitor of cholinesterases. With BuChE as enzyme, the compound seems to be only partly competitive with the substrate, preferably at higher concentrations of the substrate. Calculation of K_M from the left curve in Fig. 1 gives a value of 3.6×10^{-3} mole/l. The same value was obtained for butyrylcholinesterase acting on high concentrations of the sub-

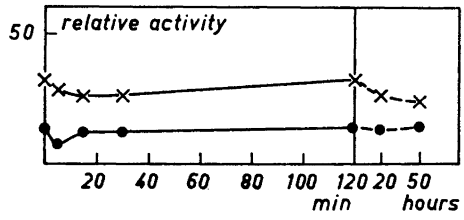

Fig. 3. Cholinesterase activity of dog erythrocytes plotted against time after injection of 1 mg Tacrin/kg body weight. Substrates: × = acetylcholine iodide, ● = acetyl-β-methylcholine iodide. The points represent mean values of two determinations.

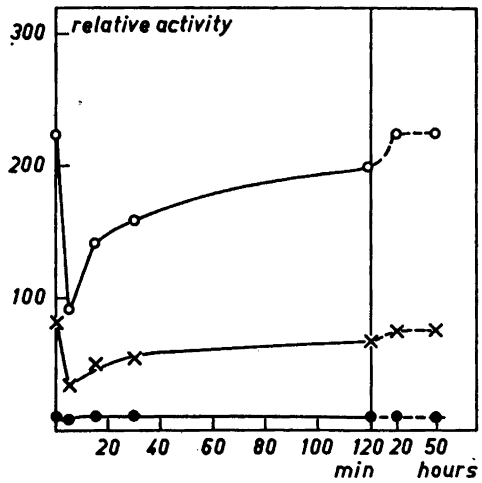

Fig. 4. Cholinesterase activity of dog plasma plotted against time after injection of 1 mg Tacrin/kg body weight. Substrates: × = acetylcholine iodide, O = butyrylcholine iodide, ● = acetyl-β-methylcholine iodide. The points represent mean values of two determinations.

strate, when pS-activity curves [11] were measured on the same enzyme preparation and the experimental values were treated as described earlier [12], *i.e.* when the preparation was supposed to contain two simultaneously acting cholinesterases.

My thanks are due to Prof. Gustaf Ljunggren, Director of Research Institute of National Defence, Department 1, for the kind interest he has shown in this work.

REFERENCES

1. Shaw, F. H. and Bentley, G. A. *Australian J. Exptl. Biol. Med. Sci.* **31** (1953) 573.
2. Shaw, F. H. and Bentley, G. A. *Australian J. Exptl. Biol. Med. Sci.* **33** (1955) 143.
3. Gordh, T. and Wåhlin, Å. *Report given at the annual meeting of Svensk Anestesiologisk förening. To be published in Nordisk medicin.*
4. Houghs, W. *Report given at the annual meeting of Svensk Anestesiologisk förening. To be published in Nordisk medicin.*
5. Larsson, L. and Hansen, B. *Svensk Kem. Tidskr.* **68** (1956) 521.
6. Tammelin, L.-E. *Scand. J. Clin. Lab. Invest.* **5** (1953) 267.
7. Strehlitz, F. *Biochem. J.* **38** (1944) 86.
8. Dixon, M. and Webb, E. C. *Enzymes*, Longmans, Green et Co, London 1958, p. 181.
9. Wilson, I. B. in Boyer, P. D., Lardy, H. and Myrbäck, K. *The Enzymes*, Academic Press, New York 1960, Vol. 4, p. 501.
10. Augustinsson, K. B. *Ibid.* Vol. 4, p. 521.
11. Heilbronn, E. *To be published.*
12. Heilbronn, E. *Acta Chem. Scand.* **12** (1958) 1879.

Received February 23, 1961.

ACTA CHEMICA SCANDINAVICA 15 (1961) 1391–1422

Short Communications

On the Adsorption of Proteins on Calcium Phosphate

BO SÖRBO

Nobel Medical Institute, Biochem. Dept., Stockholm, and Research Institute of National Defence, Dept. 1, Sundbyberg, Sweden

The use of calcium phosphate for purification of proteins is well established. There appears, however, to exist some confusion concerning the effect of pH on the adsorption of proteins on this adsorbents. Thus there are reviews [1,2] on enzyme purification which state that the adsorption always increases with a decrease of pH, whereas others [3] state that maximum adsorption occurs at the isoelectric point of the protein. In support of the latter statement Singer and Kearney [4] found that L-amino acid oxidase from snake venom was maximally adsorbed on calcium phosphate gel at the pH where the crude enzyme had its minimum solubility in ammonium sulfate solutions. However, the solubility minimum of an impure protein may not be identical with its isoelectric point due to protein-protein interaction [5] with impurities. Therefore the effect of pH on the adsorption of pure proteins of known isoelectric points on calcium phosphate gel has now been studied. An effect of certain anions on the adsorption was also noticed.

Preliminary experiments with an acid, neutral and a basic protein (Fig. 1) gave results in agreement with the theory that maximum adsorption occurred at the isoelectric point (IP) of the protein *. Thus metmyoglobin (IP 6.8) was maximally adsorbed around pH 6.8, whereas the acid protein, egg albumin (IP 4.7) showed a decrease in adsorption with increasing pH and the basic protein, cytochrome c (IP 10.7) showed the opposite effect.

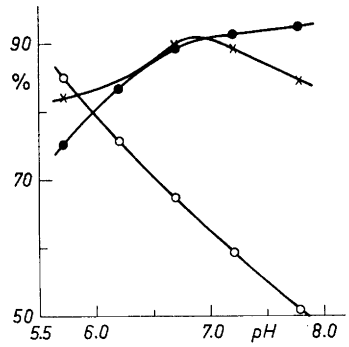

Fig. 1. Effect of pH on the adsorption of proteins on CPG. The test system, of final volume 5 ml, contained 8 mg CPG plus phosphate buffer, $\Gamma/2$ 0.01. The reaction time was 30 min. ○ Egg albumin, 2.0 mg; × Metmyoglobin, 0.66 mg; ● Cytochrome c, 0.30 mg.

Further experiments were carried out with oxyhemoglobin (IP 6.7). It was observed that the adsorption was very rapid (maximum adsorption occurred within 1 min). It was verified that the adsorption of oxyhemoglobin was reversible (the adsorbed protein could be eluted by an alkaline phosphate buffer) and that the adsorption followed Freundlich's adsorption equation[6]. When the effect of ionic strength and pH on the adsorption was studied, (Fig. 2) maximum adsorption was obtained around the isoelectric point of the protein at comparatively low ionic strength (0.01). When the latter was increased by addition of phosphate, the adsorption was diminished, but only at the higher pH values studied. At the

* The isoelectric points cited in this paper refer to electrophoretically determined values (usually at an ionic strength of 0.01). They have been compiled from review articles [7-9].

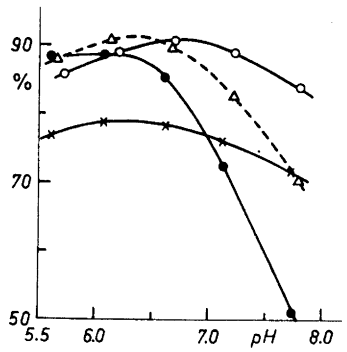

Fig. 2. Adsorption of oxyhemoglobin on CPG. The test system contained 1.67 mg horse oxyhemoglobin and phosphate or sodium chloride as indicated. The reaction time was 5 min. Other conditions as in Fig. 1. ○ phosphate, $\Gamma/2$ 0.01; △ phosphate, $\Gamma/2$ 0.02; ● phosphate, $\Gamma/2$ 0.04; × phosphate, $\Gamma/2$ 0.01 + chloride, $\Gamma/2$ 0.03.

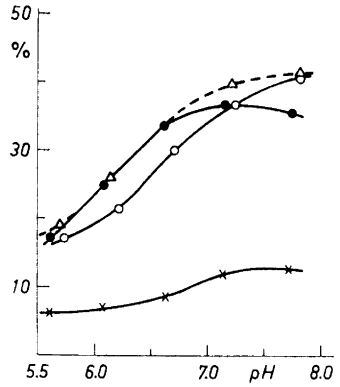

Fig. 3. Adsorption of lysozyme on CPG. The system contained 2.0 mg lysozyme instead of oxyhemoglobin with other conditions as in Fig. 2. Curves indicated as in Fig. 2.

most acid pH a slight increase in adsorption was actually observed. The result was a shift of the point of maximum adsorption to the acid side of the isoelectric point by an increase of phosphate concentration. Chloride, on the other hand, decreased the adsorption over the entire pH range studied (Fig. 2). Fluoride was found to behave as phosphate, whereas sulfate behaved as chloride.

Similar experiments were also carried out with lysozyme (IP 11.0) and bovine serum albumin (IP 4.7). Lysozyme (Fig. 3) behaved similarly to oxyhemoglobin with respect to phosphate and chloride, but serum albumin (Fig. 4) behaved differently. In the latter case, phosphate depressed the adsorption over the entire pH range studied, whereas chloride had a small depressing effect at the lower pH values, which changed to an increase in adsorption at pH 7.8.

Thus, also the results obtained with oxyhemoglobin, lysozyme and bovine serum albumin are in accordance with the theory that maximum adsorption occurs at the isoelectric point of the protein. The different behaviour of the anions studied with respect to their effect on the adsorption of certain proteins is, however, difficult to explain from the data available. Both anion-protein and anion-adsorbent interaction have to be considered. It may be recalled in this connection that phosphate ions combine with oxyhemoglobin [8], making the protein molecule more negatively charged. This could explain why the point of maximum adsorption of this protein is depressed to lower pH-values with increasing phosphate concentration.

Finally, it should be pointed out that advantage may be taken of such anion effects in purification experiments with calcium phosphate.

Material and methods. Calcium phosphate gel (CPG) was prepared according to Tsuboi and

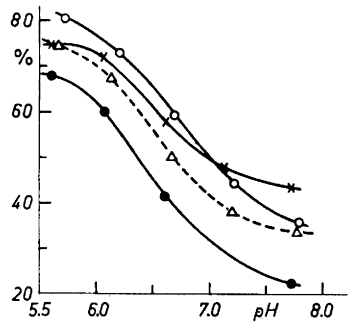

Fig. 4. Adsorption of bovine serum albumin on CPG. Test system contained 2.0 mg bovine serum albumin and only 4 mg CPG. Other conditions and curves indicated as in Fig. 2

Hudson [10], horse oxyhemoglobin was prepared according to Ferry *et al.* [11] and beef cytochrome c according to Neilands [12]. Crystalline beef metmyoglobin was a gift from Mr. Å. Åkeson. Egg albumine, lysozyme and bovine serum albumine were crystalline commercial preparations. Phosphate buffers were prepared from the sodium salts and when other anions were studied the corresponding sodium salts were also used in order to avoid a cation effect on the adsorption phenomena. The adsorption experiments were carried out at + 4°C in 10 ml centrifuge tubes which were agitated on a simple manual rotator during the incubation. The adsorbent was then centrifuged off and protein remaining in the supernatant solution was determined from the adsorption at 280 mμ (or 405 mμ in case of the heme proteins) corrected for a blank, obtained by omitting the protein from the test system. Only a rather narrow pH-range (5.6−7.8) was studied as calcium phosphate is unstable outside this range. All experiments were carried out in the presence of phosphate buffer, as it was found impossible to free the gel from free phosphate by repeated washing on the centrifuge. For an explanation of this effect se Ref. [13,14]

Preliminary experiments were carried out with a reaction time of 30 min, but as it was later observed that the adsorption of proteins on the gel was very rapid, a shorter reaction time (5 min) was used in the following experiments.

The author is much indebted to Dr. C. L. Woronick for his constructive criticism of the manuscript.

1. Colowick, S. P. *Methods in Enzymol.* **1** (1955) 90.
2. Schwimmer, S. and Pardee, A. B. *Advances in Enzymol.* **14** (1953) 375.
3. Zittle, C. H. *Advances in Enzymol.* **14** (1953) 319.
4. Singer, T. P. and Kearney, E. B. *Arch. Biochem.* **29** (1950) 190.
5. Green, A. A. and Hughes, W. L. *Methods in Enzymol.* **1** (1955) 87.
6. Freundlich, H. *Kapillarchemie*, Akademische Verlagsgesellschaft, Leipzig 1909.
7. Alberty, R. A. in Neurath, H. and Bailey, K. *The Proteins.* Academic Press, Inc., New York 1953, Vol. I, p. 511−14.
8. Haurowitz, F. and Hardin, R. L. in Neurath, H. and Bailey, K. *The proteins.* Academic Press, Inc., New York 1953, Vol. II, p. 307.
9. Wyman, J. *Advances in Protein Chem.* **4** (1948) 407.
10. Tsuboi, K. K. and Hudson, J. P. *J. Biol. Chem.* **224** (1957) 879.
11. Ferry, R. M., Cohn, E. J., Green, A. A. and Teel, E. W. *Biochem. Preparations.* **6** (1958) 51.
12. Neilands, J. B. *J. Biol. Chem.* **197** (1952) 701.
13. Eisenberger, S., Lehrman, A. and Turner, W. D. *Chem. Revs.* **26** (1940) 257.
14. Hayek, E., Müller, F. and Koller, K. *Monatsh.* **82** (1959) 959.

Received August 11, 1961.

Halogen-Metal Interconversion with Dibromobithienyls

SALO GRONOWITZ

Chemical Institute, University of Uppsala, Uppsala, Sweden

Bithienyl dicarboxylic acids are useful intermediates for a study of optically active bithienyls [1] and of thiophene analogues to fluorene. Most bithienyls have been prepared by the Ullmann reaction [2-4], which usually gives low yields, especially in the absence of activating substituents such as $-NO_2$ or $-CO_2CH_3$. The coupling of Grignard reagents with $CuCl_2$ was used in a few cases by Steinkopf *et al.*[5,6] for the preparation of bithienyls. In the thiophene series, however, organolithium compounds are available through halogen-metal interconversion, in cases where Grignard reagents are formed only with difficulty [7,8]. Thus the present author and Karlsson [9] were able to demonstrate that good yields of bithienyls can be obtained on coupling 2- and 3-thienyllithium with $CuCl_2$.

It has now been found that 4,4′-dibromo-3,3′-bithienyl (I) and 3,3′-dibromo-2,2′-bithienyl (II) are obtained in 50−60 % yield by treating 4-bromo-3-thienyllithium and 3-bromo-2-thienyllithium, respectively, with $CuCl_2$ at −70°. The NMR-spectra of the products showed that no rearrangement had occurred during the coupling. II was obtained earlier in lower yield by Steinkopf *et al.*[6] by the coupling of 3-bromo-2-thiophenemagnesium bromide, obtained through the entrainment Grignard reaction of 2,3-dibromothiophene, with $CuCl_2$.

Hudson [10], horse oxyhemoglobin was prepared according to Ferry *et al.* [11] and beef cytochrome c according to Neilands [12]. Crystalline beef metmyoglobin was a gift from Mr. Å. Åkeson. Egg albumine, lysozyme and bovine serum albumine were crystalline commercial preparations. Phosphate buffers were prepared from the sodium salts and when other anions were studied the corresponding sodium salts were also used in order to avoid a cation effect on the adsorption phenomena. The adsorption experiments were carried out at + 4°C in 10 ml centrifuge tubes which were agitated on a simple manual rotator during the incubation. The adsorbent was then centrifuged off and protein remaining in the supernatant solution was determined from the adsorption at 280 mμ (or 405 mμ in case of the heme proteins) corrected for a blank, obtained by omitting the protein from the test system. Only a rather narrow pH-range (5.6−7.8) was studied as calcium phosphate is unstable outside this range. All experiments were carried out in the presence of phosphate buffer, as it was found impossible to free the gel from free phosphate by repeated washing on the centrifuge. For an explanation of this effect se Ref. [13,14]

Preliminary experiments were carried out with a reaction time of 30 min, but as it was later observed that the adsorption of proteins on the gel was very rapid, a shorter reaction time (5 min) was used in the following experiments.

The author is much indebted to Dr. C. L. Woronick for his constructive criticism of the manuscript.

1. Colowick, S. P. *Methods in Enzymol.* **1** (1955) 90.
2. Schwimmer, S. and Pardee, A. B. *Advances in Enzymol.* **14** (1953) 375.
3. Zittle, C. H. *Advances in Enzymol.* **14** (1953) 319.
4. Singer, T. P. and Kearney, E. B. *Arch. Biochem.* **29** (1950) 190.
5. Green, A. A. and Hughes, W. L. *Methods in Enzymol.* **1** (1955) 87.
6. Freundlich, H. *Kapillarchemie*, Akademische Verlagsgesellschaft, Leipzig 1909.
7. Alberty, R. A. in Neurath, H. and Bailey, K. *The Proteins.* Academic Press, Inc., New York 1953, Vol. I, p. 511−14.
8. Haurowitz, F. and Hardin, R. L. in Neurath, H. and Bailey, K. *The proteins.* Academic Press, Inc., New York 1953, Vol. II, p. 307.
9. Wyman, J. *Advances in Protein Chem.* **4** (1948) 407.
10. Tsuboi, K. K. and Hudson, J. P. *J. Biol. Chem.* **224** (1957) 879.
11. Ferry, R. M., Cohn, E. J., Green, A. A. and Teel, E. W. *Biochem. Preparations.* **6** (1958) 51.
12. Neilands, J. B. *J. Biol. Chem.* **197** (1952) 701.
13. Eisenberger, S., Lehrman, A. and Turner, W. D. *Chem. Revs.* **26** (1940) 257.
14. Hayek, E., Müller, F. and Koller, K. *Monatsh.* **82** (1959) 959.

Received August 11, 1961.

Halogen-Metal Interconversion with Dibromobithienyls

SALO GRONOWITZ

Chemical Institute, University of Uppsala, Uppsala, Sweden

Bithienyl dicarboxylic acids are useful intermediates for a study of optically active bithienyls [1] and of thiophene analogues to fluorene. Most bithienyls have been prepared by the Ullmann reaction [2-4], which usually gives low yields, especially in the absence of activating substituents such as $-NO_2$ or $-CO_2CH_3$. The coupling of Grignard reagents with $CuCl_2$ was used in a few cases by Steinkopf *et al.*[5,6] for the preparation of bithienyls. In the thiophene series, however, organolithium compounds are available through halogen-metal interconversion, in cases where Grignard reagents are formed only with difficulty [7,8]. Thus the present author and Karlsson [9] were able to demonstrate that good yields of bithienyls can be obtained on coupling 2- and 3-thienyllithium with $CuCl_2$.

It has now been found that 4,4′-dibromo-3,3′-bithienyl (I) and 3,3′-dibromo-2,2′-bithienyl (II) are obtained in 50−60 % yield by treating 4-bromo-3-thienyllithium and 3-bromo-2-thienyllithium, respectively, with $CuCl_2$ at −70°. The NMR-spectra of the products showed that no rearrangement had occurred during the coupling. II was obtained earlier in lower yield by Steinkopf *et al.*[6] by the coupling of 3-bromo-2-thiophenemagnesium bromide, obtained through the entrainment Grignard reaction of 2,3-dibromothiophene, with $CuCl_2$.

It was shown earlier [10] that thienyllithium derivatives in which the Li is not in the most acidic position, undergo a complex series of rearrangements when they are obtained by halogen-metal interconversion. They are, however, sufficiently stable at −70° to be of great use for the preparation of substituted thiophenes. It has now been found that the Li derivatives obtained from dibromobithienyls are stable at −70°. Treatment of I with excess *n*-butyllithium at −70° followed by carbonation gave 4,4′-dicarboxy-3,3′-bithienyl, which melts with decomposition at 275−280°. Its structure is demonstrated by the occurrence in its NMR-spectrum of a coupling constant of 3.4 c/s between the two groups of equivalent ring-hydrogens. This is of the magnitude characteristic of J_{25} in 3,4-disubstituted thiophenes [11]. The properties (m.p., IR- and NMR-spectra) of this acid differ from those of 2,2- and 5,5′-dicarboxy-3,3′-bithienyl, which have been obtained through metalation of 3,3′-bithienyl with excess *n*-butyllithium [12].

Similarly reaction of II with excess *n*-butyllithium at −70° followed by carbonation, gave 3,3′-dicarboxy-2,2′-bithienyl, which melted with decomposition at 289−291°. This acid was prepared earlier in low yield by Nord *et al.*[2] by the Ullmann coupling of the less easily obtained methyl 2-bromo-3-thiophenecarboxylate. They state the m.p. to be 175−185°, but this is probably due to a printing error as the m.p. of the dimethyl ester is the same as that obtained in the present investigation.

Experimental. 4,4′-Dibromo-3,3′-bithienyl. 74 g (0.55 mole) of anhydrous $CuCl_2$ were added at −70° to a solution of 4-bromo-3-thienyllithium prepared in the usual way [13] at −70° from 570 ml of 0.92 N *n*-butyllithium and 107 g (0.44 mole) of 3,4-dibromothiophene [14]. After standing at −70° for 2 h the mixture was allowed to attain room temperature overnight, and was then treated under cooling with 4 N hydrochloric acid. The ether phase was extracted several times with 4 N hydrochloric acid in order to remove cuprous chloride and was then extracted with water. It was subsequently dried, and ether and butyl bromide were removed *in vacuo*. The residue was recrystallized from ligroin (Norit) and yielded 37 g (52 %) of pure 4,4′-dibromo-3,3′-bithienyl, m.p. 127−129°, crystallizing in large flakes. (Found: C 29.76; H 1.32; Br 49.16. Calc. for $C_8H_4Br_2S_2$: C 29.64; H 1.24, Br 49.35.) The NMR-spectrum in dimethyl sulphoxide (23 wt %) consists of two strongly coupled doublets with a splitting of 3.4 c/s. The shifts of the two groups of equivalent ring hydrogens are 5.22 ppm and 5.11 ppm relative to the solvent peak.

3,3′-Dibromo-2,2′-bithienyl. This was prepared as described above from 138 g (0.57 mole) of 2,3-dibromothiophene [15] in 100 ml of ether, 630 ml of 1.0 N *n*-butyllithium and 100 g (0.74 mole) of anhydrous $CuCl_2$. Yield 56 g (61 %) of 3,3′-dibromo-2,2′-bithienyl, which crystallized from ligroin in beautiful almost cubic crystals, m.p. 102−104° (Found: C 29.62; H 1.24; Br 49.35. Calc. for $C_8H_4Br_2S_2$: C 29.64; H 1.24; Br 49.35.) (Literature values [6]: m.p. 96−97°). The NMR-spectrum in dimethyl sulphoxide (28 wt %) consists of two doublets with a splitting of 5.4 c/s. The shifts of the two groups of equivalent ring-hydrogens are 5.23 ppm and 4.66 ppm relative to the solvent peak.

4,4′-Dicarboxy-3,3′-bithienyl. A solution of 16.2 g (0.050 mole) of 4,4′-dibromo-3,3′-bithienyl in 100 ml of anhydrous tetrahydrofuran was added over a period of 5 min to 130 ml of 1.20 N *n*-butyllithium cooled to −70°. After a few minutes the mixture was poured onto solid carbon dioxide covered with ether. The reaction mixture was hydrolyzed with water, and the ether phase was extracted with sodium carbonate solution. On acidification with dilute hydrochloric acid the crude acid precipitated out (10.1 g, 80 %). The product was washed twice with 250 ml portions of ether and then recrystallized from glacial acetic acid, yielding 7.1 g of pure 4,4′-dicarboxy-3,3′-bithienyl in small prisms, m.p. 275−280° (decomp.). (Found: C 46.80; H 2.70; S 25.23. Calc. for $C_{10}H_6O_4S_2$: C 47.23; H 2.38; S 25.21). The resonances of the ring protons in its NMR-spectrum in dimethyl sulphoxide (15 wt %) consist of two doublets with a splitting of 3.4 c/s. The shifts of the two groups of equivalent ring-hydrogens are 5.64 ppm and 4.84 ppm relative to the solvent peak.

4,4′-Dicarbomethoxy-3,3′-bithienyl was prepared through methylation with diazomethane, m.p. 147−148°.

3,3′-Dicarboxy-2,2′-bithienyl. This was prepared as described above from 10.0 (0.031 mole) of 3,3′-dibromo-2,2′-bithienyl and 76 ml of 0.92 N *n*-butyllithium. Yield 5.5 g (70 %) of crude acid. Purification as above gave 3.5 g of pure acid, m.p. 289−291° (decomp.) (Found C 46.67; H 2.50; S 25.01. Calc. for $C_{10}H_6O_4S_2$: C 47.23; H 2.35; S 25.21.) In the NMR-spectrum in dimethyl sulphoxide solution (34 wt %) the resonances of all four ring-hydrogens coincide at 4.97 ppm relative to the solvent peak.

3,3′-Dicarbomethoxy-2,2′-bithienyl was prepared through methylation with diazomethane, m.p. 150−151°. (literature value [2]: m.p. 145−147°.)

The NMR-spectra were obtained at 40 Mc/s with a Varian Associates model V-4 300 B high resolution NMR-spectrometer and a flux-stabilized 12 in. electromagnet obtained from the same company. The magnet sweep was calibrated using the modulation side-band technique.

Acknowledgements. The author wishes to express his thanks to Professor Arne Fredga for his interest in this work and for all facilities put at his disposal. Thanks are also due to Mr. Bo Gestblom for recording the NMR-spectra. The elementary analyses were carried out by Dr. A. Bernhardt, Mülheim. A grant from the *Hierta-Retzius stipendiefond* is gratefully acknowledged.

1. Gronowitz, S. and Frostling, H. *Tetrahedron Letters* **1961** No. 17.
2. Owen, L. J. and Nord, F. F. *J. Org. Chem.* **16** (1951) 1864.
3. Jean, G. N. and Nord, F. F. *J. Org. Chem.* **20** (1955) 1363.
4. Uhlenbroek, J. H. and Bijloo, J. D. *Rec. trav. chim.* **79** (1960) 1181.
5. Steinkopf, W. and Roch, J. *Ann.* **482** (1930) 251.
6. Steinkopf, W., v. Petersdorff, H.-J. and Gording, R. *Ann.* **527** (1937) 272.
7. Gronowitz, S. *Arkiv Kemi* **13** (1958) 295.
8. Gronowitz, S., Moses, P., Hörnfeldt, A.-B. and Håkansson, R. *Arkiv Kemi* **17** (1961) 165.
9. Gronowitz, S. and Karlsson, H.-O. *Arkiv Kemi* **17** (1961) 89.
10. Moses, P. and Gronowitz, S. *Arkiv Kemi* **18**(1961) 119.
11. Hoffman, R. A. and Gronowitz, S. *Arkiv Kemi* **16** (1960) 563.
12. Gronowitz, S. and Karlsson, H.-O. *To be published.*
13. Gronowitz, S., Moses, P. and Hörnfeldt, A.-B. *Arkiv Kemi* **17** (1961) 237.
14. Gronowitz, S., Moses, P. and Håkansson, R. *Arkiv Kemi* **16** (1960) 267.
15. Lawesson, S.-O. *Arkiv Kemi* **11** (1957) 373.

Received August 22, 1961.

Separation of Uronic Acids by Paper Electrophoresis

ARNE HAUG and BJØRN LARSEN

Norwegian Institute of Seaweed Research, N.T.H., Trondheim, Norway

The purpose of this work was to develop a rapid and convenient method for qualitative and quantitative analysis of mixtures of uronic acids. Paper chromatography of uronic acids in the solvents most commonly used for chromatography of sugars does not give satisfactory results. In basic solvents such as pyridine-ethyl acetate-water, the uronic acids do not move, and in acidic solvents such as acetic acid-ethyl acetate-water, the mobilities of the different uronic acids are nearly identical. The most satisfactory solvents are mixtures of both basic and acidic components, such as the solvent introduced by Fischer and Dörfel [1]: Pyridine-ethyl acetate-acetic acid-water, 5:5:1:3. However, the separation is not very satisfactory, it is not possible to distinguish between glucuronic and guluronic acid, it is time-consuming and for quantitative work it is necessary beforehand to transform all lactones to uronic acids. Paper electrophoresis of uronic acids has been used by Jayme and Kringstad [2] and Hoffman, Linker and Meyer [3] but no details of the mobilities of the different uronic acids were given. The possibility of using paperelectrophoresis for separation of uronic acids was therefore further investigated.

Materials and methods. The glucuronic and galacturonic acids used were commercial preparations. The guluronic and mannuronic acids were prepared from hydrolysates of alginic acid by chromatographic separation of the lactones [4] and transforming the lactones by addition of alkali to uronic acid salts. The determination of the pK values has been described earlier [5]. The electrophoresis was carried out in an LKB paper electrophoresis apparatus on Schleicher & Schüll 2043b paper strips. The

Table 1. pK_s values and mobilities in acidic medium.

	pK_s	M_m
Glucuronic acid	3.20	1.10
Mannuronic acid	3.38	1.00
Galacturonic acid	3.42	0.95
Guluronic acid	3.65	0.88

The NMR-spectra were obtained at 40 Mc/s with a Varian Associates model V-4 300 B high resolution NMR-spectrometer and a flux-stabilized 12 in. electromagnet obtained from the same company. The magnet sweep was calibrated using the modulation side-band technique.

Acknowledgements. The author wishes to express his thanks to Professor Arne Fredga for his interest in this work and for all facilities put at his disposal. Thanks are also due to Mr. Bo Gestblom for recording the NMR-spectra. The elementary analyses were carried out by Dr. A. Bernhardt, Mülheim. A grant from the *Hierta-Retzius stipendiefond* is gratefully acknowledged.

1. Gronowitz, S. and Frostling, H. *Tetrahedron Letters* **1961** No. 17.
2. Owen, L. J. and Nord, F. F. *J. Org. Chem.* **16** (1951) 1864.
3. Jean, G. N. and Nord, F. F. *J. Org. Chem.* **20** (1955) 1363.
4. Uhlenbroek, J. H. and Bijloo, J. D. *Rec. trav. chim.* **79** (1960) 1181.
5. Steinkopf, W. and Roch, J. *Ann.* **482** (1930) 251.
6. Steinkopf, W., v. Petersdorff, H.-J. and Gording, R. *Ann.* **527** (1937) 272.
7. Gronowitz, S. *Arkiv Kemi* **13** (1958) 295.
8. Gronowitz, S., Moses, P., Hörnfeldt, A.-B. and Håkansson, R. *Arkiv Kemi* **17** (1961) 165.
9. Gronowitz, S. and Karlsson, H.-O. *Arkiv Kemi* **17** (1961) 89.
10. Moses, P. and Gronowitz, S. *Arkiv Kemi* **18**(1961) 119.
11. Hoffman, R. A. and Gronowitz, S. *Arkiv Kemi* **16** (1960) 563.
12. Gronowitz, S. and Karlsson, H.-O. *To be published.*
13. Gronowitz, S., Moses, P. and Hörnfeldt, A.-B. *Arkiv Kemi* **17** (1961) 237.
14. Gronowitz, S., Moses, P. and Håkansson, R. *Arkiv Kemi* **16** (1960) 267.
15. Lawesson, S.-O. *Arkiv Kemi* **11** (1957) 373.

Received August 22, 1961.

Separation of Uronic Acids by Paper Electrophoresis

ARNE HAUG and BJØRN LARSEN

Norwegian Institute of Seaweed Research, N.T.H., Trondheim, Norway

The purpose of this work was to develop a rapid and convenient method for qualitative and quantitative analysis of mixtures of uronic acids. Paper chromatography of uronic acids in the solvents most commonly used for chromatography of sugars does not give satisfactory results. In basic solvents such as pyridine-ethyl acetate-water, the uronic acids do not move, and in acidic solvents such as acetic acid-ethyl acetate-water, the mobilities of the different uronic acids are nearly identical. The most satisfactory solvents are mixtures of both basic and acidic components, such as the solvent introduced by Fischer and Dörfel [1]: Pyridine-ethyl acetate-acetic acid-water, 5:5:1:3. However, the separation is not very satisfactory, it is not possible to distinguish between glucuronic and guluronic acid, it is time-consuming and for quantitative work it is necessary beforehand to transform all lactones to uronic acids. Paper electrophoresis of uronic acids has been used by Jayme and Kringstad [2] and Hoffman, Linker and Meyer [3] but no details of the mobilities of the different uronic acids were given. The possibility of using paperelectrophoresis for separation of uronic acids was therefore further investigated.

Materials and methods. The glucuronic and galacturonic acids used were commercial preparations. The guluronic and mannuronic acids were prepared from hydrolysates of alginic acid by chromatographic separation of the lactones [4] and transforming the lactones by addition of alkali to uronic acid salts. The determination of the pK values has been described earlier [5]. The electrophoresis was carried out in an LKB paper electrophoresis apparatus on Schleicher & Schüll 2043b paper strips. The

Table 1. pK_s values and mobilities in acidic medium.

	pK_s	M_m
Glucuronic acid	3.20	1.10
Mannuronic acid	3.38	1.00
Galacturonic acid	3.42	0.95
Guluronic acid	3.65	0.88

Table 2. Mobilities of uronic acids in borate buffer containing varying amounts of calcium.

Acid	M $CaCl_2$							
	0	0.0001	0.0003	0.0005	0.001	0.002	0.005	0.007
Guluronic	0.93	0.93	0.92	0.85	0.84	0.85	0.85	0.81
Mannuronic	1.00	1.00	1.00	1.00	1.00	1.00	1.00	1.00
Galacturonic	0.97	0.97	1.01	0.98	1.00	1.09	1.18	1.16
Glucuronic	1.05	1.05	1.12	1.13	1.19	1.28	1.44	1.40
Glucose	0.71	0.76	0.80	0.88	1.00	1.01	1.14	1.17

current applied was 0.5 mA/cm. A 2.5 % solution of anilinetrichloroacetate in glacial acid was used as location reagent. After dipping, the strips were heated for 2—3 minutes at 100°C. It was found to be convenient to examine the strips in ultraviolet light.

Results. Acids having sufficiently different pK values may be separated by paper electrophoresis in acid buffer. The pK values of galacturonic, glucuronic, guluronic and mannuronic acids were determined and the results are given in Table 1. The same table gives the mobilities of the four acids relative to mannuronic acid (M_m) in phthalate buffer at pH 3.15. It may be seen from the table that it is possible to separate guluronic and glucuronic acid from each other and from galacturonic and mannuronic acid, while the two latter acids are not separated.

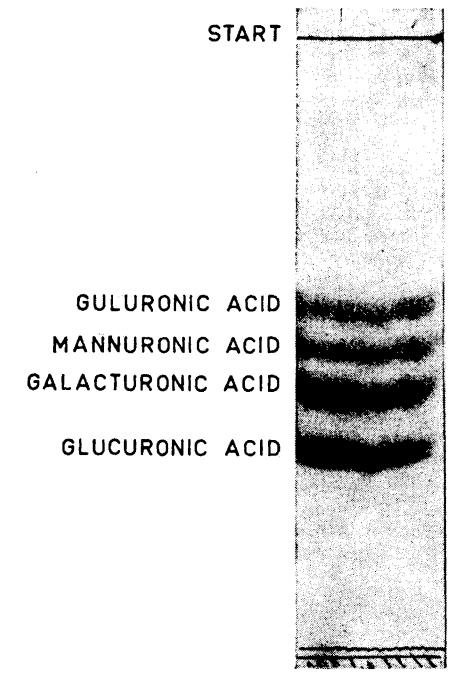

Fig. 1. Separation of uronic acids by electrophoresis in 0.01 M borax containing 0.005 M calcium chloride.

Borate buffers give good results for separation of neutral monosaccharides [6]. However, the separation of uronic acids in this buffer was not satisfactory. If the uronic acids show some tendency to complex formation with calcium at the pH of the borate buffer, the addition of small amounts of calcium to the buffer should reduce the mobility. If this tendency is different for the different uronic acids, the addition of calcium to the buffer might improve the separation. The mobilities of the four uronic acids in borate buffer containing varying amounts of calcium are given in Table 2. For comparison, the mobility of glucose is given in the same table.

As the table shows, the separation is very much improved by the addition of calcium. A 0.01 M borax solution (pH 9.2) containing 0.005 M calcium chloride gives in two hours a satisfactory separation of the four uronic acids investigated (Fig. 1). For quantitative determination the method has the advantage that the alkaline buffer automatically transforms all lactones to uronic acid salts.

1. Fischer, F. G. and Dörfel, H. *Z. physiol. Chem., Hoppe-Seyler's* **301** (1955) 224.
2. Jayme, G. and Kringstad, K. *Chem. Ber.* **93** (1960) 2263.
3. Hoffman, P., Linker, A. and Meyer, K. *Science* **124** (1956) 1252.
4. Fischer, F. G. and Dörfel, H. *Z. physiol. Chem., Hoppe-Seyler's* **302** (1955) 186.
5. Haug, A. *Acta Chem. Scand.* **15** (1961) 950.
6. Foster, A. B. *Advances in Carbohydrate Chem.* **12** (1957) 81.

Received August 9, 1961.

Separation of Uronic Acids on Anion Exchange Columns

BJÖRN LARSEN and ARNE HAUG

Norwegian Institute of Seaweed Research, N.T.H., Trondheim, Norway

Chromatography on anion exchange columns has been used for the separation of oligouronides of different molecular weight [1]. The method has also been used for the separation of monomeric uronic acids. Khym and Doherty [2] separated galacturonic and glucuronic acid on columns of Dowex 1 by elution with 0.15 M acetic acid. Mannuronic and glucuronic acid were, however, not separated. Hallén [3] separated galacturonic and glucuronic acids by chromatography on Dowex 2 columns with 0.03 M borax in 0.6 M sodium hydrogen carbonate as eluant.

The absorption of organic acids on an anionic exchange column is partly due to ionic absorption and partly to molecular absorption [4]. The ionic absorption depends on the dissociation of the acid, and if this type of absorption predominates, it is possible to separate organic acids provided that the dissociation constants are sufficiently different. A difference of 0.2 pH units will often permit a separation of the acids [4].

The dissociation constants of galacturonic, glucuronic, guluronic and mannuronic acid are given in a previous note in this journal [5]. The pK_S values indicate that it should be possible to separate guluronic and glucuronic acid from each other and from mannuronic and galacturonic acid, while the two latter should be inseparable on a laboratory column of convenient size.

Materials and methods. The samples of uronic acids used have been described earlier [5]. Dowex 1 X 8, 200–400 mesh, was used as ion exchange resin and the dimension of the column was 2 × 45 cm. Approximately 0.75 mequiv uronic acids were added to the column in each run and the flow of the liquid was 0.3–0.5 ml/min. The resin was activated with 1 N sodium hydroxide and washed with 2 N acetic acid followed by 0.2 N acetic acid. The uronic acids were applied to the column in slightly alkaline solution. The elution was carried out with acetic acid varying from 0.5 N to 2 N with a linear gradient. The elution was followed by the colour reaction with phenolsulphuric acid [6]. The figures given for optical density refer to 2 ml eluate, and have been corrected for dilution when necessary. The elution products were identified by paper electrophoresis in 0.01 borate buffer containing 0.005 M $CaCl_2$ [5].

Results. The elution curve from a typical experiment is shown in Fig. 1. Table 1 gives the identity of the elution product in the different fractions. The results show that glucuronic and mannuronic acids are separated from each other and from guluronic and galacturonic acid while the separation of the two latter acids was not satisfactory.

The order of elution of guluronic, mannuronic and glucuronic acids is in good agreement with the pK_S values of the uronic acids. Galacturonic acid forms an exception, thus indicating that the order of elution is not controlled solely by ionic absorption.

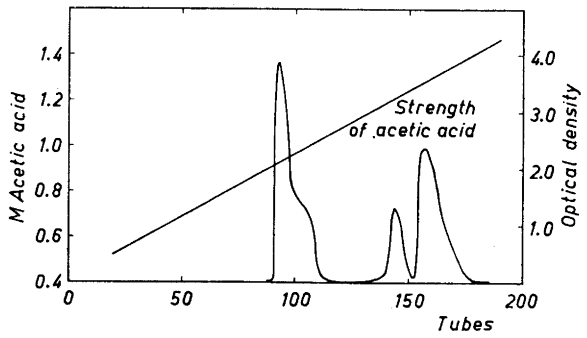

Fig. 1.

Table 1. Uronic acids eluted from anion exchange columns.

Tube	M HAc	Galacturonic acid	Guluronic acid	Mannuronic acid	Glucuronic acid
89 – 96	0.90 – 0.95	+			
97 – 103	0.95 – 1.00	+	+		
104 – 111	1.00 – 1.05		+		
139 – 150	1.20 – 1.25			+	
151 – 175	1.25 – 1.40				+

1. Derungs, R. and Deuel, H. *Helv. Chim. Acta* **37** (1954) 42.
2. Khym, J. X. and Doherty, D. G. *J. Am. Chem. Soc.* **74** (1952) 3199.
3. Hallén, A. *Acta Chem. Scand.* **14** (1960) 2249.
4. Davies, C. W. *Biochem. J.* **45** (1949) 38.
5. Haug, A. and Larsen, B. *Acta Chem. Scand.* **15** (1961) 1395.
6. Dubois, M., Gilles, K. A., Hamilton, J. K., Rebers, P. A. and Smith, F. *Anal. Chem.* **28** (1956) 350.

Received August 9, 1961.

Crystal Data of $MnO,P_2O_3Cl_4,(CH_3COOC_2H_5)_2$

JACOB DANIELSEN and
SVEND ERIK RASMUSSEN

Department of Inorganic Chemistry, University of Aarhus, Aarhus, Denmark

Bassett and Taylor[1,2] investigated 40 years ago the reactions between metal oxides and phosphorus oxychloride. Their aim was to establish the molecular structure of apatite and related compounds.

They discovered that the oxides of divalent manganese, zinc, magnesium and calcium react with phosphorus oxychloride to yield crystalline products. To a crystal chemist of to day this is somewhat surprising and these compounds deserve a structural investigation, as they certainly are not related to apatite.

Bassett and Taylor discovered also that $POCl_3$ dissolved in acetone or ethylacetate or other related compounds reacts violently with the metal oxides mentioned above.

Hydrogen chloride is evolved during the reaction and the oxides are dissolved. After cooling a crystalline product appears, *e.g.* $MnO,P_2O_3Cl_4,(CH_3COOC_2H_5)_2$.

All the compounds mentioned are rather hygroscopic, and we selected the manganous compound for an X-ray investigation as it was apparently less hygroscopic than the others. The chemical analysis confirmed the results of Bassett and Taylor: (Found: Cl 28.84; P 12.38. Calc. for $MnO,P_2O_3Cl_4$, $(C_4H_8O_2)_2$: Cl 28.45; P 12.42).

A crystal of the dimensions: 1.7 mm × 0.8 mm × 0.4 mm was sealed in a Lindemann tube. Weissenberg and precession photographs have been taken using both Cu and Mo radiation.

The crystal proved to be monoclinic. The unit cell has the following dimensions:

$$a = 14.27 \text{ Å}$$
$$b = 13.87 \text{ Å}$$
$$c = 10.04 \text{ Å}$$
$$\beta = 95°56'$$

The following spectra were absent: $h0l$ for $h = 2n + 1$, $0k0$ for $k = 2n + 1$. Thus the space group is $P2_1/a$. The density of the crystal is found as 1.671. The general point in $P2_1/a$ is fourfold so the molecular weight of the asymmetric unit is 500. The calculated molelucar weight for MnO, $P_2O_3Cl_4,(C_4H_8O_2)_2$ is 499.

A full structure determination of this compound has been started.

1. Bassett, H. and Taylor, H. S. *J. Chem. Soc.* **99** (1911) 1402.
2. Bassett, H. and Taylor, H. S. *Z. anorg. Chem.* **73** (1912) 75.

Received August 15, 1961.

Table 1. Uronic acids eluted from anion exchange columns.

Tube	M HAc	Galacturonic acid	Guluronic acid	Mannuronic acid	Glucuronic acid
89 – 96	0.90 – 0.95	+			
97 – 103	0.95 – 1.00	+	+		
104 – 111	1.00 – 1.05		+		
139 – 150	1.20 – 1.25			+	
151 – 175	1.25 – 1.40				+

1. Derungs, R. and Deuel, H. *Helv. Chim. Acta* **37** (1954) 42.
2. Khym, J. X. and Doherty, D. G. *J. Am. Chem. Soc.* **74** (1952) 3199.
3. Hallén, A. *Acta Chem. Scand.* **14** (1960) 2249.
4. Davies, C. W. *Biochem. J.* **45** (1949) 38.
5. Haug, A. and Larsen, B. *Acta Chem. Scand.* **15** (1961) 1395.
6. Dubois, M., Gilles, K. A., Hamilton, J. K., Rebers, P. A. and Smith, F. *Anal. Chem.* **28** (1956) 350.

Received August 9, 1961.

Crystal Data of $MnO,P_2O_3Cl_4,(CH_3COOC_2H_5)_2$

JACOB DANIELSEN and
SVEND ERIK RASMUSSEN

Department of Inorganic Chemistry, University of Aarhus, Aarhus, Denmark

Bassett and Taylor[1,2] investigated 40 years ago the reactions between metal oxides and phosphorus oxychloride. Their aim was to establish the molecular structure of apatite and related compounds.

They discovered that the oxides of divalent manganese, zinc, magnesium and calcium react with phosphorus oxychloride to yield crystalline products. To a crystal chemist of to day this is somewhat surprising and these compounds deserve a structural investigation, as they certainly are not related to apatite.

Bassett and Taylor discovered also that $POCl_3$ dissolved in acetone or ethylacetate or other related compounds reacts violently with the metal oxides mentioned above.

Hydrogen chloride is evolved during the reaction and the oxides are dissolved. After cooling a crystalline product appears, *e.g.* $MnO,P_2O_3Cl_4,(CH_3COOC_2H_5)_2$.

All the compounds mentioned are rather hygroscopic, and we selected the manganous compound for an X-ray investigation as it was apparently less hygroscopic than the others. The chemical analysis confirmed the results of Bassett and Taylor: (Found: Cl 28.84; P 12.38. Calc. for $MnO,P_2O_3Cl_4$, $(C_4H_8O_2)_2$: Cl 28.45; P 12.42).

A crystal of the dimensions: 1.7 mm × 0.8 mm × 0.4 mm was sealed in a Lindemann tube. Weissenberg and precession photographs have been taken using both Cu and Mo radiation.

The crystal proved to be monoclinic. The unit cell has the following dimensions:

$$a = 14.27 \text{ Å}$$
$$b = 13.87 \text{ Å}$$
$$c = 10.04 \text{ Å}$$
$$\beta = 95°56'$$

The following spectra were absent: $h0l$ for $h = 2n + 1$, $0k0$ for $k = 2n + 1$. Thus the space group is $P2_1/a$. The density of the crystal is found as 1.671. The general point in $P2_1/a$ is fourfold so the molecular weight of the asymmetric unit is 500. The calculated molelucar weight for MnO, $P_2O_3Cl_4,(C_4H_8O_2)_2$ is 499.

A full structure determination of this compound has been started.

1. Bassett, H. and Taylor, H. S. *J. Chem. Soc.* **99** (1911) 1402.
2. Bassett, H. and Taylor, H. S. *Z. anorg. Chem.* **73** (1912) 75.

Received August 15, 1961.

The Mononuclear Hydrolysis of Vanadium(V)

DAVID DYRSSEN and TATSUYA SEKINE

Department of Inorganic Chemistry, Royal Institute of Technology, Stockholm 70, Sweden

The hydrolysis of vanadium(V) has been studied by emf titrations at this laboratory [1,2]. Because of the unusual stability of the decavanadates, it was not possible to detect the mononuclear hydrolytic species in acid solutions [1]. However, in 0.5 M Na(OH,Cl) solutions Ingri and Brito [2] could calculate the equilibrium constants for the mononuclear reactions.

$$VO_3^- + H_2O \rightleftharpoons HVO_4^{2-} + H^+; pK_{a3} = 7.7$$

$$HVO_4^{2-} \rightleftharpoons VO_4^{3-} + H^+; \qquad pK_{a4} = 13.0$$

The purpose of the present work was to study the mononuclear hydrolysis of vanadium(V) in the lower pH range and to determine the acidity constants of the following equilibria at 25°C:

$$VO_2^+ + H_2O \rightleftharpoons HVO_3 + H^+; K_{a1} \qquad (1)$$

$$HVO_3 \rightleftharpoons VO_3^- + H^+; K_{a2} \qquad (2)$$

(From X-ray work on solid vanadium compounds, there is reason to believe that the vanadium(V) is five-coordinated with oxygen except in some VO_4^{3-} compounds, but we have chosen here to write the formula with as few H_2O as possible.)

To avoid polymerization of the hydrolytic species it was desirable to work with solutions of very low vanadium concentrations. (Spectrophotometric work [3] has shown that the decavanadates probably exist even at 10^{-4} M.) For this purpose, carrier-free ^{48}V was prepared by deuteron irradiation of pure titanium metal in the Swedish cyclotron at the Nobel Institute of Physics.

Methods such as emf titrations, which are based on the measurement of the amount of protons released from the vanadyl ion, cannot be used for very low metal concentrations. We, therefore, tried to find a suitable solvent extraction system. Instead of introducing a hydrophobic chelating reagent that would form an uncharged extractable VO_2^+ complex, we wished to use an organic solvent which would extract uncharged HVO_3. The alcohol, methyl-*iso*butylcarbinol (hexol), was found to give a measurable distribution ratio (*cf.* Fig. 1) and was chosen for the investigation. The aqueous phase was 0.5 M (H,Na)ClO_4 which was buffered with small amounts of sodium acetate.

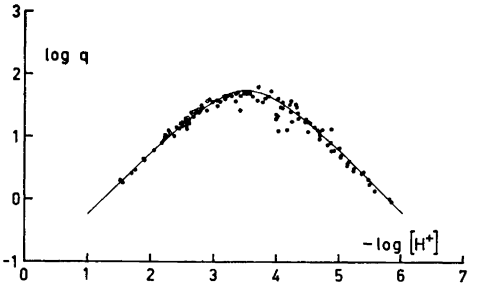

Fig. 1. The distribution of ^{48}V between hexol and 0.5 M (H,Na)ClO_4.

The results for carrier-free ^{48}V are given in Fig. 1 as log q (q = γ-activity of ^{48}V in the hexol phase/γ-activity of ^{48}V in the aqueous phase) as a function of $-\log[H^+]$. In some experiments (open circles) a solution of ^{48}V in 0.5 M $HClO_4$ was added to the aqueous layer. In other experiments (closed circles) a solution of ^{48}V in hexol was added to the organic layer. The results of these two procedures agreed quite well.

The following conclusions may be drawn from Fig. 1 even though there is considerable scattering of the points. The slope +1 shows the existence of an uncharged vanadium species in the hexol phase with one proton less than $VO_2(H_2O)_n^+$. The slope −1 shows that there exists a monovalent negative vanadium ion in the aqueous phase with one proton less than the uncharged complex in the organic phase. The rather sharp bending of the curve shows that the stability range of the uncharged complex is not very large. In each run, about the same amount of ^{48}V was added to the system and, therefore, the total vanadium concentration in each phase varies with the distribution ratio. Still the limiting slopes in Fig. 1 are exactly + 1 and −1. This indicates that no polynuclear species

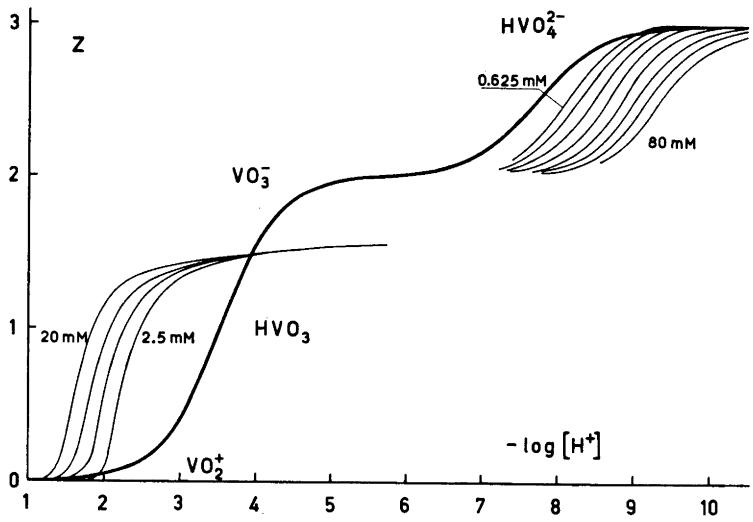

Fig. 2. The number of OH^- added to VO_2^+, as a function of $-\log [H^+]$. The thick curve represents the mononuclear hydrolysis. The thin curves are based on emf titrations [1,2] at various concentrations of V, and show the effect of the formation of polynuclear species.

are formed. This was further confirmed by the addition of inactive vanadium(V). A shift of the extraction curve was obtained by the addition of 10^{-5} M vanadium or more.

The expression for the distribution ratio q that is compatible with these observations is

$$q = \frac{[HVO_3]_{org}}{[VO_2^+] + [HVO_3] + [VO_3^-]}$$

Using the equilibrium constants of reactions (1) and (2) and the partition coefficient of HVO_3, λ, one obtains

$$q = \frac{\lambda}{K_{a1}^{-1}[H^+] + 1 + K_{a2}[H^+]^{-1}}$$

By curve-fitting [4,5], the following approximate values of λ, K_{a1}, and K_{a2} were determined:

$\log \lambda = 2.10$; $pK_{a1} = 3.30$; $pK_{a2} = 3.70$

With these acidity constants and the data of Ingri and Brito [2], it is possible to calculate the average number of hydroxyl groups attached to VO_2^+ as a function of pH (Fig. 2) for the mononuclear hydrolysis of vanadium(V). The constants will be refined by high-speed computing using the LETAGROP program [6,7]. Details will be given in the full paper.

Acknowledgements. We wish to thank Professor Lars Gunnar Sillén, Dr. Nils Ingri, Dr. Felipe Brito, and Professor Howard Evans for helpful discussions, and Dr. Denis Mc Whan for revising the English text. We also wish to thank Docent Wilhelm Forsling and Mr. Hans Rundvall for the irradition of the titanium target. The work has been supported by the *Swedish Council for Atomic Research* and by the *Air Force Division of the Air Research and Development Command, USAF, through its European Office.*

1. Rossotti, F. J. C. and Rossotti, H. *Acta Chem. Scand.* **10** (1956) 957.
2. Ingri, N. and Brito, F. *Acta Chem. Scand.* **13** (1959) 1971; *Anales fis. y quim. (Madrid)* **56 B** (1960) 165.
3. Newman, L. and Quinlan, K. P. *J. Am. Chem. Soc.* **81** (1959) 547.
4. Dyrssen, D. and Sillén, L. G. *Acta Chem. Scand.* **7** (1953) 663.
5. Sillén, L. G. *Acta Chem. Scand.* **10** (1956) 186.
6. Dyrssen, D., Ingri, N. and Sillén, L. G. *Acta Chem. Scand.* **15** (1961) 694.
7. Ingri, N. and Sillén, L. G. *Acta Chem. Scand. In print.*

Received August 11, 1961.

Thin-layer Chromatography of Some Nitramine-Explosives

J. G. LENNART HARTHON

Analytical Laboratory, Research Department of AB Bofors, Nobelkrut Bofors, Sweden

During the investigations of formation of the high explosive hexogen by nitrolysis of hexamethylene tetramine a number of nitramines closely related to hexogen were discovered. These compounds are of interest as possible reaction intermediates or side products which if present may adversely affect the properties of hexogen.

Very few papers deal with methods for chromatographic separation of these compounds. Malmberg *et al.*[1] described a column chromatographic procedure for the separation of various nitramines. This method, however, is rather tedious and does not lend itself to routine examinations. Yasuda and Rogers [2] deal with the separation of hexogen and octogen (HMX) on paper impregnated with formamide, for the determination of RDX in HMX.

The scope of this investigation was to establish if thin-layer chromatography is a suitable method for separating some of the more well-known nitramines.

Of special interest is, of course, the separation of hexogen, hexahydro-1,3,5-trinitro-*s*-triazine (III) and HMX, octahydro-1,3,5,7-tetranitro-*s*-tetrazine (V) as hexogen manufactured by the Bachmann process usually contains a few per cent of HMX. For investigation of different steps in the manufacturing process BSX, 2,4,6-trinitro-2,4,6-triazaheptane-1,7-dioldiacetate (I) AcAn, 2,4,6,8-tetranitro-2,4,6,8-tetrazanonane-1,9-dioldiacetate (II). SEX, 1-acetyloctahydro-3,5,7-trinitro-1,3,5,7-s-tetrazine (VI) and DPT, 3,7-dinitro-1,3,5,7-tetrazabicyclo-[3,3,1]-nonane (VII) were of interest and therefore included in this study.

Experimental. The thin-layer plates were prepared by coating silica gel G (Merck) on glass plates using Stahl's technique and activated at 110° for an hour. All substances tested were prepared in our laboratories and purified by several recrystallisations in suitable solvents. All spots were applied in acetone solution with an Agla burette.

The number of solvents usable for chromatography are limited as the nitramine compounds are not easily soluble in most organic solvents except for ketones. The latter, however, are so strong eluants that all substances follow the front. By addition of less polar solvents to, *e.g.*, acetone the solubility is so decreased that problems with tailing spots may easily arise. The most promising combinations of solvents were mixtures of aliphatic hydrocarbons with acetone or ethylmethylketone. With a mixture of petroleum ether (b.p. 40–60°C) and acetone, 2:1.2, as the moving phase the most efficient separation was obtained. The solubility of the nitramines in this solvent was, however, so low that spots containing more than 50 μg of each substance caused tailing.

Detection of spots. The usual way of detecting nitramines is with the Franchimont reagent [1]. This, however, is less suitable in thin-layer chromatography as the zinc-powder used is difficult to remove completely from the surface and thus may hide weak spots. The sensitivity of this reagent is otherwise excellent (approxi-

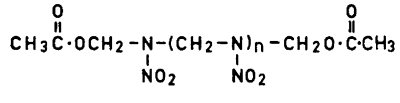

I n=2
II n=3

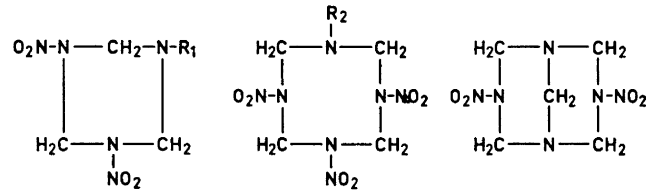

III $R_1 = -NO_2$ *IV* $R_1 = -CO{\cdot}CH_3$ *V* $R_2 = -NO_2$ *VI* $R_2 = -CO{\cdot}CH_3$ *VII*

mately 0.5 μg). With fluorescence indicators (fluorescein or diphenylbenzidine) it is possible to detect 1—2 μg by noting the reduction in the fluorescent background when irradiating with ultraviolet light.

The photochemical reaction between diphenylamine and nitrates proposed by Coldwell [3], with the nitrate ion resulting in a strongly yellow product consisting of 2- and 4-nitrodiphenylamine [4], is said to give only a very faint yellow colour difficult to distinguish from the background if applied to RDX. When spots of nitramines on silica-gel plates were sprayed with a 1 % solution of diphenylamine in ethanol and exposed for 5 min to radiation from a standard 125 W mercury lamp (black glass bulb removed) strong blue-violet spots appeared making 0.5 μg of nitramines easily detectable against a faint brownish background. The nature of this reaction is still unknown but the reaction product could be separated by chromatography into at least four compounds, two of which were violet and two yellow, the latter presumably the two nitrodiphenylamines isolated by Coldwell. By visual comparison of colour intensities with spots obtained from known standard amounts a semiquantitative estimation of nitramines was possible.

Results. Fig. 1 shows the separation of five different nitramines. About 30 μg substance was applied in each spot. The plates were developed for about 45 min at room temperature. To obtain constant R_F values the temperature is rather critical with this type of solvent. It is therefore advisable to use a reference spot of RDX. The separation was, however, always good. The two substances BSX and AcAn were not separable with this solvent. This is quite understandable due to their similar structure.

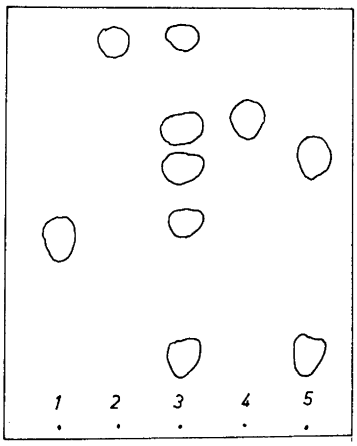

Fig. 1. Chromatogram of different nitramines 1.) HMX. 2.) BSX. 3.) From top BSX, RDX, DPT, HMX and SEX. 4.) RDX. 5.) From top HMX and SEX.

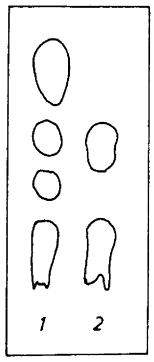

Fig. 2. To the left chromatogram of waste product from the Bachmann process. To the right reference chromatogram.

Fig. 2 shows to the left a chromatogram of a product isolated from a waste liquor of the Bachmann process. About 200 μg was applied. To the right a reference mixture of HMX and SEX was applied. The by-product was treated in such a manner that neither BSX or DPT could be present. It was evident that RDX, HMX and SEX were present. The third spot from the top is, however, still unknown, but is believed to be TAX, 1-acetylhexahydro-3,5-dinitro-*s*-triazine (IV). This has, however, not yet been proved as pure TAX is not available and no method for synthesis of this compound seems to have been published. Work is in progress to isolate the substance and to prove its identity.

Thin-layer chromatography has showed to be a most valuable tool for rapid separation of nitramines of interest in the manufacture of hexogen. No doubt further types may be separated in this way and a better quantitative estimation of the different substances after elution of the spots seems to be possible with Yasuda's colorimetric micromethod [2].

1. Malmberg, E. W., Trueblood, K. N. and Waugh, T. D. *Anal. Chem.* **25** (1953) 901.
2. Yasuda, S. K. and Rogers, R. N. *Anal. Chem.* **32** (1960) 910.
3. Coldwell, B. B. *Analyst* **84** (1959) 665.
4. Coldwell, B. B. and McLean, S. R. *Can. J. Chem.* **37** (1959) 1637.

Received August 26, 1961.

Studies on the Occurrence of Cholesterol in Water-Containing Liquid-Crystalline Form

III. Formation of Cholesterol-containing Mesomorphous Phases by the Interaction of Sodium Caprylate Solutions with Solid Cholesterol Crystals

PER EKWALL and
LEO MANDELL

Institute of Physical Chemistry, Åbo Akademi, Åbo, Finland

Whereas salts of fatty acids from nonylic acid upwards are able to cause solid crystalline cholesterol to change into the mesomorphous state already when their concentrations exceed their limiting association concentrations (LAC) [1], the same process is not effected by the sodium salt of the next lower fatty acid, caprylic acid, before the concentration of this salt exceeds the critical micelle concentration (CMC). The formation of the mesophase takes place only very slowly in caprylate solutions immediately above the CMC at room temperature. High concentrations of caprylate are necessary to cause the process to proceed rapidly at this temperature. An increase in temperature, however, accelerates the process also at low caprylate concentrations, but the mesomorphous cholesterol-containing phase is not produced by caprylate solutions even at high temperatures unless the concentration of the latter exceeds the CMC.

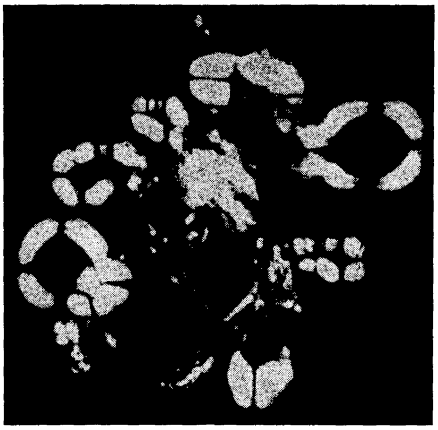

Fig. 1b. Crossed Nicols. 200 ×.

The mesomorphous substance that is formed in concentrated caprylate solutions down to that containing about 2.4 moles of sodium caprylate in 1 000 g of water consists of strongly doubly-refracting matter which rapidly coalesces to more or less spherical globules (Figs. 1a and 1b). In solutions from about 2.4 M down to the CMC, the mesomorphous matter forms long, narrow, often curved spool-shaped doubly-refracting structures (Fig. 2).



Fig. 1a. Ordinary light. 200 ×.

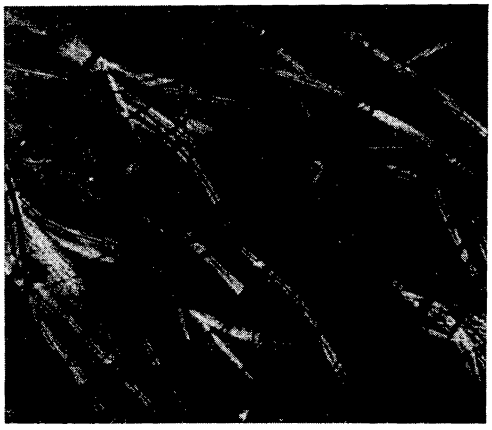

Fig. 2. Crossed Nicols. 200 ×.



Fig. 3. Crossed Nicols. 200 ×.

The appearance of the spherical particles does not change when the temperature rises, but the spool-shaped mesomorphous substance does undergo a change. When the latter substance is warmed in its mother liquor on a heated stage between 34 and 38°C, it changes into a weakly doubly-refracting semiliquid mass (Fig. 3). The same change occurs when the mesomorphous substances is first freed of its mother liquor. The temperature where the change takes place varies for the mesomorphous substances that have separated from solutions containing different caprylate concentrations: it increases from about 34°C for the substance that is formed in solutions at the highest concentration studied to about 38°C for the substance formed near the CMC of sodium caprylate.

Thus cholesterol forms at least two water-containing mesomorphous phases under the influence of caprylate solutions at 20°C. The two phases are formed at different caprylate concentrations and they differ in appearance and temperature stability. Whether the mesomorphous phase that is produced when the spool-shaped liquid crystals are warmed to 34—38°C is identical with the phase that separates from highly concentrated caprylate solutions or represents a third mesomorphous phase has not yet been investigated.

These studies confirm that the chain length of the parent fatty acid is of decisive importance in determining the properties of the water-containing cholesterol mesophases and the conditions under which these phases are produced.

Financial support from *Sigrid Juselius' Stiftelse* is gratefully acknowledged.

1. Part I of this series. *Acta Chem. Scand.* **15** (1961) 1195.

Received August 26, 1961.

Studies on the Occurrence of Cholesterol in Water-Containing Liquid-Crystalline Form

IV. The Solubility of Cholesterol in Sodium Caprylate Solutions at 20°C

PER EKWALL and
LEO MANDELL

Institute of Physical Chemistry, Åbo Akademi, Åbo, Finland

It has been stated in the literature that cholesterol is almost insoluble in water [1] and we have been unable to find any reliable solubility data for this sterol. It is, however, known that the solubility of cholesterol in water increases appreciably in the presence of association colloids of the bile salt type owing to micellar solubilisation. Thus, Bashour and Baumann have reported rather high solubilities of cholesterol in solutions of different bile acid salts [2]. Also Ekwall has found cholesterol to dissolve in appreciable amounts in sodium cholate solutions. However, the values of the latter author were much lower than the values given by the former [3]. Values of the solubility of cholesterol in solutions of fatty acid salts or other association colloids of the paraffin-chain type seem not to have been reported.

We have found that cholesterol in the finely divided form in which it exists after its solubilisation in association colloid micelles undergoes rapid oxidation at temperatures over 40°C. This confirms the observation of Bergström that cholesterol in the colloidal state (in the presence of sodium stearate) is oxidised at high tem-



Fig. 3. Crossed Nicols. 200 ×.

The appearance of the spherical particles does not change when the temperature rises, but the spool-shaped mesomorphous substance does undergo a change. When the latter substance is warmed in its mother liquor on a heated stage between 34 and 38°C, it changes into a weakly doubly-refracting semiliquid mass (Fig. 3). The same change occurs when the mesomorphous substances is first freed of its mother liquor. The temperature where the change takes place varies for the mesomorphous substances that have separated from solutions containing different caprylate concentrations: it increases from about 34°C for the substance that is formed in solutions at the highest concentration studied to about 38°C for the substance formed near the CMC of sodium caprylate.

Thus cholesterol forms at least two water-containing mesomorphous phases under the influence of caprylate solutions at 20°C. The two phases are formed at different caprylate concentrations and they differ in appearance and temperature stability. Whether the mesomorphous phase that is produced when the spool-shaped liquid crystals are warmed to 34—38°C is identical with the phase that separates from highly concentrated caprylate solutions or represents a third mesomorphous phase has not yet been investigated.

These studies confirm that the chain length of the parent fatty acid is of decisive importance in determining the properties of the water-containing cholesterol mesophases and the conditions under which these phases are produced.

Financial support from *Sigrid Juselius' Stiftelse* is gratefully acknowledged.

1. Part I of this series. *Acta Chem. Scand.* **15** (1961) 1195.

Received August 26, 1961.

Studies on the Occurrence of Cholesterol in Water-Containing Liquid-Crystalline Form

IV. The Solubility of Cholesterol in Sodium Caprylate Solutions at 20°C

PER EKWALL and
LEO MANDELL

Institute of Physical Chemistry, Åbo Akademi, Åbo, Finland

It has been stated in the literature that cholesterol is almost insoluble in water [1] and we have been unable to find any reliable solubility data for this sterol. It is, however, known that the solubility of cholesterol in water increases appreciably in the presence of association colloids of the bile salt type owing to micellar solubilisation. Thus, Bashour and Baumann have reported rather high solubilities of cholesterol in solutions of different bile acid salts [2]. Also Ekwall has found cholesterol to dissolve in appreciable amounts in sodium cholate solutions. However, the values of the latter author were much lower than the values given by the former [3]. Values of the solubility of cholesterol in solutions of fatty acid salts or other association colloids of the paraffin-chain type seem not to have been reported.

We have found that cholesterol in the finely divided form in which it exists after its solubilisation in association colloid micelles undergoes rapid oxidation at temperatures over 40°C. This confirms the observation of Bergström that cholesterol in the colloidal state (in the presence of sodium stearate) is oxidised at high tem-

peratures [4]. In order to avoid this oxidation of cholesterol we have carried out our experiments in a nitrogen atmosphere at 20°C. We saturated the association colloid solutions with cholesterol by shaking and vigorously mixing the solutions with a magnetic stirrer over long periods (1—5 weeks). The excess of solid cholesterol or cholesterol-containing mesophases that were formed under certain conditions were separated from the solution by combined centrifugation and filtration through fine membrane filters in sealed filter tubes. These precautions were found necessary to effect a complete separation of the very finely divided matter. The cholesterol in the clear solutions was determined spectrophotometrically by the method of Zlatkis, Zak and Boyle which is suitable for the measurement of cholesterol in amounts down to about 0.01—0.05 mg.[5]

The most reliable determinations gave a solubility value of only 0.06—0.07 mg of cholesterol in 1 000 g of water. We found that the solubility of cholesterol was already slightly higher (several tenths of a milligram to about one milligram in 1 000 g of solution) in sodium caprylate solutions below the critical micelle concentration (CMC). Owing to the variation of the measured solubility values, we are unable to report any reliable solubility data for this concentration range. A definite increase in solubility is, however, observed when the sodium caprylate concentration exceeds the CMC, 0.36 *M*. (In this paper *M* = moles sodium caprylate/1 000 g of cholesterol-free solution). Already in a 0.39 *M* caprylate solution, the solubility is 2 mg of cholesterol in 1 000 g of solution and in a 0.56 *M* caprylate solution the solubility is about 60 mg of cholesterol in 1000 g of solution. The solubility then increases more rapidly with increasing caprylate concentration and is 1 000 mg of cholesterol in 1 000 grams of the 1 *M* solution and about 5 000 mg in 1 000 grams of the 1.5 *M* solution. The solubility increases even more rapidly in more concentrated caprylate solutions, being about 20 g in 1 000 g of the 2 *M* solution and about 50 g in 1 000 g of the 2.4 *M* solution. In the latter range of caprylate solutions, the solubility of cholesterol is hence about 200 000—500 000 times as great as in pure water (Fig. 1).

This great increase in solubility depends, of course, on the solubilising power of sodium caprylate which increases markedly with increasing colloid concentration. The different solubilisation powers in various

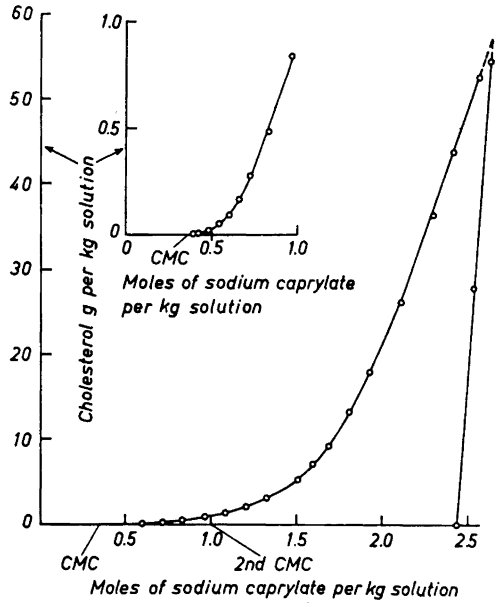

Fig. 1.

concentration ranges becomes more clearly evident if the solubility is divided by the content of micellar sodium caprylate and the increase of this ratio with the caprylate

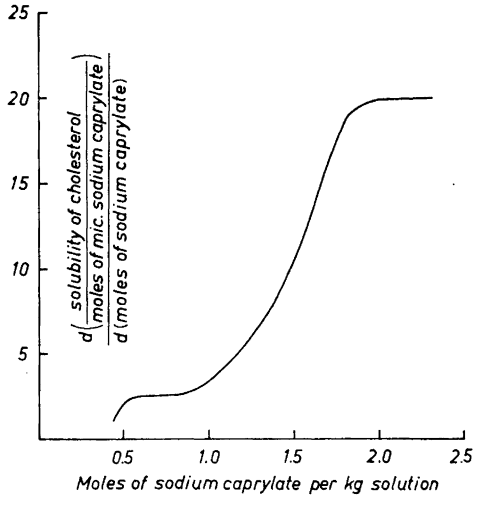

Fig. 2.

concentration is plotted as a function of the concentration (Fig. 2). A pronounced increase in the power of micellar caprylate to solubilise cholesterol is observed between 1.0 and 1.9 *M* caprylate. Below the first-mentioned and above the last-mentioned concentration the solubilising power of the micelles changes only little with the concentration. Our earlier studies have revealed that the structures of pure caprylate solutions change at approximately these same concentrations [6]. The concentration range from the CMC, at 0.36 *M*, to about 1 *M* (0.38 M → 1.2 M, *i.e.*, moles per 1 009 g of water) is known as the so-called small micelle range where the properties of the micellar substance are constant and the micelles are relative small spheres. Above the last-mentioned concentration (the so-called 2nd CMC), the properties of the micellar substance change evidently as a result of the formation of larger micelles which are no longer spherical in form. Above the concentration of about 1.9—2.0 *M* (*i.e.* 2.8—3.0 M) a further change has been observed to take place in the properties of the micellar substance and this has been attributed to the formation of micelles of cylindrical form which rapidly increase in length with increasing colloid concentration. It is of considerable interest that there is a relationship between the solubility of cholesterol and the micellar structure of the caprylate solution. Similar variations in the solubility of cholesterol with the structure of the solution would be expected with other association colloids.

In the solubilisation mixed micelles composed of caprylate ions and cholesterol are formed, but nothing definite is known about their composition. It is probable that there exists an equilibrium between these mixed micelles and pure caprylate micelles similarly as in the solubilisation of other lipophilic compounds with large molecules such as steroid hormones and polycyclic aromatic hydrocarbons [7,8]. It is also likely that the mixed micelles, at least those formed in the small micelle range, do not contain more than one cholesterol molecule to a micelle. As is usual, the large hydrocarbon part of cholesterol is incorporated within the micelle and the hydrophilic hydroxyl group, like the carboxyl groups of caprylate ions, is probably located at the surface of the micelle in contact with water. In the formation of these mixed micelles ion-dipole interactions and hydrogen-bond formation between the hydroxyl groups and the adjacent ionised carboxyl groups play a decisive part similarly as in the solubilisation of other amphiphilic compounds such as paraffin-chain alcohols and fatty acids. The mixed micelles in question are evidently sparingly soluble in water for when more cholesterol is added to the system the mixed micelle substance separates from the isotropic solution together with the excess of cholesterol as a mesomorphous phase composed of cholesterol, sodium caprylate and water. We have previously reported [9] that the mesomorphous phase that separates from caprylate solutions between the CMC and a concentration of about 1.9—2.0 *M* (*i.e.* 2.8—3.0 M) differs in type from that which separates from more concentrated caprylate solutions in which the pure caprylate micelles, and probably also the mixed micelles, have a structure different from the structure of the micelles in solutions below the last-mentioned concentration limit.

Financial support from *Sigrid Juselius' Stiftelse* is gratefully acknowledged.

1. Lettré, H., Inhoffen, H. H. und Tschesche, R. *Über Sterine, Gallensäuren und verwandte Naturstoffe*, Band I. Ferdinand Enke, Stuttgart, p. 5.
2. Bashour, J. T. and Baumann, L. *J. Biol. Chem.* **121** (1937) 1.
3. Ekwall, P. *Proc. Intern. Coll. Biochem. Probl. Lipids. Brussels* 1953, 103.
4. Bergström, S. *Arkiv Kemi Mineral. Geol.* **16A** (10) 1.
5. Zlatkis, A., Zak, B. and Boyle, A. J. *J. Lab. Clin. Med.* **41** (1953) 482.
6. Ekwall, P., Danielsson, I. and Mandell, L. *Kolloid-Z.* **169** (1960) 113; *Proc. 3rd Intern. Congr. Surface Activity*, Cologne 1960, Vol. I, Section A, 189; *Finska Kemistsamf. Medd.* (*in press*) and *unpublished experiments.*
7. Ekwall, P., Setälä, K. and Sjöblom, L. *Acta Chem. Scand.* **5** (1951) 175.
8. Ekwall, P., Lundsten, T. and Sjöblom, L. *Acta Chem. Scand.* **5** (1951) 1383.
9. Part III in this series. *Acta Chem. Scand.* **15** (1961) 1403.

Received August 26, 1961.

Studies on the Occurrence of Cholesterol in Water-Containing Liquid-Crystalline Form

V. Equilibria between Isotropic Caprylate Solutions and Cholesterol-Containing Mesophases

PER EKWALL and LEO MANDELL

Institute of Physical Chemistry, Åbo Akademi, Åbo, Finland

A brief summary of data collected hitherto in our investigations of the phase equilibria of the three-component system cholesterol-sodium caprylate-water is presented below. These data are limited to those relating to the equilibria between isotropic aqueous caprylate solutions containing cholesterol in solubilised form and mesomorphous cholesterol-caprylate-water phases.

Equilibrium is attained in the heterogeneous cholesterol-caprylate-water system more rapidly at higher temperatures than at room temperature; but the attainment of the final equilibrium state at 20°C takes a very long time. We have nevertheless preferred to carry out the experiments at room temperature only, and to promote the interaction by prolonged vigorous magnetic stirring. The cholesterol crystals are loosened up by the penetrating caprylate solution and are then readily split by the mechanical action into thin flakes which rapidly react further. The disappearance of the strongly doubly-refracting cholesterol crystals can be followed in the microscope. After all traces of solid crystals had completely disappeared, the reaction was allowed to continue for a shorter or longer period (up to 30 days). Parallel experiments carried out with different periods of reaction revealed that the true equilibrium state had been reached in each case. The equilibrated system was then centrifuged (at about 25 000 *g*) to separate the mesomorphous phase from the isotropic solution, and the cholesterol, caprylate and water contents of both phases were analysed. The cholesterol content was determined spectrophotometrically by the method of Zlatkis, Zak and Boyle [1]. The sodium caprylate contents were determined after drying the isolated phases over phosphorus pentoxide to a constant weight (the loss in weight gave an approximate value

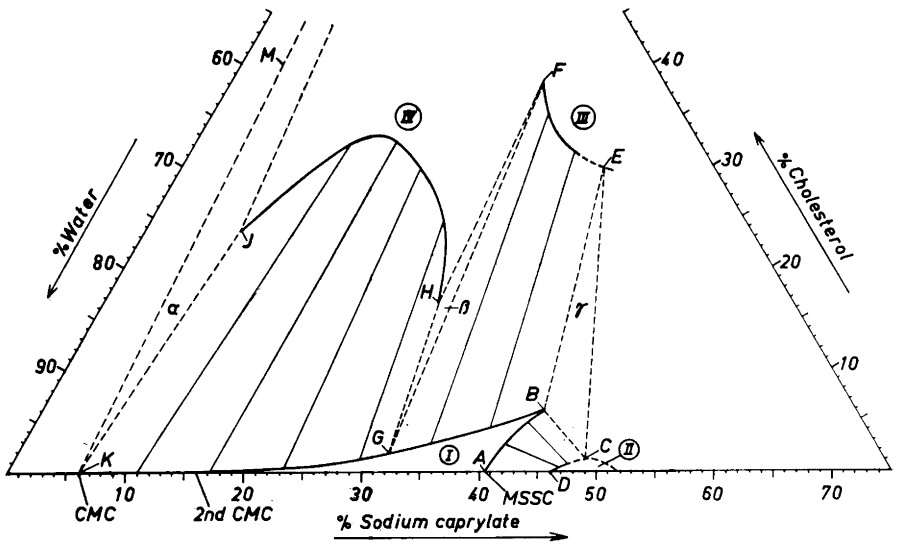

Fig. 1.

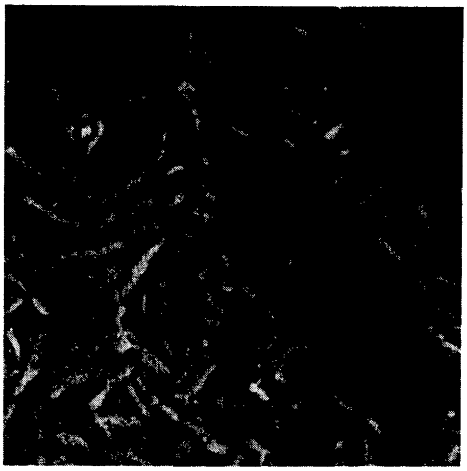

Fig. 2A. Ordinary light. 200 ×.



Crossed Nicols. 200 ×.

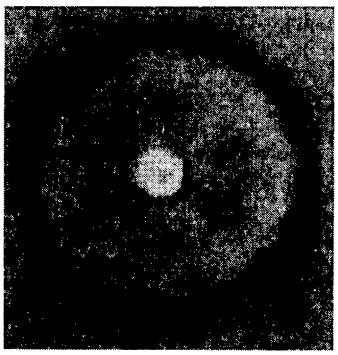

Fig. 2B.

for the water content) by dissolving the residue in glacial acetic acid and titrating it with perchloric acid employing crystal violet as indicator, and the water content either by evaporating the sample to dryness or by the Karl Fischer method. The mesomorphous phases were in addition examined with the microscope and with a X-ray diffraction camera. The X-ray photographs were taken with a Philips Norelco unit employing a copper target and Ni-filtered radiation. A small angle vacuum camera with pinhole collimators (Kiessig) and a sample to film distance of 212 mm were employed. The X-ray room was maintained at a temperature of 20°C.

Fig. 1 shows a part of the triangular diagram for the investigated three-component system. The region of homogeneous, isotropic aqueous solutions containing caprylate and solubilised cholesterol is marked I. This region naturally starts at zero caprylate concentration, but up to a caprylate concentration of about 16 % the solubility of cholesterol is so low that the isotropic region can be indicated only by a thick line lying against the caprylate axis. When the concentration of a pure sodium caprylate solution rises to 40.5 % (the "middle soap separation concentration", MSSC) the system becomes heterogeneous owing to the separation of mesomorphous middle soap. This mesophase can take up small amounts of cholesterol. The homogeneous middle soap range is marked II. The region ABCD between the homogeneous phases I and II represents a two-phase region in which the system is divided into an isotropic caprylate solution with the composition indicated by line AB and a middle soap with the composition indicated by line CD. The division is indicated by the tie lines. The appearance (focal conic texture) of the cholesterol-containing mesomorphous phase II in a microscope in ordinary light and between crossed nicols is seen in Fig. 2A. Fig. 2B shows the X-ray diagram for the same phase. The region

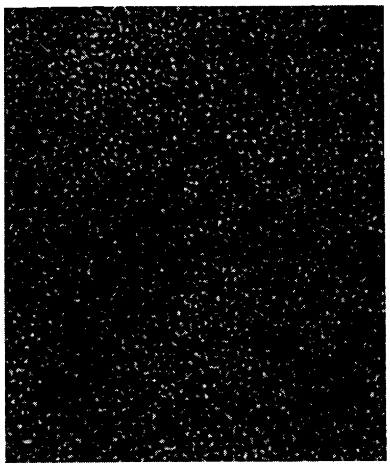

Fig. 3A. Ordinary light. 200 ×.

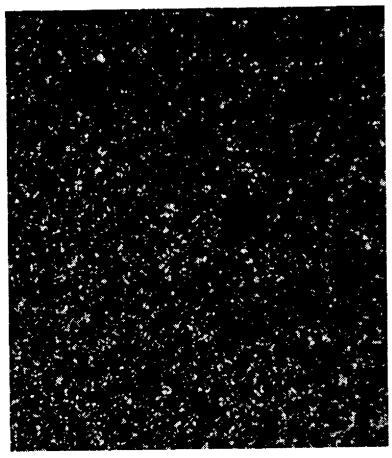

Crossed Nicols. 200 ×.

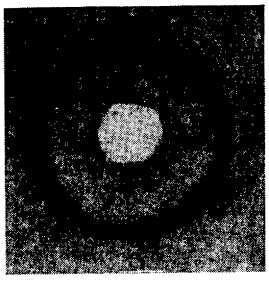

Fig. 3B.

BEFG represents another two-phase region in which the system is divided into an isotropic caprylate solution (I) with the composition given by the line BG and a mesomorphous phase with the composition given by line EF. Line EF thus represents the lower limit of the region where the homogeneous mesophase III of high cholesterol content exists. At point E this phase is composed of 30 % cholesterol, 36 % sodium caprylate, and 34 % water and at point F of 38 % cholesterol, 27 % sodium caprylate and 35 % water. The appearance (mosaic texture) of this mesomorphous phase in a microscope is shown in Fig. 3A and its X-ray diagram in Fig. 3B. In the region GHJK there is a third two-phase region in which the system is divided into an isotropic caprylate solution (I) with the composition given by line GK and a mesomorphous phase with the composition given by line HJ. The latter line represents the lower boundary of the region where a homogeneous mesophase IV of relatively high cholesterol content exists. The composition of this phase at point H is 17 % cholesterol, 28 % sodium caprylate and 55 % water, and at point I 23.5 % cholesterol, 8 % sodium caprylate and 68.5 % water. In a microscope this mesomorphous phase has the appearance shown in Fig. 4A. This phase exists as spool-shaped liquid crystals. This is the phase described previously (part III of this series; Fig. 2) which is stable only up to 34—38°C. Fig. 4B shows the X-ray diagram for this phase. A further two-phase region lies to the left of the line KM. The two phases are a dilute, isotropic sodium caprylate solution or water saturated with cholesterol and solid, crystalline cholesterol.

The triangles, α,β,γ, drawn with broken lines represent regions where three different phases coexist; their compositions are given by the points at the corners of the triangles. In the three-phase triangle α a 6 % (0.38 M) sodium caprylate solution, solid cholesterol and the mesomorphous phase IV are in equilibrium; in the triangle β an about 32 % sodium caprylate solution containing 1.7 % cholesterol and the meso-

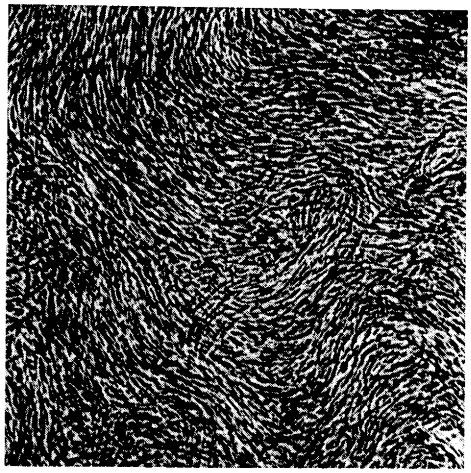

Fig. 4A. Ordinary light. 200 ×.

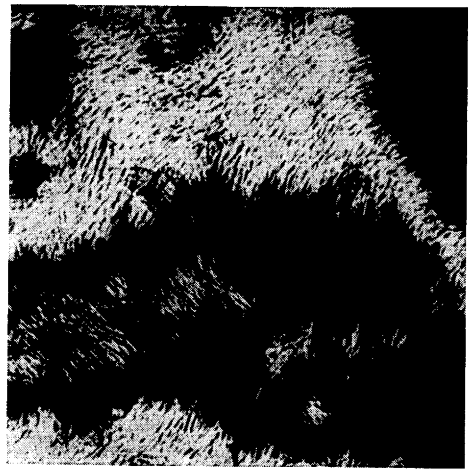

Crossed Nicols. 200 ×.



Fig. 4B.

phases IV and III are in equilibrium, and in triangle γ an about 45 % sodium caprylate solution containing about 6 % cholesterol and the mesophases III and II are in equilibrium.

Our studies thus reveal that there exists at 20°C three different mesomorphous phases composed of water, cholesterol and sodium caprylate which differ in composition and properties and in the conditions under which they are formed. It is of particular interest that each phase is in equilibrium with only a limited range of caprylate solutions and that there hence exists a relationship between the structures of the caprylate solutions and those of the mesomorphous phases. We have previosuly established that a similar relationship exists also between the structures of isotropic association colloid solutions and the water-containing mesomorphous phases that these solutions form by interaction with paraffin-chain alcohols or fatty acids [2].

Financial support from *Sigrid Juselius' Stiftelse* is gratefully acknowledged.

1. Zlatkis, A., Zak, B. and Boyle, A. J. *J. Lab. Clin. Med.* **41** (1953) 486.
2. Ekwall, P., Danielsson, I. and Mandell, L. *Kolloid-Z.* **169** (1960) 113; *Proc. 3rd Intern. Congr. Surface Activity*, Cologne 1960, Vol. I, Section A, 193, 189.

Received August 28, 1961.

Determination of the Relative Effective Area of Electrodes by Polarization Measurements

GÖSTA WRANGLÉN and ÅKE WARG

Division of Applied Electrochemistry and Corrosion, Royal Institute of Technology, Stockholm 70, Sweden

It is of great importance in many cases to have a measure of the true surface area of solid materials. Porous metal and graphite bodies may serve as examples. Their true surface area can be obtained by the wellknown BET method. When such bodies are used as electrodes there is reason to believe, however, that their electrochemically effective area is smaller than their total or BET area. Hydrated ions will not penetrate into the finest pores and the penetration of the current is limited by its throwing power. The ratio of the electrochemically effective areas of two electrodes is therefore probably different from their BET area ratio. An electrochemical method for the determination of relative surface areas would therefore seem desirable in this case.

Such a method is the capacitance method, in which the double layer capacity of the electrode/electrolyte interface is measured by an a.c. bridge or by an oscillographic analysis of square waves passed through the interface. This method is very sound in principle but the results depend on the frequency used and may thus be difficult to interpret.[1-5]

Another electrochemical method which is close at hand but of which, remarkably enough, there seems to be no published account, is the polarization method. It is based on the principle that the polarization is a definit , function of current density and hence of surface area. Two cases should be distinguished

I. At small values of the current density i, *i.e.* high values of surface area A, we have

$$\eta = c \cdot i = c \cdot I/A$$

where η = activation polarization, c = a constant and I = current. If η is recorded as a function of I for several electrodes of the same material but differing in area, we obviously obtain converging straight lines, the slopes S of which are inversely proportional to the surface area. For two electrodes we thus find $A_2/A_1 = S_1/S_2$ giving the ratio between the effective surface areas.

II. At higher values of the c.d. i, *i.e.* smaller surface area A, we have the wellknown Tafel equation

$$\eta = a + b \log i = a + b \cdot \log I/A$$
$$= a + b \cdot \log I - b \cdot \log A$$

where a and b are constants. If η is again recorded as a function of I for two electrodes of the same nature but of different area, we will expect parallel straight lines whose difference in η determines the ratio of the respective surfaces by the relation $\log (A_2/A_1) = (\eta_1 - \eta_2)/b$.

In both the cases referred to, the conditions of electrolysis should be such that the current is uniformly distributed over the effective cathode surface. This means that the electrolytic throwing power T, defined by the expression $T = (\varkappa/d)(d\eta/di)$, where $\varkappa$ = conductivity of electrolyte, $d\eta/di$ = slope of η/i-relation and d = electrode distance, should be as high as possible. An electrolyte of high conductivity can usually be found, although one requirement is that it must not corrode the electrode. The electrode process used should preferably have a high activation polarization. The choice is very limited, however. Hydrogen evolution, oxygen reduction and oxidation-reduction systems not corroding the metal may be considered. It is evidently more advantageous from this point of view to

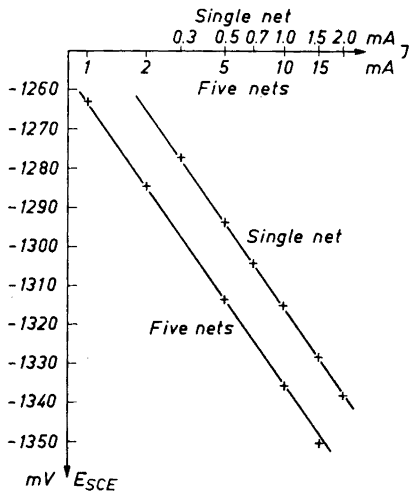

Fig. 1. Tafel lines for hydrogen evolution on nickel wire net cathodes.

Table 1. Polarization curves for hydrogen evolution on nickel wire net cathodes.

i mA	log i	Potential *vs* SCE mV	Slope, b mV	$\eta_1-\eta_2$ mV
Single net. Area = A_1				
0.3	−0.5229	−1 277.3		−52.5
0.5	−0.3010	−1 293.8	−74.4	−52.2
0.7	−0.1549	−1 304.1	−70.4	−52.3
1.0	0.0000	−1 315.1	−71.0	−52.2
1.5	0.1761	−1 328.3	−74.9	
2.0	0.3010	−1 338.0		
			M = −72.1	M = −52.4
Five nets. Area = A_2				
1	0.000	−1 263.0		
2	0.3010	−1 284.7	−72.1	−52.3
5	0.6990	−1 313.5	−72.4	−53.0
10	1.0000	−1 335.6	−73.4	−52.2
15	1.1761	−1 350.5		
			M = −72.6	M = −52.5

$$\log \frac{A_2}{A_1} = \frac{-52.4}{-72.7} = 0.720; \quad \frac{A_2}{A_1} = 5.25$$

work at a low c.d., since $d\eta/di$ is then higher due to the logarithmic nature of the η/i-relation. In applying hydrogen evolution for the purpose the method should, for the same reason, have the best prospects with metals of high hydrogen overvoltage.

In exploring the possibilities of the method, some electrolysis experiments were made with hydrogen evolution on nickel, although this is not a particularly favorable case, since nickel has a low hydrogen overvoltage. Two wire net electrodes of surface ratio 5 were used, one being a single 3 × 3 cm net with a wire diameter of 0.2 mm and having 8 meshes per cm, the other consisting of five such nets. The areas were estimated to be 9 and 45 cm² respectively. With the instruments available, the experiments had to be carried out in the logarithmic range, which is also not very favorable. The electrolyte was 27 % KOH solution, having a very good conductivity and being only slightly corroding to solid nickel. In an electrolysis cell, the cathode was placed in a horizontal position in the cathode compartment, separated by a long electrolyte path from the anode compartment. In the latter a platinum anode was placed close to the electrolyte surface. Through both the anolyte and the catholyte pure hydrogen, freed from oxygen by passing through vanadium(II)sulphate solution, was bubbled vigorously in order to prevent oxygen from entering the cathode compartment. The electrodes were pre-electrolyzed at the lowest currents used (0.3 and 1 mA, respectively) for 100 min. Cathode potentials were determined by the direct method using a saturated calomel electrode as reference. Readings were taken at 2 min intervals. The results are recorded in Table 1. The two Tafel lines obtained are shown in Fig. 1 with different log I axes. As shown in Table 1, the area ratio experimentally found is 5.25 in good accordance with the real value. The method can obviously be used for the determination of the area of irregular surfaces, a problem encountered for instance in dentistry.

Measurements on nickel powders and sintered nickel plates in the same cell and with currents of the same magnitude give good linear relations if diluted KOH solutions are used. The throwing power is, however, too low. In concentrated KOH solutions, on the other hand, the active porous nickel electrodes are corroded, in accordance with the potential-pH-diagram for nickel. This diagram suggests a less corroding electrolyte, *viz.* 1 M K_2CO_3, 1 M $KHCO_3$ with a resulting pH of 10.25. Measurements on two nickel wire nets of the kind described above and with the weight ratio 5:1 gave the surface area ratio 4.94:1. This electrolyte appears promising for porous nickel electrodes.

For porous silver electrodes, also of great potential interest, the prospects with concentrated KOH solution seem good since silver is not corroded and has, furthermore, a high hydrogen overvoltage. The investigations are being continued.

1. Brodd, R. J. and Hackerman, N. *J. Electrochem. Soc.* **104** (1957) 704.
2. Pilo, C., KTH, Stockholm, *Unpublished work.*
3. Dugdale, I. *Ph. D. Thesis*, Durham 1959.
4. Betteridge, W., INCO, London. *Personal communication.*
5. Euler, J. *Electrochim. Acta* **4** (1961) 27.

Received August 31, 1961.

Chemical Composition and Crystal Data of Some Chromium(VI) — Iodine(V) Compounds

KARL-AXEL WILHELMI and
PERCY LÖFGREN

Institute of Inorganic and Physical Chemistry, University of Stockholm, Stockholm, Sweden

In connection with crystal structure studies on *isopolyacids* of hexavalent chromium, it was found of interest to consider the possibility of the interaction of chromate(VI) with other ions, giving rise to complex *heteropolyacids*. A literature survey showed that several articles have appeared dealing with chromate(VI) complexes containing *anionic* phosphorus(V) [1-3], arsenic(V) [1], sulphur(VI) [4], iodine(V) [5] and *cationic* cerium(III) [6] and chromium(III) [7,8].

The present work has been confined to the chromate-iodate system and deals with the crystallographic and analytical data of the compounds $(NH_4)_2O{\cdot}2CrO_3{\cdot}I_2O_5$, $K_2O{\cdot}2CrO_3{\cdot}I_2O_5$, $K_2O{\cdot}2CrO_3{\cdot}I_2O_5{\cdot}H_2O$, $Rb_2O{\cdot}2CrO_3{\cdot}I_2O_5$ and $Cs_2O{\cdot}2CrO_3{\cdot}I_2O_5$. Crystallographic evidence is given for the existence of a $CrIO_6^-$ complex in the solid state.

Experimental. Analytical grade reagents were used throughout. Chromium trioxide was dried at 120°C and weighed out of contact with air.

pH measurements were made at 25°C with a Radiometer pH meter M 3, using Radiometer glass and calomel electrodes standardized against a commercial phosphate buffer, pH = 6.50.

The powder patterns were obtained in a Guinier type focusing camera of 80 mm diameter (transmission position) with strictly monochromatized Cu$K\alpha_1$ radiation. Potassium chloride (Analar, British Drug Houses, $a = 6.2919$ Å at 20°C) was added to the specimens as internal standard.

The structural investigation was based on X-ray data. The exposures were made with a commercial Nonius Weissenberg camera with CuK radiation.

The density of the crystals was determined from the apparent loss of weight in benzene.

Synthesis. The compounds were prepared according to Blomstrand [5] by dissolving *ca.* 20 g of alkali dichromate (or chromium trioxide and alkali chromate) in water and adding a stoichiometric quantity of HIO_3. Single crystals were obtained by allowing this solution to evaporate slowly at room temperature. The crystals were removed from the solutions by decanting at equal time intervals and the phase purity was controlled by X-ray and chemical analyses.

Attempts to prepare other phases than the 1:1 compounds were made by varying the proportions of chromate and iodic acid or adding HNO_3 to the solutions. These attempts were unsuccessful but two phases were observed in the potassium system, *viz.* $KCrIO_6$ and $KCrIO_6{\cdot}\frac{1}{2}H_2O$, the former crystallizing from solutions containing HNO_3, the latter from HNO_3-free solutions.

Chemical analysis. The results are given in Table 1.

Iodine. The crystals were dissolved in appr. 50 ml 10^{-3} M HCl, and SO_2 was then bubbled into the acid solution. The iodate was reduced over iodine to iodide. The reduction was stopped 1 min after the brown iodine colour had disappeared. The solution was then titrated potentiometrically with 0.015 M $AgNO_3$.

Chromium. The original solution was acidified with HCl and KI was added. Titration with thiosulphate gave the sum of chromate and iodate. The amount of chromium was calculated by difference.

Water. The sample was heated to 150°C in a Pyrex tube according to the method of Penfield [9].

Alkali. The alkali metals were determined gravimetrically with $(C_6H_5)_4BNa$ [10] or with the following technique utilizing cation exchange.

When an alkali dichromate solution is titrated potentiometrically with NaOH, the weak acid $HCrO_4^-$ is determined according to the equations:

Table 1. Analytical data.

	% Alkali		% Chromium		% Iodine		% Water	
	Found	Calc.	Found	Calc.	Found	Calc.	Found	Calc.
NH_4CrIO_6	6.23 ± 0.05	6.16	18.3 ± 0.3	17.7	43.2 ± 0.2	43.3	—	0
$KCrIO_6{\cdot}\frac{1}{2}H_2O$	11.8 ± 0.1	12.1	15.7 ± 0.3	16.1	40.1 ± 0.2	39.3	2.4 ± 0.1	2.8
$KCrIO_6$	12.5 ± 0.1	12.5	16.7 ± 0.3	16.6	40.0 ± 0.2	40.4	0.3 ± 0.1	0
$RbCrIO_6$	23.7 ± 0.1	23.7	15.1 ± 0.3	14.4	35.3 ± 0.2	35.2	0	0
$CsCrIO_6$	32.6 ± 0.1	32.6	13.3 ± 0.3	12.8	31.2 ± 0.2	31.1	0	0

Table 2. Crystallographic data.

	Probable symmetry	a (Å)	b (Å)	c (Å)	β	Formula units in the cell	Density Found	Density ($g\ cm^{-3}$) Calcd.
NH_4CrIO_6	$Pbca$	6.05	14.32	13.38	—	8	3.34	3.36
$KCrIO_6$	$P2_1/c$	9.25	4.86	14.28	108°	4	3.56	3.42
$KCrIO_6 \cdot \frac{1}{2}H_2O$	$C2/m$	14.91	5.48	15.76	95°	8	3.35	3.34
$RbCrIO_6$	$P2_1/n$	8.12	7.70	10.45	109°	4	3.85	3.86
$CsCrIO_6$	$P2_1/n$	8.26	8.08	10.75	110°	4	4.05	4.02

$$M_2Cr_2O_7(s) + H_2O = 2\ M^+ + 2\ HCrO_4^-$$
$$HCrO_4^- + OH^- = CrO_4^{2-} + H_2O$$

An aliquot part of the dichromate solution is then introduced into a cation exchange column saturated with hydrogen ions. The effluent is titrated with NaOH and a curve is obtained with two titration points. The amount of NaOH required for the first equiv. points is equivalent to the alkali ions present.

When the chromium(VI)–iodine(V) complex is dissolved in water, the compound will be hydrolyzed and the solution will contain alkali, hydrogen-, hydrogen chromate- and iodate ions.

$$MCrIO_6(s) + H_2O = M^+ + H^+ + HCrO_4^- + IO_3^-$$

The solution is titrated with NaOH before and after running through the ion exchange column. The difference between the amount of NaOH required for the two first equiv. points is equivalent to the alkali content. It is also clear from the reaction formula that the amount of NaOH required for the first titration point (without ion exchange) is equivalent to the iodate present in the compound. Thus the amounts of alkali, hexavalent chromium and pentavalent iodine could be determined from the two titrations. The equivalent points were determined by plotting $\Delta V/\Delta$pH *versus* V according to Gran[11]. The method has also been used successfully for analyzing trichromates and tetrachromates.

Crystallographic data. The unit cell parameters and probable symmetry of the various phases are summarized in Table 2. The rubidium and cesium salts present the single instance of isomorphism among these compounds. So far only the crystal structure of NH_4CrIO_6 has been investigated (*v. infra*) — studies of further phases of this group are in progress.

The crystal structure of NH_4CrIO_6. Rotation and Weissenberg photographs about all three axes were taken of a small crystal of NH_4CrIO_6 (CuK radiation). Analysis of the photographs showed a systematic absence for $0kl$ when k odd, $h0l$ when l odd and $hk0$ when h odd, indicating the space group to be No. 61, *Pbca*.

Space group No. 61 *Pbca*.

Unit cell dimensions: $a = 6.05$ Å, $b = 14.32$ Å, $c = 13.38$ Å.

Unit cell content: 8 NH_4CrIO_6.

The structure may be described as built up of $CrIO_6^-$-ions formed by a CrO_4-tetrahedron and a trigonal IO_3-pyramid sharing one corner (the O_1 atom).

The following interatomic distances are obtained:

$I-O_1 = 2.06$ Å	$Cr-O_1 = 1.90$ Å
$I-O_2 = 1.86$ Å	$Cr-O_4 = 1.62$ Å
$I-O_3 = 1.81$ Å	$Cr-O_5 = 1.64$ Å
	$Cr-O_6 = 1.65$ Å

The distances are of reasonable length throughout. The central bond distances $Cr-O_1$ and $I-O_1$ are significantly longer than the peripheral bond lengths.

The $Cr-O_1-I$ angle is $\sim 118°$.

A three-dimensional refinement process is in progress and the result with a full description of the structure analysis and a further discussion of the structure will be published elsewhere.

Acknowledgements. This investigation forms part of a research programme on the crystal chemistry of chromium compounds which is financially supported by the *Swedish Natural Science Research Council*. Part of the calculations has been carried out on the BESK, for the use of which the authors are indebted to the *Swedish Board for Computing Machinery*.

The authors wish to thank Professor Arne Ölander for his kind interest and Professor Arne Magnéli for valuable discussions in connection with this work.

1. Friedheim, C. and Mozkin, J. *Z. anorg. Chem.* **6** (1894) 273.
2. Holloway, F. *J. Am. Chem. Soc.* **74** (1952) 224.

3. Zsakó, I. *Studii cercetari chim. Filiala Cluj* **7** (1956) 53.
4. Yatsimirskii, K. B. and Vasil'eva, V. N. *Zhur. Neorg. Khim.* **1** (1956) 1983.
5. Blomstrand, C. W. *J. prakt. Chem.* [2] **40** (1889) 328.
6. Tong, J. Y. and King, E. L. *J. Am. Chem. Soc.* **76** (1954) 2132.
7. King, E. L. and Neptune, J. A. *J. Am. Chem. Soc.* **77** (1955) 3186.
8. Krauss, H.-L. and Gnatz, G. *Chem. Ber.* **92** (1959) 2110.
9. Penfield, S. L. *Am. J. Sci.* [3] **48** (1894) 30.
10. Raff, P. and Brotz, W. *Z. anal. Chem.* **133** (1951) 241.
11. Gran, G. *Acta Chem. Scand.* **4** (1950) 559.

Received September 7, 1961.

Crystallographic Data of Sr_2CrO_4

KARL-AXEL WILHELMI and
OLA JONSSON

Institute of Inorganic and Physical Chemistry, University of Stockholm, Stockholm, Sweden

Rather few compounds containing tetravalent chromium are reported in literature and the information about their crystallographic properties is incomplete. The syntheses of CrF_4 and $CrBr_4$ have been reported [1,2] but no crystallographic data are available for these substances. In 1950 the fluoro complexes M_2CrF_6 (M = K, Rb, and Cs) were prepared [3] and Bode and Voss [4] found that these complexes have the octahedral arrangement with discrete CrF_6^{2-} ions. The coordination number 6 is also found in CrO_2 which phase is of a rutile type [5,6].

Scholder and Sperka [7,8] have reported the syntheses of Ba_2CrO_4, Ba_3CrO_5 and Sr_2CrO_4, containing chromium with an average oxidation number of + 4. According to these authors, there exist structural relationships between the compounds M_2TiO_4 and M_2CrO_4 (M = Ba and Sr).

The crystal structure of Ba_2TiO_4 has been determined by Bland [9]. The space group is $P2_1/n$ and the cell dimensions are:

$a = 6.12$ Å, $b = 7.70$ Å, $c = 10.50$ Å, $\beta = 93°8'$

The structure is of the β-K_2SO_4 type and is closely related to β-Ca_2SiO_4. The environment of the titanium atom is unusual; it is approximately tetrahedral and the structure is considered as an arrangement of discrete TiO_4-groups and barium atoms.

Sr_2TiO_4 belongs according to Balz and Plieth [10] to an interesting group of oxide compounds with the same crystal structure as K_2NiF_4 and K_2MgF_4[11]. The space group is $I4/mmm$ and the cell dimensions are:

$$a = 3.88 \text{ Å} \qquad c = 12.58 \text{ Å}$$

The structure is formed by somewhat distorted TiO_6-octahedra arranged in layers with the composition TiO_2 by sharing corners. In the direction of the tetragonal c axis an alternation of two SrO-layers with one TiO_2 layer can be distinguished.

By a partial substitution of Sr^{2+} ions (about 5 mole %) in Ba_2TiO_4, specimens with the orthorhombic β-K_2SO_4 structure were obtained by Kwestroo and Paping [12]. The solid solution area ends at a composition with a Ba^{2+}/Sr^{2+} ratio of about 1:3. The structure of Sr_2CrO_4 has been investigated by the present authors and preliminary results are given in this paper.

Crystals of Sr_2CrO_4, suitable for single-crystal X-ray studies, were prepared from chromium(III)oxide, strontium chromate(VI) and carbonate-free strontium hydroxide in a platinum crucible at 900°C with argon as a protecting gas.

$$Cr_2O_3 + SrCrO_4 + 5\ Sr(OH)_2 = 3\ Sr_2CrO_4 + 5\ H_2O$$

The excess of strontium hydroxide was extracted with water-free methanol. The crystals obtained were small blue-black prisms stable in air and insoluble in hot acetic acid.

The hexavalent chromium was determined iodometrically, the total chromium after oxidation by hydrogen peroxide in alkaline solution. The strontium was determined gravimetrically as strontium sulphate in chromium-free solutions. The reproducibility of the analyses was found to be good and the results in fair agreement with the values calculated for Sr_2CrO_4.

	Chromium (VI), %	Chromium total, %	Strontium %
Found	5.88 ± 0.05	17.62 ± 0.05	60.2 ± 0.1
Calc.	5.95	17.85	60.17

3. Zsakó, I. *Studii cercetari chim. Filiala Cluj* **7** (1956) 53.
4. Yatsimirskii, K. B. and Vasil'eva, V. N. *Zhur. Neorg. Khim.* **1** (1956) 1983.
5. Blomstrand, C. W. *J. prakt. Chem.* [2] **40** (1889) 328.
6. Tong, J. Y. and King, E. L. *J. Am. Chem. Soc.* **76** (1954) 2132.
7. King, E. L. and Neptune, J. A. *J. Am. Chem. Soc.* **77** (1955) 3186.
8. Krauss, H.-L. and Gnatz, G. *Chem. Ber.* **92** (1959) 2110.
9. Penfield, S. L. *Am. J. Sci.* [3] **48** (1894) 30.
10. Raff, P. and Brotz, W. *Z. anal. Chem.* **133** (1951) 241.
11. Gran, G. *Acta Chem. Scand.* **4** (1950) 559.

Received September 7, 1961.

Crystallographic Data of Sr_2CrO_4

KARL-AXEL WILHELMI and
OLA JONSSON

Institute of Inorganic and Physical Chemistry, University of Stockholm, Stockholm, Sweden

Rather few compounds containing tetravalent chromium are reported in literature and the information about their crystallographic properties is incomplete. The syntheses of CrF_4 and $CrBr_4$ have been reported [1,2] but no crystallographic data are available for these substances. In 1950 the fluoro complexes M_2CrF_6 (M = K, Rb, and Cs) were prepared [3] and Bode and Voss [4] found that these complexes have the octahedral arrangement with discrete CrF_6^{2-} ions. The coordination number 6 is also found in CrO_2 which phase is of a rutile type [5,6].

Scholder and Sperka [7,8] have reported the syntheses of Ba_2CrO_4, Ba_3CrO_5 and Sr_2CrO_4, containing chromium with an average oxidation number of + 4. According to these authors, there exist structural relationships between the compounds M_2TiO_4 and M_2CrO_4 (M = Ba and Sr).

The crystal structure of Ba_2TiO_4 has been determined by Bland [9]. The space group is $P2_1/n$ and the cell dimensions are:

$a = 6.12$ Å, $b = 7.70$ Å, $c = 10.50$ Å, $\beta = 93°8'$

The structure is of the β-K_2SO_4 type and is closely related to β-Ca_2SiO_4. The environment of the titanium atom is unusual; it is approximately tetrahedral and the structure is considered as an arrangement of discrete TiO_4-groups and barium atoms.

Sr_2TiO_4 belongs according to Balz and Plieth [10] to an interesting group of oxide compounds with the same crystal structure as K_2NiF_4 and K_2MgF_4[11]. The space group is $I4/mmm$ and the cell dimensions are:

$$a = 3.88 \text{ Å} \qquad c = 12.58 \text{ Å}$$

The structure is formed by somewhat distorted TiO_6-octahedra arranged in layers with the composition TiO_2 by sharing corners. In the direction of the tetragonal c axis an alternation of two SrO-layers with one TiO_2 layer can be distinguished.

By a partial substitution of Sr^{2+} ions (about 5 mole %) in Ba_2TiO_4, specimens with the orthorhombic β-K_2SO_4 structure were obtained by Kwestroo and Paping [12]. The solid solution area ends at a composition with a Ba^{2+}/Sr^{2+} ratio of about 1:3. The structure of Sr_2CrO_4 has been investigated by the present authors and preliminary results are given in this paper.

Crystals of Sr_2CrO_4, suitable for single-crystal X-ray studies, were prepared from chromium(III)oxide, strontium chromate(VI) and carbonate-free strontium hydroxide in a platinum crucible at 900°C with argon as a protecting gas.

$$Cr_2O_3 + SrCrO_4 + 5\ Sr(OH)_2 = 3\ Sr_2CrO_4 + 5\ H_2O$$

The excess of strontium hydroxide was extracted with water-free methanol. The crystals obtained were small blue-black prisms stable in air and insoluble in hot acetic acid.

The hexavalent chromium was determined iodometrically, the total chromium after oxidation by hydrogen peroxide in alkaline solution. The strontium was determined gravimetrically as strontium sulphate in chromium-free solutions. The reproducibility of the analyses was found to be good and the results in fair agreement with the values calculated for Sr_2CrO_4.

	Chromium (VI), %	Chromium total, %	Strontium %
Found	5.88 ± 0.05	17.62 ± 0.05	60.2 ± 0.1
Calc.	5.95	17.85	60.17

Table 1. Crystallographic data of Sr_2CrO_4.

Laue symmetry: *mmm*
Unit-cell dimensions: $a = 14.193$ Å
$b = 10.033$ Å
$c = 5.790$ Å
Absent spectra: $hk0$ with h odd
$0kl$ with $k + l$ odd
Space group: No. 33 $Pn2_1a$
Density observed: 4.54 g cm^{-3}
Density calculated: 4.50 g cm^{-3} (for $Sr_{16}Cr_8O_{32}$)

Approximate values of the cell dimensions were obtained from Weissenberg photographs (CuK radiation). More accurate values were then obtained from a Guinier powder photograph (80 mm diameter, transmission position) with strictly monochromatized CuK_1 radiation. Potassium chloride (Analar, British Drug Houses, $a = 6.2919$ Å at 20°C, Hambling [13]) was added to the specimen as an internal standard. A few very weak extra lines showed the presence of a small content of non-identified impurities in the specimen.

Rotation photographs around [100], [010] and [001] and Weissenberg photographs (hkl: $h = 0-8$, $k = 0-6$ and $l = 0-3$) showed the crystal to be orthorhombic. There seems to be an almost exact relationship between the lengths of the cell edges $a:b:c = \sqrt{6}:\sqrt{3}:1$ (Table 1). The reflexions systematically absent are characteristic of the space groups No. 62 *Pnma* and No 33 $Pn2_1a$. All attempts to solve the structure on the basis of the space group No. 62 *Pnma* failed and it was concluded that the space group might be No. 33 $Pn2_1a$.

The present stage of the structure determination is in accordance with the latter symmetry. Thus studies of the Patterson and electron density projections have lead to a structure containing the 16 strontium and 8 chromium atoms in 6 sets of 4-fold positions (4a) of the space-group $Pn2_1a$. The distribution of the metal atoms indicates that Sr_2CrO_4 is isomorphous neither with K_2NiF_4 nor with K_2CrO_4 (low-K_2SO_4-type), but that the structure very likely contains discrete four-coordinated chromium-oxygen complexes similar to those found in K_2CrO_4. The refinement of the structure will be continued according to this assumption.

Acknowledgements. This investigation forms part of a research programme which is financially supported by the *Swedish Natural Science Research Council.*

The authors are indebted to Professor Arne Ölander for his kind interest and to Professor Arne Magnéli for stimulating discussions and criticism in connection with this work.

1. Wartenberg, H. von *Z. anorg. Chem.* **247** (1941) 135.
2. Sime, R. J. and Gregory, N. W. *J. Am. Chem. Soc.* **82** (1960) 93.
3. Huss, E. and Klemm, W. *Z. anorg. Chem.* **262** (1950) 25.
4. Bode, H. and Voss, E. *Z. anorg. Chem.* **286** (1956) 136.
5. Michel, A. and Bénard, J. *Compt. rend.* **200** (1935) 1316.
6. Wilhelmi, K.-A. and Jonsson, O. *Acta Chem. Scand.* **12** (1958) 1532.
7. Scholder, R. and Sperka, G. *Z. anorg. Chem.* **285** (1956) 49.
8. Sperka, G. Dissertation 1952, Karlsruhe.
9. Bland, J. A. *Acta Cryst.* **14** (1961) 875.
10. Balz, D. and Plieth, K. *Z. Elektrochem.* **59** (1955) 545.
11. Brehler, B. and Winkler, H. G. F. *Heidelberger Beiträge zur Mineralogie und Petrographie* **4** (1954) 6.
12. Kwestroo, W. and Paping, H. A. M. *J. Am. Ceram. Soc.* **42** (1959) 292.
13. Hambling, P. G. *Acta Cryst.* **6** (1953) 98.

Received September 7, 1961.

The Study of Horseradish Peroxidase Catalyzed Oxidations by Means of Chemiluminescence

GUNNAR AHNSTRÖM,
GÜNTHER v. EHRENSTEIN and
ROBERT NILSSON

Institute of Organic Chemistry and Biochemistry, University of Stockholm, Sweden

In the oxidation of pyrogallol coloured endproducts are formed, the main component of which is presumably purpurogallin [1]. This process is also accompanied by chemiluminescence [2].

A standard method for the determination of peroxidase activity has been the measurement of the amount of purpurogallin formed in the enzymic oxidation of pyrogallol by hydrogen peroxide. In the present investigation we have studied the above mentioned reaction by means of light emission measurements.

Experimental. The equipment used for the luminescence measurements is described in detail in a previous paper [3]. A Sigma HRP preparation of a purity corresponding to 21 purpurogallin units per mg (20 sec.) was used [1]. All other chemicals were analytically pure. To prevent autoxidation, the freshly prepared pyrogallol solutions were immediately acidified.

Phosphate buffer, pyrogallol and enzyme solutions were mixed in a Beckman standard cuvette, and the volume of the reaction mixture adjusted to 1 ml by the addition of distilled water. The reaction was initiated by injection of the peroxide. The luminescence intensity was then recorded as a function of time under varying peroxide, pyrogallol and enzyme concentrations.

Results. The effect of varying HRP-concentrations on the light intensity-time dependance curve of constant peroxide and pyrogallol concentrations is shown in Fig. 1.

It may be seen from this figure that after a certain induction period the light intensity reaches a fairly constant maximum value and then slowly decreases. This probably implies that in the enzymic oxidation of the hydrogen donor the concentration of an active, intermediate molecular species is built up which then undergoes a secondary chemiluminescent elimination without necessarily requiring the participation of the enzyme protein. This is supported by Chance's observation [4] that the formation of reaction products continues long after the active enzyme-peroxide, usually rate determinating, complex (complex II) has disappeared. However, at present no method is available for the determination of the actual concentrations of the enzyme peroxide complexes at these low HRP concentrations. The rate of production of the intermediate directly involved in the luminescent reaction is dependent upon the enzyme concentration and, in consequence, the light intensity during the steady state, when the rate of production of this species is balanced by its chemiluminescent elimination, is also a function of the same.

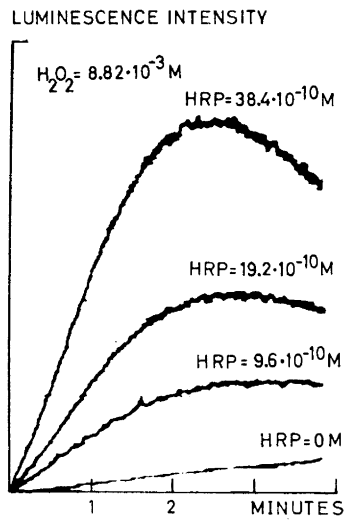

Fig. 1. Luminescence intensity as a function of time at different HRP concentrations. H_2O_2 and pyrogallol concentrations constant.

Fig. 2 shows the light intensity at the plateau as a function of the HRP concentration at four H_2O_2 levels. In the presence of a larger excess of peroxide the inhibition previously noted by Mann [5] is observed. This inhibition is illustrated in more detail in Fig. 3 which shows the variations in the light intensity at steady state for increasing peroxide concentrations at five different enzyme levels.

The effect of varying pyrogallol concentrations at constant peroxide and enzyme

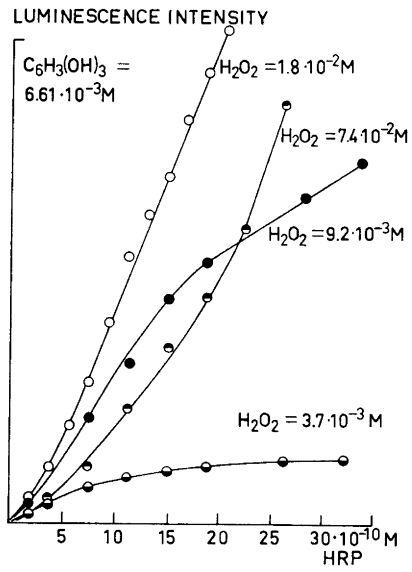

Fig. 2. Luminescence intensity at steady state as a function of HRP concentration at different H_2O_2 levels. Pyrogallol concentration constant.

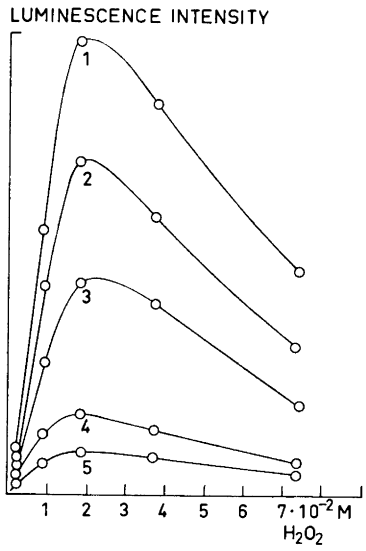

Fig. 3. Luminescence intensity at steady state as a function of H_2O_2 concentration at five different enzyme levels. Pyrogallol concentration constant = $6.61 \cdot 10^{-3}$ M. HRP = 1) $19 \cdot 10^{-10}$ M; 2) $14 \cdot 10^{-10}$ M; 3) $9.5 \cdot 10^{-10}$ M; 4) $4.7 \cdot 10^{-10}$ M; 5) $2.8 \cdot 10^{-10}$ M.

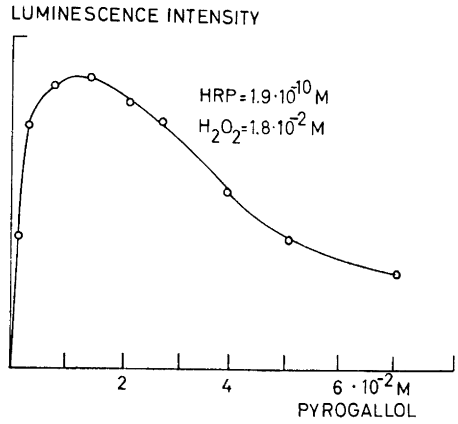

Fig. 4. Luminescence intensity at steady state as a function of pyrogallol concentration. HRP and H_2O_2 concentrations constant.

concentrations is illustrated in Fig. 4. The previously observed inhibition effect is marked at the highest donor concentrations [5].

The classical purpurogallin method has the disadvantage of being very sensitive to factors such as the presence of impurities in the reaction mixture, concentration of buffer etc.[6] We have not found these factors to influence the reproducibility of the results obtained by the luminescence measurements to any appreciable extent. Thus, ordinary tap water could be used.

In dealing with media of high optical density, the emission measurements are definitely preferable to absorption measurements, as the surface of the reaction mixture, in the former case, can be increased, resulting in an appreciable decrease in the internal absorption while retaining the photon counting efficiency.

Furthermore, this method is not restricted to the utilization of pyrogallol as reducing substrate. By the use of very low concentrations of pyrogallol in the presence of an excess of another hydrogen donor to be studied, the pyrogallol is rapidly oxidized in a nonenzymic luminescent reaction by the reaction products formed from the reducing substrate present in excess. Due to this "scavenging" property of the pyrogallol, the light emission under these conditions provides a means of investigating the oxidation of various other substances such as *o*-phenylenediamine, *p*-phenylenediamine and others.

Acknowledgement. The present investigation was supported by grants from *Kungl. Universitetets i Stockholm matematisk-naturvetenskapliga fakultets anslag för främjande av ograduerade forskares verksamhet.*

1. Willstätter, R. and Stoll, A. *Ann.* **416** (1918) 21.
2. Lenard, P. and Wolf, M. *Ann. Phys. und Chem.* 1888, xxxiv, 918.
3. Ahnström, G. *Acta Chem. Scand.* **15** (1961) 463.
4. Chance, B. *Arch. Biochem.* **24** (1949) 410.
5. Mann, P. J. G. *Biochem. J.* **24** (1931) 921.
6. Ettori, J. *Biochem. J.* **44** (1949) 35.

Received September 8, 1961.

3-Substituted Furans

SALO GRONOWITZ and
GUNNAR SÖRLIN

Chemical Institute, University of Uppsala, Uppsala, Sweden

In connection with work on the substituent effects in heterocyclic systems, a number of 3-substituted furans was needed in order to compare the chemical shifts in their NMR-spectra with those of the corresponding thiophenes [1]. Although some 3-substituted furans occur in nature [2] most compounds of this type are only obtained with difficulty. Some compounds have been prepared by modifying the carboxyl group of 3-furancarboxylic acid [3,4], which is obtained by partial decarboxylation of polycarboxyfurans [3-5]. Recently 3-hydroxytetrahydrofuran has been used for the preparation of 3-phenylfuran [6] and new methods for the synthesis of 3-methylfuran from commercially available aliphatic compounds have been worked out [7,8]. These methods give a carbon-carbon bond in the 3-position.

In the thiophene series it has been shown that 3-thienyllithium, obtained through halogen-metal interconversion between 3-bromothiophene and *n*-butyllithium at $-70°$, is a very useful intermediate both for the formation of a new carbon-carbon bond in the 3-position and also for the introduction of other types of substituents (for review *cf.* Ref.[9]). Of the two 3-halofurans which are suitable for an analogous investigation we found that 3-iodofuran [10] could be more easily and reproducibly synthesised than 3-bromofuran [11] owing to difficulties in the reduction of 4,5-dibromo-2-furancarboxylic acid to 4-bromo-2-furancarboxylic acid. Through minor changes in the Gilman process, which consists of the pyrolysis of the mercury salt of 2-furancarboxylic acid followed by reaction of the resulting chloromercury furan with iodine, the yield of 3-iodofuran was increased from 4.0 % to 5.1 %, calculated on the weight of the 2-furancarboxylic acid used. The reactions of 3-iodofuran have been investigated very briefly by Gilman and Wright only. They found that it did not give a Grignard reagent, but that with a sodium-potassium alloy it formed a metalorganic compound, which upon carbonation gave 3-furancarboxylic acid in low yield [12]. We have now found that 3-iodofuran undergoes halogen-metal interconversion with *n*-butyllithium at $-70°$ to 3-furyllithium. Upon carbonation this compound gives 3-furancarboxylic acid in good yield, and with N,N-dimethyl formamide it reacts to give 3-furaldehyde. By contrast with 2-bromo- and 2-iodofuran [13], 3-iodofuran reacts with sodium methylate in methanol in the presence of cupric oxide, to give 3-methoxyfuran. It is not considered that the yields obtained in these preliminary experiments are the best obtainable.

Thus, although 3-iodofuran is not so readily available as 3-bromothiophene [14], its halogen metal interconversion at $-70°$ with *n*-butyllithium to form 3-furyllithium (a compound sufficiently stable at this temperature) opens up the route to many 3-substituted furans. Further investigation into its potentialities as an intermediate for such compounds is in progress.

Experimental. 3-Furancarboxylic acid. A solution of 8.8 g (0.045 mole) of 3-iodofuran in 25 ml of dry ether was added to a stirred solution of 47 ml of 1.20 N *n*-butyllithium at $-70°$ in the conventional four-necked, nitrogen-swept flask. After 5 min, the mixture was poured onto solid carbon dioxide covered with ether. The reaction mixture was hydrolyzed with water and the ether phase extracted with sodium carbonate solution. The 3-furancarboxylic acid was precipitated out on acidification with dilute hydrochloric acid. One recrystallization from water yielded 3.2 g (63 %) of pure 3-furancarboxylic acid, m.p. 122–123°. (Literature value:[5] m.p. 122–123°.) The characteristic peaks

Acknowledgement. The present investigation was supported by grants from *Kungl. Universitetets i Stockholm matematisk-naturvetenskapliga fakultets anslag för främjande av ograduerade forskares verksamhet.*

1. Willstätter, R. and Stoll, A. *Ann.* **416** (1918) 21.
2. Lenard, P. and Wolf, M. *Ann. Phys. und Chem.* 1888, xxxiv, 918.
3. Ahnström, G. *Acta Chem. Scand.* **15** (1961) 463.
4. Chance, B. *Arch. Biochem.* **24** (1949) 410.
5. Mann, P. J. G. *Biochem. J.* **24** (1931) 921.
6. Ettori, J. *Biochem. J.* **44** (1949) 35.

Received September 8, 1961.

3-Substituted Furans

SALO GRONOWITZ and
GUNNAR SÖRLIN

Chemical Institute, University of Uppsala, Uppsala, Sweden

In connection with work on the substituent effects in heterocyclic systems, a number of 3-substituted furans was needed in order to compare the chemical shifts in their NMR-spectra with those of the corresponding thiophenes [1]. Although some 3-substituted furans occur in nature [2] most compounds of this type are only obtained with difficulty. Some compounds have been prepared by modifying the carboxyl group of 3-furancarboxylic acid [3,4], which is obtained by partial decarboxylation of polycarboxyfurans [3-5]. Recently 3-hydroxytetrahydrofuran has been used for the preparation of 3-phenylfuran [6] and new methods for the synthesis of 3-methylfuran from commercially available aliphatic compounds have been worked out [7,8]. These methods give a carbon-carbon bond in the 3-position.

In the thiophene series it has been shown that 3-thienyllithium, obtained through halogen-metal interconversion between 3-bromothiophene and *n*-butyllithium at $-70°$, is a very useful intermediate both for the formation of a new carbon-carbon bond in the 3-position and also for the introduction of other types of substituents (for review *cf.* Ref.[9]). Of the two 3-halofurans which are suitable for an analogous investigation we found that 3-iodofuran [10] could be more easily and reproducibly synthesised than 3-bromofuran [11] owing to difficulties in the reduction of 4,5-dibromo-2-furancarboxylic acid to 4-bromo-2-furancarboxylic acid. Through minor changes in the Gilman process, which consists of the pyrolysis of the mercury salt of 2-furancarboxylic acid followed by reaction of the resulting chloromercury furan with iodine, the yield of 3-iodofuran was increased from 4.0 % to 5.1 %, calculated on the weight of the 2-furancarboxylic acid used. The reactions of 3-iodofuran have been investigated very briefly by Gilman and Wright only. They found that it did not give a Grignard reagent, but that with a sodium-potassium alloy it formed a metalorganic compound, which upon carbonation gave 3-furancarboxylic acid in low yield [12]. We have now found that 3-iodofuran undergoes halogen-metal interconversion with *n*-butyllithium at $-70°$ to 3-furyllithium. Upon carbonation this compound gives 3-furancarboxylic acid in good yield, and with N,N-dimethyl formamide it reacts to give 3-furaldehyde. By contrast with 2-bromo- and 2-iodofuran [13], 3-iodofuran reacts with sodium methylate in methanol in the presence of cupric oxide, to give 3-methoxyfuran. It is not considered that the yields obtained in these preliminary experiments are the best obtainable.

Thus, although 3-iodofuran is not so readily available as 3-bromothiophene [14], its halogen metal interconversion at $-70°$ with *n*-butyllithium to form 3-furyllithium (a compound sufficiently stable at this temperature) opens up the route to many 3-substituted furans. Further investigation into its potentialities as an intermediate for such compounds is in progress.

Experimental. 3-Furancarboxylic acid. A solution of 8.8 g (0.045 mole) of 3-iodofuran in 25 ml of dry ether was added to a stirred solution of 47 ml of 1.20 N *n*-butyllithium at $-70°$ in the conventional four-necked, nitrogen-swept flask. After 5 min, the mixture was poured onto solid carbon dioxide covered with ether. The reaction mixture was hydrolyzed with water and the ether phase extracted with sodium carbonate solution. The 3-furancarboxylic acid was precipitated out on acidification with dilute hydrochloric acid. One recrystallization from water yielded 3.2 g (63 %) of pure 3-furancarboxylic acid, m.p. 122–123°. (Literature value:[5] m.p. 122–123°.) The characteristic peaks

of the 2-isomer were absent from its IR-spectrum.

Methyl 3-furancarboxylate. This was prepared by methylation with diazomethane, b.p. 72–73°/30 mm Hg, $n_D^{20} = 1.4677$ (literature values [5]: b.p. 160°, $n_D^{20} = 1.4676$).

3-Furaldehyde. A solution of 3-furyllithium prepared as above from 11.5 g (0.059 mole) of 3-iodofuran and 78 ml 0.90 N *n*-butyllithium was forced under a pressure of nitrogen into a stirred solution of 8 g (0.11 mole) of N,N-dimethyl formamide in 30 ml of ether. After several hours the reaction mixture was decomposed with ice-water, and the ether phase was washed with dilute hydrochloric acid and sodium bicarbonate. In order to separate the aldehyde from the *n*-butyl iodide formed, the ether layer was extracted several times with 30 % sodium bisulphite solution. The combined aqueous extracts were made alkaline and then extracted with ether. Distillation of the dried ether phase yielded 1.1 g (20 %) of 3-furaldehyde, b.p. 76°/50 mm Hg, $n_D^{20} = 1.4937$, phenylhydrazone, m.p. 148–149.5°. (Literature values[8]: b.p. 70–72°/43 mm Hg, $n_D^{20} = 1.4945$, phenylhydrazone, m.p. 149.5°.) The IR-spectrum indicated the presence of traces of furfural.

3-Methoxyfuran. 19.7 g (0.86 mole) of sodium were dissolved in 240 ml of anhydrous methanol; 58 g (0.299 mole) of 3-iodofuran and 29 g of cupric oxide were added. The mixture was then refluxed with vigorous stirring for 24 h. The cooled mixture was filtered, diluted with two volumes of water and extracted with ether. The combined ether phases were washed with water, dried and fractionated. 18.6 g (65 %) of 3-methoxyfuran, b.p. 112°, $n_D^{20} = 1.4488$, was obtained. (Found: C 61.19; H 6.17. Calc. for $C_5H_6O_2$ (98.1): C 61.21; H 6.16.) IR- and NMR-spectra showed it to be free from 3-iodofuran and 2-methoxyfuran.

Acknowledgements. The authors wish to express their thanks to Professor Arne Fredga for his interest in this work and for all facilities put at their disposal. The elementary analyses were carried out by Dr. W. Kirsten, Microanalytical Laboratory, Institute of Medical Chemistry, Uppsala. A grant from the *Swedish Natural Science Research Council* to S.G. is gratefully acknowledged.

1. Gronowitz, S. and Hoffman, R. A. *Arkiv Kemi* **16** (1960) 539.
2. Edward, J. T. *Ann. Repts. on Progr. Chem. (Chem. Soc. London)* **51** (1954) 243.
3. Gilman, H. and Burtner, R. R. *J. Am. Chem. Soc.* **55** (1933) 2903.
4. Sherman, E. and Amstutz, E. D. *J. Am. Chem. Soc.* **72** (1950) 2195.
5. Dunlop, A. P. and Peters, F. N. *The Furans.* New York 1953, pp. 560 ff.
6. Wynberg, H. *J. Am. Chem. Soc.* **80** (1958) 364.
7. Burness, D. M. *Org. Syntheses* **39** (1959) 46.
8. Cornforth, J. W. *J. Chem. Soc.* **1958** 1310.
9. Gronowitz, S. *Arkiv Kemi* **13** (1958) 295.
10. Gilman, H. and Wright, G. F. *J. Am. Chem. Soc.* **55** (1933) 3302.
11. Shepard, A. F., Winslow, N. R. and Johnson, J. R. *J. Am. Chem. Soc.* **52** (1930) 2083.
12. Gilman, H. and Wright, G. F. *J. Am. Chem. Soc.* **55** (1933) 2893.
13. Manly, D. G. and Amstutz, E. D. *J. Org. Chem.* **21** (1956) 516.
14. Gronowitz, S. *Acta Chem. Scand.* **13** (1959) 1045.

Received September 13, 1961.

Polynuclear Complexes: Criticism Invited

LARS GUNNAR SILLÉN

Department of inorganic chemistry, The Royal Institute of Technology Stockholm 70, Sweden

B. S. Jensen [1] has recently published a paper on "The determination of the composition and formation constants of polynuclear complexes", a subject to which our group in Stockholm has devoted some interest for the last ten years. He who reads and understands the various series of papers from our group [2] will find that we endeavour to start without any previous assumptions on the composition of the complexes and that our present methods — given sufficiently good "three-dimensional" data — can deal with practically any set of polynuclear complexes; they are certainly not limited to sets of the "core and links" type, which correspond to exactly parallel Z curves.

Jensen's method requires that two species predominate in the solution. If there are only two species, however, one of them can be treated as the "core" and the other as a singular "core and links" complex. Then the curves $Z(\log h)_B$ are parallel, Jensen's equation (14) or (19) is exactly valid, and the data can be treated in a much simpler way than he gives.

Let us now consider some of the chemical results that Jensen deduces from data of the Stockholm group.

Rossotti and Rossotti [3], from their data on the hydrolysis of VO^{2+}, deduced the formulas $(VO)_2(OH)_2^{2+}$ and $VOOH^+$ and the formation constants $\log^*\beta_{22} = -6.88 \pm 0.05$ and $\log^*\beta_{11} = -6.0 \pm 0.1$. Jensen finds $\log^*\beta_{22} = -6.9 \pm 0.3$; he notices the deviations that indicate another complex but fails to find its formula or formation constant.

Rossotti and Rossotti [4] from their data on the acid hydrolysis of VO_2^+ have deduced the equilibria (25°C, 1 M $(Na)ClO_4$):

$$10VO_2^+aq + 8\,H_2O \rightleftharpoons H_2V_{10}O_{28}^{4-}aq + 14H^+,$$
$$\log^*\beta_{14,10} = -6.75$$
$$H_2V_{10}O_{28}^{4-}aq \rightleftharpoons HV_{10}O_{28}^{5-}aq + H^+,$$
$$\log K = -3.6$$
$$HV_{10}O_{28}^{5-}aq \rightleftharpoons V_{10}O_{28}^{6-} + H^+,$$
$$\log K = -5.8 \qquad (1)$$

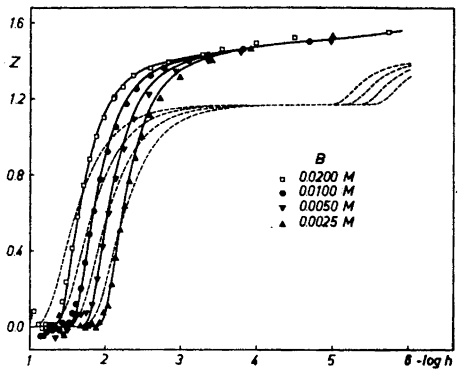

Fig. 1. Hydrolysis of VO_2^+ (1 M $(Na)ClO_4$, 25°C). Z (average number of OH^- bound per VO_2^+) as a function of log $[H^+]$ for four different values of B, the total vanadium concentration. Points: experimental data, Ref.[4] Solid curves calculated with Rossotti's theory [4] (1), dotted curves with B. S. Jensen's [1] (2).

From these same data, Jensen [1] deduces a different set of equilibria (notations below as in "Stability constants"[5])

$$6VO_2^+ + 7OH^- \rightleftharpoons (VO_2)_6(OH)_7^-,$$
$$\log \beta_{7,6} = 94.6 \pm 0.5$$
$$7(VO_2)_6(OH)_7^- + 10\,OH^- \rightleftharpoons (VO_2)_{42}(OH)_{59}^{17-},$$
$$\log K = 100 \pm 2. \qquad (2a)$$

With $\log K_w = -13.8$, which Jensen has used, this gives

$$6VO_2^+ + 7H_2O \rightleftharpoons (VO_2)_6(OH)_7 + 7H^+,$$
$$\log^*\beta_{7,6} = -2.0$$
$$7(VO_2)_6(OH)_7^- + 10\,H_2O \rightleftharpoons (VO_2)_{42}(OH)_{59}^{17-} + 10\,H^+, \log K = -38. \qquad (2b)$$

Jensen claims (p. 498) "The above conclusions are well in accord with the experimental data". Among his several diagrams, however, one does not find any comparison of the experimental data with his theory (2), and with the Rossotti's (1). Fig. 1 gives such a diagram (calculated using our computer program KUSKA) [6]. The points are the experimental data, the solid curves are calculated with Rossotti's theory (1), and the dotted curves from Jensen's (2). The reader is invited to compare the agreement.

He who is interested may then read Jensen's "general discussion" where he claims, among other things, "A distinct

advantage is that the primary polymerisation product often can be determined with certainty".

Those who would like to question (as we do ourselves sometimes) the conclusions reached by our group are cordially invited either

a) to present a better set of data (more accurate or covering a broader range of concentrations), or

b) to give another set of reactions and equilibrium constants that explain our data as well as or better than those deduced by our methods.

It is hard to see that B. S. Jensen's contribution [1] means any progress in our methodical or chemical knowledge.

1. Jensen, B. S. *Acta Chem. Scand.* **15** (1961) 487.
2. See, *e.g.*, Ingri, N. and Brito, F. *Acta Chem. Scand.* **13** (1959) 1971; Olin, Å. *Acta Chem. Scand.* **14** (1960) 126, 814; Biedermann, G. and Ciavatta, L. *Acta Chem. Scand.* **15** (1961) 1347.
3. Rossotti, F. J. C. and Rossotti, H. S. *Acta Chem. Scand.* **9** (1955) 1177.
4. Rossotti, F. J. C. and Rossotti, H. S. *Acta Chem. Scand.* **10** (1956) 957.
5. Bjerrum, J., Schwarzenbach, G. and Sillén, L. G. *Stability Constants* I—II, *Chem. Soc. Spec. Publ.* **6—7** (1957—1958).
6. Ingri, N. and Sillén, L. G. *Acta Chem. Scand. In print.*

Received August 16, 1961.

ACTA CHEMICA SCANDINAVICA 15 (1961) 1423–1428

Phosphopeptides from a Tryptic Hydrolysate of Human Casein

LARS STRID

Department of Medical Biochemistry, University of Göteborg, Göteborg, Sweden

Phosphopeptides have been isolated by anion exchange chromatography from a tryptic hydrolysate of human casein. The homogeneity of the phosphopeptide with the highest phosphorus content has been demonstrated and its amino acid composition and terminal amino acid residues determined. It contains 19 amino acid residues and 5 phosphate groups and appears to have the composition

$$Arg[Thr_2, Ser_5, Glu_5, Ileu_3, Leu, (PO_4)_5]Tyr, Lys$$

one of the glutamic acid residues possibly being in amide form.

Phosphopeptides from enzymatic hydrolysates of cow's casein have been isolated and characterized by several authors [1–8]. Phosphopeptides from human casein on the contrary have so far been investigated only by Mellander and collaborators [1–2], who studied the qualitative difference in the amino acid composition of phosphopeptone from cow, goat and human casein by a paper chromatographic method.

The aim of this investigation was to isolate phosphorylated peptides from a tryptic hydrolysate of human casein and to determine their amino acid composition.

MATERIALS AND METHODS

Preparation of human casein. Human casein was prepared according to Johansson and Strid [9]. The technical procedure was as follows:

8 l pooled human milk was defatted by centrifugation and passed through a 3.5 × 30 cm column of Amberlite IRC 50 in Na^+-form equilibrated with 0.1 M NaAc–HAc buffer pH 5.8 in order to remove the main part of calcium. The flow rate was 30 ml per min. The casein was precipitated by acidification with glacial acetic acid to pH 4.6 and heating to 35° during 30 min. After centrifugation the casein was washed with 0.1 M NaAc–HAc buffer pH 4.6, followed by methanol:chloroform (1:1), acetone and ether. Finally the casein was filtered off and airdried.

Degradation of human casein by trypsin. 20 g human casein suspended in 400 ml water was dissolved by automatic addition of 0.1 M NaOH while the pH was kept constant at 8.0. A clear solution was obtained. Trypsin (50 % $MgSO_4$, 2 × cryst. Mann Lot No. B1401) was added to give a weight ratio enzyme/substrate of 1:130. The hydrolysis was performed at 22°. The pH was maintained at 8.0 by automatic addition of 0.1 M NaOH. After 90

PREPARATION SCHEME

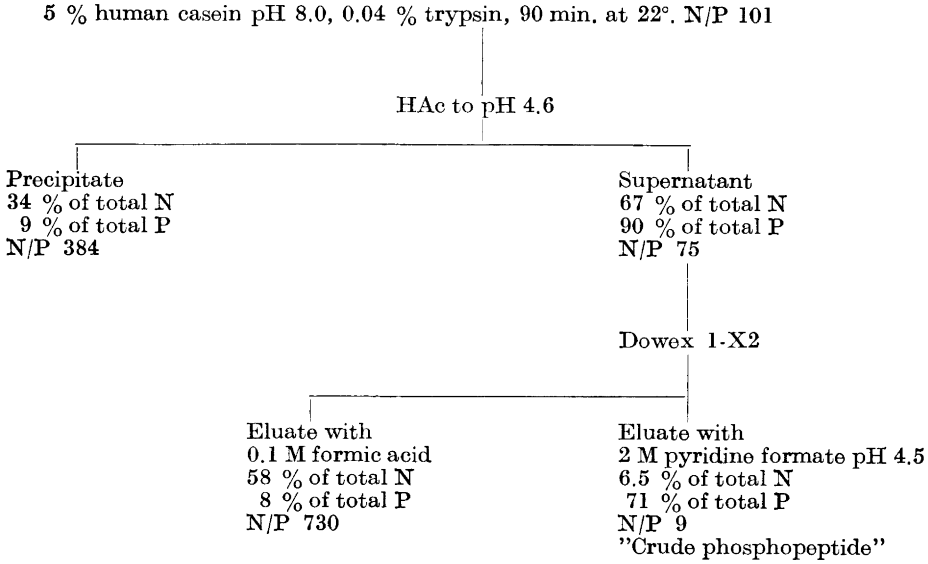

min. (50 ml 0.1 M NaOH) the reaction was interrupted by addition of 1 M HAc to pH 4.6. The precipitate obtained was removed by centrifugation and the clear supernatant lyophilized.

Separation and isolation of phosphopeptides from the tryptic hydrolysate. Column I. 10 g lyophilized hydrolysate dissolved in 150 ml water was applied to a 2.8 × 7 cm column of Dowex 1-X2 in formate form. 0.1 M formic acid was added until the effluent gave a negative ninhydrin reaction. The column was then eluted with 2 M pyridine formate at pH 4.5, whereby a fraction containing 71 % of the casein phosphorus and 7 % of the nitrogen was obtained. This fraction was lyophilized.

Column II. To separate the phosphopeptides in the crude fraction, the method described earlier was used with small modifications [10]. 850 mg of the crude fraction was dissolved in 30 ml water and 1 N NaOH was added to pH 6. The solution was applied to a 1.6 × 40 cm column of Dowex 1-X2(200–400 mesh) in formate form. A gradient elution to 2 M pyridine formate pH 4.5 was immediately started. The mixing chamber (constant volume) was filled with 1 l 0.1 M formic acid. The flow rate was 1.5 ml per min. and fractions of 12 ml were collected. 0.5 ml of each fraction was analysed with ninhydrin according to Moore and Stein [11] in order to locate the peaks (see Fig. 1). The fractions of each peak were combined and lyophilized. To remove remaining pyridine the lyophilized material was dissolved in water and added to a 1 × 3 cm column of Dowex 50-X12 (H^+). The phosphopeptides were washed through with 0.1 M formic acid and then lyophilized.

Amino acid determination. Quantitative amino acid analysis was performed with column chromatography according to Moore *et al.*[12] Samples were hydrolysed for 22.5 and 90 h at 110° in 6 N HCl.

Two-dimensional paper chromatography in the solvent systems butanol:acetic acid:water (4:1:5) and phenol containing 0.1 % ammonia was used for qualitative amino acid determination.

Paper electrophoresis. The buffer used for paper electrophoresis was 0.1 M pyridine acetate pH 5.0 [13]. Satisfactory resolution of phosphopeptides was obtained after 3 h and 10 V/cm.

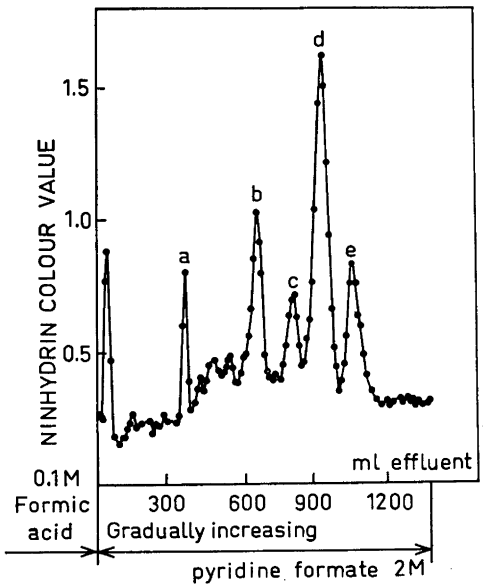

Fig. 1. Chromatogram obtained by the separation of the phosphopeptides from a tryptic hydrolysate of human casein on a 1.6 × 40 cm Dowex 1-X2 column. 0.5 ml of each fraction was used for the ninhydrin reaction [11].

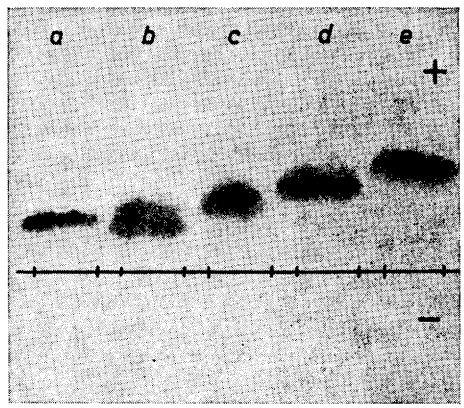

Fig. 2. Paper electrophoretic pattern of the isolated phosphopeptides, ninhydrin colour. Buffer: 0.1 M pyridine acetate pH 5.0 (10 V/cm, 3 h).

Determination of N-terminal amino acid residues. N-Terminal analysis was performed with the DNFB-method [14]. After hydrolysis liberated DNP-amino acids were identified by paper chromatography in the solvent system *tert.* amyl alcohol:biphthalate [15].

Determination of the atomic N/P ratio. Phosphorus was determined according to Dryer *et al.*[16] after combustion of the phosphopeptide with perchloric acid at 150°.

Nitrogen was determined with a colorimetric method similar to that described by Fels and Veatch [17]. 0.2 mg phosphopeptide was hydrolysed with 0.1 ml of the combustion-acid used in the Kjeldahl procedure. The hydrolysate was mixed with 3 ml 4 N sodium acetate pH 5.5 buffer [11] and finally diluted to 10 ml with water. 2 ml samples were taken for the ninhydrin reaction [11]. Ammonium sulphate was used as standard.

RESULTS AND DISCUSSION

From a 90 min. tryptic hydrolysate of human casein about 34 % of total N and 9 % of total P was precipitated by acidification to pH 4.6.

The material soluble at pH 4.6 was separated on column I in two fractions, one containing about 8 % of the total casein phosphorus and 58 % of the nitrogen and the other 71 % and 7 %, respectively. Separation of the later fraction on column II gave five well separated peaks (See Fig. 1). This showed that the previously described method for separation of small phosphopeptides involving an anion exchange resin eluted with pyridine formate [10] was applicable also to large phosphopeptides.

Table 1. Amino acid content, N/P atomic ratio and N-terminal amino acid residues of the isolated phosphopeptides.

	Phosphopeptide				
	a	b	c	d	e
Aspartic acid	Trace	Trace	Trace		
Threonine	Trace	+ +	+ +	+ +	+ +
Serine	+ + +	+ + + +	+ + + +	+ + + +	+ + + +
Glutamic acid	+ + +	+ + + +	+ + + +	+ + + +	+ + + +
Proline	+ +				
Alanine	Trace	Trace	+		
Valine + Methionine	Trace				
*Iso*leucine + leucine	+ + +	+ + + +	+ + + +	+ + + +	+ + + +
Tyrosine		+	+	+	+
Lysine		+	+	+	+
Arginine	+	+	+	+	+
Atomic ratio N/P	11	9.5	8.0	5.3	4.5
N-terminal amino acid residue	Ileu or Leu	Arg	Arg	Arg	Arg

The isolated materials from the peaks were tested by paper electrophoresis. From Fig. 2 it can be seen that the isolated compounds appeared to be electrophoretically homogeneous except peptide *b*, which gave a double-zone. The atomic ratio N/P was; fraction $a = 11$, $b = 9.5$, $c = 8.0$, $d = 5.3$ and $e = 4.5$.

N-terminal analysis showed that fraction *a* had leucine or *iso*leucine as the N-terminal amino acid residue, while the other four had arginine. The qualitative amino acid composition of the isolated compounds was determined by paper chromatography (Table 1).

The paper chromatographic amino acid analysis demonstrated that four of the five isolated phosphopeptides were very similar as regards their amino acid composition. These four were all found to have arginine as the N-terminal amino acid residue and seemed to differ only in their phosphorus content.

Phosphopeptide *e*, which had the highest phosphorus content, was selected for further investigations. Its quantitative amino acid composition was determined according to Moore *et al.*[12] after different times of hydrolysis. The results are given in Table 2. The peptide seems to contain 19 amino acid residues, 5 phosphate groups and possibly one amide group. Its minimum molecular weight is therefore 2 600.

The peptide contained one tyrosine residue and ought to be split by chymotrypsin in accordance with the specificity of this enzyme.

Chymotryptic hydrolysis of the phosphopeptide *e* (3 mg in 0.2 M THAM—HCl* buffer pH 8.7) gave two new components, which were isolated by paper elec-

* THAM = abbreviation for tris(hydroxymethyl)amino methan.

Table 2. Amino acid composition of phosphopeptide *e*.

	Duration of hydrolysis 6 N HCl, 110°C				Mean values		Molar ratio ***	Number of amino acid residues
	22.5 h		90 h					
	% amino acid	% N	% amino acid	% N	% amino acid	% N		
Threonine	7.20	0.846	5.66	0.666	7.71 *	0.906 *	1.92	2
Serine	14.65	1.952	9.16	1.222	16.48 *	2.195 *	4.65	5
Glutamic acid	25.50	2.430	24.05	2.287	24.77	2.358	5.00	5
*Iso*leucine	9.70	1.038	11.58	1.237	11.58 **	1.237 **	2.62	3
Leucine	5.10	0.543	4.87	0.520	4.99	0.531	1.11	1
Tyrosine	6.28	0.485	3.26	0.252	7.29 *	0.529 *	1.10	1
Lysine	4.96	0.953	5.19	0.995	5.07	0.974	1.03	1
Arginine	5.80	1.867	(5.01)	(1.610)	5.80	1.867	0.99	1
Ammonia	1.18	0.974	2.88	2.375	0.61	0.507	1.07	1
	80.37	11.088	71.66	11.164	84.30	11.104		

* Extrapolated to zero time.
** 90 h value.
*** Based on the glutamic acid content taken as 5.00.

trophoresis in a preparative scale. One of these moved very fast to the cathode. The other moved to the anode with somewhat higher mobility than the original phosphopeptide. Qualitative amino acid analysis showed that the compound moving to the cathode consisted of lysine only whereas the other component contained the same amino acids as the original phosphopeptide with the exception of lysine. This proved lysine to be the C-terminal amino acid residue in the phosphopeptide, which is in accordance with the specificity of trypsin and that the peptide probably contained only one lysine residue. This indicated that the molecular weight is 2 600 and not a multiple of it. The disappearing of phosphopeptide *e* in the electrophoretic pattern after chymotryptic hydrolysis appeared to indicate that this peptide fraction was homogeneous.

From a peptic hydrolysate of the phosphopeptide *e* a peptide containing only tyrosine and lysine was isolated. Thus, tyrosine appeared to be the residue next to lysine.

The results above indicated that the isolated phosphopeptide had the composition

$Arg[Thr_2, Ser_5, Glu_5, Ileu_3, Leu, (PO_4)_5]Tyr, Lys$

one of the glutamic acid residue possibly being in amide form.

A comparison between the phosphopeptide *e* and the phosphopeptides obtained in the same way from cow's casein [2-8] showed a resemblance in the high contents of glutamic acid, serine and *iso*leucine. It lacked aspartic acid, glycine

and valine, which usually are present in phosphopeptides isolated from cow's casein.

Acknowledgement. The author wishes to express sincere thanks to Professor Olof Mellander for his support in this work.

The work was supported by grants from the *Swedish Medical Research Council* to Professor Olof Mellander.

REFERENCES

1. Mellander, O. *Upsala Läkarfören. Förh.* **52** (1947) 107.
2. Mellander, O. and deVerdier, C.-H. *Acta Soc. Med. Upsaliensis* **57** (1952) 218.
3. Peterson, R. F., Nauman, L. W. and McMeekin, T. L. *J. Am. Chem. Soc.* **80** (1958) 95.
4. Pantlitschko, M. and Gründig, E. *Monatsh.* **89** (1958) 274.
5. Pantlitschko, M. and Gründig, E. *Monatsh.* **89** (1958) 489.
6. Österberg, R. *Arkiv Kemi* **13** (1959) 409.
7. Bennich, H., Johansson, B. and Österberg, R. *Acta Chem. Scand.* **13** (1959) 1171.
8. Österberg, R. *Biochim. et Biophys. Acta* **42** (1960) 312.
9. Johansson, B. and Strid, L. *Unpublished work.*
10. Strid, L. *Acta Chem. Scand.* **13** (1959) 1787.
11. Moore, S. and Stein, W. H. *J. Biol. Chem.* **211** (1954) 907.
12. Moore, S., Spackman, D. H. and Stein, W. H. *Anal. Chem.* **30** (1958) 1185.
13. Bennich, H. *Biochim. et Biophys. Acta,* **51** (1961) 265.
14. Sanger, F. and Thompson, E. O. P. *Biochem. J.* **53** (1953) 353.
15. Blackburn, S. and Lewther, A. G. *Biochem. J.* **48** (1951) 126.
16. Dryer, R. L., Tammes, A. R. and Routh, J. I. *J. Biol. Chem.* **225** (1957) 177.
17. Fels, G. and Veatch, R. *Anal. Chem.* **31** (1959) 451.

Received March 23, 1961.

ACTA CHEMICA SCANDINAVICA 15 (1961) 1429–1436

Crystal Structure of the 1:1 Addition Compound Dithiane-Iodoform

T. BJORVATTEN and O. HASSEL

Universitetets Kjemiske Institutt, Blindern - Oslo, Norway

The crystal structure of a new (1:1) addition compound formed by 1,4-dithiane and iodoform has been determined. The crystals have a melting point of 72°C and an observed density of 2.8 g·cm^{-3}.

The monoclinic unit cell (space group $P2_1/m$) containing *two* formula units has the parameters

$a = 6.56$ Å $\quad b = 21.06$ Å $\quad c = 4.47$ Å $\quad \beta = 104.4°$

The dithiane molecules are situated in centers of symmetry, the iodoform molecules in symmetry planes. Two iodine atoms belonging to a particular iodoform molecule form charge transfer bonds with sulphur atoms belonging to neighbouring dithiane molecules and the I—S distance (3.32 Å) is about 0.7 Å shorter than anticipated for a van der Waals contact. Each iodoform molecule is therefore linked to two neighbouring dithiane molecules and *vice versa* and chains of alternating donor and acceptor molecules are present in the crystal.

It has become increasingly clear that the elucidation of the structures of molecular compounds in which halides play the rôle of electron acceptors is essential for a thorough understanding of the nature of the charge transfer bond. So far, however, the crystal structure of the 3:1 compound formed by quinoline and iodoform is the only one which has been described in some detail [1]. But a number of additional structures are at present being investigated in our laboratory and detailed reports of the results obtained will be published in the near future.

We start by giving a report dealing with the crystal structure of a compound not previously described in the literature which contains dithiane and iodoform molecules in the ratio 1:1.

Crystals of this new compound may be obtained simply by slow evaporation of the solvent (*e.g.* carbon disulphide) from a saturated solution containing an equimolecular mixture of the two components.

The crystals, colourless flat needles, are monoclinic with the lattice constants

$a = 6.56$ Å; $\quad b = 21.06$ Å; $\quad c = 4.47$ Å; $\quad b = 104.4°$

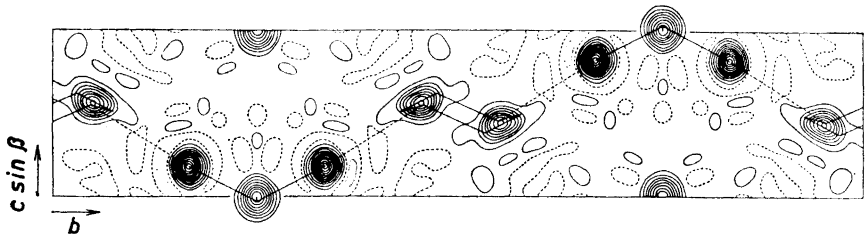

Fig. 1a. Electron density projection along the *a*-axis. Contour intervals: 4 e·Å^{-2} for for sulphur and carbon atoms. 10 e·Å^{-2} for iodine atoms.

The estimated error in the lattice constants is $\pm$ 0.5 %. The density was found equal to 2.80 giving the value $Z = 2$ for the number of molecules in the unit cell (density calculated from the lattice parameters 2.85). The space group derived from the X-ray extinctions is either $P2_1/m$ or $P2_1$. The determination of the structure was carried out assuming the former, more symmetrical space group to be the correct one.

The X-ray material on which the structure determination was based consisted of Weissenberg diagrams obtained with Cu$K\alpha$-radiation using an integrating camera of the Wiebenga type. The sections of the crystals selected for this work were approximately 0.08 × 0.08 mm^2.

Zero layer line diagrams were taken with rotation about the three principal axes using the multiple film method and the intensities (*cf.* Table 3) were measured photometrically. Corrections for absorption or extinction effects were not introduced. The number of observed reflexions in the (h00), (0k0) and [00l] zones are 93, 52, and 136, respectively. The number of reflexions compatible with the actual experimental conditions are 119, 71, and 174.

Approximate coordinates of the iodine atoms could easily be found from Patterson syntheses with projection along the *c* and *a*-axes. Choosing the structure factor signs based on these coordinates a Fourier synthesis was first

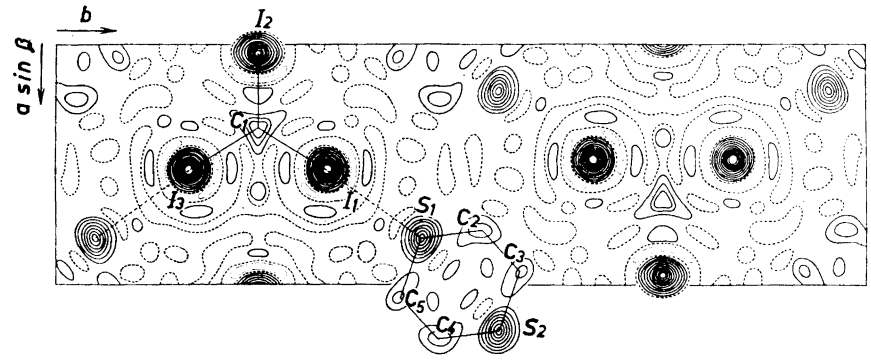

Fig. 1b. Electron density projection along the *c*-axis. Contour intervals: 4 e·Å^{-2} for sulphur and carbon atoms. 10 e·Å^{-2} for iodine atoms.

performed with projection along the *c*-axis. In the resulting map peaks giving the positions of the sulphur atoms were found besides the heavier peaks due to the iodine atoms. In the next Fourier refinement peaks belonging to the lighter atoms were also present. The data obtained from diagrams with rotation about the *a*-axis were treated correspondingly and both Fourier projections refined until no further changes of structure factor signs occurred. The final atomic coordinates based on the material obtained from Weissenberg diagrams about [001] and [100] were computed using a least squares program worked out for the Ferranti Mercury computer used throughout this investigation. As it appeared probable, however, that anisotropy in the atomic vibrations might have to be taken into account, two total difference Fourier syntheses with projection along the *c* and *a* axes were first performed, the results of which clearly showed that such anisotropic vibrations actually occur in the case of the iodine atoms which are not situated in the symmetry planes.

The correctness of this suggestion regarding the ansiotropic vibrations associated with the iodine atoms just mentioned is fully confirmed by the least squares computation, the *R* factor including only observed reflections of the projection along [100] actually dropped from 0.148 to 0.094 when this anisotropy was taken into account. In the case of the [001] projection, on the other side, the *R* factor 0.123 was not improved by such a procedure.

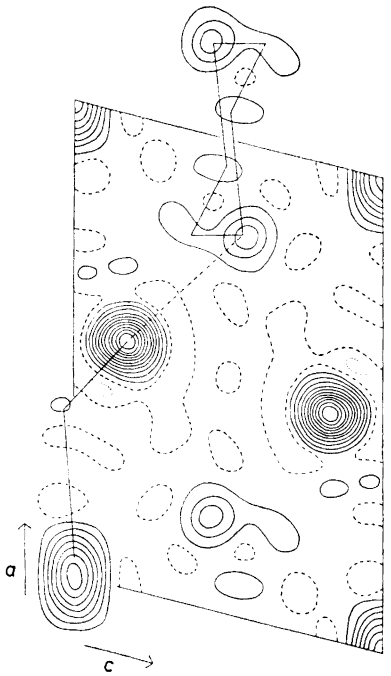

Fig. 2. Electron density projection along the *b*-axis. Contour intervals: 20 e·Å^{-2}.



Fig. 3. Structure of the iodoform-dithiane chains. Open circles indicates sulphur, closed circles iodine (large) and carbon (small) atoms.

Table 1. Atomic coordinates as fractions of cell edges.

Atom	x	y	z
I_1	0.5214	0.3339	0.1763
I_2	0.0406	0.2500	−0.0039
S_1	0.805	0.4529	0.551
C_1	0.344	0.2500	−0.037
C_2	0.775	0.5287	0.384
C_3	0.943	0.5733	0.492

Turning now to the ($0k0$) zone, least squares refinements were performed directly, starting with the coordinates obtained from the two other projections. The R factor for this zone dropped to 0.124 assuming all over isotropic vibrations and to 0.108 assuming anisotropic vibrations of the iodine atoms not situated in the symmetry planes.

The final Fourier maps are reproduced in Figs. 1 a, 1 b, and 2. The dithiane molecules are situated in centers of symmetry, the iodoform molecules in symmetry planes. Two iodine atoms belonging to a particular iodoform molecule are linked to sulphur atoms of neighbouring dithiane molecules thus producing endless chains of alternating dithiane and iodoform molecules (Fig. 3). The arrangement C—I—S appears to be nearly linear but the observed small deviation of the CIS angle from 180° is probably significant. Observed and calculated structure factors are listed in Table 3. In the calculations the analytical approximation to the atomic scattering factors computed by Forsyth and Wells [2] was employed.

The atomic coordinates finally arrived at are listed in Table 1. In this table the mean value of each coordinate obtained from the two relevant projections are given (in the case of the iodoform carbon atom the z-coordinate could only be determined from the [010] projection). The agreement between the coordinates as determined from different projections is indeed very good leading to values not differing by more than 0.05 Å for carbon, 0.03 Å for sulphur and 0.012 Å in the case of iodine.

In Table 4 the resulting interatomic distances have been listed. The observed difference in the C—I distance referring to the two types of iodine atoms is not necessarily significant, however. The S—I bond distance (3.32 Å) is about 0.7 Å shorter than the van der Waals radius sum (4.0 Å), a fact clearly indicating the presence of a charge transfer bond between these atoms. The value reported [3] for the corresponding bond in the compound formed by iodoform and three molecules of S_8 is somewhat larger (3.45 Å). It follows from the anisotropic vibration amplitudes of the iodine atoms directly linked to sulphur that these atoms are vibrating more freely in directions perpendicular to the S—I bond than along the direction of the bond. The B values actually has a maximum for a direction nearly perpendicular both to the S—I direction and

Table 2. Standard deviations for the positions of atoms.

Iodine:	$\sigma(x) = 0.0037$ Å ;	$\sigma(y) = 0.0031$ Å ;	$\sigma(z) = 0.0035$ Å
Sulphur:	$\sigma(x) = 0.013$ Å ;	$\sigma(y) = 0.011$ Å ;	$\sigma(z) = 0.012$ Å
Carbon:	$\sigma(x) = 0.039$ Å ;	$\sigma(y) = 0.043$ Å ;	$\sigma(z) = 0.060$ Å

Table 3. Observed and calculated structure factors.

(00*l*) zone

h k l	F_o	F_c	*h k l*	F_o	F_c
0 2 0	88	−130	2 15 0	< 17	− 2
0 4 0	52	37	2 16 0	18	− 15
0 6 0	76	65	2 17 0	< 18	− 10
0 8 0	47	− 31	2 18 0	63	48
0 10 0	193	−190	2 19 0	< 18	− 14
0 12 0	183	168	2 20 0	33	− 23
0 14 0	131	−121	2 21 0	< 17	− 11
0 16 0	22	− 9	2 22 0	64	− 69
0 18 0	88	61	2 23 0	36	33
0 20 0	< 18	12	2 24 0	72	69
0 22 0	60	− 58	2 25 0	< 13	− 10
0 24 0	104	98	3 0 0	97	−109
0 26 0	32	− 42	3 1 0	17	− 3
1 0 0	63	− 64	3 2 0	19	− 15
1 1 0	< 6	− 2	3 3 0	35	29
1 2 0	55	37	3 4 0	98	103
1 3 0	60	56	3 5 0	104	−108
1 4 0	158	183	3 6 0	159	−169
1 5 0	21	− 26	3 7 0	79	79
1 6 0	224	−265	3 8 0	108	114
1 7 0	61	68	3 9 0	35	− 30
1 8 0	106	124	3 10 0	38	40
1 9 0	18	− 16	3 11 0	< 16	5
1 10 0	< 12	0	3 12 0	40	− 37
1 11 0	< 7	− 6	3 13 0	< 17	20
1 12 0	89	− 77	3 14 0	23	23
1 13 0	31	− 27	3 15 0	39	39
1 14 0	22	6	3 16 0	69	73
1 15 0	17	− 12	3 17 0	44	− 46
1 16 0	105	97	3 18 0	106	−108
1 17 0	57	− 49	3 19 0	50	48
1 18 0	126	−121	3 20 0	29	34
1 19 0	< 18	10	3 21 0	< 17	− 15
1 20 0	67	67	3 22 0	< 16	2
1 21 0	< 17	− 7	3 23 0	< 14	− 13
1 22 0	30	20	3 24 0	46	− 44
1 23 0	16	12	4 0 0	148	141
1 24 0	60	− 40	4 1 0	126	−117
1 25 0	20	15	4 2 0	70	− 66
1 26 0	16	9	4 3 0	31	21
2 0 0	160	200	4 4 0	16	− 20
1 1 0	62	− 74	4 5 0	30	− 24
2 2 0	157	−184	4 6 0	73	72
2 3 0	43	44	4 7 0	< 16	− 25
2 4 0	42	− 42	4 8 0	21	− 24
2 5 0	25	23	4 9 0	42	− 47
2 6 0	72	82	4 10 0	67	− 70
2 7 0	< 12	12	4 11 0	84	94
2 8 0	< 12	0	4 12 0	83	92
2 9 0	16	− 17	4 13 0	52	− 56
2 10 0	81	− 90	4 14 0	50	− 53
2 11 0	47	54	4 15 0	43	47
2 12 0	173	183	4 16 0	30	− 24
2 13 0	60	− 60	4 17 0	19	24
2 14 0	65	− 66	4 18 0	47	48

$h\,k\,l$	F_o	F_c	$h\,k\,l$	F_o	F_c
4 19 0	< 18	0	7 13 0	< 11	13
4 20 0	21	− 13	8 0 0	< 11	0
4 21 0	20	− 23	8 1 0	52	− 58
4 22 0	33	− 36	8 2 0	< 11	− 12
4 23 0	26	37	8 3 0	14	10
5 0 0	36	− 41	8 4 0	14	− 26
5 1 0	< 17	14			
5 2 0	47	52		(h00) zone	
5 3 0	41	28	0 2 0	117	−129
5 4 0	69	58	0 4 0	41	36
5 5 0	111	−101	0 6 0	83	71
5 6 0	90	− 83	0 8 0	45	− 36
5 7 0	77	78	0 10 0	181	−185
6 8 0	32	25	0 12 0	165	163
5 9 0	35	− 31	0 14 0	141	−116
5 10 0	< 18	7	0 16 0	30	− 28
5 11 0	< 18	− 17	0 18 0	78	73
5 12 0	63	− 75	0 20 0	< 19	− 5
5 13 0	< 18	18	0 22 0	52	− 54
5 14 0	< 17	10	0 24 0	95	98
5 15 0	21	26	0 26 0	32	− 32
5 16 0	31	33	0 0 1	80	100
5 17 0	54	− 58	0 1 1	92	−133
5 18 0	52	− 43	0 2 1	176	−202
5 19 0	45	50	0 3 1	23	13
5 20 0	31	35	0 4 1	37	31
6 0 0	62	65	0 5 1	150	159
6 1 0	97	− 81	0 6 1	19	6
6 2 0	24	− 25	0 7 1	93	−104
6 3 0	54	39	0 8 1	72	73
6 4 0	21	− 22	0 9 1	24	9
6 5 0	< 18	37	0 10 1	58	− 59
6 6 0	42	48	0 11 1	102	107
6 7 0	< 18	− 9	0 12 1	128	130
6 8 0	24	− 27	0 13 1	93	− 90
6 9 0	27	− 21	0 14 1	64	− 54
6 10 0	31	− 37	0 15 1	23	− 13
6 11 0	67	68	0 16 1	< 18	13
6 12 0	36	40	0 17 1	76	74
6 13 0	67	− 73	0 18 1	< 19	9
6 14 0	< 16	− 26	0 19 1	72	− 72
6 15 0	< 16	2	0 20 1	< 19	− 4
6 16 0	17	− 18	0 21 1	< 18	− 9
6 17 0	< 13	8	0 22 1	48	− 47
6 18 0	36	39	0 23 1	58	59
7 0 0	56	− 59	0 24 1	40	35
7 1 0	< 16	27	0 25 1	42	− 46
7 2 0	< 16	12	0 26 1	23	− 29
7 3 0	39	35	0 0 2	25	26
7 4 0	< 15	9	0 1 2	98	− 98
7 5 0	60	− 60	0 2 2	< 13	4
7 6 0	23	− 28	0 3 2	33	− 27
7 7 0	86	81	0 4 2	105	115
7 8 0	< 17	20	0 5 2	67	66
7 9 0	23	− 13	0 6 2	139	−149
7 10 0	32	32	0 7 2	111	−111
7 11 0	< 14	− 22	0 8 2	65	62
7 12 0	26	− 28	0 9 2	20	− 14

$h\,k\,l$	F_o	F_c
0 10 2	30	− 32
0 11 2	68	67
0 12 2	39	− 38
0 13 2	54	− 59
0 14 2	21	− 15
0 15 2	< 19	5
0 16 2	57	60
0 17 2	71	71
0 18 2	64	− 66
0 19 2	45	− 44
0 20 2	40	44
0 21 2	< 18	2
0 22 2	19	20
0 23 2	38	44
0 24 2	18	− 17
0 0 3	67	− 69
0 1 3	34	28
0 2 3	< 17	− 10
0 3 3	22	17
0 4 3	95	85
0 5 3	22	12
0 6 3	124	−115
0 7 3	34	32
0 8 3	88	90
0 9 3	20	19
0 10 3	27	25
0 11 3	22	− 16
0 12 3	48	− 42
0 13 3	< 19	6
0 14 3	< 19	10
0 15 3	< 18	− 11
0 16 3	48	52
0 17 3	21	− 23
0 18 3	76	− 82
0 19 3	< 18	− 2
0 20 3	32	31
0 21 3	< 15	2
0 22 3	< 13	12
0 0 4	< 19	29
0 1 4	56	50
0 2 4	21	− 12
0 3 4	19	− 18
0 4 4	23	29
0 5 4	68	− 68
0 6 4	46	− 45
0 7 4	23	29
0 8 4	< 18	21
0 9 4	< 18	− 3
0 10 4	< 18	− 18
0 11 4	46	− 49
0 12 4	< 19	2
0 13 4	51	53
0 14 4	< 19	− 3
0 15 4	17	13
0 16 4	22	21
0 17 4	24	− 27
0 18 4	15	− 18
0 0 5	45	42
0 1 5	28	30
0 2 5	28	− 28
0 3 5	< 18	8
0 4 5	< 17	0
0 5 5	< 17	− 6
0 6 5	22	21
0 7 5	24	29
0 8 5	< 15	2
0 9 5	< 14	6
0 10 5	21	− 25
0 11 5	16	− 25
	(0k0) zone	
1 0 0	44	− 65
2 0 0	174	206
3 0 0	108	−112
4 0 0	177	149
5 0 0	47	− 45
6 0 0	75	76
7 0 0	73	− 71
8 0 0	< 23	12
$\bar{8}$ 0 1	55	67
$\bar{7}$ 0 1	75	− 63
$\bar{6}$ 0 1	99	86
$\bar{5}$ 0 1	120	−110
$\bar{4}$ 0 1	122	111
$\bar{3}$ 0 1	27	− 28
$\bar{2}$ 0 1	224	219
$\bar{1}$ 0 1	66	− 56
0 0 1	90	107
1 0 1	< 18	− 13
2 0 1	117	117
3 0 1	72	64
4 0 1	< 33	17
5 0 1	< 37	10
6 0 1	< 34	− 30
7 0 1	< 33	35
$\bar{8}$ 0 2	< 27	3
$\bar{7}$ 0 2	59	− 48
$\bar{6}$ 0 2	< 37	11
$\bar{5}$ 0 2	36	35
$\bar{4}$ 0 2	34	28
$\bar{3}$ 0 2	75	62
$\bar{2}$ 0 2	< 25	− 17
$\bar{1}$ 0 2	140	146
0 0 2	24	28
1 0 2	193	189
2 0 2	50	− 58
3 0 2	122	121
4 0 2	65	− 80
5 0 2	94	108
6 0 2	53	− 63
$\bar{7}$ 0 3	53	51
$\bar{6}$ 0 3	37	− 50
$\bar{5}$ 0 3	70	67
$\bar{4}$ 0 3	83	− 89
$\bar{3}$ 0 3	116	133
$\bar{2}$ 0 3	51	− 49

$h\,k\,l$	F_o	F_c	$h\,k\,l$	F_o	F_c
$\bar{1}$ 0 3	200	166	$\bar{1}$ 0 4	47	54
0 0 3	94	− 77	0 0 4	< 37	16
1 0 3	148	128	1 0 4	66	70
2 0 3	78	− 68	2 0 4	34	32
3 0 3	123	126	3 0 4	< 36	7
4 0 3	< 42	− 39	4 0 4	< 25	15
$\bar{5}$ 0 3	57	59	$\bar{5}$ 0 5	< 27	− 1
$\bar{7}$ 0 4	23	26	$\bar{4}$ 0 5	< 34	8
$\bar{6}$ 0 4	62	− 62	$\bar{3}$ 0 5	< 36	− 21
$\bar{5}$ 0 4	53	65	$\bar{2}$ 0 5	53	60
$\bar{4}$ 0 4	< 36	− 25	$\bar{1}$ 0 5	< 34	− 6
$\bar{3}$ 0 4	85	84	0 0 5	70	74
$\bar{2}$ 0 4	< 37	− 23	1 0 5	37	− 45

Table 4. Interatomic distances and angles.

	Distance (Å)		Angle (°)
C_1-I_1	2.20	$I_1-C_1-I_2$	113
C_1-I_2	2.03	$I_1-C_1-I_3$	107
I_1-I_2	3.529	$C_5-S_1-C_2$	104
I_1-I_3	3.534	$S_1-C_2-C_3$	117
S_1-C_2	1.75	$C_2-C_3-S_2$	114
C_2-C_3	1.44	$C_1-I_1-S_1$	175
S_1-C_5	1.79	$I_1-S_1-S_2$	137
S_1-S_2	3.35		
I_1-S_1	3.32		

the *b*-axis. It may be added that the direction of the S—I bond corresponds to the equatorial bond direction in *cyclo*hexane.

When the present investigation was started, some crystallographic work dealing with the 1:1 compound formed by iodoform and 1,4-dioxan [4] had already been carried out in this laboratory. It was found, however, that the preparation of sufficiently good single crystals of this compound was more problematic than in the case of the dithiane analogue and the work was therefore first concentrated on the latter. The dioxan compound is orthorhombic and not isostructural with the dithiane compound. It may, however, be stated with confidence that the general characteristics of the two structures are very similar. Thus, even in the dioxan compound chains similar to those found in the dithiane compound and consisting of alternating acceptor and donor molecules are present. Two iodine atoms of each iodoform molecule therefore form charge transfer bonds with ether oxygen atoms of adjacent dioxan molecules.

This investigation has in part been sponsored by the *United States Air Force Development Command* under contract AF 61 (052)-71.

REFERENCES

1. Bjorvatten, T. and Hassel, O. *Acta Chem. Scand.* **13** (1959) 1261.
2. Forsyth, J. B. and Wells, M. *Acta Cryst.* **12** (1959) 412.
3. Bjorvatten, T., Hassel, O. and Rømming, Chr. *Nature* **189** (1961) 137.
4. Rheinboldt, H. and Luyken, A. *J. prakt. Chem.* [2] **133** (1932) 284.

Received March 23, 1961.

ACTA CHEMICA SCANDINAVICA 15 (1961) 1437–1453

The Crystal Structure of $InOHSO_4(H_2O)_2$

GEORG JOHANSSON

Department of Inorganic Chemistry, Royal Institute of Technology, Stockholm 70, Sweden

Crystals of the basic indium sulfate $InOHSO_4(H_2O)_2$ are monoclinic with unit cell dimensions: $a = 6.06$ Å, $b = 7.89$ Å, $c = 12.66$ Å, $\beta = 107.5°$. The indium atoms are octahedrally surrounded by oxygen atoms at an average distance of 2.16 Å with no significant differences between the In—O bond lengths. The InO_6 octahedra are joined together by means of common corners, to chains running parallel to the b axis. Different indium-oxygen chains have no oxygen atoms in common but are linked together by means of hydrogen bonds to the oxygen atoms of the sulfate groups.

The preparation of a basic indium sulfate by the addition of ethanol to a solution of indium sulfate in water has been reported in the literature [1,2]. It is described as forming small bi-axial positive crystals, probably monoclinic [1]. The formula, based on indium and sulfate analysis only, has been given as $In_2O(SO_4)_2 \cdot 6H_2O$ [1] or $2InOHSO_4 \cdot 5H_2O$ [2]. The structure of a basic sulfate prepared in the same way has been investigated as part of a program on structure determinations of basic salts of some tervalent metals [3–5].

EXPERIMENTAL

Preparation of crystals. Indium sulfate was prepared from indium metal of 99.95 % purity supplied by the Consolidated Mining and Smelting Company of Canada, Ltd. Solutions of indium sulfate with concentrations ranging from 0.05 M to 1.0 M In^{3+} were mixed with one, or two times their volume of ethanol. According to powder X-ray photographs the phases precipitated in the various solutions were identical. Good crystals were obtained from 0.05 M indium sulfate solutions when these were mixed with twice the volume of ethanol. The crystallization was very slow and several weeks were required for the formation of crystals as large as 0.1 mm in length.

Analysis. An air dried sample was used for the analysis. The crystals are very slightly soluble in water but dissolve readily in warm dilute acid. Indium was determined by precipitation with ammonia, igniting, and weighing as In_2O_3. Sulfate was determined as $BaSO_4$. The water content was obtained by Brush and Penfield's method as described by Kolthoff and Sandell [6]. The density was found by comparing the weight of a specimen, in benzene and in air.

The results of the analysis (Table 1) seem to favor the formula $InOHSO_4(H_2O)_2$ rather than $InOHSO_4(H_2O)_{2.5}$. This is supported by the result of the structure determination.

Table 1.

	Found	Calculated for $InOHSO_4(H_2O)_2$	Calculated for $InOHSO_4(H_2O)_{2.5}$
% In_2O_3	52.3	52.60	50.86
% SO_3	30.4	30.34	29.34
% H_2O	17.5	17.07	19.80
Density	3.0_0	3.03	3.14

UNIT CELL AND SPACE GROUP

The crystals are rod-shaped and elongated along the *b*-direction. Rotation and Weissenberg photographs around the *b* and *c* axes showed that the unit cell is monoclinic and enabled the following approximate values of the lattice parameters to be calculated: $a = 6.1$ Å, $b = 7.9$ Å, $c = 12.6$ Å, $\beta = 107°$. More precise values were determined from powder photographs (Table 2) taken with Cu$K\alpha$ radiation in a Guinier focusing camera, using KCl ($a = 6.2929$ Å) as the internal standard. The values found were:

$$a = 6.05_8 \text{ Å}; b = 7.89_4 \text{ Å}; c = 12.66_5 \text{ Å}; \beta = 107.5°; V = 577.6 \text{ Å}^3.$$

The accuracy is estimated to about 0.1 %.

The density calculated on the basis of four formula weights in the unit cell is 3.03, that observed is 3.0_0 (Table 1).

The only systematically absent reflections are of the type $0k0$ with k odd, which indicates the space group $P2_1/m$ or $P2_1$. Since all reflections for k odd were extremely weak on the photographs, the rather few nonobserved $0k0$ reflections might have been only accidentally absent. However, nothing during the structure determination indicated a lower space group than $P2_1/m$ which was therefore assumed to be the correct symmetry.

Weissenberg photographs were taken around the *b* and *c* axes (layer lines 0—4 and 0,2,4, respectively) using the multiple film technique with CuK radiation. Intensities were estimated visually with the aid of a calibrated intensity strip and corrected for Lorentz and polarization factors. No correction for absorption was applied. For the photographs taken around the *b* axis, a crystal approximately 0.1 mm in length and 0.06 × 0.08 mm in cross-section was used. A crystal of about the same size was used for the photographs taken around the *c*-axis.

STRUCTURE DETERMINATION

All reflections for k odd or l odd are extremely weak and it does not seem likely that the In atoms make any contributions to the intensities of these reflections. Accordingly, it should be possible to describe the positions of the In atoms with a unit cell four times smaller than the actual unit cell. The x parameters are restricted to $x \approx 0$ or $x \approx \frac{1}{2}$ since the In-In peaks on the $h0l$ Patterson projection (Fig. 1) occur at $u = 0$, $w = 0$, and at $u = 0$, $w = \frac{1}{2}$. Other peaks in the projection are too small to correspond to In-In vectors. In space group $P2_1/m$ the following In positions are thus possible, if only structurally nonequivalent arrangements are included:

1.	4 In in 4(f):	$\pm(x,y,z),\pm(x,\frac{1}{2}-y,z)$	$x=0,y=0,z=1/4$
2.	2 In in 2(*e*):	$\pm(x,1/4,z)$	$x=0,z=1/4$
	2 In in 2(*e*):		$x=0,z=3/4$
3.	2 In in 2(e):		$x=0,z=0$
	2 In in 2(*e*):		$x=0,z=\frac{1}{2}$
4.	2 In in 2(*a*):	0,0,0; $0,\frac{1}{2},0$	
	2 In in 2(*c*):	$0,0,\frac{1}{2}$; $0,\frac{1}{2},\frac{1}{2}$	

Table 2. Powder photograph of $InOHSO_4(H_2O)_2$. Guinier camera. Cu$K\alpha$ radiation.

$h\,k\,l$	$10^4 \sin^2\Theta$ calc.	$10^4 \sin^2\Theta$ obs.	I obs.
0 0 2	163	165	m
1 0 0	178	179	m
1 0 $\bar{2}$	238	239	s
0 1 2	258	259	vw
1 1 0	273	275	vw
0 2 0	381	381	m
1 0 2	443	445	m
0 2 2	544	545	s
1 2 0	559	559	s
1 0 $\bar{4}$	624	625	w
0 0 4	651	653	vvw
2 0 $\bar{2}$	669	671	vw
2 0 0	711	716	vw
1 1 $\bar{4}$	719		
0 1 4	746	748	vw
2 1 0	806	805	vw
1 2 $\bar{2}$	824	825	w
1 0 $\bar{5}$	939	947	w
2 1 $\bar{1}$	949		
2 0 $\bar{4}$	952		
1 2 $\bar{4}$	1005	1005	w
0 2 4	1032	1034	vw
1 0 4	1033		
1 1 $\bar{5}$	1034		
2 2 $\bar{2}$	1050	1050	vw
1 2 3	1078	1084	vw
2 0 2	1079		
2 2 0	1092	1096	vw
1 3 $\bar{2}$	1095		
2 2 $\bar{4}$	1333	1334	w
1 0 $\bar{6}$	1335		
1 2 4	1414	1418	vw
2 2 2	1460	1464	vw
0 0 6	1464		
0 4 0	1523	1522	w
0 1 6	1560	1562	vw
2 0 $\bar{6}$	1561		
3 0 0	1600	1601	vw
3 1 $\bar{3}$	1601		
3 0 $\bar{4}$	1637	1638	vw
0 4 2	1686	1684	vw
1 4 0	1701	1701	vw
1 2 $\bar{6}$	1716	1717	vw
1 4 $\bar{2}$	1762	1759	vw
3 2 $\bar{2}$	1837	1839	vw
0 2 6	1845		
2 2 $\bar{6}$	1942	1941	vw
1 4 $\bar{2}$	1966	1966	w
3 2 $\bar{4}$	2018	2017	vw

The distance, 3.95 Å, between the mirror planes of the unit cell is too small for the sulfate groups to have positions between these planes. The sulfur atoms must therefore occupy two twofold positions, 2(*e*), on the mirror planes. The perpendicular distance from the S atom to one of the edges of the SO_4 tetrahedron should be about 0.8 Å [13]. In a Patterson projection along the *b* axis, that is perpendicular to the mirror planes, an In-S vector should then always be accompanied by a peak of two overlapping In-O vectors of approximately the same height and at a distance of about 0.8 Å.

The Patterson projection, $P(upw)$, calculated from the $h0l$ reflections,* is shown in Fig. 1. The four alternative sets of In positions all result in identical In—In vectors corresponding to the high peaks at $u = 0$, $w = 1/2$, and at the origin. $P(upw)$ also shows four double peaks which, according to the discussion above, probably represent vectors between In and atoms of the sulfate groups.

Assuming the parameters of the sulfur atoms, S_1 and S_2, to be x_1,z_1 and x_2,z_2, respectively, the following In—S vectors should appear on the $h0l$ projection if the 1st or 2nd alternative sets of In positions are applicable:



Fig. 1. Patterson projection along the *b*-axis. Dashed lines indicate negative regions. In the peaks at (0,0) and (0, ½) only every 5th contour has been drawn. The four double peaks with the approximate positions ± [0.38, 0.18] and ± [0.38, 0.68] contain the In-S vectors.

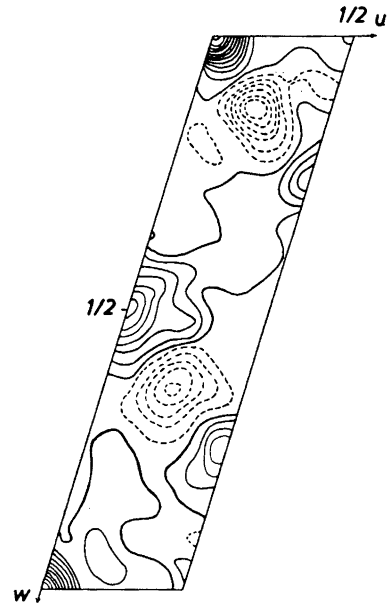

Fig. 2. The generalized Patterson projection $P_1(uw)$. Dashed lines indicate negative regions.

* All calculations were carried out on the "Besk" computer with the use of programs designed for the calculation of structure factors [7] and electron densities.[8]

$\pm[\bar{x}_1,\ 1/4-z_1]$ $\pm[\bar{x}_2,\ 1/4-z_2]$
$\pm[x_1,\ 1/4+z_1]$ $\pm[x_2,\ 1/4+z_2]$

For the 3rd and 4th alternatives the corresponding vectors are:

$\pm[x_1,\ z_1]$ $\pm[x_2,\ z_2]$
$\pm[x_1,\ 1/2+z_1]$ $\pm[x_2,\ 1/2+z_2]$

The presence of only four double peaks in $P(upw)$ within the unit cell instead of the expected eight, and the heigths of these peaks compared to the height of the origin peak, indicate the presence of overlapping In—S vectors. This can be explained by assuming: $x_2 \approx x_1$ and $z_2 \approx 1/2 + z_1$. The most likely positions of the In—S vectors are:

$$\pm\ [0.38,\ 0.68_5] \text{ and } \pm\ [0.38,\ 0.18_5]$$

The y parameters of the corresponding sulfur atoms are 1/4 or 3/4. For geometrical reasons they must be the same and can be chosen to be 1/4 since $y = 3/4$ would result in an equivalent structure.

In a generalized Patterson projection, calculated from the $h1l$ reflections to which the In atoms do not contribute, the following sulfur-sulfur vectors should then be present:

$u = 0.24,\ w = 0.13$	weight: -2
$u = 0\ \ ,\ w = 0.50$	» : $+2$
$u = 0.24,\ w = 0.63$	» : -2

As is shown on Fig. 2 the calculated vectors correspond to the three largest peaks of $P_1(uw)$, thus confirming the correctness of the assumed arrangement of sulfur atoms.

The In contributions determine the signs of the structure factors of those $h0l$ reflections for which l is even, and a Fourier projection with the In atoms subtracted was calculated using these reflections. The resulting Fourier map (Fig. 3a) gives only an average of the electron density projections of the two halves of the unit cell, but because it contains all but the very weakest reflections it still shows the main features of the structure.

Since only reflections for l even have been used, false centers of symmetry have been introduced at $x = 1/2$, $z = 1/4$ and at $x = 1/2$, $z = 3/4$ with the result that the two crystallographically non-equivalent sulfate groups of the unit cell are related by centers of symmetry in the Fourier map. The peak at $x \approx 0.29$, $z \approx 0.12$, which is not well resolved from the peak of the sulfur atom, gives the positions of those oxygen atoms of the sulfate groups (O_1 and O_4), which lie outside the mirror planes. The rather extended peak at $x \approx 0.37$, $z \approx 0.30$ at a distance of roughly 1.5 Å from the sulfur peak, indicates the positions of those oxygen atoms of the sulfate groups (O_2, O_3, O_5, and O_6) which lie on the mirror planes. The projection shows only two more peaks which probably indicate the positions of the twelve remaining oxygen atoms of the unit cell: (O_7, O_8, O_9, O_{10}). Approximate values of the corresponding y parameters can be found from geometrical considerations since the available space is restricted by the presence of mirror planes and by oxygen atoms of the sulfate groups for which approximate positions are already known. The oxygen atom corresponding to the peak at $x = 0.12$, $z = 0.05$ must then be on the

mirror plane since its distance to O_1 and O_4 would otherwise be much too short. It therefore corresponds to four oxygen atoms occupying two twofold positions (O_7 and O_8). The rather extended peak at $x \approx 0.81$, $z \approx 0.12$ must correspond to oxygen atoms outside the mirror planes since they would otherwise occupy positions too close to one of the atoms O_2, O_3, O_5, or O_6. This peak must then represent eight oxygen atoms in two fourfold positions (O_9 and O_{10}).

The positions of the atoms O_7 and O_8 eliminate the 2nd and 3rd alternative sets of In positions, that is with the In atoms on the mirror planes, since they would lead to too short In—O distances (about 0.8 Å). The remaining two alternatives both correspond to a structural arrangement consisting of InO_6 octahedra joined together by means of common corners to chains running parallel to the *b* axis. Of the oxygen atoms of the sulfate groups only the atoms outside the mirror planes (O_1 and O_4) belong to the coordination polyhedra of the In atoms. O_7 and O_8 (on the mirror planes) are in contact with two In atoms each and the remaining eight oxygen atoms of the unit cell (O_9 and O_{10}; outside the mirror planes) are each in contact with one In atom.

The shapes of the peaks in Fig. 3a suggest that the presence of the very weak reflections for *l* odd results from small displacements of the sulfate groups and of O_9 and O_{10}. Since the peaks corresponding to the sulfur atoms do not seem to be deformed the displacements of the SO_4 tetrahedra were assumed to correspond to small rotations around the sulfur atoms. The resulting trial structures, corresponding to the two remaining alternatives for the In positions, are shown in Fig. 4. They were the results of attempts to get the best fit both

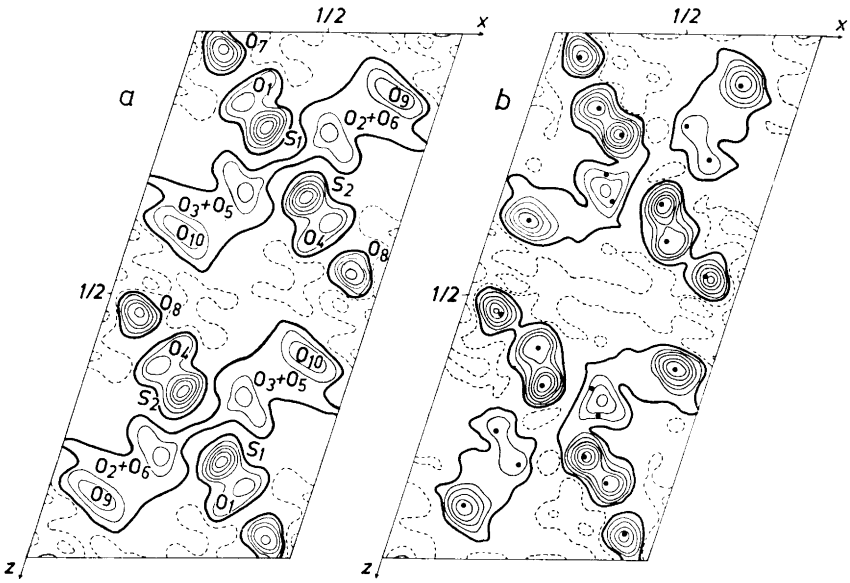

Fig. 3a. Electron density projection along the *b*-axis. Only structure factors for $l = 2n$ have been included and the contribution from the indium atoms has been subtracted.
Fig. 3b. Final electron density projection along the *b*-axis with all structure factors included and with the contribution from the indium atoms subtracted. The final positions of the sulfur and oxygen atoms are marked by dots.

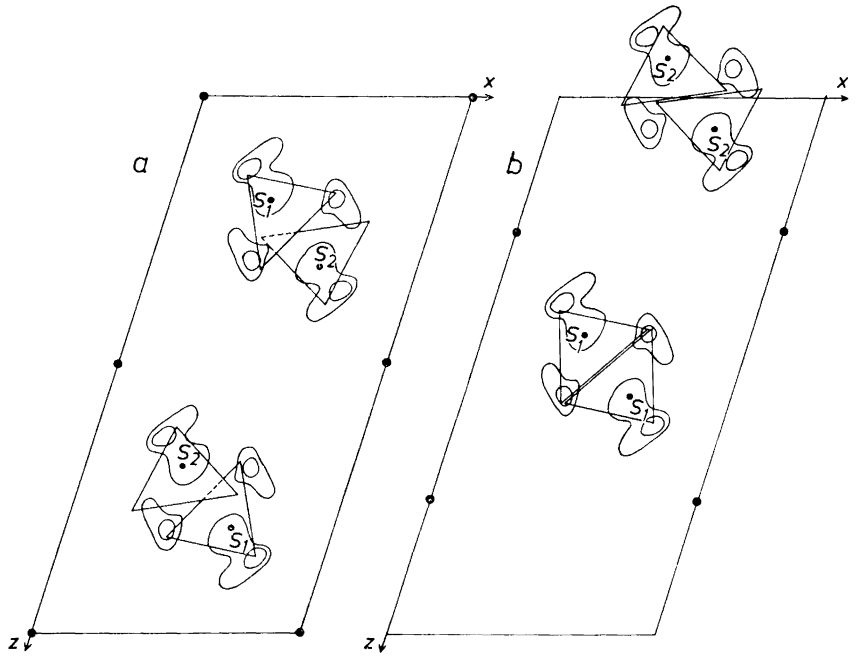

Fig. 4. The two trial structures assumed to explain the presence at the weak reflections for l odd. Black dots indicate In atoms. The sulfate groups are represented by triangles. Some of the contours from the electron density projection in Fig. 3 a are also shown in the figures:
a) In atoms assumed to be at centers of symmetry
b) In atoms assumed to occupy a fourfold position with $x = 0$, $y = 0$, $z = \frac{1}{4}$.

to the peaks of the electron density projections and to the expected In—O distance of about 2.1 Å, without making any changes in the assumed sulfur positions. If the angles of rotation of the SO_4 tetrahedra around the sulfur atoms are the same for the two trial structures, they both give the same absolute values for those structure factors for which l is even and differ only for l odd.

Structure factors were calculated for the $h1l$ and $h3l$ reflections for the two trial structures. The y parameters of O_1 and O_4 were determined by assuming the O—O distance in a SO_4 tetrahedron to be 2.4 Å [13]. The oxygen atoms O_9 and O_{10} were not included in the calculations. Their contributions to the $h1l$ and $h3l$ reflections should be small since they have positions close to the planes $y = 0$ and $y = 1/2$. Only the structure corresponding to the 4th alternative, that is with the indium atoms at centers of symmetry, gave a reasonable agreement for structure factors for l odd.

Most of the signs of the $h1l$ and $h3l$ structure factors could then be determined, and more accurate parameters were obtained from the generalized electron density projections $S_3(xz) + S_1(xz)$, to which atoms on the mirror planes do not contribute, and $S_3(xz) - S_1(xz)$, which to a large extent eliminates

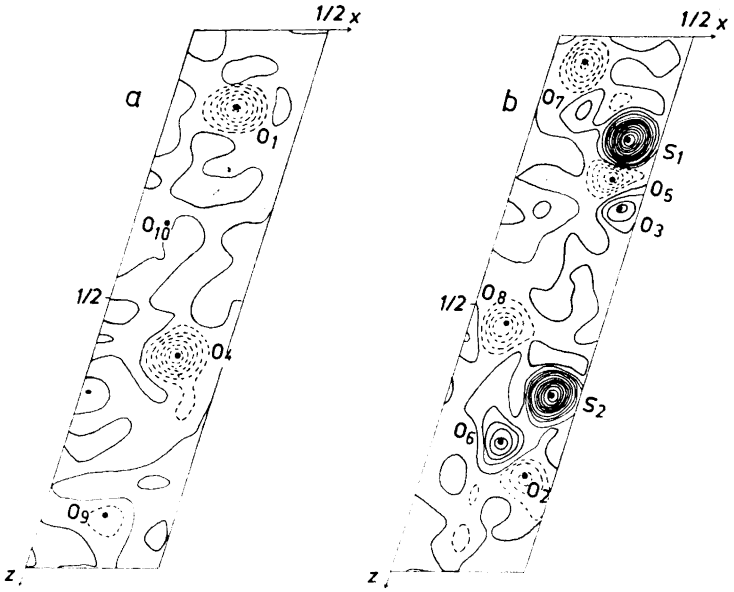

Fig. 5a. The Fourier summation $S_3(x,z) + S_1(x,z)$.
Fig. 5b. The Fourier summation $S_3(x,z) - S_1(x,z)$.

the contributions from atoms outside the mirror planes relative to those on these planes (Fig. 5). $S_1(xz)$ and $S_3(xz)$ represent the Fourier summations:

$$S_1(xz) = \sum_h \sum_l F(h1l) \sin 2\pi(hx + lz)$$

$$S_3(xz) = \sum_h \sum_l F(h3l) \sin 2\pi(hx + lz)$$

The parameters obtained were used for determining the signs of $h0l$ reflections with l odd. From $h0l$ electron density projections the positions of O_9 and O_{10} could then be determined (Fig 3b).

REFINEMENT AND ACCURACY OF THE PARAMETERS

The parameters obtained from the electron density projections were refined by means of difference maps. The refinement was carried out from the $h1l$ and the $h3l$ reflections independently. The positions of the sulfur atoms and the oxygen atoms in fourfold positions were also refined in the same way from the $h0l$ data. A single isotropic temperature factor of 1.6 Å^2, determined by a comparison of observed and calculated structure factors, was used for all the atoms. Atomic scattering factors were calculated according to the analytical expressions given by Vand, Eiland and Pepinsky [9].

The y parameters of O_9 and O_{10} were determined from the heights of the corresponding peaks on the generalized $h3l$ electron density projection. The

height of the peak at the O_9 position corresponds to $y = -0.010$. Since no peak occurs at the O_{10} position the corresponding parameter should be close to $y = 0$ (Fig. 5a). Accurate values of the y parameters of O_1 and O_4 cannot be obtained from the *h*1*l* or *h*3*l* generalized projections since the corresponding peak heights are rather insensitive to a change of y parameters; they were therefore calculated assuming the O_1-O_1 and O_4-O_4 distances to be the same as the average value of the final O_2-O_3 and O_5-O_6 distances, which are 2.38 and 2.39 Å respectively. The y parameters obtained in this way are consistent with the *h*1*l* and *h*3*l* difference maps, giving no peaks of significant heights at the O_1 and O_4 positions.

The final parameters (Table 3) were calculated by taking the average of the values obtained in the independent refinements of the *h*0*l*, *h*1*l*, and *h*3*l* data. Calculated and observed structure factors for the zones *h*0*l*, *h*1*l*, *h*2*l*, *h*3*l*, and *hk*0 are given in Table 5. If only observed reflections are included the overall R factor $\left[R = \frac{\Sigma \, ||F_o| - |F_c||}{\Sigma \, |F_o|}\right]$ is 0.127. For those 205 observed reflections to which In contributes, $R = 0.125$ (with In contributions only $R = 0.23$). For the 171 reflections without In contributions, $R = 0.132$. The R value is 0.164 for the 103 reflections with l odd which were observed. The higher R value for these reflections may probably be explained in part by the high percentage of very weak reflections for which intensities are difficult to estimate accurately.

The standard deviations of the positional parameters were calculated according to the formula given by Cruickshank [10]. For the x and z parameters the average between the results obtained from the *h*1*l* and *h*3*l* data was 0.01_1 Å for the sulfur atoms and 0.02_5 Å for the oxygen atoms except O_9 and O_{10}. The standard deviations of the x and z parameters of O_9 and O_{10}, calculated from the *h*0*l* data, were 0.04 Å. A value of 0.03_5 Å was obtained for the y parameters of O_9 and O_{10} from an estimate of the standard deviation in the electron density of the final *h*3*l* difference map.

Since the parameters were refined from the *h*1*l* and the *h*3*l* data independently, a standard deviation may also be calculated from a comparison between the refined parameters obtained from the *h*1*l* and the *h*3*l* data, respectively. This gives a value of 0.03_1 Å for the oxygen atoms (O_1 to O_8), which is nearly the same as the value given above.

These values lead to standard deviations of 0.01 to 0.04 Å in the In—O distances and of about 0.03 Å in S—O distances within the SO_4 tetrahedra. If the SO_4 groups are assumed to be regular tetrahedra the variation of the S—O distances (S_1-O_2, S_1-O_3, S_2-O_5, S_2-O_6) around the calculated mean (1.48 Å) corresponds to a standard deviation of 0.02_8 Å, which gives some support for the correctness of the values calculated above. The standard deviations in O—O distances are generally less than 0.05 Å.

DISCUSSION OF THE STRUCTURE

Interatomic distances are listed in Table 4. Projections of the structure along the *a* and *b* axes are shown in Figs. 6 and 7.

Table 3. Final paramenters.

		x	y	z
In:	2 In_1 in 2(*a*)	0	0	0
	2 In_2 in 2(*c*)	0	0	½
S:	2 S_1 in 2(*e*)	0.378	1/4	0.197
	2 S_2 in 2(*e*)	0.610	3/4	0.326
O:	4 O_1 in 4(*f*)	0.258	0.099	0.146
	2 O_2 in 2(*e*)	0.608	1/4	0.180
	2 O_3 in 2(*e*)	0.422	1/4	0.321
	4 O_4 in 4(*f*)	0.676	0.599	0.397
	4 O_5 in 2(*e*)	0.364	3/4	0.270
	2 O_6 in 2(*e*)	0.736	3/4	0.242
OH:	2 O_7 in 2(*e*)	0.121	3/4	0.050
	2 O_8 in 2(*e*)	0.142	3/4	0.540
H_2O:	4 O_9 in 4(*f*)	0.762	0.990	0.100
	4 O_{10} in 4(*f*)	0.867	0.000	0.640

Indium is octahedrally surrounded by six oxygen atoms at an average distance of 2.16 Å, with no significant differences between the indium-oxygen bond lengts. The InO_6 octahedra are joined together by means of common corners, in chains running parallel to the *b* axis. The unit cell contains two crystallographically non-equivalent chains of InO_6 octahedra; they are, however, both built up in the same way. No oxygen atoms are shared between two chains.

Table 4. Interatomic distances.

Within the InO_6 octahedra:

In_1-2O_7	2.14 Å	In_2-2O_8	2.15 Å
$-2O_9$	2.19	$-2O_{10}$	2.16
$-2O_1$	2.18	$-2O_4$	2.15
$O_7 - O_9$	3.09 Å	$O_8 - O_{10}$	3.09 Å
$O_7 - O_9$	3.02	$O_8 - O_{10}$	3.00
$O_1 - O_9$	3.16	$O_4 - O_{10}$	3.05
$O_1 - O_9$	3.01	$O_4 - O_{10}$	3.04
$O_1 - O_7$	3.03	$O_4 - O_8$	2.99
$O_1 - O_7$	3.07	$O_4 - O_8$	3.09

Within the SO_4 tetrahedra:

$S_1 -2O_1$	1.44 Å	$S_2 -2O_4$	1.47 Å
$- O_2$	1.47	$- O_5$	1.45
$- O_3$	1.51	$- O_6$	1.48
$O_2 - O_3$	2.38 Å	$O_5 - O_6$	2.39 Å
$O_1 - O_2$	2.36	$O_4 - O_5$	2.40
$O_1 - O_3$	2.45	$O_4 - O_6$	2.42
$(O_1 - O_1$	2.38)	$(O_4 - O_4$	2.38)

Short O—O distances:

$O_7 - O_5$	2.73 Å	$O_8 - O_3$	2.70 Å
$O_9 - O_2$	2.58	$O_{10} - O_3$	2.78
$O_9 - O_6$	2.65	$O_{10} - O_5$	2.85

Other O—O distances < 3.5 Å

$O_1 - O_5$	3.14 Å	$O_3 - O_4$	3.16 Å
$O_1 - O_9$	3.39	$O_4 - O_{10}$	3.27
$O_1 - O_{10}$	3.12	$O_6 - O_{10}$	3.12
$O_2 - O_8$	3.42	$O_9 - O_9$	3.41
		$O_9 - O_{10}$	3.37

Table 5. Observed and calculated structure factors.

hkl	F_o	F_c	*hkl*	F_o	F_c	*hkl*	F_o	F_c
000	—	484	$\bar{7}04$	56	63	307	15	24
1	124	132	$\bar{6}$	48	51	4	<13	8
2	85	91	$\bar{5}$	69	77	5	<10	−11
3	142	145	$\bar{4}$	97	98			
4	58	63	$\bar{3}$	138	142	$\bar{7}08$	45	40
5	84	92	$\bar{2}$	243	207	$\bar{6}$	56	72
6	55	50	$\bar{1}$	188	155	$\bar{5}$	58	67
7	46	52	0	108	100	$\bar{4}$	116	109
			1	147	143	$\bar{3}$	87	71
$\bar{7}01$	<9	−8	2	114	119	$\bar{2}$	96	85
$\bar{6}$	<13	−17	3	77	90	$\bar{1}$	146	149
$\bar{5}$	<13	−3	4	62	74	0	88	94
$\bar{4}$	18	23	5	68	76	1	82	99
$\bar{3}$	12	17	6	69	71	2	61	61
$\bar{2}$	<7	−4				3	61	77
$\bar{1}$	14	9	$\bar{7}05$	<10	0	4	97	83
0	—	−6	$\bar{6}$	24	31	5	33	25
1	<5	1	$\bar{5}$	16	−21			
2	38	−36	$\bar{4}$	20	−19	$\bar{7}09$	<8	−2
3	19	−20	$\bar{3}$	49	49	$\bar{6}$	18	−18
4	28	28	$\bar{2}$	37	−31	$\bar{5}$	17	17
5	<13	11	$\bar{1}$	51	−38	$\bar{4}$	<13	6
6	<13	−10	0	8	4	$\bar{3}$	28	−19
7	<8	−3	1	22	18	$\bar{2}$	26	13
			2	24	29	$\bar{1}$	13	15
$\bar{7}02$	45	55	3	<13	−4	0	<13	5
$\bar{6}$	71	83	4	<14	−14	1	14	−19
$\bar{5}$	47	54	5	<13	2	2	<13	−6
$\bar{4}$	113	138	6	<8	−2	3	<13	1
$\bar{3}$	98	96				4	<10	−1
$\bar{2}$	131	107	$\bar{7}06$	38	48			
$\bar{1}$	217	268	$\bar{6}$	49	57			
0	120	126	$\bar{5}$	79	84	$\bar{7}010$	26	39
1	218	203	$\bar{4}$	56	54	$\bar{6}$	48	52
2	157	179	$\bar{3}$	152	132	$\bar{5}$	85	88
3	73	86	$\bar{2}$	192	185	$\bar{4}$	74	72
4	82	90	$\bar{1}$	143	127	$\bar{3}$	98	96
5	57	65	0	153	145	$\bar{2}$	104	95
6	56	62	1	88	88	$\bar{1}$	69	58
7	39	49	2	81	96	0	81	85
			3	63	66	1	59	66
$\bar{7}03$	<10	1	4	62	61	2	54	64
$\bar{6}$	<13	−7	5	88	80	3	88	78
$\bar{5}$	<13	5	6	27	37	4	41	47
$\bar{4}$	30	−31						
$\bar{3}$	<9	−6	$\bar{7}07$	<9	0	$\bar{6}011$	11	16
$\bar{2}$	75	73	$\bar{6}$	<13	−7	$\bar{5}$	<13	−1
$\bar{1}$	40	−27	$\bar{5}$	<13	8	$\bar{4}$	<13	−13
0	11	5	$\bar{4}$	37	35	$\bar{3}$	<13	5
1	30	30	$\bar{3}$	15	−15	$\bar{2}$	27	−14
2	20	−9	$\bar{2}$	20	−14	$\bar{1}$	<13	3
3	<11	−8	$\bar{1}$	21	20	0	<13	1
4	13	−17	0	15	−16	1	<13	12
5	<13	−8	1	24	−28	2	<13	11
6	<12	14	2	<12	−5	3	<11	−16

hkl	F_o	F_c
$\bar{6}012$	38	44
$\bar{5}$	49	42
$\bar{4}$	95	79
$\bar{3}$	116	96
$\bar{2}$	70	58
$\bar{1}$	83	65
0	59	71
1	49	47
2	57	62
3	41	41
$\bar{6}013$	<7	−3
$\bar{5}$	<10	−4
$\bar{4}$	16	13
$\bar{3}$	13	−5
$\bar{2}$	<13	1
$\bar{1}$	23	−25
0	<12	−4
1	26	28
2	<9	−10
$\bar{5}014$	39	42
$\bar{4}$	77	61
$\bar{3}$	69	45
$\bar{2}$	72	61
$\bar{1}$	73	61
0	52	39
1	59	65
$\bar{4}015$	<10	−13
$\bar{3}$	<10	11
$\bar{2}$	<9	0
$\bar{1}$	<9	−3
$\bar{3}016$	29	37
$\bar{2}$	38	43
010	—	—
1	46	−50
2	61	65
3	<11	6
4	<13	−1
5	<15	−9
6	<14	−11
7	<10	9
$\bar{7}11$	<11	−1
$\bar{6}$	<15	4
$\bar{5}$	<15	−4
$\bar{4}$	<13	0
$\bar{3}$	<11	−9
$\bar{2}$	<8	6
$\bar{1}$	<6	2
0	<4	0
1	<6	13
2	25	−28
311	20	22
4	<14	3
5	<15	−9
6	<14	4
7	<9	−1
$\bar{7}12$	19	18
$\bar{6}$	<15	3
$\bar{5}$	17	−11
$\bar{4}$	25	21
$\bar{3}$	49	−50
$\bar{2}$	16	14
$\bar{1}$	11	4
0	55	−57
1	82	82
2	11	16
3	<13	−19
4	<14	5
5	20	−13
6	<13	3
7	<7	−3
$\bar{7}13$	<11	−2
$\bar{6}$	<15	5
$\bar{5}$	<15	−2
$\bar{4}$	25	−26
$\bar{3}$	34	32
$\bar{2}$	<8	−7
$\bar{1}$	<7	−5
0	<7	3
1	<8	−8
2	18	25
3	11	−16
4	<13	1
5	<15	2
6	<12	1
$\bar{7}14$	<12	−4
$\bar{6}$	<15	−5
$\bar{5}$	23	25
$\bar{4}$	39	−39
$\bar{3}$	<11	2
$\bar{2}$	<9	7
$\bar{1}$	43	−44
0	69	66
1	<10	9
2	<11	−9
3	15	14
4	25	−26
5	<15	8
6	<11	−4
$\bar{7}15$	<11	5
$\bar{6}$	<15	−6
$\bar{5}$	19	−18
$\bar{4}$	27	25
$\bar{3}$	<12	−1
$\bar{2}15$	26	−20
$\bar{1}$	13	7
0	27	29
1	13	−16
2	<12	−8
3	<14	8
4	<15	−3
5	<14	4
6	<9	−6
$\bar{7}16$	<11	1
$\bar{6}$	<15	12
$\bar{5}$	24	−24
$\bar{4}$	<14	2
$\bar{3}$	<12	4
$\bar{2}$	27	−32
$\bar{1}$	39	39
0	<11	6
1	<12	11
2	<13	7
3	30	−32
4	20	17
5	<13	−10
$\bar{7}17$	<11	2
$\bar{6}$	<14	−13
$\bar{5}$	<15	9
$\bar{4}$	<14	6
$\bar{3}$	27	−26
$\bar{2}$	34	32
$\bar{1}$	<12	12
0	27	−33
1	13	17
2	<14	−6
3	<15	3
4	<14	0
5	<11	−6
$\bar{7}18$	<10	4
$\bar{6}$	<14	−6
$\bar{5}$	<15	2
$\bar{4}$	<15	−6
$\bar{3}$	24	−23
$\bar{2}$	32	32
$\bar{1}$	<13	3
0	<13	9
1	<14	3
2	21	−20
3	21	16
4	18	−15
5	<9	−8
$\bar{6}19$	<13	6
$\bar{5}$	<15	6
$\bar{4}$	15	−20
$\bar{3}$	32	31
$\bar{2}$	<14	13
$\bar{1}$	<14	0

hkl	F_o	F_c	*hkl*	F_o	F_c	*hkl*	F_o	F_c
019	<14	10	421	<17	18	225	<15	12
1	22	−22	5	<18	8	3	<17	14
2	20	18	6	<16	1	4	<17	−10
3	<15	−9				5	<17	−13
4	<12	−1	$\bar{7}22$	45	55			
			$\bar{6}$	48	50	$\bar{7}26$	45	57
$\bar{6}110$	<12	0	$\bar{5}$	84	112	$\bar{6}$	61	68
$\bar{5}$	<14	−9	$\bar{4}$	81	98	$\bar{5}$	45	64
$\bar{4}$	<15	−10	$\bar{3}$	133	141	$\bar{4}$	96	98
$\bar{3}$	19	22	$\bar{2}$	121	105	$\bar{3}$	85	79
$\bar{2}$	<14	−6	$\bar{1}$	72	53	$\bar{2}$	133	118
$\bar{1}$	<14	5	0	220	217	$\bar{1}$	200	151
0	<15	12	1	141	133	0	92	93
1	15	−14	2	119	145	1	137	138
2	<14	5	3	132	148	2	79	83
3	<13	−10	4	60	71	3	76	80
4	<9	−7	5	80	80	4	87	79
			6	57	51	5	41	33
$\bar{6}111$	<11	0						
$\bar{5}$	<13	−9	$\bar{7}23$	<13	3	$\bar{7}27$	<12	−7
$\bar{4}$	14	17	$\bar{6}$	<18	14	$\bar{6}$	<17	4
$\bar{3}$	<14	−10	$\bar{5}$	23	−24	$\bar{5}$	<18	3
$\bar{2}$	<15	15	$\bar{4}$	23	−20	$\bar{4}$	<18	−2
$\bar{1}$	<15	−10	$\bar{3}$	17	23	$\bar{3}$	<16	12
0	<15	−13	$\bar{2}$	<17	−5	$\bar{2}$	<14	−9
1	20	20	$\bar{1}$	<9	5	$\bar{1}$	<14	3
2	14	−14	0	<9	5	0	<14	1
3	<11	1	1	29	30	1	19	−28
			2	<13	4	2	<17	8
$\bar{6}112$	<10	−6	3	28	−30	3	<18	11
$\bar{5}$	<13	−3	4	<18	−9	4	<18	2
$\bar{4}$	<14	10	5	<18	9	5	<12	6
$\bar{3}$	<15	−5	6	<14	6			
$\bar{2}$	<15	3	$\bar{7}24$	35	46	$\bar{7}28$	36	48
$\bar{1}$	18	16	$\bar{6}$	64	79	$\bar{6}$	51	61
0	<15	−11	$\bar{5}$	67	74	$\bar{5}$	87	104
1	<14	−1	$\bar{4}$	88	101	$\bar{4}$	47	47
			$\bar{3}$	141	136	$\bar{3}$	83	73
020	94	110	$\bar{2}$	195	142	$\bar{2}$	111	94
1	244	224	$\bar{1}$	153	114	$\bar{1}$	81	82
2	111	108	0	91	73	0	139	142
3	74	88	1	113	125	1	79	83
4	121	137	2	140	163	2	76	90
5	48	53	3	73	86	3	87	83
6	63	67	4	84	76	4	45	39
7	42	49	5	89	80	5	41	43
			6	35	41			
$\bar{6}21$	<17	−16						
$\bar{5}$	<18	10	$\bar{7}25$	<15	16	$\bar{7}29$	<10	−11
$\bar{4}$	<16	15	$\bar{6}$	<18	4	$\bar{6}$	<16	−4
$\bar{3}$	<13	−1	$\bar{5}$	<18	6	$\bar{5}$	<18	−6
$\bar{2}$	<10	9	$\bar{4}$	<16	−12	$\bar{4}$	<19	5
$\bar{1}$	12	−7	$\bar{3}$	23	−26	$\bar{3}$	<18	−9
0	<6	7	$\bar{2}$	15	18	$\bar{2}$	<18	0
1	<9	−16	$\bar{1}$	28	−22	$\bar{1}$	45	38
2	35	−36	0	<11	−7	0	<18	−4
3	<14	−1	1	24	21	1	<18	−13

hkl	F_o	F_c
229	<18	−8
3	<18	−3
4	<18	6
$\bar{7}210$	23	40
$\bar{6}$	52	63
$\bar{5}$	52	55
$\bar{4}$	97	91
$\bar{3}$	84	73
$\bar{2}$	65	53
$\bar{1}$	100	96
0	76	82
1	67	77
2	73	71
3	43	53
4	41	52
$\bar{6}211$	19	−16
$\bar{5}$	<16	−1
$\bar{4}$	<17	2
$\bar{3}$	<18	−13
$\bar{2}$	22	13
$\bar{1}$	<18	−13
0	<18	11
1	<18	21
2	<18	−12
3	<18	−6
$\bar{6}212$	31	38
$\bar{5}$	47	45
$\bar{4}$	75	62
$\bar{3}$	85	70
$\bar{2}$	76	81
$\bar{1}$	72	66
0	61	62
1	57	74
2	37	40
3	28	37
$\bar{5}213$	<17	0
$\bar{4}$	<16	−8
$\bar{3}$	27	23
$\bar{2}$	19	−12
$\bar{1}$	<16	−10
0	<16	5
1	<17	−7
$\bar{5}214$	37	41
$\bar{4}$	52	38
$\bar{3}$	80	58
$\bar{2}$	71	55
$\bar{1}$	63	58
0	57	66
1	57	38
030	—	—
1	28	−29
2	29	−28
330	22	23
4	18	−16
5	<14	3
6	18	15
$\bar{6}31$	<12	8
$\bar{5}$	19	16
$\bar{4}$	21	23
$\bar{3}$	<11	5
$\bar{2}$	17	20
$\bar{1}$	8	−8
0	<4	−3
1	12	−17
2	<10	15
3	<12	2
4	<14	−5
5	<14	−7
6	<12	5
$\bar{7}32$	16	−15
$\bar{6}$	<11	−4
$\bar{5}$	17	17
$\bar{4}$	19	−24
$\bar{3}$	24	22
$\bar{2}$	15	20
$\bar{1}$	16	13
0	10	−15
1	48	−48
2	21	26
3	<12	−7
4	<14	−14
5	29	25
$\bar{5}33$	17	−18
$\bar{4}$	19	17
$\bar{3}$	<11	9
$\bar{2}$	15	−9
$\bar{1}$	27	−27
0	15	19
1	<9	13
2	16	−23
3	<13	12
4	<14	−8
$\bar{5}34$	19	−23
$\bar{4}$	32	31
$\bar{3}$	<12	10
$\bar{2}$	<10	5
$\bar{1}$	<9	−6
0	59	−49
1	41	40
2	17	−13
3	32	−36
4	44	43
$\bar{5}35$	<14	4
$\bar{4}$	<13	7
$\bar{3}35$	<11	4
$\bar{2}$	21	−22
$\bar{1}$	<9	8
0	<9	0
1	<10	−1
2	<12	4
3	<13	−7
4	<13	3
$\bar{5}36$	22	25
$\bar{4}$	<14	−4
$\bar{3}$	<13	2
$\bar{2}$	19	18
$\bar{1}$	47	−41
0	22	22
1	<15	−14
2	31	−29
3	43	43
$\bar{4}37$	<14	0
$\bar{3}$	<13	−7
$\bar{2}$	21	−16
$\bar{1}$	20	20
0	<12	3
1	20	−25
2	19	21
$\bar{3}38$	28	23
$\bar{2}$	23	−26
$\bar{1}$	<13	7
0	<13	−9
1	23	−21
2	28	28
$\bar{3}39$	24	−29
$\bar{2}$	38	40
$\bar{1}$	<14	−12
0	28	−28
1	34	35
2	<13	−11
$\bar{3}310$	15	−15
$\bar{2}$	<14	1
$\bar{1}$	<14	−2
0	20	−16
1	19	13
2	<12	4
$\bar{3}311$	17	24
$\bar{2}$	<14	−19
$\bar{1}$	<14	−8
0	25	26
1	<13	−10
2	<12	−1
040	223	218
1	90	107

hkl	F_o	F_c	*hkl*	F_o	F_c	*hkl*	F_o	F_c
240	97	112	060	42	40	080	142	117
3	78	89	1	112	123	1	75	53
4	33	42	2	78	86	2	78	53
5	77	88	3	46	49	3	76	59
6	41	43	4	86	87	4	35	30
			5	48	44			
050	—	—				090	—	—
1	17	−15	070	—	—	1	<12	−2
2	24	31	1	<16	18	2	<11	12
3	<15	−4	2	27	−28	3	<9	−5
4	<15	5	3	<14	2			
5	<14	−6	4	<13	3	0100	40	37
6	<10	−10	5	<14	3	1	50	55

The hydrogen atoms of the unit cell may be approximately located from considerations of the sum of electrostatic bond strengths for the various oxygen atoms and the short O—O distances listed in Table 4. The number of short O—O contacts is the same as the number of hydrogen atoms and may probably be taken as an indication of the presence of hydrogen bonds. O_7 and O_8, which

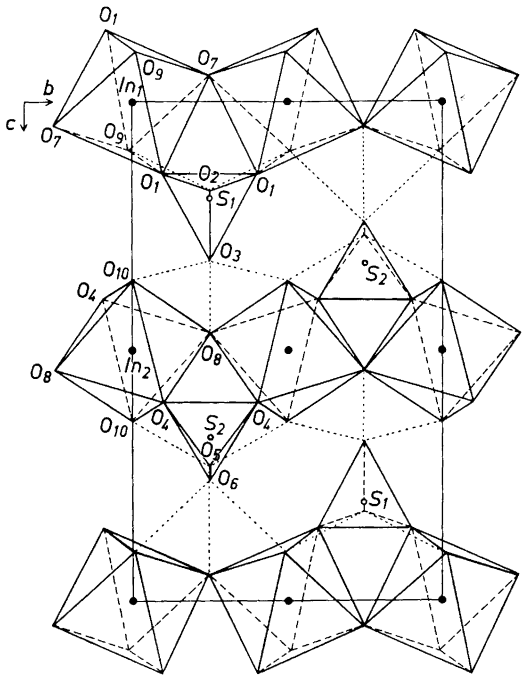

Fig. 6. Projection of the structure along the *a*-axis. Dotted lines represent short O—O distances which probably indicate hydrogen bonds. Filled circles represent indium atoms. At the lower left hand corner one of the dotted lines connects O_7 with O_5 and not with O_6 as the drawing seems to indicate.

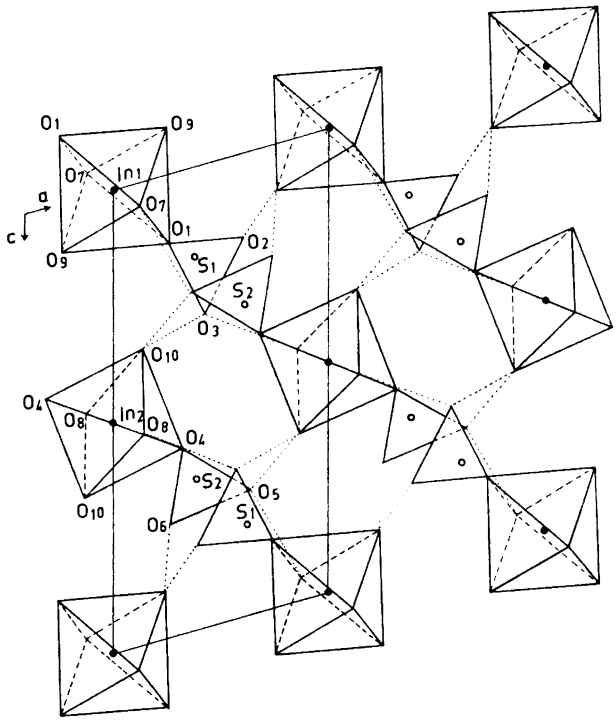

Fig. 7. Projection of the structure along the *b*-axis. Filled circles indicate indium atoms. Dotted lines represent short O—O distances.

are both in contact with two indium atoms and therefore probably associated with one hydrogen atom, are each involved in one short O—O distance. O_9 and O_{10}, which are both in contact with only one In atom and therefore are likely to be H_2O molecules, are each involved in two short O—O distances. All the hydrogen bonds are formed to those oxygen atoms of the sulfate groups which are not in contact with indium atoms. The H_2O molecules, O_9, of the In_1 chains (see Figs. 6 and 7) are bonded to O_2 and O_6; the bond lengths are 2.58 and 2.65 Å, with estimated standard deviations slightly less than 0.05 Å, and the angle $O_2—O_9—O_6$ is 102°. The H_2O molecules, O_{10}, of the In_2 chains are bonded to O_3 and O_5 with bond lengths of 2.78 and 2.85 Å; estimated standard deviations are about 0.05 Å and the angle $O_3—O_{10}—O_5$ is 91°. O_3 and O_5 are also bonded to the OH groups, O_7 and O_8. The H_2O molecules of the In_2 chains are therefore bonded to those oxygen atoms of the sulfate groups which are also involved in hydrogen bonds to the OH groups, O_7 and O_8. The H_2O molecules of the In_1 chains, on the other hand, are bonded to oxygen atoms (O_2 and O_6) which do not form other hydrogen bonds. This is the main difference between the two kinds of indium-oxygen chains in the unit cell. The $O_{10}—O_3$ and $O_{10}—O_5$ hydrogen bonds are longer than the bonds $O_9—O_2$

and O_9—O_6, and in view of the standard deviations this difference may have some significance.

The indium atoms within one of the chains of InO_6 octahedra can also be described as being joined together by means of single hydroxo bridges (O_7 and O_8). The corresponding In—O distances are the most accurately known of the indium-oxygen bond lengths in the structure; they are for In_1—O_7 2.14 Å, and for In_2—O_8 2.15 Å, with estimated standard deviations of about 0.01 Å. The shortest In—In distance within a chain is 3.95 Å, which is equal to one half of the length of the *b* axis. The O_7—In_1—O_7 and O_8—In_1—O_8 angles are exactly 180°, as required by considerations of symmetry. The corresponding angles at the oxygen atoms are about 134° for both In_1—O_7—In_1 and In_2—O_8—In_2. These angles can be compared with those found in $TlOHSO_4(H_2O)_{2.5}$[3], which contains TlO_6 chains very similar to the InO_6 chains in the structure under consideration. The corresponding O—Tl—O angle, which is not determined by symmetry, is very nearly 180°. The average value of the two Tl—O—Tl angles, which do not differ significantly, is 134°, that is the same as in the indium salt.

In—O—In chains may also be distinguished in the three dimensional framework of InO_2F_4 octahedra in the structure of $InOHF_2$, in which the In—In distances are 3.87 Å, the In—O distances are 2.08 Å, and the angles O—In—O and In—O—In are 180° and 137°, respectively[11]. In the cubic $In(OH)_3$[12] the InO_6 octahedra seem to share corners with six other octahedra; the In—In distance is 3.96 Å, which is equal to one half of the unit cell edge. These distances are similar to those found in the present structure determination.

Acknowledgements. I wish to thank Professor Lars Gunnar Sillén and Dr. Georg Lundgren for many valuable discussions. The work has been supported by the *Office of Scientific Research of the Office of Aerospace Research, USAF*, through its European Office on contract number AF 61(052)—162. Free time at the "Besk" computer has been made available by the *Swedish Board for Computing Machinery*, which is gratefully acknowledged. Dr. D. Lewis corrected the English text.

REFERENCES

1. Seward, R. P. *J. Am. Chem. Soc.* **55** (1933) 2740.
2. Ensslin, F., Lessmann, O. and Ziemeck, B. *Z. anorg. u. allgem. Chem.* **254** (1947) 83.
3. Johansson, G. *Acta Chem. Scand.* **13** (1959) 925.
4. Johansson, G., Lundgren, G., Sillén, L. G. and Söderquist, R. *Acta Chem. Scand.* **14** (1960) 769.
5. Johansson, G. *Acta Chem. Scand.* **14** (1960) 771.
6. Kolthoff, I. M. and Sandell, E. B. *Textbook of Quantitative Inorganic Analysis*, New York 1952, p. 717.
7. Åsbrink, S., Blomqvist, G. and Westman, S. *Arkiv Kemi* **14** (1959) 545.
8. Westman, S., Blomqvist, G. and Åsbrink, S. *Arkiv Kemi* **14** (1959) 535.
9. Vand, V., Eiland, P. F. and Pepinsky, R. *Acta Cryst.* **10** (1957) 303.
10. Cruickshank, D. W. J. *Acta Cryst.* **2** (1949) 65.
11. Forsberg, H. E. *Acta Chem. Scand.* **11** (1957) 676.
12. Schubert, K. and Seitz, A. *Z. anorg. Chem.* **256** (1948) 226.
13. *Tables of Interatomic Distances and Configuration in Molecules and Ions.* The Chemical Society, Special Publication No. 11, London 1958, p. 74.

Received March 8, 1961.

ACTA CHEMICA SCANDINAVICA 15 (1961) 1454–1460

Ozonolysis of Phenols

II. Catechol, Resorcinol and Quinol

ERLING BERNATEK, JAN MØSKELAND and KRISTIAN VALEN

Universitetets Kjemiske Institutt, Blindern · Oslo, Norway

Catechol, resorcinol and quinol have been ozonised in ethyl acetate at 3–4°C. The ozonolysis fragments carbon dioxide, formic and oxalic acids and glyoxal have been determined quantitatively. Possible reaction paths are proposed to explain the experimental results. Classical formulae only are assumed in this connection.

In a previous communication [1] the ozonolysis of phenol in ethyl acetate was described. It was found that phenol readily absorbed three moles of ozone and was broken down to small fragments; mainly carbon dioxide and monoxide, formic acid, glyoxal and oxalic acid. Glyoxylic acid could not be detected among the reaction products. The course of reaction could fairly satisfactorily be described as a combination of anomalous ozonolysis (or rearrangement of a normal ozonide) and acid-rearrangement. We considered it of interest to extend the reaction to the simple dihydric phenols, as a preliminary to further research on the ozonolysis of phenolic compounds as well as for its own sake.

Catechol, resorcinol and quinol have been ozonised in aqueous solution by Otto [2] in 1898. The reaction products were intractable sticky solids and besides were found considerable amounts of unreacted phenols. Consequently no definite conclusions regarding the ozonolysis could be drawn on the basis of these experiments.

The present investigation concerns the ozonolysis of the mentioned dihydric phenols in ethyl acetate. Our interest is centered upon the ozone absorption and the (qualitative and quantitative) analysis of reaction products; further the possibility of explaining the course of reaction through simple steps involving classical formulae only, and whether in the case of catechol and quinol the material passes through a quinoid stage.

ANALYTICAL METHODS AND RESULTS

Ozone was determined in the usual way by absorption in aqueous potassium iodide and titration of the liberated iodine with standard thiosulphate.

Active oxygen in the ozonised solution was determined in accordance with standard practice by reaction with sodium iodide in glacial acetic acid and titration of the iodine. Hydrogen peroxide was found in the aqueous decomposition solution by the yellow coloration with titanium reagent.

Carbon monoxide was detected with palladium chloride reagent on filter paper strips.

Carbon dioxide was detected by reaction with aqueous barium hydroxide and determined quantitatively by absorption in soda asbestos.

Formic acid was identified through its S-benzyl*iso*thiuronium salt, and because acetic acid was present, determined by oxidation with potassium permanganate as described in the preceeding communication [1].

Oxalic acid was identified and determined quantitatively through its calcium salt.

Glyoxal was identified through its *p*-nitrophenylosazone and determined quantitatively through oxidation by hydrogen peroxide to formic acid.

Formaldehyde was identified and determined quantitatively by the colour reaction with chromotropic acid.

Unreacted amounts of the dihydric phenols were determined:

a) Catechol and quinol by oxidation with ferric chloride to the corresponding quinone and extraction of this with chloroform. The quinone was then determined iodometrically [4].

b) Resorcinol by precipitation under specified conditions with furfural and weighing of the precipitate [5].

Active oxygen after ozonolysis in moles/mole reactant:

Reacted with	Catechol	Resorcinol	Quinol
1 mole O_3	0.5	0.6	0.4
2 » O_3	0.9	0.9	0.8
3 » O_3	1.6	1.2	1.1

Unreacted phenol after ozonolysis in per cent of starting material:

Reacted with	Catechol %	Resorcinol %	Quinol %
1 mole O_3	38	54	43
2 » O_3	10	8	6

After the addition of 3 moles of ozone no unreacted material could be found.

Carbon dioxide was evolved during ozonolysis as well as under decomposition of the ozonised solution with water.

Total non-volatile products (oxalic acid, glyoxal and unidentified compounds) were isolated by evaporation of the ethyl acetate and aqueous phases and drying the residues *in vacuo*. Combustion analysis gave the content of carbon.

DISCUSSION

Ozone is very readily absorbed by the dihydric phenols, only towards the end of application of three moles small amounts of unreacted gas escape from the reaction vessel. This indicates a facile reaction with the aromatic nucleus.

Table 1. Amounts of reaction products from ozonolysis of dihydric phenols with 3 moles of ozone. (The first figure gives the amount in moles/mole of starting material, while the second figure gives the percentage of recovered carbon).

Product	Catechol		Resorcinol		Quinol	
Carbon dioxide (ozonolysis)	0.46	7.7	0.60	10.1	0.64	10.7
Carbon dioxide (hydrolysis)	1.02	17.1	1.00	16.7	1.00	16.5
Formic acid	1.95	32.5	2.12	35.4	2.25	37.5
Total non-volatile compounds		36.4		29.8		24.3
Oxalic acid	0.19	6.2	0.24	7.9	0.21	7.0
Glyoxal	0.13	4.2	0.12	4.0	0.14	4.8

The figures in Table 1 are calculated from the means of the analytical values in the experimental part.

A qualitative comparison with the ozone absorption by phenol reveals an even readier absorption in the present case, which, of course, is not unexpected. In the case of phenol there was after reaction with 3 moles of ozone still present about 9 % of unreacted material. The phenols now under consideration are completely removed when three moles of ozone are absorbed. Application of one or two moles of ozone per mole of dihydric phenol left relatively large amounts of unreacted material. This is, as in the case of phenol itself, due to a greater reactivity of ozone towards the primary ozonisation products than towards starting material.

Table 1 tells that the main part of the dihydric phenols is split up to rather small fragments, the greater part of the recovered carbon occurring as carbon dioxide and formic acid. Of the non-volatile reaction products only between one half and one third of the recovered carbon can be accounted for as oxalic acid and glyoxal. The remainder has, in spite of continued efforts, not yielded to our attempts at separation and identification. It can be said, however, that the unidentified substances mainly are of aldehydic and acidic nature, both functional groups presumably being present in the same molecule. The latter statement is partly based on our repeated experiments with chromatography of the reaction products on weakly basic anion exchangers.

The total recovered carbon (whether in identified products or not) is 94 %, 92 % and 89 % for catechol, resorcinol and quinol, respectively. Since carbon dioxide, formic acid as well as carbon in the non-volatile products can be determined with a fair degree of accuracy it is reasonable to suppose that the deficiency in carbon is real, *i.e.*, that carbon has been lost in the form of a volatile compound. Formaldehyde has been detected among the reaction products, but has been estimated to occur in such minute amounts as to be without significance for the carbon balance. Further carbon monoxide has been found and albeit not determined quantitatively the amount seems to be great enough

to explain the missing carbon. If this is supposed, there is formed 0.36, 0.48 and 0.66 moles of carbon monoxide per mole of dihydric phenol from catechol, resorcinol and quinol, respectively. It is noteworthy that in no case the formation of maleic or glyoxylic acid could be demonstrated.

The analytical results show that the degradation obviously follows the same pattern in all the three phenols and it seems therefore unlikely that catechol and quinol should take a route through a quinone intermediate. In that case one would, for quinol at least, expect the occurrence of maleic and glyoxylic acids [3] among the reaction products.

When regarding the mode of reaction between the phenols and ozone one must take into consideration the three main reaction types, *viz.* anomalous ozonolysis, normal ozonide formation followed by hydrolysis, and acid-rearrangement. There is a great number of possible combinations of these reactions, especially in the case of catechol where two different Kekulé-structures can be written. We need here, however, consider only the combinations which give no glyoxylic acid.

Since carbon dioxide and formic acid are the main products it seems very likely that most of the material undergoes a complete anomalous ozonolysis. This can be depicted in the diagrams I, II and III (only one Kekulé-structure is taken into account for catechol). The primary products will be the anhydri-

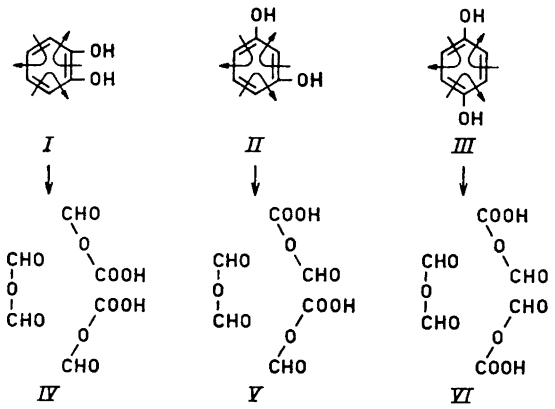

des in IV, V and VI. Such anhydrides are generally very unstable and will break down rapidly to carbon monoxide and dioxide under anhydrous conditions. With water present also formic acid will be formed. Probably most of the formic acid actually found is formed through rearrangement of an ozonide (the ozonised solution contains an appreciable amount of peroxidic material) since the anhydrides must be supposed to break down before the hydrolysis can be performed. Rearrangement of the ozonides of course leads to the same structures (IV, V and VI) as the direct anomalous ozonolysis. Total anomalous ozonolysis gives for all three phenols two moles of carbon dioxide and four moles of formic acid and/or carbon monoxide per mole of phenol. The found mole ratios are:

	Catechol	Resorcinol	Quinol
$\frac{CO_2}{HCOOH + CO}$:	$\frac{1.48}{2.31}$	$\frac{1.60}{2.60}$	$\frac{1.64}{2.91}$

The amounts of formic acid-carbon monoxide fall somewhat short of what is required by the above reaction modes. Exact agreement with any particular reaction scheme is hardly to be expected in view of the relatively large amounts of unidentified products.

Glyoxal and oxalic acid can be formed through several reaction paths. Since some hydrogen peroxide was found in the aqueous decomposition solution it seems reasonable to suppose that the reactions at some stage involve the hydrolysis of ozonides. Schematically the reactions can be visualised in the following way:

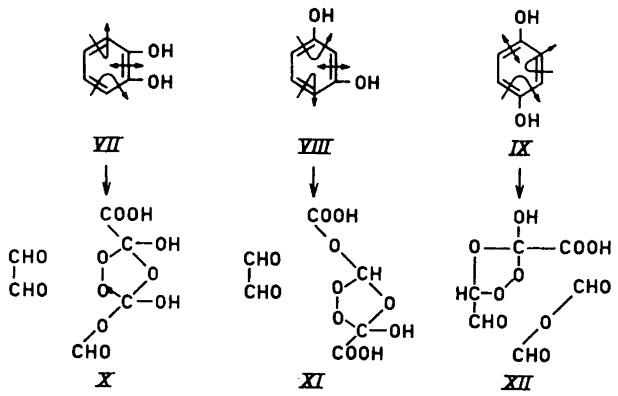

In VII, VIII and IX the arrows mean:



The anhydridic and peroxidic structures in X, XI and XII will on hydrolysis all give the same products and in the same amounts, *viz.* one molecule each of glyoxal, oxalic acid, carbon dioxide, formic acid and hydrogen peroxide. Table 1 gives the molecular ratio of oxalic acid to glyoxal closer to two than to one, but in view of the difficulties in exact determination of glyoxal this cannot be regarded as a serious argument against the operation of schemes VII, VIII and IX or something akin to it.

EXPERIMENTAL

Ozonolysis. The ozonisation technique and the decomposition with water were the same as described in the previous communication [1].

Determination of dihydric phenols: Unreacted phenols were determined after absorption of 1 and 2 moles of ozone.

(a) Resorcinol. 1.000 g of resorcinol was ozonised and hydrolysed. An aliquot of the aqueous decomposition solution (25 ml) was made up to 100 ml with hydrochloric acid and water thereby adjusting the content of mineral acid to 12 %. To this was added freshly distilled furfural (50 mg), the mixture shaken and left for 24 h. The blue-black precipitate was collected, washed and dried in a hydrogen atmosphere. The ethyl acetate phase from the decomposition was evaporated to dryness and the residue taken up in hydrochloric acid (100 ml, 12 %). Furfural (1 100 mg) was added and the mixture treated as above.

1 O_3: Found resorcinol in water 145, 164 and 172 mg. From ethyl acetate 364, 345 and 431 mg.

2 O_3: In water 1 mg. From ethyl acetate 79 mg.

(b) Quinol: 1.000 g of quinol was ozonised and hydrolysed. An aliquot of the aqueous decomposition solution was mixed with aqueous ferric chloride (15 ml, 10 %). The mixture was extracted with three portions (30 ml) of chloroform and to the combined extracts was added acidified potassium iodide solution (15 ml, 10 % + H_2SO_4 10 ml, 10 %). The heterogeneous mixture was shaken vigorously for 2 min and the liberated iodine titrated with standard thiosulphate. The ethyl acetate phase from the decomposition was evaporated to dryness and the residue taken up in water and analysed as above.

1 O_3: Found quinol in water 139, 134 and 136 mg. From ethyl acetate 269, 280 and 338 mg.

2 O_3: In water 8 mg. From ethyl acetate 50 mg.

(c) Catechol. The analysis was performed essentially in the same way as for quinol with the modification that less aqueous ferric chloride was used (5 ml) and the extraction with chloroform was repeated a fourth time.

1 O_3: Found catechol in water 64 and 53 mg. From ethyl acetate 328 and 314 mg.

2 O_3: In water 4 mg. From ethyl acetate 96 mg.

Determination of products after the absorption of 3 moles of ozone. The determinations of carbon dioxide during ozonisation and decomposition, formic and oxalic acids and glyoxal were performed as in the previous communication [1].

(a) Resorcinol. Carbon dioxide during ozonisation 284, 243 and 246 mg. During hydrolysis 409, 405 and 356, 445 and 380 mg CO_2. Formic acid 1 019, 737, 735, 971 and 866 mg. Oxalic acid 190, 200 and 190 mg. Glyoxal 61 and 65 mg.

(b) Quinol. Carbon dioxide during ozonisation 251 and 276 mg. During hydrolysis 417, 397 and 383 mg, CO_2. Formic acid 822, 1 019 and 978 mg. Oxalic acid 180, 162 and 172 mg. Glyoxal 79 and 72 mg.

(c) Catechol. Carbon dioxide during ozonisation 200, 198 and 210 mg. During hydrolysis 390, 416 and 427 mg CO_2. Formic acid 866, 722, 998 and 676 mg. Oxalic acid 165, 140 and 153 mg. Glyoxal 63, 72 and 65 mg.

(d) Non-volatile matter. The ozonised solutions were hydrolysed and extracted exhaustively with water. The combined extracts were evaporated and the residue dried to constant weight above phosphorus pentoxide and potassium hydroxide (Table 2).

Table 2.

Phenol	Weight of non-volatile matter	Per cent carbon
	mg	
Catechol	733	31.3 , 31.2
	694	35.7 , 35.6
Resorcinol	620	31.8 , 30.8
	622	31.5 , 31.4
Quinol	456	31.0 , 31.2
	530	34.5 , 34.1
	505	29.5 , 30.4

All the above determinations refers to the ozonolysis of 1.000 g of dihydric phenol. The different figures under (a), (b), (c) and (d) are independent results from separate ozonolysis runs.

REFERENCES

1. Bernatek, E. and Frengen, C. *Acta Chem. Scand.* **15** (1961) 471.
2. Otto, M. *Ann. chim. (Paris)* [7] **13** (1898) 137.
3. Bernatek, E. and Straumsgård, K. A. *Acta Chem. Scand.* **13** (1959) 178.
4. Böck, F. and Lock, G. *Monatsh.* **54** (1929) 888.
5. Votocek, E. and Potmesil, R. *Ber.* **49** (1916) 1185.

Received March 10, 1961.

ACTA CHEMICA SCANDINAVICA 15 (1961) 1461–1466

Complex Formation of Aluminium with 7-Iodo-8-hydroxyquinoline-5-sulphonic Acid (Ferron)

F. J. LANGMYHR and Å. R. STORM

University of Oslo, Chemical Institute A, Blindern, Norway

By potentiometric methods the two dissociation constants of ferron were found to be: $pK_1 = 2.50$ and $pK_2 = 7.11$ at 25.0 ± 0.1°C and in the presence of 0.10 M potassium chloride. Potentiometric titrations of mixtures of ferron (H_2A) and aluminium indicated the presence of the following complexes: AlA^+, $Al(OH)A$ (slightly soluble), $Al(OH)_2A^-$, AlA_2^-, $Al(OH)A_2^{2-}$ and AlA_3^{3-}. The stability constants of the complexes not containing hydroxyl were found to be: $\log K_{MA} = 7.6$, $\log K_{MA_2} = 7.1$ and $\log K_{MA_3} = 5.6$ at 25.0 ± 0.1°C and in the presence of 0.10 M potassium chloride. Under the same conditions the $\log K$ for the equilibrium $[AlA_2^-]/[Al(OH)A_2^{2-}]\,[H^+]$ was calculated to 5.0.

7-Iodo-8-hydroxyquinoline-5-sulphonic acid (ferron) was originally proposed as analytical reagent for iron by Yoe [1]. By colorimetric methods he studied the colour formation of ferron with various metal ions and found that aluminium did not develop any colour. Swank and Mellon [2] later investigated the interaction of ferron with aluminium and ferric iron by spectrophotometric methods and reported that aluminium interfered in the ferron method for iron. They found that the interfering effect was caused by the formation of an aluminium ferron complex with a colour similar to that of ferron itself. Davenport [3] found that this complex absorbed in the ultraviolet region (absorption maximum 370 mμ), and utilized the difference of absorption maximum of the ferric iron and aluminium complexes to determine the elements simultaneously.

By colorimetry Yoe and Hall [4] investigated in more detail ferron and its reaction with ferric iron, and found evidence of only one complex pointing to a ferron metal ratio 3:1. Nortia [5] studied the interaction of ferron with a series of metal ions including ferrous and ferric iron, and deduced from pH measurements that the ferric iron complex had the ligand metal ratio 3:1. He further predicted the existence of a ferric iron complex with the ferron metal ratio 1:1 and the composition Fe(OH)A. No references were found in the literature as to the composition and stability of the complexes formed between ferron and aluminium.

Ferron is an important reagent in the simultaneous spectrophotometric determination of aluminium and iron, and in this connection it is of interest to know the composition and stability of the complexes formed. As seen above no data are available on the system aluminium ferron, while the data on the ferric iron ferron system are inconclusive. The present paper describes a redetermination of the dissociation constants of ferron and an investigation of the system aluminium ferron.

EXPERIMENTAL

Methods. The interaction of aluminium with ferron was studied by potentiometric tiration, solutions of the ligand being titrated with standard alkali in the absence of and in the presence of aluminium ions. The ionic strength was kept relatively constant by maintaining a concentration of 0.10 M potassium chloride, and by keeping a low concentration of ligand and metal ions. The titrations were carried out at 25.0 ± 0.1°C. Mixing was obtained by passing a stream of nitrogen through the solutions. The hydrogen ion concentrations were obtained directly from the pH values measured.

Instruments. A Beckman Zeromatic pH meter (glass and calomel reference electrodes) was employed. The solutions to be titrated were placed in an ultrathermostat.

Reagents. Aluminium solutions were prepared from super pure metal (99.997 %) which contained the following amounts of impurities: silicon — 0.0014 %, iron — 0.0007 %, copper — 0.0008 % and zinc — 0.0002 %. The ferron (Hopkin and Williams) contained, according to the producer's specification, not less than 98.0 % of $C_9H_6O_4NSI$ and a maximum amount of 0.1 % of sulphated ash. All other chemicals were of reagent grade quality.

Standard solutions. A 5×10^{-3} M solution of ferron was prepared by dissolving 1.7556 g in boiled distilled water. Potassium chloride was added and the solution was diluted to 1 000 ml. Ferron solutions decompose slowly on standing and were therefore not used for more than one week. A 0.2 M solution of aluminium was prepared by dissolving 5.3942 g in hydrochloric acid and diluting to 1 000 ml. A 5×10^{-3} M standard solution of the metal was prepared by pipetting out 25 ml of 0.2 M solution, adding potassium chloride and diluting to 1 000 ml. A 0.09953 N solution of potassium hydroxide was used for the titrations.

ACID DISSOCIATION CONSTANTS OF FERRON

The acid dissociation constants were determined on the basis of potentiometric titrations of ferron with standard alkali. From the 5×10^{-3} M solution of ferron 50 ml were pipetted into a beaker placed in the thermostat. After thermal equilibrium was reached, a number of pH readings were plotted after the addition of small increments of base. The titration curve exhibited two distinct inflections, probably corresponding to the neutralization of the two hydrogen ions of ferron. The calculation of the dissociation constants was based on the following equilibria:

$$H_2A \rightleftharpoons H^+ + HA^-;\ K_1 = [H^+][HA^-]/[H_2A]$$

$$HA^- \rightleftharpoons H^+ + A^{2-};\ K_2 = [H^+][A^{2-}]/[HA^-]$$

When T_A represents the total concentration of the species of ligand present and a the number of moles of base added per mole of ligand, it follows for the lower buffer region, assuming that no A^{2-} ions were present:

$$T_A = [H_2A] + [HA^-] \text{ and } aT_A + [H^+] = [HA^-] + [OH^-]$$

Table 1. Determination of first dissociation constant of ferron.

a	pH	$[H^+] \times 10^3$	$T_A \times 10^3$	$K_1 \times 10^3$	pK_1
0.3	2.785	1.641	4.8450	2.901	2.537
0.4	2.855	1.396	4.8215	3.101	2.508
0.5	2.945	1.135	4.7983	3.173	2.498
0.6	3.050	0.8913	4.7752	3.286	2.483
0.7	3.190	0.6457	4.7524	3.288	2.483

Average value of $pK_1 = 2.50$ at 25.0 ± 0.1°C and in the presence of 0.10 M potassium chloride.

And similarly for the upper buffer region, assuming that no H_2A was present:

$$T_A = [HA^-] + [A^{2-}] \text{ and } (a-1)T_A + [H^+]-[OH^-] = [A^{2-}]$$

Substitution and solving for K_1 and K_2 gives:

$$K_1 = \frac{[H^+]\ (aT_A + [H^+]-[OH^-])}{T_A-(aT_A + [H^+]-[OH^-])} \text{ and}$$

$$K_2 = \frac{[H^+]\ ((a-1)T_A + [H^+]-[OH^-])}{T_A-((a-1)T_A + [H^+]-[OH^-])}$$

Values for K_1 and K_2 were calculated for 5 different additions of base in the lower and in the upper buffer region. In Tables 1 and 2 the experimental and calculated data are given. The pH values in Tables 1 and 2 were determined graphically to the nearest 0.005 pH from a large scale plot of the titration curves.

COMPOSITION AND STABILITY CONSTANTS OF THE ALUMINIUM FERRON COMPLEXES

For the determination of composition and stability constants, solutions containing 1:1, 2:1 and 3:1 molar ratios of ligand to metal ion were titrated with standard alkali according to the method of Bjerrum [6]. From the aluminium standard solution 25 ml were pipetted into a beaker, and 25, 50, or 75 ml

Table 2. Determination of second dissociation constant of ferron.

a	pH	$[H^+]$	$[OH^-]$	$T_A \times 10^3$	$K_2 \times 10^8$	pK_2
1.3	6.745	1.799×10^{-7}	5.559×10^{-8}	4.675	7.711	7.113
1.4	6.940	1.148×10^{-7}	8.710×10^{-8}	4.653	7.792	7.108
1.5	7.110	7.762×10^{-8}	1.288×10^{-7}	4.631	7.762	7.110
1.6	7.290	5.129×10^{-8}	1.950×10^{-7}	4.609	7.693	7.114
1.7	7.490	3.236×10^{-8}	3.090×10^{-7}	4.587	7.548	7.122

Average value of $pK_2 = 7.11$ at 25.0 ± 0.1°C and in the presence of 0.10 M potassium chloride.

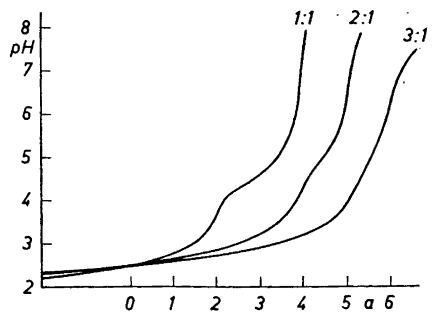

Fig. 1. Titration curves for solutions with ferron aluminium ratios 1:1, 2:1 and 3:1. a = equivalents of base added per mole of metal.

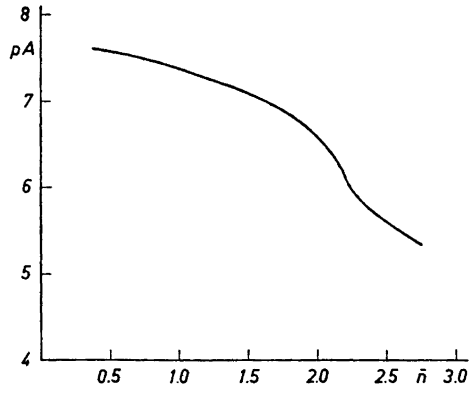

Fig. 2. Variation of degree of formation $\bar{n}$ for aluminium ferron complexes as a function of concentration of ligand pA.

of ferron standard solution were added. After thermal equilibrium was reached in the thermostat, standard alkali was added in small increments, and the corresponding pH data were recorded when constant values were obtained with the pH meter. The curves obtained by repeated titrations did not differ by more than $\pm$ 0.02 pH units. A set of curves is reproduced in Fig. 1.

The 1:1 curve. The curves obtained for equimolar amounts of ferron and aluminium showed two inflections, corresponding to the addition of two and four equivalents of alkali per mole of metal. During these titrations a precipitate also appeared after the addition of more than two equivalents of base. The precipitate disappeared again after the addition of four equivalents of alkali. The following reaction mechanism is suggested for the initial interaction of equimolar amounts of ligand and aluminium, and the later stepwise incorporation of hydroxyl:

$$Al^{3+} + H_2A \rightleftharpoons AlA^+ + 2H^+$$
$$AlA^+ + H_2O \rightleftharpoons Al(OH)A(\text{slightly soluble}) + H^+$$
$$Al(OH)A + H_2O \rightleftharpoons Al(OH)_2A^- + H^+$$

Hydroxo-complexes were thus probably not present at pH values below 3.6.

The 2:1 curve. The titration curves for solutions with ferron metal ratios 2:1 also exhibited two inflections, *viz.* after the addition of four and five equivalents of base. Precipitates were not observed during these titrations. The reactions taking place are believed to be:

$$Al^{3+} + 2H_2A \rightleftharpoons AlA_2^- + 4H^+$$
$$AlA_2^- + H_2O \rightleftharpoons Al(OH)A_2^{2-} + H^+$$

The hydroxo-complex is believed not to be formed before the addition of more than four equivalents of base, or at pH values below about 4.2.

The 3:1 curve. In these titration curves an inflection appeared after the addition of 6 equivalents of base, probably corresponding to the reaction:

$$Al^{3+} + 3H_2A \rightleftharpoons AlA_3^{3-} + 6H^+$$

Hydroxo-complexes are probably not present in the pH range investigated.

From the inflections of the titration curves it was possible to establish graphically the starting point of the titrations in the absence of acid originating from the aluminium solution, and at the same time to determine the amount of acid added. The stability constants could then be calculated both with and without taking into account the acid originally present in the aluminium solution. The stability constants were calculated for the three complexes AlA^+, AlA_2^- and AlA_3^{3-}. The calculations were based on the 3:1 curve, but the data obtained were controlled by using the acid ranges of the two other curves in which hydroxo-complexes were not present.

The average number of moles of ligand bound per mole of metal ion, designated by $\bar{n}$ were plotted against pA, the negative logarithm of the concentration of ligand. The values of pA at $\bar{n} = 0.5$, 1.5 and 2.5 were taken as $\log K_{MA}$, $\log K_{MA_2}$ and $\log K_{MA_3}$, respectively. The formation function curve obtained is reproduced in Fig. 2. The stability constants calculated were: $\log K_{MA} = 7.6$, $\log K_{MA_2} = 7.1$ and $\log K_{MA_3} = 5.6$ at 25.0 ± 0.1°C, in the presence of 0.10 M potassium chloride and with $pK_1 = 2.50$ and $pK_2 = 7.11$ as the dissociation constants of ferron.

On the basis of the 2:1 curve, and assuming that in the interval 4 to 5 equivalents of base the reaction:

$$AlA_2^- + H_2O \rightleftharpoons Al(OH)A_2^{2-} + H^+$$

takes place, the equilibrium constant:

$$K = \frac{[AlA_2^-]}{[Al(OH)A_2^{2-}][H^+]}$$

was found to be $10^{5.0}$.

Due to the presence of a solid phase, similar data for the 1:1 complexes were not calculated.

DISCUSSION

Ferron. The two sharp inflections obtained by potentiometric titration of ferron probably corresponded to the following neutralization reactions:

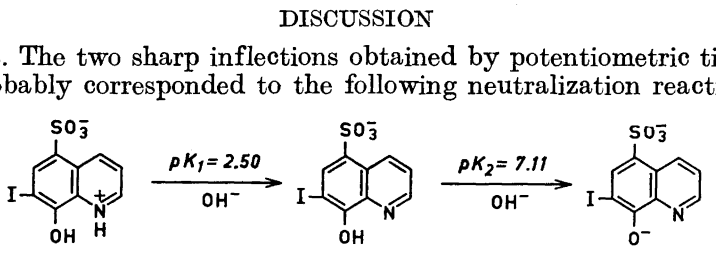

The pK values of 2.50 and 7.11 may be compared with those obtained colorimetrically by Feldman and Powell [7] and potentiometrically by Näsänen and Ekman [8]. The former authors got the values 2.45 and 7.15 without indicating the ionic strength and temperature at which the measurements were made. The latter authors obtained the values 2.42 and 7.09 at a temperature of 25°C and an ionic strength of 0.1. It is further of interest to note the increasing acidity when going from 8-hydroxyquinoline (pK values determined, *e.g.*, by

Table 3. Determined and estimated stability constants of complexes of aluminium with 7-iodo-8-hydroxyquinoline-5-sulphonic acid, 8-hydroxyquinoline-5-sulphonic acid and 8-hydroxyquinoline. The estimated data are given in parenthesis.

	log K_1	log K_2	log K_3
7-Iodo-8-hydroxyquinoline-5-sulphonic acid	7.6	7.1	5.6
8-Hydroxyquinoline-5-sulphonic acid	(10.0)	(9.5)	(8.0)
8-Hydroxyquinoline	(12.5)	(12.0)	(10.5)

Näsänen, Lumme and Mukula [9] to 5.02 and 9.81 at zero ionic strength and the temperatures 20° and 25°C, respectively), to 8-hydroxyquinoline-5-sulphonic acid (pK values determined, *e.g.*, by Richard, Gustafson and Martell [10] to 3.84 and 8.35 at 25°C and in the presence and 0.10 M potassium chloride), and to 7-iodo-8-hydroxyquinoline-5-sulphonic acid with the pK values 2.50 and 7.11.

The aluminium ferron complexes. In the literature [11] no data were found on the stability of complexes of aluminium with 8-hydroxyquinoline or its derivatives. The data published deal mainly with bivalent metals which do not form hydroxocomplexes at lower pH values.

The decreasing basicity observed when going from 8-hydroxyquinoline to 8-hydroxyquinoline-5-sulphonic acid and finally to 7-iodo-8-hydroxyquinoline-5-sulphonic acid is reflected in a correspondingly lower stability of the respective metal complexes. Richard, Gustafson and Martell [10] compared the stability constants of four bivalent metal ions with 8-hydroxyquinoline and 8-hydroxyquinoline-5-sulphonic acid, and found the average decrease of log $K_1 = 3.0$ and log $K_2 = 3.2$ when going from the former to the latter ligand. On the basis of the stability constants determined in this investigation it is possible to estimate roughly the expected stability constants for the complexes of aluminium with 8-hydroxyquinoline and 8-hydroxyquinoline-5-sulphonic acid. A Δ log$K$ value of about 2.5 was considered probable in these estimations. In Table 3 determined and estimated stability constants are given.

REFERENCES

1. Yoe, J. H. *J. Am. Chem. Soc.* **54** (1932) 4139.
2. Swank, H. W. and Mellon, M. G. *Ind. Eng. Chem., Anal. Ed.* **9** (1937) 406.
3. Davenport, W. H. *Anal. Chem.* **21** (1949) 710.
4. Yoe, J. H. and Hall, R. T. J. *J. Am. Chem. Soc.* **59** (1937) 872.
5. Nortia, T. *Ann. Acad. Sci. Fennicae, Ser. A, II*, **No. 86** (1957).
6. Bjerrum, J. *Metal Ammine Formation in Aqueous Solution*, P. Haase and Son, Copenhagen 1941.
7. Feldman, H. B. and Powell, A. L. *J. Am. Chem. Soc.* **62** (1940) 3107.
8. Näsänen, R. and Ekman, A. *Acta Chem. Scand.* **6** (1952) 1384.
9. Näsänen, R., Lumme, P. and Mukula, A. *Acta Chem. Scand.* **5** (1951) 1199.
10. Richard, C. F., Gustafson, R. L. and Martell, A. E. *J. Am. Chem. Soc.* **81** (1959) 1033.
11. Bjerrum, J., Schwarzenbach, G. and Sillén, L. G. *Stability Constants*. Part 1, The Chemical Society, London 1957.

Received March 16, 1961.

ACTA CHEMICA SCANDINAVICA 15 (1961) 1467–1476

Syntheses of N-[(4-Morpholinyl)alkyl]benzamides

NILS LÖFGREN and HANS WÅHLSTAM

Institute of Organic Chemistry and Biochemistry, University of Stockholm, Stockholm, Sweden

Twelve new N-[(4-morpholinyl)alkyl]benzamides have been synthesized and examined for their sedative and local anesthetic actions. The compounds were prepared from the corresponding 4-(aminoalkyl)-morpholines, three of which have not been described previously. The ionization constant, K_a, of one of the N-[(4-morpholinyl)alkyl]benzamides, *i.e.* N-[2-(4-morpholinyl)ethyl]-2,4-dimethylbenzamide, has been determined.

A fairly large number of N-(dialkylaminoalkyl)benzamides have been synthesized by Löfgren and Stoffel [1], and by Lüning [2]. The compounds were studied pharmacologically (toxicity, local anesthetic action) and many of them were also subjected to physico-chemical measurements (ionization constant K_a, absorption in the ultraviolet) [2]. All these benzamides possess local anesthetic action [1,2], and some of them, for instance N-(diethylaminoethyl)-2,4-dimethylbenzamide [2] (A) exhibited — when tested in white mice — a pronounced,

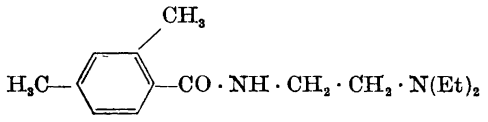

A

though not strong CNS depression (sublethal dose, no convulsions) [3]. Among the local anesthetics of the Xylocaine ® type, Xylocaine itself * and several other members [5] also show a weak though distinct sedative action. If in Xylocaine (B) or in β-diethylaminoethyl-2,6-dimethylpropionanilide (C), the diethylamino group is substituted by the morpholino group, the change in structure is accompanied by a marked increase in the depressive action, and at the same time by a pronounced decrease in local anesthetic potency [6]. With regard to these facts, it seemed of interest to synthesize and investigate pharmacologically N-[(4-morpholinyl)ethyl]-2,4-dimethylbenzamide, *i.e.* a compound that

* See for instance Wiedling [4].

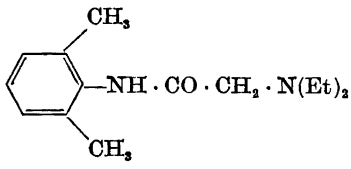

B

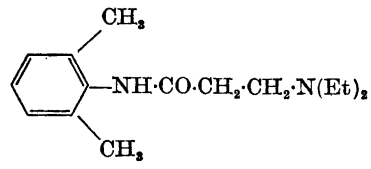

C

differs from the CNS-active benzamide A in having a morpholino group instead of a diethylamino group. It was plausible to assume that the new morpholino derivative would possess a stronger CNS-depressive action than the diethylamino derivative. The experiments showed, however, that such a prediction was false (*cf.* below).

In the present work twelve N-[(4-morpholinyl)alkyl]benzamides have been synthesized and studied with regard to their sedative and local anesthetic actions. The compounds are of the general type

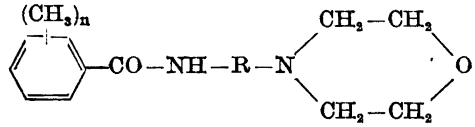

where n is 1, 2 or 3, the methyl or methyls belong to the positions 4, 2,4, 2,6, 3,5 or 2,4,6, and R is a lower straight or branched alkylene chain. The combinations of the actual groups are avident from Table 1, where the compounds (I—XII) are listed.

To obtain information of the basic strengths of these morpholino derivatives as compared with the corresponding diethylamino derivatives, one of the

Table 1. Chemical data of bases prepared (I—XII). All the bases are recrystallized from di-*iso*propyl ether.

	Compound		Yield %	M.p., °C corr.	Equivalen weight [a]	
	Name	Empirical formula			Calc.	Fou
I	N-[2-(4-Morpholinyl)ethyl]-4-methylbenzamide	$C_{14}H_{20}N_2O_2$	78	118—119	248.3	24
II	N-[2-(4-Morpholinyl)ethyl]-2,4-dimethylbenzamide	$C_{15}H_{22}N_2O_2$	64	122—124	262.3	26
III	N-[2-(4-Morpholinyl)ethyl]-3,5-dimethylbenzamide	$C_{15}H_{22}N_2O_2$	93	112—113	262.3	26
IV	N-[2-(4-Morpholinyl)ethyl]-2,6-dimethylbenzamide	$C_{15}H_{22}N_2O_2$	78	110—111	262.3	26
V	N-[2-(4-Morpholinyl)ethyl]-2,4,6-trimethylbenzamide	$C_{16}H_{24}N_2O_2$	78	111—113	276.4	27
VI	N-[3-(4-Morpholinyl)propyl]-4-methylbenzamide	$C_{15}H_{22}N_2O_2$	78	80— 81	262.3	26
VII	N-[3-(4-Morpholinyl)propyl]-2,4-dimethylbenzamide	$C_{16}H_{24}N_2O_2$	73	55— 56	276.4	27
III	N-[3-(4-Morpholinyl)propyl]-2,6-dimethylbenzamide	$C_{16}H_{24}N_2O_2$	82	82— 83	276.4	27
IX	N-[3-(4-Morpholinyl)propyl]-2,4,6-trimethylbenzamide	$C_{17}H_{26}N_2O_2$	91	111—112	290.4	29
X	N-[1-Methyl-2-(4-morpholinyl)ethyl]-2,4-dimethylbenzamide	$C_{16}H_{24}N_2O_2$	93	87— 88	276.4	27
XI[b]	N-[1,2-Dimethyl-3-(4-morpholinyl)propyl]-2,6-dimethylbenzamide	$C_{18}H_{28}N_2O_2$	41	131—132	304.4	30
XII	N-[2,2-Dimethyl-3-(4-morpholinyl)propyl]-2,6-dimethylbenzamide	$C_{18}H_{28}N_2O_2$	83	92— 93	304.4	30

a Concerning the determination of the equivalent weights of the bases, see footnote, p. 1473.

b Data given for compound XI refer to the racemate of lower solubility (in di-*iso*propyl ether; *cf.* above). It w rther purified by recrystallization from di-*n*-butyl ether. (The racemate of higher solubility was not isolated.)

twelve compounds, *i.e.* the above mentioned N-[(4-morpholinyl)ethyl]-2,4-dimethylbenzamide, was subjected to pK_a determination (see p. 1475); the ionization constant of the corresponding diethylamino derivative is known from investigations by Lüning [2] who determined pK_a values of a fairly large number of N-(diethylaminoalkyl)benzamides.

Each of the compounds I—XII was synthesized by condensing a benzoyl chloride with a 4-(aminoalkyl)morpholine in the molar ratio 1:1.6.

4-(2-Aminoethyl)morpholine was prepared according to Hultqvist and Northey [7] by reacting ethylenediamine with bis(β-chloroethyl) ether in the molar ratio 3:1. The same type of synthesis was employed to obtain 4-(3-aminopropyl)morpholine (XIII), ethylenediamine being substituted by trimethylenediamine. XIII has earlier been prepared by Uthermohlen and Hamilton [8] who obtained the compound in a low yield from a Gabriel synthesis. The three other amines, *viz.* 1-methyl-2-(4-morpholinyl)ethylamine (XIV), 1,2-dimethyl-3-(4-morpholinyl)propylamine (XV), and 2,2-dimethyl-3-(4-morpholinyl)propylamine (XVI), were prepared as outlined below under *A*, *B* and *C*.

A. 1-Methyl-2-(4-morpholinyl)ethylamine (XIV):

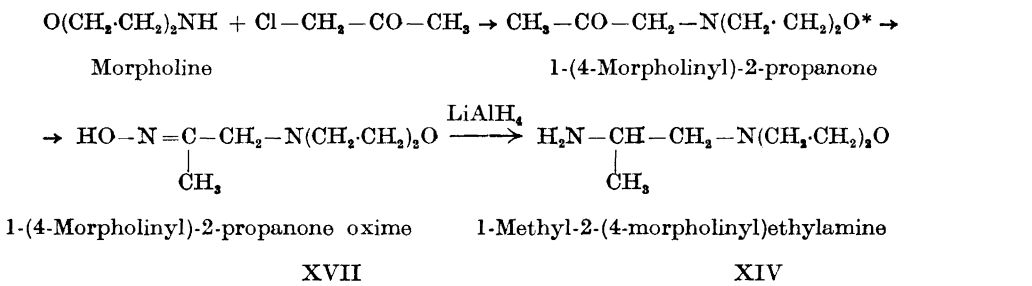

B. 1,2-Dimethyl-3-(4-morpholinyl)propylamine (XV):

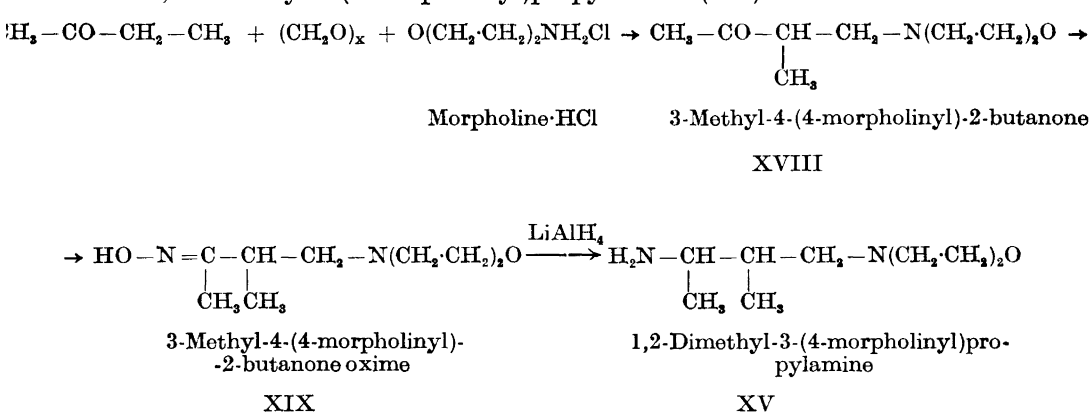

* Prepared earlier in this way by Mason and Ross [9].

Compound XVIII was prepared according to the method given by Mannich and Hof [10] for the synthesis of 4-dimethylamino-3-methyl-2-butanone. They obtained the latter compound as a main product in a yield of 80 %. The collected, higher boiling by-product, they supposed to be the linear isomer (satisfactory proof not given). Cardwell [11] has later proved the correctness of the structure of the main product, and found the by-product to be a diamine, *i.e.* either 3,3-bis(dimethylaminoethyl)-2-butanone or 1,5-bis(dimethylamino)-2-methyl-3-pentanone. Recently, Blicke and McCarty [12] were able to show that the last mentioned compound is identical with Mannich and Hof's by-product. In the literature, no evidence can be found that a linear amine is formed from methyl ethyl ketone or methyl propyl ketone in the Mannich reaction *. (*Cf.* for instance the reactions in which (a) methyl ethyl ketone and diethylamine [11,14] (b) methyl ethyl ketone and piperidine [10] or (c) methyl propyl ketone and dimethylamine [10], are involved.

C. 2,2-Dimethyl-3-(4-morpholinyl)propylamine (XVI):

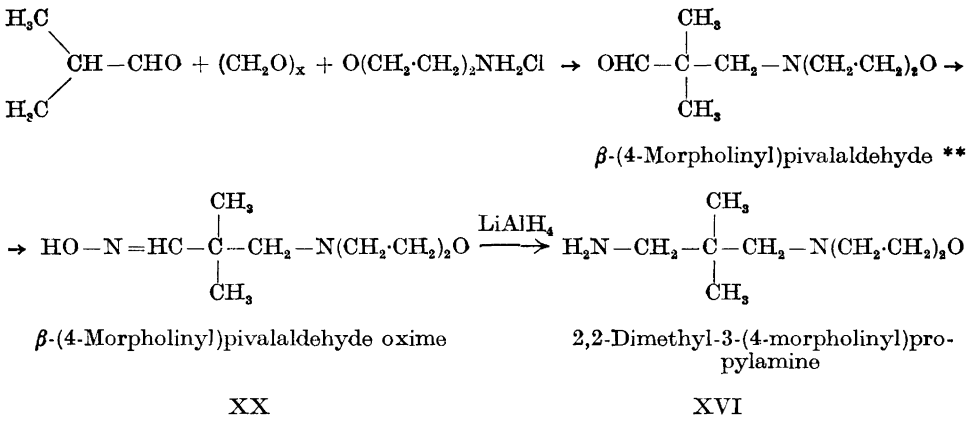

All the oximes (XVII, XIX, XX) and diamines (XIV, XV, XVI) are new compounds. The reduction of the oximes with $LiAlH_4$ in ether could not be carried out in the usual way, lumps being formed when the ethereal solution of the oxime was added dropwise to the $LiAlH_4$-suspension. However, the reaction could be performed smoothly by adding the $LiAlH_4$-suspension to the oxime solution. The best yield was obtained when two moles of $LiAlH_4$ per mole of oxime were used. Compound XI contains two asymmetric carbon atoms, and thus appeared as a mixture of two racemates. By recrystallization from di-*iso*propyl ether, the racemate of lower solubility was obtained. It was further purified by another recrystallization from di-*n*-butyl ether. The racemate of higher solubility was difficult to purify, and no definite product was isolated.

Due to the morpholino moiety, compounds I—XII should be rather weak bases. For N-(2-diethylaminoethyl)-2,4-dimethylbenzamide, the pK_a value at 25° is known from measurements by Lüning [2]. In order to compare this pK_a

* Unfortunately, Schröter [13] in a very well-known encyclopedia of synthetic organic chemistry [13] has misinterpreted the work of Cardwell, and reported the above mentioned by-product to be the linear 1-dimethylamino-3-pentanone. This mistake might, in several cases, have given rise to confusion as regards the products in the Mannich reaction with ketones.

** Prepared earlier in this way by Cheney [15].

value with that of N-[2-(4-morpholinyl)ethyl]-2,4-dimethylbenzamide (II), measurements were made on the latter compound, using the same technique as that given by Lüning [2] (*cf.* also Lindström [16], Löfgren [17]).

pH measurements at 25° were made under such conditions that the validity of the equation

$$pK_a = pH - \log \frac{C_B}{C_{BH^+}} - pf_{BH^+} \quad (1)$$

was fulfilled (*cf.* experimental part). pf_{BH^+} was computed from the Debye-Hückel formula:

$$pf_{BH^+} = \frac{0.358 \cdot z^2 \cdot \Gamma^{1/2}}{1 + 10^8 d_{BH^+} \cdot 0.2325\, \Gamma^{1/2}} \quad (2)$$

where $\Gamma = \Sigma C_i z_i^2$ is the ionic concentration, and d_{BH^+} is the effective diameter of the ion BH^+. In the actual case d_{BH^+} is set to 8×10^{-8} cm (*cf.* Löfgren [17], Lindström [16], Lüning [2]).

The apparatus used was a cell of the type:

Glass electrode/H^+(aq.)// KCl (satd.)/Hg_2Cl_2,Hg.

For this cell we have:

$$pH = \frac{E - E_o}{k} \quad (3)$$

(at 25°, $k = 59.16$)

E_o was obtained by making use of the pH values of Hitchcock and Taylor's [18] standard buffers (based on exact thermodynamic pK_a values). Accordingly, E_o may be considered as the sum of two constant quantities:

$$E_1 + E_j = E_o \quad (4)$$

E_1, which is a function of the glass electrode and of the calomel electrode, does not include the junction potential, and E_j should be regarded as the junction potential between satd. KCl and pure water.

Thus, Hitchcock and Taylor [18] standardized their buffers from an E_o value which was obtained from the relation:

$$E' = E - kpK_a + k \log \frac{C_{HA}}{C_A} + kA\sqrt{\mu} = E_o + kB\mu \quad (5)$$

The left member contains known quantities. In plotting E' against μ and drawing the best line to represent the observed points, the intercept E_o at zero ionic strength was obtained. In this way Hitchcock and Taylor derived an E_o value which almost exactly agrees with that of Bates [19] (based on measurements which are different from those of Hitchcock and Taylor).

Thus, when measuring pH in an unknown solution of *low ionic strength* (in our case $\mu \sim 5 \times 10^{-3}$, *cf.* Table 2), it may be assumed that the junction potentials included in E and E_0 should, to a high degree, cancel each other. However, it must be emphasized that it is clearly impossible to determine the

pH of a solution that is "unknown" in every sense of the word with an uncertainty less than $\pm$ 0.02 unit (*cf.* Bates [19]).

pK_a of compound II was thus found to be 6.10 (mean value of three different measurements; *cf.* experimental part). Lüning's [2] value for N-(2-diethylaminoethyl)-2,4-dimethylbenzamide is 8.92. Hence, ΔpK_a is 2.82 *. Thus, the morpholino compound is a much weaker base than the diethylamino compound. This is consistent with the theory, since the 3-oxapentamethylene radical, as compared with the two ethyl groups, must have a much smaller electron-repelling effect. — A comparison with the ΔpK_a value for *diethylamine → morpholine* is of interest. The two ΔpK_a values should, of course, not be identical, but should lie close to each other (within a few tenths). For diethylamine, Hall and Sprinkle [20] give a pK_a value (at 25°) equal to 10.98. According to Hall [21], the corresponding morpholine value is 8.36. Hence, ΔpK_a should be equal to 2.62.

The twelve compounds were investigated pharmacologically as to their sedative and local anesthetic actions. Bearing in mind the change in CNS activity that occurs with the "Xylocaines" when the morpholino group is substituted for the diethylamino group (see p. 1467) one could suppose that N-[(4-morpholinyl)ethyl]-2,4-dimethylbenzamide (II) should have a more pronounced hypnotic action than the corresponding diethylamino derivative, *i.e.* N-(diethylaminoethyl)-2,4-dimethylbenzamide (*cf.* p. 1467). However, this was not found to be the case: when tested in white mice (subcutaneous injections), the diethylamino compound gave a distinct though not strong hypnotic effect, whereas the morpholino derivative (II) showed a very weak action, if any**. Nor did the other eleven compounds (I, III—XII) exhibit a distinct positive action.

Table 2. Determination of the ionization constant of N-[2-(4-morpholinyl)ethyl]-2,4-dimethylbenzamide (II). The substance used is the *hydrochloride* (mol. wt. 298.8); NaOH-solution = 0.0333$_0$ M; test solution = 100 ml. The double e.m.f. values arise from the two glass electrodes used.

Salt weighed g	NaOH added ml	$\log \frac{C_B}{C_{BH^+}}$	$1/2\,\Gamma \times 10^3$	pf_{BH^+}	$-E_o$ mV	$+E$ mV	$E-E_o$ mV	pH	pK_a
0.1155	3.98	−0.283	3.865	0.028	157.2 152.7	189.4 193.0	346.6 345.7	5.859	6.11
0.1638	9.80	0.167	5.482	0.032	157.2 152.7	215.2 219.3	372.4 372.0	6.291	6.09
0.1202	5.87	−0.024	4.023	0.028	157.2 152.7	204.2 208.4	361.4 361.1	6.106	6.10
							Mean value =		6.10

* Both pK_a values are subjected to almost the same *systematic* error, caused by the potential at the liquid junction (*cf.* above). In ΔpK_a, however, this type of error is almost eliminated.

** The comparisons made by injections of equimolar doses per kg of body weight.

For three of the compounds, *i.e.* I, II, and X, the LD50 values were determined by subcutaneous injections in white mice. According to these experiments, all three compounds are relatively non-toxic and none of the LD50 values (in grams of the base per kg of body weight) was found to be lower than 0.8 or higher than 1.3.

As regards the local anesthetic action, none of the twelve compounds proved to be active when applied to the human tongue by rubbing *.

EXPERIMENTAL

A. Syntheses **

4-(3-Aminopropyl)morpholine (XIII). This compound was made by following the directions of Hultqvist and Northey [7], who prepared 4-(2-aminoethyl)morpholine. Instead of 57.5 % ethylenediamine, 81.5 % trimethylenediamine was used. 4-(3-Aminopropyl)morpholine distilled as a colourless oil, b.p. 139—140°/43—45 mm, n_D^{20} 1.4768. (These values agree with those given by Uthermohlen and Hamilton [8], who prepared the amine by a Gabriel synthesis). Yield 41 %.

1-(4-Morpholinyl)-2-propanone oxime (XVII). Saturated water solutions of hydroxylamine·HCl, 113 g (1.63 moles), and of $NaOAc \cdot 3H_2O$, 440 g (3.23 moles), were prepared. To 230 g (1.61 moles) of 1-(4-morpholinyl)-2-propanone [9], the hydroxylamine and the acetate solutions were consecutively added. The oxime immediately precipitated as a white crystalline mass. After cooling, the crystals were sucked off an extracted with the minimum quantity of boiling benzene. The hot combined extracts were dried with anhydrous sodium sulphate. This was removed by filtration, and on cooling colourless crystals of m.p. 103—104° (corr.) were obtained; yield 162 g (1.02 moles, 63 %). (Found: Equiv. wt. 158. Calc. for $C_7H_{14}N_2O_2$: 158.2.)

1-Methyl-2-(4-morpholinyl)ethylamine (XIV). In a three-necked 2 l flask equipped with a reflux condenser, a sealed Hershberg stirrer and a dropping funnel, 80 g (0.51 mole) of 1-(4-morpholinyl)-2-propanone oxime (XVII) were dissolved in 750 ml of absolute ether. To this solution a suspension (*cf.* p. 1470) of 40 g (1.1 moles) of $LiAlH_4$ in 500 ml of dry ether was added under rapid stirring during 3 h. The complex formed, as well as the excess of $LiAlH_4$, were decomposed as described by Amundsen and Nelson [22]. The inorganic salts were filtered off and washed with ether. After removing the solvent, the amine was distilled as a colourless oil, b.p. 96—98°/20 mm, n_D^{25} 1.4620, yield 20.5 g (0.142 mole, 28 %). (Found: Equiv. wt. 72.0. Calc. for $C_7H_{16}N_2O$ (144.2): 72.1.)

3-Methyl-4-(4-morpholinyl)-2-butanone (XVIII). According to Mannich and Hof's [10] preparation of 4-dimethylamino-3-methyl-2-butanone, a mixture of 144 g (2.00 moles) methyl ethyl ketone, 123.5 g (1.00 mole) of morpholine·HCl, 40 g of paraformaldehyde (1.3 moles of formaldehyde) and 50 ml of *iso*propyl acolhol was refluxed on the steam bath for 6 h. After cooling, the volatile products were driven off under reduced pressure. 200 g of a 50 % sodium hydroxide solution were added, and the mixture was extracted three times with 200 ml of ether. The combined extracts were dried over Na_2SO_4 and after filtering and removing the ether, the residue was purified by distillation. The main fraction (70 g) distilled at 100—115°/12 mm. After redistillation through a 30 cm asbestos-wrapped Vigreux column, 52 g of a colourless oil of b.p. 136—139°/31—32 mm were collected; n_D^{25} 1.4657. (Found: Equiv. wt. 173. Calc. for $C_9H_{17}NO_2$: 171.2.)

Hydrochloride. Colourless crystals from acetone-methyl ethyl ketone of m.p. 146—147° (corr.). (Found: Cl*** 17.1. Calc. for $C_9H_{18}ClNO_2$ (207.7): Cl 17.1.)

3-Methyl-4-(4-morpholinyl)-2-butanone oxime (XIX). This oxime was obtained from 3-methyl-4-(4-morpholinyl)-2-butanone (XVIII), hydroxylamine hydrochloride, and

* The *bases* as well as the *hydrochlorides* were tested.

** The determination of equivalent weights of the synthesized bases was made by titrating them in glacial acetic acid with 0.1 N perchloric acid; BZL-Blue (CIBA) was used as an indicator.

*** Potentiometr. titration.

sodium acetate in the same manner as described in the preparation of XVII. The oxime appeared as an oily layer, which was taken up in ether. The ethereal solution was dried over Na_2SO_4, the ether removed, and the residue distilled. The oxime was collected as a colourless viscous oil, b.p. 172—174°/24—25 mm, n_D^{25} 1.4896, yield 73 %. (Found: Equiv. wt. 186. Calc. for $C_9H_{18}N_2O_2$: 186.3.)

1,2-Dimethyl-3-(4-morpholinyl)propylamine (XV). 60 g (0.32 mole) of 3-methyl-4-(4-morpholinyl)-2-butanone oxime (XIX) in 300 ml of absolute ether was reduced with 25 g (0.66 mole) of $LiAlH_4$ in 400 ml of absolute ether as described under compound XIV. By distillation the amine was obtained as a colourless oil, b.p. 124—125°/17—18 mm, n_D^{25} 1.4672, yield 18.5 g (0.107 mole, 33 %). (Found: Equiv. wt. 86.0. Calc. for $C_9H_{20}N_2O$ (172.3): Equiv. wt. 86.1.)

β-(4-Morpholinyl)pivalaldehyde oxime (XX). This oxime was made from β-(4-morpholinyl)pivalaldehyde, hydroxylamine·HCl, and sodium acetate in the same manner as described in the preparation of XVII. The oxime separated as an oily layer, and was taken up in ether. The ethereal solution was dried over Na_2SO_4, the ether removed, and the residue distilled under reduced pressure. The main fraction which was obtained in a yield of 86 % was a colourless oil of distinct b.p., but titration of the base gave an equivalent weight (191) that differed a few per cent from the calculated one (186). Another distillation did not result in an acceptable value. Therefore, the base was dissolved in a mixture of dry acetone-dry ether and the *hydrochloride* was precipitated by adding somewhat more than the calculated amount of dry ether·HCl. The crystals were washed with a mixture of dry acetone-dry ether and then recrystallized from absolute ethanol. The salt was obtained in the form of colourless needles. On chlorine analysis the salt gave the theoretical value (*cf.* below). From this hydrochloride, the base was regenerated and isolated by distillation. Viscous colourless oil, b.p. 166—167°/24—25 mm, n_D^{25} 1.4846. The over-all yield from β-(4-morpholinyl)pivalaldehyde was 46 %. (Found: Equiv. wt. 187. Calc. for $C_9H_{18}N_2O_2$: 186.3.)

Hydrochloride. Colourless needles from absolute ethanol (*cf.* above); m.p. 186—187° (decomp., corr.). (Found *: Cl 15.9. Calc. for $C_9H_{19}ClN_2O_2$ (227.7): Cl 15.9.) **

2,2-Dimethyl-3-(4-morpholinyl)propylamine (XVI). 100 g (0.54 mole) of β-(4-morpholinyl)pivalaldehyde oxime in 500 ml of absolute ether was reduced with 42 g (1.1 moles) of $LiAlH_4$ in 500 ml of absolute ether in the same way as described under compound XIV. The amine distilled as a colourless oil, b.p. 118—120°/22—23 mm, n_D^{25} 1.4661, yield 32 g (0.19 mole, 35 %). (Found: Equiv. wt. 86.0. Calc. for $C_9H_{20}N_2O$ (172.3): Equiv. wt. 86.1.)

N-[(4-Morpholinyl)alkyl]benzamides (I—XII, *cf.* Table 1). All twelve compounds were synthesized according to the same method by reacting a benzoyl chloride with an 4-(aminoalkyl)morpholine; the composition of the reactants is evident from Table 1. (The syntheses of the 4-(aminoalkyl)morpholines are described in text above.) The following method was used: A solution of 0.059 mole of the methyl substituted benzoyl chloride in 50 ml of absolute ether is placed in a three-necked flask equipped with a reflux condenser, a dropping funnel and a teflon sealed stirrer. Under vigorous stirring, a solution of 0.094 mole of the 4-(aminoalkyl)morpholine in 50 ml of dry ether is introduced during a period of 30 min. The apparatus is then arranged for downward distillation *in vacuo*. To the turbid mixture, 50 ml of 2 M sodium hydroxide (0.10 mole) are added. Under reduced pressure and vigorous stirring, the ether is then driven off at a bath temperature of 30 °. The precipitate is sucked off, washed two times with small quantities of ice-cold 6 M ammonia and dried in a desiccator. From di-*iso*propyl ether the product is obtained as colourless crystals. The crude product of compound XI consisted of two racemates. On recrystallization from di-*iso*propyl ether, the racemate of lower solubility was easily collected and further purified by another recrystallization from di-*n*-butyl ether. The racemate of higher solubility was not isolated. Yields, melting points and analytical data of the twelve bases are shown in Table 1.

---

* Potentiometr. titration.

** The *hydrochloride* has been prepared previously by Cheney [15] who gave the m.p. 175.5° (decomp.). (The *base* has not been described previously.)

Table 3. Melting points and analytical data of the *hydrochlorides* of compounds I—XII.

Hydrochloride of	Empirical formula	M.p., °C corr.	Analysis, % Calc. Cl	Analysis, % Found Cl [a]
I	$C_{14}H_{21}ClN_2O_2$	196—197	12.5	12.6
II	$C_{15}H_{23}ClN_2O_2$	171—172	11.9	11.8
III	$C_{15}H_{23}ClN_2O_2$	193—195	11.9	11.9
IV	$C_{15}H_{23}ClN_2O_2$	157—158	11.9	11.8
V	$C_{16}H_{25}ClN_2O_2$	187—188	11.3	11.4
VI	$C_{15}H_{23}ClN_2O_2$	167—168	11.9	11.9
VII	$C_{16}H_{25}ClN_2O_2$	142—143	11.3	11.2
VIII	$C_{16}H_{25}ClN_2O_2$	190—191	11.3	11.3
IX	$C_{17}H_{27}ClN_2O_2$	211—213	10.9	10.9
X	$C_{16}H_{25}ClN_2O_2$	141—142	11.3	11.3
XI[b]	$C_{18}H_{29}ClN_2O_2$	232—234	10.4	10.5
XII	$C_{18}H_{29}ClN_2O_2$	228—230	10.4	10.5

[a] The hydrochlorides were titrated potentiometrically with 0.1 M $AgNO_3$.
[b] The hydrochloride of the racemate that has the *lower* solubility (*cf.* p. 1474).

Hydrochlorides of compounds I—XII. In 20 ml of dry acetone 0.0040 mole of the base was dissolved. To this solution 0.0060 mole of dry hydrogen chloride in dry ether was added, and the precipitation completed by the addition of absolute ether. The precipitate was filtered off and recrystallized from a solvent mixture di-*iso*propyl ether-*iso*propanol. Melting points and analytical data of the hydrochlorides are found in Table 3.

B. Determination of the ionization constant K_a for N-[2-(4-morpholinyl)ethyl]-2,4-dimethylbenzamide (II) at 25°.

As pointed out above (*cf.* p. 1471) the determination of the ionization constant, $pK_a^{25°}$, of compound II was carried out by using a cell of the type:

Glass electrode/H^+(aq.)//KCl (satg.)/Hg_2Cl_2, Hg *

To standardize the electrodes, Hitchcock and Taylor's [18] 0.1 M acetate and 0.025 M phosphate buffers were used. Calibration of the cell was made immediately before measuring the solution of unknown pH. The E_0 values (*cf.* Table 2) for the cell, obtained from the two buffer solutions, were never found to deviate more than 0.1 mV from each other. The *hydrochloride* of *N*-[2-(4-morpholinyl)ethyl]-2,4-dimethylbenzamide (II) was weighed, and dissolved in water having a specific conductivity of about 5×10^{-6} $ohm^{-1}cm^{-1}$. A suitable amount of sodium hydroxide was added, and after diluting to definite volume (ionic strength $\sim 5 \times 10^{-3}$) the solution was subjected to pH measurement. The primary data and the results are given in Table 2.

REFERENCES

1. Löfgren, N. and Stoffel, W. *Acta Chem. Scand.* **13** (1959) 1585.
2. Lüning, B. *Acta Chem. Scand.* **13** (1959) 1623, *ibid.*, **14** (1960) 321.
3. Lüning, B. *Private communication.*
4. Wiedling, S. *Xylocaine. The Pharmacological Basis of its Clinical Use*, Almqvist and Wiksell, Stockholm 1959, p. 50.

* As to the technical details of the set, see Löfgren [17], Lindström [16] or Lüning [3].

5. Smith, A. *Helv. Chim. Acta* **42** (1959) 1764, 1771.
6. Brit. P. 840361 (1960).
7. Hultquist, M. and Northey, E. *J. Am. Chem. Soc.* **62** (1940) 447.
8. Uthermohlen, W., Jr. and Hamilton, C. *J. Am. Chem. Soc.* **63** (1941) 156.
9. Mason, P. and Ross, S. *J. Am. Chem. Soc.* **62** (1941) 2882.
10. Mannich, C. and Hof, W. *Arch. Pharm.* **265** (1927) 592.
11. Cardwell, H. *J. Chem. Soc.* **1950**, 1056.
12. Blicke, F. and McCarty, F. *J. Org. Chem.* **24** (1959) 1376.
13. Schröter, R. *Methoden der organischen Chemie*, 4th Ed., Georg Thieme, Stuttgart 1957, Vol. **XI:1**, p. 739.
14. Lur'e, S. *J. Gen. Chem. U.S.S.R.* **9** (1939) 287.
15. Cheney, L. *J. Am. Chem. Soc.* **73** (1951) 685.
16. Lindström, S. *Acta Chem. Scand.* **11** (1957) 962.
17. Löfgren, N. *Studies on Local Anesthetics. Xylocaine, a New Synthetic Drug.* Dissertation, Stockholm 1948.
18. Hitchcock, D. and Taylor, A. *J. Am. Chem. Soc.* **59** (1937) 1812.
19. Bates, R. *Chem. Revs.* **42** (1948) 1.
20. Hall, N. and Sprinkle, M. *J. Am. Chem. Soc.* **54** (1932) 3469.
21. Hall, H., Jr. *J. Am. Chem. Soc.* **78** (1956) 2570.
22. Amundsen, L. and Nelson, L. *J. Am. Chem. Soc.* **73** (1951) 242.

Received March 16, 1961.

ACTA CHEMICA SCANDINAVICA 15 (1961) 1477–1484

*iso*Thiocyanates XXXIX *. Glucobenzosisymbrin, a New Glucoside Present in Seeds of *Sisymbrium austriacum* Jacq. **

ANDERS KJÆR and BO W. CHRISTENSEN

Department of Organic Chemistry, The Royal Veterinary and Agricultural College, Copenhagen, Denmark

As formerly shown, seeds of the crucifer *Sisymbrium austriacum* Jacq. contain three major glycosides (A, B, and C) the first of which, glucosisymbrin, was demonstrated to contain a 2-hydroxy*iso*propyl side-chain of established absolute configuration [1].

In the present paper, glycoside C, designated *glucobenzosisymbrin*, is shown to be a glucoside of the customary type, differing from glucosisymbrin only by containing a benzoyl grouping attached in ester linkage to the side-chain.

The mustard oil (benzosisymbrin), liberated on enzymic hydrolysis of the new glucoside, is characterized as its thiourea derivative. The deduced structure of the latter is confirmed by synthesis of the enantiomeric thiourea. The configuration around the asymmetric carbon atom of the side-chain in glucobenzosisymbrin is shown to be the same as that prevailing in glucosisymbrin. The new glucoside represents the second example of the natural occurrence of *iso*thiocyanate glucosides with benzoylated hydroxy-alkyl side-chains, glucomalcolmiin [6,7] being the first discovered of these.

In a previous communication from this laboratory [1], the distribution of *iso*thiocyanate glycosides in various members of the cruciferous genus *Sisymbrium* was discussed. Particular attention was given to the species *Sisymbrium austriacum* Jacq., a seed extract of which was demonstrated to contain three major glycosides, obviously different from all heretofore described glucosides [2] and designated A, B, and C according to increasing R_B-values [3] on paper chromatograms. It was further shown that compound A, named *glucosisymbrin*, on enzymic hydrolysis afforded (+)-4-methyl-2-oxazolidinethione with the absolute configuration presented in (I), from which a plausible structure could be deduced for the glucoside [1]. It is the purpose of the present paper to report on the chemical structure of glycoside C.

* Part XXXVIII of this series: *Acta Chem. Scand.* **14** (1960) 1226.

** Presented in abstract before the I. Scandinavian Symposium on Natural Product Chemistry, June 1961, Bornholm, Denmark.

In the course of paperchromatographic studies of methanolic seed extracts of *S. austriacum* Jacq.* it was noticed that glycoside C on treatment with aqueous ammonia was converted into a much more hydrophilic glycoside, indistinguishable from glucosisymbrin on paper chromatography. This observation suggested a chemical relationship between the two. Enzymic hydrolysis of a paperchromatographically purified solution of glycoside C was accompanied by the liberation of *glucose*, whereas acid hydrolysis was employed to demonstrate the formation of sulphate and hydroxylamine. These results indicated that glycoside C was a glucoside of the customary structural type [4]. Consequently, and in view of its chemical character, unveiled in the sequel, the designation *glucobenzosisymbrin* is proposed for glucoside C.

On a preparative scale, it proved advantageous to remove the *iso*thiocyanate (benzosisymbrin) liberated from glucobenzosisymbrin on enzymic hydrolysis by steam distillation, since glucosisymbrin and glycoside B did not give rise to volatile enzymic hydrolysis products.

In view of the limited quantities on hand, no attempts were made to distil the oily *iso*thiocyanate isolated by ether extraction of the aqueous condensate. It was noticed, however, that the crude mustard oil on treatment with alkali was converted into a compound with a positive Grote reaction, which was indistinguishable from (+)-4-methyl-2-oxazolidinethione (I) on paper chromatography. Hence, the observed lability of the glucoside to alkali apparently

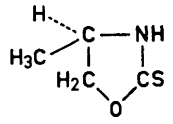

I

$C_6H_5COOCH_2CH_2CH_2NCS$

II

resided in the side-chain. The mustard oil was subjected directly to reaction with ammonia in attempts to produce a crystalline thiourea-derivative, suitable for characterization. Paperchromatographic analyses indicated that thiourea formation in aqueous or methanolic solutions of ammonia was accompanied by extensive ammonolysis, whereas treatment with anhydrous ammonia in chloroform under controlled conditions afforded the desired thiourea, yet contaminated by small amounts of an additional thiourea possessing a somewhat higher R_F-value in the solvent system: carbon tetrachloride: 30 % acetic acid (1:1)**. On a preparative scale, 165 g of seeds of *S. austriacum* Jacq. afforded 385 mg of a crystalline *dextro*rotatory thiourea (m.p. 122°) which was subjected to a 60-plate counter-current distribution in order to remove the above-mentioned thiourea contaminant. Thus, a homogeneous specimen was produced, devoid of notable acid or basic properties and possessing the elemental com-

* The present investigation was carried out on seed material propagated in 1959—1960 in *The Botanical Garden of the University of Copenhagen* from the authentic stock employed in our previous studies.

** *Added in proof:* Since this work was submitted, the contamination has been identified as the higher homologue, 1-(1-ethyl-2-benzoyloxyethyl)-thiourea, arising from the glucoside glucobenzsisaustricin [15].

position $C_{11}H_{14}O_2N_2S$. Its ultra-violet absorption spectrum displayed maxima at 238 mμ and 205 mμ, characteristic for thioureas, yet with auxiliary low-extinction shoulders at 273 mμ and 280 mμ, suggestive of the presence of an aroyl grouping. A prominent band at 1 698 cm^{-1} in the infra-red spectrum (in KBr) was accordingly assigned to the C=O stretching mode of an aromatic ester, although this value is slightly below the range commonly quoted for such esters [5]. While reasonably stable towards acid, the new thiourea was readily cleaved in aqueous alkali to *benzoic acid* and a hydroxypropylthiourea, indicating its derivation from one of the isomeric benzoyloxypropyl *iso*thiocyanates.

One of these, *viz.* 3-benzoyloxypropyl mustard oil (II), was previously established in this laboratory as a product of enzymic hydrolysis of the glucoside glucomalcolmiin, encountered in seeds of the crucifer *Malcolmia maritima* (L.) R.Br.[6,7].

The stability of benzosisymbrin-thiourea, together with its optical activity, in fact restricted the possible structural formulations to (III) and (IV). The mustard oil whence (III) derives should be converted into a 5-methyl-2-oxazoli-

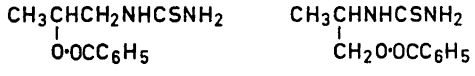

III IV

dinethione upon alkali hydrolysis of the ester grouping, whereas the isothiocyanate corresponding to (IV), subjected to the same treatment, should cyclize to a 4-methyl-2-oxazolidinethione (I). The *dextro*rotatory isomeride of the latter was previously isolated from the same seed material [1]. This fact, together with the abovementioned coinciding spots on paper chromatograms of authentic (I) and alkali-treated crude benzosisymbrin, rendered structure (IV) by far the most likely. A slight, but consistent difference in R_F-values between the 4- and 5-methyl-substituted 2-oxazolidinethiones in several solvent systems lent further support to structure (IV).

This conclusion was finally corroborated by an unambiguous synthesis of the enantiomer of benzosisymbrin-thiourea by a series of reactions providing full information as to its absolute configuration.

In the malcolmiin series it proved feasible to synthesize 3-hydroxypropyl *iso*thiocyanate which could be converted further into malcolmiin upon benzoylation [7]. The greatly enhanced tendency to intramolecular cyclization of aliphatic 2-hydroxy-substituted *iso*thiocyanates, compared to those of the 3-hydroxy-substituted series [7], made a similar approach to the desired 2-benzoyloxy*iso*propyl *iso*thiocyanate impracticable. Efforts were hence directed towards synthesis of the latter from the previously unknown 2-aminopropyl benzoate (VI), accessible as its hydrochloride from N-(2-hydroxy*iso*propyl)-benzamide (V) by acid-induced, intramolecular benzoyl migration. Despite a

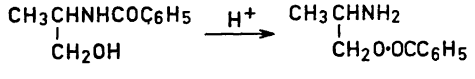

V VI

rapidly occurring reconversion of the ester base (VI) to the amide (V), conditions were found under which the rate of reaction of (VI) with thiocarbonyl chloride was sufficiently high, compared to that of the O→N migration, to produce an acceptable yield of the desired *iso*thiocyanate.

In a model experiment, DL-N-(2-hydroxy*iso*propyl)-benzamide (N-benzoyl-DL-alaninol (V)) [8] was transformed into the hydrochloride of DL-2-aminopropyl benzoate (VI) by anhydrous hydrogen chloride in ethanol, conditions similar to those previously employed in analogous reactions (*cf. e.g.* Ref.[9]). Addition of precisely three equivalents of triethylamine to a chloroform solution containing equimolar quantities of the hydrochloride of the racemic base (VI) and thiocarbonyl chloride, resulted in the formation of the racemic 2-benzoyloxy*iso*propyl *iso*thiocyanate which was, in turn, converted into the crystalline racemic thiourea (m.p. 133°) by treatment with ammonia in chloroform under controlled conditions.

Repetition of the above sequence of reactions, starting from optically pure L-alaninol [10], led to the production of *levo*rotatory 1-(2-benzoyloxy*iso*propyl)-thiourea (m.p. 122°) with the absolute configuration depicted in (VII). The synthetic specimen had the same m.p., R_F-value, ultra-violet and infra-red

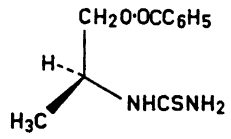

VII

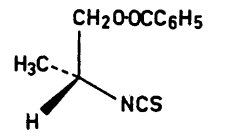

VIII

spectrum as naturally derived benzosisymbrin-thiourea, whereas its optical rotation was *similar in magnitude but opposite in sign* to that of the natural specimen. Recrystallization of a mixture of equal amounts of the natural and synthetic thiourea afforded the racemic compound, which melted undepressed in admixture with synthetic, racemic material. On the likely assumption that the enzyme-induced rearrangement leading to the *iso*thiocyanate proceeds with retention of configuration [4], structure (VIII) can be attributed to benzosisymbrin which therefore constitutes the benzoate of the hypothetic 2-hydroxy-*iso*propyl *iso*thiocyanate, liberated from glucosisymbrin on enzymic hydrolysis and undergoing spontaneous cyclization to (+)-4-methyl-2-oxazolidinethione (I). The establishment of identical absolute configurations in the cyclized and the benzoylated, noncyclizing *iso*thiocyanate, derivable from glucosides occurring in the same plant, strongly supports the view that such cyclizations proceed without configurational changes.

The combined evidence suggests that the genuine glucoside, glucobenzosisymbrin, on basis of the general structural expression of Ettlinger and Lundeen [4], possesses the structure (IX) and thus represents the second example of a natural glucoside of this type containing a benzoate grouping in the side-chain. The finding of benzoates in this series of glucosides is well in line with the frequently observed occurrence of benzoyloxy-substitutes among natural products (*e.g.* populin, coniferyl benzoate, cocaine, aconitine *etc.*). It appears

likely that the benzoyl grouping enters the glucosides at a late stage of their biosyntheses. A possible biosynthetic pathway to the 2-hydroxy*iso*propyl grouping was discussed in a previous paper[1].

The structure elucidation of glucoside B in seeds of *S. austriacum* Jacq. will form the subject of a forthcoming communication.

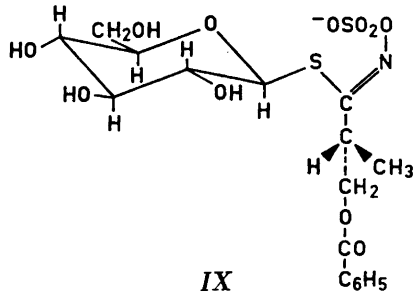

IX

EXPERIMENTAL

Melting points are determined in capillary tubes in an Anschütz-Hershberg apparatus equipped with fully immersed thermometers. Rotations are measured in a 1 dm tube. Infra-red spectra are determined in KBr pellets on a Perkin-Elmer "Infracord" instrument. Analytical specimens are dried *in vacuo* over calcium chloride at room temperature.

Exploratory paperchromatographic studies. An extract of 1.25 g of finely ground seeds of *Sisymbrium austriacum* Jacq. in 70 % methanol was evaporated to dryness, redissolved in water, filtered through Celite, and concentrated to a volume of 3 ml. This solution was applied to four sheets of filter paper (Schleicher and Schüll 2043 b) and chromatographed for 24 h with the upper layer of the solvent system *n*-butanol:ethanol:water (4:1:4) as the mobile phase. Narrow edge cuts from each sheet were sprayed with ammoniacal $AgNO_3$ in order to locate the three major glycoside bands (A, B, and C, *cf.* Ref.[1]) which were then cut out and eluted with water to a total volume of 2 ml for each glycoside. Control chromatograms of the eluate of glycoside C in the same solvent system gave an R_B-value of *ca.* 1.47, similar to the value 1.42 observed for a sample of glucomalcolmiin [7] run on the same chromatogram *.

Treatment of a 50 μl-portion of the eluate of glycoside C with conc.aqueous ammonia caused its rapid conversion into another glycoside, indistinguishable on the paper chromatogram from glucosisymbrin [1] (glucoside A). More than half of C had disappeared within one hour and after 28 h the conversion was complete.

Another 50 μl-portion of the eluate was buffered with 20 μl of a phosphate solution (pH 6.8) and 5 μl of the usual, cell-free myrosinase solution were added. Next morning, paper chromatography showed that the glycoside had been completely hydrolyzed, and other chromatograms, run in the same solvent system as well as in *n*-butanol:pyridine: water (6:4:3) and developed with the aniline-diphenylamine phosphate sugar reagent, indicated that *glucose* had been liberated during the enzymic fission.

When a 500 μl-portion of glucoside C, from here on designated *glucobenzosisymbrin*, was treated with conc. hydrochloric acid for 2 h at 60°, a hydrolytic fission took place, analogous to that described by Ettlinger and Lundeen [4] for similar glucosides. The forma-

* It has been repeatedly observed in this laboratory that R_B-values of glycosides migrating faster than glucotropaeolin may vary considerably according to the amount of glycoside applied to the paper, the type and orientation of the latter *etc.* This fact explains the observed deviations from previosuly reported R_B-values for glucomalcolmiin (1.36 [6,7]) and glycoside C (1.67 [1]) and indicates that identifications of such glycosides, solely based on R_B-values, are likely to be fallacious.

tion of sulphate and hydroxylamine was demonstrated by precipitation with Ba^{++} and paper chromatography [4], respectively.

Enzymic liberation of benzosisymbrin. Seeds of *Sisymbrium austriacum* Jacq. (165 g) were pulverized and defatted by treatment with three 400 ml-portions of carbon tetrachloride in a Waring blendor. The air-dried seed powder (115 g) was then exhaustively extracted by refluxing for 3 h with three 750 ml-portions of 70 % methanol. The combined filtrates were concentrated *in vacuo* to a dark syrup, foaming being controlled by the addition of small volumes of octanol. The residue was dissolved in water (700 ml) and the solution clarified by filtration through Celite. The dry matter in this solution amounted to 23.5 g.

The solution was now buffered to pH 6.8 by the addition of 50 ml each of 0.2 M solutions of primary and secondary phosphates. Then a few mg of ascorbic acid [11] and a cell-free myrosinase solution (10 ml) were added, and the mixture was set aside at room temperature. After a few hours, secondary phosphate was added to readjust the diminished pH-value to 6.8, and the mixture was left overnight. Next morning, it was steam-distilled and the distillate (about 1 l) was saturated with NaCl and continuously extracted for 24 h with ether. After drying, the solvent was removed through a column and the crude *iso*thiocyanate remained as a faintly yellow oil (675 mg).

The two oxazolidinethiones, deriving from glucosisymbrin [1] and glycoside B, remained unchanged in the enzymic hydrolysis mixture after steam distillation.

Formation of the thiourea derivative of benzosisymbrin. The above crude mustard oil (675 mg) was dissolved in 100 ml of a 2 N solution of anhydrous ammonia in chloroform and left standing at room temperature for 7.5 h when the volatile constituents were removed *in vacuo*. The oily residue crystallized in contact with benzene and was dissolved in this solvent (30 ml). On cooling, colourless prisms separated (385 mg), m.p. 121 – 121.5°. Paper chromatography, run with the lower layer of the solvent system CCl_4:30 % acetic acid (1:1) [12] as the mobile phase, revealed the presence of a minor thiourea (R_{Ph} 2.10) besides that of benzosisymbrin (R_{Ph} 1.50). Since attempts to remove the former by fractional crystallization were fruitless, recourse was taken to a 60-plate counter-current distribution in the same solvent system as employed for paper chromatography. Partial separation was thus achieved and a homogeneous specimen was readily obtained from the appropriate tubes in the Craig-apparatus. Before analysis, the thiourea was recrystallized once from benzene and twice from water, separating from the latter solvent in shiny plates, m.p. 121.0 – 121.5°, $[\alpha]_D^{25}$ + 65.3° (*c* 1.29, 96 % EtOH) (Found: C 55.45; H 5.99; N 11.45; S 13.39. Calc. for $C_{11}H_{14}O_2N_2S$: C 55.44; H 5.92; N 11.76; S 13.46). In 96 % ethanol, the UV-absorption spectrum exhibited a characteristic thiourea pattern, very similar to that of malcolmiin-thiourea[6]: λ_{max} 238 mμ (ε 19 500), λ_{max} 205 mμ (ε 15 000), λ_{min} 216 mμ (ε 11 000), and, in addition, two low-extinction plateaus at 273 mμ and 280 mμ. The infra-red spectrum (in KBr) showed a very strong band at 1 698 cm^{-1}, assigned to the C=O stretching mode of an aromatic ester. Other prominent bands were observed at: 3 350 s, 3 220 s, 3 110 m, 3 020 m, 2 930 m, 1 610 vs, 1 550 vs, 1 485 m, 1 445 s, 1 415 m, 1 385 m, 1 365 m, 1 345 s, 1 315 s, 1 280 vs, 1 170 s, 1 115 vs, 1 070 m, 1 020 m, 963 m, 942 w, 927 m, 858 w, 808 w, 718 vs, 688 w and 675 w cm^{-1} (vs very strong, s strong, m medium, w weak).

Alkali treatment of benzosisymbrin and its thiourea derivative. In consequence of the above-described lability of glucobenzosisymbrin towards alkali, the corresponding steam-volatile, crude mustard oil was exposed to 0.5 N NaOH in 50 % ethanol for 16 h at room temperature. The solution was then acidified and extracted with small volumes of chloroform. The organic phase gave a positive Grote reaction, and on chromatography in benzene:heptane:water (9:2:9), a spot was noticed at exactly the same position as that of a simultaneously chromatographed sample of authentic (+)-4-methyl-2-oxazolidinethione (I), derivable from glucosisymbrin. The isomeric 5-methyl-2-oxazolidinethione [6] could be excluded on basis of paper chromatograms, run with carbon tetrachloride saturated with 30 % acetic acid as the mobile phase [12]. In this solvent system, as well as others, the 4-isomeride migrated at a slightly higher rate than the 5-substituted ring compound.

When a solution of benzosisymbrin-thiourea (42 mg) in ethanol (10 ml) containing 0.1 N NaOH (10 ml) was kept for 24 h at room temperature, an acid could be extracted with ether after acidification. The solid acid was readily identified as *benzoic acid* by means of its infra-red spectrum which was indistinguishable from that of an authentic specimen.

Synthesis of DL-*1-(2-benzoyloxyisopropyl)-thiourea (IV).* DL-Alaninol was prepared by reduction of DL-alanine methyl ester with lithium aluminium hydride according to Karrer *et al.*[13] N-Benzoylation of the amino-alcohol was performed as described by Billman and Parker[8]. The crude DL-N-(2-hydroxy*iso*propyl)-benzamide (V) (3.8 g), m.p. 102—103° (reported: 107—108°[8], 104.5—106°[14]), was refluxed for 1 h with ethanol (40 ml) containing 10 mequiv. of anhydrous HCl per ml. The solution was then concentrated to about 15 ml and ether was added to precipitate the previously unknown *hydrochloride of* DL-*2-aminopropyl benzoate* (VI) (1.08 g), yet heavily contaminated with alaninol hydrochloride, formed by ethanolysis of the benzoate during the reaction, as apparent from paperchromatographic analysis in *n*-butanol:ethanol:water (4:1:4) (spray reagent:ninhydrin). Additional crops from the mother liquor raised the total yield to 1.81 g (40 %). Complete separation of the two hydrochlorides was achieved by a 60-plate countercurrent distribution with *n*-butanol:ethanol:water (4:1:4) as the solvent system. The contents of tubes No. 18—32 afforded the homogeneous ester hydrochloride which was recrystallized twice from anhydrous ethanol:ether mixtures (1:2) before analysis. The salt separated in colourless needles, m.p. 175° (Found: C 55.53; H 6.64; N 6.30; Cl 16.55. Calc. for $C_{10}H_{14}O_2NCl$: Cl 55.68; H 6.54; N 6.50; Cl 16.44). The infra-red spectrum exhibited the expected C=O ester bond at 1 710 cm^{-1}. The procedure employed is analogous to that employed by Philips and Baltzly[9] for analogous intramolecular N→O acyl migrations.

To a stirred solution of the crude ester hydrochloride (500 mg) and thiocarbonyl chloride (276 mg) in chloroform (16 ml), a total of 950 µl of triethylamine (theoretical: 980 µl) was dropwise added in the course of 5 min, resulting in disappearance of the thiophosgene colour. After 2 h at room temperature, the chloroform solution was washed with 1 N HCl and water, dried over Na_2SO_4, and made 2N with regard to ammonia (total volume 60 ml). At the end of 4 h, the solvent was removed and the semi-crystalline residue was dissolved in benzene and treated with charcoal. On cooling, almost colourless prisms separated (141 mg), m.p. 128—129°. An analytical sample of DL-*1-(2-benzoyloxyisopropyl)-thiourea* (IV) was produced on two additional crystallizations, first from benzene and then from water. The colourless prisms melted at 133° (Found: C 55.64; H 6.01; N 11.75; S 13.39. Calc. for $C_{11}H_{14}O_2N_2S$: C 55.44; H 5.92; N 11.76; S 13.46). On paper chromatography in water-saturated chloroform and carbon tetrachloride:acetic acid, the synthetic thiourea was indistinguishable from the optically active thiourea-derivative of benzosisymbrin. The infra-red spectra, however, were, as expected, distinctly different outside the "double-bond region".

Synthesis of (—)-1-(2-benzoyloxyisopropyl)-thiourea (VII). The sequence of reactions described above was employed with minor modifications in the optically active series for the synthesis of the enantiomer of benzosisymbrin-thiourea.

L-Alaninol, $[a]_D^{25}$ + 22.1° (*c* 7.2, 96 % EtOH), was produced by reduction of L-alanine with $LiAlH_4$ in tetrahydrofuran as described[10]. N-Benzoylation proceeded in 88 % yield as reported for the racemic alaninol[8] to give *(—)-N-(2-hydroxyisopropyl)-benzamide* ((—)-N-benzoyl-L-alaninol) separating from benzene in flat needles, m.p. 131.5—132.5°, $[a]_D^{25}$ —2.9° (*c* 7.4, 96 % EtOH)] (Found: C 67.04; H 7.25; N 7.81. Calc. for $C_{10}H_{13}O_2N$: C 67.02; H 7.31; N 7.82). The infra-red spectrum contained the expected C=O amide band at 1 640 cm^{-1}.

A somewhat better yield of a less contaminated product than that produced in the racemic series was obtained in the following way: an anhydrous ethanol solution (50 ml), containing the active N-benzoyl-alaninol (5.0 g) and anhydrous HCl (131 mequiv.), was heated in an open flask on the steam bath for 90 min, when about half of the solvent had evaporated. Addition of ether (100 ml) and cooling overnight yielded the *dextro*rotatory *hydrochloride* of *2-aminopropyl benzoate* (3.26 g, 54 %), including material obtained from the mother liquor. A minor contamination of alaninol hydrochloride, revealed by paper chromatography as above, could be removed by repeated recrystallizations from mixtures of anhydrous ethanol and ether (1:2). A homogeneous specimen exhibited the m.p. 195°, $[a]_D^{25}$ + 21.5° (*c* 1.73, H_2O) (Found: C 55.85; H 6.48; N 6.40; Cl 16.53. Calc. for $C_{10}H_{14}O_2NCl$: C 55.68; H 6.54; N 6.50; Cl 16.44). The infra-red spectrum possessed the expected bands.

The conversion of the aminoester hydrochloride into the *levo*rotatory thiourea (VII) was performed exactly as described above in the racemic series. A product resulted which

after two recrystallizations from benzene and two from water separated in beautiful plates of *(—)-1-(2-benzoyloxyisopropyl)-thiourea* possessing the absolute configuration depicted in (VII), m.p. 122.0—122.8° (Found: C 55.48; H 5.85; N 11.71; S 13.78. Calc. for $C_{11}H_{14}O_2N_2S$: C 55.44; H 5.92; N 11.76; S 13.46). The rotation was $[\alpha]_D^{24}$ —64.3° (*c* 1.28, 96 % EtOH), compared with the value + 65.3° of benzosisymbrin-thiourea. The naturally derived and synthetic samples possessed identical UV-spectra, R_F-values and infra-red curves. Hence, there can be no doubt as to the enantiomeric relationship of the two preparations.

When equal amounts of the two antipodes were mixed and recrystallized from benzene, small prisms separated, m.p. 130°, alone or in admixture with the synthetic racemic compound. The infra-red spectra of the two preparations were identical.

Microanalyses were performed by Messrs. G. Cornali and W. Egger. The authors are grateful to the *Botanical Garden of the University of Copenhagen* for valuable help in propagating the employed seed material.

The present work is part of investigations supported by *The Danish State Research Foundation (Statens Almindelige Videnskabsfond)* and *Kai Hansen's Fond*. One of us (A.K.) wishes to express his gratitude to *The Research Council of The Technical Sciences (Det Teknisk-Videnskabelige Forskningsråd)* for the grant of an infrared spectrophotometer.

REFERENCES

1. Kjær, A. and Christensen, B. W. *Acta Chem. Scand.* **13** (1959) 1575.
2. Kjær, A. *Fortschr. Chem. org. Naturstoffe* **18** (1960) 122.
3. Schultz, O.-E. and Wagner, W. *Z. Naturforsch.* **11b** (1956) 73.
4. Ettlinger, M. G. and Lundeen, A. J. *J. Am. Chem. Soc.* **78** (1956) 4172.
5. Bellamy, L. J. *The Infra-red Spectra of Complex Molecules*, Methuen, London 1958.
6. Kjær, A. and Gmelin, R. *Acta Chem. Scand.* **10** (1956) 1193.
7. Kjær, A. and Boe Jensen, R. *Acta Chem. Scand.* **12** (1958) 1746.
8. Billman, J. H. and Parker, E. E. *J. Am. Chem. Soc.* **65** (1943) 2455.
9. Philips, A. P. and Baltzly, R. *J. Am. Chem. Soc.* **69** (1947) 200.
10. Vogl, O. and Pöhm, M. *Monatsh.* **83** (1952) 541.
11. Nagashima, Z. and Uchiyama, M. *Bull. Agr. Chem. Soc. Japan* **23** (1959) 555.
12. Procházka, Ž., Šanda, V. and Jirousek, L. *Collection Czechoslov. Chem. Communs.* **24** (1959) 3606.
13. Karrer, P., Portmann, P. and Suter, M. *Helv. Chim. Acta* **31** (1948) 1617.
14. Berlin, A. Ya. and Sycheva, T. P. *J. Gen. Chem. U.S.S.R. (Eng. Transl.)* **20** (1950) 609.
15. Kjær, A. and Christensen, B. W. *Acta Chem. Scand. In press.*

Received March 16, 1961.

ACTA CHEMICA SCANDINAVICA 15 (1961) 1485–1506

Ion Exchange Isoformation for Spectrochemical Analysis with the Tape Method

GUSTAF SUNDKVIST*

The Research Laboratory of the Boliden Mining Company, Skelleftehamn, and the Department of Analytical Chemistry of the Royal Institute of Technology, Stockholm, Sweden

A new method of treating samples to be analyzed with the tape technique is described. The sample is dissolved, and the solution is treated with cation and anion exchangers in a batch process. The dried and ground cation exchanger is spectrochemically analyzed as a powder. Different parameters of the batch process have been studied.

The tape machine, described elsewhere [1], is a device to introduce the sample in powder form into the spark gap. The tape machine gives a very high precision. High reproducibility on the same sample is, however, of little or no use if there are large systematical errors between different samples. The main sources of such systematical errors are variation in particle size, chemical and mineral composition.

These errors can be eliminated only by a pretreatment of the sample. For this type of pretreatment the new word "isoformation" is introduced. Different types of isoformations have been summarized previously [2]. The most efficient isoformation is achieved by dissolving the sample. To make it possible to use the tape technique, the solution must be converted into powder. This can be done by evaporation to dryness or by precipitation of the elements concerned. Although these methods can be used in some cases, a general method has been looked for. Isoformation by ion exchange is a result of this effort.

1. PRINCIPLE OF ION EXCHANGE ISOFORMATION

The sample is dissolved, and internal standard element and spectroscopic buffer are added. By a batch process the solution is separated into three components. The positive ions are attached to a cation exchanger, the negative ions to an anion exchanger, and deionized solution remains. The ion exchangers

* Boliden Mining Company, Skelleftehamn, Sweden.

used are chosen to have different particle size and are therefore easily separated by sieving. The cation exchanger, which contains the elements to be analyzed, is dried, milled, and analyzed with the tape method. This isoformed sample is the most perfect one for the tape method since all the ions from the sample, the internal standard, and the spectroscopic buffer are mixed on almost an atomic scale.

2. DESCRIPTION OF ONE APPLICATION. ION EXCHANGE ISOFORMATION APPLIED AT THE ORE DRESSING PLANT OF BOLIDEN IN CONNECTION WITH TAPE MACHINE AND QUANTOMETER

Prior to the detailed discussion of the development of the ion exchange isoformation one case of application is described.

2.1 Analytical situation

At the Ore Dressing Plant of Boliden there was a need for rapid and accurate analyses. The samples are sulphides of Zn, Cu, Pb, As, and Fe, or mixtures of these and rocks in any proportions. The analytical program covers contents up to 60 % and down to hundredths of a per cent. The elements to be determined are Zn, Cu, Pb, and Fe, and in some cases Bi. There are essentially three factors that have contributed to the solution of this analytical problem: ion exchange isoformation, tape machine, and direct reading spectrograph. The tape machine was previously developed, and the direct reading spectrograph used, the Quantometer, is commercially available.

2.2 Procedure

2.2.1. Weighing and solution of samples. 200 mg of the sample are weighed within $\pm$ 0.1 mg and transferred to a 400 ml beaker. The amount of sample corresponds to a max. of 5 milliequivalents (mequiv). The sample is dissolved in 4 $\pm$ 0.5 ml diluted perchloric acid (70 % acid diluted 1:1) on a hot plate. Infrared lamps are used for additional heat. The acid is added from a "whipping flask". About one minute is required for solution. Most of the acid is evaporated to near, but not complete, dryness. It is desired to evaporate as much free acid as possible, while still avoiding the formation of insoluble oxides.

2.2.2. Ion exchange. The walls of the beaker are washed with 10—20 ml deionized water. 15.00 ml internal standard solution containing 10.00 g Cd/l as perchlorate are added from a Dettker automatic pipette. This corresponds to 2.68 mequiv. The accuracy of the pipette is better than 0.1 %.

12.00 mequiv of Dowex 50 W, X-12, 200—400 mesh cation exchanger in hydrogen form are added, and the solution is diluted with deionized water to about 150 ml. The solution with ion exchanger is heated to near boiling. The amount of cation exchanger which corresponds to 12.00 mequiv is determined by titration. The amount may vary depending on residual contents of water and acetone but is normally about 3.3 g.

After some minutes 5.0 ml of 0.60 N K_2CO_3-solution, *i.e.* 3.0 mequiv, are added with automatic pipette. As the solution is strongly acidic, there is no risk of precipitation of metal hydroxides. Potassium is used as spectroscopic buffer.

In order to take care of the acid and displace the equilibrium, 20 g of anion exchanger are added. In this way the cation exchanger can take up the positive metal ions quantitatively. The anion exchanger used is Amberlite IR-45, 20—50 mesh, which is a weak base resin. The amount corresponds to about 60 mequiv, which is a rather large excess. The excess is necessary to displace the equilibrium sufficiently and to make the reaction proceed rapidly. The amount of anion exchanger is not critical, and the addition can be performed by using volume measurement. The ion exchange is complete when pH is 3.0—3.5. This can be checked with a pH paper. The procedure of ion exchange, after the addition of the anion exchanger, takes about 5 min. This time is of course dependent on the capacity of the anion exchanger and upon the completeness of the acid fuming mentioned above.

2.2.3. Separation and drying of cation exchanger. The separation of the cation exchanger is performed at the so-called "ion exchange table" (Ref.[2], Fig. 3, p. 128) *. Use is made of specially designed plastic funnels connected to a vacuum. The funnels consist of two parts — the upper part contains a 60 mesh screen of stainless steel, the lower part contains a supporting screen. Three filter papers (OB Munktell) are placed on the supporting screen and kept in position by a plastic ring. In performing the separation the upper part of the funnel is connected to the lower part. The content of the beaker is washed into the upper part. The separation is performed by a shower of deionized water (pressure 1.2 kg/cm^2). The cation exchanger passes down to the filter paper, and the anion exchanger remains on the screen in the upper part. After the separation the upper part is removed and the anion exchanger is washed down to a container. The "ion exchange table" at Boliden has twelve funnels.

The drying of the cation exchanger is done by two treatments with acetone. Each time 10 $\pm$ 1 ml of acetone are added from a "whipping flask", and a contact time of 1 min is allowed before the acetone is removed by suction. After the second treatment with acetone, air is drawn through the cation exchanger for 3 min. Since the cation exchanger and the filter papers are now dry, the cation exchanger is easily removed from the filter paper almost quantitatively. Small losses of cation exchangers can be tolerated, as every grain contains internal standard, buffering element, and elements to be analyzed, in the same proportions.

2.2.4. Grinding of the cation exchanger. The ion exchanger must be ground to be used with the tape technique. The grinding should be performed as soon as possible so that the samples, which are not in equilibrium with the content of water in the atmosphere, do not change their composition. The grinding is performed in the swingmill manufactured by Messrs. Siebtechnik, Mühlheim (Ruhr) [Ref.[2], Fig. 1, p. 128]. The mill grinds 6 samples simultaneously for 6 min. The milling can, of course, be performed in mills having only one millhouse and in that case the milling time can be reduced. The millhouse and mill-

* Figs. 2 and 3 in Ref.[2] happened to be interchanged.

bodies are made from Avesta 739 S stainless steel. As the efficiency of the mill is dependent on the amount of material to be milled, the entire sample should be transferred to the mill. If the ground sample is to be stored it should be kept in a tight plastic box. The houses and bodies are cleaned by washing with water. They are wiped absolutely dry with towels or paper.

2.2.5. Excitation, analysis, and calculation. The isoformed samples are analyzed with an ARL Quantometer and a tape machine. The excitation is accomplished with an ARL High Precision Source Unit modified to give 50 sparks per second.

The lines used are summarized in Table 1. The Cd line 2288 is strongly self reversal, but can be used as an analytical line up to about 1 % Cd. It is mainly used for checking the self absorption conditions in the spark [3]. The intensity of this Cd line is used as a parameter for correcting other self reversal lines. Calcium gives a specific contribution to the background underneath the Zn line 3345. 20 % CaO corresponds to 0.07 % Zn. The Ca line 3179 × 2 can be used as correction parameter.

Table 1. Spectral lines.

Element	Line	Ranges
Cd	I 4799.9 G	Internal standard
»	I 2288.0	0–1 % Cd
Zn	I 2138.6	0–0.7 % Zn
»	I 3345.0	0–3, 3–15 % Zn
»	I 3345.6	
»	I 4722.2 G	15–60 % Zn
Pb	I 4057.8 G	0–3, 3–15 % Pb
»	I 2663.2	15–60 % Pb
Cu	I 3274.0 × 2 UV	0–0.5, 0.5–2.5 % Cu
»	I 5218.2 G	2–10, 10–30 % Cu
Fe	I 4260.5 G	0–50 % Fe
Bi	I 3067.7 × 2 UV	0–1 % Bi
Ca	II 3179.3 × 2 UV	0–20 % CaO
Background	4116 G	

G = glass filter, UV = UV-filter

At low levels of Pb, Zn, and Fe a higher precision is obtained, if a correction is made for variations in the general background. These variations are due mainly to variation in running times. The background measured at 4116 Å is the parameter for this correction.

Tabulated fixed working curves are used and are the same for all types of products. The values obtained are corrected against standard samples, which have been treated in the same way as the samples. This must be done as a small curve drift cannot be avoided. The corrections are based on the values obtained for a low and a high standard on the same curve.

2.2.6. Standard samples made from solutions. The standard samples are made from weakly acidic perchlorate solutions. The contents have been chosen so that 15.00 ml standard solution corresponds to 200.0 mg sample. Table 2

shows the composition of the five standard solutions which are necessary and are sufficient for a complete check of all analytical lines for Zn, Pb, Cu, and Fe. The contents given in Table 2 are not the actual ones in the solution but are the contents of the corresponding 200 mg sample.

Table 2. Standard samples.

Notation	% Zn	% Pb	% Cu	% Fe	% Bi*
A	58.00	2.00	0.50	0.00	—
B	12.00	60.00	0.00	10.00	—
C	2.00	12.00	22.00	20.00	(0.50)
D	0.50	0.00	2.00	46.00	—
E	0.00	30.00	8.00	30.00	(1.00)

* For Bi a freshly prepared solution should be added separately.

2.2.7. Preparation of internal standard solution. The internal standard solution is prepared in lots of 60 liters by dissolving CdO or $CdCO_3$ in perchloric acid. The contents are determined and adjusted by titration with EDTA.

2.2.8. Purifying and drying of cation exchanger. Since the cation exchanger Dowex 50 contains some impurities, for example Fe, it has to be purified before use. Further, it must be dried in order to weigh out a definite amount to each sample. Treatment is as follows:

a) The cation exchanger is purified by treatment with 2 N HCl and oxalic acid in a batch process.

b) If the cation exchanger is Dowex 50 W instead of Dowex 50, it should be treated with an alluviation in water of extremely finely ground Dowex 2 in OH-form (0.025 % of the amount of cation exchanger). Without this treatment Dowex 50 W shows a strong "electrostatic effect".

c) The ion exchanger is dried by treatment with acetone and by suction of air through the exchanger.

d) The ion exchanger is treated in a mixer in order to make it homogeneous with respect to the residual contents of acetone and water.

The capacity of the dried cation exchanger, which is about 3.6 mequiv per gram, is determined by titration in the following way: 1 g of ion exchanger is treated with 40 ml of warm 0.1 N NaOH for 10 min. After filtration the solution (and the wash water) is back-titrated with 0.1 N H_2SO_4 using methyl red as indicator.

2.2.9. Regeneration of anion exchanger. In this particular case there are economic reasons to use the anion exchanger over and over again. It has therefore to be purified and regenerated. The purification and regeneration is performed in a 60 liters plastic jar which contains two bottoms, the upper one being a 50 mesh stainless screen. The jar has a draining tap, which can be connected to the vacuum line *via* a large suction bottle. The treatment is performed in the following steps:

a) Treatment with neutral 0.03 M EDTA solution. After a time of contact of 30 min the solution is removed by suction as completely as possible.

b) Washing with deionized water. Time of contact is 15 min.

c) Treatment with neutral 0.03 M $Ca(ClO_4)_2$ solution to remove the surplus of EDTA.

d) Washing as above (b).

e) Regeneration with 4 N NH_3. The time of contact should be at least 12 h.

f) Washing with deionized water until the wash solution is neutral.

g) After the last washing the anion exchanger is dried by drawing air through it.

The capacity of the anion exchanger is determined in the following way: 1 g of anion exchanger is treated at 100°C with 10 mequiv acid in 100 ml H_2O. After filtration the solution is back-titrated with NaOH. The capacity should not be much less than 3 mequiv/g.

2.3. Risks of contaminations at ion exchange isoformation. Since products with widely different concentration ranges are ion exchanged, ground and run at the same time, close attention must be paid to the risk of mutual contamination. The relative effect of contamination is, of course, increased due to the very large dilution of the sample with ion exchanger. Many of these risks can be eliminated by carefulness by the operator; in other cases certain steps have to be taken.

2.3.1. Funnels and millhouses. The mills and the screens of the funnels must be stainless. Screens of brass would, of course, contaminate the samples with Cu and Zn. A usual chrome steel mill cannot be used since the elements more noble than the material of the mill will be precipitated on the mill surfaces. Even when using screens and mills of stainless steel, samples of widely different composition should be treated in different funnels and different millhouses. If a high level sample of Cu, Pb or Zn is milled, the next sample will be contaminated up to about 0.03 %.

2.3.2. Water and reagents. The reagents used and the ion exchangers shall be as pure as possible with respect to the elements to be analyzed. This holds especially for the water and the anion exchanger, where the amount as well as the impurity level may vary. Distilled water from brass apparatus is not pure enough and should be purified. A suitable method is to have the distilled water pass through a filter of cation exchanger which is in hydrogen form.

2.4. Hazards with ion exchange isoformation. Attention must be paid to possible risks when working with perchloric acid. Solution and ion exchange must be performed in different hoods. Dilution with internal standard solution and water shall be performed before the beaker is moved to the second hood. The hood, where the solution is performed, must *not* contain any wood or other organic material.

The ground ion exchanger, which contains poisonous metals, is very finely divided. Therefore, good ventilation is necessary where the millhouses are emptied.

As acetone is used attention must be paid to the risk of fire.

3. DEVELOPMENT OF THE ION EXCHANGE ISOFORMATION

3.1. Column versus batch process

The ion exchange isoformation differs from conventional analytical application of ion exchange [4,5]. The ion exchange resin must contain the ions to be analyzed with the tape technique in a homogeneous mixture. Although it might be possible to obtain a homogeneous resin by milling, the column still has some serious drawbacks. If a column process is used the cation exchanger must be quantitatively recovered. To make such a recovery without losses is very difficult. The present batch process is much more rapid than the column process both in the time of reaction and the time used for recovery of the ion exchanger. As the cation exchanger is completely homogeneous, small losses can be tolerated in connection with separation, drying, and grinding. The drawback of the batch process compared to the column process is that the cations are not completely taken up by using only a cation exchange resin. However, since quantitative recovery is possible if the equilibrium is displaced by using cation and anion exchangers simultaneously, the batch process has been chosen.

3.2. Choice of cation exchanger

3.2.1. Weak and strong cation exchangers. A cation exchanger containing the strongly acidic sulphonic acid group is completely dissociated and acts as cation exchanger at all pH levels with constant capacity of exchange. For a cation exchanger with weakly acidic groups the ion exchange equilibrium is coupled to a protolysis equilibrium. Such an ion exchanger does function only in neutral or alkaline solution.

A weak cation exchanger is unsuitable since no exchange occurs until the anion exchanger has taken up or eliminated the excess acid of the solution. Besides the fact that the ion exchange takes a long time, this means, losses of cations.

The possibility of obtaining Dowex 50 in hydrogen form and in different particle sizes and with different crosslinkings has significantly influenced the choice of this cation exchanger. The strongly acidic cation exchangers have good thermal stability and can stand 100°C even in acidic solutions.

3.2.2. Choise of grain size and crosslinking. The grain size has been chosen to be 200—400 mesh for reasons which shall be mentioned later in connection with the choice of anion exchanger. The crosslinking is not critical. Too high a crosslinking (X-16, 16 % divinyl benzene) makes the reaction slower. Too low a crosslinking (X-4, 4 % divinyl benzene) makes drying with acetone more difficult. X-12 with 12 % crosslinking has been chosen without any special investigation. X-8 is presumably equally well suited.

3.3. Cation exchange

3.3.1. Equilibrium and affinities of the cation exchange. In treating, for example, a cation exchanger in hydrogen form with a solution containing metallic ions, an equilibrium is established between the positive ions of the solution and those of the ion exchanger.

$$\underline{R \cdot SO_3^- H^+} + Me^{n+}/n \rightleftharpoons \underline{R \cdot SO_3^- Me^{n+}/n} + H^+ \quad (1)$$

where Me^{n+} are the metal ions. Although the different types of cation exchangers have different affinities for different cations the equilibrium is never quantitatively displaced in one or the other direction.

3.3.2. Displacement of the equilibrium by dilution. The ion exchange equilibrium is a Donnan equilibrium.

Using concentrations an equilibrium constant $K_{H^+}^{Me^{n+}}$ can be defined in the following way. R refers to the ion exchange phase and S to the water phase

$$\frac{[Me^{n+}]_R}{[H^+]_R^n} = \frac{[Me^{n+}]_S}{[H^+]_S^n} \times K_{H^+}^{Me^{n+}} \quad (2)$$

This formula shows that multivalent ions are more efficiently taken up at a higher dilution.

Investigations have been performed that show that an uptake above 90 % of multivalent ions can be obtained by using only cation exchanger, if the dissolved sample is fumed to near dryness and the capacity of the ion exchanger is not utilized to more than 50 %.

Although the dilution technique could be used in some cases, especially at low concentrations where a rather large relative error up to 10 % could be tolerated, it is not a satisfactory procedure in most instances. First of all this technique could not be used for monovalent ions. Furthermore, according to the formula (2) the amount of uptake of a certain ion varies with the following parameters: excess acid in the solution, excess capacity of the ion exchanger, and chemical composition of the sample.

3.3.3. Displacement of the equilibrium by removal of hydrogen ions. The equilibrium (1) is displaced completely to the right, if the hydrogen ions or other corresponding ions originally in the cation exchanger are removed from the equilibrium in some way. General methods can be based only on the use of cation exchangers in hydrogen form. The following more or less special methods can be used.

a) The equilibrium is automatically displaced if the sample is or can be transformed to salts (oxides, hydroxides, carbonates) of weak uncharged acids (water, carbonic acid). An example of such a technique is the use of K_2CO_3 solution for the addition of spectroscopic buffer.

$$2\,R{\cdot}SO_3^- H^+ + 2\,K^+ + CO_3^{2-} \rightarrow 2\,R{\cdot}SO_3^- K^+ + H_2O + CO_2 \quad (3)$$

b) Neutralization with an anion base and similtaneous precipitation of its counter cation as a very insoluble salt of the anion of the sample. For ion exchange of a sample containing no other anions than SO_4^{2-} it might be possible to titrate with $Ba(OH)_2$ to a point where all sulphuric acid is precipitated as $BaSO_4$.

c) Neutralization with an anion base or neutral base whose corresponding cation or formed cation acid cannot react in the cation exchange due to its size.

The cases (a) and (b) are special ones and very difficult to perform. A precipitation of metal carbonates is often incomplete and a filtration is necessary. A titration as in case (b) is also tedious. The case (c) has made possible a more general method by using strongly or weakly basic anion exchangers. The hydroxyl form or carbonate form of a strong anion exchanger contains the anion bases OH^- and CO_3^{2-}, respectively, whose corresponding cations are fixed in the carbon skeleton of the anion exchanger. The cations formed by protolysis of the uncharged amino groups of a weak anion exchanger are also firmly bound. The advantages of this method of equilibrium displacement is that it is universal and simple. The amount of added anion exchanger is not critical. With a surplus of anion exchanger the outer solution can, at the most, become neutral and never alkaline, and therefore hydroxides and basic salts normally are not precipitated.

3.4. Complete deionization of the solution by using both cation and anion exchangers

3.4.1. The displacement of the equilibrium using strongly or weakly basic anion exchangers. A strongly basic anion exchanger contains positively charged quaternary ammonium groups in a network polymer. Furthermore, it contains displaceable negative ions as, for example, chloride ions. It is completely dissociated at all pH levels and acts therefore as an ion exchanger in both acidic and basic environments. It can bind anions of both strong and weak acids. When used to deionize solutions, a strong anion exchanger should be in hydroxyl or carbonate form. CO_3^{2-} and OH^- combine with H^+ forming volatile CO_2 and H_2O respectively. The equilibrium (1) is therefore quantitatively displaced to the right.

In the case of weak anion exchangers, a protolysis equilibrium exists together with the ion exchange equilibrium. The ion exchanger in the base form contains free amino groups, which can bind hydrogen ions by protolysis. Electroneutrality is obtained through the fact that the acid anion is bound as counter ion. Accordingly, a weak anion exchanger acts as an acid uptaker when deionizing solutions:

$$R{\cdot}NH_2 + H^+ + ClO_4^- \rightleftharpoons \underbrace{R{\cdot}NH_3^+ \; ClO_4^-} \qquad (4)$$

The equilibrium is strongly displaced to the right in acidic solutions (up to pH 3—4).

3.4.2. Choice of anion exchanger. Weak versus strong anion exchangers. As the ion exchange is performed in acidic or neutral solutions, there are no principal reasons for choosing one or the other type. The choice of IR-45 in the Boliden application is mainly due to practical and economic considerations. As will be shown later, a strong anion exchanger should be preferred when analyzing monovalent cations.

The following anion exchangers have been investigated: Amberlite IR-4B, IR-45, and IRA-400, and Dowex 2. When choosing a suitable anion exchanger, the following factors have to be considered: losses in the final solution, losses in form of complexes on the anion exchanger, losses as precipitates, ease of

regeneration, thermal and mechanical stability, capacity, speed, electrostatic properties, and shape of grains. None of the above mentioned anion exchangers have optimum properties in all these respects and the choice is therefore a question of the best compromise.

The losses during ion exchange are discussed in detail later on. Here a summary is given of the considerations that have influenced the choice of anion exchanger in this special case. When analyzing only multivalent ions, as in the Boliden program, it is possible to reduce the losses to a negligible level when using a weak as well as a strong anion exchanger.

In the particular application described above the anion exchanger has for economic reasons to be regenerated and used several times. In respect of regeneration the weak anion exchanger has an advantage since it loses its ion exchange property due to protolysis in an alkaline solution and therefore completely gives off the acid. The regeneration can, in this case, be performed with ammonia. The equilibrium of regeneration of a strong anion exchanger is not equally strongly displaced and this type of anion exchanger is therefore more difficult to regenerate. Also the costs of chemicals are greater.

The thermal stability is different for different anion exchangers. The weak anion exchanger IR-45 has the best thermal stability and can stand 100°C without noticeable loss of capacity. Dowex 2 and Amberlite IRA-400 in OH^--forms cannot stand temperatures higher than 40°C and 60°C respectively, but at those temperatures they are almost as rapid as IR-45 at 100°C. The fact that it in practice is much easier to maintain a working temperature of 100°C than 40 or 60°C makes the use of IR-45 more attractive. According to our experience it has also shown very good mechanical stability. Because of the round form of the grains, IR-45 is easily sieved. A drawback of Amberlite IRA-400 compared to Dowex 2 and IR-45 is that this anion exchanger has a strong electrostatic affinity to the cation exchanger Dowex 50, which makes the separation more difficult.

Since the losses at the ion exchange can be kept within tolerable limits, the choice of IR-45 for the actual analytical programs is based mainly on the practical considerations discussed above.

3.4.3. Some considerations on the time required for the ion exchange. Choice of a mixed bed performance. When ion exchange isoformation is to be used for routine analysis it has to be as rapid as possible. If the anion exchanger is kept separate within a fabric container the time for ion exchange will require several hours.

This time can be reduced to about 5 min using a mixed bed performance. The cation and anion exchangers must then be separated after the ion exchange for the following reasons:

a) If the analysis is performed on a mixture of cation and anion exchanger the sensitivity is greatly reduced.

b) The matrix of the sample will not be defined, since the amount of acid varies.

c) The anion exchanger can be used several times.

The most convenient method of separation of the exchangers is sieving and therefore the exchangers must have different grain sizes. A coarse anion exchanger and a fine cation exchanger have been chosen in order to facilitate

the recovery and regeneration of the anion exchanger. The performance of sieving and drying becomes more practical when the anion exchanger remains on the screen. Undissolved gangs which are finely divided follow the cation exchanger and do not contaminate the anion exchanger.

The anion exchanger has been chosen with grain sizes 20—50 mesh, the cation exchanger 200—400 mesh. The sieving is performed with a 60 mesh stainless screen.

In addition to the influence of the preciously mentioned conditions, the speed of the ion exchange is influenced by the following factors: temperature, stirring, dilution, and amount of anion exchanger. The temperature should be as high as the stability of the exchanger allows, which means that the ion exchange should be performed at 100°C when IR-45 is used. While boiling, a certain amount of stirring also results. A small volume and a large amount of anion exchanger increase the speed but also increase the loss of ions.

The ion exchange can be interrupted at pH 3—3.5 (checked with a pH paper).

3.4.4. The degree of utilization of the cation exchanger. The capacity of the cation exchanger shall be utilized to as high a degree as is possible with regard to the consequences of the equilibrium equation (2) for a quantitative ion exchange (3.5.) and with regard to the maximum content of milliequivalents in the sample. To keep the cost low the amount of cation exchanger should be as small as possible. A limit however, is set by the fact that the weighed sample has to be large enough to cancel out possible nonhomogeneities of the sample and to allow sufficiently accurate weighing. It is not possible to take aliquots in the presence of precipitates as, for instance, $PbSO_4$. In the Boliden program it is considered most practical to have a constant amount of sample, 200 mg, for all types of samples and a constant amount of cation exchanger corresponding to 12.00 mequiv. Including internal standard and buffer, the capacity of the ion exchanger is utilized up to between 80 and 90 %, the charges on the metal ions being assumed to be the same as their valency.

This is not valid under all circumstances. For multivalent ions a higher value of the nonutilized capacity than the one theoretically expected is obtained by titration. The explanation might be that the water molecules, which coordinate around these ions split off hydrogen ions to a certain degree. Thus, the water complexes of the metal ions have a lower charge and consequently occupy fewer sites in the exchanger.

Moreover, the situation is probably that the redistribution of the charges on the ions does not occur before almost all hydrogen ions have disappeared from the cation exchanger, which is not the case at pH 3.5 according to the equilibrium (2). A good measure of the nonutilized capacity is obtained in the following way: The cation exchanger from the ion exchange is titrated with KOH by successive additions of, for example, 0.1 mequiv. After each addition a few grains of the cation exchanger are taken out of the reaction vessel and placed on a filter paper. 1 drop of neutral $Ca(ClO_4)_2$ solution containing a suitable amount of methyl orange is added. Hydrogen ions are liberated at the test only by ion exchange between Ca^{2+} ions and possibly remaining H^+ ions. A relatively sharp color change is generally obtained (the red color does not appear), when all hydrogen ions are titrated. When the cation exchanger

contains much iron the point of change is, however, not sharp. The ion exchanger is obviously buffered by the system $Fe(OH)^{2+}aq \rightleftharpoons Fe(OH)_2^{+}aq + H^+$. Estimating the average charges on the Fe ions at + 1.4 and using the normal charges for Zn, Cu, Pb, Cd, and K, a very good agreement is obtained between titrated and calculated values.

3.5. Sources of error during ion exchange. In a perfect isoformation by ion exchange all the metal ions should be 100 % on the cation exchanger. However, losses outside the resins in the form of precipitates and on the anion exchanger in the form of complexes or hydrolyzed products contribute to inaccuracy of the analysis. The losses due to complexes are the most severe. In general, it is possible to reduce them to a negligible level by taking certain steps. Furthermore, it should be remembered that it is the variation in losses that contributes to the errors and therefore the conditions of the ion exchange from sample to sample should be kept as constant as possible.

3.5.1. Losses in the solution. Such losses can be due to the following factors: Insufficient capacity of the cation exchanger, noncharged soluble complexes, too low final pH.

After the separation of the ion exchangers it is possible to check that the capacity of the cation exchanger has been sufficient by placing a few grains of the cation exchanger on a pH paper wetted with a $Ca(ClO_4)_2$ solution. The paper shall indicate a strongly acidic reaction as the Ca^{2+} ions displace the excess hydrogen ions.

Noncharged complexes can, of course, occur in the solution at the beginning, but they are, in general, dissociated rapidly due to the displacement of the equilibrium.

Losses due to the final pH being too low are, of course, largest for monovalent ions. Assuming equation (2) valid, the relative loss of ions due to incomplete deionization of the solution is

$$F = \frac{10^{-n \cdot pH} \cdot v}{K \cdot E\,(1-x)^n} \tag{5}$$

where F = loss
v = volume of water phase
E = total capacity of cation exchanger in milliequivalents
x = the degree of utilization of the cation exchanger
y = the part of the total capacity occupied by the monovalent metal ion
K = selectivity constant in relation to the hydrogen ion

The parameters which affect the losses in the solution are as follows: volume of solution in relation to amount of cation exchanger (v/E), degree of utilization x, valence n, factor of selectivity K, and pH of the solution.

According to (5) the value of (v/E) should be as low as possible. As total losses must be considered and as the losses on the anion exchanger increase when the volume decreases, there is an optimum value for the volume, the other conditions being constant and the kinetics disregarded for the moment. It should be remembered that the effect of dilution is different when only cation exchanger is used and when cation exchanger is used in combination with a

weak anion exchanger. A weak anion exchanger constitutes a buffer system and therefore the pH of the solution is almost independent of the dilution. When a weak anion exchanger is present, the losses in the solution increase with dilution. On the other hand, these losses decrease for a multivalent ion when no anion exchanger is present.

The losses in the solution are strongly dependent upon the degree of utilization when x approaches 1. The losses of a monovalent ion increase 10 times when x increases form 0 to 0.9 and of a divalent ion 10^2 times. From the point of view of the spectrochemical sensitivity x should be as high as possible. When x is 0.8 there is, however, not very much more to be gained in this respect.

The losses in the solution are influenced exponentially by the valence n and the pH of the solution. If the hydrogen ion concentration is decreased, for instance, 100 times, the concentration of another monovalent ion is decreased to the same extent but of a divalent ion 100^2 times. Using a strong anion exchanger the end pH obtained is close to the neutral point and a complete deionization is therefore obtained even for monovalent ions. When using weak anion exchangers as IR-45 the end pH will be 3.5, if the total amount of anions in the solution to be deionized corresponds to 30 % of the original capacity of the ion exchanger. Using a weak anion exchanger the end pH is dependent on the ratio, base form/acid form, in conformity with the formula for a solution buffer system:

$$\mathrm{pH} = \mathrm{p}K_s + \log \frac{[\text{base}]}{[\text{acid}]} \tag{6}$$

From this formula it is obvious that the anion exchanger ought to be as completely regenerated as possible. Furthermore, an excessive amount should be used so that the base form predominates, even when the ion exchange is finished.

The losses in the solution can be neglected in the case of multivalent ions. The choice of suitable solution volume during ion exchange is therefore in this case determined primarily by the losses on the anion exchanger and by the kinetics of the reaction. By choosing suitable conditions, it is possible to keep the solution losses of monovalent ions, too, at a sufficiently low level, even when a weak anion exchanger is used. This is especially true for Ag, which has a factor of selectivity of 18. In this case, however, other complications prevent the use of a weak anion exchanger.

3.5.2. Losses in form of precipitates which are not dissolved by the ion exchangers. This is a problem only for the few monovalent ions (Ag^+, BiO^+) that form insoluble precipitates. Precipitates of multivalent ions are relatively easily dissolved by the ion exchangers. The combination strong cation exchanger — strong anion exchanger is the most efficient one.

The important factors when considering losses in form of precipitates are end pH, the degrees of utilization of cation and anion exchangers, valence, and, of course, solubility product. Kinetics also play a most important role.

Insoluble precipitates might occur originally in the solution or be formed during the ion exchange. Examples of the first case are lead sulphate and silver chloride, which can be formed when dissolving sulphides. Examples of the

second case are the basic salts, which can be precipitated as well within the anion exchanger as in the solution. This latter case has been observed with bismuth.

If the anion exchanger contains chloride ions, which often is the case with a strong anion exchanger which is delivered in the chloride form and is very difficult to purify from residual chloride ions, then AgCl is precipitated within the anion exchanger and the precipitate cannot be dissolved in a reasonably short time. When a weak anion exchanger is used losses of the same type can occur on account of chloride ions in the solution or in the anion exchanger. It is, however, difficult to study these losses in the case of a weak anion exchanger since other types of losses more predominant occur at the same time.

Precipitates of $PbSO_4$ are no problem. The amounts of Bi to be determined at Boliden are less than 0.50 % in the samples corresponding to less than 1 mg in the cation exchanger. At these concentrations there are no difficulties, since the total losses in the solution and in form of $BiOClO_4$ are less than 2 per cent of the amount present.

If the amount of Bi is larger than around 60 mg, $BiOClO_4$ is precipitated when adding the anion exchanger.

3.5.3. Losses in form of complexes on the anion exchanger. The losses on the anion exchanger can be of the following types:

1) Losses due to precipitations. This has already been treated in 3.5.2.

2) Losses due to cations complexed directly to the active centers within the anion exchanger.

3) Losses due to negatively charged complex ions, which are bound in the same way as other anions.

Losses of the second type occur only on a weak anion exchanger and are due to the property of the amino group of complexing a positive metal ion in conformity with its ability to complex the hydrogen ion, *i.e.* to be protolyzed.

$$RNH_2 + H^+ \rightleftharpoons RNH_3^+ \tag{7}$$

$$RNH_2 + Ag^+ \rightleftharpoons RNH_2Ag^+ \tag{8}$$

By complex binding, the N-atom utilizes its ability to form a fourth electron pair bond with help of its free electron pair. On a strong anion exchanger, on the other hand, the N-atom is already bound to four other atoms by molecule bonds, and therefore the N-atom cannot act as a donor of electron pairs binding positive metal or hydrogen ions. The magnitude of the losses due to complexes directly on the anion exchanger can be expected to depend on the following factors: the valence, the magnitude of the stability constant of the complex, the degree x of utilization of the cation exchanger, the pH of the solution according to (2), the amount of anion exchanger (number of milliequivalents), and the ratio (acid/base) of the anion exchanger. Some of these factors are dependent on each other to some extent.

In addition to the above mentioned factors, the kinetics certainly play a role. The kinetics are influenced by the volume, the way of adding the anion exchanger, and the relative speeds of the exchangers. The number of multivalent ions present in the solution when adding the anion exchanger is depen-

dent on the volume of the solution and therefore the volume affects the kinetics. Furthermore, losses of multivalent ions are smaller if the anion exchanger is added in several portions. This is due to the square influence of the hydrogen ion concentration according to (2), the smaller amount of the base form in the first portion of added anion exchanger, and the irreversibility of the binding of metal ions to the amino groups. That such an irreversibility exists is obvious from the fact that the cation exchanger is not contaminated, when using an anion exchanger containing considerable amounts of such complexes. When such an anion exchanger is used, the amount of anion exchanger should, however, be added in one portion. At an excess of acid there is a protolysis even of the amino groups to which the metal ions are bound, resulting in elutriation of the metal ions. A third kinetic factor is the speed of the cation exchanger versus the speed of the anion exchanger. The cation exchanger is much more rapid than the anion exchanger, as it should be. Also, the cation exchanger is added before the anion exchanger.

Losses of the third type, *i.e.* in the form of negative complex ions may occur on a weak anion exchanger as well as on a strong one, but seem to occur to a larger extent in the latter case.

Besides the properties of the type of anion exchanger used and the factors influencing the first type of complex losses, there is essentially one additional factor affecting the losses due to negative complex ions. The concentration of the complex-forming anion in the solution and in the anion exchanger is of very large importance.

Complex ions can be assumed to be taken up on the anion exchanger in two different ways. Complex ions already in the solution are taken up by the anion exchanger or complex ions are formed within the anion exchanger due to combination of positive metal ions with anions already present in the anion exchanger. The losses in the two cases are

$$f_1 = k_1 \cdot C_{Me^{n+}} \cdot C^m_{A^-(S)} \cdot M_A \tag{9}$$

$$f_2 = k_2 \cdot C_{Me^{n+}} \cdot C^m_{A^-(R)} \cdot M_A \tag{10}$$

$MeA_m^{(m-n)-}$ is the composition of the complex, $C_{A^-(S)}$ is the concentration of the anion in the water phase, $C_{A^-(R)}$ is the concentration in the anion exchanger, and M_A is the amount of anion exchanger.

If $n > 1$ then $C_{Me^{n+}}$ is strongly dependent on pH and accordingly on the volume of the solution, when adding the anion exchanger. The same is valid for $C_{A^-(S)}$ and even to a greater extent for $C^m_{A^-(S)}$. By addition of the anion exchanger in several portions, the hydrogen concentration is reduced in steps. In this way the total losses can be diminished substantially.

The influence of the above mentioned factors is shown in Tables 3 and 4, which summarize some of the investigations made. All the investigations in Table 3 have been performed by solution and ion exchange of the same sample (22 % Cu, 14 % Zn, 23 % Fe, 5 000 ppm Ag). Deviations from the normal procedure are indicated in the table. 5 + 15 indicates that 5 g of anion exchanger have been added first and the rest after 5 min at 100°C. Dowex 2 was originally

in the chloride form, but it has been partially converted to the carbonate form by regeneration with 2 N Na_2CO_3 solution. In the investigations reported in Table 4, the ion exchange was performed on pure perchlorate, chloride, and nitrate solutions of the ions concerned (10 mequiv). Internal standard and buffer have not been added in this case. Except for this, the ion exchange was performed in the usual way.

The losses have in all cases been determined by elutriation of the anion exchanger with 150 ml 1 N $HClO_4$, fuming of the acid, and repeated ion exchange.

Table 3. Ion exchange of Cu concentrates under different conditions. $x \sim 0.75$. Losses on the anion exchanger.

Investigation number	Volume	Anion exchanger		Losses on anion exchanger, % of total amount			
		Type	g	Cu	Zn	Cd	Ag
1	50	IR-45	20	0.7	0.5	0.7	25
2	150	»	20	0.5	0.3	0.3	20
3	150	»	5 + 15	0.3	0.2	0.2	20
4	50	Dowex 2, CO_3^{2-}, Cl-form	20	2.1	2.3	2.5	>50
5	150	»	20	0.7	0.6	0.7	>50
6	150	»	5 + 15	0.5	0.4	0.5	>50

Table 4. Ion exchange of pure solutions of Cu, Pb, Zn and Cd in the form of chlorides, perchlorates, and nitrates. $x = 0.85$. Losses on the anion exchanger (IR-45).

Investigation number	Acid	Losses on anion exchanger, % of total amount			
		Cu	Zn	Pb	Cd
1—4	HCl	1.8	1.9	0.15	1.4
5—8	$HClO_4$	1.7	1.3	0.15	0.5
9—12	HNO_3	2.0	1.0	0.15	0.4

The results show that, at the conditions chosen, there are great difficulties with silver, but that the losses of the other ions are small. The final error of the analysis is dependent on the variation in these losses, which is still smaller. Table 4 indicates also that the losses in form of negative complex ions are relatively unimportant on a weak anion exchanger, the difference between different counter ions being comparatively small. The larger losses reported in Table 4, compared to those in Table 3 are explained by the fact that $(1-x)^2$ is about 3 times less.

In the following a summary is given of the steps that should be taken in order to reduce the total losses on the anion exchanger:

a) The anions of the solution should have as small a tendency as possible to complex the metal ions. This is especially important when using a strong anion exchanger. The perchlorate ion is best in this respect.

b) The anion exchanger shall not contain complex-forming anions as, for instance, chloride ions to any great extent. In conformity with (a) this holds especially for a strong anion exchanger.

Although, complex-forming anions cannot be completely avoided, the losses can often be reduced to a negligible level in the following ways:

c) The volume of the solution should be as large as possible. The limit is indicated by the increased time of ion exchange.

d) The anion exchanger can be added in several portions. When an impure weak anion exchanger is used, attention should be paid to possible elutriation of metal ions during the first step.

e) The degree of utilization of the cation exchanger can be reduced. This is the most efficient of the last three factors. By a relatively small sacrifice of spectrochemical sensitivity it is possible to reduce the losses to the order of 0.1 %.

3.6. Choice of procedure of solution. When applying the described isoformation method the sample always has to be dissolved by acids, an alkaline fusion technique introducing excessive amounts of alkali ions. In the Boliden Ore Dressing Plant application, solution with perchloric acid has been chosen mainly for the following reasons.

a) The solution is rapid (ready in 2 min).

b) The perchlorate ions do not complex the metal ions.

c) The formation of free sulphur is avoided. Free sulphur is known to give losses due to inclusions.

d) An essential part of the sulphur content vanishes as gaseous sulphur chlorides [6]. As not all sulphur is transferred to sulphate, the lead ions have a larger solubility. Table 5 shows the amount for different types of products. Solution and fuming were performed in a 400 ml beaker.

Table 5. Formation of sulphate when dissolving sulphide products.

Product	Acid	Amount of sulphate obtained	
		mg	% of theoretical amount
Zn concentrate, 200 mg	4 ml $HClO_4$ (1:1)	9	5
Cu concentrate, 200 mg	»	13	6
Pb concentrate, 200 mg	»	6	4
FeS_2 concentrate, 200 mg	»	35	12
» 200 »	2 ml $HClO_4$ (70 %)	50	17
» 200 »	Br_2 + 3 ml HNO_3 (conc.)	300	100

Free sulphur is obtained when dissolving with aqua regia. The formation of free sulphur can be avoided by dissolving with Br_2 (wetting of the sample) and nitric acid. This solution procedure is inconvenient and furthermore the sulphide is quantitatively converted to sulphate as seen in Table 5. The most convenient solution is obtained with perchloric acid (70 % acid, diluted 1:1).

The recommended use of $HClO_4$ does not exclude the use of other common acids such as HCl, HNO_3, HF, or H_2SO_4. However, at least when using a strong anion exchanger it is advantageous to fume with perchloric acid after dissolving with one of the volatile acids. If it is necessary to have a complex-forming anion to keep the metal ion in solution a weak anion exchanger should be used, possibly added in portions, and the cation exchanger should be utilized to less than 50 %.

3.7. Drying and milling of the cation exchanger. Prior to the analysis with the tape method the cation exchanger has to be dried and milled. The drying cannot be performed with heat as the cation exchanger is not stable and metallic oxides will be formed on its surfaces. It is performed with acetone and by drawing air through the exchanger. The air humidity should be relatively constant and preferably not to high. When drying is done in this way the milling has to be performed in inert mills. It should be remembered that the cation exchanger, even when dried, acts as an electrolyte. Therefore, the noble metals as, for instance, Cu are precipitated on the surfaces of a Cr 13 steel mill in agreement with the electromotive force series.

Our experience has shown that mill house and bodies of Avesta 739 S steel is the best compromise between nobility and hardness. This steel contains molybdenum. That this steel is sufficiently noble is demonstrated by the fact that even Ag is not precipitated.

When using Cr 13 steel mills, the amount of precipitated Cu varies and may reach several per cent of the amount present. By a rather complicated procedure of drying it is, however, possible to avoid these losses of Cu when milling in a Cr 13 steel mill. In principle, this is done by neutralizing the residual hydrogen ions of the cation exchanger with a $C_2H_5OH-NH_3$ mixture after removing most of the water.

The more noble molybdenum steel is, however, definitely to be recommended when the samples contain noble metals because of the much simpler procedure of drying. A hard chrome-plated mill would probably be the best solution.

The time of milling is not critical but should be kept constant.

3.8. Spectroscopic buffer. At the Boliden Ore Dressing Plant application, an inner buffer has been chosen, which means that the buffering element is added to the solution and sticks to the cation exchanger in the same way as the elements to be analyzed and the internal standard. Having a high equivalent weight and a low ionization potential potassium has been chosen as buffering element. It is also possible to use an outer buffering substance added at the milling. In this case the buffering element will not utilize any of the capacity of the cation exchanger. The only compounds containing alkali which can be used as outer buffer are the feldspars, since the ions of the buffering substance must be strongly bound so that no ion exchange can occur at the milling. This alternative procedure of buffering has been rejected for two

reasons. In the first place it is very difficult to obtain a pure feldspar. Most of the natural feldspars contain, among other things, lead. Secondly, there will be too great wear on the mills made of 739 S steel.

3.9. Pretreatment of the cation exchanger. With regard to the purifying, drying, and titration of the cation exchanger before its use there is nothing to be added to the description of the procedure.

When using Dowex 50 W a surface treatment of the cation exchanger must be performed. Dowex 50 W is less fluid than Dowex 50 after the drying with acetone and sticks together making it difficult to weigh and mix. It has been observed that Dowex 50 W obtains the same fine properties as Dowex 50, if not better, by treatment with an alluviation in water of a very small amount of extremely finely ground anion exchanger in base form.

The sticky property of the resin grains is due to hydrogen bonds. The difference between Dowex 50 W and Dowex 50 must be that the latter has much fewer sulphonic acid groups on the surface. The substitution of metal ions for hydrogen ions occurs homogeneously throughout the whole grain. The anion exchanger on the other hand cannot penetrate the cation exchanger and neutralizes therefore only the sulphonic acid groups on the surface.

3.10. Regeneration and purifying of the anion exchanger. The purifying and regeneration of the weak anion exchanger IR-45 is described in 2.2.9. This treatment is of course done especially to conform to that analytical program.

The impurities are partly in the form of cation exchanger containing metal ions, partly in the form of complexes on the anion exchanger. It can never be taken for granted that the separation of the cation and the anion exchanger is completely accomplished. Therefore, to avoid contamination, the metal ions must be removed from the cation exchanger. The metal ions, which are held on the anion exchanger as complexes do not interfere if they are not elutriated under the conditions used at the ion exchange. It is possible to purify the anion exchanger completely by treatment with a surplus of acid. The cost of chemicals will, however, in this case be relatively high due to the large amount of acid used and due to the about four times larger amount of NH_3 required for the regeneration since the anion exchanger after the acid treatment is completely in its acid form. For the above reasons, the acid treatment has been excluded as a procedure for purifying in this application.

The most efficient way of removing the cations from a cation exchanger is to treat the exchanger with an agent which forms strong complexes with the metal ions. Since the stability constants of the metal complexes of EDTA are of such magnitude that EDTA can be used for titration of metal ions, it can be expected that this complexing agent should be very efficient even when not used in a large excess. Cu, Zn, Pb, and Cd are the most important elements to be removed. Cu, Zn, and Pb have to be determined at high as well as low levels and from a practical point of view it is inconvenient to keep the anion exchangers which are used at different levels separated. Iron is to be determined only at relatively high content and the demand for accuracy is less. In any case, the accuracy of the Fe determination is limited by the fact that a steel mill is used.

In the investigation reported in Table 6 150 mg cation exchanger (200—400 mesh) containing metal ions was mixed with 100 g pure anion exchanger (20—50 mesh). The mixture was treated with EDTA solution after which the cation and anion exchangers were separated by sieving and the cation exchanger analyzed spectrochemically.

Table 6. Purifying of the anion exchanger IR-45.

Investigation number	Treatment	Time min.	Relative amounts				
			Cu	Zn	Cd	Pb	Fe
Untreated cation exchanger			100	100	100	100	100
1	100 ml 0.03 M EDTA	5	1	1	1	1	50
2	»	25	<1	<1	<1	<1	50
3	100 ml 0.03 M EDTA + 2 ml conc. NH_3	25	<1	<1	<1	50	50

Obviously it is not possible to remove the lead ions from the cation exchanger by simultaneously stripping with EDTA and regenerating the anion exchanger with ammonia. The treatments have to be performed in different steps. The treatment with EDTA is performed in neutral solution and the surplus of EDTA is complexed by adding a neutral $Ca(ClO_4)_2$ solution.

It has been observed that only part (~ 30 %) of the metal ions bound to the amino groups of the anion exchanger are removed by this procedure of purifying and regeneration. This degree of elutriation is, however, sufficient to keep the content of metal ions in the anion exchanger within tolerable limits. Investigations have shown that these metal ions are not stripped off during the ion exchange if an excess of anion exchanger is added. As the concentrates are only a small part of the whole analytical program the risks of contamination are small even when the anion exchangers are mixed.

4. DISCUSSION OF RESULTS OBTAINED

When estimating the overall accuracy of the method, random as well as systematic errors must be considered. Errors at the ion exchange process, the excitation, and the recording should be included. The first of these sources of errors has already been discussed in detail, and the errors have been shown to be very small at the conditions chosen.

Disregarding the errors at the solution of the samples it is possible to test the method with respect to precision as well as accuracy with the use of synthetic solutions. The ion exchange isoformation method is therefore independent of chemical analyses of reference samples, which is not the case with conventional spectrochemical methods. Dissolving with perchloric acid the errors

associated with the solution procedure are small as no free sulphur is formed which might contain inclusions. Further, the losses due to volatilization are negligible, which has been checked by repeated fuming.

The precision obtained at different levels is shown in an earlier paper (Ref.[3], Table 1).

The systematic errors are of two types, absolute errors due to influence from coincidences or specific backgrounds, and relative errors due to variation in relative sensitivities. The first type of error has been reduced to a large extent by using the most sensitive spectral lines as analytical lines at the lower concentration ranges. The small errors of this type, which might remain, can be corrected in a satisfactory way. Although these sensitive lines are strongly self absorbing, they can be used successfully because of the great dilution of the sample.

In this application the relative errors are very small, and it is found possible to use only one working curve for each analytical line independent of the matrix. Some results are presented in an earlier paper (Ref.[2], Tables 1, 2).

5. OTHER APPLICATIONS OF ION EXCHANGE ISOFORMATION

Although the investigation described above was made primarily with respect to a special analytical program, the method has, of course, many other applications. It can be used for all the elements, that form positive ions and have suitable spectral lines.

Ion exchange isoformation can be applied to the following elements: Li, Na, K, Rb, Cs, Cu, Ag, Be, Mg, Ca, Sr, Ba, Zn, Cd, Hg, Al, Sc, Y, La, Ga, In Tl, rare earths (if the sensitivity is sufficient), Sn(II), Pb, Sb(III), Bi, Cr, Mn, Fe, Co, and Ni. In the case of all these elements, the losses at the ion exchange can be reduced to the order of 0.1 %. To this group of elements uranium and thorium can be added. They are taken up to the same extent but do not have sensitive lines. Vanadium(V) goes to the cation exchanger after reduction, for example, with ascorbic acid. The losses might be somewhat larger in this case (around 1 %).

In the case of all the elements mentioned above except Ag, a weak anion exchanger can be used. For Ag a strong anion exchanger, substantially free from chloride ions, is necessary.

The alkali metal ions suffer no complex losses on the anion exchanger. The losses in the solution are negligible when using a strong anion exchanger, but even in the case of a weak anion exchanger these losses are easily reduced below 1 %.

The alkaline earth metal ions are the most ideal ones, the losses in as well solution as anion exchanger being negligible at all conditions.

Fe, Cr, and the third group metals (especially Al) can be lost in the anion exchanger in the form of negatively charged hydroxo complexes or uncharged precipitates.

Attention must be paid to the fact that the commercially available ion exchangers often contain Al, Ca, and Mg and have to be purified.

In the case of Sn(II) and Sb(III) a complex-forming counter ion is required to keep the metal ions in solution, and a weak anion exchanger is therefore definitely to be preferred.

For the rest of the ions mentioned above it is in principle possible to use either a weak anion exchanger or a strong one.

In this general field of application attention should be paid to some inter-element effects. In most cases they can be reduced to a negligible level by choice of suitable internal standard elements.

The ion exchange isoformation method has its universal range of application as a pretreatment method for the tape technique. In special cases, however, it can be used also in X-ray fluorescence. In this case a complete isoformation is achieved with respect to particle size and structure. It is not possible to eliminate the influence from the matrix by referring to only one internal standard. Furthermore, the sensitivity is in general too low.

Acknowledgements. The author in indebted to Dr. Axel Johansson (Assoc. Professor of the Department of Analytical Chemistry of the Royal Institute of Technology, Stockholm) and to Dr. Allan Danielsson (The Boliden Mining Company, Skelleftehamn) for valuable discussions. The author thanks the Management of the Boliden Mining Company for permission to publish this paper.

REFERENCES

1. Danielsson, A., Lundgren, F. and Sundkvist, G. *Spectrochim. Acta* **15** (1959) 122.
2. Danielsson, A. and Sundkvist, G. *Spectrochim. Acta* **15** (1959) 126.
3. Danielsson, A. and Sundkvist, G. *Spectrochim. Acta* **15** (1959) 134.
4. Kitchener, J. A. *Ion-Exchange Resins*, John Wiley & Sons. Inc. New York 1957.
5. Samuelsson, O. *Ion-Exchangers in Analytical Chemistry*, John Wiley & Sons Inc. New York 1952.
6. Smith, G. F. *Analyst* **80** (1955) 16.

Received March 6, 1961.

ACTA CHEMICA SCANDINAVICA 15 (1961) 1507–1512

Aromatic Sulfonation with Sulfur Trioxide in Nitromethane

N. HESSELBJERG CHRISTENSEN

Danish Atomic Energy Commission, Risø, Denmark

Solutions of nitromethane containing about 500 mg of SO_3 pr ml have been used for sulfonation of various aromatic hydrocarbons at 0°C. The separated reaction products have been found to be sulfonic acid anhydrides, and especially with aryl halides this method gives good yields and pure products. The paper describes various anhydrides not previously reported. The exchange reactions $H_2{}^{35}SO_4 + SO_3$ and $Ar^{35}SO_3H + SO_3$ in nitromethane have been qualitatively investigated, and a method for the preparation of pipsan, *p*-iodobenzenesulfonic acid anhydride, labelled with ^{35}S has been developed. The yield of activity has been 60–65 % in the crude product.

In search of a simple method for the preparation of labelled *p*-iodobenzenesulfonic acid anhydride, pipsan, the direct sulfonation of iodobenzene at room temperature, as described by Lukashevich [1], has been investigated. In a previous paper [2] studies on the conditions for the formation of the pipsan in oleum were reported. It was concluded that the optimal conditions correspond to the brutto-equation:

$$3\ SO_3 + 2\ C_6H_5I \rightleftharpoons (IC_6H_4)_2S_2O_5 + H_2SO_4$$

and it was shown that while the amount of free SO_3 (in excess of 100 % H_2SO_4) is critical, the H_2SO_4 appears to act as an inert solvent only.

The present paper describes a new modification in which sulfur trioxide in nitromethane is used as sulfonating agent.

Sulfonations of iodobenzene conducted on a semi-micro scale with varying amounts of SO_3 in nitromethane showed improved yields compared to those obtained with oleum (*cf.* Fig. 1). The optimal range is far broader than that of the previous method. Neither competing crystallization of the sulfonic acid nor tar-formation were observed in these experiments. Further, the low viscosity of the nitromethane solution compared to that of oleum at 0° makes the modification better suited for syntheses in micro and semi-micro scale.

Sulfonation of various aromatic compounds with nitromethane containing sulfur trioxide resulted in many cases in rapid separation of sulfonic acid anhydride, the best yields and purest products having been obtained with the halogen substitutes, *cf.* Table 1.

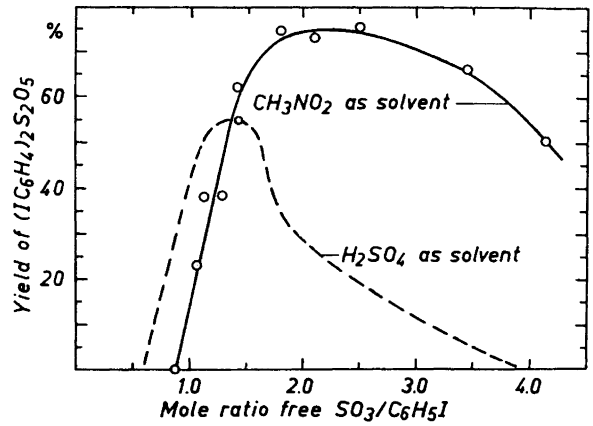

Fig. 1. Yields of iodobenzenesulfonic acid anhydride formed by sulfonation of iodobenzene with 3—5 M solution of sulfur trioxide in nitromethane (full line). Broken line indicates yields obtained with oleum as previously reported [2].

Table 1. Data for sulfonic acid anhydrides.

Sulfonated aromatic compound	Yield %	Solubility in CH_3NO_2. 0°C. mg in 1 g sat. soln.	Neutr. equiv. wt.		M.p. in °C of	
			found	calc. mono-sulf.	anhydrides	amides
Benzene	0	270[a]				
Toluene	20	27[a]	167	163		
m-Xylene	50		135	177		
Diphenyl	85		134	225		
Naphthalene	57		153	199		
Anthracene	0					
Anthraquinone	0					
Chlorobenzene	35	20	190	184	130—141	143—144
Bromobenzene	60	5.0	232	228	178.5—182	166—167
Iodobenzene	70	2.1	279	275	220—221	187—189
p-Dichlorobenzene	0					
p-Diiodobenzene	0					
us-Trichlorobenzene	14		264	253		
o-Chlorotoluene	30	15			148—151[b]	130
m-Chlorotoluene	70	14	195	198	149—150[b]	185
p-Chlorotoluene	90	1.8	199	198	210—211	143
m-Bromotoluene	60		237	242	179.5—180.5	
p-Iodotoluene	36		290	289	215—220	
1-Chloronaphthalene	50		246	234	218.5—219	
1-Bromonaphthalene	60		285	278	217—218	
2-Bromonaphthalene	20		284	278	227—229	

[a]. Solubilities of benzene- and toluene sulfonic acid anhydrides were found on samples prepared according to Bernoulli [12] and Fichter [13]

[b]. M.p. of mixture from *o*- and *m*- chlorotoluenesulfonic acid anhydrides: 124—126°C.

Generally a ratio of 1.7 mole SO_3 per mole of aryl was used in these experiments. In some cases improved yields were observed with higher SO_3/ArH-ratios.

The yields have been calculated as per cent of the theoretical from the aromatic compound.

The solubilities of some of the recrystallized samples in nitromethane have been measured at 0°C. The figures given in Table 1 indicate that the yields of the syntheses to some degree depend upon the solubilities of the anhydrides.

The anhydride character of the crude compounds was confirmed by their direct transformation to amides and anilides with ammonia and aniline.

The modification is well suited for the preparation of sulfonic acid anhydride labelled with the radioactive isotope ^{35}S. This aspect has only been investigated with $(I\text{-}C_6H_4)_2S_2O_5$, but the results will no doubt apply to aromatic sulfonic acid anhydrides in general.

A droplet of concentrated H_2SO_4 containing the radioactive isotope as $^{35}SO_4^{2-}$ was mixed at 0° with the SO_3-nitromethane solution. By sulfonation of iodobenzene with this medium, the anhydride labelled with ^{35}S was formed directly. Assays of activities showed that the original activity had exchanged completely with the sulfur trioxide *.

It was observed that neither the sulfonic acid nor its anhydride would undergo rapid exchange with sulfur trioxide in nitromethane solution, and it could be demonstrated that, with the same amounts of chemicals and activities, the specific activity of the labelled pipsan was increased about 50 % if the sulfonation was conducted in two steps instead of one: the first being the formation of the sulfonic acid by the use of the total activity and only a fraction of the calculated amount of SO_3, the second being the anhydride formation of

Table 2. Syntheses of ^{35}S-labelled pipsan in nitromethane. In each of the experiments were used 245± 10 μC of the activity, 0.02 mmole H_2SO_4 as carrier and 0.59 mmole C_6H_5I, all values referring to one mmole of total SO_3. The activity, carrier and iodobenzene were mixed with the amount of SO_3 given in the second column. To this mixture was subsequently added the quantity given in the third column.

Expt. No.	SO_3 added, mmole per mmole aromatic		Yield of crude pipsan		Spec. activity of pipsan μC/mil. equiv.	Yield of activity in crude products %
	in first step	in second step	% of total SO_3	% of C_6H_5I		
1	1.65	0	40.0	67.9	230± 10	38
2	0.83	0.83	44.5	75.3	330± 15	60
3	0.33	1.33	45.0	76.2	360± 15	66

* *Added in proof:* It has been observed that also the exchange between SO_3 and Na_2SO_4 in nitromethane is rapid, and the use of Na_2SO_4-carrier instead of conc. H_2SO_4 has proved advantageous in the synthesis of ^{35}S-pipsan.

the labelled sulfonic acid from the first step by the addition of the rest of the SO_3 (*cf.* Table 2). With the latter procedure yields of 60—65 % of the activity have been obtained in the crude pipsan.

EXPERIMENTAL

The nitromethane was from L. Light and Co, boiling range 98—101°. If the amount of free SO_3 had to be known with fair accuracy, the nitromethane was distilled over P_2O_5 prior to use. The solutions of SO_3 in nitromethane were prepared by mixing fibrous SO_3 (from Merck, p.a.) with the nitromethane. The content of SO_3 per ml was determined by weighing of the SO_3 and by assay of specific gravity of the solution. Solutions having a molarity of 7—8 can be prepared. The usual concentrations of the solutions have been 3—5 M. At room temperature the solution will gradually decompose, perhaps due to the process $CH_3NO_2 \rightarrow H_2NOH + CO$, which has been observed by Pfungst [3]. At 0°C the solution can be used for at least 4 h.

The aromatic compounds were pure preparations from Fluka and British Drug Houses. Weighed amounts of these compounds (around 0.5 g) were dissolved in 0.5—2.0 g of nitromethane in 10 ml centrifuge tubes placed in ice-water. The sulfonation mixture, which had been prepared shortly before and stored at 0°, was added with micropipettes.

In most cases the precipitation started immediately after the mixing of the components and was apparently complete after a few minutes, but occasionally, especially with the unsubstituted hydrocarbons, the precipitation did not start until several minutes after the mixing.

After one hour the precipitate was washed, dried and weighed as crude products as described previously [2], the only exception being the use of nitromethane instead of acetic anhydride as washing agent.

The melting points given in Table 1 are corrected. Since prolonged heating lowers the melting points of the anhydrides, the capillary tubes with these compounds have been immersed in the oil bath 10—20°C before the expected melting points. The rate of heating in this range was 2°C per minute.

The melting ranges of the sulfonic acid anhydrides are often fairly broad. Although the sulfonic anhydrides generally are insoluble in cold water and only slowly decomposed by hot water, they appear to be quickly hydrolysed by humid atmosphere. Therefore anhydrous conditions are necessary in order to obtain sharp melting points of these compounds.

By hydrolysis and evaporation of crude pipsan and subsequent boiling with thionyl-chloride and recrystallization from anhydrous chloroform-pentane, a pure product is consistently obtained with melting point 220—221°C. This melting point has previously been observed on the pure *p*-iodobenzenesulfonic acid anhydride [4]. In our laboratory the same melting point has sometimes been observed on products recrystallized from anhydrous chloroform or nitromethane, but quite as often this procedure results in products melting only at 200—210°. On the other hand the crude pipsan may sometimes melt as high as 218—219°.

An accelerated hydrolysis of the anhydrides is conveniently carried out by exposure to steam. The hydrolysates of the crude products have in all cases been found to be completely soluble in water indicating absence of sulfone. The neutr. equiv. weights were determined by titration with 0.1 N NaOH on crude products.

Sulfonyl chlorides were prepared from the crude sulfonic anhydrides of the mono halogen benzenes by steam hydrolysis, treating the acid with excess of PCl_5 in $POCl_3$, destruction of the excess with ice-water, extraction with benzene and finally sublimation. The following m.p's. were found: chloro- 51.5°, bromo- 75.0°, and iodo- 82.5—83.5°C. All three correspond to the *p*-halogeno-benzenesulfonyl chlorides.

The *sulfonic amides* were prepared from the crude sulfonic anhydrides by dissolving in chloroform and treating with aqueous ammonia. By evaporation of the chloroform phase and acidifying the aqueous solution, the amides separated in 60—70 % yields. The melting points in Table 1 were determined on samples recrystallized from alcohol.

In order to obtain chlorobenzenesulfoneamide it was necessary to apply a dry NH_3-$CHCl_3$ solution.

The *anilides* of the monohalogeno-benzene sulfonic acids were prepared in a similar way, the melting points being: chloro- 93.5—96.0°, bromo- 117—118°, and iodo- 142—144°C.

The pure anhydrous *sulfonic acids* are difficult to isolate by classical sulfonation. By the present method these difficulties are overcome, as the sulfonic acids are obtained merely by hydrolysis of the recrystallized sulfonic anhydride and drying. The anhydrous acids are apparently even more hydroscopic than the anhydrides. The sulfonic acids of the halogeno-benzene prepared according to this method were dried for three days over P_2O_5 *in vacuo*, and the samples in the capillary tubes intended for determination of melting points were dried for one day more in the same way. The following melting ranges were observed: chloro- 89—99°, bromo- 90—92°, and iodo- 75—77.5°C.

The *solubilities* in nitromethane at 0° of various sulfonic anhydrides were determined by shaking recrystallized samples in closed 5 ml bottles for 6 h. Samples of clear supernatants were taken at intervals to check equilibrium.

The ^{35}S-*activity* was prepared on Risø's Isotope Laboratory from KCl irradiated in the reactor DR2. It was obtained as an aqueous solution of $^{35}SO_4^{2-}$. A solution containing about 1 mC ^{35}S and 10 mg of H_2SO_4 per ml was prepared. In each of the experiments referred to in Table 2, 1 ml of this solution was transferred to the test-tubes with a micropipette. The solutions were evaporated at 100°C with a gentle stream of dry nitrogen blowing in the tube. Towards the end of the evaporation the temperature was raised to 120° and kept there for 5 min. The tube with the evaporated sulfuric acid (forming a droplet in the bottom of the tube) was transferred to an ice-bath, and the solutions of SO_3 and C_6H_5I were added with micropipettes in the amount and sequence as indicated in Table 2. The pipsan was isolated, dried and weighed.

Counting was performed with a calibrated end-window Geiger-Müller-tube. The samples for assay of activity were prepared from dilute aqueous solutions by drying 100 μl drops on alumina planchets. The labelled pipsan products were recrystallised from nitromethane prior to weighing, steam hydrolysis, dilution and sampling.

RESULTS AND DISCUSSION

If it may be assumed that the nitromethane does not interfere with the solutes, the exchange reaction between SO_3 and the H_2SO_4 possibly takes place with a polysulfonic compound as intermediate, *e.g.*

$$H_2S^*O_4 + SO_3 \rightleftharpoons H_2SS^*O_7 \rightleftharpoons H_2SO_4 + S^*O_3 \qquad \text{(i)}$$

The exchange is so rapid even at 0° that no kinetic effect can be observed with the described simple technique of synthesis.

The neutr. equiv. of the compounds so far investigated correspond to monosulfonation except for xylene, diphenyl and naphthalene. These three hydrocarbons gave all substantial amounts of precipitate, but the products were amorphous and difficult to obtain dry. By sulfonating naphthalene at 0° with SO_3 in chloroform Courtot *et al.*[5] found products with SO_3-contents varying according to the SO_3/ArH ratio in the sulfonation mixtures. Disulfonation and adducts with SO_3 were observed. An American patent [6] describes the formation of 1-naphthalenesulfonic acid anhydride by sulfonation of naphthalene with SO_3 dissolved in phosphorus oxychloride or dimethylsulfate. Blangey [7] observed formation of long anhydride-chains by sulfonation of naphthalene with oleum.

Toluene and the halogen substituted compounds form anhydrides derived from monosulfonation. The melting points of the derivatives suggest that the conditions of isomerism are identical to those obtained in classical sulfonation.

The variations in melting points from a rather large number of pipsan preparations suggest that the conditions of synthesis are not yet fully con-

trolled. It is possible that slight variations in the temperature during the sulfonation may lead to small variations in the formation of isomers. The importance of anhydrous conditions has been demonstrated by Field [8], who observed that even slight contamination with *p*-toluenesulfonic acid in the corresponding anhydride seriously depressed the melting point. Isomeric impurities present in the starting materials used in our investigation may possibly also contribute to the unsharpness of the m.p's.

The observation of increased specific activity with sulfonation starting with low values of SO_3/C_6H_5I-ratios (Table 2) shows that the *p*-iodobenzenesulfonic acid is formed in this range although it is not precipitated as in the investigations with oleum [2]. Probably the sulfonic acid is the primary product with all SO_3/C_6H_5I ratios.

In this connection attention should be paid to a kinetic investigation of aromatic sulfonation carried out by Hinshelwood and co-workers [9,10]. No formation of anhydride was observed in these investigations, probably due to the use of dilute solutions. The sulfonation at room temperature with solutions of SO_3 in nitrobenzene was found to be second order in SO_3, the rate determining reaction possibly being

$$S_2O_6 + ArH \rightarrow ArS_2O_6H \qquad \text{(ii)}$$

Lukashevich [11], assuming a very reactive pyrosulphonic acid as precursor to the anhydride formed by sulfonation with oleum, suggested the following route of reaction:

$$ArS_2O_6H \rightleftharpoons ArSO_3H + SO_3 \qquad \text{(iii)}$$

$$ArS_2O_6H + ArSO_3H \rightleftharpoons Ar_2S_2O_5 + H_2SO_4 \qquad \text{(iv)}$$

The lower yields of pipsan with oleum than with nitromethane may be due to the excess of H_2SO_4 forcing eqn.(iv) from right to left.

The described method has been used for the preparation of ^{35}S-labelled pipsan in charges of 100—200 mC, and with a specific activity of 600 mC/g or more. Products prepared by this method has proved fully applicable in analyses of steroid hormones according to Bojesen [4].

Acknowledgement. I want to thank Miss Birgit Krarup Nielsen for the precision and interest with which she carried out her part of the work.

REFERENCES

1. Lukashevich, V. O. *Doklady Akad. Nauk S.S.S.R.* **99** (1954) 995; *Chem. Abstr.* **50** (1956) 217.
2. Christensen, N. H. *Acta Chem. Scand.* **15** (1961) 219.
3. Pfungst, A. *J. prakt. Chem.* **34** (1886) 34.
4. Bojesen, E. and Degn, H. *Acta Endocr.* **37** (1961) 541.
5. Courtot, C. and Bonnet, J. *Compt. rend.* **182** (1926) 855.
6. Lecher, H. Z. and Adams, F. H. *U.S.P.*2,483,213 (1949); *Chem. Abstr.* **44** (1950) 2563.
7. Blangey, L. and Fierz-David, H. E. *Helv. Chim. Acta* **32** (1949) 631.
8. Field, L. *J. Am. Chem. Soc.* **74** (1952) 394.
9. Wadsworth, K. D. and Hinshelwood, C. N. *J. Chem. Soc.* **1944** 469.
10. Dresel, E. and Hinshelwood, C. N. *J. Chem. Soc.* **1944** 649.
11. Lukashevich, V. O. *Proc. Acad. Sci. U.S.S.R., Sect. Chem.* **112** (1957) 133, (English translation).
12. Bernoulli, A. H. and Stauffer, H. *Helv. Chim. Acta* **23** (1940) 627.
13. Fichter, Fr. and Stocker, E. *Helv. Chim. Acta* **7** (1924) 1064.

Received April 24, 1961.

ACTA CHEMICA SCANDINAVICA 15 (1961) 1513–1516

Interaction of Cobalt and Iron in the Riboflavin Production of *Candida guilliermondii*

T.-M. ENARI and VELI KAUPPINEN

Laboratory of Brewing, Helsinki, and Department of Biochemistry, University of Helsinki, Helsinki, Finland

The effect of cobalt on the production of riboflavin by *Candida guilliermondii* has been studied. The yeast was grown in a continuous culture with iron as growth limiting factor. When the iron concentration of the nutrient medium was small enough (0.5 μg/l) cobalt had no effect. At higher iron concentrations cobalt stimulated the riboflavin production and the highest riboflavin production was obtained at an iron concentration of 5 μg/l and a cobalt concentration of 15–25 mg/l. It was concluded that cobalt specifically replaces iron at the site were iron is necessary for the binding of riboflavin in the cell. Thus cobalt competes with iron and produces the same effect as iron deficiency.

Iron is known to inhibit the production of riboflavin by the yeast *Candida guilliermondii*. The optimal iron concentration in the medium is, according to Tanner *et al.*[1], 5–10 μg/l. The effect of some other divalent cations on the riboflavin production of *C. guilliermondii* has also been studied. Thus Levine *et al.*[2] found that manganese, copper, zinc, tin, nickel, and aluminium in concentrations of 1 mg/l do not affect it. Enari [3,4] showed that cobalt and, to a lesser degree, zinc stimulate riboflavin production. He found that the addition of 10^{-4} M of cobalt to the medium shifts the optimum iron concentration from about 10^{-7} M to about 10^{-5} M. On the basis of a study of the uptake of iron and cobalt and their interaction it was suggested that cobalt acted by preventing the uptake of iron into the yeast cell. The cobalt would thus cause an iron deficiency in the cell. Iron deficiency in the cell, whether caused by a low iron concentration in the medium or by the addition of cobalt, would lead to the excretion of riboflavin into the medium.

If this hypothesis is correct, cobalt should have no effect in an iron deficient medium. Attempts to test this in a closed culture were not successful. The failure was obviously due to the manner in which the iron was taken up by the yeast [4]. When grown in a medium with low iron concentration the yeast cell rapidly binds most of the iron. The iron concentration in the cell is thus

normal in the early stages of the experiment. As the yeast multiplies, the iron concentration in the cells gradually decreases until it finally becomes low enough to prevent any further growth. If cobalt is added to such a culture it inhibits the iron uptake in the beginning and an iron deficient yeast is produced much earlier than when no cobalt is added. The only way to produce a yeast culture with a constant low iron concentration is to use continuous cultivation in a chemostat with iron as growth limiting factor [5,6].

The effect of cobalt on the riboflavin production of *C. guilliermondii* when grown in a chemostat with iron as growth limiting factor was studied in order to test the hypothesis mentioned above.

EXPERIMENTAL

The yeast *C. guilliermondii* was grown with vigorous aeration in an all-glass chemostat[5] which was easy to keep free of iron. The capacity of the chemostat was 250 ml and a flow rate of 5 ml/h was used in all experiments. The nutrient medium used contained 30.0 g glucose, 3.8 g diammonium citrate, 4.1 g citric acid (H_2O), 15.2 g trisodium citrate (5 1/2 H_2O), 0.20 g KH_2PO_4, 1.0 g $(NH_4)_2HPO_4$, 0.25 g $MgSO_4 \cdot 7H_2O$, and 5 μg biotin per litre. The citrate was added to buffer the medium to pH 6.0. This buffering was necessary to keep the pH constant. Iron was removed from the medium by shaking with a chloroform solution of ferron and tributylamine [7]. Ferrous sulphate and cobaltous sulphate were then added to give the concentrations desired. In the experiments in which glucose was used as growth limiting factor the amount of glucose was reduced to 5 g/l and 200 μg/l of iron was added. The concentrations actually used in each experiment are given in connection with the results.

The riboflavin produced was determined by direct spectrophotometry of the centrifuged medium [4].

RESULTS AND DISCUSSION

The effect of iron on riboflavin production when iron was used as growth limiting substance was first studied (Fig. 1). The culture was started with an iron concentration of 5 μg/l. At this concentration the yeast produced about 2.4 μg of riboflavin per mg of yeast dry weight. When the iron concentration was gradually increased the riboflavin production decreased until it was

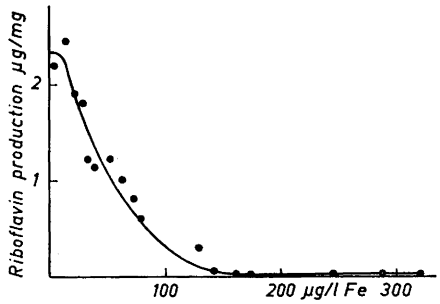

Fig. 1. Effect of iron on the riboflavin production of *C. guilliermondii*.

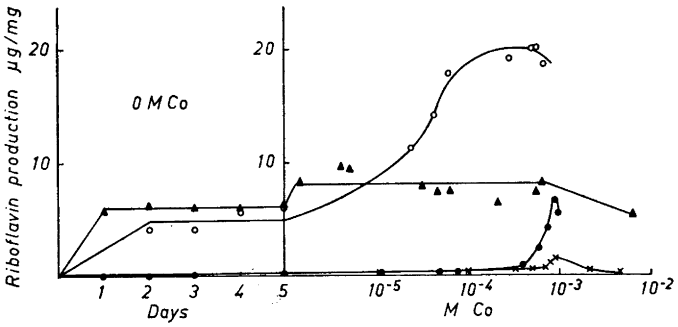

Fig. 2. Effect of cobalt on riboflavin production. × = 200 µg/l Fe in the medium, glucose growth limiting; ● = 200 µg/l Fe in the medium, Fe growth limiting; ○ = 5 µg/l Fe in the medium, Fe growth limiting; ▲ = 0.5 µg/l Fe in the medium, Fe growth limiting.

almost completely inhibited at an iron concentration of 140 µg/l. Thus also when iron is the growth limiting factor it can prevent the production of riboflavin by the yeast. This is in good agreement with our previous studies on the iron uptake of yeast [6]. In these it was found that at iron concentrations below 140 µg/l all the iron in the medium was taken up by the yeast. At iron concentrations higher than this value an excess of iron was left in the medium and the iron concentration of the yeast remained at a steady value of 15 µg/g dry yeast.

In the next experiment we studied the effect of cobalt on the riboflavin production at different iron concentrations (Fig. 2). In all the experiments the yeast was cultivated in a medium without any cobalt until a steady state was reached. After five days cobalt was added to the medium in increasing concentrations until finally a cobalt concentration of $1-8 \times 10^{-3}$ M was reached in 7—8 days. When glucose was used as growth limiting factor almost no riboflavin was produced. When iron used as growth limiting factor riboflavin was excreted into the medium. The lower the iron concentration in the medium, the lower was the cobalt concentration at which the highest riboflavin yield was obtained. Thus for an iron concentration of 200 µg/l the optimal

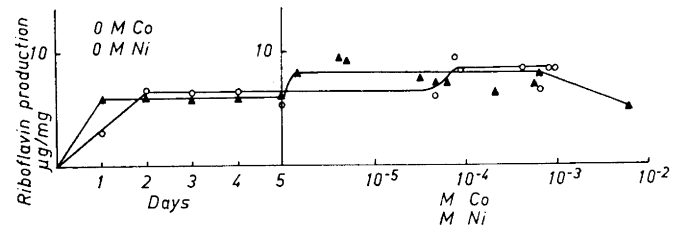

Fig. 3. Effect of nickel and cobalt on the riboflavin production of iron deficient yeast. ▲ = Co added, Fe growth limiting at 0.5 µg/l; ○ = Ni added, Fe growth limiting at 5 µg/l.

cobalt concentration was 10^{-3} M and for an iron concentration of 5 μg/l the optimal cobalt concentration was about 5×10^{-4} M. When the iron concentration was reduced to 0.5 μg/l cobalt had only a very slight effect.

The greatest amount of riboflavin was produced with an iron concentration of 5 μg/l and a cobalt concentration of about 5×10^{-4} M. With the lower iron concentration a smaller amount of riboflavin was produced. This shows that the effect of cobalt is more specific than the effect of iron deficiency. Obviously cobalt replaces iron at the site where the latter is necessary for the binding of the riboflavin in the cell. At an iron concentration of 0.5 μg/l cobalt has no effect but the iron deficiency also retards the general metabolism of the cell and hence the amount of riboflavin released is smaller.

It was suspected that the small effect of cobalt at an iron concentration of 0.5 μg/l was due to a general toxic effect. In order to test this hypothesis an experiment was performed with nickel, which, as was shown by earlier experiments [4], has no specific effect on riboflavin but exerts a general toxic effect leading to autolysis of the yeast and consequently to a higher riboflavin concentration in the medium. In this experiment it was found that the effects of cobalt and nickel were of the same order of magnitude (Fig. 3). I can be concluded that cobalt had no specific effect on the riboflavin production of the yeast when only 0.5 μg of Fe per litre was present in the medium.

It has thus been proved that the effect of cobalt on the production of riboflavin by *C. guilliermondii* is due to an interaction with iron and that cobalt produces an iron deficiency in the yeast.

REFERENCES

1. Tanner, F. W., Jr., Vojnovich, C. and Van Lanen, J. M. *Science* **101** (1945) 180.
2. Levine, H., Oyaas, J. E., Wasserman, L., Hoogerheide, J. C. and Stern, R. M. *Ind. Eng. Chem.* **41** (1949) 1665.
3. Enari, T.-M. *Acta Chem. Scand.* **9** (1955) 1726.
4. Enari, T.-M. *Ann. Acad. Sci. Fennicae A II* (1958) No. 90.
5. Enari, T.-M. and Kauppinen, V. *Suomen Kemistilehti* **B 32** (1959) 131.
6. Enari, T.-M. and Kauppinen, V. *10. Nordiska Kemistmötet, Stockholm 1959.*
7. Kauppinen, V. *Suomen Kemistilehti* **B 34** (1961) 59.

Received April 25, 1961.

ACTA CHEMICA SCANDINAVICA 15 (1961) 1517–1531

Studies on the Coagulation of Chicken Blood

II. Unidentified Nutritional Factors, Essential for Maximum Level of $\varkappa$-factor

ØYVIND SØRBYE*

Department of Biochemistry and Nutrition, Polytechnic Institute, Copenhagen, Denmark

By nutritional experiments it has been shown that the level of $\varkappa$-factor in chicken plasma depends on the composition of the diet, and that the $\varkappa$-factor level is determined by the simultaneous presence of a set of nutritional factors, six of which are of unidentified nature. Besides vitamin K, nutritional factors in barley, wheat bran, pancreas powder, corn oil, dried skimmed milk, and alfalfa are required for maximal $\varkappa$-factor activity. A diet is described which is adequate for maintaining the plasma $\varkappa$-factor concentration at a maximal level during the experimental periods. When the diet is fed to chickens with low levels of $\varkappa$-factor, their $\varkappa$-factor concentration is raised to the maximal level.

The extraction and preliminary concentration of the active principles in the essential ingredients of this diet is described. One of these factors is a lipo-soluble compound. It is non-saponifiable and may be a hydrocarbon containing a few polar groups. The other five factors are water-soluble compounds, probably containing nitrogen.

It is suggested that the factors influence the $\varkappa$-factor level of plasma by affecting the formation of $\varkappa$-factor. They may be catalysts for this process or essential parts of the $\varkappa$-factor molecule.

It was described in a previous paper [1] how mixtures of vitamin K-deficient and coumachlor plasmas could be used to distinguish between three different "types" of coagulation factors ($\varkappa$-, δ- and φ-factors). The concentrations of δ- and φ-factors appeared to be limiting for the coagulation rate of vitamin K-deficient plasmas, whereas the coagulation rate of coumachlor plasmas was limited by the concentrations of $\varkappa$- and φ-factors. A method for comparison of $\varkappa$-, δ- and φ-factor levels in different plasmas was outlined. Application of this method to plasmas from chickens on slightly different diets revealed some variations in the levels of these factors, indicating that their concentrations in plasma might depend on nutritional factors other than vitamin K.

* Fellow of the Royal Norwegian Research Council for Scientific and Industrial Research.

The present paper deals with: 1) the design of a diet which can raise the plasma ϰ-factor concentration to a maximum in chickens, where the ϰ-factor concentration is low, and is adequate for maintenance of the ϰ-factor concentration at the maximal level, and 2) extraction and preliminary concentration of the active principles in the essential ingredients of this diet.

MATERIALS AND METHODS

The materials and method for measurement of ϰ-factor activity were described in a previous paper [1].

Feeding of chickens. Chickens were raised on a commercial diet [2] for 2—3 weeks and thereafter on the same commercial diet or on various experimental diets (Table 1) for no less than 2—3 weeks. Variations in the plasma levels of ϰ-factor were thereafter followed in *individual* chickens by determination of ϰ-factor activity at intervals of 5—10 days. The effect of different diets and of changes in the composition of diets on the ϰ-factor activity could thus be followed for several weeks.

Testing of concentrates. By omission of an essential ingredient from a diet, adequate for maintenance of maximal ϰ-factor level, a reduced level of ϰ-factor was induced in 2—4 weeks. Chickens on such "deficient" diets were then used to trace the active principles of the various essential food ingredients through the extraction and fractionation procedures.

Extraction residues were tested for activity by feeding a diet where extracted material was substituted for the corresponding unextracted material in the complete diet. The effect on the ϰ-factor level was examined after 6—9 days.

Table 1. Composition of exploratory diets.

Ingredients	Composition of diets in grams					
	S-02.2A	S-04.2A	S-05.2A	S-06.2A	S-21.2A	S-25.2A
Casein, Vitamin Test [a]	70	—	—	—	—	—
Casein, Stege [b]	—	70	—	—	150	170
Gelatine	30	30	30	—	80	80
Pancreas powder [c]	—	—	70	100	80	—
Dried skimmed milk	—	—	—	100	—	—
Salt mixture[c]	50	50	50	50	50	50
Vitamin-sucrose mixture [d]	105	105	105	105	105	105
Ground corn	200	200	200	200	—	400
Ground barley	200	200	200	200	—	—
Ground oats	100	100	100	—	—	—
Wheat bran	80	80	80	80	—	—
Dried alfalfa	60	60	60	60	60	60
Refined peanut oil	50	50	50	50	50	50
Sucrose	55	55	55	55	425	85

All chickens received vitamins A and D as described by Dam and Søndergaard [2].

a) From Genatosan Ltd, Loughborough, England.
b) From A/S Dansk Mejeri Industri & Export Kompagni, Stege, Denmark.
c) As described by Dam and Søndergaard [2].
d) As described by Sørbye and Kruse [1].

Diagram 1. General scheme for extraction and fractionation.

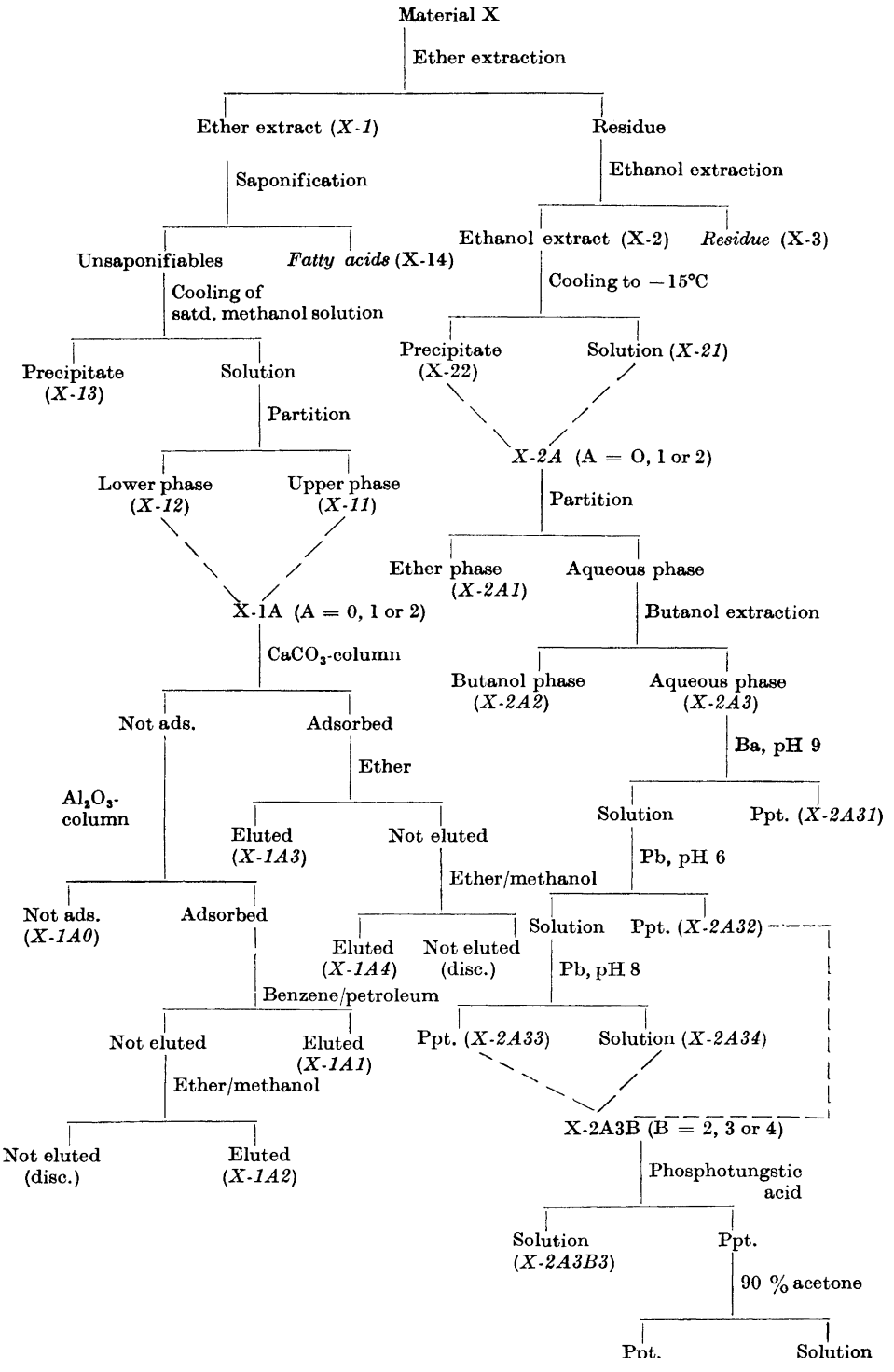

Extracts and fractions were prepared as aqueous solutions, emulsions, oils, or mixed with sugar and made into pellets. They were fed as supplements to the deficient diet for 4 (3—5) days in succession. The *x*-factor level was then examined on the 5th (4th—6th) day.

General extraction and fractionation procedures

Extraction of essential food ingredients. All food ingredients, which proved essential for maintenance of maximal *x*-factor activity, were subjected to extraction in a Soxhlet extractor. The materials were first extracted with ethyl ether for 20 h. If the active factor could not be extracted with ether, the ether-extracted material was next extracted with hot 96 % ethanol for 24 h. All active extracts were subjected to further fractionation.

Fractionation of ether extracts (Fractions 1).

Saponification was performed with 5 ml of methanol and 1 ml of 60 % potassium hydroxide per g of extract by refluxing under nitrogen for 1/2—3/4 h.

Unsaponifiable matter was isolated after addition of water to the soap solution by extraction trice with ether. The combined ether extracts were washed free from alkali and dried over sodium sulfate.

Fatty acids (fraction 14) were isolated from the ether extracted soap solution after acidification by extraction with three lots of ether. The extracts were washed free of acid and dried over sodium sulfate.

The bulk of sterols were separated from the rest of the unsaponifiable matter by dissolving the unsaponifiables in a minimum of hot methanol. The main part of the sterols separated out after storage overnight at —15°C, was filtered off and washed with cold methanol (fraction 13).

Partition. The sterol-poor, unsaponifiable matter was dissolved in a small amount of light petroleum (b.p. 40—70°C). To the petroleum solution were added 9/10 vols. of methanol and 1/10 vol. of water. The mixture was shaken and allowed to separate. The lower phase was drawn off, and the same procedure was repeated 9 more times with the upper phase. The final upper phase was washed free from methanol, dried over sodium sulfate and concentrated to a suitable volume (fraction 11). The lower phases were combined and extracted with ether after addition of water. The ether extract was washed, dried over sodium sulfate and finally dissolved in ether, or in petroleum containing a trace of ethanol (fraction 12).

Chromatography. When the activity of the unsaponifiable matter had been located to the upper- or lower-phase material, or to both, further fractionation was attempted by chromatography. The active fractions (fraction 1A) were dissolved in light petroleum and first applied to a column of calcium carbonate * (1 g of adsorbent for 2—3 g of original oil or ether extract). The column was then washed with light petroleum (6-7 ml per g of adsorbent). The material, adsorbed on the column, was eluted with ether (fraction 1A3) and/or with mixtures of ether and methanol (fraction 1A4).

The material, washed out of the calcium carbonate column by light petroleum, was concentrated and chromatographed on alumina ** (1 g of adsorbent per 1—2 g of original oil or ether extract). The column was washed with light petroleum (6-7 ml per g of adsorbent), giving fraction 1A0, and eluted with a benzene-petroleum mixture (fraction 1A1), ether and/or ether-methanol (fractions 1A2).

Fractionation of ethanol extracts (fractions 2).

Ethanol extracts, containing the active principle of an essential dietary component, were stored overnight at —15°C and thus separated into a cold-ethanol soluble (fraction 21) and a cold-ethanol insoluble part (fraction 22). In many cases the active principle was

* $CaCO_3$ (Merck, for chromatography) was heated at 125°C for 16-20 h before use.

** Al_2O_3 (Merck, for chromatography) was washed free from alkali and U.V. adsorbing material by percolation with hot water and with hot methanol. The washed product was dried at 160°C for 48 h. Before use it was activated at 190°C for 20 h.

concentrated in one of these fractions only. Usually both fractions were distributed separately in a water:ethanol:ether solvent system as follows: to the solution (fraction 21) or suspension (fraction 22) of the fractions in ethanol were added 3 vols. of ether and 3 vols. of distilled water. The mixtures were shaken and allowed to separate.

Ether layers (fractions 2A1) were evaporated to dryness under reduced pressure, and emulsified in 15 % aqueous ethanol with small amounts of Tween 80. (Ethanol was added to all aqueous fractions to prevent deterioration on storage).

Aqueous phases were concentrated on a steam bath and extracted twice by shaking with 1/2—1/3 vol. of *n*-butanol. The combined *butanol extracts* (fractions 2A2) were concentrated by evaporation under reduced pressure, washed with ether and finally dissolved in 15 % aqueous ethanol containing trace amounts of Tween 80.

The *butanol extracted solutions* (fractions 2A3) were freed from butanol by extraction with ether, concentrated and finally dissolved in 15 % aqueous ethanol.

In these studies all or the major part of the activity of an ethanol extract was found in the butanol-extracted aqueous solutions, and further fractionation of the aqueous solutions was attempted by *fractionation with metal salts.*

Aqueous fractions carrying an active principle (fraction 2A3) were further purified by precipitation with barium hydroxide: A solution of barium hydroxide was added until pH was 9.5—10. The resulting precipitate was separated by centrifugation after storage at 5°C overnight. The precipitate was regenerated by addition of dilute sulfuric acid to pH 2.5 or slightly below, heating on a steam bath for 1 h and filtration. The filtrate was adjusted to pH 6 with sodium hydroxide. To the solution was finally added 15 % ethanol (fraction 2A31).

Precipitation with lead acetates. The supernatant after precipitation with barium hydroxide was brought to pH 6 with dilute sulfuric acid. A solution of neutral lead acetate (10 %) was added until precipitation was complete. The precipitate was separated by centrifugation after storage at 5°C overnight. The precipitate was suspended in water and regenerated by addition of dilute sulfuric acid to bring pH below 2.5, heating on a steam bath for one hour and filtration. The filtrate was then treated with hydrogen sulfide gas to remove the last traces of lead. Excess hydrogen sulfide was removed by heating on a steam bath, and pH was brought to 6 with sodium hydroxide. The solution was filtered and 15 % ethanol added (fraction 2A32).

The supernatant after precipitation with neutral lead acetate at pH 6 was brought to pH 8 with barium hydroxide. A solution of basic lead acetate (10 %) was added until precipitation was complete. pH 8 was maintained by continuous addition of barium hydroxide solution. The resulting precipitate was separated by centrifugation after storage at 5°C overnight. The precipitate was regenerated as described for the neutral lead acetate precipitate and dissolved in 15 % aqueous ethanol (fraction 2A33).

The supernatant after precipitation with basic lead acetate was also regenerated in the same way as the two fractions precipitated with neutral and basic lead acetates and finally dissolved in 15 % aqueous ethanol (fraction 2A34).

When the active factor was concentrated in one or more of the fractions not precipitated by barium (fractions 2A3B), further fractionation of the active fraction(s) was attempted by

Precipitation with phosphotungstic acid. The active fraction(s) (2A3B) was dissolved in 5 % sulfuric acid, and a 10 % solution of phosphotungstic acid was added until precipitation was complete. After storage at 5°C overnight the solution was centrifuged. The precipitate was treated twice with acetone-water (9:1) and separated into a soluble fraction (2A3B1) and a fraction, insoluble in 90 % acetone (fraction 2A3B2). Both these fractions and the filtrate after precipitation with phosphotungstic acid (fraction 2A3B3) were regenerated by addition of barium hydroxide solution to pH 9—9.5, heating on a steam bath for one hour and filtration. Excess barium in the filtrate was precipitated by addition of dilute sulfuric acid and the excess of sulfuric acid was finally neutralized with sodium hydroxide. After filtration and concentration, 15 % ethanol was added to all solution.

EXPERIMENTS AND RESULTS

Through a series of experiments it became apparent that *x*-factor concentration in plasma from chickens was related to the chicken diet. The first

Table 2. $\varkappa$-factor activity of chickens on exploratory diets.

Chicken No.	Diet	$\varkappa$-factor level in % of maximal
5924	Commercial	80
6209	»	45
8024	»	75
8044	»	40
1990	S-21.2A	95
8335	»	55
6325	S-02.2A	25
6874	»	65
8839	»	60
7168	S-25.2A	40
7169	»	70
7170	»	70
2406 * First test	S-21.2A	100
2406 * Second test	S-21.2A	78
2406 * Third test	S-21.2A	73
2406 * Fourth test	S-21.2A	68

* The blood samples were taken at intervals of seven days.

experiments seemed to indicate that the $\varkappa$-factor levels of chickens on different diets were markedly different, but it was soon realized that the $\varkappa$-factor level of chickens, fed the same diet, also showed similar, individual differences (Table 2). Chickens with a high level of $\varkappa$-factor in the first plasma sample usually showed decreasing levels of $\varkappa$-factor in subsequent plasma samples taken at intervals of seven days. The supply of vitamins was above usual requirements with these diets, and it was therefore suspected that the observed variations in $\varkappa$-factor level might reflect variations in the available amounts of *other nutritional factors* which were not provided in adequate amounts with these diets.

A change of diet often resulted in a change of $\varkappa$-factor activity of the plasma (Table 3). In some cases, a dietary change was followed by an initial increase in $\varkappa$-factor concentration. On prolonged administration of the new diet the $\varkappa$-factor level, however, again declined. This course of events was also observed after supplementation of a vitamin K-deficient diet with Synkavit. The $\varkappa$-factor concentration first rose to the maximal level. On prolonged feeding of this supplemented diet, the $\varkappa$-factor level dropped below maximal. An adequate diet was finally worked out [diet No. S-06.2A). This diet was able to raise the $\varkappa$-factor concentration in all chickens to a level which appeared to be the *maximal level of* $\varkappa$*-factor* in chicken plasma, and to maintain the $\varkappa$-factor concentration at this maximal level. Diet No. S-06.2A apparently provided adequate supply of all nutrients, essential for maximal $\varkappa$-factor activity. Plasma from chickens raised on this diet, therefore, served as a reference, representing maximal or 100 % activity of $\varkappa$-factor.

After establishment of the adequate diet (S-06.2A), the importance of the various ingredients for maximal $\varkappa$-factor activity could be determined.

Table 3. Influence of dietary changes on ϰ-factor activity.

Chicken No.	Sequence of diets	Length of dietary periods	ϰ-factor level at end of period, in %
6323	No. S-02.2A	6 weeks	80
	No. S-04.2A	1 week	55
8717	Commercial	6 weeks	50
	No. S-05.2A	1 week	90
		2 weeks	70
		3 weeks	65
1981	Vitamin K-deficient [a])	2 weeks	17 [c])
	Do. + Synkavit [b])	1 week	100
	(10 mg per kg of diet)	2 weeks	80
		3 weeks	70
8715	Commercial	6 weeks	35
	No. S-02.2A	1 week	85
	No. S-06.2A	1 week	100
		2 weeks	100
9044	No. S-21.2A	4 weeks	not measured
	No. K-13.3	1 week	100
		2 weeks	100
		3 weeks	100
		4 weeks	100

a) as described by Dam and Søndergaard [2].
b) Bicalcium-2-methyl-1,4-naphthohydroquinone biphosphate (Roche).
c) Thromboplastin coagulation time of plasma was 84 min/100, compared to 24—25 for normal plasma.

A series of diets (Table 4) were prepared and tested, each lacking one of the ingredients of diet No. S-06.2A. After 2—4 weeks on these diets, chickens normally had ϰ-factor levels below 65—75 % of maximal. Diet No. K-13.3 was an exception. Chickens on this diet were able to maintain their ϰ-factor activity at 100 %. The active factor in corn could thus be supplied by corn oil alone, and ether extracted corn was found unessential for maximal ϰ-factor activity in these studies. The low ϰ-factor activity produced by diet K-5.2 proved that corn oil could not be replaced by refined peanut oil. The low ϰ-factor activity produced by diets K-6 and K-11 showed that the essential material supplied by pancreas powder was not supplied by similar amounts of dietary casein.

It was thus evident that barley, wheat bran, corn, pancreas powder, dried skimmed milk and alfalfa were supplying nutrients essential for maximal ϰ-factor activity.

The diets K-1, K-2, K-5.2, K-6 or K-11, K-12, and K-14 were adopted as basal diets since chickens, given these diets, would have plasma ϰ-factor levels

Table 4. Composition of experimental diets.

Ingredients	Composition of diets in grams							
	K-1	K-2	K-5.2	K-6	K-11	K-12	K-13	K-14
Casein, Vitamin Test [a]	—	—	—	150	—	—	—	—
Casein, Stege [b]	—	—	—	—	150	—	—	—
Pancreas powder [c]	150	150	150	—	—	150	150	150
Dried skimmed milk	100	100	100	100	100	—	100	100
Salt mixture [c]	50	50	50	50	50	50	50	50
Vitamin-sucrose mixture [d]	105	105	105	105	105	105	105	105
Ground corn	250	250	—	250	250	250	—	250
Ether-extracted ground corn	—	—	200	—	—	—	—	—
Ground barley	—	200	200	200	200	200	200	200
Wheat bran	100	—	85	85	85	85	85	85
Dried alfalfa	60	60	60	60	60	60	60	—
Refined peanut oil	—	—	50	—	—	—	—	—
Corn oil	—	—	—	—	—	—	50	—
Sucrose	185	85	—	—	—	100	200	60
Vitamins A and D[2]								

a—d *cf.* footnote to Table 1.

specifically sensitive to the active principles in barley, wheat bran, corn oil, pancreas powder, dried skimmed milk and alfalfa, respectively.

Extraction of the active principles from the various sources could thus be attempted and studies of their behavior during fractionation procedures started.

1. *Concentration of the active principles in barley.* In Table 5 are summarized the results from testing of the various fractions obtained from barley. It will be seen that the active factor was not extracted by ether (By-1), and that the residue after ethanol extraction was inactive (By-3). After partition of the ethanol extracts (By-21 and By-22), the ether phases (By-211 and By-221) were without activity. Butanol extracts (By-212 and By-222) of the lower phases were not significantly active. All activity was found in By-223, whereas By-213 was inactive. This indicated that the active factor was completely precipitated from the original ethanol extract by cooling to —15°C.

Further fractionation of By-223 revealed that the active factor could not be precipitated by barium at pH 9 (By-2231) and not with neutral lead acetate at pH 6 (By-2232), but was precipitated by basic lead acetate at pH 8 (By-2233) with no demonstrable activity being left in the filtrate (By-2234).

After treatment of By-2233 with phosphotungstic acid the filtrate fraction (By-22333) was inactive, indicating that the active factor had been completely precipitated. The slight activity of By-22331, but pronounced activity of By-22332, showed that the active factor formed a compound with phosphotungstic acid which was almost insoluble in 90 % acetone.

2. *Concentration of the active factor in wheat bran.* In Table 6 are summarized the results from testing of the various fractions obtained from wheat bran. It will be seen that the active factor was not extracted by ether (Hk-1), and

Table 5. Effect of barley fractions fed as supplements to diet No. K-1.

Supplement	Daily amounts, in equivalents of unfractionated barley	x-factor level in %	
		Before feeding of supplement	After feeding of supplement
By-1	30 g	70	50
By-3	20 % of diet	70	70
By-211 + By-221	20 g	65	55
By-212 + By-222	20 g	55	60
By-213	20 g	60	50
By-223	20 g	50	100
By-2231	15 g	65	60
By-2232	15 g	60	60
By-2233	15 g	65	100
By-2234	15 g	70	65
By-22331	15 g	60	65
By-22332	15 g	65	100
By-22333	15 g	65	65

that the residue after ethanol extraction was inactive (Hk-3). After partition of the ethanol extracts (Hk-21 and Hk-22) the ether layers (Hk-211 and Hk-221) did not contain the active factor. Butanol extracts (Hk-212 and Hk-222) of the lower phases were inactive. The butanol extracted solutions carried all activity. The slight activity of Hk-213, but pronounced activity of Hk-223, showed that the main part of the active factor had been precipitated by cooling the original ethanol extract to −15°C.

Further fractionation of Hk-223 revealed that the active factor could not be precipitated by barium at pH 9 (Hk-2231). It was not precipitated by neutral

Table 6. Effect of wheat bran fractions fed as supplements to diet No. K-2.

Supplement	Daily amounts, in equivalents of unfractionated wheat bran	x-factor level in %	
		Before feeding of supplement	After feeding of supplement
Hk-1	20 g	55	50
Hk-3	8 % of diet	70	55
Hk-211 + Hk-221	10 g	65	65
Hk-212 + Hk-222	10 g	65	60
Hk-213	10 g	60	65
Hk-223	10 g	50	100
Hk-2231	8 g	—	70
Hk-2232	8 g	65	70
Hk-2233	8 g	—	65
Hk-2234	8 g	70	100
Hk-22341	8 g	70	55
Hk-22342	8 g	75	100
Hk-22343	8 g	65	65

Table 7. Effect of pancreas powder fractions fed as supplements to diet No. K-6.

Supplement	Daily amounts, in equivalents of unfractionated pancreas powder	x-factor level in %	
		Before feeding of supplement	After feeding of supplement
Pa-3	15 % of diet	65	60
Pa-211 + Pa-221	10 g	75	60
Pa-212 + Pa-222	10 g	60	55
Pa-213	10 g	55	100
Pa-223	10 g	60	100
Pa-2031	10 g	70	65
Pa-2032	10 g	65	60
Pa-2033	10 g	75	100
Pa-2034	10 g	60	70
Pa-20331	10 g	75	60
Pa-20332	10 g	75	100
Pa-20333	10 g	65	70
Pa-20333	10 g	90	75

lead acetate at pH 6 (Hk-2232), nor with basic lead acetate at pH 8 (Hk-2233), but remained in the final filtrate (Hk-2234).

After treatment of Hk-2234 with phosphotungstic acid, the filtrate fraction (Hk-22343) was inactive, indicating that the active factor had been completely precipitated. No activity was found in Hk-22341, but pronounced activity in Hk-22342, showing that the active factor formed a compound with phosphotungstic acid which was insoluble in 90 % acetone.

3. *Concentration of the active factor in pancreas powder.* In Table 7 are summarized the results from testing of the various fractions obtained from ether extracted pancreas powder.

The active factor was not present in the residue after ethanol extraction (Pa-3). After partition of the ethanol extracts (Pa-21 and Pa-22), the ether layers (Pa-211 and Pa-221) were without activity. Butanol extracts (Pa-212 and Pa-222) of the lower phases were inactive. The butanol extracted solutions

Table 8. Effect of corn oil fractions fed as supplements to diet No. K-5.2.

Supplement	Daily amounts, in equivalents of unfractionated corn oil	x-factor level in %	
		Before feeding of supplement	After feeding of supplement
Ma-11	5 g	70	100
Ma-12	5 g	60	100
Ma-13	8 g	75	70
Ma-14	5 g	—	75
Ma-100 + Ma-101	5 g	75	65
Ma-102	5 g	60	100
Ma-103	5 g	70	60

Table 9. Effect of dried skimmed milk fractions fed as supplements to diet No. K-12.

Supplement	Daily amounts, in equivalents of unfractionated dried skimmed milk	κ-factor level in %	
		Before feeding of supplement	After feeding of supplement
Tm-1	10 g	50	60
Tm-3	10 % of diet	60	50
Tm-211 + Tm-221	10 g	65	65
Tm-212 + Tm-222	6 g	65	80
Tm-213	6 g	80	100
Tm-213	6 g	55	100
Tm-223	10 g	60	100
Tm-2031	6 g	—	60
Tm-2032	7 g	65	100
Tm-2033	7 g	75	70
Tm-2034	7 g	75	70
Tm-20321	7 g	70	85
Tm-20322	7 g	70	100
Tm-20323	7 g	80	65

carried all activity. Pa-213 and Pa-223 were both active and thus showed that the active factor had been only partly precipitated from the original ethanol extract by cooling to −15°C. The two fractions were therefore combined and designated Pa-203.

Further fractionation of Pa-203 revealed that the active factor could not be precipitated by barium at pH 9 (Pa-2031), and not with neutral lead acetate at pH 6 (Pa-2032). The precipitate obtained by addition of basic lead acetate at pH 8 (Pa-2033) contained the active factor, and very little activity, if any, was left in the filtrate (Pa-2034).

After treatment of Pa-2033 with phosphotungstic acid the filtrate was inactive (Pa-20333). The active factor had been completely precipitated. Activity was found in Pa-20332, but not in Pa-20331, showing that the active factor formed a compound with phosphotungstic acid, which was insoluble in 90 % acetone.

4. *Concentration of the active factor in corn oil.* In Table 8 are summarized the results from testing of the various fractions obtained from corn oil.

After saponification of corn oil and fractionation of the unsaponifiable matter, the active material was concentrated in the fractions Ma-11 and Ma-12. This meant that the active factor in corn oil was unsaponifiable and did not belong to the sterols. The sterol fraction (Ma-13) and the fatty acids (Ma-14) were inactive.

The two active fractions (Ma-11 and Ma-12) were combined (Ma-10) and chromatographed. After washing this solution through a calcium carbonate column the adsorbed material was eluted with ether (Ma-103) and found to be inactive. The active factor was adsorbed on an alumina column. The fraction passing through this column by washing with light petroleum (Ma-100) and the material eluted with 30 % benzene in light petroleum (Ma-101) were inac-

Table 10. Effect of alfalfa fractions fed as supplements to diet No. K-14.

Supplements	Daily amounts, in equivalents of unfractionated alfalfa	x-factor level in %	
		Before feeding of supplement	After feeding of supplement
Lu-1	5 g	60	60
Lu-3	6 % of diet	70	60
Lu-211 + Lu-221	3 g	75	65
Lu-212 + Lu-222	4 g	—	70
Lu-213	4 g	70	65
Lu-223	5 g	60	100
Lu-2231	4 g	65	60
Lu-2231	4 g	80	65
Lu-2232	4 g	65	65
Lu-2233	4 g	65	65
Lu-2234	4 g	85	100
Lu-22341	4 g	—	70
Lu-22342	4 g	65	100
Lu-22343	4 g	70	65

tive. The active factor could be eluted with 10 % methanol in ethyl ether (Ma-102).

5. *Concentration of the active factor in dried skimmed milk.* In Table 9 are summarized the results from testing of the various fractions obtained from dried skimmed milk. The active factor was not extracted with ether (Tm-1), and the residue after ethanol extraction was inactive (Tm-3). After partition of the ethanol extracts the ether layers (Tm-211 and Tm-221) were inactive. Butanol extracts (Tm-212 and Tm-222) of the lower phases contained some activity, but the main part remained in the auqeous phases (Tm-213 and Tm-223). The latter fractions were both active, and the active factor had thus only been partly precipitated by cooling the original ethanol extract to −15°C. The two fractions were combined and designated Tm-203.

Further fractionation of fraction Tm-203 revealed that the active factor could not be precipitated by barium at pH 9, but was precipitated by addition of neutral lead acetate at pH 6 (Tm-2032). No further activity was precipitated by basic lead acetate at pH 8 (Tm-2033), and no activity remained in the final filtrate (Tm-2034).

After treatment of Tm-2032 with phosphotungstic acid, the filtrate was inactive (Tm-20323). The active factor had thus been precipitated completely. Some activity was found in Tm-20321, but the main part was in Tm-20322, showing that the active factor formed a compound with phosphotungstic acid which was slightly soluble in 90 % acetone.

6. *Concentration of the active factor in alfalfa.* In Table 10 are summarized the results from testing of the various fractions obtained from dried alfalfa. The active factor could not be extracted with ether (Lu-1), and no activity was left in the residue after ethanol extraction (Lu-3).

After partition of the ethanol extracts (Lu-21 and Lu-22) the ether layers (Lu-211 and Lu-221) were found to be inactive. Butanol extracts (Lu-212 and Lu-222) of the lower phases were inactive. Of the butanol extracted solutions, only Lu-223 was active, whereas Lu-213 had no demonstrable activity. This showed that the active factor had been precipitated completely by cooling the original ethanol extract to −15°C.

Further fractionation of Lu-223 revealed that the active factor could not be precipitated by barium at pH 9 (Lu-2231). The precipitate obtained by addition of neutral lead acetate at pH 6 (Lu-2232) was inactive. So was the precipitate obtained by addition of basic lead acetate at pH 8 (Lu-2233). The active factor remained in the final filtrate (Lu-2234).

After treatment of Lu-2234 with phosphotungstic acid, the filtrate was inactive (Lu-22343). The active factor had been precipitated completely. Lu-22341 was inactive, whereas Lu-22342 carried all activity, showing that the active factor in alfalfa had formed a compound with phosphotungstic acid which was insoluble in 90 % acetone.

DISCUSSION

The experiments demonstrate that the level of $\varkappa$-factor in chicken plasma depends on dietary factors, and that $\varkappa$-factor concentration cannot by dietary means be raised above a certain level, which is regarded as the maximal level of $\varkappa$-factor in chicken plasma. $\varkappa$-factor concentrations below the maximal level have, so far, always turned out to be due to dietary deficiencies.

The design of an adequate diet — able to maintain $\varkappa$-factor at the maximal level during the experimental periods — and of deficient diets — producing lower levels of $\varkappa$-factor — permitted a study of the active principles in the various nutrients of the complete diet, which were found to be essential for maximal $\varkappa$-factor concentration in plasma. So far, work on extraction and preliminary concentration of the active principles has shown that fractions, carrying the activity, may be separated from the bulk of inactive material by conventional methods. The activity of each essential nutrient thus seems to be due to its content of a special *nutritional factor* which is not found in comparable quantities in the other ingredients of the adequate diet. Thus, the effect of corn in the diet is due to a fat-soluble substance, present in corn oil. It is non-saponifiable and does not seem to be sterol. From its behavior on partition and chromatography one might expect it to be a hydrocarbon with a relatively small number of polar groups.

The effects of the other five essential ingredients are due to alcohol-extractable, water-soluble substances. None of the factors can be precipitated from aqueous solutions by barium hydroxide. Some, however, form insoluble compounds with lead, whereas others are not precipitated from aqueous solutions on addition of lead salts. All the water-soluble factors form precipitates with phosphotungstic acid which show, at most, a limited solubility in 90 % acetone. One might therefore expect these factors to be nitrogen-containg compounds with a relatively complex structure.

It seems logical to conclude that the $\varkappa$-factor level in chicken plasma is controlled by a set of nutritional factors, each of which may act as a limiting factor for $\varkappa$-factor formation.

Depending on their previous dietary situation chickens may have greater or smaller stores of these factors. Only when these stores have been exhausted, the $\varkappa$-factor will drop and indicate a dietary insufficiency. One should therefore expect that diets may have "hidden deficiencies". If, *e.g.*, a certain diet limits $\varkappa$-factor level to 20—30 % of maximal through the amount of one essential dietary factor, the chicken will be able to build up stores of other essential dietary factors, even if these factors are provided in amounts below that required for maximal $\varkappa$-factor level. On admission of adequate amounts of the limiting factor, it might be expected that $\varkappa$-factor would show a rise, even up to 100 %. With this increased output of $\varkappa$-factor, the stores of the other essential factors, not adequately provided by the diet, would sooner or later be exhausted, whereby one of these factors would become the limiting factor for the $\varkappa$-factor level. Consequently, the $\varkappa$-factor concentration would gradually drop to a level determined by the dietary supply of this factor. This might be the explanation for the transient increases observed after changing diets. The experiment, in which a vitamin K-deficient diet was supplemented with Synkavit, was particularly illustrating. After Synkavit supplementation a rise to 100 % was observed. Then the $\varkappa$-factor level again declined, indicating that dietary factors, other than vitamin K, had become limiting factors for the $\varkappa$-factor level.

In studies of this nature one must obviously always be prepared to find $\varkappa$-factor deficiencies due to dietary insufficiencies not observed previously. The demand for dietary factors in addition to those described may in the present studies have been covered by reserves obtained from the egg, or provided by the earliest diet, or even supplied through the activities of the intestinal flora. The present work only indicates that at least six unidentified nutritional factors, in addition to vitamin K, are involved directly or indirectly in the formation of $\varkappa$-factor. The reports by Howard and co-workers [3,4] may in this connection be seen as another example of relations between dietary factors and blood coagulation factors. These workers demonstrated that plasma from scorbutic guinea-pigs was not activated by glass, showed decreased blood thromboplastin formation and had prolonged Quick time, but normal coagulation time with Russel's viper venom-cephalin. These symptoms were prevented by vitamin C. The reports indicate a role of vitamin C in the formation of the glass activable factor(s), which act in the intrinsic coagulation system, and of a factor (or factors) acting in the extrinsic system.

The present work gives no information as to the mode of action of vitamin K and the six unidentified factors in determining the $\varkappa$-factor level of plasma. However, each of these nutritional factors probably plays a specific part in the mechanism for formation of $\varkappa$-factor, since none of the six unidentified factors can replace vitamin K or any of the other five, and vitamin K cannot replace any of the six unidentified factors. In the same sense as vitamin K is regarded as a vitamin for formation of $\varkappa$-factor, prothrombin, proconvertin and other coagulation factors, it might be justified to regard the six unidentified nutritional factors as vitamins or co-vitamins for formation of $\varkappa$-factor.

Whether or not they are of importance for formation of other proteins or coagulation factors is not known at present. Their classification as true vitamins will of course, depend on determination of the quantities in which they are required, or rather by deciding whether they serve as catalysts for essential steps in the formation of $\varkappa$-factor or as structural units in the $\varkappa$-factor molecule. In the latter case the designation vitamin might not be proper. These problems must await the preparation of the pure compounds. Much work remains to be done before this eventually becomes possible.

REFERENCES

1. Sørbye, Ø. and Kruse, I. *Acta Chem. Scand.* **14** (1960) 2177.
2. Dam, H. and Søndergaard, E. *Acta Pharmacol. Toxicol.* **9** (1953) 131.
3. Flute, D. T. and Howard, A. N. *Brit. J. Haematol.* **5** (1959) 421.
4. Barkham, D. and Howard, A. N. *Brit. J. Nutrition* **13** (1959) 389.

Received March 16, 1961.

ACTA CHEMICA SCANDINAVICA 15 (1961) 1532–1544

Hydrolysis of Protolytic Esters

ALLAN ÅGREN, ULLA HEDSTEN and BRITTA JONSSON

Department of Chemistry, Royal Pharmaceutical Institute, Stockholm, Sweden

The hydrolysis of several esters with protolytic groups has been investigated in alkaline and acidic solution. The relation between reaction velocity and pH is discussed together with the best conditions for the determination of the activation energies of such esters.

In the alkaline hydrolysis of an ester of a carboxylic acid the following equation is valid

$$R_1{\cdot}COOR_2 + OH^- = R_1{\cdot}COO^- + R_2OH$$

where R_1 and R_2 are radicals. This process has been studied with a great number of esters, both aliphatic and aromatic. Almost always the process has been found to be a second order one, and thus the following equation is valid

$$-dc/dt = k_{oh} \cdot c \cdot [OH^-]$$

where c is the concentration of the ester at the time t and $[OH^-]$ is the concentration of hydroxyl ion at the same time.

If the hydrolysis is performed at a constant pH value the process is pseudo monomolecular

$$-dc/dt = k'_{oh} \cdot c$$

where

$$k'_{oh} = k_{oh} \cdot [OH^-] \quad (1)$$

In the acidic hydrolysis of the ester the reaction may be written

$$R_1{\cdot}COOR_2 + H_2O = R_1{\cdot}COOH + R_2OH$$

This process is catalyzed by hydrogen ions, and often the following equation is found to be valid

$$-dc/dt = k_h \cdot c \cdot [H^+]$$

As the hydrogen ions are not consumed in the process and the acid formed is weak, $[H^+]$ is constant and thus the equation may be written

$$-dc/dt = k'_h \cdot c$$

where

$$k'_h = k_h \cdot [H^+] \qquad (2)$$

Taking logarithms, eqns. (1) and (2) may be written

$$\log k'_{oh} = \log k_{oh} + pH - pK_w$$

and

$$\log k'_h = \log k_h - pH$$

respectively, where pK_w is the negative logarithm of the ion product of water. Thus, k'_{oh} and k'_h change with varying pH as shown in Fig. 1. In this figure log k' refers to log k'_h in the left part of the figure, and to log k'_{oh} in the right part. The two lines cross at a pH value where the two processes are equally fast. Near this point the curved line shows the true velocity of the hydrolysis. (*Cf.* Tammelin and Larsson [1].)

Sometimes R_1 or R_2 in the ester, is a protolytic group. Depending on the pH of the solution, ethyl salicylate for example, exists as a molecule or as an ion:

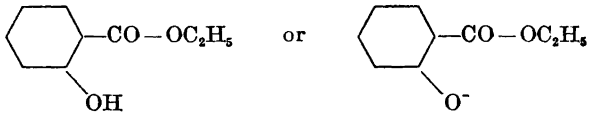

In a similar manner diethyl amino ethyl benzoate can exist as

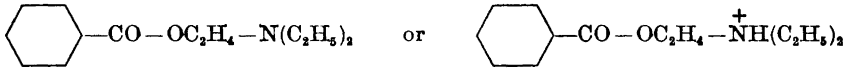

In the first example the ester may exist as an anion ester, in the second example as a cation ester.

Is such cases one may expect that the acidic form and the basic form of the ester may be hydrolyzed with different velocities. This is true in alkaline hydrolysis at least. In acidic hydrolysis there seems to be another situation. In the following, alkaline and acidic hydrolysis will be discussed separately.

ALKALINE HYDROLYSIS

In alkaline hydrolysis the reaction mechanism may be formulated in the following manner:

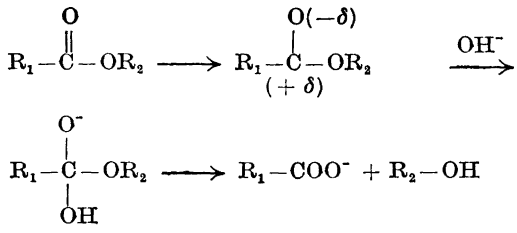

The carbonyl carbon has a partial positive charge, which attracts the hydroxyl ion. If R_1 or R_2 is a group which is electron attracting the process will be favoured. If the group is electron releasing the process will be slower. If the groups R_1 or R_2 have a positive or negative ionic charge this effect will be still more pronounced.

If the acidic and basic forms of the ester are called e_a and e_b, the reaction velocity may be written:

$$-dc/dt = k_{boh} \cdot [e_b] \cdot [OH^-] + k_{aoh} \cdot [e_a] \cdot [OH^-] \quad (3)$$

where

$$c = [e_b] + [e_a]$$

and

$$[e_a] \cdot [OH^-] = [e_b] \cdot K_b \quad (4)$$

K_b is the base constant of the ester. By combining these equations one obtains

$$-\frac{dc}{dt} = \frac{k_{boh} \cdot [OH^-]^2 + k_{aoh} \cdot K_b \cdot [OH^-]}{K_b + [OH^-]} \cdot c$$

If the hydroxyl ion concentration is constant this equation may be written

$$-dc/dt = k'_{oh} \cdot c$$

where

$$k'_{oh} = \frac{k_{boh} \cdot [OH^-]^2 + k_{aoh} \cdot K_b \cdot [OH^-]}{K_b + [OH^-]} \quad (5)$$

The reaction is pseudo monomolecular. Three different cases may be distinguished.

1. $[OH^-] \gg K_b \cdot k_{aoh}/k_{boh}$. Eqn. (5) may be transformed to

$$k'_{oh} = k_{boh} \cdot [OH^-]$$

or by taking logarithms

$$\log k'_{oh} = \log k_{boh} + pH - pK_w$$

2. $[OH^-] \ll K_b \cdot k_{aoh}/k_{boh}$. Eqn. (5) may be written

$$\log k'_{oh} = \log k_{aoh} + pH - pK_w$$

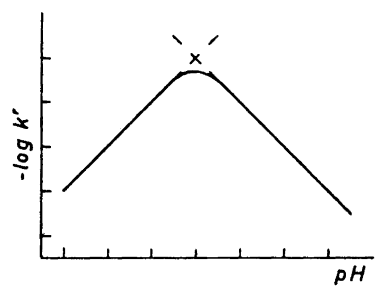

Fig. 1. log k'_h and log k'_{oh} (to the left and to the right) *vs.* pH.

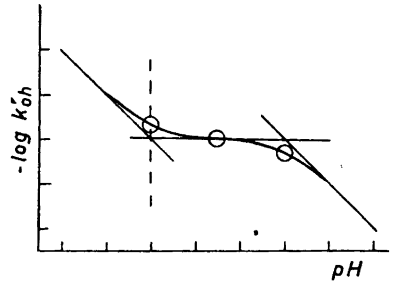

Fig. 2. log k'_{oh} *vs.* pH. Theoretical curve when log k_{aoh} = log k_{boh} + 3.

In both cases a straight line is formed when log k'_{oh} is plotted *vs.* pH. The two lines are identical only if $k_{aoh} = k_{boh}$. As has been noted before, this will not be the case in practice.

In the range where $[OH^-]$ is of the same order as $K_b \cdot k_{aoh}/k_{boh}$ the curve is bent and here the third case may be of interest.

3. $[OH^-] = K_b \cdot$ Eqn. (5) may be written

$$k'_{oh} = \frac{k_{boh} + k_{aoh}}{2} \cdot K_b$$

But k_{aoh} always is bigger than k_{boh}, and thus

$$\log k'_{oh} = \log k_{aoh} + \log K_b - \log 2$$

Now the line may be drawn for the whole range of pH as is shown in Fig. 2. The curved part of the line has its mid point at

$$\begin{cases} \mathrm{pH} = \mathrm{p}K_a + \frac{1}{2}(\log k_{aoh} - \log k_{boh}) \\ \log k'_{oh} = \log k_{aoh} + \log K_b \end{cases}$$

and if the distance between the straight lines is big enough (> 3 log units) the curve will be horizontal in this range, that is the reaction velocity is independent of pH.

This can be shown in a simpler manner from eqns. (3) and (4). By combining them one obtains

$$-\mathrm{d}c/\mathrm{d}t = k_{boh} \cdot [e_b] \cdot [OH^-] + k_{aoh} \cdot [e_b] \cdot K_b$$

or

$$-\mathrm{d}c/\mathrm{d}t = (k_{boh} \cdot [OH^-] + k_{aoh} \cdot K_b) \cdot [e_b]$$

If $k_{boh} \cdot [OH^-] \ll k_{aoh} \cdot K_b$ the expression in the brackets will be constant. Further, if $[OH^-] \gg K_b$ then $[e_b] = c$. That is, the reaction velocity will be independent of pH within a range where the following conditions are fulfilled

$$K_b \ll [OH^-] \ll K_b \cdot k_{aoh}/k_{boh}$$

This has been shown by Pekkarinen and Tommila [2], who studied alkyl salicylates.

That the reaction velocity is not a linear function of pH in alkalineh ydrolysis of some esters has also been shown by Higuchi *et al.*[3].

As already noted, an ester of the type

$$R_1\text{—}CO\text{—}OC_2H_4\text{—}N(R_2)_2$$

may add a proton and form the corresponding ammonium compound

$$R_1\text{—}CO\text{—}OC_2H_4\text{—}\overset{+}{N}H(R_2)_2 \qquad \text{(I)}$$

and this compound is more easily hydrolyzed in alkaline solution than the uncharged ester. The nitrogen atom may also acquire a positive charge by transformation to a quaternary compound of the following type

$$R_1\text{—}CO\text{—}OC_2H_4\text{—}\overset{+}{N}(R_2)_3 \qquad \text{(II)}$$

This product, as one might expect, is also more easily hydrolyzed than the primary ester. Such a case has been investigated by Butterworth *et al.*[4] who studied acetyl choline and ethyl acetate.

In order to compare reaction velocities of the different esters the bimolecular velocity constants k_{boh} and k_{aoh} must be calculated. These constants are independent of pH. This calculation can be made using eqn. (1). The effect of the positive charge is not, however, the same in both cases (I and II). A similar effect was found by Hansen [5]. The addition of a proton results in an increase of the velocity constant by about 1 000 (see for example esters Nos. 1, 4, and 10 in the experimental part of this work). The quaternary ester is hydrolyzed only about 15 times as fast as the primary ester without any ionic charge (compare esters Nos. 1 and 2 or 4 and 5). This may be explained by the following formulas

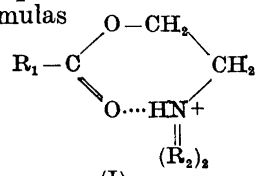

(I)

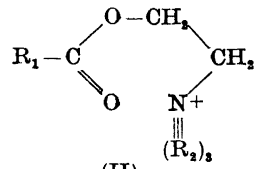

(II)

In formula I there is a hydrogen bond because of which the charge of the carbonyl carbon is more pronounced than in formula II.

Esters which have two or more protolytic groups have also been studied in this work. An example of this type is

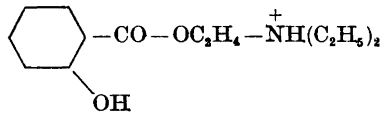

This compound is a dibasic acid and the difference between the pK_a values is relatively small. In this case the velocity constant of the positively charged ester was found to be about 10^5 times as great as that of the negatively charged ester. (Compare esters Nos. 3, 7, and 8.)

ACIDIC HYDROLYSIS

The mechanism of acidic hydrolysis of esters is usually described in the following manner

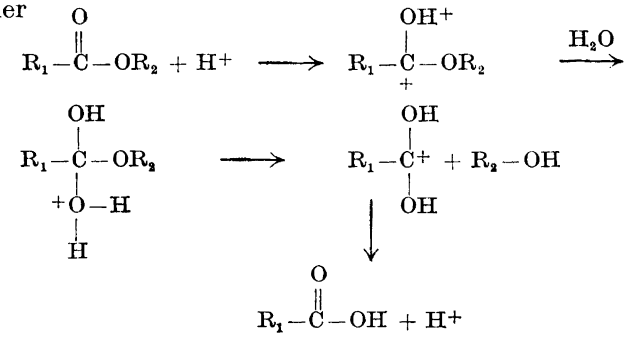

The reaction velocity is often, but not always, proportional to the hydrogen ion concentration.

In the acidic hydrolysis also, different substituents in R_1 and R_2 influence the reaction velocity. It has been found that electron attracting substituents favour the process and electron releasing substituents make the reaction slower.

However, in some cases the mechanism seems to be of another kind. Thus, when the mono ethyl ester of phthalic acid is studied there is found to be a relationship between the reaction velocity and the acid constant, of the same kind as has been described for alkaline hydrolysis. Bender [6] explains this fact by the assumption that the process is catalyzed internally by the carboxylic group. Phthalic acid anhydride is formed as an intermediate.

No matter what the mechanism may be, the experimental results (ester No. 11) show that the reaction velocity may be expressed by the following equation

$$-\mathrm{d}c/\mathrm{d}t = k_{\mathrm{bh}} \cdot [\mathrm{e_b}] \cdot [\mathrm{H^+}] + k_{\mathrm{ah}} \cdot [\mathrm{e_a}] \cdot [\mathrm{H^+}] \qquad (6)$$

where

$$c = [\mathrm{e_b}] + [\mathrm{e_a}]$$

and

$$[\mathrm{e_b}] \cdot [\mathrm{H^+}] = [\mathrm{e_a}] \cdot K_{\mathrm{a}} \qquad (7)$$

K_{a} is the acid constant of the ester. By transformations quite analogous to those shown for alkaline hydrolysis, one obtains

$$-\mathrm{d}c/\mathrm{d}t = k'_{\mathrm{h}} \cdot c$$

where

$$k'_{\mathrm{h}} = \frac{k_{\mathrm{ah}} \cdot [\mathrm{H^+}]^2 + K_{\mathrm{a}} \cdot k_{\mathrm{bh}} \cdot [\mathrm{H^+}]}{K_{\mathrm{a}} + [\mathrm{H^+}]} \qquad (8)$$

Thus, the reaction is monomolecular when the pH is constant. It can easily be shown that $\log k'_{\mathrm{h}}$ varies with varying pH as is shown in Fig. 3.

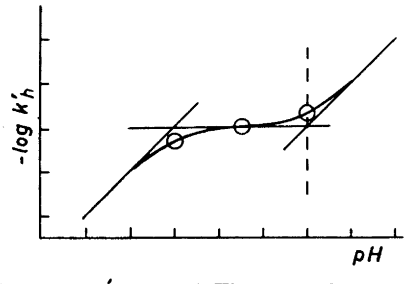

Fig. 3. $\log k'_{\mathrm{h}}$ *vs.* pH. Theoretical curve according to eqn. (8) when $\log k_{\mathrm{ah}} + 3 = \log k_{\mathrm{bh}}$.

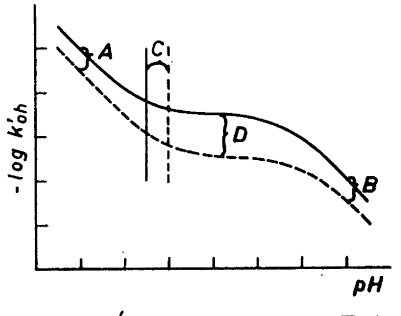

Fig. 4. $\log k'_{\mathrm{oh}}$ *vs.* pH at temp. T_1 (——) and T_2 (– – –). See text.

THE TEMPERATURE DEPENDENCE

The change of reaction velocity with temperature is given by the Arrhenius formula

$$\frac{\mathrm{d} \ln k}{\mathrm{d}T} = \frac{E}{RT^2}$$

or

$$\log k = A - \frac{E}{2.303\ RT} \tag{9}$$

where k is the velocity constant, T the absolute temperature, A is the frequency factor and E is the activation energy. A and E may be calculated when k is determined at at least two temperatures.

In the hydrolysis of an ester possessing protolytic groups, the value of the velocity constant is different for the acidic and the basic forms, that is k_{aoh} and k_{boh} in alkaline solution and k_{ah} and k_{bh} in acidic solution (at least in some cases). Each of these constants varies with T according to eqn. (9). Further, the acid constant, K_a, varies with temperature

$$\frac{\mathrm{d} \ln K_a}{\mathrm{d}T} = \frac{\Delta H}{RT^2} \tag{10}$$

where ΔH is the enthalpy increase in the dissociation.

According to eqn. (5) the monomolecular velocity constant, k'_{oh}, depends on k_{boh}, k_{aoh}, and K_b (or K_a) and further on pH. In the same manner k'_h depends on k_{bh}, k_{ah}, and K_a. Thus, the correlation between k'_{oh} (or k'_h) and the temperature is rather complicated, but it is possible to deduce the relation by differentiating eqn. (5) or (8).

These relations may be understood more simply by using graphs*. This will be illustrated only for the case of alkaline hydrolysis. Fig. 4 shows how log k'_{oh} varies with pH. The full line corresponds to the temperature T_1 and the broken line to T_2. The same figure shows the variation of k_{aoh}, k_{boh}, and K_a when the temperature is changed from T_1 to T_2:

$$A = \frac{\Delta \log k_{aoh}}{\Delta T} \qquad B = \frac{\Delta \log k_{boh}}{\Delta T}$$

$$C = \frac{\Delta \log K_a}{\Delta T} \qquad D = A + C$$

It may be seen from the figure that in the range where log k'_{oh} *vs.* pH is a straight line, eqn. (9) may be used and from the experimental results at these pH values, the activation energy (E_a or E_b, resp.) and the frequency factor (A_a or A_b, resp.) of the ester acid and the ester base may be calculated. But if the measurements are made in that range, where the lines are curved the value

* In this description the change of pK_w with T is neglected.

$$\frac{\mathrm{d} \ln k'_{oh}}{\mathrm{d}T}$$

(that is D in Fig. 4) depends upon at least two of the expressions

$$\frac{\mathrm{d} \ln k_{aoh}}{\mathrm{d}T}, \quad \frac{\mathrm{d} \ln k_{boh}}{\mathrm{d}T} \quad \text{and} \quad \frac{\mathrm{d} \ln K_a}{\mathrm{d}T}$$

In this range the values E_a and E_b can not easily be calculated. If the difference between log k_{aoh} and log k_{boh} is big enough (as is the case in Fig. 4) it can be seen that within a certain range the following equation is valid

$$\frac{\mathrm{d} \ln k'_{oh}}{\mathrm{d}T} = \frac{\mathrm{d} \ln k_{aoh}}{\mathrm{d}T} + \frac{\mathrm{d} \ln K_a}{\mathrm{d}T}$$

or

$$E' = E_a + \Delta H$$

where E' is the apparent activation energy. One concludes that the measurements have to be made in carefully chosen pH ranges, when E_a and E_b are to be estimated.

Table 1. Survey of the esters studied.

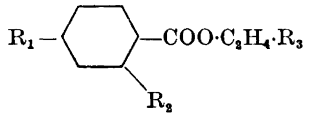

Ester No.	R_1	R_2	R_3
1	H	H	$N(C_2H_5)_2$
2	H	H	$\overset{+}{N}(C_2H_5)_3$
3	H	OH	$N(C_2H_5)_2$
4	NH_2	H	$N(C_2H_5)_2$
5	NH_2	H	$\overset{+}{N}(C_2H_5)_3$
6	NHC_4H_9	H	$N(C_2H_5)_2$
7	NH_2	OH	$N(C_2H_5)_2$
8	OH	H	$N(C_2H_5)_2$
9	OH	H	H
10	H	OH	H
11	H	COOH	H

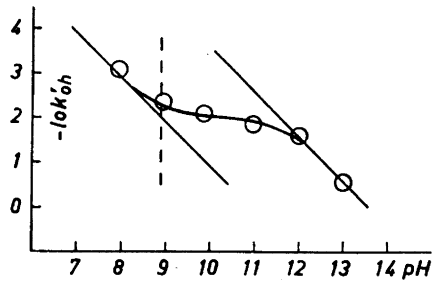

Fig. 5. Diethylaminoethyl benzoate. $pK_a = 8.84$.

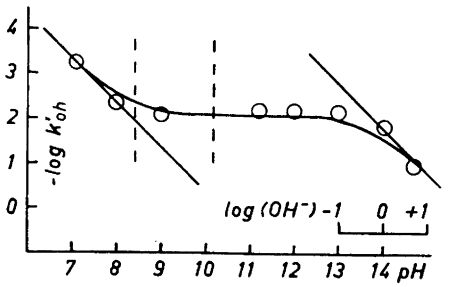

Fig. 6. Diethylaminoethyl salicylate. $pK_{a1} = 8.41$, $pK_{a2} = 10.14$.

Table 2. Diethylaminoethyl benzoate. 25.0°C. *Cf.* Fig. 5.

pH	k'_{oh} (min^{-1})
7.96	8.2×10^{-4}
8.94	4.5×10^{-3}
9.86	8.2×10^{-3}
10.95	1.40×10^{-2}
13.0	2.75×10^{-1}

Table 3. Diethylaminoethyl salicylate. 25.0°C. *Cf.* Fig. 6.

pH	k'_{oh} (min^{-1})
7.08	5.7×10^{-4}
8.00	4.4×10^{-3}
9.00	8.0×10^{-3}
11.20	6.3×10^{-3}
12.0	6.4×10^{-3}
13.0	6.8×10^{-3}
14.0	1.3×10^{-2}
14.7	1.1×10^{-1}

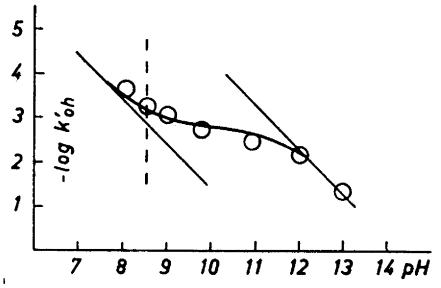

Fig. 7. Procaine. $pK_a = 8.53$.

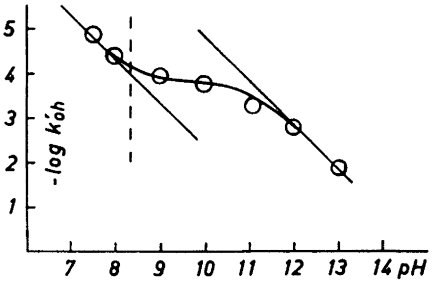

Fig. 8. Tetracaine. $pK_a = 8.33$.

Table 4. Procaine. 35.0°C. *Cf.* Fig. 7.

pH	k'_{oh} (min^{-1})
8.05	2.21×10^{-4}
8.52	5.46×10^{-4}
9.02	8.45×10^{-4}
9.52	1.48×10^{-3}
9.76	1.79×10^{-3}
10.90	3.54×10^{-3}
12.0	6.80×10^{-3}
13.0	4.82×10^{-2}

Table 5. Tetracaine. 25.0°C. *Cf.* Fig. 8.

pH	k'_{oh} (min^{-1})
7.50	1.34×10^{-5}
8.00	3.99×10^{-5}
9.00	1.15×10^{-4}
9.98	1.66×10^{-4}
11.08	5.47×10^{-4}
12.0	1.73×10^{-3}
13.0	1.43×10^{-2}

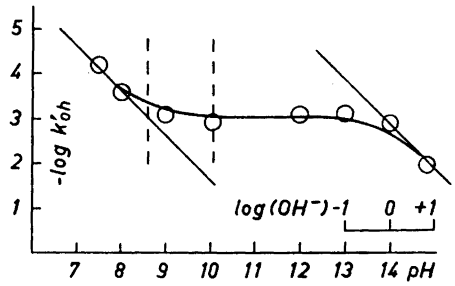

Fig. 9. Hydroxyprocaine. $pK_{a1} = 8.61$, $pK_{a2} = 10.07$.

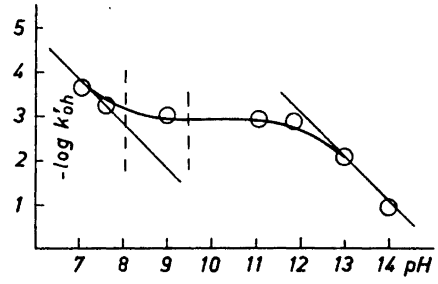

Fig. 10. Diethylaminoethyl(*p*-hydroxy) benzoate. $pK_{a1} = 8.07$, $pK_{a2} = 9.5$.

Table 6. Hydroxyprocaine. 25.0°C. *Cf.* Fig. 9.

pH	k'_{oh} (min^{-1})
7.54	2.40×10^{-4}
8.00	2.55×10^{-4}
9.00	8.52×10^{-4}
10.05	1.26×10^{-3}
12.0	8.25×10^{-4}
13.0	8.14×10^{-4}
14.0	1.69×10^{-3}
14.7	1.12×10^{-2}

Table 7. Diethylaminoethyl(*p*-hydroxy)-benzoate. 45.0°C. *Cf.* Fig. 10.

pH	k'_{oh} (min^{-1})
7.04	2.36×10^{-4}
7.60	5.87×10^{-4}
9.01	1.03×10^{-3}
11.08	1.20×10^{-3}
11.84	1.38×10^{-3}
13.0	8.96×10^{-3}
14.0	1.27×10^{-1}

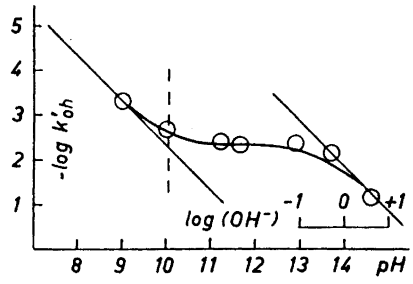

Fig. 11. Ethyl salicylate. $pK_a = 10.1$.

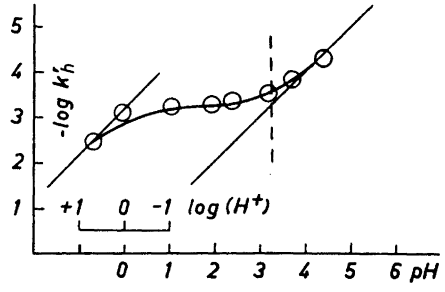

Fig. 12. Phthalic acid monoethyl ester. 60°C. $pK_a = 3.24$ (at 25°C).

Table 8. Ethyl salicylate. 25.0°C. *Cf.* Fig. 11.

pH	k'_{oh} (min^{-1})
8.02	6.31×10^{-5}
9.02	4.78×10^{-4}
9.95	2.22×10^{-3}
11.23	3.95×10^{-3}
11.64	4.15×10^{-3}
12.89	4.33×10^{-3}
13.7	7.37×10^{-3}
14.6	7.29×10^{-2}

Table 9. Phthalic acid monoethyl ester. 110°C (the pH measurements were made at 25°C). *Cf.* Fig. 12.

pH	k'_{h} (min^{-1})
− 0.7	1.87×10^{-1}
0.0	5.16×10^{-2}
1.0	3.60×10^{-2}
2.0	3.59×10^{-2}
3.00	2.91×10^{-2}
4.02	1.02×10^{-2}
5.04	2.70×10^{-3}
6.01	1.29×10^{-3}
7.10	1.21×10^{-3}
8.00	2.16×10^{-3}
9.00	1.19×10^{-2}
10.00	6.62×10^{-2}

EXPERIMENTAL

Methods. The photometric method used by Karlén and Ågren [7] has been used in this work. The extinction curve of the ester and the hydrolysis products was taken and that wave length chosen where the extinction changes are greatest. In some cases the solution was buffered to a pH value where the reaction velocity was very low.

In strongly acidic solution (pH < 2) hydrochloric acid was used, in strongly alkaline solution (pH > 12) NaOH was used. In these solutions the stoichiometric concentration of hydrogen ion or hydroxyl ion was calculated. In the pH range between 2 and 12 buffer solutions were used and pH was measured with a glass electrode and a valve potentiometer (type Radiometer PHM 4). The buffer solutions recommended in the *Swedish Pharmacopeia Ed. XI* were used and between pH 10 and 12 carbonate buffers were employed.

Table 10. Determination of the activation energies. Velocity constants (l^{-1}.mole.min^{-1}).

Ester No.	1		3		7		8	
Temp.(°C)	pH	k_{boh}	pH	k_{aoh}	pH	k_{aoh}	pH	k_{aoh}
15.0	12.00	0.975	—	—	—	—	—	—
25.0	12.00	2.48	7.08	8.26×10^{3}	7.50	200	7.04	170
35.0	12.00	5.50	7.08	9.92×10^{3}	7.50	380	7.04	310
45.0	—	—	7.08	19.05×10^{3}	7.50	780	7.04	540

Ester No.	8		9		10	
Temp.(°C)	pH	k_{boh}	pH	k_{boh}	pH	k_{aoh}
25.0	13.0	2.17×10^{-2}	13.0	1.90×10^{-2}	9.00	48
35.0	13.0	4.65×10^{-2}	13.0	3.77×10^{-2}	9.00	74
45.0	13.0	8.96×10^{-2}	13.0	7.57×10^{-2}	9.00	118

Table 11. Survey of the results.

Ester No.	Temp.	log k_{aoh}	log k_{boh}	E_a kcal.	A_a	E_b kcal.	A_b
1	25.0	3.20	0.40	—	—	15.3	11.6
2	25.0	1.84	—	—	—	—	—
3	25.0	3.67	−2.0	13.2	13.4	—	—
4	35.0	2.65	−0.20	—	—	—	—
5	25.0	0.60	—	—	—	—	—
6	25.0	1.63	−0.84	—	—	—	—
7	25.0	2.50	−2.62	12.8	11.7	—	—
8	45.0	2.73	−1.05	10.9	10.2	13.4	8.1
9	25.0	—	−1.72	—	—	13.0	7.8
10	25.0	1.50	−1.73	8.5	7.9	—	—
11	110	−1.40 *	+ 2.1 **	—	—	—	—

* log k_{ah} ** log k_{bh}

The temperature was determined with an accuracy of 0.1°.

Chemicals. The chemicals used were of analytical grade. The esters which were investigated are tabulated in Table 1. Ester No. 1 was synthesized from benzoyl chloride and diethyl amino ethanol according to Vanderhaeghe [8]. Melting point 124.5—125°. Esters Nos. 2 and 5 were synthesized as iodides by boiling diethyl amino ethyl benzoate resp. procaine with ethyl iodide according to Jones [9]. Melting points 146—150°, resp. 135—137°. Esters Nos. 3 and 8 were made according to Ref.[10]. Melting points 147°, resp. 184—186°. Ester No. 9 was made according to Cavill and Vincent [11]. Melting point 114—115°. The synthesis of ester No. 7 is given by Karlén and Ågren [7]. The other esters were commercial materials, which were purified by distillation or recrystallisation.

Results. The results are given in Tables 1—10 and Figs. 5—12. The curves are the theoretical ones from eqn. (5) or (8) which best agree with the experimental points. In the figures the pK_a values of the ester are marked by vertical lines.

Ethyl salicylate (ester No. 10) has been studied earlier by Pekkarinen and Tommila [2] who, however, worked in an acetone-water mixture. Their results agree rather well with ours. Phthalic acid mono methyl ester has been studied by Bender [6] whose results the present authors could not reproduce (in this work the ethyl ester was used). The reason for the discrepancy is not known as the experimental conditions used by Bender are very briefly described. It may be that the buffer substances used by him had a catalyzing effect. The buffers used by us had no marked catalyzing effect as was proved by varying the buffer concentration (without changing pH) between wide limits.

REFERENCES

1. Tammelin, L. E. and Larsson, L. *Svensk Farm. Tidskr.* **59** (1955) 229.
2. Pekkarinen, L. and Tommila, E. *Acta Chem. Scand.* **13** (1959) 1019.
3. Higuchi, T., Havinga, A. and Busse, L. W. *J. Am. Pharm. Assoc., Sci. Ed.* **39** (1950) 405.
4. Butterworth, J., Eley, D. D. and Stone, G. S. *Biochem. J.* **53** (1953) 30.
5. Hansen, B. *Acta Chem. Scand.* **12** (1958) 324.
6. Bender, M. L. *Chem. Revs.* **60** (1960) 53.
7. Karlén, B. and Ågren, A. *Acta Chem. Scand.* **14** (1960) 197.
8. Vanderhaeghe, H. *J. Pharm. Pharmacol.* **6** (1954) 55.
9. Jones, M. *J. Am. Chem. Soc.* **49** (1927) 1534.
10. Brit. Pat. 739, 210.
11. Cavill, G. W. K. and Vincent, J. M. *J. Soc. Chem. Ind.* **66** (1947) 175.

Received March 17, 1961.

ACTA CHEMICA SCANDINAVICA 15 (1961) 1545–1556

Formation of Free Radicals from Some Phenothiazine Derivatives as Studied by Electron Spin Resonance

CARL LAGERCRANTZ

Department of Medical Physics, University of Göteborg, Sweden

When adsorbed on the cation exchanger Dowex-50 containing a small amount of ferric iron, phenothiazine and phenothiazine derivatives such as promethazine and chlorpromazine are transformed to free radicals. The ESR-spectra of these radicals exhibit a hyperfine structure and a characteristic asymmetry. The radical spectra observed on iron-activated Dowex-50 are compared with those obtained when the phenothiazine substances are dissolved in concentrated sulphuric acid.

Michaelis and collaborators [1] have shown by potentiometric titration that certain phenothiazine dyes, such as thionine, form an intermediate between the oxidized and the reduced state analogous to the semiquinone intermediate observed in the oxidation of hydroquinone. If not dimerized, the configuration of such an intermediate involves an unpaired electron.

Depending on the pharmacological activity of several phenothiazine derivatives, it should be of interest to study the radical forming properties of these compounds. The convenience of electron spin resonance (ESR) has not been used to a great extent for such studies. The only contribution appears to be a paper by Forrest and Forrest [2], who found an ESR signal in the urine of patients treated with chlorpromazine. Free radicals could also be detected by ultraviolet irradiation of a solution of chlorpromazine. No hyperfine structure could be observed in the spectra, neither from the urine, nor from the irradiated solution. The ESR signal exhibited a certain asymmetrical shape and could only be detected in isolated solid state specimens.

In the present paper it will be shown that free radicals are formed from several phenothiazine derivatives when solutions of these compounds are poured on to the cation exchanger Dowex-50 activated with a small amount of ferric iron. The radical spectra exhibit hyperfine lines. Similar radical spectra are obtained, when the phenothiazine substances are dissolved in concentrated sulphuric acid.

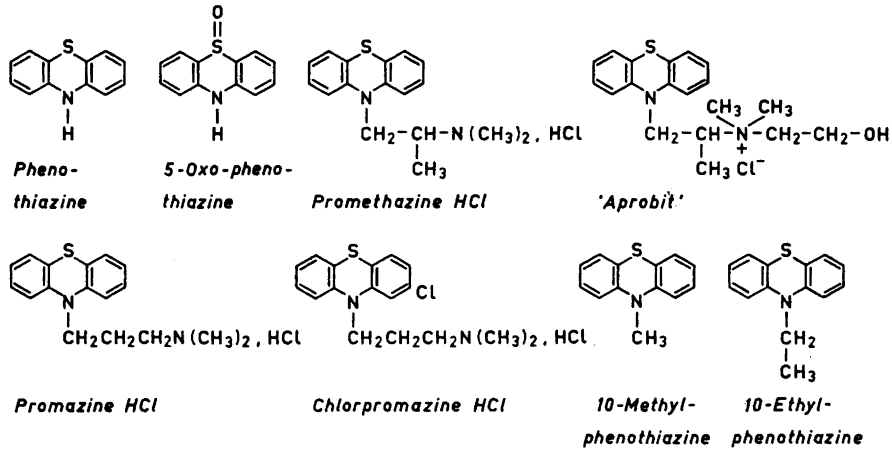

EXPERIMENTAL

The ESR-spectrometer was of a type rather similar to that described by Krongelb and Strandberg [3], and was operated at a frequency of about 9 527 Mc/s. It was equipped with a rectangular resonance cavity working in the H_{011} mode. A 100-kc sinusoidal magnetic field was superimposed on the d.c. field of the electromagnet through an internal loop located close to the specimen tube, as described by Ingram [4]. The magnet was a Varian 6″ electromagnet, type V-4007-1, equipped with ring shims. The first derivative of the absorption is recorded against the magnetic field in the ESR spectra shown. The spectra are recorded at room temperature unless otherwise stated. The experiments at liquid air temperature were performed with the aid of a glass Dewar vessel, placed inside the resonance cavity.

The structure formulae of the phenothiazine derivatives investigated are given above.

Phenothiazine. Eastman practical grade was recrystallized from *n*-butanol.

5-Oxophenothiazine was prepared from phenothiazine by oxidation with hydrogen peroxide as described by Pummerer [5].

10-Methyl- and *10-ethylphenothiazine* were prepared as described by Gilman *et al.*[6]

10-(2-Dimethylamino-1-propyl)-phenothiazine hydrochloride (promethazine hydrochloride, "Lergigan") was obtained from AB Recip, Stockholm.

10-(3-Dimethylamino-1-propyl)-phenothiazine hydrochloride (promazine hydrochloride, "Centracil") was obtained from AB Astra, Södertälje.

2-Chloro-10-(3-dimethylamino-1-propyl)-phenothiazine hydrochloride (Chlorpromazine hydrochloride) was obtained from AB Leo, Hälsingborg.

[1-(10-Phenothiazinylmethyl)-ethyl]-2-hydroxyethyl-dimethylammoniumchloride ("Aprobit") was obtained from Ab Recip, Stockholm.

The last four substances were drug preparations, and were used without further purification.

Dowex-50 × 4, 50–100 mesh, was purified according to the procedure described by Moore and Stein [7].

Concentrated sulphuric acid-d_2 (D_2SO_4) was delivered by Merck & Co. Ltd, Montreal.

The experiments with the cation exchanger were performed as follows. The specimen tube was filled with the moist ion exchanger. The solution of the substance to be studied was then poured into the tube. After removing air bubbles by shaking, the specimen was ready for recording in the spectrometer. In other experiments, the supernatant solution was removed on a Büchner funnel after equilibration, and the resin washed several times with the solvent before recording the ESR-spectrum. The concentration was 0.05 M both in the experiments on Dowex-50 and that with sulphuric acid, unless otherwise stated. The solvent used is stated in the figure captions.

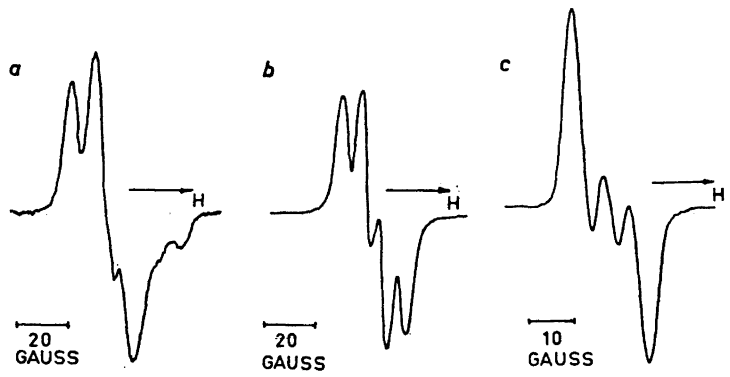

Fig. 1. Phenothiazine: *a*) on Dowex-50. Solvent: benzene. The resin was separated from the supernatant and washed with the solvent before the spectrum was recorded; *b*) in conc. H_2SO_4; *c*) in conc. D_2SO_4.

RESULTS

A. Radicals produced on activated Dowex-50 H^+. When a solution of the phenothiazine derivatives mentioned above is poured on the strongly acid, sulphonated cation exchanger Dowex-50 in the hydrogen form (H^+), ESR-spectra with a hyperfine structure are obtained which indicate the presence of free radicals. In the majority of the substances investigated, the radical concentration reached the maximum value a few minutes after the solution had been in contact with the resin. In order to obtain radicals from promethazine hydrochloride and "Aprobit", however, it was necessary to remove the solvent to some extent from the resin by drying *in vacuo* for about half an hour after the resin had been separated from the solution and washed by the solvent.

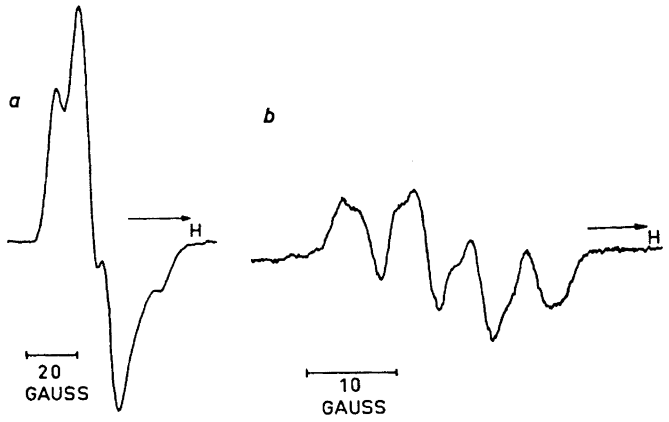

Fig. 2. 5-Oxo-phenothiazine: *a*) on Dowex-50. Solvent: ethanol. The resin was separated from the supernatant and washed with the solvent before the spectrum was recorded; *b*) in conc. H_2SO_4.

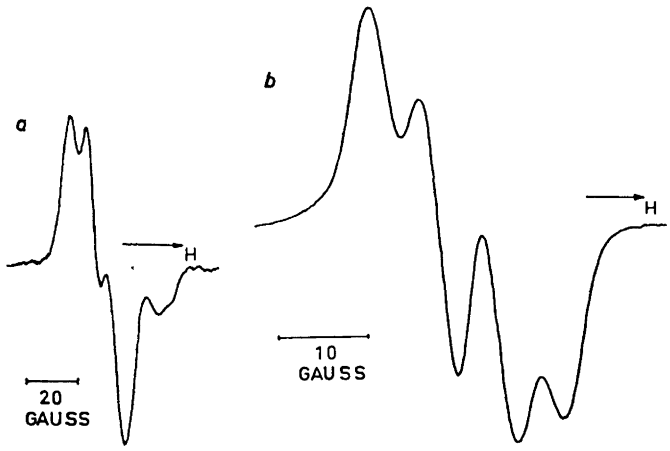

Fig. 3. Promethazine·HCl: *a*) on Dowex-50. Solvent: water. The resin was separated from the supernatant, washed with the solvent and dried for half an hour *in vacuo* before the spectrum was recorded; *b*) in conc. H_2SO_4.

The radicals formed are firmly attached to the resin-phase since the ESR-spectra remained unchanged after the resin had been separated from the solution and washed several times with the solvent.

In order to obtain free radicals, a small amount of ferric (III) iron must be present on the ion exchanger prior to absorption of the phenothiazine derivative. If the ion exchanger is washed with 4 N HCl until the wash-water is free from ferric iron, as indicated by a negative colour-reaction with alkali rhodanide, no ESR signal will be obtained. The resin can be wholly reactivated subsequent to equilibration against a 10^{-4} M $FeCl_3$ solution, followed by washing with H_2O.

With increased concentration of the ferric iron on the resin, the ESR-spectrum gradually loses the hyperfine structure, and at higher concentration a single line only is seen. When the iron concentration is rather high, as occurs after equilibration against a 0.1 M $FeCl_3$ solution, no hyperfine pattern can be observed. In this case the radicals formed are not attached to the resin, as evidenced by the nonappearance of an ESR signal subsequent to separation of the phases and after washing the resin with the solvent.

ESR-spectra similar to those registered on Dowex-50 when activated with ferric iron, can be observed when ceric (Ce^{4+}) ions are present instead of ferric iron. After treating the resin containing phenothiazine radicals with a solution of ascorbic acid in H_2O, the ESR signal is completely abolished.

Specimens of the cation exchanger with the adsorbed radicals could be stored in sealed tubes for several weeks at room temperature without any change in the ESR-spectrum.

When the resin is dried even at room temperature, unpurified preparations of Dowex-50 sometimes give rise to a single narrow ESR line without any phenothiazine substance adsorbed. This signal, which is especially pro-

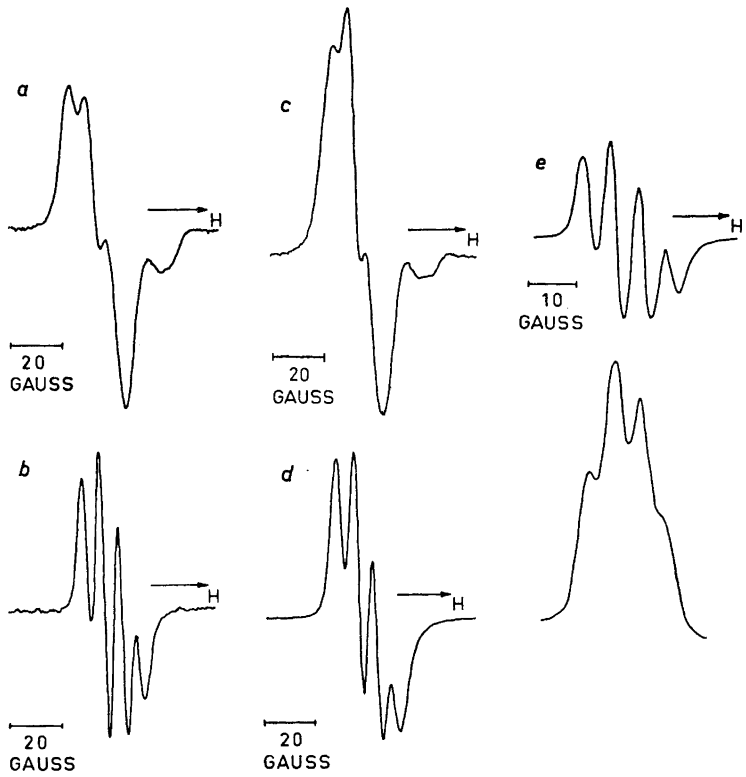

Fig. 4. Aprobit: *a*) on Dowex-50. Solvent: water. The resin was separated from the supernatant, washed with the solvent and dried for half an hour *in vacuo* before the spectrum was recorded; *b*) in conc. H_2SO_4; *c*) in conc. H_2SO_4, 77°K; *d*) in conc. D_2SO_4; *e*) in conc. H_2SO_4. Observed derivative tracing and its integrated absorption.

nounced when the resin is in the sodium form, greatly diminishes after treatment according to Moore and Stein [7]. Such a "false" signal seems in no case to have interfered in the experiments described above as indicated by control experiments.

The spectra of the radicals formed on activated Dowex-50 H^+ exhibit hyperfine splittings superimposed on a rather broad line. The extreme width of this line is about 60 gauss. A characteristic feature of the spectra is their asymmetrical shape. Introduction of a very small crystal of diphenylpicrylhydrazyl (DPPH) in the centre of a specimen tube, filled with dry cation exchanger containing adsorbed radicals, shows that the ESR signal due to DPPH is located approximately in the centre of the spectrum of the phenothiazine substance.

Phenothiazine (Fig. 1a), 5-oxophenothiazine (Fig. 2a), promethazine hydrochloride (Fig. 3a) and "Aprobit" (Fig. 4a) give rise to a four-line spectrum. Promazine hydrochloride (Fig. 5a) exhibits three lines, and chlorpromazine

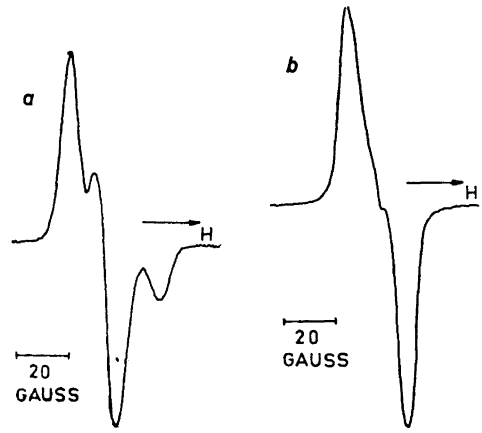

Fig. 5. Promazine · HCl: *a*) on Dowex-50. Solvent: water. The spectrum was recorded without separation of the phases; *b*) in conc. H_2SO_4.

hydrochloride (Fig. 6a) and 10-methylphenothiazine (Fig. 7a) exhibit a number of very incompletely resolved hyperfine lines.

B. Radicals produced in concentrated sulphuric acid. When the phenothiazine derivatives concerned in this case are dissolved in concentrated sulphuric acid, radicals with hyperfine splittings are produced. Compared with the corresponding spectra of the radicals formed on Dowex-50, these spectra are of a much more symmetrical shape, even if a certain asymmetry can be recognized also in these spectra. Phenothiazine (Fig. 1b), 5-oxophenothiazine (Fig. 2b), promethazine hydrochloride (Fig. 3b) and "Aprobit" (Fig. 4b) show four lines. Promazine hydrochloride (Fig. 5b) and chlorpromazine hydrochloride (Fig 6b)

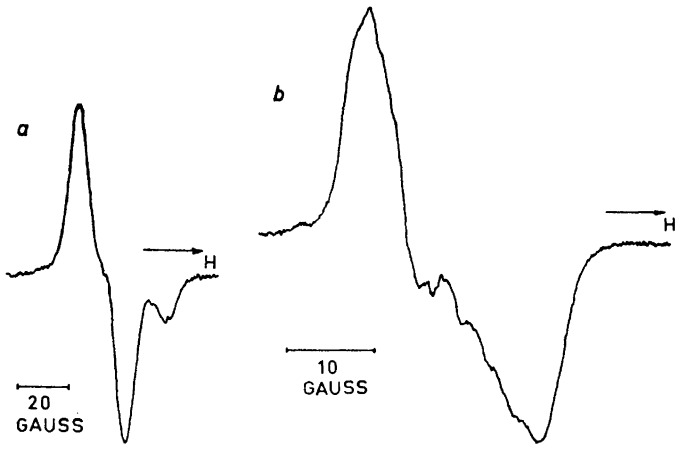

Fig. 6. Chlorpromazine·HCl: *a*) on Dowex-50. Solvent: water. The spectrum was recorded without separation of the phases; *b*) in conc. H_2SO_4.

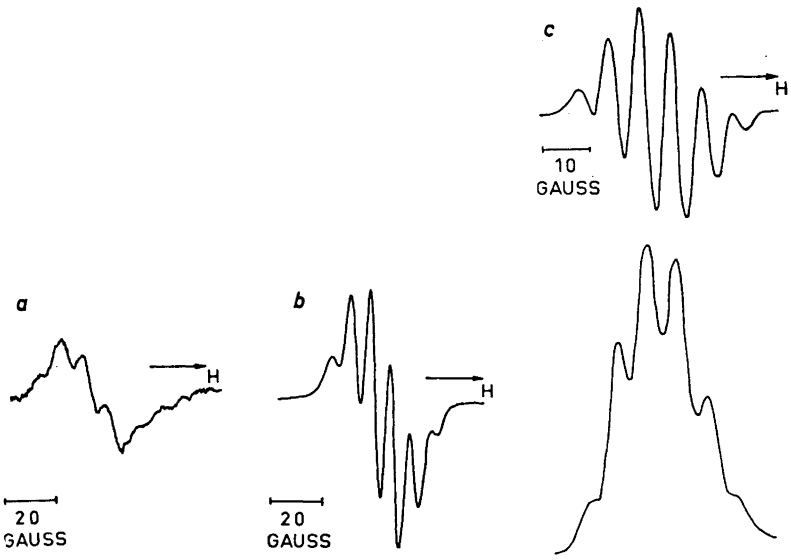

Fig. 7. 10-Methylphenothiazine: *a*) on Dowex-50. 0.1 M solution in benzene. The spectrum was recorded without separation of the phases; *b*) in conc. H_2SO_4; *c*) in conc. D_2SO_4. Observed derivative tracing and its integrated absorption.

exhibit a single line, in the centre of which an incompletely resolved hyperfine pattern can be seen.

10-Methylphenothiazine exhibits six distinct hyperfine lines both in H_2SO_4 (Fig. 7b) and in D_2SO_4 (Fig. 7c). 10-Ethylphenothiazine (Fig. 8) gives rise to an ESR-spectrum rather similar to that obtained from chlorpromazine hydrochloride, *i.e.* a single line, with an incompletely resolved hyperfine pattern in the centre. Further experiments with D_2SO_4 are described in the discussion below.

DISCUSSION

Several aromatic hydrocarbons are known to form free radicals when dissolved in concentrated sulphuric acid. The subject has been reviewed by Wertz [8] and Ingram [4]. The mechanism of the radical formation is most probably the same for the hydrocarbons and the phenothiazines here considered. The hyperfine splittings of the spectra observed when the phenothiazine substances are dissolved in concentrated sulphuric acid, will now be discussed. Consider the unsubstituted phenothiazine. By configurational interaction between the π-orbital of the odd electron and a σ-state of the ring nitrogen, the electronic levels are split into three ($M_I=1$). By further interaction with a σ-state of the hydrogen attached to the ring nitrogen, each of these levels are split in two ($M_I=\frac{1}{2}$). By overlapping of some of the last mentioned levels, four lines are produced as shown in the suggested energy level diagram in Fig. 9.

When 10-methylphenothiazine is dissolved in concentrated sulphuric acid, six lines are observed. This spectrum is consistent with the interaction between the π-orbital of the ring system, the ring nitrogen, and the three equivalent hydrogens of the methyl group (see Fig. 9).

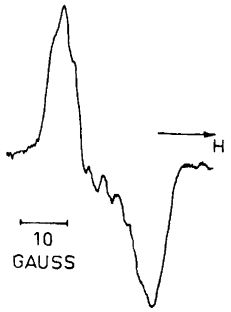

Fig. 8. 10-Ethylphenothiazine in conc. H_2SO_4.

The relative intensities of the four-line spectrum of "Aprobit" in H_2SO_4 (Fig. 4e) and of the six line spectrum of 10-methylphenothiazine in D_2SO_4 (Fig. 7c) obtained by double integration of the derivative curves are shown in Table 1 together with the theoretical intensity distribution consistent with the energy level diagram in Fig. 9. For comparison, the line intensities corresponding to the interaction of the odd electron with three and four equivalent hydrogens respectively (binomial distribution) are also shown. The distributions obtained experimentally seem to support the splitting mechanism suggested in Fig. 9, but the asymmetry of the curves and the incomplete separation make the tracing of the individual lines somewhat ambiguous. The intensity distribution obtained must therefore be considered uncertain.

The interaction of the odd electron with the methyl hydrogens in 10-methylphenothiazine is of a type different from that of the configurational interaction with an excited state, and is due to a spatial overlapping of wave functions with the same symmetry. This mechanism is generally termed hyperconjugation. In order to obtain an equal interaction with all the three methyl hydrogens, it is necessary to assume that the methyl group is rotating with a frequency faster than that of the hyperfine splitting (Ingram *et al.*[9]).

Table 1.

Relative line intensities	Four-line spectrum "Aprobit" in H_2SO_4 Fig. 4e	Six-line spectrum 10-Methylphenothiazine in D_2SO_4 Fig. 7c
Found	1 : 2.2 : 2.0 : 0.8	1 : 4.1 : 7.4 : 6.6 : 3.2 : 1.1
Calculated according to the energy level diagram in Fig. 9	1 : 2 : 2 : 1	1 : 4 : 7 : 7 : 4 : 1
Binomial distribution	1 : 3 : 3 : 1	1 : 5 : 10 : 10 : 5 : 1

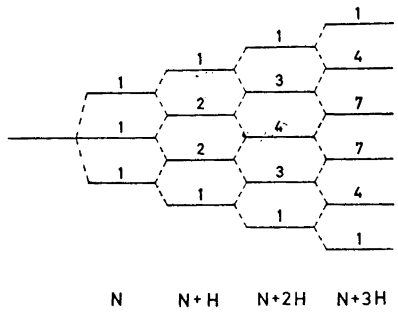

Fig. 9. Energy level diagram of the splitting due to one nitrogen, one nitrogen and one hydrogen, one nitrogen and two hydrogens, one nitrogen and three hydrogens. Only one of the two electronic levels is shown. The figures give the relative intensity distributions.

In the ethyl group of 10-ethylphenothiazine there are two different kinds of hydrogen position. Hence, the hyperfine pattern should be the combination of an interaction with two equivalent hydrogens in the methylene group and the ring nitrogen which gives rise to a five-line spectrum, and an interaction with the three methyl hydrogens which will split each of these lines into another four lines, if a non-integral relation between the coupling constants of the two kinds of hydrogen is assumed. Due to the large number of lines and perhaps also the relatively low spin density of the unpaired electron at the hydrogens most distant from the ring nitrogen, such a predicted hyperfine pattern will not be resolved. (Fig. 8). A similar interpretation seems to be valid for the incompletely resolved hyperfine spectra of promazine hydrochloride (Fig. 5b) and chlorpromazine hydrochloride (Fig. 6b), where the unpaired electron interacts with the σ-state of the hydrogens in the amino-alkyl chain. A possible interaction with the nitrogen of the side chain will further complicate the hyperfine pattern.

In none of the experiments described is there any evidence for an interaction of the unpaired electron in the π-orbital of the ring system with the edge protons of the two symmetrical side-rings of the phenothiazine nucleus. This means that the unpaired electron is distributed mainly over the central ring and in the side chain. This behavior is probably connected with the presence of the sulphur atom, which is known to have a localizing effect on the electron distribution. Naturally, such a suggestion does not exclude a further splitting due to the edge protons that will be observed, perhaps, in a highly resolved spectrum.

In order to explain the four-line pattern of promethazine hydrochloride (Fig. 3b) and "Aprobit" (Fig. 4b), it is necessary to assume a cleavage of the amino-alkyl side chain leaving, attached to the ring nitrogen of the phenothiazine nucleus, a group which makes interaction with one hydrogen possible. The presence of a branching in the carbon side chain of promethazine hydrochloride and "Aprobit" contrary to the situation prevailing in the other phenothiazine derivatives investigated, makes such a splitting probable. This assumption is further supported by the fact that there is a vigorous evolution of

SO_2 with foaming, when the promethazine hydrochloride and "Aprobit" are dissolved in concentrated sulphuric acid. Such a reaction is not observed for phenothiazine derivatives which have an unbranched side chain. The side chain is probably split between the carbons 1 and 2 according to the formula

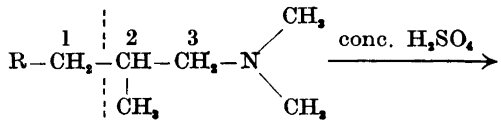

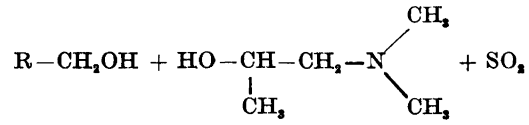

R = phenothiazine nucleus.

It is also necessary to assume a restricted rotation of the hydroxymethyl group left attached to the ring system after the splitting of the carbon side chain, thus allowing interaction with only one of the hydrogens of the hydroxymethyl group. The hypothesis of a splitting of the side chain between carbons 1 and 2 is further strengthened by the fact that when "Aprobit" is dissolved in concentrated deuterium sulphuric acid (D_2SO_4), a four-line spectrum (Fig. 4d) is observed, which appears very similar to that obtained in H_2SO_4 (Fig. 4b). In case of a split between the ring nitrogen and the alkyl chain, the four-line spectrum of "Aprobit" observed in H_2SO_4 (Fig. 4b) had to be due to a radical of a structure very similar to, or identical with, that obtained from unsubstituted phenothiazine, *i.e.* to a radical involving a hydrogen attached to the ring nitrogen. The last mentioned radical structure for "Aprobit" after splitting is not very probable, since unsubstituted phenothiazine exhibits a three-line spectrum when dissolved in D_2SO_4 (Fig. 1c) due to exchange of the hydrogen attached to the ring nitrogen. The deuterium nucleus has a magnetic moment, but this is about three times smaller than that of the proton (*cf.* Kopferman [10], p. 398). It has also a spin of 1 instead of ½ for the proton, and hence, the expected splitting of the nitrogen levels due to the deuterium atom seems to be unresolved under the actual experimental conditions. A four-line spectrum in H_2SO_4 and a three-line spectrum in D_2SO_4 might also be consistent with a radical structure in which a hydroxyl group is left attached to the ring nitrogen. However, it seems to be a general feature of ESR-spectra that no interaction is obtained with the protons of hydroxyl groups (Ingram *et al.*[11]), with the result that a four-line spectrum in H_2SO_4 and a three-line spectrum in D_2SO_4 therefore appear to be wholly consistent with a radical structure with a hydrogen attached to the ring nitrogen as in unsubstituted phenothiazine. Consequently the four-line spectrum both in H_2SO_4 and in D_2SO_4 supports the hypothesis that "Aprobit" is split between carbons 1 and 2 of the side chain, as shown in the formula. In this connection it may be pointed out that there is no evidence for an exchange of the hydrogens of the methyl group

attached to the ring nitrogen, since 10-methylphenothiazine shows a six-line spectrum both in H_2SO_4 (Fig. 7b) and in D_2SO_4 (Fig. 7c).

The main difference between the radical spectra observed in sulphuric acid and those obtained on activated Dowex-50 is the highly asymmetrical shape of the latter. The asymmetry may be due either to the presence of more than one radical species or an anisotropy of the g-value. The last alternative infers that the g-value along the symmetry axis of the radical molecule is not equal to that in an orthogonal direction. As long as the radicals are free to rotate at a frequency of the same order of magnitude as that of the microwave power used, the effect of the g-value anisotropy is blotted out. When the rotation is restricted, however, the actual ESR-spectrum is a superposition of spectra corresponding to a series of randomly orientated symmetry axes.

In radicals containing a sulphur atom, the unpaired electron is known to be incompletely delocalized and the ESR-spectrum to exhibit a g-value anisotropy. Consequently, the presence of a sulphur atom in the phenothiazines suggests that the asymmetrical shape of the radical spectra observed on Dowex-50 depends on a g-value anisotropy combined with a restricted rotation of the radicals when attached to the ion exchanger. Asymmetrical ESR-spectra analogous to those here discussed have been described by Faber and Rogers [12] in an investigation of paramagnetic ions adsorbed on cation exchangers.

In order to decide whether the asymmetry is due to a g-value anisotropy or not, "Aprobit" was dissolved in concentrated H_2SO_4 and the ESR-spectrum recorded at room temperature (Fig. 4b). It was now observed that the symmetrical spectrum changed into an asymmetrical one, which was very similar to that obtained on Dowex-50 at room temperature, when the solution in sulphuric acid was cooled to the temperature of liquid air (Fig. 4c). The rotation of the radical molecules is thus hampered both when fixed to the resin-phase at room temperature and when the solution in sulphuric acid is cooled to a very low temperature. The small asymmetry that can be recognized in the spectra of the sulphuric acid at room temperature indicates a slight degree of restricted rotation even at this temperature due to the viscosity of the solution. From the experiment described it is evident that the asymmetrical shape of the radical spectra observed on Dowex-50 very probably depends on a g-value anisotropy and a restricted rotation, and not to the presence of more than one radical species.

When comparing the radical spectra for each substance observed in sulphuric acid with those on Dowex-50, it is noted that the number of lines is equal for several of the substances. Thus phenothiazine, 5-oxophenothiazine, promethazine hydrochloride, and "Aprobit" exhibit a four-line spectrum both in sulphuric acid and on Dowex-50. This fact implies that the branched chain of promethazine hydrochloride and of "Aprobit" is split not only in sulphuric acid, but also in the redox reaction on Dowex-50. The six hyperfine lines of 10-methylphenothiazine in sulphuric acid (Figs. 7b and 7c) are not resolved on Dowex-50 (Fig. 7a) probably due to the anisotropy effect and the restricted rotation discussed above, which blur the individual lines. When comparing the radical spectra of promazine hydrochloride (Fig. 5b) and chlorpromazine hydrochloride (Fig. 6b) observed in sulphuric acid with those obtained on Dowex-50 (Figs. 5a and 6a), it is expected that the incompletely resolved hyperfine

pattern in sulphuric acid should be further impaired on Dowex-50 due to the anisotropy effect and restricted rotation. Such a state of affairs appears to prevail in the case of chlorpromazine hydrochloride (Figs. 6a and b). However, the three-line spectrum of promazine hydrochloride on Dowex-50 (Fig. 5a) is not expected and the origin is not wholly understod. It may depend on a non-interaction of the three nitrogen levels with the side chain hydrogens due to improper orientation.

From the discussion above it is obvious that the radicals formed by the one-electron oxidation with ferric iron on the cation exchanger are very probably of a structure similar to those found in sulphuric acid.

Free radicals really being formed *in vivo* from phenothiazine derivatives and the possible role of natural ferric-compounds in such a hypothetical reaction are open questions, as are the importance of such radicals for the pharmacological activity of these compounds.

Acknowledgements. The author is indebted to *Wilhelm and Martina Lundgrens Vetenskapsfond* for financial support, and to Mr. Elof Gustafsson and Mr. Lennart Persson for excellent cooperation in the construction of the ESR-spectrometer, and to Mr. Levi Claesson for making the Dewar vessel.

The author would like to express his thank to AB Recip, Stockholm, AB Astra, Södertälje, and AB Leo, Hälsingborg, for supplying various phenothiazine drugs.

REFERENCES

1. Michaelis, L., Schubert, M. P. and Granick, S. *J. Am. Chem. Soc.* **42** (1940) 204.
2. Forrest, I. and Forrest, F. *Biochim. et Biophys. Acta* **29** (1958) 441.
3. Krongelb, S. and Strandberg, M. W. P. *J. Chem. Phys.* **31** (1959) 1196.
4. Ingram, D. J. E. *Free Radicals as Studied by Electron Spin Resonance*, London 1958.
5. Pummerer, R. and Gassner, S. *Ber.* **46** (1913) 2322.
6. Gilman, H., Van Ess, P. R. and Shirley, D. A. *J. Am. Chem. Soc.* **66** (1944) 1214.
7. Moore, S. and Stein, W. H. *J. Biol. Chem.* **192** (1951) 660.
8. Wertz, J. E. *Chem. Revs.* **55** (1955) 829.
9. Ingram, D. J. E., Symons, M. C. R. and Townsend, M. G. *Trans. Faraday Soc.* **54** (1958) 409.
10. Kopferman, H. *Kernmomente*, 2nd ed., Frankfurt am Main 1956.
11. Gibson, J. F., Ingram, D. J. E., Symons, M. C. R. and Townsend, M. G. *Trans. Faraday Soc.* **53** (1957) 914.
12. Faber, R. J. and Rogers, M. T. *J. Am. Chem. Soc.* **81** (1959) 1849.

Received March 13, 1961.

ACTA CHEMICA SCANDINAVICA 15 (1961) 1557–1562

An Electron Diffraction Investigation of the Molecular Structure of Butatriene

A. ALMENNINGEN, O. BASTIANSEN and M. TRÆTTEBERG

Universitetets kjemiske institutt, Blindern - Oslo;
Institutt for teoretisk kjemi, Norges tekniske høgskole, Trondheim, Norway

The electron diffraction sector method was used to determine the structure of the butatriene molecule in the vapour phase. The molecular parameters are determined to be the following: C—H 1.083 Å (u = 0.080 Å), $C_1 = C_2$ 1.318 Å (u = 0.040 Å), and $C_2 = C_3$ 1.283 Å (u = 0.039 Å). The error limits of all the parameters are approximately ± 0.005 Å. As in several other molecules with linear equilibrium conformation, a "shrinkage effect" is observed; *i.e.* the observed non-bonded CC distances are a trifle shorter than that calculated from the sum of the individual bond distances. The effect is explained by out-of-linearity vibrations.

The present work is a part of our endeavour to collect more precise information of CC bond lengths, particularly in conjugated and cumulated systems. The molecular structure of butatriene has been studied by Stoicheff [1] in 1957, using the Raman spectroscopic method. Assuming the end C=C double bond length to be the same as he found for allene [2], namely 1.309 Å, he determined the central C=C double bond length to be 1.284 Å.

The electron diffraction method has the advantage that each individual bond length in principle can be determined independently. The central C=C double bond in butatriene with an sp—sp σ-bond, is of particular interest. The length of this bond has so far not been determined independently with particularly great accuracy.

PREPARATION OF BUTATRIENE

Butatriene was prepared by Dr. Else Kloster-Jensen by a 2-stage synthesis [3] from 2-butyne-1,4-diol. This compound was converted to 1,4-dibromobutyne-2, and treated with zinc powder to give butatriene.

1,4-Dibromobutyne-2. After recrystallization of 2-butyne-1,4-diol, 700 ml of dry benzene was added to 111 g of the diol. The solution was stirred and cooled with ice as 500 g of phosphorus tribromide were added slowly during 3 h. The reaction mixture was stirred overnight at room temperature. The mixture was then transferred to 1 000 ml ice water

and the benzene layer isolated. After extraction of the water phase with 4 × 250 ml ether, the organic extract was washed with 4 × 100 ml 10 % sodium hydrogen carbonate solution and dried over anhydrous sodium sulphate. The solvent was removed under reduced pressure, and fractionated distillation gave 127.4 g colourless liquid at 66–75°C/ 1.5–2.5 mm Hg . $n_D^{21} = 1.5898$.

Butatriene. 7.5 g zinc powder was suspended in 25 ml diethyl carbitol (distilled over metallic sodium). After evacuating the flask which was coupled to vacuum (1 mm) through a reflux cooler, 12.5 g 1,4-dibromobutyne-2 were dropped into the suspension which was stirred and heated to 80°C. A manometer showed that gas was developed. The crude distillate, collected in a liquid nitrogen cold trap, amounted to a few ml colourless solid. The redistilled product gave an infrared spectrum which was in good agreement with that published by Schubert [4].

ELECTRON DIFFRACTION STUDY

The electron diffraction diagrams were taken at the three usual distances between the scattering point and the photographic plate (approximately 48 cm, 19 cm, and 12 cm). A modified s^3 sector was used. Photometer traces of the plates were read off at intervals of $\Delta s = 1/4$ Å^{-1} and transferred into intensity values in the usual way [5].

The background scattering was subtracted by adjusting to the total intensity curve a theoretical background consisting of the atomic and incoherent scattering. After averaging the overlap regions an experimental molecular intensity curve ranging from $s = 1.25$ Å^{-1} to $s = 63.5$ Å^{-1} was obtained. Fig. 1 shows the theoretical (A) and experimental (B) molecular intensity curves. The theoretical curve is based on the final molecular model described later in this article.

It is usually difficult to obtain satisfactory correspondence between the theoretical background and the total experimental intensity curve for s values less than 5 Å^{-1} and for very large s values. An empirical correction is usually

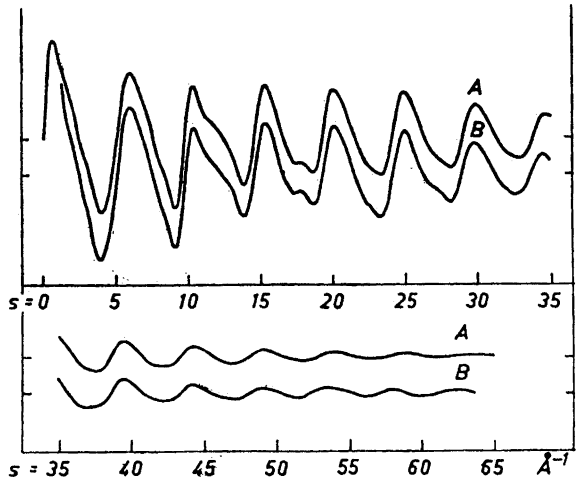

Fig. 1. Butatriene. Theoretical (A) and experimental (B) intensity curves.

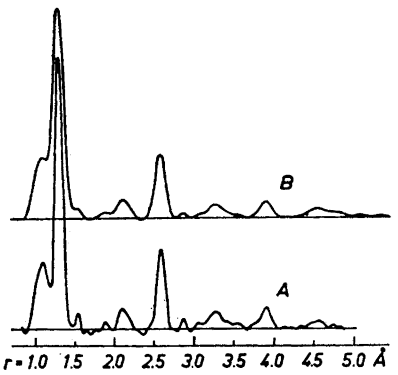

Fig. 2. Butatriene. Radial distribution curves with damping constant k equal to 0 (A) and 0.0009 (B).

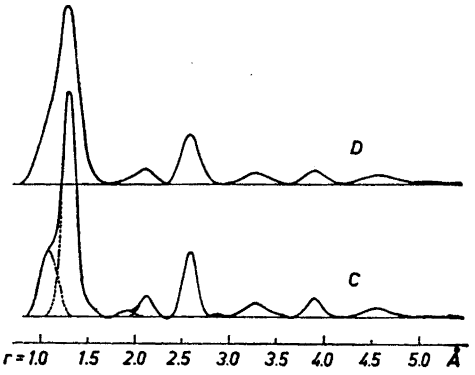

Fig. 3. Butatriene. Radial distribution curves with damping constant k equal to 0.0015 (C) and 0.0036 (D).

necessary and is carried out the following way: A preliminary background is subtracted and the molecular intensity curve thus obtained is submitted to a Fourier transformation, leading to a first radial distribution curve. From this curve a preliminary molecular model is obtained. Using this model a theoretical intensity curve is computed, and the background corrections are carried out by comparing the experimental and theoretical intensity curves. From the final experimental molecular intensity curve a series of radial distribution curves was calculated using four different k-values (0, 0.0009, 0.0015, and 0.0036). Figs. 2 and 3 show the corresponding four radial distribution curves.

From an analysis of these curves a set of internuclear distances was obtained. The correspondence between distances determined from curves with various damping factors was very good, and the mean values are listed in Table 1, second column. In the third column the observed root-mean-square deviation values for the various internuclear distances (u-values) are given.

The peak having a maximum at 1.306_5 Å is composed of contributions from the two sp^2-sp C=C double bonds and from the sp-sp double bond. The distance values of the two kinds of bonds are so close together that it is not possible to resolve the compound peak, even for the radial distribution curve of $k = 0$. The question now arises if the maximum position of the first CC peak corresponds to the arithmetical mean of the C=C double bond lengths. To check this two Gaussian curves were added, one with maximum at 1.28 Å and one with maximum at 1.31 Å, the latter one having a weight factor twice that of the first one. Both curves were based on the same u-value, namely 0.040 Å. The maximum position of the compound peak appeared to be off the value of the arithmetical mean by no more than 3×10^{-5} Å. This result shows that the following equation

$$1.306_5 = \tfrac{1}{3}[2\ r_{C_1=C_2} + r_{C_2=C_3}] \qquad (1)$$

is valid within the error of the method.

Table 1. Butatriene. Experimentally determined maxima of the radial distribution curves and the corresponding root-mean-square deviation values (u-values).

Type of distance	Observed internuclear distances	u-values
C—H	1.082_0	0.079_9
$C_1=C_2$; $C_2=C_3$	1.306_5	(0.047_0)
H_1C_2	2.114_4	0.061_8
C_1C_3	2.590_4	0.051_0
H_1C_3	3.277_4	0.102_3
C_1C_4	3.906_8	0.055_3
H_1C_4	4.571_0	0.111_6
$H_1H'_1$	1.89_2	
$H_1H'_4$	5.10_5	
H_1H_4	5.32_6	

If the butatriene molecule has a linear carbon skeleton, the C_1C_4 distance length should be equal to three times the r-value of the first CC peak. This is not so. The observed value for the C_1C_4 distance is 3.906_8 Å while three times the maximum position of the first CC peak is 3.919_5 Å. This corresponds to a shrinkage effect [6] equal to $-\delta_{C_1C_4} = 0.0127$ Å.

Examining the shape of the C_1C_3 and C_1C_4 peaks of the radial distribution curves, it is seen that the right side slope of each of the peaks is steeper than that of the left side. This is in contrast to the effect usually observed and ascribed to anharmonicity in the molecular vibrations.

The shrinkage effect has earlier been explained by out-of-linearity vibrations, assuming a linear equilibrium conformation [7,8]. These vibrations can also explain the described asymmetry of the C_1C_3 and C_1C_4 peaks.

In the electron diffraction investigation of allene a shrinkage effect of the same order of magnitude as for butatriene was observed. In the allene case the effects caused by out-of-linearity vibrations can easily be treated theoretically [8]. It is considerably more complicated to carry out the same sort of calculations for butatriene, as this molecule exhibits more complicated out-of-linearity vibrations.

The main problem and the most difficult problem in the investigation of the molecular structure of butatriene is to determine the lengths of the two different types of double bonds. If a linear and rigid molecule is assumed, the end C=C double bond could be obtained by subtracting the observed C_1C_3 distance from the corresponding C_1C_4 distance. The length of the central C=C double bond could then be calculated from eqn. (1). In the actual case, a subtraction of the observed C_1C_3 from the observed C_1C_4 distance leads to an end C=C double bond length of 1.316_4 Å. This value must be too low as the observed C_1C_4 distance probably is more influenced by out-of-linearity vibrations than is the C_1C_3 distance. By inserting 1.316_4 Å for the sp^2-sp double bond length in eqn. (1), the value 1.286_7 Å is obtained for the sp—sp double bond length, a value which according to the same line of argument must be too high.

Table 2. Results of refinement calculations for linear molecular models using: a) the observed CC distances only, b) the CC as well as the CH distances.

Parameters	CC distances	CC and CH distances
$C_1=C_2$	1.3173 Å	1.3270 Å
$C_2=C_3$	1.2730 Å	1.2572 Å
C—H		1.0834 Å
$< H-C=C$		122.5°

By a least-squares calculation based on observed interatomic distances, the molecule has to be described by a static model. Doing so it might be of interest to study the possibility of describing the molecule by a non-linear model. If butatriene is treated as a non-linear molecule and a *trans* configuration is assumed, three parameters are necessary for describing the carbon skeleton, namely the $C_1=C_2$ and $C_2=C_3$ double bond distances and the $C_1C_2C_3$ angle. There are all together three observable CC peaks in the radial distribution curves, and the corresponding maximum values may be combined in a set of three equations with the three unknown parameters. By solving these equations, the following values are obtained: $C_1=C_2$ 1.320 Å, $C_2=C_3$ 1.280 Å and $<C_1C_2C_3$ 170°, *i.e.*, a 10-degrees deviation from linearity.

Least-squares calculations were carried out by adjusting both a linear and a non-linear molecular model to the observed interatomic distances. Both models were studied using (a) only the observed CC distances, and (b) CC distances as well as CH distances. For these calculations the following zeroth order set of parameters was chosen based upon a preliminary examination of the radial distribution curves: $C_1=C_2$ 1.316_0 Å, $C_2=C_3$ 1.289_0 Å, C—H 1.082_0 Å and $<H-C=C$ 122°. In Table 2 the results of the refinements are given when a linear model is assumed. The error square sums before and after adjustment were 398.0×10^{-4} and 22.8×10^{-4} when only the CC distances were considered. In the other case treated, the same values were 1096.8×10^{-4} and 340.7×10^{-4}, respectively.

Zeroth order parameters used for the study of non-linear models were the same as for a linear molecular model, but in addition a zeroth order parameter for $<C_1C_2C_3$ of 170° was assumed. In Table 3 the results of the refinements are given when a non linear model is assumed. The error square sums before

Table 3. Results of refinement calculations for non-linear molecular models using: a) the observed CC distances only, b) the CC as well as the CH distances.

Parameters	CC distances	CC and CH distances
$C_1=C_2$	1.320 Å	1.3278 Å
$C_2=C_3$	1.280 Å	1.2693 Å
C—H		1.0827 Å
$< H-C=C$		121.76°
$< C_1C_2C_3$	170°	169.02°

and after adjustment were 25.3 $\times$ 10^{-4} to 5.2 $\times$ 10^{-4} and 307.0 $\times$ 10^{-4} to 97.6 $\times$ 10^{-4}, respectively, in the two cases.

The calculations show that the butatriene molecule neither can be described by a linear nor a non-linear static model, and the correspondence between parameters determined from the four different approaches is not satisfactory.

In order to determine the two types of C=C double bond distances the work was, at this stage of the investigation, concentrated on the peak at 1.306_5 Å on the radial distribution curves. Theoretical radial distribution curves composed of Gaussian curves with contribution from the C=C double bond distances were calculated. The four parameters, the two equilibrium C=C double bond distances and their corresponding u-values, were varied in small intervals over a large r-range. The following set of values gave a very satisfactory agreement between the theoretical and observed peak: $C_1=C_2$ 1.318 Å, $C_2=C_3$ 1.283 Å, $u_{C_1C_2}$ 0.040 Å, $u_{C_2C_3}$ 0.039 Å. In obtaining these results the u-values and bond distances were restricted to certain limitations. For instance the u-values should be in reasonable agreement with earlier obtained values for double bonds, and the bond lengths should be kept within the limits given above.

CONCLUSION

As a result of this electron diffraction investigation the following structure parameters for butatriene can be given:

C—H	1.083 Å	u_{C-H}	0.080 Å
$C_1=C_2$	1.318 Å	$u_{C_1=C_2}$	0.040 Å
$C_2=C_3$	1.283 Å	$u_{C_2=C_3}$	0.039 Å

It is very difficult to give definite statements concerning the error limits for the structure parameters. It is felt that an error limit of $\pm$ 0.005 Å can be given both for the distance parameters and for the u-values.

Acknowledgement. This investigation has been sponsored by the *United States Air Force Development Command* under contract AF 61(052)-72.

The authors wish to thank Dr. Else Kloster-Jensen, University of Oslo, who kindly prepared the butatriene used in the present investigation. The authors also wish to acknowledge the valuable advice given by Dr. A. T. Morse, Merck and Co., Montreal, in connection with the synthesis of the compound.

REFERENCES

1. Stoicheff, B. P. *Can. J. Phys.* **35** (1957) 837.
2. Stoicheff, B. P. *Can. J. Phys.* **33** (1955) 811.
3. Morse, A. T. *Private communication* (1959).
4. Schubert, W. M., Liddicoet, T. H. and Lanka, W. A. *J. Am. Chem. Soc.* **76** (1954) 1929.
5. Almenningen, A., Bastiansen, O. and Fernholt, L. *Kgl. Norske Videnskab. Selskabs. Skrifter* **1958** No. 3.
6. Almenningen, A., Bastiansen, O. and Trætteberg, M. *Acta Chem. Scand.* **13** (1959) 1699.
7. Munthe-Kaas, T. *Thesis, University of Oslo* (1955).
8. Trætteberg, M. *Thesis, Technical University of Norway*, Trondheim (1960).

Received April 7, 1961.

ACTA CHEMICA SCANDINAVICA 15 (1961) 1563–1570

Preparation of 3-*Iso*propyl-7-methyl-dibenz(ah)anthracene from Retene

EYLIF DYNESEN

Chemical Department, University of Aarhus, Denmark

Starting from 3-reteneacetic acid, 3-*iso*propyl-7-methyldibenz(ah)-anthracene has been prepared by application of the Pschorr ring closure reaction.

3-*Iso*propyl-7-methyl-benz(a)anthracene was first synthesized from retene [1] and later from dihydroretene [2] as starting material.

According to a report, cited by Newman and Joshel [3], 3-*iso*propyl-7-methyl-benz(a)anthracene has given no tumors when injected into mice, thus the high carcinogenic potency of 7-methyl-benz(a)anthracene is destroyed by the introduction of an *iso*propyl group into the 3-position.

It seemed of interest to prepare for comparison 3-*iso*propyl-7-methyl-dibenz(ah)anthracene, since 7-methyl-dibenz(ah)anthracene shows marked carcinogenic activity [4].

Several preparative methods are available for preparation of the dibenz(ah)-anthracene ring system. The most direct synthetic approach in this case, however, seemed to apply the Pschorr [5] ring closure reaction on suitable 3-substituted retene derivatives.

The intermediate *o*-nitro-*α*-(3-retenyl)cinnamic acid (Ia) was prepared [6] previously in 40—45 % yield by condensation of 3-reteneacetic acid with *o*-nitrobenzaldehyde. To increase the yield a slight modification was introduced in isolating the acid Ia. Instead of extracting the reaction product from the Perkin reaction with sodium carbonate, the product was extracted with warm benzene, in which the acid Ia was only slightly soluble. The acid Ia was pure after recrystallization from glacial acetic acid. The yield was about 50 %. Extraction of the benzene filtrate from purification of Ia and subsequent acidification gave a mixture of the acids Ia and Ib. These were separated by partial esterification with methanol. From the acid fraction the acid Ib was isolated. Fractional recrystallization of the esterified fraction gave the methyl-ester of Ib. The infrared spectra of the acids Ia and Ib are nearly identical. Other experimental facts suggest that the acid Ia has the *trans* configuration with respect to the carboxyl and *o*-nitrophenyl group and that Ib is the *cis*-

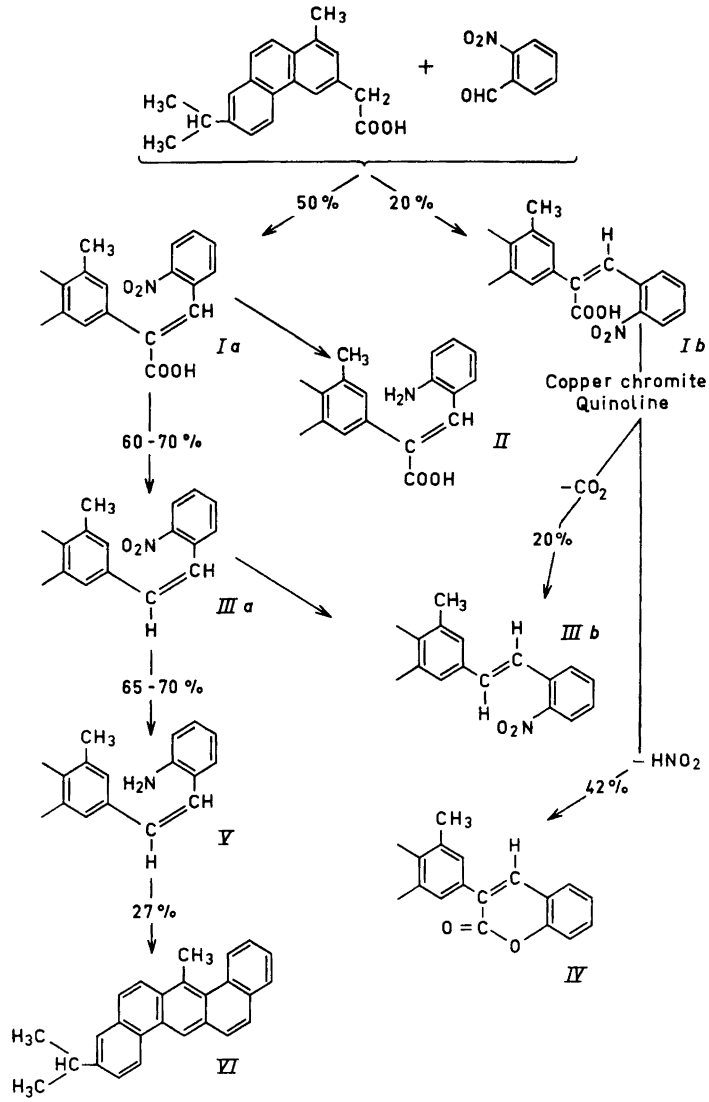

isomer. The acid Ib with the lower melting point and greater solubility is much more slowly esterified with methanol-sulphuric acid than Ia, as a result of steric hindrance from the *o*-nitrophenyl group.

The U.V. spectrum of the methylester of Ia shows two maxima, a high intensity band at 258 mμ and a maximum of lower intensity at 302 mμ. For the methylester of Ib, the 290—400 mμ range is displaced towards longer wavelengths and higher intensities, in accordance with the more elongated chromophoric system of Ib.

The usual procedure in the Pschorr reaction involves reduction of the substituted nitrocinnamic acid to the corresponding aminocinnamic acid. This reaction, however, did not appear applicable in this case, since reduction of the nitro group in Ia met with difficulties. The conventional reduction with ferrous sulphate and ammonia gave only low yields of *o*-amino-*α*-(3-retenyl)cinnamic acid (II), possibly owing to the slight solubilities of the ammonium salts of the acids Ia and II.

The carboxyl group in the substituted aminocinnamic acid is not essential to the ring closure. Ruggli and Staub [7] have shown, that phenanthrene can be prepared in good yield by the copper catalyzed decomposition of the diazoniumsalt of *cis*-*o*-aminostilbene. The function of the carboxyl group is merely to direct the aryl nuclei into the necessary *cis*-position during the Perkin reaction. This method was used as *cis*-*o*-nitro-stilbene derivatives generally are obtained in good yields by decarboxylation of the corresponding cinnamic acid derivatives.

The decarboxylation of Ia in quinoline was previously carried out on a minor scale [6] with anhydrous copper sulphate as catalyst. 3-(*o*-Nitrostyryl)-retene was isolated. Repetition of this reaction on a larger scale, using copper chromite as catalyst, gave the same substance in 60—70 % yield. In some experiments, however, rearrangement to the geometrical isomer occurs to some extent, especially when the temperature during decarboxylation is too high or the time of heating too long. In this case lower melting material was isolated and chromatography gave two substances, of which the weakest adsorbed was identical to the main product.

The U.V. and infrared spectra show that the main product from decarboxylation of Ia is *cis*-3-(*o*-nitrostyryl)-retene(IIIa), whereas the by-product is the *trans*-isomer (IIIb). The U.V. spectrum of IIIa has a maximum at 316 mμ. This maximum is shifted 11 mμ in going to the *trans*-isomer(IIIb). At the same time, the extinction coefficient is increased 1.5 times due to the more extended conjugated system of IIIb. The infrared spectrum of IIIb has a strong band at 957 cm^{-1}. This band is absent in the *cis*-isomer IIIa. The 957 cm^{-1} band is characteristic of the —CH=CH— trans structure, usually giving rise to a medium to strong band in the 990—965 cm^{-1} range.

The configuration of Ib is identical to that of IIIb, since IIIb is formed by decarboxylation of Ib in quinoline with copper chromite as catalyst. The yield of *trans*-3-(*o*-nitrostyryl)-retene(IIIb) was low. The main product was an almost white, slightly soluble compound. In solution it showed strong fluorescence in ultraviolet light. The substance contained no nitrogen and formed an orange complex with 2,4,7-trinitro-fluorenone. Analysis indicates that the substance contained two oxygen atoms. With alkali, the substance showed the characteristics of aromatic lactones. Accordingly, the substance appears to be 3-(3′-retenyl)-coumarin(IV).

The structure of IV is consistent with the infrared spectrum of the substance. There is no absorption in the 2 500—2 700 cm^{-1} region characteristic of a strongly hydrogen-bonded OH-group. The spectrum shows C=O absorption at 1 705—1 725 cm^{-1}. The position of this C=O band corresponds to that found in coumarin and some of its derivatives. In addition, the infrared spec-

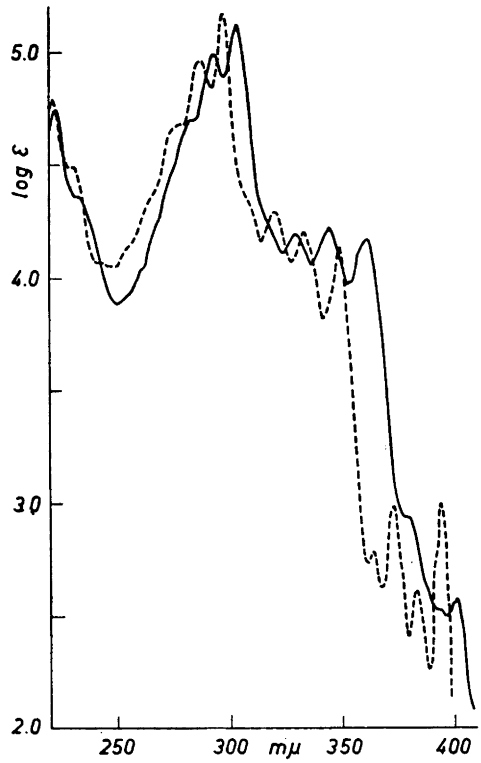

Fig. 1. Ultraviolet absorption spectra of 3-*iso*propyl-7-methyl-dibenz(ah)anthracene (———)and dibenz(ah)anthracene(------). Solvent: 96 % ethanol.

trum shows a strong band at 1 105 cm-[1], frequently observed with O-ring compounds.

Thus 3-(3′-retenyl)-coumarin(IV) is formed from Ib by elimination of nitrous acid by interaction between nitro and carboxyl groups. The reaction gives further support for the configuration of the acid Ib.

Reduction of *cis*-3-(*o*-nitrostyryl)-retene(IIIa) with ferrous hydroxide and sodium hydrosulfite did not succeed. It has, however, previously been shown that hydrazine hydrate in combination with Raney nickel [8] or palladium carbon [9] is an excellent reducing agent for polycyclic nitro compounds.

The reduction of IIIa, with hydrazine hydrate as reducing agent and palladium carbon as catalyst, was investigated. *cis*-3-(*o*-Aminostyryl)-retene(V) was obtained in a yield of 65—70 % by applying the mole ratio 1:4 for nitro compound to hydrazine hydrate.

The hydrochloride of V was diazotized in a mixture of tetrahydrofuran and water containing hydrochloric or sulphuric acid. A similar procedure was used by Buchta and Kallert [10] in the synthesis of chrysene and 2-methoxychrysene. Decomposition of the diazoniumsalt was effected by copper powder. The pure hydrocarbon was isolated by chromatography of the reaction product in 27 % yield.

Two structures are possible for the cyclization product. When ring closure takes place at the 2-position of the phenanthrene nucleus, a derivative (VI) of dibenz(ah)anthracene is obtained. On the other hand, a derivative of dibenzo(cg)phenanthrene is formed, when ring closure occurs at the 4-position. Although steric hindrance makes ring closure to the 4-position less likely, a ring closure of this type has been demonstrated in the double Pschorr reaction of *a,a'*-bis-(*o*-amino-benzylidene)-*p*-benzenediacetic acid [11]. In this reaction dibenzo(cg)phenanthrene was formed together with dibenz(ah)anthracene.

Conclusive evidence for the structure of the cyclization product is provided by the U.V. spectrum, which shows close resemblance with that of dibenz(ah)-anthracene. The spectrum of the cyclization product deviates considerably from the U.V. spectrum of dibenzo(cg)phenanthrene [12]. The U.V. spectrum of VI and that of dibenz(ah)anthracene, Fig. 1, show that the two hydrocarbons have identical band structures both for the β and for the *p*-absorption. On the other hand the structure of the *a*-absorption bands is somewhat blurred in VI. The same difference in the structure of the *a*-absorption bands is found in the U.V. spectra of benz(a)anthracene [13] and 3-*iso*propyl-7-methyl-benz(a)-anthracene [14]. The carcinogenic properties of VI have not yet been investigated.

EXPERIMENTAL

The melting points, which are uncorrected, are determined on an electric heated copper bloc with Anschütz thermometers. Microanalyses were performed by Mr. P. Hansen at the Chemical Laboratory of the University of Copenhagen. The ultraviolet spectra were determined on a Beckman spectrophotometer model DU. The infrared spectra were recorded with a Perkin Elmer model 21 instrument with a sodium chloride prism, using KBr discs.

trans-o-*Nitro-a-(3-retenyl)cinnamic acid* (Ia). A mixture of 3-reteneacetic acid (14.6 g, 0.05 mole), *o*-nitrobenzaldehyde (7.55 g, 0.05 mole), acetic anhydride (30 ml) and triethylamine (7.0 ml, 0.05 mole) was heated for 20 h at 105—110°. The excess acetic anhydride was decomposed by careful addition of water (20 ml) and heating for 45 min; the reaction mixture was then poured into 5 % hydrochloric acid (300 ml). The yellow product was filtered off, washed with water and then digested with warm benzene (75 ml) filtered and this treatment repeated twice with 50 and 60 ml benzene, respectively. After drying, the product (11.2 g) was recrystallized from glacial acetic acid (135 ml) to give 10.6 g (49.8 %) of the nitrocinnamic acid, m.p. 258.5—261.5°. U.V. absorption (in 96 % ethanol): λ max 257.5 mμ (log ε 4.76); 303 mμ (log ε 4.13). I.R. maxima (cm^{-1}): 1 343 and 1 522 (NO_2), 1 685 (C=O in CO_2H), broad absorption at 2 600 (CO_2H). Methyl *trans-o*-nitro-*a*-(3-retenyl)cinnamate, was prepared by esterification of Ia with methanol-sulphuric acid; yellow crystals from *n*-propanol, m.p. 187—189°. (Found: C 76.3; H 6.14; N 3.22. Calc. for $C_{28}H_{25}NO_4$(439.5): C 76.5; H 5.73; N 3.19). U.V. absorption (in 96 % ethanol): λ_{max} 257.5 mμ (log ε 4.77); 302 mμ (log ε 4.13). U.V. absorption (in *cyclo*hexane): λ_{max} 258.5 mμ (log ε 4.77); 302 mμ (log ε 4.14).

cis-o-*Nitro-a-(3-retenyl)cinnamic acid* (Ib). The combined benzene filtrates from purification of Ia were extracted with potassium hydroxide solution, and the alkaline solution acidified. After drying, the precipitate (7.4 g) was esterified with methanol (70 ml) and concentrated sulphuric acid (0.8 ml). The mixture was refluxed for 6.5 h and the main part of methanol distilled *in vacuo;* the dark coloured residue was dissolved in ether-benzene and the solution extracted several times with sodium carbonate solution; the alkaline solution was boiled to expel dissolved ether-benzene and then filtered. The filtrate was acidified and a yellow precipitate separated. After drying, the product (4.3 g) was recrystallized from glacial acetic acid (20 ml) (charcoal), giving 3.7 g of the pure acid Ib, m.p. 207—209°. (Found: Equiv.wt. 418; C 76.1; H 5.21; N 3.25. Calc. for $C_{27}H_{23}NO_4$ (425.5): C 76.2; H 5.45; N 3.29). I.R. maxima (cm^{-1}): 1 340 and 1 520 (NO_2), 1 688 (C=O in CO_2H), broad absorption at 2 600 (CO_2H).

Methyl cis-o-*nitro-a-(3-retenyl)cinnamate*. The remaining benzene-ether solution of the esterified fraction was dried and the solvent evaporated; the dark residue (2.5 g) was dissolved in *n*-propanol-benzene, the solution treated with charcoal and filtered; yellow crystals separated with m.p. 120—140°. Two further recrystallizations from *n*-propanol gave the pure methyl ester (0.5 g), yellow needles with m.p. 140—142°, identical with a specimen prepared by direct esterification of the pure *cis-o*-nitro-*a*-(3-retenyl)-cinnamic acid. (Found: C 76.6; H 5.96; N 3.10. Calc. for $C_{28}H_{35}NO_4$(439.5): C 76.5; H 5.73; N 3.19). U.V. absorption (in *cyclo*hexane): λ_{max} 264 mμ (log ε 4.73); 307 mμ (log ε 4.22). I.R. maxima (cm^{-1}): 1 340 and 1 520 (NO_2), 1 718 (C=O in ester).

trans-o-*Amino-a-(3-retenyl)cinnamic acid* (II). A solution of *trans-o*-nitro-*a*-(3-retenyl)cinnamic acid (Ia) (0.4 g) in concentrated ammonia (0.5 ml, 12 N) and water (25 ml) was added to a warm suspension of ferrous sulphate hydrate (3.3 g), water (125 ml) and concentrated ammonia (4 ml, 12 N). The mixture was boiled with frequent stirring for 1 hour, during which time additional water (400 ml) and concentrated ammonia (20 ml) were gradually added. To the mixture was added charcoal and the suspension filtered hot with suction; the precipitate was washed several times with dilute ammonia solution and the filtrate acidified with acetic acid. The greyish precipitate (0.1 g) had m.p. 255—257°, which was depressed on admixture with Ia; recrystallization from glacial acetic acid gave a nearly white substance with m.p. 269.5—271.5° (decomp.). (Found: N 3.56. Calc. $C_{27}H_{33}NO_2$ (395.5): N 3.54).

cis-*3-(o-Nitrostyryl)-retene*[6] (IIIa). A mixture of Ia (3.5 g) copper-chromium oxide catalyst (1 g) and quinoline (30 ml) was heated at 215—220° for 18 min. To the mixture was added benzene. The catalyst was removed after cooling by filtration and washed with benzene. The dark coloured benzene filtrate was washed several times with dilute hydrochloric acid followed by sodium carbonate solution and then dried After evaporation of the solvent the strongly coloured crystalline residue was dissolved in hot *n*-propanol (130 ml), the solution treated with charcoal and filtered. Yellow crystals separated on cooling; the yield was 2.1 g (67 %) m.p. 175—179°. Recrystallization from glacial acetic acid (65—70 ml) gave 1.85 g, m.p. 178—179.4°. U.V. absorption (in 96 % ethanol): λ_{max} 266 mμ (log ε 4.67); 316 mμ (log ε 4.22). I.R. maxima (cm^{-1}): 1 337 and 1 517 (NO_2), no *trans* —CH=CH— absorption.

trans-*3-(o-Nitrostyryl)-retene* (IIIb). A mixture of Ia (3.4 g), copper-chromium oxide catalyst (1 g) and quinoline (25 ml) was heated at 228—235° for 30 min. The reaction mixture was worked up as described above. The benzene solution of the decarboxylation product was evaporated to dryness. Recrystallization of the crystalline residue from *n*-propanol gave yellow crystals (2.07 g), melting in the range 157—167°. Fractional crystallization of this material from glacial acetic acid gave *cis*-3-(*o*-nitrostyryl)-retene 1 g (32.8 %) m.p. 176.5—179.2°.

From the mother liquor was obtained 0.67 g impure 3-(*o*-nitrostyryl)-retene, melting in the range 146—160°; 0.3 g of this material was dissolved in benzene (6 ml) and the solution poured on to a column of alumina (20 × 2 cm). The chromatogram was developed with a mixture (3:2) of light petroleum and benzene. The development was continued until all yellow material had passed into the filtrate.

cis-*3-(o-Nitrostyryl)-retene* (63 mg) was isolated from the first eluate fractions, m.p. 176—177,7° one recrystallization from glacial acetic acid raised the m.p. to 177.5—179.2°.

The succeeding fractions contained a mixture of *cis* and *trans-3-(o*-nitrostyryl)-retene (185 mg) m.p. 152—172°.

Pure *trans*-3-(*o*-nitrostyryl)-retene (IIIb) was isolated from the last eluate fractions, yellow crystals from *n*-propanol (36 mg) m.p. 174—175.5°. The m.p. was depressed on admixture with the *cis*-isomer (IIIa). (Found: C 81.5; H 5.96; N 3.65. Calc. for $C_{26}H_{23}NO_2$ (381.5): C 81.9; H 6.08; N 3.67). U.V. absorption (in 96 % ethanol): λ_{max} 254 mμ (log ε 4.65): 270 mμ (log ε 4.63); 327 mμ (log ε 4.39). I.R. maxima (cm^{-1}): 957 (*trans*-CH=CH—), 1 335 and 1 515 (NO_2).

Decarboxylation of cis-o-*nitro-a-(3-retenyl)cinnamic acid* (Ib). A mixture of Ib (1.0 g), copper-chromium oxide catalyst (0.3 g) and quinoline (15 ml) was heated at 225—230° for 12 min. Reddish brown fumes were observed in the condenser at the end of the reaction time. Quinoline was removed as described above for decarboxylation of Ia. On concentrating the benzene solution of the reaction product, a crystalline precipitate separated; filtration and washing with benzene gave almost white crystals of 3-(3′-retenyl)coumarin (IV) (0.25 g) m.p. 203—205.5°. Recrystallization from glacial acetic acid raised the m.p.

to 204.5—206°. (Found: C 85.3; H 5.95. Calc. for $C_{27}H_{22}O_2$ (378.5): C 85.7; H 5.86). I.R. maxima (cm^{-1}): 1 105 (C—O—C), 1 705—1 725 two peaks (C=O), no absorption at 2 500—2 700 (CO_2H). IV could be dissolved in alcoholic potassium hydroxide solution, but during back-titration with hydrochloric acid the lactone ring was closed and practically no uptake of base was found. A fraction of IV was converted to the trinitrofluorenone complex, which crystallized from benzene in red orange crystals, m.p. 186.5—188.5°. (Found: C 68.85; H 3.98; N 6.00. Calc. for $C_{40}H_{27}N_3O_9$ (693.6: C 69.3; H 3.93; N 6.06).

The mother liquor from the isolation of IV was evaporated *in vacuo*, and the crystalline residue treated with warm *n*-propanol. After cooling the product was filtered and washed with *n*-propanol. The yellowish crystalline product (0.5 g) was dissolved in benzene (20 ml) and adsorbed on a column (20 × 2 cm) of alumina. On development with a mixture (3:2) of light petroleum and benzene, a yellow zone passed rather quickly down the column. The development was continued until nearly all yellow material had passed into the filtrate. Pure *trans*-3-(*o*-nitrostyryl)-retene (IIIb) was isolated from the filtrate. The yield was 182 mg (20 %), m.p. 173.5—175.5°. (Found: C 81.7; H 6.12; N 3.78. Calc. for $C_{26}H_{23}NO_2$ (381.5): C 81.9; H 6.08; N 3.67). This substance is identical with the substance prepared by rearrangement of *cis*-3-(*o*-nitrostyryl)-retene, as shown by mixed melting point determination, and by similarity both in I.R. and in U.V. spectra.

The solid column showed strong fluorescence in ultraviolet light and was fractionally eluted with hot benzene-ethanol; 130 mg of 3-(3′-retenyl)-coumarin m.p. 204—206.5° were isolated from the eluates.

cis-*3-(o-Aminostyryl)-retene* (V). A mixture of *cis*-3-(*o*-nitrostyryl)-retene (IIIa) (0.85 g, 0.0022 mole), 5 % palladiumcharcoal (0.2 g), 100 % hydrazine hydrate (0.445 ml, 0.0088 mole) and alcohol (25 ml) was heated under reflux on a water bath for 45 min. The catalyst was removed by filtration, and washed with warm alcohol; from the resulting greenish fluorecent filtrate nearly colourless crystals of V separated, 0.5 g, m.p. 119.7—120.7°. A further crop of material was obtained by concentrating the mother liquor; recrystallization of this material from alcohol gave 0.042 g, m.p. 119.8—120.8°. The total yield was 70 %. (Found: C 88.8; H 7.27; N 4.09. Calc. for $C_{26}H_{25}N$ (351.5): C 88.9; H 7.17; N 3.99).

A fraction of V was converted to the picrate, yellow crystals from alcohol, m.p. 200—201° (decomp.). (Found: N 9.58. Calc. for $C_{32}H_{28}N_4O_7$ (580.6): N 9.65).

3-Isopropyl-7-methyl-dibenz(ah)anthracene (VI). The hydrochloride of V (0.4 g) (prepared by saturating an ether solution of the amine (V) with hydrogen chloride at low temperature) was dissolved in a mixture of tetrahydrofuran (6 ml) and water (2 ml). To the clear solution was added concentrated sulphuric acid (0.1 ml). The solution was cooled in an ice-salt-bath and diazotized at 0 to −5° by adding a 4 % aqueous solution of sodium nitrite (0.138 g) during 5—10 min. To the red mixture was added copper powder (0.4 g), and evolution of nitrogen began at once. After 20 min at 0° and 2.25 h at room temperature copper powder was removed by filtration and washed with warm benzene. The filtrate was washed with hydrochloric acid (6 N), dilute potassium hydrogen carbonate solution and dried; the solvent was evaporated and the red brown residue taken up in benzene (5—6 ml). The benzene solution was poured on to a column of alumina (15 × 2 cm) and the chromatogram developed by a mixture (3:2) of light petroleum and benzene. When the column was examined in ultraviolet light during the chromatographic procedure, a blue fluorescent band was observed, moving quickly down the column. The development was continued until the blue fluorescent zone had passed into the filtrate. The pure hydrocarbon was isolated by evaporation of the solvent from the colourless filtrate and recrystallization of the crystalline residue from *n*-propanol-benzene.The yield of VI was 94 mg (27.4 %), m.p. 201—203°. (Found: C 92.8; H 6.54. Calc. for $C_{26}H_{22}$ (334.4): C 93.4; H 6.63). U.V. spectrum, Fig. 1.

The orange 1,3,5-trinitrobenzene complex of VI is rather unstable and dissociates in boiling alcohol with formation of the free hydrocarbon. The best material from benzene-hexane had m.p. 180—182° and was composed of one mole hydrocarbon to two mole trinitrobenzene. (Found: C 59.6; H 3.86; N 10.96. Calc. for $C_{38}H_{28}N_6O_{12}$ (760.7): C 60.0; H 3.71; N 11.05).

The 2,4,7-trinitrofluorenone complex of VI, composed of one mole hydrocarbon to one of 2,4,7-trinitrofluorenone, was more stable than the trinitrobenzene complex and was obtained as dark red crystals from benzene, m.p. 212—214°. (Found: C 72.0; H 4.23; N 6.25. Calc. for $C_{39}H_{27}N_3O_7$ (649.6): C 72.1; H 4.19; N 6.47).

The author wishes to express his gratitude to Professor B. Bak, the Chemical Laboratory of the University of Copenhagen, for determining the infrared spectra. Thanks are also due to Miss B. Møller for valuable technical assistance.

REFERENCES

1. Adelson, D. E. and Bogert, M. T. *J. Am. Chem. Soc.* **59** (1937) 1776.
2. Fieser, L. F. and Clapp, R. C. *J. Am. Chem. Soc.* **63** (1941) 319.
3. Newman, M. S. and Joshel, L. M. *J. Am. Chem. Soc.* **62** (1940) 972.
4. Shear, M. J., Leiter, J. and Perault, A. *J. Natl. Cancer Inst.* **1** (1940) 303.
5. Pschorr, R. *Ber.* **29** (1896) 496.
6. Dynesen, E. *Acta Chem. Scand.* **13** (1959) 502.
7. Ruggli, P. and Staub, A. *Helv. Chim. Acta* **19** (1936) 1288.
8. Balcom, D. and Furst, A. *J. Am. Chem. Soc.* **75** (1953) 4334.
9. Dewar, M. J. S. and Mole, T. *J. Chem. Soc.* **1956** 2556.
10. Buchta, E. and Kallert, W. *Ber.* **576** (1952) 172.
11. Cook, J. W. *J. Chem. Soc.* **1933** 1592.
12. Clar, E. and Stewart, D. G. *J. Am. Chem. Soc.* **74** (1952) 6235.
13. Jones, R. N. *J. Am. Chem. Soc.* **62** (1940) 148.
14. Jones, R. N. *J. Am. Chem. Soc.* **63** (1941) 151.

Received April 7, 1961.

ACTA CHEMICA SCANDINAVICA 15 (1961) 1571–1574

The Crystal Structure of Ru_2Si

BERTIL ARONSSON and JAN ÅSELIUS

Institute of Chemistry, University of Uppsala, Uppsala, Sweden

The crystal structure of Ru_2Si has been refined from single crystal data. The unit cell dimensions are $a = 5.27_9$ Å, $b = 4.00_5$ Å and $c = 7.41_8$ Å. The space-group is *Pnma* and the atoms are situated in 4(*c*) positions with the following atomic parameters: Ru_I: $x = 0.8319$, $z = 0.0650$; Ru_{II}: $x = 0.9820$, $z = 0.7119$; Si: $x = 0.2964$, $z = 0.1013$. Interatomic distances in the isomorphous phases Co_2P, Co_2Si, Ru_2P and Ru_2Si are discussed.

It was reported previously [1] that a ruthenium silicide with the approximate composition Ru_2Si crystallizes in the *C*23 (anti-$PbCl_2$) type structure. The structure of Ru_2Si has now been refined and the results are presented in this paper.

EXPERIMENTAL

Alloys were prepared by arc-melting or by sintering mixtures of ruthenium (claimed purity 99.9 % from Heraeus, Hanau, Germany) and silicon (claimed purity 99.9 % from Pechiney, Paris). Powder photographs were taken in Guinier cameras with Cu*Ka*-radiation. Diffraction patterns from single crystals of Ru_2Si rotated about the *b*-axis were obtained in a Weissenberg camera using Mo*K*-radiation. The multiple film technique was employed using thin iron foil between the films, and the intensities were estimated visually. The atomic parameters were refined from successive $\varrho_o(xz)$ and $\varrho_o(xz)-\varrho_c(xz)$ electron density projections. Fourier summations and structure factor computations were made on the electronic digital computer BESK with programs available at BESK.

RESULTS

By examining the powder photographs of the arc-melted alloys which had been allowed to cool rapidly in the arc furnace, it was found that alloys with nominal compositions ranging from $RuSi_{0.33}$— $RuSi_{0.50}$ contained ruthenium and Ru_2Si (Table 1), while alloys with compositions $RuSi_{0.54}$ — $RuSi_{0.56}$ contained Ru_2Si and an unknown phase (or phases) probably more silicon-rich than Ru_2Si. In the powder photograph of $RuSi_{0.52}$ only the powder lines of Ru_2Si could be detected.

Table 1. Powder photograph of an arc-melted alloy with the nominal composition $RuSi_{0.50}$. (Cu$K\alpha$-radiation). (Only diffraction lines for which $\sin^2\Theta < 0.203$ are given).

hkl for Ru_2Si	$\sin^2\Theta_{obs}$	$\sin^2\Theta_{calc}$	I_{obs}	$p\|F\|^2_{calc} \times 10^{-3}$ *
101	—	0.0321	—	2.0
002	—	0.0432	—	0.6
011	0.0480	0.0478	m-	13.8
102	0.0646	0.0645	w+	14.1
111	0.0693	0.0692	st-	47.3
200	—	0.0853	—	1.7
201	—	0.0961	—	3.3
112	0.1015	0.1016	st-	75.4
(Ru)	0.1088		m	
103	0.1183	0.1185	m	47.0
210	0.1223	0.1223	st	99.2
202	0.1285	0.1285	st	105.0
(Ru)	0.1293		m	
211	0.1330	0.1331	vst	208.6
013	0.1337	0.1342	vst	239.7
(Ru)	0.1412		vst	
020	0.1481	0.1482	st	155.5
113	0.1555	0.1556	vw	24.6
212	0.1657	0.1656	vw	21.2
004	—	0.1728	—	2.1
121	—	0.1803	—	2.4
203	0.1825	0.1825	m	67.9
022	—	0.1914	—	0.7
104	0.1944	0.1941	vw	20.1
301	0.2027	0.2027	m-	47.9

* An isotropic temperatur factor with $B = 0.50$ Å^2 has been applied.

The powder photographs of alloys prepared by sintering mixtures of the elements at 1 100°C were complex and no phase with the $C23$ structure was present in these alloys.

Our observations show that an intermediate phase in the Ru-Si system has a composition closely corresponding to the formula Ru_2Si. This phase exists at elevated temperatures, where it is in equilibrium with the solid solution of silicon in ruthenium, and when cooled rapidly it may be retained down to room temperatures.

The powder lines of Ru_2Si were not very sharp and the l.p. (lattice parameter) reported below are only accurate to about $\pm$ 0.1 %. No l.p. variations of Ru_2Si were observed, which indicates that the homogeneity range of this phase is narrow. In the two phase alloys Ru + Ru_2Si the cell dimensions of ruthenium were found to be $a = 2.699$ Å and $c = 4.286$ Å. These values are slightly different from those quoted by Pearson [2] for pure ruthenium, $a = 2.706$ Å, $c = 4.282$ Å, indicating that there may be a small solid solubility of silicon in ruthenium. Since the determinations of cell dimensions are not very accurate, it is not possible to draw a definite conclusion on this point.

The crystal structure of Ru_2Si was refined from single crystal data until the difference synthesis did not display any gradients at the atomic positions.

Table 2. Interatomic distances in Ru_2Si (in Å). (Distances shorter than 3.75 Å are listed).

Ru_I	— 2 Ru_I	: $2.84_4(2)$
	— 6 Ru_{II}	: 2.73_7, 2.76_2, $2.77_7(2)$, $2.81_8(2)$
	— 5 Si	: 2.45(2), 2.47, 2.48, 2.84
Ru_{II}	— 6 Ru_I	: 2.73_7, 2.76_2, $2.77_7(2)$, $2.81_8(2)$
	— 4 Ru_{II}	: $2.69_9(2)$, $3.73_3(2)$
	— 6 Si	: 2.46(2), 2.52, 2.84(2), 3.33
Si	— 5 Ru_I	: 2.45(2), 2.47, 2.48, 2.84
	— 6 Ru_{II}	: 2.46(2), 2.52, 2.84(2), 3.33
	— 4 Si	: 3.30(2), 3.44(2)

There was no indication that the scattering parameters should not be proportional to 44, 44 and 14, respectively. The final R-value for the 86 observed non-equivalent $h0l$ reflexions was 6.7 %. An empirical isotropic temperature factor with $B = 0.50_0$ Å^2 was employed *. The structural data for Ru_2Si are summarized below:

Space-group: $Pnma$ (D_{2h}^{16}) $Z = 4$ (Structure type $C23$)
$a = 5.27_9$ Å $b = 4.00_5$ Å, $c = 7.41_8$ Å, $U = 156.8$ Å^3.

	x	z
4 Ru_I in 4(c)	0.8319 ± 0.0003	0.0650 ± 0.0002
4 Ru_{II} in 4(c)	0.9820 ± 0.0003	0.7119 ± 0.0002
4 Si in 4(c)	0.2964 ± 0.0013	0.1013 ± 0.0011

The standard deviations given above have been estimated using Cruickshank's formula [3].

The interatomic distances are collected in Table 2. In view of the low accuracy of the l.p. the standard deviation of Ru—Ru distances is estimated to be about 0.005 Å and that of Ru—Si distances to be about 0.015 Å.

DISCUSSION

Interatomic distances in Co_2P, Co_2Si and other phases with the $C23$ structure were recently discussed by Rundqvist [4]. The results of our study show that the relationship between Ru_2P and Ru_2Si is quite analogous to that between Co_2P and Co_2Si. The a-axis of the Me_2Si phase (Me = Co or Ru) is 12—15 % shorter than that of the corresponding Me_2P phase, while the b- and c-axes are somewhat longer (4—7 %). The unit cell volume of the silicide is slightly smaller than that of the phosphide. This is noteworthy, since the radius of the silicon atom is usually considered to be greater than that of the phosphorus atoms in metallic phases.

The immediate environments of the atoms in Co_2P and Ru_2P are very similar, but they differ considerably from those in the Me_2Si phases. This is parti-

* A list of calculated and observed structure factors may be obtained from this Institute on request.

cularly striking when the Me_I-X distances (X = P,Si) are considered. In the phosphides, each Me_I atom has four close phosphorus neighbours (*e.g.* in Ru_2P at 2.26, 2.30, and 2.40(2) Å, respectively). In the silicides the corresponding distances are much longer (*e.g.* in Ru_2Si 2.47, 2.48, and 2.45(2) Å, respectively) while a fifth silicon atom has also been brought rather close (2.84 Å in Ru_2Si) to the Me_I atoms.

Thus, in the four isomorphous phases Co_2P, Co_2Si, Ru_2P Ru_2S, the detailed atomic arrangement seems to be largely determined by the "character" of the non-metal atom.

Acknowledgement. We wish to thank Professor Hägg for his kind interest and for the facilities he has put at our disposal. This work has been supported by the *Air Force Office of Scientific Research of the Air Research and Development Command, United States Air Force,* through its European Office under Contract No. AF 61(052)-40) and by the *Swedish State Council for Technical Research.* Facilities for use of the digital computer BESK were granted by the *Swedish Board for Computing Machinery.*

REFERENCES

1. Aronsson, B., Stenberg, E. and Åselius, J. *Nature* **183** (1959) 1318.
2. Pearson, W. B. *A handbook of Lattice Spacings and Structures of Metals and Alloys.* Pergamon Press, London-New York-Paris-Los Angeles 1958.
3. Cruickshank, D. W. J. *Acta Cryst.* **2** (1949) 65.
4. Rundqvist, S. *Acta Chem. Scand.* **14** (1960) 1961.

Received April 13, 1961.

ACTA CHEMICA SCANDINAVICA 15 (1961) 1575–1582

The True Dithio-*p*-urazine and Some Related Sym-tetrazine Derivatives

JAN SANDSTRÖM

Department of Organic Chemistry, University of Lund, Lund, Sweden

Tetrahydro-*sym*-tetrazine-3,6-dithione, or dithio-*p*-urazine, has been prepared by reaction between thiocarbohydrazide and the disodium salt of dicarboxymethyl trithiocarbonate. The structure of this potentially tautomeric compound has been investigated by means of infrared and ultraviolet spectra and by nuclear magnetic resonance. The evidence tends to favour the dithione form. By reaction between dithio-*p*-urazine and organic halides in alkaline solution a series of dialkylthio-dihydrotetrazines has been prepared, from which the corresponding tetrazines have been obtained by oxidation. The dithio-*p*-urazine is rearranged by hot hydrochloric acid to the isomeric 3,5-dimercapto-4-amino-4,1,2-triazole, whereas the dialkylthio-dihydrotetrazines undergo ring-opening without recyclization under the same conditions. The ultraviolet and infrared spectra of the tetrazines are briefly discussed.

In a previous communication [1] the compound described by earlier authors as dithio-*p*-urazine (I) has been shown to be 3,5-dimercapto-4-amino-4,1,2-triazole (II). The true dithio-*p*-urazine has now been prepared in 45 % yield by reaction between thiocarbohydrazide and the disodium salt of dicarboxymethyl trithiocarbonate in aqueous solution at room temperature. All attempts to increase the yield by varying solvent, pH, or temperature have invariably led to inferior results.

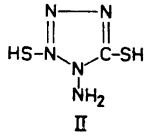

II

The general structure of dithio-*p*-urazine is demonstrated by its transformation to dihydrotetrazines and tetrazines as described later. The infrared spectrum shows no bands in the region 2 800—1 550 cm^{-1}, which indicates

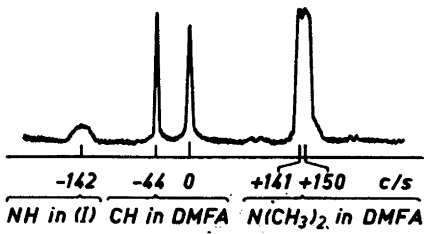

Fig. 1. NMR spectrum of dithio-*p*-urazine in DMFA solution. External standard: benzene.

that primary amino groups are absent. However, within this structural frame four protometric forms (Ia—Id) are possible, and attempts have been made to establish, which of these is the dominating one. Proton magnetic resonance has been recorded in dimethylformamide solution and shows only the broad NH signal and no sign of the sharp SH signal [2] (Fig. 1). This indicates that the form (Ia) should dominate, at least in dimethylformamide solution. However, Meyer *et al.*[3] have found the chemical shift δ-value with respect to the proton resonance in water to be -0.20 for the thiol proton in thiophenol and -0.24 for the methyl protons in dimethylformamide. Therefore, it is possible that the SH signal is not resolved from the CH_3N signal in the present case, and the conclusion must be regarded as tentative. Unfortunately, the low solubility of dithio-*p*-urazine has precluded the use of solvents other than dimethyl formamide. Recently Hoffman [4] and Gronowitz and Hoffman [5] have employed proton magnetic resonance in order to show that 2-thiouracil exists in the thione form in dimethylsulphoxide solution.

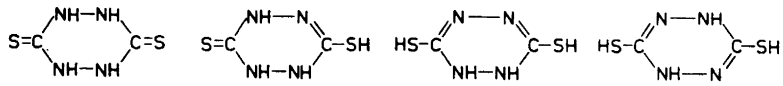

The solid state seems to be composed of the form (Ia), since, as was pointed out above, no absorption bands occur in the region 2 800—1 550 cm^{-1}, when the infrared spectrum is recorded in a potassium bromide disk. Thus, absorption bands due to S—H stretching vibration around 2 500 cm^{-1}, and to C=N stretching vibration, which appear in the spectra of the dihydrotetrazines (III) in the region 1 640—1 620 cm^{-1}, are absent.

The ultraviolet spectrum of (I) also seems to eliminate the dominance of the dithiol forms (Ic) and (Id) in ethanolic solution. The long-wave length absorption band of (I) appears at 2 985 Å with ε : 20 400, whereas the dihydrotetrazine (IIIa), which ought to have its ring protons in the same positions as the hypothetical dithiol forms of (I), has its main absorption band at 2 215 Å with ε : 13 500.

When dithio-*p*-urazine reacts with two equivalents of an organic halide in the presence of two equivalents of alkali, a dialkylthio-dihydrotetrazine (III) is formed. (For dihydrotetrazines, which are readily oxidized to tetrazines,

the 1,2-dihydro structure is generally accepted [6].) In this way the dimethylthio- and dibenzylthio-dihydrotetrazines have been prepared. When the same reaction is performed with ethyl chloroacetate, complications arise due to secondary reactions between the ethoxycarbonyl groups and the NH groups of the ring. Three compounds have been isolated, *viz.* 3,6-bis-ethoxycarbonylmethylthio-1,2-dihydrotetrazine (IIIc), the bicyclic monolactam (IV), and the tricyclic dilactam (V).

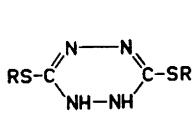

III a, R=CH_3
b, R=$PhCH_2$
c, R=$EtO_2C{\cdot}CH_2$

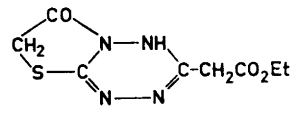

IV

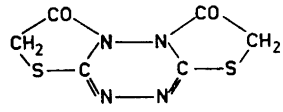

V

The pure diester (IIIc) is unchanged after boiling in ethanol for one hour. The monolactam (IV) is slowly transformed to the dilactam (V) under the same conditions. In acid solution the transformation is much more rapid. Unexpectedly, the yield of the diester (IIIc) does not increase at the expense of the lactams when the reaction is performed at 0°.

When sodium monochloroacetate and dithio-*p*-urazine react in alkaline medium, and the mixture is acidified, only the dilactam (V) is obtained. This dilactam is very slightly soluble in the common solvents and it does not melt below 300°, so a polymeric structure seems possible. However, the infrared spectrum indicates a monomeric structure. The carbonyl band of the dilactam (V) is found at 1 714 cm^{-1}, whereas that of N-acetyl-3,6-dibenzylthio-1,2-dihydrotetrazine (VI) appears at 1 650 cm^{-1} (potassium bromide disks). Five-membered lactams are known to have their carbonyl frequency near 1 700 cm^{-1}, and in a fused ring system a further increase in carbonyl frequency can be expected [7].

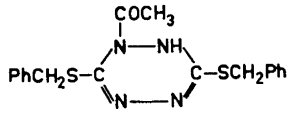

VI

Dihydrotetrazines are known to undergo ring-contraction to the isomeric 4-aminotriazoles at elevated temperatures [8] and also in hot acid medium [9,10]. The dithio-*p*-urazine (I) is rearranged by hot dilute hydrochloric acid to dimercapto-aminotriazole (II). The dihydro-tetrazines (III) show a remarkable thermal stability, and the dimethyl derivative (IIIa) sublimes unchanged at 190°. In hot dilute hydrochloric acid the dihydrotetrazines undergo hydrolytic

cleavage, and from the dibenzyl derivative (IIIb) two hydrazides, *viz.* benzylthiocarbonyl-hydrazine (VII), and 1,2-bis-benzylthiocarbonyl-hydrazine (VIII) have been isolated, but no 3,5-dibenzylthio-4-amino-triazole has been

$PhCH_2S{\cdot}CO{\cdot}NHNH_2$ VII

$PhCH_2S{\cdot}CO{\cdot}NHNH{\cdot}CO{\cdot}SCH_2{\cdot}Ph$ VIII

obtained. Dallacker [11] has investigated the corresponding reaction of 3,6-dipyridyl-dihydrotetrazine and obtained 3,5-dipyridyl-4-amino-triazole together with 1,2-dipyridoylhydrazine.

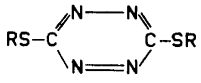

IX

a-c as in III

d, R=CH_2CO_2H

When the dihydrotetrazines (III) are oxidized with nitrous acid, bromine, hydrogen peroxide, or ferric chloride, the corresponding tetrazines (IX) are formed in good yields as bright-red solids. When the reaction mixture from sodium monochloroacetate and dithio-*p*-urazine is treated with hydrogen peroxide prior to acidification, a good yield of 3,6-dicarboxymethylthio-tetrazine (IXd) results. The same compound is formed in lower yield when the dilactam (V) is dissolved in hot alkali and treated with hydrogen peroxide and the mixture is acidified.

The ultraviolet absorption spectrum of *sym*-tetrazine has been thoroughly investigated from a theoretical point of view by Liquori and Vaciago [12], and by Mason [13–15], who have concluded that the maximum at 2 520 Å is due to a $\pi \rightarrow \pi$ transition and the one at 5 420 Å to a $n \rightarrow \pi$ transition (solvent *cyclo*hexane). Furthermore, Mason [13] has tentatively assigned a shoulder at 3 200 Å to a transition from the lowest lone-pair orbital to the second lowest

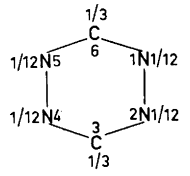

X

unoccupied π orbital. The latter has the form

$$\psi = 1/\sqrt{12}\ (2\Phi_3 - \Phi_4 - \Phi_5 - 2\Phi_6 - \Phi_1 - \Phi_2)$$

where Φ_i denote atomic orbitals, and when an electron is promoted from a non-bonding orbital to this orbital, its charge is distributed over the ring atoms according to (X). Therefore, the energy of the transition is lowered by electron-attracting substituents in the positions 3 and 6, and raised by electron-donating substituents in the same positions.

Table 1. Spectra of 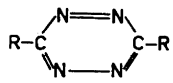

R	Solvent	λ_{max} Å	ε	λ_{max} Å	ε	λ_{max} Å	ε
CH_3S	Heptane	2 810	23 000	4 100	655	5 380	390
CH_3S	Ethanol	2 830	21 500	4 170	615	5 280	360
$PhCH_2S$	Heptane	2 875	31 200	4 125	850	5 385	520
$PhCH_2S$	Ethanol	2 890	28 000	4 160	800	5 300	490
$EtOCOCH_2S$	Ethanol	2 790	25 000	4 060	910	5 230	460
$NaOCOCH_2S$	Water	2 580	15 600	4 130	1 070	5 310	280
H [a]	*Cyclo*hexane	2 520	2 150			5 420	829
H [a]	Water (pH 7)	2 550	2 840			5 100	362
H_2N [b]	Dioxane			4 280	1 980	5 280	590
CH_3CONH [b]	Ether			3 630	1 800	5 250	520
p-Tosyl-NH [b]	Ether			3 630	1 860	5 270	560

[a] From Ref.[14] [b] From Ref.[16]

The dialkylthio-tetrazines (IX) show the two first-mentioned maxima and in addition one near 4 100 Å (Table 1). In the spectrum of the dimethylthio-tetrazine (IXa) in heptane there is a slight vibrational structure (Fig. 2). The same bands appear in the spectra of 3,6-diamino-tetrazine and some of its derivatives [16]. However, the maximum near 4 100 Å cannot be due to a transition like the one proposed by Mason, since the effect of electron-donating substituents is opposite to that expected. When the electron-donating capacity of the amino groups in diamino-tetrazine is diminished by acylation, the absorption is shifted to a shorter wavelength. A similar effect, though smaller, is obtained, when a hydrogen atom in dimethylthio-tetrazine is replaced by an ethoxycarbonyl group.

Also, the 4 100 Å band undergoes a bathochromic shift (200—400 cm^{-1}) when going from heptane to ethanol as solvent. A n → π band should give a

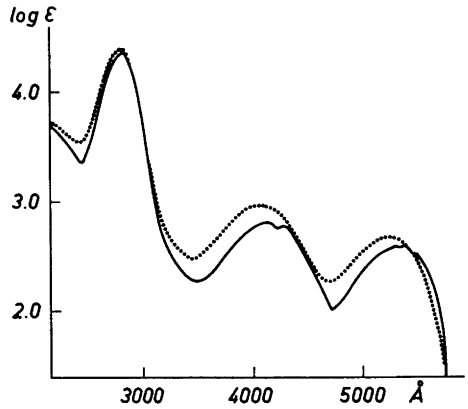

Fig. 2. Ultraviolet-visible spectra of IXa in heptane ———, and IXc in ethanol · · · · · ·

hypsochromic shift under the same conditions, since it is due to a transition, where the ground state is more stabilized with respect to the excited state in polar and particularly in hydroxylic solvents than in non-polar solvents [17,18].

The infrared spectra of diaryltetrazines have been discussed by Wiley *et al.* [19], who report absorption bands in the regions 1 390—1 375 and 925—913 cm^{-1}, which are ascribed to vibrations in the tetrazine ring. Dallacker [11,20] has prepared dipyridyl-, dithiazolyl-, and some substituted diphenyltetrazines and reports a characteristic absorption band in the region 1 430—1 335 cm^{-1}. However, the dialkylthio-tetrazines (IXa—d) do not all have absorption bands in the regions mentioned above, but all of them show strong bands in the regions 1 253—1 239 and 1 060—1 047 cm^{-1} and weaker bands in the region 980—867 cm^{-1}. The last-mentioned band may be due to a C—S strecthing vibration. This vibration is correlated with a band in the region 660—630 cm^{-1} in alkyl sulphides [21], but on conjugation it is shifted to higher frequencies, 830—710 cm^{-1} in vinyl sulphides [22], and 1 000—850 cm^{-1} in thiolesters [23]. A similar effect must be present in dialkylthio-tetrazines, since the tetrazine ring is highly π-deficient [24], and should conjugate strongly with electrondonating substituents.

EXPERIMENTAL

Dithio-*p*-urazine (I)

A solution of dicarboxymethyl trithiocarbonate (22.6 g) in N NaOH (200 ml) was added to a lukewarm solution of thiocarbohydrazide (10.6 g) in water (150 ml). The solution was cooled, and within an hour a pale yellow crystalline powder began to separate. After three days the deposition was finished, and the product (6.7 g, 45 % yield) was found to be pure dithio-*p*-urazine (I), m.p. 176° (decomp.). (Found: C 16.1; H 2.82; N 37.4; S 43.2. $C_2H_4N_4S_2$ (148.20) requires C 16.2; H 2.72; N 37.8; S 43.3).

Dithio-*p*-urazine (0.30 g) was refluxed with N HCl (5 ml) for 3 h. After cooling, colourless rods separated (0.19 g, 63 % yield), m.p. 214—214.5° (decomp.). The infrared spectrum of the product was found to be identical with that of 3,5-dimercapto-4-amino-4,1,2-triazole (II) (m.p.[1] 222°). The product (0.075 g) was dissolved in N NaOH (1.2 ml), and benzyl chloride (0.13 g) in ethanol (2 ml) was added. Colourless flakes separated (0.09 g, 55 % yield), m.p. 148—149°, identified by mixed m.p. and infrared spectrum with 3,5-dibenzylthio-4-amino-4,1,2-triazole [1].

Dialkylthio-dihydrotetrazines (III)

The 3,6-dimethylthio- and 3,6-dibenzylthio-dihydrotetrazines were prepared by dissolving dithio-*p*-urazine in two equivalents of N NaOH under nitrogen and adding two equivalents of the appropriate organic halide in sufficient ethanol to give a homogeneous solution. The *3,6-dimethylthio-dihydrotetrazine* (IIIa) was obtained in 70 % yield and crystallized from absolute ethanol as pale yellow rods, m.p 192—193°. (Found: C 27.2; H 4.59; N 32.0; S 36.2. $C_4H_8N_4S_2$ (176.26) requires C 27.3; H 4.57; N 31.8; S 36.4). The *3,6-dibenzylthio-dihydrotetrazine* (IIIb) was obtained in 65 % yield and crystallized from toluene as pale yellow plates, m.p. 165.5—166°. (Found: C 58.5; H 4.92; N 17.1; S 19.5. $C_{16}H_{16}N_4S_2$ (328.45) requires C 58.5; H 4.91; N 17.1; S 19.5).

Dithio-*p*-urazine (6.0 g) was dissolved in N NaOH (80 ml) under nitrogen, and a solution of ethyl chloroacetate (15 g) in ethanol (40 ml) was added dropwise with stirring. A colourless precipitate was formed (5.4 g), and when the filtrate was evaporated to about two thirds of the original volume, a further quantity (3.5 g) was obtained. The combined products were extracted with hot chloroform (40 ml). The undissolved material (2.9 g, 32 % yield) consisted of the dilactam (V) to be described later. The chloroform solution was added to carbon tetrachloride (40 ml), and pale yellow, pointed plates separated

(2.0 g, 18 % yield), m.p. 123—124° after recrystallization from ethanol, consisting of the *monolactam* (IV). (Found: C 35.2; H 3.75; N 20.4; S 23.4. $C_8H_{10}N_4O_3S_2$ (274.31) requires C 35.0; H 3.67; N 20.4; S 23.4.) λ_{max} 2 505 Å with ε : 20 000 in absolute ethanol.

Light petroleum (b.p. 40—60°, 80 ml) was added to the chloroform-carbon tetrachloride filtrate from (IV), and colourless, rhombic prisms separated (3.0 g, 23 % yield), m.p. 104—105°, consisting of *3,6-bis-ethoxycarbonylmethylthio-dihydrotetrazine* (IIIc). (Found: C 37.4; H 4.91; N 17.4; S 20.0. $C_{10}H_{16}N_4O_4S_2$ (320.38) requires C 37.5; H 5.03; N 17.5; S 20.0).

The monolactam (IV, 0.27 g) was refluxed for 24 h in ethanol (5 ml). Only a very small amount of the dilactam (V) had then separated. The same experiment was repeated, but N HCl (1 ml) was added. On heating a precipitate was formed, and after one hour pale yellow prisms were filtered off (0.20 g, 85 % yield). On heating they darkened without melting below 300°, and they were very slightly soluble in the common solvents. In boiling dimethylsulphoxide dissolution occurred, but probably with decomposition, since the solution was dark, and nothing crystallized on cooling. According to analysis the product was the *dilactam* (V). (Found: C 31.5; H 2.01; N 24.4; S 28.0. $C_6H_4N_4O_2S_2$ (228.24) requires: C 31.6; H 1.77; N 24.6; S 28.1).

Dithio-*p*-urazine (1.5 g) was dissolved in N NaOH (20 ml) under nitrogen, and a solution of monochloroacetic acid (2.5 g) in the equivalent amount of N NaOH was added. On the following day the solution was made acid to Congo red with 5 N HCl, and a precipitate of a pale yellow, microcrystalline powder was obtained (2.05 g, 89 % yield). The product did not melt below 300° and was shown by infrared spectrum to consist of the dilactam (V) just described.

Acetylation of 3,6-dibenzylthio-dihydrotetrazine

Dibenzylthio-dihydrotetrazine (IIIb, 0.66 g) and acetic anhydride (5 ml) were refluxed for 15 minutes. Then the acetic anhydride and acetic acid were removed *in vacuo*, and the residue crystallized from toluene as colourless rods, m.p. 141.5—142.5°, of 1-acetyl-3,6-dibenzylthio-dihydrotetrazine (VI). (Found: C 58.5; H 5.04; N 15.2; S 17.3. $C_{18}H_{18}N_4OS_2$ (370.47) requires C 58.3; H 4.90; N 15.1; S 17.3).

Hydrolysis of 3,6-dibenzylthio-dihydrotetrazine

Dibenzylthio-dihydrotetrazine (IIIb, 1.64 g) was refluxed with ethanol (50 ml) and conc. hydrochloric acid (5 ml) until after 10 h no red colour appeared when a drop of the solution was mixed with a drop of sodium nitrite solution. The solution was then evaporated to dryness on the water bath, and the residue was ground with water (20 ml) and filtered. Crystalline sodium acetate (1.5 g) was added to the aqueous extract, and a precipitate was formed, which crystallized from 50 % aqueous ethanol as colourless plates, m.p. 116—117°, of *benzylthiocarbonyl-hydrazine* (VII). (Found: C 52.9; H 5.35; N 15.2; S 17.7. $C_8H_{10}N_2OS$ (182.24) requires C 52.7; H 5.54; N 15.4; S 17.6).

The water-insoluble material (1.25 g) crystallized from ethanol (5 ml) as colourless plates (0.85 g), m.p. 155.5—156°, of *1,2-bis-benzylthiocarbonyl-hydrazine* (VIII). (Found: C 57.5; H 4.70; N 8.50; S 19.1. $C_{16}H_{16}N_2O_2S_2$ (332.43) requires C 57.8; H 4.85; N 8.42; S 19.3.)

The ethanolic mother liquor was evaporated to dryness, the semicrystalline residue was dissolved in chloroform, and the infrared spectrum was recorded. It was not very well resolved, but it showed no bands at 3 380 and 1 620 cm^{-1}, where 3,5-dibenzylthio-4-amino-4,1,2-triazole has characteristic absorption bands.

Dialkylthio-tetrazines

The dihydrotetrazines (IIIa—c) can be oxidized to tetrazines in a variety of ways. The following method was found convenient in all cases because of its rapidity. The dihydrotetrazine was dissolved in ethanol, and the calculated amount of 2 N ferric chloride was added. Water was added to precipitate all tetrazine, which came out in an almost pure state. The *3,6-dimethylthio-1,2,4,5-tetrazine* (IXa) crystallized from light petroleum

(80—100°) as bright-red rods, m.p. 83.5—84°. (Found: C 27.6; H 3.52; N 32.4; S 36.5. $C_4H_6N_4S_2$ (174.24) requires C 27.6; H 3.47; N 32.2; S 36.8).

The *3,6-dibenzylthio-1,2,4,5-tetrazine* (IXb) crystallized from ethanol as bright-red rods, m.p. 139—140°. (Found: C 58.8; H 4.42; N 17.0; S 19.5. $C_{16}H_{14}N_4S_2$ (326.43) requires C 58.9; H 4.32; N 17.2; S 19.6).

The *3,6-bis-ethoxycarbonylmethylthio-1,2,4,5-tetrazine* (IXc) crystallized from benzene-heptane as bright-red rods, m.p. 84—85°. (Found: C 37.6; H 4.38; N 17.6; S 20.1. $C_{10}H_{14}N_4O_4S_2$ (318.36) requires C 37.7; H 4.43; N 17.6; S 20.1).

Dithio-*p*-urazine and monochloroacetic acid were dissolved and mixed as above, and after one hour Perhydrol (1 ml) was added. On the following day a small amount of the dilactam (V) was removed by filtration, and the filtrate was made acid to Congo red with 5 N HCl. A precipitate of fernleaf-like, red prisms was obtained (2.1 g, 80 % yield). The product was purified by dissolution in N sodium bicarbonate solution, filtration and precipitation with 5 N HCl, and was shown by analysis to consist of *3,6-dicarboxymethylthio-1,2,4,5-tetrazine* (IXd), m.p. 255° (decomp.). (Found: C 27.6; H 2.40; N 21.2; S 24.3. $C_6H_6N_4O_4S_2$ (262.26) requires C 27.5; H 2.31; N 21.4; S 24.4.)

The same product was obtained in 25—30 % yield, when the dilactam (V) was dissolved in hot N NaOH, treated with Perhydrol, and then acidified as above.

The nuclear magnetic resonance spectrum (Fig. 1) was obtained with a Varian Associates model V-4 300-B high resolution NMR spectrometer operating at 40 Mc/s, and a flux stabilized 12″ electromagnet from the same company. The magnet sweep was calibrated by the modulation side band technique. The infrared spectra have been recorded with a Perkin-Elmer model 221 prism-grating instrument, and the ultraviolet spectra with a Beckman DU spectrophotometer.

Acknowledgements. The author is indebted to *The Swedish Natural Science Research Council* for financial support, to Miss Kristina Arvidsson and Miss Ingeborg Leutiger for valuable experimental assistance, to Miss Kerstin Kulle for recording the infrared spectra, and to civilingeniör Jan Christer Eriksson for the NMR spectrum.

REFERENCES

1. Sandström, J. *Acta Chem. Scand.* **15** (1961) 1295.
2. Abraham, R. J., Pople, J. A. and Bernstein, H. J. *Can. J. Chem.* **36** (1958) 1302.
3. Meyer, L. H., Saika, A. and Gutowsky, H. S. *J. Am. Chem. Soc.* **75** (1953) 4567.
4. Hoffman, R. A. *Svensk Kem. Tidskr.* **72** (1960) 610.
5. Gronowitz, S. and Hoffman, R. A. *Arkiv Kemi* **16** (1961) 459.
6. Wiley, P. F. in Weissberger, *The chemistry of heterocyclic compounds: The 1,2,3- and 1,2,4-triazines, tetrazines and pentazines.* Interscience Publishers, New York 1956, p. 179.
7. *The chemistry of penicillin.* Princeton University Press 1949, p. 390.
8. Curtius, Th., Darapsky, A. and Müller, E. *Ber.* **48** (1915) 1624.
9. Pinner, A. *Ber.* **30** (1897) 1871.
10. Bülow, C. and Weber, F. *Ber.* **42** (1909) 1990.
11. Dallacker, F. *Monatsh.* **91** (1960) 294.
12. Liquori, A. M. and Vaciago, A. *Gazz. chim. ital.* **86** (1956) 769.
13. Mason, S. F. *J. Chem. Soc.* **1959** 1240.
14. Mason, S. F. *J. Chem. Soc.* **1959** 1247.
15. Mason, S. F. *J. Chem. Soc.* **1959** 1263.
16. Lin, C.-H., Lieber, E. and Horwitz, J. P. *J. Am. Chem. Soc.* **76** (1954) 427.
17. Bayliss, N. S. and McRae, E. G. *J. Phys. Chem.* **58** (1954) 1002.
18. Pimentel, G. C. *J. Am. Chem. Soc.* **79** (1957) 3323.
19. Wiley, R. H., Jarboe, Jr., C.H. and Hayes, F.N. *J. Org. Chem.* **22** (1957) 835.
20. Lipp, M., Dallacker, F. and Thoma, J. *Monatsh.* **91** (1960) 595.
21. Sheppard, N. *Trans. Faraday Soc.* **46** (1950) 429.
22. Boonstra, H. J. and Rinzema, L. C. *Rec. trav. chim.* **79** (1960) 962.
23. Baker, A. W. and Harris, G. H. *J. Am. Chem. Soc.* **82** (1960) 1923.
24. Albert, A. *Heterocyclic Chemistry.* Essential Books, Fair Lawn 1959, p. 39.

Received April 2, 1961.

ACTA CHEMICA SCANDINAVICA 15 (1961) 1583–1594

On the Reactions of N-substituted Alkyltriaminosilanes. V

LEWI TANSJÖ

Department of Organic Chemistry, University of Lund, Lund, Sweden

The reactions of N-substituted alkyltriaminosilanes with water, alcohols, phenol, acetic acid, acetic anhydride and hydrogen halides are described. On the reaction with hydrogen fluoride observations were made which indicate the existence of compounds containing the alkyl- or arylpentafluorosilicate ion, $RSiF_5^{2-}$, analogous to the hexafluorosilicate ion, SiF_6^{2-}, in which silicon uses two of its five *d*-orbitals for bonding.

In this paper will be described some reactions of N-substituted alkyltriaminosilanes the preparations of which were previously published[1-4]. This purpose was partly anticipated in Parts II[2] and IV[4] of this work where their reactions with amines and their intermolecular condensations were investigated. Some of the reactions below are well known from the field of dialkyl- and trialkylaminosilanes (Ref.[5], Chapter 11) and can be treated briefly here.

When brought into solution, by adding an alcohol, for example, N-substituted *n*-propyltriaminosilanes, $n\text{-}C_3H_7Si(NHR')_3$, react with water to give high polymeric "*n*-propylsiliconic acid", but the sensitivity of hydrolysis is markedly governed by the size of the groups on the nitrogen atoms being greatest for *n*-propyltri-(methylamino)-silane and successively less for compounds with larger R′ groups. *n*-Propyltri-(*tert.*-butylamino)-silane and *n*-propyltri-(diethylamino)-silane, for example, are rather stable to 90 % alcohol, in which the corresponding methylamine and ethylamine compounds react vigorously. In acidic medium, however, even the sterically-hindered compounds above are immediately hydrolyzed which is demonstrated by the fact that they can be directly titrated with standard hydrochloric acid which involves the breaking of the Si—N bonds.

1.5 molar equivalents of water is sufficient to give complete hydrolysis of a triaminosilane according to the equation

$$RSi(NHR')_3 + 1.5\,H_2O \rightarrow RSiO_{1.5} + 3\,R'NH_2$$

Two types of condensation reactions may be involved in building up the polymeric $RSiO_{1.5}$, namely

$$\equiv SiOH + HOSi\equiv \rightarrow \equiv Si-O-Si\equiv + H_2O \qquad (a)$$

$$\equiv SiOH + R'NHSi\equiv \rightarrow \equiv Si-O-Si\equiv + R'NH_2 \qquad (b)$$

It was found that even if the hydrolysis was performed with less than 1.5 molar equivalents of water in ether solution, *n*-propyltri-(ethylamino)-silane gave very poor yields of distillable, partially hydrolysed products. This indicates that when some of the ethylamino groups are removed the intermediate hydrolysis products are much more susceptible than the remaining triaminosilane to further attack of water and/or to intermolecular condensation of the type (b) above.

n-Propyltri-(methylamino)-silane reacted spontaneously with ethanol and benzyl alcohol and complete alcoholysis was obtained on heating the reaction mixtures to reflux temperature for a short time giving the trialkoxy compounds in good yields. With the bulky *tert.*-butanol, however, only one of the methyl amino groups was replaced after prolonged heating with excess of the alcohol and the ethylamine compound was still more resistant to this alcohol.

n-Propyltri-(ethylamino)-silane reacted with phenol in a manner analogous to the reaction with alcohols to give *n*-propyltriphenoxysilane in good yield:

$$n\text{-PrSi(NHEt)}_3 + 3\ C_6H_5OH \rightarrow n\text{-PrSi(OC}_6H_5)_3 + 3\ EtNH_2$$

Miner *et al.*[6] stated that *tert.*-alkoxyaminosilanes react with organic acids to form the corresponding acyloxysilanes: *e.g.*

$$(t\text{-BuO})_2Si(NH_2)_2 + 4\ RCOOH \rightarrow (t\text{-BuO})_2Si(OCOR)_2 + 2\ RCOONH_4$$

but no experiments were described to authorize this course of reaction. Organosilicon compounds have been supposed to react in an analogous way with organic acids (Ref.[5], p. 347). It is therefore noteworthy that no alkyltriacetoxysilane could be isolated after the reaction of N-substituted alkyltriaminosilanes with acetic acid. *n*-Propyltribenzylaminosilane, for example, reacted readily with acetic acid to give a reaction mixture containing benzylamine hydroacetate, N-benzylacetamide and polysiloxanes. In another experiment ethyltriacetoxysilane was shown to react with benzylamine hydroacetate with the formation of N-benzylacetamide and acetic acid. These observations make the following course of the reaction between a N-substituted alkyltriaminosilane and acetic acid plausible: First alkyltriacetoxysilane is formed according to the equation

$$RSi(NHR')_3 + 6\ CH_3COOH \rightarrow RSi(OCOCH_3)_3 + 3\ CH_3COONH_3R'$$

which then reacts with $R'NH_2$, liberated by a small degree of dissociation of the hydroacetate:

$$\equiv Si-OCOCH_3 + R'NH_2 \rightarrow \equiv Si-OH + CH_3CONHR' \qquad (1)$$

That not all of the hydroacetate is used up to give silanol and amide according to eqn. (1) may be explained as a result of intermolecular condensation of silanol and acetoxysilane:

$$\equiv Si-OH + CH_3OCO-Si\equiv \rightarrow \equiv Si-O-Si\equiv + CH_3COOH$$

According to eqn. (1) alkyltriacetoxysilanes would act as acylating agents, the carbonyl carbons of the silyl ester being attacked by the nucleophilic $R'NH_2$. But the silicon atom of organosilicon compounds is normally very

susceptible to attack by nucleophilic agents so there would exist two possibilities for a nucleophilic replacement in an alkyltriacetoxysilane as represented in the equations (2a) (attack on the silicon) and (2b) (attack on the carbonyl carbons):

$$RSi(OCOCH_3)_3 + 6\,R'NH_2 \rightarrow RSi(NHR')_3 + 3\,CH_3COONH_3R' \quad (2a)$$

$$RSi(OCOCH_3)_3 + 3\,R'NH_2 \rightarrow RSi(OH)_3 + 3\,CH_3CONHR' \quad (2b)$$

In excess of amine (2a) and (2b) can both be expected to considerably lower the free energy of the system (and (2b), which includes the formation of "siliconic acid", can be predicted to give the lowest one). Then the reaction which is represented by the lowest energy of the transition state would first occur. If the silicon atom is more susceptible to nucleophilic attack than the carbonyl carbons Fig. 1a would give a rough picture of the energy-profiles of the reactions — curve T_1 representing reaction (2a) and curve T_2 representing (2b). According to Fig. 1b the carbonyl carbons would be more electrophilic than the silicon atom.

Experiments were performed in which ethyltriacetoxysilane was added to excess of benzylamine in benzene. A precipitate of benzylamine hydroacetate was formed immediately. In different experiments it was, however, always found that the weight of hydroacetate corresponded to 50 % of the weight calculated for the reaction (2a). N-Benzylacetamide and polysiloxanes were also found in the reaction mixture. Leaving out of consideration the possibility that the silicon atom and the carbonyl carbons would be equally susceptible to nucleophilic attack the following hypothesis can be proposed on the course of reaction:

First reaction (2a) occurs establishing very rapidly an equilibrium the composition of which corresponds to a high per cent of aminosilane. The acetoxy groups left on the silicon atom react in a slower reaction according to eqn. (2b)

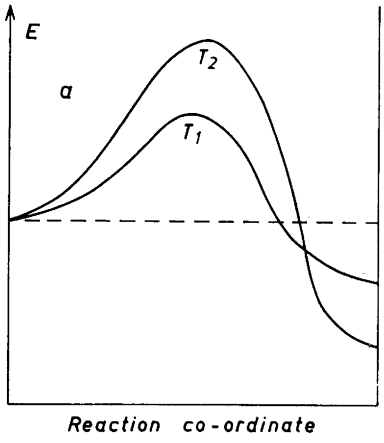

Fig. 1a.

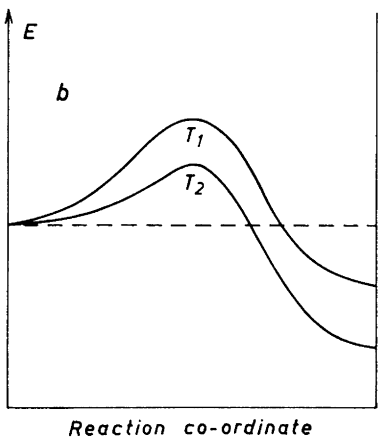

Fig. 1b.

to give silanol, and more $\equiv SiOCOCH_3$ groups are produced (by the reversal of 2a), which again are consumed according to (2b). The Si—OH groups formed will immediately condense intermolecularly with Si—N bonds:

$$\equiv Si-OH + R'NH-Si\equiv \rightarrow \equiv Si-O-Si\equiv + R'NH_2$$

and in this way just 50 % of the hydroacetate calculated for reaction (2a) will be left. This hypothesis is supported by the fact that reaction (2a) was found to be reversible. Thus *n*-propyltri-(benzylamino)-silane in benzene dissolved in a few minutes an equivalent amount of benzylamine hydroacetate with the formation of N-benzylacetamide. The fact that the weight of hydroacetate obtained when the reaction between ethyltriacetoxysilane and benzylamine was performed at −80° corresponded to more than 50 %, also gives some support to the proposed reaction pattern which is also in agreement with the finding of Dolgov *et al.*[7-8] on the reaction of acyloxysilanes with alcohols. They found that acetoxysilanes react with alcohols to give alkoxysilanes if the liberated acid is removed at reduced pressure:

$$\equiv Si-OCOCH_3 + ROH \rightarrow \equiv Si-OR + CH_3COOH$$

but silanols and the esters of acetic acid are obtained if the reaction mixtures are heated:

$$\equiv Si-OCOCH_3 + ROH \rightarrow \equiv Si-OH + CH_3COOR$$

It can therefore be concluded with some certainty that the silicon atom is more susceptible to nucleophilic attack than the carbonyl carbons in alkyltriacetoxysilanes (Fig. 1a) and the acylating ability of these compounds would then be the result only of the low energy of the products obtained after reaction at the carbonyl carbons.

In organosilicon chemistry, acetic anhydride has been used to bring about the conversion of Si—N bonds into Si—$OCOCH_3$ ones[9]: *e.g.*

$$Me_3SiNHCH_2C_6H_5 + (CH_3CO)_2O \rightarrow Me_3SiOCOCH_3 + CH_3CONHCH_2C_6H_5$$

$$Et_3SiNH_2 + (CH_3CO)_2O \rightarrow Et_3SiOCOCH_3 + CH_3CONH_2$$

$$Me_2Si(NHEt)_2 + 2\,(CH_3CO)_2O \rightarrow Me_2Si(OCOCH_3)_2 + 2\,CH_3CONHEt$$

Acetic anhydride was added to the appropriate aminosilane and on distillation of the reaction mixtures 62, 56, and 32 %, respectively, of the acetoxysilanes were obtained. Now it was found that only a very poor yield of alkyltriacetoxysilane was obtained from the reaction mixture when acetic anhydride was added to a benzene solution of a N-substituted alkyltriaminosilane. Thus *n*-propyltri-(benzylamino)-silane and excess of acetic anhydride gave less than 5 % of *n*-propyltriacetoxysilane on distillation of the reaction mixture at reduced pressure. However, at 158—62°/11 mm a fraction was obtained most of which consisted of diacetylbenzylamine. It could therefore be suspected with some reason that there had first been formed *n*-propyltriacetoxysilane according to the equation

$$n\text{-}PrSi(NHCH_2C_6H_5)_3 + 3\,(CH_3CO)_2O \rightarrow n\text{-}PrSi(OCOCH_3)_3 + 3\,CH_3CONHCH_2C_6H_5$$

which in a secondary reaction acetylated the amide:

$$\equiv Si-OCOCH_3 + CH_3CONHCH_2C_6H_5 \rightarrow \equiv Si-OH + (CH_3CO)_2NCH_2C_6H_5$$

However, a mixture of ethyltriacetoxysilane and N-benzylacetamide after standing overnight could be separated by distillation at reduced pressure without any noteworthy reaction. The only explanation of the observed reaction course would then be that during the addition of acetic anhydride to the alkyltriaminosilane a condensation between new-formed $Si-OCOCH_3$ groups and unreacted Si—N bonds had occurred:

$$\equiv Si\text{-}NHCH_2C_6H_5 + CH_3OCO-Si\equiv \rightarrow \equiv Si-O-Si\equiv + CH_3CONHCH_2C_6H_5$$

The possibility of such a reaction was confirmed by the fact that ethyltriacetoxysilane and ethyltri-(benzylamino)-silane in petroleum ether immediately gave a precipitate of N-benzylacetamide. The appearance of diacetylbenzylamine in the reaction mixture above would then be the result of acetylating — not by *n*-propyltriacetoxysilane but by acetoxysiloxanes with a few silicon atoms produced in a condensation reaction according to the last equation and/or by the excess of acetic anhydride [10]. Therefore a good yield of alkyltriacetoxysilane can only be expected if the aminosilane is added to excess of acetic anhydride and not *vice versa*. This was confirmed by the fact that a yield of almost 80 % of *n*-propyltriacetoxysilane was obtained when *n*-propyltri-(benzylamino)-silane in benzene was added to excess of acetic anhydride.

When anhydrous hydrogen chloride, bromide or iodide was passed into the ether or benzene solution of an alkyltriaminosilane, amine hydrohalide precipitated as rapidly as the gas was introduced and the appropriate alkyltrihalosilane was left in the solution. The halosilanes obtained could again be readily converted into aminosilanes by treatment with amines. These reactions point to a general method of replacing the halogen of an alkyltrihalosilane for another one and it has been used to prepare a range of alkyltriiodosilanes from the corresponding chlorosilanes [11–12].

In contrast to the other hydrogen halides the fluoride gave no ether soluble products when passed into the solution of a N-substituted alkyltriaminosilane or phenyltriaminosilane. Presumably the appropriate trifluorosilane was first formed according to the equation

$$RSi(NHR')_3 + 6\,HF \rightarrow RSiF_3 + 3\,R'NH_3F \qquad (3)$$

but was then absorbed by the precipitated amine hydrofluoride to give insoluble products, approximately corresponding to the composition $RSiF_3;3R'NH_3F$. Such an absorption is somewhat surprising in view of the finding of Booth and co-workers [13–14], that sodium fluoride did not coordinate to alkyltrifluorosilanes even on prolonged contact. The supposed reaction pattern, however, is strongly supported by the fact that amine hydrofluorides absorbed *cyclo*hexyltrifluorosilane and phenyltrifluorosilane to an extent roughly corresponding to the formation of $RSiF_3;2R'NH_3F$. These addition compounds are white, non-hygroscopic quite stable powders insoluble in common organic solvents. They dissolved in water to give acidic solutions which soon became turbid due to hydrolysis. Probably because of unfavorable conditions of reaction between

Table 1. Physical constants and analyses of the compounds I–VIII.

No.	M	B.p. °C	Pressure mm Hg	n_D^{20}	d^{20}	MR_D	% Si		Equiv. wt.	
							found	calc.	found	calc.
I	217.42	110	13	1.4381	0.8523	66.98	13.0	12.9	72.8	72.5
II	231.45	114–15	10	1.4429	0.8572	71.57	12.1	12.1	77.3	77.2
III	273.53	153	11	1.4459	0.8541	85.39	10.2	10.3	91.0	91.2
IV	375.58	250–52	4	1.5715	1.0614	116.35	7.4	7.5	125.7	125.2
V	202.41	95	11	1.4384	0.8329	63.84	13.9	13.9	101.7	101.2
VI	285.54	166–67	10	1.4672	0.9011	87.96	9.7	9.8	95.2	95.2
VII	279.49	169–70	12	1.4942	0.9358	86.98	9.8	10.0	93.0	93.2
VIII	173.37	68	11	1.4335	0.8047	56.05	16.2	16.2	174.5	173.4

the solid salts and the liquid fluorosilanes, their compositions were rather ill-defined. Yet it seems plausible to interpret them as salts containing a $RSiF_5^{2-}$ ion analogous to the hexafluorosilicate ion, SiF_6^{2-}, in which 3 sp^3d^2 hybridization of the silicon orbitals is supposed to produce six equivalent bonds constituting an octahedral arrangement of the fluorine atoms about the central silicon atom [15].

In sharp contrast to the triaminosilanes, N-substituted dialkyldiaminosilanes and trialkylaminosilanes revealed no tendency to six-coordination. Thus on passing anhydrous hydrogen fluoride into an ether solution of triethyl(-*n*-propylamino)-silane or diethyldi-(*n*-propylamino)-silane the corresponding fluorosilanes were obtained from the ether solution and no silicon was found in the precipitated amine hydrofluoride. Nor was there observed any increase in weight of amine hydrofluorides after prolonged treatment with tri- and dialkylfluorosilanes.

EXPERIMENTAL

Of the aminosilanes employed in the reactions below the following have not been described before:

I, $CH_3Si(NHC_3H_7\text{-}n)_3$; II, $C_2H_5Si(NHC_3H_7\text{-}n)_3$; III, $C_2H_5Si(NHC_4H_9\text{-}n)_3$; IV, $C_2H_5Si(NHCH_2C_6H_5)_3$; V, $(C_2H_5)_2Si(NHC_3H_7\text{-}n)_2$; VI, $C_6H_{11}Si(NHC_3H_7\text{-}n)_3$; VII, $C_6H_5Si(NHC_3H_7\text{-}n)_3$.

They were prepared as described for *n*-propylaminosilanes from the appropriate organosilicon chloride and excess of amine, the yields lying between 75 and 90 %. Their physical constants and analyses are given in Table 1. In the table are also given the data of triethyl-(*n*-propylamino)-silane, VIII, which is previously described[16] to have n_D^{20} 1.4332, d_4^{20} 0.8038.

Ethyltriacetoxysilane. This compound was prepared according to Dolgov *et al.*[8] from ethyltrichlorosilane and acetic anhydride. B.p. 108–09°/10 mm Hg, n_D^{20} 1.4123, d^{20} 1.1440, MR_D 50.99 (lit. values[8]: b.p. 107.5–108.5/8 mm, n_D^{20} 1.4123, d_4^{20} 1.1428, MR_D 51.04). (Found: Si 11.8; equiv. wt. 77.7.Calc. for $C_2H_5Si(OCOCH_3)_3$: Si 12.0; equiv.wt. 78.1).

Triethylfluorosilane. This compound was prepared according to Eaborn [17] from triethylchlorosilane and 48 % hydrofluoric acid containing alcohol to ensure a homogenous system. B.p. 110°, n_D^{20} 1.3902, d^{20} 0.8391 (lit. values: b.p. 109.5° [17], n_D^{20} 1.3910 [17], d^{20} 0.8380 [18]). Equiv. wt.: Found 135.0; calc. 134.3.

Diethyldifluorosilane was obtained according to Marans *et al.*[19] from diethyldichlorosilane and 48 % hydrofluoric acid. B.p. 63—64°, n_D^{20} 1.3400, d^{20} 0.9343 (lit. values: b.p. 62° [17], n_D^{23} 1.3393 [20], d_4^{20} 0.9348 [19]). Equiv. wt.: Found 61.8; calc. 62.1.

Phenyltrifluorosilane was prepared according to Pearlson *et al.*[21] by agitating a mixture of phenyltrichlorosilane and anhydrous hydrogen fluoride at 0°. B.p. 103—04°, n_D^{20} 1.4110, d^{20} 1.211 (lit. values: b.p. 101—02° [21], n_D^{22} 1.4103[23], d_4^{17} 1.212[22]). Equiv. wt.: Found 54.0; calc. 54.1.

Cyclo*hexyltrifluorosilane* was obtained in the way described for phenyltrifluorosilane. B.p. 106°, n_D^{20} 1.3700, d^{20} 1.106 (lit. values [20]: b.p. 106°, n_D^{25} 1.3680, d^{25} 1.1012). Equiv. wt.: Found 55.8; calc. 56.1.

The equivalent weights of these fluorosilanes were determined by dissolving the compounds in excess of standard potassium methoxide. After a few minutes water was added and the excess of alkali back-titrated with standard hydrochloric acid using thymolblue as the indicator.

Hydrolysis experiments (a) *n*-Propyltri-(methylamino)-silane and *n*-propyltri-(ethylamino)-silane were vigorously hydrolyzed in contact with liquid water and gave insoluble granular and generally intractable solids containing no nitrogen. Compounds with larger groups on the nitrogen atoms gave a liquid mixture with only a very slow reaction occurring at the interface when poured into water. This is apparently a consequense of their water insolubility for upon addition of ethanol to the amine-water mixture a homogeneous solution resulted accompanied by rapid hydrolysis of the compounds. However, the most sterically-hindered compounds, *i.e.* *n*-propyltri-(*tert.*-butylamino)-silane and the corresponding diethylamine compound were remarkably stable to the action of water. 5.8 g (0.02 mole) of *n*-propyltri-(*tert.*-butylamino)-silane (n_D^{20} 1.4427, equiv. wt. 96.7) was dissolved in 45 ml of 90 % ethanol. After standing for 2 h the solvent was evaporated at reduced pressure leaving a residue with n_D^{20} 1.4430 and equiv. wt. 99.0 from which more than 90 % of the aminosilane could be recovered by distillation.

(*b*) 20.3 g (0.1 mole) of *n*-propyltri-(ethylamino)-silane in 200 ml of dry ether were stirred rapidly and 200 ml of ether containing 0.90 g (0.05 mole) of water were added during one hour. After standing overnight the ether was removed by distillation. In the distillate was found 0.1 mole of ethylamine indicating that the intermolecular condensation had proceeded quantitatively. 12.2 g (60 %) of unreacted aminosilane were recovered by distillation. From the residue only 0.5 g of partial hydrolysis products, equiv. wt. about 200, was obtained. The remainder, 2.7 g, rapidly gelled to an insoluble resin typical of cross-linked structures and contained only traces of nitrogen.

(*c*) In the same way 1.35 g (0.075 mole) of water in 200 ml of ether liberated 0.15 mole of ethylamine from 15.3 g (0.075 mole) of n-propyl-tri-(ethylamino)-silane in 100 ml of absolute ether. 4.0 g (26 %) of unreacted aminosilane were recovered by distillation and a residue of 4.75 g of a high-polymeric resin containing less than 1 % nitrogen were left.

Reactions with alcohols. (*a*) 8.1 g (0.05 mole) of *n*-propyltri-(methyl-amino)-silane and 11.3 g (0.25 mole) of ethanol were mixed and gave a spontaneous reaction with evolution of methylamine. The reaction mixture was heated to reflux temperature until no more methylamine was liberated (2 h.). On distillation 8.0 g (77 %) of *n*-propyltriethoxysilane was obtained, b.p. 169—70° (1 atm), n_D^{20} 1.3969, d^{20} 0.8891, MR_D 55.88, calc. 55.73 (according to Smith [24]) (lit. values [25]: 170—72°, n_D^{20} 1.3956, d^{20} 0.8916). (Found: Si 13.5. Calc. for $C_9H_{22}O_3Si$: Si 13.6).

(*b*) In the same way 4.8 g (0.03 mole) of *n*-propyltri-(methylamino)-silane and 13.0 g (0.12 mole) of benzylalcohol gave 9.4 g (80 %) of *n*-propyltribenzyloxysilane, b.p. 220—22°/2 mm, n_D^{20} 1.5408, d^{20} 1.0750, MR_D 114.71, calc. 114.59. Smith does not give the group refractivity *r*-$SiOCH_2C_6H_5$, but from his value of the group refractivity *r*-$SiOCH_3$ and the atomic and structural constants of H (in CH_2) and C_6H_5 given by Vogel [26], the group refractivity *r*-$SiOCH_2C_6H_5$ was calculated to 32.61 ml. (Found: Si 7.1. Calc. for $C_{24}H_{28}O_3Si$: Si 7.2).

(*c*) A mixture of 8.1 g (0.05 mole) of *n*-propyltri-(methylamino)-silane and 14.8 g (0.2 mole) of *tert.*-butanol was heated to reflux temperature for 30 h. On distillation of the

reaction mixture 6.6 g of a product with equiv. wt. 87.3 were obtained, apparently a mixture of *n*-propyltri-(methylamino)-silane (equiv. wt. 53.8) and *n*-propyl*tert.*-butoxydi-(methylamino)-silane (equiv. wt. 102.2). 11 g of *tert.*-butanol were added to the product and the mixture was again heated to reflux temperature for 40 h. On distillation 6.0 g of a product boiling at 76—77°/10 mm were obtained, n_D^{20} 1.4273, d^{20} 0.8748, MR_D 60.02, equiv. wt. 105.6, Si 13.4. Calc. for *n*-$C_3H_7Si(NHCH_3)_2(OC_4H_9$-*t*): equiv. wt. 102.2, Si 13.7, MR_D 59.98, using the bond refractivities *r*-SiC_3H_7-*n* and *r*-$SiOC_4H_9$-*t* given by Smith [24] and the mean value 10.42 ml for *r*-SiNHMe obtained from three alkyltri-(methylamino)-silanes.[1,4]

(*d*) 10.2 g (0.05 mole) of *n*-propyltri-(ethylamino)-silane and 22.2 g (0.3 mole) of *tert.*-butanol were heated to reflux temperature for 25 h. Only a small amount of ethylamine was liberated and on distillation more than 8 g of the triaminosilane were recovered. In another experiment a mixture of 10.2 g (0.05 mole) of *n*-propyltri-(ethylamino)-silane and 22.2 g (0.3 mole) of *tert.*-butanol containing one g of sodium was heated to reflux temperature for 90 h. After filtration of the reaction mixture distillation gave 8.0 g of a product boiling at 90—100°/10 mm with equiv. wt. 83.7, apparently a mixture of *n*-propyltri-(ethylamino)-silane (equiv. wt. 67.8) and *n*-propyl*tert.*-butoxydi-(ethylamino)-silane (equiv. wt. 116.2).

Reaction with phenol. 4.6 g (0.023 mole) of *n*-propyltri-(ethylamino)-silane and 8.5 g (0.09 mole) of phenol were mixed and gave a spontaneous reaction with evolution of heat. The reaction mixture was heated to reflux temperature for 4 h. On distillation 6.0 g (74 %) of *n*-propyltriphenoxysilane were obtained, b.p. 192°C/2 mm, n_D^{20} 1.5518, d^{20} 1.1056, MR_D 101.26, calc. 101.10 (from the observed MR_D 91.84 for methyltriphenoxysilane [27] and the group refractivities *r*-$SiCH_3$ and *r*-SiC_3H_7-*n* given by Smith). (Found: Si 8.0. Calc. for $C_{21}H_{22}O_3Si$: Si 8.0.)

Reactions with glacial acetic acid. (*a*) 5.2 g (0.0133 mole) of *n*-propyltri-(benzylamino)-silane in 30 ml of benzene were added dropwise to 6.0 g (0.1 mole) of glacial acetic acid. Reaction immediately occurred with evolution of much heat. The solvent and excess of acetic acid were removed at reduced pressure from the homogeneous reaction mixture. On distillation 3.5 g of a viscous oil were obtained at 99°C/10 mm. Benzene was added to the residue in the distillation flask and the high-polymeric silicones (1.2 g) which had precipitated under the distillation were removed by filtration. When petroleum ether was added to the filtrate 2.4 g of N-benzylacetamide, m.p. 60—61° (lit.[28] 60—61°) precipitated. (Found: C 72.7; H 7.5. Calc. for $C_9H_{11}NO$: C 72.5; H 7.4). The oil obtained on distillation crystallized on cooling. It melted without definite melting point between 50 and 80°, dissolved in water to give acidic solution and contained no silicon. (Found: C 60.2; H 7.7. Calc. for $CH_3COONH_3CH_2C_6H_5$: C 64.6; H 7.8 and for $CH_3COONH_3CH_2C_6H_5$; CH_3COOH: C 58.1; H 7.5). When a mixture of benzylamine and excess of acetic acid was distilled, a viscous oil was also obtained at 99—100°/10 mm with the same properties and approximately the same analyses apparently consisting of acidic benzylamine hydroacetate of ill-defined composition.

(*b*) 4.0 g (0.0146 mole) of ethyltri-(*n*-butylamino)-silane and 7.5 g (0.125 mole) of acetic acid in the same way reacted exothermically to give a homogeneous reaction mixture and on distillation high polymeric silicones precipitated in the distillation flask. At 92°/10 mm 4.0 g of a viscous oil, n_D^{20} = 1.4365, were obtained, apparently consisting of acidic *n*-butylamine hydroacetate (Found: C 50.5; H 10.4. Calc. for $CH_3COONH_3C_4H_9$; CH_3COOH: C 49.7;H 9.9). A viscous oil (n_D^{20} = 1.4365, C 50.2; H 10.2) also distilled from a mixture of *n*-butylamine and excess of acetic acid at 92°/10 mm.

(*c*) 1.2 g (0.0072 mole) of benzylamine hydroacetate dissolved in less than one minute when added to 1.4 g (0.006 mole) of ethyltriacetoxysilane in 12 ml of benzene. The solvent and the acetic acid formed in the reaction were removed at reduced pressure and the residue was again dissolved in 10 ml of benzene. When 20 ml of petroleum ether were then added 0.7 g of N-benzylacetamide, m.p. 61—62°, precipitated.

(*d*) 3.5 (0.015 mole) of ethyltriacetoxysilane in 10 ml of benzene were added dropwise to a stirred solution of 10.7 g (0.1 mole) of benzylamine in 40 ml of benzene. Reaction immediately occurred with formation of a heavy precipitate. The reaction mixture was heated to 50° for one hour, cooled to 0° and filtered. 3.8 g (calc. for reaction (2a): 7.5 g) of benzylamine hydroacetate were left on the filter, m.p. 99—100° (lit.[29] 96.3—97.1°). (Found: C 64.6; H 7.8. Calc. for $C_9H_{13}NO_2$: C 64.6; H 7.8). The salt proved to be insoluble in benzene. When petroleum ether was added to the filtrate 2.4 g of a mixture of N-

benzylacetamide and high-polymeric silicones precipitated. The silicones were removed by heating the mixture with 75 ml of petroleum ether and 15 ml of benzene to reflux temperature. On filtration the silicones were left on the filter and N-benzylacetamide, m.p. 61—62°, precipitated from the filtrate on cooling.

(*e*) In another experiment 3.5 g (0.015 mole) of ethyltriacetoxysilane in 10 ml of benzene were rapidly added to an ice-cooled solution of 10.7 g (0.1 mole) of benzylamine in 40 ml of benzene. The reaction mixture was stirred at 0° for 5 min and then filtered. 3.7 g of benzylamine hydroacetate, m.p. 99—100°, was left on the filter and polysiloxanes and N-benzylacetamide were again found in the filtrate.

(*f*) 3.5 g (0.015 mole) of ethyltriacetoxysilane in 10 ml of toluene were slowly added to a stirred solution of 10.7 g (0.1 mole) of benzylamine in 40 ml of toluene, cooled to −80°. Thereafter the reaction mixture was stirred at the same temperature for 10 min and filtered. During the filtration the temperature increased almost to room temperature. 4.7 g of benzylamine hydroacetate, m.p. 98.5—100° — corresponding to 63 % of the amount calc. for reaction (2a) — were now left on the filter and silicones and N-benzylacetamide were found in the filtrate.

(*g*) 1.7 g (0.01 mole) of benzylamine hydroacetate dissolved in a few minutes when added to 3.9 g (0.01 mole) of *n*-propyltri-(benzylamino)-silane in 15 ml of benzene. 35 ml of petroleum ether were added and after standing overnight N-benzylacetamide, m.p. 61—62°, had precipitated.

Reactions with acetic anhydride (*a*) 21.3 g (0.21 mole) of acetic anhydride were added dropwise to an ice-cooled solution of 20.0 g (0.051 mole) of *n*-propyltri-(benzylamino)-silane in 100 ml of benzene. Reaction immediately occurred with evolution of much heat. The solvent and the excess of acetic anhydride were removed at reduced pressure. On distillation of the residue only about 0.5 g was obtained at 100—125°/11 mm where *n*-propyltriacetoxysilane can be expected to distil. 11.8 g of a viscous oil containing no silicon distilled at 158—62°. It was re-distilled and gave at 155—57°/10 mm (lit.[10] 176—78°/30 mm) 7.0 g of diacetylbenzylamine. (Found: C 68.6; H 6.9. Calc. for $C_{11}H_{13}NO_2$: C 69.1; H 6.9). When petroleum ether was added to the residue 8.0 g of N-benzylacetamide, m.p. 61—62°, precipitated.

In the same way acetic anhydride added to *n*-propyltri-(*cyclo*hexylamino)-silane, ethyltri-(*n*-butylamino)-silane, and ethyltri-(benzylamino)-silane only gave traces of the expected triacetoxysilanes.

(*b*) 15.6 g (0.04 mole) of *n*-propyltri-(benzylamino)-silane in 25 ml of benzene was added dropwise to a stirred, ice-cooled solution of 20.4 g (0.2 mole) of acetic anhydride in 50 ml of benzene. The solvent and the excess of acetic anhydride were removed at reduced pressure. On distillation of the residue 7.8 g (79 %) of *n*-propyltriacetoxysilane were obtained at 117—118°/10 mm (lit.[30] 127—31°/20 mm) with n_D^{20} 1.4148; d^{20} 1.1157; MR_D 55.71 (Found: Si: 11.2; equiv. wt. 82.6. Calc. for n-$C_3H_7Si(OCOCH_3)_3$: Si: 11.3; equiv. wt. 82.8). N-benzylacetamide was left in the distillation flask.

(*c*) 7.0 g (0.03 mole) of ethyltriacetoxysilane were mixed with 8.0 g (0.054 mole) of N-benzylacetamide. After standing overnight 6.1 g of ethyltriacetoxysilane could be recovered by distillation at 12 mm Hg.

(*d*) 1.5 g (0.0064 mole) of ethyltriacetoxysilane in 6 ml of petroleum ether were added to 2.4 g (0.0064 mole) of ethyltri-(benzylamino)-silane in 8 ml of petroleum ether. Precipitation immediately occurred. After standing for 2 h the mixture was filtered and left 0.8 g of N-benzylacetamide, m.p. 59—61°, on the filter.

n-*Propyltrichlorosilane*. 7.4 g (0.03 mole) of *n*-propyltri-(*n*-propylamino)-silane in 100 ml of absolute ether was placed in a 250 ml three-necked flask equipped with a reflux condenser, mechanical stirrer and gas inlet tube, When dry hydrogen chloride was passed into the reaction mixture amine hydrochloride was immediately formed. After excess of hydrogen chloride had been added the reaction mixture was heated to reflux temperature for 30 min. On filtration 8.6 g (calc. 8.6 g) of *n*-propylamine hydrochloride was left on the filter. Distillation of the filtrate gave 4.2 g (79 %) of *n*-propyltrichlorosilane boiling at 122—123° (1 atm) (lit.[1] 123°). Equiv. wt. 59.9; calc. 59.3.

n-Propyltribromosilane. 53.3. g (0.3 mole) of *n*-propyltrichlorosilane in 150 ml of benzene were added dropwise to an ice-cooled, vigorously stirred solution of about 90 g of ethylamine in 200 ml of benzene. After all had been added the stirring was continued for 2 h and thereafter the excess of ethylamine was removed by distillation. Filtration of the cooled mixture left 73.2 g (calc. 73.4 g) of ethylamine hydrochloride on the filter.

Hydrogen bromide which had been carefully dried over phosphorus pentoxide was then passed into the filtrate as described for the preparation of *n*-propyltrichlorosilane above. Filtration of the reaction mixture gave 112 g (calc. 113 g) of ethylamine hydrobromide on the filter. Distillation of the filtrate gave 78.0 g (83 %) of *n*-propyltribromosilane boiling at 179—81° (1 atm) lit.[31] 179—80/754 mm). Equiv. wt. 104.0 calc. 103.6 The assigned structure of the product which was a colourless liquid, fuming extensively in moist air, was confirmed by its reaction with diethylamine to give *n*-propyltri-(diethylamino)-silane[3].

n-*Propyltriiodosilane*. A small excess of hydrogen iodide which had been carefully dried over phosphorus pentoxide was passed into 15.3 g (0.075 mole) of *n*-propyltri-(ethylamino)-silane in 200 ml of benzene as described above. On filtration 38.7 g (calc. 38.9 g) ethylamine hydroiodide were left on the filter. Distillation of the filtrate gave 27.0 g (80 %) of *n*-propyltriiodosilane boiling at 118—19°/10 mm (lit.[12] 142—43°/20 mm). Equiv. wt. 151.0, calc. 150.7. The assigned structure of the product which was a colourless liquid fuming in moist air was confirmed by its reaction with *tert.*-butylamine to give *n*-propyltri-(*tert.*-butylamino)-silane[3].

Reactions with hydrogen fluoride. In Table 2 are reported the results of six experiments in which dry gaseous hydrogen fluoride was passed into an ice-cooled, stirred solution of 0.02 mole of a N-substituted alkyltriaminosilane or phenyltriaminosilane in 100 ml of ether. In all cases a white solid immediately precipitated. The introduction of hydrogen fluoride was stopped just when no more solid precipitated to avoid the formation of acidic amine hydrofluorides. Thereafter the reaction mixture was stirred for 30 min and the temperature raised to room-temperature before filtering. The products left on the filter, which were much less hygroscopic than amine hydrofluorides, were all found to contain silicon and no silicon was observed in the filtrates. The amounts obtained were considerably greater than the amounts calculated for the formation of amine hydrofluorides according to eqn. (3) but corresponded to the composition $RSiF_3;3R'NH_3F$. They dissolved in water to give acidic solutions which soon became turbid, apparently due to hydrolysis products. Their amine content (E_1 in the table) was determined by back-titrating an acid fixed condensate from a boiling solution containing the compound in excess of standard base using methylred as the indicator, and their fluorine content (E_2 in the table) was determined by back-titrating the excess of base with standard acid using phenolphthalein or thymolblue as the indicator.

When the same reaction was performed with triethyl-(*n*-propylamino)-silane or diethyldi-(*n*-propylamino)-silane the precipitates left on the filter were found to be neutral *n*-propylamine hydrofluoride containing no silicon. From the filtrates, triethylfluorosilane and diethyldifluorosilane respectively were obtained on distillation.

Table 2. N-substituted triaminosilanes and hydrogen fluoride.

	Yield, g		E_1		E_2	
	found	calc.[a]	found	calc.	found	calc.
n-$C_3H_7Si(NHC_2H_5)_3$, 4.1 g	6.3	6.5	118	108	52.5	53.9
$CH_3Si(NHC_3H_7$-$n)_3$, 4.3 g	6.8	6.8	116	112	55.4	56.2
$C_2H_5Si(NHC_3H_7$-$n)_3$, 4.6 g	6.8	7.0	120	117	56.8	58.6
n-$C_3H_7Si(NHC_3H_7$-$n)_3$, 4.9 g	7.1	7.3	126	122	62.3	60.9
$C_5H_{11}Si(NHC_3H_7$-$n)_3$, 5.7 g	7.7	8.1	135	135	69.0	67.6
$C_6H_5Si(NHC_3H_7$-$n)_3$, 5.6 g	8.2	8.0	141	133	63.5	66.6

[a] calc. for the formation of $RSiF_3;3R'NH_3F$.

The co-ordination of amine hydrofluorides to fluorosilanes. When phenyltrifluorosilane or *cyclo*hexyltrifluorosilane was added to samples of amine hydrofluorides (ethyl-, *n*-propyl-, or *n*-butylamine hydrofluoride) exothermic reactions always occurred and the liquid was absorbed by the solid salt to give a dry powder.

In one experiment excess of phenyltrifluorosilane (4.5 g; 2.8×10^{-2} mole) was added to 1.006 g (1.27×10^{-2} mole) of *n*-propylamine hydrofluoride in 35 ml of ether. The mixture was heated to reflux temperature for 3 h. After cooling, the solid was separated by filtration, carefully washed with the solvent and dried. The gain in weight was found to be 0.832 g (corresponding to 0.51×10^{-2} mole of phenyltrifluorosilane); calc. for the formation of $C_6H_5SiF_3$;2*n*-$C_3H_7NH_3F$: 1.003 g. The amine content (E_1) of the product was determined as described above but methanol was used as the solvent for the alkaline solution to ensure a homogeneous system. After the amine had been distilled off, water was added to the residue and the excess of alkali back-titrated using thymolblue as the indicator. (Found: E_1 153; E_2 62. Calc. for $C_6H_5SiF_3$;2*n*-$C_3H_7NH_3F$: E_1 160; E_2 64).

The gain in weight of 0.478 g (0.60×10^{-2} mole) of *n*-propylamine hydrofluoride after contact with excess of *cyclo*hexyltrifluorosilane as described for phenyltrifluorosilane above was 0.398 g; calc. for the formation of $C_6H_{11}SiF_3$;2*n*-$C_3H_7NH_3F$: 0.508 g. (Found: E_1 158; E_2 62. Calc. for $C_6H_{11}SiF_3$; 2 *n*-$C_3H_7NH_3F$: E_1 163; E_2 65).

Similar experiments were performed under varying conditions but well-defined products were never obtained.

When triethylfluorosilane or diethyldifluorosilane were added to samples of amine hydrofluorides the solid was immediately wet and no evolution of heat was observed. Nor was there found any gain in weight of the solid after prolonged contact with these fluorosilanes.

REFERENCES

1. Tansjö, L. *Acta Chem. Scand.* **11** (1957) 1613.
2. Tansjö, L. *Acta Chem. Scand.* **13** (1959) 29.
3. Tansjö, L. *Acta Chem. Scand.* **13** (1959) 35.
4. Tansjö, L. *Acta Chem. Scand.* **14** (1960) 2097.
5. Eaborn, C. *Organosilicon Compounds*, Butterworths Scientific Publications, London 1960 (Chapter 11).
6. Miner, C. S., Bryan, L. A., Holysz, R. P. and Pedlov, G. W. *Ind. Eng. Chem.* (Indust.) **39** (1947) 1368.
7. Dolgov, B. N., Davydova, V. P. and Voronkov, M. G. *Zhur. Obschcheĭ Khim.* **27** (1957) 921.
8. Dolgov, B. N., Davydova, V. P. and Voronkov, M. G. *Zhur. Obschcheĭ Khim.* **27** (1957) 1593.
9. Larsson, E. *Trans. Chalmers Univ. Technol. Gothenburg* No. **115** 1951.
10. Holmes, L. and Ingold, C. K. *J. Chem. Soc.* **127** (1925) 1820.
11. Anderson, H. H., Seaton, D. L. and Rudnicki, R. P. T. *J. Am. Chem. Soc.* **73** (1951) 2144.
12. Anderson, H. H. *J. Am. Chem. Soc.* **73** (1951) 2351.
13. Booth, H. S. and Carnell, P. H. *J. Am. Chem. Soc.* **68** (1946) 2650.
14. Booth, H. S. and Martin, W. F. *J. Am. Chem. Soc.* **68** (1946) 2655.
15. Keteelar, J. A. A. *Z. Krist.* **92** (1935) 155.
16. Dolgov, B. N., Kharitonov, N. P. and Voronkov, M. G. *Zhur. Obschcheĭ Khim.* **24** (1954) 678.
17. Eaborn, C. *J. Chem. Soc.* **1952** 2846.
18. Bailey, D. L., Sommer, L. H. and Whitmore, F. C. *J. Am. Chem. Soc.* **70** (1948) 435.
19. Marans, N. S., Sommer, L. H. and Whitmore, F. C. *J. Am. Chem. Soc.* **73** (1951) 5127.
20. Sowa, F. J. *U. S. Pat.* 2,477,704; *C. A.* **44** (1950) 3008.
21. Pearlson, W. H., Brice, T. J. and Simons, J. H. *J. Am. Chem. Soc.* **67** (1945) 1769.
22. Emeleus, H. J. and Wilkins, C. J. *J. Chem. Soc.* **1944** 454.
23. Spialter, L. *Tetrahedron Letters* **1960** No. 5, 11.

24. Smith, B. *Kiselorganiska studier* (Diss.) Chalmers University of Technology, Gothenburg 1951.
25. Larsson, E. *Kgl. Fysiograf. Sällskap. Lund Handl. (N.F.)* **63** (1952) No. 12.
26. Vogel, A. I. *A Textbook of Practical Organic Chemistry*, 3rd Ed. Longmans, Green and Co., London 1956.
27. George, P. D. and Newkirk, A. E. *U.S. Pat.* 2,837,552; *C.A.* **52** (1958) 17181.
28. Dermier, O. C. and King, J. *J. Org. Chem.* **8** (1943) 168.
29. Buehler, C. A., Carson, L. and Edds, R. *J. Am. Chem. Soc.* **57** (1935) 2181.
30. MacKenzie, C. A. and Schoffman, M. *U.S. Pat.* 2.537.073; *C.A.* **45** (1951) 3410.
31. Nametkin, N. S., Topchiev, A. V. and Kartasheva, L. I. *Doklady Akad. Nauk S.S.S.R.* **101** (1955) 885.

Received April 18, 1961.

ACTA CHEMICA SCANDINAVICA 15 (1961) 1595–1603

Neutron Activation Paper Chromatographic Analysis of Phospholipids in Human Liver and Bile

FUMIO NAKAYAMA* and ROLF BLOMSTRAND

The Swedish Medical Research Council, Unit for Biochemical Research for Atherosclerosis, University of Lund, Lund, Sweden

Phospholipids in human liver and bile were analyzed using a neutron activation paper chromatographic technique. Phosphatidylserine, phosphoinositide and choline plasmalogen as well as lecithin, phosphatidylethanolamine and sphingomyelin were found to be present. Further evidence for the presence of lysolecithin in normal human bile is also presented. Similar results were obtained with rat bile using radioactive phosphorus.

Lecithin comprises more than 80 % of the phospholipids in human bile in contrast to liver, where it comprises 45 %, indicating a selective secretion of phospholipid classes from liver into bile. The difference found in the fatty acid composition of the total phospholipids in human liver and bile by gas chromatography, coincides with the findings on the differences in phospholipid composition.

Phospholipids have been known to be present in bile from as early as 1862 [1]. However, the nature of the phospholipids has long remained obscure. The first attempt at characterisation of the phospholipids in bile was made in 1939 by Johnston and coworkers [2]. After careful study, they concluded that phospholipids in bile are composed solely of lecithin. This view was shared by several investigators [3,4] until quite recently. Later, in 1960, we presented evidence indicating the presence of not only lecithin but also of sphingomyelin, cephalin and lysolecithin using a combination of radioactive phosphorus, silicic acid impregnated paper chromatography, and hydrolysis with snake venom [5]. Independently, Philips [6] published paperchromatograms suggesting the presence of lysolecithin, sphingomyelin, lecithin and cephalin.

The study of the phospolipids in bile is important not only for intestinal fat absorption [7,8], but also for a better understanding of gallstone disease, since they have been shown to have a definite influence on the solubilisation of the cholesterol in bile [9–11]. Dog, a species known not to be affected by gallstone

* Visiting Investigator of the Swedish Medical Research Council. Present address: Department of Surgery I, Kyushu University, Faculty of Medicine, Fukuoka, Japan, and Department of Surgery, Wayne State University College of Medicine, Detroit, Michigan, U.S.A.

disease, has been shown to have considerably higher concentration of bile phospholipids compared with human beings [12].

The use of paper chromatography as a microanalytical tool is well established. However, in some cases its resolving power is hampered by the lack of suitable chemical methods of detection. Phospholipid analysis is a good example. In recent work [13] we have shown that after mild hydrolysis of phospholipids a combination of paper chromatography followed by neutron activation permits the separated components not only to be located and characterized but also subsequently determined quantitatively. This technique is most advantageous when phospholipid labeling with ^{32}P is not possible and only a small quantity of sample is available, as is usual in clinical investigations. This technique is therefore applied here to the qualitative and quantitative determination of phospholipids in human liver and bile.

EXPERIMENTAL

Materials. Following accidental trauma normal human hepatic bile was obtained from the bile duct of a patient using a choledochostomy tube. Radioactive rat bile was obtained from common bile duct drainage of animals given ^{32}P-orthophosphate (30 μC per g) intraperitoneally. The bile was run directly into methanol in order to prevent disintegration of biliary phospholipids which is known to occur even under refrigerated conditions [2]. Chloroform was added to the bile-methanol mixture in order to bring the ratio of bile, chloroform and methanol to 1:12:6. The mixture was brought to boiling on the water bath and filtered through a Whatman No. 1 paper. The filtrate was partitioned with one third of a volume of distilled water. The chloroform layer was concentrated under reduced pressure, the residue was taken up in a small volume of chloroform and was subjected to silicic acid column chromatography using a 2:1 mixture of silicic acid and Hyflo Super-Cel (about 100 mg of total bile lipids were run per gram of silicic acid) in order to separate the phospolipids [14].

Paper chromatography. Silicic acid impregnated paper chromatography of phospholipids was performed at room temperature according to the method of Reed *et al.*[15] using *n*-butyl ether, di*iso*butylketone, acetic acid and water (20:20:20:3).

A paper chromatography technique for deacylated phospholipid hydrolysates was used which was essentially based on the method of Dawson [16]. 3.0 mg of phospholipids was transferred into a 14 ml Pyrex tube with a glass stopper and dissolved in 0.2 ml of carbon tetrachloride. 1.9 ml of ethanol was added followed by the addition of 0.16 ml of water and 0.06 ml of 1 N aqueous sodium hydroxide solution. After the solution was thoroughly mixed by swirling, the tube was placed in a water bath maintained at 37°. After 20 min, 0.1 ml of ethyl formate was added and incubated for an additional 5 min in order to neutralize excess alkali. The solvent was evaporated under reduced pressure and the residue was partitioned by the addition of 0.5 ml of water and 1.0 ml of an *iso*-butanol/chloroform (1:2) mixture. After centrifugation, the aqueous layer containing alkali labile phospholipid hydrolysate was separated. The lower chloroform/*iso*butanol layer was washed with 0.5 ml of water twice, and the washings combined with the aqueous layer separated previously. The combined extract was concentrated under reduced pressure and the residue, dissolved in 80 % aqueous ethanol, was made up to 1.0 ml. Half the solution was quantitatively loaded on a Whatman No. 1 paper using a Carlsberg micropipette for subsequent paper chromatographic analysis [16], with the solvent system phenol saturated with water, acetic acid, and ethanol (100:10:12). When two dimensional paper chromatography was necessary, the paper chromatogram was, after drying, run using methanol, 98 % formic acid and water (80:13:7) in the second direction.

The chloroform-*iso*butanol layer was hydrolyzed at 37° by vigourously shaking with 0.2 ml 10 % aqueous trichloroacetic acid solution for 30 min. After hydrolysis 1.0 ml of petroleum ether was added, the resulting aqueous layer containing alkali stable and

acid labile phospholipid hydrolysate was concentrated and loaded on a Whatman No. 1 paper. The paper chromatogram was developed [16] using phenol saturated with water, acetic acid and ethanol (100:10:12).

The upper organic solvent layer containing alkali and acid stable phospholipids was transferred quantitatively into a Pyrex tube (190 × 18 mm). After the solvent was evaporated under reduced pressure, 0.35 ml of 0.7 N HCl in methanol was added. The tube was sealed and placed in an oven at 100°. After 4 h the hydrolysate was concentrated and one half of the hydrolysate loaded on the paper and developed with phenol saturated with water [16].

Neutron activation analysis. For neutron activation analysis the paper chromatogram was rolled and sealed in an aluminium container. After irradiation with a stream of slow neutrons of 5×10^{11} neutron/cm^2/sec for 15 h (irradiation was carried out at the Research Reactor, AB Atomenergi, Stockholm), autoradiograms were prepared using a thick plastic sheet of 10.84 mg per cm^2 as filter and standard Kodak X-ray film. After identification of the individual phospholipid hydrolysates, the corresponding spots were cut from the paper chromatogram and eluted four times with a small volume of warm 80 % ethanol. The extracts were combined and concentrated and an aliquot taken for phosphorus determinations using the method of Chen *et al.*[17]

An experiment was carried out in order to determine whether the induced radioactivity on the paper chromatogram could be used for the quantitative determination of the phospholipids separated. It was found, however, that back ground radioactivity induced in the filter paper, was too high to allow an accurate determination of the smaller components. A control experiment carried out in order to examine the extraction procedure showed a recovery of 92—95 % phosphorus. The phosphorus content of the filterpaper used was of the order of 0.02—0.03 μg per cm^2 so that it does not interfere with the final results.

When pure compounds are irradiated with neutrons, rearrangement of the chemical bonds sometimes take place [18]. However, here we have utilized neutron activation after the separation of each component by paper chromatography and thus this possibility should not interfere with the results.

Gas chromatographic analysis of fatty acids in human liver and bile. The liver biopsy sample and hepatic bile were obtained from the same patient operated on for gall-stone disease. Total fat was extracted with a chloroform/methanol (2:1) mixture according to Folch [19]. After saponification and acidification the total fatty acids from the bile were isolated. The liver lipids were separated on silicic acid into cholesterol esters, glycerides and phospholipids [20]. The fatty acids from the different lipid classes were isolated after saponification and acidification. The fatty acids isolated were methylated with diazomethane and analysed by gas-liquid chromatography using an Argon Pye apparatus with an ionisation chamber as detector. As stationary phase a polar polyester (LAC-R-296) was used, the ratio of Celite/stationary phase being 4:1. The experimental procedures used have otherwise been described earlier [20].

RESULTS

Autoradiograms prepared after neutron activation of two-dimensional paper chromatograms of alkali labile phospholipid hydrolysates of human bile, human liver and rat liver, are shown in Fig. 1 and that of a one dimensional chromatogram in Fig. 2a. The following spots were identified: GPC (glycerylphosphorylcholine, derived from lecithin), GPE (glycerylphosphorylethanolamine, from phosphatidylethanolamine), cyc-GP(cyclic glycerophosphate, from lecithin and phosphoinositide), GPS (glycerylphosphorylserine, phosphatidylserine) and GPI (glycerylphosphorylinositol, from phosphoinositide) as previously shown by Dawson [16] using the same paper chromatographic technique. All these components were found to be present in human bile as well as in human and rat liver. However, there are definite differences between these

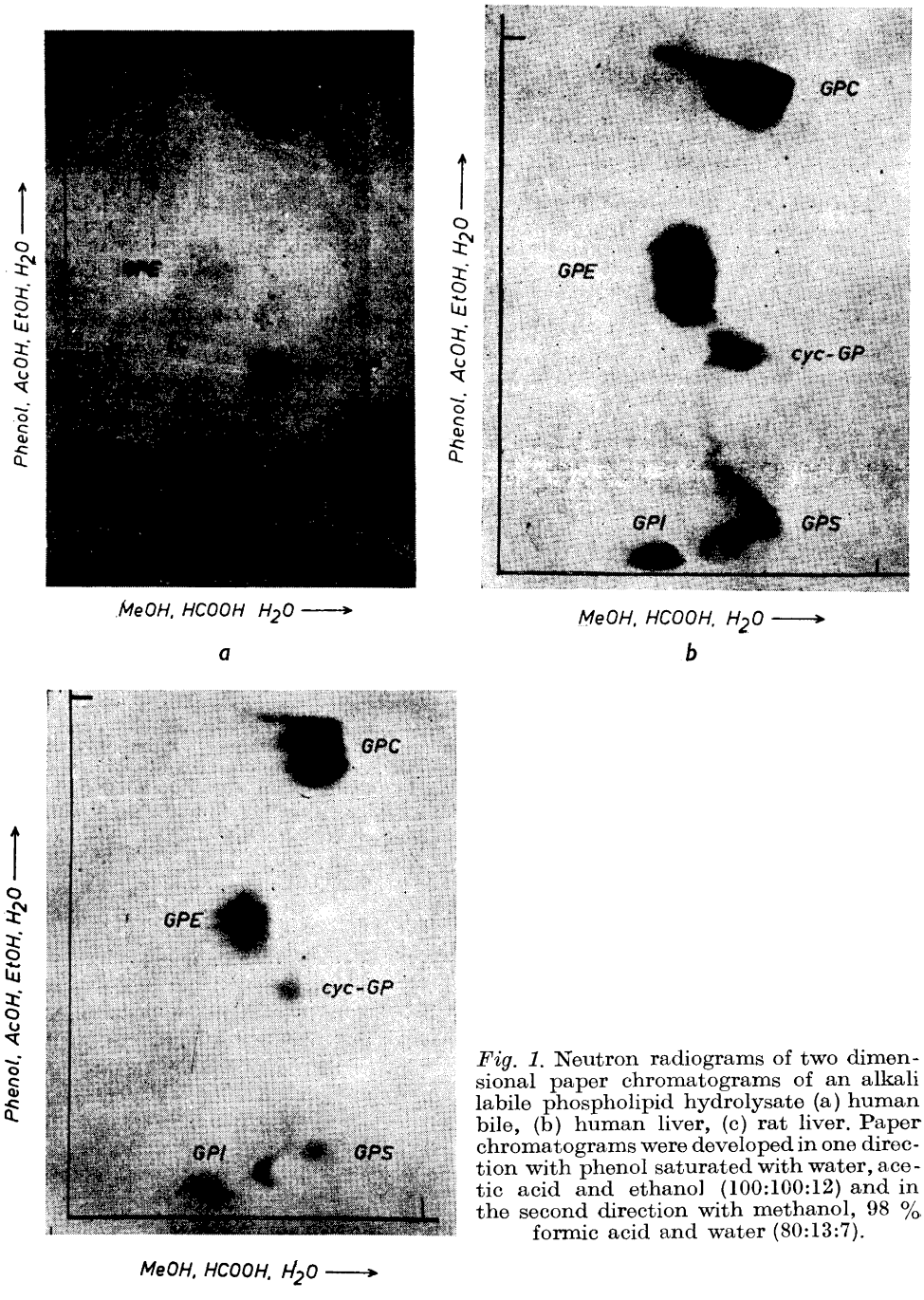

Fig. 1. Neutron radiograms of two dimensional paper chromatograms of an alkali labile phospholipid hydrolysate (a) human bile, (b) human liver, (c) rat liver. Paper chromatograms were developed in one direction with phenol saturated with water, acetic acid and ethanol (100:100:12) and in the second direction with methanol, 98 % formic acid and water (80:13:7).

autoradiograms, *e.g.* in human bile only faint glycerylphosphorylethanolamine, glycerylphosphorylserine and glycerylphosphorylinositol spots are visible as distinct from definite glycerylphosphorylcholine spot (Figs. 1 and 2a). The autoradiogram of alkali stable and acid labile phospholipid hydrolysate showed a glycerylphosphorylcholine spot indicating the presence of choline plasmalogen in human bile as well as in human and rat liver (Fig. 2b). Fig. 2c shows the autoradiogram prepared from a neutron activated paper chromatogram of alkali and acid stable phospholipid hydrolysates from human bile, human and rat liver. Phosphorylcholine, a hydrolysis product of sphingomyelin, was identified in all three. The results presented indicated the presence of lecithin, phosphatidylethanolamine, phosphatidylserine, phosphoinositide, choline plasmalogen and sphingomyelin in human bile as well as in human liver and rat liver.

Similar experiments, carried out on rats using radioactive phosphorus instead of neutron activation, indicated the presence of lecithin, phospatidylethanolamine, phosphatidylserine and phosphatidylionisitide (Figs. 3 and 4a) choline plasmalogen (Fig. 4b) and sphingomyelin (Fig. 4c).

Some preliminary quantitative data are given in Table 1. A comparison between phospholipid composition in normal human bile and liver reveals one striking difference; phospholipids in bile are predominantly composed of lecithin (over 80 %) in contrast to those in liver (48 %). Phosphatidylethanolamine, phosphatidylserine, phosphoinositide, choline plasmalogen and sphingomyelin are also present in human bile but in minute amounts.

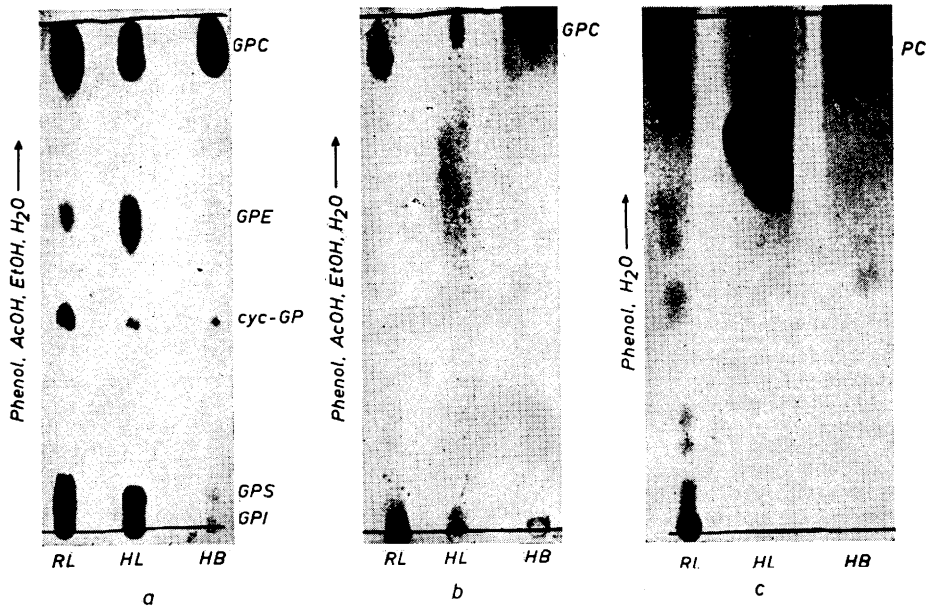

Fig. 2. Neutron radiograms of a phospholipid hydrolysate of rat liver (RL), human liver (HL) and human bile (HB), (a) alkali labile phospholipids, (b) alkali stable acid labile, (c) alkali and acid stable.

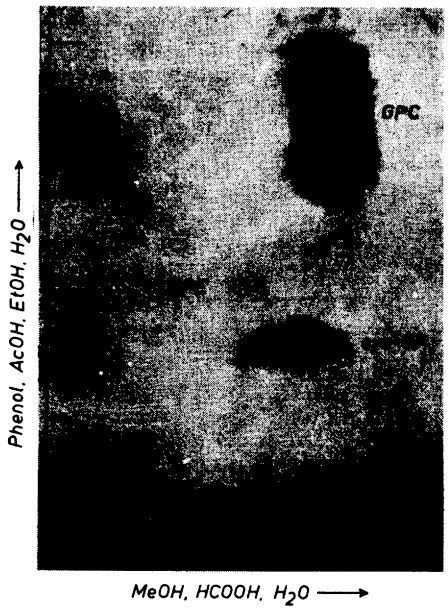

Fig. 3. Autoradiogram of two dimensional paper chromatogram of a ^{32}P-labelled alkali labile phospholipid hydrolysate of rat bile.

Similar experiments were carried out on human bile using silicic acid impregnated paper chromatography and hydrolysis with snake venom, as outlined previously [5], followed by neutron activation. Lysolecithin was also found to be present in human bile as in rat bile.

Figs. 5a and b show a comparison between the fatty acid composition in liver phospholipids and the total fatty acids in bile. Since more than 90 % of the fatty acids in bile are associated with phospholipids, the total fatty acid

Table 1. Phospholipid composition of human bile and liver as determined by neutron activation paper chromatographic analysis *.

	Human bile	Human liver	Rat liver
Alkali labile phospholipids			
Phosphoinositide	2.65	14.93	14.43
Phosphatidylserine	traces	6.54	6.09
Phosphatidylethanolamine	3.42	18.12	8.10
Phosphatidylcholine	81.36	48.36	61.57
Alkali stable acid labile phospholipids			
Choline plasmalogen	3.79	1.49	1.16
	0.36	2.35	1.48
Alkali acid stable phospholipids			
Sphingomyelin	2.52	6.93	4.97
Unidentified	5.90	1.45	3.20

* expressed as % phosphorus per total phospholipid phosphorus.

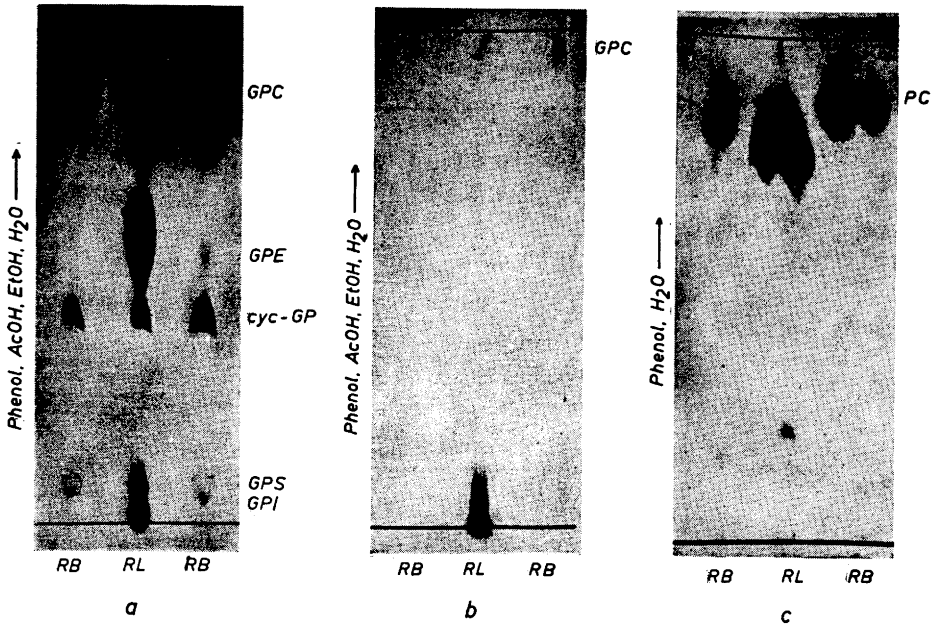

Fig. 4. Autodioragram of a ^{32}P-labelled phospholipid hydrolysate from rat liver (RL) and rat bile (RB), (b) alkali labile phospholipids, (c) alkali stable acid labile, (a) alkali and acid stable.

composition of bile could be expected to be similar to the fatty acid composition of phospholipids in bile. In fact, the fatty acid composition of purified biliary phospholipids is very similar to the total fatty acid composition of bile.

Certain differences could be seen in fatty acid composition of human liver and bile; the relative percentage of stearic acid in the liver phospholipids is greater (20.9 %) than in bile (8.5 %), while linoleic acid is smaller in liver (15.8 %) than in bile (27.8 %).

DISCUSSION

Phospholipids are secreted from the liver and enter the intestinal tract *via* bile. There are indications that phospholipids facilitate the solubilisation of the cholesterol in bile [9–11], thus preventing the formation of gall-stones. During passage in the intestinal tract, phospholipids undergo extensive hydrolysis [21,22], and may interact with fat absorption. Since bile phospholipids comprise an important part of the phospholipids present in the intestine, the mechanism of phospholipid absorption and the way phospholipids interact with fat absorption will not be fully understood, so long as the nature of the phospholipids in bile remains obscure.

The present results on the phospholipid analysis of human and rat bile confirm and extend our earlier findings [5]. Paper chromatography of phospholipids after mild hydrolysis in combination with neutron activation gives a

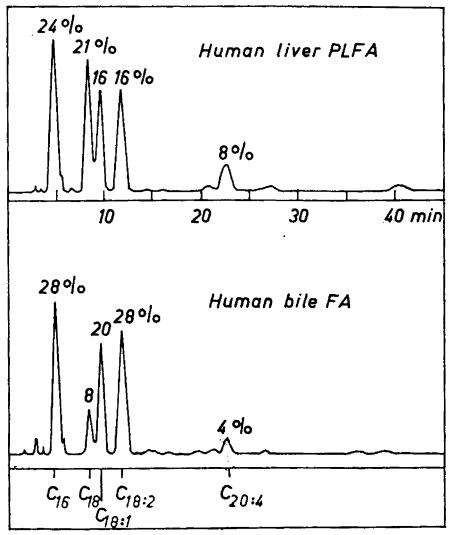

Fig. 5. Total fatty acid composition of, (a) human liver phospholipids, (b) human bile phospholipids.

better separation and identification of each of the phospholipids. Using this technique, choline plasmalogen, phosphatidylserine and phosphatidylinositol are found to be present in human bile as well as in rat bile in addition to lecithin. phosphatidylethanolamine, sphingomyelin, lysolecithin, identified earlier[6]. Gas chromatograms of fatty acids isolated from purified bile lecithin indicated the presence of several kinds of lecithins [20,23]. Among these phospholipids present in bile, the presence of a considerable amount of lysolecithin is of special interest, since this compound has been shown to have a marked solubilising effect on cholesterol [11], which is a major component of gall-stones.

A comparison between the phospholipid composition in human liver and bile reveals the presence of a much greater proportion of lecithin (phosphatidylcholine) in the bile (Table 1), which would indicate that phospholipids are selectively secreted from liver into bile. The significance of the presence of a small amount of other phospholipids has to be investigated.

Since lecithin comprises more than 80 % of bile phospholipids in contrast to that of liver (48 %) and as liver contains an appreciable amount of phospholipids other than lecithin, the differences found between liver and bile (Fig. 7) in the fatty acid composition of the total phospholipids could very well be explained by the difference in phospholipid composition in liver and bile.

This work is part of investigations supported by *The Swedish Medical Research Council.*

REFERENCES

1. Thudichum, J. L. W. *A treatise on gallstones*, John Churchil and Sons, London 1863.
2. Johnston, C. G., Irvin, J. L. and Walton, C. *J. Biol. Chem.* **131** (1939) 425.
3. Isaksson, B. *Acta Soc. Med. Upsaliensis* **56** (1952) 177.
4. Borgström, B. *Acta Chem. Scand.* **11** (1957) 749.
5. Nakayama, F. and Blomstrand, R. *Acta Chem. Scand.* **14** (1960) 1211.
6. Philips, G. B. *Biochim. et Biophys. Acta* **41** (1960) 361.
7. Nakayama, F. *Am. J. Physiol.* **196** (1959) 319.
8. Nakayama, F. and Johnston, C. G. *Am. J. Physiol.* **197** (1959) 327.
9. Isaksson, B. *On the lipids and bile acids in normal and pathological bladder bile: A study of the main cholesterol dissolving components of human bile.* Thesis, Lund, Sweden, 1954.
10. Johnston, C. G. and Nakayama, F. *Arch. Surgery* **75** (1957) 436.
11. Nakayama, F. *Solubility of cholesterol in bile in relation to gallstone formation.* Thesis, Wayne State University College of Medicine, Detroit, Michigan, U.S.A. 1957.
12. Nakayama, F. and Johnston, C. G. *Proc. Soc. Exptl. Biol. Med.* **104** (1960) 73.
13. Blomstrand, R. and Nakayama, F. *Scand. J. Clin. & Lab. Invest. In print.*
14. Borgström, B. *Acta Physiol. Scand.* **25** (1952) 101.
15. Reed, C. F., Swisher, S. N., Marinetti, G. V. and Eden, E. G. *J. Lab. Clin. Med.* **56** (1960) 281.
16. Dawson, R. M. C. *Biochem. J.* **75** (1960) 45.
17. Chen, P. A., Jr., Toribara, T. Y. K. and Warner, H. *Anal. Chem.* **28** (1956) 175b.
18. Sellers, P. S., Sato, T. R. and Strain, H. H. *J. Inorg. & Nuclear Chem.* **5** (1957) 31.
19. Floch, J., Ascoli, I., Lees, M., Meath, J. A. and Lebaron, F. N. *J. Biol. Chem.* **191** (1951) 833.
20. Blomstrand, R. *Acta Chem. Scand.* **14** (1960) 1006.
21. Blomstrand, R. *Acta Chem. Scand.* **8** (1954) 1945.
22. Blomstrand, R. and Nakayama, F. *To be published.*
23. Blomstrand, R. and Ekdahl, P. *Proc. Soc. Exptl. Biol. Med.* **104** (1960) 205.

Received April 19, 1961.

ACTA CHEMICA SCANDINAVICA 15 (1961) 1604–1628

Short Communications

Algal Carotenoids

I. Fucoxanthin Monoacetate

ARNE JENSEN

Norwegian Institute of Seaweed Research, N.T.H., Trondheim, Norway

Fucoxanthin, the characteristic carotenoid of brown algae (and of diatoms), was isolated in the crystalline state for the first time in 1914 by Willstätter and Page [1] who ascribed to it the molecular formula $C_{40}H_{54}O_6$. More recent authors have favoured the formulas $C_{40}H_{56}O_6$[2,3] and $C_{40}H_{60}O_6$[4,5]. Active hydrogen determinations have indicated between four and six hydroxyl groups in the molecule [3,6]. Attempts to determine the number of hydroxyl functions by acetylation have failed, as only about two hydroxyls could be esterified [3]. Although several investigations have been made to elucidate the structure of fucoxanthin [1-7], no satisfactory constitution has hitherto been suggested. The proposed formulations [4,8] are not in accordance with the known properties of the compound, as has been pointed out by a number of authors [5,9-11].

During a study of the content of carotenoids of Norwegian brown algae, a limited amount of chromatographically pure fucoxanthin became available. The crystalline compound, mainly isolated from *Fucus serratus*, m.p. 158–159°C (uncorr.), λ_{max} (425), 449, 478 mμ (petroleum ether), $E^{1\,\%}_{1\,cm} = 1\,650$ (449 mμ), showed main absorption bands at 3 450, 2 940, 1 930, 1 730, 1 663, 1 647, 1 610, 1 530, 1 450, 1 355, 1 240, 1 030 and 955 cm^{-1} (KBr-disc). The acetylation in pyridine-acetic anhydride at room temperature was followed by paper chromatography [12] (Table 1). The reaction came to a standstill after 3–4 h. Treatment over-night did not lead to further acetylation. After chromatography on calcium carbonate and two crystallisations from petroleum ether, the acetate melted at 118–119°C (uncorr.). The light absorption properties were very similar to those of fucoxanthin both in the visible and in the infra-red regions ($E^{1\,\%}_{1\,cm} = 1\,560$ at 449 mμ in petroleum ether). Elementary analyses gave C 74.77; H 8.84; calc. for $C_{42}H_{58}O_7$: C 74.74; H 8.66.

Partition ratios for fucoxanthin and the acetate were determined according to

Table 1. Acetylation of fucoxanthin.

Reaction time minutes	Starting material R_F[a]	Starting material Percentage[b]	Product R_F[a]	Product Percentage[b]
2	45	83	72	17
60	44	20	74	80
180	44	trace	73	100

[a] Relative mobility × 100 in petroleum ether containing 10 % of acetone.
[b] Relative amounts in the reaction mixture.

Table 2. Partition ratios[13] of fucoxanthin and fucoxanthin monoacetate.

Compound	Partition ratios in petroleum ether/aq.methanol 85 % methanol	60 % methanol	50 % methanol	R_F[a]
Fucoxanthin	2:98	72:28	92:8	49
Fucoxanthin monoacetate	29:71	—	—	73
Zeaxanthin[13]	40:60	—	—	73
Lutein[13]	43:57	—	—	78

[a] Relative mobility × 100 in petroleum ether containing 10 % of acetone.

Petracek and Zechmeister [13], and the results are given in Table 2.

The formation of a monoacetate of fucoxanthin under the conditions employed strongly indicates the presence of only one secondary (or primary) hydroxyl group in the native pigment. The infra-red spectrum of the acetate showed the presence of more hydroxyl functions, and on partition between petroleum ether and aqueous methanol the compound was more hypophasic than the dihydroxy carotenoids zeaxanthin and lutein. The R_F-value of the acetate was close to those of zeaxanthin and lutein although the former had a shorter chromophore. We therefore suggest that fucoxanthin contains at least two hindered, presumably tertiary, hydroxyl groups in the molecule. Weak absorption bands occurring at 1 140 and 900 cm^{-1} in the infra-red spectra of both fucoxanthin and the monoacetate may belong to these groups [14,15].

The spectral absorption curve of fucoxanthin (λ_{max} at (425), 449, 478 mμ in petroleum ether) is very similar in shape and position to that of β-citraurin (λ_{max} at 425, 448, 477 mμ in hexane [16]). The latter compound has eight carbon-carbon and one carbon-oxygen double bonds in conjugation. Fucoxanthin may therefore have a similar arrangement, or, if the chromophore is terminated by an allene group (the presence of which is indicated by the absorption at 1 930 cm^{-1} in the infra-red) it may consist of one terminal allene group, seven carbon-carbon and one carbon-oxygen double bonds which are all conjugated.

1. Willstätter, R. and Page, H. J. *Ann.* **404** (1914) 237.
2. Karrer, P. *Z. angew. Chem.* **42** (1929) 918.
3. Karrer, P., Helfenstein, A., Wehrli, H., Pieper, B. and Morf, R. *Helv. Chim. Acta* **14** (1931) 614.
4. Heilbron, I. M. and Phipers, R. F. *Biochem. J.* **29** (1935) 1369.
5. Torto, E. G. and Weedon, B. C. L. *Chem. & Ind.* (London) **1955** 1219.
6. Karrer, P., Wehrli, H. and Helfenstein, A. *Helv. Chim. Acta* **13** (1930) 268.
7. Liaaen, S. and Sørensen, N. A. in Braarud, T. and Sørensen, N. A. *2nd Intern. Seaweed Symposium*, Pergamon Press, London 1956, p. 25.
8. Ředrovský, R. *Collection Czechoslov. Chem. Communs* **13** (1948) 631.
9. Karrer, P. and Jucker, E. *Carotenoids*. Elsevier, New York 1950, p. 311.
10. Goodwin, T. W. *The Comparative Biochemistry of the Carotenoids*. Chapman & Hall, London 1952, p. 132.
11. Strain, H. H. in Franck, J. and Loomis, W. E. *Photosynthesis in Plants*. The Iowa State College Press, Ames 1949, p. 160.
12. Jensen, A. and Liaaen Jensen, S. *Acta Chem. Scand.* **13** (1959) 1863.
13. Petracek, F. J. and Zechmeister, L. *Anal. Chem.* **28** (1956) 1484.
14. Stamm, O. A., Schmid, H. and Büchi, J. *Helv. Chim. Acta* **41** (1948) 2006.
15. Liaaen Jensen, S. *Acta Chem. Scand.* **14** (1960) 950.
16. Karrer, P. and Würgler, E. *Helv. Chim. Acta* **26** (1943) 119.

Received September 13, 1961.

Algal Carotenoids

II. The Fucoxanthols — Reduction Products of Fucoxanthin

ARNE JENSEN

Norwegian Institute of Seaweed Research, N.T.H., Trondheim, Norway

The presence of carbonyl functions in the fucoxanthin molecule was first suggested in 1935 by Heilbron and Phipers [1] who based this assumption mainly on chemical grounds. Later [2], the poorly defined spectral absorption curve of fucoxanthin dissolved in polar solvent relative to that for the pigment dissolved in nonpolar solvent, was taken as an indication of the presence of one or more ketonic groups in the molecule. More recently absorption bands at 1 730 and 1 660 cm^{-1} in the infra-red spectrum of fucoxanthin have been demonstrated, and the presence of one conjugated and one isolated keto group [3], or of one conjugated carbonyl and one saturated carbonyl or unsaturated ester group [4] have been proposed. It should be pointed out, however, that the methyl esters of bixin and of crocetin, which each contain two identical, conjugated carbonyl groups, give rise to two separate carbonyl bands in the infra-red absorption spectrum [5] namely at approximately 1 630 and 1 730 cm^{-1}. The above assignments therefore needed some further support.

Crystalline fucoxanthin [6] (480 mg) was treated with lithium aluminium hydride, and from the reaction mixture were isolated

Petracek and Zechmeister [13], and the results are given in Table 2.

The formation of a monoacetate of fucoxanthin under the conditions employed strongly indicates the presence of only one secondary (or primary) hydroxyl group in the native pigment. The infra-red spectrum of the acetate showed the presence of more hydroxyl functions, and on partition between petroleum ether and aqueous methanol the compound was more hypophasic than the dihydroxy carotenoids zeaxanthin and lutein. The R_F-value of the acetate was close to those of zeaxanthin and lutein although the former had a shorter chromophore. We therefore suggest that fucoxanthin contains at least two hindered, presumably tertiary, hydroxyl groups in the molecule. Weak absorption bands occurring at 1 140 and 900 cm^{-1} in the infra-red spectra of both fucoxanthin and the monoacetate may belong to these groups [14,15].

The spectral absorption curve of fucoxanthin (λ_{max} at (425), 449, 478 mμ in petroleum ether) is very similar in shape and position to that of β-citraurin (λ_{max} at 425, 448, 477 mμ in hexane [16]). The latter compound has eight carbon-carbon and one carbon-oxygen double bonds in conjugation. Fucoxanthin may therefore have a similar arrangement, or, if the chromophore is terminated by an allene group (the presence of which is indicated by the absorption at 1 930 cm^{-1} in the infra-red) it may consist of one terminal allene group, seven carbon-carbon and one carbon-oxygen double bonds which are all conjugated.

1. Willstätter, R. and Page, H. J. *Ann.* **404** (1914) 237.
2. Karrer, P. *Z. angew. Chem.* **42** (1929) 918.
3. Karrer, P., Helfenstein, A., Wehrli, H., Pieper, B. and Morf, R. *Helv. Chim. Acta* **14** (1931) 614.
4. Heilbron, I. M. and Phipers, R. F. *Biochem. J.* **29** (1935) 1369.
5. Torto, E. G. and Weedon, B. C. L. *Chem. & Ind.* (London) **1955** 1219.
6. Karrer, P., Wehrli, H. and Helfenstein, A. *Helv. Chim. Acta* **13** (1930) 268.
7. Liaaen, S. and Sørensen, N. A. in Braarud, T. and Sørensen, N. A. *2nd Intern. Seaweed Symposium*, Pergamon Press, London 1956, p. 25.
8. Ředrovský, R. *Collection Czechoslov. Chem. Communs* **13** (1948) 631.
9. Karrer, P. and Jucker, E. *Carotenoids*. Elsevier, New York 1950, p. 311.
10. Goodwin, T. W. *The Comparative Biochemistry of the Carotenoids*. Chapman & Hall, London 1952, p. 132.
11. Strain, H. H. in Franck, J. and Loomis, W. E. *Photosynthesis in Plants*. The Iowa State College Press, Ames 1949, p. 160.
12. Jensen, A. and Liaaen Jensen, S. *Acta Chem. Scand.* **13** (1959) 1863.
13. Petracek, F. J. and Zechmeister, L. *Anal. Chem.* **28** (1956) 1484.
14. Stamm, O. A., Schmid, H. and Büchi, J. *Helv. Chim. Acta* **41** (1948) 2006.
15. Liaaen Jensen, S. *Acta Chem. Scand.* **14** (1960) 950.
16. Karrer, P. and Würgler, E. *Helv. Chim. Acta* **26** (1943) 119.

Received September 13, 1961.

Algal Carotenoids

II. The Fucoxanthols — Reduction Products of Fucoxanthin

ARNE JENSEN

Norwegian Institute of Seaweed Research, N.T.H., Trondheim, Norway

The presence of carbonyl functions in the fucoxanthin molecule was first suggested in 1935 by Heilbron and Phipers [1] who based this assumption mainly on chemical grounds. Later [2], the poorly defined spectral absorption curve of fucoxanthin dissolved in polar solvent relative to that for the pigment dissolved in nonpolar solvent, was taken as an indication of the presence of one or more ketonic groups in the molecule. More recently absorption bands at 1 730 and 1 660 cm^{-1} in the infra-red spectrum of fucoxanthin have been demonstrated, and the presence of one conjugated and one isolated keto group [3], or of one conjugated carbonyl and one saturated carbonyl or unsaturated ester group [4] have been proposed. It should be pointed out, however, that the methyl esters of bixin and of crocetin, which each contain two identical, conjugated carbonyl groups, give rise to two separate carbonyl bands in the infra-red absorption spectrum [5] namely at approximately 1 630 and 1 730 cm^{-1}. The above assignments therefore needed some further support.

Crystalline fucoxanthin [6] (480 mg) was treated with lithium aluminium hydride, and from the reaction mixture were isolated

three new, crystalline derivatives of fucoxanthin, for which the names fucoxanthol a (80 mg), fucoxanthol b (140 mg), and semifucoxanthol (5 mg) are proposed. Fucoxanthol a (m.p. 187–189°C, $E^{1\%}_{1\,cm}$ = 2 510 at 421 mμ) and fucoxanthol b (m.p. 181–182°C, $E^{1\%}_{1\,cm}$ = 2 150 at 421 mμ) showed identical absorption properties in the visible and infra-red regions, λ_{max} 398, 421, 448 mμ (petroleum ether) and main absorption bands at 3 340, 2 930, 1 930, 1 450, 1 360, 1 135, 1 030 and 960 cm^{-1} (KBr-disc). Elementary analyses gave C 76.47; H 9.36 and C 75.48; H 9.50 for fucoxanthol a and b, respectively. Calc. for $C_{40}H_{60}O_6$: C 75.43; H 9.50. Iodine catalysed isomerisation gave two different stereoiso-

Table 1. J_2-catalysed isomerisation of fucoxanthol a and b.

Fucoxanthol a	λ_{max}, mμ[a]	Rel.amount	R_F20 %[b]
Trans-fucoxanthol a	398, 421, 448	—	54
Equilibrium mixture	396, 419, 447	—	—
Trans	398, 421, 448	63 %	54
Neo U	395, 417, 444	37 %	52
Fucoxanthol b			
Trans-fucoxanthol b	398, 421, 448	—	—
Equilibrium mixture	396, 419, 447	—	—
Neo A	396, 418, 447	21 %	49
Trans	397, 421, 448	48 %	42
Neo U	394, 417, 442	32 %	36

[a] in petroleum ether. [b] $R_F \times 100$, 20 % acetone in petroleum ether.

Table 2. Acetylation of fucoxanthol b.

Zone No.	R_F[a]	Carotenoid in % of total after reaction time in minutes 2	15	60	200	Tentative identification
8	11	90	18.2	4.2	0	fucoxanthol b
7	26	6	20.5	9.6	0	
6	33	4	12.9	5.8	2.6	monoacetates
5	37	0	8.8	9.8	0	
4	42	0	6.0	5.6	0	
3	53	0	23.4	32.0	11.5	diacetates
2	58	0				
1	75	0	10.2	33.2	85.9	triacetate

[a] Relative mobility × 100 in petroleum ether containing 10 % of acetone.

Table 3. Partition ratios[7] of the fucoxanthols.

Compound	Partitions ratios in pet.ether/aq.methanol 85 %	60 %	50 %
Fucoxanthol a	0:100	5:95	15:85
Fucoxanthol b	0:100	5:95	15:85
Fucoxanthol b acetate	33:67	—	—
Semifucoxanthol	2:98	45:55	63:37
Zeaxanthin[7]	40:60	—	—

meric sets as shown by paper chromatography (see Table 1).

Semifucoxanthol had absorption maxima at 398, 421 and 448 mμ (petroleum ether) and showed main absorption bands at 3 340, 2 930, 1 930, 1 725, 1 450, 1 365, 1 245, 1 150, 1 030 and 960 cm^{-1} (KBr-disc.).

Acetylation of fucoxanthol b in pyridine-acetic anhydride was followed by paper chromatography. The results are shown in Table 2.

The acetate of fucoxanthol b (R_F = 75) was purified by chromatography, and melted at 168°C after two crystallisations from ether-petroleum ether, $E^{1\%}_{1\,cm}$ = 1 800 at 421 mμ, λ_{max} 398, 421, 449 mμ (petroleum ether). Elementary analyses gave C 73.39; H 8.59; CH_3CO 14.77. Calc. for the triacetate $C_{46}H_{66}O_9$: C 72.41; H 8.72; CH_3CO 16.92. (The diacetate $C_{44}H_{64}O_8$ requires CH_3CO 11.94).

Partition ratios [7] for the compounds above are given in Table 3. While solutions of fucoxanthin and its acetate in ether both gave a strong and stable blue colour reaction with 25 % hydrochloric acid, the reduction products gave a rather faint and unstable, but unmistakeable, blue colour with this reagent.

The data presented above prove that the fucoxanthin molecule contains two, non-identical carbonyl groups, one of which is conjugated with the rest of the chromophore. By reduction of the conjugated keto function, the semifucoxanthol was formed. This compound still contained one carbonyl group, as evident from the infra-red absorption at 1 725 cm^{-1}. Further reduction gave the fucoxanthols which showed no absorption in the carbonyl region of the spectrum. These three compounds exhibited pronounced fine structure absorption spectra in visible light, confirming that the conjugation with the carbonyl group had been broken. The position of the absorption maxima coincided completely with those of flavoxanthin [8], which has eight conjugated carbon-carbon double bonds in an aliphatic chromophore.

The fucoxanthols a and b were formed without loss of oxygen, a fact that rules out the suggested presence of an ester group in the fucoxanthin molecule.

The behaviour of fucoxanthol b during acetylation (Table 2) was similar to that expected for an unsymmetrical triol containing three about equally accessible hydroxyl groups, during the acetylation of which three monoacetates, three diacetates and one triacetate should occur. The formation of one single end product makes it very unlikely that any of the compounds of Table 2 were *cis-trans* isomers. Therefore the course of the acetylation of fucoxanthol b, together with the elementary analysis and the acetoxy content of the product strongly indicate that it was a triacetate. The R_F-value and the partition ratio suggest the presence of at least two free hydroxyl groups in this acetate. If the blue colour reaction of the fucoxanthols a and b with concentrated aqueous hydrochloric acid was caused by an epoxy or a furanoid function, the number of free hydroxyl groups in the acetate could not exceed two.

A detailed report of this work will be published elsewhere. Further studies on the structure of fucoxanthin is in progress.

1. Heilbron, I. M. and Phipers, R. F. *Biochem. J.* **29** (1935) 1369.
2. Strain, H. H. in Franck, J. and Loomis, W. E. *Photosynthesis in Plants.* The Iowa State College Press, Ames 1949, p. 160.
3. Liaaen, S. and Sørensen, N. A. in Braarud, T. and Sørensen, N. A. 2nd Intern. Seaweed Symposium, Pergamon Press, London 1956, p. 25.
4. Torto, E. G. and Weedon, B. C. L. *Chem. & Ind. (London)* **1955** 1219.
5. Isler, O., Gutmann, H., Montavon, M., Rüegg, R., Ryser, G. and Zeller, P. *Helv. Chim. Acta* **40** (1957) 1242.
6. Jensen, A. *Acta Chem. Scand.* **15** (1961) 1604.
7. Petracek, F. J. and Zechmeister, L. *Anal. Chem.* **28** (1956) 1484.
8. Kuhn, R. and Brockmann, H. *Z. physiol. Chem. Hoppe-Seyler's,* **213** (1932) 192.

Received September 13, 1961.

Displacement of Sulphite Groups of Polythionates by Thiosulphate

OLAV FOSS and IVAR KRINGLEBOTN

Chemical Institute, University of Bergen, Bergen, Norway

Polythionate ions higher than trithionate react with sulphite ion to give the next lower polythionate, and thiosulphate [1]. In these reactions, which are nucleophilic displacements of thiosulphate groups of polythionates by sulphite [2,3], a shortening of the divalent sulphur chain of the polythionates takes place.

The reverse reactions, *i.e.*, nucleophilic displacements of sulphite groups of polythionates by thiosulphate [4,5], correspondingly lead to a building-up of higher polythionates from lower ones:

$$S_3O_6^{--} + S_2O_3^{--} \xrightarrow{k_1} S_4O_6^{--} + SO_3^{--} \quad (1)$$

$$S_4O_6^{--} + S_2O_3^{--} \xrightarrow{k_2} S_5O_6^{--} + SO_3^{--} \quad (2)$$

$$S_5O_6^{--} + S_2O_3^{--} \xrightarrow{k_3} S_6O_6^{--} + SO_3^{--} \quad (3)$$

$$S_6O_6^{--} + S_2O_3^{--} \xrightarrow{k_4} S_7O_6^{--} + SO_3^{--} \quad (4)$$

and so forth. The equilibria lie to the left side of the equations, and so the building-up process occurs only if sulphite is removed from the equilibria, as hydrogensulphite or sulphurous acid under acid conditions [1], or by means of formaldehyde [4].

We have studied the kinetics of the reaction of potassium tetrathionate with sodium thiosulphate, eqn. (2), between 20 and 40°C in presence of formaldehyde as sulphite acceptor, in phosphate buffer to prevent the solutions from becoming alkaline. In presence of excess of formaldehyde the second step of the change, *i.e.*, the removal of sulphite as hydroxymethane sulphonate:

$$SO_3^{--} + CH_2O + H_2PO_4^- \longrightarrow HOCH_2SO_3^- + HPO_4^{--}$$

is more rapid than the first step (2) as indicated by the fact that variation in the amount of formaldehyde present (from *ca.* 0.13 M to *ca.* 0.26 M) had no influence on the rate. Neither had the addition of potassium hydroxymethane sulphonate, or variation of pH by half a unit to both sides of pH = 6.8. The reaction proceeds without change of ionic strength. It shows a positive salt effect, as expected for a reaction between ions of the same sign in the rate-determining step (2). Therefore, the experiments were carried out at a constant ionic strength of 1.15 adjusted with sodium sulphate.

The rate of disappearance of thiosulphate, as followed by iodometric titration, was found to be:

$$-dS_2/dt = k_2 a S_2 \quad (5)$$

where S_2 is the concentration of thiosulphate at time t and a is the *initial* concentration of tetrathionate. Integration, when $S_2 = b$ at $t = 0$, gives:

$$S_2 = b \exp(-k_2 a t) \quad (6)$$

At 25°C and an ionic strength of 1.15, $k_2 = 1.3 \times 10^{-3}$ l.mole^{-1}sec^{-1}, when a has been varied from 0.05 to 0.10 M and b from 0.025 to 0.05 M. The activation parameters are: $E_a = 12.0$ kcal/mole, $\Delta H^{\ddagger} = 11.4$ kcal/mole and $\Delta S^{\ddagger} = -34$ cal/mole degree.

We interpret this rate law as indicating that the pentathionate formed in the first step (2) from tetrathionate and thiosulphate, reacts with thiosulphate to give hexathionate, eqn. (3), which then reacts with thiosulphate to give heptathionate, eqn. (4), and so forth, with the same or approximately the same bimolecular rate constants: $k_2 \sim k_3 \sim k_4$. Thus, through successive S_N2 displacements of sulphite by thiosulphate, in presence of a sulphite acceptor, a building-up of higher polythionates from tetrathionate and thiosulphate takes place.

Analysis of the reaction mixtures by the sulphite method [6] showed that the sum of unreacted thiosulphate and thiosulphate produced by reaction with excess sulphite remained constant. The formation of pentathionate and hexathionate when solutions of thiosulphate and tetrathionate are mixed with simultaneous addition of formaldehyde has been demonstrated by a paper chromatographic method by Skarżyński and Szczepkowski [7].

A series of consequtive steps with equal rate constants gives for the rates of disappearance of thiosulphate and tetrathionate:

$$-dS_2/dt = k_2 S_2 (S_4 + S_5 + S_6 + S_7 + \ldots) \quad (7)$$

$$-dS_4/dt = k_2 S_2 S_4 \quad (8)$$

and for the rates of formation of pentathionate and higher polythionates:

$$dS_5/dt = k_2 S_4 S_2 - k_2 S_5 S_2 \quad (9)$$

$$dS_6/dt = k_2 S_5 S_2 - k_2 S_6 S_2 \quad (10)$$

$$dS_7/dt = k_2 S_6 S_2 - k_2 S_7 S_2 \quad (11)$$

where S_4, S_5, S_6, S_7 denote the concentrations of tetra-, penta-, hexa-, heptathionate, respectively, at time t. Here, $S_4 + S_5 + S_6 + S_7 + \cdots = a$, so that eqn. (7) becomes equal to eqn. (5). Integration of eqn. (8), inserting eqn. (6) and putting $S_4 = a$ at $t = 0$ gives:

$$S_4 = a \exp(-x/a) \qquad (12)$$

where $x = b - S_2$ is the amount of thiosulphate reacted in moles per liter at time t. Successive integrations of eqns. (9), (10) and (11), with conditions $S_5 = S_6 = S_7 = 0$ at $t = 0$, lead to:

$$S_5 = S_4\frac{x}{a};\ S_6 = S_4\frac{x^2}{2a^2};\ S_7 = S_4\frac{x^3}{6a^3}$$

where S_4 is given by eqn. (12). The general form of the expressions can be seen to be:

$$S_{4+n} = S_4\frac{x^n}{n!a^n}$$

and the sum of polythionate concentrations becomes:

$$S_4[1+\frac{x}{a}+\frac{x^2}{2a^2}+\frac{x^3}{6a^3}+\frac{x^n}{n!a^n}+\cdots]$$

The series in the bracket is the expansion of $\exp(x/a)$ so that the sum, by eqn. (12), is equal to a as should be.

Thus at any time t, the ratios of the concentrations of successively higher polythionates to that of tetrathionate are as the successively higher terms in the above series expansion of $\exp(x/a)$. The reactions were in some cases followed up to about $x/a = 0.2$ but not longer, since then often liberation of sulphur set in, probably as a result of thiosulphate-catalyzed decompositions of pentathionate and higher polythionates. At such a stage:

$$S_4 : S_5 : S_6 : S_7 = 1 : 0.2 : 0.02 : 0.0013$$

That is, the pentathionate reacting in the second step (3) amounts to 20 % of the tetrathionate present, the hexathionate reacting in the third step (4) to 2 % while the amount of heptathionate present is negligible. The kinetics followed eqn. (6) within the accuracy of the iodometric titrations up to this value of x/a. Unless reactions or effects not considered here influence the picture, the amount of pentathionate then present should be large enough to show that k_3 can not differ much from k_2.

Experiments on the reaction of potassium trithionate with sodium thiosulphate, eqn. (1), in presence of formaldehyde under the same conditions as employed for tetrathionate, indicate that, at 25°C and an ionic strength of 1.15, the bimolecular rate constant $k_1 = 1.1 \times 10^{-4}$ l·mole^{-1}sec^{-1}. Thus, the first step in the reaction sequence (1)—(4) is markedly slower than the subsequent ones. This confirms the findings of Fava and Pajaro [8]: $k_1 = 6.2 \times 10^{-4}$ l·mole^{-1}sec^{-1} at 51°C and $\mu = 0.816$ from the rate of isotopic exchange of trithionate with thiosulphate, and Fava and Bresadola [9]: $k_2 = 3.9 \times 10^{-3}$ l.mole^{-1}sec^{-1} at 50°C and $\mu = 0.94$ from the rate of thiosulphate-catalyzed rearrangement of tetrathionate.

The work has been aided by a grant from *Norges Almenvitenskapelige Forskningsråd.*

1. Gmelin's *Handbuch der anorganischen Chemie*, Vol. **9 B 2**, Verlag Chemie, Weinheim/Bergstrasse, 1960, pp. 974—975, 914—917.
2. Foss, O. *Kgl. Norske Videnskab. Selskabs Forh.* **16** (1943) 72; *Skrifter* **1945** No. 2.
3. Christiansen, J. A. and Drost-Hansen, W. *Nature* **164** (1949) 759.
4. Foss, O. *Acta Chem. Scand.* **4** (1950) 866.
5. Foss, O. *Acta Chem. Scand.* **12** (1958) 959.
6. Kurtenacker, A. *Analytische Chemie der Sauerstoffsäuren des Schwefels*, F. Enke, Stuttgart 1938.
7. Skarżyński, B. and Szczepkowski, T. W. *Nature* **183** (1959) 1413.
8. Fava, A. and Pajaro, G. *J. chim. phys.* **51** (1954) 594.
9. Fava, A. and Bresadola, S. *J. Am. Chem. Soc.* **77** (1955) 5792.

Received September 20, 1961.

Thiosulphate Catalysis on Rearrangements of Higher Polythionates

OLAV FOSS

Chemical Institute, University of Bergen, Bergen, Norway

The rearrangement of tetrathionate ion into pentathionate and trithionate:

$$2\ S_4O_6^{--} = S_5O_6^{--} + S_3O_6^{--} \quad (1)$$

is strongly catalyzed by thiosulphate ion [1]. The catalysis is due to nucleophilic displacements [2,3], of sulphite group of tetrathionate by thiosulphate:

$$S_4O_6^{--} + S_2O_3^{--} = S_5O_6^{--} + SO_3^{--} \quad (2)$$

and of thiosulphate group by sulphite:

$$S_4O_6^{--} + SO_3^{--} = S_3O_6^{--} + S_2O_3^{--} \quad (3)$$

It is the purpose of the present note to point out that thiosulphate ion should catalyze the rearrangement into a higher and a lower polythionate, not only of tetrathionate but also of pentathionate and higher polythionates:

$$2\ S_5O_6^{--} = S_6O_6^{--} + S_4O_6^{--} \quad (4)$$

$$2\ S_6O_6^{--} = S_7O_6^{--} + S_5O_6^{--} \quad (5)$$

and so forth, through the same two-step nucleophilic displacement mechanism as in the case of tetrathionate. As shown in a previous note [4], the displacement which would initiate such catalytic rearrangement, *i.e.*, the displacement of a sulphite group of pentathionate and higher polythionates by thiosulphate:

$$S_nO_6^{--} + S_2O_3^{--} = S_{n+1}O_6^{--} + SO_3^{--} \quad (6)$$

appears to take place with the same or approximately the same rate as for tetrathionate, and the subsequent displacement of a thiosulphate group of another polythionate ion by the sulphite released in the first step:

$$S_nO_6^{--} + SO_3^{--} = S_{n-1}O_6^{--} + S_2O_3^{--} \quad (7)$$

will occur rapidly [1].

Thiosulphate ion also catalyzes the change of pentathionate and higher polythionates into lower polythionate, and sulphur [1]. Perhaps therefore, the above thiosulphate catalysis on rearrangements which should simultaneously occur, has not been directly observed. However, apparently pure pentathionate has occasionally been found to rearrange into hexa- and tetrathionate [5], perhaps because of minute amounts of impurities like thiosulphate, and the formation in a mixture of tetrathionate and thiosulphate, not only of trithionate and pentathionate but also of hexathionate and probably heptathionate, has been demonstrated by Skarżyński and Szczepkowski [6].

The thiosulphate-catalyzed decomposition of pentathionate and higher polythionates into lower polythionates and sulphur [1] may be due to the displacement, in the case of pentathionate [7-9]:

$$S_5O_6^{--} + S_2O_3^{--} = S_4O_6^{--} + S{-}S_2O_3^{--} \quad (8)$$

This is then followed by a building-up of dithio- and polythio-thiosulphate ions $S_x{-}S_2O_3^{--}$ from the thio-thiosulphate ion released in the first step, through a series of consecutive nucleophilic displacements of thiosulphate by thio-thiosulphate:

$$S{-}S_2O_3^{--} + S{-}S_2O_3^{--} = S_2{-}S_2O_3^{--} + S_2O_3^{--} \quad (9)$$

$$S_2{-}S_2O_3^{--} + S{-}S_2O_3^{--} = S_3{-}S_2O_3^{--} + S_2O_3^{--} \quad (10)$$

and so forth, with ultimate ring closure to S_8:

$$S_8{-}S_2O_3^{--} = S_8 + S_2O_3^{--} \quad (11)$$

This building-up process is of the same type as proposed by Davis [10] for the decomposition of acidified thiosulphate (there displacement of sulphite or hydrogensulphite by thiosulphate). The acids corresponding to the species $S_x{-}S_2O_3^{--}$, the so-called sulphanemonosulphonic acids $HS{-}S_x{-}SO_3H$, have been prepared and studied by Schmidt [11]; they decompose into sulphur in presence of basic substances, probably due to a reaction sequence analogous to the above, *i.e.*, nucleophilic attack of the terminal divalent sulphur atom of an ion $S_x{-}S_2O_3^{--}$ on a divalent sulphur atom of another, not necessarily ionized species.

The point is that a thiosulphate-catalyzed rearrangement of pentathionate into tetrathionate and hexathionate may occur also as a result of an initial displacement (8) followed by:

$$S_5O_6^{--} + S{-}S_2O_3^{--} = S_6O_6^{--} + S_2O_3^{--} \quad (12)$$

and correspondingly for rearrangements of still higher polythionates. In fact, any species $S_x{-}S_2O_3^{--}$, occurring in the sequence (8)–(11) or released directly from a polythionate, should be expected to attack a polythionate chain to give another polythionate, preferably a higher one since thiosulphate probably is the better leaving group relative to a thio-, dithio- or poly-

thio-thiosulphate group. The $S_x-S_2O_3^{--}$ ions are probably stronger nucleophiles than thiosulphate ion, in accordance with the lower strength of the corresponding —SH acids the longer the distance from the sulphonate group.

The above interactions of thiosulphate and polythionate ions, leading to rearrangements or decompositions, involve the displacement of a sulphite group of tetrathionate or higher polythionate by thiosulphate, eqns. (2) and (6); of a thiothiosulphate group of pentathionate or higher polythionate, eqn. (8); of a dithiothiosulphate group of hexathionate or higher polythionate. The various modes of heterolysis of the sulphur-sulphur bonds of the tetra-, penta- and hexathionate ions in reactions with nucleophilic reagents have been discussed [9]; the preferred, more rapid displacement appears to be that of thiosulphate, as for example in the second step of the rearrangements, eqns. (3), (7) and (12) above.

1. Gmelin's *Handbuch der anorganischen Chemie*, Vol. **9 B 2**, Verlag Chemie, Weinheim/Bergstrasse, 1960, pp. 915—917, 1001—1028.
2. Foss, O. *Acta Chem. Scand.* **4** (1950) 866.
3. Fava, A. and Bresadola, S. *J. Am. Chem. Soc.* **77** (1955) 5792.
4. Foss, O. and Kringlebotn, I. *Acta Chem. Scand.* **15** (1961) 1608.
5. Fehér, F. *Private communication* (1959).
6. Skarżyński, B. and Szczepkowski, T. W. *Nature* **183** (1959) 1413.
7. Foss, O. *Acta Chem. Scand.* **3** (1949) 1385.
8. Fava, A. *Gazz. chim. ital.* **83** (1953) 87.
9. Foss, O. *Acta Chem. Scand.* **12** (1958) 959.
10. Davis, R. E. *J. Am. Chem. Soc.* **80** (1958) 3565.
11. Schmidt, M. *Z. anorg. u. allgem. Chem.* **289** (1957) 158.

Received September 20, 1961.

On the Oxidation of Diselenides and Related Compounds

GÖRAN BERGSON

Chemical Institute, University of Uppsala, Sweden

As a result of a number of recent investigations [1] it has been shown that disulphides are oxidized to thiolsulphinates (R—SO—S—R) under mild conditions. In addition, Calvin and his co-workers [2] have found that *α*-lipoic acid (I) is oxidized to the corresponding thiolsulphinate (II) by ammonium persulphate under conditions in which non-cyclic disulphides are not attacked; this demonstrates the increased reactivity associated with the 1,2-dithiolane ring. Further oxidation of the thiolsulphinates generally gives thiolsulphonates ($R-SO_2-S-R$), although it has been supposed that this reaction occurs *via* fission of the sulphur-sulphur bond [3].

It has been reported that diselenides are oxidized directly to seleninic acids ($R-SeO_2H$), and although several attempts to detect lower oxidation products have been made, none have ever been found [4]. The instantaneous conversion of diselenides to seleninic acids by reaction with bromine in aqueous solution has been clearly demonstrated by Fredga [5] using polarimetric methods.

In a comparative study of the properties and reactions of simple molecules containing the S—S, Se—S, or Se—Se bonds, the

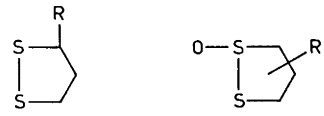

I II

R=$-(CH_2)_4-COOH$

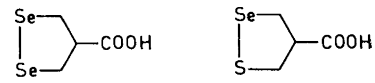

III IV

thio-thiosulphate group. The $S_x-S_2O_3^{--}$ ions are probably stronger nucleophiles than thiosulphate ion, in accordance with the lower strength of the corresponding —SH acids the longer the distance from the sulphonate group.

The above interactions of thiosulphate and polythionate ions, leading to rearrangements or decompositions, involve the displacement of a sulphite group of tetrathionate or higher polythionate by thiosulphate, eqns. (2) and (6); of a thiothiosulphate group of pentathionate or higher polythionate, eqn. (8); of a dithiothiosulphate group of hexathionate or higher polythionate. The various modes of heterolysis of the sulphur-sulphur bonds of the tetra-, penta- and hexathionate ions in reactions with nucleophilic reagents have been discussed [9]; the preferred, more rapid displacement appears to be that of thiosulphate, as for example in the second step of the rearrangements, eqns. (3), (7) and (12) above.

1. Gmelin's *Handbuch der anorganischen Chemie*, Vol. **9 B 2**, Verlag Chemie, Weinheim/Bergstrasse, 1960, pp. 915—917, 1001—1028.
2. Foss, O. *Acta Chem. Scand.* **4** (1950) 866.
3. Fava, A. and Bresadola, S. *J. Am. Chem. Soc.* **77** (1955) 5792.
4. Foss, O. and Kringlebotn, I. *Acta Chem. Scand.* **15** (1961) 1608.
5. Fehér, F. *Private communication* (1959).
6. Skarżyński, B. and Szczepkowski, T. W. *Nature* **183** (1959) 1413.
7. Foss, O. *Acta Chem. Scand.* **3** (1949) 1385.
8. Fava, A. *Gazz. chim. ital.* **83** (1953) 87.
9. Foss, O. *Acta Chem. Scand.* **12** (1958) 959.
10. Davis, R. E. *J. Am. Chem. Soc.* **80** (1958) 3565.
11. Schmidt, M. *Z. anorg. u. allgem. Chem.* **289** (1957) 158.

Received September 20, 1961.

On the Oxidation of Diselenides and Related Compounds

GÖRAN BERGSON

Chemical Institute, University of Uppsala, Sweden

As a result of a number of recent investigations [1] it has been shown that disulphides are oxidized to thiolsulphinates (R—SO—S—R) under mild conditions. In addition, Calvin and his co-workers [2] have found that *α*-lipoic acid (I) is oxidized to the corresponding thiolsulphinate (II) by ammonium persulphate under conditions in which non-cyclic disulphides are not attacked; this demonstrates the increased reactivity associated with the 1,2-dithiolane ring. Further oxidation of the thiolsulphinates generally gives thiolsulphonates ($R-SO_2-S-R$), although it has been supposed that this reaction occurs *via* fission of the sulphur-sulphur bond [3].

It has been reported that diselenides are oxidized directly to seleninic acids ($R-SeO_2H$), and although several attempts to detect lower oxidation products have been made, none have ever been found [4]. The instantaneous conversion of diselenides to seleninic acids by reaction with bromine in aqueous solution has been clearly demonstrated by Fredga [5] using polarimetric methods.

In a comparative study of the properties and reactions of simple molecules containing the S—S, Se—S, or Se—Se bonds, the

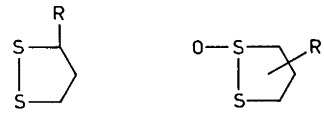

I II

R=$-(CH_2)_4-COOH$

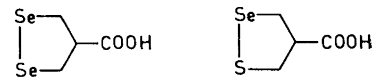

III IV

present author has made some observations which suggest the existence of lower oxidation products of diselenides and thiolselenenates (R—Se—S—R). The oxidation conditions were analogous to those used by Calvin [2], *i.e.* ammonium persulphate in aqueous ethanol was employed. The molar ratio between ammonium persulphate and diselenide or thiolselenenate was 1:1. The compounds studied were 1,2-diselenolane-4-carboxylic acid (III) and 1-thia-2-selena-cyclopentane-4-carboxylic acid (IV).

Figs. 1—3 show the course of oxidation for the compounds I, III, and IV as followed by spectrophotometric techniques. Fig. 1 confirms Calvin's results and demonstrated that after 24 h, the characteristic 1,2-dithiolane peak at 330 mμ has completely disappeared. A peak at 246 mμ due to the thiolsulphinate is then observed. The first noticeable feature in the oxidation of the diselenide (Fig. 2) is the greater speed of this reaction as compared with that for the disulphide. The most remarkable fact is, however, that the optical density of the peak at 440 mμ (characteristic of the 1,2-diselenolane ring) reaches a minimum after about 16 min. The 1,2-diselenolane peak subsequently increases again and finally attains a height approximately two-thirds of the original value. This final height corresponds to the oxidation to seleninic acid, since three oxidation equivalents are required for the oxidation of a diselenide to the corresponding seleninic acid. The pattern of the reaction as outlined above is best explained in terms of the initial formation of a product in a lower oxidation state. This product then undergoes disproportionation to seleninic acid and diselenide. Attempts to isolate the initial oxidation product have failed, presumably owing to its instability. It seems natural to suppose, however, that the reaction proceeds *via* a selenolseleninate (V) as shown in the following scheme:

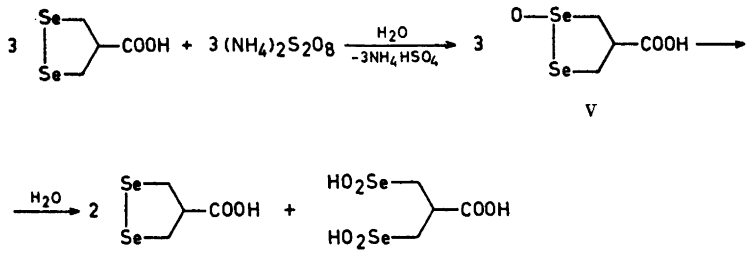

It is unlikely that the first step would result in fission of the Se—Se bond since a seleninic acid and a selenol would then be

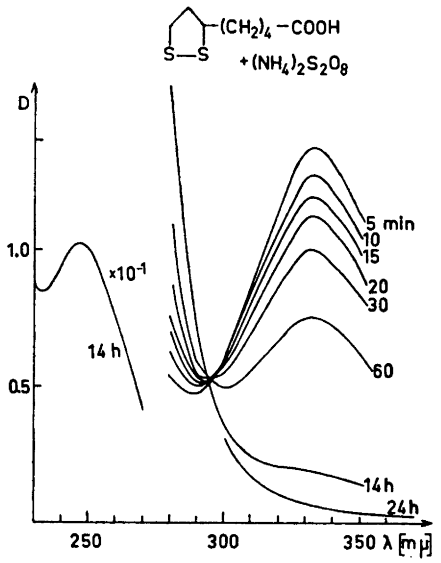

Fig. 1. Oxidation of α-lipoic acid with ammonium persulphate. Initial concentrations of both reactants: 0.01 M. Solvent: 5 parts ethanol and 1 part water. Temperature: 25.0°.

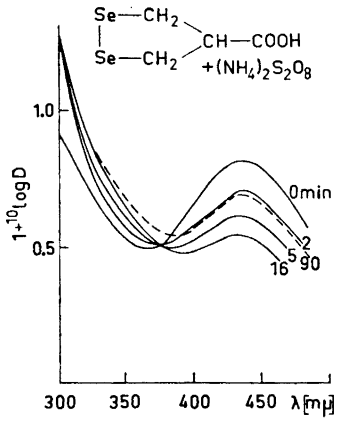

Fig. 2. Oxidation of 1,2-diselenolane-4-carboxylic acid with ammonium persulphate. Initial concentrations of both reactants: 0.005 M. Solvent as in Fig. 1. Temperature: 25.0°.

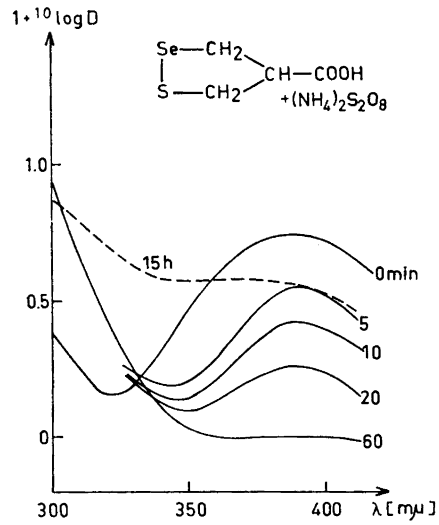

Fig. 3. Oxidation of 1-thia-2-selena-cyclopentane-4-carboxylic acid by ammonium persulphate. Initial concentrations of both reactants: 0.005 M. Solvent as in Fig. 1. Temperature: 25.0°C.

formed, and these products would at once react to form a diselenide.

Fig. 3 shows that the oxidations of the diselenide and the thiolselenenate (IV) follow closely similar paths. The speed of the thiolselenenate oxidation is not as great as that of the diselenide oxidation, but it is much greater than the oxidation of the disulphide. It is probable that in this instance the thiolseleninate is the primary oxidation product.

An investigation of the kinetics of the primary oxidation is in progress, together with a study of non-cyclic diselenides and thiolselenenates.

Experimental. DL-*α-Lipoic acid.* The sample used was synthesized by Hoffmann-La Roche & Co. Ltd, Basle (Switzerland). *1,2-Diselenolane-4-carboxylic acid* was prepared from *β,β'*-dibromo-isobutyric acid and sodium diselenide [6]; m.p. 148.5—149.5°. The synthesis of *1-Thia-2-selena-cyclopentane-4-carboxylic acid* has been described by Bergson and Biezais [7]; m.p. 105.5—107.5°.

The optical measurements were made with a Beckman Model DU (220—400 mμ) and a Beckman Model B (400—550 mμ) spectrophotometer.

1. Stoll, A. *Helv. Chim. Acta* **31** (1948) 189; Small, D., Bailey, J. H. and Cavallito, C. J. *J. Am. Chem. Soc.* **69** (1947) 1710; Bretschneider, H. and Klötzer, W. *Monatsh.* **81** (1950) 589; Backer, H. J. and Kloosterziel, H. *Rec. trav. chim.* **73** (1954) 129.
2. Barltrop, J. A., Hayes, P. M. and Calvin, M. *J. Am. Chem. Soc.* **76** (1954) 4348; Calvin, M. *Federation Proc.* **13** (1954) 697.
3. Barnard, D. and Percy, E. J. *Chem. & Ind. London* **1960** 1332.
4. Small *et al.* Ref. 1; Fromm, E. and Martin, K. *Ann.* **401** (1913) 184.
5. Fredga, A. *Uppsala Universitets Årsskrift* **1935:5** 134.
6. Bergson, G. *To be published.*
7. Bergson, G. and Biezais, A. *Arkiv Kemi* **18** (1961) 143.

Received October 5, 1961.

IPT — a New Extracting Agent for Metal Ions

DAVID DYRSSEN

Department of Inorganic Chemistry, Royal Institute of Technology, Stockholm 70, Sweden

An extensive investigation of the β-isopropyl derivative of tropolone (IPT) as a reagent for the extraction of metal ions has been carried out at our institute in cooperation with the Research Institute of National Defence and with the support of the Swedish Council for Atomic Research.

The distribution of 27 metal ions between chloroform and 0.1 M perchlorate solutions has been studied at 25°C as a function of the concentration of IPT in the chloroform phase and the hydrogen ion concentration in the aqueous phase. With an IPT concentration of 0.1 M the following metals are extracted below pH 1: Sc(III), Fe(III), Cu(II), In(III), Th(IV), U(VI) and probably Al(III) and Ga(III). Between pH 2 and 6 the following ions are extracted: Co(II), Ni(II), Zn(II), Cd(II), Y(III), the lanthanide ions and Am(III). Above pH 7 it is possible to extract Ca, Sr, Ba and some Ag. For these elements as probably also for Ni, Zn, Cd, U(VI) and large trivalent ions the extraction might be improved by the addition of TBP, quinoline or some more basic compound (*e.g.* laurylamine) to the chloroform.

IPT has a considerably larger distribution constant (K_d = 2 340 for chloroform/water) than TTA (K_d = 37 for benzene/water). IPT does not seem to undergo any such tautomeric or hydration equilibria as TTA. Furthermore, TTA decomposes rapidly in alkaline solutions while IPT does not. In addition the value of $pK_a + \log K_d$ for the IPT-chloroform system (10.41) is considerably larger than for the TTA-benzene system (7.80). An IPT-chloroform solution can therefore be used over a wider pH-range, *e.g.* for the extraction of alkaline earth metals. With some exceptions (*e.g.* Cu(II), Cd(II), U(VI), Fe(III) and In(III)) the pH values for 50 % extraction (equal phase volumes) are quite comparable for IPT and TTA as may be seen from Table 1.

The solubilities of the extractable metal chelates are often low (10^{-3} to 10^{-4} M) and this restricts the use of IPT for the extraction of large quantities of metals. In some cases (*e.g.* Cu(II), Fe(III) and U(VI)) the extinction coefficient of the extractable IPT complex is very high at 400—450 mμ where IPT itself does not absorb light.

Table 1. Values of $\log [HA]_{org} [H^+]^{-1}$ for 50 % extraction.

Element	HA = IPT org = $CHCl_3$ $[HA]_{org}$ = 0.1 M	HA = TTA[a] org = C_6H_6 $[HA]_{org}$ = 0.2 M
Ag(I)	8.71	—
Ca(II)	7.19	6.0
Sr(II)	7.58	7.1
Ba(II)	8.47	7.3
Co(II)	3.84	3.4
Ni(II)	3.86	>4.3
Cu(II)	—0.80	0.68
Zn(II)	3.13	—
Cd(II)	4.05	>7.3
U(VI)	—1.11	1.27
Sc(III)	—0.35	0.29
Fe(III)	—3.33	—0.94
Y(III)	2.46	2.50
In(III)	—1.34	1.48
La(III)	3.44	3.54
Pr(III)	2.83	2.98
Sm(III)	2.52	2.59
Eu(III)	2.41	2.59
Tb(III)	2.28	2.54
Ho(III)	2.08	2.45
Tm(III)	2.04	2.35
Yb(III)	1.96	2.27
Lu(III)	1.76	2.29
Am(III)	2.41	2.52
Th(IV)	—0.84	—0.2

[a] Values taken from a summary by Poskanzer, A. M. and Foreman, B. M., Jr. in *J. Inorg. & Nuclear Chem.* **16** (1961) 323.

IPT will probably always be a high-priced chemical. However, cedar wood or thuja may contain as much as 4 % and it is not very difficult to isolate the compound from the powdered heartwood or roots. It is possible that some other derivative of tropolone (*e.g.* nootkatin) will have still more favorable properties as an extracting agent for metal ions.

The full report of our work, which includes experimental details, distribution data, extraction curves, equilibrium constants and composition of the extractable complexes, will be published in the *Transactions of the Royal Institute of Technology*.

Received September 25, 1961.

Complexes of Divalent Tellurium with Thiourea

OLAV FOSS and SVERRE HAUGE

Chemical Institute, University of Bergen, Bergen, Norway

Square planar complexes of divalent tellurium with thiourea have been studied in this laboratory since 1959 [1]. Of the type $Te(tu)_2X_2$ where tu = thiourea, they include those with X = chloride [1], bromide [1], iodide, thiocyanate [1], and methanethiosulphonate [2]. Crystal structure determinations of the chloride [3], bromide [4] and methanethiosulphonate [5] have been carried out, and a Fourier analysis of one zone of the thiocyanate [6]. The crystals of the three halides are isomorphous; of the two possible isomers, *cis* and *trans*, of a square planar complex of this type, they represent the *cis* isomer, as does also the thiocyanate, while the methanethiosulphonate is *trans*. Of the same type and also *trans*, are two salts [7], the chloride and bromide, of a divalent tellurium cation with two thiourea and two tetramethylthiourea ligands; the two salts are isomorphous and crystallize in the space group C_{2h}^5–$P2_1/c$ with two molecules per unit cell so that the cations are centrosymmetric.

Vřeštál [8] has independently prepared the chloride and bromide, $Te(tu)_2Cl_2$ and $Te(tu)_2Br_2$, and Němec [9] has determined the unit cells and space group. Their results agree with ours [1].* The purpose of this note is to describe the iodide, and to give preparative and analytical data for the thiocyanate [1]. Salts of the cation $Te(tu)_4^{2+}$ form the subject of a following note [10].

Diiodo-dithiourea-tellurium(II), $Te(tu)_2I_2$, crystallizes from aqueous thiourea solutions of a tetrathiourea-tellurium(II) salt such as the chloride or bromide (or of $Te(tu)_2Cl_2$ or $Te(tu)_2Br_2$ which dissolve in aqueous thiourea to give these salts) and potassium iodide: 6 g of $Te(tu)_2Br_2$ was dissolved in 200 ml of 10 % aqueous thiourea at 35°, traces of tellurium were filtered off, and 10 g of potassium iodide in 50 ml of water was added. After 24 h at room temperature the brownish red crystals of $Te(tu)_2I_2$ were filtered off, and washed with ethanol containing a little thiourea, and then with ether. Yield, 4.9 g (67 %). (Found: S 10.53; Te 25.28. Calc. for $C_2H_8I_2N_4S_2Te$: S 12.02; Te 23.91.) The analytical results indicate that the samples were not quite pure, or that there is a little less than two thiourea units in the molecule. The samples on microscopic inspection appeared homogeneous, and the crystals were found to be isomorphous with those of the chloride and bromide, for which the analytical data are quite satisfactory.

The crystals occur as prisms extended along the *b* axis, or as plates {100}. The unit cell dimensions are listed below, together with, for comparison, those of the chloride and bromide [1].

	a	*b*	*c*	*β*
$Te(tu)_2Cl_2$	9.90 Å	7.62 Å	14.10 Å	100 ½°
$Te(tu)_2Br_2$	10.10	7.74	14.67	100°
$Te(tu)_2I_2$	10.24	7.93	15.59	100°

The space group is C_{2h}^6–$I2/c$, and there are four molecules per unit cell; the tellurium atoms lie on twofold axes of symmetry.

Dithiocyanato-dithiourea-tellurium(II), $Te(tu)_2(SCN)_2$, was prepared from the chloride or bromide, and ammonium thiocyanate: To a solution of 165 g of ammonium thiocyanate in 150 ml of water, at 70–80°, was added 5 g of $Te(tu)_2Br_2$ under stirring. A red solution resulted which deposited a little tellurium; after filtering, the solution was placed in a refrigerator over night. The crystals were then filtered off, and washed with ethanol containing a little concentrated hydrochloric acid, and then with ether. Yield, 2.7 g (60 %). (Found: S 32.18; Te 32.19. Calc. for $C_4H_8N_6S_4Te$: S 32.29; Te 32.22.) Similar results were obtained by use of the chloride instead of the bromide. Unit cell and space group data have been reported earlier [1]. As mentioned [1], the compound was obtained as prisms when prepared from the chloride and as plates from the bromide. The plates rapidly grew into prisms when brought in contact with aqueons or dilute ethanolic hydrochloric acid.

* Minor divergencies are: Vřeštál [8] gives m.p. 184° (decomp.) for the chloride, $Te(tu)_2Cl_2$; we found 220° (decomp.). Vřeštál [8] obtained two forms of the bromide, $Te(tu)_2Br_2$, which gave "practically identical" X-ray powder photographs: Plates (from dilute solutions) with m. p. 170° (decomp.) and density 2.57 g/cm³, and short prisms (from more concentrated solutions) with m. p. 220° (decomp.) and density 2.47 g/cm³; we found m. p. 220° (decomp.) and density 2.58 g/cm³ (X-ray density calc. 2.59 g/cm³). We have not been able to identify more than one crystalline form of any $Te(tu)_2X_2$ complex.

The TeS_2Cl_2 and TeS_2Br_2 groups in $Te(tu)_2Cl_2$ and $Te(tu)_2Br_2$ have, according to two-dimensional crystal structure analyses, the dimensions: Te—S = 2.48 Å, Te—Cl = 2.92 Å, ∠S—Te—S = 93°, ∠ Cl—Te—Cl = 93° in the chloride [3]; Te—S = 2.47 Å, Te—Br = 3.05 Å, ∠S—Te—S = 95°, ∠Br—Te—Br = 93° in the bromide[4]. The groups are almost but not exactly planar, the Te—Cl bonds being rotated 8° and the Te—Br bonds 9° out of the S—Te—S plane, to opposite sides of the plane in accordance with the twofold axis of molecular symmetry.

1. Foss, O. and Hauge, S. *Acta Chem. Scand.* **13** (1959) 1252.
2. Foss, O. and Johannessen, I.-J. *To be published.*
3. Foss, O., Johnsen, K. and Marøy, K. *To be published.*
4. Foss, O. and Maartmann-Moe, K. *To be published.*
5. Foss, O. and Marøy, K. *To be published.*
6. Marøy, K. *To be published.*
7. Foss, O. and Johannessen, W. *To be published.*
8. Vřešťál, J. *Collection Czechoslov. Chem. Communs.* **25** (1960) 443.
9. Němec, D. *Práce Brněnské základny Československ. akad. věd* **30** (1958) 27.
10. Foss, O. and Hauge, S. *Acta Chem. Scand.* **15** (1961) 1616.

Received October 8, 1961.

Tetrathiourea-tellurium(II) Salts

OLAV FOSS and SVERRE HAUGE

Chemical Institute, University of Bergen, Bergen, Norway

The salts $Te(tu)_4Cl_2 \cdot 2H_2O$ and $Te(tu)_2Br_4$ (tu = thiourea) were described and unit cell and space group data reported in 1959 [1]. The chloride dihydrate crystallizes in the space group $C_{2h}^5 - P2_1/c$ with two formula units per unit cell, which shows that the tellurium atom lies in a centre of symmetry and the TeS_4 group of the complex is thus planar. A two-dimensional structure analysis has subsequently been carried out [2]; the Te—S bonds are 2.69 Å and the S—Te—S angles 90°.

Some other salts have later been prepared and characterized, namely an anhydrous chloride, a thiocyanate, nitrate and perchlorate. Vřešťál [3] has independently prepared several tetrathiourea-tellurium(II) salts, and Němec [4] has studied the morphology and unit cells of the chloride dihydrate and perchlorate. Our results are reported below to the extent that they do not duplicate Vřešťál's and Němec's data.

Unit cell dimensions were derived from oscillation and Weissenberg photographs, using Cu$K\alpha$ radiation, λ = 1.542 Å. Axial lengths are believed to be accurate to within 0.5 %. Densities were determined by flotation in carbon tetrachloride-bromoform mixtures.

The salts are yellow, and stable in the solid state, but become black in contact with water, due to hydrolysis and subsequent dismutation into zero- and tetravalent tellurium. They hydrolyze slightly in contact with 96 % ethanol, and were on the preparative filters in most cases washed with 96 % ethanol containing a little thiourea or concentrated hydrochloric acid, and then with ether. Solutions in aqueous or ethanolic thiourea are fairly stable. The salts dissolve readily in dimethylformamide, to give orange-yellow to orange solutions, apparently stable at room temperature.

Tetrathiourea-tellurium(II) dichloride dihydrate, $Te(tu)_4Cl_2 \cdot 2H_2O$. As reported [1], and confirmed through structure analysis [2], this salt is monoclinic. Němec [4], from morphological study and rotation photographs about three axes, described it as triclinic, obviously because his a and b axes, the rotation photographs about which [4] "are quite identical, referring not only to the length of axes, but also to the distribution of diffraction spots and their intensities", were not recognized as bc diagonals in space group $P2_1/c$.

The salt can be prepared by mixing, at about 80°, a solution of 2.4 g (15 mmoles) of tellurium dioxide in 10 ml of concentrated hydrochloric acid and 10 ml of water, and a solution of 7.5 g (99 mmoles, 10 % excess) of thiourea in 50 ml of water. The mixture is allowed to cool to about 30° and the crystals then filtered off. Yield, 7.9 g (98 %). The mother liquor on further cooling deposits crystals of formamidinium disulphide dichloride. Vřešťál [3] used more dilute solutions. The salt was also prepared as follows: 5.6 g of $Te(tu)_2Cl_2$ was dissolved, under stirring and warming to 40—50°, in a solution of 24 g of thiourea in 160 ml of 48 % ethanol. Some undissolved matter and a little tellurium was filtered off, and the filtrate allowed to stand at room temperature over night. Yield, 5.5 g (64 %). Analytical data for this salt, and for the

The TeS_2Cl_2 and TeS_2Br_2 groups in $Te(tu)_2Cl_2$ and $Te(tu)_2Br_2$ have, according to two-dimensional crystal structure analyses, the dimensions: Te—S = 2.48 Å, Te—Cl = 2.92 Å, ∠S—Te—S = 93°, ∠ Cl—Te—Cl = 93° in the chloride [3]; Te—S = 2.47 Å, Te—Br = 3.05 Å, ∠S—Te—S = 95°, ∠Br—Te—Br = 93° in the bromide[4]. The groups are almost but not exactly planar, the Te—Cl bonds being rotated 8° and the Te—Br bonds 9° out of the S—Te—S plane, to opposite sides of the plane in accordance with the twofold axis of molecular symmetry.

1. Foss, O. and Hauge, S. *Acta Chem. Scand.* **13** (1959) 1252.
2. Foss, O. and Johannessen, I.-J. *To be published.*
3. Foss, O., Johnsen, K. and Marøy, K. *To be published.*
4. Foss, O. and Maartmann-Moe, K. *To be published.*
5. Foss, O. and Marøy, K. *To be published.*
6. Marøy, K. *To be published.*
7. Foss, O. and Johannessen, W. *To be published.*
8. Vřešťál, J. *Collection Czechoslov. Chem. Communs.* **25** (1960) 443.
9. Němec, D. *Práce Brněnské základny Československ. akad. věd* **30** (1958) 27.
10. Foss, O. and Hauge, S. *Acta Chem. Scand.* **15** (1961) 1616.

Received October 8, 1961.

Tetrathiourea-tellurium(II) Salts

OLAV FOSS and SVERRE HAUGE

Chemical Institute, University of Bergen, Bergen, Norway

The salts $Te(tu)_4Cl_2 \cdot 2H_2O$ and $Te(tu)_2Br_4$ (tu = thiourea) were described and unit cell and space group data reported in 1959 [1]. The chloride dihydrate crystallizes in the space group $C_{2h}^5 - P2_1/c$ with two formula units per unit cell, which shows that the tellurium atom lies in a centre of symmetry and the TeS_4 group of the complex is thus planar. A two-dimensional structure analysis has subsequently been carried out [2]; the Te—S bonds are 2.69 Å and the S—Te—S angles 90°.

Some other salts have later been prepared and characterized, namely an anhydrous chloride, a thiocyanate, nitrate and perchlorate. Vřešťál [3] has independently prepared several tetrathiourea-tellurium(II) salts, and Němec [4] has studied the morphology and unit cells of the chloride dihydrate and perchlorate. Our results are reported below to the extent that they do not duplicate Vřešťál's and Němec's data.

Unit cell dimensions were derived from oscillation and Weissenberg photographs, using Cu$K\alpha$ radiation, λ = 1.542 Å. Axial lengths are believed to be accurate to within 0.5 %. Densities were determined by flotation in carbon tetrachloride-bromoform mixtures.

The salts are yellow, and stable in the solid state, but become black in contact with water, due to hydrolysis and subsequent dismutation into zero- and tetravalent tellurium. They hydrolyze slightly in contact with 96 % ethanol, and were on the preparative filters in most cases washed with 96 % ethanol containing a little thiourea or concentrated hydrochloric acid, and then with ether. Solutions in aqueous or ethanolic thiourea are fairly stable. The salts dissolve readily in dimethylformamide, to give orange-yellow to orange solutions, apparently stable at room temperature.

Tetrathiourea-tellurium(II) dichloride dihydrate, $Te(tu)_4Cl_2 \cdot 2H_2O$. As reported [1], and confirmed through structure analysis [2], this salt is monoclinic. Němec [4], from morphological study and rotation photographs about three axes, described it as triclinic, obviously because his a and b axes, the rotation photographs about which [4] "are quite identical, referring not only to the length of axes, but also to the distribution of diffraction spots and their intensities", were not recognized as bc diagonals in space group $P2_1/c$.

The salt can be prepared by mixing, at about 80°, a solution of 2.4 g (15 mmoles) of tellurium dioxide in 10 ml of concentrated hydrochloric acid and 10 ml of water, and a solution of 7.5 g (99 mmoles, 10 % excess) of thiourea in 50 ml of water. The mixture is allowed to cool to about 30° and the crystals then filtered off. Yield, 7.9 g (98 %). The mother liquor on further cooling deposits crystals of formamidinium disulphide dichloride. Vřešťál [3] used more dilute solutions. The salt was also prepared as follows: 5.6 g of $Te(tu)_2Cl_2$ was dissolved, under stirring and warming to 40—50°, in a solution of 24 g of thiourea in 160 ml of 48 % ethanol. Some undissolved matter and a little tellurium was filtered off, and the filtrate allowed to stand at room temperature over night. Yield, 5.5 g (64 %). Analytical data for this salt, and for the

anhydrous chloride and the perchlorate are given by Vřeštál [3].

Tetrathiourea-tellurium(II) dichloride, $Te(tu)_4Cl_2$. Well developed crystals were obtained from a saturated solution of $Te(tu)_2Cl_2$ in boiling anhydrous methanol containing an excess of thiourea, by slow cooling.

The salt occurs as thin, triclinic plates {001} extended along the *a* axis, with the shorter plate edge parallel to the *b* axis: $a = 5.83$ Å, $b = 7.77$ Å, $c = 10.86$ Å, $\alpha = 95\frac{1}{2}°$, $\beta = 90°$, $\gamma = 119\frac{1}{2}°$. There is one formula unit per unit cell; density, calc. 1.96, found [3] 1.97 g/cm³. From Fourier projections along the *a* and *b* axes [5], the tellurium atom lies in a centre of symmetry of the space group $C_i^1-P\bar{1}$.

Tetrathiourea-tellurium(II) dibromide, $Te(tu)_4Br_2$, is isomorphous with the anhydrous chloride, and shows the same morphology. The unit cell dimensions are: $a = 5.95$ Å, $b = 7.86$ Å, $c = 11.10$ Å, $\alpha = 95\frac{1}{2}°$, $\beta = 89\frac{1}{2}°$, $\gamma = 119\frac{1}{2}°$. With one formula unit per unit cell, the calculated density is 2.18; found [1] 2.21 g/cm³. The space group, from isomorphism with the chloride, is $C_i^1-P\bar{1}$. The incomplete unit cell data reported earlier [1] correspond to a different choice of *b* axis.

The salt was prepared by dissolving, under stirring and warming to 30—40, 11 g of $Te(tu)_2Br_2$ in 300 ml of 10 % aqueous thiourea. After filtering, and addition of 7 g of potassium bromide in 15 ml of water, the salt rapidly crystallized. Yield, 14 g (95 %). (Found: N 18.64; Te 21.59. Calc. for $C_4H_{16}Br_2N_8Te$: N 18.93; Te 21.56.)

Tetrathiourea-tellurium(II) dithiocyanate, $Te(tu)_4(SCN)_2$, was obtained from the dithiourea compound, and thiourea: 3 g of $Te(tu)_2(SCN)_2$ was dissolved in 75 ml of 10 % aqueous thiourea at about 40°, and the solution filtered and allowed to stand over night at room temperature. Yield, 3.4 g (72 %). The salt can also be prepared from aqueous thiourea solutions of tetrathiourea-tellurium(II) dichloride or dibromide, and ammonium or potassium thiocyanate. (Found: N 25.18; S 34.84; Te 22.92. Calc. for $C_6H_{16}N_{10}S_6Te$: N 25.55; S 35.09; Te 23.27.)

The crystals occur as well developed, monoclinic prisms {011} terminated by {100}, with $a = 7.68$ Å, $b = 14.08$ Å, $c = 9.72$ Å, $\beta = 105°$, and two formula units per unit cell; density, calc. 1.79, found 1.78 g/cm³. The space group, from systematic absences, is $C_{2h}^5-P2_1/c$, and the tellurium atoms thus lie in centres ofsymmetry.

Tetrathiourea-tellurium(II) nitrate, $Te(tu)_4(NO_3)_2$, crystallizes from aqueous thiourea solutions of the chloride or bromide, on addition of aqueous potassium nitrate or nitric acid. (Found: S 23.02; Te 22.80. Calc. for $C_4H_{16}N_{10}O_6S_4Te$: S 23.06; Te 22.95.) The salt forms monoclinic prisms extended along the *c* axis and bounded by {010} and, less dominantly, by {100}, with $a = 6.14$ Å, $b = 24.70$ Å, $c = 7.44$ Å, $\beta = 120°$. The space group, from systematic absences, is $C_{2h}^5-P2_1/c$ and there are two formula units per unit cell; density, calc. 1.89, found 1.88 g/cm³. Also in this salt, therefore, the cation is centrosymmetric.

The location of the tellurium atoms in centres of symmetry in this and the preceding salt is consistent with the intensity distributions, *hkl* reflections with $k + l$ even being in most cases markedly stronger than those with $k + l$ odd.

Vřeštál [3] obtained the nitrate as a dihydrate.

Tetrathiourea-tellurium(II) perchlorate, $Te(tu)_4(ClO_4)_2$. 2 g of the bromide, $Te(tu)_4Br_2$, was dissolved in 30 ml of 10 % aqueous thoiurea, some liberated tellurium filtered off, and 5 ml of 60 % perchloric acid added to the filtrate. Yield, after one night in a refrigerator, 1.7 g (80 %).

The salt occurs as triclinic prisms extended along the *c* axis, with $a = 15.35$ Å, $b = 11.97$ Å, $c = 6.01$ Å, $\alpha = 90°$, $\beta = 91°$, $\gamma = 108°$. There are two formula units per unit cell; density, calc. 2.00, found 2.01 g/cm³. Vřeštál [3] gives the density as 2.11 g/cm³. Němec's [4] X-ray data agree well with ours; his *b* axis corresponds to the short *ab* diagonal in the above setting.

The TeS_4 group of the $Te(tu)_4^{2+}$ ion is thus, from space group requirements of centrosymmetry, exactly planar in five of the above salts: Three salts (chloride dihydrate, thiocyanate and nitrate) crystallize in the monoclinic space group $C_{2h}^5-P2_1/c$ with two formula units per unit cell, and two (anhydrous chloride and bromide) in the triclinic space group $C_i^1-P\bar{1}$ with one formula unit per unit cell.

1. Foss, O. and Hauge, S. *Acta Chem. Scand.* **13** (1959) 1252.
2. Fosheim, K. and Foss, O. *To be published.*
3. Vřeštál, J. *Collection Czechoslov. Chem. Communs.* **25** (1960) 443.
4. Němec, D. *Práce Brněnské základny Československ. akad. věd* **30** (1958) 27.
5. Foss, O. and Solheimsnes, S. *Work in progress.*

Received October 8, 1961.

Complexes of Divalent Tellurium with Ethylenethiourea

OLAV FOSS and SIGVARD FOSSEN

Chemical Institute, University of Bergen, Bergen, Norway

Divalent tellurium forms square planar complexes with thiourea [1-3]. Of the two possible isomers, *cis* and *trans*, of type $Te(tu)_2X_2$ complexes where tu = thiourea, only one has been encountered in each case. *E.g.*, the crystals of the halides and the thiocyanate (X = Cl, Br, I, SCN) represent the *cis* isomer. In a study of similar complexes with ethylenethiourea (etu) we have not been able to isolate a chloride, $Te(etu)_2Cl_2$, but have obtained at least two forms of the bromide, $Te(etu)_2Br_2$, as well as an iodide and a thiocyanate; these are described below. In one of the bromides, isomorphous with the iodide, the tellurium atom lies in a centre of symmetry, and the arrangement of ligands around tellurium is thus planar *trans*. In the other one, tellurium is located on a twofold axis, and this form, or a possible third one, may be the *cis* isomer.

The ethylenethiourea complexes are stable in the solid state, but like the thiourea complexes, they hydrolyze and become black in contact with water. X-Ray data were obtained from oscillation and Weissenberg photographs; the values for axial lengths are based on $\lambda = 1.542$ Å for Cu*Ka* radiation and are believed to be accurate to within 0.5 %.

Dibromobis(ethylenethiourea)tellurium(II), $Te(etu)_2Br_2$. Two crystalline forms have been obtained pure, an orthorhombic and a monoclinic one. The former was best prepared from tellurium dioxide and ethylenethiourea in a molar ratio of 1 : 6 as follows: 1.6 g (10 mmoles) of tellurium dioxide was dissolved in 50 ml of 48–50 % hydrobromic acid and 150 ml of water, the solution was heated almost to boiling, and 6.1 g (60 mmoles) of ethylenethiourea in 60 ml of hot water was added rapidly under stirring. From the resulting, clear solution (filtered immediately after mixing, if necessary) crystallization sets in spontaneously or on scratching of the beaker walls, and may be hastened by occasional stirring; it should take place from hot solution since if the temperature falls below about 50° some tetrakis(ethylenethiourea)-tellurium(II) dibromide dihydrate [4] may crystallize and contaminate the product. Yield, 2.6–3.8 g (53–77 %) depending on the rate of crystallization and temperature when filtering. M.p. 186° (decomp.). (Found: S 13.27; Te 25.98. Calc. for $C_6H_{12}Br_2N_4S_2Te$: S 13.04; Te 25.95.)

The brownish-yellow, *orthorhombic* crystals occur as flat prisms extended along the *c* axis with {010} dominant. The axial lengths are, $a = 14.46$ Å, $b = 31.40$ Å, $c = 12.10$ Å, and the space group, from systematic absences, is $D_{2h}^{24} - Fddd$, which has 32-fold general positions. There are 16 molecules per unit cell; density, calc. 2.38, found 2.38 g/cm³. The intensity distribution: *hkl* reflections with $h+k+l = 2n+1$ or $4n$ in most cases markedly strongest, indicates that the tellurium atoms lie on twofold axes of symmetry.

The substance is practically insoluble in glacial acetic acid, but readily soluble in dimethylformamide to give red, stable solutions. When to a warm solution of the substance in dimethylformamide, preferably less concentrated than corresponding to saturation at room temperature, an about double volume of glacial acetic acid is added, the monoclinic form crystallizes; the orthorhombic one could not be recovered even on seeding.

The *monoclinic* crystals appear a little darker reddish-yellow in colour than the orthorhombic ones. M.p. 192° (decomp.). (Found: S 13.16; Te 26.02.) They occur as prisms or plates extended along the *b* axis, bounded by {100} and {001} with the latter dominant in most cases. The unit cell dimensions are, $a = 17.30$ Å, $b = 5.89$ Å, $c = 15.57$ Å, $\beta = 120°$, and there are four molecules per unit cell; density, calc. 2.38, found 2.38 g/cm³. Systematic absences, *hkl* when $h + k$ is odd, *h0l* when *h* is odd or *l* is odd. These, together with the intensity distribution, perhaps best observed on oscillation photographs about the *bc* diagonal: *hkl* reflections with $k + l$ even generally stronger than those with $k + l$ odd, indicate that the tellurium atoms lie in symmetry centres, positions (*c*) or (*d*) [5], of the space group $C_{2h}^6 - C2/c$.

This has been confirmed by structure analysis [6], through projections along the *b* axis and along the *ab* diagonal, the repeat distance along which is halved on account of the *C*-centering and thus is 9.14 Å. The dimensions of the planar *trans* TeS_2Br_2 group of the centrosymmetric molecule are: Te–S = 2.69 Å, Te–Br = 2.78 Å, and

Complexes of Divalent Tellurium with Ethylenethiourea

OLAV FOSS and SIGVARD FOSSEN

Chemical Institute, University of Bergen, Bergen, Norway

Divalent tellurium forms square planar complexes with thiourea [1-3]. Of the two possible isomers, *cis* and *trans*, of type $Te(tu)_2X_2$ complexes where tu = thiourea, only one has been encountered in each case. *E.g.*, the crystals of the halides and the thiocyanate (X = Cl, Br, I, SCN) represent the *cis* isomer. In a study of similar complexes with ethylenethiourea (etu) we have not been able to isolate a chloride, $Te(etu)_2Cl_2$, but have obtained at least two forms of the bromide, $Te(etu)_2Br_2$, as well as an iodide and a thiocyanate; these are described below. In one of the bromides, isomorphous with the iodide, the tellurium atom lies in a centre of symmetry, and the arrangement of ligands around tellurium is thus planar *trans*. In the other one, tellurium is located on a twofold axis, and this form, or a possible third one, may be the *cis* isomer.

The ethylenethiourea complexes are stable in the solid state, but like the thiourea complexes, they hydrolyze and become black in contact with water. X-Ray data were obtained from oscillation and Weissenberg photographs; the values for axial lengths are based on $\lambda = 1.542$ Å for Cu*Ka* radiation and are believed to be accurate to within 0.5 %.

Dibromobis(ethylenethiourea)tellurium(II), $Te(etu)_2Br_2$. Two crystalline forms have been obtained pure, an orthorhombic and a monoclinic one. The former was best prepared from tellurium dioxide and ethylenethiourea in a molar ratio of 1 : 6 as follows: 1.6 g (10 mmoles) of tellurium dioxide was dissolved in 50 ml of 48–50 % hydrobromic acid and 150 ml of water, the solution was heated almost to boiling, and 6.1 g (60 mmoles) of ethylenethiourea in 60 ml of hot water was added rapidly under stirring. From the resulting, clear solution (filtered immediately after mixing, if necessary) crystallization sets in spontaneously or on scratching of the beaker walls, and may be hastened by occasional stirring; it should take place from hot solution since if the temperature falls below about 50° some tetrakis(ethylenethiourea)-tellurium(II) dibromide dihydrate [4] may crystallize and contaminate the product. Yield, 2.6–3.8 g (53–77 %) depending on the rate of crystallization and temperature when filtering. M.p. 186° (decomp.). (Found: S 13.27; Te 25.98. Calc. for $C_6H_{12}Br_2N_4S_2Te$: S 13.04; Te 25.95.)

The brownish-yellow, *orthorhombic* crystals occur as flat prisms extended along the *c* axis with {010} dominant. The axial lengths are, $a = 14.46$ Å, $b = 31.40$ Å, $c = 12.10$ Å, and the space group, from systematic absences, is $D_{2h}^{24} - Fddd$, which has 32-fold general positions. There are 16 molecules per unit cell; density, calc. 2.38, found 2.38 g/cm³. The intensity distribution: *hkl* reflections with $h+k+l = 2n+1$ or $4n$ in most cases markedly strongest, indicates that the tellurium atoms lie on twofold axes of symmetry.

The substance is practically insoluble in glacial acetic acid, but readily soluble in dimethylformamide to give red, stable solutions. When to a warm solution of the substance in dimethylformamide, preferably less concentrated than corresponding to saturation at room temperature, an about double volume of glacial acetic acid is added, the monoclinic form crystallizes; the orthorhombic one could not be recovered even on seeding.

The *monoclinic* crystals appear a little darker reddish-yellow in colour than the orthorhombic ones. M.p. 192° (decomp.). (Found: S 13.16; Te 26.02.) They occur as prisms or plates extended along the *b* axis, bounded by {100} and {001} with the latter dominant in most cases. The unit cell dimensions are, $a = 17.30$ Å, $b = 5.89$ Å, $c = 15.57$ Å, $\beta = 120°$, and there are four molecules per unit cell; density, calc. 2.38, found 2.38 g/cm³. Systematic absences, *hkl* when $h + k$ is odd, *h0l* when *h* is odd or *l* is odd. These, together with the intensity distribution, perhaps best observed on oscillation photographs about the *bc* diagonal: *hkl* reflections with $k + l$ even generally stronger than those with $k + l$ odd, indicate that the tellurium atoms lie in symmetry centres, positions (*c*) or (*d*) [5], of the space group $C_{2h}^6 - C2/c$.

This has been confirmed by structure analysis [6], through projections along the *b* axis and along the *ab* diagonal, the repeat distance along which is halved on account of the *C*-centering and thus is 9.14 Å. The dimensions of the planar *trans* TeS_2Br_2 group of the centrosymmetric molecule are: Te–S = 2.69 Å, Te–Br = 2.78 Å, and

$\angle$ S—Te—Br = 90° within the error. In the *cis* TeS_2Br_2 group of $Te(tu)_2Br_2$ the bond lengths are [2,7], Te—S = 2.47 Å, Te—Br = 3.05 Å; thus, thiourea ligands in *trans* positions to bromine, in a *cis* complex, exert a considerable lengthening effect on the Te—Br bonds with corresponding shortening of the Te—S bonds.

The bis(ethylenethiourea) complexes can be obtained also from tetrakis(ethylenethiourea)tellurium(II) dibromide dihydrate: A 0.01 M solution of this salt [4] in methanol had after three days at room temperature deposited crystals of the monoclinic form. In another, like experiment, the orthorhombic form separated, and it was found that crystallization of one or the other form could be directed by seeding.

The forms are practically insoluble in methanol, and are stable in contact with the mother liquor when formed from methanolic tetrakis(ethylenethiourea)tellurium(II) dibromide dihydrate, although methanol not containing a little ethylenethiourea or acid slowly becomes black in contact with the compounds, probably because of moisture. They were on the filters washed with methanol or 96 % ethanol containing a few drops of concentrated hydrobromic acid, and then with ether.

If, in the procedure for the preparation of the orthorhombic form from tellurium dioxide and ethylenethiourea, a molar ratio of 1 : 4 instead of 1 : 6 is employed (4.1 g ethylenethiourea in 50 ml of water, otherwise as above) the product is not a $Te(etu)_2Br_2$ complex but a compound of apparent composition $Te_7(etu)_{12}Br_{16}$. (Found: Br 38.19; S 11.42; Te 26.06. Calc. for $C_{36}H_{72}Br_{16}N_{24}S_{12}Te_7$: Br 37.63; S 11.32; Te 26.29.) The compound forms long, reddish-brown, six-sided prisms extended along [10$\bar{1}$] with a = 23.50 Å, b = 24.50 Å, c = 16.96 Å, β = 94°, and density corresponding to four formula units per unit cell; calc. 2.32, found 2.34 g/cm³. The systematic absences and the morphology indicate that the space group is C_{2h}^6—$C2/c$, which would require that of the 28 tellurium atoms in the unit cell, 4 be located in special, fourfold positions. If the above formula is correct, and should not include two hydrogen atoms more, one of the seven tellurium atoms (four per unit cell) must be tetravalent.

In some early preparations, from tellurium dioxide and ethylenethiourea in a molar ratio of 1 : 4, but where smaller volumes of hydrobromic acid and water were used as solvent for the tellurium dioxide (there is then a tendency of oil formation on mixing of the tellurium dioxide and ethylenethiourea solutions) crystals of the above substance were found, admixed with crystals of orthorhombic dibromobis(ethylenethiourea)tellurium(II) and also crystals which appear to represent a third (a second monoclinic) form of the dibromo complex: Brownish yellow, long prisms or thicker, flat prisms extended along the c axis, bounded by {100} and {110} with the former dominant, and terminated by {111}, with a = 26.76 Å, b = 11.48 Å, c = 9.38 Å, β = 102°, and density agreeing with eight $Te(etu)_2Br_2$ molecules per unit cell; calc. 2.32, found 2.30 g/cm³. The morphology indicates that a twofold axis is present, and together with the systematic absences point to the space group C_{2h}^6—$C2/c$, which here would not require any molecular symmetry. These crystals could not be obtained from solutions of the orthorhombic form in dimethylformamide-glacial acetic acid on seeding; only the monoclinic *trans* form crystallized from such solutions.

Diiodobis(ethylenethiourea)tellurium(II), $Te(etu)_2I_2$, crystallizes from solutions of the salt [4], $Te(etu)_4Cl_2 \cdot 2H_2O$, in hot methanol, on addition of methanolic sodium iodide. It is readily soluble in dimethylformamide, and better developed crystals were obtained from room temperature solutions of the crude product in this solvent, by adding about four times the volume of methanol. M.p. 198—200° (decomp.). (Found: S 11.17; Te 21.88. Calc. for $C_6H_{12}I_2N_4S_2Te$: S 10.96; Te 21.80.)

The red crystals are isomorphous with those of the monoclinic *trans* bromide, and show the same morphology. The unit cell dimensions are, a = 17.17 Å, b = 6.24 Å, c = 15.97 Å, β = 119½°, and the density, calc. 2.61 for four molecules per unit cell, found 2.60 g/cm³. From systematic absences, and isomorphism with the bromide, the space group is C_{2h}^6—$C2/c$; the tellurium atoms lie in centres of symmetry, and the TeS_2I_2 group is planar *trans*.

Dithiocyanatobis(ethylenethiourea)tellurium(II), $Te(etu)_2(SCN)_2$, was obtained from the bromide, $Te(etu)_2Br_2$, and ammonium thiocyanate: 2 g of the bromide was dissolved by heating in a solution of 7 g of ammonium thiocyanate in about 20 ml of methanol, and the resulting, red solution was allowed to cool. Yield, 0.7 g (39 %). M.p. 142—144° (decomp.). (Found: S 28.83; Te 28.43. Calc. for $C_8H_{12}N_6S_4Te$: S 28.63; Te 28.48.)

The crystals are yellow, and form short, thick prisms {011}, with a = 10.71 Å, b = 12.84 Å, c = 12.01 Å, β = 102°, and

four molecules per unit cell; density, calc. 1.84, found 1.85 g/cm³. The space group, from systematic absences, is $C_{2h}^5-P2_1/c$. No molecular symmetry is required in these crystals.

1. Foss, O. and Hauge, S. *Acta Chem. Scand.* **13** (1959) 1252.
2. Foss, O. and Hauge, S. *Acta Chem. Scand.* **15** (1961) 1615.
3. Foss, O. and Hauge, S. *Acta Chem. Scand.* **15** (1961) 1616.
4. Foss, O. and Fossen, S. *Acta Chem. Scand.* **15** (1961) 1620.
5. *International Tables for X-ray Crystallography*, Vol. I. The Kynoch Press, Birmingham, 1952, p. 101.
6. Foss, O. and Kjøge, H. *To be published.*
7. Foss, O. and Maartmann-Moe, K. *To be published.*

Received October 8, 1961.

Tetrakis(ethylenethiourea)-tellurium(II) Salts

OLAV FOSS and SIGVARD FOSSEN

Chemical Institute, University of Bergen, Bergen, Norway

In acid solutions tetravalent tellurium reacts with six moles of thiourea to give tetrathiourea-tellurium(II) salts [1,2]. This note describes corresponding salts of divalent tellurium with ethylenethiourea (etu) as ligand, *i.e.*, salts of the cation $Te(etu)_4^{2+}$. They are formed in the same way as the thiourea analogs, two moles of ethylenethiourea reducing tetravalent tellurium to divalent and thereby themselves becoming oxidized to the ethyleneformamidinium disulphide cation, $(etu)_2^{2+}$. The very soluble chloride of this disulphide cation has been described [3]; we have identified it in the mother liquor from tetrakis(ethylenethiourea)tellurium(II) dichloride dihydrate preparations through its reaction product [4,5] with potassium iodide.

In two salts of the $Te(etu)_4^{2+}$ cation namely the anhydrous bromide and the perchlorate, and probably also in the anhydrous chloride, the tellurium atoms lie in centres of symmetry, and the TeS^4 group is thus exactly planar, as in tetrathiourea-tellurium(II) salts [1,2].

Like previously described divalent tellurium complexes [1,2,6,7], the present salts hydrolyze and liberate tellurium in presence of water. Acids prevent hydrolysis; *e.g.*, the chloride and bromide can be recrystallized from 2 N hydrochloric and hydrobromic acid, respectively. On the filters the salts were washed with 96 % ethanol containing a little concentrated hydrochloric acid (hydrobromic acid in the case of the bromides) and then with ether.

The following tetrakis(ethylenethiourea)tellurium(II) salts have been characterized through single-crystal X-ray photographs, using Cu$K\alpha$ radiation, $\lambda = 1.542$ Å; values for axial lengths are probably accurate to within 0.5 %. The salts are yellow, the chlorides with a greenish, the perchlorate with a brownish tinge.

Dichloride dihydrate, $Te(etu)_4Cl_2 \cdot 2H_2O$. To 1.6 g (10 mmoles) of tellurium dioxide dissolved in 15 ml of concentrated, warm hydrochloric acid were added 6.5 g (a little more than 60 mmoles) of ethylenethiourea in 60 ml of hot water. Crystallization takes place on cooling to room temperature. Yield, 6.1—6.3 g (93—98 %). (Found: S 19.90; Te 19.84. Calc. for $C_{12}H_{28}Cl_2N_8O_2S_4Te$: S 19.94; Te 19.84. Weight loss after one hour at 110°: 5.8 %. Calc. for dihydrate: 5.6 %.) Prisms, extended along the b axis and bounded by {100}, {001} and {101}, with $a = 18.22$ Å, $b = 7.84$, $c = 21.30$ Å, $\beta = 124°$, and four formula units per unit cell; density, calc. 1.69, found 1.70 g/cm³. The space group, from systematic absences, is $C_{2h}^5-P2_1/c$.

This salt results also when a tellurium dioxide : ethylenethiourea molar ratio of 1 : 4 is used; 4.1 g ethylenethiourea in the above procedure gave 3.2 g yield. In the case of thiourea [1], this molar ratio gives the dichloro complex, $Te(tu)_2Cl_2$.

The *dibromide dihydrate*, $Te(etu)_4Br_2 \cdot 2H_2O$, is isomorphous with the dichloride dihydrate, and has $a = 19.12$ Å, $b = 7.85$ Å, $c = 21.42$ Å, $\beta = 125°$; density, calc. 1.84, found 1.87 g/cm³. The salt was prepared by dissolving 1.6 g (10 mmoles) of tellurium dioxide in 20 ml of 48—50 % hydrobromic and 30 ml of water, and adding at about 50°, rapidly under stirring, 7 g (*ca.* 70 mmoles) of ethylenethiourea in 100 ml of warm water. The resulting, orange red solution was allowed to cool to room temperature. Yield, about

four molecules per unit cell; density, calc. 1.84, found 1.85 g/cm³. The space group, from systematic absences, is $C_{2h}^5-P2_1/c$. No molecular symmetry is required in these crystals.

1. Foss, O. and Hauge, S. *Acta Chem. Scand.* **13** (1959) 1252.
2. Foss, O. and Hauge, S. *Acta Chem. Scand.* **15** (1961) 1615.
3. Foss, O. and Hauge, S. *Acta Chem. Scand.* **15** (1961) 1616.
4. Foss, O. and Fossen, S. *Acta Chem. Scand.* **15** (1961) 1620.
5. *International Tables for X-ray Crystallography*, Vol. I. The Kynoch Press, Birmingham, 1952, p. 101.
6. Foss, O. and Kjøge, H. *To be published.*
7. Foss, O. and Maartmann-Moe, K. *To be published.*

Received October 8, 1961.

Tetrakis(ethylenethiourea)-tellurium(II) Salts

OLAV FOSS and SIGVARD FOSSEN

Chemical Institute, University of Bergen, Bergen, Norway

In acid solutions tetravalent tellurium reacts with six moles of thiourea to give tetrathiourea-tellurium(II) salts [1,2]. This note describes corresponding salts of divalent tellurium with ethylenethiourea (etu) as ligand, *i.e.*, salts of the cation $Te(etu)_4^{2+}$. They are formed in the same way as the thiourea analogs, two moles of ethylenethiourea reducing tetravalent tellurium to divalent and thereby themselves becoming oxidized to the ethyleneformamidinium disulphide cation, $(etu)_2^{2+}$. The very soluble chloride of this disulphide cation has been described [3]; we have identified it in the mother liquor from tetrakis(ethylenethiourea)tellurium(II) dichloride dihydrate preparations through its reaction product [4,5] with potassium iodide.

In two salts of the $Te(etu)_4^{2+}$ cation namely the anhydrous bromide and the perchlorate, and probably also in the anhydrous chloride, the tellurium atoms lie in centres of symmetry, and the TeS^4 group is thus exactly planar, as in tetrathiourea-tellurium(II) salts [1,2].

Like previously described divalent tellurium complexes [1,2,6,7], the present salts hydrolyze and liberate tellurium in presence of water. Acids prevent hydrolysis; *e.g.*, the chloride and bromide can be recrystallized from 2 N hydrochloric and hydrobromic acid, respectively. On the filters the salts were washed with 96 % ethanol containing a little concentrated hydrochloric acid (hydrobromic acid in the case of the bromides) and then with ether.

The following tetrakis(ethylenethiourea)tellurium(II) salts have been characterized through single-crystal X-ray photographs, using Cu$K\alpha$ radiation, $\lambda = 1.542$ Å; values for axial lengths are probably accurate to within 0.5 %. The salts are yellow, the chlorides with a greenish, the perchlorate with a brownish tinge.

Dichloride dihydrate, $Te(etu)_4Cl_2 \cdot 2H_2O$. To 1.6 g (10 mmoles) of tellurium dioxide dissolved in 15 ml of concentrated, warm hydrochloric acid were added 6.5 g (a little more than 60 mmoles) of ethylenethiourea in 60 ml of hot water. Crystallization takes place on cooling to room temperature. Yield, 6.1—6.3 g (93—98 %). (Found: S 19.90; Te 19.84. Calc. for $C_{12}H_{28}Cl_2N_8O_2S_4Te$: S 19.94; Te 19.84. Weight loss after one hour at 110°: 5.8 %. Calc. for dihydrate: 5.6 %.) Prisms, extended along the b axis and bounded by {100}, {001} and {101}, with $a = 18.22$ Å, $b = 7.84$, $c = 21.30$ Å, $\beta = 124°$, and four formula units per unit cell; density, calc. 1.69, found 1.70 g/cm³. The space group, from systematic absences, is $C_{2h}^5-P2_1/c$.

This salt results also when a tellurium dioxide : ethylenethiourea molar ratio of 1 : 4 is used; 4.1 g ethylenethiourea in the above procedure gave 3.2 g yield. In the case of thiourea [1], this molar ratio gives the dichloro complex, $Te(tu)_2Cl_2$.

The *dibromide dihydrate*, $Te(etu)_4Br_2 \cdot 2H_2O$, is isomorphous with the dichloride dihydrate, and has $a = 19.12$ Å, $b = 7.85$ Å, $c = 21.42$ Å, $\beta = 125°$; density, calc. 1.84, found 1.87 g/cm³. The salt was prepared by dissolving 1.6 g (10 mmoles) of tellurium dioxide in 20 ml of 48—50 % hydrobromic and 30 ml of water, and adding at about 50°, rapidly under stirring, 7 g (*ca.* 70 mmoles) of ethylenethiourea in 100 ml of warm water. The resulting, orange red solution was allowed to cool to room temperature. Yield, about

7 g (96 %). (Found: S 17.42; Te 17.45. Calc. for $C_{12}H_{28}Br_2N_8O_2S_4Te$: S 17.52; Te 17.43.) Under slightly different conditions [6] (60 mmoles of ethylenethiourea, and crystallization from more dilute and hotter solutions) this procedure gives orthorhombic dibromobis(ethylenethiourea)tellurium(II).

The two dihydrates are readily soluble in dimethylformamide, to give yellow to orange red solutions, apparently stable at room temperature. Boiling methanol dissolves per 100 ml about 1.5 g of either of the dihydrates; on cooling, the anhydrous salts crystallize out. Also in contact with the solid dihydrates at room temperature, methanol transfers them to the anhydrous salt.

The *dibromide*, $Te(etu)_4Br_2$, forms short, thick, monoclinic prisms bounded by {100} and {110} and terminated by {001}, with $a = 18.11$ Å, $b = 8.19$ Å, $c = 16.52$ Å, $\beta = 105\frac{1}{2}°$, and four formula units per unit cell; density, calc. 1.96, found 1.95 g/cm³. Systematic absences, *hkl* when $h + k$ is odd, *h0l* when *h* is odd or *l* is odd. On oscillation photographs about the *c* axis, reflections on odd layer lines are markedly weaker than on even layer lines, particularly at large scattering angles. This indicates that the tellurium atoms lie in symmetry centres, positions (*a*) or (*b*) [8], of the space group C_{2h}^6-C2/c.

The *dichloride*, $Te(etu)_4Cl_2$, is triclinic, with $a = 9.68$ Å, $b = 7.99$ Å, $c = 8.33$ Å, $\alpha = 103°$, $\beta = 99°$, $\gamma = 109\frac{1}{2}°$, and one formula unit per unit cell; density, calc. 1.76, found 1.76 g/cm³. The *h0l* zone of reflections shows a marked similarity to the *h0l* zone of the anhydrous bromide ($\beta^* = 75\frac{1}{2}°$ in both salts, and the *a* and *c* spacings, halved in the bromide, correspond closely) also with respect to intensity distribution. This may be taken to indicate that the *h0l* zone also of the chloride is centrosymmetric, *i.e.*, that the space group is $C_i^1-P\bar{1}$, so that tellurium lies in a centre of symmetry.

The *perchlorate*, $Te(etu)_4(ClO_4)_2$, crystallizes from solutions of the dichloride dihydrate in warm 2 N hydrochloric acid, on addition of perchloric acid and cooling. (Found: S 17.38; Te 17.33. Calc. for $C_{12}H_{24}Cl_2N_8O_8S_4Te$: S 17.45; Te 17.36.) It forms flat prisms or plates {100} extended along the *b* axis, with $a = 9.61$ Å, $b = 9.78$ Å, $c = 14.64$ Å, $\beta = 92°$. There are two formula units per unit cell; density, calc. 1.78, found 1.78 g/cm³; and the space group, from systematic absences, is $C_{2h}^5-P2_1/c$. Thus, the tellurium atoms lie in centres of symmetry, and this agrees with the intensity distribution, *hkl* reflections with $k + l$ even being markedly strongest.

The *hexachlorotellurite(IV)*, $Te(etu)_4TeCl_6$, resulted from attempts to arrive at the dichloro complex, $Te(etu)_2Cl_2$. To 1.6 g (10 mmoles) of tellurium dioxide in 100 ml of warm concentrated hydrochloric acid was added 4.1 g (40 mmoles) of ethylenethiourea in 50 ml of hot water, and then 50 ml of methanol. Crystallization started on scratching of the beaker walls; to develop well-formed, not too large crystals, the solution was occasionally stirred. Yield, about 3.5 g. (Found: Cl 24.22; S 14.70; Te 28.88. Calc. for $C_{12}H_{24}Cl_6N_8S_4Te_2$: Cl 24.27; S 14.63; Te 29.11.) The salt crystallized unchanged from a solution in warm methanol, but a solution in warm 2 N hydrochloric acid, on cooling, deposited crystals of the dichloride dihydrate.

The crystals of the hexachlorotellurite(IV) are orthorhombic; bipyramidal in appearance, and occur as plates {001} bounded by {110}, sometimes with {011} developed so that the plates become extended along the *a* axis, or as short prisms {110} terminated by {001}. There is a pronounced tendency of cleavage along the *c* plane. The axial lengths are, $a = 12.09$ Å, $b = 15.84$ Å, $c = 15.08$ Å, and there are four formula units per unit cell; density, calc. 2.02, found 2.02 g/cm³. Systematic absences, *hkl* when $h + k$ is odd; furthermore, *hkl* reflections are very weak when *h* is odd or *k* is odd. Of the orthorhombic space groups consistent with these observations, $C_{2v}^{11}-Cmm2$ is perhaps the more probable one, with the tellurium atom of cation as well as anion located on the same twofold axis.

The only trithiourea-tellurium(II) salt encountered was a hydrogenfluoride [2]. In the present work, *tris(ethylenethiourea)tellurium(II) perchlorate*, $Te(etu)_3(ClO_4)_2$, was obtained, as follows: To 1.6 g (10 mmoles) of tellurium dioxide in 5 ml of concentrated hydrochloric acid was added, at room temperature, 20 ml of *ca.* 60 % perchloric acid, and then 4.1 g (40 mmoles) of ethylenethiourea in 30 ml of hot water. Crystallization set in on scratching; yield after cooling to room temperature, 4.0 g. (Found: N 13.32; S 15.20; Te 20.19. Calc. for $C_9H_{18}Cl_2N_6O_8S_3Te$: N 13.28; S 15.20; Te 20.16.) From solutions of the salt in warm methanol (in presence of a little perchloric acid) or in warm 2 N hydrochloric acid, tetrakis(ethylenethiourea)tellurium(II) salts crystallized, as perchlorate or once

from the latter solvent, as the dichloride dihydrate.

The salt forms plates {100} extended along the b axis in most cases, and bounded by {001}. There is perfect cleavage along the a plane, and a persistent tendency of twinning on this plane, but un-twinned crystals were found in a crop from a mother liquor. The unit cell dimensions are, $a = 11.96$ Å, $b = 11.48$ Å, $c = 17.08$ Å, $\beta = 112\frac{1}{2}°$, and there are four formula units per unit cell; density, calc. 1.94, found 1.93 g/cm³. The space group, from systematic absences, is $C_{2h}^5 - P2_1/c$. The reflections are very weak when $k + l$ is odd (particularly evident on oscillation photographs about the bc diagonal) which is typical for heavy atoms in centres of symmetry in this space group; however, such molecular symmetry is very improbable for stereochemical reasons. The same intensity distribution would result from tellurium atoms in general, fourfold positions x,y,z with x and $z = 0$ or $y = 0$.

1. Foss, O. and Hauge, S. *Acta Chem. Scand.* **13** (1959) 1252; **15** (1961) 1616.
2. Foss, O. and Hauge, S. *Acta Chem. Scand.* **15** (1961) 1623.
3. Freedman, L. D. and Corwin, A. H. *J. Biol. Chem.* **181** (1949) 601.
4. Johnson, T. B. and Edens, C. O. *J. Am. Chem. Soc.* **64** (1942) 2706.
5. Chase, B. H. and Walker, J. *J. Chem. Soc.* **1955** 4443.
6. Foss, O. and Fossen, S. *Acta Chem. Scand.* **15** (1961) 1618.
7. Foss, O. and Hauge, S. *Acta Chem. Scand.* **15** (1961) 1615.
8. *International Tables for X-ray Crystallography*, Vol. I, The Kynoch Press, Birmingham 1952, p. 101.

Received October 8, 1961.

Correction to "A Miniature Solubility Column and its Application to a Study of the Solubility of Red Mercury(II) Oxide in Acid 3 M $NaClO_4$ Solutions" *

DAVID DYRSSEN and VALENTINE TYRRELL

Department of Inorganic Chemistry, Royal Institute of Technology, Stockholm 70, Sweden

A systematic error in the $-\log[H^+]$ values quoted in this paper, arising from an arithmetical error, has been detected. Throughout they should be reduced by 0.142 units, *e.g.*, all points in Fig. 2 should be shifted 0.142 units to the left and $-\log[H^+]$ at the intersection of the asymptotes in Fig. 2 should be 3.08 not 3.22. As a result, the published equilibrium constants must be altered as follows:

$$\log {}^*K_1 + \log {}^*K_2 = -6.16 \pm 0.08$$

$$\log {}^*K_{s0} = 2.41 \pm 0.10$$

This new value of $(\log {}^*K_1 + \log {}^*K_2)$ agrees with Ahlberg's potentiometric value [1] within the expected limits of error. The values of $\log {}^*K_1 - \log {}^*K_2 = -0.30 \pm 0.30$ and $\log K_{s2} = -3.75 \pm 0.01$ remain unchanged.

In the calculation of the solubility product (pK_{s0}) of $Hg(OH)_2$, Lagerström's value [2] of $pK_w = 14.03$ was used. This is applicable to 3 *molal* solution of sodium perchlorate; the measured value for the 3 molar solutions used in the solubility work is 14.22 [3]. Using this and the revised value of $\log {}^*K_{s0}$, pK_{s0} becomes 26.0.

1. Ahlberg, I. *To be published.*
2. Lagerström, G. *Acta Chem. Scand.* **13** (1959) 722.
3. Ingri, N., Lagerström, G., Frydman, M. and Sillén, L. G. *Acta Chem. Scand.* **11** (1957) 1039.

Received October 12, 1961.

* *Acta Chem. Scand.* **15** (1961) 393.

from the latter solvent, as the dichloride dihydrate.

The salt forms plates {100} extended along the b axis in most cases, and bounded by {001}. There is perfect cleavage along the a plane, and a persistent tendency of twinning on this plane, but un-twinned crystals were found in a crop from a mother liquor. The unit cell dimensions are, $a = 11.96$ Å, $b = 11.48$ Å, $c = 17.08$ Å, $\beta = 112\frac{1}{2}°$, and there are four formula units per unit cell; density, calc. 1.94, found 1.93 g/cm³. The space group, from systematic absences, is $C_{2h}^5 - P2_1/c$. The reflections are very weak when $k + l$ is odd (particularly evident on oscillation photographs about the bc diagonal) which is typical for heavy atoms in centres of symmetry in this space group; however, such molecular symmetry is very improbable for stereochemical reasons. The same intensity distribution would result from tellurium atoms in general, fourfold positions x,y,z with x and $z = 0$ or $y = 0$.

1. Foss, O. and Hauge, S. *Acta Chem. Scand.* **13** (1959) 1252; **15** (1961) 1616.
2. Foss, O. and Hauge, S. *Acta Chem. Scand.* **15** (1961) 1623.
3. Freedman, L. D. and Corwin, A. H. *J. Biol. Chem.* **181** (1949) 601.
4. Johnson, T. B. and Edens, C. O. *J. Am. Chem. Soc.* **64** (1942) 2706.
5. Chase, B. H. and Walker, J. *J. Chem. Soc.* **1955** 4443.
6. Foss, O. and Fossen, S. *Acta Chem. Scand.* **15** (1961) 1618.
7. Foss, O. and Hauge, S. *Acta Chem. Scand.* **15** (1961) 1615.
8. *International Tables for X-ray Crystallography*, Vol. I, The Kynoch Press, Birmingham 1952, p. 101.

Received October 8, 1961.

Correction to "A Miniature Solubility Column and its Application to a Study of the Solubility of Red Mercury(II) Oxide in Acid 3 M $NaClO_4$ Solutions" *

DAVID DYRSSEN and VALENTINE TYRRELL

Department of Inorganic Chemistry, Royal Institute of Technology, Stockholm 70, Sweden

A systematic error in the $-\log[H^+]$ values quoted in this paper, arising from an arithmetical error, has been detected. Throughout they should be reduced by 0.142 units, *e.g.*, all points in Fig. 2 should be shifted 0.142 units to the left and $-\log[H^+]$ at the intersection of the asymptotes in Fig. 2 should be 3.08 not 3.22. As a result, the published equilibrium constants must be altered as follows:

$$\log {}^*K_1 + \log {}^*K_2 = -6.16 \pm 0.08$$

$$\log {}^*K_{s0} = 2.41 \pm 0.10$$

This new value of $(\log {}^*K_1 + \log {}^*K_2)$ agrees with Ahlberg's potentiometric value [1] within the expected limits of error. The values of $\log {}^*K_1 - \log {}^*K_2 = -0.30 \pm 0.30$ and $\log K_{s2} = -3.75 \pm 0.01$ remain unchanged.

In the calculation of the solubility product (pK_{s0}) of $Hg(OH)_2$, Lagerström's value [2] of $pK_w = 14.03$ was used. This is applicable to 3 *molal* solution of sodium perchlorate; the measured value for the 3 molar solutions used in the solubility work is 14.22 [3]. Using this and the revised value of $\log {}^*K_{s0}$, pK_{s0} becomes 26.0.

1. Ahlberg, I. *To be published.*
2. Lagerström, G. *Acta Chem. Scand.* **13** (1959) 722.
3. Ingri, N., Lagerström, G., Frydman, M. and Sillén, L. G. *Acta Chem. Scand.* **11** (1957) 1039.

Received October 12, 1961.

* *Acta Chem. Scand.* **15** (1961) 393.

Some Thiourea-tellurium(II) Fluorides

OLAV FOSS and SVERRE HAUGE

Chemical Institute, University of Bergen, Bergen, Norway

In the course of a study of complexes of divalent tellurium with thiourea [1-4], we have tried to prepare a complex $Te(tu)_2X_2$ (tu = thiourea) with X = fluoride, to complete the series [1,3] of halides of this type. In all attempts, no such fluoride was obtained; instead, tetrathiourea-tellurium(II) salts resulted, and under certain conditions a trithiourea-tellurium(II) salt, $Te(tu)_3(HF_2)_2$. The failure to obtain a difluoro-dithiourea-tellurium(II) complex, together with observations on the relative ease of formation of the corresponding complexes of the other halides, indicate that divalent tellurium belongs to the class of complex formers giving less stable fluoro than chloro, bromo and iodo complexes.

The salts obtained are described below. The preparations were performed in polythene beakers, and the products washed with ethanol containing a little thiourea, and dried on filter paper in air. The salts are yellow; the hydrogenfluorides blacken slowly on prolonged exposure to air or in contact with glass, but remain unchanged when kept in closed polythene bottles. Unit cell and space group data were obtained from oscillation and Weissenberg photographs, using Cu$K\alpha$ radiation, $\lambda = 1.542$ Å; the axial lengths are probably accurate to within 0.5 %.

The dichloro and dibromo complexes crystallize when tellurium dioxide, dissolved in hydrochloric or hydrobromic acid, reacts with four moles of thiourea [1]:
$Te^{IV} + 4\ tu + 2\ X^- = Te(tu)_2X_2 + (tu)_2^{2+}$
where X = halide. With hydrofluoric acid as a solvent, this tellurium dioxide: thiourea molar ratio (1 : 4) gave mainly monoclinic tetrathiourea-tellurium(II) di(hydrogenfluoride) in mixture with some trithiourea-tellurium(II) di(hydrogenfluoride). A molar ratio 1 : 6 gave mainly a triclinic dimorph of the tetrathiourea-tellurium(II) salt admixed with some of the monoclinic one, and a molar ratio 1 : 3 gave only the trithiourea-tellurium(II) salt.

Tetrathiourea-tellurium(II) di(hydrogenfluoride), $Te(tu)_4(HF_2)_2$. To 3.2 g (0.02 moles) of tellurium dioxide dissolved in 25 g of 38–40 % hydrofluoric acid was added, at about 50°, 9.1 g (0.12 moles) of thiourea in 30 ml of water. Yield, after 3 h at room temperature, 7.8 g (76 %). (Found: F 14.95; Te 25.74. Calc. for $C_4H_{18}F_4N_8S_4Te$: F 14.90; Te 25.02.) This sample consisted of the triclinic dimorph with only a small amount of the monoclinic one. The latter was obtained pure in an experiment as above, using 6.1 g (0.08 moles) of thiourea in 30 ml of water: After standing over night a lower layer (3.6 g) of the monoclinic dimorph (Found: F 14.60; Te 25.10) could be separated relatively cleanly from prisms (0.8 g) of the trithiourea-tellurium(II) salt which had grown on top of the layer.

The monoclinic dimorph occurs as short, thick prisms extended along the c axis, with {100} dominant, and $a = 22.32$ Å, $b = 7.92$ Å, $c = 10.16$ Å, $\beta = 91°$. Density, calc. 1.89 for four formula units per unit cell, found 1.90 g/cm³. Systematic absences, hkl when $h + k + l$ is odd, $h0l$ when h is odd or l is odd. These, together with observations that hkl reflections with l odd are in most cases very weak relative to those with l even, indicate that the tellurium atoms lie in symmetry centres of the space group C_{2h}^6-I2/c.

The triclinic dimorph forms plates extended along the a axis, with the c face dominant. With morphological axes, the unit cell dimensions are: $a = 7.59$ Å, $b = 5.84$ Å, $c = 12.41$ Å, $\alpha = 84½°$, $\beta = 116°$, $\gamma = 116°$. Density, calc. 1.92 for one formula unit per unit cell, found 1.94 g/cm³. The morphology indicates the centrosymmetric space group, $C_i^1-P\bar{1}$, which would require that the tellurium atom lies in a centre of symmetry also in this dimorph.

Tetrathiourea-tellurium(II) difluoride dihydrate, $Te(tu)_4F_2{\cdot}2H_2O$, crystallizes when the above hydrogenfluorides are dissolved in warm aqueous thiourea, and the solution allowed to cool, or on addition of potassium hydrogenfluoride solution to an aqueous thiourea solution of another tetrathiourea-tellurium(II) salt such as the chloride or bromide. (Found: F 7.70; Te 24.63. Calc. for $C_4H_{20}F_2N_8O_2S_4Te$: F 7.51; Te 25.21.) It blackens slowly if kept in a vacuum over sulphuric acid.

The salt occurs as triclinic prisms or plates {001} extended along the a axis,

with $a = 5.42$ Å, $b = 8.03$ Å, $c = 11.30$ Å, $\alpha = 103\frac{1}{2}°$, $\beta = 97°$, $\gamma = 72°$. There is one formula unit per unit cell; density, calc. 1.85, found 1.88 g/cm³. The space group $C_i^1 - P\bar{1}$ indicated by the morphology would require centrosymmetry for the cation also here. The intensity distribution along the reciprocal c axis is very similar to that of the triclinic hydrogenfluoride dimorph (c spacings 10.97 and 11.08 Å respectively).

Trithiourea-tellurium(II) di(hydrogenfluoride), $Te(tu)_3(HF_2)_2$. This salt was obtained as prisms growing on top of a layer of the monoclinic tetrathiourea-tellurium(II) salt, as recounted above, and was the only product when a tellurium dioxide: thiourea molar ratio of 1 : 3 was employed (4.5 g thiourea in 15 ml of water in the above procedure). Yield, 2.7 g (52 %). (Found: F 17.36; S 22.23; Te 29.57. Calc. for $C_3H_{14}F_4N_6S_3Te$: F 17.51; S 22.17; Te 29.40.)

The salt forms monoclinic prisms {011} with $a = 5.91$ Å, $b = 20.68$ Å, $c = 11.47$ Å, $\beta = 95°$. The space group, from systematic absences, is $C_{2h}^5 - P2_1/c$. There are four formula units per unit cell; density, calc. 2.06, found 2.05 g/cm³. The crystal structure has been solved, and will be published later.

1. Foss, O. and Hauge, S. *Acta Chem. Scand.* **13** (1959) 1252.

2. Foss, O. and Hauge, S. *Acta Chem. Scand.* **13** (1959) 2155.

3. Foss, O. and Hauge, S. *Acta Chem. Scand.* **15** (1961) 1615.

4. Foss, O. and Hauge, S. *Acta Chem. Scand.* **15** (1961) 1616.

Received October 8, 1961.

The Equilibrium Between Molten FeO—Fe_2O_3 Mixtures and O_2 Gas

H. FLOOD and K. HAGEMARK

The Royal Norwegian Council for Scientific and Industrial Research, Institute of Silicate Science, The Technical University of Norway, Trondheim, Norway

From simple energetic assumptions it is possible to calculate the equilibrium between O_2 gas, Fe(II) and Fe(III) in solid solutions of Fe_3O_4 — Fe_2O_3, Fe_3O_4 — $MgFe_2O_4$ and Fe_3O_4 — $FeCr_2O_4$ based on spinel models with a defect cation lattice (cation vacancies and interstitial cations) [1-3]. These and similar models are also applicable [1,2] for the calculation of the equilibrium between oxygen gas and molten oxide mixtures, including a larger part of the range of composition from FeO—Fe_3O_4.

In the following a more plausible model will be suggested for the molten oxide mixtures based on a spinel like structure where instead of interstitial cations a corresponding number of oxygen ion vacancies are assumed.

The structure model is thus characterized by a Schottky disorder which can be expressed by

$$\frac{n_{\boxplus}}{n_c} \times \frac{n_{\boxminus}}{n_a} = N_{\boxplus} \times N_{\boxminus} = \text{const.} \quad (1)$$

where

$n_{\boxplus}$ = number of cation vacancies
$n_{\boxminus}$ = number of anion vacancies
n_c = number of cation positions
n_a = number of anion positions

(The cation and anion vacancies are simultaneously present only in a composition range very close to stoichiometric Fe_3O_4).

The requirement for the model is that

$$\frac{n_c}{n_a} = \frac{3}{4} \quad (2)$$

where

$$n_a = n_{Fe(II)} + n_{Fe(III)} + n_{\boxplus}$$
$$n_a = n_{O^{2-}} + n_{\boxminus}$$

with $a = 5.42$ Å, $b = 8.03$ Å, $c = 11.30$ Å, $\alpha = 103\frac{1}{2}°$, $\beta = 97°$, $\gamma = 72°$. There is one formula unit per unit cell; density, calc. 1.85, found 1.88 g/cm³. The space group $C_i^1 - P\bar{1}$ indicated by the morphology would require centrosymmetry for the cation also here. The intensity distribution along the reciprocal c axis is very similar to that of the triclinic hydrogenfluoride dimorph (c spacings 10.97 and 11.08 Å respectively).

Trithiourea-tellurium(II) di(hydrogenfluoride), $Te(tu)_3(HF_2)_2$. This salt was obtained as prisms growing on top of a layer of the monoclinic tetrathiourea-tellurium(II) salt, as recounted above, and was the only product when a tellurium dioxide: thiourea molar ratio of 1 : 3 was employed (4.5 g thiourea in 15 ml of water in the above procedure). Yield, 2.7 g (52 %). (Found: F 17.36; S 22.23; Te 29.57. Calc. for $C_3H_{14}F_4N_6S_3Te$: F 17.51; S 22.17; Te 29.40.)

The salt forms monoclinic prisms {011} with $a = 5.91$ Å, $b = 20.68$ Å, $c = 11.47$ Å, $\beta = 95°$. The space group, from systematic absences, is $C_{2h}^5 - P2_1/c$. There are four formula units per unit cell; density, calc. 2.06, found 2.05 g/cm³. The crystal structure has been solved, and will be published later.

1. Foss, O. and Hauge, S. *Acta Chem. Scand.* **13** (1959) 1252.

2. Foss, O. and Hauge, S. *Acta Chem. Scand.* **13** (1959) 2155.

3. Foss, O. and Hauge, S. *Acta Chem. Scand.* **15** (1961) 1615.

4. Foss, O. and Hauge, S. *Acta Chem. Scand.* **15** (1961) 1616.

Received October 8, 1961.

The Equilibrium Between Molten FeO—Fe_2O_3 Mixtures and O_2 Gas

H. FLOOD and K. HAGEMARK

The Royal Norwegian Council for Scientific and Industrial Research, Institute of Silicate Science, The Technical University of Norway, Trondheim, Norway

From simple energetic assumptions it is possible to calculate the equilibrium between O_2 gas, Fe(II) and Fe(III) in solid solutions of Fe_3O_4 — Fe_2O_3, Fe_3O_4 — $MgFe_2O_4$ and Fe_3O_4 — $FeCr_2O_4$ based on spinel models with a defect cation lattice (cation vacancies and interstitial cations) [1-3]. These and similar models are also applicable [1,2] for the calculation of the equilibrium between oxygen gas and molten oxide mixtures, including a larger part of the range of composition from FeO—Fe_3O_4.

In the following a more plausible model will be suggested for the molten oxide mixtures based on a spinel like structure where instead of interstitial cations a corresponding number of oxygen ion vacancies are assumed.

The structure model is thus characterized by a Schottky disorder which can be expressed by

$$\frac{n_{\boxplus}}{n_c} \times \frac{n_{\boxminus}}{n_a} = N_{\boxplus} \times N_{\boxminus} = \text{const.} \quad (1)$$

where

$n_{\boxplus}$ = number of cation vacancies
$n_{\boxminus}$ = number of anion vacancies
n_c = number of cation positions
n_a = number of anion positions

(The cation and anion vacancies are simultaneously present only in a composition range very close to stoichiometric Fe_3O_4).

The requirement for the model is that

$$\frac{n_c}{n_a} = \frac{3}{4} \quad (2)$$

where

$$n_a = n_{Fe(II)} + n_{Fe(III)} + n_{\boxplus}$$
$$n_a = n_{O^{2-}} + n_{\boxminus}$$

A liquid of stoichiometric FeO thus corresponds to the structural formula $Fe_3O_3\boxminus$.

Fe(II) and Fe(III) ions are assumed to be statistically distributed over two kinds of positions, formally octahedral and tetrahedral with respect to the anion positions. The equilibrium between Fe(II), Fe(III) and O_2 gas can then be expressed by the equation

$$2\ Fe^{2+} + \tfrac{1}{2}O_2 + \boxminus = 2\ Fe^{3+} + O^{2-} \qquad (3)$$

(for Fe(III)/Fe(II) < 2. When Fe(III)/Fe(II) > 2 the corresponding equilibrium equation with cation vacancies can be applied [1]).

An additional assumption is necessary to make $p_{O_2} \neq 0$ for stoichiometric FeO. This can be accounted for by a disproportionation equilibrium

$$2\ Fe^{2+} = Fe^{+} + Fe^{3+} \qquad (4)$$

(or alternatively $3\ Fe^{2+} = Fe + 2\ Fe^{3+}$)

This equilibrium equation becomes important at compositions close to stoichiometric FeO only.

These assumptions lead to the following expression for log p_{O_2} as a function of the ratio O/Fe, (applicable in the composition range $FeO-Fe_3O_4$):

$$\log p_{O_2} = \text{const.} + 4 \log \left[\frac{x-1}{3-2x} \left(1 + \sqrt{1 + \frac{(2x-1)(3-2x)}{(x-1)^2} K_2} \right) \left(\frac{x}{\frac{1}{3}(4+y)-x} \right)^{\frac{1}{2}} \right] \qquad (5)$$

where

x = O/Fe in the melt
K_2 = the equilibrium constant of (4)
$y = 4 \cdot \frac{n_{\boxplus}}{n_{Fe}}$ (≈ 0 when $x < \frac{4}{3}$)

A calculation based on a randomly distributed cationic mixture only, without structural defects (Temkin model) leads to the following equation:

$$\log p_{O_2} = \text{const.} + 4 \log \frac{x-1}{3-2x} \qquad (6)$$

The two models are compared with the experimental values of Darken and Gurry [4] at 1 600°C as shown in Fig. 1. The superiority of the defect spinel model is evident.

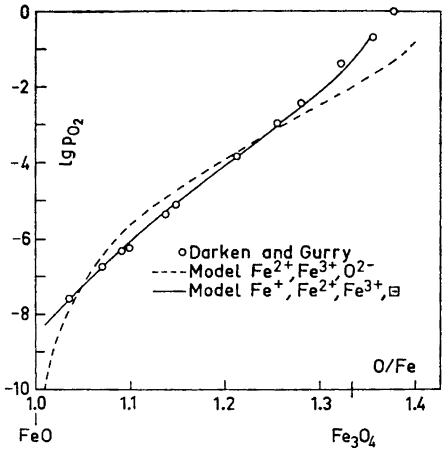

Fig. 1. lg p_{O_2} as a function of O/Fe in the melt (lg = $\log_{10}$).

A structural model of molten ionic compounds based on randomly distributed vacancies, mainly of the type which occupies the positions of the larger ion present, may possibly be of a more general applicability. This will be shown in a subsequent communication.

1. Flood, H. and Hill, D. G. *Z. Elektrochem.* **61** (1957) 18.
2. Takeuchi, S. and Furukawa, K. *Tohoku Sci. Rep. Ritu* **A 12** No. 2 (1960) 120.
3. Salmon, O. N. *J. Phys. Chem.* **65** (1961) 550.
4. Darken, L. S. and Gurry, R. W. *J. Am. Chem. Soc.* **68** (1946) 798.

Received October 2, 1961.

Are Defect Structure Models Applicable to Molten Salts?

H. FLOOD and K. HAGEMARK

The Royal Norwegian Council for Scientific and Industrial Research, Institute of Silicate Science, The Technical University of Norway, Trondheim, Norway

In a previous communication, it was shown that red-ox equilibria in molten $FeO-Fe_2O_3$ mixtures can be calculated from a simple model based on a spinel structure. In this model, the Fe(II) and Fe(III) ions are statistically distributed in the cation positions, and oxygen ions and vacancies in the anion positions [1].

One could then ask whether this model can also be applied to other systems where the radius ratio and charge ratio of the cation to anion are similar, for example when FeO is replaced by MgO (or LiF) and Fe_2O_3 by Al_2O_3 *etc.*

In the following some arguments will be presented which favour the opinion that the anion vacancy model might be better for describing the thermodynamic properties of systems of this type than for example the Temkin model.

(1) It is *well* established that on quenching molten Al_2O_3, the spinel modification γ-Al_2O_3 readily results. This would indicate that molten Al_2O_3 has a structure more similar to the spinel than to the corundum lattice.

The available data of the heat of fusion of α-Al_2O_3 compared with the $\gamma \rightarrow \alpha$ heat of transition together with the densities reported for α, γ and liquid Al_2O_3 also indicate strongly that γ-Al_2O_3 is more related to the liquid than to the corundum structure.

Another observation may also support this. It is known (compare the $MgO-Al_2O_3$ phase diagram [2]) that the spinel $MgO \cdot Al_2O_3$ at higher temperature forms solid solutions with Al_2O_3. This region of solubility increases rapidly with increasing temperature. The solid solution curve expresses the equilibrium:

$$\alpha\text{-}Al_2O_3 = \gamma\text{-}Al_2O_3 \ (MgO \cdot Al_2O_3) \text{ s.s.}$$

Extrapolation of the solid solution curve to $N_{Al_2O_3} = 1$, should give the transition temperature for $\alpha \rightleftharpoons \gamma$. It is evident that this temperature must be very close to the melting point of α-Al_2O_3 ($\approx$ 2 050°C).

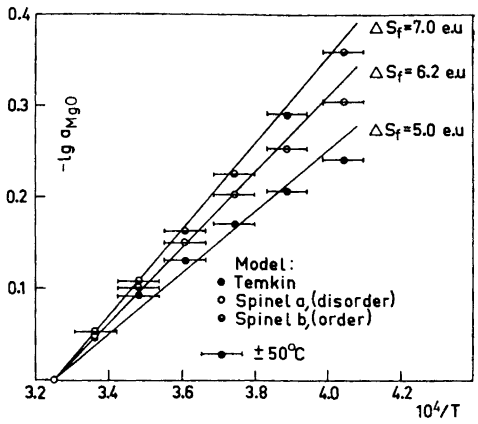

Fig. 1. lg a_{MgO} as a function of $10^4/T$. (lg = $\log_{10}$).

(2) The liquidus line of MgO in the system $MgO-Al_2O_3$ has not been accurately determined because of the extremely high temperature involved. Still an estimated position of the line is shown in the phase diagram, compare Muan and Osborn [3]. In Fig. 1 the activity of MgO is shown as a function of temperature, calculated from the following three models:

(*a*) Statistically distributed Mg^{2+} and Al^{3+} ions:

$$a_{MgO} = N_{Mg^{2+}} \cdot N_{O^{2-}}$$

where N = ionic fraction; $N_{O^{2-}} = 1$ (Temkin model)

(*b*) Spinel model with statistically distributed Mg^{2+} and Al^{3+} in the cation positions, and O^{2-} and $\square$ in the anion positions:

$$a_{MgO} = c \cdot N_{Mg^{2+}} \cdot N_{O^{2-}} \cdot N^{\frac{1}{3}}_{\square}$$

where $c = 3^{\frac{1}{3}} \cdot 4^{\frac{4}{3}}$ (from entropy of pure MgO of the chosen structure) N = ionic position fraction (Spinel model, disorder).

(*c*) Spinel model where the Al^{3+} occupy only the octahedral positions (normal spinel).

$$a_{MgO} = c' \cdot N_{Mg(IV)} \cdot N^{\frac{2}{3}}_{Mg(VI)} \cdot N_{O^{2-}} \cdot N^{\frac{1}{3}}_{\square}$$

where c' = constant; $N_{Mg(IV)} = 1$ (Spinel model, order).

(According to the latest information [4], the heat of formation of $MgO \cdot Al_2O_3$ from MgO and Al_2O_3 is < 5 kcal and hence lower than RT in the actual temperature range. An $Al^{3+}-Mg^{2+}$ disorder according to (*b*) should therefore be expected).

The three straight lines drawn in Fig. 1 are calculated from

$$\ln a_{MgO} = \frac{\Delta S_f}{R}\left(1 - \frac{T_f}{T}\right)$$

where the value of ΔS_f, the entropy of fusion, is chosen to be 5, 6.2 and 7 e.u. respectively. The MgO activity calculated with the normal value for alkali-halides, $\Delta S_f = 6.2$ e.u., are in a remarkably good agreement with the disorder model (*b*).

(3) The change in volume on melting of LiF is $\Delta V/V_f = 29.4$ % [5]. If contribution of the Li ions is neglected, the volume change according to the transition

$$LiF_{(NaCl)} \rightarrow LiF\square_{\frac{1}{3}(Spinel)}$$

should be $\Delta V/V_f = 33$ %, which is in astonishingly good agreement with the expansion on melting.

Of course this does not mean that the spinel model, as suggested above, is identical to the real structure of the liquid phase. However, it seems that an improvement in the evalution of the thermodynamic properties is possible if in addition to a Temkin statistical ion distribution one takes into account statistically distributed vacancy positions.

1. Flood, H. and Hagemark, K. *Acta Chem. Scand.* **15** (1961) 1624.
2. Roy, D. M., Roy, R. and Osborn, E. F. *Am. J. Sci.* **251** (1953) 341.
3. Osborn, E. F. and Muan, A. *Phase quilibrium diagrams of oxide systems.* Plate 3. The system $MgO—Al_2O_3—SiO_2$ (1960).
4. Altman, R. L. and Searcy, A. W. *Intern. Congr. Pure and Appl. Chem. 18th Congr.*, Montreal, Canada, 1961, p. 53.
5. Schinke, H. and Sauerwald, F. *Z. anorg. u. allgem. Chem.* **287** (1956) 313.

Received October 2, 1961.

Reversible Transformation of the Acceptor Specificity of Yeast D-Lactic Cytochrome *c* Reductase

AGNAR P. NYGAARD

Johan Throne Holst's Institute for Nutrition Research, University of Oslo, Blindern, Oslo, Norway

D-Lactic cytochrome *c* reductase (D-LcR), which is highly specific for cytochrome *c* as acceptor [1,2], is inhibited cytochrome *c*-competitively by the polyvalent cation protamine [3]. With increasing concentrations of protamine added to the assay medium, however, D-LcR acquires the ability to reduce ferricyanide. The decrease of the cytochrome *c* reduction and the increase of the ferricyanide reduction is shown in Fig. 1. The maximum rate obtained with ferricyanide as acceptor approximates that obtained with cytochrome *c* as acceptor; 2,6-dichlorophenol indophenol is not reduced.

The positively charged proteins lysozyme and ribonuclease, which likewise inhibit D-LcR in a cytochrome *c*-competitive man-

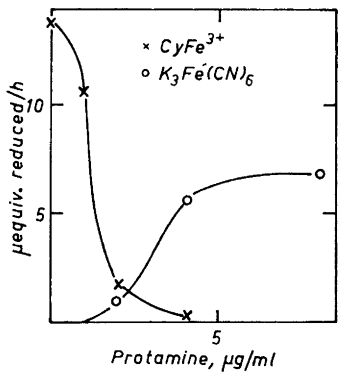

Fig. 1. Change of the acceptor specificity of D-LcR by the addition of protamine sulfate to the assay solution; the rate is expressed as μ-equiv. of acceptor reduced per hour, both when cytochrome *c* and when ferricyanide is used as acceptor. Buffer, sodium phosphate, $\Gamma/20.01$, + 0.001 M Versene; pH 6.8; D-lactate, 5×10^{-3} M; 23°; ×————×, cytochrome *c*, 4×10^{-6} M; o————o, ferricyanide, 1.4×10^{-4} M.

(According to the latest information [4], the heat of formation of $MgO \cdot Al_2O_3$ from MgO and Al_2O_3 is < 5 kcal and hence lower than RT in the actual temperature range. An $Al^{3+}-Mg^{2+}$ disorder according to (*b*) should therefore be expected).

The three straight lines drawn in Fig. 1 are calculated from

$$\ln a_{MgO} = \frac{\Delta S_f}{R}\left(1 - \frac{T_f}{T}\right)$$

where the value of ΔS_f, the entropy of fusion, is chosen to be 5, 6.2 and 7 e.u. respectively. The MgO activity calculated with the normal value for alkali-halides, $\Delta S_f = 6.2$ e.u., are in a remarkably good agreement with the disorder model (*b*).

(3) The change in volume on melting of LiF is $\Delta V/V_f = 29.4$ % [5]. If contribution of the Li ions is neglected, the volume change according to the transition

$$LiF_{(NaCl)} \rightarrow LiF\square_{\frac{1}{3}(Spinel)}$$

should be $\Delta V/V_f = 33$ %, which is in astonishingly good agreement with the expansion on melting.

Of course this does not mean that the spinel model, as suggested above, is identical to the real structure of the liquid phase. However, it seems that an improvement in the evalution of the thermodynamic properties is possible if in addition to a Temkin statistical ion distribution one takes into account statistically distributed vacancy positions.

1. Flood, H. and Hagemark, K. *Acta Chem. Scand.* **15** (1961) 1624.
2. Roy, D. M., Roy, R. and Osborn, E. F. *Am. J. Sci.* **251** (1953) 341.
3. Osborn, E. F. and Muan, A. *Phase quilibrium diagrams of oxide systems.* Plate 3. The system $MgO—Al_2O_3—SiO_2$ (1960).
4. Altman, R. L. and Searcy, A. W. *Intern. Congr. Pure and Appl. Chem. 18th Congr.*, Montreal, Canada, 1961, p. 53.
5. Schinke, H. and Sauerwald, F. *Z. anorg. u. allgem. Chem.* **287** (1956) 313.

Received October 2, 1961.

Reversible Transformation of the Acceptor Specificity of Yeast D-Lactic Cytochrome *c* Reductase

AGNAR P. NYGAARD

Johan Throne Holst's Institute for Nutrition Research, University of Oslo, Blindern, Oslo, Norway

D-Lactic cytochrome *c* reductase (D-LcR), which is highly specific for cytochrome *c* as acceptor [1,2], is inhibited cytochrome *c*-competitively by the polyvalent cation protamine [3]. With increasing concentrations of protamine added to the assay medium, however, D-LcR acquires the ability to reduce ferricyanide. The decrease of the cytochrome *c* reduction and the increase of the ferricyanide reduction is shown in Fig. 1. The maximum rate obtained with ferricyanide as acceptor approximates that obtained with cytochrome *c* as acceptor; 2,6-dichlorophenol indophenol is not reduced.

The positively charged proteins lysozyme and ribonuclease, which likewise inhibit D-LcR in a cytochrome *c*-competitive man-

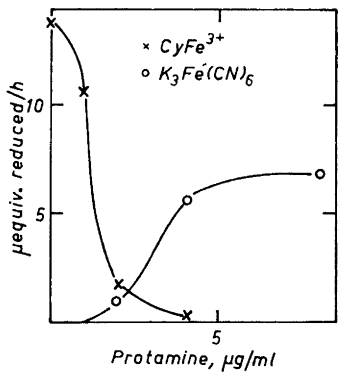

Fig. 1. Change of the acceptor specificity of D-LcR by the addition of protamine sulfate to the assay solution; the rate is expressed as μ-equiv. of acceptor reduced per hour, both when cytochrome *c* and when ferricyanide is used as acceptor. Buffer, sodium phosphate, $\Gamma/20.01$, + 0.001 M Versene; pH 6.8; D-lactate, 5×10^{-3} M; 23°; ×————×, cytochrome *c*, 4×10^{-6} M; o————o, ferricyanide, 1.4×10^{-4} M.

ner, do not form a ferricyanide reductase system with D-LcR.

The inhibition of the D-lactic cytochrome *c* reductase system is counteracted by the polyvalent anions deoxyribonucleic acid and chondroitine sulfate; the recovered D-lactic cytochrome *c* reductase system is inactive in the reduction of ferricyanide. In the absence of protamine these polyvalent anions, too, are acceptor-competitive inhibitors of cytochrome *c* reduction.

The reversible transformation of the D-lactic cytochrome *c* reductase system to a ferricyanide reductase system is interesting in view of the fact that a D-lactic ferricyanide reductase disappears and D-LcR is formed during oxygen induction of anaerobically grown yeast [4]. The D-lactic ferricyanide reductase formed from D-LcR and protamine differs from anaerobic D-lactic dehydrogenase, however. There are differences in the pH optimum, the apparent Michaelis constants for D-lactate and ferricyanide, and the reduction of 2,6-dichlorophenol indophenol; only the latter enzyme reduces this acceptor.

1. Nygaard, A. P. *J. Biol. Chem.* **236** (1961) 920.
2. Nygaard, A. P. *J. Biol. Chem.* **236** (1961) 2128.
3. Nygaard, A. P. *J. Biol. Chem.* **236** (1961) 2779.
4. Nygaard, A. P. *J. Biol. Chem.* **236** (1961) 236.

Received October 10, 1961.

ACTA CHEMICA SCANDINAVICA 15 (1961) 1629–1638

Photoreduction of Methyl Red and Tetrazolium Blue by Spinach Chloroplasts and Chromatophores of *Rhodospirillum rubrum* *

OWEN K. ASH, WALDO S. ZAUGG and LEO P. VERNON**

Department of Chemistry, Brigham Young University, Provo, Utah, U.S.A., and Medicinska Nobel-institutet, Biokemiska Avdelningen, Stockholm, Sweden

1. Chloroplasts prepared from spinach leaves have been shown to catalyze a photoreduction of both methyl red and tetrazolium blue in a regular Hill reaction. Addition of 3-(3,4-dichlorophenol)-1,1-dimethylurea (DCMU) *** at 10^{-5} M inhibited both reactions, but the further addition of ascorbate and 2,6-dichlorophenolindophenol (DPIP) restored the activity of the chloroplasts in the photoreductions.

2. Chromatophores of *Rhodospirillum rubrum* also catalyzed a photoreduction of both dyes in the presence of DPIP and ascorbate. Addition of quinacrine markedly stimulated both reactions, with half-maximal stimulation occurring at 20 μM quinacrine. Experiments performed in red light showed the quinacrine did not increase the reaction rate by itself acting as a photocatalyst in the reactions. Addition of quinacrine inhibited the succinate-supported photoreduction of DPN by the chromatophores.

3. The respiratory inhibitors antimycin A and 2-heptyl-4-hydroxyquinoline-N-oxide both failed to stimulate the photoreduction of tetrazolium blue and methyl red by *R. rubrum* chromatophores, but instead were slightly inhibitory. These inhibitors strongly inhibited the succinate-supported photoreduction of DPN. Thus in terms of inhibition characteristics with chromatophores, quinacrine did not resemble antimycin A and HQNO. The photoreductions catalyzed by chloroplasts were not affected by added quinacrine, which is a distinguishing feature of the two photosynthetic systems.

* This investigation was supported by a research grant (No. E 917-C) from the *National Institute of Allergy and Infectious Diseases, National Institutes of Health, United States Public Health Service* and was completed during the tenure of Predoctoral Fellowships from the same institute to two of the authors (O.K.A. and W.S.Z.).

** Present address: Charles F. Kettering Foundation, Yellow Springs, Ohio, USA.

*** The abbreviations used are: DPIP, 2,6-dichlorophenolindophenol; Tris, tris hydroxymethyl)aminomethane; DCMU, 3-(3,4-dichlorophenyl)-1,1-dimethylurea; FMN, flavin mononucleotide, and HQNO, 2-heptyl-4-hydroxyquinoline-N-oxide.

Experiments performed with both plant chloroplasts and chromatophores of *Rhodospirillum rubrum* have shown that with both photosynthetically active systems a photoreduction of an added electron acceptor can be coupled to a photooxidation of ascorbate [1-4]. The photooxidation of ascorbate, furthermore, was to a large degree dependent upon the presence of DPIP [2]. This oxidation-reduction dye, which is reduced directly by ascorbic acid, appears to serve as an intermediate electron carrier between the chlorophyll system and ascorbate. An extensive series of investigations by Krasnovsky and coworkers [5] has shown that ascorbate can participate in photoreduction reactions catalyzed by isolated chlorophylls and porphyrins, in which the final electron acceptors may be oxidation-reduction dyes such as methyl red or safranin T [6,7], pyridine nucleotides [8], or the chlorophyll or porphyrin itself [9]. A study of the photoreduction of selected reagents by chloroplasts, chromatophores and isolated chlorophylls is desirable, since it will allow a comparison of the various systems and may indicate to what extent the photoreactions catalyzed by isolated chlorophylls are representative of the photoreactions taking place in the organized biological systems. For purposes of comparison, the photoreductions catalyzed by the isolated chlorophylls and porphyrins should be studied in aqueous media. The present paper describes the photoreduction of two such compounds, methyl red and tetrazolium blue, by both chloroplasts and chromatophores, while the following paper describes the photoreduction of these compounds by chlorophylls and porphyrins. In the case of the chloroplasts, both dyes are photoreduced in a regular Hill reaction, in which water is oxidized to produce oxygen. The dyes are also photoreduced by either chloroplasts or chromatophores when ascorbate is the electron donor, but the presence of DPIP is also required.

MATERIALS AND METHODS

Chloroplasts were prepared from spinach as previously described [3]. The growth of *R. rubrum* cells and the preparation of chromatophores from the cells of this bacterium have been reported previously [4]. The experiments were performed in a Thunberg tube which was adapted in such a manner that two regular 1 cm Pyrex absorption cells were joined to the main part of the tube through a T joint. The two absorption cells were spaced so that they would fit into positions 1 and 4 of the cell holder of a Beckman DU spectrophotometer. A special black cardboard cover was constructed to cover the adapted Thunberg tube which extended above the cell compartment of the spectrophotometer. The reagents required for a particular experiment were added to the reaction vessel, after which anaerobicity was obtained by means of three one-minute evacuations with a vacuum pump interspaced with the admission of nitrogen gas and mixing of the nitrogen gas with the contents of the vessel. Thus, the oxygen was flushed out and replaced with nitrogen. The contents of the reaction vessel were initially at 0°C. After the evacuation procedure the contents of the reaction vessel were distributed in approximately equal amounts in the two absorption cells, the reaction vessel was placed for four minutes in a glass chamber which was maintained at the desired temperature with an immersion heater, cooling coil and thermoregulator, following which the illumination period was initiated. One of the arms of the adapted Thunberg tube was covered with a cap of black cloth, and the contents of this absorption cell served as a dark control system. Absorbancy readings were made at 5 min intervals against a blank of appropriate absorbancy so that the observed readings were on the most sensitive part of the absorbancy scale. Illumination was performed with a 150 W tungsten reflector flood lamp, which gave a light intensity of approximately 1 700 foot candles in the reaction vessel. The photoreduction of methyl

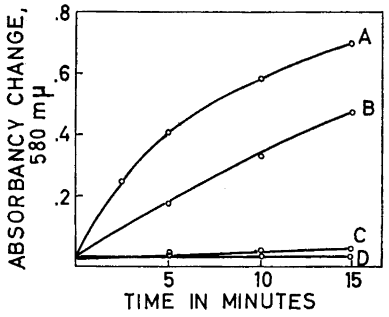

Fig. 1. Photoreduction of tetrazolium blue by spinach chloroplasts and chromatophores of *R. rubrum*. The experimental conditions were those of Tables 1 and 2, with the chlorophyll concentrations being 4.8 and 5.5 μM for the experiments with chloroplasts and chromatophores respectively. Anaerobic conditions were employed. A, chloroplasts in light; B, chromatophores in light; C, chromatophores in the dark, and D, chloroplasts in dark

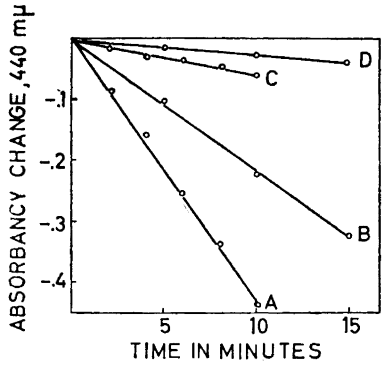

Fig. 2. Photoreduction of methyl red by spinach chloroplasts and *R. rubrum* chromatophores under anaerobic conditions. The experimental conditions were the same as given in Tables 1 and 2, including the concentrations of chlorophyll. A, chromatophores in the light; B, chloroplasts in the light; C, chromatophores in the dark; D, chloroplasts in the dark.

red was followed at 440 mμ, while tetrazolium blue was determined at 580 mμ. The reactions were run at a temperature of 30°C.

Chlorophyll was determined by the method of Vernon [10] and bacteriochlorophyll was determined by the method of van Niel and Arnold [11]. Tris and FMN were purchased from Sigma Chemical Co. of St. Louis, ascorbic acid from the Nutritional Biochemical Corp., DPIP from Eastman Organic Chemical Co., methyl red from Merck and Co., tetrazolium blue from Mann Research Laboratories, Inc., DCMU was a gift from Dr. N. Bishop, and HQNO was a gift from Dr. J. W. Lightbrown.

RESULTS

Photoreductions catalyzed by spinach chloroplasts. The photoreduction of tetrazolium blue and methyl red by spinach chloroplasts in a regular Hill reaction is shown in Figs. 1 and 2, respectively. For these reactions there was no added electron donor, and the photoreduction of the dye was presumably accompanied by an evolution of oxygen. In the case of tetrazolium blue there was no observable reduction of the dye in the dark, while a slow but detectable reduction of methyl red did take place in the dark. Apparently the chloroplast preparation contained sufficient endogenous electron donors to catalyze the slow dark reaction.

The photoreaction with methyl red was linear with time, but this was not the case with tetrazolium blue. It is difficult to make a quantitative measurement of tetrazolium blue reduction in an aqueous solution, due to the formation of the insoluble formazan. Lester and Smith [12] have solubilized the formazan by adding a detergent to the reaction mixture in their experiments. It was not possible to do so in the present case, however, due to the difficulty of removing

Table 1. Photoreduction of tetrazolium blue and methyl red by spinach chloroplasts under anaerobic conditions in the presence and absence of ascorbate and DPIP. The reaction mixture contained 83 mM Tris buffer pH 7.0, 120 μM methyl red or 67 μM tetrazolium blue and 4.8 μM chlorophyll which was contained in spinach chloroplasts. Where indicated there was also present 0.67 mM ascorbate, 34 μM DPIP and 10 μM 3-(3,4-dichlorophenyl)-1,1-dimethylurea (DCMU). The final volume was 6.0 ml and the final pH of the reaction system was 6.9. The control system contained only the dye, chloroplasts, and buffer. A photoreduction is indicated by an increase in absorbancy at 580 mμ in the case of tetrazolium blue (formation of blue color), and in the case of methyl red a decrease in absorbancy at 440 mμ indicated a photoreduction (loss of yellow color). Illumination was carried out with a 150 W tungsten reflector flood lamp.

Conditions	Change in absorbancy after 10 min (Light minus dark)	
	Methyl red 440 mμ	Tetrazolium blue 580 mμ
Control	−0.202	0.575
+ ascorbate	−0.497	0.621
+ ascorbate, DPIP	−1.23	0.701
+ DCMU	+ 0.021	0.051
+ DCMU, ascorbate, and DPIP	−0.817	0.481
+ ascorbate, DPIP, boiled chloroplasts	−0.016	0.006
Control, chloroplasts aged 100 h, 0°C.	+ 0.012	0.002
+ ascorbate, DPIP	−0.622	0.051

aliquots from the anaerobic system and maintaining the anaerobicity required. Accordingly, the data recorded for tetrazolium blue were those obtained directly, and as the reaction proceeded there was formation of the insoluble product. However, for the purposes of these experiments the reproducibility of the reaction for the short times investigated was sufficient to show the qualitative aspects of the reaction. It should be mentioned that while there was visible precipitation of the reduced dye in the experiments involving chloroplasts (and microscopically it was shown to collect on the chloroplasts), when chromatophores were used a much clearer "solution" was obtained. This was probably due to the smaller particles involved in the photoreaction in the case of the chromatophores.

The ability of chloroplasts to utilize ascorbate (in the presence of DPIP) as the electron donor for the photoreduction of both tetrazolium blue and methyl red is shown in Table 1. The addition of DCMU, a potent inhibitor of the oxygen evolving system[13], completely inhibited methyl red photoreduction in the absence of ascorbate and decreased the photoreduction of tetrazolium blue to less than 10 % of the original activity. This demonstrates that the photoreduction of the dyes in the control system was coupled to the evolution of oxygen. Addition of ascorbate increased the rates of the reactions, and further addition of DPIP gave the maximal rates. When DCMU was present in the system, ascorbate and DPIP were able to overcome the inhibitory effect of this compound, which is readily explained in terms of the ascorbate and DPIP couple serving as the electron donor for the photoreduction of the dyes.

Table 2. Photoreduction of methyl red and tetrazolium blue by chromatophores of *Rhodospirillum rubrum*. The reaction system contained 33 mM Tris buffer pH 7.2, 0.67 mM ascorbate, 34 μM DPIP, 11 μM bacteriochlorophyll (in the chromatophores) and either 44 μM tetrazolium blue or 120 μM methyl red in a final volume of 6.0 ml. Anaerobic conditions were employed. Illumination was performed with a 150 W tungsten reflector flood lamp.

Conditions	Absorbancy change in 10 min Light minus dark	
	Methyl red 440 mμ	Tetrazolium blue 580 mμ
Complete system	−0.439	0.539
− DPIP	+ 0.025	−0.011
− ascorbate, DPIP	+ 0.012	−0.009
− chromatophores	0	0
Chromatophores heated at 95°C for 10 min	+ 0.008	0.039

The behavior of the chloroplasts in these reactions is the same as was previously observed [3] for the photoreduction of TPN, DPN, indigo carmine, FMN and vitamin K_3. Thus, the chloroplast appears to be employing its usual reaction mechanisms in the present photoreductions.

As shown in Table 1, boiling the chloroplasts destroyed their ability to catalyze the photoreduction reactions in the presence of ascorbate and DPIP. The accompanying paper in this series [14] shows that isolated chlorophylls are capable of catalyzing a photoreduction of both dyes in the presence of ascorbate and DPIP. Since the isolated chlorophylls can catalyze the reactions, the boiling process apparently either causes a change in the chlorophyll molecules, or more likely, through some physical process makes the chlorophyll unavailable to the reagents in solution. The latter could be due to a structural change in the chloroplasts or a covering of some specific reaction sites by chloroplast material released by the boiling process.

Photoreductions catalyzed by R. rubrum chromatophores. The ability of *R. rubrum* chromatophores to catalyze a photoreduction of methyl red and tetrazolium blue is shown by the data presented in Figs. 1 and 2. In order for the photoreduction to proceed, the presence of ascorbate and DPIP was required, since unlike the plant chloroplast, the bacterial system cannot catalyze a photoreduction unless some electron donor is added to the reaction system. On the basis of the chlorophyll content of the chloroplasts and the chromatophores used in the experiments, it is apparent that the chloroplasts were more effective in both reactions. However, as shown below, the activity of the chromatophore system was greatly stimulated by the addition of quinacrine. The ability of the ascorbate and DPIP couple to donate electrons to the dyes used in the present experiments agrees with previously published data, in which the ascorbate-DPIP couple was shown to support the photoreduction of DPN by *R. rubrum* chromatophores [4]. The strict dependence of the photoreductions upon the presence of both DPIP and ascorbate is shown in Table 2.

Table 3. Stimulation by quinacrine of the anaerobic photoreduction reactions catalyzed by chromatophores of *R. rubrum*. The composition of the complete system was the same as given for Table 2, with 0.2 mM quinacrine also present. The reaction time was decreased to 5 min. For experiment 2 the chromatophores were heated at 95°C for 10 min.

Conditions	Absorbancy change in 5 min Light minus dark	
	Methyl red 440 mμ	Tetrazolium blue 580 mμ
1. Complete system	−1.42	0.902
— quinacrine	−0.230	0.296
— DPIP	+ 0.003	0.071
— ascorbate, DPIP	+ 0.008	0.008
2. Complete, chromatophores heated	−0.060	0.024
— quinacrine	+ 0.030	0.020

As was the case with chloroplasts, heating the chromatophores destroyed their ability to catalyze both reactions. The inability of ascorbate alone to support the photoreactions agrees with the previously advanced hypothesis that although the ascorbate serves as the ultimate electron donor, it is the reduced form of the DPIP which interacts with the chlorophyll system, and the presence of excess ascorbate insures that the DPIP remains in the reduced form and allows the reactions to proceed [3,4].

The addition of quinacrine to chromatophores of *R. rubrum* produces a marked inhibition of photosynthetic phosphorylation [15]. In this phosphorylation process ATP is formed by reactions coupled with the recombination of the electrons from the primary reducing site with the oxidized product formed *via* the primary photochemical act of the chromatophore. Since such a recombination would not favor the demonstration of a net photoreduction of tetrazolium blue or methyl red, it was thought that addition of this compound might serve to stimulate the photoreduction reactions. The data presented in Table 3 show that such was the case, and marked stimulation was observed if quinacrine was present in the reaction system. Furthermore, quinacrine was not effective in the absence of DPIP, indicating that the quinacrine did stimulate the reaction already taking place, and the increase in activity was not due to the introduction of a new type of reaction catalyzed by the quinacrine. Again, heating the chromatophores served to remove almost all of the activity.

The illumination for the preceding experiments was accomplished with white light. Since quinacrine is structurally somewhat similar to the flavins and the flavins are capable of catalyzing photoreduction reactions in white light [16], it was necessary to perform the same type of experiment using red light which was not absorbed by the quinacrine. For a comparison, the effect of FMN upon the reaction run in both white and red light was examined. The results of these experiments are shown in Table 4. Concerning the photoreduction of tetrazolium blue, the presence of either FMN or quinacrine resulted in an increased rate of photoreduction in white light. Performing the experiment in red light, however, showed that the stimulating effect of quinacrine was

Table 4. The effect of quinacrine and FMN on the anaerobic photoreduction reactions of *R. rubrum* chromatophores using red and white light. The composition of the experimental system was the same as given in Table 2, with the exception of the bacteriochlorophyll concentrations which were 3.7 μM for the experiments using tetrazolium blue and 3.0 μM for the experiments with methyl red. Also present were 83 μM FMN and 100 μM quinacrine where indicated.

Conditions	Absorbancy change, light minus dark	
	Methyl red 440 mμ 5 min	Tetrazolium blue 580 mμ 10 min
White light		
Control	−0.163	0.156
+ quinacrine	−1.16	0.693
+ FMN	−0.167	0.674
+ quinacrine, FMN	−1.04	0.745
Red light		
Control	−0.140	0.287
+ quinacrine	−1.05	0.924
+ FMN	−0.030	0.255
+ quinacrine, FMN	−0.176	0.992
+ quinacrine and 166 μM FMN	−0.340	—

retained while FMN was inactive. Thus, the stimulation by FMN in white light could be ascribed to the FMN itself acting as the photocatalyst for the reaction, while quinacrine stimulated the photoreaction catalyzed by the chlorophyll of the chromatophore. When the experiments utilizing methyl red as electron acceptor are considered, it is seen that whereas the quinacrine behaved in the same fashion as with tetrazolium blue, FMN failed to stimulate the reaction in white light, and in red light it inhibited the reaction. Furthermore, addition of both quinacrine and FMN to the system revealed that the FMN acted as an antagonist to the quinacrine and decreased the usual activation observed with quinacrine. The reason for the inhibitory effect of FMN in the case of methyl red photoreduction is not known. FMN may be acting in a competitive manner with quinacrine in the activated methyl red photoreduction, but the necessary experiments required to support this conclusion have not yet been performed. As shown in the subsequent paper of this series [14], quinacrine does not stimulate the photoreduction of either tetrazolium blue or methyl red when the photocatalyst is isolated chlorophyll or porphyrin. Thus, an explanation of its effect must be found in terms of the organized electron transport system found in the chromatophore.

The effect of quinacrine concentration upon both tetrazolium blue and methyl red photoreduction is shown in Fig. 3. Both reactions respond in a similar manner to changes in quinacrine concentration, indicating a common point of action for the quinacrine in both photoreactions. The concentrations of quinacrine active in these photoreactions are close to those which are effective in inhibiting photosynthetic phosphorylation in chromatophores of the same organism [15].

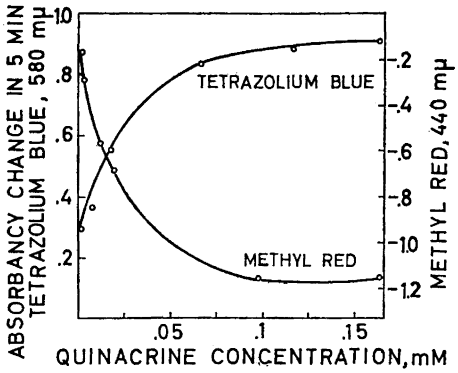

Fig. 3. The effect of quinacrine concentration upon the photoreduction reactions. The composition of the reaction systems was the same as given in Table 2, except that for the experiment with methyl red the final concentration of bacteriochlorophyll was 3.0 μM

Aside from quinacrine, other compounds are known to inhibit the photosynthetic phosphorylation process in bacterial chromatophores, notably antimycin A and 2-heptyl-4-hydroxyquinoline-N-oxide (HQNO) [4,17]. Using the same reasoning advanced above, addition of these compounds would be expected to increase the rate of the photoreduction reactions. As shown in Table 5, such was not the case, and the presence of these compounds served to slightly inhibit the photoreductions. For comparison, the effect of these compounds upon the photoreduction of DPN is included. In the case of DPN photoreduction the electron donor was succinate, which couples with the chromatophores *via* succinic dehydrogenase [18]. Of the three inhibitors, quinacrine was unique, since it inhibited only DPN photoreduction, while stimulating the other reactions. Both antimycin A and HQNO inhibited all three reactions, but only DPN photoreduction was strongly inhibited. There is not enough evidence available at present to explain these differences in terms of the electron transfer

Table 5. Effect of respiratory inhibitors upon the photoreductions catalyzed by *R. rubrum* chromatophores. The composition of the control systems was the same as given for Table 2 for methyl red and tetrazolium blue photoreduction. For the experiments on DPN photoreduction, the ascorbate and DPIP were replaced with 5 mM succinate. The inhibitor solutions added to the reaction system were all 5 mg per ml, and the antimycin A and 2-heptyl-4-hydroxyquinoline-N-oxide (HQNO) were dissolved in ethanol. Anaerobic conditions were employed.

Additions	Absorbancy change, light minus dark		
	DPN 340 mμ, 10 min	Methyl red 440 mμ, 5 min	Tetrazolium blue 580 mμ, 5 min
None	0.194	−0.251	0.254
antimycin A, 0.5 mg	−0.009	−0.211	0.156
HQNO, 0.25 mg	0.025	−0.215	0.243
quinacrine, 0.5 mg	0.043	−1.08	0.777
antimycin A and quinacrine	—	−0.819	0.368
HQNO and quinacrine	—	−0.998	0.463

components of the chromatophore. If quinacrine stimulation of tetrazolium blue and methyl red photoreduction is due to its ability to prevent the cyclization of the electrons in the chromatophore, it is difficult to see why antimycin A and HQNO do not give the same response.

In comparing the photoreduction of DPN with the other two photoreactions, the differences in the two reaction systems employed became apparent. The succinate-supported photoreduction of DPN was much more sensitive to the respiratory inhibitors. Also, in comparing the abilities of both succinate and the ascorbate-DPIP couple to support DPN photoreduction, succinate was observed to give the better reaction. Furthermore, succinate could not support a photoreduction of methyl red and produced only a slow photoreduction of tetrazolium blue. Accordingly, there are unknown aspects of both systems which must first be clarified before the mode of action of these inhibitors can be ascertained.

Preliminary experiments have been performed to see if quinacrine was capable of stimulating the photoreductions catalyzed by chloroplasts. Although a few cases were observed in which there was slight activation, the general case was that quinacrine had no effect on the photoreductions. Accordingly, one significant difference between the chloroplasts and chromatophores is their response to quinacrine.

DISCUSSION

The photoreduction of methyl red and tetrazolium blue by spinach chloroplasts in the absence of any added electron donor shows the characteristics of a regular Hill reaction. However, a simpler reaction is taking place in the presence of ascorbate and DPIP. The information presented in the following paper [14] shows that these dyes can be photoreduced by the ascorbate-DPIP couple in the presence of isolated chlorophylls or porphyrins, and there is no reason in the present case to rule out a direct photoreduction of the dyes by the chlorophyll system in the chloroplast. There is also no reason to rule out a direct reaction of the DPIP-ascorbate couple with the chlorophyll system. Indeed, in view of the data on the inability of DCMU to prevent the photoreduction of the dyes in the presence of the ascorbate-DPIP couple, a direct reaction of the couple with the chlorophyll seems most logical. Therefore, it would appear that the only part of the chloroplast utilized in these reactions is the photoactive chlorophyll system, making this reaction one of the most simple of the many photochemical reactions catalyzed by plant chloroplasts.

The ability of *R. rubrum* chromatophores to catalyze the same reactions as the plant chloroplasts again points up the basic similarity of the plant and bacterial systems. It has earlier been shown that with both chloroplasts and chromatophores a photooxidation of ascorbate and a corresponding photoreduction of DPN was possible [3]. This agrees with the concept that the bacterial chromatophores practice a more primative photosynthetic process, and under certain conditions the plant chloroplast can be forced into the same pattern [3,19].

One difference in the two systems investigated is the manner in which quinacrine affects the photoreductions catalyzed by chloroplasts and chromatophores. From the information presented in the following paper [14] it is

seen that quinacrine does not stimulate the corresponding photoreductions catalyzed by isolated chlorophylls, and therefore it does not affect the chromatophore by influencing the processes associated with the activated chlorophyll system. Therefore, it is most likely active by virtue of its ability to prevent the cyclization of electrons *via* the electron transport components of the chromatophore. However, further experimentation is required, since the differences found in the response of chromatophores to quinacrine and the respiratory inhibitors antimycin A and HQNO still cannot be explained in a satisfactory manner.

REFERENCES

1. Vernon, L. P. and Kamen, M. D. *Arch. Biochem. Biophys.* **51** (1954) 122.
2. Vernon, L. P. and Hobbs, M. O. *Arch. Biochem. Biophys.* **72** (1957) 25.
3. Vernon, L. P. and Zaugg, W. S. *J. Biol. Chem.* **235** (1960) 2728.
4. Vernon, L. P. and Ash, O. K. *J. Biol. Chem.* **235** (1960) 2721.
5. Krasnovsky, A. A. *Ann. Rev. Plant Physiol.* **11** (1960) 363.
6. Krasnovsky, A. A. and Brin, G. P. *Doklady Akad. Nauk. S.S.S.R.* **73** (1950) 1239.
7. Krasnovsky, A. A. *Doklady Akad. Nauk. S.S.S.R.* **122** (1958) 1061.
8. Krasnovsky, A. A. and Brin, G. P. *Doklady Akad. Nauk. S.S.S.R.* **67** (1949) 325.
9. Krasnovsky, A. A. *Doklady Akad. Nauk. S.S.S.R.* **60** (1948) 421.
10. Vernon, L. P. *Anal. Chem.* **32** (1960) 1144.
11. van Niel, C. B. and Arnold, W. *Enzymologia* **5** (1938) 244.
12. Lester, R. L. and Smith, A. L. *Biochim. et Biophys. Acta* **47** (1961) 475.
13. Bishop, N. I. *Biochim. et Biophys. Acta* **27** (1958) 205.
14. Vernon, L. P. *Acta Chem. Scand.* **15** (1961) 1639.
15. Baltscheffsky, H. *Biochim. et Biophys. Acta* **40** (1960) 1.
16. Vernon, L. P. *Biochim. et Biophys. Acta* **36** (1959) 177.
17. Baltscheffsky, H. and Baltscheffsky, M. *Acta Chem. Scand.* **12** (1958) 1333.
18. Vernon, L. P. and Ash, O. K. *J. Biol. Chem.* **234** (1959) 1878.
19. Arnon, D. I. *Nature* **184** (1959) 10.

Received April 27, 1961.

ACTA CHEMICA SCANDINAVICA 15 (1961) 1639–1650

Photoreduction of Methyl Red and Tetrazolium Blue by Ascorbate: Catalysis by Chlorophylls and Porphyrins in Aqueous Media *

LEO P. VERNON**

Medicinska Nobelinstitutet, Biokemiska Avdelningen, Stockholm, Sweden

1. A photoreduction of methyl red and tetrazolium blue by ascorbate has been observed in the presence of pure chlorophyll *a*, chlorophyll *b*, pheophytin *a*, pheophytin *b*, protoporphyrin IX, hematoporphyrin IX and coproporphyrin III in aqueous solutions under anaerobic conditions. The chlorophylls and pheophytins, which were added to the aqueous reaction system absorbed on sucrose, gave "solutions" which were visually clear, but were apparently suspensions of small aggregates of the pigment molecules.

2. The photoreductions of both methyl red and tetrazolium blue were stimulated (with chlorophylls or porphyrins as catalysts) if 2,6-dichlorophenolindophenol (DPIP)*** was also present. This indicates a role of intermediate electron carrier for DPIP, serving to increase the flow of electrons from ascorbate to the photocatalyst under the influence of light. Addition of quinacrine had no effect upon tetrazolium blue photoreduction, but showed slight inhibition in the case of methyl red photoreduction.

3. A comparison of a number of porphyrins and porphyrin derivatives as catalysts for these reactions has been made. Activity was observed for the chlorophylls, pheophytins and porphyrins. Iron porphyrins, hemeproteins and FMN were inactive.

4. During photoreduction of methyl red a simultaneous oxidation of ascorbate was observed. Glutathione could substitute for ascorbate but gave a slower rate of reaction.

5. In the presence of air, the chlorophylls and protoporphyrin catalyzed a photooxidation of DPNH, reduced cytochrome *c*, reduced DPIP and ascorbate. Comparative rates are given.

6. These results are discussed in relation to the same photoreduction reactions catalyzed by plant chloroplasts and bacterial chromatophores.

* This investigation was conducted during the tenure of a National Science Foundation Senior Postdoctoral Fellowship.

** Present address: Charles F. Kettering Foundation, Yellow Springs, Ohio, USA.

*** The abbreviations used are: DPIP, 2,6-dichlorophenolindophenol; Tris, tris(hydroxymethyl)-aminomethane; FMN, flavin mononucleotide, and DPNH, reduced diphosphopyridine nucleotide.

The ability of isolated chlorophylls, pheophytins and porphyrins to catalyze photochemical oxidation-reduction reactions has been shown by the extensive investigations of Krasnovsky and his coworkers [1]. Following the original paper of Krasnovsky which reported a photochemical reduction of chlorophyll by ascorbic acid in pyridine solution [2], it was shown that chlorophylls in light could transfer electrons from ascorbate to a wide variety of compounds including oxidation-reduction dyes, riboflavin, quinones, hematin, dehydroascorbic acid and pyridine nucleotides [3,5]. A chlorophyll-catalyzed photoreduction of methyl red by phenylhydrazine in methanol was demonstrated by the earlier experiments of Livingston and Pariser [6]. The photoreduction of the chlorophylls and pheophytins proceeds rapidly in the presence of pyridine, piperidine, nicotine and quinonine [7], and most of the investigations by the Krasnovsky group have involved such non-aqueous media. That some of the reactions can also proceed in aqueous media was shown by the experiments of Krasnovsky and Umrikhina [8], in which ascorbic acid, ferrous ion and ferrocyanide served as electron donors in a photochemical transfer of electrons to methyl red in the presence of chlorophyll, hematoporphyrin and protoporphyrin.

The present investigation is concerned with the photoreduction of two dyes, methyl red and tetrazolium blue, which have been shown to be readily photoreduced by plant chloroplasts and by chromatophores of *Rhodospirillum rubrum* [9]. With chromatophores, the photoreduction reactions require the presence of both ascorbate and DPIP. Accordingly, the photoreduction of these two dyes by ascorbate using chlorophylls, porphyrins and their derivatives as the photocatalyst was examined, with particular emphasis upon the role of DPIP in such photoreductions. The reactions were all performed in aqueous media, in order that a direct comparison could be made with the data obtained from the experiments with chloroplasts and chromatophores. The chlorophylls were added to the aqueous medium adsorbed on powdered sucrose, and as the sucrose dissolved, the chlorophyll remained in a fine colloidal suspension. The results obtained for methyl red photoreduction are in agreement with the previous data reported by the Krasnovsky group [8], but the presence of DPIP in the reaction system was found to stimulate the reactions.

MATERIALS AND METHODS

A description of the reaction vessels used in this experimental work has been given in the previous paper [9]. Anaerobic conditions were obtained in the manner reported, with the exception that argon gas was used for the intermediate flushings in the present investigation. Illumination was performed with either a 150 or 500 W tungsten reflector flood lamp which gave a light intensity at the reaction site of approximately 1500 or 4500 footcandles, respectively. The reactions were run in a water bath with a controlled temperature of 26°C, and the reaction vessels were illuminated through the transparent walls of the plastic container. Absorbancy readings were made on the illuminated and non-illuminated systems at 5 min intervals in the case of the tetrazolium blue experiments and at 2 min intervals for the methyl red experiments. A Beckman DU spectrophotometer was used for all measurements.

Chlorophyll *a* and chlorophyll *b* were prepared from spinach leaves by means of chromatography on a powdered sucrose column as previously reported [10]. Following the final separation of the chlorophylls on the column, the sucrose adsorbing the pure chlorophylls was dug out of the column, air dried in the dark, and stored at −20°C in the dark in a drying chamber. For the experiments involving chlorophyll *a* and chlorophyll *b*, the

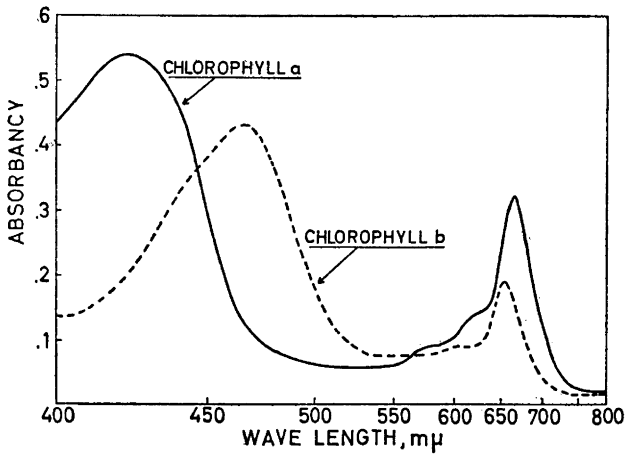

Fig. 1. Absorption spectra of pure chlorophyll *a* and chlorophyll *b* dissolved in Tris buffer solution after adsorption on sucrose. In addition to the chlorophyll the solution contained only 10 mM Tris buffer pH 8.0 and the sucrose which had adsorbed the pigment. The final sucrose concentration was approximately 0.5 M. The spectra were obtained with a Beckman DK2 automatic recording spectrophotometer.

chlorophylls were added to the reaction system on the sucrose. The sucrose quickly dissolved as the liquid was swirled around, and the chlorophyll was thus dispersed through the medium. Although not a true solution of chlorophyll, the reaction mixture containing the chlorophyll was visually clear and there was no tendency for the chlorophylls to precipitate out of solution unless it was allowed to stand for several hours. The chlorophyll adsorbed on sucrose could not be stored for extended periods without losing activity, and the experiments described in this investigation were performed with freshly prepared chlorophylls. The absorption spectra of "solutions" of chlorophyll *a* and chlorophyll *b* prepared in this manner are given in Fig. 1. The maxima of the main absorption bands of chlorophyll *a* are at 669—671 and 418—422 mμ, while for chlorophyll *b* they occur at 655—658 and 464—468 mμ. Although no experiments have been performed to determine the state of the chlorophyll in such experiments, the absorption bands of both pigments are shifted to longer wavelengths and are flattened when compared to the corresponding spectra in aqueous 80 % acetone [10], in a manner similar to the chlorophylls present in the intact leaf [1].

Pheophytins *a* and *b* were prepared from the purified chlorophylls by adding a drop of concentrated HCl to the chlorophylls in petroleum ether, allowing the solutions to stand for 5 min, following which the acid was washed out with 8 successive washings with water, and the final solution rechromatographed on a powdered sucrose column. The pheophytins were added to the reaction system in the same manner as the chlorophylls, adsorbed on powdered sucrose. The absorption maxima of pheophytin *a* under the same conditions as given in Fig. 1 were at 681—684 and 400—405 mμ for the two main bands, which were less sharp than the corresponding bands for the pigment dissolved in acetone or ether. The absorption maxima for pheophytin *b* were observed at 667—669 and 423—427 mμ. Again these bands were not sharp.

For some experiments a non-purified preparation of the chlorophylls was used. This was prepared by extracting spinach leaves with acetone, transferring the extracted pigments into petroleum ether, and adsorbing the pigments on powdered sucrose. No chromatography was performed. Consequently, this preparation contained both chlorophylls and other acetone-soluble compounds, including the carotenoids. Since the composition of such a preparation was not controlled, a variation would be expected. Whereas with some preparations an almost clear "solution" was obtained upon dissolving it into water,

with other preparations there was a tendency for the "solution" to become cloudy, and in this case the chlorophylls would precipitate. This could be avoided by adding small quantities of sodium deoxycholate to the system, and accordingly this was routinely done when using the non-purified chlorophyll preparation.

The photoreduction of tetrazolium blue was followed at 580 mμ and no attempt was made to solubilize the formazan formed in the reaction. Accordingly, the results reported for tetrazolium blue cannot be translated into quantitative terms, but are intended only to show the qualitative aspects of the reaction. The photoreduction of methyl red was followed at 440 mμ. For converting the absorbancy readings into definite quantities of methyl red, a molar extinction coefficient of 17 000 was used. This value was determined for the pH used in this investigation.

The tetrazolium blue was purchased from Mann Research Laboratories, New York, methyl red from E, Merck and Co., Darmstadt, ascorbic acid from Hoffman La Roche and Co., Basle, DPIP from Eastman Chemical Co., Rochester, glutathione from Nutritional Biochemicals Corp., Cleveland, cytochrome c, FMN, catalase and peroxidase from Sigma Chemical Co., St. Louis, and protoporphyrin IX, hematoporphyrin IX and hemin from California Corp. for Biochemical Research, Los Angeles. The protoporphyrin was substantially purified before use in these experiments. The coproporphyrin and hematoheme were obtained from Dr. B. Burnham.

Quantitative determination of photocatalysts used. The concentrations of chlorophylls *a* and *b* as well as the concentrations of pheophytins *a* and *b* were determined from absorbancy measurements made at the appropriate maxima in the red spectral region. These readings were related to concentrations by use of the specific absorption coefficients for these compounds given for aqueous 80 % acetone [10]. The concentration of chlorophylls in the nonpurified preparation was determined from the absorption maximum in the red, using the specific absorption coefficients for the chlorophylls as above and assuming a ratio of chlorophyll *a* to *b* of 2.5 [10]. The concentrations of protoporphyrin and coproporphyrin were determined from absorbancy readings, using extinction values of $E^{1\,\%}_{1\,cm} = 4900$ in dilute HCl at the Soret band maximum for protoporphyrin [11] and a molar extinction coefficient of 47 000 at 402 mμ in 1 M HCl for coproporphyrin [12]. The molar extinction coefficient given for coproporphyrin was also used for determining hematoporphyrin concentration, utilizing the Soret maximum of hematoporphyrin for the measurement. The concentrations of hemin and hematoheme were determined using the spectroscopic data given by Paul [13] for these compounds. Catalase and peroxidase concentrations were calculated by utilizing the molecular weights of the proteins, and cytochrome c and FMN concentrations were determined from absorbancy values at 550 (in the reduced form) and 450 mμ, respectively [14,15].

RESULTS

The photoreduction of tetrazolium blue by chlorophyll *a*, chlorophyll *b* and protoporphyrin IX is shown in Table 1. The activity with all three photocatalysts was maximal in the presence of both ascorbate and DPIP. As in the previous experiments there was excess ascorbate present, so that the DPIP was maintained in the reduced state, and the stimulation by the added DPIP is best explained in terms of its acting as an intermediate electron carrier between the ascorbate and photocatalyst, thereby increasing the rate of photoreduction of the photocatalyst and increasing the rate of the overall reaction. In the present case, a good rate of tetrazolium blue photoreduction was observed in the absence of DPIP, which is in contrast to the reaction catayzed with *R. rubrum* chromatophores [9]. At the pH of the reaction there was no observable reduction of tetrazolium blue in the dark. At a pH of 10 or above, a dark reduction of tetrazolium blue was observed, pointing out the fact that the photoreduction of this dye by ascorbate is a thermodynamically favorable one, and in this case there is no storage of energy as a consequence of the photochemical

Table 1. Component study for tetrazolium blue photoreduction catalyzed by chlorophyll *a*, chlorophyll *b* and protoporphyrin IX. The complete reaction system contained 3.0 mM ascorbate, 30 μM DPIP, 15 mM Tris buffer pH 7.5 and 0.1 mM tetrazolium blue in 5.5 ml of solution. When present, quinacrine and β-carotene were 36 μM and sucrose was 0.5 M. The ascorbic acid was neutralized with NaOH just prior to addition, and the tetrazolium blue was added after the ascorbate had reduced the DPIP. Illumination was with a 150 W tungsten reflector flood lamp. Anaerobic conditions were employed. The chlorophylls were added to the reaction system adsorbed on sucrose, and consequently those reaction systems were also approximately 0.5 M in sucrose.

Conditions	Absorbancy increase at 580 mμ in 20 min.		
	Chphyll *a* 2.5 μM	Chphyll *b* 3.4 μM	Protoporphyrin 4.0 μM
Complete system	0.196	0.155	0.168
— DPIP	0.156	0.061	0.094
— ascorbate, DPIP	0.001	0.001	0.006
— tetrazolium blue	0.002	0.002	0.001
+ quinacrine	0.210	0.155	0.167
+ β-carotene	0.169	0.134	0.161
+ sucrose	—	—	0.175
— photocatalyst	0.008	—	—

reaction. In view of the marked stimulating effect of quinacrine on the photoreduction of tetrazolium blue by bacterial chromatophores, this compound was tested with the isolated pigments. As shown, it had no significant effect upon the three photoreactions. Addition of β-carotene to the reaction resulted in a slight decrease in activity, which agrees with previously reported data on the inhibition of photoreactions of chlorophyll by this compound [16,17].

A similar series of experiments in which methyl red was the electron acceptor is reported in Table 2. Perusal of the table reveals that this reaction resembles

Table 2. Component study for methyl red photoreduction. The complete reaction system contained 6.0 mM ascorbate, 90 μM DPIP, 15.6 mM phosphate buffer pH 6.7 and 0.13 mM methyl red in 5.5 ml of solution. When present, quinacrine and β-carotene were 36 μM and sucrose was 0.5 M. The ascorbic acid was neutralized just prior to addition to the system, and the methyl red was added last. Illumination was with a 150 W tungsten reflector flood lamp. Anaerobic conditions were employed. The chlorophylls were added to the reaction system adsorbed on sucrose, and consequently those systems contained approximately 0.5 M sucrose.

Conditions	Absorbancy change at 440 mμ in 6 min.		
	Chphyll *a* 2.5 μM	Chphyll *b* 3.4 μM	Protoporphyrin 3.0 μM
Complete system	−0.166	−0.057	−0.812
— DPIP	−0.059	+0.008	−0.132
— ascorbate, DPIP	+0.004	+0.020	+0.023
— methyl red	+0.001	+0.001	−0.005
+ quinacrine	−0.103	−0.045	−0.131
+ β-carotene	−0.181	−0.095	−0.795
+ sucrose	—	—	−0.820
— photocatalyst	+0.012	—	—

the photoreduction of tetrazolium blue in most of the aspects investigated. Thus, the maximal reaction rate was observed when DPIP was present in addition to the ascorbate. In fact, there was no activity observed with chlorophyll *b* unless the DPIP was present. No activity was observed in the absence of both compounds, and the presence of quinacrine served to inhibit the reaction, with the reaction catalyzed by protoporphyrin being particularly susceptible. In the present case, however, the presence of β-carotene caused a slight stimulation of the reactions catalyzed by the chlorophylls. The photoreduction of methyl red was observed to take place over a wide range of pH values. Experiments run at pH 4, in which case the dye was in the red form, showed good rates of photoreduction with protoporphyrin as the catalyst. The pH used in these experiments gave maximal activity, and at this pH the dye was primarily in the alkaline yellow form.

The relative efficiency of various porphyrins and porphyrin derivatives in catalyzing the two photoreactions is shown in Table 3. It is seen that both the chlorophylls and pheophytins were active in the reactions, with chlorophyll *a* being better than chlorophyll *b*, and the chlorophylls being superior to the pheophytins. All the porphyrins investigated were active, with protoporphyrin being superior in both reactions. The presence of iron in the porphyrin caused a loss of photochemical activity. This is in accord with data reported by Krasnovsky [18]. As expected, the heme proteins examined were inactive in the reactions, as was FMN. The FMN result was also expected, since the presence of ascorbate serves to inhibit the direct photoreduction of FMN itself [19]. In comparing the two photoreductions, chlorophyll *a* was the most effecient of the

Table 3. Comparison of chlorophylls, porphyrins and porphyrin derivatives in the photoreduction reactions. The anaerobic experimental conditions utilized were the same as given for Tables 1 and 2. The observed rates have been corrected for a 4.0 μM concentration of photocatalyst. In the actual experiments the concentrations of photocatalyst were close to 4 μM with the exception of the iron porphyrins (10 μM), the hemeproteins (24 μM) and FMN (166 μM).

Photocatalyst	Absorbancy change, light minus dark	
	Methyl red 6 min 440 mμ	Tetrazolium blue 20 min 580 mμ
Chlorophyll *a*	−0.265	0.312
Chlorophyll *b*	−0.135	0.168
Pheophytin *a*	−0.174	0.097
Pheophytin *b*	−0.102	0.029
Protoporphyrin	−1.09	0.171
Hematoporphyrin	−0.568	0.026
Coproporphyrin	—	0.019
Hemin	−0.002	0.006
Hematoheme	−0.009	0.005
Cytochrome *c*	−0.001	0.001
Catalase	−0.003	0.001
Peroxidase	−0.003	0.003
FMN	—	0.001

Table 4. Substitution of glutathione for ascorbate in the photoreduction of methyl red and tetrazolium blue. Conditions were the same as given in Tables 1 and 2 with the exception that illumination was with a 500 W tungsten reflector flood lamp and where indicated, equimolar quantities of glutathione were substituted for ascorbate.

Conditions	Absorbancy change, light minus dark	
	Methyl red 6 min 440 mμ	Tetrazolium blue 10 min 580 mμ
2.5 μM chlorophyll *a*		
with ascorbate	−0.414	0.388
with glutathione	−0.286	0.208
with glutathione, minus DPIP	−0.198	0.161
3.0 μM protoporphyrin		
with ascorbate	−2.76[a]	0.200
with glutathione	−0.530	0.116
with glutathione, minus DPIP	−0.218	0.046

[a] This value was calculated by extrapolation of the rate observed for a two minute illumination period.

compounds investigated for tetrazolium blue photoreduction, while for methyl red photoreduction, protoporphyrin was most active.

The function of ascorbate in the experiments described above is that of an electron donor, since Krasnovsky has repeatedly shown that ascorbate can directly photoreduce either chlorophylls, pheophytins or porphyrins [1]. The possibility of using another compound for the electron donor was investigated. It was found that glutathione would support the photoreductions, but at a somewhat slower rate. Table 4 presents the data obtained with glutathione. For these experiments illumination at a higher light intensity was employed in order that the reactions would be in the range where they could be readily measured. As shown in the table, glutathione substituted for ascorbate in the reaction, giving about half the activity of ascorbate except in the case of methyl red photoreduction by protoporphyrin, where it was only about 1/5 as active. As was the case with ascorbate, a couple consisting of glutathione and DPIP gave more activity than the glutathione alone, indicating that here also the DPIP could serve as an intermediate electron carrier between the glutathione and photocatalyst. This is in agreement with the activity observed with glutathione in the early photooxidation experiments of Vernon and Kamen [10].

Although not systematically examined, it was observed that phenylhydrazine could also serve as an electron donor in these reactions, but it was not very effective. It should also be mentioned that in experiments designed to see if mammalian cytochrome c could serve as an electron donor in reactions of this type, there was no oxidation of the reduced cytochrome c added. However, if the oxidized form of the cytochrome was added to the chlorophylls with no other additions, a slow but consistent photoreduction of the cytochrome was

Table 5. Stoichiometry of anaerobic photoreduction involving methyl red, with ascorbate as the electron donor. The reaction system contained 1.8 mM ascorbate, 55 μM DPIP, 9.1 mM phosphate buffer pH 7.4, methyl red as indicated in the table and either 4.0 μM protoporphyrin or chlorophyll *a* in 5.5 ml of solution. The reaction was allowed to proceed until all the methyl red was reduced as shown by visual inspection, following which the ascorbate remaining in the illuminated system was determined by titration with a standard solution of DPIP. A comparison was then made with a control system which was identical in composition with the exception that it contained no methyl red. The control system was also illuminated, and the difference in ascorbate between the two systems corresponded to that which entered into the photochemical reaction with methyl red. The standard DPIP solution was prepared by standardization against a solution of ascorbic acid whose concentration was determined by the method of Hewitt and Dickes [22].

Photocatalyst	μmoles ascorbate oxidized	μmoles methyl red reduced
Protoporphyrin	1.87	1.64
Chlorophyll *a*	1.72	1.55

observed. This again agrees with previous experiments performed by Krasnovsky [21], with the reduction coming at the expense of some unknown hydrogen donor in the medium, probably protein.

In the experiments reported to date it has been assumed that the ascorbate was functioning as a hydrogen donor, and was consumed in the photochemical reaction. To show that this actually was the case, the stoichiometry of the reaction was determined, with the results of the experiments shown in Table 5. The photoreduction of methyl red was chosen, both because of the rapidity of the reaction and because of the fact that the final solution was colorless and allowed a titration of the ascorbate remaining in the medium. With both chlorophyll *a* and protoporphyrin as photocatalyst, the values obtained were close to the expected 1 to 1 ratio. In both cases there was slightly more ascorbate disappearing than would be expected, and the cause for this is not known. The experiments do show the fundamental aspects of the photoreduction, that ascorbate is oxidized in the reaction as methyl red is reduced.

Krasnovsky *et al.* have shown that it is possible to photoreduce chlorophylls, pheophytins and porphyrins in organic solvents such as pyridine or piperidine if no electron acceptor is added [1,2,23,24]. Similar experiments were performed in the present investigation, to see if the photoreduced forms of the chlorophylls and porphyrins could be demonstrated in an aqueous medium. It was possible to show changes in the absorption spectrum of hematoporphyrin in the presence of ascorbic acid. Illumination caused a visible bleaching of the hematoporphyrin, with a decrease in the absorption of the Soret band and an increase in absorption at 500 mμ. These changes were more pronounced under acid conditions. A measure of the reaction is the change in absorbancy in the vicinity of the Soret peak, and the data presented in Fig. 2 represent such changes. A rapid decrease in the absorbancy was observed in the light, and a slower reverse reaction was seen in the dark. Addition of methyl red to the system prevented the absorbancy changes related to this reaction until the methyl red was reduced, at which time photoreduction of the porphyrin commenced (however at a slower rate). In the absence of ascorbate no reaction was

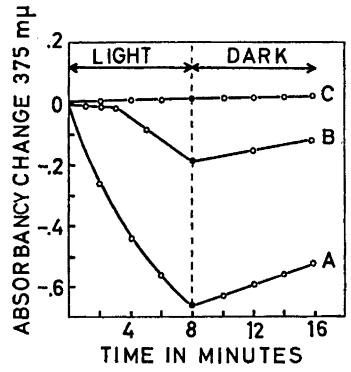

Fig. 2. Direct photoreduction of hematoporphyrin by ascorbate in the absence of other electron acceptors. The reaction mixture contained 1.8 mM ascorbate, 50 μM hematoporphyrin and 10 mM acetate buffer pH 4.6. A, Composition as given above; B, 0.2 mg of methyl red was also present; C, same as A except ascorbate was not present.

observed. Similar experiments performed with chlorophyll *a* revealed that changes in the absorbancy of the chlorophyll at its absorption maxima could be observed, but the rates were very slow, and it is questionable if they were reversible. Since protoporphyrin is not appreciably soluble at the pH utilized, it was difficult to perform experiments with this compound. However, the same general type of reaction as shown in Fig. 2 was observed with protoporphyrin, with the rate of reaction being much slower due to the low concentration of the porphyrin.

The experiments described above were all performed under anaerobic conditions, so that nothing would impede the flow of electrons to the final electron acceptor. It is well known that the chlorophylls and porphyrins are active in photooxidations in air [25], and accordingly experiments were performed to compare some of the previously investigated photocatalysts in an aerobic

Table 6. Photooxidation of various substances by chlorophylls and protoporphyrin in the presence of air. The reactions were all performed in 5.5 ml of solution which contained 10 mM phosphate buffer pH 7.4, approximately 5 μM photocatalyst and 0.1 mM DPNH, reduced cytochrome c or reduced DPIP. For the experiment with ascorbate it was present with an 1.8 mM concentration. The results have been adjusted to give the rate for 5.0 μM photocatalyst. Cytochrome *c* was reduced with hydrosulfite and DPIP was reduced with an equivalent amount of ascorbic acid. The experiment with DPIP was only run for 2 min, since there was an oxidation of the dye in the dark. The rate so obtained was projected for the 10 min period. The rates were obtained from absorbancy differences between the illuminated and non-illuminated compartments of the adapted Thunberg tubes, except that ascorbate was determined by titration with a standard solution of DPIP. Illumination was obtained with a 500 watt tungsten reflector flood lamp.

Photocatalyst	μMoles oxidized in 10 min for 5.0 μM photocatalyst			
	DPNH	Cytochrome c	$DPIPH_2$	Ascorbate
Protoporphyrin	0.159	0.170	0.465	0.38
Hemin	0.009	0.004	0.001	0
Chlorophyll *a*	0.038	0.135	0.180	0.22
Chlorophyll *b*	0.027	0.052	0.075	0.15

photooxidation of ascorbate and other reducing agents. As shown in Table 6, the same pattern of relative reactivity was shown for protoporphyrin, chlorophyll *a* and chlorophyll *b*, with activity decreasing in that order. An active photooxidation was observed for all four substrates examined, reduced cytochrome c, reduced DPIP, DPNH, and ascorbate. The oxidation of ascorbate was expected, as was the reaction with DPIP, since it stimulated the photoreductions reported above. Indeed, the demonstration of the photooxidation of reduced DPIP strengthens the concept that DPIP does function in the manner suggested in the photoreduction experiments. The photooxidation of cytochrome c has been previously described by Krasnovsky [21] in the case of chlorophyll *a* and *b*, by Vernon and Kamen [26] for chromatophores of *R. rubrum* and by Nieman *et al.* [27] for a digitonin extract of chloroplasts. In the case of the photooxidations catalyzed by both chromatophores and the digitonin preparation from chloroplasts, it was supposed that the cytochrome was oxidized directly by the chlorophyll system. The data of Krasnovsky [21] and those shown in Table 6 show that this is the case. The photooxidation of DPNH, though not as rapid as the other reactions, shows that this reaction can be catalyzed by the chlorophylls, and can explain the photooxidation of pyridine nucleotides by chloroplasts observed earlier [28].

A comparison of the rates of ascorbate oxidation using either oxygen or methyl red as the electron acceptor can be made by converting the rates for methyl red photoreduction given in Table 4, using a value of 17 000 for the molecular extinction coefficient for methyl red at this wave length. The comparable rate for methyl red photoreduction using protoporphyrin as the photocatalyst is 2.6 μmoles/10 min/5 μM photocatalyst, while the rate for chlorophyll *a* is 0.47. So in both cases, the transfer of electrons was faster with methyl red. However, in the aerobic experiments there were no special provisions made for shaking the reaction system to insure ready solution of oxygen from the air, and accordingly the rates given for the aerobic reaction are probably not maximal.

DISCUSSION

The photoreductions studied in this investigation are the same ones which have been shown to take place with both plant chloroplasts and *R. rubrum* chromatophores [9]. Although the photoreactions do not involve the storage of energy such as does the photoreduction of pyridine nucleotides, and although the compounds photoreduced are not physiological compounds, a comparison of the reactions does allow some conclusions concerning the nature of the photochemical act in the chloroplast and chromatophore. The main feature is that the organized pigment systems found in the chloroplast and chromatophore can catalyze the same relatively simple reactions as do the isolated chlorophylls. Also, in both cases, the presence of DPIP stimulates the reaction.

The photooxidation experiments performed in the presence of air show that the activated chlorophylls are not specific for ascorbate as an electron donor, but can also react with glutathione, DPNH, reduced cytochrome c and reduced DPIP. Also, a wide variety of electron acceptors can be used, as shown by Krasnovsky and Brin [5]. Thus, a wide variety of reactions could theoretically be available to the chloroplast and chromatophore, and although

the intensive study now being made of the photosynthetic phosphorylation electron transport system shows that the chloroplasts can catalyze several photoreductions, it still seems that one of the remarkable things about the chloroplast is the selectivity they maintain in the photoreactions they perform. This may well be one of the prime advantages gained by the chloroplast and chromatophore from the organization present in the photosynthetic apparatus. The removal of carotenoids from chromatophores sufficiently upsets this control so that irreversible and lethal photooxidations take place [29,30]. With the intact chloroplast there is also a high degree of selectivity concerning what can be photooxidized by the chloroplast, since only with aging or intentional damage to the oxygen evolving system can the chloroplast be made to substitute an oxidation of ascorbate in lieu of the natural reaction [31].

In comparing the various photocatalysts that have been examined, it becomes apparent that the inclusion of iron in the porphyrin molecule causes a loss in activity. On the other hand, the presence of magnesium in the chlorophylls increases the activity over that of the pheophytins. This indicates that the metal ion is not necessary for the photoreactivity of the porphyrin, and one should consider the porphyrin system itself as the active agent in these reactions. The spectroscopic changes observed when the chlorophylls and porphyrins are photoreduced by ascorbate directly also indicate a change in the porphyrin system. One might wonder why the photosynthetic apparatus could not use porphyrins as well as the chlorophylls. It must be remembered, however, that although in the mechanistic sense the reactions described here may be representative of the ones taking place in the organized chloroplast or chromatophore, they are not the ones catalyzed by the organized pigment systems in nature. One cannot extrapolate from these data to the reactions taking place in the chloroplasts where water is oxidized to produce oxygen, or in the bacteria where an accessory hydrogen donor (not ascorbate) is oxidized in the normal photosynthetic process.

Although the photoreduction experiments described in the previous paper [9] were performed in another laboratory, the conditions were approximately the same, and a general comparison of the rates of the photoreduction reactions catalyzed by the isolated photocatalysts and the chloroplasts and chromatophores can be made. Taking the data from Tables 1 and 4 of the previous paper and Table 3 of this paper, the rates for methyl red and tetrazolium blue photoreduction have been calculated and are shown in Table 7. The rates

Table 7. Comparison of photoreduction rates for the different photocatalysts.

Photocatalyst	Methyl red μmoles/h/μmole of photocatalyst	Tetrazolium blue Absorbancy change, 580 mμ per hour for μM photocatalyst
Chlorophyll *a*	51	0.27
Protoporphyrin	170	0.14
Chloroplasts	96	0.88
Chromatophores	24	0.36
Chromatophores plus quinacrine	145	1.11

obtained with the different photocatalysts are all in the same order of magnitude. The chloroplasts were more active than the chromatophores, but the addition of quinacrine stimulated the latter reaction to a rate above that for the chloroplasts. The quinacrine-stimulated chromatophores gave the highest rate for tetrazolium blue photoreduction, but protoporphyrin was the most active in methyl red photoreduction.

The activity of the porphyrins in the reactions described above may well have biological expression in the sensitization to light caused by high concentrations of porphyrins in the blood. The demonstrated ability of these compounds to photooxidize ascorbic acid, glutathione, reduced cytochrome c and DPNH suggests that their harmful effects in the case of porphyria may well be due to the photooxidation of some vital component of the cell or surrounding fluid thus upsetting the normal metabolic pattern.

Acknowledgements. The author wishes to thank Prof. H. Theorell for his generous hospitality and for his interest in this work. Thanks are also due to Dr. B. Burnham for making available samples of coproporphyrin and hematoheme for this investigation. The many helpful discussions with Dr. Burnham and Dr. R. A. Plane during the course of this work are greatly appreciated.

REFERENCES

1. Krasnovsky, A. A. *Ann. Rev. Plant Physiol.* **11** (1960) 363.
2. Krasnovsky, A. A. *Doklady Akad. Nauk S.S.S.R.* **60** (1948) 421.
3. Krasnovsky, A. A. and Brin, G. P. *Doklady Akad. Nauk S.S.S.R.* **67** (1949) 325.
4. Brin, G. P. and Krasnovsky, A. A. *Biokhimiya* **24** (1959) 6.
5. Krasnovsky, A. A. and Brin, G. P. *Doklady Akad. Nauk S.S.S.R.* **73** (1950) 1239.
6. Livingston, R. and Pariser, R. *J. Am. Chem. Soc.* **70** (1948) 1510.
7. Krasnovsky, A. A. and Brin, G. P. *Doklady Akad. Nauk S.S.S.R.* **89** (1952) 527.
8. Krasnovsky, A. A. and Umrikhina, A. V. *Doklady Akad. Nauk S.S.S.R.* **122** (1958) 1061.
9. Ash, O. K., Zaugg, W. S. and Vernon, L. P. *Acta Chem. Scand.* **15** (1961) 1629.
10. Vernon, L. P. *Anal. Chem.* **32** (1960) 1144.
11. Grinstein, M. and Wintrobe, M. M. *J. Biol. Chem.* **172** (1948) 459.
12. Mauzerall, D. and Granick, S. *J. Biol. Chem.* **232** (1958) 1141.
13. Paul, K. *Acta Chem. Scand.* **12** (1958) 1611.
14. Paléus, S. *Acta Chem. Scand.* **14** (1960) 1743.
15. Whitby, L. G. *Biochem. J.* **54** (1953) 437.
16. Krasnovsky, A. A., Drosdova, N. N. and Pakshina, E. V. *Biokhimiya* **25** (1960) 288.
17. Claes, H. *Research Comm.* **3** (1960) 585.
18. Krasnovsky, A. A. *Repts. Intern. Symposium "The Origin of Life on Earth"*, The Publishing House of the Academy of Science, U.S.S.R. Moscow (1957) 351.
19. Vernon, L. P. *Biochim. et Biophys. Acta* **36** (1959) 177.
20. Vernon, L. P. and Kamen, M. D. *Arch. Biochem. Biophys.* **51** (1954) 122.
21. Krasnovsky, A. A. *Doklady Akad. Nauk S.S.S.R.* **103** (1955) 283.
22. Hewitt, E. J. and Dickes, G. J. *Biochem. J.* **78** (1961) 384.
23. Krasnovsky, A. A. and Pakshina, E. V. *Doklady Akad. Nauk S.S.S.R.* **120** (1958) 581.
24. Krasnovsky, A. A. and Voinovskaya, K. K. *Doklady Akad. Nauk S.S.S.R.* **112** (1957) 911.
25. Rabinowitch, E. *Photosynthesis*, Vol. 1, Interscience Publishers, New York 1945.
26. Vernon, L. P. and Kamen, M. D. *Arch. Biochem. Biophys.* **44** (1953) 298.
27. Nieman, R. H., Nakamura, H. and Vennesland, B. *Plant Physiol.* **34** (1959) 262.
28. Jagendorf, A. *Arch. Biochem. Biophys.* **62** (1956) 141.
29. Cohen-Bazire, G. and Stanier, R. Y. *Nature* **181** (1958) 250.
30. Fuller, R. C. and Anderson, I. C. *Nature* **181** (1958) 252.
31. Vernon, L. P. and Zaugg, W. S. *J. Biol. Chem.* **235** (1960) 2728.

Received April 27, 1961.

ACTA CHEMICA SCANDINAVICA 15 (1961) 1651–1659

Photoreduction of Pyridine Nucleotides by Ascorbate: Catalysis by Chlorophylls and Porphyrins in Aqueous Media *

LEO P. VERNON**

Medicinska Nobelinstitutet, Biokemiska Avdelningen, Stockholm, Sweden

1. In the presence of ascorbate and partially purified photosynthetic pyridine nucleotide reductase (PPNR) ***, a photoreduction of pyridine nucleotides was catalyzed by chlorophyll *a*, chlorophyll *b*, hematoporphyrin IX, protoporphyrin IX, coproporphyrin III, and to a lesser extent by pheophytin *a* and pheophytin *b*. Iron porphyrins and hemeproteins were inactive. Phycocyanin was moderately active.

2. In general, TPN was photoreduced at a faster rate than DPN. With purified chlorophylls, however, the reverse was true.

3. Addition of 2,6-dichlorophenolindophenol or quinacrine resulted in an inhibition of the photoreductions.

4. In the absence of PPNR, hematoporphyrin catalyzed a slow photoreduction of DPN. Under the same conditions with TPN, a photoreduction of the porphyrin was observed.

The previous paper in this series describes the photoreduction of methyl red and tetrazolium blue by ascorbate in aqueous solution, which reactions are catalyzed by chlorophylls, pheophytins and porphyrins [1]. These reactions are also catalyzed by spinach chloroplasts and by chromatophores of *Rhodospirillum rubrum* [2], showing that similar reactions can be catalyzed by the chlorophylls in the free form or when contained in the organized structure found in chloroplasts and chromatophores. The reactions described have significance in terms of the mechanism of the primary photochemical act of photosynthesis, but the reagents involved are not those which take part in the natural photosynthetic process. Of more interest would be the demonstration of a photoreduction of pyridine nucleotides by the isolated chlorophylls in an

* This investigation was performed during the tenure of a National Science Foundation Senior Postdoctoral Fellowship.

** Present address: Charles F. Kettering Foundation, Yellow Springs, Ohio, USA.

*** The abbreviations used are: DPIP, 2,6-dichlorophenolindophenol; DPN, diphosphopyridine nucleotide; TPN, triphosphopyridine nucleotide; PPNR, photosynthetic pyridine nucleotide reductase; Tris, tris(hydroxymethyl)aminomethane, and FMN, flavin mononucleotide.

aqueous medium. Krasnovsky [3,4] has shown that chlorophylls dissolved in pyridine catalyze a photoreduction of pyridine nucleotides by ascorbate. The data presented in this paper show that the photoreduction of pyridine nucleotides proceeds in the presence of PPNR in an aqueous medium, and a few of the characteristics of this reaction are presented.

MATERIALS AND METHODS

The experimental methods employed, the preparative methods for chlorophylls and pheophytins, the methods used for estimation of photocatalyst concentration and a description of most of the materials used have been previously described [1]. DPN and TPN were purchased from Sigma Chemical Co. of St. Louis. PPNR was prepared from spinach leaves according to the directions of San Pietro and Lang [5], and the preparations used correspond to their "extract of acetone precipitate". The enzyme preparation was lyophylized and stored at −20°C in a drying chamber in the dark. The alcohol dehydrogenase was a twice recrystallized preparation from horse liver, and was a gift from Dr. C. L. Woronick. Illumination was with a 500 W tungsten reflector flood lamp, which gave a light intensity of approximately 4500 foot candles at the reaction site.

RESULTS

In view of the requirement for PPNR for pyridine nucleotide photoreduction with fresh chloroplasts in a regular Hill reaction [5] and by aged chloroplasts utilizing ascorbate as the electron donor [6], it would be expected that the photoreduction of pyridine nucleotides in an aqueous medium by photocatalysts outside the biological photosynthetic unit would also require the presence of

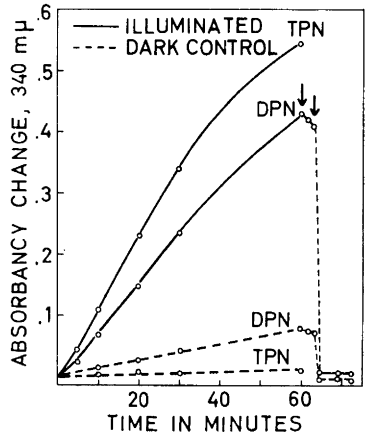

Fig. 1. Photoreduction of pyridine nucleotides by non-purified chlorophyll preparation. The chlorophyll preparation was an acetone extract of spinach which had been transferred into petroleum ether and adsorbed on sucrose. The experimental conditions were the same as given for Table 1. At the first arrow, 0.05 ml of water was added to both the illuminated and non-illuminated sides of the reaction vessel, and at the second arrow 50 μmoles of acetaldehyde and 0.05 μmole of alcohol dehydrogenase were added in sequence to both the illuminated and non-illuminated sides. The resultant sharp decrease in the optical density shows the presence of DPNH in the illuminated system.

this enzyme. Fig. 1 shows the results obtained when a non-purified chlorophyll preparation (added to the system adsorbed on sucrose) was illuminated in the presence of ascorbate, pyridine nucleotide and PPNR. A photoreduction of both DPN and TPN was observed, with TPN giving the faster reaction. This type of nucleotide preference would be expected in view of the characteristics of the PPNR preparation used [5]. To show that the absorbancy change at 340 mμ was a measure of the reduced pyridine nucleotide formed, acetaldehyde and alcohol dehydrogenase were added after illumination of the reaction system containing DPN. The immediate drop in absorbancy can be attributed to the DPNH present in the illuminated system. Similar experiments were not performed with the TPN system, but it is logical to assume that here also the absorbancy changes were an accurate measurement of the formation of reduced pyridine nucleotide.

The extensive work of Krasnovsky and coworkers [7] shows the ability of protoporphyrin and hematoporphyrin to catalyze the same photoreactions as the chlorophylls and pheophytins. Both protoporphyrin and hematoporphyrin are also active in the photoreduction of methyl red and tetrazolium blue previously reported [1]. Therefore, it is not surprising that a photoreduction of the pyridine nucleotides would also be catalyzed by these porphyrins in the presence of PPNR. Fig. 2 shows the activity of hematoporphyrin in such a reaction. Compared to the chlorophylls, higher concentrations of hematoporphyrin could be utilized, thus allowing a faster rate of pyridine nucleotide photoreduction. The addition of acetaldehyde and alcohol dehydrogenase again showed the presence of DPNH in the system geared for its production in the light. The same nucleotide preference was shown as in the case when chlorophylls were used, emphasizing that this is a function of the PPNR preparation used.

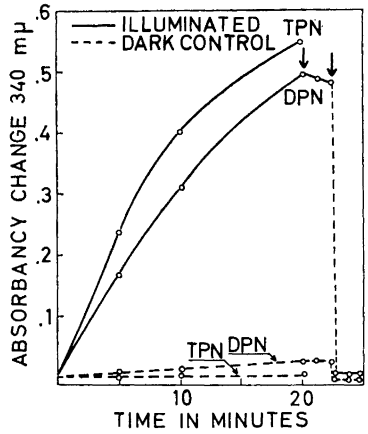

Fig. 2. Photoreduction of pyridine nucleotides catalyzed by hematoporphyrin. The experimental conditions were the same as listed in Table 1. At the first arrow 0.05 ml of water was added to both the illuminated and non-illuminated sides of the reaction vessel, and at the second arrow 50 μmoles of acetaldehyde and 0.05 μmole of alcohol dehydrogenase were added in sequence to both sides of the reaction vessel, showing the presence of DPNH.

The reaction system employed for the experiments represented in Figs. 1 and 2 contained glutathione, since as shown below, glutathione stimulated the reaction. In both experiments, there was a show rate of DPNH formation in the dark. The shorter illumination period utilized with hematoporphyrin minimized this dark reaction, but it was observed to proceed at about the same rate in both cases. This reduction in the dark was related to the PPNR preparation used, since in separate experiments removal of this compound prevented the reduction of DPN in the dark. Thus, it is apparently caused by a contaminating dehydrogenase in the PPNR preparation.

The relationship between the rate of pyridine nucleotide photoreduction and the concentration of PPNR is shown in Fig. 3. With both photocatalysts, and with both pyridine nucleotides, maxima were observed. The inhibition caused by excess enzyme was more pronounced and commenced at a lower enzyme concentration when TPN was used. One explanation for this behavior is to be found in the fact that the PPNR preparations used were not extensively purified, and probably contained glutathione reductase. Since glutathione was added to the system, a coupling of the reduced pyridine nucleotide and the glutathione system would be expected at higher enzyme concentrations. This would explain the greater decrease in activity with TPN, since glutathione reductase from plants is specific for TPN [8]. The saturation of the hematoporphyrin system at lower PPNR concentrations reflects a better interaction between the hematoporphyrin and the enzyme than occurs in the case of chlorophyll. This is logical, since the hematoporphyrin is in solution, while the chlorophyll is present as a very fine colloidal suspension. That saturation occurs in these experiments indicates that under these conditions the donation of electrons to the PPNR complex from the pigment molecules becomes the limiting factor.

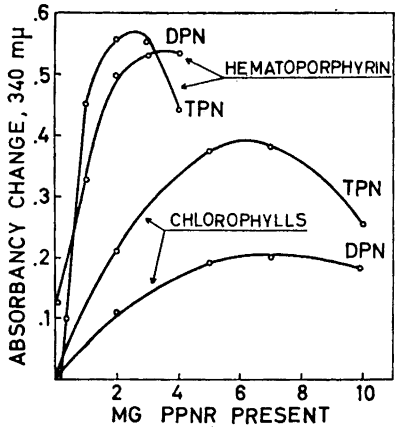

Fig. 3. The effect of PPNR concentration upon the photoreduction of pyridine nucleotides catalyzed by a non-purified chlorophyll preparation and by hematoporphyrin. The experimental conditions were the same as given in Table 1 except the chlorophyll concentration was 7.6 μM. The experiments performed with chlorophyll were for 30 min and the experiments with hematoporphyrin were 20 min in the case of DPN and 10 min in the case of TPN.

In the reactions catalyzed by chlorophylls, no photoreduction was observed when PPNR was absent. In the case of hematoporphyrin however, it was seen that with DPN there was a significant reaction in the absence of added enzyme. In the case of TPN with hematoporphyrin, negative absorbancy changes were observed in the absence of the enzyme. In the latter case, these reflect a photoreduction of the porphyrin itself by ascorbate. The previous paper [1] reports such a reaction and although the maximum absorbancy change upon hematoporphyrin photoreduction occurred at 375 mμ, there was nevertheless considerable change at 340 mμ, where pyridine nucleotide reduction was followed. In the experiments with TPN and no PPNR, a visual bleaching of the hematoporphyrin was observed.

The effect of concentration of photocatalyst upon the photoreduction reactions is shown in Fig. 4. The reactions saturated with respect to the photocatalyst, indicating that under these conditions some other component becomes rate limiting, and the most logical substance to suspect in this regard would be the enzyme. One would expect a further increase in the rate of reaction by increasing the concentration of both enzyme and photocatalyst. When such experiments were performed, a descrease in activity was noted. This suggests the presence of an inhibitor in the PPNR preparation. It is apparent that clarification of this problem depends upon the use of pure PPNR in reactions of this sort.

The requirements for the photoreduction of pyridine nucleotides by hematoporphyrin and the chlorophylls are shown in Table 1. Also included in this table are results obtained with pure chlorophyll *a*. One significant result of these experiments is the fact that DPIP inhibits the reactions. This was

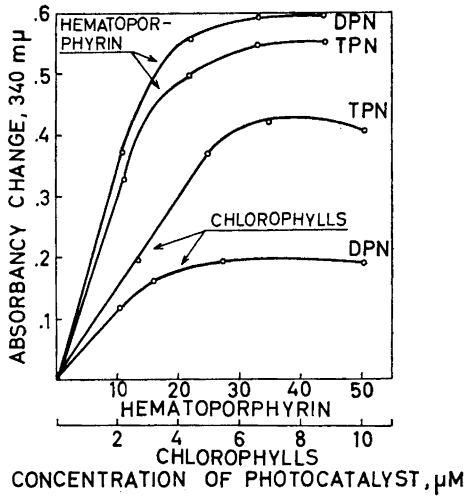

Fig. 4. The effect of photocatalyst concentration upon the photoreduction of pyridine nucleotides. The experimental conditions were the same as given for Table 1 and the exposure times were the same as set forth in Fig. 3. A non-purified chlorophyll preparation was used in these experiments, with a final concentration of 7.5 μM.

Table 1. Requirements for pyridine nucleotide photoreduction by chlorophyll and hematoporphyrin. The reaction mixture contained 5.5 mM ascorbate, 1.8 mM glutathione, 18 mM Tris buffer pH 7.8 and either 22 μM hematoporphyrin (with 2 mg PPNR), 4.2 μM chlorophyll *a* (with 5 mg PPNR) or 8.2 μM crude chlorophyll (with 5 mg PPNR). The volume was 5.5 ml and anaerobic conditions were employed. The crude chlorophyll preparation was from an acetone extract of spinach and consequently contained both chlorophylls and other acetone-soluble substances, including carotenoids. For the experiments involving the crude chlorophyll, 4 mg of sodium deoxycholate were also added, since otherwise the chlorophyll showed a tendency to precipitate from solution. When present, DPIP was 91 μM. β-carotene was 15 μM and pyridine was added to give a 1 % pyridine solution. Illumination was performed with a 500 W tungsten reflector flood lamp. The chlorophylls were added to the system dissolved on sucrose and consequently these solutions were also approximately 0.5 M in sucrose.

Conditions	Absorbancy change, 340 mμ, light minus dark				
	Hematoporphyrin 20 min		Crude Chphyll 30 min		Chphyll *a* 40 min
	DPN	TPN	DPN	TPN	DPN
Complete system	0.495	0.542	0.217	0.302	0.176
— ascorbate	0.283	0.301	0.063	0.123	0.054
— glutathione	0.328	0.410	0.169	0.207	0.113
— ascorbate and glutathione	0.024	0.015	0.011	0.016	0.007
Boiled PPNR	0.098	−0.158	0.003	0.002	0.003
— PPNR	0.118	−0.163	0.003	0.001	0.001
— pyridine nucleotide	−0.115	−0.110	0.004	0.003	0.003
— photocatalyst	0.001	0.002	0.001	0.002	0.001
+ DPIP	0.238	0.375	−0.068	−0.021	−0.135
+ pyridine	—	—	—	—	0.018
+ β-carotene	—	—	—	—	0.156

unexpected, since this compound serves to stimulate the photoreduction of tetrazolium blue and methyl red by these same photocatalysts, and is almost an absolute requirement for the photoreduction of pyridine nucleotides by ascorbate using chloroplasts which are aged or inhibited with 3-(3,4-dichlorophenyl)-1,1-dimethylurea (DCMU) [6]. The inhibition was particularly severe when the chlorophyll mixture or chlorophyll *a* were used. In both of these cases an absorbancy decrease was observed in the illuminated systems. This cannot be explained at present, but it could reflect a photoreduction of the chlorophyll molecule itself. The mode of inhibition by DPIP must await further experimentation, but it is expected that its ability to function either as as oxidant [9] or a reductant [1] to the chlorophyll system is the basis for this behavior. In this regard, it should be pointed out that DPIP is a potent inhibitor of DPN photoreduction by chromatophores of *R. rubrum*, and its action there is attributed to its ability to act as a shunt between the photoreducing and photooxidizing sites [10].

Removal of either ascorbate or glutathione from the reaction systems caused a decrease in activity, and removal of both compounds almost stopped the reactions. It should be noted that the small residual activity in the latter case is probably due to the fact that in preparation of the enzyme, sufficient glutathione was added just prior to lyophylization to make the solution mM

in this compound, and consequently some glutathione would be added with the PPNR preparation. The glutathione can function both as an electron donor [1] or as a protective agent for the PPNR, which is inactivated by illumination in the presence of chlorophyll [11].

No photoreduction of pyridine nucleotides was observed in the absence of photocatalyst. Addition of β-carotene caused a slight reduction in the activity of the chlorophyll *a* system, and addition of pyridine resulted in a marked drop in activity. Removal of the PPNR allowed no reaction to proceed in the case of the chlorophylls, but had opposite effects on the hematoporphyrin catalyzed reactions. Some photoreduction of DPN was observed with no PPNR present, while in the case of TPN an absorbancy decrease was noted subsequent to illumination. This was due to photoreduction of the hematoporphyrin itself by ascorbate as discussed above. A photoreduction of hematoporphyrin was also observed in the case where there was no pyridine nucleotide added.

In Table 2 a comparison is made of various porphyrins and porphyrin derivatives concerning their ability to catalyze the photoreduction of pyridine nucleotides. In general, the same pattern was obtained as was previously observed for the photoreduction of tetrazolium blue and methyl red [1]. In the present case, however, hematoporphyrin was more active than either protoporphyrin or coproporphyrin. For the chlorophylls, the best reaction was observed with the non-purified mixture of chlorophylls. This preparation also contained other acetone-soluble components, and it may be that these stimulate the reaction. When comparing this chlorophyll preparation with the purified

Table 2. A comparison of several porphyrins and porphyrin derivatives in pyridine nucleotide photoreduction. The experimental conditions were the same as those described in Table 1, with different photocatalysts added in the amounts indicated. The observed photoreduction rates have been adjusted to give a rate for 60 minutes with 10 μM photocatalyst.

Photocatalyst	Absorbancy change, 340 mμ for 60 min for 10 μM photocatalyst, light − dark	
	TPN	DPN
Crude chlorophyll	0.734	0.530
Chlorophyll *a*	−0.007	0.487
Chlorophyll *b*	0.135	0.428
Pheophytin *a*	0.004	0.030
Pheophytin *b*	0.038	0.056
Hematoporphyrin IX	0.740	0.676
Protoporphyrin IX	—	0.408
Coproporphyrin III	—	0.484
Hematoheme	—	0.007
Hemin	—	0.004
Cytochrome c	—	−0.008
Catalase	—	−0.002
Peroxidase	—	−0.003
FMN	—	−0.006
Bilirubin	—	0
Phycocyanin	—	1.08

Table 3. Effect of various compounds upon DPN photoreduction catalyzed by hematoporphyrin. The experimental conditions were the same as given for Table 1, with the additions as listed below. Different PPNR preparations were used during the course of these experiments, and accordingly the activities are expressed as a percent activity related to a control.

Addition	Final concentration mM	Activity %
None	—	100
Ethylenediamine tetraacetic acid	0.18	65
KCN	1.8	97
Sucrose	530	102
Quinacrine	0.17	28
Mn^{++}	0.18	76
Mg^{++}	0.18	92
Cu^{++}	0.18	69
Fe^{+++}	0.18	9
None, aerobic	—	61

chlorophylls, one significant difference is observed. With chlorophyll *a* no photoreduction of TPN was observed, and with chlorophyll *b* the rate of TPN photoreduction was less than that of DPN. This is opposite to the nucleotide preference ordinarily found [5]. The reason for this odd behavior toward TPN is not known, but it has a corollary in the fact that with hematoporphyrin and no added PPNR, a slow photoreduction of DPN was noticed, but none was observed with TPN (Table 1). Thus it would appear that in opposition to the preference of the PPNR preparation for TPN photoreduction, there is a greater potential for DPN photoreduction in the absence of the enzyme.

The results given in Table 2 again show the iron porphyrins, the hemeproteins and FMN to be inactive in the reaction. Bilirubin was also inactive, but phycocyanin was found to be moderately effective. The phycocyanin was prepared from *Cyanidium caldarium*, was chromatographically purified, and was made available by Dr. L. Bogorad. The high value reported for phycocyanin must be considered in light of the fact that the values are reported for 10 μM photocatalyst. Since the phycocyanin molecule has 8 or 16 light absorbing groups per molecule [12], the rate per absorbing group would be smaller by that factor. The phycocyanin concentration was determined from absorbancy measurements using the constant given by Lemberg and Legge [12].

The effect of various compounds upon the photoreduction of DPN by hematoporphyrin is shown in Table 3. Sucrose was included since the experiments involving the chlorophylls contained that quantity of sucrose in the reaction system. It was found to have no inhibitory effect upon the reaction catalyzed by hematoporphyrin. Quinacrine, which markedly stimulates the photoreduction of methyl red and tetrazolium blue by *R. rubrum* chromatophores [2] was inhibitory in the present case. Anaerobic conditions were best, as shown by the decreased activity in the presence of air. The presence of some selected metal ions inhibited the reaction, with iron being the most effective. Cyanide ion was without effect, while ethylenediamine tetraacetic acid was mildly inhibitory.

DISCUSSION

The data presented above show that chlorophylls and porphyrins can catalyze a photoreduction of both DPN and TPN when ascorbate is present as an electron donor and PPNR is present to facilitate electron transfer to the pyridine nucleotides. The rates of the photoreductions observed to date are relatively low when compared to the rates obtained with the intact chloroplast [13]. The data of Table 2 show that with non-purified chlorophyll, 12 moles of TPN were reduced per hour for each mole of chlorophyll. The rate observed for hematoporphyrin, the most active porphyrin, was only slightly higher. The results are significant, however, since they show this important reaction can proceed in aqueous solution in the absence of the complex organization of the chloroplast or chromatophore. The ability of the chlorophylls to function in this simplified system strongly supports the concept advanced by Krasnovsky [7] that in the chloroplast also the primary photochemical act involves the photoreduction of chlorophyll by means of some physiological electron donor (ultimately water) and a subsequent transfer of the electrons to either pyridine nucleotide or the enzymatic components of the cyclic electron transfer system. In comparing the photoreduction of pyridine nucleotides by chlorophylls and chloroplasts, two differences are noted. With the purified chlorophylls an inverse nucleotide preference is shown, with TPN being photoreduced at the lower rate (and not at all with chlorophyll *a*). Also, addition of DPIP to the chlorophyll system caused complete inhibition of the reactions, whereas it stimulates the ascorbate coupled photoreduction of pyridine nucleotides by chloroplasts [6]. As mentioned above, this is most likely due to the ability of DPIP to act as either an oxidant or a reductant with the photoactivated chlorophyll depending upon experimental conditions, and thus it has the potential of short-circuiting the electron flow and preventing any net photoreduction.

Acknowledgements. The author wishes to thank Prof. H. Theorell for his generous hospitality and for his interest in this work. Thanks are also due to Dr. W. Zaugg for the PPNR preparations used in this investigation, and to Drs. B. Burnham and L. Bogorad for many helpful discussions during the course of this work.

REFERENCES

1. Vernon, L. P. *Acta Chem. Scand.* **15** (1961) 1639.
2. Ash, O. K., Zaugg, W. S. and Vernon, L. P. *Acta Chem. Scand.* **15** (1961) 1629.
3. Krasnovsky, A. A. and Brin, G. P. *Doklady Akad. Nauk S.S.S.R.* **67** (1949) 325.
4. Brin, G. P. and Krasnovsky, A. A. *Biokhimiya* **24** (1959) 6.
5. San Pietro, A. and Lang, H. M. *J. Biol. Chem.* **231** (1958) 211.
6. Vernon, L. P. and Zaugg, W. S. *J. Biol. Chem.* **235** (1960) 2728.
7. Krasnovsky, A. A. *Ann. Rev. Plant Physiology* **11** (1960) 363.
8. Hendley, D. D. and Conn, E. E. *Arch. Biochem. Biophys.* **46** (1953) 454.
9. Hinkson, J. W. and Vernon, L. P. *Plant Physiol.* **34** (1959) 268.
10. Vernon, L. P. and Ash, O. K. *J. Biol. Chem.* **234** (1959) 1878.
11. Giovanelli, J. and San Pietro, A. *Arch. Biochem. Biophys.* **84** (1959) 471.
12. Lemberg, R. and Legge, J. W. *Hematin Compounds and Bile Pigments*, Interscience Publishers, Inc., New York 1949, pp. 146–147.
13. Davenport, H. E. *Biochem. J.* **73** (1959) 49P.

Received April 27, 1961.

ACTA CHEMICA SCANDINAVICA 15 (1961) 1660–1666

Pyridazine Studies

I. The Preparation of Some 3,6-Disubstituted 4-Methyl-pyridazines

SØREN LINHOLTER, AA. BAK KRISTENSEN, R. ROSENØRN, S. E. NIELSEN and H. KAABER

Department of Organic Chemistry, The Royal Technical University, Copenhagen, Denmark

The competitive monosubstitution of the individual chlorine atoms of 4-methyl-3,6-dichloro-pyridazine by alkoxide ions is studied. A preferential reaction at the 6-position by alkoxy groupings larger than methoxy is noticed. Reaction of 4-methyl-3,6-dichloro-pyridazine with ammonia at 120° results in the production of two isomeric amino-chloro-4-methyl-pyridazines, whereas dimethylamine affords only one product of as yet unestablished structure.

The structures of the various isomeric substitution products have been established by synthetic transformations and comparison with authentic compounds.

For some time we have been studying the reactivity of methyl groups present as substituents in various heterocyclic systems and the influence of other substituents on the reactivity of such methyl groups. In this connection some 3- and 6-substituted 4-methyl-pyridazines were desired, and 4-methyl-3,6-dichloro-pyridazine served as a useful starting material for the synthesis of such compounds. The latter was synthesised according to Mizzoni and Spoerri [1] from citraconic anhydride and hydrazine. Dehydration of itaconic acid by means of acetic anhydride [2] provided a satisfactory route to the anhydride employed. The conversion of citraconic anhydride into 4-methyl-3,6-dichloro-pyridazine was performed essentially as described [1].

Selective exchange of one halogen atom was effected by treatment of the dichloro compound with sodium alkanolate, water, ammonia and dimethylamine, as suggested by Druey *et al.*[3] For each of these reagents two isomeric compounds are possible:



After separation of the reaction products it was necessary to identify each of the components separately. The difference in solubility of the isomeric mono-

methoxy and monoethoxy substitutes was sufficiently great to allow separation of the less soluble component by repeated recrystallisations. It was difficult, however, to obtain the more soluble isomerides in homogeneous form. The methoxy compounds (see Table 1) were formed in almost equal amounts, the 5-methyl-6-methoxy-3-chloro-pyridazine (I) * being the less soluble isomer.

For the ethoxy derivatives, (IX) and (X), the proportion was displaced in favour of the 4-methyl-6-ethoxy-3-chloro-pyridazine (X). We therefore undertook a preliminary investigation of the influence of the alkyl size on the proportion between the two isomers. The reaction with sodium methanolate, ethanolate, 2-propanolate, *iso*butanolate and *cyclo*hexanolate was studied and a tendency to preferential 6-alkoxylation with increasing size of the alkyl group was noticed. It would be of interest to include sodium *tert.*-butanolate into this series of alkanolates, but according to Druey *et al.*[3] much more vigorous conditions would be needed in this case.

As mentioned above, the methoxy compounds could be separated. For the other alkoxy derivatives, however, separation was more easily achieved after hydrolysis to the pyridazinones with constant boiling hydrochloric acid. As pointed out by Druey *et al.*[3] and verified by us, the remaining chlorine atom is not attacked by this treatment. Because 4-methyl-3,6-dichloro-pyridazine is hydrolysed under these conditions, quantitative reaction of one of the chlorine atoms must be ascertained before the ratio between the two isomeric pyridazinones can be utilized for estimating the ratio between the alkoxy derivatives. Quantitative reaction was in each case established by isolating and weighing the sodium chloride separating from the solutions, before hydrolysis of the mixture of the alkoxy compounds. The two compounds. 5-methyl-3-chloro-1,6-dihydro-pyridazin-6-one (VII), (5-methyl-3-chloro-6-hydroxy-pyridazine) and 4-methyl-3-chloro-1,6-dihydro-pyridazin-6-one (VIII), (4-methyl-3-chloro-6-hydroxy-pyridazine), could be almost quantitatively separated, and the structures of the two isomeric compounds were established by unambiguous methods.

A mixture of the isomeric compounds (VII) and (VIII) was obtained in 61 % yield from 4-methyl-1,2,3,6-tetrahydro-pyridazin-3,6-dione by treating this compound with phosphoryl chloride, and, in turn, hydrolysing the crude reaction product with hydrochloric acid. Acid was found superior to alkali for the hydrolysis, giving fewer side reactions and less tar formation.

The structures of these compounds were established as outlined in the formula scheme. The methoxy-chloro compounds (I) and (II) were dehalogenated by reduction with hydrogen and Raney nickel in methanolic potassium hydroxide solution according to Kämmerer *et al.*[4] Both methyl-methoxy-pyridazines (III) and (IV) had a smell similar to that of anisole and formed addition products with picric acid. The picrates were used for analysis, because the parent compounds, one of which is liquid at room temperature, are rapidly discoloured. The methoxy compounds were hydrolysed with hydrochloric acid, and the m.p.'s of the two methyl-pyridazinones (V) and (VI) were compared with the m.p. of authentic 5-methyl-1,6-dihydro-pyridazin-6-one prepared

* In a recent publication, Steck[9] reports the preparation of a methoxy substitute with m.p. 118°, yet without structural assignment.

Table 1.

	Substituents	M.p. * °C	Formula	C Found	C Calc.	H Found	H Calc.	N Found	N Calc.	Cl Found	Cl Calc.
I	5-methyl-6-methoxy-3-chloro	113	$C_6H_7N_2ClO$	45.95	45.45	4.68	4.43	17.20	17.66	22.53	22.35
II	4-methyl-6-methoxy-3-chloro	66	$C_6H_7N_2ClO$	45.30	45.45	4.37	4.43	17.24	17.66	22.30	22.35
III	5-methyl-6-methoxy **	34	$C_{12}H_{11}N_5O_8$	40.70	40.79	3.14	3.11	19.97	19.83		
IV	4-methyl-6-methoxy **	15	$C_{12}H_{11}N_5O_8$	40.80	40.79	3.21	3.11	19.99	19.83		
V	5-methyl-6-hydroxy	156	$C_5H_6N_2O$								
VI	4-methyl-6-hydroxy	162	$C_5H_6N_2O$								
VII	5-methyl-6-hydroxy-3-chloro	170	$C_5H_5N_2ClO$	41.45	41.51	3.39	3.49	19.48	19.39	24.35	24.53
VIII	4-methyl-6-hydroxy-3-chloro	220	$C_5H_5N_2ClO$	41.40	41.51	3.49	3.49	19.57	19.39	24.46	24.53
IX	5-methyl-6-ethoxy-3-chloro	78	$C_7H_9N_2ClO$	48.65	48.72	5.13	5.36	15.80	16.24	20.51	20.94
X	4-methyl-6-ethoxy-3-chloro	49	$C_7H_9N_2ClO$	48.75	48.72	5.24	5.36	15.52	16.24	20.44	20.94
XI	5-methyl-6-amino-3-chloro	137	$C_5H_6N_3Cl$	41.90	41.83	4.26	4.21	29.42	29.26	24.67	24.69
XII	4-methyl-6-amino-3-chloro	187	$C_5H_6N_3Cl$	41.40	41.83	4.34	4.21	29.03	29.26	24.59	24.69
XIII	4-methyl-6-dimethylamino-3-chloro ***	122	$C_7H_{10}N_3Cl$	48.92	49.01	5.87	5.65	24.28	24.12		
XIV	4-methyl-6-dimethylamino ***	90	$C_7H_{11}N_3$	61.00	61.28	8.00	8.08	30.77	30.63		

Analyses by P. Hansen, The Chemical Laboratory of the University of Copenhagen.

* All the m.p.'s are uncorrected.

** Analyses on the picrates.

*** The position of the methyl group is unknown.

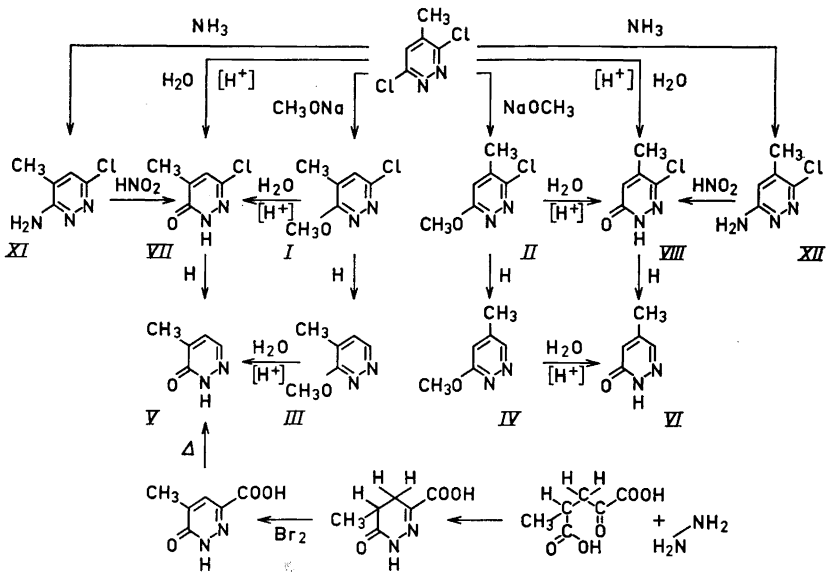

according to McMillan *et al.*[5] from α-keto-γ-methyl-glutaric acid [6] as indicated in the scheme. The identity of one of the isomeric hydrolysis products with the authentic specimen was thus established. The structure of the other isomer is therefore indirectly ascertained.

Attempts to reproduce the preparation by Druey *et al.*[3] of an aminochloro-4-methyl-pyridazine by treating 4-methyl-3,6-dichloro-pyridazine with aqueous ammonia at elevated temperature proved unsuccessful. However, reaction of the latter with anhydrous ammonia in methanol at 120° resulted in partial conversion into a mixture of amino-chloro-4-methyl-pyridazines that could be separated as N-acetyl derivatives into the two isomers (XI) and (XII). The structures of these were established by transforming them separately by diazotation into the above described hydroxy-chloro-pyridazines. On treating the dichloro derivative with aqueous or alcoholic dimethylamine at 120° only one isomer was obtained, representing 4- or 5-methyl-substituted 3-dimethylamino-6-chloro-pyridazine, of which the latter seems more likely for steric reasons. No bis-amination, as reported by Druey *et al.*[3] in the case of 3,6-dichloro-pyridazine, was observed. Reductive dehalogenation with Raney nickel proceeded smoothly to give 4-(or 5-) methyl-6-dimethylamino-pyridazine. The more facile reduction of the chloro-substituted pyridazines containing methoxy- or dimethylamino-substituents, compared to the chloro-pyridazinones, can probably be attributed to the diminished aromatic character of the latter, resulting from the lactam-lactim-tautomerism.

EXPERIMENTAL

All melting points are uncorrected.

Citraconic anhydride.[2] 43 g (1/3 mole) of itaconic acid was suspended in 68 g (2/3 moles) of acetic anhydride. After standing for about 20 h, the mixture was heated to 80° for 2 h. Acetic acid and excess acetic anhydride were removed *in vacuo*. Itaconic anhydride distilled at 12 mm and 110—115° and crystallised in the receiver as long, beautiful columns, though some of the solid was already transformed into liquid citraconic anhydride. Distillation at atmospheric pressure gave 24 g (65 %) of citraconic anhydride, b.p. 215°.

4-Methyl-1,2,3,6-tetrahydro-pyridazin-3,6-dione.[1] To a boiling suspension of 260 g (2 moles) of hydrazine sulfate in 600 ml of water, 224 g (2 moles) of citraconic anhydride were added. The reaction started spontaneously under vigorous boiling. After heating under reflux for 2 h the mixture was cooled to 0°, and the 4-methyl-1,2,3,6-tetrahydropyridazine-3,6-dione was filtered off, washed with ice-cold water and dried at 100°. Yield 99—100 %.

4-Methyl-3,6-dichloro-pyridazine.[1] To 126 g (1 mole) of 4-methyl-1,2,3,6-tetrahydropyridazine-3,6-dione, 400 ml of phosphoryl chloride were added, and the mixture heated gently under reflux for 0.5 h. Excess reagent was distilled off *in vacuo*, and the residue was poured onto a mixture of water and crushed ice. The light yellow precipitate was filtered off and dried. The filtrate was extracted with chloroform giving 7 g of the dichloro compound. The crude 4-methyl-3,6-dichloro-pyridazine was distilled at 1 mm, b.p. 130—135°. The molten distillate was poured into petroleum ether and the crystals collected after cooling in the ice-box. Yield 147 g (90 %). m.p. 86°.

5-Methyl-6-methoxy-3-chloro-pyridazine (I) and 4-methyl-6-methoxy-3-chloro-pyridazine (II). To a solution of 1 mole of sodium methoxide in 750 ml of methanol, 163 g (1 mole) of 4-methyl-3,6-dichloro-pyridazine were added. A vigorous reaction started quickly with separation of sodium chloride. After cooling to room temperature the salt was filtered off, and the methanolic solution was kept at —10° overnight. The almost pure crystals were recrystallised from methanol or ether, by far the greatest part of (I) formed being isolated in this way. The yield of 5-methyl-6-methoxy-3-chloro-pyridazine (I) was 62 g, m.p. 113°.

The filtrate was evaporated to dryness *in vacuo* and the residue extracted with 250 ml of boiling ether. The inorganic material was removed — a little (I) separated here — and 250 ml of petroleum ether were added. To complete the crystallisation, the mixture was kept at —10° overnight. The product was recrystallised from petroleum ether giving 17 g of (II), m.p. 66°. From the combined filtrates, 36 g of (II) was obtained by repeated recrystallisations from petroleum ether. The yield of 4-methyl-6-methoxy-3-chloropyridazine (II) was 53 g, m.p. 66°. Total yield 115 g (73 %).

5-Methyl-6-methoxy-pyridazine (III) and 4-methyl-6-methoxy-pyridazine (IV). 11.5 g of 5-methyl-6-methoxy-3-chloro-pyridazine (I) was partly dissolved in a mixture af 75 ml of 1 N methanolic potassium hydroxide and 50 ml of methanol [4]. 90 ml of Raney nickel suspension [7] (500 ml contained 75 g of Raney nickel) were added and the dehalogenation was carried out at atmospheric pressure. The hydrogenation proceeded rapidly during the first 30 min, and after 1 h the reaction was complete. The catalyst was filtered off — the last part, which was difficult to remove, was filtered off with sodium sulfate as filter-aid — and the solvent was removed, the last part of it *in vacuo*. The residue was extracted with dry ether, and the ethereal solution filtered and evaporated. The residue was distilled at 12 mm, b.p. about 100°. The yield of 5-methyl-6-methoxy-pyridazine (III) was 6.3 g (75 %), m.p. 34°.

The dehalogenation of (II) was carried out analogously, giving a 67 % yield of 4-methyl-6-methoxy-pyridazine (IV), m.p. 15°, b.p. about 105° at 12 mm.

5-Methyl-1,6-dihydro-pyridazin-6-one (V) and 4-methyl-1,6-dihydro-pyridazin-6-one (VI). 0.5 g of 5-methyl-6-methoxy-pyridazine (III) was dissolved in 10 ml of conc. hydrochloric acid and the solution was refluxed for about 0.5 h and then evaporated to dryness *in vacuo*. The dry residue was extracted with chloroform, the extract dried over anhydrous magnesium sulfate and concentrated to a small volume, from which 5-methylpyridazinone-6 (V) separated on addition of petroleum ether. The hydrolysis of 4-methyl-6-methoxy-pyridazine (IV) was carried out in the same way. The yields were about 100 %.

The m.p.'s found were:

m.p. of (VI)	156°
m.p. of (VI)	162°
m.p. of authentic 5-methyl-pyridazone-6 [5]	155°
m.p. of authentic 5-methyl-pyridazone-6 + (V)	156°
m.p. of authentic 5-methyl-pyridazone-6 + (VI)	110—120°

The depression of 40—50° obtained when (VI) is mixed with 5-methyl-pyridazone-6 and the lack of depression when (V) is mixed with the same substance clearly shows, that (V) is 5-methyl-pyridazone-6. For this substance McMillan *et al.*[5] indicate the m.p. 158—9°, whereas Schmidt and Druey [8] report the m.p. 151—3° for the isomeric 4-methyl-pyridazone-6.

5-Methyl-3-chloro-1,6-dihydro-pyridazin-6-one (VII) and 4-methyl-3-chloro-1,6-dihydro-pyridazin-6-one (VIII). 50 g of 4-methyl-3,6-dichloro-pyridazine was dissolved in 250 ml of conc. hydrochloric acid and the solution was heated under reflux for 1 h. The acid was removed *in vacuo* and the residue was dissolved in a minimum of boiling ethanol. After cooling to about 30° crystals of (VIII) were filtered off at this temperature, m.p. 220° (subl.). The filtrate was kept a 0° for some hours and almost pure (VII) crystallised, m.p. 167—9°. On concentrating the mother liquor, a less pure crop of (VII) separated, m.p. 140—155°, but it was impossible to obtain the pure components from this mixture.

The first two products were recrystallised from ethanol, and further recrystallisations did not raise the m.p.'s. Yield of 5-methyl-3-chloro-1,6-dihydro-pyridazin-6-one, (VII): 20 g, m.p. 170°. Yield of 4-methyl-3-chloro-1,6-dihydro-pyridazin-6-one, (VIII): 15 g, m.p. 222°. The preparation of (VII) and (VIII) from (I) and (II) was effected analogously to the hydrolysis of 5-methyl-6-methoxy-pyridazine. The yields were about 100 %.

5-Methyl-6-ethoxy-3-chloro-pyridazine (IX) and 4-methyl-6-ethoxy-3-chloro-pyridazine (X). To a solution of 0.1 mole of sodium ethoxide in 100 ml of ethanol, 16.3 g (0.1 mole) of 4-methyl-3,6-dichloro-pyridazine was added. A vigorous reaction started with separation of sodium chloride. The mixture was heated under reflux for 0.5 h, and the sodium chloride was filtered off at room temperature. The filtrate was evaporated to dryness and the residue was extracted with boiling petroleum ether. Inorganic material was filtered off and on slow cooling of the filtrate the main part of (IX) could be isolated before crystallisation of (X) started. Both components crystallised from petroleum ether as needles, but of quite different appearance. The first crop, (IX), crystallised from ether as plates with m.p. 78°, unchanged by further recrystallisations. The purification of (X) was more difficult and was achieved by several recrystallisations from ether, giving needles with m.p. 49°. Due to losses during the purification the yields were rather poor.

The hydrolysis, establishing the structure of (IX) by giving 5-methyl-3-chloro-1,6-dihydro-pyridazin-6-one (VII), m.p. 170°, was carried out analogously to the hydrolysis of (I) and (II), the corresponding methoxy compounds.

5-Methyl-6-amino-3-chloro-pyridazine (XI) and 4-methyl-6-amino-3-chloro-pyridazine (XII). 16.3 g (0.1 mole) of 4-methyl-3,6-dichloro-pyridazine was suspended in 50 ml of methanol and 150 ml liquid ammonia were added. The reaction mixture was heated at 120° in an autoclave for 5 h. After cooling to room temperature, methanol and ammonia were removed on a steam bath. The residue was dissolved in dilute hydrochloric acid, and the acid solution was extracted with chloroform to remove unchanged starting material. In this way about 50 % of the dichloro compound were recovered. To the acid solution sodium hydroxide was added until alkaline reaction. The separated crude product corresponded to about 50 % conversion. The product was dried and acetylated by dissolving it in a minimum of boiling acetic anhydride. On cooling, the acetylation product of (XII) separated, m.p. 216°. The filtrate was concentrated to about one tenth of its original volume, and on cooling the almost pure acetylation product of (XI) separated, m.p. about 140°. Without further purification, the acetylation products were hydrolysed with the equivalent amount of potassium hydroxide in aqueous-alcoholic solution. Concentration and cooling gave 4-methyl-6-amino-3-chloro-pyridazine, (XII), m.p. 187° and 5-methyl-6-amino-3-chloro-pyridazine, (XI), m.p. 137°. The ratio between the amounts of (XI) and (XII) was about 1:10.

Diazotation of the amino-chloro-pyridazines, (XI) and (XII). 100 mg of the amino compounds was dissolved in a mixture of 2 ml of water and 1 ml of conc. sulfuric acid.

A small piece of ice was added and the solution cooled to 0°. The equivalent quantity of a 10 % solution of sodium nitrite was added while the reaction flask was thoroughly shaken. The diazotized 4-methyl-6-amino-3-chloro-pyridazine (XII) gave off nitrogen spontaneously at 0°, whereas the diazotized solution of (XI) required heating to about 40—50° before evolution of nitrogen started. Then the solutions were concentrated to about half their volumes. The pyridazones, which separated on cooling, established the structures of the amino-chloro-pyridazines. From (XII), m.p. 187°, 4-methyl-3-chloro-pyridazone-6, m.p. 220°, was obtained, and from (XI), m.p. 137°, 5-methyl-3-chloro-pyridazone-6, m.p. 170°.

4-(or 5-) Methyl-6-dimethylamino-3-chloro-pyridazine (XIII). 8.15 g (0.05 moles) of 4-methyl-3,6-dichloro-pyridazine was heated in an autoclave at 120° for 20 h with 100 ml of 30 % aqueous solution of dimethylamine. After cooling, colourless needles, m.p. 122°, could be filtered off. Recrystallisation from ethanol did not raise the m.p. Yield of (XIII) 7.1 g (83 %), m.p. 122°.

4-(or 5-) Methyl-6-dimethylamino-pyridazine (XIV). 5.7 g (1/20 mole) of 4- (or 5-) methyl-6-dimethylamino-3-chloro-pyridazine (XIII) was dehalogenated with hydrogen and Raney nickel as described above for 5-methyl-6-methoxy-3-chloro-pyridazine. The theoretical amount of hydrogen was absorbed during 1 h. The Raney nickel was filtered off and the solution evaporated to dryness. The residue was extracted with chloroform and inorganic material was removed. The chloroform was evaporated off and the residue distilled at 12 mm. The distillate solidified to slightly pink crystals, but the colour disappeared on melting the crystals and pouring the melt into petroleum ether. Yield of (XIV) 3.7 g (80 %), m.p. 90°.

Acknowledgements. The authors wish to thank professor A. Kjær and professor S. Veibel for advice during the preparation of the manuscript.

REFERENCES

1. Mizzoni, R. H. and Spoerri, P. E. *J. Am. Chem. Soc.* **76** (1954) 2201.
2. Fittig, R. and Bock, K. *Ann.* **331** (1904) 174.
3. Druey, J., Meier, Kd. and Eichenberger, K. *Helv. Chim. Acta* **37** (1954) 121.
4. Kämmerer, H., Horner, I. and Beck, H. *Chem. Ber.* **91** (1958) 1376.
5. McMillan, F. H., Kun, K. A., McMillan, C. B., Schwartz, B. S. and King, J. A. *J. Am. Chem. Soc.* **78** (1956) 407.
6. Blaise, E. E. and Gault, H. *Bull. soc. chim. France* [*4*] **9** (1911) 451.
7. Vogel, A. J. *Practical Organic Chemistry*, Longmans, Green and Co, London 1956, p. 871.
8. Schmidt, P. and Druey, J. *Helv. Chim. Acta* **37** (1954) 1467.
9. Steck, E. A. U.S. 2,905,672 (1959), *cf. Chem.Abstr.* **54** (1960) 14281.

Received April 24, 1961.

ACTA CHEMICA SCANDINAVICA 15 (1961) 1667–1675

Ein Beitrag zur Kenntnis der Konfiguration und der Konformation anomerer Aldosen und deren Glykoside

JAKOB BLOM

Tuborg Brauereien, Kopenhagen, Dänemark

Das Studium der Geschwindigkeitskonstanten der Säurehydrolyse von anomeren Methyl-aldo-glykosiden mit Pyranosering resp. Furanosering sowie der Geschwindigkeitskonstanten der Bromoxydation von anomeren Aldo-pyranosen führt nach Umkehrung der in der Literatur angegebenen Konfiguration am glykosidischen Kohlenstoffatom zu plausiblen Korrelationen.

I. HYDROLYSE VON GLYKOSIDEN MIT PYRANOSERING

Die Hydrolyse anomerer Methylglykoside durch Säuren wurde zum ersten Mal eingehend von Riiber und Sørensen [1] in der klassischen Arbeit "Zur Kenntnis der anomeren Zucker" behandelt. Aus dieser Arbeit zitiere ich:

"Ohne Zweifel ist die Hydrolysengeschwindigkeit eine recht komplizierte Grösse. Und wieder zeigen die schönen Modellversuche von Max Bergmann und seinen Mitarbeitern über die Glykosidbildung und Glykosidspaltung der 2-Desoxyzucker, dass vor allem das Hydroxyl am C-2 die Reaktionen nicht nur der freien Zucker sondern auch der Zuckerderivate bestimmt. Nach den Versuchen von Bergmann, Schotte und Lechinsky [2] sowie von Bergmann und Breuers [3] sind die Verhältnisse der Hydrolysengeschwindigkeiten von zwei Glucosiden und den entsprechenden 2-Desoxyglucosiden folgende:

α-Methylglucopyranosid :	α-Methyl-2-Desoxyglucopyranosid	= 1:500
β-Methylcellobiosid :	α,β-Methyl-2-Desoxycellobiosid	= 1:500

Besonders beachtenswert ist die Tatsache, dass nach Bergmann, Schotte und Lechinsky α- und β-Methyl-glucodesoside gleich schnell hydrolysiert werden. Die von den erwähnten Forschern ausgeführten Versuche sind nur orientierend und auch wegen der grossen Säureempfindlichkeit der Desosen recht schwierig auszuführen. Nehmen wir aber den ersten Wert, bei dem die kleinste Menge 2-Desoxyglucose freigelegt worden ist, so ergibt sich:

T = 100°C, 0,01 N HCl, 15 Min. α-Methyl-2-Desoxyglucopyranosid, 66 bzw 69 % Spaltung

T = 100°C, 0,01 N HCl, 15 Min. β-Methyl-2-Desoxyglucopyranosid, 70 % Spaltung.

Daraus $k\alpha_{(10 \log)} = 0{,}033$, $k\beta_{(10 \log)} = 0{,}035$

Es scheint deshalb, als ob das Hydroxyl am C-2 nicht nur stark verlangsamend auf die Glykosidhydrolyse wirkt, sondern dass es auch für den Unterschied im Reaktionsvermögen der anomeren Zucker verantwortlich ist. Es muss deshalb der schwere Substituent des C-2 als solcher sein, der die sterische Hinderung hervorruft."

Shafizadeh [4] ist derselben Anschauung. "The hydroxyl group at C_2 being closer to the reactive center excerts the largest influence; those at C_3 and C_5 have a lesser but nevertheless significant effect."

Kreevoy und Taft [5] haben durch Versuche in wässriger Lösung, welche $H_2{}^{18}O$ enthält, gezeigt, dass die Hydrolyse der Glykoside in einer Spaltung der Hexose-Sauerstoff-Bindung besteht; es bildet sich nämlich unmarkiertes Methanol.

In dem bekannten Buch: "Chemistry of the Carbohydrates" von Pigman und Goepp (1. Auflage, 1948) sind die Geschwindigkeitskonstanten der Säurehydrolyse von Methylglykosiden zusammengestellt; und zwar einerseits die Konstanten, die in der klassischen Abhandlung von Riiber und Sørensen [1] zusammengestellt sind, anderseits die Geschwindigkeitskonstanten, die von Isbell und Frusch [6] einige Jahre später bestimmt worden sind. Diesen Arbeiten sind die Geschwindigkeitskonstanten der Säurehydrolyse der α- und β-Methylpyranoside von 2-Desoxy-D-Glucose von D-Glucose und D-Mannose, die in Tabelle 1 zusammengestellt sind, entnommen.

Alle α-Glykoside der D-Hexosen haben dieselbe Konfiguration der $-OCH_3$ Gruppe bei C_1, alle β-Glykoside dieselbe aber umgekehrte Konfiguration. In der stabilen Cl Konformation nach Reeves [7] können α-resp. β-D-Glucose als eine α- resp. β-2-Desoxyglucose betrachtet werden, in welcher das equatoriale H-Atom bei C_2 durch eine Hydroxylgruppe ausgetauscht worden ist. α- resp. β-D-Mannose können *mutatis mutandis* als eine α- resp. β-2-Desoxyglucose betrachtet werden, in welcher das axiale H-Atom bei C_2 durch eine Hydroxylgruppe ausgetauscht worden ist. Es besteht für jedes der vier Glykoside die Möglichkeit der *cis*- und der *trans*-Stellung der beiden Gruppen bei C_2 und C_1.

Tabelle 1. Hydrolyse anomerer Methyl-Pyranose-Glykoside. Geschwindigkeitskonstanten k_{10}.

		A O_2-O_1 Å	B O_2-O_1 Å	T = 100°C 0,01 N HCl k_{10}	T = 75° 0,5 N HCl k_{10}
2-Deoxy-D-Glucose	$-\alpha$ CH_3			0,033	—
»	$-\beta$ CH_3			0,035	—
D-Glucose	$-\alpha$ CH_3	*cis* e_2a_1 2,96	*trans* e_2e_1 2,85	0,000066	0,000198
»	$-\beta$ CH_3	*trans* e_2e_1 2,85	*cis* e_2a_1 2,96	0,000137	0,000379
D-Mannose	$-\alpha$ CH_3	*trans* a_2a_1 3,73	*cis* a_2e_1 2,96	0,000137	0,000471
»	$-\beta$ CH_3	*cis* a_2e_1 2,96	*trans* a_2a_1 3,73	0,000210	0,001130

Wählt man für α-D-Glucose die *cis*-Konfiguration, wie im Falle A, ergibt sich zwangsweise für β-D-Glucose wie für α-D-Mannose die *trans*-, für β-D-Mannose die *cis*-Konfiguration.

Die in der Tabelle angeführten Abstände in Å zwischen vicinalen Sauerstoffatomen sind der klassischen Arbeit "The structure of molecules containing cyclohexane or pyranose rings" von Hassel und Ottar [8] entnommen. Diese Werte sind auf eine Arbeit von Ottar [9] basiert: "The molecular structure of *cis* and *trans cyclo*hexanediol-(1,2). An electron diffraction investigation by the sector method." In α-D-Glucose und in β-D-Mannose werden im Falle A die Abstände der Sauerstoffatome equidistant. In β-D-Glucose und α-D-Mannose werden die Abstände wesentlich verschieden. Im Falle B sind alle Verhältnisse umgekehrt.

Vergleicht man die Werte für die Abstände der Sauerstoffatome bei C_1 und C_2 und die Werte der Geschwindigkeitskonstanten der Säurehydrolyse kann man nur für den Fall B eine Parallelität finden. Im Falle B sind die Abstände der O-Atome in β-D-Glucose und α-D-Mannose equidistant. Die *k*-Werte sind gleich oder nur wenig verschieden. Im Falle B sind die Abstände der O-Atome in α-D-Glucose und β-D-Mannose 2,85 Å resp. 3,73 Å. Dieser grosse Unterschied gibt sich darin zu erkennen, dass das Glykosid der β-D-Mannose 3,2 Mal resp. 5,7 Mal schneller gespalten wird als das Glykosid der α-D-Glucose.

Nimmt man also an, dass es die Hydroxylgruppe bei C_2 ist, welche "für den Unterschied im Reaktionsvermögen der anomeren Zucker verantwortlich ist" (Riiber und Sørensen [1]) kommt man zu dem Schluss, dass in α-Glykosiden der D-Hexosen die OCH_3 Gruppe equatorial an C_1, in β-Glykosiden die $-OCH_3$ Gruppe axial an C_1 gebunden sein muss.

Nach Hassel und Ottar [8] beträgt der kleinste Abstand zwischen Sauerstoffatomen bei C_1 und C_2 2.85 Å. Der Aufbau der Stuhlkonformation bedingt einen Fall, wo der Abstand zwischen zwei Sauerstoffatomen noch kleiner ist; nämlich zwischen axial-axial gebundenen Sauerstoffatomen bei C_1 und C_3. Der Abstand beträgt 2,78 Å. In den beiden anderen möglichen Kombinationen ist der Abstand viel grösser, ja grösser als 3,73 Å.

D-Galactose und D-Gulose unterscheiden sich nur in der Konfiguration bei C_3. In den Formelbildern nach E. Fischer zeigt die Hydroxylgruppe bei C_3 in der D-Galactose nach links, in der D-Gulose nach rechts. In der C1 Stuhl-Konformation hat D-Galactose eine equatorial, D-Gulose eine axial gebundene Hydroxylgruppe bei C_3.

In der Tabelle 2 sind die Abstände zwischen dem Sauerstoffatom bei C_1 und dem bei C_2 einerseits, sowie zwischen dem Sauerstoffatom bei C_1 und dem bei C_3 anderseits, sowohl für den Fall A als für den Fall B angeführt. In beiden Fällen haben wir ein Anomer der D-Gulose, dessen Sauerstoffatom bei C_1 sowohl durch ein Sauerstoffatom bei C_2 (Abstand 2.96 Å) als durch ein Sauerstoffatom bei C_3 (Abstand 2.78 Å) geschützt ist, während das andere Anomer nur den Schutz eines Sauerstoffatoms bei C_2 (Abstand 2.85 Å) hat.

Durch die Untersuchungen von Isbell und Frusch [6] kennen wir die Geschwindigkeitskonstanten der Säurehydrolyse sowohl der anomeren Methyl-D-Gulo-hexopyranoside, als auch der anomeren der Methyl-D-Gluco-D-Gulo-hepto-pyranoside. Hierzu kommt noch, dass diese Bestimmungen sowohl mit 0.05 N HCl bei 98°C als mit 0.5 N HCl bei 75°C ausgeführt worden sind. In

Tabelle 2. Hydrolyse anomerer Methyl-Pyranose-Glykoside. Geschwindigkeitskonstanten k_{10}.

		T = 98°C 0,05 N HCl k_{10}	T = 75°C 0,5 N HCl k_{10}
D-Galactose	$-\alpha$ CH_3	—	0.00104
»	$-\beta$ CH_3	—	0.00183
D-Gulose	$-\alpha$ CH_3	0.01250	0.01150
»	$-\beta$ CH_3	0.00576	0.00377
D-Gluco-D-Gulo-pyranose	$-\alpha$ CH_3	0.00486	0.00417
»	$-\beta$ CH_3	0.00219	0.00132

A

		O_2-O_1	O_3-O_1	$k_{10} \times 10^5$
D-Galactose	$-\alpha$ CH_3	*cis* e_2a_1 2,96	*trans* $e_3a_1 > 3,73$	104
»	$-\beta$ CH_3	*trans* e_2e_1 2,85	*cis* $e_3e_1 > 3,73$	183
D-Gulose	$-\alpha$ CH_3	*cis* e_2a_1 2,96	*cis* a_3a_1 2,78	1150
»	$-\beta$ CH_3	*trans* e_2e_1 2,85	*trans* $a_3e_1 > 3,73$	377

B

		O_2-O_1	O_3-O_1	$k_{10} \times 10^5$
D-Galactose	$-\alpha$ CH_3	*trans* e_2e_1 2,85	*cis* $e_3e_1 > 3,73$	104
»	$-\beta$ CH_3	*cis* e_2a_1 2,96	*trans* $e_3a_1 > 3,73$	183
D-Gulose	$-\alpha$ CH_3	*trans* e_2e_1 2,85	*trans* $a_3e_1 > 3,73$	1150
»	$-\beta$ CH_3	*cis* e_2a_1 2,96	*cis* a_3a_1 2,78	377

allen vier Fällen wird von den Glykosiden das α-Anomer der D-Gulosen wesentlich schneller hydrolysiert als das β-Anomer; während bei der D-Galactose das Umgekehrte der Fall ist.

Beide anomere Glykoside der D-Galactose haben die C1 Konformation. Beide Anomere der D-Gluco-D-Gulo-hepto-pyranose müssen ebenfalls die C1 Konformation haben, da nur in dieser der grosse Substituent bei C_5-$CHOH$-CH_2OH, die bevorzugte equatoriale Position einnehmen kann. Da unter gleichen Bedingungen der Quotient der Geschwindigkeiten der Hydrolyse der anomeren Glykoside der homomorphen Hexose und Heptose fast gleich sind:

k_α/k_β, 98°C, Hexose 2.2, Heptose 2.2
k_α/k_β, 75°C, Hexose 3.0, Heptose 3.2

ist es begründet anzunehmen, dass alle Glykoside die C1 Konformation einnehmen.

Eine plausible Erklärung aller Befunde kann nur der Fall B geben. Die homomorphen β-Methyl-D-Gulo-pyranoside tragen also in der C1 Konformation eine axial gebundene Glykosidgruppe.

II. HYDROLYSE VON GLYKOSIDEN MIT FURANOSERING.

Bis vor einigen Jahren waren nur wenige Methyl-glykoside mit Furanosering bekannt. Augestad und Berner [10] haben in 1956 durch Säulenchromatographie eine grössere Anzahl von krystallinischen Anomeren dargestellt und

Tabelle 3. Hydrolyse anomerer Methyl-Furanose-Glykoside. Geschwindigkeitskonstanten, k_{10}.

N HCl, 20°C.

		$[\alpha]_D$	$k_{10} \times 10^6$		$[\alpha]_D$	$k_{10} \times 10^6$
D-Xylose	β	− 89°	3300	α	+182°	5 600
D-Glucose	β	− 86°	5400*	α	+ 98°	10 000*
L-Arabinose	α	−127°	89	β	+118	610
D-Galactose	β	−112°	53	α	+104°	450
L-Fucose	β	+113°	65	α	−111,4°	210
D-Arabinose	α	+128°	89	β	−119°	520
D-Mannose	α	+109°	142	β	−86,5°	2 050

* Haworth, Porter und Waine [20], Äthyl-gluco-furanoside. 0.01 N Salzsäure, 55–60°C.

die Geschwindigkeit der Hydrolyse k_{10}, in N Salzsäure bei 20°C bestimmt. Die gefundenen k_{10}-Werte und $[\alpha]_D$ sind in Tabelle 3 zusammengestellt.

α-D- und β-L- referieren zu derselben absoluten Konfiguration am anomeren Kohlenstoffatom; β-D- und α-L- zu der umgekehrten. β-L-Arabinose und α-D-Galactose sind also homomorphe Zucker mit derselben absoluten Konfiguration am Kohlenstoffatom C_1.

Furanosen enthalten einen Tetrahydrofuranring der im Gegensatz zum Tetrahydropyranring als eben angesehen werden kann, (Mills [11]). Die Hydroxylgruppen in einer Furanose sind gleichartig im Verhältnis zur Ebene des Ringes an die Ringkohlenstoffatome gebunden.

Eine Klassifizierung in axial und equatorial gebundene Substituenten wie im Tetrahydro-pyranring fällt weg. Das Problem wird noch einfacher indem ein Tetrahydro-furanring nicht verschiedene Konformationen einzunehmen vermag, und eine Hydroxylgruppe bei C_3 nicht näher der Glykosidgruppe bei C_1 stehen kann, als eine Hydroxylgruppe bei C_2. Nach Reeves [7] ist der Abstand vicinaler Sauerstoffatome bei *cis*-ständiger Bindung 2,51 Å, bei *trans*-ständiger 3,45 Å.

Von jedem anomeren Paar ist das anomere Glykosid, welches am langsamsten hydrolysiert wird, in der linken Kolonne angeführt.

Nach Augestad und Berner [10] sind alle in dieser Kolonne aufgezählten Glykoside *trans*-1,2-Glykoside.

Wenn man wiederum von der Anschauung ausgeht, dass die Geschwindigkeit der Hydrolyse von Glykosiden, wenn auch nicht allein, so doch decisiv, durch den Abstand zwischen dem Reaktionscentrum und der nächststehenden Hydroxylgruppe bestimmt wird, kommt man zu dem Resultat, dass die in der linken Kolonne der Tabelle 3 aufgezählten mit geringerer Geschwindigkeit hydrolysierbaren Anomeren die *cis*-2,1-Anomeren darstellen.

Die Untersuchungen der Hydrolyse von Glykosiden mit Pyranosering und mit Furanosering geben also dasselbe Resultat.

In Tabelle 4 sind die Formelbilder und die relativen Hydrolysenkonstanten der anomeren, epimeren D-Glucose-und D-Mannose-furano-glykoside zusammengestellt. Um vergleichbare Werte zu haben, sind die relativen k-Werte der anomeren Glucoside, wie aus der Nebentabelle hervorgeht, calcu-

Tabelle 4. Relative Geschwindigkeiten der Hydrolyse anomerer epimerer Methyl-Furanose-Glykoside.

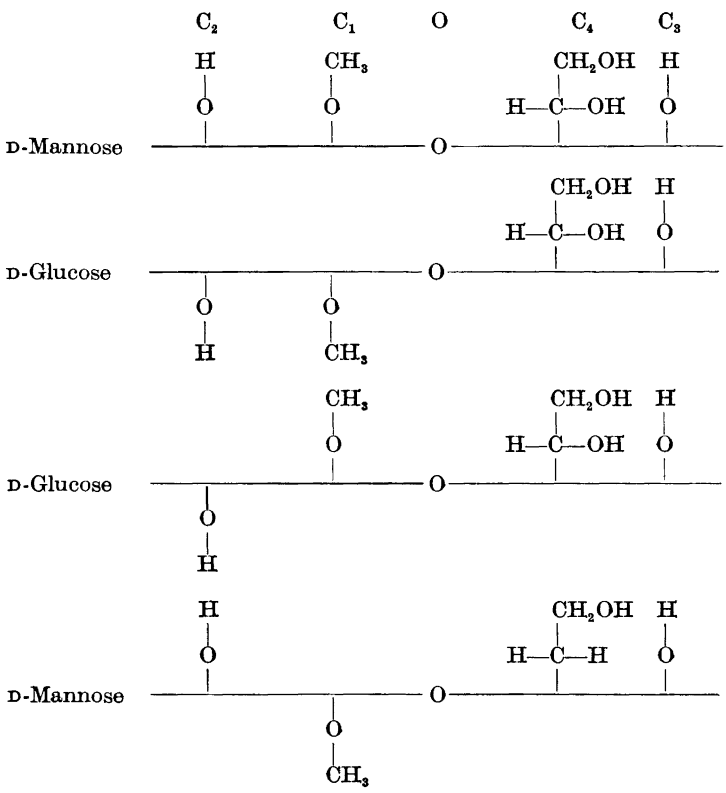

	95—100°C 0,01 N HCl $k \times 10^5$ (21)	55—60°C 0,01 N HCl $k \times 10^5$ (20)	20°C N HCl $k \times 10^5$ (10)	k rel.
D-Mannose *α*	1500		33	1
D-Glucose *β*		540		1,5
D-Glucose *α*	4500	1000		3
D-Mannose *β*			471	14

liert. Der Fall A zeigt die rel. k-Werte der Glykoside in Relation zu der von Böesecken eingeführten, heute gültigen Konfiguration der anomeren Glykoside. Der Fall B zeigt die umgekehrte Auffassung. Ist man der Anschauung, dass sterische Effekte die Geschwindigkeit der Glykosidhydrolyse decisiv beeinflussen, ist der Fall B vorzuziehen.

Tabelle 5. Relative Geschwindigkeit der Oxydation von *a*- und *β*-Aldo-Pyranosen.

Geschwindigkeit der Oxydation von *a*-D-Glucose = 1.
0.05 Mol Zucker, 0.08 Mol Br_2, Puffer $BaCO_3$ + CO_2, pH = 5,4, 0°C.

	Pentosen		Hexosen		Heptosen		OH C_2	OH C_3
	a	*β*	*a*	*β*	*a*	*β*		
D-Glucose	2.8	52	1	39	0.8	53	*e*	*e*
D-Mannose	4.9	14	1.6	24	2.3	56	*a*	*e*
D-Galactose	3.0	52	1.3	50	1.3	58	*e*	*e*
D-Talose	6.1	46	2.4	26			*a*	*e*
D-Gulose			2.2	13	1.4	12	*e*	*a*
D-Idose					0.9	11	*a*	*a*

III. OXYDATION VON ALDOSEN MIT PYRANOSERING

Die Oxydation eines sekundären Alkohols zu einem Keton besteht in der Entfernung zweier Wasserstoffatome; nämlich eines Atoms, das mit einem Sauerstoffatom und eines Atoms das mit einem Kohlenstoffatom verbunden ist. Bei der Oxydation eines cyclischen sekundären Alkohols in einem Cyclohexan- oder Tetrahydropyran-ring-system bestehen zwei Möglichkeiten; entweder sitzen das Wasserstoffatom equatorial und die Hydroxylgruppe axial oder das Wasserstoffatom axial und die Hydroxylgruppe equatorial.

Klyne [12] schreibt in "The conformations of six-membered ring systems": "In the oxidation of secondary alcohols by chromic acid or by hypobromous acid the rate-determining step is the attack on the C-H bond. Compounds carrying equatorial hydroxyl groups are in fact oxidized more slowly than their epimers carrying axial hydroxyl groups. These facts are consistent with the view that relative rates of oxidation are dependent on steric hindrance of the hydrogen atom of the carbinolgroup (axial hydrogen more hindered than equatorial hydrogen.)"

Braude und Jackman [13] schreiben in "Reaction Kinetics". "Again the chromic acid oxidation of 2-alkylcyclohexanols and 3-cholestanols proceeds more rapidly with the epimer in which the hydroxyl group has the highest axial character."

	Preferred conformation of hydrogen atom	k (min^{-1})
trans-2-Methyl*cyclo*hexanol	*a*	0,87
cis-2-Methyl*cyclo*hexanol	*e*	2,7
β-Cholestanol	*a*	1,78
a-Cholestanol	*e*	15,1

"Barton has pointed out that this is consistent with the theory providing the oxidation involves the direct attack on the C-H bond, an assumption which is amply substantiated by researches of Westheimer."

Eliel [14] schreibt: "Among substituted *cyclo*hexyl alcohols, compounds having axial hydroxyl groups and equatorial carbinol hydrogen, such as *cis*-4-*t*-butyl-*cyclo*hexanol are oxidized more readily than the isomers with equatorial hydroxyl and axial carbinol hydrogen, such as *trans*-4-*t*-butyl*cyclo*hexanol."

Heyns und Paulsen [15] haben in einer grossen Arbeit die katalytische Oxydation (Sauerstoff und Platin) von sekundären Hydroxylgruppen in Cyclitolen studiert. Scyllitol, welches nur equatoriale Hydroxylgruppen besitzt, wird nicht bei der katalytischen Oxydation angegriffen. Myo-Inositol wird dagegen oxydiert. Oxydiert wird im Myo-Inositol nur die einzige axial an einem Kohlenstoffatom des *Cyclo*hexanringsystemes gebundene Hydroxylgruppe. Es ensteht das Keton, Myo-Inosose. Weitere Untersuchungen über Cyclitole mit mehreren axial gebundenen Hydroxylgruppen, Mono-Methyl-Äther der Cyclitole und Amino-Cyclitole bestätigen "das Prinzip der Selectivität der Oxydation der axialen Hydroxylgruppen." Angyal und Anderson [16] bemerken zu dieser Arbeit: "Since, in the dehydrogenation a carbon bound hydrogen atom is removed, the selectivity for axial hydroxyl groups is readily explained. Only when the carbon atom carries the hydroxyl group in the axial position is the carbon bound hydrogen atom in the more readily accessible equatorial position."

Aldosen werden durch verschiedene Oxydationsmittel in schwach saurer, neutraler oder schwach alkalischer Lösung zu Aldonsäuren oxydiert. Der Mechanismus der Oxydation von Aldosen durch Brom in Gegenwart von Bariumcarbonat und Bromid, pH *ca.* 5,4, $T = 0°C$, ist von Isbell und Pigman [17] eingehend untersucht. Unter diesen Bedingungen ist freies Brom das aktive Oxydationsmittel; es sind die ringförmigen Halbacetale und nicht die freien Aldehydformen, die direkt oxydiert werden. Pyranosen geben δ-Lactone, Furanosen γ-Lactone in hoher Ausbeute. Bei dem einen Anomer besteht die Reaktion in der Entfernung eines equatorial direkt an C_1 gebundenen Wasserstoffatoms und eines Wasserstoffatoms einer axial an C_1 gebundenen Hydroxylgruppe. Bei dem anderen Anomer ist das umgekehrte der Fall. Beide Anomere geben dasselbe δ-Lacton.

Isbell und Pigman [17] haben für eine Reihe anomerer Aldosen die Geschwindigkeit der Reaktion bestimmt; die Resultate dieser Versuche sind in Tabelle 5 zusammengestellt und in folgender Weise geordnet: Homomorphe Pentosen, Hexosen und Heptosen sind in derselben Linie angeführt. Epimere Zucker stehen paarweise gruppiert. Die Epimerie ist durch equatoriale, respektive axiale Bindung der Hydroxylgruppe bei C_2 für die C1 Konformation angedeutet.

Die vier ersten Zucker haben eine equatorial gebundene Hydroxylgruppe bei C_3, die beiden letzten eine axial gebundene. In allen Fällen wird von einem anomeren Paar das β-Anomer schneller oxydiert als das α-Anomer. Auch andere Oxydationsmittel (Hypojodit, pH = 9,2 [18] Permanganat, pH = 2,3 [19]) oxydieren das β-Anomer schneller als das α-Anomer. Die Reaktion ist also stereospecifisch. Nach den einleitend in diesem Kapitel erwähnten Befunden, erscheint es natürlich, dem stets schneller oxydierbaren β-Anomeren ein equatorial gebundenes Wasserstoffatom und damit eine axial gebundene Hydroxylgruppe bei C_1 zuzuteilen. Wie erwähnt wird ein equatorial gebundenes Wasserstoffatom in *Cyclo*hexanringsystemen als sterisch leichter zugänglich angesehen als ein axial gebundenes. Da die Stuhlkonformationen des *Cyclo*hexans und des Tetrahydro-pyrans nur wenig verschieden sind, ist die Annahme berechtigt.

D-Gulose unterscheidet sich von D-Galactose in der Konfiguration am C_3 Atom. In den α-Anomeren dieser Zucker sind bei D-Galactose die drei Wasserstoffatome bei C_1, C_3, C_5 axial gebunden, bei D-Gulose sind nur die beiden

Wasserstoffatome bei C_1 und C_5 axial gebunden. α-D-Gulose wird schneller oxydiert als α-D-Galactose. β-D-Gulose wird langsamer oxydiert als β-D-Galactose. In β-D-Galactose ist die Hydroxylgruppe bei C_3 equatorial gebunden und steht damit so weit entfernt von der axialen Hydroxylgruppe bei C_1, dass ein sterischer Effekt nicht in Frage kommt. In β-D-Gulose ist die Hydroxylgruppe bei C_3 axial gebunden und steht dadurch der axial gebundenen Hydroxylgruppe bei C_1 so nahe, dass eine sterische Hinderung einer Reaktion mit der Hydroxylgruppe bei C_1 als logische Folge erscheint. β-D-Gulose wird *ca.* vier Mal langsamer als β-D-Galactose oxydiert. Denselben Effekt haben wir in den β-Anomeren der Heptosen mit D-Galactose- und D-Gulose-Ring. Er kommt auch zum Ausdruck in der langsameren Oxydation des β-Anomers der Heptose mit D-Idose-Ring. Ein direkter Vergleich, wie zwischen D-Gulose und D-Galactose, kann nicht durchgeführt werden, da Untersuchungen über Heptosen mit D-Talose-Ring nicht existieren. Immerhin verläuft die Oxydation der Heptose mit β-D-Idose-Ring langsamer als die Oxydation aller anderer β-Anomeren.

Die C1 Konformation ist für alle Heptosen durch die grosse CH_2OH-CHOH-Gruppe bei C_5 stabilisiert; solch grosse Gruppe bevorzugt eine equatoriale Bindung. Beide Anomere von D-Glucose und D-Galactose bevorzugen die C1 Konformation. In der C1 Konformation werden also β-Anomere schneller oxydiert als α-Anomere; eine axiale Hydroxylgruppe bei C_3 zeigt einen retardierenden Effekt.

Zum Schluss sei noch Shafizadeh [4] citiert: "Since at a low temperature (0°C) the rate of mutarotation and interconversion of the chair conformation is diminished, the reaction in certain instances exhibits a stereospecificity comparable with the specificity of enzyme systems."

LITERATUR

1. Riiber, C. N. und Sørensen, N. A. *Kgl. Norske Videnskab. Selskabs Skrifter* **1** (1938) 21.
2. Bergmann, M., Schotte, H. und Lechinsky, W. *Ber.* **55** (1922) 158.
3. Bergmann, M. und Breuers, W. *Ann.* **470** (1929) 38.
4. Shafizadeh, F. A. *Advances in Carbohydrate Chem.* **13** (1958) 9.
5. Kreevoy, M. M. und Taft, R. W. *J. Am. Chem. Soc.* **77** (1955) 5590.
6. Isbell, H. S. und Frush, H. L. *J. Research Natl. Bur. Standards* **24** (1940) 125.
7. Reeves, R. E. *Advances in Carbohydrate Chem.* **6** (1951) 107.
8. Hassel, O. und Ottar, B. *Acta Chem. Scand.* **1** (1947) 929.
9. Ottar, B. *Acta Chem. Scand.* **1** (1947) 521.
10. Augestad, I. und Berner, E. *Acta Chem. Scand.* **10** (1956) 911.
11. Mills, J. A. *Advances in Carbohydrate Chem.* **10** (1955) 13.
12. Klyne, W. *Progress in Stereochemistry* **1** (1954) 63.
13. Braude, E. A. und Jackman, L. M. in Braude, E. A. und Nachod, F. C. *Determination of Organic Structures by Physical Methods*, New York 1955, p. 692.
14. Eliel, E. L. in Newman, M. A. *Steric Effects in Organic Chemistry*, New York (1956), p. 152.
15. Heyns, K. und Paulsen, H. *Angew. Chem.* **69** (1957) 600.
16. Angyal, S. J. und Anderson, L. *Advances in Carbohydrate Chem.* **14** (1959) 148.
17. Isbell, H. S. und Pigman, W. W. in Pigman, W. W. und Goepp, R. M. *Chemistry of the Carbohydrates*, New York 1948, p. 325.
18. Ingles, O. G. und Israel, G. C. *J. Chem. Soc.* **1948** 810.
19. Kuhn, R. und Wagner-Jauregg, T. *Ber.* **58** (1925) 1441.
20. Haworth, W. N., Porter, C. R. und Waine, A. C. J. *J. Chem. Soc.* **1932** 2257.
21. Haworth, W. N. *Ber.* **65 A** (1932) 50.

Eingegangen am 22. April 1961

ACTA CHEMICA SCANDINAVICA 15 (1961) 1676–1694

The Chemistry of the Natural Order Cupressales

40 *. The Structure of Thujopsene and Hinokiic Acid

TORBJÖRN NORIN

Organisk-kemiska Institutionen, Kungl. Tekniska Högskolan, Stockholm, Sweden

The structures of thujopsene and hinokiic acid are proved to be (*1a*) and (*1b*), respectively. On catalytic hydrogenation of these compounds a conjugate addition of hydrogen takes place with formation of the corresponding dihydro-compounds (*2a*) and (*2b*), respectively.

Yano [1] and Uchida [2] found that the wood oil of the Japanese Hiba tree, *Thujopsis dolabrata* (L.f.) Sieb. et Zucc., contained a tricyclic sesquiterpene. Kawamura [3] gave this product the name thujopsene and investigated it in some detail. He also suggested two possible structures (*3* and *4*) for this compound.

Erdtman and Thomas [4] isolated a hydrocarbon, $C_{15}H_{24}$ called widdrene, from the heartwood of various species of the South African genus *Widdringtonia* and Erdtman and Pelchowicz [5] later found the same hydrocarbon in the heartwood of *Platycladus (Biota) orientalis*. On oxidation with selenium dioxide widdrene gave a crystalline α,β-unsaturated aldehyde [4]. This aldehyde can be obtained even from fairly impure widdrene fractions. Widdrene was also found in many genera belonging to the natural order Cupressales [6–9].

Hirose and Nakatsuka [10] later oxidised thujopsene from *Thujopsis* and obtained an aldehyde which was identical with that obtained from *Platycladus*. This was confirmed by Erdtman and Norin [6]. Most of the hydrocarbon fractions isolated by the Japanese authors were impure, exhibiting lower rotations than that of pure widdrene, but in view of the fact that the name thujopsene has priority over the name widdrene it was suggested that the name thujopsene should be retained for the pure hydrocarbon [6].

The α,β-unsaturated aldehyde, "widdrenal" (now thujopsenal, *1c*), could be oxidised with silver oxide to an α,β-unsaturated acid, "widdrenic acid" (now thujopsenic acid, *1b*). The identity of this acid with hinokiic acid was long suspected. Hinokiic acid was first isolated by Uchida [11] from the leaf oil of the hinoki tree, *Chamaecyparis obtusa*, and was extensively investigated by

* Part 39: *Acta Chem. Scand.* **15** (1961) 1313.

Okuda [12a–f] who suggested structure (*5*) for this acid. Hinokiic acid was later found to be a common congener of thujopsene [6].

However, due to some ambiguities in Okuda's paper, the identity of thujopsenic and hinokiic acids could not be settled. It was not until a direct comparison of both acids was made possible that Erdtman and Norin [6] were able to establish the identity of these compounds.

As the results of degradation studies and consideration of Okuda's structure (*5*) for hinokiic acid, Erdtman and Norin [6] tentatively suggested the structures (*6a*) and (*6b*) for thujopsene and hinokiic acid respectively. Independently, and almost simultaneously, Kobayashi, Nagahama and Akiyoshi [13] arrived at the same structure as regards the hydrocarbon. Without adducing any further experimental evidence Sisido and Nozaki [14] proposed structure (*7*) for thujopsene. However, continued degradative studies and spectral investigations soon indicated that the structures (*6a*) and (*6b*) for thujopsene and hinokiic acid required modification. Based on the new evidence Erdtman and Norin [15] suggested that thujopsene and hinokiic acid were correctly represented by structures (*1a*) and (*1b*), respectively.*

In this paper conclusive evidence for the revised structures (*1a*) and (*1b*) for thujopsene and hinokiic acid is presented.

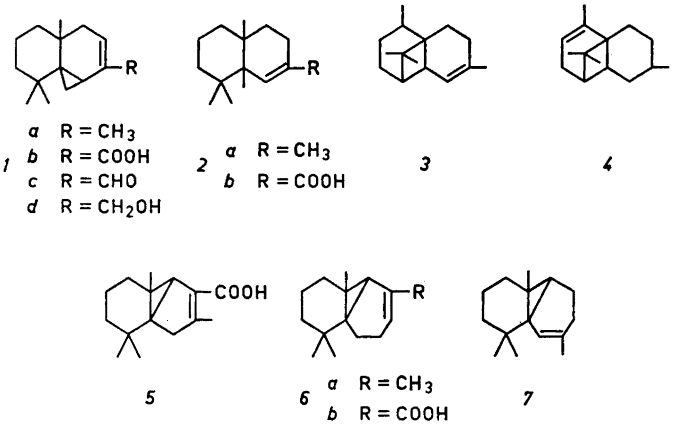

1 *a* R = CH_3; *b* R = COOH; *c* R = CHO; *d* R = CH_2OH

2 *a* R = CH_3; *b* R = COOH

3

4

5

6 *a* R = CH_3; *b* R = COOH

7

The thujopsene used for this investigation was obtained by a careful distillation of Japanese "hiba oil" and was a pure compound according to its infrared spectrum (Fig. 1) and gas-chromatogram [16].

Titration with perphthalic acid indicated the presence of only one double bond in thujopsene and, according to the oxidation of thujopsene with selenium dioxide, the hydrocarbon must contain the grouping $>C=C(CH_3)-$ [4].

On ozonisation thujopsene gave a ketocarboxylic acid (*8a*) together with small amounts of a hydroxyketocarboxylic acid (*8b*). Hypobromite oxidation

* *Added in proof.* Structure (1a) for thujopsene has now been accepted by several investigators (Kobayashi, H., Nagahama, S. and Akiyoshi, S. *Bull. Chem. Soc. Japan* **34** (1961) 1123, Sisido, K., Nozaki, H. and Imagawa, T. *J. Org. Chem.* **26** (1961) 1964 and Nozoe, T., Takeshita, H., Ito, S., Ozeki, T. and Seto, S. *Chem. and Pharm. Bull. Japan* **8** (1960) 936).

of the ketocarboxylic acid (*8a*) furnished a C_{14}-dicarboxylic acid (*9*) and bromoform. This dicarboxylic acid (*9*) could readily be converted to an anhydride (*10*) with acetic anhydride. A Dieckmann condensation of the dimethyl ester of (*9*) followed by hydrolysis and decarboxylation afforded a ketone (*11a*). Oxidation of this ketone (*11a*) with selenium dioxide gave the diketone (*12*) which on further oxidation with hydrogen peroxide gave the C_{13}-dicarboxylic acid (*13*). The latter seems to be identical with the C_{13}-dicarboxylic acid that Okuda [12e,f] obtained by an oxidation of hinokiic acid with permanganate. On heating it gave a remarkably stable anhydride (*14*).

Hinokiic acid on ozonisation followed by hypobromite oxidation gave an oil which was separated into a neutral and an acidic fraction. The neutral fraction consisted mainly of a dibromoketone (*11b*). By chromatography of the oily, acidic fraction the C_{14}-dicarboxylic acid (*9*) was obtained. The dibromoketone (*11b*) was transformed into the ketone (*11a*) by a reductive debromination with zinc and acetic acid. It was also possible to obtain the dibromoketone (*11b*) by bromination of the ketone (*11a*) although in poor yield.

Hypobromite oxidation of the ozonised hinokiic acid may appear to be a somewhat surprising procedure, but when this experiment was carried out Okuda's structure (*5*) for hinokiic acid [12f] was believed to be correct.

Hinokiic acid methyl ester gave the primary alcohol (*1d*) on reduction with lithium aluminium hydride. This alcohol on ozonisation furnished the hydroxyketocarboxylic acid (*8b*). Hypoiodite oxidation of compound (*8b*) gave the C_{14}-dicarboxylic acid (*9*). No iodoform was formed.

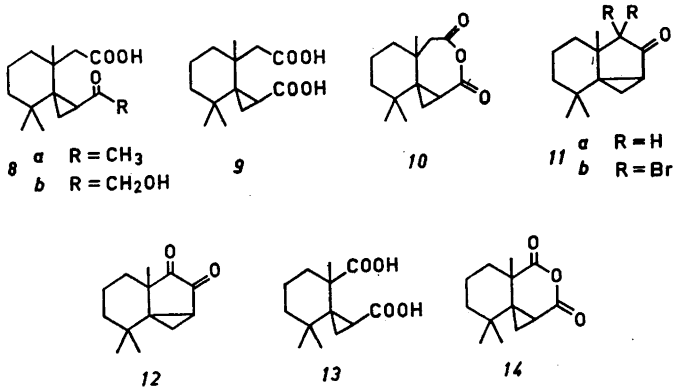

Selenium dehydrogenation of the alcohol (*15*) obtained by potassium borohydride reduction of the ketone (*11a*) furnished a crude mixture. This mixture was separated by chromatography into α-methylnaphthalene (*16*) and an oily product which according to its ultra-violet spectrum appeared to contain a tetralin derivative. Ozonisation of the latter followed by hydrogen peroxide oxidation gave α,α-dimethyladipic acid (*17*).

The ketone (*11a*) was converted to the alcohol (*18*) by treatment with methylmagnesium iodide. This alcohol gave on selenium dehydrogenation 1,6-

dimethylnaphthalene (*19*) and an oil possessing the ultra-violet characteristics of a tetralin derivative. The latter furnished *α,α*-dimethyladipic acid (*17*) on oxidation as above.

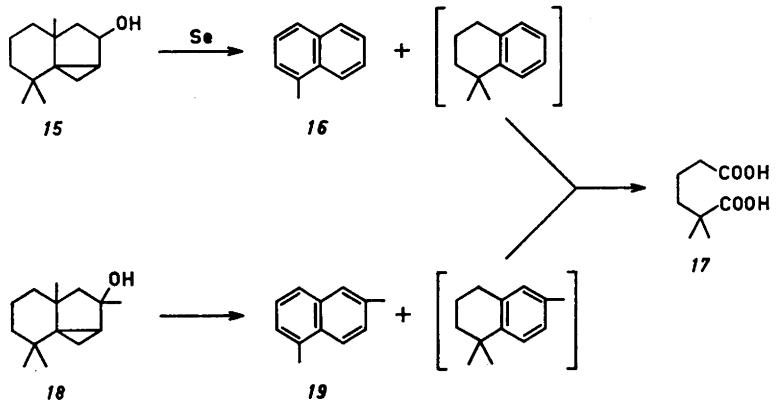

15 *16* *17* *18* *19*

On catalytic hydrogenation thujopsene (*1a*) and hinokiic acid (*1b*) readily formed di- and tetrahydroderivatives. The results of the ozonisation and titration experiments with perphthalic acid, however, indicated the presence of only one double bond in compounds (*1a*) and (*1b*). It therefore seemed probable that thujopsene and hinokiic acid contained a *cyclo*propane ring. This was also indicated by the molecular refraction ($[R_L]_D$ 64.9) which showed an exaltation compared with that of a tricyclic sesquiterpene with only one double bond ($[R_L]_D$ 64.4). Such exaltations are known from alkenyl*cyclo*propane systems (compare sabinene, *α*- and *β*-thujene, Δ^3-, Δ^4-carene and related compounds) [17]. The alcohols (*15*) and (*18*) gave pale yellow colour reactions with tetranitromethane which also indicated the presence of a *cyclo*propane ring [18,19].

Infra-red bands at 1 000—1 020 cm^{-1} and 850—860 cm^{-1} have been reported to be characteristic for *cyclo*propane rings [20–22]. The infra-red spectra of thujopsene, hinokiic acid and their degradation products exhibit absorption at these frequencies, but the bands are not characteristic enough to be assigned to a *cyclo*propane ring [20,21].

Compounds having a *cyclo*propane ring with a CH_2-group are reported to show a characteristic infra-red band at 3 050—3 090 cm^{-1} [21–23]. The reliability of this assignment has been questioned by Allen *et al.*[24] Moreover, several compounds of tricyclene type exhibit this band, *e.g.* nortricyclene (*20*) 3 085 cm^{-1} [21]. Thus, the appearance of a band at about 3 050 cm^{-1} in compounds having no interfering groups, such as olefinic hydrogens, seems to provide clear evidence for the presence of hydrogens attached to a *cyclo*propane ring, but the band does not prove the presence of a CH_2-groups in such a ring.

In thujopsene, hinokiic acid and especially in some of their degradation products such as ketone (*11a*), dibromoketone (*11b*), diketone (*12*) and alcohols (*15*) and (*18*), there is a band at about 3 050 cm^{-1} which must be due to hydrogens attached to a *cyclo*propane ring.

Thujopsene shows an ultra-violet maximum at 212 mμ (ε 4 680), which is in good agreement with a *cyclo*propane-ene chromophore. When such a chromophore is part of a seven-membered ring the observed maximum is at about 222—224 mμ (ε 4 000—6 000) and when part of a six-membered ring no maximum is observed down to 205 mμ (λ_{205} about 5 000) [25].

The spectral data of the ketone (*11a*), λ_{max}^{EtOH} 210 mμ (ε 4 900) and the infra-red band at 1 723 cm^{-1}, show the presence of a *cyclo*propane ring conjugated with the keto group. The data are in good agreement with those for dihydroumbellulone (*21*), λ_{max}^{EtOH} 210 mμ (ε 2 470); carbonyl band at 1 721 cm^{-1} [26–28] but not with those for carone (*22*), λ_{max}^{EtOH} 210 mμ (ε 3 970); carbonyl band at 1 685 cm^{-1} [22]. The *cyclo*propane ring is shown to be conjugated with the keto group of the ketocarboxylic acid (*8a*) by the spectral data of this acid, λ_{max}^{EtOH} 210 mμ (ε 4 700), and infra-red band at 1 700 cm^{-1} [29]. This is confirmed by the fact that the dicarboxylic acid (*9*), its dimethylester and a lactone (*23*), obtained by potassium borohydride reduction of the ketocarboxylic acid (*8a*), do not show any ultra-violet maxima above 205 mμ.

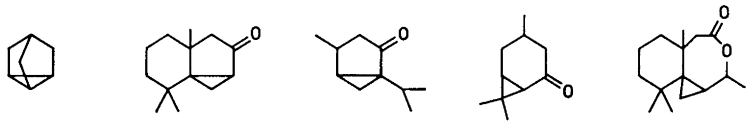

20 *11a* *21* *22* *23*

From the above results thujopsene may be formulated as (*1a*) or (*6a*). Conclusive evidence for structure (*1a*) is presented below.

In the infra-red spectra of thujopsene (Fig. 1) and hinokiic acid (Fig. 2) a band of medium intensity is observed at 1 487 cm^{-1}. This band is not present in the di- and tetrahydrocompounds. Ring strain can lead to alterations in the CH_2-deformation frequency as in ethylene oxide with one band at 1 500 cm^{-1} [30] and in *cyclo*propane with a Raman band at 1 505 cm^{-1} [31]. It has been reported that when *cyclo*propane rings are situated within larger systems,

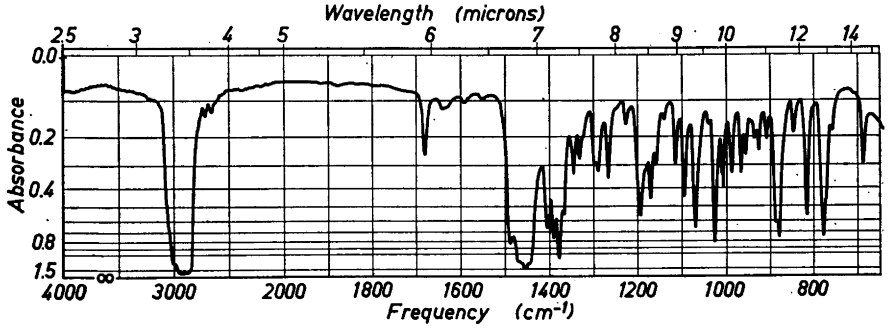

Fig. 1. Infra red spectrum of thujopsene (*1a*) as a pure oil in a 0.025 mm NaCl-cell.

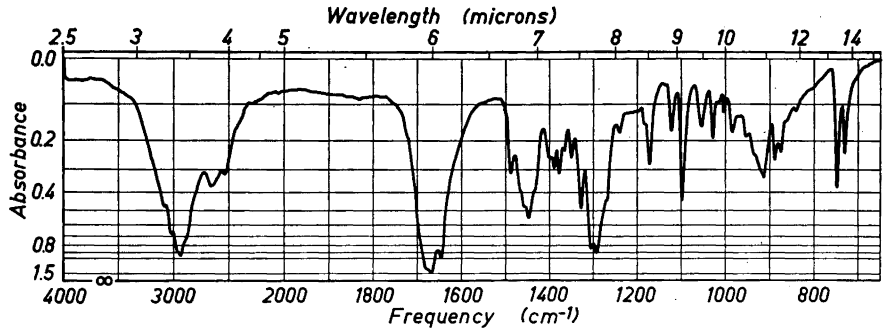

Fig. 2. Infra red spectrum of hinokiic acid (*1b*) in a KBr-disc.

such as triterpenes, the CH-deformation frequencies are not distinct enough for identification [32]. In the case of thujopsene and hinokiic acid, however, the band at 1 487 cm^{-1} may be assigned to a CH_2-group in the *cyclo*propane ring.

The diketone (*12*) did not show any tendency to enolise under neutral conditions (see experimental). If the structure (*6a*) for thujopsene was correct this compound should have furnished a diketone (*24*) which would have been expected to be more or less completely enolised [33,34].

The dibromoketone (*11b*) failed to undergo dehydrobromination with both collidine and lithium bromide in dimethylformamide. The corresponding dibromoketone (*25*) derived from structure (*6a*) for thujopsene should, on the other hand, undergo such a dehydrobromination.

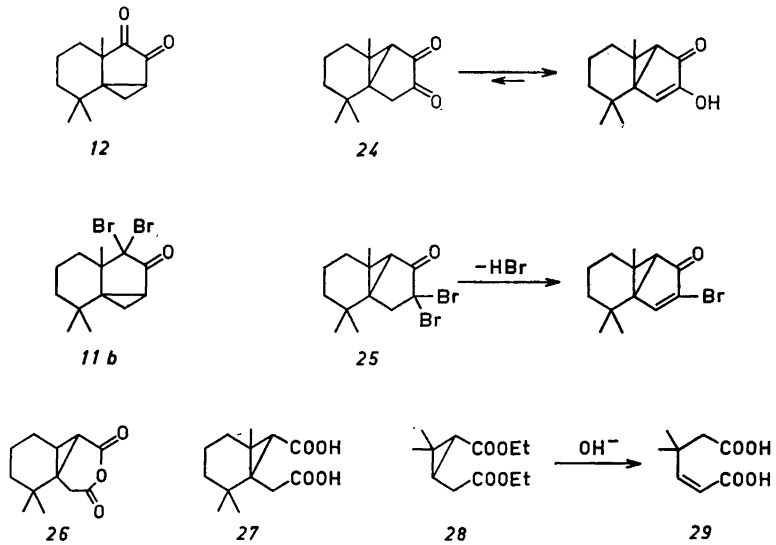

In the infra-red spectrum of the C_{14}-dicarboxylic acid anhydride (*10*) there is a band at 1 418 cm^{-1} indicating the presence of a CH_2-group adjacent to a carbonyl. The C_{13}-dicarboxylic acid anhydride (*14*) did not show such a band. If the structure (*6a*) originally proposed for thujopsene were correct this compound should have furnished a C_{13}-anhydride (*26*) exhibiting this absorption.

The C_{13}-dicarboxylic acid (*13*) is stable towards strong alkali. If structure (*27*) were correct it would be expected to rearrange as in the hydrolysis of homocaronic acid diethyl ester (*28*) to the acid (29) [35].

A proton magnetic resonance investigation on the structure of thujopsene and hinokiic acid confirmed that their structures must be (*1a*) and (*1b*), respectively [36].

On catalytic hydrogenation of thujopsene (*1a*) and hinokiic acid (*1b*) with palladised charcoal in methanol solution, a conjugate addition of hydrogen evidently takes place with formation of the corresponding dihydro-compounds (*2a* and *2b*). Further hydrogenation gave saturated tetrahydro-compounds. This type of conjugate addition of hydrogen has been observed in vinyl-*cyclo*propane systems [37,38].

The formation of a new methyl group due to fission of the *cyclo*propane ring on the catalytic hydrogenation of thujopsene and hinokiic acid has been studied in detail as it proves the presence and position of this ring. The proof of the structures (*2a* and *2b*) for the dihydro-compounds is also of importance since the hydrogenation of the alkenyl-*cyclo*propane systems in *a*-thujene (*30*), sabine (*31*) and related compounds is reported to give di- and tetrahydro-derivatives where the cleavage of the *cyclo*propane ring has occurred in another way [17]. *a*-Thujene (*30*) and sabinene (*31*) both gave the same dihydro-compound (*32*). These catalytic hydrogenations are now being reinvestigated in this Laboratory.

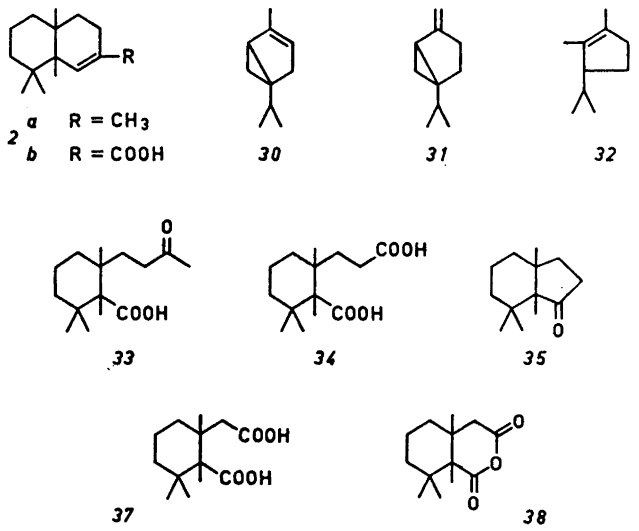

Ozonisation of dihydrothujopsene (*2a*) gave the dihydroketocarboxylic acid (*33*) which on further oxidation with hypobromite gave the dihydro-C_{14}-dicarboxylic acid (*34*) and bromoform. Dieckmann condensation of the dimethyl ester of this acid (*34*) followed by hydrolysis and decarboxylation yielded a five-membered ring ketone (*35*). Selenium dioxide oxidation of this ketone (*35*) furnished the diketone (*36*) which was further oxidised with hydrogen peroxide to the dihydro-C_{13}-dicarboxylic acid (*37*). This acid (*37*) on heating gave the dihydro-C_{13}-anhydride (*38*).

Similarly, dihydrohinokiic acid (*2b*) was ozonised to an aldehyde-acid (*39*) which on further oxidation with silver oxide gave the same dicarboxylic acid (*34*) as was obtained from dihydrothujopsene (*2a*).

The appearance of a new methyl group on hydrogenation of thujopsene and hinokiic acid is indicated by the results of Kuhn-Roth determinations. The increase in the carbon-methyl content of the dihydrocompounds compared with the non-hydrogenated products corresponds to a value expected for a new angular methyl group.

Thujopsene (*1a*) exhibits infra-red absorption at 1 380 cm^{-1} (ε 68). This band is much stronger in the dihydro-derivative (*2a*) (ε 101) as shown from Fig. 3, which also indicates the formation of a new methyl group on hydrogenation. This could be further proved by comparing the intensities of the infra-red maxima at 1 380 cm^{-1} of a dihydro-compound and its corresponding dideutero-derivative. It is known from a similar case that the number of CH_3-groups contributing to this band is proportional to its intensity [39]. Catalytic deuteration has been used for the preparation of some steroids deuterated in certain positions [40–42]. Thujopsene on catalytic deuteration formed a dideutero-derivative which, as shown from Fig. 3, had a band at 1 380 cm^{-1} of lower intensity compared with that of dihydrothujopsene.

However, it has also been shown by a mass spectrometric investigation that an extensive replacement of hydrogen by deuterium takes place on catalytic deuteration of unsaturated fatty acid esters. Deuterium was found to have entered the chain not only where the double bond was situated [43]. Such a deuterium exchange can occur during the catalytic dideuteration of thujop-

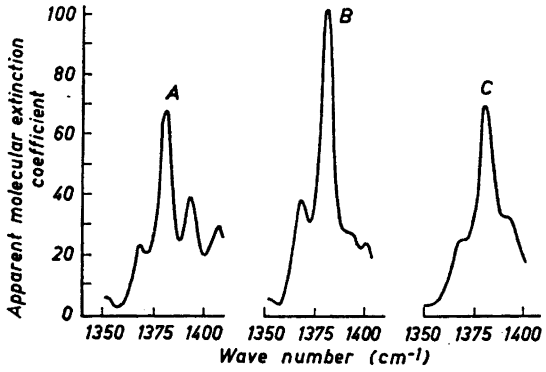

Fig. 3. Infra-red spectra in the region of the symmetrical methyl C—H bending vibration in CCl_4-solutions. A. Thujopsene (*1a*). B. Dihydrothujopsene (*2a*). C. Dideuterothujopsene.

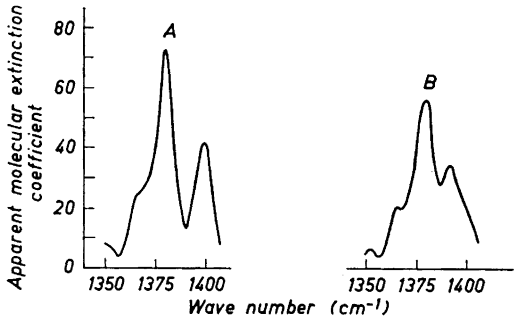

Fig. 4. Infra-red spectra in the region of the symmetrical methyl C—H bending vibration in CCl_4-solutions. A. Dimethylester of the dihydro-C_{14}-dicarboxylic acid (*34*). B. Dimethylester of the corresponding dideutero-C_{14}-dicarboxylic acid.

sene and the exchange can take place with the hydrogens of a methyl group. The results from a direct comparison of the infra-red bands at 1 380 cm^{-1} for dihydro- and dideuterothujopsene can in such a case be misleading. The methyl group attached to the double bond is, however, the only one to which the double bond can shift. Such shifts are known to occur during catalytic hydrogenation of olefins and are also believed to be the cause of the deuterium exchange[43]. This methyl group was therefore removed by degradation of the dideuterothujopsene to the dideutero-compound corresponding to the dihydro-C_{14}-dicarboxylic acid (*34*) . The dimethylester of this deutero-dicarboxylic acid showed a decrease in intensity of the infra-red band at 1 380 cm^{-1} compared with that of the dimethylester of the dihydro-C_{14}-dicarboxylic acid (*34*) as shown from Fig. 4. This proves that a new methyl group had been formed during the hydrogenation.

In the proton magnetic resonance spectrum of dideutero-thujopsene there is a signal at 224 cps (from benzene as internal standard on a 40 Mc instrument[36]) that can be assigned to a methyl group on the double bond[36]. This shows that the deuterium exchange in this methyl group is negligible. Therefore it is possible by a direct comparison of the infra-red maxima at 1 380 cm^{-1} of the dihydro- and dideuterothujopsene to determine the number of methyl groups contributing to this band. The ratio (101—69) of the intensities of this band corresponds almost to the calculated (3—2), as shown from Fig. 3.

The PMR-spectrum of dihydrothujopsene shows signals at 252, 253.5 and 254.5 cps which are assigned to four methyl groups (the average area of these signals corresponds to 12 protons)[36]. In the spectrum of dideuterothujopsene there is a decrease in the intensity of this signal group. The decrease in intensity corresponds to one methyl group (the average area corresponds almost to 9 protons). This is also in agreement with the formation of a new methyl group during hydrogenation.

The dihydroketone (*35*) contains the grouping 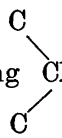 (A).

Evidence in favour of this grouping was obtained in the same way as described by Barnes *et al.*[44]

(i) The ketone did not afford a 2,4-dinitrophenylhydrazone even when refluxed for 1 h in ethanolic solution (*cf.* 2β-8β-11α-triacetoxylanan-17-one[43]) but on the other hand the ketone (*11a*) rapidly gave a 2,4-dinitrophenylhydrazone.

(ii) Quantitative bromination experiments clearly show that the dihydroketone contains only two α-hydrogen atoms replaceable by bromine. The dibromoketone was isolated.

(iii) The ketone (*11a*), which evidently has one α-CH_2-group, exhibits infrared absorption at 1 415 cm^{-1} with almost the same apparent integrated intensity ($I = 23.0$) as the dihydroketone ($I = 21.9$).

The number of hydrogen atoms in the α-position to the keto group in the dihydroketone (*35*) was also determined by deuterium exchange. A mass spectrum of the deutero-compound showed that two hydrogen atoms had been exchanged which confirms the presence of grouping (A) in the dihydroketone (*35*).

The structures of dihydrothujopsene and dihydrohinokiic acid must therefore be (*2a*) and (*2b*) respectively as shown also by Forsén and Norin[36] from a proton magnetic resonance investigation. Thus the hydrogenation experiments conclusively prove the presence and position of the *cyclo*propane ring in thujopsene and hinokiic acid and their structures must be represented by (*1a*) and (*1b*) respectively.

Application of the "octant rule"[45] to the ketone (*11a*), which exhibits a strong positive Cotton effect, suggests that the *cyclo*propane ring stands out of the plane of the paper as indicated in (*40*).* The ring junction of the dihydrothujopsene (*2a*) is proposed to be *cis* for the following reasons: (i) The dihydro-C_{13}-dicarboxylic acid (*37*) formed the anhydride (*38*) readily by heating to its melting point. (ii) The dihydro-ketone (*35*) has an extremely low carbonyl frequency (1 728 cm^{-1}, in CCl_4) for a five-membered ring ketone, which is in good agreement with a *cis* fusion of the five- and six-membered rings in this ketone[46]. From the above reasons it is believed that the angular methyl group of the ketone (*11a*) stands out of the plane of the paper as indicated in (*40*). Further work on the stereochemistry and absolute configuration of thujopsene is in progress.*

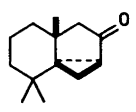

40

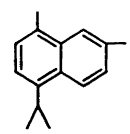

41

* See footnote p.1886.

Finally, it is of interest to note that on selenium dehydrogenation thujopsene (*1a*) affords 1,7-dimethyl-4-*iso*propylnaphthalene (*41*) in an unexpectedly high yield (15 %) together with other compounds which have not yet been completely characterised. The results of the dehydrogenation of thujopsene (*1a*) will be discussed in a following paper. Widdrol, a frequent congener of thujopsene[4,7], the structure of which is presently being investigated, also gives this naphthalene derivative on dehydrogenation [4]. Nagahama [47] recently reported that on hydration with oxalic acid thujopsene gives widdrol.*

EXPERIMENTAL

Melting points are uncorrected and were taken on a Kofler micro hot stage unless otherwise stated. The infra-red spectra were recorded on a Perkin-Elmer No. 21 instrument (NaCl-prism; liquids as pure oils in 0.025 mm NaCl-cell and solids in KBr-discs, unless otherwise stated). The ultra-violet spectra were measured in alcohol (95 %) on a Beckman DK 2 spectrophotometer. Rotations were measured in chloroform ($c \approx 2.0$ unless otherwise stated). Light petroleum refers to a fraction b.p. 40–60°. Alumina used for chromatography was supplied by Merck A.G., Darmstadt, Germany, and the degree of activity was according to Brockmann.

Thujopsene. Gas chromatographically pure thujopsene was obtained by a careful distillation of the neutral fraction of Japanese "hiba oil" (wood oil of *Thujopsis dolabrata* (L.f.) Sieb. et Zucc.) [16]. B.p. 120/10 mm, $[\alpha]_D$ −110° (*c* 2.0), n_D^{25} 1.5031, d^{24} 0.932, $[R_L]_D$ 64.9, λ_{max} 212 mμ (ε 4 680), infra-red spectrum see Fig. 1. (Found: C 88.1; H 11.8; C–CH_3 (Kuhn-Roth) 1.49 moles HOAc/mole. $C_{15}H_{24}$ requires C 88.2; H 11.8).

Hinokiic acid. A combined acidic fraction (10 g) from several *Widdringtonia* species remaining from the work of Erdtman and Thomas [4] was fractionally crystallised as described by the authors. The material which was slightly less soluble in ether gave on recrystallisation from this solvent "Widdringtonia acid II" [4] (3 g), m.p. 190–192°, $[\alpha]_D$ −79° (*c* 1.9). The more soluble material gave on recrystallisation from ether/light petroleum and then from methanol small amounts of *hinokiic acid*, "Widdringtonia acid I", (*1b*) (0.5 g), m.p. 169–170°, $[\alpha]_D$ −86° (*c* 1.8), identical with a sample of hinokiic acid kindly supplied by Dr. Okuda [13]. The infrared spectrum of hinokiic acid is shown in Fig. 2 and the ultraviolet data are λ_{max} 245 mμ (ε 5 000). (Found: C 76.8; H 9.3; C–CH_3 0.57

---

* *Added in proof:* The absolute configuration of the monoterpenes of the thujane group has recently been determined (Norin, T. *Acta Chem. Scand. In the press* and Walborsky, H. M., Sugita, T., Ohno, M. and Inouye, Y. *J. Am. Chem. Soc.* **82** (1960) 5255). The optical rotatory dispersion curves of dihydroumbellulone (i) (Djerassi, C., Riniker, R. and Riniker, B. *J. Am. Chem. Soc.* **78** (1956) 6377) and sabinaketone (ii) show negative Cotton effects. By analogy and contrary to earlier findings, the CH-group of the *cyclo*propane ring in the ketone (*11a*) lies below the plane of the paper as shown in formula (iii). The stereochemistry and absolute configuration of thujopsene will thus be represented by formula (iv) and formula (v) will represent the related alcohol widdrol [4,47], the structure of which now has been assigned (Enzell, C. *Acta Chem. Scand.* **15** (1961) 1303 and Ito, S., Endo, K., Takeshita, H., Nozoe, T. and Stother, J. B. *Chem. & Ind. London* **1961** 1618). Full details and further evidence will be presented in a separate paper.

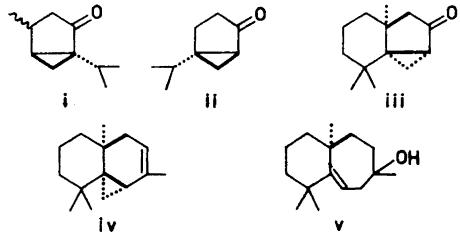

moles HOAc/mole. $C_{15}H_{22}O_2$ requires C 76.9; H 9.5). The mother liquors afforded a solid fraction which after several recrystallisations from different solvents gave a constant melting material (4 g), m.p. 137—139°. According to paper chromatography (dimethyl sulphoxide-light petroleum system)[48] this fraction consisted of a mixture of cuparenic acid [49] and hinokiic acid. The mixture was separated by chromatography on silica gel (250 g); elution with chloroform/methanol (200:1) gave hinokiic acid (3 g) m.p. 169—170°; further elution with chloroform/methanol (20:1) gave *cuparenic acid* (1 g), m.p. and mixed m.p. 158—160°, $[\alpha]_D$ + 63° (*c* 2.0), infra-red and ultra-violet spectra identical with those of an authentic sample.

The selenium dioxide oxidation of thujopsene (*1a*) was carried out according to Erdtman and Thomas [4] and the *aldehyde* (*1c*) was obtained, m.p. 75—76°, $[\alpha]_D$ —27° (*c* 1.9), λ_{max} 255 mμ (ε 6 800). Silver oxide oxidation [4] of this aldehyde (*1c*) gave hinokiic acid (*1b*), m.p. and mixed m.p. 169—170°, $[\alpha]_D$ —86° (*c* 1.9), and infra-red spectrum identical with that of an authentic sample.

Ozonisation of thujopsene (*1a*). Thujopsene (*1a*) (15 g) in ethyl acetate/methanol (6:1, 200 ml) was ozonised at —70° until a blue colour appeared. Excess ozone was removed by bubbling nitrogen through the solution until the colour disappeared. When the reaction mixture had reached room temperature zinc dust (30 g), activated with acetic acid, was added in portions. A vigorous reaction began and the mixture started to boil. After about 1 h the reaction was complete and ether (200 ml) was added followed by dilute sulphuric acid (1 %, 200 ml). The reaction mixture was filtered, the zinc residue washed with ether and the organic phase separated. The water phase was shaken with ether and the combined ether extracts washed with water, dried and taken to dryness. The residue was recrystallised from ethyl acetate and gave large crystals of the *ketocarboxylic acid* (*8a*) (11.5 g), m.p. 166—168°, $[\alpha]_D$ —129° (*c* 2.0), λ_{max} 210.5 mμ (ε 4 700), strong infra-red absorption at 1 700 cm^{-1} (double peak, carbonyl and carboxyl). (Found: C 71.2; H 9.7; C—CH_3 1.36 moles HOAc/mole, $C_{15}H_{24}O_3$ requires C 71.4; H 9.6.) *Semicarbazone* m.p. 220° (decomp.). *2,4-Dinitrophenylhydrazone* (yellow-orange) m.p. 153—154°. More of the ketocarboxylic acid (*8a*) (1 g) was obtained by working up the mother liquors and also a compound that was less soluble in ether (0.6 g, needles). The latter compound was the *hydroxyketocarboxylic acid* (*8b*) m.p. 193 (decomp.), λ_{max} 212 mμ (ε 6 050), strong infra-red absorption at 3 420 and 3 200 cm^{-1} (hydroxyl), 1 718 and 1 688 cm^{-1} (carbonyl and carboxyl). (Found: C 67.4; H 9.3. $C_{15}H_{24}O_4$ requires C 67.1; H 9.0.)

Potassium borohydride reduction of the ketocarboxylic acid (8a). The ketocarboxylic acid (*8a*) (250 mg) was dissolved in methanol (2 ml) and aqueous sodium hydroxide (10 %, 0.5 ml). This solution was added to a solution of potassium borohydride (300 mg) in methanol (2 ml) and water (4 ml). The reaction mixture was acidified and diluted with water until it became cloudy and then warmed until a clear solution was obtained. After cooling the product that crystallised was sublimed to give the *lactone* (*23*), m.p. 125—127°, characteristic infra-red bands at 3 060 cm^{-1} (hydrogens attached to the *cyclo*propane ring) and 1 720 cm^{-1} (seven-membered ring lactone), no maximum above 205 mμ in the ultra-violet spectrum (ε_{205} 150). (Found: C 77.0; H 9.4. $C_{15}H_{22}O_2$ requires C 76.9; H 9.5).

Hypobromite oxidation of the ketocarboxylic acid (*8a*). The ketocarboxylic acid (*8a*) (5 g) was dissolved in aqueous sodium hydroxide (10 %, 50 ml) and excess sodium hypobromite solution (freshly prepared from 25 g sodium hydroxide, 400 ml water and 9 ml bromine) at ice-bath temperature. The mixture was kept at room temperature for 3 h and then extracted with ether to remove bromoform. The solution was decolourised with sodium bisulphite. The solution was acidified and extracted with ether and the ether extract washed with water and evaporated. Recrystallisation of the crude product from ethyl acetate gave the *C_{14}-dicarboxylic acid* (*9*) (4.5 g), m.p. 215°, $[\alpha]_D$ —57°, (*c* 1.7), no maximum above 205 mμ in UV (ε_{205} 800). (Found: C 66.1; H 8.7; C—CH_3 0.62 moles HOAc/mole. $C_{14}H_{22}O_4$ requires C 66.1; H 8.7).

Hypoiodite oxidation of the hydroxyketocarboxylic acid (*8b*). The hydroxyketocarboxylic acid (*8b*), (100 mg) was dissolved in aqueous sodium hydroxide and aqueous iodine-potassium iodide solution (10 % iodine, 20 % potassium iodide) added until there was a slight excess of iodine present. The solution was warmed to 60° and more iodine added until the colour persisted for 2 min and then aqueous sodium hydroxide (10 %) until the colour just disappeared. The solution was allowed to cool to room temperature and water (10 ml) was added. No iodoform was obtained. Sulphuric dioxide was bubbled through the solu-

tion which was then acidified and extracted with ether. The ether extract was washed with water and evaporated to give crystals which on recrystallisation from ethyl acetate gave the *C_{14}-dicarboxylic acid* (*9*), m.p. and mixed m.p. 215° and infra-red spectrum identical with the substance obtained by hypobromite oxidation of the ketocarboxylic acid (*8a*).

Preparation of the anhydride (*10*). The C_{14}-dicarboxylic acid (*9*) (200 mg) was refluxed in acetic anhydride (10 ml) for 1 h and the reaction mixture then evaporated to dryness to give oily crystals which were sublimed *in vacuo* and crystallised from light petroleum-chloroform to give the *anhydride* (*10*), m.p. 113°, $[\alpha]_D$ + 39° (*c* 2.4), characteristic infra-red bands at 1 803 and 1 726 cm^{-1} (in CCl_4, in KBr these bands were displaced to 1 778 and 1 740 cm^{-1}) and at 1 418 cm^{-1} (CH_2-group adjacent to carbonyl). (Found: C 71.0; H 8.5. $C_{14}H_{20}O_3$ requires C 71.2; H 8.5.)

The dimethyl ester of the C_{14}-dicarboxylic acid (*9*) was prepared with diazomethane and purified by recrystallisation from methanol-water and sublimation, m.p. 71—73°, $[\alpha]_D$ —59° (*c* 1.7). (Found: C 68.3; H 9.2. $C_{16}H_{26}O_4$ requires C 68.1; H 9.3.) Saponification of the ester gave unchanged starting material; m.p. 214—215° (from ethyl acetate).

Preparation of the ketone (*11a*). The dimethyl ester of the dicarboxylic acid (*9*) (2.82 g) was dissolved in dry benzene (30 ml). Sodium methoxide (0.54 g) was added and the mixture refluxed for 3 h under an atmosphere of dry nitrogen. The solution (nearly all the sodium methoxide had dissolved) was cooled and poured into an ice-cooled mixture of ether (30 ml) and water (60 ml). The organic phase was separated and the water phase extracted with two portions (20 ml) of ether. The combined ether extracts were washed with water and dried.

The aqueous phase was acidified and extracted with ether and the extract dried and evaporated to give an oil (0.180 g) which after crystallisation from methanol-water and sublimation *in vacuo* gave needles of *a monomethyl ester of the C_{14}-dicarboxylic acid* (*9*), m.p. 115—116°. (Found: C 67.0; H 8.9. $C_{15}H_{24}O_4$ requires C 67.1; H 9.0). Saponification gave the C_{14}-dicarboxylic acid (*9*), m.p. and mixed m.p. 213—215° and infra-red spectrum identical with that of an authentic sample.

The combined organic extract was evaporated to give an oil which was dissolved in a solution of methanol (20 ml) and aqueous sodium hydroxide (10 %, 10 ml) and refluxed for 2 h. The mixture was cooled and diluted with water, acidified and extracted with ether. The dried ether extract was evaporated to give an oil which was distilled *in vacuo* to give the crystalline ketone (*11a*) (1.720 g). Crystallisation from methanol-water and sublimation *in vacuo* gave pure (*11a*). The crystals became isotropic at 49—50° (at this temperature under crossed Nicols the crystals lost their polarisability) and melted at 119—121° (sealed tube). $[\alpha]_D$ + 65°, λ_{max} 210 mμ (ε 3 490). Characteristic infra-red bands at 3 060 cm^{-1} (hydrogens attached to the *cyclo*propane ring), 1 723 cm^{-1} (carbonyl) and 1 415 cm^{-1} ($C-CO-CH_2-C$, in CCl_4 with apparent integrated intensity, *I* 23.0). (Found: C 81.3; H 10.4; $C-CH_3$ 0.65 moles HOAc/mole. $C_{13}H_{20}O$ requires C 81.2; H 10.5). *2,4-Dinitrophenylhydrazone* (orange) m.p. 215—217°. *Semicarbazone*, m.p. 225—226° (decomp.). The rotatory dispersion curve of the ketone (*11a*) (in methanol) showed a maximum at 300 mμ, [M] + 12 600°, and the lowest value recorded was 265 mμ [M] —17 800°.

Preparation of the alcohol (*1d*). Hinokiic acid (*1b*) was esterified with diazomethane and the methyl ester[4] treated with lithium aluminium hydride in the usual way. The primary *alcohol* (*1d*) so obtained was recrystallised from petroleum ether, m.p. 103—104°, $[\alpha]_D$ —102°. (Found: C 81.7; H 11.0. $C_{15}H_{24}O$ requires C 81.8; H 11.0).

Ozonisation of the alcohol (*1d*). The alcohol (*1d*) (0.30 g) was ozonised according to the method used for thujopsene (*1a*). The crystalline product obtained gave, after recrystallisation from ether-ethyl acetate, the *hydroxyketocarboxylic acid* (*8b*) (0.21 g), m.p. 190—193° (decomp.) and infra-red spectrum identical with the compound obtained as a byproduct on ozonisation of thujopsene (*1a*).

Ozonisation of hinokiic acid (*1b*). Hinokiic acid (*1b*) (1.5 g) was dissolved in ethyl acetate-methanol (5:1, 20 ml) and treated with ozone at a temperature of —70° until the solution turned blue. Excess ozone was removed with nitrogen and water added. The organic solvents were removed by distillation and aqueous sodium hydroxide (40 %, 1 ml) was added to the residue of water and oily organic material. After cooling in ice-water an excess of freshly prepared sodium hypobromite solution (from 5 g sodium hydroxide, 100 ml water and 1.5 ml bromine) was added and the mixture was allowed to stand for

3 h at room temperature. No bromoform could be isolated but a crystalline neutral product was obtained (0.21 g). This was recrystallised from methanol-water to give the *dibromoketone* (*11b*), m.p. 99—100°, $[\alpha]_D$ + 87°, λ_{max} 211 mμ (ε 4 100), characteristic infra-red bands at 3 060 cm^{-1} (hydrogens attached to the *cyclo*propanering) and 1 733 cm^{-1} (carbonyl). (Found: C 44.5; H 5.2; Br 45.9. $C_{13}H_{18}OBr_2$ requires C 44.6; H 5.2; Br 45.7). The filtrate was acidified and extracted with ether. The extract was dried and evaporated to give an oil (0.95 g) which after standing for one week gave a small amount of crystalline material (0.08 g). After recrystallisation from ethyl acetate the m.p. was 213—215° and undepressed when mixed with the *C_{14}-dicarboxylic acid* (*9*) (identical infra-red absorption). After evaporating the solvent from the mother liquors the oily residue was dissolved in chloroform (2 ml) and chromatographed on silica gel (50 g). Methanol-chloroform (4 %) eluted the *monomethyl ester* (0.150 g) of the *C_{14}-dicarboxylic acid* (*9*), m.p. 115—116°, which was also obtained as a by-product of the Dieckmann-condensation of the dimethyl ester of the C_{14}-dicarboxylic acid (*9*). (Mixed m.p. and identical infra-red spectra). Methanol-chloroform (10 %) eluted the *C_{14}-dicarboxylic acid (9)* m.p. and mixed m.p. 213—215° (identical infra-red spectra).

Reductive debromination of the dibromoketone (*11b*). A mixture of the dibromoketone (*11b*) (0.160 g) in acetic acid (3 ml), zinc dust (1.0 g) and sodium acetate (0.5 g) was refluxed for 1 h. After filtration the inorganic residue was washed with ether. The ether phase was washed with water and sodium bicarbonate, dried and evaporated to give the *ketone* (*11a*) (0.080 g). Sublimation *in vacuo* gave the pure (*11a*), m.p. and mixed m.p. 119—121° (sealed tube). Infra-red spectrum identical with that of an authentic sample.

Bromination of the ketone (*11d*). The ketone (*11a*) (0.100 g) was dissolved in carbon tetrachloride (3 ml) and bromine (0.160 g) added. The reaction mixture was stirred overnight by which time the bromine colour had disappeared. Ether (20 ml) was added and the solution dried over sodium sulphate. After evaporation of the solvents an oil remained, which, after the addition of some methanol, furnished crystals of the *dibromoketone* (*11b*) (0.020 g), m.p., mixed m.p., 99—100°. The infra-red spectrum was identical with that of an authentic sample. From the mother liquor crystals were obtained which, after recrystallisation from methanol, furnished a tribromo compound (0.040 g), m.p. 174—177° (decomp.). (Found: C 36.0; H 4.4; Br 55.9. $C_{13}H_9OBr_3$ requires C 36.1; H 4.4; Br 55.6).

The dehydrobromination experiments [50]. The dibromoketone (*11b*) (35 mg) in dimethyl formamide (2.5 ml) was heated with lithium carbonate (80 mg) and lithium bromide (95 mg) and the mixture stirred in an atmosphere of dry nitrogen. After 24 h at 100° the product was extracted with ether. After crystallisation from methanol, the product obtained was found to be unchanged starting material (28 mg), m.p. and mixed m.p. 99—100°, infrared and ultra-violet spectra identical. Even the crude product did not exhibit any ultra-violet absorption indicating the presence of an α,β-unsaturated ketone. The dibromoketone (*11b*) (20 mg) was heated under reflux with γ-collidine (1 ml). No precipitate of the collidine salt was formed even after 2 h heating. The crude residue did not exhibit any ultra-violet absorption corresponding to that of an α,β-unsaturated ketone. The crystalline material obtained from this residue was unchanged starting material.

Selenium dioxide oxidation of the ketone (*11a*). The ketone (*11a*) (0.380 g) was dissolved in acetic acid (5 ml), selenium dioxide (0.400 g) added and the mixture refluxed for 1 h. The selenium formed was removed by filtration and washed with ether. The ether solution was washed with water and sodium bicarbonate. The ether layer was dried and evaporated to give an orange oil (0.400 g). This oil was chromatographed on alumina (neutral, activity I, 40 g). Ether-light petroleum (50 %) eluted starting material (0.150 g), m.p. and mixed m.p. 119—120°, and infra-red spectrum identical with that of the ketone (*11a*). Ether eluted the *diketone* (*12*) (0.170 g) which after sublimation *in vacuo* gave pure (*12*). At 68° the crystals became isotropic (*cf.* ketone(*11a*)) and melted at 177° (sealed tube). Characteristic infra-red bands at 3 080 cm^{-1} (hydrogens attached to the *cyclo*propane ring), 1 752 and 1 727 cm^{-1} (non-enolised diketone), λ_{max} 233 mμ (ε 2 200). (Found: C 75.7; H 8.8. $C_{13}H_{16}O_2$ requires C 75.7; H 8.8).

Hydrogen peroxide oxidation of the diketone (*12*). The diketone (*12*) (0.150 g) was dissolved in methanol (5 ml) and methanolic potassium hydroxide (10 %, 5 ml) at ice-bath temperature. Hydrogen peroxide (30 %, 2 ml) was added and a white solid began to separate from the solution. After standing overnight in a refrigerator, the mixture was refluxed on a water bath for 10 min. After cooling the mixture was diluted with water

(20 ml) when the white solid obtained went into solution. The aqueous phase was acidified and extracted with ether. The ether extract was dried and evaporated to give a solid which, after sublimation *in vacuo*, gave crystals of the *C_{13}-anhydride* (*14*) (0.140 g). At 92—93° the crystals became isotropic (*cf.* ketone (*11a*)) and melted at 211—213° (sealed tube). Characteristic infra-red bands at 3070 cm^{-1} (hydrogens attached to the *cyclo*propane ring), 1795 and 1750 cm^{-1} (in CCl_4, anhydride). (Found: C 70.1; H 8.2. $C_{13}H_{18}O_3$ requires C 70.2; H 8.2).

The anhydride (*14*) could be recrystallised from methanol-water without being hydrolysed and also a rapid recrystallisation from acetic acid-water yielded unchanged anhydride. A slow crystallisation from this mixture gave large crystals of the *C_{13}-dicarboxylic acid* (*13*) which could be recrystallised from methanol-water. The acid did not analyse well probably due to partial anhydride formation on drying in a vacuum. (Found: C 66.5; H 8.3. $C_{13}H_{20}O_4$ requires C 65.0; H 8.4). On rapid heating the crystals began to melt at about 180° giving an oil which solidified and remelted at 211—213° when it also sublimed. The sublimed product showed an identical infra-red spectrum and undepressed mixed m.p. (sealed tube) with the C_{13}-anhydride (*14*).

Potassium borohydride reduction of the ketone (*11a*). A solution of potassium borohydride (0.900 g) in water (15 ml) and methanol (6 ml) was added to the ketone (*11a*) (0.500 g) in methanol (6 ml). The mixture was allowed to stand overnight at room temperature and water (25 ml) was added. Extraction with ether gave a product which was crystallised from methanol-water to give the *alcohol* (*15*) (0.425 g). At 87° the crystals became isotropic and melted at 133—135°. No absorption in the ultra-violet above 205 mμ, characteristic infra-red bands at 3360 cm^{-1} (hydroxyl) and 3060 cm^{-1} (hydrogens attached to the *cyclo*propane ring). (Found: C 80.6; H 11.5. $C_{13}H_{22}O$ requires C 80.4; H 11.4).

Selenium dehydrogenation of the alcohol (*15*). The alcohol (*15*) (0.500 g) and selenium (0.600 g) were heated under reflux in a salt bath kept at 280—290° for 24 h in an atmosphere of carbon dioxide. The product was distilled giving an oil (0.33 g) which was chromatographed on alumina (standard, activity I, 30 g). Elution was carried out with light petroleum (20 ml fractions). Fractions 3 and 4 gave an oil (0.195 g) which, according to its ultra-violet spectrum contained a tetralinic compound, λ 260 mμ (inflexion, ε 400), 263 mμ, (inflexion, ε 520), 267 mμ (maximum, ε 530), 272 mμ (minimum, ε 310), 274 mμ (maximum, ε 450) (the extinction coefficients are calculated for an assumed molecular weight of 160). The fractions 6—8 gave an oil (0.100 g) which according to its ultra-violet and infra-red spectra was identical with *α-methyl-naphthalene* (*16*); *picrate*, m.p. and mixed m.p. 139—140°.

Preparation of the alcohol (*18*). The ketone (*11a*) (0.730 g) in ether (5 ml) was added dropwise to a stirred solution of methyl magnesium iodide (from 0.250 g magnesium and 0.64 ml methyl iodide in 10 ml ether) at ice-bath temperature. The stirring and cooling were continued for 4 h. The reaction mixture was then stirred for half an hour at room temperature followed by 1 h heating under reflux. The mixture was poured into a mixture of ice (30 g) and ammonium chloride (4 g). The organic phase was separated, washed with aqueous sulphuric acid (1 %, 2 × 20 ml), and water and then dried. After evaporation of the ether, oily crystals (0.750 g) were obtained. Recrystallisation from methanol-water gave the *alcohol* (*18*), m.p. 62—63°, having characteristic infra-red bands (in CCl_4) at 3580 and 3450 cm^{-1} (hydroxyl) and 3070 cm^{-1} (hydrogens attached to the *cyclo*propane ring) (Found: C 80.7; H 11.6. $C_{14}H_{24}O$ requires C 80.7; H 11.6).

Selenium dehydrogenation of the alcohol (*18*). This reaction was carried out in the same way as with alcohol (*15*). The alcohol (*18*) (0.500 g) also gave an oily product (0.300 g) which was chromatographed on alumina as described above. Fractions 3 and 4 gave an oil (0.175 g) with tetralinic properties. λ 265 mμ (inflexion ε 590), 270 mμ (maximum, ε 700), 272 mμ (inflexion, ε 640), 276 mμ (minimum, ε 490), 278 mμ (maximum, ε 670) (the extinction coefficients were calculated for an assumed molecular weight of 174). Fractions 6—8 gave an oil which according to its ultra-violet and infra-red spectra was identical with (1,6-dimethylnaphthalene *19*). The m.p. and mixed m.p. of the styphnates, 119—120°, and of the picrates, 112—114°, were identical with those of authentic samples.

Ozonisation of the tetralinic compounds. The tetralinic compounds obtained from the selenium dehydrogenation of the alcohols (*15*) and (*18*) were treated as follows:

Ozone was passed through a solution of the compound (0.200 g) in methanol (7 ml) for 12 h at room temperature. Most of the methanol was removed by evaporation and the residue refluxed with a mixture of aqueous sodium hydroxide (5 %, 2 ml) and hyd-

rogen peroxide (30 %, 0.3 ml) on a water bath for 1 h. After cooling the mixture was extracted with ether. The alkaline solution was acidified and extracted with ether (4 × 20 ml). The ether solution was dried and the solvent removed, yielding an oil (0.120 g), which was suspended in a solution of copper acetate (0.5 g) in water (10 ml). A few drops of ether were added and the mixture stirred for 3 h. The copper salts were collected and washed with water (20 ml) and ether (25 ml), suspended in aqueous sodium hydroxide (10 %, 10 ml) and the mixture saturated with hydrogen sulphide. More sodium hydroxide was added and the mixture stirred for 2 h. The copper sulphide was removed by filtration and washed with water and the filtrate acidified and extracted with ether (5 × 15 ml). The combined ether extracts were dried and evaporated to give an oil (0.055 g) which did not crystallise. According to paper chromatography (dimethyl sulphoxide-ether system) [48] the main spot had the same R_F-value (0.15) as *a,a*-dimethyladipic acid. A sheet of paper (15 × 30 cm, Whatman 3 MM) was impregnated by passing it through a solution of dimethyl sulphoxide in toluene (25 % v/v), uniformly blotted between layers of filter paper and dried in an oven at 60° for 3 min. This process was repeated and the paper immediately placed between glass plates leaving only the starting line and the paper above it uncovered. After application of the crude oil (0.050 g) the paper was transferred to the chromatogram tank in such a manner as to prevent absorbtion of moisture. Sodium dried ether containing small amounts of dimethyl sulphoxide (4 % v/v) was used as eluent. The chromatogram was run until the diffuse ether front had moved about 20 cm. Three thin slips were cut out along the paper and developed by spraying with indicator in the usual way [18]. The part of the paper that contained the main product was cut out, extracted with ether and the combined ether extracts washed with water and dried. After evaporating the solvents an oil (0.020 g) was obtained which on standing partly crystallised giving *a,a-dimethyladipic acid* (*17*), m.p. and mixed m.p. 86—88°. The infra-red spectrum was identical with that of an authentic sample.

Catalytic hydrogenation of thujopsene (*1a*). Thujopsene (*1a*) (4.040 g, 20 mmoles) in methanol (30 ml) and ether (3 ml) was hydrogenated over a 10 % palladium on charcoal catalyst. When the theoretical amount of hydrogen (20 mmoles) had been consumed the mixture was filtered, diluted with water and extracted with ether. The ether extract was dried and the solvent evaporated to give *dihydrothujopsene* (2a), $[a]_D$ + 24°, n_D^{25} 1.5100, characteristic infra-red bands at 1 675 cm^{-1} (double bond) and in the 1 375 cm^{-1} region as shown from Fig. 3. (Found: C 87.3; H 12.7; C—CH_3 1.55 moles HOAc/mole. $C_{15}H_{26}$ requires C 87.3; H 12.7).

On further hydrogenation in the same solvent and catalyst system the rate of hydrogen uptake decreased to about one sixth of that of the first molar equivalent of hydrogen. After the uptake of a further 0.90 molar equivalent of hydrogen the reaction stopped. The *tetrahydrothujopsene* was isolated, $[a]_D$ + 27, n_D^{25} 1.4922, no infra-red bands in the range 1 600—1 700 cm^{-1}. (Found: C 86.7; H 13.4. $C_{15}H_{28}$ requires C 86.5; H 13.5).

The hydrogenation products were not completely homogeneous and there seemed to be 10 % of the normal 1:2 addition of hydrogen besides the main 1:4-addition, since only 1.9 molar equivalents of hydrogen were consumed.

Catalytic hydrogenation of hinokiic acid (*1b*). Hinokiic acid (*1b*) (0.469 g) in methanol (30 ml) was hydrogenated over a 10 % palladium on charcoal catalyst. The reaction was stopped when one molar equivalent of hydrogen had been consumed. The catalyst was filtered off. On evaporation to half the volume and addition of a little water needles of dihydrohinokiic acid separated. Recrystallisation from methanol and sublimation under reduced pressure gave pure *dihydrohinokiic acid* (*2b*), m.p. 158—160°, $[a]_D$ + 75°, λ_{max} 219 mμ (ε 9 000) characteristic infra-red bands at 1 685 and 1 640 cm^{-1} (carboxyl with conjugated double bond). (Found: C 76.1; H 10.2; C—CH_3 0.79 moles HOAc/mole. $C_{15}H_{24}O_2$ requires C 76.2; H 10.2).

With platinum in acetic acid hinokiic acid rapidly consumed 1.85 molar equivalents of hydrogen. No further hydrogen uptake took place. Evaporation under reduced pressure gave a product which after several recrystallisations from methanol gave pure tetrahydrohinokiic acid, m.p. 144—146°, $[a]_D$ + 60°. (Found: C 75.7; H 10.9. $C_{15}H_{26}O_2$ requires C 75.6; H 11.0).

Ozonisation of dihydrothujopsene (*2a*). Dihydrothujopsene (*2a*) (4.0 g) in ethyl acetate-methanol (6:1, 50 ml) was treated with ozone at —70° as described for thujopsene (*1a*).

The crystalline acidic fraction obtained (3.1 g) gave on recrystallisation from ethyl acetate pure *dihydroketocarboxylic acid* (*33*), m.p. 160–161°, $[\alpha]_D$ + 7.1°, no ultra-violet maximum above 205 mμ, characteristic infra-red bands at 1 722 cm^{-1} (carbonyl) and 1 692 cm^{-1} (carboxyl). (Found: C 70.9; H 10.2; C–CH_3 1.55 moles HOAc/mole. $C_{15}H_{26}O_3$ requires C 70.8; H 10.3). *2,4-Dinitrophenylhydrazone*, m.p. 227–228°.

Hypobromite oxidation of the dihydroketocarboxylic acid (*33*). The dihydroketocarboxylic acid (*33*) (3.0 g) was treated with sodium hypobromite as described for the ketocarboxylic acid (*8a*). The *dihydro-C_{14}-dicarboxylic acid* (*34*) (2.2 g) was obtained which on recrystallisation from acetonitrile gave pure (*34*), m.p. 185–187°, $[\alpha]_D$ –10°. (Found: C 65.8; H 9.3; C–CH_3 0.8 moles HOAc/mole. $C_{14}H_{24}O_4$ requires C 65.6; H 9.4).

Ozonisation of dihydrohinokiic acid (*2b*). The dihydrohinokiic acid (*2b*) (0.500 g) was dissolved in ethyl acetate-methanol (5:1, 10 ml) and treated with ozone at –70° until the blue colour appeared. Excess ozone was removed by bubbling nitrogen through the solution. Activated zinc (about 1 g) was added at room temperature and the mixture allowed to stand for 3 h. Ether (30 ml) and aqueous sulphuric acid (1 %, 30 ml) were added and the organic phase separated. The water phase was extracted with further amounts of ether (2 × 20 ml) and the combined organic extracts washed with water and dried. On evaporation an oil was obtained which crystallised overnight. Recrystallisation from methanol-water gave the *acid-aldehyde* (*39*) (0.310 g), m.p. 111–113.5°, characteristic infra-red bands at 1 735 cm^{-1} (aldehyde) and 1 688 cm^{-1} (carboxyl). This compound did not give a good analyses probably because of slow autoxidation.

Silver oxide oxidation of the acid-aldehyde (*39*). A saturated solution of silver nitrate (0.350 g) in water was added with stirring to a solution of aqueous sodium hydroxide (4 %, 2 ml) and dioxane (2 ml). The acid-aldehyde (*35*) (0.100 g) in dioxane (5 ml) was added to the mixture which was then heated with mechanical stirring for 24 h on a water bath. A silver mirror was formed. After filtration the filtrate was diluted with water, acidified and extracted with ether. The extract was dried and evaporated and the crystalline residue recrystallised from acetonitrile to give pure *dihydro-C_{14}-dicarboxylic acid* (*34*) (0.068 g), m.p. and mixed m.p. 185–187°. The infra-red spectrum was identical with that of an authentic sample.

Preparation of the dihydroketone (*35*). The oily dimethyl ester (1.42 g, 0.050 mole) of the dihydro-C_{14}-dicarboxylicacid obtained with diazomethane was dissolved in dry benzene (20 ml). Sodium hydride (0.050 mole) was added and the mixture refluxed for 3 h under an atmosphere of dry nitrogen. The sodium hydride passed into solution. The reaction mixture was cooled and poured into a mixture of ether (30 ml) and water (50 ml) at ice-bath temperature. The organic phase was separated and the aqueous phase extracted with ether (2 × 20 ml). The combined ether extract was washed with water, dried and evaporated to given an oil which was dissolved in methanol (20 ml) and aqueous sodium hydroxide (10 %, 10 ml) and refluxed for 2 h. The mixture was cooled, diluted with water (30 ml) and extracted with ether. The alkaline phase was acidified and extracted with ether. The dried ether extract was evaporated to give a crystalline residue which, after decarboxylation by heating on a water bath under reduced pressure, gave the *dihydroketone* (*35*) which sublimed (0.805 g), m.p. 202° (sealed tube, the crystals were isotropic at room temperature *cf.* ketone *(11a)*) $[\alpha]_D$ + 82°, characteristic infra-red bands at 1 728 cm^{-1} (in CCl_4, 5-membered ring ketone) and at 1 415 cm^{-1} (C–CO–CH_2–C, in CCl_4 with apparent integrated intensity: *I* 21.9). (Found: C 80.4; H 11.4; $C_{13}H_{22}O$ requires C 80.4; H 11.4).

Attempts to prepare the 2,4-dinitrophenylhydrazone of the dihydroketone (*35*) failed even on refluxing an ethanolic solution of the compound for 1 h in the presence of hydrochloric acid (with 70 % recovery of starting material).

Quantitative bromination experiment of the dihydroketone (*35*). A quantitative bromination experiment was carried out according to Barnes *et al.*[44] but the excess bromine was decreased to about 10 moles bromine/mole ketone. The uptake of bromine (in moles/mole ketone) was after 1 day, 2.1; 2 days, 2.0; 3 days, 2.1; 4 days, 2.1. The dibromodihydroketone was isolated and, after sublimation *in vacuo*, the pure compound was obtained, m.p. 119–120°, characteristic infra-red band at 1 755 cm^{-1} (*a,a*-dibromosubstituted 5-membered ring ketone). (Found: C 42.1; H 5.7; Br 47.9. $C_{13}H_{20}OBr_2$ requires C 41.9; H 5.4; Br 48.2).

Deuteration of the dihydroketone (*35a*)[22,51]. A mixture of the dihydroketone (*35a*) (100 mg), potassium deuteroxide (60 mg), deuterium oxide (2.5 ml) and dioxane (6 ml) was heated under reflux in an atmosphere of nitrogen for 30 min. Half the volume of the

reaction mixture was evaporated (care was taken as the dihydroketone is volatile). The mixture was cooled to room temperature and light petroleum added. The organic phase was collected, washed with two portions of deuterium oxide, dried over anhydrous magnesium sulphate and the light petroleum evaporated. Sublimation of the crystalline residue (80 mg) afforded pure *deuteroketone*, m.p. 202° (sealed tube), no infra-red band at about 1 415 cm^{-1}. The mass spectrum of the compound (kindly recorded by Dr. R. Ryhage, Laboratory for Mass Spectrometry, Karolinska Institutet, Stockholm) showed a mass peak at 196 *m/e*, corresponding to the dideuterated ketone.

Selenium dioxide oxidation of the dihydroketone (*35*). The dihydroketone (*35*) (0.300 g) was dissolved in acetic acid (3 ml) and oxidised with selenium dioxide (0.180 g) as described for ketone (*11a*). The yellowish oily product obtained was chromatographed on alumina (neutral, activity I, 15 g). Ether-light petroleum (10 %) eluted unchanged starting material (0.065 g). Ether-light petroleum (25 %) eluted the *diketone* (*36*) (0.130 g). Recrystallisation from methanol gave pure (*36*), m.p. 125—126°, λ_{max} 278 mμ (ε 1 800), characteristic infra-red bands (in CCl_4) at 1 700 and 1 600 cm^{-1} (enolised diketone). (Found: C 74.9; H 9.6. $C_{13}H_{20}O_2$ requires C 75.0; H 9.7).

Hydrogen peroxide oxidation of the diketone (*36*). The diketone (*36*) (0.100 g) was dissolved in methanolic potassium hydroxide (5 %, 10 ml) and cooled in ice water. Hydrogen peroxide (30 %, 2 ml) was added. After standing overnight in the refrigerator the mixture was refluxed on a water bath for 10 min. After cooling the mixture was diluted with water (20 ml) acidified and extracted with ether. On evaporation the dried ether extract gave oily crystals of the *dihydro-C_{13}-dicarboxylic acid* (*37*) which, after recrystallisation from methanol-water, gave the pure compound (0.070 g), m.p. 225—227° (decomp.). (Found: C 64.7; H 9.1. $C_{13}H_{22}O_4$ requires C 64.4; H 9.2).

On heating to the melting point the dihydro-dicarboxylic acid lost water and the *dihydro-C_{13}-dicarboxylic acid anhydride* (*38*) sublimed. At 64°, the crystals became isotropic (*cf.* ketone (*11a*))and melted at 216—218° (sealed tube). Characteristic infra-red bands at 1 800 and 1 760 cm^{-1} (in CCl_4, 6-membered ring anhydride). (Found: C 69.6; H 8.9. $C_{13}H_{20}O_3$ requires C 69.6; H 9.0).

Catalytic deuteration of thujopsene (*1a*). Thujopsene (*1a*) (0.741 g) in deuteromethanol (MeOD, 8 ml) and ether (2 ml) was deuterated over a 10 % palladium on charcoal catalyst (previously saturated with deuterium) until one molar equivalent of deuterium had been taken up. The dideuterothujopsene was isolated as described for dihydrothujopsene (*2a*): $[a]_D$ + 22°, n_D^{25} 1.5013. Characteristic infra-red bands at 2 185 and 2 125 cm^{-1} (carbon-deuterium stretching) 1 675 cm^{-1} (double bond). The bands in the 1 375 cm^{-1} region are shown in Fig. 3.

The nuclear magnetic resonance spectrum of dideuterothujopsene was recorded under the same conditions as for dihydrothujopsene [36]. The shifts given in the discussion are from benzene as internal standard (on a 40 Mc/s instrument).

The ozonisation of the dideuterothujopsene was carried out in the same way as described for dihydrothujopsene (*2a*) and gave the *deuteroketocarboxylic* acid, m.p. 159—160°.

The hypobromite oxidation of the deuteroketocarboxylic acid was carried out in the same way as described for the dihydroketocarboxylic acid (*33*) and gave the *deutero-C_{14}-dicarboxylic acid*, m.p. 185—187°. This acid on esterification with diazomethane gave the dimethylester with infra-red absorption in the 1 375 cm^{-1} region as shown from Fig. 4.

Acknowledgements. I wish to thank professor H. Erdtman for his interest in this work and for his kind encouragement. Thanks are also due to Dr. S. Forsén for the proton magnetic resonance spectra; to Professor W. Klyne for the optical rotatory dispersion data; to Dr. R. Ryhage for the mass spectra; to Miss G. Hammarberg for the infra-red and ultra-violet measurements. Thanks are due to Dr. I. Wellings for reading the manuscript and to *Statens Tekniska Forskningsråd* for a fellowship.

REFERENCES

1. Yano, M. *J. Soc. Chem. Ind. Japan* **16** (1913) 443.
2. Uchida, S. *J. Soc. Chem. Ind. Japan* **31** (1928) 501.
3. Kawamura, J. *Bull. Imp. For. Exp. Stn. Japan* **30** (1930) 59.
4. Erdtman, H. and Thomas, B. R. *Acta Chem. Scand.* **12** (1958) 267.

5. Erdtman, H. and Pelchowicz, Z. *Chem. Ber.* **89** (1956) 341.
6. Erdtman, H. and Norin, T. *Acta Chem. Scand.* **13** (1959) 1124.
7. Erdtman, H. *Conifer Chemistry and Taxonomy of Conifers* in *Fourth International Congress of Biochemistry*. Vol II — Biochemistry of Wood. Pergamon Press 1958.
8. Runeberg, J. *Acta Chem. Scand.* **14** (1960) 1995.
9. Enzell, C. *Acta Chem. Scand.* **14** (1960) 81.
10. Hirose, Y. and Nakatsuka, T. *J. Japan Wood Research Soc.* **4** (1958) 26.
11. Uchida, S. *J. Soc. Chem. Ind. Japan* **31** (1958) 650.
12. Okuda, O. a) *J. Pharm. Soc. Japan* **72** (1952) 703, b) *ibid.* p. 705, c) *ibid.* **73** (1953) 1, d) *ibid.* p. 4, e) *ibid.* p. 6, f) *ibid.* p. 9.
13. Kobayashi, H., Nagahama, S. and Akiyoshi, S. *Bull. Chem. Soc. Japan* **32** (1959) 203.
14. Sisido, K. and Nozaki, H. *J. Org. Chem.* **25** (1960) 275.
15. Erdtman, H. and Norin, T. *Chem. & Ind. London* **1960** 622.
16. Norin, T. and Nagahama, S. *To be published shortly.*
17. From Simonsen, J. and Barton, D. H. R. *The Terpenes* (2nd Ed.) Vol. II and III, University Press, Cambridge 1949.
18. Barton, D. H. R. *J. Chem. Soc.* **1951** 1444.
19. Zurcher, A., Jeger, O. and Ruzicka, L. *Helv. Chem. Acta* **37** (1954) 2145.
20. Bellamy, L. J. *The Infra-red Spectra of Complex Molecules*, Methuen and Co, London 1958, p. 29.
21. Paasivirta, J. *Suomen Kemistilehti B* **31** (1958) 115.
22. Büchi, G., Schach v. Wittenau, M. and White, D. M. *J. Am. Chem. Soc.* **81** (1959) 1968.
23. See Ref. 20, p. 17.
24. Allen, C. F. H., Davies, T. J., Humphlett, W. J. and Stewart, D. W. *J. Org. Chem.* **22** (1957) 1291.
25. Dauben, W. G. and Fonken, G. J. *J. Am. Chem. Soc.* **81** (1959) 4060.
26. Eastman, R. H. *J. Am. Chem. Soc.* **76** (1954) 4115.
27. Barton, D. H. R., De Mayo, P. and Shafiq, M. *J. Chem. Soc.* **1958** 140.
28. Barton, D. H. R. and Taylor, W. C. *J. Chem. Soc.* **1958** 2500.
29. Ingraham, L. L. in Newman, M. S. (Ed.) *Steric Effects in Organic Chemistry*, John Wiley and Sons, New York 1956, p. 519.
30. See Ref. 20, p. 23.
31. King, G. W., Armstrong, R. T. and Harris, L. *J. Am. Chem. Soc.* **58** (1936) 1580.
32. Cole, A. R. H. *J. Chem. Soc.* **1954** 3810.
33. Hammond, G. S. in Newman, M. S. (Ed.) *Steric Effects in Organic Chemistry*, John Wiley and Sons, New York 1956, p. 449.
34. Bredenberg, J. B. *Acta Chem. Scand.* **13** (1959) 1733.
35. Widmark, G. *Arkiv Kemi* **11** (1957) 195.
36. Forsén, S. and Norin, T. *Acta Chem. Scand.* **15** (1961) 592.
37. Ullman, E. F. *J. Am. Chem. Soc.* **81** (1959) 5386.
38. Sarel, S. and Breuer, E. *J. Am. Chem. Soc.* **81** (1959) 6522.
39. Barton, D. H. R., Page, J. E. and Warnhoff, E. W. *J. Chem. Soc.* **1954** 2715.
40. Pearlman, W. H., Pearlman, M. R. J. and Elsey, S. *J. Am. Chem. Soc.* **71** (1949) 4126.
41. Pearlman, W. H. and Pearlman, M. R. J. *J. Am. Chem. Soc.* **72** (1950) 5781.
42. Koechlin, B. A., Kritchensky, T. H. and Gallagher, T. F. *J. Biol. Chem.* **184** (1950) 393.
43. Dinh-Nguyen, N. and Ryhage, R. *Acta Chem. Scand.* **13** (1959) 1032.
44. Barnes, C. S., Barton, D. H. R., Cole, A. R. H., Fawcett, J. S. and Thomas, B. R. *J. Chem. Soc.* **1953** 571.
45. Djerassi, C. *Optical Rotatory Dispersion*, McGraw-Hill Book Company 1960, p. 178.
46. Baddeley, G. V., Halsall, T. G. and Jones, E. R. H. *J. Chem. Soc.* **1960** 1715.
47. Nagahama, S. *Bull. Chem. Soc. Japan* **33** (1960) 1467.
48. Hammarberg, G. and Wickberg, B. *Acta Chem. Scand.* **14** (1960) 882.
49. Enzell, C. and Erdtman, H. *Tetrahedron* **4** (1958) 361.
50. Djerassi, C., Cais, M. and Mitscher, L. A. *J. Am. Chem. Soc.* **81** (1959) 2386.
51. Grant, P. K. and Hodges, R. *Chem. & Ind. London* **1960** 1300.

Received April 6, 1961.

ACTA CHEMICA SCANDINAVICA 15 (1961) 1695–1700

Studies on the Chemistry of Lichens

14 *. The Structure of Calycin

BJÖRN ÅKERMARK

Organisk-kemiska institutionen, Kungl. Tekniska Högskolan, Stockholm, Sweden

Calycin has been shown to have the structure (*4*) and not, as previously supposed, the isomeric *o*-hydroxypulvinic dilactone structure (*1*). An improved synthesis of calycin is described.

The spectroscopic investigation of calycin methyl ether and its geometrical isomer furnished additional support for the proposed structure of calycin.

In 1880 Hesse [1] isolated a deep red compound, calycin, from the lichen *Lepraria candelaris* Shaer. About 50 years later Asano *et al.*[2] formulated calycin as *o*-hydroxypulvinic dilactone (*1*) on the grounds of degradative and synthetic experiments.

The high carbonyl frequencies of pulvinic dilactone (*3*) and related compounds (Table 1; *cf.* Ref.[3]) together with the easy opening of one of the lactone rings with formation of vulpinic acid (*11*) on short boiling with methanol, indicate that such lactone systems are highly strained.

Calycin has a lower carbonyl frequency (Table 1) and remains unchanged even after prolonged boiling with methanol. Either of the less strained structures (*4*) and (*6*) therefore seemed more reasonable for calcyin than (*1*). In order to study this question, an attempt was made to repeat the synthesis of calycin reported by Asano *et al.*[2]

o-Methoxybenzylcyanide was prepared in good yield by treating the corresponding benzylchloride in dimethyl sulphoxide solution with an excess of potassium cyanide at room temperature. When equimolecular amounts of *o*-methoxybenzylcyanide and diethyl oxalate were refluxed in ethanolic sodium ethoxide solution a low yield of ethyl 3-cyano-3-(*o*-methoxyphenyl)pyruvate was obtained. Subsequent condensation of this compound with benzylcyanide gave mainly 2,5-diphenyl-3,4-dioxoadiponitrile (*8*) instead of the expected 2-(*o*-methoxyphenyl)-5-phenyl-3,4-dioxoadiponitrile (*9*) which could only be isolated in poor yield by fractional crystallisation of the reaction product.

* Part *13. Acta Chem. Scand.* **13** (1959) 1855.

Table 1. Carbonyl stretching frequencies of calycin and pulvinic lactones.

Compound	ν_{CO} (cm^{-1}; in KBr)	
Calycin	1 790	1 775 1 715
Pulvinic dilactone	1 825	1 800 (sh)
o-Methoxypulvinic dilactone	1 805	1 780 (sh)
p-Methoxypulvinic dilactone	1 810	1 785 (sh)

However, when sodium hydride in 1,2-dimethoxyethane was used as the base, both condensation steps could be accomplished at room temperature and high yields of the desired products were obtained.

Hydrolysis of the dinitrile (*9*) with sulphuric acid in acetic acid-water gave *o*-methoxypulvinic dilactone (*2*), m.p. 170—171°, and hydrolysis with hydrobromic acid-acetic acid yielded calycin, m.p. 248.5—249.5°, identical with an authentic sample isolated from *Lepraria candelaris* Shaer.

Vulpinic acid (*11*) is an enol of pronounced acidity and reacts readily with diazomethane giving a colourless methylether (*cf.* Ref.[4]). Calycin reacted similarly, affording an O-methyl derivative, m.p. 174—176°, which was not identical with *o*-methoxypulvinic dilactone (*2*). Structure (*1*) for calycin must therefore be incorrect and the true structure should be either (*4*) or (*6*). The low hydroxyl and carbonyl stretching frequencies of the crystalline calycin indicate strong hydrogen bonding. Intramolecular hydrogen bonds are possible in (4)

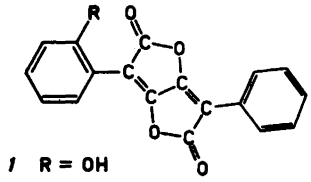

1 R = OH
2 R = OCH_3
3 R = H

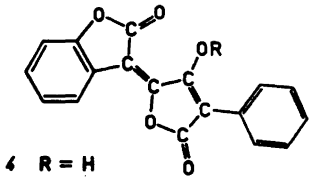

4 R = H
5 R = CH_3

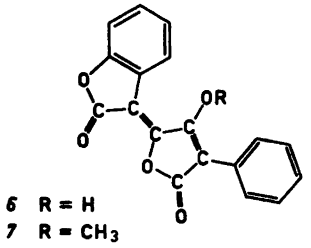

6 R = H
7 R = CH_3

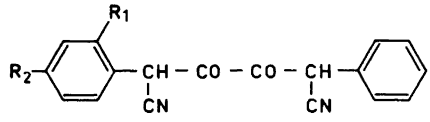

8 $R_1 = R_2 = H$
9 $R_1 = OCH_3$, $R_2 = H$
10 $R_1 = H$, $R_2 = OCH_3$

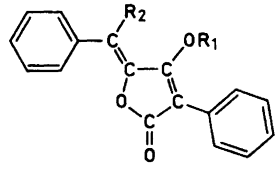

11 $R_1 = H$, $R_2 = COOCH_3$
12 $R_1 = CH_3$, $R_2 = COOCH_3$
13 $R_1 = R_2 = H$
14 $R_1 = CH_3$, $R_2 = H$

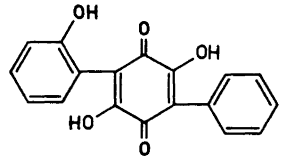

15

Table 2. Infra-red absorption of the hydrogen bonded carbonyl groups of calycin, vulpinic acid and pulvinone.

Compound	ν_{CO} (cm^{-1}; in KBr)	ν_{CO}(cm^{-1}; in dioxan)	Shift (cm^{-1})
Calycin	1 715	1 722	7
Vulpinic acid (*11*)	1 685	1 682	−3
Pulvinone (*13*)	1 697	1 767	70

but in (6) only intermolecular hydrogen bonds can be formed. The type of hydrogen bonding present can be determined [5] by measuring the carbonyl frequencies of compounds in dioxan solution and in the pure state.

Calycin, vulpinic acid (*11*) and pulvinone (*13*) were investigated by this method. Of the two latter pulvinone can form only intermolecular hydrogen bonds. Since calycin and vulpinic acid showed very nearly the same infra-red carbonyl frequencies in dioxan solution and in the pure state (Table 2), both compounds must form intramolecular hydrogen bonds. By contrast a large difference was observed for pulvinone (Table 2), indicating strong intermolecular hydrogen bonding.

Ultraviolet absorption measurements supported these conclusions. Calycin and vulpinic acid exhibited large blue-shifts on methylation but pulvinone showed only a comparatively small shift (Table 3, *cf.* Ref.[5]). Calycin must therefore have the structure (*4*).

An isomeric monomethyl ether, m.p. 235—237°, together with unchanged starting material was isolated from the attempted mild hydrolysis of calycin methyl ether (*5*) with hydrochloric acid in dilute acetic acid. The isomer was also obtained in low yield by sublimation of calycin methyl ether at 0.001 mm. The great similarities in ultraviolet and infra-red absorption strongly suggest that the high melting "*iso*calycin methyl ether" is the geometrical isomer (*7*) of calycin methyl ether. From a closer examination of the absorption spectra of calycin methyl ether and *iso*calycin methyl ether additional indirect evidence for the structure of calycin was obtained.

In calycin methyl ether the absorption band originating from the conjugated double bond has a higher frequency and a lower apparent extinction coefficient (1 635 cm^{-1}, ε 240) than *iso*calycin methyl ether (1 625 cm^{-1}, ε 410). This indicates a *trans-trans* configuration for calycin methyl ether and *cis-trans* for the isomer (*cf.* Ref.[6]).

Inspection of models shows that the hydrogen atoms of the methoxyl group will probably interact with the benzene rings in both (*5*) and (*7*), but slightly less in (*5*). Since the conjugated systems are very similar, the corresponding ultraviolet absorption should occur at longer wavelength in the compound (*5*) than in (*7*) and have a slightly higher absorption coefficient in (*5*) [7,8]. In agree-

Table 3. Ultraviolet absorption of calycin, vulpinic acid and pulvinone and their methyl ethers.

Compound	Absorption (mμ; in dioxan)	Absorption of *O*-methyl derivative (mμ; in dioxan)	Shift (mμ)
Calycin	424	391	−33
Vulpinic acid	371	324	−47
Pulvinone	337	328	−9

ment with this calycin methyl ether absorbs at 391 mμ (ε 28 000) and the isomer at 384 mμ (ε 27 400).

A similar type of hydrogen-hydrogen interaction in diphenyl polyenes [9] has been shown to cause a splitting of the IR band at 690 cm^{-1} which is due to the C—H out of plane vibrations of *mono*substituted benzene rings (*cf.* Ref.[10]). Calycin, where no such interaction is possible, absorbs at 685 cm^{-1} whereas calycin methyl ether (695, 680 cm^{-1}) and *iso*calycin methyl ether (700 and 680 cm^{-1}) exhibit two bands. The apparent extinction coefficient of the higher of these frequencies is greater in calycin methyl ether (*5*) (695 cm^{-1}, ε 100) than in the isomer (*7*) (700 cm^{-1}, ε 45).

Finally an interesting difference in infra-red carbonyl absorption was observed for calycin methyl ether and its isomer. Both compounds contain two different carbonyl functions but calycin methyl ether showed only one carbonyl band (1 775 cm^{-1}) whereas *iso*calycin methyl ether had two (1 780, 1 760 cm^{-1}). A possible explanation is that the methoxyl group increases the coumaranone carbonyl frequency in calycin methyl ether (*5*) by a dipolar field effect similar to that observed for halogen atoms [11,12]. It was not possible, however, to show that the lower carbonyl frequency of the isomer (*7*) corresponded to the coumaranone carbonyl since the frequencies did not differ appreciably for the benzalcoumaranones (1 752—1 770 cm^{-1}) and the vulpinic acid derivatives (1 760—1 785 cm^{-1}) examined.

The relation between polyporic and pulvinic acid derivatives is obvious. Polyporic acid is converted to pulvinic lactone by oxidation with lead tetraacetate [13]. The close relationship between these compounds and calycin is also indicated by the fact that some species of *Stictae* contain both calycin, pulvinic lactone, and polyporic acid [14].

It seems probable that calycin is formed in nature by oxidation of the hypothetical *o*-hydroxypolyporic acid (*15*).

EXPERIMENTAL

Melting points were determined on a Kofler block and are corrected. Infra-red absorption spectra were taken on a Perkin-Elmer spectrophotometer No. 21, fitted with a sodium chloride prism. Ultraviolet absorption spectra were recorded with a Beckman DK-2 spectrophotometer.

o-*Methoxybenzylcyanide.* (a) *o*-Methoxybenzylchloride (120 g) in dimethylsulphoxide solution (1 l) was stirred for 18 h with potassium cyanide (250 g) at 25°, then 5 min at 100°. After cooling, water (2 l) was added and the product extracted with ether. Evaporation of the solvent, steam distillation and finally distillation at reduced pressure afforded pure *o*-methoxybenzylcyanide (100 g, 89 %), m.p. 70—71° (lit.[15] 68°).

(b) *o*-Methoxybenzylchloride (300 g) in dimethylformamide-water solution (3:1, 2 l) was stirred with potassium cyanide for 18 h at 25°, then 0.5 h at 100°. After the addition of water (2 l) the product was extracted with ether. Steam distillation and subsequent distillation at reduced pressure gave *o*-methoxybenzylcyanide (220 g, 78 %), m.p. 70—71°.

Ethyl 3-cyano-3-(o-methoxyphenyl)pyruvate. Sodium hydride (50 % in oil, 57 g) was added to a mixture of dry dioxan (800 ml) and 1,2-dimethoxyethane (200 ml) under an atmosphere of dry hydrogen. *o*-Methoxybenzylcyanide (80 g) and diethyl oxalate (120 g), containing a few drops of methanol were added all at once. After a while, the reaction started with violent evolution of hydrogen. The reaction-mixture was allowed to stand overnight at room temperature, then cautiously diluted with water (2 l) and washed with ether. On acidification with acetic acid ethyl 3-cyano-3-(*o*-methoxyphenyl)pyruvate slowly deposited as long needles (105 g, 78 %), m.p. 108—109° (from acetic acid-water; lit.[2] 104—105°).

2-(o-Methoxyphenyl)-5-phenyl-3,4-dioxoadiponitrile (9). (a) Sodium hydride (50 % in oil, 37 g) was added to a solution of benzylcyanide (28 g) in 1,2-dimethoxyethane (100 ml) under an atmosphere of dry, oxygen-free nitrogen. The mixture was cooled to −10° and ethyl 3-cyano-3-(*o*-methoxyphenyl)pyruvate (55 g) in 1,2-dimethoxyethane (200 ml) containing a trace of methanol, was slowly added. The cooling bath was then removed and the mixture allowed to stand overnight at room temperature. The solution was then diluted with water (1 l) and washed with ether. On acidification with acetic acid 2-(*o*-methoxyphenyl)-5-phenyl-3,4-dioxoadiponitrile deposited as a crystalline mass (58 g, 82 %), m.p. 233—237° (decomp.) (from acetic acid, lit.[2] 262°). (Found: OCH_3 9.3. Calc. for $C_{19}H_{14}N_2O_5$: OCH_3 9.7).

(b) Ethyl 3-cyano-3-(*o*-methoxyphenyl)pyruvate (5 g) and benzylcyanide (2.5 g) were refluxed for 2.5 h with sodium ethoxide [2] (from 2.4 g sodium in 45 ml ethanol). After cooling the solution was acidified with acetic acid and the precipitate collected. Fractional crystallisation from acetic acid gave 2,5-diphenyl-3,4-dioxoadiponitrile (*8*) (0.9 g), m.p. 263—267° (decomp.) (lit.[16] 270°) and small amounts of the reported reaction product, 2-(*o*-methoxyphenyl)-5-phenyl-3,4-dioxoadiponitrile (0.2 g), m.p. 232—236° (decomp.) [*cf.* (*a*)]. The identity of the compounds was confirmed by mixed melting point determination with authentic samples prepared according to procedure (*a*) and Ref.[16], respectively, and by comparison of the infra-red absorption spectra.

o-*Methoxypulvinic lactone* (*2*). 2-(*o*-Methoxyphenyl)-5-phenyl-3,4-dioxoadiponitrile (1.7 g) was refluxed for 1 h with a mixture of acetic acid (20 ml), sulphuric acid (conc. 10 ml), and water (15 ml). After cooling water was added (50 ml). The precipitate was collected, washed with water and dried. The product was refluxed for 15 min with acetic anhydride and then poured on to ice. *o*-Methoxypulvinic dilactone (1.5 g, 88 %) was obtained, m.p. 170—171° (from acetic acid, sublimed) (lit.[17] 172—173°). (Found: C 71.0; H 4.1; OCH_3 9.7. Calc. for $C_{19}H_{12}O_5$: C 71.2; H 3.8; OCH_3 9.7).

Calycin (4). 2-(*o*-Methoxyphenyl)-5-phenyl-3,4-dioxodiponitrile (22 g) was refluxed for 1.5 h with hydrobromic acid (48 %, 200 ml) in acetic acid (1 l). On cooling calycin separated out as red needles (10.4 g, 49 %), m.p. 249—249.5° (from acetic acid), undepressed on admixture with an authentic sample isolated from *Lepraria candelaris*. λ_{max} 208 mμ (ε 19 800), 237 mμ (ε 15 700), 253 mμ (ε 7 700), 430 mμ (ε 24 700) (in *cyclo*hexane), 422 mμ (ε 17 000) (in dioxan). (Found C 70.0; H 3.3. Calc. for $C_{18}H_{10}O_5$: C 70.6; H 3.3).

Calycin methyl ether (5). Calycin (7.4 g) in ether was treated with ethereal diazomethane, containing traces of methanol, for 15 min at room temperature. Excess diazomethane was destroyed with acetic acid, and unreacted calycin (0.8 g) filtered off. Evaporation of the ether solution gave calycin methyl ether (6.8 g, 98 %), m.p. 174—176° (from acetic acid). λ_{max} 205 mμ (ε 15 700), 254,5 mμ (ε 5 800), 396 mμ (ε 12 800) (in *cyclo*hexane), 391 mμ (ε 28 000) (in dioxan). (Found: C 71.2; H 3.9; OCH_3 9.2. Calc. for $C_{19}H_{12}O_5$: C 71.2; H 3.8; OCH_3 9.7).

"Iso*calycin methyl ether" (7),* (a) Calycin methyl ether was sublimed. The most volatile part consisted mainly of calycin methyl ether, but from the least volatile part of the sublimate an isomerised product, "*iso*calycin methyl ether", (5 mg), m.p. 235—237° (from acetic acid) (preheating to 225°) was obtained. λ_{max} 205 mμ (ε 15 000), 255 mμ (ε 5 100), 387 (ε 11 000) (in *cyclo*hexane), 384 mμ (ε 27 400) (in dioxan). (Found: C 71.2; H 4.1; OCH_3 9.75. Calc. for $C_{19}H_{12}O_5$: C 71.2; H 3.8; OCH_3 9.7).

(b) Calycin methyl ether (0.28 g) was refluxed for 2 h with hydrochloric acid (2 N, 1.5 ml) in acetic acid (30 ml). On cooling, a mixture of calycin methyl ether and the isomeric ompound (0.10 g) was obtained. Fractional crystallisation from acetic acid gave "*iso*calycin methyl ether" (0.025 g), m.p. 235—237°, undepressed on admixture with a sample obtained according to (*a*).

2-(p-Methoxyphenyl)-5-phenyl-3,4-dioxoadiponitrile (10) was made from ethyl 3-cyano-3-(*p*-methoxyphenyl)pyruvate [19] (5 g) and benzylcyanide (2.5 g) using the procedure described above for 2-(*o*-methoxyphenyl)-5-phenyl-3,4-dioxoadiponitrile. The yield was 5,3 g (83 %), m.p. 259—262° (decomp.) (lit.[18] 265°).

p-*Methoxypulvinic dilactone.* Hydrolysis of 2-(*p*-methoxyphenyl)-5-phenyl-3,4-dioxoadiponitrile (5 g) with sulphuric acid (12 ml) in acetic acid (25 ml) and water (18 ml) and subsequent refluxing of the product for 15 min with acetic anhydride furnished *p*-methoxypulvinic dilactone (3.6 g, 72 %), m.p. 200—201° (from acetic acid, followed by sublimation, lit. 196—198 [2], 184—186 [18]).

2,5-Diphenyl-3,4-dioxoadiponitrile (8) was prepared according to Volhard. M.p. 263—267° (decomp.) (lit.[16] 270°).

Pulvinic dilactone (3). Hydrolysis of the dinitrile (*8*) with dilute sulphuric acid (60 %)[16] gave pulvinic dilactone, m.p. 220—221° (lit.[20] 220—221°).

Vulpinic acid (11). Pulvinic dilactone (3 g) in dry methanol (50 ml) was refluxed for 0.5 h. The acid material was taken up in ether; evaporation of the solvent gave almost pure vulpinic acid (2.7 g, 81 %), m.p. 147—149° (from aqueous methanol, lit.[21] 148—149°), ν_{CO} 1 770 cm^{-1}.

O-Methylvulpinic acid (12). Vulpinic acid (1 g) on treatment for 0.5 h with ethereal diazomethane containing a trace of methanol gave O-methylvulpinic acid (1 g), m.p. 137—139° (from methanol, lit.[22] 141°), ν_{CO} 1 785 cm^{-1}.

Pulvinone (13) was prepared according to Claisen *et al.*[23] M.p. 247—249° (from acetic acid) (lit.[23] 248—249°).

o-Methylpulvinone (14). A suspension of pulvinone in ether was treated for 0.5 h with ethereal diazomethane containing a trace of methanol. Evaporation of the solvent gave *O*-methylpulvinone (1 g), m.p. 104—106° (from methanol, lit.[24] 104—105°) ν_{CO} 1 760 cm^{-1}.

4,6-Dimethoxy-3-benzalcoumaranone[25] (ν_{CO} 1 770 cm^{-1}), *4,6-dimethoxy-3-(4-methoxybenzal)coumaranone* (ν_{CO} 1 752 cm^{-1}) and *4,6-dimethoxy-3-(3,4,5-trimethoxybenzal)coumaranone* (ν_{CO} 1 755 cm^{-1}) were all kindly supplied by Professor J. Gripenberg.

Acknowledgements. The author would like to thank Professor H. Erdtman and Docent C. A. Wachtmeister for valuable discussions. Thanks are also due to Miss G. Hammarberg for infra-red and ultraviolet absorption measurements and to Dr. I. Wellings for checking the English.

Financial support from the *Swedish Technical Research Council* is gratefully acknowledged.

REFERENCES

1. Hesse, O. *Ber.* **13** (1880) 1816.
2. Asano, M. and Kameda, Y. *Ber.* **68** (1935) 1568.
3. Bellamy, L. J. *The Infra-red Spectra of Complex Molecules*, Methuen, London 1958, p. 387.
4. Karrer, P., Gehrckens, K. A. and Heuss, W. *Helv. Chim. Acta* **9** (1926) 446.
5. Åkermark, B. *Acta Chem. Scand.* **15** (1961) 985.
6. Bellamy, L. J. *Ref.*[3], p. 38.
7. Ingraham, L. L. in Newman, M. S. (Ed.), *Steric Effects in Organic Chemistry*, John Wiley & Sons, New York 1956, p. 479.
8. Forbes, W. F. in Gray, G. W. (Ed.) *Steric Effects in Conjugated Systems*, Butterworth, London 1958, p. 62; Waight, E. S. and Erskine, R. L. *Ibid.*, p. 73.
9. Lunde, K. and Zechmeister, L. *Acta Chem. Scand.* **8** (1954) 1421.
10. Bellamy, L. J. Ref.[3], p. 77.
11. Jones, R. N. and Sandorfy, C. in Weissberger, A. (Ed.), *Technique of Organic Chemistry* IX, Interscience, New York 1956, p. 477.
12. Bellamy, L. J. Ref.[3], p. 400.
13. Frank, R. L., Clark, G. R. and Coker, J. N. *J. Am. Chem. Soc.* **72** (1950) 1824.
14. Murray, J. *J. Chem. Soc.* **1952** 1345.
15. Pschorr, R., Wolfes, O. and Buckow, W. *Ber.* **33** (1900) 162.
16. Volhard, J. *Ann.* **282** (1894) 1.
17. Mittal, O. P. and Seshadri, T. R. *J. Chem. Soc.* **1956** 1734.
18. Asano, M. and Kameda, Y. *J. Pharm. Soc. Japan* **53** (1933) 67; Chem. Zentr. **104** II (1933) 722.
19. Asano, M. and Kameda, Y. *Ber.* **67** (1934) 1522.
20. Spiegel, A. *Ann.* **219** (1883) 1.
21. Zopf, W. *Ann.* **284** (1895) 107.
22. Schenck, R. *Ann.* **282** (1894) 21.
23. Claisen, L. and Ewan, T. *Ann.* **284** (1895) 278.
24. Kögl, F. *Ann.* **465** (1928) 256.
25. Gripenberg, J. and Juselius, B. *Acta Chem. Scand.* **8** (1954) 734.

Received April 26, 1961.

ACTA CHEMICA SCANDINAVICA 15 (1961) 1701–1706

A Calorimetric Method for Determination of ΔS for a Chemical Reaction from Measurements on an Electrochemical Cell

JAN CHRISTER ERIKSSON and BJÖRN SÖDERQVIST

Division of Physical Chemistry, Royal Institute of Technology, Stockholm 70, Sweden

An equation is derived which may be used for the calculation of ΔS for a chemical reaction from rather simple calorimetric measurements on an electrochemical cell. This equation is experimentally exemplified for the lead accumulator. Further application of the method, notably the determination of Peltier heats for electrodes, is discussed.

THEORY

Consider an electrochemical cell operating at the temperature T and pressure p and at a certain voltage e and current i that may be defined as positive for an electrolyzer and as negative for a galvanic cell. e is related to η, the overpotential of the cell, by

$$\eta = e - E \tag{1}$$

where E denotes the electromotive force. η is consequently > 0 when $i > 0$ and *vice versa*. During the time of current flow $\mathrm{d}t$, the energy U of the system is changed by an amount

$$\mathrm{d}U = \delta q - p\mathrm{d}V + e\mathrm{d}Q \tag{2}$$

where $\mathrm{d}Q$ is the change of charge $i \cdot \mathrm{d}t$, d means a complete differential and δ a differential depending upon the means chosen in order to achieve a certain change of state. If, however, the same change is performed quasistatically, we have that

$$\mathrm{d}U = T\mathrm{d}S - p\mathrm{d}V + E\mathrm{d}Q \tag{3}$$

because it is then sufficient to consider only reversible energy increments. Now eqns. (2) and (3) must both be applicable assuming that all independently occurring self-discharge reactions are negligible.
Hence,

$$\delta q + e\mathrm{d}Q = T\mathrm{d}S + E\mathrm{d}Q \tag{4}$$

This equation may also be rewritten in other more convenient forms. Introduction of (1) and the definition

$$dS = \delta_e S + \delta_i S \tag{5}$$

where $T\delta_e S = \delta q$ and $T\delta_i S$ equals the Clausius uncompensated heat leads to the well-known formula [1]

$$\eta i = T\sigma = P \tag{6}$$

Here σ is the entropy production $\delta_i S/dt$ in the cell and P is the "power of irreversibility", a concept introduced by de Donder and Van Rysselberghe [2]. From the second law it follows that

$$P \geq 0 \tag{7}$$

Another formulation of (4) may be attained by dividing by dQ or by combining (5) and (6), namely

$$\dot{q}/i = T(dS/dQ) - \eta \tag{8}$$

where $\dot{q}$ denotes the rate of heat absorption $\delta q/dt$. We now define the cell reaction as the reaction which *proceeds* when a discharging current is withdrawn. dQ can thus be expressed by

$$dQ = -nF d\xi \tag{9}$$

where ξ is the extent of the cell reaction, n the participating number of moles of electrons and F the Faraday constant. However, for given T and p, dS equals $\Delta S d\xi$ and thus eqn. (8) reduces to the differential equation

$$-\dot{q}/i = T\Delta S/nF + \eta \tag{10}$$

This equation is generally valid for the system considered, *i.e.* it holds for any construction of the electrochemical cell. An equation similar although not identical to (10), has been derived by Van Rysselberghe [3]. Using eqn. (10), it is obviously possible to evaluate ΔS for the cell reaction from simultaneous measurements of the rate of heat absorption, the overvoltage and the current. Since ΔS for a reaction is a constant at fixed initial and final states, the quotient $-\dot{q}/i$ should vary linearly with η provided T, p, and the composition variables are held constant. However, a current flow generally causes both a temperature change and variations in the compositions. But it is well-known that the temperature-dependence of ΔS for a reaction is usually rather small at ordinary temperatures and so a slight change in temperature is permissible. This small change may be used for the determination of $\dot{q}$ under adiabatic conditions if a sensitive temperature-measuring device like a thermistor is utilized. In actual experiments it is also possible to maintain approximately constant compositions if the time of current flow is short enough and the amounts of electrolyte and electrodes are comparatively large.

Consider now especially the discharge of a galvanic cell at a certain resistance in the cell circuit. At the time $t = 0$, the current starts to flow and the rate of decrease of the overpotential is large. After a short time, η decreases only slowly. However, as η is a function of time, $\dot{q}$ and i are also time-dependent. Because the thermal effects at the electrodes usually have different signs and

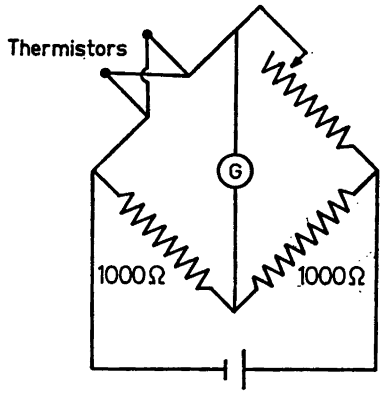

Fig. 1. The bridge system used for the determination of small temperature changes.

since it may be difficult to arrange stirring good enough to give a uniform temperature throughout the system, we may conclude that it is probably not easy to measure experimentally the proper value of $\dot{q}$ corresponding to given η- and i-values. Thus, it might be advantageous to use, instead of eqn. (10), its integrated form, *viz.*

$$-q/(i_m \cdot t) = T\Delta S/nF + \eta_m \tag{11}$$

which is valid if $T\Delta S/nF$ may be regarded as a constant during the time of current flow t. i_m is the mean value of the current defined by

$$i_m = \frac{1}{t}\int_0^t i \, dt \tag{12}$$

and η_m is given by

$$\eta_m = \frac{|1}{i_m \cdot t}\int_0^t \eta \cdot i \, dt \tag{13}$$

Consequently, instead of measuring the rate of heat absorption, it is sufficient to determine q, the total quantity of heat absorbed during the time t. It readily appears from (11) that, if discharging experiments are performed at various cell circuit resistances and approximately constant T, p, and compositions, it is required that the quantity $-q/(i_m \cdot t)$ shall depend linearly upon η_m. Disregarding the trivial case when the current is zero, q may become zero when

$$\eta_m = -T\Delta S/nF \tag{14}$$

Thus, when $-q/(i_m \cdot t)$ is determined as a function of η_m, q may in principle be measured in any arbitrary unit since the η_m-intercept gives directly the value of ΔS.

EXPERIMENTAL RESULTS

In order to illustrate the validity of eqn. (11) we have performed measurements at room temperature (21.3°C) when discharging a small, thermally insulated lead accumulator (type R2, Svenska Aktiebolaget Jungner). It has been shown that the lead accumulator [4] fulfils the condition that only *one* reaction, *viz.* the cell reaction $Pb + PbO_2 + 2H_2SO_4 \rightarrow 2PbSO_4 + 2H_2O$, occurs at discharge. The accumulator was equipped with a magnetic stirrer and two parallel-coupled thermistors ($R_{25} \approx 2\ 600\ \Omega$) were placed in the electrolyte for the determination of the temperature changes. The thermistors were connected to an ordinary resistance-bridge (Fig. 1) and so the relative temperature could be obtained as a galvanometer reading. For sufficiently small temperature intervals, the resistance of a thermistor varies linearly with the temperature. Because the galvanometer deflection was found to depend linearly upon the resistance change in the thermistor circuit, we could consequently regard the galvanometer deflection as proportional to the temperature change. From experiments with a separate heating coil it was shown that at 21.3°C one scale division corresponded to 1.034×10^{-3} °C and that the heat capacity of the accumulator was 1 050 cal/deg. From these figures the proportionality constant between q and the galvanometer deflection was calculated to be 1.086 cal/scale division.

At various resistances in the cell circuit, the galvanometer deflection, the current i and the cell voltage e were measured as functions of the time of discharging. After correction for the heat exchange with the surroundings, the absorbed heat q could be obtained from the galvanometer readings. The cell voltage was measured with a tube voltage meter (pH-meter 22, Radiometer, Copenhagen). η_m and i_m were calculated from the experimentally given e- and i-functions. The result of our measurements appears from Fig. 2. The experimental points lie all with good accuracy on a straight line which has the slope 1 as required by the theory. The intercepts on the axes are 0.0675 V corresponding to $\Delta S = 10.6$ cal/deg. During the experiments the electromotive force E decreased from 2.046 to 2.036 V implying a slight change in the composition of the electrolyte. Thus, when calculating η_m for each separate experiment, the mean value of E before and after the discharge was used. The time of discharing chosen was 5—10 min and the maximum temperature change was always less than 0.1°C. The variation of the current i during an experiment was, as might be expected, usually negligible.

According to Beck and Wynne-Jones [4] the measurements of the comparatively small ($\approx 2 \times 10^{-4}$ V/deg) temperature coefficient of the lead accumulator made by different authors are not very consistent. An obvious reason for this fact is that there are several possible sources of irreversibility in commercial accumulators. Better agreement has been attained between measurements on electrodes carefully prepared from pure substances. The mean value for ΔS when $E = 2.041$ V of such temperature-coefficient data given by Vosburghe and Craig, Craig and Vinal, Harned and Hamer is 11.2 cal/deg at 25°C [4]. The difference between this value and ours can hardly be attributed to the small difference in the temperature at which the measurements were performed. It seems more probable that the discrepancy arises from the less good accuracy in the measurements of the rather small temperature coefficient.

DISCUSSION

Compared with the temperature-coefficient method for the determination of ΔS, the procedure developed here exhibits certain advantages. The accuracy attainable seems to be more satisfactory (optimum construction conditions have, however, not been investigated) and the experimental arrangements required are comparatively simple. For the same maximum error in ΔS, it appears that a larger error in the voltage-measurements is permissible when using our method than when the temperature-coefficient method is utilized because, if other sources of errors are neglected, it is readily demonstrated on applying $\Delta S = nF\ \mathrm{d}E/\mathrm{d}T$ that an error of 0.1 cal/deg in the ΔS-value corresponds to the error 2×10^{-6} V/deg in $\mathrm{d}E/\mathrm{d}T$ whereas the same ΔS-error from eqn. (14) would be equivalent to an error in η_m amounting to 6×10^{-4} V at room temperature. Our method is also interesting from a theoretical and pedagogical point of view and on account of its possibilities for further application. Thus, *e.g.*, it should be possible to split eqn. (10) into equations referring to different parts of the lead accumulator, *viz.*

$$T\Delta S_+/nF + \eta_+ = -\dot{q}_+/i \tag{15}$$

$$T\Delta S_-/nF - \eta_- = -\dot{q}_-/i \tag{16}$$

$$T\Delta S_L/nF + \eta_L = -\dot{q}_L/i \tag{17}$$

where the accumulator is imagined to be divided into two electrode spaces (+, −) linked together by a tube (L) filled with the electrolyte. It should be

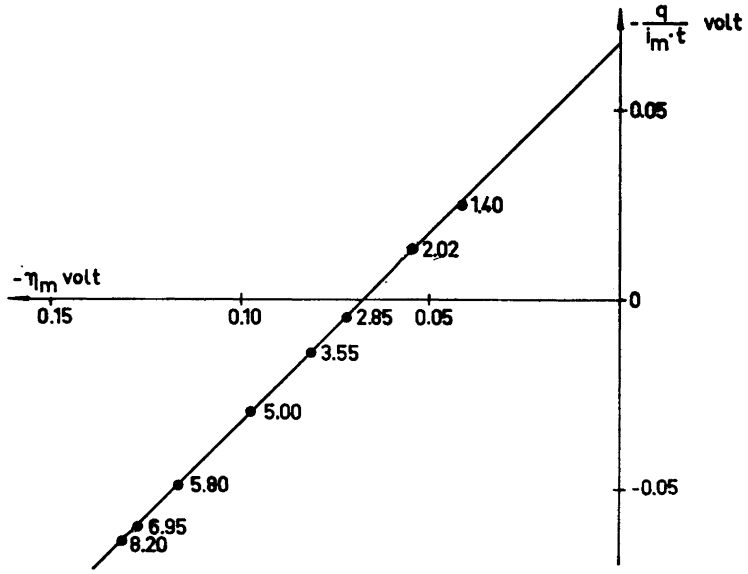

Fig. 2. $-q/(i_m \cdot t)$ plotted against η_m for the lead accumulator at $E \approx 2.04$ volt and 21.3°C. The figures at the experimental points indicate the strengths of the initial currents in amp.

noticed that if the definition (1) is extended to single electrodes, we would have $\eta = \eta_+ - \eta_- + \eta_L$. Here η_L is given by $R_L \cdot i$. On inspection of the above equations it appears that $T\Delta S_+/n$ and $T\Delta S_-/n$ are the so-called *electrolytic Peltier heats*, usually denoted by Π_+ and Π_-, of the electrodes [5]. Such heats generally occur at isothermal reversible passage of one Faraday at the junction between an electrode and its electrolyte. When there are no interfaces between the different phases within the L-space and when approximate temperature and composition constancy is maintained, it is evident that ΔS_L may be put equal to zero. Thus (17) is not interesting from our point of view because it only expresses the fact that the Joule-heat generated equals $R_L \cdot i^2$. It has been shown [6,7] that the electrolytic Peltier heat is given by

$$\Pi = -\sum_i t_i Q_i^*/z_i - Q_{e^-}^* + T\Delta S_j/n \qquad (18)$$

if the Soret effect is neglected. Here Q_i^* denotes the molar heat of transfer for the ion i and $Q_{e^-}^*$ the molar heat of transfer for an electron. z_i is the charge, t_i the transference number for the ion i and ΔS_j refers to the single electrode reaction. The heats of transfer cancel when the Peltier heats for two electrodes are added resulting in $T\Delta S/n$ for the cell reaction. The method we have developed seems to be well suited for experimental determination of electrolytic Peltier heats which have so far not been extensively measured.

Acknowledgements. The authors wish to thank the Head of the Division, Professor Ole Lamm, for his never-failing interest in this work and Dr. Gösta Wranglén for interesting discussions.

REFERENCES

1. Van Rysselberghe, P. *Electrochemical Affinity*, Hermann & Cie Editeurs, Paris 1955.
2. De Donder, T. and Van Rysselberghe, P. *Thermodynamic Theory of Affinity*, Stanford University Press 1936.
3. Van Rysselberghe, P., Ref.[1], eqn. 5.3.13, p. 97.
4. Beck, W. H. and Wynne-Jones, W. F. K. *Trans. Faraday Soc.* **50** (1954) 136, 147.
5. *Cf.* Lange, E. *Elektrochemie der Phasengrenzen, Handbuch der Experimental-Physik* XII [2], Leipzig 1933, p. 263.
6. Holtan, Jr., H. *Electric Potentials in Thermocouples and Thermocells* (Diss.) Utrecht 1953.
7. Lewis, G. N., Randall, M., Pitzer, K. S. and Brewer, L. *Thermodynamics, 2nd Ed.*, McGraw-Hill Book Company, New York, Toronto, London 1961.

Received May 29, 1961.

ACTA CHEMICA SCANDINAVICA 15 (1961) 1707–1717

Complexes of 1,3-Diamino-2-aminomethylpropane with Nickel(II): Equilibrium Constants and Visible Spectra

THOMAS G. SPIRO and C. J. BALLHAUSEN

Universitetets fysisk-kemiske Institut, Copenhagen, Denmark

From pH measurements at 22 ± 1°C, in an ionic medium whose anion concentration was kept constant at 1.0 M with potassium nitrate, pK values for 1,3-diamino-2-aminomethylpropane, (pmtn) were found to be 6.90, 8.86 and 10.51 for $pmtnH_3^{+++}$, $pmtnH_2^{++}$ and $pmtnH^{+}$, respectively. Furthermore the equilibrium constants for the reactions $Ni^{++} + pmtn = Nipmtn^{++}$ and $Nipmtn^{++} + H^{+} = NipmtnH^{+++}$ were found to be 9.23 and 7.18 log units, respectively. The complex, $Ni(pmtn)_2(NO_3)_2$ has been prepared. The spectra of the various complex species and of the crystal at room temperature are in accord with the crystal field theory for octahedral nickel(II) complexes. No splittings due to the trigonal symmetry of the complex have so far been observed.

The triamine, 1,3-diamino-2-aminomethylpropane, $CH(CH_2NH_2)_3$, (hereafter abbreviated to pmtn), possesses a three-fold symmetry axis. If the three amino groups of a pmtn molecule occupy adjacent octahedral positions on a transition metal ion, the trigonal component of the resulting ligand field would be expected to perturb the electronic structure of the purely octahedral complex. This influence might be detectable by spectral measurement.

As a first step in the exploration of this question the solution chemistry of pmtn with nickel(II) ions has been quantitatively investigated. Formation constants for the species $Ni(pmtn)^{++}$ and $Ni(pmtn)H^{+++}$, as well as the three successive dissociation constants of $pmtnH_3^{+++}$ were determined by glass electrode titration, at room temperature, 22 ± 1°C, of the triamino trihydrochloride with varying amounts of nickel(II) nitrate added. To maintain activity coefficients constant, the concentration of negatively charged counter ions (chloride plus nitrate) was kept constant at 1.0 M by addition of potassium nitrate. The formation constant for $Ni(pmtn)_2^{++}$ could not be evaluated from pH measurements alone, but the complex was isolated by precipitation from solution. Its spectrum in the visible region was measured, both in solution and in the crystalline state. Spectra of $Ni(pmtn)^{++}$ and $Ni(pmtn)H^{+++}$ were also obtained.

EXPERIMENTAL

Pure 1,3-diamino-2-methylaminopropane trihydrochloride was kindly prepared by Dr. J. Munch-Petersen of the Technical University of Denmark after the procedure of Geissman *et al.*[2] Microanalysis gave the following results: Found: C 22.55; H 7.34; N 19.74; Cl 49.90. Calc. for $C_4H_{13}N_3.3HCl$: C 22.60; H 7.59; N 19.77; Cl 50.04.

A 1.97 M potassium nitrate stock solution was prepared from the reagent grade (Merck) chemical, and its concentration was checked by conductivity measurement. Sodium hydroxide titrant was prepared by diluting a carbonate-free concentrated stock solution to 1 M (0.1 M for titration III — see below) with distilled water and the proper amount of potassium nitrate stock solution to make the titrant 1.0 M in nitrate. The hydroxide concentration was determined by titration of standard potassium acid phthalate.

Solutions for titration were made up from weighed amounts of the amine hydrochloride and reagent grade (Analar) nickel(II) nitrate by the addition of water and potassium nitrate solution to adjust the total anion concentration to 1.0 M. In all, four different titrations were performed, with the following initial (molar) concentrations of amine and nickel.

Titration	*Amine*	*Nickel*
I	0.0412	—
II	0.0313	0.0155
III	0.00368	0.0437
IV	0.0250	0.0250

Titrations were performed in the open in a room whose temperature was 22 ± 1°C. The hydrogen ion concentration was measured with a Radiometer pH-meter 4 connected to a Radiometer Type G202 B glass electrode, with shielded cable, and a K100 saturated calomel electrode with a bent capillary tip liquid junction. The electrodes were calibrated using standard hydrochloric acid solutions, with potassium nitrate added to give a total anion concentration of 1.0 M.

Absorption spectra of solutions were recorded between 325 and 800 mμ on a Carey Model 11 spectrophotometer, and between 800 and 1 000 mμ measurements were taken pointwise on a Zeiss PMQII spectrophotometer.

LIST OF SYMBOLS

(For simplicity charges will be omitted from chemical formulas).

A = ligand
M = central ion
H = hydrogen ion
C_A = formal (analytical) concentration of A
C_M = » » » » M
C_H = » » » » H

(For any point in a titration:

$$C_H = 3C_A - \frac{\text{equivalents of base added}}{\text{total volume}})$$

$$K_j = \frac{(AH_j)}{ah^j}, \beta_n = \frac{(MA_n)}{ma^n}, \delta_{nj} = \frac{(MA_nH_j)}{(MAn)n^j}, K^M_{MAH_j} = \frac{(MAH_j)}{m(AH_j)}$$

$K_w' = hb$
α_x = fraction of total central ion present as the species x.
ε_x = optical absorptivity of the species x.
E = optical absorbance per mole of total central ion per cm of path length.

EQUILIBRIUM CONSTANTS

The acidity constants for pmtn were extracted from the data yielded in titration I, by standard methods. The mass balances representing this system are

$$C_A = \sum_{j=0} (AH_j) = a \sum_{j=0} k_j h^j$$

and $$C_H = \sum_{j=0} j(AH_j) + (H^+) - (OH^-) = a \sum_{j=0} {}_jK_j h^j + h - \frac{K_w'}{h}$$

(The quantities h and K_w'/h are significant terms in the mass balance only at very low or very high pH. For all the titrations discussed herein they are entirely negligible, and will be dropped from the equations.)
Then

$$\frac{C_H}{C_A} = \frac{\sum_j K_j h^j}{\sum_{j=0} K_j h_j} = \bar{j}$$

Values of $\bar{j}$ were calculated from the titration data and plotted as a function of log h. The resulting protonation curve was analyzed graphically to determine the K_j's. Preliminary values were obtained by comparison with a family of normalized protonation curves representing a theoretical system with $j_{maximum} = 2^3$, neglecting first the region $\bar{j} > 2$ and then the region $\bar{j} < 1$. These values were then refined by the linear extrapolation method of Rossotti and Rossotti[4], to give $K_1 = 3.27 \times 10^{10}$, $K_2 = 2.36 \times 10^{19}$, $K_3 = 1.87 \times 10^{26}$. A theoretical protonation curve calculated from these constants agrees very well with the experimental points, as can be seen the Fig. 1. Expressed in another way, these results give the following pK values for AH_3, AH_2 and AH, respectively: 6.90, 8.86, and 10.51.

Titration II was then performed and an attempt was made to construct a formation curve [5] for the system M, MA, and MA_2, but it became obvious that

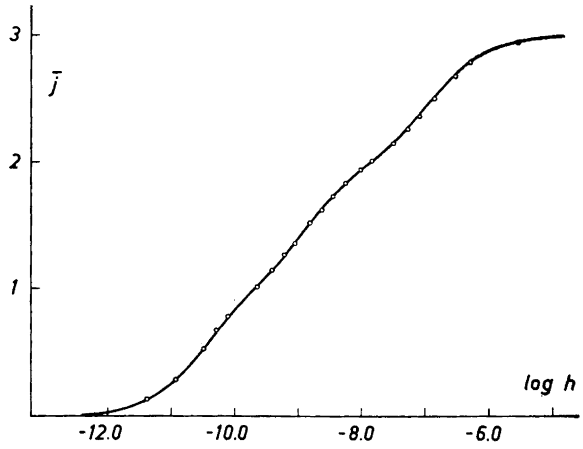

Fig. 1. Protonation curve for pmtn. The points are experimental, the curve theoretical.

the experimental points could not describe a system with only these complexes present. The distortion was thought to arise from protonated complexes, whose occurrence is common in polyamine complex systems, as shown by the studies of Prue and Schwarzenbach [6].

A convenient method for studying protonated complexes containing one molecule of ligand has been given by Schwarzenbach [7]. It consists simply in titrating the protonated ligand in the presence of a large (10 fold) excess of central ion. Under these conditions it is clear that the concentration of complexes containing more than one ligand molecule will be negligible, and the mass balances may be written as follows

$$C_A = \sum_{j=0} (MAH_j) + \sum_{j=0} (AH_j) = a \sum_{j=0} (m\beta_1\delta_{1j} + K_j)h^j$$

$$C_H = \sum_{j=0} j(MAH_j) + \sum_{j=0} j(AH_j) = \sum_{j=0} j(m\beta_1\delta_{1j} + K_j)h^j$$

Then

$$\frac{C_H}{C_A} = \frac{\sum_j c_j h^j}{\sum_{j=0} c_j h^i} = \bar{j}' \; ; \; c_j = \frac{m\beta_1\delta_{1j} + k_j}{m\beta_1 + 1}$$

The quantities c_j are constants because m remains essentially constant, the central ion being present in large excess. Therefore the c_j's may be extracted from the new protonation curve, $\bar{j}'$(log h), by the same method as described above for the amine acidity constants. Furthermore, δ_{13} must be zero, A being a triamine; therefore β_1 may be determined from c_3 (and the known values of m and K_3) and δ_{12} and δ_{11} may then be determined from c_2 and c_1 (together with K_2 and K_1.

Accordingly, titration III was performed and an experimental curve $\bar{j}'$ (log h), was constructed. Comparison of the portion $2<\bar{j}'<3$ with the normalized family of curves described above showed that, within experimental error, $c_2 = 0$, *i.e.*, the concentration of species containing two protons (such as MAH_2) was negligible. At the same time, the steepness of the curve in this

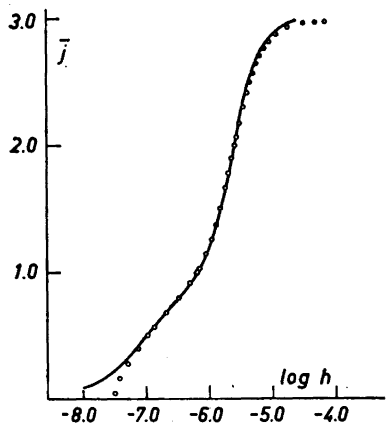

Fig. 2. Protonation curve for pmtn in the presence of excess nickel(II) ions. The points are experimental, the curve theoretical.

region allowed a reliable visual estimate of the ratio c_3/c_1 as 11.22 log units. The points below $\bar{j}' = 1$ were analyzed by the linear extrapolation method, which gave a value for c_1 of 9.87×10^6. These two constants give a theoretical curve which adequately fits the theoretical points throughout most of the range of $\bar{j}'$ (Fig. 2). There appears to be a slight systematic error for $\bar{j}' > 2.8$, and for $\bar{j}' < 0.4$, the points deviate from the theoretical curve due to the precipitation of nickel hydroxide. From the above values it was calculated that $\log \beta_1 = 9.43$ and $\log \delta_{11} = 6.99$.

As Schwarzenbach pointed out [8], the assumption that the concentration of complexes containing more than one ligand molecule is negligible should still be valid when the ligand and central ion are present in equal concentration (β_2/β_1 being appreciably lower than β_1 for most polyamines), and an "equivalent" titration provides a useful check on the results obtained by the excess central ion method. The check can be made by simply calculating a theoretical titration curve and comparing it with the experimental one. The "degree of tetration", *i.e.*, the number of moles of base added per mole of triamine trihydrochloride, can be expressed in terms of the formal concentrations as

$$f = \frac{3C_A - C_H}{C_A}$$

There being only one protonated complex in the present system, the mass balances reduce to

$$C_M = m + ma\beta_1 (1 + \delta_{11}h)$$
$$C_A = ma\beta_1 (1 + \delta_{11}h) + ap$$
$$C_H = ma\beta_1\delta_{11}h + aq$$

where $p = \sum_{j=0} K_j h^j$ and $q = \sum_{j=0} jK_j h^j$. $(q/p = \bar{j})$

Since $C_M = C_A$, $m = ap$.

$$\text{Then, } f = \frac{m\beta_1(3 + 2\delta_{11}h) + 3 - pq}{m\beta_1(1 + \delta_{11}h) + p} = \frac{3 + 2\delta_{11}h + (3-\bar{j})(\beta_1 a)^{-1}}{1 + \delta_{11}h + (\beta_1 a)^{-1}}$$

$\bar{j}$ can be read directly from Fig. 1, and a is best calculated by substituting $m = ap$ into the mass balance for C_H, and solving the resulting quadratic equation. When the theoretical curve calculated in this way was compared with the experimental curve from titration IV, it was found to have the right form, but a slight systematic deviation in the latter half of the titration indicated an error in the constants used. These were therefore recalculated, using the data from titration IV, in the following manner.

In the last part of the titration curve, when the concentration of free central ion becomes negligible, the expression for f reduces to

$$f = \frac{3 + 2\delta_{11}h}{1 + \delta_{11}h}$$

from which

$$\delta_{11} = \frac{1}{h}\,\frac{3-f}{f-2}$$

In the first part of the curve, when the concentration of MA is negligible,

$$f = \frac{2\delta_{11}h + (3-\bar{j})(a\beta)^{-1}}{\delta_{11}h + (a\beta)^{-1}}$$

from which

$$\beta\delta_{11} = \frac{1}{ah}\,\frac{f+\bar{j}-3}{2-f}$$

At the same time, the difference between C_H and C_A becomes

$$C_H - C_A = a(q-p) = ap(\bar{j}-1)$$

so that a can be calculated simply from

$$a = \frac{C_H - C_A}{p(\bar{j}-1)}$$

In this way δ_{11} was calculated for eight points on the last part of the titration curve ($f > 2.4$) and $\beta_1\delta_{11}$ was calculated from eight points on the first part ($f < 1.1$). Finally, the value for δ_{11} was refined slightly by including the terms in β_1, originally neglected in the expressions for f. The resulting values, $\log \delta_{11} = 7.18$, $\log \beta_1 = 9.23$, give a theoretical curve which is in excellent agreement with the experimental points, as can be seen in Fig. 3. These values are significantly different from those obtained from the excess central ion titration, although their product remains the same. The source of this discrepancy probably lies in the determination of c_1 in the excess central ion method *. The number of points on the protonation curve which are actually sensitive to the value of c_1 (or δ_{11}) are very few because of the early precipitation of nickel hydroxide. Any error in c_1 is reciprocated in c_3, which is calculated from the experimentally obtained ratio c_3/c_1. In the equivalent titration, on the other

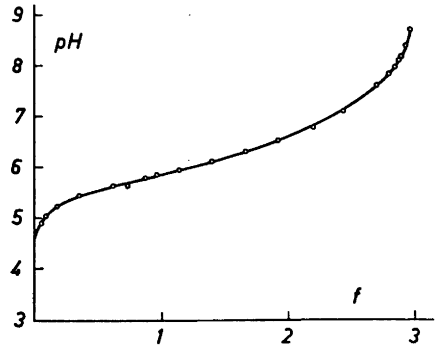

Fig. 3. "Equivalent" titration of pmtn H_3^{+3} and nickel(II) ions. The points are experimental, the curve theoretical.

* An alternative explanation, that polynuclear complexes are formed, in considered highly unlikely, in view of Schwarzenbach's [9] finding from studies of polyamines with a variety of metal ions (including nickel(II)) that only silver(I) forms such complexes.

hand, nickel hydroxide does not precipitate, and points are available over the entire titration range. The constants calculated from this titration are therefore felt to be the more reliable.

In the light of these constants, another attempt was made to analyze the data for titration II (where $C_A/C_H = 2$) in an effort to obtain the formation constant for MA_2. No satisfactory results were obtained however, probably because the number of chemical species present puts too much strain on pH data, taken alone. Schwarzenbach [10] considers it impractical to analyze pH curves when more than two complexes are formed in a given buffer region, which is certainly the case in the present system. As titration II proceeds, the solution turns from the green of aquo nickel ion, to the blue characteristic of MA (titration IV) and then on to violet, indicating the formation of di-ligand complexes. In addition to MA_2, it is quite likely that MA_2H and possibly MA_2H_2 are formed. Finally, at a pH of about 8.1 there precipitated out of solution fine pink crystals, which turned out to contain the complex MA_2. It may be possible to elucidate the di-ligand complexes by augmenting the pH titration curves with measurements of the solubility of the MA_2 crystals. However only a small amount of the triamine was available and the equilibrium work was not pursued further.

The precision of the determinations of the various equlibrium constants is probably about $\pm$ 0.05 log units.

DISCUSSION OF THE CONSTANTS

It is instructive to compare the solution chemistry of pmtn with that of the chemically similar ligand ptn, studied by Prue and Schwarzenbach [11].

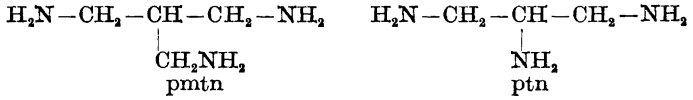

The constants for these two triamines are compared in Table 1. The association of the two ligands with nickel (as reflected in the values of β_1 and K^M_{MAH}) is seen to be practically identical, which is somewhat surprising in view of the fact that ptn can form two five membered chelate rings, while pmtn can only form six-membered rings. They do not necessarily form an exception to the general rule of increased stability for five membered rings as compared with six mem-

Table 1. Acidity constants for ptn and pmtn and their complexity constants with nickel(II)

	ptn [a]	pmtn [b]
pK_{AH_2}	3.72	6.90
pK_{AH_2}	7.95	8.86
pK_{AH}	9.59	10.51
log β_1	9.3	9.23
log δ_{11}	6.3	7.18
log K^M_{MAH}	6.0	5.90

[a] Schwarzenbach and Prue [11] measured at 20° in 0.1 M potassium chloride.
[b] This study.

bered rings [12], however. It is possible that the complex $Ni(ptn)H^{+++}$ involve protonation of the middle nitrogen on ptn, leaving the end nitrogens bonded to nickel. The resulting structure would have a six-membered chelate ring. In the complexes MA, on the other hand, where all three nitrogens are presumably bonded to nickel, it is probable that the ring structure of both ligands is somewhat strained due to the fact that all three rings are joined at a single carbon atom. It is worth noting that $\log \beta_1$ for the nickel complex of diethylenetriamine, a ligand without this steric requirement is considerably higher (10.7)[13] than for either ptn or pmtn.

The species involving pmtn appear to be somewhat stronger bases than the corresponding ones involving ptn, though part of this effect may be due to the stronger ionic medium of this study as compared with that used by Prue and Schwarzenbach. (However, the pK for H_3A is over three units higher for pmtn than for ptn, a remarkably large difference. Possibly the five membered rings which could be formed by internal hydrogen bonding in $ptnH_2^{++}$ are more stable then the six-membered rings to be expected in $pmtnH_2^{++}$).

The values of K^{M}_{MAH}, representing the association of HA with nickel ion, presumably through two of the three nitrogen atoms, are, for both ligands, smaller than the value of $\log \beta_1$, 7.66 [5], for the nickel-ethylenediamine complex, as would be expected from the charge repulsion present in the protonated triamine complexes. On the other hand, the values of β_1 for the two triamines are considerably greater than β_1 for ethylenediamine, implying that all three nitrogens are indeed bonded to nickel in the complexes MA.

SPECTRA OF MAH AND MA

The spectra of MAH and MA were obtained [5] from two solutions containing equal formal concentrations of ligand and central ion (0.025 M), adjusted to different pH values by addition of sodium hydroxide. The anion concentration was again kept at 1.0 M with potassium nitrate. For such solutions we have, from the results of the above equilibrium study, and from Beer's law, that

$$E = \varepsilon_M \alpha_M + \varepsilon_{MAH} \alpha_{MAH} + \varepsilon_{MA} \alpha_{MA}$$

The values of α_x are calculated with the aid of the equilibrium constants, and ε_M can be determined independently (from the spectrum of aquo nickel(II) ion). The result is an equation in two unknowns (ε_{MAH} and ε_{MA}) which can be determined from two sets of value of E and the fractions α_x. For the two pH values selected, 6.84 and 7.90, the following distributions of the complexes were calculated

pH	α_M	α_{MAH}	α_{MA}
6.84	0.089	0.626	0.285
7.90	0.009	0.158	0.833

The spectra of MAH and MA, calculated from the spectra of these solutions are shown in Fig. 4. The spectrum of MAH is nearly identical with that of the first ethylenediamine complex of nickel [14], while the peaks in the MA spectrum are shifted definitely to higher frequencies. Thus the spectra support the

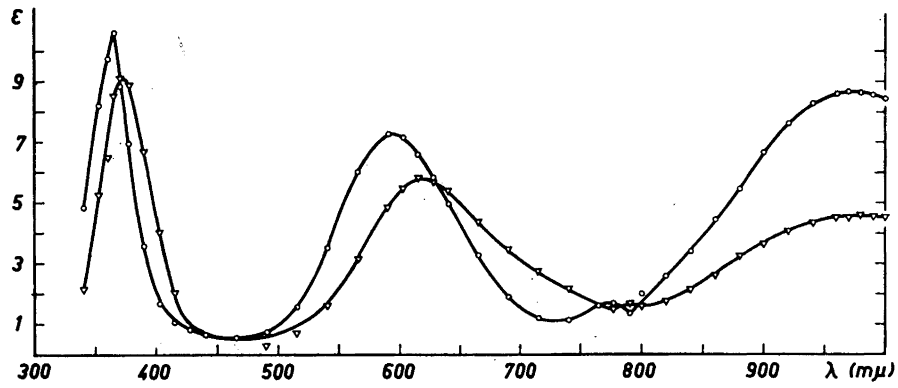

Fig. 4. Solution spectra of NiA (circles) and NiAH (triangles).

impression gained from the equilibrium constants that in MAH two nitrogens are bonded to nickel, while in MA, all three nitrogen atoms are bonded.

PREPARATION AND SPECTRA OF $Ni(pmtn)_2(NO_3)_2$

A portion of the triamine trihydrochloride was converted to the nitrate salt by dissolving it in a small quantity of water, adding a stoichiometric amount of silver nitrate, and filtering off the resulting silver chloride precipitate. One half the equivalent amount of nickel(II) nitrate was then added to the nitrate solution and sodium hydroxide was dripped in slowly until the precipitate observed in titration II appeared. This was filtered and recrystallized from water as fine, pink hexagonal plates. Microanalysis gave the following results: Found: C 24.30; N 28.55; H 6.61. Calc. for $Ni(C_4N_3H_{13})_2(NO_3)_2$: C 24.70; N 28.81; H 6.74.

A saturated solution of the complex in 1.0 M potassium nitrate, and a more concentrated one in water, were prepared and their visible spectra were recorded. Subsequent analysis of the solutions by dimethylglyoxime precipitation of nickel gave the following concentrations for the water and potassium nitrate solutions respectively: $C_M = 2.71 \times 10^{-3}$ and 9.03×10^{-3} M. It was also possible to grow a sizable crystal (about 1 mm per hexagonal edge) of the complex, which was then mounted on a microscope stage, and its absorption spectrum was recorded after focusing the microscope image on the slit of a Beckman D.U. spectrophotometer.

The spectra are shown in Fig. 5. The peaks are shifted considerably to higher frequencies relative to those of MA. On the other hand, the three spectra are also shifted relative to one another, the crystal peaks having the highest frequencies and those in the potassium nitrate having the lowest. These shifts may be due to dissociation and/or hydrolysis of MA_2, the degree of which cannot be reliably estimated as the relevant equilibrium constants are not known.

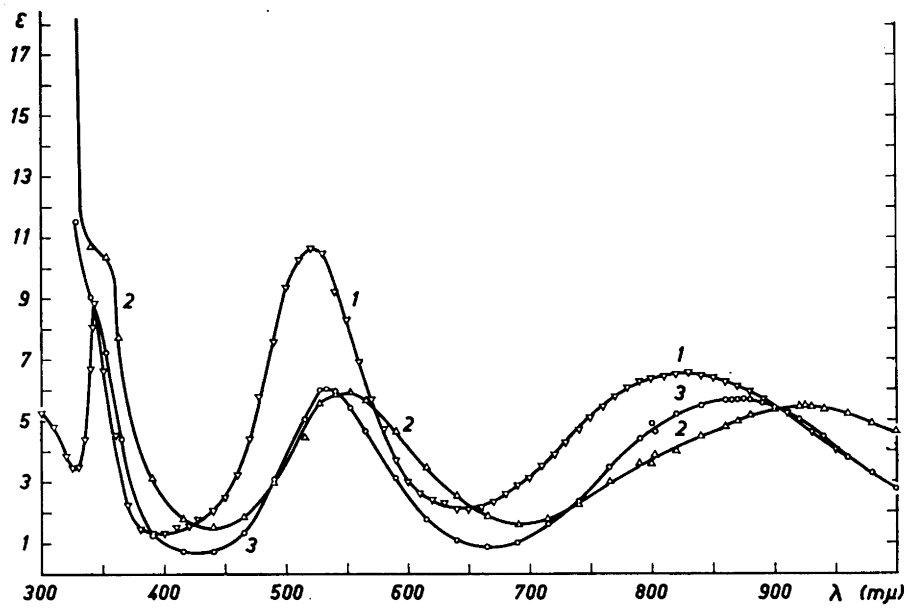

Fig. 5. Absorption spectra of (1) $NiA_2(NO_3)_2$ crystal (arbitrary absorbance units), (2) NiA_2 in 1.0 M KNO_3 and (3) NiA_2 in water.

CRYSTAL FIELD CONSIDERATIONS

In general outline, the spectra of the three species measured are adequately explained by the usual crystal field model for octahedral complexes of nickel(II) [14]. The major peaks clearly represent those transitions which have been assigned as $^3A_{2g} \rightarrow {}^3T_{2g}$, $^3A_{2g} \rightarrow {}^3T_{1g}(F)$ and $^3A_{2g} \rightarrow {}^3T_{1g}(P)$ in order of increasing frequency. The value of Dq is some 1 200 cm^{-1}, or about the value found for $Ni(en)_3$. In addition, the MA and MAH spectra also show a minor peak, between

Table 2. Octahedral transition frequencies (cm^{-1}) for pmtn complexes of nickel(II).

	MA_2 (crystal)		MA		MAH	
Transition	Exptl.	Theoret.[a]	Exptl.	Theoret.[a]	Exptl.	Theoret.[a]
$^3A_{2g} \rightarrow {}^3T_{2g}$	12 050	12 000	10 300	10 000	10 200	10 000
		−12 500		−10 800		−10 500
$^3A_{2g} \rightarrow {}^1E_g$	—	12 700	12 900(?)	12 500	12 650(?)	12 500
$^3A_{2g} \rightarrow {}^3T_{1g}(F)$	19 250	18 800	16 800	16 200	16 100	15 800
		−19 500		−17 210		−16 900
$^3A_{2g} \rightarrow {}^3T_{1g}(P)$	29 250	29 700	27 400	27 000	27 000	26 600
		−30 300		−27 400		−27 000

[a] Taken from the energy level diagram of Liehr and Ballhausen [15]. The ranges are a reflection of splittings due to spin orbit coupling.

the first two major ones, which has about the right frequency for the spinforbidden $^3A_{2g} \rightarrow {}^1E_g$ transition. The experimental and theoretical frequencies (taken from the energy level diagram of Liehr and Ballhausen [15]) for the three complexes are compared in Table 2.

The application of a trigonal perturbation to the octahedral field should produce a splitting of all three excited triplet states, and therefore the three major peaks of MA and MA_2 should all be split. Evidently the splitting is too small to be observed in solution, nor is it apparent in the crystal spectrum of MA_2. The latter was obtained with a rather crude setup, however, and the resulting uncertainty in the absorbance values might be enough to obscure any fine structure. Conceivably a more careful measurement of the spectrum at low temperatures might show the trigonal splitting. Also the trigonal symmetry of the complex should give rise to dichroism in the crystal, which could be measured if a crystal could be grown large enough to present more than one face to an incident light beam. Work on these aspects of the problem are currently underway in this laboratory.

Acknowledgements. One of us (T.G.S.) is indebted to the *Fulbright Foundation* for a study grant which made possible his study in Copenhagen. Both of us want to thank Dr. Jon Munch-Petersen of the Technical University of Denmark for having prepared our supply of the ligand, and Professor J. Bjerrum for an instructive discussion.

REFERENCES

1. Biedermann, G. and Sillén, L. G. *Arkiv Kemi* **5** (1953) 425.
2. Geissman, T. A., Schlatter, M. J. and Webb, I. A. *J. Org. Chem.* **11** (1946) 736.
3. Sillén, L. G. *Acta Chem. Scand.* **10** (1956) 194.
4. Rossotti, F. J. C. and Rossotti, H. S. *Acta Chem. Scand.* **9** (1955) 1166.
5. Bjerrum, J. *Metal Ammine Formation in Aqueous Solution* P. Haase, Copenhagen 1941.
6. Prue, J. E. and Schwarzenbach, G. *Helv. Chim. Acta* **33** (1950) 963.
7. Schwarzenbach, G. *Ibid.* **33** (1950) 954.
8. Schwarzenbach, G. *Ibid.* **33** (1950) 958.
9. Schwarzenbach, G. *Ibid.* **33** (1950) 956.
10. Schwarzenbach, G. *Ibid.* **33** (1950) 960.
11. Prue, J. E. and Schwarzenbach, G. *Ibid.* **33** (1950) 995.
12. Irving, H., Williams, R. J. P., Ferret, D. J. and Williams, A. E. *J. Chem. Soc.* **1954** 3494.
13. Prue, J. E. and Schwarzenbach, G. *Helv. Chim. Acta.* **33** (1950) 992.
14. Ballhausen, C. J. *Kgl. Danske Vidskab. Selskab. Mat. Fys. Medd.* **29** (1955) No. 8.
15. Liehr, A. D. and Ballhausen, C. J. *Ann. Phys.* **6** (1959) 146.

Received June 8, 1961.

ACTA CHEMICA SCANDINAVICA 15 (1961) 1718–1722

The Hydrolysis of Ethyl Acetoacetate and the Decarboxylation of Acetoacetic Acid in Strongly Acid Solution

KAI JULIUS PEDERSEN

Chemical Laboratory, Royal Veterinary and Agricultural College, Copenhagen, Denmark

The first-order rate constants for the hydrolysis of ethyl acetoacetate and for the decarboxylation of acetoacetic acid, k_1 and k_2, respectively, have been measured at 37°C in concentrated solutions of hydrochloric, sulphuric, and perchloric acid (in some cases added sodium or potassium salt of the strong acids). The rate constants were computed from the observed rate of production of carbon dioxide, in solutions of the ester and solutions of the free keto-acid, respectively. It was found that k_2 decreased linearly with increasing concentration of strong acid or salt, while $\log(k_1/[H^+])$ was found to increase linearly with increasing concentration of hydrochloric or sulphuric acid, but pass through a minimum in solutions of perchloric acid.

When a β-keto carboxylic ester is dissolved in an aqueous solution of a strong acid two consecutive first-order reactions, acid hydrolysis of the ester (rate constant k_1) and decarboxylation of the free keto-acid (rate constant k_2), will occur. If k_1 is not much larger than k_2, and if k_2 is known from separate experiments, it is possible to calculate k_1 from the observed rate of production of carbon dioxide. Since our knowledge of the rate of ester hydrolysis in strongly acid medium is rather scanty, it was found worth while to apply this method to the study of the hydrolysis of ethyl acetoacetate in concentrated solutions of hydrochloric, sulphuric, and perchloric acid.

The ethyl acetoacetate used for the measurements was an old preparation which had been carefully purified through the sodium hydrogen sulphite compound and by distillation [1]. The other substances were commercial *pro analysi* preparations. Experiments were carried out at the temperature 37.0°C by means of an apparatus described earlier [2]. The production of carbon dioxide was followed by observing the pressure above the solution.

RATE OF DECARBOXYLATION OF ACETOACETIC ACID

Solutions of free acetoacetic acid were prepared in the following way. Ethyl acetoacetate was dissolved in about 4/3 of the amount of sodium hydroxide solution necessary for hydrolysis. The mixture was left at room temperature

Table 1. Decarboxylation of acetoacetic acid at 37.0°C in solutions of hydrochloric acid.

[HCl]	[NaCl]	$k \times 10^5$	$k_2 \times 10^5$ calc.	[HCl]	[NaCl]	[KCl]	$k_2 \times 10^5$	$k_2 \times 10^5$ calc.
0.23	0.02	8.07	8.11	0.51	2.02		6.74	6.81
0.50	0.02	8.00	8.00	0.51	3.02		6.14	6.22
0.98	0.02	7.81	7.80	0.51	4.02		5.69	5.63
1.98	0.02	7.38	7.38	0.98	1.02		7.21	7.21
2.99	0.02	6.98	6.95	0.98	2.02		6.61	6.62
4.01	0.02	6.54	6.52	0.51	0.02	1.00	7.68	7.66
4.51	0.02	6.29	6.31	0.51	0.02	2.00	7.31	7.33
0.51	1.02	7.45	7.40	0.51	0.02	3.00	7.02	7.00

Table 2. Decarboxylation of acetoacetic acid at 37.0°C in solutions of sulphuric acid.

$[H_2SO_4]$	$[NaHSO_4]$	$k_2 \times 10^5$	$k_2 \times 10^5$ calc.
0.23	0.02	8.13	8.20
0.48	0.02	8.04	8.01
0.98	0.02	7.64	7.62
1.99	0.02	6.87	6.84
2.99	0.02	6.06	6.06
4.00	0.02	5.29	5.28
5.00	0.02	4.43	4.50
6.01	0.02	3.74	3.72
6.97	0.02	2.97	2.97
7.95	0.02	2.27	2.21
10.02	0.02	1.16	0.60

Table 3. Decarboxylation of acetoacetic acid at 37.0°C in solutions of perchloric acid.

$[HClO_4]$	$[NaClO_4]$	$k_2 \times 10^5$	$k_2 \times 10^5$ calc.
0.08	0.02	8.14	8.40
0.48	0.02	7.97	8.04
0.98	0.02	7.60	7.59
1.98	0.02	6.70	6 70
2.98	0.02	5.80	5.80
3.98	0.02	4.94	4.91
4.98	0.02	4.00	4.01
5.98	0.02	3.12	3.12
0.98	1.02	6.46	6.55
0.98	2.02	5.60	5.51

for at least 16 h after which time hydrolysis was complete. Appropriate amounts of this solution, the strong acid, and, in some experiments, salt solution were pipetted into the reaction vessel. The initial concentration of acetoacetic acid was in all the kinetic experiments about 0.015 M. The solutions contained in addition about 0.015 M ethanol produced by hydrolysis of the ester, and about 0.020 M sodium salt of the strong acid produced by neutralisation of the sodium hydroxide used for the hydrolysis. The reaction was always found to follow the first-order law. In Tables 1, 2, and 3 are given the molar concentrations of the solutions examined and the rate constants k_2 found (in sec^{-1}). The values of k_2 decrease nearly linearly with increasing concentration of strong acid or salt, and may be expressed by the formulae

$$k_2 \times 10^5 = 8.22 - 0.42[HCl] - 0.59[NaCl] - 0.33[KCl] \quad (1)$$

$$k_2 \times 10^5 = 8.38 - 0.776[H_2SO_4] \quad (2)$$

$$k_2 \times 10^5 = 8.49 - 0.895[HClO_4] - 1.04[NaClO_4] \quad (3)$$

Values of k_2 calculated from these expressions are given in the last column of the three tables. The agreement is good except for 8 and 10 M H_2SO_4 and for small concentrations of the acids where the experimental values are smaller than those calculated from the formulae (most pronounced for 0.08 M $HClO_4$). This discrepancy is not due to dissociation of the acetoacetic acid since its dissociation constant [3] is as small as 3×10^{-4}. The failure of the formulae at small concentrations is also apparent from the fact that for zero concentration of strong acid and salt they give different values of k_2. The effect of strong acids on k_2 therefore seems to be composed of two parts, a moderate increase which reaches its full value in less than 1 M solution, and the predominating linear decrease. It follows from the formulae 1—3 that there is a close similarity between the effects of the strong acids and the salts; both are salt effects.

RATE OF HYDROLYSIS OF ETHYL ACETOACETATE

The ester was weighed out in a small platinum bucket which was suspended in the apparatus above the solution of strong acid in such a way that it could be released when the apparatus had been evacuated and pressure and temperature equilibrium was attained. Pressure readings were taken from the moment when the ester was dissolved. The difference P between the final pressure reading and the reading at the time t is proportional to the sum x of the concentrations of keto-ester and free keto-acid. The rate constants for the hydrolysis and the decarboxylation, k_1 and k_2, respectively, were in most cases of the same order of magnitude. Therefore, the following formula, known from text-books on chemical kinetics, was applied (x_o denotes the initial ester concentration)

$$x = x_o \left(\frac{k_1}{k_1 - k_2} e^{-k_2 t} - \frac{k_2}{k_1 - k_2} e^{-k_1 t} \right)$$

By rearrangement is obtained

$$(x - x_o e^{-k_2 t})/k_2 = (x - x_o e^{-k_1 t})/k_1 = x_o e^{-k_2 t}(1 - e^{-(k_1 - k_2)t})/(k_1 - k_2)$$

$$(k_1 - k_2)\, t/(1 - e^{-(k_1 - k_2)t}) = k_2\, t\, e^{-k_2 t} \Big/ \left(\frac{x}{x_o} - e^{-k_2 t} \right)$$

When we remember that P is proportional to x and set

$$0.4343\ k_1 = k_1^*, \qquad 0.4343\ k_2 = k_2^*$$

$$(k_1^* - k_2^*)t = y \tag{4}$$

$$k_2^* t 10^{-k_2^* t} \Big/ \left(\frac{P}{P_o} - 10^{-k_2^* t} \right) = z \tag{5}$$

we obtain

$$z = y/(1 - 10^{-y}) \tag{6}$$

The formulae 4—6 were applied in the following way. First, z was calculated from the observed P,t-values and the known value of k_2^* by means of eqn. 5.

Table 4. Hydrolysis of ethyl acetoacetate at 37.0°C in solutions of strong acids (*c* M).

Hydrochloric acid			Sulphuric acid				Perchloric acid		
c	$k_1 \times 10^5$	$\frac{k_1 \times 10^5}{[H^+]}$	c	$[H^+]$	$k_1 \times 10^5$	$\frac{k_1 \times 10^5}{[H^+]}$	c	$k_1 \times 10^5$	$\frac{k_1 \times 10^5}{[H^+]}$
0.500	2.55	5.10	0.500	0.547	2.99	5.47	0.250	1.19	4.76
1.000	5.55	5.55	1.000	1.07	6.41	5.99	0.500	2.32	4.64
1.333	7.64	5.73	2.000	2.11	15.02	7.12	1.000	4.36	4.36
2.00	12.30	6.15	3.00	3.13	27.8	8.88	2.000	8.50	4.25
3.02	21.08	6.98	4.00	4.14	44.5	11.01	3.00	12.71	4.23
4.00	30.83	7.71	5.00	5.11	68.1	13.32	4.00	17.8	4.44
1.00 [a]	6.79	6.79					5.00	23.3	4.66
1.00 [b]	8.02	8.02					6.00	29.7	4.96

[a] The solution contained in addition 1.00 M NaCl.
[b] The solution contained in addition 2.00 M NaCl.

Then, y was found by means of a four-place table of function 6 computed for values of y from -1 to $+1$ with intervals of 0.01. Finally, k_1 was found from a plot of y against t, applying eqn. 4.

The rate constants k_1 (in sec^{-1}) found for solutions of hydrochloric, sulphuric, and perchloric acid are given in Table 4. For hydrochloric and perchloric acid $[H^+]$ may with good approximation be set equal to c. For sulphuric acid approximate values of $[H^+]$ were computed from estimates of the two dissociation constants of the acid made by Young and Blatz[4] mainly on the basis of measurements of the intensities of Raman-lines carried out by Rao[5]. As seen from Table 4, k_1 for hydrochloric and sulphuric acid increases more rapidly than $[H^+]$, while the ratio $k_1/[H^+]$ for perchloric acid at first decreases, then passes a minimum

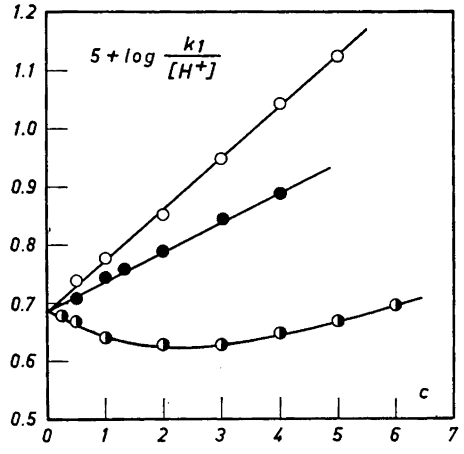

Fig. 1. Plot of $\log(k_1/[H^+])$ against c for the hydrolysis of ethyl acetoacetate in solutions of sulphuric acid (open circles), hydrochloric acid (closed circles), and perchloric acid (semi-closed circles).

(between 2 and 3 M $HClO_4$), and finally increases. Fig. 1 shows a plot of $\log(k_1/[H^+])$ for the three acids. For hydrochloric and sulphuric acid, the points fall close to straight lines with equations

for hydrochloric acid $\log(k_1/[H^+]) = 0.687-5 + 0.051\ c$
for sulphuric acid $\log(k_1/[H^+]) = 0.686-5 + 0.088\ c$

By extrapolation to $c = 0$ is for all three acids obtained

$$k_1 = 4.86 \times 10^{-5}[H^+]\ \text{sec}^{-1}.$$

A similar behaviour of the three acids was found in the hydrolytic decomposition of urethane [6]. Here, however, the value of $k/[H^+]$ found by extrapolation to $c = 0$ was higher for sulphuric acid than for the two other acids, a result which may possibly be attributed to acid catalysis by the ion HSO_4^-. Since the extrapolation for the hydrolysis of ethyl acetoacetate gives the same value for all three acids, no perceptible catalysis by the ion HSO_4^- is found in this reaction.

If the rate-determining step in ester-hydrolysis is assumed to be a bimolecular reaction between an ester molecule (E) and a *hydrated* hydrogen ion (probably $H(H_2O)_4^+$, but here for simplicity written as H^+), the first-order rate constant k may be expressed by the formula

$$k = A[H^+]f_E f_{H+}/f_{EH+}$$

where A is a constant, f denotes activity coefficient, and EH^+ the transition state. If, to a first approximation, we set

$$\log(f_E f_{H+}/f_{EH+}) = Bc$$

where B is a constant, we obtain the approximate formula

$$\log(k/[H^+]) = \log A + Bc \qquad (7)$$

It follows from the experiments in this paper that formula 7 holds for the hydrolysis of ethyl acetoacetate in solutions of hydrochloric acid (up to 4 M) and in solutions of sulphuric acid (up to 5 M) while it fails for the hydrolysis in solutions of perchloric acid. A similar result was earlier [6] obtained for the hydrolysis of ethyl urethane in solutions of the three acids.

REFERENCES

1. Pedersen, K. J. *J. Phys. Chem.* **37** (1933) 751.
2. Pedersen, K. J. *J. Am. Chem. Soc.* **53** (1931) 18.
3. Pedersen, K. J. *J. Phys. Chem.* **38** (1934) 993.
4. Young, T. F. and Blatz, L. A. *Chem. Revs.* **44** (1949) 102.
5. Rao, N. R. *Indian J. Phys.* **14** (1940) 143.
6. Pedersen, K. J. *Acta Chem. Scand.* **14** (1960) 1448; **15** (1961) 959.

Received June 3, 1961.

ACTA CHEMICA SCANDINAVICA 15 (1961) 1723–1738

On the Calculation of Complexity Constants by the Method of Least Squares *

JAN RYDBERG

University of Stockholm, and Research Institute of National Defense, Stockholm, Sweden

Some requirements for the application of the method of least squares to equations for complex equilibria are discussed, and a review is given of what so far has been done. In a number of examples, the results of least squares calculations with high-speed digital computors are compared to results obtained by graphical methods. The application of simple statistical tests as the χ^2-and t-tests are also demonstrated.

In complex chemistry — as in many other scientific fields — one is commonly faced with the problem of trying to fit theoretical equations to a number of experimental points. This fit may be done in a graphical or numerical manner. If the equations are complicated and the body of experimental data large, graphical methods seem more attractive and have been used by far more often in complex chemistry. However, with the increasing availability of high-speed digital computors, the complex chemist no longer has any reason to avoid numerical calculations.

The present paper shows how the method of least squares in combination with electronic computors can be applied to studies of complex equilibria. The results will be subjected to simple statistical tests and compared to results obtained graphically.

TYPE OF ERRORS TO BE CONSIDERED

Since the method of least squares considers the errors in the experimental data, and permits the calculation of standard errors in the constants computed, it is necessary to say a few words about errors in general.

All experiments are subject to errors. Indeed, it may be observed, that it is impossible to establish the *true* value of any constant through experiments alone. However, through careful experiments, it is possible to approach the true value of the constants to any degree of closeness. This »degree of closeness» depends on the type of errors involved in the experiments.

* Parts of this paper also appears under the same title and by the same author in Advances in the Chemistry of Coordination Compounds, Stanley Kirschner (Ed.), The Macmillan Co, New York 1961.

The most familiar type of error is *mistakes*, which are easily recognised because they always lie far off the main population of experimental data. In the following we shall assume that all mistakes have been eliminated from our data.

Accidental errors occur in all experiments, and their cause is in principle unknown. Their occurrence follows the laws of chance, and they can therefore be treated by the Mathematical Theory of Error. From the accidental errors in the experiments, this theory permits the calculation of precision in constants computed from the data. Various measures of precision are used; in this paper only the standard error (also called standard deviation or mean square error) σ shall be employed.

When the same system is investigated by various methods, and the results do not agree, this may either be due to the use of wrong theories, or to presence of unknown *systematic errors*. In principle such errors are determinate.

Before experimental data are used for computing constants, corrections for systematic errors should be applied, whether these corrections are based on empirical observations or true knowledge of the cause of the error. If such corrections are not made, *e.g.* because the presence of systematic errors is not realized by the investigator, the constants obtained will be much farther away from the true value than may be indicated by standard deviations given. The reader may view such results not only with suspicion but also regard them as being dangerous, because the standard deviations lend a false impression of exactness to the constants. However, it should be observed and strongly emphasized, that when errors are given for constants, in whatever field of science, these errors should be adequately defined. Standard errors, which are used in this paper, are exactly defined (*cf.*, *e.g.*, Refs.[1,2]) to be based only on the accidental errors in the experimental data. Thus the reader who suspects systematic errors in an investigations should, after considering the accidental errors causing the standard deviations in the constants, focus his attention on how the constants themselves have been obtained. The relative value of standard deviations in such a case will be discussed in connection with the examples at the end of the paper.

In the following, it will be assumed that all mistakes and systematic errors have been eliminated from the experimental material, provided this question is not brought up in a particular discussion.

TYPES OF EQUATIONS ENCOUNTERED IN EQUILIBRIUM STUDIES

The ultimate nature of the problem is to determine the stability constant $\beta_{m,n,p}$ as defined by

$$\beta_{m,n,p} = \frac{[\mathrm{M}_m\mathrm{A}_n\mathrm{B}_p]}{[\mathrm{M}]^m[\mathrm{A}]^n[\mathrm{B}]^p} \qquad (1)$$

for the complex $\mathrm{M}_m\mathrm{A}_n\mathrm{B}_p$, where M is the central (metal) atom and A and B are two different kinds of ligands. Brackets may here indicate activities or concentrations; in the latter case it is assumed that the ratio of the activity coefficients of the various species involved in the equilibrium are constant.

More complicated complexes may be defined (*cf.*, *e.g.*, Refs.[3–5], but these are almost entirely of theoretical interest because of the practical difficulties in investigating such complexes.

The mathematical formulation of the equations as well as methods for calculating the stability constants for *complexes of type* MA_n have been thoroughly discussed by many authors as, *e.g.*, Bjerrum [6], Sullivan and Hindman [7], and Irving and Rossotti [8]. In the general equation

$$\sum_0^N (C_A - [A] - n \cdot C_M)\beta_n[A]^n = 0 \tag{2}$$

which for reasons given later can be written

$$\sum_0^N (y - bx - a_n)\beta_n x^n = 0 \tag{3}$$

C_A and C_M are the total concentrations of ligand and metal.

Depending on the method of investigation, the symbols y, b and a_n can be given various meanings. Thus, in spectrophotometric investigations where only the metal species show measureable extinction, one may put $y = \varepsilon_M$ = molar extinction coefficient of all metal species in solution ($\varepsilon_M = E \cdot C_M^{-1} \cdot d^{-1}$, where E is measured extinction for cell length d), $b = 0$ and $a_n = \varepsilon_n$ = molar extinction coefficient of MA_n (*e.g.*, *Ref.*[9]). In partition measurements, one may put $y = Q_M$ = partition ratio of all metal species between one phase (*e.g.* resin or organic solvent) and the aqueous phase, $b = 0$, and $a_n = \lambda_n$ = partition constant for MA_n (*e.g.*, *Ref.*[11–12]).

The equations for *mixed complexes of type* MA_nB_p can be formulated in many ways, as given, *e.g.*, by Fronæus [13] and Rydberg [3]. The primary equations all contain double sums; a representative example is given by

$$\bar{n}_A = \frac{C_A - [A]}{C_M} = \frac{\sum_0^N n\beta_{np}[A]^n[B]^p}{\sum_0^N \sum_0^P \beta_{np}[A]^n[B]^p} \tag{4}$$

where $\bar{n}_A$ is the average number of ligands A bound per metal atom.

Equations for the formation of *polynuclear complexes* have been elaborated by many authors, as for type M_2A_n, *e.g.*, by N. Bjerrum [14], Leden [15] and Fronæus [9], for type M_mA_n, *e.g.*, by Bodländer and Storbeck [16], Brosset [17], Ahrland [18], Sillén [19] and Hedström [20], for type $M_mH_jA_n$ (complexes between metals and acid ligands), *e.g.*, by Schwarzenbach [21], for type $H_jM_mA_n$ (polyanions neutralized by jH^+), *e.g.*, by Rossotti and Rossotti [22] and for the core-and-link types by Granér [23] and Sillén [23,24]. The primary equations all contain double sums, as for example in

$$\bar{n}_A = \frac{C_A - [A]}{C_M} = \frac{\sum_m \sum_n n\beta_{mn}[M]^m[A]^n}{[M] + \sum_m \sum_n m\beta_{mn}[M]^m[A]^n} \tag{5}$$

where the summations are to be taken from 1.

A test of the validity of the models specified by equations (1)—(5) is outside the scope of the present paper, and it will be assumed that the equations are basically true for the given cases.

METHODS USED FOR CALCULATION OF COMPLEXITY CONSTANTS

After the experimental data have been collected, a threefold problem is encountered: (i) it is necessary to get an idea about which complexes are formed; (ii) on the basis of this idea, complexity constants are calculated; (iii) it is necessary to test if the results thus obtained are consistent with the experimental data. The first problem often involves chemical judgement. The second problem is mathematical in nature, and shall be discussed in this section. The third problem may also be a problem of judgement; it can be based both on chemical knowledge and on statistical tests, as will be further discussed in connection with the examples at the end of this paper.

At present four different approaches to the problem of computing constants in complexity equations seem to be in use. The methods are (*a*) the method of linear plots, (*b*) the method of curve fitting, (*c*) the method of averages, and (*d*) the method of least squares.

The first two methods are graphical and the last two are numerical. Each of these methods will be shortly discussed below *. It should, however, be remembered that whatever method is applied, a graph of the experimental points should first be made, partly to eliminate mistakes (and perhaps systematic errors) and partly to see if the points in any way can be represented by a smooth curve.

(*a*). *The method of linear plots.* In this method (*e.g. Ref.*[2]) which by far is the most common, the equations are transformed so that they are linear in the variables over a certain range of one of the variables. In this range, the experimental data (variables) can be plotted as straight lines.

Under limiting conditions, the intercept of this line on one of the axes, or its slope at this point, gives a value, which may be one of the constants searched for (see, *e.g.*, Leden [15]) or a parameter which is a simple function of this constant (see, *e.g.*, Rydberg [10]). It may also be an intermediate variable obtained under fixed conditions. A number of such intermediate variables may then be plotted in a similar manner, and the intercept on one of the axes of the curve through these points may yield the constant or a new intermediate variable, etc. (see, *e.g.*, Ahrland [25]).

Instead of extrapolations, interpolations may be made; a set of curves drawn trhough the set of experimental points are cut at certain fixed values of one of the variables, and the corresponding values of the other variable is further treated in a graphical or numerical manner (see, *e.g.*, Fronæus [9]).

From the accidental errors in the experiments, it is possible to calculate standard errors in the final constants. However, this is rarely done, because it is so much simpler to get acceptable *estimates* of these errors from the graphs. By introducing the final constants in the equation valid for the experiments, and comparing the graph of this equation with the plot of the experimental

* For a more comprehensive discussion, the reader is referred to the references given.

data (*cf.* next paragraph), systematic deviations between theory and experiments are easily revealed.

(*b*). *The method of curve-fitting.* In this method [26–30], the basic equations are transformed so that for each variable there is a single relationship between that particular variable and one parameter, and this relationship is the only way in which the parameter enters the equation. Curves are then calculated for given parameter values. A fitting of these curves to the experimental data, transformed into the same type of equation, will yield the parameter values. These parameters are related to the constants searched for in a simple manner.

What is said in the foregoing paragraph on accidental errors, is also valid for the curve-fitting method. This method also easily reveals systematic deviations between theory and experiments.

(*c*). *The method of averages.* The method of averages (*e.g. Ref.*[2]) is probably the shortest and easiest numerical method for finding the constants in an empirical equation, but is limited to equations linear in the unknown constants.* The method assumes that the best representative curve is that for which the algebraic sum of the residuals (*i.e.*, the difference between the computed and measured values of the dependent variable) is zero. When there are more equations (measured points) than unknown parameters, the equations are grouped together so that only as many equations as unknowns are obtained. This system of equations is then solved for the parameters in a conventional manner.

There is no rule for grouping together the equations, and as pointed out by Scarborough [2], a careless grouping may yield quite erronous results, unless each group comprises at least 3 to 4 points.

Though this method in its clear-cut form seems to be rarely applied in complex chemistry, the principle is used for example in Bjerrum's method [6] (*cf.* also Bloch and McIntyre [31] and many others), when n combinations $\bar{n}([A])$ are introduced in equation (2), and the system of equations thus obtained is solved by determinants.

Properly used, the method of averages does not introduce any systematic computational errors. On the other hand it does not permit any calculation of statistical errors in the constants obtained.

(*d*). *The method of least squares.* This method is no doubt the most commonly used in numerical calculations in which the number of measured points exceed the number of unknown constants. The principle of least squares, which is founded on the normal probability equation (the "Gaussian curve"), says that the best or most probable value of a measured quantity is that value for which the sum of the weighted squares of the residuals is a minimum. The application of this principle to curve fitting is extensively treated, *e.g.*, by Deming [32].

The method is only applicable to equations which are linear or can be reduced to a linear form in the constants. In complex chemistry this is a rather serious limitation, because it is seen that none of the equations (3)—(5) fullfill this requirement. The problem of linearity will be discussed separately in next paragraph.

* See also next paragraph on least squares.

The method of least squares does not introduce any systematic computational errors. It gives the best set of constants obtainable from the data according to the Theory of Error, and it also permits the calculation of standard errors of these constants, which make it possible to subject the results to statistical tests (see, *e.g.*, Fisher [33]), as will be demonstrated in the examples at the end of this paper. A requirement for such a test as well as the use of the method of least squares is — as pointed out earlier — that only accidental errors occur and that they have a normal statistical distribution.

EQUATIONS SUITABLE FOR LEAST SQUARES TREATMENT

The determination of many parameters from a large number of experimental data with the method of least squares leads to very extensive calculations. It is therefore understandable that few chemists have used this method until very recently, when high-speed digital computors have become easily available. The following summary of what has been done in this field is therefore necessarily meager, though this situation will certainly not last very long.

(a). Equations linear in the parameters. If in eqn. (3), $b = 0$ and only one value of a_n is greater than zero, the equation can be rearranged to give

$$z = \sum_{0}^{N} c_n x^n \tag{6}$$

which is linear in the parameter c_n, which is simply related to the constant β_n. This equation represents a number of common cases of investigations on the complex MA_n.

The method of least squares is straight forward in this case, and it has been applied by Irving and Rossotti [8] to a number of systems with $N = 2$, and by Kivalo and Rastas [34] and McMaster and Schaap [35] to polarographic studies with $N = 4$. While Irving and Rossotti, and Kivalo and Rastas made their calculations manually, McMaster and Schaap, as well as the investigators in the following references, used high-speed computor calculations. None of these authors used weighted data. Both Kivalo and Rastas, and McMaster and Schaap used an approximation technique in the calculations, and the latter authors did not calculate any standard deviations in their parameters.

Rydberg, Sullivan and Miller [11,36-38] have applied eqn. (2) to potentiometric and eqn. (6) to solvent extraction studies, while Zielen [39] has applied eqn. (6) to cation exchange data. In all cases, weighted data were used, and the computors were programmed to calculate standard deviations in the parameters.

(b). Equations non-linear in the parameter; the Gauss transformation to a linear form. The problem of using the method of least squares for determination of parameters, which do not enter the equations in a linear way, as is the case with eqns. (3)—(5), has been discussed, *e.g.*, by Moore and Zeigler [40].

In order to obtain an equation linear in the unknowns (β_n) these are replaced by a guessed or estimated value ($\hat{\beta}_n$) and its deviation ($\Delta\beta_n$) from the "true" value β_n (thus $\beta_n = \hat{\beta}_n + \Delta\beta_n$). The function is then expanded in a

Taylor's series, where higher terms of $\Delta \beta_n$ are neglected. The new function, which will take the form

$$y(\beta_n) \approx y(\widehat{\beta_n}) + \frac{\partial y(\widehat{\beta_n})}{\partial \widehat{\beta_1}} \cdot \Delta\beta_1 + \frac{\partial y(\widehat{\beta_n})}{\partial \widehat{\beta_2}} \cdot \Delta \beta_2 + \ldots \quad (7)$$

is then solved for $\Delta \beta_n$ by the method of least squares. With the $\Delta \beta_n$ values so obtained, new and better estimates of the constants are made, and these new constants are introduced into eqn. (7), and the procedure is repeated until the $\Delta \beta_n$'s are negligible to the standard errors computed for the β_n's; usually very few iterations are needed [40]. This method may be referred to as the Gauss [40] or Newton-Raphson [2] method.

The method is based on estimated values of β_n. It seems not to be clear how good these estimates have to be. Moore and Zeigler report success in cases where the estimates have been as far off as a factor of 10^5, and failures in cases where the estimates have been only 20 % off the correct value. In most cases, adequate estimates can probably be obtained from graphical plots.

This principle has (unknowingly?) been used by van Panthaleon van Eck [41] on data $n([A])$, where all weights have been taken equal to unity. It has also been used with weighted data in kinetic studies of the reduction of Np(VI) by Zielen, Sullivan and Hindman [42], and on spectrophotometric investigations of the hydrolysis of Pu(IV) by Rabideau and Kline [43].

When no approximate values of β_n are known or can easily be determined, reasonable such values of the parameters may be guessed and tried according to the Gauss method. Another approach is to use these guessed values, and to study how the sum S of the squares of the residuals vary with the variation of one parameter at a time. When the minimum of S (S_{min}) is found for one parameter, this value is retained, and the next parameter is varied until S_{min} for that parameter is found. After S has been minimized for each parameter in turn, the procedure is started over again, and continued in this manner until S is a minimum for all of the parameters. Obviously, this technique will not guarantee that one will reach a true minimum for S. Also, there may be another set of parameters, which gives an equally small value of S[40]. However, if the original estimate of the parameters is not too bad, it seems likely that this method will yield correct answers.

Another more systematic method for polynuclear complexes has recently been suggested by Dyrssen, Ingri and Sillén [44], who call the method "pit-mapping". In this case estimates of the parameters are obtained through graphical methods *.

* When mixed or polynuclear complexes are studied, the calculations will be much simplified if the experiments are carried out so that the system is studied as a function of one of the independent variables, while the other is kept constant. This situation is wellknown to all investigators in this particular field.

It was earlier indicated that eqn. (3) could be used for spectrophotometric and partition studies in which case it can be written ($b = 0$)

$$\sum_0^N (\varepsilon_M - \varepsilon_n)\beta[A]^n = 0 \quad (8a)$$

$$\sum_0^N (Q_M - \lambda_n)\beta_n[A]^n = 0 \quad (8b)$$

In these equations ε_M, Q_M and [A] are measured, while ε_n, λ_n and β_n are the unknown parameters, though usually one value of ε_n and λ_n is known: *i.e.* ε_0 for $M^{\nu+}$ or ε_N for MA_N in spectrophotometric investigations, λ_0 for $M^{\nu+}$ in cation exchange studies, or λ_r for the uncharged complex MA_r in solvent extraction work. By guessing reasonable values for ε_n and λ_n the method of least squares can be used for calculation of those β_n's which gives a minimum for S. This method, which has been used in one of the examples below, is obviously a variation of the principle described above.

SOME RESULTS OF LEAST SQUARES CALCULATIONS ON COMPLEXITY SYSTEMS

In this part, the application of the method of least squares to a number of complexity systems will be demonstrated and the discrepancies between the results and those obtained with graphical methods will be discussed. Since the method of least squares provide standard errors to the computed constants, some statistical tests have been applied and their merits analysed. It is believed that the viewpoints which are brought up in this connection are rather general in nature and shall indicate to the chemists not familiar to this field both what can be gained and what the limitations of the methods are.

(a). The Ni(II)-NH_3 system; a potentiometric investigation. The experimental data of Bjerrum [6] were directly introduced into eqn. (2) which was then solved for β_n by the method of least squares [37] using an IBM 704 computor. With the program used [45a], one run on the computor takes about one minute. In practice, it may take a much larger time to find the β_n, because if proper data are not used, it may be necessary to make several runs on the computor. The reason for this is that all errors are assumed to belong to the experimental

Table 1. The Ni(II)-NH_3 system, 2 M NH_4NO_3 at 30°C.

Gross constant *	Bjerrum	Least squares	Step-wise constant *	Bjerrum	Least squares
$\beta_1 \times 10^{-2}$	6.29	6.094 ± 0.048	$\log k_1$	2.795	2.785 ± 0.0034
$\beta_2 \times 10^{-5}$	1.084	1.111 ± 0.020	$\log k_2$	2.24	2.262 ± 0.0085
$\beta_3 \times 10^{-6}$	5.82	5.377 ± 0.173	$\log k_3$	1.73	1.686 ± 0.016
$\beta_4 \times 10^{-7}$	9.00	9.254 ± 0.414	$\log k_4$	1.19	1.249 ± 0.023
$\beta_5 \times 10^{-8}$	5.06	5.202 ± 0.262	$\log k_5$	0.75	0.737 ± 0.029
$\beta_6 \times 10^{-8}$	5.43	5.514 ± 0.396	$\log k_6$	0.03	0.026 ± 0.038

* $\beta_n = \Pi k_n$

determination of [A], and the present program cannot handle cases where the difference $C_A-[A]-nC_M$ is about the same or smaller than the error in [A]. If one wants to save computor time, such combinations have to be eliminated before running the program. In the $Ni-NH_3$ case, 3 points of 14 had to be excluded. Table 1 gives the results then obtained, and also the results of the semi-graphical ligand number method [6]. It is seen that the agreement is excellent.

The χ^2-test [33] may be applied to the data. Bjerrum estimates "the limit of experimental error" in the e.m.f. measurements to 0.2—0.5 mV (p. 124) [6], which here is interpreted to a standard error of $\pm$ (0.1—0.25) mV. A standard error of $\pm$ 0.1 mV corresponds to a 0.54 % error in [A], *i.e.* $\sigma_{[A]} = \pm 0.0054[A]$. Using this error of internal consistency [32], a χ^2-value is calculated (this calculation is incorporated in the computor program) to 4.25. Since the number of degrees of freedom here is 5 (11 points minus 6 parameters), the χ^2-test shows a high degree of consistency between the experimental points and the curve calculated with the obtained constants. This consistency, found even for the smallest possible error assumed by Bjerrum, is a strong support for the basic hypothetis, *i.e.* that all stepwise complexes from Ni^{2+} to $Ni(NH_3)_6^{2+}$ exist. For larger errors in the experimental data, the χ^2 value decreases and the probability for a good fit between the calculated function and the experimental points further increases.

The same point may be illuminated by quoting Deming [32] "The unbiased estimate of χ^2 made by external consistency is found by calculating what value of σ forces χ^2 to take its mean value G", where G is the number of degrees of freedom, which in this case, is the number of experimental points minus the number of parameters minus one. Using this criterium, one arrives at an error of 0.498 % in [A], which obviously very closely corresponds to an error of $\pm$ 0.1 mV in the e.m.f. measurements.

These results indicate that the experiments perhaps have been even more accurate than Bjerrum assumed. Even though the result of the χ^2-test here is striking, it must be realized that it probably is a rather favorable case. Some caution is also necessary, considering the small number of degrees of freedom in the system [32].

(b). The Th(IV), U(IV), Pu(IV) acetylacetone system; a solvent extraction investigation. This example may well be called "The case of the missing constants" or — as it has turned out — "The case of constant misunderstandings", as shall be explained below.

The least squares calculations of stability constants for Th(IV), U(IV) and Pu(IV) acetylacetone complexes using eqn. (6) and the IBM 704 computor has earlier been published [38] and the results are collected in Table 2. In this case a program [45b], slightly different from the previous one, was used. All errors are assumed to belong to the measured distribution ratio Q of the metal between the organic solvent and the aqueous phase. The speed of the computations are about the same as for the previous program. No points have to be excluded.

In the U(IV) case the agreement between the constants obtained by the two-parameter method and the least squares method is quite good. The number of experimental points in this case is 46 and the residuals show a normal distri-

Table 2. The Th(IV), U(IV) and Pu(IV) acetylacetone systems; 25°C.

Case	System	log k_1	log k_2	log k_3	log k_4	log λ_4
1	U(IV), par.*a)*	9.05 ± 0.16	7.97 ± 0.17	6.90 ± 0.18	5.84 ± 0.11	3.62 ± 0.05
	Least squares	9.02 ± 0.29	8.26 ± 0.15	6.52 ± 0.09	5.98 ± 0.09	3.64 ± 0.025
2	Pu(IV), Lig.*b)*	10.0 ± 1.	9.1 ± 0.2	8.5 ± 0.3	5.9 ± 0.3	2.50 ± 0.2
	Least squares	—	17.77 ± 0.12		5.91 ± 0.09	2.54 ± 0.07
3	Th(IV), Lim.*c)*	(7.82 ± 0.16)	(7.73 ± 0.09)	6.27 ± 0.05	5.00 ± 0.04	2.52 ± 0.04
	Least squares	15.57 ± 0.08		6.15 ± 0.04	5.14 ± 0.07	2.48 ± 0.06
4	Th(IV) Lim.*d)*	8.00 ± 0.17	7.48 ± 0.14	6.00 ± 0.11	5.30 ± 0.05	2.55 ± 0.03
	Least squares	—	7.43 ± 0.21	5.83 ± 0.39	5.35 ± 0.42	2.53 ± 0.20

$$k_1 = \frac{a_1}{a_0} = \frac{[MA]}{[M][A]};\ k_2 = \frac{a_2}{a_1} = \frac{[MA_2]}{[MA][A]};\ k_3 = \frac{a_3}{a_2} = \frac{[MA_3]}{[MA_2][A]};\ k_4 = \frac{a_4}{a_3}\frac{[MA_4]}{[MA_3][A]};$$

$$\lambda_4 = \frac{1}{a_4} = \frac{[MA_4]_{org}}{[MA_4]_{aq}};\ k_1k_2 = \frac{a_2}{a_0} = \frac{[MA_2]}{[M][A]^2};\ k_2k_3 = \frac{a_3}{a_1} = \frac{[MA_3]}{[MA][A]^2}$$

a) Calculated by 2-parameter method: 0.1 M $NaClO_4$
b) » » ligand number method: 0.1 M $NaClO_4$
c) » » limiting value method: 0.01 M $NaClO_4$ · Benzene solvent.
d) » » » » » 0.1 M $NaClO_4$ · Chloroform solvent.

bution around the curve. Thus it may be concluded, that the two-parameter method and the least squares method of calculation applied to good solvent extraction data yields the same results, provided the basic assumptions for the two-parameter method are valid [26].

Not so good agreement is found in the Pu(IV) case, which comprises 24 points. From a consideration of replicate experiments, a standard error of 20 % was assigned to the measured distribution ratio. The least squares calculations yielded the results in Table 3. The negative values of the parameters a_0 and a_2* indicate either a systematic deviation from the assumed equation for the system or that negative concentrations of the complexes are present. Since the standard errors are very large and negative concentrations of complexes are assumed not to exist, it seems reasonable to eliminate these parameters from the calculations.

This procedure may cause some concern among chemists, who may conclude that the elimination of a_0 and a_2 means that the corresponding chemical species (Pu^{4+} for a_0, and PuA_2^{2+} for a_2; see Table 2) do not exist. The author feels however, that constants should not be given for equilibria involving species which one has not been able to identify **. It might well be possible to identify the missing species and to determine equilibrium constants for their formation

* The parameters a_n are defined in Table 2.

** In this case, the only method of "identification" is through a fit between the experimental data and the equations involving the particular species.

Table 3. Primary parameters obtained for the Pu(IV) case.

$a_0 \times 10^{37}$	$a_1 \times 10^{26}$	$a_2 \times 10^{17}$	$a_3 \times 10^{9}$	$a_4 \times 10^{3}$	χ^2	G
-17 ± 10	1.9 ± 0.8	-0.046 ± 0.53	3.3 ± 0.6	2.9 ± 0.4	17.3	19
—	0.61 ± 0.15	—	3.6 ± 0.5	2.9 ± 0.5	22.4	21

with a better set of experimental data. In the present experimental material, Pu^{4+} and PuA_2^{2+} cannot be identified ($[Pu^{4+}]$ and $[PuA_2^{2+}]$ cannot be determined) with any reasonable degree of accuracy, though the existence of PuA_2^{2+} seems highly probable from a chemical point of view, and Pu^{4+} is known to exist. The χ^2-values indicate about equally good fits between the experimental data and the calculated curve, either Pu^{4+} and PuA_2^{2+} are assumed to be present or not. Thus the indeterminate influence of these species on the system is obvious.

A similar state of affairs exists for the Th(IV) systems in Table 2. In these systems, one expects to find the same species, even though the systems have been investigated by slightly different methods. With the graphical methods, formation constants were obtained for all stepwise complexes. Neverthelsess the least squares calculations on case 3 came out with $a_1 = (-1.3 \pm 1.3)\,10^{-22}$ and on case 4 with $a_0 = (-17 \pm 20)\,10^{-30}$. The parameters a_1 and a_0 are here eliminated simply because they cannot statistically be proven to differ from zero; this operation caused practically no change in the χ^2-values. The elimination of a_1 in case 3 and a_0 in case 4 does not mean that ThA_3^+ and Th^{4+} respectively, do not exist. In fact, the species missing in one of the systems is "found" in the other of the systems.

Tests were also carried out assuming that complexes higher than MA_4 were formed, *i.e.* MA_5 and MA_6, but the standard deviations of β_5 and β_6 far exceeded the constants. In fact, in no case where the least squares method has been tried by the author, has it been possible to identify more complexes than assumed by the original investigators.

It may thus be concluded that the method of least squares does not give any better results than can be justified by the experimental data. An advantage of this fact is that it indicates in which experimental region the data are too uncertain (too scattered, too few, *etc.*), whatever consequence this may have on the investigator.

(c). The VO^{2+}—F^- system; a potentiometric investigation. To this system [46] eqn. (2) is applicable in the same manner as for the Ni—NH_3 system described earlier. In Fig. 1, the original authors have plotted $\bar{n}([A])$. Since the points are obtained from 5 different sets of experiments, and the curve obtained with the four constants β_1, β_2, β_3 and β_4 seems to well fit all the 5 sets of points, a statistical t-test [33] seems applicable.

A general look at Table 4 reveals 3 things: (i) of the 5 sets of experiments some rather high values of χ^2/G are obtained; (ii) the β_n-values computed by the method of least squares for the various sets of experiments do not all agree

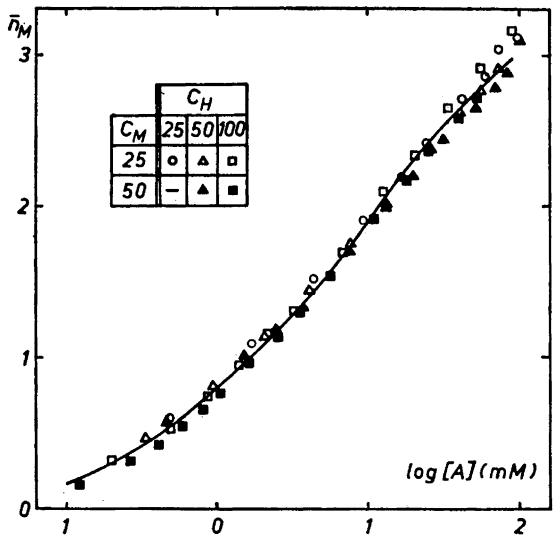

Fig. 1. The complex formation function of the vanadyl fluoride system. The points refer to titrations with different values of C_M and C_H, as indicated by the scheme given in the figure. The curve is calculated from the constants β_n finally found.

within their errors; (iii) Ahrland and Noréns β_n-values agree approximately well with the mean values calculated by the method of least squares. These points shall be discussed in turn.

If the error of external consistency is found by calculating what value forces $\chi^2/G = 1.0$, one finds that the error should be around 2 % in [A], with exception for set 4, where the error must be assumed to be about 5 %. This agrees rather well with the $\pm$ 0.2 mV error estimated for the e.m.f. measurements.

Table 4. The VO^{2+}—F-system. The errors given are mean square errors at the 95 % confidence limit (2 times standard deviation).

Set	$[H^+]\times10^2$	$C_M \times 10^3$	$\beta_1 \times 10^{-3}$	$\beta_2 \times 10^{-5}$	$\beta_3 \times 10^{-7}$	$\beta_4 \times 10^{-7}$	χ^2	G
1	25	25	2.29 ± 0.03	4.84 ± 0.07	1.75 ± 0.06	8.97 ± 0.64	0.64	4
2	50	25	2.16 ± 0.06	4.14 ± 0.16	1.31 ± 0.14	6.14 ± 1.31	5.30	5
3	50	50	2.13 ± 0.10	3.67 ± 0.28	1.15 ± 0.20	3.12 ± 1.73	41.4	6
4	100	25	1.97 ± 0.20	3.49 ± 0.60	1.53 ± 0.59	9.65 ± 9.23	198	7
5	100	50	1.53 ± 0.03	2.57 ± 0.11	0.93 ± 0.07	3.32 ± 0.90	20.6	10
Mean values of least squares calculations			2.02 ± 0.08	3.74 ± 0.24	1.34 ± 0.21	6.2 ± 2.8		
Values by Ahrland and Norén			2.0 ± 0.1	2.9 ± 0.3	1.4 ± 0.2	3.0		

A t-test was carried out on the β_r-values ($r = 1, 2, 3, 4$) to see if there were any significant deviations between them. The test was based on the assumption (1) that in each experimental set, the points have a normal statistical distribution, and (2) that all data were of the same relative weights. A constant percentage error P in [A] was assumed; thus $1/W_i = (0.01\ P[\mathrm{A}]_i)^2$.
If these assumptions are not too incorrect, the t-test indicates significant differences between the β_r-values. Thus for $10^{-5}\beta_2 = 4.84 \pm 0.07$ (set 1) and 2.57 ± 0.11 (set 5), the test shows that the probability is <1 % that the two β_2-values belong to the same normal population. As a comparison, it is found that the two values $10^{-5}\beta_2 = 4.14 \pm 0.16$ (set 2) and 3.67 ± 0.28 (set 3) may belong to the same population. After analyzing all β_r-values it must be concluded from a statistical point of view that the differences between these values must be caused by systematic differences among the five sets of experiments.

If all experimental points are taken together (*i.e.* are assumed to belong to the same normal population), the agreement between the mean values of the least squares calculations and the values obtained by Ahrland and Norén is quite reasonable (see Table 4). Fig. 1 also shows how well the computed curve fits the experimental points. It is the author's opinion that graphical methods do not permit more information to be extracted from these data than has been obtained by the original authors.

(d). The Ce(III)-SO_4^{2-} system; a cation exchange investigation. This is the only system [47] known to the author where the parameters are not linear in the equation and the trial-and-error least squares approach (see p. 1729) has been applied. In this particular case, equation 8b is applicable, and the maximum number of parameters, which have to be considered, are λ_0, λ_1, β_1, β_2 and β_3. Of these constants λ_0 is known directly from the experiments (see below). In the following treatment we shall assume that we have no knowledge of the results of Fronæus's calculations.

On the basis of the experiments, it can be assumed that all error can be attributed to the measured partition ratios Q, and are of the size $\sigma_Q = \pm 0.03\ Q$. The experimental data $Q([\mathrm{A}])$ comprise only 8 points. The curve through these points is anchored at $Q_0([\mathrm{A}] = 0) = 0.752$, which is our λ_0-value.

We now make a number of runs on the computor with equations based on the following assumptions:

Run:	Cerium species in solution	Cerium species on the resin
1	Ce^{3+}, CeA^+, CeA_2^-	Ce^{3+}
2—5	»	Ce^{3+}, CeA^+
6	Ce^{3+}, CeA^+, CeA_2^-, CeA_3^{3-}	Ce^{3+}
7—10	»	Ce^{3+}, CeA^+

Here A^{2-} stands for SO_4^{2-}. Looking at runs 1—5 in Table 5, it follows from the χ^2/G-values that the most probable λ_1 value is obtained for run 1 (χ^2/G value closest to 1.0). However, even though the χ^2/G-value for run 1 is not improbable for a fit between the assumed equation and the experimental data, one of the

Table 5. The Ce(III)—SO_4^{2-} system. $G = 5$ for runs 1—5, and 4 for runs 6—10; $\lambda_0 = 0.752$.

Run	λ_1	$10\,\beta_1$	$100\,\beta_2$	$1\,000\,\beta_3$	Q_1	Q_3	Q_7	χ^2/G
1	0.00	3.45 ± 0.14	1.65 ± 0.16	0	0.424	0.201	0.0504 *	1.51
2	0.04	3.45 ± 0.20	2.90 ± 0.20	0	0.428	0.199	0.0514 *	2.67
3	0.0787	3.46 ± 0.26	4.10 ± 0.23	0	0.430 *	0.198	0.0521 *	3.90
4	0.10	3.46 ± 0.29	4.76 ± 0.26	0	0.432 *	0.197	0.0523 *	4.58
5	0.30	3.48 ± 0.60	11.08 ± 1.09	0	0.044 *	0.191 *	0.0532 *	9.94
6	0.00	3.47 ± 0.19	0.72 ± 0.51	0.48 ± 0.26	0.418	0.205	0.0479	0.994
7	0.04	4.01 ± 0.21	1.25 ± 0.55	0.95 ± 0.32	0.418	0.205	0.0481	0.946
8	0.0787	4.29 ± 0.24	1.86 ± 0.58	1.46 ± 0.40	0.418	0.206	0.0482	0.904
9	0.10	4.47 ± 0.26	2.25 ± 0.59	1.77 ± 0.44	0.417	0.206	0.0482	0.884
10	0.30	7.05 ± 0.60	8.38 ± 0.66	6.37 ± 1.21	0.417	0.206	0.0485	0.752
Fronæus	0.0787	4.3 ± 0.3	2.2 ± 0.5	1.2 ± 0.3	0.414 ± 0.012	0.202 ± 0.006	0.0483 ± 0.014	—

* These values are outside the 3 % standard error in the measured Q-values.

computed points, $Q_7 = 0.0504$ seems somewhat too far off from the measured value 0.0483. We assume this is a significant difference, and therefore make a new set of runs, 6—10, where also CeA_3^{3-} is considered in the equation. Since χ^2/G has the same normal distribution as the sum S of the squares of the weighted residuals [30], χ^2/G shall show a minimum for the most probable value of λ_1, No such minimum is achieved in runs 6—10, and no higher λ_1 value than 0.30 was tested, because higher values seemed very improble from a chemical point of view. As compared to runs 1—5, the χ^2/G values in runs 6—10 indicate that the functional form in the latter case is more probable. From this result it may be concluded that the experimental data can be best explained by considering the species Ce^{3+}, CeA^+, CeA_2^-, and CeA_3^{3-} in the aqueous phase, and the species Ce^{3+} and CeA^+ in the resin phase. This is the same conclusion as reached by Fronæus.

Unfortunately, as the least squares calculations were made on the present data, the χ^2-test gives us very little help in finding the best λ_1 value. We are therefore forced to make a subjective judgement. Since the λ_1 value is of greater importance for the higher complexes (*i.e.* higher β_n; see left part of Table 5), which dominate at the points of highest [A] value (the [A] value increases from point Q_0 to Q_7), we shall say that the best λ_1 is that, which causes the smallest deviation between the computed and measured values of point Q_7; this value turns out to be 0.0482 (runs 8 and 9). Since we here have two such values, we chose the one which causes the smallest deviation in the Q_3-value, which turns out to be for run 8, if the trend in Q_3 is considered. This corresponds to the same λ_1-value as Fronæus has arrived at from somewhat different considerations. If should be observed, that the approach used here can be stated in a more strict mathematical form, because what we have done is only to increase the

weights of the points for the highest [A] values. It may be added that the electronic computor can easily be ordered to try the various λ_n values automatically until the λ_n value, which gives the smallest S value, is obtained.

If we compare the constants obtained by Fronæus and by the method of least squares for $\lambda_1 = 0.0787$, we find an excellent agreement. This shows that complicated graphical treatments, when carried out on good data yield results in almost complete agreement with the results of our machine calculations.

CONCLUSION

It is always necessary to check the computed results to see if they are reasonable from a chemical point of view. Of all tests, which can be applied to the data, this is the most crucial. When a sufficient number of experimental points are at hand, it should also be checked (by hand or using the computor) that the points have a normal distribution around the computed curve. Under these circumstances, the method of least squares in combination with high speed digital computors is both a powerful and time-saving tool for helping complex chemists in analyzing their experimental data.

REFERENCES

1. Cramér, H. *Mathematical Methods of Statistics*, Princeton University Press, Princeton, 1946; *Sannolikhetskalkylen och några av dess användningar*, Almqvist och Wiksell, Uppsala 1961.
2. Scarborough, J. B. *Numerical Mathematical Analysis*, 4h Ed. The John Hopkins Press, Baltimore 1958.
3. Rydberg, J. *Arkiv Kemi* **8** (1955) 101.
4. Irving, H., Rossotti, F. J. C. and Williams, R. J. P. *J. Chem. Soc.* **1955** 1906.
5. Sillén, L. G. Supplement to *La Ricerca Scientifica* **28** (1958).
6. Bjerrum, J. *Metal Amine Formation in Aqueous Solution*, P. Haase and Son, Copenhagen 1941.
7. Sullivan, J. C. and Hindman, J. C. *J. Am. Chem. Soc.* **74** (1952) 6091.
8. Irving, H. and Rossotti, H. S. *J. Chem. Soc.* **1953** 3397.
9. Fronæus, S. *Komplexsystem hos koppar*. Thesis, Lund 1948.
10. Rydberg, J. *Acta Chem. Scand.* **4** (1950) 1503.
11. Rydberg, J. and Sullivan, J. C. *Acta Chem. Scand.* **13** (1959) 1057.
12. Fronæus, S. *Acta Chem. Scand.* **5** (1951) 859.
13. Fronæus, S. *Acta Chem. Scand.* **4** (1950) 72.
14. Bjerrum, N. Thesis, Copenhagen 1908.
15. Leden, I. *Potentiometriska undersökningar av några kadmiumsalters komplexitet*. Thesis, Lund 1943.
16. Bodländer, G. and Storbeck, O. *Z. anorg. Chem.* **31** (1902) 1, 458.
17. Brosset, C. *Elektrokemisk och röntgenkristallografisk undersökning av komplexa aluminiumfluorider*. Thesis, Stockholm 1942.
18. Ahrland, S. *Acta Chem. Scand.* **3** (1949) 374.
19. Sillén, L. G. *Acta Chem. Scand.* **8** (1954) 299.
20. Hedström, B. *Acta Chem. Scand.* **9** (1955) 613.
21. Schwarzenbach, G. *Helv. Chim. Acta* **33** (1950) 947.
22. Rossotti, F. J. C. and Rossotti, H. *Acta Chem. Scand.* **10** (1956) 957.
23. Granér, F. and Sillén, L. G. *Acta Chem. Scand.* **1** (1947) 631.
24. Sillén, L. G. *Acta Chem. Scand.* **8** (1954) 318.
25. Ahrland, S. *Acta Chem. Scand.* **3** (1949) 783.
26. Dyrssen, D. and Sillén, L. G. *Acta Chem. Scand.* **7** (1953) 663.

27. Rossotti, F. J. C. and Rossotti, H. *Acta Chem. Scand.* **9** (1955) 1166.
28. Sillén, L. G. *Acta Chem. Scand.* **10** (1956) 186.
29. Rossotti, F. J. C., Rossotti, H. and Sillén, L. G. *Acta Chem. Scand.* **10** (1956) 203.
30. Sillén, L. G. *Acta Chem. Scand.* **10** (1956) 803.
31. Block, B. P. and McIntyre, Jr., G. H. *J. Am. Chem. Soc.* **75** (1953) 5667.
32. Deming, W. E. *Statistical Adjustment of Data*, J. Wiley and Son, New York 1948.
33. Fisher, R. A. *Statistical Methods for Research Workers*, 13th Ed., Hafner Publ. Co., New York 1958.
34. Kivalo, P. and Rastas, J. *Suomen Kemistilehti* **30** (1957) 128.
35. McMasters, D. L. and Schaap, W. B. *Proc. Indiana Acad. Sci.* **67** (1958) 111.
36. Rydberg, J. and Sullivan, J. C. *Acta Chem. Scand.* **13** (1959) 186.
37. Sullivan, J. C., Rydberg, J. and Miller, W. F. *Acta Chem. Scand.* **13** (1959) 2023.
38. Rydberg, J. *Acta Chem. Scand.* **14** (1960) 157.
39. Zielen, A. *J. Am. Chem. Soc.* **81** (1959) 5022.
40. Moore, R. H. and Zeigler, R. K. *The solution of the general least squares problem with special references to high-speed computors*, LA-2367, Los Alamos Scientific Laboratory, New Mexico, 1960.
41. Van Panthaleon van Eck, C. L. Thesis, Amsterdam 1958.
42. Zielen, A. J., Sullivan, J. C. and Hindman, J. C. *Private communication.*
43. Rabideau, S. W. and Kline, R. J. *J. Phys. Chem.* **64** (1960) 680.
44. Dyrssen, D., Ingri, N. and Sillén, L. G. *Acta Chem. Scand.* **15** (1961) 694.
45. a) Program 626/CHM 112. b) Program 495/CHM 104. Applied Mathematics Division, Argonne National Laboratory, Argonne, Illinois.
46. Ahrland, S. and Norén, B. *Acta Chem. Scand.* **12** (1958) 1595.
47. Fronæus, S. *Svensk Kem. Tidskr.* **64** (1952) 317.

Received May 3, 1961.

ACTA CHEMICA SCANDINAVICA 15 (1961) 1739–1746

Studies on Peptides from a Peptic Hydrolyzate of Cytochrome c from *Rhodospirillum rubrum*

KLAS LEVIN

Medicinska Nobelinstitutet, Biokemiska Avdelningen, Stockholm, Sweden

Cytochrome c (550 *Rhodospirillum rubrum*) was prepared by acid extraction, precipitation with $(NH_4)_2SO_4$ and TCA, and chromatography on DEAE and CM–W. It was studied by spectrophotometry and electrophoresis. The cytochrome c was digested with pepsin, after which two peptides were isolated by partition chromatography. They have been subjected to amino acid analysis and N-terminal end group determination. The peptides were also investigated by ultracentrifugation and spectrophotometry.

Ever since a cytochrome c * was first shown to be present in the facultative photoheterotrophic organism *Rhodospirillum rubrum* [1], a great interest has been focused on it and other heme proteins [2–4] in this type of bacteria. The remarkable similarity between the spectra of this cytochrome c and cytochrome c from mammalian sources, in spite of dissimilarities in oxidation potentials and other physio-chemical properties, has called for an elucidation of the structural similarities and differences. Paléus and Tuppy [5] were able to determine the structure of a hemopeptide containing 13 amino acids residues from a tryptic hydrolyzate of *R. rubrum* cytochrome c. They established the fact that the "core" of the peptide chain had the same structural features earlier encountered in all cytochrome c samples. The aim of the present investigation was to isolate a hemopeptide after digestion of the cytochrome c from *R. rubrum* with pepsin.

EXPERIMENTAL

Material

Rhodospirillum rubrum. The method of growing the bacteria on a large scale has been described in an earlier paper [6]. The total yield of a fermentation was 600 g of lyophilized bacteria. As was pointed out previously, a large portion of the bacteria was disrupted by

* The following abbreviations will be used: cyt. c and cytochrome c = cytochrome c (550 *Rhodospirillum rubrum*), unless otherwise stated. TCA = trichloroacetic acid, DNFB = 2,4-dinitrofluorobenzene, DNP– = dinitrophenyl-, CM–W = carboxymethyl cellulose, DEAE = diethylaminoethyl cellulose.

the harvesting procedure and by the lyophilization. The material had been stored in an evacuated desiccator at + 4° for 5 months before use.

Ion exchange material. Cellulose powder ion exchangers CM—W and DEAE types were used throughout the preparations of the cytochrome. They were prepared strictly according to the procedures recommended by Peterson and Sober [7], using Whatman cellulose powder and Solca floc as starting material.

Talc. Ordinary commercial talcum powder was washed 6 times with N HCl, allowed to settle each time, and the supernatant solution discarded. After the last sedimentation the supernatant solution was practically clear.

Silica. The commercial product "Celite analytical filter-aid" was thoroughly washed as described by Tuppy and Bodo [8], using 50 % ethanol containing 3 % ammonia, water, 2.4 N HCl and ethanol. The product was dried for 24 h at 110°C.

DNP-amino acids. For qualitative experiments, a DNP-amino acids kit purchased from Mann Research Laboratories was used. Quantitative measurements were performed on DNP-amino acids kindly supplied by Dr. Alfred Arens.

Pepsin. 3 times crystallized pepsin, lot No. P 109—060 from Sigma Chemical Co., was used.

DNFB. 2,4-Dinitro-fluorobenzene, Merck No. 2966 was used.

Paper chromatography. Whatman No. 1 papers were used throughout this investigation. The solvents for the "Toluene" mixture were purified from commercial products as recommended by Biserte *et al.*[9]

Other chemicals. Except for the chemicals used in the crude preparations, good commercial analytical grade substances were used. Ordinary distilled water was used throughout. All buffer concentrations refer to the sum of the concentrations of the acidic and basic forms of the buffer.

Methods

Electrophoresis. This was carried out in a Tiselius electrophoresis apparatus (Beckman/Spinco Model H Electrophoresis-Diffusion Instrument) at + 0.6°C. The micro (2 ml) cell was used. A tungsten lamp was used, with a red filter introduced for the exposures. The samples were equilibrated with the buffer by dialyses for 48 h at + 4°C.

The mobility was calculated by the formula $u = Sq\varkappa/ti$ where S is the apparent speed of the boundary, q is the cross-section of the electrophoresis cell, $\varkappa$ is the specific conductance of the solution, t is the time and i is the current.

Spectrophotometry. Measurements at single wavelengths were carried out in a Beckman Model DU Spectrophotometer using cuvettes of 1 cm optical light path, and with a volume of 3 ml. For smaller quantities, 0.5-ml cells were used. For complete spectra, the recording Beckman DK 2 was used with scanning set from 700 to 250 mμ. The heights of the sharper peaks were checked with the DU instrument. Measurements were usually performed in 0.066 M phosphate buffer of pH 6.8. As reducing agent, solid sodium dithionite was used.

Ultracentrifugation. This was performed in a Spinco Analytical Ultracentrifuge Model E by the method described by Yphantis and Waugh [10]. The hemopeptides were dissolved in a 0.2 M Na_2HPO_4 solution. In order to avoid polymerization, sufficient N-acetyl-L-histidine was added to form the hemochromogen. The concentrations of the hemochromogen, both in the top and bottom compartments of the cell, were determined spectrophotometrically at 320, 410 or 550 mμ. The molecular weight was calculated as described in the original method, except for the Q-values which were calculated according to the formula:

$$Q = \frac{c_t(b^2-a^2)}{c_t(r_p^2-a^2) + c_b(b^2-r_p^2)}$$

where c_t and c_b are the absorbancies of the solutions in the top and bottom compartments of the cell respectively, a is the distance from the rotor center to the meniscus, b is the distance from the rotor center to the bottom of the cell when the rotor is rotating at full speed, and r_p is the distance from the rotor center to the separating plate when the rotor is at rest.

DNP-amino acid analysis. This was carried out chiefly as described by Wallenfels and Arens [11]. The coupling with the DNFB was achieved in a small water-mantled vessel which contained a glass electrode, an agar-KCl bridge to a calomel electrode, and the outlet tube from an Agla micrometer syringe. A Radiometer pH meter (type PHM 22 p) was used. Water at 40°C was circulated through the mantle. The vessel was provided with a magnetic stirrer. 0.3 to 1 mg of material was used in each experiment. To the solution which was to be reacted was added KCl to make it 0.1 M. The pH was adjusted to 8.9 with 0.100 N NaOH from an Agla syringe, after which 0.02—0.1 ml of DNFB was added. The course of the reaction was followed by observing the amount of 0.1 N NaOH needed to keep the pH constant at 8.9. Readings were made every third minute and continued until the alkali consumption showed a linear course, which was after 90 to 120 min. The excess of DNFB was then extracted with ether.

In the case of the end-group analysis, the dinitrophenylated peptide was precipitated by acidifying the solution. The precipitate was centrifuged, and the supernatant solution discarded. The peptide was dissolved in alkaline water and reprecipitated. The precipitate was then washed with alcohol and with ether. The peptide was dried in a desiccator, and subjected to hydrolysis with 6 N HCl for 24 h at 110°C. The hydrolyzate was then evaporated to dryness in a vacuum desiccator at room temperature. The residue was dissolved in water and extracted 3 times with ether. The two fractions of DNP-amino acids were evaporated to dryness separately, and dissolved in acetone or ethyl acetate. Each of these solutions was then transferred to a separate sheet of 45 × 45 cm paper. The spots on each sheet were formed in one corner, 7 cm from each edge. The papers were subjected to descending chromatography with the solvents recommended by Levy [12]. First they were developed with the "toluene"-mixture for 7 h and, after drying in a forced-draft oven at 35°C for 6 h, developed in the 1.5 M phosphate buffer, pH 6, for 10 h. The spots were identified by comparison with runs made with known DNP-amino acids, and with other published charts [9,11,12]. In a confirmatory experiment, a mixture of 99 % formic acid:acetic anhydride:70 % perchloric acid (20:11:3 volume ratios), which is said to cause less destruction of DNP-glycine [13], was used as the hydrolyzing agent for the peptide. This hydrolysis was carried out at 100°C for 2 h. The hydrolysis was performed in a thick-walled, sealed glass tube which had to be opened very carefully to avoid explosions. The hydrolyzate was diluted 10 times and extracted 3 times with benzene that contained 10 % *tert*-amyl alcohol. The extract was then evaporated to dryness and chromatographed as described above.

In the case of the total amino acid analysis, the unreacted peptide was hydrolyzed with HCl as described above, and reacted with DNFB. The solution was then acidified, and the ether-soluble DNP-amino acids separated from the water-soluble derivatives by extraction. The solvents were evaporated, and the residues dissolved as quantitatively as possible in acetone or ethyl acetate, and transferred to spots on the papers. The chromatography was carried out as before. After identification of the spots, they were cut out, leaving 5 mm margins along the edges, and the DNP-amino acids were extracted in test tubes with 5 ml of 1 % $NaHCO_3$ solution at 60°C for 20 min. The relative concentrations were determined by reading the absorbancy at 360 mμ, and multiplying these values, after correcting them for the paper and cuvette blank values, by the factors given by Wallenfels and Arens [11] to give the corrected absorbancy readings. Since the extinction coefficients at 360 mμ of the DNP-derivatives of the common amino acids are about the same, the ratios of the absorbancy readings are approximately proportional to the molar ratios of amino acid residues in the original peptide. The DNP-aspartic acid and DNP-glutamic acid were determined together. They were separated by a second chromatogram in one dimension with 2.5 M phosphate buffer at pH 6. The mixed preliminary value was divided up in proportion to the content of each of the two.

Amino acid analysis. For this analysis, a sample of the peptide was hydrolyzed in an evacuated ampule with 6 N HCl at 110°C for 20 h. It was then dried, dissolved in water, dried again, and subjected to ion exchange chromatography as described by Moore *et al.*[14]

Preparations

Preparation of the cytochrome c. The preparation was performed at + 4°C except for the first centrifugations and the column chromatographies which were done at room tem-

perature. The extraction was performed by suspending 550 g of the lyophilized bacteria in 11 l water to which 22.9 ml concentrated H_2SO_4 had been added. The pH, after the addition of the bacteria, was 4. The suspension was stirred as vigorously as possible without causing excessive foaming. After standing for 2.5 h, the pH was adjusted to 7.0 by the addition of 4 N NH_4OH. After standing for 3 h, the suspension was centrifuged at 2 200 *g* for 1 h. To the turbid supernatant solution, 313 g of solid $(NH_4)_2SO_4$ per liter was added, and the solution allowed to stand overnight. After centrifugation for 1 h at 2 200 *g*, the supernatant solution was clear and had a reddish-brown colour.

Another 203 g of $(NH_4)_2SO_4$ was added to each liter of the resulting supernatant solution, after which it was allowed to stand overnight, and centrifuged as before. The supernatant solution was then saturated with $(NH_4)_2SO_4$, and left for 48 h with slow stirring. It was not possible to obtain a satisfactory sedimentation in the centrifuge at this stage. Therefore, 25 ml of 20 % TCA was added per liter of the suspension, after which it was immediately centrifuged for 0.5 h. The supernatant solution, which was now perfectly clear and free from any reddish colour, was discarded, and the precipitate washed with water that was saturated with $(NH_4)_2SO_4$. The brown residue was dissolved in 220 ml of 0.066 M phosphate buffer at pH 6.1. To this solution, which contained about 23 % $(NH_4)_2SO_4$ as determined by electrical resistance, was added 80.5 g solid $(NH_4)_2SO_4$ to give about 75 % saturation. The large amount of precipitate was sedimented by centrifuging at 3 500 *g*. The supernatant solution was strongly red coloured.

In order to diminish losses, all of the $(NH_4)_2SO_4$ precipitates were combined and subjected to repetition of the process, and the final red solution added to the main batch.

To the combined final red solutions was added 2.5 ml of 20 % TCA per 100 ml. The heavy gelatinous precipitate which appeared immediately was centrifuged, washed once with saturated $(NH_4)_2SO_4$ solution, and dissolved in 0.1 M phosphate buffer pH 7. A viscous, deeply red-coloured solution containing a large amount of 260-mμ-absorbing material was obtained. The solution was dialysed against water until free of salts, and mixed with half its volume of a settled suspension of DEAE which had been equilibrated with 0.01 M sodium acetate at pH 7. The suspension was transferred to a chromatography column and the solution allowed to pass through the ion exchanger twice. If not all of the red material was adsorbed by the ion exchanger, the column was washed with water once, and the solution allowed to pass through once again. The column was then carefully washed with water, and the cytochrome c eluted with 0.1 M ammonium acetate buffer of pH 5.4. The cyt. c could now, after dialysis against 0.01 M ammonium acetate buffer of pH 5.4, be adsorbed on a CM—W column which had been equilibrated with the same buffer. The column was washed with 4 volumes of buffer. When the buffer strength was increased to 0.033 M a red band moved slowly down the column. It contained the reduced cyt. c in a highly pure form. Finally, the oxidized cyt. c was eluted with 0.2 M buffer. The yield of cyt. c was about 100 mg. Recently Horio and Kamen [4] have introduced a new method of preparation, which gives a better yield of cytochrome c.

Preparation of the peptic peptide. Digestion: 51 mg of the cyt. c, prepared as described, was dissolved in 22 ml of water and adjusted to pH 1.55 with 0.3 N HCl. 5.9 mg of pepsin was dissolved in 0.01 N HCl and added to the cytochrome solution. The digestion was performed at 25°C for 22 h. After this, the pH was rapidly adjusted to 8.7 with 0.2 NaOH, and the solution was brought to 85 % saturation with solid $(NH_4)_2SO_4$ to precipitate the pigment. The solution was filtered to give a colourless filtrate. The precipitate was dissolved in a small quantity of ammoniacal water, and precipitated once more at about 80 % saturation of $(NH_4)_2SO_4$.

Desalting. A column of talc, 50 mm long and 15 mm in diameter, was prepared, and washed with 4 volumes of 0.05 M phosphate buffer pH 5.0. The pigment in ammoniacal water was adsorbed on the talc, and washed with 0.5 % acetic acid until no more sulphate ion could be demonstrated in the eluate on addition of $BaCl_2$. The pigment could then be completely eluted with a mixture of equal parts of acetone and 10 % ammonia solution. The coloured part of the eluate was evaporated in an evacuated desiccator over H_2SO_4 and NaOH.

Partition chromatography. 0.92 ml of the aqueous phase of a 20-hours-old mixture of butanol:acetic acid:water (4:1:5 volume ratios) was added to 2.50 g of washed and dried celite. This was suspended in the organic phase of the same mixture, and carefully packed in an 11 mm wide column. The pigment easily dissolved in 1 ml of the organic phase,

and was subsequently chromatographed on the column using the organic phase as the developing solvent. One main fraction of the coloured material travelled down the column as a sharp band, the R_F of which was calculated, as described by Martin and Synge [15], to be 0.7. This band was collected, and was found to contain 7.5 mg of material when dried in an evacuated desiccator over H_2SO_4 and NaOH.

RESULTS AND DISCUSSION

Analysis of the cytochrome c

Spectrophotometry. The absorption spectra were recorded on the reduced and oxidised fractions eluted from the CM—W column. They were found to be identical with the spectra published by Horio and Kamen [4], except for a small elevation of the 275 mμ maximum, probably caused by small amounts of protein contaminants. The differences in absorption in the range 250—290 mμ between the oxidised and reduced forms is considered to be of interest as it shows that the ratio $E_{550\ red}/E_{275\ ox}$, which was used as an index of the purity during the preparation, can only be used if the measured sample is fully oxidised.

Electrophoresis. The cyt. c preparation was concentrated on a CM—W column in a similar way as was described above. Solutions of 0.6 % concentration were dialyzed for 48 h against the buffers to be used. The electrophoresis were performed with acetate buffers at pH 5.02 and 5.32, and with phosphate buffers at pH 5.90 and 7.11. The ionic strength of the buffers was 0.1, and the pH was determined at 20°C. The cytochrome c was fully oxidised in all runs, as determined spectrophotometrically. The mobility was calculated after running times of between 2 and 3 h. A plot of the obtained mobilities indicates an isoelectric point close to pH 5.5 (Fig. 1). Horio and Kamen [4] have found the isoelectric point of the cyt. c to be 6.4. This might depend on dissimilarities of the protein configuration due to the different ways of preparation. The only certain difference in the experimental conditions is that they used buffers of ionic strength 0.2 instead of 0.1.

The electrophoresis showed that the preparations were not entirely homogeneous, but consisted of one main fraction and about 10 % impurities. The impurities were isolated, and upon examination showed an absorption maximum at 280 mμ and very little absorption in the Soret-band region. They were therefore considered to be uncoloured proteins.

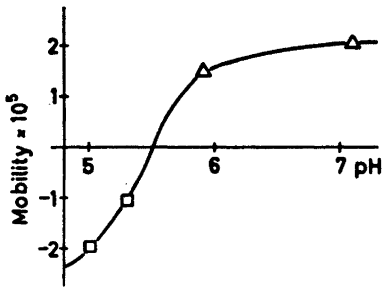

Fig. 1. Electrophoretic mobilities of oxidised cytochrome c from *R. rubrum*. △-phosphate buffers, □-acetate buffers. Ionic strength 0.1.

Analysis of the peptic hemopeptide

Spectrophotometry. The spectrum of the isolated peptide was recorded in 0.066 M phosphate buffer of pH 6.8. It showed similarities with the spectrum of the oxidised cyt. c, but there were several differences. The Soret-band had its maximum at 400 mμ whereas the 360 mμ band was seen only as a weak shoulder, obviously because of the widening of the Soret-band. Upon addition of an excess of N-acetyl-L-histidine there were several spectral changes which tended to bring the spectrum of the peptide closer to that of the cyt. c, but did not make it identical. The spectrum of the reduced N-acetyl-histidine hemochromogen was not quite identical with that of the reduced cyt. c, in contrast to what has been shown for the mammalian cyt. c peptic hemopeptide [16,17]. Another observation made in this experiment was that the molar extinction coefficient at 550 mμ was only about 50 % of that observed in other hemopeptides.

Ultracentrifugation. The Yphantis and Waugh [10] method was chosen because it required very small quantities of peptide. Different concentrations of the peptide were used. Several centrifugations were performed lasting from 1 to 5 h. Unfortunately, the peptide was not stable in these dilute solutions, but showed a decrease of extinction in the visible light region of about 10 % per 24 h upon storage at room temperature. This destruction was accelerated when the sample was introduced into the cell of the ultracentrifuge. By introducing the formula stated above, for calculating the Q value, this could be corrected for if it was postulated that the destruction took place uniformly throughout the solution being centrifuged, and that no compound of different molecular weight than the investigated peptide contributed to the extinction. The Q values thus obtained indicated a molecular weight of 2 600.

Amino acid composition. The results of the analyses are presented in Table 1. With the DNP-method, the histidine determination is very uncertain because of the formation of both α-amino-DNP-histidine and di-DNP-histidine. The same is true for the cysteine determination where only a part of it can be recov-

Table 1. Amino acid composition of the peptic hemopeptides of cytochrome c from *R. rubrum*. For details see text.

Amino acid residue	DNP-method	Stein and Moore	Number of residues
Alanine	2.06	2.10	2
Aspartic acid	0.55	0.55	0.5
Cysteine		1.28	2
Glutamic acid	0.98	0.98	1
Glycine	0.90	0.88	1
Histidine		0.94	1
Leucine	1.16	1.12	1
Lysine	3.84	2.81	3
Phenylalanine	1.09	0.97	1
Serine	1.04	1.05	1
Threonine	0.95	0.97	1
Valine	0.90	0.99	1

ered as DNP-cysteic acid and DNP-cysteine. These values are therefore omitted. The lysine determination is probably too high. This may be because the DNP-lysine spots have very low R_F values in the phosphate solvent system and therefore are probably contaminated with unhydrolyzed peptides. In the Stein and Moore analysis, the sum of the cysteine and cysteic acid gives the cysteine value and it is well known to be too low. The value of 2 residues is a minimal one and is deduced from the work of Paléus and Tuppy. Leucine cannot be distinguished from the *iso*leucine with the DNP-method but can be identified by the Stein and Moore method. Neither method makes it possible to distinguish between glutamine and glutamic acid or between asparagine and aspartic acid because they are all in the acid form after hydrolysis.

A comparison of the two methods of amino acid analysis show that they give comparable results. For the DNP-method 0.2 μmole of peptide was used whereas in the Stein and Moore analysis 0.4 μmole was required. The DNP-method may be considered easier to perform.

End group analysis. The end groups were identified as DNP-aspartic acid and di-DNP-lysine, each of which was present in only half of the amount predicted by the amount of peptide used in the experiment. The washing of the dinitrophenylated peptide made it improbable that one of them could have been present as a free impurity. It was thus concluded that the sample contained two peptides. At least one of them must be a hemopeptide, because the spectrum is that of a typical cytochrome c hemopeptide. High-voltage paper electrophoreses has failed to demonstrate the presence of any ninhydrin-positive spot other than the red-coloured hemopeptide spot. The most probable explanation therefore is that both of the peptides are hemopeptides, one having lysine as an end group, and the other having asparagine or aspartic acid as the end group, with lysine as the second residue. This is also in good accordance with the total amino acid analysis.

Paléus and Tuppy [5] established the sequence of the amino acids in the tryptic hemopeptide. The sequence CyS—Leu—Ala—CyS—His—Thr—Phe is probably included in the present hemopeptide because phenylalanine is very likely to be the C-terminal residue after digestion with pepsin. The above-mentioned authors also pointed out that due to the specific action of trypsin, the amino acid residue preceding the cysteic acid must be either lysine or arginine. As arginine was not found to be present in the peptic hemopeptides this residue must be lysine. With this in mind one can suggest the following amino acid sequence for the longer of the two hemopeptides that are assumed to be present: Asp—Lys(Ala, Glu, Gly, Lys, Ser) Lys—CyS—Leu—Ala—CyS——His—Thr—Phe. The molecular weight of this peptide, including the heme, is 2385, which is close to the value of 2 600 obtained by ultracentrifugation. The low molar extinction coefficient and the observations on the instability of the spectrum when the peptide was stored before the ultracentrifugations suggest that the hemin part of it is unusually unstable.

Acknowledgements. The author wishes to express his gratitude to Professor H. Theorell for his never-failing interest and support during this work. He also wants to thank Dr. N. Ellfolk and Doc. S. Paléus for valuable discussions and suggestions, and Dr. C. L. Woronick for reviewing the language in this manuscript.

It is a pleasure to thank Misses A.-M. Blomquist, A.-M. Fridén and G. Heimbürger for their technical assistance, and Mr. B. E. Marcussen for performing the ultracentrifugations.

REFERENCES

1. Vernon, L. P. *Arch. Biochem. Biophys.* **43** (1953) 492.
2. Vernon, L. P. and Kamen, M. D. *J. Biol. Chem.* **211** (1954) 643.
3. Kamen, M. D. and Vernon, L. P. *Biochim. et Biophys. Acta* **17** (1955) 10.
4. Horio, T. and Kamen, M. D. *Biochim. et. Biophys. Acta* **48** (1961) 266.
5. Paléus, S. and Tuppy, H. *Acta Chem. Scand.* **13** (1959) 641.
6. Hedén, C.-G. and Levin, K. *J. Biochem. Microbiol. Technol. Eng.* **1** (1959) 303.
7. Peterson, E. A. and Sober, A. *J. Am. Chem. Soc.* **78** (1955) 751.
8. Tuppy, H. and Bodo, G. *Monatsh.* **85** (1954) 1024.
9. Biserte, G., Holleman, J. W., Holleman-Dehave, J. and Santière, P. *J. Chromtography* **2** (1959) 225.
10. Yphantis, D. A. and Waugh, D. F. *J. Phys. Chem.* **60** (1956) 623.
11. Wallenfels, K. and Arens, A. *Biochem. Z.* **332** (1960) 217.
12. Levy, A. L. *Nature* **174** (1954) 126.
13. Hanes, C. S., Hird, F. J. R. and Isherwood, F. A. *Biochem. J.* **51** (1952) 25.
14. Moore, S., Spackman, D. H. and Stein, W. H. *Anal. Chem.* **30** (1958) 1185.
15. Martin, A. J. P. and Synge, R. L. M. *Biochem. J.* **35** (1941) 1358.
16. Ehrenberg, A. and Theorell, H. *Acta Chem. Scand.* **9** (1955) 1193.
17. Margoliash, E., Frohwirt, N. and Wiener, E. *Biochem. J.* **71** (1959) 559.

Received May 26, 1961.

ACTA CHEMICA SCANDINAVICA 15 (1961) 1747–17

The Crystal Structure of Lower *n*-Paraffins. I. *n*-Octane

N. NORMAN and H. MATHISEN

Central Institute for Industrial Research Blindern - Oslo, Norway

The crystal structure of *n*-octane has been determined by two-dimensional Patterson and Fourier syntheses and refined by two-dimensional difference syntheses and the method of least squares. The crystals are triclinic, space group $P\bar{1}$, with one molecule in the unit cell. The unit cell dimensions are $a = 4.16 \pm 0.02$ Å, $b = 4.75 \pm 0.02$ Å, $c = 11.00 \pm 0.02$ Å, $\alpha = 94.8 \pm 0.3°$, $\beta = 84.5 \pm 0.3°$, and $\gamma = 105.1 \pm 0.3°$. The average C–C bond length is 1.53 ± 0.01 Å, the average C– –C repeat distance along the molecular chain is 2.54 ± 0.01 Å and the average <CCC is $112.0 \pm 0.5°$. The intermolecular C– – – –C distances are all normal (*i.e.* about 4.0 Å) except for the head-to-tail $-CH_2- - - - -H_2C-$ contact, which is only 3.62 ± 0.02 Å.

Only a few X-ray investigations of the crystal structures of the lower members of the *n*-paraffin series have been reported in the literature. McLennan and Plummer [1], in their paper dating back to 1926, concluded that *n*-octane crystallizes both in the orthorhombic and the monoclinic systems, the two modifications occurring simultaneously in different proportions depending on the freezing conditions. In 1930 Müller [2] found that crystals of *n*-octane exist in what he called "the second form", the long spacing of this form being somewhat shorter than that of "the first form", which is identical with the usual orthorhombic modification where the molecular chains are normal to the basal plane. Both these investigations were made on powder samples.

In 1948 Müller and Lonsdale [3] published the unit cell parameters for the triclinic modification of *n*-$C_{18}H_{38}$. In their paper it is stated that this low-temperature modification is iso-structural with that of other even *n*-paraffins from *n*-$C_{22}H_{46}$ down to *n*-C_6H_{14}.

It seems that below *n*-$C_{18}H_{38}$ no single crystal X-ray work has been reported. It was therefore decided to study the crystal structures of some of these compounds, the particular range chosen being *n*-octane, *n*-heptane, *n*-hexane, and *n*-pentane. The work reported here forms a part of this programme [4,5].

EXPERIMENTAL

The *n*-octane sample used was supplied by the Chemical Research Laboratory, Teddington, Middlesex, England. Its purity as quoted by the manufacturer was 99.63 ± 0.18 %. The single crystals were grown in sealed capillaries of Lindeman glass mounted on the head of a Nonius Weissenberg camera equipped for low-temperature work. The inner diameter of the capillaries used was approximately 0.2 mm. The desired lowering of the temperature was obtained by passing compressed gaseous nitrogen through copper spiral tubes immersed in liquid nitrogen and further through a Dewar tube mounted along the centre line of the Weissenberg camera.

Oscillation and equi-inclination Weissenberg diagrams of zero, first, second, and third layer lines were obtained with rotation about the *a*-axis. Unfiltered Cu-radiation and multiple film technique were used.

The same cooling arrangements as described above was also used in connection with a 14.38 mm Debye-Scherrer camera. By freezing the liquid *n*-octane rapidly, a sample consisting of partly oriented needles was obtained, giving a Debye-Scherrer diagram which was dominated by coarse arcs of the (0*kl*) powder lines. Much smoother lines were obtained by dividing the total exposure time of 2 h into intervals of about 10 min, the sample being melted and refrozen between each interval. During all exposures the crystals were kept at a temperature of about 20 – 25°C below the melting point of −56.5°C.

The Weissenberg reflections were indexed in the usual way, and the blackening measured by a Jarrel-Ash-Microphotometer and converted to relative intensities. The intensities were corrected for the Lorentz-Polarization factor. The necessary correlation of intensities of reflections on different layer lines was performed by the method described by Hägg [6].

CRYSTAL DATA

The *a*-axis was determined from an oscillation diagram about this axis. The three reciprocal parameters b^*, c^*, and a^* were determined by a least squares adjustment to the observed positions of 19 different (0*kl*) reflections which could be indexed on the above-mentioned Debye-Scherrer diagram. The two remaining parameters, the reciprocal angles β^* and γ^*, were determined by observing the displacements of the (1*kl*), (2*kl*), and (3*kl*) reciprocal nets relative to the (0*kl*) net. All reciprocal parameters was refined by means of the powder method, including now reflections with $h = 0$. The crystal data are the following

$a = 4.16 \pm 0.02$ Å	$\alpha = 94.8 \pm 0.3°$
$b = 4.75 \pm 0.02$ »	$\beta = 84.5 \pm 0.3°$
$c = 11.00 \pm 0.02$ »	$\gamma = 105.1 \pm 0.3°$

Crystal system: Triclinic
Space group: $P\bar{1}$
Volume of the unit cell: 215 Å^3
Measured density (of the liquid at + 20°C) 0.7036 g/cm^3
Calculated density (of the crystal at about −70°C): 0.858 g/cm^3

The (yz)-projection. The (*yz*)-projection of the structure was solved by the two-dimensional Patterson synthesis, $P(v,w)$, shown in Fig. 1. The molecule as such is in a special position, *i.e.* a centre of symmetry. The direction of the molecular axis is determined by the position of the Patterson peak at about 2.5 Å (the $C_1 - - C_3$ repeat distance along the molecular chain), and the correct orientation of the molecule about its axis is determined by the positions and the relative heights of the two peaks at about 1.5 Å. (The multiplicities of the distances $C_1 - C_2$ and $C_2 - C_3$ are 4 and 3, respectively.)

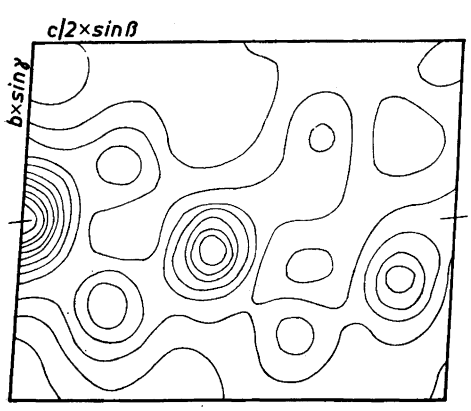

Fig. 1. Patterson projection along the *a*-axis of *n*-octane. Contours are at equal, arbitrary intervals.

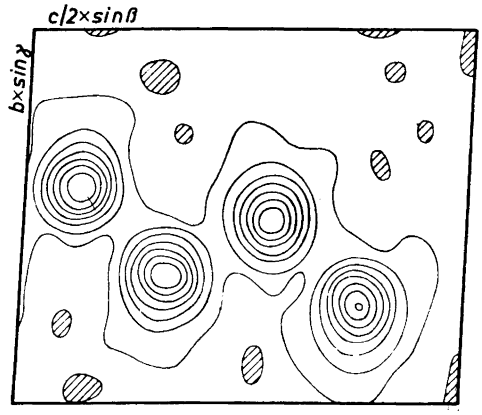

Fig. 2. The final (*yz*) electron density projection of *n*-octane. Contours are at intervals of 1 e/Å², negative areas shaded.

The projection was refined through several Fourier and difference syntheses and finally by the method of least squares. The final projection of the electron density is shown in Fig. 2. In Fig. 3 the contributions from the carbon atoms have been subtracted.

As the plane of the molecule is nearly normal to the projection axis, the two hydrogens belonging to the same CH_2-group overlap to a large extent. Such pairs of overlapping hydrogens were therefore in the refinements of this projection treated as one atom with scattering power twice that of hydrogen. In the least squares refinement the carbon atoms were treated as isotropic. The hydrogens were all given a *B*-value of 2.6.

As expected, the final *B*-values for the carbon atoms show a pronounced increase towards the ends of the molecule. The *R*-factor for the 90 observed (0*kl*)-reflections is 0.07. (The total number of theoretically observable (0*kl*)-reflections is 129.)

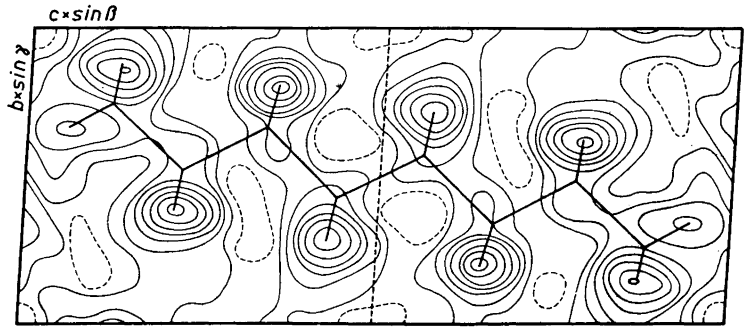

Fig. 3. ($F_o - F_{carbon}$)-map for the (*yz*)-projection of *n*-octane. Contours are at intervals of 0.2 e/Å², zero contour broken.

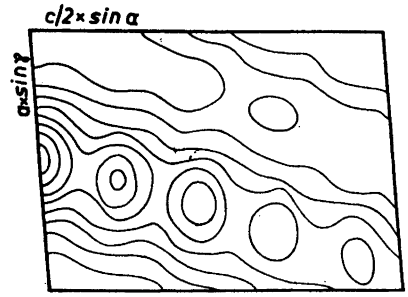

Fig. 4. Patterson projection along the *b*-axis of *n*-octane. Contours are at equal arbitrary intervals.

The two strongest reflections, $(01\bar{1})$ and (010), are considerably weakened by extinction. However, as the amplitudes of those two reflections are rather unsensitive to small changes in the atomic coordinates, their calculated values could quite safely be included in the electron density calculations. The same reflections were throughout excluded from the difference syntheses and the least squares refinements. In the *(xz)*-projection the reflections $(10\bar{1})$ and (100) for similar reasons were treated in the same way.

The (xz)-projection. The (*h*0*l*)-reflections needed for the refinement of this projection were selected from the (0*kl*), (1*kl*), (2*kl*), and (3*kl*) data.

Assuming C—C bond lengths of 1.54 Å and C—C—C bond angles of about 110° preliminary *x*-coordinates of the carbon atoms were evaluated. Practically the same values were obtained from the $P(u,w)$ Patterson projection, Fig. 4. The final electron density projection is shown in Fig. 5. As one would expect the carbon atoms show rather pronounced anisotropy in this projection. This anisotropy obviously had to be taken into account. This was effected by modifying the atomic scattering factor by the exponential factor

$$\exp\ (-u_i h^2 - v_i hl - w_i l^2)$$

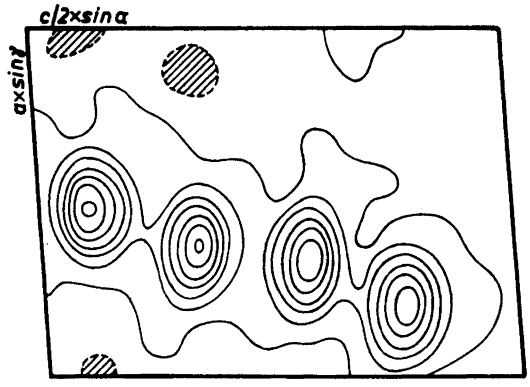

Fig. 5. The final (*xz*) electron density projection of *n*-octane. Contours are at intervals of 1 e/Å², negative areas shaded.

Table 1. Fractional atomic coordinates and temperature factor parameters for *n*-octane.

	x	y	z	$B(yz)$	$B(xz)$ *	u_{xz}	v_{xz}	w_{xz}
C_1	0.3037	0.2447	0.3811	3.22	3.35	0.0982	0.0107	0.0040
C_2	0.1715	0.0161	0.2777	2.82	2.87	0.0937	0.0174	0.0037
C_3	0.1417	0.1585	0.1620	2.78	3.09	0.0834	0.0104	0.0040
C_4	0.0176	−0.0699	0.0576	2.68	2.85	0.0803	0.0104	0.0036
H_1	0.325	0.150	0.449					
H_2	0.550	0.380	0.360					
H_3	0.117	0.379	0.390					
H_4	0.390	−0.126	0.267					
H_5	−0.083	−0.120	0.297					
H_6	0.387	0.293	0.140					
H_7	−0.033	0.295	0.166					
H_8	0.242	−0.223	0.050					
H_9	−0.235	−0.191	0.075					

* A "best fit" isotropic B-values.

The parameters u_i, v_i, and w_i are different for the different carbon atoms. They are included in the least squares refinement programme. The approximate positions of the hydrogens were determined from a difference synthesis where

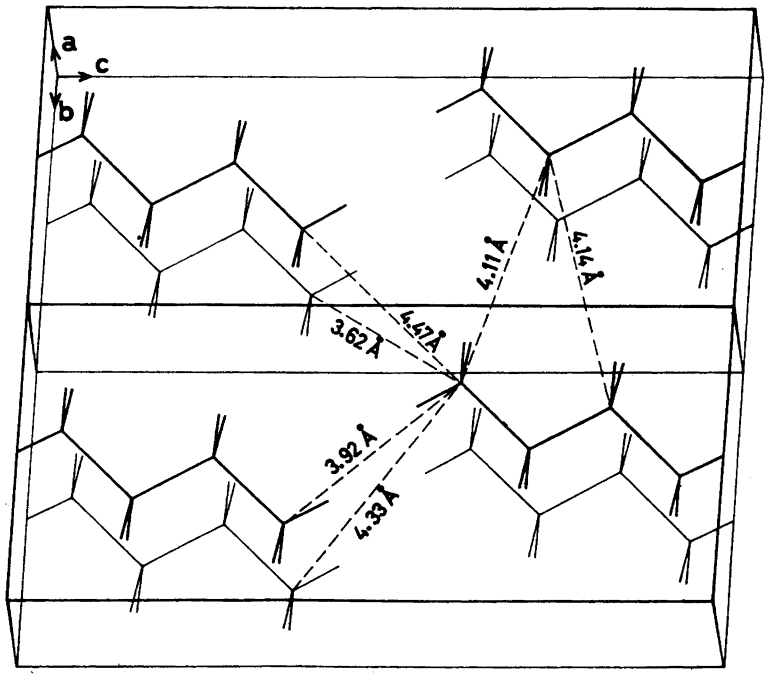

Fig. 6. A schematic drawing showing how the *n*-octane molecules pack in the crystal. Some of the shortest intermolecular carbon-carbon distances are indicated.

Table 2. Comparison of observed and calculated structure factors for the (0*kl*)- and (*h*0*l*)-zones of *n*-octane.

hkl	F_o	F_c	*hkl*	F_o	F_c	*hkl*	F_o	F_c
001	3.7	6.8	$02\bar{2}$	1.4	− 1.2	044	—	0.3
002	5.8	− 6.3	$02\bar{1}$	5.2	4.9	045	—	− 0.2
003	5.9	6.1	020	1.3	− 1.3	046	—	− 0.2
004	6.6	− 6.5	021	2.4	2.5	047	1.7	1.8
005	—	0.1	022	3.7	− 3.5	048	2.5	2.3
006	1.7	− 1.7	023	7.3	6.9	049	0.8	− 0.8
007	1.6	1.4	024	15.0	15.2	$05\bar{8}$	—	0.5
008	—	− 0.3	025	1.7	− 1.5	$05\bar{7}$	0.7	− 0.9
009	9.2	− 9.8	026	—	− 0.2	$05\bar{6}$	—	0.1
00,10	2.6	− 2.6	027	1.6	0.8	$05\bar{5}$	—	− 0.5
00,11	1.6	1.4	028	4.6	− 4.1	$05\bar{4}$	0.6	0.6
00,12	1.3	− 1.1	029	1.4	− 1.2	$05\bar{3}$	1.0	− 0.8
00,13	1.4	1.1	02,10	—	− 0.1	$05\bar{2}$	4.4	− 5.3
00,14	0.7	0.6	02,11	—	0.5	$05\bar{1}$	1.1	− 1.1
$01,\bar{1}4$	2.5	2.8	02,12	1.1	− 1.1	050	0.8	1.0
$01,\bar{1}3$	—	0.3	$03,\bar{1}2$	—	0.2	051	0.8	− 0.9
$01,\bar{1}2$	0.8	− 0.7	$03,\bar{1}1$	—	0.2	052	1.6	1.5
$01,\bar{1}1$	1.5	1.4	$03,\bar{1}0$	2.3	2.1	053	1.0	0.9
$01,\bar{1}0$	4.8	− 4.6	$03\bar{9}$	0.7	− 0.7	054	—	0.1
$01\bar{9}$	3.9	− 3.8	$03\bar{8}$	—	0.3	055	—	− 0.2
$01\bar{8}$	—	0.3	$03\bar{7}$	0.7	0.6	056	—	0.1
$01\bar{7}$	0.8	0.6	$03\bar{6}$	7.6	− 7.5	$10,\bar{1}3$	—	− 0.8
$01\bar{6}$	1.6	− 1.4	$03\bar{5}$	3.6	− 3.6	$10,\bar{1}2$	—	0.4
$01\bar{5}$	16.8	−16.1	$03\bar{4}$	1.3	1.4	$10,\bar{1}1$	—	—
$01\bar{4}$	6.0	− 5.7	$03\bar{3}$	—	− 0.7	$10,\bar{1}0$	5.5	− 7.0
$01\bar{3}$	7.4	7.6	$03\bar{2}$	—	0.0	$10\bar{9}$	2.9	− 2.6
$01\bar{2}$	10.6	−10.6	$03\bar{1}$	3.4	− 3.6	$10\bar{8}$	—	1.2
$01\bar{1}$	17.3	22.9	030	—	0.3	$10\bar{7}$	—	− 0.7
010	17.9	24.3	031	1.6	0.9	$10\bar{6}$	—	0.2
011	4.1	− 4.3	032	1.4	− 1.7	$10\bar{5}$	3.4	− 4.3
012	1.3	1.2	033	8.6	8.8	$10\bar{4}$	—	0.6
013	1.2	− 1.2	034	5.1	5.1	$10\bar{3}$	—	1.0
014	16.3	15.6	035	1.7	− 1.8	$10\bar{2}$	3.5	− 4.2
015	5.7	5.4	036	0.9	0.8	$10\bar{1}$	V.V.S.	31.9
016	3.7	− 3.6	037	—	− 0.4	100	V.S.	15.4
017	3.7	3.6	038	0.9	0.7	101	6.6	− 7.3
018	5.5	− 5.5	039	—	0.2	102	3.6	4.0
019	7.4	− 7.3	03,10	—	− 0.5	103	2.5	− 2.9
01,10	0.8	0.5	03,11	0.8	0.6	104	4.5	4.3
01,11	—	0.1	$04,\bar{1}0$	1.9	1.9	105	1.0	− 1.0
01,12	—	− 0.2	$04\bar{9}$	0.9	− 1.2	106	—	− 0.5
01,13	1.0	− 1.1	$04\bar{8}$	1.0	1.1	107	2.8	2.7
$02,\bar{1}3$	0.7	− 0.7	$04\bar{7}$	1.6	− 1.7	108	12.1	−11.6
$02,\bar{1}2$	—	0.6	$04\bar{6}$	3.6	− 4.0	109	7.8	− 7.5
$02,\bar{1}1$	—	− 0.3	$04\bar{5}$	—	− 0.2	10,10	2.9	2.7
$02,\bar{1}0$	1.4	− 1.3	$04\bar{4}$	—	0.2	10,11	1.4	− 1.3
$02\bar{9}$	—	0.1	$04\bar{3}$	—	0.5	10,12	—	0.3
$02\bar{8}$	1.1	− 1.0	$04\bar{2}$	3.3	− 3.6	10,13	0.9	0.6
$02\bar{7}$	2.5	2.2	$04\bar{1}$	3.4	− 3.8	10,14	—	0.1
$02\bar{6}$	7.0	− 6.7	040	1.4	1.7	$20,\bar{1}2$	0.6	0.6
$02\bar{5}$	12.0	−12.0	041	1.1	− 1.2	$20,\bar{1}1$	3.0	− 3.2
$02\bar{4}$	2.0	2.1	042	1.5	1.3	$20,\bar{1}0$	2.8	− 2.7
$02\bar{3}$	—	− 0.4	043	5.1	5.5	$20\bar{9}$	—	0.4

hkl	F_o	F_c	*hkl*	F_o	F_c	*hkl*	F_o	F_c
$20\bar{8}$	—	− 0.2	207	5.6	− 5.5	$30\bar{2}$	5.7	5.6
$20\bar{7}$	—	0.1	208	8.4	− 8.1	$30\bar{1}$	—	0.4
$20\bar{6}$	2.4	− 2.0	209	1.1	1.1	300	—	0.1
$20\bar{5}$	1.0	− 1.2	20,10	—	0.1	301	—	− 0.1
$20\bar{4}$	1.5	1.3	20,11	—	− 0.5	302	0.9	1.6
$20\bar{3}$	3.1	− 2.5	20,12	—	− 0.2	303	1.7	2.0
$20\bar{2}$	7.9	7.3	20,13	0.6	− 0.4	304	1.2	− 1.3
$20\bar{1}$	7.7	9.1	$30,\bar{1}0$	—	− 0.1	305	1.1	1.2
200	1.9	− 2.0	$30\bar{9}$	—	− 0.1	306	1.2	− 1.5
201	0.9	1.0	$30\bar{8}$	—	0.1	307	4.8	− 5.9
202	0.7	− 0.9	$30\bar{7}$	1.7	− 1.7	308	1.3	− 0.9
203	2.7	2.6	$30\bar{6}$	1.6	− 1.7	309	0.7	0 7
204	1.5	1.2	$30\bar{5}$	1.1	1.1	30,10	0.5	− 0.4
205	2.0	− 1.6	$30\bar{4}$	1.3	− 1.1	30,11	0.7	− 0.7
206	2.7	2.6	$30\bar{3}$	2.3	2.0	30,12	1.1	− 1.0

the carbon atoms had been subtracted. In this projection a uniform isotropic temperature factor of 2.4 was used for the hydrogen atoms.

The final R factor was 0.08 for the 62 ($h0l$)-reflections included in the least squares refinement. (The total number of theoretically observable ($00l$), ($10l$), ($20l$), and ($30l$) reflections is 92.) The final coordinates and temperature factors for the 4 carbon and 9 hydrogen atoms in the asymmetric unit are given in Table 1. In Table 2 are listed the observed and calculated structure factors.

Table 3. Interatomic distances and bond angles of *n*-octane.

Distances

C_1-C_2 = 1.542 Å	C_1-H_1 = 0.93 Å
C_2-C_3 = 1.519 »	C_1-H_2 = 1.07 »
C_3-C_4 = 1.542 »	C_1-H_3 = 1.12 »
C_4-C_5 = 1.514 »	C_2-H_4 = 1.26 »
	C_2-H_5 = 1.10 »
C_1-C_3 = 2.535 »	C_3-H_6 = 1.07 »
C_2-C_4 = 2.536 »	C_3-H_7 = 1.09 »
C_3-C_5 = 2.538 »	C_4-H_8 = 1.32 »
	C_4-H_9 = 1.07 »

Angles

$C_1-C_2-C_3$ = 111.8°	$H_1-C_1-H_2$ = 104°
$C_2-C_3-C_4$ = 111.9°	$H_1-C_1-H_3$ = 118°
$C_3-C_4-C_5$ = 112.3°	$H_2-C_1-H_1$ = 110°
$C_2-C_1\ldots C_1'$ = 173.8°	$H_4-C_3-H_5$ = 113°
	$H_6-C_3-H_7$ = 108°
	$H_8-C_4-H_9$ = 115°

Mean values

The C−C bond length	1.53 ± 0.01 Å
The C−H bond length	1.11 ± 0.10 Å
The C−C−C bond angle	112.0° ± 0.5°
The repeat distance along the molecular chain	2.54 ± 0.01 Å
The H−C−H bond angle	111° ± 5°

DISCUSSION

The interatomic distances and bond angles of the *n*-octane structure are given in Table 3. The standard deviations were calculated by use of Cruickshanks formulæ. Because of the uncertainties in cell dimensions, however, the uncertainties in bond lengths and bond angles are probably somewhat greater than indicated by these formulæ. The deviations given in Table 3 should therefore be regarded as total estimates of the uncertainties in the distances and angles given.

The *n*-octane molecules pack in the extended *trans* configuration, *i.e.* the molecules are planar. The packing is schematically visualized in Fig. 6, where some of the shortest distances between carbon atoms of different molecules are indicated. The order of magnitude of most of these distances shows good agreement with the van der Waals' radius of 2.0 $\pm$ 0.1 Å usually found for CH_2— or CH_3— groups. The rather close approach of 3.62 Å between the terminal CH_3-groups across the center of symmetry at (1/2, 1/2, 1/2) is very surprising in view of the results of Rushworth's [8] NMR investigation of *n*-pentane and *n*-hexane, which seem to indicate that the end methyl groups are freely rotating. A reinvestigation of this point will be undertaken in this laboratory.

Acknowledgement. The research reported in this document has been made possible through the support and sponsorship of the *US Department of Army*, through its European Research Office. Our thanks are also due to Mrs. L. Bryn and Mrs. T. L. Rolfsen for their help in carrying out the intensity measurement and some of the calculations, and to other members of the staff for many valuable discussions.

REFERENCES

1. McLennan, J. C. and Plummer, W. G. *Trans. Roy. Soc. Can.* **III 21** (1926) 99.
2. Müller, A. *Proc. Roy. Soc. (London)* **A 127** (1930) 417.
3. Müller, A. and Lonsdale, K. *Acta Cryst.* **1** (1948) 129.
4. Norman, N. and Mathisen, H. *The Structure of Linear Polymers. Lower* n-*Hydrocarbons*, July 1959, Final Technical Report, Contract No. DA-91-508-EUC-377.
5. Norman, N. and Mathisen, H. *The Structure of Linear Polymers. Lower* n-*Hydrocarbons*, October 1960, Final Technical Report, Contract No. DA-91-591-EUC-1166.
6. Hägg, G. *Bestämning av* /F/ *ur Weissenbergfotogram*, Uppsala 1948.
7. Cruickshank, D. W. J. *Acta Cryst.* **2** (1949) 65.
8. Rushworth, F. A. *Proc. Roy. Soc. (London)* **A 222** (1954) 526.

Received May 18, 1961.

ACTA CHEMICA SCANDINAVICA 15 (1961) 1755–1760

The Crystal Structure of Lower *n*-Paraffins. II. *n*-Hexane

N. NORMAN and H. MATHISEN

Central Institute for Industrial Research Blindern - Oslo, Norway

The crystal structure of *n*-hexane has been determined by two-dimensional ordinary and generalized Patterson syntheses and refined by ordinary and generalized Fourier projections and the method of least squares. The crystals are triclinic, space group $P\bar{1}$, with one molecule in the unit cell. The unit cell dimensions are $a = 4.17 \pm 0.02$ Å, $b = 4.70 \pm 0.02$ Å, $c = 8.57 \pm 0.02$ Å, $\alpha = 96.6 \pm 0.3°$, $\beta = 87.2 \pm 0.3°$, and $\gamma = 105.0 \pm 0.3°$. The average C—C bond length is 1.53 ± 0.01 Å, the average C- - -C repeat distance along the chain of the molecule is 2.56 ± 0.01 Å, and the average <CCC is $113.9 \pm 0.5°$. The intermolecular C- - - -C distances are all normal (*i.e.* about 4.0 Å) except for the head-to-tail $-CH_3$- - - - H_3C- contact, which is only 3.62 ± 0.02 Å.

The work reported herein forms the second part of a series of papers concerning the crystal structures of lower *n*-paraffins, the first part being our paper on *n*-octane [1].

EXPERIMENTAL

The experimental techniques used for the study of *n*-hexane were the same as described earlier [1]. In this case equi-inclination Weissenberg diagrams of zero and second layer lines were obtained with rotation about the *a*-axis.

CRYSTAL DATA

The unit cell dimensions were determined in the same way as described in the previous article [1]. The crystal data are the following

$a = 4.17 \pm 0.02$ Å	$\alpha = 96.6 \pm 0.3°$
$b = 4.70 \pm 0.02$ »	$\beta = 87.2 \pm 0.3°$
$c = 8.57 \pm 0.02$ »	$\gamma = 105.0 \pm 0.3°$

Crystal system: Triclinic
Space group: $P\bar{1}$
Volume of the unit cell: 161 Å^3
Measured density (of the liquid at + 20°C) = 0.6603 g/cm^3
Calculated density (of the crystal at about −115°C) = 0.888 g/cm^3

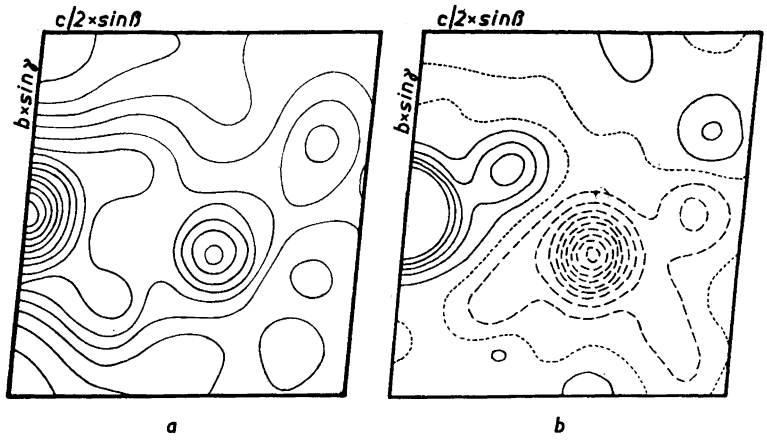

Fig. 1a. The $P_o(vw)$ ordinary Patterson projection along the *a*-axis of *n*-hexane. Contours are at equal arbitrary intervals.

Fig. 1b. The real part, $C_s(vw)$, of the $P_s(vw)$ generalized Patterson projection along the *a*-axis of *n*-hexane. Contours are at equal, arbitrary intervals zero contour dotted, negative contours broken.

The (yz)-projection. The structure was solved in this projection by means of the Patterson synthesis shown in Fig. 1a. The projection was refined through several Fourier and difference syntheses and finally by the method of least squares. The final projection of the electron density is shown in Fig. 2.

In the least squares refinements of this projection, the three pairs of overlapping hydrogens were treated as single atoms with scattering power twice that of hydrogen. Initial hydrogen coordinates were obtained from a Fourier synthesis from which the carbon atoms had been subtracted. The hydrogens were assigned a uniform, isotropic temperature factor, B, of 2.4, in accordance with the overall value as determined by Wilson's method. The carbon atoms were treated as isotropic. Three of the strongest reflections, (001), (01$\bar{1}$) and

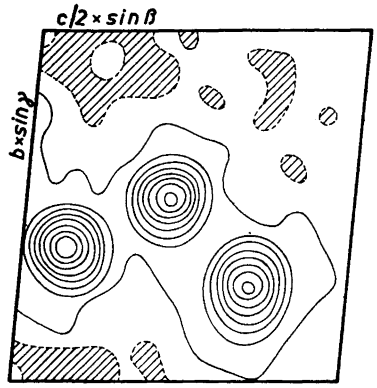

Fig. 2. The final (*yz*) electron density projection of *n*-hexane. Contours are at intervals of 1 e/Å^2 negative areas shaded.

Table 1. Comparison of observed and calculated (0*kl*) structure factors for *n*-hexane.

0*kl*	F_o	F_c	0*kl*	F_o	F_c	0*kl*	F_o	F_c
001	4.6	6.0	015	3.7	3.7	03— 1	2.9	— 2.9
2	5.9	6.4	6	5.4	— 5.3	1	1.2	1.4
3	6.3	6.7	7	5.7	— 5.9	2	7.5	— 7.3
4	0.8	— 0.9	10	0.6	0.8	3	4.4	— 4.1
5	1.6	1.7	02—10	0.8	0.5	4	1.4	1.2
6	1.1	— 1.2	— 9	1.0	— 0.3	8	1.1	— 0.4
7	7.2	— 7.9	— 8	1.0	— 0.9	04— 8	1.7	1.8
8	2.2	— 2.4	— 6	1.7	— 1.5	— 7	1.0	— 1.1
9	1.5	1.2	— 5	16.0	5.4	— 6	1.6	1.6
10	1.3	— 1.3	— 4	10.0	9.5	— 5	3.3	3.1
01—11	1.9	— 2.5	— 3	1.0	— 1.2	— 2	2.7	— 2.7
—10	1.1	— 0.7	— 2	0.9	— 0.7	— 1	3.1	— 3.2
— 9	1.2	1.0	— 1	4.4	4.6	0	1.3	1.5
— 8	3.9	— 3.8	0	1.6	— 1.4	1	1.7	— 1.5
— 7	3.0	— 2.8	1	3.1	3.1	2	4.3	— 4.3
— 5	1.4	1.4	2	6.4	— 5.9	3	0.7	— 0.5
— 4	11.9	12.3	3	12.2	—12.1	5	1.3	1.3
— 3	6.4	6.2	4	0.9	0.9	6	1.8	1.9
— 2	8.7	— 9.1	6	4.0	— 3.6	05— 6	0.6	1.0
— 1	11.0	17.3	7	1.0	— 0.9	— 3	1.1	— 0.9
0	10.0	18.6	9	1.1	1.0	— 2	3.8	— 4.1
1	2.8	— 2.8	03— 8	1.9	1.8	— 1	1.1	— 1.1
2	1.0	0.9	— 5	6.1	5.9	0	0.8	0.8
3	11.8	—11.9	— 4	3.2	3.0	1	1.5	— 1.6
4	5.0	— 4.8	— 3	0.8	— 0.8	2	0.8	— 0.7

(010), were left out because they were obviously strongly influenced by extinction.

The observed and calculated structure factors are compared in Table 1. The final agreement factor for the 75 observed (0*kl*)-reflections included in the least squares refinements is 0.064. (The total number of theoretically observable (0*kl*)-reflections is 104.)

The x-coordinates. Because the crystals always grew along the shortest axis, the *a*-axis, one was restricted to one single rotation axis for the exposures. In this case it was decided to use the method of generalized projections. This method has been developed and described by several authors, notably by Clews and Cochran [2], Dyer [3], and Cochran and Dyer [4], and later by Rumanova [5]. For details of calculation and interpretation reference should be made to one or more of these papers. The generalized Patterson projection along the *a*-axis may be expressed as

$$P_H(vw) = C_H(vw) + iS_H(vw) \tag{1}$$

where

$$C_H(vw) = \frac{a}{V} \sum_k \sum_l |F(Hkl)|^2 \cos 2\pi (kv + lw) \tag{2}$$

and

$$S_H(vw) = \frac{a}{V} \sum_k \sum_l |F(Hkl)|^2 \sin 2x (kv + lw) \tag{3}$$

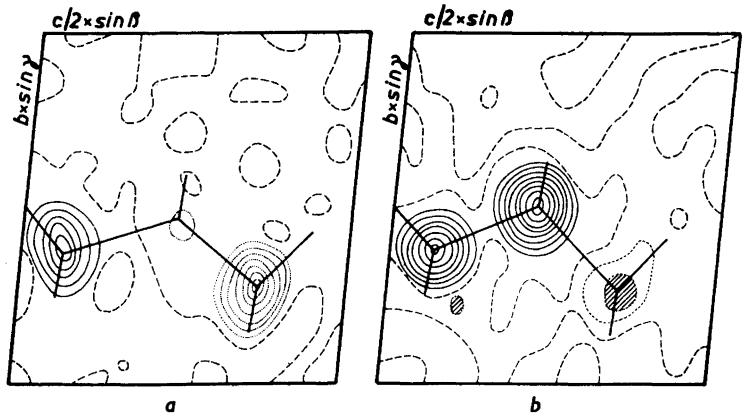

Fig. 3. a) The imaginary part, $S_2(yz)$, of the $\varrho_2(yz)$ generalized electron density projection along the a-axis of n-hexane. Contours are at equal, arbitrary intervals.
b) The real part, $C_2(yz)$, of the $\varrho_2(yz)$ generalized electron density projection along the a-axis of n-hexane. Contours are at the same intervals as in a).

where H is a whole, positive number. In the present case it was 2. Corresponding expressions apply for the generalized electron density projection of centrosymmetrical structures. By eqn. (2) a map can be calculated from which the u-coordinates of the Patterson peaks can be determined by comparing the peak heights of this map to the corresponding peak heights of the ordinary Patterson projection, provided that the two sets of data which are involved, the $|F(0kl)|^2$,s and $|F(2kl)|^2$'s, are on the same scale. Another method is to compare the heights of corresponding peaks on maps calculated according to eqns. (2) and (3). In this case no scaling is involved.

In the present case the first method was employed. The $C_2(vw)$-synthesis for n-hexane is shown in Fig. 1b. From this map and that of Fig. 1a approximate x-coordinates could be evaluated for the three carbon atoms in the asymmetric unit. Based on these coordinates generalized electron density projections were calculated. From these projections refined values for the x-coordinates were obtained, changing the signs of a few of the weak $(2kl)$-reflections. The refined generalized electron density projections are shown in Fig. 3.

Table 2. Fractional atomic coordinates and temperature parameters for n-hexane.

	x	y	z	$B(yz)$
C_1	0.2795	0.2322	0.3482	2.95
C_2	0.1366	−0.0065	0.2153	2.62
C_3	0.0723	0.1180	0.0664	2.35
H_1		0.146	0.428	
(H_2,H_3)		0.356	0.335	
(H_4,H_5)		−0.131	0.223	
(H_6,H_7)		0.248	0.057	

Table 3. Relative $F_o(2kl)$-values with calculated signs.

$2kl$	F_o	Sign	$2kl$	F_o	Sign
$2\bar{6}1$	5.7	−	$20\bar{9}$	14.6	−
$2\bar{5}3$	8.1	−	$20\bar{8}$	14.0	−
$2\bar{5}0$	10.2	−	$20\bar{5}$	13.7	+
$2\bar{5}1$	9.8	−	$20\bar{4}$	7.9	+
$2\bar{5}4$	5.8	+	$20\bar{3}$	16.1	−
$2\bar{5}7$	5.1	+	$20\bar{2}$	46.4	+
$2\bar{4}4$	10.3	−	$20\bar{1}$	45.8	+
$2\bar{4}3$	15.6	−	200	8.6	−
$2\bar{4}0$	9.3	−	201	3.5	+
$2\bar{4}3$	9.2	+	202	11.8	−
$2\bar{4}4$	17.8	+	203	8.3	−
$2\bar{4}7$	8.3	+	204	10.3	+
$2\bar{3}7$	7.3	−	205	21.1	−
$2\bar{3}4$	22.9	−	206	28.9	−
$2\bar{3}3$	10.7	−	$21\bar{9}$	9.6	−
$2\bar{3}2$	3.9	+	$21\bar{6}$	15.1	+
$2\bar{3}0$	15.3	+	$21\bar{5}$	27.9	+
$2\bar{3}3$	29.4	+	$21\bar{4}$	12.2	−
$2\bar{3}4$	16.8	+	$21\bar{2}$	44.9	+
$2\bar{3}5$	5.7	−	$21\bar{1}$	13.3	+
$2\bar{3}9$	3.9	+	211	13.0	−
$2\bar{2}8$	12.8	−	212	37.7	−
$2\bar{2}7$	11.2	−	213	5.8	+
$2\bar{2}6$	8.7	+	215	28.5	−
$2\bar{2}5$	10.5	−	216	7.4	−
$2\bar{2}4$	16.6	−	219	13.3	+
$2\bar{2}2$	3.2	−	$22\bar{6}$	27.7	+
$2\bar{2}1$	32.5	+	$22\bar{5}$	16.1	+
$2\bar{2}0$	28.8	+	$22\bar{4}$	8.1	−
$2\bar{2}1$	14.9	−	$22\bar{3}$	10.1	+
$2\bar{2}2$	14.3	+	$22\bar{2}$	8.6	+
$2\bar{2}3$	32.2	+	220	4.4	+
$2\bar{2}4$	4.1	+	221	36.5	−
$2\bar{2}5$	4.5	−	222	24.2	−
$2\bar{2}6$	6.9	−	223	10.1	+
$2\bar{2}7$	10.6	−	224	8.2	−
$2\bar{2}8$	5.0	+	228	15.3	+
$2\bar{2}9$	3.5	−	$23\bar{8}$	4.7	−
$2\bar{2}10$	13.0	−	$23\bar{7}$	8.4	+
$2\bar{1}9$	6.1	−	$23\bar{6}$	18.1	+
$2\bar{1}8$	21.2	−	$23\bar{3}$	9.1	−
$2\bar{1}5$	9.4	−	$23\bar{2}$	12.6	−
$2\bar{1}3$	8.9	−	$23\bar{1}$	8.4	+
$2\bar{1}2$	11.0	+	230	9.7	−
$2\bar{1}1$	55.0	+	231	28.7	−
$2\bar{1}1$	6.7	−	235	9.3	+
$2\bar{1}2$	20.0	+	237	4.0	+
$2\bar{1}3$	19.7	+	$24\bar{4}$	5.7	−
$2\bar{1}4$	3.0	+	$24\bar{3}$	19.9	−
$2\bar{1}5$	3.5	−	$24\bar{2}$	6.9	−
$2\bar{1}6$	26.5	−	$24\bar{1}$	3.6	+
$2\bar{1}7$	8.4	−	240	12.2	−
$2\bar{1}8$	6.9	+	241	8.8	−
$2\bar{1}9$	10.3	−	244	14.5	+
$2\bar{1}10$	6.9	−			

Table 4. Interatomic distances and bond angles of *n*-hexane.

C—C distances		*C—H distances in the* (yz-)*plane*	
C_1-C_2	= 1.530 Å	C_1-H_1	= 0.82 Å
C_2-C_3	= 1.526 »	$C_1-(H_2,H_3)$	= 0.58 »
C_3-C_4	= 1.524 »	$C_2-(H_4,H_5)$	= 0.58 »
		$C_3-(H_6,H_7)$	= 0.60 »
C_1-C_3	= 2.557 »		
C_2-C_4	= 2.559 »		

$C_1 \cdots C_1'$ = 3.62 Å (across the centre of symmetry at (1/2, 1/2, 1/2))

Angles

$C_1-C_2-C_3$ = 113.6°
$C_2-C_3-C_4$ = 114.1°
$C_2-C_1 \cdots C_1'$ = 172°

Mean values

The C—C bond length	1.53 ± 0.01 Å
The C—C—C bond angle	114 ± 1°
The repeat distance along the molecular chain	2.56 ± 0.01 Å

The final fractional atomic coordinates are given in Table 2. The observed $F(2kl)$-values and their calculated signs are listed in Table 3.

DISCUSSION

The calculated interatomic distances and bond angles are given in Table 4. The deviations quoted in the table is to be regarded as total estimates of the uncertainties in the distances and bond angles given. The *n*-hexane molecules pack in the extended *trans* configuration, *i.e.* the molecules are planar. The order of magnitude of most of the intermolecular C— — —C distances shows good agreement with the van der Waals' radius of 2.0 ± 0.1 Å usually found for CH_2- or CH_3-groups. The only exception is the rather close approach of 3.62 ± 0.02 Å between the terminal CH_3-groups across the centre of symmetry at (1/2, 1/2, 1/2). This is, however, in excellent agreement with what was found for *n*-octane [1]. The agreement in bond lengths and bond angles is also fairly good.

Acknowledgement. The research reported in this document has been made possible through the support and sponsorship of the *US Department of Army*, through its European Research Office. Our thanks are also due to Mrs. L. Bryn and Mrs. T. L. Rolfsen for their help in carrying out the intensity measurement and some of the calculations, and to other members of the staff for many valuable discussions.

REFERENCES

1. Norman, N. and Mathisen, H. *Acta Chem. Scand.* **15** (1961) 1747.
2. Clews, C. J. B. and Cochran, W. *Acta Cryst.* **2** (1949) 46.
3. Dyer, H. B. *Acta Cryst.* **4** (1951) 42.
4. Cochran, W. and Dyer, H. B. *Acta Cryst.* **5** (1952) 634.
5. Rumanova, I. M. *Soviet Physics, Crystallography* **3** (1958) 674.

Received May 18, 1961.

ACTA CHEMICA SCANDINAVICA 15 (1961) 1761–1764

Complex Dibenzofurans

III *. The Synthesis of Unsymmetrical Biphenyl Derivatives by Mixed Ullmann Coupling

HOLGER ERDTMAN, FRANK HAGLID and NILS E. STJERNSTRÖM

Organisk-kemiska Institutionen, Kungl. Tekniska Högskolan, Stockholm, Sweden

The synthesis of unsymmetrical polymethoxybiphenyls from iodophenol methyl ethers by mixed Ullmann coupling suffers from the disadvantage that, sometimes, the reaction products are difficult to separate. If, however, one of the components is an iodinated carboxylic ester and the reaction products are subjected to alkaline hydrolysis a neutral product, a mono- and a dicarboxylic acid are obtained. The acids are easily separated and decarboxylation of the monocarboxylic acid gives the unsymmetrical biphenyl. In this way 2,4,2′-trimethoxybiphenyl has been conveniently prepared.

When treated with strong acids certain derivatives of 2,2′dihydroxybiphenyl easily undergo dehydration with formation of dibenzofurans while others do not react or only react with considerable difficulty. We have been interested in the structural features necessary for facile ring closure as well as in the reaction mechanism involved.

In an earlier investigation [1] it was observed that polymethoxy-*p*-terphenyls (all being methoxylated derivatives of I) possessing methoxyl groups in 4,4″-, 5,5″- or 6,6″-positions (derivatives of *m*- and *p*-dihydroxybenzene) showed a pronounced tendency to give dioxidoterphenyls on demethylation with constant boiling hydrobromic acid.

A more suitable series of compounds, for a study of the structural requirements for ring closure, would however be substituted anisols containing in the *ortho* position a 2-methoxy-, a 2,3-dimethoxy- or a 2,4-dimethoxyphenyl group, *etc.*

Such unsymmetrical polymethoxybiphenyls can be prepared directly by mixed Ullmann couplings. Späth and Gibian [2] prepared 2,4,3′,4′-tetramethoxybiphenyl and Riedl [3] 2,4,6,3′,5′-pentamethoxybiphenyl in this way. The reaction products obtained could be separated by fractional crystallisation [2] and by chromatography on silica gel [3].

* Part II. *Acta Chem. Scand.* **14** (1960) 2191.

During attempts to prepare 2,4,2′-trimethoxybiphenyl(IIa) from 2-iodoanisol and 4-iodoresorcinol dimethyl ether by a mixed Ullmann coupling, it was found, however, that the separation of the reaction products was laborious. A general method involving less complicated separation problems was therefore devised.

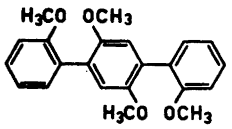

I

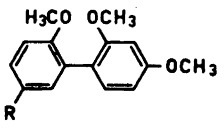

II a. R = H
II b. R = $COOCH_3$
II c. R = COOH

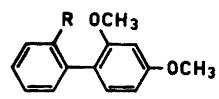

III a. R = NO_2
III b. R = NH_2

Mixed Ullmann coupling of an iodophenol methyl ether with an iodinated methyl methoxybenzoate gives, after hydrolysis, a mixture of a neutral methyl ether, a mono- and a dicarboxylic acid. These can be easily separated. Decarboxylation of the monoacid gives the required unsymmetrical polymethoxybiphenyl.

Methyl 3-iodo-4-methoxybenzoate and 4-iodoresorcinol dimethyl ether were subjected to a mixed Ullmann coupling in a ratio of 1:2 giving a mixture of mainly 2,4,2′,4′-tetramethoxybiphenyl, dimethyl 6,6′-dimethoxybiphenyl-3,3′-dicarboxylate and methyl 6,2′,4′-trimethoxybiphenyl-3-carboxylate (IIb). This mixture was saponified with alkali and the neutral tetramethoxybiphenyl was removed by extraction with ether. The mono- and dicarboxylic acids were precipitated with hydrochloric acid and separated by fractional crystallisation from methanol. The yield of the monocarboxylic acid IIc was *ca.* 40 % based on the iodo-ester. Decarboxylation of the acid IIc, with a copper chromite catalyst in quinoline, gave 2,4,2′-trimethoxybiphenyl (IIa) in good yield.

The biphenyl IIa on prolonged heating with hydrobromic acid gave 3-hydroxydibenzofuran which was also obtained directly from the acid IIc by similar treatment.

Although the following route failed to give the desired compound (IIa), certain results of interest were obtained which are recorded. Equivalent amounts of 2-bromonitrobenzene and 4-iodoresorcinol dimethyl ether were subjected to a mixed Ullmann coupling in boiling nitrobenzene. The reaction products were separated by chromatography on alumina and fractional crystallisation. The yield of the unsymmetrical product, 2-nitro-2′,4′-dimethoxybiphenyl (IIIa) was *ca.* 65 %, only minor amounts of 2,4,2′,4′-tetramethoxybiphenyl were isolated and no 2,2′-dinitrobiphenyl. Such good yields of unsymmetrical biphenyls in mixed Ullmann couplings are not common, but do occur in the preparation of 2- and especially 2,6-substituted nitrobiphenyls[4].

2-Nitro-2′,4′-dimethoxybiphenyl (IIIa) was converted to the corresponding amine (IIIb) by catalytic hydrogenation. Demethylation of this compound with boiling hydrobromic acid gave 2-amino-2′,4′-dihydroxybiphenyl in excellent yield. Demethylation with pyridine hydrochloride, however, gave a *ca.* 75 % yield of 2-hydroxycarbazole. This synthesis of a carbazole derivative is closely

analogous to the formation of dibenzofurans from substituted 2,2'-dihydroxybiphenyls. That the demethylation with hydrobromic acid occurred without ring closure is probably due to the fact that under these strongly acidic conditions the nitrogen is present exclusively as ammonium ion.

Attempts to replace the amino group in IIIb by hydroxyl *via* diazotisation invariably failed, 3-methoxydibenzofuran being formed in *ca.* 80 % yield. This is in full accordance with the findings of Mascarelli *et al.*[5] on the reactions of the diazonium salt of 2-amino-2'-methoxybiphenyl which gives dibenzofuran.

Syntheses of other unsymmetrical methoxybiphenyls are in progress as well as studies on the mechanism of the formation of dibenzofurans from 2,2'-dihydroxybiphenyls.

EXPERIMENTAL

All melting points are uncorrected.

6,2',4'-Trimethoxybiphenyl-3-carboxylic acid (IIc). Methyl 3-iodo-4-methoxybenzoate[6] (18 g), 4-iodoresorcinol dimethyl ether [1] (33 g) and copper bronze (*ca.* 120 g) were thoroughly mixed and heated to about 220° when a vigorous reaction started, which raised the temperature to about 280°. After some minutes the reaction mixture was allowed to cool and the organic products extracted with chloroform. After evaporation of the solvent the residue was distilled *in vacuo*. A fraction (b.p. 150—225°, 1 mm) was collected and saponified with ethanolic sodium hydroxide. Water was added and 2,4,2',4'-tetramethoxybiphenyl (9.2 g) removed by extracting with ether. The acids were then precipitated with dilute hydrochloric acid. The precipitate was dried and triturated with boiling methanol several times. 6,2',4'-Trimethoxybiphenyl-3-carboxylic acid (IIc) crystallised on cooling and was purified by recrystallisation from methanol. Yield 7.4 g, m.p. 214.5—215.5°. (Found: C 66.3; H 5.5; equiv.wt. 283. Calc. for $C_{16}H_{16}O_5$: C 66.7; H 5.6; equiv.wt. 288.) The less soluble acid was 6,6'-dimethoxybiphenyl-3,3'-dicarboxylic acid (4.5 g), m.p. *ca.* 310° (lit.[7] m.p. 312°).

Methyl 6,2',4'-trimethoxybiphenyl-3-carboxylate (IIb). The acid IIc was quantitatively converted to the methyl ester with diazomethane. Crystals from methanol, m.p. 81—81.5°. (Found: C 67.6; H 6.3. Calc. for $C_{17}H_{18}O_5$: C 67.5; H 6.0.)

2,4,2'-Trimethoxybiphenyl (IIa). The acid IIc (1.0 g) in quinoline (15 ml) was heated for 3 h at 200° in an atmosphere of nitrogen in the presence of a copper chromite catalyst (300 mg). The filtered reaction mixture was acidified with dilute hydrochloric acid and extracted with ether. The extract was thoroughly washed with first dilute sodium hydroxide and then water. The solution was dried over magnesium sulphate, the solvent was evaporated and the residue dissolved in a small amount of chloroform. A tenfold volume of light petroleum was added and the solution filtered through a short column of neutral alumina. After evaporation of the solvent the product was collected and recrystallised from methanol. Yield 0.7 g, m.p. 59—59.5°. (Found: C 73.3; H 6.5; OCH_3 37.0. Calc. for $C_{15}H_{16}O_3$: C 73.7; H 6.6; OCH_3 38.1.)

3-Hydroxydibenzofuran and the corresponding methyl ether. The acid IIc (2.0 g) was refluxed for 36 h with hydrobromic acid (48 %, 50 ml) in an atmosphere of nitrogen. The reaction mixture was poured into water and extracted with ether. The extract was washed first with small amounts of dilute sodium bicarbonate and then with water. After drying over anhydrous calcium sulphate and evaporation of the solvent the residual dibenzofuran was recrystallised from water. Yield 0.8 g, m.p. 141—141.5° (lit.[8] m.p. 138—138.5°). 3-Methoxydibenzofuran was obtained by methylation with dimethyl sulphate and alkali. M.p. 95—95.5° (lit.[8] m.p. 97—97.5°).

The biphenyl IIa, treated with hydrobromic acid as described above, gave 3-hydroxydibenzofuran in *ca.* 75 % yield.

2-Nitro-2',4'dimethoxybiphenyl (IIIa). A mixture of 4-iodoresorcinol dimethyl ether (20 g), 2-bromonitrobenzene (15.3 g), copper bronze (96 g) and nitrobenzene (150 ml) was boiled for 3 h with vigorous stirring (reflux). The reaction mixture was filtered and the solid washed with chloroform. The chloroform and nitrobenzene were removed by steam distillation and the residue extracted with chloroform. The extract was

dried over magnesium sulphate and concentrated to a small volume. Light petroleum (2 volumes) was added and the solution was chromatographed on neutral alumina (200 g, column constructed in a chloroform-light petroleum mixture, 1:2). The main component was eluted with the same solvent mixture. After evaporation of the solvent a dark syrup was obtained, which crystallised on scratching with light petroleum. This product was recrystallised from methanol. Yield 26 g, m.p. 101.5–102°. (Found: C 64.7; H 5.1; N 5.6. Calc. for $C_{14}H_{13}NO_4$: C 64.9; H 5.1; N 5.4.)

2,4,2',4'-Tetramethoxybiphenyl (1.5 g) was isolated from the methanolic mother liquor.

2-Amino-2',4'-dimethoxybiphenyl (IIIb). The nitro compound IIIa, in ethanol, was hydrogenated with a palladium charcoal catalyst (10 % Pd) at room temperature and atmospheric pressure. The calculated amount of hydrogen was rapidly absorbed. The amine IIIb, m.p. 68.5–69°, easily formed a picrate. Crystals from ethanol, m.p. 199–200°. (Found: C 51.8; H 4.1; N 12.3. Calc. for $C_{20}H_{18}N_4O_9$: C 52.4; H 4.0; N 12.2.)

2-Amino-2',4'-dihydroxybiphenyl. A mixture of the hydrobromide of compound IIIb (1.5 g, obtained by saturating an ether solution of the amine with dry hydrogen bromide, m.p. 155–160°) and hydrobromic acid (48 %, 30 ml) was boiled in an atmosphere of nitrogen for 24 h (reflux). During the first hours the reaction mixture was intensely green but gradually became brownish towards the end. On cooling crystals were deposited. They were dissolved in water and the free amine was precipitated with saturated sodium bicarbonate solution. Crystals from water. Yield 0.8 g, m.p. 149–149.5°. (Found: C 71.6; H 5.6; N 6.9. Calc. for $C_{12}H_{11}NO_2$: C 71.6; H 5.5; N 7.0.)

2-Hydroxycarbazole. The hydrobromide of compound IIIb (630 mg) was heated with pyridine hydrochloride (4.5 g) and pyridine (0.2 ml) at *ca.* 180° in an atmosphere of nitrogen for 3 h. The reaction mixture was poured into water and the crude product collected and dried. The substance was decolourised by shaking an ethanol-chloroform solution with charcoal and sublimed *in vacuo*. Yield 370 mg, m.p. *ca.* 260°, decomp. (lit.[9] m.p. 277°, to a black liquid with previous darkening). (Found: C 79.0; H 5.2; N 7.5. Calc. for $C_{12}H_9NO$: C 78.7; H 5.0; N 7.7.)

2-Acetoxycarbazole. The preceding phenol was acetylated with acetic anhydride and pyridine. Crystals from methanol, m.p. 183–184° (lit.[10] m.p. 188°). (Found: C 75.0; H 4.9; N 6.2. Calc. for $C_{14}H_{11}NO_2$: C 74.7; H 4.9; N 6.2.)

Attempted replacement of the amino group in compound IIIb by hydroxyl. A mixture of the amine IIIb (2.8 g) and dilute sulphuric acid (15 %, 100 ml) was treated with a solution of sodium nitrite (1.5 g) in water (20 ml) at 0–5° with stirring. Excess of nitrite was destroyed with urea and the mixture heated at 70° until nitrogen evolution ceased. The reaction mixture was then extracted with chloroform. The extract was washed with water, dried over magnesium sulphate and filtered through a short column of neutral alumina. The solvent was evaporated and the residue recrystallised from methanol. Yield 2.0 g, m.p. 95–95.5°. A mixed melting point with 3-methoxydibenzofuran (prepared from the biphenyl IIa, m.p. 95–95.5°.) showed no depression (m.p. 95–95.5°). The ultraviolet spectra of the two samples were identical.

The authors are grateful to Dr. I. Wellings for correcting the English.

REFERENCES

1. Stjernström, N. E. *Acta Chem. Scand.* **14** (1960) 1274.
2. Späth, E. and Gibian, K. *Monatsh.* **55** (1930) 342; *cf. Chem. Zentr.* **1930** II 573.
3. Riedl, W. and Imhof, F. *Ann.* **597** (1955) 153.
4. Fanta, P. E. *Chem. Revs.* **38** (1946) 139.
5. Mascarelli, L. and Pirona, M. *Gazz. chim. Ital.* **68** (1938) 117; *cf. Chem. Abstracts* **32** (1938) 6235.
6. Baddar, F. G., El-Assal, L. S. and Baghos, V. B. *J. Chem. Soc.* **1955** 1714.
7. Sugii, Y. *J. Pharm. Soc. Japan* **50** (1940) 23; *cf. Chem. Zentr.* **1930** II 253.
8. Tatematsu, K. and Kubota, B. *Bull. Chem. Soc. Japan* **9** (1934) 448; *cf. Chem. Zentr.* **1935** I 1375.
9. Cummins, J. A. and Tomlinson, M. L. *J. Chem. Soc.* **1955** 3475.
10. French Patent 666450; *cf. Chem. Zentr.* **1930** II 470.

Received May 31, 1961.

ACTA CHEMICA SCANDINAVICA 15 (1961) 1765–1771

Complex Formation of Ferric Iron with 7-Iodo-8-hydroxyquinoline-5-sulphonic Acid (Ferron)

Å. R. STORM and F. J. LANGMYHR

University of Oslo, Chemical Institute A, Blindern, Norway

The complex formation of ferric iron with 7-iodo-8-hydroxyquinoline-5-sulphonic acid (ferron) was studied by potentiometric and spectrophotometric methods. Titrations of mixtures of the ligand and metal ion with standard alkali indicated the presence of complexes with ligand metal ratios 1:1, 2:1 and 3:1. On the basis of the titrations, the stability constants at 25.0° ± 0.1°C and in the presence of 0.10 M potassium chloride were calculated to: log K_{MA} = 8.9 ± 0.2, log K_{MA_2} = 8.4 ± 0.15 and log K_{MA_3} = 7.9 ± 0.15. By spectrophotometry, absorption curves and curves of continuous variation at different pH values were plotted. The photometric measurements confirmed the results obtained by potentiometry as to the number of complexes present, and showed that in the visible range the three complexes have absorption maxima which are only 10–15 mμ apart.

In connection with the application of 7-iodo-8-hydroxyquinoline-5-sulphonic acid (ferron) in the simultaneous spectrophotometric determination of iron and aluminium it is of importance to know the composition and stability of the complexes formed. In a previous work [1] the authors studied the system aluminium-ferron and found evidence of complexes with ferron metal ratios 1:1, 2:1 and 3:1. In addition, hydroxo-compounds of the 1:1 and 2:1 complexes were found to be present.

The interaction of ferric iron with ferron has earlier been investigated by Yoe and Hall [2] and by Nortia [3]. The former authors concluded from colorimetric methods that a complex with ferron metal ratio 3:1 was formed. The latter author confirmed this result and in addition predicted the existence of a 1:1 complex with the composition Fe(OH)A.

The inconclusiveness as to the number of complexes present in the system ferric iron-ferron made further studies desirable. The present investigation was started with the purpose of determining the species present in the system, and at the same time to procure data on the stability of the compounds formed.

EXPERIMENTAL

Methods. The methods employed in this investigation were potentiometric titration and spectrophotometry. Ferron was titrated with standard alkali in the absence of and in the presence of ferric ions. During the titrations the temperature was 25.0 ± 0.1°C, and the ionic strength was kept relatively constant by maintaining a concentration of 0.10 M potassium chloride and by keeping a low concentration of ligand and metal ion. Mixing was effected by passing a stream of nitrogen through the solutions. Hydrogen ion concentrations were taken directly from the pH values measured. Absorption curves were plotted at different pH of solutions containing the ligand and the metal in the ratios 1:1, 2:1 and 3:1. To determine the composition of the complexes, curves of continuous variation were plotted at varying pH. The photometric measurements were carried out at room temperature (20 ± 2°C) and in the presence of 0.10 M potassium chloride.

Instruments. Extinction measurements were made with a Zeiss spectrophotometer PMQ II and 1.000 cm glass and quartz cells. For the potentiometric titrations and the measurement and regulation of pH a Beckman Zeromatic pH meter (glass and calomel reference electrodes) was employed. The solutions to be titrated were placed in an ultrathermostat.

Reagents. All chemicals were of reagent grade quality. The ferron used (Hopkin and Williams) contained (according to the producers' specification) not less than 98.0 % of $C_9H_6O_4NSI$ and a maximum amount of 0.1 % of sulphated ash. The iron compound applied was ferric chloride ($FeCl_3 \cdot 6H_2O$).

Standard solutions. For the potentiometric titrations the following standard solutions were prepared. A 5×10^{-3} M solution of ferron was prepared by dissolving 1.7556 g in boiled distilled water, adding potassium chloride and diluting to 1 000 ml. Solutions of ferron decompose slowly on standing and were therefore not stored for more than one week. A standard solution of ferric iron was prepared by dissolving 54.16 g of $FeCl_3 \cdot 6H_2O$ in about 100 ml of distilled water containing about 0.5 ml of concentrated nitric acid. The solution was boiled and all iron was found to be in the ferric state (no colour formed with a freshly prepared solution of potassium ferricyanide). After dilution to 1 000 ml, the concentration of iron was determined gravimetrically and was found to be 11.165 g of iron per 1 000 ml, corresponding to a 0.20 M solution. By pipetting out 25 ml of this solution, adding potassium chloride and diluting to 1 000 ml with distilled water, a 5×10^{-3} M solution of ferric iron was obtained. A 0.09953 N solution of potassium hydroxide was used for the titrations, the solution being added from a calibrated 10 ml burette graduated to 0.01 ml. For the photometric measurements 5×10^{-3} M standard solutions of ferron and ferric iron were prepared, but these solutions did not contain inert salt. Potassium chloride was, however, added later during the preparation of the separate solutions.

Acid dissociation constants of ferron. The values determined previously by the authors [1] were employed in this investigation ($pK_1 = 2.50$ and $pK_2 = 7.11$ at 25.0 ± 0.1°C and in the presence of 0.10 M potassium chloride).

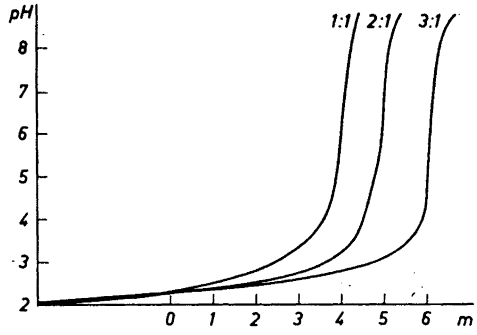

Fig. 1. Titration curves for solutions with ferron/ferric iron ratios 1:1, 2:1 and 3:1. m = equivalents of base added per mole of metal.

Potentiometric titrations. Solutions containing 1:1, 2:1 and 3:1 molar ratios of ligand to metal ion were titrated with standard alkali. From the 5×10^{-3} M solution of iron 25 ml were pipetted into a beaker and 25,50 or 75 ml of 5×10^{-3} M ferron solution were added. After thermal equilibrium was reached, standard alkali was added in small increments and the corresponding pH data were recorded as soon as constants values were obtained.

In Fig. 1 a set of titration curves is reproduced.

RESULTS

The 1:1 curves. Titration of equimolar amounts of ligand (H_2A) and metal ion resulted in a single inflection obtained after the addition of four equivalents of base per mole of metal. This result probably corresponded to the reactions:

$$Fe^{3+} + H_2A \rightleftharpoons FeA^+ + 2H^+$$
$$FeA^+ + H_2O \rightleftharpoons Fe(OH)A + H^+$$
$$Fe(OH)A + H_2O \rightleftharpoons Fe(OH)_2A^- + H^+$$

No precipitate was observed at any time during the titration. The increasing slope of the curve in the region two to four equivalents of alkali was believed to indicate that the formation of hydroxo-complexes took place by overlapping reactions. At the start of the titrations the solutions were green, but changed to red at the inflection. (A red colour is typical of iron-phenolate compounds.)

The 2:1 curves. The titration curves of solutions containing ferron and ferric iron in the ratio 2:1 exhibited one inflection corresponding to the addition of five equivalents of base per mole of metal. The following reactions probably took place:

$$Fe^{3+} + 2H_2A \rightleftharpoons FeA_2^- + 4H^+$$
$$FeA_2^- + H_2O \rightleftharpoons Fe(OH)A_2^{2-} + H^+$$

During these titrations the colour also changed from green to red. No precipitates were seen.

The 3:1 curves. These curves showed an inflection after the addition of six equivalents of base, probably corresponding to the reaction:

$$Fe^{3+} + 3H_2A \rightleftharpoons FeA_3^{3-} + 6H^+$$

Two or three titration curves were plotted of each mixture. The separate curves of one set did not differ by more than 0.01 to 0.02 pH units in the ranges employed for the calculation of the stability constants.

Stability constants. Stability constants for the complexes not containing hydroxyl were calculated according to the method by Bjerrum [4] on the basis of a titration curve of the 3:1 complex. The average number of moles of ligand bound per mole of metal ion, designated by $\bar{n}$, were plotted against pA, the negative logarithm of the concentration of ligand. In Fig. 2, the fully drawn line resulted from calculations in which the amount of acid originating from the iron solution was included in the formula employed. The initial amount of acid was determined graphically from the plot of the titration curves. To obtain data of pA at $\bar{n}$ values below about 1.5, the broken line (Fig. 2) was drawn.

The values of pA at $\bar{n} = 0.5$, 1.5 and 2.5 were taken as log K_{MA}, log K_{MA_2} and log K_{MA_3}, respectively.

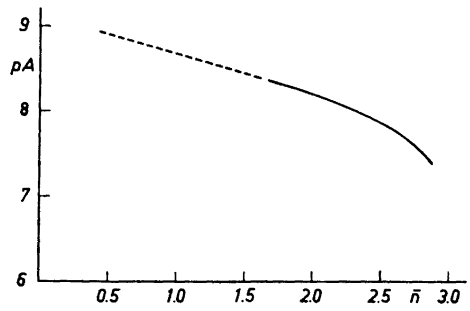

Fig. 2. Variation of degree of formation $\bar{n}$ for ferric iron/ferron complexes as a function of concentration of ligand pA.

The effect of a variation of $\pm$ 0.02 pH (the reproducibility of the pH meter) on the stability constants was calculated, and the data were used to estimate the limits of variation given below. (The pA *versus* $\bar{n}$ curve obtained by using a formula not including the amount of acid initially present, fell within the limits calculated for the pH variation of $\pm$ 0.02.)

The constants calculated were:

$\log K_{MA} = 8.9 \pm 0.2$, $\log K_{MA_2} = 8.4 \pm 0.15$ and
$\log K_{MA_3} = 7.9 \pm 0.15$.

Photometric measurements

In addition to the early colorimetric studies made by Yoe [5] and Yoe and Hall [2], spectrophotometric investigations of the system ferron-ferric iron have been carried out by Davenport [6], Swank and Mellon [7] and Nortia [3].

Davenport [6] plotted absorption curves at different pH values of some solutions containing ferric iron and excess of ligand, and recommended a pH of 5.0 for the analytical determination of iron. Swank and Mellon [7] plotted in more detail similar absorption curves, which showed, for the maximum around 600 mμ, a shift to lower wavelengths with increasing pH values. In another experiment these authors kept a constant concentration of metal ion, a contant pH of 3.0, and examined the effect of varying concentration of ferron. They found that increasing amounts of ferron increased the extinction of the solutions. A study of their absorption curves also showed that by increasing the concentration of ferron the maximum around 600 mμ shifted to lower wavelengths.

Nortia [3] studied the effect of the ligand-metal ratio on the absorption at 600 mμ by measuring the extinction of a series of unbuffered solutions. He found the resulting curves to be typical of systems where successive compounds are formed, or where the stability of the complex is not high. He also plotted absorption curves in the range 400—700 mμ and at different pH values for solutions in which hydrous ferric oxide and ferron or 8-hydroxyquinoline-5-sulphonic acid had reacted. The curves obtained for the two systems were similar in form. The curves reproduced by Nortia for the latter system also

showed that increasing pH values resulted in a shift of the maximum around 600 mμ to lower wavelengths.

The present potentiometric investigation indicated the presence of complexes with ligand metal ratios 1:1, 2:1 and 3:1. In the opinion of the authors, it seemed probable that the variations of the absorption maximum around 600 mμ with pH (*vide supra*) were due to the presence of different complexes. These complexes probably have slightly different absorption curves and different ranges of existence depending on pH. In order to confirm these assumptions, some photometric measurements were carried out.

Absorption curves. A series of solutions were prepared by pipetting into 100 ml volumetric flasks 3 ml of 5×10^{-3} M ferric iron solution, 3, 6 or 9 ml of 5×10^{-3} M ferron solution and 10 ml of 1.0 M potassium chloride. pH was regulated without the use of buffers and the solutions were diluted to volume with distilled water. The extinctions were then measured in the wavelength range 550 to 700 mμ against distilled water (ferron does not absorb in this wavelength region). The absorption curves are reproduced in Fig. 3.

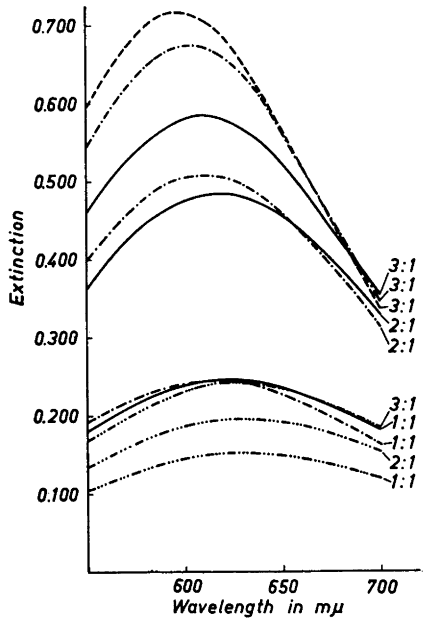

Fig. 3. Absorption curves at different pH values for solutions with ferron/ferric iron ratios 1:1, 2:1 and 3:1. Solutions with pH 1.30 —···—···—, pH 2.70 ————, pH 3.50 —·—·—·— and pH 5.0 — — — — —.

Solutions containing equimolar amounts of ligand and metal ion and having the pH values 1.30, 2.70 and 3.50 exhibited absorption curves which were similar in form and with maxima at the same wavelength, 625 mμ. The extinction of the solutions increased with pH. These solutions probably all contained mainly the 1:1 complex, the varying extinction being caused by the

difference of pH. Solutions containing ferron and metal ion in the ratios 2:1 and 3:1 and maintained at pH 1.30 exhibited curves which were similar to the 1:1 curves and with maxima at the same wavelength. At this low pH, the 2:1 and 3:1 complexes were probably not formed, the only stable compound being the 1:1 complex. The 2:1 and 3:1 curves plotted at higher pH values showed maxima at lower wavelengths and considerable higher extinctions. The maxima of the 2:1 curve at pH 2.70 and 3.50 were found at 618 and 613 mμ, respectively. In this pH range, the 2:1 complex was probably predominating. For solutions containing the ligand and metal ion in the ratio 3:1, the maximum varied considerably with pH. At pH 1.30 the 1:1 complex was believed to be formed, at intermediary pH values the 2:1 complex appeared and finally, at pH 5.00, the 3:1 complex was formed with absorption maximum at 595 mμ. Solutions of the 1:1 and 2:1 compounds at pH 5.00 probably contained phenolate compounds and the corresponding curves are not reproduced in Fig. 3.

Curves of continuous variation. Curves of continuous variation were plotted at 600 mμ for series of solutions with pH 1.25, 2.30, 3.25 and 4.90. In Fig. 4 these curves are given.

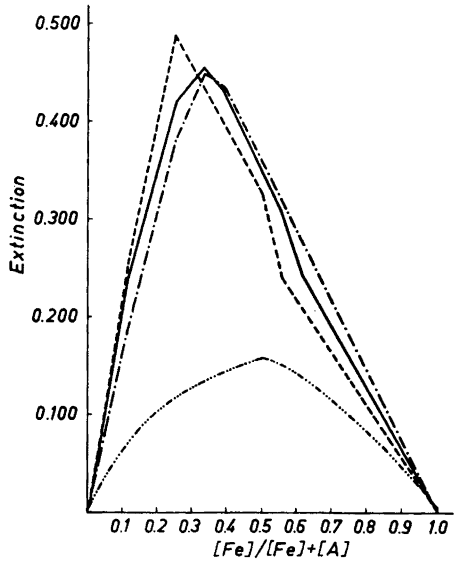

Fig. 4. Curves of continuous variation measured at 600 mμ. Solutions with pH 1.25 —···—···—, pH 2.30 —·—·—, pH 3.25 ————, and pH 4.90 — — — —.

The presence of three different complexes is indicated by the curves, the form of which also reflects the increasing stability when going from the 1:1 to the 3:1 complex.

DISCUSSION

The earlier observed change of the absorption maximum around 600 mμ with pH, or by varying the ferron metal ratio at a constant pH (*vide supra*) is explained by the presence of three complexes.

From this study conclusions can also be drawn as to the most suitable conditions for spectrophotometric determination of iron. An excess of ferron and a relatively high pH value should favour the formation of the 3:1 complex, which also has the highest extinction coefficient. The pH value given by Davenport [6], *viz.* 5.0 can thus be recommended.

It is of interest to compare the absorption curves of the present work with the data given by Phillips [8] for the complexes of ferric iron with 8-hydroxyquinoline-5-sulphonic acid. Phillips reported that the 1:1 and 3:1 complexes with 8-hydroxyquinoline-5-sulphonic acid had absorption maxima at 625 and 580 mμ, respectively, while the maxima for the ferron complexes of the same composition in the present study were found at 625 and 595 mμ. The introduction of iodine in the 7-position does therefore not seem to change the visible absorption curves of the ferric iron complexes appreciably. It is highly probable, that the system 8-hydroxyquinoline-5-sulphonic acid/ferric iron is similar to that of ferron/ferric iron, the only difference being that higher stability constants can be expected in the former system.

REFERENCES

1. Langmyhr, F. J. and Storm, Å. R. *Acta Chem. Scand.* **15** (1961) 1461.
2. Yoe, J. H. and Hall, R. T. *J. Am. Chem. Soc.* **59** (1937) 872.
3. Nortia, T. *Ann. Acad. Sci. Fennicae Ser. A*, II, No. 86 (1957).
4. Bjerrum, J. *Metal Ammine Formation in Aqueous Solution*, P. Haase and Son, Copenhagen, 1941.
5. Yoe, J. H. *J. Am. Chem. Soc.* **54** (1932) 4139.
6. Davenport, W. H. *Anal. Chem.* **21** (1949) 710.
7. Swank, H. W. and Mellon, M. G. *Ind. Eng. Chem., Anal. Ed.* **9** (1937) 406.
8. Phillips, J. P. *J. Am. Chem. Soc.* **72** (1950) 3159.

Received May 3, 1961.

ACTA CHEMICA SCANDINAVICA 15 (1961) 1772–1776

The Isolation and Identification of 2,6-Diiodohydroquinone from the Thyroid Gland

JAN-GUSTAF LJUNGGREN

Nobel Medical Institute, Biochemical Department, Stockholm, Sweden

^{131}I-labelled 2,6-diiodohydroquinone has been isolated from the thyroid gland of rabbits after a single injection of ^{131}I, and identified by the use of the reversed isotope dilution technique and by radiochromatography.

The recovery of ^{131}I in the ^{131}I-labelled diiodohydroquinone fraction was about 0.2 % of the total ^{131}I in the thyroid.

The results are discussed with respect to the compound being an intermediate between diiodotyrosine and thyroxine.

The formation of 2,6-diiodobenzoquinone from 3,5-diiodotyrosine by the action of peroxidase has been described previously [1]. It was suggested that 2,6-diiodobenzoquinone, or 2,6-diiodohydroquinone, might be an intermediate in the *in vivo* conversion of diiodotyrosine into thyroxine.

Lissitzky and Krotemberg [2] have reported that 2,6-diiodohydroquinone, or a related compound, could be isolated from the thyroid gland under certain conditions, but no detailed experimental data were given. Allegretti [3] has claimed that incubation of thyroxine with liver homogenate leads to the formation of 2,6-diiodo-*p*-benzoquinone and 3,5-diiodophenylalanine.

In this investigation 2,6-diiodobenzoquinone and 2,6-diiodohydroquinone have not been isolated separately. Before the isolation was begun the 2,6-diiodobenzoquinone was reduced to 2,6-diiodohydroquinone.

EXPERIMENTAL

Materials

The following chemicals and apparatus were used:

^{131}I. Catalogue number IBS 2, The Radiochemical Centre, England.

2,6-Diiodohydroquinone was synthetized according to Elbs and Volk [4]. A commercial product was also used. The melting point of the crystals was 144°C.

Trypsin. Unfractionated trypsin with an activity of 1.14 units/g [5,6].

All commercial chemicals were of analytical reagent quality. The solvents used for paperchromatography were freshly distilled before use.

Homogenizer. Glass homogenizer with a Teflon plunger. Catalogue number, 4288-B, Arthur H. Thomas Comp., U.S.A.

Counting equipment. ^{131}I-Labelled compounds measured were in a well-scintillation counter (type-number P-20B, Tracerlab. Inc. U.S.A.) connected to a Single Pulse Height Analyzer (type-number RLI-4, Tracerlab.) and a Superscaler (type-number SC 18 A, Tracerlab.). The high voltage was fed from a Superstable High Voltage Power Supply (type-number 312, Baird Atomic Inc., U.S.A.). The pulse-height analyzer was adjusted to count the gamma emissions of the 0.36 MeV photopeak of ^{131}I. The background was about 24 counts/min.

Methods

The following technique was routinely employed.

Isolation procedure. 100 μC ^{131}I was injected intraperitoneally into each of two rabbits. After 48 h, the animals were sacrified by injection of air in the ear veins, and their thyroid glands were removed, minced with scissors and transferred to a chilled motor driven homogenizer. The homogenizer tube was surrounded by a beaker of ice during the grinding procedure. The glands were homogenized in 15 ml 0.05 M phosphate buffer pH 7.4 and then incubated in the same solution for 72 h at 37°C with 25 mg unfractionated trypsin and one drop of toluene during continous stirring. After hydrolysis the pH was adjusted to 2 with 0.1 N sulfuric acid and SO_2-gas was bubbled through for 20 min. The homogenate was then extracted three times with 10 ml diethyl ether and the ether extracts were combined.

Identification procedure. The compound was identified by the reversed isotope dilution technique and by radiochromatography.

1. The reversed isotope dilution technique. To the combined ether fractions was added 200 mg of synthetic 2,6-diiodohydroquinone and 20 ml of water. Before adding, the pH of the water had been adjusted to 2 with 0.1 N sulfuric acid and SO_2-gas had bubbled through for 20 min at 20°C. The system was then slowly heated on a waterbath, and stirred continously until the ether evaporated and the diiodohyroquinone dissolved. The solution was filtered, and allowed to stand at 0°C to crystallize the product. The crystals were collected, and washed three times with distilled water (pH 2, SO_2-saturated, 0°C). An aliquot of the crystals was dried in a desiccator and analyzed as described below. The remaining crystals were redissolved in 15 ml distilled water (pH 2, SO_2-saturated), heated, filtered and crystallized as described above. This recrystallization procedure was repeated 10 times. The volume of solvent was gradually decreased with each recrystallization. An aliquot of the crystals were, after each crystallization, analyzed by radiochromatography, and the melting point, and specific activity (counts/min/mg dry weight) were measured. The melting point was measured in order to make sure that the carrier material was not decomposed by the recrystallization procedure.

To determine if there was any exchange between free iodine and the iodine bound to the diiodohydroquinone, the following control experiment was conducted. 15 μC ^{131}I was added to 15 ml distilled water, the pH was adjusted to 2 with 0.1 N sulfuric acid and SO_2-gas was bubbled through for 20 min. The solution was then extracted three times with 10 ml diethyl ether and the ether extracts were combined. 200 mg of synthetic 2,6-diiodohydroquinone was added, recrystallized and analyzed as described above.

2. Radiochromatography. The ether extract of the hydrolyzed homogenate was combined with 3 ml of distilled water. The pH was adjusted to 2 with 0.1 N sulfuric acid and SO_2-gas was bubbled through for 5 min at 20°C. The system was then slowly heated on a waterbath and stirred continously until the ether evaporated. The solution was filtered.

The following solvent systems have been developed for paperchromatography of 2,6-diiodohydroquinone.

A. Heptane:*n*-propanol:acetic acid:0.001 M sodium thiosulfate = 100:50:1:100 v/v (organic phase).

B. Petroleum ether (boiling range 60—80°C):acetone:0.001 M sodium thiosulfate = 3:1:3 v/v (organic phase).

C. Benzene:0.001 M soldium thiosulfate = 1:1 v/v (organic phase).

D. Acetone:acetic acid:0.001 M sodium thiosulfate = 8:1:60 v/v.

E. *n*-Propanol:acetic acid:0.001 M sodium thiosulfate = 10:1:60 v/v.

Whatman No. 1 filter paper was used and the chromatograms were run at 20°C. The spots were visualized with diazotized sulfanilic acid [7]. The diiodohydroquinone compound was also visualized with alkaline silver nitrate [8] and iodide with 0.1 N ferric nitrate + 3 % hydrogen peroxide.

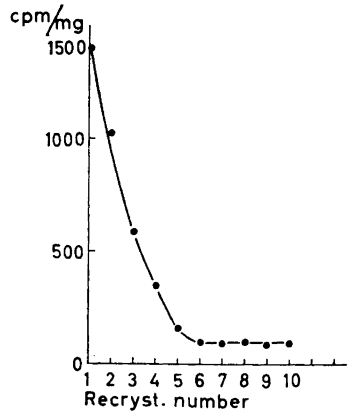

Fig. 1. The specific activity (counts/min/mg dry weight) of the diiodohydroquinone crystals from ten recrystallization experiments.

Synthetic 2,6-diiodohydroquinone was added to the solution before chromatography. In some experiments synthetic 2,6-diiodohydroquinone was not added to the solution but was placed beside the test spot. Both one- and two-dimensional systems were run. When two-dimensional chromatograms were run the order to the solvents was reversed. After visualizing, the papers were cut out in strips and their radioactivity measured. The colored and the radioactive spots were compared. The R_F values of other thyroxine precursors were also investigated.

RESULTS

The specific activity (counts/min/mg dry weight) of the diiodohydroquinone crystals obtained after each recrystallization was measured. It was found that the specific activity gradually decreased at first, but reached a constant value after the 6th recrystallization. The results, corrected for decay and background, are shown in Fig. 1.

Table 1. R_F-values of 2,6-diiodohydroquinone and other thyroxine precursors in system *A* (heptane:acetic acid:0.001 M sodium thiosulfate), *B* (petroleum ether:acetone:0.001 M thiosulfate), *C* (benzene: 0.001 M sodium thiosulfate), *D* (acetone:acetic acid:0.001 M sodium thiosulfate) and *E* (propanol:acetic acid:0.001 M sodium thiosulfate). The different systems are further described in the text.

System	*A*	*B*	*C*	*D*	*E*
Compound					
Iodide	0	0	0	0.84	0.84
L-Tyrosine	0	0	0	0.80	0-79
3-Monoiodo-L-tyrosine	0	0	0	0.70	0.71
3,5-Diiodo-L-tyrosine	0	0	0	0.59	0.59
L-Thyroxine	0	0	0	0	0
3,5,3-Triiodothyronine	0	0	0	0	0
2,6-Diiodohydroquinone	0.73	0.47	0.60	0.51	0.52

In the control experiment, when ^{131}I was added to synthetic diiodohydroquinone and then recrystallized, the crystals could be completely freed of radioactivity after the first recrystallization experiment.

The melting points for the different crystals were the same (144°C).

The recovery of ^{131}I in the ^{131}I-labelled diiodohydroquinone fraction was about 0.2 % of the total ^{131}I in the thyroid, based on the total amount of ^{131}I in the gland, the specific activity of the crystals and the added amount of synthetic diiodohydroquinone.

The R_F values obtained for 2,6-diiodohydroquinone and other thyroxine precursors are shown in Table 1.

When the colored area on the chromatograms, given by the added sample of synthetic 2,6-diiodohydroquinone, were compared to the radioactive spots a complete coincidence was found.

DISCUSSION

The time interval between injection and sacrificing was 48 h in this experiment. This time interval was chosen according to Taurog and Chaikoff[9]. They investigated the distribution of ^{131}I in rat thyroids at different time intervals and found that after 50 h about 27 % of the total ^{131}I in the thyroid gland was in the thyroxine, about 72 % in the diiodotyrosine and about 1.5 % in the non-protein-bound fraction.

Air oxidation of iodide-131 in acid solution may easily produce $^{131}I_2$, and the latter might then iodinate organic compounds, especially those added in relatively large amounts as markers for chromatography[10]. Control experiments have excluded these types of artefacts in this investigation.

Unidentified ^{131}I-labelled compounds in the thyroid gland have been reported by many authors (*e.g.* Refs.[11, 12]). It might, however, be possible that many of these unknown compounds are simple oxidation products of iodide[13], but the possible identity of some of them with 2,6-diiodohydroquinone or 2,6-diiodobenzoquinone must not be disregarded.

The formation of 2,6-diiodobenzoquinone from 3,5-diiodotyrosine by the action of peroxidase has previously been described. It might be possible that 2,6-diiodobenzoquinone or 2,6-diiodohydroquinone, is an intermediate in the conversion of diiodotyrosine into thyroxine in the thyroid gland. This conversion is now being investigated.

Acknowledgement. The author wishes to thank Professor Hugo Theorell for valuable help and criticism. Thanks are also due to Drs. N. Ellfolk, B. Sörbo and C. Woronick for instructive discussions. This work has been supported by grants from *Statens Medicinska Forskningsråd, Statens Naturvetenskapliga Forskningsråd, Karolinska Institutetes Lärarkollegium* and *Stiftelsen Therese och Johan Anderssons Minne,* and is acknowledged with grateful thanks.

REFERENCES

1. Ljunggren, J. G. *Acta Chem. Scand.* **11** (1957) 1072.
2. Lissitzky, S. and Krotemberg, W. *Compt. rend.* **242** (1956) 3002.
3. Allegretti, N. *Liječnički vjesnik* **76** (1954) 625.
4. Elbs, K. and Volk, H. *J. prakt. Chem.* **99** (1919) 271.
5. Anson, M. L. and Mirsky, A. E. *J. Gen. Physiol.* **16** (1932/33) 59.
6. Anson, M. L. and Mirsky, A. E. *J. Gen. Physiol.* **17** (1933/34) 151.
7. Ames, B. N. and Mitchell, H. K. *J. Am. Chem. Soc.* **74** (1952) 252.
8. Burton, R. B., Zaffaroni, A. and Keutmann, E. H. *J. Biol. Chem.* **188** (1951) 763.
9. Taurog, A. and Chaikoff, I. L. *J. Biol. Chem.* **169** (1947) 49.
10. Colowick, S. P. and Kaplan, N. O. (Ed.) *Methods in Enzymology,* Academic Press inc. Publishers, New York, **IV** (1957) 867.
11. Taurog, A., Tong, W. and Chaikoff, I. L. *J. Biol. Chem.* **227** (1957) 759.
12. Dobyns, B. M. and Barry, S.R. *J. Biol. Chem.* **204** (1953) 517.
13. De Groot, L. J. and Berger, J. E. *Endocrinology* **67** (1960) 657.

Received May 3, 1961.

ACTA CHEMICA SCANDINAVICA 15 (1961) 1777–1779

The Structure of Phloraspin

ANERI PENTTILÄ and JACOBUS SUNDMAN

The Research Laboratories, Medica Ltd., Helsinki, Finland

Phloraspin (I) has been shown to be a phloroglucinol methylene compound combined of methylphlorobutyrophenone and phlorobutyrophenone-4-methyl ether.

In addition to the known phloroglucinol derivatives from *Dryopteris* fern species, listed in our earlier report [1], we have now investigated the substance called phloraspin. It was first isolated by Kraft [2], who called the compound flavaspidinin, m.p. 199°. In a later paper Kraft [3] supposed flavaspidinin to be identical with phloraspin, which had been isolated and described by Boehm [4] in 1903.

According to Boehm [4] phloraspin is a light yellow or nearly colourless substance, m.p. 211°, which is very slightly soluble in most organic solvents except in acetone and chloroform. Ferric chloride causes a red brown colour in ethanol solution. Treated with diazoaminobenzene phloraspin yields benzeneazomethylphlorobutyrophenone, m.p. 182°, which reaction Boehm offered in support of phloraspin being a methylene compound with methylphlorobutyrophenone as one member. The molecular data, $C_{23}H_{28}O_8$, and the methoxyl content of phloraspin lead Boehm to assume that the other half of the phloraspin molecule is a monomethyl ether of phlorobutyrophenone. This assumption has now been confirmed by identifying the decomposition products of phloraspin whereby it was found that the phlorobutyrophenone monomethyl ether was the 4-methyl ether isomer. The structure of phloraspin is furthermore proved by synthesis. Thus, phloraspin is an exception to the other known *Dryopteris* phloroglucinols since butyrylfilicinic acid is not a part of its molecule.

Occasionally phloraspin has been isolated from *Dryopteris austriaca* (Jacq.) Woynar in amounts of about 0.002 % calculated on air dried rhizomes; phloraspin could not be found in every specimen of the same, in agreement with earlier reports [4–6]. In a pure state phloraspin has a melting point of 211—212°. It could be recrystallised from benzene and methanol as yellowish crystals.

The chromatographic behaviour of the phloroglucinol derivatives isolated from *Dryopteris* ferns has been studied by the authors [7]. This earlier study did not include phloraspin which can also be separated by the same method. On papers, buffered to pH 9.1—8.0 and impregnated with formamide, phloraspin

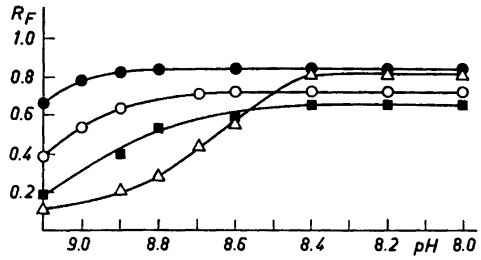

Fig. 1. Variation of the R_F-values with the pH of the papers. ● aspidinol, O florobutyrophenone-4-methyl ether, ■ florobutyrophenone-2-methyl ether, △ phloraspin.

has the R_F-values shown in Fig. 1. The chromatographing is performed with chloroform-benzene (1:1) solvent; the buffering of the papers is depending on the mixture to be separated [7].

The alkaline cleavage [8] of phloraspin yielded aspidinol (II) and desaspidinol (= phlorobutyrophenone 4-methyl ether) (III), both identified by paper chromatographic separation [7]. The R_F-curves on papers buffered to pH 9.1—8.0 were identical with the R_F-curves obtained for authentic specimens of aspidinol, m.p. 142—143°, and desaspidinol, m.p. 127—128° * (Fig. 1). The R_F-curve of phlorobutyrophenone 2-methyl ether distinctly differs from the R_F-curves obtained for the products which were formed by the alkaline cleavage of phloraspin.

These decomposition products can be explained by the phloraspin structure I: aspidinol and desaspidinol are obtained when the methylene bridge is broken along A— — —A and along B— — —B, respectively.

Phloraspin was synthesised by dissolving methylphlorobutyrophenone, m.p. 162—163°, and desaspidinol, m.p. 127—128° in dilute alkali and treating the solution with formaldehyde. The reaction product consisted of phloraspin together with the two symmetrical compounds, *i.e.*, methylene-bis-methylphlorobutyrophenone and methylene-bis-desaspidinol. Phloraspin was isolated from the mixture by recrystallisation from benzene and methanol. The melting

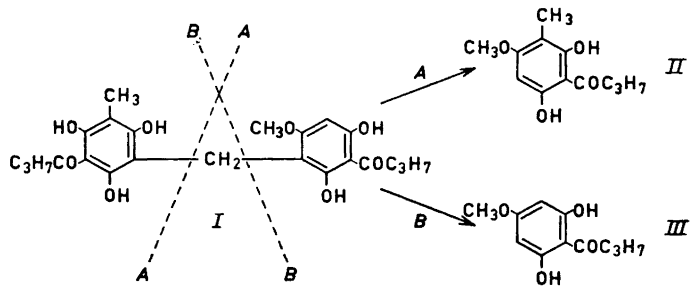

* Desaspidinol (= phlorobutyrophenone-4-methyl ether) is earlier reported to have a m.p. of 113° [10] and 121—123° [11] while the corresponding 2-methyl ether has a m.p. of 130° [10]. Proof was needed to give conclusive evidence of our desaspidinol with the m.p. of 127—128° being the true 4-methyl isomer. This proof is published elsewhere [12].

point of the synthetic phloraspin was 212—213° showing with natural phloraspin a mixed melting point of 211—212°.

In a recent report by Klevstrand [9] a melting point of 216—218° is given for phloraspin. According to our observations, as well as to an earlier report by Widén [6], phloraspin undergoes decomposition when heated to the temperature of fusion visible by a dark red colour of the fused material. When heating is carried out rapidly somewhat higher melting points may be obtained, in our case 215—216° was observed, but the lower melting point mentioned is considered to be the more correct.

EXPERIMENTAL

Isolation of phloraspin. The "raw aspidin" from *Dryopteris austriaca* rhizomes was obtained as previously described [1]. Flavaspidic acid, aspidin and albaspidin were isolated according to Aho [5]. The mother liquid was dried in vacuum and phloraspin obtained by crystallisation from benzene. Repeated recrystallisations from benzene and methanol yielded phloraspin in a pure state with a m.p. of 211—212°. (Found: C 63.90, 63.72; H 6.70, 6.65; OCH_3 7.02. Calc. for $C_{23}H_{28}O_8$: C 63.88; H 6.48; OCH_3 7.17.)

Alkaline cleavage of phloraspin. Phloraspin (300 mg) was dissolved in aqueous sodium hydroxide (2 M, 50 ml), zinc dust (600 mg) was added and the mixture heated on a steam bath for 5 min. After addition of water (50 ml) the solution was filtered, acidified with sulphuric acid (10 %) and extracted with ether. The ethereal solution was evaporated to dryness and the residue dissolved in acetone. The acetone solution was paper chromatographed [7]: aspidinol and desaspidinol were identified as the main components among the decomposition products formed.

Synthesis of phloraspin. Phloraspin was synthesised from methylphlorobutyrophenone and desaspidinol as follows: methylphlorobutyrophenone (2.1 g) and desaspidinol (2.1 g) were dissolved in potassium hydroxide (200 ml, 1 %) and formaldehyde (0.6 ml, 40 %) was added. The mixture was kept at room temperature for 15 min and made acidic with hydrochloric acid (10 %). The precipitate was filtered off, washed with water and dried. After several recrystallisations from benzene and methanol phloraspin was freed from the symmetrical compounds formed and obtained in a pure state with a m.p. of 212—213°, mixed m.p. with natural phloraspin, of 212—213°. (Found: C 63.79, 63.67; H 6.70, 6.67; OCH_3 7.06. Calc. for $C_{23}H_{28}O_8$: C 63.88; H 6.48; OCH_3 7.17.)

REFERENCES

1. Penttilä, A. and Sundman, J. *Acta Chem. Scand.* **15** (1961) 839.
2. Kraft, F. *Schweiz. Wschr. Pharm. Chem.* **40** (1902) 322.
3. Kraft, F. *Arch. Pharm.* **242** (1904) 489.
4. Boehm, R. *Ann.* **329** (1903) 338.
5. Aho, E. *Über Isolierung und tautomere Formen der Flavaspidsäure und anderer Filix-phloroglucinabkömmlinge* (Diss.) University of Turku 1958.
6. Widén, B. *Untersuchungen über die Phloroglucinderivate finnischer Farnarten* (Diss.) University of Helsinki 1944.
7. Penttilä, A. and Sundman, J. *J. Pharm. and Pharmacol.* **13** (1961) 531.
8. Boehm, R. *Ann.* **318** (1901) 230.
9. Klevstrand, R. *Medd. Norsk. Farm. Selskap* **22** (1960) 23.
10. Karrer, P. *Helv. Chim. Acta* **2** (1919) 466.
11. Aebi, A., Kapoor, A. L. and Büchi, J. *Helv. Chim. Acta* **40** (1957) 572.
12. Penttilä, A. and Sundman, J. *Finska Kemistsamfundets Medd.* **70** (1961) 61.

Received May 10, 1961.

ACTA CHEMICA SCANDINAVICA 15 (1961) 1780–1796

Short Communications

Heterocyclic Boron Compounds I

K. A. JENSEN and THORVALD PEDERSEN

Chemical Laboratory of the University of Copenhagen, Copenhagen, Denmark

In connexion with attempts to prepare boracycloheptatriene (borepin) and other heteroaromatic boron compounds it was found that acyloins (acetoin, propioin, benzoin) react smoothly with phenylboron dichloride according to the following scheme:

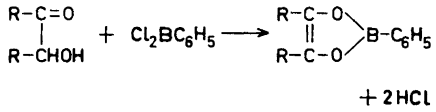

probably with the following compound as an intermediate:

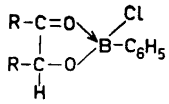

The compound derived from propioin is a colourless liquid, whereas those derived from acetoin and benzoin form colourless crystals. They are all very sensitive to humidity and are hydrolysed to the acyloin and phenylboric acid. Attempts to prepare the benzoin derivative from phenylboric acid and benzoin were unsuccessful.

The above compounds are derivatives of a ring system 1,3-dioxa-2-boracyclopentene or 1,3,2-dioxaborole which might be considered a heteroaromatic system since the grouping $-\overline{B}=\overset{+}{O}-$ is isoelectronic with the grouping $>C=C<$. The aromatic stabilisation is, however, not significant. Dewar *et al.*[1] have prepared a similar derivative of catechol, which was also very sensitive to humidity.

Phenylboron dichloride also reacts with esters of α-hydroxyacids, such as ethyl lactate. In this case the reaction proceeds according to the scheme:

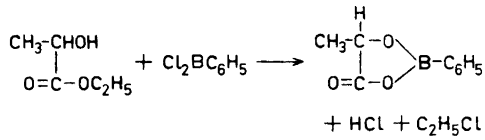

The resulting 2-phenyl-4-methyl-5-oxo-1,3,2-dioxaborolane is a colourless liquid which is extremely easily hydrolysed so that special care has to be taken to avoid hydrolysis when it is handled.

The infrared spectrum of this compound (in CCl_4 solution) shows a strong band at 1803 cm^{-1}, corresponding to a lactone C=O group, but no absorption above 3050 cm^{-1}. Accordingly the compound must have the structure assigned to it above; no tautomerisation to the 5-hydroxydioxaborole seems to occur.

The infrared spectra of the acyloin derivatives show no absorption in the double bond region. This seems to indicate that the dioxaborole ring system has some aromatic character irrespective of chemical reactivity. All the heterocyclic boron compounds studied show strong absorption bands at 1440–1445 cm^{-1} (C_6H_5–B), 1365–1375 and 1310–1320 cm^{-1} (B–O) and 1240–1270 cm^{-1} (C–O–).

Similar S- and N-containing compounds are being studied.

EXPERIMENTAL

General procedure. A solution of phenylboron dichloride (0.1 mole) in dry methylene chloride (100 ml) was placed in a three-necked flask

provided with a precision-ground stirrer, a reflux condenser with a $CaCl_2$-tube and a dropping funnel with a pressure-equalising tube. A solution of the acyloin (0.1 mole) in methylene chloride (100-400 ml, see below) was added through the dropping funnel in the course of 1 ½ h while a stream of dry nitrogen was passed through the apparatus from an inlet in the dropping funnel. Finally the solution was refluxed for 1 h. The hydrogen chloride evolved was collected in water and titrated with sodium hydroxide; usually a titer close to 95 % of the theoretical was found.

After the solution had been refluxed, the reflux condenser was replaced by a Claisen head with condenser and the solvent was distilled off. The triphenyl derivative crystallised; it was recrystallised from acetone. The other compounds were distilled *in vacuo*, moisture being carefully prevented from passing into the apparatus.

2,4,5-Triphenyl-1,3,2-dioxaborole. From 21.2 g of benzoin dissolved in 400 ml of methylene chloride. Recrystallised from dry acetone. Yield 16.7 g = 58 %. M.p. 110.5–111°C. (Found: C 79.80; H 5.05. Calc. for $C_{20}H_{15}BO_2$: C 80.50; H 5.07).

2-Phenyl-4,5-diethyl-1,3,2-dioxaborole. From 11.6 g of propioin in 100 ml of methylene chloride. Yield 10.0 g = 50 %. B.p./11 mm: 118–19°C. (Found: C 71.20; H 7.50. Calc. for $C_{12}H_{15}BO_2$: C 71.34; H 7.43).

2-Phenyl-4,5-dimethyl-1,3,2-dioxaborole. From 8.8 g of dimeric acetoin dissolved in 250 ml of methylene chloride. The reaction product, which boiled from 119 to 129°C at 11–12 mm Hg, crystallised on standing; it was recrystallised from pentane. Yield 9.3 g = 53 %. M.p. 43.5–44.5°C. The compound was very sensitive to humidity, and we did not succeed in obtaining quite correct analytical values. (Found: C 67.20; H 6.63. Calc. for $C_{10}H_{11}BO_2$: C 69.02; H 6.37).

2-Phenyl-4-methyl-5-oxo-1,3,2-dioxaborolane. From 11.8 g of ethyl lactate in 125 ml methylene chloride. Yield 8 g = 46 %, distilling from 127 to 128°C at 11 mm Hg. (Found: C 61.50; H 5.38. Calc. for $C_9H_9BO_3$: C 61.42; H 5.35).

1. Dewar, M. J. S., Kuppa, V. P. and Pettit, R. *J. Chem. Soc.* **1958** 3073, 3076.

Received October 11, 1961.

The Structure of β-Lyxose

ASBJÖRN HORDVIK

University College of Addis Ababa, Ethiopia

In 1947 Hassel and Ottar [1] advanced the assumption that the six membered pyranose ring is chair formed. The correctness of this assumption has been confirmed by the determination of several pyranose structures [2-6]. The chair formed pyranose ring, however, made it necessary to accept two possible structures for each pyranose isomer, one being formed from the other by a conversion of the ring. The existence of only one of the conversion forms of a pyranose in the crystalline state seems to be due to their different stability, and the hexa- and penta-pyranoses which so far have been determined [2-6] agree with the proposals of Reeves [7].

The purpose of the present work is to find out whether the same is valid for β-lyxose. This pentapyranose has the conversion forms 1*e*2*a*3*e*4*e* and 1*a*2*e*3*a*4*a*. According to Reeves' stability scheme the first form is the more stable, and is consequently expected to be found in β-lyxose crystals.

Crystallization of β-lyxose was tried from several different solvents, but always resulted in syrups. Eventually one crystal large enough for single crystal studies was obtained by placing some syrup on an objective glass and then making scratches in the glass. The crystals grown in this way are needle-shaped and elongated along the *c* axis.

Space group and axial lengths were determined from Weissenberg and oscillation photographs, using Cu$K\alpha$ radiation. The crystals are orthorhombic and the space group is $P2_12_12_1$. The unit cell dimensions are, a = 9.58 Å, b = 10.42 Å and c = 6.53 Å, to within 0.5 %. With four molecules in the unit cell the calculated density is 1.53 g/cm³, which agrees with the experimental value 1.54 g/cm³.

The intensities of the $hk0$ reflections were estimated visually from a series of Weissenberg photographs, using an intensity scale made from one of the reflections in this zone. 67 $hk0$ reflections were observed, representing about 52 % of the possible number observable under the experimental conditions. The intensities were corrected for the Lorenz and polarization factors in the usual way, and in order to derive the

provided with a precision-ground stirrer, a reflux condenser with a $CaCl_2$-tube and a dropping funnel with a pressure-equalising tube. A solution of the acyloin (0.1 mole) in methylene chloride (100-400 ml, see below) was added through the dropping funnel in the course of 1 ½ h while a stream of dry nitrogen was passed through the apparatus from an inlet in the dropping funnel. Finally the solution was refluxed for 1 h. The hydrogen chloride evolved was collected in water and titrated with sodium hydroxide; usually a titer close to 95 % of the theoretical was found.

After the solution had been refluxed, the reflux condenser was replaced by a Claisen head with condenser and the solvent was distilled off. The triphenyl derivative crystallised; it was recrystallised from acetone. The other compounds were distilled *in vacuo*, moisture being carefully prevented from passing into the apparatus.

2,4,5-Triphenyl-1,3,2-dioxaborole. From 21.2 g of benzoin dissolved in 400 ml of methylene chloride. Recrystallised from dry acetone. Yield 16.7 g = 58 %. M.p. 110.5–111°C. (Found: C 79.80; H 5.05. Calc. for $C_{20}H_{15}BO_2$: C 80.50; H 5.07).

2-Phenyl-4,5-diethyl-1,3,2-dioxaborole. From 11.6 g of propioin in 100 ml of methylene chloride. Yield 10.0 g = 50 %. B.p./11 mm: 118–19°C. (Found: C 71.20; H 7.50. Calc. for $C_{12}H_{15}BO_2$: C 71.34; H 7.43).

2-Phenyl-4,5-dimethyl-1,3,2-dioxaborole. From 8.8 g of dimeric acetoin dissolved in 250 ml of methylene chloride. The reaction product, which boiled from 119 to 129°C at 11–12 mm Hg, crystallised on standing; it was recrystallised from pentane. Yield 9.3 g = 53 %. M.p. 43.5–44.5°C. The compound was very sensitive to humidity, and we did not succeed in obtaining quite correct analytical values. (Found: C 67.20; H 6.63. Calc. for $C_{10}H_{11}BO_2$: C 69.02; H 6.37).

2-Phenyl-4-methyl-5-oxo-1,3,2-dioxaborolane. From 11.8 g of ethyl lactate in 125 ml methylene chloride. Yield 8 g = 46 %, distilling from 127 to 128°C at 11 mm Hg. (Found: C 61.50; H 5.38. Calc. for $C_9H_9BO_3$: C 61.42; H 5.35).

1. Dewar, M. J. S., Kuppa, V. P. and Pettit, R. *J. Chem. Soc.* **1958** 3073, 3076.

Received October 11, 1961.

The Structure of β-Lyxose

ASBJÖRN HORDVIK

University College of Addis Ababa, Ethiopia

In 1947 Hassel and Ottar [1] advanced the assumption that the six membered pyranose ring is chair formed. The correctness of this assumption has been confirmed by the determination of several pyranose structures [2-6]. The chair formed pyranose ring, however, made it necessary to accept two possible structures for each pyranose isomer, one being formed from the other by a conversion of the ring. The existence of only one of the conversion forms of a pyranose in the crystalline state seems to be due to their different stability, and the hexa- and penta-pyranoses which so far have been determined [2-6] agree with the proposals of Reeves [7].

The purpose of the present work is to find out whether the same is valid for β-lyxose. This pentapyranose has the conversion forms 1*e*2*a*3*e*4*e* and 1*a*2*e*3*a*4*a*. According to Reeves' stability scheme the first form is the more stable, and is consequently expected to be found in β-lyxose crystals.

Crystallization of β-lyxose was tried from several different solvents, but always resulted in syrups. Eventually one crystal large enough for single crystal studies was obtained by placing some syrup on an objective glass and then making scratches in the glass. The crystals grown in this way are needle-shaped and elongated along the *c* axis.

Space group and axial lengths were determined from Weissenberg and oscillation photographs, using Cu$K\alpha$ radiation. The crystals are orthorhombic and the space group is $P2_12_12_1$. The unit cell dimensions are, a = 9.58 Å, b = 10.42 Å and c = 6.53 Å, to within 0.5 %. With four molecules in the unit cell the calculated density is 1.53 g/cm³, which agrees with the experimental value 1.54 g/cm³.

The intensities of the $hk0$ reflections were estimated visually from a series of Weissenberg photographs, using an intensity scale made from one of the reflections in this zone. 67 $hk0$ reflections were observed, representing about 52 % of the possible number observable under the experimental conditions. The intensities were corrected for the Lorenz and polarization factors in the usual way, and in order to derive the

unitary structure factors of the reflections, the observed structure factors were put on an approximately absolute scale by Wilson's method [8].

The carbon and oxygen contributions to calculated structure factors are based on the atomic scattering curves of Berghuis *et al.*[9]

The Patterson *c* projection revealed the general arrangement of the molecules (rather similar to the arrangement in the *a* projection of β-arabinose [6]), and this indicated that the strong reflection 400 should have a negative sign. The signs of 210 and 790 were chosen, and probable phases of 28 reflections were deduced by Zachariassen's method [10]. Eight sets of phases were found, but the corresponding Fourier maps were difficult to interpret, as none showed a maximum corresponding to an axial hydroxyl oxygen atom. An approximate map showing such a maximum, and also giving a rough outline of the molecule, was eventually obtained by selecting 15 phases by an application of a method proposed by Woolfson [11]. These 15 phases were common for two of the phase sets. Further phases for both sets were deduced for unitary structure factors larger than 0.1 by the equation $s(\mathbf{h}) = s(\Sigma_{\mathbf{h}'} U_{\mathbf{h}} U_{\mathbf{h}+\mathbf{h}'})$ (Cochran and Woolfson [12]). The two corresponding electron density maps were very nearly mirror images of each other around $(a/8, b/4)$. For one of these structures the refinement process stopped at an R_1 value of 0.26, while the other one, with coordinates as listed in Table 1, gave $R_1 = 0.15$ and so proved to be the correct one. In $R_1 = \Sigma|F_o - F_c|/\Sigma|F_o|$ also unobserved reflections are included. An overall temperature function $\exp(-3.0 \sin^2\Theta/\lambda^2)$ was used. Contributions from hydrogen atoms to the structure amplitudes have so far been ignored.

Table 1. Atomic coordinates, in fractions of corresponding cell edges. Origin on twofold screw axis.

	x	*y*
C_1	0.090	0.124
C_2	0.117	0.262
C_3	0.087	0.357
C_4	0.179	0.326
C_5	0.144	0.187
O_1	0.134	0.028
O_2	0.259	0.260
O_3	0.124	0.486
O_4	0.133	0.409
O_5	0.180	0.109

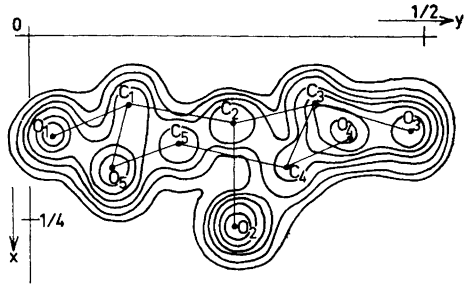

Fig. 1. Electron density projection of β-lyxose on the (001) plane, showing one asymmetric unit. Plane group *pgg*, origin at 2. Contours at arbitrary but equal intervals.

The final electron density map is reproduced in Fig. 1. It shows that β-lyxose has the configuration *1e2a3e4e* in agreement with Reeves' prediction.

An account of the crystal structure determination, when completed, and a discussion of the molecular structure will be published later.

I wish to thank *Fr. Meltzer's Höyskolefond* for a grant.

1. Hassel, O. and Ottar, B. *Acta Chem. Scand.* **1** (1947) 929.
2. McDonald, T.R.R. and Beevers, C.A. *Acta Cryst.* **5** (1952) 654.
3. McGeachin, H. McD. and Beevers, C. A. *Acta Cryst.* **10** (1957) 227.
4. Woolfson, M. M. *Acta Cryst.* **11** (1958) 393.
5. Furberg, S. *Acta Chem. Scand.* **14** (1960) 1357.
6. Hordvik, A. *Acta Chem. Scand.* **15** (1961) 16.
7. Reeves, R. E. *J. Am. Chem. Soc.* **72** (1950) 1499.
8. Wilson, A. J. C. *Acta Cryst.* **2** (1949) 318.
9. Berghuis, J., Haanappel, I. M., Potters, M., Loopstra, B. O., MacGillavry, C. H. and Veenendaal, A. L. *Acta Cryst* **8** (1955) 478.
10. Zachariassen, W. H. *Acta Cryst.* **5** (1952) 68.
11. Woolfsen, M. M. *Acta Cryst.* **10** (1957) 116.
12. Cochran, W. and Woolfson, M. M. *Acta Cryst.* **8** (1955) 1.

Received September 28, 1961.

A Theoretical Interpretation of Dale's Rule for the Position of the Absorption Bands of Linear Conjugated Polyenes

J. N. MURRELL

Department of Chemistry, University of Sheffield, Sheffield, England

Dale [1,2] has noticed that the wavelength of the pth absorption band (λ_p) of a linear conjugated polyene containing n double bonds, is almost the same as that of the first absorption band of a polyene containing n/p double bonds. If p/n is not an integer then the wavelength for this hypothetical molecule is interpolated from the experimental curve relating λ_1 to n for the real polyenes. To explain this generalization Dale postulated a selection rule for the polyene transitions, namely that only the outermost π-electron shell could be excited. In the ground state of the polyenes the first n molecular orbitals are filled, so that Dale's selection rule means that the absorption bands arise from the transitions $n \rightarrow n+1$, $n \rightarrow n+2$, $n \rightarrow n+3$, *etc.*, but that $n-1 \rightarrow n+1$, *etc.* are forbidden.

Dale's selection rule was derived from the free-electron-pattern of molecular orbital energies. He showed that the transition energy was given by the formula

$$\Delta E(n \rightarrow n+p) \propto \frac{p}{n} + \frac{p^2}{n^2} \qquad (1)$$

if the free electron path was taken to be $2n$, and this formula explains his observations. However, the transitions from the other occupied orbitals of the ground state do not fall into this pattern, thus

$$\Delta E(n+1-p \rightarrow n+1) \propto \frac{p}{n} + \frac{p(2-p)}{n^2} \qquad (2)$$

Kuhn and Bar [3] have shown that even if the effect of bond alternation on the free electron potential is allowed for, the pattern of orbital energies explains the experimental results only if Dale's selection rule is adopted. However, just because an empirical theory gives results which agree with experiment that does not mean that it is correct. The agreement may be fortuitous. On the free electron theory the second absorption band should arise from the transition $n-1 \rightarrow n+1$, whether we have bond alternation or not, and there is no theoretical justification behind Dale's selection rule, which removes this transition from the spectrum. In this note I shall show that Dale's observations can be explained without introducing any new selection rules.

Although a theory based on a one-electron Hamiltonian (*e.g.* free electron or Hückel theory) can correlate the position of a particular band (especially the first band) in a series of related molecules, it fails to explain the relative positions of successive bands in the spectrum. To do this the electron repulsion terms in the Hamiltonian have to be taken into account. A theory of polyene spectra which does include these terms, and which is justified for the polyenes because of the double bond localisation in these molecules, has been developed by Simpson [4,5]. In this theory he just considers the electronic interaction between n coupled ethylene fragments, each of which has one excited state: that giving the strong band $V \rightarrow N$ of ethylene ($\lambda \sim 1700$ Å). If there is an interaction term of the Hamiltonian H' between two adjacent double bonds, then the energy of the pth excited state can be shown to be [5]

$$E_p = E_0 - 2 \mid H' \mid \cos[\pi p/(n+1)] \qquad (3)$$

where E_0 is the excitation energy of a single double bond. This formula gives fairly good agreement for the position of the fundamental and overtone bands of the linear polyenes; it therefore follows that it must also explain Dale's observations. From expression 3, the first band of the n/p polyene has an energy

$$E_1 = E_0 - 2 \mid H' \mid \cos[\pi/\left(\frac{p}{n} + 1\right)]$$
$$= E_0 - 2 \mid H' \mid \cos([\pi p/(n+p)] \qquad (4)$$

If p is significantly smaller than n, as it must be to see a band in the accessible ultra-violet region of the spectrum, then $\cos[\pi p/(n+p)] \simeq \cos[\pi p/(n+1)]$. For example, for the 5th band of dodecapreno-β-carotene ($n = 19$), Dale calculates $\lambda_5 = 292$ mμ, and the observed value is 288 mμ. But for this case $\cos(5\pi/20) = 0.71$ and $\cos(5\pi/24) = 0.79$, which are sufficiently close to explain Dale's observations.

Since Simpson's theory gives a satisfactory qualitative account of the polyene spectra, it must be assumed that a free electron theory which includes bond alternation and electron interaction would do so also, and in this theory Dale's selection rule would not be required.

1. Dale, J. *Acta Chem. Scand.* **8** (1954) 1235.
2. Dale, J. *Acta Chem. Scand.* **11** (1957) 265.
3. Kuhn, H. *Progr. in Chem. Org. Nat. Prods.* **17** (1959) 404.
4. Simpson, W. T. *J. Am. Chem. Soc.* **73** (1951) 5363.
5. Simpson, W. T. *J. Am. Chem. Soc.* **77** (1955) 6164.

Received September 28, 1961.

On the Donor Strength of Amides

MARGARETA ZACKRISSON

Institute of Chemistry, University of Uppsala, Uppsala, Sweden

It has previously been suggested [1] that two main effects can be predicted from a comparison of the strengths of ketones and esters as donor molecules. Accordingly the inductive effect associated with the substitution of the more electronegative methoxy group for a methyl group can be expected to reduce the donor strength, while this effect may be counteracted by the delocalization of one of the two lone pairs of electrons in the ether oxygen atom. The two effects seem to balance each other in this instance.

If the carbonyl oxygen atom in an amide acts as the donor, the same two effects can be assumed to influence the donor strengths when passing from ketones to amides. The inductive effect associated with the substitution of the $(CH_3)_2N$ group for a CH_3 group should reduce the donor strength while the delocalization of the lone pair electrons of the nitrogen atom should exert an opposing influence. In order to estimate the magnitude of the donor strength of amides compared with that of ketones, some reactions between tertiary amides and acetone as donors and $SbCl_5$ or $SnCl_4$ as acceptors have been studied by qualitative thermochemical measurements. The effect of further substitution leading to tetramethylurea was also studied.

Experimental. All chemicals used were commercial products which were further purified by distillation.

The thermochemical measurements were made in ethylene chloride solutions as described earlier [2], but with different concentrations.

Results and discussion. In each case the infrared spectra of the addition compounds formed in the systems studied (unpublished) show a decrease in the carbonyl bond frequency (in the free molecules situated in the range 1690–1650 cm^{-1}). In the compound formed between $SbCl_5$ and NN-dimethylformamide, however, this decrease is not significant, whereas in the compound formed with NN-dimethylacetamide the decrease is about 20 cm^{-1}. A decrease in the carbonyl bond frequency was earlier assumed to indicate that the carbonyl oxygen atom functioned as the donor. Although the negligible shift found in NN-dimethylformamide cannot be explained without further investigation, there is no prior reason to suspect that this compound would react differently from NN-dimethylacetamide. From the infrared spectra, therefore, it appears as though the carbonyl oxygen atom acts as the donor in all these molecules. It is further suggested that the oxygen atom in these amides functions as a donor in compounds formed with BCl_3 and BBr_3[4] and with $TiCl_4$[5].

The results from the thermochemical measurements are given in Table 1. From this table it appears that the amides are much better donor molecules than the ketone. If the inductive and the delocalization effects are the main influences on the relative donor strengths when passing from ketones to amides, the delocalization effects seems to be much more significant. With $SbCl_5$ tetramethylurea is a better donor than the amides. Other effects that can influence the donor strength cannot be excluded, but a discussion of these possible influences can only be made after further investigations of the compounds formed. In this connection a structure determination of the compound $SbCl_5 \cdot HCON(CH_3)_2$ using X-ray techniques has already been started at this institute.

A grant from the *Swedish Natural Science Research Council* is gratefully acknowledged.

Table 1.

Acceptor: $SbCl_5$

$(CH_3)_2NCON(CH_3)_2 > CH_3CON(CH_3)_2 = HCON(CH_3)_2 >> (CH_3)_2CO$

Acceptor: $SnCl_4$

$(CH_3)_2NCON(CH_3)_2 = CH_3CON(CH_3)_2 = HCON(CH_3)_2 >> (CH_3)_2CO$

1. Dale, J. *Acta Chem. Scand.* **8** (1954) 1235.
2. Dale, J. *Acta Chem. Scand.* **11** (1957) 265.
3. Kuhn, H. *Progr. in Chem. Org. Nat. Prods.* **17** (1959) 404.
4. Simpson, W. T. *J. Am. Chem. Soc.* **73** (1951) 5363.
5. Simpson, W. T. *J. Am. Chem. Soc.* **77** (1955) 6164.

Received September 28, 1961.

On the Donor Strength of Amides

MARGARETA ZACKRISSON

Institute of Chemistry, University of Uppsala, Uppsala, Sweden

It has previously been suggested [1] that two main effects can be predicted from a comparison of the strengths of ketones and esters as donor molecules. Accordingly the inductive effect associated with the substitution of the more electronegative methoxy group for a methyl group can be expected to reduce the donor strength, while this effect may be counteracted by the delocalization of one of the two lone pairs of electrons in the ether oxygen atom. The two effects seem to balance each other in this instance.

If the carbonyl oxygen atom in an amide acts as the donor, the same two effects can be assumed to influence the donor strengths when passing from ketones to amides. The inductive effect associated with the substitution of the $(CH_3)_2N$ group for a CH_3 group should reduce the donor strength while the delocalization of the lone pair electrons of the nitrogen atom should exert an opposing influence. In order to estimate the magnitude of the donor strength of amides compared with that of ketones, some reactions between tertiary amides and acetone as donors and $SbCl_5$ or $SnCl_4$ as acceptors have been studied by qualitative thermochemical measurements. The effect of further substitution leading to tetramethylurea was also studied.

Experimental. All chemicals used were commercial products which were further purified by distillation.

The thermochemical measurements were made in ethylene chloride solutions as described earlier [2], but with different concentrations.

Results and discussion. In each case the infrared spectra of the addition compounds formed in the systems studied (unpublished) show a decrease in the carbonyl bond frequency (in the free molecules situated in the range 1690–1650 cm^{-1}). In the compound formed between $SbCl_5$ and NN-dimethylformamide, however, this decrease is not significant, whereas in the compound formed with NN-dimethylacetamide the decrease is about 20 cm^{-1}. A decrease in the carbonyl bond frequency was earlier assumed to indicate that the carbonyl oxygen atom functioned as the donor. Although the negligible shift found in NN-dimethylformamide cannot be explained without further investigation, there is no prior reason to suspect that this compound would react differently from NN-dimethylacetamide. From the infrared spectra, therefore, it appears as though the carbonyl oxygen atom acts as the donor in all these molecules. It is further suggested that the oxygen atom in these amides functions as a donor in compounds formed with BCl_3 and BBr_3[4] and with $TiCl_4$[5].

The results from the thermochemical measurements are given in Table 1. From this table it appears that the amides are much better donor molecules than the ketone. If the inductive and the delocalization effects are the main influences on the relative donor strengths when passing from ketones to amides, the delocalization effects seems to be much more significant. With $SbCl_5$ tetramethylurea is a better donor than the amides. Other effects that can influence the donor strength cannot be excluded, but a discussion of these possible influences can only be made after further investigations of the compounds formed. In this connection a structure determination of the compound $SbCl_5 \cdot HCON(CH_3)_2$ using X-ray techniques has already been started at this institute.

A grant from the *Swedish Natural Science Research Council* is gratefully acknowledged.

Table 1.

Acceptor: $SbCl_5$

$(CH_3)_2NCON(CH_3)_2 > CH_3CON(CH_3)_2 = HCON(CH_3)_2 >> (CH_3)_2CO$

Acceptor: $SnCl_4$

$(CH_3)_2NCON(CH_3)_2 = CH_3CON(CH_3)_2 = HCON(CH_3)_2 >> (CH_3)_2CO$

I wish to thank Dr. I. Lindqvist for suggesting the problem and for his stimulating interest during the work and also Prof. G. Hägg for all the facilities placed at my disposal.

1. Lindqvist, O. and Fjellström, B. *Acta Chem. Scand.* **14** (1960) 2055.
2. Lindqvist, I. and Zackrisson, M. *Acta Chem. Scand.* **14** (1960) 453.
3. Zackrisson, M. and Lindqvist, I. *J. Inorg. Nuclear Chem.* **17** (1961) 69.
4. Gerrard, W., Lappert, M. F., Pyszora, H. and Wallis, J. W. *J. Chem.* Soc. **1960** 2144.
5. Archambault, J. and Rivest, R. *Can. J. Chem.* **36** (1958) 1461.

Received November 1, 1961.

A Comparison between Oxygen and Sulphur as Donor Atoms

MARGARETA ZACKRISSON

Institute of Chemistry, University of Uppsala, Uppsala, Sweden

In an earlier paper [1] it was reported that ethyl sulphide has better donor properties than ethyl ether in reactions with $SbCl_5$ and $SnCl_4$. It is of interest, therefore, to know whether, in comparable compounds, sulphur is always a better donor atom than oxygen in reactions with these acceptor molecules. To obtain the relevant information a few acceptor-donor reactions have been studied by qualitative thermochemical measurements. In these reactions, $SbCl_5$ and $SnCl_4$ were used as acceptor molecules, while comparable compounds of sulphur and oxygen comprised the donor molecules. The various donor molecules studied include different ways of bonding the donor atoms.

Experimental. NN-dimethyl-thioacetamide was prepared according to Kindler [2]. M.p. 73–74°. Other chemicals used were commercial products which were further purified by distillation.

Table 1.

Acceptor: $SbCl_5$
$C_4H_8S > C_4H_8O$
$POCl_3 >> PSCl_3$

Acceptor: $SnCl_4$
$C_4H_8S > C_4H_8O$
$CH_3CON(CH_3)_2 = CH_3CSN(CH_3)_2$
$POCl_3 > PSCl_3$

The thermochemical experiments were made in ethylene chloride solutions as described earlier [1], but with different concentrations.

Results and discussion. The relative donor strengths are given in Table 1. As might be expected, tetrahydrothiophene and tetrahydrofuran show the same relative donor strengths as the ether and sulphide investigated earlier [1].

In both the amide and the thioamide studied here, the molecules contain two possible donor atoms since the nitrogen atom may also have donor properties. The infrared spectra of the addition compounds show, however, that the C=O bond frequency of the amide (1660 cm^{-1}) decreases upon adduct formation, as does the C=S bond frequency of the thioamide (1280 cm^{-1}) (unpublished results). Negative shifts in the carbonyl bond frequency were earlier assumed to indicate that the carbonyl oxygen functioned as the donor [3]. Accordingly it appears that the oxygen atom of the amide and the sulphur atom of the thioamide are the donor atoms. The addition compound formed between NN-dimethyl-thioacetamide and $SbCl_5$ is so slightly soluble in ethylene chloride that no measurements could be made. The adduct formed with $SnCl_4$ also precipitates when the molar ratio, acceptor:donor, is 1:2. However, at the molar ratio 1:1, measurements could be made. The table shows that no difference in the donor strengths could be detected.

$POCl_3$ is a better donor molecule than $PSCl_3$ and the difference is most marked when $SbCl_5$ is used as acceptor.

From the above considerations it is impossible to state that one type of atom, oxygen or sulphur, is a better donor than the other in reactions with the acceptor molecules studied. As far as these few experiments can show, the type of bonding to the donor atom is of importance to the relative donor strengths of sulphur and oxygen. At present, however, it is not possible to explain why in molecules of the ether type sulphur is a better donor atom than oxygen, why in molecules where the donor atoms are of the carbonyl type the donor strengths of oxygen and sulphur are approximately equal, and why in phosphoryl type molecules the phosphoryl oxygen is a better donor atom than sulphur in the same position.

A grant from the *Swedish Natural Science Research Council* is gratefully acknowledged.

I wish to thank Dr. I. Lindqvist for suggesting the problem and for his stimulating interest during the work and also Prof. G. Hägg for all the facilities placed at my disposal.

1. Lindqvist, O. and Fjellström, B. *Acta Chem. Scand.* **14** (1960) 2055.
2. Lindqvist, I. and Zackrisson, M. *Acta Chem. Scand.* **14** (1960) 453.
3. Zackrisson, M. and Lindqvist, I. *J. Inorg. Nuclear Chem.* **17** (1961) 69.
4. Gerrard, W., Lappert, M. F., Pyszora, H. and Wallis, J. W. *J. Chem.* Soc. **1960** 2144.
5. Archambault, J. and Rivest, R. *Can. J. Chem.* **36** (1958) 1461.

Received November 1, 1961.

A Comparison between Oxygen and Sulphur as Donor Atoms

MARGARETA ZACKRISSON

Institute of Chemistry, University of Uppsala, Uppsala, Sweden

In an earlier paper [1] it was reported that ethyl sulphide has better donor properties than ethyl ether in reactions with $SbCl_5$ and $SnCl_4$. It is of interest, therefore, to know whether, in comparable compounds, sulphur is always a better donor atom than oxygen in reactions with these acceptor molecules. To obtain the relevant information a few acceptor-donor reactions have been studied by qualitative thermochemical measurements. In these reactions, $SbCl_5$ and $SnCl_4$ were used as acceptor molecules, while comparable compounds of sulphur and oxygen comprised the donor molecules. The various donor molecules studied include different ways of bonding the donor atoms.

Experimental. NN-dimethyl-thioacetamide was prepared according to Kindler [2]. M.p. 73–74°. Other chemicals used were commercial products which were further purified by distillation.

Table 1.

Acceptor: $SbCl_5$
$C_4H_8S > C_4H_8O$
$POCl_3 >> PSCl_3$

Acceptor: $SnCl_4$
$C_4H_8S > C_4H_8O$
$CH_3CON(CH_3)_2 = CH_3CSN(CH_3)_2$
$POCl_3 > PSCl_3$

The thermochemical experiments were made in ethylene chloride solutions as described earlier [1], but with different concentrations.

Results and discussion. The relative donor strengths are given in Table 1. As might be expected, tetrahydrothiophene and tetrahydrofuran show the same relative donor strengths as the ether and sulphide investigated earlier [1].

In both the amide and the thioamide studied here, the molecules contain two possible donor atoms since the nitrogen atom may also have donor properties. The infrared spectra of the addition compounds show, however, that the C=O bond frequency of the amide (1660 cm^{-1}) decreases upon adduct formation, as does the C=S bond frequency of the thioamide (1280 cm^{-1}) (unpublished results). Negative shifts in the carbonyl bond frequency were earlier assumed to indicate that the carbonyl oxygen functioned as the donor [3]. Accordingly it appears that the oxygen atom of the amide and the sulphur atom of the thioamide are the donor atoms. The addition compound formed between NN-dimethyl-thioacetamide and $SbCl_5$ is so slightly soluble in ethylene chloride that no measurements could be made. The adduct formed with $SnCl_4$ also precipitates when the molar ratio, acceptor:donor, is 1:2. However, at the molar ratio 1:1, measurements could be made. The table shows that no difference in the donor strengths could be detected.

$POCl_3$ is a better donor molecule than $PSCl_3$ and the difference is most marked when $SbCl_5$ is used as acceptor.

From the above considerations it is impossible to state that one type of atom, oxygen or sulphur, is a better donor than the other in reactions with the acceptor molecules studied. As far as these few experiments can show, the type of bonding to the donor atom is of importance to the relative donor strengths of sulphur and oxygen. At present, however, it is not possible to explain why in molecules of the ether type sulphur is a better donor atom than oxygen, why in molecules where the donor atoms are of the carbonyl type the donor strengths of oxygen and sulphur are approximately equal, and why in phosphoryl type molecules the phosphoryl oxygen is a better donor atom than sulphur in the same position.

A grant from the *Swedish Natural Science Research Council* is gratefully acknowledged.

I wish to thank Dr. I. Lindqvist for suggesting the problem and for his stimulating interest during the work and also Prof. G. Hägg for all the facilities placed at my disposal.

1. Lindqvist, I. and Zackrisson, M. *Acta Chem. Scand.* **14** (1960) 453.
2. Kindler, K. *Ann.* **431** (1923) 209.
3. Zackrisson, M. and Lindqvist, I. *J. Inorg. Nuclear Chem.* **17** (1961) 69.

Received November 1, 1961.

6α-Trifluoromethyl-17α-acetoxyprogesterone and some Unsaturated Analogs

W. O. GODTFREDSEN and S. VANGEDAL

Leo Pharmaceutical Products, Copenhagen, Denmark

It has recently been shown [1,2], that introduction of an α-orientated fluorine, chlorine or bromine atom in the 6-position of 17α-acetoxyprogesterone causes a remarkable increase of its oral progestational activity, and that this activity is further increased by Δ^1, Δ^6 or $\Delta^{1,6}$ unsaturation of these compounds. It seemed therefore of interest to synthesize 6α-trifluoromethyl-17α-acetoxyprogesterone and some of its corresponding unsaturated analogs.

When a solution of 17α-acetoxyprogesterone-3-ethyl enol ether (I)[1] in trifluoroiodomethane [3] containing pyridine was irradiated in a quartz vessel at room temperature with ultraviolet light from a high pressure mercury lamp, 6-trifluoromethyl-17α-acetoxyprogesterone-3-ethyl enol ether (II)[m.p. 184–186°C, $[\alpha]_D^{20}$ −181° (all rot. in $CHCl_3$), λ_{max}^{EtOH} 256 mμ, ε 21 400. Found: C 66.53; H 7.66. Calc. for $C_{26}H_{35}F_3O_4$: C 66.65; H 7.53] was obtained in 60 % yield. Acid catalyzed hydrolysis of II afforded smoothly 6α-trifluoromethyl-17α-acetoxyprogesterone (III) (m.p. 206–207°C, $[\alpha]_D^{20}$ +30°, λ_{max}^{EtOH} 234 mμ, ε 15 600. Found: C 65.37; H 6.98. Calc. for $C_{24}H_{31}F_3O_4$: C 65.45; H 7.10).

The α-configuration of the trifluoromethyl group in III followed from stability toward treatment with hydrogen chloride in acetic acid [4], and from the fact, that the rotatory dispersion curve was very similar to that of 17α-acetoxyprogesterone [5].

Selenium dioxide dehydrogenation of III yielded 6α-trifluoromethyl-$\Delta^{1,4}$-pregnadiene-17α-ol-3,20-dione acetate (IV) (m.p. 213–215°C, $[\alpha]_D^{20}$ −29°, λ_{max}^{EtOH} 242 mμ, ε 17 350. Found: C 65.40; H 6.80. Calc. for $C_{24}H_{29}F_3O_4$: C 65.73; H 6.67).

6-Trifluoromethyl-$\Delta^{4,6}$-pregnadiene-17α-ol-3,20-dione acetate (V) (m.p. 233–234°C, $[\alpha]_D^{20}$ 0°, λ_{max}^{EtOH} 270 mμ, ε 20 300. Found: C 65.44; H 6.89. Calc. for $C_{24}H_{29}F_3O_4$: C 65.73; H 6.67) was synthesized from the 3-cycloethylene ketal of III [6] (m.p. 178–182°C, $[\alpha]_D^{20}$ +66°. Found: C 64.28; H 7.29. Calc. for $C_{26}H_{35}F_3O_5$: C 64.45; H 7.28) by bromination at C-7 with NBS followed by dehydrobromination in boiling collidine and hydrolysis of the ketal with methanol-sulfuric acid.

The oral progestational activities of II, III, IV, and V, determined by the Mc Phail modification of the Clauberg assay are given in Table 1.

Table 1. Oral progestational activity — Clauberg assay.

Compound	Relative activity
6α-Methyl-17α-acetoxyprogesterone	1
6α-Trifluoromethyl-17α-acetoxyprogesterone	1–2
6α-Trifluoromethyl-17α-acetoxyprogesterone-3-ethyl enol ether	0.5–1
6-Trifluoromethyl-$\Delta^{4,6}$-pregnadiene-17α-ol-3,20-dione acetate	0.5–1
6α-Trifluoromethyl-$\Delta^{1,4}$-pregnadiene-17α-ol-3,20-dione acetate	0.5–1

1. Ringold, H. J., Batres, E., Bowers, A., Edwards, J. and Zderic, J. *J. Am. Chem. Soc.* **81** (1959) 3485.
2. Bowers, A., Ibàñez, L. C. and Ringold, H. J. *J. Am. Chem. Soc.* **81** (1959) 5991.
3. The addition of trifluoroiodomethane to unsaturated systems has been extensively investigated by Haszeldine. See, *e.g.*, Walling, C. *Free Radicals in Solution*, John Wiley & Sons, New York 1957, pp. 247–272.
4. Bowers, A., Ibàñez, L. C. and Ringold, H. J. *Tetrahedron* **7** (1959) 138.
5. Djerassi, C., Osiecki, J., Riniker, R. and Rinker, B. *J. Am. Chem. Soc.* **80** (1958) 1216.
6. Prepared from III by the dioxolane method: Dauben, H. J., Löken, B. and Ringold, H. J. *J. Am. Chem. Soc.* **76** (1954) 1359.

Received October 11, 1961.

I wish to thank Dr. I. Lindqvist for suggesting the problem and for his stimulating interest during the work and also Prof. G. Hägg for all the facilities placed at my disposal.

1. Lindqvist, I. and Zackrisson, M. *Acta Chem. Scand.* **14** (1960) 453.
2. Kindler, K. *Ann.* **431** (1923) 209.
3. Zackrisson, M. and Lindqvist, I. *J. Inorg. Nuclear Chem.* **17** (1961) 69.

Received November 1, 1961.

6α-Trifluoromethyl-17α-acetoxyprogesterone and some Unsaturated Analogs

W. O. GODTFREDSEN and S. VANGEDAL

Leo Pharmaceutical Products, Copenhagen, Denmark

It has recently been shown [1,2], that introduction of an α-orientated fluorine, chlorine or bromine atom in the 6-position of 17α-acetoxyprogesterone causes a remarkable increase of its oral progestational activity, and that this activity is further increased by Δ^1, Δ^6 or $\Delta^{1,6}$ unsaturation of these compounds. It seemed therefore of interest to synthesize 6α-trifluoromethyl-17α-acetoxyprogesterone and some of its corresponding unsaturated analogs.

When a solution of 17α-acetoxyprogesterone-3-ethyl enol ether (I)[1] in trifluoroiodomethane [3] containing pyridine was irradiated in a quartz vessel at room temperature with ultraviolet light from a high pressure mercury lamp, 6-trifluoromethyl-17α-acetoxyprogesterone-3-ethyl enol ether (II)[m.p. 184–186°C, $[\alpha]_D^{20}$ −181° (all rot. in $CHCl_3$), λ_{max}^{EtOH} 256 mμ, ε 21 400. Found: C 66.53; H 7.66. Calc. for $C_{26}H_{35}F_3O_4$: C 66.65; H 7.53] was obtained in 60 % yield. Acid catalyzed hydrolysis of II afforded smoothly 6α-trifluoromethyl-17α-acetoxyprogesterone (III) (m.p. 206–207°C, $[\alpha]_D^{20}$ +30°, λ_{max}^{EtOH} 234 mμ, ε 15 600. Found: C 65.37; H 6.98. Calc. for $C_{24}H_{31}F_3O_4$: C 65.45; H 7.10).

The α-configuration of the trifluoromethyl group in III followed from stability toward treatment with hydrogen chloride in acetic acid [4], and from the fact, that the rotatory dispersion curve was very similar to that of 17α-acetoxyprogesterone [5].

Selenium dioxide dehydrogenation of III yielded 6α-trifluoromethyl-$\Delta^{1,4}$-pregnadiene-17α-ol-3,20-dione acetate (IV) (m.p. 213–215°C, $[\alpha]_D^{20}$ −29°, λ_{max}^{EtOH} 242 mμ, ε 17 350. Found: C 65.40; H 6.80. Calc. for $C_{24}H_{29}F_3O_4$: C 65.73; H 6.67).

6-Trifluoromethyl-$\Delta^{4,6}$-pregnadiene-17α-ol-3,20-dione acetate (V) (m.p. 233–234°C, $[\alpha]_D^{20}$ 0°, λ_{max}^{EtOH} 270 mμ, ε 20 300. Found: C 65.44; H 6.89. Calc. for $C_{24}H_{29}F_3O_4$: C 65.73; H 6.67) was synthesized from the 3-cycloethylene ketal of III [6] (m.p. 178–182°C, $[\alpha]_D^{20}$ +66°. Found: C 64.28; H 7.29. Calc. for $C_{26}H_{35}F_3O_5$: C 64.45; H 7.28) by bromination at C-7 with NBS followed by dehydrobromination in boiling collidine and hydrolysis of the ketal with methanol-sulfuric acid.

The oral progestational activities of II, III, IV, and V, determined by the Mc Phail modification of the Clauberg assay are given in Table 1.

Table 1. Oral progestational activity — Clauberg assay.

Compound	Relative activity
6α-Methyl-17α-acetoxyprogesterone	1
6α-Trifluoromethyl-17α-acetoxyprogesterone	1–2
6α-Trifluoromethyl-17α-acetoxyprogesterone-3-ethyl enol ether	0.5–1
6-Trifluoromethyl-$\Delta^{4,6}$-pregnadiene-17α-ol-3,20-dione acetate	0.5–1
6α-Trifluoromethyl-$\Delta^{1,4}$-pregnadiene-17α-ol-3,20-dione acetate	0.5–1

1. Ringold, H. J., Batres, E., Bowers, A., Edwards, J. and Zderic, J. *J. Am. Chem. Soc.* **81** (1959) 3485.
2. Bowers, A., Ibàñez, L. C. and Ringold, H. J. *J. Am. Chem. Soc.* **81** (1959) 5991.
3. The addition of trifluoroiodomethane to unsaturated systems has been extensively investigated by Haszeldine. See, *e.g.*, Walling, C. *Free Radicals in Solution*, John Wiley & Sons, New York 1957, pp. 247–272.
4. Bowers, A., Ibàñez, L. C. and Ringold, H. J. *Tetrahedron* **7** (1959) 138.
5. Djerassi, C., Osiecki, J., Riniker, R. and Rinker, B. *J. Am. Chem. Soc.* **80** (1958) 1216.
6. Prepared from III by the dioxolane method: Dauben, H. J., Löken, B. and Ringold, H. J. *J. Am. Chem. Soc.* **76** (1954) 1359.

Received October 11, 1961.

A McFadyen-Stevens Reaction of Thiosemicarbazides

K. A. JENSEN and ARNE HOLM

Chemical Laboratory of the University of Copenhagen, Copenhagen, Denmark

During attempts to prepare *p*-toluenesulfonylaminoguanidine from S-methyl-*p*-toluenesulfonylisothiosemicarbazide (I) and ammonia we obtained instead *p*-toluene sulfinic acid in 80–90 % yield [1]. It was assumed that a McFadyen-Stevens reaction had taken place (the acyl group being methylmercaptocarbimidoyl, $CH_3S-\underset{|}{C}=NH$):

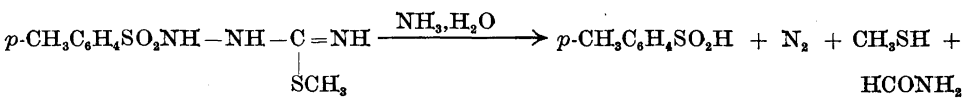

I

Such a reaction is rather surprising, both because Greer and Smith [2] have prepared sulfanilamido-methylguanidine from the corresponding S-methylthiosemicarbazide and methylamine, and because McFadyen-Stevens reactions seem only to have been observed with hydrazides containing a cyclic acyl group [3].

A closer examination of this reaction has, however, shown that it proceeds as assumed with the formation of formamide. It proved difficult to isolate pure formamide from the reaction mixture, but it was definitely identified through its xanthydrol derivative. The reaction seems to be quite general for compounds of this type. From the S-methyl derivatives of 1-*p*-toluenesulfonyl-4-methylthiosemicarbazide and 1-*p*-toluenesulfonyl-4-phenylthiosemicarbazide, N-methylformamide and formanilide were obtained. The former, which has properties similar to formamide, could only be identified by its infrared spectrum, but formanilide was isolated in a crystalline state; its melting point showed no depression on admixture with an authentic sample of formanilide and the infrared spectrum of the reaction product was in all details identical with the spectrum of formanilide. *p*-Toluenesulfinic acid was in both cases isolated in high yield.

Experimental. 1-p-Toluenesulfonyl-4-methylthiosemicarbazide (II; p-$CH_3C_6H_4SO_2NHNH$-CS-$NHCH_3$). A mixture of *p*-toluenesulfonylhydrazine (37.2 g; 0.2 mole), methylisothiocyanate (14.6 g; 0.2 mole) and benzene (350 ml) was boiled for 30 min. Generally the reactants passed into solution and then the thiosemicarbazide began to precipitate in the boiling solution. After cooling, the precipitate was filtered and washed with a little benzene and ether. Yield 40 g = 77 %. M.p. after three recrystallisations from abs. ethanol 199–202°C (decomp.). (Found: N 16.15. Calc for $C_9H_{13}N_3O_2S_2$: N 16.21).

1-p-Toluenesulfonyl-3,4-dimethylisothiosemicarbazide (III; p-$CH_3C_6H_4SO_2NHNH$-C(=NCH_3)-SCH_3). A suspension of II (38.8 g; 0.15 mole) in methyl iodide (21.3 g; 0.15 mole) and abs. ethanol (500 ml) was boiled until all had dissolved and then for a further 10 min. The ethanol was distilled off *in vacuo;* the residue was stirred with hot water and the solution was neutralised with sodium hydroxide. The solid was filtered off and washed with water. Yield 38 g = 91 %. M.p. 172.5–173°C after recrystallisation from ethanol. (Found: N 15.33. Calc. for $C_{10}H_{15}N_3O_2S_2$: N 15.38).

In the same way were prepared: *1-p-Toluenesulfonyl-4-phenylthiosemicarbazide* (IV; p-$CH_3C_6H_4SO_2NHNH$-CS-NHC_6H_5). Yield 94 %. M.p. 197–199°C (decomp.) after recrystallisation from ethanol. (Found: N 13.22. Calc. for $C_{14}H_{15}N_3O_2S_2$: N 13.08).

1-p-Toluenesulfonyl-3-methyl-4-phenylisothiosemicarbazide (V; p-$CH_3C_6H_4SO_2NHNH$-C(=NC_6H_5)-SCH_3). Yield 86 %. M.p. 169.5–170°C after recrystallisation from propanol/water. (Found: N 12.67. Calc. for $C_{15}H_{17}N_3O_2S_2$: N 12.53).

Decomposition of the isothiosemicarbazides by ammonia. (*a*) 13 g of I (0.05 mole) was boiled with 300 ml of aqueous ammonia. All went into solution with the evolution of methanethiol in the course of ½ h. The solution was boiled for 2 h with the addition of 20 ml conc. aqueous ammonia every ½ h. The solution was evaporated *in vacuo* and the residue

first extracted with ether (the ether solution left no residue on evaporation) and then with acetone. The acetone solution was dried with Na_2SO_4 and evaporated *in vacuo;* it left 1.6 g of a yellowish oil, *i.e.* 72 % calculated on formamide. After treatment with active carbon the infrared spectrum of the oil, sandwiched between two KBr discs, was recorded on a Perkin Elmer model 21 spectrophotometer. The spectrum left little doubt that the oil was formamide, although in an impure state.

The xanthydrol derivative of formamide was prepared in the following way: Xanthydrol (0.5 g) was dissolved in acetic acid (7 ml) and dure formamide (0.5 g) was added. The solution was heated for ½ h on a steam bath; after addition of water to begin crystallisation the solution was cooled and yielded a crystalline substance which was filtered off and recrystallised from dioxan/water. M.p. 187–89°C (lit.[4] 184°C). When the above-mentioned impure formamide was added to a xanthydrol solution a small amount of a solid separated at once. It was filtered off and found to be a nitrogen-free substance. The filtrate was heated on a steam bath as above and yielded on dilution with water the xanthydrol derivative of formamide. M.p. after recrystallisation from dioxan/water 184–87°C, no depression occurring on admixture with the authentic xanthydrol derivative.

The crystalline residue from the acetone extraction was almost pure ammonium *p*-toluenesulfinate (equiv. weight by titration of the ammonia 174, calc. 173). Yield 7.7 g = 89 %. On dissolution in water and addition of hydrochloric acid it yielded *p*-toluenesulfinic acid with m.p. 83–86°C.

(*b*) The isothiosemicarbazide III (9.1 g; 0.033 mole) was treated with aqueous ammonia as sub (*a*), except for the washing with ether, but the boiling was extended to 7 h. The acetone solution left on evaporation 1.3 g of a yellowish oil, *i.e.* 65 % calculated as N-methylformamide. (Found: C 40.66; H 8.53. Calc. for C_2H_4NO: C 41.70; H 7.90). The infrared spectrum showed all the bands of N-methylformamide, but in addition 4 weak bands due to impurities.

The residue from the acetone extraction was almost pure ammonium *p*-toluenesulfinate (equiv. weight by titration of the ammonia 171, calc. 173). Yield 5.2 g = 93 %. On dissolution in water and addition of hydrochloric acid it yielded *p*-toluenesulfinic acid with m.p. 84–86°C.

(*c*) The isothiosemicarbazide V (6.7 g; 0.02 mole) was treated with aqueous ammonia as above for 7 h. The residue, left after evaporation of the solution *in vacuo*, was extracted with ether, which dissolved the formanilide. The ether solution, dried with Na_2SO_4, left 1.2 g (66 %) of an oil which crystallised on seeding with formanilide. The crude product melted at 44°C, sintering beginning some degrees lower; after recrystallisation from light petroleum the m.p. was 45°C (lit. 47.5). The infrared spectrum of this sample was identical with a spectrum of pure formanilide.

The crystalline residue from the ether extraction was almost pure ammonium *p*-toluenesulfinate (equiv. weight by titration of the ammonia 171, calc. 173). Yield 2.9 g = 84 %. On dissolution in water and addition of hydrochloric acid it yielded *p*-toluenesulfinic acid with m.p. 83–85°C.

1. Jensen, K. A. and Pedersen, Chr. *Acta Chem. Scand.* **15** (1961) 991.
2. Greer, A. H. and Smith, G. B. L. *J. Am. Chem. Soc.* **76** (1954) 1141.
3. Mosettig, E. *Org. Reactions*, **8** (1954) 218.
4. Phillips, R. F. and Pitt, B. M. *J. Am. Chem. Soc.* **65** 1355 (1943).

Received October 19, 1961.

The Crystal Structure of β-Si_3N_4

O. BORGEN and H. M. SEIP

Institutt for teoretisk kjemi, Norges tekniske høgskole, Trondheim, Norway

The crystal structure of β-Si_3N_4 is known from studies by Hardie and Jack [1], and Popper and Ruddlesden [2] with X-ray data obtained from powder photographs.

Although crystals of β-Si_3N_4 have been grown[2] by heating silicon in an ammonia atmosphere at 1500°C for three days, no single crystal structure investigation has been published.

A sample of crystals formed spontaneously on a ferrosilicon alloy in air at room temperature [3] has been given us by Prof. K. Grjotheim. The sample contains both α- and β-Si_3N_4.

The crystal structure of β-Si_3N_4 has been reinvestigated by us, using X-ray intensities measured photometrically from integrated Weissenberg films and corrected in the usual way. Needle-formed crystals of diameter about 30 μ were used for this investigation.

We have reaffirmed the space group $P6_3/m$ and unit cell parameters, $a = 7.607$ Å, $c = 2.911$ Å, found by the earlier investigators [1,2].

As the z-coordinates of all atoms are determined by the space group, only the $hk0$-reflections have been utilized in this investigation.

Three cycles of least-squares refinement of the atomic coordinates were made, giving the final values for atoms in different special positions,

N in (c) $x = 1/2$ $y = 2/3$ $z = 1/4$
N in (h) $x = 0.321$ $y = 0.025$ $z = 1/4$
Si in (h) $x = 0.174$ $y = -0.234$ $z = 1/4$

The coordinates of N in (h) are somewhat different from those of Hardie and Jack [1].

N in (h) $x = 0.333$ $y = 0.033$ $z = 1/4$
Si in (h) $x = 0.172$ $y = -0.231$ $z = 1/4$

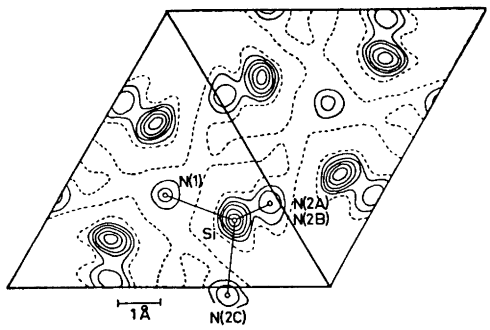

Fig. 1. Electron density projection of β-Si_3N_4 on (001).

The final reliability factor was $R = \Sigma \mid \Delta F \mid / \Sigma \mid F_0 \mid = 0.109$.

An electron density projection on (001), calculated before the least-squares refinement, is shown in Fig. 1.

The interatomic distances within the distorted SiN_4 tetrahedron (see Fig. 1) are given below.

Si – N(1)	1.72_0 Å
Si – N(2A) = Si – N(2B)	1.75_8 Å
Si – N(2C)	1.71_1 Å
N(1) – N(2A) = N(1) – N(2B)	2.89_3 Å
N(1) – N(2C)	2.77_4 Å
N(2A) – N(2B)	2.91_1 Å
N(2C) – N(2A) = N(2C) – N(2B)	2.76_7 Å

The standard deviations of the above distances are estimated to be less than 0.015 Å.

1. Hardie, D. and Jack, K. H. *Nature* **180** (1957) 332.
2. Ruddlesden, S. N. and Popper, P. *Acta Cryst.* **11** (1958) 465.
3. Grjotheim, K., Johnson, E. and Krohn, C. *Nature* **190** (1961) 23.

Received October 13, 1961.

On the Biological Activity and Amino Acid Composition of Secretin

ERIK JORPES and
VIKTOR MUTT

Chemistry Department II, Karolinska Institutet, Stockholm, Sweden

We recently reported on secretin preparations having a strength of 7500 clinical units or 150 000 Hammarsten cat units (HCU) per mg. [1,2] They behaved in paper and starch gel electrophoresis and in two-dimensional paper chromatography as an almost homogeneous protein. Before making final conclusions about the purity of the product, it was considered desirable to check its homogeneity in other solvent and buffer systems and its behaviour in the Craig counter-current analysis. This has now been done and a fraction with a still higher activity, at least 2×10^4 clinical units or 4×10^5 HCU per mg has been isolated. One mequiv. of alkali will be secreted in response to 0.250 μg of secretin. The dose necessary for the clinical secretin test in man would be about 4 micrograms.

The starting material for this purification was the secretin-pancreozymin-cholecystokinin concentrate described by Jorpes and Mutt in 1957 [3]. This was purified essentially as described by Mutt in 1959 [4], *i.e.* separation of the secretin from the bulk of the impurities by extraction into methanol followed by chromatography of the methanol soluble material on carboxymethyl cellulose at pH 8.

60 mg of the purified material with an activity of 7×10^4 HCU per mg was subjected to a 60-transfer counter-current distribution in the system 0.1 M phosphate buffer/*n*-butanol, pH 7.0, each phase 10 ml. That secretin can be distributed in this system was demonstrated several years ago in this laboratory by Anders Vestermark.

The activity was found in tubes 18—30 and the bulk of the proteinaceous impurities in the first four tubes.

The active fractions were combined and 15 volumes of water added. The activity was adsorbed on alginic acid (0.5 g dry weight), eluted with 10 ml of 0.2 M HCl and the chloride exchanged for acetate on a column of DEAE-Sephadex in acetate form. After lyophilization the material weighed 3 mg and assayed at about 4×10^5 HCU per mg, which means that 1 mg could stimulate the secretion of 40 litres of 0.1 N bicarbonate solution.

A preliminary quantitative amino acid analysis according to the Spackman, Stein and Moore technique of 1958 was carried out by Mr. Börje Lindqvist at the Central Laboratory of Mjölkcentralen, Stockholm (Head: Prof. Torsten Storgårds).

Hydrolysis in 6 N HCl in evacuated sealed tubes during 67 h at 105°C. Not the slightest discoloration occurred. The following peaks came out, calc. as μmoles/mg lyophilized substance (Fig. 1): Lys 0.05,

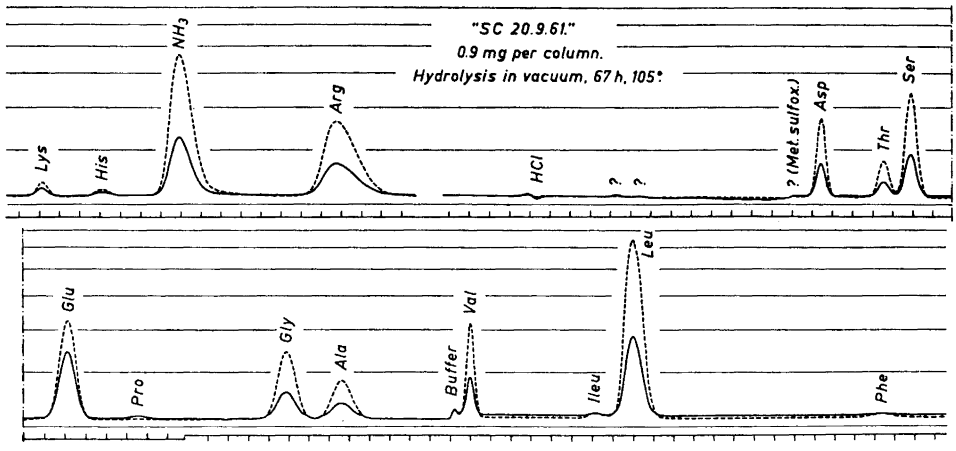

Fig 1.

His 0.03, NH_4 1.11 (3), Arg 0.96 (3), Asp 0.31 (1), Thr 0.16 (1?), Ser 0.52 (2), Glu 0.70 (2?), Gly 0.51 (2), Ala 0.29 (1), Val 0.27 (1) and Leu 1.56 (5).

This preliminary analysis seems to indicate that there are five moles of leucine, three moles of arginine and two moles each of glutamic acid and glycine per one mole of aspartic, acid, alanine and valine, and that proline, cystine, methionine, isoleucine, tyrosin and phenylalanine are absent. Tryptophane is known to be absent in preparations still containing isoleucine, tyrosin and a considerable amount of lysine [5].

At an early stage J. Sjöqvist, Lund, found that the content of leucine increased and that tyrosin disappeared during the purification process. Likewise Swan's reaction for cystine turned negative as found by A. Henschen of this laboratory. The traces of lysine and histidine still present indicate that a slight further purification could be achieved, possibly with a higher number of transfers in the counter-current distribution.

Acknowledgement. This work has been supported by Research Grant No. H-4295 (R 1 and C 1) from the *National Heart Institute, National Institutes of Health, U. S. Public Health Service* and by grants from *The Squibb Research Institute,* New Brunswick, N.J., U.S.A., *The Swedish Cancer Society* and *Magn. Bergvalls Stiftelse,* Stockholm.

The authors thanks are due to Docent Sven Paléus for valuable discussions.

1. Jorpes, E. and Mutt, V. *Ann. Internal Med.* **55** (1961) 395.
2. Jorpes, E. and Mutt, V. *Ciba Foundation Symposium on Normal and abnormal functions of the exocrine pancreas,* May 30 — June 1, London, 1961.
3. Jorpes, E. and Mutt, V. Swed. Pat. 156013/1956.
4. Mutt, V. *Arkiv Kemi* **15** (1959) 69.
5. Fishman, L. Dissert. Dep. Physiol. Sc., New York Univ., April 1, 1957. *Federation Proc.* **18** (1959) 226.

Received October 26, 1961.

Acid Phosphatases in *Escherichia coli*

BENGT v. HOFSTEN and JERKER PORATH

Institute of Biochemistry, University of Uppsala, Sweden

A cell-free extract of *Escherichia coli* will catalyze the hydrolysis of various monophosphate esters in a sodium acetate buffer at pH 4—5 [1-3]. We have found that the activity of this acid phosphatase is remarkably stable at low temperatures over a very wide pH-range. Thus no loss in enzymatic activity measured against *p*-nitrophenyl phosphate (Sigma 104) was encountered after 24 h at 4° in 0.2 M Na_2CO_3, pH about 11, or in 1 M acetic acid, pH 2.4, in the absence of salt. Repeated freezing and thawing of a crude cell extract was found to cause considerable losses of the phosphatase activity, and only 20—40 % could be recovered after lyophilization. However, solutions could be stored for several months at —10° in the presence of 60 % sucrose without detectable losses.

The interesting stability properties of the phosphatase activity prompted us to attempt its purification with the aid of gel filtration in acetic acid and zone electrophoresis. Sonicated cell-free extracts were prepared from cells grown in a succinate-inorganic salts medium essentially as described earlier by one of us [3]. The phosphatase activity was determined at a 0.01 M substrate concentration in 0.1 M sodium acetate buffer, pH 4.7. Gel filtration experiments [4] were performed on Sephadex G 75 (Pharmacia, Uppsala), and zone electrophoresis was carried out on vertical columns [5].

When an extract of *E. coli* was dialyzed against 0.1 M pyridinium acetate, pH 5, a heavy precipitate containing approximately 20 % of the total acid phosphatase activity was formed. If the supernatant solution was filtered through a column of Sephadex G75, in equilibrium with 1 M acetic acid, an interesting elution pattern was obtained. All the acid phosphatase activity was located in the region containing proteins, which pressumably have a lower molecular weight than those in the main, slightly turbid protein peak. Fig. 1 illustrates a gel filtration experiment in which 12 ml of solution was fractionated on a 22 × 500 mm Sephadex column

His 0.03, NH_4 1.11 (3), Arg 0.96 (3), Asp 0.31 (1), Thr 0.16 (1?), Ser 0.52 (2), Glu 0.70 (2?), Gly 0.51 (2), Ala 0.29 (1), Val 0.27 (1) and Leu 1.56 (5).

This preliminary analysis seems to indicate that there are five moles of leucine, three moles of arginine and two moles each of glutamic acid and glycine per one mole of aspartic, acid, alanine and valine, and that proline, cystine, methionine, isoleucine, tyrosin and phenylalanine are absent. Tryptophane is known to be absent in preparations still containing isoleucine, tyrosin and a considerable amount of lysine [5].

At an early stage J. Sjöqvist, Lund, found that the content of leucine increased and that tyrosin disappeared during the purification process. Likewise Swan's reaction for cystine turned negative as found by A. Henschen of this laboratory. The traces of lysine and histidine still present indicate that a slight further purification could be achieved, possibly with a higher number of transfers in the counter-current distribution.

Acknowledgement. This work has been supported by Research Grant No. H-4295 (R 1 and C 1) from the *National Heart Institute, National Institutes of Health, U. S. Public Health Service* and by grants from *The Squibb Research Institute,* New Brunswick, N.J., U.S.A., *The Swedish Cancer Society* and *Magn. Bergvalls Stiftelse,* Stockholm.

The authors thanks are due to Docent Sven Paléus for valuable discussions.

1. Jorpes, E. and Mutt, V. *Ann. Internal Med.* **55** (1961) 395.
2. Jorpes, E. and Mutt, V. *Ciba Foundation Symposium on Normal and abnormal functions of the exocrine pancreas,* May 30 — June 1, London, 1961.
3. Jorpes, E. and Mutt, V. Swed. Pat. 156013/1956.
4. Mutt, V. *Arkiv Kemi* **15** (1959) 69.
5. Fishman, L. Dissert. Dep. Physiol. Sc., New York Univ., April 1, 1957. *Federation Proc.* **18** (1959) 226.

Received October 26, 1961.

Acid Phosphatases in *Escherichia coli*

BENGT v. HOFSTEN and JERKER PORATH

Institute of Biochemistry, University of Uppsala, Sweden

A cell-free extract of *Escherichia coli* will catalyze the hydrolysis of various monophosphate esters in a sodium acetate buffer at pH 4—5 [1-3]. We have found that the activity of this acid phosphatase is remarkably stable at low temperatures over a very wide pH-range. Thus no loss in enzymatic activity measured against *p*-nitrophenyl phosphate (Sigma 104) was encountered after 24 h at 4° in 0.2 M Na_2CO_3, pH about 11, or in 1 M acetic acid, pH 2.4, in the absence of salt. Repeated freezing and thawing of a crude cell extract was found to cause considerable losses of the phosphatase activity, and only 20—40 % could be recovered after lyophilization. However, solutions could be stored for several months at —10° in the presence of 60 % sucrose without detectable losses.

The interesting stability properties of the phosphatase activity prompted us to attempt its purification with the aid of gel filtration in acetic acid and zone electrophoresis. Sonicated cell-free extracts were prepared from cells grown in a succinate-inorganic salts medium essentially as described earlier by one of us [3]. The phosphatase activity was determined at a 0.01 M substrate concentration in 0.1 M sodium acetate buffer, pH 4.7. Gel filtration experiments [4] were performed on Sephadex G 75 (Pharmacia, Uppsala), and zone electrophoresis was carried out on vertical columns [5].

When an extract of *E. coli* was dialyzed against 0.1 M pyridinium acetate, pH 5, a heavy precipitate containing approximately 20 % of the total acid phosphatase activity was formed. If the supernatant solution was filtered through a column of Sephadex G75, in equilibrium with 1 M acetic acid, an interesting elution pattern was obtained. All the acid phosphatase activity was located in the region containing proteins, which pressumably have a lower molecular weight than those in the main, slightly turbid protein peak. Fig. 1 illustrates a gel filtration experiment in which 12 ml of solution was fractionated on a 22 × 500 mm Sephadex column

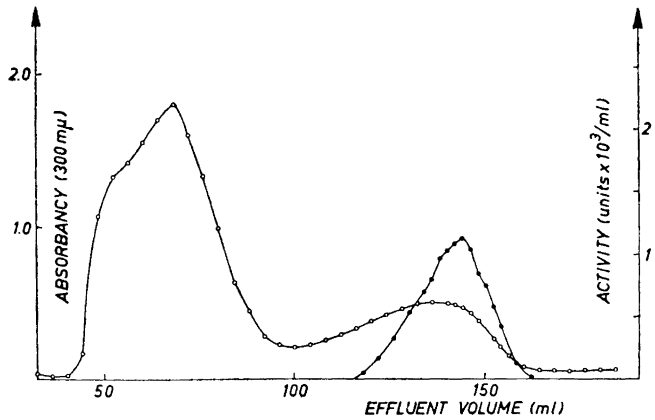

Fig. 1. Gel filtration of a partially purified acid phosphatase preparation on Sephadex G75 in 1 M acetic acid. O absorbancy at 300 mμ; ● enzymatic activity.

with 1 M acetic acid as eluent. The recovery of the enzymatic activity was usually quantitative within the limit of experimental error. The acid phosphatase activity was also assayed with substrates other than *p*-nitrophenyl phosphate, and the liberated orthophosphate was then determined according to Dryer *et al.*[6] An identical distribution of the enzymatic activity was observed with glucose-1-phosphate, glucose-6-phosphate and *o*-carboxyphenyl phosphate. When the gel filtration was carried out at a higher pH, for instance in 0,2 M pyridinium formate, pH 3.2, or in

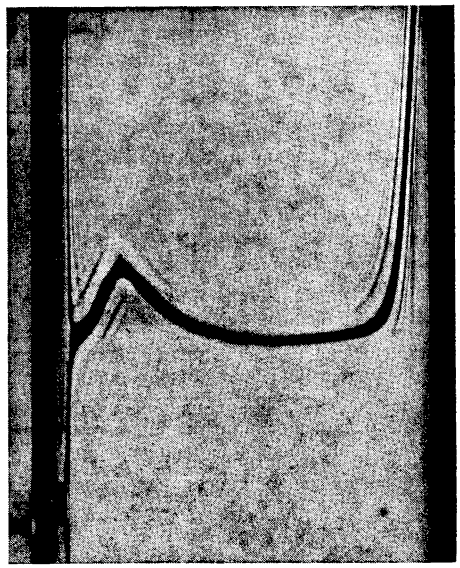

Fig. 2. Sedimentation pattern of enzyme concentrate from the experiment illustrated in Fig. 1. Spinco ultracentrifuge Model E, anal. D-rotor, 130 min after full speed (59 780 r.p.m.)

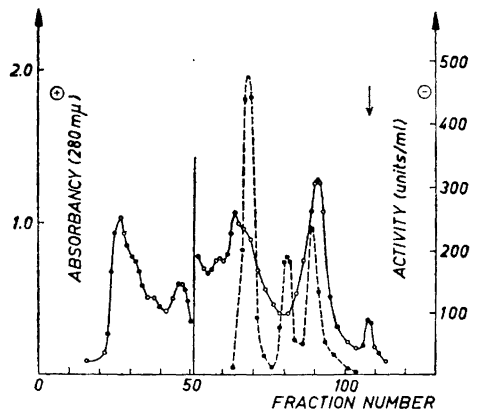

Fig. 3. Zone electropherogram of a crude extract of *E. coli* on a 20 × 250 mm column packed with formaldehyde treated cellulose in 0.05 M Tris-HCl, pH 8.2. 17 h, 27—30 mA, 600—610 V. Fractions 0—50 eluted concomitant with the electrophoresis (Ref.[5]). Position of the starting zone (2 ml) is indicated by an arrow. Fraction volume 2 ml. O absorbancy at 280 mμ; ● enzymatic activity.

Tris-HCl buffer, pH 8.2, the phosphatase activity was eluted with only slight retardation.

Ultracentrifugation of the pooled phosphatase-containing fractions obtained after gel filtration in acetic acid and subsequent concentration by ultra-filtration [7] gave the sedimentation pattern shown in Fig. 2. In addition to some gelatinous material accumulating on the bottom of the centrifuge cell, only one sedimenting boundary was observed. The uncorrected sedimentation coefficient of this component was approximately 1.0 S. We have reason to believe that the heavy gelatinous material is formed by aggregation of protein molecules in concentrated solutions.

Zone electrophoresis of the acid phosphatase preparation obtained after gel filtration revealed several different electrophoretic components. For instance, in a 0.05 M Tris-HCl buffer, pH 8.2, two phosphatase activity peaks were observed in addition to three or four inactive components. This was not surprising, since electrophoresis of the crude sonicated extract under similar conditions gave three acid phosphatase components having different electrophoretic mobilities as illustrated in Fig. 3.

Our experiments thus demonstrate that the acid phosphatase activity of *E. coli* is associated with several different proteins in the cell-free extract. This is in agreement with the results of Rogers and Reithel [2], who have partially purified five different proteins with phosphatase activity from the same organism. The gel filtration experiments in 1 M acetic acid show that the major part of the acid phosphatase activity exists as, or can be converted to, a protein of relatively low molecular weight. We are now attempting to isolate and characterize such a low-molecular weight phosphatase, in order to gain further information about the chemical background of the enzyme multiplicity.

This work has been supported by grants from the *Swedish Natural Science Research Council* to the Enzyme Chemistry Group of the Institute of Biochemistry.

1. Torriani, A. *Biochim. et Biophys. Acta* **38** (1960) 460.
2. Rogers, D. and Reithel, F. J. *Arch. Biochem. Biophys.* **89** (1960) 97.
3. v. Hofsten, B. *Biochim. et Biophys. Acta* **48** (1961) 171.
4. Porath, J. *Biochim. et Biophys. Acta* **39** (1960) 193.
5. Porath, J. and Hjertén, S. in Glick, D. *Methods of Biochemical Analysis. In press.*
6. Dryer, R. L., Tammes, A. R. and Routh, J. G. *J. Biol. Chem.* **225** (1957) 177.
7. v. Hofsten, B. and Falkbring, S. O. *Analyt. Biochem.* **1** (1960) 436.

Received November 1, 1961.

The Affinity of Some Divalent Metals to Different Types of Alginates

ARNE HAUG

Norwegian Institute of Seaweed Research, N.T.H., Trondheim, Norway

In a series of experiments, Thiele and co-workers have investigated the interaction between divalent ions and polyuronides, in particular alginic acid. They found that gels with a capillary structure were formed if divalent metals under certain conditions were allowed to diffuse into an alginate solution. The diameter of the capillaries depended on the nature of the divalent metal, and increased in the following order: Pb <Cu <Cd <Ba <Sr <Ca <Zn, Co, Ni [1]. Also other properties of mixtures of alginates and divalent metal salts, such as gel formation [2] and ion exchange [3] varied in the same (or opposite) order. For the precipitation of alginates McDowell [4] found that the amount of divalent metal ions necessary to obtain precipitation increased in the order Pb, Cu <Ca <Co, Ni, Zn <Mn.

It has recently been shown that the ion exchange properties of alginates depend on the chemical composition of the alginate [5]. Alginates rich in mannuronic acid residues, such as alginates from *Laminaria digitata*, have a lower affinity to calcium in a sodium-calcium ion exchange reaction than alginates rich in guluronic acid residues, such as alginate from *Laminaria hyperborea* stipes. It was therefore of interest to determine if the affinity of alginates to the different divalent metal ions varied in the same order for alginates with different chemical composition.

Materials and methods. The preparation of alginate from the algal samples has been described previously [6]. The sodium alginate was washed with 0.1 M hydrochloric acid to transform the alginate to alginic acid, and then carefully washed with water, dried and ground. Samples of 25 mg were suspended in water and sodium hydroxide added in an amount corresponding to half the equivalent amount of alginic acid, the total volume being maintained at 5 ml. The samples were shaken for one hour and the pH determined in a Beckman Zeromatic pH meter furnished with a glass electrode. 0.1 M solutions of divalent metal salts were added and the pH again determined after the samples had been shaken for one hour.

The selectivity coefficient for the cadmium-strontium ion exchange reaction was determined by the following method: Samples of 25 mg of sodium alginate were shaken over night with a mixture of 5 ml 0.01 M strontium nitrate, 5 ml 0.01 M cadmium nitrate and 4 ml water. The solution was separated from the alginate by decantation and the alginate washed. The combined solution and wash-water was titrated with 0.01 M EDTA solution at pH 10 with Eriochrome Black T as an indicator. After the endpoint was reached 1 ml of a 0.1 M solution of magnesium EDTA complex was added and the titration continued until the next endpoint was reached. The first endpoint corresponds to the content of cadmium in the solution, while the second corresponds to the total amount of cadmium and strontium. The alginate gel was treated twice with 10 ml 0.2 M hydrochloric acid and the content of cadmium and strontium in the acid determined as described above, after the acid had been neutralized with 1 M sodium hydroxide.

When a metal salt solution is added to a half neutralized sample of alginic acid the pH decreases and the magnitude of the decrease depends on the affinity between the alginate and the metal ion. Table 1 gives the results for two alginate samples produced from *Laminaria digitata* and *Laminaria hyperborea* stipes, respectively. Alginate from *L. digitata* contains more mannuronic than guluronic acid residues while the opposite is usually the case with alginate from *L. hyperborea* stipes. The uronic acid composition of the two alginates used are given in Table 2. The observed difference in pH for half neutralized samples is in agreement with earlier observations [7]. For alginate from *L. digitata* it was found that the magnitude of the decrease of pH depended on the divalent metal used, and that the same order of metals was found as that observed by Thiele for other properties of alginates. For alginate from *L. hyperborea* stipes, however, the order was found to be significantly different, the addition of cadmium salt leading to a smaller pH decrease than addition of barium or strontium salts.

The results thus indicate that the affinity to these divalent metals is different for alginates with different chemical composition. This point was further investigated by determining the selectivity co-

Table 1. pH of alginate solutions containing metal salts.

Metal salt	mequiv. salt / mequiv. alg. :	*L. digitata*			*L. hyperborea* stipe		
		0	0.83	1.66	0	0.83	1.66
$Pb(NO_3)_2$		3.90	2.60	2.40	4.48	2.60	2.38
$Cu(NO_3)_2$			2.85	2.75		2.95	2.65
$Cd(NO_3)_2$			2.94	2.77		3.13	2.96
$Ba(NO_3)_2$			3.00	2.80		3.05	2.85
$Sr(NO_3)_2$			3.05	2.95		3.10	2.92
$Ca(NO_3)_2$			3.21	2.98		3.25	3.02
$Co(NO_3)_2$			3.24	3.11		3.41	3.31
$Ni(NO_3)_2$			3.32	3.15		3.51	3.38
$ZnSO_4$			3.32	3.22		3.49	3.40
$MnSO_4$			3.32	3.31		3.74	3.72
$MgSO_4$			3.39	3.36		3.80	3.70

The ionotropic series of Thiele:
Pb < Cu < Cd < Ba < Sr < Ca < Zn,Co,Ni

Table 2.

Source of alginate	$k_{Cd\text{-}Sr}$	Mannuronic acid / Guluronic acid
L. digitata, Kråkvågøy 3/7	1.17	2.10
» » Espevær 8/1	0.98	1.75
L. hyperborea stipes, Reine 28/6	0.70	1.10
» » » Hustad 26/2	0.54	0.56
Ascophyllum nodosum, Være 2/3	1.19	2.45
Commercial samples:		
Protanal LF *(L. digitata)*	1.22	2.17
Manucol SS/LD *(L. hyperborea* stipes)	0.58	0.70
Manucol SA/LM *(A. nodosum)*	0.95	1.65

efficient of the cadmium-strontium ion exchange reaction:

$$k = \frac{Cd_g \cdot Sr_s}{Sr_g \cdot Cd_s}$$

where subscripts g and s refer to gel and solution, respectively. No attempt has been made to determine a true equilibrium constant involving activities. The results for a number of alginate samples of different composition are given in Table 2. The uronic acid composition was determined by hydrolysis of the alginate, separation of the two uronic acids by chromatography on an anion exchange resin [8] and determining the amounts of uronic acid in the two fractions by means of the orcinol method [9] (the detailed procedure will be published later).

The results show that a close correlation exists between the selectivity coefficient for the cadmium-strontium ion exchange reaction and the chemical composition of the alginate.

The interaction between divalent metals and alginates will be investigated further.

1. Thiele, H. and Hallich, K. *Kolloid-Z.* **151** (1957) 1.
2. Thiele, H. and Schacht, E. *Kolloid-Z.* **161** (1958) 120.
3. Thiele, H. and Schacht, E. *Z. physik. Chem.* **208** (1957) 42.
4. McDowell, R. H. *Third International Seaweed Symposium*, Galway 1958.
5. Haug, A. *Acta Chem. Scand.* **13** (1959) 1250.
6. Haug, A. *Acta Chem. Scand.* **13** (1959) 601.
7. Haug, A. *Acta Chem. Scand.* **15** (1961) 950.
8. Larsen, B. and Haug, A. *Acta Chem. Scand.* **15** (1961) 1397.
9. Brown, H. H. *Arch. Biochem.* **11** (1946) 269.

Received October 24, 1961.

Phenolic Biphenyl Derivatives from the Heartwood of *Sorbus aucuparia* (L)

HOLGER ERDTMAN, GÖRAN ERIKSSON and TORBJÖRN NORIN

Organisk-kemiska Institutionen, Kungl. Tekniska Högskolan, Stockholm, Sweden

From the heartwood of *Sorbus aucuparia*, Rosaceae, mountain ash or rowan tree (Swedish rönn), two biphenyl derivatives have been isolated by solvent extraction. They occur in almost equal amounts and constitute up to 7 % by weight of the dry heartwood. One of these compounds, aucuparin, has the composition $C_{12}H_7(OH)(OCH_3)_3$ and melts at 101–101.5°. (Methyl ether, $C_{12}H_7(OCH_3)_3$, m.p. 88–89°. Acetate, $C_{12}H_7(OCOCH_3)(OCH_3)_2$, m.p. 150–151°). The other compound, methoxyaucuparin, has the composition $C_{12}H_6(OH)(OCH_3)_3$ and melts at 120–122°. (Methyl ether $C_{12}H_6(OCH_3)_4$, m.p. 71.5–72°. Acetate $C_{12}H_6(OCOCH_3)(OCH_3)_3$, m.p. 119–120°).

On oxidation with permanganate aucuparin gives benzoic acid and methoxyaucuparin affords 2-methoxybenzoic acid. The U.V. spectra of the aucuparins show that they are hydroxybiphenyl derivatives and the N.M.R. spectra that they contain one symmetrical dimethoxy-hydroxyphenyl group. The aucuparins give no colour reaction with bisdiazotised benzidine and hence cannot be 2,6-dimethoxy-4-hydroxyphenyl derivatives. Aucuparin is therefore 3,5-dimethoxy-4-hydroxybiphenyl (I: R = H) and methoxyaucuparin is 3,5,2′-trimethoxy-4-hydroxybiphenyl (II: R = OCH_3).

Aucuparin methyl ether was synthesised by mixed Ullmann coupling of 3,4,5-trimethoxyiodobenzene and methyl 2-bromobenzoate followed by hydrolysis of the reaction product and isolation of the 2′-carboxy-3,4,5-trimethoxybiphenyl, $C_{12}H_6(OCH_3)_3COOH$, m.p. 136–137°, which was then decarboxylated with Adkins' catalyst in boiling quinoline. The 3,4,5-trimethoxybiphenyl thus obtained was identical with aucuparin methyl ether.

Similarly, using methyl 3-iodo-4-methoxybenzoate instead of methyl 2-bromobenzoate, 5′-carboxy-3,4,5,2′-tetramethoxybiphenyl, $C_{12}H_5(OCH_3)_4COOH$, m.p. 216–217.5°, was obtained. On decarboxylation this gave 3,4,5,2′-tetramethoxybiphenyl identical with methoxyaucuparin methyl ether.

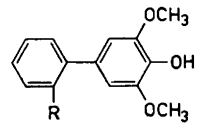

I: R = H
II: R = OCH_3

Our thanks are due to Mr. G. Alfvén for carrying out the extraction and isolation work.

Received November 9, 1961.

ACTA CHEMICA SCANDINAVICA 15 (1961) 1797–1810

Liver Alcohol Dehydrogenase

I. Kinetics and Equilibria without Inhibitors

HUGO THEORELL and JOHN S. McKINLEY-McKEE

Medicinska Nobelinstitutet, Biokemiska avdelningen, Stockholm, Sweden

Liver alcohol dehydrogenase can form all the four binary complexes possible with DPNH, DPN, aldehyde and alcohol. The ternary complexes E-DPNH-aldehyde and E-DPN-alcohol are formed and are in very rapid equilibrium with one another. From a kinetic point of view the "Theorell-Chance" mechanism was nevertheless found to obtain. This depends on the following conditions:

1. The "on" velocity constants for DPNH and DPN are nearly independent of whether the enzyme is free or already combined with the substrate reaction partner.
2. The ternary complexes are in rapid equilibrium.
3. The ternary complexes prefer to liberate the substrate first, because this is less tightly bound than the coenzyme. The dissociation velocity of the binary enzyme-coenzyme complexes in the last phase of the reaction therefore becomes rate limiting when both substrate and coenzyme are present in high concentration in the first phase.
4. Determinations of initial reaction velocities with varied concentrations of both coenzyme and substrates have given Dalziel Φ-relations which agree with the specific requirements of the T.-C.-mechanism at pH 7

The values of the Michaelis constants close to zero concentration of their reaction partner, gave thedissociation constants $K_{E,R}$, $K_{E,O}$, $K_{E,ald}$ and $K_{E,alc}$.

The reaction mechanism of the liver alcohol dehydrogenase-coenzyme-substrate system * proposed in 1951 by Theorell and Chance [1] has been subject to repeated attempts at experimental confirmation [1-4]. In general, fair agreement was found between the values for the dissociation constants of the

* Abbreviations:

LADH and YADH:	Liver and yeast alcohol dehydrogenase, respectively
E:	1/2 LADH (since each molecule of LADH has 2 independent binding sites)
R:	reduced diphosphopyridine nucleotide, DPNH
O:	oxidized » » , DPN
S:	aldehyde
S':	alcohol

binary complexes ER and EO ($K_{E,R}$ and $K_{E,O}$) as determined from fluorometric equilibrium determinations in absence of substrate, and those calculated from the relation between the kinetic "off" and "on" rate constants, as determined in kinetic experiments with the substrates, assuming the T.-C. mechanism to be valid.

However, in connection with inhibition studies to be reported in Parts II and III of this series the opportunity arose of making decisive experiments to ascertain how far former disagreements, where there were indications that the formation or interconversion of the ternary complexes was perhaps effecting the rate [3,4], were occasional or not. We now had the advantage that the fluorometric titration of E with R in the presence of excess *iso*butyramide, enabled us to make very accurate determinations of the enzyme concentration.

Dalziel [5] has derived relations which distinguish the T.-C.-mechanism from other possible alternatives. This test necessitates carrying out series of kinetic experiments with submaximal concentrations of the constant reaction partner in each series. Four types of experiments are used for the determinations of the initial velocity, v ($\mu M \cdot sec^{-1}$).

	Constant	Varied
Case 1:	S	R
Case 2:	R	S
Case 3:	S′	O
Case 4:	O	S′

The results for each case are plotted according to Lineweaver and Burk [6] in terms of e/v against 1/[varied partner].

For the T.-C.-mechanism,

$$E + R \underset{k_2}{\overset{k_1}{\rightleftharpoons}} ER$$

$$ER + S \underset{k_3'}{\overset{k_3}{\rightleftharpoons}} EO + S'$$

$$EO \underset{k_1'}{\overset{k_2'}{\rightleftharpoons}} E + O$$

a steady state treatment gives the initial rate equations

$$\text{Case 1 and 2: } \frac{e}{v} = \frac{1}{k_2'} + \frac{1}{k_1[R]} + \frac{1}{k_3[S]} + \frac{k_2}{k_1 k_3[R][S]} \quad (1a)$$

$$\text{Cases 3 and 4: } \frac{e}{v} = \frac{1}{k_2} + \frac{1}{k_1'[O]} + \frac{1}{k_3'[S']} + \frac{k_2'}{k_1' k_3'[O][S']} \quad (1b)$$

(1a) and (1b) are the special T.-C. mechanism forms of Dalziel's general equation [5]:

$$\frac{e}{v} = \Phi_0 + \frac{\Phi_1}{S_1} + \frac{\Phi_2}{S_2} + \frac{\Phi_{12}}{S_1 S_2} \qquad (2)$$

Experiments with as high as possible concentration of the constant partner will, by combination of all four cases, give values for all six rate constants. However, in this case the Φ_{12}-term is always neglected. This is permissible in cases 1 and 2, where Φ_{12} is low, but not in cases 3 and 4, where Φ_{12} is high. Furthermore, as Dalziel has pointed out, determinations of e/v with submaximal concentration of the constant reaction partner can give independent values for the Φ_{12}-term, which are very important as a check of the T.-C.-mechanism. Experiments have therefore been carried out with both maximal and submaximal concentrations of the constant partner at pH 7, and with maximal concentrations at pH 9.

Eqn. 2 on rearrangement gives

$$\text{Case 1:} \quad \frac{e}{v} = \Phi_0 + \frac{\Phi_2}{[S_2]} + \left(\Phi_1 + \frac{\Phi_{12}}{[S_2]}\right)\frac{1}{[S_1]} \qquad (3a)$$

$$\text{Case 2:} \quad \frac{e}{v} = \Phi_0 + \frac{\Phi_1}{[S_1]} + \left(\Phi_2 + \frac{\Phi_{12}}{[S_1]}\right)\frac{1}{[S_2]} \qquad (3b)$$

Due to the symmetry of the T.-C.-mechanism the introduction of primed symbols represents cases 3 and 4 for the reverse reaction. Thus in experiments where both substrates are present in concentrations low enough to be rate limiting (submaximal concentrations) [5,7], when (for various S_2 concentrations) S_1 is varied, plots of the intercepts (taken from the case 1 Lineweaver-Burk plots) against $1/S_2$ will give Φ_0 as an intercept and Φ_2 as a slope, while the slopes when plotted will give Φ_1 as intercept, and Φ_{12} as slope. When S_2 is varied (Case 2) the intercepts again give Φ_0 but with Φ_1 as slope, while the slopes give Φ_2 as intercept, with Φ_{12} as slope again. Cases 1 and 2 for the forward reaction thus give two values each for Φ_0, Φ_1, Φ_2, and Φ_{12}. Cases 3 and 4 likewise give Φ'_0, Φ'_1, Φ'_2, and Φ'_{12}. For the T.-C.-mechanism the identity of eqns. 1 and 2 for the forward and reverse reactions, give the relations $\Phi_0 = \Phi'_1\Phi'_2/\Phi'_{12}$, and $\Phi'_0 = \Phi_1\Phi_2/\Phi_{12}$, which are a sensitive way of distinguishing the T.-C.-mechanism from other mechanisms conforming to eqn. 2. Several of these mechanisms give the relation $K_{eq} = \Phi_{12}/\Phi'_{12}$, but because of the distinguishing Φ relations above, the T.-C.-mechanism has the further characteristic relation, but less sensitive test, $K_{eq} = \Phi_0\Phi_1\Phi_2/\Phi'_0\Phi'_1\Phi'_2$. It is these Dalziel relations [5] that have been tested at pH 7.

At 0.1 μ and 23.5°C the overall equilibrium constant $K_{eq} = [S_1][S_2]/[S'_1][S'_2] = 0.9 \times 10^{-4} \times [H^+]$ and therefore the forward reaction is greatly favoured from the thermodynamic point of view [8]. One would think this would lead to technical difficulties in cases 3 and 4, where the equilibrium is already reached when a very small part of [O] has reacted with [S']. However, in fluorometric determinations rather the opposite is true. In cases 1 and

2 we observe the disappearance of the fluorescence of R, and the whole reaction cycle is limited to the width of the paper, so that bent curves are often obtained. Furthermore, the highest [R] that can be used is limited by the extinction of the exciting light through absorption.

In cases 3 and 4 highest sensitivity and very small enzyme concentrations can be used, because only the very beginning of the reaction is of interest. A production of 10^{-7} M R is sufficient for determining the slope of the line, which will in this case be nearly straight. In addition, unlimited concentrations of O can be used, since it does not absorb the exciting light.

EXPERIMENTAL

Materials. DPN and DPNH were from the Sigma Chemical Co. Assay was carried out with a catalytic amount of YADH. Using an absorbancy index of 6.25×10^6 cm²/mole at 340 mμ [9], the βDPNH purity was 70—71 % by weight, 95 % on the basis of E_{340}, while the residual extinction after enzymatic oxidation was 5 % and the residual fluorescence which was corrected for was 6 %. Fig. 1 shows the relation between the concentration of DPNH solutions and their fluorescence. Quenching by absorption of the exciting light is seen and consequently concentrations above 13 μM where the correction is 8 % were seldom used. However, corrections were made where necessary, these being 6 % at 10 μM and 16 % at 26 μM. As DPNH is unstable in water or below pH 7.5, particularly when exposed to U.V. light, a stock DPNH solution was made in 0.01 M tris(hydroxymethyl)aminomethane, pH 10.6, and kept at 2°C in the dark. More dilute solutions were made with distilled water and kept at 2°C, except during actual use, when they were kept in the dark at 23.5°C. Stock solutions of concentration 1 050 μM (1 mg/ml) or greater were sometimes kept for periods of up to 30 h, but never longer or at lower concentrations, as otherwise decomposition become measurable. On the basis of an absorbancy index [10] of 18.0×10^6 cm²/mole, the βDPN purity was found to be 90—91 % by weight, and 99—100 % from the absorbancy at 260 mμ. Solutions (pH 4—7) were made in distilled water. Unless when in use, they were kept at 2°C in the dark where they were found to be stable, solutions of 1 360 μM (1 mg/ml) or more not changing for many days.

LADH was prepared from a horse liver according to Dalziel [11]. After chromatography on the carboxymethylcellulose column, the main component was twice crystallized in the presence of 30 % ethanol at −14°C and then 3 or 4 times recrystallized by dialysis against 6 % ethanol at 2°C [11]. The LADH crystals were kept at −14°C under 0.1 μ phosphate buffer, pH 7, containing 30 % ethanol. No measured or noticeable change was seen in the solutions prepared from the crystals over a two year period. Solutions were prepared by centrifuging some of the stirred suspension (~ 10 mg/ml) at 15 000 r.p.m. and −14°C, discarding the supernatant and dissolving the crystals in the same volume of 0.1 μ phosphate-ammonia buffer, pH 9. A clear solution resulted which was dialysed for 3—4 days against 0.1 μ phosphate pH 7 or 8, the buffer being changed each 12 or 24 h. Greatest stability to dialysis or standing was found between pH 8 and 9. Finally the solution was centrifuged at 15 000 r.p.m. and 2°C. Stock solutions resulted (~ 10^{-4} M) which were stable for many days; indeed on occasion the decrease in activity was less than the slight increase due to concentration by evaporation, although the enzyme was kept in a 3 ml stoppered glass bottle at 0°C. Dilute solutions were made, using either 0.1 μ phosphate buffer, pH 7 or 8. These were assayed immediately before and after an experiment, particularly when more dilute than 10^{-6} M. All enzyme solutions were maintained at 0°C or 2°C.

Enzyme solutions were assayed according to Dalziel [11,12], the enzyme concentration, $e = 1.13/(V)(t_{0.2})(84\ 000)$ moles/litre, where V is the volume (ml) of enzyme pipetted into the 3 ml assay solution (1.0 ml of 1 mg/ml DPN solution + 150 μl 0.16 M ethanol + 1.85 ml 0.1 M glycine-NaOH buffer, pH 10) in a quartz 1 cm cuvette, and t the time in seconds for the absorbancy at 340 mμ to increase by 0.2 units. The enzyme concentration used, however, was always 0.83 of this (2×0.83 μN) as in the spectrophotofluorometer the ratio of the binding sites concentration determined using excess *iso*butyramide to the μN concentration determined in the above spectrophotometric assay was 0.83. The enzyme

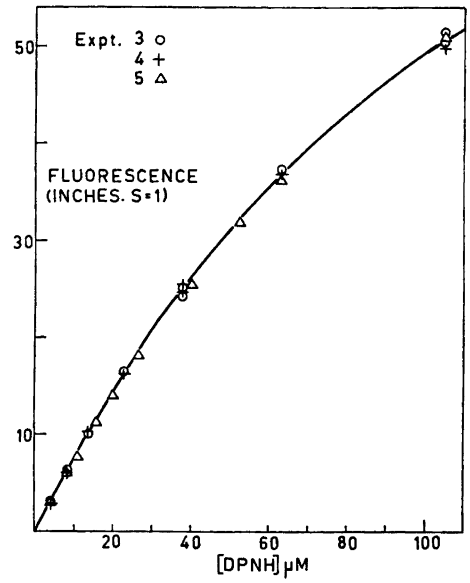

Fig. 1. Relation between the concentration of DPNH solutions and their fluorescence. Fluorimeter I. (The fluorescence has been corrected for a cuvette fluorescence of 0.1″. S = 1.)

was considered pure as stock enzyme solutions had an E_{280} which in relation to the activity had a specific extinction (1 mg/ml) of 0.41 – 0.42. The binding site concentration (as determined by titration with DPNH in the presence of *iso*butyramide) gives a specific extinction near 0.5.

All solutions were made in quartz redistilled water. This showed no fluorescence even at the highest sensitivity of the fluorometer, where there was, however, a background deflection of 0.1″ (S = 1.0) from the cuvettes. Buffer solutions were made with "analar" or "pro analysi" chemicals. At pH 7, 0.1 μ phosphate was used, while at pH 9, 0.1 μ Na_2HPO_4 + 3.6 mM glycine-NaOH buffer was used. Versene was never added to any solutions. 95 volume % alcohol ("finsprit") and Merck, Darmstadt, "puriss" acetaldehyde were distilled through 20″ Fensky helix packed columns and the middle third collected. They were kept apart at −14°C in the dark. Stock solutions were made in water by adding 200 μl, and checked by weighing and enzymatic assay. 95 volume % alcohol (5 % water) was used, as absolute alcohol on occasion contained traces of benzene.

Methods. The apparatus was essentially as described earlier [13]. A Luma Hg 125 water-cooled lamp was employed to excite the solutions with the 366 mμ mercury line, and very high sensitivity obtained by using wide entrance and exit slits (6 mm), thus enabling substrate concentrations down to 0.5 μM to be used. The LADH concentration was made low enough to give linear initial velocities. The enzyme (2 – 20 μl) and small substrate volumes (5 – 200 μl) were added from Carlsberg pipettes checked by the weight of clean mercury they held, and then calibrated from the absorption at 350 mμ of the amount of sodium dichromate they delivered, using the method of equal dilutions and calibrated volumetric glassware. Substrate solutions were kept in the dark either in the refrigerator or at 23.5°C when in immediate use. With the buffer they were added to give a final volume of 4 ml in 4.5 ml, 1 × 1 cm fluorescence- free glass cuvettes which when checked gave the same velocities as similar quartz cuvettes. pH (± 0.02) was measured at 23.5°C on a Beckman model G pH meter with microelectrodes. The enzyme was added from a glass stirrer in the dark with rapid stirring. Due to the non-fluorescence of DPN and the bluish white fluorescence of DPNH [14] the rate of DPNH oxidation or DPN reduction (e/V) can be measured by the rate of formation or disappearance of DPNH; $e/V = e\,\Delta D/(V_p \cdot S \cdot [D])$, where e = binding site enzyme concentration; V_p = recorder pen velocity-inches/sec.; S = sensitivity variable from 0.1 to 5; $[D]$ = concentration of the DPNH standard and

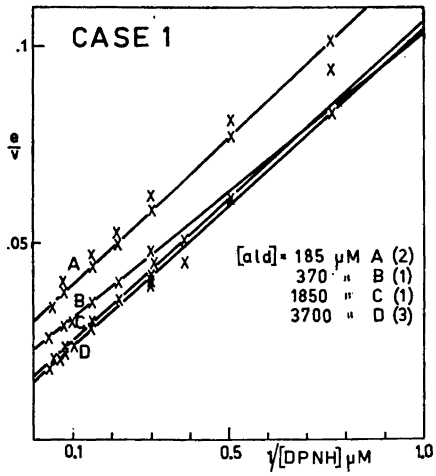

Fig. 2. Lineweaver-Burk plots for case 1. (The number of experiments on which each plot is founded is marked beside the particular plot designations.)

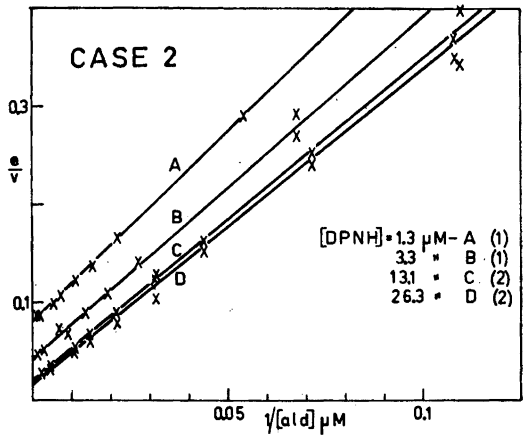

Fig. 3. Lineweaver-Burk plots for case 2.

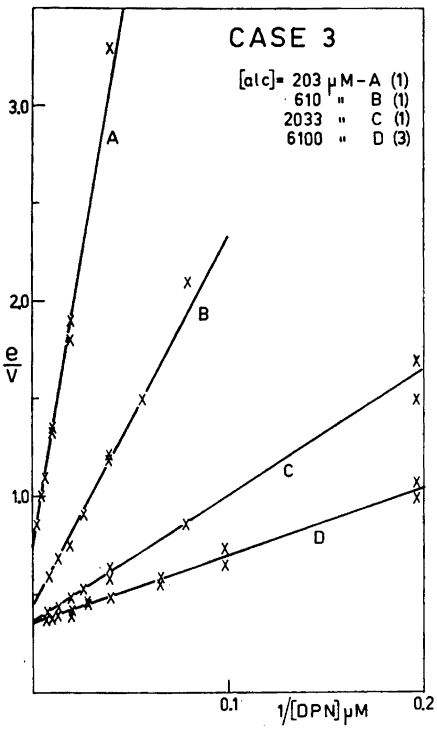

Fig. 4. Lineweaver-Burk plots for case 3.

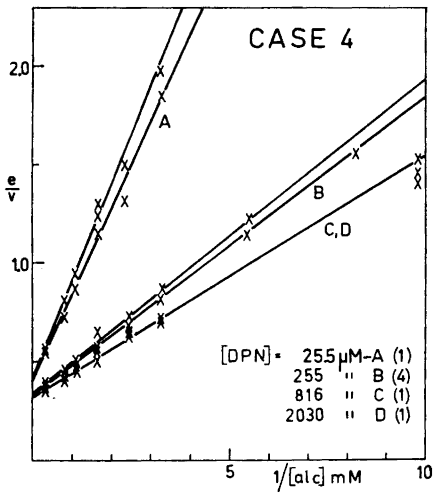

Fig. 5. Lineweaver-Burk plots for case 4.

Table 1. Φ-values and rate constants, pH 7.

Φ-values determined experimentally	Rate constants *
$\Phi_0 = 0.0135$ (0.014; 0.013) sec	$k'_2 = 74$ sec^{-1}
$\Phi_1 = 0.090$ (0.089; 0.091) sec $\times$ μM	$k_1 = 11.1$ sec^{-1} $\times$ μM^{-1}
$\Phi_2 = 3.2$ (3.2; 3.2) sec $\times$ μM	$k_3 = 0.31$ sec^{-1} $\times$ μM^{-1}
$\Phi_{12} = 0.9$ (0.96; 0.8) sec $\times$ μM^2	
$\Phi'_0 = 0.32$ (0.325; 0.32) sec	$k_2 = 3.12$ sec^{-1}
$\Phi'_1 = 1.9$ (1.9; 2.3) sec $\times$ μM	$k'_1 = 0.525$ sec^{-1} $\times$ μM^{-1}
$\Phi'_2 = 82$ (82; $\approx$ 110) sec $\times$ μM	$k'_3 = 0.0122$ sec^{-1} $\times$ μM^{-1}
$\Phi'_{12} = 10\,500$ (10 000; 11 000) sec $\times$ μM^2	

* Calculated from Φ values ($1/\Phi$).

Table 2. Equilibrium constants obtained from kinetics and equilibrium data, pH 7.

	Kinetic	Equilibrium
$K_{E,R}$	$k_2/k_1 = 0.28$ μM	0.31 μM *
$K_{E,O}$	$k'_2/k'_1 = 141$ μM	160 μM *
$K_{E,O}/K_{E,R}$	502	515
K_{eq}	$k_2k'_3k'_1 \times 10^{-7}/k'_2k_3k_1 = 0.78 \times 10^{-11}$ M.	0.90×10^{-11} M (Ref.[8])

* Part II.

Table 3. Relations between coefficients required by the Theorell-Chance mechanism according to Dalziel[5], pH 7.

$\Phi'_0 = \frac{\Phi_1\Phi_2}{\Phi_{12}}$	$\Phi'_0 = 0.32$ sec	$\frac{\Phi_1\Phi_2}{\Phi_{12}} = 0.32$ sec
$\Phi_0 = \frac{\Phi'_1\Phi'_2}{\Phi'_{12}}$	$\Phi_0 = 0.0135$ sec	$\frac{\Phi'_1\Phi'_2}{\Phi'_{12}} = 0.0149$ sec
$K_{eq} = \frac{\Phi_{12} \times 10^{-7}}{\Phi'_{12}}$	$K_{eq} = 0.90 \times 10^{-11}$ M	$\frac{\Phi_{12} \times 10^{-7}}{\Phi'_{12}} = 0.86 \times 10^{-11}$ M
$K_{eq} = \frac{\Phi_0\Phi_1\Phi_2 \times 10^{-7}}{\Phi'_0\Phi'_1\Phi'_2}$	$K_{eq} = 0.90 \times 10^{-11}$ M	$\frac{\Phi_0\Phi_1\Phi_2 \times 10^{-7}}{\Phi'_0\Phi'_1\Phi'_2} = 0.78 \times 10^{-11}$ M

ΔD its deflection in inches at $S = 1$. It was unaffected by direct exposure to the incident light for 5—10 min, a period much longer than the total time it was irridated during a series of experiments, when it was measured along with each cuvette, each exposure taking 3—4 sec. (Recently a "pure" βDPNH Sigma sample was found unsuitable in this respect as it was unstable to UV-light, ΔD decreasing during the course of an experiment). At the end of each experiment the standard was checked against unused standard taken from the refrigerator and carefully brought to 23.5°C. The fluorescence intensity of a DPNH solution changes noticeably with a 1° temperature change.

Table 4. Φ-values and rate constants, pH 9.

Rate constants	Φ-values *
k_2' = 8.15 sec^{-1}	Φ_0 = 0.122 (Φ_0 expt. = 0.122) sec
k_1 = 5.7 $sec^{-1} \times \mu M^{-1}$	Φ_1 = 0.175 sec $\times$ μM
k_3 = 0.062 $sec^{-1} \times \mu M^{-1}$	Φ_2 = 16.1 (Φ_2 expt. = 16.8) sec $\times$ μM
$\frac{k_2}{k_1 \times k_3}$ = 13.8 $sec^{-1} \times \mu M^{-2}$	Φ_{12} = 13.8 sec $\times$ μM^2
k_2 = 4.9 sec^{-1}	Φ_0' = 0.204 sec
k_1' = 0.508 $sec^{-1} \times \mu M^{-1}$	Φ_1' = 1.97 sec $\times$ μM
k_3' = 0.00885 $sec^{-1} \times \mu M^{-1}$	Φ_2' = 113 sec $\times$ μM
$\frac{k_2'}{k_1' k_3'}$ = 1 810 $sec^{-1} \times \mu M^{-2}$	Φ_{12}' = 1 810 sec $\times$ μM^2

* Calculated from rate constants. ($1/k$).

Table 5. Equilibrium constants obtained from kinetic and equilibrium data, pH 9.

	Kinetic	Equilibrium
$K_{E,R}$	k_2/k_1 = 0.86 μM	0.65 μM*
$K_{E,O}$	$k_2'k_1'$ = 16 μM	12 μM*
$K_{E,O}/K_{E,R}$	18.6	18.5
K_{eq}	$\frac{k_2k_3'k_1' \times 10^{-9}}{k_2'k_3k_1}$ = 0.77 $\times$ 10^{-11} M	0.90 $\times$ 10^{-11} M (Ref.[8])

* Part II.

RESULTS

For pH 7, Figs. 2—5 show the Lineweaver-Burk plots (to avoid uncertainty many points, several of which are done in duplicate, are usually required) for cases 1—4, while Figs. 6—13 show the plots of the intercepts and slopes which give the Φ values and resultant kinetic and equilibrium constants in Tables 1—3. Table 3 shows that the sensitive requirements of the T.-C.-mechanism are excellently fulfilled. The maximum velocities, k_2 (cases 3 and 4) and k'_2 (cases 1 and 2) are seen to be twice the 1955 value [2], which could partly be due to the titrations with *iso*butyramide giving a correct knowledge of the concentration of enzyme binding sites, along with the extrapolation of the velocities to infinite concentration of the constant reaction partner. Tables 4 and 5 give the results for pH 9, where experiments with submaximal concentrations were only performed for case 1. The older method of calculation [2] was used with the modification that the values for k_2 and k'_2 were found by crosswise extrapolation to infinite concentrations. Excellent agreement was obtained between the k_2 values from cases 3 and 4, and between the k'_2 values from cases 1 and 2.

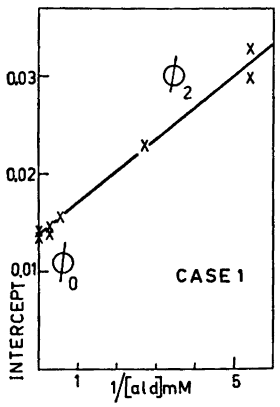

Fig. 6. Plot of intercepts, case 1.

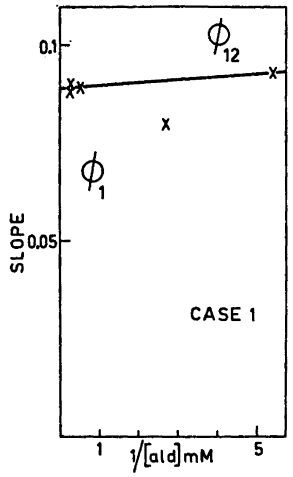

Fig. 7. Plot of slopes, case 1.

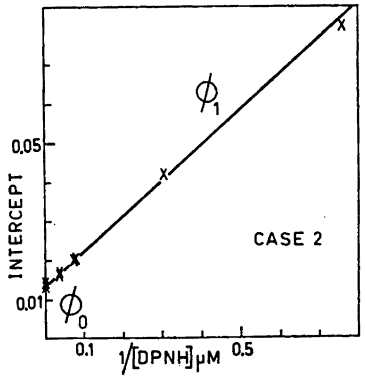

Fig. 8. Plot of intercepts, case 2.

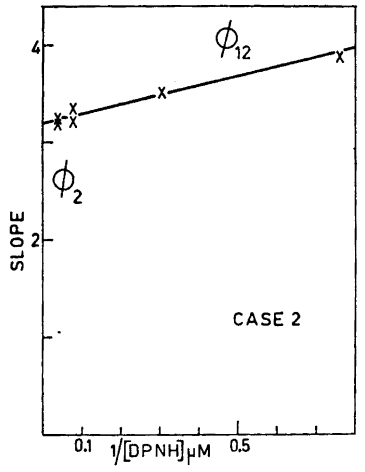

Fig. 9. Plot of slopes, case 2.

DISCUSSION

The results obtained at pH 7 and 9 give very convincing evidence that the T.-C.-mechanism obtains for the liver alcohol dehydrogenase system. All the criteria given by Dalziel agree with this mechanism. Of course, as already emphasized [1], the T.-C.-mechanism does not exclude the existence of binary ES and ES′ complexes or of the ternary complexes ERS and EOS′, dissociating and interconverting rapidly enough to not affect the maximum rate. Whether there are ternary complexes operating under these kinetic conditions or not,

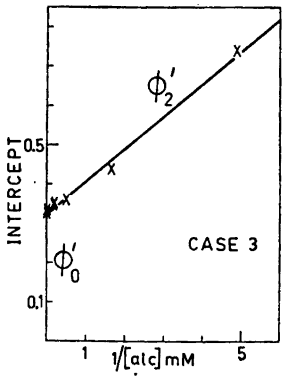

Fig. 10. Plot of intercepts, case 3.

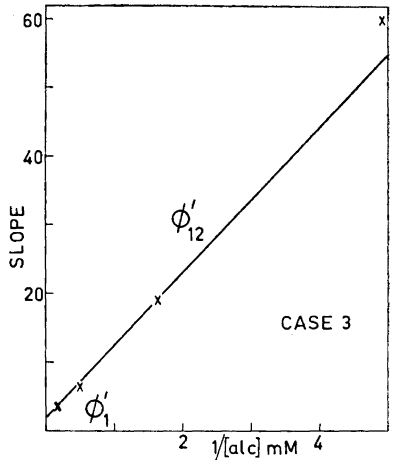

Fig. 11. Plot of slopes, case 3.

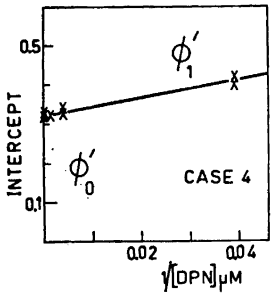

Fig. 12. Plot of intercepts, case 4.

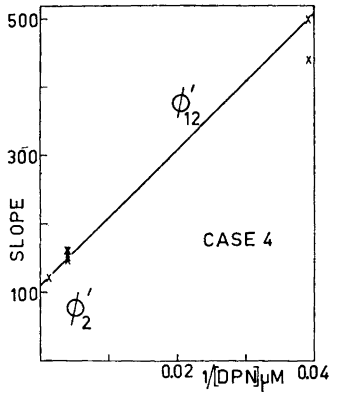

Fig. 13. Plot of slopes, case 4.

the present experiments could not indicate, although experiments where products were initially added might [15,16]. Indeed, in Part III we shall give experimental evidence for the existence of both types of complex, along with confirmatory values of the dissociation constants for ES and ES'. This means that the general mechanism I for an enzyme with two substrates is followed in the case of liver alcohol dehydrogenase, though with such restrictions that the T.-C. simplification is allowed at least at pH 7.

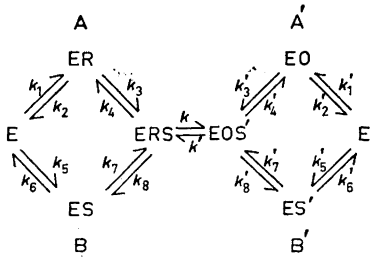

(I)

We can distinguish different phases in this reaction scheme: the first "on" phase and the second "off" phase. Between these interconversion operates. The reaction will prefer the routes in the four cases as shown in Table 6.

It is evident from Tables 2 and 5 that the dissociation constants, determined in equilibrium measurements without substrates (See Part II) agree with the values calculated from the kinetic constants, thus $K_{E,R,\,eq} = k_2/k_1 = 0.31\ \mu M$,

Table 6. Reaction pathways for cases 1—4.

Case	Conditions	First phase	Second phase
1	Constant [S] R → 0	B	A′
2	» [R], S → 0	A	A′
3	» [S′], O → 0	B′	A
4	» [O], S′ → 0	A′	A

$K_{E,O,\,eq} = k_2'/k_1' = 160\ \mu M$ and as shown below and in Part III, $K_{E,S} = 10.2\ \mu M$, $K_{E,S'} = 4.6$ mM and thus $K_{ER,S}/K_{ES,R} = K_{E,S}/K_{E,R} = 33$ and $K_{EO,S'}/K_{ES',O} = K_{E,S'}/K_{E,O} = 29$. Therefore it appears highly likely that as required by the T.-C.-mechanism the dissociation reactions of the ternary complexes in the second phase of the reaction will prefer the routes A and A′, thus

$$E\begin{matrix}R\\S\end{matrix} \rightarrow ER \rightarrow E + R \quad \text{and} \quad E\begin{matrix}O\\S'\end{matrix} \rightarrow EO \rightarrow E + R$$
$$\begin{matrix}+\\S\end{matrix} \qquad\qquad \begin{matrix}+\\S'\end{matrix}$$

In the reverse reaction, at [O] → ∞ and [S′] → ∞ practicaly all the enzyme will be in the state ER, and $V_{max} = k_2$. The kinetic determinations of V_{max} therefore will be expected to give k'_2 and k_2 rather than k'_6 and k_6, in agreement with the T.-C.-mechanism. The reaction in the first phase will follow the upper or lower routes depending on the relative concentrations of the reaction partners. The values calculated as k_1 (from case 1) and k'_1 (from case 3) will therefore rather reflect the "on" velocity constants k_7 and k'_7

for $ES + R \xrightarrow{k_7}$ and $ES' + O \xrightarrow{k'_7}$. According to Tables 2 and 5, $K_{E,R,eq} \approx K_{E,R,kin}$, and $K_{E,O,eq} \approx K_{E,O,kin}$, which means that $k_1 = k_7$ and $k'_1 = k'_7$, in agreement with an earlier discussion [17]. It is by no means obvious, why this should be so. However, as we shall show experimentally in Part III, there seems to be a more general rule saying that partners in a ternary complex do not seem to interfere appreciably with each other's "on" velocity constants, but mainly with the "off" velocity constants, resulting in mutual stabilization to the same extent as the "off" velocity decreases, or mutual repulsion resulting in an increased "off" velocity.

The interconversion phase is in both directions very fast compared with the other steps, as required by the T.-C.-mechanism.

As seen in Figs. 2—5 the Michaelis constants vary with the concentration of the other partner in opposite ways for the forward and reverse reactions. This is inherent in the T.-C. mechanism:

From equation (1a) at $R = \infty$

$$\frac{e}{V} = \frac{1}{k_2'} + \frac{1}{k_3[S]}$$

Therefore at $[DPNH] = K_M$

$$\frac{1}{k_2'} + \frac{1}{k_3[S]} = \frac{1}{k_1[R]} + \frac{k_2}{k_3[S] \times k_1[R]}$$

$$K_M = [R] = 1 + \frac{k_2}{k_3[S]} \Big/ \frac{k_1}{k_2'} + \frac{k_1}{k_3[S]}$$

This hyperbolic function $(1 + ax)/(b + cx)$ gives an asymptotic value for $K_M = k_2'/k_1 = 6.7$ μM for $[S] = \infty$, and $K_M = k_2/k_1 = 0.28$ μM for $[S] = 0$. K_M approaches infinity for the unreal condition $1/[S] = -k_3/k_2' = -0.0042$.

Table 7 shows the values of the Michaelis constants obtained by analogous considerations at infinite and zero concentrations of each reaction partner. In all cases there is a 23.8-fold relation, operating in the opposite way for the forward and reverse reactions. As can be seen from Table 7 this is k_2'/k_2 (74/3.1 = 23.8). The condition for K_M being independent of the concentration of the other partner is that $k_2' = k_2$ (which is not true in our case).

As seen from Table 7 the Michaelis constants for DPNH and DPN, when their reaction partners approach zero concentration, asymptotically become equal to the dissociation constants $K_{E,R} = k_2/k_1$ and $K_{E,O} = k'_2/k'_1$. This reflects the situation:

$$E + R \underset{k_2}{\overset{k_1}{\rightleftharpoons}} ER$$

When [E] = [ER] and [ald] is very low, the reaction velocity will be equal to half that recorded when $[R] \to \infty$, that is $[R] = K_{M,DPNH}$ and *vice versa* for $K_{M,DPN}$. This is as expected since the T.-C. mechanism assumes that binary coenzyme-enzyme complexes are formed before any reaction with the substrate occurs.

Table 7. Dependence of the Michaelis constants on the concentration of the other reaction partner [C].

	K_M (μM)	
	[C] → 0	[C] → ∞
DPNH	$k_2/k_1 = 0.28$	$k_2'/k_1 = 6.7$
Aldehyde	$k_2/k_3 = 10$	$k_2'/k_3 = 239$
DPN	$k_2'/k_1' = 141$	$k_2/k_1' = 5.9$
Alcohol	$k_2'/k_3' = 6\,060$	$k_2/k_3' = 255$

From the general two substrate mechanism A, one would expect *mutatis mutandis* $K_{M,ald} = K_{E,ald} = k_6/k_5$, and $K_{M,alc} = K_{E,alc} = k_6'/k_5'$ for [R] resp. [O] → 0, and the values found, 10 μM and 6 100 μM are close to those found (in Part II) for $K_{E,ald}$ (10 μM) and $K_{E,alc}$ (4 600 μM) in experiments ments with inhibitors. The functions k_2/k_3 and k_2'/k_3' given in Table 7 for $K_{M,ald}$ and $K_{M,alc}$ are valid only under the assumptions of the T.-C. mechanism, that no binary enzyme-substrate complexes (ES, ES') are formed. The results obtained here, however, prove that such complexes are formed in agreement with the general mechanism I. Nevertheless the relations between the rate constants are such that the T.-C. simplification of the general mechanism I is kinetically adequate.

Note added in proof. K. Dalziel [18,19] has recently reported that impurities such as adenosine-diphosphate-ribose present in some DPNH preparations may have an inhibiting action, leading to too low values for k_2'. His highest value [19] for k_2' at pH 7 was = 100 which is somewhat higher than our value 74. However, we have confidence in our value for two reasons: first, it has been obtained consistently with three different DPNH preparations; second, these preparations were thoroughly analyzed (McKee, to be published) and were found to be at least as pure as Dalziel's best one. The conformity of our data to the requirements of the T. C. mechanism, *e.g.* $\Phi_0 = \Phi_1'\Phi_2'/\Phi_{12}'$ (Table 3) could be to some extent fortuitous. It can in fact be shown that strict simplification of the complex initialrate equation [16] for the general mechanism I to the simple T. C. equations 1 (a) and 1(b) reqires contradictory assumptions for the forward and reverse reaction, but approximate simplification can under certain conditions be expected theoretically (Dalziel, in preparation).

Acknowledgements. The authors are indebted for financial support given by *Statens Medicinska Forskningsråd, Statens Naturvetenskapliga Forskningsråd, Knut och Alice Wallenbergs Stiftelse, The Rockefeller Foundation, Wenner-Grenska Samfundet* and *Institutet för Maltdrycksforskning.*

Skilful technical assistance has been given by Mr. Lars-Gunnar Falksveden.

REFERENCES

1. Theorell, H. and Chance, B. *Acta Chem. Scand.* **5** (1951) 1127.
2. Theorell, H., Nygaard, A. P. and Bonnichsen, R. *Acta Chem. Scand.* **9** (1955) 1148.
3. Dalziel, K. and Theorell, H. *Biochem. J.* **66** (1957) 34P; Theorell, H. *Advances in Enzymol.* **20** (1958) 471.

4. Theorell, H. and Winer, A. D. *Arch. Biochem. Biophys.* **83** (1959) 291.
5. Dalziel, K. *Acta Chem. Scand.* **11** (1957) 1706.
6. Lineweaver, H. and Burk, D. *J. Am. Chem. Soc.* **56** (1934) 658.
7. Alberty, R. A. *J. Am. Chem. Soc.* **75** (1953) 1928.
8. Bäcklin, K. I. *Acta Chem. Scand.* **12** (1958) 1279.
9. Rafter, G. W. and Colowick, S. P. *Methods in Enzymology,* **Vol. III,** p. 887. Academic Press, New York 1957.
10. Kornberg, A. and Pricer, W. E. *Biochem. Preparations* **3** (1953) 20; Siegal, J. M., Montgomery, G. A. and Bock, R. M. *Arch. Biochem. Biophys.* **82** (1959) 288.
11. Dalziel, K. *Acta Chem. Scand.* **12** (1958) 459.
12. Dalziel, K. *Acta Chem. Scand.* **11** (1957) 397.
13. Theorell, H. and Nygaard, A. P. *Acta Chem. Scand.* **8** (1954) 877.
14. Warburg, O. and Christian, W. C. *Biochem. Z.* **287** (1936) 287.
15. Alberty, R. A. *J. Am. Chem. Soc.* **80** (1958) 1777.
16. Dalziel, K. *Trans. Faraday Soc.* **54** (1958) 1247.
17. Winer, A. D. and Theorell, H. *Acta Chem. Scand.* **14** (1960) 1741.
18. Dalziel, K. *Nature* **191** (1961) 1098.
19. Dalziel, K. *Biochem. J.* **80** (1961) 440.

Received March 28, 1961.

ACTA CHEMICA SCANDINAVICA 15 (1961) 1811–1833

Liver Alcohol Dehydrogenase

II. Equilibrium Constants of Binary and Ternary Complexes of Enzyme, Coenzyme, and Caprate, *Iso*butyramide and Imidazole

HUGO THEORELL and JOHN S. McKINLEY-McKEE

Medicinska Nobelinstitutet, Biokemiska avdelningen, Stockholm, Sweden

Using the fluorescence of the complexes ER and ERI the dissociation constants in 0.1 μ buffer, 23.5°C, at pH 7 of the caprate complexes $K_{E,I}$, $K_{EO,I}$ and $K_{EI,O}$ and of the *iso*butyramide complexes $K_{E,I}$, $K_{ER,I}$ and $K_{EI,R}$ have been determined, as well as $K_{E,R}$, $K_{E,O}$ and the imidazole dissociation constants $K_{E,I}$, $K_{ER,I}$, $K_{EI,R}$, $K_{EO,I}$ and $K_{EI,O}$ for the pH range 6—9. Glycine used for buffering at pH 9, was found to give a binary but no ternary complex. In titrations in the presence of relatively high concentrations of alcohol, "unnatural" binary and ternary alcohol complexes were also found.

$K_{E,R}$ was similar to previous values, but higher values obtained for $K_{E,O}$ resulted now in the disappearance of previous disagreements between the equilibrium and kinetic values at lower pH's, the results now agreeing with the Theorell-Chance mechanism.

Except for $K_{E,R}$, $K_{E,O}$ and $K_{EO,I}$ the dissociation constants were essentially invarient with pH. The increase of $K_{E,R}$ at high pH suggested it was probably sulphydryl groups which joined the protein to the DPNH ring. Analysis of the pH curve for $K_{E,O}$ indicated that of the free octahedral zinc bonds which in the free enzyme presumably hold water, one at higher pH (8.6) looses a proton. The resulting attraction between zinc-OH^- and the positively charged pyridine ring of DPN, is considered responsible for the changes in $K_{E,O}$ with pH.

In a previous publication, Winer and Theorell[1] described how fatty acids (I) formed complexes EI with liver alcohol dehydrogenase (E), as well as complexes EOI with the binary complex EO of enzyme with diphosphopyridine nucleotide, DPN (O). The corresponding complexes with DPNH, ERI, were not formed with fatty acids.

Fatty acid amides, on the contrary, formed complexes of the type ERI, but not EOI.

While testing different nitrogen compounds for their ability to form ternary complexes with ER it was observed that imidazole gave highly fluorescent compounds with interesting properties. Imidazole forms complexes with zinc

ions [2,3], and LADH contains zinc [4] just as does yeast ADH [5]. It was considered interesting to make more accurate determinations of the dissociation constants of the complexes of one fatty acid and one amide than had been possible previously. Capric acid and *iso*butyramide were selected, the latter because of its highly fluorescent ternary complexes, the former because it was found in determinations of $K_{E,O}$ that DPN not only competes with DPNH but in addition causes some quenching of the fluorescence intensity of ER. Thus a redetermination of the dissociation constants of the ternary complexes of caprate with DPN was called for, as the relations between these constants are so involved that even small errors sometimes produce unexpectedly large effects. In addition, the imidazole complexes were studied, with the purpose of comparing all these equilibrium data with studies of the influence of these substances on the kinetics.

EXPERIMENTAL

Buffers. At pH 6—8, 0.1 μ phosphate buffer was used while at pH 9, (a) 0.1 μ phosphate, pH 8 + 0.1 NaOH-glycine buffer, pH 10, gave 0.1 μ phosphate + 3.64 mM glycine buffer. (b) 1 M NaOH + glycine crystals gave 0.1 μ NaOH + 811 mM glycine buffer and (c) a mixture of the above two gave a 0.1 μ phosphate + 81 mM glycine buffer. Versene was never present in these or any other solutions.

Enzyme and coenzymes. LADH prepared according to Dalziel [6] or Bonnichsen and Brink [7] was used. The two enzymes gave identical results. In step 5 the Bonnichsen enzyme was twice dissolved in ice cold 0.02 M phosphate pH 7, and precipitated with 30 % ethanol. The crystals were each time washed with a little buffer containing 6 % ethanol. The enzyme was then crystallized from 0.02 M phosphate, pH 7, at 2°C. Finally it was recrystallized several times by dialysis [6]. The enzyme was considered pure, the absorbancy index at 280 mμ being 35×10^4 cm^2/mole (specific extinction = 0.42)[8], while E_{280}/E_{260} which was independent of whether the enzyme was treated with DPN (see below) or not, was 1.30 ± 0.01. A suspension of LADH crystals in 0.1 μ phosphate and 30 % alcohol (~ 10 mg/ml) was centrifuged; the crystals were dissolved in the same volume of 0.1 μ phosphate-ammonia buffer, pH 9, centrifuged again and dialysed twice against 0.1 μ phosphate, pH 7 or 8. A few milligrams of DPN/ml were then added to the enzyme which was then kept overnight in the refrigerator. The enzyme solution was then dialysed 4—5 times (3—5 days) against phosphate buffer. The DPN treatment was made because it is essential for good titrations in the presence of DPN that the enzyme does not contain traces of alcohol [9]. If precautions are taken to ensure that the quartz distilled water (distilled water redistilled from dilute alkaline permanganate) used to make up the buffer solutions and the buffer solutions themselves never are near a room where there are traces of alcohol in the air the DPN treatment can be avoided and contrary to previous ideas [9] alcohol can be removed by dialysis alone, the resulting enzyme giving identical results with the DPN treated enzyme. The above conditions are indeed important in these experiments (as a problem is that the enzyme quickly picks up any traces of alcohol in the air). Stock enzyme solutions $0.5—0.6 \times 10^{-4}$ M resulted which were quite stable, their activity decreasing approximately 1 % each day. Enzyme assay was carried out by determining the concentration of binding sites (1.0—1.2 μN in most equilibrium experiments) through titration with DPNH in the presence of 50 mM *iso*butyramide. This was performed at the beginning and end of each day's experiments, there normally being no change. The details regarding the coenzymes were described in Part I.

Inhibitors. Potassium caprate and *iso*butyramide did not fluoresce. Most nitrogen compounds, however, like imidazole were found to fluoresce strongly due to impurities. As in both kinetic and equilibrium experiments this background fluorescence prevents the use of high apparatus sensitivity, it was necessary to prepare the nitrogen compounds as fluorescence free as possible. This was achieved by adsorbing the fluorescent impurities on Norite S X 30 charcoal. To avoid contamination with organic solvents such as ethanol from which Tris is usually recrystallized or benzene (F = 2.6, S = 1, see Table 1) from

Table 1. Fluorescence F in inches at sensitivity $S = 1$. Water = 0.1″.

Compound	Tris	Imidazole	Piperazine
2 M Solution	2.2	27.0	7.4
1st Recrystallisation	0.9		
2nd »		2.5	0.7
Norite Column	0.2	0.35	0.2

which imidazole is usually recrystallized, the nitrogen compounds even when very soluble were recrystallized from water at temperatures down to 0°C. A 2 M solution in water was then passed once or twice using a 30 cm mercury pressure, through a fresh 3—4 cm column of Norite S X 30, previously washed with 2 N HCl, 2 N ammonia and water. This treatment reduced the fluorescence of imidazole and the nitrogen compounds used to near that of water (Table 1). The process was accelerated if the 2 M solution was first heated with Norite, filtered hot and then allowed to crystallize. Water was removed around 40°C and the fluorescence-free compounds dried and kept as crystals. The liquid nitrogen compounds tried, were soluble in water and were passed directly through Norite-water columns as above.

As it was necessary to have an accurate pK for imidazole under our experimental conditions, so as to know the concentration of neutral or unionized imidazole, 0.2 M imidazole was titrated with 1 M HCl at 23.5°C, using the Beckman Model G pH meter used throughout our work. The pK of imidazole was taken as 7.10 as the titration gave 7.12 while the values in the literature when adjusted to 0.1 μ, 23.5° were 7.06[2], 7.10,[10] and 7.11 [11].

Experiments were performed with a recording Beckman spectrophotometer, DK2, to see if any addition compounds were formed between imidazole and the coenzymes under any of our conditions. None were formed.

Apparatus. The equilibrium experiments were performed using a recording spectrophotofluorimeter [12]. The activating wavelengths in light from a high pressure Xenon lamp were isolated using a Bausch and Lomb grating monochromator, passed into a 3 ml, 1 × 1 cm precision quartz cuvette containing either the experimental solution or the standard solution, and the emitted fluorescence analysed in a Beckman DU spectrophotometer with recorder. The quartz cuvette was placed in a light tight cell compartment maintained by water rapidly circulated from a thermostat at 23.5°C. This was the temperature of the experiments, the pH determinations (performed on each cuvette immediately after titration) and all solutions other than the concentrated enzyme and coenzyme solutions which were kept at 0°C. The standard (10.5 μM DPNH in 0.01 M Tris) was measured immediately before and after each experimental cuvette to ensure there had been no apparatus drift. In determining the dissociation constants, the activation wavelength was 330 mμ, the isosbestic point for DPNH and DPNH-LADH, while the fluorescence was measured at 410 mμ where the fluorescent ratio of DPNH-LADH/DPNH (Q) is 13.1. Using calibrated Carlsberg pipettes (3—200 μl), enzyme, coenzymes and inhibitor solutions were added either directly or on a glass rod to give a final cuvette volume of 2 ml.

METHOD OF CALCULATION

For all the inhibitors $K_{ER,I}$ was determined directly by titration of E in the presence of excess R with the inhibitor. (The ternary complexes comprising E, R and I can be written ERI or EIR. However, $K_{ER,I}$ represents I dissociating from the complex while $K_{EI,R}$ represents R dissociating from the same complex. The same terminology applies to the dissociation constants for the ternary complexes comprising O). Otherwise the constants were determined

from titrations with R. These gave a Q and an apparent dissociation constant D_{app} from which the true dissociation constants were calculated depending on how the titrations were set up and the fact that only the complexes ER and ERI fluoresce [1].

I. Titration of E with R. ($K_{E,R}$)

The cuvette only contains buffer and enzyme and as in all these titrations eight additions of R are made on a glass rod. Table 2 illustrates a typical calculation of Q and D_{app}. C (μN) = LADH concentration; R (column 1) = μM DPNH/addition; F (column 3) = $Q' - 1$, where Q' = deflection in inches for each addition of R/r; r = deflection that each addition of R would by itself give = (S—B) × 0.525/10.5; (S—B) = the deflection of 10.5 μM DPNH, S and B (see Figs. 4—5) being the deflection of the 10.5 μM standard and the buffer.

The eight additions of R have to be listed with the F values calculated for each resultant fluorescence increment. Column 2 is the summation of R and column 4 that for FR. Z (column 5) is the solution of the equation [12]

$$C\left(\frac{\Sigma R''}{\Sigma FR''} - \frac{\Sigma R'}{\Sigma FR'}\right)Z^2 - (\Sigma R'' - \Sigma R')\,Z + (\Sigma FR'' - \Sigma FR') = 0$$

for the particular pairs of ΣR and ΣFR values 1—5, 2—6, 3—7, 4—8. $Q = Z + 1$, an average of the four Z values being taken.

Our calculations were greatly simplified throughout by the use of a Wegematic 1 000 electronic calculating machine. Table 2 is typical of those it produced, as it had been programmed so that it was only necessary to feed in C and the columns R and F.

II. Titration of E + O with R ($K_{E,O}$)

In the titration of the enzyme with R in the presence of O, there is present in the cuvette at any stage E, ER and EO. If E_t, R_t, and E_f, R_f, respectively, represent total added or free E or R present, then

$$K_{E,R} = E_f \times R_f/ER = (E_t - ER - EO)(R_t - ER)/ER \qquad (1)$$

and $D_{app} = (E_t - ER)\,(R_t - ER)/ER$. D_{app}, the apparent dissociation constant, is the value given by the computor in the last column, see Table 2. Only when no other complexes than ER are present does this value represent a simple dissociation constant, $K_{E,R}$.

Putting $E_t = 1.0$ and ER = 0.5, EO is obtained from eqn. 2.

$$K_{E,R}/D_{app} = (0.5 - EO)/0.5 \qquad (2)$$

$E_f = E_t - ER - EO = 0.5 - EO$ and $K_{E,O} = E_f[O]/EO$.

Table 2. $K_{E,R}$ (0.1 μ, pH 7, 23.5°C). Expt. F IV, $C = 0.890$.

	R	ΣR	F	ΣFR	Z	ΣFR/Z	$K_{E,R}$
1	0.525	0.525	8.030	4.216	12.482	0.336	0.311
2	0.525	1.050	5.090	6.888	12.484	0.549	0.311
3	0.525	1.575	2.670	8.290	12.565	0.661	0.317
4	0.525	2.100	1.380	9.014	12.633	0.719	0.329
5	0.525	2.625	1.000	9.539		0.761	0.317
6	0.525	3.150	0.570	9.838		0.785	0.318
7	0.525	3.675	0.430	10.064		0.803	0.313
8	0.525	4.200	0.280	10.211		0.814	0.315
				Average	12.541		0.316

III. Titration of E + I with R ($K_{ER,I}$, $K_{E,I}$ and $K_{EI,R}$)

Whenever ERI is not formed and the only fluorescent complex is therefore ER eqn. 2 applies. If instead of O, it is I which is present, giving EI, then $K_{E,I}$ instead of $K_{E,O}$, results. This situation occurs with glycine and caprate.

When ERI can be formed, as with *iso*butyramide or imidazole, in titrations of E plus various amounts of I with R the complexes ER, EI and ERI are present. ER and ERI are fluorescent with different intensities, Q_{ER} and Q_{ERI}, and have different dissociation constants. Q and D_{app} are consequently found to vary with the concentration of I.

(a) Q_∞ and $K_{ER,I}$

From the variation of Q with [I] and knowing that at zero [I] $Q = Q_{ER}$, $Q_{ERI} = Q_\infty$ ([I] = ∞) can be caculated for pairs of Q values since

$$K_{ER,I} = \frac{ER}{ERI}[I] = \frac{Q_\infty - Q_x}{Q_x - Q_{ER}}[I] \quad (3)$$

and for any two concentrations of I

$$\frac{Q_\infty - Q_1}{Q_1 - Q_{ER}}[I_1] = \frac{Q_\infty - Q_2}{Q_2 - Q_{ER}}[I_2] \quad (4)$$

From the mean Q_∞, $K_{ER,I}$ is calculated directly using formula 3, or by plotting $\log \frac{Q_\infty - Q_x}{Q_x - Q_{ER}}$ against log [I], the value of log [I] at zero ordinate being log $K_{ER,I}$.

(b) D_{app}, $K_{E,I}$ and $K_{EI,R}$:

Put the total concentration of fluorescent complexes = ER′ = ER + ERI. Then by combining with (3):

$$ER = ER' \times K_{ER,I}/([I] + K_{ER,I}) \quad (5)$$

Knowing $K_{ER,I}$, and putting $E_t = 1.0$ and ER′ = 0.5, ER and ERI can be calculated for each concentration of I. Then

$$D_{app} = (E_t - ER')(R_t - ER')/ER' = (R_t - ER') = R_f \quad (6)$$

$$E_f = K_{E,R} \times ER/R_f \qquad (K_{E,R} = E_f \times R_f/ER) \tag{7}$$

$$EI = 0.5 - E_f \qquad (E_f = E_t - ER' - EI) \tag{8}$$

giving $K_{E,I} = E_f \times [I]/EI$ and $K_{EI,R} = EI \times R_f/ERI$

IV. Titration of E + I + O with R ($K_{EO,I}$ and $K_{EI,O}$)

Q and D_{app} depend on the various concentrations of both I and O. All the possible complexes may be present (ER, EO, EI, ERI, and EOI) but again only ER and ERI fluoresce. Eqn. 5 applies, giving ER and ERI which only depend on $K_{ER,I}$ and I.
Again

$$D_{app} = R_f \tag{6}$$

$$E_f = K_{E,R} \times ER/R_f \tag{7}$$

Now

$$EO = E_f \times [O]/K_{E,O}$$

$$EI = E_f \times [I]/K_{E,I}$$

$$EOI = E_t - (ER + ERI + EI + EO + E_f) = 0.5 - (EI + EO + E_f)$$

giving $K_{EO,I} = EO \times [I]/EOI$ and $K_{EI,O} = EI \times [O]/EOI$

Relations between the dissociation constants. All the dissociation constants are interdependent and have to fulfill relations 8 and 9

$$\frac{K_{ER,I}}{K_{E,I}} = \frac{K_{EI,R}}{K_{E,R}} \tag{8}$$

$$\frac{K_{EO,I}}{K_{E,I}} = \frac{K_{EI,O}}{K_{E,O}} \tag{9}$$

RESULTS

Table 3 gives the values at pH 6, 7, and 8 of K_{ER} at 23.5° and 0.1 ionic strength. As expected they do not differ very much from the earlier values [12]. The constancy of Q_{ER} both at these pH's and at pH 9 (Table 5) is noticeable and a mean $Q_{ER} = 13.1$ could have been used in these calculations. Indeed it is often best to use an average Q particularly when Q is dependent on small ER′ values as in the case of $K_{E\text{-capric}}$ in Table 8.

Table 4 gives the values for $K_{E,O}$ at pH 6—8. These have been calculated using the tabulated Q values from the computor, as in Fig. 1 the mean Q values obtained in $K_{E,O}$ determinations at pH 6—9 (Tables 4 and 6) in the presence of different amounts of DPN are plotted, and the resulting curve shows that there is a drop in Q with increasing concentration of DPN from 13.1 at zero DPN to around 11 at 1 mM, DPN obviously quenching the fluorescence somewhat. Though apparently not very large this decrease leads to considerably higher values for $K_{E,O}$, now for example at pH 7, 160 μM instead of 84 μM as calculated with an average Q previously [12]. In calculating D_{app} whenever DPN is present, each particular computor Q has always to be used.

Table 3. $K_{E,R}$ (μ = 0.1, 23.5°C)

pH	Expt.	Q	$K_{E,R}$ μM
6	F VI, E 3	13.70	0.225
	4	13.46	0.227
	F XA 12	12.66	0.226
		13.27 ± 0.26	0.226
7	F II, E 26	12.40	0.29
	III, 3 + 4	12.6	0.26
	IV, 5 + 6	13.94	0.317
	7 + 8 + 9	13.54	0.316
	F XA, 5	13.17	0.300
	6	13.31	0.367
	F XB, 3	12.43	0.359
		13.18 ± 0.17	0.310 ± 0.03
8	F VII, E 4	12.22	0.395
	5	12.67	0.425
	39	14.03	0.378
	46	13.65	0.433
	F XA 13	12.88	0.370
	14	14.32	0.467
		13.30 + 0.3	0.411 + 0.016

Glycine. At pH 9 glycine was used as buffering substance in earlier determinations [12]. As seen from Table 5 the values obtained for $K_{E,R}$ are strongly dependent on the glycine concentration. This was explained by assuming formation of an enzyme-glycine compound (EI) which does not combine with R or O. In agreement herewith Q is not at all dependent on the glycine concentration, and $K_{ER,app}$ is influenced to the same degree as $K_{EO,app}$. Calculations under this assumption with eqn. 2, gave $K_{E,glycine}$ = 230 mM. $K_{E,R}$ = 0.64 μM, and $K_{E,O}$ = 12 μM at zero [glycine] as shown in Table 7. Previous values for $K_{E,R}$ of 0.9—1.0 μM were all made in 100 mM glycine [12] and agree with the present results. The equilibrium and kinetic values can now be said to agree, not only for $K_{E,R}$ from pH 6—9 but also for $K_{E,O}$, the discrepancies for $K_{E,O}$ at neutral and acid pH previously [12] having disappeared. It was found practical to use in the kinetic experiments 3.6 mM glycine + phosphate. This small amount of glycine does not appreciably alter the kinetics but contributes to the buffering capacity which is very low for phosphate at pH 9.

Caprate. The dissociation constants $K_{E,I}$, $K_{EO,I}$ and $K_{EI,O}$ were redetermined for K-caprate. As seen from Table 8, $K_{E,I}$ now came out to be 45 ± 3 μM. This value is considerably lower than 200—250 μM obtained by Winer and Theorell [1]. It should be noted that the values for $K_{E,I}$ showed no drift with increasing concentration of caprate. This proves that a ternary ERI

Table 4. $K_{E,O}$ (0.1 μ, 23.5°C)

pH	Expt.	[DPN] μM	Q	D_{app} μM	$K_{E,O}$ μM
6	F VI, E 5	204	12.17	0.392	282
	6	408	12.13	0.573	266
	7	408	11.37	0.566	272
	8	1 020	10.0	1.166	246
	15	408	11.38	0.559	277
	16	408	10.95	0.595	250
	18	612	11.02	0.787	248
					266 ± 5
7	F III, E 5	136	11.7	0.495	191
	F IV, 10	136	13.16	0.635	135
	12	408	11.0	1.17	147
	14	408	11.0	1.05	171
	24	408	10.88	1.056	170
	25	408	11.23	0.995	165
	30	408	12.58	1.062	173
	26	816	11.39	1.957	157
	27	816	11.70	1.900	147
	28	816	11.10	1.55	187
	F XIV, 4	130	12.62	0.581	149
	11	128	13.40	0.584	144
	12	128	11.81	0.541	172
	13	320	10.66	1.008	143
					160 ± 4
8	F VII, E 9	68	13.30	1.134	38
	41	68	12.33	0.871	60
	43	68	13.64	1.052	43
	6	136	12.00	1.314	61
	7	136	12.41	1.414	55
					51 ± 5

Table 5. pH 9, $K_{E,R}$

Expt.	[Glycine] mM	Q	$K_{E,R}$ μM	$K_{E,R}$ average μM
F XII, 7	0	13.12	0.534	0.613
9	0	12.82	0.691	
F XII A, 10	3.6	13.08	0.714	
11	3.6	13.03	0.609	0.655
26	3.6	13.33	0.642	
F VIII, 6	81	13.66	0.884	
7	81	13.38	0.858	0.868
F IX, 23	81	12.66	0.891	
24	811	12.42	0.838	
F IX B, 44	811	14.12	2.94	2.63
46	811	13.02	2.33	
	Average	13.15		

Table 6. pH 9, $K_{E,O}$ in glycine-phosphate, 0.1 μ.

Expt.	[Glycine] mM	Q	D_{app}	[DPN] μM	$K_{E,O,app}$ μM
F XII, 12	3.6	10.66	2.663	34	11.1
13	3.6	11.26	1.689	17	11.1
F VIII, 8	81	11.88	4.172	68	17.9
9	81	12.78	4.75	68	15.2
10	81	13.93	4.13	34	18.0
11	81	12.81	1.82	17	15.4
F IX, 26	81	12.50	4.62	66	15.7
F IX B, 48	811	13.5	5.4	66	49
49	811	13.5	8.0	132	53
51	811	13.5	8.85	132	63

$K_{E,O}$, 3.6 mM: 11.1 ± 0 (2 values)
81 » : 16.4 ± 0.7 (5 values)
811 » : 55 ± 5 (3 values)

Table 7. pH 9, $K_{E,glycine}$ in glycine-phosphate, 0.1 μ.

[Glycine] mM	$K_{E,R,app}$ mM	$K_{E,O,app}$ mM	$K_{E,glycine}$ From $K_{E,R,app}$	$K_{E,glycine}$ From $K_{E,O}$	$K_{E,R}$ * [glycine]=0 μM	$K_{E,O}$ * [glycine]=0 μM
0	0.64 *	12 *			0.64	12
3.6	0.655	11.1			0.645	11.0
81	0.868	16.4	226	222	0.642	12.2
811	2.63	55	259	226	0.582	12.2
			Average 231 mM			

* Calc. values if $K_{E,glycine}$ = 231 mM.

Table 8. Caprate, $K_{E,I}$ (0.1 μ, pH 7, 23.5°C). Q_{ave} = 12.4.

Expt.	[Caprate] μM	D_{app} μM	$K_{E,I}$ μM
F XIV, E 15	50	0.59	55
5	100	0.89	53
6	100	1.19	35
7	100	1.10	39
8	200	1.68	45
9	200	1.59	49
10	400	2.90	48
11	400	3.32	41
		Average	45 ± 3

Table 9. Caprate, $K_{EI,O}$ and $K_{EO,I}$ (0.1 μ, pH 7, 23.5°C).

Expt.		[Caprate] μM	[DPN] μM	D_{app} μM	Q	$K_{EO,I}$ μM	$K_{EI,O}$ μM
F XVI, E	12	100	13.6	1.95	10.44	2.85	10
	13	100	6.8	1.60	11.24	2.25	6.9
	14	50	6.8	1.23	14.22	1.2	4.2
F XIV,	6	10	130	1.61	12.1	2.55	9.1
	8	5	65	0.96	12.1	1.3	4.6
				Average	12.0	2	7

complex is not formed with caprate, for in such case with increasing caprate D_{app} would asymptotically approach a constant value $= K_{EI,R}$. In agreement herewith the caprate caused no change in the Q-value.

The experiments for determining $K_{EI,O}$ and $K_{EO,I}$ which are interdependent through the relation $K_{E,O} \times K_{EO,I} = K_{E,I} \times K_{EI,O}$ (eqn. 9) are summarized in Table 9. In these experiments it was found difficult to get precise results, due to the great differences between $K_{E,O}$ and $K_{EI,O}$, $K_{E,I}$ and $K_{EO,I}$, respectively. Whatever the concentrations of DPN and caprate used, the complexes will be present in very different concentrations.

As seen from Table 9 a wide range of concentrations of both DPN and caprate were used. The values of the ternary complex constants are somewhat scattered, but entirely at random and the averages should not be far from correct. The values of Winer and Theorell, $K_{EO,I} = 3.8$, $K_{EI,O} = 1.6$ μM were calculated from $K_{E,O} = 84$ μM, $K_{E,I} = 200$ μM. If these determinations are recalculated using $K_{E,O} = 160$, $K_{E,I} = 45$ μM, we obtain: $K_{EO,I} = 1.7$ and $K_{EI,O} = 6.0$ μM, in agreement with the present determinations.

Iso*butyramide* (IB). Because of the strong fluorescence of the ternary ERI complex ($Q = 40$) the constant $K_{ER,I}$ could be determined by adding an

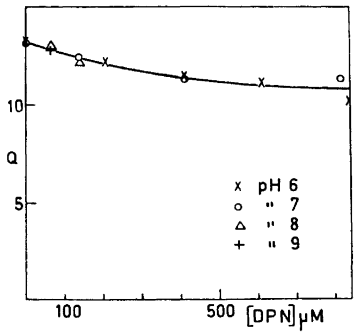

Fig. 1. Variation of Q with DPN concentration in $K_{E,O}$ determinations.

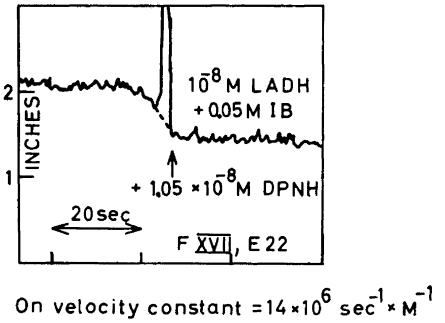

Fig. 2. Reaction cycle for E-*iso*butyramide associating with DPNH.

excess of R to E and then titrating with successive additions of either 10 or 50 μM IB. The results are given in Table 10.

The average value at pH 7, for $K_{ER,I}$ of 140 $\pm$ 5 μM, is definitely lower than the value 450 μM obtained earlier[1]. At pH 9, however, the earlier value $K_{ER,I}$ = 120 μM is in agreement with the present of 116 μM.

The influence of pH in changing from 7 to 9 is small, if it exists at all, for the values 116 and 115 at pH 9 were obtained in the same series and lie between the pH 7 values of 117 and 133 as can be seen from the experiment numbers.

Because of the very low value for $K_{EI,R}$, the direct titration of E + excess I with R implied working at extremely high dilutions. However, due to the high Q value we could when using highest sensitivity get deflections of around 2 inches when 10^{-8} M R was added to 2 $\times$ 10^{-8} N (10^{-8} M) E. The values for $K_{EI,R}$ (Table 10) now came out still lower than before, 5.5 $\times$ 10^{-9} M instead of 20 $\times$ 10^{-9} M.[1]

The value for $K_{E,I}$ was calculated from the values for $K_{E,R}$, $K_{ER,I}$ and $K_{EI,R}$. It was expected to be high; the earlier value was 5.75 mM. It now came out

*Table 10. Iso*butyramide. I. Direct titration of ER with 8 $\times$ 10 μM (or 50 μM in E 38—41) additions of *Iso*butyramide. μ = 0.1, 23.5°C.

pH	Expt.		[DPNH] μM	[LADH] μN	$K_{ER,I}$ μM
7	F XIV E	25	2.5	0.45	163
		26	5.0	0.45	152
		23	5.0	0.45	156
		29	10.0	0.90	135
		38	10.0	0.94	117
		41	10.0	0.94	133
	F XVI	16	10.5	0.85	145
		17	10.5	0.85	131
				Average	140 $\pm$ 5
9	F XIV	39	10.0	0.94	116
		40	10.0	0.94	115
				Average	116

II. Direct titration of EI with R ($K_{EI,R}$).

[LADH] = 2 $\times$ 10^{-8} N. [DPNH] Additions = 1.05 $\times$ 10^{-8} M. (0.1 μ, phosphate pH 7, 23.5°C).

Expt.		[*Iso*butyramide]	$K_{EI,R}$ M $\times$ 10^{9}	k_0 μM^{-1} $\times$ sec^{-1} [13] (from cycles)
F XVII	E 23	50 mM	6.0	13
	24	»	7.8	15
	25	»	4.0	15
F XVIII	27	»	4.6	
	29	»	4.5	
	33	»	6.0	
			5.5 $\pm$ 0.6	14

Table 11. Equilibrium constants (μM) for caprate and *iso*butyramide: 0.1 μ phosphate, 23.5°C, pH 7.

	$K_{E,I}$	$K_{ER,I}$	$K_{EI,R}$	$K_{EO,I}$	$K_{EI,O}$
Caprate	45	—	—	7	2
IB.	9 300	140	0.005	—	—

still higher, so that the 50 mM IB used in the experiment was not high enough to make corrections for free E in equilibrium with EI unnecessary. When these were done, $K_{E,I}$ was 9.3 mM, and the corrected $K_{EI,R} = 4.7 \times 10^{-9}$ M. This may be the lowest value for a dissociation constant ever determined by direct titration, illustrating the great sensitivity of fluorimetry.

An interesting observation was made in these titration experiments. At the high dilutions used the association of R with EI was slow enough to give measurable "on" cycles on the recorder (Fig. 2) from which the second order "on" velocity constant of R to EI could be calculated [13]. The value 14 $\mu M^{-1} \times sec^{-1}$ in Table 10 is close to the value of k_1 ($E + R \xrightarrow{k_1} ER$) = 11

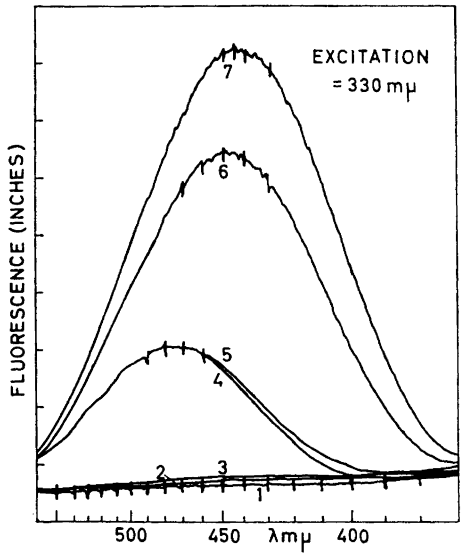

Fig. 3. Fluorescence emission curves for LADH, DPNH and imidazole.

1. Buffer (0.1 μ phosphate, pH7, 23.5°C)
2. » + 0.1 M imidazole
3. » + » + 2.2 μN LADH
4. » + 2.1 μM DPNH
5. » + » + 0.1 M imidazole
6. » + » + 2.2 μN LADH
7. » + » + » + 0.1 M imidazole

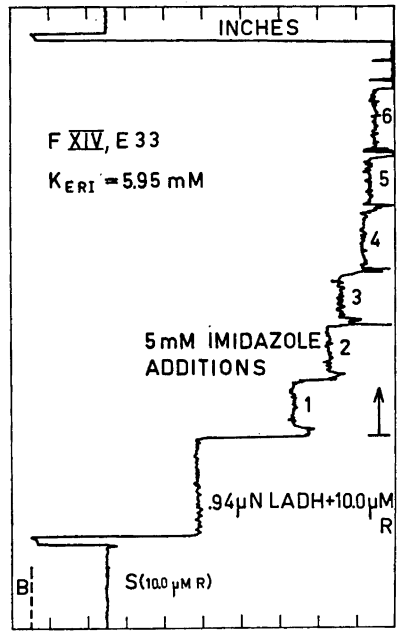

Fig. 4. Direct titration of LADH + DPNH with imidazole.

$\mu M^{-1} \times sec^{-1}$, obtained by kinetic experiments (see Part I). The great difference between $K_{EI,R} = 5 \times 10^{-9}$ M and $K_{E,R} = 310 \times 10^{-9}$ M must therefore be practically exclusively dependent on the "off" velocity constants. It should be emphasized that the association of DPNH to LADH is a very fast reaction of the same order of magnitude as the catalase reaction with hydrogen peroxide [14]. The association velocity constant of FMN to the apoprotein of the old yellow enzyme is under optimal conditions 1 $\mu M^{-1} \times sec^{-1}$.[13]

Imidazole. Fig. 3 shows the fluorescence emission curves for DPNH and its binary and tertiary complexes with enzyme and imidazole. The increase

Table 12. Imidazole; direct titration of $K_{ER,I}$, $\mu = 0.1$, 23.5°C, pH = 7.0.

Expt.		[DPNH] μM	[LADH] μN	$K_{ER,I}$ mM
F XIV, E	31	10	0.94	4.98 [a]
	33	10	0.94	5.93 [a]
	37	10	0.94	4.82 [b]
F XVI	18	10.5	0.85	5.5 [c]
	19	10.5	0.85	5.8 [c]
				5.41

a 5 mM additions
b 2 » »
c 2.5 » »

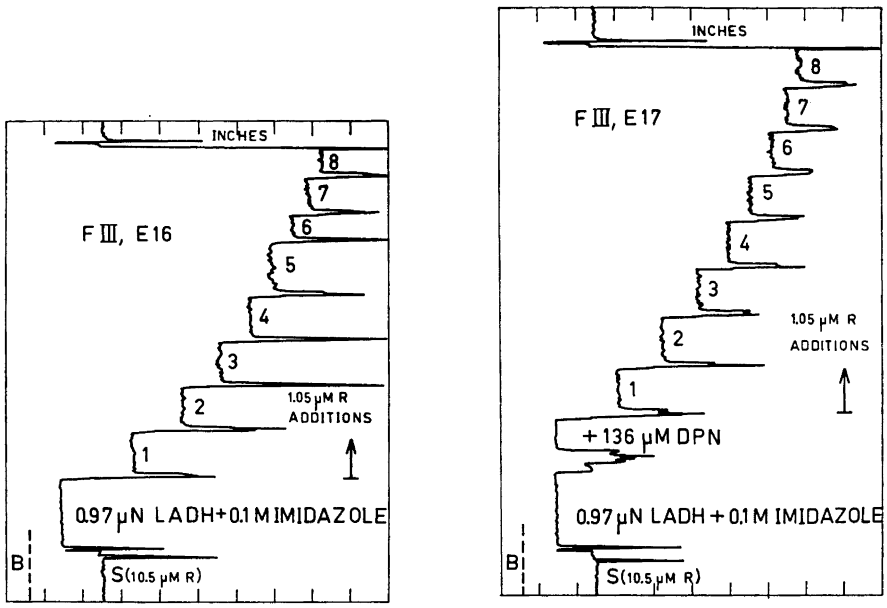

Fig. 5. (a) Titration of LADH + imidazole with DPNH. (b) Titration of LADH + imidazole + DPN with DPNH.

due to the formation of the ternary complex is particularly noticeable in view of the fact that although ERI is highly dissociated its fluorescence is still greater than that of the binary complex ER. The fluorescence emission curve for buffer, buffer with imidazole, or imidazole + enzyme could have been omitted as these are seen to be almost identical. The formation of the binary and ternary complexes is underlined by the change from 475—6 mμ (R) to 447 and 442 mμ in λ_{max} of their emission spectra. The maxima shown, however, are uncorrected for variations with wavelength of the intensity of the exciting light and photocell sensitivity and are 13 mμ too high, the true maxima being 462 (R), 432 (ER) and 429 (ERI) although the ternary complex being dissociated the latter value may be somewhat too high.

Fig. 4 shows a direct titration of E and excess R with imidazole at pH 7. Table 12 gives the values from these direct titrations, the mean $K_{ER,I}$ being 5.4 mM. This value is not too far from the value of 8 mM (Table 13) obtained as a mean of several determinations using the method of titrating E + various amounts of imidazole with R. The direct titration value for $K_{ER,I}$ might be expected to be most accurate as it does not involve Q_∞ which is sometimes difficult to obtain accurately. Fig. 5 shows two typical titrations with R, where compared with the titration of enzyme alone, imidazole markedly enhances the deflection per addition of R, and the total deflection, although these are both decreased again when O is present. In Figs. 4 and 5, B and S are the deflections of the buffer and the standard, the difference in the levels corres-

Table 13. Variation of Q and D_{app} with imidazole concentration at pH 7, 0.1 μ and 23.5°C.

Expt.	[Imidazole] mM	Q	D_{app}	$K_{ER,I}$(mM)	$K_{E,I}$(mM)	$K_{EI,R}$(mM)
FII, E 10	100	45.4	2.33	8.0	1.04	2.49
11	100	44.5	2.20	8.0	1.05	2.35
FIII, 16	100	43.8	2.12	8.0	1.05	2.26
18 + 20	100	44.3	2.12	8.0	1.05	2.26
		44.5				
FII, 20	30	38.4	1.51	8.0	1.35	1.83
21	30	38.0	1.59	8.0	1.28	1.93
22	30	39.9	1.63	8.0	1.25	1.98
FIII, 13 + 14	30	36.7	1.43	8.0	1.43	1.73
		37.9				
FII, 13	10	32.1	1.32	8.0	1.17	2.12
15	10	34.5	1.10	8.0	1.43	1.73
FIV, 16	10	35.7	1.29	8.0	1.19	2.08
20	10	33.6	1.19	8.0	1.31	1.90
		34.0				
FII 24	3	22.3	0.75	8.0	1.30	1.92
FIII 8	3	23.8	0.73	8.0	1.35	1.85
		23.1				
	∞	47.0	Average	8.0	1.23	2.03

ponding to the deflection of the DPNH in the standard solution, thus matching the apparatus sensitivity. Tables 13 and 14 summarize the results of the titrations with R at pH 7, while Table 13 also shows how markedly Q and D_{app} vary with imidazole concentration. Throughout all our experiments

Table 14. Variation of Q and D_{app} with imidazole concentration at pH 7, 0.1 μ and 23.5°C.

Expt.	[Imidazole] mM	[DPN] μM	Q	D_{app}	$K_{EO,I}$mM	$K_{EI,O}\mu$M
FII, E 12	100	136	43.0	2.54	3.06	393
FIII, 17 + 19	100	136	44.0	2.85	2.06	276
FII, 23	30	136	36.9	2.10	4.10	535
FIII, 15	30	136	36.8	2.11	4.11	535
FII, 16 + 18	10	136	31.8	1.71	3.46	452
FIII, 11	10	136	31.1	1.91	2.16	281
12	10	136	28.0	1.68	3.86	502
FIV, 18	10	136	33.1	1.72	3.40	443
17	10	408	31.2	2.46	4.20	545
22	10	408	29.7	2.42	4.20	545
23	10	816	27.0	3.87	3.68	478
FIII, 9	3	136	22.1	1.19	2.61	341
				Average	3.30	430

Table 15. Dissociation constants for complexes of LADH with the coenzymes and imidazole. $\mu = 0.1$ 23.5°C.

pH	Q	$K_{E,R}$ μM	$K_{ER,I}$ mM	$K_{ER,I}$ mM (Corr)*	$K_{E,I}$ mM	$K_{E,I}$ mM (Corr)*	$K_{EI,R}$ μM	$K_{E,O}$ mM	$K_{EO,I}$ mM	$K_{EO,I}$ mM (Corr)*	$K_{EI,O}$ μM
6	63	0.23	57	4.2	6.43	0.47	2.01	266	10.8	0.80	448
7	47	0.31	8	3.5	1.23	0.55	2.03	160	3.3	1.45	430
8	49	0.41	4	3.6	0.76	0.68	2.20	51	6.7	5.9	440
9	48	0.65	3	3.0	0.68	0.67	2.91	12	24.6	24.2	435
											440

* The total imidazole concentrations are corrected to the concentration of unionized imidazole using pK 7.10.

μ has been maintained constant at 0.1 except in some of these experiments at pH 7 where μ was > 0.1 due to the added contribution of imidazole-phosphate not having been allowed for. Consequently Q and D_{app} were corrected to $\mu = 0.1$ from plots of their variation with $\sqrt{\mu}$. It was found that a ten-fold increase in μ doubled D_{app} and the D_{app} values had to be reduced. Likewise with $\mu > 0.1$, Q was too low due to quenching by phosphate.

The mean values of the dissociation constants and their variation with pH, are given in Table 15. It is seen that the Q value of 63 is higher at pH 6 than at pH 7—9, where it is around 48. The reason for this is unknown. At pH 6 ER is a thousand fold more stable than EO, at pH 9 only twenty-fold, this fifty-fold change being caused by a 2- to 3-fold decrease in the stability of ER, and a twenty-fold increase in the stability of EO. $K_{ER,I}$ means that the total imidazole concentrations are used in the calculations. When reduced to the concentration of the neutral or unionized form of imidazole, using $pK = 7.10$, as described in the experimental part, it is seen that the drift in $K_{ER,I}$, with pH disappears, and $K_{ER,Icorr.}$ is perhaps independent of pH. The irregular variations are certainly within the limits of error. Indeed it is noticeable that the dissociation of DPNH and imidazole from the enzyme ($K_{E,R}$ and $K_{E,I}$), and the dissociation of I, R or O from ER and EI ($K_{ER,I}$; $K_{EI,R}$; and $K_{EI,O}$) are intensitive to pH changes. However, the dissociations of O from EO ($K_{E,O}$) and of I from EO ($K_{EO,I}$) are interdependent and pH sensitive, $K_{E,O}$ and

Table 16.

pH	$K_{E,I} \times K_{EI,R} = K_{E,R} \times K_{ER,I}$	$K_{E,I} \times K_{EI,O} = K_{E,O} \times K_{EO,I}$
6	0.95	212
7	1.10	233
8	1.49	292
9	1.95	292

Table 17. Experiments XII B and X B. Alcohol inhibition. Equilibrium experiments.

Q	$K_{ER,alc}$	$K_{E,alc}$ *	$K_{Ealc,R}$
7.7	40 mM	100 mM	0.12 μM

$K_{EO,I}$ changing in a reciprocal way due to the relation $K_{E,I} \times K_{EI,O} = K_{E,O} \times K_{EO,I}$ (eqn. 9) and the relative pH insensitivity of $K_{E,I}$ and $K_{EI,O}$. Table 16 shows the inverse relation between $K_{E,O}$ and $K_{EO,I\ corr}$. There may be an upward trend but the values are not strongly (if at all) pH dependent.

Several other nitrogenous compounds were preliminarily tested for their ability to form complexes with E or ER. Histidine seemed to form a weak complex ($K_{E,I} \approx 0.1$ M); piperazine was somewhat stronger. Pyridine was considerably stronger and formed both an EI and an ERI complex less strongly fluorescent than ER. Veronal, and particularly collidine, formed strong EI-complexes. Preliminary experiments with YADH and pyridine indicated complex formation similar to that with LADH. In kinetic experiments the *ionized* form of pyridine bases was stated to inhibit YADH [15]. Experiments with lactic dehydrogenase and imidazole gave no indication of any complex formation, which would support imidazole and certain nitrogen compounds being joined to the zinc of LADH or YADH, and lactic dehydrogenase not containing zinc in agreement with Pfleiderer [16].

Ethanol. It has been known for many years [4] that concentrations of ethanol higher than 10 mM cause considerable inhibition of the reaction with liver-ADH and DPN. This is the reason why in our kinetic experiments concentrations of ethanol higher than 6.1 mM were not exceeded*. It wast herefore considered interesting to investigate whether additions of relatively high concentrations of alcohol to ER caused any changes in fluorescence intensity and $K_{ER,app}$ indicating the formation of an ERI complex at pH 7.

Fig. 6 shows this to be the case. $K_{E,R,app}$ and Q both changing along what can be considered to be a monovalent dissociation curve with 50 % dissociation at around 40 mM. With increasing alcohol concentration, $K_{E,R,app}$ went down from 0.31 to 0.12 μM, and Q from 12.5 to 8, indicating that a ternary complex ERalc is formed.

The values of the dissociation constants are shown in Table 17. It was found that 1 M ethanol gave a 10 % fluorescence increase for DPNH and in calculating Q and D_{app} the effect of this on r and hence on the F values in the programmes had to be allowed for. In these experiments alcohol behaves like imidazole in forming complexes ERI, EI, and EIR (I = alcohol) and the dissociation constants were similarly calculated from the variation of Q ($K_{ER,alc}$) and D_{app} ($K_{E,alc}$ and $K_{Ealc,R}$) with alcohol concentration using eqns. 3—7. For eqn. 4, Q values taken from a smooth curve drawn through the experimental points were used to obtain Q_∞. $K_{ER,alc}$ is also the mid point of the dissociation curve (Fig. 6). E,alc * is denoted with an asterisk to distin-

* Winer nnd Schwert [16a] reported evidenec for the existence of a LADH-DPNH-alcohol complex being formed at acidic pH values.

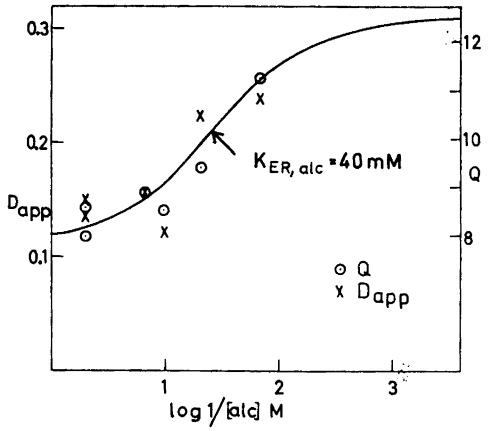

Fig. 6. Experiments with high [alcohol]. Variation of D_{app} and Q with alcohol concentration.

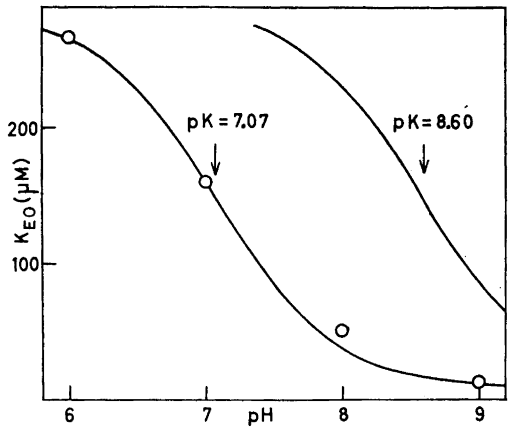

Fig. 7. Experimental values of $K_{E,O}$ at pH 6, 7 and 9 adapted to fit a dissociation curve with asymptotes 288 and 8.5 μM. pK 7.07. The titrable group in the free enzyme then has a pK of 8.60.

guish it from the ordinary, binary E,alc complex ($K_{E,alc}$ = 4.6 mM) described in Part III. The implications of these findings will be discussed together with some kinetic experiments in Part III.

DISCUSSION

$K_{E,R}$. The present values for K_{ER} on the whole agree with the previous ones obtained by both kinetic and equilibrium measurements [12]. The glycine effect described above should, however, be corrected for at pH 9 to 10. At pH 9 this reduced $K_{E,R}$ from 0.9 to 0.65 μM. Higher pH-values were not used in the present study, but it would be logical to assume that the glycine effect would be higher at pH 10 than at pH 9, since it probably is proportional to the concentration of $NH_2—CH_2—COO^-$, assuming that $—NH_2$, but not $—NH_3^+$ is coordinated with zinc.

In Table 15, $K_{E,R}$ is essentially pH independent. However, above pH 9, $K_{E,R}$ changes rapidly from 0.65 μM at pH 9 to near 5 μM at pH 10 where it is already half $K_{E,O}$ [12]. This sudden change with pH would seem to indicate that the pyridine ring in DPNH is bound to the protein by groups with a pK around 10. SH groups are known to add across the 2—3 position of DPNH model compounds but not DPN [19]. Previously the participation of SH groups in the binding of DPNH to LADH was suggested from the shift on addition of *p*-chloromercuribenzoate, of the 325 mμ peak of the binary complex to 340 mμ [17], although the mercurial could have liberated the DPNH by breaking down the enzyme's own tertiary structure rather than specific enzyme SH — coenzyme bonds. In the above, the protein SH groups would account for

the pH sensitivity of ER at alkaline reaction. The pH variation of $K_{E,O}$ is here considered due to a zinc-pyridinium rather than an SH-pyridinium interaction [4,15,20].

$K_{E,O}$. The new values for $K_{E,O}$ differ from the earlier ones partly because of the quenching effect of DPN on the fluorescence of ER. It should be noticed that the differences are largest in acid solution, decreasing towards pH 9, where there is complete agreement between the present value of $K_{E,O} = 16$ μM and the previous value 15 ± 1.4 μM, both in ~100 mM glycine buffer. The reason for this is obvious: at the low pH values $K_{E,R}$ is low, $K_{E,O}$ high, so that large concentrations of DPN of up to 1 000 μM or more were required to give suitable competition with DPNH. Therefore, the quenching through DPN caused large errors. At pH 9 the situation was the opposite; non-quenching DPN-concentrations around 10—20 μM DPN were high enough in these experiments.

The conclusion drawn in 1959 [12] that the postulated Theorell-Chance mechanism was half right and half wrong, with agreement between kinetic and equilibrium values at alkaline pH, disagreement at acid pH [12,18], must now in view of the higher $K_{E,O}$ values from equilibria at acid reaction be corrected to say that satisfactory agreement is observed at acid as well as alkaline pH, as discussed in Part I.

The $K_{E,O}$ values from 1959 conformed to a dissociation curve with a pH ~ 7.5 and already in 1951 [17] the redox potential-pH curve, calculated from the value of $K_{E,O}/K_{E,R}$, gave indication of a DPN-linked group in the enzyme with a p$K \approx 7.8$.

It was therefore of interest to analyse the present values somewhat closer. The general trend of the points indicated that towards extremely acid pH, $K_{E,O}$ would approach an upper asymptote, disregarding secondary effects that could enter into the picture at such high activity. Towards the alkaline side a lower asymptote must be assumed since $K_{E,O}$ cannot reasonably go down to zero, and the earlier value was 15 μM at pH 9 and 10 μM at pH 10, both in 100 mM glycine [12].

Since 3 values with a consistent trend can always be brought to fit a dissociation curve it was decided to use the values of $K_{E,O}$ at pH 6, 7 and 9, as probably being the most accurate ones for finding the upper and lower asymptotes and the pK value.

Since according to these assumptions the binary compound EO is not entirely dissociated at any of the pH values, DPN must be assumed to be attached to the enzyme by two or more bonds. In the case of DPN, but not DPNH, one of these is a titrable, acid group in the protein, contributing to the sta-

Table 18. Monovalent dissociation curve made to fit the experimental values of $K_{E,O}$ at pH 6, 7 and 9. $K_{E^-H^+,O} = 288$ μM, $K_{E^-,O} = 8.5$ μM, p$K = 8.60$.

pH	6	7	8	9
$K_{E,O}$ exp	266	160	51	12
$K_{E,O}$ calc	266	160	37	12

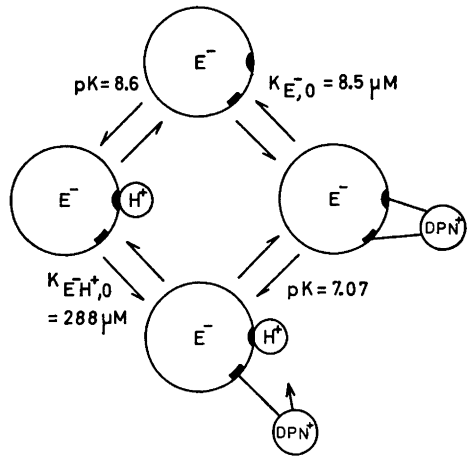

Fig. 8. The equilibrium between LADH, DPN and H^+ and the mode of attachment of DPN.

bility as a result of the coulombic attraction between a negatively charged group in the protein and the positively charged pyridine ring of DPN, as suggested previously. There would thus be a competition between protons and the pyridine ring for this negative group.

It was found that the $K_{E,O}$, values 266 μM (pH 6); 160 μM (pH 7) and 12 μM (pH 9) fitted with a dissociation curve if the acid asymptote was 288 μM, the alkaline one 8.5 μM and the pK of the acid group in the free enzyme = 8.60 and the pK of the same group in the binary EO complex was 7.07 (Table 18). The relation between these numbers is defined by the equation:

$$\log \frac{288}{8.5} + 7.07 = 8.60$$

The dissociation curves of the negative group in the free enzyme (pK 8.60) and in LADH—DPN (pK 7.07) are seen from Fig. 7. The value of $K_{E,O}$ for pH 8 falls close to the theoretical curve; $K_{E,O}$ exptl. = 51, $K_{E,O}$ required by theory = 37 μM. It must be noted that all the errors inherent in the values at 6, 7 and 9 are by this procedure imposed on $K_{E,O}$ at pH 8. Allowing small errors in all four constants could give a much closer approach to a dissociation curve within the limits of error for all four constants. The equilibrium and attachments assumed are illustrated in Fig. 8.

In Part IV it is concluded that Zn is bound by more than two bonds to the protein, where "more than two" is most likely 3. In the free enzyme the zinc seems to be bound in an octahedral complex[21]. A free zinc ion cannot readily attach more than 4 molecules of imidazole as unidentate ligands[2,3]. It is therefore logical to assume that a zinc atom with three bonds to the protein

cannot attach more than one molecule of imidazole, and indeed the equilibrium measurements could all be interpreted on the basis of assuming one molecule imidazole per binding site. The values for $K_{E,I}$ and $K_{ER,I}$ came out practically constant in the presence of from 3 mM to 100 mM imidazole (Tables 13 and 14).

The free bonds of the zinc in the free enzyme are very probably attached to water molecules in neutral or acid solution, and one or more would give hydroxo groups in alkaline solution. It seems entirely reasonable that this transition could occur with a pK of 8.60, as calculated. In the natural β-isomer of DPNH the pyridine ring is so close to the adenine that energy transfer takes place between the two [22,23], and since adenine is presumably bound to Zn, the pyridine ring must be rather close to the Zn as well. Coulombic attraction between the $-OH^-$ and the positively charged pyridine ring in DPN could explain the increase in stability of the DPN—ADH complex with increasing pH, which is not operative in DPNH—ADH. Introduction of imidazole instead of OH^- would eliminate this attraction effect, as is indeed observed.

In EO at high pH DPN uses all three bonds to the Zn, two for the adenine and one for $Zn-OH^--N^+ C_5H_5$. This last bond is the same that imidazole has to use for the formation of the ternary EOI complex. There is thus competition between imidazole and the positively charged pyridine ring for this bond. Alkaline reaction favours the hydroxo group formation, which stabilizes the bond to pyridine$^+$ but not to neutral imidazole. This explains why $K_{EO,I}$ increases with pH in the same proportion as $K_{E,O}$ decreases. The bonding of DPN to ADH in acid solution ($K_{E,O} = 288\,\mu M$) is about equally strong as DPN to ADH-imidazole ($K_{EI,O} = 440\,\mu M$): two bonds from adenine to Zn, the third bond holding water in the first case, neutral imidazole in the second. In addition to this other bonds between DPN and the protein may contribute to the stabilization of both.

In alkaline solution there is a parallel situation between ADH-DPN ($K_{E,O} = 8.5\,\mu M$) and ADH-DPN-caprate ($K_{EI,O} = 7\,\mu M$). The negatively charged caprate ion seems to have the same stabilizing effect as the hydroxo group at the zinc atom. Variations in the length of the carbon chain of fatty acids (C_1 to C_{15}) [1] have no great influence on $K_{EI,O}$, the charge effect being roughly the same in all of them. The dramatic changes in $K_{EO,I}$ with the chain length must reasonably be attributed to a lipofilic binding site.

For *iso*butyramide $K_{ER,I}$ and $K_{EI,R}$ when compared with $K_{E,I}$ and $K_{E,R}$ showed 66—70 fold mutual stabilization to operate between I and R. In the ternary complex EOI with DPN and caprate there is a 22—23 fold mutual stabilization. Imidazole which forms both ERI and EOI complexes on the contrary causes *de*stabilization. This is 6—7 fold for ERI, 3 fold for EOI at pH 7. With the DPNH complexes the destabilization is rather insensitive to pH changes, whereas with the DPN complexes the destabilization increased with pH due to the additional effect of the N^+-OH^--Zn interaction.

We think $K_{E,I}$ for imidazole is comparatively insensitive to pH changes, because imidazole with the free enzyme can attach to any of the free Zn bonds. The slight increase in $K_{E,I}$ with pH may result from the hydroxo group being more tightly bound to Zn than is a water molecule.

In the ternary complex ERI no charge effects operate between the neutral pyridine ring in DPNH and the neutral imidazole. As discussed in Part III we think that in ERI all three of the free Zn bonds are occupied, two by the adenine moiety and one by neutral imidazole, leaving no opportunity for pH effects to occur by formation of hydroxo groups in alkaline solution.

The increased fluorescence of ER compared with R has been attributed to the greater rigidity of R attached to the enzyme [20,28], and in particular to the interaction between the pyridine ring and zinc. Why there is a further increase in the ternary complexes with imidazole and with *iso*butyramide (but not with most of the other amides) we do not know yet.

Due to the stereospecific nature of the LADH reaction with regard to the plane of the pyridine ring [24,25] (it is also stereospecific towards the substrates) it has been suggested that the amide group in the pyridine ring gives the ring its stability by joining to the enzyme, possibly the zinc [4,26]. It is possible that the amide group is bound to the protein at a site other than zinc, but this is not necessary with LADH as the protein SH addition to pyridine in DPNH and the pyridinium-Zn bond in DPN would suffice to give the pyridine ring its stereospecific rigidity.

Further discussion on the bonding of coenzymes, substrates and inhibitors will be found in Part III.

Acknowledgements. The authors are indebted for financial support given by *Statens Medicinska Forskningsråd, Statens Naturvetenskapliga Forskningsråd, Knut och Alice Wallenbergs Stiftelse, The Rockefeller Foundation, Wenner-Grenska Samfundet* and *Institutet för Maltdrycksforskning.*

Generous assistance with a Wegematic 1 000 Computer was offered by Mr. Bo Nyman, Director of ABN Bolagen, Stockholm.

Skilful technical assistance has been given by Mr. Lars-Gunnar Falksveden.

REFERENCES

1. Winer, A. D. and Theorell, H. *Acta Chem. Scand.* **14** (1960) 1729.
2. Edsall, J. T., Felsenfeld, G., Goodman, D. S. and Gurd, F. R. N. *J. Am. Chem. Soc.* **76** (1954) 3054.

3a. Nozaki, Y., Gurd, F. R. N., Chen, R. F. and Edsall, J. T. *J. Am. Chem. Soc.* **79** (1957) 2123; 3b Koltun, W. L, Dexter, R. N., Clark, K. E. and Gurd, F. R. N. *J. Am. Chem. Soc.* **80** (1958) 4188.

4. Theorell, H., Nygaard, A. P. and Bonnichsen, R. *Acta Chem. Scand.* **9** (1955) 1148.
5. Vallee, B. L. and Hock, F. L. *Proc. Natl. Acad. Sci. U.S.* **41** (1955) 327; Wallenfels, K., Sund, H., Faessler, A. and Burchard, W. *Biochem. Z.* **239** (1957) 31.
6. Dalziel, K. *Acta Chem. Scand.* **12** (1958) 459.
7. Bonnichsen, R. and Brink, N. G. *Methods in Enzymology*, **Vol. I**, P 495, Academic Press, New York 1955.
8. Ehrenberg, A. and Dalziel, K. *Acta Chem. Scand.* **12** (1958) 465.
9. Kaplan, N. O. and Ciotti, M. M. *J. Biol. Chem.* **211** (1954) 431.
10. Mickel, B. L. and Andrews, A. C. *J. Am. Chem. Soc.* **77** (1955) 5291.
11. Tanford, C. and Wagner, M. L. *J. Am. Chem. Soc.* **75** (1953) 434.
12. Theorell, H. and Winer, A. D. *Arch. Biochem. Biophys.* **83** (1959) 291.
13. Theorell, H. and Nygaard, A. P. *Acta Chem. Scand.* **8** (1954) 885.
14. Chance, B. *Acta Chem. Scand.* **1** (1947) 236; Chance, B., Greenstein, D. S. and Roughton, F. J. W. *Arch. Biochem. Biophys.* **37** (1952) 301.
15. Van Eys, J. and Kaplan, N. O. *Biochim. et Biophys. Acta* **23** (1957) 574.

16. Pfleiderer, G., Jeckel, D. and Wieland, T. *Biochem. Z.* **330** (1958) 296.
16a. Winer, A. and Schwert, G. *Biochim. et Biophys. Acta* **29** (1958) 424.
17. Theorell, H. and Bonnichsen, R. *Acta Chem. Scand.* **5** (1951) 1105.
18. Theorell, H. *Advances in Enzymol.* **20** (1958) 47.
19. Wallenfels, K. and Schüly, H. *Angew. Chem.* **69** (1957) 505.
20. Shifrin, S. and Kaplan, N. O. *Advances in Enzymol.* **22** (1960) 353.
21. Vallee, B. L. and Coombs, T. L. *J. Biol. Chem.* **234** (1959) 2615; Theorell, H. and Plane, R., *This Journal*, Part IV.
22. Weber, G. *Nature* **180** (1957) 1409; *J. chim. phys.* **55** (1958) 878.
23. Shifrin, S. and Kaplan, N. O. *Nature* **183** (1959) 1529.
24. Fisher, H. F., Conn, E. E., Vennesland, B. and Westheimer, F. H. *J. Biol. Chem.* **202** (1953) 687.
25. Vennesland, B. *Discussions Faraday Soc.* **20** (1955) 240.
26. Vallee, B. L. and Williams, R. J. P. *Discussions Faraday Soc.* **20** (1955) 246; Mahler, H. R. and Douglas, J. *J. Am. Chem. Soc.* **79** (1957) 1159; Wallenfels, K. and Sund, H. *Biochem. Z.* **329** (1957) 59.
27. Kaplan, N. O., Ciotti, M. M. and Stolzenbach, F. E. *Arch Biochem. Biophys.* **69** (1957) 441; *J. Biol. Chem.* **221** (1956) 840.
28. Shifrin, S. and Kaplan, N. O. *Proc. Natl. Acad. Sci. U.S.* **44** (1958) 177.
29. Karreman, G., Steele, R. H. and Szent-Györgyi, A. *Proc. Natl. Acad. Sci. U.S.* **44** (1958) 140.

Received March 28, 1961.

ACTA CHEMICA SCANDINAVICA 15 (1961) 1834–1865

Liver Alcohol Dehydrogenase

III. Kinetics in the Presence of Caprate, *Iso*butyramide and Imidazole

HUGO THEORELL and JOHN S. McKINLEY-McKEE

Medicinska Nobelinstitutet, Biokemiska avdelningen, Stockholm, Sweden

1. The effects on the kinetics of the LADH-coenzyme-substrate system of caprate and *iso*butyramide at pH 7 are described. Caprate and *iso*butyramide have only inhibitory actions, which were localized to different parts of the reaction cycle and used for the calculations of various velocity constants. The results were in agreement with the equilibrium data from Part II.

2. Likewise, the effects of imidazole at pH 7 and 9 were studied in detail. It was found that imidazole could either increase (5 – 10 fold) or decrease the reaction velocity depending on the concentration of coenzymes and substrates. These effects were explained from the properties of the ternary enzyme-coenzyme-imidazole complexes.

3. It was found to be a general rule that the attachment of substrates or competing inhibitors to the substrate binding sites do not interfere appreciably with the "on" velocity constants of the coenzymes. The sometimes very large changes in dissociation constants, observed in equilibrium measurements, were parallelled by changes in the "off" velocity constants.

4. The mode of attachment of coenzymes, substrates and inhibitors is discussed. Zinc seems to be bound to the protein by three out of six octahedral bonds. The free bonds presumably hold water molecules, one of which at higher pH (pK 8.60) looses a proton. The resulting attraction between $Zn-OH^-$ and the positively charged pyridine ring of DPN is held responsible for the changes in $K_{E,O}$ with pH. This does not operate in the case of $K_{E,R}$ where the pyridine ring carries no charge.

5. It is concluded that in both ER and EO, the adenine moieties are attached to Zn by two bonds as third bidentate ligands, which as in the case of ethylene diamine are weak. Zinc is implicated as the center of a ternary complex with three bonds to the protein, two to the adenine and one to the substrates. In the binary complexes this latter bond is in EO joined to the pyridinium ring ($Zn-OH^--N^+$) but not in ER when it is occupied by a water molecule or at high pH a hydroxo group.

The two coenzymes select with great preference their partners by switching during interconversion to free one or the other of two out of three bonds, while each imposes by its different nature different properties on the third bond.

6. An abortive ternary complex ERalc formed at high alcohol concentrations is more stable than the binary ER complex. This

explains the inhibition of reaction velocity observed at high concentrations of alcohol in the LADH system.

7. Glycine like *ortho*phenanthroline and *aa'*-dipyridyl forms a binary complex with LADH but no ternary complexes including the coenzymes. It is assumed that glycine acts as a third bidentate ligand, excluding the adenine moieties of the coenzymes from being bound to the zinc.

It was earlier found that fatty acids form compounds of the type EI and EOI, but not ERI, and that fatty acid amides form compounds EI and ERI, but not EOI, and it was considered that the ternary complexes possessed a similar structure to the reactive complexes containing alcohol or aldehyde [1]. It was shown in Part II that imidazole and other nitrogenous compounds form compounds with both EO and ER. Whereas in the case of fatty acids and amides the ternary complexes are more stable than the binary ones, the opposite was found for imidazole. It was therefore of obvious interest to study the influence of these three different types of inhibitors on the kinetics in the hope of finding new facts on the nature of the binding sites for co-enzymes and substrates. Knowledge from Part II of the dissociation constants for imidazole provided an understanding of the stimulation rather than inhibition found with imidazole at high substrate concentrations, a phenomenon previously encountered with chloride [2].

Materials and methods were the same as those used in Parts I and II. In all but two of the sets of experiments the fluorometer rather than the spectrophotofluorometer was used due to greater sensitivity and stability.

RESULTS

It is customary to distinguish between three types of inhibition; competitive, noncompetitive and uncompetitive. In a system with two substrates, and the reaction occurring in two phases with alternative pathways, as is the case with alcohol dehydrogenase, the results do not always conform with any of these categories, and the interpretation of the experiments to be presented below therefore requires some comment.

Some inhibitors interfere only in the first reaction phase, and these have no influence on the break down of the complexes in the second phase. An interference of inhibitors with the breakdown of ternary complexes has never been observed and is not to be expected since the binding sites for coenzymes and substrates are already occupied. However, after the dissociation of the substrates, the binary EO (case 1 and 2, the "forward" reaction) and ER (case 3 and 4, the "reverse" reaction) can form EOI or ERI complexes which leads to a "second phase effect"; inhibition if the breakdown is retarded, as with caprate (EOI, Figs. 1 and 2) or *iso*butyramide (ERI, Figs. 7 and 8), or stimulation, if it is accellerated, as with imidazole (Figs. 11—13 b etc). These second phase effects appear near the intercepts with the ordinate, where both coenzyme and substrate are in high concentration, and the decomposition of the complexes in the second phase is more or less rate-limiting. When the inhibitor is unable to form ternary complexes with the second phase binary complexes, for

example *iso*butyramide with EO (case 1 and 2), or caprate with ER (case 3 and 4), no second phase effects occur. When both ERI and EOI can be formed, (as is the case with imidazole), second phase effects will always occur, but will not influence the reaction velocity in the special case when the decomposition rate of EO is the same as for EOI, as is not far from true with imidazole at pH 7 (case 1 and 2, Figs. 9a and 10.).

The second phase effects interfere only with the terms $1/k_2$ or $1/k_2'$ in the T.-C. formula (equations 1a and 1b, Part I), which are independent of coenzyme and substrate concentrations and changes in decomposition velocity by complex formation with inhibitors will therefore cause a parallel displacement of the Lineweaver-Burk plots upward (inhibition) or downward (stimulation). Thereby it may happen that plots result, which would normally be taken for un- or noncompetitive, or mixed *e.g.* Fig. 1. The correct interpretation, however, is in this case competitive first + uncompetitive second phase inhibition. It should be pointed out that unless equilibrium measurements have proved the formation of ternary complexes in the second phase, the distinction between the different inhibition types may be very difficult.

The relations between the types of inhibition in the T.-C. mechanism are determined by both rate and equilibrium constants in the following way. *Noncompetitive* means that the degree of inhibition is independent of the concentration of the varied reaction partner. The Lineweaver-Burk plots cross on the abscissa at a negative value for 1/[C]. An example of this is caprate, case 3 (Fig. 3). Caprate gives complexes with E (EI) and with EO (EOI), but not with ER. Second phase inhibition therefore does not occur and alcohol and caprate are strictly competitive (Fig. 4). In Fig. 3, at the intercept with the ordinate [DPN] = ∞, and every enzyme molecule, E, when liberated from the second phase reaction will immediately form EO that will either react with caprate (I) to form EOI, or with alcohol:

$$\mathrm{EOI} \rightleftharpoons \mathrm{EO} + \mathrm{alc} \xrightarrow{k_3'} \mathrm{ER} \xrightarrow{k_2'} \mathrm{E} + \mathrm{R} \qquad (1)$$

Since the k_3' and k_2' reactions are consecutive:

$$[\mathrm{EO}]\,[\mathrm{alc}]\,k_3' = [\mathrm{ER}]k_2' \qquad (2)$$

If [I] is chosen to give 50 % inhibition:

$$[\mathrm{EOI}] = [\mathrm{EO}] + [\mathrm{ER}] \qquad (3)$$

From (2) and (3): $[\mathrm{EO}]/[\mathrm{EOI}] = k_2/(k_2 + k_3\,[\mathrm{alc}])$ (4)

and $K_{\mathrm{EO,I}} = [\mathrm{I}]k_2/(k_2 + k_3'\,[\mathrm{alc}])$ (5)

Now the condition for noncompetitive, 50 % inhibition is that [alc] is such that half inhibition should also be found when [DPN]$\rightarrow$0, which requires:

$$[\mathrm{alc}]/[\mathrm{I}] = K_{\mathrm{E,alc}}/K_{\mathrm{EI}} \qquad (6)$$

Combining (5) and (6) gives:

$$\frac{1}{[\mathrm{alc}]} = \frac{K_{\mathrm{EI}}}{K_{\mathrm{E,alc}} \times K_{\mathrm{EO,I}}} - \frac{k_3'}{k_2} \qquad (7)$$

Introducing the experimental values for [alc] = 6100 μM, K_{EI} = 45 μM, $K_{EO,I}$ = 2 μM (see Part II), k_3' = 0.0122 $\mu M^{-1} \times sec^{-1}$, k_2 = 3.1 sec^{-1} (Part I) gives $K_{E,alc}$ = 5500 μM, which agrees with the value 4600 μM obtained (see below p. 1842) from the slopes. This confirms that the results presented in Fig. 3 closely conform with noncompetitive conditions. Since $K_{E,I}/K_{E,alc} \times K_{EO,I}$ (0.00406) is only a little larger than k_3'/k_2 (0.00390) the values for [alc] required for strict noncompetition is very sensitive to small errors. If $K_{E,alc}$ is taken 4600 μM (see below), [alc] becomes 1000 μM. This means that very nearly noncompetitive behaviour will be expected with [alc] in the whole region from 1000 μM up to those concentrations where substrate inhibition begins to occur. The [I] required for 50 % inhibition with 6100 μM alcohol is 50 μM according to (6) when $K_{E,alc}$ = 5500 and $K_{E,I}$ = 45 μM. This agrees with the experiments.

The *vice versa* case to caprate, case 3, would be expected to be *iso*butyramide, case 1, since *iso*butyramide gives complexes EI and ERI but not EOI. However, the experimental results, (Fig. 5 a and b), show practically completely *un*competitive behaviour with parallel L-B plots. Substituting $K_{ER,I}$ for $K_{EO,I}$, k_2' for k_2, k_3 for k_3', [ald] for [alc], equation (5) and (7) gives [ald] = 0.15 μM, [I] = 140 μM.

These concentrations, unlike the experiments with caprate, case 3, are very far from the concentrations actually used in the experiments (Fig. 5 a and b). The [ald] used, 370 and 3700 μM, are far above $K_{E.ald}$ (10 μM), and I concentrations are below $K_{E,I}$ (9.3 mM). This is the reason for the different competition pictures.

Rearrangements of the above equations give:

$$\text{Caprate, case 3: } \frac{1}{[I]} = \frac{1}{K_{EO,I}} - \frac{K_{E,alc}}{K_{E,I}} \times \frac{k_3'}{k_2} \qquad (8)$$

where $1/K_{EO,I} = 0.500$ and $K_{E,alc} \times k_3'/K_{E,I} \times k_2 = 0.481$

$$\textit{Iso}\text{butyramide, case 1: } \frac{1}{[I]} = \frac{1}{K_{ER,I}} - \frac{K_{E,ald}}{K_{E,I}} \times \frac{k_3'}{k_2} \qquad (9)$$

where $1/K_{ER,I} = 0.00715$ and $K_{E,ald} \times k_3/K_{E,I} \times k_2' = 0.45 \times 10^{-5}$.
In (8) the first and second terms are nearly equal. Therefore, noncompetition occurs when $K_{EO,I} \approx (K_{E,I} \times k_2)/K_{E,alc} \times k_3')$
In (9) the second term is negligible compared with the first. Therefore
[I] = $K_{ER,I}$ = 140 μM, and [ald] = 0.15 μM
is required to give noncompetitive plots. This experiment cannot be conveniently carried out; [ald] = 0.15 μM is unsufficient to give observable initial reaction rates with excess of DPNH. Therefore possible experiments in case 1 always give more or less uncompetitive plots. In case 3, on the contrary, the constants are of favourable magnitude for giving $\approx$ noncompetitive plots.

As seen from (7), when it happens that

$$k_3'/k_2 > K_{E,I}/(K_{E,alc} \times K_{EO,I})$$

the substrate concentration should have to be $> \infty$ to fulfil the conditions for noncompetitive inhibition. In such cases mixed noncompetitive-competitive pictures occur. *Ortho*phenanthroline (OP) case 4, is an example of this. In Fig. 1

(Part IV), OP, case 4 approaches competitive behaviour, the [DPN] being 107 μM. The same case done by Vallee *et al.*[6] is also mixed competitive -non-competitive rather than non-competitive as claimed, but the [DPN] being 4000 μM, it is nearer to non-competitive behaviour than with 107 μM DPN. Mixed non- and uncompetitive behaviour results when the substrate concentration is higher than that calculated (eqn. 7) for strict noncompetition.

The possible equilibria between enzyme, substrates and inhibitors are represented by the general mechanism I.

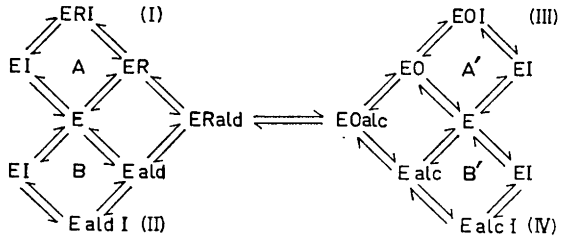

(I)

Only two of the four ternary complexes I—IV are however formed by each of the following inhibitors.

Caprate:	E ald I	and	EOI	(omit I-complexes in A and B′)
IB:	ERI	»	E alc I	(» » » B » A′)
Imidazole:	ERI	»	EOI	(» » » B » B′)
OP:	E ald I	»	E alc I	(» » » A » A′)

In interpreting the results for each inhibitor the above scheme with the appropriate complexes omitted may be useful. Wherever three compounds are on a straight line those at the ends compete for the middle one. First and second phase effects are also readily apparent. Caprate in the forward reaction gives first phase inhibition through B, second phase inhibition through A′. In the reverse reaction first phase inhibition occurs through A′, but no second phase inhibition occurs, as no ERI is formed.

Table 1. Caprate cases 1 and 2, intercepts. (Corrected to infinite [DPNH] and infinite [ald]).

$[C_{10}]$ μM	e/V		V/e (average) sec^{-1}
	Case 1	Case 2	
0	0.0133	0.0137	74
12.5	0.034		29.4
50	0.086	0.085	11.7
125		0.173	5.8
∞	$1/X$	$1/X$	X

Potassium caprate (C_{10})

Cases 1 and 2, intercepts. The intercepts (Figs. 1 and 2) were first corrected to give the value for $1/V_{max} = 1/k_2'$ at [DPNH] = ∞ and [aldehyde] = ∞, using for case 1 the corresponding slopes in case 2 and the [aldehyde] in case 1, and *vice versa* for case 2. In case 1, the corrections were very small, in case 2, $\sim$ 10 %. The results are given in Table 1. Since [DPNH] is infinite, and ERI is not formed, the inhibition at the intercept must be caused by formation of EOI in the second phase of the reaction:

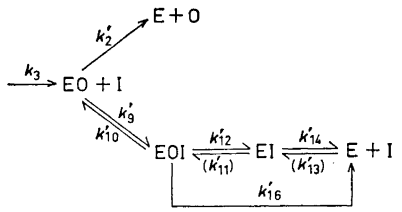

(A)

If k_9' and k_{10}' are both $\gg k_2'$ and k_{12}', EO and EOI should be in true equilibrium, and the inhibition constant should be $K_{EO,I} = 2$ μM, as determined in equilibrium measurements (see Part II), and confirmed in case 3, *vide infra.*

In case the assumption does not hold, the inhibition constant, calculated from the intercepts, in cases 1 and 2 should be $> K_{EO,I}$, and k_9', k_{10}' and k_{16}' can be calculated.

As seen from scheme A, the free enzyme is regenerated along two pathways, the normal upper one with $V_{max} = k_2' = 74$, the lower, inhibited one with V_{max} = X. The observed V will be the sum of both and as is easily derived, if V_{max}, V/e, and X are the velocities at inhibitor concentrations of zero, I and infinity. Then

$$\frac{V}{e} = \frac{K_I}{[I] + K_I} \times V_{max} + \frac{[I]}{[I] + K_I} \times X \qquad (10)$$

Using equation 10:

$$12.5\ \mu M\ C_{10}\text{: } 29.4 = \frac{K_I}{12.5 + K_I} \times 74 + \frac{12.5}{12.5 + K_I} \times X$$

$$50\ \mu M\ C_{10}\text{ : } 11.7 = \frac{K_I}{50 + K_I} \times 74 + \frac{50}{50 + K_I} \times X$$

$K_I = 7.6$ and $X = 2.23$

Taking the values for 12.5 and 125 μM, C_{10} gives $K_I = 7.8$ and $X = 1.6$. The average is $K_I = 7.7$ μM and $X = 1.9$ sec^{-1} for V_{max} at I = ∞.

In the steady state and at [C_{10}] = 7.7 μM, [EO] = [EOI] + [EI], (E, ER, E ald R and EO alc = 0) and assuming that [EOI] > [EI] which is not unlikely since $K_{E,I}$ (45 μM) is > $K_{EI,O}$ (7 μM) then, as $7.7\ k_9' - k_{10}' = 1.9$ and $k_{10}'/k_9' = 2$ μM = $K_{EO,I}$,
$k_9' = 0.33$ μM^{-1} sec^{-1}, and $k_{10}' = 0.66$ sec^{-1}, $k_{16}' = 1.9$ sec^{-1}.

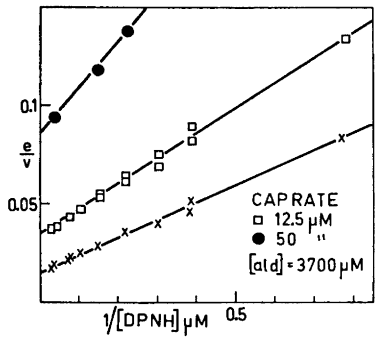

Fig. 1. Case 1. Caprate inhibition. 0.1 μ, 23.5°C and pH 7.
(Points marked × in Figs. 1—16 represent experiments without added inhibitor).

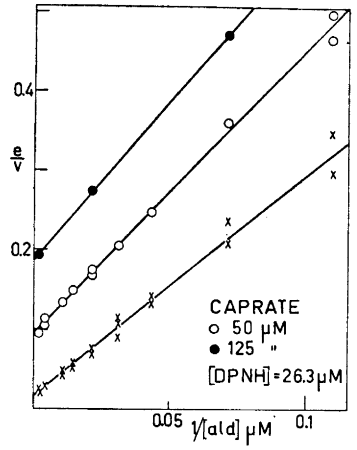

Fig. 2. Case 2. Caprate inhibition. 0.1 μ, 23.5°C and pH 7.

If [EOI] $\gg$ [EI] $k_{12}' = k_{16}'$ ($k_{14}' = \infty$) and as $K_{EI,O} = 7\ \mu M$ (Part II) $= k_{12}'/k_{11}'$, therefore $k_{11}' = 0.27\ sec^{-1}\ \mu M^{-1}$.

k_{11}', the "on" velocity constant for DPN binding with EI, is not far therefore from k_1', the "on" velocity constant for DPN binding with E, 0.5 sec^{-1} μM^{-1}. Since $K_{E,O} = 160\ \mu M$ and $K_{EI,O}$ is 7 μM this means that the introduction of the fatty acid into the enzyme molecule only causes a small, if any decrease in "on" velocity, but a drastic reduction of the "off" velocity, from 74 to 1.9 sec^{-1}. Similar examples of what may be a general rule will be given below.

Case 1, slopes (Fig. 1). In addition to the second phase effect on the intercepts already commented upon, there is an increase in slope with increasing concentrations of C_{10}.

The difference in intercepts above was shown to be a second phase effect. The slopes therefore may indicate competition between DPNH and C_{10} in the first phase. This is very likely because DPNH and C_{10} do not form ternary complexes with the enzyme, which is most easily explained by assuming competition for the same binding site. The constant aldehyde concentration is very

Table 2. Caprate, case 1, slopes.

$[C_{10}]\ \mu M$	Slopes, $\mu M \times sec$	K_I
0	0.088	—
12.5	0.126	29
50	0.244	31
		Average 30 μM

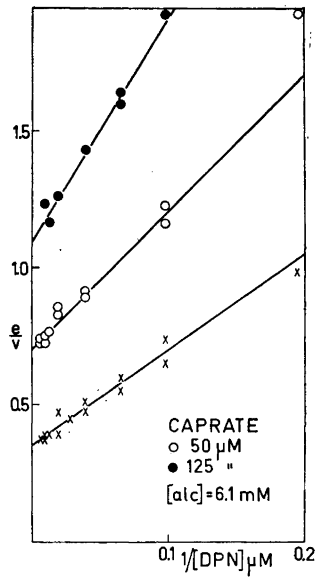

Fig. 3. Case 3. Caprate inhibition. 0.1 μ, 23.5°C and pH 7.

high compared with $K_{E,ald}$ (see below) and there will be very little free enzyme. The enzyme at low concentrations of DPNH starts a new cycle by forming the binary Eald complex which at low [DPNH] could be in equilibrium with C_{10} as E ald I. K_I would then reflect E ald + I $\rightleftharpoons$ E ald I and be $K_{Eald,I}$. The value 30 μM (Table 2) is close to $K_{E:I}$ (45 μM).

Case 2, slopes. The slopes show nearly uncompetitive inhibition caused by the formation of EOI in the second phase. The small differences in the slopes are due to some EI being formed since [DPNH] is not infinite, and a small part of E will be free to be inhibited as EI.

Case 3, intercepts. At the intercept (Fig. 3) 50 μM caprate causes just 50 % inhibition that occurs in the first phase, since only EOI can be formed. The situation in the steady state may be described as follows. When [DPN] goes to infinity, all free E will immediately form EO. The alcohol concentration is high (6100 μM) but not infinite. When the overall reaction velocity is reduced to half by 50 μM C_{10}, 50 % of the total enzyme appears as inactive EOI. Using the rate constants from Part I, $k_3' = 0.0122\ \mu M^{-1} \times sec^{-1}$ and $k_2 = 3.12\ sec^{-1}$, $0.0122 \times 6100 \times EO = 3.12 \times ER$, (because EO + alc $\rightarrow$ and ER $\rightarrow$ E + R are consecutive) and as [ER] + [EO] = 0.5 [E_t] = [EOI], therefore [EO] = 0.02 [E_t], [ER] = 0.48 [E_t] and $K_{EO,I} = 0.02 \times 50\ \mu M/0.50 = 2\ \mu M$, in agreement with the equilibrium value reported in Part II.

Case 4, intercepts. Figure 4 a and particularly 4 b show strict competition of C_{10} with alcohol, with intercept at the same point on the ordinate. This is to be expected since ERI is not formed, and no interference in the second phase is therefore to be expected, in agreement with the earlier results.

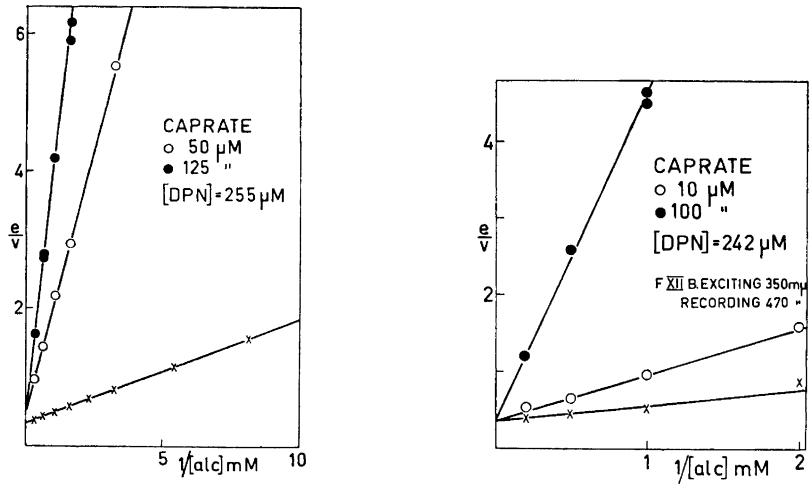

Fig. 4 a and b. Case 4. Caprate inhibition. 0.1 μ, 23.5°C and pH 7. In 4b the experiment was performed on the spectrophotofluorometer.

Case 3, slopes. Since C_{10} and alcohol are competitive, when [DPN] → 0, with [alc] = 6100 μM, and $[C_{10}]$ = 104 μM (Table 3), the following equilibrium will prevail

E alc ⇌ E ⇌ EI,

where [E alc] + [E] = [EI], [EI] = 0.5 $[E_t]$ and [E] = X $[E_t]$.

Therefore [E alc] = (0.5—X) × $[E_t]$, and taking $K_{E,I}$ = 45 μM, gives X = 0.216 and $K_{E.alc}$ = 4600 μM. This is not far from the value $K_{E,alc}$ = 6100 μM, obtained from the Michaelis constants (see part I).

Case 4, slopes. The contrast between this strict competition and the uncompetitive behaviour of caprate and aldehyde is marked and emphasizes that aldehyde and alcohol must have different binding sites. When [alc] → 0 the following equilibria will prevail

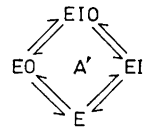

Table 3. Caprate, case 3, slopes.

$[C_{10}]$ μM	Slopes, sec × μM	K_I
0	3.5	
50	5.1	113
125	8.1	95
		Average 104 μM

Table 4. Caprate, case 4, slopes.

Expt.	$[C_{10}]$ μM	Slopes, μM × sec	K_I
R XXVI (fluorometer)	0	150	
	50	1 544	4.8
	125	3 560	5.2
F XII B (spectrophotofluorometer)	0	200	
	10	600	5.0
	100	4 320	4.9
			Average 5.0 μM

When [I] = 5.0 μM (Table 4); [EI] + [EIO] = [E] + [EO]. With $K_{E,O}$ = 160 μM, [DPN] = 255 μM and $K_{E,I}$ = 45 μM: $K_{EO,I}$ = 3.2 μM, in fair agreement with the values of 2 μM obtained from both equilibrium measurements (Part II) and from the intercepts in case 3.

*Iso*butyramide (IB)

*Case 1, intercepts. Iso*butyramide causes an uncompetitive type of inhibition which is dependent on the aldehyde concentration (IB and DPNH can both go on to the enzyme). As can be seen from Fig. 5 a and 5 b, it is much larger with 370 μM than with 3700 μM aldehyde. Table 5 gives the values obtained by extrapolation of the intercepts to infinite [aldehyde], using the slopes in case 2.

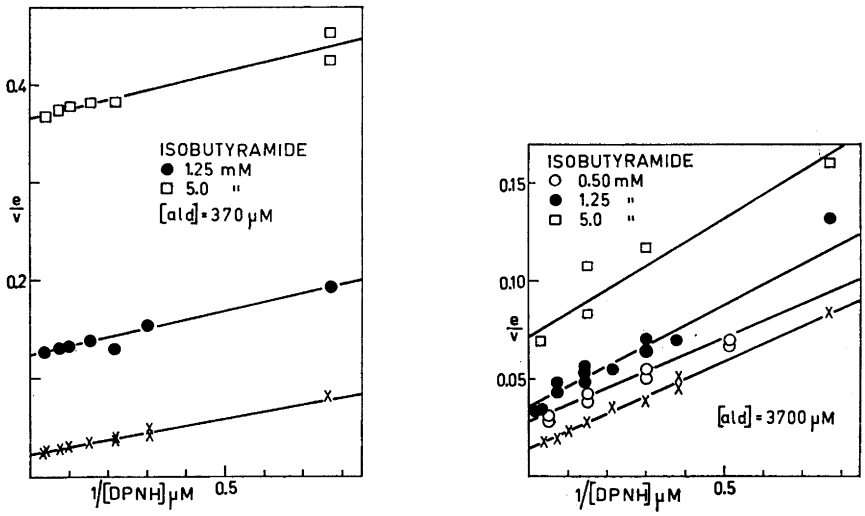

Fig. 5 a and b. Case 1. *Iso*butyramide inhibition. 0.1 μ, 23.5°C and pH 7.

Table 5. Isobutyramide, case 1 intercepts (Uncorrected and corrected to infinite [DPNH] and [ald])

[IB.] mM	e/V			
	A (370 μM [ald])		B (3 700 μM [ald])	
	Uncorr.	Corr.	Uncorr.	Corr.
0	0.022	0.015	0.0145	0.0132
1.25	0.124	0.025	0.036	0.029
5	0.366	0.030	0.071	0.044

The values for e/V_{max} at [ald] = ∞ in the presence of IB, do not quite go down to the values without IB, but the corrections are large and the results therefore uncertain. In case the difference between V_{max} with and without IB are real, they would indicate formation of EOI ($K_{EO,I} \approx 5$ mM) at high concentrations of IB. However, since the Lineweaver-Burk plots in case 2 seem to cross on the ordinate, and as the equilibrium measurements gave no indication of EOI formation [1], the earlier conclusion seems valid, that EOI is not formed, or perhaps only at such high concentrations that EOI plays no essential role in the kinetics.

The intercepts obtained in case 1a, (Fig. 5) can be used for checking either $K_{ER,I}$ or k_3 as follows.

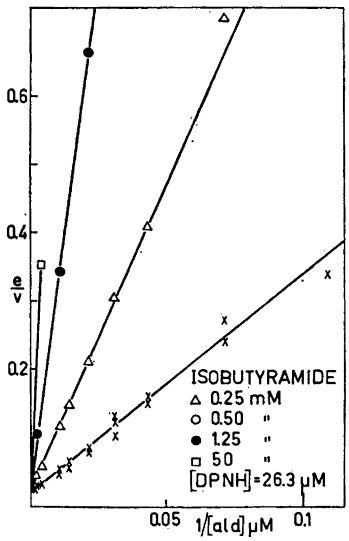

Fig. 6. Case 2. *Iso*butyramide inhibition. 0.1 μ, 23.5°C and pH 7.

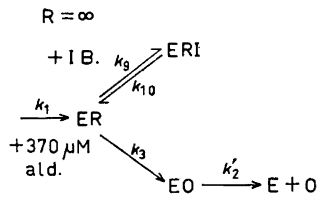

(B)

From the intercepts K_I = 300 μM, $K_{ER,I}$ (Part II) = 140 μM, and thus ER/ERI = 0.466. At half inhibition [ERI] = [ER] + [EO] = 0.5 [E_t] and therefore [ER] = 0.233 [E_t], and [EO] = 0.267 [E_t]. As k'_2 = 74 sec^{-1},
370 × 0.233 × k_3 = 74 × 0.267, and therefore
k_3 = 0.23 $\mu M^{-1} \times sec^{-1}$
in fair agreement with the value 0.31 obtained from the kinetic measurements without inhibitors (Part I).

Case 1, slopes. The inhibition is nearly uncompetitive for reasons discussed above p. 1836, or in other worlds $K_{E,I} >> K_{ER,I}$.

Case 2, intercepts. Fig. 6 shows competitive inhibition as found earlier [1], the intercepts meeting at the same point on the ordinate and no EOI being formed.

Case 2, slopes. Since the concentration of DPNH is high compared with $K_{E,R}$, and $K_{E,I}$ is very high, the inhibition constant K_I = 143 mM (Table 6) in this case is $K_{ER,I}$, in excellent agreement with the value (140 mM) obtained from the equilibrium determinations (Part II).

Cases 3 and 4, intercepts (Figs. 7 and 8). Inhibition occurs in the second phase due to the presence of ERI. The data in Table 7 when treated as for caprate, cases 1 and 2 (above), gave X = 0.077 sec^{-1} and K_I = 200 μM. Therefore, $k_{12} = k_{16}$ = 0.077 sec^{-1} (scheme C), since in this case it can be taken for certain that $k_{14} >> k_{12}$: $K_{E,I}$ (9300 μM, Part II) is 2 million times greater than $K_{EI,R}$ (0.005 μM). In Part II, a value for k_{11} = 14 sec^{-1} μM^{-1} was obtained from direct reaction cycles in very dilute solutions, thus $K_{EI,R}$ = 0.077/14 = 5.5 × 10^{-3} μM, in excellent agreement with the equilibrium titrations in Part II.

Table 6. Isobutyramide, case 2, slopes.

[IB] mM	Slope, μM × sec	$K_I = K_{EE,I}$
0	2.8	
0.25	7.8	138
0.50	12.3	145
1.25	26	148
		Average 143 μM

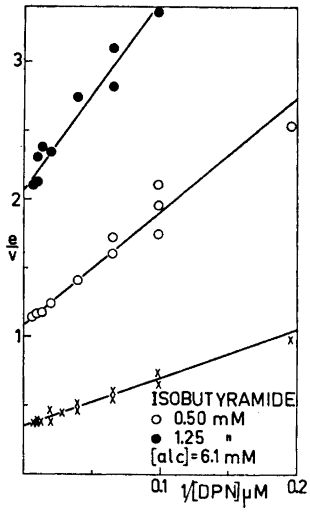

Fig. 7. Case 3. *Iso*butyramide inhibition. 0.1 μ, 23.5°C and pH 7.

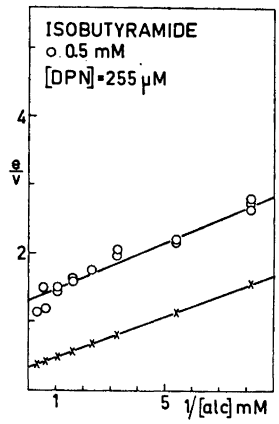

Fig. 8. Case 4. *Iso*butyramide inhibition. 0.1 μ, 23.5°C and pH 7.

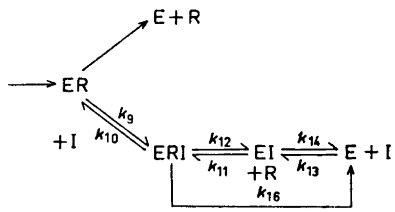

(C)

Taking $K_{ER,I\,eq} = k_{10}/k_9 = 140$ μM, and [I] = 200 μM, where [ER] = [ERI]; $0.077 = 200\ k_9 - k_{10} = k_{16}$

$k_9 = 1.3$ sec$^{-1} \times$ mM^{-1} and $k_{10} = 0.18$ sec^{-1}.

Case 3, slopes. No EOI is formed and Fig. 7 accordingly shows first phase competition between DPN and IB. Since I and alcohol do not compete with one another, it may be that a ternary complex E alc I can be formed. Consider-

*Table 7. Iso*butyramide, cases 3 and 4, intercepts (Corrected to infinite [DPN] and [alc]).

[IB] mM	e/V			V/e
	Case 3	Case 4	Average	
0	0.330	0.329	0.33	3.0
0.5	1.045	1.145	1.10	0.91
1.25	2.01	2.14	2.08	0.48
∞				X

Table 8. Isobutyramide, case 3, slopes.

[IB] mM	Slopes, μM × sec	K_I
0	3.5	
0.5	8.3	365 μM
1.25	15.8	355 "

ing that $K_{E,I}$ is 9.3 mM, very little inhibition would occur at [I] = 0.5 and 1.25 mM, if only EI were formed. In the equilibrium

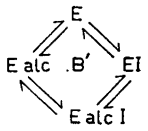

when [DPN] → 0, and when [I] = 360 μM (Table 8), [E] + [E alc] = [EI] + [E alc I]. From this equation, and from the values for $K_{E,I}$ = 9300 and $K_{E,alc}$ = 4600 μM, [Ealc I] can be calculated, giving $K_{EI,alc}$ = 103 μM and $K_{E\,alc,I}$ = 209 μM. Thus there is high stabilisation operating between alcohol and isobutyramide; the stabilisation factor being 4600/103 = 45. This is different from the complex E alc caprate (see p. 1841) where the stabilization was very low.

Case 4, slopes. No appreciable change in slope (uncompetitive and no inhibition in the first phase) occurs on addition of *iso*butyramide (Fig. 8) because EOI is not formed, and the concentrations of I used were too low compared with $K_{E,I}$ to cause the formation of more than a small fraction of EI.

Imidazole, pH 7

Cases 1 and 2, intercepts. Case 1 was carried out with two different concentrations of aldehyde, 370 μM (Fig. 9 a) and 3700 μM (Fig. 9 b).

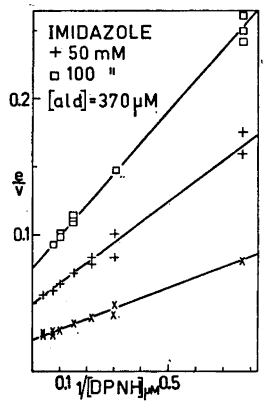

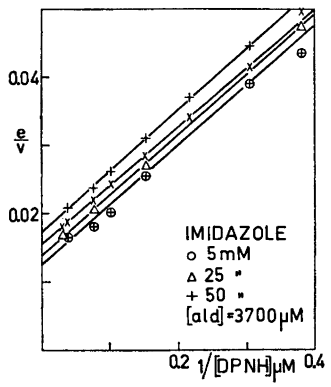

Fig. 9 a and b. Case 1. Imidazole. 0.1 μ, 23.5°C and pH 7.

Table 9. Imidazole, cases 1 and 2, intercepts (Corrected to infinite [DPNH] and [ald]).

[Im] mM	e/V (average)	V/e
0	0.0135	74
5	0.0096	104
10	0.0097	103
20	0.0086	116
25	0.0083	120

Fig. 9 b shows an uncompetitive picture with smaller concentrations of imidazole causing slight stimulation, higher ones some inhibition. However, if the intercepts were corrected to infinite [ald], then the results shown in Table 9 for the averages of cases 1 and 2 were obtained. There is thus a slight increase in reaction velocity in the last phase, but as seen below the influence of imidazole is slight as EO here decomposes almost as fast as EOI. At pH 9 the presence of EOI will be seen to be much more noticeable, the stimulation observed being much greater. Using the values for 5 and 20 mM imidazole in eqn. 10, $X = 122$ and $K_{EO,I\,kin} = 3.1$ mM; 5 mM and 25 mM gave $X = 126$ and $K_{EO,I\,kin} = 3.8$ mM.

The value for 10 mM did not fit with these values. It should be remembered, however, that the errors in these experiments are such that better agreement cannot always be expected. The values for $K_{EO,I}$ fit with the value $K_{EO,I}$ (uncorr.) at pH 7 of 3.3 mM obtained by equilibrium measurements in Part II.

The destabilization factor operating between I and DPN at pH 7 is from the equilibrium data in Part II: $K_{EI,O}/K_{E,O} = 440/160 = 2.75$.
Taking V_{max} for the decomposition

$$EIO \underset{k_{11}'}{\overset{k_{12}'}{\rightleftharpoons}} EI \underset{k_{13}'}{\overset{k_{14}'}{\rightleftharpoons}} E = 124 \text{ sec}^{-1} \text{ (see scheme A)}$$

$$\text{then } \frac{1}{k_{12}'} + \frac{1}{k_{14}'} = \frac{1}{124}$$

Since $K_{EI,O} = 440$ μM and $K_{E,I\,corr} = 550$ μM (Part II) are of the same order of magnitude, it is reasonable to assume that k_{12}' and k_{14}' should in this case be of similar order of magnitude and both contribute to the time needed for the liberation of E from EOI. If the "on" velocity constant k_{11}' ($EI + O \xrightarrow{k_{11}'}$) is assumed to be the same as k_1' ($E + O \xrightarrow{k_1'}$) $= 0.53$ sec^{-1} $\times$ μM^{-1} (which is probably not far from true, *cf.* caprate, cases 1 and 2, and *iso*butyramide cases 3 and 4) then $k_{12}' = 0.53 \times 440 = 234$ sec^{-1}. Since V_{max} for [I] $= \infty$ is 124 sec^{-1}, $1/234 + 1/k_{14}' = 1/124$ and $k_{14}' = 257$ sec^{-1}, $K_{E,I} = 550\,\mu M = k_{14}'/k_{13}'$, therefore $k_{13}' = 0.47$ μM^{-1} $\times$ sec^{-1}.

These values are only to be taken as a general confirmation of the mechanism. However, if we assume k_{14}' and k_{13}' both to be very large, $k_{12}' = 124$ sec^{-1} and $k_{11}' = 0.28$ μM^{-1} $\times$ sec^{-1}, which is not very far from the values

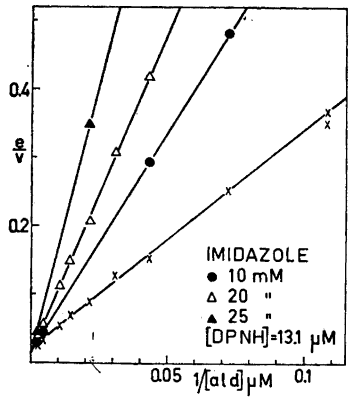

Fig. 10. Case 2. Imidazole 0.1. μ, 23.5°C and pH 7.

of $k_{11}' = 0.53$ under the first assumption of $k_{11}' = k_1'$. Whereas k_{11}' is thus reasonably well defined the absolute values of k_{13}' and k_{14}' are in fact unknown. They are only bound by the relation $k_{14}'/k_{13}' = 550$ μM.

Case 1a, slopes: With 370 μM aldehyde (Fig. 9a), nearly noncompetitive inhibition happens to occur at this [ald]. Compare the same case at pH 9 (Fig. 13 a and b).

As case 2 shows, imidazole competes strictly with aldehyde. At very low [DPNH] most of the enzyme exists in the equilibrium E ald $\rightleftharpoons$ E $\rightleftharpoons$ EI, where [E] is very small. The slopes give $K_I = 44.5$ mM imidazole. At 370 μM aldehyde and 44.5 mM imidazole therefore [E ald] = [EI], and $K_{E,ald} = 10.2$ μM ($K_{E,I\ uncorr.}$ being 1.23 mM). This value agrees with $K_{E,ald} = 10.0$ μM, obtained from the Michaelis constants (see Part I).

Case 2, slopes. These (Fig. 10) give $K_{ER,I}$, since the enzyme is at low [ald] essentially in the equilibrium ER + I $\rightleftharpoons$ ERI. The value of 8.9 mM (Table 10) agrees rather well with the value obtained in Part II ($K_{ER,I\ uncorr.} = 8$ mM).

Cases 3 and 4, intercepts. As seen from Figures 11 and 12 the plots without or with different concentrations of imidazole cross one another in an interesting way. At high concentrations of both DPN and alcohol, imidazole causes a considerable increase in reaction velocity, which at the intercepts, when corrected to infinite concentration of both DPN and alcohol, is 4—5 fold for 10 mM imidazole, 7—10 fold for 20 mM.

Table 10. Imidazole, case 2, slopes.

[Im] mM	Slope, μM × sec	$K_I = K_{ER,I}$
0	2.99	—
10	5.98	10.0
20	8.70	10.4
25	16.0	6.3
		Average 8.9 mM

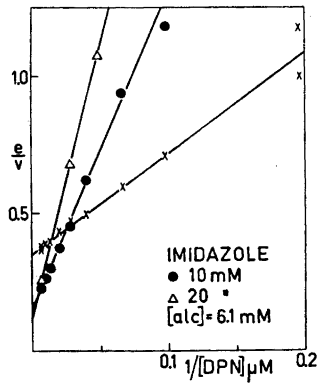

Fig. 11. Case 3. Imidazole. 0.1 μ, 23.5°C and pH 7.

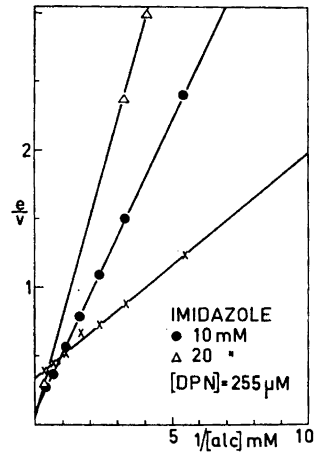

Fig. 12. Case 4. Imidazole. 0.1 μ, 23.5°C and pH 7.

This is explained by the fact that under these conditions without imidazole practically all of the enzyme is in the form of ER, and the dissociation velocity of

$ER \xrightarrow{k_2} E + R$, is rate limiting.

In the presence of imidazole, ERI is formed, which is less stable than ER. At pH 7, the destabilization factor is (*cf.* Part II) $K_{EI,R}/K_{E,R} = 2.01/0.31 = 6.5$, in general agreement with the extent of rate increase observed. As already discussed for caprate inhibition (cases 1 and 2) and *iso*butyramide inhibition (cases 3 and 4), the changes in dissociation constants caused by ternary complex formation are caused essentially by changes in the dissociation rate constants; the association rate constants seem rather independent of the presence or absence of another ligand.

The intercept data in this case do not allow accurate calculations because the extrapolations to infinite concentrations of DPN and alcohol become quite large at pH 7, where alcohol cannot be added in sufficient excess because of the inhibition effects described in Part II. Conditions are more favorable at pH 9, where such calculations are made (see below).

Case 3, slopes. It is noteworthy that imidazole and DPN compete, although as seen later from the stimulation shown at pH 9 (cases 1 and 2) and as shown in Part II, EOI is also formed. This competition is probably due to a charge effect, as discussed below, p. 1859.

In Fig. 11, $K_I = 4.7$ mM for both 10 and 20 mM imidazole. As in the case of aldehyde, assuming a complex E-alc-imidazole to be formed led to unreasonable results. Assuming strict competition, $K_I = 4.7$, $K_{E,I} = 1.23$ and [alc] = 6.1 mM gives $K_{E,alc} = 2.2$ mM.

This value is considerably lower than $K_{E,alc}$ obtained from the caprate inhibition (4.6 mM). The latter value is considered more likely to be true, since it is closer to the value $K_{E,alc} = 6$ mM obtained from the Michaelis constant in Part I.

Case 4, slopes (Fig. 12). There is strict competition with alcohol along with a second phase effect. At very low alcohol concentration, the following equilibria are assumed to prevail:

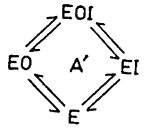

The concentration of imidazole expected to give half inhibition, where [E] + [EO] = [EI] + [EIO] was calculated from the data given in Parts I and II; $K_{E,O} = 160$ mM, $K_{E,I\ uncorr.} = 1.23$ mM, $K_{EO,I\ uncorr.} = 3.3$ mM, and $K_{I,calc}$ was found to be 2 mM. However, the experimental K_I is considerably higher, being 6.2 for 10 mM imidazole, 5.8 for 20 mM. The average $K_I = 6$ mM, is thus three times higher than the value calculated from the equilibrium measurements.

Imidazole pH 9

Cases 1 and 2, intercepts. The intercepts in Figs. 13 and 14 were corrected to infinite concentrations of DPNH and aldehyde (Table 11). Calculations using eqn. 1 gave $K_{EO,I} = K_I = 30.8$ mM and $X = 44.4$ sec^{-1}.

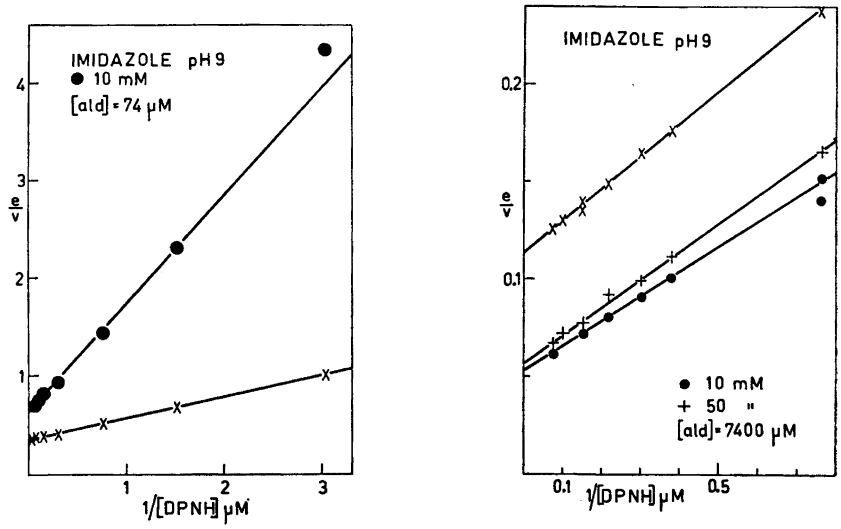

Fig. 13 a and b. Case 1. Imidazole. 0.1 μ, 23.5°C and pH 9.

Table 11. Imidazole, pH 9, cases 1 and 2, intercepts (corrected to infinite [DPNH] and [ald]).

[Im] mM	V/e, average
0	8.1
2	10.3
10	17.0
50	30.6
∞	X

A 5-fold stimulation of the reaction velocity is thus produced, due to the formation of EOI, which decomposes at a faster rate, 44 sec^{-1}, than EO, 8.1 sec^{-1}.

$K_{EO,I}$ (Part II) = 24.2 mM = k_{10}'/k_9' and $k_9' \times 30.8 - k_{10}' = 44.4$. Therefore $k_9' = 7\ mM^{-1} \times sec^{-1}$ and $k_{10}' = 168\ sec^{-1}$.

The relation between k_{12}' and k_{14}' in this case cannot be predicted since $K_{E,I}$ (670 μM) and $K_{EI,O}$ (440 μM) are rather equal. Probably both k_{12}' and k_{14}' contribute to the time factor e/V in the equation

$e/V = 1/k_{12}' + 1/k_{14}' = 1/k_{16}' = 1/44.4$

which obtains for infinite [DPNH], [aldehyde] and [imidazole].

Fig. 13 a, with 74 μM aldehyde, is interpreted as a stimulating second phase effect, combined with a non-competitive first phase effect.

Second phase effect: The reciprocals of the intercepts were 2.8 sec^{-1} without and 1.4 sec^{-1} with 10 mM imidazole. This can be used to calculate $K_{ER,I}$. Since R = ∞ at the intercept, the reaction may be considered to be:

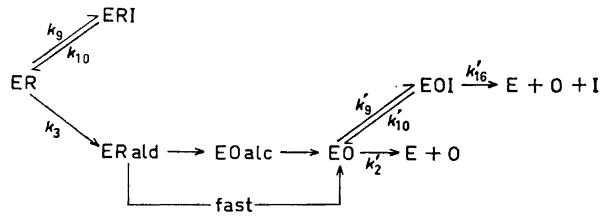

(D)

The decomposition of EO needs to be considered only as the summarized rate constant = 1.4 sec^{-1}. As $k_3 = 0.062\ \mu M^{-1}\ sec^{-1}$ (Part I), and the enzyme exists only in the three forms ER, EO and ERI, where at half inhibition, caused by 10 mM imidazole, [ERI] = [ER] + [EO]. Therefore $0.062 \times 74 \times [ER] = 1.4 \times [EO]$, from which $K_{ER,I}$ = 2.4 mM, in reasonable agreement with the equilibrium value 3.0 mM (See Part II, Table 15).

Case 1, slopes. The slopes as at pH 7 are nearly independent of [Im] when [ald] is high (Fig. 13 b).

First phase effect: When [ald] is lower as in Fig. 13 a where [ald] is 74 μM, the slopes differ due to competition between imidazole and aldehyde. Without imidazole the slope is 0.22 μM × sec, while with 10 mM imidazole it is 1.10 μM × sec, giving K_I = 2.5 mM.

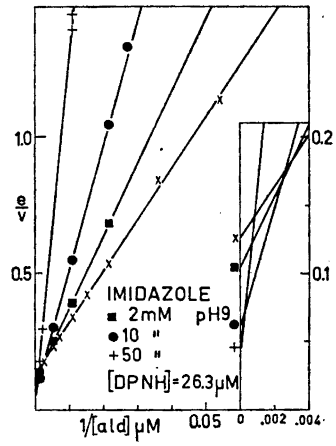

Fig. 14. Case 2. Imidazole. 0.1 μ, 23.5°C and pH 9. The intercepts enlarged and corrected to infinite [DPNH] are also shown.

When [DPNH] goes to zero with [I] = 2.5 mM and [ald] = 74 μM, [EI] = [E] + [Eald] and $K_{E,I\ uncorr.} = 0.68 = 2.5[E]/[EI]$.
Therefore [EI] = 3.7 [E], [E ald] = 2.7 [E], and $K_{E,ald} = 27$ μM.*

Case 2, slopes. The slopes in Fig. 14 indicate competition between imidazole and aldehyde. K_I (Table 12) would be expected to correspond to $K_{ER,I}$ in this case, which was found to be 3 mM in the equilibrium experiments.

The drift with [Im] and the not too good agreement with the equilibrium value may depend upon oversimplified assumptions.

Cases 3 and 4, intercepts (Fig. 15 and 16). The intercepts (Table 13) were corrected to infinite [DPN] and [alc], using eqn. 1.
2 and 10 mM imidazole: $K_I = 10.4$ mM, $X = 22$ sec^{-1}
10 and 50 mM imidazole: $K_I = 10.6$ mM $= 22.2$ sec^{-1}
Thus at 10.5 mM imidazole, [ER] = [ERI] (see scheme C) in the "second phase" of the reaction.

$K_{ER,I}$ (Part II) = 3 mM $= k_{10}/k_9$ and $k_9 \times 10.5 - k_{10} = 22.1$. Therefore $k_9 = 3$ mM$^{-1} \times$ sec^{-1} (cf. 7 mM$^{-1} \times$ sec^{-1} at pH 7 and $k_{10} = 9$ sec^{-1}). The "destabilization factor" for ERI is $K_{ER,I}/K_{E,I} = 3/0.67 = 4.5$.

Table 12. Imidazole, pH 9, case 2, slopes.

[Im] mM	Slope, μM × sec	K_I
0	18.8	
2	26.4	5 mM
10	45.2	7
50	126	9

* Recent determinations of Φ-values and rate constants at pH 9 (H. T. and L.-G. Falksveden) gave $K_{m,ald}$ (DPNH → O) = $K_{E,ald} = k_2/k_3 = 5.0/0.096 = 52$ μM. The value found from the competition between aldehyde and imidazole is again some two times lower.

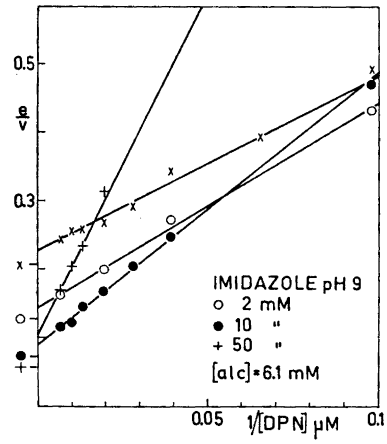

Fig. 15. Case 3. Imidazole. 0.1 μ, 23.5°C and pH 9. The position the intercept has when corrected to infinite [alcohol] is shown.

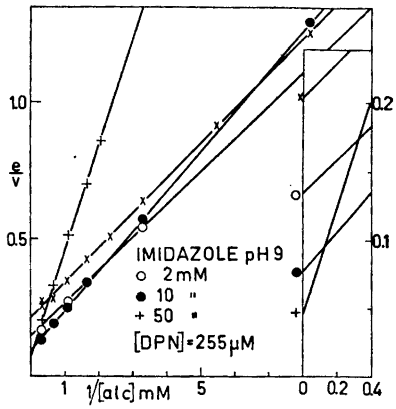

Fig. 16. Case 4. Imidazole. 0.1 μ, 23.5°C and pH 9. The intercepts enlarged and corrected to infinite [DPN] are also shown.

If it is assumed that the "on" velocity constants for R being attached to E (k_1) and to EI (k_{11}) are equal, the ratio between the dissociation constants should depend entirely on a corresponding difference in the "off" velocities.

In this case k_{12} should be $4.5 \times k_2 = 4.5 \times 4.9 = 22$ sec^{-1}. The agreement is surprisingly good; assuming that k_{14} is $\gg k_{12}$, which is reasonable since $K_{E,I} = 680$ μM and $K_{EI,R} = 2.91$ μM, $k_{12} = k_{16} = 22$ sec^{-1}. Again it appears probable that the changes in dissociation constants occurring on ternary complex formation are predominantly caused by changes in the "off" velocity constants of the ligands.

Case 3, slopes. As seen from Fig. 15, the slopes indicate competition by charge effect between DPN and imidazole, as was the case at pH 7. Presuming that when [DPN] approaches zero the equilibrium EI $\rightleftharpoons$ E $\rightleftharpoons$ E alc is maintained, then using $K_{E,I\ uncorr.} = 0.68$ mM, $K_I = 17.8$ mM (Table 14) and [alc] = 6.1 mM, $K_{E,alc}$ is found to be 0.23 mM. This value is again lower than that expected from K_m at [DPN] $\rightarrow 0$; $k_2'/k_3' = 1$ mM.

Case 4, slopes. The slopes in Fig. 16 again show competition. They differ markedly from the slope without imidazole (128 μM $\times$ sec) only in the presence

Table 13. Imidazole, pH 9, cases 3 and 4 intercepts (uncorrected and corrected to infinite [alc] and [DPN]).

	e/V				Average	
[Im] mM	Case 3		Case 4		*e/V*	*V/e*
	Uncorr.	Corr.	Uncorr.	Corr.		
0	0.225	0.209	0.210	0.200	0.204	4.9
2	0.144	0.128	0.145	0.134	0.131	7.6
10	0.090	0.0736	0.090	0.0766	0.075	13.3
50	0.104	0.057	0.080	0.046	0.052	19.2
∞						*X*

Table 14. Imidazole, pH 9, case 3, slopes.

[Im] mM	Slopes, μM × sec	K_I
0	2.58	—
(2	3.0)	—
10	4.0	18.2
50	10	17.4
		Average 17.8 mM

of 50 mM imidazole (384 μM × sec), from which K_I = 25 mM. From the equilibrium measurements in Part II it was known that EOI is formed. Calculating the [Im] that would be needed for fulfilling the half inhibition condition when [alc] → zero, [E] + [EO] = [EI] + [EOI] (see pH 7), using the equilibrium constants from Part II gives $[Im]_{50\ \%\ inhibition}$ = 9.8 mM. This value is again ~ 3 times lower than the experimentally found 25 mM, just as was the case at pH 7. On the other hand K_I = 25 mM happens to agree with $K_{EO,I}$ = 24.6 mM, found in Part II.

Ethanol

In Part II the formation of a complex ER alc at high concentrations of alcohol, with $K_{ER,alc}$ = 40 mM, $K_{E,alc}$* = 100 mM, and $K_{E,alc,R}$ = 0.12 μM was observed. Kinetic experiments presented in Fig. 17 indicated that at infinite alcohol concentration e/V is = 0.75 instead of the value 0.3 obtained by straight line extrapolation from values at [alc] < 10 mM. Mutual stabilization thus occurs with a factor of 2.5, ($K_{ER}/K_{E,alc,R}$ = 0.31/0.12 = $K_{E,alc}$*/$K_{ER,alc}$ = 2.5), which corresponds to the decrease in reaction velocity at infinite alcohol concentration, 0.75/0.3 = 2.5. As already found for the ternary complexes with caprate, *iso*butyramide and imidazole, the introduction of one ligand does not interfere with the "on" velocity constant of the other, but only with the "off" velocity constant:

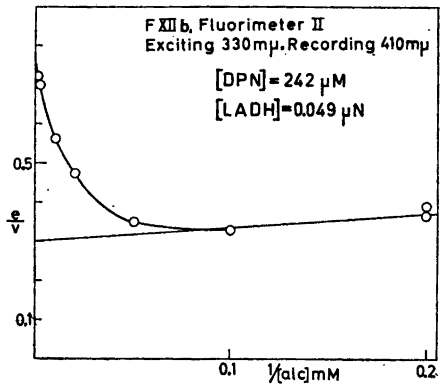

Fig. 17. Kinetics in the presence of relatively high concentrations of alcohol. The spectrophotofluorometer was used.

$$\text{E alc}^* + \text{R} \underset{k_{off}}{\overset{k_{on}}{\rightleftharpoons}} \text{E alc R}$$

$1.25/k_{on} = 0.12$; $k_{on} = 10.4\ \mu M^{-1} \times sec^{-1}$ in agreement with $k_1 = 11.2\ \mu M^{-1} \times sec^{-1}$ (Part II).

Half inhibition, $e/V = 0.525$, occurs at 75 mM alcohol. This kinetic value is, as expected, somewhat higher than the equilibrium value ($K_{ER,alc} = 40$ mM) and the differences could be used for calculating the "on" and "off" velocity constants for alcohol in equilibrium with ER, as was done above for example with *iso*butyramide (scheme B, I = alcohol). This would give $k_9 = 0.036\ mM^{-1} \times sec^{-1}$, $k_{10} = 1.4\ sec^{-1}$. However, the value 40 mM is uncertain, so that no great attention should be paid to the absolute magnitude, but it should be noticed that k_9 is very low, perhaps reflecting the low probability of a successful collision between ER and alcohol to form the abortive ER alc complex.

DISCUSSION

"On" and "off" velocities in binary and ternary complexes

$K_{E,ald}$ and $K_{E,alc}$ determined from the imidazole case 1, and caprate, case 3, experiments, agreed with the values determined in Part 1 from $K_{M,ald}$ and $K_{M,alc}$ when the coenzyme concentration approached zero. This further substantiates the existance of the complexes E ald and E alc, and the general two substrate mechanism A (Part I).

As discussed in Part I the "on" velocity constants for DPNH and DPN are nearly independent of whether DPNH is attached to E or to E,ald (k_1, resp. k_7), or DPN to E or to E alc (k_1', resp. k_7').

There is convincing evidence to believe that the maximum velocity in the forward reaction is k_2' ($EO \xrightarrow{k_2'} E + O$) and in the backward reaction, k_2 ($ER \xrightarrow{k_2} E + R$). The values found for k_2' were at pH 7, 74 sec^{-1}; at pH 9, 8.2 sec^{-1}; for k_2 at pH 7, 3.1 sec^{-1}; at pH 9, 4.9 sec^{-1}.

The dissociation constants $K_{E,R}$ and $K_{E,O}$, determined by equilibrium experiments in the absence of substrate (see Part II), together with the "off" velocity constants from the kinetic experiments allowed the calculation of the "on" velocity constants k_1 ($E + R \xrightarrow{k_1} ER$) and k_1' ($E + O \xrightarrow{k_1'} EO$).

The kinetic "on" velocity constants, as discussed in Part I, reflect k_7 ($E\ ald + R \xrightarrow{k_7} E\ ald\ R$) and k_7' ($E\ alc + O \xrightarrow{k_7'} E\ alc\ O$). The relations found between these constants were:

	k_7/k_1	k_7'/k_1'
pH 7	0.90	0.88
pH 9	0.76	0.75

The conclusion was that substrates on their binding sites at the enzyme only slightly affect the association velocity of their coenzyme partner. Nothing could be said, however, from these experiments as to how the presence of substrates in ternary complexes would affect the "off" velocity of the coenzyme, because these ternary complexes are rapidly transformed to other products and their dissociation constants therefore still unknown. This is not the case with ternary complexes of enzyme, coenzyme and inhibitors, and the experiments reported herein show that whereas the "on" velocity for the coenzyme is scarcely changed by inhibitors at the substrate site, the "off" velocity for the coenzyme is greatly affected, being decreased with caprate and *iso*butyramide, but increased with imidazole. For *caprate* at pH 7, k_{11}' (EI + O $\xrightarrow{k_{11}'}$ EIO) is at least = 0.54 × k_1' ,and k_{11}' may easily be $k_1' \cdot k_{16}'$ (EIO $\xrightarrow{k_{16}'}$ E + I + O), on the contrary, is only = 0.026 × k_2', so that the dissociation velocity of DPN is reduced fortyfold by caprate attached to the binding site of alcohol.

In the case of iso*butyramide* the constant k_{11} (EI + R $\xrightarrow{k_{11}}$ EIR) could be determined directly from reaction cycles at 10^{-8} M concentrations along with $K_{EI,R}$. k_{11} was found to be 14 μM^{-1} sec^{-1}, which is $\approx k_1$, whereas k_{16} was 0.025 × k_2, a fortyfold decrease just as in the case of caprate.

Imidazole forms ternary complexes corresponding to both ERI and EOI. At pH 7 the formation of EOI in the second phase of the forward reaction causes a slight increase in the maximal reaction velocity, from 74 to 124 sec^{-1}. This increase (the "destabilization factor"), 124/74 = 1.7, agrees with the increase in $K_{E,O}$ when the pH is lowered from 7 to approach the acid asymptote (288/160 = 1.8). Both cases may reflect the same thing, cancellation of the attraction between DPN^+ and $ZnOH^-$ in the former case by imidazole substituting OH^-, in the latter by H^+ neutralizing it.

In the "backward" reaction, imidazole accelerates the reaction at high [DPN] and high [alc] 5 to 10-fold in agreement with the destabilization factor $K_{EI,R}/K_{E,R}$ = 2.01/0.31 = 6.5.

At pH 9, the maximal acceleration caused by imidazole in the forward reaction was found to be 5.5-fold (44/8.1). In this case the destabilization factor $K_{EI,O}/K_{E,O}$ = 435/12 = 36. was much higher. The reason for this will be discussed below. In the backward reaction it was 4.5-fold (k_{16}/k_2 = 22/4.9) in perfect agreement with the destabilization factor ($K_{ER,I}/K_{E,I}$ = 3/0.67 = 4.5).

All the facts mentioned here concerning the influence of inhibitors, caprate, *iso*butyramide and imidazole (and alcohol!), on the dissociation constants and reaction velocities, conforms with the idea *that the entrance of a ternary ligand into a coenzyme-enzyme complex in most cases influences the "off" velocity but hardly at all the "on" velocity of the coenzyme.* Furthermore, the fact that the binding of both DPN and of DPNH to zinc is weakened by imidazole, in both cases resulting in stimulation of the reaction velocity, favours the suggestion of Wallenfels and Sund [3] that the adenine moiety which is equal in DPN and DPNH, is bound to Zn, rather than the pyridine ring, which is different in DPN and in DPNH. The amino group at C (6) and the N (7) was assumed

Table 15. Competitive features of the kinetics. Competition = +.

Case:	1	2	3	4
Caprate	+	−	−	+
*Iso*butyramide	−	+	+	−
Imidazole	−	+	+	+
o-Phenanthroline (Part IV)	+	−	+	±

to form a bidentate chelate with zinc. This forms a five membered ring, with zinc between two nitrogen atoms, and with two carbons, just as in ethylenediamine. Ethylenediamine as third bidentate ligand to zinc in octahedral bonds forms only weak complexes with association constants around 10^1, which is in agreement with the data for LADH + ethylenediamine reported in Part IV, and is also in agreement with the kinetic and equilibrium data for imidazole.

Along with the velocity constants the competitive features of the kinetics (Table 15) are illustrative. Caprate competed with DPNH and alcohol and the kinetic experiments, in agreement with the equilibrium data, showed that EI and EOI, but not ERI are formed. *Iso*butyramide was the opposite, being competitive with aldehyde and DPN, there being no real indication of effects due to the presence of EOI, only EI and ERI being formed. These differences in behaviour would indicate that alcohol and caprate have a different site of attachment compared with aldehyde and *iso*butyramide [1], and suggest the idea of different bonds for the substrates. Imidazole competes with both substrates and forms both the ternary complexes ERI and EOI. This behaviour of imidazole, a well known complexer with zinc, strongly suggests that zinc plays a central role in the binding of the substrates [3,4]. The formation by glycine of only the binary E-glycine, but no ternary coenzyme complexes in the equilibrium experiments of Part II, and the competition of *o*-phenanthroline (OP) and 2,2'-dipyridyl with DPNH and DPN (Part IV) show the importance of zinc attaching the coenzyme as bidentate ligands through the adenine moiety [3,4]. The mixed type of inhibition caused by o-phenantroline when alcohol (case 4) is varied will be discussed below (see p. 1862).

The structure of the binary and ternary complexes

The assumption of octahedral bond type with zinc attached to the protein by three coordinative valencies, and with three free from the protein was discussed in Part II. It explains why zinc is very firmly bound to the protein. Furthermore, the zinc is rigidly fixed at the protein, and the three free valencies directed to constant positions are not necessarily equivalent. They may be denoted A, B and C:

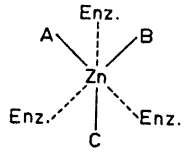

In neutral or acid solution the free valencies as usual carry water molecules, one or more of them losing protons at increasing pH:

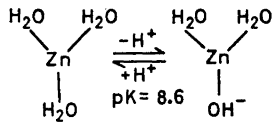

As discussed in Part II, only one of the water molecules or hydroxo groups can be replaced by imidazole.

The attachment of DPN to zinc by the adenine moiety as bidentate ligand, with the pyridine ring close to the adenine (and hence to the zinc also, *i.e.* N^+ and OH^- in proximity) could be schematically represented as

LADH-DPN (EO)

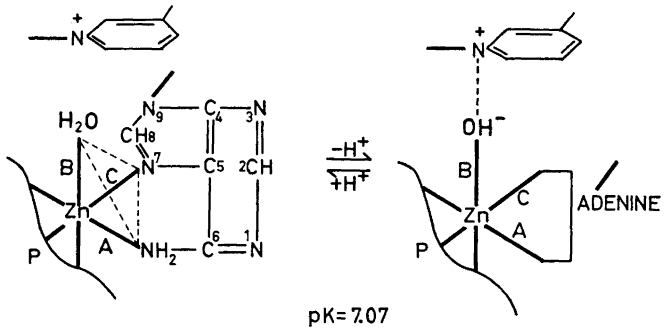

(E)

$K_{E,O}$ = 288 μM (H_2O on bond B) $K_{E,O}$ = 8.5 μM
$K_{EI,O}$ = 440 μM (Imidazole on bond B) $K_{EI,O}$ = 440 μM

The introduction of imidazole at bond B instead of an hydroxo group abolishes the stabilization of the binary EO complex in alkaline solution, presumably caused by attraction between N^+ and OH^-. This is illustrated by the observation that at pH 9 the "off" velocity of DPN from EIO is only 5.3 times higher than that from EO. From the destabilization factor $K_{EI,O}/K_{E,O}$ = 440/12 one would have expected a 36—fold increase. The discrepancy could be explained if it is assumed that the coulombic attraction between $Zn—OH^-$ and N^+ (DPN), operating in the absence, but not in the presence of imidazole, would result in a higher "on" velocity in the former case. The increase would be required to be 36/5.5 = 6.5-fold.

As shown in Part II, $K_{EI,O}$ for caprate (7 μM) and long chain fatty acids was essentially the same as the alkaline asymptote value of $K_{E,O}$ (8.5 μM) which deponds upon the Zn — OH^- — N^+ interaction. Therefore there is reason to believe that the ternary EOI complexes with fatty acids have a similar structure with the carboxyl group interposed between Zn and the pyridine N^+, Zn — COO^- — N^+.

R

The strict competition between fatty acids and alcohol suggests that alcohol could be similarly attached as an alcoholate ion. The dissociation of the proton from alcohol which is required by the reaction mechanism receives an explanation as it must be favoured by the positive charge of pyridinium, and the interaction to the zinc. This effect will not operate with aldehyde or fatty acid amides, which do not ionize. Thus the positively charged pyridinium ring would seem sufficient to explain the formation of EOalc, and why the complexes EOald and EOamide are not formed.

The kinetic results, while substantiating the octahedral binding of zinc discussed above, also implicated it as the center of a ternary complex [3,4] where along with the three bonds to the protein and the two to adenine [3], the last now attaches the substrates. It is this bond which in the binary complex EO was joined to the pyridinium ring (Zn—OH^-—N^+) but in ER was occupied by a water molecule. It was also suggested previously that Zn in LADH was octahedral [5], but it was by some authors considered not to attach the substrates [6,7] or to be the center of a ternary complex [6]. Indeed zinc attachment to coenzyme pyrophosphate groups has been suggested [7,8]. although pyrophosphate does not affect the activity [9].

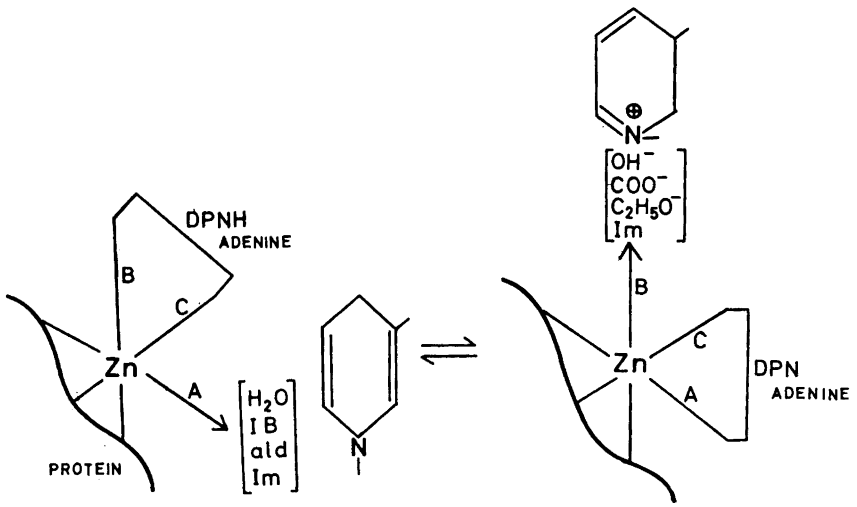

(F)

The ternary complexes and the interconversion phase

Since imidazole and caprate are both competitive with alcohol, bond B (scheme E) presumably can be used for attaching any of these. Aldehyde and *iso*butyramide, on the contrary, do not seem to be able to use this bond; the complexes EOIB, or EOald are not formed. Imidazole and *iso*butyramide in the kinetic experiments both compete with aldehyde, but there is no immediate reason why imidazole should not be able to use any one of the bonds A, B, or C. This brings up the question whether the adenine bonds could both move or one flick over ("edge shift") from A to B when DPN is reduced to DPNH, thus leaving bond A free for aldehyde or *iso*butyramide.

This hypothesis involves that during the rapid interconversion EOalc ⇌ ERald the substrate as alcohol uses bond B, as aldehyde bond A. Thus with DPN on the zinc bonds A and C, only alcohol, caprate or imidazole can compete at or go on the third bond B. DPN changing to DPNH implies bond shift so that A becomes free, which only accepts aldehyde, *iso*butyramide and imidazole. Thus as a result of a presumably small intramolecular rearrangement the coenzyme determines which of two bonds is available and so what can attach. This concept gains some support from the stereospecific requirement that due to their different structures the substrates must change their position somewhat relative to the enzyme surface [10]. However, while the competitive features of Table 15 generally agree with this model, it does imply that imidazole in case I should be competitive with DPNH (Figs. 9 and 13). With bond A saturated by a high [aldehyde], imidazole is prevented from attaching there, and therefore the imidazole should compete with DPNH for bonds B or C. This is not so, imidazole does not show competition with DPNH, and in agreement herewith ERimidazole complexes are formed (see Part II).

In the ternary complexes either negative or neutral ligands appear to be attached to the zinc in the vicinity of the DPN pyridinium or DPNH pyridine rings respectively. The charge interaction between N^+ and zinc makes alcohol much more negative in the complexes than in the free state as discussed on p. 1860. Imidazole, perhaps due to its conjugated structure, behaved in an intermediate way (see Part II). While R and IB mutually stabilized each other in the ternary complex, O and IB completely destabilized each other. Caprate behaved in the reverse way. Imidazole, however, caused partial destabilization with both R and O, but formed ternary complexes with both. This effect was parallelled in the competition experiments.

The competition experiments taken as a whole (Table 15) confirm that the three free zinc bonds are not used at random by the coenzymes, substrates and inhibitors. Restrictions on which bonds each can use obviously prevail, steric, charge forces or binding sites in addition to the bonds with zinc resulting in orientation on the enzyme surface. Caprate case 1 and IB case 3 (Figs. 1 and 7); caprate case 2 and IB case 4 (Figs. 2 and 8); caprate case 4, IB case 2, and imidazole case 2 and 4 (Figs. 4, 6, 10 and 12) are seen to be similar. In these cases there is either competition at the bond they can both attach at, or else they are not competing where one cannot attach.

The effect of bidentate ligands

The bidentate ligands, like *ortho*phenanthroline (OP), 2,2′-dipyridyl, ethylenediamine (or glycine, as indicated by the equilibrium data), are all strictly competitive with both DPN and DPNH, as would be expected when only three bonds are free and the coenzyme-adenine forms a bidentate itself. This confirms that the adenine bonds to Zn are essential for the activity. As these inhibitors would not be expected to have additional bonds to other sites, restrictions unless for steric reasons would not be expected, but independent of which two bonds out of three are used, competition with the adenine would result. Nevertheless it is possible that OP and the bidentate ligands might be only attaching at the coenzyme bonds. The lack of strict competition with both substrates and the nature of the competition between OP and the substrates which shows that EIald and EIalc (mechanism 1) must be formed, may indicate this. If OP and DPNH are restricted to use the same two bonds then in agreement with the experiments, case 2 would not be competitive. The mixed competition in case 4, might be influenced by a stabilizing effect of DPN^+ and $alcohol^-$ on each other ($N^+—alc^-—Zn$), in the equilibrium

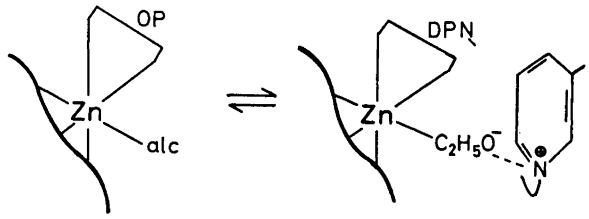

(G)

increasing [alc] shifting the equilibrium to the right, thus simulating a certain degree of competition between alc and OP. If OP would be able to compete at any two bonds, competition or mixed competition would be expected in both cases 2 and 4. The experiments with OP and the bidentate inhibitors are fortunate in giving excellent support for the necessity that the coenzymes be attached as bidentates to zinc.

LADH thus emerges as a protein where zinc is held by three bonds, water molecules being on the other three zinc bonds. In the binary complexes two of these water molecules are replaced by bidentate ligand inhibitors or by the coenzyme adenine moeity acting as a bidentate ligand, the state of the remaining water molecule depending on the pH, it being more dissociated in EO than in ER. In the ternary complexes this latter water molecule or OH^- is substituted by substrates or unidentate ligands (Fig. 18). In the binary and ternary complexes with DPN, there is an additional enzyme-coenzyme-pyridine ring attachment through the $N^+—X^-—Zn$ interaction. The great stability of the DPNH complexes may be caused by bond formation between enzyme SH-groups and the pyridine ring [2].

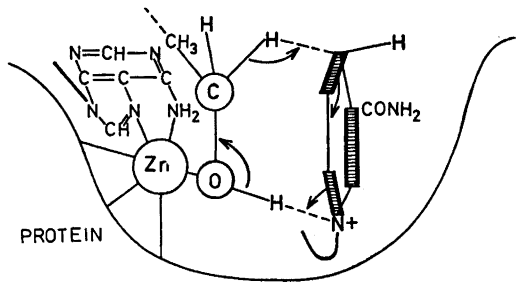

Fig. 18. Schematic representation of the LADH ternary complexes.

The theory presented here concerning how coenzymes and substrates are bound to Zn has the advantage of giving a possible explanation of how enzymes make coenzymes and substrates to select with great preference their active reaction partners, and reject those like ER alc, EO ald with which no reaction can occur.

The assumed shift of bonds (edge shift) from adenine to Zn on oxidoreduction of both coenzymes and substrates requires some shift in the conformation of the molecules, which one can easily imagine to take place with the coenzymes but less easily with the substrates. However, weak bonds and small displacements on the enzyme surface are probably involved.

While it is easy to envisage the positive charge of the pyridine ring in DPN being strong enough to bring about great preference for ligands with negative charge, e.g. fatty acids and alcohols, which may at least partly react as alcoholate ions, it is not so easy to visualize why aldehydes should be prevented from using the same bond, or why the neutral pyridine ring in DPNH should prefer aldehydes and amides. However, a zinc atom and the charge atmosphere around it would be expected to be very different in bonding or complexing properties to negative, neutral or conjugated molecules when a positive charge was present or absent in proximity, and of course even small differences in geometry and charge may be of importance in the crowded neighbourhood of the Zn atom in a ternary complex.

The abortive ERalc complex formed at very high alcohol concentrations may represent alcohol attached to the aldehyde zinc bond. The complex ERalc, which according to Winer and Theorell [1] should not be formed at all, shows that the formation of unreactive ternary complexes with both coenzyme and substrate is difficult, but not always entirely impossible. The specificity of fatty acids for EO, amides for ER may also be relative rather than absolute.

The inhibition of the reaction rate by very high concentrations of alcohol has now found an obvious explanation. Alcohol is the substrate in the first phase, an inhibitor in the second, acting there just as isobutyramide in forming a ternary complex, from which DPNH is dissociated more slowly than from DPNH-LADH.

The remarkable effect of imidazole stimulating the reaction velocity manifold at high substrate concentrations through the formation of labile ternary complexes in the second phase of the reaction, but inhibiting at lower substrate concentrations by effects in the first phase, could have a physiological significance. Substances of this kind would have a homeostatic function to maintain substrates at a suitable concentration. An excess would be rapidly removed, but the process would be strongly inhibited when lower concentrations were reached.

Note added to the proof December 16, 1961 by Hugo Theorell. An alternative theory which in some ways fits better with the experimental data is the following.

The zinc atoms in the free enzyme are held by three bonds to the enzyme, as assumed before. All other numbers than three are in fact controversial with experimental data. But in the free enzyme and in the binary complexes with monodentate ligands the arrangement could be *tetrahedral* instead of octahedral, leaving one bond free for attaching water, OH^-, imidazole, aldehydes, alcohols, amides or fatty acids.

This would explain why pH changes give a monovalent dissociation curve ($pK = 8.6$) for the free enzyme, and why only one molecule of imidazole can be attached, also giving a monovalent dissociation curve. $K_{E,Im,corr} = 0.6$ mM corresponds to an association constant = 3.2 which is not far from the value $k^4 = 2{,}65$ for free zinc ions in equilibrium with imidazole given in the literature (Part II, Ref. 3 b). Some difference must of course be expected from the probability that some of the three enzyme-zinc bonds are not imidazole residues.

Monodentate ligands which unlike water, hydroxo- or imidazole, are attached to the protein by additional groups, for example the lipofilic binding site operating with alcohols, aldehydes, fatty acids or amides may introduce some strain on the zinc bond, bending it somewhat in one or the other direction. The assumption of tetrahedral configuration with monodentate ligands readily explains why complexes with both imidazole and alcohol or aldehyde were not formed (*cf.* p. 1849), and why imidazole competes with both. On the other hand this theory would not allow the complexes E ald, caprate or E alc, *iso*butyramide to be formed.

Certain bidentate ligands like 1:10-phenanthroline and 2,2′-dipyridyl readily give quite strong octahedral complexes with zinc. It might therefore be possible that bidentate ligands can change the Zn bonds from tetrahedral to octahedral in LADH. The ternary complexes of LADH would therefore consist of one tridentate (LADH), one bidentate (adenine moiety of coenzymes or bidentate inhibitors) and one monodentate ligand (substrates or monodentate inhibitors).

Bidentate inhibitors forming octahedral complexes compete with the bidentate adenine of the coenzymes (*cf.* 1,10-phenanthroline in Part IV). Monodentate inhibitors compete with the substrates: imidazole competes with both alcohol and aldehyde, but not with DPNH. The competitive pictures between DPN and imidazole are caused by the inductive effect of the positively charged pyridine ring (*cf.* p. 1859). Aldehydes and amides by virtue of their lipofilic binding sites could distort the direction of the two bonds appearing on transformation to octahedral configuration enough to fit only the adenine moiety of DPNH; and alcohols or fatty acids — both negatively charged — could make them fit instead to the adenine of DPN. This direction change obviously substitutes the more complicated assumption of an "edge shift".

Acknowledgements. The authors with to thank Dr. H. Sund for many useful discussions. They are indebted for financial support given by *Statens Medicinska Forskningsråd, Statens Naturvetenskapliga Forskningsråd, Knut och Alice Wallenbergs Stiftelse, The Rockefeller Foundation, Wenner-Grenska Samfundet* and *Institutet för Maltdrycksforskning.*

Skilful technical assistance has been given by Mr. Lars-Gunnar Falksveden.

REFERENCES

1. Winer, A. D. and Theorell, H. *Acta Chem. Scand.* **14** (1960) 1729.
2. Theorell, H., Nygaard, A. P. and Bonnichsen, R. *Acta Chem. Scand.* **9** (1955). 1148.
3. Wallenfels, K. and Sund, H. *Biochem. Z.* **329** (1957) 59.
4. Mahler, H. R. and Douglas, J. *J. Am. Chem. Soc.* **79** (1957) 1159.
5. Vallee, B. L. and Coombs, T. L. *J. Biol. Chem.* **234** (1959) 2615.
6. Vallee, B. L., Williams, R. J. P. and Hoch, F. L. *J. Biol. Chem.* **234** (1959) 2621; Vallee, B. L. *The Enzymes, Vol. 3*, Academic Press 1960 p. 247.
7. van Eys, J., Pietro, A. San and Kaplan, N. O. *Science*, **127** (1958) 1443.
8. van Eys, J., Ciotti, M. M. and Kaplan, N. O. *Biochim. Biophys. Acta* **23** (1957) 574, 581.
9. Wallenfels, K. and Sund, H. *Biochem. Z.* **329** (1957) 48.
10. Gierer, A., *Biochim. Biophys. Acta* **17** (1955) 111.

Received March 28, 1961.

ACTA CHEMICA SCANDINAVICA 15 (1961) 1866–1874

Liver Alcohol Dehydrogenase

IV. Kinetics in the Presence of Zinc Binding Agents

ROBERT A. PLANE* and HUGO THEORELL

Medicinska Nobelinstitutet, Biokemiska avdelningen, Stockholm, Sweden

Measurements of the kinetics of both the oxidation of alcohol by DPN ** and the reduction of aldehyde by DPNH have been made in the presence of a variety of zinc binding agents. These substances show a varied pattern of behavior, which is summarized as follows. Binding of inhibitors to the enzyme parallels the binding of the third bidentate ligand to free zinc, indicating the zinc to be bound in the enzyme octahedrally at more than two of its coordination positions. Bidentate ligands compete with DPN and DPNH, thus indicating that at least one of their normal binding sites are at the zinc. In addition ternary complexes are formed between enzyme-substrate-inbibitor which show markedly increased affinity of inhibitor and substrate for the enzyme. Furthermore, monodentate ligands compete with substrate in forming ternary complexes with enzyme-coenzyme complexes. Both these results are taken to indicate that the substrates may also be bound to the zinc.

It has been shown that a number of species capable of binding to the zinc atoms of the enzyme liver alcohol dehydrogenase act as inhibitors for the enzyme [1-3]. In one case, that of 1,10-phenanthroline, the actual binding of the inhibitor was determined spectrophotometrically [4], and the kinetics of the inhibition studied in detail [3]. Studies of this type, if extended to cover a wide range of inhibitors, might provide considerable information as to the role played by zinc atoms in the enzyme. For this reason the present study was undertaken. Specifically, three topics were investigated. By studying in some detail the kinetics of both the forward (reduction of aldehyde by DPNH) and reverse (oxidation of alcohol by DPN) processes, it was hoped to obtain an indication as to the role of the zinc atom in binding the various reactants. By using as inhibitors species whose affinities for free Zn^{++} are known, it was hoped to confirm or deny the importance of Zn in the enzyme activity and furthermore

* U.S. Public Health Service Special Fellow.

** Abbreviations: DPNH and DPN, reduced and oxidized diphosphopyridine nucleotide, respectively, which are also abbreviated in dissociation constants as R and O.

to gain information concerning the state of the zinc in the enzyme. Finally, it was hoped that a study of several different anions would shed some light on the relatively large and apparently specific effects on the enzyme shown by negative ions [1].

For the present study, the following species were used as possible enzyme inhibitors: 1,10-phenanthroline, 2,2'-dipyridyl, ethylenediamine, oxalate ion, pyrophosphate ion, sulfate ion, thiosulfate ion, thiocyanate ion, fluoride ion, bromide ion, and perchlorate ion. For all, except perchlorate, the affinity for free zinc ion is known [5]. Perchlorate ion shows no measurable affinity for Zn^{++} or other positive ions in aqueous solution. Thus the series should be ideal for revealing any correlations between zinc binding and inhibitor action.

EXPERIMENTAL

Crystalline alcohol dehydrogenase was prepared according to the method of Bonnichsen and Brink [6]. After three recrystallizations, the assay of Dalziel [7] showed the purity to be 106 %. DPN and DPNH were obtained from Sigma Chemical Company and assayed spectrophotometrically. Acetaldehyde and ethanol were redistilled and assayed enzymatically. Ethylenediamine was redistilled just prior to its use and NaSCN was recrystallized from water. All other inhibitors and the buffer salts ($NaH_2PO_4 \cdot 2H_2O$, $Na_2HPO_4 \cdot 12\ H_2O$) were of the purest grade commercially available, used without further purification. All water was redistilled in an all glass system.

Initial rates were determined by following the change in DPNH concentration as reflected by the change of its fluorescence. Both the apparatus used [8] and the general technique have been described previously [1]. Rates were determined from tangents at the time of mixing and it was found that the values so obtained were precise, judging from duplicate experiments, to within a mean deviation of ± 5 %. For each inhibitor four sets of experiments were carried out. In the first, case 1, aldehyde concentration was relatively high and constant, while DPNH was varied from experiment to experiment. In the second, case 2, DPNH was constant while aldehyde was varied. Similarly, case 3 consisted of constant alcohol with varied DPN, and case 4 of constant DPN and varied alcohol. The temperature was 23.5° and the total ionic strength 0.1 μ. The pH was maintained at 7.1 in all experiments.

Table 1. Inhibitor effects.

Inhibitor	DPNH varied [Ald.] = 3.0 mM	Ald. varied [DPNH] = 9.8 μM	DPN varied [Alc.] = 8.0 mM	Alc. varied [DPN] = 200 μM
Ethylene-diamine	No effect I = 3.5 mM	Competitive $K_I > 3$ mM	No effect I = 3.4 mM	No effect I = 3.4 mM
Sodium oxalate	No effect I = 2.1 mM	Noncompetitive $K_I > 2$ mM	No effect I = 3.4 mM	Competitive $K_I = 30$ mM
Sodium pyrophosphate	No effect I = 2.7 mM	No effect I = 2.7 mM	No effect I = 3.0 mM	No effect I = 3.0 mM
Sodium sulfate	No effect I = 2.5 mM	No effect I = 2.5 mM	Competitive $K_I = 8$ mM	No effect I = 3.0 mM
Sodium thiosulfate	Competitive $K_I = 6$ mM	Noncompetitive $K_I > 20$ mM	Competitive $K_I = 4$ mM	No effect I = 3.5 mM

RESULTS

Figs. 1—4 show results obtained for the four sets of experiments run in the absence of inhibitors (lower lines, with actual points shown in Fig. 4) and in the presence of six of the inhibitors tested. Each set of experiments was duplicated with good agreement; however, for clarity, only one set of points is shown. The remaining five inhibitors showed very small effects and the results found with them are summarized in Table 1.

From the figures, or Table 1, it is seen that the various inhibitors display various patterns of behavior. Within the entire set, the most common is that shown, for example, by 1,10-phenantroline. The same pattern, competition with three of the reactants, but not with aldehyde, is shown by 2,2′-dipyridyl, Br^-, and ClO_4^-. On the other band, SCN^- and F^- seem to compete only with alcohol, although as will be discussed below, the apparent non-competition is probably illusory.

The inhibitor 1,10-phenanthroline has been studied in the greatest detail both in the present investigation and in a previous one [3]. Both investigations show strict competition with DPNH and DPN, non-competition with aldehyde

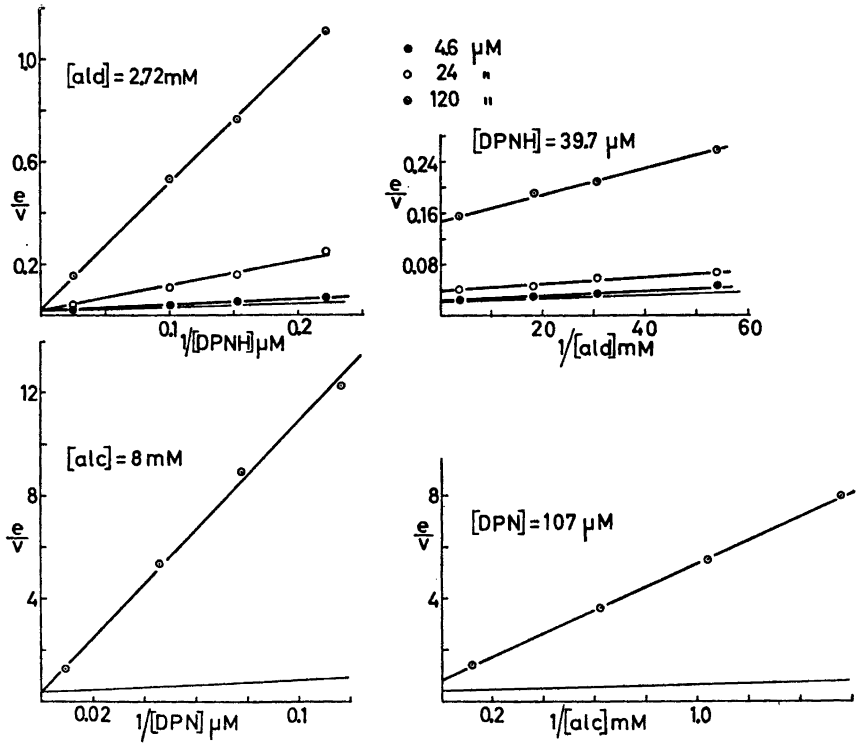

Fig. 1. Kinetic behavior with 1,10-phenanthroline. Closed circles refer to inhibitor = 4.6 μM, open circles, 24 μM, circles with dot, 120 μM. Enzyme concentrations are in terms of active sites.

and mixed inhibition with alcohol. The results for the latter case seem to differ somewhat between the two studies. However, the difference is not large and probably arises as follows. The results of Vallee *et al.* were obtained using alcohol in excess of 10 mM which causes some substrate inhibition [9] and thus biases the curves somewhat toward non-competitive behavior. The present results were obtained at lower DPN concentration, which because of the competition between DPN and the inhibitor emphasizes the competition between alcohol and 1,10-phenanthroline. For further discussion, see Part III, p. 1862.

In interpreting the 1,10-phenanthroline results, the simplest mechanism is to postulate the binding of free enzyme by the inhibitor thus preventing it from entering the reaction. This hypothesis can be tested by seeing whether the dissociation constants calculated from the various plots give the same value for the dissociation constant of the enzyme inhibitor complex ($K_{E,I}$). It should be noted that $K_{E,I}$ is not in general equal to the inhibitor constant, K_I (recorded in Table 1 for all competitive cases), which is merely the concentration of inhibitor necessary to halve the rate. The reason for the difference is that in most experiments only a small fraction of the total enzyme is present as free enzyme, the majority being present as binary complexes containing one of the four reactant species (alcohol, aldehyde, DPN, or DPNH).

It is thus necessary to calculate the fraction of free enzyme, prior to calculating $K_{E,I}$. To do so requires a knowledge of the dissociation constants of the various binary constants. These values have been determined (see Parts II and III) and the values used in calculating the present results are $K_{E,ald} = 10.2$ μM, $K_{E,R} = 0.31$ μM $K_{E,alc} = 4\,600$ μM, $K_{E,O} = 160$ μM[10]. Using these values, apparent values of $K_{E,I}$ can be calculated for 1,10-phenanthroline. These turn out to be 1.3×10^{-8} M (from the first series, high aldehyde), 3.0×10^{-6} (high alcohol), 1.1×10^{-5} (both from the series shown in Fig. 1, DPN = 107 μM, and from a separate experiment with DPN = 200 μM). Comparison of the three values obtained show that they vary widely and that only the last agrees at all reasonably with the value (3.3×10^{-5} M) determined directly by Vallee and Coombs [4]. Thus, we are forced to conclude that the situation is more complicated and that ternary complexes involving the inhibitor are indicated, *cf.* Parts II and III.

The data for the forward reaction (case 1) can be accounted for by assuming the presence of the ternary complex E ald I with dissociation constant $K_{E\,ald,\,I} = 4$ μM. The value seems of reasonable magnitude since the presence of aldehyde might be expected to stabilize the binding of 1,10-phenanthroline. The data for the reaction from the alcohol side (case 3) seems likewise to require the postulation of at least one ternary complex, this time between enzyme, alcohol and inhibitor. The value resulting for $K_{E\,alc,I}$ is 4.0 μM. This number is again of reasonable magnitude especially since it is the same as that for the ternary complex differing only by the substitution of aldehyde for alcohol.

K_I obtained from the slopes, in cases 2 and 4, is interesting, being 17 μM and 6.6 μM. The slopes reflect the situation when [ald] or [alc] are approaching zero, and thus competition between *o*-phenanthroline and the adenine moiety of DPNH or DPN (*cf.* Part III). The adenine is so weakly bound that the values are close to 14 μM, the third dissociation constant for *o*-phenanthroline and free zinc ions, the corresponding association constant k_3 being 4.85 [5]. This gives

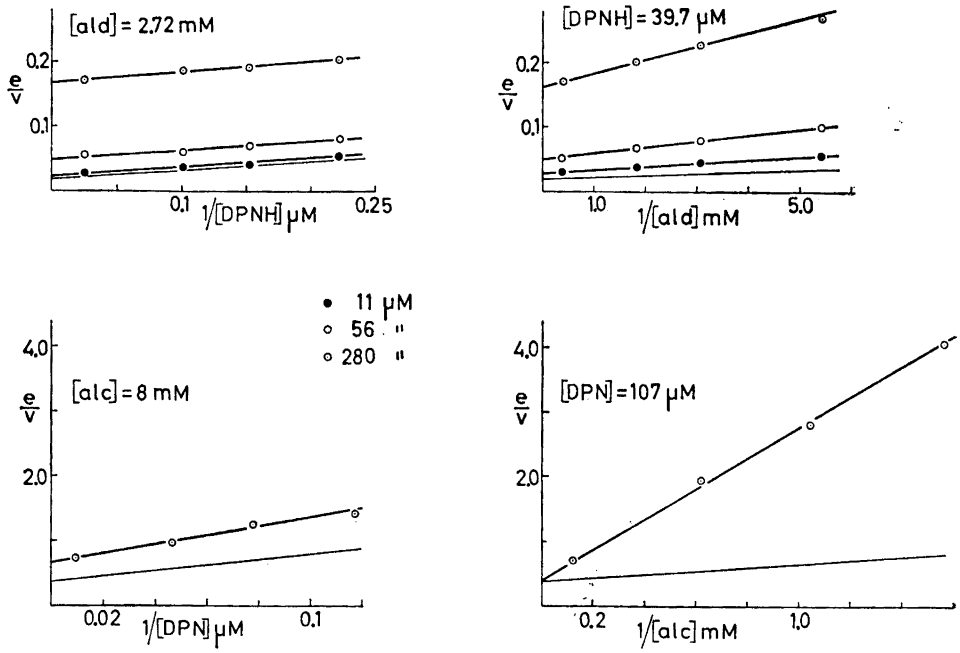

Fig. 2. Kinetic behavior with SCN^-. Closed circles refer to inhibitor = 1.1×10^{-5} M, open circles 5.6×10^{-5} M, circles with dots, 2.8×10^{-4} M.

additional evidence that the weak adenine-zinc bonds are essential for the activity.

As discussed in Part III the complexes could be pictured (omitting attachments of Zn to the enzyme) as follows:

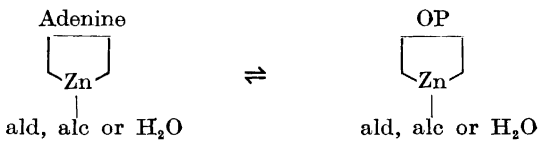

The conclusion of Vallee [3] that the aldehyde and ethanol are not attached to the zinc rests upon his statement of non competition of OP and these substrates. However, this conclusion is clearly invalid. The three free valencies of the zinc allow ternary complexes with substrates and OP to be formed. The mixed competition occurring in case 4 is explained in Part III.

The results for 2,2'-dipyridyl are as follows. If no ternary complexes form, the apparent values for $K_{E,I}$ are 5.4×10^{-7} M (from competition with DPNH), 5.2×10^{-4} (from competition with DPN) and 6.3×10^{-4} M (from competition with alcohol). Agreement between the last two values is completely satisfactory and thus there is no reason to postulate ternary complexes for the reverse

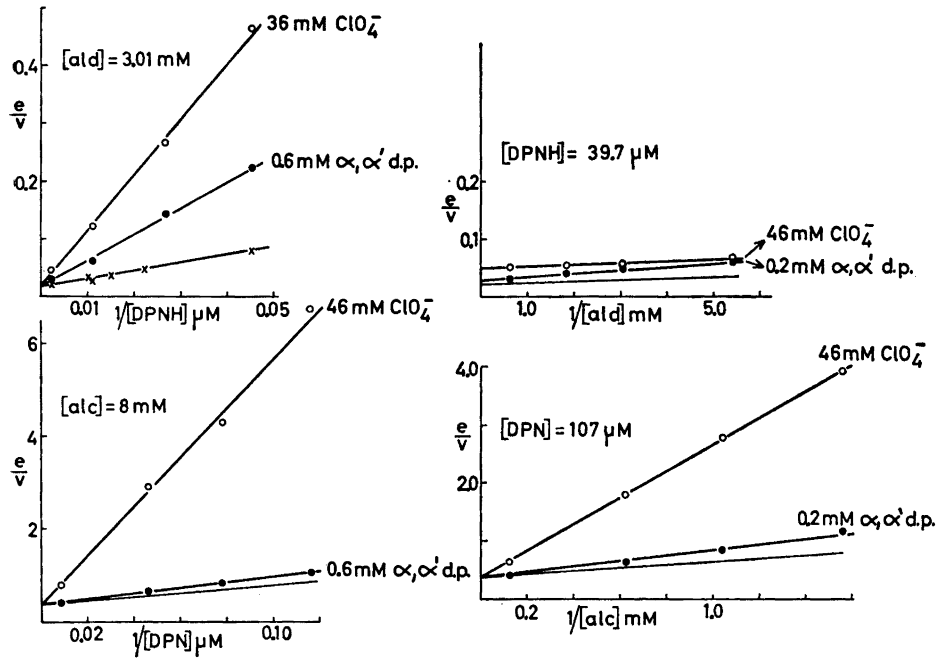

Fig. 3. Kinetic behavior with 2,2'-dipyridyl and ClO_4^-. Closed circles refer to 2,2'-dipyridyl = 6.0×10^{-4} M in cases 1 and 3, 2×10^{-4} M in others, open circles to ClO_4^- = 0.036 M in case 1 and 0.046 M in others.

reaction. However, the value 5.4×10^{-7} M is much too small and again the ternary complex enzyme-aldehyde-inhibitor is indicated. For this case, $K_{\text{Eald,I}} = 1.6 \times 10^{-4}$ M which represents a reasonable enhancement by aldehyde of the affiniy of the inhibitor.

For perchlorate inhibition the $K_{\text{E,I}}$ calculated from DPNH competition, 2.0×10^{-6} M, is again much the smallest, indicating a ternary complex with $K_{\text{Eald,I}} = 6.0 \times 10^{-3}$ M. The values obtained from the reverse reaction, 2.5×10^{-3} M and 9.1×10^{-3} M, do not clearly decide whether E alc I forms or not.

The case of Br^- (Fig. 4) is similar to that found earlier [1] for Cl^-, and differs from the cases just described in that at high concentration of alcohol and DPN, the reaction is accelerated. This is probably due to the presence of the ternary complex enzyme-DPNH-bromide whose decomposition is faster than that of enzyme-DPNH (under these conditions the rate limiting step). In addition Br^- seems to form another ternary complex with $K_{\text{E ald, Br}} = 2.3 \times 10^{-2}$ M. Apparent values for $K_{\text{E, Br}}$ obtained from the reverse reaction are 2.3×10^{-2} M and 6.9×10^{-2} M, sufficiently equal to make the decision as to additional ternary complexes difficult from the present data.

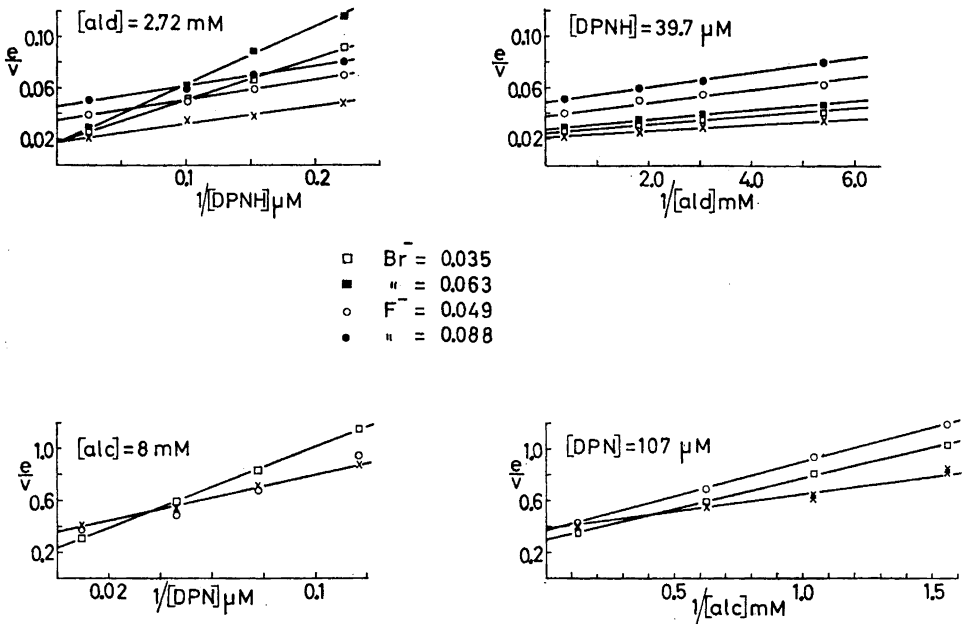

Fig. 4. Kinetic behavior with F^- and Br^-. Open squares refer to Br^- = 0.035 M closed squares, Br^- = 0.063 M; open circles, F^- = 0.049 M, closed circles, F^- = 0.088 M; × refers to no inhibitor.

The pattern of behavior shown by the thiocyanate ion, Fig. 2, is considerably different from that of the cases thus far discussed. Its uncompetitive behavior with DPNH suggests the formation of a ternary complex between enzyme, DPN, and SCN^-, which decomposes very much slower than the enzyme-DPN complex. On this assumption, the various concentrations of SCN^- are useful in calculating the dissociation constant $K_{EO,I} = 3.2 \times 10^{-5}$ M and its relative rate of decomposition, which is less than 1 % of that of EO. Finally, an independent check is given by the competition with alcohol which gives a value for $K_{EO,I}$ of 3.8×10^{-5}. This single species accounts for the entire behavior except for the apparent non-competitive behavior with aldehyde. Since the inhibition at infinite aldehyde is attributed to the last stage complex, enzyme-DPN-SCN, it seems this cannot be non-competitive inhibition in the early stage. It can, however, be due to a combination of a second phase effect with a first phase competitive effect. This first phase competition could either be between I and aldehyde for ER, with a resulting $K_{ER,I} = 3 \times 10^{-5}$ M, or competition for E, with $K_{E,I} = 2 \times 10^{-7}$ M. If the ternary complex, enzyme-DPNH-SCN^-, offers the correct explanation, it must decompose at the same rate as enzyme-DPNH, in order not to interfere with the kinetics of the reverse reaction. However, its dissociation constant seems of a more reasonable magnitude than that demanded for $K_{E,I}$, especially since its value is nearly the same as the similar constant $K_{EO,I}$. Finally, fluoride behaves in a manner quite

similar to SCN^-. From the case 1 type of experiments $K_{EO,I} = 5 \times 10^{-2}$ M with EOI decomposing less than 5 % as fast as EO. This value is checked by the fourth case (competition with alcohol) which gives $K_{EO,I} = 5.4 \times 10^{-2}$ M. As with SCN^-, the experiments with varied aldehyde can be accounted for either by assuming competition for free enzyme, with $K_{E,I} = 4 \times 10^{-4}$ M, or by competition for enzyme-DPNH, with $K_{ER,I} = 5 \times 10^{-2}$ M. Again $K_{ER,I} = K_{EO,I}$ which lends support to the existence of the ternary complex enzyme-DPNH-inhibitor for both F^- and SCN^-.

CONCLUSIONS

The results obtained with the inhibitor 1,10-phenanthroline show clearly that binding of the inhibitor blocks the binding of both DPN and DPNH. This gives strong indication, as Vallee, Williams, and Hoch have pointed out that coenzymes are bound to zinc [3]. However, the apparent lack of strict competition with the substrates need not indicate that they are not also bound to zinc. In fact the observed enhancement of the binding of inhibitor by the simultaneous presence of aldehyde or alcohol indicates that the substrate cannot be far removed from the zinc atom and quite likely is also bound to it. The ternary complexes, enzyme-coenzyme-inhibitor, indicated for SCN^-, F^-, and Br^- are significant in that no such complexes were formed with the larger, and bidentating ligands. If indeed the smaller, ionic inhibitors bind to zinc, these results mean that even when bound to coenzyme, zinc is able to coordinate small monodentate ligands as for example also imidazole (See Part II), although not large, bidentate ones. Furthermore, the competition shown between SCN^- or F^- and the substrates indicates that these ions are bound at the substrate site. However, a complete analysis of the results with ionic inhibitors is not possible from the present data. It should be noted that even in relatively dilute solutions, certain ions have significant effects and that these effects are remarkably specific. Thus, the enzyme system is affected differently by F- and Br-, which would not be at all true if the results were due merely to an ionic atmosphere, or general salt effects. The inhibition noted for perchlorate seems especially marked and this represents the anion least likely to coordinate to zinc (or any other metal) [5]. Quite possibly perchlorate affects a different portion of the enzyme and thus exerts its influence.

The very small inhibition shown by several of the zinc complexing agents, ethylene-diamine, oxalate, and pyrophosphate, should be noted. Judging from the affinity of each of these species for a free zinc atom, large inhibitions would be expected for the concentrations tested. However, each of these species seems to coordinate best to free zinc and in each case the affinity of zinc already bound to two (bidentate) ligands is extremely small [5]. Thus for ethylene diamine, for example, the first and second association constants are of the order of 10^6 and 10^5, respectively while the third is much smaller (about 10 [1]. Vallee and Coombs have noted, that the affinity of 1,10-phenanthroline for Zn in liver alcohol dehydrogenase most closely equals the third association constant of 1,10-phenathroline for aqueous zinc ion. This same correlation is noted throughout the present work, thus the $K_{E,I}$ found for 2,2'-dipyridyl (6×10^{-4}) agrees best with the dissociation constant of Zn (2,2'-dipyridyl)$^{++}$

which is 2×10^{-4}, rather than with the smaller values of the mono-[3] and di-complexes [5], as well as the poor inhibition caused by ligands whose third affinity constant for zinc is slight. The explanation for the correlation may be that the zinc in the enzyme is octahedrally coordinated to the enzyme and is bound at more than two coordination positions.

In conclusion, a consistent picture of the behavior indicated in the present study is that zinc in alcohol dehydrogenase binds both the coenzymes and substrates, while it is itself bound octahedrally to the enzyme at several points of attachment (for further discussion se Parts II and III).

Acknowledgements. Thanks are due to Mr. L. G. Falksveden for skilful technical assistance.

The authors are indebted for financial support given by *Statens Medicinska Forskningsråd, Statens Naturvetenskapliga Forskningsråd, Knut och Alice Wallenbergs Stiftelse, The Rockefeller Foundation* and *Institutet för Maltdrycksforskning.*

REFERENCES

1. Theorell, H., Nygaard, A. P. and Bonnichsen, R. *Acta Chem. Scand.* **9** (1955) 1148.
2. Vallee, B. L. and Hoch, F. L. *J. Biol. Chem.* **225** (1957) 185.
3. Vallee, B. L., Williams, R. J. P. and Hoch, F. L. *J. Biol. Chem.* **234** (1959) 2621.
4. Vallee, B. L. and Coombs, T. L. *J. Biol. Chem.* **234** (1959) 2615.
5. *Stability Constants,* Ed. Bjerrum, N., Schwartzenbach, G. and Sillén, L. G. Chem. Soc. London 1957.
6. Bonnichsen, R. K. and Brink, N. G. in Colowick, S. P. and Kaplan, N. O. *Methods in Enzymology,* **Vol. I,** p. 495, Academic Press, New York, 1955.
7. Dalziel, K. *Acta Chem. Scand.* **11** (1957) 397; **12** (1958) 459.
8. Theorell, H. and Nygaard, A. P. *Acta Chem. Scand.* **8** (1954) 877.
9. Theorell, H. and McKinley McKee, J. S. *Ibid.* **15** (1961) 1811. (*Paper II of this series*).
10. *Ibid.* **15** (1961) 1797. (*Paper I of this series*).

Received March 28, 1961.

ACTA CHEMICA SCANDINAVICA 15 (1961) 1875–1884

Studies on the Hydrolysis of Metal Ions

37. Application of the Self-Medium Method to the Hydrolysis of Beryllium Perchlorate

BIRGITTA CARELL and ÅKE OLIN

Department of Inorganic Chemistry, Royal Institute of Technology, Stockholm 70, Sweden

The hydrolysis of beryllium perchlorate has been studied in the concentration range $B = 0.04-1$ M by measurements of $\log h$ at 25°C. The same set of complexes as found by Kakihana and Sillén at low beryllium concentrations, namely Be_2OH^{3+} and $Be_3(OH)_3^{3+}$, can also explain the present data.

$3\ Be^{2+} + 3\ H_2O \rightleftharpoons Be_3(OH)_3^{3+} + 3\ H^+$; $\log\beta_{3,3} = -8.66 \pm 0.03$ ($B = 0.04$ to 1 M)

$2\ Be^{2+} + H_2O \rightleftharpoons Be_2OH^{3+} + H^+$; $\log\beta_{1,2} = -3.22 \pm 0.05$ ($B = 0.04$ to 0.32 M), -3.18 ± 0.03 ($B = 0.64$ M), -3.15 ± 0.03 ($B = 1$ M).

In a recent study [1] on the hydrolysis of lead perchlorate in concentrated solutions, evidence was presented for the formation of Pb_2OH^{3+} and $Pb_4(OH)_4^{4+}$. When the average number of OH^- per Pb(II), Z, exceeded about 0.1 however, deviations between the experimental data and the calculated curves $Z(\log h)_B$ occurred. It was suspected then that the cause was variations in the activity factors.

From emf studies on the hydrolysis of Be(II), Kakihana and Sillén [2] found evidence for the formation of Be_2OH^{3+}, $Be_3(OH)_3^{3+}$ and in addition small amounts of $Be(OH)_2$ at low concentrations. Although the case of beryllium is not strictly analogous to that of Pb(II) it was thought to be of interest to study concentrated $Be(ClO_4)_2$ solutions to see if similar deviations were observed for this metal.

SYMBOLS

B	total concentration of Be(II)
b	concentration of free Be^{2+}
H	analytical hydrogen ion concentration, often negative
h	actual hydrogen ion concentration
Z	average number of OH^- split off by one Be(II)
$\beta_{p,q}$	equilibrium constant of the reaction

$$qBe^{2+} + pH_2O \rightleftharpoons Be_q(OH)_p^{(2q-p)+} + pH^+$$

$y(x)_v$ y as a function of x at constant v

All concentrations are expressed in M (moles/l) and equilibrium constants are given on the M scale.

METHOD

The hydrolysis has been followed by measurements of log h using the cells

Ref/B M Be(II), H M H^+, (3−H−2B) M Na^+, 3 M ClO_4^-/glass (I)

$$E = E_I^0 + 59.15 \log h + 59.15 \log f_{H^+} + E_j \quad (1)$$

Ag, AgCl/0.015 M Ag^+, B M Be(II), H M H^+, (2.985−H−2B) M Na^+, 3 M ClO_4^-/glass (II)

$$E = E_{II}^0 + 59.15 \log h - 59.15 \log [Ag^+] + 59.15 \log f_{H^+}/f_{Ag^+} \quad (2)$$

The reference half-cell in (I) was

/3 M $NaClO_4$/0.01 M Ag^+, 2.99 M Na^+, 3 M ClO_4^-/Ag, AgCl (III)

In some of the experiments with cell (I) the glass electrode was replaced by a quinhydrone electrode.

The experiments were carried out as potentiometric titrations and log h was varied by addition of $HClO_4$ or $NaHCO_3$.

EXPERIMENTAL

Materials and analysis. $HClO_4$, $NaClO_4$ and $AgClO_4$ were prepared and analysed as described in Refs.[3,4].

$NaHCO_3$ solutions were prepared from $NaHCO_3$ (Merck p.a.) and, after filtration, were used without further purification.

$Be(ClO_4)_2$ was prepared *via* the chloride. Beryllium metal (Pechiney) was dissolved in redistilled HCl, the chloride solution was evaporated to a thick syrup and finally the perchlorate was formed by the addition of $HClO_4$ which completely displaced the HCl. The $Be(ClO_4)_2$ was once recrystallised from $HClO_4$. Beryllium was determined as BeO by precipitating $Be(OH)_2$ with gaseous NH_3 in a platinum vessel and igniting the precipitate at 1 000−1 100°C.

$[ClO_4^-]$ was found by ion exchange methods, and the analytical hydrogen ion concentration, H, was calculated as $[ClO_4^-] - 2B$. The value of H was checked by emf methods as described later.

Glass electrodes. Beckman glass electrodes (No. 1 190−808) were used. They were checked against the hydrogen electrode as described in Ref.[4]

Experimental details. In order to obtain an overlap between the measurements of Kakihana and Sillén and our own, we started the series of measurements with fairly dilute solutions. The values of B used were, 0.03973; 0.07944; 0.1589; 0.3178; 0.64 and 1 M.

The composition of the equilibrium solutions was

$$B \text{ M Be(II)}, H \text{ M } H^+, (3-H-2B) \text{ M } Na^+, 3 \text{ M } ClO_4^-$$

H was often negative so that the solutions were deficient in hydrogen ions. The titrations were started either from slightly hydrolysed solutions ($Z \simeq 0.01$), adding $NaHCO_3$ solution, or from solutions with $Z \simeq 0.4$, adding $HClO_4$. The last procedure was found to be best suited for the highest values of B, since the bubbles of CO_2 formed on the introduction of HCO_3^- sometimes adhered to the glass electrode, thereby causing erroneous emf's.

In all runs B and $[ClO_4^-]$ (= 3 M) were kept constant. After each addition of acid or base the potential was followed till it reached a constant value. This seemed to be the

case after a few minutes. Since the sensitivity of the potentiometer used (Radiometer PHM 4a) is only 0.1 mV, we waited at least 15—20 min before the final reading was taken, to make sure that no slow drift in potential occurred. The agreement between the results obtained from titrations with increasing and decreasing Z seems to indicate that equilibrium was established in the Z range studied here.

The salt bridge was of the "Wilhelm" type and filled with 3 M $NaClO_4$. In self-medium studies it has been customary (*cf.* cells (I) and (III) above) to have in the salt bridge a solution which also contains the metal ion being investigated and at the same concentration as in the test solution. At low values of B one would expect that the choice of solution for the salt bridge is of less importance. When, however, B has a high value the choice may become important. In the present study we have chosen instead to eliminate the liquid junction potential when studying the highest values of B and have added Ag^+ to the solutions and made use of the cell (II).

The evaluation of log h from eqns. (1) and (2) necessitates a knowledge of $E°$. $E°$ can be determined at low values of B, simply by adding enough acid to repress the hydrolysis sufficiently, so that it is permissible to set $h = H$. For the two highest values of B studied here, this is no longer feasible since the hydrolysis is so strong that $h = H$ only at high acidities. This means that $E°$ is determined in a solution quite different from that where the main hydrolysis takes place and that for cell (I) the measured emf involves a large and unknown liquid junction potential. The $E°$ determined in these acid solutions was therefore regarded as only provisional and the final $E°$ was determined by the method described by Hietanen and Sillén [5]. The details of these calculations will be presented later.

RESULTS AND CALCULATIONS

It will be convenient for the sake of presentation of the data to consider first the results obtained with the four lowest values of B. For these concentrations E^0 was determined by suppressing the hydrolysis with $HClO_4$ till $h = H$

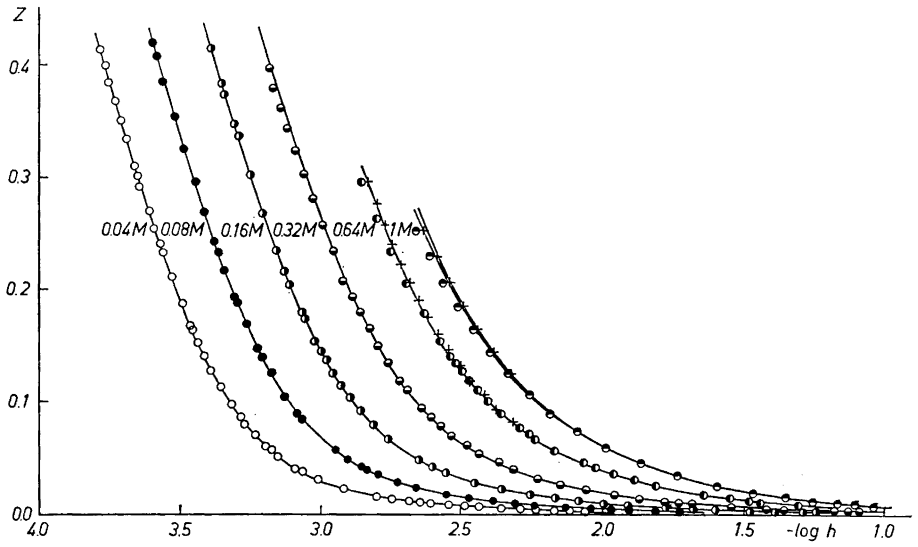

Fig. 1. Z as a function of log h. Circles represent data from measurements with cell(I) and crosses data from cell(II). The curves are calculated with the equilibrium constants given in Table 3.

Table 1. Corresponding values of $-\log h$ and Z from Cell (I).

B = 0.03972 M;	$-\log h$,	Z;	2.115,	0.003;	2.167,	0.003;	2.232,	0.004;	
2.287,	0.004;	2.353,	0.005;	2.435,	0.006;	2.484,	0.007;	2.541,	0.008;
2.607,	0.009;	2.645,	0.010;	2.682,	0.011;	2.745,	0.013;	2.808,	0.015;
2.917,	0.022;	3.009,	0.030;	3.063,	0.038;	3.090,	0.040;	3.149,	0.050;
3.152,	0.051;	3.176,	0.057;	3.196,	0.060;	3.235,	0.070;	3.269,	0.082;
3.284,	0.086;	3.318,	0.097;	3.356,	0.113;	3.390,	0.127;	3.391,	0.129;
3.418,	0.140;	3.438,	0.152;	3.458,	0.163;	3.463,	0.167;	3.489,	0.185;
3.531,	0.211;	3.560,	0.233;	3.570,	0.241;	3.595,	0.254;	3.609,	0.270;
3.614,	0.274;	3.646,	0.292;	3.651,	0.301;	3.661,	0.310;	3.686,	0.331;
3.690,	0.334;	3.712,	0.350;	3.729,	0.367;	3.724,	0.371;	3.754,	0.384;
3.764,	0.399;	3.779,	0.410;						
B = 0.07944 M;	$-\log h$,	Z;	1.724,	0.002;	1.810,	0.002;	1.905,	0.003;	
1.968,	0.004;	2.040,	0.005;	2.128,	0.006;	2.240,	0.007;	2.307,	0.009;
2.385,	0.011;	2.469,	0.014;	2.555,	0.017;	2.643,	0.022;	2.658,	0.023;
2.724,	0.028;	2.795,	0.035;	2.836,	0.039;	2.855,	0.042;	2.905,	0.048;
2.945,	0.057;	3.068,	0.084;	3.085,	0.089;	3.127,	0.104;	3.176,	0.125;
3.208,	0.139;	3.223,	0.147;	3.265;	0.169;	3.296,	0.188;	3.308,	0.193;
3.345,	0.217;	3.364,	0.233;	3.379,	0.243;	3.416,	0.269;	3.446,	0.296;
3.487,	0.325;	3.519;	0.354;	3.564,	0.385;	3.583,	0.407;	3.605,	0.417;
B = 0.1589 M;	$-\log h$,	Z;	1.293,	0.002;	1.392,	0.002;	1.480,	0.003;	
1.599,	0.004;	1.678,	0.004;	1.777,	0.005;	1.907,	0.007;	1.987,	0.008;
2.084,	0.011;	2.165,	0.014;	2.253,	0.017;	2.354,	0.022;	2.447,	0.027;
2.552,	0.036;	2.598,	0.042;	2.631,	0.045;	2.648,	0.048;	2.748,	0.064;
2.753,	0.067;	2.812,	0.079;	2.853,	0.091;	2.897,	0.103;	2.926,	0.114;
2.934,	0.117;	2.958,	0.125;	2.980,	0.136;	3.000,	0.145;	3.022,	0.154;
3.058,	0.174;	3.066,	0.179;	3.112,	0.204;	3.130,	0.216;	3.161,	0.235;
3.198,	0.263;	3.208,	0.268;	3.250,	0.302;	3.293,	0.336;	3.308,	0.347;
3.345,	0.373;	3.353,	0.383;	3.392,	0.414;				
B = 0.3178 M;	$-\log h$,	Z;	1.086,	0.003;	1.127,	0.004;	1.177,	0.004;	1.243,
0.003;	1.296,	0.004;	1.357,	0.005;	1.418,	0.005;	1.489,	0.006;	1.541,
0.007;	1.609,	0.007;	1.685,	0.009;	1.730,	0.010;	1.781,	0.011;	1.869,
0.013;	1.957,	0.017;	2.050,	0.019;	2.058,	0.021;	2.139,	0.024;	2.151,
0.026;	2.229,	0.031;	2.303,	0.037;	2.312,	0.040;	2.363,	0.046;	2.434,
0.053;	2.476,	0.061;	2.569,	0.078;	2.604,	0.086;	2.638,	0.094;	2.691,
0.110;	2.718,	0.118;	2.758,	0.134;	2.797,	0.149;	2.826,	0.165;	2.858,
0.179;	2.883,	0.193;	2.920,	0.207;	2.954,	0.233;	2.993,	0.257;	3.027,
0.280;	3.059,	0.302;	3.090,	0.323;	3.120,	0.343;	3.142,	0.361;	3.171,
0.379;	3.184,	0.396;							
B = 0.64 M;	$-\log h$,	Z;	1.177,	0.007;	1.248,	0.007;	1.306,	0.008;	
1.368,	0.009;	1.443,	0.011;	1.483,	0.012;	1.550,	0.015;	1.811,	0.025;
1.884,	0.030;	1.959,	0.035;	2.026,	0.041;	2.063,	0.046;	2.170,	0.056;
2.238,	0.066;	2.261,	0.072;	2.292,	0.076;	2.350,	0.088;	2.356,	0.090;
2.403,	0.100;	2.439,	0.110;	2.471,	0.119;	2.496,	0.127;	2.518,	0.134;
2.538,	0.140;	2.574,	0.154;	2.631,	0.179;	2.696,	0.205;	2.750,	0.233;
2.800,	0.263;	2.853,	0.295;						
B = 1 M;	$-\log h$,	Z;	0.988,	0.006;	1.038,	0.007;	1.104,	0.008;	1.168, 0.010;
1.257,	0.011;	1.351,	0.015;	1.470,	0.018;	1.596,	0.025;	1.734,	0.034;
1.865,	0.045;	1.988,	0.058;	2.087,	0.073;	2.186,	0.089;	2.260,	0.106;
2.335,	0.125;	2.396,	0.144;	2.457,	0.164;	2.511,	0.184;	2.564,	0.206;
2.611,	0.229;	2.660,	0.252;						

Corresponding values of $-\log h$ and Z from Cell (II). Data are given only for $Z > 0.1$.

B = 0.64 M;	$-\log h$,	Z;	2.417,	0.106;	2.467,	0.118;	2.501,	0.132;	
2.545,	0.147;	2.581,	0.160;	2.618,	0.175;	2.650,	0.190;	2.682,	0.206;
2.713,	0.222;	2.743,	0.240;	2.772,	0.257;	2.800,	0.276;	2.838,	0.295;
B = 1 M;	$-\log h$,	Z;	2.255,	0.106;	2.326,	0.125;	2.384,	0.144;	2.441, 0.164;
2.489,	0.184;	2.541,	0.206;	2.629,	0.252				

and calculating E^0 from the emfs in these solutions with E_j values obtained from the calibration of the glass electrode. With E_0 known, log h was calculated from the emfs in hydrolysed solutions. The results are presented in Table 1 and as a set of curves $Z(\log h)_B$, where $Z = (h-H)/B$.

The set of curves $Z(\log h)_B$ is shown in Fig. 1. It may be characterized as follows. For $0.2<Z<0.4$ the curves are parallel with a spacing along the log h axis at constant Z

$$t = (\Delta \log B/\Delta \log h)_Z \simeq 1.5 \tag{3}$$

For $Z<0.2$ the value of t tends to decrease, this tendency being more pronounced the higher the value of B. Z apparently approaches 0 slowly, indicating that the last surviving complex contains only one or two OH^- groups. This characteristic was also shown by the set of $Z(\log h)_B$ curves obtained by Kakihana and Sillén. At the outset therefore, it seemed likely that the same complexes, namely Be_2OH^{3+} and $Be_3(OH)_3^{3+}$, proposed to explain their data, could also explain ours. We decided, however, not to make use of their findings and have started with our data, to determine what complexes are formed, although these data were obtained with solutions in which the activity factors may be expected to vary on account of the fairly large change in medium on going from 0.04 to 0.32 M Be(II). The computational methods have been deliberately chosen to be different from theirs.

Complexes formed at low Z. We shall start by considering the data for $Z<0.01$. Putting $b \simeq B$ we find for the formation of a set of complexes $Be_q(OH)_p^{(2q-p)+}$

$$Z = \Sigma p\beta_{p,q}B^{(q-1)}h^{-p} = \Sigma K_p h^{-p} \tag{4}$$

For each value of p we may construct a set of normalised curves $Z(-\log X)$, where $X = K_p^{1/p}/h$, and compare these with the experimental curves $Z(\log h)_B$. Only for $p = 1$ a satisfactory agreement is found and the last surviving complex is thus $Be_qOH^{(2q-1)+}$. Information on the value of q can be obtained from the relative positions of the $Z(\log h)_B$ curves. One way of doing this, which at the same time offers a check on H, will be given.

The analytical hydrogen ion concentration was calculated from the analysis of Be and ClO_4^- as $H' = [ClO_4^-]-2B$. These analyses may be somewhat in error and we shall put the error so caused in H equal to εB, corresponding to ε H^+ per Be(II). For a given value of B we have

$$H = H' + \varepsilon B \tag{5}$$

$$h = H' + \varepsilon B + \beta_{1,q}B^q h^{-1} \tag{6}$$

where h is found from the measured emf. $(h-H')$ is plotted as a function of h^{-1} and the intercept on the $(h-H')$-axis (εB) and the slope ($\beta_{1,q}B^q$) of the line are determined. A similar method has been used by Hedström [6].

In order to obtain sufficient accuracy log h was measured with the quinhydrone electrode. ε was found to be 0.0035 ± 0.0005, which corresponds to an error in the beryllium analysis of 0.2 %.

q was found to be 2, by plotting the logarithm of the numerical value of the slope against log B. The complex is thus Be_2OH^{3+}.

Be_2OH^{3+} can only account for the data at low Z, and larger complexes must be formed when Z increases. Information on these complexes has been obtained by calculating

$$\bar{p} = \frac{\Sigma p[Be_q(OH)_p]}{\Sigma[Be_q(OH)_p]} \quad ; \quad \bar{q} = \frac{\Sigma q[Be_q(OH)_p]}{\Sigma[Be_q(OH)_p]} \qquad (7),\ (7a)$$

$\bar{p}$ and $\bar{q}$ are thus average values of p and q for the complexes formed. A set of formulas for these calculations have been given by Sillén [7]. Of these the following have been used.

$$R = b/B + \Sigma[Be_q(OH)_p]/B = 1 - \int_0^Z (\partial \log h/\partial \log B)_Z \, dZ \qquad (8)$$

$$\ln b = R + \ln B - 1 - \int_{\ln h}^{\infty} Z \, d\ln h \qquad (9)$$

The integral in (9) was calculated from the experimental data starting from $Z = 0.005$ onwards. The residual integral was found on the assumption that Be_2OH^{3+} is the only complex present at $Z < 0.005$, and with a provisional value of $\beta_{1,2}$ (5.75×10^{-4})

$$\int_{\ln h}^{\infty} Z \, d\ln h = \int_h^{\infty} \beta_{1,2} B \, h^{-2} \, dh = \beta_{1,2} B \, h^{-1} \qquad (10)$$

$\bar{p}$ and $\bar{q}$ was then obtained from

$$\bar{p} = BZ/(RB-b) \quad ; \quad \bar{q} = (B-b)/(RB-b) \qquad (11),\ (11a)$$

A straight line drawn through the points $(\bar{q},\bar{p})$ passes close to (2,1) and (3,3). The complexes formed are thus shown to be Be_2OH^{3+} and $Be_3(OH)_3^{3+}$, in agreement with the findings of Kakihana and Sillén.

Whereas there is no choice at the lower end of the line other than Be_2OH^{3+}, higher complexes than $Be_3(OH)_3^{3+}$ might also form at the other end of the line. In order to satisfy the equation of the line these would be $Be_4(OH)_5^{3+}$ ($p/q = 1.25$), $Be_5(OH)_7^{3+}$ ($p/q = 1.4$), *etc.* In order to test this possibility we have calculated the ratio $\bar{p}/\bar{q}$ for the complexes other than Be_2OH^{3+}. [Be_2OH^{3+}] was calculated using three provisional values of log $\beta_{1,2}$ for each B value (-3.20, -3.25, -3.30, obtained from curvefitting at low values of Z). The results obtained for $B = 0.03973$ M is shown in Table 2 and it may be concluded that complexes with $p/q = 1$ predominate. The complexes present are thus Be_2OH^{3+} and $Be_3(OH)_3^{3+}$. The formation constants $\beta_{1,2}$ and $\beta_{3,3}$ have been determined by curve-fitting.

Method I. Comparison of experimental curves $Z(\log h)_B$ with normalized curves $Z(-\log v)_l$.

Normalized curves $Z(-\log v)_l$ have been calculated from

$$Z = v^{-1}(\sqrt{1 + v(1-Z)} - 1)^2 + l(\sqrt{1 + v(1-Z)} - 1)^3 \qquad (12)$$

Table 2. $B = 0.03973$ M.

		$\bar{q}/\bar{p}$ for complexes other than Be_2OH^{3+}	
Z	$\log \beta_{1,2} = -3.20$	-3.25	-3.20
0.15	0.95	1.00	1.03
0.16	0.96	1.00	1.03
0.17	0.97	1.00	1.04
0.18	0.96	1.00	1.03
0.19	0.96	1.00	1.03
0.20	0.98	1.01	1.04
0.22	0.97	1.00	1.02
0.24	0.97	1.00	1.02
0.26	0.97	0.99	1.02
0.28	0.98	1.00	1.02
0.30	0.98	1.00	1.01
0.32	0.99	1.01	1.02
0.34	0.98	1.00	1.01
0.36	0 99	1.00	1.02
0.38	0.98	0.99	1.01
0.40	1.00	1.01	1.02

for a number of different values of l. Eqn. (12) may be derived from the two basic eqns. (13) and (14)

$$B = b + 2\beta_{1,2}b^2h^{-1} + 3\beta_{3,3}b^3h^{-3} \tag{13}$$

$$BZ = \beta_{1,2}b^2h^{-1} + 3\,\beta_{3,3}b^3h^{-3} \tag{14}$$

by elimination of b and introduction of

$$v = 4B\beta_{1,2}h^{-1} \text{ and } l = 3\beta_{3,3}/(8B\beta_{1,2}^3) \tag{15), (16}$$

By comparing the experimental $Z(\log h)_B$ curve with the set of normalized curves $Z(-\log v)_l$ a best value of l is found and in the position of overlap between the two curves $\log \beta_{1,2}$ and $\log \beta_{3,3}$ are found from

$$\log \beta_{1,2} = \log v + \log h - \log (4B) \tag{15a}$$

and

$$\log \beta_{3,3} = \log l + 3\log \beta_{1,2} + \log (8B/3) \tag{16a}$$

This method has the great advantage that it involves a direct comparison of the experimental and normalized curves. From eqn. (16a) we see, however that when $\beta_{3,3}$ is calculated 3 times the uncertainty in $\log \beta_{1,2}$ is transferred to the value of $\log \beta_{3,3}$. But displacing the curves along the $\log h$ axis often calls for a new value of l. In this way $\log \beta_{3,3}$ stays more constant than would be expected from eqn. (16a).

Method II. Comparison of experimental curves $y(x)_Z$, ($\log B - \log h = y$; $\log B - 1.5 \log h = x$), with normalized $Y(X)_Z$. Method II provides a means of finding $\log \beta_{3,3}$ and $\log \beta_{1,2}$ independently and simultaneously. We have

$$B = b(1 + 3\beta_{3,3}\, b^2h^{-3} + 2\beta_{1,2}\, bh^{-1}) \tag{17}$$

$$Bh^{-1} = bh^{-1}(1 + 3\beta_{3,3}b^2h^{-3} + 2\beta_{1,2}bh^{-1}) \tag{18}$$

$$Bh^{-3/2} = bh^{-3/2}\ (1 + 3\beta_{3,3}b^2h^{-3} + 2\beta_{1,2}bh^{-1}) \tag{19}$$

and

$$Z = \frac{\beta_{1,2}bh^{-1} + 3\beta_{3,3}b^2h^{-3}}{1 + 2\beta_{1,2}bh^{-1} + 3\beta_{3,3}b^2h^{-3}} \tag{20}$$

which can be normalized by the following substitutions

$$k^2 = 3\beta_{3,3};\ u = kbh^{-3/2}\ ;\ v = \beta_{1,2}bh^{-1} \tag{21}$$

to give

$$X = x + \log k = \log u + \log (1 + 2v + u^2) \tag{22}$$

$$Y = y + \log\beta_{1,2} = \log v + \log (1 + 2v + u^2) \tag{23}$$

$$Z = \frac{v + u^2}{1 + 2v + u^2} \tag{24}$$

where x and y are the corresponding experimental coordinates

$$x = \log B - 1.5 \log h \tag{25}$$

$$y = \log B - \log h \tag{26}$$

Normalized curves $Y(X)_Z$ are calculated for a set of values of Z and compared with the experimental $y(x)_Z$. In position of best fit the equilibrium constants are found from eqns. (22) and (23).

Treatment of data for B = *0.64 and 1 M.* For the highest values of B, the E^0's in cells (I) and (II) were determined as described by Hietanen and Sillén [5]. From the analytical data (B and H), h was calculated using provisional values of $\log \beta_{1,2}$ and $\log \beta_{3,3}$. $\log \beta_{1,2}$ was varied between -3.11 and -3.23 with a 0.02 unit interval, whereas $\log \beta_{3,3}$ was kept constant at -8.66.

For cell (I) ($E - 59.15 \log h$) was plotted as a function of h. A linear plot was taken as a criterion for a correct choice of $\log \beta_{1,2}$, and E_I^0 was determined by extrapolation to $h = 0$. For cell (II) ($E - 59.15 \log h$) was also calculated and the criterion would here be a constant value for this quantity.

With $B = 1$ M, $\log \beta_{1,2} = -3.15$ gave values of ($E - 59.15 \log h$) for cell (I) and cell (II) which fulfilled the above requirements. With $B = 0.64$ M $\log \beta_{1,2} = -3.19$ gave best agreement for cell (I). For cell (II), however, no choice could be made since the determination of E_{II}^0 in this case was done in so acid solution that variations in $\log \beta_{1,2}$ did not produce a trend in E_{II}^0.

Values of the equilibrium constants. In Table 3 the values of the formation constants are given. They represent mean values of the results obtained by

Table 3.

B M	log $\beta_{1,2}$	log $\beta_{3,3}$	Z	
0.03973	−3.23 ± 0.04	−8.67 ± 0.03	> 0.4	
0.07944	−3.23 ± 0.04	−8.68 ± 0.03	> 0.4	
0.1589	−3.21 ± 0.03	−8.64 ± 0.03	0.4	
0.3178	−3.21 ± 0.03	−8.65 ± 0.03	0.3	(cell (I))
0.3178	−3.21 ± 0.03	−8.65 ± 0.03	0.4	(cell (II))
0.64	−3.18 ± 0.03	−8.64 ± 0.03	0.18	(cell (I))
0.64	−3.18 ± 0.03	−8.64 ± 0.03	0.25	(cell (II))
1	−3.15 ± 0.03	−8.66 ± 0.03	0.15	(cell (I))
1	−3.15 ± 0.03	−8.62 ± 0.03	0.2	(cell (II))

methods (I) and (II). The last column gives the highest value of Z at which these constants agree with our experimental results within 0.002—0.003 Z-units.

DISCUSSION

From Table 3 we see that the values of the equilibrium constants stay constant despite the fairly large change in medium. The trend in log $\beta_{1,2}$ towards higher values with increasing B is probably real, whereas for log $\beta_{3,3}$ no trend is seen. At low B the values of the constants agree well with those of Kakihana and Sillén, who found log $\beta_{1,2} = -3.24$ and log $\beta_{3,3} = -8.66$. An approximate constancy of the β's has also been found for other cations [1,5,8]. This fact suggests that the relative positions of the curves $Z(\log h)_B$ on the log h axis at large B's can be used to find the q values of the complexes formed.

The range in Z which can be accounted for is seen to diminish with increasing B. The calculated curves $Z(\log h)_B$ are seen to lie above the experimental ones. The case of Be(II) is thus quite similar to that of Pb(II) and the deviations start at about the same values of Z. A definite increase in the range of validity seems to occur with the measurements from cell (II).

The variation of E of cell (II) is expressed by eqn. (2). If $f_{H^+} = f_{Ag^+}$ in these solutions the measurements from this cell would give log h. Evidence for this comes from the fact that constant E^0s were obtained when h was varied at constant B. Also the E^0s obtained at different values of B seemed to be the same, as is seen from the table below which gives the results for the two glass electrodes , "A" and "B", both used with cell II.

B M	E^0_A mV	E^0_B mV
0.3178	−105.7	−135.2
0.64	−105.7	−135.3
1	−106.0	−135.1

For cell (I) the variation of E is expressed by eqn. (1). "E^0_I" is usually determined by plotting

$$(E - 59.15 \log h) = E^0_I + 59.15 \log f_{H^+} + E_j \qquad (27)$$

as a function of h and extrapolating to $h = 0$. Denoting the quantities relating to the solution with $h = 0$ with primes, we have

$$E_I^{0\prime} = E_I^0 + 59.15 \log f_H' + E_j' \quad (28)$$

Inserting this into eqn. (1) we find

$$E = E_I^{0\prime} + 59.15 \log h + 59.15 \log f_{H^+}/f_{H^+}' + E_j - E_j' \quad (29)$$

The measurements will therefore give log h only if $f_{H^+} = f_{H^+}'$ and the difference between E_j and E_j' is negligible or can be corrected for. At a high value of B the change in the composition of the medium is considerable even at moderate values of Z. We need not therefore be surprised that somewhat different results are obtained from measurements of the two cells for $Z > 0.1$.

Acknowledgements. The authors wish to thank Professor L. G. Sillén for his interest in our work and Mr. Frans Ericson for construction of the apparatus. The English of this paper has been corrected by Dr. Derek Lewis. This work has been supported by *Statens Tekniska Forskningsråd (Swedish Technical Research Council)*.

REFERENCES

1. Olin, Å. *Acta Chem. Scand.* **14** (1960) 814.
2. Kakihana, H. and Sillén, L. G. *Acta Chem. Scand.* **10** (1956) 985.
3. Olin, Å. *Acta Chem. Scand.* **11** (1957) 1445.
4. Olin, Å. *Acta Chem. Scand.* **14** (1960) 126.
5. Hietanen, S. and Sillén, L. G. *Acta Chem. Scand.* **13** (1959) 533.
6. Hedström, B. O. A. *Arkiv Kemi* **5** (1952) 457.
7. Sillén, L. G. *Mimeographed lecture sheets. Studies on chemical equilibria* (MIT, 1957).
8. Hietanen, S. and Sillén, L. G. *Acta Chem. Scand.* **13** (1959) 1828.

Received May 19, 1961.

ACTA CHEMICA SCANDINAVICA 15 (1961) 1885–1891

Studies Related to Naturally Occurring Acetylene Compounds

XXIX. Preliminary Investigations in the Genus *Bidens*: I. *Bidens radiata* Thuill and *Bidens ferulaefolia* (Jacq.) DC.

SYNNÖVE LIAAEN JENSEN and NILS ANDREAS SÖRENSEN

Institutt for Organisk Kjemi, Norges Tekniske Högskole, Trondheim, Norway

A preliminary investigation of 2 species of the genus *Bidens*, *viz. B. radiata* Thuill and *B. ferulaefolia* (Jacq.) DC. has revealed the occurrence of a number of the polyacetylenes previously isolated from several members of the genus *Coreopsis*. The diene-tetrayne I was found both in the nonpolar form I, R = H, and as a polar derivative supposed to be I, R = $OCOCH_3$. Further the trideca-1,3,5,11-tetraene-7,9-diyne II could be isolated in crystalline form. The presence of 1-phenylhepta-1,3,5-triyne could be demonstrated only spectroscopically. *B. radiata* furnished two fractions containing substances with broad absorption bands in the ultraviolet. One of them could be obtained pure, and preliminary constitutional work indicated the structure IV = 5-methyl-5′-buta-1,3-dienyl-2,2′-dithienyl.

Among the numerous genera of the *Compositae* family which have turned out to contain acetylenic compounds, the genus *Coreopsis* is leading as to the number of isolated polyacetylenes [1–4]. The genus *Coreopsis* belongs to the tribus *Heliantheae*, subtribus *Coreopsidinae*. In this subtribus the botanists have since long ago placed the genera *Coreopsis*, *Bidens* and *Cosmos* close together. As a matter of fact the opinion of the botanical experts has varied very much as to where in the three genera a given species has to be placed, and the examples are numerous where a species has synonymous names in all three genera [5]. So it was tempting to investigate some members of the genus *Bidens* to see if they did contain polyacetylenes, and if so, whether they were of the types earlier found in *Coreopsis*.

The UV spectra of the crude essential oils or acetone extracts of *Bidens ferulaefolia* Thuill and *B. radiata* (Jacq.) DC. at once revealed the presence of compounds with polyacetylenic chromophores. By chromatography some of these could be isolated in a pure state.

The trideca-1,11-diene-3,5,7,9-tetrayne (I, R = H) which was first isolated from some annual *Coreopsis* species [1]

$$R-CH_2-CH=CH-C\equiv C-C\equiv C-C\equiv C-C\equiv C-CH=CH_2 \quad (I)$$

$$CH_3-CH=CH-C\equiv C-C\equiv C-CH=CH-CH=CH-CH=CH_2 \quad (II)$$



$$-C\equiv C-C\equiv C-C\equiv C-CH_3 \quad (III)$$

was found in the root and the flowers as well as in the green parts of both the *Bidens* species investigated.

In the root extract of *B. radiata* and *B. ferulaefolia* and in the essential oil of the green parts of the latter there was found a polar compound with exactly the same UV spectrum as I. A similar compound has recently been isolated by J. Stene Sörensen from some perennial *Coreopsis* species, and is supposed to be I, R = $OCOCH_3$. In no case so far the amount of this polar form of I has been sufficient for isolation of the substance in pure, crystalline form.

From the essential oil of the flowers and green parts of *B. ferulaefolia* a crystalline compound of m.p. 70°C could be isolated which through its UV spectrum and the spectrum of its maleic anhydride adduct could be identified with the diyne-tetraene II first isolated [1] from the green part of some annual *Coreopsis* varieties.

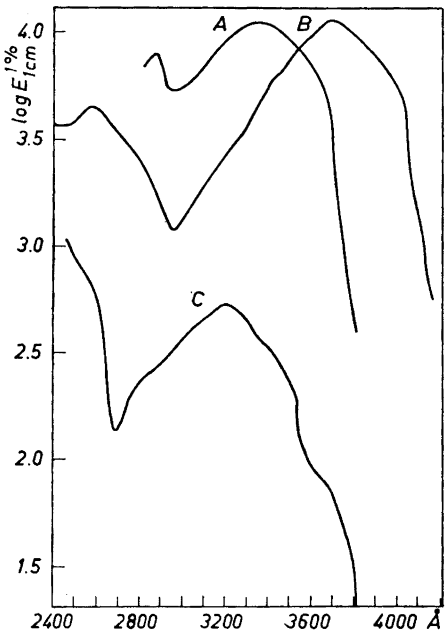

Fig. 1. Ultraviolet absorption in hexane of:

A. Compound with λ_{max} at 3 350 Å.
B. Compound with m.p. 42°C.
C. Compound with m.p. 42°C after hydrogenation.

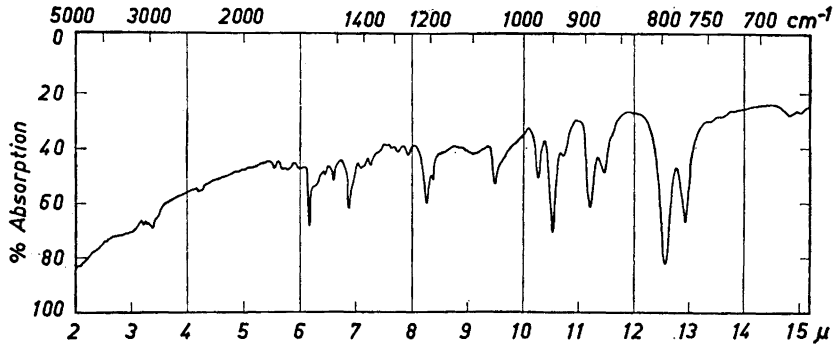

Fig. 2. Infrared absorption in KBr of compound with m.p. 42°C.

The green parts of *B. ferulaefolia* gave some fractions with UV spectra which seemed to indicate mixtures of II with phenyl-heptatriyne III characteristic of some perennial *Coreopsis* species [3]. The amount of these fractions was too small to allow the isolation of III in pure form. J. Stene Sörensen has, however, isolated III in a pure form from members of the genus *Bidens* [6], *viz. B. cernua* L. and *B. pilosa* L., thus III is also a polyacetylenic compound common to the genera *Coreopsis* and *Bidens*.

When the extracts from leaves and flowers of *B. radiata* were chromatographed on deactivated alumina, fractions were obtained on elution with 10—50 % benzene in petroleum ether which had only one very broad maximum in UV. From the 10 %-benzene eluates there could be isolated very small amounts of a substance with one broad maximum in UV in hexane solution at 3 350 Å, *cf.* Fig. 1. The amount of substance was too small for further investigations.

The eluates with 25 and 50 % benzene on evaporation afforded slightly yellow crystals, m.p. 42°C (evacuated tube). When tested in an open melting point tube, the substance only darkened without melting below 350°C.

The UV spectrum in hexane is reproduced in Fig. 1 and shows no relationship to the fine-structure spectra of polyacetylenic compounds. The IR spectrum had no absorption in the triple bond region, but maxima at 3 120, 1 513, 1 210 and 771 cm^{-1} were indicative of 2,5-disubstituted thiophene. Other bands characteristic of double bonds were present, but carbonyl or other characteristic groups were absent.

That the substance was really a sulphur containing compound, was confirmed by a quantitative sulphur determination (J.S.S.) giving 26.4 % S. This sulphur content is so high that the molecule must contain 2 sulphur atoms, since the molecular weight of about 120 calculated for one sulphur atom is too low to build up a chromophore with first maximum at 3 690 Å.

By catalytic hydrogenation with $Pd/BaSO_4$ the UV maximum moved down to 3 190 Å. A similar displacement was found in the reaction with maleic anhydride; first maximum of the crude adduct at 3 150 Å. The new substance thus seems to contain a butadienyl-grouping linked with a chromophore resistant to mild hydrogenation.

According to Sease and Zechmeister [7] dithienyl has one broad UV maximum at 3 010 Å. One alkyl group displaces this maximum 40—50 Å towards longer wavelengths; thus a 5,5′-dialkyl-2,2′-dithienyl should absorb around 3 100 Å.

The meagre experimental evidence thus point to a general formula IV.

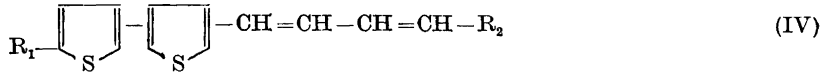

(IV)

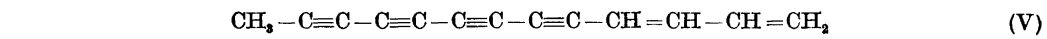

(V)

Bands of medium strength at 890 and 976 cm^{-1} in the IR spectrum of IV may indicate a vinyl group, that is $R_2 = H$. The sulphur content gives a molecular weight for 2 S intermediate between $R_1 = CH_3$ (232.35) and $R_1 = C_2H_5$ (246.47). Since all the polyacetylenic compounds from *Coreopsis* have C_{13} skeletons, and 4 of these, as mentioned above, occur in *B. radiata* and *B. ferulaefolia* we are inclined to assume that $R_1 = CH_3$, and that the compound, m.p. 42°C, is 5-methyl-5′-buta-1,3-dienyl-2,2′-dithienyl=IV, R_2=H, R_1= CH_3.

As the content of IV in the essential oil of *B. radiata* is rather small, and it thus would take a long time to collect enough of the natural substance for further constitutional work, IV was synthesized by Lars Skatteböl, and, as shown in a later communication [8], synthetic IV agrees in most properties well with those observed for the *B. radiata* substance. A minor difference in the IR spectra might be due to the fact that the natural substance because of the small amount available had to be measured as solid in a potassium bromide disk, whereas the synthetic substance was measured in carbon disulphide solution.

IV Is the first derivative of dithienyl to be found in nature *. Since the thiophene derivatives found in the *Compositae* seem to be closely related to aliphatic poly-ene-ynic compounds [4], attention might be drawn to the formal relationship between IV, $R_1 = CH_3$, $R_2 = H$ and trideca-1,3-diene-5,7,9,11-tetrayne V. V Has not so far been identified with a naturally occurring compound. In previous investigations [9,2] we have demonstrated that isomeric compounds R—C≡C—CH=CH—CH=CH_2 and R—  occur in *Compositae* plants indicating their possible origin from a common precursor. The phenyl isomer corresponding to V is the 1-phenylhepta-1,3,5-triyne III which so far is known only from *Bidens* and *Coreopsis* species.

EXPERIMENTAL

General method. The essential oils of the flowers and the green parts were isolated by steam distillation, whereas the roots were given 3 successive extractions with acetone on standing at room temperature for one day. The bulk of the acetone was removed in a vacuum, and the remaining solution shaken with petroleum ether after dilution with much water. The combined petroleum ether extracts were washed with water and dried over anhydrous sodium sulphate. Petroleum ether solutions were chromatographed on

* Since this work was carried out in 1955, another derivative of dithienyl has been isolated from *Tagetes* (African Marigolds) by J. H. Uhlenbroek and J. D. Bijloo [*Rec. trav. chim.* **78** (1959) 382].

alumina, slightly deactivated according to the method of Mancera *et al.*[10]; retention volume of the packed column 200 ml. Elution was carried out with mixtures of petroleum ether containing benzene in stepwise increasing amounts. At every concentration level 450 ml eluant were added, and the eluate was cut into three fractions of 150 ml each.

Bidens radiata Thuill.

Seed sample (*Hort. Bot. Univ. Osloensis*) cultivated on open ground at N.T.H. during the summer 1955.

Flowers. 1.2 kg of fresh flowers afforded 1.32 % of essential oil. A solution in petroleum ether was chromatographed on deactivated alumina. The first fraction with 10 % benzene in petroleum ether gave 2.2 mg of residue with a UV spectrum of pure I; calculated content in the fraction 0.82 mg. The residue crystallised, but the small amount of crystals which rapidly became dark in light, could not be investigated further.

The following fractions with 10 % benzene showed only two broad and undistinct absorption bands in UV. The total amount of substance in these fractions was only some 10 mg. But from these residues a small amount of white crystals could be isolated which in UV showed two broad maxima at 3 395 and 2 900 Å and some slight inflexions presumably caused by chromophore I. The amount was insufficient for further work.

The first fraction with 50 % benzene showed only one broad absorption band in UV at 3 650 Å. From the small residue (23.2 mg) a slightly yellow crystalline compound, m.p. 42°C, could be isolated by crystallisation from petroleum ether. According to the m.p. and the UV spectrum it is identical with one of the substances from the leaves, *vide infra.*

Leaves and stems. 2.3 kg of the green parts furnished 0.05 % of essential oil. Chromatography on alumina was carried out as above. The eluate with petroleum ether showed on absorption above 2 200 Å. The first fractions with 10 % benzene in petroleum ether gave UV spectra conform with that of I. From the absorption spectra a total content of 2.8 mg I was calculated, that is 0.24 % of the essential oil.

The final fraction with 10 % benzene in petroleum ether contained the same broad-banded chromophore as found in the flowers, first maximum at 3 350 Å; Fig. 1, curve A. The amount of material was small (5.3 mg), and the substance could not be obtained in the crystalline state.

The eluates with 25 % and with 50 % benzene in petroleum ether contained the other broad-banded chromophore found in the flowers. The total amount of material was about 55 mg. When this oily residue was dissolved in low boiling petroleum ether (40—60°C) and the solution stored at —10°C, 7.5 mg of slightly yellow crystals resulted. Attempts to do a m.p. determination in the usual open tube was unsuccessful; the crystals only darkened and turned slowly into carbonaceous material without melting. In an evacuated tube a rather sharp m.p. of 42°C was observed. UV spectrum, Fig. 1, curve B, λ_{max} = 3 690 Å, log $E^{1\%}_{1\,cm}$ = 4.04, λ_{max} = 2 580, log $E^{1\%}_{1\,cm}$ = 3.63; IR spectrum Fig. 2.

Maleic anhydride adduct: 1 mg of crystals was dissolved in 0.5 ml of pure benzene with 55 mg of freshly sublimed maleic anhydride in a tube and sealed under pure nitrogen. It was left in a water bath at 70°C for 4 h. The reaction solution was measured directly in the spectrometer; the maximum at 3 690 Å had disappeared. The solvent and the excess of maleic anhydride was removed in a vacuum at room temperature. The minute residue dissolved in alcohol showed λ_{max} at 3 150, inflexion at 3 050 Å.

Catalytic hydrogenation: 4.9 mg of crystals were hydrogenated in alcoholic solution with a Pd-catalyst. A quantitative determination of the consumption of hydrogen could not be carried out. The hydrogenation product was a viscous oil, UV spectrum, see Fig. 1, curve C.

Roots. 0.57 kg of fresh roots were extracted with acetone, and the extract transferred to petroleum ether, yield of crude extract 0.14 %.

Chromatography on alumina was carried out as above. The eluate with petroleum ether had no selective absorption in UV. The first fraction with 10 % benzene gave 25.4 mg of oily residue with the characteristic spectrum of I, calculated content 0.56 mg, that is 0.07 % of the root extract. Small amounts of the characteristic, unstable crystals of I could be isolated from petroleum ether in a refrigerator.

The further fractions with 10 % to 50 % benzene in petroleum ether appeared to contain a complicated mixture of compounds with different chromophoric systems. The material was insufficient for isolation of any of these in a pure state. When more starting material becomes available, a reinvestigation will be attempted.

Undiluted benzene eluted some 180 mg of an oil with a very indistinct spectrum of I. The calculated amount of this chromophore using the extinction coefficient of I, R = H, was only about 1.5 mg. As, however, it was of interest to ascertain that a polar compound with the diene-tetrayne-chromophore was present, a rechromatography was carried out, taking three fractions with 70 % benzene in petroleum ether and then three with undiluted benzene. The whole of the compound with the diene-tetrayne-chromophore was obtained in the third of the 70 % benzene fractions. The total amount of substance in this eluate was only a few mg. The UV spectrum was completely conform to I, R = H, and the calculated concentration in this fraction was 31 %. The residue was a viscous oil. The amount of substance was too small for further experiments.

Bidens ferulaefolia (Jacq.) DC.

Seed sample *(Hort. Bot. Univ. Osloensis)* cultivated on open ground at N.T.H. during the summer 1955.

Flowers. 530 g of fresh flowers gave a 0.053 % yield of essential oil, which was chromatographed on alumina as above. The eluate with petroleum ether showed no selective absorption in the UV region. The first fraction with 10 % benzene showed the characteristic spectrum of I, R = H, calculated content 0.8 mg, that is 0.3 % of the essential oil.

The subsequent fractions with 10 % benzene in petroleum ether and the first fraction with 25 % benzene had rather indistinct spectra in UV, but some of the main maxima agreed with those of the diyne-tetraene II. By crystallisation from petroleum ether in a refrigerator some 4 mg of slightly yellow crystals were obtained which showed a somewhat unsharp m.p. of 68 – 69°C; pure II has m.p. 71 – 72°C. The UV spectrum of this crystalline compound agreed very well with that of II.

Maleic anhydride adduct: 2.5 mg of the crystals were dissolved in 0.5 ml of pure benzene and 53 mg of maleic anhydride were added. The solution was prepared in a tube which was sealed under pure nitrogen. The tube was left for 5 h at 72°C and worked up as above. The residue was washed with cold petroleum ether which removed unreacted II. The insoluble residue showed the characteristic maxima of an ene-diyne-ene-grouping.

Leaves. 2.7 kg of green parts (leaves and stems) gave 0.14 % of essential oil separated by chromatography as above. As with the flowers the eluate with petroleum ether showed no selective absorption in the UV region.

The first fraction with 10 % benzene in petroleum ether showed the characteristic spectrum of I, R = H. The calculated amount of I was only 0.3 mg and was insufficient for further investigation.

The following fractions with 10 % benzene in petroleum ether had UV spectra in which very sharp peaks in the positions characteristic of III were superimposed on the indistinct spectrum of the diyne-tetraene II. Although crude crystals of II could be obtained, they always contained small amounts of III which gave extra peaks in the UV spectra.

Rechromatography using 8, 10 and 20 % benzene in petroleum ether as eluants gave a fairly complete separation. The first eluates showed UV spectra conform to that of phenylheptatriyne III whereas the final ones were conform to that of II.

The eluate with 50 % benzene had no selective absorption. With undiluted benzene there appeared small amounts of a substance with the distinct spectrum of the diene-tetrayne I. Thus also in this case a derivative of I with a polar substituent (R = $OCOCH_3$?) is present.

Roots. 530 g of fresh roots were extracted with acetone, and the lipoids transferred to petroleum ether; crude extract 0.34 %. Chromatography carried out as above gave an unusually simple picture. The characteristic spectrum of the diene-tetrayne I appeared in the first fraction with 10 % benzene, and the final fraction with 10 % benzene and all fractions with 25 % and with 50 % benzene showed no selective absorption. Undiluted benzene then eluted a compound with UV spectrum identical with that of I. The roots thus seem to contain only two polyacetylenic compounds, a non-polar and a polar type of I. The amount of polar I was too small for further study.

REFERENCES

1. Sørensen, J. Stene and Sørensen, N. A. *Acta Chem. Scand.* **8** (1954) 1741.
2. Sørensen, J. Stene and Sørensen, N. A. *Acta Chem. Scand.* **12** (1958) 756.
3. Sørensen, J. Stene and Sørensen, N. A. *Acta Chem. Scand.* **12** (1958) 765.
4. Sørensen, J. Stene and Sørensen, N. A. *Acta Chem. Scand.* **12** (1958) 771.
5. Sherff, E. E. *The Genus Bidens*. Botanical Series. Field Museum of Natural History, Vol. **XVI** , Chicago 1937.
6. Sørensen, J. Stene. *Unpublished.*
7. Sease, J. W. and Zechmeister, L. *J. Am. Chem. Soc.* **69** (1941) 270.
8. Skattebøl, L. *Acta Chem. Scand. To be published.*
9. Sørensen, J. Stene and Sørensen, N. A. *Acta Chem. Scand.* **8** (1954) 1763.
10. Mancera, O., Barton, D. R. H., Rosenkranz, V. and Djerassi, C. *J. Chem. Soc.* **1952** 1025.

Received May 2, 1961.

ACTA CHEMICA SCANDINAVICA 15 (1961) 1892–1904

Studies on Derivatives of Malachite Green. Protolytic Equilibria and Reaction-Rate Constants of *m*-Hydroxy and *m*-Methoxy Malachite Green

RUNE CIGÉN

Department of Inorganic and Physical Chemistry, Chemical Institute, University of Lund, Lund, Sweden

Dyestuffs of the Malachite Green type give in water solutions five species, two coloured (B and G) and three colourless (C, S′, and S″) between which the following reversible reactions take place:

$B + H^+ \rightleftharpoons G$; $C + 2H^+ \rightleftharpoons S' + H^+ \rightleftharpoons S''$; $G + H_2O \rightleftharpoons S''$; $B + H_2O \rightleftharpoons S'$; $B + OH^- \rightleftharpoons C$. The equilibria between B and G and between C, S′, and S″ are reached instantaneously whereas the hydration equilibria are reached only after a certain time.

Through spectrophotometric measurements dissociation, hydration and reaction-rate constants for the above indicated reactions have been determined for *m*-hydroxy and *m*-methoxy Malachite Green in water solutions having a constant ionic strength 0.5 M at 20°C. The method was the same as that used by the author in previous investigations of a similar nature.

A comparison between the constant values obtained shows that there is a marked difference between the *m*-hydroxy and *m*-methoxy derivatives only in strongly alkaline solutions.

A comparison between Malachite Green and the dyes now investigated shows that the influence of a *m*-hydroxy or a *m*-methoxy substituent is relatively small in acid and weakly alkaline solutions.

Previously, Malachite Green (MG) and a number of its *ortho* and *para* derivatives, with the substituent in the amino free phenyl group, were investigated [1]. In the present paper the corresponding investigations on the *m*-hydroxy MG and *m*-methoxy MG are reported. Further, the measurements have now been extended to also include the reactions in strongly alkaline solutions.

The reactions of the dyestuffs now investigated can be expressed with the same equilibrium scheme that was previously used by the author [2] in studies

on the influence of temperature on protolytic equilibria and reaction rates of Methyl Green.

m-Hydroxy and *m*-methoxy MG show very great similarities in regard to absorption curves, protolytic constants, and reaction rates. Only in strongly alkaline solutions is there found a marked difference between the two compounds. Previously investigated *p*-hydroxy and *p*-methoxy MG (Ref.[1]) show a striking mutual similarity when pH <6. At a higher pH the *p*-hydroxy derivative, on account of its acidic —OH group, can give rise to two additional forms, one coloured and one colourless, which cannot be formed by the corresponding methoxy compound. *o*-Hydroxy MG and *o*-methoxy MG have also been investigated and the results will soon be published in this journal. Like the corresponding *para*-derivatives the *ortho*-derivatives show great similarities in acid solutions and striking dissimilarities in alkaline solutions where the hydroxy compound can form two additional species, one coloured and one colourless.

Malachite Green can give two coloured ionic species,

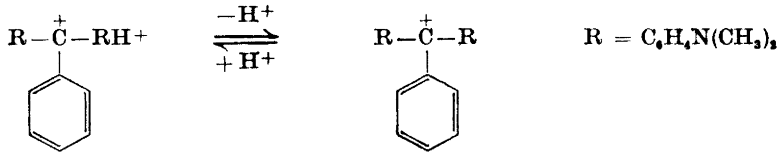

strongly acid solution (yellow) — weakly acid solution (blue-green)

p-Hydroxy and *o*-hydroxy MG can give another coloured from through splitting off a proton from the OH-group. The following quinoid structures then become possible:

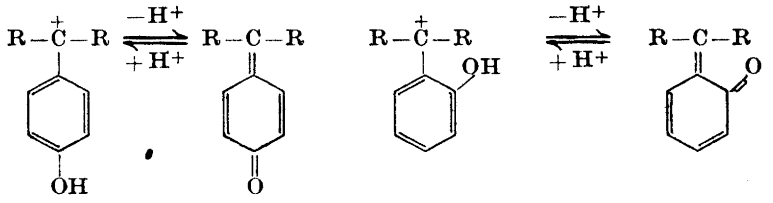

weakly acid solution — alkaline solution — weakly acid solution — alkaline solution

On the other hand, *m*-hydroxy MG can not give rise to a certain coloured form through splitting off a proton from the OH-group, since this does not give any possibility of an additional quinoid structure. Therefore we can formally use the same equilibrium scheme as for the *m*-methoxy derivative. In the Discussion part some differences in strongly alkaline solutions will be treated.

Neutral water solutions of the dyestuffs now investigated are beautifully blue-green. In strongly acid solutions they at first turn yellow and then are strongly discoloured. In alkaline solutions they are colourless. The reactions may be written schematically in the following way, where $R = C_6H_4N(CH_3)_2$ and $R_1 = C_6H_4OH$ or $C_6H_4OCH_3$

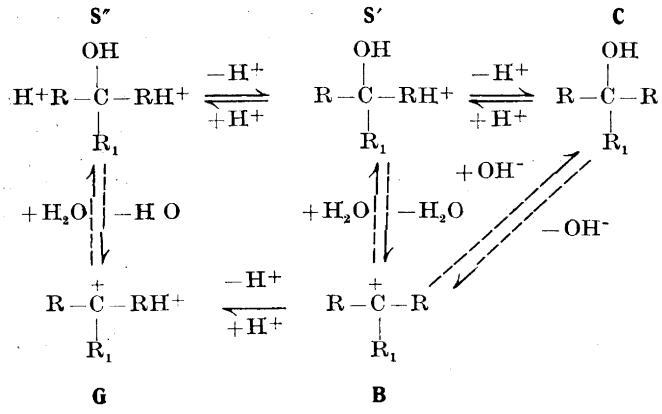

Definitions of constants and symbols

$$K_1 = \frac{[G]}{[B][H^+]} \; ; \; K_2 = \frac{[S'']_\infty}{[G]_\infty} \; ; \; K_3 = \frac{[S'][H^+]}{[S'']} \; ; \; K_4 = \frac{[C][H^+]}{[S']} \; ; \; K_6 = \frac{[B]_\infty}{[S']_\infty}$$

h $= [H^+]$; oh $= [OH^-]$; $K_w = [H^+][OH^-]$
k_1 = rate constant for the reaction $G + H_2O \rightarrow S''$
k_2 = » » » » » $S'' \rightarrow G + H_2O$
k_3 = » » » » » $B + H_2O \rightarrow S'$
k_4 = » » » » » $S' \rightarrow B + H_2O$
k_5 = » » » » » $B + OH^- \rightarrow C$
k_6 = » » » » » $C \rightarrow B + OH^-$
k = rate constant for the total reaction

ε_B, ε_G = the molar extinction coefficient of B and G
e_0, e_t, e_∞ = the absorbance per cm of a solution at the times 0 and t and at equilibrium (thickness of absorbing layer $d = 1$ cm)
E_0, E_t, E_∞ = the absorbance when $d \neq 1$ cm
e_B, e_G = the absorbance per cm of a solution containing only B or G
C_M = the total concentration of dyestuff

The constants in the equilibrium scheme can be calculated if the following data are determined for a large number of solutions with varying pH: (1) The absorbance, e_0, at the moment of mixing a dye stock solution with appropriate

buffers; (2) The absorbance, e_∞, when equilibrium is reached; (3) The pH of the solutions; (4) The total rate constant, k, for the reactions that change the intensity of the colour of the solutions either through hydration of the coloured forms (B and G) to the colourless (C, S′, and S″) or vice versa.

The following equation for e_0 can be derived

$$e_0 = \frac{e_B + hK_1e_G}{1 + hK_1} \tag{1}$$

Eqn. (1) requires that the dyestuffs are present only as the coloured form B (or G) when it is mixed with the buffer solution. This can not be realized for *m*-hydroxy MG or *m*-methoxy MG in water solutions. In acetate buffers, pH ≈ 5, these dyestuffs have a maximum colour intensity when about 97 % of the individual dye is present as the coloured ion B while the remaining 3 % is distributed among the colourless forms S″, S′, and C. Such dye-solutions, very weakly buffered, were used as stock solutions.

We can transform eqn. (1) and at the same time replace e_B and e_G with e_B' and e_G', where

$$\frac{e_B'}{e_B} = \frac{e_G'}{e_G} = \frac{[B]_0 + [G]_0}{[B]_0 + [G]_0 + [S'']_0 + [S']_0 + [C]_0}$$

and we obtain

$$\frac{h}{e_B' - e_0} = \frac{h}{e_B' - e_G'} + \frac{1}{K_1(e_B' - e_G')} \tag{2}$$

The terms K_1 and e_G' can be obtained from eqn. (2) by a graphical method when h, e_0, and e_B' have been determined.

For the equilibrium absorbance, e_∞, the following equation can be derived

$$e_\infty = \frac{e_B + hK_1e_G}{1 + 1/K_6 + K_4/hK_6 + hK_1(1 + K_2)} \tag{3}$$

In acid solutions, pH <2, we can approximate eqn. (3) and write

$$K_2 = \frac{e_G}{e_\infty} + \frac{e_B - e_\infty(1 + hK_1 + 1/K_6)}{hK_1e_\infty} \tag{4}$$

From eqn. (4) K_2 can be determined when e_B and e_G are known.

In weakly alkaline solutions eqn. (3) is approximated and transformed to

$$\frac{h}{e_\infty} = h\frac{1 + K_6}{K_6e_B} + \frac{K_4}{K_6e_B} \tag{5}$$

Eqn. (5) gives a straight line from which $(1 + K_6)/K_4$ is obtained.

KINETIC MEASUREMENTS

The equilibrium between the two coloured forms B and G is reached instantaneously. The same is true for the equilibrium between the colourless forms C, S′, and S″. The hydration equilibrium between a coloured and a corresponding colourless form and the equilibrium $B + OH^- \rightleftharpoons C$, on the other hand, are reached only after a measureable time. The following rate expression can be derived (*cf.* Refs.[2-3]).

$$k = \frac{k_2h^2 + k_4hK_3 + k_6K_3K_4}{h^2 + hK_3 + K_3K_4} + \frac{k_1hK_1 + k_3 + k_5oh}{hK_1 + 1} = \frac{1}{t} \ln \frac{e_0 - e_\infty}{e_t - e_\infty} \quad (6)$$

In strongly acid solutions eqn. (6) is approximated to

$$k = k_2 + \frac{k_1hK_1 + k_3}{hK_1 + 1} \quad (7)$$

and in strongly alkaline solutions to

$$k = k_3 + k_6 + k_5oh \quad (8)$$

Between these two extreme approximations we can make a smaller approximation of eqn. (6) in the pH-range 4—8.

$$k = \frac{k_4K_3h}{h^2 + hK_3 + K_3K_4} + k_3 \quad (9)$$

Eqn. (9) can be simplified further to

$$k = k_4h/K_4 + k_3 \quad (10)$$

when pH = 7—8.

Approximate values of k_1, k_2, and k_4 can be determined from eqns. (7) and (9) while eqns. (8) and (10) give exact values of k_3 and k_5 but not of k_6 since $k_6 \ll k_3$. Then non-approximated values of k_1, k_3, and k_4 can be calculated from eqn. (6). The rate constant k_6 is obtained from the expression $k_6 = k_5K_wK_6/K_4$. Finally K_3, K_4, and K_6 are obtained from eqns. (5) and (6) by combining equilibrium measurements with kinetic measurements.

EXPERIMENTAL

Chemicals and solutions. m-*Hydroxy Malachite Green.* The leuco compound was prepared in a nitrogen atmosphere, through condensation of *m*-hydroxybenzaldehyde with *p*-dimethylaniline in conc. hydrochloric acid and urea. The leuco compound was recrystallized from benzene-ethanol. Light green needles, m.p. 134°C, were obtained. The dyestuff was prepared by oxidizing, with lead dioxide, and the leuco compound dissolved in a calculated amount of 5 M HCl and diluted with 10 % acetic acid. From the oxidized product a perchlorate was prepared that was obtained as small green crystals after repeated recrystallizations from 2 % acetic acid. (Found: C 62.6; H 5.68; O 17.6; N 6.22; Cl 7.72. Calc. for $C_{23}H_{25}O_5N_2Cl$: C 62.1; H 5.66; O 17.98; N 6.30; Cl 7.97).

m-*Methoxy Malachite Green* was prepared in the same manner as the *m*-hydroxy derivative. The leuco compound was obtained as white needles, m.p. 126°C, and the perchlorate of the dyestuff as small dark green crystals. (Analysis of the perchlorate. Found: C 63.1; H 5.87; O 17.60; N 6.14; C 7.73. Calc. for $C_{24}H_{27}O_5N_2Cl$: C 62.8; H 5.93; O 17.43; N 6.11; Cl 7.72).

Stock solutions of the dyes were prepared by weighing and dissolving the perchlorates in acetone that then was diluted with a potassium chloride solution giving a final solution with ionic strength 0.5 M and containing 4 % of acetone. The stock solutions, with $C_M = 2 \times 10^{-5}$ M, were buffered very weakly with an acetate buffer, pH ≈ 5, and were diluted, when necessary, with 0.5 M potassium chloride containing 4 % of acetone. The perchlorates are so slightly soluble in water that it is almost impossible to prepare reproducible stock solutions with a fixed C_M by dissolving the perchlorates directly in 0.5 M KCl.

Hydrochloric acid, sodium acetate, disodium hydrogen phosphate, potassium dihydrogen phosphate, and *sodium hydroxide,* all of analytical grade, were used in the buffer solutions. *Potassium chloride* of analytical grade was added to keep the ionic strength constant (0.5 M).

Apparatus. The determinations of $[H^+]$ were carried out titrimetrically ($pH \leq 2$ and $pH \geq 12$) and potentiometrically ($2 < pH < 12$). For the potentiometric measurements a reference solution (pH = 2) having the composition 0.01 M HCl + 0.49 M KCl was used. In the present paper pH always means $-\log[H^+]$ and not $-\log a_{H^+}$. For the electrodes quinhydrone and platinumplate were used for $pH \leq 8$ and platinum-black and hydrogen gas for $pH > 8$. The temperature was kept at 20.0°C.

For the spectrophotometric measurements a modified Beckman DU quartz spectrophotometer with photomultiplier was used. The absorption cell house was kept at 20.0°C by pumping water from a thermostat through its walls and the whole apparatus was placed in a room kept constant at 20°C. Further details of the experimental technique may be found in Refs.[2,3].

MEASUREMENTS AND RESULTS

The absorption curves of the two dyestuffs now investigated show such a similarity that only curves for one of the dyestuffs have been drawn in Fig. 1. In Fig. 1 the absorption curves are seen for the blue-green ion B in acetate buffer, pH ≈ 5, and the yellow ion G in dilute hydrochloric acid. The molecular extinction coefficients were calculated from experimentally determined absorption curves and eqn. (3). ($e_B = C_M \varepsilon_B$ and $e_G = C_M \varepsilon_G$). The following values were obtained:

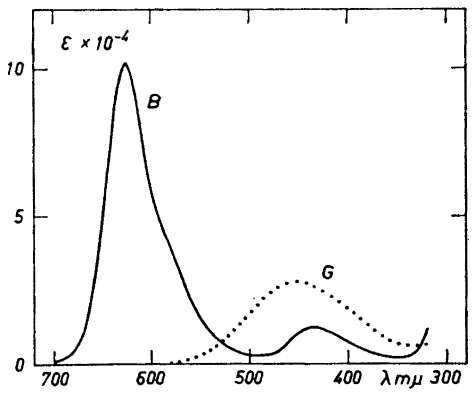

Fig. 1. *m*-Hydroxy Malachite Green. Absorption curves for the blue-green ion, B, in acetate buffer and the yellow ion, G, in dilute hydrochloric acid.

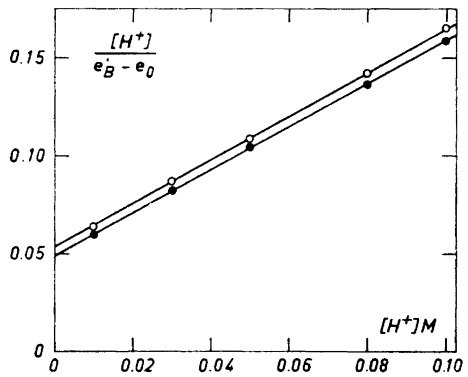

Fig. 2. $[H^+]/(e'_B - e_0)$ as a function of $[H^+]$ for the determination of K_1 for *m*-hydroxy MG (●) and *m*-methoxy MG (○).

m-hydroxy MG

$\lambda_{Bmax} = 621$ mμ resp. 430 mμ
$\varepsilon_{Bmax} = 9.4 \times 10^4$ resp. 1.8×10^4
$\lambda_{Gmax} = 454$ mμ
$\varepsilon_{GMax} = 2.9 \times 10^4$

m-methoxy MG

$\lambda_{Bmax} = 622$ mμ resp. 430 mμ
$\varepsilon_{Bmax} = 9.5 \times 10^4$ resp. 1.8×10^4
$\lambda_{Gmax} = 455$ mμ
$\varepsilon_{Gmax} = 2.9 \times 10^4$

Determination of K_1. The dye stock solutions were mixed with an equivalent volume of suitable HCl + KCl-buffers and e_0 was determined by extrapolation of the absorbancies to $t = 0$. The measurements were carried out at the wavelengths $\lambda = 621$ and 622 mμ where *m*-hydroxy MG and *m*-methoxy MG, respectively, have an absorption maximum. In Fig. 2 $[H^+]/(e'_B - e_0)$ is plotted against $[H^+]$. We get linear relations, and the slopes, l, and the intercepts, y, on the y-axis give according to eqn. (2) for *m*-hydroxy MG ($e'_B = 0.918$): $y = 0.0492$ M, $l = 1.096$, $e_G = 0.006$, $\mathbf{K_1 = 22.3 \pm 0.3\ M^{-1}}$ and for *m*-methoxy MG ($e'_B = 0.912$): $y = 0.0540$ M, $l = 1.104$, $e_G = 0.006$, $\mathbf{K_1 = 20.4 \pm 0.3\ M^{-1}}$.

Determination of $K_4/(K_6 + 1)$. The dye stock solutions were mixed with appropriate phosphate buffers and the equilibrium absorbancies, E_∞, were read off after 24 h. Table 1. $C_M = 5 \times 10^{-6}$ M, $d = 2$ cm. In Fig. 3 $[H^+]/E_\infty$ is plotted as a function of $[H^+]$. According to eqn. (5) linear relations are obtained which give for *m*-hydroxy MG: $y = 1.20 \times 10^{-7}$ M, $l = 1.088$, $K_4/(K_6 + 1) = 1.103 \times 10^{-7}$ M and for *m*-methoxy MG: $y = 1.31 \times 10^{-7}$ M, $l = 1.070$, $K_4/(K_6 + 1) = 1.224 \times 10^{-7}$ M.

Table 1. *m*-Methoxy and *m*-hydroxy Malachite Green. Determination of $K_4/(K_6 + 1)$. $C_M = 5 \times 10^{-6}$ M, $d = 2$ cm, $\lambda = 622$ mμ, $T = 20.0$°C.

	m-methoxy MG	*m*-hydroxy MG
$[H^+] \times 10^7$ M	$E_\infty = 2\,e_\infty$	$E_\infty = 2\,e_\infty$
14.48	0.858	0.857
8.32	0.812	0.812
5.30	0.758	0.761
3.45	0.689	0.696
2.26	0.605	0.617
1.400	0.500	0.513
0.824	0.376	0.390
0.372	0.215	0.229
0.1844	0.122	

Determination of K_2. The dye stock solutions were mixed with suitable HCl + KCl-buffers. The solutions were thermostatted and the equilibrium absorbancies, E_∞, were measured in 5 cm absorption cells. The constant K_2 was calculated from eqn. (4) when e_B, e_G, and K_6 were determined. The results

Table 2. *m*-Hydroxy Malachite Green. $e_\infty -$, $e_o -$, and k-values for determination of K_2, K_1, and k_1. $\lambda = 621$ mμ, $C_M = 1 \times 10^{-5}$ M, $d = 1$, 2, and 5 cm, $e_B = 0.946$, $e_B' = 0.918$.

[H+] M	e_∞	K_2	e_o	k min^{-1}	k_1 min^{-1}
0.010	0.1190	30.2	0.750	0.0403	0.152
0.020	0.0630	30.5			
0.030	0.0440	29.8	0.553	0.0728	0.152
0.040	0.0330	30.2			
0.050	0.0270	29.8	0.439	0.0917	0.152
0.060	0.0226	29.8			
0.080	0.0174	29.3	0.330	0.1091	0.152
0.100	0.0140	29.3	0.287	0.1163	0.151
Mean		29.9			0.152

are recorded in Tables 2 and 3. From these tables the following mean values are obtained: *m*-hydroxy MG, $\mathbf{K_2 = 29.9 \pm 0.6}$; *m*-methoxy MG, $\mathbf{K_2 = 33.7 \pm 0.7}$.

Kinetic measurements. If the dye stock solutions are mixed with NaOH + KCl-buffers, the solutions are decolourized with a rate that is directly proportional to [OH^-]. In Fig. 4 the rate constants of the decolourization, k in eqn. (8), are plotted against [OH^-]. Straight lines are obtained which pass almost through the origin. This means that in this pH-range $k_3 + k_6 \ll k_5 oh$. Therefore, only k_5 can be determined from Fig. 4. For *m*-hydroxy MG, $\mathbf{k_5 = 11.7 \pm 0.2\ min^{-1}\ M^{-1}}$ and for *m*-methoxy MG, $\mathbf{k_5 = 32.0 \pm 0.5\ min^{-1}\ M^{-1}}$.

The rate constant k_3 was determined from kinetic measurements in phosphate buffers, pH = 7—8. The approximate eqn. (10) permits a good determination of k_3 but not of k_4/K_4. In Fig. 5 k is plotted as a function of [H^+]. The straight lines give the following k_3 values: *m*-hydroxy MG, $\mathbf{k_3 = 0.00654 \pm 0.00010\ min^{-1}}$; *m*-methoxy MG, $\mathbf{k_3 = 0.00622 \pm 0.00010\ min^{-1}}$.

Table 3. *m*-Methoxy Malachite Green. $e_\infty -$, $e_o -$, and k-values for determination of K_2, K_1, and k_1. $\lambda = 622$ mμ, $C_M = 1 \times 10^{-5}$ M, $d = 1$, 2, and 5 cm, $e_B = 0.948$, $e_B' = 0.912$.

[H+] M	e_∞	K_2	e_o	k min^{-1}	k_1 min^{-1}
0.010	0.1170	33.9	0.755	0.0373	0.151
0.020	0.0624	33.9			
0.030	0.0428	33.7	0.568	0.0689	0.152
0.040	0.0324	33.8			
0.050	0.0264	33.5	0.451	0.0894	0.155
0.060	0.0220	33.6			
0.080	0.0166	33.7	0.349	0.1050	0.152
0.100	0.0134	33.6	0.307	0.1131	0.152
Mean		33.7			0.152

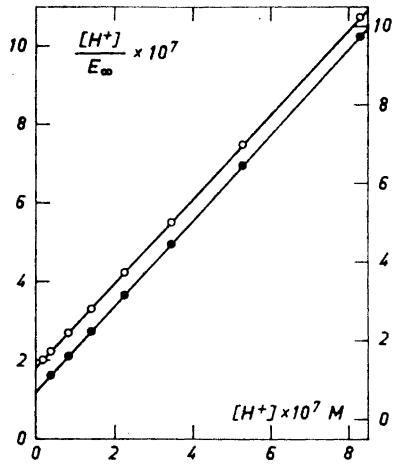

Fig. 3. $[H^+]/E_\infty$ as a function of $[H^+]$ for the determination of $K_4/(K_6 + 1)$ for *m*-hydroxy MG (●), ordinate left, and *m*-methoxy MG (○), ordinate right.

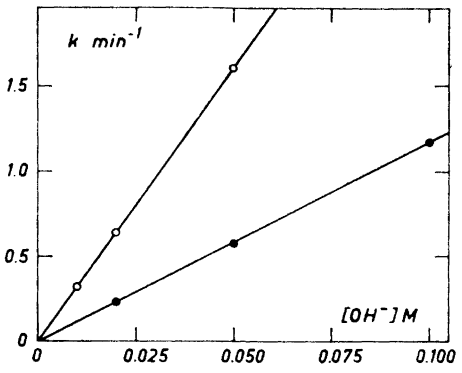

Fig. 4. k plotted against $[OH^-]$ for the determination of k_5. *m*-Hydroxy MG (●), *m*-methoxy MG (○).

Determination of k_1 *and* k_2. These rate constants were determined by kinetic measurements in HCl + KCl-buffers. The fading rate was determined and approximative values of k_1 and k_2 were initially calculated from eqn. (7). Tables 2 and 3 contain the k-values and the correct values of k_1 and k_2 calculated later from eqn. (6). The following values were obtained: *m*-hydroxy MG, $\mathbf{k_1 = 0.152 \pm 0.002\ min^{-1}}$ and $\mathbf{k_2 = 0.00508 \pm 0.00015\ min^{-1}}$; *m*-methoxy MG, $\mathbf{k_1 = 0.152 \pm 0.002\ min^{-1}}$ and $\mathbf{k_2 = 0.00451 \pm 0.00015\ min^{-1}}$.

Determination of k_4, K_3, K_4, *and* K_6. If k is differentiated with respect to $[H^+]$ in eqn. (9) k is found to have a maximum when $[H^+] = \sqrt{K_3 K_4}$. The dye stock solutions were partially decolourized by making them 0.02 M with respect to hydrochloric acid. The following reactions then occur $B + H^+ + H_2O \rightarrow G + H_2O \rightarrow S''$ and $B + H^+ + H_2O \rightarrow S' + H^+ \rightarrow S''$. These partially decoloured dye solutions were then quickly mixed with acetate buffers, and the colour was restored owing to the reactions $S'' \rightarrow S' + H^+ \rightarrow B + H^+ + H_2O$ and $S'' \rightarrow G + H_2O \rightarrow B + H^+ + H_2O$. The rate constants for the restoring of the colour were determined.

In Fig. 6 k is plotted as a function of pH. The following values are obtained: for *m*-hydroxy MG, $k_{max} = 0.167$ min^{-1} when pH = 4.88 which gives $K_3K_4 = 1.74 \times 10^{-10}$ M^2 and for *m*-methoxy MG, $k_{max} = 0.160$ min^{-1} when pH = 4.87 which gives $K_3K_4 = 1.82 \times 10^{-10}$ M^2.

If K_6 is fixed, K_4 can be determined from the known value of $K_4/(K_6 + 1)$, and K_3 from the known value of K_3K_4. Further, k_4 can be obtained from $k_4 = k_3K_6$ and k_6 from $k_6 = k_5K_wK_6/K_4$. Different values of K_6 were tried using eqn. (6). Within the pH-range 4—6 the terms k_4hK_3 and k_3 are dominating in eqn. (6). Therefore the approximate values of k_1 and k_2, obtained from

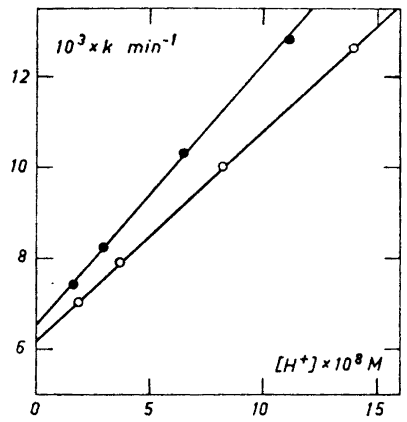

Fig. 5. k plotted against [H$^+$] for the determination of k_3. *m*-Hydroxy MG (●), *m*-methoxy MG (○).

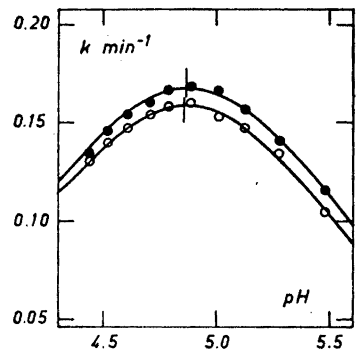

Fig. 6. k as a function of pH. The solid curves have been calculated from eqn. (6). The symbols have been determined by kinetic measurements in acetate buffers. *m*-Hydroxy MG (●), *m*-methoxy MG (○).

eqn. (7) by earlier measurements, can be used. The values of K_6 were chosen so that the curve calculated from eqn. (6) coincides best with the experimentally found k-values.

The best coincidence was found for *m*-hydroxy MG when $\mathbf{K_6 = 42.0 \pm 0.5}$ which gives $\mathbf{K_3 = (3.68 \pm 0.05) \times 10^{-5}\ M}$, $\mathbf{K_4 = (4.73 \pm 0.06) \times 10^{-6}\ M}$, $\mathbf{k_4 = 0.275 \pm 0.008\ min^{-1}}$ and for *m*-methoxy MG when $\mathbf{K_6 = 44.0 \pm 0.5}$ which gives $\mathbf{K_3 = (3.32 + 0.05) \times 10^{-5}\ M}$, $\mathbf{K_4 = (5.49 + 0.07) \times 10^{-6}\ M}$, $\mathbf{k_4 = 0.274 \pm 0.008\ min^{-1}}$. From a previous investigation we have $K_w = 1.24 \times 10^{-14}$ M^2 and k_6 can now be calculated from the relation $k_6 = k_5 K_w K_6 / K_4$. Thus for *m*-methoxy MG, $\mathbf{k_6 = (1.29 \pm 0.06) \times 10^{-6}\ min^{-1}}$ and for *m*-methoxy MG, $\mathbf{k_6 = (3.18 \pm 0.15) \times 10^{-6}\ min^{-1}}$.

In Fig. 6 it can be seen that the curves calculated from the non-approximated eqn. (6) agree with the experimentally obtained k-values.

By definition, $K_1K_2K_3K_4 = 1$. The values of this product that were determined are as follows: *m*-hydroxy MG, $K_1K_2K_3K_6 = 1.03$ and *m*-methoxy MG, $K_1K_2K_3K_6 = 1.00$.

DISCUSSION

A comparison between the values of the constants of *m*-hydroxy MG and *m*-methoxy MG shows a very great similarity when pH < 8. Corresponding values differ only by 0—16 %. On the other hand, in strongly alkaline solutions, there is a marked difference between the rate constants. The rate constants k_5 and k_6 for *m*-methoxy MG are, respectively, 2.7 and 2.5 times as great as those for *m*-hydroxy MG.

The explanation of the difference in strongly alkaline solutions is probably that the equilibrium scheme on page 1894 does not cover all of the possible reactions of *m*-hydroxy MG. The hydroxy-group gives off a proton in alkaline solutions, and the following reactions are obtained some of which can not be established by measurements.

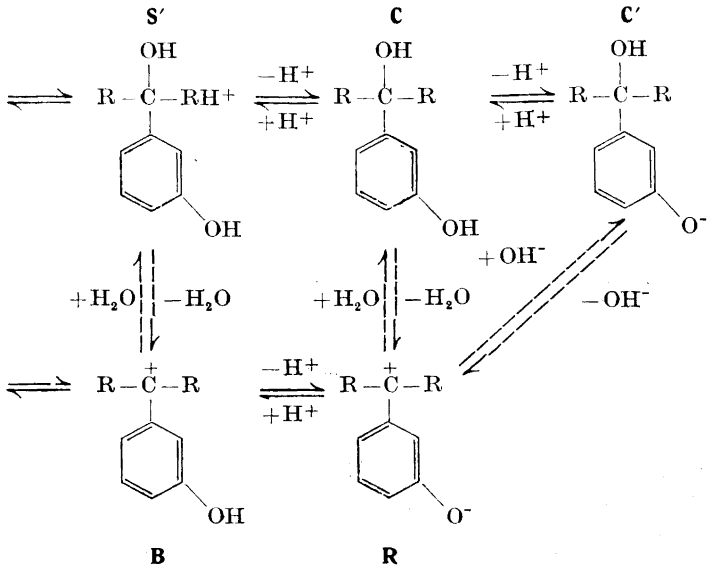

The following constants are defined as follows:

$$K_7 = \frac{[R][H^+]}{[B]} \; ; \; K_8 = \frac{[C'][H^+]}{[C]} \; ; \; K_9 = \frac{[C]_\infty}{[R]_\infty}$$

If B and R have a different colour, K_7 can be determined in the same way as K_1. However, B and R do not show any noticeable difference in colour and K_7 can not be determined. An idea of K_7 might be obtained if the equilibrium measurement were influenced by K_7 in the pH-range 7—8 where $K_4/(K_6 + 1)$ was determined. This is not the case and therefore pK_7 is certainly >9. Nor are the kinetic measurements in strongly alkaline solutions (pH $\gtrsim$ 12) appreciably influenced by K_7 which means that pK_7 is certainly < 11.

When pH >9 *m*-hydroxy MG, at requilibrium, is present only in the form of the colourless species S', C, and C' and this is the reason why K_8 and K_9 can not be determined. For the *para*- and *ortho*-derivatives the following values of the constants were obtained: *p*-hydroxy MG, $K_7 = 1.1 \times 10^{-7}$ M, $K_8 = 1.20 \times 10^{-10}$ M, and $K_9 = 8.4$ (Ref.[1]); *o*-hydroxy MG, $K_7 = 2.7 \times 10^{-9}$ M, $K_8 = 6.1 \times 10^{-10}$ M, and $K_9 = 0.15$ (to be published). For *m*-hydroxy MG both pK_7 and pK_8 probably lie in the range 9—10 which gives a value of 100—1 000 for K_9.

The reason why k_5 and k_6 are considerably greater for *m*-methoxy MG than for *m*-hydroxy MG, therefore, probably lies in the fact that the kinetic measurements at pH $\gtrsim$ 12 for the latter dyestuff give the total rate-constant for the reaction

$$R + OH^- \underset{k_6'}{\overset{k_5'}{\rightleftharpoons}} C'$$

From the kinetic measurements k_5' is obtained which is numerically identical with k_5 on page 1899. Of the two structures, corresponding to B and R, R has the greater electron density on the central methane carbon atom. Therefore it seems reasonable that the reaction $R + OH^- \rightarrow C'$ has a smaller rate constant than the reaction $B + OH^- \rightarrow C$. The latter reaction may be assumed to proceed with approximately the same speed for *m*-hydroxy MG as for *m*-methoxy MG. However, the rate constants of the reactions $B + OH^- \rightleftharpoons C$ or $R + H_2O \rightleftharpoons C$ can not be determined, for *m*-hydroxy MG as K_7, K_8 or K_9 are not known and the reaction $R + OH^- \rightarrow C'$ dominates the fading reactions at high pH.

Table 4. Comparasion between corresponding constants of Malachite Green and its *m*-hydroxy and *m*-methoxy derivatives.

	K_1	K_2	$K_3 \times 10^5$	$K_4 \times 10^6$	K_6	k_1 min^{-1}	k_2 min^{-1}	k_3 min^{-1}	k_4 min^{-1}
Malachite Green	28	22	2.7	5.8	68	0.168	0.00783	0.00647	0.439
m-Hydroxy »	22	30	3.7	4.7	42	0.152	0.00507	0.00654	0.275
m-Methoxy »	20	34	3.3	5.5	44	0.152	0.00451	0.00622	0.274

If the values of the constants of Malachite Green, *m*-hydroxy MG, and *m*-methoxy MG are compared, it is found from Table 4 that a *m*-hydroxy or a *m*-methoxy group in the amino free phenyl ring has a comparatively small influence on the equilibrium and reaction-rate constants. The meta-substituents do not give any marked resonance or steric effects. The inductive influence of the negative groups —OH and $-OCH_3$ may be seen in an about 30 % increase in the acid constants $1/K_1$ and K_3 and a somewhat greater increase in the hydration constants K_2 and $1/K_6$.

The author is indebted to Mr Olle Nilsson for valuable help in preparing the dyes and to Fil.mag. Gösta Bengtsson for assistance in some of the kinetic measurements.
The English has been revised by Dr. D. Karipides (USA).

REFERENCES

1. Cigén, R. *Protolysengleichgewichte und Reaktionsgeschwindigkeiten einiger basischer Triphenylmethanfarbstoffe* (Diss.), University, Lund 1956.
2. Cigén, R. *Acta Chem. Scand.* **14** (1960) 979.
3. Cigén, R. *Acta Chem. Scand.* **12** (1958) 1456.
4. Cigén, R. *Acta Chem. Scand.* **15** (1961) 1905.

Received May 26, 1961.

ACTA CHEMICA SCANDINAVICA 15 (1961) 1905–1912

Studies on Derivatives of Malachite Green. Protolytic Equilibria and Reaction Rate Constants of *o*-Methoxy Malachite Green

RUNE CIGÉN

Department of Inorganic and Physical Chemistry, Chemical Institute, University of Lund, Lund, Sweden

Previous investigations on protolytic and hydration equilibria and reaction rates of basic triphenylmethane dyes have been continued with the investigations of *o*-methoxy Malachite Green.

Three protolytic, two hydration, and six reaction rate constants have been determined by spectrophotometric measurements in aqueous solutions with the ionic strength 0.5 M at 20.0°C.

In earlier investigations on derivatives of Malachite Green [1], with the substituent *ortho* or *para* to the central carbon atom, electrostatic and steric effects were observed in the hydration reactions similar to those shown below for Malachite Green (R = C_6H_4—NMe_2)

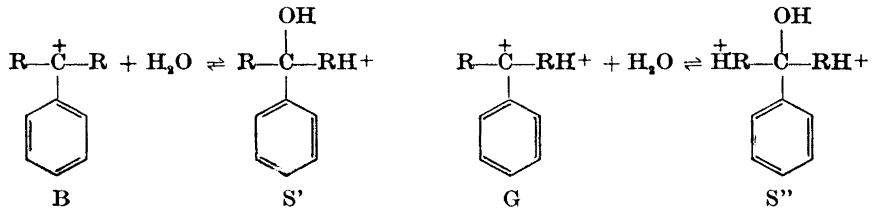

B S' G S''

In comparison with Malachite Green, the dyes with the electron attracting substituents —Cl and —NO_2 in the *para* position increases the tendency of the central carbon atom to bond a polarized water molecule which then splits off a proton by an intermolecular proton transfer.

With the same substituents in the *ortho* position the adding of a water molecule is made more difficult. Thus the rate constants of the reactions from left to right, stated above, are 30—50 times smaller for the *ortho* than for the *para* derivatives in adding a water molecule to the ion B, with one positive charge, and 70—300 times smaller in adding to the ion G, with two positive

charges. At the same time the equilibria are displaced towards the coloured species B and G. This indicates a strong steric hinderance. The conditions are analogous to the previously investigated sulfonated dyestuffs of the Malachite Green type [2], "Lichtgrün SF" and its *o*-chloro-derivative, "Brillantsäuregrün 6B".

Two *m*-derivatives, *m*-hydroxy MG and *m*-methoxy MG have been investigated up to the present time [3]. The effect of a substituent in the *m*-position is, as a rule, small and this proved to be true for the two investigated *m*-derivatives. Rate constants as well as dissociation and hydration constants differ only 0—30 per cent from the corresponding constants of Malachite Green.

Previous investigations (Ref.[1]) on *p*-hydroxy MG and *p*-methoxy MG have been continued now with investigations on *o*-methoxy MG. (The corresponding *o*-hydroxy-derivative has also been investigated and the results will be published soon.)

The "*ortho*"-effect of the group $-OCH_3$ (and $-OH$) is marked but not as pronounced as the effect of the groups $-Cl$ and $-NO_2$. The rate constants of the hydration and dehydration reactions of the *ortho*-methoxy- and *ortho*-hydroxyderivatives are only about a third of those of the corresponding *para*-derivatives.

o-Methoxy MG is beautifully blue-green in neutral water solutions, becomes yellow in strongly acid solutions and is colourless in alkaline solutions. The reactions which take place when the pH of a solution of *o*-methoxy MG is changed can be indicated schematically in the following manner, where $R = C_6H_4NMe_2$ and $R_1 = C_6H_4OCH_3$

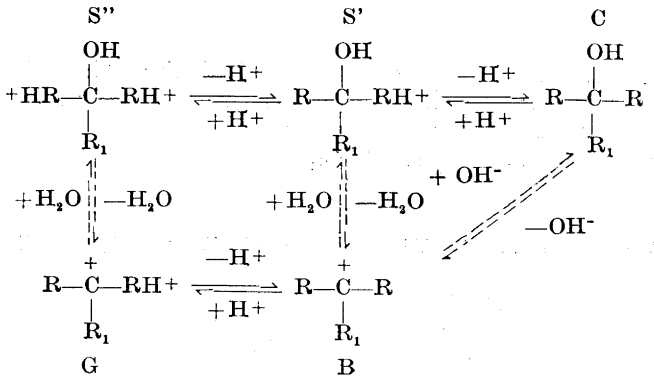

Definitions of constants and symbols, *cf.* a previous article by the author (*Acta Chem. Scand.* **15** (1961) 1892).

The constants in the equilibrium scheme can be calculated if the following data are determined for a large number of solutions with varying pH: (1) The absorbance, e_0, at the moment of mixing a dye stock solution with the appropriate buffers; (2) The absorbance, e_∞, when equilibrium is reached; (3) The pH of the solutions; (4) The total rate constant, k, for the reactions that change the intensity of the colour of the solutions either by hydration of the coloured forms (B and G) to colourless (C, S', and S") or *vice versa*.

EQUATIONS

The following equation for e_0 can be derived

$$e_0 = \frac{e_B + hK_1e_G}{1 + hK_1} \quad (1)$$

Eqn. (1) requires that the dyestuff is present only as the coloured form B (or G) when it is mixed with the buffer solutions. This can be realized in a dye stock solution that is buffered very weakly with acetate buffer, pH $\approx$ 5. In such a stock solution the dyestuff is present to $>>$ 99 % as the ion B.

Determination of K_1. Eqn. (1) is transformed to

$$\frac{h}{e_B - e_0} = \frac{h}{e_B - e_G} + \frac{1}{K_1(e_B - e_G)} \quad (2)$$

The terms K_1 and e_G can be obtained from eqn. (2) by a graphical method when h, e_0, and e_B have been determined.

The following equation for the equilibrium absorbance, e_∞, can be derived

$$e_\infty = \frac{e_B + hK_1e_G}{1 + 1/K_6 + K_4/hK_6 + hK_1(1 + K_2)} \quad (3)$$

In acid solutions, pH $\leq$ 2, eqn. (3) can be approximated and written

$$K_2 = \frac{e_G}{e_\infty} + \frac{e_B - e_\infty(1 + hK_1 + 1/K_6)}{hK_1e_\infty} \quad (4)$$

The constant K_2 can be determined from eqn. (4) when e_B, e_G and an approximate value of K_6 ($K_6 >> 1$) are known.

In very weakly alkaline solutions eqn. (3) is approximated and transformed to

$$\frac{h}{e_\infty} = \frac{h(1 + K_6)}{K_6e_B} + \frac{K_4}{K_6e_B} \quad (5)$$

Eqn. (5) gives a straight line from which e_B and $(1 + K_6)/K_4$ are obtained.

KINETIC MEASUREMENTS

The equilibrium between the two coloured forms B and G is reached instantaneously. The same is true for the equilibrium between the colourless forms C, S', and S''. The hydration equilibrium between a coloured and a corresponding colourless form and the equilibrium $B + OH^- \rightleftharpoons C$, on the other hand, are reached only after a measurable time. The following rate expression can be derived (*cf.* Ref.[1,4]).

$$k = \frac{k_2h^2 + k_4hK_3 + k_6K_3K_4}{h^2 + hK_3 + K_3K_4} + \frac{k_1hK_1 + k_3 + k_5oh}{hK_1 + 1} = \frac{1}{t} \ln \frac{e_0 - e_\infty}{e_t - e_\infty} \quad (6)$$

In strongly acid solutions eqn. (6) is approximated to

$$k = k_2 + \frac{k_1 h K_1 + k_3}{h K_1 + 1} \tag{7}$$

and in strongly alkaline solutions to

$$k = k_3 + k_6 + k_5 oh \tag{8}$$

Between these two extreme approximations we can make a smaller approximation of eqn. (6) in the pH-range 4—8.

$$k = \frac{k_4 h K_3}{h^2 + h K_3 + K_3 K_4} + k_3 \tag{9}$$

When pH = 7—8 eqn. (9) can be simplified further to

$$k = k_4 h / K_4 + k_3 \tag{10}$$

Approximate values of k_1, k_2, and k_4 can be determined from eqns. (7) and (9) while eqns. (8) and (10) give exact values of k_3 and k_5 but not of k_6 since $k_6 \ll k_3$. Then non-approximated values of k_1, k_2, and k_4 can be calculated from eqn. (6) when K_3 and K_4 have been determined. The rate constant k_6 is obtained from the expression $k_6 = k_5 K_w K_6 / K_4$.

The constants K_3, K_4, and K_6 are obtained from eqns. (9) and (5) in the following way. If k is differentiated with respect to $[H^+]$ in eqn. (9), k is found to have a maximum when $[H^+] = \sqrt{K_3 K_4}$

$$k_{max} = \frac{k_4 K_3}{K_3 + 2\sqrt{K_3 K_4}} + k_3 \tag{11}$$

Eqn. (11) can be written

$$k_{max} = \left(\frac{K_6}{K_4} \cdot \frac{K_4 K_3}{K_3 + 2\sqrt{K_3 K_4}} + 1 \right) k_3 \tag{12}$$

since $k_4 = k_3 K_6$. From eqn. (5) $(K_6 + 1)/K_4$ is obtained. But since $K_6 \gg 1$ for *o*-methoxy MG the expression $(1 + K_6)/K_4 \approx K_6/K_4$ can be used with sufficient accuracy. In eqn. (12) K_6/K_4, $K_3 K_4$, k_{max}, and k_3 are known and therefore K_3 can be calculated.

The K_4 is obtained from $\sqrt{K_3 K_4} = [H^+]_{k\ max}$ and K_6 from eqn. (5).

As a control of the correctness of the approximations undertaken the k-values can be calculated from the non-approximated eqn. (6), using values of the constants obtained, and the calculated results compared with those experimentally found. Further, by definition, $K_1 K_2 K_3 K_6 = 1$ which gives another possibility of control.

EXPERIMENTAL

Chemicals and solutions. o-Methoxy Malachite Green. The leuco compound was prepared in a nitrogen atmosphere by refluxing for 18 h *o*-methoxybenzaldehyde, (0.1 mole), *p*-dimethylaniline (0.3 mole), conc. hydrochloric acid (0.3 mole), and urea (0.1 mole). The leuco compound was recrystallized from benzene-ethanol. White needles, m.p. 152°C, were obtained. The dyestuff was prepared by oxidizing 3.6 g of the leuco compound dissolved in 5 ml of 5 M hydrochloric acid and diluted with 500 ml of 10 % acetic acid.

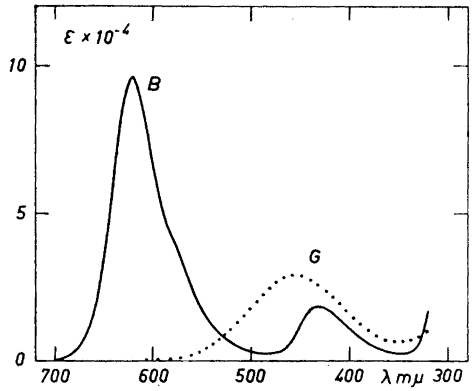

Fig. 1. *o*-Methoxy Malachite Green. Absorption curves: B is the curve for the blue-green ion $[(Me_2NC_6H_4)_2CC_6H_4OMe]^+$ in acetate buffer, G is the curve for the yellow ion $\left[\begin{matrix} Me_2NC_6H_4 \\ Me_2HNC_6H_4 \end{matrix}\right\rangle CC_6H_4OMe\Big]^{2+}$ in dilute hydrochloric acid.

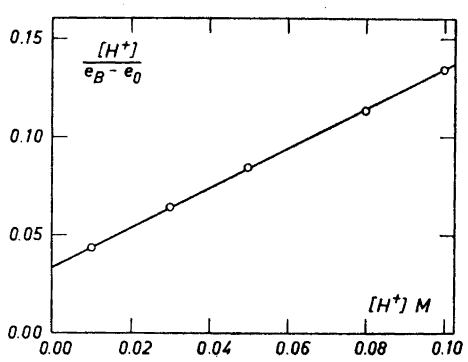

Fig. 2. $[H^+]/(e_B - e_0)$ plotted against $[H^+]$ for the determination fo K_1.

For an oxidizing agent 3.0 g of lead dioxide was used. From the oxidized product a perchlorate was prepared that was obtained as small green balls of needle-like crystals. (Found: C 62.7; H 6.01; O 17.45; N 5.89; Cl 7.51. Calc. for $C_{24}H_{27}O_5N_2Cl$: C 62.8; H 5.93; O 17.43; N 6.11; Cl 7.72).

Stock solutions of the dye were prepared in the same manner as in Ref.[3] Chemicals used for the buffer solutions and apparatus used for the measurements were the same as in Ref.[3]

MEASUREMENTS AND RESULTS

In Fig. 1 the absorption curves are seen for the blue-green ion B in acetate buffer and for the yellow ion G in dilute hydrochloric acid. The molecular extinction coefficients were calculated from the experimentally obtained absorption curves and eqn. (3) ($e_B = C_M \cdot \varepsilon_B$ and $e_G = C_M \cdot \varepsilon_G$). The following values were obtained: $\lambda_{B\ max} = 624$ mμ and 435 mμ; $\varepsilon_{B\ max} = 1.02 \times 10^5$ and 1.20×10^4, resp. $\lambda_{G\ max} = 452$ mμ; $\varepsilon_{G\ max} = 2.75 \times 10^4$.

Determination of K_1. The dye stock solution was mixed with an equivalent volume of suitable HCl + KCl-buffers and e_0 was determined by extrapolation of the absorbancies to $t = 0$. The measurements were carried out at the wavelength $\lambda = 620$ mμ, where $\varepsilon_B = 9.80 \times 10^4$. In Fig. 2 $[H^+]/(e_B - e_0)$ is plotted against $[H^+]$. A straight line is obtained. The slope l and the intercept y on the y-axis of this line and eqn. (2) give ($e_B = 0.980$): $y = 0.0335$ M; $l = 1.015$; $\boldsymbol{K_1 = 30.3 \pm 0.5\ M^{-1}}$.

Determination of K_2. The dye stock solution was mixed with HCl + KCl-buffers and the equilibrium absorbancies, e_∞, were measured in 1 and 5 cm absorption cells. K_2 was calculated from eqn. (4) where $K_1 = 30.3$ is known and $K_6 \gg 1$. $e_B = 0.980$ and $e_G \approx 0$ at the wavelength used, 620 mμ. The

Table 1. *o*-Methoxy Malachite Green $\lambda = 620$ mμ; $e_B = 0.980$; $T = 20.0$°C. Determination of K_1, K_2, and k_1.

[H+] M	e_∞	K_2	e_0	k min^{-1}	k_1 min^{-1}
0.010	0.359	4.71	0.748	0.0248	0.0487
0.020	0.220	4.70			
0.030	0.159	4.67	0.512	0.0361	0.0491
0.040	0.124	4.70			
0.050	0.1026	4.65	0.385	0.0426	0.0497
0.060	0.0878	4.59			
0.080	0.0674	4.58	0.272	0.0477	0.0496
0.100	0.0546	4.59	0.232	0.0516	0.0514
Mean		$K_2 = 4.65$			$k_1 = 0.0497$
					$k_2 = 0.0107$

Table 2. *o*-Methoxy Malachite Green. E_∞-values for determination of $K_4/(K_6 + 1)$. $\lambda = 624$ mμ; $C_M = 2.5 \times 10^{-6}$ M; $d = 2$ cm; $T = 20.0$°C.

[H+] $\times 10^8$ M	E_∞
14.00	0.453
8.24	0.427
3.72	0.360
1.844	0.280
0.774	0.168

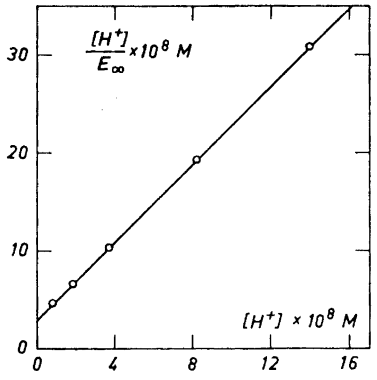

Fig. 3. [H+]/E_∞ plotted against [H+] for the determination of $K_4/(K_6 + 1)$.

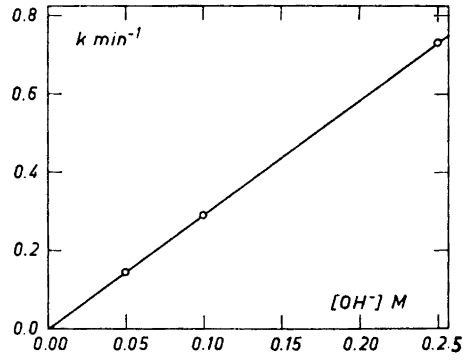

Fig. 4. The total rate constant k plotted against [OH^-] for the determination of k_5.

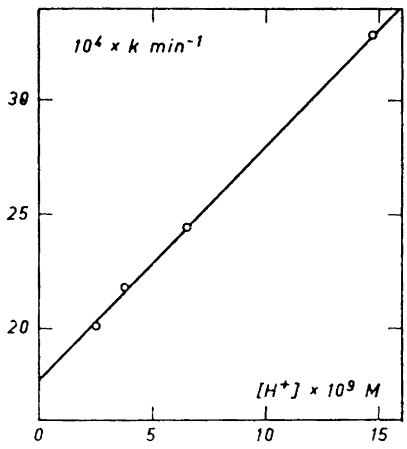

Fig. 5. The total rate constant k as a function of [H+] for the determination of k_3.

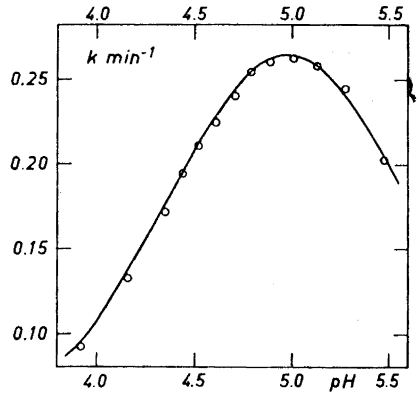

Fig. 6. The total rate constant k as a function of pH. The points represented by the symbols, O, are obtained experimentally; the full drawn curve is calculated from the non-approximated eqn. (6).

results are recorded in Table 1. From this table the mean value $K_2 = \mathbf{4.65 \pm 0.10}$ is obtained.

Determination of $K_4/(K_6 + 1)$. The dye stock solution was mixed with appropriate phosphate buffers and the equilibrium absorbancies, E_∞, (Table 2) were read off after 42 h. $C_M = 2.5 \times 10^{-6}$ M, $d = 2$ cm, $\lambda = 624$ mμ, $T = 20.0$°C. In Fig 3 $[H^+]/E_\infty$ is plotted as a function of $[H^+]$. A straight line is obtained which gives $l = 1.988$, $y = 2.90 \times 10^{-8}$ M and from eqn. (5) $K_4/(K_6 + 1) = 1.46 \times 10^{-8}$ M is obtained.

Kinetic measurements. If the dye stock solution is mixed with NaOH + KCl-buffers, the solutions are decolourized with a rate that is directly proportional to $[OH^-]$. In Fig. 4 the rate constants of the decolourization are plotted against $[OH^-]$. A straight line is obtained which passes almost through the origin. This means that in this pH-range $k_3 + k_6 \ll k_5 \cdot$ oh. Therefore, only k_5 can be determined from Fig. 4; $\boldsymbol{k_5 = 2.90 + 0.03}$ **min^{-1} M^{-1}**.

The rate constant k_3 was determined from kinetic measurements in borate buffers, pH = 7.8—8.6. The approximate eqn. (10) can be used since $k_6 + k_5$oh $\ll k_3$ in this pH range. In Fig. 5 k is plotted as a function of $[H^+]$. From the straight line $\boldsymbol{k_3 = 0.00177 \pm 0.00002}$ **min^{-1}** is obtained.

Determination of k_1 *and* k_2. These rate constants were determined by kinetic measurements on the fading which is caused by the reactions G + $H_2O \rightleftharpoons$ S'' and B + $H_2O \rightleftharpoons$ S' in HCl + KCl-buffers. Table 1 contains k-values experimentally found and values of k_1 and k_2 calculated from eqn. (6) (Approximate values of k_1 and k_2 were calculated initially from eqn. (7).) The following values were obtained: $\boldsymbol{k_1 = 0.0497 \pm 0.0010}$ **min^{-1}** and $\boldsymbol{k_2 = 0.0107 \pm 0.0003}$ **min^{-1}**.

Determination of k_4, K_3, K_4, *and* K_6. The dye stock solution was partially decoloruized by making it 0.02 M with respect to hydrochloric acid. The following reactions then occur in the forward direction (→):
$B + H^+ + H_2O \rightleftharpoons G + H_2O \rightleftharpoons S''$ and $B + H^+ + H_2O \rightleftharpoons S' + H^+ \rightleftharpoons S''$. This partially decolourized dye solution was then quickly mixed with acetate buffers and the colour was more or less restored owing to the reactions above in the reverse direction. The rate constants for the restoring of the colour were determined.

In Fig. 6 k is plotted as a function of pH. The following values are obtained: $k_{max} = 0.263$ min^{-1} when pH = 4.99 which gives $\sqrt{K_3K_4} = 1.024 \times 10^{-5}$ M since k has a maximum when $[H^+] = \sqrt{K_3K_4}$. Then $K_3 = \mathbf{(2.83 \pm 0.04) \cdot 10^{-5}\ M}$ is obtained from eqn. (12) since $K_4/(K_6 + 1) = 1.46 \times 10^{-8}$ M and $K_6 + 1 \approx K_6$. The expression $K_3K_4 = 1.05 \times 10^{-10}$ gives $K_4 = \mathbf{(3.71 \pm 0.05) \times 10^{-6}\ M}$ and K_6 is calculated from the determined value of $K_4/(K_6 + 1)$; $K_6 = \mathbf{253 \pm 4.}$

The remaining rate constants k_4 and k_6 are calculated from $k_4 = k_3K_6$ which gives $k_4 = \mathbf{0.448 \pm 0.010\ min^{-1}}$ and from $k_6 = k_5K_wK_6/K_4$ which gives $k_6 = \mathbf{(2.45 \pm 0.10) \times 10^{-6}\ min^{-1}}$.

As can be seen in Fig. 6 the agreement between the experimentally determined k-values and those calculated from the non-approximated eqn. (6) is good. By definition, $K_1K_2K_3K_6 = 1$. The determined values of these constants give $K_1K_2K_3K_6 = 1.01$.

The author is indebted to Mr Olle Nilsson for valuable help in preparing the dye and to Fil.Mag. Gösta Bengtsson for assistance in some of the kinetic measurements.
The English has been revised by Dr D. Karipides (USA).

REFERENCES

1. Cigén, R. *Protolysengleichgewichte und Reaktionsgeschwindigkeiten einiger basischer Triphenylmethanfarbstoffe. (Diss.)* University, Lund 1956.
2. Cigén, R. *Acta Chem. Scand.* **13** (1959) 1113.
3. Cigén, R. *Acta Chem. Scand.* **15** (1961) 1892.
4. Cigén, R. *Acta Chem. Scand.* **12** (1958) 1456.

Received June 5, 1961.

ACTA CHEMICA SCANDINAVICA 15 (1961) 1913–1922

Paper Electrophoresis of Carbohydrates in Sulphonated Phenylboronic Acid Buffer

PER J. GAREGG and BENGT LINDBERG

Svenska Träforskningsinstitutet, Träkemiska avdelningen, Stockholm Ö, Sweden

The paper electrophoresis of some carbohydrates in sulphonated phenylboronic acid buffers is described. These allow electrophoresis to be run at neutral pH values and are therefore useful for the separation and characterisation of alkali-labile carbohydrate derivatives. Specific configurations are required for the hydroxyls for complex formation and information of structural significance can be obtained for unknown carbohydrates. The new buffers are a useful complement to those previously described, especially for the separation of glycitols.

In the course of investigations on acetylated carbohydrates it was found desirable to separate various acetylated xylose derivatives by paper electrophoresis. The electrolytes commonly used, borate buffer [1], arsenite [2], basic lead acetate [2], sodium hydroxide [2], and recently germanate buffer [3] are inapplicable to acetylated carbohydrates; due to the alkalinity of these buffer solutions deacetylation or acyl migration may occur during the electrophoresis. Decreasing the pH leads to too low mobility of the carbohydrate derivatives. Paper electrophoresis in molybdate [4] at pH 5 was inapplicable, as xylose and its derivatives show insignificant mobilities in this buffer system. A new concept was therefore tried, namely, the use of phenylboronic acid instead of boric acid in borate electrophoresis, and further by substitution in the benzene ring of a group that dissociates in aqueous solution, the production of increased mobility of the complexes formed between carbohydrates and the hydroxylated boron atom at neutral pH values. At pH 7 no significant increase in the rate of mobility of the sugars tried was found by using phenylboronic acid instead of boric acid. Nitration in the *ortho* [5] or the *meta* [5] position of the benzene ring gave significantly higher mobilities, highest for the *m*-derivative; the poor water solubility of these compounds, however, rendered them unsuitable. Treatment of phenylboronic acid in 25 % oleum [6] at 0° yielded sulphonated phenylboronic acid; the sodium salt of the acid was very soluble in water and gave satisfactory mobilities for a number of carbohydrates at pH values about 7. The present paper deals with an investigation of the rates of migra-

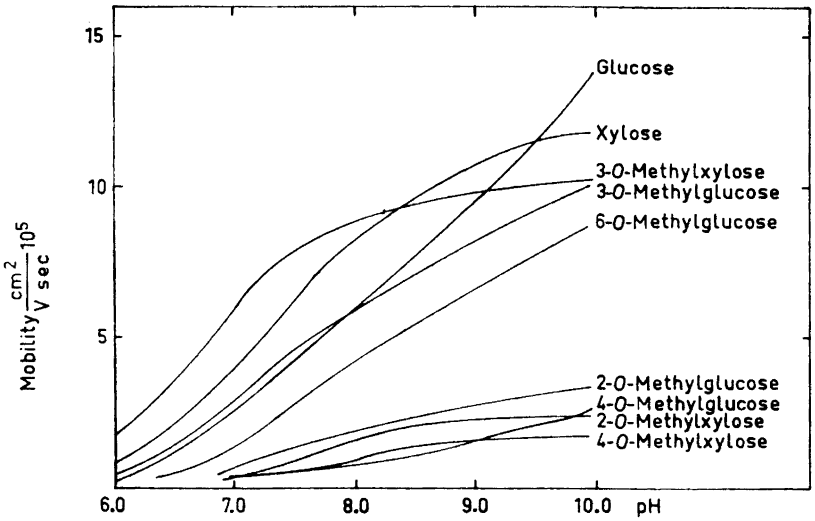

Fig. 1. The mobilities of xylose, glucose and monomethyl ethers in sulphonated phenylboronic acid at various pH values.

tion of various carbohydrates in buffers containing sulphonated phenylboronic acid.

The infrared spectrum, using the potassium bromide pellet technique, of the mono sodium salt of the sulphonated phenylboronic acid gave some indication of the position of substitution. The absorption at 6.25 μ and the weak one at 6.7 μ are typical of mono-, *ortho-* and *meta*-substituted benzene [7,8] the bands

Table 1. Monosaccharides.

$$M_G = \frac{\text{true distance of migration of the substance}}{\text{true distance of migration of glucose}}$$

Substance	M_G in sulphonated phenylboronic acid pH 6.5	M_G in germanate pH 10.7	M_G in borate pH 10.0
D-Xylose	1.8	1.4	1.00
D-Lyxose	2.3	1.9	0.71
L-Arabinose	2.4	1.5	0.96
D-Ribose	4.7	2.1	0.77
L-Rhamnose	0.50	1.3	0.52
D-Glucose	1	1	1
D-Mannose	1.1	1.4	0.72
D-Galactose	1.8	1.3	0.93
D-Altrose	5.8		0.97
L-Sorbose	8.5	2.0	0.95
D-Tagatose	8.6	2.4	0.95
D-Fructose	9.3	2.1	0.90

Table 2. Glycosides.

Substance	M_G in sulphonated phenylboronic acid pH 6.5	M_G in germanate pH 10.7	M_G in borate pH 10.0
Methyl α-D-xylofuranoside	2.3	0.05	0.33
Methyl β-D-xylopyranoside	0.0	0.0	0.0
Methyl β-D-glucofuranoside	2.0	—	—
Methyl α-D-glucopyranoside	0.0	0.0	0.11
Methyl α-D-mannofuranoside	16.0	1.4	—
Methyl β-D-mannopyranoside	0.0	0.4	0.31
Methyl β-D-galactofuranoside	0.4	0.2	0.31
Methyl β-D-galactopyranoside	0.0	0.5	0.38

at 14.15 μ and possibly at 14.45 μ are typical of mono- and *meta*-substituted benzene, the strong absorption band at 13.55 μ is characteristic for *ortho*-substitution only, a weaker diffuse band at 12.3—12.6 μ is typical of *m*-substitution only, while the absence of absorption at 6.10 μ and 6.60 μ rules out *para*-substitution. It therefore seems probable that the sulphonic acid is largely the *ortho*-sulphonic acid while a smaller part is the *meta*-isomer; it seems improbable that the *para*-isomer is present.

The buffers were 0.05 M aqueous solutions of sulphonated phenylboronic acid containing the requisite amount of sodium hydroxide for the desired pH. Additional pH stability of the buffers was obtained by the addition of monopotassium phosphate and sodium hydroxide. Electrophoreses were run at 40° and 500 V (about 10 V/cm). Under these conditions the mobility of glucose ranged from 0.08 cm/h at pH 6.0 to 4.5 cm/h at pH 10 as shown in Fig. 1. At pH 6.5, which was generally used throughout this work, the average mobi-

Table 3. Methyl ethers of glucose and xylose.

Substance	M_G in sulphonated phenylboronic acid pH 6.5	M_G in germanate pH 10.7	M_G in borate pH 10.0
D-Xylose	1.8	1.4	1.00
2-*O*-Methyl-D-xylose	0.0	0.0	0.39
3-*O*-Methyl-D-xylose	2.9	1.7	0.66
4-*O*-Methyl-D-xylose	0.0	0.3	0.21
5-*O*-Methyl-D-xylose	13.0	—	—
3,5-Di-*O*-methyl-D-xylose	9.3	—	—
D-Glucose	1	1	1
2-*O*-Methyl-D-glucose	0.0	0.0	0.23
3-*O*-Methyl-D-glucose	1.3	1.4	0.80
4-*O*-Methyl-D-glucose	0.0	0.3	0.24
6-*O*-Methyl-D-glucose	0.5	0.96	0.80

Table 4. Glycitols.

$$M_M = \frac{\text{true distance of migration of the substance}}{\text{true distance of migration of mannitol}}$$

Substance	M_M in sulphonated phenylboronic acid pH 6.5	M_M in germanate pH 10.7	M_M in borate pH 10.0
Glycol	0.0	0.0	—
Glyceritol	0.0	0.2	0.54
Erythritol	0.1	0.5	0.83
L-Threitol	0.3	—	0.83
erythro Butane 2,3-diol	0.0	—	0.14
threo Butane 2,3-diol	0.3	—	0.56
D-Ribitol	0.3	0.6	0.93
L-Arabinitol	0.6	0.9	0.96
Xylitol	0.9	0.9	0.87
D-Glucitol	1.3	1.0	0.91
D-Mannitol	1	1	1
L-Iditol	1.4	—	0.89
Galactitol	1.0	1.1	1.07
2-*O*-Methyl-L-arabinitol	0.1	0.1	
4-*O*-Methyl-L-arabinitol	0.5	0.5	
2-*O*-Methyl-D-xylitol	0.4	0.6	
3-*O*-Methyl-xylitol	0.1	0.3	
5-*O*-Methyl-D-xylitol	0.6	—	
1-Deoxy-D-glucitol	0.9		
2-*O*-Methyl-D-glucitol	1.2	0.8	
3-*O*-Methyl-D-glucitol	0.1	0.4	
4-*O*-Methyl-D-glucitol	1.3	0.7	
6-*O*-methyl-D-glucitol	0.6		
6-Deoxy-L-mannitol (Rhamnitol)	0.8	—	
1,6-Di-*O*-acetyl-D-mannitol	0.8	—	
2-*O*-Methyl-D-galactitol	0.5	0.9	
3-*O*-Methyl-D-galactitol	1.0	0.7	
6-*O*-Methyl-D-galactitol	0.8	0.8	

lity of glucose was 0.38 cm/h and that of mannitol, used as standard for measuring the relative mobility of sugar alcohols was 3.4 cm/h. The mobilities for the carbohydrates and related compounds are shown in Tables 1 to 6 and in Figs. 1, 2 and 3. The M_G and $M_{mannitol}$ (M_M) values in germanate are taken from Lindberg and Swan [3] and those in borate from Foster [1] and Frahn and Mills [2].

As will be seen from Table 1 the spread in mobilities of monosaccharides in sulphonated phenylboronic acid is much greater than in either germanate or borate. In borate pairs of aldopentoses and aldohexoses with similar configura-

tion, *e.g.* arabinose and galactose, xylose and glucose, lyxose and mannose have very similar mobilities. In both sulphonated phenylboronic acid and in germanate the pentoses are the faster in each pair, and, except for L-rhamnose, glucose is the slowest sugar in both buffers while being the fastest in borate. The high mobility of the three ketohexoses in sulphonated phenylboronic acid probably, as discussed below in connection with Table 2, reflects the high proportion of the furanose forms of these sugars present in aqueous solution since most of the mobility is due to furanosidic 1,2-*cis*-diols, as is the case in germanate [3]. Similarly the differences in the mobilities of the aldopentoses and the aldohexoses possibly reflect the stability of the most stable pyranosidic chair form of these sugars. The differences in mobility among the three ketohexoses is small in all three buffers.

In Table 2 are given the mobilities of a few glycosides. The very high mobility of the mannofuranoside indicates that furanosidic *cis*-1,2-diols are by far the most important in complex formation. In mannofuranoside the hydroxyls on $C_{(2)}$, $C_{(3)}$ and $C_{(5)}$ also are situated for a possible tridental complex formation with boron [1]. The much lower mobility of the xylofuranose is probably due to complex formation on $C_{(3)}$ and $C_{(5)}$.

The possibility of contribution to the mobility of the furanosides by the $C_{(5)}$ and $C_{(6)}$ hydroxyls [1] is unlikely as glyceritol does not migrate (see Table 4).

No contribution to the mobility of the sugars comes from pyranosidic *cis*-1,2-diols or from pyranosidic *cis*-1,3-diols as shown by the lack of mobility of the mannopyranoside, galactopyranoside, and D-inositol, likewise no contribution is given by the $C_{(4)}$ and $C_{(6)}$ hydroxyls in the glucoside configuration.

These results are different to those obtained with germanate and borate where, apart from the interactions mentioned above, contributions are given by pyranosidic *cis*-1,2-diols and possibly also by 1,3-diols of suitable configuration, *e.g.* $C_{(4)}$ and $C_{(6)}$ in glucopyranose.

The results obtained for methyl ethers of xylose and glucose, Table 3, can with the exception of the 3-*O*-substituted sugars be explained as for the furanosides and pyranosides. Blocking of the $C_{(2)}$ and $C_{(4)}$ hydroxyls yields derivatives which are immobile in sulphonated phenylboronic acid. The lack of mobility of the 2-*O*-methyl ethers indicates, as has been discussed by Foster [1], that these derivatives are not to any appreciable degree present in the furanose form; substitution in the 4-position entails pyranose forms with which no interaction occurs.

As in germanate buffer, 3-substitution yields enhanced mobility of the two sugars. This is difficult to interpret on the basis of present knowledge and will be the subject of a subsequent investigation. Substitution on the $C_{(6)}$ hydroxyl in glucose leads to decreased mobility in sulphonated phenylboronic acid, more so than in borate, while in germanate this has little effect. While the reduction in mobility in borate may be attributed to blocking the interactions with the 4,6- or 5,6-hydroxyls this should not be the case in sulphonated phenylboronic acid, since α-D-glucopyranoside and glycerol are immobile on electrophoresis; the explanation possibly lies in the furanose-pyranose and/or in the α-β-equilibria of glucose and 6-*O*-methylglucose. A similar example is the slower mobility of rhamnose compared to mannose. (Table 1). As would be expected, the mobilities of 5-*O*- and 3,5-di-*O*-methylxylose are high in

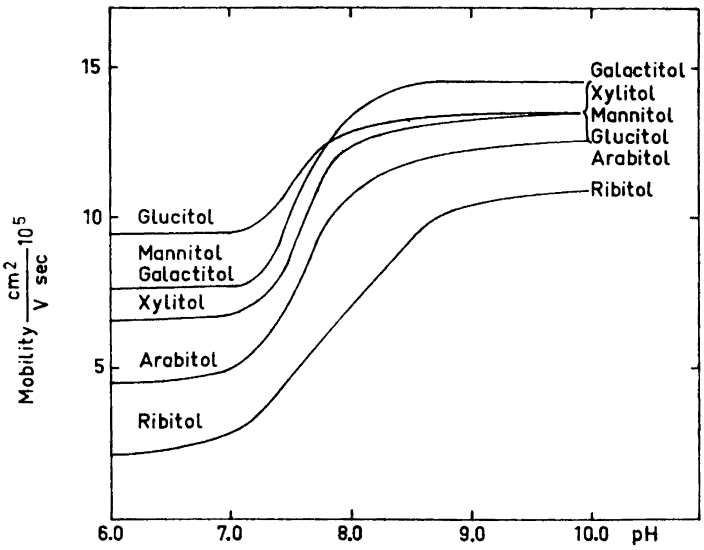

Fig. 2. The mobilities of some glycitols in sulphonated phenylboronic acid at various pH values.

sulphonated phenylboronic acid, this again reflects the importance of furanosidic *cis*-1,2-diols in complex formation. The differences between the two methyl ethers may reflect different α-β-equilibria under the conditions used.

In Fig. 1 are given the results of runs in sulphonated phenylboronic acid at various pH values for xylose, 2-, 3- and 4-*O*-methyl-xylose and the similar series for glucose including the 6-*O*-methyl ether. At pH 9 to 10 the relative mobilities strongly resemble those obtained with borate. As the pH decreases, fewer possibilities for complex formation exist, and important differences in relative mobilities arise, *e.g.* for the sugars glucose, xylose, 3-*O*-methyl-glucose and 3-*O*-methylxylose. Superimposed on this is the general decrease in mobility of all sugars with decreasing pH due to decreasing ionisation of the boronic acid.

A series of runs similar to the one described in connection with Fig. 1, but where each sugar and methyl sugar was dissolved in buffer solution at the appropriate pH and kept for a minimum period of 24 h did not give any difference to the mobilities depicted in Fig. 1, outside that due to experimental error, indicating that the equilibria between the various forms of the sugars and the complex were rapidly established.

Better separations are obtained for sugar alcohols run in sulphonated phenylboronic acid than those obtained in both borate and germanate (Table 4); the separations at low pH values are better than those obtained at higher pH as will be seen from Fig. 2. At pH 10 the relative mobilities in sulphonated phenylboronic acid resemble those in borate at the same pH. A lowering of the pH of borate does not lead to separations as good as those obtained with

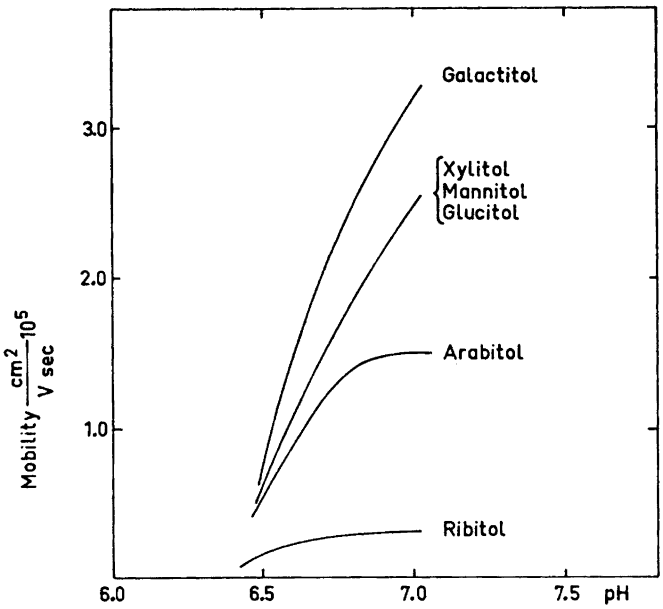

Fig. 3. The mobilities of some glycitols in boric acid below pH 7.

phenylboronic acid as shown in Fig. 3; at low pH values the rate of migration in borate of the glycitols approaches zero and relative differences in mobility between the substances cannot be observed. The lack of restriction on the conformations of the glycitols and their derivatives makes the rationalisation of their relative mobilities in sulphonated phenylboronic acid rather difficult. From a study of the M_M values of the glycitols and their methyl ethers it does however seem probable that 1,2-*trans*-diols are important in complex formation as shown by the mobilities of the glycitols up to and including the pentitols, and also by the high mobility of iditol.

From the lack of mobility of glycol and glycerol it may be inferred that primary 1,2-diols as well as 1,2-diols with one primary hydroxyl do not form complexes. That primary hydroxyl groups play some part in complex formation is, however, indicated by the reduction in mobility by substituting xylitol on $C_{(1)}$ (or $C_{(5)}$) and by 1-deoxy-D-glucitol, 6-*O*-methyl-D-glucitol as well as 1,6-di-*O*-acetyl-D-mannitol and L-rhamnitol which all move slower than their parent hexitols. Substitution on the primary hydroxyls in threitol has no effect on the mobility while in erythritol this leads to a mobility too low to measure, as indicated by the mobilities of *threo*- and *erythro*-butane-2,3-diol. The importance of 1,2-*trans*-diols is reflected by the low mobilities of 2-*O*-methyl-L-arabinitol, 2-*O*-methyl-D-galactitol, 3-*O*-methyl-xylitol and 3-*O*-methyl-D-sorbitol. In the hexitol series however, the M_M values for the glycitols and their derivatives indicate that the situation is too complex to be accounted for by the number of 1,2-*trans*-diol groupings only. It might be possible that tridental

Table 5. Reduced disaccharides.

Substance	Linkage	M_M in sulphonated phenylboronic acid pH 6.5
Sophoritol	β (1→2)	1.2
Laminaribiitol	β (1→3)	0.1
Cellobiitol	β (1→4)	1.1
Gentiobiitol	β (1→6)	0.6

Table 6. Inositols.

Substance	M_M in sulphonated phenylboronic acid pH 6.5	M_M in germanate	M_M in borate
myo-Inositol	0.0	0.1	0.59
D-Inositol	0.0	0.4	0.70
epi-Inositol	1.8	0.9	0.81

complex formation occurs with at least some of the glycitols; that tridental complex formation is possible is also indicated by the high mobility of *epi*-inositol (Table 6).

The relative mobilities of the reduced disaccharides in sulphonated phenylboronic acid in Table 5 closely correspond to those of the corresponding methyl glycitols. This might be useful for the characterisation of disaccharides and glycityl glycosides.

The rate of migration of three inositols is shown in Table 6. Of these, *myo*-inositol and *epi*-inositol in one of the chair conformations have three axial *cis*-hydroxyls in 1,3,5-positions that may form tridental complexes [1]. *Myo*-inositol with 5 axial hydroxyls in this conformation is immobile while *epi*-inositol with 4 axial hydroxyls has a high mobility. The high mobility of *epi*-inositol may however be due to a complex with the two axial hydroxyls in the 1,3-position in its most stable chair form. D-Inositol has in its most stable chair form two axial hydroxyls, these however are 1,2-*trans* and D-inositol does not migrate.

Buffers containing sulphonated phenylboronic acid have proved useful for separating mono-acetylated monosaccharides [9] at sufficiently low pH values to avoid deacetylation, the mobilities closely correspond to those of the corresponding methyl ethers under the same conditions.

DISCUSSION

The substitution of phenylboronic acid with an ionisable group and paper electrophoresis with this substance at neutral pH values, thus decreasing the ionisation of the boric acid residue of the molecule, leads to much more selective complex formation than is the case with borate at pH 10. At the

same time, reasonable rates of migration of the complexes are obtained. With reducing sugars and glycosides by far the largest contribution to the mobilities is given by furanosidic 1,2-*cis*-diols. A smaller contribution is given by 3,5-hydroxyls, *e.g.* in the xylofuranose structure. No contributions to the mobilities are given by pyranosidic *cis*-1,2-diols or by the $C_{(4)}$ and $C_{(6)}$ hydroxyls in the glucose configuration. The very fast rate of movement of *epi*-inositol suggests either tridental complex formation with inositols with a *cis-cis*-1,3,5-triol grouping in one of its chair conformations provided no more than four of the hydroxyls are axial in this conformation, or a complex involving two axial hydroxyls in 1,3-position.

Substitution on $C_{(3)}$ in xylose and glucose gives enhanced mobility; this phenomenon is not perfectly understood and is currently being investigated *.

The number of conformations possible makes the rationalisation of the mobilities of the glycitols difficult. It is however obvious that *trans*-1,2-diol groupings are important in complex formation, and it is possible that tridental complexes are present in the equilibrium mixtures.

Electrophoresis in sulphonated phenylboronic acid at neutral pH values makes possible a number of separations of carbohydrates substituted with alkali-labile groups. Some separations are better in this than in other buffer systems due to the specific configurations required for the hydroxyls for complex formation with sulphonated phenylboronic acid. With reducing sugars and glycosides the separations obtained resemble those in germanate at pH 10.6, although the steric requirements for complex formation are more extreme than for germanate.

With the glycitols, however, the separations are much better than those obtained with borate [1] or germanate [3]. The separations to some extent resemble those reported for sodium arsenite [2] and basic lead acetate [2] buffers but is different from those obtained in molybdate buffer [4] and sulphonated phenylboronic acid can be regarded as a complement to these buffers.

Sulphonated phenylboronic acid buffers should also prove useful for separating compounds that form strong complexes with this buffer from those that form weak complexes on anion exchange resins.[10]

EXPERIMENTAL

Evaporations were performed at 40° in a vacuum.

Sulphonation of phenylboronic acid [6]. Phenylboronic anhydride (100 g) was added in small portions during 1 h to 25 % oleum (600 g) cooled in an ice-salt or dry ice-alcohol bath to −5 to 0° under vigorous mechanical stirring, the temperature was maintained at about 0° to control the exothermic reaction. At the end of the additions the mixture was stirred at 0° for a further 10 min and then poured into crushed ice (3 l) under vigorous stirring. The precipitate (probably biphenyl sulphone) was filtered off and the filtrate neutralised to pH 7 with aqueous sodium hydroxide under external cooling. Some precipi-

* *Added in proof.* Bishop and Cooper [15] have studied the equilibrium mixtures in the Fischer syntheses starting from xylose and from some of its methyl ethers. They found that the percentages of the furanosides were much higher with 3-*O*-methyl-D-xylose than with D-xylose as starting material. If this reflects the equilibrium mixture of the two sugars in aqueous solutions, the high mobility of 3-*O*-methylxylose in sulphonated phenylboronic acid and in germanate solution would seem to be explained.

tated sodium sulphate was filtered off and the filtrate concentrated to dryness under reduced pressure. The sodium salt of the sulphonated phenylboronic acid was extracted with several portions of boiling 80 % aqueous ethanol, the combined extracts were evadorated to dryness. The crystalline residue was extracted with several portions of boiling 90 % aqueous ethanol, the combined extracts were concentrated and poured into absolute ethanol and kept at −4° overnight. The precipitate was collected by filtration and air dried. The yield of sodium sulphate-free material varied between 80 to 120 g depending upon the temperature control of the sulphonation.

Buffer. The buffers were 0.05 M solutions of sulphonated phenylboronic acid containing sodium hydroxide to give the desired pH and also monopotassium phosphate and sodium hydroxide in the ratio giving the same pH; the molarity of the solution was 0.06 with respect to phosphate.

Method. The apparatus was similar to that described by Kunkel and Tiselius [11] and the procedure as described by Foster [1]. Whatman No. 1 filter paper was used, the starting line was placed 20 cm from the cathode end of the cooling plate. Hydroxymethylfurfural was used to mark the starting line and glucose or mannitol as standard references for the relative rates of migration. Water at 40° was passed through the cooling plate. The voltage applied was 0.5 kV corresponding to about 10 V/cm and the time was 3 or 6 h. The electrolytes in the two electrolyte vessels were mixed again after each run, and after running electrophoresis for each 3 h at 0.5 kV the electrophoresis was interrupted and the solutions in the two vessels were mixed again to avoid too large pH variations. Good reproducibility for the relative rates of migration at various pH values was obtained.

The reducing sugars were located by spraying with anisidine hydrochloride [12] and the non-reducing sugars and inositols with periodate-benzidine [13]. Distinct, although occasionally somewhat elongated spots were obtained, and migration distances were measured from the centres of the spots.

Substances. Most of the substances were available at this laboratory or at the Institution of Wood Chemistry, The Royal Institute of Technology [3]. The partially methylated glycitols not previously available [3] were obtained from the corresponding reducing sugars by reduction with Raney nickel [14].

Acknowledgement. The authors are indebted to Miss Hillevi Svensson for her skilful assistance and to Dr. K. Torssell for a gift of the sodium salt of sulphonated phenylboronic acid, and for directions concerning its preparation.

REFERENCES

1. Foster, A. B. *Advances in Carbohydrate Chem.* **12** (1957) 81.
2. Frahn, J. L. and Mills, J. A. *Australian J. Chem.* **12** (1959) 65.
3. Lindberg, B. and Swan, B. *Acta Chem. Scand.* **14** (1960) 1043.
4. Bourne, E. J., Hutson, D. H. and Weigel, H. *Chem. & Ind., London* **1959** 1047; *J. Chem. Soc.* **1961** 35.
5. Saeman, W. and Johnson, J. R. *J. Am. Chem. Soc.* **53** (1931) 711.
6. Torssell, K. *Private communication.*
7. Colthup, N. B. *J. Opt. Soc. Am.* **40** (1950) 397.
8. McMurry, H. L. and Thornton, V. *Anal. Chem.* **24** (1952) 318.
9. Garegg, P. J. *Unpublished results.*
10. Khym, J. X. and Zill, L. P. *J. Am. Chem. Soc.* **73** (1951) 2399; **74** (1952) 2090.
11. Kunkel, H. G. and Tiselius, A. *J. Gen. Physiol.* **35** (1951) 89.
12. Hough, L., Jones, J. K. N. and Wadman, W. H. *J. Chem. Soc.* **1950** 1702.
13. Cifonelli, J. A. and Smith, F. *Anal. Chem.* **26** (1954) 1132.
14. Karabinos, J. V. and Ballun, A. T. *J. Am. Chem. Soc.* **75** (1953) 4501.
15. Bishop, C. T. and Cooper, F. P. *Abstract Papers Am. Chem. Soc.* **140** (1961) 3 D.

Received May 17, 1961.

ACTA CHEMICA SCANDINAVICA 15 (1961) 1923–1926

Quantitative Polarographic Determination of Aliphatic Esters

TH. ØSTERUD and MILDA PRYTZ

Yrkeshygienisk Institutt, Blindern — Oslo, Norway

Reaction mixtures of pure aliphatic esters with hydroxylamine have been polarographed at well defined concentrations in ethanol-water solutions of tetrabutylammonium iodide, buffered with tetraethylammonium hydroxide. The height of the resulting hydroxamic acid curves show proportionality with the original concentration of ester.

A series of esters were treated with hydroxylamine in alcoholic sodium hydroxide solutions as described in our paper on polarographic reduction of aliphatic esters [1]. After the addition of the hydroxyl amine solution the concentration of ester in the reaction mixture was 0.031 M. The supporting electrolyte had a pH of about 12.5. To 10 ml of the supporting electrolyte in the electrolytic cell was added respectively 5, 10, and 15 drops of the reaction mixture. This gave for the acetic acid ethyl ester (ethyl ethanoate) the concentrations 3.1×10^{-4} M, 6.2×10^{-4} M and 9.3×10^{-4} M. The molar concentrations of the other esters were of the same order of magnitude.

The solutions were polarographed, and the height of the polarographic waves (steps) was found to vary proportionally with the amount of ester. When the concentration of ester was doubled the height of the corresponding wave became twice as large as originally.

EXPERIMENTAL

The same apparatus was used as in our earlier study [1]. The experimental procedure was similar to that already described and the chemicals used were the same. To 10 ml of supporting electrolyte in the electrolytic cell was added, respectively, 5 drops, 10 drops, and 15 drops of the reaction mixture and the pH was kept at approximately 12.5. 5 drops or 10 drops of the reaction mixture were weighed and the molarity of the polarographed solutions calculated accordingly. They were of the order of magnitude of 10^{-4} M. After addition of, respectively, 5 and 10 drops (molar concentrations 3.1×10^{-4} to 6.2×10^{-4}) the waves were quite regular with very good, measurable plateaus. On addition of 15 drops of reaction mixture, however, the resulting third wave was apt to show a maximum. This might have been due either to the higher concentration or to the solution having been polarographed twice already. We therefore added 15 drops of reaction mixture directly to 10 ml of supporting electrolyte and polarographed in the usual way. Also by this method we got an ill-defined plateau. As to be expected the halfwave

potentials were not influenced by concentration; the same values were obtained as given in the above mentioned paper [1]. It seems practical for quantitative purposes not to exceed a concentration of 6×10^{-4} M in order to evade plateaus with maxima. By all these experiments we used a sensitivity of 7:1 000.

In order to test the usability of an ester solution with known concentration in comparison with an ester solution of unknown concentration we ran some parallels. In one case we heated two reaction mixtures with the same amount of ester similtaneously in the same waterbath and polarographed both at room temperature. The waves were of equal height. In another case one of the reaction mixtures contained one and a half as much ester as the other. The wave heights varied according to concentration.

One has to keep in mind that the reaction between ester and hydroxylamine is reversible, and one should always treat an ester solution of known strength and the one of unknown concentration identically in every detail if one wishes to measure the concentration of the latter by comparison with the former.

RESULTS

Firstly we tested the variation of wave heights with concentration by adding increasing amounts of one and the same reaction mixture to an electrolytic cell with 10 ml of the above mentioned supporting electrolyte. Seven different aliphatic esters have been treated in this way. These experiments showed that the wave heights increased proportionally with the concentration within the limits $\pm$ 5 %. The results are given in Table 1.

Fig. 1. gives the diagram for acetic acid *iso*propyl ester.

We also found it important to ascertain if two different reaction mixtures of equal concentration gave equally high waves when treated under exactly similar conditions. The result was satisfactory as shown in Fig. 2. Two different reaction mixtures with acetic acid *iso*propyl ester show exactly the same shape of curve and have the same wave height.

Eventually we found it expedient to test if the proportionality between concentration and wave height which had been found when we added increasing amounts of a reaction mixture to one and the same polarographic cell would be evident if we added increasing amounts of reaction mixture (4 and 6

Table 1. Relationship between concentration and wave height in polarographic determination of aliphatic esters.

Ester	Mol. conc. × 10^{-4}			Relative concentration			Wave heights in mm			Relative heights measured		
	1	2	3	1	2	3	1	2	3	1	2	3
Acetic acid ethyl ester	3.1	6.2	9.3	1	2	3	27	55	81	1	1.9	3
Acetic acid *iso*propyl ester	3.1	6.2	9.3	1	2	3	23	43	68	1	2	3
Acetic acid octyl ester	3.1	6.2	9.3	1	2	3	24	47	74	1	2	3.1
Propionic acid ethyl ester	3.1	6.2	9.3	1	2	3	23	45	72	1	2	3.1
Butyric acid ethyl ester	3.1	6.2	9.3	1	2	3	27	54	79	1	2	2.9
Butyric acid butyl ester	3.1	6.2	9.3	1	2	3	26	54	78	1	2.1	3
Valeric acid ethyl ester	3.1	6.2	9.3	1	2	3	23	45	68	1	2	3

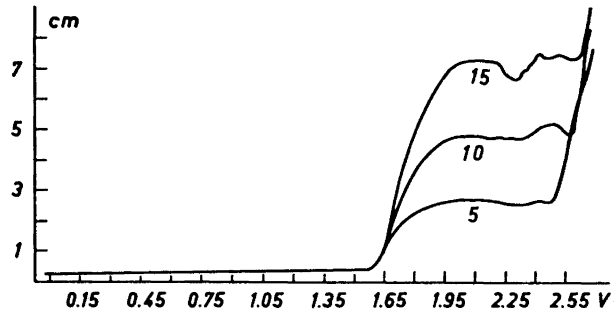

Fig. 1. Variation of wave height with concentration for acetic acid *iso*propyl ester. Concentrations: 3.1, 6.2 and 9.3 × 10^{-4} M.

drops, respectively) to different cells, each with 10 ml of supporting electrolyte. The results for acetic acid *iso*propyl ester are shown in Fig. 3. The figure shows that also with this procedure we got proportionality.

DISCUSSION

We presume to have shown that our method for indication of aliphatic esters by conversion to hydroxamic acid and polarographic determination of the reaction mixture also may be used for quantitative determination of the same. The results are reliable within the limits of ± 10 %.

One must always keep in mind that the reaction

$$\text{ester} + \text{hydroxylamine} \rightleftharpoons \text{hydroxamic acid} + \text{alcohol}$$

is reversible, so that reaction mixtures for quantitative use must be made very carefully. Comparisons between different reaction mixtures are only allowed when these have been prepared under exactly similar conditions.

Water solutions with alkali salts as supporting electrolyte can not be used, because of the high decomposition potentials of the hydroxamic acids.

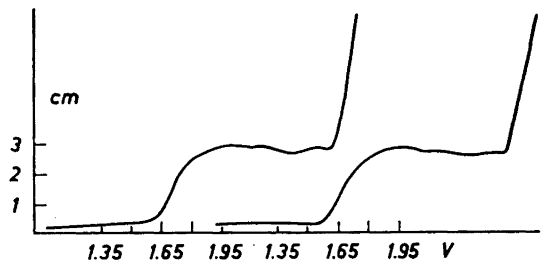

Fig. 2. Polarographic waves for two different reaction mixtures similarly treated, showing the same wave height. Conc. of acetic acid *iso*propyl ester: 3.1 × 10^{-4} M.

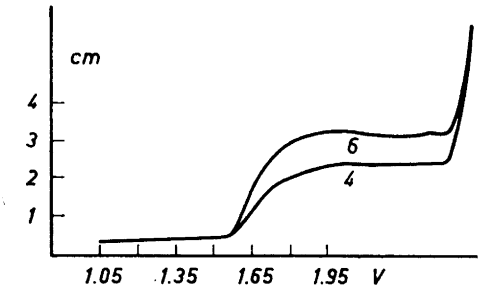

Fig. 3. Polarographic waves of acetic acid *iso*propyl ester showing proportionality between concentration and wave height even when different electrolytic cells were used. Concentrations: 2.5 and 3.7 $\times$ 10^{-4} M.

The authors are greatly indebted to Dr. Karl Wülfert for giving us working facilities at *Yrkeshygienisk Institutt*. Likewise to cand. mag. Nicolay Soteland for the recording of the polarograms.

REFERENCE

1. Prytz, M. and Østerud, Th. *Acta Chem. Scand.* **15** (1961) 1285.

Received May 10, 1961.

ACTA CHEMICA SCANDINAVICA 15 (1961) 1927–1931

On the Determination of Lipoperoxides in Animal Tissues

J. GLAVIND and S. HARTMANN*

Department of Biochemistry and Nutrition, Polytechnic Institute, Copenhagen, Denmark

The determination of lipoperoxides in animal tissues was studied through recovery experiments. Quantities of peroxides up to about 0.1 μequiv./g tissue added during the extraction of liver vith chloroform disappeared during the determination. Lung and muscle destroy amounts of peroxides of the same order, whereas with blood and pancreas the recovery is better. Improved recoveries were obtained by adding large amounts of hydrogen peroxide. The principles disturbing the determination of lipoperoxides do not interfere with the thiobarbituric acid reaction.

The occurrence of lipoperoxides has been demonstrated in the adipose tissue of nutritionally deficient experimental animals [1], in subcutaneous tissue of man with peripheral venous diseases [2], and in the atherosclerotic human aorta [3]. Lipoperoxides may also occur as normal constituents of the organism. Gomori [4] has postulated that the presence of lipoperoxides in leucocytes are responsible for the histochemical, so-called stable nadi-reaction; yet, the present authors were able to find, by chemical methods, only small amounts of lipoperoxides in the leucocytes [5].

The determination of lipoperoxides, *e.g.*, in adipose tissue, is simple since only an extraction with a peroxide-free solvent is needed before the usual chemical methods can be carried out. However, the peroxide-group is, chemically, highly reactive. Consequently, a general survey of the presence and function of lipoperoxides in physiology and pathology will have as a necessary prerequisite a study of the applicability of the methods for peroxide determination, especially their use for organs consisting to a major extent of parenchymatous tissue. Such a study was the purpose of this work.

MATERIAL AND METHODS

The organs and other tissues, generally from pigs, were freshly brought from slaughter. Extracts were prepared by grinding 40 g portions of tissue with 120 g anhydrous sodium sulfate and 200 ml chloroform in a Waring blendor. In the recovery studies, known amounts of lipoperoxides in the form of lard were added in the chloroform. The extracts were filtered, and 100 ml evaporated *in vacuo* at low temperature to a small volume which was adjusted to 5 ml with chloroform.

* Deceased May 1959.

Table 1. The disappearance of lipoperoxides during the extraction of pig liver. Colorimetric peroxide determinations carried out on liver lipids, the triglyceride and phospholipid fractions of liver lipids, and liver lipids extracted with the addition of lard containing a known amount of peroxides.

Material	Extinction at 530 mμ
Liver extract	0.095
Triglyceride fraction	0.055
Phospholipid fraction	0.040
Liver extract	0.095
Lard	0.170
Liver extract with added lard	0.100

Determinations of lipoperoxides were carried out both by the thiocyanate and the indophenol methods. Generally the latter method was used since, in the presence of high amounts of phospholipids, it gives more quantitative results than the thiocyanate method. Both methods were carried out as described in a previous paper [6]. A Beckman spectrophotometer was used for colorimetry, and corrections made for reagent blanks and for the yellow color of the extracts.

Separate determinations of peroxide groups in the triglyceride and the phospholipid fractions were carried out as described in an earlier paper [7].

The thiobarbituric acid reaction was carried out essentially as described by Wilbur *et al.*[8]: Two g tissue was homogenized with 3 ml 10 % trichloroacetic acid, the mixture centrifuged, and 2 ml of the clear supernatant mixed with 0.67 % thiobarbituric acid. The mixture was heated for 10 min in a boiling water-bath, the tubes cooled, and the optical densities read at 530 mμ.

RESULTS

Attempts to determine lipoperoxides in liver. When the indophenol method for determination of lipoperoxides was carried out on liver, as a rule a distinct, but low value was obtained (Table 1). When triglyceride and phospholipid peroxides were determined separately, small values were usually obtained for both fractions. When, however, a known quantity of lipoperoxide was added

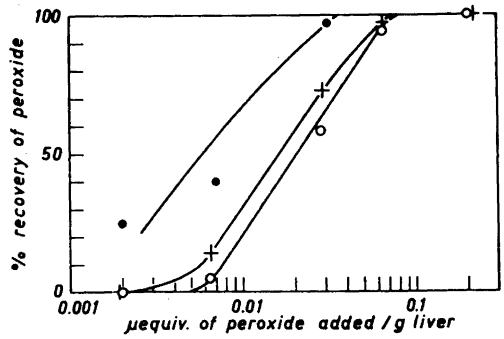

Fig. 1. Recovery of peroxide. Tests carried out on liver with the addition of known amounts of peroxide. Peroxide added before extraction O, after filtration +, and after absorption ●.

with the chloroform during the extraction of liver lipids, sometimes only a very small, sometimes a larger part of the peroxide was recovered.

The disappearance of lipoperoxides was studied in recovery experiments of the type exemplified in Fig. 1. Graded amounts of lipoperoxides were added, (1) in the chloroform, (2) in the filtrate after extraction, and (3) in the solution obtained after absorption on alumina.

These results show that amounts of added lipoperoxide of about 0.01 μequiv./g liver disappeared during the determination, whereas a good recovery was obtained when amounts above 0.1 μequiv./g liver were added. The filtered chloroform extract gave almost as great an inhibition, but only slight losses occurred in the filtrate obtained after absorption of the extract on alumina.

The influence on the destruction of lipoperoxides of varying the experimental conditions, adding enzyme poisons, *etc.*, was studied in further recovery experiments. The peroxide-destroying effect of liver was not affected by heating the liver for half an hour in a boiling water-bath. Likewise, freezing the liver and cooling the chloroform with solid carbon dioxide gave the same result as carrying out the experiment at room temperatures. The use of petrol ether or ethanol instead of chloroform as solvent, or the addition of hydrocyanic acid, ethylenediaminetetraacetic acid, formalin, or sulfosalicylic acid did not influence the peroxide recovery.

An improved recovery was obtained by the addition of large amounts of certain hydroperoxides which probably acted by saturating lipoperoxide-reducing systems. The best results were obtained by adding 20—50 mg perbenzoic acid in the chloroform, and afterwards filtering through alumina which removed the acid. Unfortunately, the instability of perbenzoic acid complicates the use of this substance for routine analysis. Peracetic and monoperphthalic acids destroy the peroxide group. An improved recovery was obtained by the addition of 5—10 ml 30 % hydrogen peroxide. Amounts of lipoperoxide down to 0.01 μequiv./g liver could be recovered, but smaller amounts disappeared.

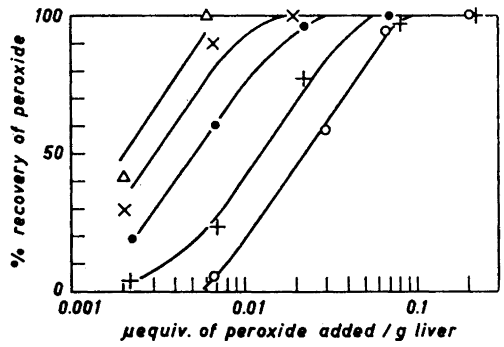

Fig. 2. Recovery of peroxide. Tests carried out on different organs with the addition of known amounts of peroxide. Liver O, muscle +, lung ●, pancreas ×, and blood △.

Thus, the elaboration of a method which gave under all circumstances a quantitative recovery, was not achieved. The best approach resulting from our studies was the following method elaborated for use on chick livers:

Two ml 30 % hydrogen peroxide and 30 g anhydrous sodium sulfate were finely ground in a mortar. 5 g liver were added and ground until the mass was homogeneous. The mixture was extracted with 10 ml chloroform, filtered through a column (12 × 50 mm) of purified alumina [6], the column washed with more chloroform, and the filtrate used for the determination which was carried out as usual.

The use of this method enabled the demonstration of lipoperoxides in livers of chicks receiving a special, vitamin E-deficient diet [9]. Values corresponding to a content of up to 0.1 μequiv. of peroxide per g liver were found while only about 0.01 μequiv. was found in the livers of a control group fed the same diet supplemented with vitamin E.

The lipoperoxide-destroying properties of different organs. Other tissues and organs were examined in the same way as liver, *e.g.*, in recovery experiments with graded amounts of lipoperoxides (Fig. 2). It appears from these results that muscle and lung have peroxide-destroying properties of a potency similar to that of liver, whereas the effects of blood and pancreas are weaker.

The influence of the peroxide-destroying principles on other methods. When recovery experiments were carried out on liver using the thiocyanate method for lipoperoxide determination instead of the indophenol method, similar results were obtained.

A comparison with the thiobarbituric acid reaction was carried out in the following way: Liver was stored in a refrigerator. Samples were taken daily and tested by the thiobarbituric acid reaction. The fresh liver gave no reaction, but an increasingly strong color appeared when the liver was stored for some days. Recovery experiments with the indophenol method were carried out on a sample of liver giving a strongly positive thiobarbituric acid reaction without incubation (optical density 0.6). Peroxide-reducing properties in the stored liver similar to those in fresh liver were found.

DISCUSSION

The peroxide-destroying properties of liver have been profoundly studied by Dubouloz and his co-workers [10]. However, since our procedures differ from theirs, it cannot be settled whether the disappearance of lipoperoxides found here is due to the same peroxide-destroying principles as described by these investigators.

The presence of peroxide-destroying properties in a filtered chloroform extract, and the fact they were influenced neither by hydrocyanic acid, *etc.*, nor by heating, suggest that they are not of enzyme character, but due more likely to some fat-soluble reducing substances. Substances present in the extract might interfere with the peroxide determination in other ways than by reducing the peroxides, or ferric iron, but since the same results were found both with the indophenol and the thiocyanate methods, the reductive effect seems to be the most logical explanation. The nature of the reducing substances is

unknown. Tocopherols, vitamin A, and carotenoids, *etc.*, are oxidized by lipoperoxides and by ferric ions. The reactions are, however, very slow at room temperatures unless catalyzed by heme pigments, and such catalysis seems improbable since hydrocyanic acid does not interfere.

The presence of reducing substances complicates the determination of lipoperoxides which may be present in the same tissue, *e.g.*, deposited in other microscopic structures. In liver amounts less than 0.1 μequiv. per g probably cannot be determined by the usual methods. When hydrogen peroxide is added, to neutralize the reducing substances, the limit concentration which can be determined is probably about 0.01 μequiv. per g liver.

In recent years many studies on the formation of lipoperoxides have been conducted with the thiobarbituric acid reaction of Kohn and Liversedge [11]. A major portion of these studies have been carried out on tissue samples after incubation in the presence of oxygen. Carried out in this way the method gives an expression of the tendency to lipoperoxide formation by the tissue, rather than an estimate of its lipoperoxide content. When the thiobarbituric acid reaction is carried out without incubation, obviously only preformed substances can give the reaction. However, this reaction is not given by the peroxide group proper but by secondary reaction products, and consequently it cannot replace a proper peroxide determination method when quantitative information is required.

It appears from our experiments that the substances interfering with methods for the determination of the peroxide group do not inhibit the thiobarbituric acid reaction. The stability of this reaction towards reducing substances is a definite advantage. Therefore, the thiobarbituric acid reaction, carried out without previous incubation, should be tried when reducing substances impede the use of methods for the determination of lipoperoxides proper.

Acknowledgement. This investigation was supported by a grant from *P. Carl Petersens Fond.*

REFERENCES

1. Dam, H. and Granados, H. *Acta Physiol. Scand.* **10** (1945) 162.
2. Jessen, K. E., Glavind, J., Hartmann, S. and Dam, H. *Acta Pathol. Microbiol. Scand.* **29** (1951) 73.
3. Glavind, J., Hartmann, S., Dam, H., Clemmesen, J. and Jessen, K. E. *Acta Pathol. Microbiol. Scand.* **30** (1952) 1.
4. Gomori, G. *Microscopic Histochemistry, Principles and Practice,* Univeristy of Chicago Press, Chicago 1952, p. 157.
5. Glavind, J. and Hartmann, S. *II. Congr. Intern. Biochim.* Paris 1952, *Résumés des Communs.*, p. 356.
6. Glavind, J. and Hartmann, S. *Acta Chem. Scand.* **9** (1955) 497.
7. Glavind, J. and Hartmann, S. *Acta Chem. Scand.* **10** (1956) 1298.
8. Wilbur, K. M., Bernheim, F. and Shapiro, O. W. *Arch. Biochem.* **24** (1949) 305.
9. Glavind, J. *IV. Congr. Intern. Nutrition,* Paris 1957, *Résumés des Communs.*, p. 228.
10. Dubouloz, P., Fondarai, J. and Lagarde, C. *Biochim. et Biophys. Acta* **3** (1949) 371.
11. Kohn, H. I. and Liversedge, M. *J. Pharmacol. Exptl. Therap.* **82** (1944) 292.

Received June 20, 1961.

ACTA CHEMICA SCANDINAVICA 15 (1961) 1932–1938

Studies on Sulphates, Selenates and Chromates of Mercury(II)

KARIN AURIVILLIUS and BIRGITTA MALMROS

Institute of Inorganic and Physical Chemistry, University of Stockholm, Stockholm, Sweden

For some mercury(II)salts containing tetrahedral anions (Table 2) the cell edges, cell contents and probable space groups are given.

Investigations of the crystal chemistry of mercury(II), which have been made at this Institute, have revealed that infinite —O—Hg—O— chains are fundamental constituents in a number of phases comprising the oxides and some oxide halides. The present investigation of the sulphates, selenates and chromates of mercury(II) was undertaken in order to find out whether such chains are also compatible with the presence of tetrahedral anions. This note will present a few results obtained during the preparative work and also some X-ray data.

In the literature, the existence of several sulphates, selenates and chromates of mercury(II) has been reported, *viz.*

Table 1. Observed and calculated values for the analyses and the densities. Calculated values are given within brackets.

Formulae	% Hg	% S	% Se	% Cr	% H_2O	Density $g \cdot cm^{-3}$
$HgSO_4$	67.3(67.6)	10.8(10.8)				6.49(6.50)
$HgSO_4 \cdot H_2O$	63.5(63.7)	10.2(10.2)			5.69(5.72)	5.44(5.45)
$Hg_3O_2SO_4$	82.3(82.5)	4.41(4.39)				8.32(8.43)
$HgSeO_4$	58.0(58.4)		24.0(23.0)			6.88(6.92)
$HgSeO_4 \cdot H_2O$	55.4(55.4)		22.4(21.8)		5.01(4.98)	5.60(5.61)
$Hg_3O_2SeO_4$	76.4(77.5)		10.9(10.2)			8.63(8.69)
$HgCrO_4$	63.3(63.4)			15.9(16.4)		6.06(6.10)
$HgCrO_4 \cdot (H_2O)_{\frac{1}{2}}$	61.3(61.6)			15.6(16.0)	2.76(2.76)	5.51(5.53)
$Hg_3O_2CrO_4$	79.9(80.2)			6.78(6.94)		8.39(8.46)

Table 2. Cell dimensions, cell volumes, cell contents, systematically absent spectra and probable space groups. The cell edges are given in Å, the cell volume in Å^3 and the cell content in formula units.

Formulae	a	b	c	β	V	Cell content	Systematically absent spectra (n is an integer)	Probable* space group
$HgSO_4$	4.817	6.577	4.783		151.5	2	$hk0: h+k=2n+1$	$Pmmn$ (No. 59)
$HgSO_4 \cdot H_2O$	7.881	5.419	8.976		383.3	4	$0kl: k+l=2n+1$ $hk0: h=2n+1$	$Pnma$ (No. 62)
$Hg_3O_2SO_4$	7.049		10.017		431.0	3	$00l: l \neq 3n$	$P3_121$ (No. 152)
$HgSeO_4$	4.979	6.721	4.928		164.9	2	$hk0: h+k=2n+1$	$Pmmn$ (No. 59)
$HgSeO_4 \cdot H_2O$	7.769	7.712	8.249	120.0°	428.1	4	$h0l: l=2n+1$ $0k0: k=2n+1$	$P2_1/c$ (No. 14)
$Hg_3O_2SeO_4$	7.146		10.070		445.3	3	$00l: l \neq 3n$	$P3_121$ (No. 152)
$HgCrO_4$	7.346	8.527	5.514	93.9°	344.5	4	$h0l: h+l=2n+1$ $0k0: k=2n+1$	$P2_1/n$ (No. 14)**
$HgCrO_4 \cdot (H_2O)_{\frac{1}{2}}$	11.837	5.526	14.638	120.9°	782.8	8	$hkl: h+k=2n+1$ $h0l: l=2n+1$	$C2/c$ (No. 15)
$Hg_3O_2CrO_4$	7.132		10.019		441.3	3	$00l: l \neq 3n$	$P3_121$ (No. 152)

* The probable space groups have been deduced from the Laue symmetry and the observed extinctions in the Weissenberg photographs. In the cases where the observed extinctions are characteristic of several space groups we have chosen the one with the highest symmetry as the probable one.

** Orientation different from that given in the *International Tables*.

$Hg_nO_{n-1}SO_4 \cdot mH_2O$ with $n = 1$, $m = 0$; $n = 1$, $m = 1$; $n = 3$, $m = 0$; $n = \frac{3}{2}$, $m = 1$ (Refs.[1-3])

$Hg_nO_{n-1}SeO_4 \cdot mH_2O$ with $n = 1$, $m = 0$; $n = 1$, $m = 1$; $n = 3$, $m = \frac{1}{2}$ (Ref.[4])

$Hg_nO_{n-1}CrO_4 \cdot mH_2O$ with $n = 1$, $m = 0$; $n = 3$, $m = 0$ (Refs.[5-7])

Apart from the above compounds reported by other authors, we have found $Hg_3O_2SeO_4$ and $HgCrO_4(H_2O)_{\frac{1}{2}}$ which have not been reported before to our knowledge. On the other hand we have not yet been successful in preparing $Hg_3O(SO_4)_2(H_2O)_2$ reported by Hoitsema[1] and Paiĉ[3] and $Hg_3O_2SeO_4 \cdot (H_2O)_{\frac{1}{2}}$ reported by Cameron and Davy[4].

The substances $HgSO_4$, $HgSO_4 \cdot H_2O$, $HgSeO_4$, $HgSeO_4 \cdot H_2O$, $HgCrO_4$ and $HgCrO_4(H_2O)_{\frac{1}{2}}$ were synthesized by conventional methods starting from yellow HgO and H_2SO_4, H_2SeO_4 or CrO_3 and H_2O, respectively, while the oxide salts $Hg_3O_2SO_4$, $Hg_3O_2SeO_4$ and $Hg_3O_2CrO_4$ were obtained from $Hg(C_2H_3O_2)_2$ and the appropriate acid. By boiling yellow HgO with CrO_3 and H_2O, not only $HgCrO_4$ but also the new compound $HgCrO_4(H_2O)_{\frac{1}{2}}$ was prepared. $HgCrO_4(H_2O)_{\frac{1}{2}}$ looses its water of crystallization at about 200°C. An X-ray

Table 3. Part of the powder photographs of $HgSO_4$, $HgSeO_4$, $HgSO_4 \cdot H_2O$, $HgSeO_4 \cdot H_2O$, $HgCrO_4$, $HgCrO_4(H_2O)_{\frac{1}{2}}$, $Hg_3O_2SO_4$, $Hg_3O_2SeO_4$ and $Hg_3O_2CrO_4$. Guinier focusing camera of 80 mm diameter with $CuKa_1$ radiation and potassium chloride as internal standard (a (KCl) = 6.2930 Å).

$HgSO_4$				$HgSeO_4$			
$h\,k\,l$	$10^4\sin^2\Theta$ obs	$10^4\sin^2\Theta$ calc	I obs	$h\,k\,l$	$10^4\sin^2\Theta$ obs	$10^4\sin^2\Theta$ calc	I obs
0 0 1	0260	0261	m	0 0 1	0244	0246	m
1 1 0	0394	0395	st	1 1 0	0371	0373	st
0 1 1	0398	0399	st	0 1 1	0378	0378	m
1 0 1	0518	0518	vst	1 0 1	0487	0486	vst
0 2 0	0550	0552	vst	0 2 0	0528	0528	vst
1 1 1	0655	0656	st	1 1 1	0618	0618	vst
0 2 1	0812	0813	vw	0 2 1	0772	0774	w
2 0 0	1028	1028	m	2 0 0	0961	0962	st
0 0 2	1043	1042	w	0 0 2	0982	0982	m
1 2 1	1070	1070	st	1 2 1	1014	1014	vst
0 1 2	1181	1180	m	0 1 2	1115	1114	vst
2 0 1	1289	1289	vw	1 0 2	1223	1223	m
1 0 2	1300	1299	w	2 1 1	1338	1340	m
2 1 1 *	1426	1427	st	1 3 0 }	1431	1429 }	m
1 1 2 *	1438	1437	vw	0 3 1 }		1434 }	
1 3 0 }	1500	1499 }	m	2 2 0	1490	1490	st
0 3 1 }		1503 }		0 2 2	1510	1510	vw
0 2 2	1594	1594	vw	1 3 1 *	1675	1674	st
1 3 1 *	1757	1760	m	1 2 2	1750	1751	m
1 2 2 *	1852	1851	m	2 0 2	1944	1944	w
2 0 2 *	2069	2070	w	2 1 2 *	2075	2076	st
0 4 0 }	2210	2208 }	st	0 4 0	2110	2112	st
2 1 2 }		2208 }		0 3 2	2169	2170	st

* By careful examination these lines were found to be faintly split.

powder photograph of a pure sample of $HgCrO_4(H_2O)_{\frac{1}{2}}$ which had been heated to 170°C for about 70 h gave only the lines of $HgCrO_4$ and showed the corresponding loss of weight. Upon studying commercial »mercuric chromates» from well-known manufacturers, it was found by chemical analyses and X-ray photography that some of them consisted of $HgCrO_4$ and others consisted of $Hg_3O_2CrO_4$.

The pure samples were analysed for Hg, S, Se, Cr and H_2O. The mercury analyses were made using electrolysis or by titrating Hg(II) with a standard solution of KSCN using Fe(III) as an indicator, and the sulphur analyses by precipitation of $BaSO_4$. The selenium analyses were performed by reducing the selenate ion to metallic selenium by adding a saturated solution of SO_2 to a strongly acid (HCl) solution of the salt. This method was, however, found to give slightly too high values. Chromium was determined titrimetrically by conventional methods with standard solutions of $Fe(NH_4)_2(SO_4)_2(H_2O)_6$ and

$HgSO_4 \cdot H_2O$			
h k l	$10^4 \sin^2\Theta$ obs	$10^4 \sin^2\Theta$ calc	*I* obs
1 0 1	0171	0170	m
0 1 1	0278	0277	st
0 0 2	0297	0296	m
1 1 1	0374	0373	m
1 0 2	0393	0392	w
2 0 1	0458	0458	st
2 1 0	0587	0587	st
2 1 1	0661	0661	vw
1 0 3	0763	0762	st
0 2 0	0813	0812	m
0 1 3	0870	0869	m
2 1 2	0881	0883	st
3 0 1	0937	0938	vw
1 1 3	0966	0965	m
1 2 1	0981	0982	m
2 0 3	1051	1050	m
0 2 2	1107	1108	m
3 0 2	1161	1160	vw
0 0 4	1184	1184	w
2 2 1	1268	1270	st
1 0 4	1280	1280	w
3 1 2	1363	1363	m
1 1 4	1484	1483	m
4 0 0	1535	1536	m
1 2 3	1573	1574	m
3 1 3	1735	1733	m
2 1 4	1772	1771	w
4 0 2	1833	1832	m
2 2 3	1861	1862	m

$HgSeO_4 \cdot H_2O$			
h k l	$10^4 \sin^2\Theta$ obs	$10^4 \sin^2\Theta$ calc	*I* obs
1 0 0	0131	0132	m
0 1 1	0216	0217	m
1 1 0	0232	0232	st
1 0 $\bar{2}$	0350	0351	w
0 2 0	0400	0401	st
1 1 $\bar{2}$	0451	0451	vst
0 0 2	0465	0467	w
1 1 1	0472	0473	vw
2 1 $\bar{1}$	0497	0496	m
2 0 $\bar{2}$		0498	
1 1 $\bar{1}$	0527	0526	vst
2 0 0		0527	
1 2 0	0533	0533	vw
0 1 2	0565	0568	vw
2 1 0	0628	0627	m
1 2 $\bar{2}$	0750	0752	m
1 2 1	0772	0774	m
2 2 $\bar{1}$	0796	0797	m
1 0 2	0846	0847	vw
0 2 2	0867	0868	st
2 2 $\bar{2}$	0899	0899	st
3 0 $\bar{2}$	0911	0909	w
1 1 $\bar{3}$		0911	
2 2 0	0929	0928	m
1 1 2	0948	0947	st
3 1 $\bar{2}$	1010	1009	m
3 1 $\bar{1}$	1034	1031	st
1 3 0		1034	
0 1 3	1148	1152	vw
1 2 $\bar{2}$	1251	1248	m
1 3 $\bar{2}$		1253	
1 3 1	1272	1275	w
3 1 0	1287	1286	w
3 2 $\bar{2}$	1311	1310	m
3 2 $\bar{1}$	1335	1332	m
2 3 $\bar{2}$	1403	1400	m
2 0 $\bar{4}$		1404	
2 3 0	1429	1429	w
0 2 3	1448	1452	w
2 1 $\bar{4}$	1501	1504	m
1 0 $\bar{4}$		1505	
3 2 3	1525	1522	vw
3 0 $\bar{4}$	1567	1567	w
2 1 2	1591	1590	st
0 4 0	1602	1604	m
1 1 $\bar{4}$		1605	

$HgCrO_4$				$HgCrO_4(H_2O)_{\frac{1}{2}}$			
h k l	$10^4\sin^2\Theta$ obs	$10^4\sin^2\Theta$ calc	*I* obs	*h k l*	$10^4\sin^2\Theta$ obs	$10^4\sin^2\Theta$ calc	*I* obs
1 1 0	0192	0193	vst	0 0 2	0149	0151	vw
1 0 $\bar{1}$	0288	0288	st	2 0 0	0229	0231	m
0 2 0	0328	0328	st	1 1 0	0271	0273	st
1 0 1		0328		1 1 $\bar{2}$	0325	0328	w
1 1 1	0369	0370	vw	1 1 1	0357	0359	w
2 0 0	0443	0444	st	2 0 4	0448	0450	m
0 2 1	0525	0525	vst	1 1 $\bar{3}$	0466	0468	vw
2 1 0		0526		1 1 2	0518	0520	vw
1 2 $\bar{1}$	0616	0616	vst	2 0 2	0575	0574	vw
1 2 1	0657	0656	vst	3 1 1	0626	0629	vw
2 0 1	0683	0681	vst	1 1 $\bar{4}$	0683	0684	vst
2 1 $\bar{1}$		0683		4 0 2	0689	0692	vw
2 1 1	0765	0763	vst	3 1 0	0735	0735	vst
0 0 2	0790	0788	st	4 0 $\bar{4}$	0760	0760	vst
1 3 0	0848	0849	m	3 1 $\bar{4}$		0762	
1 0 $\bar{2}$	0861	0859	vw	0 2 0	0860	0860	m
0 1 2	0871	0870	w	4 0 0	0926	0925	m
2 2 $\bar{1}$	0928	0929	w	3 1 5	0954	0956	vw
1 0 2	0941	0939	w	1 1 $\bar{5}$	0975	0975	vw
1 1 $\bar{2}$		0941		2 2 1	1029	1032	vvw
1 3 $\bar{1}$	1023	1026	w	1 1 4	1071	1068	m
1 1 2		1021		2 2 0	1090	1091	m
1 3 1	1064	1066	w	2 2 $\bar{3}$	1142	1143	vw
3 1 0	1080	1081	st	2 2 1	1225	1225	w
0 2 2	1118	1116	m	3 1 $\bar{6}$		1228	
2 0 $\bar{2}$	1151	1152	vw	5 1 $\bar{4}$	1303	1303	m
2 3 0	1180	1182	w	2 2 $\bar{4}$	1310	1310	w
2 1 2	1233	1234	w	1 1 $\bar{6}$	1346	1342	vvw
1 2 2	1270	1267	w	5 1 $\bar{5}$	1399	1403	vvw
2 0 2	1312	1312	w	0 2 4	1468	1465	m
3 1 1	1337	1336	w	6 0 4	1531	1532	w
3 2 0		1339		4 2 $\bar{3}$	1552	1548	w
2 1 2	1396	1394	vw	4 2 $\bar{2}$		1552	
2 3 1	1422	1419	m	2 2 $\bar{5}$		1554	
1 4 0		1423		4 2 $\bar{4}$	1620	1620	m
2 2 2	1478	1480	vw				
0 4 1	1508	1508	m				

$KMnO_4$. The water analyses were made according to Penfield[8]. The results of the analyses are in good agreement with the values calculated for the formulae of the compounds given (Table 1).

The densities of the substances were determined from the loss of weight in benzene. From Table 1 it is seen that the agreement between observed and calculated values is very good.

$Hg_3O_2SO_4$			
h k l	$10^4\sin^2\Theta$ obs	$10^4\sin^2\Theta$ calc	*I* obs
1 0 0	0158	0160	m
1 0 1	0218	0219	st
1 0 2	0396	0398	w
1 1 0	0479	0480	vw
0 0 3	0535	0535	vst
2 0 0	0639	0640	m
2 0 1	0700	0699	vst
1 1 2	0717	0718	m
2 0 2	0878	0879	vst
1 1 3	1015	1015	w
1 0 4	1110	1111	st
1 2 0	1121	1120	st
1 2 1	1179	1179	m
1 2 2	1358	1358	m
3 0 1	1502	1499	m
2 0 4	1593	1591	vst
3 0 2	1679	1678	m
2 2 0	1922	1920	st
1 1 5	1966	1966	m
2 2 1	1979	1981	m
1 3 0	2080	2079	m
2 0 5	2127	2126	st
1 3 1 / 0 0 6	2140	2139 / 2139	m
2 2 2	2160	2158	m

$Hg_3O_2SeO_4$			
h k l	$10^4\sin^2\Theta$ obs	$10^4\sin^2\Theta$ calc	*I* obs
1 0 0	0155	0156	m
1 0 1	0213	0214	m
1 0 2	0389	0391	vw
0 0 3	0529	0529	vst
2 0 0	0622	0622	m
2 0 1	0682	0681	vst
1 1 2	0702	0702	m
2 0 2	0857	0857	vst
1 1 3	0995	0996	vw
1 0 4	1096	1096	st
1 2 1 / 2 0 3	1150	1148 / 1151	m
1 2 2	1325	1324	vw
1 1 4	1407	1407	vw
3 0 1	1460	1459	vw
2 0 4	1565	1562	vw
1 0 5	1623	1625	st
3 0 2	1636	1635	st
2 2 0	1870	1867	m
1 1 5	1934	1936	m
1 2 4	2032	2029	vw
2 0 5	2094	2091	st
2 2 2	2105	2102	m
0 0 6	2118	2116	w
1 0 6	2274	2272	w

All of the compounds synthesized in this work were characterized by X-ray (powder and single crystal) methods. The cell dimensions, cell volumes, cell contents, systematically absent spectra and probable space groups are given in Table 2. Part of the powder patterns are given in Table 3.

The compounds $HgSO_4$ and $HgSeO_4$ were found to be isomorphous, likewise the compounds $Hg_3O_2SO_4$, $Hg_3O_2SeO_4$ and $Hg_3O_2CrO_4$. For $HgSO_4$, the same cell edges within the limits of experimental error have been recently reported by Kokkoros and Rentzeperis [9]. A faint splitting of some of the lines *hkl* and *h0l* in the X-ray powder photographs taken in a Guinier focusing camera may, however, indicate a lower symmetry. For $HgSO_4 \cdot H_2O$, the same cell edges and symmetry were found as those recently reported by Bonifačić[10].

The authors wish to thank Professor A. Ölander and Professor A. Magnéli for their very kind interest in our work.

These studies form part of a research program on mercury(II)salts, financially supported by the *Swedish Natural Science Research Council.*

$Hg_3O_2CrO_4$			
h k l	$10^4\sin^2\Theta$ obs	$10^4\sin^2\Theta$ calc	*I* obs
1 0 0	0156	0156	m
1 0 1	0215	0215	st
1 0 2	0393	0394	vw
1 1 0	0469	0469	vw
0 0 3	0534	0535	vst
2 0 0	0625	0625	w
2 0 1	0686	0685	vst
1 0 3	0690	0691	m
1 1 2	0706	0707	m
2 0 2	0863	0863	vst
1 1 3	1004	1004	vw
1 2 0	1095	1094	m
1 0 4	1106	1106	m
1 2 1	1154	1153	w
2 0 3	1161	1160	w
1 2 2	1331	1332	vw
1 1 4	1419	1419	vw
3 0 1	1466	1466	vw
2 0 4	1576	1575	vst
1 2 3	1628	1629	m
1 0 5 3 0 2	1643	1641 1645	w
2 2 0	1876	1876	m
2 2 1	1934	1935	m
1 1 5	1954	1954	m
1 3 0	2032	2032	vw
1 2 4	2045	2044	w
1 3 1	2091	2091	w
2 0 5 2 2 2	2112	2110 2114	st
0 0 6	2137	2138	w

REFERENCES

1. Hoitsema, C. *Z. physik. Chem.* **17** (1895) 651.
2. Paič, M. *Bull. soc. chim. France* **47** (1930) 1254.
3. Paič, M. *Ann. Chim.* **19** (1933) 427.
4. Gmelin-Kraut, *Handbuch der anorganischen Chemie*, 7. Aufl., Heidelberg 1914, Vol. V:2, p. 625.
5. Cox, A. I. *Z. anorg. Chem.* **40** (1904) 146.
6. Cox, A. I. *Z. anorg. Chem.* **50** (1906) 226.
7. Montignie, E. *Bull. soc. chim. France Memoires* **3** (1936) 460.
8. Kolthoff, I. M. and Sandell, E. B. *Textbook of Quantitative Inorganic Analysis*, 3rd Ed., New York 1952, p. 717.
9. Kokkoros, P. A. and Rentzeperis, P. J. *Acta Cryst.* **14** (1961) 329.
10. Bonifačić, A. *Acta Cryst.* **14** (1961) 116.

Received June 9, 1961.

ACTA CHEMICA SCANDINAVICA 15 (1961) 1939—1948

Short Communications

Complexes of Tellurium Tetrachloride and Tetrabromide with Tetramethylthiourea

OLAV FOSS and
WERMUND JOHANNESSEN

Chemical Institute, University of Bergen, Bergen, Norway

In the course of a study of complexes of divalent tellurium with tetramethylthiourea (tmtu) we have encountered two derivatives of tetravalent tellurium, the presumably six-coordinated complexes $Te(tmtu)_2Cl_4$ and $Te(tmtu)_2Br_4$. The crystals of the two compounds are isomorphous, and unit cell and space group data indicate that the tellurium atom lies in a centre of symmetry. Similar complexes have been described earlier; for example, of tellurium tetrachloride with thiourea [1,2], pyridine and aniline [1], and dimethylaniline [3], and of tellurium tetrabromide with thiourea [2], aniline, dimethylaniline and diphenylamine [4], but no structural data appear to be available.

Tetravalent tellurium in six-coordinated complexes has six bonding electron pairs and one non-bonding one in its valency shell. The stereochemistry of such complexes will depend on whether the lone pair is stereochemically active, in which case a pentagonal-bipyramidal arrangement of six bonding pairs and one lone pair is expected [5], or stereochemically inert [6,7], as in the octahedral [8,9] hexachloro- and hexabromotellurite(IV) ions. Although the centre of symmetry in the tetramethylthiourea complexes does not impose regular octahedral symmetry on the bonding pairs, it is in accord with octahedral symmetry and not with a lone pair in one of seven positions. The compounds would represent the *trans* isomer of octahedral complexes of this type.

The crystals are dark red in colour, and are stable when kept in closed bottles. On prolonged exposure to humid air the surface becomes whitish, and water hydrolyzes them rapidly to white tellurous acid. X-Ray crystallographic data were obtained from oscillation and Weissenberg photographs; the axial lengths quoted below are based on $\lambda = 1.542$ Å for Cu*Ka* radiation and are believed to be accurate to within 0.5 %.

Tellurium tetrachloride complex, $Te(tmtu)_2Cl_4$. To 1.6 g (10 mmoles) of tellurium dioxide in 6 ml of concentrated hydrochloric acid was added, rapidly with swirling, at room temperature, 5.3 g (40 mmoles) of tetramethylthiourea in 20 ml of methanol. The resulting red solution was, to remove some oily material, decanted into another beaker, and 10 ml of methanol was added to the decantate. On standing, the complex slowly crystallized. Yield, 1.8 g (34 %). M.p. 153—154°. (Found: Cl 26.55; S 12.15; Te 23.96. Calc. for $C_{10}H_{24}Cl_4N_4S_2Te$: Cl 26.56; S 12.01; Te 23.90.)

Tellurium tetrabromide complex, $Te(tmtu)_2Br_4$. To 1.6 g (10 mmoles) of tellurium dioxide in 5 ml of concentrated hydrochloric acid and 10 ml of water was added 2.7 g (20 mmoles) of tetramethylthiourea in 20 ml of methanol, and then, rapidly under swirling, a hot mixture of 10 ml of 48—50 % hydrobromic acid, 50 ml of water and 50 ml of methanol. If hydrobromic instead of hydrochloric acid is used to dissolve the tellurium dioxide, rather extensive oil formation occurs on addition of the tetramethylthiourea solution. Yield, after cooling to room temperature, 5.2 g. The product was a mixture of about equal amounts of the tetrabromide complex and the divalent tellurium complex [10] $Te(tmtu)Br_2$; the crystals of the two compounds could be readily discerned and picked out under a microscope. Although the tetrabromide complex thus was not obtained pure and not analyzed,

identity was established through single-crystal X-ray photographs showing isomorphism with the tetrachloride complex. M.p., of picked-out crystals, 176–177°.

The crystals are orthorhombic; those of the tetrachloride complex occur as prisms along the c axis bounded by {010} and {100} and those of the tetrabromide complex as six-sided plates {010} a little extended along the c axis. The axial lengths are, for $Te(tmtu)_2Cl_4$: a = 14.74 Å, b = 13.87 Å, c = 10.06 Å, and for $Te(tmtu)_2Br_4$: a = 14.98 Å, b = 13.88 Å, c = 10.40 Å. There are four molecules per unit cell; densities, calc. 1.72 and 2.19, respectively, found 1.70 and 2.21 g/cm³. The space group, from systematic absences, is D_{2h}^{15} – $Pbca$, which has eightfold general positions, and requires that the four tellurium atoms lie in centres of symmetry. This is consistent with the intensity distribution of the hkl reflections, those with $h + k$, $k + l$ and $l + h$ even being strongest, particularly in the case of the tetrachloride complex.

1. Tronev, V. G. and Grigorovich, A. N. *Zhur. Neorg. Khim.* **2** (1957) 2400; *C. A.* **53** (1959) 3967.
2. Aynsley, E. E. and Campbell, W. A. *J. Chem. Soc.* **1958** 3290.
3. Morgan, G. T. and Burgess, H. *J. Chem. Soc.* **1929** 1103.
4. Lowy, A. and Dunbrook, R. F. *J. Am. Chem. Soc.* **44** (1922) 614.
5. Gillespie, R. J. and Nyholm, R. S. *Quart. Revs. (London)* **11** (1957) 339.
6. Sidgwick, N. V. *Ann. Repts. on Progr. Chem. (Chem. Soc. London)* **30** (1933) 120.
7. Pauling, L. *The Nature of the Chemical Bond*, 2nd. Ed., Cornell Univ. Press, Ithaca, New York, 1940, pp. 183–5.
8. Engel, G. *Z. Krist.* **90** (1935) 341.
9. Bagnall, K. W., D'Eye, R. W. M. and Freeman, J. H. *J. Chem. Soc.* **1955** 3959.
10. Foss, O. and Johannessen, W. *Acta Chem. Scand.* **15** (1961) 1940.

Received October 17, 1961.

Complexes of Tellurium Dichloride and Dibromide with One Mole of Tetramethylthiourea

OLAV FOSS and
WERMUND JOHANNESSEN

Chemical Institute, University of Bergen, Bergen, Norway

The tetravalent tellurium complex described in a preceding note [1], $Te(tmtu)_2Cl_4$ where tmtu = tetramethylthiourea, when dissolved in warm 4 N hydrochloric acid-methanol 2 : 1 (30 ml per g) and the solution kept near boiling temperature, forms a divalent tellurium complex, $Te(tmtu)Cl_2$, which in the course of a few hours separates out as dark red crystals. Presumably tetramethylthiourea acts as the reducing agent, being itself oxidized to the disulphide cation, $(tmtu)_2^{2+}$, of which salts are known [2,3].

The tellurium dichloride complex, and the corresponding bromide, may also be prepared directly from tellurium dioxide and tetramethylthiourea, as described below. The X-ray crystallographic data have been obtained from oscillation and Weissenberg photographs; the axial lengths, believed to be accurate to within 0.5 %, are based on $\lambda(CuK\alpha)$ = 1.542 Å.

Tellurium dichloride complex, $Te(tmtu)Cl_2$. To a warm solution of 1.6 g (10 mmoles) of tellurium dioxide in 20 ml of concentrated hydrochloric acid and 40 ml of water was added 2.7 g (20 mmoles) of tetramethylthiourea dissolved in 40 ml of methanol. The resulting, red solution was heated to near boiling temperature, and kept at this temperature some hours, while crystallization took place; the crystallization starts on scratching of the beaker walls, or on seeding, and is rather slow. Yield, about 2.2 g. M.p. 207°. (Found: Cl 21.32; S 9.69; Te 38.67. Calc. for $C_5H_{12}Cl_2N_2STe$: Cl 21.44; S 9.70; Te 38.58.) The compound, and the dibromide complex, are stable in the solid state, but liberate tellurium in contact with water like other complexes of divalent tellurium. They were on the filters washed with methanol containing a little concentrated hydrochloric acid or hydrobromic acid, respectively, and then with ether.

identity was established through single-crystal X-ray photographs showing isomorphism with the tetrachloride complex. M.p., of picked-out crystals, 176–177°.

The crystals are orthorhombic; those of the tetrachloride complex occur as prisms along the c axis bounded by {010} and {100} and those of the tetrabromide complex as six-sided plates {010} a little extended along the c axis. The axial lengths are, for $Te(tmtu)_2Cl_4$: a = 14.74 Å, b = 13.87 Å, c = 10.06 Å, and for $Te(tmtu)_2Br_4$: a = 14.98 Å, b = 13.88 Å, c = 10.40 Å. There are four molecules per unit cell; densities, calc. 1.72 and 2.19, respectively, found 1.70 and 2.21 g/cm³. The space group, from systematic absences, is D_{2h}^{15} – $Pbca$, which has eightfold general positions, and requires that the four tellurium atoms lie in centres of symmetry. This is consistent with the intensity distribution of the hkl reflections, those with $h + k$, $k + l$ and $l + h$ even being strongest, particularly in the case of the tetrachloride complex.

1. Tronev, V. G. and Grigorovich, A. N. *Zhur. Neorg. Khim.* **2** (1957) 2400; *C. A.* **53** (1959) 3967.
2. Aynsley, E. E. and Campbell, W. A. *J. Chem. Soc.* **1958** 3290.
3. Morgan, G. T. and Burgess, H. *J. Chem. Soc.* **1929** 1103.
4. Lowy, A. and Dunbrook, R. F. *J. Am. Chem. Soc.* **44** (1922) 614.
5. Gillespie, R. J. and Nyholm, R. S. *Quart. Revs. (London)* **11** (1957) 339.
6. Sidgwick, N. V. *Ann. Repts. on Progr. Chem. (Chem. Soc. London)* **30** (1933) 120.
7. Pauling, L. *The Nature of the Chemical Bond*, 2nd. Ed., Cornell Univ. Press, Ithaca, New York, 1940, pp. 183–5.
8. Engel, G. *Z. Krist.* **90** (1935) 341.
9. Bagnall, K. W., D'Eye, R. W. M. and Freeman, J. H. *J. Chem. Soc.* **1955** 3959.
10. Foss, O. and Johannessen, W. *Acta Chem. Scand.* **15** (1961) 1940.

Received October 17, 1961.

Complexes of Tellurium Dichloride and Dibromide with One Mole of Tetramethylthiourea

OLAV FOSS and
WERMUND JOHANNESSEN

Chemical Institute, University of Bergen, Bergen, Norway

The tetravalent tellurium complex described in a preceding note [1], $Te(tmtu)_2Cl_4$ where tmtu = tetramethylthiourea, when dissolved in warm 4 N hydrochloric acid-methanol 2 : 1 (30 ml per g) and the solution kept near boiling temperature, forms a divalent tellurium complex, $Te(tmtu)Cl_2$, which in the course of a few hours separates out as dark red crystals. Presumably tetramethylthiourea acts as the reducing agent, being itself oxidized to the disulphide cation, $(tmtu)_2^{2+}$, of which salts are known [2,3].

The tellurium dichloride complex, and the corresponding bromide, may also be prepared directly from tellurium dioxide and tetramethylthiourea, as described below. The X-ray crystallographic data have been obtained from oscillation and Weissenberg photographs; the axial lengths, believed to be accurate to within 0.5 %, are based on $\lambda(CuK\alpha)$ = 1.542 Å.

Tellurium dichloride complex, $Te(tmtu)Cl_2$. To a warm solution of 1.6 g (10 mmoles) of tellurium dioxide in 20 ml of concentrated hydrochloric acid and 40 ml of water was added 2.7 g (20 mmoles) of tetramethylthiourea dissolved in 40 ml of methanol. The resulting, red solution was heated to near boiling temperature, and kept at this temperature some hours, while crystallization took place; the crystallization starts on scratching of the beaker walls, or on seeding, and is rather slow. Yield, about 2.2 g. M.p. 207°. (Found: Cl 21.32; S 9.69; Te 38.67. Calc. for $C_5H_{12}Cl_2N_2STe$: Cl 21.44; S 9.70; Te 38.58.) The compound, and the dibromide complex, are stable in the solid state, but liberate tellurium in contact with water like other complexes of divalent tellurium. They were on the filters washed with methanol containing a little concentrated hydrochloric acid or hydrobromic acid, respectively, and then with ether.

Tellurium dibromide complex, $Te(tmtu)Br_2$. To 1.6 g of tellurium dioxide, dissolved by heating in 6 ml of concentrated hydrochloric acid, was added 20 ml of water and then 2.7 g of tetramethylthiourea in 40 ml of methanol. The solution was heated, and a hot mixture of 20 ml of 48–50 % hydrobromic acid, 100 ml of water and 100 ml of methanol was added under stirring. Crystallization takes place from hot solution as in the case of the dichloride complex. Yield, about 2.7 g of dark red crystals. M. p. 226°. (Found: S 7.61; Te 30.46. Calc. for $C_5H_{12}Br_2N_2STe$: S 7.64; Te 30.41.) More concentrated solutions and lower crystallization temperature [1] gave mixtures of the compound with the tetravalent tellurium complex, $Te(tmtu)_2Br_4$.

The crystals of the tellurium dichloride and dibromide complexes are isomorphous. The dimensions of the triclinic unit cells are, for $Te(tmtu)Cl_2$: a = 8.01 Å, b = 8.57 Å, c = 9.43 Å, α = 108°, β = 110½°, γ = 93½°, and for $Te(tmtu)Br_2$: a = 8.12 Å, b = 8.74 Å, c = 9.65 Å, α = 108½°, β = 110°, γ = 94½°. There are two formula units per unit cell; densities, calc. 1.94 and 2.33, respectively, found 1.94 and 2.34 g/cm³.

The crystal structure of $Te(tmtu)Cl_2$ has been determined through projections along the a and b axes [4]. The space group is the centrosymmetric one, $C_i^1 - P\bar{1}$. Planar $TeSCl_2$ groups, joined two and two over a centre of symmetry through two unsymmetrical, rather weak Te–Cl–Te bridges, occur in the crystals. Each tellurium atom forms, in a planar, approximately square arrangement, one Te–S bond, two *trans* Te–Cl bonds and a third, longer Te–Cl bond *trans* to the Te–S bond.

1. Foss, O. and Johannessen, W. *Acta Chem. Scand.* **15** (1961) 1939.
2. Lecher, H., Graf, F., Heuck, C., Köberle, K., Gnädinger, F. and Heydweiller, F. *Ann.* **445** (1925) 35.
3. Sahasrabudhey, R. H. *J. Indian Chem. Soc.* **28** (1951) 341.
4. Foss, O. and Scheie, A. *To be published.*

Received October 17, 1961.

Complexes of Divalent Tellurium with Tetramethylthiourea

OLAV FOSS and
WERMUND JOHANNESSEN

Chemical Institute, University of Bergen, Bergen, Norway

The tellurium dichloride and dibromide complexes [1], $Te(tmtu)Cl_2$ and $Te(tmtu)Br_2$ where tmtu = tetramethylthiourea, dissolve in warm methanolic tetramethylthiourea to give red solutions from which the compounds, $Te(tmtu)_2Cl_2$ and $Te(tmtu)_2Br_2$, crystallize on cooling. These are divalent tellurium complexes of the same type as $Te(tu)_2X_2$ (tu = thiourea, X = Cl, Br, I, SCN) [2,3] and $Te(etu)_2X_2$ (etu = ethylenethiourea, X = Br, I, SCN) [4]. We have also obtained the iodide, $Te(tmtu)_2I_2$, in two crystalline forms, and, from the thiourea compounds $Te(tu)_2Cl_2$ and $Te(tu)_2Br_2$ dissolved in warm methanolic tetramethylthiourea, on cooling, the chloride and bromide of a divalent tellurium cation with two thiourea and two tetramethylthiourea ligands. In all of these $Te(tmtu)_2X_2$ complexes, except one of the forms of the iodide, unit cell and space group data indicate that the tellurium atom lies in a centre of symmetry, and they thus represent the *trans* isomer of a square planar complex of this type. *Trans* forms have otherwise been found in the case of $Te(etu)_2Br_2$ and $Te(etu)_2I_2$ [4] and a series of complexes of divalent tellurium thiosulphonates with thioureas [5].

We have not been able to isolate any salt of a $Te(tmtu)_4^{2+}$ cation, although $Te(tu)_4^{2+}$ and $Te(etu)_4^{2+}$ salts are easily formed [2,6,7]. The reason may lie in the steric requirements of the methyl groups, as may also the preferred occurrence of *trans* forms of the $Te(tmtu)_2X_2$ complexes. Scale models indicate, however, that a planar arrangement of four tetramethylthiourea groups around tellurium, or a *cis* arrangement of two groups, should be possible.

The crystals of the dichloride and dibromide complexes are orange yellow to red in colour, those of the diiodide complex dark red, and those of the cation complexes yellow. They are stable in the solid state, but liberate tellurium in presence of water. Single-crystal X-ray data were obtained using Cu$K\alpha$ radiation, λ = 1.542 Å; values

Tellurium dibromide complex, $Te(tmtu)Br_2$. To 1.6 g of tellurium dioxide, dissolved by heating in 6 ml of concentrated hydrochloric acid, was added 20 ml of water and then 2.7 g of tetramethylthiourea in 40 ml of methanol. The solution was heated, and a hot mixture of 20 ml of 48–50 % hydrobromic acid, 100 ml of water and 100 ml of methanol was added under stirring. Crystallization takes place from hot solution as in the case of the dichloride complex. Yield, about 2.7 g of dark red crystals. M. p. 226°. (Found: S 7.61; Te 30.46. Calc. for $C_5H_{12}Br_2N_2STe$: S 7.64; Te 30.41.) More concentrated solutions and lower crystallization temperature [1] gave mixtures of the compound with the tetravalent tellurium complex, $Te(tmtu)_2Br_4$.

The crystals of the tellurium dichloride and dibromide complexes are isomorphous. The dimensions of the triclinic unit cells are, for $Te(tmtu)Cl_2$: a = 8.01 Å, b = 8.57 Å, c = 9.43 Å, α = 108°, β = 110½°, γ = 93½°, and for $Te(tmtu)Br_2$: a = 8.12 Å, b = 8.74 Å, c = 9.65 Å, α = 108½°, β = 110°, γ = 94½°. There are two formula units per unit cell; densities, calc. 1.94 and 2.33, respectively, found 1.94 and 2.34 g/cm³.

The crystal structure of $Te(tmtu)Cl_2$ has been determined through projections along the a and b axes [4]. The space group is the centrosymmetric one, $C_i^1 - P\bar{1}$. Planar $TeSCl_2$ groups, joined two and two over a centre of symmetry through two unsymmetrical, rather weak Te–Cl–Te bridges, occur in the crystals. Each tellurium atom forms, in a planar, approximately square arrangement, one Te–S bond, two *trans* Te–Cl bonds and a third, longer Te–Cl bond *trans* to the Te–S bond.

1. Foss, O. and Johannessen, W. *Acta Chem. Scand.* **15** (1961) 1939.
2. Lecher, H., Graf, F., Heuck, C., Köberle, K., Gnädinger, F. and Heydweiller, F. *Ann.* **445** (1925) 35.
3. Sahasrabudhey, R. H. *J. Indian Chem. Soc.* **28** (1951) 341.
4. Foss, O. and Scheie, A. *To be published.*

Received October 17, 1961.

Complexes of Divalent Tellurium with Tetramethylthiourea

OLAV FOSS and
WERMUND JOHANNESSEN

Chemical Institute, University of Bergen, Bergen, Norway

The tellurium dichloride and dibromide complexes [1], $Te(tmtu)Cl_2$ and $Te(tmtu)Br_2$ where tmtu = tetramethylthiourea, dissolve in warm methanolic tetramethylthiourea to give red solutions from which the compounds, $Te(tmtu)_2Cl_2$ and $Te(tmtu)_2Br_2$, crystallize on cooling. These are divalent tellurium complexes of the same type as $Te(tu)_2X_2$ (tu = thiourea, X = Cl, Br, I, SCN) [2,3] and $Te(etu)_2X_2$ (etu = ethylenethiourea, X = Br, I, SCN) [4]. We have also obtained the iodide, $Te(tmtu)_2I_2$, in two crystalline forms, and, from the thiourea compounds $Te(tu)_2Cl_2$ and $Te(tu)_2Br_2$ dissolved in warm methanolic tetramethylthiourea, on cooling, the chloride and bromide of a divalent tellurium cation with two thiourea and two tetramethylthiourea ligands. In all of these $Te(tmtu)_2X_2$ complexes, except one of the forms of the iodide, unit cell and space group data indicate that the tellurium atom lies in a centre of symmetry, and they thus represent the *trans* isomer of a square planar complex of this type. *Trans* forms have otherwise been found in the case of $Te(etu)_2Br_2$ and $Te(etu)_2I_2$ [4] and a series of complexes of divalent tellurium thiosulphonates with thioureas [5].

We have not been able to isolate any salt of a $Te(tmtu)_4^{2+}$ cation, although $Te(tu)_4^{2+}$ and $Te(etu)_4^{2+}$ salts are easily formed [2,6,7]. The reason may lie in the steric requirements of the methyl groups, as may also the preferred occurrence of *trans* forms of the $Te(tmtu)_2X_2$ complexes. Scale models indicate, however, that a planar arrangement of four tetramethylthiourea groups around tellurium, or a *cis* arrangement of two groups, should be possible.

The crystals of the dichloride and dibromide complexes are orange yellow to red in colour, those of the diiodide complex dark red, and those of the cation complexes yellow. They are stable in the solid state, but liberate tellurium in presence of water. Single-crystal X-ray data were obtained using Cu$K\alpha$ radiation, λ = 1.542 Å; values

for axial lengths are probably accurate to within 0.5 %.

Tellurium dichloride complex, $Te(tmtu)_2Cl_2$. M. p. 167° (decomp.). (Found: Cl 15.57; S 13.82; Te 27.68. Calc. for $C_{10}H_{24}Cl_2N_4S_2Te$: Cl 15.32; S 13.85; Te 27.56.) The crystals occur as triclinic plates {001} with plate edges parallel to the *ab* diagonals and the *a* axis. The unit cell dimensions are, a = 10.64 Å, b = 11.46 Å, c = 9.07 Å, α = 102°, β = 120°, γ = 84½°, and there are two molecules per unit cell; density, calc. 1.64, found 1.64 g/cm³. A striking feature, for example on oscillation photographs about the *ab* diagonals, are the weak *hkl* reflections for odd values of $h + k$. This indicates that the tellurium atoms are centered on the *c* plane; instead of occupying a twofold set of general positions of the space group $C_i^1 - P\bar{1}$, they are located in symmetry centres at 0,0,0 and ½,½,0. The asymmetric unit thus consists of two half molecules.

Tellurium dibromide complex, $Te(tmtu)_2Br_2$. M. p. 192° (decomp.). (Found: S 11.64; Te 23.15. Calc. for $C_{10}H_{24}Br_2N_4S_2Te$: S 11.62; Te 23.12.) The crystals are isomorphous with those of the dichloride complex, and show the same morphology and the same intensity distribution: Weak *hkl* reflections when $h + k$ is odd, although less pronounced than in the case of the dichloride complex in accordance with the presence of the heavier bromine in general positions. The unit cell dimensions are, a = 10.89 Å, b = 11.66 Å, c = 9.07 Å, α = 101½°, β = 120°, γ = 84°, and the density, calc. 1.88 for two molecules per unit cell, found 1.89 g/cm³.

About 2.5 g of tetramethylthiourea in 50 ml of methanol was used per g of $Te(tmtu)Cl_2$ and $Te(tmtu)Br_2$ in preparing the dichloride and dibromide complexes. The methanolic tetramethylthiourea was heated to about 60° and stirred with the powdered substances for some minutes, until no more dissolved, then filtered while warm and allowed to cool to room temperature, in the case of the dichloride complex after addition of a few drops of concentrated hydrochloric acid and about the double volume of ether. The crystals of the dichloride complex were washed on the filter with methanol-ether 1 : 1 and those of the dibromide complex with methanol, containing a little hydrochloric or hydrobromic acid, respectively, and then with ether.

The dibromide complex was also obtained directly from tellurium dioxide and tetramethylthiourea in a molar ratio of 1 : 4 by the procedure [6] which with a molar ratio of 1 : 2 gave a mixture of $Te(tmtu)_2Br_4$ and $Te(tmtu)Br_2$. Yield, from 1.6 g (10 mmoles) of tellurium dioxide, 4–5 g (72–91 %). The crystals of the crude product were poorly developed, and twinned; better ones were obtained on recrystallization from methanolic tetramethylthiourea.

Tellurium diiodide complex, $Te(tmtu)_2I_2$. M. p. 172–3° (decomp.). (Found: I 39.57; S 9.93; Te 19.65. Calc. for $C_{10}H_{24}I_2N_4S_2Te$: I 39.30; S 9.93; Te 19.76.) The samples were mixtures of two types of crystals, which could be picked out under a microscope; they are both monoclinic.

One of the forms occurred as plates {101} bounded by {011} and {110}, often like cut-off, oblique pyramids, with a = 8.00 Å, b = 10.81 Å, c = 11.96 Å, β = 97½°, and two molecules per unit cell; density, calc. 2.09, found 2.10 g/cm. The space group, from systematic absences, is $C_{2h}^5 - P2_1/n$, which requires that the tellurium atoms lie in centres of symmetry.

The second type of crystals were prisms {021} terminated by {110}, with {010} developed in most cases, and a = 9.23 Å, b = 18.98 Å, c = 11.94 Å, β = 102°. The space group is the same as for the first form, $C_{2h}^5 - P2_1/n$, but there are four molecules per unit cell; density, calc. 2.10, found 2.10 g/cm³, so that no molecular symmetry is required. In view of the finding of only *trans* forms of other tetramethylthiourea complexes, this is probably not the *cis* isomer of the diiodide, but a *trans* dimorph.

The diiodide complex was prepared from warm methanolic tetramethylthiourea solutions of the dichloride or dibromide complex, by addition of methanolic sodium or potassium iodide. It was recrystallized by dissolving it in boiling methanolic tetramethylthiourea (a rather large volume and long heating time is required because of low solubility) and allowing the solution to cool.

The *dichloride*, $[Te(tu)_2(tmtu)_2]Cl_2$. M. p. 157° (decomp.). (Found: Cl 11.50; S 20.94; Te 20.79. Calc. for $C_{12}H_{32}Cl_2N_8S_4Te$: Cl 11.53; S 20.85; Te 20.74.) The salt forms monoclinic prisms extended along the *c* axis, bounded by {100} and {010} with the former dominant, and terminated by {011}. The unit cell dimensions are, a = 8.83 Å, b = 14.40 Å, c = 9.90 Å, β = 94°, and there are two formula units per unit cell; density, calc. 1.63, found 1.63 g/cm³.

The space group, from systematic absences, is C_{2h}^5 — $P2_1/c$, which requires that the tellurium atoms lie in centres of symmetry. This is consistent with the intensity distribution of the *hkl* reflections, those with $k + l$ even being in most cases markedly stronger than those with $k + l$ odd.

The *dibromide*, $[Te(tu)_2(tmtu)_2]Br_2$, is isomorphous with the dichloride, and has $a = 8.78$ Å, $b = 15.02$ Å, $c = 10.04$ Å, $\beta = 94°$, and density, calc. 1.77 for two formula units per unit cell, found 1.79 g/cm³. M. p. 150° (decomp.). (Found: S 18.52; Te 18.09. Calc. for $C_{12}H_{32}Br_2N_8S_4Te$: S 18.22; Te 18.12.) The crystals occurred as short prisms {011}.

The same procedure as above for the dichloride and dibromide complexes was used in preparing the dithioureabis(tetramethylthiourea)tellurium(II) salts; here, about 2 g of tetramethylthiourea in 20 ml of methanol was employed per g of $Te(tu)_2Cl_2$ and $Te(tu)_2Br_2$, and no ether except for the last washings. The methanolic mother liquors, which contain the excess of tetramethylthiourea, can be used for further preparations of the same substance.

1. Foss, O. and Johannessen, W. *Acta Chem. Scand.* **15** (1961) 1940.
2. Foss, O. and Hauge, S. *Acta Chem. Scand.* **13** (1959) 1252.
3. Foss, O. and Hauge, S. *Acta Chem. Scand.* **15** (1961) 1615.
4. Foss, O. and Fossen, S. *Acta Chem. Scand.* **15** (1961) 1618.
5. Foss, O. and Johannessen, I.-J. *Acta Chem. Scand.* **15** (1961) 1943.
6. Foss, O. and Hauge, S. *Acta Chem. Scand.* **15** (1961) 1616.
7. Foss, O. and Fossen, S. *Acta Chem. Scand.* **15** (1961) 1620.
8. Foss, O. and Johannessen, W. *Acta Chem. Scand.* **15** (1961) 1939.

Received October 17, 1961.

Complexes of Divalent Tellurium Thiosulphonates with Thioureas

OLAV FOSS and INGER-JOHANNE JOHANNESSEN

Chemical Institute, University of Bergen, Bergen, Norway

Thiosulphonates of divalent tellurium, $Te(S_2O_2R)_2$ with R = methyl, phenyl and *p*-tolyl, have been prepared earlier by one of us[1,2], and their crystal structures determined[3-5]. Divalent tellurium in these compounds readily releases the thiosulphonate groups in displacement reactions with thio ions of higher nucleophilic reactivity, such as thiosulphate and dialkyldithiocarbamate ions [1,2]:

$$Te(S_2O_2R)_2 + 2\ YS^- = Te(SY)_2 + 2\ RSO_2S^-$$

This note reports the finding that with thioureas as nucleophiles, in most cases only an addition and not a displacement takes place. Divalent tellurium adds two molecules of thiourea (tu), ethylenethiourea (etu), or tetramethylthiourea (tmtu), to give four-coordinated, planar complexes $Te(tu)_2X_2$, $Te(etu)_2X_2$ and $Te(tmtu)_2X_2$, where X = thiosulphonate. Five representatives are described below, one in two crystalline forms. In all but one of the crystals, unit cell and space group data indicate that the tellurium atom lies in a centre of symmetry. They thus are the *trans* isomers.

The compounds are yellow, with a greenish tinge in the case of the ethylenethiourea derivatives, except the tetramethylthiourea-benzenethiosulphonate complex which is red. In contact with methanol the latter complex gives off tetramethylthiourea, leaving yellow crystals of tellurium dibenzenethiosulphonate. Water destroys the complexes with liberation of tellurium. In the solid, dry state they are quite stable.

Unit cell and space group data were derived from oscillation and Weissenberg photographs, using Cu*Kα* radiation, λ = 1.542 Å. The values for axial lengths are believed to be accurate to within 0.5 %.

Dimethanethiosulphonato-dithiourea-tellurium(II), $Te(tu)_2(S_2O_2CH_3)_2$, crystallizes from solutions made by dissolving powdered tellurium dimethanethiosulphonate in methanolic thiourea, under stirring and heating to near boiling temperature. Some

The space group, from systematic absences, is C_{2h}^5 — $P2_1/c$, which requires that the tellurium atoms lie in centres of symmetry. This is consistent with the intensity distribution of the *hkl* reflections, those with $k + l$ even being in most cases markedly stronger than those with $k + l$ odd.

The *dibromide*, $[Te(tu)_2(tmtu)_2]Br_2$, is isomorphous with the dichloride, and has $a = 8.78$ Å, $b = 15.02$ Å, $c = 10.04$ Å, $\beta = 94°$, and density, calc. 1.77 for two formula units per unit cell, found 1.79 g/cm³. M. p. 150° (decomp.). (Found: S 18.52; Te 18.09. Calc. for $C_{12}H_{32}Br_2N_8S_4Te$: S 18.22; Te 18.12.) The crystals occurred as short prisms {011}.

The same procedure as above for the dichloride and dibromide complexes was used in preparing the dithioureabis(tetramethylthiourea)tellurium(II) salts; here, about 2 g of tetramethylthiourea in 20 ml of methanol was employed per g of $Te(tu)_2Cl_2$ and $Te(tu)_2Br_2$, and no ether except for the last washings. The methanolic mother liquors, which contain the excess of tetramethylthiourea, can be used for further preparations of the same substance.

1. Foss, O. and Johannessen, W. *Acta Chem. Scand.* **15** (1961) 1940.
2. Foss, O. and Hauge, S. *Acta Chem. Scand.* **13** (1959) 1252.
3. Foss, O. and Hauge, S. *Acta Chem. Scand.* **15** (1961) 1615.
4. Foss, O. and Fossen, S. *Acta Chem. Scand.* **15** (1961) 1618.
5. Foss, O. and Johannessen, I.-J. *Acta Chem. Scand.* **15** (1961) 1943.
6. Foss, O. and Hauge, S. *Acta Chem. Scand.* **15** (1961) 1616.
7. Foss, O. and Fossen, S. *Acta Chem. Scand.* **15** (1961) 1620.
8. Foss, O. and Johannessen, W. *Acta Chem. Scand.* **15** (1961) 1939.

Received October 17, 1961.

Complexes of Divalent Tellurium Thiosulphonates with Thioureas

OLAV FOSS and INGER-JOHANNE JOHANNESSEN

Chemical Institute, University of Bergen, Bergen, Norway

Thiosulphonates of divalent tellurium, $Te(S_2O_2R)_2$ with R = methyl, phenyl and *p*-tolyl, have been prepared earlier by one of us[1,2], and their crystal structures determined[3-5]. Divalent tellurium in these compounds readily releases the thiosulphonate groups in displacement reactions with thio ions of higher nucleophilic reactivity, such as thiosulphate and dialkyldithiocarbamate ions [1,2]:

$$Te(S_2O_2R)_2 + 2\ YS^- = Te(SY)_2 + 2\ RSO_2S^-$$

This note reports the finding that with thioureas as nucleophiles, in most cases only an addition and not a displacement takes place. Divalent tellurium adds two molecules of thiourea (tu), ethylenethiourea (etu), or tetramethylthiourea (tmtu), to give four-coordinated, planar complexes $Te(tu)_2X_2$, $Te(etu)_2X_2$ and $Te(tmtu)_2X_2$, where X = thiosulphonate. Five representatives are described below, one in two crystalline forms. In all but one of the crystals, unit cell and space group data indicate that the tellurium atom lies in a centre of symmetry. They thus are the *trans* isomers.

The compounds are yellow, with a greenish tinge in the case of the ethylenethiourea derivatives, except the tetramethylthiourea-benzenethiosulphonate complex which is red. In contact with methanol the latter complex gives off tetramethylthiourea, leaving yellow crystals of tellurium dibenzenethiosulphonate. Water destroys the complexes with liberation of tellurium. In the solid, dry state they are quite stable.

Unit cell and space group data were derived from oscillation and Weissenberg photographs, using Cu*Kα* radiation, λ = 1.542 Å. The values for axial lengths are believed to be accurate to within 0.5 %.

Dimethanethiosulphonato-dithiourea-tellurium(II), $Te(tu)_2(S_2O_2CH_3)_2$, crystallizes from solutions made by dissolving powdered tellurium dimethanethiosulphonate in methanolic thiourea, under stirring and heating to near boiling temperature. Some

liberated tellurium was filtered off, and the filtrate allowed to cool to room temperature. The compound can also be prepared from the thiourea complexes $Te(tu)_2Br_2$ or $Te(tu)_4Br_2$ and methanolic sodium methanethiosulphonate monohydrate. The crystals were on the filters drained well, and washed with ether; washing with methanol sometimes caused slight blackening. M. p. 130–131° (decomp.). (Found: S 38.52; Te 25.36. Calc. for $C_4H_{14}N_4O_4S_6Te$: S 38.31; Te 25.41.)

The crystals occur as monoclinic prisms extended along the *b* axis, with $a = 12.50$ Å, $b = 5.60$ Å, $c = 12.80$ Å, $\beta = 98°$, and two molecules per unit cell; density, calc. 1.88, found 1.89 g/cm³. The space group, from systematic absences, is $C_{2h}^5 - P2_1/n$; the tellurium atoms lie in centres of symmetry.

From Fourier projections along the *b* and *c* axes [6], the Te–S(thiosulphonate) bonds are 2.68 Å, as compared with 2.36 Å in the parent, uncomplexed compound [3]. The Te–S(thiourea) bonds are 2.65 Å, and the S–Te–S angles of the planar TeS_4 group are 90° within the error.

Dimethanethiosulphonatobis(ethylenethiourea)tellurium(II), $Te(etu)_2(S_2O_2CH_3)_2$, crystallized when to 1.3 g of tetrakis(ethylenethiourea)tellurium(II) dichloride dihydrate [7] dissolved in 20 ml of warm methanol was added a filtered solution of 0.65 g (*ca.* 7 % excess) of sodium methanethiosulphonate monohydrate in 8 ml of methanol. Yield, 1.0 g (89 %). These crystals, and those of the ethylenethiourea-benzenethiosulphonate complex below, were on the filters washed with methanol and then with ether. M. p. 168–169° (decomp.). (Found: S 34.63; Te 23.02. Calc. for $C_6H_{18}N_4O_4S_6Te$: S 34.71; Te 23.02.) Microscopic examination of the samples showed that they consisted of two types of crystals, long prisms and rather small plates, both monoclinic; the latter seemed to predominate in preparations from more dilute methanol solutions.

The prisms were extended along the *b* axis, with $a = 18.35$ Å, $b = 5.41$ Å, $c = 20.16$ Å, $\beta = 102°$, and four molecules per unit cell; density, calc. 1.88, found 1.89 g/cm³. Systematic absences, *hkl* when $h + k$ is odd, *h*0*l* when *h* is odd or *l* is odd. A Fourier projection along the *b* axis has been carried out, which shows that the space group is $C_{2h}^6 - C2/c$, and outlines clearly a centrosymmetric, *trans* molecule.

The plates had edges parallel to the *bc* diagonals, and $a = 9.61$ Å, $b = 10.86$ Å, $c = 10.67$ Å, $\beta = 119°$. There are two molecules per unit cell; density, calc. 1.89, found 1.89 g/cm³. From systematic absences, and weak *hkl* reflections when $k + l$ is odd, the tellurium atoms lie in symmetry centres of the space group $C_{2h}^5 - P2_1/c$. This is thus a dimorph of the *trans* isomer.

Dibenzenethiosulphonatobis(ethylenethiourea)tellurium(II), $Te(etu)_2(S_2O_2C_6H_5)_2$, was prepared like the methanethiosulphonate analog, from 1.6 g of tetrakis(ethylenethiourea)tellurium(II) dichloride dihydrate in 50 ml of warm methanol, to which was added a filtered solution of 1.25 g (*ca.* 15 % excess) of potassium benzenethiosulphonate dihydrate in 20 ml of methanol. Yield, 1.6 g (95 %). M. p. 147° (decomp.). (Found: C 32.09; S 28.40; Te 18.76. Calc. for $C_{18}H_{22}N_4O_4S_6Te$: C 31.87; S 28.36; Te 18.81.)

The crystals are triclinic prisms extended along the *c* axis, with $a = 7.08$ Å, $b = 10.60$ Å, $c = 8.98$ Å, $\alpha = 102½°$, $\beta = 91°$, $\gamma = 94°$, and one molecule per unit cell; density, calc. 1.72, found 1.71 g/cm³. The centrosymmetric space group, $C_i^1 - P\bar{1}$, would place the tellurium atom in a centre of symmetry also here.

Dimethanethiosulphonatobis(tetramethylthiourea)tellurium(II), $Te(tmtu)_2(S_2O_2CH_3)_2$. 1.3 g of powdered tellurium dimethanethiosulphonate was dissolved, under stirring and heating to near boiling temperature, in 15 ml of methanol containing 1.2 g (*ca.* 20 % excess) of tetramethylthiourea. Some liberated tellurium was filtered off, and 5 ml of ether added to the warm filtrate. There was a tendency for the product to separate as an oil; crystallization could be effected through scratching of the beaker walls, or by seeding. The crystals were washed on the filters with methanol-ether 1:1 and then with ether. Yield, 1.4 g (60 %). M. p. 85°. (Found: C 23.65; S 31.42; Te 20.68. Calc. for $C_{12}H_{30}N_4O_4S_6Te$: C 23.46; S 31.31; Te 20.77.)

The compound forms prisms extended along the *b* axis and flattened along the *a* axis. They are monoclinic, with $a = 9.52$ Å, $b = 12.62$ Å, $c = 10.46$ Å, $\beta = 98°$, and two molecules per unit cell; density, calc. 1.64, found 1.64 g/cm³. The systematic absences, 0*k*0 when *k* is odd, indicate the space group $C_2^2 - P2_1$ or $C_{2h}^2 - P2_1/m$. The tellurium atoms do not lie in symmetry centres of the latter, since *hkl* reflections are not systematically weak when *k* is odd. There is perfect cleavage along the *b* plane.

Dibenzenethiosulphonatobis(tetramethylthiourea)tellurium(II), $Te(tmtu)_2(S_2O_2C_6H_5)_2$.

was prepared by treating 0.95 g of powdered tellurium dibenzenethiosulphonate with 15 ml of methanol containing 0.9 g (*ca.* 90 % excess) of tetramethylthiourea, under stirring and heating to boiling temperature. Undissolved thiosulphonate and some liberated tellurium were filtered off, and the solution allowed to cool to room temperature, after scratching or seeding to start crystallization. The crystals were drained well on the filters and washed with ether. Yield, about 0.2 g (14 %). M p. 121°. (Found: C 35.80; S 26.02. Calc. for $C_{22}H_{34}N_4O_4S_6Te$: C 35.78; S 26.05.)

The crystals show varying habit and many faces, one was a prism extended along the *b* axis, another a thick plate {100} extended along the *bc* diagonal. The dimensions of the monoclinic unit cell are, a = 10.26 Å, b = 10.07 Å, c = 15.98 Å, β = 110°, and there are two molecules per unit cell; density, calc. 1.58, found 1.58 g/cm³. The systematic absences, and weak *hkl* reflections when $k + l$ is odd, show that the tellurium atoms lie in symmetry centres of the space group $C_{2h}^5 - P2_1/c$.

1. Foss, O. *Acta Chem. Scand.* **5** (1951) 115.
2. Foss, O. *Acta Chem. Scand.* **6** (1952) 521.
3. Foss, O. and Vihovde, E. H. *Acta Chem. Scand.* **8** (1954) 1032.
4. Øyum, P. and Foss, O. *Acta Chem. Scand.* **10** (1956) 279.
5. Foss, O. and Øyum, P. *Acta Chem. Scand.* **9** (1955) 1014.
6. Foss, O. and Marøy, K. *To be published.*
7. Foss, O. and Fossen, S. *Acta Chem. Scand.* **15** (1961) 1620.

Received October 17, 1961.

Complexes of Divalent Tellurium with Propylenethiourea

OLAV FOSS and KJARTAN MARØY

Chemical Institute, University of Bergen, Bergen, Norway

The work reported here and in a following note [1] terminates a series of preparative and preliminary X-ray studies of complexes of divalent tellurium with thioureas, now with propylenethiourea (prtu) as ligand. Four $Te(prtu)_2X_2$ complexes are described, namely with X = chloride, bromide, thiocyanate and methanethiosulphonate; the two former represent the *cis* and the two latter the *trans* isomer of four-coordinated planar complexes of this type. This is the first *trans* thiocyanate found; the established or indicated *trans* isomers of other TeX_2Y_2 complexes are: With thiourea [2,3] only the methanethiosulphonate, with ethylenethiourea [3,4] the bromide, iodide, methane- and benzenethiosulphonate, with tetramethylthiourea [3,5] the chloride, bromide, iodide and benzenethiosulphonate, and two salts [5] of a cation with two thiourea and two tetramethylthiourea ligands. The assignment of planar *trans* structure is based on unit cell and space group data, which indicate that in all the above representatives the tellurium atom lies in a crystallographic centre of symmetry, and in some cases on structure analysis.

Propylenethiourea (hexahydropyrimidine-2-thione) was prepared from 1,3-diaminopropane and carbon disulphide [6,7], and recrystallized from water. In acid solutions it reduces tetravalent tellurium to divalent, and becomes thereby itself probably oxidized to a disulphide cation, $(prtu)_2^{2+}$, like other thioureas.

The compounds are yellow, and stable in the solid state, but hydrolyze and liberate tellurium in contact with water. They were on the preparative filters washed with methanol to which in the case of the dichloride complex a little concentrated hydrochloric acid had been added, and then with ether. Single-crystal X-ray data were obtained using Cu$K\alpha$ radiation, λ = 1.542 Å; values for axial lengths are probably accurate to within 0.5 %.

Tellurium dichloride complex, $Te(prtu)_2Cl_2$. To 1.6 g (10 mmoles) of tellurium dioxide in 15 ml of concentrated hydrochloric acid was added, rapidly under stirring, 4.7 g (40 mmoles) of propylenethiourea in 15 ml of hot water. Crystallization set in on scratching of the beaker walls. Yield, after cooling to room temperature, 3.5 g (81 %). M. p. 199° (decomp.). (Found: Cl 16.54; Te 29.67. Calc. for $C_6H_{16}Cl_2N_4S_2Te$: Cl 16.46; Te 29.61.)

The crystals occur as monoclinic prisms extended along the *b* axis and often flattened along the *c* axis. The unit cell dimensions are, a = 16.49 Å, b = 7.64 Å, c = 14.52 Å, β = 120°, and there are four molecules per unit cell; density, calc. 1.81, found 1.81 g/cm³. From systematic absences, and a Fourier projection along the *b* axis, the

was prepared by treating 0.95 g of powdered tellurium dibenzenethiosulphonate with 15 ml of methanol containing 0.9 g (*ca.* 90 % excess) of tetramethylthiourea, under stirring and heating to boiling temperature. Undissolved thiosulphonate and some liberated tellurium were filtered off, and the solution allowed to cool to room temperature, after scratching or seeding to start crystallization. The crystals were drained well on the filters and washed with ether. Yield, about 0.2 g (14 %). M p. 121°. (Found: C 35.80; S 26.02. Calc. for $C_{22}H_{34}N_4O_4S_6Te$: C 35.78; S 26.05.)

The crystals show varying habit and many faces, one was a prism extended along the *b* axis, another a thick plate {100} extended along the *bc* diagonal. The dimensions of the monoclinic unit cell are, a = 10.26 Å, b = 10.07 Å, c = 15.98 Å, β = 110°, and there are two molecules per unit cell; density, calc. 1.58, found 1.58 g/cm³. The systematic absences, and weak *hkl* reflections when $k + l$ is odd, show that the tellurium atoms lie in symmetry centres of the space group $C_{2h}^5 - P2_1/c$.

1. Foss, O. *Acta Chem. Scand.* **5** (1951) 115.
2. Foss, O. *Acta Chem. Scand.* **6** (1952) 521.
3. Foss, O. and Vihovde, E. H. *Acta Chem. Scand.* **8** (1954) 1032.
4. Øyum, P. and Foss, O. *Acta Chem. Scand.* **10** (1956) 279.
5. Foss, O. and Øyum, P. *Acta Chem. Scand.* **9** (1955) 1014.
6. Foss, O. and Marøy, K. *To be published.*
7. Foss, O. and Fossen, S. *Acta Chem. Scand.* **15** (1961) 1620.

Received October 17, 1961.

Complexes of Divalent Tellurium with Propylenethiourea

OLAV FOSS and KJARTAN MARØY

Chemical Institute, University of Bergen, Bergen, Norway

The work reported here and in a following note [1] terminates a series of preparative and preliminary X-ray studies of complexes of divalent tellurium with thioureas, now with propylenethiourea (prtu) as ligand. Four $Te(prtu)_2X_2$ complexes are described, namely with X = chloride, bromide, thiocyanate and methanethiosulphonate; the two former represent the *cis* and the two latter the *trans* isomer of four-coordinated planar complexes of this type. This is the first *trans* thiocyanate found; the established or indicated *trans* isomers of other TeX_2Y_2 complexes are: With thiourea [2,3] only the methanethiosulphonate, with ethylenethiourea [3,4] the bromide, iodide, methane- and benzenethiosulphonate, with tetramethylthiourea [3,5] the chloride, bromide, iodide and benzenethiosulphonate, and two salts [5] of a cation with two thiourea and two tetramethylthiourea ligands. The assignment of planar *trans* structure is based on unit cell and space group data, which indicate that in all the above representatives the tellurium atom lies in a crystallographic centre of symmetry, and in some cases on structure analysis.

Propylenethiourea (hexahydropyrimidine-2-thione) was prepared from 1,3-diaminopropane and carbon disulphide [6,7], and recrystallized from water. In acid solutions it reduces tetravalent tellurium to divalent, and becomes thereby itself probably oxidized to a disulphide cation, $(prtu)_2^{2+}$, like other thioureas.

The compounds are yellow, and stable in the solid state, but hydrolyze and liberate tellurium in contact with water. They were on the preparative filters washed with methanol to which in the case of the dichloride complex a little concentrated hydrochloric acid had been added, and then with ether. Single-crystal X-ray data were obtained using Cu$K\alpha$ radiation, λ = 1.542 Å; values for axial lengths are probably accurate to within 0.5 %.

Tellurium dichloride complex, $Te(prtu)_2Cl_2$. To 1.6 g (10 mmoles) of tellurium dioxide in 15 ml of concentrated hydrochloric acid was added, rapidly under stirring, 4.7 g (40 mmoles) of propylenethiourea in 15 ml of hot water. Crystallization set in on scratching of the beaker walls. Yield, after cooling to room temperature, 3.5 g (81 %). M. p. 199° (decomp.). (Found: Cl 16.54; Te 29.67. Calc. for $C_6H_{16}Cl_2N_4S_2Te$: Cl 16.46; Te 29.61.)

The crystals occur as monoclinic prisms extended along the *b* axis and often flattened along the *c* axis. The unit cell dimensions are, a = 16.49 Å, b = 7.64 Å, c = 14.52 Å, β = 120°, and there are four molecules per unit cell; density, calc. 1.81, found 1.81 g/cm³. From systematic absences, and a Fourier projection along the *b* axis, the

space group is C_{2h}^6 $-C2/c$. The tellurium atoms lie on twofold axes of symmetry (not in centres of symmetry since there are no systematically weak *hkl* reflections) and the nearly but not quite planar TeS_2Cl_2 group is *cis*. Its projection along the *b* axis (twofold axis) is very like the corresponding projection [8] of the TeS_2Cl_2 group in $Te(tu)_2Cl_2$ and[9] of the TeS_4 group in $Te(tu)_2(SCN)_2$ which also are *cis* isomers.

Tellurium dibromide complex, $Te(prtu)_2Br_2$. To 1.6 g of tellurium dioxide in 5 ml of warm concentrated hydrochloric acid was added, rapidly under stirring, 4.7 g of propylenethiourea in 20 ml of hot water, then 10 ml of methanol and, under stirring, 20 ml of hot *ca.* 25 % hydrobromic acid. Yield, after scratching or seeding, and cooling to room temperature, 5 g (96 %). M. p. 190° (decomp.). (Found: Br 30.57; Te 24.74. Calc. for $C_8H_{16}Br_2N_4S_2Te$: Br 30.75; Te 24.55.) It can be recrystallized by dissolving 5 g in 30 ml of dimethylformamide at about 60° and adding three to four times the volume of methanol.

The compound forms thick monoclinic plates {100} with a = 16.11 Å, b = 7.91 Å, c = 14.31 Å, β = 117½°, and four molecules per unit cell; density, calc. 2.13; found 2.13 g/cm³. Systematic absences, *hkl* when $h + k + l$ is odd, *h*0*l* when h is odd or l is odd. The *h*0*l* and *hk*0 zones of reflections are very similar to the corresponding zones of the dichloride complex, indicating that the compounds are isostructural in the projections along the *b* and *c* axes. The space group of the dibromide complex is therefore very probably C_{2h}^6-I2/c, the same as for the dichloride complex, but *I*- instead of *C*-centered once the *a* axes and β angles in the two compounds are chosen so as to conform dimensionally. This is the same relationship as between the crystals of *racem*-1,2-dithiane- and *racem*-1,2-diselenane-3,6-dicarboxylic acid [10].

The *tellurium dithiocyanate complex*, $Te(prtu)_2(SCN)_2$, was prepared from the dichloride complex, and ammonium thiocyanate: 2.2 g of powdered $Te(prtu)_2Cl_2$ was dissolved in 50 ml of methanol containing 10 g of ammonium thiocyanate, under stirring and heating to near boiling temperature. Some liberated tellurium was filtered off, and the solution allowed to cool. Yield, 1.8 g (89 %). M. p. *ca.* 214° (decomp.). (Found: N 17.15; Te 26.84. Calc. for $C_{10}H_{16}N_6S_4Te$: N 17.65; Te 26.80.)

The crystals occur as monoclinic prisms {110} with a = 13.27 Å, b = 14.43 Å, c = 9.76 Å, β = 108½°, and four molecules per unit cell; density, calc. 1.78, found 1.78 g/cm³. The systematic absences, and very weak *hkl* reflections when l is odd, indicate that the tellurium atoms lie in symmetry centres, positions (*a*) or (*b*)[11], of the space group C_{2h}^6-C2/c.

The *tellurium dimethanethiosulphonate complex*, $Te(prtu)_2(S_2O_2CH_3)_2$, crystallized when to 2.8 g of tetrakis(propylenethiourea)tellurium(II) dichloride dihydrate [1] in 8 ml of methanol was added, at room temperature, a filtered solution of 1.4 g (15 % excess) of sodium methanethiosulphonate monohydrate in 8 ml of water. Yield, 2.0 g (86 %). M. p. 172° (decomp.). (Found: N 9.57; Te 21.65. Calc. for $C_{10}H_{22}N_4O_4S_6Te$: N 9.62; Te 21.91.)

The crystals are orthorhombic, and occur as prisms along the *c* axis bounded by {100} and {001}, with a = 12.95 Å, b = 18.92 Å, c = 8.80 Å, and four molecules per unit cell; density, calc. 1.79, found 1.78 g/cm³. The space group, from systematic absences, is D_{2h}^{10} — *Pccn*, so that twofold molecular symmetry is required. The *hkl* reflections are weak when $h + k$, $k + l$ and $l + h$ are odd, and not when l is odd, which shows that the tellurium atoms lie, not on twofold axes but in symmetry centres.

1. Foss, O. and Marøy, K. *Acta Chem. Scand.* **15** (1961) 1947.
2. Foss, O. and Hauge, S. *Acta Chem. Scand.* **13** (1959) 1252; **15** (1961) 1615.
3. Foss, O. and Johannessen, I.-J. *Acta Chem. Scand.* **15** (1961) 1943.
4. Foss, O. and Fossen, S. *Acta Chem. Scand.* **15** (1961) 1618.
5. Foss, O. and Johannessen, W. *Acta Chem. Scand.* **15** (1961) 1941.
6. Schacht, W. *Arch. Pharm.* **235** (1897) 441.
7. Staudinger, H. and Niessen, G. *Chem. Ber.* **86** (1953) 1223.
8. Foss, O., Johnsen, K. and Marøy, K. *To be published.*
9. Marøy, K. *To be published.*
10. Foss, O. and Schotte, L. *Acta Chem. Scand.* **11** (1957) 1424.
11. *International Tables for X-ray Crystallography*, Vol. I, The Kynoch Press, Birmingham 1952, p. 101.

Received October 17, 1961.

Some Propylenethiourea-tellurium(II) Salts

OLAV FOSS and KJARTAN MARØY

Chemical Institute, University of Bergen, Bergen, Norway

Thiourea [1,2] and ethylenethiourea [3], but not tetramethylthiourea [4], give cation complexes TeA_4^{2+} where A is an electroneutral thiourea ligand. Here, we describe two salts, a dichloride dihydrate and a perchlorate, of the cation $Te(prtu)_4^{2+}$ where prtu = propylenethiourea; unit cell and space group data show that, like in the $Te(tu)_4^{2+}$ and $Te(etu)_4^{2+}$ cations [1-3], the TeS_4 group is planar. Also, two crystalline modifications of a tris(propylenethiourea)-tellurium(II) perchlorate have been characterized; these represent the third example of a salt of apparently tri-coordinated divalent tellurium, among the prevailingly four-coordinated ones.

Unit cell and space group data were obtained from oscillation and Weissenberg photographs; the values for axial lengths are based on $\lambda = 1.542$ Å for Cu$K\alpha$ radiation and are believed to be accurate to within 0.5 %.

The *tetrakis dichloride dihydrate*, $Te(prtu)_4Cl_2 \cdot 2H_2O$, was prepared, like the corresponding thiourea and ethylenethiourea salts, from tellurium dioxide and propylenethiourea in a molar ratio of 1:6. To a warm solution of 1.6 g (10 mmoles) of tellurium dioxide in 10 ml of concentrated hydrochloric acid was added, rapidly with stirring, 7.5 g (*ca.* 8 % in excess of 60 mmoles) of propylenethiourea in 20 ml of hot water. Yield, after scratching of the beaker walls or seeding, and cooling to room temperature, 6.5—6.7 g (93—96 %). The salt is readily soluble in methanol, and was washed on the filter with a small amount of cold 4 N hydrochloric acid. (Found: Cl 10.09; Te 18.12. Calc. for $C_{16}H_{36}Cl_2N_8O_2S_4Te$: Cl 10.14; Te 18.25.)

The crystals are yellow with an orange tinge, and form short, monoclinic prisms extended along the *a* axis. The unit cell dimensions are, $a = 9.31$ Å, $b = 18.78$ Å, $c = 9.73$ Å, $\beta = 118°$, and there are two formula units per unit cell; density, calc. 1.55; found 1.55 g/cm³. The space group, from systematic absences, is C_{2h}^5—$P2_1/c$, which requires that the tellurium atoms lie in centres of symmetry. This is consistent with the intensity distribution of the *hkl* reflections, those with $k + l$ even being in most cases markedly strongest.

The *tetrakis perchlorate*, $Te(prtu)_4(ClO_4)_2$, crystallizes on addition of dilute perchloric acid to methanol solutions of the dichloride dihydrate. Yield, from 3 g of the latter salt in 15 ml of methanol, and an equal volume of *ca.* 10 % perchloric acid, 2.9 g (86 %). The crystals showed irregular growth, and better developed ones were obtained on recrystallization from methanol. (Found: N 14.11; Te 16.17. Calc. for $C_{16}H_{32}Cl_2N_8O_8S_4Te$: N 14.16; Te 16.13.)

The crystals occur as plates {010} or as six-sided prisms along the *a* axis, bounded by {010}, {001} and {011}. They are triclinic, with $a = 10.03$ Å, $b = 9.41$ Å, $c = 9.82$ Å, $\alpha = 118\frac{1}{2}°$, $\beta = 90\frac{1}{2}°$, $\gamma = 107°$, and one formula unit per unit cell; density, calc. 1.71, found 1.71 g/cm³. In view of the centrosymmetry shown by the cation in the dichloride dihydrate and the majority of analogous salts [1-3], the space group is probably C_i^1—$P\bar{1}$.

The *tris perchlorate*, $Te(prtu)_3(ClO_4)_2$, was best prepared from methanol solutions of equal molar amounts of dichlorobis-(propylenethiourea)tellurium(II)[5] and propylenethiourea, or of the former compound and the tetrakis dichloride dihydrate, by addition at room temperature of about one fifth the volume of *ca.* 60 % perchloric acid. (Found: N 12.43; Te 19.01. Calc. for $C_{12}H_{24}Cl_2N_6O_8S_3Te$: N 12.45; Te 18.90.) The previously encountered analogs are trithiourea-tellurium(II) di(hydrogenfluoride)[2] and tris(ethylenethiourea)tellurium-(II) perchlorate [3].

The salt occurs in two modifications, one monoclinic and one triclinic, both are greenish yellow in contrast to the tetrakis perchlorate which is brownish yellow. The above procedure gave, on seeding, the monoclinic dimorph. It can be recrystallized from methanol; on cooling of the warm solution without seeding the monoclinic dimorph crystallized; on seeding with the triclinic one about equal amounts of the two dimorphs and of the tetrakis perchlorate were obtained. The equilibrium in solution between tellurium(II) cations with three, four and probably also two propylenethiourea ligands showed also when to methanol solutions of the tetrakis dichloride dihydrate was added, at room temperature, about one fifth the volume of *ca.* 60 % perchloric acid: On scratching

without seeding, the tetrakis perchlorate crystallized, once admixed with a little of the triclinic tris perchlorate. On seeding with one of the tris perchlorates, the dimorph employed for seeding crystallized first, accompanied in the case of the triclinic by the monoclinic one, and then except once when seeding with the monoclinic dimorph, the tetrakis perchlorate.

The monoclinic crystals occur as long prisms {011}, with $a = 12.22$ Å, $b = 14.74$ Å, $c = 14.27$ Å, $\beta = 106\frac{1}{2}°$, and four formula units per unit cell. The space group, from systematic absences, is $C_{2h}^5 - P2_1/c$.

The triclinic dimorph forms small, relatively thick plates with edges parallel to the a and c axes, and a pronounced tendency of cleavage along the b plane. The unit cell has the dimensions, $a = 12.62$ Å, $b = 10.03$ Å, $c = 10.03$ Å, $\alpha = 96\frac{1}{2}°$, $\beta = 93°$, $\gamma = 78\frac{1}{2}°$, and contains two formula units. Densities, calc. and found 1.82 g/cm³ for both dimorphs.

1. Foss, O. and Hauge, S. *Acta Chem. Scand.* **13** (1959) 1252; **15** (1961) 1616.
2. Foss, O. and Hauge, S. *Acta Chem. Scand.* **15** (1961) 1623.
3. Foss, O. and Fossen, S. *Acta Chem. Scand.* **15** (1961) 1620.
4. Foss, O. and Johannessen, W. *Acta Chem. Scand.* **15** (1961) 1941.
5. Foss, O. and Marøy, K. *Acta Chem. Scand.* **15** (1961) 1945.

Received October 17, 1961.

ACTA CHEMICA SCANDINAVICA 15 (1961) 1949–1962

X-Ray Study of Titanium Selenides

FREDRIK GRØNVOLD and F. J. LANGMYHR

Kjemisk Institutt A, Universitetet i Oslo, Blindern, Norway

Three intermediate phases have been characterized in titanium-selenium samples heat-treated at 800 and 600°C: the $TiSe_{0.95}$-phase, the $TiSe_{1.05}$-phase and the $TiSe_{1.20-2.00}$-phase. The $TiSe_{0.95}$-phase has an orthorhombic, NiAs-like structure, a = 3.494 Å, c = 6.462 Å, space group $Pcmn$ (D_{2h}^{16}) with ~4Ti and ~4 Se atoms in positions $\pm(x,1/4,z;\ 1/2+x,3/4,1/2-z)$, x_{Ti} = 0.19, z_{Ti} = 0.01, x_{Se} = 0.58 and z_{Se} = 0.22. The $TiSe_{1.05}$-phase is hexagonal of NiAs-like type, a = 3.571 Å c = 6.297 Å, for a sample heat-treated at 600°C, with 5 % vacant titanium positions probably distributed at random. The phase is presumably identical with a phase earlier designated as Ti_3Se_2. The $TiSe_{1.20-2.00}$-phase is hexagonal at the titanium-rich limit, undergoes a monoclinic deformation with increasing selenium content, and is hexagonal again in the range from about $TiSe_{1.4}$ to $TiSe_{2.00}$. From $TiSe_{1.20}$ to $TiSe_{1.30}$ the changes in structure are so large that some discontinuity in the form of a two-phase region might be expected at lower temperatures. A low-symmetric structure is observed for $TiSe_{1.60}$ when heat-treated at 800°C. Observed densities are only between one and two per cent lower than those calculated from the X-ray data assuming a subtractive solid solution, $Ti_{2-x}Se_2$ with $0.17 < x < 1$, in the range $TiSe_{1.20-2.00}$.

In the titanium selenium system Ehrlich [1] described the existence of a solid solution in the range TiSe to $TiSe_2$ with hexagonal structure and continuously changing lattice constants. The structure was found to be of NiAs-like type at the composition TiSe, and of $Cd(OH)_2$-like type at the composition $TiSe_2$. The structure of $TiSe_2$ had earlier been determined by Oftedal [2]. In two respects Ehrlich's results differed from those obtained for the related selenides of vanadium [3], chromium [4], iron [5], cobalt [6] and nickel [7]; *viz.* that no deformation of the hexagonal structure was observed in the range around $MeSe_{1.3}$, and that the discrepancy between observed densities and those calculated on the basis of the X-ray data in the TiSe-region was considerably larger than for any of the other systems. It therefore became one of the objects of this investigation, which was started in 1947 as part of a series of investigations on transition metal chalcogenides, to study these points in more detail by means of X-ray methods and density measurements.

The presence of a deformed structure in the composition range $TiSe_{1.2}$ to $TiSe_{1.4}$ was soon established [8], but the density determinations were inconsistent, indicating the presence of a varying amount of impurities, either picked up during preparation, or due to the instability of the samples under atmospheric conditions. A reinvestigation of the titanium selenium system in the range TiSe to $TiSe_2$ was therefore carried out using titanium of higher purity, and improved experimental technique. In the meantime, new results were reported by Hahn * and Ness, first in a short note [9], and afterwards in more detail [10]. They found that the composition of the TiSe-phase extended on the titanium-rich side of TiSe to about $TiSe_{0.75}$. The structure was reported as hexagonal with lattice constants twice as large as found by Ehrlich [1] both in the *a*- and *c*-directions, but without any change with composition from TiSe to $TiSe_{0.75}$. A second modification of TiSe was obtained in the form of crystals grown from the vapor phase. The symmetry was reported as trigonal, and the dimensions of the hexagonal cell about the same as of the first modification in the *a*-direction, but somewhat more than twice as large in the *c*-direction. In the composition range $TiSe_{0.70}$ to $TiSe_{0.50}$ a new phase was observed with simple NiAs-like structure. The phase was formally designated as Ti_3Se_2 ($TiSe_{0.67}$) and structurally, with support from density determinations, as $Ti_2(Ti_{0.4}Se_{1.6})$, *i.e.*, as a NiAs-type structure with the excess Ti atoms occupying vacant Se-positions. Investigations of samples with composition TiSe, Ti_2Se_3 and $TiSe_2$ have also been carried out by McTaggart and Wadsley [11], who reported good agreement between their results and those of Hahn and Ness on the superstructure of TiSe, and the results of Ehrlich for the two other samples.

There is a rather striking discrepancy between the cell dimensions given by Hahn and Ness for the subcell of TiSe and those given by Ehrlich [1], indicating that the TiSe of the former is equivalent to $TiSe_{1.2}$ of the latter. Thus, if Ehrlich's samples represent the correct compositions more closely than those by Hahn and Ness, the unexpected occurrence of a NiAs-type structure way over on the metal-rich side among the chalcogenides might be explained on the basis of impure samples. In order to get an answer to this question, additional samples had to be prepared in the titanium-rich region.

EXPERIMENTAL

High purity titanium prepared by the iodide (van Arkel) process, and containing more than 99.9 % Ti was obtained from the Imperial Chemical Industries, Ltd. By spectrographic analysis the following amounts of impurities were found: about 0.01 % Fe, Mg, Si and Sn, and about 0.001 % Al and Cu. The titanium came in form of a bar, from which small turnings were made. Highly refined selenium was kindly placed at our disposal by Bolidens Gruvaktiebolag. According to their analysis it contained 0.0002 % Cu, 0.0007 % Fe, 0.01 % S, 0.003 % Te and 0.003 % non volatile matter.

The alloys were prepared by heating accurately weighed quantities of the elements in small crucibles of alumina placed inside silica tubes, 15 mm i.d. and 50 mm high, which

* According to an agreement between Professor Hahn and Professor Haraldsen to avoid unnecessary duplication of work we have concentrated our investigation on titanium selenides in the range TiSe to $TiSe_2$. The diverging results obtained for samples with composition around TiSe made further studies in this range necessary.

were then evacuated and sealed. In the course of the present investigation samples with the following compositions were prepared: $TiSe_{0.60}$, $TiSe_{0.95}$, $TiSe_{1.00}$, $TiSe_{1.05}$, $TiSe_{1.10}$, $TiSe_{1.20}$, $TiSe_{1.30}$, $TiSe_{1.40}$, $TiSe_{1.50}$, $TiSe_{1.60}$, $TiSe_{1.70}$, $TiSe_{1.80}$, $TiSe_{1.90}$, $TiSe_{2.00}$ and $TiSe_{2.50}$.

Preparations in the composition range $TiSe_{1.10}$ to $TiSe_{2.50}$ were heated slowly to 1000°C, kept at this temperature for 24 h, and afterwards at 800°C for 48 h. The sample tubes were then cooled to room temperature with the furnace. To prevent reactions with the atmosphere, the opening of the silica tubes and crushing and other handling of the alloys was done under pure nitrogen in a dry-box. About two-thirds, or 2 g, of each sample was transferred to a pycnometer for density measurements, and the rest to small silica tubes for annealing at 600°C for one month. In some cases the silica tubes were opened after the initial treatment at 1 000°C and the content transferred to a new tube for annealing at 800°C. The annealed alloys were cooled with the furnace and then examined by X-rays.

Alloys richer in titanium than $TiSe_{1.10}$ were difficult to equilibrate by this method, and different techniques were tried. The reaction mixture was first heated at 400 to 500°C until selenium could no longer be observed and then transferred to a carbon resistance (Tammann) furnace. Heating for one hour at about 1 250°C was tried without success, and finally a heating for 3 to 5 min at about 1 500°C was adopted. To prevent the silica tubes from collapsing at this temperature, argon gas at a pressure of 10 to 12 cm Hg was let into the tubes before sealing them off. The samples were cooled to about 1 100°C with the furnace and then quenched in ice-water to avoid cracking of the silica tubes. The further treatment was as described above.

The titanium-rich samples were sintered products with greyish, metallic luster. With increasing selenium content the color changed to violet. The only titanium-rich alloy that was partly melted after heating to 1 500°C was $TiSe_{0.60}$. Single crystals were present in some of the alloys.

X-ray powder photographs were taken of all samples at about 20°C in 11.48 cm diameter cameras with asymmetric film mounting using iron radiation. The lattice constants are expressed in Å units on the basis of $\lambda FeK\alpha_1$ = 1.93597 Å. The probable error in the lattice constants is estimated to be 0.02 % for the hexagonal structures, and 0.04 % for the monoclinic structure. Lattice constants taken from earlier investigations have been transformed from kX to Å by multiplication by the factor 1.00202.

Density determinations were carried out at 25°C in a pycnometer that could be filled with kerosene under vacuum. Approximately 2 g of substance were used in each experiment. The standard error in the density measurements is estimated to be of the order of 0.3 %.

RESULTS AND DISCUSSION

Samples in the range $TiSe_{0.60}$ to TiSe gave X-ray powder photographs showing the presence of a phase with structure different from what had been earlier reported by Ehrlich [1] and by Hahn and Ness [8] as major constituent. Although the structure was of NiAs-like type, it showed considerable line splitting, indicating lower symmetry than hexagonal. No other phases were observed in the $TiSe_{0.95}$ samples, whether they had been heat-treated at 800 or 600°C, while both $TiSe_{0.60}$ and TiSe were two-phase preparations. The photographs of $TiSe_{0.60}$ contained many weak lines that were not from metallic titanium, and thus perhaps from a sub-selenide of titanium. The origin of these lines has not been pursued further, the attention being primarily focused on the range $TiSe_{0.95}$ to $TiSe_2$. Only small differences between the X-ray photographs of samples heated at 800 and 600°C were observed in most cases; only for $TiSe_{1.05}$, $TiSe_{1.40}$ and $TiSe_{1.60}$ marked influences of temperature were noted (see below).

TiSe was found to contain some lines from a structure of the NiAs-type, in addition to those from the lower symmetric structure, and the composition of the lower symmetric phase should thus be close to $TiSe_{0.95}$. Its range of homo-

geneity is probably rather narrow, since there are only slight shifts in the positions of the X-ray reflections. A reservation with regard to its composition must be made, however, as the titanium selenides in this composition range are rather reactive and easily oxidizable. A slight reaction with the sintered alumina crucibles, which contain about 0.5 % of silica, would lower the titanium content of the titanium selenides, due to the formation of compounds between titanium, silicon, aluminum and oxygen. The composition of the titanium selenide phase in $TiSe_{0.95}$ might thus be closer to TiSe. With this reservation, the phase is provisionally designated as *the $TiSe_{0.95}$-phase.*

Attainment of equilibrium in the TiSe-range was rather difficult to achieve. This was apparent from the fact that the slight differences between powder photographs obtained of samples heated at 1000 and 800°C persisted after the 600°C heat-treatment. The results obtained for the 600°C series were thus in some cases dependent upon the previous history of the sample and corresponded to those obtained by the original heat-treatment at 1000°C for the titanium-rich samples. In this series $TiSe_{1.05}$ was found to be a one-phase preparation with a hexagonal structure of the NiAs-type. At the composition $TiSe_{1.10}$ a two-phase region was again observed, and the composition of the phase with NiAs-type structure thus lies around $TiSe_{1.05}$. This phase will be called *the $TiSe_{1.05}$-phase* until its unit cell content can be more precisely determined. In the 800°C series this phase was not present except as one constituent of the $TiSe_{1.10}$ sample. This indicates that the $TiSe_{1.05}$-phase is only stable at higher temperatures. At the composition $TiSe_{1.20}$ a single phase is again observed, with cell dimensions gradually changing with composition. Its upper limit is close to the composition $TiSe_{2.00}$, in agreement with the results by Ehrlich. This phase will be called *the $TiSe_{1.20-2.00}$-phase.* At higher selenium contents elemental selenium was observed. Each of the three intermediate phases will now be discussed in more detail.

The $TiSe_{0.95}$-phase. Small crystals of the $TiSe_{0.95}$-phase were found in a sample that had been heated at about 1500°C for 5 min. By means of oscillation and Weissenberg photographs the symmetry was found to be orthorhombic. The unit cell dimensions were more accurately determined from powder photographs, and found to be:

$$a = 6.222 \text{ Å}, \quad b = 3.494 \text{ Å}, \quad c = 6.462 \text{ Å}.$$

This refers to a sample of $TiSe_{0.95}$ that had been annealed at 800°C for one week. Powder photograph data for this compound are listed in Table 1.

Small variations in lattice constants due to the heat treatment were noted, as can be seen from the values listed in Tables 2 and 3 for the 800°C and 600°C series, respectively. The differences between the values for $TiSe_{0.60}$ and $TiSe_{0.95}$ are within the limits of error, indicating that the titaniumrich limit of the phase is above $TiSe_{0.95}$. The TiSe-samples show lattice constants that differ somewhat from those of $TiSe_{0.95}$, and also the presence of small amounts of another phase. Thus it can be concluded that the phase has a narrow range of homogeneity between the composition $TiSe_{0.95}$ and $TiSe_{1.00}$.

The unit cell was assumed to contain four TiSe formula units, which require a density of 5.997 g cm^{-3}. The observed density of TiSe, 5.80 g cm^{-3}, was considered to agree well with the calculated value in view of the reactivity of

Table 1. Powder photograph data of $TiSe_{0.95}$ taken with iron radiation, α_2 and β-lines omitted.

$\sin^2\Theta \times 10^4$	I_{obs}	*hkl*	I_{calc}	$\sin^2\Theta \times 10^4$	I_{obs}	*hkl*	I_{calc}
—	—	101	1.2	6285	vw	501	3.4
911	vw	002	5.5	6552	st—	314	13
—	—	200	0.4	—	—	205	2.6
—	—	110	0.8	—	—	115	2.7
—	—	102	0.9	6676	st	413	15
1201	st	201	55			024	11
1244	vst	111	100	6816	vw	510	4.1
1680	w	012	8.5	6921	vw	124	3.0
1874	st	202	32	—	—	420	1.0
1918	vst	112	72	—	—	502	0.4
1970	m	211	22	7053	w+	511	10
2272	w	103	17	—	—	130	0.0
2420	w(+β)	301	7.9	7178	w+	421	10
—	—	212	0.8	7282	vw	323	3.4
2955	st	310	27	7358	w+	131	10
3003	vw	203	6.7	7386	st	215	17
3042	m	113	18	—	—	404	0.1
3081	m	020	20	—	—	224	0.0
		302	1.7	7723	vw	512	2.0
—	—	311	0.3	—	—	032	1.5
—	—	121	0.1	7847	vw	305	2.4
3610	w	004	8.6			422	2.9
—	—	213	0.1	8058	m	132	16
3858	m	104	2.4	—	—	503	0.1
		312	10	—	—	006	0.1
—	—	400	0.8	—	—	414	1.6
—	—	022	1.2	—	—	106	0.5
—	—	220	1.0	—	—	315	0.8
4113	w+	401	8.8	—	—	600	1.9
4204	vw	303	2.4			513	7.0
		122	0.2	8869	st	224	0.0
4279	m	221	14			016	13
4376	w—	014	2.6	8926	vw	033	0.0
—	—	204	0.0			125	5.3
—	—	114	0.6	8963	st	601	2.6
4773	vw	402	1.5			423	17
4867	vw	411	2.8	9080	st	206	4.6
4955	st—	222	13			330	18
		313	0.0	9121	m	116	12
5347	m—	123	6.8	9165	m	133	15
		214	1.0	9345	m	331	0.0
5504	w+	321	4.2			521	14
—	—	412	0.4	—	—	405	2.0
5779	w	304	2.6	9611	st	602	3.1
—	—	105	1.7	9645	st(+α_2)	504	2.5
5908	w+	403	5.2			225	16
6071	m	223	5.4	9705	w	611	9.7
6153	vw	322	2.2	—	—	216	6.4

Table 2. Lattice constants of the titanium selenides after annealing for one week at 800°C.

Composition	a ($b\sqrt{3}$) in Å	b in Å	c in Å	β
$TiSe_{0.60}$	6.222	3.494	6.462	(90°)
$TiSe_{0.95}$	6.222	3.494	6.462	(90°)
$TiSe_{1.00}$	6.223	3.488	6.469	(90°)
	(6.18)	3.57	6.21	(90°)
$TiSe_{1.05}$	(6.185)	3.571	6.189	(90°)
$TiSe_{1.10}$	(6.185)	3.571	6.30	(90°)
	(6.185)	3.571	6.21	(90°)
$TiSe_{1.20}$	(6.187)	3.572	6.195	(90°)
$TiSe_{1.30}$	6.378	3.564	2 × 6.012	90.92°
$TiSe_{1.40}$	6.353	3.572	2 × 6.006	90.61°
$TiSe_{1.50}$	(6.226)	3.598	5.989	(90°)
$TiSe_{1.60}$	—	—	—	(90°)
$TiSe_{1.70}$	(6.185)	3.571	5.992	(90°)
$TiSe_{1.80}$	(6.163)	3.558	5.992	(90°)
$TiSe_{1.90}$	(6.144)	3.547	5.997	(90°)
$TiSe_{2.00}$	(6.126)	3.537	6.005	(90°)

Table 3. Lattice constants of the titanium selenides after annealing for one month at 600°C.

Composition	a ($b\sqrt{3}$) in Å	b in Å	c in Å	β
$TiSe_{0.60}$	6.223	3.485	6.469	(90°)
$TiSe_{0.95}$	6.222	3.494	6.467	(90°)
$TiSe_{1.00}$	6.223	3.488	6.469	(90°)
	(6.18)	3.57	6.30	(90°)
$TiSe_{1.05}$	(6.185)	3.571	6.301	(90°)
$TiSe_{1.10}$	(6.185)	3.571	6.30	(90°)
	(6.185)	3.571	6.21	(90°)
$TiSe_{1.20}$	(6.185)	3.571	6.188	(90°)
$TiSe_{1.30}$	6.389	3.561	2 × 5.995	90.83°
$TiSe_{1.40}$	(6.235)	3.600	5.987	(90°)
$TiSe_{1.50}$	(6.228)	3.596	5.979	(90°)
$TiSe_{1.60}$	(6.185)	3.571	5.983	(90°)
$TiSe_{1.70}$	(6.171)	3.563	5.985	(90°)
$TiSe_{1.80}$	(6.154)	3.553	5.990	(90°)
$TiSe_{1.90}$	(6.135)	3.542	5.994	(90°)
$TiSe_{2.00}$	(6.126)	3.537	6.002	(90°)
$TiSe_{2.50}$	(6.130)	3.539	5.999	(90°)

the sample. It was not felt that the observed densities could give more reliable informations about the stoichiometry and unit cell content of the $TiSe_{0.95}$-phase.

The structure of $TiSe_{0.95}$ was obviously NiAs-like and closely related to that of FeAs[12] and MnP[13]. When choosing the axial orientation as above, so that the relationship with the NiAs-type structure is clearly brought out, the missing reflections are $hk0$ when $h + k = 2n + 1$, and $0kl$ when $l = 2n + 1$. The highest symmetric space group is thus $Pcmn$ (D_{2h}^{16}). In this space group

Table 4. Interatomic distances in the structure of $TiSe_{0.95}$ (in Å).

Ti — Se = 2.52	Ti — 2 Ti = 3.21	Se — 2 Se = 3.48
Ti — 2 Se = 2.56	Ti — 2 Ti = 3.49	Se — 2 Se = 3.49
Ti — 2 Se = 2.70	Ti — 2 Ti = 4.00	Se — 4 Se = 3.59
Ti — Se = 2.78	Ti — 2 Ti = 4.43	Se — 2 Se = 3.89
		Se — 2 Se = 4.14

the NiAs-type structure is realized by placing all atoms in the fourfold positions $x,1/4,z$; $\bar{x},3/4,\bar{z}$; $1/2+x$, $3/4$, $1/2-z$; $1/2-x,1/4,1/2+z$; with $x_1 = 1/4$ and $z_1 = 0$ for the metal atoms and $x_2 = 7/12$ and $z_2 = 1/4$ for the non-metal atoms. For complete superposition the origin has to be translated to 1/4,1/4,0.

Intensities of the reflections were calculated using the formula

$$I = \text{const} \times F^2 \times Lp \times \nu$$

The best agreement between calculated and observed intensities was obtained with $x_{Ti} = 0.19$, $z_{Ti} = 0.01$, $x_{Se} = 0.58$ and $z_{Se} = 0.22$. The results of the calculations are listed in Table 1, with the intensity of the strongest reflection adjusted to 100.

The interatomic distances calculated for this structure are listed in Table 4, and a projection of the structure on (010) is shown in Fig. 1. As can be seen, the regular octahedral arrangement of metal atoms around the non-metal atoms, characteristic of the NiAs-type structure is distorted with half of the selenium atoms being definitely closer to the titanium atom than the rest. No strong titanium-titanium bonds are present in this structure, as evidenced by the shortest distance being 3.21 Å.

The $TiSe_{1.05}$-phase. As far as it can be judged from the X-ray powder photographs of samples heat-treated at 600°C, this phase has a hexagonal structure of the NiAs-type with lattice constants:

$a = 3.571$ Å, $c = 6.301$ Å.

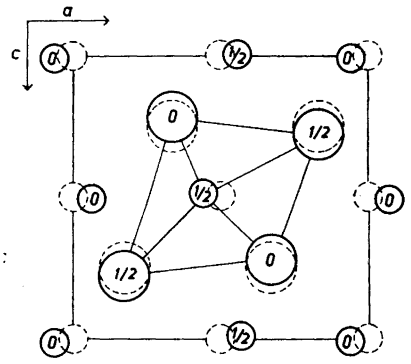

Fig. 1. Projection of the orthorhombic TiSe-structure on (010). Fully drawn large circles indicate selenium atoms and small circles titanium atoms. Broken circles show ideal positions for a NiAs-type structure.

The powder photograph data are listed in Table 5. The density of this phase, as estimated from the observed values for TiSe and $TiSe_{1.10}$ given in Table 8, is 5.77 g cm^{-3}. The corresponding cell content is 1.88 Ti atoms and 1.97 Se atoms and indicates that the selenium positions are virtually completely occupied, while about 5 % of the titanium positions are empty.

The absence of superstructure reflections makes it reasonable to assume a certain randomness in the distribution of the vacancies, in accordance with observations made in other chalcogenide systems at about the same composition. Thus, Grønvold and Haraldsen [14] found no superstructure lines for iron sulfides with composition around $FeS_{1.10}$. The only extra reflections observed by Jellinek [15] for $CrS_{1.12}$ ("Cr_7S_8") were 001 and 111. Their presence were interpreted to mean that the vacancies on the metal lattice were confined to every other layer perpendicular to the *c*-axis. This conclusion presupposes that the chromium positions are 0,0,0 and 0,0,1/2 and the sulfur positions $\pm$ (1/3,2/3,1/4) exactly. This assumption, although probable, has not yet been verified.

The quality of the intensity data obtained for $TiSe_{1.05}$ precludes a decision between ordered and random distribution of the vacancies. Intensities have been calculated for two possibilities, one assuming random distribution of vacancies over the 0,0,0 and 0,0,1/2 positions, the other assuming all vacancies in one of these positions. The former alternative can be described in terms of the space group $C6/mmc$ (D_{6h}^4) with 1.9 Ti atoms in (*a*) 0,0,0; 0,0,1/2, and 2 Se atoms in (*d*) 1/3,2/3,3/4; 2/3,1/3,1/4, the latter in terms of the space group $C\bar{3}m1$ (D_{3d}^3) with 1 Ti atom in (*a*) 0,0,0, 0.9 Ti atoms in (*b*) 0,0,1/2 and 2 Se atoms in (*d*) 1/3,2/3,*z*; 2/3,1/3,$\bar{z}$, with $z = 1/4$. The intensities calculated for these two alternatives differ practically only in that reflections *hhl* for $l = 2n + 1$ are not completely extinct for the latter. They are found under the same heading I' in Table 5, and both are equally well in accord with the observed data since no such reflections were observed.

Table 5. Powder photograph data for $TiSe_{1.05}$, taken with iron radiation, and results of intensity calculations.

$\sin^2\Theta \times 10^4$	*hkl*	I_{obs}	I'	I''	$\sin^2\Theta \times 10^4$	*hkl*	I_{obs}	I'	I''
—	001	—	0.01	0	4878	202	6	5.9	5.8
945	002	3	1.9	1.1	—	113	—	0.00	0
—	100	—	0.2	0.8	—	005	—	0.00	0
1221	101	35	35	30	6048	203	4	3.3	2.7
1925	102	30	26	26	6718	114	12	11	10
—	003	—	0.00	0	—	210	—	0.02	0.08
2942	110	12	14	13	6881	105	3	3.4	2.8
3107	103	8	7.7	6.4	7089	211	10	6.8	5.7
—	111	—	0.01	0	—	204	—	0.02	0.08
3782	004	3	3.0	2.8	7803	212	10	11	11
3871	112	1	1.3	0.7	—	006	—	0.2	0.1
—	200	—	0.02	0.07	8816	300	5	8.2	7.7
4149	201	6	4.8	4.1	—	115	—	0.01	0
—	104	—	0.02	0.1	8980	213	10	11	9.2

The good overall agreement indicates, however, that the main features of the proposed structure are correct. In this structure each titanium atom is octahedrally surrounded by six selenium atoms at distances of 2.59 Å. Each titanium atom is further surrounded by two titanium atoms at a slightly shorter distance (3.15 Å) than in the orthorhombic $TiSe_{0.95}$-structure (3.21 Å).

The X-ray data obtained for the $TiSe_{1.05}$-phase showed striking similarities with the data for the Ti_3Se_2-phase reported by Hahn and Ness [10]. This phase had a hexagonal NiAs-like structure with unit cell dimensions $a = 3.574 \pm 0.005$ Å, $c = 6.322 \pm 0.005$ Å. On the basis of the observed density, 5.54 g cm^{-3}, Hahn and Ness concluded that the cell content was 2.4 Ti atoms and 1.6 Se atoms and stated that the calculated intensities of the X-ray reflections assuming 2 Ti atoms in 0,0,0 and 0,0,1/2, and 0.4 Ti + 1.6 Se atoms in ±(1/3, 2/3,1/4) agreed so well with the observed data that the correctness of the proposed structure seemed ascertained. In our opinion this conclusion is unwarranted and the intensities calculated for this assumption — see column labelled *I* in Table 5 — are in no better agreement with the observed intensities than those for the two other alternatives, which both refer to a much higher selenium to titanium atom ratio.

A serious discrepancy apparently exists with regard to the composition of the titanium-rich selenides, and we assume that this must be sought in the methods of preparation. Certainly, the utmost care needs to be taken in order to avoid oxide and silicide formation of the samples. In the present research, turnings of "iodide" titanium were used in the reaction and the greatest care taken to keep the samples out of contact with air and moisture. Hahn and Ness [10] used titanium in the form of decomposed hydride (for which no analytical data was given). It seems to us that in the work by Hahn and Ness side reactions might have seriously reduced the amount of titanium available for selenide formation and increased the selenium content of the titanium selenides accordingly.

The $TiSe_{1.20-2.00}$-phase. At the composition $TiSe_{1.20}$ another phase with hexagonal structure is observed in pure state. The *a*-axis is equal to that for the $TiSe_{1.05}$-phase within the limits of experimental error, while the *c*-axis is about 2 % shorter. For $TiSe_{1.20}$ the *c*-axis is slightly below the value found in the two-phase region, indicating that $TiSe_{1.20}$ is within the homogeneity range of the phase. No superstructure reflections were seen on the powder photographs, but that does not prove their non-existence. Especially in the 600°C sample some ordering might be expected.

A pronounced change in the appearance of the X-ray photographs is seen from $TiSe_{1.20}$ to $TiSe_{1.30}$. The basic structure is no longer hexagonal but monoclinic, and the cell dimensions determined are listed in Tables 2 and 3 for samples annealed at 800 and 600°C, respectively. Powder photograph data for the 600°C series sample are given in Table 6. They indicate clearly a doubling of the *c*-axis. The dimensional changes for the *a*- and *c*-axes are so large from $TiSe_{1.20}$ to $TiSe_{1.30}$, see Fig. 2, that a two-phase region might be expected at lower temperatures.

From the composition $TiSe_{1.30}$ on, the unit cell dimensions change more regularly, but in a somewhat different way depending upon the heat treatment. For the 600°C series, the monoclinic deformation has disappeared already

Table 6. Powder photograph data of $TiSe_{1.30}$, 600°C series, taken with iron radiation, α_2- and β-lines omitted.

I_{obs}	$\sin^2\Theta \times 10^4$		*hkl*	I_{obs}	$\sin^2\Theta \times 10^4$		*hkl*
	obs	calc			obs	calc	
vw	819	803	011	w−	4120	4120	$\bar{2}22$
w	1054	1029	$\bar{1}11$	st	4140	4148	222
		1040	004	vw	4660	4656	$\bar{4}04$
		1037	111	w	4773	4768	404
w	1178	1164	$\bar{2}02$	m	4878	4886	$\bar{2}24$
w+	1204	1192	202	w	4948	4942	224
st	1238	1221	$\bar{1}12$	w−	5937	5932	$\bar{4}06$
w−	1249	1235	112	w+	6108	6100	406
w−	1340	1325	013	w	6197	6176	$\bar{2}26$
w−	1743	1729	211	w	6277	6260	226
w−	1887	1903	$\bar{2}12$	vw	6392	—	?
w+	1938	1930	$\bar{2}04$	w−	6710	6702	$\bar{5}12$
m	2005	1986	204	w−	6792	6772	512
		1994	$\bar{1}14$	st	6886	6890	$\bar{3}18$
m	2036	2022	114	m	7062	7058	318
vw	2100	2120	$\bar{3}01$	st	7133	7133	$\bar{1}32$
w−	2153	2140	301			7147	132
w−	2233	2222	$\bar{2}13$	m	7443	7453	$\bar{1},1,10$
vw	2629	2630	$\bar{3}03$	m	7497	7508	2,0,10
st	2808	2803	310	w	7612	7612	$\bar{4}24$
m	2970	2956	020	m	7728	7724	424
w	3216	3216	022	st	7932	7934	134
		3220	$\bar{2}06$	w	8264	8264	600
w+	3290	3291	$\bar{1}16$	vw	8612	—	?
		3304	206	st	8714	8716	$\bar{5}16$
w	3336	3333	116			8716	330
vw	3380	3394	$\bar{1}07$	m	8897	8888	$\bar{4}26$
w	3804	3802	$\bar{3}14$	w+	9045	9056	426
w	3884	3886	314	m	9188	9203	$\bar{1}36$
		3902	$\bar{4}02$	st	9245	9245	136
vw	3940	3958	402				
vw	3995	3996	024				

at the composition $TiSe_{1.40}$. The *a*-axis decreases steadily towards the composition $TiSe_{2.00}$, while the *c*-axis goes through a minimum in the range $TiSe_{1.50}$ to $TiSe_{1.60}$ with a very slight increase towards the limiting value for $TiSe_{2.00}$. For the 800°C series, the monoclinic deformation still exists at the composition $TiSe_{1.40}$, but $TiSe_{1.50}$ gives photographs showing a hexagonal structure only. At the composition $TiSe_{1.60}$ the structure is no longer of the simple hexagonal type. The powder photographs show considerable line splitting, indicating the presence of a phase with low-symmetric structure and perhaps more than one phase. Powder photograph data for the new structure are found in Table 7. By heating a sample showing this line splitting to 960°C and quenching it in ice-water the hexagonal structure is obtained, and it persists after heat-treatment for one month at 600°C. Similarly, a sample showing the low-

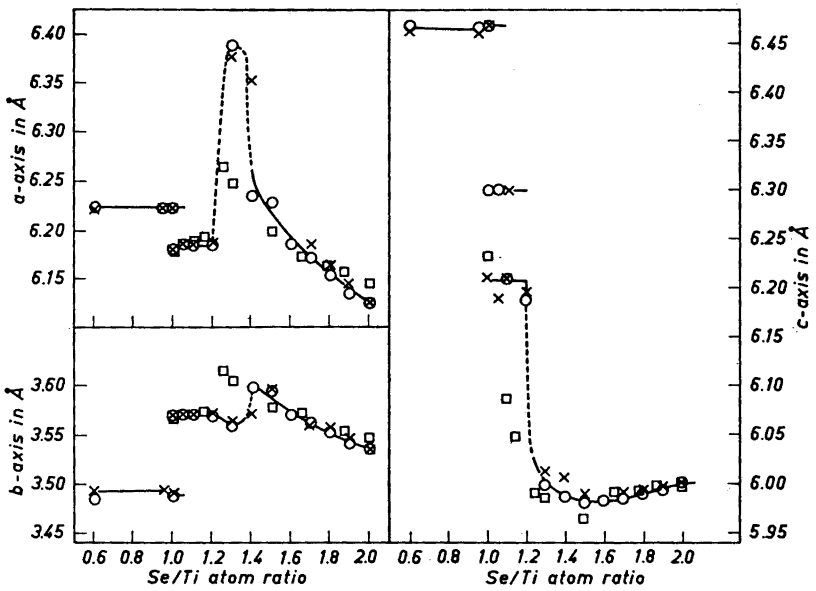

Fig. 2. Variations in lattice constants of titanium selenides as function of composition in the range $TiSe_{0.60}$ to $TiSe_{2.00}$. Results both for the 800°C series (×) and 600°C series (○) are shown, and likewise earlier results by Ehrlich (□). The slight monoclinic distortions for $TiSe_{1.30}$ and $TiSe_{1.40}$, and the doubling of the *c*-axis in that range are not shown. Added in proof: The circle coinciding with the cross for the *b*-axis at the composition $TiSe_{0.95}$ was inadvertently omitted.

symmetric structure before the 600°C annealing also shows it afterwards. This is another indication that true equilibrium is not attained at 600°C. In the composition range $TiSe_{1.70}$ to $TiSe_{2.00}$ only slight differences between the lattice constants determined for the two series of samples occur, and they are supposedly mainly due to variable success in preventing the samples from decomposing during heat-treatment and cooling. The results from the 600°C series are considered to be the most reliable.

A comparison of the present results with those obtained by Ehrlich[1] shows reasonable agreement in the range above $TiSe_{1.4}$, see Fig. 2. For samples richer in titanium the divergences with regard to the length of the *c*-axis are rather large and indicate close relationships between Ehrlich's $TiSe_{1.00}$ sample and the present $TiSe_{1.20}$ sample. The cell dimensions reported by McTaggart and Wadsley[11] for $TiSe_{1.5}$ (a = 3.595, c = 5.994 Å) and for $TiSe_2$ (a = 3.535, c = 6.004 Å) and those by Oftedal[2] for $TiSe_2$ (a = 3.533, c = 5.995 Å) agree well with those reported here. The powder photograph data presented by Hahn and Ness[10] for the TiSe-phase "1. Modifikation" indicate close relationships with our samples in the range $TiSe_{1.20}$ to $TiSe_{1.30}$. The length of the *c*-axis changes enormously with composition from $TiSe_{0.95}$ to $TiSe_{1.3}$ and lets us conclude that neither the $TiSe_{1.0}$ nor the $TiSe_{0.75}$ preparation by Hahn and Ness were richer in titanium than our $TiSe_{1.20}$. With regard to the "2. Modifikation" of

Table 7. Powder photograph data of $TiSe_{1.60}$, taken with iron radiation, α_2 and β-lines omitted.

I_{obs}	$\sin^2\Theta \times 10^4$	I_{obs}	$\sin^2\Theta \times 10^4$	I_{obs}	$\sin^2\Theta \times 10^4$
w	269	w	3364	st	7097
vw	320	w	3389	m	7181
vw	805	w	3951	w+	7485
m	1066	vw	4021	m	7557
v st	1248	w+	4146	st–	7796
vw	1777	m	4223	w	7911
vw	1918	w	4918	m	8692
m	2023	w	4953	st	9081
w	2051	w+	6190	m	9131
w	2065	w	6277	w	9217
st	2927	st	7034	m	9254
m	3328				

the TiSe-phase, the listed X-ray powder data show more resemblance to our data for $TiSe_{1.30}$ than for $TiSe_{1.00}$, the only two compositions for which a quadrupling of one of the axes ($4c$ = 25.8 Å for $TiSe_{1.00}$, $4a$ = 25.6 Å for $TiSe_{1.30}$) would give some agreement with the data by Hahn and Ness (c = 27.4 Å), but no conclusions can be reached at present.

Results of the density determinations are presented in Table 8 and in Fig. 3. Data were only obtained for samples heat-treated at 800°C. The observed values are in reasonable agreement with those calculated on the basis of subtraction of titanium atoms only with changing composition from Ti_2Se_2 to $TiSe_2$. It can be seen that the observed densities are considerably higher than those by Ehrlich, except for compositions close to $TiSe_2$, where the preparation of pure and well defined samples offers no special problems. The density value reported by McTaggart and Wadsley for $TiSe_2$ agrees with the theoretical value, while those for $TiSe_{1.5}$ and TiSe are low. Values reported by Hahn and Ness for two TiSe samples are also low. The discrepancies found by Ehrlich between observed

Table 8. Observed and calculated densities in g cm^{-3} for the titanium selenides. The atomic weight unit is taken to be 1.6602×10^{-23} g.

Sample	D_{obs}	D_{calc}	Sample	D_{obs}	D_{calc}
$TiSe_{0.95}$	5.93	6.116	$TiSe_{1.50}$	5.41	5.484
$TiSe_{1.00}$	5.80	5.997	$TiSe_{1.60}$	5.34	—
$TiSe_{1.05}$	—	5.848	$TiSe_{1.70}$	5.27	5.376
$TiSe_{1.10}$	5.73	—	$TiSe_{1.80}$	5.26	5.335
$TiSe_{1.20}$	5.66	5.758	$TiSe_{1.90}$	5.20	5.294
$TiSe_{1.30}$	5.54	5.622	$TiSe_{2.00}$	5.17	5.252
$TiSe_{1.40}$	5.45	5.514			

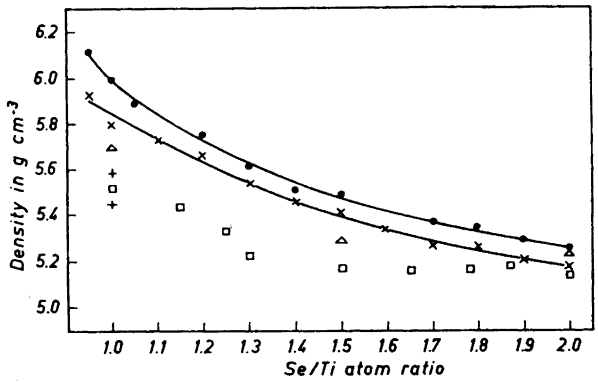

Fig. 3. Observed (×) and calculated (●) densities for titanium selenides heat-treated at 800°C. Earlier observed values by Ehrlich (□), McTaggart and Wadsley (△) and Hahn and Ness (+) are also shown.

and calculated densities for titanium selenides and tellurides ($D_{obs}/D_{calc} = 0.90$ for TiSe and 0.86 for TiTe) were interpreted by him [16] as caused by vacant lattice sites and due to the presence of strong "atomic bonds" between the metal atoms. In view of the data presented here this conclusion seems unwarranted, and the present authors ascribe the large differences between observed and calculated densities for the titanium selenides observed by earlier investigators as mainly due to experimental errors. It should also be remarked that for the iron selenides where the principle of both empty metal and non-metal positions was first thought to apply [5], the low density in the range around FeSe can be accounted for by the presence of the phase $FeSe_{0.96}$ with lower density.

The interatomic distances change comparatively little within the range of the $TiSe_{1.20-2.00}$-phase. In the range $TiSe_{1.30}$ to $TiSe_{1.40}$ some distortion of the octahedral arrangement around the titanium atoms apparently takes place, and further work is needed to clear up the details. It is expected, however, that the deformation of the structures are closely related to those for $NiSe_{1.25}$ [17] and Cr_3S_4 [15]. For $TiSe_{1.20}$, $TiSe_{1.50}$ and $TiSe_{2.00}$ the following interatomic distances are found, see Table 9.

Table 9. Interatomic distances in the structures of $TiSe_{1.20}$, $TiSe_{1.50}$ and $TiSe_{2.00}$ (in Å).

$TiSe_{1.20}$	$TiSe_{1.50}$	$TiSe_{2.00}$
Ti — 6 Se = 2.58	Ti — 6 Se = 2.56	Ti — 6 Se = 2.54
Ti — 1.3 Ti = 3.09	Ti — 0.7 Ti = 2.99	—
Se — 5 Ti = 2.58	Se — 4 Ti = 2.56	Se — 3 Ti = 2.54
Se — 6 Se = 3.57	Se — 6 Se = 3.60	Se — 6 Se = 3.54
Se — 6 Se = 3.69	Se — 6 Se = 3.64	Se — 6 Se = 3.63

The titanium-selenium distances decrease with increasing selenium content as is expected due to the lowering of the number of coordinated titanium atoms around selenium. Using the metallic radii derived by Pauling [18], the following radius sums ($r_{Ti} + r_{Se}$) are obtained: $TiSe_{1.20}$, 1.377 + 1.286 = 2.663 Å; $TiSe_{1.50}$, 1.377 + 1.257 = 2.634 Å; $TiSe_{2.00}$, 1.377 + 1.219 = 2.596 Å. For TiSe the expected distance for six-coordination would be 1.377 + 1.31 = 2.687 Å, while the average distance in the $TiSe_{0.95}$-phase is 2.63 Å, and the distances in the $TiSe_{1.05}$-phase are 2.59 Å. The shorter distances observed in all cases might indicate a metallic valence higher than four for titanium.

Acknowledgments. The authors wish to thank Professor Haakon Haraldsen for his interest in this study and for making laboratory facilities available. They express thanks to Bolidens Gruvaktiebolag for generous supply of high-purity selenium, to siv.ing. Sigurd Rutlin, Sentralinstitutt for Industriell Forskning, for spectrographic analysis of the titanium, and to Mr. Arne Henriksen and Mr. John Krause for help with preparation and density measurements of the samples.

REFERENCES

1. Ehrlich, P. *Z. anorg. Chem.* **260** (1949) 1.
2. Oftedal, I. *Z. physik. Chem.* **134** (1928) 301.
3. Hoschek, E. and Klemm, W. *Z. anorg. u. allgem. Chem.* **242** (1939) 49; Grønvold, F. *Unpublished work.*
4. Haraldsen, H. and Mehmed, F. *Z. anorg. u. allgem. Chem.* **239** (1938) 369.
5. Hägg, G. and Kindström, A.-L. *Z. physik. Chem.* **B22** (1933) 453; for further references see Grønvold, F. and Westrum, E. F., Jr. *Acta Chem. Scand.* **13** (1959) 241.
6. Bøhm, F., Grønvold, F., Haraldsen, H. and Prydz, H. *Acta Chem. Scand.* **9** (1955) 1510.
7. Grønvold, F. and Jacobsen, E. *Acta Chem. Scand.* **10** (1956) 1440.
8. Langmyhr, F. J. *Thesis*, University of Oslo, 1951.
9. Hahn, H. and Ness, P. *Naturwiss.* **44** (1957) 581.
10. Hahn, H. and Ness, P. *Z. anorg. u. allgem. Chem.* **302** (1959) 17.
11. McTaggart, F. K. and Wadsley, A. D. *Australian J. Chem.* **11** (1958) 445.
12. Hägg, G. *Nova Acta Regiae Soc. Sci. Upsaliensis* **7** (1929) No. 1.
13. Fylking, K. E. *Arkiv Kemi Mineral. Geol.* **B11** (1934) No. 48.
14. Grønvold, F. and Haraldsen, H. *Acta Chem. Scand.* **6** (1952) 1452.
15. Jellinek, F. *Acta Cryst.* **10** (1957) 620.
16. Ehrlich, P. *Z. anorg. Chem.* **260** (1949) 19.
17. Grønvold, F. Paper presented at the 2. Scandinavian Structure Symposium, Oslo 1955. *Tidskr. Kjemi, Bergvesen Met.* **15** (1955) 49.
18. Pauling, L. *J. Am. Chem. Soc.* **69** (1947) 542.

Received May 3, 1961.

ACTA CHEMICA SCANDINAVICA 15 (1961) 1963–1974

The Apparent Acid Ionization Constants of L-Seryl-L-Lysine, L-Seryl-L-Glutamic Acid and their O-Phosphorylated Analogues. Proposed Mechanism for the Absence of Tryptic Action on O-Phosphorylated Lysine Peptides *

GEORG FÖLSCH and RAGNAR ÖSTERBERG

Department of Medical Biochemistry, University of Göteborg, Göteborg, Sweden

1. The peptides L-seryl-L-lysine and O-phosphoryl-L-seryl-L-lysine have been synthesized.

2. Apparent acid ionization constants have been determined at 25° in 0.15 M KCl for L-seryl-L-lysine, L-seryl-L-glutamic acid and their corresponding O-phosphorylated analogues.

3. The effect of the phosphate group on the ionization of the other acid groups in these peptides is discussed in relation to previous studies on synthetic phosphopeptides.

4. Some of the pK values obtained are discussed in relation to pK values and possible amino acid sequences of phosphopeptides prepared from whole-casein and α-casein.

5. Electrostatic interaction between the phosphate and ε-amino groups in O-phosphorylseryllysine is shown to be present. It is proposed that this interaction is the reason for the observed inability of trypsin to hydrolyse peptide bonds involving a lysine carboxyl group, when O-phosphorylserine is attached to the lysine residue.

As a part of a study of phosphorus linkages in casein and its degradation products [2,3], a phosphopeptide, containing seven phosphate groups was isolated in two different ways from α-casein [4,5]. The type of phosphate bonds in this peptide has been studied by means of acid-base titration [6]. The analysis of the titration data in the form of pK-values for different acid groups assumed to be present, required information about acid ionization constants of these groups in similar peptides of known structure. A preceding paper [3] reported acid-base properties of the α-amino, α-carboxyl-, and O-phosphoryl groups in selected synthetic peptides. In the present work peptides containing γ-carboxyl- and ε-amino groups have been prepared and the ionization con-

* Synthesis of phosphopeptides, Part IV. For Parts II and III see Ref.[1]

stants of these groups determined. The peptides investigated are listed in Fig. 1. One of these peptides, O-phosphoryl-L-seryl-L-lysine, was of special interest with regard to hydrolysis of peptide bonds in phosphopeptides, as it is known that trypsin is unable to hydrolyse lysyl peptide bonds, when the peptide contains negatively charged groups [7] such as O-phosphoryl [5,8] or carboxyl groups [9–11] near the lysine residue.

The synthesis of L-seryl-L-glutamic acid [1,12] and O-phosphoryl-L-seryl-L-glutamic acid [1,13] have been reported previously. Free and O-phosphorylated L-seryl-L-lysine were obtained as follows (reaction scheme, Fig. 2): N^{α}-(N-carbobenzoxy)-L-seryl-N^{ε}-carbobenzoxy-L-lysine benzyl ester (I) was prepared by condensation of the appropriate derivatives with N,N′-di*cyclo*hexyl-carbodiimide. Hydrogenolysis of (I) in *tert*-butanol-water-hydrochloric acid gave L-seryl-L-lysine as the *mono*-hydrochloride. Phosphorylation of (I) in pyridine with dibenzylphosphoryl chloride gave N^{α}-(O-dibenzylphosphoryl-N-carbobenzoxy)-L-seryl-N^{ε}-carbobenzoxy-L-lysine benzyl ester (III). Unchanged (I) could be removed from (III) by means of fractional crystallization, but the main portion of crude (III) was hydrogenolyzed directly to a mixture of the two peptides (II) and (IV), and these were separated easily by means of ion exchange chromatography.

Before titration, all peptides (except II, hydrochloride) were freed from acetate and formate ions by means of chromatography on a cation exchange resin, Dowex 50-X2.

Peptide		Abbreviation	Formula
L-Seryl-L-lysine	(a)	Ser-Lys	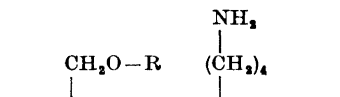
O-Phosphoryl-L-seryl-L-lysine	(b)	SerP-Lys	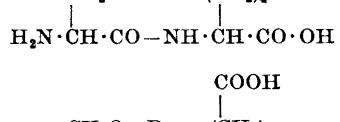
L-Seryl-L-glutamic acid	(c)	Ser-Glu	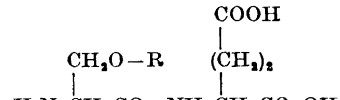
O-Phosphoryl-L-seryl-L-glutamic acid	(d)	SerP-Glu	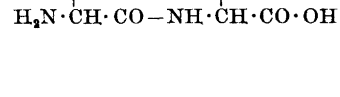

Compounds: a,c : R = —H

b,d : R = 

Fig. 1. Structure and symbols of peptides investigated.

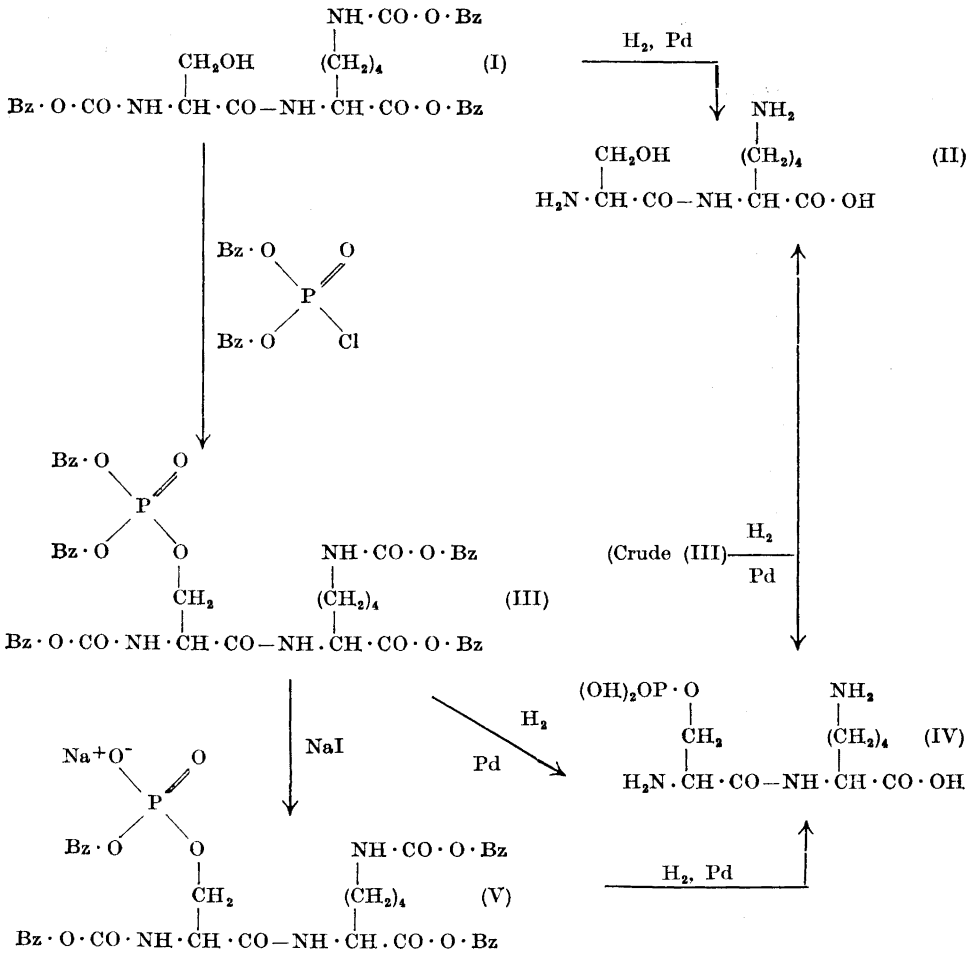

Fig. 2. Reaction scheme. Bz = $-CH_2 \cdot C_6H_5$.

EXPERIMENTAL *

Peptide synthesis

Nα-(N-carbobenzoxy-)-L-seryl-Nε-carbobenzoxy-L-lysine benzyl ester (Compound I, Fig. 2)

N,N′-Di*cyclo*hexylcarbodiimide (6.3 g = 30 mmoles) was added to a solution of 7.2 g (30 mmoles) N-carbobenzoxy-L-serine [12], 12.2 g (30 mmoles) Nε-carbobenzoxy-L-lysine benzyl ester hydrochloride [14] and 4.2 ml (30 mmoles) triethylamine in 150 ml of tetrahydrofuran-acetonitrile (2:1). The next day the precipitated di*cyclo*hexylurea was removed

* Solvents systems used in the paper (Whatman No. 1) chromatography: (a) phenol-water (80:20, v/v), ascending, 6 h; and (b) *n*-butanol-acetic acid-water (40:10:50, v/v/v), descending, 18 h. All papers were sprayed first with ninhydrin and then with phosphate (ammonium molybdate) reagents.

by filtration, and the solvent distilled off *in vacuo*. The residue was dissolved in ethyl acetate and the solution washed successively with water, 2 M H_2SO_4, $KHCO_3$ solution and water. After drying (Na_2SO_4), the solution was concentrated to a small volume. Light petroleum was added causing crystallization. The product was recrystallized from ethyl acetate-light petroleum, yielding 15.5 g (87 %) of (I). M.p. 112–113° (Found: C 64.7; H 6.3; N 7.1; Calc. for $C_{32}H_{37}N_3O_8$ (591.6): C 65.0; H 6.3; N 7.1).

L-*Seryl*-L-*lysine (Compound II)*

a) *From (I).* To a solution of 3.0 g (5 mmoles) of (I) in 50 ml *tert*-butanol, water was added to slight turbidity. After adding 5 ml of 1 M HCl, the solution was shaken in an atmosphere of pure hydrogen together with 0.5 g 10 % palladium on charcoal catalyst. In 2 h, 340 ml hydrogen was consumed. The catalyst was filtered off and the solution evaporated to dryness *in vacuo*. The solid residue was dissolved in 5 ml water and precipitated with acetone, yielding (II) as the *mono*-hydrochloride (1.25 g = 93 % after drying over P_2O_5 at room temperature).

$[\alpha]_D^{19}$ −5.9 (1 M HCl, *c* 3.9); R_F 0.45 (solvent a); R_F 0.20 (solvent b). (Found: C 40.1; H 7.8; N 14.9; Calc. for $C_9H_{19}N_3O_4 \cdot HCl$ (269.4) : C 40.1; H 7.5; N 15.6). The hydrochloride was strongly hygroscopic.

b) *From crude (III).* After hydrogenolysis and chromatographic separation (see below, compound IV), 2.5 g of (II) was isolated as the diformate salt. (Found: C 40.5; H 7.1; N 13.2; Calc. for $C_9H_{19}N_3O_4.2CH_2O_2$ (325.3): C 40.6; H 7.1; N 12.9). The compound moved on paper chromatography exactly as the above-mentioned hydrochloride. The formate salt was less hygroscopic than the latter.

Nα-(O-Dibenzylphosphoryl-N-carbobenzoxy-)-L-*seryl-Nε-carbobenzoxy*-L-*lysine benzyl ester (Compound III)*

A solution of 11.8 g (20 mmoles) of (I) in 20 ml dry pyridine was cooled to just above the freezing point. Dibenzylphosphoryl chloride, freshly prepared from 10.5 g (40 mmoles) dibenzylphosphite was added. After shaking 15 min at this temperature the flask was left at 4° over night. The reaction product, which had turned pale yellow, was poured into a cold mixture of 100 ml ethyl acetate and 100 ml water. The ethyl acetate layer was washed successively with 5 M H_2SO_4, water, $KHCO_3$ solution and water. After drying (Na_2SO_4), evaporation of the solvent yielded 15.5 g of a slowly solidifying mass. Analysis (Found: N 6.9; P 2.8) indicated that the product contained large amounts of (I) *. A sample of 1 g was recrystallized four times from ethyl acetate-light petroleum, yielding 0.30 g of fairly pure (III) with m.p. 92–93°. (Found: C 63.5; H 6.0; N 5.3; P 3.4; Calc. for $C_{46}H_{50}O_{11}N_2P$ (851.9): C 64.8; H 5.9; N 4.9; P 3.6). Most of the material was hydrogenolyzed directly (see below, compound IV).

O-Phosphoryl-L-*seryl*-L-*lysine (Compound IV)*

a) *From crude (III)* by direct hydrogenolysis. To a solution of 12.0 g of crude (III) in 100 ml *tert*-butanol, water was added to slight turbidity. The solution was shaken with 2.0 g 10 % Pd/C in an atmosphere of pure hydrogen. In 4 h, 930 ml was consumed. The filtered solution was worked up as under (II a), yielding 4.8 g of a solid product. This was found by paper chromatography to be a mixture of (II) and (IV). The product was dissolved in a small amount of water and applied to a column (2.7 × 14 cm) of Dowex 1-X2, 200–400 mesh (formate form) (*cf.* Ref.[16]). Fractions were collected as given in Table 1 and evaporated immediately to dryness *in vacuo*.

---

* The N and P analyses as well as the hydrogenolysis below (compound IV) indicated a yield of about 50 % of (III). Careful low temperature phosphorylations of serine derivatives with freshly prepared dibenzyl phosphoryl chloride may yield 60–75 % of phosphate triester [1]. Higher yields are obtained with diphenylphosphoryl chloride [1,13] but the hydrogenolytic elimination of phenyl groups is usually slow. Theodoropoulos *et al.*[15] obtained very low yields with any phosphorylation method tried except when imidazole was added to the phosphorylation mixture.

Table 1. Separation of O-phosphoryl-L-seryl-L-lysine and L-seryl-L-lysine on Dowex 1-X2, 100—200 mesh.

Fraction No.	H_2O ml	Grams	Fraction No.	1 M HCOOH ml	Grams
1	20	0.1	5	20	0
2	20	2.2	6	20	0.1
3	20	0.2	7	20	0.8
4	30	0.1	8	20	1.5
			9	50	0.1
			10	50	0

The fractions were analysed by paper chromatography in solvent II. Fractions 2, 3 and 4 (R_F 0.20), contained compound (II), whereas fractions 6, 7, and 8 (R_F 0.03), contained the expected phosphopeptide (IV). After drying *in vacuo* at room temperature over P_2O_5, the latter had $[\alpha]_D^{19}$ −4.7 (1 M HCl, *c* 3.4). Analyses indicated it to be *mono*-formate salt. (Found: C 34.7; H 6.7; N 12.5; P 8.5; Calc. for *mono*-formate salt ($C_9H_{20}O_7N_3P \cdot CH_2O_2$) (359.3): C 33.4; H 6.2; N 11.7; P 8.7. Calc. for free phosphopeptide ($C_9H_{20}O_7N_3P$) (313.3): C 34.5; H 6.4; N 13.4; P 9.9).

The sample to be titrated was converted to its hydrochloride by means of a cation exchange column (Dowex 50-X2, 200—400 mesh) in H^+-form. This had the dimensions 1.5 × 40 cm, and 250 mg peptide was applied. The column was eluted first with 2 l of water and then with 0.5 M HCl. After 1.2 l of the latter eluent the peptide came out, as indicated with Moore and Stein's ninhydrin method [17]. After immediate freeze-drying 150 mg of O-phosphoryl-L-seryl-L-lysine dihydrochloride was obtained. The compound moved as a single spot in paper chromatography; R_F 0.08 (solvent a); R_F 0.04 (solvent b). (Found: C 28.0; H 5.8; N 10.0; P 7.8; Calc. for $C_9H_{20}O_7N_3P$ (386.2): C 28.0; H 5.7; N 10.8; P 8.0). The hydrochloride was hygroscopic.

b) *From pure (III).* Hydrogenolysis of 100 mg of (III) as described for compound (IIa) yielded 35 mg (77 %) of compound (IV), paper chromatographically homogeneous in solvents a (R_F 0.08) and b (R_F 0.04).

c) *From (III) via mono-debenzylation.* A solution of 1.5 g of crude (III) in 10 ml dried acetone was refluxed for 15 min with 0.2 g anhydrous NaI. The expected sodium salt (V) did not separate from the acetone solution within 48 h at 4°. The solvent was distilled off and the residue poured into ethyl acetate and $KHCO_3$ solution. Acidification of the aqueous phase gave an oily acid. This was extracted with ethyl acetate, the solvent distilled off and the residue hydrogenolyzed as above. Thereby 110 mg of compound (IV) was obtained; R_F = 0.04 (solvent b).

L-*Seryl*-L-*glutamic acid.*

Palladium-catalyzed hydrogenolysis of N-carbobenzoxy-L-seryl-L-glutamic acid dibenzyl ester [1] in glacial acetic acid solution (to avoid any ester exchange [19],) resulted in a peptide, which contained strongly bound acetic acid *. The acetic

* The presence of acetic acid was indicated by titration. After drying *in vacuo* over KOH at room temperature, the ratio between KOH consumed for ionization of carboxyl groups (below pH 6) and that for the amino group (pH 6—10) was 1.6. Drying over KOH at 1 mm Hg, 5 h at 75° lowered this ratio to 1.18. Further 8 h drying at 100°, however, resulted in a large decrease in free amino groups, and the ratio increased to 4.0. Diketopiperazine formation or polymerisation (involving amino- and α- or γ-carboxyl groups) may have occurred.

acid was removed by applying the original peptide (407 mg) to an 1.5 × 19 cm column of Dowex 50-X2, 200—400, mesh, in H^+-form. The column was first eluted with water and then with 0.12 M HCl. After 120 ml (in 10 ml fractions) of the latter effluent the peptide appeared as indicated by ninhydrin [17]. After freeze-drying and drying *in vacuo* over P_2O_5 at room temperature 341 mg of peptide hydrochloride was obtained. (Found: C 35.2; H 5.5; N 10.5; Calc. for $C_8H_{14}O_6N_2$. HCl (270.7): C 35.5; H 5.6; N 10.4).

O-Phosphoryl-L-seryl-L-glutamic acid

This phosphopeptide, prepared as described previously [1], was finally purified by cation exchange chromatography (Dowex 50-X2, 200—400 mesh, 1.5 × 40 cm column in H^+-form). After elution with 250 ml of water, the peptide appeared, and the solution was freeze-dried. R_F 0.04 (solvent I) and R_F 0.06 (solvent II). (Found: C 30.6; H 5.0; N 9.0; P 9.9: Calc. for $C_8H_{15}O_9N_2P$ (314.2): C 30.6; H 4.8; N 8.9; P 9.9).

In attempts to crystallize O-phosphoryl-L-seryl-L-glutamic acid from ethanol the product obtained showed at least two new ninhydrin- and phosphate-positive spots in paper chromatography (solvents a and b). These moved appreciably faster (R_F 0.9 and R_F 0.4 in solvent a; R_F 0.3 and R_F 0.2 in solvent b) than the original peptide. Ethyl esters seem to be formed *. Ester interchange during hydrogenolysis of benzyl esters in ethanolic solvent has been observed by Crofts, Markes and Rydon [19], and *tert*-butyl alcohol recommended as solvent. Therefore, hydrogenolysis has been performed in either glacial acetic acid or in *tert*-butanol-water, and acetone has been preferred for precipitation of acidic peptides. With these precautions no esterification has been detected.

Titration

Potassium hydroxide, 0.25 M, containing 0.15 M KCl, and *hydrochloric acid*, 0.30 M, were prepared and standardized as described [2]. All reagents in this work were of analytical grade.

Titration procedure. Acid-base titrations were carried out for each peptide by successive addition of standard KOH or HCl to the experimental solution (initial volume 10 ml), containing peptide (approximately 2×10^{-3} M) and 0.15 M KCl, and the pH measured after each addition. In respect of the lysine peptides, the compounds IIa and IVa (hydrochlorides) were titrated. Every titration was reproduced at least once. The true concentration of peptide, used in the calculations, was obtained from the titration curve. As measuring instrument a Radiometer PHM 4a valve potentiometer, equipped with a Radiometer glass electrode G202 B and a calomel electrode K 100 was used. The rest of the apparatus was the same as described previously [3]. All titrations were made at 25.00 ± 0.03°. Activity coefficients were assumed to be constant owing to the presence of 0.15 M KCl. Standardization of the pH-meter, conversion of measured pH to correspond to hydrogen ion concentration, pcH (*cf.* Ref.[20]), and the routine calibration of the measuring system were made as before [3]. The reproducibility of the measurements was within 0.01 pH unit.

Calculations **. Apparent ionization constants were computed for the peptides investigated as described [3] with the exception of the overlapping constants of serylglutamic acid and phosphorylserylglutamic acid.

The ionization constants (K_{H_3A} and K_{H_2A}) of the α- and γ-carboxyl groups in serylglutamic acid were resolved by comparing the experimental data with a family of normalized curves [21]. The constant, K_{H_3A}, was normalized and determined the position of the experimental function $\bar{n}_H$ (pcH) on the abscissa, while the ratio K_{H_3A}/K_{H_2A} determined the shape. The constants obtained thereby were refined by the projection strip method developed by Rossotti *et al.*[22]

---

* Contrary to O-phosphorylserylglutamic acid, O-phosphorylserine is very resistant to esterification and can be crystallized from boiling methanol.

** The same symbols have been used as in the preceding paper [3]. Thus, any constant K_{H_jA} is defined $h(H_{j-1}A)/(H_jA)$; A = conjugate base of the polybasic acid H_jA with all dissociable protons removed; h = molar free hydrogen ion concentration; $\bar{n}_H$ = average number of protons bound per all different species of A; Y(X)z means Y as a function of X with Z constant.

Table 2. Apparent ionization constants of the peptides at 25° in 0.15 M KCl.

Compound	α-COOH	γ-COOH	$-PO_3H^-$	$\alpha\text{-}NH_3^+$	$\varepsilon\text{-}NH_3^+$
Ser–Lys	$pK_{H_3A} = 2.92 \pm 0.02$			$pK_{H_2A} = 7.16 \pm 0.01$	$pK_{HA} = 10.49 \pm 0.03$
SerP–Lys	$pK_{H_4A} = 2.98 \pm 0.01$		$pK_{H_3A} = 5.34 \pm 0.01$	$pK_{H_2A} = 7.58 \pm 0.02$	$pK_{HA} = 11.05 \pm 0.03$
Ser–Glu	$pK_{H_3A} = 2.94 \pm 0.02$	$pK_{H_2A} = 4.34 \pm 0.01$		$pK_{HA} = 7.42 \pm 0.01$	
SerP–Glu	$pK_{H_4A} = 3.02 \pm 0.02$	$pK_{H_3A} = 4.39 \pm 0.01$	$pK_{H_2A} = 5.69 \pm 0.005$	$pK_{HA} = 8.25 \pm 0.005$	
Ser–Gly *	$pK_{H_2A} = 3.10 \pm 0.01$			$pK_{HA} = 7.33 \pm 0.02$	
SerP–Gly *	$pK_{H_3A} = 3.13 \pm 0.01$		$pK_{H_2A} = 5.41 \pm 0.01$	$pK_{HA} = 8.01 \pm 0.01$	
Ser–Leu *	$pK_{H_2A} = 3.08 \pm 0.01$			$pK_{HA} = 7.45 \pm 0.01$	
SerP–Leu *	$pK_{H_3A} = 3.11 \pm 0.02$		$pK_{H_2A} = 5.47 \pm 0.005$	$pK_{HA} = 8.26 \pm 0.01$	

* Data compiled from the preceding paper [3].

The constants (K_{H_4A}, K_{H_3A} and K_{H_2A}) related to the α-carboxyl-, γ-carboxyl- and second phosphate groups of phosphorylserylglutamic acid were computed by one of the elimination methods described by Sillén [21] for two parameter systems. A preliminary value of K_{H_3A} was, however, first obtained from extrapolation of the plot, $\log[h(4-\bar{n}_H)/(\bar{n}_H-1)]$ as a function of $(\bar{n}_H-1)$, to $(\bar{n}_H-1)$ equal to zero (for details see Ref.[3]). Holding K_{H_4A} constant, K_{H_3A} and K_{H_4A} were then determined by plotting $K_{H_4A}^{-1}$ as a function of h, for different K_{H_3A}. With two similar plots the constants were refined: K_{H_3A} and K_{H_3A} were computed from $K_{H_3A}(h)K_{H_3A},K_{H_4A}$ curves with different K_{H_3A}, and values of K_{H_3A} and K_{H_4A} were computed from $K_{H_3A}(h)K_{H_4A},K_{H_3A}$ curves with different K_{H_4A}. The latter two plots gave only a minor change in the values of the constants (less than 0.01 pK unit).

RESULTS AND DISCUSSION

In Table 2 are listed the apparent ionization constants, expressed as pK values, obtained in this investigation, as well as those reported [3] for some analogous peptides. The titrations are shown in Fig. 3. The constants in Table 2 are referred to individual groups, even though they are not true intrinsic constants [23]. The pK value of the first ionization of the phosphate group is not included, as it cannot be determined under the experimental conditions used. Due to some possible overlapping of the ionization of this group and the α-carboxyl group, less weight was given to experimental data below pcH 3 for the phosphorylated peptides.

No acid-base data are available in the literature for any of the present compounds. The ionization constants obtained for serylglutamic acid and seryllysine may, however, be compared with those of similar peptides, if differences in experimental conditions and chemical structure are considered. The following constants have been reported: glutaminylglutamic acid [24]: pK (α—COOH) 3.14, pK (γ—COOH) 4.38; lysylglutamic acid [24]: pK (α—COOH) 2.93, pK (γ—COOH) 4.47, pK (ε—NH_3^+) 10.50; lysyllysine [25]: pK (α—COOH) 3.01; and alanyllysylalanine [25]: pK (ε—NH_3^+) 10.30 (all L-configurations).

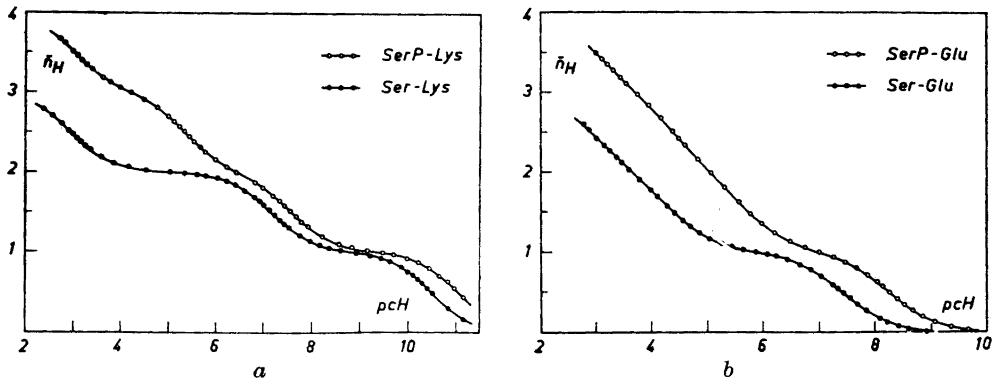

Fig. 3. Potentiometric titration data of serine peptides at 25° in 0.15 M KCl.
a. L-Seryl-L-lysine, ●; O-phosphoryl-L-seryl-L-lysine, O.
b. L-Seryl-L-glutamic acid, ●; O-phosphoryl-L-seryl-L-glutamic acid, O.
The drawn curves have been computed from the constants in Table 1.

From Table 2 can be seen that the introduction of an O-phosphoryl group in serylglutamic acid and seryllysine results in a similar slight increase in pK of the α-carboxyl group as in the analogues, serylglycine and serylleucine. The increase in p$K(\alpha-NH_3^+)$ of phosphorylserylglutamic acid relative to serylglutamic acid is also almost as great as that obtained by phosphorylation of serylglycine and serylleucine (0.7—0.8 pK units). This may therefore be due to the same effects in all three peptides, reasonably the combined direct field (+ D) and inductive effects [26] (*cf.* Fig. 4, conformation a). The γ-carboxyl group seems, thus, to have no measurable effect on the rise in pK $(\alpha-NH_3^+)$, caused by the phosphate group.

The other pK values obtained for phosphorylserylglutamic acid do not allow any further discussion owing to overlap of the ionization of the α-carboxyl, γ-carboxyl- and second phosphate groups. However, the pK values of the carboxyl groups may be compared with the corresponding values for the phosphopeptides prepared from α-casein [6] * and whole-casein [2] **. The p$K(\gamma-COOH)$ value obtained in this study agrees roughly with the intrinsic pK value (= 4.1) for the ten free side-chain carboxyl groups present in the α-casein peptide *, especially as these groups may constitute both β-aspartic and γ-glutamic carboxyl groups. The titration data of the whole-casein peptide[2] suggest a lower intrinsic pK value (about 3.8) for its γ-carboxyl groups. This may be properly explained by the fact that one of the glutamyl residues occupies the N-terminal position and one other possibly being neighbour to the basic histidyl residue. The pK $(\alpha-COOH)$-values of the synthetic peptides studied (see Ref.[3] and Table 2) further indicate that this histidyl residue may be C-terminal in the whole-casein peptide, due to the apparently low pK (= 2.7) of its α-carboxyl group.

In contrast to the other phosphopeptides in Table 2, the increase in pK of the α-amino group of phosphorylseryllysine relative to unphosphorylated peptide is much less (0.4 pK units). The pK of the second phosphate ionization in this compound is only slightly lower than that of phosphorylated serylglycine and serylleucine. Furthermore, the pK of the ε-amino group in phosphorylseryllysine is appreciably higher (0.5 pK units) than that of the unphosphorylated peptide and other lysine derivatives [24,25,27]. This suggests that the phosphate group is shared between the two amino groups, when they are charged; schematically by a combination of the forms (a) and (b) of Fig. 4. The approach between the charged side-chains is not sterically hindered according to Stuart-Briegleb molecular models. Owing to the isolated position of the ε-amino group, differences around this group in inductive, mesomeric or solvation effects between seryllysine and phosphorylseryllysine may be eliminated. Therefore the increase in pK of the ε-amino group will be due almost exclusively to the + D effect of the negatively charged phosphate group.

This interaction between the ε-amino- and phosphate groups may now be discussed in relation to trypsin action. At pH 8.5—10.0 involving an uncharged α-amino group, conformation of type (b) in Fig. 4 will dominate. Fig. 4 c

* $Asp(Asp_3, Thr, Ser_6, Glu_{10}, Pro, Gly, Ala_2, Val_2, Met_2, Ileu_4, Lys)Lys; (NH_3)_4;(H_3PO_4)_7$.
** $Glu(Thr,Ser_3,Glu_2,Val, Ileu_2,His); (H_3PO_4)_3$.

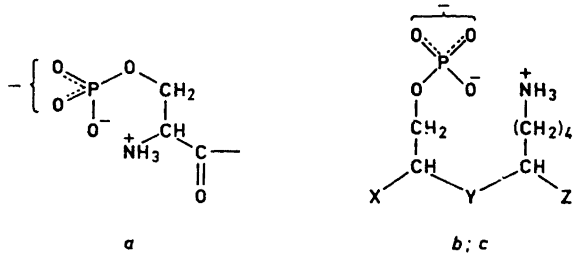

Fig. 4. Probable conformations due to charge interaction in O-phosphorylated serine peptides at pH 6—7 (a), and pH 7—10 (b, c) according to acid-base data.

a. N-terminal O-phosphorylserine residue
b. Amino acid sequence -SerP-Lys-; X = NH; Y = CO-NH; Z = CO
c. » » » -Lys-SerP-; X = CO; Y = NH-CO; Z = NH

as well as molecular models show that the above discussion will apply also to the reversed amino acid sequence, lysyl-(O-phosphoryl)-serine. As in larger peptides and proteins the α-amino- and α-carboxyl groups of these sequences are involved in peptide bonds, the phosphate group interacts with the ε-amino group in the pH optimum region of trypsin. Trypsin requires, however,

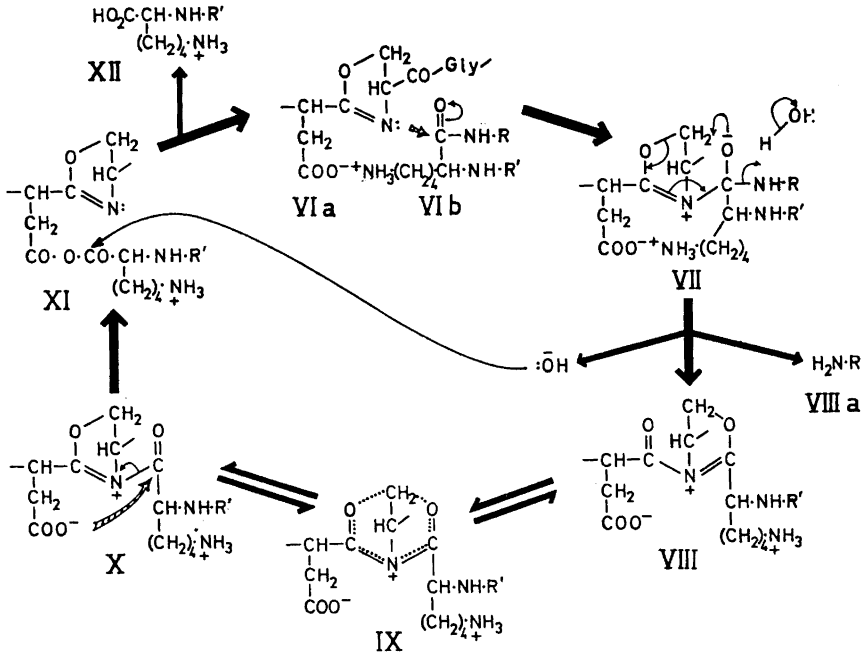

Fig. 5. Tryptic hydrolysis mechanism according to Rydon [34], adapted for lysine peptides. VI a = active center of enzyme. The serine carbonyl group and the glycine residue are indicated by a bond line only in VII—XI.

a free ε-amino group for action on a peptide bond involving the lysine carboxyl group [7]. A plausible mechanism taking in account this specificity and the absence of hydrolysis of O-phosphorylated lysine peptides may be formulated as follows:

The amino acid sequence in the "active center" of trypsin [28,29] and several other esterases [28,30–33] has been shown to be ···—Asp—Ser—Gly—···. Rydon [34] has formulated a mechanism for the trypsin catalyzed hydrolysis of esters, assuming a Δ^2-oxazoline structure for the active serine residue. The adaption of his mechanism to peptides and proteins is suggested in Fig. 5. In this figure, (VI a) represents the active center of the enzyme and (VI b) the substrate with a free, positively charged ε-amino group of lysine. We tentatively propose that the function of this basic group is to bind the substrate to the aspartic acid residue in the active center of the enzyme *. As shown in Fig. 5, the approach of the ε-amino group to the aspartic acid β—COO^- may bring the peptide bond carbonyl group in favourable position for a nucleophilic attack by the oxazoline N atom, forming (VII). Rearrangement of (VII) and proton transfer from a water molecule would liberate the amino acid or peptide chain (H_2N—R) attached to the lysine carboxyl group and result in (VIII), having a positive charge on the oxazoline N atom. This charge may then repel the ε-amino group from the aspartic acid carboxyl group and thus enable an attack on the lysine carbonyl group in the tautomeric isomer (X). Finally, the anhydride (XI) so formed would undergo hydrolysis, formally by the uptake of the OH^- released in stage (VII)→(VIII), and so liberate the lysyl part of the peptide chain (XII) under simultaneous regeneration of the enzyme (VIa).

The observed inability of trypsin to hydrolyse O-phosphorylated peptides ** may then be attributed to a hindrance of the enzyme-substrate complex formation involving the enzyme β-carboxyl group and the substrate ε-amino group. The positive charge on the latter is preferentially taken into account by the phosphate group. Furthermore, the negatively charged enzyme carboxyl- and substrate phosphate groups may repel each other ***.

We are indebted to Miss Görel Larsson for valuable technical assistance. The investigation was aided by grants from the *Swedish Medical Research Council* to Professor O. Mellander and by grants from the *Medical Faculty, University of Göteborg* to R.Ö.

* On the basis of kinetic data it has been suggested that the combination between enzyme and substrate is essentially electrostatic in character [7,p.108]. The differences in specificity between different esterases, apparently with the same active centers, may be explained by a different mechanism for the enzyme-substrate complex formation; *e.g.* chymotrypsin may combine with the substrate through hydrogen bonds [7,p.118]. The validity of the electrostatic binding mechanism described below is not dependant on the presence of an oxazoline structure; an unmodified serine residue may undergo similar reactions, when suitably activated, e.g. by a histidine residue.

** In Fig. 5, R = $-CH(CH_2OPO_3^{2-})CO-$ in a sequence —lysyl-(O-phosphoryl-)serine; R′ = $-CO\cdot CH(CH_2OPO_3^{2-})NH-$ in a sequence —(O-phosphoryl-)seryl-lysine.

*** A mechanism for the inhibition of trypsin by polyelectrolytes as, *e.g.*, poly-α-L-glutamic acid, has been proposed by Kornguth and Stahmann [35]. In that case the inhibition is entirely independant of the substrate.

REFERENCES

1. Fölsch, G. *Acta Chem. Scand.* **13** (1959) 1407, 1422.
2. Österberg, R. *Arkiv Kemi* **13** (1959) 409.
3. Fölsch, G. and Österberg, R. *J. Biol. Chem.* **234** (1959) 2298.
4. Bennich, H., Johansson, B. and Österberg, R. *Acta Chem. Scand.*, **13** (1959) 1171.
5. Österberg, R. *Biochim. et Biophys. Acta* **42** (1960) 312.
6. Österberg, R. *Biochim. et Biophys. Acta* **54** (1961) 424.
7. Neurath, H. and Schwert, G. W. *Chem. Revs.* **46** (1950) 69.
8. Theodoropoulos, D., Bennich, H., Fölsch, G. and Mellander, O. *Nature* **184** (1959) 187.
9. Geschwind, I. I., Li, C. H. and Barnafi, L. *J. Am. Chem. Soc.* **79** (1957) 620.
10. Jollès Thaureaux, J., Jollès, P. and Fromageot, C. *Biochim. et Biophys. Acta* **27** (1958) 298.
11. Hirs, C. H. W., Moore, S. and Stein, W. H. *J. Biol. Chem.* **219** (1956) 623.
12. Fruton, J. S. *J. Biol. Chem.* **146** (1942) 463.
13. Riley, G., Turnbull, J. H. and Wilson, W. *J. Chem. Soc.* **1957** 1373.
14. Erlanger, B. F. and Brand, E. *J. Am. Chem. Soc.* **73** (1951) 4025.
15. Theodoropoulos, D., Gazopoulos, J. and Souchleris, I. *Nature* **185** (1960) 606; **188** (1960) 489; *J. Chem. Soc.* **1960** 5257.
16. Strid, L. *Acta Chem. Scand.* **13** (1959) 1787.
17. Moore, S. and Stein, W. H. *J. Biol. Chem.* **211** (1954) 907.
18. Zervas, L. and Dilaris, I. *J. Am. Chem. Soc.* **77** (1955) 5354.
19. Crofts, P. C., Markes, J. H. H. and Rydon, H. N. *J. Chem. Soc.* **1959** 3610.
20. Bates, R. G. and Schwarzenbach, G. *Helv. Chim. Acta* **37** (1954) 1069.
21. Sillén, L. G. *Acta Chem. Scand.* **10** (1956) 186.
22. Rossotti, F. J. C., Rossotti, H. and Sillén, L. G. *Acta Chem. Scand.* **10** (1956) 203.
23. Edsall, J. T. and Wyman, J. *Biophysical Chemistry*, Academic Press, New York 1958, Vol. I, p. 481.
24. Cohn, E. J. and Edsall, J. T. *Proteins, Amino Acids and Peptides*, Reinhold Publishing Co., New York 1943, p. 85–86.
25. Ellenbogen, E. *J. Am. Chem. Soc.* **74** (1952) 5198.
26. Ingold, C. K. *Structure and Mechanism in Organic Chemistry*, Ithaca, New York 1953, Chapter XIII.
27. Steinhardt, J. and Zaiser, E. M. *Advances in Protein Chem.* **10** (1955) p. 163.
28. Oosterbaan, R. A., Jansz, H. S. and Cohen, J. A. *Biochim. et Biophys. Acta* **20** (1956) 402.
29. Dixon, G. H., Kauffman, D. L. and Neurath, H. *J. Am. Chem. Soc.* **80** (1958) 1260; *J. Biol. Chem.* **233** (1958) 1373.
30. Turba, F. and Gundlach, G. *Biochem. Z.* **327** (1955) 186.
31. Schaffer, N. K., Simet, L., Harshman, S., Engle, R. R. and Drisko, R. W. *J. Biol. Chem.* **225** (1957) 197.
32. Oosterbaan, R. A., Kunst, P., Van Rotterdam, J. and Cohen, J. A. *Biochim. et Biophys. Acta* **27** (1958) 549.
33. Naughton, M. A., Sanger, F., Hartley, B. S. and Shaw, D. C. *Biochem. J.* **77** (1960) 149.
34. Rydon, H. N. *Nature* **182** (1958) 928.
35. Kornguth, S. E. and Stahmann, M. A. *Arch. Biochem. Biophys.* **91** (1960) 32.

Received June 6, 1961.

ACTA CHEMICA SCANDINAVICA 15 (1961) 1975–1980

The Components of Orosomucoid

JOHN GOA

Department of Clinical Chemistry, Rikshospitalet, Oslo, Norway *

Orosomucoid has been prepared by fractional precipitation with perchloric acid followed by chromatography on DEAE-cellulose. All the components of which the protein is built up, have been determined. Special attention is paid to the amino acids and amide nitrogen. The number of carbohydrate and amino acid residues in orosomucoid are calculated.

Extensive studies have been made on the chemistry of orosomucoid. This protein is interesting because of its high carbohydrate content (40 %), and because the structure, and especially the linkage between the protein and the carbohydrate is unknown. The individual carbohydrate components of orosomucoid are well known; however, fewer data have been published about the amino acid part.

Amino acid analysis of orosomucoid presents special problems. During the acid hydrolysis of this protein a massive humin formation makes the results uncertain. It is shown that humin formation does not take place in the presence of titanium trichloride.

EXPERIMENTAL

Preparation of orosomucoid

The preparation of seromucoids from human serum by fractional precipitation with perchloric acid and fractionation on DEAE-cellulose has been described previously [1]. Three fractions were obtained, called A, B and C. Fraction B was eluted with 0.05 M phosphate + 0.1 N sodium chloride, pH 6.8, and consisted of two components in the ratio of about 9:1, called B-1 and B-2. When fraction B was rechromatographed in the same system three times, the B-1 fraction became pure as tested by paper electrophoresis and immunologically by the method of double diffusion in agar according to Ouchterlony [2,3]. Fraction B-1 was shown to be identical with orosomucoid tested immunologically and by determination of hexose, hexosamine and nitrogen [1].

An almost ash-free preparation was obtained by passing the protein through a column of Dowex 2 in OH-form followed by Dowex 50 in H-form. The preparation was finally lyophilized.

* Present address: Central Laboratory, Hospital of Norrköping, Norrköping, Sweden.

Table 1.

Hydrolysis	Weighted protein-N mg	Analyzed N in the hydrolysate mg	Per cent recovery	Mean
24 h 110°C	17.0	15.8	93	95
44 h 110°C	19.5	18.9	95	
72 h 110°C	18.0	17.3	96	
24 h, 110°C with $TiCl_3$	15.0	15.2	101	99
44 h, 110°C with $TiCl_3$	18.4	17.3	94	
72 h, 110°C with $TiCl_3$	17.8	18.2	102	

Amino acid analysis

The amino acids were determined according to Moore, Spackman and Stein [4] by chromatography on Amberlite IR-120. Cysteine plus cystine was determined by means of hydrazinolysis [5] and tryptophane with *p*-dimethylaminobenzaldehyde and sodium nitrite as described by Spies and Chambers [6].

Special attention was paid to the hydrolysis of the protein because of the humin formed. It was observed that all the sialic acid and a large part of the hexosamine was destroyed. It could also be expected that part of the amino acids had been lost. An attempt was made, therefore, to reduce the humin formation by means of catalysts. Titaniumtrichloride, of the metal salts tried, was found to eliminate the humin without destruction of amino acids.

The hydrolysis was performed as follows: In six Pyrex test tubes about 15 mg of orosomucoid with a nitrogen content of 10.7 % was dissolved in 2 ml redistilled 6 N hydrochloric acid. To three of the tubes were added three drops of titaniumtrichloride ($TiCl_3$, 15 %, Merck). The tubes were evacuated and sealed, and hydrolysis was carried out at 110 ± 2°C for 25, 44, and 72 h. The tubes without $TiCl_3$ contained a considerable amount of humin, which seemed to be coal particles. In the tubes with $TiCl_3$, however, the solutions were almost clear, and the small amount of particles were of inorganic origin.

The contents were transferred quantitatively through filter papers into small beakers by means of distilled water and dried in a desiccator over sodium hydroxide. Finally the residues were dissolved in 5 ml of pH 3.25 buffer for chromatography. Aliquots were taken out for nitrogen determination (micro Kjeldahl). The results are given in Table 1. The difference from the theoretical values was about 5 % and may be due to technical errors during the different procedures. There is, however, a tendency to better yield when $TiCl_3$ is used. This also applies to the amino acid analysis.

Chromatography was performed with 1 ml hydrolysate on the long column and 0.6 or 0.7 ml on the short one. In Table 2 the values are given as amino acid residues in per cent of hydrolyzed protein. Glucosamine which emerged as a free peak from the short column before lysine, had undergone partial destruction and was found in amounts of about 5 %. Ammonia was found in amounts of 13—15 %, given as ammonia nitrogen in per cent of hydrolyzed nitrogen. These values are not given in the table.

Table. 2

Hydrolysis time and conditions	24 h	24 h +$TiCl_3$	44 h	44 h +$TiCl_3$	72 h	72 h +$TiCl_3$	Extrapolated values of residues	Moles per 46 000 g orosomucoid	Grams per 100 g protein
Components	% amino acid residue of orosomucoid								
Aspartic acid	6.40	6.56	6.08	6.69	6.11	6.11	6.5	26	7.5
Threonine	4.31	4.31	3.91	4.52	4.02	3.99	4.3	19	4.7
Serine	1.71	1.66	1.37	1.69	1.57	1.55	1.7	9	2.1
Glutamic acid	8.95	8.55	8.30	8.92	8.39	8.88	8.9	31	10.1
Proline	2.45	2.48	2.10	2.63	2.35	2.47	2.5	12	3.0
Glycine	1.16	1.25	1.13	1.25	1.08	1.08	1.2	9	1.6
Alanine	2.33	2.30	1.81	1.96	1.86	1.88	2.3	15	2.8
Valine	2.13	2.18	2.28	2.38	2.22	2.46	2.3	11	2.7
Methionine	0.42	0.44			0.44	0.79	0.5	2	0.5
Isoleucine	2.64	2.73	2.73	2.86	2.69	2.70	2.7	11	3.1
Leucine	4.50	4.74	(3.33)	4.85	4.72	4.74	4.7	19	5.4
Tyrosine	3.70	3.92	3.43	3.79	3.84	3.59	3.8	11	4.3
Phenylalanine	3.96	4.05	(3.14)	3.94	3.69	(3.24)	4.0	12	4.5
Lysine	4.71	4.53	4.52	4.80	4.98	(3.43)	4.7	17	5.5
Histidine	1.07	1.29	1.12	0.97	1.24	0.87	1.2	4	1.4
Arginine	2.84	2.94	3.19	3.38	3.17	2.80	3.1	9	3.5
Tryptophan							1.4	4	1.5
Cystine/2							1.4	6	1.7
Acetyl glucosamine							12.8	29	14.0
N-acetyl neuraminic acid							12.0	19	12.8
Hexoses							14.6	41	16.2
Fucose							1.0	3	1.1

The amino acids have also been determined microbiologically by Weimer *et al.*[7] and by Caputo and Santoro [8] by means of high voltage electrophoresis. The agreement between these values and those in Table 2 is not very good.

Determination of amide nitrogen

The amide nitrogen content of orosomucoid is extremely difficult to determine due to the instability of sialic acid during hydrolysis, and because amino sugars as well as sialic acid are deaminated to some degree under the alkaline conditions generally used for liberation of ammonia.

Five different procedures for hydrolysis have been used in this study.

1. *Hydrolysis in 1 N sulphuric acid for 30 and 60 min. in sealed tubes at 120°C.* The hydrolysates were transferred to Conway chambers and made alkaline by addition of sodium hydroxide with phenolphthalein as indicator. The liberated ammonia was determined by titration after diffusion into boric acid for 5 h at 4°C. At this low temperature there is no destruction of hexosamine under alkaline conditions (Tracey [9]). This procedure gave a massive humin formation. The values found were equivalent to 13 to 20 residues per 46 000 g of protein.

2. *Hydrolysis in 0.1 N sulphuric acid for 1 to 4 h at 80°C.* This procedure has been used by Zilliken *et al.*[10] for liberation of sialic acid. Liberated ammonia was determined by diffusion in Conway chambers as described under procedure 1.

After half an hour of hydrolysis the liberated ammonia was less than 1 residue. After 2 and 4 h of hydrolysis the values rose to about 2 residues. Humin formation could be seen after about 2 h.

3. *Hydrolysis according to Rees* [11] *with 10 N hydrochloric acid for different time periods at 37°C, followed by diffusion in Conway chambers.* The humin formation started after some hours. After 4 days of hydrolysis, about 5 residues were liberated, after 8 days about 10 residues, and then the values rose slowly to about 22 residues after 28 days.

4. *Hydrolysis is 10 N hydrochloric acid as under procedure 3, but with addition of* $TiCl_3$. The humin formation was inhibited and first seen after 12 days. The amount of ammonia liberated was greater the first days compared with procedure 3, after 25 days it was about the same. After 2, 5, 12, and 25 days 4, 12, 14, and 19 moles of ammonia were liberated per 46 000 g of orosomucoid.

5. *Hydrolysis in 2 N HCl at 110°C.* Humin was formed after one hour and 19 residues were found. The values then rose slowly to 23 residues after 3 h and were found nearly constant for the following 3 h.

Thus it has not been possible to hydrolyze orosomucoid without destruction of sialic acid, and the liberated ammonia is more an expression of destruction than of amide nitrogen. According to Popenoe and Drew [12] a modified orosomucoid may be obtained by splitting off the sialic acid by means of sialidase from *Clostridium perfringens*. This modified protein has a slightly lower molecular weight, but as far as we know there is no other chemical change in the molecule than the absence of sialic acid. The modified protein was prepared as described by Popenoe and Drew [12]. Sialic acid was split off to a degree of 85 %, and the reaction mixture was separated on DEAE-Cephadex * in phosphate buffer pH 6.2. By stepwise elution with increasing ionic strength a fraction was obtained that was homogeneous in paper electrophoresis and free of sialic acid. This protein was used for determination of amide nitrogen as described under procedures 3 and 5. Only traces of humin were formed.

With procedure 3 hydrolysis was performed up to 10 days. After one day of hydrolysis 3—4 residues were liberated. After 2 days the number was 7, and this value was almost constant up to 6 days. After 10 days, however, the liberated ammonia corresponded to about 12 residues per 40 500 g of modified orosomucoid. The value 40 500 is calculated from the assumed molecular weight of orosomucoid by substraction of 19 sialic acid residues.

With procedure 5, *i.e.* 2 N HCl and 110°C, about 10 residues were found after one hour of hydrolysis. The value rose slowly to about 12 residues after 3—6 h. In all experiments the values after more than one hour of hydrolysis were within 12 ± 2 residues or 0.42 ± 0.07 per cent amide nitrogen.

With the assumption that the only change in orosomucoid treated with sialidase, is that sialic acid has been split off, it may be concluded that the number of 12 ± 2 amide groups are also present in native orosomucoid.

Determination of acid groups

This was determined by the dye-binding method of Fraenkel—Conrat and Cooper [13]. Using safranine 0 at pH 11.5 a total number of 83 ± 2 acid groups was found.

Basic groups could not be determined as orosomucoid was not precipitated by the dye orange G at pH 2.2.

Determinations of the carbohydrate components

Hexosamine was determined by the method of Morgan and Elson as described by Svennerholm [14]. Hexoses by anthrone [15], sialic acid by Bials reaction according to Svennerholm [16] and fucose by the cysteine method of Gibbons [17]. The hexosamines were found to be only glucosamine, determined by means of chromatography on Dowex 50 according to Gardell [18]. Test for glucoronic acid was negative. The values are given in Table 3 together with those of some other authors.

* DEAE-Cephadex was a gift from Pharmacia, Uppsala, Sweden.

DISCUSSION

All the components of which orosomucoid is built up, are now known. The number of residues are given in Table 3, assuming a molecular weight of 46 000. This value agrees well with the values calculated from the minimum molecular weight for each component. It is also known that glucosamine as well as sialic acid is N-acetylated. Sialic acid can be split off by enzymes from *Clostridium perfringens* [12] or other micro-organisms without affecting the rest of the molecule. About the same was obtained by cold concentrated hydrochloric acid [24]. It seems likely, therefore, that sialic acid is in end-position.

No N terminal amino acid could be found by the fluorodinitrobenzene- or the phenyl*iso*cyanate-method [25].

The C-terminal amino acid was found by Schmid *et al.*[24] to be serine. Only one mole C-terminal amino acid was found, indicating a single peptide chain.

The most interesting problem is the number of carbohydrate groups and the nature of linkage. One of the possibilities is the linkage to amino groups. Popenoe and Drew [12] found, however, 17 amino nitrogen groups by the method af Van Slyke [26], and the same value was found by the author. Thus the free amino groups correspond to the 17 ε-amino groups of lysine. Still the possibility exists that the carbohydrate component is linked to the N-terminal amino group as a single polysaccharide chain. This is not very likely, however.

Another possibility is linkage to one of the acid groups. Linkage between the phenol group in tyrosine and carbohydrate or between SH-groups and carbohydrate, has not been reported, but linkage between dicarboxylic amino acids and carbohydrate, has been found in egg albumin by Johansen *et al.*[27]. They were able to isolate a fragment containing only carbohydrate and aspartic acid.

The number of acid groups in orosomucoid are 26 β-aspartic acid carboxyl groups, 31 β-glutamic acid carboxyl groups, 19 sialic acids, 11 phenol groups

Table 3.

Author	Nitrogen %	Hexosamine %	Hexose %	N-acetyl neuraminic acid %	Fucose %	Mol. weight
Weimer *et al.*[7]	10.1	11.9	16.4			
Smith *et al.*[19]						44 100
Schmid [20]	10.7	11.5	17.2			
Werner and Odin [21]		11.5	14.1	9.8		
Schultze [22]		11.3[a]	14.7	12.1	0.7	41 000
Winzler [23]	10.1	11.9	16.4	10.6	1.3	44 100
Caputo and Santoro [8]	11.1	10	17			41 000[b]
						46 000[c]
Present author	10.7	11.3	16.2	12.6	1.1	

a) Recalculated from 13.9 % N-acetyl hexosamine.
b) By ultracentrifugation.
c) By refractive index measurements.

of tyrosine, 6 SH-groups of cysteine and 1 carboxyl group of the C-terminal serine. 12 of the β-carboxyl groups are bound to amide groups, and the calculated total number of free acid groups are thus about 82. The dye-binding method gave a value of 83 ± 2 free acid groups, which is in agreement with the value of 86 ± 2 found by Popenoe and Drew [12]. Thus, there is no real difference between calculated and estimated acid groups. The value of the acid groups is not exact, as it has been calculated from many different determinations, all of which are connected with errors. If the assumed linkage between carbohydrate and β-carboxyl exists, however, the number of polysaccharide units is very low.

Acknowledgements. This work has been supported by a grant from "*Norges almenvitenskapelige forskningsråd*". The author is greatly indebted to Miss Åse Ström for skiltul technical assistance.

REFERENCES

1. Goa, J. *Acta Chem. Scand.* **14** (1960) 1790.
2. Ouchterlony, Ö. *Arkiv Kemi, Mineral. Geol.* **26** (1948) 1.
3. Ouchterlony, Ö. *Acta Pathol. Microbiol. Scand.* **26** (1949) 507.
4. Moore, S., Spackman, D. H. and Stein, W. H. *Anal. Chem.* **30** (1958) 1185.
5. Goa, J. *Acta Chem. Scand.* **15** (1961) 853.
6. Spies, J. R. and Chambers, D. C. *Anal. Chem.* **21** (1949) 1249.
7. Weimer, H. E., Mehl, J. W. and Winzler, R. J. *J. Biol. Chem.* **185** (1950) 561.
8. Caputo, A. and Santoro, M. *Clin. Chim. Acta* **5** (1960) 559.
9. Tracey, M. V. *Biochem. J.* **52** (1952) 265.
10. Zilliken, F., Braun, G. A. and György, P. *Arch. Biochem. Biophys.* **54** (1955) 564.
11. Rees, M. V. *Biochem. J.* **40** (1946) 632.
12. Popenoe, E. A. and Drew, R. M. *J. Biol. Chem.* **228** (1957) 673.
13. Fraenkel-Conrat, H. and Cooper, M. *J. Biol. Chem.* **154** (1944) 239.
14. Svennerholm, L. *Acta Soc. Med. Upsaliensis* **61** (1957) 287.
15. Goa, J. *Scand. J. Clin. Lab. Invest.* **7** Suppl. 22 (1955) 19.
16. Svennerholm, L. *Arkiv Kemi* **10** (1957) 577.
17. Gibbons, M. N. *Analyst* **80** (1955) 268.
18. Gardell, S. *Acta Chem. Scand.* **7** (1953) 207.
19. Smith, E. L., Brown, D. M., Weimer, H. E. and Winzler, R. J. *J. Biol. Chem.* **185** (1950) 569.
20. Schmid, K. *J. Am. Chem. Soc.* **75** (1953) 60.
21. Werner, I. and Odin, L. *Acta Soc. Med. Upsaliensis* **57** (1952) 230.
22. Schultze, H. E. *Deut. med. Wochschr.* **83** (1958) 1742.
23. Winzler, R. J. *Ciba Foundation Symposium, London* (1958) 245.
24. Schmid, K., Bencze, W. L., Nussbaumer, T. and Wehrmüller, J. O. *J. Biol. Chem.* **234** (1959) 529.
25. Schmid, K. *Biochim. et Biophys. Acta* **14** (1954) 437.
26. Van Slyke, D. D. *J. Biol. Chem.* **83** (1929) 425.
27. Johansen, P., Marshall, R. D. and Neuberger, A. *Nature* **181** (1958) 1345.

Received June 13, 1961.

ACTA CHEMICA SCANDINAVICA 15 (1961) 1981–1992

On Equilibria in Systems with Polynuclear Complex Formation

V. Some Useful Differential Expressions

LARS GUNNAR SILLÉN

Department of Inorganic Chemistry, Royal Institute of Technology, Stockholm 70, Sweden

A general method is indicated for deriving the relationships that hold between the free and total concentrations of the reagents in an equilibrium mixture, regardless of the reactions taking place in it. Equations are given for calculating, from measurements (A, B, b) or (A, B, a), the average $\bar{p}$ and $\bar{q}$ for complexes A_pB_q formed by two reagents A and B. These equations have already been used repeatedly in this laboratory.

The appearance of a precipitate of constant or variable ratio $A/B = Z_s$ can be detected, and its composition determined, from diagrams $A(B)_a$. The equations derived for a solution hold also for an equilibrium mixture of solution and precipitate.

The extension to cases with several reagents, and to distribution equilibria with two phases are indicated.

Since the first papers in this series appeared [1,2] some experience has accumulated in this laboratory how to study equilibria of polynuclear complexes experimentally, and how to treat the experimental data. We have found it advisable to apply as many independent experimental and mathematical-graphical methods as possible to reach our primary aim: to find the formulas of the predominant complexes and the equilibrium constants for their formation.

One of our methods is based on equations (19,21,22) below and allows one to calculate the average composition of the complexes, without any previous assumption except that the law of mass action is obeyed in its simple form (activity coefficients held constant by ionic medium).

This method was derived by the present author many years ago and has been applied, among other things, to equilibria of polyborate [3], and polyvanadate [4] ions. In these cases as in many others, the method has given valuable hints for the following treatment.

A general proof for the equations used — which can also be applied for deriving a number of other relationships — was given [5] in my lectures at MIT

in the spring of 1957. The equations are founded on the simple law of mass action, there is nothing difficult or unusual about them, and equations related to some of them have been given earlier for instance by Hedström [6], Byé [7] and Lefebvre [8].

The latter two workers, in the opinion of the present writer, may not use the most convenient variables and symbolism for treating these systems. The differences in our conclusions on specific systems may partly reflect a difference in the accuracy of our data. The French workers, besides the data, sometimes also use their chemical intuition for concluding on the formulas of the complexes.

It was hoped that it might help some chemists if a rather general approach were given, which could be applied to other situations as well. In the following, the main stress will be on the principles and it will in general be left to the reader to make those smaller transformations that will simplify the calculations, such as transforming natural to decadic logarithms.

TWO REAGENTS: ASSUMPTIONS AND DEFINITIONS

A solution contains two reagents, A and B, with the free concentrations

$$[A] = a \; ; \; [B] = b \tag{1}$$

A and B form one or more complexes, of the general formula A_pB_q, with p and q integral. In the equilibria we need not consider any other species than A, B, and the various A_pB_q. As usual, a formula like $[A_pB_q]$ stands for the total of all species containing pA, qB, and in addition an indefinite number of solvent and medium ions.

For brevity we shall write

$$[A_pB_q] = c_{pq} \tag{2}$$

The total concentrations of A and B we shall as usual denote by

$$A = a + \Sigma p c_{pq} \; ; \qquad B = b + \Sigma q c_{pq} \tag{3a, b}$$

We shall find it useful to introduce the »complexity sum» S, which is the sum of the concentrations of all complexes:

$$S = \Sigma c_{pq} \tag{4}$$

The average composition of the complexes can be described using the average values $\bar{p}$ and $\bar{q}$:

$$\bar{p} = \frac{\Sigma p c_{pq}}{\Sigma c_{pq}} = \frac{A-a}{S}; \qquad \bar{q} = \frac{\Sigma q c_{pq}}{\Sigma c_{pq}} = \frac{B-b}{S} \tag{5a, b}$$

Eqns. (1) through (5) are symmetrical in A and B. In the definitions (6—8) below, we shall arbitrarily denote one of the reagents, say B, as the »nucleus» or »central group» whereas A is the »ligand». All formulae deduced below will also be valid if the roles of the two reagents are interchanged.

The average number of A bound per B we shall call Z.

$$Z = \frac{A-a}{B} \tag{6}$$

For mononuclear complexes A_nB, Z is often denoted by $\bar{n}$, which is quite logical: it is the average value for n. For polynuclear complexes the notation $\bar{n}$ would have no direct meaning. It is often advantageous to consider the number of moles of bound A per liter, from (3 a) and (6):

$$BZ = \Sigma p c_{pq} \tag{6a}$$

The total molar concentration of species containing B we shall denote by BR:

$$BR = b + \Sigma c_{pq} = b + S \tag{7}$$

The fraction of B that is present as free B we denote by α_0

$$[B] = b = \alpha_0 B \tag{8}$$

Equilibrium conditions

If the system is at equilibrium, and if the activity coefficients can be assumed to be kept constant (for instance by means of an ionic medium), the formation »constants» β_{pq} of the various complexes are really constant, and we have

$$c_{pq} = \beta_{pq} a^p b^q \tag{9}$$

Inserting (9) into (3a, 3b, 4, 6a) we find

$$A - a = BZ = \Sigma p \beta_{pq} a^p b^q; B - b = \Sigma q \beta_{pq} a^p b^q \tag{10a, 10b}$$

$$S = \Sigma \beta_{pq} a^p b^q \tag{11}$$

Differentiating (11) with respect to the variables a and b we easily find using (10 a) and (10 b)

$$\mathrm{d}S = \Sigma p \beta_{pq} a^{p-1} b^q \mathrm{d}a + \Sigma q \beta_{pq} a^p b^{q-1} \mathrm{d}b = (A-a)\mathrm{d} \ln a + (B-b)\mathrm{d} \ln b \tag{12}$$

Differentiating (10a) and (10b), one will obtain similar equations where, however, the sums $\Sigma p^2 c_{pq}$, $\Sigma pq c_{pq}$ and $\Sigma q^2 c_{pq}$ appear. These equations could be used for finding more complicated averages.

We shall now center our attention on eqn. (12).

GENERAL METHOD: AUXILIARY EQUATIONS

Perhaps the simplest way of deriving the differential expressions we will need is by means of total differentials. Let us assume that F is a function of two independent variables x and y, and that its total differential can be expressed by

$$\mathrm{d}F(x,y) = G(x,y)\, \mathrm{d}x + H(x,y)\, \mathrm{d}y \tag{13}$$

where the partial derivatives, G and H, are functions of x and y. The second partial derivative of F, $(\partial^2 F/\partial x \partial y)$ gives

$$\left(\frac{\partial G}{\partial y}\right)_x = \left(\frac{\partial H}{\partial x}\right)_y \tag{14}$$

From (13) we may derive the total differential for $(F-Hy)$, which is also a function of x and y:

$$\mathrm{d}(F-Hy) = G\mathrm{d}x - y\mathrm{d}H \tag{13a}$$

In the same way as (14) was derived from (13), we find from (13a)

$$\left(\frac{\partial G}{\partial H}\right)_x = -\left(\frac{\partial y}{\partial x}\right)_H \tag{14a}$$

From (14) and (14a) we find by integration, at constant x:

$$G = \text{const} + \int_{x\ \text{const}} \left(\frac{\partial H}{\partial x}\right)_y \mathrm{d}y = \text{const} - \int_{x\ \text{const}} \left(\frac{\partial y}{\partial x}\right)_H \mathrm{d}H \tag{15,15a}$$

In the equilibrium case we are considering, we have used a and b as independent variables, but we could have chosen practically any pair out of a, b, A, B, Z, R, S, α_0 or other convenient variables that can be defined by means of a, b and sums, $\Sigma\ p^r q^s c_{pq} (r, s = \text{integer})$.

We shall not bother about degenerate cases such as systems with no complexes, or with only mononuclear complexes: they are easily and joyfully recognized, and treated by simpler methods.

If it is desired to calculate one of the variables mentioned above from measurements of some other variables, one should try to transform (12) or some analogous differential equation into another expression of the form (13); to the left should stand a total differential, the unknown quantity searched for would be in the place of G, and H, x and y would be experimentally known quantities. Then, one easily derives the desired expressions for partial derivatives (14, 14a) and integrals (15, 15a)

DATA (A, B, a)

Let us assume that we know the total concentrations A and B and can measure the free concentration a, for instance by emf methods. It is then practical to eliminate A and use $BZ = A-a$ (6), so that (12) takes the form

$$\mathrm{d}S = BZ\ \mathrm{d}\ln a + (B-b)\ \mathrm{d}\ln b$$

which we may transform using (7):

$$\mathrm{d}(BR) \equiv \mathrm{d}\,(S+b) = BZ\ \mathrm{d}\ln a + B\ d\ln b \tag{16}$$

If we introduce the identity $\mathrm{d}(BR) = B\mathrm{d}R + R\mathrm{d}B$, into (16), divide through B, and rearrange, we find

$$\mathrm{d}(\ln b - R) = R\ \mathrm{d}\ln B - Z\ \mathrm{d}\ln a \tag{17}$$

Adding $\mathrm{d}(Z \ln a)$ to both sides of (17) we can alternatively use

$$\mathrm{d}(\ln b - R + Z\ln a) = R\ \mathrm{d}\ln B + \ln a\ \mathrm{d}Z \tag{17a}$$

Both (17) and (17a) are total differentials and analogous to equations (13) and (13a); in analogy to (14) and (14a) we obtain:

$$\left(\frac{\partial R}{\partial \ln a}\right)_B = -\left(\frac{\partial Z}{\partial \ln B}\right)_a ; \left(\frac{\partial R}{\partial Z}\right)_B = \left(\frac{\partial \ln a}{\partial \ln B}\right)_Z = \left(\frac{\partial \log a}{\partial \log B}\right)_Z \tag{18a, 18}$$

(In the following, transformations from natural to decadic logarithms will be left to the reader).

We may, in passing, see from (18) or (18a) that if these expressions are = 0, thus $Z(a)$ is independent of B, for a single value for a, then R has a maximum or minimum there. If they are zero for all values for a, then R is independent of a; which is possible in general only of the system is homonuclear.

Integration, by analogy with (15) and (15a) gives

$$R = \text{const} - \int_{B\ \text{const}} \left(\frac{\partial Z}{\partial \ln B}\right)_a \mathrm{d} \ln a = \text{const} + \int_{B\ \text{const}} \left(\frac{\partial \log a}{\partial \log B}\right)_Z \mathrm{d}Z \qquad (19,\ 19a)$$

Usually the last formula, (19a), is more convenient for use: the partial derivative $(\partial \log a/\partial \log B)_Z$ is obtained directly as the inverted value of the slope of the curves $\log B$ ($\log a)_Z$ in »projection maps»[9], and in many systems it tends to be more constant and thus easier to interpolate than $(\partial Z/\partial \log B)_a$.

Finding the integration constant. In an integration at constant B according to (19) or (19a), one should start at a point with a known value for R, in order to obtain the integration constant.

Sometimes the data extend or can easily be extrapolated into a range with low A where free B predominates, so that $b \approx B$, and $R = 1$. For instance, the derivative in (19a) often behaves well on extrapolation.

In other cases, the extrapolation is uncertain, or at any rate, accuracy is gained by integrating only from some point where one can presume that only two species, say B and A_PB_Q, exist in appreciable amounts. In such case we have:

$$B = b + Qc_{PQ}\ ;\ BR = b + c_{PQ}\ ;\ BZ = Pc_{PQ} \qquad (20)$$

By elimination of c_{PQ} and b in (20) we obtain

$$R = 1 - Z(Q - 1)P^{-1} \qquad (20a)$$

From Z in the first experimental point that is to be used, R for that point can be calculated from (20a) and used as the integration constant in (19a). Usually, P and Q can be deduced from the shape of the experimental curves at low values for Z, but it is conceivable that in some cases alternative sets (P, Q) might be tried. A similar procedure can be used in any range where only two species can be presumed to predominate.

Eliminating c_{PQ} in (20) we may also deduce.

$$\alpha_0 = b/B = 1 - ZQP^{-1} \qquad (20b)$$

Calculation of b or α_0 from data (A, B, a). One may integrate (17) directly at constant B, add ($-\ln B$) to both sides and introduce it into the constant to the right; after rearranging one obtains

$$\ln\alpha_0 \equiv \ln b - \ln B = \text{const} + R - \int_{B\ \text{const}} Z\, \mathrm{d} \ln a \qquad (21)$$

Inserting the expression for R from (19) we get

$$\ln a_0 \equiv \ln b - \ln B = \text{const} - \int_{B\ \text{const}} \left[Z + \left(\frac{\partial Z}{\partial \ln B} \right)_a \right] \mathrm{d} \ln a \qquad (21a)$$

Eqn. (21a) can also be deduced from (16) *via* the transformation

$$\mathrm{d}\,(B \ln b - BR) = \ln b\, \mathrm{d}\, B - BZ\, \mathrm{d} \ln a$$

The integration constant in (21) or (21a) can be obtained either by extrapolation, or using (20b), if B and $A_P B_Q$ predominate at one limit of integration.

As usual, it depends on the data which of the expressions (21) and (21a) is the most practical one to use.

Average composition of complexes

Now that R and b (or a_0) are known, one may calculate the average composition of the complexes (5a, 5b, 6, 7, 8): ,

$$\bar{p} = \frac{BZ}{S} = \frac{BZ}{BR-b} = \frac{Z}{R-a_0}\,; \bar{q} = \frac{B-b}{S} = \frac{B-b}{BR-b} = \frac{1-a_0}{R-a_0} \qquad (22a,\ b)$$

Thus we can, in principle, determine the average composition of the complexes from data (A, B, a), without any more assumption about the system than that the law of mass action holds.

Elimination of mononuclear species. For special cases, a still more straightforward calculation may be devised. In several systems (such as for instance the borates [3] and arsenates (III)), the mononuclear species predominate at low values for B, so that the functions pertaining to mononuclear species, $f_1(a)$ and $Z_1(a)$ in (23a, b), are accurately known. The polynuclear complexes are indicated by deviations at the higher values for B. One might use (19) and (21), but a higher accuracy may be obtained if one calculates directly B_1, the total concentration of B in the form of mononuclear species. For the mononuclear species we have:

$$B_1 = b\,(1 + \Sigma \beta_{p1} a^p) = b f_1(a) \qquad (23a)$$

$$B_1 Z_1 = b\, \Sigma p \beta_{p1} a^p = b \mathrm{d} f_1(a)/\mathrm{d} \ln a \qquad (23b)$$

Thus we have

$$Z_1 = \mathrm{d} \ln f_1 / \mathrm{d} \ln a \qquad (23c)$$

$$\mathrm{d} \ln B_1 = \mathrm{d} \ln b + \mathrm{d} \ln f_1 = \mathrm{d} \ln b + Z_1\, \mathrm{d} \ln a \qquad (24)$$

We integrate (24) at constant B and introduce the expression for ln b from (21a):

$$\ln B_1 = \text{const} + \int \left[Z_1 - Z - (\partial Z/\partial \ln B)_a \right] \mathrm{d} \ln a \qquad (25)$$

In (25), Z_1 is known before as a function of a, whereas $Z(a, B)$ differs for each value of B chosen.

The integration constant is found in a way analogous to (20 a,b). If we may assume that at one integration limit, there is only one polynuclear complex of importance, say A_PB_Q, we have

$$B = B_1 + Qc_{PQ}\ ;\ BZ = B_1Z_1 + Pc_{PQ}\ ;\ B_1 = B(P-QZ)\ (P-QZ_1)^{-1} \qquad (26)$$

If the polynuclear complexes may be neglected at this limit, we have $B_1 = B$.

Having calculated B_1 from (25), we may then subtract from B, BZ and BR the contributions from the mononuclear species, which leaves the polynuclear terms:

$$B_{\text{poly}} = B - B_1\ ;\ B_{\text{poly}}\ Z_{\text{poly}} = BZ - B_1Z_1\ ;\ B_{\text{poly}}\ R_{\text{poly}} = BR - B_1 \qquad (27)$$

For any experimental point we may then calculate the average composition of the polynuclear complexes ($\bar{p}$ and $\bar{q}$ in eqn. (22) include also the mononuclear complexes):

$$Z_{\text{poly}} = \frac{BZ-B_1Z_1}{B-B_1}\ ;\ \bar{p}_{\text{poly}} = \frac{Z_{\text{poly}}}{R_{\text{poly}}} = \frac{BZ-B_1Z_1}{BR-B_1}\ ;\ \bar{q}_{\text{poly}} = \frac{1}{R_{\text{poly}}} = \frac{B-B_1}{BR-B_1} \qquad (28)$$

In (28), the average composition has been obtained from the data (A, B, a) without any other assumption than the validity of the law of mass action. B and Z are obtained from the experiments, Z_1 is known as a function of a, and B_1 calculated by means of (25).

DATA (A, B, b)

From (12) we obtain by easy transformations:

$$\mathrm{d}\,(A \ln a + B \ln b - S - a - b) = \ln a\,\mathrm{d}A + \ln b\,\mathrm{d}B \qquad (29)$$

$$\mathrm{d}\,(A \ln a - S - a - b) = \ln a\,\mathrm{d}A - B\,\mathrm{d}\ln b \qquad (29a)$$

The two differentials in (29) and (29a) give

$$\left(\frac{\partial \ln a}{\partial B}\right)_A = \left(\frac{\partial \ln b}{\partial A}\right)_B \text{ or } \left(\frac{\partial \ln(aA^{-1})}{\partial B}\right)_A = \left(\frac{\partial \ln (bB^{-1})}{\partial A}\right)_B \qquad (30)$$

$$\left(\frac{\partial \ln a}{\partial \ln b}\right)_A = -\left(\frac{\partial B}{\partial A}\right)_b \qquad (30a)$$

Integrals for practical evaluation can be written in several forms, for instance

$$\ln\left(\frac{a}{A}\right) = \text{const} + A^{-1}\int_{A\ \text{const}}\left(\frac{\partial \ln (b/B)}{\partial \ln A}\right)_B \mathrm{d}B \qquad (31)$$

$$\ln a = \text{const} - \int_{A\ \text{const}}\left(\frac{\partial B}{\partial A}\right)_b \mathrm{d}\ln b \qquad (31a)$$

Eqns. (30) and (30a) have been derived in other ways by Hedström [6] and McKay[10].

DATA (a, B, b)

In some systems, both b and a can be measured, but the difference $(A - a)$ is too small for an accurate treatment. Such cases are for instance the hydrolysis of metal ions in very acidic solutions, where the metal ion activity can be measured by means of amalgam electrodes.

By transformation of (16) we obtain using (8)

$$\mathrm{d}(S+b-B) = BZ\,\mathrm{d}\ln a + B\,\mathrm{d}\ln \alpha_0 \tag{32}$$

$$\mathrm{d}(S+b-B-B\ln \alpha_0) = BZ\,\mathrm{d}\ln a - \ln \alpha_0 \mathrm{d}\,B \tag{32a}$$

From the total differentials (32) and (32a) we find

$$\left(\frac{\partial(BZ)}{\partial \ln \alpha_0}\right)_a = \left(\frac{\partial B}{\partial \ln a}\right)_{\alpha_0};\left(\frac{\partial(BZ)}{\partial B}\right)_a = -\left(\frac{\partial \ln \alpha_0}{\partial \ln a}\right)_B \tag{33, 33a}$$

$$BZ = \text{const} + \int_{a\ \text{const}}\left(\frac{\partial B}{\partial \ln a}\right)_{\alpha_0} \mathrm{d}\ln\alpha_0 = \text{const} - \int_{a\ \text{const}}\left(\frac{\partial \ln\alpha_0}{\partial \ln a}\right)_B \mathrm{d}\,B \tag{34, 34a}$$

Thus we can obtain Z; S and R are obtained directly from (32) which gives us, for a constant a:

$$BR - B = S + b - B = \text{const} + \int_{a\ \text{const}} B\,\mathrm{d}\ln \alpha_0 \tag{35}$$

Eqns. (34) and (35) can be transformed in various ways for convenience in calculations. The integration constant can usually be found by starting in a region where only two species predominate.

SPECIAL EQUATIONS FOR HYDROLYSIS

An important case of polynuclear complex formation is the hydrolysis of metal cations B. The ligand A may be considered to be OH^-, but since one measures

$$h = [\mathrm{H}^+] \tag{36}$$

it is often practical[10a] to describe the ligand, instead, as $(-\mathrm{H}^+)$. Eqn. (9) is replaced by

$$c_{pq} = [\mathrm{H}_{-p}\mathrm{B}_q] = \beta_{pq}\, h^{-p} b^q \tag{37}$$

Instead of A we must introduce the total analytical excess of H^+, H, and then find, instead of (3a) and (6a)

$$BZ = h - H = \Sigma p c_{pq} \tag{38}$$

Eqns. (3b) and (4) are valid as before:

$$B - b = \Sigma\, q c_{pq}\ ;\ S = \Sigma\, c_{pq} \tag{3b, 3c}$$

Differentiation gives

$$d S = (B-b)\, d \ln b - (h - H)\, d \ln h \quad (39)$$

Introducing (38) into (39) we find

$$d(S+b) = B\, d \ln b - BZ\, d \ln h \quad (40)$$

This is equivalent to eqn. (16). If we have data (H, B, h), to apply eqns. (18) – (22) we need only replace a by h^{-1}, or ln a by $-\ln h$.

In the treatment of data (H, B, b) we can rewrite (39) to the form

$$d S = (H-h)\, d \ln h + (B-b) d \ln b \quad (39a)$$

which is obviously analogous to (12). In using (31) and corresponding equations, we need then only replace A by H and a by h.

SOLID PHASE PRESENT

An important and challenging task for the future seems to be the study of micellar systems by the methods of equilibrium analysis. Perhaps the micelles of various long-chain ions can be described as a sort of solid solution, thus a separate phase [11], perhaps they are better described as very large complexes, of definite or variable composition. Previous experience [2,12] has shown that it is rather hard, without a high accuracy of measurement, to distinguish between large complexes and a solid phase (infinite complexes).

Let us assume that for each liter of solution, A_s mole A and B_s mole B are present as bound in a solid phase so that

$$A_s = B_s Z_s \quad (41)$$

The ratio Z_s may be a constant, but we shall consider the general case where Z_s is a function of a; because of the equilibrium condition, b will also be a function of a in the presence of a solid phase.

Equations (3a, 3b, 4) are now replaced by

$$A = a + \Sigma p c_{pq} + A_s\,;\; B = b + \Sigma q c_{pq} + B_s\,;\; S = \Sigma c_{pq} \quad (42a,\ b,\ c)$$

In the presence of a solid phase, b and Z_s, and hence $(A - A_s)$ and $(B - B_s)$ are functions of a (cf. 42 a and b). It follows immediately that

$$\left(\frac{\partial A}{\partial B}\right)_a = \left(\frac{\partial A_s}{\partial B_s}\right)_a = Z_s \quad (43)$$

A plot $A(B)_a$, thus of $A(B)$ for a constant a-value, should thus give a straight line, of slope Z_s, when a solid is present; this may be used to find out whether a new phase is separated. In equilibria with only homonuclear complexes, and no solid, $A(B)_a$ is also a straight line since Z is a function of a only. There should be no difficulty distinguishing this case from that of precipitation.

We shall now apply the Gibbs-Duhem law to the new phase: $n_A d\mu_A + n_B d\mu_B = 0$. Inserting $n_A = A_s$, $n_B = B_s$, $\mu_A = \text{const} + \mathbf{R}T \ln a$, $\mu_B = \text{const} + \mathbf{R}T \ln b$, and dividing by $\mathbf{R}T$, we obtain

$$A_s \, d \ln a + B_s \, d \ln b = 0, \tag{44}$$

or using (41) $Z_s \, d \ln a + d \ln b = 0$ (44a)

Differentiation of (42 c) and insertion of (42 a, b), gives:

$$d S = \Sigma p c_{pq} \, d \ln a + \Sigma q c_{pq} \, d \ln b = (A - a - A_s) \, d \ln a + (B - b - B_s) \, d \ln b$$

Inserting (44) we find

$$dS = (A - a) \, d \ln a + (B - b) \, d \ln b \tag{12}$$

Thus, eqn. (12) is also valid if a solid phase exists in equilibrium with the solution, and eqns. (19), (21) *etc.* can be applied. One must, however, remember (42 a, b, c) that S is valid for the solution, whereas A and B also contain terms for the solid phase. So, $R = (S + b)/B$ for the mixture of solution and solid will come out lower than what corresponds to the solution only.

It is true that b is a function of a, so that (a, b) are not independent. The system is determined instead by, say (a, B) or (Z, B) which are really independent.

One might proceed to derive a number of equations, which could be used to determine the various equilibrium constants involved. However, in a real case it will not be hard to derive the equations one needs. The most important task is to obtain reliable experimental data over a broad concentration range.

SEVERAL REAGENTS

The treatment may be extended to equilibria with several reagents. We shall arbitrarily denote one of them as the »central group» B, whereas the others are »ligands» A_1, A_2... A_n... Denoting, as before, total concentrations by capital letters and free concentrations by lower case letters, we have for any complex

$$c_i = [(A_1)_{p_1} (A_2)_{p_2} ... B_q] = \beta_i a_1^{p_1} a_2^{p_2} ... b^q \tag{45}$$

and, with easily understood symbols

$$S = \Sigma \, c_i \tag{46}$$

$$A_n - a_n = \Sigma p_n c_i = \bar{p}_n S \, ; \, B - b = \Sigma \, q c_i = \bar{q} S \tag{46a, 46b}$$

Differentiation of (46) gives, introducing (46a, 46b):

$$dS = \Sigma \, (A_n - a_n) \, d \ln a_n + (B - b) \, d \ln b \tag{47}$$

or $$d \ln S = \Sigma \, \bar{p}_n d \ln a_n + \bar{q} d \ln b \tag{48}$$

$$d(S + b + \Sigma a_n - \Sigma A_n \ln a_n) = B d \ln b - \Sigma \ln a_n d A_n \tag{49}$$

Keeping all A_n constant except A' we find from (49)

$$d(S + b + \Sigma a_n - \Sigma A_n \ln a_n + A' \ln a') = B d \ln b + A' d \ln a' \tag{49a}$$

Eqns. (47) — (49) can be used as a basis for deriving useful relationships between the variables, if satisfactory data are available.

In differentiating eqn. (46 b), weighed averages $\widetilde{p_n}$ and $\widetilde{q}$ occur (Rossotti[13]), defined by

$$B\widetilde{p_n} = \Sigma p_n q c_i \; ; \; B\widetilde{q} = b + \Sigma \, q^2 c_i \qquad (50a, 50b)$$

Differentiating (46 b) we find

$$dB = B \, d \ln B = \Sigma\Sigma p_n q c_i d \ln a_n + (b + \Sigma q^2 c_i) \, d \ln b$$

or, after transformation using (50a, 50b)

$$d \ln B = \Sigma \widetilde{p_n} d \ln a_n + \widetilde{q} \, d \ln b \qquad (51)$$

DISTRIBUTION EQUILIBRIA

Let us assume that there are two solution phases at equilibrium, say one aqueous (no subscript) and one organic (subscript "$_o$"). There will then be two sets of equations, one for each phase. For instance, the counterpart to (51) is (51_o):

$$d \ln B_o = \Sigma \widetilde{p}_{no} d \ln a_{no} + \widetilde{q}_o d \ln b_o \qquad (51_o)$$

The equilibrium between the phases requires that for each reagent the distribution ratio, a_n/a_{no} or b/b_o, remains constant so that

$$d \ln a_{no} = d \ln a_n \; ; \; d \ln b_o = d \ln b \qquad (52)$$

The distribution ratio for B, Q, is defined by

$$B_o = BQ, \text{ thus } d \ln B_o = d \ln Q + d \ln B \qquad (53)$$

Eliminating d ln b and d ln B_o from (51), (51_o) and (53), using (52), we find

$$d \ln Q = \widetilde{q}_o(\widetilde{q}^{-1} - \widetilde{q}_o^{-1}) \, d \ln B + \Sigma \, \widetilde{q}_o(\widetilde{p}_{no}\widetilde{q}_o^{-1} - \widetilde{p}_n\widetilde{q}^{-1}) \, d \ln a_n \qquad (54)$$

In special cases we may set

$$a_n \approx A_n \qquad (55)$$

for instance when B is present in small or tracer amounts. From (54) and (55) we then find

$$\left(\frac{\partial \ln Q}{\partial \ln B}\right)_{\text{all } A_n} \approx \widetilde{q}_o\left(\frac{1}{\widetilde{q}} - \frac{1}{\widetilde{q}_o}\right); \left(\frac{\partial \ln Q}{\partial \ln A'}\right)_{B, \text{ all other } A_n} \approx \widetilde{q}_o\left(\frac{\widetilde{p}_{no}}{\widetilde{q}_o} - \frac{\widetilde{p}_n}{\widetilde{q}}\right) \qquad (55a, 55b)$$

These equations are essentially the same as those given by Rossotti [13]. They can be simplified if $\widetilde{q}_o$ and $\widetilde{q}$ can be treated as constant, or even as equal.

We shall not further develop the cases of many ligands, or distribution equilibria. It is not hard to deduce a number of differential and integral expressions. The real difficulty is to get data over a broad range of concentrations for each reagent, data that are sufficiently reliable to allow valid conclusions to be drawn from such calculations.

Acknowledgement. I am indebted to a number of friends and co-workers who have provided data of sufficient accuracy to make this treatment worthwhile, have discussed the applications with me in detail, and have urged me to publish this paper. I would especially like to mention Drs. George Biedermann, Sirkka Hietanen, Nils Ingri and Åke Olin, still in Stockholm, and Drs. Hazel and Francis Rossotti, now in Oxford. Dr Derek Lewis kindly corrected the English of the manuscript.

This is part of a program supported by *Statens naturvetenskapliga forskningsråd (Swedish natural science research council)* and *Statens råd för atomforskning (Swedish atomic research council)*.

REFERENCES

1. Sillén, L. G. *Acta Chem. Scand.* **8** (1954) 299.
2. Sillén, L. G. *Acta Chem. Scand.* **8** (1954) 318.
3. Ingri, N., Lagerström, G., Frydman, M. and Sillén, L. G. *Acta Chem. Scand.* **11** (1957) 1034.
4. Ingri, N. and Brito, F. *Acta Chem. Scand.* **13** (1959) 1971; Brito, F. and Ingri, N. *Anales fis. quim.* **56 B** (1960) 165.
5. Sillén, L. G. *Studies on chemical equilibria*, mimeographed lecture sheets, MIT spring 1957.
6. Hedström, B. *Acta Chem. Scand.* **9** (1955) 613.
7. Byé, J. *Compt. rend.* **221** (1945) 99; **238** (1954) 239; *Bull. soc. chim. France* **1952** 1075.
8. Lefebvre, J. *J. Chim. Phys.* **54** (1957) 553.
9. Sillén, L. G. *Acta Chem. Scand.* **10** (1956) 803.
10. McKay, H. A. C. *Trans. Faraday Soc.* **49** (1953) 237.

10 a Hietanen, S. and Sillén, L. G. *Acta Chem. Scand.* **8** (1954) 1607.

11. Seim, J., Sillén, L. G. and Ulfvarsson, U. *Acta Chem. Scand.* **10** (1956) 683.
12. Brosset, C., Biedermann, G. and Sillén, L. G. *Acta Chem. Scand.* **8** (1954) 1917.
13. Rossotti, F. J. C. *Rec. trav. chim.* **75** (1956) 743.

Received June 7, 1961.

ACTA CHEMICA SCANDINAVICA 15 (1961) 1993–1998

On the Stability Relations and Solubilities of Hexagonal and Orthorhombic Mercury(II)oxide

KARIN AURIVILLIUS and OLOV von HEIDENSTAM

Institute of Inorganic and Physical Chemistry, University of Stockholm, Stockholm, Sweden

The hexagonal modification of mercury(II)oxide is found to be metastable with regard to the orthorhombic oxide, from at least room temperature and up to the decomposition temperature, from experiments transforming the hexagonal oxide into the orthorhombic modification and from solubility measurements in water.

The solubility obtained for the hexagonal modification is 2.55×10^{-4} mole/l at 25°C. For the transition HgO(hexagonal) = HgO (orthorhombic, red) at 25°C an approximate value is calculated for the Gibbs energy change, $\Delta G = -72 \pm 10$ cal/mole. Approximate values of ΔH and ΔS were determined: $\Delta H = -300 \pm 200$ cal/mole, $\Delta S = -1 \pm 1$ cal/mole · degree.

In connection with studies of the crystal structures of orthorhombic and hexagonal mercury(II)oxide [1,2], it seemed of interest to study the stability relations between these different modifications. The relationship between the red and yellow modifications of the orthorhombic oxide has been studied earlier by several methods [3–7] which seemed to indicate that the two oxides were identical, the discrepancies in colour and solubility being due to a difference in particle size.

PREPARATIONS AND ANALYSES

The hexagonal mercury(II)oxide was synthesized by mixing one part of 0.1 M K_2HgI_4, containing an excess of 0.025 M KI, with two parts of 5.5 M NaOH at about 50°C (Ref.[3]). After a few hours the resulting precipitate was decanted and washed with hot water. In spite of numerous experiments, no other method of preparation has been devised.

Red mercury(II) oxide was prepared by ignition of the pure nitrate on a sand bath until it was completely decomposed, and the resulting product was then carefully washed. The mercury(II)nitrate was prepared by dissolving redistilled reagent quality mercury in nitric acid, *pro analysi*, and partially crystallizing the solution.

Commercial yellow mercury(II)oxide, *e.g.* reagent quality from J. T. Baker, Phillipsburg, N. J., was found to give reproducible solubilities in agreement with values found by previous authors and was therefore used in the experiments.

All samples of the mercury(II)oxides (checked for purity by means of amply exposed X-ray powder photographs) were agitated for several weeks in conductivity water that was frequently changed. This washing procedure was done to eliminate the finest particles and to remove possible traces of impurities that were not discovered in the powder diagrams.

Table 1. Hydrothermal heating of hexagonal HgO in 5 M NaOH at different temperatures.

Temperature °C	Time of heating	Resulting phases in the sample
		5 M NaOH
200	2 days	HgO_{rh}, HgO_{hex}
170	2 days	HgO_{rh}, HgO_{hex}
130	2 days	HgO_{rh}, HgO_{hex}
100	2 days	HgO_{hex}, HgO_{rh}
60	6 weeks	HgO_{hex}, HgO_{rh}
35	8 weeks	HgO_{hex}, HgO_{rh}
25	8 weeks	HgO_{hex}

The analyses of mercury were carried out by titrating Hg(II) with a standard solution of KSCN using Fe(III) as an indicator (principally according to Kolthoff and Sandell [8]) or by potentiometric titration [7] with a standard solution of KI. The thiocyanate method is considerably quicker than the potentiometric one but does not give the same precision, the reproducibilities being estimated to be 0.8 and 0.2 % respectively. The results of the thiocyanate titration and of the potentiometric method were found to agree within the limits of experimental error.

THE STABILITY RELATIONS OF HEXAGONAL AND ORTHORHOMBIC MERCURY(II)OXIDE

By heating the hexagonal oxide to temperatures above 200°C, Laruelle [9] was able to convert it into the orthorhombic modification. We also obtained the same result above 200°C and have furthermore succeeded in performing the conversion at temperatures down to 35°C. However, the fact that the reaction velocity of the transition decreases greatly with decreasing temperature made it necessary to use another method than the dry heating of the samples. We were able to perform the conversion within a reasonable time by means of hydrothermal heating. A small amount of pure hexagonal oxide in a gold tube was sealed off in a thick walled glass tube together with a quantity of 5 M NaOH. At temperatures above 100°C, the samples were kept in

Table 2. Solubilities of red and yellow orthorhombic HgO in water at 25°C. The solubilities are given in 10^{-4} mole/l.

Investigator	Ref.	Year	Red HgO	Yellow HgO
Ostwald, W.	3	1900		2.41
Hulett, G. A.	10	1901	2.34	
Schick, K.	11	1903	2.37	2.39
Fuseya, G.	12	1920	2.33	
Garrett, A. B. and Hirschler, A.E.	7	1938	2.25	2.37
Ragg, M.	13	1950	2.88	2.92
Bruja, N. Z.	14	1954	2.52	4.20

an electric oven while, below this temperature, the samples were agitated in a thermostat. After cooling, the samples were washed and X-ray powder photographs were taken. At all temperatures from 35 to 200°C, proof was obtained of a partial conversion of the hexagonal oxide into the orthorhombic modification (Table 1). In this table, the predominant component is the first mentioned one. Later on (Table 6), it was shown by experiments that the hexagonal modification is more soluble than the orthorhombic ones down to at least 25°C.

Since an estimation of the particle sizes of some samples (Table 5) indicates that the finest particles of the hexagonal oxide are of a size somewhere between those of the two orthorhombic modifications, the differences in the particle sizes cannot be the reason for the higher solubility of the hexagonal oxide.

Thus, from these experiments, the conclusion can be drawn that the hexagonal mercury(II)oxide is metastable with regard to the orthorhombic modifications from room temperature up to the decomposition temperature ($\sim$ 500°C).

THE SOLUBILITY OF HEXAGONAL AND ORTHORHOMBIC MERCURY(II)OXIDE

The solubility values at 25°C of the red and yellow modifications of orthorhombic HgO found in the literature are given in Table 2.

To check our experiments, we at first redetermined the solubilities of the orthorhombic modifications of HgO at 25°C and obtained 2.26×10^{-4} and 2.36×10^{-4} mole/l, respectively, practically the same values as those found by the other authors with the exception of Ragg and Bruja.

EXPERIMENTAL

The samples, 0.1—2 g oxide and about 100 ml conductivity water, were sealed in glass flasks and rotated in a water thermostat at 25.00° and 35.00°C or in an air thermostat at 50.0° and 60.0°C. The accuracy of the water thermostat was ± 0.03° and of the air thermostat ± 0.1°. A preliminary study of the reaction velocity indicated that the mercury(II) oxide attained its equilibrium solubility in water at 25°C within a few days but the samples were always rotated for two to four weeks. At higher temperatures a shorter time was used.

The flasks were opened and placed in a metal vessel at the proper temperature. The solutions were filtered by nitrogen pressure through sintered glass filters of porosity G4 and analysed for Hg(II).

Table 3. The solubilities (in 10^{-4} mole/l) of different samples of red orthorhombic HgO in water at 25°C. The experiment was repeated for each sample up to three times. The mean value is $(2.26 \pm 0.03) \times 10^{-4}$ mole/l with 95 % confidence.

Run	Sample				
	a	b	c	d	e
1	2.24	2.25			
2	2.26	2.22	2.29	2.23	2.35
3	2.24	2.22	2.27	2.26	2.31

Table 4. The solubilities (in 10^{-4} mole/l) of yellow orthorhombic HgO in water at 25°C, the equilibrium being approached from both undersaturation and supersaturation. The mean value is $(2.36 \pm 0.03) \times 10^{-4}$ mole/l with 95 % confidence.

From undersaturation			From supersaturation		
2.28	2.30	2.36	2.32	2.34	2.37
2.38	2.40	2.41	2.38	2.39	2.39
	2.36			2.37	

Table 5. Estimated particle sizes of some samples of HgO at a magnification of 800 times.

Sample	Particle diameter (μ)		
	Main body of the sample	Smallest observed	Value given by Garrett and Hirschler
Hexagonal HgO	5 – 35	~0.5	–
Yellow orthorhombic HgO	0.5 – 14	<0.5	<0.5 – 10
Red orthorhombic HgO	10 – 60	~1.0	10 – 30

Table 6. The solubilities (in 10^{-4} mole/l) of the hexagonal, yellow orthorhombic and red orthorhombic modifications of HgO in water at different temperatures. The number of experiments at the different temperatures are given. The errors are reported for 95 % confidence.

Temp. °C	HgO hexagonal	Number of expts.	Yellow HgO orthorhombic	Number of expts.	Red HgO orthorhombic	Number of expts.
60.0	7.75 ± 0.07	10	7.57 ± 0.09	12	7.34 ± 0.09	12
50.0	5.55	5	5.42	5	5.17	5
35.00	3.42	5	3.25	5	3.16	5
25.00	2.55 ± 0.04	18	2.36 ± 0.03	12	2.26 ± 0.03	12

The solubility of the hexagonal modification was often abnormally high in the first few runs, a fact that probably was due to traces of impurities not revealed in the X-ray diagrams. The solubilities of the samples decreased when the impurities were washed out and a constant value was attained.

A check of the X-ray powder pattern of some hexagonal samples used in a great number of experiments revealed their partial conversion into the orthorhombic modification. As the solubility of the hexagonal oxide has been found in this investigation to exceed the solubility of the orthorhombic oxide, this partial transition does not have any importance as long as there is some of the hexagonal oxide left. To get a reliable connection between the solubilities of a modification at different temperatures, most samples were run at all the temperatures investigated. The results of the experiments are given in the following tables. Table 3 gives a survey of a series of experiments with different samples of red orthorhombic HgO at 25.00°C and Table 4 a comparison between measurements of the solubilities of yellow orthorhombic HgO, some of the samples being allowed to approach the equilibrium from undersaturation and the others from supersaturation. Microscopic measurements of some of the samples at a magnification of 800 times led to an estimation of the particle sizes given in Table 5.

Table 6 shows the resulting solubilities of red and yellow orthorhombic HgO and of hexagonal HgO at different temperatures (25.0°—60.0°C). As seen, the hexagonal modification is at all temperatures investigated, the most soluble one. It is also evident that the yellow modification of orthorhombic mercury(II)oxide is more soluble than the red one. This difference in the solubility can of course be considered as depending on the difference in particle size as stated in the literature [7]. By microscopic measurements (Table 5) such a difference in the particle size was also revealed in the present investigation. However, a possible difference in the arrangement of the oxygen atoms in the structures of the two orthorhombic modifications may also give a difference in the solubility. The X-ray powder diffractograms of the red and yellow oxides are identical, indicating the positions of the heavy mercury atoms are the same but giving no knowledge about an eventual difference in the oxygen atom arrangements. Such a difference might be revealed by neutron powder diffractograms of these two modifications. Therefore a neutron diffraction investigation of a powder sample of the yellow modification is being done; the red modification has been investigated by neutron diffraction methods before [1].

THE THERMODYNAMIC FUNCTIONS FOR THE REACTION HgO (HEXAGONAL) = HgO (ORTHORHOMBIC, RED)

According to Garrett and Hirschler [7], Hietanen and Sillén [15] and Dyrssen and Tyrrell [16] the mercury-containing species in the aqueous solution are mononuclear. Accepting this view, a value of the Gibbs energy change, $\Delta G = -72 \pm 10$ cal/mole, can be calculated for the transition HgO (hexagonal) = HgO (orthorhombic, red) from the solubility data at 25.0°C. The values of ΔG calculated for the other temperatures investigated are given in Table 7.

From the solubility values at different temperatures an approximate value of $\Delta H = -300 \pm 200$ cal/mole and of $\Delta S = -1 \pm 1$ cal/mole · degree were estimated, the variation of ΔG with temperature approximated to a straight line. These values are of the same order as those calculated from values given in the literature [17] for the reaction HgO (orthorhombic, yellow) = HgO (orthorhombic, red). A preliminary value of $\Delta H = -0.2 \pm 1.0$ kcal/mole for the transition above was also obtained from calorimetric measurements of the heats of solution in 4 M HCl of hexagonal and of orthorhombic, red mercury(II)oxide. The potential difference between the electrodes

$$\mathrm{Hg,HgO(hexagonal)}\,|\,\mathrm{OH^-}\ \text{and}\ \mathrm{Hg,HgO(orthorhombic,\ red)}\,|\,\mathrm{OH^-}$$

Table 7. Calculated values of the Gibbs energy change ΔG for the transition HgO (hexagonal) = HgO (orthorhombic, red) at different temperatures.

Temperature °C	25.00	35.00	50.0	60.0
ΔG cal/mole	−72	−47	−42	−32

was calculated to $e_{hex} - e_{rh} = 1.5$ mV from the Gibbs energy change, given above. However, this will not influence the values hitherto measured with the electrode Hg,HgO(orthorhombic, red) | OH^- as there is no proof that orthorhombic mercury(II)oxide synthesized by conventional methods contains any hexagonal mercury(II)oxide.

DISCUSSION

From crystallographic point of view, the hexagonal and orthorhombic modifications of mercury(II)oxide are very much alike. The hexagonal oxide is built up of infinite spiral chains —O—Hg—O— while the orthorhombic one contains infinite planar zig-zag chains —O—Hg—O—. The distances and angles between the mercury and oxygen atoms and the coordination of the atoms are almost the same in both structures. The single crystals of these two modifications show very often an epitaxial growth which could be interpreted as being due to a transition of the infinite spiral chain into the infinite planar zig-zag chain. This structural resemblance suggests that physical properties such as solubility should be nearly the same, which is also supported by the experimental values obtained in this work. There seems, however, from crystallographic point of view to be no obvious reason for the orthorhombic form to be more stable than the hexagonal one which is the unambiguous result from the present investigation.

The authors wish to thank Professor Arne Ölander and Professor Arne Magnéli for their kind interest in our work. Thanks are also due to Dr. Kurt Schlyter for valuable help with the calorimetric measurements.

These studies form part of a research program on mercury(II)oxide salts, financially supported by the *Swedish Natural Science Research Council.*

REFERENCES

1. Aurivillius, K. *Acta Chem. Scand.* **10** (1956) 852.
2. Aurivillius, K. and Carlsson, I.-B. *Acta Chem. Scand.* **12** (1958) 1297.
3. Ostwald, W. *Z. physik. Chem.* **34** (1900) 495.
4. Cohen, E. *Z. physik. Chem.* **34** (1900) 69.
5. Taylor, G. B. and Hulett, G. A. *J. Phys. Chem.* **17** (1913) 565.
6. Levi, G. R. *Gazz. chim. ital.* **54** (1924) 709.
7. Garrett, A. B. and Hirschler, A. E. *J. Am. Chem. Soc.* **60** (1938) 299.
8. Kolthoff, I. M. and Sandell, E. B. *Textbook of Quantitative Inorganic Analyse.* 3rd Ed. New York 1952, p. 547.
9. Laruelle, P. *Compt. rend.* **241** (1955) 802.
10. Hulett, G. A. *Z. physik. Chem.* **37** (1901) 406.
11. Schick, K. *Z. physik. Chem.* **42** (1903) 172.
12. Fuseya, G. *J. Am. Chem. Soc.* **42** (1920) 369.
13. Ragg, M. *Farbe und Lack* **56** (1950) 435.
14. Bruja, N. Z. *Rev. chim. Bucharest* **5** (1954) 173.
15. Hietanen, S. and Sillén, L. G. *Acta Chem. Scand.* **6** (1952) 747.
16. Dyrssen, D. and Tyrrell, V. *Acta Chem. Scand.* **15** (1961) 393.
17. *National Bureau of Standards circular* 500 (1952), p. 199.

Received June 9, 1961.

ACTA CHEMICA SCANDINAVICA 15 (1961) 1999–2011

Lösungsmitteleinfluss und Elektrolytwirkung bei der Einwirkung von Chlorwasserstoff auf *n*-Propanol in *n*-Propanol-Wassergemischen

S. KILPI und EVA LINDELL

Chemisches Institut der Universität Helsinki, Finnland

Die Geschwindigkeitskoeffizienten k_1 und k_2 der Einwirkung von HCl auf *n*-Propanol bzw. der Solvolyse des gebildeten Propylchlorids wurden in wasserarmen Propanol-Wassergemischen bei verschiedenen Temperaturen bestimmt. Der auf unendliche Verdünnung extrapolierte und auf ein Mol Propanol bezogene Geschwindigkeitskoeffizient k_0 befriedigt die Gleichung (1). Die Zunahme des Ionenabstands beim Steigen des Wassergehalts und die dabei stattfindende Veränderung der Aktivierungsenergie und Aktivierungsentropie wurden in Beziehung zu der Solvatation diskutiert. Beim Darstellen der Elektrolytwirkung mit der Debye-Hückelschen Gleichung wurde statt 2Bm ein empirisch entwickelter elektrostatischer Ausdruck verwendet, mit dem die Wirkung der Veränderung der Dielektrizitätskonstante und des Ionenabstands auf den Aktivitätskoeffizienten thermodynamisch berechnet werden kann. Der Ionenabstand von HCl ist nach den Messungsresultaten in konzentrierter Lösung gleich 1.84 Å entsprechend dem Wert des Ionenabstands in nichtsolvatisiertem Zustand.

LÖSUNGSMITTELEINFLUSS

Der auf unendliche Verdünnung extrapolierte und auf ein Mol Äthanol bezogene Geschwindigkeitskoeffizient k_0 der Einwirkung von Bromwasserstoff auf Äthanol und der Ionenaktivitätskoeffizient γ_0 befriedigen nach unseren Messungen die folgenden Gleichungen: [1]

$$\left.\begin{aligned} 2 \log \gamma_0/\gamma_0' &= \frac{e^2}{2{,}303\, kT}\left(\frac{1}{Da} - \frac{1}{D'a'}\right) \\ \log k_0/k_0' &= 2 \log \gamma_0/\gamma_0' \end{aligned}\right\} \qquad (1)$$

wenn mit D und D' die Dielektrizitätskonstanten der miteinander verglichenen Gemische bezeichnet werden. Beim Ausdrücken des Ionenabstands a in Å-Einheiten ergibt sich:

$$2 \log \gamma_0/\gamma_0' = \frac{7{,}25 \times 10^4}{T}\left(\frac{1}{Da} - \frac{1}{D'a'}\right) \qquad (1')$$

In einer früheren reaktionskinetischen Arbeit über die Einwirkung von HCl auf Propanol in Propanol-Wassergemischen wurde von einem [2] von uns die beobachtete starke Zunahme des Geschwindigkeitskoeffizienten beim Zunehmen des Propanolgehalts mit der Veränderung des theoretisch berechneten Aktivitätskoeffizienten verglichen. Der Aktivitätskoeffizient wurde mit einer Gleichung berechnet, die mit der obigen Gleichung (1) kvantitativ identisch ist. Die Werte der mittleren Ionenradien wurden auf Grund der Elektrolytwirkung mit Anwendung der Gleichung von Gronwall, La Mer und Sandved berechnet. Die Konzentration der verdünntesten Lösung war zu gross um genaue Werte für a zu bekommen. Trotzdem war die Übereinstimmung der Veränderung des Geschwindigkeitskoeffizienten mit der berechneten Veränderung des Aktivitätskoeffizienten deutlich.

Beim Untersuchen der Einwirkung von HCl auf Propanol wird im folgenden für a des HCl in Propanollösung der Wert 1,84 Å angenommen, welchen Wert man mit der Gleichung (1) in Äthanollösung erhält [3] auf Grund der potentiometrischen Messungen von Scatchard und von Harned und Mitarbeitern, wenn für den Ionenabstand in Wasserlösung 4,22 Å verwendet wird. Die Übereinstimmung des Wertes 1,84 mit dem von Pauling für den Ionenradius von Cl^- berechneten Wert 1,81 ist zu erklären als verursacht durch die kleinere Solvatation des Protons in Alkohollösung in Vergleich mit der Solvatation in Wasserlösung.

In der Tabelle 1 sind die auf Grund der in den Propanol-Wassergemischen ausgeführten kinetischen Messungen mit Hilfe von (1) ermittelten Werten des Ionenabstands a_0 angegeben.

Tabelle 1. Die ermittelten Werte des Ionenabstands a_0 von HCl in den Wasser-Propanolgemischen.

Gew. % Propanol	99,82	97,09	95,24	90,91
$[H_2O]:[C_3H_7OH]$		1:10	1:6	1:3
T°C	a_0 in Å			
85	1,84	1,98	2,02	2,06
75	1,84	2,016	2,066	2,08
65	1,84	2,062	2,11	—
55	1,84	2,092	2,18	—

Die auf Grund der gemessenen Werte k_0 berechnete Veränderung des Ionenaktivitätskoeffizienten beim Variieren des Wassergehalts und die nach Åkerlöf [4] berechneten Werte der Dielektrizitätskonstante der Gemische sind in der Tabelle 2 dargestellt. Bei den untersuchten verhältnismässig niedrigen Temperaturen konnte der Geschwindigkeitskoeffizient Propanol-Wasser-Gemische, die weniger als 90,91 % Propanol enthielten, nicht mit genügender Genauigkeit bestimmt werden. Die früher bei 110°C ausgeführten Messungen [2] zeigen

Tabelle 2. Die Werte $-2 \log \gamma_0/\gamma_0' = pk_0/k_0'$ in den Propanol-Wassergemischen und die Werte der Dielektrizitätskonstante der Gemische nach Åkerlöf [4].

Gew. % Propanol	99,82		97,09		95,24		90,91	
T°C	D_0	pk_0/k_0'	D_0	pk_0/k_0'	D_0	pk_0/k_0'	D_0	pk_0/k_0'
85	13,42	0	13,97	0,878	14,33	1,21	15,21	1,74
75	14,36	0	14,93	0,965	15,31	1,30	16,24	1,72
65	15,36	0	15,96	1,072	16,36	1,38	17,33	—
55	16,43	0	17,07	1,12	17,48	1,51	18,50	—

jedoch, dass der Geschwindigkeitskoeffizient k_0 bei Zunahme des Wassergehalts regelmässig in den wasserreicheren wie in den wasserärmeren Gemischen stark abnimmt.

Die aus der Tabelle 1 ersichtliche Vergrösserung des Ionenabstands beim Zunehmen des Wassergehalts ist zu erklären als verursacht durch die Zunahme der Solvatation. Der beim Erhöhen der Temperatur stattfindenden Verminderung der Solvatation entsprechend ist die Veränderung des Ionenabstands bei verändertem Wassergehalt um so kleiner je höher die Temperatur ist. Der grösseren Solvatation bei niedrigeren Temperaturen entsprechend nimmt der Geschwindigkeitskoeffizient, wie aus der Tabelle 2 ersichtlich, beim Zunehmen des Wassergehalts um so stärker ab, je niedriger die Temperatur ist.

AKTIVIERUNGSENERGIE UND AKTIVIERUNGSENTROPIE

In der Tabelle 3 sind die auf Grund der in den Propanol-Wassergemischen ermittelten Werte k_0 berechneten Werte der Aktivierungsenergie E der Arrheniusschen Gleichung

$$k = A\, e^{-E/RT}$$

Tabelle 3. Aktivierungsenergie und Aktivierungsentropie der Einwirkung von HCl bzw. HBr auf Äthanol in den Äthanol-Wassergemischen und die betreffenden Werte der Einwirkung von HCl auf Propanol in den Propanol-Wassergemischen.

Lösungsmittel	HX	E(kcal)	log$A$	ΔS^* (333°K)
Äthanol	HCl	30,686	15,34	+11,4 cal
$[H_2O] : [C_2H_5OH] = 0$	HBr	31,119	16,015	+14,6 »
» = 1:10	»	37,614	18,88	+27,8 »
» = 1:6	»	36,252	17,74	+22,6 »
Propanol	HCl	34,573	18,226	+24,8 »
$[H_2O] : [C_3H_7OH] = 1:10$	»	39,068	20,065	+33,5 »
» = 1:6	»	39,828	20,201	+32,9 »
» = 1:3	»	39,37	19,41	+30,3 »

angegeben. Die Aktivierungsentropie ΔS^* in der Tabelle ist aus A dieser Gleichung nach [9]

$$A = 2{,}1 \times 10^{10} T \, e^{\Delta S^*/R}$$

ermittelt worden. Vergleichsweise sind in der Tabelle auch die früher [1] ermittelten Werte der Aktivierungsenergie und der Aktivierungsentropie für die Einwirkung von HCl auf Äthanol in Äthanollösung und von HBr auf Äthanol in den Äthanol-Wassergemischen angegeben. Die Aktivierungsenergie und Aktivierungsentropie sind in reiner Alkohollösung kleiner als in wässrigen Alkohollösungen. Die grössere Aktivierungsenergie in den Wasser-Alkohollösungen ist zu erklären als verursacht durch die Zunahme der Solvatation, weil das H^+-Ion und die Alkoholmoleküle dadurch auf ein niedrigeres Energieniveau sinken.

Nach dem positiven Wert der Aktivierungsentropie besitzen die reagierenden Komponenten einen grösseren Ordnungsgrad und eine niedrigere Entropie als der Übergangskomplex. In den wasserärmsten Gemischen, in denen der Geschwindigkeitskoeffizient k_0 bei allen untersuchten Temperaturen mit genügender Genauigkeit bestimmt werden konnte, steigt die Aktivierungsentropie der Einwirkung von HBr und HCl auf Alkohol beim Zufügen von Wasser. Demnach wächst hierbei der Ordnungsgrad der reagierenden Komponente, was durch die Zunahme der Solvatation zu erklären ist.

Die Veränderung der Aktivierungsenergie und der Aktivierungsentropie stimmt nach dem obigem mit der auf Grund der Ionenaktivitätswerte nach (1) berechneten Zunahme des Ionenabstands beim Steigen des Wassergehalts überein.

Die Geschwindigkeit der Solvolyse ist bei den untersuchten Temperaturen verhältnismässig gering. Der Geschwindigkeitskoeffizient k_2 konnte deshalb nur in den wasserreicheren Gemischen gemessen werden, in denen $[H_2O]$: $[C_3H_7OH] = 1{:}6$ bzw. $1{:}3$ war. Wie aus der Tabelle 4 ersichtlich, sind die in diesen Gemischen ermittelten Werte der Aktivierungsenergie und Aktivierungsentropie der Solvolyse von derselben Grössenordnung wie bei der Äthanolyse und der Hydrolyse von Äthylbromid [4] in den Wasser-Äthanolgemischen.

Tabelle 4. Aktivierungsenergie und Aktivierungsentropie der Solvolyse von C_2H_5Br und C_3H_7Cl in den Wasser-Alkoholgemischen.

Reaktion	Lösungsmittel	E(kcal)	log$A$	ΔS^* (333°K)
Äthanolyse von C_2H_5Br	Äthanol	24,05	7,90	−22,8 cal
» » »	$[H_2O]:[C_2H_5OH]$ $\frac{1}{10}$ bis $\frac{1}{3}$	25,11	8,59	−19,6 »
Hydrolyse von »	» » = 1/10	23,28	8,28	−21,0 »
» » »	» » = 1/6	21,98	7,38	−25,2 »
» » »	» » = 1/3	21,79	7,30	−25,5 »
» » »	» » = 1/1	22,17	7,65	−23,9 »
Solvolyse von C_3H_7Cl	$[H_2O]:[C_3H_7OH]$ = 1/6	23,24	7,06	−26,6 »
» » »	» » = 1/3	22,07	6,56	−28,9

Nach dem negativen Wert der Aktivierungsentropie ist der Ordnungsgrad des Übergangskomplexes bei der Solvolyse grösser als der Ordnungsgrad der reagierenden Komponente.

VERGLEICH MIT FRÜHEREN MESSUNGEN

Es war von Interesse, die obigen bei den Temperaturen 55—85°C erhaltenen Messungsresultate mit den von einem [2] von uns bei 110°C ausgeführten kinetischen Messungen zu vergleichen. Die Geschwindigkeitskoeffizienten in der genannten Arbeit ($C_{1,0}/[C_3H_7OH] \rightarrow k_0$) wurden mit den angegebenen Werten d_0 auf die in Mol pro 1000 g Lösung ausgedrückte Konzentration bezogen und die Zeit in Sekunden statt in Minuten gerechnet. Die Tabelle 5 enthält die in obiger Weise berechneten Werte k_0 und die nach (1) auf Grund der Werte k_0 ermittelten Werte des Ionenabstands von HCl. Für a in dem wasserärmsten Gemisch mit 96,87 Gew. % Propanol wurde der Wert 1,84 Å angenommen, weil die Dehydratation von HCl in diesem Gemisch bei 110° wahrscheinlich vollständig ist.

Tabelle 5. Der Ionenabstand von HCl in den wasserarmen Propanol-Wassergemischen bei 110°C nach den Messungen von Kilpi [2]. N_a bezeichnet die Molfraktion von Propanol.

N_a	Gew. % Propanol	d_0	D_0	pk_0	a(Å)
0,903	96,87	0,812	11,87	2,05	1,84
0,823	94,00	0,818	12,35	2,55	1,88
0,693	88,30	0,830	13,45	3,20	1,87

Nach den Werten der Tabelle wächst der Ionenabstand auch bei 110°C beim Zunehmen des Wassergehalts; doch ist die Zunahme von a merkbar geringer als bei niederen Temperaturen nach den in der Tabelle 1 angegebenen Werten.

Die bei den Temperaturen 55—85°C gemessenen Geschwindigkeitskoeffizienten wurden mit den betreffenden Parametern der Arrchenius'schen Gleichung auf 110°C extrapoliert. Ungeachtet des weiten Temperaturintervalls stimmen die durch Extrapolation erhaltenen Werte k_0 mit den auf Grund der Werte der Tabelle 5 nach (1) berechneten Werten überein, wie aus der Tabelle 6 ersichtlich ist.

Tabelle 6. Ein Vergleich der bei 55—85°C in dieser Arbeit gemessenen Geschwindigkeitskoeffizienten mit den bei 110°C früher gemessenen Werten.

Gew. % Propanol	D_0	pk_0	pk_0 (ber. nach Tabelle 5)
97,09	11,82	2,08	2,02
95,24	12,14	2,38	2,38
90,91	12,93	2,89	2,89

ELEKTROLYTWIRKUNG

Die Aktivitätskoeffizienten der Alkalichloride, die von Harned und Mitarbeitern potentiometrisch gemessen worden sind, können nach einem [3,6] von uns beim Steigen der Konzentration durch die folgenden Gleichungen dargestellt werden, in denen der empirische Term 2 Bm der Debye-Hückelschen Gleichung durch 2 log γ ersetzt worden ist:

$$\left.\begin{aligned} -2\log f &= -2\log\gamma + \frac{2A\sqrt{m}}{1+a\sqrt{m}} \\ 2\log\gamma &= \frac{7{,}25\times10^4}{Ta}\left(\frac{1}{D_m}-\frac{1}{D_o}\right) \\ A &= 1{,}82\times10^6\,(D_mT)^{-3/2} \\ a &= 50{,}3\,a(D_mT)^{-1/2} \end{aligned}\right\} \quad (2)$$

Für a wurden die nach den von Pauling berechneten Ionenradien ermittelten Ionenabstände verwendet. Die mit der Konzentration veränderliche D_m wird interativ berechnet mit Anwendung von (2) und den folgenden Gleichungen:

$$\left.\begin{aligned} 2\log\gamma &= 2(\log\gamma)_{lin} + 2\delta(m-m_o)^2 \\ 2(\log\gamma)_{lin} &= \frac{7{,}25\times10^4}{Ta}\left(\frac{1}{D_M}-\frac{1}{D_o}\right)\frac{mM}{1000} \\ D_{lin} &= D_o\left(1+\frac{mM}{1000}\times\frac{D_o-D_M}{D_M}\right)^{-1} \\ 2\delta(m-m_o)^2 &= \frac{7{,}25\times10^4}{Ta}\left(\frac{1}{D_m}-\frac{1}{D_{lin}}\right) \end{aligned}\right\} \quad (3)$$

Der nach den in den verdünntesten Lösungen ausgeführten Messungen empirisch zu bestimmende Hilfsparameter D_M bezeichnet die Dielektrizitätskonstante des Elektrolyten in verdünnter Lösung und D_0 die des reinen Lösungsmittels. Die Konzentration wird hierbei in Mol pro 1000 g Lösung berechnet. Wenn D_M empirisch nicht zu ermitteln ist, kann statt dessen der Wert des reinen Elektrolyten verwendet werden. 2δ bleibt in den Alkalichloridlösungen konstant, unabhängig von der Konzentration. Insbesondere ist dies der Fall betreffend CsCl, dessen Hydratation im Vergleich mit den niederen Alkalichloriden am geringsten ist. In den Gleichungen (2) sind D_M und D_{lin} eliminiert worden.

Im Gegensatz zu den nichtsolvatisierten Elektrolyten muss bei den solvatisierten Elektrolyten neben D_m auch die Veränderung des Ionenabstands mit der Konzentration beachtet werden. Nach den Messungen nehmen D_m und a_m beim Steigen der Konzentration ab. Die hierdurch verursachte Veränderung der Ionenaktivität kann unter gewissen Voraussetzungen für D und a voneinander getrennt berechnet werden. Dies ist der Fall, wenn die Aktivitätsmessungen von verdünnten Lösungen an bis zu genügend konzentrierten Lö-

sungen ausgeführt werden können, in denen der Ionenabstand des Elektrolyten einen dem nichtsolvatisierten Zustand entsprechenden kleinsten Wert hat.

Bei solvatisierten Elektrolyten wird log γ mit der Gleichung

$$2\log\gamma = 2(\log\gamma)_{\text{lin}} + \frac{7{,}25\times10^4}{Ta_o}\left(\frac{1}{D_m}-\frac{1}{D_{\text{lin}}}\right) + \frac{7{,}25\times10^4}{TD_m}\left(\frac{1}{a_m}-\frac{1}{a_o}\right) \quad (4)$$

dargestellt. Es sei angenommen, dass beim Variieren der Konzentration bei solvatisierten Elektrolyten dem Verhalten der nichtsolvatisierten Elektrolyten entsprechend die folgende Formel anzuwenden ist:

$$2\delta m^n = \frac{7{,}25\times10^4}{Ta_o}\left(\frac{1}{D_m}-\frac{1}{D_{\text{lin}}}\right) \quad (5)$$

Wenn in der Gleichung (4) a_m in der konzentriertesten Lösung als gleich dem Ionenabstand des nichtsolvatisierten Elektrolyten gesetzt wird, können durch Variieren der Konzentration die Parametern δ und n der Gleichung (5) empirisch bestimmt werden.

Mit bekannten Werten von δ und n kann D_m bei beliebiger Konzentration nach der Formel

$$2(\log\gamma)_{\text{lin}} + 2\delta m^n = \frac{7{,}25\times10^4}{T\ a_o}\left(\frac{1}{D_m}-\frac{1}{D_o}\right) \quad (6)$$

ermittelt werden. Die Werte a_m sind darauf mit den Gleichungen (2) und

$$2\log\gamma = \frac{7{,}25\times10^4}{T}\left(\frac{1}{D_m a_m}-\frac{1}{D_o a_o}\right) \quad (7)$$

durch Iteration zu berechnen.

Im folgenden wird die Berechnung von D_m und a_m auf Grund der bei 65°C ausgeführten kinetischen Messungen in dem Propanol-Wassergemisch $[H_2O]:[C_3H_7OH] = 1:6$ dargestellt. Für den Ionenabstand von HCl wurde in der konzentriertesten Lösung ($m\sim2$) 1,84 Å des nichtsolvatisierten Zustands angenommen. Die in der Berechnung erforderlichen Werte a_o, D_o und der Wert des Hilfsparameters D_{HCl} sind in den Tabellen 1, 2 und 8 angegeben. Mit den empirisch ermittelten Werten

$$\begin{cases} 2\delta = 2{,}070 \\ n = 3/2 \end{cases}$$

lauten die Gleichungen zur Berechnung von G_m und a_m auf Grund der gemessenen Werte des Aktivitätskoeffizienten im vorhandenen Fall:

$$\left.\begin{aligned} -2\log f = \mathrm{p}k_1 - \mathrm{p}k_{1,0} &= -2\log\gamma + \frac{2A\sqrt{m}}{1+a\sqrt{m}} \\ 0{,}7918\ m + 2{,}070\ m^{3/2} &= \frac{101{,}66}{D_m} - 6{,}214 \\ 2\log\gamma &= \frac{214{,}5}{D_m a_m} - 6{,}214 \end{aligned}\right\} \quad (8)$$

Die Formeln zur Berechnung von A und a sind unter (2) angegeben.

Die Möglichkeit der Berechnung von D_m und a_m auf Grund der Messresultate beruht wesentlich darauf, dass die Veränderung derselben mit der Konzentration in der Formel (4) für $2\log \gamma$ getrennt voneinander in verschiedenen Ausdrücken dargestellt ist.

In der Tabelle 9 sind die Berechnungsresultate von der Elektrolytwirkung angegeben. Die Veränderung sowohl von a_m als von D_m mit der Konzentration entspricht den gemachten Voraussetzungen. Bemerkenswert ist, dass in dem untersuchten Propanol-Wassergemisch der Ionenabstand von HCl schon von $m \sim 0{,}5$ an gleich dem Ionenabstand im nichtsolvatisierten Zustand ist und von da ab bis zu der konzentriertesten untersuchten Lösung innerhalb der Messungsgenauigkeit konstant bleibt.

Mit den Formeln (2) kann der Aktivitätskoeffizient eines 1—1-wertigen unsolvatisierten Elektrolyten berechnet werden, wenn die Dielektrizitätskonstante der betreffenden Elektrolytlösungen und der Ionenabstand des Elektrolyten bekannt sind. Bei solvatisierten Elektrolyten müssen die Werte a_m bei bekannten Werten D_m empirisch nach (2) und (7) auf Grund der Aktivitätsmessungen bestimmt werden.

MESSUNGEN

Die in den Messungen verwendeten Lösungsmittel waren 99,82 % *n*-Propanol (d_4^{30}=0,79628. Fluka AG, Buchs, Schweiz) und die aus diesem bereiteten Wasser-Propanolgemische mit 97,09; 95,24 und 90,91 Gew. % Propanol ($[H_2O]:[C_3H_7OH]$=1:10, 1:6 und 1:3). Zur Bereitung der HCl-Lösungen wurde durch konz. Schwefelsäure geleitetes HCl-Gas in Propanol und in die genannten Wasser-Propanolgemische eingeleitet. In Lösungen, in denen $k_{1,0}$ durch Extrapolation des gemessenen k_1 auf unendliche Verdünnung berechnet wurde, war die Konzentration von HCl *ca.* 0,02 M.

Die Temperaturen der in den Messungen verwendeten Thermostaten waren 45, 55, 65, 75, und 85°C mit einer Variation der Temperatur innerhalb ±0,01°. Beim grösseren Wassergehalt als in $[H_2O]:[C_3H_7OH]$=1:3 war die Bestimmung von k_1 bei den obigen Temperaturen zu ungenau, um die betreffenden Messresultate zu dem vorhandenen Zweck verwenden zu können.

Die Messung der Solvolysegeschwindigkeit von *n*-Propylchlorid wurde ausgeführt mit Anwendung von *n*-Propylchlorid von Schering-Kahlbaum, Sp. 47,6—48,1°(770,9 mm Hg) und d_4^{20} = 0,8834. Die Konzentration der in den kinetischen Messungen verwendeten Lösungen war *ca.* 0,1 M. Bei der Berechnung des Geschwindigkeitskoeffizienten k_1 der Einwirkung von HCl auf Propanol musste der Wert des Geschwindigkeitskoeffizienten der Solvolyse nur in den Gemischen $[H_2O]:[C_3H_7OH]$ = 1:6 und 1:3 berücksichtigt werden. Auch in diesen Gemischen war die Geschwindigkeit der Solvolyse verhältnismässig klein.

Bei den Messungen wurden gewogene Mengen (*ca.* 10 g) des Gemisches in zugeschmolzenen Ampullen aus Pyrexglas in Thermostaten von gewünschter Temperatur gehalten, bis bei der Einwirkung von HCl auf Propanol *ca.* 10 % des HCl reagiert hatten, und bei der Solvolyse des Propylchlorids, bis die Konzentration des gebildeten HCl auf 0,005—0,01 M gestiegen war. Die in

den Tabellen angegebenen Geschwindigkeitskoeffizienten sind Mittelwerte aus 10 verschiedenen Messungen. Der mittlere Fehler in den Mess-serien war $\pm 0{,}011$ pk-Einheiten.

Der Verlauf der Reaktion wurde durch Titrieren mit 0,02 N Bariumhydroxydlösung verfolgt. Wenn die HCl-Konzentration klein ist, ist beim Anwenden von Phenolphthalein als Indikator der Titrationswert dafür zu korrigieren, dass zu dem betreffenden Wasser-Propanolgemisch ein wenig Bariumhydroxydlösung zuzufügen ist, bevor die Lösung rot wird. Die anzubringende Korrektion wurde experimentell gemessen. Hierbei wurde wie in den kinetischen Messungen zu dem Reaktionsgemisch von *ca.* 10 ml soviel Wasser zugesetzt, dass das Gesamtvolumen der Lösung am Ende der Titration 50 ml beträgt. Unter diesen Verhältnissen war die für HCl anzubringende Titrationskorrektion -0.0008 g Äquiv./Lit.

BERECHNUNG DER GESCHVINDIGKEITSKOEFFIZIENTEN

Der Geschwindigkeitskoeffizient k_1 wurde nach der die Geschwindigkeit der Reaktion darstellenden Gleichung[7] bestimmt. In der Gleichung bezeichnet

$$\begin{aligned} dy/dt &= k_1(b'-y)^2 - k_2 y \\ &= k_{1,0} f^2 (b'-y)^2 - k_2 y \end{aligned} \tag{9}$$

b' die Anfangskonzentration von HCl und y die Konzentration des zur Zeit t gebildeten Propylchlorids. Wie durch graphische Integration konstatiert wurde, kann die Veränderung des Aktivitätskoeffizienten beim Vermindern der Konzentration von HCl vernachlässigt werden, wenn die Konzentration sich während der Reaktion nur um 10 % vermindert. (Vgl. Tabellen 12 und 13). Mit dieser Voraussetzung und mit der Anfangsbedingung $y = 0$ bei $t = 0$ lautet die Formel zur Berechnung von k_1[7]:

$$\left.\begin{aligned} k_1 &= \frac{2{,}303}{(y_1 - y_2)\,t} \log \frac{y_2(y_1 - y)}{y_1(y_2 - y)} \\ y_1 &= b' + \frac{k_2}{2k_1} + \sqrt{\frac{k_2}{k_1}\left(b_1 + \frac{k_2}{4k_1}\right)} \\ y_2 &= b' + \frac{k_2}{2k_1} - \sqrt{\frac{k_2}{k_1}\left(b' + \frac{k_2}{4k_1}\right)} \end{aligned}\right\} \tag{10}$$

Weil der Aktivitätskoeffizient bei den kleinsten Konzentrationen beim Steigen der Konzentration stark abnimmt, wurde k_2 durch graphische Integration nach der Gleichung

$$k_2 = \frac{1}{t}\int_0^x [(a'-x) - \frac{k_{1,0}}{k_2} f^2 x^2]\,dx \tag{11}$$

mit der Anfangskonzentration a' des Propylchlorids berechnet.

In Propanollösung und in dem Wasser-Propanolgemisch mit $[H_2O]:[C_3H_7OH] = 1:10$ kann k_1 wegen der kleinen Geschwindigkeit der Solvolyse in denselben mit der Gleichung

$$k_1 = \frac{1}{t} \cdot \frac{y}{b'(b'-y)} \qquad (12)$$

berechnet werden. Mit dieser Gleichung wurde auch bei grösserer Solvolysengeschwindigkeit ein Annäherungswert für k_1 berechnet, um darauf mit den Gleichungen (10) und (11) durch Iteration die Werte k_1 und k_2 zu ermitteln.

Die zur Berechnung des Aktivitätskoeffizienten nötigen Werte der Dielektrizitätskonstante der Wasser-Propanolgemische bei den Messungstemperaturen wurden nach Åkerlöf [4] mit der Gleichung

$$\log D_t = \log D_0 - \beta (t - t_0)$$

berechnet. Mit einer Gleichung derselben Form wurden auch die Werte von D_{HCl} berechnet, die als Hilfsparametern bei der Berechnung des Aktivitätskoeffizienten nach (2) und (3) verwendet wurden. Die Ermittelung von D_0 und β der obigen Formel geschah nach den von Schaefer und Schlundt [8] gemessenen Werten der Dielektrizitätskonstante von HCl im flüssigen Zustand:

t°C	D_{HCl}
27,7	4,60
−90	8,85

Die ermittelten Werte von log D_0 und β in den betreffenden Medien sind in der Tabelle 8 wiedergegeben

Tabelle 8.

Medium	t°C	log D_0	β
Propanol	20	1,3183	0,00293
$[H_2O]:[C_3H_7OH]$ = 1:10	»	1,3336	0,00290
» » = 1:6	»	1,3434	0,00288
» » = 1:3	»	1,3662	0,00283
HCl	25	0,6693	0,00241

DIE MESSRESULTATE

In den die gemessenen Geschwindigkeitskoeffizienten darstellenden Tabellen 9—16 ist die Konzentration in Mol pro 1000 g Lösung angegeben. b' und a' bezeichnen die Anfangskonzentration von HCl bzw. C_3H_7Cl; y bezeichnet die Konzentration des zur Zeit t gebildeten C_3H_7Cl bei der Einwirkung von HCl auf Propanol und x die Konzentration des zur Zeit t gebildeten HCl bei der Solvolyse von Propylchlorid. k_1 ist der gemessene Geschwindigkeitskoeffizient mit der Anfangskonzentration b' des HCl und $k_{1,0}$ der auf unendliche Verdünnung extrapolierte Wert von k_1. $k_{1,0}/[C_3H_7OH]$ ist mit k_0 bezeichnet worden. Die bei der Extrapolation verwendeten Werte der Dielektrizitätskonstante sind in der Tabelle 2 angegeben. Die berechneten Werte k_0 der Tabellen sind mit Anwendung der in der Tabelle 3 angegebenen Werte der Parameter der Arrheniuss'schen Gleichung $k = A^{-E/RT}$ ermittelt worden.

Tabelle 9. Elektrolytwirkung auf Grund der Messungen von k_1. T = 65°C; pk_2 = 7,873; [C_3H_7OH] = 15,85; [H_2O] = 2,642.

m	t(Sek.) × 10^{-5}	y	pk_1	D_m	a(Å)	2 log γ	p$k_{1,0}$
0,0199	11,23	0,0025	5,187	16,30	2,11	0,023	4,165
0,0354	9,576	0,0042	5,396	16,25	2,092	0,097	4,166
0,0510	8,766	0,0062	5,508	16,19	2,066	0,200	4,167
0,0729	7,776	0,0087	5,620	16,11	2,036	0,325	4,164
0,1015	8,712	0,0147	5,713	15,99	2,02	0,432	4,165
0,2487	6,039	0,0330	5,990	15,25	1,92	1,116	4,165
0,4916	4,374	0,0688	6,120	13,90	1,86	1,955	4,165
0,9893	1,809	0,1088	6,157	11,25	1,83	4,228	4,168
1,6030	1,044	0,1979	6,075	8,70	1,83	7,258	4,156
2,0048	0,864	0,2786	6,031	7,43	1,84	9,465	4,168

Tabelle 10. k_1 in 99,82 %igem n-Propanol. [C_3H_7OH] = 16,64; a = 1,84 Å.

T°C	b'	t(Sek.)	y	pk_1	p$k_{1,0}$	pk_0	pk_0 ber
85							2,741
75	0,02467	1,620 × 10^4	0,00306	3,451	2,130	3,351	3,343
65	»	6,840 × 10^4	0,00359	3,995	2,744	3,965	3,981
55	0,02169	2,628 × 10^5	0,00288	4,571	3,447	4,668	4,658
45	»	10,37 × 10^5	0,00258	5,222	4,156	5,377	5,378

Tabelle 11. k_1 in 97,09 %igem n-Propanol. [C_3H_7OH] = 16,16; [H_2O] = 1,616.

T°C	b'	t(Sek.)	y	pk_1	a (Å)	p$k_{1,0}$	pk_0	pk_0 ber
85	0,02072	3,24 × 10^4	0,00284	3,626	1,98	2,411	3,619	3,629
75	»	1,548 × 10^5	0,00319	4,248	2,016	3,100	4,308	4,308
65	0,02077	6,012 × 10^5	0,00267	4,928	2,062	3,845	5,053	5,030
55	»	2,16 × 10^6	0,00212	5,596	2,092	4,570	5,778	5,794

Tabelle 12. k_1 in 95,25 %igem n-Propanol. [C_3H_7OH] = 15,85; [H_2O] = 2,642.

T°C	b'	t(Sek.)	y	pk_2	pk_1	a(Å)	p$k_{1,0}$	pk_0	pk_0 ber
85	0,02025	7,20 × 10^4	0,00303	7,037	3,917	2,02	2,761	3,961	3,953
75	»	3,348 × 10^5	0,00334	7,431	4,536	2,066	3,444	4,644	4,646
65	0,01986	11,23 × 10^5	0,00250	7,873	5,187	2,11	4,163	5,363	5,382
55	»	4,241 × 10^6	0,00173	8,325	5,941	2,18	4,975	6,175	6,162

Tabelle 13. Berechnung von $k_{1,0}$ durch graphische Integration in 95,25 %igem Propanol während des Verlaufes der Reaktion. Die angebrachte Titrationskorrektion für HCl war −0,001 g Äquiv./Lit. T = 85°C. Der für $k_{1,0}$ erhaltene Wert stimmt mit dem in der Tabelle 12 angegebenen bei 85°C erhaltenen Wert überein.

b'	t(Sek.) × 10^{-5}	y	p$k_{1,0}$
0,01925	0,720	0,00303	2,775
»	1,620	0,00612	2,775
»	10,44	0,01631	2,774

Tabelle 14. Der Geschwindigkeitskoeffizient k_2 der Solvolyse von *n*-Propylchlorid in 95,25 % igem *n*-Propanol. Die angebrachte Titrationskorrektion für HCl war −0,001 g Äquiv./Lit.

T°C	a'	t(Sek.) × 10^{-5}	x	a (Å)	p$k_{1.0}$	pk_2	pk_2 ber
85	0,1274	5,112	0,00392	2,02	2,762	7,042	7,037
75	0,11625	10,30	0,00367	2,066	3,444	7,431	7,441
65	0,09986	35,28	0,00406	2,11	4,163	7,875	7,872
55	»	71,68	0,00320	2,18	4,975	8,325	8,325

Tabelle 15. k_1 in 90,91 %igem *n*-Propanol; [C_3H_7OH] = 15,13; [H_2O] = 5,046.

T°C	b'	t(Sek.) × 10^{-7}	y	pk_2	pk_1	p$k_{1.0}$	pk_0
85	0,02885	1,653	0,00369	6,823	4,512	2,06	3,288
75	»	7,812	0,00415	7,207	5,127	2,08	3,973

Tabelle 16. Der Geschwindigkeitskoeffizient der Solvolyse von *n*-Propylchlorid in 90,91 %igem *n*-Propanol. Die für HCl angebrachte Titrationskorrektion war −0,0008 g Äquiv./Lit.

T°C	a'	t(Sek.) × 10^{-5}	x	a (Å)	p$k_{1.0}$	pk_2
85	0,1222	1,033	0,01188	2,06	3,288	6,823
75	»	2,16	0,01282	2,08	3,973	7,207

Die Ausführung dieser Arbeit ist von der *Staatlichen Naturwissenschaftlichen Kommision* mit Stipendien unterstützt worden, wofür wir hiermit unseren Dank aussprechen.

LITERATUR

1. Kilpi, S. *Suomen Kemistilehti* B **31** (1958) 121; Kilpi, S. und Lindell, E. *Suomen Kemistilehti* B **33** (1960) 17.
2. Kilpi, S. *Z. physik. Chem.* A **166** (1933) 285.
3. Kilpi, S. *Suomen Kemistilehti* B **31** (1958) 375; *Svensk Kem. Tidskr.* **72** (1960) 178. Vgl. die daselbst angegebene Literatur.
4. Åkerlöf, G. *J. Am. Chem. Soc.* **54** (1932) 4125.
5. Kilpi, S. *Acta Chem. Scand.* **11** (1957) 1143.
6. Kilpi, S. *Suomen Kemistilehti* B **32** (1959) 125; B **34** (1961) 12.
7. Kilpi, S. *Z. physik Chem.* **86** (1914) 427.
8. Schaefer, O. G. und Schlundt, H. *J. Phys. Chem.* **13** (1909) 669. Zitiert nach Critical Tables VI, 76.
9. Glasstone, S., Laidler, K. J. und Eyring, H. *The Theory of Rate Processes.* New York 1941, S. 416, 452.

Eingegangen am 8. Juni 1961.

ACTA CHEMICA SCANDINAVICA 15 (1961) 2012–2020

Mechanism of the Molybdate Catalyzed Reductions of Perchlorate and Nitrate Ions at the Dropping Mercury Electrode

G. P. HAIGHT, Jr.

Department of Chemistry, Swarthmore College, Swarthmore, Pa., U.S.A., and Kemisk Laboratorium A, Danmarks Tekniske Højskole, Copenhagen, Denmark

Data on the catalytic waves found for molybdate in acid solutions containing nitrate and perchlorate have been reexamined and extended. Various theories of catalytic polarographic currents are applied. The conclusion from studies in homogeneous systems (that Mo(IV) is the catalyst) is introduced and the consequence tested. Given this assumption it is possible to determine the order of magnitude of rate constants for the bimolecular reactions of Mo(IV) with nitrate, perchlorate, and chloride, and for the disproportionation of Mo(IV).

The powerful catalytic effect of molybdate toward the reduction of perchlorate and nitrate has been observed to occur when reduction is effected by stannous ion [1], zinc [2], or at the dropping mercury electrode [3,4]. By showing that Mo(VI), Mo(V), and Mo(III) are not the catalyst, Haight and Sager concluded [1] that the unstable Mo(IV) state is the catalytically active form of molybdenum in these systems. It has been interesting for the author, in connection with studies of the reduction of nitrate in homogeneous systems [5], to reexamine the polarographic data [3,4] in the framework of the theories of polarographic catalytic currents developed by Koutecky [6], Delahay and Stiehl [7], and Orlemann and Kern [8] in order to test the assumption that Mo(IV) which disproportionates is the catalytic species.

EXPERIMENTAL

Much of the data used in drawing the conclusions of this paper have been drawn from Refs.[3,4]. Additional data reported here were obtained in conventional manner using Radiometer model PO-4 recording polarograph. Since the primary interest is in limiting currents, mercury pool anodes were employed. Polarographic cells were thermostated at 25°C.

THEORETICAL

Considering a sequence of reactions giving a catalytic polarographic wave:

$$A + ne \longrightarrow B \text{ (Diffusion controlled)} \quad (1)$$

$$B + Z \xrightarrow{k_2} A \quad (2)$$

Delahay and Stiehl [7] derived an equation for the catalytic current

$$i_c = 0.753 \times 10^6 nm^{2/3}t^{2/3}D_A^{1/2}C_A C_Z^{1/2}k_2^{1/2} \quad (I)$$

where i_c is the catalytic current in microamperes; n is the number of electrons in the electrochemical reduction (1); m is the number of milligrams of mercury per second flowing from the capillary; t is the time, in seconds, of formation of each drop of mercury; D_A is the diffusion coefficient of substance A in $cm^2/sec.$; C_A is the concentration in moles per liter of substance A in the bulk of the solution; C_Z is the concentration in moles per liter of substance Z, and k_2 is the rate constant in liters per mole per second for reaction (2). Koutecky, considering spherical, rather than linear diffusion, for the same chemical situation, derived the equation

$$i/i_d = 0.812\ (C_Z k_2 t)^{1/2} \quad (II)$$

where i is the total current observed and i_d is the current if no catalysis takes place. If one considers the situation when $i_c \gg i_d$, division of eqn. (I) by the Ilkovic equation [7] for i_d gives

$$i_c/i_d = 1.2(C_Z k_2 t)^{1/2} \quad (III)$$

Thus k_2 is 2.25 times as great if eqn. (II) is employed as it is if eqn. (I) is used. Delahay and Stiehl require $C_Z k_2 > 100$ reciprocal seconds for their equation to be valid. Koutecky requires $C_Z k_2 t > 100$, which is considerably less restrictive since t is generally between 2 and 6 sec. It should be noted that k_2 in Koutecky's derivation is replaced by $(k_f + k_b)$ where k_f is k_2 and k_b is the rate constant for the reverse reaction;

$$A \longrightarrow B + Z \quad (-2)$$

PROPOSED MECHANISM FOR CATALYTIC CURRENTS

The evidence for Mo(IV) as the catalytic species of molybdenum should be presented since most of the analysis and discussion hinges on this assumption. As stated, it has been shown [1] that the other common valence states are not catalytically active. Further, the author has observed [13] that 10^{-4} M Mo(VI) in 0.5 M hydrochloric acid gives a single polarographic wave with the characteristics of a reversible two-electron reduction. This wave is enhanced by the presence of either perchlorate or nitrate indicating that the product, which is assumed to be Mo(IV), is the catalyst. Further evidence is found in the nature of the catalytic waves themselves. Mo(III) is inert toward catalysis. Thus the catalytic waves should cease at potentials where Mo(III) is produced. (Such a discontinuity is observed in the tungstate catalyzed reduction of perchlorate [14]). In this case no such discontinuity occurs, indicating that the Mo(V)→ Mo(III) wave, which is enhanced by the catalysis in question, consists of electroreduction of Mo(V) to Mo(IV) followed by rapid disproportiona-

tion of Mo(IV). Mo(III) is not produced by electro-reduction, thus the steady state concentration of Mo(IV) is unaffected by increasing the potential of the electrode beyond that needed to give a limiting current. The principle evidence for Mo(IV) as the catalytic species continues to be the evidence against the other valence states, however. The following reactions are proposed as contributing to the observed catalytic effects.

$$\text{Mo(VI)} + 2\ e \longrightarrow \text{Mo(IV)} \text{ or } \text{Mo(V)} + e \longrightarrow \text{Mo(IV)} \quad (3)$$

$$\text{Mo(IV)} + \text{Z} \xrightarrow{k_4} \text{X} * \quad (4)$$

$$\text{X} + ne \longrightarrow \text{Mo(IV)} + \text{D (fast)} \quad (5)$$

$$2\ \text{Mo(IV)} \xrightarrow{k_6} \text{Mo(V)} + \text{Mo(III)} \quad (6)$$

Z will be either nitrate or perchlorate ion. X is an electroreducible species which may be Mo(VI), Mo(V), or a complex of Mo(IV) with Z which allows the electroreduction of nitrate or perchlorate. The kinetics of homogeneous reductions has suggested complexes [1,9], but no choice can be made on the nature of X nor the value of n. D would be chloride ion if perchlorate is electrolytically reduced and one of many reduction products if nitrate is so reduced. It is seen that n may be any integer from 1 to 8. It will most likely be 2, if Mo(IV) is oxidized to Mo(VI); 8, if perchlorate is reduced to chloride, or 4, if nitrate is reduced to N_2O, the product with this catalyst and Sn(II) as reducing agent in solutions containing sulfate [5]. Eqns. 3, 4, and 5 are seen to give the same pattern as eqns. 1 and 2. Thus the catalytic current should be proportional to the concentration of Mo(VI) in the bulk of the solution and proportional to the half power of the concentration of perchlorate or nitrate. If disproportionation becomes important at high Mo(VI) concentrations the catalytic current should become dependent upon the square root of the bulk concentration of Mo(VI), as follows.

Consider a steady state for Mo(IV) at the surface of the mercury drop. Mo(IV) will be formed at the same rate at which Mo(VI) diffuses from the bulk of the solution into the reaction layer at the surface of the drop. Mo(IV) will leave the reaction layer by diffusion and by disproportionation into Mo(V) and Mo(III).

$$\mathrm{d}N/\mathrm{d}t = k_\mathrm{D}A[\text{Mo(VI)}] - k_\mathrm{D}A[\text{Mo(IV)}] - k_6[\text{Mo(IV)}]^2V = 0 \quad \text{(IV)}$$

where N is the number of atoms of Mo(IV) in the reaction layer at the drop surface, k_D is a diffusion rate constant, A is the area of the mercury drop, V is the volume of the reaction layer, [Mo(VI)] is the concentration in moles per liter of molybdate in the bulk of the solution, and [Mo(IV)] is the concentration in moles per liter in the reaction layer at the surface of the mercury drop. From the Ilkovic equation [10] it can be calculated that

$$k_\mathrm{D} = 1.27(D/t)^{1/2} \quad \text{(V)}$$

where D is the diffusion coefficient in cm²/sec (assumed to be the same for Mo(VI) and Mo(IV) and t is the time required for the formation of each mer-

* k_4 and k_2 correspond to one another.

cury drop. Letting $V = A\mu$, where μ is the thickness of the reaction layer, and solving for Mo(IV) we find

$$[\text{Mo(IV)}] = \frac{-k_D}{4\,\mu k_6} + \left(\frac{k_D^2}{4\,\mu^2 k_6^2} + \frac{k_D}{\mu k_6}\,[\text{Mo(VI)}]\right)^{1/2} \qquad \text{(VI)}$$

Thus, at high concentration of Mo(VI), the second term under the square root sign in eqn. (VI) becomes dominant. A plot of catalytic current *vs.* $[\text{Mo(VI)}]^{1/2}$ should give a straight line, the slope and intercept of which will yield values of the product μk_6. The validity of this reasoning was checked by applying it to the disproportionation of U(V) studied by Orlemann and Kern [8]. The equations which they used were directly derivable and the values of constants found to be identical. We shall assume that reaction (4) leading to catalytic current does not remove Mo(IV) from the reaction layer, and that disproportionation removes only one Mo(IV) atom, the one which becomes Mo(III). If Mo(VI) or Mo(V) are formed by either or both of these reactions it is assumed that they will be electrolytically reconverted to Mo(IV) at rates which are very high compared with the purely chemical processes.

Effect of chloride ion on catalytic waves

Inhibition of catalytic waves by foreign anions such as chloride ion can best be ascribed to competitive reaction for sites on the catalytically active Mo(IV):

$$\text{Mo(IV)} + \text{Z} \xrightarrow{k_4} \text{C} \qquad (4)$$

$$\text{Mo(IV)} + \text{Cl}^- \xrightarrow{k_7} \text{Mo(IV)Cl} \qquad (7)$$

Let α be the fraction of Mo(IV) reacting with Z to give catalytic current. If $(i_c)_o$ is the catalytic current for ClO_4^- in the absence of chloride

$$\alpha = \frac{k_4[\text{Mo(IV)}][ClO_4]}{k_4[\text{Mo(IV)}][ClO_4] + k_7[\text{Mo(IV)}][Cl^-]} = \frac{i_c}{(i_c)_o} \qquad \text{(VII)}$$

Table 1. Effect of changing perchlorate and nitrate concentrations on catalytic current *. 8.95×10^{-5} M Mo(VI), $m = 1.01$ mg/sec, $t = 6.0$ seconds, $T = 25°C$.

i_c μA	$[ClO_4^-]$ m/l	$i_c/[ClO_4^-]^{1/2}$
1.35	0.05	6.0
1.78	0.10	5.7
4.05	0.50	5.7
5.65	1.00	5.7
8.30	2.00	5.9
	$[NO_3^-]$	$i_c/[NO_3^-]^{1/2}$
20.6	1.00	20.6
6.9	0.10	21.8

* Ion strength could not be maintained constant.

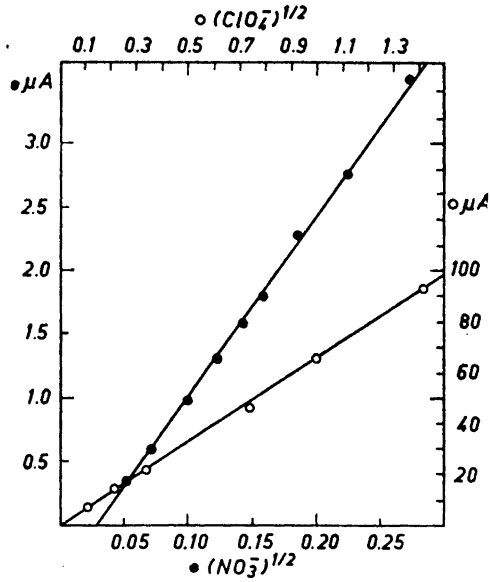

Fig. 1. Dependence of catalytic currents on the square root of the concentrations of nitrate (closed circles) and of perchlorate (open circles).

Eqn. (VII) rearranges to

$$\frac{(i_c)_o}{i_c} = 1 + \frac{k_7[Cl^-]}{k_4[ClO_4^-]} \qquad \text{(VIII)}$$

Thus, if k_4 has been determined, k_7 is readily calculable from observed catalytic currents in the presence of chloride.

Table 2. Rate constants from kinetic currents.

Reaction	Medium	k_4 l m^{-1}sec^{-1}	Data source
Mo(IV) + NO_3^-	0.1 M HNO_3 1.0 M HNO_3	$2700/n^2$	New
Mo(IV) + NO_3^-	0.05 M HNO_3 0.10 M H_2SO_4 0.20 M Na_2SO_4	$2370/n^2$	Ref.[4]
Mo(IV) + ClO_4^-	1.0 M $HClO_4$	$250/n^2$	Ref.[3]
	1.0 M $HClO_4$ 0.75 M H_2SO_4	$180/n^2$	Ref.[3]

$D = 6.88 \times 10^{-6}$ cm^2/sec for Mo(VI) in 0.2 M $NaHSO_4$ used for nitrate calculations.
$D = 5.76 \times 10^{-6}$ cm^2/sec for Mo(VI) in 1 M H_2SO_4 used for perchlorate calculations.
$m^{2/3}t^{1/6}$ had to be estimated for nitrate calculations.
3.45 cm^2 was used. Only $m^{2/3}t^{1/6}$ values are available.
k_4 values determined from eqn. (1), then multiplied by 2.25.

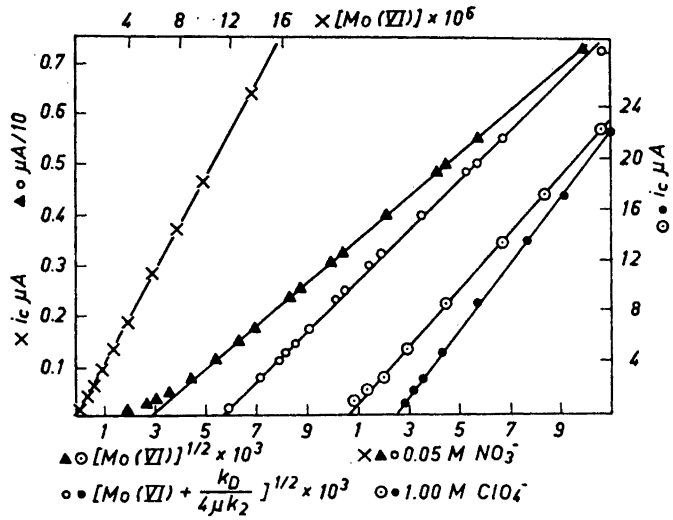

Fig. 2. Dependence of i_c on molybdate concentration. At low concentration (crosses) i_c is directly proportional to [Mo(VI)]. The test of eqn. (VI) at higher concentrations of Mo is shown in the other plots. The points represented by open and closed circles are estimated from the adjacent lines.

EXPERIMENTAL TESTS OF THEORETICAL PREDICTIONS

The term $m^{2/3}t^{2/3}$ in eqn. (I) requires that catalytic currents be independent of the head of mercury in the reservoir of the dropping electrode. This test has been made in several instances in the case of the perchlorate catalysis and found to be true. One rough measurement in 1 M nitric acid showed that the catalytic current was independent of head of mercury. However, this test was not applied under the conditions used to obtain the data on the nitrate reduction upon which calculations in this study are based [4].

Previously unreported data on the dependence of i_c on perchlorate concentration is given in Table 1.

Figs. 1 and 2 show clearly the dependence of catalytic currents on the square root of nitrate and perchlorate ion concentrations, and on the first power of the molybdate concentration when it is lower than 10^{-5} M. The plot of i_c *vs.* $[NO_3^-]^{1/2}$ reflects the fact that the nitrate concentrations were below those required to maintain $k_2C_Zt > 100$ at the lower values.

For [Mo(VI)] $> 10^{-5}$ M a dependence of i_c on $[Mo(VI)]^{1/2}$ as predicted by eqn. (V) is found. However, slope and intercept give disparate values of $k_D/k_6\mu$ because the two terms under the square root sign in eqn. (V) are of comparable magnitude. It is possible to estimate μk_6 from the slope of the plot which is insensitive to the changes to be made and then to plot i_c *vs.* $\frac{k_6}{4k_6\mu} + [Mo(VI)]$. Such a procedure brings slope and intercept into fair agreement. The analysis has ignored the possibility of polymerization of Mo(VI) and the possibility

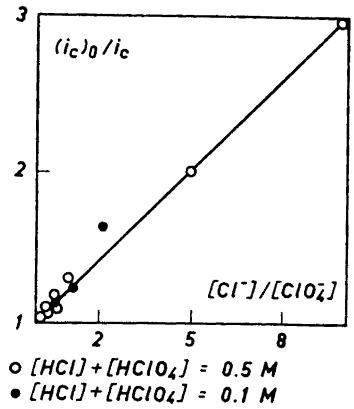

Fig. 3. Chloride inhibition of catalysis. A test of eqn. (VIII).

of reoxidation of Mo(III). High acidity and low concentrations of molybdate justify ignoring polymerization and the absence of catalysis when Mo is introduced in the trivalent state justifies the latter assumption. However, freshly formed Mo(III) may be much more reactive than that previously prepared and subsequently added to solutions to be polarographed.

Fig. 3 shows a plot of $(i_c)_0/i$ *vs.* $[Cl^-]/[ClO_4^-]$ using the intercept at $[Cl^-] = 0$ as the origin. New data (summarized in Table 3) has been obtained for ion strength 0.5 and combined with that reported for ion strength 0.1 in Ref.[3]. The previous observation that i_c was proportional to perchlorate concentration is seen to be a fortuitous result in which the combined effects of perchlorate dilution and chloride inhibition participate.

Evaluation of rate constants. k_4 may be determined from eqn. (I) using data obtained under conditions where i_c is proportional to [Mo(VI)]. Values of the diffusion coefficient, D, for molybdate used in the calculation were derived from non-catalytic currents obtained in similar media. Sources are indicated in Table 1. Only $m^{2/3}t^{1/6}$ was recorded for Robinson and Johnson's data [4] on the nitrate waves and not individual values of m and t. For purposes of estimating k_1 and k_2 from these data, the values 3.5 for $m^{2/3}t^{2/3}$ and 3 sec. for the drop time have been selected arbitrarily in order to obtain the order of magnitude of the constants.

Table 3. Disproportionation constants for Mo(IV).

Medium	μ/n (cm) = $[D/k_1C_Z]^{1/2} \times 10^4$	nk_6 (l $m^{-1}sec^{-1}$) $\times 10^{-4}$
0.05 M HNO_3	2.58	5.78 (intercept)
0.20 M $NaHSO_4$		6.5 (slope)
1.0 M $HClO_4$	1.52	0.91 (intercept)
		0.70 (slope)
1.0 M $HClO_4$	1.80	2.4 (intercept)
0.75 M H_2SO_4		2.61 (slope)

In the case of perchlorate an estimate of the equilibrium constant $K = [Mo(IV)ClO_4]/[Mo(IV)][ClO_4^-]$ is available from the kinetic data of Haight and Sager [1]. In 2.5 M sulfuric acid $K = 8.15$ l mole^{-1} if the rate constants for disproportionation of different Mo(IV) species are assumed to be the same. Thus if $k_4 = k_f + k_b$, k_f is about 89 % of k_4 and k_b about 11 %. For strict comparison a polarographic study must be undertaken in the same medium used for the homogeneous kinetics [1]. It is likely that K is larger in the polarographic case here reported since sulfate may be expected to decrease complex formation with perchlorate.

The values of k_4 reported in Table 1 are the results of such calculation multiplied by 2.25 to give the result consistent with Koutecky's treatment of spherical diffusion. Values of k_4 for reactions involving nitrate and perchlorate ions in various media are summarized in Table 1. Given values of k_4, k_7 can be readily calculated from eqns. (VII) and (VIII). Individual results for k_7 are included in Table 3. The slope of the line in Fig. 3 gives $k_7 = 50/n^2$ l/m/sec.

Values for the disproportionation rate constant, k_6 depend on the assignment of a value for the thickness of the reaction layer, μ. Comparing Koutecky's theoretical result [6] with that of Brdicka and Wiesner [11] based on the concept of the reaction layer, μ is found to be equal to $D^{1/2}/k_1^{1/2}C_Z^{1/2}$(Ref.[12]). Orlemann and Kern [8] evaluated μ for the case of a simple disproportionation reaction giving catalytic current and obtained the value $\mu = 0.3D^{1/2}t^{1/2}$. Normally these values will differ by about a factor of 10. Since the main effect being studied is the catalytic current due to reaction with Z, the reaction layer will be assigned the former value, which is the smaller, on the assumption that only disproportionation within this smaller region affects the catalytic current. Values of k_6 and of μ based on these assumptions are recorded in Table 2.

Table 4. Effect of chloride ion on catalytic currents for perchlorate. [Mo(VI)] = 10^{-6} M, $m = 4.24$ mg/sec, $t = 2.0$ sec. $(i_c)_o$ is calculated on the basis of the square root law for perchlorate concentration.

i_c	$(i_c)_o$	a	$[ClO_4^-]$	$[Cl^-]$	$k_7\ n^2$
4.88	4.88	1	0.5	0.0	—
4.58	4.66	0.982	0.455	0.045	44
4.08	4.46	0.916	0.417	0.083	105
4.20	4.46	0.943	0.417	0.083	74
3.70	4.09	0.904	0.35	0.15	62
3.56	4.09	0.871	0.35	0.15	85
2.68	3.46	0.775	0.25	0.25	72
1.00	2.00	0.500	0.083	0.417	50
0.50	1.48	0.338	0.0455	0.455	49
2.01	2.01	1	0.10	0.0	—
1.46	1.65	0.885	0.067	0.033	66
1.14	1.42	0.803	0.05	0.05	61
0.71	1.16	0.612	0.033	0.067	77
Average $k_7 = 67/n^2$					

The accuracy is extremely limited by the inherent difficulty in making precise polarographic measurements. K values depend on small differences in these measurements. Note — a difference of 3 % in i_c in the 3rd and 4th lines makes a 30 % difference in k_7. See Fig. 3.

DISCUSSION

The figures show that the proposed mechanism is clearly consistent with available data. The straight line plots confirm the form of the equations consistent with the theory. It is unfortunate that lack of knowledge of n values and the inaccessibility of details of capillary characteristics leaves doubt as to values for the rate constants. However, the results give added weight to a general pattern for the manner in which molybdenum functions as a catalyst in the reduction of oxy-ions. In papers to follow dealing with the homogeneous catalysis of the reduction of hydroxylamine and nitrate, it will be observed that disproportionation becomes an effective part of kinetics at concentrations of molybdenum (added as V or VI) in the neighborhood of 10^{-5} M consistent with the polarographic finding. Direct information about the disproportionation from polarographic data in the absence of catalysis may be difficult to obtain in view of the low concentrations at which it becomes important. Polymerization of Mo(VI) leads to changing character of polarographic waves with changing molybdate concentration and such effects will be difficult to sort out from others such as those due to disproportionation.

The author wishes to thank the Climax Molybdenum Company for financial assistance, and Professor Jannik Bjerrum and Dr. Hakon Nord for helpful discussions.

REFERENCES

1. Haight, Jr., G. P. and Sager, W. F. *J. Am. Chem. Soc.* **74** (1952) 6056.
2. Haight, Jr., G. P. *Anal. Chem.* **25** (1953) 642.
3. Haight, Jr., G. P. *Anal. Chem.* **23** (1951) 1505.
4. Johnson, M. G. and Robinson, R. J. *Anal. Chem.* **24** (1952) 366.
5. Haight, Jr., G. P. *Acta Chem. Scand.* **16** (1962). *In press.*
6. Koutecky, J. *Chem. Listy* **47** (1953) 9; *Collection Czechoslov. Chem. Communs* **18** (1953) 311.
7. Delahay, P. and Stiehl, G. *J. Am. Chem. Soc.* **74** (1952) 3500.
8. Orlemann, E. F. and Kern, D. M. H. *J. Am. Chem. Soc.* **75** (1953) 3058.
9. Haight, Jr., G. P. *J. Am. Chem. Soc.* **76** (1954) 4718.
10. Ilkovic, D. *Collection Czechoslov. Chem. Communs* **6** (1934) 498.
11. Brdicka, R. and Wiesner, K. *Collection Czechoslov. Chem. Communs* **12** (1947) 39.
12. Delahay, P. *New Instrumental Methods in Electrochemistry*, Interscience, New York 1954.
13. Haight, Jr., G. P. *Paper submitted for publication.*
14. Laitinen, H. A. and Zeigler, W. *J. Am. Chem. Soc.* **75** (1953) 3045.

Received June 10, 1961.

ACTA CHEMICA SCANDINAVICA 15 (1961) 2021–2025

Mean Amplitudes of Vibration and Shrinkage Effects of Acetylene from Spectroscopic Data

E. MEISINGSETH and S. J. CYVIN

Institutt for teoretisk kjemi, Norges tekniske høgskole, Trondheim, Norway

Force constants, mean-square amplitude matrix elements, mean amplitudes of vibration and shrinkage effects for the acetylene molecule have been calculated from spectroscopic data. Small harmonic vibrations have been assumed. The shrinkage effects at the temperature of 298°K came out with the values 0.019 Å and 0.041 Å for the C···H and H···H distances, respectively. In particular some studies have been made on certain approximation methods. By transferring the CC stretching frequency from acetylene to the simple two-particle model CH·CH, a very good approximation for the CC mean amplitude of vibration was produced.

The theory of vibrational mean-square amplitudes for linear symmetrical X_2Y_2 molecules [1] has been applied to acetylene. It would have been interesting to compare the presently calculated mean amplitudes of vibration and shrinkage effects with those from electron-diffraction, but the latter ones are unfortunately not available at present. Anyhow the spectroscopic calculations for acetylene (H—C≡C—H) along with those of cyanogen [2] (N≡C—C≡N) are believed to be of great interest in connection with some recent electron-diffraction experiments on the H—C≡C—C≡N molecule.

An additional reason for undertaking this work was the desire of making a study of the effect of certain approximation methods. In this connection the acetylene molecule has been treated tentatively as a two-particle structure CH·CH.

RIGOROUS TREATMENT

The adopted values for the equilibrium interatomic distances are [2–4] $R = 1.058_5$ Å for C—H and $D = 1.204_7$ Å for C≡C. The fundamental frequencies from Herzberg [5] were applied and are not much different from some later observations [6]. The normal frequencies (ω) were computed from the fundamentals (ν) by means of approximately estimated anharmonicity constants (x), following the method of Dennison [7,8]. The anharmonicity constants are defined by

$$\nu_i = (1 - x_i)\omega_i$$

and the assumption

$$x_i/x_i^* = \nu_i/\nu_i^*$$

is made. Here the asterisk is used to identify the appropriate quantities of acetylene-d_2. The resulting numerical values are presented in Table 1.* The

Table 1. Fundamentals (ν), anharmonicity constants (x), and normal frequencies (ω) for acetylene and acetylene-d_2.

C_2H_2	No.	ν(cm^{-1})	x[a]	ω(cm^{-1})
Σ_g^+	1	3373.7	0.03939	3512.0
	2	1973.8	0.02[b]	2014.1
Σ_u^+	3	3287	0.02107	3357.7
Π_g	4	611.8	0.01[b]	618.0
Π_u	5	729.1	0.02634	748.8
C_2D_2	No.	ν(cm^{-1})	x[a]	ω(cm^{-1})
Σ_g^+	1	2700.5	0.03153	2788.4
	2	1762.4	0.01786	1794.5
Σ_u^+	3	2427	0.01555	2465.3
Π_g	4	510.9[c]	0.00835	515.2
Π_u	5	539.1	0.01947	549.7

[a] Approximate computations. All of the reported decimals are not significant.
[b] Assumed.
[c] Calculated.

value of $x_2 = 0.02$ has been chosen within the limited range making $x_1 > x_2$ and both of these constants positive. The calculated value of $\nu_4^* = 510.9$ cm^{-1} is well compatible with the corresponding value of 505 cm^{-1} obtained from a combination band, as quoted by Herzberg [5].

Table 2. Force constants and mean-square amplitude matrix elements for acetylene.

Symbol [a]	Force constant (mdyne/Å)	Symbol [a]	Mean-square amplitude (Å^2)[b] $T = 0$	298°K
F_1	6.412	Σ_1	0.006860	
F_2	29.561	Σ_2	0.001285	
F_{12}	9.194	Σ_{12}	−0.001473	
F_3	6.175	Σ_3	0.005400	
F_4	0.1216	Σ_4	0.05046	0.05586
F_5	0.2699	Σ_5	0.02756	0.02908

[a] For explanation of symbols, see Ref.[1]
[b] For the figures in the middle column the temperature dependence is insignificant.

* Similar corrections for anharmonicity in acetylene have been performed previously by many workers; *cf.* Refs. [5,6] and references cited therein. Special reference is made to a paper of Wu and Kiang.[9] From their reported values the calculated anharmonicity constants x_1, x_2, x_3 and x_4 for C_2H_2 (in the present notation) are 0.0404, 0.0159, 0.0295, and 0.0322, respectively. The agreement is satisfactory.

The force constants (which reproduce the normal frequencies for acetylene and acetylene-d_2 given in Table 1) are shown in Table 2, along with the mean-square amplitude matrix elements at $T = 0$ and 298°K for C_2H_2. The calculated mean amplitudes of vibration and shrinkage effects are presented in Table 3.

Table 3. Mean amplitudes of vibration and shrinkage effects for acetylene.

Distance	Symbol [a]	Mean amplitude of vibration (Å)[b,c] $T = 0$	298°K
CH	u_r	0.0783	
CC	u_d	0.0358	
C··H	u_{r+d}	0.0730	
H··H	u_{2r+d}	0.1041	
Distance	Symbol[a]	Shrinkage effect (Å) $T = 0$	298°K
C··H	δ^g_{r+d}	0.017	0.019
H··H	δ^g_{2r+d}	0.038	0.041

[a,b] See footnotes to Table 2.
[c] The values show good correspondence with those of Bakken.[10]

APPROXIMATE TREATMENTS

Separation of frequencies. The approximate method of separating high and low frequencies developed by Wilson [11] may be applied to the Σ_g^+ species of acetylene. The corresponding simplified F and G matrices read

$$F^\circ = \begin{bmatrix} F_1^\circ & 0 \\ 0 & F_2^\circ \end{bmatrix} \; ; \; G^\circ = \begin{bmatrix} (m_C + m_H)/m_C m_H & 0 \\ 0 & 2/(m_C + m_H) \end{bmatrix}$$

Hence the following equations are obtained for the force constants of the F° matrix:

$$F_1^\circ = 4\pi^2 c^2 \omega_1^2 \; m_C m_H/(m_C + m_H) \quad (1)$$

$$F_2^\circ = 2\pi^2 c^2 \omega_2^2 \; (m_C + m_H) \quad (2)$$

$$F_{12}^\circ = 0 \quad (3)$$

The resulting equations for the mean-square amplitudes of vibration according to this approximation are given in the following.

$$(u_r^\circ)^2 = (h/16\pi^2 c)[(m_C + m_H)/m_C m_H][(1/\omega_1)\coth(hc\omega_1/2kT) + (1/\omega_3)\coth(hc\omega_3/2kT)] \quad (4)$$

$$(u_d^\circ)^2 = (h/4\pi^2 c\omega_2)[1/(m_C + m_H)]\coth(hc\omega_2/2kT) \quad (5)$$

$$(u_{r+d}^\circ)^2 = (u_r^\circ)^2 + (u_d^\circ)^2 \quad (6)$$

$$(u_{2r+d}^\circ)^2 = (h/4\pi^2 c\omega_1)[(m_C + m_H)/m_C m_H]\coth(hc\omega_1/2kT) + (u_d^\circ)^2 \quad (7)$$

Symbols:

m_C = mass of the C atom,
m_H = mass of the H atom,
c = velocity of light,
h = Planck's constant,
k = Boltzmann's constant,
T = absolute temperature.

For the numerical results, see Table 4.

Table 4. Approximate mean amplitudes of vibration for acetylene after separation of frequencies.

Distance	Symbol	Value	Difference [a]
CH	u_r	0.0727	−0.0056
CC	u_d	0.0359	+ 0.0001
C··H	u_{r+d}	0.0810	+ 0.0080
H··H	u_{2r+d}	0.0178	+ 0.0037

[a] Compared with the values in Table 3.

Table 5. Approximate results for some quantities related to the CC bond of acetylene.

Approximation	ω_2 (cm^{-1})	H_2[a] (Å/mdyne)	F_2 (mdyne/Å)	u_d (Å)
1. alternative $\omega = \omega_2$	2014.1	0.06434	15.543	0.0359
2. alternative $1/F = H_2$	2067.4	0.06106	16.376	0.0354
3. alternative $F = F_2$	2777.6	0.03383	29.561	0.0305

[a] From the rigorous calculation: $H_2 = 0.06106$ Å/mdyne.

Simplified model. The approximate treatment based on simplified molecular models has been discussed elsewhere.[12] The method has been applied previously to allene [13], benzene [14], *cyclo*propane [12], and other molecules. In the present case of acetylene the simplified treatment turns out to be extremely simple, as the molecule may be regarded as a two-particle structure and treated as a diatomic molecule $(CH)_2$. Hence the following equations apply to the force constant and the mean-square amplitude of vibration:

$$F = 2\pi^2 c^2 \omega^2 \ (m_C + m_H) \tag{8}$$

$$u^2 = (h/4\pi^2 c\omega)[1/(m_C + m_H)]\coth(hc\omega/2kT) \tag{9}$$

It may be assumed that if the CC normal frequency from acetylene (*viz.* ω_2) is inserted as ω in eqn. (9), the resulting u^2 value will represent an approximation for the mean-square amplitude of vibration for the CC distance (*viz.* u_d^2). This approximation will be referred to as the first alternative and is seen to be coincident with the result from the separation of frequencies (*cf.* eqn. 5).

It is interesting to notice that the force constant F from the first-alternative approximation, being identical with F_2° of eqn. (2), deviates largely from the rigorously calculated F_2 (*cf.* Tables 2 and 5). This feature may be attributed to the fact that F_2 is not a pure CC stretching force constant, as is apparent from the comparatively high value of the interaction constant F_{12} (see Table 2). However, the *inverse* force constant H_2, *i.e.* the appropriate element of the matrix $H = F^{-1}$, is seen to be not so much affected by the approximation in question. As pointed out by Cyvin and Slater [15] the inverse force constants do possess the property of being pure constants for defined coordinates.

The above considerations give a clue to another approximation, namely that obtained by putting the inverse of F in eqn. (8) equal to H_2, i.e.

$$1/F = F_1/(F_1F_2-F_{12}^2) \tag{10}$$

The numerical results from this approximation, referred to as the second alternative, are included in Table 5. The approximation is seen to be very good.

For the sake of completeness the calculations with

$$F = F_2 \tag{11}$$

have also been carried through, the results being found in Table 5 as the third alternative. These calculations are seen to give a much poorer approximation for the CC mean amplitude of vibration, compared to the results from the first and second alternatives.

REFERENCES

1. Cyvin, S. J. and Meisingseth, E. *Acta Chem. Scand.* **15** (1961) 1289.
2. Overend, J. and Thompson, H. W. *Proc. Roy. Soc. (London).* **A 232** (1955) 291; **A 234** (1956) 306.
3. Christensen, M. T., Eaton, D. R., Green, B. A. and Thompson, H. W. *Proc. Roy. Soc. (London)* **A 238** (1956) 15.
4. Callomon, J. H. and Stoicheff, B. P. *Can. J. Phys.* **35** (1957) 373.
5. Herzberg, G. *Infrared and Raman Spectra of Polyatomic Molecules*, D. van Nostrand, New York 1945.
6. Bell, E. E. and Nielsen, H. H. *J. Chem. Phys.* **18** (1950) 1382; **19** (1951) 136.
7. Dennison, D. M. *Revs. Modern Phys.* **12** (1940) 175.
8. Hansen, G. E. and Dennison, D. M. *J. Chem. Phys.* **20** (1952) 313.
9. Wu, T. Y. and Kiang, A. T. *J. Chem. Phys.* **7** (1939) 178.
10. Bakken, J. *Acta Chem. Scand.* **12** (1958) 594.
11. Wilson, E. B., Jr. *J. Chem. Phys.* **9** (1941) 76.
12. Cyvin, S. J. *Acta Polytechn. Scand.* Ph 6 (279/1960).
13. Cyvin, S. J. *J. Chem. Phys.* **30** (1959) 337.
14. Cyvin, S. J. *J. Mol. Spectroscopy* **3** (1959) 467.
15. Cyvin, S. J. and Slater, N. B. *Nature* **188** (1960) 485.

Received May 26, 1961.

ACTA CHEMICA SCANDINAVICA 15 (1961) 2026–2036

The Molybdenum Catalyzed Reduction of Hydroxylamine with Stannous Chloride

G. P. HAIGHT, Jr.* and CARL von FRANKENBERG**

Kemisk Laboratorium A, Technical University of Denmark, Copenhagen, Denmark, and Swarthmore College, Swarthmore, Pa., U.S.A.

Hexavalent molybdenum in the presence of stannous chloride has previously been shown to be a powerful catalyst for the reduction of oxyanions such as perchlorate and nitrate. This paper reports conditions for catalytic reduction of hydroxylamine and the kinetics of the reaction:

$$SnCl_3^- + NH_3OH^+ \xrightarrow{\text{Mo(VI) or Mo(V)}} SnOCl_3^- + NH_4^+$$

Reactions initiated by Mo(V) showed a much shorter induction period than in the case of perchlorate reductions. Reactions initiated by Mo(VI) gave an initial surge as with perchlorate. The two cases gave the same final steady state kinetics with Mo(V) as the dominant form of molybdenum remaining except in cases where reactions initiated by Mo(VI) were completed without reaching steady state conditions. The kinetics apart from induction periods and initial surges gave the rate law:

$$d[Sn(II)]/dt = k'[Sn(II)]^{1/2}[NH_3OH^+]^{1/4}[Mo(V)]^{1/2}[H^+]^2/(1 + k''[NH_3OH^+])$$

Since k' is a maximum where $SnCl_3^-$ is at maximum concentration relative to other $SnCl_n^{2-n}$ species, $SnCl_3^-$ is judged to be the most reactive form of Sn(II) present. A mechanism is deduced based on the assumption that Mo(IV) is the catalyst and compared with a mechanism previously deduced for the reduction of perchlorate.

Interest in the previously observed ability of molybdate to catalyze the reduction of oxyanions [1–4] such as perchlorate and nitrate has been heightened by the discovery that molybdate is a necessary participant in the enzymatically catalyzed conversion of nitrate to ammonia in biochemical systems.[5] We have accordingly undertaken a study of the catalytic removal of oxygen

* On leave from Chemistry Department, Swarthmore College, Swarthmore, Pa., U.S.A., 1960–1.

** Chemistry Department, University of Pennsylvania, Philadelphia 4, U.S.A.

from nitrate and its oxygen containing reduction products, nitrite and hydroxylamine. The reduction of hydroxylamine reported here has been studied in dilute hydrochloric acid. The rate of the catalytic reduction has been found to be significant only over a very narrow range of hydrochloric acid concentration (in the vicinity of 3.0 M) suggesting that conditions for conversion of nitrate as well as hydroxylamine to ammonia must be very carefully specified.

EXPERIMENTAL

Reagent grade chemicals were used without further purification. Solutions were prepared as follows:

$SnCl_2.2H_2O$ was dissolved in standard hydrochloric acid and diluted to give 3.0 M H^+ assuming no hydrolysis. Hydroxylamine hydrochloride was dissolved in standard hydrochloric acid and the solution diluted to give 3.0 M chloride ion. Sodium molybdate dihydrate was dissolved in 3.0 M hydrochloric acid. These solutions with total ion concentrations of 3.0 M were used for the more significant experiments. Some results with other concentrations of H^+ and Cl^- are reported in the tables.

Reactions initiated by Mo(VI) were started by adding sodium molybdate solution to a predetermined mixture of the Sn(II) and hydroxylamine solutions. Reactions initiated by Mo(V) were started by adding the hydroxylamine last, enabling the Sn(II) to reduce Mo(VI) to Mo(V). All reactions were carried out under nitrogen to prevent air oxidation of stannous chloride. The concentration of Sn(II) remaining at various times was determined by titration with iodine. A few runs were made in which the reaction was quenched in solutions of 0.1 M Mo(VI) in concentrated hydrochloric acid. The green Mo(V) species produced by the reaction

$$\text{Sn(II)} + 2\,\text{Mo(VI)} = \text{Sn(IV)} + 2\,\text{Mo(V)}$$

was measured spectrophotometrically at 720 mμ with a Beckmann model DU spectrophotometer. Both analytical methods gave the same kinetics. Hydroxylamine does not react with iodine in the time required for a titration at the acidities used in this study, and reacts too slowly with Mo(VI) in concentrated hydrochloric acid to interfere with the spectrophotometric measurement. Tests of each procedure showed no interference from hydroxylamine. Although iodine is used to titrate hydroxylamine to nitrous oxide in neutral solutions [6], one drop of 0.01 molar iodine gave a permanent starch test in 0.5 M hydroxylamine in solutions 1.0 to 3.0 M in hydrochloric acid.

RESULTS

Runs containing an excess of Sn(II) all proceeded until the Sn(II) concentration had decreased an amount equal to the initial concentration of hydroxylamine indicating that each substance changes two equivalents in oxidation number. For convenience we shall write the equation for the reaction:

$$SnCl_3^- + NH_3OH^+ = SnOCl_3^- + NH_4^+ \qquad (I)$$

No evidence of formation of intermediates such as hydrazine was found.

Reliable kinetics were obtained only with runs initiated by Mo(V) although some runs initiated by Mo(VI) gave the same kinetics following an initial surge. A suggestion of an induction period covering 1—5 min was observed in several reactions initiated by Mo(V), following which the kinetics to be described were valid for up to 95 % completion of the reaction. Similar runs initiated by Mo(VI) are illustrated in Table 1.

Determination of the empirical rate law. In runs containing a high excess of hydroxylamine, plots of [Sn(II) $^{1}/_{2}$ *vs.* time gave straight lines as illustrated in

Table 1. Comparison of runs started with Mo(V) and Mo(VI).

Run 13 $[NH_2OH]$ = 0.659 M Added [Mo(VI)] = 1.6×10^{-5}			Run 22 $[NH_2OH]$ = 0.665 M Added [Mo(V)] = 1.7×10^{-5}	
Time min.	[Sn(II)], M		Time min.	[Sn(II)], M
0	0.0338	Initial surge	0	0.0327
1	0.0253		1.2	0.0320
3.17	0.0210		5	0.0287
6	0.0145		10	0.0249
9	0.0133		20.25	0.0174
14	0.0107		40	0.00700
17	0.0090		50	0.00425
25	0.0061		60	0.00255

Note. Kinetics for run 13 are the same as run 22 after the first 6.0 minutes.

Fig. 1. These plots have slopes proportional to $[Mo(V)]^{½}$ as shown by runs 20, 21, and 22 in Table 2. These results suggest the reaction is 1/2 order in respect to Sn(II) and in respect to Mo(V).

In runs containing equimolar Sn(II) and hydroxylamine plots of 1/[Sn(II)] *vs.* time give straight lines as illustrated in Fig. 2. (The correction term in Fig. 2 is required by the final rate law.) These results suggest the rate law:

$$d[Sn(II)]/dt = k[Sn(II)]^{½}[NH_3OH^+]^{½}[Mo(V)]^{½} \quad (1)$$

The results of runs 5 and 24 (Table 2) with the same chloride concentration and fairly similar hydroxylamine concentrations suggest that k is proportional to the square of the hydrogen ion concentration. If this is true a comparison of runs 20, 21, and 22 with run 38 requires that

$$k = k'[H^+]^2/(1 + k''[NH_3OH^+]). \quad (2)$$

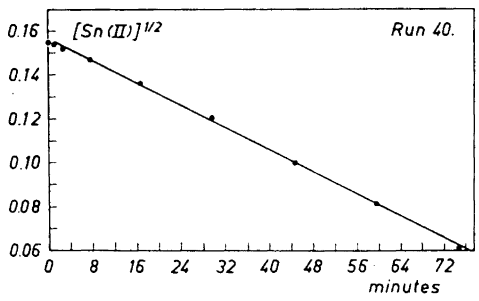

Fig. 1. Plot showing the reaction to be half order in Sn(II) in the presence of excess hydroxylamine. Details of run 40 are shown in Table 2.

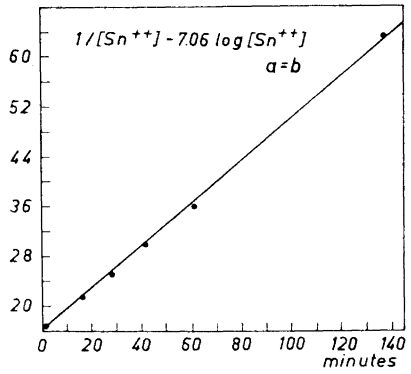

Fig. 2. Plot showing the reaction to be second order in Sn(II) when concentrations of Sn(II) and hydroxylamine are equal.

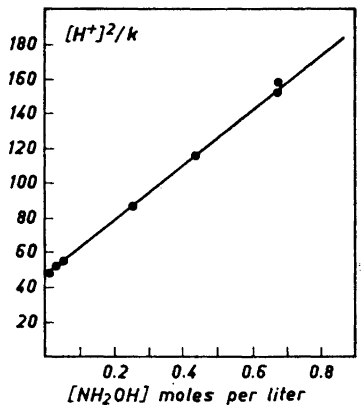

Fig. 3. Plot showing calculation of k' and k'' from the dependence of k on concentrations of hydrogen ion and hydroxylamine for runs containing 2.9 M chloride ion. Intercept = 48 = $1/k'$; k' = 2.08 × 10^{-2}; slope = 148 = k''/k'; k'' = 3.07.

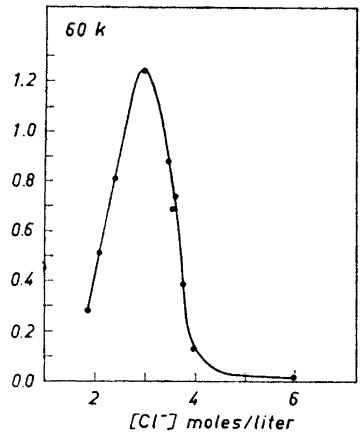

Fig. 4. Variation of k' with changing chloride ion concentration, k'' assumed to be constant.

All runs performed at $[Cl^-]$ = 2.90 M (allowing for 3.0 combined chloride ions per tin atom) were used to test eqn. (2). Fig. 3 shows a plot of $[H^+]^2/k$ *vs.* $[NH_3OH^+]$. From the slope and intercept of the straight line obtained k' and k'' were evaluated. In all other cases k' was evaluated assuming k'' = 3.07. If $[NH_3OH^+]_0$ <0.03, the term containing k'' can be ignored. The final empirical rate law thus obtained is

$$\mathrm{d[Sn(II)]/d}t = \frac{k'[\mathrm{Sn(II)}]^{1/2}[\mathrm{NH_3OH^+}]^{1/4}[\mathrm{Mo(V)}]^{1/2}[\mathrm{H^+}]^2}{1 + k''[\mathrm{NH_3OH^+}]} \qquad (3)$$

The values of the constants for $[Cl^-]$ = 2.90 M are k' = 0.020 and k'' = 3.07 if concentrations are in moles per liter and time is in seconds. The rate law is valid for concentrations of Sn(II) from 0.1 to 0.002 M, of hydroxylamine from 0.67 to 0.020 M, of Mo(V) from 5 × 10^{-3} to 10^{-5} M, and of hydrogen ion

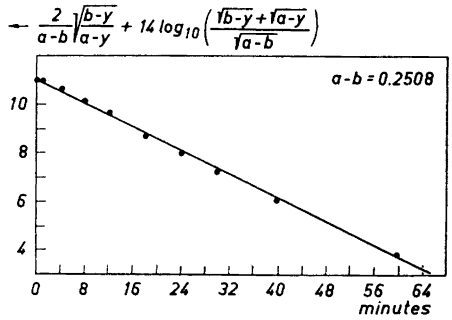

Fig. 5. Plot showing validity of eqn. 3 at chloride ion concentration of 2.3. Run 37 in Table 2.

Table 2. Data on runs giving characteristic Mo(V) kinetics in moles/liter $k'' = 3.07$, time in seconds

Run	Sn(II)	NH_3OH^+	H^+	Cl^-[a]	Mo(V)	Plot vs. t	Slope	k'	
38	0.1000	0.0999	2.81	2.81	1.62×10^{-3}	1a	5.77×10^{-3}	0.0182	
9	0.0309	0.421	2.60	2.93	1.32×10^{-3}	2	2.73×10^{-5}	0.0198	
12	0.0300	0.296	2.70	2.97	1.58×10^{-4}	2	2.00×10^{-5}	0.0165	
20	0.0370	0.665	2.28	2.90	7.50×10^{-5}	2	7.70×10^{-5}	0.0198	
21	0.0280	0.665	2.28	2.90	6.24×10^{-4}	2	2.37×10^{-4}	0.0198	
22	0.0330	0.665	2.28	2.90	1.74×10^{-5}	2	3.83×10^{-5}	0.0215	
34	0.0311	0.311	2.61	2.89	7.50×10^{-5}	2	4.50×10^{-5}	0.0167	
36	0.0211	0.0311	2.97	2.96	2.03×10^{-3}	3a	4.38×10^{-5}	0.0222	
40	0.0246	0.248	1.91[c]	2.91	6.00×10^{-5}	2	2.08×10^{-5}	0.0208	
51[b]	0.1157	0.1157	2.88	2.88	4.63×10^{-4}	1a	3.68×10^{-3}	0.0204	25°C
52[b]	0.1000	0.1000	2.90	2.90	4.00×10^{-4}	1	6.25×10^{-3}	0.0377	35°C
53[b]	0.1000	0.0400	2.90	2.90	4.00×10^{-4}	3a	6.67×10^{-4}	0.0076	13°C
39	0.248	0.248	1.11	1.11	1.62×10^{-3}	1a	2.33×10^{-4}	0.00471	
42	0.0247	0.249	1.78	2.00	6.00×10^{-5}	2	8.12×10^{-5}	0.00853	
19	0.545	0.545	2.31	2.31	1.30×10^{-4}	1a	6.40×10^{-4}	0.0104	
37	0.304	0.620	2.94	2.32	2.45×10^{-3}	3b	7.47×10^{-2}	0.0116	
41	0.247	0.498	2.96	2.46	2.70×10^{-3}	3b	1.20×10^{-1}	0.0148	
17	0.382	0.382	2.51	2.51	1.30×10^{-4}	1a	8.67×10^{-4}	0.0116	
18	0.348	0.348	2.56	2.56	1.31×10^{-4}	1a	8.90×10^{-4}	0.0118	
10	0.329	0.329	2.57	2.57	1.60×10^{-3}	1a	3.47×10^{-4}	0.0122	
35	0.308	0.311	2.64	2.67	7.50×10^{-3}	1a	7.45×10^{-4}	0.0124	
5	0.030	0.400	2.84	3.21	5.2×10^{-5}	2	5.83×10^{-5}	0.0175	
24	0.0283	0.313	1.11*	3.27	7.5×10^{-5}	2	7.00×10^{-6}	0.0147	
11	0.0310	0.296	3.15	3.45	1.6×10^{-5}	2	1.60×10^{-5}	0.00115	
43	0.025	0.249	3.75	4.00	1.2×10^{-4}	2	1.21×10^{-4}	0.0022	
44	0.025	0.249	5.75	6.00	1.2×10^{-4}	2	6.00×10^{-7}	3×10^{-6}	

[a]. Assuming 3 combined Cl- per Sn(II).
[b]. Runs at varying temperature, analyzed by spectrophotometric method. [c]. LiCl present

Plots *vs.* time: 1. $1/[Sn(II)]_0$ 2. $[Sn(II)]^{1/2}$ 3a. $\frac{[Sn(II)]^{1/2}}{NH_3OH^+]^{1/2}}$

1a. $1/[Sn(II)] + 7.06 \log_{10}[Sn(II)]$.

3b. $2/(a-b)\sqrt{(b-y)/(a-y)} + 14 \log_{10}(\sqrt{(b-y)} + \sqrt{(a-y)})/\sqrt{(a-b)}$.

All reactions at 25°C unless otherwise indicated.

from 1.0 to 3.0 M. The form of the rate law holds for [Sn(II)] up to 0.5 M with changing k' values caused by changes in the concentration of free chloride ion.

Effect of other ions present in the solution on the rate constant k'. The products, Sn(IV) and NH_4^+ had no effect on the reaction kinetics. Increasing chloride ion concentrations accelerated the reaction if $[Cl^-] < 3.0$ M, and inhibited the reaction for $[Cl^-] > 3.0$ M, as shown by the graph in Fig. 4. The effect could not be studied at constant ion normality since no anion could be found which was inert toward the system.

Effect of temperature. The results of runs carried out at three different temperatures are summarized in Table 2, runs 51—53. These runs were of the type where the term involving k'' was unimportant. Therefore the temperature dependence of k' only has been determined. The results are described by the equation:

$$k' = 1.6 \times 10^7 \, e^{-13600/RT} \qquad (4)$$

The activation energy of 13.6 kcal. may be compared with an activation energy of 23.0 kcal. found for the direct oxidation of Mo(V) by hydroxylamine in 3.0 M hydrochloric acid.[9]

Tests of the rate law.

Let y = the number of transformations in moles per liter
a = initial concentration of hydroxylamine
b = initial concentration of Sn(II).
t = time in seconds following the start of reaction.
$A = k''/(k'[\mathrm{Mo(V)}]^{½}[\mathrm{H^+}]^2)$
$B = A/k''$

From eqn. (3)

$$\mathrm{d}t/\mathrm{d}y = A/(a-y)^{½}(b-y)^{½} + B/(a-y)^{3/2}(b-y)^{½} \qquad (5)$$

Integrating (5)

$$t = Af_1 + Bf_2 \qquad (6)$$

where

$$f_1 = 2\ \ln(\sqrt{a} + \sqrt{b})/(\sqrt{a-y} + \sqrt{b-y})$$

and

$$f_2 = (2/(a-b))(\sqrt{b/a} - \sqrt{(b-y)/(a-y)})$$

When $a = b$

$$f_1 = \ln(a/(a-y))$$
$$f_2 = 1/(a-y) - 1/a$$

The quantities f_1 and f_2 may be evaluated for each experimental point from the measured quantity $(b-y)$, the time t calculated and compared with observed times. Initial discrepancies between calculated and observed times were in general due to the occurrence of either initial surges of reaction or short induction periods. Such discrepancies could be removed by taking one of the early points as representing $t = 0$. Later deviations occurred most frequently when a and b were of comparable magnitude. In such cases small errors due to the difficulty in handling stannous chloride solutions would be magnified. Calculated and observed times for several representative runs of different types are shown in Tables 3 and 4. In all cases where hydroxylamine was in large excess, the correlation is extremely good.

DISCUSSION

Derivation of a reaction mechanism. A plausible mechanism for reaction (I) must not only allow derivation of the empirical rate law (3), but must also explain the observed initial surges and induction periods and be consistent with the known chemistry of Sn(II) and Sn(IV), of hydroxylamine and ammonia, and of the various oxidation states of molybdenum.

The knowledge of species of the various reagents in 3.0 M hydrochloric acid is limited, and this will to some extent limit the discussion.

Table 3. Comparison of calculated and observed times for runs with excess hydroxylamine. Symbols are those used in eqn. 4. All concentrations are in moles per liter.

Run 20. $A = 3\,420$ $B = 1\,110$ $a = 0.665$ $b = 0.0370$ $\sqrt{a} + \sqrt{b} = 1.01$ $2/(a-b) = 3.18$ $\sqrt{b/a} = 0.236$.

$t_{obs.}$ sec.	b-y	$\sqrt{a\text{-}y} + \sqrt{b\text{-}y}$	f_1	$\sqrt{(a\text{-}y)/(b\text{-}y)}$	f_2	$t = Af_1 + Bf_2$ sec.
60	0.0350	1.003	0.0125	0.230	0.0191	64
240	0.0295	0.983	0.0360	0.212	0.0765	208
480	0.0247	0.960	0.1010	0.195	0.131	490
780	0.0180	0.939	0.145	0.167	0.219	739
1 080	0.0117	0.908	0.212	0.135	0.321	1 081
1 440	0.0065	0.879	0.276	0.101	0.429	1 421

Run 21[a]. $A = 1\,190$ $B = 385$ $a = 0.665$ $b = 0.0247$ $\sqrt{a} + \sqrt{b} = 0.972$ $2/(a\text{-}b) = 3.12$ $\sqrt{b/a} = 0.193$.

180	0.0147	0.928	0.092	0.146	0.146	169
300	0.0080	0.895	0.166	0.111	0.256	297
390	0.0046	0.872	0.216	0.0843	0.339	387
480	0.0022	0.850	0.266	0.0592	0.417	478
600	0.0008	0.831	0.313	0.0358	0.490	562

Run 36[b] $A = 390$ $B = 127$ $a = 0.0286$ $b = 0.0198$ $\sqrt{a} + \sqrt{b} = 0.310$ $2/(a\text{-}b) = 227$ $\sqrt{b/a} = 0.832$.

480	0.0177	0.296	0.092	0.817	3.40	470
780	0.0162	0.286	0.160	0.806	5.9	812
1 200	0.0144	0.273	0.260	0.787	10.2	1 400
2 280	0.0121	0.244	0.478	0.744	20.1	2 740
3 480	0.0078	0.217	0.709	0.687	32.9	4 430

[a]. Second or third point used for t_0 to eliminate induction period.
[b]. Run most subject to large deviations late in run due to small initial errors.

Mo(VI) is either H_2MoO_4 or $HMoO_3Cl$. It is probably completely depolymerized.

Mo(V) is a dimer of unknown structure [10].

Mo(IV) is unstable.

Mo(III) has an unknown structure derived from the hydrolysis of $MoCl_6^{3-}$.

NH_2OH is basic enough to be completely protonated to NH_3OH^+.

Sn(II) is a mixture of $SnCl_n^{2-n}$. Average $n = 3.0$ [7,8].

Sn(IV) is some species resulting from hydrolysis of $SnCl_6^{2-}$. For convenience, we assume $SnOCl_3^-$ as a product of oxidation of $SnCl_3^-$.

The following reactions have been observed among the various species above.

$$Sn(II) + Mo(IV) = Sn(IV) + Mo(IV) \quad \text{(II) Ref.[11]}$$
$$2\,Mo(IV) = Mo(V) + Mo(III) \quad \text{(III) Ref.[11]}$$
$$2\,Mo(VI) + Mo(III) = 3\,Mo(V) \quad \text{(IV)}$$
$$2\,Mo(VI) + Sn(II) = (Mo(V))_2 + Sn(IV) \quad \text{(V)}$$

Table 4. Comparison of calculated and observed times for runs with $a = b$.

Run 38 $A = 488$ $B = 159$ $a = 0.100 = b$

t_{obs} sec.	$a-y$	$\ln(a/(a-y))$	Af_1	$1/(a-y)$	Bf_2	t_{calc} seconds	Δt_{obs}	Δt_{calc}.
180	0.0954	0.046	22.5	10.5	80	103	180	103
375	0.0875	0.133	65	11.4	226	291	195	189
900	0.0735	0.308	150	13.6	575	725	525	434
1 620	0.0604	0.506	270	16.5	1 045	1 315	720	590
2 400	0.0479	0.735	358	20.9	1 730	2 088	820	773
3 600	0.0385	0.950	465	26.0	2 540	3 000	1 200	912
8 160	0.0195	1.630	795	51.4	6 570	7 365	4 560	4 365
14 340	0.0111	2.210	1 075	90.0	12 720	13 800	6 200	6 435

There is definitely an induction period of slow reaction initially. All but the last point give a better fit with the individual k' recorded for this run in Table 2, increasing t_{calc} by about 10 %.

Run 51 $A = 860$ $B = 280$ $a = b = 0.1157$.

708	0.0901	0.248	214	11.1	680	894	708	894
2 658	0.0557	0.650	560	16.67	2 240	2 780	1 950	1 886
3 798	0.0484	0.780	672	12.0	3 360	4 032	1 140	1 252
4 728	0.0436	0.975	840	15.0	4 200	5 040	930	1 008
6 120	0.0366	1.150	990	18.6	5 200	6 190	1 392	1 150

This run started with Mo(V), indicating a gross error in measurement of the first point. The last four points fit the rate law.

Reaction (V) is the overall process observed in 3.0 M HCl, but reactions (II), (III), and (IV) are thought to be intermediates.[11]

$$(Mo(V))_2 + NH_3OH^+ + 2\,H^+ = 2\,Mo(VI) + NH_4^+ + H_2O \qquad (VI)$$

The rate of (VI) is independent of [Mo(VI)] and of $[NH_4^+]$.[9] In addition, Mo(VI) reacts extremely slowly with hydroxylamine forming yellow complexes of unknown composition. Hydroxylamine shifts the absorption band for Mo(V) in the same manner as additional hydrochloric acid, suggesting intermediate complex formation between NH_2OH and $(Mo(V))_2$[9].

Mo(IV) catalyzes the reduction of perchlorate [2].

Assumptions.

Mo(IV) is the catalytically active state of molybdenum.

The slow step involves breaking of the N—O bond since hydroxylamine is kinetically inert towards most reducing agents.

Half powers in the rate low may be derived from (*a*) the existence of an equilibrium

$$(Mo(V))_2 = Mo(VI) + Mo(IV) \qquad (VII)$$

or (*b*) the possibility that Mo(IV) disappears mainly through disproportionation. Of these the second possibility is most difficult to find fault with. It is hard to visualize how equilibrium (VII) can be the source of Mo(IV) in view of

the tendency of the reaction under discussion and other reactions to exhibit induction periods when initiated by Mo(V). In addition Mo(VI) plays no part in the kinetics of reaction (VI). We therefore conclude that (VII) plays no part in the steady state kinetics, though it may serve as an initial source of Mo(IV) during the so-called induction period.

Assuming that Mo(IV) disproportionates, the half powers in each reactant suggest a concerted process leading to the formation of Mo(IV). It is assumed that hydroxylamine oxidizes Mo(IV) to Mo(VI), which is rapidly reduced back to Mo(IV) by Sn(II). The oxidation of Mo(IV) by hydroxylamine is very slow compared with the disproportionation of Mo(IV). These assumptions have led to the following reaction scheme.

		Assumptions
$(Mo(V))_2 + NH_3OH^+ \rightleftharpoons X_1$	(± 1)	$k_{-1} \gg k_2$
$Sn(II) + X_1 \rightarrow 2\,Mo(IV) + NH_3OH^+ + Sn(IV)$	(2)	
$Mo(IV) + NH_3OH^+ \rightleftharpoons X_2$	(± 3)	$k_{-3} \gg k_4$
$2\,H^+ + X_2 \rightarrow NH_4^+ + Mo(VI) + H_2O$	(4)	Slow step
$Mo(VI) + Sn(II) \rightarrow Sn(IV) + Mo(IV)$	(5)	$k_5 \gg k_4$
$2\,Mo(IV)^* \rightarrow Mo(V) + Mo(III)$	(6)	$k_6 \gg k_4$
$Sn(IV) + Mo(V) \rightarrow Mo(V) + Sn(II)$	(7)	fast
$2\,Mo(V) \rightarrow (Mo(V))_2$	(8)	fast

Net reaction

$$Sn(II) + NH_3OH^+ + 2H^+ \rightarrow Sn(IV) + NH_4^+ + H_2O$$

Only valence states are indicated where formulas are not known or where mixtures exist as with $SnCl_2^{2-n}$ complexes. Hydrogen ion is introduced in reaction (4) and in the net reaction only to preserve the notation and balance atoms. The participation of hydrogen and chloride ions may not be rigorously included until the structures of the various species involved are better known.

Derivation of the empirical rate law from the reaction scheme.

K's are equilibrium constants.

k's are rate constants.

$$\text{Rate} = K_3k_4[NH_3OH^+][Mo(IV)][H^+]^2$$

If a steady state exists for all forms of Mo(IV), and reaction (5) does not effectively decrease the concentration of Mo(IV),

$$d([Mo(IV)^*]/dt = 0 = K_1k_2[Sn(II)][NH_3OH^+][(Mo(V))_2] - k_6[Mo(IV)^*]^2$$

$$[Mo(IV)^*] = (K_1k_2)^{1/2}[Sn(II)]^{1/2}[NH_3OH]^{1/2}[(Mo(V))_2]^{1/2}$$

$$[Mo(IV)^*] = [Mo(IV)] + [X]$$

$$[Mo(IV)] = [Mo(IV)^*]/(1 + K_3([NH_3OH^{1/2}])$$

$$\text{Rate} = \frac{k'[NH_3OH^+]^{3/4}[Sn(II)]^{1/2}[(Mo(V))_2][H^+]^2}{1 + k''[NH_3OH^+]}$$

as given by eqn. (3).

Discussion of the reaction scheme. Evidence for reaction (± 1) has been observed [9]. Reaction 2 is postulated to fit the kinetics. If reaction (± 1) were to give Mo(VI) followed by reduction of the latter by Sn(II), the term $[Sn(II)]^{1/2}$

* Indicates all species containing Mo(IV)

drops out of the rate expression. Equilibrium (± 3) is postulated in order to obtain the denominator term in the final rate expression. Reaction (5) is known to be very fast compared with *the* net catalytic reaction. Reaction (6) is postulated on the assumption that all Mo(IV) disproportionation reactions have comparable rate constants. Oxidation of Mo(III) might be accomplished by hydroxylamine or by hydrogen ion. However, reaction (7) is most consistent with the stoichiometric studies involving Mo(VI) and Sn(II) described in the Ph.D. thesis of A. Bergh [11], as is the assumption that it is fast. Reaction 8 is known to be very fast [10].

Virtual equilibrium is assumed in reactions (± 1) and (± 3) because of the general lability of H—O bonds and Mo—O bonds as compared with the N—O bond in hydroxylamine. The dimer of Mo(V) is also rather inert toward reduction.

In reactions initiated by Mo(VI) reaction (5) serves as a source of Mo(IV) leading to the initial surge observed. In the steady state reaction (5) merely restores Mo(IV) consumed by reaction (4). Apparently some time is needed to build [Mo(IV)] up to its steady state level when $(Mo(V))_2$ is the initiator.

The concentration of hydrogen ion has been introduced into the reaction scheme in a purely arbitrary manner. It may be involved in any or all of the steps to give the net effect observed. The effect of chloride ion on the rate is extremely interesting. The peak in value of k' occurs at the same hydrochloric acid concentration as the minimum solubility [8] of $(CH_3)_4NSnCl_3$. This means that the concentration of $SnCl_3^-$ is at a maximum at exactly the same concentration that the rate is a maximum, suggesting that $SnCl_3^-$ is by far the most reactive of the $SnCl_n^{2-n}$ species present as found by Duke and Peterson [12]. It is interesting also that an assumption that k'' is constant in varying concentrations of chloride does not lead to departures from linearity for plots of the integrated form of equation 3 *vs.* time (Fig. 5). This adds weight to the suggestion that the whole of the chloride effect is due to varying relative concentration of $SnCl_3^-$ *vs.* other Sn(II) species. In any case it appears that the effect of changing chloride ion concentration on the disproportionation of Mo(IV) is negligble.

Comparison of the kinetics and mechanism with that observed for the reduction of perchlorate.[2] Both the kinetics and proposed mechanisms are understandably similar in the two cases. Two differences stand out and require explanation, however. The first is the decrease in the length of the induction period when $(Mo(V))_2$ initiates the reaction, and the second is the decrease in order of Sn(II) by one in the case of hydroxylamine reduction. The decrease in induction period is probably related to the greater reactivity of hydroxylamine over perchlorate both as an oxidant and as a ligand in the formation of complex ions. Actually, if disproportionation rate constants are about the same for all species, K_3 is less than half for hydroxylamine than it is for perchlorate suggesting that the qualitative argument above is not entirely valid. The oxidation of Mo(V) by hydroxylamine is faster than that by perchlorate. The change in order for Sn(II) comes about through the failure of Sn(II) to participate in the rate determining step in the present case. If the hydroxylammonium ion is coordinated to Mo(IV) through its oxygen atom, it is effectively protected from attack by Sn(II). No such protection exists for Cl—O bonds in perchlorate

coordinated to Mo(IV). Thus $H_3N-O-Mo$ (IV) must undergo internal oxygen transfer to reduce the hydroxylamine, while $O_3Cl-O-Mo(IV)$ has three oxygen atoms attached to chlorine which are vulnerable to attack by Sn(II). Further evidence that species X_2 does not undergo reduction by external reducing agents is the failure by the authors to find a catalytic polarographic reduction for hydroxylamine similar to those observed for perchlorate and nitrate.

The kinetics of a very complicated reaction and a possible mechanism for the reaction have been described. This reaction is of interest as a possible step in the conversion of nitrate to ammonia and for the way it fits an emerging pattern for reactions involving oxygen-transfer catalyzed by molybdenum. The tendency for molybdenum to undergo one step divalent changes is seen once again as in the reduction of perchlorate. The acceleration of reactions of Sn(II) by chloride ion [12-14] has again been vividly demonstrated. The rather specific conditions of 3.0 M chloride found for maximum catalytic effect suggest that this medium might be suitable for reduction of nitrate to ammonia. Such has been found to be the case and this reaction is discussed in a following paper.

The reaction studied is quantitative as is the uncatalyzed reduction of hydroxylamine by stannous chloride at elevated temperatures [15,16]. However, application to analysis for hydroxylamine would have to be in the absence of reducible oxy-anions such as nitrate and perchlorate which are also catalytically reduced by Sn(II) in the presence of molybdate.

The authors are indebted to the Wagner Free Institute of Science in Philadelphia, and to the Climax Molybdenum Company for financial support. Mr. Philip Littleford did the chemical analyses for runs 51–53. We especially thank Prof. J. A. Christiansen and Dr. Hakon Nord for helpful discussions.

REFERENCES

1. Haight, Jr., G. P. *Anal. Chem.* **23** (1951) 1505.
2. Haight, Jr., G. P. and Sager, W. F. *J. Am. Chem. Soc.* **74** (1952) 6056.
3. Haight, Jr., G. P. *Anal. Chem.* **25** (1953) 642.
4. Johnson, M. G. and Robinson, R. J. *Anal. Chem.* **24** (1952) 366.
5. Nicholas, J. D. and Nason, A. *J. Biol. Chem.* **207** (1954) 353; *J. Bacteriol.* **67** (1954) 58; *Plant Physiol.* **30** (1955) 135. *J. Biol. Chem.* **211** 183; Nicholas, J. D., Nason, A. and McElroy, W. D. *J. Biol. Chem.* **207** (1954) 341.
6. Yost, D. M. and Russell, Jr., H. *Systematic Inorganic Chemistry*. Prentice Hall, New York 1944, p. 92.
7. Vanderzee, C. E. and Rhodes, D. E. *J. Am. Chem. Soc.* **24** (1952) 3552.
8. Haight, Jr., G. P. and Evans, W. *Acta Chem. Scand. In press.*
9. Haight, Jr., G. P. and Carroll, A. *J. Phys. Chem.* **65** (1961) 1921.
10. Sacconi, L. and Cini, R. *J. Am. Chem. Soc.* **76** (1954) 4239.
11. Bergh, A. *Ph. D. Thesis*, University of Pennsylvania (1959).
12. Duke, F. R. and Peterson, N. C. *J. Phys. Chem.* **63** (1959) 2077.
13. Gorin, M. H. *J. Am. Chem. Soc.* **58** (1936) 1787.
14. Duke, F. R. and Pinkerton, R. C. *J. A. Chem. Soc.* **73** (1951) 3045.
15. Dumreicher, V. *Monatsh.* **1** (1880) 724.
16. Milligan, L. H. and Gillette, G. R. *J. Phys. Chem.* **28** (1924) 747.

Received June 10, 1961.

ACTA CHEMICA SCANDINAVICA 15 (1961) 2037–2042

An Example of the Influence of Intraparticle Diffusion on the Kinetics of Consecutive Heterogeneous Catalytic Reactions

KNUD ØSTERGAARD

Laboratoriet for almen teknisk Kemi, Danmarks tekniske Højskole, Copenhagen, Denmark

In mathematical language is described how diffusion in the pore structure of a solid catalyst can influence the over-all kinetics of a series of consecutive first order reactions. Expressions are derived in which the maximum conversion to the first intermediate product is related to the resistance to intraparticle diffusion. The maximum conversion, *i.e.* the selectivity of the process, decreases with increasing diffusion resistance and approaches a lower limit, whereas the time of reaction required to reach the maximum conversion increases steadily.

The pioneer workers in the field of diffusion and heterogeneous catalysis, Thiele [1], Wagner [2], Wicke and Brötz [3], Smith and Amundson [4], and others, have been concerned mainly with the influence of intraparticle diffusion on the rate of simple reactions such as

$$M_1 \rightarrow M_2 \text{ or } M_1 \rightleftharpoons M_2$$

For more complex reaction schemes the mathematical development rapidly becomes quite involved and such reactions apparently have not been treated in greater detail.

Wheeler [5,6] studied several cases of simultaneous reactions and concluded that diffusion in the pore structure can markedly influence catalyst selectivity. He thus examined a case of two consecutive first order reactions

$$M_1 \rightarrow M_2 \rightarrow M_3$$

catalyzed at the wall of a cylindrical pore and found that the maximum conversion to the unstable intermediate decreases with increasing resistance to axial diffusion of reactant.

The subject of the present paper is the first order reaction sequence

$$M_1 \rightarrow M_2 \rightarrow \cdots M_n \rightarrow \cdots$$

The purpose is to evaluate concentrations as functions of residence time in a fixed bed flow reactor and quantitatively to determine the influence of the diffusion process in the porous catalyst pellets.

The catalytic reactor is operated under isothermal conditions. Flow rates are assumed constant throughout the reactor and longitudinal mixing and diffusion is neglected. Only the steady state will be considered.

The catalyst is used in the form of spherical, homogeneous pellets. It is assumed that the reactions are not accompanied by volume changes, that diffusion coefficients remain constant, that the individual catalyst pellet is surrounded by a reaction mixture of constant composition, that pressure drop across the catalyst pellet can be disregarded, and that there is no resistance to mass transfer at the pellet surface.

The concentration distributions inside the catalyst must be determined before the rate equations can be derived.

NOTATION

$C_1', C_2', \cdots$	concentrations in catalyst pore
$C_1, C_2, \cdots$	concentrations at pellet surface
$C_{1,0}$	concentration of M_1 at reactor entrance
$C_{2,\,max}$	maximum concentration of M_2
$D_1, D_2, \cdots$	coefficients of diffusion in catalyst pellet
$E_1, \cdots$	dimensionless factors as defined by eqn. (6)
$k_1', k_2', \cdots$	reaction rate constants per unit volume of catalyst pellet
$k_1, k_2, \cdots$	reaction rate constants per unit volume of catalyst bed
$m_1, m_2, \cdots$	Thiele moduli as defined by eqn. (3)
R_p	radius of catalyst pellet
S	selectivity ratio
t	residence time in flow reactor
x	distance from center of catalyst pellet
ϱ_p, ϱ_b	density of catalyst pellet and of catalyst bed
τ	dimensionless residence time

CONCENTRATION DISTRIBUTIONS

The components of the reaction mixture are subjected to a diffusion process into the catalyst and to a chemical reaction at the intrinsic catalytic surface. The material balance in a spherical element of catalyst volume of radii x and $x + dx$ comprises the following equations:

$$D_1 \, (d^2C_1'/dx^2 + (2/x) \, dC_1'/dx) = k_1'C_1' \tag{1.1}$$

$$D_2 \, (d^2C_2'/dx^2 + (2/x) \, dC_2'/dx) = k_2'C_2' - k_1'C_1' \tag{1.2}$$

$$\cdot \quad \cdot \quad \cdot$$

$$D_n \, (d^2C_n'/dx^2 + (2/x) \, dC_n'/dx) = k_n'C_n' - k_{n-1}C_{n-1} \tag{1.n}$$

$$\cdot \quad \cdot \quad \cdot$$

The first of these equations was solved by Thiele [1]. The others can be solved by the method of variation of parameters. In determination of the arbitrary constants use is made of the initial conditions:

$$C_1' = C_1;\ C_2' = C_2;\ \cdots\ C_n' = C_n;\ \cdots$$

when

$$x = R_p$$

and of the physically obvious condition that concentrations must remain finite at the center of the pellet.

The solutions to eqns. (1) are:

$$C_1' = \frac{R_p}{x}\, C_1\, \frac{\sinh(xm_1/R_p)}{\sinh\ m_1} \tag{2.1}$$

$$C_2' = \frac{R_p}{x}\left(C_2\,\frac{\sinh(xm_2/R_p)}{\sinh\ m_2} + C_1\,\frac{k_1'}{k_2'}\left(\frac{m_2^2}{m_2^2-m_1^2}\,\frac{\sinh(xm_1/R)_p}{\sinh\ m_1} + \frac{m_2^2}{m_1^2-m_2^2}\,\frac{\sinh(xm_2/R_p)}{\sinh\ m_2}\right)\right) \tag{2.2}$$

$$C_n' = \frac{R_p}{x}\left(C_n\,\frac{\sinh(xm_n/R_p)}{\sinh\ m_n} + C_{n-1}\,\frac{k_{n-1}'}{k_n'}\left(\frac{m_n^2}{m_n^2-m_{n-1}^2}\,\frac{\sinh(xm_{n-1}/R_p)}{\sinh\ m_{n-1}} + \frac{m_n^2}{m_{n-1}^2-m_n^2}\,\frac{\sinh(xm_n/R_p)}{\sinh\ m_n}\right) + \cdots\right.$$

$$\left. + C_1\,\frac{k_1'}{k_n'}\left(\frac{m_2^2m_3^2\cdots m_n^2}{(m_2^2-m_1^2)\cdots(m_n^2-m_1^2)}\,\frac{\sinh\ (xm_1/R_p)}{\sinh\ m_1} + \cdots\,\frac{m_2^2m_3^2\cdots m_n^2}{(m_1^2-m_2^2)\cdots(m_{n-1}^2-m_n^2)}\,\frac{\sinh\ (xm_n/R_p)}{\sinh\ m_n}\right)\right) \tag{2.n}$$

$m_1, m_2, \cdots m_n$ are the dimensionless Thiele moduli:

$$m_i = R_p\sqrt{k_i'/D_i} \tag{3}$$

REACTION RATES

The differential rate of formation of M_n is calculated as the rate of diffusion out of a catalyst pellet multiplied by the number of pellets in unit volume of catalyst bed:

$$\mathrm{d}C_n/\mathrm{d}t = -(3D_n\varrho_b/R_p\varrho_p)(\mathrm{d}C_n'/\mathrm{d}x)_{x=Rp} \tag{4}$$

$\mathrm{d}C_n'/\mathrm{d}x$ is derived from eqns. (2) and inserted into (4).

The result is the following system of equations:

$$\mathrm{d}C_1/\mathrm{d}t = -k_1E_1C_1 \tag{5.1}$$

$$\mathrm{d}C_2/\mathrm{d}t = -k_2E_2C_2 + k_1E_{1,2}C_1 \tag{5.2}$$

. . .

$$dC_n/dt = -k_n E_n C_n + k_{n-1} E_{n-1,n} C_{n-1} + \cdots k_1 E_{1,2\ldots n} C_1 \qquad (5.n)$$

. . .

where

$$E_i = (3/m_i^2)(m_i \coth m_i - 1) \qquad (6)$$

$$E_{i,i+1,\ldots n} = -m_{i+1}^2 m_{i+2}^2 \cdots m_{n-1}^2 \left(\frac{m_i^2 E_i}{(m_{i+1}^2 - m_i^2)\cdots(m_n^2 - m_i^2)} + \cdots + \frac{m_n^2 E_n}{(m_i^2 - m_n^2)\cdots(m_{n-1}^2 - m_n^2)} \right)$$

and

$$k_i = k_i' \varrho_b / \varrho_p$$

By solution of eqns. (5) by a standard method for linear first order differential equations concentrations become expressed as functions of residence time in the reactor. The initial conditions (the concentrations at the reactor entrance) are:

$$C_1 = C_{1,0};\ C_2 = C_3 = \ldots . C_n = 0$$

when

$$t = 0$$

For the first three equations (5) are obtained the solutions:

$$C_1 = C_{1,0} \exp(-k_1 E_1 t) \qquad (7.1)$$

$$C_2 = C_{1,0} k_1 E_{1,2} \left(\frac{\exp(-k_1 E_1 t)}{(k_2 E_2 - k_1 E_1)} + \frac{\exp(-k_2 E_2 t)}{(k_1 E_1 - k_2 E_2)} \right) \qquad (7.2)$$

$$C_3 = C_{1,0} k_1 E_{1,2} k_2 E_{2,3} \left(\frac{\exp(-k_1 E_1 t)}{(k_2 E_2 - k_1 E_1)(k_3 E_3 - k_1 E_1)} + \frac{\exp(-k_2 E_2 t)}{(k_1 E_1 - k_2 E_2)(k_3 E_3 - k_2 E_2)} + \frac{\exp(-k_3 E_3 t)}{(k_1 E_1 - k_3 E_3)(k_2 E_2 - k_3 E_3)} \right) + C_{1,0} k_1 E_{1,2,3} \left(\frac{\exp(-k_1 E_1 t)}{(k_3 E_3 - k_1 E_1)} + \frac{\exp(-k_3 E_3 t)}{(k_1 E_1 - k_3 E_3)} \right) \qquad (7.3)$$

It is assumed that all the Thiele moduli and all the reaction rate constants are of different magnitude. If this is not the case the expressions can still be derived in the way described, the results becoming somewhat different. An example is presented below.

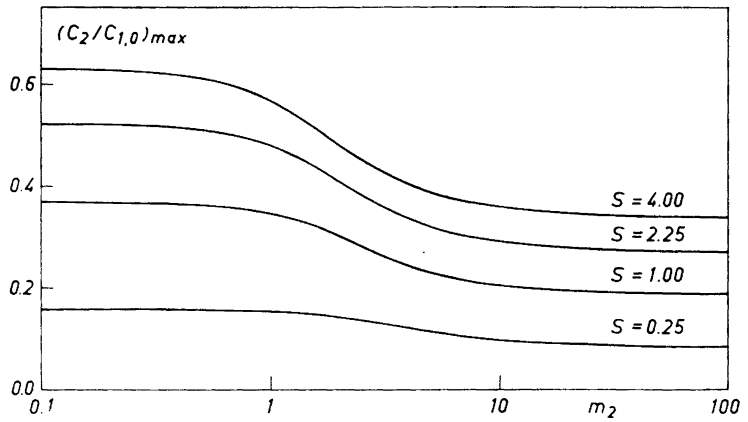

Fig. 1.

SELECTIVITY

As residence time is increased the concentration of any intermediate product in a series of consecutive reactions passes through a maximum. It is of technical importance to determine the magnitude of this maximum concentration as well as of the residence time required to reach the maximum. It is also of interest to examine how these factors are influenced by intraparticle diffusion.

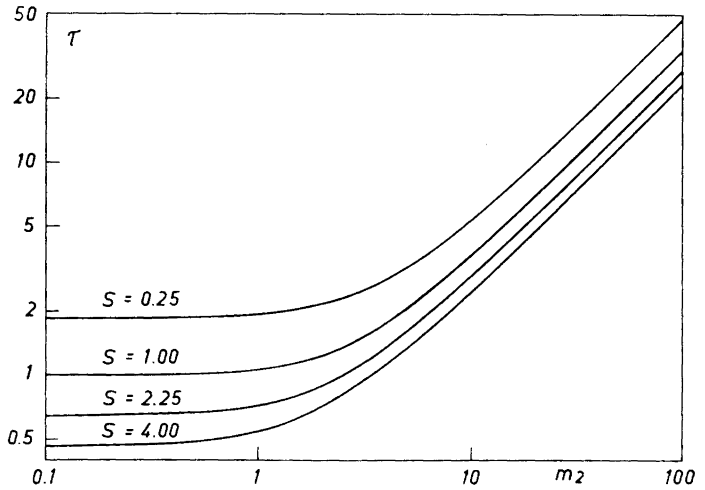

Fig. 2.

This can be done analytically only for the first intermediate product, M_2. The condition:

$$d(C_2/C_{1,0})/dt = 0$$

is fulfilled when

$$\tau = k_2 t = \ln(SE_1/E_2)/(SE_1 - E_2) \quad (8)$$

τ being a dimensionless time of reaction and

$$S = k_1/k_2$$

Insertion of (8) into (7.2) yields the following expression for the maximum fraction of initial reactant which can be converted to the first intermediate product:

$$(C_2/C_{1,0})_{max} = (E_{1,2}/E_1)(SE_1/E_2)^{-1/((SE_1/E_2)-1)} \quad (9)$$

If $S = 1$ and $m_1 = m_2$ (*i.e.* $D_1 = D_2$) eqns. (8) and (9) are transformed into

$$\tau = 1/E_2 \quad (8a)$$

$$(C_2/C_{1,0})_{max} = (E'_{1,2}/E_1)\ \exp(-1) \quad (9a)$$

where

$$E'_{1,2} = \tfrac{3}{2}\ (1 + (\coth m_2)/m_2 - \coth^2 m_2)$$

The relationships expressed in eqns. (8), (8a), (9), and (9a) are shown graphically in Figs. 1 and 2. It has been assumed that $D_1 = D_2$ and, consequently, $m_1 = \sqrt{S} m_2$. $(C_2/C_{1,0})_{max}$ decreases from an upper limit, $S^{-1/(S-1)}$ when diffusion has no rate determining influence, to a lower limit, $(\sqrt{S}/(\sqrt{S}+1))(\sqrt{S})^{-1/(\sqrt{S}-1)}$. The residence time required to reach the maximum conversion increases steadily with increasing diffusion resistance.

CONCLUSION

The influence of intraparticle diffusion upon the reaction kinetics of a series of n consecutive first order reactions catalyzed by spherical catalyst pellets can be evaluated analytically, reaction conditions being idealized to some extent.

The selectivity of the first reaction step, defined as the maximum conversion to M_2, depends only upon the dimensionless factors S, m_1 and m_2. For fixed values of S and increasing values of m the selectivity decreases towards a lower limit. This relationship is illustrated in Fig. 1.

REFERENCES

1. Thiele, E. W. *Ind. Eng. Chem.* **31** (1939) 916.
2. Wagner, C. *Z. physik. Chem.* **A 193** (1944) 1.
3. Wicke, E. and Brötz, W. *Chem. Ing. Tech.* **21** (1949) 219.
4. Smith, N. L. and Amundseon, N. R. *Ind. Eng. Chem.* **43** (1951) 2156.
5. Wheeler, A. *Advances in Catalysis* **3** (1951) 249.
6. Wheeler, A. In Emmett, P. H. *Catalysis* **2** (1955) 105.

Received June 20, 1961.

ACTA CHEMICA SCANDINAVICA 15 (1961) 2043–2046

N-Alkyl-3-piperidyl Phenothiazine-10-carboxylates

RICHARD DAHLBOM and BO BJÖRKQVIST

Department of Chemistry, Royal Institute of Pharmacy, Stockholm, and Research Laboratories, AB Astra, Södertälje, Sweden

A number of N-alkyl-3-piperidyl esters of some phenothiazine-10-carboxylic acids have been synthesised.

N-Alkyl-3-piperidyl esters have recently aroused great pharmacological interest. For example N-ethyl-3-piperidyl diphenylacetate and N-ethyl-3-piperidyl benzilate methobromide have found clinical use as spasmolytic agents [1,2] and N-alkyl-3-piperidyl esters of benzilic acid and phenyl*cyclo*alkylglycolic acids have been reported to exert strange hallucinogenic effects [3,4].

In an earlier paper from these laboratories the synthesis of a number of β-dialkylaminoalkyl phenothiazine-10-carboxylates with pronounced antispasmodic and nicotinolytic properties was described [5], one of which, β-diethylaminoethyl phenothiazine-10-carboxylate (Transergan®) has found use as an antispasmodic [6] and antiparkinsonism [7] drug.

The present paper deals with the synthesis of a series of N-alkyl-3-piperidyl phenothiazine-10-carboxylates of the general formula shown below.

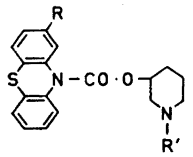

R = H, CH_3, C_2H_5, CH_3O, Cl, CH_3CO

R' = CH_3, C_2H_5

The preparation of these esters seemed worth while, not only because of their potential spasmolytic properties, but also owing to the combination in one molecule of two structural elements of psychopharmacological interest, *viz.* an N-alkyl-3-piperidyl and a phenothiazine residue, which in most cases is substituted in the important 2-position.

The new compounds were readily obtained by the reaction of a phenothiazine-10-carbonyl chloride with N-methyl-, and N-ethyl-3-hydroxypiperidine in the presence of triethylamine.

The 2-substituted phenothiazine-10-carbonyl chlorides used as starting materials were prepared from the appropriate 2-substituted phenothiazine and phosgene with the exception of 2-acetylphenothiazine-10-carbonyl chloride, which was obtained from phenothiazine-10-carbonyl chloride and acetyl chloride by the Friedel—Crafts reaction.

That the acetyl group had entered the 2-position in the phenothiazine nucleus was proved by the treatment of the reaction product with alcoholic potassium hydroxide which yielded 2-acetylphenothiazine.

Results from the pharmacological tests will be published elsewhere.

EXPERIMENTAL

2-Methyl-, 2-ethyl-, 2-methoxy- and 2-chlorophenothiazine were obtained from Société des Usines Chimiques Rhône-Poulenc, France. N-Methyl- and N-ethyl-3-hydroxypiperidine were obtained from Lakeside Laboratories, Inc., U.S.A.

Phenothiazine-10-carbonyl chlorides

2-Methylphenothiazine-10-carbonyl chloride. 2-Methylphenothiazine (42.4 g, 0.2 mole) was dissolved in toluene (750 ml) and a solution of phosgene in toluene (330 ml containing 10 % v/v) was added. The mixture was heated at 90° under efficient reflux for 4 h. After cooling, ethanol (50 ml) was added to destroy excess of phosgene. The solvent was evaporated *in vacuo* and the residue, a dark oil which soon crystallised, was recrystallised from ethyl acetate giving light grey crystals (54 g, 98 %) of m.p. 120—121°. Further recrystallisation from the same solvent raised the m.p. to 122—122.5°. (Found: C 60.5; H 3.66; N 4.95. Calc for $C_{14}H_{10}ClNOS$: C 61.0; H 3.66; N 5.08).

2-Ethylphenothiazine-10-carbonyl chloride was prepared by the same method. As it was impossible to get the product in crystalline form, it was used as starting material for syntheses without further purification.

2-Methoxyphenothiazine-10-carbonyl chloride was obtained in 88 % yield in the same way. This compound has earlier been prepared [8] by heating 2-methoxyphenothiazine and phosgene in a sealed vessel. M.p. 94—95° (from methanol), (lit.[8] 96—97°.)

2-Chlorophenothiazine-10-carbonyl chloride. 2-Chlorophenothiazine reacted with phosgene more sluggishly than the foregoing 2-substituted phenothiazines. The reaction mixture (46.5 g of 2-chlorophenothiazine in 750 ml of toluene and 330 ml of 10 % phosgene in toluene) was heated at 140° in an oil bath for 6 h under effective reflux. A further quantity (130 ml) of phosgene in toluene was then added and the reaction mixture was heated at 140° for further 8 h. The solvent was removed *in vacuo* and the solid residue was extracted with benzene to remove the unreacted 2-chlorophenothiazine which is sparingly soluble in this solvent. After evaporation of the benzene the residue was crystallised from ethyl acetate to give crystals (35.0 g, 59 %) melting at 100—101°. (Found: C 52.9; H 2.36; N 4.70. Calc. for $C_{13}H_7Cl_2NOS$: C 52.7; H 2.38; N 4.73).

2-Acetylphenothiazine-10-carbonyl chloride. To a suspension of phenothiazine-10-carbonyl chloride (131 g, 0.5 mole) in carbon disulphide (800 ml) was added with stirring anhydrous aluminium chloride (200 g, 1.5 mole), and the mixture was heated to reflux to dissolve the phenothiazine compound. After cooling to room temperature acetyl chloride (54.9 g, 0.7 mole) was added in portions and the reaction mixture was heated slowly. At 30° a vigorous reaction started and external heating was stopped. The colour of the mixture changed from pink to green and hydrogen chloride was evolved. The reaction subsided in one hour and the reaction mixture was then refluxed for 3 h. A dark viscous oil was gradually formed at the bottom of the reaction flask. After cooling the bottom layer was separated and poured on *ca.* 1 kg of crushed ice and 25 ml of conc. hydrochloric acid. A greyish precipitate separated which was collected by filtration and dried to give 150 g of product (99 %) melting at 108—110°. Two recrystallisations from ethyl acetate raised the m.p. to 120—122°. This compound has been prepared from 2-

Table 1.

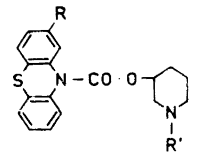

No.	R	R′	Yield [a] %	Derivative	M.p. °C	Recryst. Solvent [b]	Formula	Calc. %			Found %		
								C	H	N	C	H	N
1	H	CH_3	72	Base	88–90	P	$C_{19}H_{20}N_2O_2S$	67.0	5.92	8.23	66.7	5.98	8.17
				HCl	230–232 d.	M–E	$C_{19}H_{20}N_2O_2S \cdot HCl$	60.5	5.62	7.43	60.5	6.06	7.18
			86	CH_3Br	273–274 d.	M	$C_{19}H_{20}N_2O_2S \cdot CH_3Br$	55.2	5.32	6.44	54.8	5.41	6.17
2	H	C_2H_5	55	HCl	222–223 d.	A–E	$C_{20}H_{22}N_2O_2S \cdot HCl$	61.4	5.93	7.17	61.3	6.18	7.20
			67	CH_3Br	232–233 d.	A–E	$C_{20}H_{22}N_2O_2S \cdot CH_3Br$	56.1	5.61	6.24	56.0	5.72	6.20
			71	C_2H_5I	220–221 d.	A–E	$C_{20}H_{22}N_2O_2S \cdot C_2H_5I$	51.8	5.33	5.49	51.9	5.49	5.12
3	CH_3	CH_3	92	HCl	242–244 d.	A–E	$C_{20}H_{22}N_2O_2S \cdot HCl$	61.4	5.93	7.17	61.3	6.11	6.91
4	CH_3	C_2H_5	69	HCl	223–224 d.	A–E	$C_{21}H_{24}N_2O_2S \cdot HCl$	62.3	6.22	6.92	62.3	6.31	6.65
5	C_2H_5	CH_3	80	HCl	240–242 d.	M	$C_{21}H_{24}N_2O_2S \cdot HCl$	62.3	6.22	6.92	61.7	6.31	7.01
6	C_2H_5	C_2H_5	57	HCl	202–203 d.	A–E	$C_{22}H_{26}N_2O_2S \cdot HCl$	63.1	6.50	6.69	62.5	6.80	6.42
7	CH_3O	CH_3	80	HCl	242–244 d.	M–E	$C_{20}H_{22}N_2O_3S \cdot HCl$	59.0	5.70	6.89	59.3	6.23	6.66
8	CH_3O	C_2H_5	66	HCl	230–231 d.	M–E	$C_{21}H_{24}N_2O_3S \cdot HCl$	59.9	5.99	6.66	59.9	6.18	6.59
9	Cl	CH_3	77	HCl	235–237 d.	M–E	$C_{19}H_{19}ClN_2O_2S \cdot HCl$	55.5	4.90	6.81	56.0	5.09	6.57
10	Cl	C_2H_5	64	HCl	220–222 d.	A–E	$C_{20}H_{21}Cl\ N_2O_2S \cdot HCl$	56.5	5.21	6.59	56.7	5.44	6.28
11	CH_3CO	CH_3	80	Base	112–114	A	$C_{21}H_{22}N_2O_3S$	65.9	5.80	7.33	66.2	5.66	7.22
				HCl	236–238 d.	A	$C_{21}H_{22}N_2O_3S \cdot HCl$	60.2	5.53	6.69	60.3	5.68	6.38
12	CH_3CO	C_2H_5	49	HCl	188–189 d.	A–E	$C_{22}H_{24}N_2O_3S \cdot HCl$	61.0	5.82	6.47	61.0	5.70	6.23

[a] Calculated on the recrystallised products.
[b] A, ethanol; E, ether; M, methanol; P, petroleum ether.

acetylphenothiazine and phosgene by Schmitt *et al*[8]., who report the m.p. 116—117°. (Found: C 58.8; H 3.28; N 4.57. Calc. for $C_{15}H_{10}ClNOS$: C 59.3; H 3.32; N 4.61).

Treatment of this compound with potassium hydroxide in ethanol yielded 2-acetylphenothiazine, m.p. 188—189° undepressed on admixture with an authentic specimen.

N-Alkyl-3-piperidyl phenothiazines-10-carboxylates

A solution of the appropriate phenothiazine-10-carbonyl chloride (0.05 mole), N-alkyl-3-hydroxypiperidine (0.05 mole) and triethylamine (0.075 mole) in toluene (50 ml) was heated under reflux. The reflux times were 4 h in syntheses using N-methyl-3-hydroxypiperidine and 8 h with the N-ethyl homologue. After cooling the triethylamine hydrochloride was removed by filtration and the toluene solution was washed thoroughly with water and then extracted with N hydrochloric acid. The slightly soluble hydrochloride of the reaction product usually separated as a semi-crystalline oil. The hydrochloride was separated, dissolved in water and combined with the acid water extract. The extract was made alkaline with sodium carbonate solution. The reaction product usually separated as a viscous oil which in two cases (compounds 1 and 11) crystallised. When it was impossible to obtain the base in crystalline form it was dissolved in ether and converted to the hydrochloride by the addition of ethereal hydrogen chloride. Some of the bases were quaternised with alkyl halides according to the method earlier described for β-dialkylaminoalkyl phenothiazine-10-carboxylates [5].

Physical constants and analytical data are collected in Table 1.

Before analysis the compounds were dried at 50° and 0.05 mm. The elemental analyses were performed by Dr. A. Bernhardt, Mülheim, Germany.

REFERENCES

1. Biel, J. H., Friedman, H. L., Leiser, H. A. and Sprengler, E. P. *J. Am. Chem. Soc.* **74** (1952) 1485.
2. Necheles, H., Jefferson, N. C. and Sporn, J. *Am. J. Gastroenterol.* **26** (1956) 464.
3. Abood, L. A., Ostfeld, A. M. and Biel, J. *Proc. Soc. Exptl. Biol. Med.* **97** (1958) 483.
4. Abood, L. A., Ostfeld, A. M. and Biel, J. *Arch. intern. pharmcodynamie* **125** (1959) 186.
5. Dahlbom, R. *Acta Chem. Scand.* **7** (1953) 879.
6. Johnson, S. R. *Nord. Med.* **53** (1955) 265.
7. Eliasson, S. and Tejning, S. *Acta Med. Scand.***154** (1956) 375.
8. Schmitt, J., Boitard, J., Comoy, P., Hallot, A. and Suquet, M. *Bull. soc. chim. France* **1957** 938.

Received June 19, 1961.

ACTA CHEMICA SCANDINAVICA 15 (1961) 2047–2066

Short Communications

Studies Related to Naturally Occurring Acetylene Compounds XXX. The Synthesis of 5-Methyl-5′(buta-1,3-dienyl)-2,2′-bithienyl

LARS SKATTEBÖL*

Institutt for Organisk Kjemi, Norges Tekniske Högskole, Trondheim, Norway

In the preceding communication of this series Liaaen Jensen and Sörensen [1] described the isolation of a number of polyacetylenes and of a sulphur containing compound from plants of the genus *Bidens*. The latter was obtained as a crystalline compound, m.p. 42°, from *Bidens radiata* and assigned the structure 5-methyl-5′-(buta-1,3-dienyl)-2,2′-bithienyl (III). Because of the very small amount available and the low stability of the compound the structural assignment was based mainly on spectroscopic evidence. Hence, in order to confirm the proposed structure a synthesis of III was undertaken and this was achieved using the following sequence of reactions:

5-Methyl-2,2′-bithienyl (I) was prepared according to Steinkopf, Leitsmann and Hofmann [2] from 2-iodothiophene and 2-iodo-5-methyl-thiophene with copper bronze. A Vilsmeier reaction on (I) using phosphorus oxychloride and N-methyl-formanilide gave the desired aldehyde (II) in a reasonable yield. This compound has recently been prepared by Lescot, Buu-Hoï and Xuong [3] in excellent yield using slightly different conditions. A Wittig reaction of this aldehyde with allyltriphenyl phosphonium bromide yielded III as pale yellow needles, m.p. 46–47°. The compound was extremely unstable and a satisfactory elementary analysis was not obtained. It was, however, characterized as the stable maleic anhydride adduct, m.p. 135°.

The infrared spectrum of III in carbon disulfide solution is shown in Fig. 1. A band at 992 cm^{-1} indicates that the double bond has the *trans* configuration.

At the time this synthesis was completed none of the naturally occurring substance was unfortunately available for a mixed melting point determination.

Experimental. All melting points are uncorrected. The ultraviolet absorption data were obtained using a Beckman, Model DK recording spectrophotometer. A Perkin Elmer Model 21 spectrophotometer was used for the infrared measurements. Elementary analysis was car-

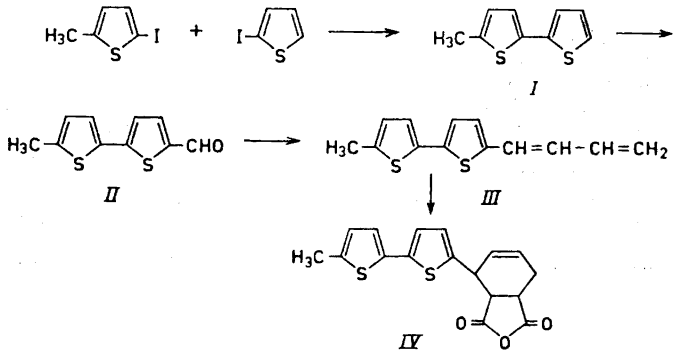

I II III IV

* Present address: European Research Associates, s.a., 95, rue Gatti de Gamond, Brussels 18, Belgium.

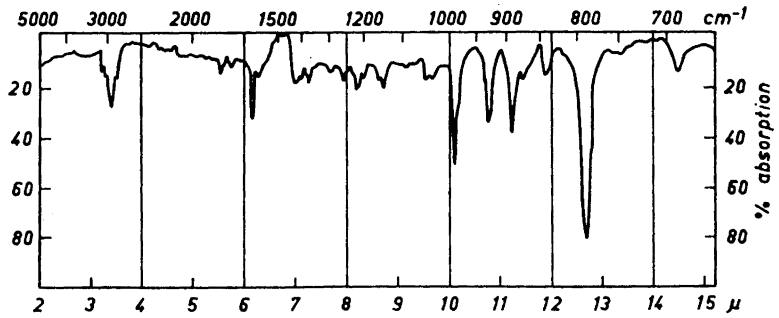

Fig. 1.

ried out by Dr. A. Elek, Los Angeles, Calif., U.S.A.

5-Methyl-2,2'-bithienyl (I) was prepared according to Steinkopf, Leitsmann and Hofmann [2]. I was separated from the reaction mixture by chromatography on alumina.

5-Formyl-5'-methyl-2,2'-bithienyl (II). I (2.2 g), phosphorus oxychloride (2.3 g) and N-methylformanilide (2.1 g) were mixed together and heated until hydrogen chloride was evolved. The mixture was then cooled in ice-water until the vigorous reaction had ceased and was finally heated at 100° for 20 min. The reaction mixture was poured into water and extracted with ether. The extract was washed with sodium bicarbonate and water until neutral and dried over sodium sulphate. Evaporation of the ether gave a crystalline residue which after recrystallization from ethanol gave pale yellow crystals (500 mg), m.p. 98—99° (Lescot, Buu-Hoï and Xuong [3] report m.p. 98°). Ultraviolet absorption (in *n*-hexane):

λ_{max} 3550 Å, ε = 28 000.

5-Methyl-5'(buta-1,3-dienyl)-2,2'-bithienyl (III). Allyltriphenylphosphonium bromide (650 mg) was suspended in 10 ml of dry ether and methyllithium (6.5 ml; 0.23 M in ether) was added. After 2 h at room temperature the aldehyde (II, 30 mg), dissolved in dry ether-tetrahydrofuran (1:1; 5 ml), was added and the mixture shaken mechanically for some minutes. After 24 h at room temperature the mixture was heated under reflux for 15 min and filtered. The filtrate was subsequently washed with 2 N hydrochloric acid and water and dried over sodium sulphate. The solvents were evaporated under vacuum and the crystalline residue chromatographed on alumina (deactivated with ethyl acetate). A crystalline compound was eluted with petroleum ether 20—30 % benzene and recrystallization from hexane gave III as highly unstable, pale yellow crystals, m.p. 46—47° (evacuated tube). Ultra violet absorption (in *n*-hexane): λ_{max}2215, 2568, 2608 and 3650 Å, ε = 17 500, 13 700, 14 000 and 32 000, respectively.

Maleic anhydride adduct (IV). The bithienyl derivative (III, 30 mg) and maleic anhydride (100 mg) were dissolved in 2 ml of dry benzene and heated at 70° in a sealed tube for 4 h. The benzene was evaporated and the unreacted maleic anhydride sublimed in high vacuum (50°, 10^{-4} mm). The residue was recrystallized from acetone-petroleum ether to give slightly yellow needles (15 mg), m.p. 135° (Found: C 61.86; H 4.38. Calc. for $C_{17}H_{14}O_3S_2$; C 61.82; H 4.27). Ultraviolet absorption (in ethanol): λ_{max} 2450 and 3150 Å, ε = 6 800 and 20 000 respectively.

1. Liaaen Jensen, S. and Sörensen, N. A. *Acta Chem. Scand.* **15** (1961) 1885.
2. Steinkopf, W., Leitsmann, R. and Hofmann, K. H. *Ann.* **546** (1941) 180.
3. Lescot jr., E., Buu-Hoï, Ng. Ph. and Xuong, N. D. *J. Chem. Soc.* **1959** 3234.

Received November 7, 1961.

Fluorometric Studies of the Coupling of Reduced Diphosphopyridine Nucleotide to Lactic Dehydrogenase from Rabbit Skeletal Muscle

ANDERS CARLSTRÖM

Medicinska Nobelinstitutet, Biokemiska avdelningen, Stockholm, Sweden

Boyer and Theorell [1] in 1956 reported a shift in the fluorescence spectrum of DPNH * on binding to liver alcohol dehydrogenase. Since that time similar results have been described for many other pyridine nucleotide-requiring dehydrogenases [2-7]. Winer *et al.* have reported a shift in the fluorescence spectrum of DPNH when it is bound to beef heart lactic dehydrogenase [6] as well as to the lactic dehydrogenase from rabbit skeletal muscle [7]. The observations concerning the skeletal muscle enzyme could not be confirmed by other workers [8], but have now been confirmed in this laboratory. We have also found that these enzyme preparations have the peculiar property of totally quenching the fluorescence of the first part of DPNH added, whereas the fluorescence of subsequently added DPNH is increased. The nonfluorescing part of the coenzyme still exists, however, in its reduced form.

The change in the fluorescence spectrum of DPNH is further strengthened upon addition of sodium oxalate to the skeletal muscle LDH-DPNH complex. Similar results have been obtained for beef heart LDH [9].

Experimental Rabbit skeletal muscle LDH was obtained from C. F. Boehringer und Soehne, G.m.b.H. ** The enzyme, which was assayed according to the method of Pfleiderer and Jeckel [10], was recrystallized from ammonium sulfate as described by Beisenhertz *et al.* [11] Protein concentrations were estimated spectrophotometrically at 280 mμ (e_{280} = 1.27 $cm^2 \times mg^{-1}$) [11]. The molecular weight was assumed to be 100 000. Alcohol dehydrogenase from horse liver was a gift from Dr. C. L. Woronick of this institute whereas DPNH and sodium pyruvate were purchased from the Sigma Chemical Co., sodium oxalate, reagent grade, from J. T. Baker Chemical Co., and isobutyramide from Eastman Kodak Co. The titrations were performed at 23.5° in sodium phosphate buffers, pH 7.0, μ = 0.1 (unless otherwise indicated), using a spectrophotofluorometer which previously has been described [12]. The exciting wavelength was 340 mμ and the fluorescence was recorded at 410 mμ. Emission maxima in the fluorescence spectra are uncorrected for variations with wavelength in the intensity of the exciting light and sensitivity of the photocell. The correction would move

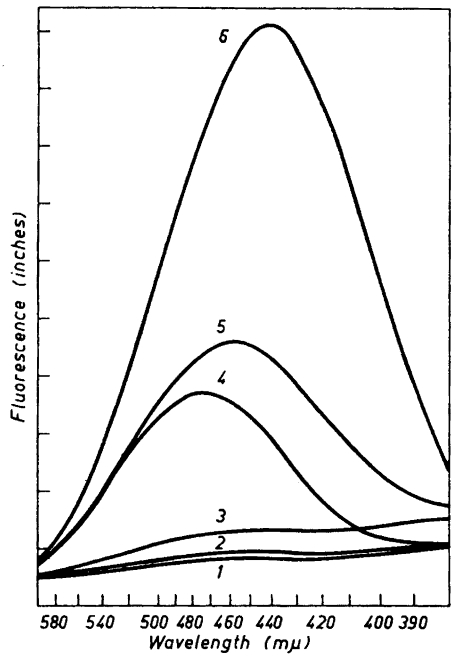

Fig. 1. Fluorescence emission spectra of the DPNH-LDH complex and the DPNH-LDH-oxalate complex. Curve (1): sodium phosphate buffer, μ = 0.1, pH 7.0. Curve (2): 0.01 M sodium oxalate. Curve (3): LDH, 0.107 mg/ml. Curve (4): 1.17 × 10^{-6} M DPNH. Curve (5): LDH, 0.107 mg/ml plus 1.17 × 10^{-6} M DPNH. Curve (6): LDH, 0.107 mg/ml plus 1.17 × 10^{-6} M DPNH plus 0.01 M sodium oxalate. Activating wavelength 340 mμ. Temp. 23.5°. Final volume 2 ml.

* Abbreviations: LDH, lactic dehydrogenase. DPNH, reduced diphosphopyridine nucleotide.

** We would like to thank C. F. Boehringer und Soehne, G.m.b.H. for the very generous gift of lactic dehydrogenase which was used in these studies.

the maxima about 15 mμ towards shorter wavelengths on this apparatus. Electrophoreses and ultracentrifugation were carried out in the Spinco Model H and Model E apparatus, respectively. CM-W cellulose for column chromatography was prepared according to Peterson and Sober [13], the ethanoldrying step, however, being excluded.

Results and discussion. On binding of DPNH to LDH from rabbit skeletal muscle, the emission maximum for DPNH is shifted from 478 mμ to 460 mμ, and the intensity of the emitted light is increased (Fig. 1). In the presence of 0.01 M sodium oxalate this effect is very much increased (*cf.* Fig. 1). The fluorescence maximum is shifted another 20 mμ towards shorter wavelengths and the maximal fluorescence intensity is increased about 3 times. In 1959 Winer and Schwert [7] reported the same results concerning the binary complex, whereas Shifrin and Kaplan [8] were not able to find any changes in the fluorescence spectrum of DPNH on binding to this enzyme. The spectral shift first found by Winer and Schwert, and now confirmed by us, should enable determinations of dissociation constants of LDH-coenzyme complexes [13]. However, upon titration of LDH with concentrations of DPNH which were small compared with the LDH concentration, the first added coenzyme gave smaller increments in the fluorescence intensity than that produced by free DPNH alone (Fig. 2). By decreasing the concentration of DPNH in each addition, it could be seen that the fluorescence is completely quenched for amounts of DPNH corresponding to about 1/10 or less of the total concentration of LDH. Six times recrystallization of the commercial enzyme preparation did not change this ratio, nor did prolonged dialysis against phosphate buffer, pH 7.0, $\mu = 0.1$. There was a possibility that the disappearance of fluorescence could be caused by oxidation of DPNH. Therefore the following experiments were made. The supernatant from heat-inactivated enzyme did not increase the quenching. Adding liver alcohol dehydrogenase and isobutyramide, which from a very tight complex with DPNH [14], to an LDH-DPNH solution, liberated all the added DPNH in its reduced form. This means that the DPNH was not oxidized by any substrate that may have been present as an impurity in the enzyme preparation. Moving-boundary electrophoresis of the enzyme in phosphate buffers, pH 6.0–8.0, $\mu = 0.1$, gives an asymmetric peak which does not separate into definite peaks even after 24 h. The asymmetry corresponds to about 15 % of impurity which is in good agreement with the results of Ankel *et al.* [15] In the ultracentrifuge, the protein appears homogeneous at pH 7.1, $\mu = 0.1$. On chromatography of the enzyme on CM-W cellulose with stepwise elution with phosphate buffers, pH 6.0–6.9, $\mu = 0.05$, the protein exhibits a very pronounced "tailing" with no sharp protein peak in the eluate. In one experiment, some of the enzyme which was eluted at pH 6.8, $\mu = 0.05$, upon titration in the same buffer, showed a considerable increase in the relative proportion of nonfluorescent complex formed with DPNH (nonfluorescent complex: fluorescent complex ~ 1:1).

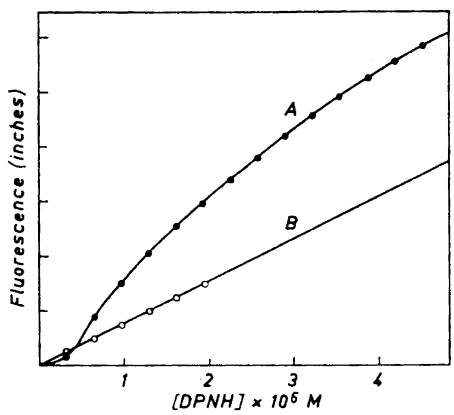

Fig. 2. Titration of LDH with DPNH (A). DPNH blank (B). The concentration of LDH is 0.087 mg/ml.

A small fraction with a typical nucleic acid absorption spectrum was removed on the CM-W cellulose column. This fraction had no influence on the ability of LDH to quench the fluorescence of DPNH. Performing the chromatography a second time, an enzyme fraction was obtained which caused no detectable quenching of DPNH, but already from the beginning gave an increase in fluorescence. This enzyme fraction was obtained by an elution procedure similar to that in the first experiment. The specific activities of these enzyme preparations were about the same as those for the unchromatographed enzyme. The errors in the estimations of the specific activities of the chromatographed

LDH are, however, quite large, because the eluted enzyme is very dilute, and the determinations of protein concentrations therefore inexact. If the enzyme is eluted in a more concentrated form no fractionation is produced. Higher specific activites are then obtained, but the large variations in the quenching of the DPNH fluorescence are not obtained.

These observations could be explained in several ways, a few of which will be mentioned. The LDH preparations used contain a protein impurity, which has a higher affinity for DPNH than has LDH, and it quenches the fluorescence of DPNH on complexing. A second explanation is that a small molecule is bound to the enzyme, which together with enzyme and DPNH forms a non-fluorescent ternary complex. The enzyme could also contain two different binding sites, one binding the coenzyme tightly and quenching its fluorescence, along with another site which binds it more loosely and enhancing its fluorescence. There is also a possibility that the conformation of the LDH is changed upon chromatography, thereby unmasking hidden binding sites. Polymerization or depolymerization could also explain our observations.

The present results might possibly explain the diverging results of different workers on this enzyme.

Work is continued in this laboratory to purify the enzyme and to determine some of its physical-chemical properties.

Acknowledgements. The author wishes to express his thanks to Professor Hugo Theorell for his interest and many helpful discussions during the course of this work, and to Dr. C. L. Woronick for valuable advice and corrections of the English language.

1. Boyer, P. D. and Theorell, H. *Acta Chem. Scand.* **10** (1956) 447.
2. Duysens, L. N. M. and Kronenberg, G. H. M. *Biochim. et Biophys. Acta* **26** (1957) 437.
3. Theorell, H. and Langan, T. A. *Acta Chem. Scand.* **14** (1960) 933.
4. Langan, T. A. *Acta Chem. Scand.* **14** (1960) 936.
5. Winer, A. D. and Schwert, G. W. *Biochim. et Biophys. Acta* **29** (1958) 424.
6. Winer, A. D., Novoa, W. B. and Schwert, G. W. *J. Am. Chem. Soc.* **79** (1957) 6571.
7. Winer, A. D., Schwert, G. W. and Millar, D. B. S. *J. Biol. Chem.* **234** (1959) 1149.
8. Shifrin, S. and Kaplan, N. O. *Advances in Enzymol.* **22** (1960) 337, p. 366.
9. Winer, A. D. and Schwert, G. W. *J. Biol. Chem* **234** (1959) 1155.
10. Pfleiderer, G. and Jeckel, D. *Biochem. Z.* **329** (1957) 370.
11. Beisenhertz, G., Boltze, H. J., Bücher, Th., Czok, R., Garbade, K. H., Meyer-Arend, E. and Pfleiderer, G. *Z. Naturforsch.* **8 B** (1953) 555.
12. Theorell, H. and Winer, A. D. *Arch. Biochem. Biophys.* **83** (1959) 291.
13. Peterson, E. A. and Sober, H. A. *J. Am. Chem. Soc.* **78** (1956) 751.
14. Winer, A. D. and Theorell, H. *Acta Chem. Scand.* **14** (1960) 1729.
15. Ankel, H., Bücher, Th., Czok, R., Schmiedtberger, R. and Schulze, H. Unpublished results, *cf.* Ref [16].
16. Czok, R. and Bücher, Th. *Advances in Protein Chem.* **15** (1960) 315, p. 367.

Received November 16, 1961.

Correction to "Microdetermination of Polyenoic Fatty Acids" *

JENS G. NØRBY

Biokemisk Institut, Århus Universitet, Århus, Denmark

On p. 529, last line (the eqn. for diene fatty acids) the term $-k'_5 \times 0.961$ is incorrect and should read $-k'_5 \times 0.091$.

Received December 7, 1961.

* *Acta Chem. Scand.* **15** (1961) 525.

Determination of the Stability Constant of the Bismuth-DCTA Complex

A. R. SELMER-OLSEN

University of Oslo, Chemical Institute A, Blindern, Norway

1,2-Diaminocyclohexanetetra-acetic acid (DCTA) forms stable complexes with many metal ions. The complexes are in general more stable than the corresponding EDTA complexes.

In the present communication the composition and the stability constant of the complex formed between bismuth(III) and DCTA have been determined polarographically. No information on these data were found in the literature.

A displacement method, previously applied by Schwarzenbach *et al.* [1], was used. The method is based upon the displacement in the complex of one metal ion by another, according to the equilibrium:

$$MR + M' \rightleftharpoons M'R + M$$

$$K = \frac{K_{M'R}}{K_{MR}} = \frac{[M'R] \cdot [M]}{[MR] \cdot [M']}$$

where [] represent molar concentration, R the chelating agent and K the displacement equilibrium constant. K is equal to the ratio of the stability constants.

Pribil *et al.* [2] suggested a polarographic method by which it was possible to determine the concentrations of bismuth- and copper-DCTA complexes in the presence of each other. The stability constant of the copper-DCTA complex was determined by Schwarzenbach [1] to be $10^{21.36}$.

Experimental. Polarograms were recorded with an Atlas Tast-polarograph, Selector D. A conventional type of dropping mercury electrode was used. A saturated calomel electrode (S.C.E.) served as a reference electrode. Oxygen-free nitrogen was bubbled through the solution for 10 min in order to remove dissolved air.

Solutions containing varying amounts of bismuth, DCTA and copper, were prepared. A constant pH of 4.30 and an ionic strength of about 0.1 was maintained by the addition of acetic acid/sodium acetate buffer.

Polarographic measurements were carried out after different times of standing. The concentrations of copper and bismuth complexes were found from the polarograms. All experiments were performed at 20.0 ± 0.2°C.

Results. Amperometric titrations showed that the composition of the bismuth-DCTA complex was 1:1.

The stabilities of the copper- and bismuth-DCTA complexes are of the same order. Because of this, copper will displace some bismuth from the complex. The equilibrium was indicated by constant diffusion currents.

A mean value of the stability constant was found to be: $K_{Bi\text{-}DCTA} = 1.3 \times 10^{24}$.

1. Schwarzenbach, G., Gut, R. and Anderegg, G. *Helv. Chim. Acta* **37** (1954) 937.
2. Pribil, R., Roubal, Z. and Svatek, E. *Collection Czechoslov. Chem. Communs.* **18** (1953) 43.

Received November 13, 1961.

Table 1. Determination of the stability constant of the bismuth-DCTA complex.

Total molar concentrations × 10^4			Molar concentrations found × 10^4				log $K_{Bi\text{-}DCTA}$
DCTA	Bi	Cu	Bi-DCTA	Bi	Cu-DCTA	Cu	
3.6	3.00	3.52	2.86	0.14	0.19	3.33	23.9
2.3	2.00	5.28	1.77	0.23	0.09	5.19	23.9
4.8	4.00	7.04	3.67	0.33	0.27	6.77	23.7
4.7	3.00	7.04	2.76	0.24	0.07	6.97	24.4
4.2	4.00	7.04	3.72	0.28	0.06	6.98	24.5

A Method for Gas-Liquid Multiplicative Distribution on a Preparative Scale

ÖRN WAHLROOS

Laboratory of the Foundation for Chemical Research, Biochemical Institute, Helsinki, Finland

When traces of a volatile compound dissolved in other volatile materials have to be isolated for further identification, the amount of material may be too small, and the number of components too many, to be dealt with conveniently in a column for extractive distillation. On the other hand, a preparative gas chromatographic column having the large effective plate volume needed requires a gas flow rate [1] at which it may be impossible to condense eluted trace components efficiently. In the case of known substances, it is desirable to be able to calculate accurately the plate numbers needed for a separation, and the position of the elution bands. An approach to these problems has been made by constructing a simple apparatus for multiplicative gas-liquid distribution together with a device for the rapid determination of gas-liquid distribution coefficients over a wide concentration range.

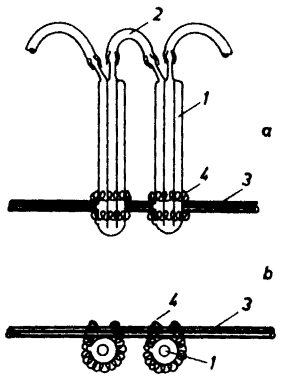

Fig. 1. Section of the distribution apparatus. a. Side view. b. View from above. 1. Glass tube. 2. Teflon tubing. 3. Steel rod. 4. Spring.

Experimental. The countercurrent distribution apparatus differs from an apparatus for extractive distillation [2] in that the liquid phase is efficiently stirred. The apparatus consists of a train of glass tubes (inner Ø = 1.2 cm, length = 11 cm) connected to each other by capillary tubes (Fig. 1). Two kinds of capillaries have been tried: (*a*) steel capillary, inner Ø = 0.4 mm; in this case the tubes must be closed with screw lids to which the capillaries are silver soldered, because of the pressure gradient; (*b*) Teflon tubing, inner Ø = 2 mm. The simple Teflon-to-glass seal (Fig. 1) is well able to withstand the pressure needed to drive the mobile phase through the train. The glass tubes are attached to a steel rod (Ø = 6.6 mm) by means of spiral springs made of 0.6 mm steel thread. The force constant of a spring is about 460 Newton/m. One end of the steel rod is connected to an electromagnetic vibrator (type "Vibromix", 40 W, frequency 100 c/sec), so that the rod oscillates in the longitudinal plane. The vibrator can take a load of 100 tubes weighing about 19 g each. The tubes are attached 5 cm below their centre of gravity. When the liquid content of each tube is between 0 and 5 cm^3, the tubes' own frequency is sufficiently near to that of the vibrator for resonance to occur between the tubes and the vibrating rod. Then efficient mixing of the tube contents is achieved. With prolonged vibration steel capillaries may be broken by fatigue whereas the Teflon tubing withstands the vibration. Either the gas or the liquid may be used as the mobile phase.

For the rapid determination of gas-liquid distribution coefficients, and for the evaluation of the liquid phases for use in the countercurrent distribution apparatus, an exponential dilution method modified from that described by Lovelock [3] for the calibration of gas chromatographic detectors is developed. Carrier gas is passed through a vessel with the gas volume V_g, containing a known volume V_L of the "nonvolatile" liquid to be tested, to a vapour detector. The detector should have as large a linear range as possible; a hydrogen flame ionization detector is suitable for this purpose. If efficient mixing is provided for the gas and the liquid phases within the vessel, and a volatile substance is introduced into the vessel, the relation between the concentration C_g of the substance in the gas phase and time is given by

$$\ln C_g = \ln C_{go} - \frac{U}{V_g + kV_L} \cdot t \qquad (1)$$

where C_{go} is the concentration at time $t = 0$, U the gas flow velocity and k the distribution coefficient $C_{L\,liquid}/C_{gas}$. Thus, a plot of the

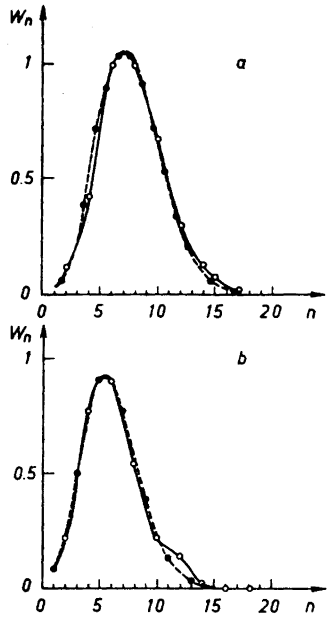

Fig. 2. The distribution of benzene between nitrogen and eucalyptol. 0.5 ml liquid phase/tube. Total amount of benzene: 0.25 ml. Room temperature. Capillary Ø: 0.4 mm. Ordinate: Amount of benzene/tube, arbitrary units. Abscissa: Tube number. O Experimental values. ● Calculated Poisson distribution assuming 1 plate/tube. a) Flow rate: 3 cm³ N_2/min. Time: 27 h. b) Flow rate: 150 cm³ N_2/min. Time: 1 h.

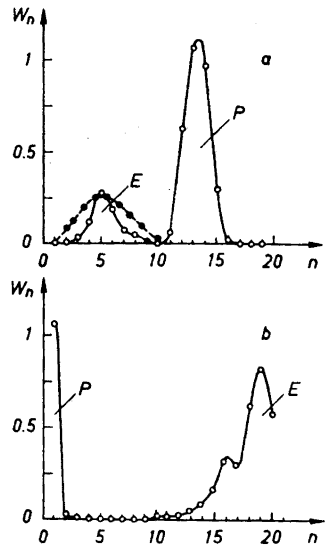

Fig. 3. Separation of ethyl ether (E) and *n*-pentane (P). Ordinate: Amount of substance/tube, arbitrary units. Abscissa: Tube number. Total amount of mixture: 20 mg. Room temperature. Capillary Ø: 2 mm. a) Mobile phase: nitrogen, flow rate 32.5 cm³/min. Stationary phase: water, 1 cm³/tube. Time: 5.5 min. O Experimental values. ● Calculated Poisson distribution assuming 1 plate/tube. b) Mobile phase: water, average flow rate 2 cm³/min. Time: 24 min. Average amount of water/tube: 1 ml. Stationary phase: air.

logarithm of the recorder signal against time gives a straight line in the case of linear distribution, and k is obtained from the slope of this line.

Some properties of the distribution apparatus described are listed below:

One plate or slightly more per tube is obtained over at least a gas velocity range of from 3 cm³/min to 150 cm³/min at room temperature when the capillaries connecting the tubes have an inner Ø of 0.4 mm (Fig. 2). With the tubes shown in Fig.1, five plates/tube have been observed (Fig. 3a). According to preliminary experiments, the gas velocity need not be more than just sufficient to overcome the rate of diffusion in the gas phase, which is rather slow.

When gas is the mobile phase, a pressure difference of 1.6 atm between the ends of the apparatus does not seem seriously to diminish the number of plates obtained, though such an effect might be expected when the distribution isotherm is influenced by pressure.

"Reversed phase" gas liquid distribution is easily performed with this apparatus (capillary Ø = 2 mm). In this case the pressure gradient has a visible effect upon the distribution owing to the compressibility of the gas; the amount of liquid per tube gradually decreases towards the end of the apparatus (Fig. 3b).

The liquid phases used must not be too viscous.

The sample is introduced into the apparatus in liquid form.

To perform a separation, a specific liquid phase is chosen with the aid of the dynamic method for the determination of distribu-

tion coefficients. With quinoline as the stationary phase (5 cm³/tube), 10 g of benzene-cyclohexane mixture (1:1) was separated in one run, the efficiency being equivalent to slightly more than one plate per tube (tube number = 20; room temperature).

To get a separation with the least possible number of tubes, use should also be made of the fact that the separation factor a^* for two compounds (1 and 2) increases with the absolute value of their distribution constants towards the limiting value given by the ratio of the distribution constants (k_1 and k_2):

$$a^* = \frac{n_1}{n_2} = \frac{V_G/V_L + k_2}{V_G/V_L + k_1} \quad (2)$$

(V_G and V_L are the gas and the liquid volumes; n_1 and n_2 are the tubes containing the maxima of compounds 1 and 2, respectively). Eqn. (2) is easily derived from the formula $V_R = n\ (V_G + kV_L)$, where V_R is the retention volume [4]. Eqn. (2) also applies if a^* is considered as the ratio between the retention volumes. The effect of the absolute values of the distribution constants, and of the volume ratio between the mobile and the stationary phases, upon the separation is exemplified by the separation of ethyl ether and *n*-pentane (Fig. 3a, b). With water as the stationary phase, their separation factor was 2.7, while with air it was about 19.

From the distribution coefficients determined, the number of plates required for a given separation is obtained by use of the following expression:

$$n_2 = \left(\frac{b}{a^* - 1}\right)^2 \quad (3)$$

$$\text{and } n = \sqrt{n_1 n_2} = \left(\frac{b}{a^* + (1/a^*) - 2}\right)^2 \quad (4)$$

Here, n_2 is the plate containing the maximum of the slower component, and b is the number of standard deviations that separates the two maxima from each other. Eqn. (3) is obtained by putting $n_1 - n_2 = b\sqrt{n_2}$ and eliminating n_1 with the aid of (2).

Purnell [5] has given a formula for the number of plates required in GLC to just separate a pair of compounds.

This formula gives higher values for the required plate number than (4). However, with the apparatus described here, experimental agreement with formula (4) has been obtained.

This work is being continued.

The author is greatly indebted to Professor A. I. Virtanen for his kind interest in this work. The investigation is a part of a research project under U. S. Public Law No. 480, 83rd Congress.

1. Bayer, E., Hupe, K. P. and Witsch, H. G. *Angew. Chem.* **73** (1961) 525.
2. Huppes, N. *Chem. Weekblad* **57** (1961) 113.
3. Lovelock, J. E. *Anal. Chem.* **33** (1961) 162.
4. Keulemans, A. I. M. *Gas Chromatography*, Reinhold, New York 1960, p. 122.
5. Purnell, J. H. *J. Chem. Soc.* **1960** 1268.

Received November 13, 1961.

A Method for Kinetic Study of "Moderately Fast" Reactions. Rate of Dissociation of Monoamminenickel(II) Ion in Aqueous Solution

CLIFFORD S. GARNER* and JANNIK BJERRUM

Department of Inorganic Chemistry, University of Copenhagen, Copenhagen, Denmark

Rates of formation and dissociation of labile complex ions are often too great at room temperature to follow by conventional methods. Semi-quantitative studies [1,2] of such reactions in methanol at low temperatures (*e.g.*, −75°C) have given useful information. For certain systems and purposes it is also desirable to investigate reactions in aqueous solution. Although excellent methods exist for the study of such "moderately fast" reactions, *e.g.*, the stopped-flow and quenched-flow methods, they involve the construction and calibration of complicated apparatus.

We report here a method adaptable for many reactions and especially useful for kinetic and equilibrium studies of formation and dissociation reactions of ammine and amine metal complexes, using only commercially available instruments. The principle is to use an appropriate non-complexing salt to depress the freezing

* John Simon Guggenheim Fellow, 1960, on leave from the University of California, Los Angeles.

tion coefficients. With quinoline as the stationary phase (5 cm³/tube), 10 g of benzene-cyclohexane mixture (1:1) was separated in one run, the efficiency being equivalent to slightly more than one plate per tube (tube number = 20; room temperature).

To get a separation with the least possible number of tubes, use should also be made of the fact that the separation factor a^* for two compounds (1 and 2) increases with the absolute value of their distribution constants towards the limiting value given by the ratio of the distribution constants (k_1 and k_2):

$$a^* = \frac{n_1}{n_2} = \frac{V_G/V_L + k_2}{V_G/V_L + k_1} \quad (2)$$

(V_G and V_L are the gas and the liquid volumes; n_1 and n_2 are the tubes containing the maxima of compounds 1 and 2, respectively). Eqn. (2) is easily derived from the formula $V_R = n\ (V_G + kV_L)$, where V_R is the retention volume [4]. Eqn. (2) also applies if a^* is considered as the ratio between the retention volumes. The effect of the absolute values of the distribution constants, and of the volume ratio between the mobile and the stationary phases, upon the separation is exemplified by the separation of ethyl ether and *n*-pentane (Fig. 3a, b). With water as the stationary phase, their separation factor was 2.7, while with air it was about 19.

From the distribution coefficients determined, the number of plates required for a given separation is obtained by use of the following expression:

$$n_2 = \left(\frac{b}{a^* - 1}\right)^2 \quad (3)$$

$$\text{and } n = \sqrt{n_1 n_2} = \left(\frac{b}{a^* + (1/a^*) - 2}\right)^2 \quad (4)$$

Here, n_2 is the plate containing the maximum of the slower component, and b is the number of standard deviations that separates the two maxima from each other. Eqn. (3) is obtained by putting $n_1 - n_2 = b\sqrt{n_2}$ and eliminating n_1 with the aid of (2).

Purnell [5] has given a formula for the number of plates required in GLC to just separate a pair of compounds.

This formula gives higher values for the required plate number than (4). However, with the apparatus described here, experimental agreement with formula (4) has been obtained.

This work is being continued.

The author is greatly indebted to Professor A. I. Virtanen for his kind interest in this work. The investigation is a part of a research project under U. S. Public Law No. 480, 83rd Congress.

1. Bayer, E., Hupe, K. P. and Witsch, H. G. *Angew. Chem.* **73** (1961) 525.
2. Huppes, N. *Chem. Weekblad* **57** (1961) 113.
3. Lovelock, J. E. *Anal. Chem.* **33** (1961) 162.
4. Keulemans, A. I. M. *Gas Chromatography*, Reinhold, New York 1960, p. 122.
5. Purnell, J. H. *J. Chem. Soc.* **1960** 1268.

Received November 13, 1961.

A Method for Kinetic Study of "Moderately Fast" Reactions. Rate of Dissociation of Monoamminenickel(II) Ion in Aqueous Solution

CLIFFORD S. GARNER* and JANNIK BJERRUM

Department of Inorganic Chemistry, University of Copenhagen, Copenhagen, Denmark

Rates of formation and dissociation of labile complex ions are often too great at room temperature to follow by conventional methods. Semi-quantitative studies [1,2] of such reactions in methanol at low temperatures (*e.g.*, −75°C) have given useful information. For certain systems and purposes it is also desirable to investigate reactions in aqueous solution. Although excellent methods exist for the study of such "moderately fast" reactions, *e.g.*, the stopped-flow and quenched-flow methods, they involve the construction and calibration of complicated apparatus.

We report here a method adaptable for many reactions and especially useful for kinetic and equilibrium studies of formation and dissociation reactions of ammine and amine metal complexes, using only commercially available instruments. The principle is to use an appropriate non-complexing salt to depress the freezing

* John Simon Guggenheim Fellow, 1960, on leave from the University of California, Los Angeles.

point of water to a temperature low enough to increase the reaction half-time to at least *ca.* 20 seconds, and to inject quickly into the equilibrium reaction system a small volume of a reagent, *e.g.* acid, which displaces the equilibrium and then to measure with a suitable detector the time rate of change to the new equilibrium state. As detector a Radiometer TTT-1 titrator has been used in conjunction with a micro syringe, electronic relay and recorder (Radiometer SBR2 Titrigraph) functioning as a potentiostat to determine the rate of addition of acid required to titrate the amine as it is released by a dissociating metal complex and thereby maintain constant the pH in the solution. This requires that a suitable EMF cell be devised that will respond rapidly to changes in the amine concentration at the low temperatures involved.

This method has been used to determine the rate constant k of the reaction:

$$NiNH_3^{2+} \rightarrow Ni^{2+} + NH_3$$

in aqueous solution at -25°C. Of those salts tested for depression of the freezing point, the most satisfactory was $Mg(NO_3)_2 \cdot 6H_2O$, which has a eutectic point at -29°C[3], and which does not form complexes with NH_3 to a considerable extent ($K_1 \sim 2$)[4]. Glass electrodes are not usable for our purpose at -25°C *, therefore a specially constructed mercuric half-cell:

$$Hg \mid Hg(NH_3)_2^{2+}, NH_3, NH_4^+ \mid$$

was used in combination with a modified calomel reference electrode (KCl solution replaced with 8.0 g $MgCl_2 \cdot 6H_2O$ in 10 ml water, usable at -29°C); this cell was found to respond rapidly at -25°C to changes in $p[NH_3]$ as well as in pH at constant ammonium ion concentration. Reaction solutions (30 ml) were made with the following molar total concentrations: $C_{Ni(NO_3)_2} = 0.100$, $C_{NH_3} = 0.00624$, $C_{NH_4NO_3} = 0.10$, $C_{Hg(NO_3)_2} = 0.000095$, $C_{Mg(NO_3)_2} = 2.7$ at -25°C, and from the data of Bjerrum [4] ($K_1/K_2 = 3.6$) estimated to have $[NiNH_3^{2+}] = 0.0058$, $[Ni(NH_3)_2^{2+}] \sim 0.0001$. To solutions of this composition 0.091 ml 0.198 M HNO_3, 2.7 M $Mg(NO_3)_2$ were rapidly injected to displace the equilibrium (pH drops abruptly from *ca.* 6 to *ca.* 3, and EMF changes by *ca.* 130 mV). The $Hg(NH_3)_2^{2+}$ present as potential indicator for NH_3 is only 1.7 % of the $NiNH_3^{2+}$ concentration, and is furthermore practically unchanged during the reaction ($K_1 \sim 10^9$, $\beta_2 \sim 10^{18}$, $\beta_3 = 10^{19}$)[4]. The rate of addition of HNO_3 (equal to the rate of dissociation of $NiNH_3^{2+}$) required to keep the pH constant was recorded by the Titrigraph. For a first-order dissociation the Titrigraph volume reading (% of syringe capacity) at time t can be shown to be

$$V\% = (100\, C_o V_R / M V_S)\,(1 - e^{-kt}),$$

where C_o = initial concentration of $NiNH_3^{2+}$, M = molarity of HNO_3 titrating agent, V_R = volume (ml) of reaction solution, and V_S = volume (ml) delivered by syringe in moving from 0 to 100 % on Titrigraph volume scale. Hence, the dissociation rate constant k can be evaluated from the Titrigraph curve. Equivalently, values of the dissociation half-time $t_{½}$ can be read directly off the Titrigraph curve by noting the times required for $V\%$ to go half-way from different arbitrary values to the infinite-time value. Since, the reaction was not carried to completion, the rate constant obtained is $(k + k')$, where k' is the pseudo first-order rate constant for the association reaction at constant $p[NH_3]$. From the complexity constant for $NiNH_3^{2+}$ at -25°, estimated from the data of Bjerrum [4] to be $K_1 = 10^{3.1}$, k' ranges from $10^{-1.4}k$ to $10^{-4.1}k$ between $p[NH_3] = 4.5$ and 7.2; thus the observed $(k + k')$ is essentially k itself.

Values of $t_{½}$ (sec) found at the pH given inside parentheses were: 70 (3.1), 70 (3.7), 64 (4.8), 54 (5.4), 70 (5.8), 59 (5.8), 63 (5.8). There is no clear trend of $t_{½}$ with pH; the range of values more likely corresponds to random errors arising from technical problems (including diffusion of reaction solution through the sintered-Pyrex disc of the reaction vessel) which could be reduced with improved design. The average $t_{½} = 64$ sec, corresponding to $k = 0.011$ sec^{-1} at -25°C.

Wilkins [6] has recently studied the dissociation of $NiNH_3^{2+}$ at 25° and 5° using a stopped-flow method with spectrophotometric detection. Under his conditions of $C_{Ni(NO_3)_2} = 0.18$, $C_{NH_3} = 0.10$, $C_{NH_4NO_3} = 0.04$, $C_{Mg(NO_3)_2} = 0$, 0.8 or 1.5 M, $t_{½} = 0.12$ sec at 25° and the Arrhenius activation energy $E_a = 14.3$ kcal. Extrapolation to

* Modified glass and calomel electrodes for use down to -30° have been reported recently [5].

$-25°$ gives $t_{½} = 16$ sec. Wilkins estimates his errors such that $t_{½} \leqslant 32$ sec at $-25°$, so there is an apparent discrepancy between his and our values. We estimate the nickel ammine concentrations in his solutions to be $[NiNH_3^{2+}] = 0.07$, $[Ni(NH_3)_2^{2+}] = 0.014$. Aside from the somewhat different conditions (especially the much higher relative concentration of $Ni(NH_3)_2^{2+}$ and lower ionic strength in Wilkins' experiments), the discrepancy may arise from a nonlinear Arrhenius plot and the long extrapolation to $-25°$; accurate experiments on first-order reactions in aqueous solution show that dE_a/dT is negative [7], which would be in the right direction to account for the difference in the two k values (*ca.* 30 % increase in E_a would be required). Either k value shows that the dissociation of $NiNH_3^{2+}$ in aqueous solution is faster, as expected, than dissociation of other Ni(II) monoamines, such as $Ni(en)^{2+}$, $Ni(bn)^{2+}$, etc.[8]

Experimental. The reaction vessel was a Pyrex half-cell having a Pt-wire electrode sealed in through the bottom and a side arm equipped with a stopcock and a G4 sintered-Pyrex disc separating the side arm from the rest of the vessel. The side arm was filled with 2.7 M $Mg(NO_3)_2$, 0.14 M NH_4NO_3 solution up to the disc, then 5.00 ml Hg delivered into the vessel and the reaction solution synthesized by careful delivery of the necessary amounts of stock solutions of $Mg(NO_3)_2$, NH_4NO_3, $Ni(NO_3)_2$, and NH_3, then water on top of the Hg (with care to avoid solution getting below the Hg meniscus) up to a mark so calibrated that, after mixing and adding the necessary amount of $Hg(NO_3)_2$ solution and cooling to $-25°C$, the volume would be 30.0 ml. The vessel was next connected via its side arm to a vial containing $Mg(NO_3)_2$ solution and stoppered with a 3-hole stopper containing the calomel electrode and a vertical tube which allowed for volume change in the vial and half-cell side arms on cooling to $-25°C$. Stopcocks in the side arms were left closed until the entire assembly, immersed in a thermostated bath at $-25.0 \pm 0.2°C$, came to bath temperature (*ca.* 20 min). The 0.5-mm ID capillary delivery tube of the 0.45-ml syringe burette (Radiometer SBU1), already filled with 0.4956 M HNO_3, 2.7 M $Mg(NO_3)_2$, was then inserted through a 3-hole rubber stopper into the reaction solution with the delivery tip *ca.* 5 mm above the Hg surface; at the same time a stirring propeller was placed through a second hole of the stopper into the reaction solution next to the delivery tip (placement of both tip and stirrer is fairly critical for proper action of the potentiostat). With the stirrer on and the potentiostat set for operation at a predetermined voltage (corresponding to a given pH), and after a further 10-min temperature equilibration (during which the EMF remained constant to < 1 mV), 0.091 ml 0.198 M HNO_3, 2.7 M $Mg(NO_3)_2$ "initiator" was injected quickly from a micropipette into the reaction solution and the Titrigraph recording switch turned to "pH-STAT-ON" and the Titrigraph allowed to maintain constant pH by controlled delivery of HNO_3 into the reaction solution at a recorded rate corresponding to the rate of release of NH_3 by the dissociating $NiNH_3^{2+}$. Recording was continued until no further HNO_3 was added by the Titrigraph. The Titrigraph was operated with chart gear A = 10 mm/rev, chart motor B = 4 rpm, pen motor C = 30 rpm and pen gear D = 2 or 4 %/rev (4 1-cm chart divisions/min, checked with a stop watch). Change in volume of the reaction solution during a run was < 1.5 %, and change in temperature from the added titrating agent was negligible. The pH at which the reaction was run could be varied by setting the controlling EMF of the potentiostat accordingly.

We thank Dr. R. G. Wilkins for his kindness in making several runs with added $Mg(NO_3)_2$ and for his permission to quote his results in advance of their publication.

1. Bjerrum, J. and Poulsen, K. G. *Nature* **169** (1952) 463.
2. Bjerrum, J., Poulsen, K. G. and Poulsen, I. *Proc. Symposium Co-ordination Chemistry*, Copenhagen, August 1953, p. 51–56.
3. Lange, N. A. (Ed.) *Handbook of Chemistry*, 9th ed., Handbook Publishers, Inc., Ohio 1956, p. 1191.
4. Bjerrum, J. *Metal Ammine Formation in Aqueous Solution*. Thesis 1941. Reprinted 1957, P. Haase and Son, Copenhagen.
5. Van den Berg, L. *Anal. Chem.* **32** (1960) 628.
6. Wilkins, R. G. *Private communication.*
7. Moelwyn-Hughes, E. A. *Physical Chemistry*, Pergamon Press, London 1957, p. 1205; 2nd ed., 1961, p. 1246.
8. Ahmed, A. K. S. and Wilkins, R. G. *Proc. Chem. Soc. (London)* **1959** 399; *J. Chem. Soc.* **1960** 2895.

Received November 29, 1961.

Bacterial Carotenoids

IX. The Constitution of the Third Member of the P481-Group (3,4-Dehydro-Rhodopin)

L. M. JACKMAN and S. LIAAEN JENSEN

Imperial College of Science and Technology, London S.W.7, England, and Organic Chemistry Laboratories, Norges Tekniske Høgskole, Trondheim, Norway

Goodwin [1,2] has shown that several species of the photosynthetic purple bacteria contain two carotenoids previously referred to as P481 and OH-P481. Work on the chemical constitution of these carotenoids has led to the suggestions of structures (I or II) for P481 [3,4,12] and (III or IV) for OH-P481 [5]. The latter carotenoid is assumed to be identical with rhodovibrin described by Karrer, Solmssen and Koenig [6-8,9,5]. On the basis of the structural relationship between rhodovibrin (III or IV) and P481 (I or II) the name anhydrorhodovibrin has been suggested for P481 [4,10].

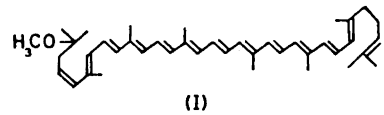

(I)

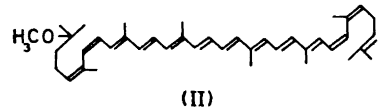

(II)

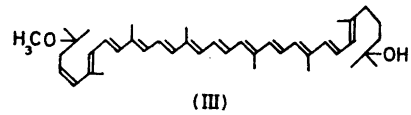

(III)

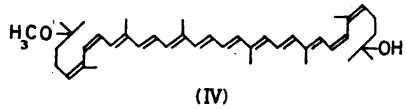

(IV)

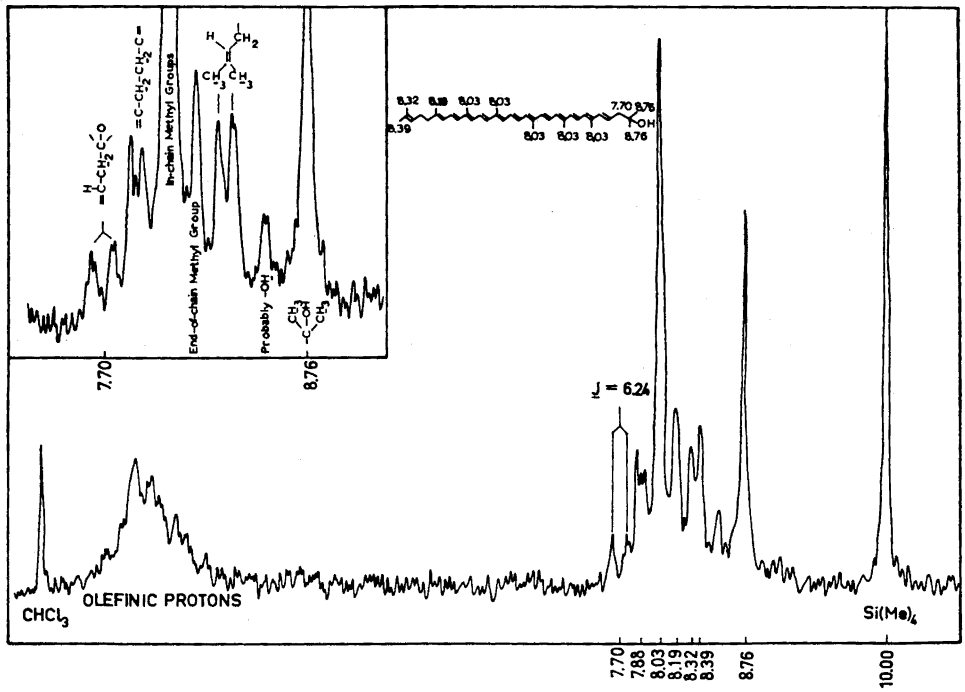

Fig. 1. The proton spectrum of 3,4-dehydro-rhodopin. 4.1 mg/0.19 ml $CDCl_3$ at 60 Mc/s.

For biochemical reasons, the structures (I) and (III), with unsymmetrically located chromophores, for anhydro-rhodovibrin and rhodovibrin respectively, have been preferred [10,11], although the chemical evidence does not support such a preference. It was hoped that conclusive evidence for the position of the chromophore could be obtained from the NMR-spectrum of rhodovibrin. Such a study was therefore performed on a specimen isolated from a strain of *Rhodopseudomonas palustris*. This strain had been isolated in pure culture by C. B. van Niel from an impure culture provided by H. Gaffron, and which Gaffron had designated as *Rhodovibrio parvus*. The isolation was carried out as described elsewhere [5,11]. The yield obtained was 11.5 mg, m.p. 186–190°C (evacuated tube), λ_{max} (358) (374) 455, 483 and 517 mμ in petroleum ether, with pronounced fine-structure, $E^{1\%}_{1\,cm} = 3\,100$ at 483 mμ.

The NMR-spectrum at 60 Mc/s, recorded in $CDCl_3$ from which traces of acid had been removed, is presented in Fig. 1. The doublet (J = 6.2 c/s.) at 7.70*, and the sharp singlet at 8.76 are characteristic of the end groups of spirilloxanthin [12,14], while the absorptions at 7.88, 8.19, 8.32 and 8.39 correspond closely to the end group absorptions of lycopene [13,15]. That the spectrum exhibits no absorption between 5.0 and 7.0 proves the absence of a methoxyl group. These facts, together with the visible light absorption data, lead unambigously to (V) as the structure of the compound investigated.

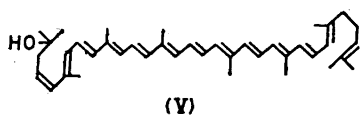

(V)

The question immediately arises as to whether this carotenoid is identical with rhodovibrin, for which structures (III or IV) had been suggested [5]. The isopropylidene value and hydrogenation data obtained for rhodovibrin [5] are not in favour of this identity. Furthermore, the infrared absorption band at 1 078 cm^{-1} (KBr), characteristic of tertiary methoxyl groups [5,11], and the methoxyl value obtained [5], would require the capture of one molecule of methanol of crystallization during the saponification procedure. To check the latter possibility, lutein, crystallized from ether-methanol, was prepared. When crystallized from this solvent lutein is known to retain one molecule of methanol per carotenoid molecule [16]. The infrared spectrum of such lutein exhibited a weak band at 1 120 cm^{-1} when measured in $CHCl_3$. This difference in the methoxyl region of the infrared spectra of lutein·CH_3OH and of rhodovibrin thus supports the contention that rhodovibrin possesses a methoxyl group.

A clear demonstration of the non-identity of (V) and rhodovibrin (III or IV) was obtained by mixed chromatography on Schleicher and Schüll No. 287 paper [17]. *Trans* rhodovibrin and *trans* (V) showed R_F-values 0.54 and 0.70, respectively, when the chromatogram was developed with 10 % acetone in petroleum ether. That this discrepancy in R_F-values was not detected before was due the similarity in other properties, together with the fact that, at the time when compound (V) was isolated, a new batch of paper with weaker adsorptive properties was used.

The elementary analysis reported for rhodovibrin [5] (C 85.88; H 10.16; O indirect 3.96; direct 3.61) was obtained on substance (V). It is seen that the result fits better with the calculated values for (V) ($C_{40}H_{56}O$: C 86.90; H 10.21; O 2.89). The calculated values for rhodovibrin ($C_{41}H_{60}O_2$) are C 84.20; H 10.34; O 5.47. Also the extinction coefficient reported for rhodovibrin [5] ($E^{1\%}_{1\,cm} = 3\,100$ at 483 mμ in petroleum ether) was measured on substance (V). For rhodovibrin itself the corresponding highest extinction value observed was $E^{1\%}_{1\,cm} = 2\,910$. Thus the molar extinction coefficients at the main maximum for compound (V) (ε = 17 110) and rhodovibrin (ε = 17 000) are in good agreement.

Compound (V) was isolated from the above mentioned strain of *Rhodopseudomonas palustris*, whereas rhodovibrin (III or IV) was isolated from *Rhodospirillum rubrum* strain 1, 1, 1, and also from *Rhodopseudomonas palustris* strain 5 (all strains of Prof. C. B. van Niels collection). An inspection of the biosynthetic scheme suggested for the transformation of lycopene to spirilloxanthin in photosynthetic purple bacteria [4,10,11], reveals that compound (V) represents the hypothetical intermediate, not isolated before. Thus there is good reason to believe that compound (V)

* Line positions are quoted as τ-values.

can be found at suitable stages of development in all the organisms where these transformations take place. The adsorptive and solubility properties of rhodovibrin (III or IV) and of (V) are probably such that under similar conditions the isolation of rhodovibrin is more readily obtained.

The compound described in this paper is the third member of the P481-group of carotenoids, and structurally is a 1,2-dihydro-3,4-dehydro-1-hydroxy-lycopene. On the basis of structure (VI) ascribed to rhodopin [18,19], it can also be considered as a 3,4-dehydro-rhodopin.

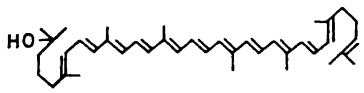

(VI)

The existence of (V) strengthens the biochemical arguments [10,11] in support of the unsymmetrical location of the chromophores in anhydro-rhodovibrin and rhodovibrin. The known members of the P481-group of bacterial carotenoids can then be represented as follows:

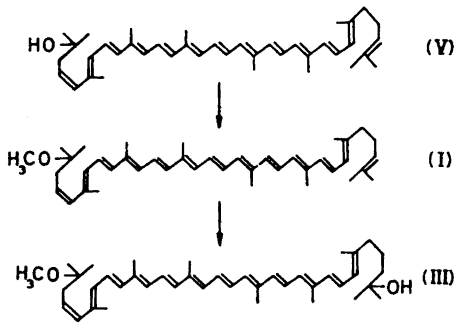

(V) (I) (III)

The biosynthetic relationship between these three members is discussed elsewhere [4,10,11].

The authors wish to stress that the isolation of 3,4-dehydro-rhodopin is wholly due to the success of Prof. C. B. van Niel, Hopkins Marine Station, Pacific Grove, California, in isolating the strain used in pure culture and to his generosity in providing dried cells for pigment extraction. One of us (SLJ) is grateful to *Norges Teknisk-Naturvitenskapelige Forskningsråd* for a maintenance grant.

1. Goodwin, T. W. *Arch. Mikrobiol.* **24** (1956) 313.
2. Goodwin, T. W. *Soc. Biol. Chemists, India. Silver Jubilee Souvenir* **1955**, 271.
3. Liaaen Jensen, S. *Acta Chem. Scand.* **12** (1958) 1698.
4. Liaaen Jensen, S. *Acta Chem. Scand.* **15** (1961) 1182.
5. Liaaen Jensen, S. *Acta Chem. Scand.* **13** (1959) 2143.
6. Karrer, P. and Solmssen, U. *Helv. Chim. Acta* **19** (1936) 3.
7. Karrer, P. and Solmssen, U. *Helv. Chim. Acta* **19** (1936) 1019.
8. Karrer, P., Solmssen, U. and Koenig, H. *Helv. Chim. Acta* **21** (1938) 454.
9. Goodwin, T. W. and Land, D. G. *Arch. Mikrobiol.* **24** (1956) 305.
10. Liaaen Jensen, S., Cohen-Bazire, G. and Stanier, R. Y. *Nature.* **192** (1961) 1167.
11. Liaaen Jensen, S. *To be published.*
12. Barber, M. S., Jackman, L. M. and Weedon, B. C. L. *Proc. Chem. Soc.* **1959** 96.
13. Barber, M. S., Davis, J. B., Jackman, L. M. and Weedon, B. C. L. *J. Chem. Soc.* **1960** 2870.
14. Jackman, L. M. *Applications of Nuclear Magnetic Resonance Spectroscopy in Organic Chemistry.* Pergamon Press, London 1959, p. 108.
15. Davis, J. B., Jackman, L. M., Siddons, P. T. and Weedon, B. C. L. *Proc. Chem. Soc.* **1961** 261.
16. Karrer, P. and Jucker, E. *Die Carotinoide.* Birkhäuser, Basel 1948, p. 207.
17. Jensen, A. and Liaaen Jensen, S. *Acta Chem. Scand.* **13** (1959) 1863.
18. Liaaen Jensen, S. *Acta Chem. Scand.* **13** (1959) 842.
19. Liaaen Jensen, S. *Acta Chem. Scand.* **13** (1959) 2142.

Received November 20, 1961.

Titration of Polythionates by Means of a Standard Sodium Hypochlorite Solution

NIELS HOFMAN-BANG and
MARGIT TANG CHRISTIANSEN

Chemistry Department A, Technical University of Denmark, Copenhagen, Denmark

Several titrimetric methods have been tried for the oxidation of polythionates to sulfate. Already in 1848 Gélis [1] used a standard sodium hypochlorite solution for the titration of sodium trithionate and barium tetrathionate. The polythionate solution was acidified and titrated with hypochlorite until the smell of chlorine was detectable or until indigo was decolourized. This method does not yield accurate results. Oxidation of polythionates with hypochlorite in excess in basic solution, addition of potassium iodide, acidifying, and backtitration with thiosulfate would seem a better possibility for an accurate method *.

Already Gélis [1] noticed that the oxidation of polythionates by means of hypochlorite is rather slow in basic solution, and he discarded the possibility of using the basic oxidation. Kitchener, Liberman and Spratt [2] have shown that basic solutions of pure hypochlorites may be boiled without decomposition. They used a solution 0.4 M with respect to sodium hydroxide and 0.1 N with respect to sodium hypochlorite, which was made by passing chlorine into the alkali until the required titre was reached. The titre of this solution was determined thiosulfatometrically, and the effect of boiling on the titre was investigated. During the first two minutes' boiling there was a loss of titre amounting to 0.7 %. Thereafter the titre remained constant within 0.1 % during a further 8 minutes' boiling. The initial loss was believed to be due to reaction with traces of dust. The hypochlorite solution could be kept for many months without appreciable change of titre when stored in a dark bottle to avoid photochemical decomposition.

The present investigation deals with the problem whether it is possible to estimate the amount of tri-, tetra- and pentathionate by oxidation with an excess of sodium hypochlorite in basic solution at 100°C, addition of iodide and sulfuric acid, and backtitration with thiosulfate. In the case of trithionate the expected reaction is

$$S_3O_6^{2-} + 4\,ClO^- + 4\,OH^- \rightarrow$$
$$4\,Cl^- + 3\,SO_4^{2-} + 2\,H_2O$$

and analogously for tetra- and pentathionate. As standards were used $K_2S_3O_6$, $K_2S_4O_6$ and $K_2S_5O_6 1\,\frac{1}{2}H_2O$, all of which correspond to the given formulae within 0.1 %.

Experimental procedure. 30 ml 0.05 M sodium hypochlorite [2] was boiled in a flask for 3 min. To the hot solution was added 20 ml of a freshly prepared solution of the polythionate (corresponding to about 2/3 of the hypochlorite used). The mixture was heated again and allowed to boil for 30 sec. After cooling with water, 2 g potassium iodide, 10 ml 2 M sulfuric acid and 200 ml oxygen-free water were added, and the iodine formed backtitrated with standard thiosulfate using starch as indicator. The hypochlorite solution was analyzed correspondingly, *i.e.* was boiled for 3 min, cooled, potassium iodide and sulfuric acid added, etc.

Results. To a first approximation dithionate is not oxidized. Trithionate is not oxidized quantitatively, but only to a degree varying from 30 to 40 %. Tetrathionate, however, is oxidized quantitatively (99.9, 99.8, 100.8 and 100.4 % was found by experiments). Pentathionate yields results which are 1.9 to 2.2 % too low. The explanation is possibly that a small percentage of dithionate is formed by the oxidation.

Conclusion. The method described yields excellent results in case of tetrathionate, whereas it cannot be used for di-, tri- and pentathionate.

* After the present investigation was carried out, Sharada and Vasudeva Murthy have published a paper "Oxidation of Polythionates with Chloramine-T", *Z. anal. Chem.* **177** (1960) 401.

1. Gélis, F. *Ann. chim. et phys.* **3** (1848) 60; *J. prakt Chem.* **43** (1848) 449.
2. Kitchener, J. A., Liberman, A. and Spratt, D. A. *Analyst* **76** (1951) 509.

Received December 4, 1961.

Inhibition of Liver Alcohol Dehydrogenase by Amides

CHARLES L. WORONICK

Medicinska Nobelinstitutet, Biokemiska avdelningen, Stockholm, Sweden

Winer and Theorell [1] have reported that fatty acid amides form complexes of the type EI ** and EIR with horse liver alcohol dehydrogenase. The saturated straight chain hydrocarbon amides from C_1 to C_6, as well as the branched chain amides isobutyramide and isovaleramide, were found to form complexes. Isobutyramide was tested for inhibition and was found to be a competitive inhibitor for acetaldehyde. The present communication reports the results of kinectic experiments using a group of amides with widely different steric and polar properties as inhibitors for acetaldehyde.

Experimental. Alcohol dehydrogenase from horse liver was prepared essentially according to the method of Bonnichsen and Brink [2], and was recrystallized 3 times. β-DPNH was purchased from Sigma. It was found to be 90 % pure by weight when based on total absorbancy at 340 mμ, and 85 % pure by weight when based on enzymatic oxidation at pH 7 in the presence of a large excess of substrate. Reagent grade salts were used for the buffer solutions. The acetaldehyde and water were redistilled from a glass still.

Some amides were purchased from commercial sources and were recrystallized 2—3 times. The following reports the amide, melting point in °C, and solvent used for recrystallization: acetamide, 81—82, ethylacetate; propionamide, 81—82, ethylacetate; isobutyramide, 129—130, $CHCl_3$; acrylamide, 85.7—86, ether; α-methylacrylamide, 110—112, ether; thioacetamide, 114—114.5, benzene-ether; fluoroacetamide, 108—109, $CHCl_3$; chloroacetamide, 121, water; trichloroacetamide, 142—143, ether-petroleum ether; iodoacetamide, 94—95.7, water.

The other amides were synthesized by adding dry NH_3 gas to an ice-cold solution of the appropriate intermediate in anhydrous ether [3]. The starting materials were commercial products. The following gives the starting material, the synthesized amide, the melting point of the amide in °C, and the solvent used for recrystallization: difluroacetic acid, difluoroacetamide [4], 51—52, $CHCl_3$; trifluoroacetic acid, trifluoroacetamide [3], 75, ether; trimethylacetic acid, trimethylacetamide [5], 160—160.5, water; tiglic acid, tiglic amide [6], 69—71, benzene; dichloroacetyl chloride, dichloroacetamide, 100, $CHCl_3$; bromoacetyl bromide, bromoacetamide, 91, $CHCl_3$; ethyldibromoacetate, dibromoacetamide, 159, ethylacetate; α,α-diethylacetyl chloride, α,α-diethylacetamide, 113.5—114, water; and *trans*-crotonyl chloride, *trans*-crotonamide, 159.5—160, $CHCl_3$.

The reactions were performed in duplicate at 23.0±0.1° in 0.11 μ sodium phosphate buffer, pH 7.15±0.05. Four to five different aldehyde concentrations were used. The reaction was followed by measuring the rate of change of fluorescence when DPNH was oxidized [7]. The enzyme concentration in the stock solution was determined by a modification of the method of Dalziel [8], in which the enzyme concentration obtained by Dalziel's method is multiplied by 0.83 as described by Theorell [9]. The enzyme concentrations in this article refer to the normality of the enzyme, a 1 M solution being 2 N with respect to the number of active sites on the enzyme molecule at pH 7 [10]. The DPNH was determined by its absorbancy at 340 mμ using an absorption coefficient of 6.22×10^6 cm^2/mole [11], and the aldehyde concentrations were determined enzymatically.

Results and dicussion. The results of these experiments, presented in Table 1, show that in almost all cases mixed inhibition occurs. The competitive inhibitor constants were determined, as decribed by Theorell *et al.*[12,13] for similar cases, from the slopes of the Lineweaver-Burk plots according to eqn. 1:

$$K_I = [I] / \frac{\text{Slope with I}}{\text{Slope without I}} - 1 \qquad (1)$$

---

* Regular Postdoctoral Fellow of the National Science Foundation, Washington, D.C.

** Abbreviations used: E = Free enzyme; I = Inhibitor; R = DPNH = Reduced diphosphopyridine nucleotide; O = DPN^+ = Oxidized diphosphopyridine nucleotide; EI, EIO, etc. = Enzyme-Inhibitor complex, Enzyme-Inhibitor-DPN^+ complex, etc.;

$K_{E,I}$, $K_{ER,I}$, etc. = [E][I]/[EI], [ER][I]/[EIR], etc.;

e = total concentration of enzyme including that combined in complexes.

Table 1. Summary of Experiments.

Expt.	[β-DPNH] μM	Amide	[Amide] mM	K_m Aldehyde mM	Observed $V_{max}/[e]$ sec^{-1}	Competitive K_I mM
I	10.4	None	0.00	0.110	41.5	—
		Acetamide	12.35		37.7	10.5
		Propionamide	12.35		16.7	0.439
		Isobutyramide	12.35		19.3	0.169
		Trimethylacetamide	12.35		20.8	2.16
II	10.1	None	0.0	0.114	40.3	—
		Chloroacetamide	12.5		28.1	6.29
		Dichloroacetamide	12.5		18.3	4.69
		Dichloroacetamide	25.0		16.6	4.78
		Trichloroacetamide	10.0		32.4	12.8
III	9.4	None	0.0	0.105	37.0	—
		Acrylamide	12.5		37.3	5.32
		α-Methylacrylamide	12.5		23.4	0.814
		α,α-Diethylacetamide	12.5		16.3	0.290
IV	9.1	None	0.0	0.105	39.4	—
		Bromoacetamide	12.5		19.2	3.86
		Iodoacetamide	12.5		9.48	1.83
V	9.4	None	0.0	0.103	36.8	—
		Tiglic amide	12.5		19.4	0.501
		Dibromoacetamide	12.5		13.2	2.72
VI	9.3	None	0.0	0.106	38.2	—
		Crotonamide	12.5		29.2	1.01
		Fluoroacetamide	62.5		27.4	31.4
		Difluoroacetamide	62.5		30.1	59.2
		Trifluoroacetamide	62.5		27.3	39.6
		Thioacetamide	125		23.8	230

The observed values for V_{max}/e were obtained from the e/v intercepts of the Lineweaver-Burk plots, and are reported without extrapolation to infinite DPNH concentration. The competitive K_I values obtained in this way are independent of the inhibitor concentration, as can be seen in the case of dichloracetamide. The maximum velocity, on the other hand, depends on the inhibitor concentration. These results can be explained on the following basis:

The increases in the slopes of the Lineweaver-Burk plots represent competition with aldehyde in the first phase of the Theorell-Chance [14] mechanism:

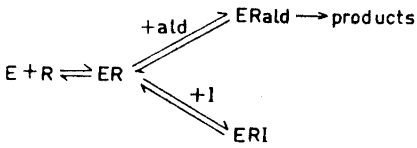

This scheme is supported by the fact that the K_I values obtained under these conditions are found to be equal, within the limits of experimental error, to $K_{ER,I}$ [15].

The changes in the intercepts of the Lineweaver-Burk plots can be explained by assuming the formation of an EOI complex in the last phase of the reaction.

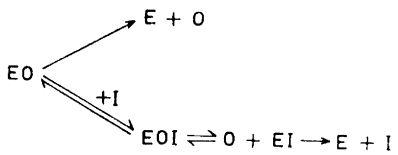

In the absence of I, the breakdown of EO is rate-limiting [14]. In the presence of I, part of the EO breaks down to E + O, and part of it forms EOI. If the breakdown of EOI in the forward direction is slower than the breakdown of EO, the observed maximum velocity will be reduced. A similar case involving an EO-imidazole complex, which breaks down at a faster rate, has been studied by Theorell [12].

The formation of an EOI complex containing an amide was not observed with the low amide concentrations employed by Winer and Theorell [1], although Theorell [12] later suggested that such a complex might form in the presence of a high concentration of amide. The data presented here indicate that EO-amide complexes do form, and that $K_{EO,I}$ is much larger than either $K_{EI,R}$ or $K_{ER,I}$ for most of the amides studied so far. In fact, $K_{EO,I}$ would appear to be of the same order of magnitude as $K_{E,I}$, thereby indicating that a mutual stabilization of I and O in the complex does not occur to any great extent. A more detailed report will be submitted for publication at a later date.

Acknowledgements. The author wishes to thank Professor Hugo Theorell for helpful discussions and advice. The technical assistance of Mr. Lars-Gunnar Falksveden is gratefully acknowledged. Financial support has been generously given by *Knut och Alice Wallenbergs Stiftelse.*

1. Winer, A. D. and Theorell, H. *Acta Chem. Scand.* **14** (1960) 1729.
2. Bonnichsen, R. K. and Brink, N. G. in Colowick, S. P. and Kaplan, N. O. *Methods in Enzymology* **1** (1955) 495.
3. Gilman, H. and Jones, R. G. *J. Am. Chem. Soc.* **65** (1943) 1458.
4. Park, J. D., Gerjovich, H. J., Lycan, W. R. and Lacher, J. R. *J. Am. Chem. Soc.* **74** (1952) 2189.
5. Gaylord, N. G. and Caul, L. D. *J. Am. Chem. Soc.* **77** (1955) 3132.
6. Barger, G., Martin, W. F. and Mitchell, W. *J. Chem. Soc.* **1937** 1820.
7. Theorell, H., Nygaard, A. P. and Bonnichsen, R. *Acta Chem. Scand.* **8** (1954) 1490.
8. Dalziel, K. *Acta Chem. Scand.* **11** (1957) 397.
9. Theorell, H. and McKinley-McKee, J. S. *Acta Chem. Scand.* **15** (1961) 1797.
10. Theorell, H. and Bonnichsen, R. *Acta Chem. Scand.* **5** (1951) 1105.
11. Horecker, B. L. and Kornberg, A. *J. Biol. Chem.* **175** (1948) 385.
12. Theorell, H. and McKinley-McKee, J. S. *Acta Chem. Scand.* **15** (1961). 1834.
13. Plane, R. A. and Theorell, H. *Acta Chem. Scand.* **15** (1961) 1866.
14. Theorell, H. and Chance, B. *Acta Chem. Scand.* **5** (1951) 1127.
15. Woronick, C. L. *Manuscript in preparation.*

Received November 21. 1961.

Notiz über die Addition von Thioharnstoff an Citraconsäure

ERIK LARSSON und
LARS-ERIK HAGERHALL

Abteilung für organische Chemie, Chemisches Institut, Universität, Lund, Schweden

Nach Andreasch [1] wird Thioharnstoff in der Mercaptoform an Citraconsäure unter Bildung eines Zwischenproduktes Ia addiert, das unter Wasserabspaltung zu Ib cyclisiert wird:

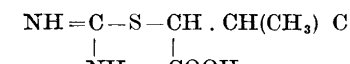

(Ia)

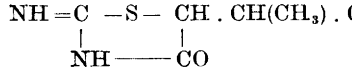

(Ib)

Die Verbindung Ib wurde zu der Mercaptosäure Ic hydrolysiert, die dann durch Benzylieren die S-Benzylmercaptosäure Id ergab:

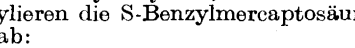

(Ic)

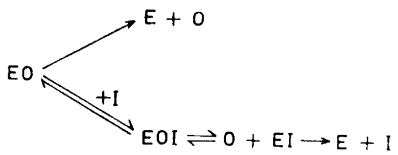

In the absence of I, the breakdown of EO is rate-limiting [14]. In the presence of I, part of the EO breaks down to E + O, and part of it forms EOI. If the breakdown of EOI in the forward direction is slower than the breakdown of EO, the observed maximum velocity will be reduced. A similar case involving an EO-imidazole complex, which breaks down at a faster rate, has been studied by Theorell [12].

The formation of an EOI complex containing an amide was not observed with the low amide concentrations employed by Winer and Theorell [1], although Theorell [12] later suggested that such a complex might form in the presence of a high concentration of amide. The data presented here indicate that EO-amide complexes do form, and that $K_{EO,I}$ is much larger than either $K_{EI,R}$ or $K_{ER,I}$ for most of the amides studied so far. In fact, $K_{EO,I}$ would appear to be of the same order of magnitude as $K_{E,I}$, thereby indicating that a mutual stabilization of I and O in the complex does not occur to any great extent. A more detailed report will be submitted for publication at a later date.

Acknowledgements. The author wishes to thank Professor Hugo Theorell for helpful discussions and advice. The technical assistance of Mr. Lars-Gunnar Falksveden is gratefully acknowledged. Financial support has been generously given by *Knut och Alice Wallenbergs Stiftelse.*

1. Winer, A. D. and Theorell, H. *Acta Chem. Scand.* **14** (1960) 1729.
2. Bonnichsen, R. K. and Brink, N. G. in Colowick, S. P. and Kaplan, N. O. *Methods in Enzymology* **1** (1955) 495.
3. Gilman, H. and Jones, R. G. *J. Am. Chem. Soc.* **65** (1943) 1458.
4. Park, J. D., Gerjovich, H. J., Lycan, W. R. and Lacher, J. R. *J. Am. Chem. Soc.* **74** (1952) 2189.
5. Gaylord, N. G. and Caul, L. D. *J. Am. Chem. Soc.* **77** (1955) 3132.
6. Barger, G., Martin, W. F. and Mitchell, W. *J. Chem. Soc.* **1937** 1820.
7. Theorell, H., Nygaard, A. P. and Bonnichsen, R. *Acta Chem. Scand.* **8** (1954) 1490.
8. Dalziel, K. *Acta Chem. Scand.* **11** (1957) 397.
9. Theorell, H. and McKinley-McKee, J. S. *Acta Chem. Scand.* **15** (1961) 1797.
10. Theorell, H. and Bonnichsen, R. *Acta Chem. Scand.* **5** (1951) 1105.
11. Horecker, B. L. and Kornberg, A. *J. Biol. Chem.* **175** (1948) 385.
12. Theorell, H. and McKinley-McKee, J. S. *Acta Chem. Scand.* **15** (1961). 1834.
13. Plane, R. A. and Theorell, H. *Acta Chem. Scand.* **15** (1961) 1866.
14. Theorell, H. and Chance, B. *Acta Chem. Scand.* **5** (1951) 1127.
15. Woronick, C. L. *Manuscript in preparation.*

Received November 21. 1961.

Notiz über die Addition von Thioharnstoff an Citraconsäure

ERIK LARSSON und
LARS-ERIK HAGERHALL

Abteilung für organische Chemie, Chemisches Institut, Universität, Lund, Schweden

Nach Andreasch [1] wird Thioharnstoff in der Mercaptoform an Citraconsäure unter Bildung eines Zwischenproduktes Ia addiert, das unter Wasserabspaltung zu Ib cyclisiert wird:

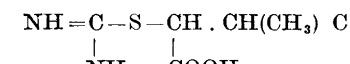

(Ia)

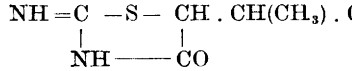

(Ib)

Die Verbindung Ib wurde zu der Mercaptosäure Ic hydrolysiert, die dann durch Benzylieren die S-Benzylmercaptosäure Id ergab:

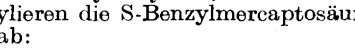

(Ic)

$$Bz \cdot S \cdot CH(COOH) \cdot CH(CH_3) \cdot COOH \quad (Id)$$

Die Bildung von Ia bedeutet, dass die Additionsrichtung des Thioharnstoffes an Citraconsäure entgegengesetzt derjenigen der Halogenwasserstoffe ist. Dieses scheint etwas eigentümlich zu sein, da die Additionsrichtungen des Thioharnstoffes und der Halogenwasserstoffe an Acrylsäure nach Behringer und Zillikens [2] dieselben sind. Eine umgekehrte Addition des Thioharnstoffes an Citraconsäure würde eine Reihe von Verbindungen IIa—IId ergeben:

$$\begin{array}{l} NH{=}C \;-S-\; C(CH_3) \cdot CH_2 \cdot COOH \\ \quad\;\; | \qquad\qquad\;\; | \\ \quad\;\; NH_2 \qquad\;\; COOH \end{array} \quad (IIa)$$

$$\begin{array}{l} NH{=}C \;-S-\; C(CH_3) \cdot CH_2 \cdot COOH \\ \quad\;\; | \qquad\qquad\;\; | \\ \quad\;\; NH \text{———} CO \end{array} \quad (IIb)$$

$$HS \cdot C(CH_3)\,(COOH) \cdot CH_2 \cdot COOH \quad (IIc)$$

$$Bz \cdot S \cdot C(CH_3)\,(COOH) \cdot CH_2 \cdot COOH \quad (IId)$$

Es gibt in Andreaschs Arbeit keinen Beweis dafür, dass die Bildung von Ia und Ib wahrscheinlicher als diejenige von IIa und IIb sein soll.

Wir haben nun das Additionsprodukt von Citraconsäure und Thioharnstoff näher untersucht. Es zeigte sich, dass es bei der Hydrolyse ein Gemisch von Mercaptosäuren ergab. Aus diesem konnte leicht eine Mercaptosäure (Ac) von der Zusammensetzung Ic oder IIc und dem Schmelzpunkt 189° abgetrennt werden. Weiter wurde eine nichtkrystallisierender Rest (Bc) erhalten, aus dem durch Benzylieren eine Säure (Bd) von der Zusammensetzung Id oder IId und dem Schmelzpunkt 152—153° erhalten wurde. Die 189°-Säure ergab durch Benzylieren ein Benzylderivat vom Schmelzpunkt 156—157° (Ad).

In der Literatur sind die folgenden Schmelzpunkte angegeben

Für Ic1 [3]	108—110°; Ic2 [3] 189—190°	(zwei *racem*-Säuren)
» IIc [4]	116—118°	
» Id1 [3]	141—142°; Id2 [3] 156—157°	(zwei *racem*-Säuren)
» IId [3]	153—154,5°	

(Id1 entspricht Ic1 und Id2 entspricht Ic2) Die drei Benzylderivate wurden nach Holmberg und Schjånberg [3] hergestellt und mit denjenigen verglichen, die aus dem nach Andreasch dargestellten Additionsprodukt erhalten wurden. Ein Vergleich der Schmelzpunkte und Bestimmung von Mischschmelzpunkten ergab, dass

Ac	die Säure	Ic2,	β-Methylthioäpfelsäure,
Ad	» »	Id2,	S-Benzyl-β-methyl thioäpfelsäure,
Bd	» »	IId,	S-Benzylthiocitramalsäure,

war. Eine gewisse Unsicherheit liegt darin, dass die Schmelzpunkte für die Benzylderivate nach Holmberg und Schjånberg [3] sowie nach unseren eigenen Erfahrungen von der Erhitzungsweise bei ihrer Bestimmung abhängig sind.

Eine Strukturbestimmung der Benzylverbindungen Ad und Bd kann man auch erhalten, in dem man ihre IR-Spektra in KBr in dem Gebiete 6,5—8 μ und 10—15 μ mit denjenigen von Id1, Id2 und IId vergleicht. Man findet, dass Ad und Bd zu mindestens 90 % aus Id2 bzw. IId bestehen. Hieraus folgt, dass Thioharnstoff an Citraconsäure in zwei Richtungen unter Bildung von Ib und IIb addiert wird. IIb wird in grösserer Menge als Ib gebildet. Die überwiegende Additionsrichtung ist entgegengesetzt der von Andreasch angenommenen.

Das Additionsprodukt aus Thioharnstoff und Citraconsäure wurde nach Andreasch [1] hergestellt.

Die Mercaptosäuren (Ac, Bc). 7,5 g (0,04 Mol) Additionsprodukt und 8,5 g (0,15 Mol) Natriumhydroxyd in 100 ml Wasser wurden während 30 Min auf dem Wasserbad erwärmt. Danach wurde das Reaktionsgemisch mit Schwefelsäure im Überschuss versetzt und mit Äther mehrmals extrahiert. Die ersten Extrakte ergaben eine nichtkrystallisierende Säure (Bc), dann folgten Extrakte, die eine Säure (Ac) vom Schmelzpunkte 189° ergab. Durch Titration der Säuren — teils direkt teils nach Zusatz von $HgCl_2$ und KBr — wurde festgestellt, dass sie Mercaptosäuren von der erwarteten Zusammensetzung waren. In drei verschiedenen Versuchen wurden Ac und Bc in einer Ausbeute von im Mittel etwa 8 + 32 = 40 % erhalten.

Das Benzylderivat Ad. 1,6 g (0,01 Mol) Ac wurden in 15 ml 2,5 N Natriumhydroxyd und 35 ml Wasser gelöst. Die Lösung wurde mit 1,3 g (0,01 Mol) Benzylchlorid versetzt und 24 Stunden geschüttelt. Danach wurde sie mit Äther extrahiert und mit Schwefelsäure im

Überschuss versetzt. Dabei fiel eine Säure aus, die nach Umkristallisation aus Wasser bei 156—157° schmolz und mit einer der bekannten S-Benzyl-β-methylthioäpfelsäuren (Id2) identisch war (Schmp, IR-Spektrum, Äquiv.-Gew.).

Das Benzylderivat Bd. Dieses wurde in derselben Weise wie Ad aus Ac dargestellt. Schmp 153—154°. Es war mit der bekannten S-Benzylthiocitramalsäure identisch (Schmp, Mischschmp, IR-Spektrum, Äquiv.-Gew.).

Gemisch der Benzylderivate Ad und Bd. 9,4 g (0,05 Mol) des Additionsproduktes in 200 ml 2 N Natriumhydroxyd (0,4 Mol) wurden 24 Stunden mit 12,7 g (0,1 Mol) Benzylchlorid geschüttelt. Die alkalische Lösung wurde mit Äther ausgeschüttelt und dann mit Schwefelsäure im Überschuss versetzt. Es fiel 9,8 g Säure aus, die nach Umkristallisieren aus Wasser-Alkohol den Schmp. 136—141° und das Äquiv.-Gew. 127,3 hatte. Das IR-Spektrum zeigte ein Gemisch der beiden Säuren Id2 und IId.

1. Andreasch, R. *Sitz.-Ber. Wiener Akad. Math.-naturwiss. Klasse II b* **56** (1897) 64.
2. Behringer, H. und Zillikens, P. *Ann.* **574** (1951) 140.
3. Holmberg, B. und Schjånberg, E. *Arkiv Kemi, Mineral Geol.* **14A** (1940) No 7.
4. Holmberg, B. *Ber.* **69** (1936) 115.

Eingegangen am 20. November 1961.